

Cardiopulmonary Monitoring

Basic Physiology, Tools,
and Bedside Management
for the Critically Ill

Sheldon Magder
Atul Malhotra
Kathryn A. Hibbert
Charles Corey Hardin
Editors

 Springer

Cardiopulmonary Monitoring

Sheldon Magder
Atul Malhotra
Kathryn A. Hibbert
Charles Corey Hardin
Editors


Cardiopulmonary Monitoring

Basic Physiology, Tools, and Bedside
Management for the Critically Ill

 Springer

Editors

Sheldon Magder
Royal Victoria Hospital
(McGill University Health
Centre), Departments of
Critical Care and Physiology
McGill University
Montreal, QC
Canada

Kathryn A. Hibbert 
Division of Pulmonary and
Critical Care Medicine
Massachusetts General Hospital
Boston, MA
USA

Atul Malhotra
UC San Diego
Department of Medicine
La Jolla, CA
USA

Charles Corey Hardin
Division of Pulmonary and
Critical Care Medicine
Massachusetts General Hospital
Boston, MA
USA

ISBN 978-3-030-73386-5 ISBN 978-3-030-73387-2 (eBook)
<https://doi.org/10.1007/978-3-030-73387-2>

© Springer Nature Switzerland AG 2021

This work is subject to copyright. All rights are solely and exclusively licensed by the Publisher, whether the whole or part of the material is concerned, specifically the rights of translation, reprinting, reuse of illustrations, recitation, broadcasting, reproduction on microfilms or in any other physical way, and transmission or information storage and retrieval, electronic adaptation, computer software, or by similar or dissimilar methodology now known or hereafter developed. The use of general descriptive names, registered names, trademarks, service marks, etc. in this publication does not imply, even in the absence of a specific statement, that such names are exempt from the relevant protective laws and regulations and therefore free for general use.

The publisher, the authors, and the editors are safe to assume that the advice and information in this book are believed to be true and accurate at the date of publication. Neither the publisher nor the authors or the editors give a warranty, expressed or implied, with respect to the material contained herein or for any errors or omissions that may have been made. The publisher remains neutral with regard to jurisdictional claims in published maps and institutional affiliations.

This Springer imprint is published by the registered company Springer Nature Switzerland AG
The registered company address is: Gewerbestrasse 11, 6330 Cham, Switzerland

This book is dedicated to the memory of Dr Brian Kavanagh who sadly died during its preparation. He was our friend, colleague, and another lover of physiology. The book is also dedicated to all the healthcare personnel who worked tirelessly and risked their own health to help others during the COVID 19 scourge.

Acknowledgements

We would like to thank all the authors of this book who spent time preparing their wonderful scholarly contributions. Together we made a whole.

SM: I would like to acknowledge Dr Maurice McGregor and Dr Solbert Permutt who shaped my thoughts and lay the basis for this book. I would also like to thank my wife Annette Lefebvre who encouraged me for years to write this book and supported me through the adventure.

AM: I would like to thank my family, my teachers, my patients and my students for providing inspiration and motivation over the years.

CCH: I am grateful to all my teachers including my co-editors and contributors to this volume.

KAH: I would like to thank all of the mentors who have so generously given their time to teaching me physiology and challenging me to find a deeper understanding. And to the many patients who have inspired me to become better in all ways.

Contents

1	Introduction: To the Love of Physiology	1
	Sheldon Magder, Atul Malhotra, C. Corey Hardin, and Kathryn A. Hibbert	
Part I Physiological Basics: Cardiovascular Basics		
2	Volume and Regulation of Cardiac Output	7
	Sheldon Magder	
3	Function of the Right Heart	21
	Sheldon Magder	
4	Function of the Left Heart	49
	Keith R. Walley	
5	Pulmonary Vascular Resistance	61
	Wayne Mitzner	
6	Fluid Filtration in the Microcirculation	71
	FitzRoy E. Curry	
7	Physiology of Heart Rate	87
	T. Alexander Quinn and Sheldon Magder	
8	Physiological Aspects of Arterial Blood Pressure	107
	Sheldon Magder	
9	Pulsatile Haemodynamics and Arterial Impedance	123
	David Fitchett and Michael F. O'Rourke	
10	Basics of Fluid Physiology	137
	Sheldon Magder and Alexandr Magder	
11	Cerebral Hemodynamics	153
	Christine E. Yeager and Thomas P. Bleck	
Part II Physiological Basics: Pulmonary Basics		
12	Stress, Strain, and the Inflation of the Lung	167
	C. Corey Hardin and James P. Butler	
13	Physiology of PEEP and Auto-PEEP	177
	John J. Marini	

14	Basics of Ventilation/Perfusion Abnormalities in Critically Ill Ventilated Patients	189
	Jeremy E. Orr and Susan R. Hopkins	
15	Control of Breathing	205
	Esteban A. Moya, Tatum S. Simonson, Frank L. Powell, Robert L. Owens, and Atul Malhotra	
16	Respiratory Muscle Blood Flow and Heart–Lung Interactions	219
	Sheldon Magder	
17	Surfactant Activity and the Pressure-Volume Curve of the Respiratory System	235
	Charles Corey Hardin, Roger G. Spragg, and Atul Malhotra	
Part III Physiological Basics: Interactions		
18	Heart-Lung Interactions	245
	Sheldon Magder and Atul Malhotra	
Part IV The Tools: Cardiovascular		
19	Evaluation of Devices for Measurement of Blood Pressure	273
	Agnes S. Meidert and Bernd Saugel	
20	Measurement of Cardiac Output	283
	Konstantinos D. Alexopoulos, Sheldon Magder, and Gordan Samoukovic	
21	Evaluations of Devices for Measurement of Cardiac Output	309
	Pierre Squara	
22	Basics of Hemodynamic Measurements	319
	Sheldon Magder	
23	Cerebral Hemodynamic Monitoring Techniques	337
	Ivan Da Silva and Thomas P. Bleck	
24	Transthoracic Echocardiography for Monitoring Cardiopulmonary Interactions	359
	Michel Slama	
25	Transesophageal Echocardiography for Monitoring Cardiopulmonary Interactions	375
	Antoine Vieillard-Baron	
26	Extra-cardiac Doppler Hemodynamic Assessment Using Point-of-Care Ultrasound	385
	William Beaubien-Souligny and André Denault	

- 27 Measurements of Fluid Requirements with Cardiovascular Challenges. 405**
Xavier Monnet and Jean-Louis Teboul
- 28 CO₂-Derived Indices to Guide Resuscitation in Critically Ill Patients. 419**
Francesco Gavelli, Jean-Louis Teboul, and Xavier Monnet
- 29 Microcirculatory Monitoring to Assess Cardiopulmonary Status 429**
Goksel Guven and Can Ince
- 30 Clinical Assessment and Monitoring of Peripheral Circulation During Shock and Resuscitation 443**
Bernardo Lattanzio and Vanina Kanoore Edul
- 31 Optimizing Oxygen Delivery in Clinical Practice 461**
Marat Slessarev and Claudio M. Martin

Part V The Tools: Respiratory

- 32 Measuring Volume, Flow, and Pressure in the Clinical Setting 473**
Jason H. T. Bates
- 33 Measurement of Pleural Pressure 485**
Nadia Corcione, Francesca Dalla Corte, and Tommaso Mauri
- 34 Ultrasound Assessment of the Lung 493**
Alberto Goffi, Emanuele Pivetta, and Richelle Kruisselbrink
- 35 Diaphragm Ultrasound: Physiology and Applications 521**
Ewan C. Goligher
- 36 Monitoring Respiratory Muscle Function 533**
Franco Laghi and Martin J. Tobin
- 37 Basics of Electrical Impedance Tomography and Its Application 585**
Christian Putensen, Benjamin Hentze, and Thomas Muders
- 38 Clinical Monitoring by Volumetric Capnography 601**
Gerardo Tusman and Stephan H. Bohm
- 39 MRI in the Assessment of Cardiopulmonary Interaction 619**
Ritu R. Gill and Samuel Patz

Part VI The Tools: Interaction

- 40 Respiratory Function of Hemoglobin: From Origin to Human Physiology and Pathophysiology 635**
Connie C. W. Hsia

41 Acid-Base and Hydrogen Ion	653
Sheldon Magder and Raghu R. Chivukula	
Part VII Applications	
42 Use of Maintenance and Resuscitation Fluids	669
Sheldon Magder	
43 Identifying and Applying Best PEEP in Ventilated Critically Ill Patients	685
Takeshi Yoshida, Lu Chen, Remi Coudroy, and Laurent J. Brochard	
44 Cardiopulmonary Monitoring in the Prone Patient	699
Hernan Aguirre-Bermeo and Jordi Mancebo	
45 Cardiopulmonary Interactions in the Management of Acute Obstructive Disease	707
Charles Corey Hardin and Julian Solway	
46 Evaluation and Management of Ventilator-Patient Dyssynchrony	715
Enrico Lena, José Aquino-Esperanza, Leonardo Sarlabous, Umberto Lucangelo, and Lluís Blanch	
47 Cardiopulmonary Monitoring in the Patient with an Inflamed Lung	729
Tommaso Tonetti and V. Marco Ranieri	
48 Ventilation During Venovenous Extracorporeal Membrane Oxygenation	741
Jacopo Fumagalli, Eleonora Carlesso, and Tommaso Mauri	
49 Vasopressor Support for Patients with Cardiopulmonary Failure	751
Daniel De Backer and Pierre Foulon	
50 Cardiogenic Shock Part 1: Epidemiology, Classification, Clinical Presentation, Physiological Process, and Nonmechanical Treatments	759
Sheldon Magder	
51 Cardiogenic Shock Part 2: Mechanical Devices for Cardiogenic Shock	793
Sheldon Magder and Gordan Samoukovic	
52 Pathophysiology of Sepsis and Heart-Lung Interactions: Part 1, Presentation and Mechanisms	821
Sheldon Magder	
53 Pathophysiology of Sepsis and Heart-Lung Interactions: Part 2, Treatment	849
Sheldon Magder and Margaret McLellan	

54	Cardiopulmonary Monitoring of Patients with Pulmonary Hypertension and Right Ventricular Failure	871
	Ryan A. Davey, Ahmed Fathe A. Alohal, Sang Jia, and Sanjay Mehta	
55	Monitoring and Management of Acute Pulmonary Embolism	905
	Jenna McNeill and Richard N. Channick	
56	Clinical Neurologic Issues in Cerebrovascular Monitoring	917
	Thomas P. Bleck	
57	Delirium in the Critically Ill Patient	923
	Alex K. Pearce, Jamie Labuzetta, Atul Malhotra, and Biren B. Kamdar	
58	Obesity in Critically Ill Patients	935
	Kathryn A. Hibbert and Atul Malhotra	
 Part VIII Epilogue		
59	The Future	951
	Sheldon Magder, Charles C. Hardin, Kathryn A. Hibbert, and Atul Malhotra	
	Index	959

Contributors

C. Corey Hardin, MD, PhD Division of Pulmonary and Critical Care Medicine, Massachusetts General Hospital, Boston, MA, USA

Hernan Aguirre-Bermeo, MD, PhD Intensive Care Unit, Hospital Santa Inés, Cuenca, Ecuador

Konstantinos D. Alexopoulos, MD Department of Critical Care, Royal Victoria Hospital – McGill University and McGill University Health Centre, Montreal, QC, Canada

Ahmed Fathe A. Alohalí, MBBS Southwest Ontario PH Clinic, Division of Respirology, London Health Sciences Centre, London, ON, Canada

Department of Medicine, Schulich School of Medicine, Western University, London, ON, Canada

Internal Medicine, Adult Pulmonary Medicine and Pulmonary Hypertension, Adult Critical Care and Cardiovascular Critical Care, King Fahad Medical City Hospital, Critical Care Services Administration, Riyadh, Kingdom of Saudi Arabia

Daniel De Backer, MD, PhD Department of Intensive Care, CHIREC Hospitals, Université Libre de Bruxelles, Brussels, Belgium

Jason H. T. Bates, Ph.D., D.sc. Department of Medicine, Larner College of Medicine, University of Vermont, Burlington, VT, USA

William Beaubien-Souligny, MD Division of Nephrology, Department of Medicine, Centre Hospitalier de l'Université de Montréal, Montreal, QC, Canada

Department of Anesthesia, Montreal Heart Institute, Université de Montréal, Montreal, QC, Canada

Lluís Blanch, MD, PhD Critical Care Center, Hospital Universitari Parc Taulí, Institut d'Investigació i Innovació Parc Taulí I3PT, Sabadell, Spain

Biomedical Research Networking Center in Respiratory Diseases (CIBERES), Instituto de Salud Carlos III, Madrid, Spain

Thomas P. Bleck, MD, MCCD Northwestern University Feinberg School of Medicine, Davee Department of Neurology, Chicago, IL, USA

Rush Medical College, Chicago, IL, USA

The Ken & Ruth Davee Department of Neurology, Northwestern University Feinberg School of Medicine, Chicago, IL, USA

Departments of Neurological Sciences, Neurosurgery, Internal Medicine, and Anesthesiology, Rush Medical College, Chicago, IL, USA

Division of Stroke and Neurocritical Care, Davee Department of Neurology, Northwestern University Feinberg School of Medicine, Chicago, IL, USA

Stephan Hubertus Bohm, MD Department of Anesthesiology and Intensive Care Medicine, Rostock University Medical Center, Rostock, Germany

Laurent J. Brochard, MD Interdepartmental Division of Critical Care Medicine, University of Toronto, St. Michael's Hospital, Toronto, ON, Canada

Keenan Research Centre for Biomedical Science, Li Ka Shing Knowledge Institute, St. Michael's Hospital, Unity Health Toronto, Toronto, ON, Canada

James P. Butler, PhD Harvard TH Chan School of Public Health and Harvard Medical School, Boston, MA, USA

Eleonora Carlesso, MSc Dipartimento di Fisiopatologia Medico-Chirurgica e dei Trapianti, Università degli Studi di Milano, Milan, Italy

Richard N. Channick, MD UCLA Medical Center, UCLA David Geffen School of Medicine, Pulmonary and Critical Care Division, Los Angeles, CA, USA

Lu Chen, MD Interdepartmental Division of Critical Care Medicine, University of Toronto, St. Michael's Hospital, Toronto, ON, Canada

Keenan Research Centre for Biomedical Science, Li Ka Shing Knowledge Institute, St. Michael's Hospital, Unity Health Toronto, Toronto, ON, Canada

Raghu R. Chivukula, M.D., Ph.D. Harvard Medical School, Massachusetts General Hospital, Division of Pulmonary and Critical Care Medicine, Department of Medicine, Boston, MA, USA

Nadia Corcione Department of Anesthesia, Critical Care and Emergency, Fondazione IRCCS Ca' Granda Ospedale Maggiore Policlinico, University of Milan, Milan, Italy

Francesca Dalla Corte Department of Anesthesia, Critical Care and Emergency, Fondazione IRCCS Ca' Granda Ospedale Maggiore Policlinico, University of Milan, Milan, Italy

Remi Coudroy, PhD Interdepartmental Division of Critical Care Medicine, University of Toronto, St. Michael's Hospital, Toronto, ON, Canada

Keenan Research Centre for Biomedical Science, Li Ka Shing Knowledge Institute, St. Michael's Hospital, Unity Health Toronto, Toronto, ON, Canada

FitzRoy E. Curry, BE, PhD Department of Physiology and Membrane Biology, School of Medicine, University of California, Davis, CA, USA

Ryan A. Davey, MD, FRCPC, FACC St. Josephs Hospital PH Clinic, London, ON, Canada

Heart Failure Service, Division of Cardiology, London Health Sciences Centre and St. Josephs Healthcare Centre, London, ON, Canada

André Denault, MD, PhD Department of Anesthesia, Montreal Heart Institute, Université de Montréal, Montreal, QC, Canada

Division of Intensive Care, Montreal Heart Institute, Université de Montréal, Montreal, QC, Canada

Division of Intensive Care, Centre Hospitalier de l'Université de Montréal, Montreal, QC, Canada

Vanina Kanoore Edul, MD, PhD Facultad de Ciencias Médicas, Universidad Nacional de La Plata, Cátedra de Farmacología Aplicada, La Plata, Argentina

Intensive Care Department, Hospital Juan A. Fernández, Buenos Aires, Argentina

José Aquino-Esperanza, MD Critical Care Center, Hospital Universitari Parc Taulí, Institut d'Investigació i Innovació Parc Taulí I3PT, Sabadell, Spain

Universitat de Barcelona, Facultat de Medicina, Barcelona, Spain

Biomedical Research Networking Center in Respiratory Diseases (CIBERES), Instituto de Salud Carlos III, Madrid, Spain

David Fitchett, MD, FRCP© Department of Cardiology, St Michael's Hospital, University of Toronto, Toronto, ON, Canada

Pierre Foulon Department of Intensive Care, CHIREC Hospitals, Université Libre de Bruxelles, Brussels, Belgium

Jacopo Fumagalli, MD Dipartimento di Fisiopatologia Medico-Chirurgica e dei Trapianti, Università degli Studi di Milano, Milan, Italy

Fondazione IRCCS Ca' Granda Ospedale Maggiore Policlinico, Department of Anesthesia, Critical Care and Emergency, Milano, Italy

Francesco Gavelli, MD Université Paris-Saclay, AP-HP, Service de médecine, intensive-réanimation, Hôpital de Bicêtre, DMU CORREVE, Inserm UMR S_999, FHU SEPSIS, Groupe de recherche clinique CARMAS, Le Kremlin-Bicêtre, France

Emergency Medicine Unit, Department of Translational Medicine, Università degli Studi del Piemonte Orientale, Novara, Italy

Ritu R. Gill, MD, MPH Department of Radiology, Beth Israel Deaconess Medical Center, Harvard Medical School, Boston, MA, USA

Alberto Goffi, MD Interdepartmental Division of Critical Care Medicine, University of Toronto, Toronto, ON, Canada

Department of Medicine and Department of Critical Care Medicine, St. Michael's Hospital, Toronto, ON, Canada

Li Ka Shing Knowledge Institute, St. Michael's Hospital, Toronto, ON, Canada

Ewan C. Goligher, MD, PhD Interdepartmental Division of Critical Care Medicine, University of Toronto, Toronto, ON, Canada

Department of Medicine, Division of Respiriology, University Health Network, Toronto, ON, Canada

Toronto General Hospital Research Institute, Toronto, ON, Canada

Goksel Guven, MD Department of Intensive Care, Erasmus MC University Medical Centre, Rotterdam, The Netherlands

Charles Corey Hardin, MD, PhD Division of Pulmonary and Critical Care Medicine, Massachusetts General Hospital, Boston, MA, USA

Benjamin Hentze, Dipl.-Ing Department of Anesthesiology and Intensive Care Medicine, University Hospital Bonn, Bonn, Germany

Kathryn A. Hibbert, MD Division of Pulmonary and Critical Care Medicine, Massachusetts General Hospital, Boston, MA, USA

Susan R. Hopkins, MD, PhD Department of Medicine and Radiology, University of California, San Diego, La Jolla, CA, USA

Connie C. W. Hsia, MD Department of Internal Medicine, Pulmonary and Critical Care Medicine, University of Texas Southwestern Medical Center, Dallas, TX, USA

Can Ince, PhD Department of Intensive Care, Erasmus MC University Medical Centre, Rotterdam, South Holland, The Netherlands

Sang Jia, MD Department of Medicine, University of Manitoba, Winnipeg, MB, Canada

Biren B. Kamdar, MD, MBA, MHS Division of Pulmonary, Critical Care, Sleep Medicine and Physiology, University of California San Diego, La Jolla, CA, USA

Richelle Kruisselbrink, BMus MD FRCPC Department of Anesthesia, Grand River Hospital and St. Mary's General Hospital, Kitchener, ON, Canada

Department of Anesthesia, McMaster University, Hamilton, ON, Canada

Jamie Labuzetta, MD, MSc, MPhil Division of Neurocritical Care, Department of Neurosciences, University of California San Diego, La Jolla, CA, USA

Franco Laghi, MD Division of Pulmonary and Critical Care Medicine, Hines Veterans Administration Hospital, Hines, IL, USA

Loyola University of Chicago Stritch School of Medicine, Maywood, IL, USA

Bernardo Lattanzio, MD Facultad de Ciencias Médicas, Universidad Nacional de La Plata, Cátedra de Farmacología Aplicada, La Plata, Argentina
Critical Care Unit, Clínica Bazterrica y Santa Isabel, Buenos Aires, Argentina

Enrico Lena, MD Department of Perioperative Medicine, Intensive Care and Emergency, Cattinara Hospital, Trieste University, Trieste, Italy

Umberto Lucangelo, MD Department of Perioperative Medicine, Intensive Care and Emergency, Cattinara Hospital, Trieste University, Trieste, Italy

Alexandr Magder, MD, B.Sc Department of Pediatrics, Bernard and Millie Duker Childrens Hospital, Albany Medical Center, Albany, NY, USA

Sheldon Magder, MD Royal Victoria Hospital (McGill University Health Centre), Departments of Critical Care and Physiology McGill University, Montreal, QC, Canada

Atul Malhotra, MD UC San Diego, Department of Medicine, La Jolla, CA, USA

Jordi Mancebo, MD, PhD Intensive Care Unit, Hospital de la Santa Creu i Sant Pau, Barcelona, Spain

John J. Marini, MD, BES University of Minnesota, Minneapolis, MN, USA

Claudio M. Martin, MSc, MD, FRCPC Division of Critical Care Medicine, Department of Medicine, University of Western Ontario, London, ON, Canada

Tommaso Mauri, MD Department of Anesthesia, Critical Care and Emergency, Fondazione IRCCS Ca' Granda Ospedale Maggiore Policlinico, University of Milan, Milano, Italy

Dipartimento di Fisiopatologia Medico-Chirurgica edei Trapianti, Università degli Studi di Milano, Milano, Italy

Dipartimento di Anestesia, Rianimazione ed Emergenza, Fondazione IRCCS Ca' Granda Ospedale Maggiore Policlinico, Milano, Italy

Agnes S. Meidert, MD Department of Anaesthesiology, University Hospital of Munich (LMU), Munich, Germany

Margaret McLellan, MD, FRCPC Department of Anesthesia and Critical Care, McGill University and McGill University Health Centre, Montreal, QC, Canada

Jenna McNeill, MD Massachusetts General Hospital, Department of Pulmonary and Critical Care, Boston, MA, USA

Sanjay Mehta, MD, FRCPC Southwest Ontario PH Clinic, Division of Respiriology, London Health Sciences Centre, London, ON, Canada

Department of Medicine, Schulich School of Medicine, Western University, London, ON, Canada

Pulmonary Hypertension Association (PHA) of Canada, Vancouver, BC, Canada

Western University, London Health Sciences Centre, Department of Medicine/Respirology, Victoria Hospital, London, ON, Canada

Wayne Mitzner, PhD Department of Environmental Health & Engineering, Johns Hopkins Bloomberg School of Public Health, Baltimore, MD, USA

Xavier Monnet, MD, PhD Université Paris-Saclay, AP-HP, Service de médecine intensive-réanimation, Hôpital de Bicêtre, DMU CORREVE, Inserm UMR S_999, FHU SEPSIS, Groupe de recherche clinique CARMAS, Le Kremlin-Bicêtre, France

Esteban A. Moya, PhD Section of Physiology, Division of Pulmonary, Critical Care & Sleep Medicine, Department of Medicine, University of California San Diego, La Jolla, CA, USA

Thomas Muders, MD, DESA Department of Anesthesiology and Intensive Care Medicine, University Hospital Bonn, Bonn, Germany

Michael F. O'Rourke, MD DSc St. Vincent's Hospital, Department of Cardiology, St Vincent's Clinic, Sydney, NSW, Australia

Jeremy E. Orr, MD Department of Medicine, Division of Pulmonary Critical Care and Sleep Medicine, University of California, La Jolla, CA, USA

Robert L. Owens, MD University of California San Diego, Division of Pulmonary, Critical Care, and Sleep Medicine, Department of Medicine, La Jolla, CA, USA

Samuel Patz, PhD Department of Radiology, Harvard Medical School, Brigham & Women's Hospital, Boston, MA, USA

Alex K. Pearce, MD Division of Pulmonary, Critical Care, Sleep Medicine and Physiology, University of California San Diego, La Jolla, CA, USA

Emanuele Pivetta, M.D., M.Sc., Ph.D Division of Emergency Medicine and High Dependency Unit, Department of Medical Sciences, University of Turin, Turin, Italy

Cancer Epidemiology Unit and CRPT U, Department of Medical Sciences, University of Turin, Turin, Italy

Frank L. Powell, PhD Section of Physiology, Division of Pulmonary, Critical Care & Sleep Medicine, Department of Medicine, University of California San Diego, La Jolla, CA, USA

Christian Putensen, MD Department of Anesthesiology and Intensive Care Medicine, University Hospital Bonn, Bonn, Germany

T. Alexander Quinn, PhD Dalhousie University, Department of Physiology & Biophysics, Halifax, NS, Canada

V. Marco Ranieri, MD Alma Mater Studiorum – Università di Bologna, Dipartimento di Scienze Mediche e Chirurgiche, Anesthesia and Intensive Care Medicine, IRCCS Policlinico di Sant'Orsola, Bologna, Italy

Gordan Samoukovic, MD, MSc, FRCPC, FRCSC, FASE Department of Critical Care, Royal Victoria Hospital – McGill University and McGill University Health Centre, Montreal, QC, Canada

Leonardo Sarlabous, PhD Critical Care Center, Hospital Universitari Parc Taulí, Institut d'Investigació i Innovació Parc Taulí I3PT, Sabadell, Spain
Biomedical Research Networking Center in Bioengineering, Biomaterials and Nanomedicine (CIBER-BBN), Instituto de Salud Carlos III, Madrid, Spain

Bernd Saugel, MD Department of Anesthesiology, Center of Anesthesiology and Intensive Care Medicine, University Medical Center Hamburg-Eppendorf, Hamburg, Germany

Ivan Da Silva, MD, PhD Rush Medical College, Chicago, IL, USA
Rush University Medical Center, Department of Neurological Sciences, Chicago, IL, USA

Tatum S. Simonson, M.D., Ph.D. Section of Physiology, Division of Pulmonary, Critical Care & Sleep Medicine, Department of Medicine, University of California San Diego, La Jolla, CA, USA

Michel Slama, MD, PhD Medical Critical Care Unit, Amiens University Hospital, Amiens, France

CHU Sud Amiens Hospital, Department of Medical Intensive Care, Place du Professeur Christian Cabrol, Amiens, France

Marat Slessarev, MD, MSc FRCPC Division of Critical Care Medicine, Department of Medicine, University of Western Ontario, London, ON, Canada

Julian Solway, MD Department of Medicine, Section of Pulmonary/Critical Care, University of Chicago, Chicago, IL, USA

Roger G. Spragg, MD Division of Pulmonary, Critical Care and Sleep Medicine, University of California San Diego, La Jolla, CA, USA

Pierre Squara, MD ICU and Cardiology Department, Clinique Ambroise Paré, Neuilly-sur-Seine, Hauts de Seine, France

Jean-Louis Teboul, MD, PhD Université Paris-Saclay, AP-HP, Service de médecine intensive-réanimation, Hôpital de Bicêtre, DMU CORREVE, Inserm UMR S_999, FHU SEPSIS, Groupe de recherche clinique CARMAS, Le Kremlin-Bicêtre, France

Martin J. Tobin, MD Division of Pulmonary and Critical Care Medicine, Hines Veterans Administration Hospital, Hines, IL, USA

Tommaso Tonetti, MD Alma Mater Studiorum – Università di Bologna, Dipartimento di Scienze Mediche e Chirurgiche, Anesthesia and Intensive Care Medicine, IRCCS Policlinico di Sant'Orsola, Bologna, Italy

Gerardo Tusman, MD Department of Anesthesiology, Hospital Privado de Comunidad, Mar del Plata, Buenos Aires, Argentina

Antoine Vieillard-Baron, MD, PhD Publique-Hôpitaux de Paris, University Hospital Ambroise Paré, Intensive Care Unit, Boulogne-Billancourt, France

Medical and Surgical Intensive Care Unit, University Hospital Ambroise Paré, APHP, Boulogne-Billancourt, France

Keith R. Walley, MD Division of Critical Care Medicine, Centre for Heart Lung Innovation, University of British Columbia, St. Paul's Hospital, Vancouver, BC, Canada

Christine E. Yeager, MD Department of Neurology, University of Minnesota, Minneapolis, MN, USA

Takeshi Yoshida, MD, PhD Osaka University Graduate School of Medicine, Department of Anesthesiology and Intensive Care Medicine, Yamadaoka, Suita, Osaka, Japan

Interdepartmental Division of Critical Care Medicine, University of Toronto, St. Michael's Hospital, Toronto, ON, Canada

Keenan Research Centre for Biomedical Science, Li Ka Shing Knowledge Institute, St. Michael's Hospital, Unity Health Toronto, Toronto, ON, Canada



Introduction: To the Love of Physiology

1

Sheldon Magder, Atul Malhotra, C. Corey Hardin,
and Kathryn A. Hibbert

We begin this introduction to *Cardiopulmonary Monitoring: Basic Physiology, Tools, and Bedside Management* with a statement of bias. We love physiology. It is why we are intensivists. Physiology is at the core of our approach to management of our critically ill patients, and managing critically ill patients provides continuous feedback for our understanding of physiological processes. It is for this reason that physiological considerations are the central part of this book.

We hope that the reader will find the chapters enlightening and will be able to access important information from a single source. In the process of putting together this book, we sought out authors who share our belief in the importance of physiology in the management of the critically ill. These authors have made important contributions to our understanding of the underlying pro-

cesses and how to better manage them. Our objective was to immortalize these fundamental concepts in a single source to ensure their availability to the critical care community.

The first section of the book deals with the underlying fundamental physiological concepts that we believe are necessary for rational management of the critically ill. The chapters are grouped into sections addressing the cardiovascular and respiratory systems with a smaller “overlap” section. A theme throughout the book, though, is that the cardiovascular and respiratory systems are always interacting, and in the final analysis of pathological processes, both must be considered. Some of the concepts in this section are repeated in parts two and three because some review is inevitably necessary to understand the applications. The second section deals with the tools that are available to monitor critically ill patients. It again is divided into separate sections that deal with the cardiovascular and respiratory systems. The third section provides the clinical integration of the physiologic concepts from the first section with the data available from the tools described in the second section. The objective of the third section is to provide a rational physiological approach to the management of the critically ill. An underlying principle in this section is that clinical responses only can be in the realm of the physiologically possible.

A few words about what we have not included in this book. We have chosen not to include more cellular and molecular science in these chapters.

S. Magder (✉)

Royal Victoria Hospital (McGill University Health Centre), Departments of Critical Care and Physiology
McGill University, Montreal, QC, Canada
e-mail: sheldon.magder@mcgill.ca

A. Malhotra

UC San Diego, Department of Medicine,
La Jolla, CA, USA
e-mail: amalhotra@health.ucsd.edu

C. C. Hardin · K. A. Hibbert

Division of Pulmonary and Critical Care Medicine,
Massachusetts General Hospital, Boston, MA, USA
e-mail: Charles.hardin@mgh.harvard.edu;
KAHIBBERT@mgh.harvard.edu

We are big believers in the advances molecular sciences have brought and fully appreciate the myriad ways in which knowledge of a particular molecule or receptor is illuminating. However, understanding integrated function is crucial for overall understanding of patient pathophysiology. In the end, biochemical processes have their effects by altering organ functions, and it is necessary to know how those organ functions affect the overall homeostasis of the body. We note that the majority of improvements in patient care in the ICU have not come from molecular studies divorced from the larger context, but rather from the better understanding of the underlying physiology and unified pathophysiological processes. As such, we argue that physiology is not dead but is alive and well, and we emphasize that integrated function is what should guide bedside decisions and management.

We have also not spent much time in this book discussing evidence from clinical trials. Clinical trials are clearly essential for the rigorous practice of medicine, but we also recognize that the majority of clinical trials in the ICU have failed to show positive outcomes. We do not regard these observations as a failure, but rather as a reminder of the complexity of ICU patients. Furthermore, a failed trial still provides information – in this case what is not useful, or at least not useful the way the study was done. Understanding why a trial is negative thus can lead us to generate new hypothesis on how best to treat our patients. Moreover, negative trials have been instrumental in identifying important sources of heterogeneity (e.g., high PEEP in ARDS). Beyond study design failure, a strong understanding of the underlying physiology may give new insights into why the trial results were negative and therefore how to better approach the problem in the future.

As physicians working in the intensive care unit, we have the privilege of being able to observing the basic physiology constantly unfold in front of us. Bedside tools we have today allow us to make measurements that previously only could have been possible in an animal laboratory.

A basic part of the approach to a clinical problem is the generation of a hypothesis to explain the observed pathology. As clinicians, we act on that hypothesis by performing tests that give results that are either consistent with the hypothesis or inconsistent, in which case we consider rejecting the hypothesis or modifying it. We also apply treatments that are thought to be effective for the hypothesized disordered process. The information from our monitoring tools give us constant feedback of the response to the treatments that we have tried. This allows us to constantly test whether or not our hypothesis is correct. Therapy then can be adjusted based on the response. This approach can be called “responsive therapy” rather than goal-directed therapy. As a final step, good clinicians should always consider whether or not the patient’s outcome is consistent with the initial beliefs, and by this process clinicians should constantly modify their understanding of human biology so as to manage the next patient better.

When choosing the authors and topics of this book, our goal was to summarize classic concepts that are not always easy to find in traditional textbooks or in the literature. In addition, we sought to bring new concepts and techniques to the reader which were not available when some of the classics were completed.

We have learned many of these concepts over the years by talking to colleagues, drawing on the backs of napkins and piecing together studies from the literature. However, the strongest source for our knowledge has come from the day to day management of patients. This approach has provided constant feedback of proposed theories. When the bedside experience contradicts the common belief, it has led us to review the underlying source of these beliefs and to discuss our experiences with colleagues. Knowledge is not static and needs to be constantly modified by experience. An important principle in biological science is that unlike mathematics, physics, and chemistry, nothing is always precisely the same. Exceptions are what allows biological species to evolve. For this reason, we must remember that our patients are rarely the “mean” value but

instead they are some standard deviation from that value. The exceptions also allow us to better understand the rules that determine normal function. The key to being a good clinician, and to being a good clinical scientist, is to constantly observe and reflect on what is seen at the bedside.

We view this book as a consolidation of this knowledge and hope that this book provides a legacy for concepts that we hope will never be lost. If even a portion of the readers of the book help pass the knowledge along to the next generation, we would view the book as a major success. Enjoy the reading.

Part I

Physiological Basics: Cardiovascular Basics



Volume and Regulation of Cardiac Output

2

Sheldon Magder

A fundamental biological need for all animals is that there be sufficient delivery of oxygen and nutrients to tissues and removal of metabolic wastes. In single-cell organisms, this occurs by simple diffusion of substances across the cell wall, as well as membrane channels and active transport mechanisms. In initial multicellular organisms (\approx approximately 800–700 million years ago), this occurred by circulation of sea water, nutrient absorption, and reproduction, all being combined in pathways through the organisms (Moorman and Christoffels 2003; Bishopric 2005; Pascual-Anaya et al. 2013). When a symmetric body plan evolved, a passage formed through the center of the organism. This channel had pulsatility but no directionality to flow. Insects developed an early cardio-aortic valve and pericardial cells which allowed directionality of fluid flow; however, they still did not have a separate gas exchange system (\approx 600 million years ago) (Bishopric 2005). It is at the level of Chordata, \approx 550 million years ago, that the gut and gas exchange units separated and there was development of early myocardial cells and the beginning of the cardiovascular system (Xavier-Neto et al. 2007). With the evolution of vertebrates around 550 million years ago, the full

circulatory system began to develop (Simoes-Costa et al. 2005). This started with a single ventricle and no separate pulmonary circulation. The final development of the mammalian and avian circulations with a four chamber heart and fully separated pulmonary and systemic circulations occurred between 220 and 170 million years ago and is thus a very late development in the history of evolution (Bishopric 2005).

Flow through a closed circuit is governed by three variables: pressure, volume, and time. These are related to each other through two primary relationships: the pressure-volume relationship, which describes the elastic properties of the compartments of the system, and the pressure-flow relationship, which describes the resistance to flow between compartments. These two primary relationships also describe movements of air in the respiratory system and thus this analysis of pressure-volume and pressure-flow for the circulation has direct parallels to volume and flow in the respiratory system. A principle underlying the discussion in this chapter is that the volume that stretches the elastic structures of the vasculature is the key independent variable for the flow of blood (Magder 2016). This volume is called stressed volume and over the short run is constant, although it can be increased by intake or loss (Magder and De Varennes 1998; Rothe 1983a). Stretch of the elastic walls of vascular structures by the stressed volume creates pressures in the system; importantly, the pressure

S. Magder (✉)

Royal Victoria Hospital (McGill University Health Centre), Departments of Critical Care and Physiology
McGill University, Montreal, QC, Canada
e-mail: sheldon.magder@mcgill.ca

does not determine the volume but rather the volume determines the pressure. Pressure is present with or without flow. However, when the pressure created by the volume in one region is greater than the pressure in a downstream compartment, flow occurs. Some of these concepts have been reviewed previously (Magder 2016; Magder and Scharf 2001).

Pressure-Volume Relationship

The force created by stretching walls of vascular structures is based on Hooke's law, which says that if a substance is homogeneous, stress increases linearly with a change in the length (Fig. 2.1). Below a certain length, elastic structures do not have a tension. Tension only arises when the substance is straightened to a length above which the substance is stretched. This length is called L_0 (Fig. 2.1a). The slope of a plot of a change in stress against change in length is called elastance. This can be thought of as a "recoil" force; when the force stretching the structure is released, the substance snaps back to the resting length.

In curved vascular structures, stress is described by the term pressure, which is the force over the surface area (Fig. 2.1b). The

inverse of elastance is compliance. Elastance and compliance will be used interchangeably in this chapter, but in general, I will use compliance when considering the uptake of volume and elastance when discussing the expulsion of volume. Elastance and compliance are static measurements, which means that they must be measured under steady state condition. If not, the measured pressure includes resistive and inertial components of the force. In the physiological range, the elastance of veins is linear, but at low pressures, it is curvilinear because some vessels collapse, which decreases the overall surface area (Fig. 2.1b) and because of inhomogeneities of components of the vessel walls. At high pressures, the elastance of arterial vessels increases, i.e., the slope becomes steeper (see Chap. 8 on blood pressure), whereas in veins the slope is curvilinear at low volumes because new channels open, but venous compliance is linear in the physiological range.

The compliance (elastance) of the walls of vessels is a function of the properties of the wall, specifically the collagen and elastin, and it does not change acutely. A change requires changes in the matrix of the wall, which takes time. The total compliance of a system that has compartments in a row that have different compliances is simply the sum of the compliances of each compartment

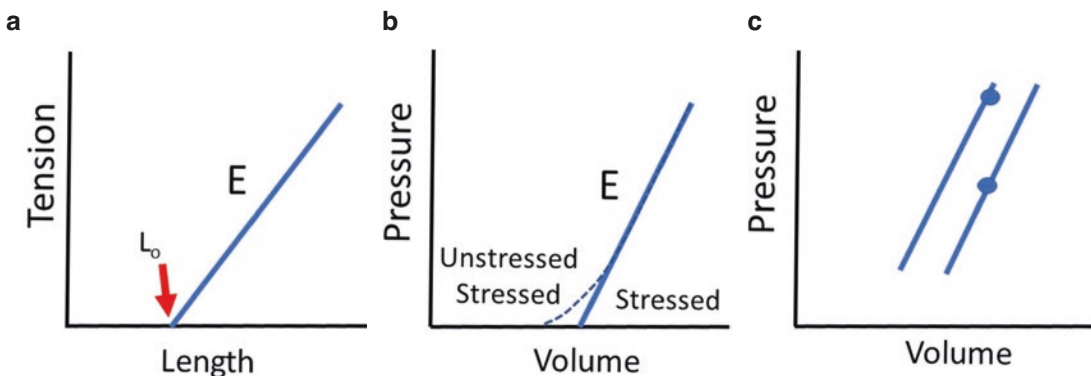


Fig. 2.1 Pressure volume relationships. The first panel (a) shows the change in tension for change in length as per Hooke's law. If the substance is homogeneous, the slope is linear. It starts from an unstretched length (L_0). The slope of the line is elastance (E , elastic modulus), which is the constant for the relationship. In the middle panel (b), the length

is replaced by volume (L^3) and the tension by pressure (force per cross-sectional area). The slope is still elastance. The right panel (c) shows a decrease in capacitance. The vessels' circumference is reduced by contraction of vascular smooth muscle, which shifts the elastance curve to the left. The same volume (circles) now has a greater pressure

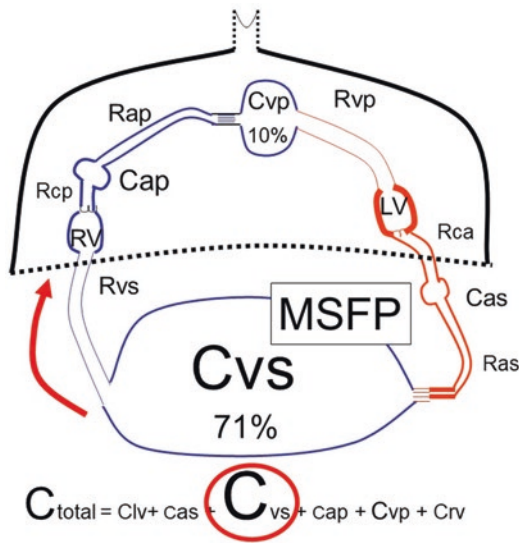


Fig. 2.2 General schema of the circulation. The six regions are roughly drawn in proportion to their size. Regions above the dotted line are in the thorax. C refers to the compliance and R to the resistance. RV = right ventricle, LV = left ventricle, vs = systemic venous compartment, ap = pulmonary arterial compartment, vp = pulmonary venous compartment, as = systemic arterial compartment. When flow is zero, 71% of volume is in the systemic venous compartment (for a total stressed volume, this is 1022 ml) and 10% in the pulmonary venous compartment (137 ml). The total compliance (C_{total}) is the sum of the compliances of the six regions

(Fig. 2.2). Thus, the total compliance of the circulatory system is the sum of the compliance of the arterial, arteriolar, capillary, small veins, large veins, and the pulmonary components. However, the compliance of venules and veins is 40 times that of the arterial compartment. Although the capillaries have a very large cross section area, their compliance, too, is very low, and thus the venous compartments dominate the magnitude of the overall vascular compliance (Permutt and Caldini 1978; Guyton et al. 1956). As will be seen later, this allows for a “lumped parameter” model for the analysis of cardiac output, which leaves out the compliance of the arterial system. This simplification produces about a 10% error in the quantitative analysis but makes the mathematical analysis much simpler.

Capacitance

Total blood volume in a 70- to 75-kg male is in the range of 5.5 L, but not all of the blood volume stretches vessel walls and creates the pressure in vessels; a portion of the volume just makes vessels round. This portion of blood volume is called unstressed volume and it is the equivalent of the x -intercept (L_0) in Hooke’s assessment of tension versus length (Rothe 1983a, b) (Fig. 2.1). As already noted, the proportion of volume that stretches vessel walls and creates the pressure in vessels is called stressed volume (Rothe 1983a). Under conditions of minimum vascular tone in humans and in animal studies, the stressed portion of blood volume is approximately 30% of the total blood volume (Magder and De Varennes 1998). This means that only about 1.3–1.4 L of blood volume actually is involved in making the blood go around.

The advantage of having a reserve of unstressed volume is that this volume can be recruited into stressed volume by contraction of the vascular smooth muscle in the walls of veins and venules (Drees and Rothe 1974). This occurs primarily in the splanchnic circulation. Importantly, a change in capacitance changes the position of the vascular volume-pressure curve, but it does not affect the slope of the relationship, which is $1/\text{compliance}$ (Fig. 2.1c). A strong sympathetic discharge through baroreceptor mechanisms can recruit from 10 to 18 ml/kg of unstressed into stressed volume and this occurs in seconds (Deschamps and Magder 1992). To achieve a similar increase in stressed volume by giving an intravenous crystalloid would require an infusion of almost 2 L because the crystalloid distributes between the vascular and interstitial spaces, whereas the change in capacitance is a pure vascular phenomena. Importantly, the opposite, removal of sympathetic tone that was maintaining stressed volume in someone with a reduced total blood volume, very rapidly decreases stressed volume and produces a marked fall in venous return and cardiac output.

Uniqueness of Volume-Pressure Relationship of the Cardiac Chambers

During diastole, cardiac chambers have a curvilinear pressure-volume relationship which is related to the structural components of the walls of the vascular chambers. However, unlike all other components of the circulation, the elastance of cardiac chambers rhythmically markedly decrease, and thus cardiac chambers have a “dynamic compliance” or what Sagawa called a time-varying elastance. The transient decrease in the elastance of the cardiac chambers markedly increases the pressure in their contained volume. The rise in pressure results in the ejection of the volume into the next region which had a lower pressure. This is the systemic arteries for the left heart and pulmonary arteries for the right heart. Blood flows in one direction because of the cardiac valves. The volume ejected from the left heart transiently increases aortic pressure, which then passes the volume to the arteries, to the capillaries, to the venules and veins, and finally to the vena cavae and back to the right heart. Ultimately, though, the cardiac chambers only can pump out what they get back on each beat (Sylvester et al. 1983). The same process occurs from the right ventricle back to the left atrium. The cyclic changes in ventricular elastic pressures are discussed further in the chapters on the right (Chap. 3) and left ventricles (Chap. 4).

Pressure-Flow Relationship

The pressure-flow relationship describes the frictional energy loss of the flow of fluid through tubes as described by Poiseuille’s law:

$$Q = \frac{\Delta P}{R} = \frac{l\eta\delta}{r^4\pi} \quad (2.1)$$

Where Q is the flow, R is the resistance, l is the length, η is the viscosity, r is the radius, and Δ indicates the difference of pressure between upstream and downstream regions. Important assumptions in Poiseuille’s law are that the fluid is “Newtonian” which requires that a steady state

flow in the tube be established, and that the flow is “laminar”, in that it has a parabolic profile due to the friction between layers of the fluid and the vessel walls. These assumptions are not true for flows through valves and at major branch points where turbulence can develop. They also are not true in regions in which vessel diameters are very small and the velocity is high. However, for this discussion about flow between major parts of the circulation, the relationship is adequate for the description of total cardiac output.

Importance of Compliance for Blood Flow

Although compliance is a static property, it is essential for flow, which is a dynamic property. This is illustrated in Fig. 2.3a, which shows a circuit with rigid tubes (extremely low compliance), a bellows that can be pumped to produce flow, and valves that control the direction of the flow. The resistance through the tubes has a value of $1 \text{ L} \times \text{min}^{-1} \times \text{mmHg}$. The maximum possible flow in this simple system is zero. This is because as soon as the bellows is compressed, the pressure instantly rises everywhere in the system and there is no pressure difference to allow a pulse of volume to travel through the system. For pulsatile flow to occur, there needs to be an area which transiently can take up the volume with a rise in pressure, here simulated by a change in height of the fluid in the open area, for flow to occur (Fig. 2.3b). Height is a measure of pressure because of the force of gravity on the mass of the fluid. If the compliant region has a very high compliance, here simulated by a large surface area relative to the height (Fig. 2.3c), the pulsations are very small.

Flow from a Single Compliant Region

Even when there is no blood flow in the circulation, the volume stretching the elastic walls of circulatory structures creates a stored elastic energy that can be released when the system is

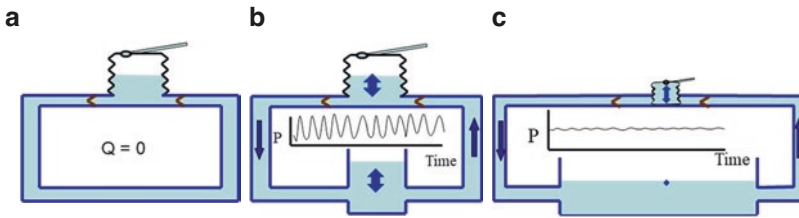


Fig. 2.3 Significance of compliance in the circulation. In each of the figures, a bellows can create a pressure to move the fluid. Valves control the direction. The tubes are rigid (very low compliance). In the top left (a), no flow ($Q = 0$) can occur because when the bellows is compressed, pressure is instantaneously transmitted through the system and there is no pressure difference for flow. On the upper right

(b), there is an opening that can transiently take up volume and then let it flow out again; it allows a change in volume for a change in pressure which is compliance. The flow has pulsations. At the bottom (c), the area with opening has a large surface area compared to the volume in the bellows. Pulsations are thus very small. Similarly, there is little change in MSFP during the cardiac cycle

open to the surrounding pressure, even without any pumping by the heart. This is illustrated in Fig. 2.4 which shows a balloon-like structure filled with a volume that stretches the wall above the unstressed volume and a tube draining the balloon. In “A,” a clamp prevents the balloon from emptying; in “B,” when the clamp is released, the balloon expels the volume until it reaches the pressure surrounding the outside of the balloon which in this case is atmospheric pressure. The determinants of flow are given by:

$$Q = \frac{\gamma}{RC} \quad (2.2)$$

Where Q is the flow, γ is the stressed volume, and R is the resistance to drainage. $R \times C$ gives the time constant of drainage which is the time it takes to get to a 63% of the new steady state, which in this case is the time it takes to expel 63% of the volume. This simple equation indicates the importance of the total stressed volume as a major determinant of flow around the system.

Bathtub Concept

As already indicated, the bulk of the volume in the circulation is in small veins and venules (Fig. 2.2). The pressure in this region normally is in the range of 8–10 mmHg indicating that the compliance is very large. The implication of this can be understood by considering the analogy of

drainage from a bathtub (Magder and De Varennes 1998). Drainage from a bathtub is determined by the height of the water above the hole at the bottom, the resistance draining the tub, and the downstream pressure of the drain. The inflow to the tub only can increase the outflow by increasing the height of the water in the tub. Thus, only the flow from the tap, which is the volume per minute, and not the pressure coming out of the tap, determines the emptying of the tub. Since the surface is so large compared to the volume coming in, shutting off the tap in the short run has little effect on drainage from the tub. At the extreme, when the tub is fully filled, increasing the inflow will not increase outflow from the drain, although it will certainly fill the bathroom floor! This is in a sense what occurs when excess fluid is given to patients; there is a marked increase in vascular leak but no increase in the venous drainage back to the heart.

Blood volume in veins and venules provides the equivalent of the bathtub because they have a large volume with a low pressure. This means that the arterial pressure upstream from the veins and venules does determine the outflow from the venous compartment. Only the volume coming from the arteries per minute determines venous outflow. Furthermore, because the bulk of blood volume exists in veins and venules, there is very little other volume that can be recruited from other vascular regions to increase the pressure in the veins, the body’s equivalent of a bathtub. Even the vascular components of the pulmonary

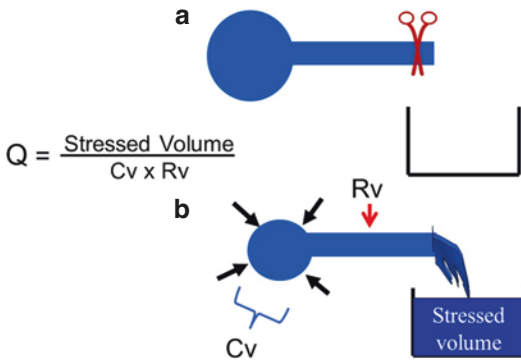


Fig. 2.4 Generation of flow (Q) in a simple system which is similar to the venous compartment; it has a compliance (C_v), downstream resistance (R_v) and is filled with a stressed volume. When the clamped is released, the elastic recoil of the walls of the compliant region pushes the volume out through the downstream resistance. The volume that remains is the unstressed volume. The equation for this simple system is given in the figure. See text for further discussion

compartments cannot contribute much volume because the total compliance of pulmonary vessels only is about one-seventh of that of the systemic venous compliance (Guyton et al. 1956).

When there is no flow in the system, the pressure is the same everywhere in the vasculature. This pressure is called mean *circulatory* filling pressure (MCFP) and it was first appreciated as a major determinant of blood flow by Weber in the nineteenth century and later considered by Ernest Starling (Patterson et al. 1914) and almost 50 years later by Arthur Guyton (Guyton et al. 1954). When there is blood flow around the circulation, volume redistributes based on the compliance and resistance draining each region (Fig. 2.2). However, the pressure in veins and venules changes only by a very small amount because it accounts for such a large proportion of the total vascular compliance. The pressure in this region under flow conditions is called mean *systemic* filling pressure (MSFP), and it is a major determinant of the return of flow back to the heart. The other factor is the total resistance of the vessels draining the veins and venules (Fig. 2.2) (Guyton et al. 1957). This is called the resistance to venous return. Importantly, vascular compliances (not to be confused with vascular capacitance) do not actively change acutely, and

thus do not act in the regulation of blood flow. However, as will be seen later, distribution of blood flow to regions with different compliances can affect the venous return.

In the steady state, cardiac output must equal venous return. Furthermore, stroke volume out from the heart must be matched by stroke return when heart rate is constant. This means that under steady state conditions, only the equivalent of one stroke volume moves around the circulation per cardiac pulsation. The total flow obviously is then determined by the number of pulsations per minute.

Since output from the heart cannot have much effect on the stressed volume in the veins and venules, it becomes apparent that the only way the actions of the heart can increase steady state blood flow is by lowering the outflow pressure for venous drainage by lowering right atrial pressure relative to MSFP. Thus, the primary role of the heart in the circulation is a “permissive function.” By lowering right atrial pressure, the heart allows more blood to come back to be pumped out again. The heart also has a second very important role which is a “restorative” function by which I mean that it must put the blood it gets back again. The drainage function of venous return back to the heart (Eq. 2.2) interacts with cardiac function as described by Starlings law, and as discussed in detail in Chap. 3, and together these two functions determine the steady state cardiac output, venous return, and right atrial pressure.

Difference Between Hydraulic and Electrical Models of the Circulation

It is now possible to come back to the principle laid out in the introduction that volume is the independent variable for blood flow and not the arterial pressure. Note that Eq. 2.1 which describes the outflow from an elastic balloon has no pressure term. The circulation often is described with electrical models based on Ohm’s law:

$$V = I \times R \quad (2.3)$$

Where V is the voltage and analogous to pressure differences, I is the current and analogous to blood flow, and R is the resistance as in the hydraulic model. The voltage difference is based on the difference between the source charge and the “ground value.” The voltage is thus a fixed, independent variable. It initially is not obvious where volume fits into this relationship. The “volume” is the number of electrons in the system, and since the current varies with resistance, this means that the volume of electrons changes with changes in current, and volume is not a fixed value in an electrical model as is the case in the hydraulic model of circulation presented in this chapter. This fundamental limitation of electrical models must always be considered. For example, an electrical model does not easily deal with changes in vascular capacitance. Of note, in an electrical model, “capacitance” is the equivalent of “compliance” in a hydraulic model and “unstressed” volume has no meaning because it has no force.

Guyton’s Analysis

Arthur Guyton created a very effective way of analyzing the regulation of cardiac output by building on the work of Ernest Starling who also appreciated the importance of the return of blood to the heart as a determinant of cardiac output (Guyton 1955; Guyton et al. 1973). The basis of Guyton’s analysis is that two functions determine the steady state cardiac output. One is the cardiac function as described by Starling (Patterson et al. 1914) and includes heart rate and the determinants of stroke volume which are the preload of the heart, afterload, and contractility (Fig. 2.5). Starling’s function curve describes the output of the heart based on the preload of the right ventricle (right atrial pressure or P_{ra}) and the properties of the flow to the aorta and all the structures in between, including the pulmonary arterial and venous compliances and resistances, and the right and left ventricles.

Guyton’s original contribution was to add another function that describes the return of blood from the venous compliant regions back to

the heart (Guyton et al. 1957). In an elegant set of experiments, he showed that venous return is determined by stressed volume, venous compliance, and venous resistance (as in Eq. 2.1), as well as the downstream pressure for venous outflow which is the right atrial pressure. Right atrial pressure, or central venous pressure, can be used interchangeably because their resistance from the great veins to the right heart normally is negligible. The stressed vascular volume and venous compliance determine the upstream MSFP:

$$\text{MSFP} = \frac{\gamma}{C_v} \quad (2.4)$$

Where γ is the stressed volume and C_v is the venous compliance. With a constant blood volume and constant venous resistance, venous return is determined by the right atrial pressure which in turn is determined by the function of the heart. The venous return function is thus:

$$VR = \frac{\text{MSFP} - P_{ra}}{R_v} \quad (2.5)$$

where R_v is the venous resistance. The equation also can be written in terms of volume without pressure by substituting Eq. 2.4 into 2.5:

$$VR = \frac{\gamma - P_{ra} C_v}{R_v C_v} \quad (2.6)$$

The product of R_v and C_v is the time constant of drainage. It becomes evident that P_{ra} is common to both the cardiac function, where it acts as preload, and to the return function where it is the downstream pressure for venous outflow. In his elegant experiments, Guyton examined the determinants of these two functions and how they interact.

Guyton’s, Graphical Approach

A major contribution of Guyton’s was the development of a graphical approach to mathematically solve the interaction of the cardiac and return functions (Guyton 1955). He developed a

function curve to describe the return of blood to heart (venous return curve) (Fig. 2.6) and combined it with Starling’s cardiac function curve (Fig. 2.5). He reasoned that the key role of the heart in the regulation of the return of venous blood is to lower right atrial pressure (Pra). He thus plotted his venous return curve with Pra on the x-axis and the associated return of venous blood on the y-axis (Fig. 2.6). The x-intercept of this plot is the MSFP and the slope is the negative inverse of venous resistance ($-1/R_v$). This curve is a simple pressure-flow relationship but has the reversed pattern from the usual curve, because instead of flow being plotted against the inflow pressure, flow is plotted against the outflow pressure. This because the inflow pressure for venous return, MSFP remains relatively constant.

Since the venous return curve has the same axis as the cardiac function curve, they can be plotted on the same graph and the intersection of the two curves gives the solution for the working right atrial pressure, working cardiac output, and working venous return (Fig. 2.7). An important point of confusion that often occurs when considering Guyton’s analysis is the difference between cardiac *output* and cardiac *function* and venous return and the venous return *function*. The functions describe a set of outputs or returns for a

given set of conditions, whereas cardiac output and venous return describe actual values based on the intersection of these two functions. The following sections show how this analysis works. They are given as a pure change in one variable which of course does not happen in life because of reflex adjustments, but they still describe the dominant process that occurs when there is a primarily a change in cardiac function, return function, or both (Magder 2012).

Change in Cardiac Function Cardiac function is increased by an increase in heart rate, increase in contractility, or decrease in afterload (Fig. 2.5). All three of these shift the cardiac function curve upward and to the left. If there is no change in the return function, cardiac output increases and right atrial pressure falls (Fig. 2.8). It acts as if

Increase in Cardiac Function Curve

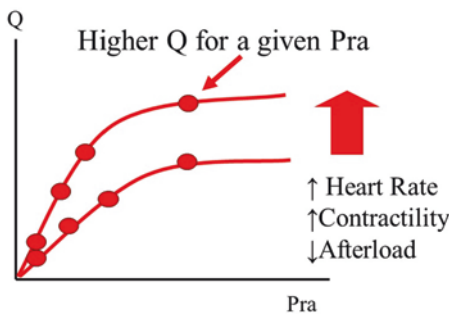


Fig. 2.5 Starling’s cardiac function curve. The greater the Pra, the greater the cardiac output (Q) until a plateau is reached, and a further increase in Pra does not change Q . Each curve assumes a constant heart rate, contractility, and afterload. An increase in heart rate, or contractility, or a decrease in afterload shifts the curve upward so that for the same Pra, Q is higher. This indicates an increase in cardiac function

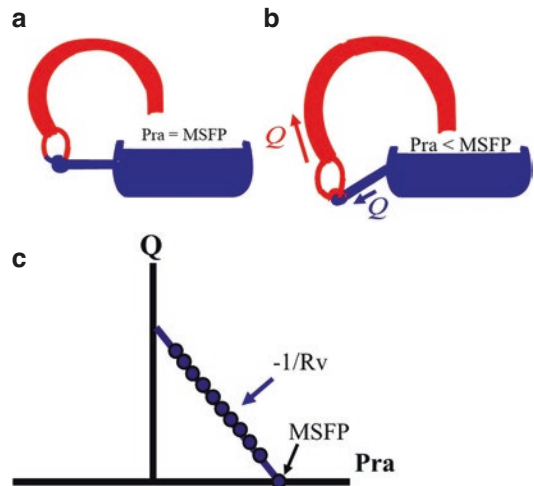


Fig. 2.6 Guyton’s venous return function. In the circulation model on the left (a), the right atrial pressure (Pra) equals MSFP and flow is zero. On the right (b), Pra is less than MSFP and flow can occur. The bottom (c) shows the graphical solution to the interaction of the pump and return functions. The beating heart lowers Pra and allows blood to come back to the heart; the heart here has a “permissive function” (blue downward arrow). The heart then pumps the blood out and back to the compliant region and thus has a “restorative” function (upward red arrow). In the graph, the x-axis is pressure and the x-intercept is the MSFP. The slope is the negative value of the inverse of venous resistance. When Pra is less than the surrounding pressure (i.e., atmosphere when breathing spontaneously), the veins collapse when they enter the chest and there is flow limitation. The downstream pressure for the return function then remains at ~ 0 mmHg

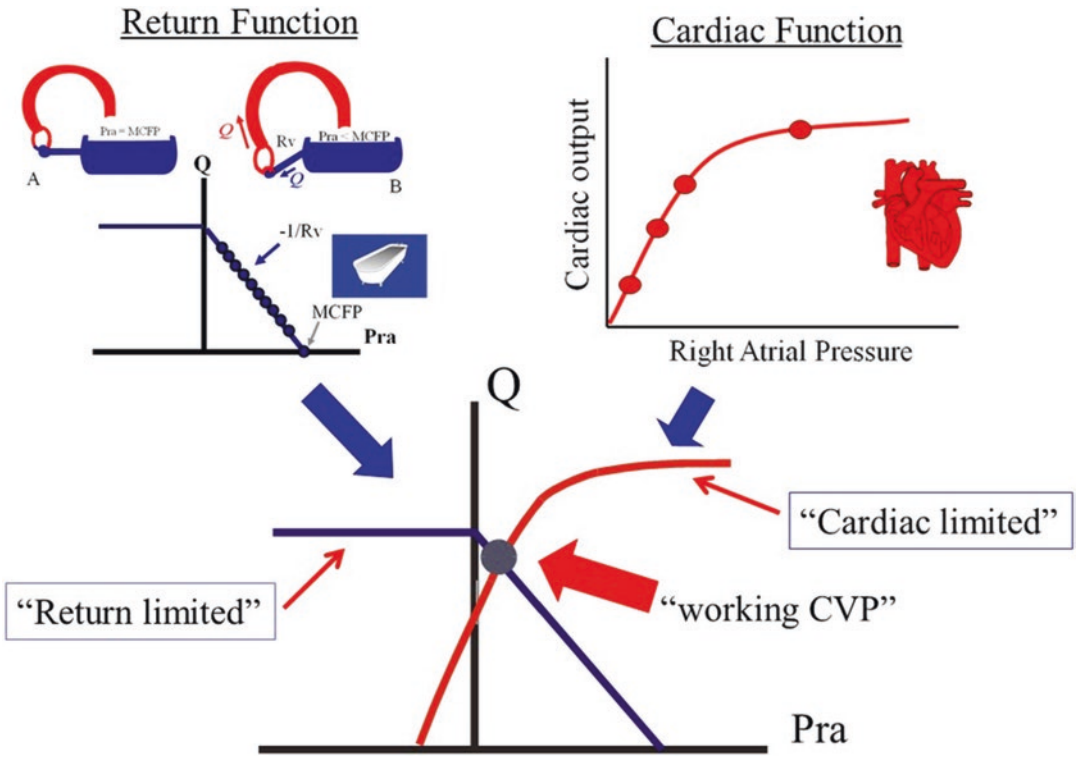


Fig. 2.7 Determination of CVP (P_{ra}) by the interaction of the pump function (“Starling curve”) and the return function (“Guyton venous return function”). The limits of the cardiac and return functions also are marked. See text for details

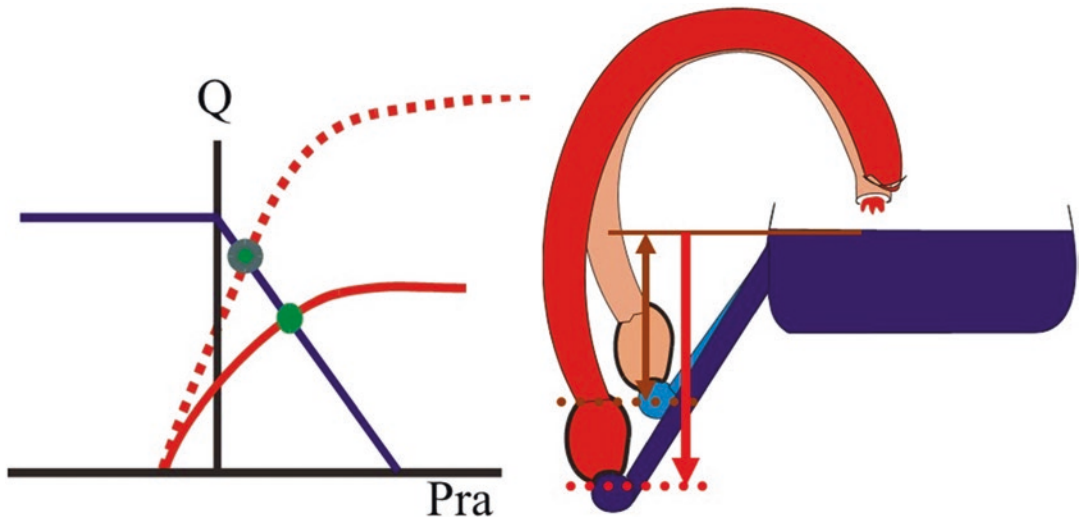


Fig. 2.8 Change in cardiac output by change in cardiac function. The left side shows an increase in cardiac function with the same venous return curve. Cardiac output rises and P_{ra} falls. It is as if the heart was lowered relative to the rest of the body and increased the pressure difference for venous return

the heart is lowered relative to the rest of the body. If cardiac function decreases, the opposite is seen; cardiac output falls and right atrial pressure rises.

Change in Stressed Volume If stressed volume is increased by a bolus of intravenous fluid, MCFP and MSFP increase but not equally because the volume distributes through all compartments including the pulmonary vessels. Under normal physiological conditions, the difference is very small but the difference becomes more important if cardiac function is decreased, especially if left heart function is decreased. I am emphasizing this difference because measurements of MCFP and MSFP depend upon the experimental technique used to obtain them. What matters for cardiac output is MSFP because this is the upstream force driving the flow of blood back to the heart. A rise in MSFP, the x-intercept of the venous return curve, shifts the venous return to the right and intersects the cardiac function curve at a higher right pressure and higher cardiac output (Fig. 2.9b). If stressed volume is lost, for example because of a major hemorrhage, aggressive fluid removal, or large gastro-intestinal losses, MSFP falls and the venous return curve is shifted to the left. Cardiac output falls with a fall in Pra.

Change in Venous Resistance Venous resistance can be decreased pharmacologically by beta-agonists and nitrates (Deschamps and Magder 1992; Green 1977; Mitzner and Goldberg 1975). The overall resistance to venous return also can be decreased by redistribution of proportion of blood flow going to the splanchnic circulation versus the muscle compartment (Deschamps and Magder 1992; Mitzner and Goldberg 1975). This is discussed further in a later section. A decrease in venous resistance is likely a major factor for the increase in cardiac output that occurs in sepsis, but this has not been well established because almost all animal models of sepsis do not show the characteristic high output state seen in humans with sepsis (Magder and Quinn 1991). A decrease in venous resis-

tance does not change the x-intercept, i.e., MSFP, but rotates the venous return curve upward. This produces a rise in cardiac output with a rise in Pra as is seen with a fluid bolus (Fig. 2.9c).

Change in Capacitance As discussed above, a decrease in vascular capacitance recruits unstressed volume into stressed volume (Rothe 1983a, b; Rothe et al. 1990). This increases MSFP without changing total blood volume. The effect on cardiac output and Pra, however, is identical to what is seen with a volume bolus (Fig. 2.10). Cardiac output rises with a rise in Pra. An increase in vascular capacitance, which commonly occurs with sedation, results in a decrease in cardiac output with a fall in Pra and looks identical to a loss of total active blood volume (Green et al. 1978).

Summary of Interaction of Cardiac and Return Functions

An increase in cardiac output that occurs with a decrease in Pra indicates that the primary physiological change was an improvement in cardiac function (Fig. 2.8) (Magder 2012). If cardiac output falls with an increase in Pra, the primary problem was a fall in cardiac function. This could be from a decrease in right heart function, increase in pulmonary vascular resistance, or a decrease in left heart function. This analysis does not distinguish these and other tests or clinical assessments are needed. If cardiac output increases with a rise in Pra, the primary physiological change was an increase in the return function (Fig. 2.9). This could be due to an increase in total blood volume, a decrease in venous capacitance, or a decrease in venous resistance. A fall in cardiac output with a fall in Pra indicates that the primary physiological change was a decrease in the return function, which could be because of a loss of total blood volume, an increase in capacitance by removal of vascular tone, or an increase in venous resistance. These simple relationships between cardiac output and CVP can allow rapid assessment of the primary pathophysiological process and provide a physiological approach to management.

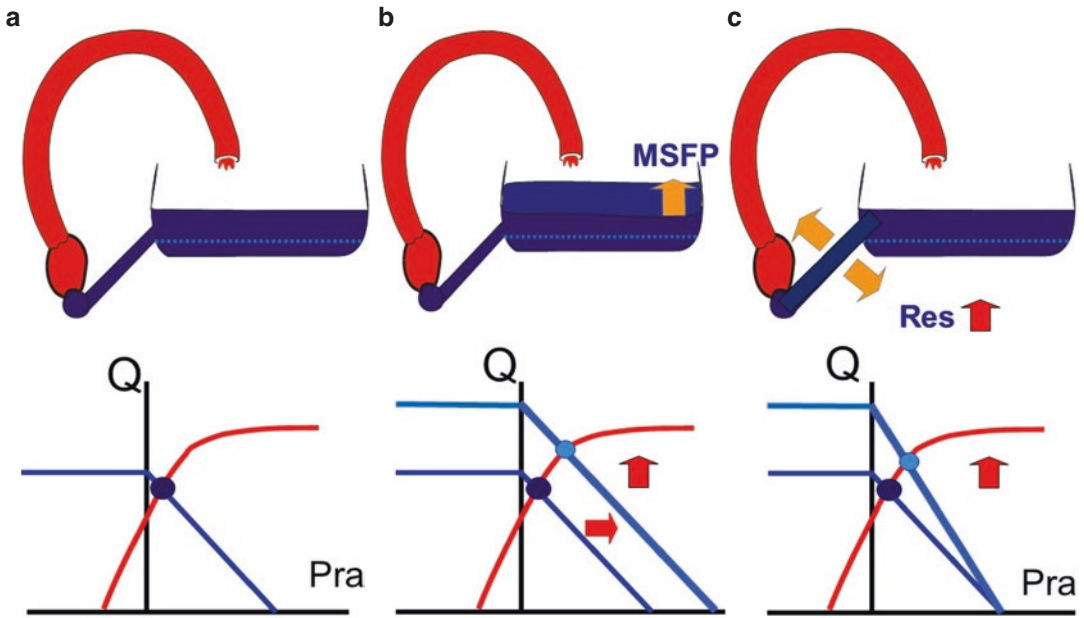


Fig. 2.9 Change in cardiac output by a change in the return function. The first panel (a) shows the basic interaction of the cardiac and return functions. In the second panel (b), vascular volume is increased which raises MSFP. The venous return curve shifts to the right and

intersects the cardiac function curve at a higher Pra and a higher Q . In the last panel (c), the slope of the return function increases which indicates a decrease in venous resistance. Q again rises with a rise in Pra, but in this case, MSFP is unchanged

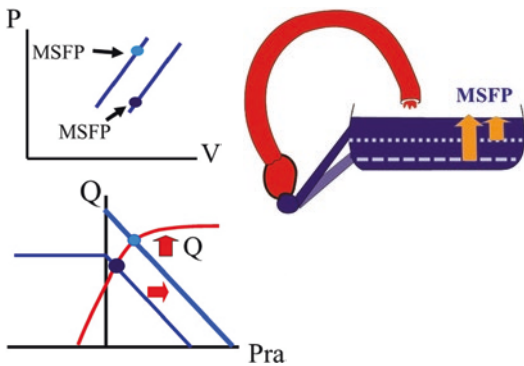


Fig. 2.10 A decrease in vascular capacitance. A decrease in vascular capacitance tightens up veins and venules (decrease in circumference). It is as if the opening of the container was lowered. More volume becomes stressed, which increases MSFP. This is seen as a shift to the left of the volume vs pressure relationship of the vasculature. A given volume then has a higher pressure. The venous return curve is shifted to the right and Q rises with a rise in Pra just as occurred when volume was given. This is the body's way of giving an auto-transfusion

Limits of the Cardiac and Return Functions

Both the cardiac and return functions have important limits (Fig. 2.7). The Starling mechanism requires that there be an increase in the length of cardiac myofibers during diastole for there to be an increase in stroke volume. However, cardiac muscle evolved differently from skeletal muscle so that it cannot be overstretched. If this were not the case, at high rates of venous return, stroke volume would decrease which would be highly disadvantageous. Under normal conditions, the pericardium constrains acute dilatation of the heart even before the sarcomere limit is reached (Holt et al. 1960). This produces a sharp break to the passive filling curve of the right heart which is seen as the flat part of Starling's cardiac function curve (Figs. 2.5 and 2.7). When right heart filling

is limited, increasing the venous return function increases P_{ra} but does not increase cardiac output. When cardiac filling is limited, only an increase in heart rate, increase in contractility, or a decrease in afterload can increase cardiac output.

The venous return function has a limitation, too, because of flow limitation in large veins returning blood to the heart. In contrast to arteries, walls of veins are floppy, and when the pressure inside a vein is less than surrounding pressure, the vessel collapses (Permutt and Riley 1963). When breathing spontaneously, pleural pressure is less than atmospheric pressure. As discussed in the chapter on heart-lung interactions, the heart is surrounded by pleural pressure so that cardiac pressure, too, becomes negative relative to atmospheric pressure. It is important to appreciate that P_{ra} is not actually “negative,” it just is negative relative to atmospheric pressure, which is around 760 mmHg at sea level. When the great veins enter the thorax, the pressure inside these veins is less than the surrounding pressure and they collapse. When this happens, lowering P_{ra} further does not increase cardiac output. This brings up a rather subversive point. The maximum possible venous return, and thus maximum possible cardiac output, occurs when the heart is removed and the great veins just drain to atmosphere. This indicates that most of the time the heart just gets in the way. However, this glorious situation only lasts for an instant as blood volume drains from the body and is not returned to the upstream reservoir. When venous return is limited, only an increase in stressed volume or a decrease in venous resistance can increase cardiac output (Fig. 2.11).

There is an important evolutionary rationale for why veins developed with floppy walls and are collapsible, whereas arteries have rigid walls and are not easily collapsible. As discussed in the chapter on blood pressure, in the upright posture, the pressures in the veins draining the cerebral circulation are very negative relative to the heart, i.e., less than -40 mmHg relative to P_{ra} in an average sized person. If the veins in the head were as stiff as arteries, and thus did not collapse and limit flow, every time a person stood up the stressed and unstressed blood volume in the head

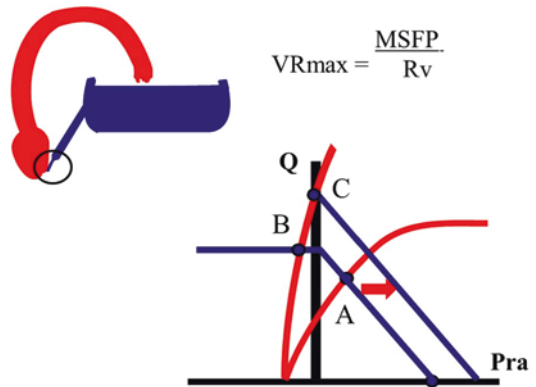


Fig. 2.11 The limit to venous return. When the pressure in the great veins is less than the atmospheric pressure (or pleural pressure in someone on positive pressure ventilation), the vessels collapse and produce the equivalence of a vascular water fall. When this happens, a further lowering of P_{ra} (B) does not increase Q . Only giving volume and shifting the venous return curve to the right increase Q

would almost instantly be sucked out and severely damage cerebral tissues.

Krogh's Two-Compartment Model of the Circulation

So far in this chapter, the analysis has been based on a model with all venous compliance lumped in one compartment. However, in 1914, August Krogh introduced a model that indicated that if there are venous regions in parallel that have different compliances and different time constants of drainage, the distribution of flow between the compartments alters the rate of flow return (Permutt and Caldini 1978; Krogh 1912; Caldini et al. 1974) (Fig. 2.12). Remember that the time constant of drainage is the product of the compliance of the region and the resistance draining it. The analysis is simpler if just two general types of compartments are considered, one with a fast and one with a slow time constant of drainage. Furthermore, it is the compliance term that has the most significant difference among different regions (Deschamps and Magder 1992; Caldini et al. 1974). The splanchnic circulation has been shown to have a slow time constant of drainage, which is in the range of 20–24 seconds, whereas

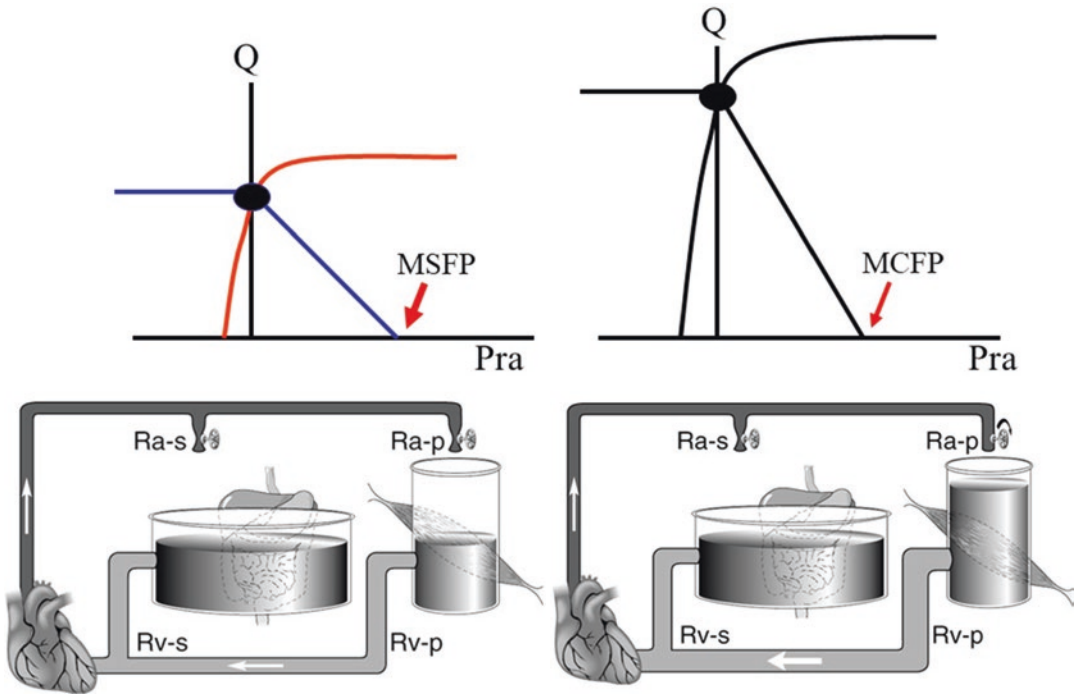


Fig. 2.12 Krogh's two-compartment model and the effect of a change in the fractional distribution of cardiac output on venous return. In A, the distribution of flow is equal to the splanchnic bed (Ra-s) and the peripheral (muscle) bed (Ra-p). In B, the fractional flow to the

peripheral bed is increased. As a result, the resistance to venous return is decreased and venous return is higher for the same total volume. (From reference Magder and Scharf 2001). Used with permission of Taylor & Francis Group LLC)

the peripheral muscle bed has a fast time constant of drainage, which is in the range of 3–6 seconds (Deschamps and Magder 1992; Green 1977; Mitzner and Goldberg 1975). A shift in the fraction of the total blood flow to the fast time constant muscle vasculature increases venous return (Caldini et al. 1974). This occurs because the increase in flow to the less compliant muscle results in an accumulation of volume and, consequently, an increase in the regional equivalent of MSFP. This increases the gradient for venous return from this region. In the Guyton analysis, this is evident as an increase in the slope of the venous return function (decrease in resistance) with no change in the x-intercept. An increase in the fraction of flow to the splanchnic bed does the opposite. Venous return decreases because the splanchnic bed can accumulate more blood with a smaller increase in regional equivalent of MSFP. This is evident as a decrease in the slope of the venous return curve.

Summary

The primary force driving flow around the circulation is the elastic energy produced by the distention of the elastic walls of the circulation by the volume they contain. When the closed circulatory loop is opened to atmosphere, this force can create flow even without a cardiac contraction. The heart cannot produce a flow rate higher than the instantaneous flow that would occur when the non-beating system is opened to atmosphere. Cardiac chambers act by transiently increasing the elastance of their walls in systole. This increases the pressure in the volume they contain and displaces that volume into the next compartment. This volume is then passed around the system as the pressure rises in each section compared to the next downstream section until the pulse of volume is back to the emptied right ventricle. Another key role of the heart is thus to reduce its elastance back to the resting state and

allow the equivalent of the ejected bolus to come back to the heart. The pressure difference required for the stroke return from the veins is much smaller than that required for the ejection of the forward stroke volume, which makes the right atrial pressure a key determinant of flow around the system.

References

- Bishopric NH. Evolution of the heart from bacteria to man. *Ann N Y Acad Sci.* 2005;1047:13–29.
- Caldini P, Permutt S, Waddell JA, Riley RL. Effect of epinephrine on pressure, flow, and volume relationships in the systemic circulation of dogs. *Circ Res.* 1974;34:606–23.
- Deschamps A, Magder S. Baroreflex control of regional capacitance and blood flow distribution with or without alpha adrenergic blockade. *J Appl Physiol.* 1992;263:H1755–H63.
- Drees J, Rothe C. Reflex venoconstriction and capacity vessel pressure-volume relationships in dogs. *Circ Res.* 1974;34:360–73.
- Green JF. Mechanism of action of isoproterenol on venous return. *Am J Physiol.* 1977;232(2):H152–H6.
- Green JF, Jackman AP, Krohn KA. Mechanism of morphine-induced shifts in blood volume between extracorporeal reservoir and the systemic circulation of the dog under conditions of constant blood flow and vena caval pressures. *Circ Res.* 1978;42(4):479–86.
- Guyton AC. Determination of cardiac output by equating venous return curves with cardiac response curves. *Physiol Rev.* 1955;35:123–9.
- Guyton AC, Polizo D, Armstrong GG. Mean circulatory filling pressure measured immediately after cessation of heart pumping. *Am J Phys.* 1954;179(2):261–7.
- Guyton AC, Armstrong GG, Chipley PL. Pressure volume curves of the arterial and venous systems in live dogs. *Am J Physiol.* 1956;184:253–8.
- Guyton AC, Lindsey AW, Bernathy B, Richardson T. Venous return at various right atrial pressures and the normal venous return curve. *Am J Phys.* 1957;189(3):609–15.
- Guyton AC, Jones CE, Coleman TG. In: Guyton AC, editor. *Circulatory physiology: cardiac output and its regulation.* Philadelphia: W.B. Saunders Co.; 1973.
- Holt JP, Rhode EA, Kines H. Pericardial and ventricular pressure. *Circ Res.* 1960;VIII:1171–80.
- Krogh A. The regulation of the supply of blood to the right heart. *Skand Arch Physiol.* 1912;27:227–48.
- Magder S. An approach to hemodynamic monitoring: Guyton at the bedside. *Crit Care.* 2012;16:236–43.
- Magder S. Volume and its relationship to cardiac output and venous return. *Crit Care.* 2016;20:271.
- Magder S, De Varennes B. Clinical death and the measurement of stressed vascular volume. *Crit Care Med.* 1998;26:1061–4.
- Magder S, Quinn R. Endotoxin and the mechanical properties of the canine peripheral circulation. *J Crit Care.* 1991;6:81–8.
- Magder S, Scharf SM. Venous return. In: Scharf SM, Pinsky MR, Magder SA, editors. *Respiratory-circulatory interactions in health and disease.* 2nd ed. New York: Marcel Dekker, Inc.; 2001. p. 93–112.
- Mitzner W, Goldberg H. Effects of epinephrine on resistive and compliant properties of the canine vasculature. *J Appl Physiol.* 1975;39(2):272–80.
- Moorman AF, Christoffels VM. Cardiac chamber formation: development, genes, and evolution. *Physiol Rev.* 2003;83(4):1223–67.
- Pascual-Anaya J, Albuixech-Crespo B, Somorjai IM, Carmona R, Oisi Y, Alvarez S, et al. The evolutionary origins of chordate hematopoiesis and vertebrate endothelia. *Dev Biol.* 2013;375(2):182–92.
- Patterson SW, Piper H, Starling EH. The regulation of the heart beat. *J Physiol.* 1914;48(6):465–513.
- Permutt S, Caldini P. Regulation of cardiac output by the circuit: venous return. In: Boan J, Noordergraaf A, Raines J, editors. *Cardiovascular system dynamics*, vol. 1. Cambridge and London: MIT Press; 1978. p. 465–79.
- Permutt S, Riley S. Hemodynamics of collapsible vessels with tone: the vascular waterfall. *J Appl Physiol.* 1963;18(5):924–32.
- Rothe C. Venous system: physiology of the capacitance vessels. In: Shepherd JT, Abboud FM, editors. *Handbook of physiology. The cardiovascular system.* Section 2. III. Bethesda: American Physiological Society; 1983a. p. 397–452.
- Rothe CF. Reflex control of veins and vascular capacitance. *Physiol Rev.* 1983b;63(4):1281–95.
- Rothe CF, Flanagan AD, Maass-Moreno R. Reflex control of vascular capacitance during hypoxia, hypercapnia, or hypoxic hypercapnia. *Can J Physiol Pharmacol.* 1990;68:384–91.
- Simoës-Costa MS, Vasconcelos M, Sampaio AC, Cravo RM, Linhares VL, Hochgreb T, et al. The evolutionary origin of cardiac chambers. *Dev Biol.* 2005;277(1):1–15.
- Sylvester JT, Goldberg HS, Permutt S. The role of the vasculature in the regulation of cardiac output. *Clin Chest Med.* 1983;4(2):111–26.
- Xavier-Neto J, Castro RA, Sampaio AC, Azambuja AP, Castillo HA, Cravo RM, et al. Parallel avenues in the evolution of hearts and pumping organs. *Cell Mol Life Sci.* 2007;64(6):719–34.



Function of the Right Heart

3

Sheldon Magder

Introduction

Right heart dysfunction is common in critically ill patients. Causes include sepsis, dysfunction following cardiac surgery, chronic lung diseases, chronic pulmonary vascular disease, and pulmonary vascular obstructive processes. Right heart dysfunction can occur acutely or as an acute on chronic process. Acute processes occur primarily when there is an excessive pressure load for right ventricular (RV) ejection as with an acute pulmonary embolism or during mechanical ventilation, and it also can occur when cardiac function is decreased as in sepsis or after cardiac surgery. Failure from chronic right heart processes occurs when adaptive mechanisms reach their limits as in end stages of primary pulmonary hypertension or secondary causes of pulmonary hypertension. The right heart also can limit cardiac output because of iatrogenic actions, such as excessive volume loading, even without intrinsic dysfunction of cardiac muscle. There have been several recent excellent reviews on RV dysfunction. These have emphasized acute right heart failure (Harjola et al. 2016), overloaded right heart and ventricular interdependence (Naeije and Badagliacca 2017), right versus left ventricular

failure in congenital heart disease (Friedberg and Redington 2014), and right ventricular hypertrophy and right heart failure (van der Bruggen et al. 2017). The emphasis in this chapter is on physiological and pathological implications for the management of the RV in the critically ill. Some of these ideas have been previously discussed (Magder 2007). This chapter will refer to principles in Chap. 2 on volume and regulation of cardiac output, Chap. 4 on the left ventricle function, Chap. 50 on cardiogenic shock, and Chap. 18 on heart-lung interactions.

Origins of the Right Heart

The earliest forms of the four-chamber mammalian heart evolved in vertebrates (Simoes-Costa et al. 2005; Xavier-Neto et al. 2007; Bishopric 2005; Pascual-Anaya et al. 2013). Knowledge of the evolution of the heart helps understand why the right heart functions the way it does and what limits its output. The heart had its evolutionary beginnings with a single circuit that had an atrium and ventricle in series (Simões-Costa et al. 2005). As an early example, in fish, blood is pumped from the equivalents of an atrium and a ventricle through a gas-exchange mechanism in the gills that oxygenates the blood and removes carbon dioxide (CO₂). Upon exiting the gills, the circuit delivers oxygen (O₂) and removes waste products from the rest of the body and the de-oxygenated blood

S. Magder (✉)
Royal Victoria Hospital (McGill University Health Centre), Departments of Critical Care and Physiology
McGill University, Montreal, QC, Canada
e-mail: sheldon.magder@mcgill.ca

returns to the heart. In sedentary fish, the heart obtains its needed O_2 from the returning blood by diffusion through trabeculations in the walls of the heart. Accordingly, this blood is the most deoxygenated in the body. In more active fish species, up to 35% of the O_2 for the heart comes directly from the gills through a primitive coronary circulation (Bettex et al. 2014). Although this simple system is adequate for the low aerobic needs of lower level organisms, and for modest rapid burst in species with primitive coronaries, it does not allow for the high aerobic power of mammals and birds. Furthermore, gas-exchange vessels in the gills receive blood ejected from the heart with the highest vascular pressure in the organism. These species thus could not have the delicate alveolar structures that exist in birds and mammals. An adaptation that helps protect the gas-exchange region is the conus arteriosus just after the ventricle. This not only dampens the ejected pulse pressure that flows into the gills but also dampens the arterial pressure for the rest of the body.

A three-chamber heart with two atria and one ventricle emerged in amphibians when species began to move on to the land and breathe air. This allowed the evolution of a separate pulmonary circuit. Respiratory function now could be separated from other organ function, and fully oxygenated blood returns to the heart, although this blood still is mixed with returning deoxygenated venous blood from the rest of the body (Bishopric 2005). This stage could be considered the dawn of the era of heart-lung interactions! At the reptilian stage, things became more complicated and various approaches evolved. Some reptiles, such as turtles, still have a three-chamber heart and low arterial pressure. Pythons and some lizards have almost complete separation of the ventricles and the outflow to the lungs is occluded during systole, thus separating the return of oxygenated and deoxygenated blood. Other reptiles, such as crocodiles, have true four-chamber hearts, but there are two aortic arches, which allow varying ratios of pulmonary to systemic flows (Bettex et al. 2014). Their arterial pressures generally are lower than in mammals and their aerobic power is much lower. Fully separated right (RV) and left ventricles (LV) only appeared with the evolution

of birds and mammals. This fully evolved structure allowed development of a low-pressure pulmonary system that has delicate high efficiency gas-exchange structures, coronary blood flow with a high-pressure source and fully oxygenated blood, and a high-pressure systemic circulation that allows rapid changes in regional flows by decreasing regional arterial resistances based on local metabolic needs (Chap. 8). It is noteworthy that a separate pulmonary gas exchange region only evolved when systemic arterial pressure exceeded 50 mmHg (Bettex et al. 2014).

During fetal life, the RV functions as the systemic ventricle and provides more than half of the cardiac output to the body as it supplies blood to the lower part of the body and the placenta. Little blood flow is needed for the low-pressure pulmonary circuit because there is no ventilation (Friedberg and Redington 2014). After birth, the RV just has to face the pressure in the low-resistance pulmonary circuit, and its walls become thinner right after birth. Based on studies in animals, it has been argued that loading the RV early in life can maintain the right heart's fetal transcriptional program and prevent RV muscle regression. This potentially can facilitate the development of RV hyperplasia in children who have congenital heart problems that are associated with rising pulmonary artery pressures later in life (Friedberg and Redington 2014; van der Bruggen et al. 2017; Apitz et al. 2012). Evidence for this is supported by the observation that children with Eisenmenger's syndrome, or corrected transposition of the great arteries, tolerate increased pulmonary pressure for prolonged periods better than children with other congenital or pathological conditions in which the pulmonary load develops later in life (Hopkins 2005; Hopkins et al. 1996; Dos et al. 2005).

Differences Between RV and LV

In 1998, it was discovered that the embryological development of the RV is directed by the transcription factor Hand 2, whereas that of the LV is directed by Hand 1, which actually evolved after Hand 2 (Thomas et al. 1998; Srivastava and

Olson 2000). The LV develops from an anterior heart field, whereas the RV evolves from a genetically more primitive field (Zaffran et al. 2004). These differences in transcriptional programs produce differences in the electrophysiological, pharmacological, and contractile properties of the RV and LV (Table 3.1).

Electrophysiological Sarcomeres from RV and LV respond differently to changes in frequency of contractions. When the frequency of sarcomere contractions is suddenly slowed, those from the RV have a small increase in their length of shortening, whereas those from the endocardial surface of the LV have a large increase in the length of shortening. Sarcomeres from the LV epicardium are more similar to those of the RV, and they only shorten a little with a decrease in frequency (Kondo et al. 2006). These differences in shortening patterns are associated with different electrophysiological properties in cell mem-

branes, which ultimately contribute to differences in the force production of the RV and LV. LV myocyte potassium currents turn off faster than those of the RV; the density of potassium channels, too, is greater in the LV. These properties allow more time for calcium ions to enter LV myocytes during the fixed time of the action potential and result in the greater LV force production than that of the RV.

Endocardial endothelial cells (EEC) Just as all blood vessels have a layer of endothelial cells, cardiac chambers, too, are lined by a layer of cells with properties that are similar to those of vascular endothelial cells, although they evolved from cardiac fields rather than the mesenchymal field, which is the source of vascular endothelial cells (Brutsaert et al. 1996; Brutsaert 2003). EEC have membrane receptors that allow peptide signaling from both the blood inside the cardiac chambers and peptides that come from the underlying cardiomyocytes (Jacques et al. 2003, 2006a, b, c). These cells also secrete peptides such as endothelin-1 and neuropeptide Y, which can have both autocrine and paracrine effects on these cells. There are many differences in EEC of the right and left sides of the heart, which result in differences in the regulation of the blood-heart barrier on the two sides of the heart (Abdel-Samad et al. 2012, 2016). EEC from the RV are thinner and have a lower baseline calcium ion concentration in both their cytoplasm and nuclei than EEC from the LV (Fig. 3.1). The increase in intracellular calcium ions in response to the same concentration of peptides, such as human polypeptide Y and endothelin, is much greater in right-sided EEC compared to left-sided EEC (Abdel-Samad et al. 2016). These differences in right- and left-sided EEC properties can allow each side of the heart to have its own regulatory responses to circulating vascular signaling molecules, as well as metabolic factors, such as tension of O₂ and CO₂ and hydrogen ion concentration.

Pharmacological Differences Although alpha-adrenergic agonists are thought in general to have

Table 3.1 Differences in properties of right and left ventricles

	Right ventricle	Left ventricle
Transcriptional factor	Hand-2	Hand-1
Electrophysiological	Less sarcomere shortening when contraction frequency slows	Greater sarcomere shortening when contraction frequency slows
	Lower density of K ⁺ channels and they turn off more slowly	Greater density of K ⁺ channels and they turn off faster
Response to α -agonists	Decrease myofiber shortening	Small increase in myofiber shortening
Endocardial endothelial cells	Thinner; lower baseline intracellular [Ca ²⁺]	Wider; greater baseline Ca ²⁺
Normal resting end-systolic elastance	4–6 mmHg/ml	1.3–2.0 mmHg/ml
Coronary flow	Diastole and systole	Primarily diastole

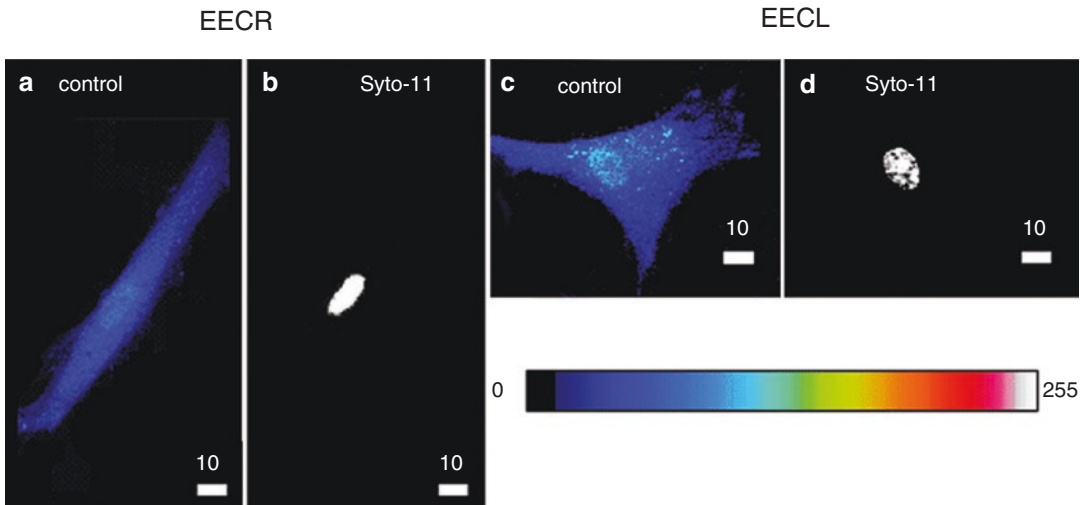


Fig. 3.1 Higher basal intracellular Ca^{2+} level in left ventricular endothelial cells compared to those from the right ventricle. 3D quantitative confocal microscopy images (top view) showing the basal intracellular distribution and levels of Ca^{2+} -Fluo 3 complexes in endothelial cells derived from the right (EEER, **a**)

and left (EEEL, **c**) ventricles. Panels (**b**) and (**d**) show labeling of the nuclei of cells in panels (**a**) and (**c**) respectively using the nucleic acid probe syto-11. The white scale bar is in μm . (Unpublished data. Used with permission of Dr Danielle Jacques)

little effect on cardiac myocytes, there are striking differences between their actions on the RV and LV. Phenylephrine, a pure α -agonist, produces a small increase in the degree of shortening of LV muscle in situ, but it produces a marked decrease of RV muscle shortening (Wang et al. 2006). A chronic infusion of norepinephrine increases LV but not RV mass (Irlbeck et al. 1996), although this could be because norepinephrine produces only a small increase in pulmonary artery pressure, but a large increase in systemic arterial pressure and thus produces a greater afterload effect on the LV (Datta and Magder 1999). The significance of this is that pharmacological agents can potentially affect the RV and LV differently.

Shape and Load Differences Between the Ventricles The implications of these will be discussed in the next section but some brief points need to be made here. The LV has the appearance of an American football cut in half at its widest diameter, whereas the normal RV wraps around the LV and functions more like a bellows than a constricting circle (Friedberg and Redington 2014; Voelkel et al. 2006) (Fig. 3.2).

RV diastolic compliance is much greater than that of the LV so that there only are small changes in RV pressure with an increase in RV volume. The diastolic filling curve of the RV, though, has a sharp break at which pressure rises steeply with little change in volume. Pressure loads on the RV and LV, too, are very different. The LV generates systolic pressures greater than 100 mmHg, whereas RV systolic pressure is usually 20 mmHg or less (Fig. 3.3). Accordingly, the LV wall normally is much thicker than the RV wall (Fig. 3.2). The peak-generated pressure for a given volume of the RV is only half that of the LV. These differences are obvious when the pressure-volume curves of the RV and LV are compared (Fig. 3.3).

Right Ventricular Ejection

Basic Principles

It is important to start with statements of some basic underlying principles (Table 3.2). These may seem obvious, but they often are forgotten in the circular reasoning which is at the core of

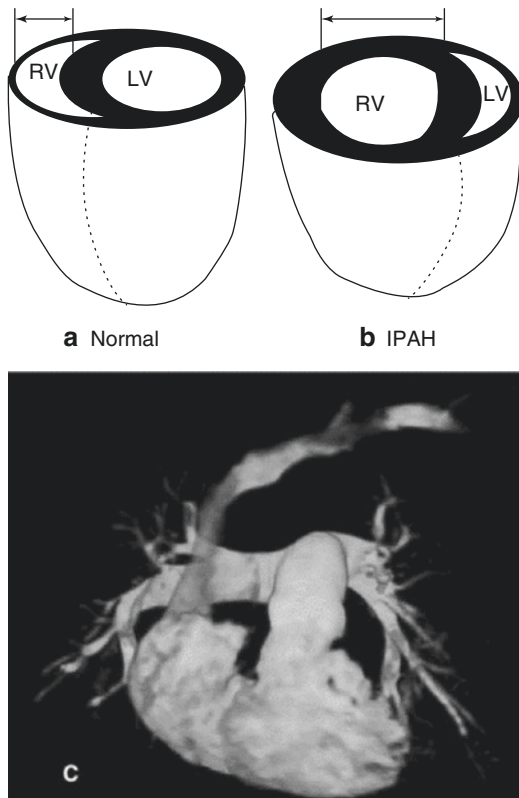


Fig. 3.2 Cast of the right ventricle indicating its complicated shape with a base and infundibular portion. The top shows the relative sizes of the RV and LV; on the left (a) a normal situation, and on the right (b) a markedly hypertrophied ventricle with a greatly reduced LV and the septum curved to the left. Bottom (c) shows MR angiogram of the RV and pulmonary arteries in a subject with idiopathic pulmonary hypertension. The RA and RV are prominent with heavy RV trabeculations. (From Voelkel *et al.* (2006). Used with permission of Wolters Kluwer Health, Inc.)

an understanding cardiovascular physiology. First, the LV only can put out what the RV gives it, and the RV only can put out what returns to it from the upstream venous reservoir. The cyclic nature of cardiac function sets the time available for filling and ejection from the ventricles. Normally, the RV does not reach its volume limit. Rather, filling of the RV in diastole is determined by the time available for the RV to fill and how fast blood comes back to it. In pathological conditions, RV filling can reach the maximum RV diastolic volume, and when this happens, it has major repercussion for the interaction of RV and LV and sets the limit of stroke volume. Finally, conservation of mass must

always be considered; if a distended RV decreases filling of the LV, the volume must accumulate somewhere else in the circulation, which means that pressure must increase somewhere else in the vasculature.

Basic mechanisms of flow generation are similar for the RV and LV. During diastole, ventricular walls are stretched by the returning blood. The pressure created by the stretched ventricular walls is their preload and sets the length of cardiac myocytes based on the diastolic compliance of the walls. The return of blood is driven by energy from the elastic recoil of the compliant upstream venous region. For the RV, the upstream pressure is in the systemic veins and is called mean systemic filling pressure (MSFP) (Chap. 2, Magder). In a parallel way, blood returns to the LV from the elastic recoil of the pulmonary venous compartment. The total compliance of pulmonary vessels (arterial and venous), though, only is about one-seventh of that of the systemic veins and, accordingly, the volume reserve in the pulmonary veins is small (Lindsey and Guyton 1959). Thus, filling of the LV is dependent upon what the right heart gives it, whereas the large volume reserve in the systemic venous compliance means that the RV is not directly dependent upon LV output.

The RV is considered by some to normally function below its stressed volume. However, this is unlikely because the RV demonstrates an active length-tension relationship and a force is needed to stretch the sarcomeres (Maughan *et al.* 1979; Redington *et al.* 1988a). More likely, what is happening is that in the range of normal stroke volumes, the passive filling curve of the RV is very compliant, and the very small changes in its diastolic pressure are hard to detect unless properly amplified. Since changes in diastolic volume produce changes in the generated systolic pressure, there must be some increase in stress on right-sided sarcomeres for them to detect a change and this indicates that a force has to be present. It also is important to appreciate that negative values relative to atmosphere do not mean that the transmural pressure is negative as the heart is in the sub-atmospheric pleural space (Slinker *et al.* 1987; Watkins and LeWinter 1993).

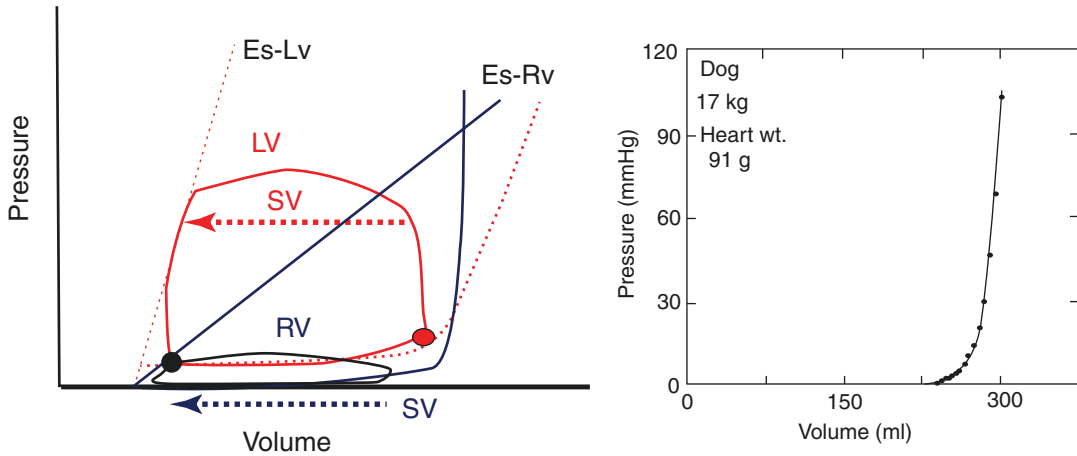


Fig. 3.3 Pressure-volume relationships of the right and left ventricles (left) and the pericardium (right). Details are in the text. Note that the end-systolic left ventricular pressure-volume (Es-LV) is much steeper than the end-systolic pressure-volume line (Es-Rv). The diastolic passive filling curve of the RV breaks more sharply than that

of the LV. Although the LV systolic pressure is much higher than that of the RV, their stroke volumes are equal. The right side shows the steep break to the pressure volume relationship of the pericardium. (From Holt *et al.* 1960). Used with permission of Wolters Kluwer Health, Inc.)

Table 3.2 Characteristics of ventricular pressure-volume relationship

	Right ventricle	Left ventricle
Systolic peak pressure	120 mmHg	20 mmHg
Diastolic filling	Low diastolic pressure (-2 to 4 mmHg)	Moderate diastolic pressure (5–10 mmHg)
	Low initial slope (high compliance)	Moderate slope (moderate compliance)
	Sharp break in diastolic filling curve at peak volume	Gradually increasing slope of diastolic filling curve at peak volume
Initial systolic rise in pressure	Curvilinear initial P-V curve	Isovolumetric initial phase
End of systole	Can have hang-out phase of stroke volume	Sharp end to stroke volume at max Es
Stroke volume	Large changes with either positive or negative inspiratory activity	Moderate effects from either positive or negative inspiratory efforts

In most people, the RV passive filling curve becomes very stiff at around 10 mmHg referenced to the middle of the right atrium, although there is a lot of individual variability of the actual value at the break of the curve (Magder and Bafaqeeh 2007). Pericardial tissue is very non-compliant and when intact, it creates a sharp limit to RV filling. This limit usually occurs before the steep part of the passive filling curve of the RV wall itself is reached (Fig. 3.3) (Watkins and LeWinter 1993; Holt *et al.* 1960). However, even without a pericardium, the cardiac cytoskeleton still sharply limits RV filling. In contrast to the diastolic properties of the RV, the compliance of the LV passive filling curve has a steeper slope even at low pressures, and the increase at higher values is less sharp (Fig. 3.3). The LV thus has a more progressive increase in diastolic pressure with volume, and the filling curve becomes much steeper and limiting at around 18 mmHg. However, when the pericardium is in place, or when the lungs, the RV itself, or the space available in the mediastinum becomes limited, LV filling, too, can become sharply limited by these other structures (Butler 1983).

Under normal conditions, the limit of RV filling provides a protective mechanism for the lungs by preventing excessive RV output from over-filling the LV. This prevents flooding of the lungs by excessive increases in LV diastolic pressure. This safety mechanism fails when RV function is maintained, and LV function is severely depressed. In this situation, the functioning RV keeps transferring volume to the pulmonary vasculature but the depressed LV cannot handle the volume and maintain the normally low pulmonary capillary pressure. This especially can be a problem in someone in whom the RV and LV are supported by mechanical devices, and the right-sided device generates more flow than the left-sided device.

Ejection from both the right and left ventricles occurs by what Sagawa called, a time-varying elastance (Sagawa 1978; Suga et al. 1977) which is discussed more fully in Chap. 4 for the LV. Unlike other vascular tissues, the elastances of ventricular walls (and atria), i.e., change in pressure for change in volume, rhythmically increase during the cardiac cycle; this rising phase of the elastance of ventricular walls defines systole. The rise in elastance increases the pressure of the volume in the ventricles and is described by the slope of a line on a pressure versus volume plot (Figs. 3.3 and 3.4). The maximum slope of the end-systolic pressure-volume line is the maximum elastance (E_{s-max}) during the cycle and is considered the best volume-independent indicator of ventricular function.

Details of the time-varying elastance in the RV were nicely documented by Maughan et al. and Sagawa (Fig. 3.4) (Maughan et al. 1979). The process occurs at a much lower scale in the RV than in the LV (Maughan et al. 1979; Redington et al. 1988a; Dell'Italia and Walsh 1988a; Dell'Italia et al. 1985; Redington et al. 1990) (Fig. 3.4). When the outflow from the RV is blocked, the pressure rises to the value on the E_{s-max} line for that volume (upper part of Fig. 3.4). When the pulmonary valve opens, the RV pressure rises until the pressure is greater than pulmonary arterial pressure. This opens the pulmonary valve and blood is ejected. Blood con-

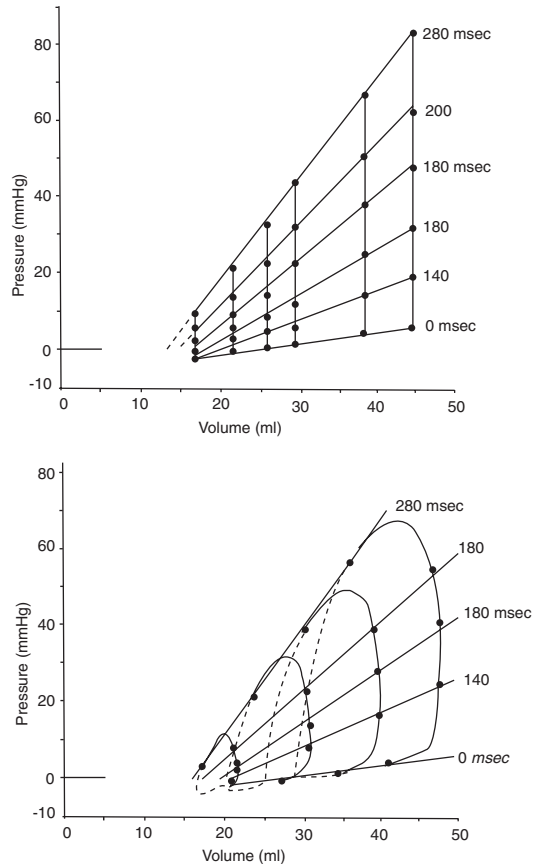


Fig. 3.4 Time-varying elastance of the RV. The upper figure shows isovolumetric (clamped pulmonary artery) and pressure volume loops with RV ejection (bottom) obtained by Maughan et al. (1979) in rabbit hearts. The lines indicate the changing elastance over time (numbers in msec) indicating that cardiac muscle elastance progressively increases during systole. The final line, the end-systolic pressure-volume line, gives the maximum pressure that can be generated from any initial volume. Unlike the pressure-volume curves of the LV, the “isotonic” phase of the pressure volume loop is curvilinear, indicating that filling of the RV continues after the onset of systole (From Maughan et al. (1979). Used with permission of Wolters Kluwer Health, Inc.)

tinues to flow out of the ventricle until the ventricular elastance begin its cyclic fall. The time available for ventricular ejection is largely determined by the time it takes for the pressure at a given volume to reach the E_{s-max} produced in a cycle (lower part of Fig. 3.4). This time is determined by the time available for Ca^{2+} to be released and taken up again by cardiac myocytes. This

time in turn is determined by the length of the plateau of the ventricular action potential (Chap. 7). RV systolic pressure (and LV pressure) peaks and begins to fall before Es-max is reached. This happens because the rising ventricular and pulmonary pressures increase the flow of volume out of the pulmonary artery and the flow out becomes faster than the flow of volume entering it. When RV cavity pressure falls below pulmonary artery pressure, the pulmonary valve closes and prevents backflow into the ventricle. This usually is considered the end of systole. However, the end of systole theoretically should be considered as the end of the active rise of ventricular elastance (i.e., at Es-max) and the beginning of relaxation of ventricular elastance. In the LV, this most often corresponds to aortic valve closure but this is not necessarily so in the RV. Timing of pulmonary valve closure sometimes can be delayed past the time that RV elastance has started to decrease. This occurs because closure of the ventricular outflow valve depends upon the pressure differences across the valve. When pulmonary arterial volume run-off is sufficiently rapid because of very low pulmonary vascular resistance, or if the RV stroke volume is small and only adds a small amount of volume to the pulmonary vasculature, pulmonary artery pressure can fall faster than RV cavity pressure falls. This is seen as a “hang-out” of the ventricular systolic pressure tracing and can make it difficult to identify the end of systole, as defined by the period of actively produced ventricular elastance. Consistent with this, Dell’Italia et al. showed that the hang-out is determined by the rate of pulmonary artery emptying and the size of the stroke volume that it receives (Dell’Italia and Walsh 1988b). A hang-out is not seen when pulmonary vascular resistance is increased because pulmonary pressure remains higher than RV cavity pressure and the pulmonary valve closes more quickly as is more typical for the LV. The important point to take away from this discussion is that the value of the pressure and volume at closure of the pulmonary valve is not necessarily a point on the RV Es-max line. This complicates the assessment of the contractile function of the RV. In summary, Es-max is a very important physiological concept but it is

difficult to define in an intact organism. It is especially a problem when a single pressure-volume point is used to estimate RV Es-max (Trip et al. 2013).

The Starling curve provides an accessible way of evaluating cardiac function. This function plots cardiac output against right atrial pressure (Pra). The derivation is shown in Fig. 3.5. The plot indicates that Pra is the preload for everything from the right atrium to the aorta. Cardiac output on the plot is what comes out of the aorta assuming a constant heart rate, constant afterload, and constant contractility for both the RV and LV and a constant pulmonary resistance. An advantage of this plot is that it emphasizes the importance of the RV in determining cardiac output because this plot also is the function curve for the RV. However, it does not represent the LV function curve because that requires left atrial pressure on the x-axis. The plot emphasizes that the LV only can put out what the RV gives it.

Pressure-Volume Loops of the Right and Left Ventricles

There are important differences between pressure-volume loops of the RV and LV. The diastolic compliance of the RV is higher than that of the LV and the diastolic volume capacity at low pressures is much higher than that of the LV. The most striking difference between the RV and LV sides is that the slope of RV Es-max is much flatter than LV Es-max (Fig. 3.3). Thus, peak RV pressure is much lower than that of the LV, even though the two ventricles pump out the same stroke volume. The RV can do this because it ejects its stroke volume through the very low pulmonary vascular resistance. This is the evolutionary advantage for having a separate RV and pulmonary vasculature, in that it allowed the development of delicate gas-exchange structures. Unlike the systemic circuit, the pulmonary circuit also does not have to make major changes in distribution of flow by lowering regional resistances. Its systolic pressure thus can be kept low. Blood flow in the lung can be increased with little change in pressure by recruitment and distention

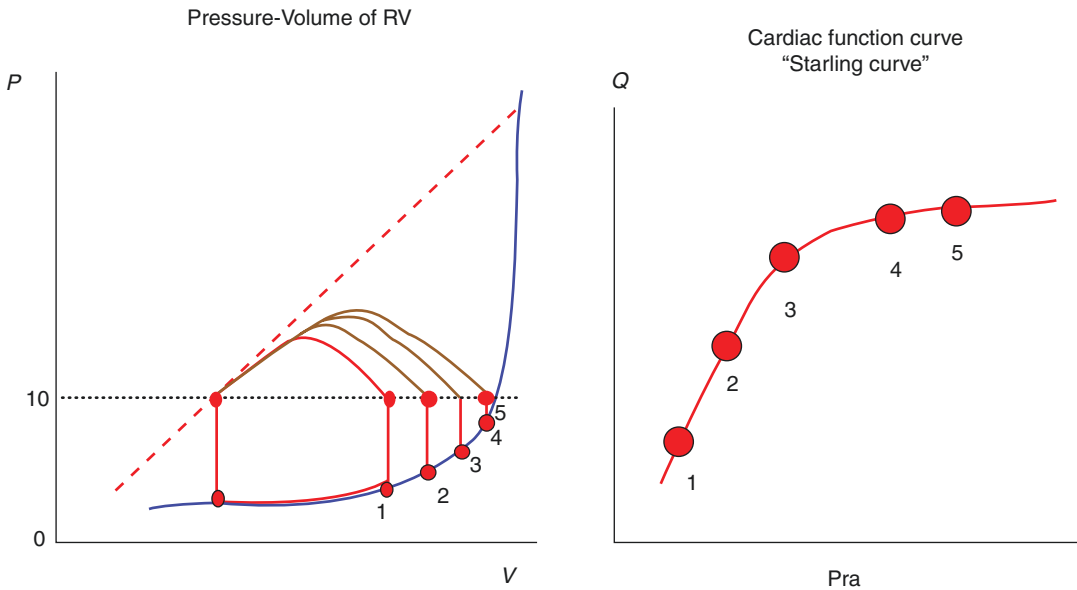


Fig. 3.5 Derivation of the cardiac function curve from the pressure-volume relationship, in this case, of the RV. The cardiac function curve indicates that cardiac output from the heart increases with increases in preload

(#1–5) while afterload (dotted line), “contractility” (slope of the end-systolic pressure volume line), and constant heart rate. The function curve has a sharp plateau when the limit of diastolic filling is reached

of vessels (see Chap. 5) (Mitzner and Goldberg 1975). However, when pulmonary pressure is higher than normal, the increased pressure cannot easily be acutely produced because the flatter Es-max line of the RV intersects the steep part of the passive filling curve at a much lower low pressure than the Es-max of the LV (Fig. 3.3). Because of this, when the required pulmonary arterial pressure is high for a normal flow, just dilating the RV is not enough to achieve the required higher systolic pressure, i.e., there is less preload reserve. Adaptations in both the diastolic pressure-volume relationship and the slope of Es-max must occur (Figs. 3.6 and 3.7) and are discussed further below.

In the LV, pressure rises at the onset of systole without a change in volume until the aortic valve opens; this is called isovolumetric ventricular contraction. In contrast, the RV diastolic volume continues to increase after the onset of systole and the rising part of RV pressure-volume relationship is curved (Fig. 3.4). This has been attributed to distortions of the RV wall based on its complex structure with an inflow region and infundibular outflow region (Figs. 3.2 and 3.7).

However, this explanation is unlikely. Heart muscle acts as syncytium, and pressure is produced by the marked rise in the systolic elastance of all myocytes. A major delay in depolarization of one region would likely result in major arrhythmias (Vogel et al. 2001). Also, if one region of the heart failed to significantly increase its elastance sufficiently fast enough, that region would expand as the pressure rises and would not produce efficient ejection. RV volume also would not increase unless more volume came in. Consistent with this reasoning, computer simulations that used linear equations to describe the rising elastance during systole to describe RV ejection still showed the same phenomena, that is, a curvilinear shape to the initial systolic rise in RV pressure (Fig. 3.8).

What then can explain the continuing increase in RV volume at the onset of systole? Careful analysis of the curves reveals that continued RV inflow likely occurs because MSFP is still higher than the low RV end-diastolic pressure and this keeps the tricuspid valve open until the generated RV pressure is greater than MSFP, which usually is in the range of 8–10 mmHg (Fig. 3.8). This

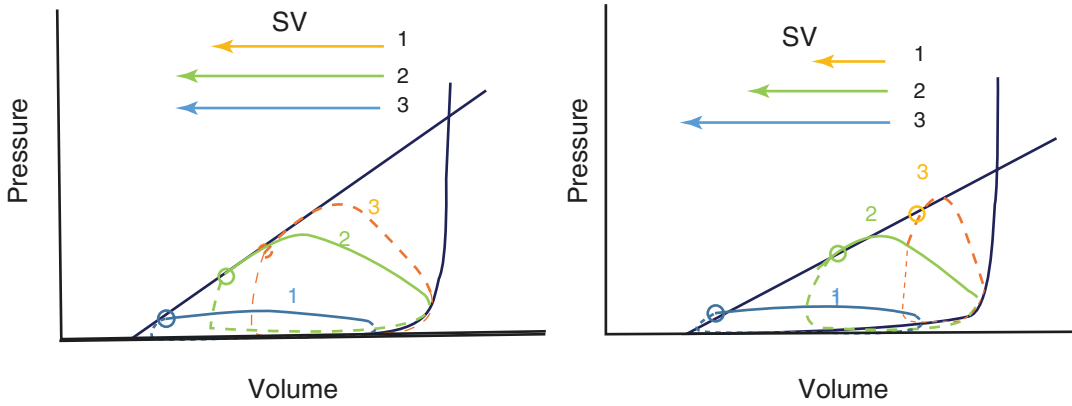


Fig. 3.6 Implications of the slope of the intersection of the RVEs and passive filling curve with normal, contractile function (left) and decreased RV-Es (right). When systole begins on the flatter part of the pressure-volume line, an increase in afterload (higher systolic peak pressure) can be accommodated by an increase in diastolic volume (#2) until the end-diastolic volume reaches the steep part

of the diastolic passive filling curve. This indicates cardiac limitation without dysfunction. When that happens (Friedberg and Redington 2014), stroke volume must fall with a further rise in afterload. On the right, the RVEs is flatter and the end-diastolic needs to be higher to maintain normal stroke volume. Accordingly, the limit of RV filling is reached earlier, indicating RV dysfunction

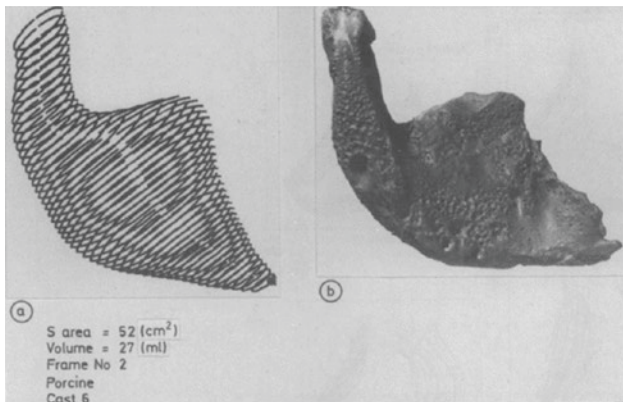


Fig. 3.7 Pressure-volume relationship of the RV obtained from angiograms and pressure measurements in a child. Note again the continuous filling of the RV after the onset of systole. The reconstructed loops (left side) also show



the complex shape of the RV. (From Redington et al. (1988a). Used with permission of BMJ Publishing Group Ltd.)

phenomenon is very evident in the notching of the ascending pressure in the RV P-V loops obtained by Redington et al. (Fig. 3.7) (Redington et al. 1988a, 1990).

Pulmonary arterial diastolic pressure is normally only in the range of 10–15 mmHg. Thus, shortly after the tricuspid valve closes, the pulmonary valve opens, ejection begins, and RV vol-

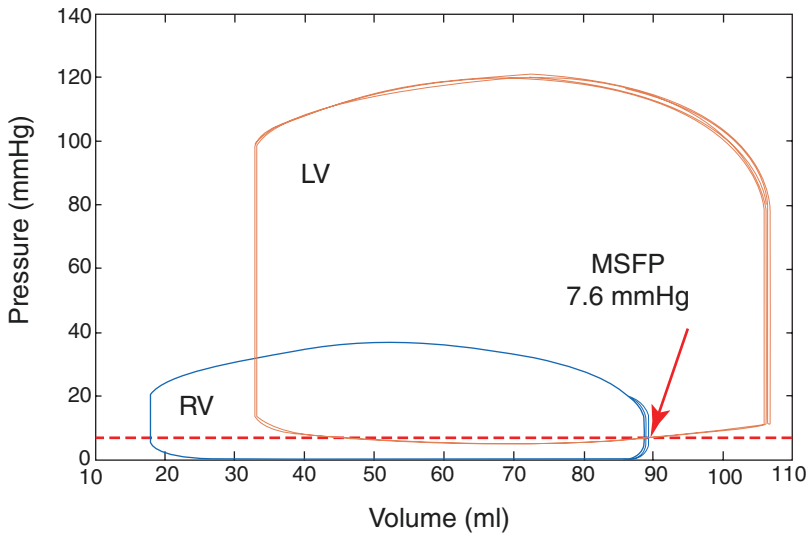


Fig. 3.8 Comparison of pressure vs volume loops of RV and LV. In these computer-generated P-V loop of the RV and LV, which are generated by equations with no geometric factors, in contrast to the LV, the P-V loop has a curvilinear initial rise in pressure instead of the isovolumetric

rise for the LV. Filling of the RV continues until the pressure in the RV is $>$ MSFP. This value is close to the opening pressure of the pulmonary valve and RV ejection so that volume then begins to decrease with the rising pressure

ume begins to decrease as blood is ejected into the low-resistance pulmonary circuit. This further contributes to the concave curve of the rising systolic pressure in contrast to the isovolumetric rise seen in the LV (Figs. 3.4, 3.7, and 3.8). A lack of a curvilinear rise in the LV occurs because the much greater pressure rise in the LV obscures any slight delay of closure of the mitral valve, and the much lower compliance of the pulmonary venous system compared to systemic veins produces faster pulmonary venous drainage into the left atrium.

Function of the RV often is considered in terms of coupling of the ventricular and pulmonary circuits (Vonk Noordegraaf et al. 2017, 2019; Vonk-Noordegraaf et al. 2013; Fourie et al. 1992). This also can be examined in terms of the impedance to RV ejection. Although the impedance analysis is useful for characterizing the shape of the pulmonary pulse pressure, a factor that likely affects RV and pulmonary vascular transcriptional signaling (Urashima et al. 2008), it is less useful for understanding volume ejection from the RV and what limits stroke output by the

RV, which is discussed next. The dominant factor in pulmonary artery impedance is the pulmonary vascular resistance and this is what dominates the load on the RV. In modeling studies, it can be pulse pressure.

Flow from the RV is determined by the pressure difference between the walls of the RV and pulmonary artery, plus a small kinetic energy component, and some dampening of the pressure by the expansion of the walls of pulmonary vessels. As already discussed, the pressure generated in the ventricles during systole is determined by Es-max which is a function of the contracting cardiac myocytes. This point is evident at the extreme condition. When the pulmonary artery is clamped, peak RV systolic pressure solely is determined by the starting end-diastolic volume in the RV, which sets sarcomere length, and the pressure value associated with that volume on the Es-max line. In this case, peak isometric RV pressure is not affected by pulmonary elastance because it does not “see” it (Fig. 3.4). Second, when the RV ejects at a pressure below Es-max, blood is ejected until the volume in the ventricle

reaches the Es-max line in the time that is available for systole, although, as already noted, some volume may continue to empty due to the rapid run-off of blood from the pulmonary vasculature in the “hang-out” period (Dell’Italia and Walsh 1988b).

A key factor limiting RV output is the limitation to its filling which occurs because of the sharp upward break of the diastolic passive pressure-volume curve (Bishop et al. 1964). As long as the diastolic volume of the RV is on the relatively flat part of the passive diastolic filling curve, stroke volume can be increased through the Frank Starling mechanism by increases in end-diastolic volume with only small increases in Pra (Figs. 3.5 and 3.6). However, when the steep part of the passive filling curve is reached, end-diastolic volume cannot increase further to any significant degree (Figs. 3.5 and 3.6). This state can be called the “volume limited” state of the RV. The consequence is that any further rise in pulmonary arterial pressure, and thus rise in RV afterload, cannot be accommodated by the Starling mechanism. RV stroke volume will then decrease with any further rise in pulmonary artery pressure and so must cardiac output. Furthermore, the RV end-systolic pressure must rise, and so will RV end-diastolic pressure, which reduces the venous return of blood to the RV and lowers the steady-state cardiac output. When pulmonary artery pressure increases in the volume-limited state, stroke volume and cardiac output only can be maintained by an increase in heart rate or RV contractility.

An important component of volume limitation is the interaction of the passive filling curve with RV Es-max. The maximum possible pressure that the ventricle can produce is where the RV Es-max line intersects the steep part of the passive filling curve because the ventricle cannot increase its volume to reach a higher pressure point on the line (Figs. 3.5 and 3.6). This explains the well-recognized clinical experience that an unconditioned RV cannot tolerate a pulmonary arterial systolic pressure much above 50–60 mmHg. This pressure is the upper limit of the intersection of the RV Es-max and RV passive filling curve in most people. The flatter the RV Es-max line, the

lower the tolerable pulmonary artery pressure. Also, the flatter the Es-max line, the less the benefit of an increase in systolic pressure on stroke volume with an increase in RV diastolic volume. Use of inotropes can produce some increase in RV Es-max in the short run and allow higher RV systolic pressure. Over time, there needs to be adaptation of RV muscle that increases the slope of RV Es-max which allows tolerance of higher RV systolic pressures (Redington et al. 1988a; Faber et al. 2006; Leeuwenburgh et al. 2001; Redington 2006) (Fig. 3.9).

Role of Pulmonary Arterial Compliance

Sunagawa and co-workers introduced the term “effective arterial elastance” (E_a) (Sunagawa et al. 1983, 1985) to describe the ventricular-independent measure of arterial function which creates an outflow load on the ejecting LV, and this analysis has been applied to the interaction of the RV with the pulmonary circulation (Vonk-Noordegraaf et al. 2013; Vonk-Noordegraaf et al. 2017). I will not go into the detail of all of the problems with this analysis, and I only make a few comments. The primary determinant of force generation of the RV is the slope of Es-max and this slope is independent of the pressure load on the ventricle. The term E_a refers to a “dynamic” elastance in that it has both resistive and elastic components. The primary determinant of flow through the pulmonary vasculature is the resistance draining it and the downstream pressure of the pulmonary circuit which is the left ventricular diastolic pressure when the mitral valve is intact or the left atrial pressure when it is not; in the presence of non-West Zone III conditions it is alveolar pressure. In modeling studies, it can be shown that even large changes in pulmonary arterial compliance do not have much effect on flow from the RV in the steady state, although compliance changes do affect the pulse pressure. There are major problems in making measurements of pulmonary arterial compliance in the intact human because to truly measure this static property, flow needs to be stopped to eliminate

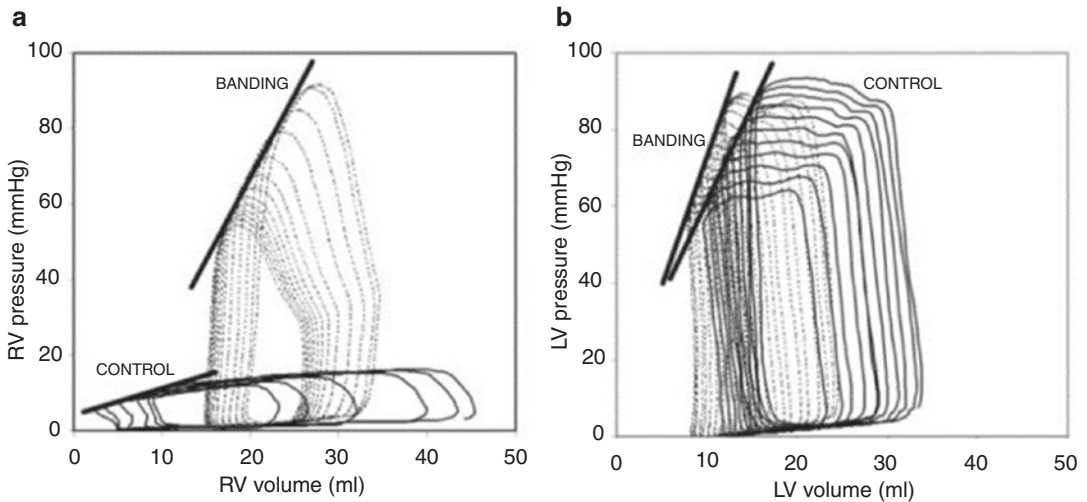


Fig. 3.9 Pressure-volume loops of RV (left, **a**) and LV (right, **b**) during vena cava occlusion with and without pulmonary artery banding. Solid lines indicate control animals and dotted lines animals with pulmonary artery banding. The black solid line indicates end-systolic P - V

relationship (E_{es}). RV E_{es} markedly increased with pulmonary banding but stroke volume fell. There was only a small increase in LV E_{es} with pulmonary artery banding. (From Leeuwenburgh et al. (2001) Used with permission of The American Physiological Society)

changes due to volume loss through the downstream resistance and to identify the value of the downstream pressure. This latter factor is often dealt with by considering the value zero which creates a large error with small pressure difference across the pulmonary circuit. Another major limitation of the analysis is that it only considers what goes out of the heart but does not consider what is coming in and what likely is most important, the significance of RV volume limitation on the potential stroke volume (Fourie et al. 1992; Vonk Noordegraaf et al. 2017; Morimont et al. 2008).

Pressure Load vs. Volume Load

Decreased RV function often is considered in terms of either a volume load, which is defined by an increased RV diameter, or a pressure load, which relates to the potential of the RV to generate a pulmonary arterial pressure. To start, it should be clear that these cannot be separated because both an increase in pulmonary arterial pressure and a decrease in E_{s-max} will increase end-diastolic volume and pressure. If cardiac output is decreased, and RV end-diastolic pressure is

increased without an enlarged RV end-diastolic volume, there is a restrictive problem such as tamponade or a myocardial infiltrative process, rather than true mechanical failure of RV muscle shortening and pressure generation.

In his seminal work on the law of the heart, Ernest Starling realized that even when the right heart stops pumping, RV end-diastolic pressure cannot be higher than the upstream MSFP, which normally is in the range of 8–10 mmHg (referenced to the mid-point of the right atrium) (Patterson and Starling 1914) (see Chap. 2). Thus, a central venous pressure greater than the normal values of MSFP only can occur generally two ways; either volume was given by the clinician or the normal volume intake orally was retained by decreased renal function.

An initial adaptive process for the RV in the face of limited RV function also can be an increase in right atrial size. The large atrium then acts as a volume reservoir, which adds to the compliance of the venous system. This reduces venous pressures and allows for faster filling of the RV. It acts somewhat like the sinus venosus in fish and in the human fetal circulation. However, the consequence is dilatation of the tricuspid annulus and progressively increasing tricuspid

regurgitation, which eventually makes the efficiency of the RV worse (Dos et al. 2005; Prieto et al. 1998).

Definitions of Right Ventricular Limitation, Dysfunction, Failure

An issue that arises from this discussion is how should right ventricular *dysfunction* and right ventricular *failure* be defined? A simpler term first needs to be introduced – right ventricular *limitation* (Table 3.3). This term indicates that the end-diastolic volume is at the steep part of the RV

passive filling curve and end-diastolic volume cannot increase (Figs. 3.3, 3.4, 3.5, and 3.6). As already indicated, when that happens, only an increase in heart rate, increase in contractility, or a decrease in RV afterload (i.e., pulmonary artery pressure) can increase cardiac output. Limitation can occur in someone who is volume overloaded but does not have RV “dysfunction”; in someone with decreased force production by the RV (flattening of RV Ees); or in someone with an increase in Es-max, but the increase is not sufficient to accommodate a markedly increased pressure load. However, the consequence is the same; when RV filling is limited, giving volume to increase Pra will not increase cardiac output. This is what more frequently is called fluid non-responsiveness. Of importance, echocardiography cannot detect right ventricular limitation because it is not possible to know that the diastolic volume did not change with a volume infusion because of a limitation to filling or because the infused volume was insufficient. Only a pressure change can identify that filling is limited. Right-sided volume limitation only becomes evident on an echocardiogram when the right-sided pressure increases sufficiently to shift the intra-ventricular septum to the left, but that is too late. Volume limitation of the RV is best identified by a rise in right atrial pressure without a rise in cardiac output.

I define *right ventricular dysfunction* as the condition in which the RV is enlarged, a higher RV diastolic pressure and volume are required for a normal cardiac output, and the limit of right heart filling occurs at a cardiac output value lower than normal. This occurs because of a decrease in RV Es (contractile force of the ventricle). By this terminology, a low stroke output from the RV because of high pulmonary pressure would be *limitation unless the load on the RV resulted in a subsequent decrease in the RV Es*.

This is similar to *right ventricular dysfunction*, but should be used to define a situation in which cardiac limitation also is present, the RV is enlarged, the cardiac index is <2.2 L/min/m², and there is evidence of inadequate cardiac output for tissue needs including rising lactate, falling central venous saturation, hypotension, decreased urine output, and decreased sensorium.

The definitions of failure and dysfunction are thus relative.

Table 3.3 Definitions for limited output by the right ventricle

1. Right ventricular limitation

End-diastolic volume is on the steep part of the diastolic passive filling curve. This can be due to limitation by the pericardium, the myocardial cytoskeleton, or other mediastinal and thoracic structures.

End-diastolic volume cannot increase with a further increase in diastolic pressure. This does not necessarily indicate dysfunction and can be due to excess use of volume, inability of the heart to sufficiently adapt to an increasing volume return, or because of right ventricular dysfunction and a failure to adequately empty RV volume.

2. Right ventricular dysfunction

The RV is enlarged, a higher RV diastolic pressure and volume are required for a normal cardiac output, and the limit of right heart filling occurs at a value of cardiac output lower than normal.

This occurs because of a decrease in RV Es (contractile force of the ventricle). By this terminology, a low stroke output from the RV because of high pulmonary pressure would be *limitation unless the load on the RV resulted in a subsequent decrease in the RV Es*.

3. Right ventricular failure

This is similar to *right ventricular dysfunction*, but should be used to define a situation in which cardiac limitation also is present, the RV is enlarged, the cardiac index is <2.2 L/min/m², and there is evidence of inadequate cardiac output for tissue needs including rising lactate, falling central venous saturation, hypotension, decreased urine output, and decreased sensorium.

The definitions of failure and dysfunction are thus relative.

See text for further details

cardiogenic shock studies (Thiele et al. 2019), but this depends upon the device used for measurement. An enlarged RV can be defined by it being larger than the LV on imaging. A complication of the terminology occurs in chronic pulmonary hypertension. These patients are able to generate higher-than normal RV systolic pressures (Fig. 3.9) which means that RV function is in fact higher than normal. The problem is that this increase is not sufficient to provide the force necessary to overcome the load, and RV limitation becomes the problem until the RV begins to truly fail, meaning that Es-max is falling.

The term *right ventricular failure* is similar to *right ventricular dysfunction*, but it should be used to define a situation in which cardiac limitation is present, the RV is enlarged, the cardiac index is $<2.2 \text{ L/min/m}^2$, and there is evidence of inadequate cardiac output for tissue needs including rising lactate, falling central venous saturation, hypotension, decreased urine output and decreased sensorium. The definitions of failure and dysfunction are thus relative, whereas *right ventricular limitation* is a broader term that does not necessarily indicate dysfunction and even can be induced by inappropriate use of fluids. It also sometimes is purposely created as part of goal-directed protocols (Pearse et al. 2014), although I do not recommend these approaches because, to repeat, when right heart output is volume limited, a further increase in cardiac output only can occur with an increase in heart rate, increase in contractility, or a decrease in afterload. If RV filling is pushed too far, and limitation is present, true RV dysfunction or even failure can result because of the strain on the RV wall.

Right and Left Ventricular Interactions

There has been much discussion about mechanical interactions between the RV and LV, which should not be unexpected, because they share a common space in the mediastinum, they have overlapping myofibers, especially in the intra-ventricular septum (Smerup et al. 2009), and they are both surrounded by the pericardium.

Interactions between the ventricles can occur through volume distention of one side, which takes up some of the common space in the pericardium, and thereby changes the compliance of the other side. This is primarily a diastolic-volume interaction. Interactions also can occur during systole by the contraction of one ventricle aiding, or failing to aid, the other side. However, as shown by Olsen et al. in conscious dogs, the primary interaction between the RV and LV is by far dominated through what is called the series effect (Olsen et al. 1983) and this always needs to be considered. The underlying principle of the series effect is that whatever comes out of the LV had to first have come out of the RV, i.e., conservation of mass. Furthermore, what comes out of the RV had to come back from the venous reservoir. When RV filling is limited, filling of the LV, too, is volume limited because more blood cannot get to it, and a change in performance of the LV has a minimal effect on cardiac output.

Appleyard and Glanz developed a theoretical model to determine the transmission time for changes in either ventricle to affect the other (Appleyard and Glantz 1990). They used a simple three-compartment model of the pulmonary circuit that comprised arterial and venous resistance and a compliant region between the two and calculated a time constant of 0.26 sec, which would predict that an effect would occur in less than one heart beat at a normal heart rate. However, during the ventilation cycle with mechanical breaths, RV output decreases transiently to almost zero, while the decrease in LV output is much more modest (Katira et al. 2017). A modeling study with two pulmonary compliances, one in the arterial and one in the venous vasculature, and three resistances connecting them faithfully reproduced this observation. This indicates that pulmonary venous volume what has been called “pulmonary buffering” capacity that can sustain LV output during the transient loss of RV output (Magder and Guerard 2012).

Interdependence due to volume effects has been studied in a number of animal studies by selectively filling one ventricle and observing the effect on the pressure-volume relationship of the other ventricle (Laks et al. 1967; Taylor et al.

1967; Taquini et al. 1960; Santamore et al. 1976; Bove and Santamore 1981; Mouloupoulos et al. 1965). Generally, the effects are modest and unlikely to have a significant impact clinically.

Interest in the effect of RV volume on LV function increased with the onset of echocardiography, likely because it became easy to observe a left shift of the septum (Weyman et al. 1976). One of the first reports described a shift of the normal septal curve toward the LV when a strong negative inspiration was applied against a closed glottis in what is called a Mueller maneuver (Brinker et al. 1980). The fall in pleural pressure during the inspiratory effort with a Mueller maneuver increases RV filling. It was argued that this shifts the intraventricular septum leftward and reduces LV volume during the inspiratory phase by compromising LV diastolic compliance. However, a study of subjects with markers placed directly into the LV wall showed that LV volume actually increases during a Mueller maneuver (Buda et al. 1979), and the increase in LV end-diastolic pressure likely was due to the combination of increased venous return and limited LV output due to the higher afterload. The shift seen in the septum also was likely due to an early phase of increased RV filling before the accumulation in LV volume that occurred with the series effect which passed the increased RV filling to the LV filling and the increased LV afterload. Animal studies also have shown an increase in LV volume during the equivalent of a Mueller maneuver (Robotham and Mitzner 1979; Summer et al. 1979). The increase in RV volume likely impacted left-sided pressure but cannot explain the actual increase in LV volume that occurs. For example, in a study in humans, left atrial transmural pressure increased to more than 30 mmHg (Magder et al. 1983). Large left-sided 'v' waves also developed indicating decreased left atrial compliance as would be expected as the increase in volume moves the left atrial passive filling up the steeper part of its pressure-volume curve. Thus, failure of the LV to eject volume was likely the major factor and consistent with the enlarged LV rather than the septal shift, but a decrease in mediastinal space by the RV also likely contributed to the rise in left atrial transmural pressure.

The role of septal shift also has arisen in magnetic resonance imaging studies (Gan et al. 2006). A recent study of patients with enlarged RV because of advanced pulmonary hypertension demonstrated a marked leftward septal shift that impaired early diastolic filling of the LV and the authors speculated that this might have caused the decrease in cardiac output. However, as the authors noted, the series and direct effects cannot be separated. Given the need to consider the conservation of mass, it is likely that the series effect dominates unless the RV increases LV diastolic pressure, which then results in an increase in PA pressure and a decrease in RV output through a mechanism discussed below where preload becomes afterload.

As shown by Maughan et al. in isolated canine hearts (Maughan et al. 1987), and modeled by Santamore et al. (1990), transmission of pressures between the RV and LV is not just dependent on the elastance of the septum but on the elastances of all cardiac walls. The basic observation was that the normal septal elastance is higher than that of the external walls of the chambers so that pressure is not easily transmitted across the septum, but this can change with ischemic injury to the septum or a cardiomyopathy. The compliances of the walls also can change with injury or can be restricted by the lungs and pericardium.

A key determinant of the potential significance of interventricular interaction is where RV volume is on the steep part of diastolic filling curve. On the flat part of the RV passive filling curve, RV diastolic pressure is low and likely does not affect the LV. It only is when the diastolic volume reaches the steep part of the passive filling curve that diastolic pressure can be high enough to be transmitted to the LV. When the steep part of the filling curve is reached, RV diastolic pressure greatly increases with any further increase in volume and effects can be greatly magnified (Mitzner et al. 1976). Accordingly, if the RV volume is large, but RV diastolic pressure is low, there should be little interaction. However, a small further change in volume could rapidly change things. The other important variable is the presence of the pericardium; without it, the effect of the RV on the LV is minimal (Maughan et al.

1979; Robotham and Mitzner 1979). Finally, the compliances of the walls of all the cardiac chambers must be considered.

From a quantitative point of view, it should be evident that in general, the effect of RV-LV diastolic interactions is small. If the RV compromises LV filling or ejection, volume distribution in the circulation must change because the volume must go somewhere, at least over the short-run, to maintain the conservation of mass. Changes in the distribution of volume change pressure differences among all regions and result in a new steady state. As long as diastolic filling of the RV is not limited, cardiac output can at least be partially restored through the Frank-Starling mechanism.

Excessive filling of the RV can produce an unfortunate situation in which RV preload becomes RV afterload. What happens is that when RV diastolic pressure is sufficiently elevated, right-sided diastolic pressure is more easily transmitted to the left heart, especially when the pericardium is intact, but even when not. The consequent rise in left-sided diastolic pressure raises the downstream pressure for return of pulmonary blood flow to the left heart. To maintain the same cardiac output, pulmonary arterial pressure must rise to maintain the same pulmonary vascular pressure difference. This increases the afterload on the RV, which further decreases right heart output and leads to a further rise in RV diastolic pressures which gets transmitted to the left side, and the cycle goes on. When this happens, the RV diastolic pressures need to be decompressed by actively removing ineffective preload, or by increasing RV function by increasing heart rate or contractility.

Clinical and physiological significance of diastolic ventricular interaction was nicely demonstrated by Atherton et al. (1997a, b) (Fig. 3.10). They applied lower body pressure to pool venous blood volume in that region and examined the effect on LV volume and cardiac output in three groups: subjects with normal cardiac function, subjects with compensated heart failure, and subjects with decompensated heart failure (symptomatic). As predicted, lower body pressure decreased LV volume in the normal and compen-

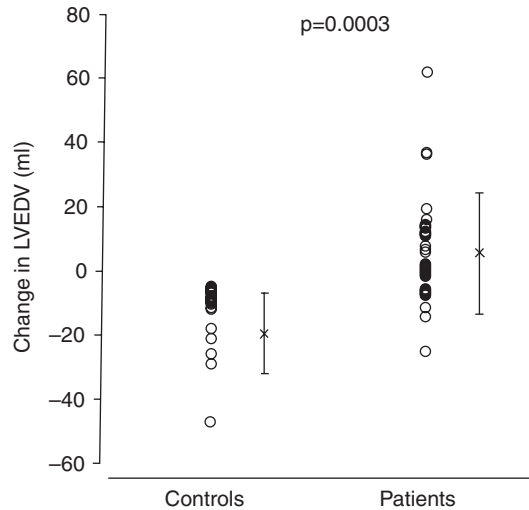


Fig. 3.10 Change in left ventricular diastolic volume obtained by echocardiography in response to lower body negative pressure in patients with compensated RV (left) and decompensated RV failure (right). Pooling blood in the legs when the RV was not overloaded results in a decrease in left-ventricular end-diastolic volume (LVEDV) as occurs when the heart is normal (not shown). However, in subjects with overfilled right hearts, application of lower body negative pressure increased LVEDV. (From Atherton et al. (1997a). Used with permission of Elsevier)

sated subjects, but surprisingly, it increased LV size and cardiac output in patients with decompensated heart failure. The argument was that decompressing the RV in the fixed volume of the cardiac cavity, and removing what I like to call wasted preload, allowed improved LV filling and output.

An example of RV dysfunction that is due to dilatation that is not because of a systolic pressure load, is the progressive dilatation that occurs with pulmonary insufficiency. This often arises after surgical repair of tetralogy of Fallot (Friedberg and Redington 2014; Babu-Narayan et al. 2006) because the pulmonary valve often has to be removed or is damaged when the surgeon needs to enlarge the PA outflow tract to prevent a high load on the RV. The amount of pulmonary regurgitation can be analyzed with P-V plots as shown in Fig. 3.11. The P-V plot on the left shows that of a normal child. The P-V on the right shows what it would look like if the child had severe pulmonary regurgitation based on the studies of Redington

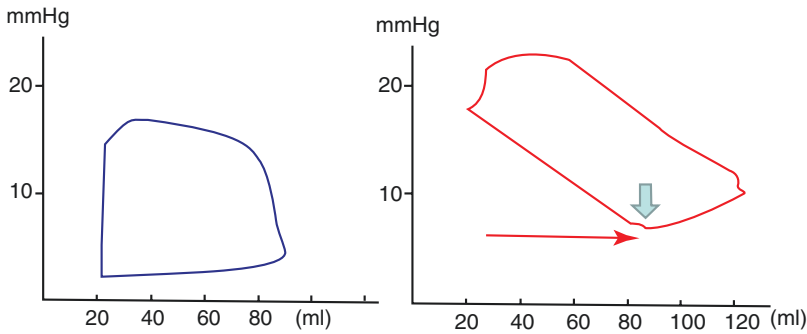


Fig. 3.11 Schematic pressure-volume loops (P-V) of RV of child without (left) and with (right) severe pulmonary regurgitation. The schematic P-V on the left is typical of a normal RV in a child. The right side shows a predicted P-V with severe pulmonary regurgitation. The normal isovolumetric fall in RV pressure at the end of systole does not occur. Instead the RV volume increases with a fall in diastolic pressure (indicated by the long straight arrow).

The downward wider arrow indicates opening of the tricuspid valve opens, venous return to the RV and start of in this case at about 7 mmHg, and end-diastolic pressure rises to 10 mmHg. The isovolumetric contraction phase also is greatly distorted because of the lowered pulmonary artery pressure post-systole due to the regurgitated volume. The patterns are based on the work of Redington et al. (1988b)

et al. (Redington et al. 1988b). There is no isovolumic diastolic phase. Instead, RV diastolic volume increases with the fall in RV pressure. This phase is marked by a long arrow. When the right atrial pressure rises above RV diastolic pressure, the tricuspid valve opens, venous return enters the ventricle, and the pressure rises (marked by a downward arrow). There also is no isovolumic contraction phase. The volume begins to fall with the onset of systole because the RV pressure quickly becomes greater than the PA pressure that was reduced by the regurgitated volume.

Marked RV dilatation overtime crowds the LV in the limited mediastinal space. The dilated RV also develops increasing tricuspid regurgitation which further dilates the RV. Increasing RV fibrosis develops with decreased RV function and ultimately failure. A phenomenon worth noting has been documented in the long-term outcome of children with repair of tetralogy of Fallot (Redington 2006). Children who have more restrictive RV function early after surgery have a higher mortality. However, over time, ventricles of survivors did not dilate with pulmonary insufficiency because of the intrinsic RV diastolic stiffness, and they thus better handle the pulmonary insufficiency later in life (Fig. 3.12).

The following are some general rules for diastolic interaction of the RV and LV. If the septum is stiff and the LV free wall is compliant, a raising RV diastolic pressure by itself has little effect on the pressure and volume of the LV, although the shape could change. If the increase in right-sided pressure is associated with increased right-sided volume, the situation is more complex. The diastolic pressure rise in the RV is affected by the RV free wall stiffness. If the pericardium is intact and the free wall is effectively very stiff, the increase in RV volume takes up more mediastinal space, and if the pericardium is in place, more of the pericardial space. The effect on the LV then depends upon the septal elastance as well as the elastance of the LV free wall. If the septal elastance is reduced by a previous myocardial infarction, or a cardiomyopathy, RV pressure is more easily transmitted to the left side, and there will be more bowing of the septum into the left side. If the LV free wall is damaged, this not only will allow more of the right-sided transmitted pressure to be dissipated through the more compliant LV free wall but also will allow more bowing of the septum into the left side. All these effects will be modified by the presence or absence of the pericardium and by the size of the mediastinal space left by the lungs (Butler 1983).

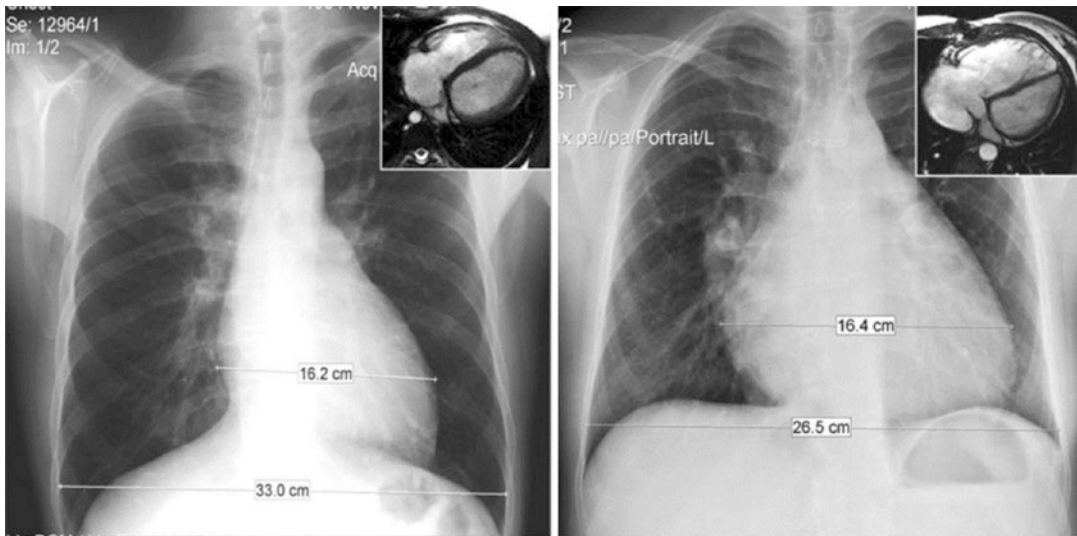


Fig. 3.12 Chest X-ray and magnetic resonance imaging (MRI inserts) from two patients 20 years following repair of Tetralogy of Fallot. Both patients were treated with a pulmonary artery patch and did not have pulmonary artery stenosis. The patient on the left had restrictive physiology on the RV and there was only a mild increase in RV size.

The patient on the left had a normal RV diastolic compliance. There is a marked increase in RV size based on the increase in the cardiothoracic ratio and the MRI image which shows the septal flattening. (From Redington (2006). Used with permission of Elsevier)

The RV and LV also can interact during systole. Increased left-sided contractions can aid RV ventricular pressure production in two ways. LV systolic pressure can be directly transmitted to the RV (Santamore et al. 1976; Bove and Santamore 1981; Yamaguchi et al. 1991; Hoffman et al. 1994) but the effect is small. More significantly, septal contraction during LV contractions can assist RV contraction. The septum is common to both ventricles and shares fibers from both. The greater the force generated by the LV, the greater the shortening of the shared right and left septal myofibers. One way this was demonstrated was by giving a bolus of volume into the LV and observing an instantaneous increase in RV systolic pressure, but the magnitude was small, and this is hardly physiologically possible because the LV gets its volume from the RV (Bove and Santamore 1981).

The importance of LV support through the septum for RV ejection becomes potentially important when the LV is unloaded by an LV assist device. An experimental difficulty in

studying this phenomena is the isolation of the effect of ventricular systolic interactions from the series effect. This was elegantly done by Farrar et al. in normal animals and animals with pacing-induced cardiomyopathy (Farrar et al. 1993). They applied an assist device to the LV and measured the generated RV pressure on a single unload LV beat. By the study design, this occurred from unchanged RV and LV diastolic volumes. The effect was modest when the RV and LV had normal function but it was greater in animals with the cardiomyopathy. In myopathic animals, generated RV systolic pressure decreased by 17% versus 10% in the normal animals and the stroke volume fell by 37% and 18% respectively. However, in this study, LV systolic pressure was decreased by 60%, which is never observed clinically. They thus demonstrated a clear decrease in RV output on the single beat, but it is hard to know whether this was a function of an overall change in the RV P-V relationship or just due to loss of LV septal contraction. Furthermore, sustained measurements over time were not obtained.

In other experimental studies, the consistent response is a reduction in RV afterload, an increase in RV diastolic compliance, and a decrease in RV contractility but, importantly, no change in cardiac output. A left shift of the septum also is commonly seen (Santamore and Gray Jr. 1996). All these are not surprising responses to the reduction of the downstream pressure faced by the RV. If cardiac output does not change, the RV must be handling what comes back. The decrease in LV force function thus most likely is not a major clinical concern. However, a potential clinical problem is that the improvement in LV production could be associated with an increase in cardiac output as part of a restoration of an oxygen deficit from previous underperfusion, or because of excessive volume resuscitation. The increased venous return could then result in RV volume limitation and produce all the associated problems of this state. It would then appear that there is RV dysfunction when it really was limitation by the excessive returning volume. Inotropic therapy, increasing the output from the LV assist device or decreasing vascular volume, may be necessary.

In the presence of pulmonary hypertension, the RV must generate greater systolic pressure, and it might be considered that this could increase left-sided output through the common septum. However, the effect is small (Yamaguchi et al. 1991) as is evident in Fig. 3.9 (Leeuwenburgh et al. 2001) in which a marked increase E_s because of RV loading over time only produced a very small increase in the LV E_s -max.

Is the Right Ventricle Necessary for Normal Aerobic Function?

The initial response likely would seem to be an obvious yes. The RV must put out the same cardiac output as the LV, which at peak exercise in a young male can be greater than 20–25 L/min; this is a very respectable job! In an often quoted study, Starr et al. cauterized the free wall of the RV of dogs and reported no difference in heart function and long-term survival, arguing that the RV is not essential (Starr et al. 1943). However,

in the actual paper, only three dogs survived and only one lasted more than 24 hours. Furthermore, cardiac function was simply based on the absence of a significant rise in central venous pressure at rest, which, as already discussed, could only raise P_{ra} to MSFP, which normally should be in the 8–10 mmHg range. Other similar canine studies followed and similar results were observed (Donald and Essex 1954a, b). One study even included a chronic follow-up and showed that the animals could exercise at moderate levels that were similar to that of control animals (Donald and Essex 1954a). A criticism of these studies was that perhaps not enough RV free wall was removed. Accordingly, a series of complex studies were performed in which the free wall was electrically isolated from the rest of the RV during surgery (Damiano et al. 1991). Pacing wires were then attached to the electrically isolated area of the RV, which allowed contractions of the RV with or without contractions in the isolated region. Again, there was little loss of cardiac output when there was no longer a functioning RV free wall. This was true as long as pulmonary vascular resistance was not increased, but the loss of the RV free wall was important when RV load was increased. Based on these studies, it was argued that the LV contributes more than 50% of the force generated by the RV (Santamore et al. 1990; Donald and Essex 1954a; Damiano et al. 1990, 1991). However, the criticism still remains that the septum also is a rich part of the RV contractile mechanism, and it still was intact. It even has been argued that the septum is a disproportionately important component of RV ejection because it is at the bottom of the effective bellows system of RV (Geva et al. 1998). It thus is not fair to argue that all of the septal actions are related to the LV.

Insight into the role of the RV can be gained from children born without a functional right heart because of tricuspid atresia or failure of the RV to develop (Gewillig and Brown 2016). To maintain pulmonary perfusion, early in life, the vena cava is connected directly to the pulmonary artery in what is called a Fontan procedure (Fontan and Baudet 1971). Strikingly, these people can be very functional aerobically, at least in their youth.

We tested a 22-year-old subject who reached over 80% of his predicted maximum aerobic capacity. Since cardiac output normally increases linearly with O_2 consumption, this implies that his cardiac output was in the range of 80% of his predicted value based on his body size. The ability of Fontan patients to obtain near-normal maximal cardiac outputs emphasizes an important principle of cardiovascular physiology. Flows are related to pressure differences through a resistance between different vascular compartments (Magder et al. 2019). The same flow can be produced with a high pressure and high resistance as with the LV in the systemic circulation, or a low pressure and low resistance as with the RV in the pulmonary circulation. What the RV does during exercise is it keeps P_{ra} low (Notarius et al. 1998). This allows the necessary increased venous return to occur. In a recent report, we postulated that exercising muscle could contribute to this function by transiently compressing the venous compartment in muscle (Magder 1995; Notarius and Magder 1996) and providing the extra force needed to decompress venous pressures in Fontan patients. However, there is a price to pay. During exercise, and even without, Fontan subjects need to have higher-than-normal venous pressures to provide a sufficient pressure difference for the return of blood to the LV. This has long-term consequences in that these patients often develop congestive cirrhosis and protein-losing enteropathies when they age (d'Udekem et al. 2014; Khairy et al. 2008), and their aerobic capacity steadily decreases with age at a much higher rate than normal subjects (Giardini et al. 2008). They also cannot tolerate a rise in pulmonary vascular resistance or an increase in left ventricular end-diastolic pressure, because in the absence of a RV, only a greater MSFP can maintain flow and that results in congestion of tissues. In summary, Fontan physiology emphasizes that the primary role of the normal RV is to reduce P_{ra} and thereby allow more efficient venous return (Furey et al. 1984). Generation of high systolic pressure is not the usual job of the RV. Normal pulmonary vascular resistance is very low and high right-sided flows can be generated at very low systolic pressures. The normal RV is actually designed to avoid generating a high pul-

monary artery pressures in order to protect the delicate pulmonary gas-exchange structures.

In a number of congenital cardiac abnormalities, the morphological RV substitutes for the morphological LV. This can occur not only when there is failure of the LV to develop but also when there is transposition of the great vessels. In this congenital abnormality, the aorta and systemic circulation come off the morphological RV, and the pulmonary artery comes off the morphological LV. To survive, these newborns require an atrial or ventricular defect, or a surgically induced shunts to mix the pulmonary and systemic parallel circulations. In an early surgical correction, a baffle was placed in the atrium so that the systemic venous return was diverted to the morphological LV, which then pumped the returning venous blood into the pulmonary circulation; the pulmonary venous return was diverted to the morphological RV, which pumped the blood out through the aorta at systemic pressure (Dos et al. 2005). Children surviving this procedure can have close to normal aerobic function. However, in their fourth or fifth decades, the morphological RV pumping at systemic pressure gradually fails and heart transplantation often is required (Dos et al. 2005; Prieto et al. 1998). A significant component of the progressive dilatation is tricuspid regurgitation, which accelerates the process (Prieto et al. 1998). This indicates the inherent difference in the load tolerance of the RV and LV, which is related to the differences in their transcriptional program as discussed above (Srivastava and Olson 2000). Today, ejection from the ventricles is redirected to their appropriate outflow tract so that the LV and not the RV pumps blood into the systemic circulation (Jatene et al. 1975).

Importance of Right Coronary Blood Flow

A component of ventricular interactions is related to coronary flow. Blood flow to the LV is restricted during systole by the high pressure that develops in the LV walls, but this does not occur in coronary vessels supplying the low-pressure RV. However, when pulmonary hypertension

develops, coronary flow to the RV also occurs primarily during systole and coronary flow becomes much more pressure dependent. To make matters worse, flow in the right coronary artery comes off the aorta and aortic pressure is dependent upon LV output. When LV output decreases, the energy demand of the LV at least decreases too. However, when the RV faces a high pulmonary artery pressure and the systemic arterial pressure falls because of decreased RV output, a very dangerous situation evolves. Inadequate coronary perfusion of the RV decreases RV output and thus decreases LV output, and there is a further fall in systemic arterial pressure. The dependence of RV load tolerance on systemic arterial pressure was elegantly shown by Salisbury (1955). They showed that the RV load tolerance progressively increased with increasing systemic arterial pressure; at a systolic aortic pressure of 200 mmHg,

dog hearts were able to produce pulmonary systolic arterial pressures of 150 mmHg, although some of the benefits also could have been due to the higher generated LV pressure as discussed below (Fig. 3.13).

The clinical importance of this is that in a patient with severe pulmonary hypertension, a fall in systemic arterial pressure and the resultant decrease in RV coronary blood flow can rapidly lead to a death spiral (Guyton et al. 1954; Brooks et al. 1971). Furthermore, as the RV fails, the rise in RV end-diastolic pressure decreases venous return and leads to limitation of RV filling so that the Starling mechanism can no longer compensate for the decrease in the RV contractile state. It thus is extremely important to maintain systemic arterial pressure in patients with severe pulmonary hypertension. Great caution should be used with any treatment that decreases systemic vascu-

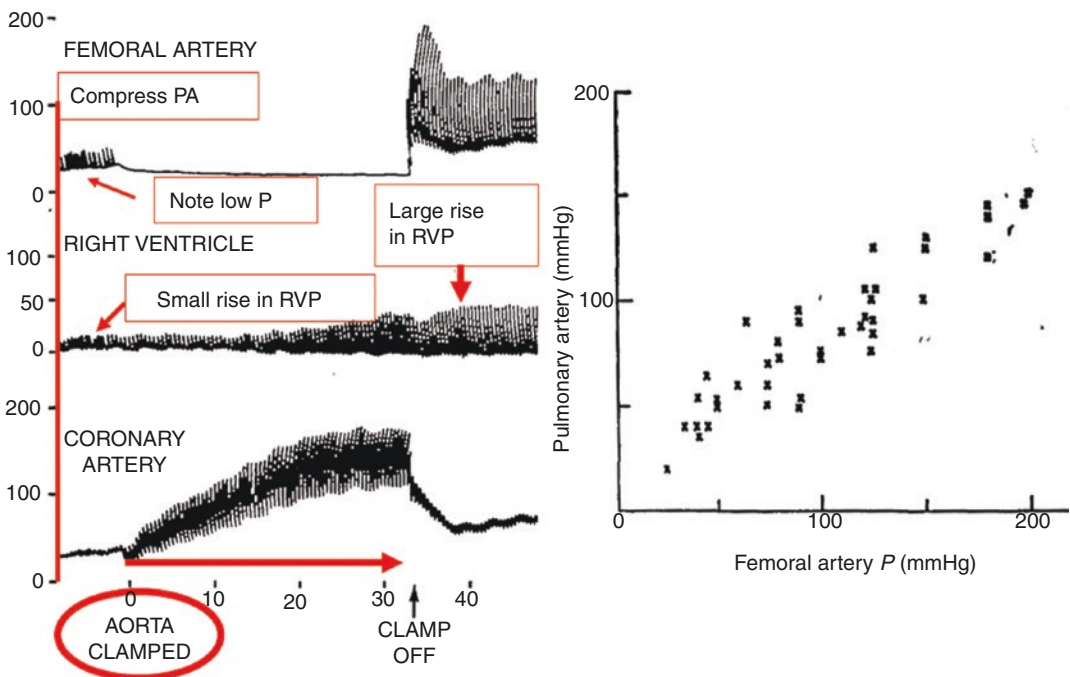


Fig. 3.13 Importance of maintenance of coronary flow for RV load tolerance in a dog. The pulmonary artery was compressed which resulted in a marked fall in arterial pressure in the femoral artery (presumably from the fall in cardiac output). The right coronary artery was cannulated and perfused. Increasing the coronary artery pressure resulted first in a small rise in right ventricular generated pressure (RVP), but when arterial pressure was high

enough, there was a larger increase in RVP. When the compression was released, a marked increase in RV function can be seen. The right side of the figure shows the increase in pulmonary artery pressure with a rise in femoral artery pressure after release of the pulmonary compression. (From Salisbury (1955). Used with permission of Wolters Kluwer Health, Inc.)

lar resistance, including anesthetic agents and drugs that vasodilate systemic resistance vessels, or a rapid decrease in stressed vascular volume by increasing venous capacitance. It also is important to avoid a mode of mechanical ventilation that increases the load on the RV. Although dobutamine has been shown to be more effective than norepinephrine for increasing the force of RV contraction in an animal study (Kerbaul et al. 2004), this only is clinically applicable if the dobutamine infusion does not vasodilate systemic arterial vessels, lowers systemic blood pressure, and causes the downward spiral discussed above. In my opinion, dobutamine only should be used in patients who have pulmonary hypertension when norepinephrine is standing by.

Systemic arterial pressure is not just necessary for right coronary flow when pulmonary artery pressure is elevated. Generation of a higher systemic arterial pressure requires greater pressure generation by the LV. The increase in the force of LV ejection can then aid RV ejection by increasing the force produced by the common septum. Evidence for this comes from studies in which higher systemic pressures increased RV load tolerance, even when the right coronary artery was cannulated and coronary flow was held constant (Page et al. 1992; Belenkie et al. 1989). In other studies it was shown that even though coronary flow did not change when arterial pressure was raised RV load tolerance increased, again indicating that it is increase in the LV force of contraction and not the increase in coronary flow that is important (Apitz et al. 2012; Scharf and Bromerger-Barnea 1973). This further emphasizes the importance of maintaining adequate systemic arterial pressure in patients with pulmonary hypertension.

Why Is Presence of a Dysfunctional Right Ventricle Often Worse than No Right Ventricle?

If patients can live and function almost normally without an RV, why do patients do so poorly with a dysfunctional RV? Part of the answer is that people who do not have an RV only have normal

function as long as they do not have an increase in pulmonary vascular resistance, pulmonary vascular critical closing pressure, or an elevated LV end-diastolic pressure. However, a dysfunctional RV can even be a problem when pulmonary pressures are not high. A key factor is the limit to RV diastolic filling. This sets a limit to the potential RV stroke volume during each cardiac cycle and thus limits left-sided stroke volume. In contrast, when there is no RV, venous return is not constrained by the limited time of RV diastolic filling, and venous return can continue right through the cardiac cycle. Another factor could be that as the RV fails to keep up with returning blood and dilates, tricuspid regurgitation develops. The RV then produces a backward wave which actively inhibits venous return as demonstrated by Guyton many years ago (Guyton et al. 1976). Since the pressure is less in the upstream venous compartment than in the pulmonary circuit, it is easier for the RV contraction to pump blood backward than forward. The consequent increased filling of the RV leads to further dilatation and further tricuspid regurgitation. Finally, the volume of the RV takes up space in the mediastinum.

Conclusion

The electrical, pharmacological, and filling characteristics of the RV are different from those of the LV. These derive not only from its more primitive transcriptional program but also from its proximal coupling to the compliant systemic venous system. The major role of the RV is to keep P_{ra} low and thereby allow adequate return of blood to the heart without the upstream venous reservoir pressure having to be excessively elevated. Despite producing a low systolic pressure under normal conditions, the RV puts out the same stroke volume as the LV. This is what it evolved to do for normal function. The diastolic RV filling curve, too, is very compliant until it breaks steeply and then strongly limits further filling. This not only protects the lungs but also limits the maximum possible stroke volume and cardiac output for a given heart rate. Most com-

monly, the pericardium limits RV filling, even before the limit of RV wall limits end-diastolic volume. These characteristics make the presence of a dysfunctional RV worse than no RV at all.

References

- Abdel-Samad D, Perreault C, Ahmarani L, Avedanian L, Bkaily G, Magder S, et al. Differences in neuropeptide Y-induced secretion of endothelin-1 in left and right human endocardial endothelial cells. *Neuropeptides*. 2012;46(6):373–82.
- Abdel-Samad D, Bkaily G, Magder S, Jacques D. ETA and ETB receptors contribute to neuropeptide Y-induced secretion of endothelin-1 in right but not left human ventricular endocardial endothelial cells. *Neuropeptides*. 2016;55:145–53.
- Apitz C, Honjo O, Friedberg MK, Assad RS, Van Arsdell G, Humpl T, et al. Beneficial effects of vasopressors on right ventricular function in experimental acute right ventricular failure in a rabbit model. *Thorac Cardiovasc Surg*. 2012;60(1):17–23.
- Appleyard RF, Glantz SA. Pulmonary model to predict the effects of series ventricular interaction. *Circ Res*. 1990;67(5):1225–37.
- Atherton JJ, Moore TD, Lele SS, Thomson HL, Galbraith AJ, Belenkie I, et al. Diastolic ventricular interaction in chronic heart failure. *Lancet*. 1997a;349:1720–4.
- Atherton JJ, Thomson HL, Moore TD, Wright KN, Muehle GWF, Fitzpatrick LE, et al. Diastolic ventricular interaction. A possible mechanism for abnormal vascular responses during volume unloading in heart failure. *Circulation*. 1997b;96:4273–9.
- Babu-Narayan SV, Kilner PJ, Li W, Moon JC, Goktekin O, Davlouros PA, et al. Ventricular fibrosis suggested by cardiovascular magnetic resonance in adults with repaired tetralogy of fallot and its relationship to adverse markers of clinical outcome. *Circulation*. 2006;113(3):405–13.
- Belenkie I, Dani R, Smith ER, Tyberg JV. Effects of volume loading during experimental acute pulmonary embolism. *Circulation*. 1989;80:178–88.
- Bettex DA, Pretre R, Chassot PG. Is our heart a well-designed pump? The heart along animal evolution. *Eur Heart J*. 2014;35(34):2322–32.
- Bishop VS, Stone HL, Guyton AC. Cardiac function curves in conscious dogs. *Am J Physiol*. 1964;207(3):677–82.
- Bishopric NH. Evolution of the heart from bacteria to man. *Ann N Y Acad Sci*. 2005;1047:13–29.
- Bove AA, Santamore WP. Ventricular interdependence. *Prog Cardiovasc Dis*. 1981;23(5):365–88.
- Brinker JA, Weiss JL, Lappe DL, Rabson JL, Summer WR, Permutt S, et al. Leftward septal displacement during right ventricular loading in man. *Circulation*. 1980;61:626.
- Brooks H, Kirk ES, Vokonas PS, Urschel CW, Sonnenblick EH. Performance of the right ventricle under stress: relation to right coronary flow. *J Clin Invest*. 1971;50(10):2176–83.
- Brutsaert DL. Cardiac endothelial-myocardial signaling: its role in cardiac growth, contractile performance, and rhythmicity. *Physiol Rev*. 2003;83(1):59–115.
- Brutsaert DL, De Keulenaer GW, Franssen P, Mohan P, Kaluza GL, Andries LJ, et al. The cardiac endothelium: functional morphology, development, and physiology. *Prog Cardiovasc Dis*. 1996;39(3):239–62.
- Buda AJ, Pinsky MR, Ingels NB, Daughters GT II, Stinson EB, Alderman EL. Effect of intrathoracic pressure on left ventricular performance. *N Engl J Med*. 1979;301:453.
- Butler J. The heart is in good hands. *Circulation*. 1983;67(6):1163–8.
- d'Udekem Y, Iyengar AJ, Galati JC, Forsdick V, Weintraub RG, Wheaton GR, et al. Redefining expectations of long-term survival after the Fontan procedure: twenty-five years of follow-up from the entire population of Australia and New Zealand. *Circulation*. 2014;130(11 Suppl 1):S32–8.
- Damiano RJ Jr, Cox JL, Lowe JE, Santamore WP. Left ventricular pressure effects on right ventricular pressure and volume outflow. *Catheter Cardiovasc Diagn*. 1990;19(4):269–78.
- Damiano RJ Jr, La Follette P Jr, Cox JL, Lowe JE, Santamore WP. Significant left ventricular contribution to right ventricular systolic function. *Am J Phys*. 1991;261(5 Pt 2):H1514–24.
- Datta P, Magder S. Hemodynamic response to norepinephrine with and without inhibition of nitric oxide synthase in porcine endotoxemia. *Am J Resp Crit Care Med*. 1999;160(6):1987–93.
- Dell'Italia LJ, Walsh RA. Application of a time varying elastance model to right ventricular performance in man. *Cardiovasc Res*. 1988a;22(12):864–74.
- Dell'Italia LJ, Walsh RA. Acute determinants of the hangout interval in the pulmonary circulation. *Am Heart J*. 1988b;116(5 Pt 1):1289–97.
- Dell'Italia LJ, Starling MR, Blumhardt R, Lasher JC, O'Rourke RA. Comparative effects of volume loading, dobutamine, and nitroprusside in patients with predominant right ventricular infarction. *Circulation*. 1985;72(6):1327–33.
- Donald DE, Essex HE. Studies on chronic effects of ligation of the canine right coronary artery. *Am J Phys*. 1954a;176(3):431–8.
- Donald DE, Essex HE. Pressure studies after inactivation of the major portion of the canine right ventricle. *Am J Phys*. 1954b;176(1):155–61.
- Dos L, Teruel L, Ferreira IJ, Rodriguez-Larrea J, Miro L, Girona J, et al. Late outcome of Senning and Mustard procedures for correction of transposition of the great arteries. *Heart*. 2005;91(5):652–6.
- Faber MJ, Dalinghaus M, Lankhuizen IM, Steendijk P, Hop WC, Schoemaker RG, et al. Right and left ventricular function after chronic pulmonary artery banding in rats assessed with biventricular pressure-volume loops. *Am J Physiol Heart Circ Physiol*. 2006;291(4):H1580–6.

- Farrar DJ, Woodard JC, Chow E. Pacing-induced dilated cardiomyopathy increases left-to-right ventricular systolic interaction. *Circulation*. 1993;88(2):720–5.
- Fontan F, Baudet E. Surgical repair of tricuspid atresia. *Thorax*. 1971;26(3):240–8.
- Fourie PR, Coetzee AR, Bolliger CT. Pulmonary artery compliance: its role in right ventricular-arterial coupling. *Cardiovasc Res*. 1992;26(9):839–44.
- Friedberg MK, Redington AN. Right versus left ventricular failure: differences, similarities, and interactions. *Circulation*. 2014;129(9):1033–44.
- Furey SA 3rd, Zieske HA, Levy MN. The essential function of the right ventricle. *Am Heart J*. 1984;107(2):404–10.
- Gan C, Lankhaar JW, Marcus JT, Westerhof N, Marques KM, Bronzwaer JG, et al. Impaired left ventricular filling due to right-to-left ventricular interaction in patients with pulmonary arterial hypertension. *Am J Physiol Heart Circ Physiol*. 2006;290(4):H1528–33.
- Geva T, Powell AJ, Crawford EC, Chung T, Colan SD. Evaluation of regional differences in right ventricular systolic function by acoustic quantification echocardiography and cine magnetic resonance imaging. *Circulation*. 1998;98(4):339–45.
- Gewillig M, Brown SC. The Fontan circulation after 45 years: update in physiology. *Heart*. 2016;102(14):1081–6.
- Giardini A, Hager A, Napoleone CP, Picchio FM. Natural history of exercise capacity after the Fontan operation: a longitudinal study. *Ann Thorac Surg*. 2008;85(3):818–21.
- Guyton A, Lindsey AW, Gilluly JJ. The limits of right ventricular compensation following acute increase in pulmonary circulatory resistance. *Circ Res*. 1954;II(July):326–32.
- Guyton RA, Andrews MJ, Hickey PR, Michaelis LL, Morrow AG. The contribution of atrial contraction to right heart function before and after right ventriculotomy. Experimental and clinical observations. *J Thorac Cardiovasc Surg*. 1976;71(1):1–10.
- Harjola VP, Mebazaa A, Celutkiene J, Bettex D, Bueno H, Chioncel O, et al. Contemporary management of acute right ventricular failure: a statement from the Heart Failure Association and the Working Group on Pulmonary Circulation and Right Ventricular Function of the European Society of Cardiology. *Eur J Heart Fail*. 2016;18(3):226–41.
- Hoffman D, Sisto D, Frater RW, Nikolic SD. Left-to-right ventricular interaction with a noncontracting right ventricle. *J Thorac Cardiovasc Surg*. 1994;107(6):1496–502.
- Holt JP, Rhode EA, Kines H. Pericardial and ventricular pressure. *Circ Res*. 1960;VIII:1171–80.
- Hopkins WE. The remarkable right ventricle of patients with Eisenmenger syndrome. *Coron Artery Dis*. 2005;16(1):19–25.
- Hopkins WE, Ochoa LL, Richardson GW, Trulock EP. Comparison of the hemodynamics and survival of adults with severe primary pulmonary hypertension or Eisenmenger syndrome. *J Heart Lung Transplant*. 1996;15(1 Pt 1):100–5.
- Irlbeck M, Muhling O, Iwai T, Zimmer HG. Different response of the rat left and right heart to norepinephrine. *Cardiovasc Res*. 1996;31(1):157–62.
- Jacques D, Sader S, Perreault C, Fournier A, Pelletier G, Beck-Sickinger AG, et al. Presence of neuropeptide Y and the Y1 receptor in the plasma membrane and nuclear envelope of human endocardial endothelial cells: modulation of intracellular calcium. *Can J Physiol Pharmacol*. 2003;81(3):288–300.
- Jacques D, Sader S, Perreault C, Abdel-Samad D, Provost C. Roles of nuclear NPY and NPY receptors in the regulation of the endocardial endothelium and heart function. *Can J Physiol Pharmacol*. 2006a;84(7):695–705.
- Jacques D, Sader S, Perreault C, Abdel-Samad D, Jules F, Provost C. NPY, ET-1, and Ang II nuclear receptors in human endocardial endothelial cells. *Can J Physiol Pharmacol*. 2006b;84(3–4):299–307.
- Jacques D, Sader S, Perreault C, Abdel-Samad D. NPY and NPY receptors: presence, distribution and roles in the regulation of the endocardial endothelium and cardiac function. *EXS*. 2006c;(95):77–87.
- Jatene AD, Fontes VF, Paulista PP, de Souza LC, Neger F, Galantier M, et al. Successful anatomic correction of transposition of the great vessels. A preliminary report. *Arq Bras Cardiol*. 1975;28(4):461–4.
- Katira BH, Giesinger RE, Engelberts D, Zabini D, Kornecki A, Otulakowski G, et al. Adverse heart-lung interactions in ventilator-induced lung injury. *Am J Respir Crit Care Med*. 2017;196(11):1411–21.
- Kerbaul F, Rondelet B, Motte S, Fesler P, Hubloue I, Ewalenko P, et al. Effects of norepinephrine and dobutamine on pressure load-induced right ventricular failure. *Crit Care Med*. 2004;32(4):1035–40.
- Khairy P, Fernandes SM, Mayer JE Jr, Triedman JK, Walsh EP, Lock JE, et al. Long-term survival, modes of death, and predictors of mortality in patients with Fontan surgery. *Circulation*. 2008;117(1):85–92.
- Kondo RP, Dederko DA, Teutsch C, Chrast J, Catalucci D, Chien KR, et al. Comparison of contraction and calcium handling between right and left ventricular myocytes from adult mouse heart: a role for repolarization waveform. *J Physiol*. 2006;571(Pt 1):131–46.
- Laks MM, Garner D, Swan HJ. Volumes and compliances measured simultaneously in the right and left ventricles of the dog. *Circ Res*. 1967;20(5):565–9.
- Leeuwenburgh BP, Helbing WA, Steendijk P, Schoof PH, Baan J. Biventricular systolic function in young lambs subject to chronic systemic right ventricular pressure overload. *Am J Physiol Heart Circ Physiol*. 2001;281(6):H2697–704.
- Lindsey AW, Guyton AC. Continuous recording of pulmonary blood volume: pulmonary pressure and volume changes. *Am J Phys*. 1959;197:959–62.
- Magder S. Venous mechanics of contracting gastrocnemius muscle and the muscle pump theory. *J Appl Physiol*. 1995;79(6):1930–5.

- Magder S. The left heart can only be as good as the right heart: determinants of function and dysfunction of the right ventricle. *Crit Care Resusc.* 2007;9(4):344–51.
- Magder S, Bafaqeeh F. The clinical role of central venous pressure measurements. *J Intensive Care Med.* 2007;22(1):44–51.
- Magder S, Guerard B. Heart-lung interactions and pulmonary buffering: lessons from a computational modeling study. *Respir Physiol Neurobiol.* 2012;182(2–3):60–70.
- Magder SA, Lichtenstein S, Adelman AG. Effects of negative pleural pressure on left ventricular hemodynamics. *Am J Cardiol.* 1983;52(5):588–93.
- Magder S, Famulari G, Garipey B. Periodicity, time constants of drainage, and the mechanical determinants of peak cardiac output during exercise. *J Appl Physiol* (Bethesda, MD: 1985). 2019;127(6):1611–9.
- Maughan WL, Shoukas AA, Sagawa K, Weisfeldt ML. Instantaneous pressure-volume relationship of the canine right ventricle. *Circ Res.* 1979;44(3):309–15.
- Maughan WL, Sunagawa K, Sagawa K. Ventricular systolic interdependence: volume elastance model in isolated canine hearts. *Am J Phys.* 1987;253(6 Pt 2):H1381–H90.
- Mitzner W, Goldberg H. Effects of epinephrine on resistive and compliant properties of the canine vasculature. *J Appl Physiol.* 1975;39(2):272–80.
- Mitzner W, Goldberg H, Lichtenstein S. Effect of thoracic blood volume changes on steady state cardiac output. *Circ Res.* 1976;38(4):255–61.
- Morimont P, Lambermont B, Ghuysen A, Gerard P, Kolh P, Lancellotti P, et al. Effective arterial elastance as an index of pulmonary vascular load. *Am J Physiol Heart Circ Physiol.* 2008;294(6):H2736–42.
- Moulopoulos SD, Sarcas A, Stamatelopoulos S, Arealis E. Left ventricular performance during bypass or distension of the right ventricle. *Circ Res.* 1965;17(6):484–91.
- Naeije R, Badagliacca R. The overloaded right heart and ventricular interdependence. *Cardiovasc Res.* 2017;113(12):1474–85.
- Notarius CF, Magder S. Central venous pressure during exercise: role of muscle pump. *Can J Physiol Pharmacol.* 1996;74(6):647–51.
- Notarius CF, Levy RD, Tully A, Fitchett D, Magder S. Cardiac vs. non-cardiac limits to exercise following heart transplantation. *Am Heart J.* 1998;135:339–48.
- Olsen CO, Tyson GS, Maier GW, Spratt JA, Davis JW, Rankin JS. Dynamic ventricular interaction in the conscious dog. *Circ Res.* 1983;52(1):85–104.
- Page RD, Harringer W, Hodakowski GT, Guerrero JL, LaRaia PJ, Austen WG, et al. Determinants of maximal right ventricular function. *J Heart Lung Transplant.* 1992;11(1 Pt 1):90–8.
- Pascual-Anaya J, Albuixech-Crespo B, Somorjai IM, Carmona R, Oisi Y, Alvarez S, et al. The evolutionary origins of chordate hematopoiesis and vertebrate endothelia. *Dev Biol.* 2013;375(2):182–92.
- Patterson SW, Starling EH. On the mechanical factors which determine the output of the ventricles. *J Physiol.* 1914;48(5):357–79.
- Pearse RM, Harrison DA, MacDonald N, Gillies MA, Blunt M, Ackland G, et al. Effect of a perioperative, cardiac output-guided hemodynamic therapy algorithm on outcomes following major gastrointestinal surgery: a randomized clinical trial and systematic review. *JAMA.* 2014;311(21):2181–90.
- Prieto LR, Hordof AJ, Secic M, Rosenbaum MS, Gersony WM. Progressive tricuspid valve disease in patients with congenitally corrected transposition of the great arteries. *Circulation.* 1998;98(10):997–1005.
- Redington AN. Physiopathology of right ventricular failure. *Semin Thorac Cardiovasc Surg Pediatr Card Surg Annu.* 2006;9:3–10.
- Redington AN, Gray HH, Hodson ME, Rigby ML, Oldershaw PJ. Characterisation of the normal right ventricular pressure-volume relation by biplane angiography and simultaneous micromanometer pressure measurements. *Br Heart J.* 1988a;59(1):23–30.
- Redington AN, Oldershaw PJ, Shinebourne EA, Rigby ML. A new technique for the assessment of pulmonary regurgitation and its application to the assessment of right ventricular function before and after repair of tetralogy of Fallot. *Br Heart J.* 1988b;60(1):57–65.
- Redington AN, Rigby ML, Shinebourne EA, Oldershaw PJ. Changes in the pressure-volume relation of the right ventricle when its loading conditions are modified. *Br Heart J.* 1990;63(1):45–9.
- Robotham SL, Mitzner W. A model of the effects of respiration on left ventricular performance. *J Appl Physiol.* 1979;46:411.
- Sagawa K. The ventricular pressure-volume diagram revisited. *Circ Res.* 1978;43:677–87.
- Salisbury PF. Coronary artery pressure and strength of right ventricular contraction. *Circ Res.* 1955;3(6):633–8.
- Santamore WP, Gray LA Jr. Left ventricular contributions to right ventricular systolic function during LVAD support. *Ann Thorac Surg.* 1996;61(1):350–6.
- Santamore WP, Lynch PR, Heckman JL, Bove AA, Meier GD. Left ventricular effects on right ventricular developed pressure. *J Appl Physiol.* 1976;41(6):925–30.
- Santamore WP, Shaffer T, Papa L. Theoretical model of ventricular interdependence: pericardial effects. *Am J Phys.* 1990;259(1 Pt 2):H181–9.
- Scharf SM, Bromerger-Barnea B. Influence of coronary flow and pressure on cardiac function and coronary vascular volume. *Am J Physiol.* 1973;224(4):918–23.
- Simoes-Costa MS, Vasconcelos M, Sampaio AC, Cravo RM, Linhares VL, Hochgreb T, et al. The evolutionary origin of cardiac chambers. *Dev Biol.* 2005;277(1):1–15.
- Simões-Costa MS, Vasconcelos M, Sampaio AC, Cravo RM, Linhares VL, Hochgreb T, et al. The evolutionary origin of cardiac chambers. *Dev Biol.* 2005;277(1):1–15.
- Slinker BK, Ditchey RV, Bell SP, LeWinter MM. Right heart pressure does not equal pericardial pressure in

- the potassium chloride-arrested canine heart in situ. *Circulation*. 1987;76(2):357–62.
- Smerup M, Nielsen E, Agger P, Frandsen J, Vestergaard-Poulsen P, Andersen J, et al. The three-dimensional arrangement of the myocytes aggregated together within the mammalian ventricular myocardium. *Anat Rec (Hoboken)*. 2009;292(1):1–11.
- Srivastava D, Olson EN. A genetic blueprint for cardiac development. *Nature*. 2000;407(6801):221–6.
- Starr I, Jeffers WA, Meade RH Jr. The absence of conspicuous increments of venous pressure after severe damage to the right ventricle of the dog, with a discussion of the relation between clinical congestive failure and heart disease. *Am Heart J*. 1943;26(3):291–301.
- Suga H, Saeki Y, Sagawa K. End-systolic force-length relationship of nonexcised canine papillary muscle. *Am J Phys*. 1977;233(6):H711–H7.
- Summer WR, Permutt S, Sagawa K, Shoukas AA, Bromberger-Barnea B. Effects of spontaneous respiration on canine left ventricular function. *Circ Res*. 1979;45:719.
- Sunagawa K, Maughan WL, Burkhoff D, Sagawa K. Left ventricular interaction with arterial load studied in isolated canine ventricle. *Am J Phys*. 1983;245(5 Pt 1):H773–80.
- Sunagawa K, Maughan WL, Sagawa K. Optimal arterial resistance for the maximal stroke work studied in isolated canine left ventricle. *Circ Res*. 1985;56(4):586–95.
- Taquini AC, Feroso JD, Aramendia P. Behavior of the right ventricle following acute constriction of the pulmonary artery. *Circ Res*. 1960;8:315–8.
- Taylor RR, Covell JW, Sonnenblick EH, Ross J Jr. Dependence of ventricular distensibility on filling of the opposite ventricle. *Am J Physiol*. 1967;213(3):711–8.
- Thiele H, Ohman EM, de Waha-Thiele S, Zeymer U, Desch S. Management of cardiogenic shock complicating myocardial infarction: an update 2019. *Eur Heart J*. 2019;40(32):2671–83.
- Thomas T, Yamagishi H, Overbeek PA, Olson EN, Srivastava D. The bHLH factors, dHAND and eHAND, specify pulmonary and systemic cardiac ventricles independent of left-right sidedness. *Dev Biol*. 1998;196(2):228–36.
- Trip P, Kind T, van de Veerdonk MC, Marcus JT, de Man FS, Westerhof N, et al. Accurate assessment of load-independent right ventricular systolic function in patients with pulmonary hypertension. *J Heart Lung Transplant*. 2013;32(1):50–5.
- Urashima T, Zhao M, Wagner R, Fajardo G, Farahani S, Quertermous T, et al. Molecular and physiological characterization of RV remodeling in a murine model of pulmonary stenosis. *Am J Physiol Heart Circ Physiol*. 2008;295(3):H1351–h68.
- van der Bruggen CEE, Tedford RJ, Handoko ML, van der Velden J, de Man FS. RV pressure overload: from hypertrophy to failure. *Cardiovasc Res*. 2017;113(12):1423–32.
- Voelkel NF, Quaipe RA, Leinwand LA, Barst RJ, McGoon MD, Meldrum DR, et al. Right ventricular function and failure: report of a National Heart, Lung, and Blood Institute working group on cellular and molecular mechanisms of right heart failure. *Circulation*. 2006;114(17):1883–91.
- Vogel M, Sponring J, Cullen S, Deanfield JE, Redington AN. Regional wall motion and abnormalities of electrical depolarization and repolarization in patients after surgical repair of tetralogy of Fallot. *Circulation*. 2001;103(12):1669–73.
- Vonk Noordegraaf A, Westerhof BE, Westerhof N. The relationship between the right ventricle and its load in pulmonary hypertension. *J Am Coll Cardiol*. 2017;69(2):236–43.
- Vonk Noordegraaf A, Chin KM, Haddad F, Hassoun PM, Hennes AR, Hopkins SR, et al. Pathophysiology of the right ventricle and of the pulmonary circulation in pulmonary hypertension: an update. *Eur Respir J*. 2019;53(1):1801900.
- Vonk-Noordegraaf A, Haddad F, Chin KM, Forfia PR, Kawut SM, Lumens J, et al. Right heart adaptation to pulmonary arterial hypertension: physiology and pathobiology. *J Am Coll Cardiol*. 2013;62(25 Suppl):D22–33.
- Wang GY, McCloskey DT, Turcato S, Swigart PM, Simpson PC, Baker AJ. Contrasting inotropic responses to alpha1-adrenergic receptor stimulation in left versus right ventricular myocardium. *Am J Physiol Heart Circ Physiol*. 2006;291(4):H2013–H7.
- Watkins MW, LeWinter MM. Physiologic role of the normal pericardium. *Annu Rev Med*. 1993;44:171–80.
- Weyman AE, Wann S, Feigenbaum H, Dillon JC. Mechanism of abnormal septal motion in patients with right ventricular volume overload: a cross-sectional echocardiographic study. *Circulation*. 1976;54(2):179–86.
- Xavier-Neto J, Castro RA, Sampaio AC, Azambuja AP, Castillo HA, Cravo RM, et al. Parallel avenues in the evolution of hearts and pumping organs. *Cell Mol Life Sci*. 2007;64(6):719–34.
- Yamaguchi S, Harasawa H, Li KS, Zhu D, Santamore WP. Comparative significance in systolic ventricular interaction. *Cardiovasc Res*. 1991;25(9):774–83.
- Zaffran S, Kelly RG, Meilhac SM, Buckingham ME, Brown NA. Right ventricular myocardium derives from the anterior heart field. *Circ Res*. 2004;95(3):261–8.



Function of the Left Heart

4

Keith R. Walley

The heart contracts and ejects blood into the circulation at a sufficient rate to deliver adequate amounts of oxygen and metabolites to meet the demands of all organs and tissues in the body. Depending on activity and organ function, the demand for oxygen and metabolites can vary enormously. But the heart is made up of fairly simple muscle tissue that contracts and relaxes. Here, I explore how these simple muscle characteristics, when assembled into a fully functioning heart, are able to meet widely varying demands.

Basic Cardiac Muscle Characteristics

The contractile apparatus of cardiac muscle is composed of thin helical polymeric actin filaments interdigitated with heavy myosin filaments as a unit termed a sarcomere. Cardiac muscle fibers are made of many sarcomeres in series and in parallel. Sliding of myosin filaments over actin filaments results in sarcomere shortening or lengthening. The conformationally active head of a myosin filament is an ATPase that can reversibly bind to actin filaments (Guhathakurta et al. 2018). The myosin head (in its short conformation, bound to actin) can cleave ATP which then

detaches the myosin head from actin and fully extends the myosin head to its greatest length. The extended myosin head can now bind further along on the actin filament and, when bound, the myosin head undergoes reverse conformational change resulting in shortening while attached to the actin filament. Repeated more than a thousand times per heartbeat, this cycle results in shortening of the sarcomere and, hence, shortening of cardiac muscle during systole. The systolic shortening interaction of myosin with actin requires unimpeded access of the myosin ATPase head to the adjacent actin filament helix. Access of myosin to actin is regulated by the additional sarcomere proteins making up the troponin/tropomyosin complex. Troponin/tropomyosin is a regulatory protein complex that lies immediately adjacent to the helical structure of actin filaments. When calcium concentration is high in the intracellular cytosol, calcium binds to the troponin C component of troponin/tropomyosin. This results in a conformational change so that tropomyosin moves away from the binding site of the myosin head to the actin filament so that systolic contraction cycles can occur. However, during diastole when cytosolic calcium is pumped into, and sequestered within, the sarcoplasmic reticulum, calcium leaves its troponin C binding site and tropomyosin undergoes reverse conformational change, moves toward the binding site of myosin to actin, and sterically hinders this interaction. Since myosin can no longer bind the actin

K. R. Walley (✉)
Division of Critical Care Medicine, Centre for Heart Lung Innovation, University of British Columbia, St. Paul's Hospital, Vancouver, BC, Canada
e-mail: Keith.Walley@hli.ubc.ca

filament, the thick and thin filaments are unbound and slide freely past each other allowing relaxed lengthening of the sarcomere, driven by low dis-tending/lengthening tension within diastolic sarcomeres.

Cardiac Muscle Tension-Length Relationships

Elastic elements are also incorporated into the sarcomere (Glantz 1975). Some of the elastic characteristics of the sarcomere are intrinsic to actin and myosin and are therefore in series with the actin-myosin contractile apparatus. Structures connecting sarcomeres and cells together in series also contribute to a “series elastic element” (Herzig 1978). Cytosolic calcium allows actin-myosin shortening which increases tension within these series elastic elements resulting in systolic wall tension (Fabiato and Fabiato 1978). Additional elastic elements within and surrounding cardiac muscle cells provide “parallel elastic elements.” During diastole, when myosin is not bound to actin, diastolic wall tension lengthens the sarcomere against parallel elastic elements (Fester and Samet 1974; Glantz 1974).

The tension-length characteristics of a trabecular strip of ventricular muscle are shown in Fig. 4.1. Ventricular muscle lengthens under minimal tension along a diastolic tension-length relationship which becomes stiffer at increasing length due to the parallel elastic elements. When the muscle is stimulated to contract, tension within series elastic elements rises to an end-systolic tension-length point. Contractions starting at increasing length yield increasing end-systolic tension and all end-systolic tension-length points lie along an approximately linear end-systolic tension-length relationship (Fig. 4.1). When intrinsic contractility is increased (in this example, by two electrical depolarizations in quick succession which result in a greater release of calcium into the cytosol and, hence, more myosin-actin interactions), the key feature is that the slope of the end-systolic tension-length relationship increases (Fig. 4.1). The strength of contraction is primarily depen-

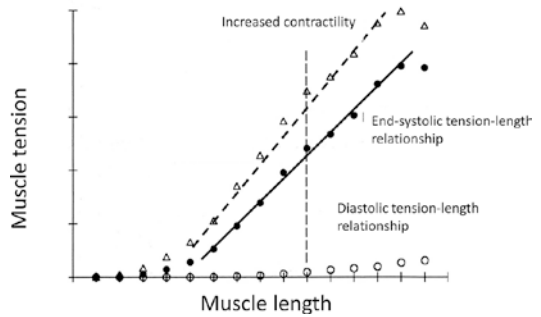


Fig. 4.1 Cardiac trabecular muscle tension-length relationships. Diastolic tension-length points (open circles) are measured in relaxed diastolic muscle over a range of lengths. At each length, the muscle strip is electrically stimulated and tension increases (for example, along the dashed vertical line) to end-systolic points (closed circles). Over a range of lengths, these end-systolic tension-length points approximately lie along a straight line (solid line). When systolic contractility is increased (by two electrical stimuli in quick succession), end-systolic tension-length points (open triangles) shift up so that the end-systolic tension length relationship (dashed line) shifts to the left with increased slope

dent on the number of actin-myosin cross bridges which, in turn, is dependent on the release and then uptake of calcium by the ryanodine receptor and then the sarcoplasmic reticulum Ca^{2+} -ATPase pump. In contrast, the speed of contraction is dependent on the load on the muscle and the rate of turnover of actin-myosin bonds which, in turn, depends on the availability of oxygen and, hence, ATP (Walley et al. 1991).

Whether in diastole or systole, the key mechanical feature of sarcomeres, cardiac muscle cells, muscle strips, and the ventricular wall is the tension generated at each length (Suga et al. 1977). Tension-length relationships within these underlying muscle elements become pressure-volume relationships of the integrated three-dimensional structure of the ventricle (Glantz and Kernoff 1975; Suga and Sagawa 1972). Therefore, the fundamental mechanical feature of the ventricle is the relationship of ventricular pressure to ventricular volume. Ventricular volume divided by pressure is “compliance” and conversely ventricular pressure divided by volume ($\Delta P/\Delta V$) is “elastance.” It follows that shortening of the contractile element of the sarcomere results in increasing elastance of the

ventricle. To understand how shortening of the sarcomere is converted into ventricular function, it is useful to consider the pressure-volume relationship of the left ventricle and changes in ventricular elastance that generate these features.

Ventricular Pressure-Volume Relationships

To understand events during a cardiac cycle, it is useful to plot the trajectory on a ventricular pressure-volume diagram (Sagawa 1984). During diastole, actin and myosin filaments are prevented from binding by steric hinderance provided by calcium-deplete troponin/tropomyosin. The actin and myosin filaments are free to slide past each other, so blood entering the ventricle through the mitral valve fills the diastolic ventricle at low diastolic pressures (labeled “1” in Fig. 4.2a). The diastolic pressure-volume relationship is curvilinear, becoming stiffer at increasing volume (Glantz and Kernoff 1975). This relationship is fit well by an exponential equation (Glantz and Parmley 1978) or by a similar relationship: $P = S \times \log[(V_m - V)/(V_m - V_0)]$, where S represents the diastolic myocardial stiffness, V_m is the maximum diastolic ventricular volume, and V_0 is the diastolic volume at a pressure of zero (Nikolic et al. 1988). Maximum volume is limited by muscle characteristics and the pericardium (Tyberg and Smith 1990; Holt et al. 1960; Glantz et al. 1978). Above the maximum volume, the ventricle would rupture since the ventricle cannot expand indefinitely (Walley and Cooper 1991). The key characteristic of the diastolic ventricle is that it fills easily at low volume because compliance is high but becomes much less compliant near maximum diastolic volume.

Upon electrical depolarization of cardiomyocytes, calcium is released from the sarcoplasmic reticulum via the ryanodine receptor into the cytosol bathing actin, myosin, and troponin/tropomyosin. Calcium binds the troponin C subunit of the troponin/tropomyosin complex causing it to move away from the actin-myosin binding site so that the myosin head ATPase is free to bind actin, shorten, release, and bind actin

again, causing systolic shortening. Early in systole, the mitral and aortic valves are closed so that sarcomere shortening results in an increase in ventricular pressure with no change in volume, which is termed isovolumic systole (labeled “2” in Fig. 4.2a). When intraventricular pressure exceeds aortic pressure, the aortic valve is pushed open and the ventricle ejects blood into the aorta. During this systolic ejection phase (labeled “3” in Fig. 4.2a), intraventricular volume decreases until end-systolic volume is reached. Toward the end of systole, intracellular cytosolic calcium is pumped back into the sarcoplasmic reticulum by the sarcoplasmic reticulum Ca^{2+} – ATPase pump, SERCA. At low cytosolic calcium concentrations, calcium is no longer bound to troponin/tropomyosin, which therefore moves back into a position inhibiting the interaction of myosin with actin. Since actin and myosin filaments are now free to slide past each other, tension generated by sarcomere shortening in systole decreases rapidly and so intraventricular pressure falls (Raff and Glantz 1981). The aortic valve closes and the mitral valve remains closed during this isovolumic relaxation phase of the cardiac cycle (labeled “4” in Fig. 4.2a). Then, when intraventricular pressure falls below left atrial pressure, the mitral valve is pushed open and the ventricle rapidly fills in diastole for its next cardiac cycle.

The End-Systolic Pressure-Volume Relationship (ESPVR) and E_{\max}

Different loading conditions result in different pressure-volume loops (Sagawa 1984; Suga et al. 1973, 1979). However, for the same contractile state, all end-systolic pressure-volume points lie along an approximately linear relationship, the end-systolic pressure volume relationship (ESPVR) having a slope of E_{\max} (Fig. 4.2a) (Sagawa 1984; Suga et al. 1973). The ESPVR is similar to, and a direct consequence of, the end-systolic tension-length relationship of cardiac muscle (Fig. 4.1) (Suga et al. 1977). The slope of the ESPVR has the units of Δ pressure divided by Δ volume, which is elastance (the inverse of compliance). The ESPVR intersects the volume

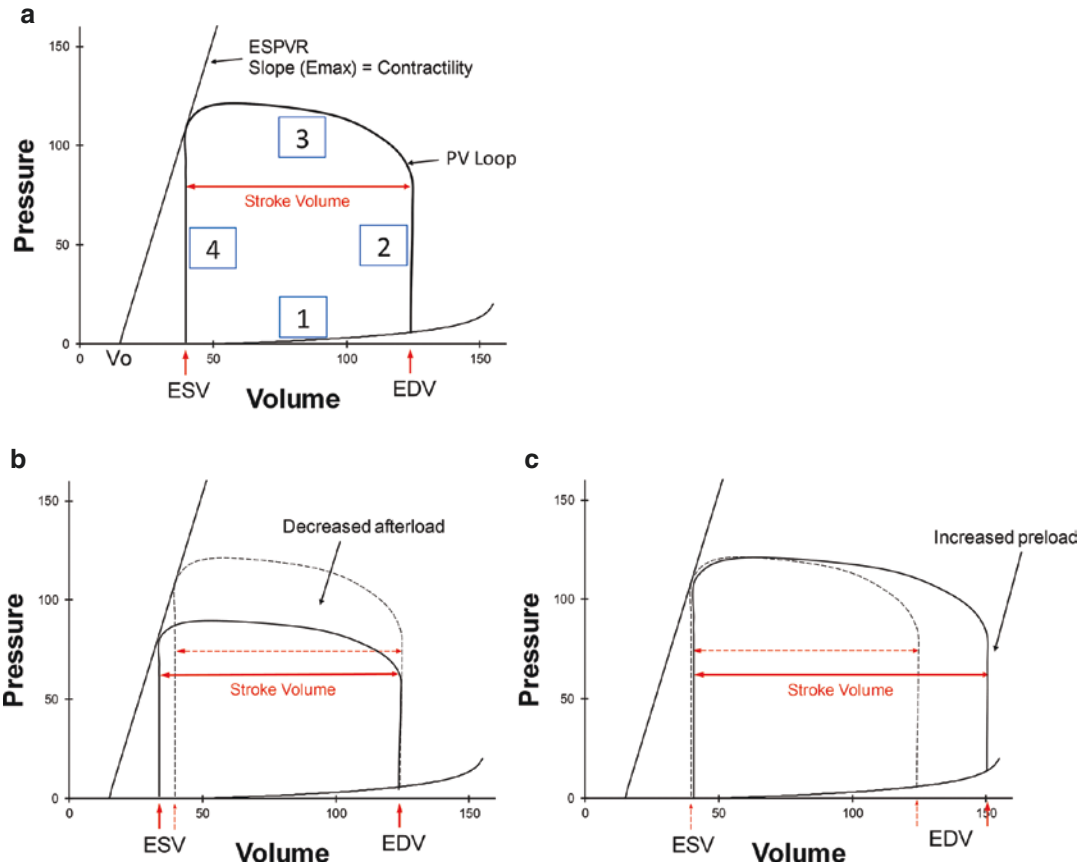


Fig. 4.2 (a) Cardiac cycle on a ventricular pressure-volume diagram. During diastole (labeled “1”), the ventricle fills from end-systolic volume (ESV) at low pressure along a compliant diastolic pressure-volume relationship to end-diastolic volume (EDV). Early systolic contraction (labeled “2”) causes ventricular pressure to rise but volume does not change because both mitral and aortic valves are closed. Ejection occurs (labeled “3”) when ventricular pressure exceeds aortic pressure so that the aortic valve is pushed open. Ejection continues up until the end-systolic pressure-volume relationship (ESPVR) when the ventricle begins to relax so that pressure falls during isovolumic

relaxation (labeled “4”). The volume of blood ejected is the stroke volume which equals $EDV - ESV$. (b) Effect of decreased afterload on stroke volume. When the ventricle is ejecting against a decreased afterload, it is able to eject further so that stroke volume increases. The end-systolic pressure-volume point of the unloaded ejection still falls on the same ESPVR, but at a lower ESV. (c) Effect of increased EDV on stroke volume. The end-systolic pressure-volume point of the ejection that starts at an increased EDV still falls on the same ESPVR so that stroke volume increases

axis at a volume that is somewhat above absolute zero ventricular volume termed V_0 .

Since the ESPVR is sloped, if aortic pressure (pressure afterload) increases, then the ventricle is not able to eject as far (end systole is higher up on the ESPVR) resulting in a greater end-systolic volume (Weber et al. 1974). Conversely, if afterload decreases, then the ventricle is able to eject to a lower end-systolic volume (Fig. 4.2b). Importantly, over a wide range of loading condi-

tions, the end-systolic pressure-volume point of any cardiac cycle lies along the same ESPVR (Suga et al. 1973).

The ESPVR is also insensitive to changes in preload. For example, at higher left atrial pressures, the left ventricle will fill more along the compliant diastolic pressure-volume relationship (Giantz and Kernoff 1975). This more completely filled diastolic ventricle ejects more during systole – down to the same end-systolic volume as a

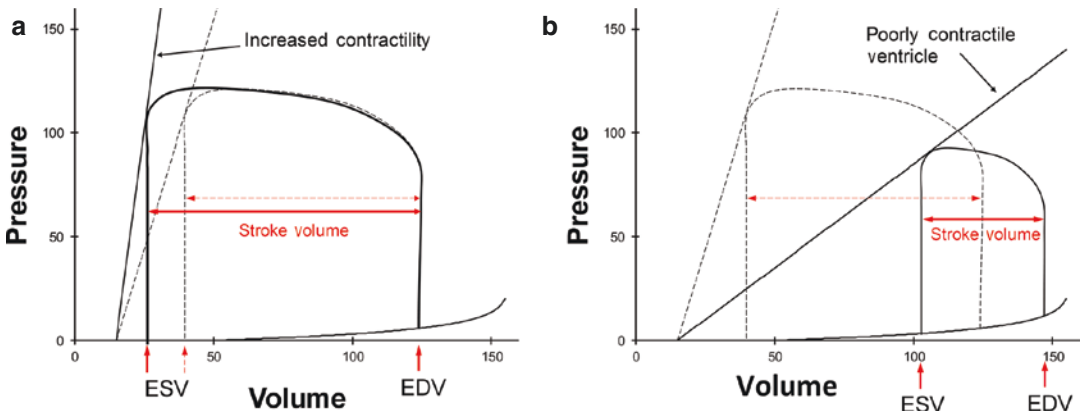


Fig. 4.3 (a) An increase in systolic contractility is synonymous with a shift up and to the left of the end-systolic pressure-volume relationship (ESPVR), primarily due to an increase in slope, E_{max} . For the same preload and afterload conditions, this results in an increase in stroke volume. (b) Conversely, a decrease in systolic contractil-

ity is a decrease in slope of the ESPVR so that end-systolic volume (ESV) increases. To maintain a sufficient stroke volume to support life, compensatory changes must occur which generally include a decrease in afterload and an increase in preload (EDV)

less-filled diastolic ventricle (Fig. 4.2c) (Suga et al. 1979). This characteristic of ventricular ejection is the basis of Starling's law of the heart, where greater diastolic filling results in greater systolic ejection. This allows the heart to rapidly adapt to changing demand for cardiac output. For example, during exercise, increased demand for cardiac output to deliver more oxygen and metabolites is sensed by the peripheral vasculature. The peripheral vasculature responds by redistributing blood flow to lower resistance vascular beds (for example, skeletal muscle) which increases blood flow back to the heart (venous return) (Goldberg and Rabson 1981; Mitzner and Goldberg 1975). The heart accommodates this by increasing ejection and cardiac output in exact proportion to the increase in venous return of blood. The underlying basis is, as mentioned, the fact that the end-systolic pressure-volume point remains on the same ESPVR even when end-diastolic volume increases due to increased venous return of blood to the heart (Suga et al. 1979).

While the slope of the ESPVR, E_{max} , is insensitive to changes in preload and afterload, it increases with an increase in intrinsic systolic contractility (Sagawa 1984; Sagawa et al. 1977), just like the slope of the end-systolic tension-length relationship increased with an increase in

systolic contractility (Fig. 4.1). An increase in systolic contractility means that, at the same preload and afterload, the ventricle gets to a steeper E_{max} , i.e., has a faster systolic increase in elastance, a steeper slope, and the left ventricle can eject further (Fig. 4.3a) (Sagawa et al. 1977). Conversely, when systolic contractility is decreased, the left ventricle reaches a lower maximum slope of the ESPVR (Fig. 4.3b). The volume axis intercept of the ESPVR, V_0 , also impacts end-systolic volume. V_0 is typically a small fraction of normal end-diastolic volume and does not change substantially with inotropic interventions that increase systolic contractility (Sagawa 1984). However, hypoxia, which decreases the velocity of sarcomere shortening (Walley et al. 1991), decreases the speed of ventricular contraction, thereby reducing ventricular ejection at any afterload, which results in an increase in V_0 (Walley et al. 1988).

Time-Varying Elastance and Maximum Elastance (E_{max})

This slope of the ESPVR has units of elastance and is termed E_{max} for "maximum elastance." Elastance is not a characteristic confined to end

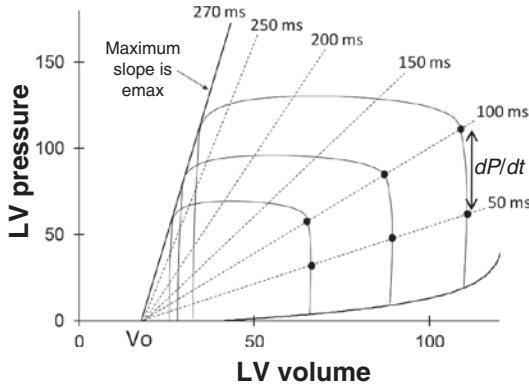


Fig. 4.4 Time-varying elastance and maximum elastance. Pressure-volume points (black circles) at times throughout systolic contraction can be connected by lines whose slope is instantaneous elastance ($\Delta P/\Delta V$). Elastance increases over the course of systole and is maximum, E_{max} , very near the end of systole. Thus, the ventricular chamber has the physical property of time-varying elastance. That is, throughout systole, the ventricle becomes increasingly stiff to a maximum stiffness (elastance) very near the end of systole. The rate of change of pressure during isovolumic systole is indicated as dP/dt which, as shown, depends on the rate of change of ventricular elastance and end-diastolic volume

systole (Suga 1971). Indeed, the elastance of all pressure-volume states throughout a cardiac cycle can be calculated as pressure/(volume- V_o) at every time point. For a wide variety of cardiac loading conditions, pressure-volume points at the same time point within the systolic contraction can be connected with an “elastance” line (Fig. 4.4) (Suga et al. 1973; Suga and Sagawa 1974). When this is done, it can be seen that the ESPVR is not a unique pressure-volume relationship but rather just one of many. The ESPVR is simply the pressure-volume relationship with the maximum slope or maximum elastance (E_{max}) (Suga et al. 1980). That is, during diastole, the ventricle is in its lowest elastance state. The curvilinear diastolic pressure-volume relationship is determined by the parallel elastic elements of the sarcomere, by parallel myocardial connective tissue such as elastin and titin, and by surrounding parallel elastic structures such as the pericardium. When elastance of sarcomeres starts to rise at the initiation of systole due to shortening of

sarcomere contractile elements (which raise tension by stretch of series elastic elements), elastance of the ventricular chamber (pressure/volume of the ventricular chamber) rises. With inflow and outflow valves to the ventricle closed, pressure rises at a constant volume. Ventricular elastance continues to rise during systole, so when ventricular pressure exceeds aortic pressure, the ejection phase begins. Ventricular elastance reaches its peak, E_{max} , near the end of systole. With sequestration of calcium into the sarcoplasmic reticulum by SERCA near the end of systole, elastance falls, ventricular pressure falls, and the aortic valve closes. The elastance at the time of aortic valve closure (end systole), E_{es} , occurs very shortly after elastance is maximum and, therefore, E_{es} is very slightly less than E_{max} .

Thus, the ventricular can be regarded as a muscle with time-varying elastance provided by contraction of sarcomeres which contain intrinsic series and parallel elastic elements. The presence of inflow and outflow valves converts time-varying elastance of this muscular chamber into the four phases of the cardiac cycle (Fig. 4.2a). Elastance is at its minimum during diastole. Careful examination of the diastolic pressure-volume relationship demonstrates that these relationships are not exactly linear and, therefore, are not fully characterized by a single value of elastance, since the ventricle becomes stiffer at increased ventricular volumes (steeper slope of the elastance line) due to the nonlinear characteristics of parallel elastic elements (Glantz 1974; Glantz and Kernoff 1975). Elastance then rapidly rises during isovolumic systole while the closed mitral and aortic valves do not allow a change in volume (Suga and Sagawa 1974). Elastance continues to rise, though at a slightly slower pace, during the ejection phase of systole when the open aortic valve allows ejection of blood so that ventricular volume decreases. During the isovolumic relaxation phase, elastance rapidly falls while the closed mitral and aortic valves do not allow a change in ventricular volume.

Isovolumic Measures of Ventricular Contractility

Measures of contractility during isovolumic systole were developed because the ventricle is isolated by closed valves from preload and afterload pressures. It was hoped that these isovolumic systole measures would be more load-independent (Kass et al. 1987). Ventricular pressure is relatively easily measured during isovolumic systole using an intraventricular catheter. As elastance increases during isovolumic systole, pressure rises at a constant end-diastolic volume. The maximum rate of change of ventricular pressure, dP/dt_{\max} , occurs late in isovolumic systole and is one simple measure of contractility during isovolumic systole that reflects increasing ventricular elastance (Fig. 4.4) (Noble 1972). dP/dt_{\max} increases as end-diastolic volume increases (Mahler et al. 1975), so a modified version less sensitive to preload is dP/dt_{\max} divided by end-diastolic volume (Little 1985). Alternatively, for a simple sarcomere model consisting of a contractile element and a series elastic element, the maximum velocity of contractility element shortening, V_{\max} (Chiu et al. 1989), can be calculated by plotting dP/dt versus ventricular pressure and extrapolating dP/dt to a zero load to yield an estimate of sarcomere V_{\max} (Wolk et al. 1971). dP/dt_{\max} and V_{\max} have been used as measures of contractility that can be made using only a pressure transducer, which can be implemented in clinical practice during cardiac catheterization. While clinically useful, these isovolumic phase measures of intrinsic ventricular contractility are more load-dependent than the ESPVR (Kass et al. 1987).

Measures such as dP/dt_{\max} reflect the time course of sarcoplasmic reticulum calcium release and uptake, while E_{\max} only reflects the net effect at end systole. The time of calcium availability to bind troponin/tropomyosin is reflected as phase 3 of the action potential. This time is dependent on the rate of release of calcium from the sarcoplasmic reticulum and then by the rate of uptake of calcium back into the sarcoplasmic reticulum by SERCA. For example, the same increase in contractility at end systole can be

achieved by post-extrasystolic potentiation, a beta-agonist, or caffeine (Chiu et al. 1989). Post-extrasystolic potentiation increases contractility by increasing the amount of sarcoplasmic reticulum calcium release without a substantial change in time course of contraction. However, the beta-agonist increases both the rate of release and uptake of sarcoplasmic reticulum calcium and, therefore, reduces the duration of the action potential. In contrast, caffeine reduces the rate of uptake by SERCA and thus prolongs the action potential. Thus, contractility is more complex than just the end-systolic result (Chiu et al. 1989).

Thus, examination of pressure-volume relationships at many time points during the cardiac cycle yields the understanding that the ventricle is a muscular chamber characterized by a time-varying elastance (Sagawa 1984). E_{\max} is the most accurate measure to characterize the intrinsic ventricular contractile state, but understanding of time-varying elastance also yields additional, easier, measures of ventricular contractility such as dP/dt_{\max} and V_{\max} (Kass et al. 1987). Further examination of the ventricular pressure-volume diagram starts to reveal how this energetic work is accomplished.

Ventricular Energetics

The study of thermodynamics was motivated by the desire to understand how energy is related to, and converted into, external mechanical work. This is highly relevant in the heart where energy depends on the delivery of oxygen to the heart, and the external mechanical work generated by the heart drives cardiac output and oxygen delivery to the entire body, including the heart.

Area on a pressure-volume diagram has units of energy or work. It follows that the external mechanical work done by the ventricle during a cardiac cycle is simply the area within a ventricular pressure-volume loop (Khalafbeigui et al. 1979). External mechanical work is the work done ejecting the stroke volume into the high-pressure aorta. However, a number of investigators found that this external mechanical work and related indices are not particularly closely corre-

lated with myocardial oxygen consumption (Yasumura et al. 1987). Suga and others recognized that a fraction of the total mechanical work that the ventricle performs is not elaborated as external mechanical work (Suga et al. 1981a, b). For example, if the aorta is briefly cross-clamped for one cardiac cycle and no blood is ejected, no external mechanical work is done. However, it is obvious that the heart expended energy during the contraction against the clamped aorta (Suga et al. 1981b). Suga proposed that the total mechanical work done during a contraction was the sum of external mechanical work (area of the ventricular pressure-volume loop) PLUS potential mechanical work (the additional area subtended by the ESPVR) (Fig. 4.5) (Suga et al. 1981a, b, 1991). One rationale to support this conjecture arises by considering a theoretically “perfectly” unloaded ejection (which is not possible in reality). Consider that, as the ventricle ejects near end systole, the pressure-volume point nears the ESPVR. If the ventricle were theoretically perfectly unloaded by a small amount, then

further ejection to a slightly lower end-systolic volume would occur. Then, consider that many other perfect unloading steps could occur. This perfectly unloaded ventricle would eject near end systole along the ESPVR. Therefore, the theoretical maximum amount of external mechanical work that could be obtained is the area within a normal ventricular pressure-volume loop plus the additional area subtended by the ESPVR. This total area is termed pressure-volume-area, PVA (Suga et al. 1981a, b, 1991)

Myocardial oxygen consumption (MVO_2) plotted against PVA yields a remarkably clean straight line under a wide variety of loading conditions and contractile states (Suga et al. 1981b). The slope of the line represents the fraction of energy derived from myocardial oxygen consumption that is converted into total mechanical work, as measured by PVA. Under a wide variety of circumstances, the slope of this MVO_2 -PVA relationship is constant at approximately 40% indicating that the heart converts energy derived from oxygen metabolism into total mechanical work (PVA work) with approximately a 40% efficiency (Suga et al. 1986). However, oxygen-derived energy is used by cardiomyocytes for more than just mechanical work so that the MVO_2 -PVA relationship intercepts the MVO_2 axis at a positive value of myocardial oxygen consumption. That is, even if the ventricle is doing no mechanical work, energy is still required. One component of this baseline oxygen consumption is used to provide basal metabolic needs to keep the cells alive. Another component of this baseline oxygen consumption increases when contractility is increased, for example by administration of a catecholamine (Suga et al. 1983). This second component of baseline oxygen consumption is related to excitation-contraction coupling. That is, energy is required to pump calcium from the cytosol back into the sarcoplasmic reticulum at the end of systole. This and related ion channel energy consumption is the excitation-contraction coupling work that increases as contractility increases (Suga et al. 1983).

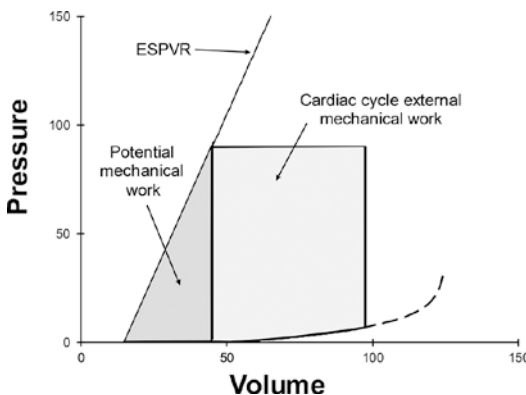


Fig. 4.5 PVA defined on a ventricular pressure-volume diagram. The area within a cardiac cycle pressure-volume loop (light shading) is the external mechanical work done by the ventricle during a cardiac cycle. The additional area subtended by the ESPVR (gray shading) is considered potential mechanical work. Pressure-volume-area (PVA) is the sum of these areas – the sum of external mechanical work and potential mechanical work. Myocardial oxygen consumption (MVO_2) is linearly related to PVA

Myocardial Oxygen Consumption

The PVA concept allows myocardial oxygen consumption to be parsed into a component required for basic cellular metabolism, a component that provides energy to pump calcium and other ions involved in coupling of electrical depolarization with contraction and a component associated with mechanical work (Suga et al. 1986). The component supporting basic cellular metabolism is fairly constant across a variety of states, the component providing for excitation-contraction coupling is highly dependent on the contractile state of the myocardium, and the component providing the energy to produce external mechanical work is highly dependent on loading conditions of the heart. Increased preload and increased afterload both increase the area within the ventricular pressure-volume loop and, therefore, increase PVA. This analysis describes the fate of energy derived from oxygen consumption for a single heartbeat. Therefore, the amount of oxygen consumed per minute is also directly proportional to heart rate.

Myocardial oxygen consumption is clinically a highly important issue. For example, partial or complete occlusion of a coronary artery may limit oxygen delivery below that necessary to meet oxygen demand. In that instance, anaerobic sources of ATP are turned on resulting in myocardial lactate production. Next, ventricular pressure-volume work must decrease because not enough ATP is delivered. Then, damage and even infarction of myocardium may occur. Relieving the coronary occlusion is the first line of therapy. But it also follows that strategies to decrease myocardial oxygen demand are an important part of the clinical armamentarium when treating patients with acute coronary syndromes due to myocardial oxygen supply that is inadequate to meet myocardial oxygen demand. It is not feasible to estimate PVA at the bedside; therefore, it is important to consider how the MVO_2 -PVA relationship can be simplified for easy clinical use.

Among a variety of proposed indexes, PVA is most closely correlated with MVO_2 in human hearts (Takaoka et al. 1993). Heart rate and systolic blood pressure are factors in the MVO_2 and

PVA calculations that are readily measurable (Sonnenblick et al. 1968; Braunwald 1999; Ardehali and Ports 1990). The tension-time index is therefore a simplification that is readily calculated as the product of heart rate and systolic blood pressure (Lewartowski et al. 1980). This simplification omits the impact of stroke volume and the slope of the ESPVR, yet the tension-time index is reasonably linearly related to MVO_2 .

Connection of Pressure-Volume Relationships with Ventricular Function

Cardiac output (the key energy output of the heart) and myocardial oxygen consumption (the key energy input of the heart) are both highly dependent on external loading conditions of the heart. Therefore, consideration of pressure-volume characteristics is incomplete without considering ventricular pump function. Left ventricular function has been characterized in many different ways (Suga et al. 1991; Glower et al. 1985; Sarnoff and Berglund 1954), but the predominant approach is to construct ventricular pump function curves (Elzinga and Westerhof 1979). The output of the ventricle is plotted as a function of input (Fig. 4.6a). A wide variety of inputs to the heart could be considered but ventricular end-diastolic pressure is often used. Similarly, a wide variety of outputs could be considered but among the simplest and most clinically relevant is cardiac output. A plot of end-diastolic pressure versus cardiac output is a classic pump function curve of the ventricle. As input increases output increases, termed Starling's law of the heart (Katz 2002). That is, cardiac output increases as greater ventricular filling is accomplished by increased ventricular end-diastolic volume. Starling's law guarantees that what goes in must go out and thus perfectly matches right and left ventricular stroke volumes over time. The relationship is curvilinear so that further increases in cardiac output diminish as the ventricle becomes fully distended at high end-diastolic pressures (Sarnoff and Berglund 1954).

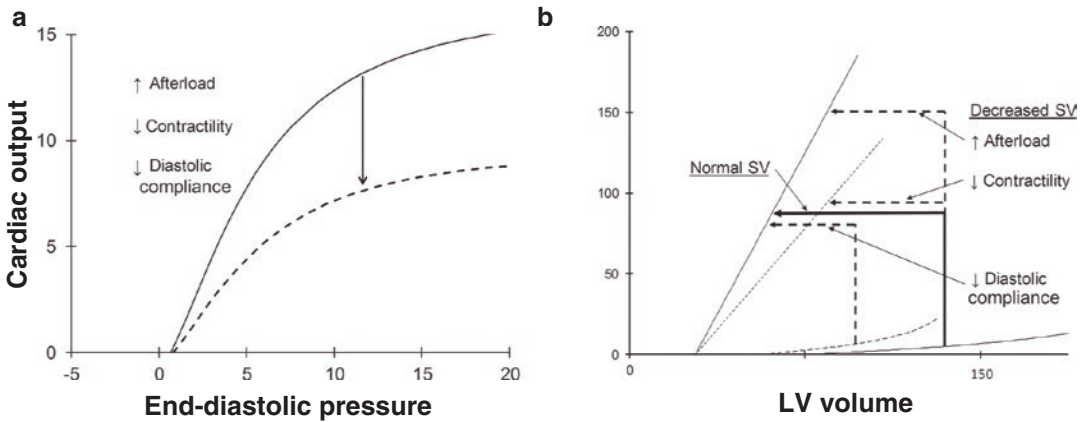


Fig. 4.6 (a) Ventricular pump function curve (solid black curve) is a plot of pump output (in this example, cardiac output) versus pump input (in this example, ventricular end-diastolic pressure). As ventricular input increases, output increases. Pump function can be decreased (dashed curve) by increased afterload that the ventricle must pump against, decreased ventricular intrinsic contractility, and decreased diastolic compliance which impairs ventricular diastolic filling. (b) Pressure-volume relationships underlie ventricular pump function curves. The decrease in ven-

tricular pump function illustrated in panel A is a direct consequence of pressure-volume characteristics shown here. If afterload increases, the normal stroke volume (length of the solid horizontal arrow) must decrease. If contractility decreases (decrease in slope of the ESPVR from the solid straight line to the dashed straight line), the stroke volume will also decrease. Stroke volume will also decrease if ventricular diastolic filling is impaired by decreased diastolic compliance (dashed diastolic pressure-volume relationship)

Cardiac output is heart rate multiplied by stroke volume. Stroke volume is determined by pressure-volume characteristics of the ventricle, specifically end-diastolic volume and end-systolic volume. In turn, end-diastolic volume is determined by the compliance of the diastolic pressure-volume relationship and end-diastolic pressure preload. End-systolic volume is determined by the ESPVR and end-systolic pressure afterload. It can be seen that ventricular pump function output is derived from consideration of pressure-volume characteristics and loading conditions. Important corollaries are that ventricular pump function can be decreased by an increase in afterload (Imperial et al. 1961), a decrease in contractility, or a decrease in diastolic compliance (Fig. 4.6b), and vice versa.

Normal valve function is essential for efficient overall cardiac function. However, abnormal valve function is an additional topic not considered here. Heart rate also impacts overall cardiac function although, within the range of normal heart rates, the effect is relatively minor because stroke volume decreases if heart rate is artificially increased (e.g., using ventricular pacing) with

minimal change in cardiac output. However, at very low and very high values, heart rate becomes important. At very low heart rates (less than ~40 beats per minute), additional filling of the diastolic ventricle cannot compensate for the reduced number of ventricular ejections per minute so that cardiac output becomes directly dependent on heart rate (cardiac output = heart rate \times stroke volume). At very high heart rates (greater than ~140 beats per minute), the diastolic ventricle does not have time to fully relax and diastolic filling time becomes very short so that diastolic filling becomes increasingly impaired resulting in an overall decrease in cardiac output.

Summary

Shortening and relaxation cycles of actin-myosin sarcomeres yield a ventricular chamber with time-varying elastance. That is, elastance ($\Delta P / \Delta V$) increases during systole to a maximum value and then decreases back to the minimum diastolic value. Maximum elastance (E_{max})

defines an end-systolic pressure-volume relationship (ESPVR). The existence of the ESPVR means that the end-systolic ventricle has the property of ejecting more stroke volume at low blood pressure afterload and ejecting less stroke volume and high blood pressure afterload. Since maximum elastance, and therefore the ESPVR, does not depend on diastolic loading, the existence of the ESPVR means that the ventricle also has the property of ejecting more stroke volume in exact proportion to any increase in diastolic filling – the heart ejects the venous return that is delivered to it.

Since the product of pressure and volume is work, examination of the ventricular pressure-volume relationships also yields a thermodynamically sound understanding of the relationship of myocardial oxygen consumption (~energy input) to the external mechanical work that the heart performs (~energy output).

Acknowledgments Support: Canadian Institutes of Health Research FDN 154311.

The author has no conflicts of interest with respect to this manuscript.

References

- Ardehali A, Ports TA. Myocardial oxygen supply and demand. *Chest*. 1990;98:699–705.
- Braunwald E. 50th anniversary historical article. Myocardial oxygen consumption: the quest for its determinants and some clinical fallout. *J Am Coll Cardiol*. 1999;34:1365–8.
- Chiu YC, Walley KR, Ford LE. Comparison of the effects of different inotropic interventions on force, velocity, and power in rabbit myocardium. *Circ Res*. 1989;65:1161–71.
- Elzinga G, Westerhof N. How to quantify pump function of the heart. The value of variables derived from measurements on isolated muscle. *Circ Res*. 1979;44:303–8.
- Fabiato A, Fabiato F. Myofilament-generated tension oscillations during partial calcium activation and activation dependence of the sarcomere length-tension relation of skinned cardiac cells. *J Gen Physiol*. 1978;72:667–99.
- Fester A, Samet P. Passive elasticity of the human left ventricle. The "parallel elastic element". *Circulation*. 1974;50:609–18.
- Glantz SA. A constitutive equation for the passive properties of muscle. *J Biomech*. 1974;7:137–45.
- Glantz SA. A three-element model describes excised cat papillary muscle elasticity. *Am J Phys*. 1975;228:284–94.
- Glantz SA, Kernoff RS. Muscle stiffness determined from canine left ventricular pressure-volume curves. *Circ Res*. 1975;37:787–94.
- Glantz SA, Parmley WW. Factors which affect the diastolic pressure-volume curve. *Circ Res*. 1978;42:171–80.
- Glantz SA, Misbach GA, Moores WY, Mathey DG, Lekven J, Stowe DF, Parmley WW, Tyberg JV. The pericardium substantially affects the left ventricular diastolic pressure-volume relationship in the dog. *Circ Res*. 1978;42:433–41.
- Glower DD, Spratt JA, Snow ND, Kabas JS, Davis JW, Olsen CO, Tyson GS, Sabiston DC Jr, Rankin JS. Linearity of the frank-starling relationship in the intact heart: the concept of preload recruitable stroke work. *Circulation*. 1985;71:994–1009.
- Goldberg HS, Rabson J. Control of cardiac output by systemic vessels. Circulatory adjustments to acute and chronic respiratory failure and the effect of therapeutic interventions. *Am J Cardiol*. 1981;47:696–702.
- Guhathakurta P, Prochniewicz E, Grant BD, Peterson KC, Thomas DD. High-throughput screen, using time-resolved fret, yields actin-binding compounds that modulate actin-myosin structure and function. *J Biol Chem*. 2018;293:12288–98.
- Herzig JW. A cross-bridge model for inotropism as revealed by stiffness measurements in cardiac muscle. *Basic Res Cardiol*. 1978;73:273–86.
- Holt JP, Rhode EA, Kines H. Pericardial and ventricular pressure. *Circ Res*. 1960;8:1171–81.
- Imperial ES, Levy MN, Zieske H. Outflow resistance as an independent determinant of cardiac performance. *Circ Res*. 1961;9:1148–55.
- Kass DA, Maughan WL, Guo ZM, Kono A, Sunagawa K, Sagawa K. Comparative influence of load versus inotropic states on indexes of ventricular contractility: experimental and theoretical analysis based on pressure-volume relationships. *Circulation*. 1987;76:1422–36.
- Katz AM. Ernest henry starling, his predecessors, and the "law of the heart". *Circulation*. 2002;106:2986–92.
- Khalafbeigui F, Suga H, Sagawa K. Left ventricular systolic pressure-volume area correlates with oxygen consumption. *Am J Phys*. 1979;237:H566–9.
- Lewartowski B, Michalowski J, Sedek G, Krynska E, Wasilewska-Dziubinska E. Directly measured tension-time index as a correlate of myocardial oxygen consumption. *Eur J Cardiol*. 1980;11:61–70.
- Little WC. The left ventricular dp/dtmax-end-diastolic volume relation in closed-chest dogs. *Circ Res*. 1985;56:808–15.
- Mahler F, Ross J Jr, O'Rourke RA, Covell JW. Effects of changes in preload, afterload and inotropic state on ejection and isovolumic phase measures of contractility in the conscious dog. *Am J Cardiol*. 1975;35:626–34.
- Mitzner W, Goldberg H. Effects of epinephrine on resistive and compliant properties of the canine vasculature. *J Appl Physiol*. 1975;39:272–80.

- Nikolic S, Yellin EL, Tamura K, Vetter H, Tamura T, Meisner JS, Frater RW. Passive properties of canine left ventricle: diastolic stiffness and restoring forces. *Circ Res.* 1988;62:1210–22.
- Noble MI. Problems concerning the application of concepts of muscle mechanics to the determination of the contractile state of the heart. *Circulation.* 1972;45:252–5.
- Raff GL, Glantz SA. Volume loading slows left ventricular isovolumic relaxation rate. Evidence of load-dependent relaxation in the intact dog heart. *Circ Res.* 1981;48:813–24.
- Sagawa K. End-systolic pressure-volume relationship in retrospect and prospect. *Fed Proc.* 1984;43:2399–401.
- Sagawa K, Suga H, Shoukas AA, Bakalar KM. End-systolic pressure/volume ratio: a new index of ventricular contractility. *Am J Cardiol.* 1977;40:748–53.
- Sarnoff SJ, Berglund E. Ventricular function. I Starling's law of the heart studied by means of simultaneous right and left ventricular function curves in the dog. *Circulation.* 1954;9:706–18.
- Sonnenblick EH, Ross J Jr, Braunwald E. Oxygen consumption of the heart. Newer concepts of its multifactorial determination. *Am J Cardiol.* 1968;22:328–36.
- Suga H. Theoretical analysis of a left-ventricular pumping model based on the systolic time-varying pressure-volume ratio. *IEEE Trans Biomed Eng.* 1971;18:47–55.
- Suga H, Sagawa K. Mathematical interrelationship between instantaneous ventricular pressure-volume ratio and myocardial force-velocity relation. *Ann Biomed Eng.* 1972;1:160–81.
- Suga H, Sagawa K. Instantaneous pressure-volume relationships and their ratio in the excised, supported canine left ventricle. *Circ Res.* 1974;35:117–26.
- Suga H, Sagawa K, Shoukas AA. Load independence of the instantaneous pressure-volume ratio of the canine left ventricle and effects of epinephrine and heart rate on the ratio. *Circ Res.* 1973;32:314–22.
- Suga H, Saeki Y, Sagawa K. End-systolic force-length relationship of nonexcised canine papillary muscle. *Am J Phys.* 1977;233:H711–7.
- Suga H, Kitabatake A, Sagawa K. End-systolic pressure determines stroke volume from fixed end-diastolic volume in the isolated canine left ventricle under a constant contractile state. *Circ Res.* 1979;44:238–49.
- Suga H, Sagawa K, Demer L. Determinants of instantaneous pressure in canine left ventricle. Time and volume specification. *Circ Res.* 1980;46:256–63.
- Suga H, Hayashi T, Shirahata M. Ventricular systolic pressure-volume area as predictor of cardiac oxygen consumption. *Am J Phys.* 1981a;240:H39–44.
- Suga H, Hayashi T, Suehiro S, Hisano R, Shirahata M, Ninomiya I. Equal oxygen consumption rates of isovolumic and ejecting contractions with equal systolic pressure-volume areas in canine left ventricle. *Circ Res.* 1981b;49:1082–91.
- Suga H, Hisano R, Goto Y, Yamada O, Igarashi Y. Effect of positive inotropic agents on the relation between oxygen consumption and systolic pressure volume area in canine left ventricle. *Circ Res.* 1983;53:306–18.
- Suga H, Igarashi Y, Yamada O, Goto Y. Cardiac oxygen consumption and systolic pressure volume area. *Basic Res Cardiol.* 1986;81(Suppl 1):39–50.
- Suga H, Goto Y, Futaki S, Kawaguchi O, Yaku H, Hata K, Takasago T. Systolic pressure-volume area (pva) as the energy of contraction in starling's law of the heart. *Heart Vessel.* 1991;6:65–70.
- Takaoka H, Takeuchi M, Odake M, Hayashi Y, Hata K, Mori M, Yokoyama M. Comparison of hemodynamic determinants for myocardial oxygen consumption under different contractile states in human ventricle. *Circulation.* 1993;87:59–69.
- Tyberg JV, Smith ER. Ventricular diastole and the role of the pericardium. *Herz.* 1990;15:354–61.
- Walley KR, Cooper DJ. Diastolic stiffness impairs left ventricular function during hypovolemic shock in pigs. *Am J Phys.* 1991;260:H702–12.
- Walley KR, Becker CJ, Hogan RA, Teplinsky K, Wood LD. Progressive hypoxemia limits left ventricular oxygen consumption and contractility. *Circ Res.* 1988;63:849–59.
- Walley KR, Ford LE, Wood LD. Effects of hypoxia and hypercapnia on the force-velocity relation of rabbit myocardium. *Circ Res.* 1991;69:1616–25.
- Weber KT, Janicki JS, Reeves RC, Hefner LL, Reeves TJ. Determinants of stroke volume in the isolated canine heart. *J Appl Physiol.* 1974;37:742–7.
- Wolk MJ, Keefe JF, Bing OH, Finkelstein LJ, Levine HJ. Estimation of v_{max} in auxotonic systoles from the rate of relative increase of isovolumic pressure: $(dp-dt)_{kp}$. *J Clin Invest.* 1971;50:1276–85.
- Yasumura Y, Nozawa T, Futaki S, Tanaka N, Goto Y, Suga H. Dissociation of pressure-rate product from myocardial oxygen consumption in dog. *Jpn J Physiol.* 1987;37:657–70.



Pulmonary Vascular Resistance

5

Wayne Mitzner

Introduction

This chapter will discuss the resistance to flow through the pulmonary circulation. Pulmonary vascular resistance is a variable that reflects the physical size (diameter and length) of the vessels at any moment in time. Resistances are commonly obtained in both physiological and clinical studies. The resistance changes with lung inflation, in response to various stimuli, and in many lung pathologies, and it can play an important role in the study of heart–lung interactions. Although the definition of pulmonary resistance is simple, the underlying basis of the final measure is complex, and it is important to understand the limitations of this measurement.

Definitions

Traditionally, the relation between resistance, blood flow, and pressure is defined by a mechanical extrapolation of Ohm's law, which states that the pressure difference along the path of flow ($P_{in} - P_{out}$) equals the vascular resistance (R) times the blood flow (F), as in Eq. 5.1a.

$$P_{in} - P_{out} = R \times F. \quad (5.1a)$$

And with regard to the focus of this chapter on pulmonary vascular resistance (PVR), the notation we will use changes P_{in} into pulmonary artery pressure, P_{pa} , and P_{out} is pulmonary venous pressure, P_{pv} , resulting in

$$P_{pa} - P_{pv} = PVR \times F \quad (5.1b)$$

In electrical circuits where Ohm's law is defined, the electrical resistance is generally considered to be a constant independent of the driving voltage or current. And if this were the case for vascular systems, there would be little need for this chapter. However, vascular resistance can be a useful metric, since it reflects the anatomical size of the vessels. Wider and shorter vessels have lower resistance, and the relation between vascular resistance and vessel diameter and length is given by Poiseuille's Law, as shown in Eq. 5.2:

$$R = \frac{128\mu L}{\pi D^4}, \quad (5.2)$$

where L is the vessel length, μ is blood viscosity, and D is vessel diameter.

It is important to emphasize that the derivation of this equation makes several assumptions (laminar or Newtonian flow, rigid tubes, and constant viscosity), *none of which* are valid in the pulmonary vasculature. Nevertheless, this equation is ubiquitously applied, since it provides some intuition about how the resistance should change

W. Mitzner (✉)
Department of Environmental Health & Engineering,
Johns Hopkins Bloomberg School of Public Health,
Baltimore, MD, USA
e-mail: wmitzner@jhu.edu

with structural changes. If the diameter of a vessel constricts, then the resistance will increase in proportion to the fourth power of diameter or at least approximately so. There is often an implicit desire for functions to behave in a linear fashion, where coefficients are constant and events can be simply added. However, much of the problems in understanding and interpreting vascular resistance arises because the circulation is often far from linear. It is perhaps relevant to note here that when Ohm first presented his now famous equation in 1827, suggesting the radical idea that electrical resistance might be constant over a range of voltages, he was so severely criticized that he resigned from his academic position, spending the next 6 years in obscurity as a private tutor (Behrens 1995). With regard to the vascular adaptation of his equation dealing with resistance in distensible vessels, there is also the additional problem of gravity.

Nonlinearities in the Pulmonary Circulation

Vascular Distensibility

If the vasculature was comprised of rigid cylindrical vessels, then the relation between inflow pressure (P_{pa}) and flow would be a straight line. The slope of this line drawn from the pulmonary venous intercept (P_{pv}) would be $1/RVR$, as shown in Fig. 5.1.

Now imagine a real biologic vessel which can distend if its transmural pressure increases. Then, the vessel would no longer be a cylinder, since the pressure at the inlet must be higher than the pressure downstream. So the vessel takes on a tapered shape. The pressure–flow curve for such a vessel would look something like that in Fig. 5.2. With such a PF curve, it should be clear that the resistance is not going to be constant. If we use Eq. 5.1b, then the line from P_v to whatever the P_a is will be increasing in slope as P_a increases. This means that the resistance will continually decrease, and this is what is expected since the vessel is being dilated at higher pressure. In Fig. 5.2, two straight lines

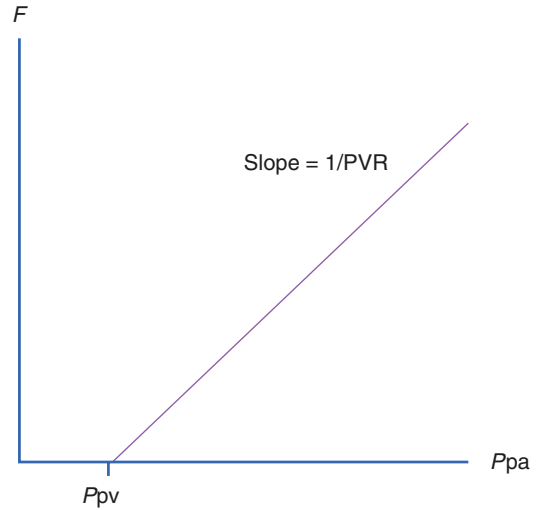


Fig. 5.1 Graph of pulmonary artery pressure (P_{pa}) vs. pulmonary blood flow (F) if the vasculature were comprised of rigid tubes. Pulmonary vascular resistance (PVR) is constant as pressure or flow increases

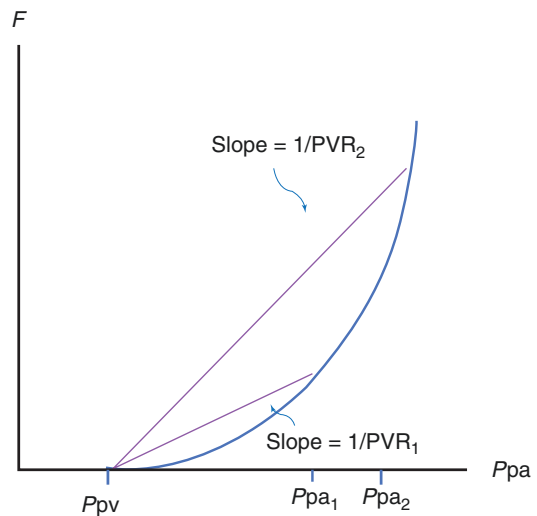


Fig. 5.2 Graph of pulmonary artery pressure (P_{pa}) vs. pulmonary blood flow (F) if the vasculature were comprised of distensible tubes. Pulmonary vascular resistance (PVR) decreases as pressure or flow increases

are shown with different P_a , and the slope ($1/R$) is greater at the higher pressure, and the PVR is lower.

In addition to increasing the inflow pressure, another way to raise the distending pressure in the vasculature is to raise the outflow pressure, P_{pv} . If blood flow stays constant, this may also

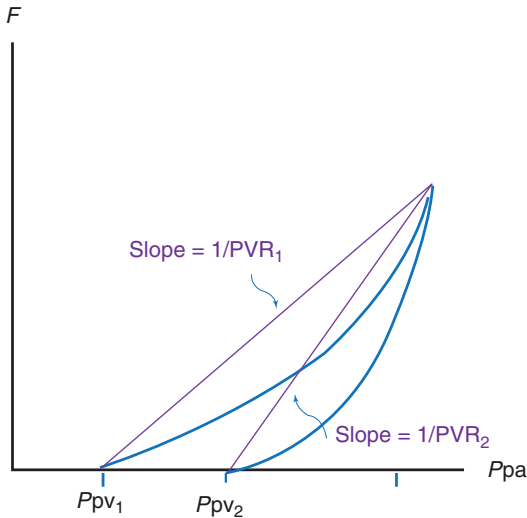


Fig. 5.3 Graph of pulmonary artery pressure (P_{pa}) vs. pulmonary blood flow (F) at two different pulmonary outflow pressures (P_{pv1} and P_{pv2}). Vascular distensibility makes pulmonary vascular resistance (PVR) lower at the elevated P_{pv} . This is true even if the inflow P_{pa} is the same

raise the P_a , but even if P_a were to remain constant, the mean transmural pressure in the vasculature would still increase. This would result in wider vessels and a lower resistance, as illustrated in Fig. 5.3.

Starling Resistors

In the preceding paragraph, the issue was raised about increases in venous pressure. In a relaxed vessel on a level plane perfused with constant flow, any increase in the outflow pressure would always result in some increase in the inflow pressure. If the vessel was rigid (i.e., constant R), every incremental increase in outflow pressure would be matched by an identical increase in inflow pressure. If the vessel were distensible, the increase in inflow pressure would be less than the increase in outflow pressure. In the pulmonary circulation, there is another important factor that distinguishes its hemodynamics from that in the systemic circulation, and that is the effect of gravity. In an upright human, the earth's gravity creates a pressure gradient due to the vertical col-

umn of blood, and this is essentially independent of the pressures generated with the blood flow. This gravitational effect would be of little consequence in the lung if the alveolar capillaries were not surrounded by alveolar air which is at atmospheric pressure (on average). Even then, it would be of little importance if the capillaries had some structure that could keep them open under slightly negative transmural pressure. However, the lung capillaries have very little structure and are very collapsible, essentially unable to withstand any negative transmural pressure. So, if we imagine the right heart generating pressure to pump blood to the upper regions of the lung, the pressure will decrease as one moves up the lung for two reasons: (1) the pressure fall from the flow through the vascular resistance; and (2) the fact that the blood is being pumped uphill, where the pressure will fall 1 cmH₂O for every cm of elevation.

In the lung, it is important to emphasize that not only will the pulmonary artery pressure decrease as one moves up the gravitational field, but also the pulmonary venous pressure will decrease to the same degree. The pulmonary venous pressure as it enters the left atrium will be a little greater than left atrial pressure, typically a few cmH₂O above zero (atmospheric). So as one moves up the lung, at some point the pulmonary venous pressure will reach zero. When this happens, further elevations make the pulmonary venous pressure negative, and since the capillaries are surrounded by a zero alveolar pressure, they will try to collapse. However, they cannot fully collapse, since the pulmonary artery pressure at the capillary inlet is still greater than zero, so it will open the capillary. So we have a conundrum – is the capillary open or is it closed?

The answer to the question is very very complex from a fluid dynamical perspective. However, from a more intuitive practical perspective, it can be simply explained. In fact, a physical device consisting of a thin-walled collapsible tube passing through a sealed box was devised by Ernest Starling over 100 years ago to allow him to do his pivotal experiment on an isolated perfused heart (Knowlton and Starling 1912). By adjusting the surrounding pressure in

the box, he was able to show that the load the heart pumped against was essentially equal to the pressure in the box surrounding the collapsible tube. These experiments provided insights into cardiac contractility that led to what is commonly known as Starling's Law of the Heart. However, this physical model is conceptually similar to what occurs in the pulmonary capillaries, where the collapsible vessels are surrounded by alveolar pressure. And applying the same logic, the downstream pressure that the right heart sees will thus be equal to the alveolar pressure.

These concepts applied to the pulmonary vasculature were developed many years ago by Permutt's group (Permutt et al. 1962; Permutt and Riley 1963) and were then adapted by West in a classic paper that outlined three zones in the pulmonary circulation, defined by the gravitational field (West et al. 1964). In the bottom of the lung (zone 3) where both pulmonary artery and venous pressures are greater than zero, the driving pressure for flow is P_{pa} minus P_{pv} . In the very top of the lung (zone 1) where both P_{pa} and P_{pv} are less than zero, there is no flow. And between these regions at the top and bottom is the situation discussed above (zone 2), where the capillary wants to be both open and closed at the same time. In zone 2, the driving pressure for flow is P_{pa} minus alveolar pressure (P_{alv}), and if the average P_{alv} is zero, then the driving pressure is simply P_{pa} . As one moves up the lung, the P_{pa} will continually decrease, and thus the flow continually decreases until the P_{pa} equals zero, when flow will equal zero (zone 1).

Pulmonary Vascular Resistance in Presence of Starling Resistors

With these different gravitational determined regions, how can we interpret pulmonary vascular resistance? In zone 3, the situation is as described in Fig. 5.2, where we have a distensible fluid pathway all open, the resistance is the inverse slope of the line connecting the P_{pv} intercept on the abscissa and the point on the PF curve for any particular P_{pa} . In zone 2, however, we have a different situation, and this is shown in

Fig. 5.4. Here, there is no flow until P_{pa} exceeds P_{alv} , and then there is a nonlinear curve reflecting the distensibility of vessels upstream from the capillaries. A resistance calculation in this situation (PVR^*) then will also be only of the vascular segment upstream from the capillaries, as shown by the straight line drawn from the P_{alv} intercept to the P_{pa} pressure. One point worth noting here is that, although we say the resistance upstream from the capillaries is what is relevant, this segment includes the capillaries. And while the capillaries are normally considered to have a low vascular resistance (and are commonly ignored), to the extent they are compressed by the alveolar pressure, they can assume an increasingly important fraction of the total resistance. For example, if we assume that a capillary is not distensible and thus has a constant perimeter, then simply compressing this constant perimeter into an elliptical shape with the smaller ellipse diameter made equal to the *radius* of the original round capillary will increase the laminar flow resistance to flow by a factor of about 3.5. (The capillary blood volume will also be reduced by about 40%.) These changes in the capillary bed thus

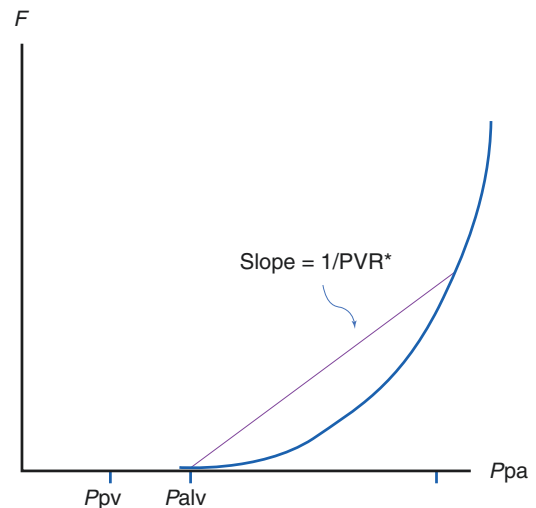


Fig. 5.4 Graph of pulmonary artery pressure (P_{pa}) vs. pulmonary blood flow (F) in a zone 2 condition. Here, alveolar pressure (P_{alv}) is the effective downstream pressure, and the resistance measured by the inverse slope of the line shown (PVR^*) is the resistance upstream from the pulmonary capillaries

can have a significant impact on the slope of the pressure flow curve.

One important feature of the zone 2 situation is the fact that what happens downstream from the capillaries is essentially not seen on the inflow side. For this reason, the situation has been likened to a waterfall, where the flow over the falls is entirely a function of the upstream river bed and completely independent of the height of the falls (i.e., events downstream of the falls). Thus, changes in left atrial pressure will not impact the flow unless the pressure rises sufficiently to begin to transition vessels into a zone 3 situation.

In a normal upright human lung, it has been estimated that there is very little zone 1, with about 60% of the lung being in zone 3 and 40% in zone 2. This fraction is very rough as it will depend on the P_{la} and the height of the lung. Also, this fraction will change substantially when the height of the lung changes relative to the gravitational field, as when one goes from upright to supine. This situation makes it difficult to both calculate and interpret the PVR, since the effective downstream pressure in the formula for flow in the two zones is different.

Figure 5.5 shows what a pressure flow curve would look like in a lung comprised of idealized regions in zone 3 and zone 2. For P_{pa} less than P_{pv} , there is no forward flow. When P_{pa} exceeds P_{pv} , flow begins in zone 3. When P_{pa} increases

above P_{alv} , then flow begins in zone 2, and flow then will continue to increase. However, if we try to calculate PVR by connecting a line between P_{pv} and the P_{pa} , we will be in error, because the regions of the lung in zone 2 will be calculated incorrectly. One would have to do a complicated subtraction on the curve to remove the zone 3 flow, so that one could calculate the resistance line from P_{alv} to P_{pa} . But this would be very impractical if even possible.

Vascular Compliance

The issue of pulmonary vascular compliance has been both implicit and explicit in the preceding discussion. It is thus worth a closer look at how this compliance could impact the pulmonary pressure flow curve quantitatively. It is important to note that there are two aspects of vascular compliance relevant to the pulmonary circulation. One is its role in blood storage – a more compliant vasculature will hold more blood volume, and there have been many so-called lumped parameter models that partition the vasculature into resistive segments in series with compliant segments. The other aspect of vascular compliance relates to the distensibility of the actual resistance vessels. While the former aspect is important in its own right, for the focus of this

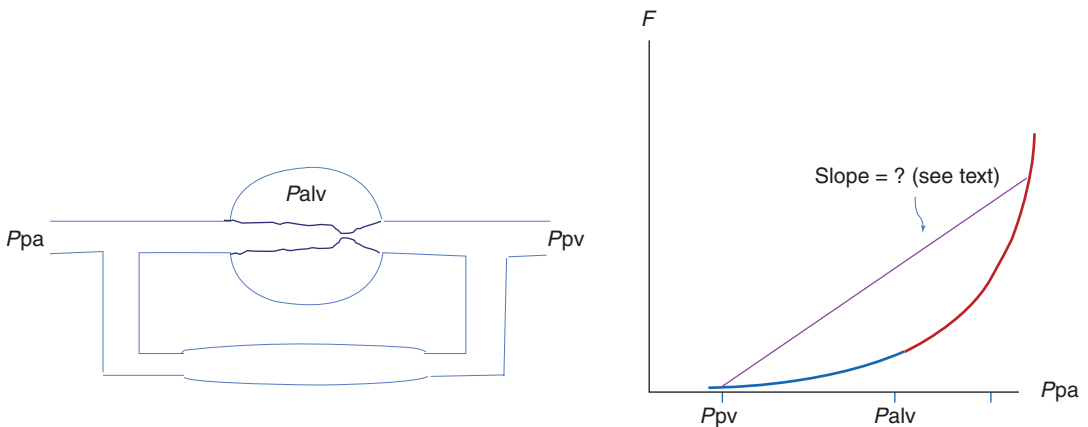
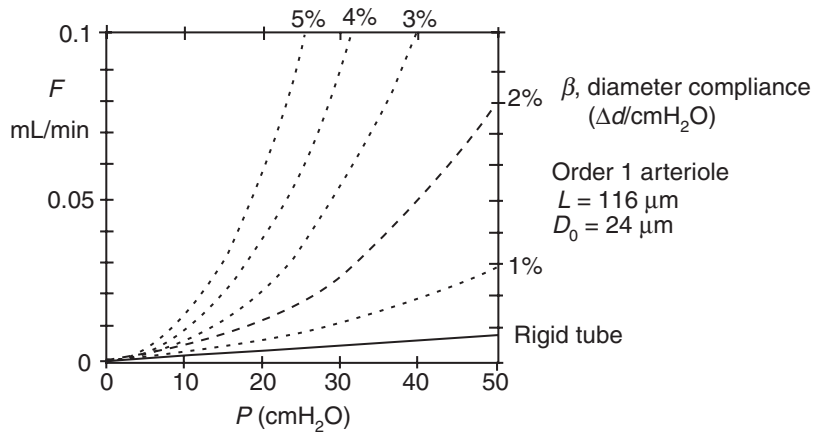


Fig. 5.5 Graph of pulmonary artery pressure (P_{pa}) vs. pulmonary blood flow (F) in a lung with both zone 3 and zone 2 conditions, as in the flow diagram on the left. Blood flow starts in the zone 3 regions when P_{pa} exceeds

P_{pv} (blue). When P_{pa} exceeds P_{alv} , the flow is then the sum of parallel flow from all regions (red). The resistance measured by the inverse slope of the line shown is not easily interpreted

Fig. 5.6 Effect of vessel distensibility (β) on the shape of the PF curve. A nominal value of β is 2%, but it can vary from 1% to 5% diameter change per cm water. Curves were derived from the equations for flow through a distensible vessel derived by Zhuang et al. (1983)



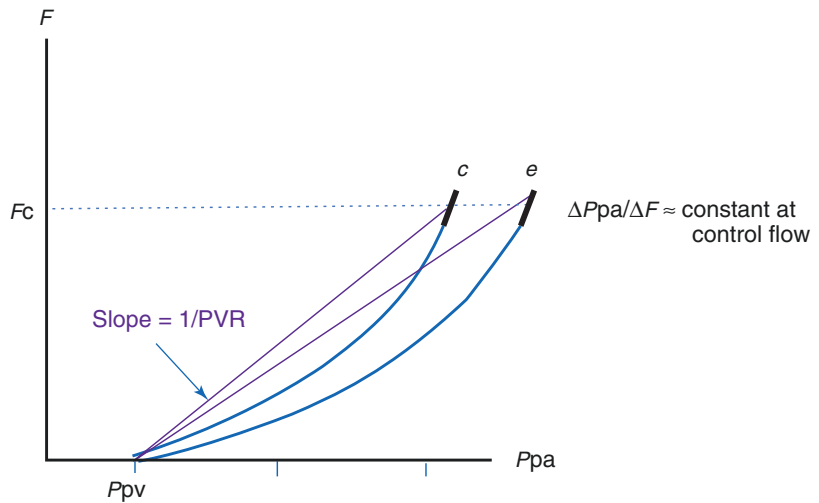
chapter on vascular resistance, it is this latter aspect that will be discussed below.

In 1983, Zhuang et al. first published an analysis of how vascular distensibility would affect the pressure flow curve (Zhuang et al. 1983). They showed how perfusion through a distensible tube would assume a tapered shape and that the laminar flow was now proportional to the average diameter to the fifth power rather than the fourth power determined by the Poiseuille formula for laminar flow through a rigid tube. This work was developed further by Krishnan, et al. who used it to graph the distribution of local resistance and compliance through the lung from large arteries to large veins (Krishnan et al. 1986). One important result from this analysis was that the major site of pulmonary vascular resistance is in the smallest arterioles. A key parameter in this analysis is the percent change in vascular diameter per change in transmural pressure. This variable, sometimes designated β , has been shown to nominally vary from 1% to 4%/cmH₂O. Figure 5.6 shows pressure flow curves derived from the equations generated by Zhuang et al. (1983). This figure shows the P-F curves for the smallest arteriole (order 1 in the Strahler ordering system). Six curves are shown, one being for a rigid tube, and the others for varying distensibility from 1 to 5% per cm water. This figure emphasizes just how sensitive the curves are to small changes in distensibility. At a constant flow, reducing β from 5 to 1% can increase the driving pressure over four-fold.

The fact that the resistance vessels are compliant can also lead to some difficulties in interpretation of resistance calculations. Figure 5.7 shows an example where there has been a shift in the PF curve. The upper regions of the curves are shown as being nearly parallel. In the real world, a change in vascular compliance from say 5–3% as shown in Fig. 5.6 might easily appear as a parallel shift. If PVR is calculated from the P_{pv} , and flow is constant, then in going from curve c to curve e, an increase will be measured. However, if one had assumed that shift was caused by a shift in critical pressure in a zone 2, then one might be tempted to measure the slopes of the curves. Here there would be no change. This example emphasizes an important cautionary point. Although the slope ($\Delta P/\Delta Q$) has units of resistance, it is not a resistance. A resistance reflects the area and length of the vessel, but the slope reflects a distensibility and has little relation to the absolute size of the vessels. Of course, if there were an ideal Starling resistor, with an upstream rigid vasculature, then this slope would be the resistance of that vasculature. However, the pulmonary circulation is quite far from an idealized Starling resistor.

In addition to the importance of the distensibility of the vascular resistance vessels discussed above, vascular compliance will play a role in the pulmonary vascular impedance. Impedance is, in its simplest definition, the ratio of driving pressure to flow as a function of frequency. The resistance that is the focus of this chapter is simply the

Fig. 5.7 Graph of pulmonary artery pressure (P_{pa}) vs. pulmonary blood flow (F) at control (c) and hypothetical experimental (e) conditions. The shift of the experimental curve shows an increased resistance, but the slope of the curve can often be unchanged



impedance at zero frequency. While it should be clear that a higher resistance will increase the load on the right ventricle, an increased impedance will also contribute to this load. A discussion of the relative importance of the resistance and impedance to the function of the right ventricle is well beyond the scope of this chapter. However, the compliance of the major resistance vessels will surely have to play a major role in this cardiac loading, since as is clear in Fig. 5.6, small changes in this local distensibility can have major effects on the driving pressure even at a constant flow.

Interpretation of Overall PVR

So where does this leave us if we want to determine the resistance to blood flow through the lungs? There is no good answer to this question. Based on the above discussion, it is clear that a simple measure of resistance is not only difficult to compute, but also difficult to interpret. What is clear, however, is that if one simply calculates PVR from the $(P_{pa} - P_{pv})$ pressure difference, then a higher number would reflect a greater load on the right ventricle. It is clear from Fig. 5.5 that as flow or P_{pa} increases the calculated PVR would decrease. This calculated decrease would occur from both the distensibility of the blood vessels and the fact that the wrong downstream

pressure is being used for the portion of the lung in zone 2.

The best way to interpret the resistance to flow through the pulmonary vasculature requires knowledge of the PF curve. Unfortunately, this is rarely available in preclinical models and almost never in clinical practice. Even so, if the curve is highly nonlinear, it would not be possible to separate the zone 2 regions from the zone 3 regions. Nonetheless, if one does the PVR calculation based on a knowledge of cardiac output, P_{pa} , and P_{pv} (estimated from left atrial pressure), the value does reflect the load on the right ventricle. If something were to cause vessels to narrow, it would surely show as an increase in this calculated PVR.

Ultimately, the measurement of PVR depends on knowing the P_{pa} and some effective downstream pressure. If the lung is all in zone 3 as might occur in a supine human, then this downstream pressure would be the left atrial pressure (P_{la}). However, in humans, P_{la} is not simple to obtain, so this has been estimated by wedging a catheter into a small artery often with a surrounding balloon to seal it off. With no distal flow, the pressure in this wedged catheter will measure the pressure at the closest downstream point where there are connecting vessels from a non-wedged vasculature. This pulmonary wedge pressure (PWP) also goes by a variety of names, including pulmonary capillary wedge pressure (PCWP) or

pulmonary artery wedge pressure (PAWP). Since there are always vascular anastomoses proximal to the left atrium, all of these wedge pressures will measure a pressure higher than P_{la} . How much higher depends on the vascular resistance in the pulmonary veins, but this is often assumed to be small. PWP can be used to measure PVR, but this measurement will clearly not include the resistance of the larger pulmonary veins. In an upright human or one with mechanical ventilation, where there can be a significant fraction in zone 2, the measurement of PWP will very much depend on whether the capillary bed distal to the wedged vessel is in zone 2 or zone 3.

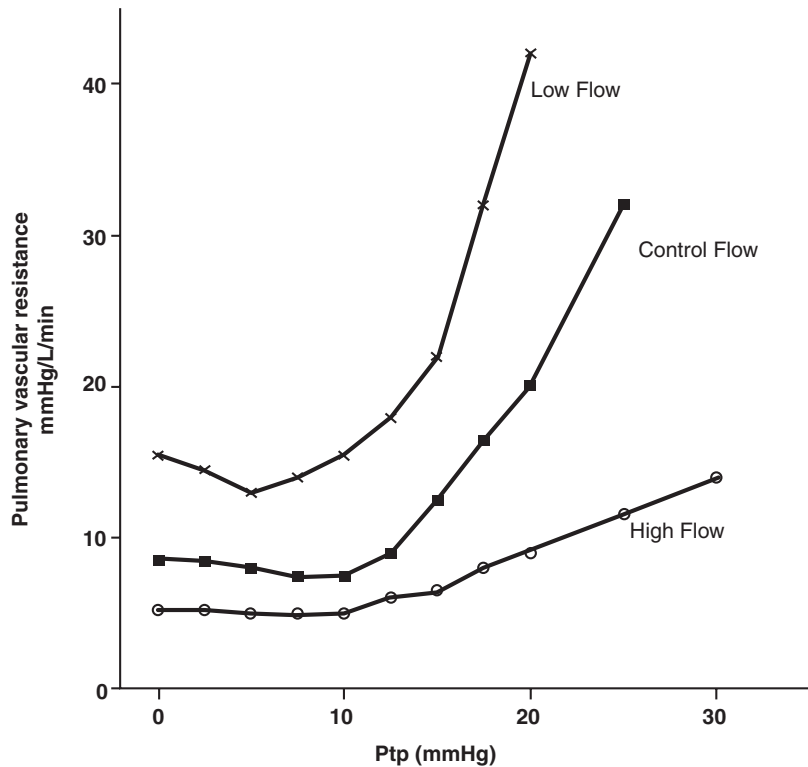
Effect of Lung Inflation on PVR

The lung vasculature is unique in that it courses through an elastic inflatable structure. Seminal work by Macklin (1946) and Permutt and colleagues (Howell et al. 1961; Permutt et al. 1961) showed that the vasculature can be partitioned into two major regions where lung inflation behaves differently. The two regions are the capillary and non-capillary regions, and these have subsequently been designated as the alveolar and extra-alveolar vasculatures, respectively. The pressure surrounding capillaries in alveoli is the alveolar pressure (P_{alv}), and with lung inflation (and constant vascular pressure) there will be an increasing compressive stress pressure on the capillaries. (Note that this explanation assumes both alveolar and vascular pressures are referenced to the pleural pressure, P_{pl} .) In contrast, the effective pressure surrounding extra-alveolar vessels is close to P_{pl} (Pare and Mitzner 2012; Smith and Mitzner 1983), and with inflation, this pressure can decrease relative to vascular pressure. Thus, there is a compressive pressure on capillaries and a distending pressure on the extra-alveolar vessels as the lung inflates. This will be true whether the lung is inflated with a positive airway pressure or in situ with a negative (subatmospheric) pleural pressure. The net effect of these internal stresses has long been known to lead to biphasic changes in lung volume as the lung is inflated, with the blood volume in extra-alveolar vessels first increasing as

the lung is inflated from very low lung volumes, and then with blood volume in alveolar vessels decreasing with increasing compression of alveolar capillaries as the lung volume (and transpulmonary pressure) increases (Howell et al. 1961). These biphasic changes in regional vascular volumes, however, do not translate directly to changes in PVR, since as emphasized above, the sites of vascular resistance may not be coincident with the sites of volume storage, and a small volume change in the smallest resistance vessels could have a big change in resistance. An understanding of this complexity has not been widely appreciated, and this has led to a common misrepresentation expressed in graphs showing a U-shaped relation between PVR and lung volume (West 2000). The relationship is in fact much more complex, depending on the magnitude of vascular pressures and especially pulmonary blood flow. This complexity was appreciated in one of the first studies by Whittenberger et al. (1960), which showed an increase in PVR in most situations even starting from low lung volumes. Figure 5.8 shows results redrawn from this original work. This figure emphasizes the major importance of blood flow on the slope of this sensitivity to inflation pressure (P_{tp}). While they did find an occasional fall in PVR with lung inflation, this only occurred at very low blood flow, and at inflation pressures below what would be FRC in an intact animal. Indeed, these results showing a steadily increasing PVR with lung inflation were subsequently supported by others in experiments in intact animals (Scharf et al. 1977).

One additional factor to consider in interpreting these relationships is that the importance of the vascular pressure depends on what reference pressure is used. Thus, while (Hakim et al. 1982) showed one figure with a U-shaped PVR vs. lung inflation graph, this was only found with “negative pressure inflation.” With positive pressure inflation, there was no decrease in PVR at low lung volumes. However, since transpulmonary pressure is always positive, and the lung can only inflate with an increasing transpulmonary pressure, the different appearances reported by Hakim et al. simply reflect a different reference pressure for the pulmonary vascular pressures.

Fig. 5.8 Relation between pulmonary vascular resistance and transpulmonary pressure (P_{tp}), at three different flow ranges. The increase in PVR with lung inflation is greatly lessened at high blood flows. (Adapted from data in Whittenberger et al. (1960); see text)



And finally, it is important to note that in this whole discussion of the effects of lung inflation, we are using PVR with the aforementioned caveats involving the effective downstream pressure, and this situation becomes even more complex with the addition of anatomic resistance compartments in series.

Summary

Given all the concerns raised above, including uncertainty about what downstream pressure to use (and how to measure it), the effect of lung inflation on different serial regions of the pulmonary vasculature and the nonlinear distensibility of the elastic vessels, does it make sense to even bother to measure PVR? As with most complex questions, there may be several conditional interpretations, the answer is that it depends. In a supine human, the amount of the lung in zone 2 is likely small, so using the left atrial pressure as the down-

stream pressure is reasonable. A measurement of PVR using Eq. 5.1b will provide a measure of how hard the right lung must work to pump blood through the lung. If PVR is found to be increased in the absence of an increased lung volume, then this surely indicates an impediment to flow in the vasculature. So as a metric for pulmonary vascular disease, the PVR may be useful. It will not be able to say anything about where the pathology might be, as this knowledge would require further testing. In a sense, the PVR has some similarities to the ubiquitous use of spirometric variables to evaluate lung function. Decrements in say, FEV1 or FVC, clearly indicate a loss of lung function, but additional tests are needed to determine which pathology might be causing this. Of course, spirometric variables are far more easily obtained than PVR, which requires invasive measurements of vascular pressure and flow. This likely limits the utility of PVR in humans to instrumented patients, but if such data can be obtained, the PVR can provide a useful index.

References

- Behrens I, in Bahr LS, Johnston B, editors. *Colliers encyclopedia*, vol. 18. New York: P.F. Collier; 1995. p. 93.
- Howell JB, Permutt S, Proctor DF, Riley RL. Effect of inflation of the lung on different parts of pulmonary vascular bed. *J Appl Physiol*. 1961;16:71–6.
- Knowlton FP, Starling EH. The influence of variations in temperature and blood pressure on the performance of the isolated mammalian heart. *J Physiol*. 1912;44:206–19.
- Krishnan A, Linehan JH, Rickaby DA, Dawson CA. Cat lung hemodynamics: comparison of experimental results and model predictions. *J Appl Physiol* (1985). 1986;61:2023–34.
- Macklin C. Evidences of increase in the capacity of the pulmonary arteries and veins of dogs, cats, and rabbits during inflation of the freshly excised lung. *Rev Can Biol*. 1946;5:199–232.
- Hakim TS, Michel RP, Chang HK. Effect of lung inflation on pulmonary vascular resistance by arterial and venous occlusion. *J Appl Physiol: Respirat Environ Exercise Physiol*. 1982;53(5):1110–115.
- Pare PD, Mitzner W. Airway-parenchymal interdependence. *Compr Physiol*. 2012;2:1921–35.
- Permutt S, Riley RL. Hemodynamics of collapsible vessels with tone: the vascular waterfall. *J Appl Physiol*. 1963;18:924–32.
- Permutt S, Howell JB, Proctor DF, Riley RL. Effect of lung inflation on static pressure-volume characteristics of pulmonary vessels. *J Appl Physiol*. 1961;16:64–70.
- Permutt S, Bromberger-Barnea B, Bane HN. Alveolar pressure, pulmonary venous pressure, and the vascular waterfall. *Med Thorac*. 1962;19:239–60.
- Scharf SM, Caldini P, Ingram RH Jr. Cardiovascular effects of increasing airway pressure in the dog. *Am J Phys*. 1977;232:H35–43.
- Smith JC, Mitzner W. Elastic characteristics of the lung perivascular interstitial space. *J Appl Physiol*. 1983;54:1717–25.
- West J. *Respiratory physiology: the essentials*. 6th ed. Baltimore: Lippincott Williams & Wilkins; 2000.
- West JB, Dollery CT, Naimark A. Distribution of blood flow in isolated lung; relation to vascular and alveolar pressures. *J Appl Physiol*. 1964;19:713–24.
- Whittenberger JL, Mc GM, Berglund E, Borst HG. Influence of state of inflation of the lung on pulmonary vascular resistance. *J Appl Physiol*. 1960;15:878–82.
- Zhuang FY, Fung YC, Yen RT. Analysis of blood flow in cat's lung with detailed anatomical and elasticity data. *J Appl Physiol: Respirat Environ Exercise Physiol*. 1983;55:1341–8.



Fluid Filtration in the Microcirculation

6

FitzRoy E. Curry

Abbreviations

A	Surface area for microvascular exchange
J_s	Plasma protein flux
J_v	Water flux
L_p	Hydraulic conductivity
P	Pressure
PBR	Peripheral boundary layer; region from which red cells are excluded in microvessels
Pe	Peclet number, the ratio of velocity of a solute dragged by water flows to its diffusion velocity
P_p, P_g, P_i	Hydrostatic pressure in capillaries, sub-glycocalyx, and interstitial space
R_a, R_v	Resistance to blood flow in arteriolar and venular vasculature segments proximal and distal to capillaries
Π	Colloid osmotic pressure
Π_p, Π_g, Π_i	Colloid osmotic pressures in plasma, sub-glycocalyx space, and interstitial space
$\Delta P, \Delta \Pi$	Difference in pressure or colloid osmotic pressure
σ	Osmotic reflection coefficient

Introduction

The plasma volume is maintained in a steady state established by fine homeostatic regulation of filtration out of the vascular compartment and return of the filtered fluid to the vascular space by a range of reabsorption mechanisms. The mechanism of passive filtration has been well understood for more than a century: the driving force for fluid movement out of the vascular system is the difference between the hydrostatic pressure of the fluid in microvessels and the colloid osmotic pressure exerted by the plasma proteins (also known as the oncotic pressure of the plasma proteins). This is a statement of the Starling principle, accounting (in a human subject) for an ultrafiltration of nearly 2 liters of plasma per day from microvessels with continuous endothelium (skin, muscle, heart, lung); up to 8 liters per day from the discontinuous capillaries of the liver and fenestrated capillaries in the GI tract (secretory glands, saliva, pancreas); and over 100 liters per day at the renal glomerulus. Some of the filtered fluid is lost (urine, feces, respiration, sweating) from the body and replaced by fluid and food intake, but most of the filtered fluid must be reabsorbed directly into the plasma or returned via the lymphatics (Michel et al. 2016; Michel 1984; Kviety and Granger 2010; Renkin 1986)). The first part of this chapter summarizes progress in our understanding of the balance between filtration and reabsorption based on the idea that the

F. E. Curry (✉)
Department of Physiology and Membrane Biology,
School of Medicine, University of California,
Davis, CA, USA
e-mail: fecurry@ucdavis.edu

Starling forces that regulate transvascular fluid exchange act primarily across the endothelial glycocalyx. Of particular significance to the topic of cardiopulmonary monitoring is the emphasis that this revised Starling principle places on: (1) the importance of capillary pressure to determine both filtration rate and the effective colloid osmotic pressure difference that determines this filtration rate; (2) the asymmetry in effectiveness of plasma protein oncotic pressure relative to tissue oncotic pressures to maintain fluid in the vascular space; (3) the development of methods to monitor the integrity of the endothelial glycocalyx as an index of microvascular dysfunction. For additional detailed reviews, see (Michel et al. 2016; Curry et al. 2016; Curry 2018; Levick and Michel 2010).

The Revised Starling Principle: Basic Science Principles

The Endothelial Glycocalyx: Primary Barrier to Circulating Plasma Proteins

The key idea is that the colloid osmotic pressure of the plasma proteins opposing filtration is across the endothelial glycocalyx ($\Pi p - \Pi g$), not the colloid osmotic pressure difference between plasma and the interstitial fluid ($\Pi p - \Pi i$). Πp is the osmotic pressure of the plasma proteins, Πg is the osmotic pressure of the plasma proteins in a space beneath the glycocalyx (sub-glycocalyx space), and Πi the osmotic pressure of the plasma proteins in the interstitial space (Levick and Michel 2010). Thus the net force determining filtration ($\Delta P - \sigma \Delta \Pi$) in the revised Starling principle is:

$$\Delta P - \sigma \Delta \Pi = [(Pp - Pg) - \sigma (\Pi p - \Pi g)] \quad (6.1)$$

where Pp is the hydrostatic pressures of circulating plasma in the microvessels where fluid exchange takes place, Pg is the pressure in the sub-glycocalyx space, and σ is the osmotic reflection coefficient of the plasma proteins in the glycocalyx and measures the fraction of the full osmotic pressure that would be exerted if the

membrane excluded all the protein. Because the endothelial glycocalyx forms the primary molecular sieve at the vascular wall, σ for plasma proteins in the glycocalyx is close to 1 and determined by the composition and arrangement of the molecular components of the glycocalyx that lies in series with the main pathways for water and solutes across the endothelial cells.

In contrast, the balance of hydrostatic and plasma protein oncotic forces across the microvascular wall for the classical Starling principle is:

$$\Delta P - \sigma \Delta \Pi = [(Pp - Pi) - \sigma (\Pi p - \Pi i)] \quad (6.2)$$

where Pi and Πi are the hydrostatic and plasma protein osmotic pressures in interstitial space, and the molecular selectivity of the vascular wall is usually associated with structures within the intercellular junctions.

The Sub-Glycocalyx Space

The ultrafiltrate of plasma exiting the glycocalyx has a plasma protein concentration which is lower than the average protein concentration in the interstitial fluid whose composition is also determined by additional plasma protein exchange across the endothelial cells via vesicle transport and occasional large pores, i.e., ($\Pi g < \Pi p$). This glycocalyx ultrafiltrate modifies the composition of interstitial fluid in the space beneath the glycocalyx. Several important consequences follow: One is that the osmotic force opposing filtration acting across the glycocalyx ($\Pi p - \Pi g$) is larger than would be predicted from the classical Starling principle ($\Pi p - \Pi i$) and resulting filtration rates are smaller; a second consequence is that the composition of the fluid in the space beneath the glycocalyx rapidly adjusts to changes in filtration rate. Thus, as filtration rates change, Πg is neither constant nor an independent variable. This is in contrast to the usual assumption that Πi is constant, or changes only slowly because the volume of the interstitial space is large compared to filtration rates. The effectiveness of the so-called “safety factors against edema,” which buffers increased

filtration, is greatly increased when the ultrafiltrate and interstitial fluid mix in the small subglycocalyx space.

A third and most radical consequence is that reabsorption of fluid from the interstitial space to circulating plasma cannot be sustained. While a sudden drop in capillary pressure favors reabsorption of fluid, plasma proteins in this interstitial fluid are carried into the space beneath the glycocalyx and accumulate there. The colloid osmotic forces favoring reabsorption are thereby reduced. Reabsorption ceases, and a new fine balance between hydrostatic and osmotic pressures is established that favors very slow filtration. According to the revised Starling principle, this is the condition of normal steady state filtration in the tissues including the lung, heart, muscle, skin. It follows that the common picture in standard textbooks showing reabsorption on the venular side of the microvascular bed that closely balances filtration on the arterial side of a microvascular bed never occurs over any sustained period (steady state). Because of the importance of this change, some of the key steps in the evolution of ideas from the classic Starling principle to the revised Starling principle are outlined in the next section.

Classical Versus Revised Starling Principle

Because capillary pressure at heart level (supine individual) falls from close to 30 mmHg on the arterial side of microvascular beds to values of the order of 10 mmHg on the venular side, and the normal colloid osmotic of the plasma proteins (25 mmHg) lies between these values, the idea that there is a transition from filtration on arterial side of the microvascular bed to reabsorption on the venous side was accepted as a logical extension of the Starling principle. Classical experiments to directly measure rates of filtration and reabsorption as a function of pressure by Landis in individual microvessels (Landis 1927) and Pappenheimer and colleagues in mammalian hindlimbs (Pappenheimer 1948) confirmed reabsorption when capillary pressures were less than

the osmotic pressure of the plasma proteins, and similar observations have been repeated and confirmed to the present day (Michel et al. 2016; Michel 1997). However, when applying these observations in intact tissue, the limitation is that these experiments were carried out under conditions where interstitial protein concentrations were low (constant washing of the tissue with protein-free solution in the Landis-type experiments on mesentery, or after a period of higher pressure ultrafiltration to locally dilute the interstitial plasma protein concentration in experiments by Pappenheimer and Soto-Rivera). Such low protein levels are not characteristic of the undisturbed interstitial space, where protein concentrations average close to 40% of plasma protein concentration and the effective colloid osmotic pressure difference opposing filtration can be smaller than capillary pressure on the venular side of the microvascular bed.

All the solid points in Fig. 6.1 represent tissues where the sum of hydrostatic pressure on the venular side of their microvascular beds exceeds the effective colloid osmotic and tissue pressures $\{\sigma(\Pi_p - \Pi_i) + P_i\}$ opposing filtration calculated from the classical Starling principle (Levick and Michel 2010; Levick 1991). Furthermore, the filtered volume (J_v) that results from the estimated forces favoring filtration in Fig. 6.1 is very large. J_v depends not only on the balance of hydrostatic pressures and colloid osmotic forces but also on the water conductivity (L_p , hydraulic conductivity) and surface area for exchange (A). The product $L_p A$ is a whole organ capillary filtration coefficient.

$$J_v = L_p A [(P_p - P_i) - \sigma(\Pi_p - \Pi_i)] \quad (6.3)$$

For example, in a 70 kg person with 40% BW muscle, a 4–5 mm Hg pressure difference applied across the vascular wall of muscle tissue with filtration coefficient $L_p A$ in the range 0.0025–0.004 ml/min/100gm predicts filtration of 4–8 liters per day. This is a minimum estimate as the mean pressure across the whole microvascular bed would be larger and the volume that would result many times the resting filtration rate estimated to be of the order of 1.5 liters per day (Michel et al.

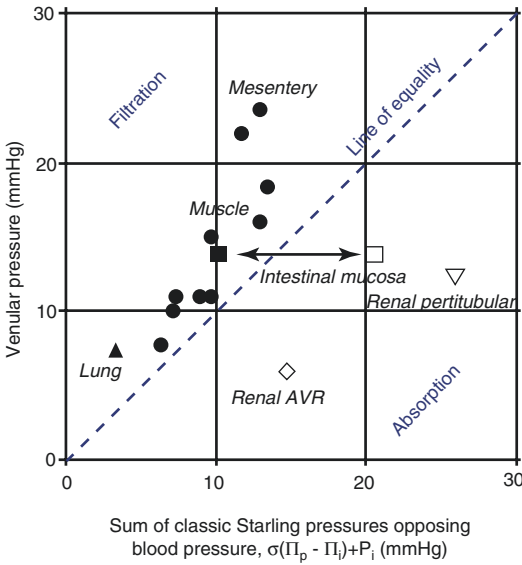


Fig. 6.1 Hydrostatic pressures on the venular side of the microvasculature of different tissues are plotted against the sum of the pressures in those tissues that oppose fluid filtration. The line of equality represents the balance of classical Starling forces. The data representing most tissues lie above this line indicating that the classical Starling principle predicts significant filtration in venules and small veins. The only points that lie below the line represent the renal cortex and medulla and intestinal mucosa during fluid absorption. (Reprinted with permission of Oxford University Press (Levick and Michel 2010))

2016). It follows that the forces favoring filtration must be much smaller than those in Fig. 6.1. There are also important exceptions in Fig. 6.1 (open symbols) representing the peritubular capillaries, vasa recta, and absorbing intestinal mucosa. The revised Starling principle in these organs is discussed in a later section.

Filtration Rate as a Function of Microvascular Pressure in the Revised Starling Principle

The relation between the filtration rate per unit area of vessel wall J_v/A and capillary pressure when the concentration of plasma proteins in the sub-glycocalyx space is itself dependent on the filtration rate, as described above, was derived by Michel (Michel 1984; Michel and Phillips 1987). The assumption is that the plasma protein concen-

tration exiting the glycocalyx (C_{gcx}) is equal to the protein flux across the glycocalyx (J_s) divided by the water flux J_v , i.e., $C_{gcx} = J_s/J_v$. This is simply a statement of mass balance across the glycocalyx. Thus, the filtration rate across the glycocalyx is found by rewriting Eq. 6.1 to describe J_v at each value of capillary pressure in terms of the Starling forces acting across the glycocalyx:

$$J_v / A = Lp_{g_{cx}} \left[(P_p - P_g) - \sigma (\Pi_p - \Pi_g) \right] \quad (6.4)$$

Although Eq. 6.4 retains the form of the classical Starling balance, the relation between filtration rate J_v and capillary pressure is nonlinear. Figure 6.2a shows the so-called “hockey-stick”-shaped curve that results using the relation $C_{gcx} = J_s/J_v$ when the transport of the plasma protein across the glycocalyx involves both diffusive and convective transports. At high pressures, the relation between J_v/A and P is linear with a slope Lp and an intercept on the pressure axis of $\sigma^2 \Pi_p$. Under these conditions, the protein flux across the glycocalyx (J_s) is carried by a solvent drag and is equal to $J_v(1-\sigma)C_p$, where C_p is the plasma protein concentration and σ is the solvent drag reflection coefficient (assumed equal to the osmotic reflection coefficient used in Eqs. 6.1 and 6.2). The plasma protein in the ultrafiltrate exiting the glycocalyx is $C_p(1-\sigma)$. Thus, $C_p - C_{gcx} = \sigma C_p$, and the effective colloid osmotic pressure opposing filtration $\sigma(\Pi_p - \Pi_g)$ is equal to $\sigma^2 \Pi_p$ (assuming the osmotic pressures are proportional to the concentration). For an osmotic reflection coefficient of the order of 0.95, the predicted osmotic pressure opposing filtration is close to 90% of the plasma colloid osmotic pressure, not less than 60% if the average interstitial is 40% of plasma.

As the filtration rate is reduced at lower pressures, C_{gcx} increases above the high filtration limit of $C_p(1-\sigma)$ and approaches C_p so that a balance of forces favoring reabsorption is never established. At all capillary pressures below the effective osmotic pressure of the plasma proteins, the colloid osmotic pressure difference is only slightly less than that of the capillary pressure difference and there is a small steady state filtration. In this range of pressures, the slope of the relation between filtration rate and capillary pressure is very flat. It is this relative insensitivity of filtra-

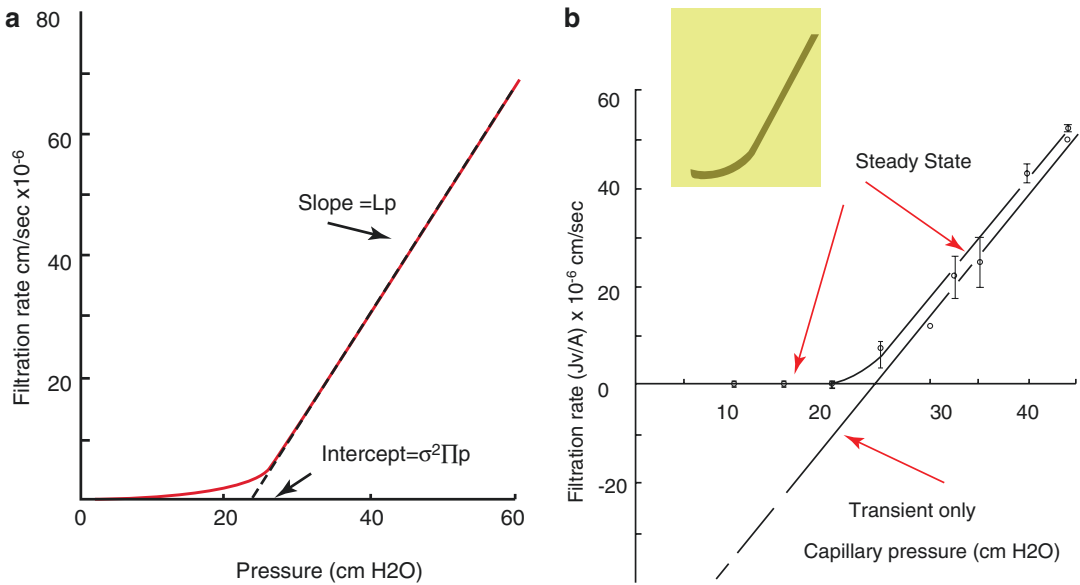


Fig. 6.2 (a) The steady state relation between filtration rate and hydrostatic pressure difference across the glycocalyx or a microvessel where the glycocalyx is the principal determinant of colloid osmotic pressures difference between circulating plasma and the interstitial fluid. At low pressures, steady state filtration increases very slowly with increased pressure reflecting fine adjustment in the concentration of plasma proteins exiting the glycocalyx so that the hydrostatic pressures and effective colloid osmotic pressures are in a fine balance favoring slight filtration. At pressure sufficiently above the effective colloid osmotic pressure of the plasma proteins, filtration rate increases linearly with increments of pressure because the plasma protein concentration difference σCp reaches a constant value of σCp . The slope of the linear relation is Lp and the intercept on the pressure axis is

$\sigma^2 \Pi p$ (Modified from (Michel et al. 2016) with permission of Springer Nature). (b) An experiment on an individually perfused capillary in the mesentery demonstrating the steady state relation between filtration rate per unit area and capillary pressure. Steady states were measured after the vessel was perfused with each pressure maintained for 5–10 minutes. The nonlinear curve fitted to the steady state data has the same shape (hockey stick) as (a). In contrast, when filtration rates were measured as rapidly as possible (within 5–10 seconds) after a sudden drop in pressure from an initial high filtration rate (pressure 40 cm H₂O), the linear relation to the right of the steady state curve was obtained. This is the result expected when the effective osmotic pressure difference remains approximately constant. (Reprinted with permission of John Wiley and Sons (Michel and Phillips 1987))

tion rates to changes in capillary pressures below the osmotic pressure of the plasma proteins that is key to understanding the application of the revised Starling relation to fluid exchange in the peripheral microvasculature. In other words,

there is very little loss of fluid from the vascular space when capillary pressures fall in the range of the flat region of the curve (see clinical example below). The relation that describes the whole curve in Fig. 6.2a is:

$$Jv / A = Lp \left\{ \Delta P - \sigma^2 \Pi p \left[1 - \exp(-Pe) \right] / \left[1 - \sigma \exp(-Pe) \right] \right\} \quad (6.5)$$

where Pe is the Péclet number equal to $(Jv/A) / (1-\sigma)/Ps$. Ps is the permeability coefficient for diffusive albumin transport through the main water pathway across the endothelial barrier.

Figure 6.2b contrasts the steady state relation between Jv/A and capillary pressure, where Πg

varies with filtration rate with the linear relation where the colloid osmotic pressure difference is constant. Michel and Phillips (Michel and Phillips 1987) established steady state by perfusing single capillaries at constant pressure before measuring filtration rates. Figure 6.2b also shows

that the curvilinear hockey stick relation between J_v/A and pressure P is preserved in microvessels in which L_{pgcx} is replaced by the whole vessel L_p , and tissue pressure is close to zero.

Both experimental and theoretical investigations have confirmed these results and provided further insights into key mechanisms. Figure 6.3a is a schematic describing the revised Starling principle with plasma proteins entering the interstitial space not only via the glycocalyx but also via additional transcapillary pathways such as vesicle shuttle or specific uptake and large pores (Levick and Michel 2010). Figure 6.3b is a specific example of a series of glycocalyx-endothelial junction pathways. The quasi-periodic structure of the glycocalyx close to the endothelial cell membrane and the geometry of the endothelial junction in rat venular microvessels as observed in ultrastructural investigations are used for quantitative evaluation of the revised Starling principle (Michel et al. 2016; Curry et al. 2016; Adamson et al. 2004).

A key observation from detailed reconstruction from serial section electronmicrographs is that the strands are not continuous. There are infrequent discontinuities in the junctional strands (150–350 nm long, the distance $2d$ in Fig. 6.3b), where adjacent endothelial cell membranes are not sealed and adjacent membrane are separated by up to 20 nm, much larger than the maximum dimensions of an albumin molecule. These discontinuities occupy less than 10% of the total junction length (estimated from the mean spacing between discontinuities, distance $2D$, in Fig. 6.3b). Thus, at least 90% of these junctions between adjacent endothelial cells are sealed by junctional strands that are not penetrated by solutes larger than 500 daltons and which offer high resistance to water, and the discontinuities form the main pathway for water and solutes. The discontinuities also serve to protect the composition of sub-glycocalyx space because the ultrafiltrate exiting the glycocalyx is funneled through them driven by a small pressure difference between the sub glycocalyx space and the interstitial space. As a result, water velocity at the discontinuities can be more than 10 times that across the glycocalyx. This convective flow opposes back diffusion of plasma proteins from the interstitial fluid. Thus, the concentration of

plasma proteins below the glycocalyx is maintained lower than tissue concentration and $(\Pi_p - \Pi_g) > (\Pi_p - \Pi_i)$ even at low capillary pressures.

Fig. 6.3c shows measured values of filtration rate as a function of pressure when the fluid bathing the capillary had an osmotic pressure equal to that in the plasma. Under this extreme form of tissue protein loading, the classical form of the Starling principle states that $(\Pi_p - \Pi_i)$ is zero, whereas direct measurement of filtration rates at a series of pressures demonstrated that plasma proteins in the microvessel lumen exert 70% of their colloid osmotic pressure across these microvessel wall (Adamson et al. 2004). This example illustrates the important fact that plasma proteins in the circulating blood are more effective oncotic agents than plasma proteins in the interstitial fluid. The same result was demonstrated both experimentally and theoretically in fenestrated microvessels (Levick and McDonald 1994; Levick 1994); see also (Curry 2018). It is also noted that, as shown in Fig. 6.2b, a requirement for the steady state is that the interstitial plasma proteins are carried from the tissue by the lymphatic system.

Recap and a Textbook Figure to Forget

Fig. 6.4 summarizes much of the above by contrasting the incorrect textbook diagram of filtration/reabsorption in a microvascular bed with the profile of microvessel pressure and colloid osmotic pressure difference along the same vascular bed based on the revised Starling principle. As expected from both the classical Starling principle and the revised Starling principle, significant filtration occurs only when microvessel pressure exceeds the colloid osmotic of the plasma proteins. At all pressures less than the effective plasma oncotic pressure, transvascular hydrostatic and colloid osmotic pressure are in a fine balance (mean difference <1 mmHg), such that very slow filtration occurs along the whole vascular bed. This difference accounts for the expected basal filtration rate from muscle of about 1.5 liters per day. A reduction in the pressure on the capillaries due to increased smooth muscle tone in arterioles will result in transient

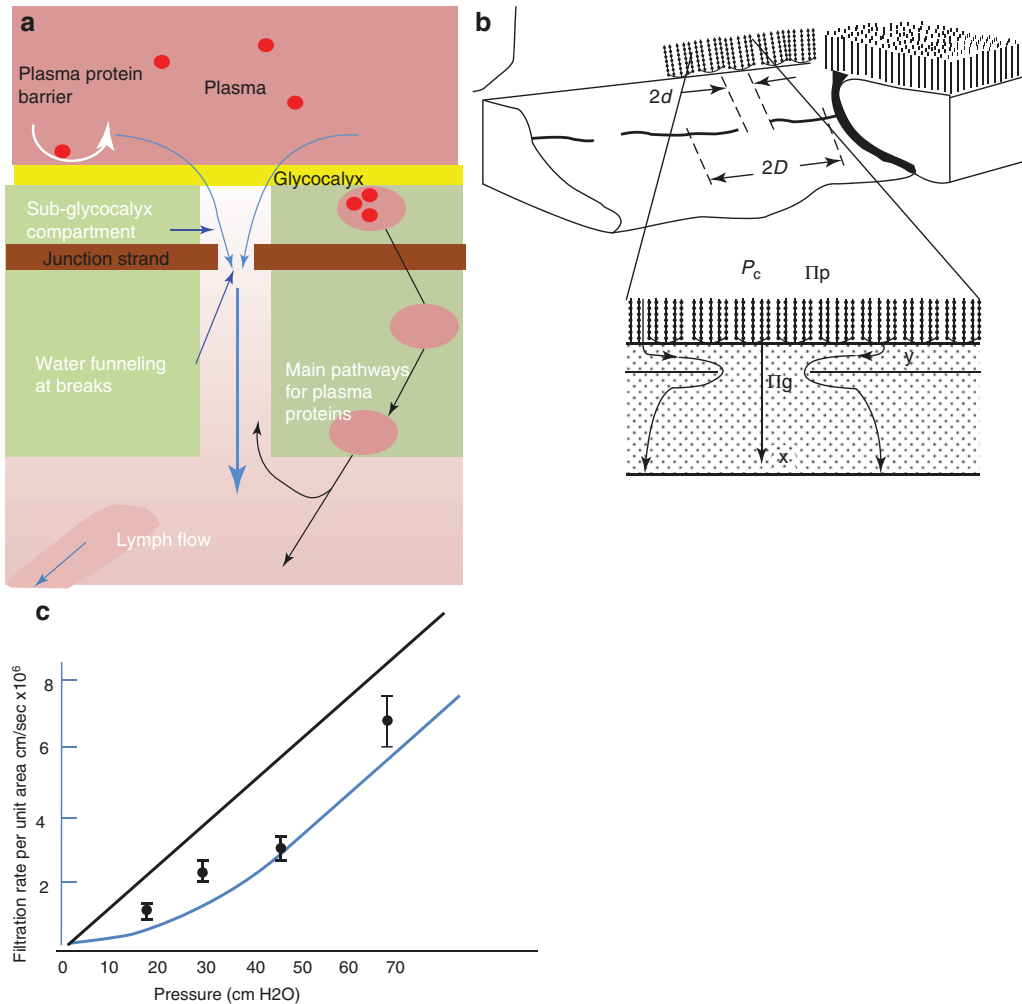


Fig. 6.3 (a) The glycocalyx-cleft model of the endothelial barrier. In part A, the glycocalyx (yellow layer overlying the endothelial cells) is identified as the primary barrier (molecular filter) to plasma proteins such as albumin. The colloid osmotic pressure that opposes filtration is between plasma and the fluid on the underside of the glycocalyx, i.e., inside the intercellular cleft and close to the glycocalyx. After crossing the glycocalyx, the plasma ultrafiltrate is funneled through infrequent breaks in the junctional strands (brown band). During steady state filtration, the difference in colloid osmotic pressure across the glycocalyx is always larger than the difference between plasma and the bulk interstitial fluid. The composition of the bulk interstitial fluid reflects the contributions from other pathways for plasma protein exchange across the endothelial barrier (vesicles, large pores, etc.). (Modified from Curry (Curry 2018) with permission of Springer Nature). (b) is a specific example of the glycocalyx-junction model in (a). The interendothelial cell cleft segment reconstructed from serial sections of a rat mesentery microvessels enabled the position of junction strands in the endothelial cleft and distance between gaps in the junction strands to be measured. The exploded

view is an idealized diagram representing the mathematical model used to evaluate fluxes of water and albumin across the glycocalyx-junction segments using values of junction geometry, junction gap frequency, and glycocalyx thickness characteristic of rat mesenteric microvessels. (From Curry (Curry 2018) with permission of Springer Nature). (c) shows the results of an experiment similar to (b), but with the interstitial fluid surrounding a rat mesenteric microvessels loaded with albumin at the same concentration as in the lumen (50 mg/ml). The solid black line shows the predicted filtration rates expected when Π_p and Π_i were set equal so that here was not colloid osmotic pressure difference opposing filtration between lumen and tissue. The measured filtration rates fall significantly below this line, indicating that a colloid osmotic pressure difference was established across the glycocalyx. The effective osmotic pressure exerted by the plasma proteins was close to 70% of the osmotic pressure of the perfusate osmotic pressure. The blue line describes filtration in the absence of tissue albumin loading. Directly measured filtration rates in the presence of albumin loading are expressed as mean \pm SEM. (Original data from Adamson et al. (Adamson et al. 2004))

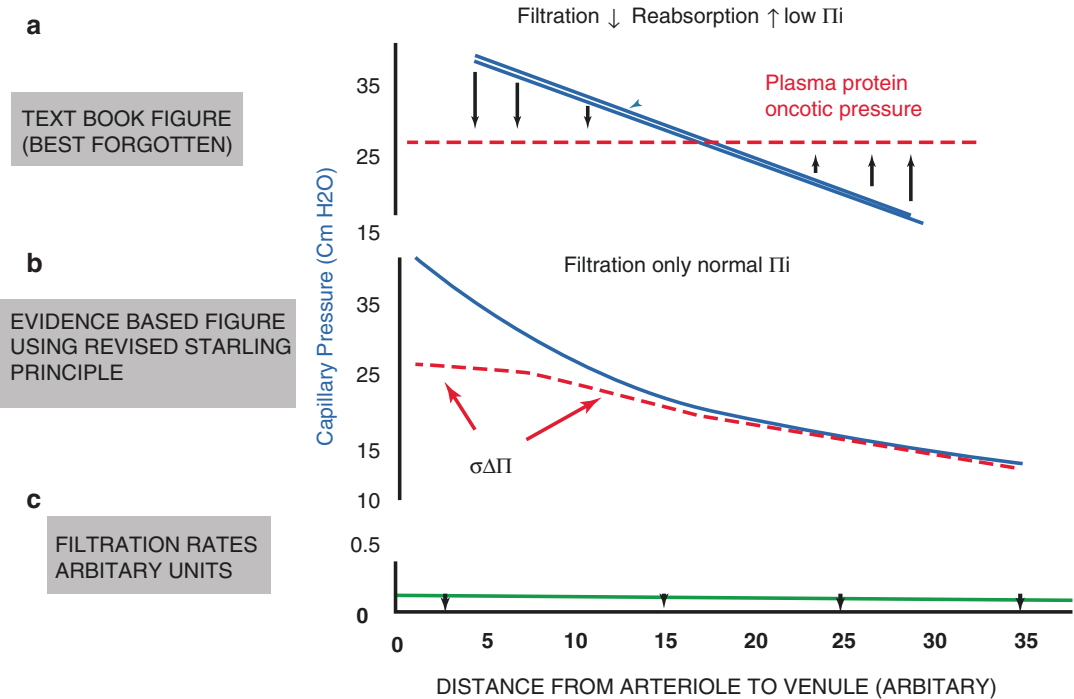


Fig. 6.4 The contrast between the common textbook diagram to illustrate filtration and reabsorption along a microvascular bed (**a**) and the steady state filtration across a microvascular bed such as muscle is shown in (**b**). The revised Starling principle describes ΔP greater than $\sigma\Delta\Pi$ at all points, although the difference is less than 1 mm Hg for most points (**b**). Although $\Delta P - \sigma\Delta\Pi$ may be larger than

1 mmHg close to the arterial side, the lower L_p in this region and higher surface area for exchange on the venular side result in near constant, but very low filtration into the tissue across the microcirculation (part **c**). (Modified from Michel et al. (Michel et al. 2016) with permission of Springer Nature)

fluid reabsorption, which rapidly returns to slow filtration. An example from the active area of current investigations to apply these concepts to the clinic is discussed in the end of the chapter.

Passive Coupling Ensures Epithelial-Endothelial Fluid Reabsorption

Filtration and Reabsorption in the Kidney

The glycocalyx of the fenestrated glomerular capillaries is now recognized as the primary molecular sieve in the renal glomerulus, responsible for the ultrafiltration of 100–120 liters per day. The structure and composition of the glomerulus is an area of active investigations (Satchell 2013; Haraldsson 2014; Arkill et al. 2010). Having demonstrated that sustained reabsorption cannot be

maintained when transvascular colloid osmotic pressure difference of plasma proteins is determined only by the coupling of water and plasma protein fluxes under the glycocalyx, the mechanisms responsible for sustained reabsorption of the large volume of glomerular filtrate require detailed evaluation. While an increase in the colloid osmotic pressure of the plasma proteins resulting from increased concentration of plasma protein by glomerular filtration favors reabsorption in distal capillaries, this mechanism would not sustain reabsorption in the peritubular capillaries unless an additional mechanism acted to reduce plasma protein accumulation beneath the glycocalyx of these fenestrated capillaries during reabsorption. The key insight with respect to the revised Starling principle is that the addition of protein free water to the interstitial space of the kidney, resulting from absorption of water across adjacent renal tubular epithelial cells, maintains a

low interstitial plasma protein concentration and, in conjunction with renal lymphatics, prevents accumulation of plasma proteins that would otherwise prevent sustained reabsorption. It can be argued that the narrow space between epithelial and endothelial barriers acts in a manner somewhat similar to the sub-glycocalyx space so that, in this case, $\Pi_p - \Pi_g$ is sufficient to support sustained reabsorption into the vascular space. In the absence of the energy used by the renal tubule epithelium to maintain transport of electrolytes and small solutes such as glucose, and associated transepithelial water flows, the passive coupling linking transepithelial and transendothelial water reabsorption would be abolished.

Filtration and Reabsorption in the Intestinal Mucosa

In the mucosal microvessels of the large intestine, the resting (non-absorbing state) favors net filtration along the microvessel bed. This fluid is removed by intestinal lymph flow. During fluid and nutrient absorption, up to 8 liters of water is reabsorbed across the epithelial barrier. This fluid not only dilutes the plasma protein in the interstitial space to maintain a low interstitial protein concentration (as in the renal cortex) but also increases interstitial pressure. Both mechanisms favor sustained reabsorption from the mucosal interstitium into the vascular space. As in the renal tissue, only a small net driving force is required to maintain reabsorption of large fluid volumes because of the large hydraulic conductivity of the fenestrated capillaries in the intestinal mucosa. In the few experimental animal models where this process has been investigated, about 70% of the reabsorbed water is returned to the circulation and 30% is returned via lymphatics (Kvietys and Granger 2010).

Reabsorption in the Lymph Nodes

While there is no sustained reabsorption in the capillaries of continuous capillaries in tissue such as the muscle and skin, the concentration of plasma protein leaving the peripheral lymph nodes in these tissues is increased, demonstrating

sustained reabsorption of lymph fluid to the vascular space. Although peripheral lymph has significant plasma protein concentrations, it is the sustained delivery of the peripheral lymph propelled by the energy of lymphatic contractions that counters the tendency of the increased plasma protein concentration in the node interstitial space to accumulate and limit reabsorption. As a result, about half of the fluid filtered into the muscle interstitial space per day is reabsorbed in the lymph nodes (Michel et al. 2016).

In summary, the lesson from all the examples of reabsorption in the kidney, gut, and lymph nodes is that there must be a supply of fluid that can dilute plasma proteins that accumulate beneath the glycocalyx layer to maintain reabsorption.

Regulation of Microvascular and Tissue Pressures

Before discussing some practical applications of the revised Starling principle, it is important to review the additional determinants of the transvascular-filtered volume. These include the regulation of microvessel pressure, regulation of the number of microvessels perfused, and modulation of interstitial pressure.

Microvascular Pressure

Mean microvascular pressure (P_p) relative to arterial pressure (P_a) and venular pressure (P_v) is determined by the ratio of the resistance to blood flow in the arteriolar vessels proximal to the microvessels (R_a) to the resistance to blood flow in venular microvessel (R_v) distal to the exchange vessels according to the following relation (Landis and Pappenheimer 1963):

$$P_p = [P_a + (R_a / R_v) P_v] / (1 + R_a / R_v) \quad (6.6)$$

The primary determinant of R_a is the action of vascular smooth muscle to control arteriolar diameter. The following representative calculations demonstrate the range of values over which Eq. 6.6 can apply. First, for P_a 100 mmHg and P_v 10 mmHg, mean capillary pressure at heart level

(for Ra/Rv close to 5–6) is 20–25 mm Hg. If after blood loss Pa fell to 65 mmHg, Pp would also fall (17–19 mm Hg) if there was no change in Ra . However, increased sympathetic stimulation of vascular smooth muscle would increase Ra to restore mean arterial pressure (e.g., 70–75 mm) and Pp would fall further (e.g., for Ra/Rv of 14, capillary pressure would fall below 15 mmHg). Capillary pressures in this range are well within the flat region of the hockey-stick-shaped curve of Fig. 6.2, and an understanding of transvascular fluid balance in this region of the curve provides new insight into strategies for fluid therapy.

An important consequence of increases and decreases in Ra is the regulation of the number of microvessels perfused. For example, reduced Ra due to local withdrawal of sympathetic tone (e.g., $Ra/Rv = 3$) would increase capillary pressure to 32.5 mmHg and increase the surface area for exchange by increasing the number of capillaries perfused. Such a mechanism regulates filtration in the capillaries of secretory glands to provide interstitial fluid for secretion. On the other hand, increased Ra reduces perfusion and the number of perfused vessels. While this may reduce the surface area for exchange, it also reduces the washout of metabolites. Accumulation of metabolites acts locally to relax vascular smooth muscle and oppose the effectiveness of sympathetic vasoconstriction.

Regulation of Interstitial Pressure

While beyond the scope of this chapter, it should be noted that while passive change in interstitial pressure results from increases and decreases in the fluid accumulation in the interstitial space, there is also growing awareness of the importance of active regulation of interstitial pressure as the result of contraction and relaxation of interstitial cells such as fibrocytes that attach to the extracellular matrix (Reed and Rubin 2010). The tension in these interstitial cells opposes the tendency of the extracellular matrix to swell due to the osmotic effects of the matrix components. Both tissue injury (burn) and inflammatory conditions reduce tension in interstitial fibrocytes

and transiently lower interstitial pressure (by tens of mmHg). The result is rapid filtration and localized edema.

Clinical Examples

Blood Loss and Saline Infusion

Michel et al. (Michel et al. 2016) recently used the following example to illustrate the differences between the classical and revised Starling principles to understand the strategies for fluid replacement therapy. Consider the loss of 20% blood volume with no change in plasma protein colloid osmotic pressure. Strong sympathetic vasoconstriction would result in reduced Pp as discussed above. The subsequent response, according to the classical Starling principle, would be reabsorption of interstitial fluid to expand the plasma volume until the dilution of the plasma proteins reduced the plasma colloid osmotic pressure to a level comparable with that of mean Pp . Further, it is argued that crystalloid infusion under these conditions should be avoided because dilution of the plasma protein would compromise the reabsorption capacity. Also volume expansion with a crystalloid solution would be short lived as the crystalloid solution is lost from the plasma volume. For example, at normal capillary pressures, within 10 minutes of infusion, only about 60% of the infused fluid is expected to be retained in the circulation (Michel et al. n.d.) and after 40 minutes less than 20% of the infused fluid would remain. The revised Starling principle also predicts that, after a fall in Pp due to vasoconstriction, there would be an initial brisk uptake of fluid from the tissues. The rate of fluid uptake, however, would diminish and in about 30 min revert to a very low level of filtration as a new steady state is approached. As emphasized above, because Pp is below $\sigma\Delta\Pi_p$, the filtration rate J_v lies on the flat portion of the steady state curve in Fig. 6.2. The revised interpretation predicts that after 10 minutes, 90% of the crystalloid infusions should be retained and after 40 minutes close to 80% be retained in the circulation, the result

being almost as effective as colloid solutions. This prediction may explain the outcomes of clinical trials that show that crystalloid infusions are as effective as colloid solutions in maintaining plasma volume (Bayer et al. 2012; Jabaley and Dudaryk 2014).

Lung Fluid Balance

The revised Starling principle points to the importance of capillary pressure as a determinant of filtration. Filtration rates are stable in the region of hockey-stick curve where microvessel pressure is below the effective colloid osmotic pressure of the plasma proteins. While capillary pressures in different parts of the body are difficult to monitor, an important threshold is the pressure in the microvessels of the lungs. Michel et al. 2016 note that the effective hydrostatic pressures for filtration in the lungs (the sum of microvessel pressure and slightly negative interstitial pressure) usually lies close to, or below 10 mm Hg. The lungs of normal individuals will be protected provided that colloid osmotic pressure of the plasma protein does not fall below 12 mmHg. This estimate assumes that there is no pulmonary hypertension and that the osmotic reflection coefficient of the glycocalyx barrier to plasma protein is of the order of 0.9–0.95.

Further Considerations

The above clinical example illustrates the importance of understanding the status of microvascular pressures, integrity of the glycocalyx, and the permeability of the vascular wall to plasma proteins as the determinants of fluid exchange when evaluating fluid therapy, not just arterial and venous pressures. Much remains to be understood about situations in which microvascular permeability is increased. The most serious problems arise when the glycocalyx layer is damaged. This will cause the subglycocalyx plasma protein concentration to be increased and the glycocalyx plasma protein osmotic reflection coefficient to

be reduced. Thus the effective osmotic pressure exerted of plasma proteins is reduced. These changes shift the hockey-stick-shaped curve to the left and likely increase the slope of the linear part of the curve. Microvascular pressures above this effective osmotic pressure conditions favor extravascular plasma protein and fluid accumulation. At microvascular pressures below the effective plasma protein oncotic pressure, a key question is whether the pressure still lies within the relatively flat part of the hockey-stick-shaped relation between filtration rate and pressure. It is also important to emphasize that interstitial protein concentration may increase without significant damage to the glycocalyx (e.g., increased vascular permeability resulting from localized inter-endothelial cell gaps). This may increase tissue plasma protein concentrations (as in conditions where tissue plasma protein was experimentally increased, Fig. 6.3(c), but Adamson et al. (Adamson et al. 2004) demonstrated that the plasma proteins still exert close to 70% of their effective osmotic pressure across the glycocalyx. These observations point to the need to preserve the integrity of glycocalyx and to understand conditions where its structure is damaged. New strategies should include ways to repair or replace damaged glycocalyx layer. Some of the ways to monitor the integrity of the glycocalyx and the limits of current attempts to measure changes in whole body glycocalyx are reviewed below.

Monitoring the Stability of the Endothelial Glycocalyx

A reduction in plasma osmotic reflection coefficient reduces the effective colloid osmotic pressure of the plasma proteins. While it is recognized that both acute and chronic inflammatory conditions modify adhesion between endothelial cells and disturb both the adhesion between adjacent endothelial cells and the glycocalyx close to the junctions, there is a growing interest in monitoring the stability of the glycocalyx. Reduced integrity of the glycocalyx is one of the earliest indications of endothelial barrier dysfunction.

Circulating Glycocalyx Components

Measurement of glycocalyx components in circulating plasma is one way to evaluate the integrity of the glycocalyx. The general chemical composition of the glycocalyx has been described in detail elsewhere (for review, see (Weinbaum et al. 2007)), and it is assumed that loss of some of these components and increased levels in circulating plasma or urine provide a clinically useful measure of glycocalyx breakdown even if the location of the site of damage cannot be determined from such measurements. Glycocalyx damage has been described in several conditions including hypovolemia, leading to poor tissue perfusion and subsequent ischemia/reperfusion injury (Rehm et al. 2007), in diabetes (Nieuwdorp et al. 2006), and exposure to a range of infections and inflammatory agents including tumor necrosis factor- α , cytokines, proteases, and other enzymes including heparanase (Becker et al. 2015; Broekhuizen et al. 2009; Lipowsky 2011; Henry and Duling 2000). Analytical methods (based on ELISA) have been used to monitor increased syndecan-1 and heparan sulfate in patients undergoing major vascular surgery (Rehm et al. 2007) and increased syndecan-1 and hyaluronic acid in dialysis patients (Vlahu et al. 2012). Similarly, an increased level of plasma hyaluronic acid in type 1 diabetes is associated with an increased circulating level of hyaluronidase. Current methods to improve the specificity of these analytic methods include attempts to identify glycocalyx component characteristic of specific organs (Schmidt et al. 2014). This approach is supported by an elegant investigation in mouse models which demonstrated that leukocyte interaction with the endothelial surface requires disruption of the endothelial surface layer (Schmidt et al. 2012).

Optical Methods

The model of a quasi-periodic structure in Fig. 6.3b used to describe the inner glycocalyx as the primary osmotic barrier at the endothelial surface is based on detailed investigation of gly-

cocalyx structures revealed by electron microscopy under a variety of fixation conditions (Curry et al. 2016; Arkill et al. 2010). This structure extends between 100 and 300 nm from the endothelial surface and is stabilized by electrostatic and chemical interactions between components directly attached to the endothelial cytoskeleton as well as binding of plasma proteins such as albumin (Curry 2018). A range of optical methods used in an animal model of microvascular function clearly demonstrated an endothelial surface layer that is thicker than the inner layer described above. The extended layer (best called a endothelial surface layer, ESL, to distinguish it from the inner layer) has been investigated using approaches that include binding of fluorescent probes, the exclusion of high molecular weight tracers at a distance from the vessel wall, and the exclusion of red cells and other large flow markers away from the microvessel wall (Curry et al. 2016; Weinbaum et al. 2007; Vink and Duling 2000). There is growing evidence that this outer ESL is more porous to macromolecules, including plasma proteins, than the inner layer and can have a resistance to the flow of water that is an order of magnitude lower than that of the inner layer (Curry et al. 2016; Curry and Adamson 2012) but still sufficient to support a lubricating layer for red cells.

In the clinical setting, the most advanced optical methods are based on an adaption of orthogonal polarization spectral imaging known as sidestream dark field imaging. This enhances the contrast between circulating red cells and the vessel wall and has been used to visualize microvessels and microvascular flows. With the use of specialized software, it has been adapted to measure the mean distance between flowing red cells and the vessel wall in sublingual and conjunctival blood vessels. A reduction in the thickness of this layer (called a peripheral boundary thickness, PBR) is interpreted as a loss of the endothelial surface layer and an index of glycocalyx dysfunction. A striking feature of reports using this approach is PBR thickness measurements of more than 2–3 microns in vessels up to 50 microns in diameter (Nieuwdorp

et al. 2006; Becker et al. 2015; Broekhuizen et al. 2009; Lipowsky 2011; Henry and Duling 2000; Vlahu et al. 2012; Schmidt et al. 2014; Schmidt et al. 2012; Vink and Duling 2000; Curry and Adamson 2012; Dane et al. 2014; Mulders et al. 2013; Donati et al. 2013). The authors claim some positive correlation between changes in PBR thickness and corresponding changes in other markers of inflammation. However, the relatively small magnitude of the reported reductions in PBR thickness, and the limited understanding of the mechanism that results in large baseline values for PBR thickness, means that the ability of the approach to discriminate between normal and diseases states may be limited (Curry et al. 2016; Amraoui et al. 2014). For example, while there is reasonable evidence that increased penetration of red cells toward the endothelial cell membrane in microvessels 4–5 microns in diameter is associated with loss of the inner glycocalyx, in larger vessels, the peripheral boundary layer thickness may also be disturbed by changes in red cell mechanics, the presence of platelets, and vessel geometry. Furthermore, it is possible to demonstrate using a theoretical model of the endothelial surface as a two-layer structure that, at normal microvascular pressures, steady state filtration through an intact inner layer may not be significantly modified by mechanism that effect loss of only the outer ESL. Some of these issues are areas of active evaluation, in addition to more recent clinical evaluations in sublingual and conjunctival microvessels (Pranskunas et al. 2018; Rovas et al. 2018).

Measurement of Whole Body Glycocalyx Volume

A third approach to evaluation of the glycocalyx and ESL is the measurement of the distribution volume of a tracer using the dilution principle. The tracer is assumed to distribute in the circulating plasma and also penetrate the glycocalyx. This volume is compared to the plasma volume calculated from measurement of the red cell volume and a large vessel hematocrit. The difference

between these two volume estimates is often quite large and has been called a “whole body glycocalyx volume” or a “non-circulating plasma volume.” Michel and Curry (Michel and Curry 2009) demonstrated that current methods to apply the dilution principle and use large vessel hematocrit as a basis for estimating a “circulating plasma volume” significantly overestimate the apparent glycocalyx volume. They showed that there is no tracer small enough to enter the glycocalyx to reach the same concentration as in the plasma (as required by the dilution principle) and still be retained within the plasma volume. Further, any higher molecular weight tracer that is reasonably well retained in the circulation has a lower concentration in the glycocalyx than in the plasma due to steric and electrostatic partitioning. Finally, the “circulating plasma volume” calculated from the red cell volume (measured using labeled red cell) and a large vessel hematocrit underestimated the true plasma volume by 10% under normal conditions. When the errors associated with these problems are used to reinterpret the published values of glycocalyx volume, reported values in glycocalyx volume of the order of 4.7 liters (clinical dextran as tracer, (Nieuwdorp et al. 2006)) are reduced to significantly less than 1 liter. Further, the claim that hemodilution reduces the noncirculating plasma volume (Jacob et al. 2007) could be reinterpreted as an indication of mechanisms whereby hemodilution causes the larger vessel hematocrit to more closely measure the whole body hematocrit. For further review of current methods to study the structure of the glycocalyx, see references (Michel et al. 2016; Curry et al. 2016). On the basis of the arguments outlined above, it is reasonable to conclude that there is no valid theoretical or experimental basis for measurement of whole body glycocalyx volume or a non-circulating plasma volume using the dilution principle and available tracers under condition where the tracers enter the glycocalyx by diffusion alone. Further investigations are required to understand the changes in the microvascular that, to date, have been interpreted as changes in glycocalyx volume or a non-circulating plasma volume.

References

- Adamson RH, Lenz JF, Zhang X, Adamson GN, Weinbaum S, Curry FE. Oncotic pressures opposing filtration across non-fenestrated rat microvessels. *J Physiol.* 2004;557(Pt 3):889–907.
- Amraoui F, Olde Engberink RH, van Gorp J, Ramdani A, Vogt L, van den Born BJ. Microvascular glycocalyx dimension estimated by automated SDF imaging is not related to cardiovascular disease. *Microcirculation.* 2014;21(6):499–505.
- Arkill KP, Knupp C, Michel CC, Neal CR, Qvortrup K, Rostgaard J, Squire JM. Similar endothelial glycocalyx structures in microvessels from a range of mammalian tissues: evidence for a common filtering mechanism? *Biophys J.* 2010;101:1046–56.
- Bayer O, Reinhardt K, Kohl M, Kabisch B, Marshall J, Sakr Y, et al. Effects of fluid resuscitation with synthetic colloids or crystalloids alone on shock reversal, fluid balance and patient outcomes in patients with severe sepsis: a prospective sequential analysis. *Crit Care Med.* 2012;40:2543–51.
- Becker BF, Jacob M, Leipert S, Salmon AH, Chappell D. Degradation of the endothelial glycocalyx in clinical settings: searching for the sheddases. *Br J of Pharmacol.* 2015;80(3):389–402.
- Broekhuizen LN, Mooij HL, Kastelein JJ, Stroes ES, Vink H, Nieuwdorp M. Endothelial glycocalyx as potential diagnostic and therapeutic target in cardiovascular disease. *Curr Opin Lipidol.* 2009;20(1):57–62.
- Curry FE. The molecular structure of the endothelial glycocalyx layer (EGL) and surface layers (ESL). Modulation of transvascular exchange. In *Molecular, Cellular, and Tissue Engineering in the Vascular System*. Editor Fu B Wright E Springer Nature Adv Exp Med Biol. 2018;1097:29–49
- Curry FE, Adamson RH. Endothelial glycocalyx: permeability barrier and mechanosensor. *Ann Biomed Eng.* 2012;40(4):828–39.
- Curry FE, Arkill KP, Michel CC. The Functions of Endothelial Glycocalyx and their Effects on Patient's Outcomes during the Perioperative Period. A review of current methods to evaluate structure-function relations in the glycocalyx in both basic research and clinical settings, Chapter 3. In: Farag E, Kunz A, editors. *Perioperative fluid management*. Cham, Switzerland: Springer; 2016. p. 75–116.
- Dane M, Khairoun M, Lee DH, van den Berg BM, Eskens B, Boels MG, et al. Association of kidney function with changes in the endothelial surface layer. *Clin J AmSoc Nephrol.* 2014;9(4):698–704.
- Donati A, Damiani E, Domizi R, Romano R, Adrario E, Pelalaia P, et al. Alteration of the sublingual microvascular glycocalyx in critically ill patients. *Microvasc Res.* 2013;90:86–9.
- Haraldsson BS. The endothelium as part of the integrative glomerular barrier complex. *Kidney Int.* 2014;85(1):8–11.
- Henry CB, Duling BR. TNF-alpha increases entry of macromolecules into luminal endothelial cell glycocalyx. *Am J Physiol Heart Circ Physiol.* 2000;279(6):H2815–23.
- Jabaley C, Dudaryk R. Fluid resuscitation for trauma patients: crystalloids versus colloids. *Curr Anesthesiol Rep.* 2014;4:216–24.
- Jacob M, Conzen P, Finsterer U, Krafft A, Becker BF, Rehm M. Technical and physiological background of plasma volume measurement with indocyanine green: a clarification of misunderstandings. *J Appl Physiol.* 2007;102(3):1235–42.
- Kvietys PR, Granger DN. Role of intestinal lymphatics in interstitial volume regulation and transmucosal water transport. *Ann N Y Acad Sci.* 2010;1207(Suppl 1):E29–43.
- Landis EM. Microinjection studies of capillary permeability. II. The relation between capillary pressure and the rate of which fluid passes through the walls of single capillaries. *Am J Phys.* 1927;82(2):217–38.
- Landis EM, Pappenheimer JR. Exchange of substances through the capillary walls, chap. 29. In: Hamilton WF, Dow P, editors. *Handbook of physiology*, sect. 2, vol. 2. Circulation. Washington, DC: American Physiological Society; 1963. p. 961–1034.
- Levick JR. Capillary filtration-absorption balance reconsidered in the light of extravascular factors. *Exp Physiol.* 1991;76:825–57.
- Levick JR. An analysis of the interaction between interstitial plasma protein. Interstitial flow and fenestral filtration and its application to synovium. *Microvasc Res.* 1994;47:90–124.
- Levick JR, McDonald JN. Viscous and osmotically mediated changes in fluid movement across synovium in response to intraarticular albumin. *Microvasc Res.* 1994;47:68–89.
- Levick JR, Michel CC. Microvascular fluid exchange and revised starling principle. *Cardiovasc Res.* 2010;87:198–210.
- Lipowsky HH. Protease activity and the role of the endothelial glycocalyx in inflammation. *Drug Discov Today Dis Models.* 2011;8(1):57–62.
- Michel CC. Fluid movements through capillary walls. In: Renkin EM, Michel CC, editors. *Handbook of physiology. The cardiovascular system*, vol. 4, Microcirculation, part 1. Bethesda: American Physiological Society; 1984. p. 375–409.
- Michel CC. Starling: the formulation of his hypothesis of microvascular fluid exchange and its significance after 100 years. *Exp Physiol.* 1997;82(1):1–30.
- Michel CC, Arkill KP, Curry FE. The revised Starling Principle and its relevance to peri-operative fluid management, Chapter 2. In: Farag E, Kunz A, editors. *Perioperative fluid management*. Cham, Switzerland: Springer; 2016;31–74.
- Michel CC, Curry FR. Glycocalyx volume: a critical review of tracer dilution methods for its measurement. *Microcirculation.* 2009;16(3):213–9.

- Michel CC, Phillips ME. Steady state fluid filtration at different capillary pressures in perfused frog mesenteric capillaries. *J Physiol*. 1987;388:421–35.
- Mulders TA, Nieuwdorp M, Stroes ES, Vink H, Pinto-Sietsma SJ. Non-invasive assessment of microvascular dysfunction in families with premature coronary artery disease. *Int J Cardiol*. 2013;168(5):5026–8.
- Nieuwdorp M, van Haefen TW, Gouverneur MC, Mooij HL, van Lieshout MH, Levi M, et al. Loss of endothelial glycocalyx during acute hyperglycemia coincides with endothelial dysfunction and coagulation activation in vivo. *Diabetes*. 2006;55(2):480–6.
- Pappenheimer JR. Soto-Rivera an effective osmotic pressure of the plasma proteins and other quantities associated with the capillary circulation in the hind limbs of cats and dogs. *Am J Phys*. 1948;152:471–91.
- Pranskunas A, Tamosuitis T, Balciuniene N, Damanskyte D, Sneider E, Vitkauskienė A, Sirvinskis E, Pilvinis V, Boerma EC. Alterations of conjunctival glycocalyx and microcirculation in non-septic critically ill patients. *Microvasc Res*. 2018;118:44–8.
- Reed RK, Rubin K. Transcapillary exchange: role and importance of the interstitial fluid pressure and the extracellular matrix. *Cardiovasc Res*. 2010;87:211–7.
- Rehm M, Bruegger D, Christ F, Conzen P, Thiel M, Jacob M, et al. Shedding of the endothelial glycocalyx in patients undergoing major vascular surgery with global and regional ischemia. *Circulation*. 2007;116(17):1896–906.
- Renkin EM. Some consequences of capillary permeability to macromolecules: Starling's hypothesis reconsidered. *Am J Phys*. 1986;250(5 Pt 2):H706–10.
- Rovas A, Lukasz AH, Vink H, Urban M, Sackarnd J, Pavenstädt H, Kumpers P. *Scand J Trauma Resusc Emerg Med*. 2018;26(1):16.
- Satchell S. The role of the glomerular endothelium in albumin handling. *Nat Rev Nephrol*. 2013;12:717–25.
- Schmidt EP, Li G, Li L, Fu L, Yang Y, Overdier KH, et al. The circulating glycosaminoglycan signature of respiratory failure in critically ill adults. *J Biol Chem*. 2014;289(12):8194–202.
- Schmidt EP, Yang Y, Janssen WJ, Gandjeva A, Perez MJ, Barthel L, Zemans RL, Bowman JC, Koyanagi DE, Yunt ZX, et al. The pulmonary endothelial glycocalyx regulates neutrophil adhesion and lung injury during experimental sepsis. *Nat Med*. 2012;18(8):1217–23.
- Vink H, Duling BR. Capillary endothelial surface layer selectively reduces plasma solute distribution volume. *Am J Physiol Heart Circ Physiol*. 2000;278(1):H285–9.
- Vlahu CA, Lemkes BA, Struijk DG, Koopman MG, Krediet RT. Damage of the endothelial glycocalyx in dialysis patients. *J Am Soc Nephrol*. 2012;23(11):1900–8.
- Weinbaum S, Tarbell JM, Damiano ER. The structure and function of the endothelial glycocalyx layer. *Annu Rev Biomed Eng*. 2007;9:121–67.



Physiology of Heart Rate

7

T. Alexander Quinn and Sheldon Magder

One might wonder about the need for a chapter on heart rate. A change in heart rate is one of the most basic ways that the heart regulates cardiac output. Rapid heart rates also often trigger clinical interventions. However, there is a much more basic reason for examining heart rate in more detail. The ‘periodicity’ that comes with rhythmic beating of the heart creates important restrictions on the cardiovascular system. It sets the fixed time available for ejection of stroke volume from the left ventricle and the time available for the stroke return to the right heart. Because of these fixed times, the rate of return and rate of ejection are important determinants of how much blood flow can leave and return during each cycle and how much the rate of blood flow needs to accelerate to reach its target. The fixed period of each cycle also means that the ratio of ejection time to the return time (i.e. diastole) is an important determinant of cardiac output. At faster heart rates, both of these are shortened, but the proportions of time for each can vary. We will start with the concept of time constants and their impor-

tance for the discussion of the periodicity of cardiac contractions. We will then review the complex membrane processes in the heart’s intrinsic pacemaker that determine heart rate, as well as the factors that determine the length of the ventricular action potential. The length of the action potential is important because it sets the amount of time for the entry of calcium ions (Ca^{2+}) to produce the contraction phase. We follow with a discussion of basic mechanisms involved in regulation of the intrinsic heart rate, and heart rate during exercise which gives insight into the regulation of heart rate at the extremes. This is followed by the significance of the fixed filling times for normal function and in pathological considerations. Finally, we review the implications for changes in heart rate on the supply and demands of the heart for oxygen. Some of these issues have been covered previously (Magder 2012).

Time Constants and Volume Constraints

To appreciate the significance of the periodicity of cardiac output, it is first necessary to understand the concept of a time constant. When there is a step change in the flow or pressure in a system that has stretchable walls, a proportion of the initial increased input volume stretches the walls of the vessels and does not contribute to distal

T. A. Quinn
Dalhousie University, Department of Physiology &
Biophysics, Halifax, NS, Canada
e-mail: alex.quinn@dal.ca

S. Magder (✉)
Royal Victoria Hospital (McGill University
Health Centre), Departments of Critical Care and
Physiology McGill University, Montreal, QC, Canada
e-mail: sheldon.magder@mcgill.ca

flow (Fig. 7.1). Once the force across the wall matches the new pressure, a new steady state in flow is reached and what goes in is matched by what goes out. In a vessel, the time taken to reach a new steady state is determined by the amount of volume the vessel takes up with the change in pressure, which is based on the compliance of the vessel wall, and how easily volume flows out of the vessel, which is determined by the downstream resistance. Mathematically, this is described by an exponential raised to the power of the product of downstream compliance and resistance divided by time (Fig. 7.1). The product of the compliance and resistance gives a time constant, which indicates the time taken to get to 63% of the new steady state. The greater the downstream resistance, or the greater the compliance of the vessel, the longer it takes to get to a new steady state. The significance of this in a pulsatile system is that when the duration of each pulse is less than the time constant, the change in flow for a change in pressure may be less than predicted from just the change in peak pressure because there is not enough time to reach the steady state (Fig. 7.2). This is especially an issue on the venous side because the change in pressure for a change in flow is so low. At faster heart rates, blood must come back faster to allow an increase in return and increase in cardiac output.

The primary process allowing this is a decrease in venous resistance because the compliance vessels do not change, but during exercise compression of peripheral veins by the contracting muscles likely gives the equivalent of a decrease in venous compliance and resistance (Magder 1995; Magder et al. 2019).

A consequence of increased heart rate is that if the duration of systole remains constant, diastolic time must become progressive shorter. This reduces diastolic filling time and the limit for return per beat (stroke return). The heart thus has to reach the peak end-systolic elastance (end-systolic pressure volume line – see Chaps. 3 and 4) faster at higher heart rates, and accordingly, the action potential needs to shorten. Ventricular relaxation time also must shorten to allow more time for diastole.

Cardiac Rhythmicity at the Cellular Level

Sinoatrial Node Control

Excitation of the heart is initiated in the sinoatrial node (SAN), the natural pacemaker of the heart. It is located adjacent to the *crista terminalis* at the junction of the right atrium and the superior

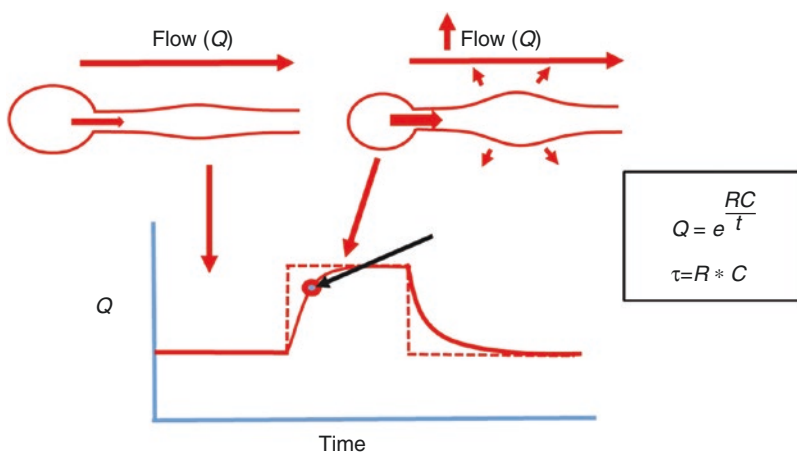


Fig. 7.1 Concept of a time constant (τ). When a step (square) change is made in a tube with a compliance, initially some of the added volume is taken up by stretching the walls and flow does not immediately reach the steady

state. The small circle indicates the time taken to reach 63% of the new steady state ($= \tau$ the time constant) as indicated by the equation in the figure. Q refers to flow, R resistance, C compliance of the chamber, and t time

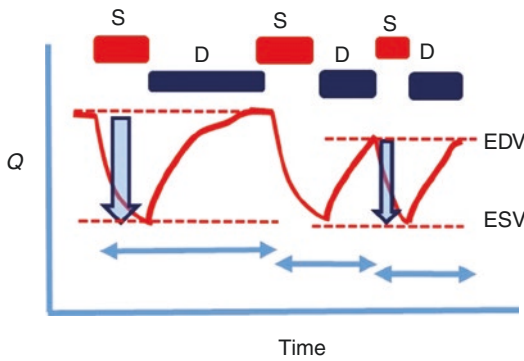


Fig. 7.2 Importance of time constant for RV filling and stroke volume. An increase in heart rate reduces the time for diastolic filling and if the rate of filling does not increase, stroke returns, and thus stroke volume must fall

vena cava. The SAN spontaneously generates action potentials (AP) in a rhythmic pattern, which propagate through the myocardium and the heart's specialised conduction system. This spontaneous, cyclic firing of the SAN (automaticity) is what determines heart rate (HR) and ultimately results in cardiac contraction, making the SAN fundamental to survival. Because of its critical importance, multiple overlapping mechanisms exist to ensure proper SAN function. These are highly regulated to allow for rapid adaptation of HR to large changes in physiological demand (Irisawa et al. 1993).

It is worth noting that there is no set point for HR (i.e. a 'targeted' value). Thus, function of the SAN is not *regulated*, but rather is *controlled* (Cabanac 1997) – engineering logic which has applications to physiology going back at least as far as Arthur Guyton's classic *Textbook of Medical Physiology* (Guyton 1956). For a system to maintain a variable within a narrow range around its set point, sensory feedback is needed for regulation. This occurs by changes in controlled variables that are allowed to vary widely (Modell et al. 2015). In the cardiovascular system, blood pressure is a critically *regulated* variable (with a clear set point). Changes in the set point are sensed by baroreceptors. Cardiac output and systemic vascular resistance are adjusted accordingly, but they also are determined by metabolic activity. HR and SAN activity, though, are affected by multiple factors. These are both

external and intrinsic to the heart. Extrinsic control is primarily through the central nervous system but also by circulating factors in the blood. Intrinsic control is within the heart itself and acts primarily through intracardiac nerves but also through release of local paracrine factors and changes in mechanical load. Both processes ultimately control HR by affecting the mechanisms responsible for SAN automaticity (Quinn and Kohl 2012; MacDonald et al. 2017, 2020; Mangoni and Nargeot 2008).

Mechanisms of SAN Automaticity

Unlike cells of the working myocardium, which have a stable negative resting membrane potential (V_m) in diastole, SAN cells spontaneously depolarise in the diastolic phase of the cardiac cycle ('diastolic depolarisation'). This depolarisation drives V_m towards the threshold for excitation and is responsible for automaticity in the SAN. Two major systems regulate V_m . These are the 'membrane-clock', which is dependent upon ion channels in the cell membrane of SAN cells, and the 'calcium-clock', which is driven by intracellular calcium (Ca^{2+}) cycling (Fig. 7.3a).

Membrane Clock

One of the principal systems driving diastolic depolarization is a collection of membrane ion channels that are responsible for inward, depolarising currents, collectively known as the membrane clock (Maltsev et al. 2006). In the initial portion of diastole, depolarization is primarily driven by cations moving out of the cell. This creates a non-specific current called the 'funny' current, (I_f). These ions pass through channels that open as the cell membrane becomes more hyperpolarised (i.e. more negative) and begin to reverse the depolarized state. They are called hyperpolarisation-activated cyclic nucleotide-gated (HCN) channels. There are four isoforms of HCN; HCN4 is the most prominent in humans (Chandler et al. 2009; DiFrancesco 2010). I_f decreases with depolarisation of V_m and at the next stage in diastole, Ca^{2+} begins to enter the cell and this current begins to contribute to diastolic

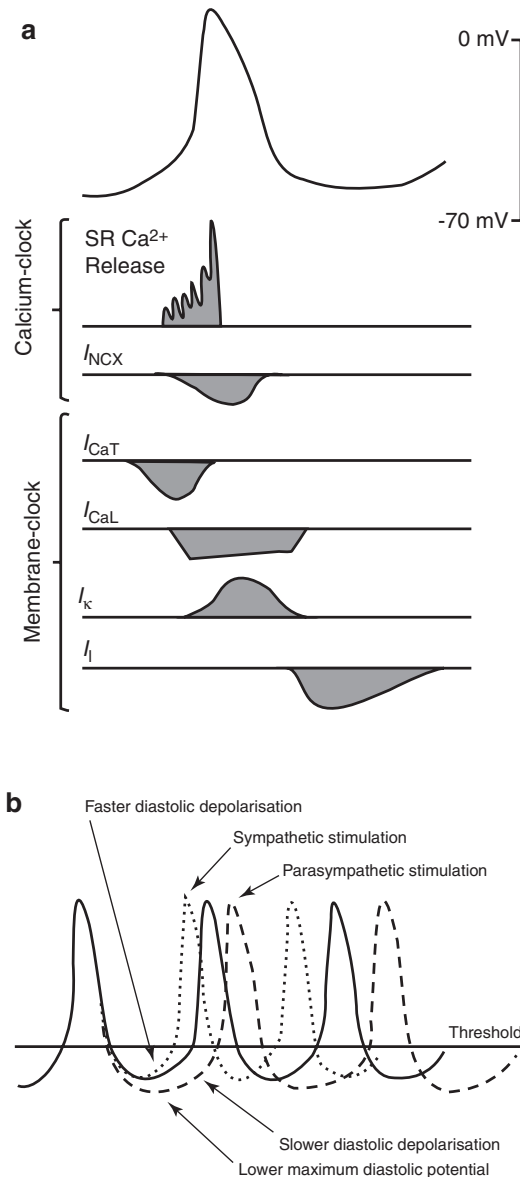


Fig. 7.3 (a) Sinoatrial node cell action potential and associated ionic fluxes. (b) Effect of sympathetic and parasympathetic stimulation on sinoatrial node cell action potential. Ca²⁺ calcium, I_{CaL} long-lasting L-type calcium current, I_{CaT} transient T-type calcium current; sodium-calcium exchanger current, I_f “funny” current, I_K repolarising potassium current, I_{NCX} sodium-calcium exchanger current, SR sarcoplasmic reticulum

depolarisation. The influx of Ca²⁺ first occurs through transient T-type current Ca²⁺ (I_{CaT}), which is created by Ca_v3.1 channels, and then by a long-lasting L-type current Ca²⁺ (I_{CaL}) created by

Ca_v1.3 which takes over (Mangoni and Nargeot 2008; Bartos et al. 2015). Once the threshold for Ca_v1.2-mediated I_{CaL} is reached at ~ -40 mV, Ca_v1.2 channels are activated, SAN cells are excited, and an AP occurs. This process differs from that of the working cardiac myocytes in which a fast sodium (Na⁺) current (I_{Na}) passing through Na_v1.5 channels is responsible for excitation (Mesirca et al. 2015). SAN also express Na_v1.5 channels, but these have only a minor, indirect action on HR (Lei et al. 2007), as do a few other currents (Zhang et al. 2002; Ju et al. 2007).

Another important consideration for SAN and the determination of HR are the currents that are responsible for repolarisation of SAN cells. Unlike working cardiac myocytes, SAN have few Kir2.1 channels so they do not have the robust inward rectifier potassium (K⁺) current (I_{K1}) to maintain the resting V_m (Chandler et al. 2009). However, similar to working cardiac myocytes, repolarisation occurs primarily through rapid (I_{Kr}) and slow (I_{Ks}) delayed rectifier K⁺ currents, along with minor contributions from currents activated late in the AP upstroke. These include the transient outward K⁺ current (I_{to}), the ultra-rapid delayed rectifier K⁺ current (I_{Kur}), and an inwardly rectifying chloride current (I_{Cl}). Ultimately, these currents determine the maximum diastolic V_m (MDP), which is the most negative membrane diastolic potential occurring during the cardiac cycle (Mangoni and Nargeot 2008; Bartos et al. 2015). Importantly, the magnitude of these repolarising currents continuously decays after maximal activation. This allows inward currents to drive diastolic depolarisation.

Calcium Clock

Intracellular Ca²⁺-cycling contributes to diastolic depolarisation through a system known as the calcium clock (Maltsev et al. 2006). Late in diastole, a small amount of Ca²⁺ is released from the sarcoplasmic reticulum (SR) in SAN cells via ryanodine receptors (RyR). This can occur spontaneously or be triggered by Ca_v1.3-mediated I_{CaL} (Torrente et al. 2016). Some of the Ca²⁺ is removed from the cell by the Na⁺-Ca²⁺ exchanger (NCX), which extrudes one Ca²⁺ ion while

bringing in three Na^+ ions, thus generating a net inward current (I_{NCX}) that causes SAN depolarisation. The remainder of the Ca^{2+} is returned to the SR by the sarco/endoplasmic reticulum Ca^{2+} -ATPase, SERCA, pump (Lakatta et al. 2008). Diastolic SR Ca^{2+} release also occurs in cells of the working myocardium but the release is enhanced in SAN cells due to a higher basal level of cyclic adenosine monophosphate (cAMP), which through a number of downstream processes, results in a higher uptake of Ca^{2+} by SERCA, and therefore, the potential for greater SR Ca^{2+} release (Vinogradova et al. 2006; Li et al. 2016).

It is still much debated whether diastolic depolarization of the SAN is driven primarily by the membrane or calcium clock (Rosen et al. 2012; DiFrancesco and Noble 2012; Maltsev and Lakatta 2012). However, because the sarcolemmal-bound NCX plays a critical role in the Ca^{2+} -clock by generating the required transmembrane depolarising current, these two ‘clocks’ are intricately linked. It is now generally accepted that overlapping and redundant mechanisms combine to cause SAN automaticity by forming a coupled system (Rosen et al. 2012; Lakatta et al. 2010) which is under tight extrinsic and intrinsic control.

Extrinsic SAN Control

Central Nervous System

The primary extrinsic mediator of SAN activity is the central nervous system, which acts through direct extracardiac sympathetic and parasympathetic innervation of intracardiac neural circuits and SAN cells (Gordan et al. 2015). Postganglionic sympathetic neurons that project from sympathetic ganglia directly to SAN cells release norepinephrine. This stimulates sarcolemmal $\text{G}\alpha_s$ -coupled β -adrenergic receptors (β -AR) and increases intracellular cAMP levels. By binding to the C-terminals of HCN channels and increasing their phosphorylation by PKA, cAMP increases HCN channel open probability, increases I_f , and thereby increases the rate of dia-

stolic depolarisation and HR (Larsson 2010). β -AR stimulation also has effects on other components important for SAN automaticity, all of which will increase the rate of diastolic depolarisation and thus HR (Fig. 7.3b).

In contrast to sympathetic neurons, preganglionic parasympathetic neurons project from brainstem vagal motor nuclei to postganglionic parasympathetic neurons within the heart. These release acetylcholine, which stimulate intracardiac neurons that project to SAN cells to also release acetylcholine, which activates sarcolemmal $\text{G}\alpha_{i/o}$ -coupled cholinergic M_2 muscarinic receptors. Stimulation of these receptors results in reduced intracellular cAMP concentration, as well as rapid $\text{G}_{\beta\gamma}$ subunit activation of an acetylcholine-activated K^+ current (I_{KACH}) through G-protein-regulated K^+ (GIRK) channels, which negatively shift MDP, reduce the rate of diastolic depolarization, and decrease HR (Accili et al. 1998; Renaudon et al. 1997) (Fig. 7.3b).

Circulating Factors

SAN function also is affected by circulating biogenic amines such as norepinephrine, epinephrine, histamine, serotonin, thyroid hormone (Gordan et al. 2015). Circulating catecholamines released by the adrenal glands (epinephrine, norepinephrine, and dopamine, when converted to epinephrine or norepinephrine) bind to α - or β -ARs and cause an increase in HR through similar mechanisms to neurotransmitters released by sympathetic neurons. Histamines are released primarily from mast cells in the heart, but also from basophils, and cause an increase in HR by activating G protein-coupled receptors that increase intracellular cAMP and PKA levels. It also acts as a neuromodulator by stimulating the release of norepinephrine from sympathetic nerves (Kevelaitis et al. 1994). The response to serotonin (5-HT) is complex. It binds to many different receptor types (Saxena and Villalon 1990), both directly on cardiac tissue and also on autonomic nerve terminals. Thus, it can cause both an increase or a decrease in HR (Linden et al. 1999; Villalon

and Centurion 2007; James 1964; Centurion et al. 2002; Gothert et al. 1986). Thyroid hormones act on nuclear hormone receptors and alter expression of cardiac ion channels. They influence HR over a longer timescale. High thyroid hormone levels cause an increase in HR by increasing I_f by increasing HCN channel expression (Renaudon et al. 2000; Pachucki et al. 1999; Gloss et al. 2001). Similarly, parathyroid hormone, synthesized by the parathyroid gland, acts on parathyroid receptors to increase intracellular cAMP and PKA (Potthoff et al. 2011; Chorev 2002), which increases the amplitude of I_f (Critchley et al. 2010), and thus the rate of diastolic depolarization and HR (Shimoni 1999).

In summary, HR is influenced by multiple extrinsic factors, some of which increase HR, primarily by increasing I_f and diastolic depolarisation through enhanced cAMP and PKA production, and some which decrease HR, primarily by lowering MDP and inhibiting diastolic depolarization. Together, these processes maintain HR at closely controlled levels.

Intrinsic SAN Control

Intracardiac Nervous System

As is the case with extrinsic control of the SAN, intrinsic control occurs partly through neuronal mechanisms, mediated by the intracardiac nervous system (ICNS). The ICNS comprises a collection of efferent, interconnecting, and afferent neurons within the heart (Ardell and Armour 2016). Functional and anatomical data have shown that the ICNS not only receives input from extrinsic efferent neurons, but also from local interneurons and afferent neurons from other locations within the heart. It thus forms intracardiac circuits, which are important for the internal processing and reflex control of cardiac function (Beadling et al. 1999; Gagliardi et al. 1988). As a result, even after acute (Gagliardi et al. 1988) or chronic (Hodgin et al. 2001) isolation of the heart from the central nervous system (decentralization), the ICNS remains responsive to changes in

the cardiac environment. It has been estimated that less than 20% of intracardiac neurons receive direct inputs from extrinsic nerves, and instead act as interconnecting neurons (Armour 2008).

Myogenic Peptides

Locally released peptides from cardiac myocytes, fibroblasts, and endothelial cells within or in close proximity to the SAN can modulate HR by paracrine or autocrine actions. They often are released as neurotransmitters and act in conjunction with the autonomic nervous system as neuropeptides, neuromodulators, or neurohormones (Beaulieu and Lambert 1998). For instance, vasoactive intestinal polypeptide (VIP) is a neuropeptide co-released with acetylcholine from parasympathetic neurons. It has the opposite effect of acetylcholine and thus moderates its effect. VIP binds to GPCRs that activate G_s -protein cascades that increase cAMP and PKA and which shifts the activation curve of I_f . The result is increase in the rate of diastolic depolarisation and HR (Hoover 1989; Chang et al. 1994; Accili et al. 1996). Release of VIP potentially could be a factor in the persistent tachycardia often seen in patients with pancreatitis without being related to volume status. Another example is the calcitonin gene-related peptide (CGRP), a neuromodulator that increases HR by blocking vagal stimulation (Bell and McDermott 1996), but in the presence of autonomic antagonists, also acts directly on SAN cells (Beaulieu and Lambert 1998). Another example of a locally synthesized peptide with both neuromodulatory and direct SAN cell effects is angiotensin II, which is highly concentrated at the level of the SAN artery (Saito et al. 1987). Angiotensin II can stimulate the release of catecholamines from sympathetic neurons (Torrente et al. 2016), but also stimulates type 1 angiotensin II receptors to decrease I_{CaL} and HR (Lambert 1995; Habuchi et al. 1995; Sheng et al. 2011; Kobayashi et al. 1978; Lambert et al. 1991; Sechi et al. 1992). Similarly, endothelin-1 and -3, produced and secreted by endothelial cells and acting through endothelin

receptors A and B, can cause an increase or decrease in HR (Saito et al. 1987; Ono et al. 2001; Tanaka et al. 1997; Ishikawa et al. 1988; Ju et al. 2011; Minkes et al. 1990).

Perhaps the most important myogenic peptides in terms of their HR effects are natriuretic peptides (NP), one of the primary factors released by atrial cells (Potter and Magder 2006; Reinhart et al. 2004). Three principal NPs are present in cardiac myocytes and fibroblasts, atrial NP (ANP), B-type NP (BNP), and C-type NP (CNP), which act on three NP receptors (NPR), NPR-A, NPR-B, and NPR-C (Moghtadaei et al. 2016). NPR-A, which binds ANP and BNP, and NPR-B, which is selectively activated by CNP, are guanylyl cyclase-linked receptors and enhance cGMP signalling (Lucas et al. 2000). NPR-C, which binds all NPs with similar affinity, is coupled to inhibitory G-proteins which inhibit adenylyl cyclase and thus cAMP signalling (Rose and Giles 2008; Anand-Srivastava 2005). Among their other functions, NPs affect HR through direct effects on SAN cells (Rose and Giles 2008; Springer et al. 2012; Azer et al. 2012). By acting on NPR-A, BNP and CNP, they increase I_f and total $I_{Ca,L}$ and thus the rate of diastolic depolarisation and HR (Springer et al. 2012; Lonardo et al. 2004). In contrast, activation of NPR-C does not affect SAN activity in basal conditions, but in the presence of β -AR activation it decreases $I_{Ca,L}$ (but interestingly not I_f), the rate of diastolic depolarisation, and HR (Springer et al. 2012; Azer et al. 2012; Rose et al. 2004). Thus, NPs can modulate the SAN via activation through both stimulatory NPR-A/B and inhibitory NPR-C, which elicit opposing effects that increase HR in some conditions but decrease it in others. The net results depend on the extent of β -AR activation and the relative contribution of each NPR under varying physiological conditions (Moghtadaei et al. 2016; Azer et al. 2012, 2014).

Tissue Stretch

Cardiac function is affected by feedback from the myocardium's mechanical state to its electrical activity. This phenomenon known as mechano-

electric feedback or coupling (Quinn et al. 2014; Quinn and Kohl 2016). The SAN specifically responds on a beat-by-beat basis to changes in hemodynamic load (Quinn and Kohl 2012; Quinn et al. 2011). This was first recognized as an increase in HR with atrial distension by intravenous fluid injection (Crystal and Salem 2012). Similar effects have since been observed in a wide variety of vertebrates (Pathak 1973), including human (Donald and Shepherd 1978). Stretch-induced increases in HR occur also in the isolated heart (Blinks 1956), SAN tissue (Blinks 1956; Deck 1964), and SAN cells (Cooper and Kohl 2005), indicating that the response is intrinsic to the heart. Furthermore, the response is insensitive to ablation of intracardiac neurons (Wilson and Bolter 2002), blockage of neuronal sodium channels (Wilson and Bolter 2002; Chiba 1977), as well as adrenergic and cholinergic blockade (Blinks 1956; Wilson and Bolter 2002; Chiba 1977; Brooks et al. 1966). This implies that non-neuronal mechanisms are involved. The increase in HR with stretch is associated with both an increase in MDP and the rate of diastolic depolarisation allowing for shorter time to an AP (Deck 1964). This can be explained by a mechano-sensitive whole-cell current presumably carried by cation non-selective stretch-activated channels (Cooper and Kohl 2005; Cooper et al. 2000; Peyronnet et al. 2016), although a stretch-induced increase in the current and activation and deactivation rate of HCN channels also has been observed (Lin et al. 2007; Calloe et al. 2005).

There appears to be an interaction between mechanical and autonomic HR modulation. In intact animals (Bolter and Wilson 1999; Bolter 1994) and isolated atria (Bolter 1996; Wilson and Bolter 2001; Barrett et al. 1998), an increase in atrial pressure induces both HR acceleration and a significant reduction in the percentage response to vagal stimulation. Vice versa, when HR is first reduced by vagal stimulation, the HR response with stretch is augmented which could have value for a more rapid increase in heart rate with the onset of exercise in well-conditioned persons who usually have high basal cholinergic tone.

Determinants of the Heart Rate Dependence of the Length of the Action Potential

As already discussed, if the duration of systole does not shorten at fast heart rates, diastolic filling is compromised. For systole to shorten, AP duration (APD) must shorten (Fig. 7.4). After an increase in HR, or an early excitation, there first is an immediate change in APD, followed by a slower transient change if the new faster HR is maintained, after which APD eventually reaches a new steady state. Different mechanisms account for each.

Immediate Change in APD After a Sudden Decrease in HR or a Premature Excitation

In general, the first APD after a sudden increase in HR, or a premature excitation, is shortened, an effect known as restitution. The degree of the initial change in APD depends on how soon after repolarisation of the previous AP the early excitation occurred ('coupling interval'). This is

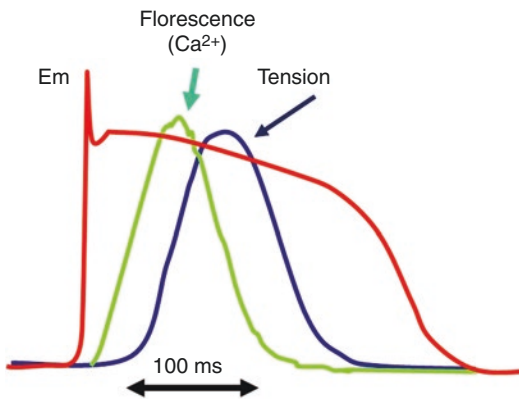


Fig. 7.4 Significance of the plateau of the myocardial action potential for cardiac contractions. Ca^{2+} enters myofibres, and is released from the sarcoplasmic reticulum during the plateau of the action potential and results in contraction. Ca^{2+} entry can be visualized by fluorescent probes, and this is seen to follow by contraction (tension) of the myofibre. The process ends when the myofiber repolarized which means that the plateau of the AP sets the limit of time for contraction and the peak force obtained during the cycle

explained by considering the dynamics (activation/inactivation and deactivation/re-priming) of ion currents in cardiac cells. When there is an early excitation, ion currents that inactivate during an AP have a decreased amplitude during the early excitation. The effect on the amplitude progressively increases with an increase in coupling interval. In working myocytes, this impacts the inward I_{Na} and I_{CaL} currents, and results in faster repolarisation and thus APD shortening. In contrast, reduced amplitude of outward currents that undergo inactivation (i.e. I_{to} and I_{Kur}) prolongs APD. However, during most of the AP, other key outward currents that do not inactivate (i.e. I_{Kr} and I_{Ks}) undergo mainly activation, and do not deactivate until the diastolic phase. As a result, when a premature excitation occurs, these currents remain partly active and accumulate with the additional AP and contribute to faster repolarisation and APD shortening (Carmeliet 2004; Carmeliet 2006).

While these are the dominant ion current changes for the immediately shortening of APD with early excitation, there also is a contribution of rapid changes in ion fluxes carried by transporters. During premature excitation, the amplitude of the inward I_{NCX} is markedly decreased because it depends primarily on the amount of Ca^{2+} released from the SR, which is reduced during early excitation because of incomplete SR refilling (Janvier et al. 1997). Similar to the decrease in other inward currents, this reduction in I_{NCX} results in a shorter AP.

In summary, with a sudden increase in HR or a premature excitation, the combined action of I_{Na} and I_{CaL} inactivation and I_{Kr} and I_{Ks} accumulation accelerate repolarisation, leading to an immediate shortening of APD (Carmeliet 2004, 2006). It should be noted, however, that the restitution process is highly species-dependent; this chapter deals with humans.

Along with the effects of increased HR or early excitation on APD being species-dependent, effects vary regionally across the heart (i.e. differences between the atria and ventricles and the sub-endocardium and -epicardium) due to differences in channels and transporters. For instance, in the ventricle, I_{to} is more highly expressed and

recovers from inactivation faster in sub-epicardial compared to sub-endocardial cells, resulting in a greater decrease in APD (Nabauer et al. 1996).

Transient Change in APD After a Decrease in HR

The initial shortening of APD when there is a sudden increase in HR generally followed by a slow, gradual decrease in APD that occurs over a few seconds to minutes although in the first few seconds oscillations in APD (alternans) can occur, due to the diastolic interval alternating in a short-long sequence before gradually reaching a steady state. The transient decrease in APD is principally driven by: (i) increased intracellular Na^+ concentration ($[\text{Na}^+]_i$, due to the increased influx of Na^+ at the increased HR; (ii) increased intracellular Ca^{2+} concentration ($[\text{Ca}^{2+}]_i$, due to the decrease in the diastolic interval, which alters the equilibrium between Ca^{2+} influx via I_{CaL} during the AP and Ca^{2+} efflux via the NCX during diastole, as well as Ca^{2+} influx via reverse-mode NCX activity driven by the increase in $[\text{Na}^+]_i$ with the increased HR; and (iii) increased extracellular concentration of K^+ ($[\text{K}^+]_o$) (Carmeliet 2004, 2006). These changes in ion concentrations affect APD by altering the flux of ions through various channels and transporters (Carmeliet 2004, 2006).

In addition to changes in ion concentrations, transmembrane ion fluxes also are altered by the increased sympathetic nervous system activity that often drives the increase in HR. Activation of PKA by stimulation of β -ARs results in phosphorylation of RyR, and SERCA. This increases the load of Ca^{2+} in the SR which facilitates Ca^{2+} release (Carmeliet 2004, 2006). The increased SR Ca^{2+} -release causes Ca^{2+} -induced inactivation of I_{CaL} and activation of I_{Cl} and protein kinase C (PKC), which further increase I_{Kr} and I_{NaK} and inhibits the slowly inactivating (also known as the late, sustained, or persistent) Na^+ current whose magnitude is further reduced due to accumulation of intracellular Na^+ with an increase in HR (Tateyama et al. 2003). Combined, these β -AR-driven changes contribute further to more rapid repolarisation and a subsequent decrease in APD.

APD at a New Steady State

Once steady state is reached after an increase in HR, APD generally is decreased in a HR-dependent manner. This relationship, however, does not hold true at lower HRs (of around 60 beats per minute or less). In this range, little change in APD occurs with a change in HR.

Intrinsic Heart Rate

In a classic paper, Jose and Collison determined the spontaneous intrinsic beating frequency of hearts of healthy individuals without any autonomic activity (Jose and Taylor 1969; Jose and Collison 1970). To do so, they inhibited parasympathetic activity by blocking muscarinic receptors with atropine, and sympathetic activity by blocking beta-adrenergic receptors with propranolol. The average heart rate in 25 year-old-subjects was 106/minute. Intrinsic heart rate declined with age at a rate of 0.057 beats/min per year. By the age of 60, intrinsic heart rate was 90 beats/min. They also found that subjects with myocardial dysfunction had an additional loss of the intrinsic rate not accounted for by age alone.

Normal resting heart rate in humans with resting autonomic activity is 70 beats/min and often lower in active individuals. This indicates that parasympathetic activity must dominate the resting state. However, there also must be resting sympathetic activity because beta-blockade lowers the resting heart rate (Jose and Taylor 1969). This is an example of nature driving with her foot on the gas and break at the same time (Magder 2012). The advantage of having opposite processes active at the same time is that it allows a more rapid change. For example, at the start of exercise, the parasympathetic output is quickly withdrawn and the sympathetic output increased so that there is a rapid acceleration of the heart rate which then can accommodate a rapid increase in venous return (Notarius and Magder 1996).

The ratio of heart mass to body weight of 0.6% is consistent throughout all mammals, including humans (Dobson 2003, Bettex 2014). Heart mass

ranges from around 0.5 kg in a normal male to 600 kg in a blue whale. Resting heart rate is inversely proportional to body size and ranges from 600 min^{-1} in a shrew (2–5 g) to $6\text{--}12 \text{ min}^{-1}$ for blue whale (Levine 1997). Life expectancy is also related to heart rate (Levine 1997), which means that the total number of heart beats in a lifetime is relatively constant at 1.1 billion and the total body O₂ consumed per body weight is also similar.

Normal Control of Heart Rate During Exercise

The importance of parasympathetic withdrawal at the onset of exercise was demonstrated by Fagraeus and Linnarsson (1976). They used combined parasympathetic and sympathetic blockade to determine the role of these systems in the change in heart rate from rest to light exercise. The increase in heart rate was primarily due to vagal withdrawal and occurred in approximately 10 s. Over the ensuing 20 s, vagal tone increased and produced some slowing of the heart rate, indicating an initial overshoot and a dynamic

interaction between sympathetic and parasympathetic systems.

Maximal aerobic exercise is one of the greatest challenges to the cardiovascular system, and the adaptations of cardiac output and heart rate provide important insights into how the system is regulated (Magder et al. 2019). Peak exercise is determined by the amount of oxygen that can be consumed by the working muscle (VO_2). VO_2 can increase 12-fold at peak performance in a healthy young male (Åstrand 1976). The rise in VO_2 is associated with a linear increase in cardiac output, which can increase to 4–5 times the normal resting value (Åstrand et al. 1964) (Fig. 7.5). The relationship of cardiac output to VO_2 is so tight that if the oxygen consumption is known, and the haemoglobin is normal, the increase in cardiac output can be estimated with an accuracy of about $\pm 5\%$. This indicates that under normal physiological activity, cardiac output tightly follows the energy demands which is represented by VO_2 .

The control of heart rate, though, is very different. Heart rate, too, increases relatively linearly with energy demands, but not as precisely as cardiac output. More importantly, heart rate

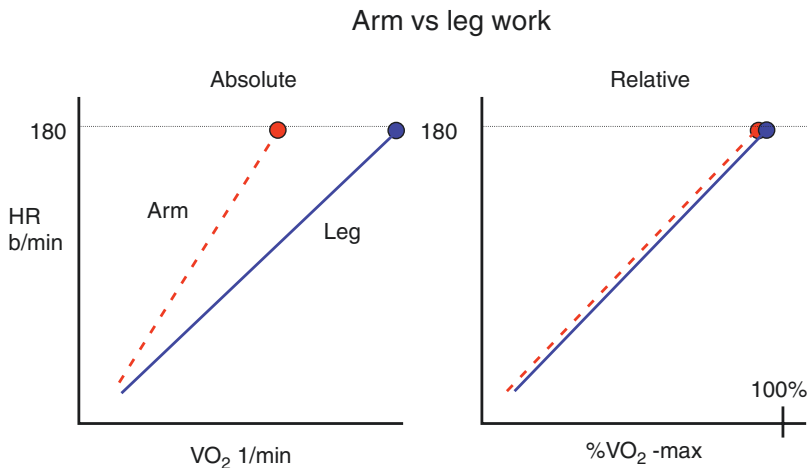


Fig. 7.5 Concept of relative work load and illustrated by arm versus leg exercise. Because legs are much larger than arms, they can generate a higher workload and thus a higher oxygen consumption (VO_2). Heart rate increases linearly with VO_2 . However, maximum heart rate is the same with leg and arm exercise. Accordingly, the slope of

the increase in heart rate with VO_2 is flatter with leg exercise than arm exercise. However, if instead of the x-axis being VO_2 in absolute numbers, it is instead plotted as a percent of maximal capacity of the muscle (i.e. relative capacity), the two curves overlap

increases in proportion to what is called the ‘relative workload’. To understand these concepts, it first needs to be appreciated that maximum heart rate is related to age. Thus, at the same age, male and females, tall versus short, high aerobic capacity versus low aerobic capacity, and fit versus unfit persons, all have the same maximum heart rate, assuming that they are healthy. However, they obviously do not have the same aerobic capacity. Thus, at any given workload and VO_2 in L/min (not normalized to body size), the heart rate is lower in a person who has a higher maximum VO_2 than in a person who has a lower maximum VO_2 (Fig. 7.5) because the workload is a lower percent of the person’s capacity. Based on this, most women have a higher heart rate at a given workload than men because they are on average smaller and have a lower maximum VO_2 max. However, if heart rate is normalized to the percent of the individual’s capacity, that is, the person’s work load as a percentage of their maximum VO_2 , the lines of heart rate versus percent of capacity for all subjects are superimposable. The usefulness of this is that if you know your maximum heart rate, then the percent of your maximum heart rate at which you are exercising indicates what the percentage the workload is of your maximum capacity. A useful training rate is around 70% of peak aerobic capacity because that is a rate that can be sustained for more prolonged periods; above that rate, lactate increases and steady-state conditions usually cannot be sustained (Åstrand and Rodahl 1977).

A likely explanation for the relationship of heart rate to the ‘relative’ workload is that output from the sympathetic nervous system increases in proportion to muscle effort through both central command and afferent signals from peripheral muscle (Mitchell and Shephard 1993). As discussed above, increased beta-adrenergic activity is a major factor in increasing the SAN depolarization.

There are important pathophysiological consequences of these basic concepts. Cardiac output is the product of heart rate and stroke volume. Heart rate is controlled by the relative workload and cardiac output by the VO_2 . Since heart rate and cardiac output are controlled variables, it fol-

lows that stroke volume must be a dependent variable. There is no central sensor for stroke volume; changes in stroke volume occur through the Frank-Starling length–tension relationship.

The increase in heart rate is a predominant factor for the increase in cardiac output during exercise. In a young male, heart rate can increase almost threefold, whereas the stroke volume in the upright posture increases by 60–90% (Åstrand et al. 1964; Cassidy and Mitchell 1981) and only about 10% when supine (Magder et al. 1987). The increase in heart rate creates a steep rise to the cardiac function curve. As a consequence, the heart becomes much more preload responsive because every stroke volume is affected and there are more stroke volumes per minute (Fig. 7.6). The effect of heart rate on the preload responsiveness is likely a variable that should be accounted for when examining the sensitivity of predictors of fluid responsiveness. The percent change in cardiac output for the same change in preload likely is higher at higher heart rates because of the steeper slope to the cardiac function curve, although this has not been tested.

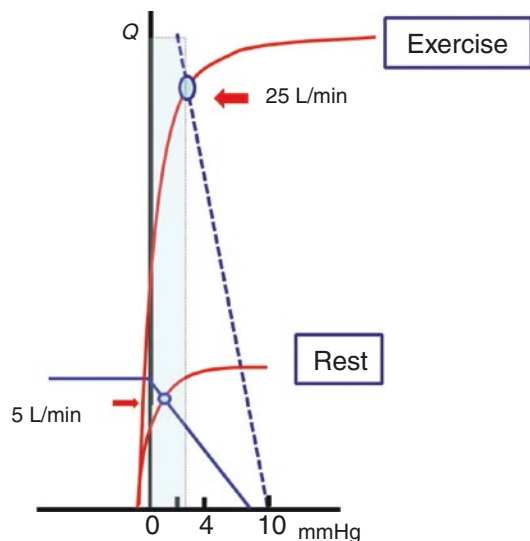


Fig. 7.6 Illustration of the dependence of the change in cardiac output for a change in preload to an increase in heart rate. An increase in heart rate makes the upslope of the cardiac function curve steeper and the plateau higher. Thus, the change in cardiac output is much large for a change in preload

Heart rate during exercise is driven by three mechanisms: central drive, baroreceptor feedback, and afferent signals from working muscle (Mitchell and Shephard 1993; McCloskey and Mitchell 1972). In addition, other central nervous system outputs (i.e. conscious thoughts), hormones, and generalized metabolic signals can change heart rate through the many currents discussed in the section on regulation of the SAN. As a consequence, based on the discussion above, changes in stroke volume are much less predictable than changes in cardiac output. Central drive describes the process by which motor signals descending to muscles from the parietal cortex and spillover into hypothalamic and medullary centres that regulate autonomic activity. This increases sympathetic output and inhibits vagal output. The initial vasodilation in the working skeletal muscle produces a large decrease in systemic vascular resistance which would markedly decrease arterial pressure except for the rapid response by the carotid baroreceptors, which decreases output from the cardio-inhibitory parasympathetic pathway and decreases the inhibition of the cardio-stimulatory centre (Raven et al. 2019). The net effect is increased sympathetic output, including direct stimulation of the sinus node. The third factor is relevant to the critically ill patient. Type III and IV thin unmyelinated afferent nerve fibres are activated by metabolic signals in working muscles (McCloskey and Mitchell 1972; Kaufman et al. 1982; Kaufman et al. 1985; Magder 2001). These signals include mechanical stretch, increased concentration of K^+ and arachidonic acid metabolites, osmolality, hypoxia, and hydrogen ions (Kaufman et al. 1982). The diaphragm and other respiratory muscles also have these afferents. When the work of breathing is increased, afferent signals from these tissues increase central sympathetic output and contribute to an increased heart rate. These afferent signals also increase the drive to breathe which produces the rapid shallow breathing associated with fatigued respiratory muscles (Magder 2001; Teitelbaum et al. 1993; Hussain et al. 1991). Adding to this the patient's mental distress and a tachycardia is inevitable. Small unmyelinated afferents in other organs, too. They are par-

ticularly dense in the region of the celiac axis. These can be activated by inflammation in this region, and also can drive an increase in heart rate. Likely, for this reason, patients with pancreatitis often have sustained high sinus rates. As discussed above, release of vasoactive peptide by the pancreas and its surrounding sympathetic fibres may also contribute (Said 1986). Their heart rates often can be in the 120–130 beats/min range, and it is important to appreciate that this does not indicate hypovolemia even though these patients often are intravascular volume-depleted.

Heart Rate, Beta Blockers, and Ejection Fraction

As already noted, cardiac output is tightly related to metabolic demand. This means that venous return, too, is regulated by metabolic demand, and the heart handles this return through its heart rate and stroke volume. This has an important consequence when pharmacologically manipulating heart rate with, for example, a beta blocker. Except for perhaps some adjustments when a beta blocker is first started, cardiac output usually does not change with chronic beta blocker therapy. Thus, venous return also must be the same. If venous return is the same and heart rate is slowed, the end-diastolic volume must be increased and the stroke volume then is increased through the Frank-Starling mechanism. This normal response can happen as long as right ventricular end-diastolic volume is not limited and the heart is functioning on the flat part of the cardiac function curve. Because both stroke volume and end-diastolic volume increase, the calculated ejection fraction increases, but this does not mean that there actually was any change in cardiac function as often is argued. The increase in ejection fraction is simply a mathematical result of the changing ratio of stroke volume to end-diastolic pressure. On the other side, in distributive shock, venous return is increased but there are no central command signals to produce the usual increase in heart rate (except perhaps from the hypotension and baroreceptor activation as well as through direct cytokine activation); the myocardium often

also is depressed in sepsis. Consequently, right-sided filling pressures usually are increased and the right ventricle becomes limited at an end-diastolic volume that is not sufficient to provide the necessary higher blood pressure to match the decrease in peripheral resistance. Blood pressure then decreases.

Another important consequence of the interaction of heart rate, stroke volume, and cardiac output is the addition of the cyclic heart–lung interactions from ventilation. As discussed in the chapters on right ventricular function and heart–lung interactions, the independent respiratory effects on filling and loading of the right and left ventricles, and time delay for changes in the right ventricle to reach the left ventricle, are modified by the phasic interactions of the cardiac cycle. In the background is the return of blood, which is relatively constant over time since it is based on the metabolic activity of the body, that is, flow follows metabolic need. A modification of this is needed when there is active recruitment of abdominal muscles because the changing peritoneal pressure can alter emptying of the splanchnic venous reservoir, as well as the return of blood from the legs. The implication is that the final magnitude of the impact of ventricular and ventilator interactions cannot be studied in isolation. The dominant variable is the steady-state flow need, and moment-to-moment changes in ventricular size may be measureable but likely have only modest effects on overall oxygen delivery.

Tachycardia and Hypovolemia

Medical personnel often react to tachycardia as a sign of hypovolemia, but heart rate bears a poor relationship to hypovolemia because there are no ‘volume’ receptors in the system except for some mild afferent fibers in the atria and ventricles (Coleridge and Coleridge 1980). More than likely the increase in heart rate with hypovolemia is due to local receptors that are activated by the ischemia from inadequate tissue perfusion, or by direct action of the cytokines involved in inflammation acting on the cardiac excitatory centres in

the brain and directly on the SAN. A number of studies have examined the sensitivity of heart rate and the blood pressure response to hypovolemia. One study compared the detection of hypovolemia by measurement of the pH in the stomach wall by gastric tonometry (pHi) to changes in heart rate and blood pressure. To do so, they removed 20% of predicted blood volume in normal subjects (Hamilton-Davies et al. 1997). In 5 of the 6 subjects, heart rate and blood pressure did not change, and in the sixth heart rate slowed because he became vasovagal. The gastric tonometer, however, detected a decrease pH in the gastric mucosa in all subjects indicating that splanchnic perfusion was impaired despite the lack of change in heart rate and blood pressure. If the subjects had stood up, though, they likely would have been tachycardic because the gravitational stress would have increased the effect of the hypovolemia and induced a baroreceptor response. These observations indicate that loss of volume has to be severe to activate an increase in heart rate in a supine patient. In trauma, pain and anxiety are more likely to be the cause of the tachycardia than hypovolemia.

An accelerated heart rate allows a more rapid increase in cardiac output. This is seen especially in racing animals, but also can be seen in humans as an ‘anticipatory’ response. The faster heart rate means that the diastolic volume is lower than normal and can immediately handle an increase in venous return per beat.

Bainbridge Reflex

Another factor that can increase heart rate is called the Bainbridge reflex (Crystal and Salem 2012; Bainbridge 1915; Hakumaki 1987). As discussed in the section on regulation of the SAN, stretch of atrial tissue can directly alter the rate of SAN depolarization, even in isolated SAN cells without innervation (Blinks 1956; Cooper and Kohl 2005). This unusual reflex is a feed-forward mechanism. A sudden increase in right atrial distension triggers an increase in heart rate. It also blocks normal baroreceptor activity that would have suppressed the heart rate increase. This was

made evident by showing that inactivation of the baroreceptors does not alter the heart rate response (Vatner et al. 1975). In the intact person, a reflex pathway also is active. The mechanism for the reflex is thought to be activation of atrial type B receptors by atrial stretch (Crystal and Salem 2012; Hakumaki 1987). Afferent signals from these cells increase sympathetic discharge to the heart and decrease vagal activity. Sympathetic activity to peripheral resistance vessels also increases and maintains the increased arterial pressure. As originally proposed by Bainbridge, the reflex allows the heart rate to respond faster to a sudden increase in venous return as occurs at the onset of exercise as discussed under the rapid vagal withdrawal at the onset of exercise (Notarius and Magder 1996; Fagraeus and Linnarsson 1976; Linnarsson 1974). As will be seen later, the consequent shortened diastolic time also limits the distension of the right heart. Finally, the suppression of baroreceptor reflex prevents it from countering the increase in heart rate. The activity of this reflex likely is minor in critically ill patients receiving volume boluses. In one study, there was only an average decrease of 1 mmHg whether a colloid or crystalloid was given (Magder and Bafaqeh 2007).

Heart Rate and the Interaction of Venous Return and Cardiac Function in the Guyton Analysis

The impact of a change in heart rate on cardiac output can be analysed with Guyton's venous return cardiac function diagram, which was discussed in Chap. 2. An increase heart rate shifts the cardiac function upward and to the left. As a consequence, the cardiac function curve intersects the venous return curve at a lower right atrial pressure and higher cardiac output. This effectively makes the heart more 'permissive', in that it allows more blood to come back. The cardiac function curve shifts because at the same right atrial pressure, that is, same preload, there are more stroke volumes per minute. An

increase in heart rate also means that there are more plateaus of the action potential which results in greater intracellular calcium influx, a major determinant of cardiac contractility. This increases the peak slope of the end-systolic pressure–volume relationship (end-systolic elastance).

However, there are limits to these processes, and these have clinical implications. When right atrial pressure is below atmospheric pressure, and the pressure inside a floppy vein is less than the pressure outside, the vessel collapses. This creates a plateau on the venous return curve and flow does not increase when right atrial pressure is lowered further. This means that in the steady state an increase in cardiac function may lower right atrial pressure but does not increase cardiac output. Furthermore, if cardiac output does not change, and heart rate increases, stroke volume has to decrease. This is the normal state when sitting or standing, but not when moving (Notarius et al. 1998). The cardiac function curve also frequently intersects the plateau of the venous return curve in patients who are on positive pressure ventilation because the limitation to venous return occurs at pressures above atmospheric pressure. A clinical consequence of this physiological point is that when cardiac output is measured with a device that is based on a stroke volume measurement, a fall in stroke volume does not mean that there necessarily has been a fall in cardiac output; the product of heart rate and stroke volume must be examined.

At the other end of the spectrum, that is, when the venous return curve intersects the plateau of the cardiac function, giving volume cannot increase stroke volume and an increase in heart rate, an increase in contractility, or a decrease in afterload are required to increase cardiac output by shifting the cardiac function upwards. However, what is not evident with the Guyton venous return curve is that the heart rate effect can be limited if the inevitably shortened diastolic time limits venous return per beat. In this case, cardiac output falls. This would 'appear' as an increase in venous resistance.

Heart Rate and Diastolic Limitation

Heart rate is especially important when there is left ventricular diastolic dysfunction and end-diastolic pressure needs to be higher for a given end-diastolic volume. As discussed above, slowing the heart rate by beta blocker requires an increase in stroke volume to maintain cardiac output. In a heart with decreased diastolic capacity, this can significantly increase end-diastolic pressure. This is especially a problem during exercise because the stroke volume needs to increase even more. It is important to determine if a patient's dyspnea on exertion is due to myocardial ischemia, in which case limiting the heart rate is a good therapeutic option, or whether it is due to a stiff left ventricle, in which case a beta blocker will make congestive symptoms worse.

The limit of diastolic filling in the right heart and the decline in peak heart with aging is a major factor for the decline in VO_2 with age. An estimate of the age-related peak heart rate is: $\text{Max heart} = 220 - \text{age}$ in beats per minute. Based on this, the peak heart rate of a 20-year old is close to 200 and in a 60-year old, it only is 160 beats per minute. Normally, exercise that is prolonged for more than 5–10 minutes only can be sustained at approximately 70–80% of the person's maximum aerobic capacity; in a 60-year old male, 80% of peak heart rate is 128 b/min compared to 160 in the 20-year old.

The significance of heart rate limitation can be seen in a quantitative analysis. If the aerobic demand requires a cardiac output of 20 L/min, and the peak heart rate is only 120 b/min, the stroke volume would have to be 168 ml. However, in an average-sized person, the limit of diastolic filling is less than 140 ml so that this is not possible.

A low heart rate has different effects on the right and left ventricles. On the right side, diastolic filling pressures generally are low until the limit of right-sided filling is reached. Assuming a right ventricular end-diastolic volume of 130 ml, and a cardiac output of 5 L/min to meet metabolic needs, the lowest tolerable heart rate would be 38 b/min; a heart beat lower than this will

lower the cardiac output because the stroke volume would be limited. On the left side, because of the steeper diastolic filling curve, and especially in subjects with diastolic dysfunction, a low heart rate can markedly increase end-diastolic pressure and the likelihood of pulmonary congestion.

Supply Demand of the Heart

The risk of myocardial ischemia is analysed by considering the factors determining myocardial oxygen demand and the factors affecting the supply of oxygen. Myocardial oxygen consumption (MVO_2) is determined by a baseline need to maintain cell function and the need for the work done by the heart. The three determinants of oxygen for cardiac work are heart rate, contractility, and wall tension, the latter of which is determined by the peak systolic pressure and the radius of curvature of the ventricular walls (Katz 1992). Heart rate and systolic pressure are easy to obtain, and contractility usually rises with a rise in heart rate. Thus, the product of heart rate and systolic pressure gives a good indication of MVO_2 . This is the rationale behind standard exercise testing. Most of the information is given by just the heart rate but adding the systolic pressure gives what is called the rate-pressure product, which gives a pretty good indication of myocardial oxygen demand.

O_2 is supplied to the heart by coronary flow. Just as occurs in the whole body, coronary blood flow is tightly related to MVO_2 . 'Rest state', means a heart rate of approximately 70 b/min, where the heart extracts about 70% of the oxygen content in the coronary blood. In comparison, only about 25% is extracted from the blood for the whole body. Because of this, the heart is especially dependent upon coronary flow. There is little reserve for more extraction and anaerobic metabolism provides too little energy to maintain the working heart. Besides coronary flow, the other factors affecting O_2 delivery to the heart are haemoglobin concentration and arterial oxygen saturation. Coronary flow is determined by the pressure difference between the aorta and a

downstream critical pressure of 25–30 mmHg (Bellamy 1978), which is dependent upon the diastolic pressure in the ventricle and activity of the heart.

The range of coronary flows in the heart is huge. Resting coronary blood flow is in the range of 80 ml/min/100 g of tissue. At peak exercise in a young male, this can increase to 500 ml/min/100 g, a greater than fivefold increase (Bellamy 1978, 1980). In comparison, flow in resting skeletal muscle is 5–7 ml/min/100 g, and at peak exercise blood flow in aerobically active muscles reaches around 200 ml/min/100 g. The implication of this is that coronary reserves are very large and as long as there is no proximal coronary artery stenosis, the myocardium can handle a large increase in heart rate. Furthermore, most of the resistance in the coronary vasculature is at the level of arterioles. Only about 5% of the pressure drop occurs in the large epicardial coronary vessels seen on an angiogram. It can be shown that it requires more than a 70% proximal stenosis of a coronary vessel to impact significantly on maximum coronary flow.

Conclusion

Control of heart rate is a complex process that is affected by the autonomic activity of the sympathetic and parasympathetic systems as well as the impact of many endogenous and other circulatory factors directly on the SAN. Under normal conditions, the heart rate increases according to the relative external workload, whereas the cardiac output increases according to the absolute workload. This means that stroke volume becomes a dependent variable based on the cardiac output venous return and the heart rate. The heart rate sets the time available for filling and ejection by the heart, which ultimately determines what the heart can pump out. When the heart rate is increased by factors not related to aerobic workload, adaptations in the return of blood to heart, and in the ratio of diastolic to systolic time, may not be adequate for optimal cardiac filling and emptying. Both ends of the spectrum of heart rates are important for cardiac

output. If the heart rate is too fast for the rate of venous return, stroke volume is decreased. If the heart rate is too slow for the rate of returning blood, stroke volume becomes limited. Heart rate is the major factor for large normal increases in cardiac output but it also is a major factor in the energy needs of the heart. With normal coronary circulation, this is not a problem because of the large coronary reserves but it can be a problem when coronary oxygen delivery is limited.

References

- Accili EA, Redaelli G, DiFrancesco D. Activation of the hyperpolarization-activated current (if) in sino-atrial node myocytes of the rabbit by vasoactive intestinal peptide. *Pflugers Arch.* 1996;431(5):803–5.
- Accili EA, Redaelli G, DiFrancesco D. Two distinct pathways of muscarinic current responses in rabbit sino-atrial node myocytes. *Pflugers Arch.* 1998;437(1):164–7.
- Anand-Srivastava MB. Natriuretic peptide receptor-C signaling and regulation. *Peptides.* 2005;26(6):1044–59.
- Ardell JL, Armour JA. Neurocardiology: structure-based function. *Compr Physiol.* 2016;6(4):1635–53.
- Armour JA. Potential clinical relevance of the 'little brain' on the mammalian heart. *Exp Phys.* 2008;93(2):165–76.
- Astrand PO. Quantification of exercise capability and evaluation of physical capacity in man. In: Sonnenblick EH, Lesch M, editors. *Exercise and heart disease. A progress in cardiovascular disease reprint.* New York: Grune and Stratton; 1976. p. 87–103.
- Astrand PO, Rodahl K. *Physiological bases of exercise. Textbook of work physiology.* Montreal: McGraw-Hill; 1977.
- Åstrand P-O, Cuddy TE, Saltin B, Stenberg J. Cardiac output during submaximal and maximal work. *J Appl Physiol.* 1964;19(2):268–74.
- Azer J, Hua R, Vella K, Rose RA. Natriuretic peptides regulate heart rate and sinoatrial node function by activating multiple natriuretic peptide receptors. *J Mol Cell Cardiol.* 2012;53(5):715–24.
- Azer J, Hua R, Krishnaswamy PS, Rose RA. Effects of natriuretic peptides on electrical conduction in the sinoatrial node and atrial myocardium of the heart. *J Physiol.* 2014;592(Pt 5):1025–45.
- Bainbridge FA. The influence of venous filling upon the rate of the heart. *J Physiol.* 1915;50(2):65–84.
- Barrett CJ, Bolter CP, Wilson SJ. The intrinsic rate response of the isolated right atrium of the rat, *Rattus norvegicus.* *Comp Biochem Physiol A Mol Integr Physiol.* 1998;120(3):391–7.
- Bartos DC, Grandi E, Ripplinger CM. Ion channels in the heart. *Compr Physiol.* 2015;5(3):1423–64.

- Beadling C, Druey KM, Richter G, Kehrl JH, Smith KA. Regulators of G protein signaling exhibit distinct patterns of gene expression and target G protein specificity in human lymphocytes. *J Immunol.* 1999;162(5):2677–82.
- Beaulieu P, Lambert C. Peptidic regulation of heart rate and interactions with the autonomic nervous system. *Cardiovasc Res.* 1998;37(3):578–85.
- Bell D, McDermott BJ. Calcitonin gene-related peptide in the cardiovascular system: characterization of receptor populations and their (patho)physiological significance. *Pharmacol Rev.* 1996;48(2):253–88.
- Bellamy RF. Diastolic coronary artery pressure-flow relations in the dog. *Circ Res.* 1978;43(1):92–101.
- Bellamy RF. Calculation of coronary vascular resistance. *Cardiovasc Res.* 1980;14:261–9.
- Blinks JR. Positive chronotropic effect of increasing right atrial pressure in the isolated mammalian heart. *Am J Phys.* 1956;186(2):299–303.
- Bettex DA, Pretre R, Chassot PG. Is our heart a well-designed pump? The heart along animal evolution. *Eur Heart J.* 2014;35(34):2322–32.
- Bolter CP. Intrinsic cardiac rate regulation in the anaesthetized rabbit. *Acta Physiol Scand.* 1994;151(4):421–8.
- Bolter CP. Effect of changes in transmural pressure on contraction frequency of the isolated right atrium of the rabbit. *Acta Physiol Scand.* 1996;156(1):45–50.
- Bolter CP, Wilson SJ. Influence of right atrial pressure on the cardiac pacemaker response to vagal stimulation. *Am J Phys.* 1999;276(4 Pt 2):R1112–7.
- Brooks CM, Lu HH, Lange G, Mangi R, Shaw RB, Geoly K. Effects of localized stretch of the sinoatrial node region of the dog heart. *Am J Phys.* 1966;211(5):1197–202.
- Cabanac M. Regulation and modulation in biology. A reexamination of temperature regulation. *Ann N Y Acad Sci.* 1997;813:21–31.
- Calloe K, Elmedy P, Olesen SP, Jorgensen NK, Grunnet M. Hypoosmotic cell swelling as a novel mechanism for modulation of cloned HCN2 channels. *Biophys J.* 2005;89(3):2159–69.
- Carmeliet E. Intracellular Ca(2+) concentration and rate adaptation of the cardiac action potential. *Cell Calcium.* 2004;35(6):557–73.
- Carmeliet E. Action potential duration, rate of stimulation, and intracellular sodium. *J Cardiovasc Electrophysiol.* 2006;17(Suppl 1):S2–7.
- Cassidy S, Mitchell J. Effects of positive pressure breathing on right and left ventricular preload and afterload. *Fed Proc.* 1981;40:2178–81.
- Centurion D, Ortiz MI, Saxena PR, Villalon CM. The atypical 5-HT2 receptor mediating tachycardia in pithed rats: pharmacological correlation with the 5-HT2A receptor subtype. *Br J Pharmacol.* 2002;135(6):1531–9.
- Chandler NJ, Greener ID, Tellez JO, Inada S, Musa H, Molenaar P, et al. Molecular architecture of the human sinus node: insights into the function of the cardiac pacemaker. *Circulation.* 2009;119(12):1562–75.
- Chang F, Yu H, Cohen IS. Actions of vasoactive intestinal peptide and neuropeptide Y on the pacemaker current in canine Purkinje fibers. *Circ Res.* 1994;74(1):157–62.
- Chiba S. Pharmacologic analysis of stretch-induced sinus acceleration of the isolated dog atrium. *Jpn Heart J.* 1977;18(3):398–405.
- Chorev M. Parathyroid hormone 1 receptor: insights into structure and function. *Receptors Channels.* 2002;8(3–4):219–42.
- Coleridge HM, Coleridge JC. Cardiovascular afferents involved in regulation of peripheral vessels. *Annu Rev Physiol.* 1980;42:413–27.
- Cooper PJ, Kohl P. Species- and preparation-dependence of stretch effects on sino-atrial node pacemaking. *Ann N Y Acad Sci.* 2005;1047:324–35.
- Cooper PJ, Lei M, Cheng LX, Kohl P. Selected contribution: axial stretch increases spontaneous pacemaker activity in rabbit isolated sinoatrial node cells. *J Appl Physiol.* 2000;89(5):2099–104.
- Critchley LA, Lee A, Ho AM. A critical review of the ability of continuous cardiac output monitors to measure trends in cardiac output. *Anesth Anal.* 2010;111(5):1180–92.
- Crystal GJ, Salem MR. The Bainbridge and the "reverse" Bainbridge reflexes: history, physiology, and clinical relevance. *Anesth Analg.* 2012;114(3):520–32.
- Deck KA. Dehnungseffekte am spontanschlagenden, isolierten Sinusknoten. *Pflugers Arch Gesamte Physiol Menschen Tiere.* 1964;280:120–30.
- DiFrancesco D. The role of the funny current in pacemaker activity. *Circ Res.* 2010;106(3):434–46.
- DiFrancesco D, Noble D. The funny current has a major pacemaking role in the sinus node. *Heart Rhythm.* 2012;9(2):299–301.
- Dobson GP. On being the right size: heart design, mitochondrial efficiency and lifespan potential. *Clinical and experimental pharmacology & physiology.* 2003;30(8):590–7.
- Donald DE, Shepherd JT. Reflexes from the heart and lungs: physiological curiosities or important regulatory mechanisms. *Cardiovasc Res.* 1978;12(8):446–69.
- Fagraeus L, Linnarsson D. Autonomic origin of heart rate fluctuations at the onset of muscular exercise. *J Appl Physiol.* 1976;40(5):679–82.
- Gagliardi M, Randall WC, Bieger D, Wurster RD, Hopkins DA, Armour JA. Activity of in vivo canine cardiac plexus neurons. *Am J Phys.* 1988;255(4 Pt 2):H789–800.
- Gloss B, Trost S, Bluhm W, Swanson E, Clark R, Winkfein R, et al. Cardiac ion channel expression and contractile function in mice with deletion of thyroid hormone receptor alpha or beta. *Endocrinology.* 2001;142(2):544–50.
- Gordan R, Gwathmey JK, Xie LH. Autonomic and endocrine control of cardiovascular function. *World J Cardiol.* 2015;7(4):204–14.
- Gothert M, Schlicker E, Kolleck P. Receptor-mediated effects of serotonin and 5-methoxytryptamine on noradrenaline release in the rat vena cava and in the heart of the pithed rat. *Naunyn Schmiedeberg's Arch Pharmacol.* 1986;332(2):124–30.

- Guyton AC. Textbook of medical physiology. 1st ed. Philadelphia: W.B. Saunders; 1956.
- Habuchi Y, Lu LL, Morikawa J, Yoshimura M. Angiotensin II inhibition of L-type Ca²⁺ current in sinoatrial node cells of rabbits. *Am J Phys.* 1995;268(3 Pt 2):H1053–60.
- Hakumaki MO. Seventy years of the Bainbridge reflex. *Acta Physiol Scand.* 1987;130(2):177–85.
- Hamilton-Davies C, Mythen MD, Salmon JB, Jacobson D, Shukla A, Webb AR. Comparison of commonly used clinical indicators of hypovolaemia with gastrointestinal tonometry. *Intensive Care Med.* 1997;23:276–81.
- Hodgin JB, Kregel JH, Reddick RL, Korach KS, Smithies O, Maeda N. Estrogen receptor alpha is a major mediator of 17 beta-estradiol's atheroprotective effects on lesion size in Apoe^{-/-} mice. *J Clin Investig.* 2001;107(3):333–40.
- Hoover DB. Effects of guinea pig vasoactive intestinal peptide on the isolated perfused guinea pig heart. *Peptides.* 1989;10(2):343–7.
- Hussain SNA, Chatillon A, Comtois A, Roussos C, Magder S. Chemical activation of thin-fiber phrenic afferents: (2) the cardiovascular responses. *J Appl Physiol.* 1991;70:159–67.
- Irisawa H, Brown HF, Giles W. Cardiac pacemaking in the sinoatrial node. *Physiol Rev.* 1993;73(1):197–227.
- Ishikawa T, Yanagisawa M, Kimura S, Goto K, Masaki T. Positive inotropic action of novel vasoconstrictor peptide endothelin on guinea pig atria. *Am J Physiol Heart Circ Physiol.* 1988;255:H970–H3.
- James TN. The chronotropic action of serotonin studied by direct perfusion of the sinus node. *J Pharmacol Exp Ther.* 1964;146:209–14.
- Janvier NC, McMorn SO, Harrison SM, Taggart P, Boyett MR. The role of Na(+)-Ca²⁺ exchange current in electrical restitution in ferret ventricular cells. *J Physiol.* 1997;504(Pt 2):301–14.
- Jose AD, Collison D. The normal range and determinants of the intrinsic heart rate in man. *Cardiovasc Res.* 1970;4(2):160–7.
- Jose AD, Taylor RR. Autonomic blockade by propranolol and atropine to study intrinsic myocardial function in man. *J Clin Invest.* 1969;48(11):2019–31.
- Ju YK, Chu Y, Chaulet H, Lai D, Gervasio OL, Graham RM, et al. Store-operated Ca²⁺ influx and expression of TRPC genes in mouse sinoatrial node. *Circ Res.* 2007;100(11):1605–14.
- Ju YK, Liu J, Lee BH, Lai D, Woodcock EA, Lei M, et al. Distribution and functional role of inositol 1,4,5-trisphosphate receptors in mouse sinoatrial node. *Circ Res.* 2011;109(8):848–57.
- Katz AM. Energy utilization (work and heat). *Physiology of the heart.* 2nd ed. New York: Raven Press; 1992. p. 129–50.
- Kaufman MP, Iwamoto GA, Longhurst JC, Mitchell JH. Effects of capsaicin and bradykinin on afferent fibers with endings in skeletal muscle. *Circ Res.* 1982;50:133–9.
- Kaufman MP, Rybicki KJ, Mitchell JH. Hindlimb muscular contraction reflexly decreases total pulmonary resistance in dogs. *J Appl Physiol.* 1985;59:1521–6.
- Kevelaitis E, Abraitis R, Lazauskas R. Histamine and pacemaker shift in the sinoatrial node. *Agents Actions.* 1994;41 Spec No:C87–8.
- Kobayashi M, Furukawa Y, Chiba S. Positive chronotropic and inotropic effects of angiotensin II in the dog heart. *Eur J Pharmacol.* 1978;50(1):17–25.
- Lakatta EG, Vinogradova TM, Maltsev VA. The missing link in the mystery of normal automaticity of cardiac pacemaker cells. *Ann NY Acad Sci.* 2008;1123:41–57.
- Lakatta EG, Maltsev VA, Vinogradova TM. A coupled SYSTEM of intracellular Ca²⁺ clocks and surface membrane voltage clocks controls the timekeeping mechanism of the heart's pacemaker. *Circ Res.* 2010;106(4):659–73.
- Lambert C. Mechanisms of angiotensin II chronotropic effect in anaesthetized dogs. *Br J Pharmacol.* 1995;115(5):795–800.
- Lambert LE, Whitten JP, Baron BM, Cheng HC, Doherty NS, McDonald IA. Nitric oxide synthesis in the CNS, endothelium and macrophages differs in its sensitivity to inhibition by arginine analogues. *Life Sci.* 1991;48:69–75.
- Larsson HP. How is the heart rate regulated in the sinoatrial node? Another piece to the puzzle. *J Gen Physiol.* 2010;136(3):237–41.
- Lei M, Zhang H, Grace AA, Huang CL. SCN5A and sinoatrial node pacemaker function. *Cardiovasc Res.* 2007;74(3):356–65.
- Levine HJ. Rest heart rate and life expectancy. *Journal of American College of Cardiology.* 1997;30(4):1104–6.
- Li Y, Sirenko S, Riordon DR, Yang D, Spurgeon H, Lakatta EG, et al. CaMKII-dependent phosphorylation regulates basal cardiac pacemaker function via modulation of local Ca²⁺ releases. *Am J Physiol Heart Circ Physiol.* 2016;311(3):H532–44.
- Lin W, Laitko U, Juranka PF, Morris CE. Dual stretch responses of mHCN2 pacemaker channels: accelerated activation, accelerated deactivation. *Biophys J.* 2007;92(5):1559–72.
- Linden A, Desmecht D, Amory H, Lekeux P. Cardiovascular response to intravenous administration of 5-hydroxytryptamine after type-2 receptor blockade, by metrenperone, in healthy calves. *Vet J.* 1999;157(1):31–7.
- Linnarsson D. Dynamics of pulmonary gas exchange and heart rate changes at start and end of exercise. *Acta Physiol Scand.* 1974;415:1–68.
- Lonardo G, Cerbai E, Casini S, Giunti G, Bonacchi M, Battaglia F, et al. Atrial natriuretic peptide modulates the hyperpolarization-activated current (If) in human atrial myocytes. *Cardiovasc Res.* 2004;63(3):528–36.
- Lucas KA, Pitari GM, Kazerounian S, Ruiz-Stewart I, Park J, Schulz S, et al. Guanylyl cyclases and signaling by cyclic GMP. *Pharmacol Rev.* 2000;52(3):375–414.
- MacDonald EA, Stoyek MR, Rose RA, Quinn TA. Intrinsic regulation of sinoatrial node function and

- the zebrafish as a model of stretch effects on pacemaking. *Prog Biophys Mol Biol.* 2017;130(Pt B):198–211.
- MacDonald EA, Rose RA, Quinn TA. Neurohumoral control of sinoatrial node activity and heart rate: experimental insight and findings from human. *Front Physiol.* 2020;11:170.
- Magder S. Venous mechanics of contracting gastrocnemius muscle and the muscle pump theory. *J Appl Physiol.* 1995;79(6):1930–5.
- Magder S. Effects of respiratory muscle afferent on the breathing and the afferent hypothesis. In: Scharf SM, Pinsky MR, Magder S, editors. *Respiratory-circulatory interactions in health and disease.* 2nd ed. New York: Marcel Dekker, Inc.; 2001. p. 405–25.
- Magder SA. The ups and downs of heart rate. *Crit Care Med.* 2012;40(1):239–45.
- Magder S, Bafaqeeh F. The clinical role of central venous pressure measurements. *J Intensive Care Med.* 2007;22(1):44–51.
- Magder SA, Daughters GT, Hung J, Savin WM, Alderman EL, Ingels NB Jr. Adaptation of human left ventricular volumes to the onset of supine exercise. *Eur J Appl Physiol.* 1987;56:467–73.
- Magder S, Famulari G, Garipey B. Periodicity, time constants of drainage and the mechanical determinants of peak cardiac output during exercise. *J Appl Physiol.* 2019;127(6):1611–9.
- Maltsev VA, Lakatta EG. The funny current in the context of the coupled-clock pacemaker cell system. *Heart Rhythm.* 2012;9(2):302–7.
- Maltsev VA, Vinogradova TM, Lakatta EG. The emergence of a general theory of the initiation and strength of the heartbeat. *J Pharmacol Sci.* 2006;100(5):338–69.
- Mangoni ME, Nargeot J. Genesis and regulation of the heart automaticity. *Physiol Rev.* 2008;88(3):919–82.
- McCloskey DI, Mitchell JH. Reflex cardiovascular and respiratory responses originating in exercising muscle. *J Physiol (Lond).* 1972;224(1):173–86.
- Mesirca P, Torrente AG, Mangoni ME. Functional role of voltage gated Ca(2+) channels in heart automaticity. *Front Physiol.* 2015;6:19.
- Minkes RK, Bellan JA, Saroyan RM, Kerstein MD, Coy DH, Murphy WA, et al. Analysis of cardiovascular and pulmonary responses to endothelin-1 and endothelin-3 in the anesthetized cat. *J Pharmacol Exp Ther.* 1990;253(3):1118–25.
- Mitchell JH, Shephard JT. Control of the circulation during exercise. In: Paul McNeil H, editor. *Exercise – the physiological challenge.* Auckland: Conference Pub.; 1993. p. 55–85.
- Modell H, Cliff W, Michael J, McFarland J, Wenderoth MP, Wright A. A physiologist's view of homeostasis. *Adv Physiol Educ.* 2015;39(4):259–66.
- Moghtadaei M, Polina I, Rose RA. Electrophysiological effects of natriuretic peptides in the heart are mediated by multiple receptor subtypes. *Prog Biophys Mol Biol.* 2016;120(1–3):37–49.
- Nabauer M, Beuckelmann DJ, Uberfuhr P, Steinbeck G. Regional differences in current density and rate-dependent properties of the transient outward current in subepicardial and subendocardial myocytes of human left ventricle. *Circulation.* 1996;93(1):168–77.
- Notarius CF, Magder S. Central venous pressure during exercise: role of muscle pump. *Can J Physiol Pharmacol.* 1996;74(6):647–51.
- Notarius CF, Levy RD, Tully A, Fitchett D, Magder S. Cardiac vs. non-cardiac limits to exercise following heart transplantation. *Am Heart J.* 1998;135:339–48.
- Ono K, Masumiya H, Sakamoto A, Christe G, Shijuku T, Tanaka H, et al. Electrophysiological analysis of the negative chronotropic effect of endothelin-1 in rabbit sinoatrial node cells. *J Physiol.* 2001;537(Pt 2):467–88.
- Pachucki J, Burmeister LA, Larsen PR. Thyroid hormone regulates hyperpolarization-activated cyclic nucleotide-gated channel (HCN2) mRNA in the rat heart. *Circ Res.* 1999;85(6):498–503.
- Pathak CL. Autoregulation of chronotropic response of the heart through pacemaker stretch. *Cardiology.* 1973;58(1):45–64.
- Peyronnet R, Nerbonne JM, Kohl P. Cardiac mechanogated ion channels and arrhythmias. *Circ Res.* 2016;118(2):311–29.
- Potter B, Magder S. Protocol performance of randomized trial of colloid vs crystalloid for fluids after cardiac surgery. *Proc Am Thorac Soc.* 2006;3(April):A651.
- Potthoff SA, Janus A, Hoch H, Frahnert M, Tossios P, Reber D, et al. PTH-receptors regulate norepinephrine release in human heart and kidney. *Regul Pept.* 2011;171(1–3):35–42.
- Quinn TA, Kohl P. Mechano-sensitivity of cardiac pacemaker function: pathophysiological relevance, experimental implications, and conceptual integration with other mechanisms of rhythmicity. *Prog Biophys Mol Biol.* 2012;110:257–68.
- Quinn TA, Kohl P. Rabbit models of cardiac mechano-electric and mechano-mechanical coupling. *Prog Biophys Mol Biol.* 2016;121(2):110–22.
- Quinn TA, Bayliss RA, Kohl P. Mechano-electric feedback in the heart: effects on heart rate and rhythm. In: Tripathi ON, Ravens U, Sanguinetti MC, editors. *Heart rate and rhythm: molecular basis, pharmacological modulation and clinical implications.* 1st ed. Heidelberg: Springer; 2011. p. 133–51.
- Quinn TA, Kohl P, Ravens U. Cardiac mechano-electric coupling research: fifty years of progress and scientific innovation. *Prog Biophys Mol Biol.* 2014;115(2–3):71–5.
- Raven PB, Young BE, Fadel PJ. Arterial baroreflex resetting during exercise in humans: underlying signaling mechanisms. *Exerc Sport Sci Rev.* 2019;47(3):129–41.
- Reinhart K, Kuhn HJ, Hartog C, Bredle DL. Continuous central venous and pulmonary artery oxygen saturation monitoring in the critically ill. *Intensive Care Med.* 2004;30(8):1572–8.

- Renaudon B, Bois P, Bescond J, Lenfant J. Acetylcholine modulates I(f) and IK(ACh) via different pathways in rabbit sino-atrial node cells. *J Mol Cell Cardiol.* 1997;29(3):969–75.
- Renaudon B, Lenfant J, Decressac S, Bois P. Thyroid hormone increases the conductance density of f-channels in rabbit sino-atrial node cells. *Receptors Channels.* 2000;7(1):1–8.
- Rose RA, Giles WR. Natriuretic peptide C receptor signalling in the heart and vasculature. *J Physiol.* 2008;586(2):353–66.
- Rose RA, Lomax AE, Kondo CS, Anand-Srivastava MB, Giles WR. Effects of C-type natriuretic peptide on ionic currents in mouse sinoatrial node: a role for the NPR-C receptor. *Am J Physiol Heart Circ Physiol.* 2004;286(5):H1970–7.
- Rosen MR, Nargeot J, Salama G. The case for the funny current and the calcium clock. *Heart Rhythm.* 2012;9(4):616–8.
- Said SI. Vasoactive intestinal peptide. *J Endocrinol Investig.* 1986;9(2):191–200.
- Saito K, Gutkind JS, Saavedra JM. Angiotensin II binding sites in the conduction system of rat hearts. *Am J Phys.* 1987;253(6 Pt 2):H1618–22.
- Saxena PR, Villalon CM. Cardiovascular effects of serotonin agonists and antagonists. *J Cardiovasc Pharmacol.* 1990;15(Suppl 7):S17–34.
- Sechi LA, Griffin CA, Grady EF, Kalinyak JE, Schambelan M. Characterization of angiotensin II receptor subtypes in rat heart. *Circ Res.* 1992;71(6):1482–9.
- Sheng JW, Wang WY, Xu YF. Angiotensin II decreases spontaneous firing rate of guinea-pig sino-atrial node cells. *Eur J Pharmacol.* 2011;660(2–3):387–93.
- Shimoni Y. Hormonal control of cardiac ion channels and transporters. *Prog Biophys Mol Biol.* 1999;72(1):67–108.
- Springer J, Azer J, Hua R, Robbins C, Adamczyk A, McBoyle S, et al. The natriuretic peptides BNP and CNP increase heart rate and electrical conduction by stimulating ionic currents in the sinoatrial node and atrial myocardium following activation of guanylyl cyclase-linked natriuretic peptide receptors. *J Mol Cell Cardiol.* 2012;52(5):1122–34.
- Tanaka H, Habuchi Y, Yamamoto T, Nishio M, Morikawa J, Yoshimura M. Negative chronotropic actions of endothelin-1 on rabbit sinoatrial node pacemaker cells. *Br J Pharmacol.* 1997;122(2):321–9.
- Tateyama M, Kurokawa J, Terrenoire C, Rivolta I, Kass RS. Stimulation of protein kinase C inhibits bursting in disease-linked mutant human cardiac sodium channels. *Circulation.* 2003;107(25):3216–22.
- Teitelbaum J, Vanelli G, Hussain SNA. Thin-fibre phrenic afferents mediate the ventilatory response to diaphragmatic ischemia. *Respir Physiol.* 1993;91:195–206.
- Torrente AG, Mesirca P, Neco P, Rizzetto R, Dubel S, Barrere C, et al. L-type Cav1.3 channels regulate ryanodine receptor-dependent Ca²⁺ release during sino-atrial node pacemaker activity. *Cardiovasc Res.* 2016;109(3):451–61.
- Vatner SF, Boettcher DH, Heyndrickx GR, McRitchie RJ. Reduced baroreflex sensitivity with volume loading in conscious dogs. *Circ Res.* 1975;37(2):236–42.
- Villalon CM, Centurion D. Cardiovascular responses produced by 5-hydroxytryptamine: a pharmacological update on the receptors/mechanisms involved and therapeutic implications. *Naunyn Schmiedeberg's Arch Pharmacol.* 2007;376(1–2):45–63.
- Vinogradova TM, Lyashkov AE, Zhu W, Ruknudin AM, Sirenko S, Yang D, et al. High basal protein kinase A-dependent phosphorylation drives rhythmic internal Ca²⁺ store oscillations and spontaneous beating of cardiac pacemaker cells. *Circ Res.* 2006;98(4):505–14.
- Wilson SJ, Bolter CP. Interaction of the autonomic nervous system with intrinsic cardiac rate regulation in the guinea-pig, *Cavia porcellus*. *Comp Biochem Physiol A Mol Integr Physiol.* 2001;130(4):723–30.
- Wilson SJ, Bolter CP. Do cardiac neurons play a role in the intrinsic control of heart rate in the rat? *Exp Physiol.* 2002;87(6):675–82.
- Zhang H, Holden AV, Boyett MR. Sustained inward current and pacemaker activity of mammalian sinoatrial node. *J Cardiovasc Electrophysiol.* 2002;13(8):809–12.



Physiological Aspects of Arterial Blood Pressure

8

Sheldon Magder

Blood pressure is measured by almost all health care professionals and is one of the most basic vital signs. However, little attention is given to the physics of the measurement and its physiological implications. As an example of a common error in reasoning, low values of arterial pressure frequently are used to identify inadequate tissue perfusion and then used to provide targets for titration of vasopressor therapy. However, arterial pressure does not predict cardiac output or indicate adequate tissue perfusion. The arterial pressure of a septic patient may be less than 80 mmHg, and cardiac output be twice normal. At peak exercise, a young male can have a cardiac output that is five times normal, but only have a small change, or even a fall, in mean arterial pressure. Blood pressure in patients with cardiogenic shock can be higher than normal even though cardiac output is critically low. Blood pressure in women often is 90 mmHg or less with a normal cardiac output and normal perfusion. To understand why these variations occur requires a better understanding of the determinants of arterial

pressure, which is the subject of this chapter. Many of these concepts have been covered elsewhere (Magder 2014, 2018).

Physical Principles

The flow of a Newtonian fluid through a rigid tube, that is, a fluid that develops laminar flow, was described by Poiseuille as (Burton 1965a):

$$\text{Flow} = \frac{\Delta P}{R} \quad (8.1)$$

where ΔP is the difference between the inflow and outflow pressure, and R is the resistance to flow along the tube. R is defined as:

$$R = \frac{l\eta 8}{\pi r^4} \quad (8.2)$$

where l is length between the two pressure measurements, η is viscosity, and r is radius of the tube. When Poiseuille's law is written the way it appears in Eq. 8.1, it appears that the pressure

S. Magder (✉)
Royal Victoria Hospital (McGill University Health Centre), Departments of Critical Care and Physiology
McGill University, Montreal, QC, Canada
e-mail: sheldon.magder@mcgill.ca

difference determines the flow. However, in the circulation, cardiac output injected into the aorta

determines the arterial pressure, so that the relationship is:

$$\text{Arterial pressure} = \text{Cardiac output} \times \text{systemic vascular resistance} \text{ (i.e. } BP = Q \times R \text{)} \quad (8.3)$$

More precisely, flow is determined by the product of cardiac output and systemic vascular resistance minus a downstream number, which will be discussed later because in Poiseuille's law it is the difference in pressure, not just the upstream pressure. Equation 8.3 can be very useful diagnostically because it indicates that if blood pressure is decreased, it is either because the cardiac output is decreased or because the systemic vascular resistance is decreased. Since systemic vascular resistance is a derived value and cardiac output is either measured or estimated, when assessing a hypotensive patient the primary question should be: is the cardiac output normal or elevated, in which case the primary problem is a decrease in systemic vascular resistance; or is the cardiac output decreased, in which case the decrease in cardiac output is the primary problem. Causes of a decrease in systemic vascular resistance include a systemic inflammatory response due to infection or other causes of cytokine release, anaphylaxis, hepatic failure, endocrine conditions (hyperthyroid, adrenal insufficiency), spinal shock, spinal anaesthesia, a major arteriovenous fistula, vasodilating drugs, or Beriberi and thiamine deficiency. Treatment should then be directed at correcting the condition that caused the low resistance state, and if necessary, treating the decrease in systemic vascular resistance with a vasopressor to try to restore flow to regions that need a greater percent of total flow such as the heart, brain, kidney, and bowel. If the cardiac output is decreased, as discussed in Chap. 2 (Magder volume), this could be because of a decrease in pump function or a difference in the return function. If the problem is a decrease in pump function, treatment should be directed at correcting the pump problem by using therapies to increase pump function. If the problem is the return function, this usually means that a volume infusion is required. Abnormalities in the pump function versus return function often

can be identified by examining the change that occurred in central venous pressure because this is where the cardiac and return functions intersect.

Poiseuille's law makes it look like a pressure difference is the only force driving flow, but flow is really determined by the total fluid energy difference from the inflow to outflow of a vessel (Burton 1965a, b):

$$E = P + \rho gh + 1/2 \rho v^2 \quad (8.4)$$

where ρ is density, g is the acceleration due to gravity, and v is the velocity of blood. All values are normalized to volume so that this represents energy per volume ($\rho/\text{volume} = \text{mass}$, and $P \times \text{Volume} = E$). The first term of Eq. 8.4 is elastic energy. It is the lateral force that stretches the vascular walls and is the most important determinant of all vascular pressures. The second term, gravitational energy, becomes especially important in the upright posture and when making measurements with fluid-filled systems. The third term, kinetic energy, is the energy produced by the movement of blood. What counts for flow is the difference in total energy from the start of the system to the end. This point will become important when considering the kinetic and gravitational components.

Elastic Energy

Elastic energy is the primary type of energy in the cardiovascular system and the value we usually are referring to when we consider arterial pressure, venous pressure, capillary pressure, ventricular pressures, preload, afterload, and many others. It is based on Hooke's law that says that an increase in length of a substance above a resting length produces a force that is proportional to the change in length (Fig. 8.1) (Burton 1965a).

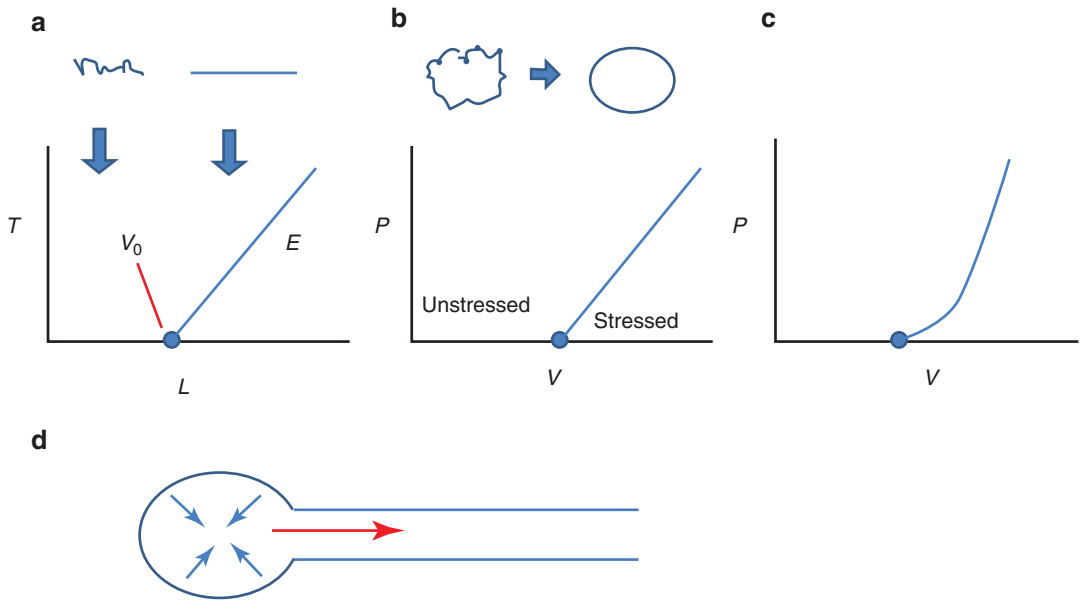


Fig. 8.1 Length tension and pressure–volume relationships and elastic energy. (a) Hooke’s law: change in tension (T), or stress if normalized to cross-sectional area, with a change in length of an elastic substance. The slope of the line is elastance (E); V_0 indicates the limit of unstressed length, that is, a length that does not cause tension. Tension only occurs above V_0 . (b) Pressure and volume are used for the length–tension relationship in a round structure; V is volume and P is pressure (force per

cross-sectional area). When the structure is homogeneous, the relationship is linear. (c) Pressure–volume (P - V) relationship of vessels in the body. The lower end of the P - V relationship is curvilinear because of recruitment of parallel elements and differences in the elastance of the components of the vessel wall. At greater volumes, the relationship tends to be more linear, especially in veins, because collagen becomes the dominant factor. (d) The recoil of an elastic structure can produce flow

The proportionality constant is called elastance, and the units are force per length. If the substance is homogeneous, the relationship is linear. In the vasculature, we deal with curved structures so that the term pressure is used to describe the force per cross-sectional area. Pressure can be considered as a kind of “potential energy” in a fluid-filled vessel. Volume in a vessel distends the elastic wall and thus changes its length. This creates a recoil force that tends to push the volume out of the vessel when it is opened to atmosphere (Fig. 8.1). The walls of vascular structures are not homogeneous and thus their relationships of force per length, or pressure to volume, are not linear. At lower lengths elastin dominates, which is very “stretchable,” whereas collagen domi-

nates at higher lengths, and it is much less stretchable so that the elastance greatly increases and then remains constant.

Kinetic Energy

Kinetic energy contributes only a small component to the arterial pressure, but it has important implications on how blood pressure is measured as well as the elastic force acting on vessel walls (Burton 1965b). The key to understanding this is the distinction between blood flow, which is volume per time, and blood velocity, which is volume per distance. Flow is related to velocity by the following ($l = \text{length}$):

$$\text{Flow (L/min)} = \text{Velocity (L/l)} \times \text{cross-sectional area (l}^2\text{)} \tag{8.5}$$

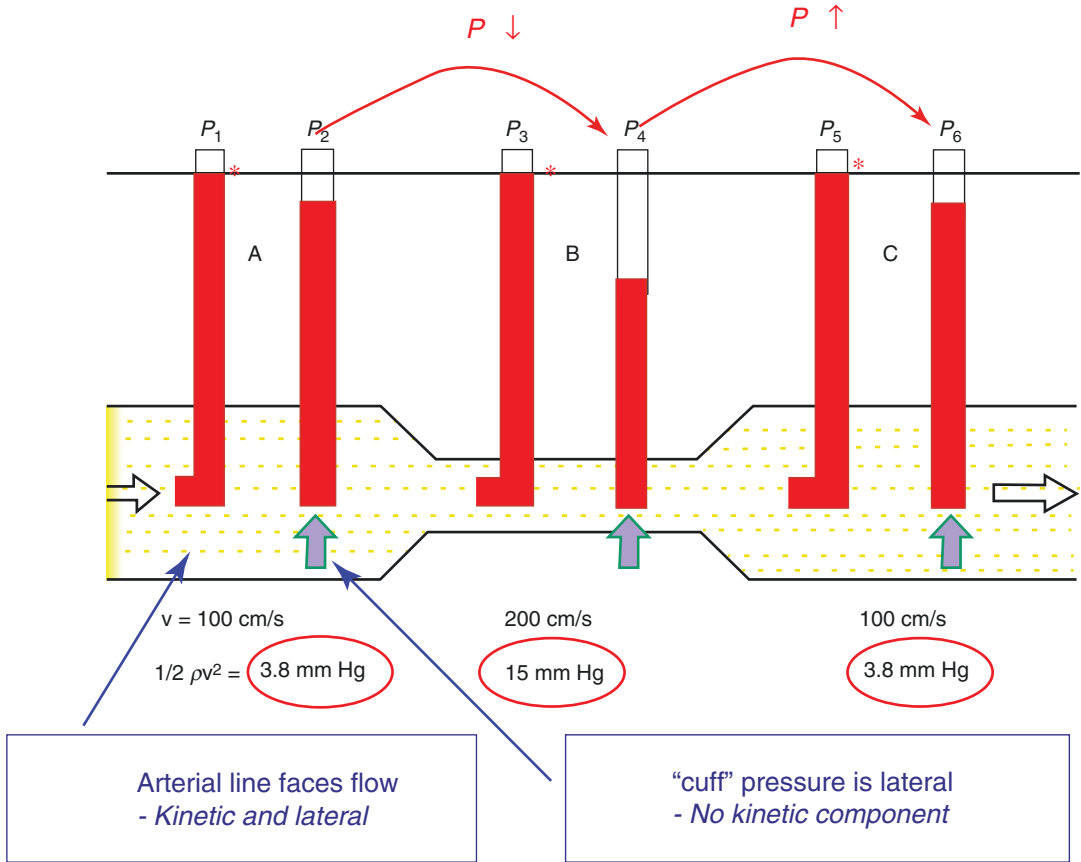


Fig. 8.2 The importance of elastic and kinetic energies for measurements of pressure and for pathological processes. The schematic represents flow through a tube with minimal loss of energy due to friction over its length. The velocity (v) at the start is 100 cm/s and kinetic energy per volume ($1/2 \rho v^2$, where ρ is density and v is velocity) is 3.8 mmHg. This energy is detected by the catheter at P1 which has an opening facing the flow because it stops the flow and the kinetic energy is converted into elastic energy. P2 only measures the lateral pressure and thus

gives a lower pressure value than P1. In the constricted region, velocity must increase to conserve the same volume over time as comes in as goes out (conservation of mass), which increases the kinetic energy component. P4 is thus much lower than P3. In the last section, the vessel is wider and velocity goes back to the initial rate, and the difference between P5 and P6 is the same as at the start. When just looking at the lateral measurements, it looks like the pressure is increasing from P4 to P6 but the total energy has not changed

Figure 8.2 shows a tube that is narrowed in its middle. Pressures are measured with two types of manometers. In one type, the opening of the tube faces the direction of flow and in the other the opening is perpendicular (lateral) to the flow. There only is a negligible resistive drop from the beginning to the end of the tube. In the first section, the pressure is higher (height of the manometer) when measured with the tube that has its opening facing the oncoming flow than the pressure measured with the tube that has its opening

perpendicular to the flow (lateral pressure). This is because the fluid that directly hits the open part of the tube facing the flow is stopped, and the kinetic energy must be turned into elastic energy to maintain the conservation of energy. In the narrowed section, to conserve the movement of the same mass of blood (volume/time) from the beginning to the end of the tube, blood flow must speed up (volume/distance) to allow the same mass to pass through. This means that elastic energy must be converted into kinetic energy.

This is evident by the decrease in the lateral elastic pressure with no change in the pressure measured with the tube opening facing the oncoming flow because it includes both the kinetic and elastic energies. When the tube again widens, the velocity of blood decreases and so does the kinetic energy. The lateral pressure is back to where it was before the narrowing, and this makes it look like the flow went from a lower to higher pressure. However, the total energy remained constant throughout the tube except for a trivial loss of energy due to friction against the walls of the tube and the “layers” of flowing fluid.

From this example, it should be evident that blood pressure measured with an inflated cuff should be slightly lower than that measured with an arterial line in which the opening of the catheter faces the flow and thus “senses” the conversion of kinetic energy to elastic energy. The inverse of the example in Fig. 8.2, a tube that is wider in the middle as is the case with an arterial aneurysm, has the opposite consequence. Blood velocity in the dilated region is reduced, and kinetic energy is converted into lateral elastic energy. The lateral pressure in the aneurysm then becomes much higher than in the upstream and downstream regions. This effect is even worse when the person exercises and flow significantly increases because the velocity and thus kinetic component is even greater. The lateral force promotes further dilatation of the aneurysmal section and creates a vicious cycle. For this reason, the aneurysm must be repaired when the vessel diameter is beyond a critical size.

Kinetic energy contributes only about 3% to arterial systolic pressure (Burton 1965b). However, it potentially plays a larger role in some circumstances. In a septic patient who has a cardiac output that is twice normal, for example, 10 L/min, and the systolic blood pressure only is 80 mmHg, the kinetic component could be close to 10% of the pressure and could have a significant impact on how the pressure is measured and interpreted. As another example, the cross-sectional area of the pulmonary artery is similar to that of the aorta, and the blood flow is the same, so that the velocity of flow is the same. However, because

pulmonary artery pressure is much lower than aortic pressure, the kinetic component makes up a larger proportion of the pressure. This is not measured with opening of most catheters facing away from the flow, whereas catheters measuring aortic pressure most often face the flow. If a catheter with a transducer at the tip or a fluid-filled catheter with a hole placed laterally, the kinetic component is not detected. Kinetic energy also makes up a greater proportion of venous pressures. This is because the sizes of the inferior and superior venae cavae are similar to the descending aorta. This means that flows and velocities are similar and thus the kinetic energy is the same, but the lateral pressures are lower.

Gravitational Energy

The third energy type is gravitational energy (Burton 1965a). Our bodies always are being accelerated towards the centre of the earth by gravity, but this force is resisted by the structures below us. This force is all around us all the time but we do not think about it because it is our baseline state. However, it is very noticeable to astronauts returning from space. Gravity does not have a major impact on haemodynamics when in the supine position because the height differences are small and all parts of the body are affected fairly equally. However, even when supine, there still is a significant force difference between the top and bottom of the body that can affect fluid filtration from capillaries. Where gravity really counts is in the upright posture, which is how we as bipeds spend most of our time. The key variable in the force of gravity is height. Figure 8.3 shows a man in the supine position. The mean pressure at the level of the heart is 100 mmHg. There is only a small pressure drop due to resistance along the major vessels so that in this case, the pressure in the arteries of the feet and head only are 5 mmHg lower than at the level of the heart. Gravity plays no significant role. However, things are dramatically different when the person stands up. In this example, the man is 180 cm in height (71 inches). The height of a column of

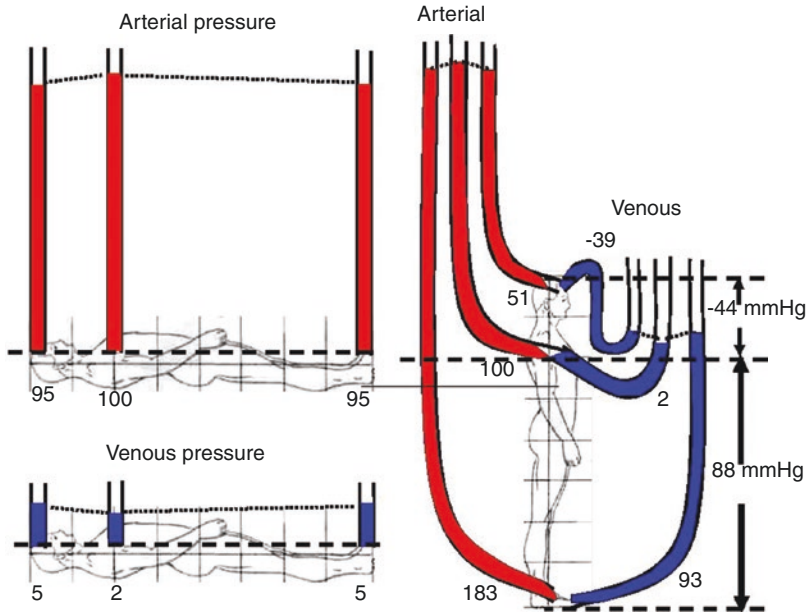


Fig. 8.3 Gravitation effect on arterial and venous pressures. On the left side, in the supine position, the effect of gravity is minimal. The dotted lines indicate the reference level at the midpoint of the right atrium. The arterial pressure is 100 at the level of the heart and the venous pressure is 2 mmHg. There is a 5 mmHg arterial pressure drop from the heart to the head and foot due to resistance and 2 mmHg for the returning venous blood. The right side of the figure indicates the person in the upright posture. His height is 182 cm. The dotted line again indicates the refer-

ences at the heart. The numbers on the right in mmHg indicate added gravitational energy to the pressures in the feet and loss of energy to vessels in the head with the same arterial pressure of 100 mmHg at the level of the heart and 2 mmHg of venous pressure. The arterial pressure is this example is 183 mmHg in the foot and 51 mmHg in the head. See text for further details. (From Magder 2014. Used with permission of Wolters Kluwer Health, Inc.)

fluid has a weight because of the acceleration due to gravity of the mass of the fluid in the column. The density of water is 1 (mass/volume) so that the force is simply the height in cm of water times the gravitational constant. This can be converted to the usual mmHg unit by multiplying by the density of mercury which is 13.6 times the density of water and accounting for the conversion from cm to mm which gives 1.36. Accordingly, the addition of the gravitational force to the elastic force gives an arterial pressure of 183 mmHg in the foot. More strikingly, the pressure in the arteries perfusing the top of the head only is 51 mmHg. In someone who is 198 cm tall (6' 6") and has a pressure of 120/80 mmHg at the level of the heart, the systolic pressure at the top of the head only is 69/29 mmHg. This likely imposes a limit on how tall humans can be.

Why Is Mammalian Arterial Pressure Set So High Compared to Lower Species?

After the previous discussion, it may seem that at high pressure is needed to perfuse the head. However, the arterial pressures of mice and rats are similar to humans, and they do not have a gravitational challenge. It is higher in all mammals, and even higher in birds, than any other animals. A high pressure also is not simply necessary to maintain cardiac output in the range of 5 L/min. The right heart of the averaged-sized male heart pumps 5 L/min through the lungs with a systolic pressure of less than 20 mmHg. Blood pressure also is not higher in whales and elephants. There are two important advantages for high aerobic mammals and birds to have high systemic arterial pressures. First, by starting with a high arterial

pressure, blood flow can be selectively increased to different regions of the body by decreasing the local resistance in the area of need (Magder 2018; Burton 1965a). The alternative approach would have required decreasing the already very low resistances in the areas that need more flow. This would have required producing a very large increase in the vessel diameters of the regions in need of more flow. More space would be needed for the dilated vessels and blood volume would be sequestered thereby decreasing the effective volume for venous return. The pulmonary circuit actually increases its flow through recruitment and dilatation of pulmonary vessels when flow increases but this works because the whole organ dilates with only a modest redistribution of blood flow; the net effect is an increase in flow with little change in pressure. Another strategy could have been to significantly vasoconstrict all regions except for the region that requires more flow. However, this would compromise local metabolic regulation of the non-working regions and require a lot more central neural coordination. The second advantage of starting with a high arterial pressure is that the load on the left ventricle can remain relatively constant. This is important because generating pressure is a much greater stress on heart muscle than ejecting volume. Even at peak exercise and the need for high tissue flow the arterial pressure of a healthy young person does not increase much above the normal value. This increase in flow can occur because the major vasodilation in the working muscles. This brings us to the next topic, and the most difficult one, which is the distribution of regional flows.

Regional Distribution of Flow

I will first begin with some basic principles. When resistances are in series, the total resistance is the sum of all the resistances in the series (Ross 1985):

$$R_{\text{total}} = R_1 + R_2 + R_3 + R_4 + \mathbf{n} \quad (8.6)$$

For example, the total resistance from the aorta to the capillaries is the sum of the resistance in the aorta, large arteries, smaller arteries, arterioles, and pre-capillary sphincters. The significance of

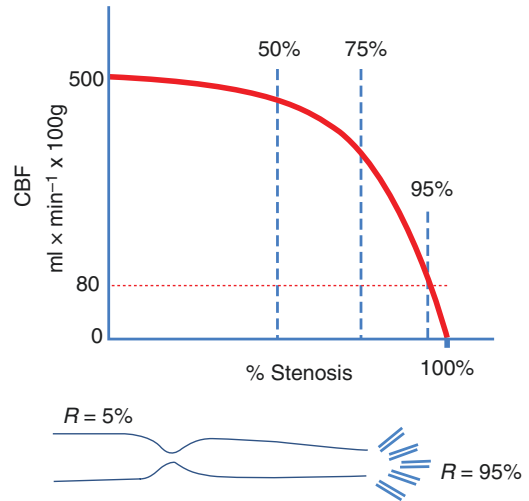


Fig. 8.4 Effect of stenosis in epicardial coronary artery on coronary blood flow (CBF). The bottom of figure indicates that the epicardium contributes only 5% of the total coronary arterial resistance and the arterioles (100–200 μm) make up $\sim 95\%$. Thus, a proximal stenosis can be adequately compensated by downstream dilation (until there is a $>75\%$ proximal stenosis. Resting flow (dotted line) is not compromised when the stenosis is $>95\%$

this is that the narrowest region dominates the pressure drop. The major resistance, and thus major pressure drop, occurs at the level of small arteries and arterioles, which are in the 100–200 μm size. The significance of this is very evident in coronary artery disease (Fig. 8.4). Coronary stenoses occur in the large epicardial conductance vessels, which normally contribute very little to the pressure drop along the coronary arteries. Thus, a major narrowing of epicardial vessels can be readily compensated by dilation of the major downstream resistance vessels (Ross 1985; Gould et al. 1975; Gould and Lipscomb 1974; Gould 2009). Because of this, a coronary stenosis of 50% only has a minimal effect on maximum coronary flow, and coronary flow does not become limited enough to be symptomatic until there is a greater than 70% stenosis. Resting symptoms are not present until the proximal stenosis is $>90\%$.

Blood flows to the different organs are in parallel. Total resistance through a vascular bed with parallel resistances is given by (8.5):

$$1/R_{\text{total}} = 1/R_1 + 1/R_2 + 1/R_3 + 1/R_4 + \mathbf{n} \quad (8.7)$$

The rationale is that the greater the number of parallel channels, the greater the total cross-sectional area and the lower the total resistance.

The greatest flow occurs in the path of least resistance (i.e., greatest cross-sectional area). The distribution of blood flow to different parts of the body is based on the relative vascular resistances of the different parts as represented in Fig. 8.5a by their individual pressure vs flow lines, which represent conductance or 1/resistance (Ross 1985). At rest, the greatest proportion of flow goes to the muscle region because it comprises the large proportion of total body mass, and its vessels have the largest cross-sectional area. The next largest proportion is the splanchnic region because it is metabolically active and has a large area. Although the kidneys are small, only about 250 g each, they have a large blood flow because of their role in filtering blood. Brain blood flow accounts for ~15% of the total because of its active metabolic rate. In comparison, at resting heart rates of around 70 b/min, the heart only takes up about 5% of cardiac output because of its small mass.

The pattern looks quite different when the flows are normalized to tissue mass; this allows the importance of local metabolic activity of the tissues to be more evident (Fig. 8.5b). In this analysis, resting flow to the muscle is very low and flow to the heart is proportionally higher. Proportional flows per weight to the brain and splanchnic regions are not as high because although they are active regions, they are not as metabolically active as the heart and the flow to the kidney is not related to metabolic activity.

Flows to regions can increase by decreasing their local resistances. The minimal resistance (or greatest conductance) of a region determines the maximum possible flow for a given blood pressure (Magder 1986). Renal resistance is close to its minimum at baseline and it thus only has a small reserve to increase its flow (Figs. 8.5 and 8.6). This makes it very vulnerable to a fall in pressure. The splanchnic bed and brain, too, change little with increased metabolic activity because the range of changes in their metabolic activity is small. Skeletal muscle has a very large

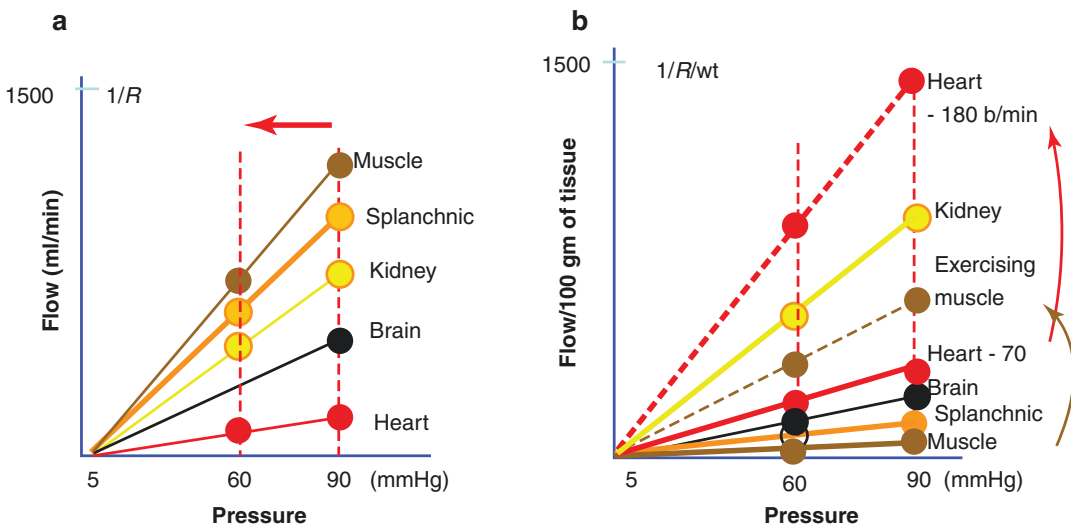


Fig. 8.5 Hypothetical pressure flow relationships of major vascular regions. (a) Regional pressure–flow (P - F) relationships for muscle, splanchnic region, kidney, brain, and heart (based on data from Magder 1986; Hoffman 1984) based on actual flow. The slope of the lines is conductance or 1/resistance. (b) The same relationships with flow are normalized by the weight (100 g) of the organ.

The slope of the muscle P - F now is small; it increases markedly with exercise (curved arrow) as does that to heart with an increase in heart rate from 70 to 180 b/min (curved arrow). The heart has the highest flow capacity per weight of tissue of the major vascular beds and has a marked capacity to increase vascular conductance (decrease in resistance)

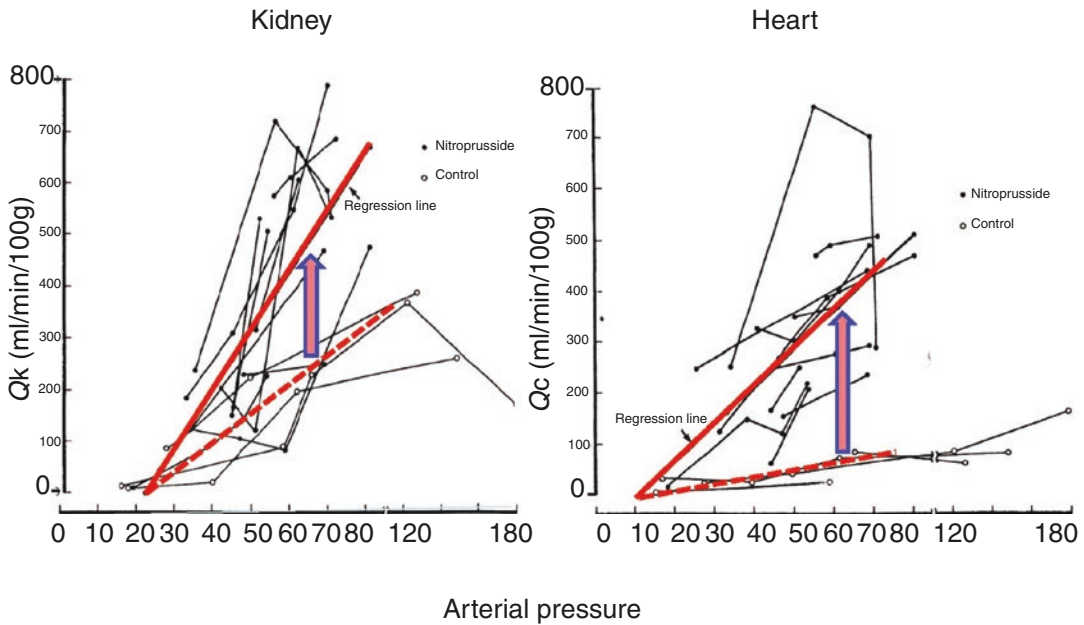


Fig. 8.6 Pressure-flow (P - F) lines for kidney (left) and heart (right) obtained in dogs under baseline condition and after maximal dilatation of the vasculature with nitroprusside. P - F relations were obtained by haemorrhaging the animals and blood flow was measured with radio-labelled microspheres. The solid line indicates the P - F for the maximally dilated state and the hashed lines the non-dilated

state. The peak flows at a given pressure are higher in the kidney than in the heart. However, the kidney starts close its maximal P - F line and thus has much less reserve. The coronary vasculature heart has a very large capacity to dilate. Note that the dilated coronary flow was still above the non-dilated value at very low arterial pressures. (From Magder 1986, *APS journal* – no permission needed)

capacity to increase its flow (Fig. 8.5b). During exercise, blood flow to large working muscles can go from less than 5–10 ml/min/100 g to 200 ml/min/100 g. The heart is the most impressive of all. Its resting flow is in the range of 80 ml/min/100 g of tissue and can reach 500 ml/min/100 g of tissue at peak heart rate (Figs. 8.4, 8.5, and 8.6) (Hoffman 1984). It thus has a very large vasodilatory reserve, which is far larger than any other tissue (Magder 1986). Of course, this assumes that there is no proximal coronary artery stenosis.

The issue of relative resistances brings up a very important point for resuscitation. Equation 8.3 indicates that arterial pressure is approximated by the product of cardiac output and systemic vascular resistance. If arterial pressure falls because cardiac output falls (Fig. 8.5), and only a vasopressor is given to increase arterial pressure, total flow does not change, nor will the flow in any region change unless the distribution of flow changes (Fig. 8.7) (Magder 2011; Thiele et al. 2011a, b). This emphasizes the earlier point that pressure

does not indicate flow, and vasoconstriction by itself only produces what is called a “tangible bias” in that the pressure on the monitor increases but O_2 delivery to tissues does not change. This is most evident with the use of phenylephrine, a pure alpha agonist with no significant effect on cardiac contractility (Thiele et al. 2011a, b). The only way that a region can benefit by vasopressor therapy is for that region to constrict less proportionally than other regions. This could happen if its local regulatory mechanisms override the effect of the exogenous vasoconstrictor (Berne 1964a, b; Guyton et al. 1964), but this is hard to predict and less likely to be the case at high doses of vasopressors. It also means that some other regions lost out. The message is that if the blood pressure falls because of a fall in cardiac output, cardiac output must rise to correct the perfusion deficit. At the other extreme, if all regional resistances decrease proportionately, the same cardiac output can be delivered at a lower pressure (Fig. 8.8). As an example, as noted at the start of this chapter, it is not uncommon to see women, and sometimes

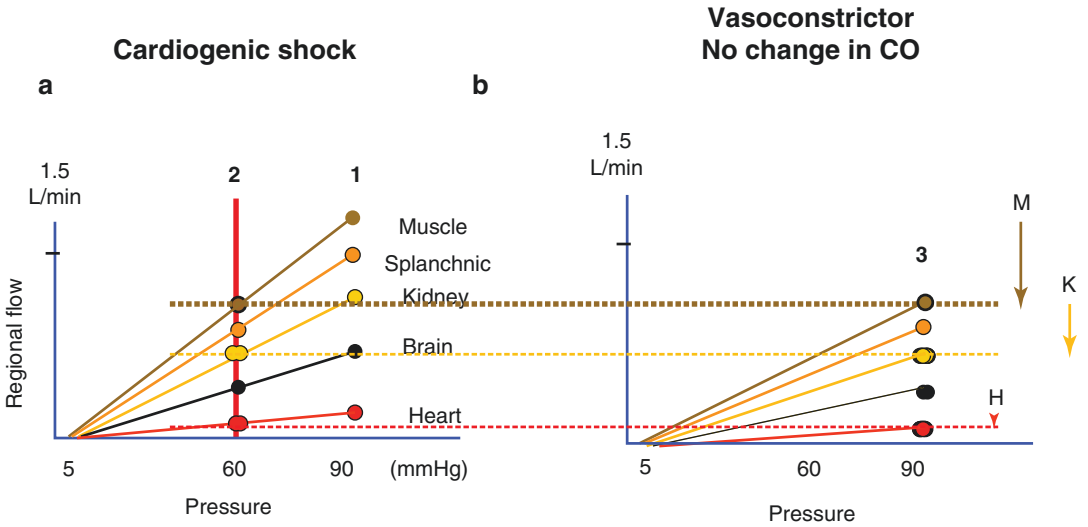


Fig. 8.7 Hypothetical regional pressure–flow relationships during cardiogenic shock and in response to a vasoconstrictor. Regional flows are based values from ref. (Magder 1986). The *x*-axis is arterial pressure (mmHg) and the *y*-axis flow (L/min). The slope of the lines is conductance, the inverse of resistance ($1/R$). (a) The initial values are at (1). At (2) cardiac output falls without any reflex adjustment. The graph (b) shows what would happen if resis-

tance increased by a similar amount in all regions but without any change in cardiac output. (3) The vasoconstrictor restored the mean pressure to 90 mmHg but flows in each region remain the same as indicated by the dotted lines. The downward arrows mark the decrease in flow from baseline for the muscle (M), kidney (K), and heart (H) that would occur without any local autoregulation

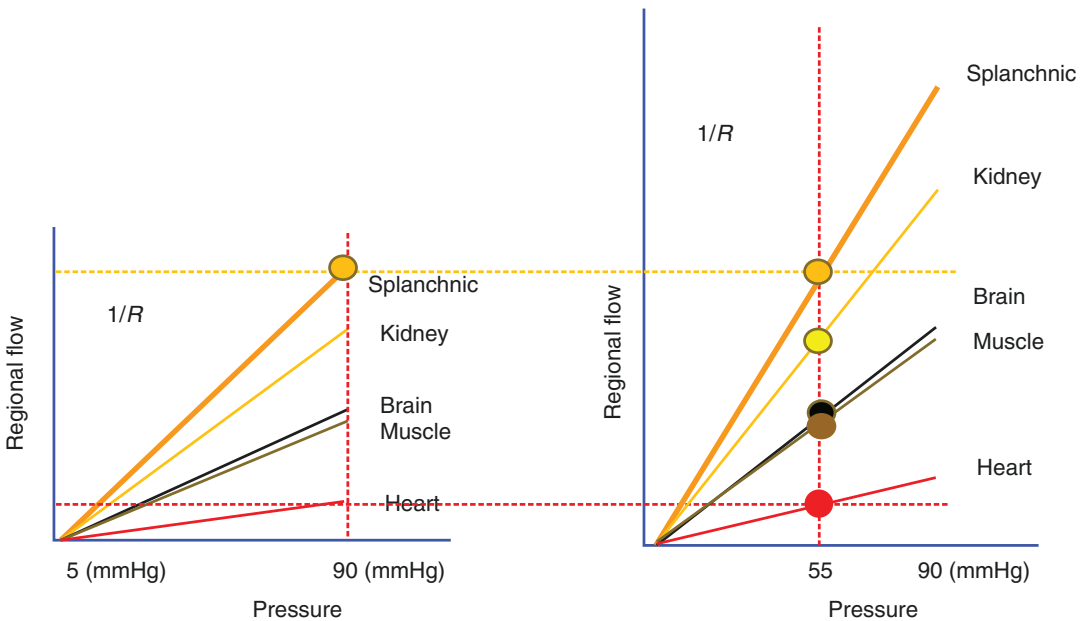


Fig. 8.8 Hypothetical regional *P-F* relationships with a proportionally equal dilation of all vascular regions. The left side shows the same starting *P-F* relationships as in Fig. 8.5. On the right side, all the *P-F* slopes have been increased (decreased resistance) proportionately. The dot-

ted lines show that the same initial resting flows can be maintained at 55 mmHg (the splanchnic and cardiac flows are marked by dotted lines). However, it is worth noting that the kidney likely does not have the vasodilatory reserve to reach this value

men, with systolic pressures less than 90 mmHg and still be perfused normally. This indicates that all their regional resistances are proportionally lower than normal and this allows their normal distribution of blood flow. This has important implications for the management of the markedly reduced systemic vascular resistance in patients with septic shock. If resistances have decreased proportionally in all regions, even low blood pressures can be tolerated. However, it is more likely that resistance does not decrease proportionally and that the greatest decrease is in the peripheral muscle bed because it has a large proportional mass and large dilatory reserves. It also is possible that mitochondrial dysfunction sends signals which are equivalent of normal metabolic signals. In contrast to the muscle bed, renal resistance starts close to its minimum value and cannot dilate much more (Fig. 8.6). The kidney, thus, is the most vulnerable of all organs and usually the first to fail. Because it is so sensitive, renal function may not be the best target in resuscitation protocols because trying to protect it may compromise other more important regions for survival.

The concept of regional resistances potentially is important when considering use of high doses of vasoactive drugs. The typical baroreceptor response to hypotension is an increase in systemic vascular resistance. This vasoconstriction is greater in peripheral muscle beds than in the splanchnic region (Hainsworth et al. 1983), which from an evolutionary point of view makes sense because the constriction will have less consequences for muscles than on the metabolically active and more delicate splanchnic region. The difference responses in the two regions is most likely due to differences in receptor densities. Presumably, the same selectivity occurs when exogenous vasoconstrictors are given at moderate doses, which provides a more physiologically appropriate response. However, although speculative, it is quite possible that this selectivity is lost at higher vasopressor doses and consequently there is increased vasoconstriction everywhere which disturbs normal flow distribution and compromise perfusion of vital organs, especially if there is no increase in cardiac output. Furthermore, vasoconstrictors also can increase the resistance

to venous return which decrease cardiac output and makes matters worse. The problem for clinicians is that it is currently not known what constitutes a “high” dose of vasopressors which would produce a loss of vasopressor selectivity.

Critical Closing Pressure

Systemic vascular resistance classically is calculated from the difference between mean aortic pressure and central venous pressure. However, it has been shown that there is a critical closing pressure (Permutt and Riley 1963), or flow limitation, at the arteriolar level. Starling understood the importance of this for the regulation of flow and the constancy of the load on the heart (Patterson and Starling 1914) (Fig. 8.9). He inserted a floppy tube, which is now called a Starling resistor, in the arterial circuit of his heart-lung preparation. By controlling the pressure around the floppy tube, he could regulate the downstream pressure faced by the heart and thereby study the effects of changes in afterload. The value of critical closing pressures varies throughout the vasculature. A critical closing pressure of about 25–30 mmHg has been demonstrated in the coronary circulation under baseline conditions (Bellamy 1978; Kloche et al. 1981; Dole et al. 1984) and a value greater than 60 mmHg in resting skeletal muscle (Magder 1990). An average for the whole body has been demonstrated in dogs by obtaining pressure–flow relationships of cardiac output versus arterial pressure; the value was around 30 mmHg (Sylvester et al. 1981). The critical closing pressure in the hind limb of a dog has been shown to decrease with exercise (Magder 1990), reactive hyperemia (Magder 1990), adenosine (Shrier and Magder 1997), calcium channel blockers (Shrier and Magder 1995a), and is raised by alpha agonists (Shrier and Magder 1995b), a reduction in baroreceptor tone (Shrier et al. 1991), by myogenic response in response to a local increase in arterial pressure (Shrier and Magder 1993) which thereby tries to keep flow constant, and by inhibition of nitric oxide synthase (Shrier and Magder 1995b).

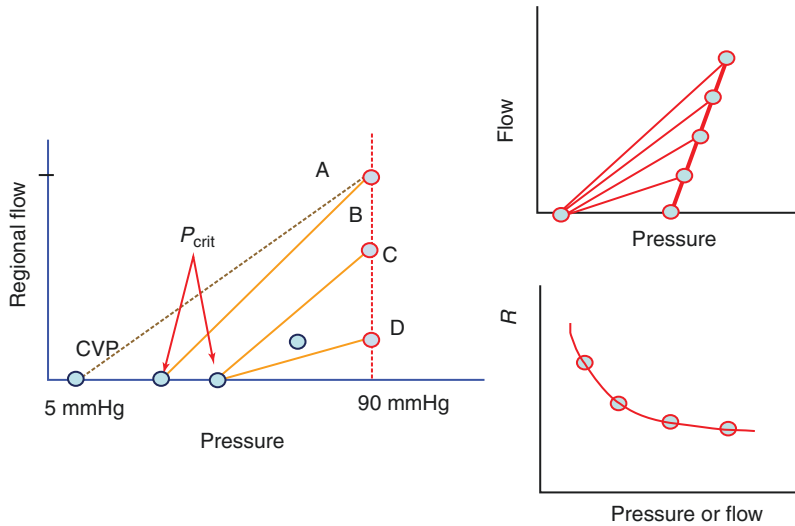


Fig. 8.9 Hypothetical P - F lines and significance of a downstream critical closing pressure on the measurement of vascular resistance. The vertical dotted line indicates three pressure values with the same arterial pressure. In A, resistance is measured in the standard way as the inverse of P - F line from the arterial pressure to the central venous pressure (CVP). In B, there is a critical closing pressure which means that the resistance (i.e., inverse of the slope of the P - F line) is actually much lower than measured by calculating the pressure difference from the arterial pres-

sure to the CVP. The right upper figure shows how the error in the slope of the P - F relationship increases as the pressure and flow fall and the bottom right shows how the resistance “appears” to increase even without any actual vasoconstriction. At C, the critical closing pressure increased without a change in the slope of the P - F line ($1/\text{resistance}$); the flow falls for the same arterial pressure. At D, the arterial resistance increased with the same critical closing pressure, and there is a further fall in flow at the same arterial pressure

When a circuit has a critical closing pressure, the pressures and the resistances downstream from the site no longer affects total flow into the region. However, factors downstream from the critical closing pressure still can affect capillary filtration and the distributions of flow in the microcirculation. The consequence of a critical closing pressure in systemic arteries is that total systemic vascular resistance (SVR) should be calculated from mean aortic to mean critical closing pressure and not to the central venous pressure because factors below the critical pressure do not affect the flow into the region. The standard calculation of SVR gives a resistance value that is much higher than the SVR calculated in the usual way and introduces an important artefact when the true resistance changes. If the critical closing pressure does not change, and the difference in pressure between the CVP and critical closing pressure do not change, the error produced by neglecting the critical closing pressure

as the true downstream pressure increases as the arterial pressure or cardiac output decrease. This makes it look like the arterial resistance is increasing when flow or pressure decrease, which would make sense physiologically, but because of the error it also could just be an artefact. As an example, milrinone has been considered by some to have no inotropic effect and to only act as a vasodilator because when milrinone is administered the SVR falls with the rise in cardiac output. However, based on the artefact just described, any increase in cardiac output will produce a decrease in calculated SVR without any actual dilation. This is not to say that milrinone does not dilate vessels, or for that matter, lower the critical closing pressure, but rather that the effects cannot be distinguished without having a number of points on a pressure-flow line. The presence of critical closing pressures also impacts on measurements of impedance and dynamic aortic elastance.

What Determines Pulse Pressure?

As discussed in Chap. 2, a pressure exists throughout the vasculature even without cardiac contractions, although it only is in the range of 8 to 10 mmHg. With each cardiac contraction, the heart pumps a stroke volume into the aorta which stretches its walls and produces a rising pressure that is modified by the run-off of volume to downstream regions with a lower pressure. The distended elastic walls of the aorta recoil after the end of systole and allow aortic flow to continue in diastole and lengthen the pulse pressure. This is called a Windkessel effect based on the mechanism in early steam engines. When the elastance of the aorta is normal, during early diastole a pressure wave moves in the opposite direction to blood flow because of reflected waves from downstream bifurcation points. These backward

waves further augment aortic pulse pressure. When aortic elastance is increased by hypertension or aging, the speed of reflected waves increase and they can come back to the heart during the ejection phase and increase the load on the left ventricle.

The primary determinants of systolic pressure in the aorta are the amount of volume entering per beat, that is, the stroke volume, and the elastance of the aortic wall. Because the elastance of the aorta is curvilinear, another variable is the volume remaining in the aorta at the onset of systole (Fig. 8.10). The greater the initial volume, the greater the pressure for a given stroke volume. The volume left in the aorta at the end of diastole is dependent upon the downstream resistance and critical closing pressure. It also can be affected by heart rate because a faster heart rate reduces the diastolic time for aortic emptying and

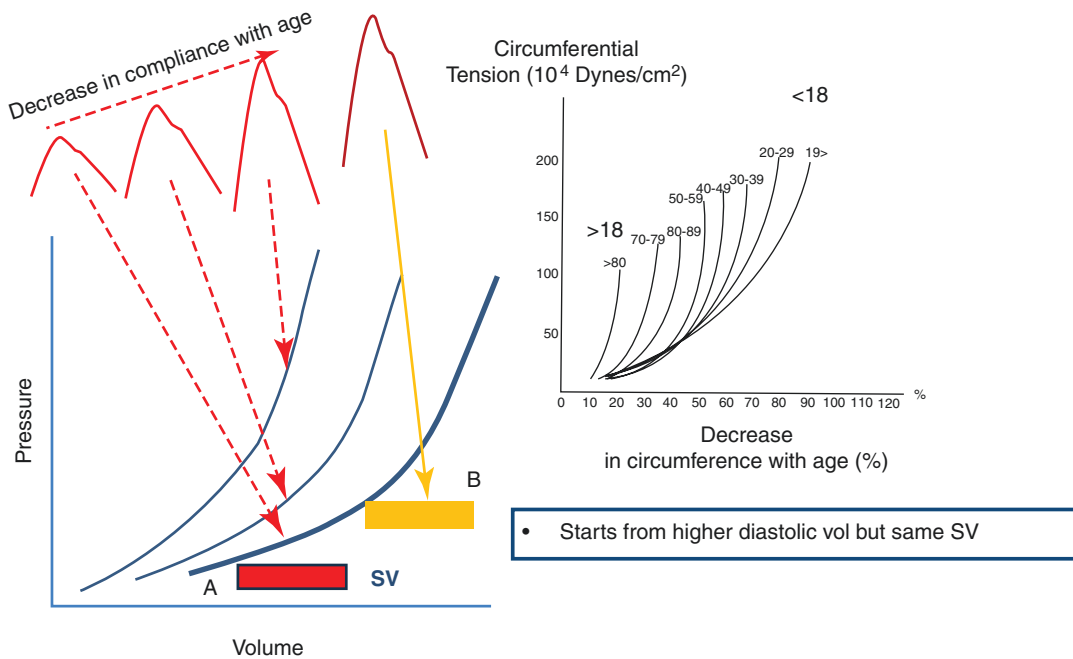


Fig. 8.10 Effect of age and initial volume on thoracic aortic elastance. Schematic pulse pressures are shown above a graph of hypothetical pressure–volume relationships in the aorta on the left and actual data of the aorta showing an increase in circumferential tension versus increases in aortic circumference in % from age <18 to >80 mmHg. (From Nakashima and Tanikawa 1971, with permission of SAGE Publications). The slope of lines in

the graphs is elastance or 1/compliance. With aging, the aorta becomes stiffer and shifts to the left. This results in increasing pulse pressure (top) for the same size SV (A) and from the same starting diastolic volume. The SV at B is the same size but starts from a higher initial diastolic volume and thus is on a steeper part of the aortic P–F curve. This results in a much larger pulse pressure for the same SV

increases the aortic volume at the end of diastole much the same way that a rapid breathing rate can lead to hyperinflation in the lungs, especially if arterial resistance is high (see Chap. 7, Heart Rate). Higher pressures also can produce a myogenic effect and increase critical closing pressures (Shrier and Magder 1993). The shape of the elastance curve also is important. Although true aortic elastance likely does not change acutely, the aorta becomes stiffer with age, with chronic hypertension, and potentially, with other chronic processes (Nakashima and Tanikawa 1971). A stiffer aorta produces a larger pulse pressure and the increased pressure leads to further increases in aortic elastance by the induction of compensatory transcriptional mechanisms in vascular walls. For all these reasons, pulse pressure is related to stroke volume, but the relationship is not direct.

Impedance

The arterial waveform is determined by a pressure wave, a velocity wave, downstream resistance, the capacitance effect from the arterial elastance, and reflected waves (O'Rourke 1971, 1990). It thus is argued that the load on the heart is best evaluated by assessing the impedance to flow in the frequency domain instead of the time domain. This allows a decomposition of the various components of the waveform and is discussed in detail in Chap. 9. However, in the intensive care unit, we mostly are concerned with determinants of cardiac output, and the major determinant of this in the impedance analysis is the arterial resistance and the downstream critical closing pressure. The aortic elastance is a major determinant of the wave patterns, but elastance is a function of the make-up of the walls of the vessels and does not change rapidly in acute illness because changes are required in the composition of the vascular walls. In some studies, attempts have been made to assess arterial elastance under acute conditions, but what most likely is being observed is a change in downstream resistance or the critical closing pressures. Factors in the impedance analysis can affect the magnitude of

the pulse pressure, shape of the pulse, and the pattern of downstream transmission, but these only have a small impact on cardiac output and thus on O₂ delivery, which is the primary concern for tissue perfusion. I thus have not included impedance as a major factor in this chapter (for discussion see Chap. 9). Its analysis also is not feasible in most critically ill patients.

Where Should Pressure Be Measured and Which Pressure?

Because of reflected waves, the pulse pressure increases the farther away the pulse is from the aortic valve. It thus has been argued that aortic pressure ideally should be measured at the aortic valve, and a tonometric technique has been developed to estimate this value. This central aortic pressure likely is important for understanding the physical forces that induce cardiac hypertrophy, but this pressure likely is not very significant determinant of regional flows. The assumptions required to estimate the central pressure in critically ill also likely are not valid in patients with distributive shock.

More proximal sites for pressure measurement, such as the femoral artery or brachial artery, often are recommended for monitoring patients in shock. This is based on the potential for the more peripheral radial artery pressure to be damped. There also is data indicating that when these more proximal sites are used, less catecholamines are needed, especially in cardiac surgery patients (Lee et al. 2015; Dorman et al. 1998; Kim et al. 2013). However, I have found that this often is just another tangible benefit. If it is known that proximal values are higher than a radial artery pressure, then why not just accept the lower radial artery value and save potential complications from the more proximal sites!

The question also arises as to which pressure to use: systolic, mean, or diastolic. The mean is the most frequently used with indwelling catheters and today the mean is commonly obtained with automated cuff-compression techniques. Use of the mean avoids under or over-damping errors with indwelling catheters (Gardner 1981). It also is

thought that it better indicates organ perfusion pressures. Much of this has come from studies examining the ideal perfusion pressure for the kidney (Bersten and Holt 1995), and most from studies that were performed with some kind of controlled renal blood flow with a relatively non-pulsatile pump. However, most tissues in the body receive the largest percent of their flow during systole. Furthermore, the mean is very much affected by diastolic run-off and a low diastolic pressure lowers the mean. However, for the diastolic pressure to be disproportionately lower than expected based on the observed systolic pressure, flow must continue to be emptying from the aorta during diastole and thus some regions are still being perfused.

I thus prefer the use of systolic pressure. To begin, this was the traditional measure in the emergency department or on the ward that triggered the call for the patient to be assessed when blood pressure was measured by a sphygmomanometer. There are few caveats though. When using systolic pressure with an arterial cannula, it is essential to ensure that the waveform is valid. When I am concerned about the systolic pressure, especially if it is low, I compare it to a cuff pressure. For me the gold standard is not an oscillometer, which calculates the systolic pressure, but rather the auscultated pressure or palpated pressure with a cuff. I will often use the cuff pressure as my reference and use the arterial line to rapidly detect changes in the patient's condition, which likely is the most important thing to know. In my experience, this leads to less catecholamine use than occurs with use of the mean pressure. However, there is no outcome data to know if this is valid.

There is a school of thought that argues that diastolic pressure is an important value to monitor (Hamzaoui and Teboul 2019). The basis of the argument is that diastolic pressure is important for coronary blood flow, and therefore there is a minimal coronary perfusion pressure that needs to be maintained. On the other hand, coronary flow reserves are very large and can be maintained with very low pressures (Magder 2019). However, this assumes that there are no significant proximal coronary lesions which then require higher perfusion pressures. My approach is to not follow the diastolic pressure because this leads to higher

concentrations of vasopressors, which also have been found to be harmful. However, if signs of myocardial ischemia appear, arterial pressure likely should be increased. Of note, an increase in troponin is not a reliable measure of this. These issues were recently reviewed in an online debate (Hamzaoui and Teboul 2019; Magder 2019).

Conclusion

I have not dealt in this chapter with the subject of what is the best clinical arterial target for blood pressure in the critically ill. This is because currently there is no satisfactory empiric data. An appropriate physiological prediction also cannot be made because of the complex determinants of what we measure. A crucial point is that pressure is not flow and what counts for tissue function is the flow that they receive. A central factor in the assessment of the ideal pressure is how flow is distributed based on arterial resistances feeding different organs. Unfortunately, this currently cannot be obtained in an intact person. It is likely that only carefully planned empiric studies which take into account the physiological principles linking pressure and flow will allow recommendations for best targets for blood pressure. These likely also will have to be specific for different patho-physiologies because best pressure targets will be different for haemorrhagic shock, septic shock, and cardiogenic shock. Even with general recommendations, target values will likely still need to be individualized based on the individual patient's needs. In difficult cases, an estimate of cardiac output as well as tissue perfusion should help individualize care.

References

- Bellamy RF. Diastolic coronary artery pressure-flow relations in the dog. *Circ Res.* 1978;43(1):92–101.
- Berne RM. Metabolic regulation of blood flow. *Circ Res.* 1964a;15(Suppl):261–8.
- Berne RM. Regulation of coronary blood flow. *Physiol Rev.* 1964b;44:1–29.
- Bersten AD, Holt AW. Vasoactive drugs and the importance of renal perfusion pressure. *New Horiz.* 1995;3(4):650–61.

- Burton AC. Total fluid energy, gravitational potential energy, effects of posture. *Physiology and biophysics of the circulation: an introductory text*. Chicago: Year Book Medical Publishers Incorporated; 1965a. p. 95–111.
- Burton AC. Kinetic energy in the circulation. *Physiology and biophysics of the circulation: an introductory text*. Chicago: Year Book Medical Publishers Incorporated; 1965b. p. 102–12.
- Dole WP, Alexander GM, Campbell AB, Hixson EL, Bishop VS. Interpretation and physiological significance of diastolic coronary artery pressure-flow relationships in the canine coronary bed. *Circ Res*. 1984;55(2):215–26.
- Dorman T, Breslow MJ, Lipsett PA, Rosenberg JM, Balsler JR, Almog Y, et al. Radial artery pressure monitoring underestimates central arterial pressure during vasopressor therapy in critically ill surgical patients. *Crit Care Med*. 1998;26(10):1646–9.
- Gardner RM. Direct blood pressure measurement—dynamic response requirements. *Anesthesiology*. 1981;54(3):227–36.
- Gould KL. Does coronary flow trump coronary anatomy? *JACC Cardiovasc Imaging*. 2009;2(8):1009–23.
- Gould KL, Lipscomb K. Effects of coronary stenoses on coronary flow reserve and resistance. *Am J Cardiol*. 1974;34(1):48–55.
- Gould KL, Lipscomb K, Calvert C. Compensatory changes of the distal coronary vascular bed during progressive coronary constriction. *Circulation*. 1975;51(6):1085–94.
- Guyton AC, Carrier O Jr, Walker JR. Evidence for tissue oxygen demands as the major factor causing autoregulation. *Circ Res*. 1964;15(Suppl):60–9.
- Hainsworth R, Karim F, McGregor KH, Rankin AJ. Effects of stimulation of aortic chemoreceptors on abdominal vascular resistance and capacitance in anaesthetized dogs. *J Physiol*. 1983;334:421–31.
- Hamzaoui O, Teboul JL. Importance of diastolic arterial pressure in septic shock: PRO. *J Crit Care*. 2019;51:238–40.
- Hoffman JJ. Maximal coronary flow and the concept of coronary vascular reserve. *Circulation*. 1984;70(2):153–9.
- Kim WY, Jun JH, Huh JW, Hong SB, Lim CM, Koh Y. Radial to femoral arterial blood pressure differences in septic shock patients receiving high-dose norepinephrine therapy. *Shock*. 2013;40(6):527–31.
- Kloche FJ, Weinstein IR, Klocke JF, Ellis AK, Kraus DR, Mates RE, et al. Zero-flow pressures and pressure-flow relationships during single long diastoles in the canine coronary bed before and during maximum vasodilation. *J Clin Invest*. 1981;68:970–80.
- Lee M, Weinberg L, Pearce B, Scurrah N, Story DA, Pillai P, et al. Agreement between radial and femoral arterial blood pressure measurements during orthotopic liver transplantation. *Crit Care Resusc*. 2015;17(2):101–7.
- Magder SA. Pressure-flow relations of diaphragm and vital organs with nitroprusside-induced vasodilation. *J Appl Physiol*. 1986;61:409–16.
- Magder S. Starling resistor versus compliance. Which explains the zero-flow pressure of a dynamic arterial pressure-flow relation? *Circ Res*. 1990;67:209–20.
- Magder S. Phenylephrine and tangible bias. *Anesth Analg*. 2011;113(2):211–3.
- Magder SA. The highs and lows of blood pressure: toward meaningful clinical targets in patients with shock. *Crit Care Med*. 2014;42(5):1241–51.
- Magder S. The meaning of blood pressure. *Crit Care*. 2018;22(1):257.
- Magder S. Diastolic pressure should be used to guide management of patients in shock: PRO. *J Crit Care*. 2019;51:241–3.
- Nakashima T, Tanikawa J. A study of human aortic distensibility with relation to atherosclerosis and aging. *Angiology*. 1971;22(8):477–90.
- O'Rourke MF. The arterial pulse in health and disease. *Am Heart J*. 1971;82(5):687–702.
- O'Rourke RA. The measurement of systemic blood pressure; normal and abnormal pulsations of the arteries and veins. In: Hurst JW, Schlant RC, Rackley CE, Sonnenblick EH, Kass Wenger N, editors. *The heart*. 7th ed. New York: McGraw-Hill; 1990. p. 158–60.
- Patterson SW, Starling EH. On the mechanical factors which determine the output of the ventricles. *J Physiol*. 1914;48(5):357–79.
- Permutt S, Riley S. Hemodynamics of collapsible vessels with tone: the vascular waterfall. *J Appl Physiol*. 1963;18(5):924–32.
- Ross J Jr. Dynamics of the peripheral circulation. In: West J, editor. *Best and Taylor's physiological basis of medical practice*. 11th ed. London/Baltimore: Williams and Wilkins; 1985. p. 119–31.
- Shrier I, Magder S. Response of arterial resistance and critical closing pressure to change in perfusion pressure in canine hindlimb. *Am J Physiol*. 1993;265:H1939–H45.
- Shrier I, Magder S. The effects of nifedipine on the vascular waterfall and arterial resistance in the canine hindlimb. *Am J Physiol*. 1995a;268:H372–H6.
- Shrier I, Magder S. N G -nitro-L-arginine and phenylephrine have similar effects on the vascular waterfall in the canine hindlimb. *Am J Physiol*. 1995b;78(2):478–82.
- Shrier I, Magder S. Effects of adenosine on the pressure-flow relationships in an in vitro model of compartment syndrome. *J Appl Physiol*. 1997;82(3):755–9.
- Shrier I, Hussain SNA, Magder S. Carotid sinus stimulation influences both arterial resistance and critical closing pressure of the isolated hindlimb vascular bed. *Clin Invest Med*. 1991;14(4):A13.
- Sylvester JL, Traystman RJ, Permutt S. Effects of hypoxia on the closing pressure of the canine systemic arterial circulation. *Circ Res*. 1981;49:980–7.
- Thiele RH, Nemergut EC, Lynch C III. The physiologic implications of isolated alpha 1 adrenergic stimulation. *Anesth Analg*. 2011a;113(2):284–96.
- Thiele RH, Nemergut EC, Lynch C III. The clinical implications of isolated alpha 1 adrenergic stimulation. *Anesth Analg*. 2011b;113(2):297–304.



Pulsatile Haemodynamics and Arterial Impedance

9

David Fitchett and Michael F. O'Rourke

The arterial system acts as a conduit to deliver oxygenated blood to the tissues, and as a compliant cushion to dampen pressure and flow oscillations and convert the intermittent flow input from the left ventricle into a near-continuous flow output at tissue level. The intermittent ejection of blood from the left ventricle into the aorta results in pulsatile pressure and flow throughout the arterial system. The time sequence and magnitude of left ventricular ejection is determined by the coupling between the hydraulic load imposed by the arterial system and the contractile status of the left ventricle. The instantaneous value of the pulsatile pressure and flow in the arterial system is, in turn, determined by both the left ventricular ejection and the properties of the arterial system.

In this chapter, we will consider the properties and models of the arterial system that provide a quantitative description of the observed physiology. The chapter will discuss how changes to both the arterial system and cardiac function influence pressure and flow waves measured at various locations in the arterial tree, to better understand problems of left ventricular/arterial

interaction which occur with ageing and in disease.

The elastic properties of the arterial system afford a buffer or cushion, to limit the rise in pressure that occurs as the heart ejects the stroke volume into the aorta. Stephen Hales in the eighteenth century likened the arterial system to the air reservoir of a fire engine which changed the intermittent input of water from the hand pump, to a steady flow at the nozzle. (Fig. 9.1) – now termed the Windkessel model.

While the Windkessel model of the arterial system provides a simple quantitative description of pressure measurements resulting from intermittent flow, it fails to reproduce observed changes in arterial pressure and flow waves throughout the arterial network. In particular, pressure and flow waves travel at a finite speed in the arterial tree, and are reflected at points of discontinuity, particularly at the entry to high resistance, low-calibre arterioles (as originally suggested by William Harvey 1957).

Figure 9.2 shows pressure in the ascending aorta of a rabbit under three conditions, which are also seen in humans when (1) blood pressure is high, the aorta is stiff and the rate at which the pressure wave travels (the pulse wave velocity) is high, (2) normal conditions where reflection from points of discontinuity is apparent as a prominent diastolic wave, and (3) an arteriolar dilating drug has decreased wave reflection (Wetterer 1954; O'Rourke 1970a). These pressure and flow waves

D. Fitchett (✉)
Department of Cardiology, St Michael's Hospital,
University of Toronto, Toronto, ON, Canada

M. F. O'Rourke
St. Vincent's Hospital, Department of Cardiology, St
Vincent's Clinic, Sydney, NSW, Australia
e-mail: m.orourke@unsw.edu.au

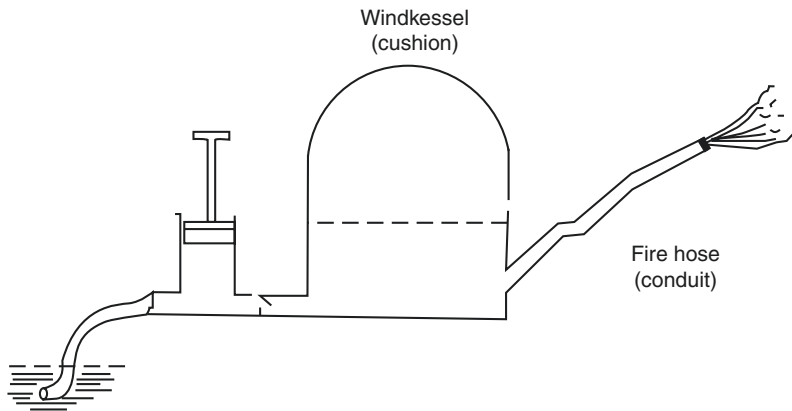


Fig. 9.1 The arterial system was compared to the fire engine of the eighteenth century by Stephen Hales. The ejection of water into the dome results in compression of the air – storing elastic energy which is returned between

pump strokes converting the intermittent flow from the pump into a continuous flow delivered to the fire hose. (Reprinted from Hales 1769)

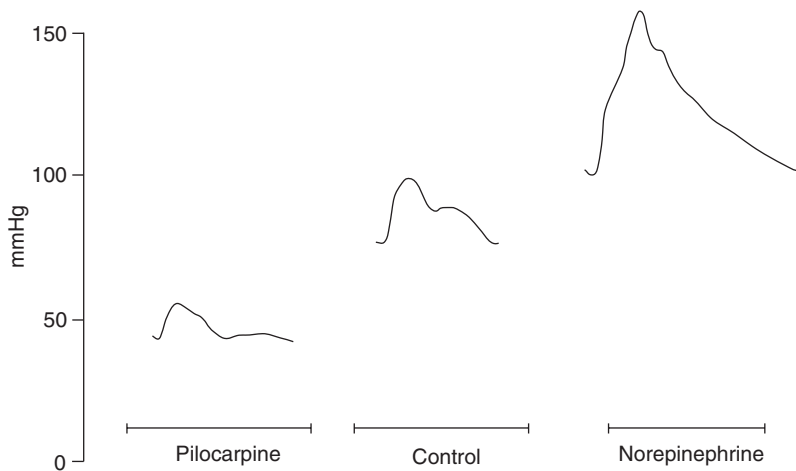


Fig. 9.2 Changes in ascending aortic pressure and flow in a rabbit (1) with severe hypertension induced with norepinephrine, (2) Control state (3) with hypotension induced with pilocarpine. Under normal resting states there is a prominent diastolic wave due to wave reflec-

tions. With severe hypertension the reflected wave returns earlier enhancing systolic pressure. During hypotension reflected waves are reduced. (Data from Wetterer (1954). Reproduced from O'Rourke (1970a) with permission of Wolters Kluwer Health, Inc.)

were recorded in the same animal just minutes apart. It is clear that the Windkessel model is inappropriate when blood pressure, heart rate, vasomotor tone, and cardiac properties are changing. The Windkessel model is of no value where it is needed most – in humans monitored during surgery and in intensive care units.

Arterial Wall Properties and Pulsatile Haemodynamics

Increased arterial stiffness and an increase of peripheral resistance are the hemodynamic determinants of hypertension (Ting et al. 1995). Hypertension increases the load on the heart and

stress on the arteries, and results in left ventricular hypertrophy, an increased risk of stroke, heart failure, renal failure and dementia.

The arterial wall shows viscoelastic properties, which can be quantified *in vivo*. Arterial compliance is the change in volume for a unit change in pressure ($\Delta V/\Delta P$). Distensibility is the compliance normalized for the initial volume of the arterial segment ($\Delta V/\Delta P)/V_0$. Peterson's elastic modulus (E_p) is the distensibility described in terms of arterial diameter: $E_p = D_o (P_s - P_d) / (D_s - D_d)$; where P_s and P_d are the systolic and diastolic arterial pressures, and D_s and D_d the systolic and diastolic diameters of the artery. The arterial stiffness or elastance is the inverse of arterial compliance or distensibility. Calculation of local arterial E_p is readily determined by vascular ultrasound measurements of systolic and diastolic arterial diameter (Baltgaile 2012) with simultaneous pressure measurements and is applicable to measurements in the aorta (ascending, arch, and descending), carotid, brachial, radial, iliac, and femoral arteries. Ideally, pressure changes should be measured at the same location as the dimension change, or using calculated central pressure determined from peripheral pressure as described below.

Arterial distensibility decreases in the axial direction (increasing when measured at a distance further from the heart) and as mean arterial pressure increases. At lower levels of distension, the elastic properties of the arterial wall result from extension of the arterial elastin, yet with greater stretch the less distensile collagen fibres take the load. Consequently, comparative measurements of elasticity, distensibility, or pulse wave velocity should be made at the same distending pressure.

Pulse wave velocity (C_o) in an elastic tube is related to the arterial elastance by the Moens-Korteweg or Bramwell-Hill equations:

$$C_o = \sqrt{V(\Delta P / \Delta V)} \quad \text{or} \quad C_o = \sqrt{(Eh / 2r\rho)}$$

where E is Young's modulus of elasticity of the artery, h wall thickness, V arterial volume, ΔP pulse pressure, and ΔV change in arterial volume. Pulse wave velocity should be distinguished from

blood flow velocity: Pulse wave velocity measures the speed of transfer of energy through the arterial wall (velocity range 4–12 m/s), whereas blood flow velocity measures the transfer of mass along the blood column (velocity range 10–100 cm/s).

Using measurements of the change of arterial radius (dR) between diastole and systole in an arterial segment, pulse pressure (dP), and blood density (ρ), the wave velocity can be calculated:

$$C_o = \sqrt{RdP / \rho 2dR}$$

Arterial pulse wave velocity is usually measured using external pressure transducers, from the time difference between the foot of the pressure wave over long arterial segments (e.g. carotid (as a surrogate for central pressure wave) to femoral) (Nichols and O'Rourke 1998). Local arterial pulse wave velocity can be determined using either ultrasound or MRI measurements of arterial flow and dimensions, in the aorta and peripheral arteries. From the central aorta to the conduit arteries in the legs, the arteries become far more numerous, smaller, and have less elastin and more smooth muscle: consequently, pulse wave velocity increases. These changes are most marked in the thoracic and abdominal aorta, and least marked in the upper limb vessels. Increasing arterial pressure reduces distensibility of the arteries, resulting in an increase in pulse wave velocity.

With ageing and hypertension, arteries become less distensile, consequently pulse wave velocity increases.

Current indices of arterial distensibility are non-linear. We seek indices which have linear relationships or where non-linearities are small, or can be controlled or allowed for. Even peripheral resistance (Mean pressure / Mean flow) is non-linear.

Up until 1960, the approach to pulsatile haemodynamics in arteries concentrated on measurements of arterial stiffness. Anatomists however pointed out how the dimensions of animals could alter wave transmission and result in reflected waves as well as waves traveling forward by increasing the number of peripheral

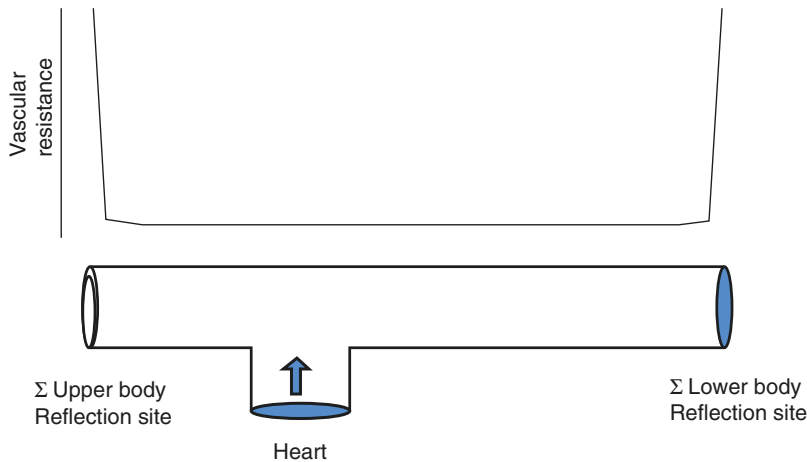


Fig. 9.3 Asymmetric T model of the arterial circulation showing the location and very abrupt change of resistance over a very short distance. (Resistance is shown on a logarithmic scale). These marked impedance mismatches provide multiple reflecting sites that can be lumped into upper and lower body sites. In this model, the lower body is the major reflection site with less intense reflections

returning from the upper body as a consequence of the low resistance cerebral vasculature. The measured pressure and flow waves result from the interaction of forward and reflected waves from both sites. (Reproduced based on diagram from O'Rourke et al. (2018) with permission of Oxford University Press)

branches, their distance from the heart and their cross-sectional area (Milnor 1979). Moreover, such reflected waves have the potential to interfere with outgoing pulse wave in the proximal arteries augmenting systolic pressure and reducing mean diastolic pressure on the pulse wave velocity. The nature and degree of such augmentation will depend on the pulse wave velocity.

Of great significance is the recent recognition of the importance of the location of the peripheral resistance vessels being just a few millimetres from the low resistance conduit arteries (O'Rourke et al. 2018). This confirms the work of Hamilton, Dow (Hamilton 1939), Remington (Remington and Wood 1956), and others that the peripheral resistance is the site of strong wave reflection (Fig. 9.3).

Vascular Impedance

A large jump in the field took place in the 1960s with the introduction of frequency domain analysis of the arterial pulse by an English group of McDonald, Womersley, and Taylor, and a US group at the NIH in Bethesda led by Donald Fry. Michael Taylor liaised with the UK and US

groups on his return from London to Sydney. Up until 1960, Taylor sought information on optimal function of the arterial tree as based upon optimal distensibility (Taylor 1967). He progressed to anatomical as well as physical preparations as required for a comprehensive study. Taylor pressed the search for answers through determination of vascular impedance in animals of different size and shape, and in humans; Michael O'Rourke was his graduate student with training in anaesthesiology and intensive care.

The pressure developed by the contracting heart is determined by the force of contraction of the heart muscle and the external opposition to ventricular outflow. Characterization of the external opposition to left ventricular ejection needs to take into account the major components of the arterial load: (1) resistance, (2) blood viscosity, (3) arterial wall visco-elasticity, (4) inertia, and (5) wave reflection. The implications of pulsatile haemodynamics on left ventricular/arterial *coupling* will be discussed in a later section of this chapter.

Arterial resistance is determined by blood viscosity and is inversely proportional to the fourth power of the radius of the vessel.

$$R = 8\mu L / \pi r^4 \quad \mu \text{ viscosity, } L \text{ vessel length, } r \text{ radius}$$

Consequently, the most important component of peripheral arterial resistance is at the level of the smallest vessels or arterioles. If flow from the heart was constant, the steady pressure (P_{mean}) generated would depend only on arterial resistance: $P_{\text{mean}} = R Q_{\text{mean}}$ where P_{mean} and Q_{mean} are the mean pressure and flow, respectively. However, the intermittent nature of left ventricular ejection presents a more complex case. In addition to the peripheral resistance, in the intermittent case, there is the possibility of reflected waves from more distant points in the vascular tree as well as the elastic nature of the arteries (which distend and recoil in systole and diastole respectively, resulting in a time-dependent elastic contribution to pressure). The pulsatile hydraulic load on the heart will reflect contributions from all of these.

The pulsatile left ventricular hydraulic load on the heart could be described in either the time or frequency domains. Time domain assessments of the pulsatile arterial load include measures of total arterial compliance (e.g. stroke volume/pulse pressure) or effective arterial elastance (end systolic pressure / stroke volume).

However, frequency domain assessment of the arterial load by the aortic input impedance provides the best description of the components of steady state and pulsatile arterial load. Impedance is a frequency-dependent measure of opposition to pulsatile flow. Resistance is the opposition to steady or non-oscillatory flow and is the impedance at zero frequency. Input impedance is determined by the properties of the arterial system, which include peripheral arteriolar resistance, the viscoelastic properties of the arteries, inertial forces associated with changing flow, the viscosity of the blood and the impact of reflected waves, as well as the size and shape of the animal.

Characteristic Impedance (Z_c) It is the relationship between pulsatile pressure and pulsatile flow ($\Delta P/\Delta V$) measured at the same site in the absence of reflected waves. Z_c is determined by the physical properties of the arterial system such as the elastic modulus of the artery and the

inverse of the cross-sectional area. Consequently, Z_c is linearly related to the pulse wave velocity (C_o) and is also directly related to blood density.

$$Z_c = \rho C_o / \pi r^2$$

Wave velocity (C_o), in turn, is directly related to $\Delta P/\Delta V$ by the “Water Hammer” equation

$$C_o = \Delta P / \rho \Delta V$$

where ΔV is the change in blood flow velocity, ΔP the change in pressure, and ρ is blood density.

Z_c can be estimated from the change in pressure occurring simultaneously with peak flow.

$$Z_c = \Delta P_o / \Delta Q = (P_i - P_d) / \text{peak flow}$$

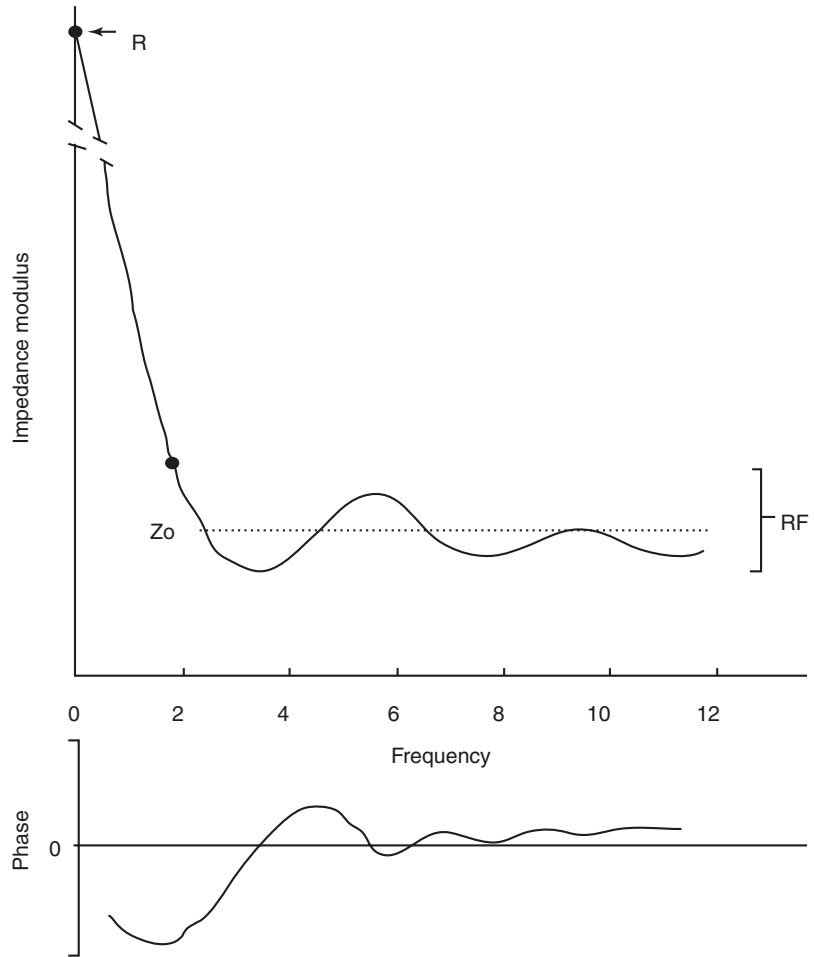
where P_i is the pressure at the inflection point of aortic pressure where peak flow occurs (see Fig. 9.4), P_d is end diastolic pressure. This estimate assumes that aortic pressure up to this time point is not changed by wave reflections.

Z_c may also be obtained by Fourier analysis of arterial pressure and flow (as described below) by averaging the moduli of impedance at frequencies above the first minimum. There is good correlation between the peak flow method and the results obtained by Fourier analysis (Dujardin and Stone 1981).

When Z_c is determined from flow change in volume units of cm^3/s , Z_c has the same units as arterial resistance ($\text{dyne}\cdot\text{s}/\text{cm}^5$). However, characteristic impedance is not a true resistance and can only be considered in the context of oscillatory phenomenon. Z_c is best expressed in terms of velocity (cm/sec) as $\text{dyne}\cdot\text{s}\cdot\text{cm}^{-3}$. Z_c numerically (in volume units) is about 5–7% of peripheral vascular resistance. Measurements of Z_c in man show increasing Z_c (in velocity units) with age, hypertension, and in patients with heart failure, as one would expect, on account of the relationship of Z_c with pulse wave velocity and arterial stiffness.

Input Impedance (Z_I) It describes the actual relationship between observed pressure and flow,

Fig. 9.4 Hypothetical aortic input impedance spectrum. The first minimum of the impedance modulus occurs close to the frequency where the phase crosses zero. The characteristic impedance (Z_c) is the average of the impedance moduli beyond the first minimum. A measure of wave reflection (RF) is the amplitude of the impedance moduli variation above the first minimum. (From Yin 1987. Reproduced with permission of Springer Nature)



in the frequency domain. The measured pressure and flow waves are the summation of incident and reflected backward traveling waves. Thus, input impedance (Z_i)

$$Z_i = (P_f + P_b) / (Q_f + Q_b)$$

in contrast to Z_c reflects the effect of reflected waves in addition to the physical properties of the arterial system such as vessel radius and visco-elastic properties. In the ascending aorta, the aortic input impedance describes the actual arterial hydraulic load on the ejecting left ventricle.

Fourier transform analysis of pressure and flow recordings taken in the arterial system yields a Fourier series – a weighted sum of sine waves at specified frequencies which would yield the observed pressure and flow recordings. These

frequencies are harmonics – multiples of the fundamental frequency (60/HR where HR is heart rate in beats/minute). The observed waveforms can be reconstructed with increased accuracy by including more harmonics.

Z_i is determined for each individual harmonic (h) as an amplitude (modulus) $Z_i(h)$ and a phase angle ($\theta(h)$). The phase angle ($\theta(h)$) is the phase difference between the pressure (β) and flow (ϕ) harmonic and is positive when the flow harmonic leads the pressure harmonic.

$$Z_i(h) = |P(h)| / |Q(h)| \quad \theta(h) = \phi - \beta$$

An aortic input impedance spectrum is a graphical representation of the phase angle and impedance moduli for each frequency (Fig. 9.4).

Impedance values decline from a high value at 0 Hz (the peripheral vascular resistance) to a minimum at approximately 3.5 Hz. At about this frequency, the phase angle crosses zero. A negative phase angle indicates that the flow harmonic leads the pressure harmonic. The impedance modulus over a range of frequencies oscillates around a mean value due to the impact of wave reflections. The magnitude of the oscillations of impedance moduli approximates the reflection index. The mean value of input impedance at frequencies above approximately 3 Hz is taken to represent the characteristic impedance (Z_c).

The frequency at which the first minimum of impedance modulus and the zero crossing point of the phase angle allows calculation of the wavelength of the travelling wave and, consequently, the distance to the major site for wave reflection. The reflection site is at a quarter of a wavelength ($\lambda/4$) where $\lambda = C_o/f$, C_o is the pulse wave velocity and f the frequency of the first impedance modulus minimum. The distance to the effective reflecting site is $d = C_o/4f$. In normal human studies, with an impedance minimum at 3.5 Hz and an average aortic pulse wave velocity of 750 cm/sec, the distance from the ascending aorta to the effective reflecting site is 54 cm.

The significance of the effect of wave reflections on the measured pressure depends upon their magnitude and the phase difference between reflected and incident waves, which in turn depends upon both the distance from the reflection site and the wave velocity. If the phase difference is 0° , the reflected wave will increase the net pressure (constructive interference), whereas if the phase difference is 180° the reflected wave will decrease the measured pressure (destructive interference).

The validity of impedance as a measure of the relationship between pressure and flow and the application to transmission line theory depends upon the linearity of the relationship between pressure and flow. For example, in the Fourier analysis, each harmonic of pressure and flow is considered to be uniquely related and not dependent upon other frequency components, that is, there is no harmonic interaction. Theoretical and experimental studies have demonstrated that any

non-linearities between pressure and flow are surprisingly small and can be neglected as a first-order approximation.

Arterial Wave Reflections

The arterial system is a network of distensible tubes with multiple branches. The arterial pressure wave is transmitted along the conduit arteries at the local pulse wave velocity. On encountering the branching points and the arteriolar network, a proportion of the wave energy is reflected back. Such reflecting points are termed points of impedance mismatch. As above, the reflected backward travelling wave interacts with the forward wave with the resulting observed wave dependent on both the magnitude and the phase difference of the forward and backward waves. Using parameters acquired from impedance data, the arterial pressure and flow waves can be analysed into forward and reflected waves (Fig. 9.5).

Reflected waves are seen in arterial pressure recordings, especially in animals and young people in whom the amplification is more pronounced and the wave velocity slower such that reflected waves return later and after the initial impulse (Fig. 9.6).

Wave reflection is responsible for the increase in systolic pressure observed as the pressure wave travels from the central aorta to the periphery. Over the same distance, diastolic pressure falls with a consequent greater fluctuation of pressure around a slightly lower mean pressure (by just 1–2 mmHg) (Pauca et al. 1992).

Wave reflection can be quantified by the magnitude of the variation of the input impedance at frequencies above the first minimum. An estimate of wave reflection can also be made by calculation of a reflection coefficient (Γ): $\Gamma = (Z_T - Z_C)/(Z_T + Z_C)$, where Z_T is the peripheral resistance and Z_C is characteristic impedance. However, Γ is frequency dependent and falls from a value of approximately 0.8 at the fundamental heart rate frequency to very low levels above the first impedance maximum.

Wave reflection can be modified by physiological, pathological, and pharmacological influ-

Fig. 9.5 Measured aortic pressure is analysed into forward and backward (reflected) waves. The reflected wave results in the late systolic peak of pressure. (From Yin 1987. Reproduced with permission of Springer Nature)

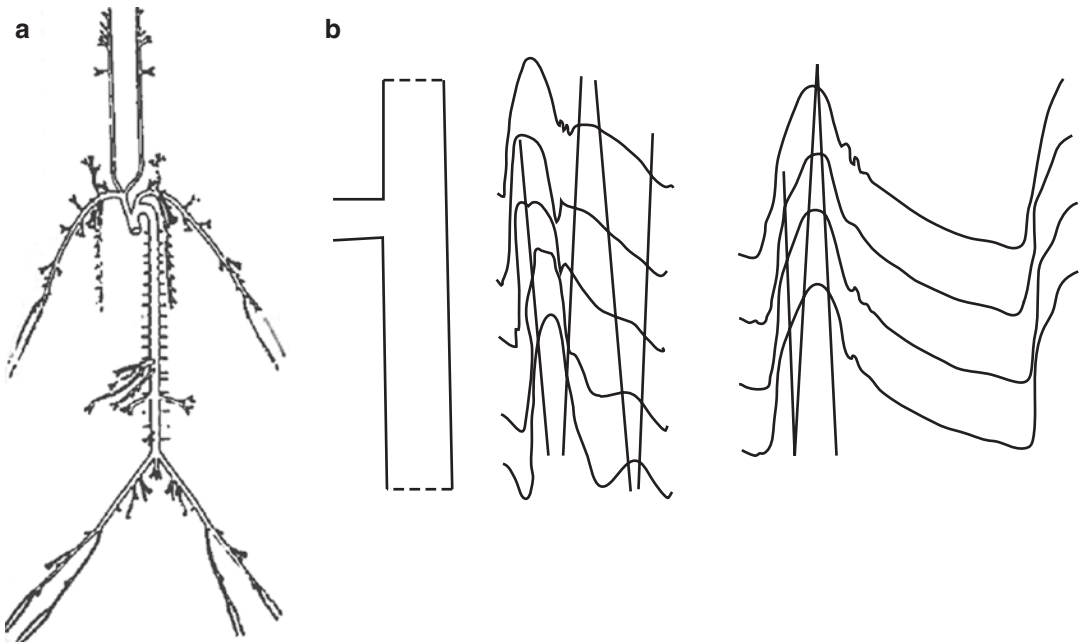
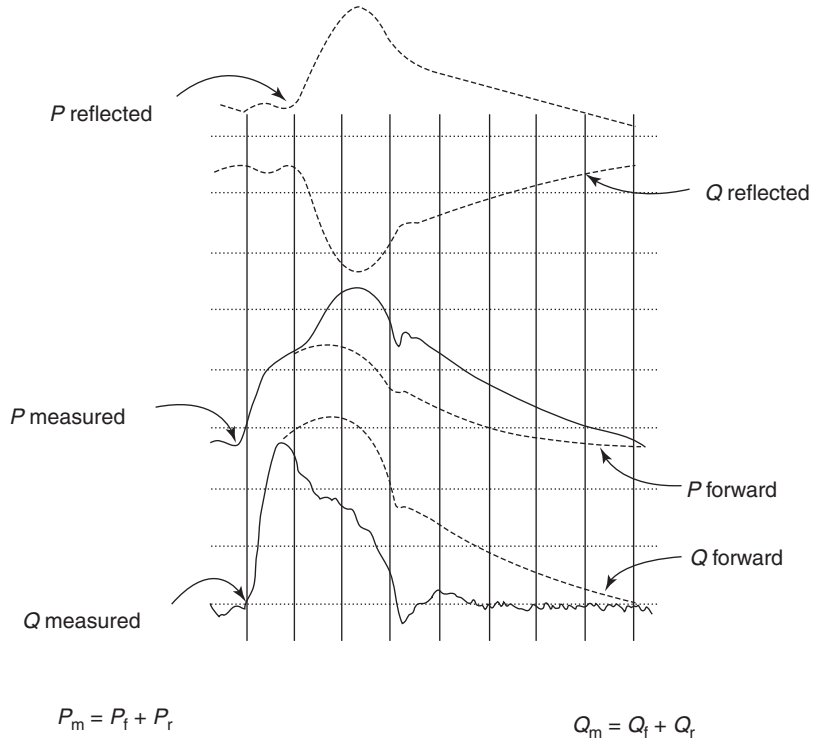


Fig. 9.6 The arterial system is modelled as an asymmetric *T* with reflections originating in the upper and lower parts of the body. (a) In a young subject or in animals, systolic and pulse pressure increase as the pressure wave is transmitted from the central aorta to the periphery due to the impact of wave reflections. (b) In an older human

subject with stiffened arteries wave reflections return earlier augmenting late systolic pressure and a lesser effect on pressure amplification between central and peripheral pressures. (From Wave Travel and Reflection in the Arterial System. O'Rourke 1971. Modified with permission of Elsevier Science & Technology Journals)

ences. Ageing and arterial disease are associated with an increase in late systolic aortic pressure due to increased wave reflection arriving early during systole as consequent to the increased pulse wave velocity.

Laskey and Kussmaul (1987) show that exercise reduces the magnitude of the reflected wave. The reduction of the late systolic peak of aortic pressure observed during a Valsalva maneuver is associated with reduced fluctuation of the impedance spectrum indicating a reduction of wave reflections (Murgo et al. 1981).

Vasodilators such as nitroprusside reduce mean arterial pressure and peripheral vascular resistance (Merillon et al. 1982). As a result of the reduction of pulse wave velocity, the input impedance curve is shifted to the left, suggesting a delay in the timing of wave reflections. In addition, the amplitude of the impedance modulus of the first two harmonics is reduced, indicating an overall reduction of wave reflections. In contrast, nitroglycerin reduces late systolic pressure in the ascending aorta as well as the fluctuations of the modulus of the impedance spectrum with little effect on peripheral arterial resistance or change in the frequency of the modulus minima (Fitchett et al. 1988a; Yaginuma et al. 1986). These observations indicate that nitroglycerin reduces wave reflection without changing peripheral arteriolar resistance.

Changes of Waveforms in the Arterial System

Differences between peripheral and central arterial pressures have important practical consequences. Pressure measured in the radial artery differs from both central aortic and intra-cranial arterial pressure. Central aortic pressure is both the pressure load encountered by the ejecting left ventricle and the driving pressure for coronary perfusion in diastole, while carotid arterial pressure is the cerebral perfusion pressure.

Differences in central and peripheral pressures become accentuated during procedures that cause hypotension as shown in Fig. 9.7.

Radial arterial pressure is frequently used for patient monitoring in critically ill patients. With vasoconstriction in patients with shock, wave reflections can be increased, potentially increasing pressure amplification and exaggerating the difference between central aortic and radial arterial systolic pressure (Fig. 9.8).

However, radial arterial pressure can underestimate central aortic pressure in these patients possibly due to peripheral arterial vasoconstriction. Consequently, measurement of peripheral arterial pressure by radial arterial pressure monitoring provides only a limited assessment of aortic systolic pressure. There is a need for fur-

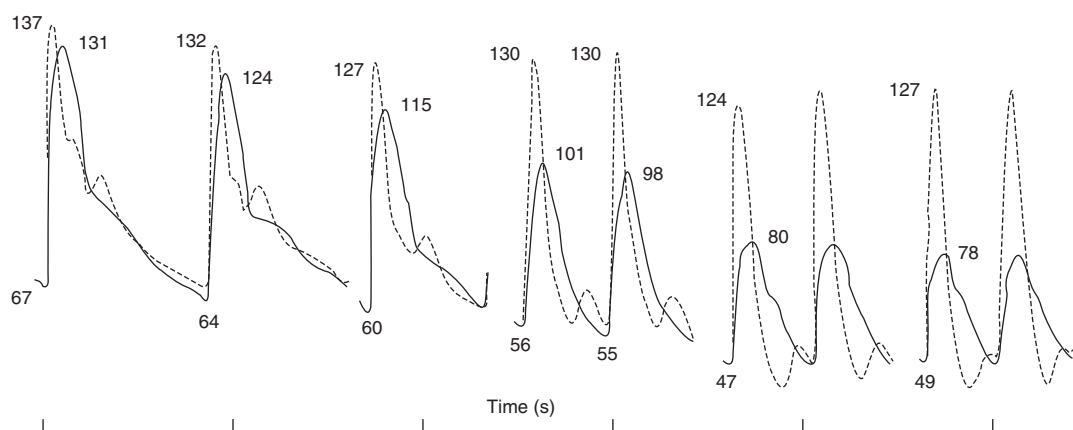
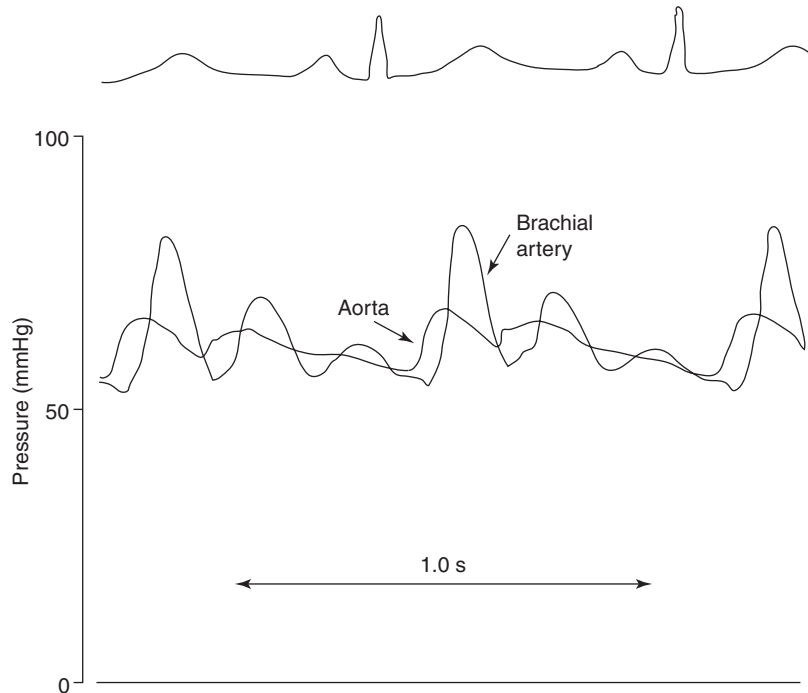


Fig. 9.7 Pressure waves simultaneously recorded from the radial artery (dashed line) and from the abdominal aorta (solid line) during the course of a hypotensive reaction to rapid intra-aortic injection of isotonic electrolyte

solution (numbers represent mmHg). (From Remington and Wood 1956. Reproduced with permission of American Physiological Society)

Fig. 9.8 Radial and aortic pressures in a patient with hypotension, vasoconstriction, and an obstructed carotid artery, showing the exaggerated diastolic pressure waves in the radial arterial pressure due to delayed wave reflection. Note the substantial difference between peak radial and aortic pressure indicating that radial arterial systolic pressure can overestimate central systolic pressure. (From O'Rourke 1970b. Reproduced with permission of Oxford University Press)



ther studies of pressure wave transmission between the central aorta and radial artery in patients with shock, to better understand the changes and clinical implications. Anaesthetists and intensivists are well aware of such problems which can also damp the pressure waveform. The appropriate action is to replace the radial cannula with a short catheter and advance it to the subclavian artery.

Vasodilators such as nitroglycerine reduce ascending aortic systolic pressure more than is apparent from changes of radial arterial pressure (Fig. 9.9) due to the reduction of reflected waves as indicated by the changes of aortic input impedance without any significant reduction in systemic vascular resistance (Fig. 9.10).

Non-invasive Assessment of Pulsatile Haemodynamics and Central Aortic Pressure

Analysis of the radial arterial pressure contour can provide information about the transmission of the pressure pulse from the aorta to the periph-

ery. The radial arterial pulse characteristically has an early systolic peak followed by a late systolic shoulder and another wave after the diastolic notch as shown in Fig. 9.9.

The relationship between recordings of aortic and radial arterial pressure waves and the moduli and phase of the individual Fourier harmonics – the output of any given input – can be expressed as a transfer function for each harmonic. In the upper limb, the transfer function is remarkably constant over a wide range of ages (Karananoglu et al. 1997) and after the administration of vasodilators such as nitroglycerine (O'Rourke et al. 1990). Consequently, the same transfer function can be used to generate central aortic pressure from recordings of the radial pressure wave in a wide range of conditions.

The radial arterial pressure wave can be reliably recorded non-invasively using applanation tonometry (Drzewiecki et al. 1983). By applying the transfer factor to the radial pressure harmonics, central aortic pressure may thus be synthesized from recordings of peripheral arterial pressure. Using this technique, it is possible to determine the impact of therapy (e.g. antihyper-

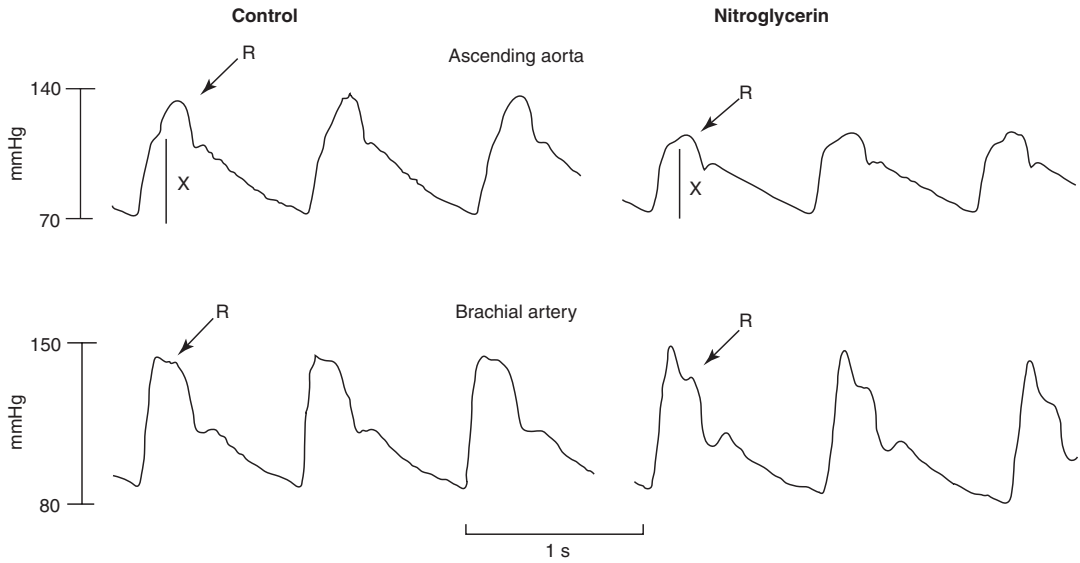
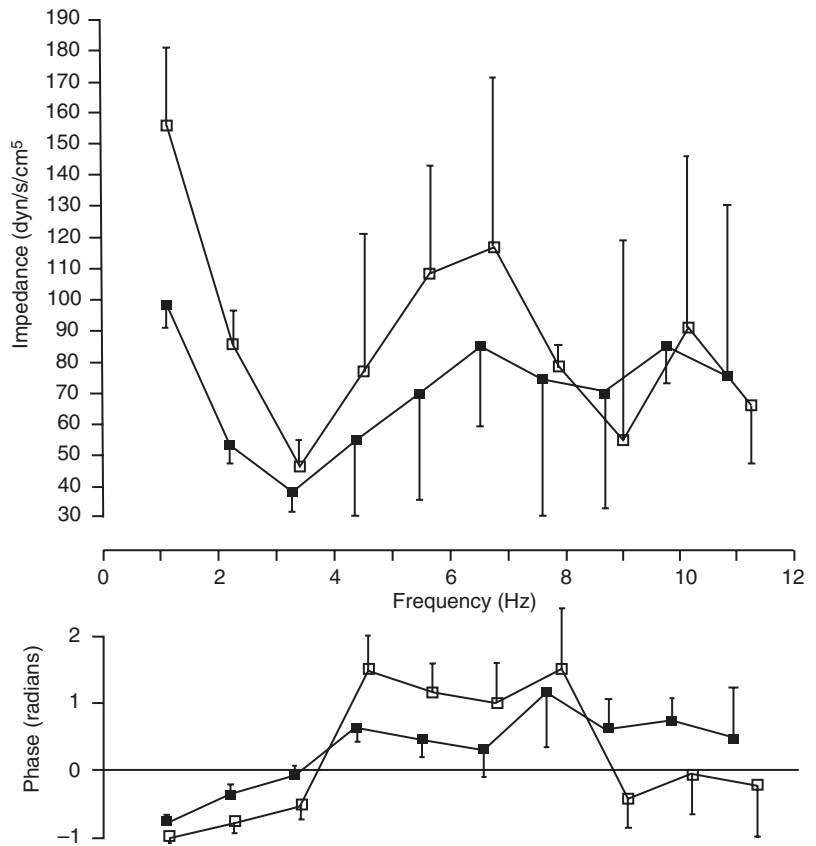


Fig. 9.9 Pressure waves recorded in the ascending aorta and brachial artery under control conditions (left) and after 0.3 mg sublingual nitroglycerine (right) in a human adult. *X*, height the pressure pulse would be without reflection (*R*). (From Kelly et al. 1990, Fig. 9.2. Reproduced with permission of Oxford University Press)

Fig. 9.10 The effect of nitroglycerin 15 μ g on the aortic input impedance modulus and phase, before and during nitroglycerine infusion. Systemic vascular resistance was unchanged. There was a significant reduction in the modulus of impedance of the first harmonic and less oscillation of the modulus and phase angle spectrum indicating nitroglycerine reduces peak systolic pressure consequent to a reduction of reflections with no reduction of systemic vascular resistance. (From Fitchett et al. 1988b. Reproduced with permission of Oxford University Press)



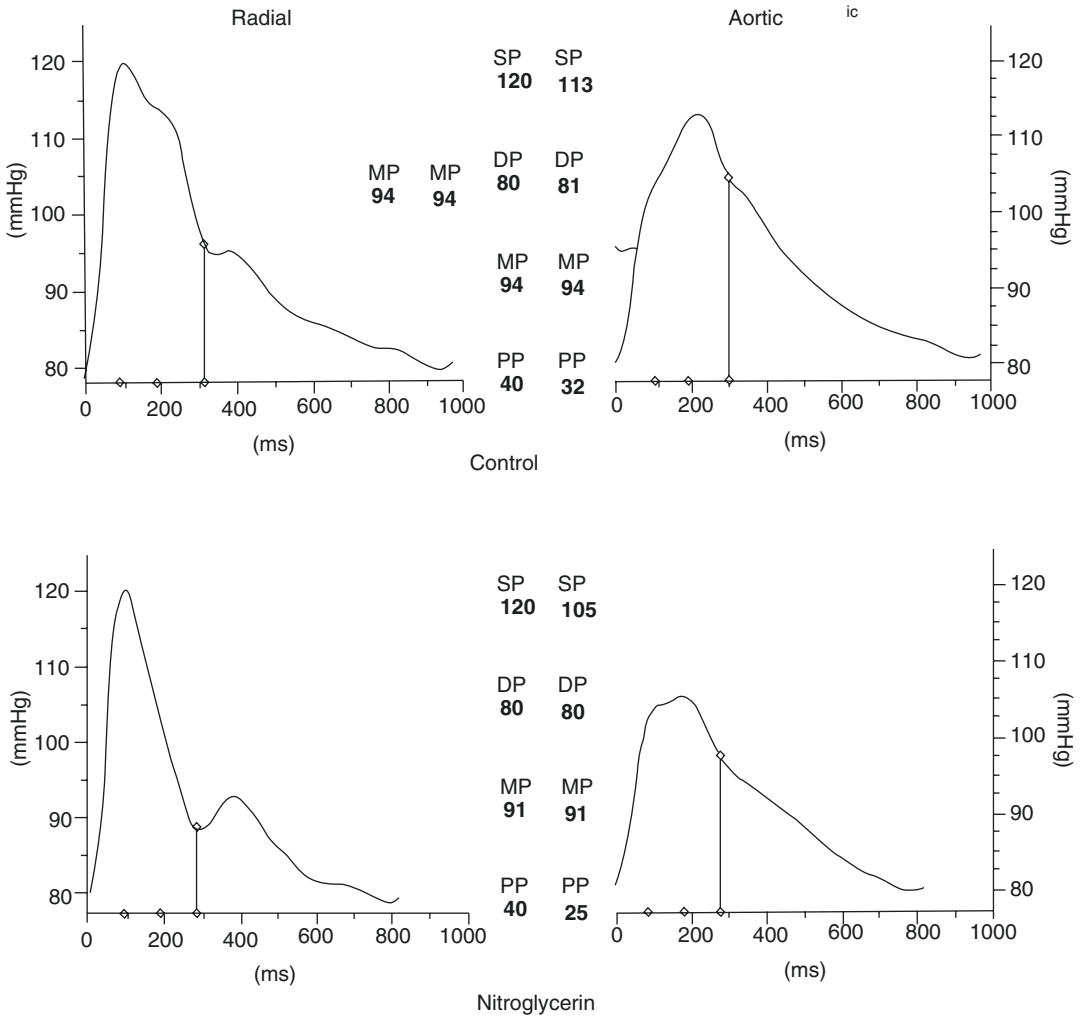


Fig. 9.11 Tonometric recordings of radial artery pressure with synthesized aortic pressure using the transfer function before and after the administration of *s/l* nitroglycerine. Similar pressure pulse changes in both the radial artery and aorta are observed to those measured with intra-arterial measurements as shown in Fig. 9.9. (From O'Rourke et al. 1993. Modified with permission of Informa UK Limited through PLSclear)

tensive and heart failure medications) on central BP and hence the impact on left ventricular loading (Fig. 9.11).

Pulsatile Haemodynamics and Ventricular Arterial Coupling

The external work performed by the heart in a cardiac cycle (or stroke work) is the integral of the pressure and flow over a cardiac cycle:

$$W(\text{stroke}) = \int P Q dt$$

Total external work has two components: (1) steady flow power (W_s).

$W_s = P_m \cdot Q_m$, where P_m is the mean arterial pressure and Q_m the mean ascending aortic flow and (2) oscillatory power (W_o) $W_o = \frac{1}{2} \sum (Q_n)^2 Z_n \cos \theta_n$.

Where Q_n is the n th harmonic of flow and Z_n the n th harmonic of impedance, and θ_n the phase angle of impedance for the n th harmonic. The

total hydraulic power is the sum of W_s and W_o . In the left ventricle, the oscillatory contribution to total power output is less than 20% of the total power (Nichols et al. 1977).

The hydraulic power of blood flow (work/time) in the ascending aorta is dependent upon (1) the ability of the left ventricle to perform external work and (2) the hydraulic load of the arterial system. Consequently, the hydraulic power generated is dependent upon both ventricular performance and the impedance to flow. The steady state achieved defines the coupling of the ventricle to the arterial system.

As shown previously, ageing, the development of atherosclerosis, and hypertension decrease arterial distensibility and increase wave reflections which arrive back early in the ascending aorta during left ventricular ejection and boost systolic pressure. Consequently, both total and oscillatory power are increased, with a larger proportion of oscillatory power in the individuals with atherosclerosis and hypertension. (oscillatory/total power normal group $13 \pm 1\%$, atherosclerosis and hypertension $19 \pm 2.5\%$) (Nichols et al. 1977). In the oldest group with the highest characteristic impedance, the pulsatile component was 26% of total power.

Exercise increases both steady flow and oscillatory power. In dogs, there was a modest increase in the proportion of oscillatory to total power during exercise 19–22% (Unpublished data presented in (Milnor 1989)). In man especially with exercise-induced systolic hypertension, it is likely that there is a greater proportion of oscillatory power/total power during exercise.

Conclusions

1. The arterial system is more than a conduit to deliver oxygenated blood to the organs. It acts both as a buffer to limit the rise of pressure and to deliver a more constant flow to the tissues.
2. The hydraulic load encountered by the left ventricle is the consequence of arteriolar resistance (constant flow) and both the elastance of the arterial system and the impact of reflected waves (pulsatile flow).
3. The arterial system behaves as a distributed network of distensible vessels with wave reflections originating from impedance mismatches that occur mainly at the arterial/arteriolar interface.
4. Characterization of the arterial load is best expressed in the frequency domain as the aortic input impedance. It allows assessment of both steady flow impedance (arteriolar resistance) and pulsatile impedance as determined by the characteristic impedance and the impact of wave reflections.
5. Arterial pressure and flow waves change during their transit through the arterial system due to their interaction with reflected waves. Consequently, pressures measured distally in a limb (e.g. radial arterial pressure) may not accurately reflect central aortic pressure: the pressure determining left ventricular afterload, coronary and cerebrovascular perfusion. Central aortic pressures can be synthesized from recordings of radial artery pressure waveforms.

For further in-depth reading, see

McDonald's Blood Flow in Arteries. Theoretical, Experimental and Clinical Principles, 6th Edition, 2011. WW Nichols, MJ O'Rourke, and C Vlachopoulos. CRC Press, Boca Raton, USA.
Hemodynamics, WR Milnor, 2nd edition 1989. Williams and Wilkins, Baltimore.

References

- Baltgaile G. Arterial wall dynamics. *Perspect Med.* 2012;1:146–51.
- Drzewiecki GM, Melbin J, Noordergraaf A. Arterial tonometry: review and analysis. *J Biomech.* 1983;16:141–52.
- Dujardin JP, Stone DN. Characteristic impedance of the proximal aorta determined in the time and frequency domain: a comparison. *Med Biol Eng Comput.* 1981;19:565–8.
- Fitchett DH, Simkus G, Genest J, Marpole D, Beaudry P. Effect of nitroglycerin on left ventricular hydraulic load. *Can J Cardiol.* 1988a;4:72–5.
- Fitchett DH, et al. Reflected pressure waves in the ascending aorta: effect of glyceryl trinitrate. *Cardiovasc Res.* 1988b;22:494–500.

- Hales S S *Statical essays*. Printed for W. Innys and R. Manby, at the west-end of St. Paul's, and T. Woodward, at the Half-Moon between Temple-Gate, Fleetstreet, London. 1769.
- Hamilton WFD. An experimental study of the standing waves in the pulse propagated through the aorta. *Am J Phys*. 1939;125:48–59.
- Karamoglu M A system for analysis of arterial blood pressure waveforms in humans. *Computers and Biomedical Research* 1997;30:244–55
- Kelly RP, et al. Nitroglycerin has more favourable effects on left ventricular afterload than apparent from measurement of pressure in a peripheral artery. *Eur Heart J*. 1990;11:138.
- Laskey WK, Kussmaul WG. Arterial wave reflection in heart failure. *Circulation*. 1987;75:711–22.
- Merillon JP, Fontenier GJ, Lerallut JF, Jaffrin MY, Motte GA, Genain CP, Gourgon RR. Aortic input impedance in normal man and arterial hypertension: its modification during changes in aortic pressure. *Cardiovasc Res*. 1982;16:646–56.
- Milnor WR. Aortic wavelength as a determinant of the relation between heart rate and body size in mammals. *Am J Phys*. 1979;237:R3–6.
- Milnor WR. *Hemodynamics*. Baltimore: Williams and Wilkins; 1989.
- Murgo JP, Westerhof N, Giolma JP, Altobelli SA. Manipulation of ascending aortic pressure and flow wave reflections with the Valsalva maneuver: relationship to input impedance. *Circulation*. 1981;63:122–32.
- Nichols WW, O'Rourke MF. McDonald's blood flow in the arteries. Theoretical, experimental and clinical principles. 4th ed. London: Arnold Publishers; 1998.
- Nichols WW, Conti CR, Walker WE, Milnor WR. Input impedance of the systemic circulation in man. *Circ Res*. 1977;40:451–8.
- O'Rourke MF. Arterial hemodynamics in hypertension. *Circ Res*. 1970a;27(Suppl 2):123. +
- O'Rourke MF. Influence of ventricular ejection on the relationship between central aortic and brachial pressure pulse in man. *Cardiovasc Res*. 1970b;4(3):291.
- O'Rourke MF. The arterial pulse in health and disease. *Am Heart J*. 1971;82:687–702.
- O'Rourke MF, Avolio AP, Karamaoglu M, Kelly RP. Derivation of ascending aortic pressure waveform from brachial pressure pulse in man. *Aust NZ J Med*. 1990;20:328.
- O'Rourke MF, Safar M, Dzau V, editors. *Arterial vasodilatation. Mechanisms and therapy*. London: Edward Arnold; 1993. p. 222.
- O'Rourke MF, Adji A, Safar ME. Structure and function of systemic arteries: reflections on the arterial pulse. *Am J Hypertens*. 2018;31:934–40.
- Pauca AL, Wallenhaupt SL, Kon ND, Tucker WY. Does radial artery pressure accurately reflect aortic pressure? *Chest*. 1992;102:1193–8.
- Remington JW, Wood EH. Formation of peripheral pulse contour in man. *J Appl Physiol*. 1956;9:433–42.
- Taylor MG. The elastic properties of arteries in relation to the physiological functions of the arterial system. *Gastroenterology*. 1967;52:358–63.
- Ting CT, Chen JW, Chang MS, Yin FC. Arterial hemodynamics in human hypertension. Effects of the calcium channel antagonist nifedipine. *Hypertension*. 1995;25:1326–32.
- Wetterer E. Flow and pressure in the arterial system, their hemodynamic relationship, and the principles of their measurement. *Minnesota Medicine*. 1954;37:77–86; passim.
- William Harvey. *De Circulatione Sanguinis* 1649. Translated by Franklin KJ. Oxford: Blackwell; 1957.
- Yaginuma T, Avolio A, O'Rourke M, Nichols W, Morgan JJ, Roy P, Baron D, Branson J, Feneley M. Effect of glyceryl trinitrate on peripheral arteries alters left ventricular hydraulic load in man. *Cardiovasc Res*. 1986;20:153–60.
- Yin FCP, editor. *Ventricular/vascular coupling. Clinical, physiological and engineering aspects*. New York: Springer Verlag; 1987.



Sheldon Magder and Alexandr Magder

Introduction

Administration of intravenous fluids is one of the commonest medical acts in hospitalized patients. This chapter will emphasize the physiological role of fluids, principles behind the movement and distribution of water and its solutes, and the characteristics of different kinds of commonly infused fluids. In Chap. 42, use of fluids for both resuscitation and maintenance of normal fluid balance is discussed. Some of these issues have been covered previously (Magder 2001), but in this review the principles are updated. An important influence on this discussion is the excellent review by Bhave and Neilson (Bhave and Neilson 2011a). We will emphasize four basic concepts. (1) Elements, especially sodium ion (Na^+) and chloride ion (Cl^-), have unique importance when compared to metabolizable organic molecules. (2) The amount of an element in the body can be regulated only by absorption or excretion. (3) The vascular space is in a dynamic equilibrium with the interstitial and other “third” spaces, such

as the pleural and peritoneal compartments. Because of this, they all have approximately the same osmolality. This means that any administration of resuscitation fluids, or de-resuscitation of fluid, shifts water and elements between all compartments. Thus, volume management must not be confined to just the vascular space. (4) Colloids play a unique role in the maintenance of intravascular and intracellular volumes because they do not readily cross cell membranes.

What Is the Role of Water in Organisms?

Organic molecules and elements need to be in solution to react with each other and to move by bulk flow or diffusion from one region to another (Rawn 1989). With the odd exception, water is the solvent for all biological solutions. Life as we know it would not exist without water. This is because water has a unique property which readily allows dissolved substances to become part of its structure (Rawn 1989; Ball 2001). Bodily solutions are essentially mixtures of salts, with dissolved proteins, carbohydrates, lipids, and other small organic molecules.

When original cell walls formed, and solutions of organic substances became walled off from the surrounding milieu, regulation of cell volume became an important physiological process. This is because cell walls are imbedded

S. Magder (✉)
Royal Victoria Hospital (McGill University Health Centre), Departments of Critical Care and Physiology
McGill University, Montreal, QC, Canada
e-mail: sheldon.magder@mcgill.ca

A. Magder
Department of Pediatrics, Bernard and Millie Duker
Childrens Hospital, Albany Medical Center,
Albany, NY, USA
e-mail: AlexandrMagder@rcsi.ie

with complex protein structures, including channels, exchangers, and receptors (O'Neill 1999). A change in cell volume stresses the cell walls and alters the tertiary structure of these large membrane molecules (Macknight and Leaf 1977). Changes in their shape can lead to intracellular transcriptional and non-transcriptional processes that are directed at restoring steady state volume as part of the body's stress response (O'Neill 1999; Orlov and Hamet 2006). *A key message is that, independent of the role water has in altering intravascular volume, infusion of a fluid that results in changes in intracellular volume significantly alters intracellular signaling processes (key messages are listed in Table 10.1)* Unfortunately, these processes are complex and not predictable; the consequences can be determined only by empirical studies on whole organisms or cells. These studies likely should be done on human tissues because of species and even cellular specificities.

When multi-celled organisms developed an envelope that excluded interior structures from the surrounding environment, it became necessary to evolve systems to regulate the volume and

concentration of substances in this interior space which is inside the outer integument but outside cells (Stein 2002). This is called the interstitial space (Pitts 1968; Magder 2014; Aukland and Nicolaysen 1981). Without regulation of the concentration of electrolytes in this space, water would be lost or gained from the milieu outside the organism's outer barrier. *Thus, a key message is that in fluid management, even though we only make assessments based on the plasma space, consideration must be given to the consequences of administered fluids for the vascular, interstitial, and intracellular spaces.* Furthermore, it needs to be appreciated that the volume in red cells is not part of the extracellular volume, but it is part of the total intracellular volume, although its properties are different from other cells.

Volume and the Generation of Blood Flow

In small organisms, O₂ and nutrients can be adequately supplied, and waste excreted, by diffusion from the surrounding environment. However, in large multicellular organisms, diffusion is not adequate and a distribution system is required to allow more rapid conductive flow. This was provided by evolution of the cardiovascular system (Bishopric 2005). The role of volume in the regulation of cardiac output is covered in Chap. 2. In essence, cardiac output is controlled by the interaction of the return of blood to the heart (return function) and cardiac function. The primary force in both of these functions is the stretch of the elastic walls of cardiovascular structures by volume.

As emphasized in Chap. 2, some of the blood volume in vessels simply rounds out vessel walls, and some of the volume stretches the walls, but only the portion that stretches the walls produces the elastic recoil force. This is called stressed volume. The remaining volume rounds out vessels but does not stretch their elastic walls; this is called unstressed volume. In a standard size male, total blood volume is approximately 5.5 L. Under resting conditions, about 30%, or 1.3 to 1.4 L, is

Table 10.1 Key principles from physiology of fluid

- | |
|---|
| 1. Independent of the role water has in altering intravascular volume, infusion of a fluid that results in changes in intracellular volume significantly alters intracellular signaling processes |
| 2. In fluid management, even though we only make assessments based on the plasma space, consideration must be given to the consequences of administered fluids for the vascular, interstitial, and intracellular spaces |
| 3. A volume bolus of more than 1 to 1.5 L is not likely to remain in the vascular space because the vessels do not have the capacity to hold it |
| 4. When considering volume therapy, the volume and composition of fluids in all extracellular compartments must be considered because they all are in equilibrium with the plasma space in the steady state |
| 5. One must distinguish the concentration of elements from their actual amount in the body. The total amount of an element in the body is related to the total amount of the volume of water and the concentration of the element and the amount only can be regulated by absorption or excretion because elements cannot be created or metabolized |
| 6. Edema can produce further edema, and large volume resuscitation can make things worse |

stressed and an elastic recoil pressure is created in vessels (Magder and De Varennes 1998). The rest of the volume is unstressed and provides a reserve that can be recruited to produce the equivalent of an auto-transfusion as discussed below. Furthermore, with a hematocrit of 40% and a total blood volume of 5.5 L, the plasma volume is about 3.3 L. The proportions of red cell mass and plasma volume in the total blood is the same in the stressed and unstressed volumes. Thus, only about 1 liter of plasma contributes to stressed volume. This means that the normal plasma component of stressed volume is only about 1 liter. *A key point is that a volume bolus of more than 1 to 1.5 L is not likely to remain in the vascular space because the vessels do not have the capacity to hold it.*

Compartments

Water makes up 60% of total body mass of an average male below the age of 40 and 50% in females and older males (West 1985; Mudge 1980). The differences between young males and females and older males are due to differences in the proportion of muscle mass relative to total body mass (Bhave and Neilson 2011b). In a 70 kg male, total body water is ~42 L. Of this total, approximately two-thirds of the water, i.e., ~ 28 L, are intracellular fluid (ICF) and 14 L are extracellular fluid (ECF) (Fig. 10.1). The ECF can be subdivided into five sub-compartments. These include plasma volume, interstitial and lymph fluid, dense connective tissue and bone fluids, transcellular fluids within cavities such as the pleural and peritoneal fluids, and the cerebrospinal fluid (Bhave and Neilson 2011a). Plasma volume accounts for 3–4 L of the ECF, and the other 10 to 12 L of the ECF, at least the exchangeable part, is primarily in the interstitial space. Adipose tissue can contain a large amount of water by weight. When body mass index is normal, and there is not a lot of fat, adipose tissue contributes a small amount to total ECF. However, it can account for a very large proportion of total body water in the morbidly obese (Bhave and Neilson 2011a). Interstitial

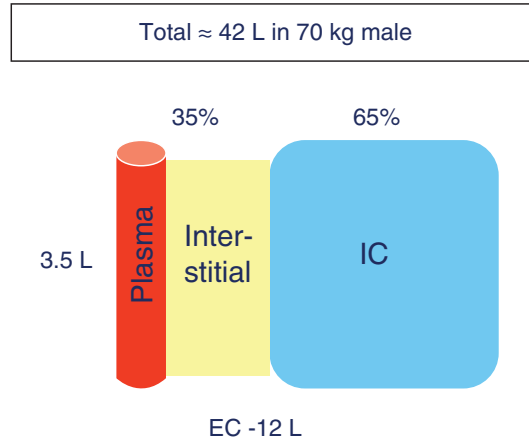


Fig. 10.1 Distribution of water in the body. See text for details. (EC extracellular volume, IC intracellular volume. The arrows indicate that plasma volume and the interstitial space are constantly interacting)

volume as a percentage of total body water can increase dramatically when edema develops. Fluid that accumulates in body cavities, such as the pleural and peritoneal spaces, also freely communicates with the interstitial and plasma spaces, and they all should be considered as one compartment. This becomes very important for understanding the distribution of an infused crystalloid solution. As will be discussed below, the volume and electrolytes in all compartments must equilibrate with the vascular space. *A key point is that when considering volume therapy, the volume and composition of fluids in all extracellular compartments must be considered because they all are in equilibrium with the plasma space in the steady state.*

Regulation of the Distribution of Body Water and Electrolytes

Distribution of water between the extracellular (EC) and intracellular (IC) compartments is determined by hydrostatic pressure and osmosis. Steady state water distribution reflects the balance of these two forces across compartments:

$$P_{ic} - P_{ec} = \Pi_{ic} - \Pi_{ec} \quad (10.1)$$

where P is the hydrostatic pressure and Π is the osmotic pressure inside (ic) and outside (ec) cells. Early life forms such as bacteria, fungi, and plants have rigid cell walls that are impermeable to water and produce hydrostatic pressure differences by pumping electrolytes into or outside of their intracellular compartment to maintain their volume. In contrast, animal species evolved non-rigid cell walls that are permeable. This gave these cells flexibility of movement, but it also meant that their intracellular volume needs to match the extracellular osmolality. Essentially, $P_{ic} - P_{ec}$ becomes zero and $\Pi_{ic} = \Pi_{ec}$. In this case, the whole organism is separated from the outside world by a surrounding barrier (i.e., skin) and all inner compartments have the same osmolality. This is expressed in the principle of iso-osmolality (West 1985; Freedman 1997) which states that all compartments of the body have essentially the same osmolality. This occurs because capillary endothelium, and almost all cell membranes, are freely permeable to water, which easily moves from areas of lower concentrations of osmoles to areas of higher concentrations of osmoles by osmosis. As will be discussed, there is a small exception to this; osmolality of the plasma is slight greater than that of the rest of the body.

What Are Osmoles?

Osmoles are discrete particles dissolved in a solution. They alter the properties of water such as its freezing and vaporization temperatures. Osmolality is the number of particles per mass (weight) of the solution; osmolarity is the number of particles per volume. The preferred term is osmolality because mass is a fixed property of a substance, whereas volume can vary with temperature and external pressure. However, volume is easier to measure and thus osmolarity is commonly used. The osmolality of a solution produces a pressure, which is defined by the Van't Hoff equation (West 1985; Freedman 1997):

$$\text{Osmotic pressure} = n(c/M)RT \quad (10.2)$$

where n is the number of particles, c is the concentration of the substances, M is the molecular weight of the substances, R is the ideal gas constant, and T is the absolute temperature. The expression c/M defines the molar concentration. One mOsmol generates 19.34 mmHg at 37 °C (Fig. 10.2). Of importance, the size of the particle does not matter so that the osmotic effect of a 69 kD albumin molecule is the same as that of a single Na^+ atom. Osmotic pressure from an electrolyte is modified by the valence (z) and the nonideality of the solution (ϕ),

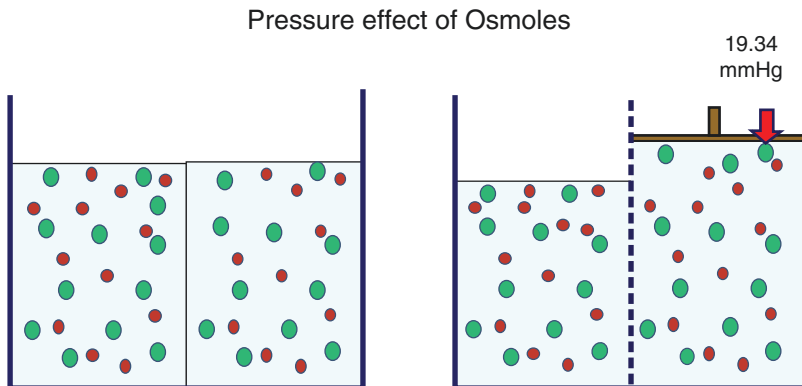


Fig. 10.2 Pressure effect of osmoles. In the panel on the left, the number of particles is equal on both sides of a semipermeable membrane that does not allow the particles to cross. On the right side, 1 mOsmol (one particle)

was added and water moves from the left to make the concentrations equal. 19.34 mmHg of pressure would need to be added to make the heights of water equal on both sides of the membrane

which indicates the deviation of the effective osmolality of a substance in a solution from that predicted simply by its mass and particle number. The osmotic pressure from one osmole in the body is thus:

$$\Pi_{ec} (37^\circ, mmHg) = 19.34 * \varphi * Z * [c] \quad (10.3)$$

$$\text{Osmolality (mOsm / kg)} = \varphi * Z * [c] \quad (10.4)$$

Osmotic water movement is determined by how easily water can pass through a membrane, which is called hydraulic permeability (L_p) and the solute concentration gradient ($\Delta[c]$) between two solutions on either side of a membrane.

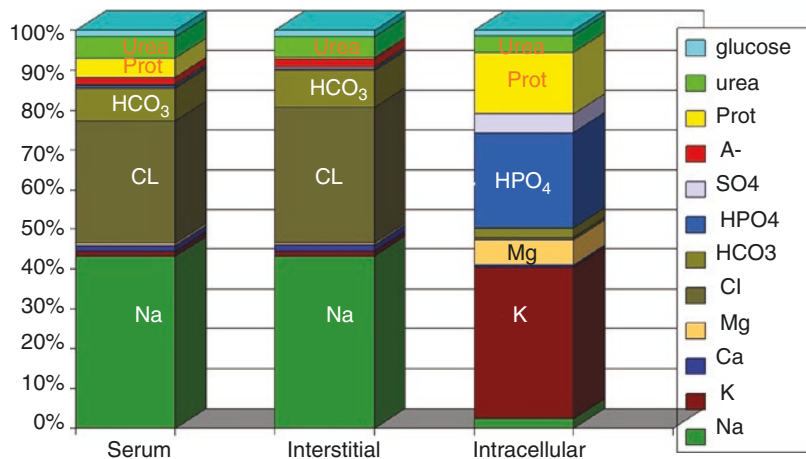
$$\text{Osmotic flux} = L_p \times 19.34 * \varphi * \Delta[c] \quad (10.5)$$

Most solutes are at least partially permeable across the cell membrane and undergo convective transport with water, but their ability to cross membranes varies. This is described by the reflection coefficient, σ , which is a dimensionless number between 0 and 1. When a solute has $\sigma = 1$, no particles move across the membrane, and the observed osmotic gradient produces the maximal osmotic force as predicted based on the difference in the number of particles on each side of the membrane. When there is a difference in the concentration of substances on the two sides of the membrane, the system is in a more “ordered” state and has a lower entropy. This attracts water to

reduce the overall ordered state, thus increasing the overall entropy of the system in the same way as the energy in the form of heat moves from an area of higher temperature to an area of lower temperature. If some particles manage to cross the membrane, the osmotic force is reduced and $\sigma < 1$. When the particles easily cross the membrane, and σ is close to 0, there is no osmotic water movement (Bhave and Neilson 2011a). For a substance that has $\sigma < 1$, and is leaking across the membrane, another variable is that the gradient for osmosis requires that the concentration gradient develop faster than the solute flux across the membrane (Bhave and Neilson 2011a). For most of the discussion in this chapter, water movement between the extracellular and intracellular fluid (ICF) is primarily related to the concentrations of Na^+ , K^+ , and Cl^- which have σ close to 1 over short periods of time.

The compositions of plasma, interstitial, and extracellular fluid are shown in Fig. 10.3. Positive elements such as Na^+ , K^+ , Ca^{2+} , and Mg^{2+} and the negative element Cl^- play the major roles in regulating water balance by determining the osmolality of body fluids (West 1985; Freedman 1997). *A key point is that one must distinguish the concentration of elements from their actual amount in the body. The total amount of an element in the body is related to the total amount of the volume of water and the concentration of the element and the amount only can be regulated by absorption or excretion because elements cannot be created or*

Fig. 10.3 Contents of serum and interstitial and intracellular spaces: Gamblegram



metabolized. Na⁺ is by far the dominant cation in serum. Once mechanisms evolved to regulate Na⁺ concentration (Stein 2002), the amount of negatively charged substances, such as Cl⁻, had to follow Na⁺ concentration to maintain electrical neutrality. Thus, by having Na⁺ concentration controlled Cl⁻ concentration tends to be controlled, although there are some independent regulators of Cl⁻ concentration itself because of its importance in acid-base balance (Magder 2014; Magder and Emami 2015). To allow for independent control of intracellular volume from the extracellular space, there needed to be another cation to replace Na⁺ and K⁺ filled this role. However, K⁺ concentration must still follow the concentration of Na⁺ in keeping with the principle of iso-osmolality because water can generally move in and out of cells. The presence of K⁺ allowed the distribution of water to be controlled despite differences in the electrolyte compositions of the extracellular and intracellular spaces. The regulation of these differences in concentrations occur through the activity of selective channels and exchangers that control the influx or efflux of these key elements across membranes. Na⁺ has the central role for the whole body regulation of osmolality because Na⁺ ions are directly taken in or excreted from outside the organism (Hollenberg 1980; Manning Jr. and Guyton 1982). This sets the osmolality of plasma and the interstitial space. The concentration of K⁺ inside cells, too, is dependent upon the osmolality of the surrounding interstitial space. The concentration of K⁺ is regulated by the exchange with Na⁺, gated channels in the membrane that allow influx and efflux of K⁺ and the movement of water from the space outside cells, i.e., interstitial space. K⁺ also has evolved with the important role of maintaining transmembrane potentials. Because of this, the concentration of K⁺ across cell membranes must be controlled in a tight range to protect life-sustaining cell functions.

Water movement due to non-charged molecules is divided into a diffusive component down a concentration gradient that does not involve water movement and a convective component that occurs with water flux. The two factors for movement of a non-charged substance are the ease with which the substance can cross a mem-

brane, which is called the diffusive permeability (P_D), and its reflection coefficient, σ .

$$\text{Solute flux } (J_s) = \underset{\text{Diffusive}}{P_d * \Delta [c]} + \underset{\text{Convective}}{(1 - \sigma) * J_v * [C]_m} \quad (10.6)$$

where J_s is the solute flux, J_v is the volume flux, and P_d is the diffusive permeability. P_d can be high because a substance is lipophilic and can diffuse across membranes or because the substance is carried by active transport mechanisms.

Glucose is an example of a substance that can be osmotically active, i.e., has a σ close to 1, but normally does not create an osmotic gradient because of the many mechanisms that transport glucose into cells and its rapid metabolism. However, in type II diabetes, increases in glucose concentration can produce osmotic activity and water shifts. An important example is hyperosmolar hyperglycemia (Bear and Neil 1983). In this condition, a stress, such as an infection or myocardial infarction, triggers a rapid increase in plasma and interstitial glucose concentration because of uncontrolled glucose production, primarily by the liver, and decreased peripheral glucose uptake. Both of these are related to insulin resistance. The increase in extracellular osmolality pulls intracellular water out of cells and into the extracellular space. Plasma Na⁺ concentration is diluted and there is a hyperosmolar plasma but hyponatremia. Most often, true total body Na⁺ is reduced because Na⁺ and water are lost by glucose-induced osmotic diuresis. When glucose is subsequently decreased, Na⁺ concentration rises because there is a greater loss of water than Na⁺ and the dehydration becomes obvious. It is clinically important to determine what the true Na⁺ concentration will be when the hyperosmolar glucose state is dealt with because this predicts how much and what type of water is needed during resuscitation. This expected increase can be estimated in mMol by subtracting 5 from the measured glucose and dividing by 3.5 (Katz 1973). There are a number of assumptions in this calculation including that the extracellular osmolality does not completely equilibrate with intracellular osmolality, extracellular water is 14 L, the solute in cells does not change, there is no Na⁺ in cells,

and the cells have no free glucose, all of which are not true but still allow an approximation.

Urea illustrates the difference between P_d and σ . Urea is hydrophobic. It normally has a σ close to 1 and a low P_d . However, along the inner medullary collecting ducts, there are urea transporters and aquaporin for the movement of water molecules. These allow independent urea and water movement under the control of antidiuretic hormone (Bhave and Neilson 2011a). P_d thus can be high and σ near 1, and urea then can create an osmotic gradient. An important variable for permeability is the surface area for the movement of a substance (Sands 1999). Although urea normally has a low P_d and σ near 1, the total area of cell membranes is large and urea production is relatively low, so that normally a concentration difference across cell membranes does not build up. In capillaries, σ also is <0.01 , because urea can pass easily through inter-endothelial pores producing a high P_d . However, this is not true in the brain and this can produce an important clinical problem. Cerebral capillaries have a low diffusive permeability, i.e., low P_d , because they lack urea transporters. They also have a σ of 0.5. During dialysis, urea in the blood can fall rapidly and this can produce a sufficient concentration difference between the brain interstitial space and plasma which creates an osmotic force that makes the water move into the brain. The result can be what is called dialysis disequilibrium syndrome (Silver et al. 1996).

A special type of osmotic pressure is called colloid osmotic or oncotic pressure. This force is due to large molecules in the plasma space that cannot readily move across vascular walls. Their osmotic force thus is limited to the plasma space. The presence of colloids in the blood results in the osmotic pressure in the blood being slightly higher than that of the interstitial and intracellular spaces. The presence of this positive osmotic pressure gradient between the plasma and interstitial space creates an inward pressure difference that counteracts the outward hydrostatic pressure. The result is a reduction of fluid filtration out of capillaries and maintenance of plasma volume (Levick and Michel 2010; Adamson et al. 2004). The plasma oncotic pressure normally is

approximately 25 mmHg, and 65 to 75% of this value is accounted for by albumin (Bhave and Neilson 2011a; Diem and Lentner 1970). Even though albumin is a large molecule with a concentration of ~ 40 g/L in the plasma, recall that osmotic pressure is dependent upon particle number and not mass. To calculate its osmotic effect, the total mass is converted to moles by dividing by the molecular weight of albumin which is 69 kDa. This gives the number of moles of albumin, which normally is around 0.58 mmol/kg. As a result, albumin produces an osmotic pressure of 11.2 mmHg. However, this value is less than the full effect of albumin in resisting the outward hydrostatic force.

Albumin molecules can dissociate and have a negative charge (Figge et al. 1992). The charge depends upon its isoelectric point (pKa), which for albumin is ~ 5 , relative to normal plasma pH of 7.4. The negative charge creates an electrical force that attracts oppositely charged ions, which in plasma is primarily countered by Na^+ . This results in a slightly higher concentration of Na^+ in plasma than in the interstitial space. By the same argument, Cl^- concentration is higher in the interstitial space than in plasma. The final concentrations of Na^+ and Cl^- in the plasma and interstitial spaces depend upon the equilibrium of their concentration gradients, the charge differences, the osmolality differences, and oncotic pressure, all of which affect water movement. The interaction of oncotic forces and charge forces is described by what is known as the Gibbs-Donnan relationship (West 1985; Sperelakis 1997; Overbeek 1956) (Kellum and Elbers 2009). The electrical component adds an inward force of 5.8 mmHg, which increases the net oncotic effect of albumin to 16 to 18 mmHg. In total, albumin accounts for 65 to 75% of the total plasma oncotic inward pressure. Although the same factors in the Gibbs-Donnan relationship exist across cell walls, the $\text{Na}^+\text{-K}^+$ adenosine triphosphate pump creates a much stronger force that easily overrides the Gibbs-Donnan relationship across cell walls (West 1985).

Albumin can be consumed rapidly during inflammatory states because it is part of the acute phase reaction. The fall in albumin con-

centration markedly reduces effective plasma oncotic pressure and allows increased fluid filtration. Other proteins in plasma are less osmotically effective because their molecular weights generally are even larger than albumin's, so that they have less particles per mass. Somewhat surprisingly, there is a condition called congenital analbuminemia in which sufferers have no albumin, yet these patients still survive without major edema (Koot et al. 2004; Kallee 1996). This occurs because the concentrations of smaller sized globulins increase. These smaller globulins also increase to some extent in inflammatory hypoalbuminemia because small $\alpha 1$ and $\alpha 2$ globulins are also part of the acute phase reaction, too, (Vavricka et al. 2009), although their effect is less efficient than in analbuminemia, because the large β fraction is unchanged and the larger γ fraction increases with chronicity of the inflammatory process (Kaysen 1993). Because of these changes in plasma protein concentration with hypoalbuminemia, the concentration of all plasma protein need to be assessed to predict the effect of the albumin loss on plasma oncotic pressure (Bhave and Neilson 2011a; Barclay and Bennett 1987).

A final determinant of plasma volume is the number of red cells and their size.

Large proteins, such as albumin, become part of the solution and create an effective osmotic force. This is not the case for red cells. They are not in solution, but rather act as a suspension in the plasma and do not contribute to plasma osmotic pressure. This means that an increase in the number of red cells does not "draw" water into the plasma space as occurs with the oncotic effect of proteins. Two simple considerations should make this obvious. In the initial stage of a large bleed, hemoglobin concentration does not change because plasma and red cells are lost equally. It is only when fluid is recruited from the interstitial space back into the plasma space, or a crystalloid solution is infused, that the loss of red cells and the decrease in the total amount of hemoglobin become obvious. On the other side, administration of packed red blood cells would not change the hemoglobin concentration if red cells had an osmotic drew water from the interstitial space into the plasma space. What red cells

do is create a mass effect in vessels by taking up space. This mass still contributes to the hydrostatic pressure on the vascular wall and thus contributes to blood pressure. However, the effect of a transfusion is proportionally smaller than what occurs with an increase in the fluid component because red cell mass is a smaller fraction of the total blood volume than plasma volume. For example, if the initial blood volume is 5 L, a change in Hct from 20 to 25 would increase blood volume by 5%, whereas a change in plasma volume from 3 L to 3.5 L would change it by 10%.

Extracellular Fluid Dynamics

This is discussed in detail in Chap. 6 (Dr. Curry), but a few points relative to edema formation will be reviewed here. As indicated by Dr. Curry, the revised understanding of Starling's forces is that there is a net filtration of fluid from the capillaries under normal conditions (Levick and Michel 2010; Adamson et al. 2004). This is determined by the positive outward hydrostatic gradient across the capillaries which is produced by the intravascular capillary pressure of approximately 24 mmHg and hydrostatic pressure in the interstitial space of close to zero. This force is countered by the inward gradient in oncotic pressure of the intravascular space relative to the oncotic pressure in the ECF, which is primarily due to the presence of albumin. It was initially thought that the albumin concentration in the interstitial space is very low, but it now is evident that 10 g of albumin moves into the interstitial space and then the into the lymphatics per hour (Renkin 1986). The concentration of albumin in the ICF is 10 to 15 g/L and accounts for 25 to 50% of total body albumin (Renkin 1986). Based on these numbers, the interstitial albumin normally turns over approximately twice per day. However, the interstitial space is not a simple system and actually comprises three systems: a free flowing fluid that contains albumin, a gel phase that contains glycosaminoglycans (CAGs), and a collagen-based matrix. Water and small solutes move through all three compartments (Maroudas 1970), but albumin

only is found in the free flowing component (Reed et al. 1989). This produces an effective albumin concentration in the interstitial space of 20 to 30 g/L and an oncotic force that is 30 to 60% of that of the plasma (Bhave and Neilson 2011a).

The discovery that interstitial albumin is not close to zero, but rather almost 50% that of plasma, created a challenge to the classic Starling hypothesis for fluid filtration from capillaries. This has been resolved by the understanding the role of the glycocalyx on the vascular surface of endothelial cells. This region provides an area with a lower albumin concentration than the whole ECF and can alter filtration rates as discussed in detail in Chap. 6 (Dr. Curry) (Levick and Michel 2010).

A number of local counter-regulatory mechanisms prevent excessive volume loss by excessive filtration. When filtration is high, water flux outstrips albumin flux, and interstitial albumin concentration is diluted. This increases the net oncotic gradient across vascular walls, which reduces net filtration rate. By this mechanism, interstitial Π is kept at about 50% of plasma Π . Another feature of the interstitial space also helps. Normal hydrostatic pressure in the interstitial space is close to zero. However, the ISF space normally is very non-compliant (Wiig and Reed 1981; Reed and Wiig 1981; Guyton 1965). Thus, an increase in interstitial volume because of increased fluid filtration quickly increases the interstitial space hydrostatic pressure. This decreases the hydrostatic pressure gradient from the plasma to the interstitium and reduces capillary filtration rate (Reed et al. 1989). Unfortunately, the effect is limited. When interstitial volume increases by more than 20 to 50%, and the interstitial pressure rises above approximately 4 mmHg, the interstitial space becomes very compliant and edema can rapidly increase with little change in the interstitial hydrostatic pressure (Wiig and Reed 1981; Reed and Wiig 1981; Guyton and 1965). This increase in interstitial compliance occurs through the interaction of cell surface integrin receptors with the extracellular collagen

matrix and force generating actin tension in the cytoskeleton (Berg et al. 2001; Lund et al. 1989; Lund et al. 1988; Reed et al. 2001; Reed and Rubin 2010; Pozzi and Zent 2003). The same increase in the interstitial compliance also occurs in inflammatory states or thermal injury by cytokine action and greatly increases capillary leak. *A key message from this section is that edema can produce further edema, and large volume resuscitation can make things worse.*

Nephrotic syndrome demonstrates a number of challenges to vascular fluid balance. Aside from the presence of hypoalbuminemia, the proportion of high molecular weight proteins increases because small-sized proteins are preferentially lost. Thus, unlike what occurs in analbuminemic subjects, plasma oncotic pressure falls in proportion to the fall in albumin. The fall in plasma oncotic pressure leads to increased capillary filtration. As described above, the increased fluid flux increases interstitial P_i and lowers interstitial oncotic pressure so that the interstitial oncotic pressure remains at about 50% of the plasma oncotic pressure or about 12 mmHg (Koomans et al. 1986). However, when interstitial oncotic pressure falls to zero, it cannot be lowered further. When that happens, a further fall in plasma albumin cannot be defended by a further fall in interstitial oncotic pressure. The ratio of plasma to interstitial oncotic pressure falls and edema is inevitable. This can result in a rapid decrease in intravascular volume and is known as a nephrotic crisis in pediatrics (Van de Walle et al. 1996).

Movement and Distribution of Fluids

In this section, I will discuss the distribution of infused exogenous fluids among the different water compartments. So far in this chapter, the discussion of water movement largely has been based on osmotic forces, but as was evident in the discussion on colloids, not all osmoles have the same effect on cell volumes, which is a major homeostatic processes (Levick and

Michel 2010). In this regard, there are osmoles that are effective and others that are ineffective for the regulation of cell volume. At this time, it is necessary to introduce the term tonicity. This term is used to describe only effective osmolality across membranes (Gennari 1984; Mange et al. 1997). An isotonic solution can be defined pragmatically as one in which added red cells, with a normal intracellular osmolality, do not shrink or swell. When plasma osmolality is normal (~290 mOsm/kg), the terms iso-osmolar and isotonic are equivalent. However, a good example of the difference between isotonicity and iso-osmolality is what happens when ethanol is added to plasma. Ethanol elevates osmolality but does not alter tonicity because it rapidly diffuses across cell membranes and increases intracellular osmolality to the same extent as in the extracellular space and cell volumes do not change (Bhave and Neilson 2011a). Iso-tonicity thus is more physiologically relevant than iso-osmotic.

The abundance of molecules inside cells that only poorly permeate to the outside, substances that interact with other molecules inside the cell, and the large K^+ concentration that acts as a counter ion to Na^+ outside cells, create a large Gibbs-Donnan effect. This produces an osmotic gradient that favors persistent water intake by cells. However, this does not happen because it is countered by the $Na^+-K^+-ATPase$, which actively extrudes Na^+ and, consequently, also draws Cl^- out of the cell to preserve electrical neutrality (Levick and Michel 2010). This process effectively makes the cell impermeable to Na^+ , Cl^- , and K^+ ions because these ions are regulated by exchangers and gated channels (Bhave and Neilson 2011a). Water passively distributes between ECF and ICF based on Na^+ and K^+ concentrations and osmotic equilibrium (tonicity) to preserve cell volume.

An important assumption in the following discussion is that the patient's initial plasma osmolality is normal, but in clinical practice, this frequently is not the case. Thus, solutions considered to be iso-osmotic or iso-oncotic relative to normal plasma are often not so in relation to the patient's plasma.

Pure Water and Dextrose in Water

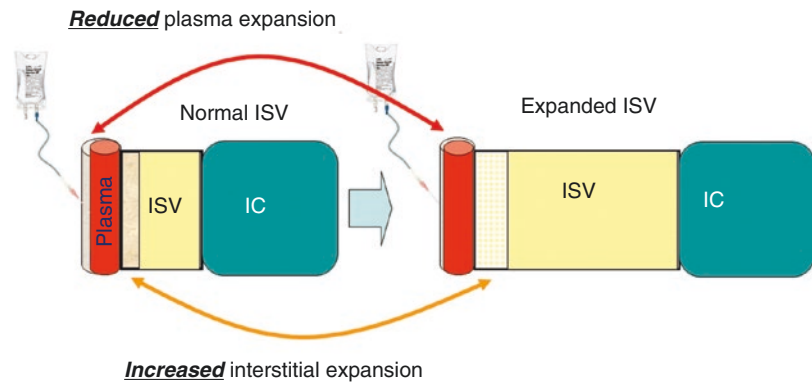
Water in the gastrointestinal tract is taken up by the intestinal walls and then is passed into the vasculature. This decreases the osmolality of plasma relative to that of the interstitial space so that the water moves to the higher osmolality in the interstitial space. This in turn lowers the osmolality of the interstitial space relative to the intracellular space and water moves into cells until osmolality is again equal in all compartments, except for the slightly higher plasma osmolality produced by the colloid oncotic pressure and Gibbs-Donnan effect (Bhave and Neilson 2011a; Overbeek 1956). The same occurs when 5% dextrose in water (D5W) is infused into the plasma space. Initially, the osmolality of D5W is the same as that of normal plasma and no movement of the water is expected. However, the dextrose moves into the interstitial space and cells and is metabolized. The plasma osmolality becomes diluted by the added water. The water then moves into the interstitial space and cells by osmosis just as with pure water coming from the gut. There also is some dilution of the concentration of Na^+ and Cl^- which will have transient effects on the charge and concentrations in different compartments until water is in equilibrium in all compartments.

Two other things happen when water is added to the plasma space. The increase in volume increases the hydrostatic pressure in the micro-circulation and decreases plasma oncotic pressure by diluting the concentration of albumin and other proteins. Both of these processes increase filtration across the vascular walls (Levick and Michel 2010).

Normal Saline

Normal saline is a 0.9% solution and is made so that it is isotonic to normal plasma. Na^+ is 154 mEq/L in the normal saline rather the 140 mEq/L in normal plasma, because to make it isotonic to plasma, a higher concentration of Na^+ is needed to account for the other substances dissolved in plasma. Isotonic normal saline

Fig. 10.4 Normal saline infusion with normal interstitial volume (ISV) (left) and expanded ISV (right). Plasma expansion is much less and ISV greater when ISV is expanded above normal values. *IC* intracellular volume



should primarily increase the plasma volume. However, the normal saline solution increases plasma Cl^- concentration which moves down its concentration gradient into the interstitial space. This drags some Na^+ with it for electrical neutrality and some water to maintain osmolality. The saline also dilutes plasma proteins and decreases oncotic pressure, which allows more filtration. In the end, the saline solution should distribute between the plasma and interstitial spaces based on their initial relative volumes and the Gibbs-Donnan equilibrium. The usual distribution based on the relative sizes of normal plasma and interstitial volumes is said to be one-third plasma and two-thirds interstitial (Fig. 10.1). Intracellular volume should not change because it has the same osmolality as the interstitial space, and at equilibrium the osmolality of the interstitium will be the same as in plasma because the normal saline was isotonic. However, if the osmolality of the plasma and interstitial spaces is lower than normal, the normal saline will be hypertonic relative to the patient's plasma and cells, and some volume will be drawn out of cells. This effect should be small because the added Na^+ and Cl^- are distributed in the whole extracellular volume. If the extracellular space is greatly expanded because of retained fluid, the proportion of volume of the infused saline that remains in the vascular space is greatly decreased. For example, in a person who has 30 L of ascites and 12 L of interstitial volume, the total extracellular volume is 42 L, but the plasma volume likely still is only

~3 L. Thus, only about 70 ml of the 1 L of added normal saline will remain in the vascular space, and this amount gets smaller each time more crystalloid volume is added (Fig. 10.4).

Hypertonic Sodium Chloride Solutions

There has been a lot of interest in the use of hypertonic NaCl solutions because of their potential to expand intravascular volume faster and with less volume than normal saline (Santry and Alam 2010). These solutions have been especially studied for use in blunt and hemorrhagic trauma, but studies have failed to show a benefit (Bulger et al. 2011; Bulger et al. 2010). It is worth emphasizing again that volume balance really is about Na^+ balance. Consideration of the distribution of these solutions can help understand why they have failed to provide a benefit. The final effect of hypertonic saline depends upon the initial concentration of Na^+ in plasma, the plasma volume, the rate of bleeding, the renal function, and the amount given, for in the end what counts is how much the plasma concentration of Na^+ and osmolality change. The 7.5% solution of NaCl used in some of these studies (Bulger et al. 2011; Bulger et al. 2010) contains 129 mEq/100 ml of Na^+ compared to 15 mEq/100 ml in 0.9 saline. Thus, each 250 ml bolus adds 321 mEq of Na^+ to the plasma and also greatly increases Cl^- , which will have a marked acidifying effect. If this solution stays in

the plasma space, it would increase the plasma Na^+ concentration to over 200 mEq/L, but instead the Na^+ and Cl^- rapidly move into the interstitial space. Typical Na^+ concentrations in the first 2 hours were in the 150 mEq/L range (Han et al. 2015), but very high concentrations were reached with repeated use (Wells et al. 2012). Initial values are not reported in the publications, but the very large Na^+ load on the system would likely have quickly drawn water out of the interstitial space, and Na^+ and Cl^- would rapidly move down their concentration gradients, increase interstitial osmolality, and pull water out of cells. As discussed above, this will induce intracellular transcriptional processes and the consequences cannot reliably be predicted because this is as much a pharmacological effect as a volume effect.

Iso-oncotic Colloids

A 5% solution of albumin is iso-oncotic and iso-osmotic compared to normal blood. Infusion of this solution expands the intravascular space and, theoretically, should not affect other compartments. The solvent for the solution is most often normal saline and distributes accordingly. If the patient's baseline albumin concentration is less than normal, the 5% solution is hyper-oncotic relative to that patient's plasma and behaves to some degree as a hyper-oncotic solution, which is discussed in the next section.

Starch solutions come in many different concentrations and molecular sizes (Treib et al. 1999). The precise oncotic value of a starch solution is difficult to assign because the oncotic effect is related to the number of particles, and serum amylase rapidly breaks starches into smaller particles. As the particle number goes up, so does the oncotic effect. When the particles are small enough, they are excreted by the kidney, which lowers the number of particles and the oncotic effect. The rate of breakdown of starch molecules can be changed by engineering the number of hydroxyethyl groups and where these are placed on glucose molecules (Treib et al. 1999). Starches therefore can function between iso-oncotic and hyperoncotic colloids, and the

effect depends upon the initial concentration and size of the starch molecules, the rate of breakdown, which is dependent upon the substitution of the hydroxyethyl groups on the glucose molecules (Treib et al. 1999) and the plasma amylase activity.

Hyper-oncotic Solutions

A solution of 25% albumin is the prototypic example of a hyper-oncotic solution, i.e., one that has an oncotic effect greater than normal blood. The added volume expands the vascular space by a small amount, but because it also increases the oncotic pressure, it draws fluid from the interstitial space. As an example, an infusion of 100 ml of a 25% solution (25 g/100 ml) into someone with a plasma volume of 3.5 L and an albumin concentration of 25 g/L would theoretically increase the albumin concentration by 36% and the oncotic pressure by 25% (assuming albumin accounts for 70% of the total plasma oncotic pressure). This sudden increase in oncotic pressure likely transiently pulls water from the interstitial space into the plasma space, or at least significantly reduces filtration. Na^+ and Cl^- will follow the water, although not necessarily at the same rate, because initially the solutions have the same electrolyte composition, but a new Gibbs-Donnan equilibrium will ensue because of the higher albumin concentration. The shrinkage of the interstitial space and possible change in interstitial electrolyte composition could then result in loss of water from cells. Furthermore, the albumin is most often in a normal saline solution so that shifts associated with Na^+ and Cl^- also occur. Some leak of the albumin into the interstitial space should also be expected. This will increase the oncotic pressure in the interstitial space and could draw more water out of the intracellular space. The consequence of all these process is activation of intracellular stress signaling pathways and expression of stress molecules (O'Neill 1999; Shrode et al. 1970). Thus, 25% albumin does not act only as a volume expander, but it produces a "pharmacologic" effect by the associated fluid and elec-

trolyte shifts from cells (Magder and Lagonidis 1999). Hyper-oncotic hetastarches might act in a similar way (Potter et al. 2013). In addition, albumin binds many substances and can act as an antioxidant, which could further produce non-volume effects (Vincent et al. 2014). In support of this, 25% albumin has been shown to produce an apparent increase in cardiac function independent of its volume expansion (Magder and Lagonidis 1999).

Sodium Bicarbonate Solution

As a way of giving Na^+ without Cl^- , a solution can be made by putting three ampoules containing 44 mEq of sodium bicarbonate (NaHCO_3) in D5W. The final concentration of Na^+ is 132 mEq/L which is slightly hypotonic. This Na^+ of the solution should distribute between the plasma and interstitial space as occurs with Na^+ in normal saline, and the excess water will distribute in all fluid compartments. The HCO_3^- will be in equilibrium with H_2CO_3 and dissolved CO_2 in serum. PCO_2 is regulated by ventilation and so the added HCO_3^- is cleared by ventilation. However, if the patient is mechanically ventilated, and has no spontaneous efforts, CO_2 in the body will increase and be distributed in total body water with a consequent fall in pH (Jones 2008).

Summary

The major point covered in this chapter is that the total amount of Na^+ in the body dictates the amount of water in the body. Fluid balance thus is about Na^+ balance. Elements such as Na^+ , K^+ , and Cl^- only can be absorbed or excreted, and thus intake and output of Na^+ in particular needs to be followed carefully when managing critically ill patients. All fluid-filled compartments are connected in a dynamic equilibrium so that movement of fluids and electrolytes across all spaces needs to be considered when managing fluid balance. Finally, it is important to distinguish between the concentration and the total amount of substances.

References

- Adamson RH, Lenz JF, Zhang X, Adamson GN, Weinbaum S, Curry FE. Oncotic pressures opposing filtration across non-fenestrated rat microvessels. *J Physiol.* 2004;557(Pt 3):889–907.
- Aukland K, Nicolaysen G. Interstitial fluid volume: local regulatory mechanisms. *Physiol Rev.* 1981;61(3):556–643.
- Ball P. A biography of water: life's matrix. University of California Press; 2001.
- Barclay SA, Bennett D. The direct measurement of plasma colloid osmotic pressure is superior to colloid osmotic pressure derived from albumin or total protein. *Intensive Care Med.* 1987;13(2):114–8.
- Bear RA, Neil GA. A clinical approach to common electrolyte problems. 1. Hyponatremia. *Can Med Assoc J.* 1983;128(10):1171–4.
- Berg A, Rubin K, Reed RK. Cytochalasin D induces edema formation and lowering of interstitial fluid pressure in rat dermis. *Am J Physiol Heart Circ Physiol.* 2001;281(1):H7–13.
- Bhave G, Neilson EG. Body fluid dynamics: back to the future. *J Am Soc Nephrol JASN.* 2011a;22(12):2166–81.
- Bhave G, Neilson EG. Volume depletion versus dehydration: how understanding the difference can guide therapy. *American Journal of kidney Diseases : The Official Journal of the National Kidney Foundation.* 2011b;58(2):302–9.
- Bishopric NH. Evolution of the heart from bacteria to man. *Ann NY Acad Sci.* 2005;1047:13–29.
- Bulger EM, May S, Brasel KJ, Schreiber M, Kerby JD, Tisherman SA, et al. Out-of-hospital hypertonic resuscitation following severe traumatic brain injury: a randomized controlled trial. *JAMA.* 2010;304(13):1455–64.
- Bulger EM, May S, Kerby JD, Emerson S, Stiell IG, Schreiber MA, et al. Out-of-hospital hypertonic resuscitation after traumatic hypovolemic shock: a randomized, placebo controlled trial. *Ann Surg.* 2011;253(3):431–41.
- Diem K, Lentner C. Composition and functions of the body. Scientific tables. 7th ed. Basle: Ciba-Geigy Limited; 1970. p. 526.
- Figge J, Mydosh T, Fencl V. Serum proteins and acid-base equilibria: a follow-up. *J Lab Clin Med.* 1992;120:713–9.
- Freedman JC. Biophysical chemistry of physiological solutions. In: Sperelakis N, editor. *Cell physiology source book.* 2nd ed. Toronto: Academic Press; 1997. p. 3–17.
- Gennari FJ. Current concepts. Serum osmolality. Uses and limitations. *N Engl J Med.* 1984;310(2):102–5.
- Guyton AC, INTERSTITIAL FLUID PRESSURE. II. Pressure-volume curves of interstitial space. *Circ Res.* 1965;16:452–60.
- Han J, Ren HQ, Zhao QB, Wu YL, Qiao ZY. Comparison of 3% and 7.5% hypertonic saline in resuscitation after traumatic hypovolemic shock. *Shock.* 2015;43(3):244–9.

- Hollenberg NK. Set point for sodium homeostasis: surfeit, deficit, and their implications. *Kidney Int.* 1980;17(4):423–9.
- Jones NL. An obsession with CO₂. *Appl Physiol Nutr Metab.* 2008;33(4):641–50.
- Kallee E. Bennhold's analbuminemia: a follow-up study of the first two cases (1953–1992). *J Lab Clin Med.* 1996;127(5):470–80.
- Katz MA. Hyperglycemia-induced hyponatremia—calculation of expected serum sodium depression. *N Engl J Med.* 1973;289(16):843–4.
- Kaysen GA. Plasma composition in the nephrotic syndrome. *Am J Nephrol.* 1993;13(5):347–59.
- Kellum JA, Elbers PWG. Peter Stewart's Textbook of Acid-Base: www.acidbase.org; 2009.
- Koomans HA, Geers AB, Dorhout Mees EJ, Kortlandt W. Lowered tissue-fluid oncotic pressure protects the blood volume in the nephrotic syndrome. *Nephron.* 1986;42(4):317–22.
- Koot BG, Houwen R, Pot DJ, Nauta J. Congenital analbuminaemia: biochemical and clinical implications. A case report and literature review. *Eur J Pediatr.* 2004;163(11):664–70.
- Levick JR, Michel CC. Microvascular fluid exchange and the revised Starling principle. *Cardiovasc Res.* 2010;87(2):198–210.
- Lund T, Onarheim H, Wiig H, Reed RK. Mechanisms behind increased dermal imbibition pressure in acute burn edema. *Am J Phys.* 1989;256(4 Pt 2):H940–8.
- Lund T, Wiig H, Reed RK. Acute postburn edema: role of strongly negative interstitial fluid pressure. *Am J Phys.* 1988;255(5 Pt 2):H1069–74.
- Macknight AD, Leaf A. Regulation of cellular volume. *Physiol Rev.* 1977;57(3):510–73.
- Magder S. Physiologic principles of fluid management. *Pediatr Crit Care Med.* 2001;2([suppl.] (3)):s4–9.
- Magder S. Balanced versus unbalanced salt solutions: what difference does it make? *Best Pract Res Clin Anaesthesiol.* 2014;28:235–47.
- Magder S, De Varennes B. Clinical death and the measurement of stressed vascular volume. *Crit Care Med.* 1998;26:1061–4.
- Magder S, Emami A. Practical approach to physical-chemical acid-base management. *Stewart at the bedside Ann Am Thorac Soc.* 2015;12(1):111–7.
- Magder S, Lagonidis D. Effectiveness of albumin versus normal saline as a test of volume responsiveness in post-cardiac surgery patients. *J Crit Care.* 1999;14(4):164–71.
- Mange K, Matsuura D, Cizman B, et al. Language guiding therapy: the case of dehydration versus volume depletion. *Ann Intern Med.* 1997;127(9):848–53.
- Manning RD Jr, Guyton AC. Control of blood volume. *Rev Physiol Biochem Pharmacol.* 1982;93:70–114.
- Maroudas A. Distribution and diffusion of solutes in articular cartilage. *Biophys J.* 1970;10(5):365–79.
- Mudge GH. Agents affecting volume and composition of body fluids. In: Goodman-Gilman A, Goodman LS, Gilman A, editors. *The Pharmacological basis of therapeutics*. 6th ed. New York: Macmillan Publishing Co., Inc; 1980. p. 848–84.
- O'Neill WC. Physiological significance of volume-regulatory transporters. *Am J Physiol.* 1999;276(45):C995–C1011.
- Orlov SN, Hamet P. Intracellular monovalent ions as second messengers. *J Membr Biol.* 2006;210(3):161–72.
- Overbeek J. The Donnan equilibrium. *Prog Biophys Biophys Chem.* 1956;6:57–84.
- Pitts RF. Mechanisms of Reabsorption and Excretion of Ions and Water. *Physiology of the Kidney and Body Fluids: an introductory text*. second. Chicago: Year Book Medical Publishers Incorporated; 1968. p. 94–128.
- Potter BJ, Deverenne B, Doucette S, Fergusson D, Magder S. Cardiac output responses in a flow-driven protocol of resuscitation following cardiac surgery. *J Crit Care.* 2013;28(3):265–9.
- Pozzi A, Zent R. Integrins: sensors of extracellular matrix and modulators of cell function. *Nephron Exp Nephrol.* 2003;94(3):e77–84.
- Raw JD. Water. In: Daisy LP, Hodgins KC, O'Quin TL, Olsen S, Swan JA, editors. *Biochemistry*. Burlington: Neil Patterson Publishers; 1989. p. 27–47.
- Reed RK, Berg A, Gjerde EA, Rubin K. Control of interstitial fluid pressure: role of beta1-integrins. *Semin Nephrol.* 2001;21(3):222–30.
- Reed RK, Lepsoe S, Wiig H. Interstitial exclusion of albumin in rat dermis and subcutis in over- and dehydration. *Am J Phys.* 1989;257(6 Pt 2):H1819–27.
- Reed RK, Rubin K. Transcapillary exchange: role and importance of the interstitial fluid pressure and the extracellular matrix. *Cardiovasc Res.* 2010;87(2):211–7.
- Reed RK, Wiig H. Compliance of the interstitial space in rats. I. Studies on hindlimb skeletal muscle. *Acta Physiol Scand.* 1981;113(3):297–305.
- Renkin EM. Some consequences of capillary permeability to macromolecules: Starling's hypothesis reconsidered. *Am J Phys.* 1986;250(5 Pt 2):H706–10.
- Sands JM. Urea transport: It's not just "freely diffusible" anymore. *News Physiol Sci.* 1999;14:46–7.
- Santry HP, Alam HB. Fluid resuscitation: past, present, and the future. *Shock.* 2010;33(3):229–41.
- Shrode LD, Klein JD, Douglas PB, O'Neill WC, Putnam WC. Shrinkage-induced activation of Na⁺/H⁺ exchange: role of cell density and myosin light chain phosphorylation. *Am J Physiol.* 1970;272:C1968–C79.
- Silver SM, Sterns RH, Halperin ML. Brain swelling after dialysis: old urea or new osmoles? *American Journal of Kidney Diseases* : The Official Journal of the National Kidney Foundation. 1996;28(1):1–13.
- Sperelakis N. Gibbs-Donnan equilibrium potentials. In: Sperelakis N, editor. *Cell physiology source book*. 2nd ed. Toronto: Academic Press; 1997. p. 202–6.
- Stein WD. Cell volume homeostasis: ionic and nonionic mechanisms. The sodium pump in the emergence of animal cells. *Int Rev Cytol.* 2002;215:231–58.

- Treib J, Baron JF, Grauer MT, Strauss RG. An international view of hydroxyethyl starches. *Intensive Care Med.* 1999;25(3):258–68.
- Van de Walle JG, Donckerwolcke RA, Greidanus TB, Joles JA, Koomans HA. Renal sodium handling in children with nephrotic relapse: relation to hypovolaemic symptoms. *Nephrology, dialysis, transplantation : official publication of the European Dialysis and Transplant Association - European Renal Association.* 1996;11(11):2202–8.
- Vavricka SR, Burri E, Beglinger C, Degen L, Manz M. Serum protein electrophoresis: an underused but very useful test. *Digestion.* 2009;79(4):203–10.
- Vincent J-L, Russell JA, Jacob M, Martin G, Guidet B, Wernerman J, et al. Albumin administration in the acutely ill: what is new and where next? *Critical Care.* 2014;18(4):231.
- Wells DL, Swanson JM, Wood GC, Magnotti LJ, Boucher BA, Croce MA, et al. The relationship between serum sodium and intracranial pressure when using hypertonic saline to target mild hypernatremia in patients with head trauma. *Crit Care.* 2012;16(5):R193.
- West JB. *Physiology of the body fluids. Physiological basis of medical practice.* 11th ed. Baltimore/London: Williams & Wilkins; 1985. p. 438–50.
- Wiig H, Reed RK. Compliance of the interstitial space in rats. II. Studies on skin. *Acta Physiol Scand.* 1981;113(3):307–15.



Christine E. Yeager and Thomas P. Bleck

Introduction to Intracranial Physiology

The brain is unique in that despite contributing only 2% of overall body mass, it receives 12% of the cardiac output and accounts for about 20% of resting oxygen demand (Madhok et al. 2018; Meng et al. 2015). Understanding intracranial physiology starts with the Monro-Kelli hypothesis, which states that the total volume of brain parenchyma (about 85% of the intracranial compartment), cerebrospinal fluid (about 5%), and blood (about 10%) remains constant; therefore, a shift in one component must cause a shift in another (Madhok et al. 2018). This concept is not completely true, as total intracranial volume varies during the cardiac cycle (le Roux et al. 2013) and further research has revealed the presence of additional components in the brain such as the glymphatic system. The glymphatic is the proposed waste elimination pathway of the central nervous system (Jessen et al. 2015). The brain consists primarily of water, with the majority of the water intracellular and the rest interstitial

(Ropper et al. 2004). Typically, volumetric changes of the brain parenchyma develop over time, in contrast to the relatively rapid changes that can occur to in the volume of blood or cerebrospinal fluid (Kim et al. 2012). Two mechanisms can increase the water content of the brain: cytotoxic edema and vasogenic edema. However, only vasogenic edema causes a net increase in brain volume (Ropper et al. 2004).

Cerebral Blood Flow and Circulation

Since blood is one of the three main intracranial components, it is important to understand the complexity of the cerebral circulation. A major determinant of cerebral blood volume (CBV) is cerebral blood flow (CBF)(Ropper et al. 2004). CBV is the volume of intravascular blood within the brain, and CBF represents the volume of blood which moves through the brain per unit of time (mL/min) (le Roux et al. 2013). In general, when CBF is increased, CBV also is increased and vice versa; however, pathologic states can change this relationship (le Roux et al. 2013). CBF is approximately 50 to 75 mL per 100 g brain tissue per minute under normal circumstances. Critical thresholds of CBF are needed to maintain normal tissue health and cellular integrity (le Roux et al. 2013; Ropper et al. 2004). At about 20 to 30 mL/100 g/min, patients typically develop neurologic symptoms, and below 10 mL/100 g/min,

C. E. Yeager (✉)
Department of Neurology, University of Minnesota,
Minneapolis, MN, USA

T. P. Bleck
Northwestern University Feinberg School of
Medicine, Davee Department of Neurology,
Chicago, IL, USA

Rush Medical College, Chicago, IL, USA

complete metabolic failure occurs and membrane integrity is compromised; this is one definition of ischemia (Madhok et al. 2018; le Roux et al. 2013). One of the most important determinants of CBF is vessel caliber, as resistance, and thus flow, changes with the fourth power of the radius; for example, 20% constriction can reduce the CBF by 60% if other factors stay the same (le Roux et al. 2013). Regional variations in CBF are tightly controlled to match these metabolic demands (Ropper et al. 2004). Substances that can alter vascular tone and local perfusion include carbon dioxide, potassium, adenosine, nitric oxide, histamine, neuropeptide Y, vasoactive intestinal peptide, calcitonin gene-related peptide, and prostaglandins (Verweij et al. 2007). Alteration of vascular tone by these mediators is termed metabolic autoregulation, and in general it is still poorly understood.

CPP and Pressure Autoregulation

Cerebral Perfusion Pressure

Cerebral perfusion pressure (CPP) is the blood pressure gradient across the brain vasculature or, in other words, the difference between arterial inflow and venous outflow pressure (le Roux et al. 2013; Ropper et al. 2004). Since the intracranial pressure (ICP) usually determines the venous outflow pressure, CPP is clinically estimated as the difference between mean arterial pressure (MAP) and ICP.

$$\text{CPP} = \text{MAP} - \text{ICP}$$

This is the driving pressure for CBF (le Roux et al. 2013), and the cerebrovascular resistance (CVR) can be estimated from Ohm's law, i.e., CPP divided by CBF (Madhok et al. 2018)

$$\text{CVR} = \text{CPP} / \text{CBF}$$

Pressure Autoregulation

CBF is maintained over a range of cerebral perfusion pressures via changes in arteriolar diameter and thus CVR, a process termed pressure auto-

regulation (le Roux et al. 2013; Ropper et al. 2004). This autoregulation is impaired by brain trauma and other pathologic processes (Ropper et al. 2004). As CPP falls, the arterioles in the brain dilate, reducing CVR in order to maintain CBF with an increased CBV (Ropper et al. 2004). Alternatively, when cerebral perfusion pressure is elevated, the arterioles constrict to maintain CBF with a reduced CBV (Ropper et al. 2004). Autoregulation in a normal adult is normally maintained when the MAP is between 50 mmHg and 150 mmHg; outside these limits, CBF and CBV passively follow CPP (le Roux et al. 2013; Ropper et al. 2004). Chronically hypertensive patients experience increases in both the lower and upper values of autoregulation (Ropper et al. 2004). When MAP exceeds the upper limits of autoregulation, it produces segmental dilation of arterial vessels, leading to disruption of the blood-brain barrier and causing cerebral edema; this is the genesis of hypertensive encephalopathy (le Roux et al. 2013). When MAP is below the lower limit, CBF is not maintained and ischemia occurs (Castro et al. 2018). In addition to brain trauma pressure, autoregulation may be impaired in pathological states including ischemic stroke, subarachnoid hemorrhage, and other etiologies of brain injury (Madhok et al. 2018; Ropper et al. 2004).

Elevated ICP and Relationships/Targets of CPP

According to the Monro-Kelli hypothesis, since the intracranial volume is fixed, any increase in total brain volume causes an increase in pressure (le Roux et al. 2013; Ropper et al. 2004). If pressure is elevated too high or for too long a period, intracranial contents will shift among one or more compartments, this leads to a herniation syndrome from displacement of brain parenchyma, or the development of ischemia and infarction from vascular compression (Cadena et al. 2017). Intracranial hypertension is currently defined as an elevation of ICP to above 22 mmHg for greater than 5 minutes (Cadena et al. 2017).

There is level IIB evidence that ICP above 22 mmHg should be treated, as a level higher than this has been shown to be associated with increased mortality (Carney et al. 2017). There is also level IIB evidence for targeting a CPP value between 60 and 70 mmHg to improve survival and favorable outcomes, but this target is often highly dependent on the degree to which cerebral autoregulation is intact (Carney et al. 2017). Intervention for a CPP less than 60 mmHg or an ICP greater than 22 mmHg should always be considered in the context of the patient; if a patient is stable and intact neurologically, there may be no need for intervention despite these values (Cadena et al. 2017).

Cerebral Metabolic Rate of Oxygen

As noted above, the brain requires significant energy due to its high metabolic demand, and as it does not have its own energy stores, it needs a constant supply of oxygen and glucose (Madhok et al. 2018). Cerebral blood flow is important for maintenance of intracranial physiology, but oxygen delivery is also important, and disruptions in this also contribute to ischemia (Verweij et al. 2007). The difference between oxygen content in the arterial blood supplying the brain and the venous blood exiting the brain is called the arteriovenous oxygen difference (AVDO₂) (Verweij et al. 2007). During the normal resting state with preserved CBF, the brain is estimated to extract 50 percent of oxygen from the arterial blood supply (Madhok et al. 2018). The cerebral metabolic rate of oxygen (CMRO₂) is the rate of oxygen consumption by the brain and is defined by the equation $CMRO_2 = CBF \times AVDO_2$ (Madhok et al. 2018). This equation is expanded as follows:

$$CMRO_2 = CBF \times (Y_a - Y_v) \times C_a$$

Where Y_a is the arterial oxygen saturation and Y_v is the venous oxygen saturation. C_a is the oxygen concentration of blood per 100 mL (Liu and Li 2016). Cerebral arterial blood contains about 13 volume % (ml O₂ / 100 ml blood) of O₂ and

venous blood contains about 6.7 volume%, which yields an AVDO₂ of about 6.3 volume % (Verweij et al. 2007). Using the first equation and estimating a CBF of about 50 mL/100 g brain tissue/min, the typical value of CMRO₂ is 3.2 mL of O₂/100 g of brain tissue/min (Verweij et al. 2007).

Cerebral Oxygenation and CO₂ Reactivity

Ischemia

One of the major goals in treating brain injury is to prevent the irreversible damage associated with infarction and brain ischemia. Our understanding of which patients will develop cerebral ischemia and how we detect it is still very limited. There is some evidence that CBF reductions are coupled to decreases in CMRO₂, at least when autoregulation is intact (Menon 2006). This coupling fails when CPP is outside of the limits of the autoregulatory plateau. CBF thresholds for irreversible cell injury have been shown to vary based on disease pathology, at least when considering ischemic stroke and traumatic brain injury (Cunningham et al. 2005). This suggests that other variables contribute to infarction and irreversible brain injury, but these have not been well defined. It is difficult to detect ischemia and prevent infarction with currently available tools. Jugular vein oximetry is seldom used in practice any more, and brain tissue oximetry and microdialysis are limited in that they only detect highly localized abnormalities (Menon 2006). When CBF is reduced, oxygen extraction fraction (OEF) is increased in an attempt to maintain oxygen consumption to the tissues and to prevent ischemia (le Roux et al. 2013). It has been suggested that one definition of regional ischemia could be an increase in local OEF because **this** suggests that CBF is inadequate for oxygen demand. (Menon 2006). When OEF is increased and CBF is inadequate, the brain may not be able to compensate for further reduction in oxygen delivery, and infarction subsequently develops (le Roux et al. 2013).

Mitochondria

When discussing brain oxygenation, it is important to understand mitochondrial function and how impairment can contribute to damage in the brain. Mitochondrial dysfunction decreases aerobic metabolism, thus decreasing oxygen demand, and results in a lower OEF (Ragan et al. 2013). Neuronal mitochondria require an intracellular oxygen tension of at least 1.5 mmHg to carry out aerobic metabolism, and when the partial pressure of oxygen in brain tissue ($P_{bt}O_2$) is reduced, there is inadequate oxygen delivery to mitochondria (Verweij et al. 2007). $P_{bt}O_2$ is dependent on arterial oxygen tension or PaO_2 (le Roux et al. 2013), and with a typical PaO_2 of 90 mmHg and a cerebral venous partial pressure of about 35 mmHg, $P_{bt}O_2$ exists in a continuum that varies from 90 mmHg to 34 mmHg depending on proximity to the capillary bed (Verweij et al. 2007). $P_{bt}O_2$ can be approximated to equal the product of CBF and $AVDO_2$ ($P_{bt}O_2 = CBF \times AVDO_2$) (Rosenthal et al. 2008). Based on this understanding, $P_{bt}O_2$ is not only dependent on PaO_2 and CBF but also related to hemoglobin concentration and diffusion of oxygen into mitochondria (le Roux et al. 2013). When the PaO_2 falls below 65 mmHg, humans experience difficulty carrying out complex tasks; when less than 55 mmHg, short-term memory is impaired; and when less than 30 mmHg, loss of consciousness occurs (Verweij et al. 2007). Microdialytic studies show that infarction occurs when the $P_{bt}O_2$ is less than 10 to 15 mmHg (le Roux et al. 2013). In brain injury states that limit diffusion or impair mitochondrial oxygen metabolism, a higher tissue oxygen tension may be required to maintain sufficient tissue oxygen supply (Verweij et al. 2007).

Carbon Dioxide and Hyperventilation

The blood vessels in the brain are very sensitive to changes in carbon dioxide; this is termed CO_2 reactivity (le Roux et al. 2013). The major determinant of this response is not CO_2 itself, but the change in pH which it produces. CO_2 is freely permeable across the blood–brain barrier, but

other forms of CO_2 in solution such as bicarbonate ion are not. A change in $PaCO_2$ of 1 mmHg can cause an increase or decrease in CBF of approximately 4% (Rangel-Castilla et al. 2008). Hypocapnia causes cerebral vasoconstriction and decreases CBF, while the reverse occurs with hypercapnia (le Roux et al. 2013). CO_2 reactivity differs from autoregulation in that these changes are not in response to metabolic demands (le Roux et al. 2013).

Hyperventilation has long been considered as a possible treatment option for elevated intracranial pressure because of the associated vasoconstriction and decrease in CBF (le Roux et al. 2013). However, there is concern that prolonged hyperventilation can lead to global cerebral ischemia (Muizelaar et al. 1991). There is support of this notion from studies with patients who have had traumatic brain injuries and were treated with hyperventilation within the first 24 hours who were noted to have evidence of ischemia (Diringer et al. 2000). Hyperventilation can decrease CBF by reducing vessel diameter; however, some studies suggest that the reduction in CBF is coupled with an increase in oxygen extraction fraction, with no net reduction in $CMRO_2$. If the increase in OEF is sufficient, there still may be adequate substrate available to maintain the metabolic demands of the neurons and glia (Diringer et al. 2000). However, at some point, CBF will be reduced to levels at which increased OEF is unable to compensate for the decrease in oxygen delivery, thereby resulting in ischemia (Diringer et al. 2000).

Pharmacologic Regulation

Several pharmacologic interventions can be considered when attempting to alter cerebral hemodynamics. It is important to understand how each intervention works and also what the contraindications and limitation of each are in order to safely administer them. At this time, pharmacologic interventions primarily target improvements in ICP and CPP; however, as newer targets are identified, additional therapies may emerge.

Osmotherapy

Osmotherapy is the core of therapy for raised intracranial pressure. The Neurocritical Care Society considers mannitol and hypertonic saline as tier 1 interventions for raised intracranial pressure (Cadena et al. 2017). Mannitol has been the mainstay of osmotherapy for some time; however, with increased interest in hypertonic saline, there is much debate over which is more effective. There is no level I evidence showing that osmotherapy improves neurologic outcomes (Fink 2012); however, the recommendation for use in elevated intracranial pressure is almost universal.

Mannitol

Mannitol is a sugar alcohol that has been used since the 1960s; it is excreted rapidly by the kidney when given intravenously and functions primarily by raising serum osmolality (Ropper et al. 2004; Fink 2012). The most commonly used concentration is 20% but is also available in 10% concentration. Mannitol does not cross the intact blood–brain barrier and it acts as a hyperosmolar agent by creating an osmolar gradient that pulls fluid from the brain into the intravascular compartment (Burgess et al. 2016; Grape and Ravussin 2012). Mannitol is also thought to have a rheological effect, improving oxygen transport by decreasing blood viscosity and increasing red blood cell deformability (Grape and Ravussin 2012). The reduction in blood viscosity causes reflex vasoconstriction, which reduces cerebral blood volume and intracranial pressure (Diringer et al. 2012); however, this may be limited to patients whose autoregulation remains intact (Grape and Ravussin 2012). Additionally, the fluid shift caused by the hyperosmolarity causes plasma expansion and subsequently can increase cardiac output, mean arterial pressure, and increased cerebral perfusion pressure (Grape and Ravussin 2012). The overall mechanism by which mannitol improves intracranial pressure is thus still under debate, with some studies suggesting that the decrease in cerebral blood volume occurs within first minutes after administration, and the reduction in water vol-

ume occurring later (Diringer et al. 2012). In addition to reducing intracranial pressure, mannitol may be a free radical scavenger and it may reduce programmed cell death (Diringer and Zazulia 2004). However, these mechanisms need further study (Grape and Ravussin 2012).

Mannitol is administered in doses of 0.5 to 1.0 g/kg by an IV bolus and does not require a central venous catheter (Cadena et al. 2017). It has been showed to have an effect on ICP that lasts for over two hours (Francony et al. 2008) and possibly up to six hours (Grape and Ravussin 2012); repeated doses are recommended every 4–6 hours (Cadena et al. 2017). It has been suggested that serum osmolality should be monitored when using repeated doses of mannitol. The previous held belief was that there is no appreciable benefit when osmolality went above 320 mOsm/L (Cadena et al. 2017) and exceeding this value could precipitate worsening kidney function; however, more recent studies have shown that patients tolerate a serum osmolality up to 340 mOsm/L (Diringer and Zazulia 2004). Another way to monitor mannitol administration is to calculate the osmolal gap prior to administration of a repeated dose, and if the value exceeds 20 mOsm/L, the next dose should be delayed because it indicates that the previous dose of mannitol has not been cleared from the system (Ropper et al. 2004). Theoretically repeated doses can also cause mannitol to cross the blood–brain barrier and potentially worsen cerebral edema; (Fink 2012) however, this has not been demonstrated in clinical practice (Freeman 2015). Another concern is that mannitol preferentially reduces water in the normal brain tissue and can thereby potentially worsen midline shift in brains with hemispheric lesions (Diringer and Zazulia 2004). One proposed complication is that the mannitol crosses the disrupted blood–brain barrier and then remains in the brain interstitium, while the intravascular mannitol is rapidly cleared from the system, creating a reverse osmolar gradient (Kaufmann and Cardoso 1992). This, too, has yet to be demonstrated in clinical practice. Contraindications to mannitol use include impaired renal function (since it is not removed by hemodialysis), progressive heart failure, and

severe dehydration (Freeman 2015). The transient expansion of the plasma volume that can exacerbate heart failure is relieved by the diuretic effect that soon follows (Freeman 2015). It is important to monitor diuresis when using mannitol, as hypotension may occur without volume replacement (Diringer and Zazulia 2004). Additionally, mannitol can be nephrotoxic by causing direct tubular damage, so that monitoring of kidney function and electrolytes is recommended (Grape and Ravussin 2012).

Hypertonic Saline

Although the first documented use of hypertonic saline was in 1919, its clinical use became more prevalent several decades later due to concerns with the potential side effects of mannitol and contraindications to its use (Surani et al. 2015). Hypertonic saline is available in various concentrations that range from 2% to 23.4%. Concentrations higher than 2% are usually administered via a central venous catheter (Grape and Ravussin 2012). Hypertonic saline has a similar osmotic effect to mannitol, although the mechanism is slightly different. The increase in serum osmolality causes fluid to move across the blood–brain barrier in a manner similar to that of mannitol; however, there is also some evidence that hypertonic saline down-regulates aquaporin 4 channels, which have been implicated in the development of cerebral edema (Zeynalov et al. 2008). Hypertonic saline expands the plasma volume, which increases cardiac output and mean arterial pressure, and potentially increases cerebral blood flow similar to the initial increase in plasma volume by mannitol; however, it is not a potent diuretic and so this effect is not followed by rapid diuresis (Fink 2012). Hypertonic saline has a rheological effect similar to mannitol, which reduces hematocrit and improves red cell deformability (Tseng et al. 2003). Additional benefits suggested by animal studies on the actions of hypertonic saline include a reduction in apoptosis in ischemic areas of the brain, and potential attenuation of reperfusion injury, but these mechanisms are difficult to confirm in humans (Grape and Ravussin 2012).

Hypertonic saline can be administered via a bolus or continuous infusion. The typical sodium goal ranges between 145 and 155 mmol/L, and it is recommended that sodium concentration should not exceed 160 mmol/L (Francony et al. 2008); however, in cases of refractory elevated intracranial pressure, concentrations as high as 180 mmol/L have been tolerated (Fink 2012). Hypertonic saline is not recommended for patients with severe heart failure because it can lead to pulmonary edema due to expansion of the plasma volume, and it does not have the same diuretic effect as mannitol. There is also concern of precipitating osmotic demyelination in patients with preexisting hyponatremia if serum sodium concentration is raised too quickly.

Many studies have been performed to assess which agent is more effective in reducing intracranial pressure; however, they have mostly been shown to have equivalent effects in reducing ICP (Francony et al. 2008). Small studies have been performed and have not shown a difference between neurologic outcomes or mortality between the two agents (Burgess et al. 2016).

Sedation

Sedation can be effective for managing patients with brain injury. In addition to lowering intracranial pressure by decreasing oxygen demand, and therefore CBF, sedatives can also alter intracerebral physiology by other mechanisms. Sedation can attenuate patient responses that increase cerebral metabolic rate and raise intracranial pressure, such as pain, anxiety, fear, and ventilator dyssynchrony (Ropper et al. 2004). Sedatives have been shown to reduce CMRO₂ (Oddo et al. 2016), which improves tolerance to ischemia. Sedatives can be administered either by using a continuous infusion or by administering the agents on an as-needed basis. The use of sedatives, however, can be problematic. Many studies have shown that minimizing sedation in ICU patients can lead to shorter duration of mechanical ventilation and reduced length of hospital stay (Oddo et al. 2016). Sedation holidays are often employed in critically ill patients;

however, they are often contraindicated in patients with brain injuries because they may cause critical increases in intracranial pressure and even precipitate herniation. Picking the ideal sedative should be based on the individual characteristics of the patient and the potential side effects of the sedative. The different categories of sedatives appear to be equally efficacious in their effects on intracranial pressure and cerebral perfusion pressure (Roberts et al. 2011).

Propofol

Propofol is often used in the intensive care unit as a sedative because of its favorable pharmacokinetic profile. Propofol exerts its effects by interacting with the GABA_A receptor and also by inhibiting excitatory glutamate release (Adembri et al. 2007). It is rapidly distributed from blood into tissues, which allows for rapid onset and emergence (Adembri et al. 2007). It is primarily metabolized by the liver but there is some extrahepatic metabolism as well; it does not appear to be affected by hepatic or renal failure (Adembri et al. 2007). Propofol decreases cerebral metabolism and cerebral blood flow while maintaining carbon dioxide reactivity, so it can be an ideal choice in patients with brain injury (Van Hemelrijck et al. 1990). Propofol also is effective at lowering intracranial pressure and decreasing cerebral electrical activity, so it often is used as the first-line sedative in patients with elevated intracranial pressure or in those with concern for seizure activity (Oddo et al. 2016). When compared to benzodiazepines, propofol has a faster wake up time and permits more rapid extubation (le Roux et al. 2013). There are, however, disadvantages to its use and these include lack of amnestic effect, lack of an analgesic effect, and development of tolerance/tachyphylaxis (Oddo et al. 2016). Propofol can also cause hypotension, hepatic dysfunction, and metabolic acidosis (Ropper et al. 2004). Propofol infusion syndrome is a severe adverse event that can occur in patients with high doses of propofol for long durations and is characterized by metabolic acidosis, and/or rhabdomyolysis, and progressive myocardial failure (Adembri et al. 2007). Therapeutic hypothermia may precipitate this often-fatal compli-

cation by reducing hepatic metabolism (Oddo et al. 2016).

Benzodiazepines

Midazolam and lorazepam are the two benzodiazepines most often considered for sedation. Lorazepam has a longer half-life than midazolam, so it is less suitable for continuous infusion. Its use can be limited due to metabolic acidosis related to propylene glycol toxicity (Horinek et al. 2009). When compared to propofol and midazolam, lorazepam leads to more oversedation (le Roux et al. 2013). Midazolam has a shorter half-life than many sedatives; however, its high lipid solubility leads to accumulation in the tissues, which can prolong clearance and delay awakening (Oddo et al. 2016). Depending on duration of use, patients can develop withdrawal symptoms if benzodiazepines are discontinued too rapidly (Oddo et al. 2016). Midazolam has been shown to decrease CMRO₂ and cerebral blood flow (CBF), with slight decrease in intracranial pressure while preserving CO₂ reactivity and cerebral autoregulation (Oddo et al. 2016). One positive side effect of midazolam is its anti-epileptic effect, which is also seen with propofol but not with opioids. Midazolam also exerts an amnestic effect which may seem less important in the ICU setting but can have significant implications for the patient in the future and the potential for psychological conditions to develop after critical illness (le Roux et al. 2013).

Opioids

Opioids are often used to treat processes that can increase intracranial pressure such as coughing, pain, and intolerance to the endotracheal tube (Ropper et al. 2004). Untreated pain or discomfort can lead to an increased stress response with tachycardia, increased oxygen consumption, hypercoagulability, immunosuppression, increased catecholamine activity, and increased ICP as previously reported (le Roux et al. 2013). Commonly used opioid infusions in the ICU are fentanyl, sufentanil, and remifentanil. Morphine was commonly used in the past; however, with its longer half-life, and potential redistribution and accumulation in renal failure, its use has declined in

favor of the newer shorter acting agents (de Nadal et al. 2000).

However, there can be a transient increase in ICP and transient decrease in MAP after fentanyl or sufentanil administration, leading to a reduction in CPP (Oddo et al. 2016; Flower and Hellings 2012). Some studies have shown this response in boluses of morphine at a dose of 0.2 mg/kg, but there are studies with the newer agents such as remifentanyl and sufentanil that suggest this response to be dose dependent (de Nadal et al. 2000; Flower and Hellings 2012). Some studies have shown that if the transient reduction in MAP is prevented, then the transient spike in ICP is not seen (de Nadal et al. 2000). Remifentanyl has been shown to not alter ICP or CBF during its administration; however, it can cause hyperalgesia at cessation (Oddo et al. 2016) which is important to consider when weaning because its withdrawal can lead to tachycardia and hypertension that may be harmful to the patient (le Roux et al. 2013). Many of the sedatives used in the ICU do not have analgesic properties (e.g., propofol), so opioids should be used in conjunction with these agents to optimize patient management. Disadvantages to use of opioids for sedation include reduced gastrointestinal motility and prolonged mechanical ventilation (Ropper et al. 2004).

Barbiturates

Barbiturates can be used for secondary treatment of refractory elevated intracranial pressure and to eliminate critical elevations in ICP (Alnemari et al. 2017); but, similar to other agents, it is not clear whether reduction in ICP improves outcomes. Barbiturates are considered third tier therapy for increased ICP (le Roux et al. 2013). Two medications that can be considered from this class are pentobarbital and thiopental; however, thiopental is no longer available in the United States. Pentobarbital is effective at reducing ICP by suppressing brain metabolic demand, and also decreasing cerebral blood flow and blood volume (Wolahan et al. 2018) by causing cardiac depression and hypotension. However, this effect can lead to cerebral hypoxia which may be associated with worse outcomes than elevated intracranial

pressure (Alnemari et al. 2017). Thiopental has been shown to be more effective than pentobarbital in reducing ICP, and there is some evidence that it may provide additional neuroprotective effect by reducing cerebrospinal fluids such as glutamate and lactate (Alnemari et al. 2017). Barbiturates can be considered in patients with brain injury who also develop refractory status epilepticus as they are effective in treating seizures. Barbiturate use, however, is associated with significant side effects and these must be considered when using this class of medications. A Cochrane review found that one in four patients developed hypotension when on a continuous infusion of pentobarbital (Roberts and Sydenham 2012), and patients often required vasopressor support (Cadena et al. 2017). Other complications of pentobarbital use include respiratory depression, cardiovascular instability, immune suppression, and paralytic ileus (Cadena et al. 2017). Pentobarbital clearance is very prolonged and it may take days after discontinuation of therapy for a patient to arouse (Cadena et al. 2017).

Dexmedetomidine

Dexmedetomidine is an alpha-2-agonist that can also be used in the ICU to provide sedation. It has several advantages including exerting an anxiolytic effect (Mantz et al. 2011) typically without depressing ventilatory drive and preserving sleep architecture, and it allows for arousable sedation (le Roux et al. 2013; Mantz et al. 2011). Some research studies also suggest that dexmedetomidine exerts neuroprotective effects against ischemia (Mantz et al. 2011; Liu et al. 2017) and that it may have favorable effects on ICP as well (Schomer et al. 2019). Adverse effects of dexmedetomidine include bradycardia and hypotension.

Neuromuscular Junction Blockers

Neuromuscular junction blockers have been used to eliminate responses that can elevate intracranial pressure such as coughing or ventilator dys-

synchrony. However, in the absence of a need for completely controlled mechanical ventilation, their use should be limited, and studies have not shown evidence of improved ICP control with their use (Ropper et al. 2004). They also have many side effects including increased incidence of critical illness such as polyneuropathy, longer ICU stay, and a higher incidence of pneumonia (Ropper et al. 2004).

Conclusion

Brain injury is a significant cause of disability in the world (Kochanek et al. 2014; Taylor et al. 2017). Cerebral physiology and hemodynamics is an ever-growing field and there is still a great deal more to learn in order to improve patient outcomes. Further research into this is ongoing and will provide future physiologic targets and potential pharmacologic innovations.

References

- Adeabri C, Venturi L, Pellegrini-Giampietro DE. Neuroprotective effects of propofol in acute cerebral injury. *CNS Drug Rev.* 2007;13(3):333–51. <https://doi.org/10.1111/j.1527-3458.2007.00015.x>. <http://www.ingentaconnect.com/content/bpl/cns/2007/00000013/00000003/art00005>.
- Alnemari AM, Krafcik BM, Mansour TR, Gaudin D. A comparison of pharmacologic therapeutic agents used for the reduction of intracranial pressure after traumatic brain injury. *World Neurosurg.* 2017;106:509–28. <https://doi.org/10.1016/j.wneu.2017.07.009>. <https://www.sciencedirect.com/science/article/pii/S1878875017311087>
- Burgess S, Abu-Laban RB, Slavik RS, Vu EN, Zed PJ. A systematic review of randomized controlled trials comparing hypertonic sodium solutions and mannitol for traumatic brain injury. *Ann Pharmacother.* 2016;50(4):291–300.
- Cadena R, Shoykhet M, Ratcliff J. Emergency neurological life support: intracranial hypertension and herniation. *Neurocrit Care.* 2017;27(S1):82–8. <https://www.ncbi.nlm.nih.gov/pubmed/28913634>. <https://doi.org/10.1007/s12028-017-0454-z>.
- Carney N, Totten AM, O'Reilly C, et al. Guidelines for the management of severe traumatic brain injury, fourth edition. *Neurosurgery.* 2017;80(1):6–15. <https://www.ncbi.nlm.nih.gov/pubmed/27654000>. <https://doi.org/10.1227/NEU.0000000000001432>.
- Castro P, Azevedo E, Sorond F. Cerebral autoregulation in stroke. *Curr Atheroscler Rep.* 2018;20(8):1–12. <https://www.ncbi.nlm.nih.gov/pubmed/29785667>. <https://doi.org/10.1007/s11883-018-0739-5>.
- Cunningham AS, Salvador R, Coles JP, et al. Physiological thresholds for irreversible tissue damage in contusional regions following traumatic brain injury. *Brain J Neurol.* 2005;128(Pt 8):1931–42.
- de Nadal M, Munar F, Poca MA, Sahuquillo J, Garnacho A, Rosselló J. Cerebral hemodynamic effects of morphine and fentanyl in patients with severe head injury: absence of correlation to cerebral autoregulation. *Anesthesiology.* 2000;92(1):11–9. <https://doi.org/10.1097/0000542-200001000-00008>. <https://www.ncbi.nlm.nih.gov/pubmed/10638893>.
- Diringer M, Zazulia A. Osmotic therapy. *Neurocrit Care.* 2004;1(2):219–33. <https://www.ncbi.nlm.nih.gov/pubmed/16174920>. doi: 219.
- Diringer MN, Scalfani MT, Zazulia AR, Videen TO, Dhar R, Powers WJ. Effect of mannitol on cerebral blood volume in patients with head injury. *Neurosurgery.* 2012;70(5):1215–9. <https://www.ncbi.nlm.nih.gov/pubmed/22089753>. <https://doi.org/10.1227/NEU.0b013e3182417bc2>.
- Diringer MN, Yundt K, Videen TO, et al. No reduction in cerebral metabolism as a result of early moderate hyperventilation following severe traumatic brain injury. *J Neurosurg.* 2000;92(1):7–13.
- Fink M. Osmotherapy for intracranial hypertension: mannitol versus hypertonic saline. *Continuum.* 2012;18(3, Critical Care Neurology):640–54. <https://doi.org/10.1212/01.CON.0000415432.84147.1e>. <http://ovidsp.ovid.com/ovidweb.cgi?T=JS&NEWS=n&CSC=Y&PAGE=fulltext&D=ovft&AN=00132979-201206000-00013>.
- Flower O, Hellings S. Sedation in traumatic brain injury. *Emerg Med Int.* 2012;2012:637171–11. <https://doi.org/10.1155/2012/637171>. <https://www.ncbi.nlm.nih.gov/pubmed/23050154>.
- Francony G, Fauvage B, Falcon D, et al. Equimolar doses of mannitol and hypertonic saline in the treatment of increased intracranial pressure. *Crit Care Med.* 2008;36(3):795–800. <https://www.ncbi.nlm.nih.gov/pubmed/18209674>. <https://doi.org/10.1097/CCM.0B013E3181643B41>.
- Freeman W. Management of intracranial pressure. *CONTINUUM: Lifelong Learn Neurol.* 2015;21(5, Neurocritical Care):1299–1323i. <https://doi.org/10.1212/CON.0000000000000235>. <http://ovidsp.ovid.com/ovidweb.cgi?T=JS&NEWS=n&CSC=Y&PAGE=fulltext&D=ovft&AN=00132979-201510000-00008>.
- Grape S, Ravussin P. PRO: osmotherapy for the treatment of acute intracranial hypertension. *J Neurosurg Anesthesiol.* 2012;24(4):402–6. <https://www.ncbi.nlm.nih.gov/pubmed/22955194>. <https://doi.org/10.1097/01.ana.0000419729.52363.64>.
- Horinek EL, Kiser TH, Fish DN, MacLaren R. Propylene glycol accumulation in critically III patients receiving continuous intravenous lorazepam infusions. *Ann*

- Pharmacother. 2009;43(12):1964–71. <https://doi.org/10.1345/aph.1M313>. <https://journals.sagepub.com/doi/full/10.1345/aph.1M313>.
- Jessen N, Munk A, Lundgaard I, Nedergaard M. The glymphatic system: a beginner's guide. *Neurochem Res.* 2015;40(12):2583–99. <https://doi.org/10.1007/s11064-015-1581-6>.
- Kaufmann AM, Cardoso ER. Aggravation of vasogenic cerebral edema by multiple-dose mannitol. *J Neurosurg.* 1992;77(4):584–9. <https://doi.org/10.3171/jns.1992.77.4.0584>. <https://www.ncbi.nlm.nih.gov/pubmed/1527619>.
- Kim D, Czosnyka Z, Kasprowitz M, et al. Continuous monitoring of the monro-kellie doctrine: is it possible? *J Neurotrauma.* 2012;29(7):1354–63. <https://www.liebertpub.com/doi/abs/10.1089/neu.2011.2018>. <https://doi.org/10.1089/neu.2011.2018>.
- Kochanek KD, Murphy SL, Xu J, Arias E. Mortality in the United States, 2013. *NCHS Data Brief.* 2014;178:1–8. <https://www.ncbi.nlm.nih.gov/pubmed/25549183>
- le Roux P, Levine J, Kofke W. Monitoring in neurocritical care. 1st ed. Elsevier Health Sciences; 2013. <http://www.r2library.com/resource/title/9781437701678>.
- Liu Y, Wang D, Yang Y, Lei W. Effects and mechanism of dexmedetomidine on neuronal cell injury induced by hypoxia-ischemia. *BMC Anesthesiol.* 2017;17(1):117–0. <https://doi.org/10.1186/s12871-017-0413-4>. <https://www.ncbi.nlm.nih.gov/pubmed/28854873>.
- Liu Z, Li Y. Cortical cerebral blood flow, oxygen extraction fraction, and metabolic rate in patients with middle cerebral artery stenosis or acute stroke. *AJNR.* *Am J Neuroradiol.* 2016;37(4):607–14. <https://www.ncbi.nlm.nih.gov/pubmed/26680459>. <https://doi.org/10.3174/ajnr.A4624>.
- Madhok D, Vitt J, Nguyen A. Overview of neurovascular physiology. *Curr Neurol Neurosci Rep.* 2018;18(12):1–6. <https://doi.org/10.1007/s11910-018-0905-8>. <https://search.proquest.com/docview/2124108243>.
- Mantz J, Josserrand J, Hamada S. Dexmedetomidine: new insights. *Eur J Anaesthesiol.* 2011;28(1):3–6. <https://doi.org/10.1097/EJA.0b013e32833e266d>. <https://www.ncbi.nlm.nih.gov/pubmed/20881501>.
- Meng L, Hou W, Chui J, Han R, Gelb A. Cardiac output and cerebral blood flow: the integrated regulation of brain perfusion in adult humans. *Anesthesiology.* 2015;123(5):1198–208. <https://doi.org/10.1097/ALN.0000000000000872>. <http://ovidsp.ovid.com/ovidweb.cgi?T=JS&NEWS=n&CSC=Y&PAGE=fulltext&D=ovft&AN=00000542-201511000-00034>.
- Menon DK. Brain ischaemia after traumatic brain injury: lessons from 15O2 positron emission tomography. *Curr Opin Crit Care.* 2006;12(2):85–9. <https://www.ncbi.nlm.nih.gov/pubmed/16543781>. <https://doi.org/10.1097/01.ccx.0000216572.19062.8f>.
- Muizelaar JP, Marmarou A, Ward JD, et al. Adverse effects of prolonged hyperventilation in patients with severe head injury: a randomized clinical trial. *J Neurosurg.* 1991;75(5):731–9. <https://www.ncbi.nlm.nih.gov/pubmed/1919695>. <https://doi.org/10.3171/jns.1991.75.5.0731>.
- Oddo M, Crippa IA, Mehta S, et al. Optimizing sedation in patients with acute brain injury. *Crit Care.* 2016;20 <https://doi.org/10.1186/s13054-016-1294-5>. https://www.openaire.eu/search/publication?articleId=dedup_wf_001::83ab60f3c6d0ad5aa172627b18d29142.
- Ragan DK, McKinstry R, Benzinger T, Leonard JR, Pineda JA. Alterations in cerebral oxygen metabolism after traumatic brain injury in children. *J Cereb Blood Flow Metab.* 2013;33(1):48–52. <https://doi.org/10.1038/jcbfm.2012.130>. <https://journals.sagepub.com/doi/full/10.1038/jcbfm.2012.130>.
- Rangel-Castilla L, Gasco J, Nauta HJW, Okonkwo DO, Robertson CS. Cerebral pressure autoregulation in traumatic brain injury. *Neurosurg Focus.* 2008;25(4):E7.
- Roberts DJ, Hall RI, Kramer AH, Robertson HL, Gallagher CN, Zygun DA. Sedation for critically ill adults with severe traumatic brain injury: a systematic review of randomized controlled trials. *Crit Care Med.* 2011;39(12):2743–51. <https://doi.org/10.1097/CCM.0b013e318228236f>. <http://ovidsp.ovid.com/ovidweb.cgi?T=JS&NEWS=n&CSC=Y&PAGE=fulltext&D=ovft&AN=00003246-201112000-00022>.
- Roberts I, Sydenham E. Barbiturates for acute traumatic brain injury. *Cochrane Database Syst Rev.* 2012;12:CD000033. <https://doi.org/10.1002/14651858.CD000033.pub2>. <https://www.ncbi.nlm.nih.gov/pubmed/23235573>.
- Ropper AH, Diringer MN, Green DM, Mayer SA, Bleck TP. Neurological and neurosurgical intensive care. 4th ed. Philadelphia [u.a.]: Lippincott Williams & Wilkins; 2004.
- Rosenthal G, Hemphill IJ, Sorani M, et al. Brain tissue oxygen tension is more indicative of oxygen diffusion than oxygen delivery and metabolism in patients with traumatic brain injury. *Crit Care Med.* 2008;36(6):1917–24. <https://www.ncbi.nlm.nih.gov/pubmed/18496376>. <https://doi.org/10.1097/CCM.0b013e3181743d77>.
- Schomer KJ, Sebat CM, Adams JY, DUBY JJ, Shahlaie K, Louie EL. Dexmedetomidine for refractory intracranial hypertension. *J Intensive Care Med.* 2019;34(1):62–6. <https://doi.org/10.1177/0885066616689555>. <https://journals.sagepub.com/doi/full/10.1177/0885066616689555>.
- Surani S, Lockwood G, Macias MY, Guntupalli B, Varon J. Hypertonic saline in elevated intracranial pressure. *J Intensive Care Med.* 2015;30(1):8–12. <https://doi.org/10.1177/0885066613487151>. <http://journals.sagepub.com/doi/full/10.1177/0885066613487151>.
- Taylor CA, Bell JM, Breiding MJ, Xu L. Traumatic brain Injury–Related emergency department visits, hospitalizations, and deaths — United States, 2007 and 2013. Morbidity and mortality weekly report. Surveillance summaries (Washington, D.C.: 2002). 2017;66(9):1–16. <https://doi.org/10.15585/mmwr.ss6609a1>. <https://www.ncbi.nlm.nih.gov/pubmed/28301451>.
- Tseng M, Al-Rawi PG, Pickard JD, Rasulo FA, Kirkpatrick PJ. Effect of hypertonic saline on cerebral

- blood flow in poor-grade patients with subarachnoid hemorrhage. *Stroke*. 2003;34(6):1389–96. <https://doi.org/10.1161/01.STR.0000071526.45277.44>. <http://stroke.ahajournals.org/cgi/content/abstract/34/6/1389>.
- Van Hemelrijck J, Fitch W, Mattheussen M, Van Aken H, Plets C, Lauwers T. Effect of propofol on cerebral circulation and autoregulation in the baboon. *Anesth Analg*. 1990;71(1):49–54. <https://doi.org/10.1213/0000539-199007000-00008>. <http://ovidsp.ovid.com/ovidweb.cgi?T=JS&NEWS=n&CSC=Y&PAGE=fulltext&D=ovft&AN=0000539-199007000-00008>.
- Verweij BH, Amelink GJ, Muizelaar JP. Current concepts of cerebral oxygen transport and energy metabolism after severe traumatic brain injury. In: *Progress in brain research*, vol. 161. Netherlands: Elsevier Science & Technology; 2007. p. 111–24. [https://doi.org/10.1016/S0079-6123\(06\)61008-X](https://doi.org/10.1016/S0079-6123(06)61008-X). <https://www.sciencedirect.com/science/article/pii/S007961230661008X>.
- Wolahan SM, Lebbly E, Mao HC, et al. Novel metabolic comparison of arterial and jugular venous blood in severe adult traumatic brain injury patients and the impact of pentobarbital infusion. *J Neurotrauma*. 2018; <https://doi.org/10.1089/neu.2018.5674>. <https://www.liebertpub.com/doi/abs/10.1089/neu.2018.5674>.
- Zeynalov E, Chen C, Froehner S, et al. The perivascular pool of aquaporin-4 mediates the effect of osmotherapy in postischemic cerebral edema. *Crit Care Med*. 2008;36(9):2634–40. <https://doi.org/10.1097/CCM.0b013e3181847853>. <http://ovidsp.ovid.com/ovidweb.cgi?T=JS&NEWS=n&CSC=Y&PAGE=fulltext&D=ovft&AN=00003246-200809000-00022>.

Part II

Physiological Basics: Pulmonary Basics



Stress, Strain, and the Inflation of the Lung

12

C. Corey Hardin and James P. Butler

Introduction

Basic to the function of the lung is its inflation in response to the application of a pressure or stress (Fredberg and Kamm 2006). In the case of spontaneous breathing, this stress is applied to the pleural surface by the respiratory muscles. In the case of mechanical ventilation, this stress is applied at the airway opening. In either case, stress is subsequently transmitted through the lung connective tissue and its adherent cells (Mead et al. 1970). The lung is a complex mechanical structure whose response to applied stress is influenced not only by the mechanical properties of cells and connective tissue (Suki et al. 2005) but also that of the surface tension at the air–liquid interface (Bachofen et al. 1970) and the potentially complex interaction between each of these components. Lung inflation in response to applied stress can be spatially heterogeneous and may exhibit features of viscoelasticity (Fredberg and Stamenovic 1989) with deformation varying in time even in the setting of constant applied stress. For most clinical pur-

poses, much of this complexity may be overlooked, but in others the full details of inflating forces and resultant lung tissue deformation are essential for a complete understanding. Here, we describe the nature of lung inflation and stretch during the respiratory cycle moving from the simplest one-dimensional descriptions of the lung as an elastic structure in series with an airway resistance to a more complex description which incorporates the oscillatory nature of applied stress during lung inflation and the time-varying response of lung tissue. In the interest of brevity, we will not attempt to address several important mechanical topics including the non-uniform distribution of pleural pressure (West and Matthews 1972), the parenchymal stress distribution surrounding airways and blood vessels (Lai-Fook 1979), and deformations of the alveolar duct during inflation and under the influence of surface tension (Wilson and Bachofen 1982). Readers are referred to the cited texts for a full discussion of these important topics. Furthermore, in this chapter, we make only superficial reference to the role of the air–liquid interface and surfactant in determining lung elastic behavior as this topic is addressed in the chapter by Hardin, Spragg, and Malhotra in this volume (Chap. 17).

C. C. Hardin (✉)

Division of Pulmonary and Critical Care Medicine,
Massachusetts General Hospital, Boston, MA, USA
e-mail: Charles.Hardin@mgh.harvard.edu

J. P. Butler

Harvard TH Chan School of Public Health and
Harvard Medical School, Boston, MA, USA
e-mail: jbutler@hsph.harvard.edu

Stress and Strain in 1D: Pressure and Volume

In clinical practice, we generally conceive of the lung as a series of tubes which serve to conduct air to and from the distensible gas exchange surfaces. The flow of air through the tubes follows the formation of a pressure gradient between the airway opening and the gas exchange region, the alveolar space. The simplest realization of this idea is that of a single tube connected to a balloon (Fig. 12.1).

The volume of this balloon is a function of the pressure difference between the airway opening and the pleural pressure acting on the outside surface – the transpulmonary pressure (Mead et al. 1970). The lung is a pressure-supported structure (Kimmel and Budiansky 1990; Suki et al. 2011). In normal circumstances, the lung maintains a positive transpulmonary pressure and thus a non-zero volume. In the context of pulmonary

mechanics, the preexisting stress – the transpulmonary pressure which exists prior to an increase in lung volume above the resting volume is referred to as the prestress. It is therefore more convenient to describe inflation as change in volume from some reference state V_0 rather than an absolute volume. We can thus imagine a relationship between the transmural pressure and displacement of the volume from its reference state. Pressure is a force per unit area so that this relationship describes the one-dimensional displacement of the volume as a function of an applied force and is analogous to Hooke's law describing an increment in length in response to an imposed force: $\sigma = Y(x - x_0)$. The magnitude of the change in length is proportional to a constant, which is determined by the physical properties of the material being stretched and is represented by the constant term, Y . The force divided by the cross-sectional area of the material is the stress, and the resultant increment in length per initial

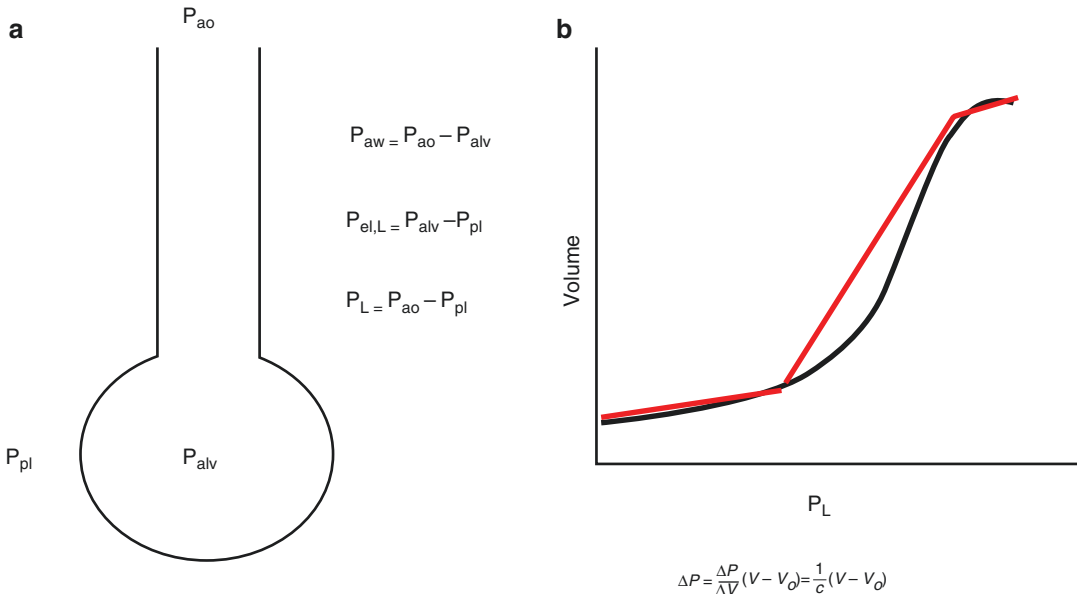


Fig. 12.1 One-dimensional model of the lung. **(a)** The transpulmonary pressure incorporates both the resistive pressure drop across the airway and the elastic distending pressure across the alveolus. **(b)** The relationship between pressure and volume is nonlinear, with the slope of the curve given by compliance or $\frac{\Delta V}{\Delta P}$. However, the pressure–volume curve may be approximated as linear over appropriate ranges of volume as indicated by the red lines

tangent to the curve. The pressure–volume curve also indicates that the lung has a nonzero volume at zero transpulmonary pressure so that when describing stress and strain during inflation volume is considered as an increment in volume from the unstressed reference state. (Abbreviations: P_{aw} , pressure drop across the airway, P_{ao} , pressure at the airway opening, P_{alv} , pressure in the alveolus, P_{pl} , pleural pressure, $P_{el,L}$ = elastic distending pressure of the lung, P_L transpulmonary pressure, C , compliance, V_0 , volume at zero transpulmonary pressure)

length is the strain. Y is specified by the ratio of stress to strain defined as the fractional change in length. In the case of the 1D lung model, the stress is the pressure across the lung (the transpulmonary pressure) and the strain is the fractional increment in volume:

$$\Delta P = E(V - V_0) \quad (12.1)$$

Note that above we have ignored the portion of the transpulmonary pressure, which is dissipated across the airway resistance. A fuller treatment results in the familiar one-compartment lung model equation of motion (Bates 2009; Otis et al. 1950):

$$\Delta P = R \frac{dV}{dt} + E(V - V_0) \quad (12.2)$$

The above description may be recommended by its simplicity but even here a hidden complexity lurks. If a real material is deformed in one direction – by applying stress parallel to its long axis – it will also deform along another axis, for example, by contracting along the axis perpendicular to the applied stress. The full mechanical behavior, even in this very simple case, therefore requires the specification of not just one but of two material constants (Atkin and Fox 2005) – Y (which is referred to as the Young’s or elastic modulus) and ratio of strain in the perpendicular direction to that in the parallel direction. This ratio is referred to as Poisson’s ratio.

More Complicated Models of Lung Inflation

The simple description above breaks down in several respects when used to describe actual lung stress and strain. The first is the problem of length scale. At the level of the alveolus, the pulmonary parenchyma is composed of elastic tissue alternating with airspaces. The stress is therefore well defined only on a length scale which averages over these discontinuities (Solid Mechanics 2011). Such a coarse-grained approach risks overlooking important events such as cellular mechanical transduction (Ingber 2003), which may depend on forces at the level of single cells (Butler et al. 2002). Secondly, Eq. 12.1 is a linear equation which implies that the relationship between stress and strain is linear – the constants being fixed. That the lung, in reality, has a nonlinear relationship between stress and strain is clear from an inspection of the pulmonary pressure–volume loop (Fig. 12.1) in which the slope clearly depends on lung volume. Third, the lung is a three-dimensional structure. Whereas the vectorial description of the forces acting on the 1D system required the specification of only one force vector, the description of the relationship between stress and strain in three dimensions requires the specification of six independent stress components (Fig. 12.2[a]). These may be resolved into those that act to expand (contract) an arbitrary cube of lung tissue (referred to as normal stresses) and those which distort its shape

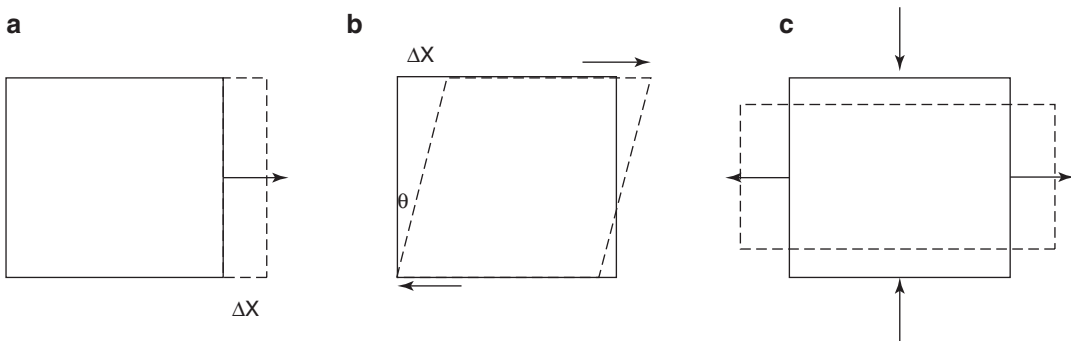


Fig. 12.2 Shear and normal stress. Any arbitrary deformation may be described by an appropriate combination so-called normal stress (contraction or elongation, **a**) and shear stress (change in shape without change in

volume, **b**). In real materials, a deformation along one axis will result in a deformation along another as well so that, for example, an elongation in the x-direction will also result in a contraction along the y-axis (**c**)

without changing its volume – referred to as shear stresses. The material constant appropriate for normal deformation is the bulk, or elastic modulus defined as the ratio of normal stress to fractional volume change (V/V_0). The material constant appropriate for shear deformation is the shear modulus defined as the ratio of the shear stress to the shear strain which may be measured by the tangent of the angle through which the material is deformed (Fig. 12.2).

Experimental measurements of lung material properties generally yield a bulk modulus that is 3–4 times larger than the shear modulus (Stamenović 1990). Any arbitrary deformation of a deformable material may be described by an appropriate combination of normal and shear deformations. Fourth, the response to imposed stress in the lung may be nonuniform. By nonuniform displacement it is meant that the application of a force at a particular location causes portions of the lung to be displaced relative to other portions of the lung, a form of strain quite different from uniform volume enlargement or elongation envisioned by Hooke's law.

Prestress and the Shear Modulus

We previously alluded to the fact that the lung is a pressure-supported structure – its nonzero volume depends upon a nonzero transpulmonary pressure. The transpulmonary pressure at the resting volume of the lung (roughly speaking, the functional residual capacity or FRC) is the prestress. By coarse graining the stress acting on lung tissue, defining it as an average over a sufficiently large length scale that the discrete nature of tissue components is ignored, we gloss over a critical consequence of the prestress. If one assumes that macroscopic deformations are faithfully transmitted to the microscopic scale (deformations which meet this requirement are referred to as affine deformations in mechanics) and attempts to predict the lung shear modulus from the properties of the individual components, one arrives at a number that is significantly larger than the measured shear modulus of lung tissue, which is approximately 0.7 times the

transpulmonary pressure (Lai-Fook et al. 1976). The resolution of this discrepancy lies in the relaxation of the assumption of affine deformation. At the microscopic level, lung tissue may be modeled as a series of connective tissue “struts” joined at discrete points to form a polyhedral structure (Fredberg and Kamm 2006; Stamenović 1990; Kimmel et al. 1987). When subjected to shear stress, this structure will not just undergo a large-scale deformation but the individual structural members may move relative to each other. This additional degree of freedom results in a structure which is less resistant to shear deformation than bulk expansion or contraction. The tendency of internal elements to move relative to each other will be less if the overall structure is under a greater degree of stress. In the lung, this results in a situation in which an applied stress results in a greater tendency to change shape than volume and one in which the shear modulus is a constant fraction of the transpulmonary pressure (Stamenović 1990).

Stress Transmission in the Lung

In keeping with the above discussion, the most comprehensive description of stress and strain will specify each at each point in the lung. Mathematically, this may be done by specifying a stress field – a mathematical construct which associates to every point in space a stress which has a magnitude along each of the three spatial axes. In response to this stress field, the lung will develop a displacement field in which each point in the lung is displaced relative to its position prior to the application of the stress field. Which leads to the question of what a typical distribution of stress and strain is obtained within the lung? Ultimately, the macroscopic material constants such as the bulk and shear modulus mostly arise from the microscopic structure of lung tissue (Kimmel et al. 1987). In the case of uniform inflation, the distribution of stress takes a particularly simple form (Mead et al. 1970). Consider an arbitrary, assumed spherical, surface within the lung (Fig. 12.3). The forces acting on this surface will consist of the forces applied to it

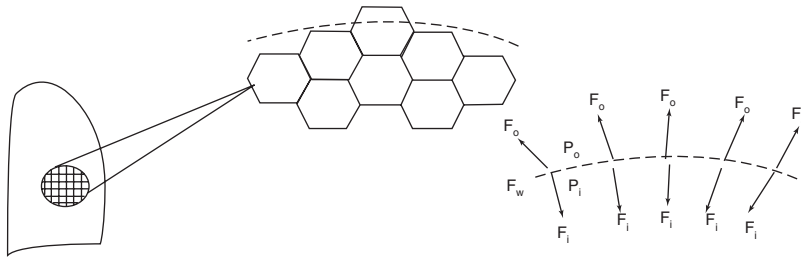


Fig. 12.3 Force balance and pulmonary stability. Any region of the pulmonary parenchyma will be composed of airspaces and connective tissue attachments (ignoring, for simplicity, the air–liquid interface and local distortions due to blood vessels or airways). For the lung to be stably inflated, all forces must balance. Imagining an arbitrary

spherical surface somewhere in the lung, the relevant forces are the pressure difference across the surface ($P_i - P_o$), the force from tissue attachments pulling inward on the surface (F_i), the force from tissue attachments pulling outward on the surface (F_o), and the tension in the wall of the surface, F_w , approximated by the law of Laplace

by all of the alveolar units through which it passes. These can be described as the sum of tissue attachments on each side of the surface (F_i and F_o , respectively), the pressure difference across the wall ($P_i - P_o$) and the radial stress that results from the elastic recoil of the surface (P_w). In equilibrium, forces must sum to zero. Note that if the tissue forces are divided by the area over which they act, they may be expressed as pressures. The radial stress for a sufficiently small surface may be determined from the law of Laplace (Mead et al. 1970) as $P_w = 2F_w/r$, where r is the radius of curvature.

for the external pressure. This expression may be read as a partial justification for the one-dimensional model discussed above in which lung stretch results from the transpulmonary pressure and is opposed by the elastic properties of the tissue.

Away from the pleural surface, the above simplifications do not apply. However, inside the lung, the gas pressures will be everywhere equal so that the first term in Eq. 12.3 will be zero. The force balance will then be:

$$0 = (P_i - P_o) + \left(\sum \frac{F_o}{A} - \sum \frac{F_i}{A} \right) + P_w \quad (12.3)$$

$$\sum \frac{F_o}{A} = \sum \frac{F_i}{A} + P_w \quad (12.5)$$

The general expression above may be simplified with respect to specific portions of the lung. At the pleural surface, there are no outward tissue forces acting to distend the lung. The radius of curvature at the pleural surface is quite large, so we are left with an expression which specifies the total distending stress as the transpulmonary pressure and the recoil forces as the sum of inward acting tissue forces:

where the outward acting tissue forces are opposed by inward acting forces and the elastic recoil due (primarily) to surface tension. In a homogenous lung, the stress tending to stretch the lung, the distending stress, has a particularly simple form. If the lung is homogeneously inflated and the pulmonary parenchyma is regarded as homogenous, the sum of outward acting forces is just the number of attachments times the (uniform) force per attachment: nF/A . The assumption of homogeneity implies the stress everywhere is the same. In particular, at the pleural surface the outward acting stress is the transpulmonary pressure, so this argument implies that the distending stress is everywhere the transpulmonary pressure – a further justification for the simple model of Eq. 12.1.

$$P_a - P_{pl} = \sum \frac{F_i}{A} \quad (12.4)$$

where we have substituted the alveolar pressure for the internal pressure and the pleural pressure

Nonuniform Inflation: Stress Multipliers

In arguing for the centrality of the transpulmonary pressure above, we assumed homogenous inflation. Even under normal circumstances, however, the lung is not uniformly inflated (Wilson 1983) as there exists a vertical gradient of pleural pressure (Lai-Fook 2004). Moreover, disease states such as the Acute Respiratory Distress Syndrome may result in partial lung collapse (Gattinoni and Pesenti 2005). In the setting of nonuniform inflation, stress transmission is altered as follows: if we postulate the collapse of a spherical region and assume that the magnitude of tissue forces does not change (they may, in fact, increase as connective tissue fibers are stretched. However, the assumption provides a lower bound on the change in forces associated with collapse). The force acting at the junction of collapsed and inflated lung then is no longer the transpulmonary pressure but instead is a multiple of it (Mead et al. 1970):

- Initial stress: nF_0/A_0
- Resultant stress: nF_0/A

Assuming spherical collapse, the area is the volume to $2/3$ power, and the ratio of resultant stress to initial stress is:

$$\frac{nF_0}{V^{2/3}} \times \frac{nF_0}{V_0^{2/3}} = \left(\frac{V_0}{V} \right)^2 \quad (12.6)$$

On the basis of the above relationship, junctions between inflated and non-inflated lung have been referred to as stress raisers and the number of such stress raisers is correlated with the severity of lung injury in the Acute Respiratory Distress Syndrome (Cressoni et al. 2014) Note that the above argument is explicitly predicated on the geometry of the local collapsed region and the subsequent change in the area on which tissue forces are acting. There are common situations of nonhomogeneous inflation – plate-like atelectasis in the lung bases, for example, in which the area does not change and would not be expected to lead to significant stress multiplication (Fung 1975).

Barotrauma and Volutrauma

Lung injury and ARDS are said to result from multiple sources (Curley et al. 2016) – barotrauma (overly large distending pressure), volutrauma (excessive lung stretch), biotrauma (inflammatory injury which may not be confined to the lung), and atelectrauma (repeated opening and closing of lung units which may result in shear stress on epithelial cells). It is apparent, however, that barotrauma and volutrauma should not be considered as separate mechanisms as changes in volume result from changes in pressure according to the equation of motion. The term barotrauma is frequently used to describe gross tissue rupture such as pneumothorax, but as these events involve displacement of tissue elements (a change of volume or shape), this is more accurately described as volutrauma. Indeed, in most circumstances, soft tissues such as the lung parenchyma may be treated as incompressible – their density is constant – so that the only possible result of an application of pressure is a displacement. The possibility of mechanotransduction (Wang et al. 1993) (the initiation of a biologic signaling cascade by the application of a mechanical stimulus) and subsequent biotrauma is beyond the scope of this chapter except to say that such events are likely to involve displacement of macromolecular complexes or protein domains.

Viscoelasticity, Respiratory Rate, and Mechanical Power

It is well established that the pulmonary parenchyma, like other biologic tissues, is not a purely elastic material (Bayliss and Robertson 1939). Elastic materials deform reproducibly and instantaneously when subjected to external stresses while most biologic materials dissipate some of the imposed stress in a manner analogous to the resistance of a flowing liquid. As in a liquid, the friction which occurs when elements of a tissue under load move relative to each other will be proportional to the rate of application of the external load and are referred to as viscous stresses. Materials which respond to an imposed load with

both elastic strain and viscous stresses (proportional to rate of deformation) are said to be viscoelastic. Viscoelastic materials may also develop other, complex, time-dependent behavior such as creep (defined as increasing strain despite constant stress) and stress relaxation (defined as continuous change in stress in response to constant strain). The precise structural origin of creep and stress relaxation is complex and material dependent but ultimately results from the complex structure of biologic materials in which constituent parts (proteins, proteoglycans, etc.) may rearrange relative to each other in response to external loading (Suki and Lutchen 2006). As the material structure changes, so may the strain at constant stress or stress at constant strain.

The viscoelasticity of lung tissue raises the possibility that the respiratory rate (the frequency of cyclic loading) will be mechanically important. It has even been suggested (Tonetti et al. 2017) that rate-dependent processes are clinically important. In particular, it has been suggested that respiratory rate can be a contributor to lung injury on par with strain. An expression which quantifies both the elastic strain in response to stress and the rate-dependent viscous stress is the mechanical power. To derive an expression for the mechanical power, investigators typically start by modifying the equation of motion (Eq. 12.2) as follows:

$$\Delta P = R \frac{dV}{dt} + E(V - V_0) + \text{PEEP} \quad (12.7)$$

explicitly including the prestress in the form of positive end-expiratory pressure (PEEP), setting the volume increment above resting ($V - V_0$) equal to V_t , the tidal volume, and letting $\frac{dV}{dt}$ be equal to the flow. Instead, here we will follow the practice of Huhle et al. (Huhle et al. 2018) in omitting the PEEP term as it represents an energy which is not applied at each cycle (see below for further discussion of PEEP and mechanical power). This equation determines the relationship between pressure and volume and integrating it over a volume change will yield the work done on the respiratory system with each breath. Writing the flow in terms of the tidal volume, respiratory rate,

and I:E ratio and carrying out the integration yields (Gattinoni et al. 2016):

$$\text{Work}_{\text{breath}} = \left(R \cdot \left(\frac{IE + 1}{IE \cdot 60} \right) + \frac{1}{2} E \right) \cdot V_t^2 \quad (12.8)$$

Power is work per unit time so that the expression for mechanical power becomes:

$$\text{MP} = \left(R \cdot \left(\frac{IE + 1}{IE \cdot 60} \right) \cdot \text{RR} + \frac{1}{2} E \right) \cdot V_t^2 \cdot \text{RR} \quad (12.9)$$

A few clinical objections may be raised against the above expression (Huhle et al. 2018). PEEP, a hallmark of clinical management of lung injury is difficult to incorporate. Including PEEP in the power is misleading (for the reasons stated above as justification for omitting it). However, cyclic stress is not independent of static stress. The justification for PEEP, a purely static stress, in the setting of lung injury is to prevent tidal recruitment and de-recruitment. Tidal recruitment is expected to increase the harm of dynamic (cyclic) stress so that PEEP should decrease cyclic lung injury (Protti et al. 2014) yet even with PEEP included, the power equation does not take this interdependence into account in a simple way. Mechanical power always increases with increasing PEEP, which suggests PEEP should always be harmful. Secondly, the expression above for mechanical power is clearly more complicated than a model of lung injury which considers only strain, so it can only be recommended if it adds explanatory power. Currently, there is no convincing clinical evidence that mechanical power offers superior prognostic information to that provided by driving pressure or tidal volume alone.

More fundamentally, the association between energy applied to the respiratory system and the development of lung injury is not straightforward owing to the complex structural origin of pulmonary viscoelasticity. It seems apparent that the dissipation of energy via flow across the resistance provided by airways should not be expected to result in strain or tissue injury. Less obvious is that energy dissipated in the tissue is also not of necessity associated with tissue

injury. Viscous dissipation in lung tissue is often described phenomenologically as akin to resistive dissipation in a flowing liquid, as we have done above. However, at the molecular level, viscous dissipation in biologic tissue is quite distinct. Formally, a frequency-dependent stress-strain relationship in the lung may be given by (Hantos et al. 1992):

$$Z = (G - ixH / \omega^\alpha) \quad (12.10)$$

Where Z is the impedance (ratio of cyclic stress to cyclic strain), ω is the frequency i is the unit imaginary number, and α is a characteristic exponent that depends on G and H . G and H are coefficients which represent the viscous and elastic stresses, respectively. Two observations which have been repeatedly validated in lung tissue are that dissipation during cyclic deformation depends on the magnitude but not the rate of deformation – quite in contrast to fluid dissipation – and that the ratio of viscous to elastic stresses (G/H) is invariant. Together, these observations support a model of pulmonary tissue called the constant phase model (Hantos et al. 1990), which describes systems in which viscous and elastic forces arise from the same structural components of a material. The precise molecular nature of viscous dissipation in the lung is still debated but it is plausibly related to internal rearrangement of the complex network of large biopolymers (Mijailovich et al. 1993; Suki et al. 1994) which comprise the ECM and even the cell cytoskeleton. Energy which is dissipated by rearrangements like this may result in stress relaxation, and in any case need not result in any tissue injury.

Finally, it is possible to imagine that even absent viscoelastic effects repeated cycles of strain may result in greater injury in a manner analogous to fatigue and crack propagation in non-biologic materials (Bouchbinder et al. 2010). However, this analogy breaks down on inspection as, unlike non-biologic materials, living materials are active – in the sense that cells and the extracellular matrix (ECM) are actively repaired and remodeled on a continuous basis. Fatigue and accumulation of injury must follow very dif-

ferent laws than those developed to describe cyclic loading in passive materials, if they occur at all. Thus, in the absence of new clinical evidence, there is little to recommend the mechanical power concept as a guide for clinical management.

Conclusion

Breathing involves the change in volume of the lung in response to the imposition of a transpulmonary pressure. The lung is a structurally complex, nonlinear, viscoelastic material which responds to the imposition of the transpulmonary pressure in nonhomogenous ways. Fortunately, in the healthy, homogeneously inflated lung, most of these complexities may be overlooked and the lung's motion treated as a one-dimensional strain given by the increment in volume above the resting state that results from the application of a single stress (the transpulmonary pressure). Important deviations from this simple behavior occur in the setting of nonhomogenous inflation. The microscopic details of lung structure remain important in understanding the resistance of the lung to changes in shape (shear deformation) and in considering its time-dependent, viscoelastic behavior.

References

- Atkin RJ, Fox N. An introduction to the theory of elasticity. Courier Corporation; 2005.
- Bachofen H, Hildebrandt J, Bachofen M. Pressure-volume curves of air- and liquid-filled excised lungs-surface tension in situ. *J Appl Physiol.* 1970;29:422–31.
- Bates JHT. Lung mechanics: an inverse modeling approach (Cambridge University Press, 2009).
- Bayliss LE, Robertson GW. The visco-elastic properties of the lungs. *Quarterly Journal of Experimental Physiology and Cognate Medical Sciences: Translation and Integration.* 1939;29:27–47.
- Bouchbinder E, Fineberg J, Marder M. Dynamics of simple cracks. *Annu Rev Condens Matter Phys.* 2010;1:371–95.
- Butler JP, Tolić-Nørrelykke IM, Fabry B, Fredberg JJ. Traction fields, moments, and strain energy that cells exert on their surroundings. *Am J Physiol Cell Physiol.* 2002;282:C595–605.

- Cressoni M, et al. Lung inhomogeneity in patients with acute respiratory distress syndrome. *Am J Respir Crit Care Med*. 2014;189:149–58.
- Curley GF, Laffey JG, Zhang H, Slutsky AS. Biotrauma and ventilator-induced lung injury: clinical implications. *Chest*. 2016;150:1109–17.
- Fredberg JJ, Kamm RD. Stress transmission in the lung: pathways from organ to molecule. *Annu Rev Physiol*. 2006;68:507–41.
- Fredberg JJ, Stamenovic D. On the imperfect elasticity of lung tissue. *J Appl Physiol*. 1989;67:2408–19.
- Fung YC. Stress, deformation, and atelectasis of the lung. *Circ Res*. 1975;37:481–96.
- Gattinoni L, Pesenti A. The concept of ‘baby lung’. *Intensive Care Med*. 2005;31:776–84.
- Gattinoni L, et al. Ventilator-related causes of lung injury: the mechanical power. *Intensive Care Med*. 2016;42:1567–75.
- Hantos Z, Daroczy B, Csendes T, Suki B, Nagy S. Modeling of low-frequency pulmonary impedance in dogs. *J Appl Physiol*. 1990;68:849–60.
- Hantos Z, Daroczy B, Suki B, Nagy S, Fredberg JJ. Input impedance and peripheral inhomogeneity of dog lungs. *J Appl Physiol*. 1992;72:168–78.
- Huhle R, Serpa Neto A, Schultz MJ, Gama de Abreu M. Is mechanical power the final word on ventilator-induced lung injury?—no. *Ann Transl Med*. 2018;6:394.
- Ingber DE. Mechanobiology and diseases of mechanotransduction. *Ann Med*. 2003;35:564–77.
- Kimmel E, Budiansky B. Surface tension and the dodecahedron model for lung elasticity. *J Biomech Eng*. 1990;112:160–7.
- Kimmel E, Kamm RD, Shapiro AH. A cellular model of lung elasticity. *J Biomech Eng*. 1987;109:126–31.
- Lai-Fook SJ. A continuum mechanics analysis of pulmonary vascular interdependence in isolated dog lobes. *J Appl Physiol*. 1979;46:419–29.
- Lai-Fook SJ. Pleural mechanics and fluid exchange. *Physiol Rev*. 2004;84:385–410.
- Lai-Fook SJ, Wilson TA, Hyatt RE, Rodarte JR. Elastic constants of inflated lobes of dog lungs. *J Appl Physiol*. 1976;40:508–13.
- Mead J, Takishima T, Leith D. Stress distribution in lungs: a model of pulmonary elasticity. *J Appl Physiol*. 1970;28:596–608.
- Mijailovich SM, Stamenović D, Fredberg JJ. Toward a kinetic theory of connective tissue micromechanics. *J Appl Physiol*. 1993;74:665–81.
- Otis AB, Fenn WO, Rahn H. Mechanics of breathing in man. *J Appl Physiol*. 1950;2:592–607.
- Protti A, Votta E, Gattinoni L. Which is the most important strain in the pathogenesis of ventilator-induced lung injury: dynamic or static? *Curr Opin Crit Care*. 2014;20:33–8.
- Solid Mechanics. In: Terjung R, editor. *Comprehensive physiology*, Vol. 41 8. John Wiley & Sons, Inc.; 2011.
- Stamenović D. Micromechanical foundations of pulmonary elasticity. *Physiol Rev*. 1990;70:1117–34.
- Suki B, Lutchen KR. Lung Tissue Viscoelasticity. *Wiley Encyclopedia Biomed Eng*. 2006; <https://doi.org/10.1002/9780471740360.ebs0701>.
- Suki B, Barabási AL, Lutchen KR. Lung tissue viscoelasticity: a mathematical framework and its molecular basis. *J Appl Physiol*. 1994;76:2749–59.
- Suki B, Ito S, Stamenovic D, Lutchen KR, Ingenito EP. Biomechanics of the lung parenchyma: critical roles of collagen and mechanical forces. *J Appl Physiol*. 2005;98:1892–9.
- Suki B, Stamenović D, Hubmayr R. Lung parenchymal mechanics. *Compr Physiol*. 2011;1:1317–51.
- Tonetti T, et al. Driving pressure and mechanical power: new targets for VILI prevention. *Ann Transl Med*. 2017;5:286.
- Wang N, Butler JP, Ingber DE. Mechanotransduction across the cell surface and through the cytoskeleton. *Science*. 1993;260:1124–7.
- West JB, Matthews FL. Stresses, strains, and surface pressures in the lung caused by its weight. *J Appl Physiol*. 1972;32:332–45.
- Wilson TA. Nonuniform lung deformations. *J Appl Physiol*. 1983;54:1443–50.
- Wilson TA, Bachofen H. A model for mechanical structure of the alveolar duct. *J Appl Physiol*. 1982;52:1064–70.



John J. Marini

Introduction and Definitions

The end expiratory airway pressure is the platform upon which the forces of inflation are superimposed. When positive pressure helps drive inflation, the positive end-expiratory pressure is designated “PEEP.” If natural muscular effort is the sole motive force for breathing, the end-expiratory airway pressure baseline is known as “CPAP” (*continuous* positive airway pressure), as airway pressure changes minimally. In practice, CPAP has come to imply that the patient provides some or all of ventilating power, while PEEP suggests that the ventilator carries most or all of the breathing workload. The terms are often interchanged, however, as they will be in this chapter—the key principles underlying PEEP and CPAP are identical. With or without effort, the absence of positive end-expiratory pressure is designated “zero end-expiratory pressure, or ZEEP”. Under static conditions, airway pressure at end exhalation is equivalent throughout the entire branching network of communicating (open) channels even to the alveolar level. Alveolar pressure may exceed the pressure measured at the airway opening, however, if measurable expiratory flow continues until interrupted by the next inflation or is blocked by early airway

closure during deflation. Under such conditions, the positive end-expiratory *alveolar* pressure or “total PEEP” ($PEEP_T$) is the sum of PEEP applied intentionally at the airway opening (PEEP or “extrinsic” PEEP) and “auto-PEEP” (sometimes also designated “occult,” “inadvertent,” or “intrinsic”) PEEP (Marini 2011). When two levels of PEEP are alternated, with spontaneous breaths occurring during each phase, the mode is termed “biphasic positive airway pressure” or “BIPAP.” If the lower level of BIPAP is maintained only transiently (i.e., within the span of a single exhalation), the mode is referred to as “airway pressure release ventilation or APRV.”

Fundamental Concepts

Transmural Pressure

To interpret the physiologic effects of PEEP on heart and lungs, several key concepts must be understood regarding the relationships among cardiopulmonary pressures and volumes. By convention, it is assumed that the pressure that surrounds the heart, blood vessels, and alveoli is the pleural pressure, even for structures imbedded far from the pleural surface. Transmural pressure, the inside minus surrounding value, is the *effective* pressure applied across the structure, whether it be lung, chest wall, blood vessel, or heart (Fig. 13.1a). Regarding the respiratory system,

J. J. Marini (✉)
University of Minnesota, Minneapolis, MN, USA
e-mail: marin002@umn.edu

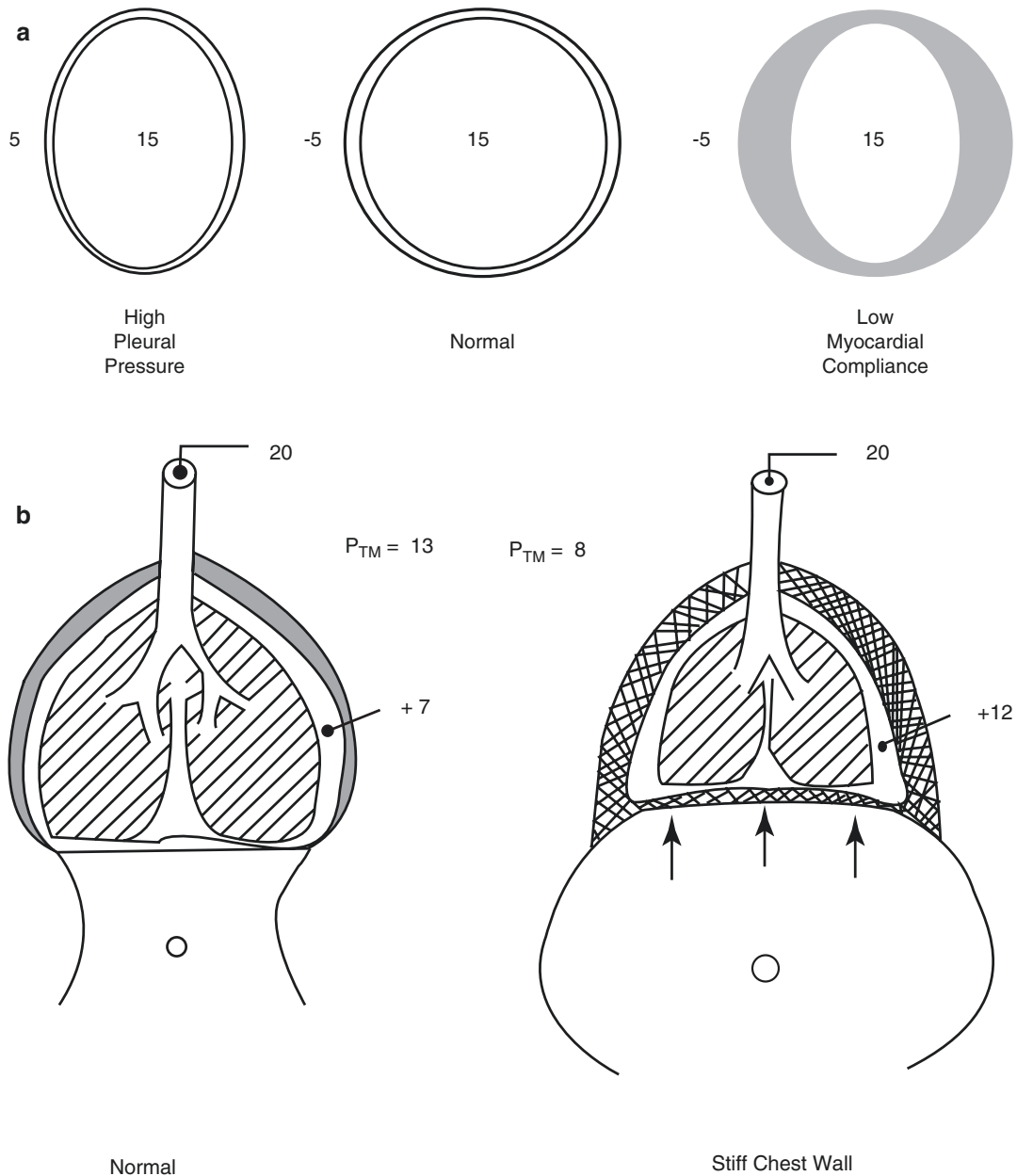


Fig. 13.1 (a) Concept of transmural pressure as applied to the heart and respiratory system. The same measured intracavitary or airway pressure may be associated with a range of chamber volumes, depending on transmural pressure (inside minus outside pressure difference) and the

compliance of the structure. (b) Influence varying chest wall compliance on the transmural pressures and volume that develop during ventilation with PEEP. Applying a PEEP of 20 cmH₂O distends the lungs much less in the presence of a stiff chest wall (right)

increased PEEP is the increment of transmural pressure applied between alveolus and atmosphere, and this increment partitions across the lungs and chest wall (Fig. 13.1b). It is not the entire PEEP but the difference in transmural pres-

sure across these structures in excess of their baseline values that determines the actual increment of stretching force applied to these individual structures by the boost in airway pressure. Thus, the transmural pressure applied across a lung unit

is the alveolar pressure (e.g., PEEP) minus the local pressure in the pleural space. For the central blood vessels and heart, it is the intravascular or intracardiac pressure minus the interstitial pressure. For the passive chest wall, it is pleural pressure minus atmospheric pressure, or simply Ppl. How much the lung and chest wall actually expand under the influence of their individual transmural pressures depends upon the individual compliances of each of these components of the respiratory system. In the absence of pleural effusion or air, the volumes of both lung and chest wall are identical, while their transmural pressures differ. Because the lung and heart are both enclosed within the chest cavity, a decrease of chest wall compliance will raise the fraction of a given airway pressure (e.g., PEEP) that translates into increased pleural pressure. Simultaneously, higher pleural pressure means that the same level of PEEP is associated with less transpulmonary pressure and volume of the always passive lung. The equation that encapsulates these relationships when airflow stops is the following:

$$\Delta P_{pl} = [C_L / (C_L + C_W)] \times \Delta P_{aw}$$

When pleural pressure is lowered by active inspiratory breathing effort, the negative change from end-expiratory baseline sums with the alveolar pressure to increase the transpulmonary pressure. Such increases of transpulmonary pressure generally affect the peri-diaphragmatic regions more than lateral and apical ones.

PEEP is applied to the lung surrounded by a chest wall with regionally different and body position-sensitive compliance characteristics. During passive inflation, the near-flaccid diaphragm allows pleural and abdominal pressures (P_{ab}) to rise by similar amounts, that is, the abdomen effectively forms part of chest wall. If intra-abdominal pressure is selectively raised (as during intra-abdominal hypertension), approximately half ΔP_{ab} is transmitted across the diaphragm to the pleural space to raise Ppl. A given PEEP value is then associated with a lower transpulmonary pressure and FRC. During *active expiration*, a phasic increase of P_{ab} means that any PEEP provides a boost for inspiration upon its release, helping to share the *inspiratory* workload. Interestingly,

when the aerated lung's external environment is made asymmetrical by a large pleural effusion or by contralateral atelectasis or consolidation, local pleural pressures differ but changes in Ppl are sensed rather uniformly throughout the chest cavity (Keenan et al. 2016; Cortes-Puentes et al. 2014; Cortes-Puentes et al. 2015).

These basic principles of transpulmonary pressures and breathing kinetics strongly influence the cardiovascular system as well (see below). Although the heart is never truly passive due to its unceasing muscular activity during both phases of its cycle, similar principles apply. The familiar Frank-Starling relationship that relates stroke volume to preload ideally allows for the surrounding pleural pressure, which is influenced by increases of airway pressure over baseline. Muscle fiber stretch—not intracavitary or even transmural pressure alone—determines the loading conditions prior to and during contraction.

Regional Heterogeneity

As already outlined, the lung and passive chest wall are serially linked structures that oppose any rise in alveolar pressures, such as PEEP. While alveolar pressure is everywhere the same in alveoli that communicate with the central airway, the local pleural pressures that surround the lung are nonuniform, with higher pleural pressures (and lower transmural pressures and net alveolar distending forces) usually encountered in more dependent zones. This nonuniformity is explained not only by the influence of gravity, but also by inherent shape differences between the two structures that must share the same dimensions of the thoracic compartment – the lungs (truncated cone-shaped) and the chest wall (cylinder-shaped) (Gattinoni et al. 2013). As implied by the previous discussion, regional differences of chest wall and respiratory system compliance cause local expansions and regional ventilations to differ. For similar reasons, the absolute pressures that surround the heart are not entirely uniform. However, the magnitude of regional differences in pericardiac and transmural pressures are much less for the heart than for the lung (O'Quin et al. 1985; Marini et al. 1982; Pelosi et al. 2001).

Careful studies using flexible surface sensors have shown that the lateral pressure adjacent to the heart is similar to that at the lung's same horizontal level (Yoshida et al. 2018) and marginally lower than that sensed by an esophageal balloon that lies beneath the heart and mediastinum in the supine position (Cortes-Puentes et al. 2015; O'Quin et al. 1985). By comparison, the great vessels (the superior and inferior *vena cavae* and aorta) are more strongly influenced by the regional pleural pressures that surround them.

PEEP, Mean Airway Pressure, and Hemodynamics

Under passive conditions, the mean airway pressure (mPaw) averaged over the entire respiratory cycle closely reflects the mean alveolar pressure (Marini and Ravenscraft 1992). Although increments of inspiratory pressure and inspiratory time fraction increase mPaw, PEEP has a proportionally greater influence on the numerical value, as PEEP serves as the steady baseline for both

phases of the respiratory cycle. Elevating mPaw influences the loading conditions of the heart, tending to reduce effective filling pressures and left ventricular afterload while having a less consistent directional influence on right ventricular afterload (see following).

Interaction of the Venous Return and Starling Curves

Vascular filling and tone are integral to cardiac output regulation – the heart cannot pump what it fails to receive in venous return, and vasoconstriction is a key determinant of afterload as well as the capacitance of the systemic vasculature. In fact, cardiac output determinants may be viewed strictly from a vascular perspective, as originally brought to our attention by Arthur Guyton (Guyton 1955) (Fig. 13.2). In steady-state conditions, venous return is proportional to the quotient of venous driving pressure and venous resistance. (Were the P_{RA} to rise suddenly to equal the P_{MSFP} , all venous return and cardiac output would stop.) Under most

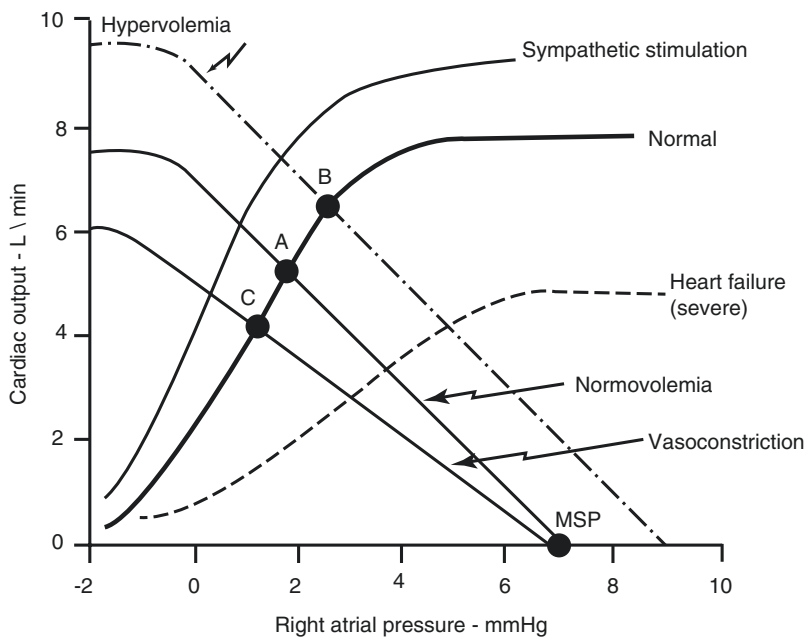


Fig. 13.2 Determinants of cardiac output. Conceptually, cardiac output is determined by the intersection of the venous return curve and the Starling curve that characterizes the right ventricle's response to the preload. The difference between mean systemic pressure (MSP) and right

atrial pressure provides the motive force for venous return. The normal intersection point (a) can be influenced by alterations of either curve by vascular filling (b), impaired or augmented contractility, or increased resistance to venous return in the large veins (c)

circumstances, the downstream pressure for venous return is the intravascular (not transmural) right atrial pressure. The upstream pressure that drives venous return, the mean systemic filling pressure (P_{MSFP}), is the volume-weighted average of intravascular pressures throughout the entire systemic vascular network. Because a much larger fraction of the total circulating volume is contained on the venous side of the circulation, P_{MS} is much closer to the right atrial pressure (P_{RA}) than to MAP. (One reasonable estimate for normal P_{MS} is 12–14 mmHg.) Mean systemic filling pressure is influenced by the circulating blood volume and vascular capacitance, which in turn is influenced by vascular tone. Thus, P_{MSFP} tends to rise under conditions of hypervolemia, polycythemia, and right-sided CHF; conversely, it tends to decline during vasodilation, sepsis, hemorrhage, diuresis.

The measured P_{MSfp} is also influenced by the downstream intravascular backpressure that opposes it (the P_{RA}) (Fessler et al. 1992). Up to a certain point, lowering P_{RA} while preserving P_{MSfp} increases driving pressure for venous blood flow and improves venous return. However, when P_{RA} is reduced below its surrounding tissue pressure, the thin-walled vena cava tends to collapse near the thoracic inlet (Fessler et al. 1993). Effective downstream pressure for venous return

then becomes the pressure just upstream to the point of collapse, rather than the P_{RA} itself.

Raising P_{RA} has the opposite effect, impeding venous return and dropping cardiac output unless P_{MS} rises sufficiently to maintain the flow-driving gradient. Therefore, a rising P_{RA} exerts the twin effects of increasing the heart's intracavitary filling pressure while impeding venous return. At any given moment, the cardiac output is determined by the intersection of the venous return curve and the Starling curve that characterizes the filling of the right heart (Guyton 1955; Fessler et al. 1991). In the analysis of a depressed cardiac output, both aspects of circulatory control must be considered, and each is affected by PEEP.

Influence of PEEP on the Determinants of Cardiac Output

By altering both intracavitary and transmural pressures as well as the pulmonary vascular resistance, PEEP may influence both the venous return and the loading conditions of the right and left ventricles (Fig. 13.3). Except where otherwise noted, the following discussion assumes a *passive* respiratory system unaided by muscular effort.

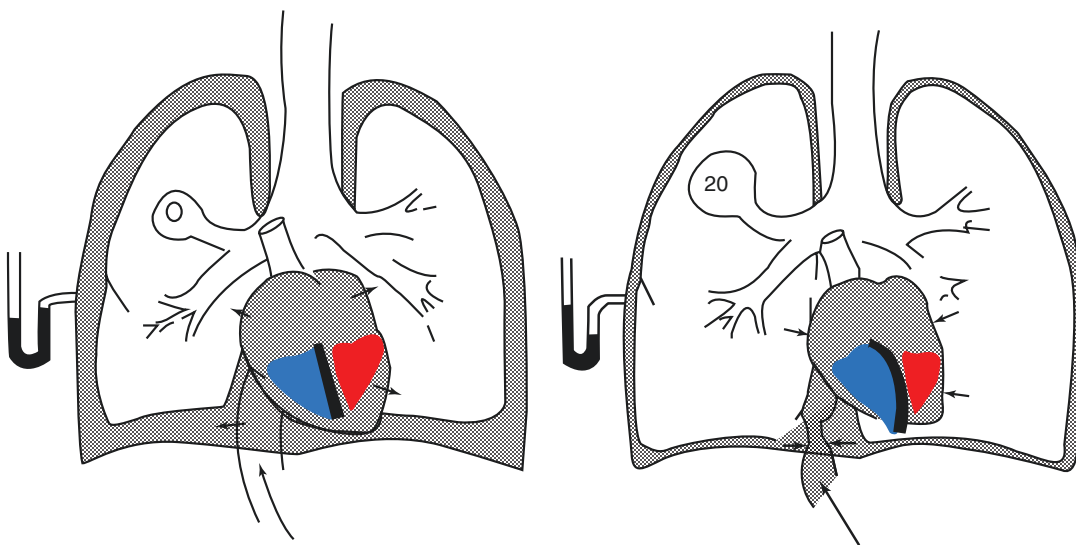


Fig. 13.3 Effects of adding PEEP on the determinants of cardiac loading conditions and output. When the lung expands under the influence of high PEEP (20 cmH20), right ventricular afterload rises and preload tends to fall. Septal shift (dark black line) may crowd the left ventricle,

restricting its filling while left ventricular afterload falls marginally. Diaphragmatic descent during lung expansion may narrow the inferior vena cava and impede venous return to some extent as well

PEEP and Transmural Cardiac Pressures

Invariably, PEEP will raise the intrapleural pressure by an amount influenced by the relative elastances of the series-coupled lungs and chest wall: $E_{\text{tot}} = E_L + E_W$. In this expression, the total elastance opposes the expanding effect of PEEP, while E_L and E_{CW} oppose expansion of the transmural pressures generated by PEEP across the lungs and chest wall, respectively. Thus, $\Delta P_{\text{pl}} = [E_W/E_{\text{tot}}] \times \Delta \text{PEEP}$. Recast into the more familiar clinical terms of lung and chest wall compliances (the inverse of their elastances), we arrive at a variant of the same algebraic relationship already described above: $\Delta P_{\text{pl}} = [C_L/(C_L + C_W)] \times \Delta \text{PEEP}$. In computing transmural vascular and cardiac pressures, which are customarily expressed in units of mmHg, the airway and pleural pressures need expression in similar units: $1.34 \text{ cmH}_2\text{O} = 1.0 \text{ mmHg}$. As a simplified and convenient example, if the compliances of the lungs and chest wall were equal (as they are near FRC in normal humans), the “transmission fraction” would approximate $1/2$, and a $13.4 \text{ cmH}_2\text{O}$ increment of PEEP would boost pleural pressure by 5 mmHg . Therefore, a right (or left) atrial pressure measured at 10 mmHg would correspond to a *volume* similar to that of 5 mmHg at ZEEP. In practice, of course, the interpretation of what this “correction” represents is less precise. The associated myocardial muscle fiber tension that better correlates with effective preload is simultaneously affected by ventricular interdependence (see Effects on Myocardial Contractility and Compliance).

PEEP and Afterload

Although afterload is often equated with elevations of blood pressure or vascular resistance, it is better defined as the muscular tension that must be developed during systole per unit of blood flow. As such, the systolic wall stress is affected by blood pressure, wall thickness, and ventricular volume. The dilated chambers of a *failing* heart—both right and left—are inherently afterload sensitive.

Left Ventricular Afterload

For a given systemic systolic blood pressure, any rise in pleural pressure consistently helps the left

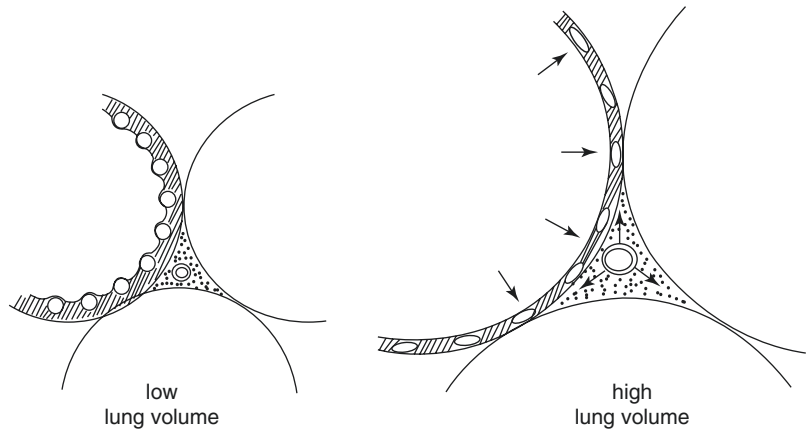
ventricle achieve the requisite systolic and mean pressure targets that are customarily measured at the periphery against atmospheric, rather than pleural, pressure. The levels of PEEP used clinically have a negligible direct effect, as is expected from a comparison of associated pleural and systemic arterial pressures. Rising pleural pressure in response to PEEP, however, may reduce right ventricular filling sufficiently to improve effective compliance of the interdependent left ventricle and myocardial wall tension, an important determinant of afterload to both ventricles. PEEP has little predictable effect on systemic vascular resistance, apart from secondary effects of compensatory reflexes.

Right Ventricular Afterload

Right ventricular (RV) afterload tends to rise nonlinearly with increasing lung volume (Pinsky et al. 1992; Vieillard-Baron et al. 2016). The pulmonary vascular pressure–flow relationship may differ slightly for positive versus negative pressure breathing. However, the RV afterload corresponding to any given lung volume is not greatly influenced by changes of pleural pressure, because the vessel that accepts its outflow (the pulmonary artery) is subjected to similar variations in pressure (Pinsky et al. 1992). Unlike its left ventricular counterpart, however, the lung volume increment in response to PEEP may significantly boost RV afterload by affecting the pulmonary vascular resistance (PVR). In both healthy and diseased lungs, progressive lung expansion by PEEP compresses the alveolar capillaries as it dilates the extra-alveolar vessels (Fig. 13.4). Consequently, PEEP increments without counterbalancing recruitment raise PVR in nonlinear fashion at all volumes that exceed functional residual capacity.

For diseased lungs, the PVR response to PEEP is often complicated by the simultaneously competing process of lung unit recruitment. Regional differences of compliance are accentuated by supine positioning, so that a PEEP increment that helps open one zone over-distends another. In early ARDS or congestive heart failure, for example, low to moderate increments of PEEP (generally $<10 \text{ cmH}_2\text{O}$) may leave PVR

Fig. 13.4 Differential behaviors of alveolar capillaries and interstitial microvessels during lung expansion. As the lung inflates, capillaries compress and the interstitial microvessels dilate under the influence of their respective transmural pressures



unchanged or even reduce it. These benefits of recruitment and attenuation of hypoxic vasoconstriction sharply decline as PEEP is raised into its higher clinical range, so that RV afterload predictably increases in progressive fashion with further PEEP increases. Recent work suggests that for a given level of PEEP, prone positioning helps even the distribution of transpulmonary pressures as well as reduce regional disparities of vascular resistance, especially if prone positioning recruits lung units and relieves the cardiac compression of the dorsal lung zones (Jozwiak et al. 2013; Albert and Hubmayr 2000).

PEEP Effects on Myocardial Contractility and Compliance

In the past, concern had been raised that PEEP might impair myocardial contractility, based primarily on the observation of marginally higher-than-expected values for left atrial transmural pressure (Scharf et al. 1979). Exactly how such proposed depression might occur remained obscure, and transmural pressures based on esophageal pressure were later shown to be influenced by ventricular interdependence and regional pleural pressure measurement artifact during lung expansion (Robotham et al. 1980; Marini et al. 1981). Unlike contractility, the effective *compliance* of the left ventricle can be influenced at high levels of PEEP-related lung distention, owing to its interdependence with the afterloaded right ventricle (Fig. 13.3). PEEP-accentuated interdependence is produced by their

shared interventricular septum, interwoven circumferential myocardial fibers, and the stretched pericardium (Jardin et al. 1981; Feihl and Broccard 2009). Moreover, because the heart is enclosed within the juxtacardiac fossa, its weight is partially supported by more dorsally positioned lung tissue. Lung expansion in the supine position may lift the heart a small amount and exert centrally directed compressive forces that are marginally higher than measured at the lateral lung surface (Marini et al. 1982). Large caudal displacement of the diaphragm may distort or narrow the inferior vena cava at the thoracic inlet, increasing its resistance to venous return to a minor degree (Fessler et al. 1992; Fessler et al. 1993; Fessler et al. 1991).

The compliance and even the contractility of the right ventricle are placed more at risk from high PEEP than is the left ventricle, especially in the supine position. The more distensible and innately afterload-sensitive RV dilates under the influence of PEEP-increased PVR, rapidly approaching its elastic limit as its transmural pressure rises (Pinsky et al. 1992). Dilation crowds the pericardium and shifts the interventricular septum toward the left. Increased muscular wall tension due to dilation not only accentuates RV afterload but also increases the pressure surrounding the embedded coronary vessels, potentially contributing to ischemic stress and impairing contractility. Simultaneously, any PEEP-related reduction of coronary perfusion pressure caused by lower mean arterial pres-

sure adds to the hazard, as the coronary vessels have little innate ability to dilate.

“Braking” Effect of PEEP on Heart Rate

A common clinical observation is that stroke volume and cardiac output may fall as PEEP is applied, whereas heart rate remains relatively unchanged. The lack of this normal adaptive response, although potentially explainable on the basis of innate pathology, anesthesia or drug intervention, may also be partially explained by a vagal reflex related to lung distention. Laboratory data indicate the presence of such a rate- “braking” reflex in relation to moderately high PEEP that is not observed when cardiac output is reduced to a similar extent by other types of reduction in preloading, such as hemorrhage and partial inferior vena caval obstruction. Selective afferent vagal blockade restores appropriate parity of heart rate response to PEEP (Marini et al. 1985).

PEEP and Lung Edema

PEEP exerts multiple effects that influence the amount and distribution of lung water (Paré et al. 1983; Luecke et al. 2003). Extra-alveolar microvessels are fluid-permeable, so that increases of alveolar pressure that raise pre-

capillary hydrostatic pressure accentuate leakage from those sites. External pressures that compress alveolar capillaries are increased by PEEP-induced lung distention, whereas pressures that surround extra-alveolar vessels are reduced (Permutt and Riley 1963). The net result of these offsetting effects of boosting PEEP is usually neutral, so that total lung water remains unaffected while its distribution shifts from alveolar to extra-alveolar compartments (Paré et al. 1983; Luecke et al. 2003). Pulmonary lymphatic drainage, although difficult to measure, is unlikely to be improved, as the pressure within the SVC and right atrium present increased backpressure to the sump (Frostell et al. 1987).

Spontaneous Vs. Passive Inflation and PEEP’s Cardiopulmonary Effects

The hemodynamics of spontaneous breathing differs markedly from those of passive inflation. (Fig. 13.5) Normally, the Pmsfp to RA pressure gradient that drives venous return is increased during inspiration, as diaphragmatic descent simultaneously raises intra-abdominal pressure as it lowers pleural pressure. When the respiratory muscles are silenced, mean alveolar pressures rise markedly. At the same time, the phasic boost to venous return characteristic of spontaneous breathing is attenu-

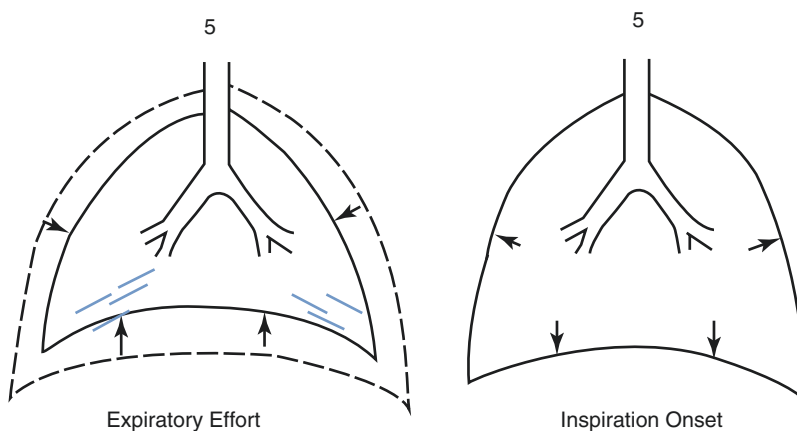


Fig. 13.5 The inspiratory “work sharing” concept during vigorous breathing. PEEP may serve as a spring against which expiratory muscular energy can be stored. In this illustration, PEEP is not allowed to distend the lung to its

passive end-expiratory dimensions (left). Upon expiratory muscle relaxation, the chest wall recoils to its passive position, helping PEEP to assist the inspiratory muscles at the onset of inspiratory effort

ated or eliminated, rendering increments of intrathoracic (pleural) pressure caused by PEEP more potent inhibitors of venous return and cardiac output, especially when the systemic vasculature is underfilled and/or adaptive venoconstriction is attenuated, as by sepsis (Nanas 1992).

Selected Clinical Applications

From the foregoing, it should be clear that the observed hemodynamic and monitoring impacts of PEEP may differ widely among varied clinical conditions; PEEP holds joint potential for benefit, harm, and interpretive confusion, depending on its level, the clinical condition, and the vigor of the breathing rhythm.

Hemodynamic Monitoring

Elevations of end-expiratory alveolar pressure not only affect hemodynamics but influence the evaluation of monitored information (O'Quin and Marini 1983). As already described, for the same distension, intracavitary vascular pressures are raised by the associated increase of pressure that surrounds the compliant blood vessel or cardiac chamber. Central venous pressure (CVP), PA pressures, and pulmonary artery occlusion pressures (Pw) should be interpreted with these effects in mind. The stiffer the chest wall and the more compliant the lung, the greater is the magnitude of the "offset" (O'Quin et al. 1985). It should be noted that the importance of these PEEP-related increases of pleural pressure fade if the ventilated lung is significantly smaller than its enclosing chest wall – as it is in ARDS. While the relative effect of PEEP on PVR may be amplified because the aerated alveoli are more distended while the major portion of blood flows through a lung with lesser capacity, the associated pleural pressure increments and their effects on Pw and CVP are sharply attenuated. In the setting of acute lung injury, this result is less a consequence of a stiffened lung than of the size mismatch between the aerated lung and its surrounding enclosure (Gattinoni et al. 2013).

Somewhat the opposite applies when PEEP is applied to the atelectatic lungs of a patient with massive obesity. Here, the chest wall is relatively stiff and the lungs have near-normal capacity to expand. Consequently, increases of alveolar pressure are disproportionately distributed to the pleural space and the vascular structures that they surround. Relatively high CVP and Pw may be recorded with little evidence for pulmonary edema. PEEP-caused elevations of pleural pressure do tend to impede venous return, however, even though Pmsfp may rise by a nearly commensurate amount in patients with intact venoconstricting reflexes (Fessler et al. 1991).

Dynamic Hyperinflation and Auto-PEEP

Positive pressure may persist at end expiration even when it is not externally applied as set PEEP. This phenomenon occurs as a consequence of insufficient time allotted for exhalation to recover relaxed functional reserve capacity. An invariable accompaniment of this enhanced recoil is gas flow that persists to the very end of exhalation period, driven by the end-expiratory flow-driving differential between auto-PEEP and the central airway pressure (Marini 2011). This elevation of alveolar pressure, which raises the effective mean pressure, tends to expand the lung and chest wall in the same way as PEEP. Although the spectrum of alveolar pressures may vary from region to region, depending on their individual deflation time constants and whether the local air channels remain open or experience early closure (as in the supine obese individual) (Lemyze et al. 2013), generation of auto-PEEP keeps the lung unit from experiencing tidal collapse. This principle of alveolar splinting is integral to inverse ratio ventilation and APRV. Persistence of auto-PEEP mandates an increase of inspiratory workload from patient or machine.

Auto-PEEP was first clinically defined and recognized in acutely decompensated COPD as a consequence of the impressive hemodynamic effects and monitoring artifacts of dynamic hyperinflation uncovered during the transition to

passive breathing (Pepe and Marini 1982). Spontaneously breathing patients maintain adequate forward output and venous return even at high levels of end-expiratory intrathoracic pressure, due to the negative pressures developed during inspiration that lower mean airway pressure and the net backpressure to venous return. Examination of the arterial pressure tracing of the vigorously breathing obstructed patient frequently demonstrates the effects of the respiratory half-cycles on the undulating stroke volume. When not flow-limited, expiratory muscle activity can also be called into play so as to speed expiratory airflow and avoid or attenuate dynamic hyperinflation. (Normal vigorous exercise also makes use of this “work sharing” mechanism.) (Henke et al. 1988) (Fig. 13.6) When auto-PEEP is accompanied by dynamic hyperinflation, as it invariably is during passive mechanical ventilation, the expanding lung increases RV afterload and boosts pleural pressure. The less the dynamic hyperinflation, the less the hemodynamic consequences associated with measured auto-PEEP (Marini 2011).

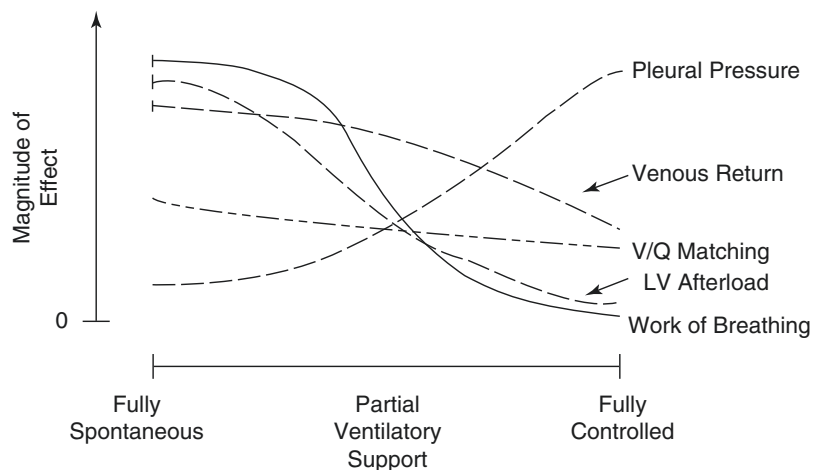
With these principles in mind, it becomes easy to see why transitioning to passive breathing exerts such impressive effects on cardiac output, blood pressure, and monitored intrathoracic vascular pressures (CVP and Pw) in COPD. Under passive conditions, relatively high lung compliance limits recoil, allowing unfettered dynamic hyperinflation that raises RV afterload, elevates

pleural pressure, and impedes venous return (Pepe and Marini 1982). These effects emerge rather suddenly as spontaneous breathing ceases, as during airway intubation.

PEEP on Auto-PEEP

It is reasonable to wonder what happens to the hemodynamic profile as PEEP is added to auto-PEEP in a patient with unchanging respiratory mechanics. The answer depends not only on whether spontaneous efforts are made and on the level of PEEP applied but also on the extent of tidal flow limitation (Henke et al. 1988) (Fig. 13.7). If auto-PEEP develops in a passively ventilated normal lung, for example, due to high minute ventilation, external PEEP simply adds to the preexisting auto-PEEP, proportionally adding to hyperinflation and increasing the hemodynamic consequences already outlined (Smith and Marini 1988). By contrast, PEEP added to a flow-limited patient essentially counterbalances the alveolar pressure until the original level of auto-PEEP is approached. Therefore, little additional hemodynamic impact usually results until the added PEEP exceeds the original auto-PEEP value (Baigorri et al. 1994). In fact, well-titrated PEEP may help keep open airways that otherwise undergo premature collapse. If the patient is breathing spontaneously, the inspiratory work of breathing declines during this intervention, as

Fig. 13.6 Influence of breathing mode on various cardiopulmonary parameters during breathing with PEEP. General trends are depicted for each parameter and are not quantitatively scaled relative magnitudes



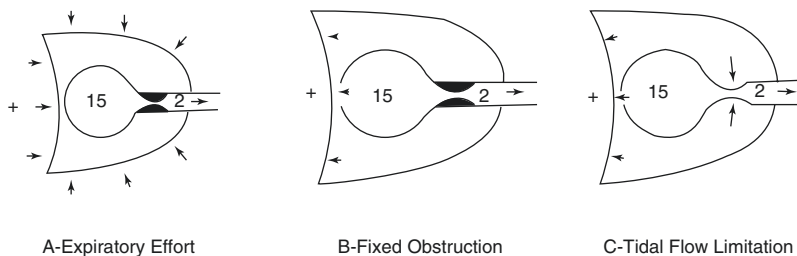


Fig. 13.7 Three forms of auto-PEEP that have differing implications for cardiopulmonary physiology. Adding PEEP to (a) (end-expiratory effort) or (c) (tidal expiratory flow limitation) may yield benefit to breathing workload without further hyperinflation or hemodynamic consequences. Conversely, external PEEP added to (b) (obstruc-

tion without flow limitation simply distends the lung and risks adverse cardiac loading. All three mechanisms may operate simultaneously in different zones of the lung and each may predominate at different phases of acute illness)

reversal of auto-PEEP is no longer necessary to initiate the breath (Feihl and Broccard 2009). In pressure-targeted modes such as PCV, offsetting auto-PEEP makes the true inspiratory driving pressure more apparent.

Conclusion

Whether deliberately applied or unintentionally developed, PEEP influences numerous determinants of hemodynamics as well as the interpretation of monitored hydrostatic pressures. Prominent among these are the loading conditions of both ventricles, heart rate, backpressure to venous return, and to a lesser degree, heart rate, left ventricular compliance, and perhaps, right ventricular contractility (Table 13.1). Understanding the key physiologic concepts of global and regional lung and vascular transmural pressures, interactions between the heart's Frank-Starling and venous return curves, and the determinants of dynamic hyperinflation primes the clinician to interpret and address many of PEEP's hemodynamic consequences at the bedside.

Table 13.1 Effects of PEEP on Hemodynamics

Impeded venous return
Increased pulmonary vascular resistance
Increased venous resistance
Diminished left ventricular compliance and afterload
Restrained heart rate increase (?)
Coronary ischemia (?)

References

- Albert RK, Hubmayr RD. The prone position eliminates compression of the lungs by the heart. *Am J Respir Crit Care Med.* 2000;161(5):1660–5.
- Baigorri F, de Monte A, Blanch L, Fernández R, Vallés J, Mestre J. Hemodynamic responses to external counterbalancing of auto-positive end-expiratory pressure in mechanically ventilated patients with chronic obstructive pulmonary disease. *Crit Care Med.* 1994 Nov;22(11):1782–91.
- Cortes-Puentes GA, Gard K, Keenan JC, Adams A, Dries D, Marini JJ. Unilateral mechanical asymmetry: positional effects on lung volume and transpulmonary pressure. *Intens Care Med Exp (ICMx).* 2014;2(4):2–9.
- Cortes-Puentes G, Keenan J, Dries DJ, Adams AB, Faltesek KA, Anderson CP, Marini JJ. Impact of chest wall modifications and lung injury on the correspondence between airway and transpulmonary driving pressures. *Crit Care Med.* 2015;43(8):e287–95.
- Feihl F, Broccard AF. Interactions between respiration and systemic hemodynamics. Part II: practical implications. *Intensive Care Med.* 2009;35:198–205.
- Fessler HE, Brower RG, Wise RA, Permutt S. Effects of positive end-expiratory pressure on the gradient for venous return. *Am Rev Respir Dis.* 1991;143(1):19–24.
- Fessler HE, Brower RG, Wise RA, Permutt S. Effects of positive end-expiratory pressure on the canine venous return curve. *Am Rev Respir Dis.* 1992;146(1):4–10.
- Fessler HE, Brower RG, Shapiro EP, Permutt S. Effects of positive end-expiratory pressure and body position on pressure in the thoracic great veins. *Am Rev Respir Dis.* 1993;148(6 Pt 1):1657–64.
- Frostell C, Blomqvist H, Hedenstierna G, Halbig I, Pieper R. Thoracic and abdominal lymph drainage in relation to mechanical ventilation and PEEP. *Acta Anaesthesiol Scand.* 1987;31(5):405–12.
- Gattinoni L, Taccone P, Carlesso E, Marini JJ. Prone position in acute respiratory distress syndrome. *Am J Respir Crit Care Med.* 2013;188(11):1286–93.

- Guyton AC. Determination of cardiac output by equating venous return curves with cardiac response curves. *Physiol Rev.* 1955;35:123–9.
- Henke KG, Sharratt M, Pegelow D, Dempsey JA. Regulation of end-expiratory lung volume during exercise. *J Appl Physiol* (1985). 1988;64(1):135–46.
- Jardin F, Farcot JC, Boisante L, Curien N, Margairaz A, Bourdarias JP. Influence of positive end-expiratory pressure on left ventricular performance. *N Engl J Med.* 1981;304(7):387–92.
- Jozwiak M, Teboul JL, Anguel N, Persichini R, Silva S, Chemla D, et al. Beneficial hemodynamic effects of prone positioning in patients with acute respiratory distress syndrome. *Am J Respir Crit Care Med.* 2013;188(12):1428–33.
- Keenan JC, Cortes-Puentes GA, Adams AB, Dries DJ, Marini JJ. The effect of compartmental asymmetry on the monitoring of pulmonary mechanics and lung volumes. *Respir Care.* 2016;61(11):1536–42.
- Lemyze M, Mallat J, Duhamel A, Pepy F, Gasan G, Barrailler S, et al. Effects of sitting position and applied positive end-expiratory pressure on respiratory mechanics of critically ill obese patients receiving mechanical ventilation. *Crit Care Med.* 2013;41(11):2592–9.
- Luecke T, Roth H, Herrmann P, Joachim A, Weisser G, Pelosi P, Quintel M. PEEP decreases atelectasis and extravascular lung water but not lung tissue volume in surfactant-washout lung injury. *Intensive Care Med.* 2003;29(11):2026–33.
- Marini JJ. Auto-PEEP and dynamic hyperinflation—Lessons learned over 30 years. *Am J Respir Crit Care Med.* 2011;184(7):756–62.
- Marini JJ, Ravenscraft SA. Mean airway pressure: physiological determinants and clinical importance. Part 1: physiological determinants and measurements. *Crit Care Med.* 1992;20(10):1461–72.
- Marini JJ, Culver BH, Butler J. Effect of positive end-expiratory pressure on canine ventricular function curves. *J Appl Physiol: Respirat Environ Exercise Physiol.* 1981;51(6):1367–74.
- Marini JJ, O'Quin R, Culver BH, Butler J. Estimation of transmural cardiac pressures during ventilation with PEEP. *J Appl Physiol: Respirat Environ Exercise Physiol.* 1982;53(2):384–91.
- Marini JJ, Culver BH, Butler J. An inflation reflex limits heart rate during PEEP-induced reduction in cardiac output (abstract). *Am Rev Respir Dis.* 1985;131(4):A146.
- Nanas S, Magder S. Adaptations of the peripheral circulation to PEEP. *Am Rev Respir Dis.* 1992;146(3):688–93.
- O'Quin R, Marini JJ. Pulmonary artery occlusion pressure: clinical physiology, measurement, and interpretation. *Am Rev Respir Dis.* 1983;128:319–26.
- O'Quin R, Marini JJ, Culver BH, Butler J. Transmission of airway pressure to the pleural space during lung edema and chest wall restriction. *J Appl Physiol: Respirat Environ Exercise Physiol.* 1985;59(4):1171–7.
- Paré PD, Warriner B, Baile EM, Hogg JC. Redistribution of pulmonary extravascular water with positive end-expiratory pressure in canine pulmonary edema. *Am Rev Respir Dis.* 1983;127(5):590–3.
- Pelosi P, Goldner M, McKibben A, Adams A, Eccher G, Caironi P, Losappio S, Gattinoni L, Marini JJ. Recruitment and Derecruitment during acute respiratory failure. An experimental study. *Am J Resp Crit Care Med.* 2001;164(1):122–30.
- Pepe PE, Marini JJ. Occult positive end-expiratory pressure in mechanically ventilated patients with airflow obstruction (the auto-PEEP effect). *Am Rev Respir Dis.* 1982;126:166–70.
- Permutt S, Riley S. Hemodynamics of collapsible vessels with tone: the vascular waterfall. *J Appl Physiol.* 1963;18:924–32.
- Pinsky MR, DeSmet JM, Vincent JL. Effect of positive end-expiratory pressure on right ventricular function in humans. *Am Rev Respir Dis.* 1992;146:681–7.
- Robotham JL, Lixfeld W, Holland L, MacGregor D, Bromberger-Barnea B, Permutt S, Rabson JL. The effects of positive end-expiratory pressure on right and left ventricular performance. *Am Rev Respir Dis.* 1980;121(4):677–83.
- Scharf SM, Brown R, Saunders N, Green LH, Ingram RH Jr. Changes in canine left ventricular size and configuration with positive end-expiratory pressure. *Circ Res.* 1979;44(5):672–8.
- Smith TC, Marini JJ. Impact of PEEP on lung mechanics and work of breathing in severe airflow obstruction. The effect of PEEP on auto-PEEP. *J Appl Physiol.* 1988;65(4):1488–99.
- Vieillard-Baron A, Matthay M, Teboul JL, Bein T, Schultz M, Magder S, Marini JJ. Experts' opinion on management of hemodynamics in ARDS patients: focus on the effects of mechanical ventilation. *Intensive Care Med.* 2016;42(5):739–49.
- Yoshida T, Amato MBP, Grieco DL, Chen L, Lima CAS, Roldan R, et al. Esophageal manometry and regional transpulmonary pressure in lung injury. *Am J Respir Crit Care Med.* 2018;197(8):1018–26.



Basics of Ventilation/Perfusion Abnormalities in Critically Ill Ventilated Patients

14

Jeremy E. Orr and Susan R. Hopkins

Introduction

The fundamental role of the pulmonary system is the delivery of oxygen to the bloodstream and removal of carbon dioxide. As inspired air travels through the upper airways, it is warmed and humidified. Continuing its path to the alveolus, it is mixed with resident gas that is left at the end of the previous expiration. Finally, after reaching the alveolus, oxygen diffuses into and carbon dioxide diffuses out of the blood by the passive processes of diffusion and is circulated to the capillary beds. This process of pulmonary gas exchange is remarkably efficient in young healthy humans and the difference between the partial pressure of oxygen in the alveolus (PAO_2) and the arterial blood (PaO_2) is at most a few mmHg. However, a majority of lung diseases are characterized by reduced gas exchange efficiency, manifest as an increase in the alveolar-arterial difference for

oxygen ($AaDO_2$). The goal of this chapter is to provide a basic physiologic understanding of ventilation-perfusion matching and how it can be disrupted in critically ill patients.

Ventilation-perfusion, \dot{V}_A/\dot{Q} , matching refers to the matching of the delivery of fresh inhaled air into the alveolar regions of the lung to the delivery of deoxygenated capillary blood to the same regions. The precise matching of ventilation and perfusion in the lung is required for efficient transfer of both oxygen into and carbon dioxide out of the body. Under normal resting conditions, the mean \dot{V}_A/\dot{Q} ratio of the lung is close to 1; almost equal minute volumes of air and blood are delivered to the gas-exchanging regions of the lung (Prisk and Hopkins 2013). This is not surprising because the oxygen content of room air (20.9 ml/100 ml) and of normally oxygenated blood (~20.6 ml/100 ml) are almost equal, necessitating equal volume delivery. In a single lung unit such as an alveolus, gas exchange is determined by the local \dot{V}_A/\dot{Q} ratio (Riley and Cournand 1949) (Fig. 14.1). However, in the human lung, there are several thousand acini, which are the primary gas exchange units of the lung. Each has a unique \dot{V}_A/\dot{Q} ratio which include units that are perfused but not ventilated which comprise shunts, and units which are ventilated but not perfused which form dead space.

In an individual lung unit, there is diffusion equilibrium in all but a few exceptional circumstances (see Agusti et al. 1991; Crawford et al.

J. E. Orr (✉)

Department of Medicine, Division of Pulmonary
Critical Care and Sleep Medicine, University of
California, La Jolla, CA, USA
e-mail: jlorr@health.ucsd.edu

S. R. Hopkins

Department of Medicine, Division of Pulmonary
Critical Care and Sleep Medicine, University of
California, La Jolla, CA, USA

Department of Medicine and Radiology, University
of California, San Diego, La Jolla, CA, USA
e-mail: shopkins@ucsd.edu

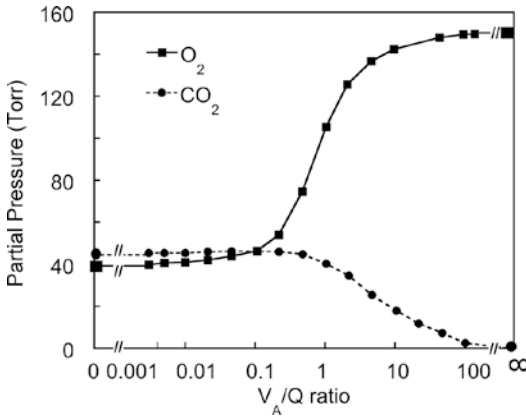


Fig. 14.1 The relationship between the partial pressure of oxygen and carbon dioxide and \dot{V}_A/\dot{Q} ratio. At a low \dot{V}_A/\dot{Q} ratio, the partial pressures of oxygen and carbon dioxide are close to mixed venous blood. At a high \dot{V}_A/\dot{Q} ratio, the partial pressure approaches that of inspired air. (Redrawn from West (1977). Adapted with permission of the American Thoracic Society. Copyright © 2020 American Thoracic Society. All rights reserved. Cite: West (1977). The American Review of Respiratory Disease* is an official journal of the American Thoracic Society. Readers are encouraged to read the entire article for the correct context at https://www.atsjournals.org/doi/10.1164/arrd.1977.116.5.919?url_ver=Z39.88-2003&rfr_id=ori:rid:crossref.org&rfr_dat=cr_pub%20%20pubmed. The authors, editors, and The American Thoracic Society are not responsible for errors or omissions in adaptations. *Now titled American Journal of Respiratory and Critical Care Medicine)

1995) but ventilation-perfusion mismatch increases the AaDO₂. As discussed in more detail below, this is because the alveolar gas composition is the ventilation-weighted average of all the lung units, but the arterial blood is the perfusion-weighted average from these same units. A majority of lung diseases are characterized by an increase in \dot{V}_A/\dot{Q} mismatch, including chronic obstructive pulmonary disease (COPD) (Wagner et al. 1977), pulmonary hypertension (Melot et al. 1983), asthma (Wagner et al. 1978), pulmonary edema (Podolsky et al. 1996), pulmonary fibrosis (Agusti et al. 1991), and acute respiratory distress syndrome (Ralph et al. 1985).

General Considerations and Theoretical Basis of Gas Exchange

Ventilation–Perfusion Relationships

Rahn and Fenn (1955), Riley and Cournand, and others (Riley and Cournand 1949, 1951; Riley et al. 1951) developed a series of simple equations to describe the relationships between alveolar gas concentrations and \dot{V}_A/\dot{Q} ratio. These are briefly outlined below and described in more detail elsewhere (Hopkins and Wagner 2017; Stickland et al. 2013; Farhi and Tenney 1977). These equations, which apply to steady-state conditions, are written for oxygen, but can be applied to any gas such as carbon dioxide or inert gases such as nitrogen and others (more about inert gases later). They assume that there is no diffusion limitation that is, that alveolar gas and end-capillary partial pressures of the gas in equilibrium, which is not always true for oxygen but is true for inert gases and likely true for CO₂. The first is a simple statement of mass balance: the amount of oxygen taken up by the body (the minute volume of oxygen uptake ($\dot{V}O_2$)) must equal the difference between what enters the lung in inspired air and what leaves the lung in expired air, that is:

$$\dot{V}O_2 = (\dot{V}_I \cdot F_I O_2) - (\dot{V}_E \cdot F_E O_2) \quad (14.1)$$

\dot{V}_I is inspired ventilation, \dot{V}_E expired ventilation, $F_I O_2$ the fractional concentration of oxygen in inspired gas, and $F_E O_2$ the fractional concentration in expired gas. Note that \dot{V}_I does not equal \dot{V}_E identically except when the respiratory exchange ratio is 1, because the volume of carbon dioxide diffusing into the alveolar space is not matched by the volume of oxygen diffusing out of the alveolus into the blood stream. This is a small effect and introduces an error only of ~1% under resting conditions. Dead space in the lung is due to unperfused areas and thus is not involved in gas exchange, so the relationship in Eq. (14.1)

can be simplified by expressing it for alveolar ventilation (\dot{V}_A) and assuming that the respiratory exchange ratio is equal to 1 so \dot{V}_I is equal to \dot{V}_E :

$$\dot{V}O_2 = (\dot{V}_A \cdot F_I O_2) - (\dot{V}_A \cdot F_A O_2) \quad (14.2)$$

Rearranging Eq. (14.2) gives a simple mass balance equation describing oxygen uptake on the ventilation side:

$$\dot{V}O_2 = \dot{V}_A \cdot [F_I O_2 - F_A O_2] \quad (14.3)$$

Mass balance for oxygen also dictates oxygen leaving the lung must also appear in the blood, where uptake is described by the Fick principle:

$$\dot{V}O_2 = \dot{Q} \cdot [C_c' O_2 - C_{\bar{v}} O_2] \quad (14.4)$$

where \dot{Q} is cardiac output, $C_c' O_2$ is the oxygen concentration in blood leaving the lungs, that is, end-capillary blood (and $C_{\bar{v}} O_2$ is the oxygen concentration in blood entering the lung (i.e., mixed venous). Under steady-state conditions, the amount of oxygen lost from the lungs must be

balanced by that being taken up into the blood so that Eq. (14.3) = Eq. (14.4):

$$\dot{V}_A \cdot [F_I O_2 - F_A O_2] = \dot{Q} \cdot [C_c' O_2 - C_{\bar{v}} O_2] \quad (14.5)$$

This can be rearranged to give:

$$\dot{V}_A / \dot{Q} = [C_c' O_2 - C_{\bar{v}} O_2] / [F_I O_2 - F_A O_2] \quad (14.6)$$

Converting the fractional concentrations of inspired and expired oxygen to partial pressures:

$$\dot{V}_A / \dot{Q} = [C_c' O_2 - C_{\bar{v}} O_2] / [F_I O_2 - F_A O_2]. \quad (14.7)$$

k is a constant and equals $7.60 \times (273 + T)/273$ where T is body temperature in degrees Celsius. k is required to account for alveolar gas variables which are typically expressed as BTPS (body temperature pressure saturated) and blood variables which are expressed as STPD (standard temperature, pressure, dry). At 37 °C, k equals 8.63.

An almost identical equation can be written using CO₂ elimination instead of oxygen uptake as:

$$\dot{V}_A / \dot{Q} = \text{kg} [C_{\bar{v}} \text{CO}_2 - C_c' \text{CO}_2] / [P_A \text{CO}_2 - P_I \text{CO}_2]. \quad (14.8)$$

Equations (14.7) and (14.8) show that when mixed venous and inspired O₂ and CO₂ concentrations and the oxygen hemoglobin dissociation curve are known, local PO₂ and CO₂ are determined by the \dot{V}_A / \dot{Q} ratio. These relationships can be solved for different \dot{V}_A / \dot{Q} ratios giving rise to Fig. 14.1, as shown previously. However, one caveat is that O₂ and CO₂ cannot be considered independently. This is because of the Bohr effect (Bohr 1891; Riggs 1988) whereby local CO₂ and pH alters the affinity of hemoglobin for oxygen, thus affecting the oxygen concentration in blood from a unit, and the Haldane effect (Christiansen et al. 1914) where the CO₂ carrying capacity of hemoglobin is affected by the local oxygen content.

It can be seen that when ventilation is low relative to perfusion, the values of alveolar gas approach mixed venous concentrations (PO₂ ~ 40, PCO₂ ~ 45, under normal sea level resting condi-

tions). Conversely, when alveolar ventilation is high relative to perfusion, the alveolar gas approaches inspired (PO₂ ~ 150, PCO₂ ~ 0). As seen in Fig. 14.1, the partial pressures of oxygen and CO₂ change the most between \dot{V}_A / \dot{Q} ratios 0.1–10. While PCO₂ continues to fall with higher \dot{V}_A / \dot{Q} ratios, PO₂ changes little.

In a perfectly uniform lung (without shunt or dead space), the alveolar-arterial difference would be zero. However, because the lung is not uniform, the alveolar gas composition is the weighted contributions of ventilation from each unit such that units with high ventilation will contribute more to expired gas. However, end-capillary gas concentration is weighted by perfusion so that units of high perfusion will have a greater effect on end-capillary blood, giving rise to an alveolar-arterial difference. Figure 14.2 shows how ventilation-perfusion mismatch

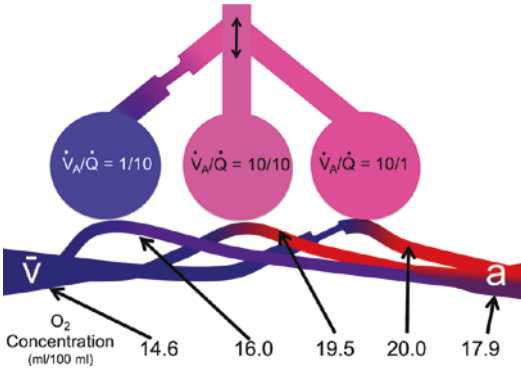


Fig. 14.2 Pulmonary gas exchange in a three-compartment lung, showing how regions of low \dot{V}_A / \dot{Q} ratio contribute to venous admixture and hypoxemia. Due to the nonlinear shape of the O_2 -Hb dissociation curve, the increase in the oxygen content of a region of high ventilation-perfusion ratio, in this case $\dot{V}_A / \dot{Q} = 10$ does not balance the low O_2 concentration in blood leaving the low ventilation-perfusion ratio (0.1) unit, resulting in reduced arterial oxygen content. (Modified with permission of Wolters Kluwer Health, Inc)

affects gas exchange efficiency in a simple three-compartment idealized lung.

Shunt

Shunt is one extreme of the ventilation-perfusion distribution and represents areas of the lung that are perfused but not ventilated (intrapulmonary shunt), or blood that bypasses the lungs altogether (extrapulmonary shunt). Shunt can be quantified during hyperoxic gas breathing, typically 100% oxygen breathing (Berggren 1942). If breathed for a sufficient period of time, blood leaving regions of low \dot{V}_A / \dot{Q} ratio will be fully oxygenated, and any venous admixture overcome. Also, in the presence of 100% oxygen, any diffusion limitation for oxygen is eliminated. This leaves shunt as the only potential source of deoxygenated blood in the arterial circulation. To calculate shunt, arterial and pulmonary mixed venous oxygen content is measured and end-capillary content, $C_c \cdot O_2$, is calculated by assuming the end capillary PO_2 is the same as alveolar PO_2 . This is a reasonable assumption because as noted above the effects of diffusion limitation and low \dot{V}_A / \dot{Q} ratio on the arterial blood are eliminated in the presence of 100% oxygen.

First, alveolar PO_2 is calculated from the barometric pressure, P_{bar} , the saturation vapor pressure of water (47 mmHg at 37 °C), the inspired oxygen concentration $F_I O_2$, the arterial PCO_2 ($P_a CO_2$) and the respiratory exchange ratio (R ; often assumed to be 0.8–1.0) as:

$$P_A O_2 = (P_{bar} - 47) \cdot F_I O_2 - P_a CO_2 \quad (14.9)$$

The saturation of arterial blood and mixed venous blood are estimated from the arterial and mixed venous PO_2 , from the equation of Severinghaus (1979).

$$SO_2 = \left(23,400 \cdot (pO_2^3 + 150 \cdot pO_2)^{-1} + 1 \right)^{-1} \quad (14.10)$$

While breathing 100% oxygen, end-capillary blood hemoglobin is essentially 100% saturated. Using the $P_A O_2$ as the end-capillary PO_2 , $C_c \cdot O_2$ is calculated from

$$C_c \cdot O_2 = 1.39 \cdot [Hb] \cdot SO_2 + 0.003 PO_2 \quad (14.11)$$

The arterial and mixed venous oxygen contents are similarly calculated from the saturation and PO_2 using equation 14.11 above. The total cardiac output (\dot{Q}_T) is divided into the portion of flow that participated in gas exchange in the capillaries (\dot{Q}_p) and that flowing through shunted regions (\dot{Q}_s):

$$\dot{Q}_T = \dot{Q}_p + \dot{Q}_s \quad (14.12)$$

Mass balance dictates that the oxygen content in arterial blood is the weighted sum of the fully oxygenated blood leaving the lung in the pulmonary end-capillary blood ($C_p \cdot O_2$) and the shunted deoxygenated mixed venous blood ($C_{\bar{v}} O_2$):

$$\dot{Q}_T \cdot C_a O_2 = \dot{Q}_p \cdot C_c \cdot O_2 + \dot{Q}_s \cdot C_{\bar{v}} O_2 \quad (14.13)$$

By substituting $\dot{Q}_T - \dot{Q}_s$ for \dot{Q}_p , and rearranging

$$\frac{\dot{Q}_s}{\dot{Q}_T} = \frac{C_c \cdot O_2 - C_a O_2}{C_c \cdot O_2 - C_{\bar{v}} O_2} \quad (14.14)$$

where \dot{Q}_s / \dot{Q}_T is the fraction of cardiac output that can be attributed to shunt.

Bohr Dead Space

Dead space, the other extreme of ventilation-perfusion matching, represents areas of the lung that are ventilated but not perfused. Dead space was first quantified by Bohr (1891) who measured dead space arising from not only the conducting airways but also an additional component arising from lung units of very high \dot{V}_A / \dot{Q} ratio (i.e., regions of the lung that receive alveolar ventilation but are un-perfused). Combined, these two components are termed physiologic or Bohr dead space (i.e., anatomic plus alveolar dead space). Bohr dead space can be calculated using the relationship between alveolar ventilation, carbon dioxide production, and dead space as follows (Bohr 1891). Rewriting Eq. (14.1) above for CO₂ elimination:

$$\dot{V}CO_2 = (\dot{V}_E \cdot F_E CO_2) - (\dot{V}_I \cdot F_I CO_2) \quad (14.15)$$

The fraction of inspired CO₂, $F_I CO_2$, is negligible so this simplifies to:

$$\dot{V}CO_2 = (\dot{V}_E \cdot F_E CO_2) \quad (14.16)$$

Assuming that all CO₂ exchange takes place in the alveoli, mass balance dictates that the volume of CO₂ eliminated from the alveoli must balance that in the expired air

$$(\dot{V}_A \cdot F_A CO_2) = \dot{V}CO_2 = (\dot{V}_E \cdot F_E CO_2) \quad (14.17)$$

Total expired ventilation is the sum of alveolar ventilation and dead space ventilation, \dot{V}_D

$$\dot{V}CO_2 / \dot{V}O_2 = (\dot{V}_A \cdot [F_A CO_2 - F_I CO_2]) / (\dot{V}_A \cdot [F_I O_2 - F_A O_2]) \quad (14.22)$$

The ratio of $\dot{V}CO_2$ to $\dot{V}O_2$ is the respiratory exchange ratio, R , assuming the concentration of CO₂ in inspired gas is negligible, and since \dot{V}_A appears in both the numerator and denominators, this simplifies to:

$$R = ([F_A CO_2]) / ([F_I O_2 - F_A O_2]) \quad (14.23)$$

Rearranged and expressed in terms of partial pressures (these gases follow Dalton's law of partial pressures, i.e., that "the total pressure exerted

$$\dot{V}_E = \dot{V}_A + \dot{V}_D \quad (14.18)$$

Substituting into Equation and rearranging the Eq. (14.17):

$$\dot{V}_D / \dot{V}_E = (F_A CO_2 - F_E CO_2) / F_A CO_2 \quad (14.19)$$

Partial pressures of CO₂ can be substituted for $F_A CO_2$ and $F_E CO_2$ and assuming $P_a CO_2 = P_A CO_2$ and then fractional dead space (\dot{V}_D / \dot{V}_E) can be calculated using measured $P_a CO_2$ and mixed expired CO₂, $P_E CO_2$:

$$\dot{V}_D / \dot{V}_E = (P_a CO_2 - P_E CO_2) / P_a CO_2 \quad (14.20)$$

If \dot{V}_E and respiratory frequency are known, this can be converted to a dead space volume by multiplying by the tidal volume.

The Alveolar-Arterial Difference (AaDO₂)

The AaDO₂ is a measure of pulmonary gas exchange efficiency. Ventilation-perfusion mismatch, diffusion limitation, and shunt are the only contributors to the AaDO₂. The derivation of the equation of the AaDO₂ is as follows: Returning to Eq. (14.3) and rewriting it for CO₂:

$$\dot{V}CO_2 = \dot{V}_A \cdot [F_A CO_2 - F_I CO_2] \quad (14.21)$$

And dividing by Eq. (14.1)

by the gases is the sum of the individual pressures"), this becomes:

$$P_A O_2 = P_I O_2 - P_A CO_2 / R \quad (14.24)$$

This will be recognized as the simplified version of the alveolar gas equation, simplified because of the assumption that the inspired ventilation, \dot{V}_I equals expired ventilation, \dot{V}_E . Without this simplification (see (Rahn and Fenn 1955) for more information), the full equation is written as:

$$P_A O_2 = P_I O_2 - P_A CO_2 / R + P_A CO_2 \cdot F_I O_2 \cdot (1 - R) / R \tag{14.25}$$

And the alveolar-arterial difference AaDO₂ is:

$$AaDO_2 = P_A O_2 - P_a O_2 \tag{14.26}$$

$$P_A / P_{\bar{V}} = P_a / P_{\bar{V}} = \lambda / [\lambda + \dot{V}_A / \dot{Q}] \tag{14.27}$$

Where λ is the blood: gas partition coefficient. This is the ratio of concentrations of the gas in blood and gas at equilibrium. Thus, they have the same partial pressure in gas and blood but may have very different concentrations depending on how soluble the gas is in blood. Equation (14.27) is derived from Eq. (14.7) shown previously. The full derivation is beyond the scope of this chapter but can be found here: (Hopkins and Wagner 2017). By solving Eq. (14.27) for gases of different λ , the extent of ventilation-perfusion inequality can be estimated. This is done by modeling the measured data to fit a 50-compartment model with the first compartment being shunt, and the last compartment being dead space (Hopkins and Wagner 2017). To express heterogeneity, ventilation and perfusion are plotted vs \dot{V}_A / \dot{Q} ratio. This plot is shown for a healthy normal subject and a patient with ARDS in Fig. 14.3. The typical metrics used to describe \dot{V}_A / \dot{Q} heterogeneity are the widths of this distribution as expressed by the LogSD, \dot{V} referring to the standard deviation on a log scale of the \dot{V}_A vs. \dot{V}_A / \dot{Q} distribution and the LogSD, \dot{Q} referring to the standard deviation on a log scale of the \dot{Q} vs. \dot{V}_A / \dot{Q} distribution,

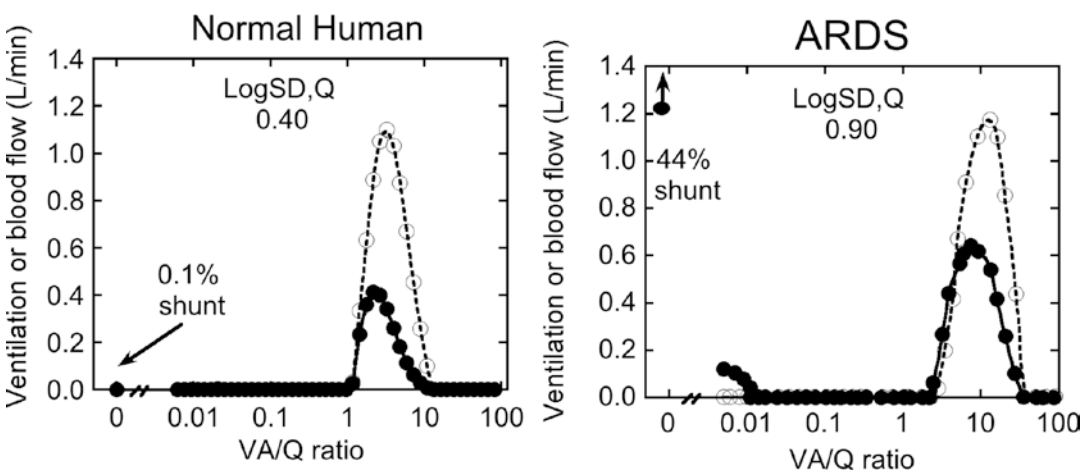


Fig. 14.3 Ventilation-perfusion matching measure by MIGET in a normal subject (left) and a patient with ARDS (right). In ARDS, there are large areas of shunt and some

broadening of the \dot{V}_A / \dot{Q} distribution along with some regions of very low \dot{V}_A / \dot{Q} ratio. (Modified from Hopkins and Wagner (2017))

respectively. These calculations of heterogeneity exclude the shunt and dead space compartments which are quantified separately. A limitation of MIGET is that the ventilation and perfusion distributions recovered from MIGET can only be expressed relative to \dot{V}_A / \dot{Q} ratio (\dot{V}_A vs. \dot{V}_A / \dot{Q} and \dot{Q} vs. \dot{V}_A / \dot{Q}). Additional metrics for describing heterogeneity that do not depend on the fit to a 50-compartment model have been described (Hopkins and Wagner 2017; Hlastala 1984), but are not as commonly used. The amount of diffusion limitation of oxygen transport can be also be indirectly estimated from MIGET data (Hammond et al. 1986). The technical challenges and moderately invasive nature of MIGET has largely limited it to a research tool, but as discussed below it has provided great insights into ventilation-perfusion matching in health and disease.

Clinical Assessment of Ventilation-Perfusion Matching

Pulmonary gas exchange problems are encountered commonly in a wide variety of clinical settings. Assessment of ventilation-perfusion

matching is essential for evaluating hypoxemia and hypercapnia, determining appropriate treatments, and as a marker of disease severity and prognosis. It should be noted that while pulse oximetry is useful for identifying impaired oxygenation, in isolation it provides limited information regarding the status of ventilation-perfusion matching. Arterial blood gas testing, in contrast, allows the calculation of several useful metrics.

The alveolar to arterial oxygen difference (AaDO₂, also referred to as the A-a gradient) is a well-known measure that reflects contributions from ventilation-perfusion heterogeneity, diffusion limitation of oxygen transport, and shunt in the lung. Alveolar PO₂ is estimated using the alveolar gas equation (Eq. 14.25 above), and arterial PO₂ is measured directly from the arterial sample. The arterial PCO₂ is used as an estimate of P_ACO₂. The measure requires an assumed respiratory exchange ratio unless it is directly measured (normally 0.8–1.0 under resting conditions) and the assumption of steady-state conditions.

In a normal adult, A-a difference is approximately 5–20 mmHg, with predicted values varying by age. This can be estimated as:

$$(\text{Predicted AaDO}_2 = 2.5 + (0.21 \times \text{age [in years]}) \text{ (Mellemaard 1966)}). \quad (14.28)$$

It should be noted that, as mentioned earlier, of three contributors to the AaDO₂, diffusion limitation whereby there is incomplete equilibrium between alveolar gas and pulmonary end capillary blood, is extremely uncommon except in patients with interstitial lung disease (Agusti et al. 1991). Other situations where diffusion limitation of oxygen transport can be present include heavy/maximal exercise in some highly trained athletes (Hopkins et al. 1998; Hopkins et al. 1994) and during exercise at high altitude (Torre-Bueno et al. 1985; Wagner et al. 1987). This leaves ventilation-perfusion mismatch and shunt as the usual causes of an increased AaDO₂. Increased ventilation-perfusion mismatch is ubiquitous in patients with lung disease, and a large AaDO₂ is common. Large shunts are also common in many critically ill patients and can

be assessed using 100% oxygen as described above.

The P_aO₂/F_IO₂ ratio (“P/F ratio”) is another measure commonly used in mechanically ventilated patients (particularly in the setting of ARDS), in whom the F_IO₂ is known (and often higher than room air). This measure is simple to calculate at bedside, but utility in assessment of gas exchange is limited due to confounding effects of barometric pressure, respiratory exchange ratio, and PaCO₂. In addition, if the inspired F_IO₂ is high, and close to 100%, the P/F ratio will only reflect shunt and not other \dot{V}_A / \dot{Q} abnormalities.

The effects of ventilation-perfusion matching on carbon dioxide exchange may also be clinically relevant. Evaluation of carbon dioxide elimination can provide information regarding

dead space, which may contribute to hypercapnia and excessive ventilatory demand, and may also have prognostic utility in some situations. For example, several studies have reported that dead space ventilation is higher in non-survivors of ALI/ARDS than in survivors (Cepkova et al. 2007). For every 0.05 increase in dead space to tidal volume ratio, the odds of death increase by 45% (Nuckton et al. 2002; Kallet et al. 2004). Interestingly, when prone position results in a reduction in dead space, survival rates are improved (Gattinoni et al. 2003).

Physiologic dead space can be calculated using the $P_a\text{CO}_2$ determined from arterial blood, as well as mixed expired CO_2 concentrations, as discussed previously (Eq. 14.20). To estimate the alveolar dead space fraction, the same principle is applied using exhaled gas capnography to measure the end-tidal (i.e., end-expiratory, thus reflecting alveolar) CO_2 ($P_{\text{ET}}\text{CO}_2$), using the equation:

$$\dot{V}_D / \dot{V}_T = (P_a\text{CO}_2 - P_{\text{ET}}\text{CO}_2) / P_a\text{CO}_2 \quad (14.29)$$

Note that the end-tidal value may not measure alveolar gas from slowly emptying lung units, which may artificially increase the dead space estimate in that an error may be introduced because of uncertainty in determining end tidal values. Measurement of anatomic dead space (i.e., volume of conducting airways) can be determined via the Fowler method (see Fowler 1948, 1949; Fowler and Comroe 1948; Verbanck and Paiva 2011). Overall, the physiological dead space is most commonly reported in patients with ARDS given its ease of measurement and (Robertson 2015) value as a marker of disease severity (as above).

Ventilation-Perfusion Matching in Healthy Young Subjects

In young healthy individuals, one would expect that ventilation and perfusion are closely matched throughout the lung, and there is a minimal difference between alveolar and arterial PO_2 . However, although the structure of the healthy

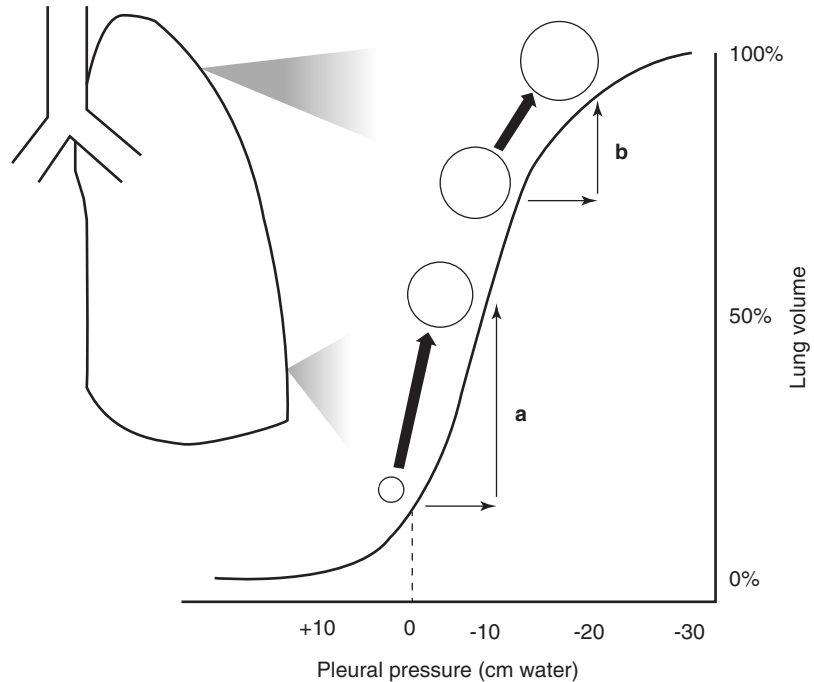
lung is well-suited towards efficient exchange of gases, regional ventilation and perfusion are nonetheless not completely uniform due to factors including airway and vascular geometry, as well as gravity and posture (see (Glenny and Robertson 2011) for review). As such, there is a distribution of ventilation-perfusion ratios within even the healthy lung, although the variability is fairly low. Data from MIGET and other techniques have shown that in normal subjects most ventilation and blood flow goes to areas with ventilation-perfusion ratios of 0.3 and 2.1, and there appears to be no appreciable shunt or diffusion limitation while breathing air (Wagner et al. 1974).

Ventilation and perfusion matching is not a completely passive process that is based on lung airway and vascular geometry and posture; mismatch in \dot{V}_A / \dot{Q} activates compensatory mechanisms that attempt to “normalize” local matching. For areas with low \dot{V}_A / \dot{Q} ratio or shunt, the presence of alveolar hypoxemia activates hypoxic pulmonary vasoconstriction (HPV) (Dunham-Snary et al. 2017). Working on the timescale of seconds to minutes, HPV leads to constriction of small intrapulmonary arterioles, diverting blood away from these areas. Nitric oxide, endothelin, and prostaglandins are vasoactive substances and thus modulators of HPV (reviewed in (Moudgil et al. 2005)), while a number of exogenous drugs lessen HPV (calcium channel blockers, volatile anesthetics) (Moudgil et al. 2005; Sylvester et al. 2012) and a few, such as almitrine, may enhance it (Reyes et al. 1988; Prost et al. 1991).

Effects of Gravity and Posture

Alveolar pressure is generally uniform throughout the lung at the beginning of inhalation and again at the end of inhalation. However, lung deforms under its own weight, and this means that there is a gradient in alveolar size from the gravitationally dependent (i.e., posterior in supine posture) to the nondependent (i.e., anterior in supine posture) lung (Glazier et al. 1967). As a result, there is a pleural pressure gradient and different portions of the lung are on different

Fig. 14.4 Explanation of the regional differences of ventilation down the lung. Because of the weight of the lung, the intrapleural pressure is less negative at the base than at the apex. As a consequence, the basal lung is relatively compressed in its resting state compared to the apex (circles represent alveolar sizes). However, the lung is more compliant at this volume, so for a given swing in pleural pressure, there is a larger change in alveolar volume (i.e., higher ventilation) in the basal lung (a) compared to the apical lung (b)



parts of the nonlinear pressure volume curve (Fig. 14.4) (Hogg and Nepszy 1969). The net result is that on inspiration the gravitationally dependent lung is preferentially ventilated (Bryan et al. 1966) compared to the nondependent lung because the nondependent alveoli are already at a higher resting volume. Of note, this physiology assumes a normal chest wall and attendant pleural pressures; in those with a heavy chest wall such as obesity, the opposite may be true due to an overall increase in pleural pressure and reduction in lung volume (Holley et al. 1967). Importantly, heterogeneity of ventilation within these gravitational planes is also present due to the geometric configuration of the lung (e.g., airway branching structure) (Glenny and Robertson 2011).

With respect to perfusion, gravitational gradients drive perfusion to dependent lung zones via hydrostatic gradients, an effect accentuated in the upright position. Local perfusion is also affected by alveolar pressure, as conceptualized by the West zone model (West and Dollery 1960; West et al. 1964); specifically, in Zone 2 where $P_{\text{arterial}} > P_{\text{alveolar}} > P_{\text{venous}}$, perfusion pressure is dependent on arterial and alveolar pressure, but not down-

stream venous pressure via a Starling-resistor mechanism (i.e., waterfall effect) (Permutt et al. 1962). Similar to the airways, the geometry of branching vessels results in substantial variability independent of gravitational forces (Glenny and Robertson 2011). Experiments in parabolic flight in which gravity is temporarily abolishing have in fact suggested that this geometric configuration is more important to perfusion than gravity, although a bias is introduced in these measurements because all estimates are made in air-dried lungs at total lung capacity (see Hopkins et al. (2007) for explanation). Nonetheless, gravity clearly plays an important role in ventilation-perfusion relationships and substantially accounts for the variability in regional \dot{V}_A / \dot{Q} matching observed in normal healthy individuals.

The prone posture has important effects on both ventilation and perfusion, with an overall effect of improving ventilation-perfusion matching in both healthy lungs and those with ARDS (see below). Modeling studies predict that the gravitational distribution of ventilation and ventilation-perfusion matching is expected to be more uniform in the prone position, and this is supported by imaging studies (Henderson et al.

2013a), showing a reduction in regions of high ventilation-perfusion ratio. Similarly, animal studies in prone posture have shown a reduction in regional ventilation-perfusion heterogeneity compared to supine posture, and indicate the effect is largely because of a reduction in the gravitational gradient in ventilation (Mure et al. 2000; Treppo et al. 1997). Compared with supine positioning, in healthy lungs prone positioning leads to more uniform ventilation across the ventral to dorsal axis, reflecting more homogenous pleural pressure (Henderson et al. 2013b; Prisk et al. 2007). Several factors appear to mediate this effect, including shifting the mediastinal weight to the dependent position and removing abdominal pressure from the dorsal-caudal lung (Fig. 14.5). It should be noted, however, that modeling studies (Tawhai et al. 2009) show these effects even in the absence of the effects of the abdomen and mediastinum, and thus the asym-

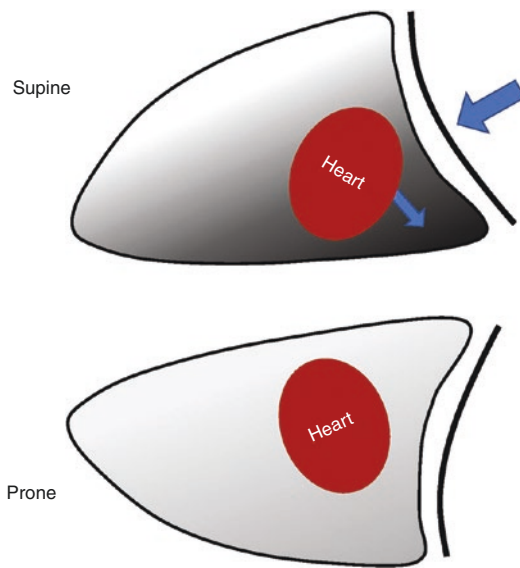


Fig. 14.5 The effect of prone posture on pleural pressure. In the supine posture, the most dependent lung has high pleural pressures alveoli due to the weight of the lung, lung shape, compression from the heart, and extrinsic compression from abdominal contents. In comparison, pleural pressures are more uniform in the prone posture. The distribution of local ventilation is more uniform in the prone posture in large part because the pleural pressures and resulting alveolar volumes are more uniform at the initiation of each breath. See reference Johnson et al. (2017)

metric lung shape between prone and supine postures is thought to play a major role (Fig. 14.6). With respect to perfusion, as discussed above, perfusion continues to follow gravitational dependence when an individual is turned prone such that the gravitationally dependent lung is better perfused than nondependent lung. (Henderson et al. 2013a; Prisk et al. 2007; Musch et al. 2002), although some report that the gradient is less (Nyrén et al. 1999; Beck et al. 1992). Nonetheless, in prone posture \dot{V}_A/\dot{Q} matching may become more spatially uniform (Henderson et al. 2013a), which may translate into more functionally uniform \dot{V}_A/\dot{Q} matching (i.e., a reduction in LogSD, \dot{Q} and LogSD, \dot{V}) and more efficient gas exchange (Beck et al. 1992; Mure et al. 1998) and a reduction in shunt (Pappert et al. 1994).

Effect of Aging

Aging of the lung is characterized by a loss of elastic recoil, leading to small airway closure in a process that to an extent resembles mild chronic obstructive lung disease (COPD). Increased \dot{V}_A/\dot{Q} mismatch is observed in older individuals, often clinically recognized on the basis of an increased arterial-alveolar oxygen difference even in healthy aging. Studies using MIGET have demonstrated overall mildly increased \dot{V}_A/\dot{Q} mismatch with aging, and no relationship between age and shunt (Cardús et al. 1997). Both ventilation (Verbanck et al. 2012) and perfusion (Levin et al. 2007) become more heterogeneous. Overall, even in this nonsmoking healthy group, most differences in \dot{V}_A/\dot{Q} matching across individuals was not attributable to differences in age, rather due to undetermined factors.

Effect of Obesity

Mild hypoxemia is often observed in obese individuals, which may reflect hypoventilation (obesity hypoventilation syndrome) and/or abnormal ventilation-perfusion matching. Obese patients appear to have not only increased ventilation-

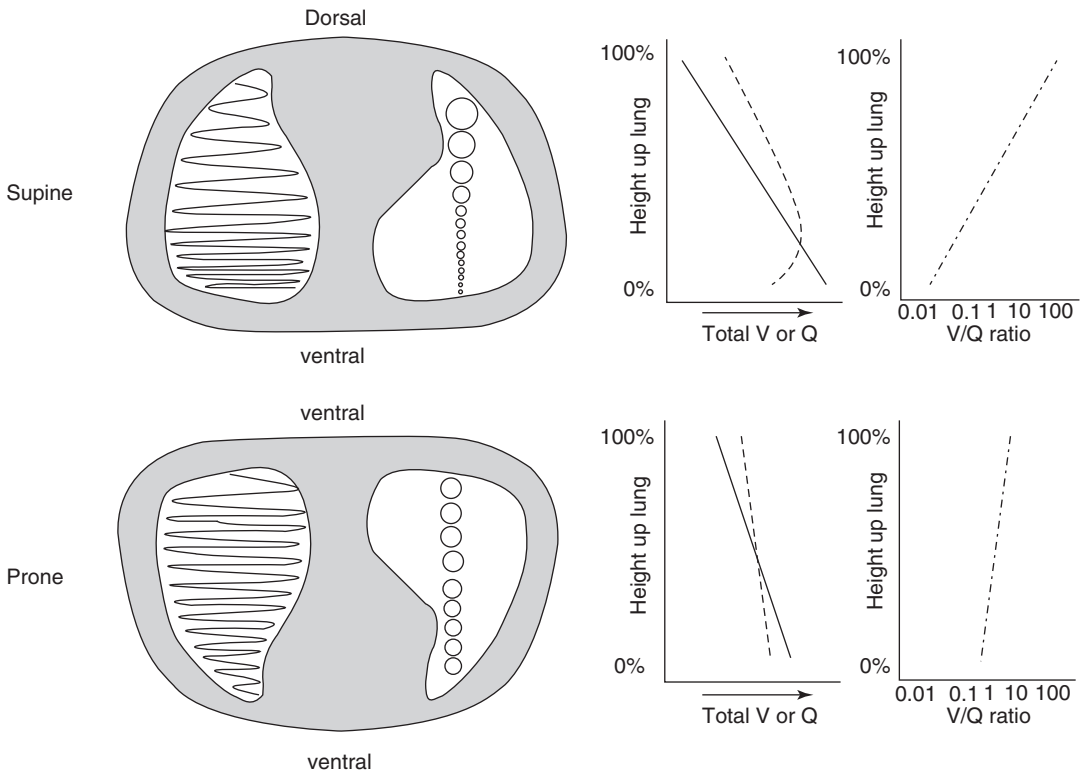


Fig. 14.6 Gravitational effects in the lung in the supine and prone postures. Considering the lung as a triangular-shaped spring, the combined effects of gravity and the greater tissue mass suspended from a larger dorsal chest wall produce more equal distribution of stress and strain in the lung (shown as curved lines inside a lung), resulting in more uniform end-expiratory lung volume and alveolar size (shown as circles inside a lung). On the right, the distribution of ventilation (dashed lines), perfusion (solid

lines), and ventilation/perfusion ratios (dot-dashed lines) across the dependent to nondependent lung are shown. In the supine posture, there is excess ventilation relative to perfusion in the ventral (nondependent) lung, and excess perfusion in the dorsal lung, leading to markedly poor ventilation/perfusion matching. In the supine posture, ventilation and perfusion are more closely matched throughout, resulting in a tighter distribution of ventilation/perfusion ratios

perfusion mismatch but also increased shunt (Barrera et al. 1969; Rivas et al. 2015). It is suspected that these abnormalities are largely seen in the dependent and particularly dorsal-caudal lung, due to compression and increased pleural pressure that occur due to increased weight of the chest wall and elevated abdominal pressure.

Effect of Lung Disease

Chronic lung disease causes disruption in both ventilation and perfusion. When substantial mismatch exists (particularly when low ventilation-perfusion regions or shunt is present), patients

often have systemic hypoxemia and may require supplemental oxygen. However, milder mismatch is often present well before the onset of appreciable abnormalities in oxygenation. Ventilation-perfusion relationships have been studied in a number of lung diseases including COPD (Wagner et al. 1977), asthma (Wagner et al. 1978) and pulmonary arterial hypertension (Melot et al. 1983). In patients with COPD, data suggest that substantial changes in ventilation-perfusion mismatch are present even in individuals with normal spirometric parameters, which might reflect subclinical changes to small airways and/or pulmonary vasculature (Bhatt et al. 2019; Estepar et al. 2013).

\dot{V}_A / \dot{Q} Relationships in Acute Respiratory Distress Syndrome (ARDS)

ARDS is characterized by non-cardiogenic pulmonary edema resulting in increased density of the lung. However, the pattern of injury itself may be relatively homogenous or heterogeneous throughout the lung on a gross scale. One of the hallmarks of ARDS is disruption of ventilation-perfusion matching. The severity of mismatch combined with the extent of shunt (see below) is included in the definition and severity grading of ARDS as the *P/F* ratio (Mild: 200–300, Moderate: 100–200, Severe: <100), with increasing severity strongly associated with worsening prognosis.

\dot{V}_A / \dot{Q} matching in ARDS has been the subject of substantial research; a complete summary is beyond the scope of this chapter, but the major conclusions are presented. In ARDS, a substantial proportion of perfusion is directed at areas of minimal to no ventilation (shunt), reaching up to 50% of cardiac output in some studies (Dantzker et al. 1979; Santos et al. 2000), and this is the major cause of hypoxemia in these patients. Surprisingly, there are regions of lung where \dot{V}_A / \dot{Q} matching is relatively well preserved (Fig. 14.3). Physiological dead space is increased in ARDS and provides additional prognostic information (Nuckton et al. 2002), as discussed above.

Treatment of ARDS involves supportive care focused on maintaining adequate oxygenation and avoidance of ventilator-induced lung injury. It should be noted that while some interventions that improve \dot{V}_A / \dot{Q} matching are associated with improved outcomes, \dot{V}_A / \dot{Q} matching is not a universal treatment target per se. For example, low tidal volume ventilation is associated with an initial worsening of oxygenation (presumably increased low \dot{V}_A / \dot{Q} and/or shunt regions) but improved mortality (Amato et al. 1998).

Prone positioning has shown to be particularly helpful in severe ARDS, both in terms of improving gas exchange and reducing mortality (Guérin et al. 2013). The prone position promotes more uniform pleural pressures (Figs. 14.5 and 14.6) (discussed above), which particularly in the setting of a heavy lung may help to prevent serious

issues related to atelectasis, including shunting, cyclical opening-closing of alveoli, and a reduction in overall lung volume and compliance. By maintaining more uniform ventilation, overdistension of some lung units is reduced and low \dot{V}_A / \dot{Q} areas may be lessened (Cornejo et al. 2013).

Effect of Positive Airway Pressure

Positive end-expiratory pressure (PEEP) is well recognized to improve oxygenation in patients with acute hypoxemic respiratory failure and is particularly used in ARDS. Studies suggest that the improvement in oxygenation is directly related to the ability to “recruit” open areas of previously atelectatic lung (Gattinoni et al. 1995), which comes with a reduction of areas of low \dot{V}_A / \dot{Q} ratio and shunt (Ralph et al. 1985). However, PEEP appears to come at the cost of increased areas of high \dot{V}_A / \dot{Q} ratio, possibly reflecting overdistension of healthy lung units (Ralph et al. 1985). In addition, PEEP may alter pulmonary blood flow via a reduction in cardiac output, by increasing overall pulmonary artery pressures, and also by shifting “up” West zones (e.g., zone 2 becomes zone 1, with a drop in perfusion) (Hermle et al. 2002). Given this recognition of potential positive and negative effects of PEEP, strategies to match individual PEEP settings to underlying physiology have been under investigation, although the focus has been generally on assessment of lung mechanics rather than \dot{V}_A / \dot{Q} changes. Emerging technologies such as electrical impedance tomography may facilitate setting the ventilator based on individual physiology, but are not yet supported by clinical trial data.

Tidal Volume, Ventilation Mode, and Cardiac Output

Low tidal volume ventilation is a mainstay of ARDS treatment based on clinical trials demonstrating improvements in mortality (Amato et al. 1998). From the standpoint of gas exchange, this leads to a reduction in lung expansion and a rise

in PaCO₂, with the effect of a reduction in PaO₂ through the Haldane effect. Other reasons for worsening gas exchange include atelectasis and an increase in cardiac output associated with hypercapnia (discussed below).

The effect of different ventilator modes on gas exchange has been the subject of a few studies. No consistent differences have been shown with volume versus pressure-cycled modes of ventilation in terms of gas exchange or lung mechanics (Muñoz et al. 1993; Ziebart et al. 2014); the decision between these ventilation strategies depends on issues such as patient synchrony and the desire to “target” a specific tidal volume versus driving pressure. High-frequency oscillatory ventilation appears to result in similar \dot{V}_A / \dot{Q} distributions to pressure-controlled ventilation (Dembinski et al. 2002). Despite the ability to achieve similar gas exchange with potentially less bulk changes in lung volume, clinical trials have indicated adverse effects on outcomes and thus it is not recommended (Fan et al. 2017). Biphasic and airway pressure release ventilation (APRV) have also been investigated, with the potential advantages of sustained lung recruitment and the facilitation of spontaneous efforts without leading to excessive volumes (as would be seen in volume ventilation due to breath stacking issues).

Spontaneous breathing superimposed on pressure-limited mechanical ventilation has been found to improve \dot{V}_A / \dot{Q} relationships by decreasing shunt and dead space (Putensen et al. 1994a, b). Nonetheless, mechanisms are unclear, as classical concepts would suggest that transpulmonary pressure swings should be the same for identical tidal volumes, and thus the distribution of ventilation is expected to be unchanged. One hypothesis is that in the setting of lung injury, spontaneous breathing leads to occult intrapulmonary ventilation from nondependent to dependent zones (pendelluft) contradicting the concept that pleural pressure swings are uniform across the lung (Yoshida et al. 2013; Neumann et al. 2005). Whether this phenomenon is harmful has been debated, but perhaps supported by the observation that abolishing respiratory effort via neuromuscular blockade may improve ARDS

outcomes (National Heart, Lung, and Blood Institute PETAL Clinical Trials Network and Moss 2019; Papazian et al. 2010).

Cardiac output and mixed venous oxygenation have been recognized as having an effect on oxygenation in the setting of ARDS. Studies in dogs have shown that increased cardiac output in the presence of lung injury does not lead to diffusion limitation; rather, there is worsening \dot{V}_A / \dot{Q} matching which might be due to increased blood flow to shunt areas or increased edema generation (Breen et al. 1982). It is possible that the corresponding increase in mixed venous oxygen tension itself might account for increased shunt, although mechanisms are unclear and data are conflicting (Rossaint et al. 1995; Sandoval et al. 1983). Clinical data support that increases in cardiac output lead to increase in shunt and worsening oxygenation (Feihl et al. 2000). Finally, decreased mixed venous oxygen tension (seen with low cardiac output or high oxygen consumption) can worsen oxygenation by increasing venous admixture (i.e., not via changes in \dot{V}_A / \dot{Q}).

References

- Agusti AG, Roca J, Gea J, Wagner PD, Xaubet A, Rodriguez-Roisin R. Mechanisms of gas-exchange impairment in idiopathic pulmonary fibrosis. *Am Rev Respir Dis.* 1991;143(2):219–25.
- Amato MBP, Barbas CSV, Medeiros DM, Magaldi RB, Schettino GP, Lorenzi-Filho G, et al. Effect of a protective-ventilation strategy on mortality in the acute respiratory distress syndrome. *N Engl J Med.* 1998;338(6):347–54.
- Barrera F, Reidenberg MM, Winters WL, Hungspreugs S. Ventilation-perfusion relationships in the obese patient. *J Appl Physiol.* 1969;26(4):420–6.
- Beck KC, Vettermann J, Rehder K. Gas exchange in dogs in the prone and supine positions. *J Appl Physiol* (1985). 1992;72(6):2292–7.
- Berggren SM. The oxygen deficit of arterial blood caused by non-ventilating parts of the lung. Stockholm: Kungl. Boktryckeriet; 1942. p. 92.
- Bhatt SP, Washko GR, Hoffman EA, Newell JD Jr, Bodduluri S, Diaz AA, et al. Imaging advances in chronic obstructive pulmonary disease. Insights from the genetic epidemiology of chronic obstructive pulmonary disease (COPDGene) study. *Am J Respir Crit Care Med.* 2019;199(3):286–301.
- Bohr C. Ueber die Lungenathmung 1. Skandinavisches Archiv für Physiologie. 1891;2(1):236–68.

- Breen PH, Schumacker PT, Hedenstierna G, Ali J, Wagner PD, Wood LD. How does increased cardiac output increase shunt in pulmonary edema? *J Appl Physiol Respir Environ Exerc Physiol.* 1982;53(5):1273–80.
- Bryan AC, Milic-Emili J, Pengelly D. Effect of gravity on the distribution of pulmonary ventilation. *J Appl Physiol.* 1966;21(3):778–84.
- Cardús J, Burgos F, Diaz O, Roca J, Barberá JA, Marrades RM, et al. Increase in pulmonary ventilation–perfusion inequality with age in healthy individuals. *Am J Respir Crit Care Med.* 1997;156(2):648–53.
- Cepkova M, Kapur V, Ren X, Quinn T, Zhuo H, Foster E, et al. Pulmonary dead space fraction and pulmonary artery systolic pressure as early predictors of clinical outcome in acute lung injury. *Chest.* 2007;132(3):836–42.
- Christiansen J, Douglas CG, Haldane JS. The absorption and dissociation of carbon dioxide by human blood. *J Physiol.* 1914;48(4):244–71.
- Cornejo RA, Díaz JC, Tobar EA, Bruhn AR, Ramos CA, González RA, et al. Effects of prone positioning on lung protection in patients with acute respiratory distress syndrome. *Am J Respir Crit Care Med.* 2013;188(4):440–8.
- Crawford AB, Regnis J, Laks L, Donnelly P, Engel LA, Young IH. Pulmonary vascular dilatation and diffusion-dependent impairment of gas exchange in liver cirrhosis. *Eur Respir J.* 1995;8(12):2015–21.
- Dantzker DR, Brook CJ, Dehart P, Lynch JP, Weg JG. Ventilation-perfusion distributions in the adult respiratory distress syndrome. *Am Rev Respir Dis.* 1979;120(5):1039–52.
- Dembinski R, Max M, Bensberg R, Bickenbach J, Kuhlen R, Rossaint R. High-frequency oscillatory ventilation in experimental lung injury: effects on gas exchange. *Intensive Care Med.* 2002;28(6):768–74.
- Dunham-Snary KJ, Wu D, Sykes EA, Thakrar A, Parlow LRG, Mewburn JD, et al. Hypoxic pulmonary vasoconstriction: from molecular mechanisms to medicine. *Chest.* 2017;151(1):181–92.
- Estepar RS, Kinney GL, Black-Shinn JL, Bowler RP, Kindlmann GL, Ross JC, et al. Computed tomographic measures of pulmonary vascular morphology in smokers and their clinical implications. *Am J Respir Crit Care Med.* 2013;188(2):231–9.
- Fan E, Del Sorbo L, Goligher EC, Hodgson CL, Munshi L, Walkey AJ, et al. An official American Thoracic Society/European Society of Intensive Care Medicine/Society of Critical Care Medicine clinical practice guideline: mechanical ventilation in adult patients with acute respiratory distress syndrome. *Am J Respir Crit Care Med.* 2017;195(9):1253–63.
- Farhi LE, Tenney SM. Section 3. The respiratory system, Volume 4 Gas exchange. In: Geiger SR, editor. Bethesda: American Physiological Society; Distributed by Williams & Wilkins; 1977. volumes p.
- Feihl F, Eckert P, Brimiouille S, Jacobs O, Schaller MD, Mélot C, et al. Permissive hypercapnia impairs pulmonary gas exchange in the acute respiratory distress syndrome. *Am J Respir Crit Care Med.* 2000;162(1):209–15.
- Fowler WS. Lung function studies. II. The respiratory dead space. *Am J Physiol.* 1948;154(3):405–16.
- Fowler WS. Lung function studies. III. Uneven pulmonary ventilation in normal subjects and in patients with pulmonary disease. *J Appl Physiol.* 1949;2(6):283–99.
- Fowler WS, Comroe JH. Lung function studies. I. The rate of increase of arterial oxygen saturation during the inhalation of 100 per cent O₂. *J Clin Invest.* 1948;27(3):327–34.
- Gattinoni L, Pelosi P, Crotti S, Valenza F. Effects of positive end-expiratory pressure on regional distribution of tidal volume and recruitment in adult respiratory distress syndrome. *Am J Respir Crit Care Med.* 1995;151(6):1807–14.
- Gattinoni L, Vaggini F, Carlesso E, Taccone P, Conte V, Chiumello D, et al. Decrease in PaCO₂ with prone position is predictive of improved outcome in acute respiratory distress syndrome. *Crit Care Med.* 2003;31(12):2727–33.
- Glazier JB, Hughes JM, Maloney JE, West JB. Vertical gradient of alveolar size in lungs of dogs frozen intact. *J Appl Physiol.* 1967;23(5):694–705.
- Glenny RW, Robertson HT. Spatial distribution of ventilation and perfusion: mechanisms and regulation. *Compr Physiol.* 2011;1(1):375–95.
- Guérin C, Reignier J, Richard J-C, Beuret P, Gacouin A, Boulain T, et al. Prone positioning in severe acute respiratory distress syndrome. *N Engl J Med.* 2013;368(23):2159–68.
- Hammond M, Gale G, Kapitan K, Ries A, Wagner P. Pulmonary gas exchange in humans during exercise at sea level. *J Appl Physiol.* 1986;60(5):1590–8.
- Henderson AC, Sa RC, Theilmann RJ, Buxton RB, Prisk GK, Hopkins SR. The gravitational distribution of ventilation-perfusion ratio is more uniform in prone than supine posture in the normal human lung. *J Appl Physiol* (1985). 2013a;115(3):313–24.
- Henderson AC, Sá RC, Theilmann RJ, Buxton RB, Prisk GK, Hopkins SR. The gravitational distribution of ventilation-perfusion ratio is more uniform in prone than supine posture in the normal human lung. *J Appl Physiol.* 2013b;115(3):313–24.
- Hermle G, Mols G, Zugel A, Benzing A, Lichtwarck-Aschoff M, Geiger K, et al. Intratidal compliance-volume curve as an alternative basis to adjust positive end-expiratory pressure: a study in isolated perfused rabbit lungs. *Crit Care Med.* 2002;30(7):1589–97.
- Hlastala MP. Multiple inert gas elimination technique. *J Appl Physiol Respir Environ Exerc Physiol.* 1984;56(1):1–7.
- Hogg JC, Nepszy S. Regional lung volume and pleural pressure gradient estimated from lung density in dogs. *J Appl Physiol.* 1969;27(2):198–203.
- Holley HS, Milic-Emili J, Becklake MR, Bates DV. Regional distribution of pulmonary ventilation and perfusion in obesity. *J Clin Invest.* 1967;46(4):475–81.

- Hopkins SR, Wagner PD. The multiple inert gas elimination technique (MIGET). New York: Springer; 2017. xiii, 329 pages.
- Hopkins SR, McKenzie DC, Schoene RB, Glenny RW, Robertson HT. Pulmonary gas exchange during exercise in athletes. I. Ventilation-perfusion mismatch and diffusion limitation. *J Appl Physiol* (1985). 1994;77(2):912–7.
- Hopkins SR, Gavin TP, Siafakas NM, Haseler LJ, Olfert IM, Wagner H, et al. Effect of prolonged, heavy exercise on pulmonary gas exchange in athletes. *J Appl Physiol* (1985). 1998;85(4):1523–32.
- Hopkins SR, Henderson AC, Levin DL, Yamada K, Arai T, Buxton RB, et al. Vertical gradients in regional lung density and perfusion in the supine human lung: the Slinky effect. *J Appl Physiol* (1985). 2007;103(1):240–8.
- Johnson NJ, Luks AM, Glenny RW. Gas exchange in the prone posture. *Respir Care*. 2017;62(8):1097–110.
- Kallet RH, Alonso JA, Pittet JF, Matthay MA. Prognostic value of the pulmonary dead-space fraction during the first 6 days of acute respiratory distress syndrome. *Respir Care*. 2004;49(9):1008–14.
- Levin DL, Buxton RB, Spiess JP, Arai T, Balouch J, Hopkins SR. Effects of age on pulmonary perfusion heterogeneity measured by magnetic resonance imaging. *J Appl Physiol* (1985). 2007;102(5):2064–70.
- Mellemegaard K. The alveolar-arterial oxygen difference: its size and components in normal man. *Acta Physiol Scand*. 1966;67(1):10–20.
- Melot C, Naeije R, Mols P, Vandenbossche JL, Denolin H. Effects of nifedipine on ventilation/perfusion matching in primary pulmonary hypertension. *Chest*. 1983;83(2):203–7.
- Moudgil R, Michelakis ED, Archer SL. Hypoxic pulmonary vasoconstriction. *J Appl Physiol* (1985). 2005;98(1):390–403.
- Muñoz J, Guerrero JE, Escalante JL, Palomino R, De La Calle B. Pressure-controlled ventilation versus controlled mechanical ventilation with decelerating inspiratory flow. *Crit Care Med*. 1993;21(8):1143–8.
- Mure M, Glenny RW, Domino KB, Hlastala MP. Pulmonary gas exchange improves in the prone position with abdominal distension. *Am J Respir Crit Care Med*. 1998;157(6 Pt 1):1785–90.
- Mure M, Domino KB, Lindahl SG, Hlastala MP, Altemeier WA, Glenny RW. Regional ventilation-perfusion distribution is more uniform in the prone position. *J Appl Physiol*. 2000;88(3):1076–83.
- Musch G, Layfield JD, Harris RS, Melo MF, Winkler T, Callahan RJ, et al. Topographical distribution of pulmonary perfusion and ventilation, assessed by PET in supine and prone humans. *J Appl Physiol*. 2002;93(5):1841–51.
- National Heart, Lung, and Blood Institute PETAL Clinical Trials Network, Moss M, et al. Early neuromuscular blockade in the acute respiratory distress syndrome. *N Engl J Med*. 2019;380(21):1997–2008.
- Neumann P, Wrigge H, Zinserling J, Hinz J, Maripuu E, Andersson LG, et al. Spontaneous breathing affects the spatial ventilation and perfusion distribution during mechanical ventilatory support*. *Crit Care Med*. 2005;33(5):1090–5.
- Nuckton TJ, Alonso JA, Kallet RH, Daniel BM, Pittet JF, Eisner MD, et al. Pulmonary dead-space fraction as a risk factor for death in the acute respiratory distress syndrome. *N Engl J Med*. 2002;346(17):1281–6.
- Nyrén S, Mure M, Jacobsson H, Larsson SA, Lindahl SG. Pulmonary perfusion is more uniform in the prone than in the supine position: scintigraphy in healthy humans. *J Appl Physiol*. 1999;86(4):1135–41.
- Papazian L, Forel J-M, Gacouin A, Penot-Ragon C, Perrin G, Loundou A, et al. Neuromuscular blockers in early acute respiratory distress syndrome. *N Engl J Med*. 2010;363(12):1107–16.
- Pappert D, Rossaint R, Slama K, Gruning T, Falke KJ. Influence of positioning on ventilation-perfusion relationships in severe adult respiratory distress syndrome. *Chest*. 1994;106(5):1511–6.
- Permutt S, Bromberger-Barnea B, Bane HN. Alveolar pressure, pulmonary venous pressure, and the vascular waterfall. *Respiration*. 1962;19(4):239–60.
- Podolsky A, Eldridge MW, Richardson RS, Knight DR, Johnson EC, Hopkins SR, et al. Exercise-induced VA/Q inequality in subjects with prior high-altitude pulmonary edema. *J Appl Physiol* (1985). 1996;81(2):922–32.
- Prisk GK, Hopkins SR. Pulmonary gas exchange. 2013. Available from: Morgan & Claypool. Restricted to UCB, UCD, UCI, UCLA, UCM, UCSB, UCSC, UCSD, and UCSF <https://doi.org/10.4199/CO0087ED1V01Y201308ISP041>.
- Prisk GK, Yamada K, Henderson AC, Arai TJ, Levin DL, Buxton RB, et al. Pulmonary perfusion in the prone and supine postures in the normal human lung. *J Appl Physiol*. 2007;103(3):883–94.
- Prost JF, Desche P, Jardin F, Margairaz A. Comparison of the effects of intravenous almitrine and positive end-expiratory pressure on pulmonary gas exchange in adult respiratory distress syndrome. *Eur Respir J*. 1991;4(6):683–7.
- Putensen C, Räsänen J, López FA. Ventilation-perfusion distributions during mechanical ventilation with superimposed spontaneous breathing in canine lung injury. *Am J Respir Crit Care Med*. 1994a;150(1):101–8.
- Putensen C, Räsänen J, López FA, Downs JB. Effect of interfacing between spontaneous breathing and mechanical cycles on the ventilation-perfusion distribution in canine lung injury. *Anesthesiology*. 1994b;81(4):921–30.
- Rahn H, Fenn WO. Graphical analysis of the respiratory gas exchange: the O₂ CO₂ diagram. American Physiological Society: Bethesda; 1955.
- Ralph DD, Robertson HT, Weaver LJ, Hlastala MP, Carrico CJ, Hudson LD. Distribution of ventilation and perfusion during positive end-expiratory pressure

- in the adult respiratory distress syndrome. *Am Rev Respir Dis.* 1985;131(1):54–60.
- Reyes A, Roca J, Rodriguez-Roisin R, Torres A, Ussetti P, Wagner PD. Effect of almitrine on ventilation-perfusion distribution in adult respiratory distress syndrome. *Am Rev Respir Dis.* 1988;137(5):1062–7.
- Riggs AF. The Bohr effect. *Annu Rev Physiol.* 1988;50(1):181–204.
- Riley RL, Cournand A. Ideal alveolar air and the analysis of ventilation-perfusion relationships in the lungs. *J Appl Physiol.* 1949;1(12):825–47.
- Riley RL, Cournand A. Analysis of factors affecting partial pressures of oxygen and carbon dioxide in gas and blood of lungs; theory. *J Appl Physiol.* 1951;4(2):77–101.
- Riley RL, Cournand A, Donald KW. Analysis of factors affecting partial pressures of oxygen and carbon dioxide in gas and blood of lungs; methods. *J Appl Physiol.* 1951;4(2):102–20.
- Rivas E, Arismendi E, Agustí A, Sanchez M, Delgado S, Gistau C, et al. Ventilation/perfusion distribution abnormalities in morbidly obese subjects before and after bariatric surgery. *Chest.* 2015;147(4):1127–34.
- Robertson HT. Dead space: the physiology of wasted ventilation. *Eur Respir J.* 2015;45(6):1704–16.
- Rossaint R, Hahn SM, Pappert D, Falke KJ, Radermacher P. Influence of mixed venous PO₂ and inspired O₂ fraction on intrapulmonary shunt in patients with severe ARDS. *J Appl Physiol.* 1995;78(4):1531–6.
- Sandoval J, Long GR, Skoog C, Wood LD, Oppenheimer L. Independent influence of blood flow rate and mixed venous PO₂ on shunt fraction. *J Appl Physiol Respir Environ Exerc Physiol.* 1983;55(4):1128–33.
- Santos C, Ferrer M, Roca J, Torres A, Hernandez C, Rodriguez-Roisin R. Pulmonary gas exchange response to oxygen breathing in acute lung injury. *Am J Respir Crit Care Med.* 2000;161(1):26–31.
- Severinghaus JW. Simple, accurate equations for human blood O₂ dissociation computations. *J Appl Physiol Respir Environ Exerc Physiol.* 1979;46(3):599–602.
- Stickland MK, Lindinger MI, Olfert IM, Heigenhauser GJ, Hopkins SR. Pulmonary gas exchange and acid-base balance during exercise. *Compr Physiol.* 2013;3(2):693–739.
- Sylvester JT, Shimoda LA, Aaronson PI, Ward JP. Hypoxic pulmonary vasoconstriction. *Physiol Rev.* 2012;92(1):367–520.
- Tawhai MH, Nash MP, Lin CL, Hoffman EA. Supine and prone differences in regional lung density and pleural pressure gradients in the human lung with constant shape. *J Appl Physiol.* 2009;107(3):912–20.
- Torre-Bueno JR, Wagner PD, Saltzman HA, Gale GE, Moon RE. Diffusion limitation in normal humans during exercise at sea level and simulated altitude. *J Appl Physiol* (1985). 1985;58(3):989–95.
- Treppo S, Mijailovich SM, Venegas JG. Contributions of pulmonary perfusion and ventilation to heterogeneity in V(A)/Q measured by PET. *J Appl Physiol.* 1997;82(4):1163–76.
- Verbanck S, Paiva M. Gas mixing in the airways and air-spaces. *Compr Physiol.* 2011;1(2):809–34.
- Verbanck S, Thompson BR, Schuermans D, Kalsi H, Biddiscombe M, Stuart-Andrews C, et al. Ventilation heterogeneity in the acinar and conductive zones of the normal ageing lung. *Thorax.* 2012;67(9):789–95.
- Wagner PD, Laravuso RB, Uhl RR, West JB. Continuous distributions of ventilation-perfusion ratios in normal subjects breathing air and 100 per cent O₂. *J Clin Invest.* 1974;54(1):54–68.
- Wagner PD, Dantzker DR, Dueck R, Clausen JL, West JB. Ventilation-perfusion inequality in chronic obstructive pulmonary disease. *J Clin Invest.* 1977;59(2):203–16.
- Wagner PD, Dantzker DR, Iacovoni VE, Tomlin WC, West JB. Ventilation-perfusion inequality in asymptomatic asthma. *Am Rev Respir Dis.* 1978;118(3):511–24.
- Wagner PD, Sutton JR, Reeves JT, Cymerman A, Groves BM, Malconian MK. Operation Everest II: pulmonary gas exchange during a simulated ascent of Mt. Everest. *J Appl Physiol* (1985). 1987;63(6):2348–59.
- West JB. State of the art: ventilation-perfusion relationships. *Am Rev Respir Dis.* 1977;116(5):919–43.
- West J, Dollery C. Distribution of blood flow and ventilation-perfusion ratio in the lung, measured with radioactive CO₂. *J Appl Physiol.* 1960;15(3):405–10.
- West JB, Dollery CT, Naimark A. Distribution of blood flow in isolated lung; relation to vascular and alveolar pressures. *J Appl Physiol.* 1964;19(4):713–24.
- Yoshida T, Torsani V, Gomes S, Santis RRD, Beraldo MA, Costa ELV, et al. Spontaneous effort causes occult pendelluft during mechanical ventilation. *Am J Respir Crit Care Med.* 2013;188(12):1420–7.
- Ziebart A, Hartmann EK, Thomas R, Liu T, Duenges B, Schad A, et al. Low tidal volume pressure support versus controlled ventilation in early experimental sepsis in pigs. *Respir Res.* 2014;15(1):101.



Control of Breathing

15

Esteban A. Moya, Tatum S. Simonson,
Frank L. Powell, Robert L. Owens,
and Atul Malhotra

Key Points

- *Negative feedback systems* control ventilation to maintain normal arterial blood gases and minimize the work of breathing in response to changes in the environment, activity, and lung function.
- The basic respiratory rhythm is generated by neurons in the brainstem, and this rhythm is modulated by ventilatory reflexes.
- Arterial P_{CO_2} is the most important factor determining ventilatory drive in resting humans.
- The ventilatory response to hypoxia depends strongly on arterial P_{CO_2} , and it is not appreciable in normal individ-

uals until arterial P_{O_2} drops below 60 mm Hg.

- *Arterial chemoreceptors* sense changes in arterial P_{O_2} , P_{CO_2} , and pH, but *central chemoreceptors* sense changes primarily in arterial P_{CO_2}/pH .
- Vagal nerve endings sensitive to stretch in the lungs mediate reflexes that fine-tune the rate and depth of breathing.
- Vagal nerve endings sensitive to mechanical and chemical irritation of the airways and lungs stimulate coughing, mucous production, bronchoconstriction, and rapid shallow breathing.
- The ventilatory response to arterial blood gases changes with time during chronic hypoxemia at high altitude or with lung disease.

E. A. Moya · T. S. Simonson · F. L. Powell
Section of Physiology, Division of Pulmonary,
Critical Care & Sleep Medicine, Department of
Medicine, University of California San Diego,
La Jolla, CA, USA
e-mail: eamoya@ucsd.edu

R. L. Owens
University of California San Diego, Division of
Pulmonary, Critical Care, and Sleep Medicine,
Department of Medicine, La Jolla, CA, USA

A. Malhotra
UC San Diego, Department of Medicine,
La Jolla, CA, USA
e-mail: amalhotra@health.ucsd.edu

Control of Breathing

Control of breathing is important to maintain proper arterial O_2 levels (PaO_2) to ensure tissue oxygenation and eliminate arterial CO_2 ($PaCO_2$) produced by cellular metabolism. This is particularly important in physiologically stressful environments with low O_2 conditions, such as high altitude, and pathological conditions of lung disease. For example, clinicians in the

intensive care unit (ICU) need to consider control of breathing as it relates to use of sedation, paralytics, patient/ventilator dyssynchrony, and ventilator weaning.

Limitations in lung function or gas exchange are compensated by physiological control systems acting to maintain *homeostasis*. Either during extreme pathophysiological situations or in daily routines (e.g., running to catch a bus, swimming), the control systems are designed to (Smith et al. 1991) maintain pH and PaCO₂ within normal limits (Feldman 1995), satisfy O₂ demands of the tissues (Feldman 2011), minimize mechanical work of breathing (Plataki et al. 2013), and prevent exposure to various irritants. It is necessary to distinguish abnormalities in the respiratory control system from primary disturbances in lung function (i.e., cannot breathe vs will not breathe) (see Figs. 15.1 and 15.2).

Respiratory Rhythm Generation

Skeletal muscles (i.e., diaphragm, intercostal muscles) that drive ventilation do not contract sponta-

neously as does cardiac muscle. Rhythmic breathing results from periodic activation of the ventilatory muscles via motor nerves from the central nervous system (CNS). A *central pattern generator* composed of neuronal networks generates this basic respiratory rhythm (Smith et al. 1991; Feldman 1995, 2011). Early observations by Galen revealed that Roman gladiators with injuries in the upper neck stopped breathing; however, breathing continued if the spinal injury occurred below the neck. In the 1800s, physiologists identified most of the important respiratory centers by making discrete lesions in the *pons* and *medulla* in experimental animals. A specific region within the medulla called the *pre-Bötzinger complex* is the central pattern generator for ventilation (Smith et al. 1991). Other nearby respiratory centers integrate afferent information and fine-tune the motor output to ventilatory muscles. For example, higher brainstem and even cortical influences can modulate breathing to coordinate speech, swallowing, and voluntary breathing exercises such as pulmonary function tests. Lesions in the medulla and pons often result in abnormal breathing patterns. For example, *apneusis* (abnormally long inspiration) can occur if the pons is injured in humans.

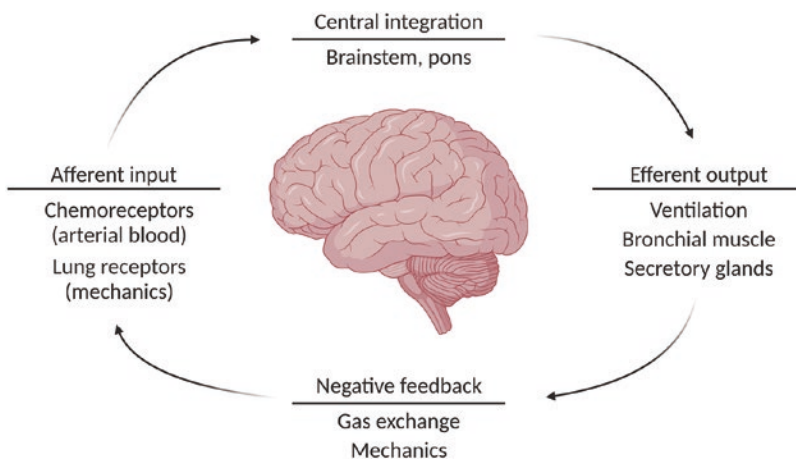


Fig. 15.1 The negative feedback loop involved in control of breathing. There are afferent inputs from the chemoreceptors and mechanoreceptors which are integrated centrally. The effectors influence ventilation via respiratory pump muscles which influence gas exchange. During pas-

sive mechanical ventilation, the respiratory rate and tidal volume are influenced by the provider although the loop remains intact for patients with spontaneous breathing (whether ventilated or not)

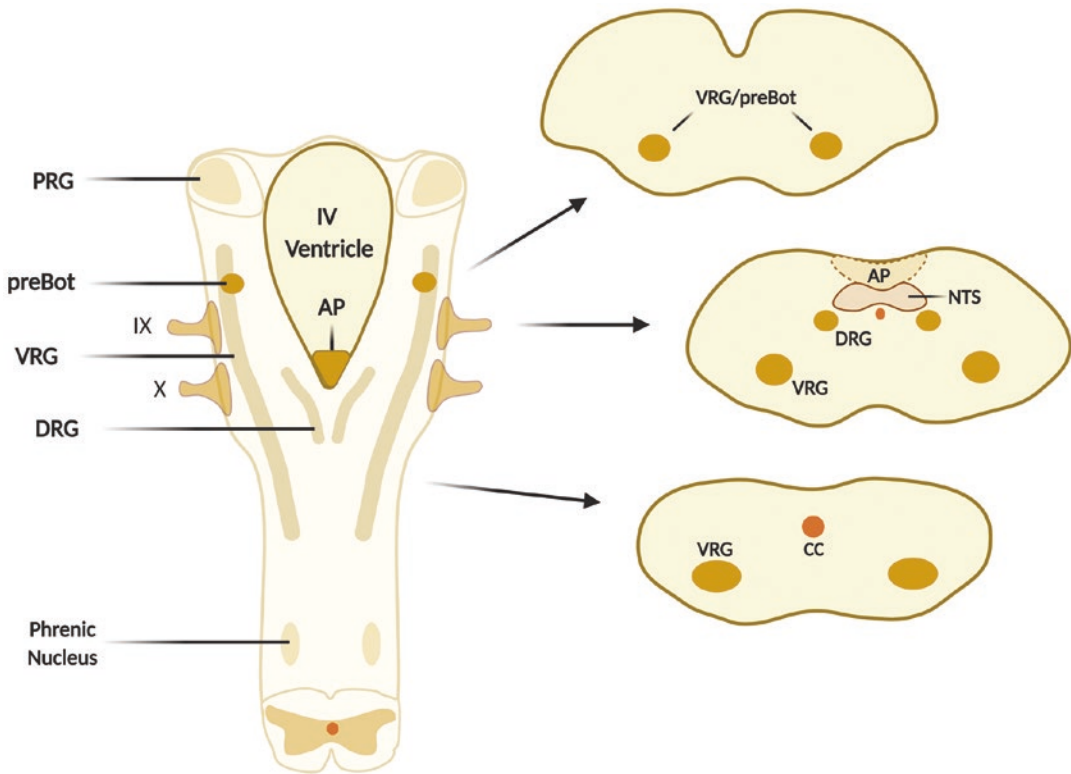


Fig. 15.2 Respiratory centers in the brainstem with functions described in text. Left-dorsal view of the pons and medulla with the cerebellum removed. Right-transverse sections from three levels of the medulla. PRG pontine respiratory group, preBot pre-Bötzinger complex, respon-

sible for generating the normal respiratory rhythm, VRG ventral respiratory group, DRG dorsal respiratory group, IX cranial nerve (glossopharyngeal), X cranial nerve (vagus), AP area postrema, NTS nucleus tractus solitarius, CC central canal

Modulation: Chemoreflex, Mechanoreflex, and Negative Feedback

The respiratory rhythm is shaped by several afferent reflexes that modulate timing and amplitude in response to changes in respiratory system function. The primary controlled variable PCO_2/pH must be maintained within a normal range; these variables are regulated via negative feedback control loops. In a physiological control system, a *sensor* can detect changes in a *physiological stimulus* and send the information through an *afferent input* to a *central integrator* that processes the information from a single or multiple input(s). The central integrator sends information

through an *efferent output* to an *effector organ*, which activates a response in order to keep the physiological stimulus value closer to the centrally set range (Plataki et al. 2013). When the response of the control system is contrary to the initial change in the physiological stimulus, this situation constitutes a negative feedback system. These concepts of a control system and negative feedback explain why a sudden increased level of PaCO_2 activates sensors that trigger hyperventilation to restore the PaCO_2 levels back to normal (Younes et al. 2001; Meza et al. 1998a; Dempsey et al. 2010; Skatrud and Dempsey 1983).

There are two main classes of sensory control systems that convey afferent input information in the respiratory system: the chemoreceptors and the

mechanoreceptors. *Chemoreceptors* monitor changes in arterial P_{O_2} , P_{CO_2} , and pH, while *mechanoreceptors* monitor pressure and stretch (volume) in the lungs and airways to provide afferent information about pulmonary mechanics. Generally, mechanoreceptors induce reflex changes in the rate and depth of breathing that aim to minimize the work of breathing under different mechanical conditions and at different levels of ventilation. Mechanoreceptors, as well as other sensory nerves from the lungs and airways, are also involved in airway smooth muscle and secretory responses that defend the lungs from environmental insult (note that *receptor in this context refers to a specialized sensory nerve ending* and not a neurotransmitter or drug receptor) (See also Chap. 16).

Efferent Pathways: CNS-Processed Signal Targeting Effector Respiratory Muscles

During resting ventilation, the output from breathing centers leads to rhythmic contraction of the diaphragm during inspiration that ceases during

expiration and allows passive elastic recoil of the lung and chest wall. The modulated rhythm from the central pattern generator is transmitted through synapses to phrenic motor neurons at the third through fifth cervical levels of the spinal cord (C3–C5). Injuries that disrupt the normal flow of information between the medulla and C3–C5 result in respiratory paralysis; therefore, “high” quadriplegics require artificial ventilation. Phrenic nerve activity reflects basic features of the central pattern generator, including (1) a sudden onset of inspiratory activity, (2) a ramp-like increase in activity during inspiration, and (3) a relatively sudden termination of activity at the onset of expiration. Low levels of phrenic activity at the onset of expiration (Fig. 15.3) allow the diaphragm to transition smoothly to passive expiration.

Inspiratory and expiratory intercostal muscles are innervated by spinal nerves from all levels of the thoracic spinal cord (T1–T11). The pattern of electrical activity in the external intercostal nerves is similar to that in the phrenic nerve, although the internal intercostals are activated during forced expiration. Electrical activity in lower thoracic and upper lumbar spinal nerves,

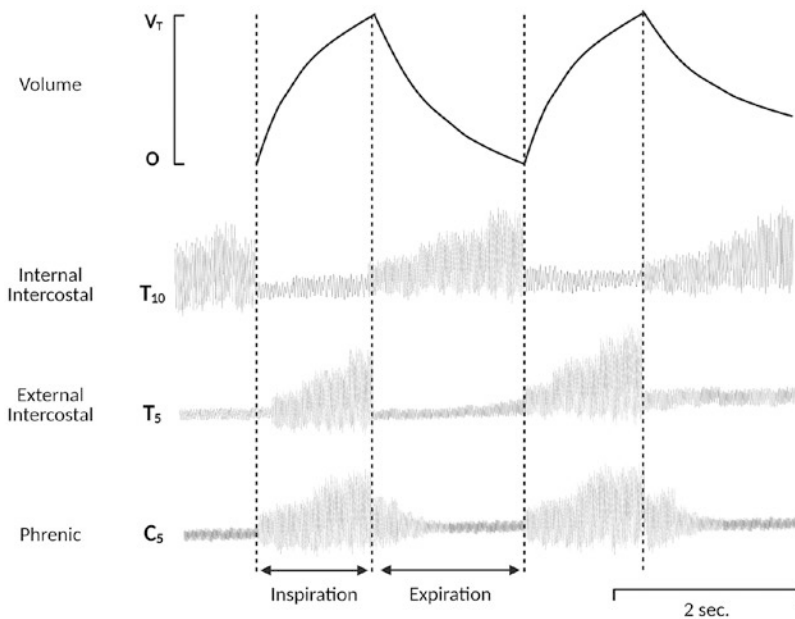


Fig. 15.3 Graphical example of changes in volume due to ventilation and motor nerve activity of one expiratory muscle (internal intercostal, recorded from 10th thoracic spinal

nerve), and two inspiratory muscles (external intercostal and diaphragm, recorded from 5th thoracic spinal nerve and from phrenic/5th cervical spinal nerve respectively)

which innervate the *abdominal expiratory muscles*, is similar to the internal intercostal activity shown in Fig. 15.3. Inspiratory and expiratory activity in the vagus and *hypoglossal (XII cranial) nerves*, which innervate the upper airway muscles in the *larynx* and *pharynx*, are also similar to the patterns shown in Fig. 15.3 (Horner 1996, 2000, 2008).

Ventilatory Response to Arterial P_{O_2} , P_{CO_2} , and pH

Arterial P_{O_2} , P_{CO_2} , and pH are sensed directly by arterial or peripheral chemoreceptors, and P_{aCO_2} is sensed indirectly by central chemoreceptors in the CNS. There is no strong evidence for mixed-venous or alveolar chemoreceptors affecting breathing.

Central Chemoreceptors

A ventilatory response to increases in P_{aCO_2} can be observed in experimental animals that have no

afferent input to the CNS from any peripheral sensory nerves. This response to P_{aCO_2} is mediated by *central chemosensitive areas* of the medulla, including the retrotrapezoid nucleus, raphé, nucleus of the solitary tract, and the ventral surface of the medulla at the fourth ventricle.

A common feature of central chemosensitive neurons is that they have dendrites with endings near cerebral blood vessels. These vessels and nerve endings are also frequently near the surface of the brain, which is bathed in *cerebrospinal fluid (CSF)* (Fig. 15.4). Specialized chemosensitive nerve endings depolarize in response to decreased *intracellular* pH, which occurs when arterial P_{CO_2} increases. CO_2 is very soluble in lipids, so it moves easily across the capillaries and membranes in the brain and generates H^+ inside central chemosensitive neurons, as well as in the extracellular space and CSF around these neurons. Glial cells, such as astrocytes present in the central chemosensitive areas, may contribute to sensing changes in CO_2 and pH. For example, astrocyte-induced release of ATP, lactate, or

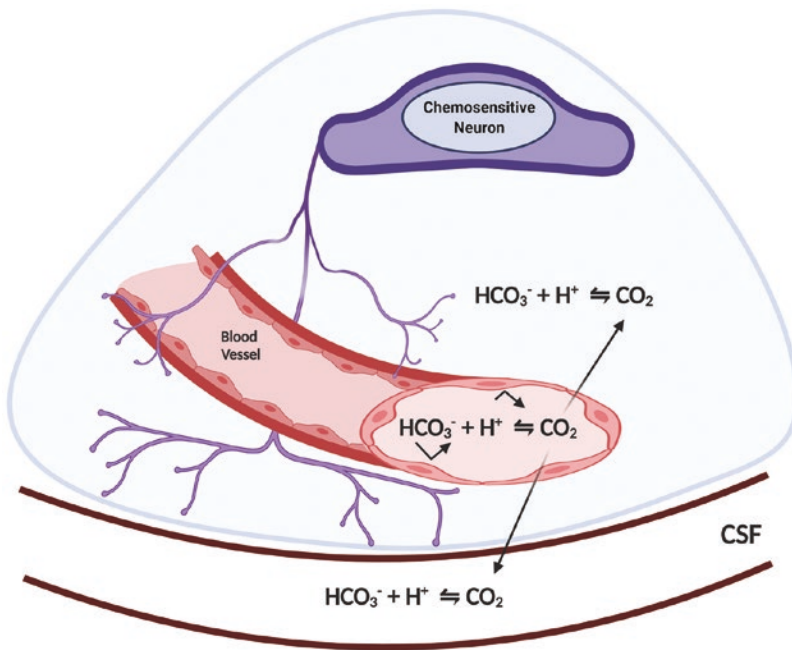


Fig. 15.4 The importance of carbonic anhydrase in catalyzing the equilibrium involving CO_2 , H_2O , and HCO_3^- . CO_2 diffuses from vessel and influences CSF and chemosensitive neurons as shown

glutamate in response to changes in CO_2/pH can modulate breathing patterns.

Although the mechanism is unknown, central chemosensitive neurons may decrease CO_2 sensitivity in response to long-term increases in arterial P_{CO_2} (e.g., in some chronic lung disease patients) and increase CO_2 sensitivity in response to chronic reduction in arterial P_{CO_2} (e.g., in some individuals exposed to chronic hypoxia at altitude). Previously, it was thought that changes in central CO_2 sensitivity could be explained by metabolic compensation for respiratory disturbances in CSF pH. However, the pH of CSF does not show complete compensation to its normal value (7.3) during chronic respiratory acidosis or alkalosis but remains slightly acidic or alkaline. Nevertheless, ventilatory reflexes from central chemoreceptors can adapt to chronic changes in P_{CO_2} “as if” the H^+ stimulus changed in parallel with metabolic compensations of arterial pH, at least under some conditions.

Arterial Chemoreceptors

Arterial chemoreceptors is a generic term for both the *carotid body chemoreceptors* and *aortic body chemoreceptors*, although most knowledge about the arterial chemoreceptors is based on studies of the carotid body. The carotid bodies are small (diameter ≈ 2 mm) sensory organs located near the carotid sinus at the bifurcation of the common carotid artery at the base of the skull. The aortic bodies are located on the aortic arch near the baroreceptors. Afferent nerves travel from the carotid bodies via the *glossopharyngeal (IX cranial) nerve* and from the aortic bodies in the *vagus (X cranial) nerve* to the CNS.

Carotid bodies have high blood flow per unit mass, and this rich blood supply makes them efficient at sensing changes in arterial blood gases. While carotid bodies respond to changes in arterial P_{O_2} , P_{CO_2} , and pH (Dempsey et al. 1990), they are the most important chemoreceptors for ventilatory sensitivity to Pa_{O_2} . This response is specific to O_2 partial pressure but *not* changes in O_2 content nor hemoglobin saturation. This concept is critical for understanding

clinical problems such as anemia or carbon monoxide poisoning. In these cases, ventilation will not be stimulated because Pa_{O_2} is normal, or even elevated, and there is no major sensory system for decreases in O_2 content of hemoglobin saturation. However, in extreme situations, such as lactic acidosis, breathing will be clearly stimulated (Duffin et al. 2000).

The mechanism of P_{O_2} sensing in the carotid bodies is not completely understood. The carotid body consists of specialized neurosecretory *glomus (chief or type I) cells* that contain several types of neurotransmitters and neuropeptides, glial-like *sustentacular (sheath or type II) cells*, capillary endothelial cells, afferent nerve endings from the glossopharyngeal nerve, and even sympathetic efferent nerve endings. Specialized NADP(H) oxidases, cytochromes, and O_2 -sensitive potassium channels are candidate molecular O_2 sensors, and O_2 sensing appears to further involve reactive oxygen species signaling. Hypoxia depolarizes glomus cells, causing release of an (unknown) excitatory neurotransmitter and excitation of afferent nerve endings that sends action potentials to respiratory centers in the brain.

Changes in Pa_{O_2} are coded as changes in the frequency of action potentials. Carotid body afferent nerve activity has a low level of tonic activity with normal Pa_{O_2} (100 mm Hg) and Pa_{CO_2} (40 mm Hg). Arterial chemoreceptor activity does not increase until Pa_{O_2} falls below normal levels *if* Pa_{CO_2} is normal. However, carotid body chemoreceptors are also sensitive to Pa_{CO_2} . If Pa_{CO_2} is below normal levels, Pa_{O_2} must decrease even further below normal to excite carotid body chemoreceptors. Conversely, carotid body chemoreceptors can be stimulated at higher P_{O_2} levels if Pa_{CO_2} is increased. The interaction between P_{O_2} and P_{CO_2} at carotid body chemoreceptors is synergistic, so hypoxia and hypercapnia increase the effect of each other as chemoreceptor stimuli. This synergistic effect at arterial chemoreceptors is important because it explains the multiplicative effect of Pa_{O_2} and Pa_{CO_2} (hypoxemia plus hypercapnia) on ventilation. The physiological advantage of this effect is that combined hypoxia and hypercapnia, which usually occur together with

limitations of gas exchange, increase ventilation more than either stimulus could alone. During the COVID-19 pandemic, considerable discussion about “silent hypoxemia” led to revisiting of these concepts (Simonson et al. 2021). In brief, in the absence of hypercapnia, the Pa_{O_2} may fall to varying degrees among individuals before a substantial increase in dyspnea or ventilation (Moosavi et al. 2004).

The synergistic effect of O_2 and CO_2 can also explain environmental and clinical observations. At extreme high altitude, low barometric pressure leads to low Pa_{O_2} and increased ventilation. However, the reduced arterial levels of CO_2 may produce apneic events during sleep, also known as high-altitude central sleep apnea (periodic breathing) (Orr et al. 2018; Heinrich et al. 2019; Swenson 2016). Another example is patients assisted with mechanical ventilators in the intensive care unit. *If mechanical ventilation decreases the CO_2 below the chemical apneic threshold, central apnea would be predicted even if the Pa_{O_2} also falls. This situation occurs commonly during spontaneous breathing trials as the patient may be apneic and labeled as “failing” their spontaneous breathing trial (see clinical note)* (Meza et al. 1998a, b; Skatrud et al. 1990; Meza and Younes 1996).

Arterial chemoreceptors respond within seconds to changes in Pa_{O_2} , Pa_{CO_2} , and pH. Changes in arterial blood gases that occur in phase with breathing, especially during conditions such as exercise, can be sensed by arterial chemoreceptors and may stimulate ventilation. This rapid response explains how ventilation can be altered within a single breath when arterial blood gases change. Carotid body chemoreceptors contain *carbonic anhydrase*, which increases the speed of response to Pa_{CO_2} based on the intracellular pH-sensing mechanisms described above (Dempsey 1995; Dempsey et al. 1972).

Reflexes from the Lungs and Airways

Reflexes from the upper airways and lungs are primarily defense reflexes, which protect the lung from injury and environmental insults to the

body. Pulmonary reflexes also adjust frequency and tidal volume to stabilize ventilation. The vagus nerve forms the afferent limb for most of these reflexes. The following sections describe reflexes associated with different types of pulmonary receptors:

Nose and Upper Airways

The *nose* has sensory nerves that transmit afferent information to the respiratory centers via the *trigeminal (V)* cranial nerve. The ends of these sensory nerves respond to mechanical and chemical irritants in the nasal mucosa, so they are called *mechanoreceptors* and *chemoreceptors*, respectively. The *sneeze reflex* occurs when nasal mechanoreceptors are stimulated, for example, by inhaled dust, or nasal chemoreceptors are stimulated by noxious gases. Sneezing is a strong inspiration followed immediately by strong expiration, which directs air mainly through the nose to remove the offending stimuli. Stimulation of nasal chemoreceptors with water elicits the *diving reflex*. The diving reflex causes *apnea (breath holding)*, laryngeal closure, and bronchoconstriction to protect the airways from water inhalation. A secondary cardiovascular reflex response to arterial chemoreceptor stimulation also occurs during apnea, slows the heart rate, and diverts blood flow to vital organs such as the brain. This is considered an important part of the diving reflex because it conserves O_2 supplies in the body until breathing can resume safely.

The *pharynx and epipharynx* (the nasal passages just above the pharynx) contain vagal mechanoreceptors. Mechanical irritants in the epipharynx stimulate the *aspiration*, or *sniff reflex*, consisting of several short and strong nasal inspirations in rapid succession. This reflex sends material down into the pharynx where it can be coughed out or swallowed. Mechanoreceptor stimulation in the pharynx causes the *swallowing reflex*. Swallowing inhibits inspiration and closes the larynx, which protects the lungs, while the tongue and other muscles move food or liquid into the esophagus.

The *larynx* contains mechanoreceptors and chemoreceptors from the *recurrent laryngeal and superior laryngeal nerves*, which are branches of the vagus. The laryngeal chemoreceptors are sensitive to inhaled noxious gases (e.g., ammonia and sulfur dioxide) and smoke, which stimulate coughing and the expiratory reflex. The *expiratory reflex* is a short and strong expiratory effort, but *coughing* also involves inspiratory activity. Liquid can also stimulate laryngeal chemoreceptors to cause apnea, which protects the lungs from inhaling fluids.

Laryngeal mechanoreceptors respond to changes in airway pressure, upper airway muscle contraction, and temperature (Horner et al. 1991; Horner 2001; Mathew 1985; Mathew et al. 1982a, b). Airway temperature can change with inspired gas temperature, ventilation rate, and the velocity of air flow, as well as mouth versus nose breathing. Stimulation of laryngeal mechanoreceptors causes reflex changes in upper airway muscle tone, which decreases *airway resistance* and prevents *upper airway collapse* with negative pressures during inspiration. A short and strong inspiratory effort results in either a *sigh* or a *hiccup*, depending on whether or not the upper airway muscles are simultaneously activated.

Lungs and Lower Airways

Vagal sensory nerves from the lungs and lower airways fall into two functional groups: *myelinated* and *nonmyelinated pulmonary receptors*. Myelinated nerves conduct action potentials rapidly and are generally involved in fine motor control and rapid defense responses. Nonmyelinated nerves conduct action potentials more slowly and are involved in slower defense reflexes.

Pulmonary Stretch Receptors

The vagus contains myelinated afferents called *slowly adapting pulmonary stretch receptors* (sometimes abbreviated PSR or SAR), which are stimulated by changes in lung volume. These

mechanoreceptors are located in the smooth muscle of the trachea and intrapulmonary airways. Stretch depolarizes these receptors, sending action potentials to respiratory centers in the brain via the vagus nerve. If volume is increased rapidly and maintained at a new level, the frequency of action potentials increases rapidly and then settles to a slightly lower frequency. However, the steady-state frequency is proportional to the steady-state volume, and the receptors are described as slowly adapting because frequency does not completely adapt back to the basal rate. Slowly adapting pulmonary stretch receptors are tonically active at functional residual capacity (FRC), so they can send to the CNS afferent information about increases *or* decreases in lung volume.

Slowly adapting pulmonary stretch receptors are involved in the control of tidal volume and respiratory frequency through the *Hering-Breuer, or inflation inhibitory, reflex*. Increasing lung volume causes increased action potential frequency from pulmonary stretch receptors. This afferent signal inhibits further inspiratory nerve activity and terminates an inspiration through synaptic mechanisms in the pons and medulla. Hence, the inflation inhibitory reflex limits a breath from being larger or longer than necessary to achieve a given level of ventilation. This reflex is of historic interest because it was the first description of negative feedback in a physiologic control system in 1868. It is of physiologic interest because it explains the effect of the vagus on the pattern of breathing.

The pattern of ventilation can also be irregular in lung transplant patients. This situation also occurs in *awake* lung transplant patients and experimental animals with pulmonary denervation. Hence, *pulmonary stretch receptors decrease breath-to-breath variations in tidal volume and frequency* for a given level of ventilation. This fine-tuning of the ventilatory pattern is hypothesized to reduce the mechanical work of breathing.

Pulmonary stretch receptors also are involved in the *deflation reflex*, which increases respiratory rate at low lung volumes. Recall that pulmonary stretch receptors are tonically active at FRC, so at low lung volumes the afferent input to respiratory centers is decreased.

Bronchial C-Fibers

C-fiber is another term for a nonmyelinated fiber, where the C designates conduction velocity in an alphabetical system ($C \leq 2.5$ m/sec). Pulmonary C-fibers can be defined further by their blood supply. *Bronchial C-fibers* are supplied by the systemic circulation, in contrast to juxtacapillary C-fibers, which are supplied by the pulmonary capillaries. Bronchial C-fibers can be stimulated by chemicals injected in the bronchial circulation, such as capsaicin (the hot ingredient in red chilies) and phenyldiguanide (a serotonin receptor agonist). Physiologically, bronchial C-fibers are probably stimulated by local release of cytokines, such as histamine, prostaglandin, and bradykinin in the airways.

The reflex response to bronchial C-fiber stimulation is an airway defense reflex, which includes rapid shallow breathing, bronchoconstriction, and mucous secretion. Bronchial C-fibers may contribute to the cough reflex too. Finally, bronchial C-fibers are involved in bronchoconstriction and changes in vascular permeability in the airways with airway inflammation. Bronchoconstriction involves both autonomic effectors (see Autonomic Nervous System in the Lungs) and a local axon reflex.

Juxtacapillary Receptors

Pulmonary vagal C-fibers that can be stimulated by chemicals in the pulmonary circulation are called *juxtacapillary receptors*, or *J-receptors* because of their presumed location next to the pulmonary capillaries. J-receptors can be stimulated by capsaicin injected into the pulmonary artery, and the reflex response is *tachypnea*, or rapid shallow breathing. *Apnea* (no breathing) may precede tachypnea depending on the dose and timing of chemical stimulation.

Physiologically, J-receptor stimulation occurs with pulmonary embolism, congestion, and edema and causes the rapid shallow breathing observed in these conditions. J-receptor stimulation probably explains the tachypnea and sensation of breathlessness (*dyspnea*) with interstitial

lung disease also. Nonmyelinated vagal afferents are responsible for all sensation, including pain, from the lower airways.

Autonomic Nervous System in the Lungs

The airways in the lungs receive both *parasympathetic* and *sympathetic* innervation, which controls bronchial smooth muscle constriction, mucous secretion, vascular smooth muscle, fluid transport across the airway epithelium, and vascular permeability in the pulmonary and bronchial circulations. In normal conditions, parasympathetic control of bronchial smooth muscle tone is the most important of these functions. Acetylcholine released from the vagus nerve causes bronchoconstriction and tonic vagal activity determines bronchial smooth muscle tone. Sympathetic innervation of the lung is less important. Circulating epinephrine from the adrenal medulla causes bronchodilation through *β -adrenergic receptors* on airway smooth muscle. Norepinephrine released from sympathetic nerves in the airways can cause bronchodilation indirectly via *α -adrenergic receptors* on parasympathetic ganglia in the lung. Activating these *α -adrenergic receptors* inhibits parasympathetic activity and cholinergic bronchoconstriction.

These different autonomic mechanisms provide a physiological basis for treating bronchoconstriction in lung disease. Chronic bronchoconstriction from chronic obstructive pulmonary disease is treated with *acetylcholine receptor* antagonists to reduce the effects of vagal tone. Acute and severe bronchoconstriction during an asthma attack is treated with *β_2 -adrenergic agonists*. *β_2 -adrenergic agonists* are selective for bronchial smooth muscle and have fewer cardiac effects.

Neuropeptides are also important in controlling airway function. The bronchoconstriction from *substance P* released directly from sensory nerves by the axon reflex were described above (see Bronchial C-Fibers). This is also called the *excitatory nonadrenergic, noncholinergic system (e-NANC)* to distinguish it from autonomic control. In contrast, the neuropeptide *VIP*

(*vasoactive intestinal peptide*) causes bronchodilation. VIP is released from nerves arising from parasympathetic ganglia, which are called the *inhibitory nonadrenergic, noncholinergic system* (i-NANC). *Nitric oxide* (NO) may also be involved in i-NANC bronchodilation.

Patients in the Intensive Care Unit

Intensivists need to consider control of breathing because it has many important clinical implications. Control issues are important in how the patient presents clinically, and thus influences subsequent diagnostic testing (Kikuchi et al. 1994). In addition, control of breathing is important in the pathophysiology affecting respiratory disease, for example, high vs. low respiratory drive which can affect lung injury and/or weaning from mechanical ventilation. Thus, therapeutic decisions including sedation, use of paralytics, and setting the ventilator to optimize patient/ventilator synchrony are best considered in the context of the control of breathing (Mascheroni et al. 1988).

In terms of clinical presentation and diagnostics, healthcare professionals often reassure patients that they are healthy based on an easily measured normal O₂ saturation, but decisions that consider O₂ saturation without other important factors can be deceiving (Moosavi et al. 2004). Oxygen tension is just one input into the respiratory control system that helps health care providers make appropriate care decisions but the evaluation also should consider findings on physical exam such as breathing and speech patterns (“2–3 word dyspnea”), accessory muscle use, and additional laboratory data such as Pa_{CO2} (Manning and Schwartzstein 1995).

Breathing drive is highly variable across individuals. Notable examples are reported among high-altitude residents whereby many Tibetan but few Andean individuals exhibit an augmented ventilatory response to hypoxia. This may be attributed to different adaptive genetic profiles (Beall et al. 1997a, b; Simonson et al. 2010; Song et al. 2020). In the clinical setting, patients at the extremes of sensitivity may be more susceptible to critical illness. For example, patients susceptible to near-fatal asthma had the lowest drives and poorest perception of dyspnea, whereas on the other hand, high drive might pre-

dispose to lung stretch and further lung damage (Kikuchi et al. 1994; Mascheroni et al. 1988). The transpulmonary pressure determines stretch on the lung and is defined by the pressure difference between airway opening pressure (Pao) and the pleural space (Ppl) (Mead et al. 1970). While providers measure and control Pao (by setting pressures from noninvasive ventilation or invasive mechanical ventilation), few measure pleural pressures that contribute substantially to lung stretch. Thus, lung protective settings on the ventilator may not be truly protective depending on ventilatory drive. A patient with very high ventilatory drive can have very negative pleural pressure swings which produce high inspiratory transpulmonary pressures and lung stretch. Lung injury could theoretically result in the context of parenchymal heterogeneity (Mead et al. 1970). However, this concept of self-inflicted lung injury has been controversial as it remains largely untested (Esnault et al. 2020; Tobin 2020; Tobin et al. 2020; Gattinoni et al. 2020). Additionally, while many health care providers routinely ask patients about pain, few providers assess and treat dyspnea, which might be equally distressing and might be relieved in many cases by adequate ventilatory support and pharmacotherapy. As will be discussed, there are different underlying causes of ventilator dyssynchrony, and an understanding of control of breathing may help assess and treat patient and ventilator dyssynchrony.

Clinical Implications

A number of clinical situations occur in the ICU where the above concepts become important for clinical care of patients as illustrated by the few examples that apply the points above.

- (a) Apnea. A common scenario in the ICU is that a patient receiving mechanical ventilation triggers the apnea alarm, which frequently leads the treating team to change the patient to volume cycled ventilation while providing increased sedation and/or paralysis (Meza et al. 1998a). In fact, the pathogenesis of apnea during mechanical ventilation is complex and should prompt consideration of the differential

diagnosis and a search for underlying cause. One situation which was best described by Younes is during pressure support ventilation (PSV). When patients are weaning from mechanical ventilation, they sometimes trigger apnea alarms, which prompts some practitioners to conclude that the patient “is not ready to wean” and the ventilator settings are returned back to baseline with a backup rate (Meza et al. 1998a, b; Meza and Younes 1996; Younes 2002; Tobert et al. 1997). In reality, the tidal volume achieved during PSV is a function of the resistance and compliance of the respiratory system, but what also matters is the patient’s ventilatory drive (P_{mus}). A gradual rise in PSV level leads to an instantaneous increase in tidal volume followed by a gradual return of tidal volume to V_{tmin} (based on the resistance and compliance of the respiratory system) as the respiratory muscles are gradually unloaded with increasing PSV. At some level of PSV, however, the tidal volume starts to increase, which can contribute to hyperventilation. Because minute ventilation is a function of respiratory rate and tidal volume, some reduction in respiratory rate may be expected but, in general, high flow rates promote tachypnea and thus hypocapnia can frequently occur (Tobert et al. 1997). As a result, the occurrence of apnea during PSV is frequently a manifestation of excessive pressure support and can be effectively managed by either reducing the PSV level or extubation. In contrast, the apnea alarm frequently triggers the opposite response where the patient is sedated and/or paralyzed and put back on volume-controlled ventilation. Thus, simple concepts underlying control of breathing may have a major impact on patient care and likely ICU outcomes.

(b) Another scenario in which control of breathing issues become important in the ICU is in the case of patient/ventilator dyssynchrony. Recent studies have shown a high prevalence of dyssynchrony with the potential for a major mechanical impact on the lung which can influence ICU outcomes (see Chap. 47). For instance, patients receiving volume-targeted ventilation may receive an injurious tidal volume if double triggering occurs, that

is, breath stacking dyssynchrony. Many authors have suggested that the outcome benefits observed with cisatracurium vs. placebo by Papazian et al. in *NEJM* were a result of reductions in breath stacking dyssynchrony (Papazian et al. 2010; Hibbert et al. 2012). Although the most recent data from the ROSE study in *NEJM* were not confirmatory, the concept that there is heterogeneity in the mechanisms underlying dyssynchrony is likely to be true (Moss et al. 2019). For example, a patient with ineffective triggering due to auto-PEEP may benefit from the application of extrinsic PEEP as a means of reducing the so-called inspiratory threshold load. On the other hand, some patients with ventilator-induced diaphragm contraction – so-called reverse triggering – occasionally benefit from reduced sedation while other patients may require paralytics to reduce the risk of breath stacking (Akoumianaki et al. 2013). One manifestation of air hunger can be double triggering whereby patients with high drive feel they are receiving insufficient airflow from the ventilator. Depending on the ventilator and the set mode, efforts that increase the airflow provided or reduce ventilatory drive (e.g., relief of hypoxia or reduced extravascular lung water) may be well effective, rather than simply paralyzing patients who are dyssynchronous. Thus, the approach to patient–ventilator dyssynchrony can be complex and influenced by the sedation level, the mechanical ventilator settings, and the underlying control of breathing of the patient. Efforts to adjust ventilator settings/strategy based on these principles may be required in an individualized manner, given that a “one size fits all” approach (e.g., give early paralytics to all ARDS patients) has not been generally fruitful to date (Beitler et al. 2016; Bergard et al. 2016).

(c) Dyspnea. Another important concept which is frequently overlooked in the ICU is related to dyspnea. Patients who are short of breath often look uncomfortable, which can prompt bedside practitioners to provide increased sedation and/or narcotic. In some scenarios, this solution may be appropriate, but in other

situations addressing the underlying cause may be advantageous for the patient. The relief of dyspnea, for example, can occur with bronchodilation or with diuresis, both of which provide improvement to the mechanics of the respiratory system. The corollary discharge hypothesis has been proposed whereby dyspnea is generally a function of a “disconnect” between what the brain/control centers are expecting and what the respiratory system is actually able to deliver (Moosavi et al. 2004; Manning and Schwartzstein 1995). Thus, in the scenario that a bronchodilator leads to relief of dyspnea, the delivered tidal volume becomes more in line with the brain’s expectations as compared to that received prior to the bronchodilator. One factor of importance also pertains to the inspiratory flow rate. One reflex which has been observed by Younes and Hubmayr and others is that high inspiratory flow rates can lead to termination of neural inspiration (Tobert et al. 1997; Younes 1989). During pressure-targeted ventilation, high flow rates can thus lead to tachypnea whereas during volume-cycled ventilation, this reflex can lead to respiratory alkalosis. Of note, for the patient with rapid shallow breathing which has been induced by high inspiratory flow rates, the breathing pattern can normalize with reductions in the delivered inspiratory flow. In contrast, for patients with air hunger, higher inspiratory flows can be helpful to meet the inspiratory flow demands of the patient. Thus, a sophisticated understanding of control of breathing has important clinical implications and may well be helpful in individualizing therapy and avoiding unnecessary interventions.

- (d) In some patients with chronic hypercapnia, the application of supplemental oxygen can lead to worsening respiratory acidosis (Malhotra et al. 2001). The typical context where this phenomenon has been reported is during acute exacerbation of COPD, in which patients develop profound respiratory acidosis when given moderate amounts of supplemental oxygen. The reasons why this

deterioration occurs are unclear, but in some cases likely reflects progression of the underlying acute illness. However, a number of physiological mechanisms have been suggested to be important at least in some cases. First, central drive to breathe is likely impaired in patients with chronic hypercapnia. Dunn et al. measured the P_{CO_2} recruitment threshold (RT), that is, the CO_2 value at which breathing resumes after severe hypocapnia (Dunn et al. 1991). The $P_{CO_2}RT$ was importantly impacted by supplemental oxygen, such that the only logical conclusion was the oxygen was affecting central drive to breathe in patients with chronic hypercapnia. Second, the Haldane effect describes the changes in Hb binding affinity for CO_2 in the context of supplemental oxygen. The release of CO_2 from Hb can thus occur in this context leading to worsening hypercapnia. Third, the changes in ventilation perfusion (V_A/Q) relationships with supplemental oxygen can lead to worsening hypercapnia. Robinson et al. performed MIGET (multiple inert gas elimination technique) studies with and without supplemental oxygen and observed increases in dead space with supplemental oxygen (Robinson et al. 2000). The supplemental oxygen led to release of hypoxic pulmonary vasoconstriction in low V_A/Q lung units. The perfusion was thus being stripped from high V_A/Q lung units leading to increased dead space. CO_2 -induced bronchodilation was also thought to be important in increasing ventilation to high V_A/Q ratio lung units. Fourth, patients with acute exacerbations of COPD are typically sleep-deprived, and thus the administration of oxygen can contribute to sleep onset by relieving both anxiety and dyspnea. Worsening hypercapnia is commonly observed in obese patients who likely have underlying obstructive sleep apnea/obesity hypoventilation syndrome. Loss of the wakefulness drive to breathe can thus contribute to worsening hypercapnia. Fifth, the inspiratory flow demand can have an important impact on the actual FIO_2 being delivered to the lung. The administration of

noninvasive oxygen can thus lead to highly variable FIO_2 depending on the breathing pattern and the amount of room air entrainment. Via all of the above mechanisms, as inspiratory flow demand is reduced (e.g., at sleep onset), there is a progressive increase in the actual FIO_2 reaching the lung even with no change in wall oxygen settings. The result of these mechanisms can occasionally be the development of a vicious cycle of worsening hypercapnia from supplemental oxygen yielding profound respiratory acidosis in some cases. The overreliance on pulse oximeters can contribute to this problem since major changes in CO_2 can occur without appreciable changes in SpO_2 depending on the clinical context. The use of noninvasive ventilation in COPD exacerbations has helped mitigate some of the deteriorating gas exchange, which was previously observed more commonly during acute exacerbation.

In summary, control of breathing is an important subject for the critical care practitioner to consider. Although a major expansion in our knowledge of neural control mechanisms has occurred in the past years, some ICU training programs neglect many of these important topics. In a number of common clinical scenarios, a sophisticated knowledge of control of breathing can have a big impact on patient care.

References

- Akoumianaki E, Lyazidi A, Rey N, Matamis D, Perez-Martinez N, Giraud R, Mancebo J, Brochard L, Richard JM. Mechanical ventilation-induced reverse-triggered breaths: a frequently unrecognized form of neuromechanical coupling. *Chest*. 2013;143:927–38.
- Beall CM, Strohl KP, Blangero J, Williams-Blangero S, Almasy LA, Decker MJ, Worthman CM, Goldstein MC, Vargas E, Villena M, Soria R, Alarcon AM, Gonzales C. Ventilation and hypoxic ventilatory response of Tibetan and Aymara high altitude natives. *Am J Phys Anthropol*. 1997a;104:427–47.
- Beall CM, Strohl KP, Blangero J, Williams-Blangero S, Decker MJ, Brittenham GM, Goldstein MC. Quantitative genetic analysis of arterial oxygen saturation in Tibetan highlanders. *Hum Biol*. 1997b;69:597–604.
- Beitler JR, Sands SA, Loring SH, Owens RL, Malhotra A, Spragg RG, Matthay MA, Thompson BT, Talmor D. Quantifying unintended exposure to high tidal volumes from breath stacking dyssynchrony in ARDS: the BREATHE criteria. *Intensive Care Med*. 2016;42:1427–36.
- Bergard SC, Beitler JR, Malhotra A. Personalizing mechanical ventilation for acute respiratory distress syndrome. *J Thorac Dis*. 2016;8:E172–4.
- Dempsey JA. Exercise hyperpnea. Chairman's introduction. *Adv Exp Med Biol*. 1995;393:133–6.
- Dempsey JA, Forster HV, Birnbaum ML, Reddan WG, Thoden J, Grover RF, Rankin J. Control of exercise hyperpnea under varying durations of exposure to moderate hypoxia. *Respir Physiol*. 1972;16:213–31.
- Dempsey JA, et al. Regulation of ventilation and respiratory muscle function in NREM sleep. *Prog Clin Biol Res*. 1990;345:145–54; discussion 154–145. available.
- Dempsey JA, Veasey SC, Morgan BJ, O'Donnell CP. Pathophysiology of sleep apnea. *Physiol Rev*. 2010;90:47–112.
- Duffin J, Mohan RM, Vasilou P, Stephenson R, Mahamed S. A model of the chemoreflex control of breathing in humans: model parameters measurement. *Respir Physiol*. 2000;120:13–26.
- Dunn WF, Nelson SB, Hubmayr RD. Oxygen-induced hypercarbia in obstructive pulmonary disease. *Am Rev Respir Dis*. 1991;144:526–30.
- Esnault P, Cardinale M, Hraiech S, Goutorbe P, Baumstrack K, Prud'homme E, Bordes J, Forel JM, Meaudre E, Papazian L, Guervilly C. High respiratory drive and excessive respiratory efforts predict relapse of respiratory failure in critically ill patients with COVID-19. *Am J Respir Crit Care Med*. 2020;202:1173–8.
- Feldman JL. Neurobiology of breathing control. Where to look and what to look for. *Adv Exp Med Biol*. 1995;393:3–5.
- Feldman JL. Chapter 14--looking forward to breathing. *Prog Brain Res*. 2011;188:213–8.
- Gattinoni L, Coppola S, Cressoni M, Busana M, Rossi S, Chiumello D. COVID-19 does not lead to a "typical" acute respiratory distress syndrome. *Am J Respir Crit Care Med*. 2020;201:1299–300.
- Heinrich EC, Djokic MA, Gilbertson D, DeYoung PN, Bosompra NO, Wu L, Anza-Ramirez C, Orr JE, Powell FL, Malhotra A, Simonson TS. Cognitive function and mood at high altitude following acclimatization and use of supplemental oxygen and adaptive servoventilation sleep treatments. *PLoS One*. 2019;14:e0217089.
- Hibbert K, Rice M, Malhotra A. Obesity and ARDS. *Chest*. 2012;142:785–90.
- Horner RL. Motor control of the pharyngeal musculature and implications for the pathogenesis of obstructive sleep apnea. *Sleep*. 1996;19:827–53.
- Horner RL. Impact of brainstem sleep mechanisms on pharyngeal motor control. *Respir Physiol*. 2000;119:113–21.
- Horner RL. The neuropharmacology of upper airway motor control in the awake and asleep states: impli-

- cations for obstructive sleep apnoea. *Respir Res.* 2001;2:286–94.
- Horner RL. Pathophysiology of obstructive sleep apnea. *J Cardiopulm Rehabil Prev.* 2008;28:289–98.
- Horner RL, Innes JA, Murphy K, Guz A. Evidence for reflex upper airway dilator muscle activation by sudden negative airway pressure in man. *J Physiol (Lond).* 1991;436:15–29.
- Kikuchi Y, Okabe S, Tamura G, Hida W, Homma M, Shirato K, Takishima T. Chemosensitivity and perception of dyspnea in patients with a history of near-fatal asthma. *N Engl J Med.* 1994;330:1329–34.
- Malhotra A, Schwartz DR, Ayas N, Stanchina M, White DP. Treatment of oxygen-induced hypercapnia. *Lancet.* 2001;357:884–5.
- Manning HL, Schwartzstein RM. Pathophysiology of dyspnea. *N Engl J Med.* 1995;333:1547–53.
- Mascheroni D, Kolobow T, Fumagalli R, Moretti MP, Chen V, Buckhold D. Acute respiratory failure following pharmacologically induced hyperventilation: an experimental animal study. *Intensive Care Med.* 1988;15:8–14.
- Mathew OP. Maintenance of upper airway patency. *J Pediatr.* 1985;106:863–9.
- Mathew OP, Abu-Osba YK, Thach BT. Influence of upper airway pressure changes on genioglossus and muscle respiratory activity. *J Appl Physiol.* 1982a;52:438.
- Mathew OP, Abu-Osba YK, Thach BT. Genioglossus muscle response to upper airway pressure changes: afferent pathways. *J Appl Physiol.* 1982b;52:445.
- Mead J, Takishima T, Leith D. Stress distribution in lungs: a model of pulmonary elasticity. *J Appl Physiol.* 1970;28:596–608.
- Meza S, Younes M. Ventilatory stability during sleep studied with proportional assist ventilation (PAV). *Sleep.* 1996;19:S164–6.
- Meza S, Mendez M, Ostrowski M, Younes M. Susceptibility to periodic breathing with assisted ventilation during sleep in normal subjects. *J Appl Physiol (1985).* 1998a;85:1929–40.
- Meza S, Giannouli E, Younes M. Control of breathing during sleep assessed by proportional assist ventilation. *J Appl Physiol (1985).* 1998b;84:3–12.
- Moosavi SH, Banzett RB, Butler JP. Time course of air hunger mirrors the biphasic ventilatory response to hypoxia. *J Appl Physiol (1985).* 2004;97:2098–103.
- Moss M, Ulysse CA, Angus DC, National Heart L, Blood Institute PCTN. Early neuromuscular blockade in the acute respiratory distress syndrome. Reply. *N Engl J Med.* 2019;381:787–8.
- Orr JE, Heinrich EC, Djokic M, Gilbertson D, Deyoung PN, Anza-Ramirez C, Villafuerte FC, Powell FL, Malhotra A, Simonson T. Adaptive servoventilation as treatment for central sleep apnea due to high-altitude periodic breathing in nonacclimatized healthy individuals. *High Alt Med Biol.* 2018;19:178–84.
- Papazian L, Forel JM, Gacouin A, Penot-Ragon C, Perrin G, Loundou A, Jaber S, Arnal JM, Perez D, Seghboyan JM, Constantin JM, Courant P, Lefrant JY, Guerin C, Prat G, Morange S, Roch A, Investigators AS. Neuromuscular blockers in early acute respiratory distress syndrome. *N Engl J Med.* 2010;363:1107–16.
- Plataki M, Sands SA, Malhotra A. Clinical consequences of altered chemoreflex control. *Respir Physiol Neurobiol.* 2013;189:354–63.
- Robinson TD, Freiberg DB, Regnis JA, Young IH. The role of hypoventilation and ventilation-perfusion redistribution in oxygen-induced hypercapnia during acute exacerbations of chronic obstructive pulmonary disease. *Am J Respir Crit Care Med.* 2000;161:1524–9.
- Simonson TS, Yang Y, Huff CD, Yun H, Qin G, Witherspoon DJ, Bai Z, Lorenzo FR, Xing J, Jorde LB, Prchal JT, Ge R. Genetic evidence for high-altitude adaptation in Tibet. *Science.* 2010;329:72–5.
- Simonson T, Baker T, Banzett R, Bishop T, Dempsey J, Feldman J, Guyenet P, Hodson E, Mitchell G, Moya EA, Nokes B, Orr J, Owens R, Poulin M, Rawlings J, Schmickl C, Watters J, Younes M, Malhotra A. Silent hypoxemia in COVID-19. *J Physiol (Lond).* 2021;599(4):1057–65.
- Skatrud JB, Dempsey JA. Interaction of sleep state and chemical stimuli in sustaining rhythmic ventilation. *J Appl Physiol.* 1983;55:813–22.
- Skatrud JB, et al. A sleep-induced apneic threshold. *Prog Clin Biol Res.* 1990;345:191–9; discussion 199–200. available.
- Smith JC, Ellenberger HH, Ballanyi K, Richter DW, Feldman JL. Pre-Botzinger complex: a brainstem region that may generate respiratory rhythm in mammals. *Science.* 1991;254:726–9.
- Song D, Navalsky BE, Guan W, Ingersoll C, Wang T, Loro E, Eeles L, Matchett KB, Percy MJ, Walsby-Tickle J, McCullagh JSO, Medina RJ, Khurana TS, Bigham AW, Lappin TR, Lee FS. Tibetan PHD2, an allele with loss-of-function properties. *Proc Natl Acad Sci U S A.* 2020;117:12230–8.
- Swenson ER. Hypoxia and its acid-base consequences: from mountains to malignancy. *Adv Exp Med Biol.* 2016;903:301–23.
- Tobert D, Simon PM, Stroetz RW, Hubmayr RD. The determinants of respiratory rate during mechanical ventilation. *Am J Respir Crit Care Med.* 1997;155:485–92.
- Tobin MJ. Basing respiratory management of COVID-19 on physiological principles. *Am J Respir Crit Care Med.* 2020;201:1319–20.
- Tobin MJ, Laghi F, Jubran A. Why COVID-19 silent hypoxemia is baffling to physicians. *Am J Respir Crit Care Med.* 2020;202:356–60.
- Younes M. The physiologic basis of central apnea and periodic breathing. *Curr Pulmonol.* 1989;10:265–326.
- Younes M. Proportional assist ventilation. In: Mancebo J, Net A, Brochard L, editors. *Update in intensive care and emergency medicine.* New York: Springer; 2002. p. 39–73.
- Younes M, Ostrowski M, Thompson W, Leslie C, Shewchuk W. Chemical control stability in patients with obstructive sleep apnea. *Am J Respir Crit Care Med.* 2001;163:1181–90.



Respiratory Muscle Blood Flow and Heart–Lung Interactions

16

Sheldon Magder

Introduction

The cardiovascular and respiratory systems are the two dominant systems maintaining the body's basic vegetative functions. They are intricately linked through the function of the respiratory muscles. The circulatory system must provide the blood flow that delivers oxygen (O₂) and nutrients to the working respiratory muscles and clears carbon dioxide (CO₂) and other waste products produced by the working muscles. In turn, respiratory muscles must maintain airflow into and out of the lungs so that the blood carried by the cardiovascular system is adequately oxygenated and CO₂ removed. Lack of adequate blood flow can compromise respiratory muscle function. In turn, inadequate activity of the respiratory muscle and gas exchange can compromise cardiac function. The activity of the respiratory muscles also produces afferent neural signals that can affect the pattern of breathing and central sympathetic output, which can affect the distribution of organ blood flow and the activity of the heart.

S. Magder (✉)

Royal Victoria Hospital (McGill University Health Centre), Departments of Critical Care and Physiology
McGill University, Montreal, QC, Canada
e-mail: sheldon.magder@mcgill.ca

The Respiratory Muscles

Anatomy

Respiratory muscles are classified as being inspiratory or expiratory. Inspiratory activity is dominated by the diaphragm, which has two components, the crural or central region, and the costal or lateral region. Most of diaphragmatic blood flow comes from the phrenic artery but blood flow also comes from branches of the intercostal arteries and internal mammary arteries (Lockhat et al. 1985). These form a plexus that provides the flow. Other inspiratory muscles have more minor roles during normal breathing. They include the external intercostals, scalenes, and the serratus anterior (Robertson et al. 1977a; Viiris et al. 1983; Rutledge et al. 1988). Expiration usually is passive and does not require muscle activity, but it can be active under a number of circumstances, some of which are physiological and some pathological. Normal uses of expiratory muscles include exercise (Aliverti et al. 1997) in which active expiration can speed expiration as well as decrease lung volume below functional residual capacity and thus expand the maximum tidal volume for high aerobic needs, walking (Sanna et al. 1999), playing musical instruments (Cossette et al. 2008), mechanical loading (Martin and De 1982), and defecating. Abnormal actions of expiratory muscles include forced expiration in patients with obstructed

airways (Parthasarathy et al. 1998; Yan et al. 2000), in which case the extra force does not increase expiratory volume because of flow limitation, in the period in which patients are regaining consciousness from deep sedation (Yan et al. 2000; Magder et al. 2016), and anxiety. The primary expiratory muscles are the internal intercostals; others include the transverse abdominal, internal oblique, external oblique, and the rectus abdominis (Robertson et al. 1977a).

Energetics and Mechanics

Normal resting ventilation is in the range of 7 L/min but at peak aerobic exercise in a young 75 kg male, total ventilation can be greater than 140 L/min (Astrand and Rodahl 1977; Astrand 1976). Muscle performance can be evaluated based on work, which is given by the product of the total pressure generated (area under the pressure curve over time) and the volume moved per breath (i.e., tidal volume). Power is the work per time and takes into account frequency. During a normal breath, the diaphragm descends and lowers pleural pressure (Ppl) and increases abdominal pressure. Force generated by the respiratory system is the positive pressure developed in the abdomen minus the negative change in Ppl. This gives a positive number that is called the transdiaphragmatic pressure, Pdi. The area under a curve of Pdi over time gives the pressure–time index (PTI). Peak Pdi per breath is proportional to PTI because the change in Pdi over a breath is almost triangular, and so Pdi can be used to track changes in PTI. Bellemare et al. (Bellemare et al. 1983) introduced the term tension time index of the diaphragm (TTdi), which is the product of Pdi and the duty cycle. Duty cycle is the proportion of a contraction cycle, that is, inverse of respiratory rate, spent in contraction and is expressed as a fraction. The normal duty cycle is about one third of the cycle. TTdi is similar to the tension time index used for assessing the energy demand of cardiac muscle (Brazier et al. 1974). As is the case with cardiac muscle and other skeletal mus-

cles (Cingolani et al. 2013), diaphragmatic O₂ consumption, and thus diaphragmatic blood flow, is more closely related to the PTI than to work as long as the contractions are intermittent and the duty cycle is constant. Thus, PTI is the more useful indicator of diaphragmatic blood flow needs than diaphragm than work (Buchler et al. 1985a; Rochester and Bettini 1976; Robertson et al. 1977b). The duty cycle is important, too, because contraction with a high diaphragmatic muscle tension can limit the blood flow during the contraction phase as occurs with coronary blood flow in the left ventricle during systole, when there may not be enough time to reach the necessary higher flows (Bellemare et al. 1983; Buchler et al. 1985a).

Frequency of contraction at a fixed tension and duty cycle has a marked effect on diaphragmatic blood flow; when the frequency of contraction was increased from 18 to 74 per minute in diaphragms of dogs, blood flow increased from 147 ± 13 ml/min/100 g to 265 ± 15 ml/min/100 g (Buchler et al. 1985a). Blood flow in tissues, especially in working muscle, is tightly linked to O₂ consumption so that a high flow indicates that the O₂ consumption is high. This also is true in the diaphragm, and there is a linear relationship between PTI and diaphragmatic O₂ consumption. The blood flow values per tissue weight in the diaphragm are much higher than in most other skeletal muscles during exercise (Laughlin et al. 2012). One explanation for the high energy cost with increases in diaphragmatic frequency is that each contraction requires a heat of activation to initiate the contraction. This energy cost then is added to the energy cost of generating pressure. Since the heat of activation occurs on each beat, its component increases linearly with the increase in frequency of contractions (Buchler et al. 1985a). The important point from this discussion is that a high respiratory frequency is energetically expensive and maladaptive in a critically ill patient.

When normal, trained, and adapted subjects breathed against a high resistance, they breathed more slowly and with larger tidal volumes.

However, when they breathed against an elastic load, they breathe with a rapid rate and shallow tidal volumes (Freedman and Campbell 1970). This makes sense physiologically. When there is a resistive load, for example, breathing through a straw, breathing slowly reduces the peak flow rate, which reduces the resistive pressure difference required for airflow and less energy is required per breath. The larger tidal volume taken slowly maintains total ventilation. In contrast, when subjects breathe against an elastic load, increasing frequency means that tidal volumes can be smaller and less energy is needed to stretch the lung and chest wall, and the increased rate maintains the required total ventilation. However, in the clinical setting, patients most often respond to both resistive and elastic loads with rapid shallow breathing as occurs with the elastic load. This maladaptive pattern greatly increases the work of breathing, especially in patients who have a high airway resistance, a very common type of increased respiratory load in the critically ill, especially when intubated with a smaller diameter endotracheal tube. This increased work increases their respiratory distress and the anxiety drives the rate higher and creates a vicious cycle. When blood flow to the diaphragm was measured in animals given a resistive (Robertson et al. 1977c) or an elastic respiratory load (Magder et al. 1983), diaphragmatic blood flow is the same at the same PTI. However, an increase in respiratory rate increases the number of PTI per minute and thus the energy cost. When an elastic load was applied, blood flow to the diaphragm even remained the same when cardiac output was reduced by tamponade (Rutledge et al. 1985) meaning that the working muscle got preferential flow.

The effects of Ppl and abdominal pressure on diaphragmatic flow were studied in a canine model. Sustained tetanic contractions of the diaphragm with creation of either negative Ppl or positive abdominal pressure obstructed diaphragmatic blood flow; the effect was greater with negative Ppl than positive abdominal pressure

(Buchler et al. 1982). Intermittent contractions did not reduce mean blood flow with either mode because the obstruction to diaphragmatic blood flow during contraction was compensated during the relaxation phase as long as the duty cycle was not too long (Buchler et al. 1982; Hussain et al. 1988a).

Normal Resting Respiratory Muscle Blood Flow and the System at Peak Effort

Based on normalization of data obtained in animals, normal resting respiratory blood flow in a 70 kg human (Arora and Rochester 1982) is estimated to be around 100 ml/min and accounts for about 2% of normal resting cardiac output. The largest proportion of the respiratory muscle blood flow goes to the diaphragm, which at resting ventilation is around 10 to 15 ml/min/100 g of tissue (Robertson et al. 1977a, 1977b; Viiris et al. 1983; Rutledge et al. 1985). Assuming a diaphragmatic weight of 180 g, this accounts for about 25% of total respiratory muscle flow. In comparison, blood flow to the external (inspiratory) and internal (expiratory) intercostal muscles are each about 5 to 7 ml/min/100 g (Robertson et al. 1977a, b; Viiris et al. 1983; Rutledge et al. 1985). Blood flow to the other respiratory muscles is much lower per weight, but they still contribute a large percentage of the total of respiratory muscle blood flow because of their large size (Viiris et al. 1983; Robertson et al. 1977c; Rutledge et al. 1985). During high diaphragmatic activity, such as working against a high resistive load, diaphragmatic blood flow can increase more than 20-fold, whereas blood flow to the intercostal muscles only increases about sixfold (Robertson et al. 1977c) (Fig. 16.1).

Some basic principles about the relationship of blood flow demand and the role of blood pressure are illustrated in Fig. 16.2. These principles hold true for the relationship of cardiac output to O₂ consumption for any muscle, and even the

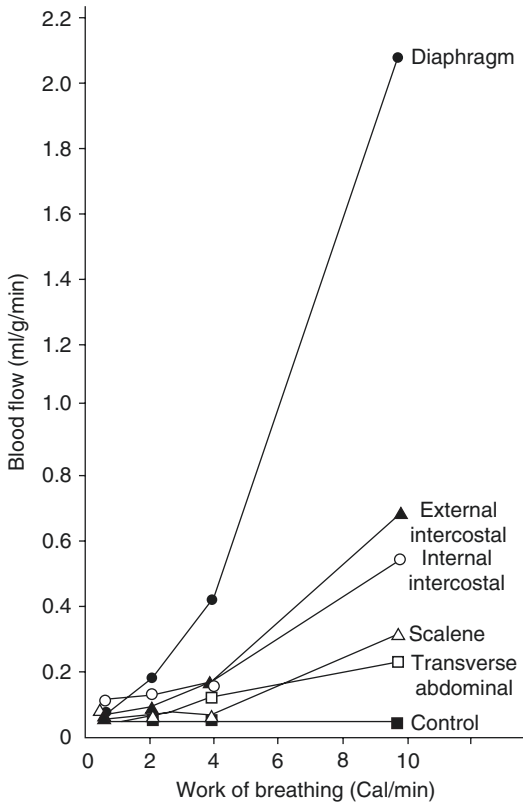


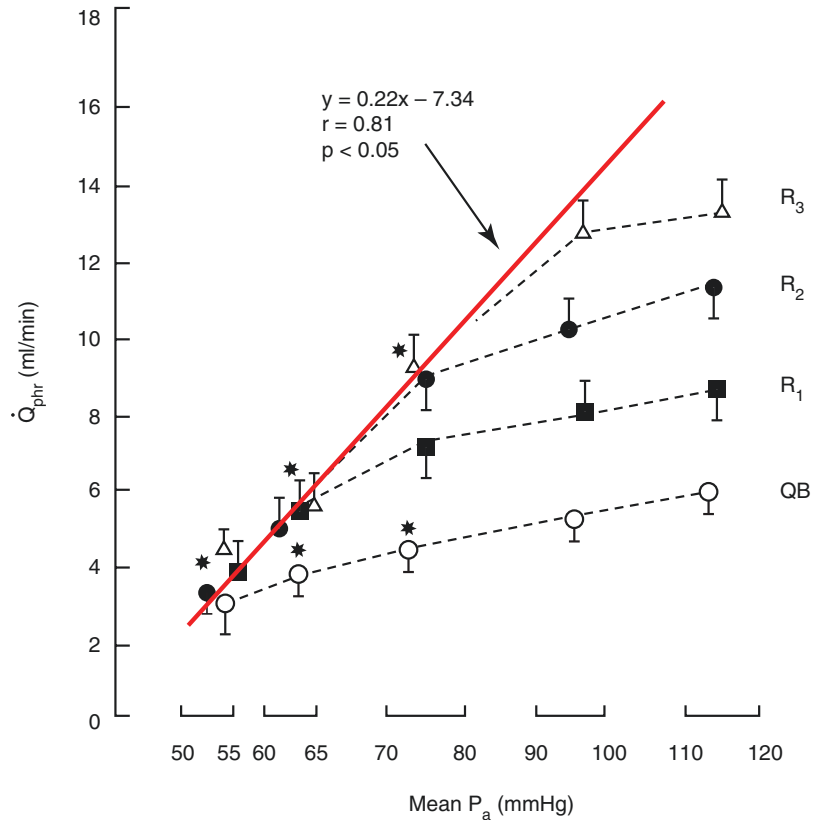
Fig. 16.1 Changes in blood flows to respiratory muscles with increasing resistance loading. The diaphragm has the greatest response and reached over 2 ml/min/g of tissue. (From Robertson et al. (1977c) Used with permission of the American Society of Clinical Investigation)

whole body during exercise (Åstrand et al. 1964). In this study, blood flow to the diaphragm was measured with a flow probe on the phrenic artery, and arterial pressure was varied between 50 to 110 mmHg by infusing or removing blood. Diaphragmatic contractions were spontaneous. Measurements were made at quiet breathing and three levels of increasing airway resistance. Diaphragmatic blood flow increased with each increase in the load, and the flow remained constant over a range of arterial pressures indicating that flow was being regulated to match the O_2 demand that was required for that level of energy consumption. For this to occur, the phrenic vascular resistance vessels had to dilate to keep the flow constant. However, an arterial pressure eventually was reached at which the vessels could not dilate more. This gives the maximal conduc-

tance (or minimal resistance) for this vasculature. Once this value is reached, a further fall in arterial pressure must be associated with a fall in blood flow.

Field et al. attempted to measure O_2 consumption of respiratory muscles in patients with cardiorespiratory disease who were mechanically ventilated and close to being weaned (Field et al. 1982). Measurements first were made while all breaths were triggered. The respiratory rate then was increased so that all breaths were fully supported. The authors argued that the difference in VO_2 between the two conditions indicated the energy consumption of the respiratory muscles. However, it also is possible that their general condition changed when they were put back on mechanical support. For example, mechanical ventilation could have reduced anxiety from the respiratory distress-associated breathlessness when they were breathing on their own, and this could have contributed to the energy cost by altering the tone of non-respiratory muscles. VO_2 decreased from 312 ± 90 ml/min to 246 ± 38 ml/min, which by their estimate gave an respiratory muscle VO_2 consumption of 75 ± 82 ml/min, but the range with this crude measure was large - 8 to 286 ml/min. In comparison, in normal resting adults, VO_2 is thought to be 5 to 10 ml/min, or about 1 to 3% of total body VO_2 . On the basis of their work, the authors concluded that in these patients respiratory muscles consumed 24% of total VO_2 . They further concluded that in patients with limited cardiac reserves and increased work of breathing, or inefficient work of breathing, mechanically supporting ventilation could leave a considerable amount of O_2 to be distributed to other tissues. This led to the hypothesis that when blood supply is limited in shock, and the work of breathing is increased because of pulmonary edema, respiratory acidosis, and increased central drive, inability to increase respiratory muscles blood flow can lead to respiratory muscle fatigue and failure, which without mechanical support would be an important cause of death in shock. Second, if the respiratory muscles take up a significant proportion of the limited blood flow in shock, mechanical ventilation could free up blood flow for vital organs. To analyze this

Fig. 16.2 Blood flow versus pressure relationship of isolated diaphragmatic vasculature with airway resistances. The different blood pressures were obtained by removing or infusing blood. Increasing the load shifted the flow–pressure relationship upward. Phr = phrenic artery. QB = quiet breathing, R1 to R3 indicates increasing resistive loading. The red line indicates the maximal vascular conductance (minimal resistance). When reached, a fall in arterial pressure decreases blood flow. See text for details. (From Hussain et al. (1988a)). <https://journals.physiology.org/author-info.permissions>



hypothesis, it is worthwhile to first put these numbers into a quantitative context. A normal young male of average body size can achieve a peak $\dot{V}O_2$ in the 3000 to 4000 ml/min range. Thus, an additional cost of even 300 ml/min of O_2 per minute, which is higher than in any of the subjects in the study by Field et al. (Field et al. 1982), is still very small compared to the aerobic reserves of the body as a whole. The aerobic capacity of a patient would have to be severely limited before this would become clinically significant. In any case, this hypothesis led to a number of experiments to provide more quantitative data that has allowed us to better understand the constraints of the system.

The question of respiratory muscle fatigue as a cause of respiratory muscle failure was addressed in a case series by Cohen et al. (Cohen et al. 1982). Muscle fatigue is defined in physiological terms as a failure of motor output for a given neural input and reversible by rest. As such, the hallmark of fatigue is evidence of

decreasing muscle force despite the same or increasing neural electrical activity. This pattern indicates that the problem is at or beyond the neural-muscular junction. It was not possible in the study to wait for true physiological respiratory fatigue to actually develop for the obvious clinical reason that the patients would have been apneic. Instead, a change in the ratio of high- to low-frequency EMG signals was used as an early warning sign of impending fatigue. I will come back to this point later. The authors found that 7 of the 12 patients met their fatigue criteria. PCO_2 rose and pH fell in all subjects. The clinical manifestations of their “pre-failure” state are still relevant today. The respiratory rate and minute ventilation progressively increased before muscles started to fail (Fig. 16.3). This indicates that the work of breathing actually increased. Normally, the abdomen goes outward with spontaneous breaths because the descent of the diaphragm increases abdominal pressure, but when the diaphragm does not contract, and only inter-

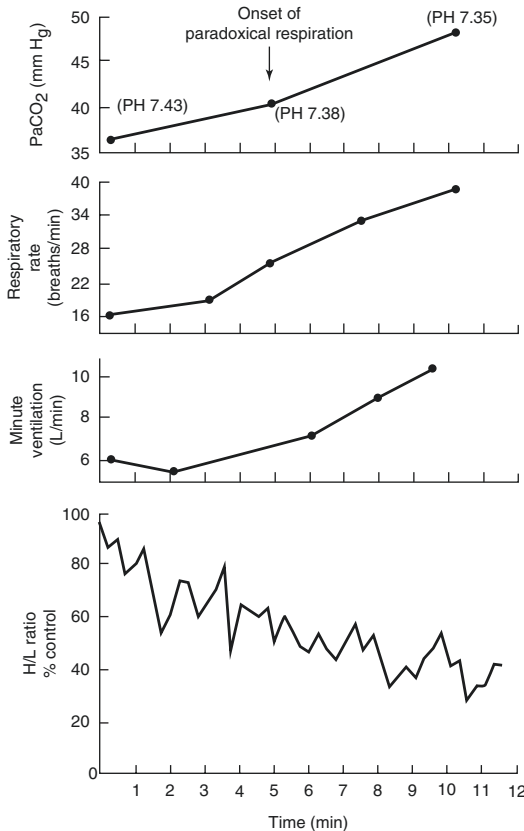


Fig. 16.3 Changes in respiratory parameters during a weaning trial. Example of one subject over 12 minutes. The arterial PCO₂ (PaCO₂) progressive increases and pH falls (top). Within 3 minutes, the respiratory rate began to increase (second tracing). Despite the increase in respiratory rate, total ventilation did not change until 6 minutes, indicating a likely fall in tidal volume (third tracing). There was a progressive decline in the high to low frequency of the EMG right from the start of the trial. (From Cohen et al. (1982). Used with permission of Elsevier)

costal muscles are used, the decrease in Pp with inspiration pulls the abdomen inward. This is called “abdominal paradox” and it occurred in 6 of the 7 subjects who were said to have fatigue. The third sign was respiratory alternans in which there is alternating abdominal and rib cage breathing; this occurred in 4 of the 7 subjects classified as having fatigue. Although not calculated in the study, based on the change in ventilation and change in respiratory rate, it is likely that tidal volumes also fell, as shown by others (Tobin et al. 1986), (Yang and Tobin 1991).

The fatigue hypothesis was studied in an animal model of cardiogenic shock which was produced by creating a controlled cardiac tamponade (Aubier et al. 1981). Following the tamponade, total ventilation increased and PCO₂ initially decreased. Of clinical importance, prior to death, the mean PCO₂ rose back to the normal 40 mmHg, and animals generally suddenly became apneic before PCO₂ increased above normal. The clinical message is that patients need to be intubated when in distress, and clinicians should not wait for PCO₂ to rise above normal. In this model, there were clear signs of respiratory muscle fatigue as indicated by a rise in phrenic neural activity and electrical activity of the diaphragmatic muscle with a decrease in diaphragmatic pressure generation (Fig. 16.4).

In a subsequent study, the authors used the same model to measure respiratory muscle and major organ blood flow during shock with and without mechanical ventilation (Fig. 16.5) (Viiris et al. 1983). This represented a direct test of the Cohen et al. hypothesis (Cohen et al. 1982). In the non-ventilated animals, blood flow measurements were made before respiratory muscles failed. During shock, total respiratory muscle blood flow doubled from approximately 60 ml/min at rest to 127 ml/min and because of the severe reduction of cardiac output to only 30% of the baseline level, these muscles consumed 21% of the total available cardiac output. It may seem that this is similar to what was observed by Cohen et al. (Cohen et al. 1982), but it must be appreciated that in this case cardiac output only was about 25% of normal. When mechanical ventilation was instituted, total respiratory muscle blood flow markedly decreased to 21 ml/min and accounted only for 3% of cardiac output (Fig. 16.5). However, because the total cardiac output was very low, the amount of blood flow redistributed to vital organs was very modest (Fig. 16.5). The rate of rise of lactate was reduced by mechanical ventilation but it still rose. This emphasizes that the primary role of mechanical ventilation is to ensure maintenance of ventilation when there is impending respiratory failure and death, but mechanical ventilation only pro-

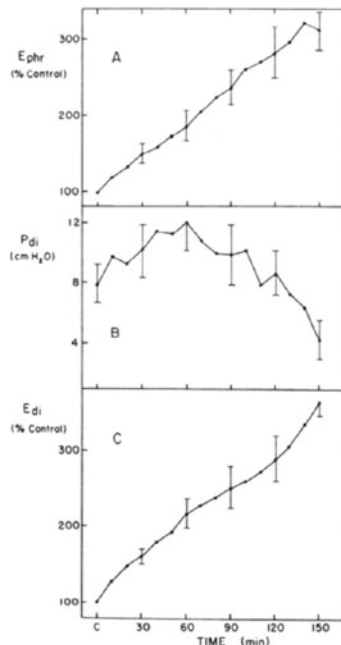
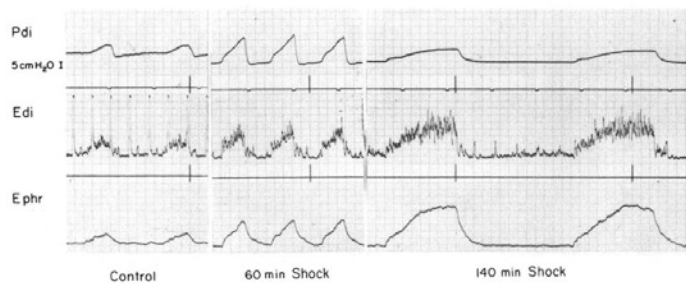


Fig. 16.4 Development of diaphragmatic fatigue following induction of cardiogenic shock with a controlled tamponade. The left shows a sample tracing from an animal in cardiogenic shock. Pdi = transdiaphragmatic pressure, Edi = diaphragm electromyogram (% of relaxed state), and Ephr = phrenic nerve electrogram. At 140 min, the Pdi

decreased with an increase in Edi and Ephr. The right side shows the mean data. After 60 minutes of tamponade, there was a steady decrease in Pdi while Ephr and Edi continued to increase. These are the classic signs of the development of muscle fatigue. (From Aubier et al. (1981). Used with permission of The American Physiological Society)

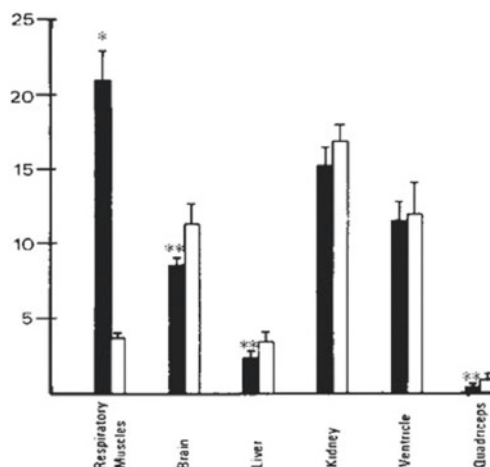
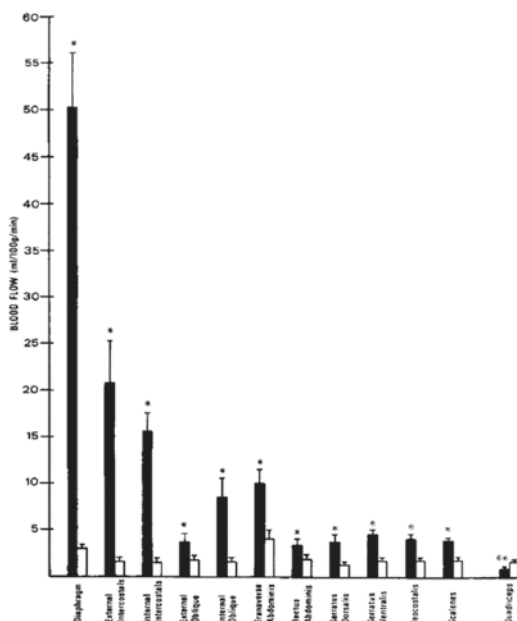


Fig. 16.5 Blood flow to respiratory muscles and selected organs during cardiogenic shock induced by tamponade with and without mechanical ventilation. On the left, respiratory muscle blood flow is markedly reduced by mechanical ventilation. However, on the right, the increase

in flow to other tissues in these animals with mechanical ventilation were modest and only significant in the brain, liver, and skeletal muscle (quadriceps). (From Viiris et al. (1983). Used with permission of the American Society for Clinical Investigation)

vides minimal blood flow support to other organs. Protection of other organs requires an increase in cardiac output. As will be discussed below, mechanical ventilation may have an unanticipated role. By stopping respiratory muscle activity, it decreases thin fiber afferent activity from respiratory muscles and their negative impact on the drive to breathe and distribution of blood flow (Magder 2001). It also is worth noting that the blood flow to the diaphragm in this study was still much less than the maximum flow that can be achieved when the diaphragm is paced at a high frequency (Buchler et al. 1985b) or with a very high resistance (Robertson et al. 1977c), which means that there still were reserves in blood flow. As also observed by Casan et al., maximal O₂ consumption by the respiratory muscles did not reach an estimated critical common value with the two types of maximal loading of respiratory muscle, and the increased energy demand was not a cause of dyspnea (Casan Pere et al. 1997).

Similar studies were performed by Hussain et al. in animals with septic shock induced by endotoxin (Hussain et al. 1986). In their animal study, endotoxin produced a marked fall in cardiac output which is not the case in most human cases of sepsis. There was a consequent rise in ventilation, likely due to direct central stimulation plus the rising lactic acidemia. The pattern of respiratory failure was very similar to that seen in tamponade-induced shock (Aubier et al. 1981); the neural output and EMG activity of the diaphragm increased, but force generation decreased. The authors argued that respiratory muscle failure is the major cause of death in sepsis unless mechanical ventilation support is instituted. Just as in the case of cardiogenic shock, clinicians should not wait for a rise in PCO₂ before deciding to intubate a patient with septic shock.

These investigators also measured respiratory muscle blood flow in the septic animals (Hussain and Roussos 1985). Of note, the fall in cardiac output was not as severe as in the cardiogenic shock study by Aubier et al. (Aubier et al. 1981) and Viiris et al. (1983). Respiratory muscle blood flow rose to 100 ml/min, which is similar to what was seen in cardiogenic shock and the distribution of blood flow to other organs, too, was simi-

lar. In most of the animals, the flow to the diaphragm was close to the maximum conductance value for diaphragmatic flow, as assessed by Reid and Johnson (Reid and Johnson Jr. 1983). The authors further studied the effect of mechanical ventilation on the distribution of blood flow during the induced septic shock. As with cardiogenic shock, mechanical ventilator support markedly decreased respiratory blood flow and redistributed blood flow to other regions (Hussain and Roussos 1985). However, regulation of the redistributed blood flow was disturbed. Blood flow to the brain and gut increased, but renal blood flow did not change and blood flow to a sample nonworking skeletal muscle increased, which indicates maldistribution of blood flow. Blood flow to the myocardium also did not increase but this likely was due to decreased demand for blood flow with the mechanical respiratory support.

Boczkowski et al. showed that force generation in response to repeated stimulation fell much faster in isolated strips of diaphragm from septic rats than in control animals (Boczkowski et al. 1988). Similarly, DeBoisblanc et al. found that the maximal strength of the diaphragmatic strips in vivo from rats fell by 40% at 270 minutes after an injection of *E. coli*. These studies in isolated strips of muscle indicate that the fall in diaphragm force production is not just flow-related.

The message from this review of muscle failure in sepsis is that respiratory failure is related to the intrinsic failure of muscle function and likely is not related to a limitation of blood flow. This means that there is little to be gained from the redistribution of blood flow to other regions by mechanical ventilation. Mechanical ventilator support is needed in sepsis because the limited functional capacity of the muscles as part of the generalized inflammatory process results in respiratory muscles failure. In my experience, it can be quite striking how quickly respiratory muscle function recovers once the inflammatory process recedes. In less than 12 to 24 h, a patient who had limited diaphragmatic function from sepsis has sufficient respiratory muscle function to be extubated. This indicates that the reason for muscle weakness is not damaged tissue but rather

impairment of the contractile machinery, which seems to be a rapidly reversible biochemical process. Importantly, muscle inactivity can rapidly result in muscle atrophy. It thus is important to recognize that muscle function has improved and allowed the patient to begin triggering breaths, which has been shown to reduce muscle atrophy (Sassoon et al. 2002). Prolonging mandatory mechanical unnecessarily may just end up prolonging the recovery period.

Respiratory muscle blood flow also was studied in a model that combined pulmonary edema and cardiogenic shock (Rutledge et al. 1988). Lung injury was induced by injecting oleic acid intravenously. This produces a capillary leak syndrome; cardiac depression was created with a controlled tamponade (Rutledge et al. 1985). In the first step, when pulmonary edema was created but cardiac function still was normal, respiratory efforts markedly increased, and blood flow to the diaphragm increased almost threefold, similar to what was seen in the shock studies (Fig. 16.6) (Viiris et al. 1983; Hussain and Roussos 1985), but there was no significant changes of blood flow to any of the other respira-

tory muscles, except for the internal intercostal (an expiratory muscle). With the strong respiratory effort, VO_2 of the diaphragm doubled, but VO_2 for the whole body increased only by 13%. When tamponade was applied, blood flowed to all regions of the body, but only by moderate amounts in respiratory muscles. When the respiratory muscle began to fail, and PTI decreased, there was little change in respiratory muscle blood flow. However, blood flow to the kidney decreased further. This might have been due to a sympathetic effect on the distribution of blood flow induced by an increase in diaphragmatic afferent signals as discussed further below. In this study, since respiratory muscle blood flow did not change much with the addition of the tamponade, respiratory muscle blood flow became a larger percent of the total cardiac output. As in the Viiris study (Viiris et al. 1983), reducing blood flow to the respiratory muscles with use of mechanical ventilation only would have provided an additional 70 ml/min to other tissues. Blood flow to the diaphragm in this study was compared to maximal diaphragmatic arterial conductance, which as discussed above, indicating the O_2

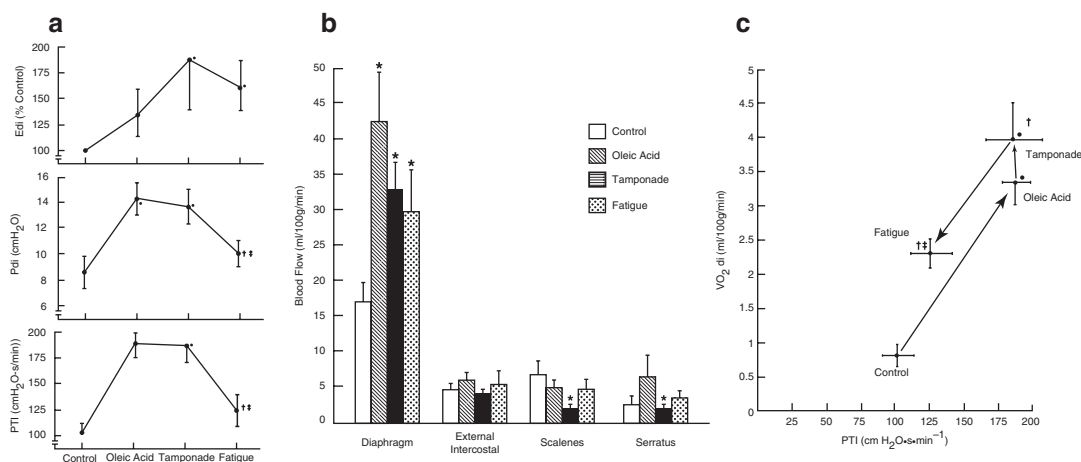


Fig. 16.6 Diaphragmatic energetics and blood flow during pulmonary edema and hypotension (tamponade). (a) Diaphragmatic electromyogram (Edt) as percent of baseline, inspiratory diaphragmatic generated pressure (Pdi), and pressure time index (PTI) at baseline, with pulmonary edema induced by oleic acid, with the addition of cardiac tamponade to reduce cardiac output to 25% of baseline, and when the muscle fails as indicated by the same EMG but falling pressure generation. (b) Blood flow

to inspiratory muscles. Diaphragmatic blood flow tripled with pulmonary edema fell somewhat with addition of tamponade (this was not significant in the study) and was not lower at the time of fatigue. (c) shows diaphragmatic O_2 consumption (VO_2 di) versus PTI. VO_2 di increased fourfold with pulmonary edema, changed further by only a small amount during tamponade and fell considerably with muscle failure. (From Rutledge et al. (1988)). <https://journals.physiology.org/author-info/permissions>

delivery value at which blood flow becomes dependent upon arterial pressure. During the tamponade condition, the flow–pressure values were very close to this predicted limit (Chapters 8 and 31) (Magder 1986). It is not possible to know if at this stage the diaphragm needed more flow but could not obtain it, or if it just did not need it. However, the results indicate that when cardiac output is normal, even under conditions in which there is a marked increase in respiratory muscle demand, there still likely are adequate blood flow reserves to supply the respiratory muscles, even without a large increase in cardiac output. It thus is unlikely that respiratory muscle blood flow is a limiting factor for respiratory muscle function unless there is a very marked decrease in cardiac output, in which case every other organ fails too. It also has been shown that the diaphragm has large anaerobic reserves and can continue to contract at basal levels for a few hours with its flow cut off (Teitelbaum et al. 1992a).

In these severe animal models, the falling TTdi with rising neural input clearly indicate that respiratory muscle fatigue was present. However, the progressively rising respiratory rate and fall in tidal volume are major factors in and of themselves because this pattern of breathing greatly increased the energy demands of the respiratory muscle. Thus, it is not that that muscles fail at some constant high-energy demand, but rather there is a progressive increase in energy demand that “drives” the animals to the limit of the capacity of their respiratory muscles. A careful study of the fatigue hypothesis which addresses this issue was undertaken by Laghi et al. (2003) in patients being weaned from a ventilator. They measured transdiaphragmatic twitch pressures by stimulating the phrenic nerves and found that in most of the patients who had failing respiratory muscles the diaphragms were weaker at the start and the force generated by the twitches did not decrease during the weaning trial, arguing against true muscle fatigue being the cause. Instead, the respiratory load and demand on the diaphragm increased with no development of low-frequency fatigue on the diaphragmatic EMG.

As discussed above, a rise in respiratory rate is very energy demanding (Buchler et al. 1985b). It shortens the time for diaphragmatic blood flow (Hussain et al. 1988a; b), increases dead space, and perhaps most importantly, when there is increased airway resistance it leads to air trapping, hyperinflation, and consequent decreased thoracic compliance. All these increase the load on the respiratory system and lead to respiratory distress and muscle failure. Thus, patients likely “drive” themselves into fatigue if they are allowed to continue. The failure occurs because of an excess respiratory load and work of breathing rather than inadequate blood flow.

Role of Afferent Fibers

Since rapid shallow breathing is so inefficient, and can actually “drive” a patient into respiratory failure, why does it happen? All skeletal muscles have thin-fiber afferent nerves that respond to noxious signals in the muscle such as increased potassium ion, lactate, arachidonic acid, increased osmolality, as well as mechanical stretch. These afferents send signals to central nuclei in the brain that send efferent signals to increase the drive to breath, and also increase sympathetic activity which can change the distribution of blood flow (Magder 2001; Kaufman et al. 1983a, b; Hussain and Roussos 1995; Teitelbaum et al. 1993a, b; Hussain et al. 1991a). During normal exercise, the metabolites that accumulate in the skeletal muscles activate these nerve terminals and provide important feedback to the brain that helps match respiratory activity to the metabolic needs and helps maintain normal PCO_2 and pH. This includes increased respiratory rate and total ventilation to deal with the increased PCO_2 production, and increased sympathetic activity that constricts vessels in nonworking tissues and redistributes blood flow to the working muscles, including the working respiratory muscles. During exercise, these afferent responses are appropriate and adaptive. However, when these afferents only are activated in respiratory muscles because of the increased respiratory activity in shock or with

compromised respiratory function, a vicious cycle can develop. The increasing respiratory muscle activity drives a further increase in respiratory muscle activity, which generates more afferent signaling, until the patient is driven into respiratory failure from the increase in respiratory rate and low tidal volumes. The activity of this pathway has been demonstrated by injecting capsaicin into the whole animal or into the isolated vasculature of the diaphragm (Figs. 16.7 and 16.8). Capsaicin causes discharge of the neurotransmitter Substance P, which is the central mediator of the afferent pathway. Of importance, once Substance P is depleted, it takes weeks for it to be restored to normal levels and during that time, the afferent signals are no longer present (Teitelbaum et al. 1993b; Hussain et al. 1991a, b). This allowed use of capsaicin in experimental models to evaluate the role of these afferent pathways. At low doses, capsaicin can be used to activate afferent activity and observe the ventilator and vascular responses reflexes (Hussain et al. 1990a; b). At

high doses, capsaicin can be used to deplete Substance P in the pathways and thereby “deafferent” an organ or even the whole animal (Teitelbaum et al. 1993a, b). This shows that in the absence of thin fiber afferent activity there is no increase in respiratory rate and drive when the diaphragm is made ischemic and is failing (Teitelbaum et al. 1992b). Thus, the action of the afferent pathway provides a plausible mechanism to explain the progressively increasing inefficient breathing pattern that drives patients into respiratory failure. The respiratory muscles are not failing because of the inability to handle the workload but rather because the afferent activity is driving them to require even higher levels of respiratory muscle activity which become truly beyond their capacity. This hypothesis is consistent with the effectiveness of weaning index during a spontaneous breathing trial as a predictor failure of extubation (Yang and Tobin 1991). The two key components of this index are the increase in respiratory rate and decrease in tidal volume. The

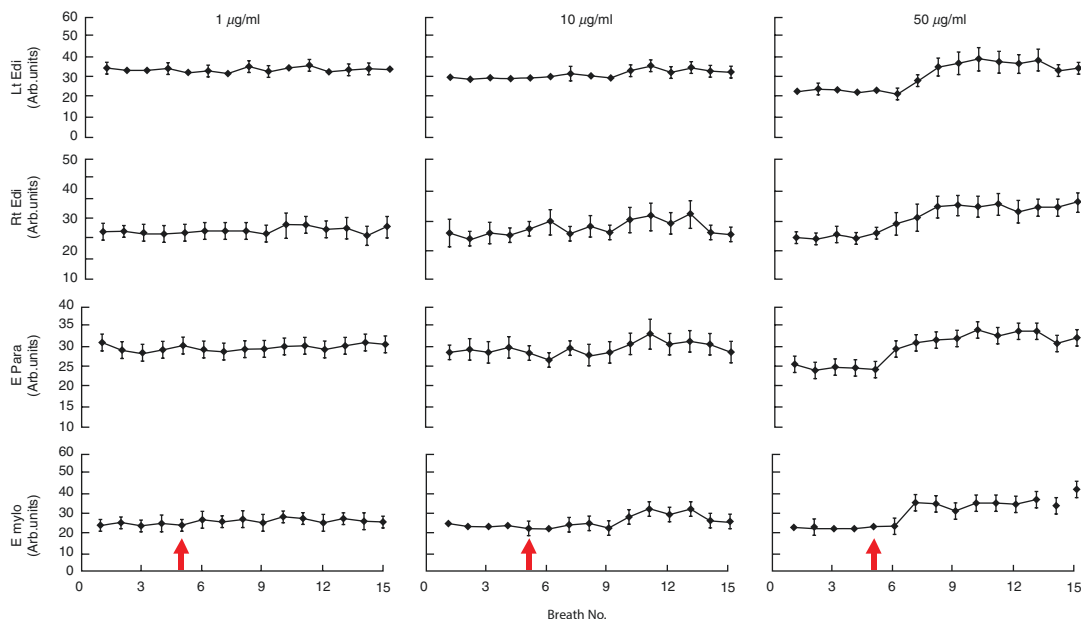


Fig. 16.7 Effect of activation of diaphragmatic afferents and the consequent increase in respiratory drive after injection of capsaicin into the phrenic artery. Changes in electromyogram activity (E) of inspiratory muscles. Three doses of capsaicin were given in 1, 10, and 50 µg. The top is the left (Lt) and next line the right (Rt) sides of the dia-

phragm, the third the parasternal muscle (para) and the last the mylohyoid (mylo). There was a dose response to capsaicin. The arrow marks the time of the ejection. (From Hussain et al. (1990c)). <https://journals.physiology.org/author-info/permissions>

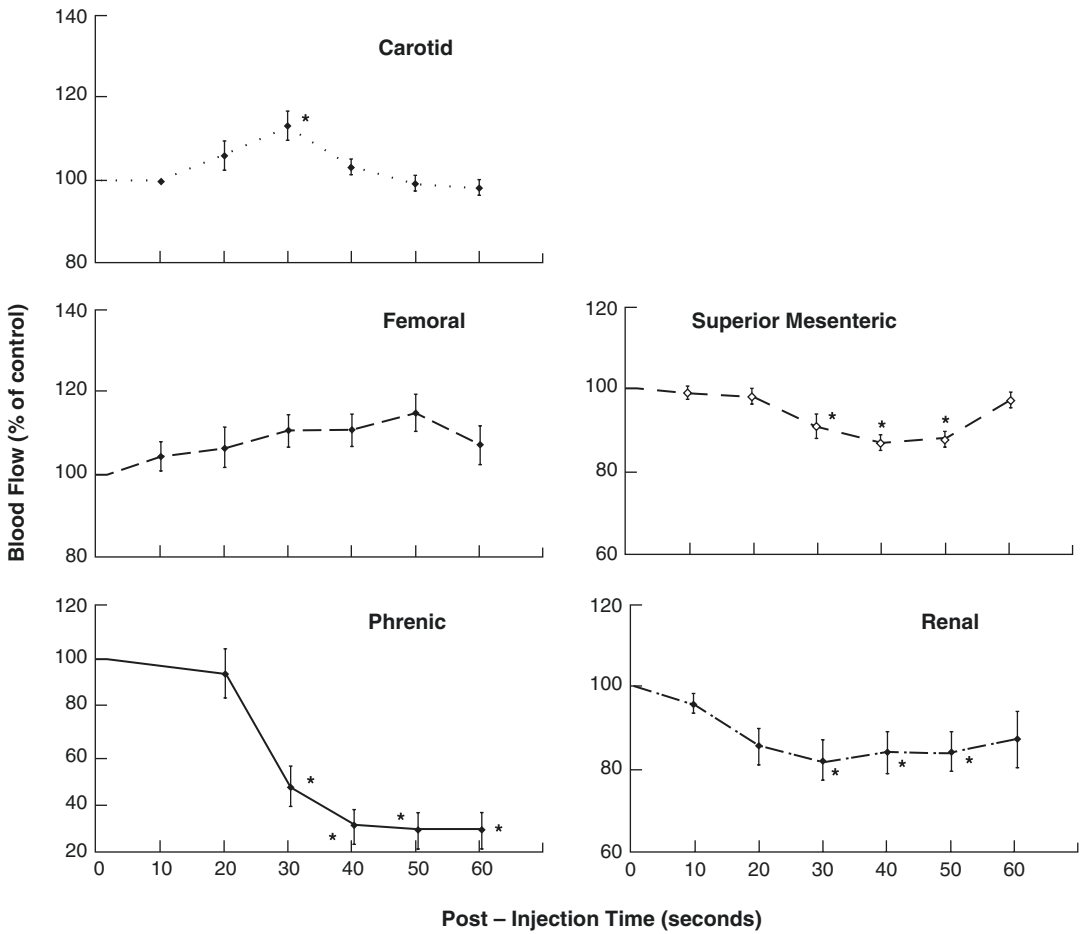


Fig. 16.8 Effect of activation of diaphragmatic afferents with capsaicin on blood flow distribution. 1 mg of capsaicin was injected into the phrenic artery. The mean arterial pressure rose from 96 to 120 mmHg, the heart rate went from 133 b/min to 146, and there was no change in aortic flow. Blood flows were measured with Doppler flow probes. Blood flow went up in the carotid and femoral

arteries, likely because of the induced rise in arterial pressure, it went down in the phrenic artery because of the local effect of capsaicin. It went down in the superior mesenteric and renal arteries, likely because of the centrally increased sympathetic activity in these regions. (From Hussain et al. (1990d)). <https://journals.physiology.org/author-info/permissions>

afferent reflex would be expected to increase the respiratory rate, and for a constant need for ventilation, decrease tidal volume and thus augment the maladaptive process for this situation. It also is quite likely that the activation of respiratory muscle afferents changes the distribution of blood flow as seen in the animal studies on cardiogenic shock (Viiris et al. 1983; Rutledge et al. 1985) (Fig. 16.5) and sepsis (Hussain and Roussos 1985). The redistribution with mechanical ventilation thus could have been due to suppression of afferent signals from the working respiratory muscles rather than a simple passive redistribu-

tion of blood flow. A clinical caveat from the afferent hypothesis is that sedation can be used to blunt the maladaptive response from the afferent signals and prevent respiratory muscle failure when weaning a patient with limited reserves.

Conclusion

In summary, the blood flow reserve of the respiratory muscles is large and it is likely that blood flow limitation is a significant cause of respiratory muscle failure only when cardiac output is

markedly reduced and all other organs are failing too. It also means that there likely is little benefit from blood flow redistribution to other organs when a patient in shock is mechanically ventilated and their own respiratory effort is removed. Accordingly, this should not be a rationale for instituting mechanical ventilation. However, the mechanical ventilation has other important effects for a patient in shock. First, the inability of the respiratory muscles to maintain adequate ventilation will result in respiratory arrest, and mechanical ventilation is essential to maintain life. Second, mechanical ventilation reduces the metabolic activity of the respiratory muscles, which reduces their afferent traffic and its negative effect on respiratory drive and distribution of blood flow. Third, in the septic patient, mechanical ventilation is critical because of the reduced force capacity of respiratory muscles, which means that they have a greatly reduced fatigue threshold. Failure of respiratory muscles is sepsis, which is not based on inadequate blood flow but rather due to intrinsic muscle failure. It can occur rapidly and without warning. Fourth, reducing large respiratory efforts can be very important for avoiding large changes in pleural and transpulmonary pressure, which can have important consequences for heart–lung interaction (Chap. 18).

References

- Aliverti A, Cala SJ, Duranti R, Ferrigno G, Kenyon CM, Pedotti A, et al. Human respiratory muscle actions and control during exercise. *J Appl Physiol* 1985; 1997;83(4):1256–69.
- Arora NS, Rochester DF. Effect of body weight and muscularity on human diaphragm muscle mass, thickness, and area. *J Appl Physiol Respir Environ Exerc Physiol*. 1982;52(1):64–70.
- Astrand PO. Quantification of exercise capability and evaluation of physical capacity in man. In: Sonnenblick EH, Lesch M, editors. Exercise and heart disease. A progress in cardiovascular disease reprint. New York: Grune and Stratton; 1976. p. 87–103.
- Astrand PO, Rodahl K. Physiological bases of exercise. *Textbook of work physiology*. Montreal: McGraw-Hill; 1977.
- Åstrand P-O, Cuddy TE, Saltin B, Stenberg J. Cardiac output during submaximal and maximal work. *J Appl Physiol*. 1964;19(2):268–74.
- Aubier M, Trippebach T, Roussos C. Respiratory muscle fatigue during cardiogenic shock. *J Appl Physiol*. 1981;51:494–8.
- Bellemare F, Wight D, Lavigne CM, Grassino A. Effect of tension and timing of contraction on the blood flow of the diaphragm. *J Appl Physiol Respir Environ Exerc Physiol*. 1983;54(6):1597–606.
- Boczkowski J, Dureuil B, Brauger C, Aubier M. Effects of sepsis on diaphragmatic function in rats. *Am Rev Respir Dis*. 1988;138:260–5.
- Brazier J, Cooper N, Buckberg G. The adequacy of subendocardial oxygen delivery: the interaction of determinants of flow, arterial oxygen content and myocardial oxygen need. *Circulation*. 1974;49(5):968–77.
- Buchler B, Magder SA, Roussos C. Effect of positive abdominal and negative pleural pressure on diaphragmatic blood flow during intermittent contraction. *Physiologist*. 1982;
- Buchler B, Magder SA, Roussos C. Effects of contraction frequency and duty cycle on diaphragmatic blood flow. *J Appl Physiol*. 1985a;58(1):265–73.
- Buchler B, Magder S, Roussos C. Effects of contraction frequency and duty cycle on diaphragmatic blood flow. *J Appl Physiol*. 1985b;58:265–73.
- Casan P, Carlos C, Kearon Clive, Campbell EJ, Kieran J Killian Kieran Contribution of respiratory muscle oxygen consumption to breathing limitation and dyspnea. *Can Respir J* 1997;2(2):6.
- Cingolani HE, Pérez NG, Cingolani OH, Ennis IL. The Anrep effect: 100 years later. *Am J Phys Heart Circ Phys*. 2013;304(2):H175–H82.
- Cohen CA, Zigelbaum G, Gross D, Roussos C, Macklem PT. Clinical manifestations of inspiratory muscle fatigue. *Am J Med*. 1982;73:308–16.
- Cossette I, Monaco P, Aliverti A, Macklem PT. Chest wall dynamics and muscle recruitment during professional flute playing. *Respir Physiol Neurobiol*. 2008;160(2):187–95.
- Field S, Kelly SM, Macklem PT. The oxygen cost of breathing in patients with cardiorespiratory disease. *Am Rev Respir Dis*. 1982;126(1):9–13.
- Freedman S, Campbell EJ. The ability of normal subjects to tolerate added inspiratory loads. *Respir Physiol*. 1970;10(2):213–35.
- Hussain SNA, Roussos C. Distribution of respiratory muscle and organ blood flow during endotoxic shock in dogs. *J Appl Physiol*. 1985;59:1802–8.
- Hussain SNA, Roussos C. The role of small-fiber phrenic afferents in the control of breathing. In: Roussos C, editor. *The thorax*. 2nd ed. New York: Marcel Dekker Inc.; 1995. p. 860.
- Hussain SNA, Graham R, Rutledge F, Roussos C. Respiratory muscle energetics during endotoxic shock in dogs. *J Appl Physiol*. 1986;60:486–93.
- Hussain S, Roussos C, Magder SA. Autoregulation of diaphragmatic blood flow in dogs. *J Appl Physiol*. 1988a;64:329–36.
- Hussain SNA, Roussos C, Magder S. Autoregulation of diaphragmatic blood flow in dogs. *J Appl Physiol*. 1988b;64:329–36.

- Hussain SNA, Chatillon A, Magder S, Roussos C. The respiratory and vascular responses evoked by chemical activation of small fiber phrenic nerve afferents in dogs. *Chest*. 1990a;97:44s–5s.
- Hussain SNA, Magder SA, Chatillon A, Roussos C. Chemical activation of thin-fiber phrenic afferents: respiratory responses. *J Appl Physiol*. 1990b;69(3):1002–11.
- Hussain S, Magder S, Chatillon A, Roussos C. Chemical activation of thin-fiber phrenic afferents: the respiratory responses. *J Appl Physiol*. 1990c;69(3):1002–11.
- Hussain S, Chatillon A, Comtois A, Roussos C, Magder SA. Chemical activation of thin-fiber phrenic afferents: the vascular responses. *Am Rev Respir Dis*. 1990d;141:A64.
- Hussain SNA, Chatillon A, Comtois A, Roussos C, Magder S. Chemical activation of thin-fiber phrenic afferents: the cardiovascular responses. *J Appl Physiol*. 1991a;70:159–67.
- Hussain S, Ward M, Gatensby A, Roussos C, Deschamps A. Respiratory muscle activation by limb muscle afferent stimulation in anesthetized dogs. *Resp Physiol*. 1991b;84:185–98.
- Kaufman MP, Longhurst JC, Rybicki J, Wallach JH, Mitchell JH. Effects of static muscular contraction on impulse activity groups III and IV afferents in cats. *J Appl Physiol Res Environ Exerc Physiol*. 1983a;55:105–12.
- Kaufman MP, Longhurst JC, Rybicki KJ, Wallach JH, Mitchell JH. Effects of static muscular contraction on impulse activity of groups III and IV afferents in cats. *J Appl Physiol*. 1983b;55(1 Pt 1):105–12.
- Laghi F, Cattapan SE, Jubran A, Parthasarathy S, Warshawsky P, Choi YS, et al. Is weaning failure caused by low-frequency fatigue of the diaphragm? *Am J Respir Crit Care Med*. 2003;167(2):120–7.
- Laughlin MH, Davis MJ, Secher NH, van Lieshout JJ, Rce-Esquivel AA, Simmons GH, et al. Peripheral circulation. *Compr Physiol*. 2012;2(1):321–447.
- Lockhat D, Magder SA, Roussos C. Collateral sources of costal and crural diaphragmatic blood flow. *J Appl Physiol*. 1985;59(4):1164–70.
- Magder SA. Pressure-flow relations of diaphragm and vital organs with nitroprusside-induced vasodilation. *J Appl Physiol*. 1986;61:409–16.
- Magder S. Effects of respiratory muscle afferent on the breathing and the afferent hypothesis. In: Scharf SM, Pinsky MR, Magder S, editors. *Respiratory-circulatory interactions in health and disease*. 2nd ed. New York: Marcel Dekker, Inc.; 2001. p. 405–25.
- Magder SA, Lockhat D, Luo BJ, Ducas D, Roussos C. Blood flow distribution in hypotensive (tamponade) and inspiratory elastic loading. *Fed Proc*. 1983;42:1855.
- Magder S, Serri K, Verscheure S, Chauvin R, Goldberg P. Active expiration and the measurement of central venous pressure. *J Intensive Care Med*. 2016;
- Martin JG, De TA. The behaviour of the abdominal muscles during inspiratory mechanical loading. *Resp Physiol*. 1982;50(1):63–73.
- Parthasarathy S, Jubran A, Tobin MJ. Cycling of inspiratory and expiratory muscle groups with the ventilator in airflow limitation. *Am J Respir Crit Care Med*. 1998;158(5 Pt 1):1471–8.
- Reid MB, Johnson RL Jr. Efficiency, maximal blood flow, and aerobic work capacity of canine diaphragm. *J Appl Physiol*. 1983;54:763–72.
- Robertson CH, Eschenbacher WL, Johnson RL. Respiratory muscle blood flow distribution during expiratory resistance. *J Clin Invest*. 1977a;60:473–80.
- Robertson CH, Pagel MA, Johnson RL. The distribution of blood flow, oxygen consumption and work output among the respiratory muscles during non-obstructed hyperventilation. *J Clin Invest*. 1977b;59:43–59.
- Robertson CH, Foster GH, Johnson RL. The relationships of respiratory failure to the oxygen consumption, lactate production by, and distribution of blood flow among respiratory muscles during increasing inspiratory resistance. *J Clin Invest*. 1977c;59:31–42.
- Rochester DF, Bettini G. Diaphragmatic blood flow and energy expenditure in the dog. Effects of inspiratory airflow resistance and hypercapnia. *J Clin Invest*. 1976;57(3):661–72.
- Rutledge F, Hussain S, Roussos C, Magder SA. Diaphragmatic blood flow and oxygen delivery in pulmonary edema and hypotension. *Clin Invest Med*. 1985;8:183.
- Rutledge F, Hussain S, Roussos C, Magder SA. Diaphragmatic energetics and blood flow during pulmonary edema and flow hypotension. *J Appl Physiol*. 1988;64(5):1908–15.
- Sanna A, Bertoli F, Misuri G, Gigliotti F, Iandelli I, Mancini M, et al. Chest wall kinematics and respiratory muscle action in walking healthy humans. *J Appl Physiol* (1985). 1999;87(3):938–46.
- Sassoon CS, Caiozzo VJ, Manka A, Sieck GC. Altered diaphragm contractile properties with controlled mechanical ventilation. *J Appl Physiol*. 2002;92(6):2585–95.
- Teitelbaum JS, Magder SA, Roussos C, Hussain SNA. Effects of diaphragmatic ischemia on the inspiratory motor drive. *J Appl Physiol*. 1992a;72:447–54.
- Teitelbaum JS, Magder SA, Roussos C, Hussain SNA. Effects of diaphragmatic ischemia on the inspiratory motor drive. *J Appl Physiol*. 1992b;72(2):447–54.
- Teitelbaum J, Borel CO, Magder S, Traystman RJ, Hussain SNA. Effect of selective diaphragmatic paralysis on the inspiratory motor drive. *J Appl Physiol*. 1993a;74:2261–8.
- Teitelbaum J, Vanelli G, Hussain SNA. Thin-fiber phrenic afferents mediate the ventilatory response to diaphragmatic ischemia. *Resp Physiol*. 1993b;91:195–206.
- Tobin MJ, Perez W, Guenther SM, Semmes BJ, Mador MJ, Allen SJ, et al. The pattern of breathing during successful and unsuccessful trials of weaning from mechanical ventilation. *Am Rev Respir Dis*. 1986;134(6):1111–8.

- Viiiris N, Sillye G, Aubier M, Rassidakis A, Roussos C. Regional blood flow distribution in dog during induced hypotension and low cardiac output. Spontaneous breathing versus artificial ventilation. *J Clin Invest.* 1983;72(3):935–47.
- Yan S, Sinderby C, Bielen P, Beck J, Comtois N, Sliwinski P. Expiratory muscle pressure and breathing mechanics in chronic obstructive pulmonary disease. *Eur Respir J.* 2000;16(4):684–90.
- Yang KL, Tobin MJ. A prospective study of indexes predicting the outcome of trials of weaning from mechanical ventilation. *N Engl J Med.* 1991;324:1445–50.



Surfactant Activity and the Pressure-Volume Curve of the Respiratory System

Charles Corey Hardin, Roger G. Spragg, and Atul Malhotra

Introduction

The mechanics of the lung and chest wall are important considerations in managing critically ill patients particularly those requiring mechanical ventilation. Throughout the respiratory cycle, the lung has a nonzero volume and a positive transpulmonary pressure, which is to say that pressure is required in order to overcome the tendency of the lung to collapse – its elastic recoil. Important insight into the nature of lung elastic recoil is gained by noting that the relationship between lung volume and transpulmonary pressure changes qualitatively when the lung is inflated with liquid instead of air (Fig. 17.1a). The pressure-volume curve of the air-filled lung is characterized by substantial hysteresis. Hysteresis is defined technically as work which is not recoverable but in practical terms for the lung reflects the fact that inspiration and expiration

can differ considerably on a pressure-volume curve; the pressure needed to maintain a given lung volume is less on deflation than on inflation. The pressure-volume curve of the liquid-filled lung, on the other hand, has very little hysteresis (Neergaard 1929). This observation points to a central role of the air-liquid interface and its associated surface tension in determining lung elastic recoil. The properties of the alveolar air-liquid interface are heavily determined by a specialized material, called surfactant, which is secreted by the type II alveolar epithelial cells (Orgeig et al. 2007). Pulmonary surfactant is a complex mixture of phospholipids and specialized surfactant proteins which dynamically modify alveolar surface tension and maintain alveolar stability – thus facilitating gas exchange. In this chapter we will review the concept of surface tension, the dynamics of the alveolar surfactant layer, the chemical nature of surfactant and surfactant proteins, the determinants of pulmonary stability, and the clinical experience with surfactant replacement.

C. C. Hardin (✉)

Division of Pulmonary and Critical Care Medicine,
Massachusetts General Hospital, Boston, MA, USA
e-mail: Charles.hardin@mgh.harvard.edu

R. G. Spragg

Division of Pulmonary, Critical Care and Sleep
Medicine, University of California San Diego,
La Jolla, CA, USA
e-mail: rspragg@ucsd.edu

A. Malhotra

UC San Diego, Department of Medicine,
La Jolla, CA, USA
e-mail: amalhotra@health.ucsd.edu

Surface Tension

For an alveolus with nonzero volume, the alveolar gas pressure is greater than the pressure at the pleural surface (Loring et al. 2016). That the alveolar pressure is positive relative to pleural pressure implies that the lung possesses a posi-

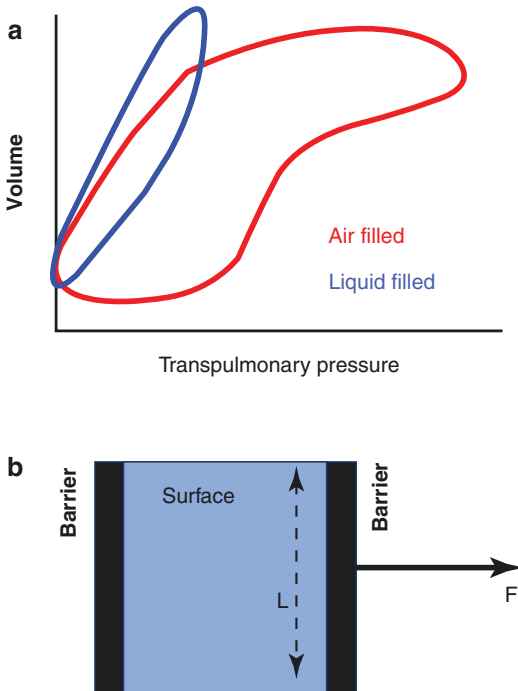


Fig. 17.1 (a) Pressure-volume curve for air-filled (red) and liquid-filled lung (blue). Filling with liquid abolishes the air-liquid interface and much of the hysteresis. (b) Relationship between surface tension and surface energy. See text for detailed discussion

tive elastic recoil pressure – a force per unit area which would tend to decrease volume where it is not opposed by $P_{ip} = P_{ao} - P_{pl}$ (Loring et al. 2009). In 1929 Van Neergaard (1929) established – by measuring the inflation pressure-volume curve of degassed lungs filled with saline and with air (Fig. 17.1) – that a major portion of this elastic recoil pressure arose from surface tension associated with the alveolar air-liquid interface. A liquid such as water is stabilized by extensive non-covalent interactions among water molecules – interactions which are less available to water molecules exposed on one side to air (Granger 2012). This situation provides an energetic driving force for returning molecules at the air-liquid interface to the bulk liquid phase and thus shrinking the area of the interface (Terjung 2011). Equivalently, it requires energy to increase the size of the interface. If a molecule that interacts less strongly with water molecules than water molecules interact with themselves is intro-

duced to a solution, its accumulation at the surface will lower the energetic cost of expanding the interface (Possmayer et al. 2001). Phospholipids – amphiphilic molecules composed of a polar head group – and hydrophobic lipid tails have this property (Rugonyi et al. 2008). That the energetic cost of the interface is equivalent to a surface tension (a force per unit length) is best seen by a thought experiment such as depicted in Fig. 17.1b. Here a bubble or liquid surface is stretched between two supports. Moving one support by dx expands the surface area by dA which requires a force to be applied to the bar – a force which is equivalent to the surface tension \times the length of the bar:

$$\sigma \times dA = F \times L \times dx$$

$$L \times dx = dA$$

$$\sigma = F$$

Thus, the energetic cost of the interface may be expressed as a surface energy or a surface tension, interchangeably. For pure water this surface tension is 72.8 dynes/cm at 20 °C (Terjung 2011). A surface tension as high as that of pure water is incompatible with normal lung function. The expansion of an alveolar surface with a surface tension that high would present a large load to the respiratory muscles and thus a large increase in the work of breathing. Introduction of phospholipids will decrease the surface tension. The equilibrium state of an aqueous solution of phospholipids is one in which the phospholipids accumulate at the surface until the entire available surface is coated (Nagle 1973). Introduction of an additional phospholipid molecule at that point will only displace a preexisting one, and the solution has reached its stable, equilibrium surface tension. The air-liquid interface of the lung consists of a thin film consisting primarily of the phospholipid dipalmitoylphosphatidylcholine (DPPC), as well as a mixture of proteins and additional lipids. Pure DPPC films have an equilibrium surface tension of approximately 20 mN/m (Rugonyi et al. 2008), but the equilibrium surface tension of lung surfactant, composed as it is of a mixture of lipids and cholesterol, is somewhat higher (Piknova et al. 2002).

Pressure-Volume Behavior, Recruitment, and Static Surface Tension

The elastic recoil pressure of the lung, influenced by alveolar surface tension, acts to shrink the size of an alveolus and is opposed by the transpulmonary pressure. Consider a simple model of the lung as a “bubble on a straw” (Fig. 17.2).

The surface tension (elastic recoil) shrinking the bubble is opposed by the transmural pressure (analogous to transpulmonary pressure) across the bubble wall. The bubble is stable when the forces are equal:

$$(P_i - P_o)\pi r^2 = \sigma 2\pi r \tag{17.1}$$

where σ is the surface tension and geometric terms (r , the radius of curvature of the bubble, πr the projected circumference, and πr^2 the projected area) are required to convert from pressures (force/area) and tension (force/length) to forces. This expression may be rearranged to yield the familiar law of Laplace:

$$\Delta P = \frac{2\sigma}{r} \tag{17.2}$$

In the case of an alveolus inflating at the end of an airway, however, the above expression predicts a region of negative compliance and thus pulmonary instability (Fig. 17.2b). At the start of inflation, an inflating bubble (or alveolus) will comprise a horizontal film across the airway and thus have an infinite radius of curvature. As the alveolus inflates, its radius of curvature decreases, and the distending pressure required to maintain that radius (and thus volume) increases, consistent with the Eq. 17.2. However (Fig. 17.2b), beyond the point at which the radius of the inflating alveolus equals that of the airway, the radius of curvature will begin to increase again, and the required distending pressure will decrease. At this point, the system can decrease its energy by increasing its volume, and it will thus be unstable.

This model is oversimplified in that it omits any contribution from pulmonary parenchymal tissue. A glance at the saline-filled pressure-volume curve in Fig. 17.1 reveals a relatively linear pressure-volume behavior, presumably attributable to the pulmonary tissue alone as there is no air-liquid interface. Such a linear curve, in series with the air-liquid interface, yields a curve (Fig. 17.3) which still possesses a region of nega-

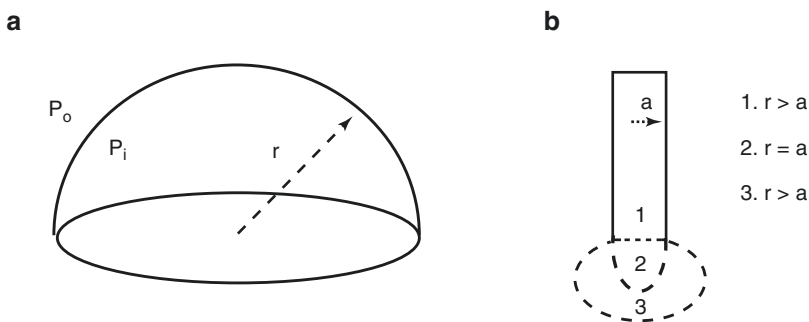


Fig. 17.2 (a) Simplified model of an alveolus as a bubble. The recoil force tending to collapse the bubble is equal to the surface tension \times the length of the air-liquid interface. The force opposing the recoil and stabilizing the bubble volume is equal to the transmural pressure \times the projected area of the bubble. (b) Model of a lung as a bubble on a straw. This model has three different regions which may be defined by the sign of the compliance (slope of the pressure-volume curve). In region 1, prior to inflation, the bubble is a horizontal air-liquid interface

across the end of the straw – its radius of curvature is infinite. Inflation from this point will decrease the radius of curvature of the bubble and requires an increasing transmural pressure according to the law of Laplace (Eq. 17.2). This is true until the radius of the bubble (r) equals the radius of the straw (a). Region 2 is the point at which $r = a$. After that point, inflation will increase the radius of curvature of the bubble and decrease the required transmural pressure. Thus, in region 3, compliance is negative

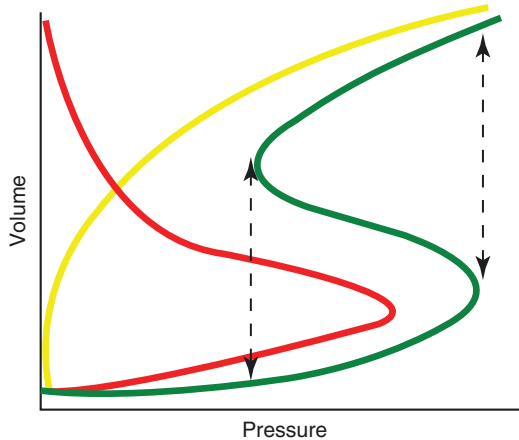


Fig. 17.3 Schematic illustrating the relationship between alveolar pressure-volume curve (green), recoil due to surface tension (red) and recoil due to elastic pulmonary tissue (yellow). The tissue component and the surface component add to yield to the total alveolar curve. The green curve contains regions of negative compliance bounded by regions of positive compliance. This leads to discontinuous jumps in volume – recruitment and derecruitment

tive compliance, but that region is now bounded by a region of positive compliance at (finite) higher volume (Fig. 17.3).

Recruitment and the Origin of Crackles

The presence of bounded regions of negative compliance in the pressure-volume curve of Fig. 17.3 leads to the possibility of sudden airway opening and closing events – recruitment and derecruitment. As the curve is transited during inflation, the inflection point between regions of positive and negative curvature will be reached which will result in a sudden airway opening event corresponding to a jump from one region of the curve with positive compliance to the next region of the curve with positive compliance (Nath and Capel 1974; Munakata et al. 1986; Fredberg and Holford 1983). Nath and colleagues demonstrated (later verified by others) that this will result in the propagation of a stress wave in

the pulmonary tissue that is manifested as a crackle or acoustic wave at the chest surface. A similar point of inflection exists on deflation, but the curve displays hysteresis so that the point of inflection on deflation occurs at a lower transpulmonary pressure and so will be less energetic and more difficult to detect. The existence of both inspiratory and expiratory crackles with expiratory crackles being less energetic than inspiratory crackles has been experimentally confirmed (Fredberg and Holford 1983).

Surfactant Composition

Pulmonary surfactant is primarily, though not exclusively, composed of phospholipid. The most abundant of the lipids are phosphatidylcholine, phosphatidylglycerol, and phosphatidylinositol (Nath and Capel 1974). In addition to the phospholipids, surfactant contains a small amount of neutral lipids such as cholesterol and four proteins, termed surfactant proteins A–D (Possmayer et al. 2001). Surfactant protein A and D are hydrophilic and proteins B and C are hydrophobic. B and C are synthesized and secreted along with phospholipids in the alveolar type II (ATII) cell. A and D are members of a family of proteins termed collectins which function in the innate immune system. Members of the collectin family possess a C-terminal domain that binds carbohydrates found on bacterial and viral surfaces (Han and Mallampalli 2015). Mice deficient in surfactant protein A have impaired clearance of bacterial and viral infections, and both protein A and protein D have been shown to increase directly the membrane permeability of bacterial and viral pathogens. Surfactant protein D is not thought to play a great role in the surface activity of surfactant. Protein A plays a role in promoting the association of reserve structures in the subphase (see below). The hydrophobic proteins B and C facilitate the rapid spreading of surfactant across the alveolar surface once it reaches the air-liquid interface (Han and Mallampalli 2015).

Surfactant Activity

Inspection of the lung pressure-volume curve highlights the opposing biophysical challenges presented by normal respiration. During expiration, the radius of curvature of the alveolus and its associated air-liquid interface decreases. This will be associated with an increase in the elastic recoil pressure, according to the law of Laplace (Eq. 17.2) regardless of the starting value of the surface tension. Thus, if the only effect of pulmonary surfactant was to lower the absolute value of surface tension, there would be an increasing tendency toward alveolar collapse on expiration (Hills 1999). A separate problem arises on inspiration where there is a need for rapid expansion of the surface film to accommodate the expansion of the interfacial area. These challenges are overcome, respectively, by the effects of compression of the phospholipid bilayer and the dynamics of the subphase and the action of surfactant proteins.

Surfactant Secretion and the Subphase

Surfactant is synthesized by alveolar type II cells (ATII) (Dietl and Haller 2005). ATII cells are enriched in endoplasmic reticulum (Rooney et al. 1994) where surfactant lipids are packaged into membrane-bound vesicles known as lamellar bodies. Lamellar bodies leave the ATII cells by exocytosis. Hydrophobic surfactant proteins (surfactant proteins C and B) are similarly secreted by the ATII cells. Once free of the ATII cell, lamellar bodies lose their outer membrane and combine with surfactant proteins and are assembled into a highly packed state known as tubular myelin (Knudsen and Ochs 2018). Lamellar bodies, tubular myelin, and complexes of previously secreted lipid recycled from the actual air-liquid interface form a subphase that is closely associated with surfactant monolayer and likely serves as a reserve source of phospholipid (Goerke 1998) that can be mobilized to facilitate rapid spreading of the surfactant film on alveolar expansion (Pérez-Gil and Keough 1998). In this

way, the phospholipid monolayer at the air-liquid interface is created and maintained by transfer of reserve lipid from the subphase, in a process which is not yet fully understood (Rugonyi et al. 2008). It is thought that replacement of surfactant molecules at the air-liquid interface occurs through multiple steps starting with approach of reserve structures to the surface film, association of the reserve structures with surface via protein-protein and ionic interactions, and then transfer of surface active lipids to the film (Dietl and Haller 2005; Pérez-Gil and Keough 1998; Lopez-Rodriguez and Pérez-Gil 2014). Once new lipid molecules are present at the air-liquid interface, they must rapidly spread over the whole of the alveolar surface – a process which is facilitated by the protein components of surfactant.

Alveolar Collapse and Phase Transitions in Surfactant Lipid Layers

As discussed above, at equilibrium, a phospholipid bilayer at an air-liquid interface fully covers the surface so that movement of a phospholipid molecule from the bulk liquid to the surface displaces one already there. The interface is then characterized by a single equilibrium surface tension that is lower than that of a bare surface. It is possible to lower the surface tension below this equilibrium value. Indeed, Pattle has estimated that surfactant-containing lung extracts are capable of reducing surface tension to near zero (Possmayer et al. 2001) during expiration. This is possible because phospholipid bilayers undergo a phase transition at some sufficiently low temperature between a relatively unordered state, the liquid-crystalline phase, and an ordered phase termed the gel phase (Daniels and Orgeig 2003). In the gel phase, molecules are tightly packed into a quasi-crystalline array so that they possess little translational freedom. In the liquid-crystalline phase, individual molecules possess a high degree of translational and rotational freedom (Lopez-Rodriguez and Pérez-Gil 2014). Transitions between the disordered, fluid state and the tightly packed, quasi-solid state may

occur with increasing compression as well as decreasing temperature. A compressed surface is associated with a loss of translational freedom but also a greater number of phospholipid molecules present for a given surface area and thus a lower surface tension. In the case of the alveolus, compression on deflation leads to a greater lowering of surface tension as alveolar radius decreases. The compressibility of a phospholipid layer is a function of its precise lipid content. Fully saturated proteins such as DPPC lipids are highly compressible whereas addition of unsaturated phospholipids or neutral lipids such as cholesterol decreases the compressibility (and thus increases fluidity). A maximally compressed, pure DPPC film is capable of reducing surface tension to near zero, as observed in films composed of surfactant extract (Lopez-Rodriguez and Pérez-Gil 2014; Daniels and Orgeig 2003). Such a film, however, is less able to spread rapidly over an expanding alveolar surface on inspiration than one that contains a mixture of neutral, saturated, and unsaturated lipids.

Current View of Surfactant Function

As a mixture of saturated, unsaturated, and neutral lipids, naturally occurring surfactant is composed of lipids with different transition temperatures and compressibility. Once present at the air-liquid interface, this heterogeneous composition is thought to lead to a phase separation which results in the surfactant films consisting of separate ordered and disordered regions with the ordered regions enriched in DPPC (de la Serna et al. 2004). On compression, the disordered, DPPC-poor islands are squeezed out so that at the end of expiration the alveolar film is a relatively pure DPPC film capable of reducing surface tension to near zero (Keating et al. 2012). The fate of squeezed out lipids is not well understood, with some evidence that they assemble into multilayered structures in the subphase and add to the lipid reserve (Schürch et al. 1998). During inspiration, the process of inspiration is facilitated by surfactant proteins and reserve structures that together allow for rapid transfer of lipid to the expanding air-liquid interface.

Transfer from a subphase structure to the air-liquid interface potentially involves exposure of hydrophobic lipids to the aqueous subphase. This energetically unfavorable process is potentially facilitated by the hydrophobic surfactant proteins B and C (Lopez-Rodriguez and Pérez-Gil 2014).

Surfactant Function and Replacement in Acute Respiratory Distress Syndrome (ARDS)

Surfactant function is impaired in a variety of lung pathologies. In adults, the best studied of these is ARDS in which both the function and absolute amount of surfactant are diminished. These changes are due to a reduction in surfactant production by alveolar type II cells, inactivation by plasma proteins in alveolar edema fluid, and inactivation by reaction with reactive nitrogen and oxygen species, proteases, and phospholipases. Loss of surfactant function results in decreased pulmonary compliance and functional residual capacity, atelectasis, increased right-to-left shunt and hypoxemia, and possibly enhanced edema formation.

As these changes are all features of ARDS, it is reasonable to postulate that loss of surfactant function may contribute to the pathophysiology of ARDS. Exogenous surfactant is effective in improving oxygenation in animal models of ARDS as well as in treatment of premature neonates in whom surfactant production is limited. For these reasons, multiple clinical trials of instilled surfactant derived from animal lungs or produced synthetically have attempted to show benefit to patients with ARDS. However, meta-analysis of 11 prospective randomized clinical trials involving 1038 patients has failed to demonstrate mortality or oxygenation benefit (Meng et al. 2019). While surfactant treatment of ARDS is not indicated currently, it is possible that future investigation targeting specific patient subgroups (based on mechanism or underlying endotype), using alternative methods of administration such as delivery by aerosol, or using synthetic surfactants that are resistant to inhibition in the inflamed lung may demonstrate benefit. For

example, adaptive clinical trials are now being designed whereby therapies can be changed based on patient characteristics and responses to therapy. In theory, patients with recruitability (i.e., who experience opening of collapsed alveoli with applied pressure) may be amenable to exogenous surfactant; however, clinical trials will clearly be required to test this hypothesis.

Conclusion

The existence of an air-liquid interface is a minimal requirement for gas exchange, and the mechanical properties of the air-liquid interface determine, to a large degree, the pressure-volume behavior of the lung. These mechanical properties are, in turn, influenced by the presence of the pulmonary surfactant layer. Surfactant dynamically lowers surface tension. Thus, surfactant activity, the dynamic change in the chemical and physical properties of the surfactant layer with changes in lung volume, is a major determinant of lung mechanical behavior.

References

- Daniels CB, Orgeig S. Pulmonary surfactant: the key to the evolution of air breathing. *News Physiol Sci.* 2003;18:151–7.
- de la Serna JB, Perez-Gil J, Simonsen AC, Bagatolli LA. Cholesterol rules: direct observation of the coexistence of two fluid phases in native pulmonary surfactant membranes at physiological temperatures. *J Biol Chem.* 2004;279:40715–22.
- Dietl P, Haller T. Exocytosis of lung surfactant: from the secretory vesicle to the air-liquid interface. *Annu Rev Physiol.* 2005;67:595–621.
- Fredberg JJ, Holford SK. Discrete lung sounds: crackles (rales) as stress-relaxation quadrupoles. *J Acoust Soc Am.* 1983;73:1036–46.
- Goerke J, Clements JA. Alveolar Surface Tension and Lung Surfactant. In *Comprehensive Physiology*, R. Terjung (Ed.). 2011. <https://doi.org/10.1002/cphy.cp030316>.
- Goerke J. Pulmonary surfactant: functions and molecular composition. *Biochim Biophys Acta.* 1998;1408:79–89.
- Granger RA. *Fluid Mechanics*. Dover Publications, NY 2012.
- Han S, Mallampalli RK. The role of surfactant in lung disease and host defense against pulmonary infections. *Ann Am Thorac Soc.* 2015;12:765–74.
- Hills BA. An alternative view of the role(s) of surfactant and the alveolar model. *J Appl Physiol.* 1999;87:1567–83.
- Keating E, et al. A modified squeeze-out mechanism for generating high surface pressures with pulmonary surfactant. *Biochim Biophys Acta.* 2012;1818:1225–34.
- Knudsen L, Ochs M. The micromechanics of lung alveoli: structure and function of surfactant and tissue components. *Histochem Cell Biol.* 2018;150:661–76.
- Lopez-Rodriguez E, Pérez-Gil J. Structure-function relationships in pulmonary surfactant membranes: from biophysics to therapy. *Biochim Biophys Acta.* 2014;1838:1568–85.
- Loring SH, Garcia-Jacques M, Malhotra A. Pulmonary characteristics in COPD and mechanisms of increased work of breathing. *J Appl Physiol.* 2009;107:309–14.
- Loring SH, Topulos GP, Hubmayr RD. Transpulmonary pressure: the importance of precise definitions and limiting assumptions. *Am J Respir Crit Care Med.* 2016;194:1452–7.
- Meng S-S, et al. Effect of surfactant administration on outcomes of adult patients in acute respiratory distress syndrome: a meta-analysis of randomized controlled trials. *BMC Pulm Med.* 2019;19:9.
- Munakata M, et al. Production mechanism of crackles in excised normal canine lungs. *J Appl Physiol.* 1986;61:1120–5.
- Nagle JF. Lipid bilayer phase transition: density measurements and theory. *Proc Natl Acad Sci U S A.* 1973;70:3443–4.
- Nath AR, Capel LH. Inspiratory crackles and mechanical events of breathing. *Thorax.* 1974;29:695–8.
- Neergaard K. Neue Auffassungen über einen Grundbegriff der Atemmechanik. *Z Gesamte Exp Med.* 1929;66:373–94.
- Orgeig S, et al. The anatomy, physics, and physiology of gas exchange surfaces: is there a universal function for pulmonary surfactant in animal respiratory structures? *Integr Comp Biol.* 2007;47:610–27.
- Pérez-Gil J, Keough KMW. Interfacial properties of surfactant proteins. *Biochim Biophys Acta Mol Basis Dis.* 1998;1408:203–17.
- Piknova B, Schram V, Hall SB. Pulmonary surfactant: phase behavior and function. *Curr Opin Struct Biol.* 2002;12:487–94.
- Possmayer F, Nag K, Rodriguez K, Qanbar R, Schürch S. Surface activity in vitro: role of surfactant proteins. *Comp Biochem Physiol A Mol Integr Physiol.* 2001;129:209–20.
- Rooney SA, Young SL, Mendelson CR. Molecular and cellular processing of lung surfactant 1. *FASEB J.* 1994;8:957–67.
- Rugonyi S, Biswas SC, Hall SB. The biophysical function of pulmonary surfactant. *Respir Physiol Neurobiol.* 2008;163:244–55.
- Schürch S, Green FH, Bachofen H. Formation and structure of surface films: captive bubble surfactometry. *Biochim Biophys Acta.* 1998;1408:180–202.

Part III

Physiological Basics: Interactions



Introduction

The pattern of breathing has direct effects on cardiovascular performance. Spontaneous inspiratory efforts normally have a small transient effect on the steady-state cardiac output, although the effect can be large at peak exercise (Miller et al. 2005). When patients are managed with mechanical ventilation, the positive pressure during inspiration, whether triggered by the patient or completely by the machine, has important effects on cardiovascular function. The converse also is true; changes in cardiovascular status can affect the lungs. Support of cardiovascular function with volume resuscitation and vasoactive and inotropic drugs can increase extravascular lung water, decrease lung compliance, and increase airflow resistance through their effects on cardiac filling pressures. Also, cardiovascular therapies that increase pulmonary artery pressure and the load on the right ventricle (RV) can lead to limitation of RV filling and dampen variations of sys-

temic arterial pressure during the ventilator cycle. Understanding the complex interactions of the heart and respiratory system in health and disease thus is a cornerstone of ICU management (Table 18.1).

The importance of heart-lung interactions is often underappreciated by the limitations of reductionist experiments in which the circulation and lungs are separated. Much work has been done on lung stretch and injury, but the isolated impact of lung stretch in a petri dish misses the significance of the important hemodynamic influences on the changing flow patterns that occur in vivo during the ventilation cycle (Katira et al. 2017). Similarly, the extensive investigations of myocardial contractile function in reduced preparations do not account for important influences of expiratory variations on cardiac performance. Furthermore, the lungs sit between the outputs of the RV and LV, and respiratory efforts can transiently dissociate on the filling and outputs of the two ventricles that occupy a common space in the pericardium.

We have structured this chapter to review spontaneous versus passive ventilation and how these impact the inflow and outflow of the RV and LV. Key underlying principles are that mass must be conserved and that output from the heart is predicated on the input to the RV, such that the heart can only eject what it receives. It will be emphasized that the effects of ventilation on the RV dominate heart-lung interactions. This is

S. Magder (✉)
Royal Victoria Hospital (McGill University
Health Centre), Departments of Critical Care and
Physiology McGill University, Montreal, QC, Canada
e-mail: sheldon.magder@mcgill.ca

A. Malhotra
UC San Diego, Department of Medicine,
La Jolla, CA, USA
e-mail: amalhotra@health.ucsd.edu

Table 18.1 Clinical implications of respiratory and cardiovascular variations

<i>Respiratory</i>	
Increased Raw: Asthma COPD Secretions Tracheal narrowing Endotracheal tube	Increased fall in Ppl with spontaneous inspiration Air-trapping and creation of auto-PEEP Decreased rise in Ppl with mechanical breath Greater potential for developing non-zone II conditions
Increased pulmonary compliance: COPD	Greater transmission of Paw to Ppl with mechanical breath
Reduced lung compliance: ARDS Pulmonary edema	Need for greater transpulmonary pressure
Increased inspiratory threshold load: e.g., auto-PEEP	Increased fall in Ppl with spontaneous inspiration
Reduced chest wall compliance: kyphoscoliosis – chest wall disease	Greater transmission of airway to pleural pressure
Increased lung and chest wall inflation	Increased vagal activity and slowing of heart rate via pulmonary afferents
Rise in pleural pressure	Increase sympathetic activity if venous return is decreased and blood pressure falls
Reduction in RV output during inspiration with mechanical breath	Increased flow swings and shear stress in the pulmonary vasculature with consequent endothelial damage
<i>Cardiovascular</i>	
Volume overload	Greater increase in RV filling with spontaneous inspiration Greater risk of RV limitation during spontaneous inspiration
RV limitation	Less tolerance of non-zone III conditions Greater interaction between RV and LV
Increased pulmonary vascular resistance	Greater tendency for non-zone III because of greater PA to LA pressure diff
Decreased LV contractility	Greater sensitivity to LV afterload from negative inspiratory effort
Inadequate tissue perfusion	Local tissue afferents (especially muscle) increase central drive to breath
Rapid heart rate	Faster transfer of changes in RV filling during ventilation to the left heart
Slow heart rate	Greater dependence of LV filling on pulmonary venous reserves, for “pulmonary vascular buffering”

Raw airway resistance, Paw airway pressure, Ppl pleural pressure, PA pulmonary artery, LA left atrium

because it is at the RV that the heart interacts with the blood coming back from the rest of the body, and the RV must pass this blood on to the LV. Furthermore, during the ventilation cycle, the pressure in the RV changes relative to its upstream volume reservoir, that is, the systemic veins and venules, because the environment around the RV changes relative to atmospheric pressure. Flow out of the RV, though, is not affected because the RV and pulmonary circuit are surrounded by the same environment. In contrast, filling of the LV is not altered by changing intrathoracic pressure because its upstream volume reservoir, the pulmonary venous compartment, has the same pressure environment as that of the LV. However, the output from the LV is affected during the ventilation cycle because the environment around the LV

changes relative to its outflow pressure, the aorta, which delivers blood to vessels surrounded by atmospheric pressure.

Guyton's Graphical Analysis of the Regulation of Cardiac Output

Arthur Guyton's graphical approach to the analysis of the interaction of a function that describes the return of blood to heart with a function that determines the blood pumped out by the heart (Chap. 2) provides a useful format for understanding the interactions of the heart and lungs during the ventilation cycle (Guyton 1955; Guyton et al. 1973). The key factor that makes the understanding of heart-lung interac-

tions difficult is that pressures are made relative to a reference value, and the reference value for pressures of vascular structure inside the thorax is different from vascular structures outside the thorax. Vessels outside the thorax are surrounded by atmospheric pressure, whereas vascular structures in the thorax are surrounded by pleural pressure (Ppl). Even more so, the reference pressure for intrathoracic structures, i.e., Ppl, changes relative to atmospheric pressure which surrounds systemic vessels during the ventilation cycle. On the other hand, the blood returning to the heart from the rest of the body is surrounded by atmospheric pressure which does not change throughout the respiratory cycle. Importantly, for practical reasons, devices that are used for measuring vascular pressures are referenced relative to atmospheric pressure.

Two other factors further complicate things. Pulmonary vessels passing between the alveoli (intra-alveolar vessels) are surrounded by airway pressure, which is at atmospheric pressure during spontaneous breaths but is a positive value in mechanically ventilated patients who are receiving positive end-expiratory pressure (PEEP). Furthermore, abdominal pressure surrounds the abdominal venous reservoir, and an increase in abdominal pressure during the ventilation cycle alters the pressure surrounding the abdominal venous reservoir. These changes in reference pressures can easily be examined in Guyton’s graphical analysis by adjusting the x-intercept of the relevant function.

A detailed discussion of Guyton’s analysis of the interaction of cardiac and return functions is provided in Chap. 2, but some key concepts need to be reviewed here (Fig. 18.1). First, venous

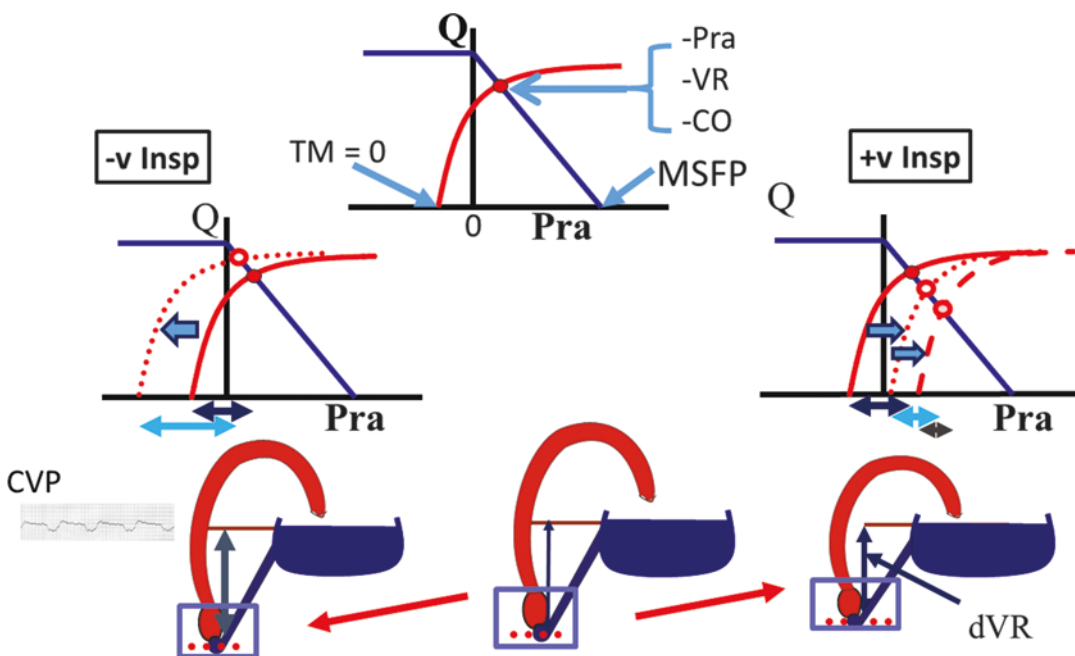


Fig. 18.1 Guyton’s cardiac function and venous return curves and general model of the circulation. The top shows typical baseline conditions. The cardiac function curve (red) starts below zero (atmospheric pressure) because the heart is surrounded by negative pleural pressure. TM, transmural pressure. The cardiac function curve intersects the venous return curve (blue) which gives the working right atrial pressure (Pra), the venous return (VR), and cardiac output (CO) ($Q = \text{flow}$). The left side

shows a spontaneous negative pressure breath (–ve Insp). With each inspiration, the cardiac function curve moves to the left of the venous return curve. Pra falls and CO rises. The right side shows a mechanical (positive, +ve) inspiration. Positive end-expiratory pressure (PEEP) shifts the cardiac function curve to the right. There is a rise in Pra (open circle) and fall in Q. With each +ve breath, the cardiac function moves further to the right, and there is a further rise in Pra and fall in Q

return is a function of the pressure difference between the mean systemic filling pressure (MSFP, i.e., pressure in the venous compliant region) and the central venous pressure (CVP) or right atrial pressure (Pra). These two terms will be used interchangeably because, in the absence of a central stenosis, they are essentially the same (Guyton 1955; Guyton et al. 1954, 1973). In addition, the resistance to venous return to the right atrium, generally simply called venous resistance, is another important determinant of venous return (Guyton et al. 1957). MSFP is determined by the volume filling the systemic small veins and venules and the compliance of these vessels. Stressed volume is the volume that actually stretches the walls of vessels, whereas unstressed volume is the volume that just rounds out vessel walls but does not stretch them. Unstressed volume thus does not produce intravascular pressure. However, as will be seen, this volume can be recruited by active vasoconstriction of venous vessels and provides an important volume reservoir when increased vascular volume is needed. Second, the cardiac function curve is defined by the filling of the right heart and the output from the LV into the aorta. The function of everything in between is included, which includes the RV, pulmonary vasculature, and the LV. Each of these components can be influenced by respiratory processes, emphasizing again the interactive nature of the cardiac and pulmonary systems, but in the analysis, they are assessed by how they change the cardiac function curve. Guyton showed that superimposing the return and cardiac functions on the same graph provides a simple mathematical solution to how changes of either function alter the steady-state Pra, venous return, and cardiac output, which are defined by the single point at which the two functions intersect on the graph.

When measuring the pressure of an elastic structure, what matters is the difference between the pressure inside the structure and the pressure outside the structure because this is the force that determines how much the elastic structure is distended. This pressure difference is called the transmural pressure, and the outside pressure is

considered the reference value. Since our bodies are surrounded by atmospheric pressure, we generally make measurements of vascular pressures relative to the surrounding atmospheric pressure and call that value zero. For example, a systolic blood pressure of 120 mmHg means that the pressure inside the vessel is 120 mmHg relative to atmosphere which we have called the zero reference and thus equals 120 mmHg. However, a measurement of a transmural vascular pressure inside the thorax is more complicated. At functional residual capacity (FRC), Ppl has a negative value relative to atmospheric pressure. This negative value occurs because of the balance between outward chest wall recoil and inward lung recoil.

The reference value for pressure on Guyton's plot is atmospheric pressure, which, as we already have said, we call "zero." However, cardiac function is based on structures in the thorax, and the reference pressure for these structures should be the intrathoracic pressure. This is easily handled in Guyton's graphical analysis by having the x-intercept of the cardiac function not start at zero but rather from a value that represents Ppl. With spontaneously normal breathing, Ppl at end expiration and functional residual capacity normally is around -2 mmHg. Thus, the cardiac function curve begins at a Pra of approximately -2 mmHg. At this value, the pressure across the walls of the heart, that is, the transmural pressure, is zero. When Ppl changes during the ventilator cycle, the x-intercept of the cardiac function curve must move accordingly, and this results in changes in the intersection point of the cardiac and return function curves (Fig. 18.1).

The RV and LV can be affected by a steady-state change in the intrathoracic pressure, such as occurs with the application of PEEP, but also dynamically with each breath. In this situation the inputs and outputs of the RV and LV can be transiently different. The actions on the RV and LV can be separated further to examine these effects in isolation, but treating them as one unit makes it much easier to understand the average blood flow going in and average going out of the

who pulmonary vascular unit, which is what counts in the end for the tissues.

Changes in Ppl

Most often, changes in Ppl are the dominant factor accounting for changes in cardiac output during the ventilation cycle. The effects of changes in Ppl on cardiovascular function can be divided into two types. There can be a fall in Ppl, or “negative” change in Ppl, as occurs with a spontaneous inspiratory effort and activation of inspiratory muscles but also with an iron-lung, which lowers the pressure around the whole body, except for the airway. Or, there can be a rise in Ppl, or “positive” change in Ppl, as occurs with a mechanical inspiration and passive lung inflation, as well as from an increase in the baseline airway pressure by the application of positive end-expiratory pressure (PEEP).

To emphasize the point again, the heart is anatomically situated in the chest cavity. It is surrounded by Ppl and thus is subject to changes in Ppl. When examining the pressure-volume relationship of an elastic structure, a fall in pressure inside the structure means that there has been a decrease in volume, and the magnitude of the change in pressure or volume is a function of the compliance of the walls of the structure. A rise in pressure means that there has been a rise in volume. However, these relationships only are true if the transmural pressure is used. This error was missed in a classic review of heart-lung interactions in the first version of the *Handbook of Respiratory Physiology*. The error resulted in the author trying to explain why left heart volumes decrease during spontaneous inspiration when in fact they actually increase (Sharpey-Schafer 1965).

Fall in Ppl: Spontaneous Breath

During spontaneous breathing, Ppl falls relative to atmospheric pressure. Since the heart is surrounded by pleural space, the pressure in the heart, as measured by a catheter going from inside the heart to a transducer outside the chest, falls

with the fall in the surrounding Ppl. Based on the relationship of pressure to volume, the fall in pressure seen on a monitor would appear to indicate that the volume in the heart fell during this phase, but this is an error due to the way the cardiac chamber measurement was made. If intracardiac pressure falls by the same amount as the fall in pressure outside of the heart, transmural pressure (inside minus outside) does not change, and there is no change in volume. The importance of this concept is illustrated on the cardiac function-venous return curves (Fig. 18.1). As already indicated, on this graph, the pressure values for the venous return and cardiac function curves are referenced to atmospheric pressure, but what is important for cardiac output as defined by the Starling curve is the transmural pressures, which is the difference in pressure from the x-intercept of the cardiac function curve to Pra at the intersection of the cardiac and return functions. With a spontaneous breath, the x-intercept of the cardiac function curve shifts to the left based on the magnitude of the fall in Ppl. However, as a point of emphasis, without any change in abdominal pressure, the venous return curve does not move. As observed in Fig. 18.1, as a result of the leftward shift of the cardiac function curve, the intersection of the cardiac function and venous return curves occurs at a higher Pra relative to atmospheric pressure and also a higher transmural pressure on the cardiac function curve. This occurs because the pressure difference for venous return, defined as the x-intercept of the venous return curve (MSFP) to Pra, is increased and allows more blood to come back to the heart. This increases the transmural diastolic filling pressure of the heart, and cardiac output increases through the Frank-Starling mechanism. In effect, it is as if the heart is lowered relative to the venous reservoir, which “allows” more blood volume to return to the RV. The normal gradient for venous return usually only is 4–8 mmHg; thus, a decrease in pleural pressure of 4 mmHg can have a major impact on venous return and cardiac output. The increase in RV output is passed through the pulmonary circulation within a few beats to the LV and leads to the increased cardiac output as seen on the cardiac function-venous return curve. This usual pattern of changes of venous return with spontaneous

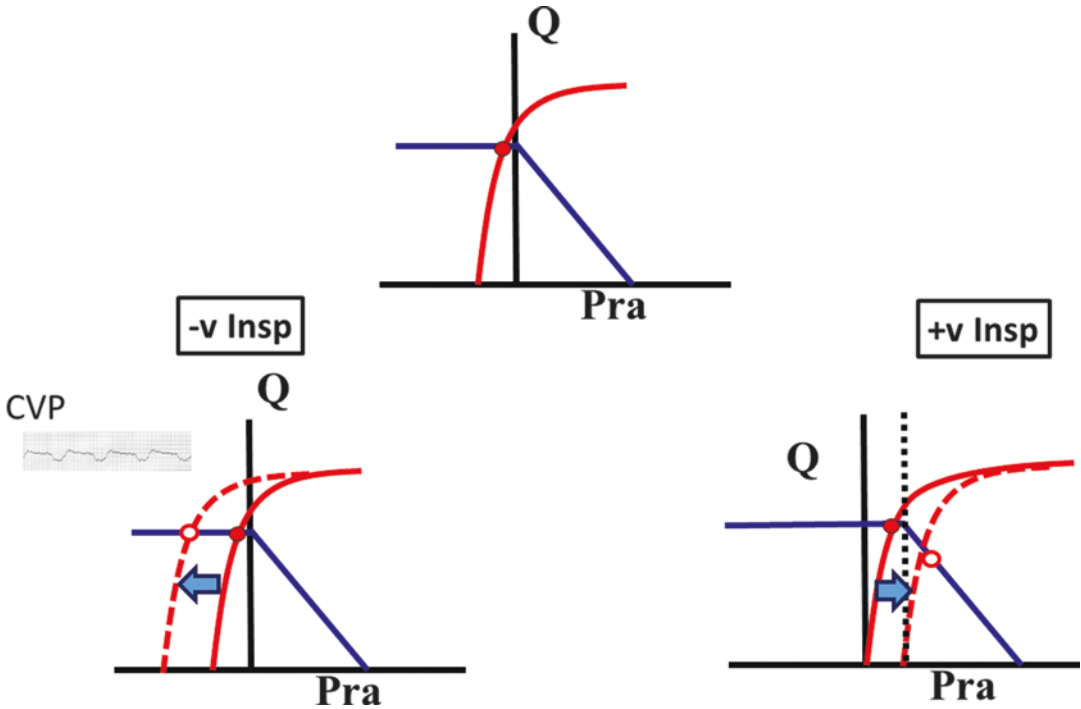


Fig. 18.2 Condition when cardiac function intersects the plateau of the venous return curve. The top shows the situation with no breathing. The left shows a spontaneous breath. The insert shows that there are still inspiratory variations in CVP but no change in Q. The right side

shows a mechanical breath with PEEP. Collapse of the vena cava occurs at a positive value. With each mechanical breath, Pra rises and return to the right heart (Q) decreases. Abbreviations are the same as Fig. 18.1

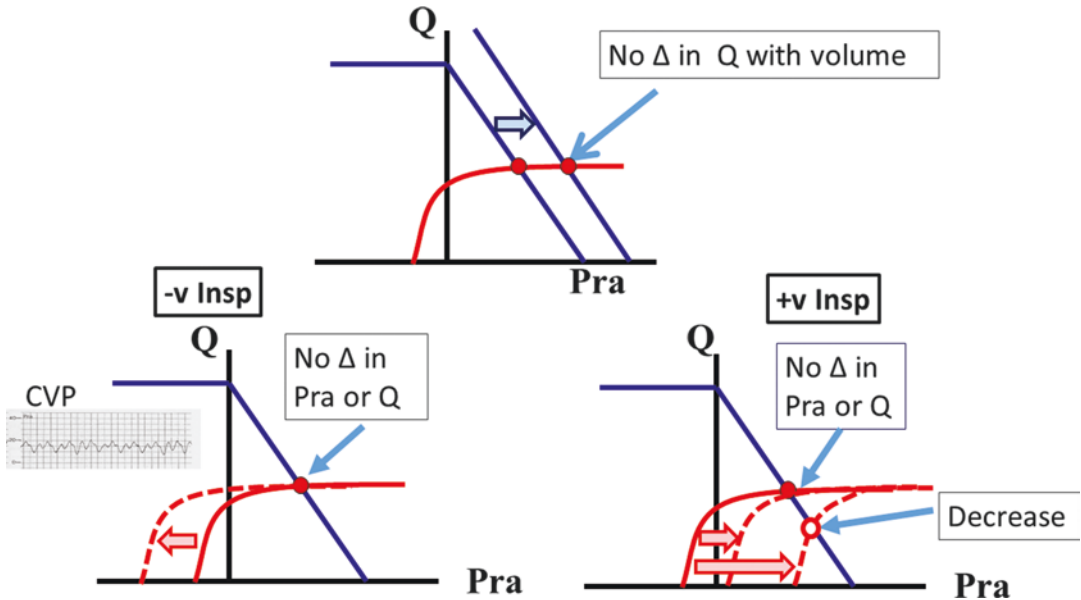


Fig. 18.3 Condition when venous return function intersects the plateau of the cardiac function curve. The top shows that increasing MSFP by giving volume does not change cardiac output. On the left, the insert shows that there is no inspiratory fall in CVP. With inspiration there

is no change in Pra or Q. On the right, raising intrathoracic pressure at lower levels does not change Pra or Q, but Q falls when the rise in intrathoracic pressure is sufficient to raise Pra. Abbreviations are the same as Fig. 18.1

breaths does not occur under two conditions: when the cardiac function curve intersects the plateau of the venous return curve (Fig. 18.2) or when the venous return curve intersects the plateau of the cardiac function curve (Fig. 18.3).

The venous return curve becomes flat just below a P_{ra} of zero, or atmospheric pressure, when breathing spontaneously. This is because the great veins have floppy walls, and when the pressure inside is negative relative to atmospheric pressure, they collapse and limit any further increase in venous return with lower values of P_{ra} . This has been called the equivalent of a vascular waterfall (Permutt and Riley 1963). When vessels collapse, flow does not stop, but rather further increases in flow do not occur when P_{ra} pressure is lowered further. This likely evolved through evolution as a safety mechanism that prevents the heart from overfilling with very large swings in P_{pl} . The implication of the collapse pressure is that the magnitude of the inspiratory increase in venous return depends upon the mag-

nitude of the P_{ra} before the onset of the breath. The greater the initial P_{ra} , the greater the potential rise in transmural pressure before venous collapse occurs because there is a greater range for P_{ra} to fall before the collapse.

As shown in Figs. 18.1, 18.2, and 18.3, the cardiac function curve has a sharp plateau which occurs because of the limits of diastolic filling either from the cardiac cytoskeleton or more often because of the pericardium. The interaction of the cardiac and return functions completely changes when the venous return curve intersects this plateau of the cardiac function curve (Fig. 18.3). When this happens, the shift to the left of the cardiac function curve with a fall in P_{pl} with a spontaneous inspiration no longer changes cardiac filling or cardiac output. P_{ra} also stays the same relative to atmospheric pressure, although the transmural pressure increases.

These observations lead to a clinical application whereby the change in CVP as measured during spontaneous inspiration (Fig. 18.4) can

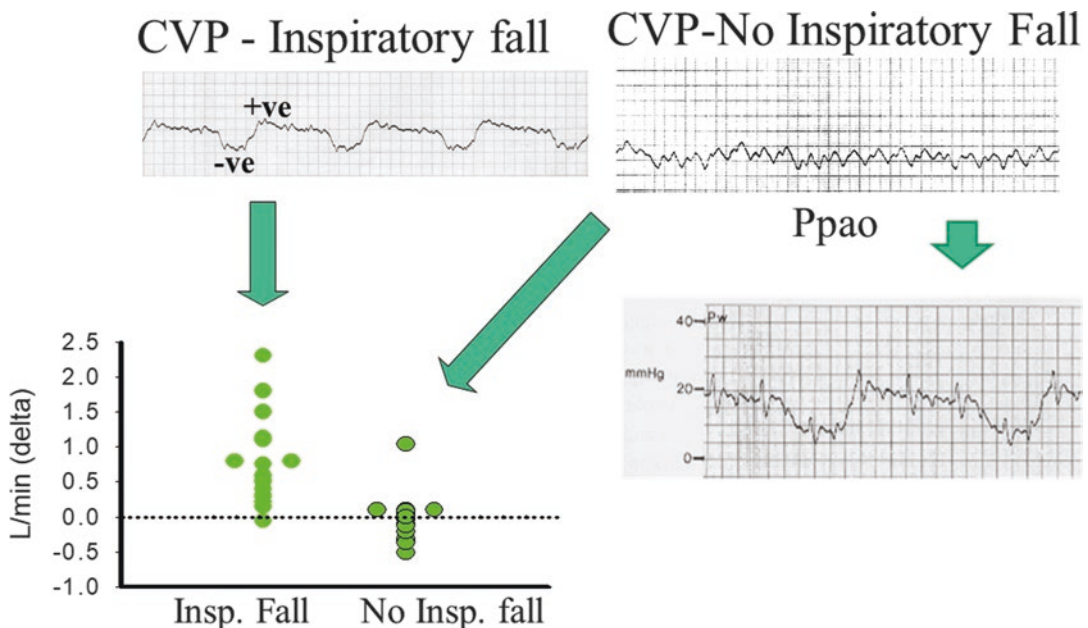


Fig. 18.4 Use of fall in CVP with a spontaneous inspiration to predict fluid responsiveness. The top left is an example of a large inspiratory swing in CVP, and the right side shows a CVP with no respiratory variation (except for mild increase in CVP from active expiration). The bottom right shows the inspiratory fall in the pulmonary artery occlusion for the same subject who had no change in CVP with the breath indicating that he has a good inspiratory

effort. The bottom graph shows that some patients with an inspiratory fall in CVP had an increase in cardiac output in response to a volume bolus, but not all. In those without an inspiratory fall in CVP, only one responded (in retrospect, the inspiratory effort likely was inadequate). (Adapted from Magder et al. (Magder et al. 1992) with permission of Elsevier)

be used to predict responsiveness to volume resuscitation (Magder et al. 1992). In patients in whom CVP does not fall with an inspiratory effort that is adequate to lower Ppl, the patient is unlikely to be volume responsive, i.e., “the tank is full.” In contrast, in patients in whom CVP falls with an adequate spontaneous inspiration, the response to volume is more variable and depends on where the system “sits” on the cardiac function/venous return curve. Thus, the pattern of changes in CVP during spontaneous inspiratory efforts has good predictive value in the negative sense. The lack of an inspiratory fall predicts that the patient will not have an increase in cardiac output if a fluid bolus is given, but the presence of an inspiratory fall in CVP is not a strong predictor that cardiac output will increase with a volume bolus. This is because the effect depends upon how close the venous return function is to the plateau of the cardiac function curve, which is not evident from the CVP because the inspiration only indicates left ward effects. The same is seen with the use of respiratory variations in vena caval blood flow to predict fluid responsiveness (Barbier et al. 2004) although changes in vessel diameter are harder to evaluate than the more precise changes in pressure. It needs to be noted that test requires an adequate fall in Ppl. This means the test still can be used on a ventilated patient if the patient has an adequate fall in Ppl while triggering the mechanical breath. For the test to be valid, the fall in Ppl with spontaneous breathing must carefully be distinguished from an active exhalation that increased abdominal pressures. This is because when the active expiratory force is released on inspiration, it may look like CVP fell from the inspiration, whereas the pressure fell because of the release of the abdominal pressure. It also is important to not use the inspiratory increase in a “y” decent as indicating a change in the baseline. However, the increase in the “y” descent marks the inspiratory effort, and a “y” descent of greater than 4 mmHg also likely indicates that the person will not be volume responsive (Magder et al. 2000).

Effect of Decrease in Ppl on the LV

A fall in Ppl also has important effects on the LV. These effects are primarily on the output from the LV rather than the input. When the heart becomes more negative relative to aortic pressure during inspiration, the LV must still generate the same pressure relative to atmosphere to open the aortic valve (McGregor 1979) (Fig. 18.5). The LV must overcome the negative pressure in the chest and add on the same change in arterial in pressure that was needed before the LV pressure was lowered relative to atmospheric pressure. The LV afterload thus is increased and the stroke volume during the inspiration is decreased. The end-systolic pressure-volume relationship is shifted to the right, and the end-systolic volume rises as does the end-diastolic volume. If the airway resistance is increased and there is a greater than normal inspiratory effort, a greater negative Ppl is needed to inflate the lungs. The effect of this on the LV can be very significant, and patients have been known to go into pulmonary edema because of large inspiratory swings in LV transmural pressure (Timby et al. 1990). The situation is worse if the LV end-systolic pressure-volume line is depressed because of a decrease in left ventricular contractility. The flatter slope results in a greater decrease in stroke volume with an increase in afterload. In summary, a fall in Ppl produces an increase in the forces filling the RV and, at the same time, increases the force opposing LV emptying so that there can be significant increases in all cardiac pressure and volumes, including those of pulmonary capillaries, during the phase of negative Ppl. This is discussed further below under the Mueller maneuver.

Rise in Ppl: PEEP and Mechanical Ventilation

The effect of an increase in Ppl with positive pressure on the heart is the opposite of the effect of a spontaneous, negative Ppl breath. The rise in Ppl raises P_{ra} relative to atmosphere and the venous

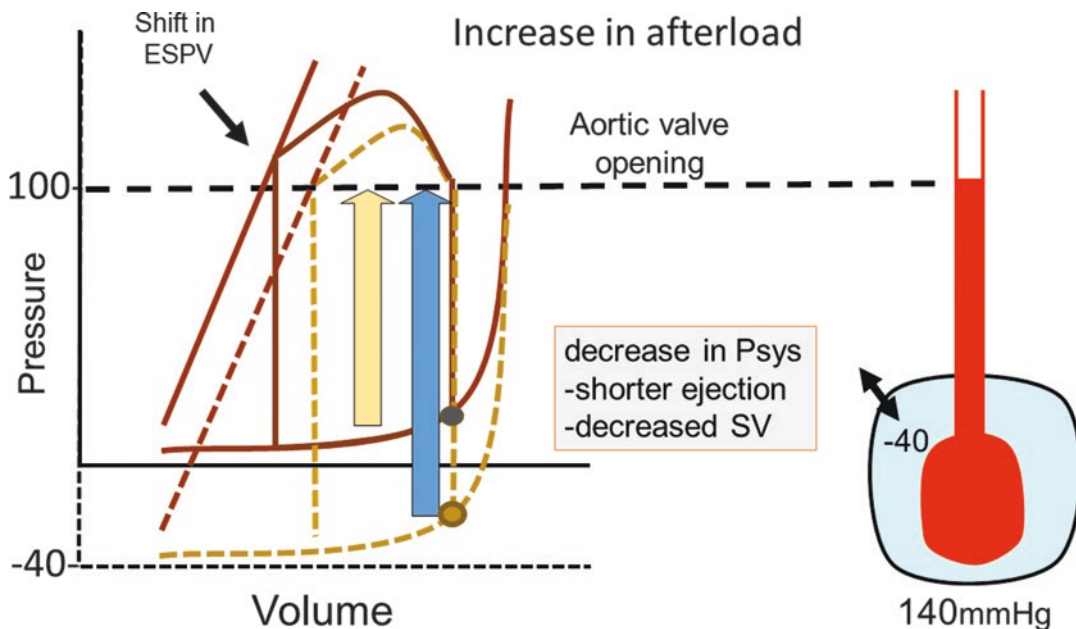


Fig. 18.5 Effect of a decrease in Ppl on the left ventricular pressure-volume relationship. A decrease in Ppl shifts the pressure-volume loop of the LV downward. On the first beat, the aortic valve opening is unchanged. This increases the isovolumetric part of ventricular contraction (blue arrow), increases LV afterload, and shortens ejection (i.e., stroke volume). The end-systolic P-V relationship is

shifted to the right because of the change in the referencing of the intracardiac pressures relative to atmosphere. The right side of the figure shows the equivalent of an isolated heart surrounded by a negative pressure of 40 mmHg and ejecting to an aortic pressure of 100 mmHg. It must generate 140 mmHg to do so instead of 100 mmHg

reservoir. This reduces the pressure difference for venous return. RV output and then LV output fall. On the Guyton venous return-cardiac function curve, this is seen as a shift of the cardiac function curve to the right, and it now intersects the venous return curve at a higher Pra but a lower value of venous return and lower cardiac output (Fig. 18.1).

Where the cardiac function curve intersects the venous return curve is again important (Figs. 18.1, 18.2, and 18.3). Collapse of the great veins occurs when the inside pressure is less than the outside pressure. When Ppl is positive the collapse no longer occurs at atmospheric pressure but at a positive value (Fig. 18.1). The maximum possible venous return is thus decreased and so is the maximum possible cardiac output. Cardiac output only then can be increased by a shift of the venous return curve to the right by an increase in stressed volume, which produces a higher intercept on both the x and y axes. This can occur by giving the patient volume but also can occur by

reflex constriction of the smooth muscle in the venous capacitance bed, which then converts unstressed volume into stressed volume (Fig. 18.6) (Nanas and Magder 1992; Fessler et al. 1992a, b). For this to happen, there needs to be sufficient reserves in unstressed volume to recruit. It also has been shown that at higher values of Ppl there can be flattening of the diaphragm which increases venous resistance which can further depress the maximum venous return (point of flow limitation) (Fessler et al. 1992b).

When the cardiac function curve intersects the flat part of the venous return curve, it is possible for there to be an increase in Ppl with no change in cardiac output, just as there was no change in cardiac output with a fall in Ppl when the cardiac function curve was in that position (Fig. 18.3). However, when the rise in Ppl is sufficient so that the venous return curve again intersects the ascending part of the cardiac function curve, cardiac output again falls.

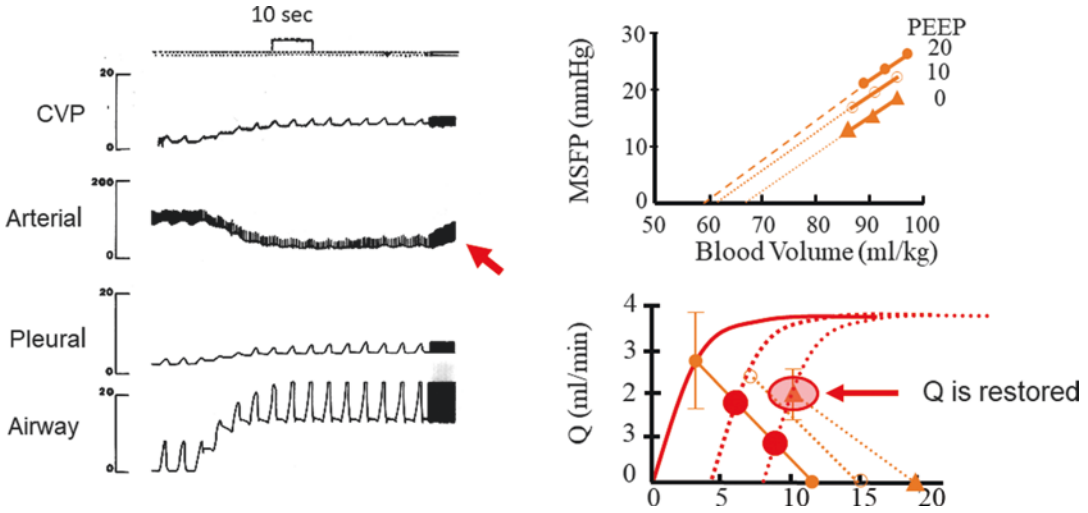


Fig. 18.6 Effect of PEEP on venous return and the adaption by a decrease in vascular capacitance. On the left side, 10 mmHg of PEEP was applied to an animal. The airway pressure rose to 10 cmH₂O, Ppl by 3 cmH₂O, and CVP rose too. Arterial pressure markedly fell, but after 1 minute, it began to increase because of reflex adjustments. The upper right shows MSFP versus the blood volume (ml/kg) at 0, 10, and 20 cmH₂O of PEEP. Application of PEEP resulted in a shift the P-V relationships to the left (decrease in capacitance). The slope is compliance and was produced by rapid bolus of volume which was then removed. Note the linearity of the P-V relationships in the measured range. The bottom right shows presumed cardiac function curves intersecting the venous return curves

which shift to the right with the increase in MSFP because of a decrease in capacitance. The closed circles indicate what would have happened to cardiac output without the decrease in capacitance – it would have fallen markedly. The larger open circle shows how the decrease in capacitance greatly reduced the fall. A small increase in the resistance to venous return can be seen at PEEP = 20 mmHg. (Reprinted with permission of the American Thoracic Society. Copyright © 2020 American Thoracic Society. All rights reserved. Cite: Nanas and Magder (1992). American Review of Respiratory Disease* is an official journal of the American Thoracic Society. *Now titled the American Journal of Respiratory and Critical Care Medicine)

As was the case with the use of the inspiratory pattern of CVP with spontaneous inspirations to predict fluid responsiveness, an inspiratory fall in CVP with the fall in Ppl with the inspiratory effort that triggers the mechanical breath should indicate that the heart is functioning on the ascending part of its function curve. This then should predict that cardiac output will fall when PEEP is applied and the cardiac function curve is shifted to the right along the x-axis of the Guyton plot. Conversely, if there is no fall in CVP during the trigger, this should predict that the patient is on the flat part of the cardiac function curve and may not have a fall in cardiac output with the application of PEEP. We used the words “may not,” because if the rise in Ppl with the PEEP and mechanical

breaths is high enough, the ascending part of the cardiac function curve will again be intersected and cardiac output will fall with further increases in Ppl. However, the test failed to be helpful (Magder et al. 2002). Although cardiac output fell more frequently in patients who had an inspiratory fall in CVP during a spontaneous effort when PEEP was applied, cardiac output did not fall in all of these patients with the application of PEEP. The explanation is that the fall in cardiac output with PEEP induces a reflex sympathetic response that contracts the capacitance veins and venules and recruits unstressed in to stressed volume (Fig. 18.6). The effectiveness of the reflex response depends upon the reserves in unstressed volume and the responsiveness of the baroreceptors.

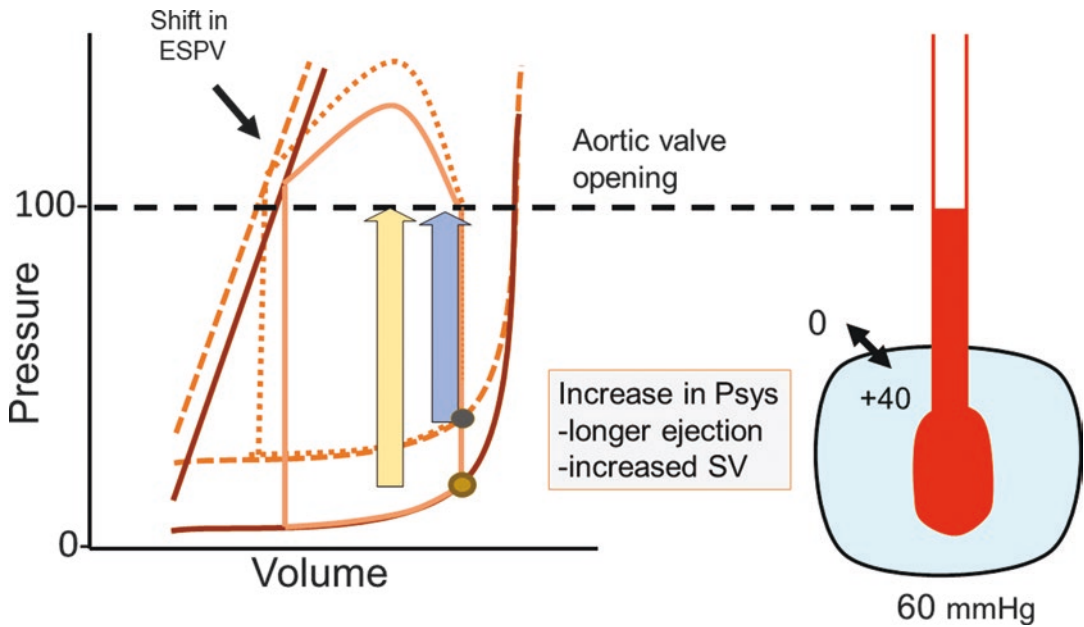


Fig. 18.7 Effect of an increase in Ppl on the left ventricular pressure-volume relationship. An increase in Ppl shifts the P-V loop upward, but as in Fig. 18.5, the aortic valve initially opens at the same pressure. This shortens the isovolumetric part of ventricular contraction (blue arrow), decreases LV afterload, and increases ejection (i.e., stroke volume). The end-systolic P-V relationship is shifted to

the left because of the change in the referencing of the intracardiac pressures relative to atmosphere. The right side of the figure shows the equivalent of an isolated heart surrounded by a positive pressure of 40 mmHg and ejecting to an aortic pressure of 100 mmHg. It now only has to generate 60 mmHg to do so instead of 100 mmHg

Effect of Increase in Ppl on the LV

In contrast to the decrease in LV ejection with a fall in Ppl, a rise in Ppl increases LV ejection because the afterload on the LV is reduced as the heart is effectively raised relative to the rest of body (Fig. 18.7). However, the effect of an increase in Ppl on the LV is much less than the effect of a decrease in Ppl for two reasons. First, during a decrease in Ppl, filling of the RV increases, and ejection from the LV decreases, and both work to increase cardiac volume. On the other hand, during an increase in Ppl, RV filling is decreased and lowers the available preload. On the left side, the rise in Ppl only mildly increases LV ejection because the changes in Ppl are generally smaller than the potentially large decrease in Ppl with a strong inspiratory effort. The effective change in afterload and benefit for LV ejection thus is small, and the large decrease in RV filling dominates the response.

Effect of Transpulmonary Pressure

The second major way that ventilation can affect cardiac output is as a consequence of lung inflation (Fig. 18.8). With a spontaneous breath, the descent of the diaphragm and outward movement of the intercostal muscles decrease Ppl relative to airway pressure. Application of a positive pressure to the airway expands the lungs by the raising airway pressure relative to Ppl. In both cases the pressure across the alveoli increases to inflate the lungs. This is called transpulmonary pressure and it always is positive for the lungs to inflate. In a normal lung, about half the applied airway pressure with positive pressure inflation is transmitted through the elastic walls of the alveoli to the pleural space, and Ppl becomes more positive during lung inflation but less positive than alveolar pressure. The pressure from the airway to atmospheric pressure is called the transthoracic pressure, and it, too, always is a positive value.

that do not affect pulmonary blood flow, but above a critical value of pressure in intra-alveolar vessels, the load on the RV increases 1:1 with the increase in transpulmonary pressure. Factors that effect this “break” point include the initial pulmonary arterial pressure, which is affected by the output from the RV and the resistance in the pulmonary artery to the alveolar vessels; the downstream left atrial pressure, which is affected by blood volume; the function of the LV; and the compliance of the lung, which determine the change in transpulmonary pressure needed to inflate the lung. It is likely that zone II conditions can develop in many patients at peak inspiration with mechanical breaths and with tidal volumes between 6–8 ml/kg and may be a major reason why lower tidal volumes have been shown to be advantageous (The Acute Respiratory Distress Syndrome N 2000). It also argues for keeping the driving pressure below 15 cmH₂O (Amato et al. 2015).

Effect of Lung Inflation

Lung inflation itself has a small effect on LV filling (Fig. 18.9). Besides there being blood vessels between the alveoli, there also are

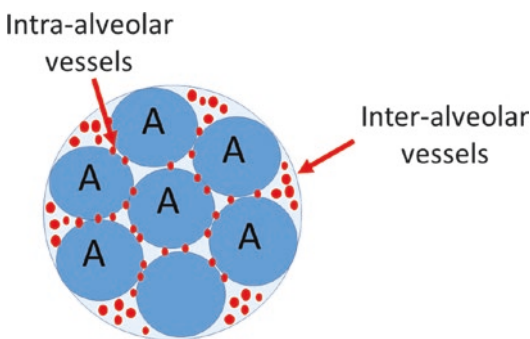


Fig. 18.9 Inter- and intra-alveolar vessels in the lungs. An alveolus. With lung inflation, whether with negative or positive inspiratory efforts, the intra-alveolar vessels are exposed to alveolar pressure but only are compressed when alveolar pressure is greater than the pressure inside the vessels (relative to atmospheric pressure). The inter-alveolar vessels are expanded during a breath and can take up volume, but this likely does not occur after a left atrial pressure of <3 mmHg because they are then fully expanded

blood vessels in the corner spaces outside of the alveoli (interalveolar spaces). When lungs inflate, the intra-alveoli are compressed and a small volume of blood is expelled into the left atrium. This produces a rise in left atrial filling pressure of ~2 mmHg. On the other hand, the corner interalveolar vessels expand and can take up volume. Experiments on isolated rabbit lungs showed that once left atrial pressure is greater than ~2 mmHg, these veins are fully distended and do not take up more volume so that, in general, the net effect is expulsion of pulmonary blood volume with lung inflation and a small increase in left atrial pressure (Howell et al. 1961).

Lung inflation can also produce a local effect on the heart by compressing it. The late John Butler nicely described this in his delightful Dickinson Richards lecture entitled “The heart is in good hands” (Butler 1983). An example is illustrated in Fig. 18.10 in which marked variations in CVP and Ppao are present in this patient who had an open chest. In the bottom half of the figure, the chest is closed, and the respiratory variations in CVP and Ppao are small, likely because the mediastinum was less swollen and packings were removed.

Respiratory Variations in Heart Rate

The change in arterial pressure that occurs during the ventilator cycle is sensed by the arterial baroreceptors. This produces variations in heart rate and, potentially to some extent, systemic vascular resistance. These changes can alter the magnitude of the pulse pressure because of their consequent effects on stroke volume. The magnitude of the effect depends upon the gain of the baroreceptors, as well as the magnitude of the change in arterial pressure. The magnitude of this sinus arrhythmia tends to be greater in younger patients and in those who have increased vagal tone. It is possible that there also is some direct input into the central regulators of autonomic activity from the respiratory center.

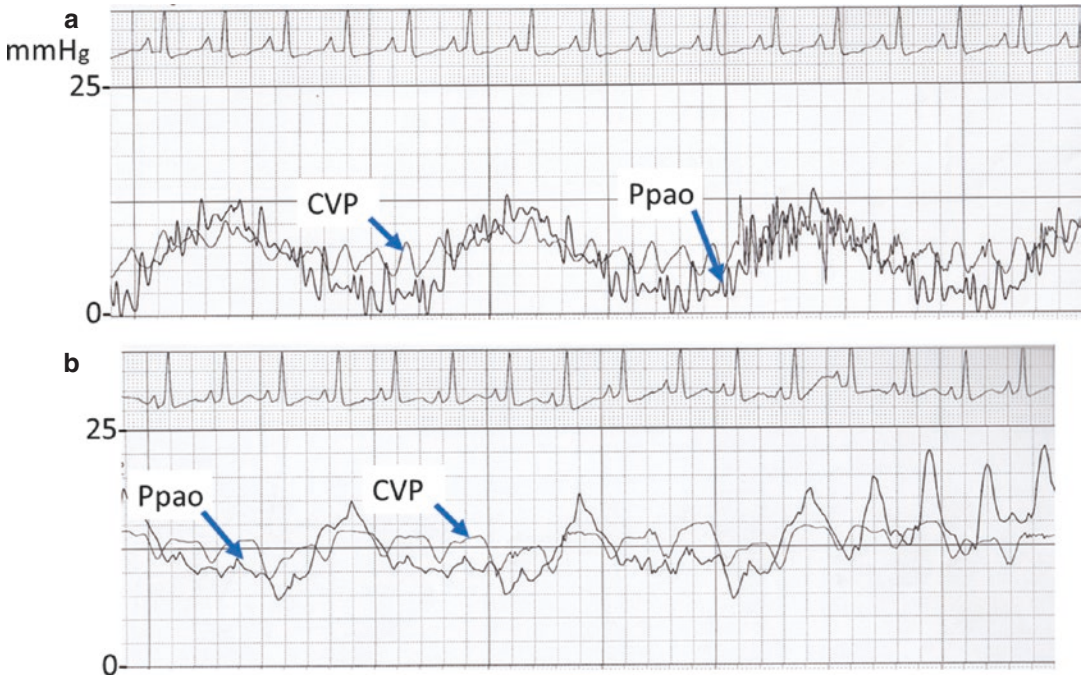


Fig. 18.10 Respiratory variations in CVP and Ppao in a patient with an open chest and controlled mechanical breaths – example of chest compression of the heart. In A, the chest is open, and both the CVP and Ppao increase together indicating that the lung inflation can produce local changes in Ppl and cardiac compression. In B the

chest was closed. There is a modest decrease in Ppao with inspiratory efforts but no change in CVP indicating the patient's RV still is volume limited. On the right side of the figure, the balloon is deflated and pulmonary artery pressure is seen

RV-LV Interactions During Ventilation

Interactions of the RV and LV are discussed in detail in the Chap. 3 on RV function. In this chapter we will deal with these interactions as they relate to the phasic changes in the status of the ventricles during the ventilation cycle.

Changes in filling and emptying of the RV and LV during the ventilation cycle are out of phase with each other. During a spontaneous breath and a fall in Ppl, and assuming that the heart is not working on the flat part of its function curve (Fig. 18.3), RV transmural diastolic pressure and volume increase and so does RV stroke volume. LV diastolic volume also increases, but this is not because of increased return of blood to the heart; the inspiratory increase in RV volume has not yet reached the LV. Rather, it is because of the inspiratory increase in LV afterload and the conse-

quent decrease in stroke volume. There also is the small increase in LV filling because of lung inflation as discussed above. The relative effects on the two sides of the heart depend upon the magnitude of volume increase to the RV, how close the RV is to the limit of its filling, how big the afterload effect is on the LV, and the contractile status of the LV. During a mechanical breath and a rise in Ppl, RV transmural diastolic pressure and volume decrease and so does RV stroke volume. LV diastolic volume goes down, too, but this is not due to decreased filling. It rather is because of the decrease in LV afterload and the consequent increase in stroke volume with a small modification from the blood squeezed out of the lungs during lung inflation (Howell et al. 1961). If non-zone III conditions develop in the lung, the situation is more complicated. This is more evident during mechanical breaths. In this situation, depending upon the relative magnitude

of the increased load on RV ejection and the magnitude of decreased RV filling during lung inflation, the RV diastolic pressure and volume may even increase. However, the RV load from the development of non-zone III conditions has no direct effect on the LV.

From the above it is evident that the volumes and pressures of the two ventricles transiently differ during the ventilation cycle, and this creates the potential for changing pressure differences between the two sides which could alter the diastolic and systolic function of the other side. The magnitude of these interactions depends upon the magnitude of the pressure differences between the ventricles and the elastance of the septal wall, as well as the elastance of the free walls of both ventricles because the force from ventricular distension is distributed to them as well (Maughan et al. 1987; Santamore et al. 1990; Bove and Santamore 1981). The interaction of the two ventricles is greatly magnified when the pericardium limits cardiac filling (Takata et al. 1990a). This is because pericardium is very stiff, and when its limit of filling is reached, it becomes the common elastance of all the free ventricular walls. The septum then becomes the easiest region to stretch.

Another factor in the interaction between the two ventricles is that cardiac muscle in the intra-ventricular septum contributes to force production of both the RV and LV (Santamore and Dell'Italia 1998). Thus changes in the force of contraction in the septum due to a change in the afterload of one ventricle can potentially affect the force produced by the other ventricle. This, too, is highly dependent upon the function of the ventricles as well as the respective pressures they have to eject against (Yamaguchi et al. 1991). Under normal conditions, pulmonary systolic pressure is very low compared to that of the LV, and the effect of LV contraction on the RV is trivial, especially because the normal RV has a large range to adapt. However, the situation potentially can be very different when the RV afterload is greatly increased. As reviewed in the chapter on RV function (Chap. 3), the interaction effect still likely is small and is primarily an issue when RV filling is limited.

There is a third factor that likely dominates RV and LV interactions and overrides the effect of the other two factors (Olsen et al. 1983). The RV and LV are in series. This means that whatever comes out of the RV during the cyclic respiratory variations must eventually come out of the LV so that based on the conservation of mass there is an average state over time. For example, a transient increase in the load on the RV from lung inflation with zone II conditions will increase RV diastolic pressure and volume and, if large enough, can shift the septum to the left. The leftward shift of the septum takes up space in the LV and decreases its diastolic compliance, which potentially can alter LV filling. However, after the load on the RV is dissipated following inspiration, and the septum is no longer displaced, the backed-up RV volume is transferred to the LV in subsequent beats, and the following LV stroke volumes increase. In the end, the volumes all must be conserved and accounted for because the system is a closed circuit. Echocardiographic or MRI images may look impressive with shifting volumes, but in the end the mean outputs cannot be different unless there is an increase in the mean P_{ra} , which then results in reduction in venous return and cardiac output.

An example of how complex the analysis can be for these interactions is the situation in which an inspiratory increase in the lung volume is sufficient to produce West zone II conditions, increases the load on the RV, and consequently increases RV diastolic volume as part of the compensation process, and this then results in RV diastolic limitation. When RV limitation occurs, any further rise in RV systolic pressure markedly increases RV diastolic pressure without a change in volume, except by shifting the septum into the LV. In the fixed pericardial space, this reduces LV diastolic volume and, consequently, decreases LV stroke volume (Takata et al. 1990a, 1997). However, the bowing of the septum occurs because RV filling is limited by pericardial constraint, or the cardiac cytoskeleton itself, so that the real problem is the inability to get more blood into and out of the RV. It also means that P_{ra} will rise during the inspiratory phase without a change in volume. This will reduce venous return during

this phase. It is the rise in Pra that really reduces the steady-state cardiac output, and the left heart is not the primary problem because the volume cannot get into the heart as a unit. The solution is to increase RV function, which will lower RV end-systolic pressure and allow more blood return. If that is not possible, decrease total blood volume so that the RV is no longer functioning on the flat part of the cardiac function curve and with what can be called “wasted preload”.

Another issue that is underappreciated is that large transient changes in pulmonary flow during the respiratory cycle can potentially have important effects on the pulmonary vasculature. As shown by Katira et al. (2017), as well as in modeling studies (Magder and Guerard 2012), RV output can go to almost zero at peak inspiration with a mechanical breath because of the rise in Pra relative to atmosphere, as well as development of zone II conditions and the consequent decrease in RV ejection. On the subsequent beats, there can be very large increases in pulmonary flow, and it is possible that the resulting shear stress has an important impact on the pulmonary vessels. This could potentially be an important factor for the lung injury associated with large tidal volumes. As shown by Webb and Tierney (Webb and Tierney 1974) and subsequently by Katira et al. (Katira et al. 2017), the lung injury with ventilation is primarily perivascular and not around the alveoli indicating that there likely is an important vascular component.

It has been argued that changes in the force of contraction of one ventricle can affect the other, and this could occur during the fluctuation in pulmonary and arterial pressures during ventilation. For example, a large transient fall in arterial pressure in someone with pulsus paradoxus will cause significant changes in the loading on the LV and thus forces generated by the septum. It might then be argued that this could lead to transient decreases in the performance of the RV, which would potentially lose some of its LV assistance. In general, this effect has not been shown to be very significant in the majority of patients who have had major unloading of the LV by a mechanical device (Santamore and Gray Jr. 1996), and it is unlikely that this would be

clinically significant with breathing. Where it may be of importance is when the decrease in septal contraction reduces the pressure tolerance of an already dysfunctional RV enough so that the limit of RV filling is reached. When that happens, any further increase in the RV load will reduce cardiac output as discussed above. Furthermore, the rising right-sided diastolic pressures can be transferred to the LV in diastole which also is limited by the pericardium. Even though the LV may look under-filled, its diastolic pressure rises with the rise in Pra. This raises pulmonary venous pressure, which raises pulmonary artery pressure and further increases the load on the RV. However, for all of this to happen, vascular volume needs to be sufficiently increased to put Pra in the range of limited RV filling and that Pra is high enough for the consequent increase in left atrial pressure to affect the RV.

In summary, analysis of the effects on cardiac output of ventricular interactions that occur during the ventilation cycle must take into account the conservation of mass, the interaction of the cardiac and return functions, and the dominance of total vascular compliance by the volume in systemic venules and veins. Based on these factors, a decrease in steady-state cardiac output must inevitably be associated with an increase in the mean value of Pra because the interactions are effectively acting to flatten the cardiac function curve in the Guyton graphical approach. Too often the interactions are evaluated by taking observations during a phase of the ventilation cycle without considering the necessary subsequent correction phase.

Pulsus Paradoxus

A readily evident effect of heart-lung interaction is seen in the variation of arterial pressure during the respiratory cycle (McGregor 1979). When breathing spontaneously, arterial systolic, diastolic, and pulse pressures fall on inspiration (Fig. 18.11). The primary factor is that the pressure around the heart, that is, Ppl, has fallen relative to atmospheric pressure so that the heart is

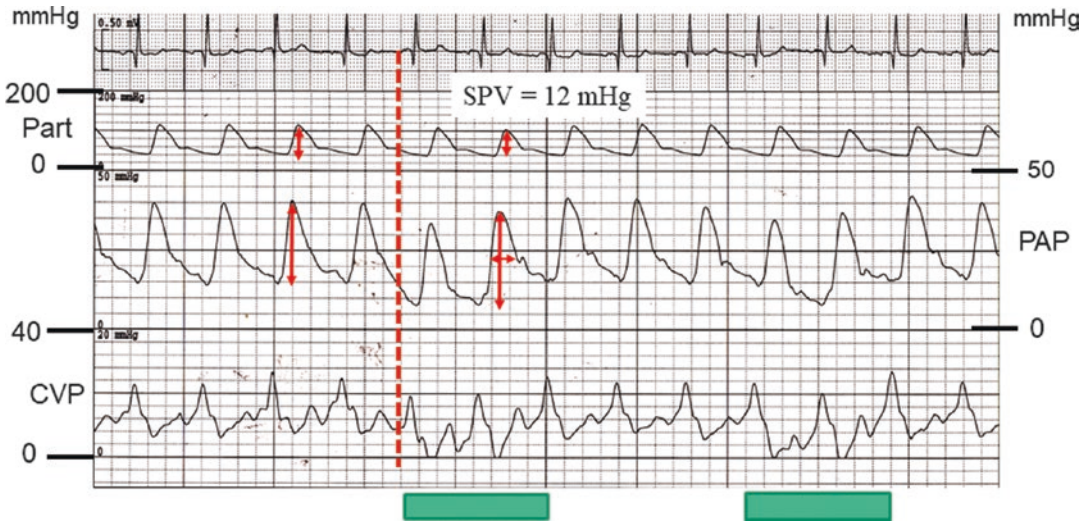


Fig. 18.11 Normal arterial pulse pressure variation with inspiration. The bars below the tracing indicate inspiration. During inspiration the CVP falls and the “y” descent increases (cutoff); PA falls relative to atmosphere, but its pulse pressure and its width increase, whereas the arterial pulse pressure falls

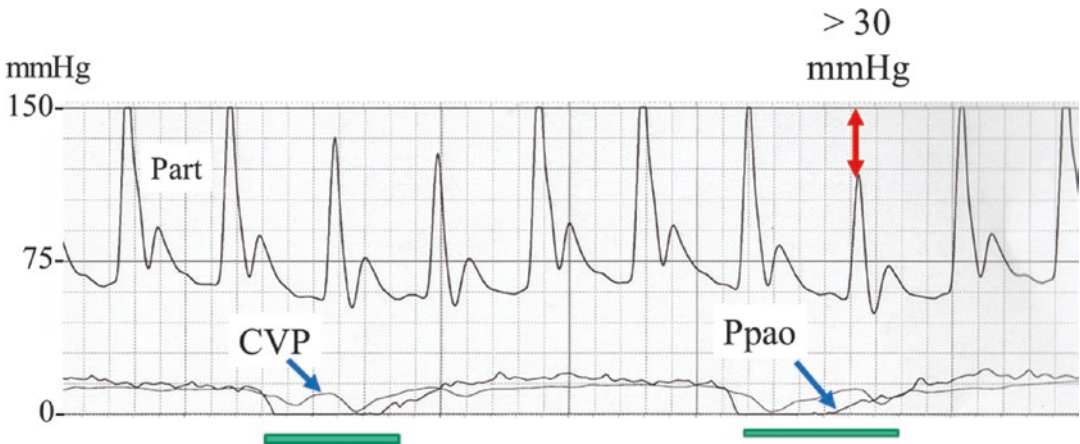


Fig. 18.12 Pulsus paradoxus with corresponding CVP and Ppao. Large inspiratory efforts as indicated by the negative swing in Ppao and active expiration contribute the marked swings in arterial pressure. The bars mark inspiration

effectively lowered relative to the rest of the body. However, if that were the only thing happening, systolic and diastolic pressures should fall equally, and the pulse pressure should not change. The pulse pressure falls because, as discussed above, the heart starts contracting from a lower arterial pressure relative to atmosphere. It thus must first overcome this negative pressure difference and then generate a sufficient pressure for the baroreceptors to maintain their normal set point. This increases the afterload on the

LV, and pulse pressure falls transiently, but the heart still generates a higher systolic transmural pressure. Furthermore, during inspiration, filling of the RV increases. Through the series effect, the increased RV filling is passed to the LV after a few beats, which then raises arterial pressures during expiration. The term pulsus paradoxus was originally coined by Kussmaul to describe larger than normal swings in arterial pulse pressure (Fig. 18.12) because he noted that the peripheral pulse got weaker whereas the heart

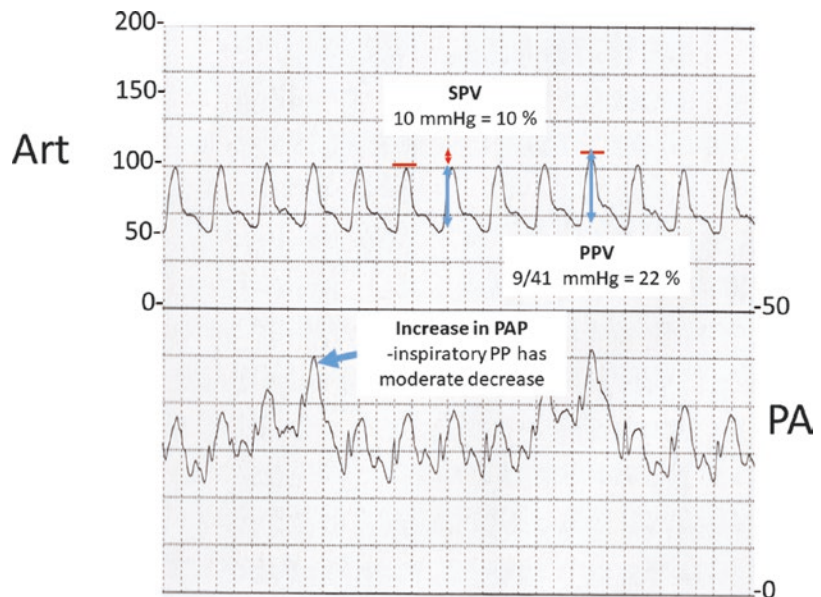
sounds got stronger (Swami and Spodick 2003). The upper normal range of systolic pressure variation with a breath is 10 mmHg. The greater the fall in Ppl pressure with inspiration, the greater the potential pulse pressure variation. The arterial pressure variation also is greater when cardiac contractility is decreased because of the flatter slope of the LV end-systolic pressure.

An exaggerated pulsus paradoxus is seen when there is cardiac tamponade (Swami and Spodick 2003). The mechanism for this starts with the understanding that during tamponade, the total volume of all compartments in the pericardium, that is, right atrium, RV, left atrium, and LV, is fixed because the pressure in diastole is determined by volume in the pericardium surrounding the heart and it does not change. During normal cardiac function, both the atrium and ventricles fill during diastole, and the whole heart gets bigger. In tamponade, the atrium only can fill during systole when the ventricles empty. The atrial volume is then passed to the ventricles during diastole, and the total pericardial volume does not change. Furthermore, during inspiration, the pressure difference filling the RV is increased because the pressure in the heart decreases relative to atmosphere, whereas this does not happen on the left side. During inspiration, the RV thus has an advantage over the LV

and compromises LV filling so that LV stroke volume falls. The LV afterload also increases which further lowers its stroke volume. After a few beats, depending upon the heart rate, the increased stroke volume from the RV passes to the LV though the series effect. RV filling is then reduced, and LV stroke volume transiently goes up which gives the exaggerated respiratory variation in arterial pressure seen in this condition. A classic sign seen in tamponade is the loss of “y” descents on the CVP. This is because the “y” descent in the CVP is due to emptying of the atrium into the relatively empty and low-pressure RV followed by the rapid rise in pressure as the RV fills. However, as already noted, in tamponade, the diastolic pressure in the pericardium does not change so the volume only can shift from the right atrium to RV with no overall change pericardial pressure.

When RV filling is limited and the heart is functioning on the flat part of the cardiac function curve pulse, pressure variations are reduced. This is because there is no inspiratory increase of RV filling (although the diastolic transmural pressure increases). However, there is still the transmission of the reduction of Ppl to the LV and the increase in afterload which can cause some variation in the arterial pressures due to direct pressure effects without a change in volume.

Fig. 18.13 Reverse paradox. SPV, systolic pressure variation. The value was 10 mmHg which was 10% of the systolic pressure of 100 mmHg. During inspiration, there is a small increase in the arterial pulse pressure (PP) and decrease in the pulmonary artery pressure (PA) PP. The pulse pressure variation is calculated from the difference between the highest and lowest PP and the mean of the two



Inverse Pulsus Paradoxus

During mechanical breaths and positive pressure ventilation, the arterial variations are reversed; the systolic and pulse pressures rise during inspiration and fall during expiration (Fig. 18.13). Exaggerations of this pattern have been used to identify patients who will be fluid responsive (Michard et al. 1999, 2000; Michard and Teboul 2002; Perel 1998; Perel et al. 1987; Pizov et al. 1988). Importantly, it needs to be emphasized that fluid responsiveness does not mean that the patient needs fluids (Magder 2004). In this situation, the inspiratory rise in Ppl reduces the return of blood to the heart which is effectively “raised” relative to the rest of the body. RV stroke volume decreases. At the same time, the rise in Ppl raises the LV pressure relative to the systemic arterial pressure. This lowers LV afterload and allows a larger stroke volume. In a few beats by the series effect, the decreased RV stroke volume is passed to the LV, and its stroke volume decreases during expiration. If the venous return curve intersects the flat part of the cardiac function curve, the

inspiratory reduction of RV filling is reduced; the farther the intersection of the venous return-cardiac curve is from the ascending part of the cardiac function curve, the greater the effect. The magnitude of the respiratory change in arterial systolic, or pulse pressure, depends upon the magnitude of the change in Ppl with the breath, which in turn depends upon the tidal volume and the compliance of the thorax (Magder and Guerard 2012). It also is affected by the size of the stroke volume and heart rate because these affect how large the change in stroke volume can be to alter the arterial pressure (Magder and Guerard 2012). Volume reserves in the pulmonary venous compartment and the pulmonary vascular resistance also affect the magnitude of the effect. The measure thus has a qualitative value, but quantitative predictions of volume responsiveness should be limited to very controlled situations such as patients in the operating room (Magder 2004). Because the effects of negative and positive pressure inspiratory efforts are 180° from each other, only changes with pure mechanical breath should be used.

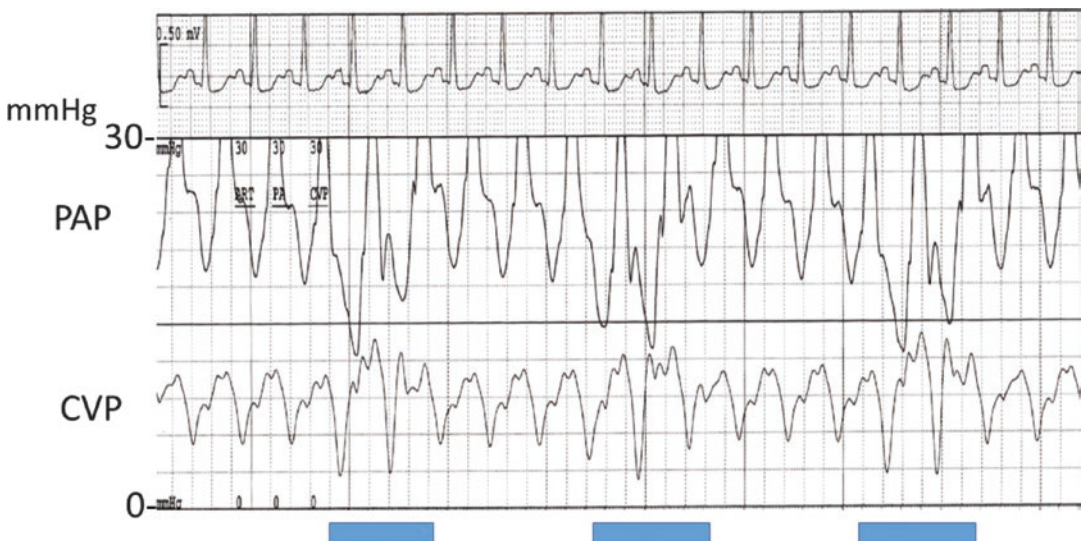


Fig. 18.14 Example of Kussmaul’s sign. The middle tracing is the pulmonary artery (PAP) pressure and the lower tracing CVP. The blue bars indicate inspiration which also is evident from the fall in PAP. On inspiration CVP rose but did not change on expiration. The fall in PAP also indicates that Ppl fell, and it is unlikely that there

could have been simultaneous contractions of abdominal muscles. For this to occur, the descending diaphragm had to have compressed the abdominal venous compartment and increased venous return to the RV that was volume limited and only could have an inspiratory rise in pressure without a change in outflow

HJR

Hepatojugular reflux is defined by a sustained elevation of jugular venous pressure after abdominal pressure is applied (Fig. 18.14) (Ducas et al. 1983). The increase in venous return that occurs with abdominal pressure increases CVP in patients who are at their volume limit of right heart filling. Because of the limit to RV filling, the increased volume cannot be passed on from the RV (Takata et al. 1990b). This test can be helpful in guiding volume resuscitation or diuretic therapy by providing a functional assessment of right heart function and identifying RV limitation.

Active Expiration

An important confounder when investigating the effect of respiratory variations, either in the Pra/CVP or with arterial pulse pressure variations, is the presence of active expiration. When present, abdominal contractions increase abdominal pressure and potentially can shift the venous return to a more positive value (i.e., rightward shift) (Magder et al. 2018; Verscheure et al. 2016). This transiently increases venous return as occurs with the hepatojugular reflux (Ducas et al. 1983) and produces an effect on the arterial pressure with a

respiratory frequency. The change in stroke volume depends upon whether the venous return function intersects the flat part of the cardiac function curve or the ascending part. The increase in abdominal pressure also can be directly transmitted to the pleural space and increase intrathoracic pressure, and this can transiently increase arterial systolic and pulse pressures (Takata et al. 1990b, c).

The shift in volume to the chest with an increase in abdominal pressure is complex (Takata et al. 1990c; Takata and Robotham 1992). First, there needs to be an adequate volume to shift. However, this need not be just stressed volume. The increase in intra-abdominal pressure also can transfer unstressed volume. The second variable is whether the cardiac function curve is functioning on its plateau. If it is, the CVP will rise but diastolic volume will not change. The third factor is the magnitude of the venous pressure. If the abdominal pressure is higher than the pressure in abdominal veins, the abdominal veins will collapse as they leave the abdomen and produce flow limitation or a vascular waterfall effect (Takata et al. 1990c). This can occur at the level of the return of blood from the legs to the abdominal veins or at the level of the abdominal veins to the chest, which makes predictions of the volume shifts variable and very sensitive to changes in the total body volume status.

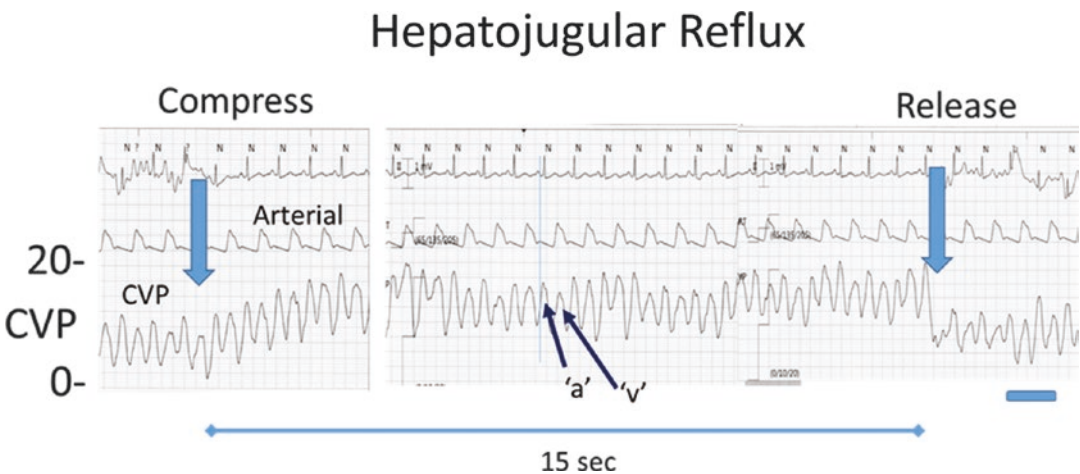


Fig. 18.15 Example of a hepatojugular reflux. Compression of the abdomen with ~20 mmHg pressure produced a sustained increase in CVP. This indicates that

there was a limit to RV filling. The compression produced a small increase in arterial pressure suggesting that there likely was a small initial RV volume increase

Kussmaul's Sign

Kussmaul's sign is defined as an inspiratory increase in CVP which is in contrast to the normal inspiratory fall in CVP (Fig. 18.15) (Takata et al. 1990a, b, c; Takata and Robotham 1992). For this to occur, RV filling needs to be limited. During inspiration, the diaphragm descends and abdominal pressure moderately increases. If the abdominal volume reserve is large and the inspiratory descent of the diaphragm is sufficiently large, the inspiratory rise in intra-abdominal pressure can be sufficient to compress the abdominal venous compliant region and transiently increase the venous return to the RV (Takata et al. 1990a, 1997). This still will not produce an inspiratory rise in CVP relative to atmosphere. For this to occur, RV filling

needs to be limited for then there can be a pressure rise without an increase in forward flow. Kussmaul's sign needs to be distinguished from contraction of expiratory muscles which also raise intra-abdominal pressure and recruit venous volume to the right heart as occurs with a hepatogastric reflux. The difference is that active contraction occurs during expiration, whereas Kussmaul's sign occurs during inspiration.

Mueller Maneuver

A Mueller maneuver is an inspiration against a closed glottis. It gives a good physiological demonstration of the potential effects of large negative swings in Ppl on LV ejection. Because the airway

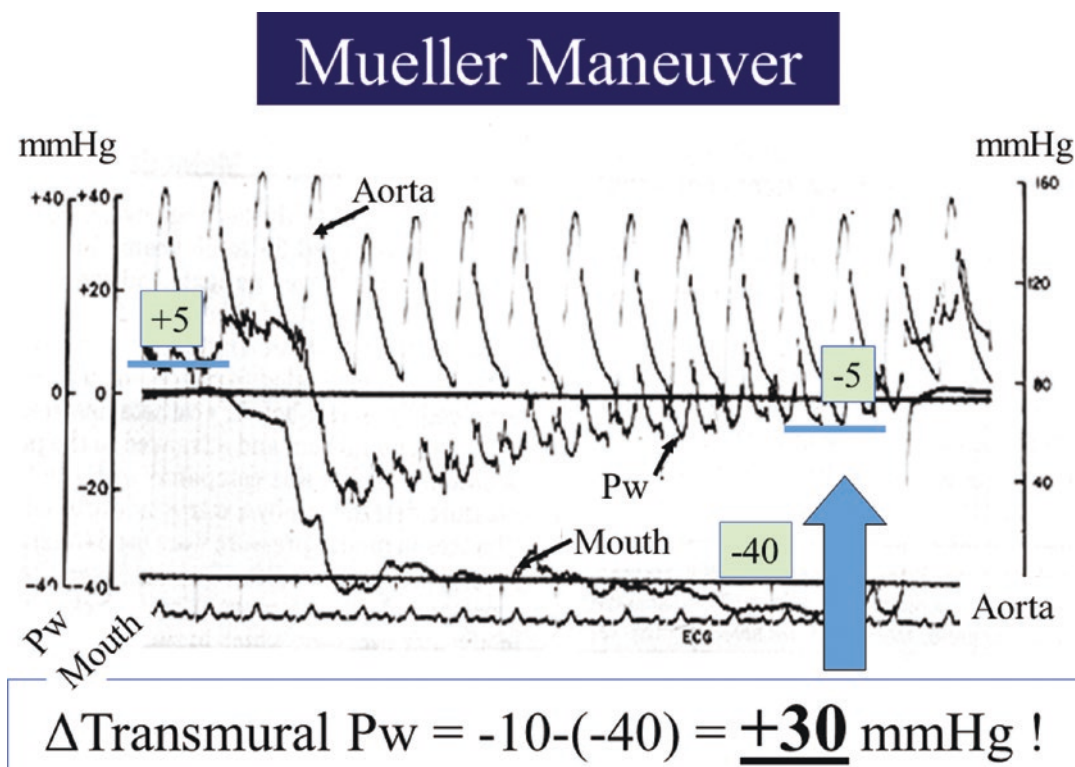


Fig. 18.16 Transmural pressure change during a Mueller maneuver. Pw refers to pulmonary capillary wedge pressure. Mouth pressure was measured with pressure gauge attached to a transducer. At the start of the Mueller, mouth pressure fell by 40 mmHg, Pw fell below zero (note that zero for Pw is in the middle of the tracing), and there was a small fall in aortic pressure. At the end of the maneuver,

Pw was -5 mmHg, and therefore the net change in Pw was -10 mmHg. Since mouth pressure fell by -40 mmHg, the transmural Pw actually rose by 30 mmHg, and the real net value is 35 mmHg. See text for further details. (Adapted from Magder et al. (1983) with permission of Elsevier)

occlusion does not allow a change in lung volume, the change in airway pressure during the maneuver reflects the change in Ppl so that *change* in Ppl can be measured without directly accessing the pleural space. This maneuver allows a calculation of change in transmural pressure by subtracting the change in Ppl from the change in vascular pressure as seen in Fig. 18.16. At the start of the maneuver, there is a moderate transient fall in arterial pressure, which within a few beats returns to the baseline value. In the figure, the airway pressure and thus Ppl fell by 40 mmHg. This means that when the arterial pressure returned back to the baseline level, LV afterload was increased by 40 mmHg. The pulmonary artery occlusion pressure as an estimate of the left atrial pressure did not fall as much as the Ppl indicating that left atrial and LV diastolic transmural pressure and volume increased. As the negative Ppl was maintained, there was a progressive increase

in the left atrial pressure, and large “v” waves developed indicating a decrease in left atrial compliance as the left atrium became more distended. The final pulmonary artery occlusion pressure decreased by 10 mmHg from the end-expiratory pre-maneuver value when measured relative to atmospheric pressure, but the outside Ppl decreased by 40 mmHg so that the final change in left atrial transmural pressure was 30 mmHg. The actual transmural left atrial pressure was the original 5 mmHg plus the 30 mmHg increase, which gives a left atrial transmural pressure of 35 mmHg and explains the large “v” waves!

Valsalva

The series effects of an increase Ppl are seen with a Valsalva maneuver (Fig. 18.17) which is an expiration against a closed glottis, the opposite of

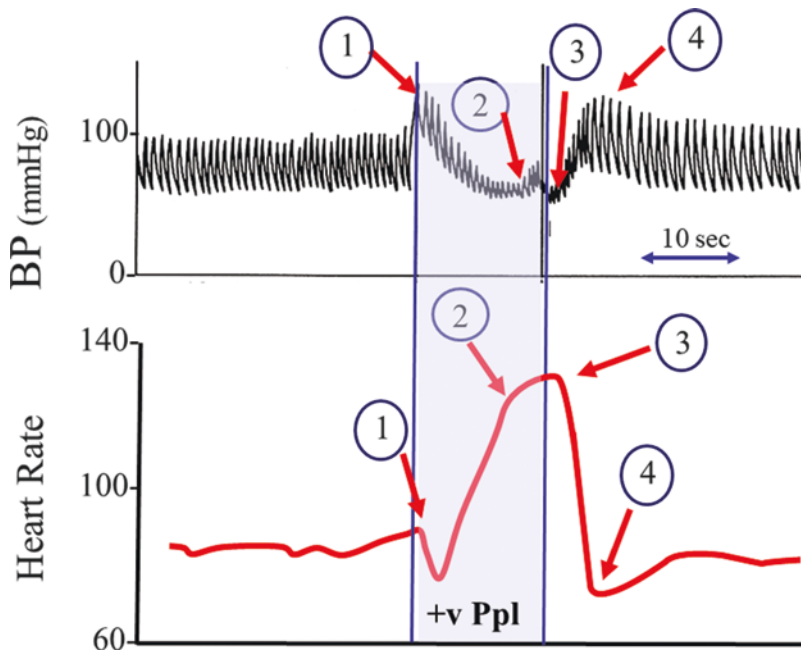


Fig. 18.17 Example of a Valsalva maneuver. The top shows the arterial pressure (BP) and the bottom the heart rate. At 1, the subject bears down by expiring against a closed glottis. There is an initial increase in arterial pressure because of the transmitted pleural pressure (Ppl) but also because of decreased LV afterload as in Fig. 18.7. The rise in BP triggers a baroreceptor response and heart rate slows. The positive Ppl decreases venous return and

BP progressively falls. The reduced baroreceptor pressure reduces cardiovascular inhibition, stage 2, and there is a rise in heart rate and rise in SVR. At 3, the Valsalva is released. There is an abrupt further fall in BP because of the decreased Ppl surrounding the heart and a further small increase in heart rate. In stage 4 backed-up venous blood can now return to the heart. BP again rises, heart rate slows, and values settle back to the baseline state

a Mueller maneuver. It also shows reflex adjustments to the effect on the vasculature of an increase in Ppl. At the start of the maneuver, phase 1, arterial pressure transiently rises because of transmission of Ppl to the LV and the resultant reduction of LV afterload and increase in stroke volume. This only lasts for a few beats. The increase in arterial pressure produces a small baroreceptor-induced decrease in heart rate. During phase 2, the increase in Ppl quickly leads to a decrease in venous return and cardiac output as evident by the fall of arterial pressure as well as arterial pulse pressure. This induces a baroreceptor-mediated increase in heart rate and systemic vascular resistance. These produce some restoration of blood pressure. There likely also is some recruitment of unstressed into stressed volume which helps support RV filling. The expiratory force is released in phase 3. The sudden decrease in Ppl leads to a further fall in arterial pressure and a further baroreceptor-mediated rise in heart rate, but this is reversed quickly in phase 4 as the backed up venous volume rapidly increases RV filling and increases cardiac output. The arterial pressure quickly rises, especially because the SVR at first still is elevated. The increase in arterial pressure results in a vagal-induced decrease in heart rate and reduction in SVR and the system settles back to baseline values.

Summary

The key principle emphasized in this review is that heart-lung interactions are dominated by changes in Ppl, which essentially change the position of the heart relative to the rest of the body. Both negative and positive changes in Ppl have major effects on RV filling, and negative changes in Ppl can have large effects on LV ejection. Volume status and limitation of RV filling by the pericardium or cardiac cytoskeleton are important moderators of the magnitude of heart-lung interactions. Low levels of changes in lung volume with small changes in transpulmonary pressure have a minimal effect on RV output, but when a critical value of transpulmonary pressure

is reached, changes in transpulmonary pressure have a one to one pressure effect on the load to the RV. The effect of this is especially important when RV function is decreased and, even more so, when RV filling is limited. The cyclic effects of the alteration of filling of the RV/LV are dominated by the series effect so that mass is conserved. Activation of expiratory muscles adds an extra level of complication to heart-lung interactions, as do reflex changes both from the carotid baroreceptors and afferent nerves in the lungs and peripheral tissues, although these generally are small unless the hemodynamic change from a heart-lung interaction is sustained.

References

- Amato MBP, Meade MO, Slutsky AS, Brochard L, Costa ELV, Schoenfeld DA, et al. Driving pressure and survival in the acute respiratory distress syndrome. *N Engl J Med*. 2015;372(8):747–55.
- Barbier C, Loubières Y, Schmit C, Hayon J, Ricôme JL, Jardin F, et al. Respiratory changes in inferior vena cava diameter are helpful in predicting fluid responsiveness in ventilated septic patients. *Intensive Care Med*. 2004;30(9):1740–6.
- Bove AA, Santamore WP. Ventricular interdependence. *Prog Cardiovasc Dis*. 1981;23(5):365–88.
- Butler J. The heart is in good hands. *Circulation*. 1983;67(6):1163–8.
- Ducas J, Magder SA, McGregor M. Validity of the hepato-jugular reflux as a clinical test for congestive heart failure. *Am J Cardiol*. 1983;52(10):1299–304.
- Fessler HE, Brower RG, Wise RA, Permutt S. Effects of positive end-expiratory pressure on the gradient for venous return. *Am Rev Respir Dis*. 1992a;146:4–10.
- Fessler HE, Brower RG, Wise RA, Permutt S. Effects of positive end-expiratory pressure on the canine venous return curve. *Am Rev Respir Dis*. 1992b;146(1):4–10.
- Guyton AC. Determination of cardiac output by equating venous return curves with cardiac response curves. *Physiol Rev*. 1955;35:123–9.
- Guyton AC, Polizo D, Armstrong GG. Mean circulatory filling pressure measured immediately after cessation of heart pumping. *Am J Physiol*. 1954;179(2):261–7.
- Guyton AC, Lindsey AW, Bernathy B, Richardson T. Venous return at various right atrial pressures and the normal venous return curve. *Am J Physiol*. 1957;189(3):609–15.
- Guyton AC, Jones CE, Coleman TG. In: Guyton AC, editor. *Circulatory physiology: cardiac output and its regulation*. Philadelphia: W.B. Saunders Co.; 1973.
- Howell JB, Permutt S, Proctor DF, Riley RL. Effect of inflation of the lung on different parts of pulmonary vascular bed. *J Appl Physiol*. 1961;16:71–6.

- Katira BH, Giesinger RE, Engelberts D, Zabini D, Kornecki A, Otulakowski G, et al. Adverse heart-lung interactions in ventilator-induced lung injury. *Am J Respir Crit Care Med.* 2017;196(11):1411–21.
- Lopez-Muniz R, Stephens NL, Bromberger-Barnea B, Permutt S, Riley RL. Critical closure of pulmonary vessels analyzed in terms of Starling resistor model. *J Appl Physiol.* 1968;24(5):625–35.
- Magder S. Clinical usefulness of respiratory variations in arterial pressure. *Am J Respir Crit Care Med.* 2004;169(2):151–5.
- Magder S, Guérard B. Heart-lung interactions and pulmonary buffering: lessons from a computational modeling study. *Respir Physiol Neurobiol.* 2012;182(2–3):60–70.
- Magder SA, Lichtenstein S, Adelman AG. Effects of negative pleural pressure on left ventricular hemodynamics. *Am J Cardiol.* 1983;52(5):588–93.
- Magder SA, Georgiadis G, Cheong T. Respiratory variations in right atrial pressure predict response to fluid challenge. *J Crit Care.* 1992;7:76–85.
- Magder S, Erice F, Lagonidis D. Determinants of the 'y' descent and its usefulness as a predictor of ventricular filling. *J Intensive Care Med.* 2000;15:262–9.
- Magder S, Lagonidis D, Erice F. The use of respiratory variations in right atrial pressure to predict the cardiac output response to PEEP. *J Crit Care.* 2002;16(3):108–14.
- Magder S, Serri K, Verscheure S, Chauvin R, Goldberg P. Active expiration and the measurement of central venous pressure. *J Intensive Care Med.* 2018;33:430–5.
- Maughan WL, Sunagawa K, Sagawa K. Ventricular systolic interdependence: volume elastance model in isolated canine hearts. *Am J Physiol.* 1987;253(6 Pt 2):H1381–H90.
- McGregor M. Current concepts: pulsus paradoxus. *N Engl J Med.* 1979;301(9):480–2.
- Michard F, Teboul JL. Predicting fluid responsiveness in ICU patients: a critical analysis of the evidence. *Chest.* 2002;121(6):2000–8.
- Michard F, Chemla D, Richard C, Wysocki M, Pinsky MR, Lecarpentier Y, et al. Clinical use of respiratory changes in arterial pulse pressure to monitor the hemodynamic effects of PEEP. *Am J Respir Crit Care Med.* 1999;159:935–9.
- Michard F, Boussat S, Chemla D, Anguel N, Mercat A, Lecarpentier Y, et al. Relation between respiratory changes in arterial pulse pressure and fluid responsiveness in septic patients with acute circulatory failure. *Am J Respir Crit Care Med.* 2000;162:134–8.
- Miller JD, Pegelow DF, Jacques AJ, Dempsey JA. Skeletal muscle pump versus respiratory muscle pump: modulation of venous return from the locomotor limb in humans. *J Physiol.* 2005;563(Pt 3):925–43.
- Nanas S, Magder S. Adaptations of the peripheral circulation to PEEP. *Am Rev Respir Dis.* 1992;146:688–93.
- Olsen CO, Tyson GS, Maier GW, Spratt JA, Davis JW, Rankin JS. Dynamic ventricular interaction in the conscious dog. *Circ Res.* 1983;52(1):85–104.
- Perel A. Assessing fluid responsiveness by the systolic pressure variation in mechanically ventilated patients. *Anesthesiology.* 1998;89:1310–2.
- Perel A, Pizov R, Cotov S. Systolic blood pressure variation is a sensitive indicator of hypovolemia in ventilated dogs subjected to graded hemorrhage. *Anesthesiology.* 1987;67:498–502.
- Permutt S, Riley S. Hemodynamics of collapsible vessels with tone: the vascular waterfall. *J Appl Physiol.* 1963;18(5):924–32.
- Permutt S, Howell JBL, Proctor DF, Riley RL. Effect of lung inflation on static pressure volume characteristics of pulmonary vessels. *J Appl Physiol.* 1961;16:64–70.
- Permutt S, Bromberger-Barnea B, Bane HN. Alveolar pressure, pulmonary venous pressure, and the vascular waterfall. *Med Thorac.* 1962;19:239–60.
- Pizov R, Ya'ari Y, Perel A. Systolic pressure variation is greater during hemorrhage than during sodium nitroprusside-induced hypotension in ventilated dogs. *Anesth Analg.* 1988;67:170–4.
- Sharpey-Schafer EP. Effect of respiratory acts on the circulation. In: Field J, editor. *Handbook of Physiology: a critical, comprehensive presentation of physiological knowledge and concepts* Circulation 3. *Handbook of Physiology.* Washington: American Physiological Society; 1965:1875–86.
- Santamore WP, Dell'Italia LJ. Ventricular interdependence: significant left ventricular contributions to right ventricular systolic function. *Prog Cardiovasc Dis.* 1998;40(4):289–308.
- Santamore WP, Gray LA Jr. Left ventricular contributions to right ventricular systolic function during LVAD support. *Ann Thorac Surg.* 1996;61(1):350–6.
- Santamore WP, Shaffer T, Papa L. Theoretical model of ventricular interdependence: pericardial effects. *Am J Physiol.* 1990;259(1 Pt 2):H181–9.
- Swami A, Spodick DH. Pulsus paradoxus in cardiac tamponade: a pathophysiologic continuum. *Clin Cardiol.* 2003;26(5):215–7.
- Takata M, Robotham JL. Effects of inspiratory diaphragmatic descent on inferior vena caval venous return. *J Appl Physiol.* 1992;72(2):597–607.
- Takata M, Mitzner W, Robotham JL. Influence of the pericardium on ventricular loading during respiration. *J Appl Physiol.* 1990a;68(4):1640–50.
- Takata M, Beloucif S, Shimada M, Robotham JL. Superior and inferior vena caval flows during respiration: pathogenesis of Kussmaul's sign. *Am J Physiol.* 1990b;262:H763–H70.
- Takata M, Wise RA, Robotham JL. Effects of abdominal pressure on venous return: abdominal vascular zone conditions. *J Appl Physiol.* 1990c;69(6):1961–72.
- Takata M, Harasawa Y, Beloucif S, Robotham JL. Coupled vs. uncoupled pericardial constraint: effects on cardiac chamber interactions. *J Appl Physiol.* 1997;83(6):1799–813.
- The Acute Respiratory Distress Syndrome N. Ventilation with lower tidal volumes as compared with traditional tidal volumes for acute lung injury and the

- acute respiratory distress syndrome. *N Engl J Med.* 2000;342(18):1301–8.
- Timby J, Reed C, Zeilender S, Glauser FL. “Mechanical” causes of pulmonary edema. *Chest.* 1990;98(4):974–9.
- Verscheure S, Massion PB, Gottfried S, Goldberg P, Samy L, Damas P, et al. Measurement of pleural pressure swings with a fluid-filled esophageal catheter vs pulmonary artery occlusion pressure. *J Crit Care.* 2016;37:65–71.
- Webb HH, Tierney DF. Experimental pulmonary edema due to intermittent positive pressure ventilation with high inflation pressures. Protection by positive end-expiratory pressure. *Am Rev Respir Dis.* 1974;110(5):556–65.
- West JB, Dollery CT, Naimark A. Distribution of blood flow in isolated lungs: relation to vascular and alveolar pressures. *J Appl Physiol.* 1964;19:713–24.
- Whittenberg JL, McGregor M, Berglund E, Borst HG. Influence of state of inflation of the lung on pulmonary vascular resistance. *J Appl Physiol.* 1960;15:878.
- Yamaguchi S, Harasawa H, Li KS, Zhu D, Santamore WP. Comparative significance in systolic ventricular interaction. *Cardiovasc Res.* 1991;25(9):774–83.

Part IV

The Tools: Cardiovascular



Evaluation of Devices for Measurement of Blood Pressure

19

Agnes S. Meidert and Bernd Saugel

Introduction

Blood pressure measurement is the basis of hemodynamic monitoring in anesthesia and intensive care medicine. Hemodynamic instability and hypotension put a patient at risk; therefore, the timely detection of low blood pressure is crucial. In addition, maintaining individual blood pressure targets is only possible by accurate blood pressure measurement. Besides the direct invasive measurement using an arterial catheter, a variety of technologies are available for blood pressure assessment (Fig. 19.1). Traditionally, non-invasive blood pressure measurement employs an inflatable upper arm cuff that occludes blood flow in the extremity. Blood pressure is then obtained in an intermittent fashion by auscultatory method, by palpating the pulse, or automatically by an oscillometric technique. In the past decade, technologies that measure blood pressure continuously and also in a non-invasive manner have become available for patient monitoring. In order to choose the appropriate way of blood pressure monitoring for an individual

patient, the clinician needs to understand the measurement principle, indications, and limitations of each technique.

Invasive Arterial Blood Pressure Measurement (Arterial Catheter)

Measurement of blood pressure by using a catheter in an artery, connected to a fluid-filled tube and an electronic pressure transducer, is called invasive or direct blood pressure measurement. Since a continuous waveform and blood pressure values can be obtained directly from the vessel, this method is considered the clinical reference standard or “gold standard,” the most accurate method available to the physician.

Routinely, arterial cannulation for the monitoring of blood pressure is performed in critically ill patients and perioperatively in high-risk patients or high-risk procedures. Most commonly, the radial artery is used for catheter placement, but the femoral, brachial, or dorsalis pedis access is also possible. Performed by a well-trained operator, the placement of the catheter is usually unproblematic; however, it can be challenging in children or patients with conditions such as arteriosclerosis or peripheral vasoconstriction. It has been suggested to use ultrasound guidance to achieve a higher success rate (Gu et al. 2014). In general, the placement of an arterial catheter has a low complication rate.

A. S. Meidert
Department of Anaesthesiology, University Hospital
of Munich (LMU), Munich, Germany

B. Saugel (✉)
Department of Anesthesiology, Center of
Anesthesiology and Intensive Care Medicine,
University Medical Center Hamburg-Eppendorf,
Hamburg, Germany

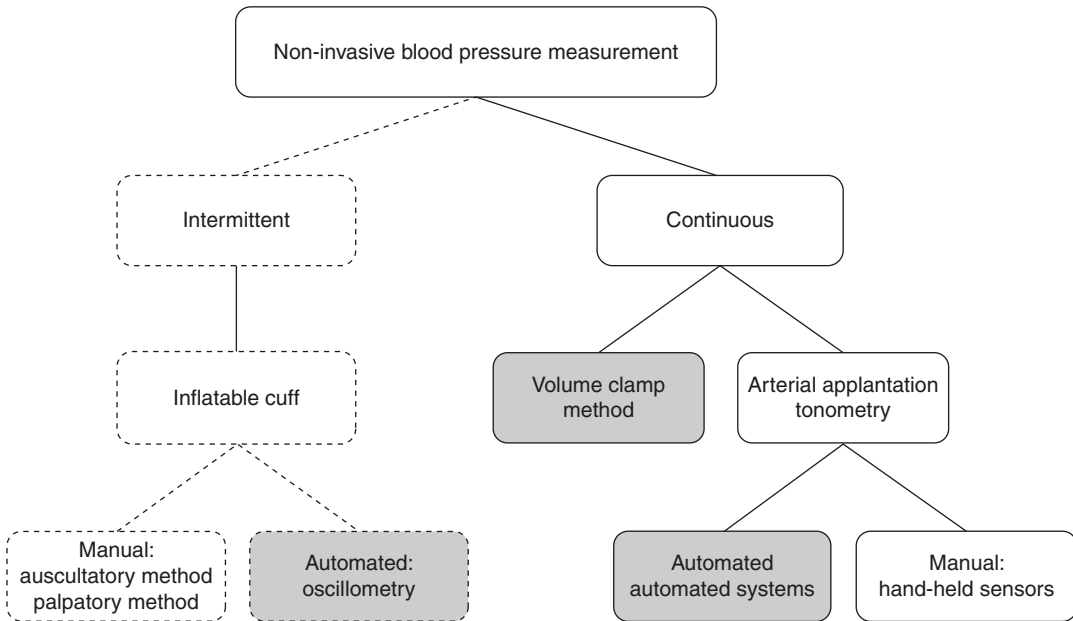


Fig. 19.1 Methods for noninvasive blood pressure monitoring. (With permission from Meidert and Saugel (2018)). With permission from Meidert AS and Saugel B (2018) Techniques for Non-Invasive Monitoring of

Arterial Blood Pressure. *Front. Med.* 4:231. <https://doi.org/10.3389/fmed.2017.00231>. <https://creativecommons.org/licenses/by/4.0/>. No changes made

However, severe conditions such as embolism, ischemic limbs, bleeding, pseudoaneurysm, or infection sometimes occur after cannulation of an artery (Scheer et al. 2002). In addition, blood flow distal to the catheter is evidently decreased (Numaguchi et al. 2015).

Blood pressure is a pressure wave, caused by the ejection of the left ventricle into the vascular system. Apart from the strength of the heart, the pressure depends on the individual resistance of the vascular tree. The shape of the pulse wave at the measurement site is also influenced by the reflection phenomenon from the previous heart beats. An arterial catheter and the connected tubes are filled with fluid, which is incompressible. Therefore, it transmits the blood pressure wave until it reaches the impermeable diaphragm of the pressure transducer (Ortega et al. 2017). The electrical resistance of the diaphragm is picked up by attached strain gauges. The other side of the diaphragm is open to atmospheric pressure. The pressure wave deforms the diaphragm physically (Ortega et al. 2017).

As a result of deformation, the electrical resistance changes in a linear relationship to intra-arterial pressure. The changes are mathematically translated into a waveform. Thus, the mechanic signal converted into an electric signal is processed by the monitor and translated into blood pressure waveform and numeric blood pressure values. The maximum of the wave is the systolic arterial pressure, the minimum the diastolic arterial pressure, and the area under the curve is the mean arterial pressure. Most processing software in the patient monitor average several heart beats, because averaging avoids big changes from heart beat to heart beat in case of arrhythmia. As with every monitoring device, the operating staff needs to be familiar with the pitfalls to avoid erroneous blood pressure readings. First, the tubes connecting the catheter to the transducer must be filled without any air bubbles since gas has different transmitting properties than fluid. Second, the pressure transducer has to be placed correctly. The correct level of the transducer for measurement and

zeroing is at the anatomic projection of the patients' right atrium on the thorax (Ortega et al. 2017; McGhee and Bridges 2002). Since the correct leveling in clinical practice is a matter of discussion, the phlebostatic axis located at the fourth intercostal space in the middle between the anterior and posterior chest walls is a pragmatic approximation for referencing the transducer. It is important to know that due to hydrostatic pressure, incorrect leveling of only 10 cm too high or too low results in a pressure difference of 7.5 mmHg at the patient monitor. The leveling of the transducer has to be checked frequently, especially when the position of the patient changes, which is often the case during operations. In certain clinical settings, e.g., beach chair positioning or patients with raised intracranial pressure, the effect of hydrostatic pressure may lead to higher blood pressure targets to ensure adequate brain perfusion.

A third source of erroneous measurement is zeroing of the transducer. For zeroing, the pressure transducer is opened to atmospheric pressure. Then, the zeroing button of the monitor is pressed. This sets the transducer level as the hydrostatic zero reference point. Furthermore, it ensures that the monitor uses atmospheric pressure as reference point (Ortega et al. 2017; McGhee and Bridges 2002).

Another prerequisite for reliable blood pressure readings is the testing of the dynamic response of the catheter and its connected tubing system. A fluid-filled system has a natural frequency and damping coefficient, which determines the dynamic response. If the damping properties are too high, the blood pressure readings can be falsely low (flat waveform), and if the damping properties are too low, readings can be too high (also known as systolic overshoot) (Gardner 1981).

Natural frequency and damping of direct blood pressure monitoring can be verified by the fast flush test (Ortega et al. 2017; McGhee and Bridges 2002; Kleinman et al. 1992; Saugel et al. 2014). It is performed by flushing the system with 300 mmHg, abruptly terminating the maneuver and inspection of the waveform directly after termination of flushing.

Whether a patient needs arterial cannulation has to be decided individually, carefully balancing the risks (due to potential complications caused by catheter placement and maintenance) and the advantages of an arterial catheter, namely the reliable continuous measurement (even in hemodynamically unstable situations) and the possibility of arterial blood withdrawals (important for patients with cardiopulmonary problems).

Intermittent Non-invasive Arterial Blood Pressure Measurement

For intermittent BP measurement (manually or automated), air-filled cuffs connected to a manometer indicating the applied pressure are used. The cuff occludes the artery at the extremity where the blood pressure is taken, most commonly the upper arm. In order to get valid results, the cuff has to be wide enough, depending on the circumference of the extremity (Petrie et al. 1986).

There are two methods of manual determination of blood pressure while gradually releasing the pressure in the occluding cuff: the palpatory and the auscultatory methods (Geddes et al. 1982). By the first method, the palpatory method, only systolic arterial pressure can be determined. The pulse distal to the occluding cuff is palpated. During the inflation, it vanishes when the pressure in the cuff becomes higher than systolic pressure. The systolic pressure equals the pressure, at which the pulse can be felt by the examiner while slowly deflating of the cuff. In contrast, the auscultatory method provides both systolic and diastolic arterial pressures. The examiner auscultates the Korrotkoff sounds over the artery distal to the occluding cuff during slow deflation. Systolic arterial pressure is determined at the onset of the sounds and diastolic arterial pressure at the disappearance of the sounds.

Apart from manual determination, automated noninvasive intermittent blood pressure is possible by a technique called oscillometry (Ogedegbe and Pickering 2010). The technique detects oscillations of the arterial wall, which occur

when the artery is obstructed by the occluding cuff. The amplitude of the oscillations varies depending on the pressure applied. In principle, oscillations are small when the pressure in the cuff is higher than systolic pressure. When the cuff is deflated, the amplitude increases until its maximum at the mean arterial blood pressure (Ramsey 3rd. 1979) and then again decreases toward the diastolic BP (Saugel et al. 2014; Nichols et al. 2011). The most accurate value derived by devices embedding oscillometric techniques is the mean arterial blood pressure. Algorithms integrate changes of oscillations, amplitude, waveform, etc., and derive systolic and diastolic pressures (Smulyan and Safar 2011). These algorithms are proprietary and are in most cases not made publicly available for independent study by the manufacturers (Smulyan and Safar 2011; van Montfrans 2001; Alpert et al. 2014). It is important to understand that, therefore, oscillometry is not a standardized technique. Today, automatic oscillometric devices are commonly used in anesthesiology and intensive care units, in ambulatory medicine, general wards, for 24-hour blood pressure assessment, and for blood pressure monitoring at home. Blood pressure monitoring using oscillometric devices has several advantages: there is no need for trained personnel, it is applied fast and easily and provides readings automatically. However, there are pitfalls that can lead to erroneous measurements. First, the correct cuff size is of paramount importance, since too small cuffs (in relation to the circumference of the arm) result in falsely high measurements and too large cuffs result in falsely low measurements (Pickering et al. 2005). Furthermore, active or passive movement of the measurement site causes artifacts that potentially result in false blood pressure measurement (Alpert et al. 2014). Equally important to know is the tendency of oscillometric devices to overestimate low blood pressure and underestimate high blood pressure when compared with invasively obtained blood pressure (Picone et al. 2017).

In critically ill patients, the use of oscillometric devices to guide therapy is controversially debated.

Some investigators studying the measurement performance of oscillometry proposed its use in intensive care unit patients with hypotension or vasopressor infusion (Lakhal et al. 2018a) and even in the presence of cardiac arrhythmia (Lakhal et al. 2015, 2018b). On the other hand, Lehman et al. (Lehman et al. 2013) revealed, after comparing oscillometric BP values with direct BP measurements (arterial catheter) intensive care unit patients in a big database, marked and clinically relevant discrepancies between the methods. In a group of non-cardiac surgery patients, Wax et al. (2011) found that oscillometric BP measurements were generally higher compared with invasive BP measurements during hypotension and lower during hypertension.

Non-invasive Continuous Arterial Blood Pressure Measurement

For continuous non-invasive automated determination and analysis of the blood pressure waveform, two technologies exist: the volume clamp method (also referred to as “vascular unloading technology” or “finger cuff technology”) and radial artery applanation tonometry (Saugel et al. 2014). The techniques are often described as new and innovative, although the basic underlying principles of both methods have been published quite some time ago (Penaz et al. 1976; Pressman and Newgard 1963).

A single or double inflatable finger cuff, with integrated infrared light and transmission plethysmograph is used by the volume clamp method. The finger cuff adjusts its pressure constantly (many times per second) in order to keep the diameter of the finger artery and hence the volume in it constant. From the pressure changes, which are necessary for the constant volume in the finger artery, a blood pressure curve can be calculated. This technique was first described in 1973 by the physiologist Peñáz (Penaz et al. 1976). The method has been developed and refined (Wesseling et al. 1985; Takazawa et al. 1996; Imholz et al. 1992; Fortin et al. 2006) which led to now commercially available monitoring systems for bedside use. One of them is the

ClearSight system (Edwards Lifesciences, Irvine, California, USA) using a transfer function; its embedded algorithm “PhysioCal” corrects the finger blood pressure changes due to changes in vasomotor tone and automatically adjusts for hydrostatic differences between the level of the finger and the heart (Wesseling et al. 1985; Wesseling 1996; Martina et al. 2012; Gizdulich et al. 1997). The other one is the CNAP system (CNSystems Medizintechnik GmbH, Graz, Austria), in which a proprietary algorithm uses oscillometric upper arm blood pressure measurement to calibrate systolic and diastolic blood pressure values obtained by the finger cuff. Adjustment and correction for long-term tracking of the finger blood pressure with this system are achieved by the use of concentrically interlocking control loops (Fortin et al. 2006).

The limitations of the volume clamp method lie within the site of measurement. In some clinical conditions, altered or impaired finger perfusion does occur. Examples are edema in the finger, peripheral vasoconstriction, peripheral vascular disease, or hypothermia, which can reduce the quality of the blood pressure signal. Furthermore, blood pressure derived by a finger cuff can be disturbed by excessive movement of the patient – both active and passive. Since devices using a finger cuff technology impair venous return from the finger which leads to venous congestion, this can cause discomfort or even pain in non-sedated patients. While the mentioned limitations hold true for both systems, the CNAP system in general has one more limitation due to its method of calibration. Since this system uses brachial oscillometric blood pressure values for calibration of systolic and diastolic blood pressures, the limitations discussed above regarding measurement performance and clinical applicability of oscillometric techniques also apply to the CNAP technology.

Technologically different is the radial artery applanation tonometry. This technique was first described by Pressman and Newgard in the 1960s (Pressman and Newgard 1963) and further improved by others (Stein and Blick 1971; Drzewiecki et al. 1983); this uses a pressure sensor, positioned over the radial artery.

In principle, the flattening (applanation) of the arterial wall by external pressure leads to a maximization of the pulse pressure amplitude that is detected with a sensor positioned over the artery. Sufficient applanation of an artery requires the artery to lie superficially and is supported by a rigid structure (e.g., the radial artery with the styloid bone underneath).

By this technology, the mean arterial BP is measured directly and the systolic and diastolic BP values are calculated (e.g., using population-based algorithms) (Meidert et al. 2013). Non-automatic systems with hand-held sensors have been used for estimation of central vascular pressures for many years by cardiologists (Nelson et al. 2010). For BP monitoring in the intensive care unit or the operating room, automatic radial artery applanation tonometry systems using a sensor attached to the patient’s wrist have been developed (Kemmons et al. 1991). In order to obtain optimal BP signal, an automatic artery applanation tonometry system needs to constantly adjust the pressure of the sensor that flattens the underlying artery with the optimal pressure. The T-Line system (Tensys Medical, San Diego, CA, USA) is a device for automatic radial applanation tonometry. It uses a disposable wrist splint for positioning the wrist and hand in slight extension combined with a “bracelet” with an embedded sensor. The sensor is electromechanically driven by two motors that are able to adjust the sensor’s position over the artery, until the position and applanation pressure obtaining the best signal are found (Saugel et al. 2014; Dueck et al. 2012).

Mean BP is derived from the maximal pulse pressure, while systolic and diastolic BP are obtained after scaling the BP waveform using a proprietary algorithm based on biometric data and a large database containing invasive radial artery reference data (Dueck et al. 2012; Drzewiecki et al. 1994).

The limitation of the radial artery applanation tonometry method is mainly its sensitivity to motion artifacts due to movements of the arm or hand. There are validation data for this device in a variety of clinical settings (Meidert et al. 2013; Dueck et al. 2012; Saugel et al. 2012, 2013; Meidert et al. 2014; Szmuk et al. 2008).

The measurement performance of these innovative non-invasive technologies for continuous BP monitoring has been evaluated in several validation studies in comparison to invasive reference measurements (Bartels et al. 2016; Kim et al. 2014; Ameloot et al. 2015).

These studies revealed contradicting results for all the devices and technologies described above. On the one hand, numerous studies demonstrated good agreement between reference and test methods, and subsequently recommended the broad clinical use of these non-invasive technologies as an alternative to invasive BP monitoring.

On the other hand, some studies showed poor agreement between test method and reference, so they did not support the use of these technologies in clinical routine to monitor BP and guide therapy.

Eventually a meta-analysis including 28 studies assessed the accuracy and precision of the different continuous non-invasive BP monitoring technologies. It revealed an overall random-effect pooled mean of differences of 3.2 mmHg, with a standard deviation of ± 8.4 mmHg and 95% limits of agreement -13.4 – 19.7 mmHg for mean BP (Kim et al. 2014). After stratifying the results depending on the different devices, this analysis resulted in a mean differences \pm standard deviation of 3.5 ± 6.8 mmHg, 5.5 ± 9.3 mmHg, and 1.3 ± 5.7 mmHg, for the ClearSight (volume clamp method), CNAP (volume clamp method), and T-Line system (radial artery applanation tonometry), respectively (Kim et al. 2014).

However, the question of the optimal definition of clinically acceptable agreement between a non-invasive test method and a reference method is still a matter of debate (Saugel and Reuter 2014). Besides testing a new non-invasive device against the invasive gold standard, it is advisable to test against an intermittent non-invasive BP monitoring technology (e.g., oscillometry) additionally. Recently, Vos and colleagues (2014) drew the conclusion, that compared with an oscillometric technique monitoring with the non-invasive continuous BP monitoring with the ClearSight system was interchangeable.

The Future of Arterial Blood Pressure Measurement

Innovative tiny sensors that record BP and heart rate might change the methods of BP monitoring both at home and at hospital in future.

For example, the use of flexible pressure-sensitive organic thin film transistors in the recording of non-invasive continuous radial artery BP has already been demonstrated (Schwartz et al. 2013).

Furthermore, BP signals can be registered and analyzed by thin piezoelectric pressure sensors placed on the skin (Dagdeviren et al. 2014).

Another promising approach is the use of nanocomposites (graphene added to polysilicon) as electromechanical sensor, which is highly sensitive and therefore able to detect pulse and blood pressure (Boland et al. 2016).

All these novel developments may eventually lead to flexible and wearable monitoring systems for innovative transcutaneous BP recording. With regard to the concepts of “mobile health monitoring” or “mobile biomonitring,” wireless and wearable sensors are an important step toward the intriguing possibility of long-term continuous monitoring of the cardiovascular status (Michard 2016, 2017; Michard et al. 2017a, b).

Thus, innovative sensor technology developments might fundamentally change ambulatory and clinic BP monitoring, which offers a variety of application in critical care, anesthesiology, emergency medicine, and cardiology (Michard 2017; Michard et al. 2017a, b).

Which Device Is Suitable for My Patient?

In our daily routine, the question of what type of BP monitoring is the best choice is answered best after considering many factors, most importantly the patient-specific ones. Regarding advantages and shortcomings of every technology in combination with the clinical requirements, the choice of the optimal monitoring equipment has to be made individually.

In case of a critically ill patient in circulatory shock, invasive direct BP monitoring with an arterial catheter is necessary and advisable (Teboul et al. 2016). Apart from the direct mea-

surement of BP, frequent arterial blood sampling allows laboratory testing and blood gas analysis that are inevitable for guidance of therapy.

The aforementioned advantages of having an arterial access also apply in patients undergoing high-risk surgery (e.g., cardiothoracic surgery, major abdominal surgery) and high-risk patients undergoing low- or intermediate-risk surgery.

Perioperatively, most remaining patients will be monitored using non-invasive BP monitoring techniques. In certain surgical patients, the use of continuous non-invasive BP monitoring is beneficial with regard to better stability of BP instead of intermittent BP monitoring (Benes et al. 2015; Meidert et al. 2017; Iliès et al. 2012). To identify specific clinical settings where continuous non-invasive BP monitoring can contribute to better care or patient safety compared to intermittent non-invasive BP measurements is the task of future research in this area. Since periods of intra-operative hypotension – even as short as a few minutes - are associated with postoperative organ dysfunction or failure (Walsh et al. 2013), continuous BP monitoring or even usage of a closed-loop system might help to reduce hypotension-related postoperative complications in the future.

Patients who are treated in an emergency department due to acute illness or patients who undergo diagnostic or therapeutic interventions (Nowak et al. 2011; Wagner et al. 2014; Siebig et al. 2009) might benefit from continuous non-invasive BP monitoring as circulatory depression can be detected earlier with continuous monitoring than with serial intermittent BP measurement.

Conclusion

BP is a fundamental hemodynamic variable in the critically ill. A profound knowledge of BP-monitoring technologies and their limitations is inevitable in order to choose the optimal BP monitoring method for the individual patient and to avoid inaccurate BP monitoring. In critically ill patients, the placement of an arterial catheter in order to directly measure invasive continuous BP remains the method of choice. In hemodynamically stable patients, BP may be monitored

in an intermittent fashion by using an oscillometric technique. Non-invasive technologies that continuously monitor BP are now available in daily clinical routine. An aim of current research is to evaluate whether these technologies for continuous non-invasive BP monitoring can contribute to improved patient outcome or to better quality of care in certain clinical settings (perioperative medicine, emergency medicine).

Conflict of Interest BS collaborates with Pulsion Medical Systems SE (Feldkirchen, Germany) as a member of the medical advisory board and has received institutional-restricted research grants, honoraria for giving lectures, and refunds of travel expenses from Pulsion Medical Systems SE. BS has received research support and honoraria for giving lectures from Edwards Lifesciences (Irvine, CA, USA). BS has received institutional-restricted research grants, honoraria for giving lectures, and refunds of travel expenses from CNSystems Medizintechnik GmbH (Graz, Austria). BS has received institutional-restricted research grants, honoraria for consulting, and refunds of travel expenses from Tensys Medical Inc. (San Diego, CA, USA). BS has received institutional-restricted research grants from Retia Medical LLC. (Valhalla, NY, USA). BS has received honoraria for giving lectures from Philips Medizin Systeme Böblingen GmbH (Böblingen, Germany).

ASM has no conflict of interest.

References

- Alpert BS, Quinn D, Gallick D. Oscillometric blood pressure: a review for clinicians. *J Am Soc Hypertens.* 2014;8(12):930–8.
- Ameloot K, Palmers PJ, Malbrain ML. The accuracy of noninvasive cardiac output and pressure measurements with finger cuff: a concise review. *Curr Opin Crit Care.* 2015;21(3):232–9.
- Bartels K, Esper SA, Thiele RH. Blood pressure monitoring for the anesthesiologist: a practical review. *Anesth Analg.* 2016;122(6):1866–79.
- Benes J, Simanova A, Tovarnicka T, Sevcikova S, Kletecka J, Zatloukal J, et al. Continuous non-invasive monitoring improves blood pressure stability in upright position: randomized controlled trial. *J Clin Monit Comput.* 2015;29(1):11–7.
- Boland CS, Khan U, Ryan G, Barwich S, Charifou R, Harvey A, et al. Sensitive electromechanical sensors using viscoelastic graphene-polymer nanocomposites. *Science.* 2016;354(6317):1257–60.
- Dagdévire C, Su Y, Joe P, Yona R, Liu Y, Kim YS, et al. Conformable amplified lead zirconate titanate sensors with enhanced piezoelectric response for cutaneous pressure monitoring. *Nat Commun.* 2014;5:4496.

- Drzewiecki GM, Melbin J, Noordergraaf A. Arterial tonometry: review and analysis. *J Biomech.* 1983;16(2):141–52.
- Drzewiecki G, Hood R, Apple H. Theory of the oscillometric maximum and the systolic and diastolic detection ratios. *Ann Biomed Eng.* 1994;22(1):88–96.
- Dueck R, Goedje O, Clopton P. Noninvasive continuous beat-to-beat radial artery pressure via TL-200 applanation tonometry. *J Clin Monit Comput.* 2012;26(2):75–83.
- Fortin J, Marte W, Grullenberger R, Hacker A, Habenbacher W, Heller A, et al. Continuous non-invasive blood pressure monitoring using concentrically interlocking control loops. *Comput Biol Med.* 2006;36(9):941–57.
- Gardner RM. Direct blood pressure measurement-dynamic response requirements. *Anesthesiology.* 1981;54(3):227–36.
- Geddes LA, Voelz M, Combs C, Reiner D, Babbs CF. Characterization of the oscillometric method for measuring indirect blood pressure. *Ann Biomed Eng.* 1982;10(6):271–80.
- Gizdulich P, Prentza A, Wesseling KH. Models of brachial to finger pulse wave distortion and pressure decrement. *Cardiovasc Res.* 1997;33(3):698–705.
- Gu WJ, Tie HT, Liu JC, Zeng XT. Efficacy of ultrasound-guided radial artery catheterization: a systematic review and meta-analysis of randomized controlled trials. *Crit Care.* 2014;18(3):R93.
- Ilies C, Kiskalt H, Siedenhans D, Meybohm P, Steinfath M, Bein B, et al. Detection of hypotension during Caesarean section with continuous non-invasive arterial pressure device or intermittent oscillometric arterial pressure measurement. *Br J Anaesth.* 2012;109(3):413–9.
- Imholz BP, Parati G, Mancia G, Wesseling KH. Effects of graded vasoconstriction upon the measurement of finger arterial pressure. *J Hypertens.* 1992;10(9):979–84.
- Kemmotsu O, Ueda M, Otsuka H, Yamamura T, Okamura A, Ishikawa T, et al. Blood pressure measurement by arterial tonometry in controlled hypotension. *Anesth Analg.* 1991;73(1):54–8.
- Kim SH, Lilot M, Sidhu KS, Rinehart J, Yu Z, Canales C, et al. Accuracy and precision of continuous non-invasive arterial pressure monitoring compared with invasive arterial pressure: a systematic review and meta-analysis. *Anesthesiology.* 2014;120(5):1080–97.
- Kleinman B, Powell S, Kumar P, Gardner RM. The fast flush test measures the dynamic response of the entire blood pressure monitoring system. *Anesthesiology.* 1992;77(6):1215–20.
- Lakhal K, Ehrmann S, Martin M, Faiz S, Reminiac F, Cinotti R, et al. Blood pressure monitoring during arrhythmia: agreement between automated brachial cuff and intra-arterial measurements. *Br J Anaesth.* 2015;115(4):540–9.
- Lakhal K, Ehrmann S, Boulain T. Non-invasive blood pressure monitoring in the critically ill: time to abandon the intra-arterial catheter? *Chest.* 2018a;153(4):1023–39.
- Lakhal K, Martin M, Ehrmann S, Faiz S, Rozec B, Boulain T. Non-invasive blood pressure monitoring with an oscillometric brachial cuff: impact of arrhythmia. *J Clin Monit Comput.* 2018b;32:707–15.
- Lehman LW, Saeed M, Talmor D, Mark R, Malhotra A. Methods of blood pressure measurement in the ICU. *Crit Care Med.* 2013;41(1):34–40.
- Martina JR, Westerhof BE, van Goudoever J, de Beaumont EM, Truijzen J, Kim YS, et al. Noninvasive continuous arterial blood pressure monitoring with Nexfin(R). *Anesthesiology.* 2012;116(5):1092–103.
- McGhee BH, Bridges EJ. Monitoring arterial blood pressure: what you may not know. *Crit Care Nurse.* 2002;22(2):60–4, 6–70, 3 passim.
- Meidert AS, Saugel B. Techniques for non-invasive monitoring of arterial blood pressure. *Front. Med.* 2018;4:231. <https://doi.org/10.3389/fmed.2017.00231>.
- Meidert AS, Huber W, Hapfelmeier A, Schofthaler M, Muller JN, Langwieser N, et al. Evaluation of the radial artery applanation tonometry technology for continuous noninvasive blood pressure monitoring compared with central aortic blood pressure measurements in patients with multiple organ dysfunction syndrome. *J Crit Care.* 2013;28(6):908–12.
- Meidert AS, Huber W, Muller JN, Schofthaler M, Hapfelmeier A, Langwieser N, et al. Radial artery applanation tonometry for continuous non-invasive arterial pressure monitoring in intensive care unit patients: comparison with invasively assessed radial arterial pressure. *Br J Anaesth.* 2014;112(3):521–8.
- Meidert AS, Nold JS, Hornung R, Paulus AC, Zwissler B, Czerner S. The impact of continuous non-invasive arterial blood pressure monitoring on blood pressure stability during general anaesthesia in orthopaedic patients: a randomised trial. *Eur J Anaesthesiol.* 2017;34:716–22.
- Michard F. Hemodynamic monitoring in the era of digital health. *Ann Intensive Care.* 2016;6(1):15.
- Michard F. A sneak peek into digital innovations and wearable sensors for cardiac monitoring. *J Clin Monit Comput.* 2017;31(2):253–9.
- Michard F, Pinsky MR, Vincent JL. Intensive care medicine in 2050: NEWS for hemodynamic monitoring. *Intensive Care Med.* 2017a;43(3):440–2.
- Michard F, Gan TJ, Kehlet H. Digital innovations and emerging technologies for enhanced recovery programmes. *Br J Anaesth.* 2017b;119:31–9.
- Nelson MR, Stepanek J, Cevette M, Covalciuc M, Hurst RT, Tajik AJ. Noninvasive measurement of central vascular pressures with arterial tonometry: clinical revival of the pulse pressure waveform? *Mayo Clin Proc.* 2010;85(5):460–72.
- Nichols WW, Nichols WW, McDonald DA. McDonald's blood flow in arteries : theoretic, experimental, and clinical principles. 6th ed. London: Hodder Arnold; 2011. xiv, p. 755.
- Nowak RM, Sen A, Garcia AJ, Wilkie H, Yang JJ, Nowak MR, et al. Noninvasive continuous or intermittent

- blood pressure and heart rate patient monitoring in the ED. *Am J Emerg Med.* 2011;29(7):782–9.
- Numaguchi A, Adachi YU, Aoki Y, Ishii Y, Suzuki K, Obata Y, et al. Radial artery cannulation decreases the distal arterial blood flow measured by power Doppler ultrasound. *J Clin Monit Comput.* 2015;29(5):653–7.
- Ogedegbe G, Pickering T. Principles and techniques of blood pressure measurement. *Cardiol Clin.* 2010;28(4):571–86.
- Ortega R, Connor C, Kotova F, Deng W, Lacerra C. Use of pressure transducers. *N Engl J Med.* 2017;376(14):e26.
- Penaz J, Voigt A, Teichmann W. Contribution to the continuous indirect blood pressure measurement. *Z Gesamte Inn Med.* 1976;31(24):1030–3.
- Petrie JC, O'Brien ET, Littler WA, de Swiet M. Recommendations on blood pressure measurement. *Br Med J.* 1986;293(6547):611–5.
- Pickering TG, Hall JE, Appel LJ, Falkner BE, Graves J, Hill MN, et al. Recommendations for blood pressure measurement in humans and experimental animals: part 1: blood pressure measurement in humans: a statement for professionals from the Subcommittee of Professional and Public Education of the American Heart Association Council on High Blood Pressure Research. *Circulation.* 2005;111(5):697–716.
- Picone DS, Schultz MG, Otahal P, Aakhus S, Al-Jumaily AM, Black JA, et al. Accuracy of cuff-measured blood pressure: systematic reviews and meta-analyses. *J Am Coll Cardiol.* 2017;70(5):572–86.
- Pressman GL, Newgard PM. A transducer for the continuous external measurement of arterial blood pressure. *IEEE Trans Biomed Eng.* 1963;10:73–81.
- Ramsey M 3rd. Noninvasive automatic determination of mean arterial pressure. *Med Biol Eng Comput.* 1979;17(1):11–8.
- Saugel B, Reuter DA. Are we ready for the age of non-invasive haemodynamic monitoring? *Br J Anaesth.* 2014;113(3):340–3.
- Saugel B, Fassio F, Hapfelmeier A, Meidert AS, Schmid RM, Huber W. The T-Line TL-200 system for continuous non-invasive blood pressure measurement in medical intensive care unit patients. *Intensive Care Med.* 2012;38(9):1471–7.
- Saugel B, Meidert AS, Hapfelmeier A, Eyer F, Schmid RM, Huber W. Non-invasive continuous arterial pressure measurement based on radial artery tonometry in the intensive care unit: a method comparison study using the T-Line TL-200pro device. *Br J Anaesth.* 2013;111(2):185–90.
- Saugel B, Dueck R, Wagner JY. Measurement of blood pressure. *Best Pract Res Clin Anaesthesiol.* 2014;28(4):309–22.
- Scheer B, Perel A, Pfeiffer UJ. Clinical review: complications and risk factors of peripheral arterial catheters used for haemodynamic monitoring in anaesthesia and intensive care medicine. *Crit Care.* 2002;6(3):199–204.
- Schwartz G, Tee BC, Mei J, Appleton AL, Kim DH, Wang H, et al. Flexible polymer transistors with high pressure sensitivity for application in electronic skin and health monitoring. *Nat Commun.* 2013;4:1859.
- Siebig S, Rockmann F, Sabel K, Zuber-Jerger I, Dierkes C, Brunnler T, et al. Continuous non-invasive arterial pressure technique improves patient monitoring during interventional endoscopy. *Int J Med Sci.* 2009;6(1):37–42.
- Smulyan H, Safar ME. Blood pressure measurement: retrospective and prospective views. *Am J Hypertens.* 2011;24(6):628–34.
- Stein PD, Blick EF. Arterial tonometry for the atraumatic measurement of arterial blood pressure. *J Appl Physiol.* 1971;30(4):593–6.
- Szmuk P, Pivalizza E, Warters RD, Ezri T, Gebhard R. An evaluation of the T-Line Tensymeter continuous non-invasive blood pressure device during induced hypotension. *Anaesthesia.* 2008;63(3):307–12.
- Takazawa K, O'Rourke MF, Fujita M, Tanaka N, Takeda K, Kurosu F, et al. Estimation of ascending aortic pressure from radial arterial pressure using a generalised transfer function. *Zeitschrift fur Kardiologie.* 1996;85 Suppl 3:137–9.
- Teboul JL, Saugel B, Cecconi M, De Backer D, Hofer CK, Monnet X, et al. Less invasive hemodynamic monitoring in critically ill patients. *Intensive Care Med.* 2016;42(9):1350–9.
- van Montfrans GA. Oscillometric blood pressure measurement: progress and problems. *Blood Press Monit.* 2001;6(6):287–90.
- Vos JJ, Poterman M, Mooyaart EA, Weening M, Struys MM, Scheeren TW, et al. Comparison of continuous non-invasive finger arterial pressure monitoring with conventional intermittent automated arm arterial pressure measurement in patients under general anaesthesia. *Br J Anaesth.* 2014;113(1):67–74.
- Wagner JY, Prantner JS, Meidert AS, Hapfelmeier A, Schmid RM, Saugel B. Noninvasive continuous versus intermittent arterial pressure monitoring: evaluation of the vascular unloading technique (CNAP device) in the emergency department. *Scand J Trauma Resusc Emerg Med.* 2014;22:8.
- Walsh M, Devereaux PJ, Garg AX, Kurz A, Turan A, Rodseth RN, et al. Relationship between intraoperative mean arterial pressure and clinical outcomes after noncardiac surgery: toward an empirical definition of hypotension. *Anesthesiology.* 2013;119(3):507–15.
- Wax DB, Lin HM, Leibowitz AB. Invasive and concomitant noninvasive intraoperative blood pressure monitoring: observed differences in measurements and associated therapeutic interventions. *Anesthesiology.* 2011;115(5):973–8.
- Wesseling KH. Finger arterial pressure measurement with Finapres. *Zeitschrift fur Kardiologie.* 1996;85 Suppl 3:38–44.
- Wesseling KH, Settels JJ, van der Hoeven GM, Nijboer JA, Butijn MW, Dorlas JC. Effects of peripheral vasoconstriction on the measurement of blood pressure in a finger. *Cardiovasc Res.* 1985;19(3):139–45.



Konstantinos D. Alexopoulos, Sheldon Magder,
and Gordan Samoukovic

Once species evolved from single-cell organisms, the ability to deliver nutrients and remove waste products became an essential function for survival; the circulatory system evolved into the complex structure that exists in humans. Simply, the role of human circulation is to deliver and remove substances. In critical care, it is paramount to monitor the bulk flow of circulation as an indicator of overall circulatory function. Being able to identify patients who are on the steep part of the Frank-Starling curve and subsequently would be fluid responsive is a core principle in clinical practice. Traditionally, this information was provided solely by the invasive pulmonary artery catheter (PAC). Recent advances in technology have been able to provide this information in a less invasive or completely noninvasive manner. Using both macro- and microcirculatory monitoring allows the practitioner to determine the extent of circulatory homeostasis, which can be maintained with fluids, with or without inotropic or vasopressor support. Utilizing continuous

assessment of cardiac output is one of the fundamental requirements for assessing overall function of a complex biological machine and for guiding therapy.

Cardiac Output and Clinical Decision-Making

The measurement of cardiac output (CO) aids for clinical decision-making when faced with the common problem of hypotension in the intensive care unit (ICU). The determinants of blood pressure are the CO and systemic vascular resistance (SVR), which is assumed to be relatively constant – or with negligible changes compared with changes in the total decrease in pressure. Using this fundamental concept, a decrease in blood pressure is due either to a decrease in CO or a decrease in SVR. SVR is governed by the blood pressure, right atrial pressure (RAP), and CO; therefore, CO is an independent variable in this relationship. If CO is normal or increased above normal, then the decrease in blood pressure must be a result of a decrease in SVR. Diagnostic efforts should be thus directed at determining the cause of the loss of vascular tone, and therapy should then be directed accordingly. If blood pressure is decreased in a low CO state, then the decrease in cardiac output is the resultant cause of the hypotension. The low CO state can manifest for a variety of reasons such as circuit factors,

K. D. Alexopoulos · G. Samoukovic (✉)
Department of Critical Care, Royal Victoria
Hospital – McGill University and McGill University
Health Centre, Montreal, QC, Canada
e-mail: gordan.samoukovic@mcgill.ca

S. Magder
Royal Victoria Hospital (McGill University
Health Centre), Departments of Critical Care and
Physiology McGill University, Montreal, QC, Canada
e-mail: sheldon.magder@mcgill.ca

decrease in intravascular volume or increase in venous resistance, or a decrease in cardiac function (i.e., decreased contractility, decreased heart rate, or an increased afterload). The value of CO is paramount for delineating the various causes of hypotension encountered in the ICU (Magder 1992, 1997).

Normalization of Cardiac Output Measurement

Cardiac output refers to the bulk flow going through the circulatory system and is given in the units mL/s in SI units or L/min in traditional units. The flow velocity is given in cm/s. The product of flow velocity and the cross-sectional area of a vessel allows for the determination of volume flow.

Under normal metabolic conditions, CO is directly related to metabolic rate and oxygen consumption (VO_2). An increase in VO_2 is directly associated with an increase in CO. For example, during exercise, there exists a linear relationship between cardiac output and VO_2 , and it is sustained until the end of exercise. The variation among subjects is small, and the change in VO_2 can be used to predict cardiac output with an error of approximation of 5 percent (Ekelund and Holmgren 1967). In patients with severe cardiac disease, the relationship remains linear in all subjects, although the y-intercept on the ordinate may be shifted up or down based on the hemoglo-

bin. The linear relationship between bulk blood flow and oxygen consumption is also present in working skeletal muscle and in cardiac muscle, strongly suggesting that blood flow is determined by the aerobic metabolic activity of tissues.

In a physiologically normal subject, a decrease in CO does not translate to a decrease in VO_2 as oxygen extraction by the tissues can increase to maintain VO_2 . Conversely, in pathologic conditions, a decrease in CO may be of such magnitude that in spite of an increase in oxygen extraction, there is insufficient oxygen provided to the tissues. Under these conditions, the heart is unable to generate an adequate CO to meet the metabolic demands of the tissues, and changes in CO lead to changes in VO_2 , which is then said to be dependent on the CO.

Since CO varies with VO_2 and VO_2 is influenced by the body mass, CO varies with body mass. To compare individuals of different body sizes, it is necessary to normalize cardiac output in relation to body size. Unfortunately, it is not adequate to simply divide cardiac output by body weight because of the disproportionate amount of adipose tissue related to muscle differences among individuals. Adipose tissue has a lower metabolic rate than muscle and other body tissues, and thus VO_2 does not rise in proportion to body weight. It has been observed that the metabolic rate varies with body surface areas and body surface area can be estimated by a formula developed by Dubois (Berkson Jm Boothby 1936):

$$\text{Body surface area (m}^2\text{)} = \text{weight (kg)}^{0.425} \times \text{height (cm)}^{0.72184} \quad (20.1)$$

Although body surface has become the standard for normalizing cardiac output, as noted by Guyton et al. (1973), the correlation between cardiac output and body surface area in humans is not strong and even weaker in animals. Based on the work of Kleiber (1947), Guyton et al. argued that relationship of the metabolic rate and a power function of weight is much better (Guyton et al. 1973) but accepted that normalization by body surface area has become the standard.

The Fick Principle

General Theory

The principle enunciated by Adolph Fick in 1870 remains the basis for many of the techniques used for measuring CO (Fishman and Richards 1975). It is essentially a statement of the law of conservation of mass. It postulates that the amount of a given substance at the outflow of a system must

equal the sum of the amount of the substance at the inflow and the amount added or removed between the inflow and outflow ends of the system. An analogy may be helpful. Consider an observer standing in front of a conveyor belt. Every minute a 1 L bottle of milk passes in front of them. The person picks up each bottle that passes and drinks $100 \text{ mL} \times (0.1 \text{ L})$. Since one bottle passes each minute and 100 mL is removed from each bottle, the rate of milk consumption is 100 mL/min. Conversely, if the rate of bottles moving along the conveyor belt is not known and exactly 100 mL is still poured from each bottle

into a large graduated cylinder and this is continued for 10 min, 1 L of milk would accumulate in the cylinder over that 10 minute period. Since 100 mL came from each 1 L bottle, then 10 bottles must have gone by in those 10 minutes, or 1 bottle per minute.

The Fick principle requires an indicator that is added at a constant rate. One of the better indicator substances is O_2 because both the rate of oxygen uptake by the lung and the amount of O_2 on either side of the lung can be measured fairly easily. The specific formula for CO using O_2 as the indicator is:

$$\text{CO(L/min)} = \frac{\text{O}_2 \text{ consumption (mL/min)}}{\text{arterial O}_2 - \text{venous O}_2 \text{ content (mL/L)}} \quad (20.2)$$

The consumption of O_2 is determined by applying the same principle to the inflow and outflow of O_2 in the air from the lungs. The flow in this case is that of air going in and out of the lungs and is given by the minute ventilation. The consumption of O_2 is then determined from the difference between O_2 content in the inspired and expired air. The O_2 content of the inspired air is equal to the product of the fraction of O_2 in the inspired air (FiO_2) and volume of inspired air. Similarly, the O_2 content of the expired air (FeO_2) is the product of fraction of O_2 in the expired air and the expired volume. Normally, only the

expired volume is measured. Unfortunately, inspired and expired volumes are not equal as CO_2 is added to the expired air. The expired air value can still be utilized to calculate the inspired volume by correcting for the addition of CO_2 through the Haldane transformation, which takes into account the expired CO_2 concentration (Jones and Campbell 1982).

The arterial O_2 content is obtained by taking a sample of blood from any arterial site, since there is essentially no extraction of O_2 until small vessels are reached. The arterial O_2 content is given by the formula:

$$\text{C}_a \text{O}_2 = \left(\text{Hgb} * 1.34 * \frac{\text{S}_a \text{O}_2}{100} \right) + (0.0031 * p_a \text{O}_2) \quad (20.3)$$

Determination of the venous O_2 sample is more problematic. It must come from a site where there is complete mixing of all venous blood. The only places where this is valid are the right ventricle (RV) and pulmonary arteries (PA). Thus, this technique requires a right heart catheterization and sampling of blood from the PA.

Sources of Error Using the Fick Principle

Sources of error with the Fick principle can be considered under the following three categories: (1) errors in sampling and analysis, (2) errors caused by changes in cardiac output, and (3) errors caused by changes in respiration.

Errors of Sampling and Analysis

A requirement for use of the Fick principle is that the indicator must be thoroughly mixed with the fluid flowing at the site of sampling. This is not a problem on the arterial side of the circulation, but it is a problem on the venous side. As noted above, application of the Fick principle using O_2 requires a right heart catheterization and sample of blood from the RV or PA. Samples of blood from the right atrium (RA) or vena cava are not sufficiently mixed to allow for accurate calculation of CO by the Fick principle. A problem arises in patients who have intracardiac shunts, because pulmonary arterial blood no longer represents the mixed venous O_2 content. In this situation, blood samples need to be taken from the superior and inferior venae cavae, and the mixed venous oxygen is calculated from a weighted average of these two samples, although a precise value cannot be determined.

As is evident when one looks at signals from continuous measurements of pulmonary artery saturation, O_2 saturation of the pulmonary blood is pulsatile and variable. To avoid errors caused by this variation, the sample should be withdrawn over 5–10 seconds to even out the variations. The same is true with arterial samples, especially when the arterial PO_2 is below 40–50 mmHg, as this places the hemoglobin on the steep part of the oxygen-dissociation curve, and slight changes in PO_2 can have a profound effect on the O_2 saturation, and even the fluctuations in the PO_2 with each heartbeat can affect the O_2 content.

A number of errors in measurement must be considered. The calculation of O_2 content given above ignores dissolved oxygen. At a normal alveolar PO_2 , this results in only a very small error. For every 1 mmHg PO_2 , 0.03 mL/L of O_2 is dissolved in plasma. Therefore, at a PO_2 of 100 mmHg arterial blood, the dissolved O_2 content is 3 mL/L. In the PA, the dissolved O_2 content is only about 1.2 mL/L of O_2 . Since the arteriovenous O_2 difference is in the range of 40–50 mL/L, the error for neglecting this is negligible (i.e., less than 5 percent) and falls within the errors associated with measuring O_2 saturation and hemoglobin concentration. When the

FiO_2 is high, this error poses a significant problem. Matters are even worse if the arteriovenous difference is narrowed, as occurs in sepsis. When the FiO_2 is 1.0, the dissolved O_2 in a normal subject can be almost 40 percent of the arteriovenous O_2 difference; under hyperbaric conditions this error is even greater.

Errors in the assessment of hemoglobin concentration can cause a problem in correct estimation of O_2 content. The O_2 saturation is generally a very reliable measurement, but the hemoglobin measurement on a CO-oximeter is prone to errors in analysis. The factors affecting the measurement of hemoglobin include excessive use of heparin in the sample syringe, which dilutes the blood sample and thus decreases the hemoglobin concentration, as well as insufficient heparin, which can result in formation of clots, thus artificially lowering the hemoglobin concentration.

Errors also can occur because of problems with measurement of VO_2 . A common problem is a “leak” in the system used to collect expired gases so that not all of the expired air is collected. Errors also arise at high FiO_2 values, because the difference between FiO_2 and fraction of expired oxygen (FeO_2) becomes very small compared with their actual values, and analytic errors in the measurement of O_2 have a greater effect. Alteration in the FiO_2 is another confounding factor, because most analytical methods assume the FiO_2 to be constant. Finally, VO_2 is very much affected by changes in ventilation. This error is described below.

Errors due to Changes in Cardiac Output

If CO changes during the measurement, one might consider taking the average arteriovenous O_2 difference. However, the relationship of CO to the arteriovenous O_2 difference is rectilinear; therefore, the change in CO and the arteriovenous O_2 difference is not directly proportional. Fortunately, this only becomes an issue with very large changes in the arteriovenous O_2 difference. This potential error should be considered if the patient does a Valsalva maneuver, is receiving a

transfusion that changes the hemoglobin concentration during the measurement, or has a change in inotropic therapy during the measurement.

Errors due to Changes in Respiration

Changes in ventilation introduce a potentially significant error when relying on the Fick method. An essential assumption is that the measurement of $\dot{V}O_2$ is a measure of the amount of O_2 entering the blood each minute, and this is violated when the volume of air entering the lungs each minute is variable. Under steady-state conditions, the O_2 entering the blood must be equal. However, because the lungs are a large volume reservoir, over short time periods, the volume of O_2 entering or leaving the lungs can be greater or less than the amount of O_2 entering the blood. This is particularly important when the FiO_2 is high, because a greater proportion of the pulmonary gas volume is O_2 and the impact of the pulmonary O_2 volume is therefore greater. At an FiO_2 of 1.0, a given change in pulmonary gas volume produces an error five times greater than that which would occur with room air. This error is potentially greater in patients with larger lung volumes. For example, if a patient has a $\dot{V}O_2$ of 250 mL/ O_2 per minute and the pulmonary O_2 volume is increased by 250 mL in 1 minute, the apparent measured $\dot{V}O_2$ would be 500 mL/min, and the calculated CO would be double the actual value. To reduce the effect of changes in lung volume, expired gases are collected over a period of 3–5 minutes, but even with this precaution, changes in pulmonary gas volume can have a substantial effect on the measurement of $\dot{V}O_2$. A unique problem arises in patients with bronchopleural fistulas, because an unknown amount of expired O_2 always is lost in the air and Fick principle cannot be applied without somehow temporarily stopping the gas leak.

Increases in respiratory rate also affect the measurement of CO. When respiratory rate increases, alveolar PCO_2 falls, and alveolar PO_2 increases; thus, more O_2 is stored in the lung, and $\dot{V}O_2$ is overestimated. This error can potentially create a very large problem in patients with

Cheyne-Stokes respirations and episodes of apnea, as occurs in those with sleep apnea, congestive heart failure, or central nervous system disorders.

An error that affects calculated CO by the Fick method can occur in the $\dot{V}O_2$ measurement in patients with a pulmonary inflammatory process. When lung inflammation is severe, consumption of O_2 by the lung before it reaches the site of alveolar gas exchange with blood can be significant. Consequently, cardiac output calculated by the Fick method is less than that obtained by dilution techniques or direct measurements of cardiac output by electromagnetometry (Light 1988). For example, Light found that $\dot{V}O_2$ could be overestimated by as much as 15% in a canine model of pneumonia (Light 1988).

Continuous Cardiac Output BT the Fick Method

Considering the importance of CO measurements, attempts have been made to acquire continuous measurements of CO using the Fick method (Guyton et al. 1973; Keinanen et al. 1992; Wippermann et al. 1996). The basic approach is to use a continuous measurement of $\dot{V}O_2$, either on a breath-by-breath basis or from a mixed expired gas sample. Continuous sampling of pulmonary venous O_2 saturation can be obtained with an oximetric catheter and continuous measurement of arterial saturation with a pulse oximeter placed on an extremity. The same errors discussed above can apply to these methods. The major concern is that each of the signals is variable on an instantaneous basis, and synchrony with the other three measurements may be a problem. Changes in pulmonary volume or CO will produce spikes in the signal, which should be apparent, and cardiac output can be discerned by taking the average signal in trends over time. The ability to collect these average signals allows for a greater accuracy in discerning the mean value of CO. Nevertheless, one should exercise caution when interpreting dynamic signals with this approach. This technique has been successfully used in a pediatric population

(Wippermann et al. 1996). When compared with the thermodilution measurements, the bias was -4.4 percent, and the precision was 0.32 L/min or 21.3 percent, which is significant; however, it should be appreciated that a single thermodilution measurement may not be sampling the same value as that obtained by the average value using the continuous measurement of CO. The difference was most apparent in the neonatal population, largely in part because their VO_2 is so low that it was at the level of detection of the metabolic monitor.

Indicator Dilution Methods

The basic procedure in this technique is to inject an indicator substance into the venous blood and measure its concentration continuously in the blood at an arterial site. The substance must not affect circulatory dynamics, must not disappear from the blood before it passes the point of detection, and must be readily detectable. There are two different approaches: a single injection in which the indicator is rapidly injected and the continuous method, in which a continuous infusion of an indicator is given and the arterial blood is analyzed over a long enough period of time afterward to ensure a steady-state concentration in the arterial blood. In the first reported use of an indicator dilution technique in 1897, Stewart employed the continuous dilution method (Stewart 1975). He gave a sudden infusion of hypertonic saline in the right side of the heart and measured the change in the electrical conduction of the arterial blood by placing an electrode over an artery. When the arterial blood conductivity reached a plateau, a sample of arterial blood was withdrawn and the concentration of saline measured. CO was then calculated by application of the Fick principle. The rate of injection of hypertonic saline was used for the rate of addition of the indicator substance, in this case, saline. The normal saline concentration in the venous blood of the initial sample was considered zero or baseline, and the increase in concentration in the arterial blood

could then be used to represent the arteriovenous difference. The rate of injection divided by the arteriovenous difference gave the cardiac output according to the Fick principle. Obvious problems with this are that the increase in blood volume could change cardiac output and the increased salt can affect vascular tone.

Hamilton and colleagues are given credit for working out the technique for the single-injection method and the rigorous analysis of its possible errors (Kinsman et al. 1975). This technique is the one most commonly used today, since it is the basis of the measurement of CO using the thermodilution catheter, which is discussed below. The basis of single-bolus-indicator dilution technique is that after an indicator is rapidly injected into the blood, the concentration transiently rises and then decreases over time. The area under the curve (AUC) gives the mean concentration time to return to baseline temperature according to the formula:

$$\text{Cardiac output} = I / \text{integral of } Cdt \quad (20.4)$$

where I is the amount of indicator injected, C is the concentration of indicator, and t is time in seconds. The formula can be reduced to:

$$\text{Cardiac output (L/min)} = 60 \times I / CT \quad (20.5)$$

where C is the mean concentration, T is the time to equilibration of temperature, and 60 converts seconds to minutes. The amount of indicator injected divided by the average concentration of indicator during time T gives the total volume that passed through the site of complete mixing –i.e., the heart. When multiplied by 60 and dividing by the number of seconds, duration of the curve gives the CO in liters per minute. The rationale for this comes from the realization that the amount of indicator passing the detector each second is given by the product of flow in liters per second and the concentration in grams per milliliter for that second period. A further assumption is that the concentration is the same everywhere in the major arteries. The sum of all the intervals therefore gives the total amount of indicator injected (M); thus:

$$M = \text{cardiac output} \times \text{integral } Cdt,$$

which simply is the rearrangement of Cardiac output = $I / \text{integral of } Cdt.$ (20.6)

The major technical problem that must be overcome with this technique is the recirculation of the indicator, which affects the tail end of the concentration curve and makes it difficult to predict T accurately and thus also the area under the concentration curve. Hamilton et al. provided the basis for the elimination of the recirculation time. They plotted the concentration-versus-time on semilogarithmic paper and then drew a straight line for the descending part of the curve. The rationale for this is that the concentration of the indicator disappears as a single exponential, such that:

$$dc / dt = -kC \text{ and therefore } C = C_0 e^{(-kt)} \quad (20.7)$$

The upstroke of the curve is complicated by the lack of instantaneous mixing and a dispersion of washout curves as the substance moves along the vascular tree, but the initial part of the downslope indeed matches a washout curve and hence supports the rationale behind the semilogarithmic approach (Guyton et al. 1973). Alternative approaches today, with computer technology, allow curve-fitting techniques to predict the downslope of the curve from the measurement of dye concentration versus time.

Basic requirements in the indicator dilution technique are that the substance must completely mix with all the blood and most of the indicator must pass a sampling site before recirculation of the indicator begins. Potential errors can occur from changes in the rate of blood flow due to either changes in CO or changes in the fraction of flow going to the sampling site, although the latter is exceedingly rare. Another potential problem occurs if the course of blood follows different parallel channels with different velocities of flow and different dispersions, since the recombination of these channels may occur unevenly and affect the downslope of the curve.

Thermodilution Technique

General Theory

Today, the most common indicator substance is a cold saline aliquot, and the thermodilution technique has become the predominant method for measuring CO in the ICU. Excellent detailed reviews have been published (Jansen 1995; Nishikawa and Dohi 1993). The basic principle is that cold saline injected into the blood at a proximal site in the circulation produces a change in temperature, which can then be sampled downstream. A bolus of the solution that is cooler than the temperature of the blood produces a change in temperature over time, which appears as the inverse of a dye-dilution curve. Advantages to this approach over the dye-dilution technique are that the change in temperature is easy to measure, it can be done in vivo, and, importantly, there is no recirculation of the cold solution, which makes the analysis of the downslope of the dilution curve much simpler. There is also no accumulation of the indicator, so that repeated measurements can easily be performed.

The original principle was described by Fegler in 1954 (Fegler 1954), but it was not until the development of flotation catheters that easily can be advanced into the pulmonary artery that this technique flourished. In the past, the standard approach was to inject 10 mL of ice-cold dextrose in water with the assumption that the water was approximately 0 °C, but currently it has become easy to measure the temperature of the injected dextrose with a thermistor at the site of injection so that room-temperature water can be used. The solutions are injected through a port in the right atrium of a multilumen catheter. The change in temperature is sampled by a thermistor located at the distal end of the catheter in the pulmonary artery. The change in temperature from baseline is recorded by a microprocessor, and CO

is calculated by the integration of the change in temperature over time (Weisel et al. 1975).

Although, there is no problem with recirculation with this technique, the return of the temperature to baseline is delayed. This is believed to result from the slow washout of cold from the myocardium, endothelial surface, and catheter (Weisel et al. 1975). The down part of the change-in-temperature curve must thus still be extrapolated by a curve-fitting technique. This is usually done when the change in temperature is less than 30 percent of the peak change. Repeat measurements cannot be performed until the baseline returns to a steady value.

Sources of Variability

Sources of variability in thermodilution measurements can be considered under (1) technical factors in the injection, such as errors in injectate volume and injection technique; (2) errors due to variations in the physiologic and pathophysiologic conditions, such as changes in pulmonary temperature and changes in cardiac output; and (3) analytic errors related to determination of the area under the temperature-change curve.

Errors Related to the Injectate

The integrated temperature is the difference between the baseline temperature and the temperature recorded during the passage of the cold injectate. There are always fluctuations in the baseline temperature; if these changes are large and the change in temperature with the injectate is small, then the signal-to-noise ratio is small, and accuracy is reduced. To maximize the signal-to-noise ratio, it was initially thought that an ice-cold solution should be used, because this would give the maximum possible change in temperature (Goodyer et al. 1959; Ganz et al. 1971). An ice-cold injectate however increases the potential heat gain before the fluid is injected. For example, the temperature of an ice-cold 10 mL syringe held in the hand will increase by 1 degree every 13 seconds, and each change in degree centigrade

produces an error in CO measurement of 2.86 percent (Nishikawa and Dohi 1993). The syringes should also be left in an ice bucket for at least 15–20 mins to ensure that they are cooled evenly. This means that syringes must be prepared in advance, which decreases the convenience of this technique and the ability to perform rapidly repeated measurements. Since syringes must be prepared separately and individually iced and many syringes are needed, this potentially increases the risk of contamination. Finally, using a colder injectate also means that a longer period of time is needed for the washout of cold from the tissues, and this increases the time delay between measurements (Pearl et al. 1986). With all of these potential problems, it might be expected that cold injectate is less effective than that at room temperature, but the reported variability of measurements is low. It should be appreciated that these measurements are obtained in studies in which greater rigor is probably applied than is often the case with multiple operators in an ICU.

It has now been demonstrated that the use of a solution at room temperature is just as accurate and much more convenient than use of an ice-cold solution (Pearl et al. 1986; Shellock and Riedinger 1983; Vennix et al. 1984; Stetz et al. 1982). Because the solution is at room temperature, the syringes do not have to be prepared in advance, and there is no change in temperature when the syringes are not used immediately. The syringes will still warm in the operator's hand; therefore, the operator must take caution to not handle the syringes for an extended period of time.

An important factor in the thermodilution technique is to have an accurate measure of the injectate temperature. When an ice-cold solution is used, the syringes are put on ice, and the injectate solution temperature is assumed to be zero. With the use of injectates at room temperature, two bags of solution are kept at the bedside; the thermistor probe is inserted into one, and the other is used for the withdrawal of sterile samples. The two bags should thus have the same temperature. A common setup includes connecting the thermistor to a bag of dextrose in water, which is left at the bedside, and injectate is

drawn from a bag attached to the manifold connected to the ports of the thermodilution catheter/PAC. This bag is also used for flushing the catheter. This approach makes it easier to keep the samples sterile, allows for repeated injections, and requires only one syringe. An error can arise when a fresh bag of injectate is prepared, especially if it is taken from a refrigerated source, since time is needed to equilibrate the injectate bag with room temperature. As indicated above, currently, it has become common to measure the injected temperature through the catheter used for the injection.

Problems can arise with the use of room-temperature solutions if the environment is very hot (i.e., a burn ICU greater than 30 degrees Celsius (86 degrees Fahrenheit) because the signal-to-noise ratio will then be very small). The same problem also arises if the patient's temperature is very low, as occurs in patients who have undergone cardiac surgery or those resuscitated from hypothermia. As opposed to an iced-cold solution, a room-temperature solution also produces more variable results when the cardiac output is low because of the low signal-to-noise ratio in the dilution curve (Nishikawa and Dohi 1993).

The volume of the solution is another important variable (Pearl et al. 1986; Elkayam et al. 1983). CO is directly proportional to the injectate volume, and whatever percent of error is introduced by an inaccurate volume of the injectate gives the same percent of error in CO. There is always a potential for error in volume measurement because of the volume being trapped in the dead space of the catheter system or because of small air bubbles in the syringe and from the stopcocks. The error will tend to be of the same magnitude whether the injectate is 3 or 10 mL; therefore, the percent of error is greater with small volumes of injectate. For this reason, it is recommended that 10 mL of solution be used in the adult patient. The volume should be adjusted accordingly in children. If the injectate volume is too large, especially with ice-cold solutions, the precipitation of cardiac dysrhythmias is possible (Harris et al. 1985; Nishikawa and Namiki 1988).

The theory assumes that the indicator mixes with the blood at the site of injection. If the injec-

tion is too slow, then this condition is not met, and the CO will be overestimated (Bazaraal et al. 1992), because the longer washout curve will increase the denominator of Eq. 20.4 by thermodilution.

An important source of potential error to be wary of is the use of a large infusion of fluids through a central catheter at the same time as the measurements are made, for this will add another large source of cool indicator. If the infusion produces a steady-state reduction of pulmonary artery temperature, the CO will be underestimated. However, if the PA temperature is still falling, CO will be overestimated. This may be the cause of inaccurate thermodilution CO measurements as compared with electromagnetometry reported in dogs undergoing rapid blood loss (Nishikawa 1993).

Errors Related to Physiologic and Pathophysiologic Factors

During the respiratory cycle, there are variations of pulmonary temperature that produce fluctuations in the baseline signal at the thermistor. CO measurements thus vary depending on when in the respiratory cycle the measurement is initiated (Delhaas et al. 1992; Jansen et al. 1981). There are also physiologic variations in the pulmonary blood flow related to changes in the pleural pressure. It has been suggested that it might, therefore, be advantageous to standardize the time in the respiratory cycle in which the injection is made. Changes in CO during the respiratory cycle are not uniform in all individuals; even if they were, this would give the CO for only part of the cycle. It has been found that the measurement of three randomly placed injections in the respiratory cycle is just as accurate as trying to choose a fixed point, and it is definitely simpler. Therefore, the present recommendation is not to try and inject during any specific point in the cycle (Jansen 1995; Nishikawa and Dohi 1993; Delhaas et al. 1992; Jansen et al. 1981).

Changes in CO during the measurement will no doubt have an effect on the measurement. This must be considered when using an ice-cold solu-

tion, since it can cause slowing of the heart rate by as much as 10 percent and can consequently result in decreased pulmonary blood flow, which will lead to an underestimation of the CO (Harris et al. 1985). The change in heart rate with a solution at room temperature is only 4 percent. Arrhythmia, particularly atrial fibrillation, also produce an irregular stroke volume, leading to artifactual thermodilution measurements. In this case, the actual stroke volume/flow at each second is variable, but there is also a variability produced by an increase in noise in the signal, which produces less accuracy in measuring the area under the temperature curve.

A very common cause of inaccurate CO measurements in the ICU is tricuspid regurgitation (TR) (Heerd et al. 1992; Boerboom et al. 1993). This can affect the measurement in a myriad of ways. The regurgitant fraction of the right ventricular output exposes the blood to a greater volume of tissue, including that in the inferior vena cava, and this warms the blood faster than usual, before it can be measured at the distal thermistor. CO is thus overestimated because the washout of the cold temperature is faster. If the regurgitant fraction is very large, there can be a delay of delivery of the indicator to the distal thermistor as well as an increase in the variability of the signal, which makes the integration of the change-in-temperature curve less accurate. The slow release of cold blood from the atrium because of the regurgitant fraction results in an underestimation of cardiac output because it prolongs the descending part of the curve and increases the denominator of the equation listed above.

Most reports demonstrate an increased variability and inaccuracy of CO measurements in patients with TR (Nishikawa and Dohi 1993; Heerd et al. 1992). There have been several reports that have failed to find a difference between Fick and thermodilution output measurements in patients with TR and without TR. The difference between CO measurements has been small, or the CO was quite low in all patients; the variability was thus already large, and it would have been difficult to detect a difference between techniques in patients with TR.

An advantage of the thermodilution technique over the dye-dilution technique in the absence of

an intracardiac shunt is that there is no recirculation. The presence of an intracardiac shunt allows for recirculation to occur, and the descending part of the thermodilution curve cannot be properly integrated with the standard automatic cardiac output computers, although techniques are available for use with the actual thermodilution curve. Note that the problem with a left-to-right shunt is not the addition of flow distal to the injection site, because the injection can be from a proximal site with dilution techniques. Rather, the problem arises in the recirculation of cold blood through the shunt. Right-to-left shunts produce a different problem. They result in a loss of indicator and inadequate mixing as the stream of cold solution separates and reforms.

Analytical Problems

A major analytic problem in all dilution techniques is the proper assessment of the downward part of the dilution curve. This problem is prominent in low CO states, because the washout curve is very slow and it is difficult to distinguish the washout of cold from the blood from the washout of cold from the tissues (Van Grondelle et al. 1983). The tissue component is also greater because of the longer contact time of the cold injectate with the tissues.

An interesting and potentially clinically important problem arises in patients after cardiac surgery. Following aortocoronary bypass procedures, the core temperature can be as low as 33–34 degrees centigrade. This results in a much smaller signal-to-noise ratio with the use of injectate at room air temperature. More importantly, there is also an initial change to the temperature when the patient comes off bypass (Bazaraal et al. 1992) and then again during rapid rewarming. These changes in baseline temperature can significantly decrease the measured cardiac output.

Another technical problem that can potentially arise is the wedging of the catheter tip during the measurement. This blocks the thermistor from the bloodstream and produces an erroneous recording of the blood temperature. It can be avoided by ensuring that a good pulmonary artery

tracing is present on the monitor before conducting a measurement.

A number of simple procedures can be of help in evaluating the validity of thermodilution CO measurements in a patient whose results appear spurious. Firstly, the dilution curve should always be examined for artifacts or unusual shape, particularly a long “tail.” Secondly, repeated measurements should produce consistent results. Finally, one can obtain a mixed venous sample and determine if it is appropriate for the measured cardiac output and observed clinical status. For example, if the CO is high and sepsis is suspected, the mixed venous oxygen content should be high. If the CO is high and the mixed venous oxygen content is also low, these values are concordant. The mixed venous oxygen saturation, the arterial saturation, and cardiac output can be used to calculate the VO_2 from the Fick equation, and this value can be assessed to determine if it is consistent with the patient’s condition and whether the results correlate with the patient’s clinical condition.

Reliability

Stetz et al. (1982) reviewed nine studies that addressed the reproducibility and accuracy of the thermodilution method. They found that with three injections, the reproducibility data indicate that there should be a 12–15 percent difference in the measured cardiac outputs before the change in cardiac output can be considered to be significant. This value increases to 20–26 percent if only one injection is performed.

Continuous Thermodilution Technique

Techniques have also been developed to obtain continuous measurements of cardiac output by the thermodilution approach (Yelderman et al. 1992; Haller et al. 1995). With this approach, a thermal catheter is placed at the usual site of the injectate port. This filament gives a transient burst of heat. A distal thermistor then monitors the change in temperature in the blood, and the thermodilution-time

curve is used to determine cardiac output as in the usual method of thermodilution cardiac output determination. Bursts of heat are given repeatedly. The on/off times of the thermistor can be randomized to a stochastic approach, which reduces the signal-to-noise ratio and allows for smaller boluses of heat (Yelderman et al. 1992). The advantage of obtaining multiple CO measurements by this technique is that atypical measurements become more obvious and the trends can be more readily followed. The system has yielded very good accuracy and precision when compared to the Fick method and bolus thermodilution as demonstrated in a swine model (Thrush et al. 1995). It was subsequently tested on patients following aortocoronary bypass procedure (Bottiger et al. 1995). The precision and accuracy were excellent before and 45 minutes after surgery but not in the immediate postoperative period, presumably due to changes in the baseline temperature. In one study, this technique was compared with cardiac output measurement by an electromagnetic flow probe on the ascending aorta in patients undergoing cardiac surgery (Hogue Jr et al. 1994). The bias was -0.48 L/min and precision was 0.56 L/min. The difference was greater than 20 percent in 11 percent of measurements.

Use of Expired Gases and the Fick Principle to Measure Cardiac Output

The Fick principle can be applied to expired gases to noninvasively measure cardiac output. This requires manipulating the expired gases so that the mixed venous concentration of the indicator can be obtained. A commonly used indicator is carbon dioxide (CO_2). This can be done with a rebreathing technique or a single-breath technique.

Rebreathing Technique

In this approach, CO_2 is used instead of O_2 for the direct Fick method. Cardiac output is then expressed as:

$$\dot{V}CO_2 = \frac{VCO_2}{\text{Venous } CO_2 - \text{arterial } CO_2 \text{ content}} \quad (20.8)$$

In the rebreathing method (Jones and Campbell 1982), subject rebreathes from a bag containing from 6% to 10% CO₂ in air. The expired CO₂ is continuously measured until the concentration reaches a plateau. When this occurs, CO₂ in the alveoli should be in equilibrium with CO₂ in the pulmonary arterial blood and thus gives a measure of the mixed venous CO₂. The PCO₂ in the bag at the plateau can then be used to calculate the pulmonary arterial CO₂ content from the hemoglobin-CO₂ dissociation curve. This, in turn, can be calculated from the PCO₂ and hemoglobin concentration because the blood CO₂ content-PCO₂ relationship is relatively linear above a PCO₂ of 30 mmHg. The arterial PCO₂ can be obtained by appreciating that arterial PCO₂ is approximately equal to alveolar CO₂. Therefore, end-expiratory CO₂ gives a measure of arterial PCO₂. Finally, VCO₂ is obtained by collecting the expired gases over a fixed time and measuring the volume and CO₂ concentration. Since the inspired CO₂ is essentially zero, the CO₂ production, VCO₂, is the concentration of CO₂ in the lung multiplied by the expired volume divided by the time of collection (Jones and Campbell 1982).

Potential Problems

The selection of the initial PCO₂ for the rebreathing bag is very important. If this value is too high, the plateau in the expired PCO₂ will never be reached because there is recirculation of the CO₂ which will continuously increase the value because of the continual production by the body. If the initial PCO₂ is not high enough, it will take too long for the subject to reach a plateau, or a plateau may never be reached.

The major problem with this approach is that, under resting condition, the difference between mixed venous and arterial PCO₂ only is about 6 mmHg. Therefore, small errors in the analysis of PCO₂ have a large impact on the measurement. For example, with an arteriovenous difference in

PCO₂ of 6 mmHg, a 1 mmHg error in analysis of either signal will result in almost a 15% error. For this reason, this approach is much more effective when cardiac output is elevated and the arteriovenous CO₂ difference is increased, as is the case during exercise. On the other side, the technique should be more accurate in patients with a low cardiac output state because they have a larger arteriovenous CO₂ gradient than normal subjects.

The estimate of arterial CO₂ also is a potential source of large error when there are inhomogeneities of washout of pulmonary gases. This is because the peak of the expired CO₂ curve does not necessarily indicate arterial blood CO₂ in this case. This obviously is a major issue in the ICU, where many patients have acute or chronic lung disease. This problem can be ameliorated easily since most patients in the ICU have an arterial line in the ICU and arterial PCO₂ can be directly measured from an arterial sample. When this is done, the bias, compared with thermodilution, was -0.06 L/m^2 per minute, and confidence intervals were -0.120 – 0.001 L/m^2 per minute, indicating very good precision (Neviere et al. 1994). This study was also performed in patients with chronic obstructive pulmonary disease; however, it is likely that these patients did not have a large shunt component, because otherwise the bias should have been more negative. The presence of significant shunts could significantly limit the value of this technique in the ICU.

Another potential error is that the breathing maneuver required to obtain a plateau during the rebreathing from the bag can alter the cardiac output. Another assumption with this technique is that the CO₂-hemoglobin dissociation curve is linear. This is true only at values of PCO₂ above 30 mmHg. If the patient hyperventilates markedly and the PCO₂ is much below 30 mmHg, this assumption is no longer valid. Finally, this technique measures only pulmonary capillary flow in contact with the alveoli, and shunted blood is not measured. Bing and coworkers actually used this fact to measure shunt flow by comparing the direct and indirect Fick calculations of cardiac output.

Single-Breath Technique

The CO₂ rebreathing technique requires time and patient cooperation and thus is not very useful in the ICU. The rapid breathing required to obtain the plateau in expired CO₂ can also affect patient hemodynamics. Therefore, efforts have been made to try and obtain cardiac output from a single long expiration. These approaches do not require an estimate of arterial PCO₂ from “normal” alveolar air. The basic principle is as follows. Oxygenated blood carries less CO₂ than deoxygenated blood, and when the venous blood is oxygenated in the lungs, CO₂ is liberated. It can be shown that when the respiratory exchange ratio (*R*) of VO₂ to VCO₂ reaches 0.32, arterial and venous PCO₂ are equal, even though the venous CO₂ content is greater. During a long expiration, alveolar CO₂ progressively rises and the *R* value decreases. When the *R* value reaches 0.32, alveolar, arterial, and mixed venous CO₂ tensions are equal, and the alveolar sample can be used to obtain the mixed venous PCO₂. The arterial PCO₂ can be obtained by taking the alveolar PCO₂ and the patient’s *R* value. The *R* value is calculated from the VO₂ and VCO₂ prior to initiating the maneuver. The CO₂ content is then obtained from the CO₂ dissociation curve for the subject. This curve is calculated using the patient’s PCO₂ and hemoglobin (Jones and Campbell 1982). Cardiac output then can be calculated using the Eq. 20.8. This procedure can be automated so that the rapid analysis of PO₂ and PCO₂ of each breath gives the cardiac output on a breath-by-breath basis.

This approach is attractive in that it allows noninvasive and continuous measurement of cardiac output. As is the case with the CO₂ rebreathing method, abnormalities in ventilation-perfusion matching and pulmonary function markedly affect the accuracy of this technique and greatly limit its potential usefulness in the ICU. Currently no studies employ the single-breath technique with CO₂ as the indicator gas in the ICU.

Foreign Gas Method

The concentration of a highly diffusible gas such as acetylene is the same in the alveoli and systemic arterial blood assuming that there is no intrapulmonary shunting. The concentration in the systemic blood (*C*_{sa}) can then be calculated from:

$$C_{sa} = P_{al} \times k \quad (20.9)$$

where *C*_{sa} is the concentration of the gas in the systemic arterial blood in milliliters per liter, *P*_{al} is the partial pressure of the gas in the alveoli in mmHg, and *k* is the solubility coefficient of the gas in milliliters per liter per mmHg.

Inert soluble gases can be used in the single-breath or rebreathing technique. With either approach, the objective is to measure the washout of the soluble gas from the lung. In rebreathing techniques (Hsia et al. 1995; Nielsen et al. 1994; Pierce et al. 1987), the subject breathes from a bag with an indicator gas for approximately 15 seconds to allow an equilibrium to be reached with the gas in the bag, the alveoli, and the arterial blood; the washout of gas is then monitored. The end-expired gas samples give a measure of the arterial concentration, and the mixed venous concentration is assumed to be zero as long as the measurement is conducted before there is significant rebreathing. CO can then be calculated as follows:

$$CO = Q_g / k \times P_{al} \quad (20.10)$$

where *Q*_g is the rate of uptake of the gas (or washout) and *k* and *P*_{al} are as described above.

In the single-breath technique (Nielsen et al. 1994; Pierce et al. 1987; Zenger et al. 1993; Elkayam et al. 1984), the subject breathes in from a bag with a known concentration of the inert gas, and the initial value is extrapolated from the value at zero time of the concentration versus time.

A problem with this technique is the assessment of the exposure of the inert gas to the blood interface because this affects the rate of uptake of gas. To account for this, another gas also is mea-

sured so that the ratio of the change in that gas to change in the soluble gas, such as acetylene, can be used to determine the rate of washout of acetylene. Various gases have been used. Initially O₂ was used, but investigators have used insoluble gases like helium (Elkayam et al. 1984), methane (Ramage Jr et al. 1987), and argon (Pierce et al. 1987). These are added to the rebreathing bag and have a different rate of uptake or no uptake, which allows an accounting of volume changes and allows the calculation of the rate of clearance of acetylene. The decay curve of acetylene concentration gives the rate of loss of acetylene, which is the source of the numerator in the cardiac output calculation. This curve is then extrapolated back to time zero, which gives the initial arterial concentration of acetylene. Since the venous sample is assumed to have a zero concentration of acetylene, cardiac output can be determined from the ratio of the rate of loss of acetylene and the arterial content.

The advantage of the single-breath technique is that it allows rapid repeated measurements and requires less cooperation (Crapo and Morrish 1987). Its accuracy tends to be less than that of rebreathing methods. The single-breath and rebreathing approaches with acetylene have been compared in a number of studies. Wendelbow et al. concluded in dogs that the single-breath technique is inferior, which is not surprising, considering the potential for greater variability in the extrapolation of the initial arterial concentration and the greater assumptions required in this assessment (Nielsen et al. 1994). Others have also found that the single-breath measurements of cardiac output agree well in patients with normal lung physiology but less well in patients with obstructive lung pathology (Pierce et al. 1987). In one study of patients with coronary artery disease (Zenger et al. 1993), the bias compared to thermodilution was 0.03 L/min, and the standard deviation of the difference was 0.76 L/min. The accuracy was less in patients with an FEV₁/FVC < 60 percent. In another study (Zenger et al. 1993), the bias compared to thermodilution was only -0.39 L/min with a precision of 0.94 L/min. This was improved by adding a correction for shunt. The error produced by shunt with obstructive

lung disease greatly limits the potential value of these techniques in the ICU.

Pulse Contour Analysis

Devices have been developed to use arterial pressure obtained from an intra-arterial catheter to measure cardiac output by pulse contour analysis (PCS). These systems allow CO to be estimated continuously after an optional external calibration with some systems. The systems measure stroke volume (SV), and CO is calculated by multiplying SV by heart rate (HR). HR is typically equal to the pulse rate. The device takes the arterial pressure waveform as an input. The pulse rate is the number of upstrokes on the arterial pressure curve over time. To calculate SV the pressure measurement is converted into a volume measurement by integrating the pressure over time which gives volume. The systems use the Otto Frank's Windkessel model from 1899 that has been modified to incorporate arterial impedance (Z_a), arterial compliance (C_a), and systemic vascular resistance (SVR) (Frank 1899).

Arterial impedance is then the ratio of pressure to flow in the central arteries and is determined by the physical properties of the arterial walls. It represents the forces opposing the propagation of the pressure wave transmitted along the arterial system. The compliance of the arterial system is defined as the difference in blood volume induced by a difference in pressure and is mainly affected by the elastic properties of the arterial walls. The SVR is the resistance of the total systemic vasculature to the blood flow. A limitation of this approach is that arterial impedance and compliance have to be assumed. To do so all systems but one do this with the use of internal nomograms or databases that are based on demographic data, such as age and gender.

Vigileo™-FloTrac System

The Vigileo™ monitor employs the proprietary FloTrac™ (Edwards Lifesciences, Irvine, CA) attached to a standard radial or femoral arterial

line. There is no external calibration. The system samples the arterial waveform at 100 Hz and determines CO in 20-second intervals by a multiplication of the pulse rate with the standard deviation (SD) of the arterial pressure over a period of time (σ) and “conversion factor” χ , which accounts for both vascular resistance and compliance and is calculated by a complex multivariate polynomial function. This function uses pulse rate, BSA, predicted aortic compliance, mean arterial pressure, and the SD of the arterial pressure over a fixed time, as well as the shape of the arterial waveform. The aortic compliance is determined using an internal demographic database (age, sex, height, and weight) and mean arterial pressure. The flow or SV is then calculated based on the following:

$$\text{APCO} = \text{PR} \times (\sigma_{\text{AP}} \times \chi) \quad (20.11)$$

where PR is the pulse rate and χ is the multivariate polynomial function.

The FloTrac™ algorithm has been refined multiple times since its introduction. The internal database has been expanded, and the tracking of SV has been improved by electronically eliminating and interpolating abnormal or premature beats.

The accuracy of this arterial-based technology is questionable during hemodynamically unstable states although the precision likely is reasonable. More robust algorithms will be required to compensate for states of low- and high-peripheral vascular resistance.

LiDCO plus® System

This system (Fig. 20.1) also uses analysis of a pulse contour from an arterial pressure waveform from an arterial line to determine SV and CO. It differs from the above-described system in that it utilizes a lithium-based dye-dilution technique to calibrate its pulse contour analysis algorithm referred to as pulse CO. After calibration, the LiDCO plus® system (LiDCO, London, UK) can generate CO measurements using analysis of the pulse contour and the gen-

erated algorithm; however, recalibration is recommended every 8 hours.

There also is a LiDCO rapid® system which uses an algorithm based on predicted arterial compliance and impedance as is the case with the FloTrac. A difference between the two devices is that the LiDCO uses a reverse approach. The algorithm subtracts the calculated stroke volume from the predicted value rather than correcting the calculated from the predicted. The results seem to be similar.

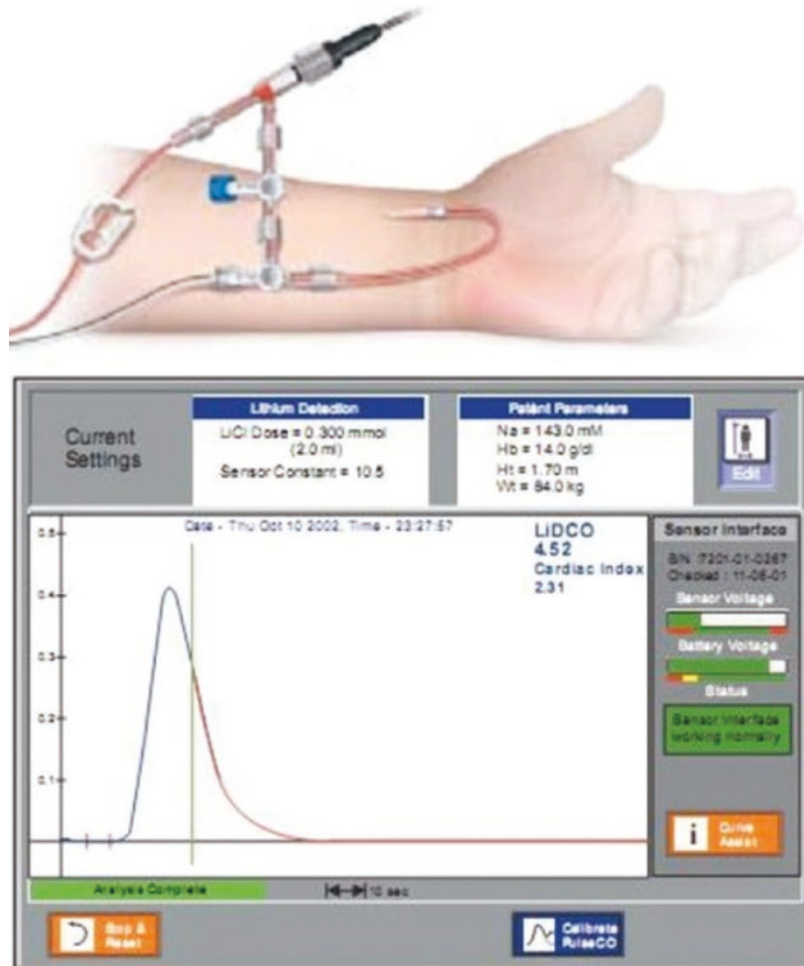
PiCCO System

This device, too, calculated CO by pulse contour analysis of the arterial pressure waveform but in addition uses a thermodilution measurement to calibrate the signal and thus provides a more accurate measurement than the devices that just use the pulse contour. To do this a cold solution is injected in a central vein and detected by an arterial catheter. This needs to be in a large vessel and is thus usually put in a femoral artery, but a brachial artery also can be used but with some loss of accuracy. Although the thermodilution provides more reliability, the need for cannulation of a larger artery makes it more invasive, and when positioned in the femoral artery, it reduces mobility. The PiCCO monitor (Pulsion Medical Systems, Munich, Germany) uses the thermodilution signal to obtain several other measurements including global end-diastolic volume of all four heart chambers and extravascular lung water measurements (Oren-Grinberg 2010). As with other PCS, periods of significant hemodynamic variability may result in inaccuracy in CO measurement which would necessitate frequent recalibration. Small single-center studies, different settings, and different standards of reference make generalization difficult (Boyle et al. 2007).

Esophageal Doppler

The esophageal Doppler produced by Deltex Medical (Fig. 20.2) is a flexible probe that has a Doppler transducer (4 MHz continuous or 5 MHz

Fig. 20.1 LiDCO plus® system for measuring cardiac output from www.lidco.com. (Used with permission of LiDCO Ltd)



pulsed wave, according to manufacturers) at the tip that is placed in the esophagus to obtain an aortic velocity signal in the descending aorta. The technology allows an assessment of cardiac preload by examining the velocity time integral (VTI) of the aortic flow (normal range, 330–3360 msec) (Fig. 20.2b). A decrease in this value indicates a decrease in preload of the left ventricle. This can be due to a true decrease in blood volume but also can be due to right ventricular limitation of cardiac output. The esophageal Doppler allows for quantification of myocardial contractile function by assessing peak velocity of the aortic VTI signal (normal >70 cm/sec). Finally, the technology is able to derive vascular tone by analysis of the VTI waveform. A meta-analysis by Dark and Singer demonstrated an

86% correlation between CO as determined by esophageal Doppler and pulmonary artery catheter (Dark and Singer 2004).

Clinical studies have demonstrated that trans-esophageal Doppler-guided protocols compared to conventional approaches of volume replacement (clinical assessment and/or CVP alone) conclusively reported beneficial effects in the Doppler-optimized groups (Noblett et al. 2006; Wakeling et al. 2005; McFall et al. 2004; McKendry et al. 2004; Conway et al. 2002; Gan et al. 2002; Venn et al. 2002; Sinclair et al. 1997). This included a reduced risk of postoperative morbidity and a shorter length of hospital or ICU stay. The resulting waveform, however, is highly dependent on correct positioning and requires frequent adjustments in depth, orientation, and gain to optimize

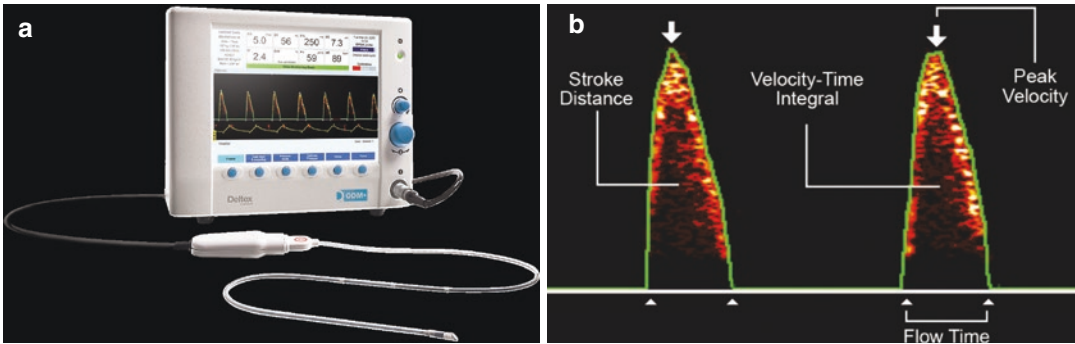


Fig. 20.2 Deltex Medical esophageal Doppler system (a) with a corresponding velocity time integral trace (b) from <https://www.deltexmedical.com>. (Used with permission of Deltex Medical Limited)

the signal. Therefore, while esophageal Doppler has utility in aiding in the assessment of the hemodynamic status of critically ill patients, this technology has been slow to be adopted. This is likely due to the high amount of continuous operator involvement required to produce accurate data.

Echocardiographic Techniques

In recent years, the use of ultrasound and particularly point-of-care ultrasound (POCUS) has become pervasive in critical care medicine. Current technologies used to achieve the goal of measuring cardiac output include transthoracic echocardiography (TTE), transesophageal echocardiography (TEE), and hemodynamic transesophageal echocardiography (hTEE).

The improvements in Doppler technology have greatly increased the ability to obtain a CO measurement by this method. Although reproducibility is very good, studies have challenged the accuracy. Recent reports suggest that Doppler techniques allow for the monitoring of relative changes in flow (Bernstein 1987). The rationale behind this technique is fairly simple. A Doppler beam is used to determine the velocity of blood by directing the ultrasound beam at the flowing column of blood. The frequency of the reflected sound waves is different than that of the transmitted sound waves. This produces a Doppler shift. The magnitude of the Doppler shift is proportional to the velocity of blood flow. If the cross-sectional area (CSA) at the site of the flow

measurement is determined, the stroke volume can be calculated for each beat because flow is the product of velocity and cross-sectional area. The product of the stroke volume and heart rate gives cardiac output in L/min. Using this information, a transthoracic image can provide left ventricular CO by measuring the velocity time integral through the aortic valve (Fig. 20.3).

Since stroke volume is calculated as the product of velocity of each heart beat and the cross-sectional area, accurate determination of CSAs is crucial. Using the hydraulic principle, assuming a constant mean flow velocity through a rigid circular tube of constant diameter, and therefore fixed CSA, volumetric flow can be expressed by the hydraulic equation:

$$Q = V \times \text{CSA} \quad (20.13)$$

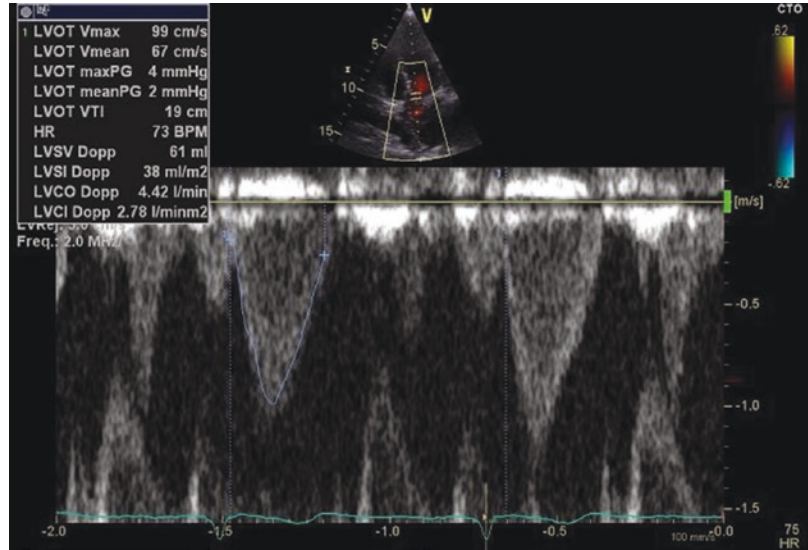
where Q is the volumetric flow rate (L/sec), V is the mean velocity (cm/s), and CSA is the cross-sectional area of the orifice (cm²).

During periods of pulsatile blood flow, volumetric flow is calculated using the velocity time integral (VTI), the stroke distance reached by the column of blood during the flow period, and calculation of volumetric flows is equivalent to determining the volume of a cylinder, where:

$$\text{Volume} = \text{CSA} \times \text{Length} = \text{CSA} \times \text{VTI} \quad (20.13)$$

If we assume a circular orifice, the CSA can be obtained using an echocardiographic diameter (d) or radius (r) at the site of the flow measurement – for example, the aorta – and the area is computed from:

Fig. 20.3 Stroke volume and cardiac output estimation from pulsed Doppler across the left ventricular outflow tract by transthoracic echocardiography. (From Royal Victoria Hospital McGill University Health Center, Dr. Gordan Samoukovic)



$$CSA = \pi (r)^2 = 0.785d^2 \quad (20.14)$$

where CSA is the cross-sectional area (cm^2), r is the radius of the circular orifice (cm), and d is the diameter of the circular orifice (d).

A number of technical problems with this approach need to be considered. They are related to the measurement of the CSA of the vessel and the assumption of laminar flow with a blunt velocity profile in the vessel (Bernstein 1987).

Any error in the diameter measurement due to resolution problems or selection of a site that is not the true CSA for the flow will result in an error that is squared and then multiplied by the heart rate or VTI. It seems that the assumption that the aorta is circular is also not valid, for in reality it is more oval. The vessel and chamber diameters also change during systolic ejection (Stewart et al. 1985), and the magnitude of change is greater in hypervolemic patients and patients on positive-pressure ventilation, because the magnitude of their aortic pulse pressure tends to be larger. Furthermore, the measured anatomic CSA may be different from the functional area for flow, particularly during the large increase in flow during stroke volume ejection. This can result in an overestimation of CSA, which could falsely increase the calculated cardiac output.

The proper assessment of aortic flow velocity requires that the Doppler beam be within 20

degrees of the axial flow; otherwise, a correction must be applied to the measured velocity (Hausen et al. 1992; Siegel et al. 1991; Sahn 1985). Within this range, the error introduced is less than 6 percent, but it is not always easy to ensure that the Doppler beam is within this range, and this likely accounts for the inaccuracies of some other Doppler approaches such as transtracheal Doppler flow measurements (Hausen et al. 1992). Furthermore, the velocity profile may be skewed relative to the aortic outflow axis. It also is possible that the velocity profile is not symmetrical in all three dimensions. If the beam is parallel to the axial flow in two dimensions, but not the third, flow likely is underestimated. Conversely, if the highest frequency is picked in the third dimension and the velocity in this axis is greater than in the other axes, flow could be grossly overestimated (Bernstein 1987).

The flow of the column of blood is assumed to be laminar, but this is not always the case in the proximal ascending aorta in patients who have a hyperdynamic circulation, such as patients with anemia or tachycardia, patients on inotropic support, and those with aortic valve disease and a dilated aortic root.

Doppler studies can be performed with pulsed or continuous Doppler (Come 1986). In the pulsed-wave Doppler technique (PW), the probe is combined with two-dimensional imaging

transducer, and the transducer samples an operator-chosen area with the field. The advantage is that the site of flow can be localized, but there are a number of pitfalls. The primary issue is the inability to detect high frequencies before aliasing occurs. The column of blood ejected from the left ventricle into the systemic circulation has a high velocity and frequency. The maximal detectable shift in frequency is one-half the pulse repetition frequency of the transducer. Since the signal is pulsed, there is a finite limit to this frequency. When the frequency limit is reached, higher velocities cannot be detected. This is called aliasing. The number of pulses admitted is also dependent upon the distance of the sample site from the transducer; longer distances require slower sampling frequencies, which compound the problem of aliasing.

In the continuous wave Doppler method (CW), there is no limit to the frequencies that can be used; therefore, this technique can detect high velocities of flow. However, CW Doppler does not allow simultaneous assessment of the cross-sectional area being sampled. It also does not allow for the distinction between two jets of flow located close together. Technological advances in ultrasound transducers have allowed for the combination of both CW and PW to be obtained using the same probe.

Using the above principles, volumetric flow across any cross-sectional area, such as a cardiac valve of an outflow tract, either during systole or diastole, can be calculated from the diameter, VTI, and a Doppler beam. When using the atrioventricular valves, the flow is examined during diastole, and the VTI is measured by tracing the PW spectral Doppler trace modal velocity. When using the semilunar valves (aortic and pulmonary), the VTI is obtained during systole by tracing the other edge of the CW spectral Doppler trace. Annular measurements are obtained when the valves are open. The stroke volume (SV) of blood ejected during one cardiac cycle is therefore calculated as:

$$SV = 0.785d^2 \times VTI, \quad (20.15)$$

where d is the diameter of orifice (cm) and VTI is the velocity time integral (cm).

SV estimates obtained using a Doppler technique do not make any geometric assumptions about the LV cavity size or function. In assessing an asymmetric LV, where geometric assumptions introduce errors, SV measured by Doppler may present a theoretical advantage when compared to two-dimensional echocardiography. The calculation of LVEF using the method of Dumesnil et al. (Dumesnil et al. 1995) combines the measurement of SV by Doppler volumetric and the end-diastolic volume using Teichholz's formula. To enhance accuracy, it is recommended to trace and average the VTI of at least 3–5 beats in normal sinus rhythm and at least 8–10 beats in atrial fibrillation. By measuring the time interval between two consecutive beats, either on the EKG or Doppler trace, the heart rate is determined by:

$$HR = 60,000 / \text{time}, \quad (20.16)$$

where "time" is the interval between two consecutive heart beats in milliseconds. Therefore, CO can be calculated using the following equation:

$$CO = 0.785d^2 \times VTI \times H \quad (20.17)$$

Now that the principles of echocardiography applicable to both TTE and TEE approaches are established, a site for the measurement must be selected. Historically, the original approach was to place a CW transducer in the suprasternal notch (Donovan et al. 1987). This approach requires operator expertise and experience to properly identify the maximum beam. Even when used with a dual beam (CW and PW), the Doppler measurement underestimates cardiac output, especially when cardiac output is increased and during spontaneous ventilation (Castor et al. 1994). Various other sites have subsequently been proposed for measurement of CO (Sahn 1985). These include the pulmonary outflow tract (Stewart et al. 1985; Maslow et al. 1996; Muhiudeen et al. 1991; Shimamoto et al. 1992), mitral valve, and aortic valve (Dittmann et al. 1987; Stoddard et al. 1993; Darmon et al. 1994; Katz et al. 1993; Descorps-Declère et al. 1996). The best site appears to be the center of the aortic annulus (Dittmann et al. 1987), although even

this measurement is subject to a lot of error. Use of the transgastric approach has been found to improve the view of the center of the aortic annulus. However, the mean bias in one study was still 0.42 L/min, with confidence intervals of 0.89 to -1.74 L/min (Descorps-Declère et al. 1996). TTE approaches are limited by the difficulty of imaging the heart in many patients on ventilators. The best approach is likely use of TEE because this removes the interference from the lungs. However, the choice between TTE or TEE for measuring cardiac output depends upon operator expertise/training, equipment availability, and status of the patient. As an example, it is very difficult to obtain TTE images on a postoperative cardiac surgery patient due to inadequate imaging windows and especially because of the dressings, tubes, and wires in the person's chest.

Transthoracic Echocardiography

Traditionally, performing a TTE required an experienced echocardiographer and a rather large machine to acquire images. Furthermore, the quality of the images depends on patient factors that may limit or obfuscate echocardiographic windows. It is, however, possible with proper training to perform a focused TTE and glean useful information such as cardiac output in the intensive care unit. The advances in POCUS devices have allowed for the clinician to directly visualize the cardiac anatomy and assess flow dynamics, while allowing for a global assessment of structural abnormalities and intravascular volume status. Historically, echocardiography required extensive specialty training and was limited to cardiologists and anesthesiologists. Recent literature has supported the ability to train a non-cardiologist to perform and interpret a limited focused TTE (Manasia et al. 2005; Mazraeshahi et al. 2007).

Key points of these guidelines include:

1. Central venous pressure (CVP) estimate via inferior vena cava (IVC) diameter and respiratory variation
2. Estimation of preload

3. Global assessment of ventricular function
4. Recognition of pericardial effusion and tamponade
5. Global assessment of valvular function via Doppler

With this in mind, there was a need to standardize objectives for learning and examination of competence. The National Board of Echocardiography Examination of Special Competence in Critical Care Echocardiography (CCEeXAM) will now be offered as of 2020. The modern intensivist will integrate the valuable information from a focused TTE exam to guide therapy in the critically ill patient.

Mercado et al. recently published on the level of agreement between cardiac output (CO-TTE) estimated by CO-TTE and that measured by the accepted gold standard reference method, pulmonary artery catheter (CO-PAC) (Mercado et al. 2017). They demonstrated that CO-TTE is both an accurate and precise method for estimating CO. The two measurements were significantly related with a median bias of 0.2 L/min; the limits of agreement were -1.3 and 1.8 L/min, and the percentage error was 25%. The precision was 8% for CO-PAC and 9% for CO-TTE. When using CO-TTE to detect a change in cardiac output measured by PAC of more than 10%, the area under the receiving operator characteristic curve (95% CI) was 0.82. A change CO-TTE of more than 8% yielded a sensitivity of 88% and a specificity of 66% for detecting a change in CO-PAC of more than 10%. Thus, not only is CO-TTE an accurate and precise method for estimating CO, but it can accurately track variations in CO (Mercado et al. 2017).

Transesophageal Echocardiography

Occasionally, it is not feasible to obtain adequate echocardiographic windows due to mechanical ventilation, recent chest closure from cardiac surgery, and body habitus. Cardiac anesthesiologists routinely employ TEE in the intraoperative management of the cardiac surgery patient. As in TTE, there exist barriers that preclude every patient from having an individual TEE probe left

in place while they are mechanically ventilated. These are cost, risk of mechanical complication such as esophageal tear, and a dedicated ultrasound machine for each patient.

Recent advances have allowed for the miniaturization of the TEE probe (mTEE) down to the size of an NG tube. This allows the probe to be left in place for up to 72 hours. The probe detaches from the handle of the ultrasound machine and allows you to use multiple probes in multiple patients.

A feasibility study by Cioccarri et al. demonstrated that with 6 hours of training, intensivists were able to perform focused bedside echocardiographic examinations that were feasible and of sufficient quantity in a majority of ICU patients with good inter-rater reliability between mTEE operators and an expert cardiologist (Luca et al. 2013).

Methods that Assess Changes in Thoracic Volume

Intrathoracic volume changes with each stroke volume; this change can be detected by changes in thoracic electrical bioimpedance and, more recently, by inductive plethysmography (“thoracocardiography”). Similar problems, however, plague both these techniques, and they suffer from poor accuracy, particularly in pathologic conditions. Both, however, have potential for monitoring trends.

Thoracic Electrical Bioimpedance

Attempts to use this technique have been made since the 1960s. The basic theory is given in detail by Bernstein (1987). In the original approach, the thorax was treated as a cylinder with a base circumference equal to the circumference of the thorax at the level of the xyphoid. The cylinder has an electrical length which is the measured distance between circumferential band electrodes placed at the base of the neck and at the level of the xyphoid process. A low-amplitude, high-frequency alternating current is applied by electrodes placed outside the cylinder, allowing

the calculation of the steady-state impedance based on the specific resistivity of the cylinder. Respiratory variations in the signal are filtered out, yielding analysis of the cardiac component. Increased aortic flow during systole decreases the thoracic impedance. The maximum value of the rate of change of the cardiac component of impedance is proportional to the peak ascending aortic flow. The product of peak aortic flow and left ventricular ejection time gives stroke volume, and the product of stroke volume and heart rate gives cardiac output. The original model has been modified so that the thorax is modeled as a truncated cone. The monitoring system (Stewart et al. 1985) has also been improved by using spot electrodes rather than Malar bands and by diastolic clamping of the electric signal as well as better baseline stabilization.

The efficacy of this technique has been assessed in a number of trials (Katz and Feigl 1988; Lyon et al. 1980; Thulesius and Johnson 1966). The technology appears to perform well during exercise (Belardinelli et al. 1996). In a multicenter trial (Shoemaker et al. 1994), the latest technology was compared with thermodilution in 68 critically ill patients with a wide variety of diagnoses. The bias was -0.013 L/min, and the limit of agreement (precision) was 1.4 L/min with a mean difference between the techniques of 16.6 ± 12.9 percent. In a series of patients following aortocoronary bypass surgery, the bias was 0.33 L/min and the precision was 3.14 L/min; in only 62 percent of patients was the cardiac output by this technique within 20 percent of the thermodilution value (Sageman and Amundson 1993). The accuracy when compared with thermodilution was poor in patients with dynamic circulations undergoing kidney transplantation. The bias was 1.36 L/min and precision 1.10–1.54 L/min, indicating very poor agreement. In another study, agreement was worse in patients with high systemic vascular resistances and low cardiac outputs and thus presumably low stroke volumes (Doering et al. 1995).

There are many technical factors that affect the measurement of cardiac output by this technique (Castor et al. 1994). An important assumption is that the ejection velocity is constant when, in fact,

at high velocities the ejection slows near the end. Changes in lung volume do not affect the signal, but large variations in intrathoracic blood volume with ventilation could be a factor and may explain why there is greater consistency during apnea than with intermittent positive-pressure breathing (Castor et al. 1994). It is not possible to use this device on patients with valvular regurgitation because the bidirectional flow alters the baseline impedance signal. It is also not accurate at high heart rates, because the pulsatile component is reduced relative to the baseline, and this decreases the signal-to-noise ratio. Inaccurate measures of body size or improper placement of the electrodes can have a very significant impact on the measurement (Castor et al. 1994). This may explain the poor performance of this technique in patients following an aortocoronary bypass procedure, as bandages and chest tubes make placement of the electrodes more difficult (Shoemaker et al. 1994). Other factors in these patients could include alterations in thoracic impedance by collections of extravascular volume, such as pericardial and pleural effusions or changes in cutaneous blood flow because of the use of vasopressors. Sternal wires, mediastinal tubes, and chest tubes may also alter thoracic impedance. Improper gating of the electrocardiogram (ECG) results in major errors because the upstroke of the impedance signal is not properly identified. The potential effects of pulmonary edema fluid on the signal (Shoemaker et al. 1994) are particularly worrisome as this is such a common problem in the ICU. Thus, the authors of the multicenter trial (Shoemaker et al. 1994) and others (Clarke and Raffin 1993) concluded that this technique is a promising approach for continuous tracking of cardiac output. However, the large potential for artifactual measurements limits its usefulness at the moment, particularly in the ICU (Fuller 1992).

Thoracocardiography

Another approach for the measurement of CO uses inductive plethysmography and is based on an approach that has been successfully used to monitor changes in lung volume. The basic pre-

mise is that inductive plethysmography represents the sum of all changes in volume enclosed by the transducers on the chest (Bloch et al. 1997a; Sackner et al. 1991). At the level of the xiphoid, respiratory movements account for 95% of the signal, and stroke volume accounts for 5% of waveform amplitude. By digital band-pass filtering and ECG-triggered ensemble averaging, the respiratory component can be filtered out, and cardiac output is left. The relative change in stroke volume is determined from this signal. To obtain the actual stroke volume and cardiac output, however, the initial value must be calibrated with stroke volume measured by another technique.

The volume that is measured by this technique is derived from the change in cross section of the heart through a short access cut. An important assumption is thus that the shape of the heart is uniform in all directions. Changes in shape of the heart or dyskinesia in the longitudinal plane will produce inaccurate results. It is likely that this technique will not be accurate in patients who have intermittent ischemia. Because this technique requires averaging to separate cardiac output from respiratory change, oscillations in the cardiac output will affect the signal. The device is not valid in the presence of arrhythmia and valvular regurgitation. Given the multitude of technical difficulties and limitations of the approach, it is not surprising that the limit of agreement is around 1.4–1.8 L/min as compared with thermodilution (Bloch et al. 1997b).

Interestingly and in contrast to electrical impedance method, the limits of agreement with thoracocardiography were worse in spontaneously breathing patients than in ventilated patients. This is likely due to ventilated patients being sedated with fewer movements of the chest wall and subsequent distortion of the chest wall with each breath. This indicates that any movement will cause great distortions in signal and will therefore greatly limit the use of this technique in many patients, especially since an objective is to obtain continuous measurements. As with electrical impedance methods, the present potential for this technique is large for trend analysis.

Conclusions and Future Directions

Despite the plethora of available techniques for estimation of CO, it is difficult to argue which one should be the gold standard. Historically, PACs have found their way to a vast number of ICUs and operating rooms. They have the advantage of being able to see the dilution curves that are used to make the measurements so that artifacts can be more easily identified. Advances in arterial-based and impedance-based technologies and utilization of echocardiography continuously show promise for less invasive approaches. As a basic principle, it is likely that the less invasive the device the lower the accuracy. However, the less accurate device may have reasonable precision and thus allow monitoring trends which is also an important component of hemodynamic monitoring because it allows an assessment of responses to therapeutic interventions. Furthermore, although the less invasive approaches have many potential interferences that decrease their accuracy, many of these can be identified at the bedside such as impacts from lung inflation, fluid in the chest, and for Doppler approaches, distortions in the signal.

A paradigm shift may be underway with these new technologies. It is possible that in the future, besides physical exam and hemodynamic monitoring, commencement of fluid and inotropic therapy will require an initial assessment cardiac output by use of an accepted gold standard method including real-time POCUS echocardiography or other noninvasive approach and then by following the response to that therapy to make more rational decisions.

References

- Bazaraal MG, Petre J, Novoa R. Errors in thermodilution cardiac output measurements caused by rapid pulmonary artery temperature decreases after cardiopulmonary bypass. *Anesthesiology*. 1992;77:31–7.
- Belardinelli R, Ciampani N, Costantini C, et al. Comparison of impedance cardiography with thermodilution and direct Fick methods for noninvasive measurement of stroke volume and cardiac output during incremental exercise in patients with ischemic cardiomyopathy. *Am J Cardiol*. 1996;77:1293–301.
- Berkson Jm Boothby WM. Studies of energy of metabolism of normal individuals: comparison estimation of basal metabolism from linear formula and “surface area”. *Am J Phys*. 1936;116:485–94.
- Bernstein DP. Noninvasive cardiac output, Doppler flowmetry, and gold-plated assumptions. *Crit Care Med*. 1987;15:886–8.
- Bloch KE, Baumann PC, Stocker R, Russi EW. Noninvasive monitoring of cardiac output in critically ill patients with thoracocardiography. *Am J Respir Crit Care Med*. 1997a;155:26–31.
- Bloch KE, Baumann PC, Stocker R, Russi EW. Noninvasive monitoring of cardiac output in critically ill patients with thoracocardiography. *Am J Respir Crit Care Med*. 1997b;155:26–31.
- Boerboom LE, Kinney TE, Olinger GN, Hoffmann RG. Validity of cardiac output measurement by the thermodilution method in the presence of acute tricuspid regurgitation. *J Thorac Cardiovasc Surg*. 1993;106:636–42.
- Bottiger BW, Rauch H, Bohrer H, et al. Continuous versus intermittent cardiac output measurement in cardiac surgical patients undergoing hypothermic cardiopulmonary bypass. *J Cardiothorac Vasc Anaesth*. 1995;9:405–11.
- Boyle M, Lawrence J, Belessis A, Murgo M, Shehavi Y. Comparison of dynamic measurements of pulse contour with pulsed heat continuous cardiac output in postoperative cardiac surgical patients. *Aust Crit Care*. 2007;20(1):27–32.
- Castor G, Klocke RK, Stoll M, et al. Simultaneous measurement of cardiac output by thermodilution, thoracic electrical bioimpedance and Doppler ultrasound. *Br J Anaesth*. 1994;72:133–8.
- Clarke DE, Raffin TA. Thoracic electrical bioimpedance measurement of cardiac output – not ready for prime time. *Crit Care Med*. 1993;21:1111–2.
- Come PC. The optimal Doppler examination: pulsed, continuous wave or both? *J Am Coll Cardiol*. 1986;7:886–8.
- Conway DH, Mayall R, Abdul-Latif MS, Gilligan S, Tackaberry C. Randomised controlled trial investigating the influence of intravenous fluid titration using oesophageal Doppler monitoring during bowel surgery. *Anaesthesia*. 2002;57(9):845–9.
- Crapo RO, Morrish AH. Using the lungs to measure cardiac output. *Chest*. 1987;92:3–4.
- Dark PM, Singer M. The validity of trans-esophageal Doppler ultrasonography as a measure of cardiac output in critically ill adults. *Intensive Care Med*. 2004;30(11):2060–6.
- Darmon P, Hillel Z, Mogtader A, et al. Cardiac output by transesophageal echocardiography using continuous-wave Doppler across the aortic valve. *Anesthesiology*. 1994;80:796–805.
- Delhaas T, Mook GA, Zijlstra WG. Respiration and measurement of cardiac output by thermodilution and central or peripheral dye dilution. *J Appl Physiol*. 1992;53:706–8.
- Descorps-Declère A, Smail N, Vigué B, et al. Transgastric, pulsed Doppler echocardiographic determination of cardiac output. *Intens Care Med*. 1996;22:34–8.
- Dittmann H, Völker W, Karsch K, Seipel L. Influence of sampling site and flow area on cardiac output mea-

- surements by Doppler echocardiography. *J Am Coll Cardiol.* 1987;10:818–23.
- Doering L, Lum E, Dracup K, Friedman A. Predictors of between method differences in cardiac output measurement using thoracic electrical bioimpedance and thermodilution. *Crit Care Med.* 1995;23:1667–73.
- Donovan KD, Dobb GJ, Newman MA. Comparison of pulsed Doppler and thermodilution methods for measuring cardiac output in critically ill patients. *Crit Care Med.* 1987;15:853–7.
- Dumesnil JG, Dion D, Yvorchuk K, et al. A new simple and accurate method for determining ejection fraction by Doppler echocardiography. *Can J Cardiol.* 1995;11:1007–14.
- Ekelund LG, Holmgren A. Central hemodynamics during exercise. *Circ Res.* 1967;20:133–43.
- Elkayam U, Berkley R, Azen S, et al. Cardiac output by thermodilution techniques: effect of injectate volume and temperature on accuracy and reproducibility in the critically ill patient. *Chest.* 1983;84:418–22.
- Elkayam U, Wilson AF, Morrison J, et al. Non-invasive measurement of cardiac output by a single breath constant expiratory technique. *Thorax.* 1984;39:107–13.
- Fegler G. Measurement of cardiac output in anaesthetized animals by a thermo-dilution method. *Q J Exp Physiol.* 1954;39:153–64.
- Fishman AP, Richards DW. Report on the work of A. Fick to the Wurzburg Physikalische-Medizinische Gesellschaft (1870). In: Warren JV, editor. *Cardiovascular physiology.* Stroudsburg, Halsted Press; 1975 p. 45–46.
- Frank O. Die Grundform des arteriellen Pulses. *Z Biol.* 1899;37:483–526.
- Fuller HD. The validity of cardiac output measurement by thoracic impedance: a meta-analysis. *Clin Invest Med.* 1992;15:103–12.
- Gan TJ, Soppitt A, Maroof M, et al. Goal-directed intraoperative fluid administration reduces length of hospital stay after major surgery. *Anesthesiology.* 2002;97(4):820–6.
- Ganz W, Donoso R, Marcus HS, et al. A new technique for measurement of cardiac output by thermodilution in man. *Am J Cardiol.* 1971;27:392–6.
- Goodyer AVN, Huvos A, Eckhardt WF. Thermal dilution curves in the intact animal. *Circ Res.* 1959;7:432–41.
- Guyton AC, Jones CE, Coleman TG. *Circulatory physiology: cardiac output and its regulation.* Philadelphia: Saunders; 1973.
- Haller M, Zollner C, Briegel J, Forst H. Evaluation of a new continuous thermodilution cardiac output monitor in critically ill patients: a prospective criterion standard study. *Crit Care Med.* 1995;23:860–6.
- Harris AP, Miller CF, Beattie C, et al. The slowing of sinus rhythm during thermodilution cardiac output determination and the effect of altering injectate temperature. *Anesthesiology.* 1985;63:540–1.
- Hausen B, Schäfers H, Rohde R, Haverich A. Clinical evaluation of transtracheal doppler for continuous cardiac output monitoring. *Anaesth Analg.* 1992;74:800–4.
- Heerdt PM, Pond CG, Blessios GA, Rosenbloom M. Inaccuracy of cardiac output by thermodilution during acute tricuspid regurgitation. *Ann Thorac Surg.* 1992;53:706–8.
- Hogue CW Jr, Rosenbloom M, McCawley C, Lappas DG. Comparison of cardiac output measurement by continuous thermodilution with electromagnetometry in adult cardiac surgical patients. *J Cardiothorac Vasc Anaesth.* 1994;8:631–5.
- Hsia CCW, Ramanathan LF, Ramanathan M, Johnson RL. Cardiac output during exercise measured by acetylene rebreathing, thermodilution, and Fick techniques. *J Appl Physiol.* 1995;78:1612–6.
- Jansen JRC. The thermodilution method for the clinical assessment of cardiac output. *Intens Care Med.* 1995;21:691–7.
- Jansen JRC, Schreuder JJ, Bogaard JM, et al. Thermodilution technique for measurement of cardiac output during artificial ventilation. *J Appl Physiol Respir Environ Exerc Physiol.* 1981;50:584–91.
- Jones NL, Campbell EJ. Calculation of results. In: Jones NL, Campbell EJ, editors. *Clinical exercise testing.* 2nd ed. Philadelphia: Saunders; 1982. p. 231–42.
- Katz SA, Feigl EO. Systolic has little effect on diastolic coronary artery blood flow. *Circ Res.* 1988;62:443–51.
- Katz WE, Gasior TA, Quinlan JJ, Gorcsan J. Transgastric continuous-wave Doppler to determine cardiac output. *Am J Cardiol.* 1993;71:853–7.
- Keinanen O, Takala J, Kari A. Continuous measurement of cardiac output by the Fick principle: clinical validation in the intensive care. *Crit Care Med.* 1992;20:360–5.
- Kinsman JM, Moore JW, Hamilton WF. Studies on the circulation: I. Injection method: physical and mathematical considerations. In: Warren JV, editor. *Cardiovascular physiology.* Stroudsburg: Halsted Press; 1975. p. 78–86.
- Kleiber M. Body size and metabolic rate. *Physiol Rev.* 1947;27:511–41.
- Light RB. Intrapulmonary oxygen consumption in experimental pneumococcal pneumonia. *J Appl Physiol.* 1988;64:2490–5.
- Luca C, Hans-Rudolf B, David B, Jan W, Jukka T, Tobias M. Hemodynamic assessment of critically ill patients using a miniaturized transesophageal echocardiography probe. *Crit Care (London, England).* 2013;17:R121. <https://doi.org/10.1186/cc12793>.
- Lyon CK, Scott JN, Wang CY. Flow through collapsible tubes at low Reynolds numbers: applicability of the waterfall model. *Circ Res.* 1980;47:68–73.
- Magder S. Shock physiology. In: Pinsky MR, Dhainault JF, editors. *Physiological foundations of critical care medicine.* Baltimore: Williams & Wilkins; 1992. p. 140–60.
- Magder S. Heart-lung interactions in sepsis. In: Dantzker DR, Scharf SM, editors. *Cardiopulmonary critical care.* Philadelphia: Saunders; 1997. In press.
- Manasia AR, Nagaraj HM, Kodali RB, et al. Feasibility and potential clinical utility of goal-directed trans-thoracic echocardiography performed by noncardi-

- ologist intensivists using a small hand-carried device (SonoHeart) in critically ill patients. *J Cardiothorac Vasc Anesth.* 2005;19(2):155–9.
- Maslow A, Comunale ME, Haering JM, Watkins J. Pulsed wave Doppler measurement of cardiac output from the right ventricular outflow tract. *Anaesth Analg.* 1996;83:466–71.
- Mazraeshahi RM, Farmer JC, Porembka DT. A suggested curriculum in echocardiography for critical care physicians. *Crit Care Med.* 2007;35(8):S431–3.
- McFall MR, Woods WG, Wakeling HG. The use of oesophageal Doppler cardiac output measurement to optimize fluid management during colorectal surgery. *Eur J Anaesthesiol.* 2004;21(7):581–3.
- McKendry M, McGloin H, Saberi D, Caudwell L, Brady AR, Singer M. Randomised controlled trial assessing the impact of a nurse delivered, flow monitored protocol for optimisation of circulatory status after cardiac surgery. *Br Med J.* 2004;329(7460):258.
- Mercado P, Maizel J, Beyls C, et al. Transthoracic echocardiography: an accurate and precise method for estimating cardiac output in the critically ill patient. *Crit Care.* 2017;21(1):136. Published 2017 Jun 9. <https://doi.org/10.1186/s13054-017-1737-7>.
- Muhiudeen IA, Kuecherer H, Lee E, et al. Intraoperative estimation of cardiac output by transesophageal pulsed Doppler echocardiography. *Anesthesiology.* 1991;74:9–14.
- Neviere R, Mathieu D, Riou Y, et al. Carbon dioxide rebreathing method of cardiac output measurement during acute respiratory failure in patients with chronic obstructive pulmonary disease. *Crit Care Med.* 1994;22:81–5.
- Nielsen OW, Hansen S, Gronlund J. Precision and accuracy of a noninvasive inert gas washing method for determination of cardiac output in men. *J Appl Physiol.* 1994;76:1560–5.
- Nishikawa T. Hemodynamic changes associated with thermodilution cardiac output determination in canine acute blood loss or endotoxemia. *Acta Anaesthesiol Scand.* 1993;37:602–6.
- Nishikawa T, Dohi S. Errors in the measurement of cardiac output by thermodilution. *Can J Anaesth.* 1993;40:142–53.
- Nishikawa T, Namiki A. Mechanism for slowing of heart rate and associated changes in pulmonary circulation by cold injectate during thermodilution cardiac output determination in dogs. *Anesthesiology.* 1988;68:221–5.
- Noblett SE, Snowden CP, Shenton BK, Horgan AF. Randomized clinical trial assessing the effect of Doppler-optimized fluid management on outcome after elective colorectal resection. *Br J Surg.* 2006;93(9):1069–76.
- Oren-Grinberg A. The piCCO monitor. *Int Anesthesiol Clin.* 2010;48(1):57–85.
- Pearl RG, Rosenthal MH, Nielson L, et al. Effect of injectate volume and temperature on thermodilution cardiac output determination. *Anesthesiology.* 1986;64:791–801.
- Pierce RJ, McDonald CD, Thuys CA, et al. Measurement of effective pulmonary blood flow by soluble gas uptake in patients with chronic airflow obstruction. *Thorax.* 1987;42:604–14.
- Ramage JE Jr, Coleman RE, MacIntyre NR. Rest and exercise cardiac output and diffusing capacity assessed by a single slow exhalation of methane, acetylene, and carbon monoxide. *Chest.* 1987;92:44–9.
- Sackner MA, Hoffman RA, Stroh D, Krieger BP. Thoracocardiography. Part 1. Noninvasive measurement of change in stroke volumes compared to thermodilution. *Chest.* 1991;99:613–22.
- Sageman WS, Amundson DE. Thoracic electrical bioimpedance measurement of cardiac output in post-aortocoronary bypass patients. *Crit Care Med.* 1993;21:1139–42.
- Sahn DJ. Determination of cardiac output by echocardiogram doppler methods: relative accuracy of various sites for measurement. *J Am Coll Cardiol.* 1985;6:663–4.
- Shellock FD, Riedinger MS. Reproducibility and accuracy of using room-temperature vs. Ice-temperature injectate for thermodilution cardiac output determination. *Heart Lung.* 1983;12:175–6.
- Shimamoto H, Kito H, Kawazoe K, et al. Transesophageal Doppler echocardiographic measurement of cardiac output by the mitral annulus method. *Br Heart J.* 1992;68:510–5.
- Shoemaker WC, Wo CCI, Bishop MJ, et al. Multicenter trial of a new thoracic electrical bioimpedance device for cardiac output estimation. *Crit Care Med.* 1994;22:1907–12.
- Siegel LC, Fitzgerald DC, Engstrom RH. Simultaneous intraoperative measurement of cardiac output by thermodilution and transtracheal doppler. *Anesthesiology.* 1991;74:664–9.
- Sinclair S, James S, Singer M. Intraoperative intravascular volume optimisation and length of hospital stay after repair of proximal femoral fracture: randomised controlled trial. *Br Med J.* 1997;315(7113):909–12.
- Stetz CW, Miller RG, Kelly GE, Raffin TA. Reliability of the thermodilution method in the determination of cardiac output in clinical practice. *Am Rev Respir Dis.* 1982;126:1001–4.
- Stewart GN. Researches on the circulation time and on the influences which affect it. In: Warren JV, editor. *Cardiovascular physiology.* Stroudsburg, PA: Halsted Press; 1975. p. 73–5.
- Stewart WJ, Jiang L, Mich R, et al. Variable effects of changes in flow rate through the aortic, pulmonary and mitral valves on valve area and flow velocity: impact on quantitative Doppler flow calculations. *J Am Coll Cardiol.* 1985;6:653–62.
- Stoddard MF, Prince CR, Ammash N, et al. Pulsed Doppler transesophageal echocardiographic determination of cardiac output in human beings: comparison with thermodilution technique. *Am Heart J.* 1993;126:956–62.
- Thrush D, Downs JB, Smith RA. Continuous thermodilution cardiac output: agreement with Fick and bolus

- thermodilution methods. *J Cardiothorac Vasc Anaesth.* 1995;9:399–404.
- Thulesius O, Johnson PC. Pre- and post capillary resistance in skeletal muscle. *Am J Phys.* 1966;210:869–72.
- Van Grondelle A, Ditchey RV, Groves BM, et al. Thermodilution method overestimates low cardiac output in humans. *J Thorac Cardiovasc Surg. Am J Phys.* 1983;245:H690–2.
- Venn R, Steele A, Richardson P, Poloniecki J, Grounds M, Newman P. Randomized controlled trial to investigate influence of the fluid challenge on duration of hospital stay and perioperative morbidity in patients with hip fractures. *Br J Anaesth.* 2002;88(1):65–71.
- Vennix CV, Nelson DH, Pierpont GL. Thermodilution cardiac output in critically ill patients: comparison of room-temperature and iced injectate. *Heart Lung.* 1984;13:574–8.
- Wakeling HG, McFall MR, Jenkins CS, et al. Intraoperative oesophageal Doppler guided fluid management shortens postoperative hospital stay after major bowel surgery. *Br J Anaesth.* 2005;95(5):634–42.
- Weisel RD, Berger RL, Hechtman HB. Measurement of cardiac output by thermodilution. *N Engl J Med.* 1975;292:682–4.
- Wippermann CF, Huth RG, Schmidt FX, et al. Continuous measurement of cardiac output by the Fick principle in infants and children: comparison with the thermodilution method. *Intens Care Med.* 1996;22:467–71.
- Yelderman M, Quinn MD, McKown RC, et al. Continuous thermodilution cardiac output measurement in sheep. *J Thorac Cardiovasc Surg.* 1992;104:315–20.
- Zenger MR, Brenner M, Haruno M, et al. Measurement of cardiac output by automated single-breath technique and comparison with thermodilution and Fick methods in patients with cardiac disease. *Am J Cardiol.* 1993;71:105–9.



Evaluations of Devices for Measurement of Cardiac Output

21

Pierre Squara

Quality Criteria Common to Measurements and Devices

A measurement method is based on a measurement principle, i.e., a physical, chemical, or biological phenomenon serving to obtain one or more values that can reasonably be attributed to the measurand: examples for CO include pulse pressure wave, chest changes in bioimpedance, and blood dilution of an indicator. A reference measurement procedure (reference method) provides measurement results fitted for their intended use. Although it has no international definition, a gold standard is supposed to be the best practically available reference method. The measurement error is the difference between a single measurement and a reference value. When this term is used without further information, it combines all types of errors and qualifies the accuracy (by definition for a single measurement).

A device is used for making repeated measurements of the measurand. It is most often a transducer, providing an output quantity (an electric signal) that has a specific relationship with an input quantity (a physiologic signal). The measuring interval is the set of values of the same kind that can be measured by a given device with specified instrumental uncertainty, under defined conditions. A device is characterized by different

properties or quality criteria in the measuring interval.

Although the properties of measurements (facts) and measuring devices (method) should not be confounded, trueness and precision can be studied together for clarity.

1. *The measurement accuracy* is the closeness of agreement between a single measured value and a true or reference value. Accuracy is a quality and cannot be expressed as a numerical value. A measurement with a small measurement error is said to be accurate.
2. *The measurement trueness* is the closeness of agreement between the average of an infinite number of replicate measured values (CO indications from a tested device) and the true or reference value of the measurand (reference CO). Trueness is also a quality and cannot be expressed as a numerical value. Since the mean random error of an infinite number of replicates is zero, the mean of the differences between the measured values and the reference values (also called measurement bias) is, therefore, an estimate of the systematic measurement error (Fig. 21.1). Consequently, the measurement trueness is inversely related to the systematic measurement error but not to the random measurement error. A correction can be applied to compensate for a known systematic error.

In analogy to the measurement bias, the instrumental bias is the average of replicate

P. Squara (✉)
ICU and Cardiology Department, Clinique Ambroise
Paré, Neuilly-sur-Seine, Hauts de Seine, France

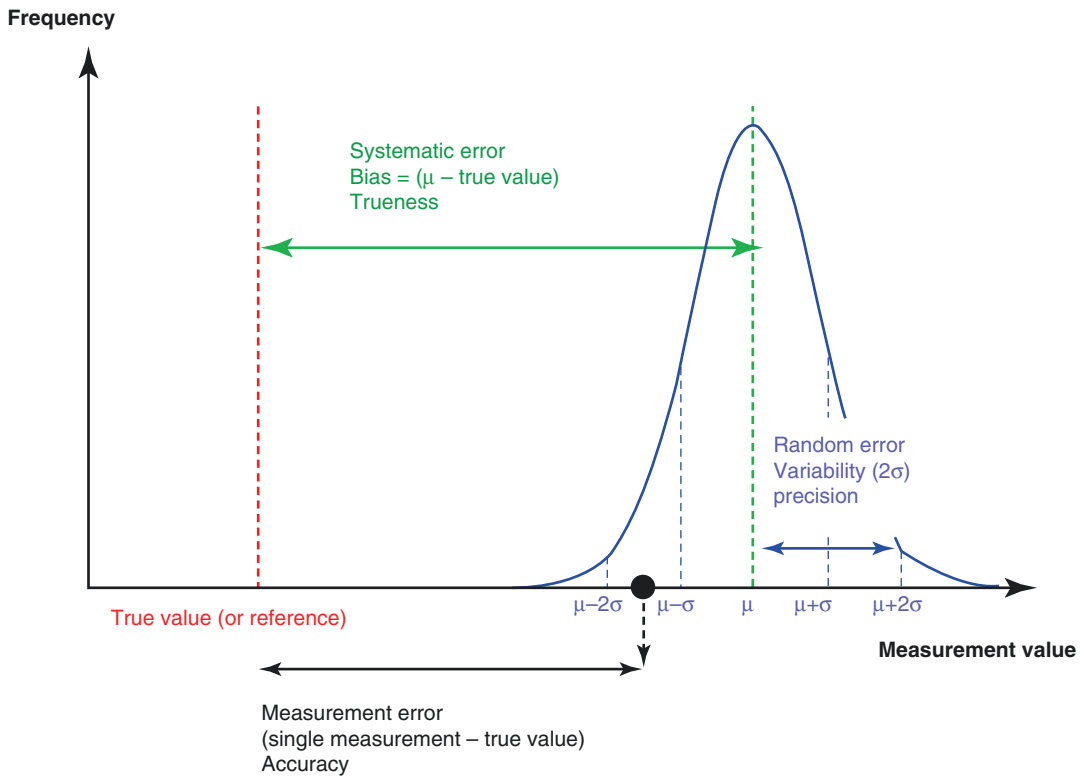


Fig. 21.1 Schematic representation of the different types of measurement errors and the corresponding quality criteria. The black point represents a single measurement value, the blue curve is the frequency distribution of the

values in case of replicate measurements of the same object under the same conditions, μ = mean, and σ = standard deviation

indications minus a reference value. It estimates the systematic error of the device.

3. *The measurement precision* is the closeness of agreement between measured values obtained by replicate measurements on the same or similar quantities under specified and stable conditions (Joint Committee for Guides in Metrology 2012; Hapfelmeier et al. 2016; Squara et al. 2015). In other words, precision describes the pattern of distribution of replicate measurements of a given CO value, without reference to a true or reference value. The measurement precision is related to the random measurement error and can be expressed as a number by measures of imprecision, such as standard deviation (σ) and variance (σ^2), of repeated measurement and assuming mean random error = zero (Fig. 21.1). The coefficient of variation ($2\sigma/\text{mean}$) can also be

derived using the mean CO value to express the precision in %. The term “precision” has many confusing connotations. Especially in intensive care medicine, it is often used to describe the interpatient variability of the bias or confounded with the 95% limits of agreement between two devices. The specified conditions of precision estimation may add variabilities of different kinds (Hapfelmeier et al. 2016). Repeatability is the precision under conditions that include the same measurement procedure, same operators, same measuring system, same operation conditions, same location, and replicate measurements on the same or similar patients over a short period of time (Joint Committee for Guides in Metrology 2012). Reproducibility is the precision under a set of conditions that include different locations, operators, measuring sys-

tems, and replicate measurements on the same or similar patients. Although it has no international acceptance in the VIM, the term precision is also frequently encountered in instrument specifications. In analogy to the measurement precision, the instrumental precision is therefore the variability of replicate indications obtained from the same CO value. It estimates the random error of the device (Hapfelmeier et al. 2016).

4. *The measurement uncertainty.* This concept is broader than precision and may add uncertainty due to the reference method, time drift, definitional uncertainty, and other uncertainties. The objective of measurement in the uncertainty approach is not to determine a true value as closely as possible but to reduce the range of values that can reasonably be attributed to the measurand.

Since “accuracy,” “trueness,” and “precision” are frequently misused in the medical literature, one solution would be to ban these quality terms for which no specified numerical values are given and to be descriptive, speaking of “measurement error,” “systematic measurement error,” and “random measurement error.” This is especially the case when using Bland-Altman analyses for two main reasons. First, the Bland-Altman plot has been proposed to compare two devices “when neither provides an unequivocally correct measurement” (Bland and Altman 1986). The second reason is that one important condition for estimating trueness and precision is to average replicate measurements of the same quantity. Therefore, when several intra- or interpatient measurements are done under different conditions, the estimation of the bias and precision is impossible, and the criterium that is studied is the systematic discordance between the two devices and its variability under different conditions.

Specific Quality Criteria for Devices

1. *The sensitivity* is the quotient of the change in a CO indication and the corresponding change of the real CO. The change considered must

be large compared with the resolution (defined below). The metrological sensitivity should not be confounded with the statistical sensitivity. The linearity which has no VIM definition usually refers to the capability of maintaining the sensitivity constant over the measuring interval. In other words, the linearity is also the capability of maintaining the instrumental bias constant (Fig. 21.2). Preferably, the linearity should be close to the identity line.

2. *The selectivity* is a property, used with a specified measurement procedure, whereby it provides measured values for one or more measurands such that the values of each measurand are independent of others (Fig. 21.3).
3. *The resolution* is the smallest change in a measurand that causes a perceptible change in the corresponding indication. The concept of resolution is linked to the discrimination threshold, the largest change in the measurand that causes no detectable change in the corresponding indication. Since a device indication is always the result of an averaging of several elementary measurements, both resolution and discrimination threshold depend on the standard error of the mean which is proportional to the variability (σ) and of the number (n) of replicates ($2 \text{ SEM} = 2\sigma/\sqrt{n}$). All these properties are therefore linked to the measurement precision. Lower precision mandates to average more measurements to identify a significant change in the indication (Fig. 21.4). In other words, using a given number of measurements, higher measurement precision will allow higher resolution. The concept of least significant change that can be considered as statistically significant ($2\sqrt{2} \text{ SEM}$) is linked to resolution.
4. *The step response time* is the duration between the instant when CO is subjected to an abrupt change and the instant when the corresponding indication of a device settles within specified limits around its final steady value. The way by which the final steady value is determined may be different: for example, the inflection point between two regression curves, or the first point of a flat curve slope, or the first point where the σ becomes below specified limits. Step response time is also

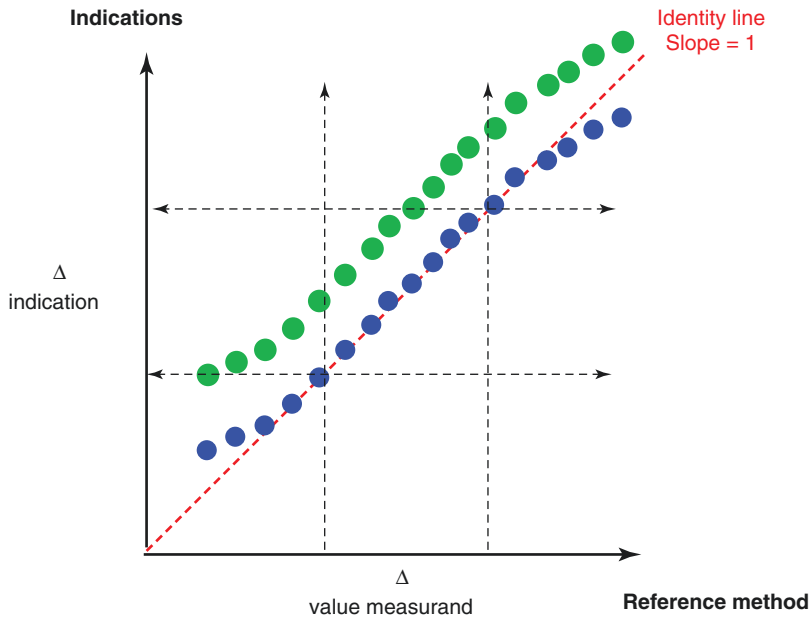


Fig. 21.2 Schematic representation of the sensitivity. The blue points represent the indications of a device when the CO is increasing. Within the range figured by the dotted arrows (measuring interval), the sensitivity is good and constant (linearity). In this example, under and over

the measuring interval, the sensitivity/linearity is altered with over- and underestimation of the true changes, respectively. The green points represent the indication of another device with the same sensitivity but with a positive instrumental bias

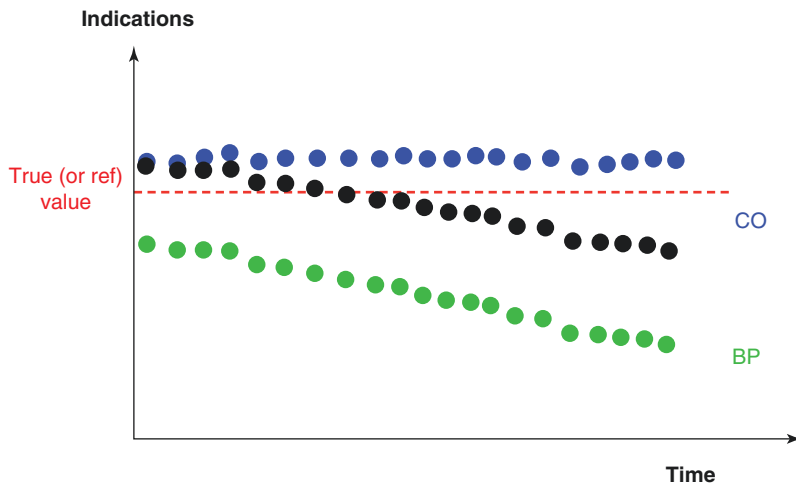


Fig. 21.3 Schematic representation of the selectivity. In this example, the indications from two different devices for CO assessment (COa blue points and COb black points) are collected when blood pressure (BP green points) is decreasing while the true CO is maintained con-

stant (red line). The COa device, although systematically overestimating the true CO, is selective since indications are independent of the BP. The COb device, although assessing CO more truly at the onset of the test, is not selective since its indications covary with BP

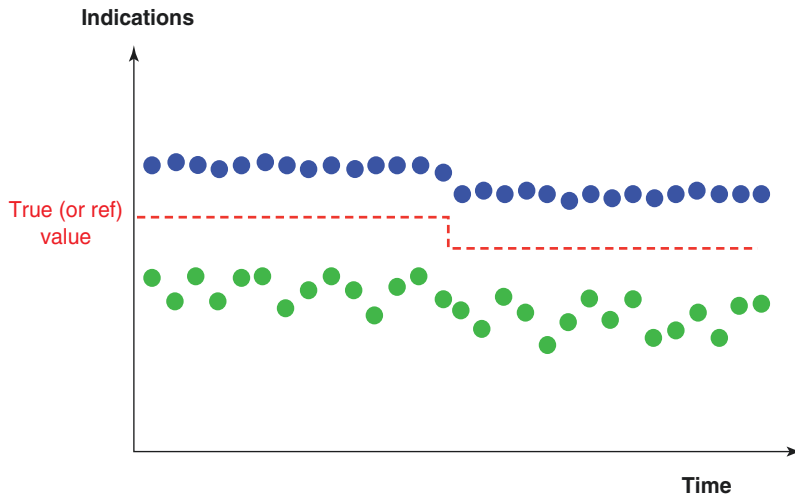


Fig. 21.4 Schematic representation of the resolution. The blue indications show a systematic overestimation of the measurand (untrueness) and small random error (high precision) allowing perceiving a small change of the mea-

surand (high resolution). The green indications show a systematic underestimation of the measurand (untrueness) and high random error (low precision) hiding a small change of the measurand (low resolution).

linked to the measurement precision since low precision increases the number of indications needed to establish the final steady state.

5. *The stability* is the property of a measuring instrument, whereby its metrological properties remain constant in time. An instrumental drift is a continuous or incremental change over time of the indication due to change in metrological properties.

Procedures for the Device Validation

Verification is a provision of objective evidences that a given measuring instrument fulfills specified requirements. Validation is a verification, where the specified requirements are adequate for the intended use. Therefore, validating devices mandates first determining the intended use.

1. *Intended use.* In intensive care medicine, we measure CO with basically three main objectives.
 1. For monitoring purposes, we use CO indications for triggering an alarm when its value is outside a specified range, for example, $5 < \text{CO} < 2 \text{ L}\cdot\text{min}^{-1}\cdot\text{m}^{-2}$.

2. For diagnosis and prognosis purposes, we compare CO indications to the expected value, with specified uncertainty. For example, we can define a low flow state as $\text{CO} < 1.8 \text{ L}\cdot\text{min}^{-1}\cdot\text{m}^{-2}$.
3. For therapeutic purpose, we look at improving CO up or down to a predetermined target value. For example, in a specific patient, we can decide to titrate $\text{CO} > 2.2 \text{ L}\cdot\text{min}^{-1}\cdot\text{m}^{-2}$.

These three objectives have different requirements regarding measurement properties or device quality criteria. For monitoring purpose, indications are compared to their initial value, measured under similar conditions, and the delay to indicate significant changes generally matters. Therefore, resolution and step response time (all linked to random errors of measurements) are the first quality criteria, whereas instrumental bias, sensitivity, linearity, and even stability may be seen of lesser importance. In contrast, for diagnostic and therapeutic purposes, the measured CO is compared with a predetermined absolute value, established from measurements in other conditions. The indications must be as close as possible to the true value. Therefore, instrumental bias, sensi-

tivity, linearity, and stability (all linked to systematic errors of measurements) are the key quality criteria, whereas resolution and step response time may be seen of lesser importance if the delay to reach an adequate indication is not critical. For all purposes, selectivity is necessary.

Although not impossible, it is quite difficult to imagine promoting and validating a given device for a restricted use (monitoring, diagnosis, or therapy). Consequently, the manufacturers of these tools most often try to reach an acceptable compromise between measurement properties (i.e., optimal compensation of systematic and random errors). However, until now, no consensual independent validation procedure addressing all these quality criteria has been suggested. Finally, the metrological properties of a device depend on the combined uncertainty of each elementary measurement, the sampling time, and the averaging method to display a value. The final compromise is always aimed at compensating the intrinsic limitations of the technologic chain used to sense CO. Basically, when the physiologic signal is poorly linked to real CO, the precision of measurements is low. This leads to an increase in the sampling time and need for sophisticated averaging methods. The consequence is always lower resolution and step response time.

2. *Choice of the reference method.* For each specific measurand and each quality criterion, a reference method that is usable in clinical conditions must be identified. The reference method must be recently and appropriately calibrated in an official national reference laboratory, used in the appropriate conditions, and in its validated measuring interval. Its uncertainty must be known, traceable, and presumably small as compared to the uncertainty of the test device. For example, for testing a new CO device, an artificial heart or an extracorporeal circuit with a measurable flow may be chosen. If the test device requires a beating heart, an ultrasonic flow probe positioned

around the pulmonary artery or the aorta during an open chest surgery may be preferred (Keren et al. 2007). If the test device requires a closed chest and standard clinical conditions, bolus indicator dilution may be chosen. Most often, the true value of the measurand is obtained by averaging several measurements from the reference method. The appropriate number of replicates must be chosen for reaching, at least, an uncertainty four times less (at best 10 times less) than that of the test device. The number of replicate reference measurements needed to derive the true value of the CO, with the prescribed uncertainty, is determined by the standard error of the mean (SEM) according to the formula: $2 \text{ SEM} = 2\sigma/\sqrt{n}$ if the uncertainty is limited to imprecision. For example, if the test device has a presumable imprecision of 20%, the reference value must, at best, have imprecision $\leq 2\%$ (10 times less). If the reference method has an imprecision of 10% (2σ), then the reference value (true value used for comparison with the test device) must average at least 25 reference measurements of the same quantity to reach a $\text{SEM} = 10\%/\sqrt{25} = 2\%$. In contrast, if an uncertainty ratio of 4 were considered as acceptable, four reference measurements would be needed (objective $20\%/4 = 5\%$, obtained by $\text{SEM} = 10\%/\sqrt{4}$). Hence, a reference CO value can be theoretically taken from continuous CO measurements when the high variability can be compensated by the large amount of data collected, therefore leading to acceptable SEM (Squara et al. 2007). In all cases, a critical issue is the constancy of the CO during the time necessary to collect the needed number of replicate values to determine the reference value.

3. *The measurements properties.* Since accuracy is qualifying a single measurement without numerical values, strictly speaking, it is not a suitable term for assessing a device performance. Moreover, accuracy depends on two types of measurement errors: random and systematic errors that should not be confounded because they have different impacts and corrections.

- 3a. *Assessment of the random error.* In a unique patient in hypothetical clinical steady state, the needed number of replicate CO indications must be collected using the reference method and the test device in parallel, during a short period of time to ensure a constant value of the measurand (real CO). If we theoretically assume that the real CO is constant, the mean CO obtained from the test device (μ) can be derived with its variability ($2\sigma_{TD}$). This variability is due to random errors of measurements or indications. The mean value of random error is 0 if normally distributed around the mean value of the measurand (μ) and refers to as the instrumental precision of the test device. This is an internal property that needs no reference to be estimated (Fig. 21.4).
- 3b. *Assessment of the systematic error.* The difference between μ and T evaluates the systematic error and refers to as trueness. The uncertainty on the systematic error depends on the respective SEMs, therefore on the con-

fidence interval attributed to the reference method and to the confidence interval attributed to the test device (Fig. 21.5). The significance of the mean difference (instrumental bias) may be tested using Welch's t -test. Indeed, the Student's t -test (and ANOVA) assumes that the two populations have normal distributions with equal variances. Welch's adaptation is designed for unequal variance but still with the assumption of normality.

- 3c. *Assessment of the sensitivity and linearity.* A device that allows CO measurements with high precision and trueness may be considered as having high instrumental precision and low instrumental bias. Once these properties have been studied for one central value of the real CO, other values must be tested, at best the minimum and the maximum values of the prescribed measuring interval. In our example, other experiments must be done to verify the same quality criteria for low and high values (e.g., CO = 1.5 and 4.5 L/min). This allows estimating the sensitivity and lin-

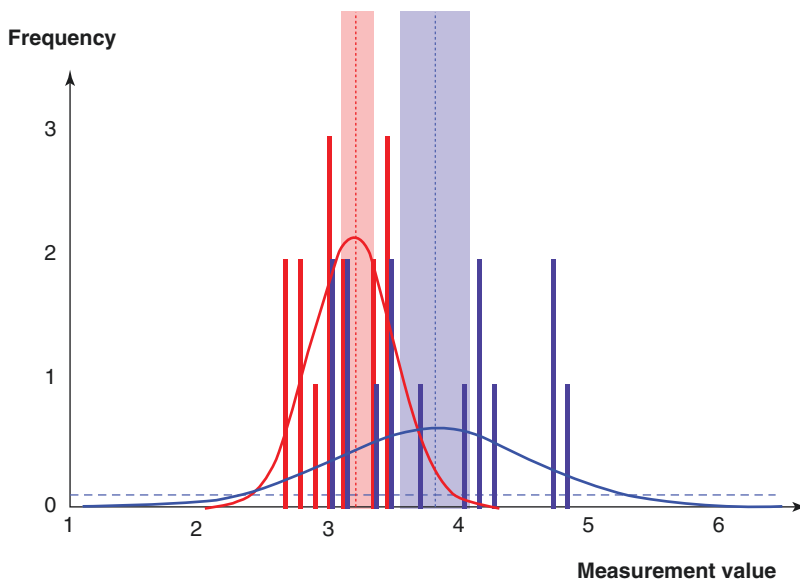


Fig. 21.5 Comparison of a test CO device (blue) against a reference method (red). In this example, it was chosen to collect the same number of measurements (15) in a single stable patient, using the reference method and using the test device. The figure shows the frequency distributions of indications with a step = 0.1. The normal adjustment (plain curve), the mean value (dotted line), and the 95%

confidence interval $\pm 2SEM$ area around the mean value (colored areas) are figured. In this example, the systematic error (instrumental bias) is 0.63 L/min., the uncertainty on this systematic error is given by the formula $(SEM_{ref}^2 + SEM_{TD}^2)^{0.5} = 0.33$, and the confidence interval is [0.31–0.96], significant with $p < 0.001$ using Welch's t -test

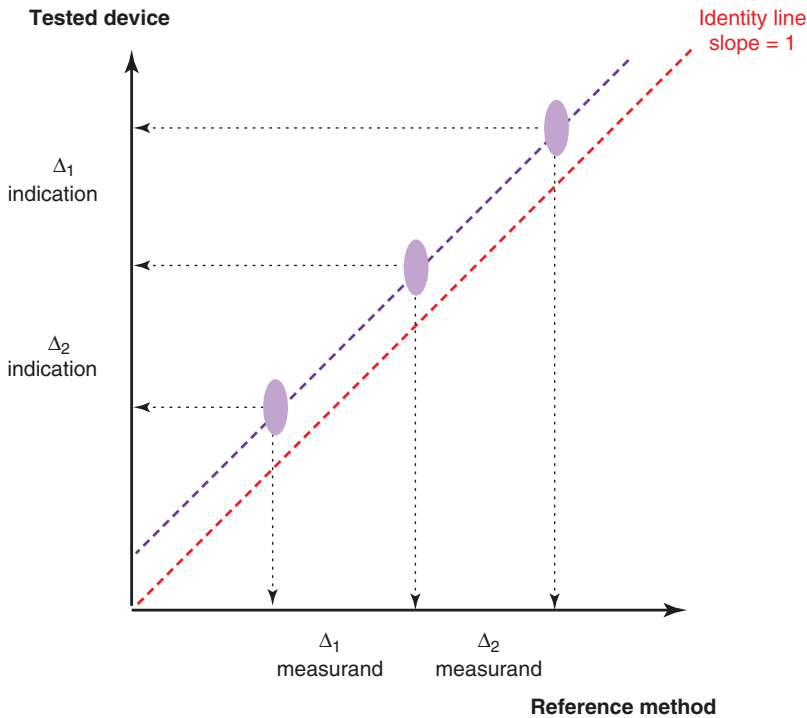


Fig. 21.6 Comparison between the test device and the reference method, based on three sets of paired measurements representing the whole measuring interval (1.5–4.5 L/min). Purple areas show the uncertainty as derived by 2SEM of the reference method on the x -axis and 2SEM of the test device on the y -axis. In this example, the precisions of both technologies remain constant over the mea-

suring interval (same purple areas). The test device shows a good sensitivity (Δ_1 indication/ Δ_1 measurand = Δ_2 indication/ Δ_2 measurand = 1) with a regression curve (purple dotted line) close to the perfect identity shown by the red dotted line. Therefore, the instrumental bias shown by the test device is constant (offset)

earity of the test device (Fig. 21.6). This figure shows a set of experiments on the same patient, in the same location, with the same investigator and the same device. Adding more diversity in each of the three last parameters will enlarge the area of imprecision which is referred to as reproducibility of measurements. Adding more than one patient (referred to as the interpatient variability) represents another source of variability and another component of a device uncertainty.

Since it very difficult to imagine the validation of a single device, covering the whole measuring interval (at least three sets of measurements) in a given patient, it is impossible to test different investigators, different devices, and different locations (reproducibility) on the same patient. That is why we are often limited to testing a technology by using different

devices, in different locations, calibrated with different chains, compared to different references, with different investigators, and in different patients. In this situation, each piece of diversity adds its own variability, and it becomes critical (even inappropriate) to speak of the instrumental bias or the instrumental precision of a technology. It would be preferable to use the general term of uncertainty, with its systematic component and its random component and respective variability.

Moreover, since it is often difficult to manipulate the CO of a patient, we are often limited to assessing the whole measuring interval by using interpatient physiological or pathological CO variability. Paired measurements of the measurand using a reference method and a device to be tested may be pooled together and come from different patients, locations,

investigators, devices, etc. A regression line between the reference and the test device or a modified Bland and Altman representation may be used by plotting on the y-axis the difference between the reference and the test devices but only the reference value on the x-axis, since it is supposed to represent the true value (Fig. 21.7) (Bland and Altman 1986). Again, in that case, the term uncertainty is more appropriate than precision.

3d. *The step response time validation* requires a constant quantity of the measurand, followed by a sudden change (at best instantaneous) at a known start time. In clinical practice, this sudden change may be not easy to provoke and to prove. Natural changes can be used if the test device can be compared with a reference method with a known fast response time. The reference method for validating a measuring device may be different for each property. For example, for validating the step response time of a CO device, changes in the mixed venous blood oxygen saturation (SvO₂) or invasive blood pressure can be chosen as the reference.

3e. *Assessment of stability.* Although instrumental drift is easier to identify, stability may affect all properties of a measuring device and contributes to the uncertainty of measurements. A complete analysis of stability requires restarting the validation process after a certain delay to verify that the same performances are obtained. The specified period of time in which stability must be checked depends on the clinical use of the measuring device and can range from several hours (blood pressure, SpO₂, SvO₂, cardiac output measuring devices) to months (blood gas analyzers, thermometers, mechanical ventilators, and so on). This is easier to do when the measurand is well known (based on a bench or a calibrated device). When the validation process involves real patients, the interpatient variability necessarily enlarges the precision and may hide a small systematic drift.

In summary, most often we find in the literature, global comparisons between two technologies (a new and old one), both having different and specific nonidealities for the different quality

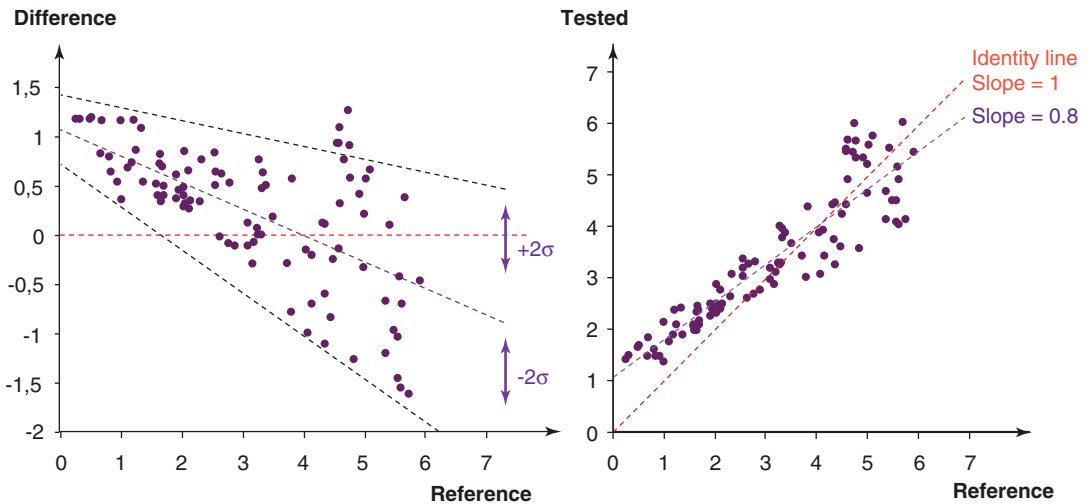


Fig. 21.7 On the left panel, a modified Bland and Altman representation. Hundred inter- and inpatient-paired measurements are reported. In this example, the systematic error is decreasing from low to high values of CO. In contrast, the uncertainty (combining imprecision, non-sensitivity, and interpatient variability of the bias) is

increasing proportionally to the value of CO. On the right panel, same data reported on a regression plot showing the same nonidealities (with different scales). The imperfect sensitivity is shown by a regression slope <1 and indicates the need for a better gain

criteria, for the different pathologies, and for the different patients. This does not allow an analysis of the limitation of a technology and to identify potential ways of improvement. Therefore, testing a new device must take first into consideration a credible reference method for the considered quality criteria: i.e., the reference method can be different for each quality criteria. At a first validation step, comparing two technologies where none of them can be considered as a reference is not acceptable. A second important requirement is to clearly distinct systematic and random errors of measurements. Evaluating random error requires no reference method but a stable physiologic signal. A stable CO can be taken from patients under stable conditions or under mechanical circulation. Large random errors indicate that the physiologic signal is not properly isolated or that the signal mixes different inputs. It mandates averaging a lot of data to compensate and affects the step response time and the resolution (ability to detect small changes). The last key point is the linearity. Most devices using a poorly calibrated signal necessarily used a “calibration factor” based on age, gender, and other morphologic data. This indicates that an important part of the indication is dependent of constant values. Such devices necessarily minimize the pathological variation of values and therefore underestimated high values and overestimated low values.

Conclusion

When evaluating CO measurement devices, it is imperative that physicians share the international metrology vocabulary with other scien-

tists, apply to consensus metrological quality criteria, and develop specific validation procedures accordingly. The comparison of two technologies neither of which provides a perfectly correct measurement is not an adequate validation process. The reference method is not only specific to the measurand (CO) but also to a quality criterion for an intended use. Therefore, different reference methods can be chosen to evaluate the different basic quality criteria, including systematic error (instrumental bias), random error (instrumental precision), sensitivity, linearity, step response time, and stability.

References

- Bland JM, Altman DG. Statistical methods for assessing agreement between two methods of clinical measurement. *Lancet*. 1986;1(8476):307–10.
- Hapfelmeier A, Cecconi M, Saugel B. Cardiac output method comparison studies: the relation of the precision of agreement and the precision of method. *J Clin Monit Comput*. 2016;30(2):149–55.
- Joint Committee for Guides in Metrology. International vocabulary of metrology – Basic and general concepts and associated terms (VIM). 3rd ed. Paris: Bureau International des Poids et Mesures; 2012. Available from: www.bipm.org/utis/common/documents/jcgm/JCGM_200_2012.pdf.
- Keren H, Burkhoff D, Squara P. Evaluation of a noninvasive continuous cardiac output monitoring system based on thoracic bioimpedance. *Am J Physiol Heart Circ Physiol*. 2007;293(1):H583–9.
- Squara P, Denjean D, Estagnasie P, Brusset A, Dib JC, Dubois C. Noninvasive cardiac output monitoring (NICOM): a clinical validation. *Intensive Care Med*. 2007;33(7):1191–4.
- Squara P, Imhoff M, Cecconi M. Metrology in medicine: from measurements to decision, with specific reference to anesthesia and intensive care. *Anesth Analg*. 2015;120(1):66–75.



Basics of Hemodynamic Measurements

22

Sheldon Magder

After obtaining a comprehensive history and performing a proper physical examination of a critically ill patient, hemodynamic monitoring is a central part of the management. However, proper use of monitoring tools requires a good understanding of the basic principles of hemodynamic measurements and the errors that can arise when making measurements. Arterial blood pressure, cardiac output, and heart rate are covered in separate chapters. This chapter deals with central hemodynamic measurements and issues related to measuring devices. It also includes issues caused by heart-lung interactions.

Hemodynamic monitoring evaluates two basic physical properties – volume and pressure. Vascular volumes are primarily evaluated by ultrasound techniques. Radiological and magnetic resonance imaging (MRI) also can provide important information but not on an ongoing basis. Movement of volume over time, which is cardiac output, is discussed in Chaps. 20 and 21. Total blood volume can be assessed by dilution techniques, but this generally is not helpful clinically. This chapter deals primarily with vascular pressure measurements.

Volume Versus Pressure Measurements

The differences between information for evaluating cardiac status obtained with a pressure versus a volume measurement (echocardiography, nuclear study, or MRI) are often not appreciated. Pressure and volume are linked by the compliance of the chamber, which defines the change in volume for a change in pressure so that it might first be thought that one can substitute for the other. However, this is not valid for a number of reasons. First, compliance usually is not known, and thus pressure or volume cannot be inferred from just one of these values unless there is an estimate of compliance. For example, an estimate of compliance can be obtained by developing a regression of left atrial volumes measured by echocardiography versus left atrial pressures; the slope of this relationship is related to compliance of the atria (change in volume for change in pressure) (Bytyçi et al. 2019). However, this measurement has a variance around a mean value and although it gives a reasonable group prediction it does not give accurate individual values because the compliance is not the same in everyone; in particular, it varies with body size. The estimation of compliance also assumes that it is linear over the range of studied values which likely also is not true. Pressures also are estimated by relating a set of measured pressures to velocities. An example is the estimate of

S. Magder (✉)
Royal Victoria Hospital (McGill University Health Centre), Departments of Critical Care and Physiology McGill University, Montreal, QC, Canada
e-mail: sheldon.magder@mcgill.ca

pulmonary artery pressure from tricuspid regurgitation velocity and an estimate of right atrial pressure (Augustine et al. 2018). Again, this approach cannot give precise values of pressure and more importantly, does not easily allow assessment of changes in pressure, which often is the key information for clinical decisions. When the limit of stretch of the elastic structures that make up vascular walls is reached, the relationship of pressure to volume becomes exponentially steeper. This cannot be detected with only a volume measurement because the volume is not changing despite the large changes in pressure. Third, the accuracy and precision of properly performed pressure measurements are very high, but volume measurements are not because of their three-dimensional structures, difficulties with resolution of boundaries and complex-shaped structures. Fourth, pressure and volume vary over time so that it is important to pick a specific time during the cardiac cycle to make the measurement. This is much more difficult to do precisely with a measurement of volume over time than with pressure over time. Finally, the difference between volume and pressure also relates to the question being asked. When the question is what is the effect of volume on the wall of a chamber, what is the energy differences for flow, what is the significance of gravitational forces, or what are the forces driving fluid filtration from vessels, a measure of pressure is needed. Volume measurements can give important information on how efficiently the heart is functioning by giving the fractional difference between volume ejected by the heart and the volume that remains, that is, the ejection fraction, but this does not indicate actual blood flow to tissues, which is what matters for metabolism. Volume per distance, i.e., velocity, also does not indicate tissue perfusion unless it is converted to flow by multiplying by cross-sectional area of the vessel. The ejection fraction also does not indicate how the heart handles different volumes for the same filling pressure. This is given by the cardiac function curve, which has pressure on the x-axis and cardiac output (or stroke volume) on the y-axis. Finally, it is worth remembering that vascular pressures have the same magnitude

regardless of size, age, or even mammalian species, whereas volumes must always be normalized to body size and formulas for this are not accurate.

Importance of Understanding Pressure Measurements

In 1996 Connors et al. published a paper that rocked the critical care community (Connors Jr. et al. 1996a). Based on an evaluation of a database from a group of intensive care units, they observed that survival was worse in patients who had a pulmonary artery catheter inserted as part of their management compared to those who did not. They accounted for the potential obvious selection bias in an observational study by performing a propensity analysis. There were two reactions to their publication. One was to ban all use of pulmonary artery catheters until randomized data showed that the catheter has value and does not produce harm (Dalen and Bone 1996). The other was that the results indicated that physicians do not understand how to properly make pressure measurements and, even more importantly, how to use the measurements, in which case better education is the solution. In support for this position, Iberti et al. found that the average score for physicians tested on a set of basic hemodynamic measurements that were expected to be known by all physicians only was 67% (Iberti et al. 1990). Nurses had a similar score (Fisher Jr. et al. 1994). I favor the latter interpretation, that is, physicians lack a basic knowledge of hemodynamic measurements. I encourage the reader to honestly test his-/herself by studying Fig. 22.1 and indicating the value that would appear on the monitor. The figure is adapted from a paper in which two questions on hydrostatic measurements were asked of ten American Board-certified cardiologists (Courtois et al. 1995). In the paper, 8/10 got the first question right and 0/10 got the second one right! The answers are at the end of this chapter. Precision in pressure measurements is especially important for central venous pressures (CVP). This is because the range of clinically important

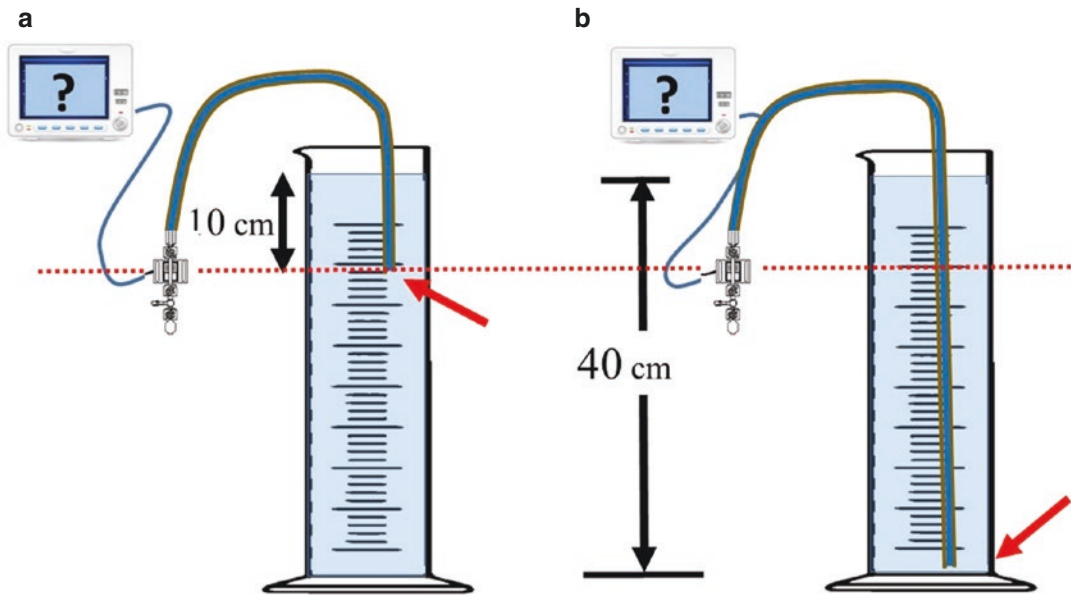


Fig. 22.1 Measurement challenge. The two cylinders are filled with water to a height of 40 cm. The transducers are placed 10 cm below the surface of the water. In (a) a fluid-filled catheter goes from the transducer to a position 10 cm below the water surface (arrow). The transducer is

connected to a monitor. What is the pressure in cmH_2O ? In (b) the tip of the fluid-filled catheter is passed to the bottom of the cylinder (arrow). What is the pressure in cmH_2O ? The answer is at the end of the chapter

pressures only is 0–10 mmHg. Thus, measurement errors that produce small differences in CVP can lead to major changes in the clinical approach, whereas on the arterial side, a pressure difference of the same magnitude is not clinically significant, although it still might be important at the lower end of arterial pressures.

The first approach to the challenge raised by the Connor et al. paper (Connors Jr. et al. 1996b), that is, perform randomized trials, was done in three large studies (Harvey et al. 2005; Richard et al. 2003; Wheeler et al. 2006). In contrast to Connor's study, there was no increased harm with use of the PA catheter; however, there also was no benefit. There are two important criticisms of these trials. They did not have algorithms that could have made use of the measurements that were obtained, and secondly, the protocols did not adhere to many of the principles of measurement covered in this chapter. My argument is that if you do not know how to properly use the device and if you are not testing an actual therapeutic algorithm, how can a device by itself change outcome?

How to Measure a Pressure

Pressure is force per cross-sectional area. As such, measuring pressures requires a device to quantify the produced force compared to a standard. This can be as simple as comparing the pressure to the force created by a column of water of a known height (Fig. 22.2). The mass of water in the column is accelerated toward the center of the earth by gravity. It might seem surprising that this gravitational force is so significant over the small height of the column, but gravity is acting on us all the time, and we do not “sense” it. However, astronauts who have returned to earth after a week in space report feeling the weight of a hand wipe on the back of their hand and the force needed to hold up their heads. The greater the height of water, the greater the force of gravity because the mass is bigger and force is mass times acceleration. Water is especially useful for the measurement because it has a density of 1 so that mass can easily be known by just measuring the volume. The actual volume of water does not matter because the force is per cross-sectional

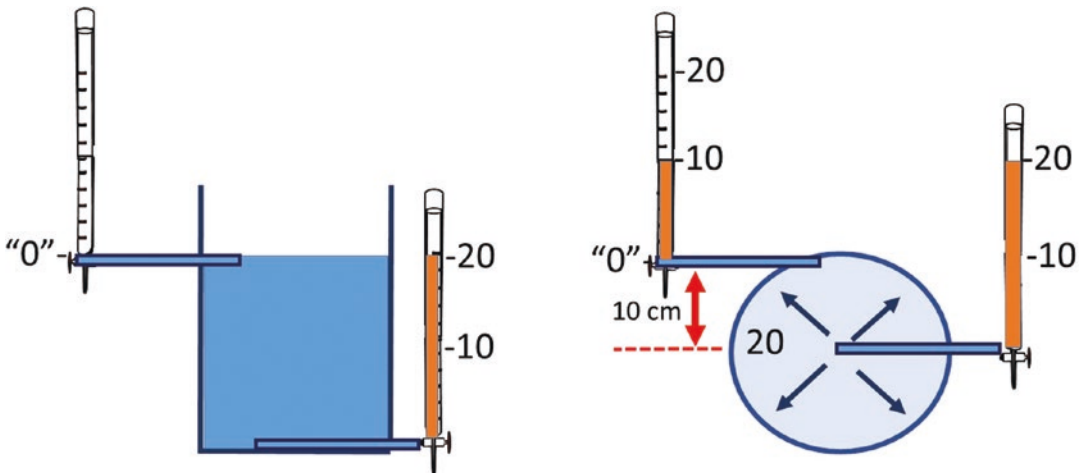


Fig. 22.2 Understanding the importance of leveling by use of fluid manometers. On the left is a tank open to the air. When the bottom of the manometer is placed at the top of the water in the tank, water does not increase the height of water in the manometer which is measured in cmH_2O , and the value on the manometer is zero. When the bottom of the manometer is positioned at the bottom of the tank, the weight of water in the tank raises the height of the water in the manometer to 20 cmH_2O . On the right is a

fluid-filled balloon that has a distending pressure of 20 cmH_2O across the wall based on a manometer leveled at the middle of the balloon. The pressure measured in the middle of the manometer leveled to the top of the balloon is only 10 cmH_2O because of the loss of gravitational force in the measuring device. Message: pressure values obtained with fluid-filled systems are relative to the arbitrary level of the measuring device

area; volume divided by the cross-sectional area gives height so that the height of water is the unit of pressure. The pressure in this case is in units of cmH_2O . As a small technical point, if the cross-sectional area is too small, forces created by the surface tension of the column come into to play as occurs in a capillary tube.

A problem with gravitational units is that the force is based on the distance from the center of the earth so that it varies the farther one is from the earth's center. Fortunately, this only is a trivial difference compared to the magnitude of vascular pressures; even on the top of Mount Everest, the difference is in the decimal point range. The more precise measurement of force is the Pascal units ($\text{Newton} \times \text{meter}^2$). This requires use of a standard force to make a measurement, but again, for vascular pressures, this does not add needed precision.

A water-based reference is fine for smaller pressures but not large pressures. Arterial blood pressure would require a column of about 1.6 m. Thus, instead of water, mercury is used for arterial gravitationally based measurement because mercury is 13.6 times denser than water and a smaller column can be used to measure the high arterial pressures. Blood has a density close to

that of water and its density can be considered essentially 1. As an example, if the CVP is 10 cmH_2O , it would be $10/1.36$ which gives 7.4 mmHg. The division is by 1.36 and not 13.6 because of the conversion of cm to mm.

Once electronic systems became available, it was much more practical to measure pressures with a transducer, although, I recommend always thinking about the column measurement to avoid some of the errors discussed below. A transducer is a device that has a thin membrane that provides a resistance to the flow of electrons across it. The voltage across the membrane is kept constant by resistors surrounding it. Distortion of the membrane by an external force changes its shape, which changes the resistance across the membrane. Since the voltage is kept constant, the change in resistance produces a change in current which can be detected by an amp meter and displayed on a monitor.

Three factors always need to be considered when making a pressure measurement: zero, calibration, and level. The zero is an arbitrary starting value. When a fluid-filled column is used, the bottom of the empty column is labeled as zero (Figs. 22.2 and 22.3). However, the force on the membrane is not really zero. We are surrounded

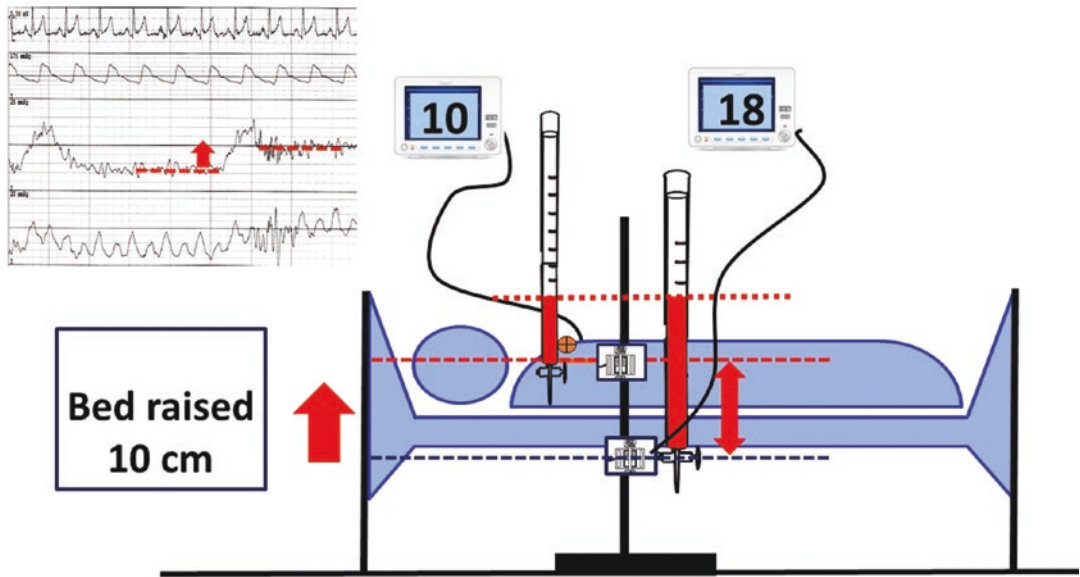


Fig. 22.3 Example of change in pressure due to change in level. The pressure tracing shows what happens when the transducer is abruptly lowered relative to the patient by 10 cm. It is useful to consider what happens when the position of the base of a fluid column is changed. In this example, the transducer position is fixed on a pole independent of the bed. Raising the bed relative to the transducer (lower transducer) resulted in a higher column of

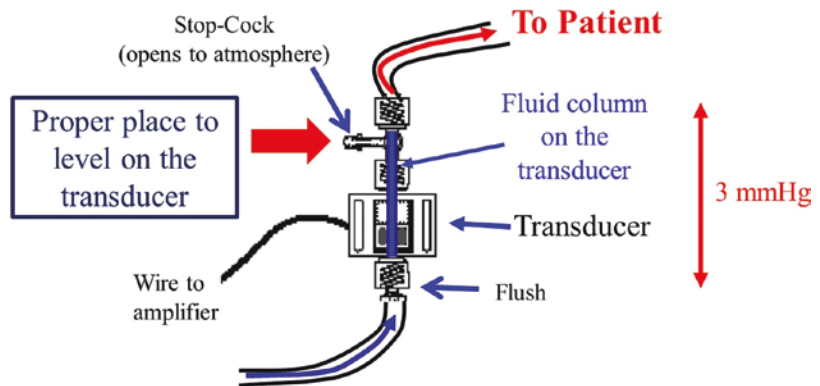
fluid acting on the transducer and gives a pressure of 18 mmHg. The proper position at 5 cm below the sternal angle (marked with round circle) gives a value of 10 mmHg. The difference is only 8 mmHg and not 10 mmHg because of the conversion from cmH_2O to mmHg which requires dividing by the density of mercury which is 13.6 times that of water and also changing cm to mm

by atmospheric pressure so that the force on the empty column at standard temperature pressure is 760 mmHg, but it is far too clumsy to use this absolute value. For example, at standard conditions, if the monitor says the central venous pressure (CVP) is -1 mmHg, it actually is 759 mmHg. If the arterial blood pressure (BP) is 120 mmHg, it actually is 880 mmHg! Furthermore, the measured value will continuously change with the weather because the barometric pressure surrounding us changes! A column of fluid used for the measurement is “zeroed” by emptying it. Similarly, the spring-based pressure gauge of a blood pressure cuff is “zeroed” by emptying out any air stretching the wall of the inflatable the cuff. The transducer is zeroed by opening up the system to the surrounding atmosphere (air). This needs to be done with fluid in the transducer up to the point where the system is open to air. If this fluid column is not taken into account, the pressure from this fluid is added to the measurement, but it is not from the patient. If there is air between

the transducer and where the system is open to air, this creates an air bubble when the system is connected to the patient, and it dampens the signal. Older transducers used to have a “drift” meaning that the zero value would gradually rise or fall; as a consequence, the transducers had to be zeroed before every measurement. This is much less of a problem today with modern electronics, but the zero should still periodically be checked by opening the system to atmosphere, especially if there is a sudden unexpected change in the displayed pressure value.

The second term is calibration. This simply indicates the change in pressure associated with a change in current through the transducer and how it is presented on a graphic display on a monitor. Calibration is established by applying a known force and observing the change in current. An important quality of a transducer is whether the relationship of the change in pressure for change in current is linear over a range of clinically important pressures. For currently used transduc-

Fig. 22.4 Proper leveling position on the transducer. The level should be where the stopcock opens to atmospheric pressure at the top of the column of fluid needed to fill the transducer and to avoid air bubbles. The difference in leveling from the correct site to the bottom at the “flush” device is 3 mmHg



ers, linearity is maintained well over the clinical range. If the signal is linear, calibration can be done with just two points, the zero value and a second value, such as 100 mmHg. Calibration of electronic devices is used to be done by actually attaching a column of water or mercury to the transducer, but this now is done with an internal electronic “force.”

The third term is leveling. This is what causes the greatest errors when making pressure measurements with fluid-filled catheters. The key point is that a pressure measured with a fluid-filled device is relative to an arbitrary reference level. This is because the fluid in the catheter has a mass that adds to the measurement because it too is being accelerated by gravity. The position of the measuring device thus becomes critical for the measured value. This is not a problem when measuring air pressures because the air in the measuring system has a trivial mass and does not contribute to the measurement. It generally is accepted that the reference level for hemodynamic measurements is the midpoint of the right atrium because this is where the blood comes back to the heart and then is pumped out again by the heart. On physical exam this positions can be found by identifying the sternal angle (also called angle of Louis), which is a small bump on the sternum where the second rib attaches to it (Bickley and Hoekelman 1999) and by knowing that the midpoint of the right atrium is 5 cm vertically below this point (Fig. 22.3). This remains true whether the subject is lying flat or sitting at up to at least 60° because the right atrium is a relatively round structure and its center remains

at the same vertical distance below the sternal angle. In our unit we use this value for setting the level of hemodynamic transducers. The sternal angle is identified and a carpenter’s level device is placed on it. A tongue depressor with a line drawn 5 cm below the leveling device is attached, and the transducer is leveled to this position at the level on the transducer where the system can be opened to air (Fig. 22.4). More often, the mid-thoracic (or midaxillary) line at the fourth intercostal position is used. However, this measurement only is valid when the subject is lying flat. On average, depending upon the chest size, measurements at the mid-thoracic level are 3 mmHg higher than the sternal angle-based measurement (Magder and Bafaqeeh 2007). With any of the approaches to leveling, the most important issue is to always use the same level so that trends in the measured values can be followed. The advantage of the sternal angle-based measurement is that it encourages the healthcare team to be more precise in identifying the reference level and it can be used in semi-upright positions as recommended for patients being fed, patients with pulmonary edema, or patients bleeding following cardiac surgery. The reader should now understand Fig. 22.1 (answer is at end of chapter).

Transmural Pressure

The pressure that matters in any hemodynamic assessment is the pressure across the wall of the elastic structure, because that is the force that

Patient extubated post thoracotomy

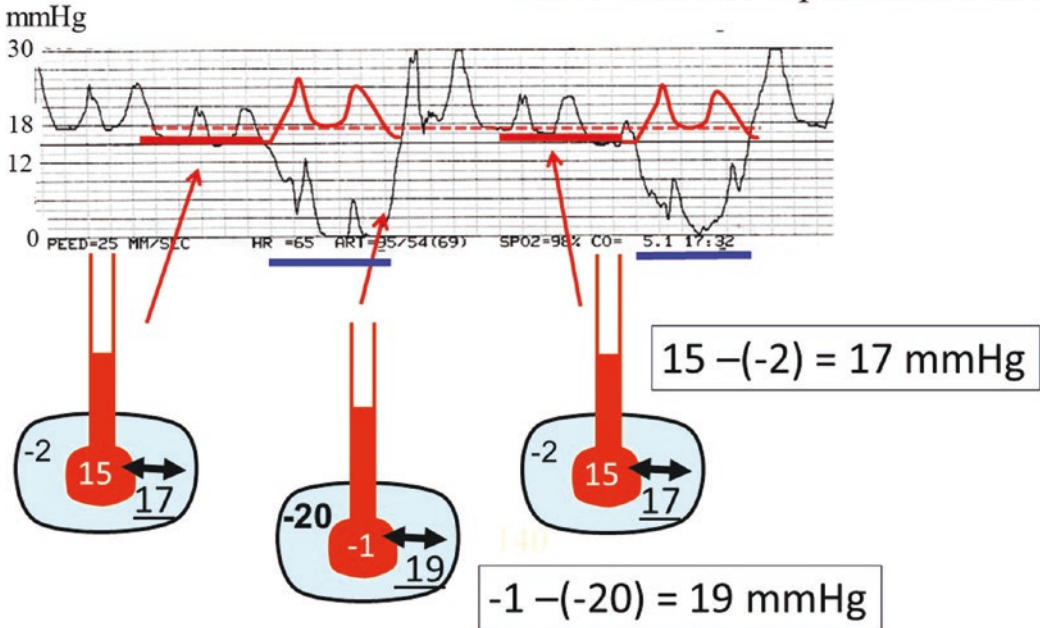


Fig. 22.5 Measurement of pulmonary artery occlusion pressure (Ppao). In a spontaneously breathing person, Ppao falls during inspiration. The proper place to measure Ppao or CVP is at end expiration or just before the inspiratory fall in pressure (these two terms are equivalent). Ppao is measured at the base of the “a” and “v” wave. In this example the value is 15 mmHg. There is an initial short rise in Ppao during expiration likely due to the inspiratory increase in right heart filling being passed to the left side. The bottom shows the equivalent of a heart (round red ball) with a column for measuring the pressure. The heart is surrounded by the equivalent of the chest and Ppl.

At end expiration, Ppl normally is approximately -2 mmHg. The true value at end expiration is then $15 - (-2) = 17$ mmHg. During inspiration Ppl falls. The change in Ppl can be estimated by the change in Ppao which closely matches the fall in Ppl except that it usually is 2 mmHg less because lung inflation increases filling of the left atrium (Bellemare et al. 2007). Thus, the new Ppl at peak inspiration is -16 , the fall in Ppl then is -18 , and it started from -2 so that the value is -20 mmHg. The inside pressure is -1 mmHg relative to atmospheric pressure so that the transmural pressure is 19 mmHg

distends the wall. It also is the force that drives fluid across the capillary walls. Transmural pressure is defined as the difference between the inside and outside pressures of a structure. As an example, for arterial pressure of 120 mmHg, the transmural pressure is 120 mmHg minus the outside pressure of 0 mmHg, and this seems like a trivial point. However, transmural pressure is not trivial when interpreting intrathoracic vascular pressures. The pressure surrounding the heart and vessels inside the chest is pleural pressure (Ppl) and not atmospheric pressure, and Ppl continuously changes during the respiratory cycle. As an example, when CVP or pulmonary artery occlusion pressure (Ppao) is measured with a device outside the chest, the waveform usually falls with a spontaneous inspiratory

effort, and one might conclude that right heart volume decreased. An example of the respiratory changes in Ppao is shown in Fig. 22.5. What really is happening is that the transducer is zeroed to atmospheric pressure and not the surrounding Ppl. If Ppl had been measured (also relative to atmosphere), it would have been apparent that Ppao fell less than Ppl because left atrial filling actually increases during inspiration because some volume is squeezed out of the lungs during inflation. As a consequence, transmural Ppao actually most often rises during a spontaneous inspiration (Fig. 22.5). The same most often occurs with the CVP. The return of blood to the right heart increases because of the increased gradient for venous return with inspiration, and this raises the transmural CVP. With

a positive pressure breath, the opposite occurs. The CVP generally rises less than Ppl because during inspiration the positive Ppl decreases venous return, right heart volume decreases, and the CVP transmural pressure decreases. The transmural Ppao, though, still usually rises because of the increased return from the lungs to the left atrium still occurs with the positive pressure lung inflation. The difference between the pressure of an intrathoracic vascular structure measured relative to atmosphere and true transmural pressure may seem small, but it must be remembered that the pressure difference for venous return only is in the 4–8 mmHg range. Furthermore, in most people, right ventricular filling becomes limited at a right ventricular transmural filling pressure measured relative to 5 cm below the sternal angle at around 10 mmHg (Magder and Bafaqeeh 2007). These principles apply to all intrathoracic vascular structures.

Changes in Ppl can be estimated with a balloon catheter placed in the esophagus, but this is not readily available most of the time, and is too inconvenient for routine measurements. The solution is to make hemodynamic measurements at end expiration because at that time in the respiratory cycle, Ppl is closest to atmospheric pressure with some important exceptions discussed below. This is true for both positive and negative pressure respiratory efforts. It should be appreciated that the end-expiratory pressure still underestimates the transmural pressure with spontaneous breathing because, at end expiration, Ppl is subatmospheric (Fig. 22.5). During a mechanical breath with positive end-expiratory pressure (PEEP), the end-expiratory value is overestimated because Ppl is greater than atmospheric pressure. However, these differences are small and create a relatively consistent bias. The problem becomes more significant when high levels of PEEP are used. There is no simple way to deal with this. It first should be appreciated that in normal lungs, a little less than half the airway pressure is transmitted to the pleural space. With a PEEP of 10 cmH₂O, this means that Ppl would increase by about 4 cmH₂O or < 3 mmHg, which is in the range of the accuracy of measurement and likely only has a small hemodynamic

effect. Furthermore, higher levels of PEEP usually are used when the lung is less compliant, which means that less airway pressure is transmitted to the pleural space. It might be considered that the effect of PEEP on the measurement could be assessed by just transiently removing the PEEP, but this does not work for measurement of CVP because the lower pressure relative to atmosphere increases right heart filling in the next diastole. Quickly removing PEEP, though, can give an indication of the effect of PEEP on the left atrial pressure because both the upstream venous pressure and the left atrial pressure are affected equally and left atrial filling does not change right away (Pinsky et al. 1991). The only real clinical solution is to chart the value as it is measured relative to atmosphere and then estimate a likely transmural pressure range by considering the magnitude of the PEEP and the lung compliance. This holds for external PEEP and intrinsic PEEP.

The significance of transmural pressure also can be important during expiration. Most often expiration is passive during spontaneous breathing, and there is little change in intrathoracic and intra-abdominal pressures. During a mechanical breath, there is a progressive decrease in the positive thoracic pressure created by the mechanical breath and then a plateau in the CVP and Ppao measurements when back to baseline. However, patients not infrequently have active expiratory efforts, especially when sedation is decreased, but also if they experience increased expiratory loads. This can result in two patterns which I have called A and B (Fig. 22.6a, b) (Magder et al. 2016). In A, Ppl is increased at the beginning of expiration by an active expiratory effort and progressively falls during expiration as the air in the thorax is emptied. In this situation, CVP and Ppao should be measured in a ventilator cycle with the longest expiratory time or when a clear expiratory plateau is identified. In the B type (Fig. 22.6b), the expiratory effort increases during expiration so that CVP and Ppao progressively increase, too. In this situation, it is wrong and misleading to make the measurement at end-expiration because Ppl at that time has the greatest deviation from atmospheric pressure. The

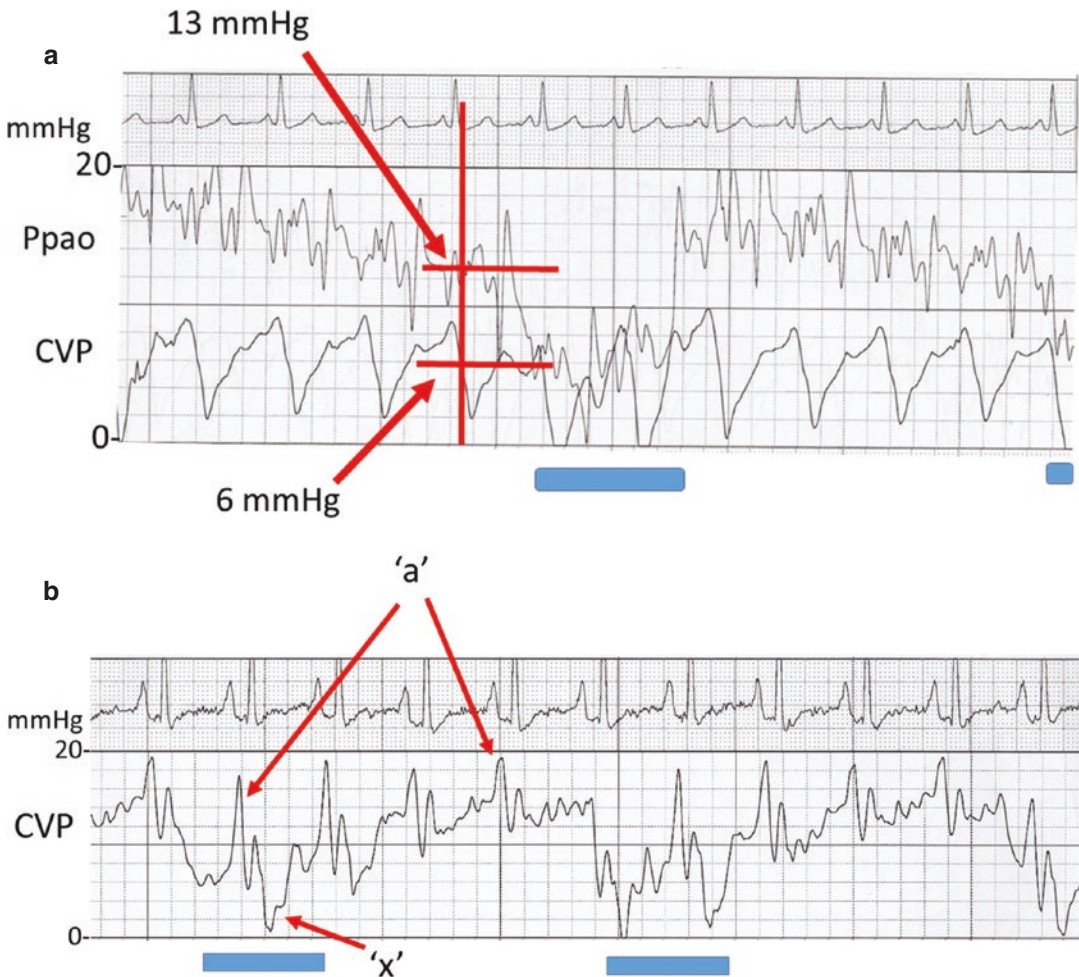


Fig. 22.6 (a) Example of forced (i.e., active) expiration type A in spontaneously breathing patient. The middle tracing shows the pulmonary artery occlusion pressure (Ppao) and the bottom the CVP. The scale is 20 mmHg for both. The horizontal bar at the bottom indicate inspiration. The Ppao progressively decreases during expiration and CVP does too but more mildly. The breath is identified by the large fall in Ppao and smaller fall in CVP. The CVP tracing shows very large *x* descents indicating right ventricular diastolic dysfunction (Mark 1991; Goldstein

et al. 1990). The red lines indicate the proper place to make the Ppao and CVP measurements. The Ppao is 13 mmHg. (b) Active expiration type B. In this spontaneously breathing patient, inspiration as indicated by the bars can be identified by the fall in CVP. During expiration there are progressive increases in CVP indicating active expiration. Note how the *a* wave decreases during expiration, likely indicating decreased right atrial filling during this phase

correct measurement only can be an estimate and should be made at the beginning of expiration when the expiratory effort is just starting (Magder et al. 2016). Other things that can be tried are to examine multiple cycles to find one in which there is no strong expiratory effort, have the patient talk even with a tube in place because this usually stops the expiratory effort, or even sedation (Magder et al. 2016).

Where on the Tracing Do You Make the Measurement?

In patients who have prominent “a” and “v” waves, the question arises where on the tracing should the pressure measurement be made. In Fig. 22.7, the top of the “a” wave is almost 10 mmHg, the bottom is almost 0 mmHg, and the middle is about 5 mmHg. At 10 mmHg fluids

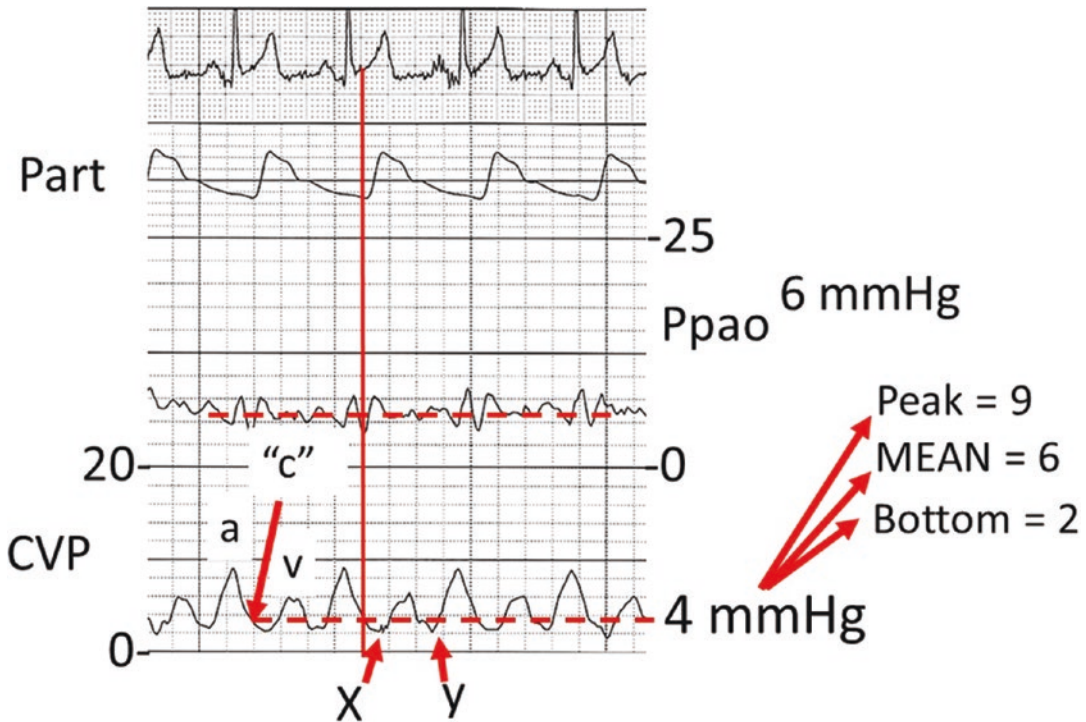


Fig. 22.7 Proper place to measure CVP. The tracing is during expiration. The top shows the ECG, the next tracing is the arterial pressure (Part), the third is the pulmonary artery occlusion pressure (Ppao), and the bottom tracing is the CVP. The *a* and *v* waves and *x* and *y* descents are marked. The place of the *c* wave is marked but it is not clear in this example. It can be located by a perpendicular

line drawn from the *S* wave on the QRS complex of the ECG. The line is shifted to the right because of time difference between an electrical (ECG) and fluid (CVP) signal. The onset of the upstroke of part also indicates the onset of systole and the proper place to measure CVP. The CVP in this example is 4 mmHg. In comparison the peak value is 9, mean 6, and bottom 2 mmHg. Ppao is 6 mmHg

might be held and a diuretic give, whereas at 0 mmHg fluids might be given! The proper place is at the base of the “*c*” wave, and if it cannot be identified, the base of the “*a*” wave is a close approximation. If the ECG signal can be synchronized with the CVP tracing, another approach is to draw a vertical line from the “*s*” wave of the QRS on the ECG to where it intersects the CVP. Unfortunately, this is not always easy on newer monitors because the ECG and pressure waves are often not synchronized without difficulty (such as the popular Philips devices).

Frequency Response

Systems that are used to measure pressure are characterized by their frequency response which is a measure of how quickly the system (pressure transducer and catheter) responds to changes in

pressure (Moxham 2003; Shapiro and Krovetz 1970). The maximum frequency in Hz that the pressure sensor can pass into its signal without distortion is called the flat frequency (Moxham 2003).

Measurement of a pressure with a catheter and transducer is characterized as second-order underdamped systems. A useful analogy is that of a bouncing ball. If there was no loss of energy, it would keep bouncing with the same height and frequency each time, but instead, frequency of bouncing stays the same with what is called the “characteristic frequency,” but the height gradually decreases. The time it takes to come to rest is its damping coefficient.

Pulse waves can be broken down into different component sine waves that have oscillations that are fractions of the dominant wavelength. These are called harmonics. For an arterial pulse, the first harmonic is the heart rate. Harmonics ideally

should not have a phase shift but a small shift related to frequency is acceptable. The natural frequency, i.e., equivalent of the bounce of the measuring device, must be greater than the first six to ten harmonics of the frequencies that make up the pressure wave being measured. Based on this, a heart rate of 140 b/min would require that the measuring system respond at up to 20 Hz. The faster the heart rate and the steeper the systolic pressure upstroke, the greater the natural frequency response required for the measuring system. On the other hand, venous waves do not have steep upstrokes, and they are composed of waves with resonant frequencies that are ten times that of arterial pressures. They thus require frequency responses of 150 Hz. This, though, is not practical and damping must be added. When the frequency of the measurement (i.e., arterial pressure) approaches the natural frequency of the measuring system, the system will start to resonate and exaggerate the amplitude of the true signal. If the frequency response of the measuring system is reduced by the friction and viscosity in the fluid being measured, the amplitudes of the signals are reduced. This usually is done to some extent electronically to avoid overestimation of the pressure signal, but typically signals are underdamped.

A high-frequency response and sensitivity are mutually exclusive, so it is important to use a system that responds to what is being measured. CVP measurements need a low-frequency response (10 Hz) but high sensitivity, whereas devices for measuring arterial pressure, especially when the arterial waveform is being used to estimate cardiac output, should have higher-frequency response (20 Hz). If dP/dt max is being measured in ventricle, a very high-frequency response (>30 Hz) is required. Importantly, systolic pressure is overestimated by an underdamped system. Diastolic pressure is less sensitive to sub-optimal dynamic response because it falls more slowly than the upstroke in systole, but it still is underestimated by underdamped systems and overestimated by overdamped systems. The mean pressure is the least affected by the dynamic response of the measuring system, but it still can be altered because of

the different effect of the frequency response on systolic and diastolic measurements. Most noninvasive pressure monitoring systems have dynamic response limitations, thus it is expected that intra-arterial measurements of systolic arterial pressure usually exceed the indirect noninvasive measurement. Modern transducers have excellent frequency response ranges with electronically regulated dampening, and they provide reliable systems as long as the catheter system is adequate. A large bore arterial cannula improves the frequency response but also increases the risk of arterial damage. If possible, less stopcocks, as well as stopcocks with wider bore taps, should be used. Catheters should regularly be flushed to minimize blood clots that will increase resistance or air that increases compliance and the signal.

The frequency response of the system can be tested by flushing the catheter system and observing the frequency of the response and the time to stabilize as shown in Fig. 22.8.

Use of CVP

Use of CVP is often criticized by arguing that it is a “static” measure, that it does not indicate blood volume, and that its value does not predict fluid responsiveness. The first of these, i.e., that it only is a static measurement, is true, but only if one looks at just one value; but why would any reasonable clinician do that? If changes in CVP over time are compared to changes in blood pressure, cardiac output, urine output, changing lactate, oxygenation, and even wakefulness, CVP is as “dynamic,” a measure as any other dynamic measures.

The other two points are true and CVP should not be used for these purposes. CVP only is determined by stressed volume, which, as discussed in Chap. 2, constitutes a little less than 30% of total blood volume. This means that 70% of blood volume does not affect the CVP. Second, CVP does not even indicate the pressure in the upstream large venous-compliant region because between the two there is a resistance that varies with neurohumoral activity. Third, the measured CVP is determined by the interaction of cardiac

Part (mmHg)

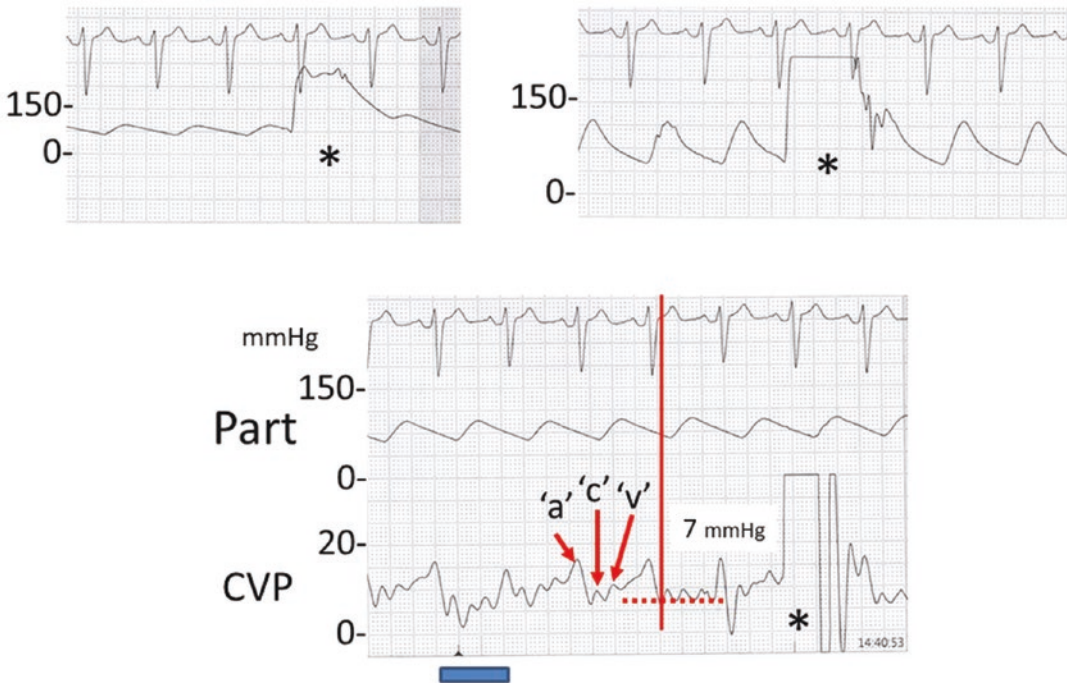


Fig. 22.8 Assessment of frequency response with flush test. The top shows a damped arterial pressure on the left. The flush test (*) shows a slow return to the base signal. The line was kinked and when the arm was strained the proper signal returned. The flush test shows brisk, narrow waves

post-flush. The bottom shows a normal brisk flush test for the CVP (it also shows the same damped part of the arterial tracing seen in the upper left but with a larger scale). Patient was on pressure support. The *a*, *c*, and *v* waves are marked (*v* is very small). The bar marks inspiratory trigger

function and return function, both of which are constantly changing, and when that happens, CVP at the same blood volume changes. In fact, these changes are the real clinical usefulness of the CVP measurement and will be discussed below.

The third statement, which is that CVP does not predict fluid responsiveness, also is true, but misses the usefulness of CVP as a pretest predictor of the likelihood of a response, which when combined with clinical judgment, can be very helpful. Factors that affect the pressure at which the RV filling is limited include the space taken up by other structures in the thorax and potentially compress the heart, the presence of PEEP, the intrinsic compliance of the RV during diastole, and even the precise position of the right heart relative to where it is assumed to be for the reference level. This likely is a greater problem with

the mid-thoracic measurement than the measurement based on 5 cm below the sternal angle because the heart is an anterior structure; just ask a cardiac surgeon who has to do midline sternotomies. The right atrium thus maintains a relatively constant position relative to the sternal angle. In contrast the mid-thoracic value is affected by the depth of the chest, and difference between the two leveling sites increases with increased depth of the chest.

A single patient meta-analysis of the predictive value of CVP for fluid responsiveness did not find a cutoff value that could reliably predict fluid responsiveness (Eskesen et al. 2015). However, details were not given for how patients were leveled, where in the cycle measurements were made, and how expiratory efforts were used. All of these can affect the CVP values which only occur over a very small range. One of my papers

was included in the meta-analysis, and no adjustment was made by the authors for the fact that we use a level of 5 cm below the sternal angle instead of the more commonly used midaxillary level (Magder and Bafaqeeh 2007). In contrast to the result of the meta-analysis, we found a very clear decrease in the percentage of patients responding to fluids with increases in CVP (Magder and Bafaqeeh 2007). There were few fluid responders above 10 mmHg, and we therefore called values above this as a “high” CVP. In reality, any CVP above 2–4 mmHg is likely abnormal, although the patient still could be fluid responsive because fluid need and fluid responsive are not the same. It also is important to appreciate that there is an inherent bias in almost all fluid challenge studies, including our own. The standard experimental approach is to obtain values of CVP and cardiac output after a fluid bolus is given. This fluid bolus most often was given based on the clinician’s belief that volume might improve the clinical condition. Accordingly, when fluids are given at higher CVP values there is a greater likelihood of responses because from a Bayesian point of view, potential responders are preselected. The dogmatic statement that CVP does not predict a fluid response also ignores some simple clinical situations. If a patient is in shock and a pulmonary embolism is considered but the CVP is zero, yes, a pulmonary embolism is still possible, but some creative pathophysiology also is required. For example, does the patient have a gastrointestinal bleed with the pulmonary embolism or even sepsis and a pulmonary embolism? On the other side, if a patient is in shock and this is thought to be due to a massive gastrointestinal bleed and the CVP is 20, yes, the shock could be because of the bleed, but the high CVP indicates that something else is happening, such as perhaps cardiac tamponade at the same time.

As indicated above, the best way to use of the CVP is to combine it with an indicator of flow. Generally, blood pressure is not a good indicator of cardiac output with the exception of the acute, severely hypotensive patient in whom the cardiac output usually is low. The ideal is to have a cardiac output measurement. The need for accuracy of a measurement of a cardiac output varies with

the severity and refractoriness of the shock. The pulmonary artery catheter and PiCCO systems still are the most reliable devices for measuring cardiac output but are more invasive. An esophageal Doppler probe can provide a reliable measure of aortic flow but requires some experience in properly positioning the probe (Dark and Singer 2004). It can be difficult to be confident with Doppler signal at low flow rates because it is hard to know whether the low signal is because of technical reasons or whether the flow is truly low, which is unfortunate because that is the question that the clinician wants to know. Changes in the signal are easy to observe, so if the system is working, the response to an intervention can help separate an inadequate signal from a true low value. An increase of the velocity signal also can be useful for identifying changes in flow in response to a therapy (McKendry et al. 2004). Echo-Doppler approaches can be noninvasive or less invasive if esophageal echocardiographic measurements are obtained but are not easily used serially. Metabolic values can give an indirect, but sometimes sufficient indication of a response to therapy. These include decreasing lactate and rising central venous saturation. An increasingly mentally responsive patient with a stabilizing blood pressure is likely one of best indicators of a good clinical response to a therapy.

The approach to use of the CVP and flow measurement is based on the appreciation that CVP indicates how cardiac function is handling the venous return as discussed in Chap. 2 (Table 22.1). An improvement in cardiac function alone makes the heart more “permissive” for the return of blood and results in a fall in CVP with a rise in cardiac output. The reverse, a decrease in cardiac function, results in a rise in CVP with a fall in cardiac output, i.e., changes in CVP and cardiac output go in opposite directions and indicate that the heart is more or less “permissive.” An improvement alone in the return function results in a rise in CVP with a rise in cardiac output, and the reverse, a fall in the return function, which usually means a fall in stressed vascular volume, results in fall in CVP with a fall in cardiac output, i.e., they move in the same direction. These rela-

Table 22.1 Clinical significance of change in CVP and change in cardiac output

CVP	Cardiac output	Functional change	Process
Increase	Increase	Increase in return function	Change in volume, capacitance, or venous resistance
Decrease	Decrease	Decrease in return function	
Increase	Decrease	Decrease in pump function	Change in HR, contractility, or afterload of RV or LV
Decrease	Increase	Increase in pump function	
No change	Increase	Increase in both pump and VR	E.g., increased NE
No change	Decrease	Decrease in both pump and VR	E.g., decreased NE

VR venous return function, HR heart rate, NE norepinephrine

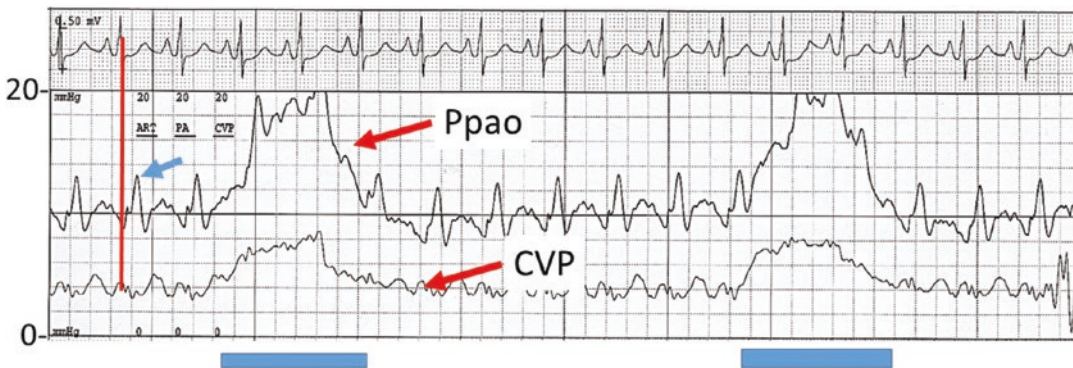


Fig. 22.9 Inspiratory increase in Ppao and CVP indicating decreased chest wall compliance. There is a prominent rise in Ppao and CVP during the mechanical breath (marked by the blue bar). There also is an unusually large

early v wave on the Ppao tracing which could indicate mitral regurgitation or a noncompliant left atrium. The blue arrow marks the v wave and the red line the onset of systole

tionships can be used diagnostically. For example, if blood pressure falls, CVP falls, and cardiac output falls, this is primarily a return problem and most likely a loss of volume. If the blood pressure falls, CVP rises, and cardiac output falls, the primary problem is a decrease in pump function. This could be a right heart, pulmonary circuit, or left heart problem, but the approach now can then be more focused. On the therapeutic side, if a bolus of fluid is given and CVP falls, the cardiac output rises, the fluid bolus cannot explain the rise in cardiac output by itself. Here also had to be an increase in cardiac function. Perhaps a catecholamine was given at the same time or maybe the patient woke up or just improved!

A useful clinical tip when following CVP tracings on the monitor is that increased positive inspiratory swings in patients receiving mechani-

cal ventilation are an indicator of decreased chest wall compliance (Fig. 22.9). This type of patient may require a higher PEEP than expected to maintain good oxygenation. An example would be an obese patient. On the other side, inspiratory falls in CVP are not as good at estimating the inspiratory fall in pleural pressure when compared to the Ppao. This is because the left heart receives blood from the pulmonary venous reservoir and the change in pressure in that region follows the change in left heart pressure during the ventilator cycle. In contrast, the venous reservoir for the right heart is outside the thorax, so the environment of the right heart changes relative to its reservoir during the ventilator cycle, and accordingly, its filling changes more than on the left (Bellemare et al. 2007). However, a large inspiratory fall in CVP indicates that there was indeed a large fall in Ppl.

Use of Ppao

I will start with a comment on nomenclature. The first publication on pulmonary artery catheterization was by Cournand and co-workers (Cournand et al. 1948). They used an end-hole catheter and passed it through the right heart, to the pulmonary artery, and then distally until it “wedged” in the vessel. When a pulmonary floatation catheter is used, the balloon near the tip occludes the vessel, and the tip is free and not “wedged.” This means that it is in slightly larger vessels which could result in some minor differences. These likely are of little clinical significance, but for the sake of preciseness, the balloon value is called an occlusion pressure instead of a “wedge” pressure although in both cases forward arterial flow in the vessel is presumed to be stopped so that only the distal pressure is measured. A potential error that is unique to a Ppao measurement is that the signal can be dampened but the artery is not actually occluded. This gives a falsely elevated estimate of left atrial pressure Fig. 22.10.

The pulmonary artery catheter was created by Swan and Ganz because they appreciated that in most patients with a myocardial infarction, CVP does not identify an elevated left atrial pressure. It was thus necessary to directly measure the left heart filling pressures to better classify the patient’s status and to plan treatments (Table 22.2) (Forrester et al. 1971; Swan et al. 1970; Laks et al. 1967). This still remains the primary use of a Ppao. In a patient in whom it is determined that a decrease in cardiac function is the primary problem, Ppao can be used to determine whether the primary problem is in the left heart or in the right heart. If the problem is primarily in the left heart, the differential diagnosis is limited to coronary artery disease, mitral or aortic valve disease, or severe hypertension, which should be obvious! Equal elevations of CVP and Ppao indicate a global cardiac problem such as a cardiomyopathy, tamponade, or restrictive process, although this, too, can occur if there is a primary left heart problem and excessive fluids have been given to the point where there also is right heart limitation

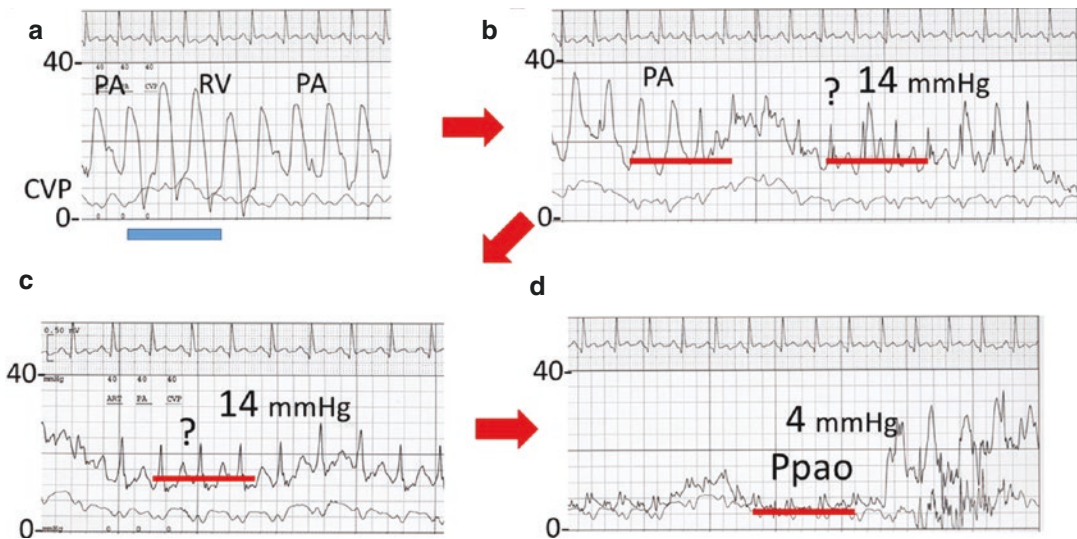


Fig. 22.10 Faulty measurement of pulmonary artery occlusion pressure (Ppao) with pulmonary artery catheter. Panel (a) shows pulmonary artery (PA) and CVP. In this patient the end of the catheter slips back into the right ventricle (RV) with a mechanical breath (bar at bottom). The arrows mark the sequence of events. In (b) the balloon is inflated and the tracing is altered. However, the diastolic

pressure has not changed and it has a prominent spike. In (c) the tracing looks like it could be Ppao but it still has the prominent spike. In (d) the proper Ppao is finally seen. The pressure is only 4 mmHg instead of 14 mmHg. At the end of (d), the balloon is deflated and the PA tracing returns

Table 22.2 Clinical prediction from combined CVP and pulmonary artery occlusion pressure (Ppao)

<i>Ppao greater than CVP</i>
Coronary artery disease
Aortic valve disease
Mitral valve disease
Severe arterial hypertension
CVP greater than Ppao
Excess fluid and RV limitation
Chronic fluid retention
Excess fluid given
Left to right shunt
Ruptured VSD with AMI
RV dysfunction
Elevated PAP
Decreased contractile function (depressed end-systolic pressure-volume relationship) (but still require excess fluid be given)
CVP and Ppao both elevated
Global dysfunction
Cardiomyopathy
Diffuse coronary disease
Volume overload
Right ventricular dysfunction with CVP transmitted to left atrium
Restrictive heart disease
Tamponade
Pericardial fluid
Mediastinal constraint

as discussed in Chap. 3. A CVP greater than Ppao indicates that the problem is primarily with the right heart such as a pulmonary embolism, primary pulmonary hypertension, chronic pulmonary disease, or even increased right heart loading to the ventilator settings (Table 22.3).

Ppao values should never be used to determine if a fluid bolus will increase cardiac output. This is because it is the CVP that indicates how the heart as a whole is interacting with the return function and volume increases cardiac output by acting on the return function. Furthermore, when right heart filling is limited and Ppao is low, more volume cannot get to the LV to fix the problem because more volume per beat cannot leave the right heart. However, Ppao can be used to indicate that one needs to be cautious about giving more fluids. Ppao gives an indication of capillary pressure and thus the risk to the lungs when giving more fluid. When Ppao values are above

Table 22.3 Guide to responses to a fluid challenge

CVP	Cardiac Index	Response
Change ≥ 2 mmHg	Increase ≥ 0.3 L/min per m ²	+ve fluid response
Change < 2 mmHg	Increase ≥ 0.3 L/min per m ²	+ve fluid response
Change < 2 mmHg	Increase < 0.3 L/min per m ²	Inadequate test – repeat
Change ≥ 2 mmHg	Increase < 0.3 L/min per m ²	Not fluid responsive no matter what the CVP value

Outcomes are independent of amount of fluid given and starting CVP

18 mmHg, fluids should be used cautiously, especially if the albumin is low or capillaries are leakier than normal.

An indirect value of the Ppao when it is in place is that the peak changes during the respiratory cycle give an indication of the change in pleural pressure with either a negative or positive inspiratory effort (Bellemare et al. 2007; Verscheure et al. 2016). The values are not exactly the same because lung inflation squeezes some blood out of the lungs and increases left atrial filling transmural Ppao by about 2 mmHg. Thus, the fall in Ppl during a spontaneous breath is underestimated by about 2 mmHg during inspiration and with a mechanical breath overestimated by 2 mmHg.

Pulmonary Artery Pressure

The primary technical issues related to pulmonary artery (PA) measurements are the same as those for the CVP and Ppao. The respiratory variations, though, can be more of a problem, especially when respiratory effort is increased. This is because there is the natural large PA pulse pressure swings at the heart rate frequency combined with the respiratory frequency. It is even worse when there is active expiration (Magder and Verscheure 2014).

Mean PA pressure often is required to evaluate the load on the right heart and the driving pressure for pulmonary artery blood flow. This is

done by smoothing out of the tracing and ignores the artifact in the estimate of transmural pressure from the changing reference value of PA compared to the atmospheric pressure used for the transducer (Magder and Verscheure 2014). This error is magnified when either inspiratory or expiratory efforts are increased. It would make more sense to make a measurement of PA pressure at end expiration and calculate a mean. High respiratory frequencies increase the problem and may make it very difficult to identify end expiration. It can become almost impossible to assess true transmural values. From a pragmatic point of view, it might be better to just use the pressure difference from the pulmonary diastolic pressure to the pulmonary artery occlusion pressure, if it can be measured, to assess PA vascular resistance. These both move with same reference system so that the difference is valid.

Conclusion

The simple CVP provides a lot of clinically useful information if it is properly understood and used in the clinical context and especially when used with a flow measurement. If used this way, it hardly can be considered a “static” measurement as it marches across the screens of many critically ill patients. CVP, Ppao, and pulmonary artery pressures generally are much smaller than arterial pressures, and there needs to be great care in using the appropriate level, zero, and calibration. Inappropriate changes in management easily can be made based on faulty measurements. The effect of respiration on Ppl always needs to be considered when making pressure measurement on intrathoracic structures. It may not always be evident that a change in pleural pressure has occurred and that it is altering the measurements. A simple short disconnect from the ventilator can sometimes detect this problem. Leveling, zeroing, and checking the calibration should always be done before any major changes are made in hemodynamic management.

The answer to the two examples in Fig. 22.1 is 10 cmH₂O for both A and B.

References

- Augustine DX, Coates-Bradshaw LD, Willis J, Harkness A, Ring L, Grapsa J, et al. Echocardiographic assessment of pulmonary hypertension: a guideline protocol from the British Society of Echocardiography. *Echo Res Pract.* 2018;5(3):G11–g24.
- Bellemare P, Goldberg P, Magder S. Variations in pulmonary artery occlusion pressure to estimate changes in pleural pressure. *Intensive Care Med.* 2007;33(11):2004–8.
- Bickley LS, Hoekelman RA, editors. *Bates guide to physical examination and history taking.* Philadelphia: Lippincott; 1999. p. 299–303.
- Bytyçi I, Bajraktari G, Lindqvist P, Henein MY. Compromised left atrial function and increased size predict raised cavity pressure: a systematic review and meta-analysis. *Clin Physiol Funct Imaging.* 2019;39(5):297–307.
- Connors AF Jr, Speroff T, Dawson NV, Thomas C, Harrell FE Jr, Wagner D, et al. The effectiveness of right heart catheterization in the initial care of critically ill patients. SUPPORT Investigators. *J Am Med Assoc.* 1996a;276(11):889–97.
- Connors AF Jr, Speroff T, Dawson NV. The effectiveness of right heart catheterization in the initial care of critically ill patients. *J Am Med Assoc.* 1996b;18:1294–5.
- Cournand A, Motley HL, Werko L, Richards DW Jr. Physiological studies of the effects of intermittent positive pressure breathing on cardiac output in man. *Am J Physiol.* 1948;152:162–74.
- Courtois M, Fattal PG, Kovacs SJ, Tiefenbrunn AJ, Ludbrook PA. Anatomically and physiologically based reference level for measurement of intracardiac pressures. *Circulation.* 1995;92:1994–2000.
- Dalen JE, Bone RC. Is it time to pull the pulmonary artery catheter? *J Am Med Assoc.* 1996;276(11):916–8.
- Dark PM, Singer M. The validity of trans-esophageal Doppler ultrasonography as a measure of cardiac output in critically ill adults. *Intensive Care Med.* 2004;30(11):2060–6.
- Eskesen TG, Wetterslev M, Perner A. Reanalysis of central venous pressure as an indicator of fluid responsiveness. *Intensive Care Med.* 2015;42:324.
- Fisher CJ Jr, Dhainaut JF, Opal SM, Pribble JP, Balk RA, Slotman GJ, et al. Recombinant human interleukin 1 receptor antagonist in the treatment of patients with sepsis syndrome. Results from a randomized, double-blind, placebo-controlled trial. Phase III rhIL-1ra sepsis Syndrome Study Group. *J Am Med Assoc.* 1994;271(23):1836–43.
- Forrester JS, Diamond G, McHugh TJ, Swan HJ. Filling pressures in the right and left sides of the heart in acute myocardial infarction. A reappraisal of central-venous-pressure monitoring. *N Engl J Med.* 1971;285(4):190–3.
- Goldstein JA, Barzilay B, Rosamond TL, Eisenberg PR, Jaffe AS. Determinants of hemodynamic compromise

- with severe right ventricular infarction. *Circulation*. 1990;82(2):359–68.
- Harvey S, Harrison DA, Singer M, Ashcroft J, Jones CM, Elbourne D, et al. Assessment of the clinical effectiveness of pulmonary artery catheters in management of patients in intensive care (PAC-Man): a randomised controlled trial. *Lancet*. 2005;366(9484):472–7.
- Iberti TJ, Fisher EP, Leibowitz AB, Panacek EA, Silverstein JH, Albertson TE. A multicenter study of physicians' knowledge of the pulmonary artery catheter. Pulmonary artery catheter study group. *J Am Med Assoc*. 1990;264(22):2928–32.
- Laks MM, Garner D, Swan HJ. Volumes and compliances measured simultaneously in the right and left ventricles of the dog. *Circ Res*. 1967;20(5):565–9.
- Magder S, Bafaqeeh F. The clinical role of central venous pressure measurements. *J Intensive Care Med*. 2007;22(1):44–51.
- Magder S, Verscheure S. Proper reading of pulmonary artery vascular pressure tracings. *Am J Respir Crit Care Med*. 2014;190(10):1196–8.
- Magder S, Serri K, Verscheure S, Chauvin R, Goldberg P. Active expiration and the measurement of central venous pressure. *J Intensive Care Med*. 2016;33:430.
- Mark JB. Central venous pressure monitoring: clinical insights beyond the numbers. *J Cardiothorac Vasc Anesth*. 1991;5(2):163–73.
- McKendry M, McGloin H, Saberi D, Caudwell L, Brady AR, Singer M. Randomised controlled trial assessing the impact of a nurse delivered, flow monitored protocol for optimisation of circulatory status after cardiac surgery. *BMJ*. 2004;329(7460):258–0.
- Moxham IM. Physics of invasive blood pressure monitoring. *S Afr J Anaesth Anal*. 2003;9(1):33–8.
- Pinsky M, Vincent JL, De Smet JM. Estimating left ventricular filling pressure during positive end-expiratory pressure in humans. *Am Rev Respir Dis*. 1991;143(1):25–31.
- Richard C, Warszawski J, Anguel N, Deye N, Combes A, Barnoud D, et al. Early use of the pulmonary artery catheter and outcomes in patients with shock and acute respiratory distress syndrome: a randomized controlled trial. *J Am Med Assoc*. 2003;290(20):2713–20.
- Shapiro GG, Krovetz LJ. Damped and undamped frequency responses of underdamped catheter manometer systems. *Am Heart J*. 1970;80(2):226–36.
- Swan HJC, Ganz W, Forrester J, Marcus H, Diamond G, Chonette D. Catheterization of the heart in man with use of a flow-directed balloon-tipped catheter. *N Engl J Med*. 1970;282(9):447–51.
- Verscheure S, Massion PB, Gottfried S, Goldberg P, Samy L, Damas P, et al. Measurement of pleural pressure swings with a fluid-filled esophageal catheter vs pulmonary artery occlusion pressure. *J Crit Care*. 2016;37:65–71.
- Wheeler AP, Bernard GR, Thompson BT, Schoenfeld D, Wiedemann HP, deBoisblanc B, et al. Pulmonary-artery versus central venous catheter to guide treatment of acute lung injury. *N Engl J Med*. 2006;354(21):2213–24.



Cerebral Hemodynamic Monitoring Techniques

23

Ivan Da Silva and Thomas P. Bleck

Introduction

Invasive and noninvasive monitoring of the central nervous system (CNS) has been a cornerstone of neurocritical care since the conception of neural critical care units. However, there is little evidence to support the idea that monitoring-based care in neurologically ill patients translates into improved outcomes. The aim of this chapter is to review the technology and physiology behind the most commonly used techniques and to highlight the potential utility, limitations, and device-related complications of the tools.

Background

Monitoring the brain, its diseases, and metabolic processes has been an obsession since the advent of neurocritical care, even when treatment

options are limited or not significantly effective. The original motivation for the development of neurocritical care units was to place patients with critical neurological conditions in the same area, in order to allow physicians and nurses to frequently check the patient's clinical status (Wijdicks 2017). The neurological exam has been the pillar of neurocritical care since those early days and remains the gold standard assessment of the CNS function. A neurological examination that identifies preserved mechanisms of alertness, awareness, cognitive function, and complex motor responses is more accurate and reassuring than any other type of brain monitoring, and clinicians should question any "abnormality" detected by ancillary devices when the exam is close to normal. All monitoring technologies are primarily of use in patients in whom a reliable neurological exam is not possible such as someone in whom significant brain injury has already occurred; the devices are being used to help prevent further neurological demise.

The term multimodal intracranial monitoring was coined within the last decade to further discuss the multitude of CNS monitoring techniques that have been developed and the challenge of how to integrate them. Excess nonintegrated information can lead to confusion and medical decisions that may cause more injury. As previously shown with the worldwide scrutiny and bashing of invasive pulmonary artery monitoring a few decades ago (Marik 2013), monitoring

I. Da Silva (✉)

Rush Medical College, Chicago, IL, USA

Rush University Medical Center, Department of Neurological Sciences, Chicago, IL, USA

e-mail: ivan_dasilva@rush.edu

T. P. Bleck

The Ken & Ruth Davee Department of Neurology, Northwestern University Feinberg School of Medicine, Chicago, IL, USA

Departments of Neurological Sciences, Neurosurgery, Internal Medicine, and Anesthesiology, Rush Medical College, Chicago, IL, USA

devices do not change patients' outcomes, and medical decisions based solely on numbers, and in the hands of inexperienced clinicians, can definitely lead to further harm. Previous studies have shown that neurocritically ill patients can experience improved outcomes if treated in units dedicated to such conditions (Egawa et al. 2016; Samuels et al. 2011; Soliman et al. 2018; Suarez et al. 2004; Varelas et al. 2008), reinforcing the idea that the best monitoring is having a specialized team at the bedside.

Intracranial Pressure

Anatomy and Physiology

The intracranial components are surrounded by a relatively rigid container, the skull. Recent research has shown that the skull diameter can vary during heart beats, but this volumetric difference is minimal (Mascarenhas et al. 2012). The intracranial components are comprised roughly of 1100–1300 cm³ of brain tissue (83%), 130–150 cm³ of cerebrospinal fluid (CSF) (11%), and 60–80 cm³ of blood (6%) inside the intracranial vessels (mostly within venous sinuses) (Zhang et al. 2017). CSF is produced and reabsorbed at approximately 15–20 cc/h. In theory the entire reservoir is renewed three times a day. CSF is mostly produced by the choroid plexuses (through filtering of blood by arterial pulsations) situated in the lateral ventricles. It flows through the third and fourth ventricles and accesses the cervical subarachnoid space through the foramina of Luschka and Magendie. From there, CSF flows down the spinal canal to the lumbar thecal sac and flows back to the cranium, where it is reabsorbed by the arachnoid granulations (connected to the venous system). Therefore, there is an intricate correlation of CSF production, flow, and reabsorption with the arterial and venous systems. It is important to emphasize that there is a natural downward pressure gradient from the brain to the spine that facilitates CSF flow, but this can become problematic when mass effect develops; it guides the pressure vectors toward

downward herniation. The intracranial compartment is further subdivided by meningeal leaflets, such as the tentorium and falx, and these divisions often compartmentalize distribution of pressure vectors and create pressure gradients. The doctrine attributed to Alexander Monro (1783) and George Kellie (1824) stated that the brain and its contained blood were incompressible, enclosed in a rigid and inextensible skull, of which the total volume remained constant (Monro 1823; Kellie 1824). Originally, the doctrine did not consider the CSF volume; this concept was introduced in 1846 by George Burrows (Burrows 1848). Also, the doctrine only referred to volumes, with the intracranial pressure component later being described by Francois Magendie and further established by Harvey Cushing (Cushing 1926). As a result, the pressure inside of the intracranial compartment is dictated by the volume of its three most important components (blood volume, CSF, and brain tissue); an increase in one of them should cause a decrease in one or both of the remaining two volumes. The doctrine itself suffers some criticism, as the volumes are dynamic (CSF is produced at every heart beat and flows toward the cervical spine, and intracranial vessels change the diameter during systole/diastole); the brain itself moves caudally during heart beats; the dural sac in the lumbar channel expands slightly against the surrounding venous plexuses. The skull also is not as rigid as previously thought (Mascarenhas et al. 2012; Greitz et al. 1992; Kasprovicz et al. 2016; Wilson 2016). But generically, it can be said that in cases where the brain parenchyma volume is increased due to hemorrhage, edema, or a tumoral lesion, first CSF is displaced to the spinal subarachnoid space to further compensate the intracranial compliance, followed by compression of the venous sinuses. After the buffering mechanism is exhausted, the intracranial pressure (ICP) starts to rise steeply, as the intracranial reserve is compromised, and not long after brain herniation ensues. Compliance has been the term used to describe the changes in intracranial pressure due to changes in the volume of intracranial components, but in a stricter way, the term elastance would be more correct or

the more neutral pressure-volume index described by Marmarou (Shapiro et al. 1980). Even though ICP monitoring is probably the hallmark of modern neurocritical care, it can be very misleading, as we try to indirectly infer intracranial volumes and elastance through a pressure monitor and use it as an indicator of resistance to blood flow to the brain (using estimated cerebral perfusion pressure).

History

Early references on CSF date as far back as the *Edwin Smith Papyrus*, which described “spillage of clear fluid from the interior of the brain” (approximately 1500 BCE) (Wilkins 1964). Hippocrates conducted the first postmortem ventricle access by needle in a case of hydrocephalus in the sixth century BC (Livramento and Machado 2013). Thomas Willis described in 1664 the production of CSF by the choroid plexuses, and later in 1705, Antonio Pacchioni reported for the first time the arachnoid granulations (Srinivasan et al. 2014). The first documented external ventricular drainage of CSF was performed by Claude-Nicolas Le Cat in October 1744 using a cannula with a stopple in an infant suffering from hydrocephalus (Korbakis and Bleck 2014). As the procedure in other attempts resulted in a number of complications and facing significant resistance from the medical community (Whytt 1768), it suffered a decline in its use until the 1880s, when Carl Wernicke and William Keen described techniques to mitigate infectious complications (Srinivasan et al. 2014). Even though consecrated in medical history as a pioneer of thyroid surgery (winning a Nobel Prize), Theodor Kocher described in 1894 in his *Textbook of Operative Surgery* the ventricular puncture through an anatomical landmark in the midpupillary line 10 cm posterior to the nasion, the most commonly used approach nowadays (Kocher’s point) (Schultke 2009). Those initial attempts used catheters made of horsehair, metal, rubber, and catgut wick, but the field advanced substantially after the plastics revolution in the 1950s (Srinivasan et al. 2014). In the late nineteenth century, interest in physio-

logical exploration of CSF surged, including the measurement of ICP by lumbar punctures (LP). Heinrich Quincke in Germany was the first to describe the needle cannulation technique for lumbar puncture (although he himself credited his London colleague Walter Essex Wynter for the initial concept), publishing on standardized techniques to measure CSF pressure (Andrews and Citerio 2004).

The use of LP to monitor increased pressure later fell into disuse due to the theoretical risk of inducing brain herniation and also with the work of Langfitt, who demonstrated that it would not accurately reflect ICP if the systems did not communicate (Langfitt et al. 1964) (i.e., CSF flow obstruction). Harvey Cushing published in 1901 what is considered his landmark study describing the clinical signs of raised ICP, also known as the Cushing triad: bradycardia, hypertension, and irregular respirations (Cushing 1901). Finally, in 1960 Nils Lundberg from Sweden published landmark studies using modern EVD cannulation and described in detail the ICP waveform, its components, temporal trends, variations with cardiac and respiratory cycles, as well as possible interventions (Lundberg 1960). His work was so comprehensive (almost 200 pages long) that his manuscripts received an issue of the journal dedicated only to his experiments. He established the feasibility and safety of prolonged drainage, as well as the association between elevated ICP and neurological decline.

Waveform Analysis and Trends

Monitoring of the ICP waveform is of essence, as it not only provides a pressure value but also information on intracranial elastance/reserve, cerebrovascular reactivity, and reliability of the measurement, among others. The “mean” ICP is a time average of the ICP waveform, consisting of mostly three components; the respiratory waveforms, which are a reflection of the respiratory cycle on cerebral venous blood flow at 0.1–0.3 Hz and consistent with the respiratory cycle; the pulse pressure waveform which is at the frequency of the heart rate; and slow vasogenic

waves, which reflect autoregulation-derived cyclic fluctuations of arterial blood volume (Lundberg waves) (Harary et al. 2018; Hall and O’Kane 2016). The ICP pulse pressure waveform occurs milliseconds after the electrocardiogram and arterial pressure waves, as it is in intimate relation with the cardiac cycle. The waveform can be grossly divided into three peaks: P1, P2, and P3 (Cardoso et al. 1983). P1 is also called the percussion wave and is believed to be produced by the arterial impulse in the choroid plexus during systole. In support of this, removal of the choroid plexuses in animals substantially decreases the P1 component (Bering Jr. 1955). P2 is named the tidal wave and reflects the degree of brain elastic properties. Finally, P3, named the dicrotic wave, is deemed to reflect the closure of the aortic valve. P2 is believed to be produced during the peak of cerebral blood volume flowing from proximal conductive large arterial vessels to distal high-resistance arterioles. An increase in its peak amplitude correlates with a high sensitivity to increased brain elastance (decreased compliance) but with a low specificity (Czosnyka et al. 2017; Chesnut 2013). Under normal conditions with preserved elastance, P1 is the tallest component of the pulse waveform, but if the intracranial elastance is further exhausted, P2 can become taller. Also, with increased elastance, the ICP waveform tends to become more apiculate, with a greater amplitude and a narrow base, due to increased resistance to cerebral blood flow during systole and compromise of effective cerebral blood volume during diastole (Hall and O’Kane 2016; Calviello et al. 2017). If the ICP rises even further, the amplitude progressively decreases due to disturbed CBF and the collapse of the cerebral microvasculature (Harary et al. 2018). Patients with abnormal waveforms have worse outcomes (Chesnut 2013), and more recently researchers have been trying to develop analytical tools to assess intracranial elastance/reserve and cerebrovascular autoregulation by using the ICP pulse waveform. Examples are the RAP and AMP indices (Czosnyka et al. 1994). These analyze the amplitude of the ICP pulse versus the mean ICP and are used as a measurement of intracranial reserve. The PRx (Czosnyka et al.

1997) plots mean ICP values temporally against mean systemic arterial pressure, to derive measurements of the cerebral autoregulation. Of great importance clinically is that the ICP pulse waveform be checked frequently because progressive dampening of the waveform with loss of its characteristic peaks puts limits to the validity and accuracy of the mean ICP value recorded and should alert the team for the need of troubleshooting the ICP measurement system.

Among the slow-frequency ICP waves/oscillations described by Lundberg in prolonged continuous ICP recordings (Lundberg 1960), the most clinically relevant are the A waves or plateau waves. These represent ICP surges with amplitudes of 50–100 mmHg, lasting 5–20 minutes, rarely hours, and are always associated with intracranial pathology. Rosner and Becker have proposed the most accepted mechanism; they supposedly are initiated as a vasodilatory cascade in response to a drop in CBF in the setting of a significant compromise of intracranial elastance and decreasing systemic arterial blood pressure (ABP) (Rosner and Becker 1984). The initial vasodilation leads to increased cerebral blood volume, which increases ICP, and subsequently decreases cerebral perfusion pressure (CPP). The fall of CPP triggers further vasodilation and a positive feedback loop ensues. Eventually, a vasoconstriction cascade occurs, possibly due to correction of CBF or exhaustion of the mechanism, and the ICP drifts back to baseline. Some researchers postulate that these phenomena are not necessarily associated with worse outcomes, because they occur in roughly 40% of patients with traumatic brain injuries and they might even signify fairly well-preserved cerebrovascular autoregulation (Chesnut et al. 2014). Others argue that when they are frequent and longer duration; they likely represent loss of autoregulation, and this potentially could lead to further ischemia and an unfavorable outcome (Castellani et al. 2009). A recent study in which multimodal monitoring was utilized suggested that autoregulation is temporarily lost during the peak of the A waves, followed by decrease of the partial pressure of cerebral oxygen, with subsequent normalization of both during the resolution phase (Lang

et al. 2015); “A” waves can be terminated at the bedside with correction of ABP, boluses of hypertonic saline, or transient hyperventilation (Czosnyka et al. 2017).

The B waves are slow oscillations usually with an amplitude up to 50 mmHg, lasting seconds to minutes and with a frequency of 0.5–2/min. They are considered to be the result of cerebral vasocycling, caused by fluctuations in the baroreceptor and chemoreceptor control mechanisms (Czosnyka et al. 2017). B waves have been correlated with the presence of chronic hydrocephalus (Stephensen et al. 2005). Finally, the C waves can oscillate up to 20 mm Hg of ICP and have a frequency of 4–8/min, last seconds, and have been previously documented in healthy volunteers as fluctuations due to interaction between the respiratory and cardiac cycles (Andrews and Citerio 2004). These two waves are of minimal clinical significance in general.

Modes of Measurement

Invasive intracranial monitoring methods can be classified based on the technology used and the place of insertion. Three major technologies for pressure reading are currently most commonly used: (a) an intraventricular catheter connected to a fluid-coupled external strain gauge pressure transducer (EVD), (b) miniaturized strain gauge device in a catheter tip (pressure microsensors), and (c) fiber-optic pressure sensor in a catheter tip. Air-coupled sensors were used in the past but seldom currently. Intraventricular monitoring with the capability of CSF drainage is considered the gold standard for monitoring, as it allows a more central pressure measurement (close to the foramina of Monro) and optional drainage of CSF for ICP management. It is most commonly used with a fluid-coupled external pressure transducer which is similar to the ones used for invasive arterial pressure monitoring, connected to a collection system.

One of the advantages of a fluid-coupled system is the possibility of measuring the ICP with a water column as is performed with a lumbar

puncture. This allows measurements even in cases of transducer failure, power outage, or in low-resource settings. Some modern catheters combine the capability of CSF drainage and pressure microsensor/fiber-optic sensor in its tip, which allows for ICP measurements even in situations where continuous CSF drainage is necessary (not possible with an external transducer) or in cases of obstruction of the fluid-filled system. ICP monitoring also can be performed with a catheter placed in the brain parenchyma with use of microsensor and fiber-optic technologies. In those situations, the tip of a much thinner catheter normally sits roughly 2 cm below the inner table of the skull and allows for a more peripheral pressure measurement, but no CSF drainage. Due to separation of the intracranial space into compartments by meningeal leaflets, it has been shown that intraparenchymal catheters might not fully detect pressure gradients (Sahuquillo et al. 1999; Piek and Bock 1990), but the clinical significance is still uncertain. Despite those disadvantages, they are much easier to place, they do not require specific anatomical landmarks, they are safer even when placed by non-neurosurgeons (Sadaka et al. 2013; Ehtisham et al. 2009), and they do not require frequent zeroing/recalibration. Overall, some previous studies reported that intraparenchymal probes are just as accurate at measuring pressure as the intraventricular ones (Bratton et al. 2007; Lang et al. 2003; Raboel et al. 2012), and a recent meta-analysis showed that in TBI patients, even though EVDs were associated with a slightly higher chance of intracranial infection, mortality and functional outcomes did not differ (Volovici et al. 2018). Table 23.1 compares the pros and cons of the intraventricular versus intraparenchymal techniques. Sensors placed in the epidural and subdural spaces are considerably less accurate and only are used in very special situations. Subdural sensors are sometimes used for ICP monitoring in patients with acute liver failure because of the bleeding risk, and epidural sensors are used occasionally in combat zones or in regions with no access to a neurosurgeon (easiest technique, not requiring dural puncture).

Table 23.1 Comparison of ICP monitoring techniques

Intraventricular catheters (fluid-coupled)	Intraparenchymal catheters
More central pressure measurements	More peripheral measurements (less accurate for pressure gradients?)
Allow CSF drainage and sampling	Do not allow CSF drainage
Requires several anatomical landmarks for placement	Easier placement (literature disclosing safety of placement by non-neurosurgeons)
Higher chance of infection	Lower chance of infection
Higher chance of procedural bleeding	Lower chance of bleeding
Less expensive	More expensive
Easier to troubleshoot pressure waveform dampening	Usually require exchange in case of pressure misreading
Less prone to ICP values drift	Drift of ICP values after a few days
Transducer can be zeroed at any time	Zeroing only allowed during placement
Preferred in cases involving hydrocephalus and/or intraventricular hemorrhage	Preferred in cases with severe ventricular anatomy distortion (TBI)
Requires higher nursing expertise and frequent maintenance of drainage system	Low expertise required, almost no maintenance.
Transducer normally compatible with most bedside monitors	Usually requires its own monitoring device
Administration of intrathecal medications	N/A

Clinical Application

ICP can be understood as the relationship between changes in intracranial volume and the ability of the craniospinal compartment to compensate for such changes. It also can be interpreted as the difference between CSF pressure and atmospheric pressure. It is important to emphasize the role of atmospheric pressure, because it can influence the drainage of CSF in patients with low-pressure hydrocephalus, the development of pneumocephalus in patients with resolving cerebral edema, and the “negative” ICP readings. In patients with resolving mass effect,

when positioned sitting up to 45 degrees, occasionally intraparenchymal pressure probes can read negative values (Czosnyka and Pickard 2004). This occurs as the pressure vector is more vertical than perpendicular to the microsensor/fiber-optic sensor vector of detection. When atmospheric pressure communicates through the craniotomy site in the presence of a downward movement of the brain in this position, the reading can be negative (in relation to the leveling, done at the atmospheric pressure).

It is hard to define what is considered the “normal” range of ICP values, as it would depend on body position during measurement, age, and clinical condition, among other factors (Czosnyka et al. 2017). Also, ICP can present slight and transient increments with Valsalva and Queckenstedt maneuvers such as coughing and sneezing. In healthy individuals, in the horizontal position, the normal values are within the range of 7–15 mm Hg (Albeck et al. 1991), and in the vertical position, it is negative with a mean of around –10 mm Hg, but not exceeding –15 mm Hg (Chapman et al. 1990). In a study with 1500 patients with neurological diseases, but without presumed lesions with a mass effect, the mean value of CSF pressure with the puncture of the cisterna magna was 11.9 cm of water, and the limits for the physiological variations were 4.1 and 19.7 cm of water (Spina-Franca 1963). The question is what is considered elevated enough in patients with intracranial pathology to merit further interventions. For a long time, it has been taught and written in textbooks that an elevated pressure greater than 20 mmHg for at least 5 minutes should be treated. However, this presents some problems: is the goal of management solely ICP control or is it maintenance of adequate cerebral perfusion? Are all patients the same regarding perfusion, elastance, and severity of injury? Should one number fit all? More importantly, what is the rationale for using 20 mmHg as the threshold?

It is not very clear when and how the threshold of 20 mmHg was consecrated as the holy grail of neurocritical care. Merritt and Fremont-Smith described in 1937 in their book *The Cerebrospinal Fluid* that after assessing the opening pressure during LPs of 1033 patients, they considered that

20 cmH₂O was an accurate threshold for high CSF pressure (Merritt and Fremont-Smith 1937). Of note, they reported the units in cm of water, but mercury is 13.6 times heavier than water. Millimeters of mercury generally have been used for ICP measurements to facilitate the calculation of the cerebral perfusion pressure, which takes into consideration the mean arterial pressure. W. Sharpe stated in 1920 in his book *Diagnosis and Treatment of Brain Injuries with and Without a Fracture of the Skull* that his principal indication for the operation of subtemporal decompression was a spinal fluid pressure above 15 mmHg (Sharpe 1920). In the 1960s Lundberg noticed that patients who sustained ICP values between 20 and 40 mmHg had worse outcomes when compared to those with ICP lower than 20 mmHg (Lundberg 1960). Douglas Miller and Donald Becker in the 1970s studied standardized treatments for ICP in traumatic brain injury (TBI) to keep ICP <30 mmHg and had significant improvement of outcomes. They observed a high mortality in patients who reached an ICP greater than 20 mmHg despite maximal therapy (Becker et al. 1977). Of note, the therapy included steroids and hyperventilation, methods shown later to worsen outcomes. Soon after, Lawrence Marshall used the threshold of 20 mmHg for therapy in a case series of TBI patients treated with pentobarbital (Marshall et al. 1979a), a study that many believe helped solidify this ICP threshold, as its initial findings were promising.

Finally, a landmark analysis of the Traumatic Coma Data Bank conducted by Anthony Marmarou identified 428 monitored patients and concluded that the proportion of total monitoring time that the pressure was higher than 20 mm Hg was an independent predictor of 6-month outcome (Marmarou et al. 1991). It is worth mentioning that the collected data reflect the care at that time and include therapies that are no longer used proscribed such as frequent mannitol doses, hyperventilation and steroids, as well as different approaches to cerebral perfusion pressure, such as using either induced hypotension to control ICP (Lund protocol (Asgeirsson et al. 1994)) or induced hypertension for supranormal CPP values (Rosner protocol (Rosner et al. 1995)), both of which are no longer used.

Not only is the fixed threshold of 20 mmHg based on scarce evidence, it also is not based on a strong physiological ground. As previously said, intracranial pressure measurement is used to indirectly infer intracranial volumes and elastance and is used as a surrogate indicator of resistance to blood flow into the brain by estimating CPP. In the end, what is essential for outcome is the maintenance of an appropriate CBF to help prevent further brain injury. In previous studies in which cerebral metabolism and oxygenation were measured, they demonstrated that brain metabolism can become deranged even when ICP and CPP are within the “normal” range (Le Roux et al. 1997; Purins et al. 2014; Stiefel et al. 2006). Since the 1980s, some authors have defended the concept of permissive intracranial hypertension and allow slight elevations of ICP as long as cerebral metabolism/oxygenation measured with the aid of additional monitoring is preserved (Chesnut et al. 2014; Miller 1985). This concept derives from the idea that treatment of excess of ICP can also be detrimental. Other important factors are the speed at which ICP increases and the compartmentalization of pressure, which both depend upon the disease process. Patients with brain tumors might progressively develop significant amount of mass effect but slowly, which allows for the compensatory mechanism to act and avoid major disturbances of CBF. Also, diffuse, non-compartmentalized high ICP such as in patients with idiopathic intracranial hypertension usually is well tolerated.

The landmark BEST TRIP trial was designed to further question reactive ICP therapy in severe TBI patients based on a fixed threshold. It compared two management protocols, one that involved ICP monitoring and the other that involved serial computed tomography (CT) brain imaging and neurologic examination. Neurological and mortality outcomes were similar (Chesnut et al. 2012). This trial should not discourage the use of ICP monitoring but rather question how we interpret it and how we react to it. ICP should be treated, but whether it should be performed in a proactive fashion, based on concerning findings on imaging and neuro exam, or if it should be used in reaction to a prespecified

threshold of pressure is still a matter of debate. It has been known for a long time that high ICP is a predictor for worse outcomes and higher mortality (Lundberg 1960; Becker et al. 1977; Marmarou et al. 1991; Marshall et al. 1979b), but the sensitivity of ICP values is low. The potential for worse outcomes increases at an ICP of 10 mmHg but only reaches 61% by 30 mmHg and with a cutoff value of around 35 mmHg which varied with the imaging classification in a study utilizing receiver-operating characteristic curves (Chambers et al. 2001). However, when death is excluded, intracranial hypertension is not independently predictive of morbidity (Chesnut et al. 2014). It also still is debated whether outcomes are affected by the way ICP is treated because of conflicting retrospective studies (Akopian et al. 2007; Shafi et al. 2008; Farahvar et al. 2012; Shen et al. 2016). Trials that focused on ICP control using hypothermia (Andrews et al. 2015), decompressive craniectomy (Hutchinson et al. 2016; Cooper et al. 2011), and barbiturates (Roberts and Sydenham 2012), among others, have been very successful in improving the pressure value but not outcome. A problem is that in several of these trials therapy only was initiated after a few minutes of ICP > 20 mmHg, in which case it is expected that the predictive value is low. Some researches defend the use of time-averaged ICP, or ICP “dose,” as being a better guide than single isolated measurements (Colton et al. 2016). It also has been argued that the therapies themselves are hurting patients or even that early brain injury plays a decisive role and after that further therapy is not helpful.

As the goal of therapy is to preserve CBF and prevent further brain insults, use of adjunct monitoring to assess brain metabolism (cerebral oxygenation, cerebral microdialysis) and tailor ICP is more physiologically sound. Based on this rationale, the recent BOOST II trial compared two treatment protocols in patients with severe TBI, one based on maintaining ICP lower than 20 mmHg and the other arm based on maintaining adequate brain oxygenation in conjunction with ICP control (Okonkwo et al. 2017). Even though this was a phase II trial, it showed a

remarkable benefit in the group that focused on cerebral oxygenation. Moreover, this group received less ICP therapy than the conventional arm, meaning that either further brain injury was prevented and less cerebral edema was generated or clinicians felt comfortable with lower levels of ICP elevations when cerebral oxygenation was preserved. Other studies have also suggested that individualized ICP therapy based on other variables such as cerebrovascular autoregulation (Lazaridis et al. 2014), ICP waveform (Balestreri et al. 2004; Kirkness et al. 2000), and intracranial compliance (Maset et al. 1987; Piper et al. 1993) might also be feasible. Nonetheless, the current evidence indicates that most likely one value does not fit all needs for every patient.

Current guidelines have challenged this notion. The 2014 Neurocritical Care Society (NCS) International Multidisciplinary Consensus Conference on Multimodality Monitoring proposed that “ICP and CPP monitoring be used to guide medical and surgical interventions and to detect life-threatening imminent herniation; however, the threshold value of ICP is uncertain based on the literature” (strong recommendation, high quality of evidence) (Chesnut et al. 2014). They also recommend tailoring the indications to the underlying brain pathology, avoiding use of ICP in isolation as a prognostic marker and, most importantly, to consider raising the treatment threshold for ICP in TBI patients when clinical evidence supports such a decision (i.e., ancillary oxygenation and metabolic monitoring of the brain, clinical exam, and neuroimaging). These recommendations were very innovative, as this was the first guideline not to reinforce strict adherence to a fixed threshold of ICP. Recently, the 2016 Brain Trauma Foundation *Guidelines for the Management of Severe Traumatic Brain Injury 4th Edition* brought more controversy to the management of ICP in TBI patients (Carney et al. 2017). Based on level IIB evidence that management of severe TBI patients with information from ICP monitoring reduces in-hospital and 2-week post-injury mortality, they recommended its use. More importantly, also based on level II B evidence, they suggested that “treating ICP above 22 mm Hg is recommended

because values above this level are associated with increased mortality.” This statement produced significant criticism as it was based solely on one level II study with 459 patients which used pressure reactivity index (PRx, which measures cerebrovascular autoregulation by plotting ICP versus mean arterial pressure in real time) and ICP to identify thresholds for unfavorable outcomes (Sorrentino et al. 2012). The guideline recognized the limitation and stated that “this study provides an overall low quality of the body of evidence about the target values for ICP when treating patients with severe TBI.” Finally, in line with the BEST TRIP trial results, it is also stated that there is level III evidence that a combination of ICP values and clinical and brain CT findings may be used to make management decisions.

Indications

ICP is an important variable in patients with an acute neurological disease. Monitoring ICP should not be discouraged, but rather needs to be interpreted appropriately. A device does not harm or save a patient and is highly dependent on the person interpreting the information and making decisions. Previous study analyses of the use of pulmonary artery catheters have taught us this lesson as well (Marik 2013). ICP is an epiphenomenon, likely reflecting several nonexclusive underlying pathophysiological processes (Chesnut 2015). ICP monitoring aids early detection of patients at risk of herniation due to ongoing worsening of a mass effect due to worsening edema or hemorrhage expansion, allows for CPP calculation, and offers adjunctive information for prognostication and decision-making for surgical interventions (Chesnut 2013). The 2014 NCS guidelines on multimodal monitoring suggest that ICP monitoring should be considered in patients “at risk for intracranial hypertension, i.e., patients in coma with CT imaging evidence of mass lesion(s), midline shift, dilatation of the contralateral ventricle, loss of the third ventricle, and obliteration of the perimesencephalic cisterns” (Chesnut et al. 2014). Also, an initial admission head CT may be normal in up to 50%

of patients who later develop raised ICP (Eisenberg et al. 1990). Narayan identified that among patients who had a normal CT scan on admission and who developed elevated ICP, the presence of age greater than 40 years, admission systolic blood pressure lower than 90 mmHg, or early uni- or bilateral motor posturing were predictive variables (Narayan et al. 1982). The incidence of elevated ICP was 60% when two or three of these variables were present, in comparison to 4% when none were present, which led to the suggestion in the NCS guidelines (but not anymore in the 2016 4th edition of the BTF guidelines) to consider this predictive model when deciding for ICP monitoring in TBI patients. Finally, while there is evidence that ICP above a threshold that is refractory to treatment is associated with poor outcome, some recent studies have reported that among young patients, 40% may survive and experience a favorable outcome, despite persistently elevated ICP (Resnick et al. 1997; Young et al. 2003).

Cerebral Perfusion Pressure

Perfusion pressure is defined, for most organs, as the difference between the inlet (arterial) and outlet (venous) pressures (Czosnyka et al. 2017). Because the brain sits inside the rigid skull, there is an intimate relation between ICP and venous pressure (VP). Normally, VP is higher than ICP in healthy individuals, but when ICP rises above venous pressure, compression occurs near the junction between the cortical veins and the draining sinuses. Blood flowing proximally will temporarily dilate the veins slightly above ICP to allow for drainage which leads to a fluttering diameter and critical closing pressure, with minimal difference between VP and ICP (Miller et al. 1972) as the collapse point. As a consequence, Douglas Miller in 1972 described that $CPP = MAP - ICP$ (Miller et al. 1972). He also showed in an animal model that CPP and CBF have a close relationship, depending upon whether cerebral autoregulation is preserved. In animals with intact regulation, CBF remained constant between CPP values of 50–150 mmHg,

a concept initially suggested by Lassen in 1959 (Lassen 1959). Conversely, in animals with compromised regulation (in a TBI model), CBF and CPP assumed a linear correlation (Miller et al. 1972).

The theory behind maintaining a target CPP is to try to minimize brain ischemia in cases of high ICP. There are some limitations to its use. We assume that the cerebral venous pressure is negligible to calculate the perfusion pressure, which is not always true depending on head positioning and elevation, cerebral venous sinus or jugular thrombosis, intrathoracic and intra-abdominal pressure, and neck compression (i.e., cervical collar). It also is presumed that the mean arterial pressure in the limbs (where it usually is measured) is the same that which reaches the circle of Willis. In his seminal work, Douglas Miller emphasized the need to use the MAP that likely reached the circle of Willis for an accurate calculation (Miller et al. 1972). The arterial pressure transducer should be leveled at the same height of the ICP transducer (both aiming for the tragus, an external anatomical landmark at the height of the foramina of Monro), in patients with an EVD. When utilizing an intraparenchymal probe, the arterial transducer should be leveled at the tragus. There can occur a difference as great as 10 mmHg of CPP depending if the arterial transducer is leveled at the level of the heart versus the brain (Depreitere et al. 2018; Livesay et al. 2017). In reality, there is no consistency when measuring CPP. A systematic review analyzed the 11 studies used in the BTF guidelines to determine thresholds for CPP (Depreitere et al. 2018). Head of bed elevation at 30° was part of the protocol in only five studies, patients were kept flat in one study, and in five studies, the head elevation was not even described. The arterial pressure transducer was leveled at the heart in merely five studies, at brain level in three studies, and was unknown in three studies. In another study, among 58 neurosurgical centers, there was high variability in how to measure MAP and the target CPP (Rao et al. 2013).

The BTF and NCS guidelines recommend aiming for a CPP value between 60 and 70 mmHg (Chesnut et al. 2014; Carney et al. 2017) although

this value could be affected by the relative positions of the ICP and arterial transducers. Previous studies have shown that values below 50 mmHg are associated with brain ischemia and above 70 mmHg with respiratory complications and worse outcomes (Rosner et al. 1995; Carney et al. 2017; Robertson et al. 1999). It is noteworthy that the approach to CPP in some of the studies was heterogeneous, as some centers utilize a protocol of decreasing vascular volume and adjusting systemic arterial pressure to control ICP (Asgeirsson et al. 1994), but other centers induce hypertension and hypervolemia to achieve supraphysiologic values of CPP (Rosner et al. 1995). Previous studies comparing an ICP-based approach versus a CPP-based approach in TBI patients did not show any significant difference in outcomes (Robertson et al. 1999).

More recently, researchers have been aiming to find the best method to identify the optimal CPP for each patient and at each time point. The physiologic background is solid, as CPP/CBF relationship is highly variable, depending on the state of autoregulation, intracranial elastance, and vessel resistance/elastic properties (highly age dependent), among other factors. In a recent study that compared PR_x (correlation between ICP and MAP), PA_x (correlation between pulse amplitude of ICP and MAP), and RAC (correlation between MAP and CPP), PR_x was the most accurate for detecting optimal CPP and had the best association with outcomes in TBI patients (Zeiler et al. 2018). Previous literature supports this finding by showing that when a U-shaped curve is drawn with PR_x values plotted against CPP at different values of MAP, the CPP values at which autoregulation is best preserved indicate the optimal CPP goal (Czosnyka et al. 2017). PR_x has been validated by utilizing transcranial Doppler and positron emission tomography scans (Czosnyka et al. 2017); negative values suggest preserved autoregulation, and positive values are associated with compromised regulation. Finally, another physiologic approach is to utilize the CPP range where cerebral oxygenation (Filippi et al. 2000) and metabolism (Zeiler et al. 2017) is preserved by utilizing methods such as described later in this chapter.

Cerebral Oxygenation

Even though the brain only represents 2–3% of body weight, it can consume up to 15–20% of the cardiac output (Arshad and Suarez 2013). Cerebral tissue predominantly uses glucose for energy and functions with a very high rate of oxygen consumption (CMRO₂), which means that even a subtle disruption of blood flow, oxygen delivery, and/or energetic crises can quickly lead to cell injury. Maintenance of adequate cerebral oxygenation is of the essence, and to monitor it requires information about oxygen supply and utilization in the CNS. Brain deoxygenation can be caused by many mechanisms, which include ischemic, cytopathic, anemic, diffusion, and hypoxic hypoxia. In many disease processes, brain hypoxia is one of the major drivers for secondary brain injury. For example, hypoxemia in TBI patients can almost double mortality (Carney et al. 2017). Moreover, ICP and CPP values within the “normal” range do not exclude the occurrence of brain hypoxia (Stiefel et al. 2006; Eriksson et al. 2012a; Gracias et al. 2004).

There are four major methods for measuring brain oxygenation: invasive probe placed in brain tissue to measure oxygen tension, near-infrared spectroscopy (NIRS), oxygen-15 positron emission tomography (PET), and jugular venous bulb oximetry.

Brain tissue O₂ can be defined as the partial pressure of O₂ in the interstitial space of the brain. There is some controversy in the literature as to whether the technique measures tissue oxygen pressure, which is the independent pressure exerted by a gaseous component of a multi-gaseous mixture, or tension (Le Roux and Oddo 2013) which is specific to O₂ dissolved in blood plasma. Furthermore, it is not known whether the Licox device measure reflects O₂ that diffused in brain parenchyma or if it reflects nearby vessels. Several abbreviations have been used in publications in the past to refer to the brain tissue oxygenation, including PtiO₂, PbrO₂, PbtO₂, PbO₂, and BTO₂, but a consensus conference in 2007 proposed that PbtO₂ should be used as the standard abbreviation (Le Roux and Oddo 2013). Previous studies have shown that the concentra-

tion of O₂ in brain tissue is <2%, with the vast majority of O₂ flowing intravascularly (Rosenthal et al. 2008). It is not completely understood how the balance between O₂ delivery and consumption affects PbtO₂, but Rosenthal studied TBI patients with probes for PbtO₂ and cerebral blood flow and demonstrated a multivariable analysis that PbtO₂ is primarily dependent on the cerebral blood flow times the difference in arterial and venous oxygen tension ($PbtO_2 = CBF \times AVTO_2$) (Rosenthal et al. 2008). Therefore, PbtO₂ somewhat reflects the dissolved O₂ within the plasma that readily diffuses across the blood-brain barrier rather than the entire O₂ content or cerebral metabolism (Rosenthal et al. 2008). With this, PbtO₂ is not an ischemia monitor per se, but low values imply that CBF and systemic PaO₂ are not appropriate for the patient in that specific time. In a lesser way, increased O₂ consumption by the brain in certain situations like fever, seizures, and shivering can also affect PbtO₂, as well as factors that influence the amount of dissolved plasma O₂ (temperature, PaCO₂, altitude, pH), cerebral autoregulation, and CO₂ reactivity.

There are two invasive methods that can be used to measure brain PbtO₂, the polarographic technique (using a Clark electrode) and optical luminescence. The first is the most commonly used. The PbtO₂ probe is inserted into the brain parenchyma in a similarly way as the insertion of an intraparenchymal ICP monitor; it generally is 3.0–3.5 cm below the dura mater. It continuously monitors an area of 13 mm² of white matter, while also providing information on brain temperature which is used to correct the PbtO₂ measurements. The probe normally is placed in a tissue at risk for injury, such as a specific vascular territory in a subarachnoid hemorrhage patient or the most injured hemisphere in a TBI patient, but catheters placed too close to a perilesional area may not work properly, as shown in some animal studies (Hawryluk et al. 2016).

Clinically, low PbtO₂ values (refer to Table 23.2 for threshold values in the literature) have been associated with worse neurological outcomes and increased mortality in TBI (Nangunoori et al. 2012; Oddo et al. 2011; Eriksson et al. 2012b; Meixensberger et al. 2004), intracerebral hemor-

Table 23.2 Threshold values for PbtO₂ from the published literature

Condition	PtiO ₂ values
Normal	25–50 mmHg
Hypoxic thresholds	
Mild/moderate	15–25 mmHg
Critical	<15 mmHg
Severe	<10 mmHg
Elevated	>50 mmHg

Table 23.3 Clinical situations associated to PbtO₂ value changes

Low PtiO ₂ (<20 mmHg)	High PtiO ₂ (>50 mmHg)
Increased consumption: Fever Seizures Cortical spreading depolarization Pain, shivering, agitation	Decreased consumption: Sedation Anesthesia Hypothermia
Decreased delivery: High intracranial pressure Decreased cardiac output Severe anemia Systemic deoxygenation Hypovolemia Hypotension Vasospasm, vessel obstruction	Increased delivery: Hyperperfusion (vasodilation, immediate reperfusion, or hyperdynamic state)

rhage (ICH) (Ko et al. 2011), and SAH (Ramakrishna et al. 2008) cohorts. As previously cited, a protocol of ICP-PbtO₂ compared to isolated ICP management has been shown to improve neurological outcomes in a phase II trial (Okonkwo et al. 2017), and in retrospective studies, PbtO₂-guided therapy seemed to help improve long-term functional outcomes in poor-grade SAH patients (Bohman et al. 2013). Also, PbtO₂ can be used to help investigate cerebral autoregulation (Hecht et al. 2011; Jaeger et al. 2006; Jaeger et al. 2007), with significant success in small clinical studies, including its use to identify optimal CPP targets (Ko et al. 2011; Radolovich et al. 2010). Table 23.3 describes clinical situations associated to PbtO₂ value changes.

Jugular venous bulb oximetry (JVBO) and NIRS are other ways of assessing intracranial oxygenation continuously in the neurocritical care patient, but they are much less used than the PbtO₂. JVBO was the first used bedside monitor of cerebral oxygenation, but its use suffered a fast decline in the past years due to several technical difficulties and the fact that it monitors a global measure of cerebral oxygenation and only provides a rough estimate of the adequacy of cerebral perfusion. Its physiological basis is that unmatched cerebral O₂ demand in relation to inadequate supply leads to increase O₂ extraction and a lower saturation of the jugular blood. No studies have confirmed a significant benefit of S_{jv} O₂-based protocols on outcomes. NIRS is a noninvasive technique that is based on the transmission and absorption of near-infrared light as it travels through the tissues. Most commercially available devices measure regional cerebral oxygen saturation (rSc O₂) with high temporal and spatial resolution, which allows for continuous and simultaneous monitoring of several areas of interest. Some of the disadvantages are the fact that threshold values for hypoxia/ischemia are largely unknown and that the technique calculates the rSc O₂ based on arterial, venous, and capillary blood within the field of view and algorithms that compensate for signal contamination from extra-cerebral blood (e.g., subcutaneous and skull tissues). There is no evidence that NIRS has impacted outcomes of neurological patients. Table 23.4 compares the three bedside techniques of cerebral oxygenation monitoring. The utilization of PET scans for cerebral oxygenation monitoring is beyond the scope of this chapter, as it provides a static measurement and it mostly is utilized for research purposes.

A brain O₂ monitor is not intended to be used alone, and it should be used as a complement to other techniques, such as ICP monitoring. It can help determine if the therapies offered to a patient, including ICP control, hemodynamic goals such as targeted cardiac output, MAP, PaO₂/SpO₂, hemoglobin concentration, temperature control, and shivering, among others, are adequate for a fine balance of brain oxygenation.

Table 23.4 Comparison of different techniques of cerebral oxygenation monitoring

Advantages	Limitations
PbtO₂: Continuous measurements Provides brain temperature Local tissue information Can be placed in the same bolt with ICP and microdialysis Method with most evidence support (including intervention-based therapies) Help assess cerebral autoregulation High correlation with CBF and AVTO ₂	Invasive Complications: bleeding and infection (rare) Focal monitoring (highly dependent on area of interest) Prone to dislocation of the catheter Drift of values after a few days Less influenced by CMRO ₂
SjvO₂ (jugular venous bulb oximetry): Continuous measurements (if using oximetry catheter) Global cerebral oximetry monitor	Invasive Complications: jugular thrombosis, hematoma, carotid puncture, infection Global cerebral monitor (insensitive to focal ischemia) Results might be confounded by venous blood from facial veins Jugular veins normally drain different areas of the brain (one side the superficial veins and the contralateral side the deep venous system) Frequent blood draws (if oximetry catheter not available) Assumes stable CMRO ₂ to infer CBF changes
NIRS: Noninvasive Continuous measurements Able to monitor several areas simultaneously Mostly utilized in the OR in carotid and cardiac surgeries	Frequent loss of signal Threshold levels for ischemia/hypoxia unknown Signal can be contaminated by vessels superficial to the brain Signal can be contaminated by venous vessels Only monitor relative changes in oxygenation rScO ₂ algorithms utilized by commercial devices vary substantially and are largely unpublished

Cerebral Microdialysis

Cerebral microdialysis (CMD) is an invasive method for the assessment of brain metabolism. It is used clinically to measure extracellular interstitial concentrations of small molecules (around 20 kDa in a regular CMD probe). It uses an extremely thin catheter (0.9 mm in diameter), with a semipermeable membrane at its tip. A pump infuses a dialysate through the catheter which is later drained back and analyzed in a point-of-care device. The substrates present within the extracellular fluid in a volume of 1 mm³ of subcortical white matter (roughly 2 cm from the inner table of the skull) reach concentration equilibrium with the dialysate, which allows detection of molecules highly dependent on their size and the speed utilized in the CMD pump (usually 0.3microL/min). The microvial with dialysate is analyzed normally every hour and requires substantial bedside work. Technically,

any molecule that can cross the semipermeable membrane can be measured. Usually glucose, lactate, and pyruvate are the ones of highest interest, but many institutions also measure glutamate and glycerol in their protocols. Physiologically, CMD measures the response of brain tissue to insults (ischemia, hypoxia, ICP elevations, changes in temperature, seizures, etc.). In a very simplified manner, the PbtO₂ catheter monitors what is offered to the mitochondria, and the CMD probe analyzes how its metabolism is affected. As with the PbtO₂ monitor, CMD only monitors a small area of white matter, being a regional monitor of cerebral metabolism. As example of metabolic derangements, ischemia can lead to increases in lactate and decrease in pyruvate concentrations through disruption of the Krebs cycle and induction of anerobic metabolism from an energetic crisis. This leads to an increase in the lactate-to-pyruvate ratio (LPR), which is the most sensitive measurement of ischemia detection

with CMD. Table 23.5 shows cutoff values for some CMD measurements, and Table 23.6 further depicts common metabolic derangements encountered and the most probable causes. The concentrations of glutamate (an excitotoxic neurotransmitter) and glycerol (a component of the cell wall) can be elevated after some insults, but they are less sensitive to acute metabolic changes and not as clearly associated with neurological outcomes as the other substrates. In patients with SAH, LPR has been shown to detect delayed cerebral ischemia (DCI) with a very high sensitivity (Sarrafzadeh et al. 2002), with values increasing as early as 11–13 hours prior to the clinical onset (Skjoth-Rasmussen et al. 2004). CMD can aid in the detection of CPP thresholds in neurologically critically ill patients (Ko et al. 2011; Schmidt et al. 2011) and detect energetic crisis that can occur when ICP and CPP are within “normal” values and thus provide a more

patient-based approach (Chen et al. 2011). In a recent systematic review involving TBI patients, the occurrence of metabolic derangements was associated with a worse functional outcome (Zeiler et al. 2017). CMD monitoring also has allowed interesting insights into brain metabolism, such as occurrence of cerebral hypoglycemia with systemic euglycemia (Helbok et al. 2010), that strict glucose control can lead to cerebral energetic crisis (Schmidt et al. 2012), that red blood cell transfusions lead to better cerebral oxygenation but do not improve ischemia markers (Kurtz et al. 2016), that cortical spreading depressions trigger metabolic derangements (Pinczolics et al. 2017), and that elevations of pyruvate and lactate in TBI patients are a mechanism of neuroprotection (Sala et al. 2013). CMD probe can be technically placed almost anywhere in the skull, either through a bolt or by tunneling.

A Consensus Meeting on Microdialysis in Neurointensive Care which involved several European centers was published in 2004 and suggested that CMD should be placed in the tissue at risk (most likely the parent vessel territory) in SAH patients and for TBI, “in patients with diffuse injury one catheter may be placed in the right frontal region. In patients with focal mass lesions one catheter should be placed in pericontusional tissue. A second catheter may be placed in normal tissue. The catheter should not be placed in contusional tissue” (Bellander et al. 2004). Several institutions have adopted the placement of a three-port bolt, simultaneous placement of an ICP monitor, CMD, and Pb O₂ catheters. The advantage of this approach is

Table 23.5 Threshold values for CMD from the published literature

Microdialysis	Value
Glucose	<0.8 mmol/L = warning <0.2 mmol/L = critical
Lactate	>4 mmol/L
Pyruvate	<70 μmol/L indicates ischemia (also hypoglycemia) Normal-to-elevated (>120 μmol/L) indicates hyperglycolysis and/or mitochondrial dysfunction
LPR	>25 warning >40 = critical
Others: glycerol, AA, glutamate	

Table 23.6 Interpretation of some metabolic derangements in CMD

Measurement	Cause	Comment
Low glucose	Serum hypoglycemia Ischemia/hypoxia Consumption: fever, seizures	Check peripheral glucose
Increased LPR	Ischemia/hypoxia Consumption: fever, seizures	Best marker for ischemia/hypoxia Most studied outcomes and detection
High lactate and pyruvate	Adaptive mechanism	Neuroprotection (TBI)
Normal glucose, raised lactate, normal/low pyruvate	Mitochondrial dysfunction (?), inflammation (?)	Drug related (?) TBI (?)

ability to monitor the delivery of CBF/O₂ and the response of brain cells to the applied treatment which helps further clarify the clinical situations were a single measure might miss conditions such as:

- Low CMD glucose: systemic hypoglycemia vs ischemia
- High CMD LPR: mitochondrial dysfunction vs ischemia
- Low PbtO₂: ischemia vs diffusion hypoxia
- Low PbtO₂ and normal ICP: hypoxia/ischemia vs increased consumption

Electrophysiology

In 1924, the German psychiatrist Hans Berger made the first recording of the electric field of the human brain in patients with skull defects; he called the measurement the electroencephalogram (EEG) (Stone and Hughes 2013). The EEG represents the spontaneous electrical activity of the brain, and the evoked potentials represent the components of the EEG that arise in response to specific stimuli, such as auditory, visual, or tactile.

EEG can be performed intermittently (iEEG), in periods of 20–120 minutes, or continuously (cEEG), often for several days. cEEG has become more popular in the late 1990s with the popularization of digital platforms to replace the previous analog systems and databases that allow storing of the enormous amounts of digital information (Horn et al. 2013).

The most common indication for cEEG in the ICU is the suspicion of seizure activity. Clinical seizures are for the most part easy to identify and do not require EEG to initiate therapy, but in patients who do not fully recover consciousness after a clinical seizure or in critically ill patients with impaired consciousness in whom clinical diagnosis of a seizure may be difficult, EEG is of essence to further evaluate the presence of non-convulsive seizures (NCS) or subclinical seizures. NCS can occur in 11–55% of patients admitted in an ICU primarily due to a brain injury (Claassen et al. 2004, 2013; Jordan 1995;

Kramer et al. 2012; Lowenstein and Aminoff 1992). The actual prevalence is not clear because older studies used different definitions for electrographic epileptic activity and some studies included sedated patients, but NCS is an entity that cannot be disregarded in modern critical care. NCS is most commonly observed among patients with SAH, ICH, TBI, ischemic stroke, encephalitis, and after therapeutic hypothermia post-cardiac arrest (Claassen et al. 2013), but it has been also reported in patients with sepsis (Hosokawa et al. 2014) and hepatic encephalopathy (Prabhakar and Bhatia 2003), among other disease processes. Also, NCS has been reported in roughly 8–10% of patients with unexplained coma or impaired consciousness and with no prior history of clinical seizures (Herman et al. 2015). Finally, NCS has been associated in small observational and retrospective studies with increased ICP (Vespa et al. 2007), increased cerebral edema and midline shift (Vespa et al. 2003), occurrences of cortical spreading depression (Dreier et al. 2012), metabolic disturbances in CMD (Vespa et al. 2002, 1998), and decreases in cerebral oxygenation (Witsch et al. 2017), suggesting that it might be involved in secondary brain injury.

In comatose patients, cEEG should be monitored for at least 24–48 h to exclude NCS, as roughly 50% of the seizures occur within the first hour of monitoring (Horn et al. 2013); in 88% of patients, seizures are recorded within the first 24 hours, and the remaining 5% occur within the first 48 h with 7% beyond that (Claassen et al. 2004). The progress in software and digital transformation of EEG data has allowed great progresses in electrophysiology monitoring and creation of the quantitative analysis of cEEG. This has been a groundbreaking achievement in the area of electroencephalography and has permitted a rapid and sensitive analysis of massive amounts of EEG data, which would have required hours or days to process if only an analogical analysis was performed. One of the most commonly used analytical methods is color density spectral array, a technique that applies fast-Fourier transformation to convert raw EEG data into a time-compressed and color-coded display (Horn et al. 2013). This

allows rapid visual detection of possible seizure activity, even by healthcare personnel without dedicated training in electrophysiology. Quantitative analysis also more recently has permitted the use of monitoring to tailor levels of sedation and perform real-time ischemia monitoring. Electroencephalography is also of great aid in the diagnosis of brain death and of neurological prognostication in post-cardiac arrest survivors. More recently, EEG has become a tool for identifying patients in minimally conscious state (Engemann et al. 2018). Finally, a recent study has suggested that patients monitored with cEEG leads to lower mortality, primarily among patients with SAH and ICH, but it is not clear if the monitoring itself changed outcomes or whether it was because cEEG is performed in critical care units that are more dedicated to the care of neurologically ill patients (Hill et al. 2019).

Take-Home Points

Multimodal monitoring is a reality in modern neurocritical care. In the near future, it might aid further development of precision medicine (Shrestha et al. 2018). However, the excess of information could also lead to increased confusion for the non-experienced clinician, potentially resulting in further injuries, as shown with the demise of invasive pulmonary artery pressure monitoring. Devices do not change outcomes, but they can provide vital information for decision-making in complicated patients. Finally, the pillar of neurocritical care, and the gold standard technique for monitoring neurologically ill patients, is a trained and dedicated team who has skills in the neurological exam.

References

Akopian G, Gaspard DJ, Alexander M. Outcomes of blunt head trauma without intracranial pressure monitoring. *Am Surg.* 2007;73:447–50.
 Albeck MJ, Borgesen SE, Gjerris F, Schmidt JF, Sorensen PS. Intracranial pressure and cerebrospinal fluid out-

flow conductance in healthy subjects. *J Neurosurg.* 1991;74:597–600.
 Andrews PJ, Citerio G. Intracranial pressure. Part one: historical overview and basic concepts. *Intensive Care Med.* 2004;30:1730–3.
 Andrews PJ, Sinclair HL, Rodriguez A, et al. Hypothermia for intracranial hypertension after traumatic brain injury. *N Engl J Med.* 2015;373:2403–12.
 Arshad S, Suarez J. Why monitor and principles of neurocritical care. In: Le Roux P, Levine J, Kofke A, editors. *Monitoring in Neurocritical care.* Philadelphia: Elsevier; 2013.
 Asgeirsson B, Grande PO, Nordstrom CH. A new therapy of post-trauma brain oedema based on haemodynamic principles for brain volume regulation. *Intensive Care Med.* 1994;20:260–7.
 Balestreri M, Czosnyka M, Steiner LA, et al. Intracranial hypertension: what additional information can be derived from ICP waveform after head injury? *Acta Neurochir.* 2004;146:131–41.
 Becker DP, Miller JD, Ward JD, Greenberg RP, Young HF, Sakalas R. The outcome from severe head injury with early diagnosis and intensive management. *J Neurosurg.* 1977;47:491–502.
 Bellander BM, Cantais E, Enblad P, et al. Consensus meeting on microdialysis in neurointensive care. *Intensive Care Med.* 2004;30:2166–9.
 Bering EA Jr. Choroid plexus and arterial pulsation of cerebrospinal fluid; demonstration of the choroid plexuses as a cerebrospinal fluid pump. *AMA Arch Neurol Psychiatry.* 1955;73:165–72.
 Bohman LE, Pisapia JM, Sanborn MR, et al. Response of brain oxygen to therapy correlates with long-term outcome after subarachnoid hemorrhage. *Neurocrit Care.* 2013;19:320–8.
 Bratton SL, Chestnut RM, Ghajar J, et al. Guidelines for the management of severe traumatic brain injury. VII. Intracranial pressure monitoring technology. *J Neurotrauma.* 2007;24(Suppl 1):S45–54.
 Burrows G. *On disorders of the cerebral circulation and on the connection between affections of the brain and diseases of the heart.* Philadelphia: Lea & Blanchard; 1848.
 Calviello LA, de Riva N, Donnelly J, et al. Relationship between brain pulsatility and cerebral perfusion pressure: replicated validation using different drivers of CPP change. *Neurocrit Care.* 2017;27:392–400.
 Cardoso ER, Rowan JO, Galbraith S. Analysis of the cerebrospinal fluid pulse wave in intracranial pressure. *J Neurosurg.* 1983;59:817–21.
 Carney N, Totten AM, O'Reilly C, et al. Guidelines for the management of severe traumatic brain injury, fourth edition. *Neurosurgery.* 2017;80:6–15.
 Castellani G, Zweifel C, Kim DJ, et al. Plateau waves in head injured patients requiring neurocritical care. *Neurocrit Care.* 2009;11:143–50.
 Chambers IR, Treadwell L, Mendelow AD. Determination of threshold levels of cerebral perfusion pressure

- and intracranial pressure in severe head injury by using receiver-operating characteristic curves: an observational study in 291 patients. *J Neurosurg.* 2001;94:412–6.
- Chapman PH, Cosman ER, Arnold MA. The relationship between ventricular fluid pressure and body position in normal subjects and subjects with shunts: a telemetric study. *Neurosurgery.* 1990;26:181–9.
- Chen HI, Stiefel MF, Oddo M, et al. Detection of cerebral compromise with multimodality monitoring in patients with subarachnoid hemorrhage. *Neurosurgery.* 2011;69:53–63; discussion.
- Chesnut R. Intracranial pressure. In: Le Roux P, Levine J, Kofke A, editors. *Monitoring in neurocritical care.* Philadelphia: Elsevier; 2013.
- Chesnut RM. What is wrong with the tenets underpinning current management of severe traumatic brain injury? *Ann N Y Acad Sci.* 2015;1345:74–82.
- Chesnut RM, Temkin N, Carney N, et al. A trial of intracranial-pressure monitoring in traumatic brain injury. *N Engl J Med.* 2012;367:2471–81.
- Chesnut R, Videtta W, Vespa P, Le Roux P. Intracranial pressure monitoring: fundamental considerations and rationale for monitoring. *Neurocrit Care.* 2014;21(Suppl 2):S64–84.
- Claassen J, Mayer SA, Kowalski RG, Emerson RG, Hirsch LJ. Detection of electrographic seizures with continuous EEG monitoring in critically ill patients. *Neurology.* 2004;62:1743–8.
- Claassen J, Taccone FS, Horn P, Holtkamp M, Stocchetti N, Oddo M. Recommendations on the use of EEG monitoring in critically ill patients: consensus statement from the neurointensive care section of the ESICM. *Intensive Care Med.* 2013;39:1337–51.
- Colton K, Yang S, Hu PF, et al. Pharmacologic treatment reduces pressure times time dose and relative duration of intracranial hypertension. *J Intensive Care Med.* 2016;31:263–9.
- Cooper DJ, Rosenfeld JV, Murray L, et al. Decompressive craniectomy in diffuse traumatic brain injury. *N Engl J Med.* 2011;364:1493–502.
- Cushing H. Concerning a definite regulatory mechanism of the vasomotor centre which controls blood pressure during cerebral compression Johns Hopkins Hospital. *Bulletin.* 1901;12:290–2.
- Cushing H. *The third circulation in studies in intracranial physiology and surgery.* London: Oxford University Press; 1926.
- Czosnyka M, Pickard JD. Monitoring and interpretation of intracranial pressure. *J Neurol Neurosurg Psychiatry.* 2004;75:813–21.
- Czosnyka M, Price DJ, Williamson M. Monitoring of cerebrospinal dynamics using continuous analysis of intracranial pressure and cerebral perfusion pressure in head injury. *Acta Neurochir.* 1994;126:113–9.
- Czosnyka M, Smielewski P, Kirkpatrick P, Laing RJ, Menon D, Pickard JD. Continuous assessment of the cerebral vasomotor reactivity in head injury. *Neurosurgery.* 1997;41:11–7; discussion 7–9
- Czosnyka M, Pickard JD, Steiner LA. Principles of intracranial pressure monitoring and treatment. *Handb Clin Neurol.* 2017;140:67–89.
- Depreitere B, Meyfroidt G, Guiza F. What do we mean by cerebral perfusion pressure? *Acta Neurochir Suppl.* 2018;126:201–3.
- Dreier JP, Major S, Pannek HW, et al. Spreading convulsions, spreading depolarization and epileptogenesis in human cerebral cortex. *Brain.* 2012;135:259–75.
- Egawa S, Hifumi T, Kawakita K, et al. Impact of neurointensivist-managed intensive care unit implementation on patient outcomes after aneurysmal subarachnoid hemorrhage. *J Crit Care.* 2016;32:52–5.
- Ehtisham A, Taylor S, Bayless L, Klein MW, Janzen JM. Placement of external ventricular drains and intracranial pressure monitors by neurointensivists. *Neurocrit Care.* 2009;10:241–7.
- Eisenberg HM, Gary HE Jr, Aldrich EF, et al. Initial CT findings in 753 patients with severe head injury. A report from the NIH Traumatic Coma Data Bank. *J Neurosurg.* 1990;73:688–98.
- Engemann DA, Raimondo F, King JR, et al. Robust EEG-based cross-site and cross-protocol classification of states of consciousness. *Brain.* 2018;141:3179–92.
- Eriksson EA, Barletta JF, Figueroa BE, et al. Cerebral perfusion pressure and intracranial pressure are not surrogates for brain tissue oxygenation in traumatic brain injury. *Clin Neurophysiol.* 2012a;123:1255–60.
- Eriksson EA, Barletta JF, Figueroa BE, et al. The first 72 hours of brain tissue oxygenation predicts patient survival with traumatic brain injury. *J Trauma Acute Care Surg.* 2012b;72:1345–9.
- Farahvar A, Gerber LM, Chiu YL, Carney N, Hartl R, Ghajar J. Increased mortality in patients with severe traumatic brain injury treated without intracranial pressure monitoring. *J Neurosurg.* 2012;117:729–34.
- Filippi R, Reisch R, Mauer D, Pernecky A. Brain tissue pO₂ related to SjvO₂, ICP, and CPP in severe brain injury. *Neurosurg Rev.* 2000;23:94–7.
- Gracias VH, Guillaumondegui OD, Stiefel MF, et al. Cerebral cortical oxygenation: a pilot study. *J Trauma.* 2004;56:469–72. discussion 72–4
- Greitz D, Wirestam R, Franck A, Nordell B, Thomsen C, Stahlberg F. Pulsatile brain movement and associated hydrodynamics studied by magnetic resonance phase imaging. The Monro-Kellie doctrine revisited. *Neuroradiology.* 1992;34:370–80.
- Hall A, O’Kane R. The best marker for guiding the clinical management of patients with raised intracranial pressure—the RAP index or the mean pulse amplitude? *Acta Neurochir.* 2016;158:1997–2009.
- Harary M, Dolmans RGF, Gormley WB. Intracranial pressure monitoring—review and avenues for development. *Sensors (Basel, Switzerland).* 2018;18

- Hawryluk GW, Phan N, Ferguson AR, et al. Brain tissue oxygen tension and its response to physiological manipulations: influence of distance from injury site in a swine model of traumatic brain injury. *J Neurosurg*. 2016;125:1217–28.
- Hecht N, Fiss I, Wolf S, Barth M, Vajkoczy P, Woitzik J. Modified flow- and oxygen-related autoregulation indices for continuous monitoring of cerebral autoregulation. *J Neurosci Methods*. 2011;201:399–403.
- Helbok R, Schmidt JM, Kurtz P, et al. Systemic glucose and brain energy metabolism after subarachnoid hemorrhage. *Neurocrit Care*. 2010;12:317–23.
- Herman ST, Abend NS, Bleck TP, et al. Consensus statement on continuous EEG in critically ill adults and children, part I: indications. *J Clin Neurophysiol*. 2015;32:87–95.
- Hill CE, Blank LJ, Thibault D, et al. Continuous EEG is associated with favorable hospitalization outcomes for critically ill patients. *Neurology*. 2019;92:e9–e18.
- Horn P, Oddo M, Schmitt S. Electroencephalography. In: Le Roux P, Levine J, Kofke A, editors. *Monitoring in neurocritical care*. Philadelphia: Elsevier; 2013.
- Hosokawa K, Gaspard N, Su F, Oddo M, Vincent JL, Taccone FS. Clinical neurophysiological assessment of sepsis-associated brain dysfunction: a systematic review. *Crit Care (London, England)*. 2014;18:674.
- Hutchinson PJ, Kolias AG, Timofeev IS, et al. Trial of decompressive craniectomy for traumatic intracranial hypertension. *N Engl J Med*. 2016;375:1119–30.
- Jaeger M, Schuhmann MU, Soehle M, Meixensberger J. Continuous assessment of cerebrovascular autoregulation after traumatic brain injury using brain tissue oxygen pressure reactivity. *Crit Care Med*. 2006;34:1783–8.
- Jaeger M, Schuhmann MU, Soehle M, Nagel C, Meixensberger J. Continuous monitoring of cerebrovascular autoregulation after subarachnoid hemorrhage by brain tissue oxygen pressure reactivity and its relation to delayed cerebral infarction. *Stroke*. 2007;38:981–6.
- Jordan KG. Neurophysiologic monitoring in the neuroscience intensive care unit. *Neurol Clin*. 1995;13:579–626.
- Kasprowicz M, Lalou DA, Czosnyka M, Garnett M, Czosnyka Z. Intracranial pressure, its components and cerebrospinal fluid pressure-volume compensation. *Acta Neurol Scand*. 2016;134:168–80.
- Kellie G. An account of the appearances observed in the dissection of two of the three individuals presumed to have perished in the storm of the 3rd, and whose bodies were discovered in the vicinity of Leith on the morning of the 4th November 1821 with some reflections on the pathology of the brain. *Trans Med Chir Sci*. 1824;1:84–169.
- Kirkness CJ, Mitchell PH, Burr RL, March KS, Newell DW. Intracranial pressure waveform analysis: clinical and research implications. *J Neurosci Nurs*. 2000;32:271–7.
- Ko SB, Choi HA, Parikh G, et al. Multimodality monitoring for cerebral perfusion pressure optimization in comatose patients with intracerebral hemorrhage. *Stroke*. 2011;42:3087–92.
- Korbakis G, Bleck T. The evolution of neurocritical care. *Crit Care Clin*. 2014;30:657–71.
- Kramer AH, Jette N, Pillay N, Federico P, Zygun DA. Epileptiform activity in neurocritical care patients. *Can J Neurol Sci Le journal canadien des sciences neurologiques*. 2012;39:328–37.
- Kurtz P, Helbok R, Claassen J, et al. The effect of packed red blood cell transfusion on cerebral oxygenation and metabolism after subarachnoid hemorrhage. *Neurocrit Care*. 2016;24:118–21.
- Lang JM, Beck J, Zimmermann M, Seifert V, Raabe A. Clinical evaluation of intraparenchymal Spiegelberg pressure sensor. *Neurosurgery*. 2003;52:1455–9. discussion 9
- Lang EW, Kasprowicz M, Smielewski P, Pickard J, Czosnyka M. Changes in cerebral partial oxygen pressure and cerebrovascular reactivity during intracranial pressure plateau waves. *Neurocrit Care*. 2015;23:85–91.
- Langfitt TW, Weinstein JD, Kassell NF, Simeone FA. Transmission of increased intracranial pressure. I. Within the craniospinal axis. *J Neurosurg*. 1964;21:989–97.
- Lassen NA. Cerebral blood flow and oxygen consumption in man. *Physiol Rev*. 1959;39:183–238.
- Lazaridis C, DeSantis SM, Smielewski P, et al. Patient-specific thresholds of intracranial pressure in severe traumatic brain injury. *J Neurosurg*. 2014;120:893–900.
- Le Roux P, Oddo M. Brain oxygen. In: Le Roux P, Levine J, Kofke A, editors. *Monitoring in neurocritical care*. Philadelphia: Elsevier; 2013.
- Le Roux PD, Newell DW, Lam AM, Grady MS, Winn HR. Cerebral arteriovenous oxygen difference: a predictor of cerebral infarction and outcome in patients with severe head injury. *J Neurosurg*. 1997;87:1–8.
- Livesay SL, McNett MM, Keller M, Olson DM. Challenges of cerebral perfusion pressure measurement. *J Neurosci Nurs*. 2017;49:372–6.
- Livramento JA, Machado LR. The history of cerebrospinal fluid analysis in Brazil. *Arq Neuropsiquiatr*. 2013;71:649–52.
- Lowenstein DH, Aminoff MJ. Clinical and EEG features of status epilepticus in comatose patients. *Neurology*. 1992;42:100–4.
- Lundberg N. Continuous recording and control of ventricular fluid pressure in neurosurgical practice. *Acta Psychiatr Scand Suppl*. 1960;36:1–193.
- Marik PE. Obituary: pulmonary artery catheter 1970 to 2013. *Ann Intensive Care*. 2013;3:38.

- Marmarou A, Anderson R, Ward J. Impact of ICP instability and hypotension on outcome in patients with severe head trauma. *J Neurosurg.* 1991;75:S159–S66.
- Marshall LF, Smith RW, Shapiro HM. The outcome with aggressive treatment in severe head injuries. Part II: acute and chronic barbiturate administration in the management of head injury. *J Neurosurg.* 1979a;50:26–30.
- Marshall LF, Smith RW, Shapiro HM. The outcome with aggressive treatment in severe head injuries. Part I: the significance of intracranial pressure monitoring. *J Neurosurg.* 1979b;50:20–5.
- Mascarenhas S, Vilela GH, Carlotti C, et al. The new ICP minimally invasive method shows that the Monro-Kellie doctrine is not valid. *Acta Neurochir Suppl.* 2012;114:117–20.
- Maset AL, Marmarou A, Ward JD, et al. Pressure-volume index in head injury. *J Neurosurg.* 1987;67:832–40.
- Meixensberger J, Renner C, Simanowski R, Schmidtke A, Dings J, Roosen K. Influence of cerebral oxygenation following severe head injury on neuropsychological testing. *Neurol Res.* 2004;26:414–7.
- Merritt H, Fremont-Smith F. *The cerebrospinal fluid.* Philadelphia: W. B. Saunders Co; 1937.
- Miller JD. Intracranial pressure monitoring. *Arch Neurol.* 1985;42:1191–3.
- Miller JD, Stanek A, Langfitt TW. Concepts of cerebral perfusion pressure and vascular compression during intracranial hypertension. *Prog Brain Res.* 1972;35:411–32.
- Monro A. Observations on the structure and function of the nervous system. Creech & Johnson: Edinburgh; 1823.
- Nangunoori R, Maloney-Wilensky E, Stiefel M, et al. Brain tissue oxygen-based therapy and outcome after severe traumatic brain injury: a systematic literature review. *Neurocrit Care.* 2012;17:131–8.
- Narayan RK, Kishore PR, Becker DP, et al. Intracranial pressure: to monitor or not to monitor? A review of our experience with severe head injury. *J Neurosurg.* 1982;56:650–9.
- Oddo M, Levine JM, Mackenzie L, et al. Brain hypoxia is associated with short-term outcome after severe traumatic brain injury independently of intracranial hypertension and low cerebral perfusion pressure. *Neurosurgery.* 2011;69:1037–45; discussion 45.
- Okonkwo DO, Shutter LA, Moore C, et al. Brain oxygen optimization in severe traumatic brain injury phase-II: a phase II randomized trial. *Crit Care Med.* 2017;45:1907–14.
- Piek J, Bock WJ. Continuous monitoring of cerebral tissue pressure in neurosurgical practice--experiences with 100 patients. *Intensive Care Med.* 1990;16:184–8.
- Pinczolits A, Zdunczyk A, Dengler NF, et al. Standard-sampling microdialysis and spreading depolarizations in patients with malignant hemispheric stroke. *J Cereb Blood Flow Metab.* 2017;37:1896–905.
- Piper IR, Chan KH, Whittle IR, Miller JD. An experimental study of cerebrovascular resistance, pressure transmission, and craniospinal compliance. *Neurosurgery.* 1993;32:805–15; discussion 15–6.
- Prabhakar S, Bhatia R. Management of agitation and convulsions in hepatic encephalopathy. *Indian J Gastroenterol.* 2003;22(Suppl 2):S54–8.
- Purins K, Lewen A, Hillered L, Howells T, Enblad P. Brain tissue oxygenation and cerebral metabolic patterns in focal and diffuse traumatic brain injury. *Front Neurol.* 2014;5:64.
- Raboeuf PH, Bartek J Jr, Andresen M, Bellander BM, Romner B. Intracranial pressure monitoring: invasive versus non-invasive methods-a review. *Crit Care Res Pract.* 2012;2012:950393.
- Radolovich DK, Czosnyka M, Timofeev I, et al. Transient changes in brain tissue oxygen in response to modifications of cerebral perfusion pressure: an observational study. *Anesth Analg.* 2010;110:165–73.
- Ramakrishna R, Stiefel M, Udoetuk J, et al. Brain oxygen tension and outcome in patients with aneurysmal subarachnoid hemorrhage. *J Neurosurg.* 2008;109:1075–82.
- Rao V, Klepstad P, Losvik OK, Solheim O. Confusion with cerebral perfusion pressure in a literature review of current guidelines and survey of clinical practice. *Scandinavian J Trauma Resusc Emerg Med.* 2013;21:78.
- Resnick DK, Marion DW, Carlier P. Outcome analysis of patients with severe head injuries and prolonged intracranial hypertension. *J Trauma.* 1997;42:1108–11.
- Roberts I, Sydenham E. Barbiturates for acute traumatic brain injury. *Cochrane Database Syst Rev.* 2012;12:Cd000033.
- Robertson CS, Valadka AB, Hannay HJ, et al. Prevention of secondary ischemic insults after severe head injury. *Crit Care Med.* 1999;27:2086–95.
- Rosenthal G, Hemphill JC 3rd, Sorani M, et al. Brain tissue oxygen tension is more indicative of oxygen diffusion than oxygen delivery and metabolism in patients with traumatic brain injury. *Crit Care Med.* 2008;36:1917–24.
- Rosner MJ, Becker DP. Origin and evolution of plateau waves. Experimental observations and a theoretical model. *J Neurosurg.* 1984;60:312–24.
- Rosner MJ, Rosner SD, Johnson AH. Cerebral perfusion pressure: management protocol and clinical results. *J Neurosurg.* 1995;83:949–62.
- Sadaka F, Kasal J, Lakshmanan R, Palagiri A. Placement of intracranial pressure monitors by neurointensivists: case series and a systematic review. *Brain Inj.* 2013;27:600–4.
- Sahuquillo J, Poca MA, Arribas M, Garnacho A, Rubio E. Interhemispheric supratentorial intracranial pressure gradients in head-injured patients: are they clinically important? *J Neurosurg.* 1999;90:16–26.

- Sala N, Suys T, Zerlauth JB, et al. Cerebral extracellular lactate increase is predominantly nonischemic in patients with severe traumatic brain injury. *J Cereb Blood Flow Metab.* 2013;33:1815–22.
- Samuels O, Webb A, Culler S, Martin K, Barrow D. Impact of a dedicated neurocritical care team in treating patients with aneurysmal subarachnoid hemorrhage. *Neurocrit Care.* 2011;14:334–40.
- Sarrafzadeh AS, Sakowitz OW, Kiening KL, Benndorf G, Lanksch WR, Unterberg AW. Bedside microdialysis: a tool to monitor cerebral metabolism in subarachnoid hemorrhage patients? *Crit Care Med.* 2002;30:1062–70.
- Schmidt JM, Ko SB, Helbok R, et al. Cerebral perfusion pressure thresholds for brain tissue hypoxia and metabolic crisis after poor-grade subarachnoid hemorrhage. *Stroke.* 2011;42:1351–6.
- Schmidt JM, Claassen J, Ko SB, et al. Nutritional support and brain tissue glucose metabolism in poor-grade SAH: a retrospective observational study. *Crit Care (London, England).* 2012;16:R15.
- Schultke E. Theodor Kocher's craniometer. *Neurosurgery.* 2009;64:1001–4; discussion 4–5
- Shafi S, Diaz-Arrastia R, Madden C, Gentilello L. Intracranial pressure monitoring in brain-injured patients is associated with worsening of survival. *J Trauma.* 2008;64:335–40.
- Shapiro K, Marmarou A, Shulman K. Characterization of clinical CSF dynamics and neural axis compliance using the pressure-volume index: I. The normal pressure-volume index. *Ann Neurol.* 1980;7:508–14.
- Sharpe W. Diagnosis and treatment of brain injuries with and without a fracture of the skull. Philadelphia: J. B. Lippincott; 1920.
- Shen L, Wang Z, Su Z, et al. Effects of intracranial pressure monitoring on mortality in patients with severe traumatic brain injury: a meta-analysis. *PLoS One.* 2016;11:e0168901.
- Shrestha GS, Suarez JI, Hemphill JC 3rd. Precision medicine in neurocritical care. *JAMA Neurol.* 2018;75:1463–4.
- Skjoth-Rasmussen J, Schulz M, Kristensen SR, Bjerre P. Delayed neurological deficits detected by an ischemic pattern in the extracellular cerebral metabolites in patients with aneurysmal subarachnoid hemorrhage. *J Neurosurg.* 2004;100:8–15.
- Soliman I, Aletreby WT, Faqih F, et al. Improved outcomes following the establishment of a neurocritical care unit in Saudi Arabia. *Crit Care Res Prac.* 2018;2018:2764907.
- Sorrentino E, Dieder J, Kasprovicz M, et al. Critical thresholds for cerebrovascular reactivity after traumatic brain injury. *Neurocrit Care.* 2012;16:258–66.
- Spina-Franca A. Physiological variations in cerebrospinal fluid pressure in the cisterna magna. *Arq Neuropsiquiatr.* 1963;21:19–24.
- Srinivasan VM, O'Neill BR, Jho D, Whiting DM, Oh MY. The history of external ventricular drainage. *J Neurosurg.* 2014;120:228–36.
- Stephensen H, Andersson N, Eklund A, Malm J, Tisell M, Wikkelso C. Objective B wave analysis in 55 patients with non-communicating and communicating hydrocephalus. *J Neurol Neurosurg Psychiatry.* 2005;76:965–70.
- Stiefel MF, Udoetuk JD, Spiotta AM, et al. Conventional neurocritical care and cerebral oxygenation after traumatic brain injury. *J Neurosurg.* 2006;105:568–75.
- Stone JL, Hughes JR. Early history of electroencephalography and establishment of the American Clinical Neurophysiology Society. *J Clin Neurophysiol.* 2013;30:28–44.
- Suarez JI, Zaidat OO, Suri MF, et al. Length of stay and mortality in neurocritically ill patients: impact of a specialized neurocritical care team. *Crit Care Med.* 2004;32:2311–7.
- Varelas PN, Schultz L, Conti M, Spanaki M, Genarrelli T, Hacein-Bey L. The impact of a neuro-intensivist on patients with stroke admitted to a neurosciences intensive care unit. *Neurocrit Care.* 2008;9:293–9.
- Vespa P, Prins M, Ronne-Engstrom E, et al. Increase in extracellular glutamate caused by reduced cerebral perfusion pressure and seizures after human traumatic brain injury: a microdialysis study. *J Neurosurg.* 1998;89:971–82.
- Vespa P, Martin NA, Nenov V, et al. Delayed increase in extracellular glycerol with post-traumatic electrographic epileptic activity: support for the theory that seizures induce secondary injury. *Acta Neurochir Suppl.* 2002;81:355–7.
- Vespa PM, O'Phelan K, Shah M, et al. Acute seizures after intracerebral hemorrhage: a factor in progressive midline shift and outcome. *Neurology.* 2003;60:1441–6.
- Vespa PM, Miller C, McArthur D, et al. Nonconvulsive electrographic seizures after traumatic brain injury result in a delayed, prolonged increase in intracranial pressure and metabolic crisis. *Crit Care Med.* 2007;35:2830–6.
- Volovici V, Huijben JA, Ercole A, et al. Ventricular drainage catheters versus intracranial parenchymal catheters for intracranial pressure monitoring-based management of traumatic brain injury: a systematic review and meta-analysis. *J Neurotrauma.* 2018.
- Whytt R. Observations on dropsy in the brain. *J. Balfour: Edinburgh;* 1768.
- Wijdicks EF. The history of neurocritical care. *Handb Clin Neurol.* 2017;140:3–14.
- Wilkins RH. Neurosurgical classic. XVII. *J Neurosurg.* 1964;21:240–4.
- Wilson MH. Monro-Kellie 2.0: the dynamic vascular and venous pathophysiological components of intracranial pressure. *J Cereb Blood Flow Metab.* 2016;36:1338–50.

- Witsch J, Frey HP, Schmidt JM, et al. Electroencephalographic periodic discharges and frequency-dependent brain tissue hypoxia in acute brain injury. *JAMA Neurol.* 2017;74:301–9.
- Young JS, Blow O, Turrentine F, Claridge JA, Schulman A. Is there an upper limit of intracranial pressure in patients with severe head injury if cerebral perfusion pressure is maintained? *Neurosurg Focus.* 2003;15:E2.
- Zeiler FA, Thelin EP, Helmy A, Czosnyka M, Hutchinson PJA, Menon DK. A systematic review of cerebral microdialysis and outcomes in TBI: relationships to patient functional outcome, neurophysiologic measures, and tissue outcome. *Acta Neurochir.* 2017;159:2245–73.
- Zeiler FA, Ercole A, Cabeleira M, et al. Comparison of performance of different optimal cerebral perfusion pressure parameters for outcome prediction in adult TBI: a CENTER-TBI study. *J Neurotrauma.* 2018.
- Zhang X, Medow JE, Iskandar BJ, et al. Invasive and non-invasive means of measuring intracranial pressure: a review. *Physiol Meas.* 2017;38:R143–r82.



Transthoracic Echocardiography for Monitoring Cardiopulmonary Interactions

24

Michel Slama

Introduction

Echocardiography is one of the primary non-invasive tool for the assessment of hemodynamics in ICU patients (Expert Round Table on Echocardiography in ICU 2014; Expert Round Table on Ultrasound in ICU 2011). Both transthoracic (TTE) and transesophageal echocardiography (TEE) can be used depending upon the skills and preferences of the team, although they each have some specific uses (de Backer et al. 2011). TTE is a technique that not only provides accurate cardiac imaging but also allows estimates of hemodynamic parameters such as cardiac output, pulmonary artery pressure and left ventricular filling pressure (Mercado et al. 2019; Mercado et al. 2017; Vignon et al. 2008; Vieillard-Baron 2009). We have developed the concept of critical care echocardiography (CCE), which is defined as echocardiography performed by an intensivist at the bedside of critical ill patients (Mayo et al. 2009). France and Europe were the first to use this technique in ICU patients, but now this tool is used in ICUs all over the world. In collaboration with many critical care societies around the world, we have defined recommendations for a proper utilization

and training of TTE and TEE (Expert Round Table on Echocardiography in ICU 2014; Expert Round Table on Ultrasound in ICU 2011). A comprehensive list of the competencies required by intensive care physicians using ultrasonography has been formulated and published in a competency statement emanating from two critical care societies (Mayo et al. 2009). We defined three levels of expertise on CCE: basic, advanced and expert. One of the difficulties is that the teaching of these techniques has not yet been incorporated into formal training curriculums; Formal training is needed to avoid pitfalls and a misutilization of this technique.

TTE Imaging

TTE is the only non-invasive technique that can image the heart and provide access to measures of the cardiac function. TEE permits assessment of left and right heart function.

Left Heart Function

One of the main uses of TTE is the assessment of left ventricle by measuring the size, thickness of the walls, and diastolic and systolic function. All echo windows and all the possible views should be used including subcostal view, which is some-

M. Slama (✉)
Medical Critical Care Unit, Amiens University
Hospital, Amiens, France
e-mail: Slama.michel@chu-amiens.fr

time the only window that can be accessed to analyze the heart (Maizel et al. 2013).

The left ventricular (LV) dimension should be assessed either by measuring the diastolic diameter, which normally is less than 50 mm, or diastolic volume (Lang et al. 2015) (Fig. 24.1). Left ventricular dilation is usually associated with chronic cardiac disease (dilated cardiomyopathy, ischemic heart disease or severe valvular disease). In contrast, in the presence of acute cardiac dysfunction (myocardial infarction, severe valvular regurgitation, septal cardiomyopathy) left ventricle size usually is normal. Left ventricular wall thickness normally is <1.2 cm and should be assessed from parasternal long axis view (Fig. 24.1a). To complete the left heart assessment, left atrial (LA) volume or area could be measured from an apical 4-chamber view (Fig. 24.1c and is normally $\leq 34\text{m}^2$). LA is dilated in patients with atrial fibrillation, chronic heart failure, diastolic dysfunction and in patients with chronic or sometimes even acute pressure or

volume overload such as mitral valve disease or volume overload due to acute renal failure.

A global assessment of LV Systolic function usually is evaluated by measuring the ejection fraction (EF) from an apical view (Fig. 24.1c or by measuring a surrogate such as the area shortening fraction from a short axis view (Fig. 24.1b). This is done by visual assessment or formal measurement. Systolic longitudinal strain obtained with the use of speckle tracking has been evaluated in ICU patients (Velagapudi et al. 2019; Chang et al. 2015; Chan et al. 2017; Menting et al. 2016). In chronic cardiac failure longitudinal strain is the first measurement to be impaired and is evident despite a normal left ventricular ejection fraction (Fig. 24.2). Huang et al. provided a simplified way to assess longitudinal strain with the use of M-mode which closely correlated with longitudinal strain (Fig. 24.3) (Huang et al. 2017).

Diastolic function is harder to assess than systolic function in ICU patients (Clancy et al.

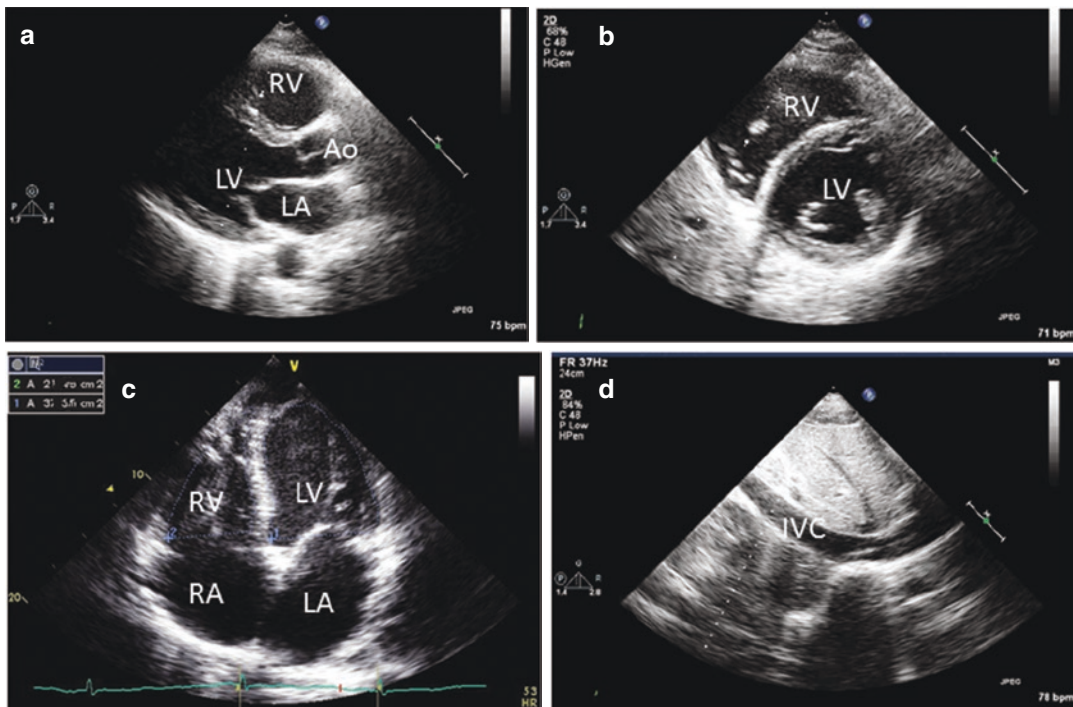


Fig. 24.1 Transthoracic echocardiographic views. (a) Parasternal long axis view; (b) parasternal short axis view at the papillary muscles level; (c) apical 4-chamber view;

(d) subcostal view of the inferior vena cava. LV left ventricle, RV right ventricle, LA left atrium, RA right atrium, Ao aorta, IVC inferior vena cava

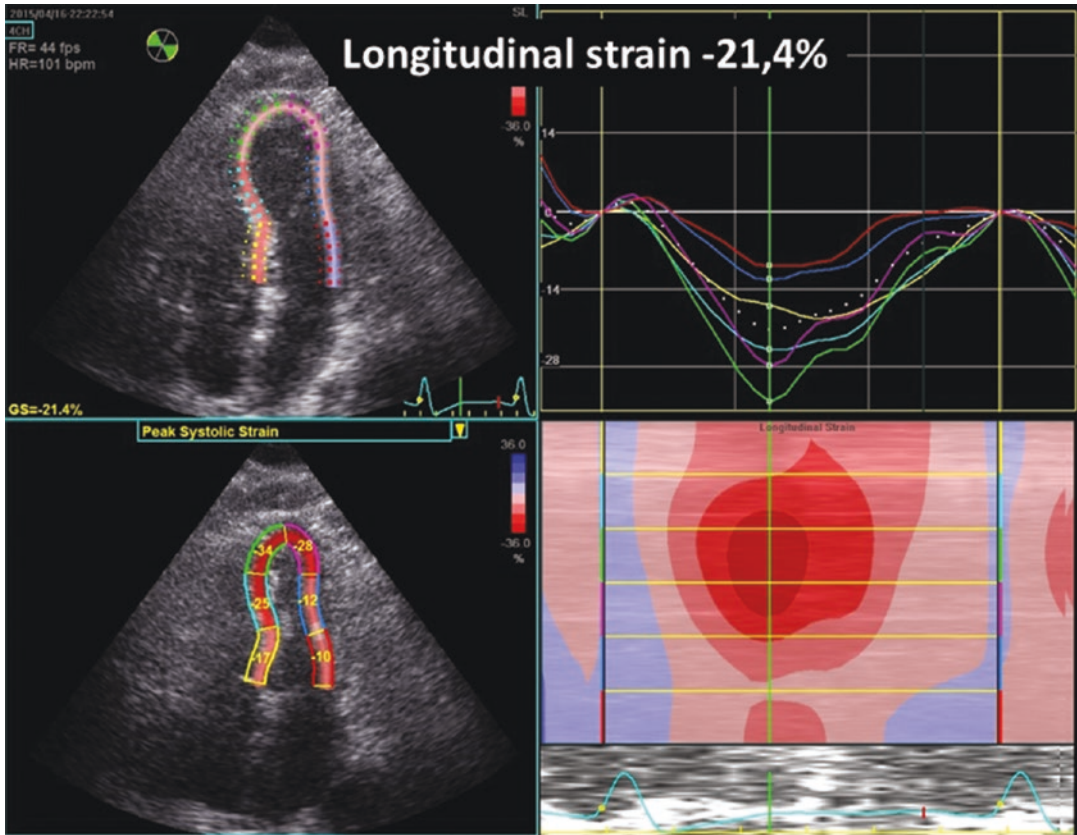


Fig. 24.2 Left ventricular longitudinal strain analyzed using speckle tracking

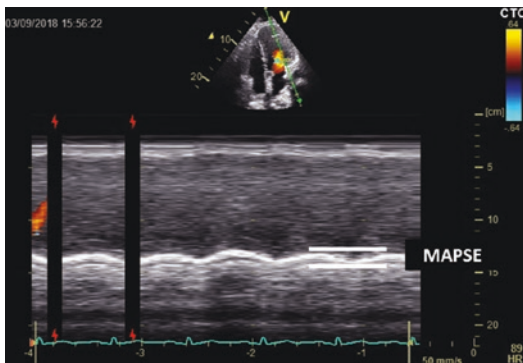


Fig. 24.3 MAPSE. Mitral Annular Plane Systolic Excursion

2017), and the criteria used in cardiological evaluations (Nagueh et al. 2016) are not applicable in critically ill patients. This is because diastolic function and left ventricular filling pressure are not related to each other. One of the best and simplest parameter for evaluation of LV relaxation is

early mitral annulus velocity (E') recorded from an apical 4-chamber view (Slama et al. 2005), and this has been used in many clinical studies in ICU patients (Fig. 24.4) (Brown et al. 2012; Landesberg et al. 2012; Okada et al. 2011; Sturgess et al. 2010; Sanfilippo et al. 2017).

Right Heart Function

Right ventricular (RV) size is hard to analyze due to its complex geometry. The RV wraps around the LV, and because of this multiple incidences and views are needed to do properly assess its function. Cardiologists have proposed assessing the RV from many windows and with many parameters (Lang et al. 2015). Intensivists have proposed a simpler evaluation from an apical 4-chamber view and measurement of the area of the RV and of the LV. RV/LV ratio has been demonstrated to be a good

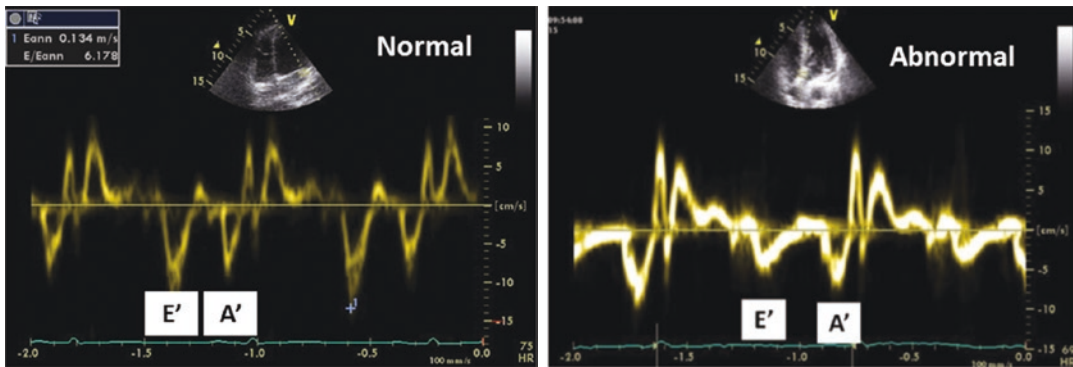


Fig. 24.4 Mitral annulus velocities using Doppler Tissue Imaging (DTI). *E'* early diastolic velocity of mitral annulus, *A'* late diastolic velocity of mitral annulus

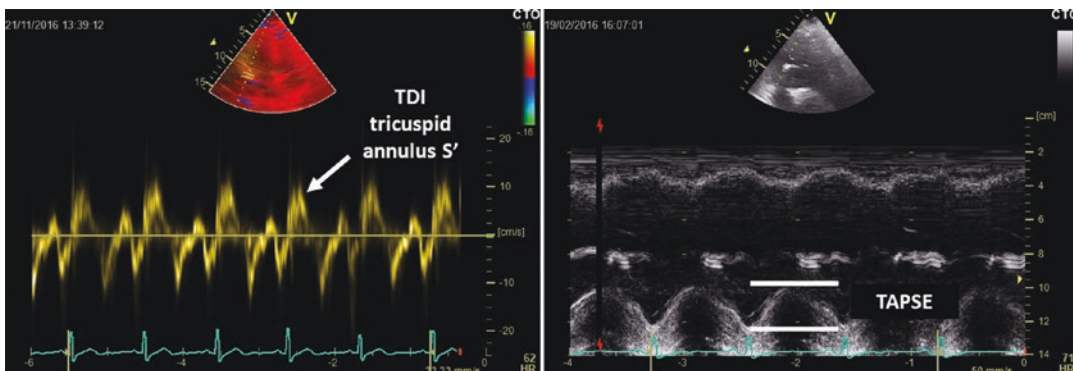


Fig. 24.5 Right ventricular systolic function. Left: tricuspid annulus systolic velocity *S'* using Tissue Doppler imaging (TDI); Right: tricuspid annular plane systolic excursion (TAPSE)

parameter in critically ill patients; the normal value is <0.6 (Vieillard-Baron 2009) (Fig. 24.1c). The septum should be analyzed from a short axis view to determine if there is paradoxical septal motion (Fig. 24.1b). Right ventricular wall thickness should be measured (normal <4 mm) when there is RV dilation due to cor pulmonale in-order to discriminate chronic from acute pulmonary hypertension (the normal is <4 mm). The RV is very sensitive to load changes and dilates when either afterload or preload increases. Thus, a normal RV size usually rules out any acute RV dysfunction.

The size of the right atrium (RA) and inferior vena cava sizes should be measured; dilation indicates that right heart pressure is increased (Fig. 24.1d).

Longitudinal contraction is the most significant contributor to the RV stroke volume. Thus

the best assessment of RV systolic function is the measurement of the apex to the base contraction. In daily practice many authors propose the use of tricuspid annular plane systolic excursion (TAPSE), or the lateral tricuspid annulus systolic velocity (*S'*) measured by tissue Doppler imaging (TDI), to evaluate right ventricular function (Fig. 24.5). Longitudinal contraction also can be accurately assessed with the use of speckle tracking (Fig. 24.6) (Vieillard-Baron 2009; Tadic et al. 2017; Orde et al. 2015).

Pericardium

The pericardium should be analyzed from all views to rule out a localized haematoma or a pericardial effusion and tamponade (Fig. 24.7).

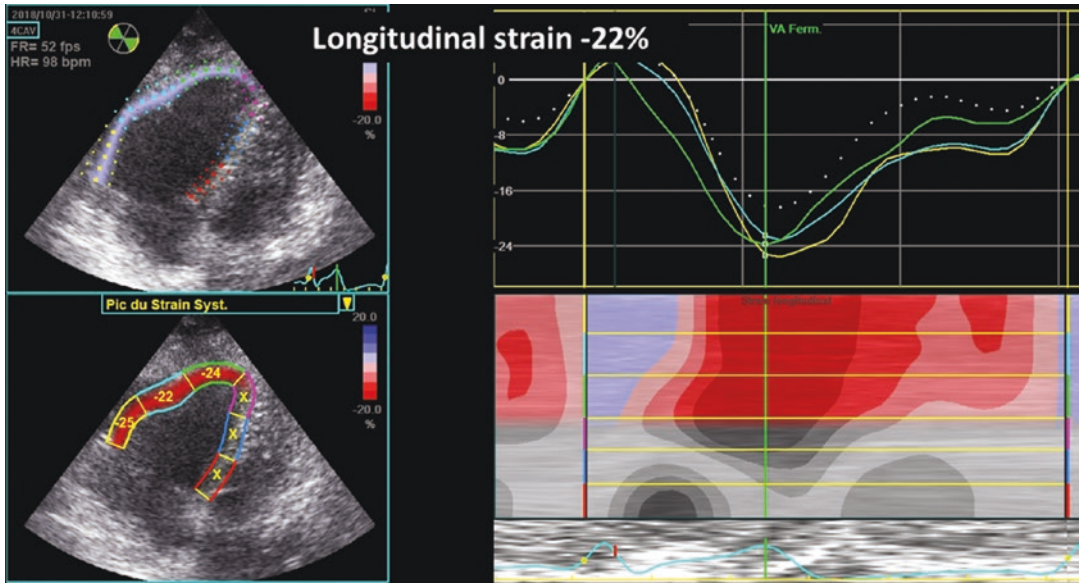


Fig. 24.6 Right ventricular longitudinal strain using speckle tracking

Valves

All valves should be explored as well to rule out severe valvular stenosis or regurgitation, and to check for the presence of abnormal structures such as an abscess or vegetation.

Classical Hemodynamical Parameters

By using Doppler measurements, cardiac output, pulmonary pressures and pulmonary artery occlusive pressure (PAOP a surrogate of wedge left ventricular filling pressures) can be evaluated with TTE.

Cardiac Output and Stroke Volume

Cardiac output is most often assessed at the level of the left ventricular outflow tract. The diameter of aortic annulus (*D*) is first measured at the base of the aortic valves from parasternal long axis view, and aortic flow velocity is recorded from an apical 5-chamber view with the use of pulsed Doppler, by placing the sample volume just

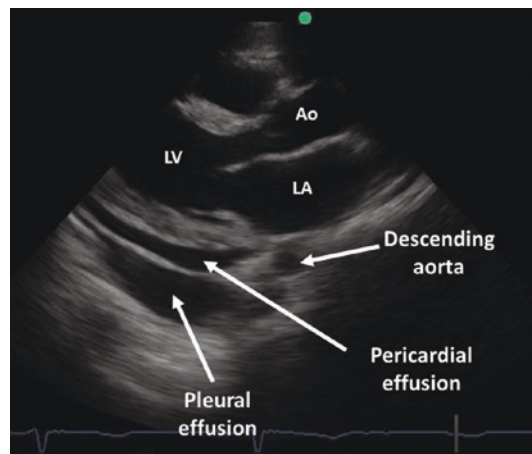


Fig. 24.7 Pericardial effusion. LV left ventricle, LA left atrium, Ao aorta

behind the aortic valves at the level of the aortic annulus and aortic velocity time integral is measured (VTI) (Fig. 24.8). Then, the cardiac output (*Qc*) could be calculated as follows: $Qc = (\pi D^2/4) \times VTI \times HR$ where HR is heart rate. Despite some criticisms (Wetterslev et al. 2016), this method has been demonstrated to be very accurate when compared to simultaneous measurements with gold standard method (Mercado et al. 2017; McLean et al. 2011).

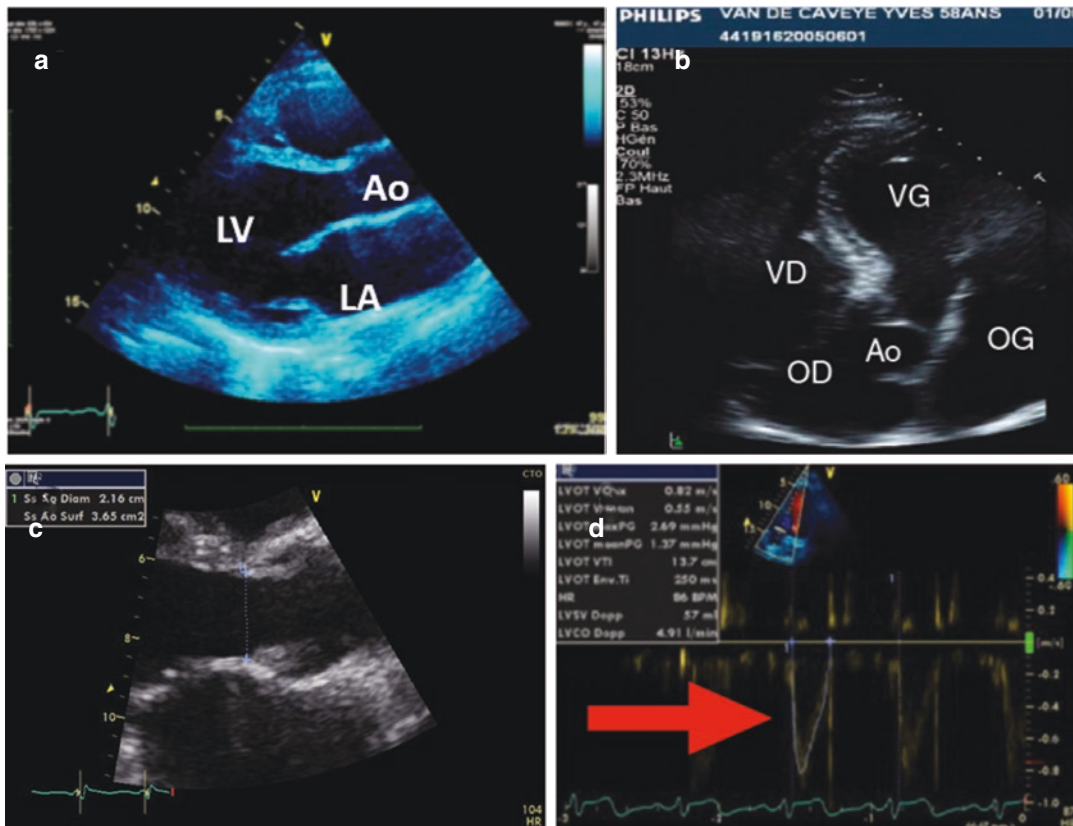


Fig. 24.8 Cardiac output measurement. (a, d) measurement of aortic annulus diameter. (b) Apical 5-chamber view. (c) Aortic annulus measurement from parasternal long axis view focused on the left ventricular outflow tract.

(d) Aortic blood flow recorded using pulsed Doppler. LV left ventricle, RV right ventricle, LA left atrium, RA right atrium, Ao aorta, IVC inferior vena cava

Pulmonary Artery Pressures

It was established many years ago that Doppler recorded velocities are closely correlated with pressure differences measured by fidelity catheters. Maximal velocity of tricuspid regurgitation represents the maximal pressure difference between the right ventricle and right atrium in systole. Adding to this maximal pressure gradient the right atrial pressure permits to have a good estimation of the pulmonary artery systolic pressure. When recorded by experienced operators, this measurement was demonstrated to be very accurate, especially when compared with a simultaneous invasive method (Mercado et al. 2019). The best correlations were obtained when CVP was measured from a central venous line; this value is easily obtained in ICU patients

because they frequently have central venous catheters (Fig. 24.9a, c). If tricuspid regurgitation is present, pulmonary artery flow velocity still can be recorded and the indexed or even non-indexed acceleration time be used to rule out pulmonary hypertension (Yared et al. 2011). Pulmonary diastolic, mean and systolic pressures might be assessed by measuring the maximal and the minimal velocities on pulmonary regurgitation flow recorded using continuous wave Doppler (Fig. 24.9b, d) (Ge et al. 1992; Lei et al. 1995).

Pulmonary Artery Occlusive Pressure (PAOP)

Ratio of early to late velocity of mitral flow recorded using pulsed Doppler (E/A), and ratio of

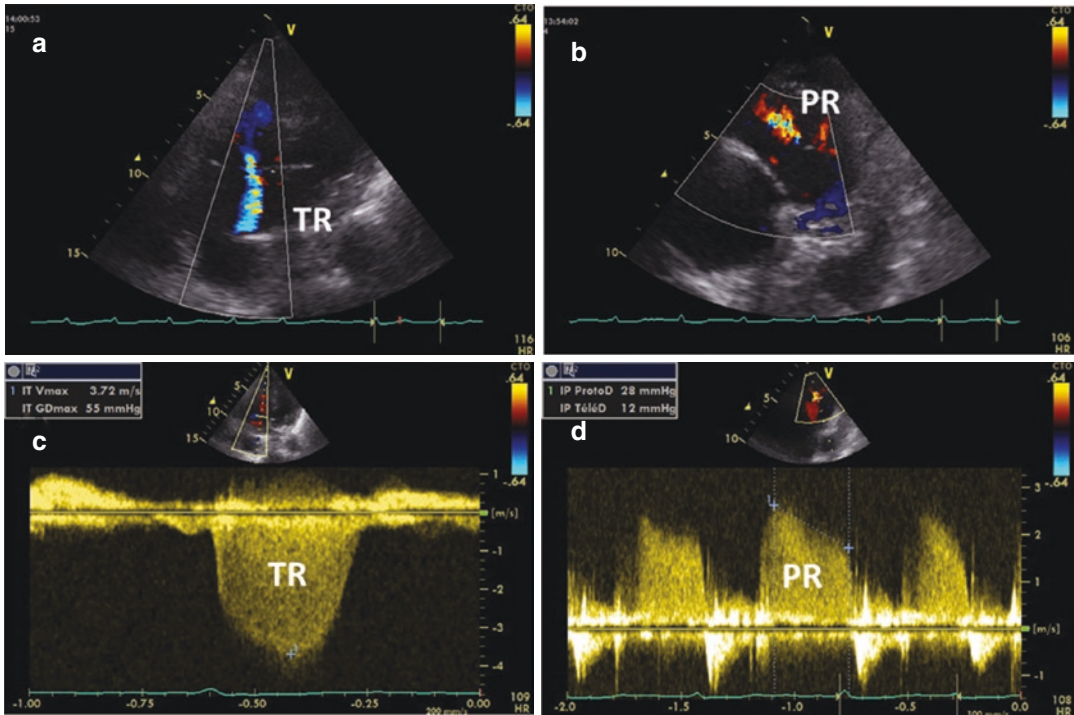


Fig. 24.9 Pulmonary artery pressures. (a) Tricuspid regurgitation imaging (TR) with colour Doppler. (b) Pulmonary regurgitation (PR) imaging with colour

Doppler. (c) Tricuspid regurgitation recorded using continuous wave Doppler. (d) Pulmonary regurgitation recorded using continuous wave Doppler

early velocity of mitral flow (E) to early velocity of mitral annulus recorded using Tissue Doppler Imaging E' (E/E') together with pulmonary venous flow have been used to estimate PAOP. Recommendations published in 2016 have an algorithm that includes the use of many parameters to assess PAOP (Nagueh et al. 2016). Although some studies have reported a good accuracy of Doppler echocardiographic measurements, recent studies have generally found that there is a large grey zone PAOP could be accurately assessed only for a small number of patients (Vignon et al. 2008; Bouhemad et al. 2003).

Clinical Conditions

General Assessment of Patients with Shock

Echocardiography is an important tool for the initial assessment of the pathophysiology of the

shock and together with the clinical situation may help the intensivist to manage patients with shock. but the and to assess needs assessment needs to be interpreted in the context of the clinical situation because as is the case with all tests predictability is very dependent upon the pretest probability. The clinical context also allows the operator to more carefully identify the most likely abnormalities. However, the investigation still should be performed with a systematic approach.

The first step is to rule out pericardial tamponade because this condition can be treated with a life-saving pericardiocentesis. This diagnosis usually is obvious, but it can be more difficult to demonstrate after cardiac surgery, because it can be due to a haematoma behind the right or the left atrium, and this is better detected with a transesophageal examination (Fig. 24.10).

The second step is the assessment of fluid-responsiveness of the patient and the determination of whether the problem is hypovolemic shock or septic shock with hypovolemia. Small cardiac

cavities with left ventricular hyperkinesia (with kissing walls), left ventricular pseudo-hypertrophy (increased wall thickness which disappears after volume expansion and an restored left ventricular size), and/or a small or collapsed inferior vena cava can be sufficient to diagnose severe hypovolemia and likely fluid-responsiveness. It also is important to determine if left ventricular outflow tract obstruction is associated with a response of fluid expansion. However, in many cases, these static parameters fail to assess fluid-responsiveness and dynamic parameters should be useful. A good method is the passive leg raising manoeuvre while simultaneously recording aortic blood flow velocity and observing a change in stroke volume change). This can be used in either spontaneously breathing patients or mechanically ventilated patients. In mechanically

ventilated patients respiratory variations in the inferior vena cava, superior vena cava, aortic flow velocities and their surrogates such as jugular venous, carotid and femoral flow velocities can be used to assess the potential for fluid expansion to increase cardiac output which remains a clinical decision (Fig. 24.11).

Left and right cardiac function are analyzed in the third step. Both LV diastolic and systolic function should be analyzed. Cardiac output, ejection fraction should be recorded as well as E' (evaluation of left ventricular relaxation) and E/E' ratio (PAOP evaluation). It is also important to determine if there are any segmental wall abnormalities that indicate the presence of ischemic heart disease.

Findings in Specific Shocks

Septic Shock

Patients with septic shock often have a relative hypovolemia, vasoplegia, and systolic and diastolic dysfunction of both the left and right ventricles. Acute cor pulmonale is frequently associated with acute respiratory distress syndrom (ARDS) is often present. Left ventricular obstruction needs to be ruled out with the use of continuous wave Doppler aligned through the LV from the apex to the left ventricular outflow tract. In the very early phase of septic shock, the left ventricle could be hyperkinetic and small. in up to 20% of cases an obstruction of left ventricular

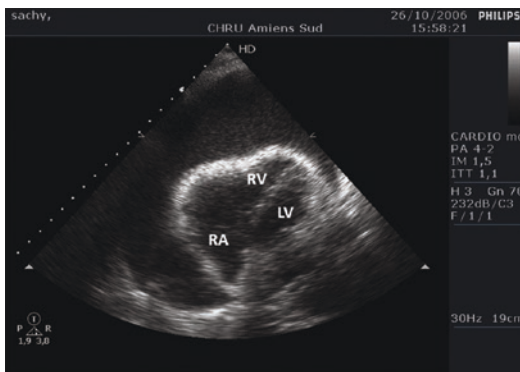


Fig. 24.10 Pericardial tamponade. LV left ventricle, RV right ventricle, RA right atrium

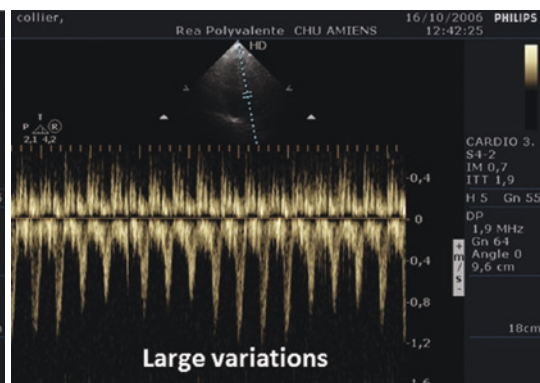
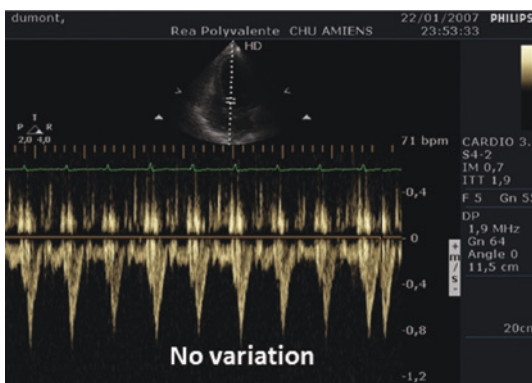


Fig. 24.11 Respiratory variations of aortic blood flow

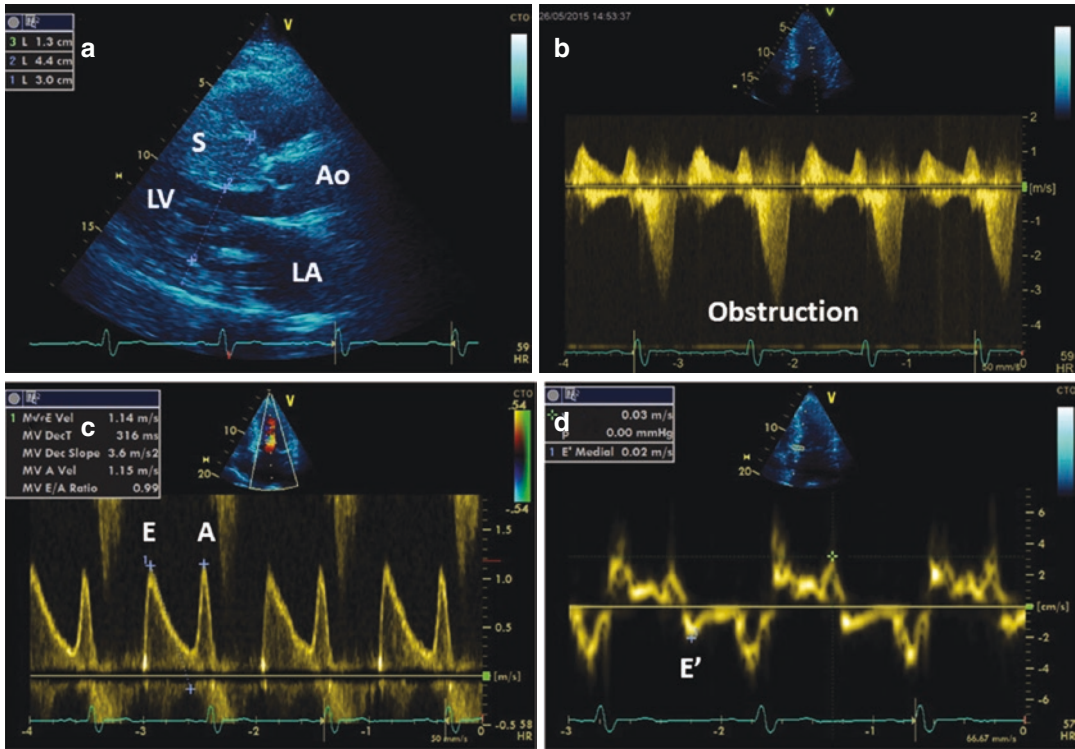


Fig. 24.12 Hypertrophic cardiomyopathy with left ventricular (LV) obstruction. (a) Parasternal long axis view with septum hypertrophy; (b) left ventricular obstructive flow recorded using continuous wave Doppler; (c) Mitral flow; (d) mitral annulus velocities recorded using tissue

Doppler imaging. E' early diastolic velocity of mitral annulus, E early diastolic velocity of mitral flow, A late diastolic velocity of mitral flow, LV left ventricle, LA left atrium, Ao aorta, S inter ventricular septum

outflow tract due to a systolic anterior motion of the mitral valve, which induces a dynamic left ventricular obstruction could be observed and recorded using continuous wave Doppler LV Diastolic dysfunction is frequent and associated with a worse prognosis. LV systolic dysfunction may occur in 20–40% of cases as indicated by a low ejection fraction and low cardiac output. LV filling pressure assessed by E/E' ratio is usually normal. The LV systolic dysfunction in sepsis usually regresses in less than 7 days with a complete recovery (Cecconi et al. 2014; Slama et al. 1996; McLean 2016; Boissier et al. 2017).

Cardiogenic Shock

Myocardial infarction is the primary cause of cardiogenic shock and is due to extensive infarction of the ventricular wall or to a mechanical

complication such as cardiac rupture, severe acute mitral regurgitation, an interventricular defect, or extension into the right ventricle. Non-ischemic cardiomyopathies causing cardiogenic shock present with global systolic dysfunction and a globally dilated heart or with apical ballooning which is called Tako-Tsubo (McLean et al. 2018). Severe acute aortic or mitral regurgitation should be ruled out by using colour Doppler. Acute pulmonary embolism should be suspected in the presence of dilation of the right cavities, a large non-compliant IVC, paradoxical septal motion and a small and restricted left ventricle (Fig. 24.13). Observation of the presence of a thrombus in the right atrium, ventricle or pulmonary artery is rare but permits starting treatment without performing CT-scan. A normal echocardiogram does not exclude pul-

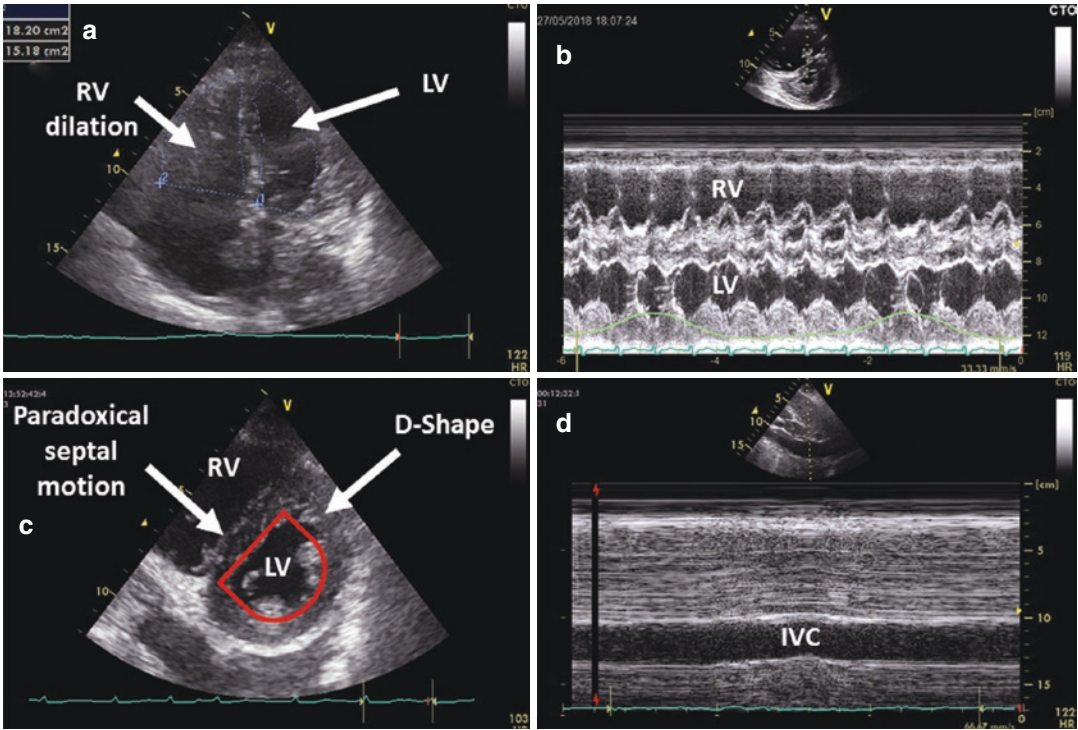


Fig. 24.13 Acute cor pulmonale. (a) Apical 4-chamber view with right ventricular dilation; (b) M-mode with dilation of right ventricle (RV); (c) D-shape of left ven-

tricle (LV) due to right ventricular systolic overload; (d) dilated inferior vena cava (IVC)

monary embolism, but in the presence of shock, absence of RV dilation makes the diagnosis of pulmonary embolism a very unlikely cause of the shock except in very rare cases of associated severe hypovolemia.

Respiratory Failure

Respiratory failure is a frequent clinical situation in ICU. In case of suspicion of pulmonary oedema E/E' ratio is useful to estimate left ventricular filling pressure and echocardiography helps to find the cause of this respiratory failure. Left ventricular systolic dysfunction could be due to myocardial infarction, dilated cardiomyopathy, myocarditis or Tako-Tsubo. When systolic function is normal, severe valvulopathy, especially mitral regurgitation, must be ruled out. This is mainly done with colour Doppler and continuous wave Doppler. In the absence of valvular disease, diastolic dysfunction can be a cause of pulmo-

nary oedema when there is a fluid overload or atrial fibrillation. When LV filling pressure is low (low E/E' ratio) ARDS or already treated cardiogenic oedema should be suspected (de Backer et al. 2011).

In the absence of pulmonary oedema, hypoxemia could be due to pneumonia, COPD/asthma or pulmonary embolism. Cardiac function can be either normal or impaired with acute and/or chronic cor pulmonale, with RV dilation, pulmonary hypertension, paradoxical septal motion and LV diastolic impairment (Fig. 24.13).

Addition of contrast examination to the TTE (or TEE) examination should be done to rule out intra-cardiac or intra-pulmonary shunt as a cause of explaining the hypoxemia.

Other Clinical Situations

TTE can be useful in many different clinical situations such as endocarditis, chest pain and

peripheral embolism and should be performed if needed with help of echocardiographic experienced intensivist.

Pitfalls and Limitations of Echocardiography

The many pitfalls and limitations of TTE need to be known by the intensivist performing critical care echocardiography.

The main limitation of TTE is bad echogenicity. Tapes and tubes can limit access windows to view the heart when using TTE. The subcostal window may be the only useful window in many patients, especially in those with COPD, high PEEP or even after thoracic surgery (Maizel et al. 2013). When the response to the clinical question cannot be obtained by TTE, a TEE needs to be performed and is especially useful in mechanically ventilated patients. In some circumstances TEE is mandated. These include suspicion of endocarditis, peripheral non-explained embolism and suspicion of aortic dissection or rupture.

Fluid-responsiveness parameters were recently re-evaluated in a large multi-centred study. All of these had much lower performance for the assessment of fluid-responsiveness in patients with shock than in earlier publications. Aortic flow variation seems to be the more sensitive based on ROC curve analysis and SVC variations the most specific. IVC variations had a very low predictive value for fluid-responsiveness and are not recommended (Vieillard-Baron et al. 2018; Vignon et al. 2017). As well although IVC size has been used for years for the assessment of central venous pressure, it too poorly correlated with measured invasive central venous pressure (Vieillard-Baron et al. 2018). Further, these parameters can be used only in mechanically ventilated patients and are inaccurate in spontaneously breathing patients. A good interpretation also requires that the patient is well sedated, should have tidal volume > 6 ml/kg (which is no longer frequently used) and should not have right cardiac dysfunction (Mahjoub et al. 2009). When using passive leg raising, which is considered as

the best method to assess fluid-responsiveness, to be accurate it needs to be done as in the original study by mobilizing the bed from semi-recumbent position to flat position with raising legs (Jabot et al. 2009). The presence of high intra-abdominal pressure or elastic compressive stocking invalidates the passive leg raising manoeuvre (Mahjoub et al. 2010; Zogheib et al. 2018). There also can be false negatives in severely hypovolemic patients who do not have volume to recruit from the lower limbs.

The ejection fraction usually is evaluated by the Simpson method, which integrates the sum of disc volume inside the left ventricle in diastole and in systole. However, this method is hard to use in ICU patients because the endocardial edge is hard to define. For this reason, eye-balling the EF estimation is most commonly used in ICU patients. Because EF estimation can have an important impact on patient management, ventricular loops should be recorded and reviewed by expert in case of low echogenicity. The mitral annular plane systolic excursion (MAPSE) and Huang index, which both assess contraction of the left ventricle from the base to the apex (mitral annulus displacement toward the apex in systole), may replace EF in this case (Huang et al. 2017). As well, the EF is dependent not only on contractility but also on the end-diastolic volume and afterload. Presence of systolic dysfunction as assessed by EF can be masked by low LV afterload. EF increases when end-diastolic volume is increased simply by the mathematics of the calculation. This can result in an increase in EF when the heart rate is lowered and diastolic volume increases without any true change in contractile function. Thus a change in EF needs to be interpreted in the context of other hemodynamic parameters. For example, in the early phase of a septic shock, EF can be normal despite a severe systolic dysfunction (Robotham et al. 1991).

Assessment of right ventricular systolic function is another difficult area. The right ventricle is wrapped around the left ventricle and is thus affected by the systolic function of the LV. Teboul et al. demonstrated a correlation between the TAPSE and the LVEF (Lamia et al. 2007). Assessment of the right ventricular systolic func-

tion independently from the LV function seems almost impossible. Another problem occurs because the crescent shape of the RV makes estimations of RV size difficult, and the size can be easily overestimated.

All hemodynamic variations have their own limitations and pitfalls. Cardiac output can be dramatically over- or under-estimated. The measurement of aortic annulus diameter is squared in the calculation and thus an error in this measurement is squared which explains the lack of precision in this measurement. Aortic blood flow measurements can be faulty in the presence of left ventricular obstruction (Chauvet et al. 2015; Orde et al. 2017) or aortic regurgitation (Chauvet et al. 2015; Orde et al. 2017). Accurate measurement of pulmonary artery pressures require carefully recorded tricuspid regurgitation velocity with a good definition of the external envelope. Otherwise, there will be an over- or under-estimation of the pressure (Fig. 24.9). It has been shown that the higher the skill and competence of the operator, the better the correlation between invasive and non-invasive evaluations of the pulmonary arterial systolic pressure based on the tricuspid regurgitant flow. As well, accurate assessment of the pulmonary artery pressures requires a proper measurement of the right atrial pressure. A false right atrial pressure estimation produces under- or over-estimation of the pulmonary pressures (Mercado et al. 2019). In case of massive laminar tricuspid regurgitation, pulmonary pressures cannot be assessed using Doppler.

Practical Problems (Monitoring, Number of Echo Machines, Price, Quality of the Machines, Time Constraints)

Many practical problems arise when a team decides to start using echocardiography at the bedside to manage critically ill patients. Apart from the problem with trying to convince the administration to buy the echocardiographic machines, it also is challenging trying to convince all team members to participate in an educational program. Time consumption is another

problem for the use of CCE in ICU patients. It takes 15–30 minutes to perform a good CCE. When this is multiplied by the number of patients who need to have at least one hemodynamic evaluation, and considering the follow-up of any interventions, the time required for this activity can be an important practical limitation of its use for the critical management in the ICU (Orde et al. 2017). Protocols based on pre-test probabilities will need to be established to prioritize the use of this potentially very helpful tool.

Education

Education is an important challenge in the coming years and should take place in countries all over the world. The ACCP, SRLF (Société de Réanimation de Langue Française) was started 10 years ago to put together a program of basic critical care echocardiography (Mayo et al. 2009). Since this first publication in the critical field, other recommendations have come out and used to propose educational program for CCE. We defined three levels of competency: basic, which should be included in the curriculum of all intensivists and anaesthetists over the world; advanced, which is optional, but should be done by a large majority of medical doctors in charge of critically ill patients; and expert level, which should be reached by at least one physician in each ICU. To avoid misinterpretation of echocardiography examinations which can lead to the wrong patient management, this education is mandated, and limitations and pitfalls should be well known by all doctors practicing CCE (Expert Round Table on Echocardiography in ICU 2014; Expert Round Table on Ultrasound in ICU 2011; Orde et al. 2017).

Echocardiography a Continuous Monitoring Technique?

Because the transthoracic technique is non-invasive tool and can be repeated as many times as needed, it should be considered as a semi-continuous monitoring technique. For this

purpose, after an initial comprehensive evaluation, focused echocardiographic should be done to follow up the effect of any therapeutic change. As well, TTE should be performed as soon as any clinical change occurs. For instance, in the case of volume expansion, aortic VTI could be assessed to measure stroke volume-induced changes and to control the tolerance of the fluid infusion. On the other hand, left ventricular systolic function should be assessed after starting Dobutamine infusion in patient with cardiac dysfunction in septic shock and in cardiogenic shock. Another example is PEEP titration in ARDS patient. Monitoring of right ventricular function is needed to avoid acute cor-pulmonale induced by a too high an airway pressure. These few examples demonstrate that echocardiography should be used as a semi-continuous monitoring tool in the patients with hemodynamic compromise in ICU patients.

Conclusion

Echocardiography is a cornerstone of the hemodynamic evaluation of critically ill patients and should be practiced by all intensivists and anaesthetists with enough competencies to reach useful conclusions to manage and follow ICU patients.

References

- Boissier F, Razazi K, Seemann A, Bedet A, Thille AW, de Prost N, et al. Left ventricular systolic dysfunction during septic shock: the role of loading conditions. *Intensive Care Med.* 2017;43(5):633–42.
- Bouhemed B, Nicolas-Robin A, Benois A, Lemaire S, Goarin J-P, Rouby J-J. Echocardiographic Doppler assessment of pulmonary capillary wedge pressure in surgical patients with postoperative circulatory shock and acute lung injury. *Anesthesiology.* 2003;98(5):1091–100.
- Brown SM, Pittman JE, Hirshberg EL, Jones JP, Lanspa MJ, Kuttler KG, et al. Diastolic dysfunction and mortality in early severe sepsis and septic shock: a prospective, observational echocardiography study. *Crit Ultrasound J.* 2012;4(1):8.
- Cecconi M, De Backer D, Antonelli M, Beale R, Bakker J, Hofer C, et al. Consensus on circulatory shock and hemodynamic monitoring. Task force of the European Society of Intensive Care Medicine. *Intensive Care Med.* 2014;40(12):1795–815.
- Chan J, Shiino K, Obonyo NG, Hanna J, Chamberlain R, Small A, et al. Left ventricular global strain analysis by two-dimensional speckle-tracking echocardiography: the learning curve. *J Am Soc Echocardiogr Off Publ Am Soc Echocardiogr.* 2017;30(11):1081–90.
- Chang W-T, Lee W-H, Lee W-T, Chen P-S, Su Y-R, Liu P-Y, et al. Left ventricular global longitudinal strain is independently associated with mortality in septic shock patients. *Intensive Care Med.* 2015;41(10):1791–9.
- Chauvet J-L, El-Dash S, Delastre O, Bouffandeau B, Jusserand D, Michot J-B, et al. Early dynamic left intraventricular obstruction is associated with hypovolemia and high mortality in septic shock patients. *Crit Care Lond Engl.* 2015;19:262.
- Clancy DJ, Scully T, Slama M, Huang S, McLean AS, Orde SR. Application of updated guidelines on diastolic dysfunction in patients with severe sepsis and septic shock. *Ann Intensive Care.* 2017;7(1):121.
- Daniel de Backer et al. (eds) Hemodynamic monitoring using echocardiography in the critically ill [Internet]. Heidelberg: Springer; 2011 [cité 21 févr 2019]. Disponible sur: <https://doi.org/10.1007/978-3-540-87956-5>.
- Expert Round Table on Echocardiography in ICU. International consensus statement on training standards for advanced critical care echocardiography. *Intensive Care Med.* 2014;40(5):654–66.
- Expert Round Table on Ultrasound in ICU. International expert statement on training standards for critical care ultrasonography. *Intensive Care Med.* 2011;37(7):1077–83.
- Ge Z, Zhang Y, Ji X, Fan D, Duran CM. Pulmonary artery diastolic pressure: a simultaneous Doppler echocardiography and catheterization study. *Clin Cardiol.* 1992;15(11):818–24.
- Huang SJ, Ting I, Huang AM, Slama M, McLean AS. Longitudinal wall fractional shortening: an M-mode index based on mitral annular plane systolic excursion (MAPSE) that correlates and predicts left ventricular longitudinal strain (LVLS) in intensive care patients. *Crit Care Lond Engl.* 2017;21(1):292.
- Jabot J, Teboul J-L, Richard C, Monnet X. Passive leg raising for predicting fluid responsiveness: importance of the postural change. *Intensive Care Med.* 2009;35(1):85–90.
- Lamia B, Teboul J-L, Monnet X, Richard C, Chemla D. Relationship between the tricuspid annular plane systolic excursion and right and left ventricular function in critically ill patients. *Intensive Care Med.* 2007;33(12):2143–9.
- Landesberg G, Gilon D, Meroz Y, Georgieva M, Levin PD, Goodman S, et al. Diastolic dysfunction and mortality in severe sepsis and septic shock. *Eur Heart J.* 2012;33(7):895–903.
- Lang RM, Badano LP, Mor-Avi V, Afilalo J, Armstrong A, Ernande L, et al. Recommendations for cardiac chamber quantification by echocardiography

- in adults: an update from the American Society of Echocardiography and the European Association of Cardiovascular Imaging. *J Am Soc Echocardiogr Off Publ Am Soc Echocardiogr*. 2015;28(1):1–39.e14.
- Lei MH, Chen JJ, Ko YL, Cheng JJ, Kuan P, Lien WP. Reappraisal of quantitative evaluation of pulmonary regurgitation and estimation of pulmonary artery pressure by continuous wave Doppler echocardiography. *Cardiology*. 1995;86(3):249–56.
- Mahjoub Y, Pila C, Friggeri A, Zogheib E, Lobjoie E, Tinturier F, et al. Assessing fluid responsiveness in critically ill patients: false-positive pulse pressure variation is detected by Doppler echocardiographic evaluation of the right ventricle. *Crit Care Med*. 2009;37(9):2570–5.
- Mahjoub Y, Touzeau J, Airapetian N, Lorne E, Hijazi M, Zogheib E, et al. The passive leg-raising maneuver cannot accurately predict fluid responsiveness in patients with intra-abdominal hypertension. *Crit Care Med*. 2010;38(9):1824–9.
- Maizel J, Salhi A, Tribouilloy C, Massy ZA, Choukroun G, Slama M. The subxiphoid view cannot replace the apical view for transthoracic echocardiographic assessment of hemodynamic status. *Crit Care Lond Engl*. 2013;17(5):R186.
- Mayo PH, Beaulieu Y, Doelken P, Feller-Kopman D, Harrod C, Kaplan A, et al. American College of Chest Physicians/La Société de Réanimation de Langue Française statement on competence in critical care ultrasonography. *Chest*. 2009;135(4):1050–60.
- McLean AS. Echocardiography in shock management. *Crit Care Lond Engl*. 2016;20:275.
- McLean AS, Huang SJ, Kot M, Rajamani A, Hoyling L. Comparison of cardiac output measurements in critically ill patients: FloTrac/Vigileo vs transthoracic Doppler echocardiography. *Anaesth Intensive Care*. 2011;39(4):590–8.
- McLean AS, Slama M, Chew M. Does this patient have takotsubo syndrome? *Intensive Care Med*. 2018;44(6):904–7.
- Menting ME, McGhie JS, Koopman LP, Vletter WB, Helbing WA, van den Bosch AE, et al. Normal myocardial strain values using 2D speckle tracking echocardiography in healthy adults aged 20 to 72 years. *Echocardiogr Mt Kisco N*. 2016;33(11):1665–75.
- Mercado P, Maizel J, Beyls C, Titeca-Beauport D, Joris M, Kontar L, et al. Transthoracic echocardiography: an accurate and precise method for estimating cardiac output in the critically ill patient. *Crit Care Lond Engl*. 2017;21(1):136.
- Mercado P, Maizel J, Beyls C, Kontar L, Orde S, Huang S, et al. Reassessment of the accuracy of cardiac Doppler pulmonary artery pressure measurements in ventilated ICU patients: a simultaneous Doppler-catheterization study. *Crit Care Med*. 2019;47(1):41–8.
- Nagueh SF, Smiseth OA, Appleton CP, Byrd BF, Dokainish H, Edvardsen T, et al. Recommendations for the evaluation of left ventricular diastolic function by echocardiography: an update from the American Society of Echocardiography and the European Association of Cardiovascular Imaging. *Eur Heart J Cardiovasc Imaging*. 2016;17(12):1321–60.
- Okada K, Mikami T, Kaga S, Onozuka H, Inoue M, Yokoyama S, et al. Early diastolic mitral annular velocity at the interventricular septal annulus correctly reflects left ventricular longitudinal myocardial relaxation. *Eur J Echocardiogr J Work Group Echocardiogr Eur Soc Cardiol*. 2011;12(12):917–23.
- Orde SR, Behfar A, Stalboerger PG, Barros-Gomes S, Kane GC, Oh JK. Effect of positive end-expiratory pressure on porcine right ventricle function assessed by speckle tracking echocardiography. *BMC Anesthesiol*. 2015;15:49.
- Orde S, Slama M, Hilton A, Yastrebov K, McLean A. Pearls and pitfalls in comprehensive critical care echocardiography. *Crit Care Lond Engl*. 2017;21(1):279.
- Robotham JL, Takata M, Berman M, Harasawa Y. Ejection fraction revisited. *Anesthesiology*. 1991;74(1):172–83.
- Sanfilippo F, Corredor C, Arcadipane A, Landesberg G, Vieillard-Baron A, Cecconi M, et al. Tissue Doppler assessment of diastolic function and relationship with mortality in critically ill septic patients: a systematic review and meta-analysis. *Br J Anaesth*. 2017;119(4):583–94.
- Slama MA, Novara A, Van de Putte P, Diebold B, Safavian A, Safar M, et al. Diagnostic and therapeutic implications of transesophageal echocardiography in medical ICU patients with unexplained shock, hypoxemia, or suspected endocarditis. *Intensive Care Med*. 1996;22(9):916–22.
- Slama M, Ahn J, Peltier M, Maizel J, Chemla D, Varagic J, et al. Validation of echocardiographic and Doppler indexes of left ventricular relaxation in adult hypertensive and normotensive rats. *Am J Physiol Heart Circ Physiol*. 2005;289(3):H1131–6.
- Sturgess DJ, Marwick TH, Joyce C, Jenkins C, Jones M, Masci P, et al. Prediction of hospital outcome in septic shock: a prospective comparison of tissue Doppler and cardiac biomarkers. *Crit Care Lond Engl*. 2010;14(2):R44.
- Tadic M, Pieske-Kraigher E, Cuspidi C, Morris DA, Burkhardt F, Baudisch A, et al. Right ventricular strain in heart failure: clinical perspective. *Arch Cardiovasc Dis*. 2017;110(10):562–71.
- Velagapudi VM, Pidikiti R, Tighe DA. Is left ventricular global longitudinal strain by two-dimensional speckle tracking echocardiography in sepsis cardiomyopathy ready for prime time use in the ICU? *Healthc Basel Switz*. 2019;7(1).
- Vieillard-Baron A. Assessment of right ventricular function. *Curr Opin Crit Care*. 2009;15(3):254–60.
- Vieillard-Baron A, Evrard B, Repessé X, Maizel J, Jacob C, Goudelin M, et al. Limited value of end-expiratory inferior vena cava diameter to predict fluid responsiveness impact of intra-abdominal pressure. *Intensive Care Med*. 2018;44(2):197–203.
- Vignon P, AitHssain A, François B, Preux P-M, Pichon N, Clavel M, et al. Echocardiographic assessment of pulmonary artery occlusion pressure in ventilated

- patients: a transoesophageal study. *Crit Care Lond Engl.* 2008;12(1):R18.
- Vignon P, Repessé X, Bégot E, Léger J, Jacob C, Bouferrache K, et al. Comparison of echocardiographic indices used to predict fluid responsiveness in ventilated patients. *Am J Respir Crit Care Med.* 2017;195(8):1022–32.
- Wetterslev M, Møller-Sørensen H, Johansen RR, Perner A. Systematic review of cardiac output measurements by echocardiography vs. thermodilution: the techniques are not interchangeable. *Intensive Care Med.* 2016;42(8):1223–33.
- Yared K, Noseworthy P, Weyman AE, McCabe E, Picard MH, Baggish AL. Pulmonary artery acceleration time provides an accurate estimate of systolic pulmonary arterial pressure during transthoracic echocardiography. *J Am Soc Echocardiogr Off Publ Am Soc Echocardiogr.* 2011;24(6):687–92.
- Zogheib E, Maizel J, Cherradi N, Benammar A, Labont B, Hchikat A, et al. The presence of elastic compression stockings reduces the fluid responsiveness of patients in the operating room. *Minerva Anesthesiol.* 2018;84(11):1279–86.



Transesophageal Echocardiography for Monitoring Cardiopulmonary Interactions

Antoine Vieillard-Baron

Abbreviations

ARDS	acute respiratory distress syndrome
PEEP	positive end-expiratory pressure
PPV	pulse pressure respiratory variation
PWD	pulsed wave Doppler
RAP	right atrial pressure
SVC	superior vena cava
TEE	transesophageal echocardiography
TTE	transthoracic echocardiography
VTI	velocity time integral

Introduction

Monitoring cardiopulmonary interactions in the critical care setting fulfills two needs. It allows the treating team to evaluate how the patient's cardiovascular system is tolerating the stresses imposed by a disordered ventilation system. The impact of ventilation is greatest on the pulmonary circulation (Versprille 1990), especially when patients are submitted to positive pressure venti-

lation for respiratory failure and also are hemodynamically compromised. As a consequence, a second role for monitoring cardiopulmonary interactions is to guide management and treatment by optimizing central blood volume and respiratory settings in accordance with right (RV) and left (LV) ventricular function. Management of acute respiratory distress syndrome (ARDS) is one of the more difficult tasks facing physicians, and improved understanding of how changes in ventilator setting and the respiratory system properties affect hemodynamics can be especially useful (Writing Group for the Alveolar Recruitment for Acute Respiratory Distress Trial (ART) 2017). The diagnosis and management of many other common clinical situations, too, are directly or indirectly driven by cardiopulmonary interactions, i.e., ventilator weaning failure, hypovolemia, and cardiac failure.

Cardiopulmonary interactions initially were mainly evaluated at the bedside by measuring vascular and cardiac pressures as well as cardiac output with the pulmonary artery catheter (Jardin et al. 1983). However, a limitation of only using pressure measurement is that cardiac pressures are submitted to changes in intrathoracic pressure, whereas the pressures are made relative to atmospheric pressure and the two can be very different during strong inspiratory and expiratory efforts and with the application of large inspiratory pressures. Two "types" of cardiac pressures are key to understanding and analyzing cardio-

A. Vieillard-Baron (✉)
Medical and Surgical Intensive Care Unit, University
Hospital Ambroise Paré, APHP,
Boulogne-Billancourt, France
e-mail: antoine.vieillard-baron@aphp.fr

pulmonary interactions: the intravascular and transmural pressures. Intravascular pressure differences generate flow between two cavities based on their difference in pressure. The transmural pressure is the difference between the pressure inside the vessel and outside the vessel and reflects blood volume in the cavity. A good example of the potential dissociation between these two types of pressure is the spontaneously breathing patient with acute asthma. There is a large negative inspiratory swing in intrathoracic pressure which is most often associated with a fall in right atrial pressure (RAP) measured relative to atmospheric pressure, but the actual transmural pressure and RV preload increase (Jardin et al. 1982) (Fig. 25.1). Monitoring esophageal pressure, as a surrogate of intrathoracic pressure, can help physicians calculate the transmural (distending) pressure, as intravascular pressure minus esophageal pressure, but this is far from perfect in supine ventilated patients and has many limitations and pitfalls in clinical practice (Repressé et al. 2018). Echocardiography provides another possibility for separating intravascular pressure effects from transmural pressure. Visualizing and

measuring the size of the cardiac cavities and great vessels with the 2-D mode can give a surrogate of their respective likely transmural pressures. A small cavity usually indicates that transmural pressure is low, while a large cavity indicates that the transmural pressure is high. However, there needs to be a point of caution, especially for the right heart. In diastole, the right ventricle normally is very compliant and works close to its stressed volume in which case even when filled the diastolic pressures are low. However, even in a normal right ventricle, there is a steep part to the passive filling curve, and when reached, the filling pressure rises rapidly with little change in volume. This occurs with a smaller volume in the failing right ventricle (Patterson and Starling 1914). By combining an evaluation of flow with the pulsed wave Doppler (PWD) mode, echocardiography can provide a surrogate of the pressure difference between two cavities by using the Bernoulli equation (White 1986) (Fig. 25.2), while this mode is much less used by critical care physicians than 2-D mode. By combining both approaches, a physician adequately trained in physiology and critical care

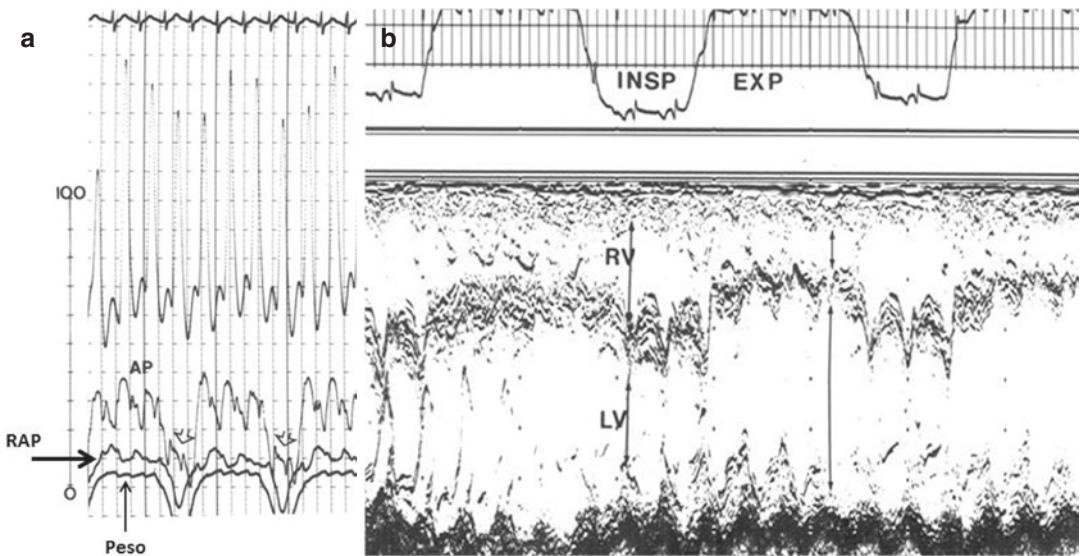


Fig. 25.1 Spontaneously breathing patients with acute asthma monitored by PAC (panel a) and transthoracic echocardiography (panel b). Note in panel a the huge decrease in intravascular right atrial pressure (RAP), suggesting a decrease in RV preload, while the right ventricle

actually dilates (panel b). This decrease in RAP is due to the transmission of the very negative intrathoracic pressure (Peso) during deep inspiration. Insp inspiration, exp expiration, RV right ventricle, LV left ventricle

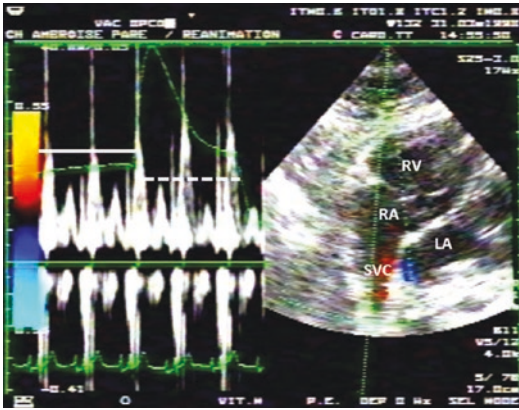


Fig. 25.2 Transthoracic echocardiography by a subcostal approach in a ventilated patient. The pulsed wave Doppler sample is placed at the entry of the superior vena cava (SVC) in the right atrium (RA). It shows a decrease in maximal velocity of the flow into the SVC during tidal ventilation (full white line) compared to expiration (dotted white line). The airway pressure trace is in green on the screen. RV right ventricle, LA left atrium

echocardiography would be fully able to accurately monitor and understand cardiopulmonary interactions: 2-D echo will give information on changes in distending pressures (preload) during ventilation, while PWD will give information on changes in flow (pressure gradient).

Transesophageal echocardiography (TEE) has the advantage over transthoracic echocardiography (TTE) in intubated and ventilated patients because factors that limit the quality and reproducibility of the transthoracic views, and consequently the reproducibility of Doppler flows and cavity sizes in the critically ill patients under positive pressure ventilation, are frequent. These include tissue edema, obesity, high PEEP, and thoracic drains (Cook et al. 2002). Another factor that has not been fully evaluated is that adequate and reproducible TTE images require more skill and training than TEE, in which optimal views are quite easy to obtain in most patients. TTE also is much more operator-dependent than TEE. Finally, TEE allows visualization of essential structures for cardiopulmonary interactions, as the superior vena cava (SVC) and the left and upper pulmonary vein, which are not possible or very challenging by TTE.

A limitation of echocardiography is that it does not provide continuous hemodynamic mon-

itoring and therefore should not be used to continuously detect an “abnormal” cardiopulmonary interaction, but rather to diagnose the main mechanism supporting this interaction, when clinically suspected, with the objective of correcting it in order to improve the patient’s condition. In other words, TEE should be performed when a warning signal suggests to the clinician that there is compromising interaction between the heart, lung, and ventilator. Thus, TEE cannot substitute for continuous invasive blood pressure monitoring which remains mandatory in severely ill patients. Significant respiratory variations of systolic arterial pressure or pulse pressure can indicate that there is a negative cardiopulmonary interaction and that the hemodynamic effects are much more than a simple preload-responsiveness status that can be corrected by fluid administration (Vieillard-Baron et al. 2016), as described more extensively below. Addition of an airway pressure tracing to the screen of the echocardiography machine when evaluating flow and cardiac beat-to-beat variation in cavity size can greatly improve the TEE evaluation of cardiopulmonary interactions.

Because this chapter is not dedicated to how to practically perform a TEE study, readers of this book may read a recent paper on 10 reasons for performing hemodynamic monitoring using TEE (Vignon et al. 2017a). Three main views are recommended: the mid-esophageal view at 0°, the short-axis view (at 0° and at 110° to visualize the LV outflow tract), and the upper esophageal view at 0° and 90°. These are briefly described below.

Monitoring Cardiac Flows by Doppler

Bernoulli’s law can be applied to the recording of the maximal velocity (V_{max}) of a flow between two chambers using PWD, to evaluate the pressure difference between these two cavities using the formula:

$$\text{Pressure difference} = (4 \times V_{max}^2).$$

When there is sufficient tricuspid regurgitation, V_{max} from the regurgitant flow gives the

pressure difference between the RV end-systolic pressure and RAP. Accordingly, this value is elevated when there is pulmonary hypertension.

A measurement of V_{max} through the aortic outflow tract gives the pressure difference between the left ventricle and the aorta, which when elevated not only represents aortic valve stenosis but also subvalvular stenosis which can occur in critically ill patients with hypertrophic cardiomyopathy and a profound underfilled left ventricle due to volume loss, right ventricular limitation, and even in sepsis. This process is usually a dynamic obstruction in the left ventricle due to systolic anterior motion of the mitral valve as visualized by 2-D mode. This problem is usually corrected by fluid expansion as long as there is not a concurrent limitation to RV volume making it unresponsive to a volume bolus (Chauvet et al. 2015).

On the right side, the transverse (0°) upper esophageal view is used to visualize the great vessels. From this view, ejection RV flow from the right ventricle to the pulmonary artery is recorded with the PWD sample placed in the main pulmonary artery just above the pulmonary valve (Fig. 25.3). Tidal ventilation induces a decrease in V_{max} across the pulmonary valve, which reaches a minimal value at the plateau of inspiration. The magnitude of the decrease varies according to the hemodynamic status of the RV (Fig. 25.3, panel a). This is supported by a decrease in the pressure difference during the ejection between the right ventricle and the pulmonary artery, which is especially due to elevation of the pulmonary artery pressure (Scharf and Ingram Jr. 1977; Scharf et al. 1980) or a decrease in RV pressure. At the same time, this is usually associated with a decrease in the velocity-time integral (VTI) of the flow, which reflects the decrease in RV stroke volume.

On the left side, LV ejection flow can be recorded when the PWD sampled in the LV outflow tract. In a mechanically ventilated patient, the LV ejection flow is 180° out of phase with the RV ejection flow, and LV outflow maximal velocity and VTI increase at end-inspiration (Fig. 25.4, panel a). This increase is due to an increase in the pressure difference between the left ventricle and

the aorta because of the transmission of the positive intrathoracic pressure to the left ventricle (McGregor 1979; Buda et al. 1979) and also because of an increase in the pulmonary venous return and consequent increase in the LV preload (Vieillard-Baron et al. 2003), as further described below. This increase in LV preload can be visualized by also placing the PWD sample in the left and upper pulmonary vein and is related to an increase in the pressure difference between the pulmonary venous circulation and the left atrium induced by the tidal ventilation (Fig. 25.4, panel b). This is due to the compression of intra-alveolar vessels in the lungs during lung inflation whether with positive or with negative pressure ventilation (Howell et al. 1961).

Monitoring Transmural Cardiac Pressures by 2-D TEE

Although there is not a good relationship between diastolic volumes and the diastolic filling pressures, especially on the right side, the cavity size can give an indication that there is at least adequate filling for the Starling effect but is not very good at indicating that there is an excessive filling pressure because the diastolic filling curve becomes very steep at the limit of RV filling. However, a small volume in association with a small stroke volume or a low blood pressure likely indicates that filling is inadequate. Furthermore, small cardiac volumes with high filling pressures indicate that the transmural pressure is likely low because of tamponade (Bodson et al. 2011) or compression by the pleural pressure or lungs. Performing this evaluation of the respiratory changes in cardiac size using 2-D TEE sheds light on different mechanisms explaining the respiratory variations in right and left ventricular flows described above.

Respiratory variations in RV ejection flow can be related to an obstruction of the pulmonary circulation during tidal ventilation due to compression of pulmonary capillaries by the distending alveoli (West et al. 1964). This produces an “afterload effect” from mechanical ventilation. Under this condition, the right ven-

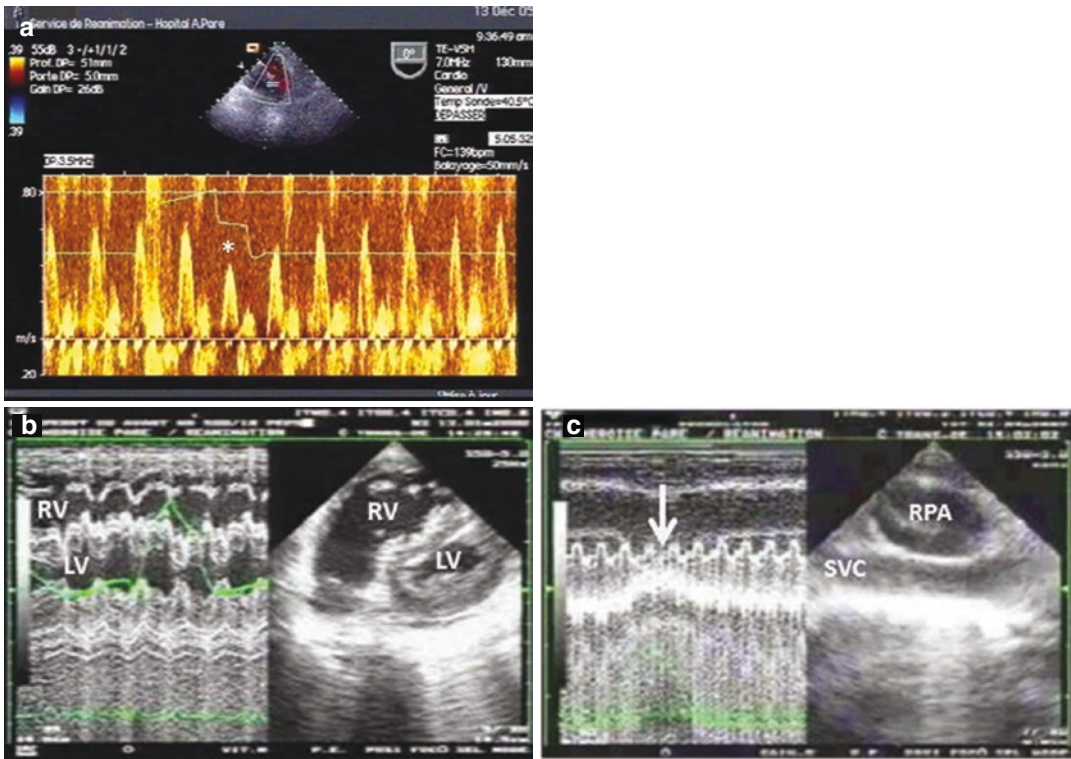


Fig. 25.3 TEE in a ventilated patient with pulse pressure respiratory variations. Panel **a**: pulsed wave Doppler in the main pulmonary artery demonstrating significant decrease in RV ejection (Vmax and VTI) during tidal ventilation (asterisk). Panel **b**: Time-motion study in a short-axis transgastric view in a patient ventilated for ARDS

tricle cyclically dilates (Fig. 25.3, panel b). Conversely, when the variation in RV ejection flow is primarily due to a decrease in systemic venous return during tidal ventilation, which is called the “preload effect” of mechanical ventilation, the right ventricle does not dilate, but the SVC partially or completely cyclically collapses (Fig. 25.3, panel c).

One of the causes of respiratory variation of LV ejection flow is the augmentation of the pulmonary venous return, the tidal ventilation pushing blood from the pulmonary capillaries to the left atrium (Vieillard-Baron et al. 2003; Howell et al. 1961). In this situation, TEE visualizes an increase in the left atrium size (Fig. 25.4, panel c) (Vieillard-Baron et al. 1999). This effect is much more related to tidal volume than to airway pressure, since the higher the tidal volume, the more

and presenting an “afterload” effect. Note that the right ventricle (RV) dilates during each insufflation. Panel **c**: Upper esophageal view of the superior vena cava (SVC) in a patient with a “preload” effect. Note the collapse of the vessel during each insufflation (white arrow). LV left ventricle, RPA right pulmonary artery

this effect is observed for the same plateau pressure (Vieillard-Baron et al. 1999). Another and perhaps more important factor is a decrease in left ventricular afterload with the onset of inspiration because the pressure in the left ventricle is raised by the mechanical breath relative to the abdominal aorta.

Clinical Applications

As reiterated above, continuous invasive blood pressure monitoring is required in most severely ill patients. In the absence of any pulse pressure respiratory variation (PPV), physicians may think that there are no significant cardiopulmonary interactions requiring a specific intervention, but this may not always be the case. For

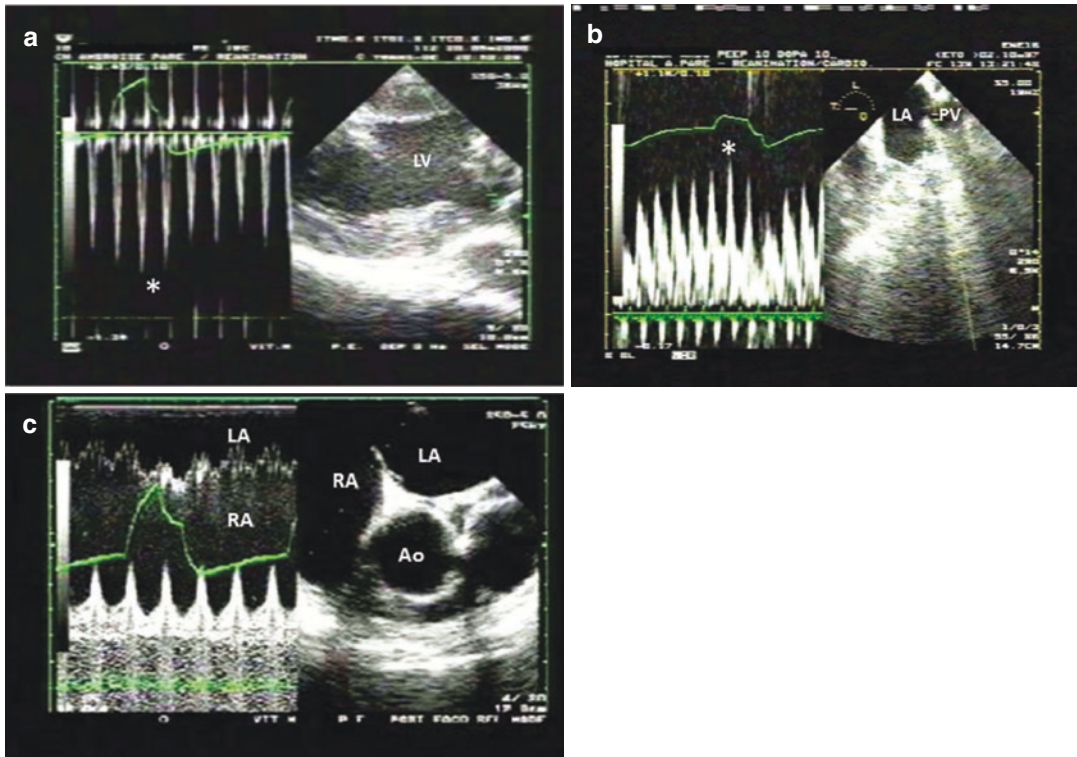


Fig. 25.4 TEE in a ventilated patient. Note that the airway pressure trace appears in green on the screen. Panel a: pulsed wave Doppler in the left ventricular outflow tract in (transgastric view) demonstrated an increase in LV ejection flow during tidal ventilation (asterisk). Panel b: the pulsed wave Doppler in the left and upper pulmonary vein

showed an increase in the pulmonary venous return during tidal ventilation (asterisk). Panel c: Time motion study across the interatrial septum showed an increase in left atrial size during tidal ventilation. LV left ventricle, LA left atrium, RA right atrium, PV pulmonary vein, Ao ascending aorta

example, overloading the right ventricle by the application of high PEEP might still decrease the steady-state RV stroke volume even without there being a PPV because the RV filling is already limited. However, this means that the steady-state cardiac output must be decreased unless the heart rate changed. A TEE could reveal a dilated RV which may be improved by lowering the PEEP or at least confirming that total pulmonary compliance is optimal. When there is significant PPV, there is no “magic” cutoff for what is “significant” PPV; it rather depends on the clinical situation, and physicians should appreciate that there are significant cardiopulmonary interactions, and a TEE should be considered to evaluate the mechanism of this interactions, specifically, how much is “preload” and how much “afterload” effect, so that management can be optimized.

There are numerous clinical situations in which monitoring of cardiopulmonary interactions by TEE in a ventilated patient is relevant. As we cannot be exhaustive in this chapter, we will discuss two classical situations: first is a septic patient whom the physician considers giving more fluid (Fig. 25.5), and second is a patient with severe ARDS in which adaptation of the respiratory strategy is required to improve hemodynamics (Fig. 25.6).

As briefly discussed in the first part of this chapter, PWD allows visualization of respiratory changes in V_{max} and VTI of the RV ejection flow in subjects with PPV (Fig. 25.3, panel a). There are three differences between the “preload” effect (which may require the administration of more fluid to the patient) and the “afterload” effect (which may not require the

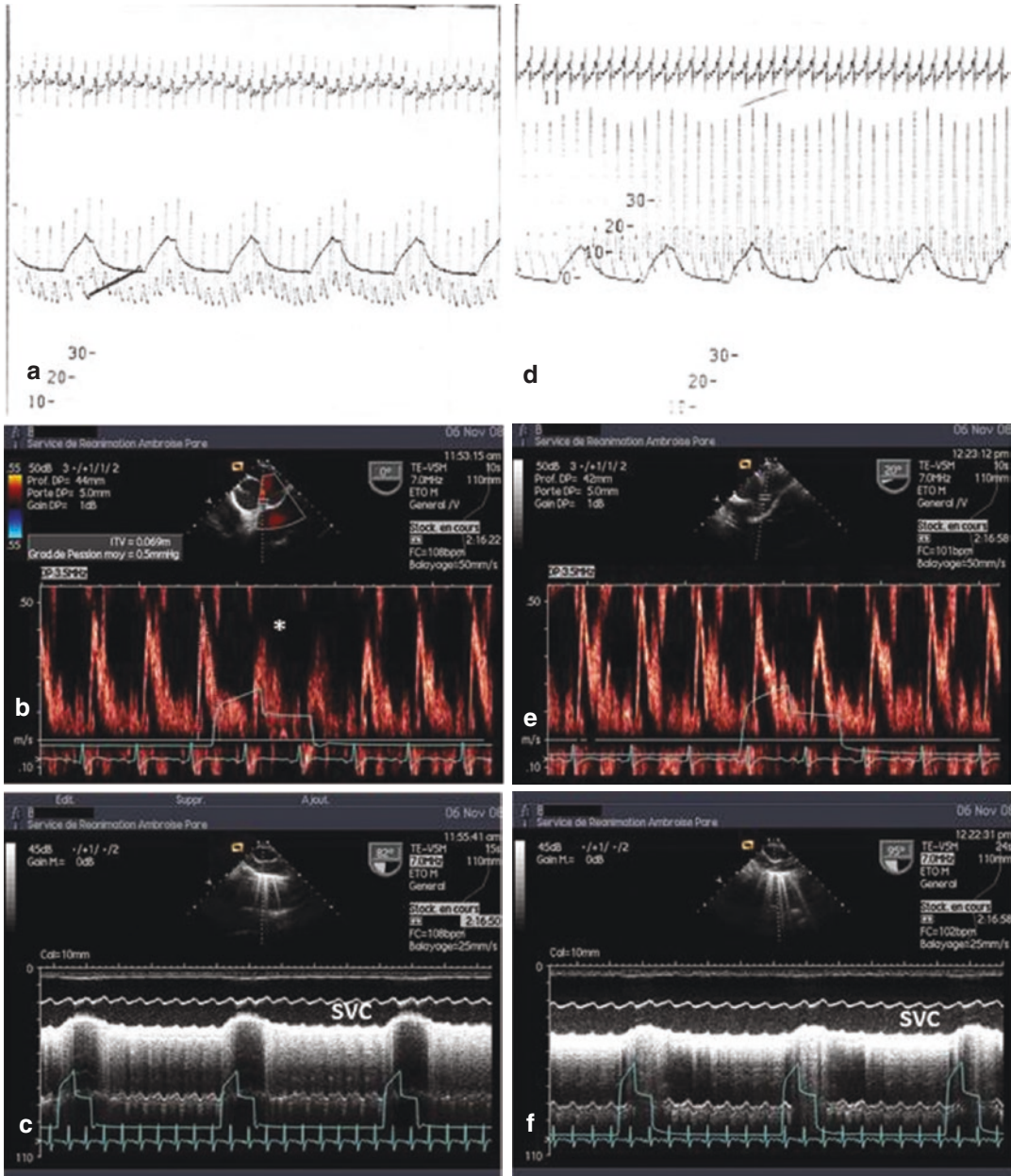


Fig. 25.5 Pulse pressure variations (panels **a**, **d**) and TEE evaluation in a septic patient. Panels **a–c** at baseline; panels **d–f** after fluid expansion. At baseline, the patient had a significant decrease in RV ejection flow during tidal ventilation using the pulsed wave Doppler in the main pulmonary artery (panel **b** asterisk, upper esophageal view),

which disappeared after fluid expansion (panel **e**). This was associated with a cyclic collapse of the superior vena cava (SVC) (panel **c**, upper esophageal view at 90° using the time motion study), which also disappeared after fluid expansion (panel **f**)

administration of more fluid, but rather a change in respiratory strategy). The first difference is that the magnitude of PPV and the magnitude of respiratory variations of RV ejection flow are

probably higher in the case of the “preload” effect, although they have been never carefully compared. In the case of the “afterload” effect, the magnitude of potential PPV depends on how

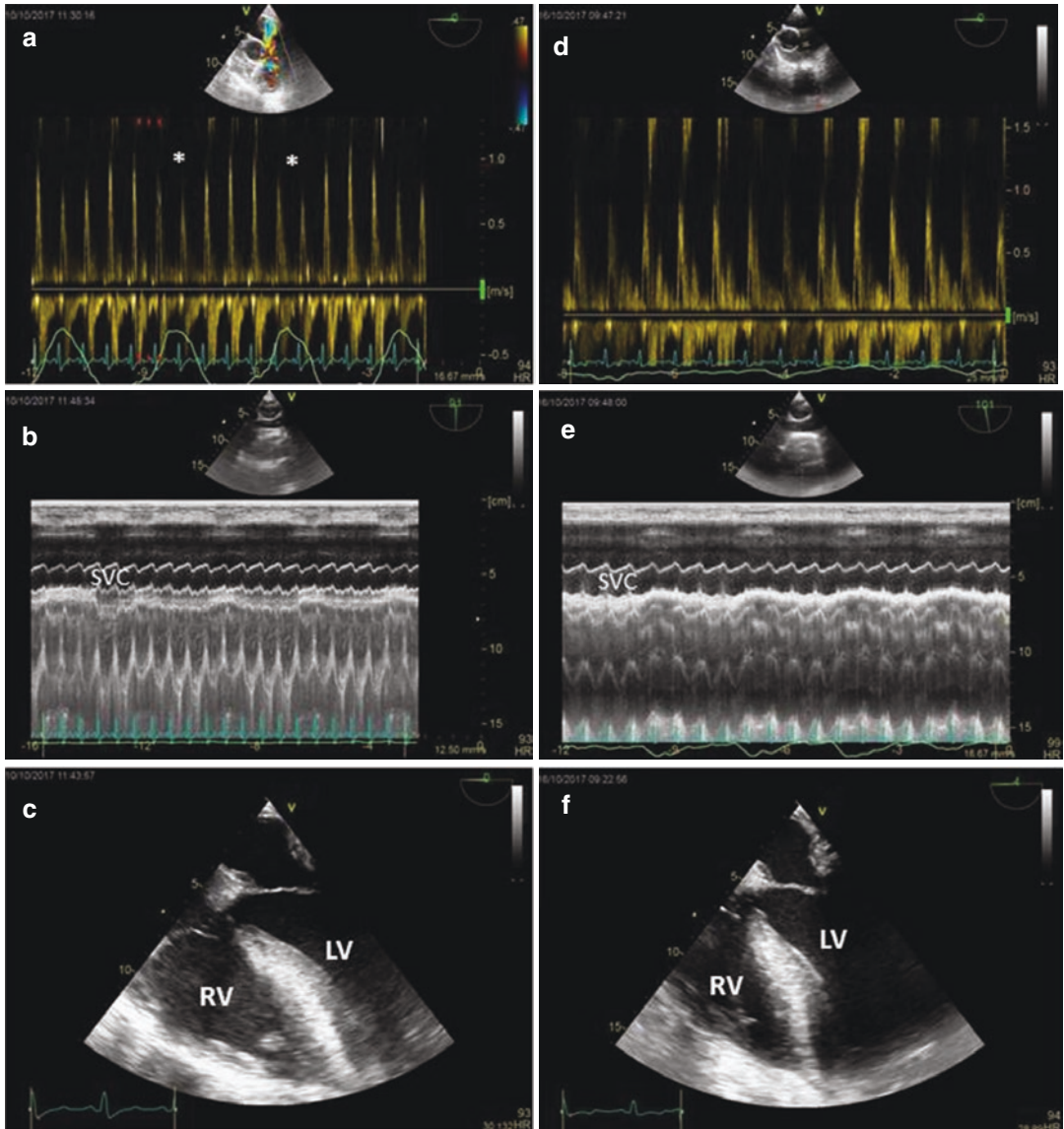


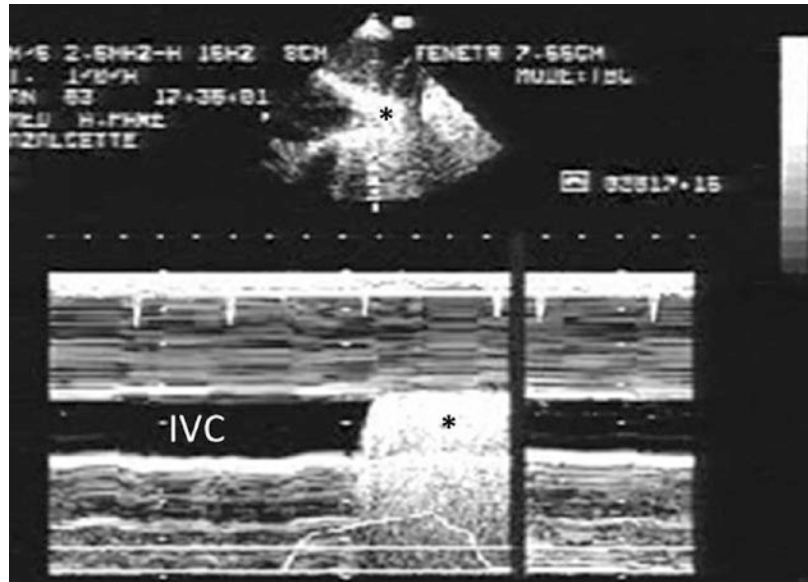
Fig. 25.6 TEE in a patient ventilated for severe ARDS with a plateau pressure of 30 cmH₂O (panels a–c) and after a significant decrease in plateau pressure (panels d–f). Initially, TEE showed a significant decrease in RV ejection flow during tidal ventilation (panel a), without collapse of the superior vena cava (SVC, panel b) and a

moderate dilatation of the right ventricle (RV). After the decrease in tidal volume and plateau pressure, no further significant decrease in RV ejection flow and RV dilatation (panels d, f) was present. SVC did not change (panel e). LV left ventricle

low the stroke volume is decreased. If no significant PPV is observed, one could argue that obstruction of the RV ejection by tidal ventilation has no clinical impact. While no data may support this assertion, it might indicate the first step in the process leading to RV failure. The

second difference is that in the case of the “pre-load” effect, there should be evident respiratory variations of SVC (Δ SVC) on the TEE, but not in the case of the “afterload” effect. To evaluate this, the TEE needs to visualize the SVC in its long axis at the upper esophageal view after

Fig. 25.7 Subcostal view in a ventilated patient with RV failure in whom agitated saline (contrast) was injected. During tidal ventilation (see the airway pressure trace in white), the 2D and time motion mode visualized a back flow into the inferior vena cava and sub hepatic veins (asterisk). IVC inferior vena cava



rotating the ultrasound beam by 90° (Vieillard-Baron et al. 2004) (Figs. 25.3, panel c, 25.5, panel c, f, 25.6, panel c, e). Accuracy and cutoff values of the change in SVC diameter were recently reported to predict fluid responsiveness in a large population of ventilated patients in shock (Vignon et al. 2017b). The third difference is that the right ventricle is usually not significantly dilated in the “preload” effect, but it is with the “afterload” effect (Figs. 25.3, panel b, 25.6, panel c, f). These three TEE differences can be used to accurately analyze the mechanisms of PPV, thereby avoiding inappropriate use of fluids which have been shown to impair RV function (Patterson and Starling 1914). Support for this was recently reported in an experimental study of RV failure related to acute obstruction of the pulmonary circulation. In that study, fluids impaired RV function, whereas hemodynamics support with norepinephrine improved RV function (Ghignone et al. 1984). The presence of a slightly dilated right ventricle, in association with significant tricuspid regurgitation, no SVC respiratory variations, and a bulging of the interatrial septum toward the left atrium (reflect of high pressure) are good warning signs that more fluids should not be given.

The effect of lung inflation on tricuspid regurgitation is easy to report with the potent observation of a backflow into the inferior vena cava and subhepatic veins when injecting agitated saline for contrast. This can be nicely observed using TTE by a subcostal approach (Fig. 25.7). It is likely too late to hold fluids when the interventricular septum is bulging toward the left ventricle. For all these reasons, critical care echocardiography and especially TEE should be part of the initial assessment in all severely ill and ventilated patients as it may get numerous information.

Conclusion

Echocardiography, as well as especially TEE in a ventilated patient, is a fantastic device to evaluate mechanisms of cardiopulmonary interactions (“preload” or “afterload” effect), if not contraindicated. Indeed, the association of size and flows, using 2-D and PWD, allows TEE to evaluate transmural pressures and pressure gradients, respectively. TEE has to be combined with continuous invasive monitoring of blood pressure, which may allow physicians to detect such interactions in the case of PPV.

References

- Bodson L, Bouferrache K, Vieillard-Baron A. Cardiac tamponade. *Curr Opin Crit Care*. 2011;17:416–24.
- Buda AJ, Pinsky MR, Ingels NB Jr, Daughters GT 2nd, Stinson EB, Alderman EL. Effect of intrathoracic pressure on left ventricular performance. *N Engl J Med*. 1979;301:453–9.
- Chauvet JL, El-Dash S, Delastre O, et al. Early dynamic left ventricular obstruction is associated with hypovolemia and high mortality in septic shock patients. *Crit Care*. 2015;19:262.
- Cook CH, Praba AC, Beery PR, Martin LC. Transthoracic echocardiography is not cost-effective in critically ill surgical patients. *J Trauma*. 2002;52:280–4.
- Ghignone M, Girling L, Prewitt RM. Volume expansion versus norepinephrine in treatment of a low cardiac output complicating and acute increase in right ventricular afterload in dogs. *Anesthesiology*. 1984;60:132–5.
- Howell JB, Permutt S, Proctor DF, Riley RL. Effect of inflation of the lung on different parts of pulmonary vascular bed. *J Appl Physiol*. 1961;16:71–6.
- Jardin F, Farcot JC, Boisante L, Prost JF, Gueret P, Bourdarias JP. Mechanism of paradoxical pulse in bronchial asthma. *Circulation*. 1982;66:887–94.
- Jardin F, Farcot JC, Gueret P, Prost JF, Ozier Y, Bourdarias JP. Cyclic changes in arterial pulse during respiratory support. *Circulation*. 1983;68:266–74.
- McGregor M. Current concepts: pulsus paradoxus. *N Engl J Med*. 1979;301:480–2.
- Patterson SW, Starling EH. On the mechanical factors which determine the output of the ventricles. *J Physiol*. 1914;48:357–79.
- Repressé X, Vieillard-Baron A, Geri G. Value of measuring esophageal pressure to evaluate heart-lung interactions. Applications for invasive hemodynamic monitoring. *Ann Transl Med*. 2018;6:351.
- Scharf SM, Ingram RH Jr. Effects of decreasing lung compliance with oleic acid on the cardiovascular response to PEEP. *Am J Phys*. 1977;233:H635–41.
- Scharf SM, Brown R, Saunders N, Green LH. Hemodynamic effects of positive pressure inflation. *J Appl Physiol Respir Environ Exerc Physiol*. 1980;49:124–31.
- Versprille A. The pulmonary circulation during mechanical ventilation. *Acta Anaesthesiol Scand*. 1990;34:51–62.
- Vieillard-Baron A, Loubieres Y, Schmitt JM, Page B, Dubourg O, Jardin F. Cyclic changes in right ventricular output impedance during mechanical ventilation. *J Appl Physiol* (1985). 1999;87:1644–50.
- Vieillard-Baron A, Chergui K, Augarde R, Prin S, Page B, Beauchet A, Jardin F. Cyclic changes in arterial pulse during respiratory support revisited by Doppler echocardiography. *Am J Respir Crit Care Med*. 2003;168:671–6.
- Vieillard-Baron A, Chergui K, Rabiller A, Peyrouset O, Page B, Beauchet A, Jardin F. Superior vena caval collapsibility as a gauge of volume status in ventilated septic patients. *Intensive Care Med*. 2004;30:1734–9.
- Vieillard-Baron A, Matthay M, Teboul JL, Bein T, Schultz M, Magder S, Marini JJ. Expert's opinion on management of hemodynamics in ARDS patients: focus on the effects of mechanical ventilation. *Intensive Care Med*. 2016;42:739–49.
- Vignon P, Merz TM, Vieillard-Baron A. Ten reasons for performing hemodynamic monitoring using transesophageal echocardiography. *Intensive Care Med*. 2017a;43:1048–51.
- Vignon P, Repessé X, Bégot E, Léger J, Jacob C, Bouferrache K, Slama M, Prat G, Vieillard-Baron A. Comparison of echocardiographic indices used to predict fluid responsiveness in ventilated patients. *Am J Respir Crit Care Med*. 2017b;195:1022–32.
- West JB, Dollery CT, Naimark A. Distribution of blood flow in isolated lung; relation to vascular bed and alveolar pressure. *J Appl Physiol*. 1964;19:713–24.
- White FM. *Fluids mechanics*. 2nd ed. New York: McGraw-Hill; 1986.
- Writing Group for the Alveolar Recruitment for Acute Respiratory Distress Trial (ART). Effect of lung recruitment and titrated positive end-expiratory pressure (PEEP) vs low PEEP on mortality in patients with acute respiratory distress syndrome: a randomized clinical trial. *JAMA*. 2017;318:1335–45.



Extra-cardiac Doppler Hemodynamic Assessment Using Point-of-Care Ultrasound

26

William Beaubien-Souligny and André Denault

Abbreviations

A	vessel cross-sectional area	CO	cardiac output
ICU	intensive care unit	CPB	cardiopulmonary bypass
CVP	central venous pressure	d	diameter
ICU	intensive care unit	D	diastolic
IVC	inferior vena cava	DAP	diastolic arterial pressure
POCUS	point-of-care ultrasound	ECA	external carotid artery
Q	blood flow	EDV	end-diastolic velocity
ΔP	pressure difference	HITS	high intensity transient signals
PF	pulsatility fraction	HR	heart rate
PI	pulsatility index	HV	hepatic vein
R	resistance	IABP	intra-aortic counterpulsation balloon pump
RI	resistive index	HR	hazard ratio
V	velocity	ICA	internal carotid artery
TVI	time-velocity integral	ICU	intensive care unit
Ao	aorta	IVC	inferior vena cava
AR	atrial reversal	LA	left atrium
CI	confidence interval	LV	left ventricle
		LVOT	left ventricular outflow tract
		MPA	main pulmonary artery
		MV	mean velocity
		PDV	peak systolic velocity
		PF	pulsatility fraction
		Pfa	femoral arterial pressure
		Pms	mean systemic venous pressure
		Pra	radial arterial pressure
		Pra	right atrial pressure
		PIC	intra-capsular renal pressure
		Ppa	pulmonary artery pressure
		Rvr	resistance to venous return
		RA	right atrium
		RI	resistance index

W. Beaubien-Souligny
Division of Nephrology, Department of Medicine,
Centre Hospitalier de l'Université de Montréal,
Montreal, QC, Canada

Department of Anesthesia, Montreal Heart Institute,
Université de Montréal, Montreal, QC, Canada

A. Denault (✉)
Department of Anesthesia, Montreal Heart Institute,
Université de Montréal, Montreal, QC, Canada

Division of Intensive Care, Montreal Heart Institute,
Université de Montréal, Montreal, QC, Canada

Division of Intensive Care, Centre Hospitalier de
l'Université de Montréal, Montreal, QC, Canada

RPA	right pulmonary artery
RV	right ventricle
S	systolic
SaO ₂	oxygen saturation
SAP	systolic arterial pressure
SVC	superior vena cava
V	velocity
V _d	diastolic velocity
V _m	mean velocity
V _{max}	maximal velocity during the cardiac cycle
V _{min}	minimal velocity during the cardiac cycle
V _s	systolic velocity
VTI	velocity-time integral

Introduction

Ultrasound imaging technology has become ubiquitous in intensive care unit (ICU) and is now being rapidly integrated in primary care due to improvement and miniaturization of the technology (Narula et al. 2018). Currently, Point-of-Care UltraSound (POCUS) is used to rapidly exclude life threatening conditions and to guide procedures at the bedside to a decrease the risk of complications. While most of the ultrasound devices possess Doppler technology, this mode is largely underutilized in the clinical setting. Doppler ultrasound enables clinicians to assess blood velocity in various blood vessels, offering a unique window into the hemodynamic status of the patient. In this chapter, we review the basic principles required for the interpretation of the Doppler assessment and offer examples on how Doppler assessment can provide important information in common clinical settings that are frequently encountered in the ICU.

Principles of Doppler Ultrasound

Pulse wave Doppler produces a time-velocity waveform during the cardiac cycle at the site of

assessment. Blood flow (Q) in a vessel is determined by the pressure difference between the ends of the vascular network (ΔP) and by the resistance (R) between the ends of the bed:

$$Q = \frac{\Delta P}{R}$$

Blood velocity depends on the blood flow and the vessel cross-sectional area (A) at the point of assessment:

$$V = \frac{Q}{A} = \frac{\Delta P}{R \times A}$$

Therefore, blood flow velocity depends on three specific variables: the pressure difference across the vessel, the resistance and the area of the vessel. The vascular system is a complex structure which includes five broad sections that can be assessed using Doppler ultrasound. Each of these sections have different properties. These characteristics will determine the normal appearance of the pulse wave Doppler waveform as shown in Fig. 26.1. As will be discussed, some variations in flow patterns can be seen depending upon the organ that is assessed. The main parameters used in routine ICU care and the indices derived from the arterial and venous waveform are summarized in Fig. 26.2 and include: pulsatility index (PI), resistive index (RI), systolic to diastolic index, systolic filling fraction, and pulsatility fraction (PF). Some parameters are qualitative in nature (e.g., continuous vs. discontinuous) while some rely on precise measurements. In order to accurately measure absolute blood velocity inside a vessel, the optimal Doppler assessment must be aligned parallel to the blood flow. In large vessels, angle correction can be performed when the angle of interrogation is $<60^\circ$. However, this is challenging to do in small vessels. Consequently, absolute blood velocity measurements in peripheral arteries and veins often are unreliable. The use of indices such as RI and PI are not subject to this problem. By using a ratio of absolute velocities, these measurements are less dependent on the angle of assessment.

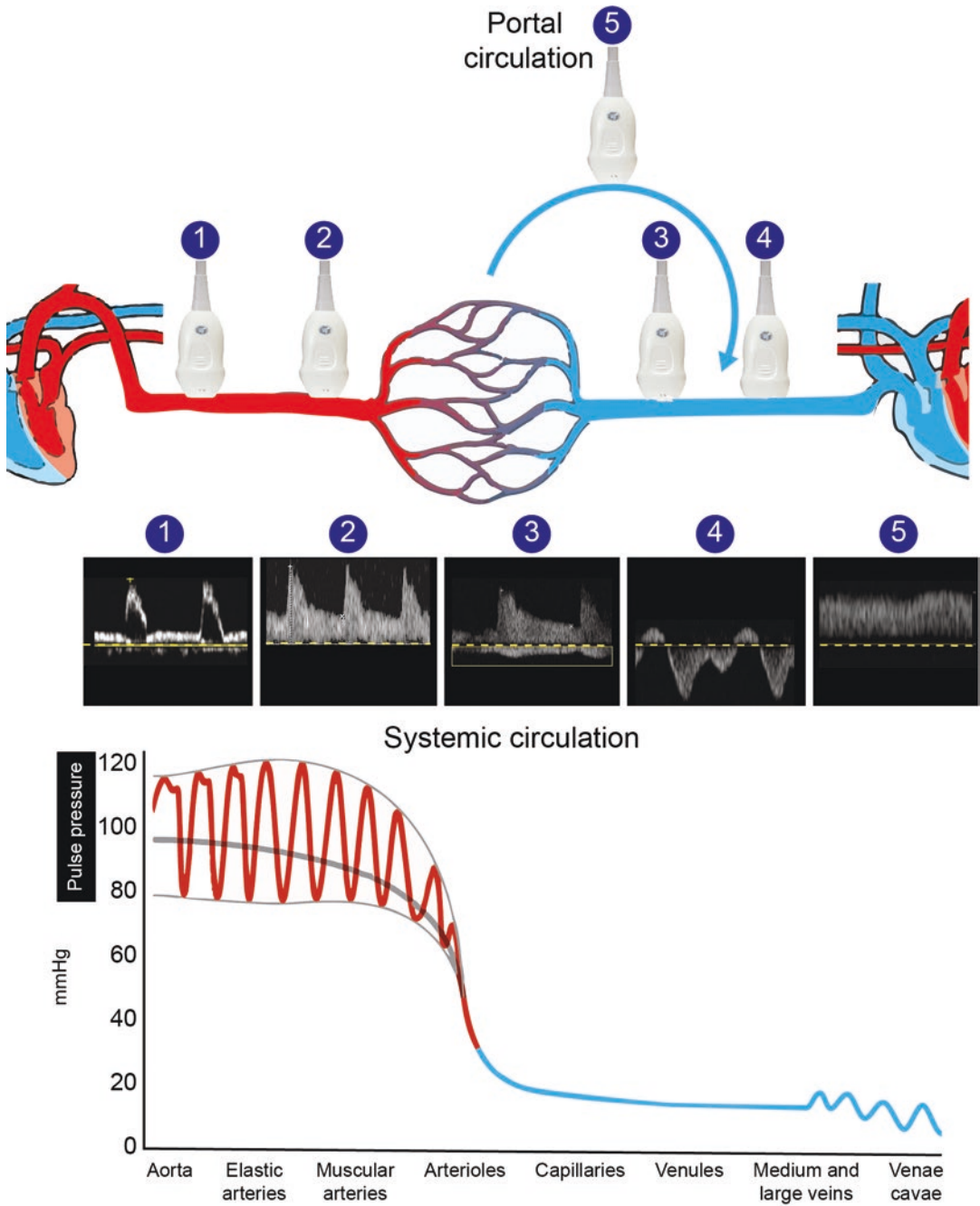


Fig. 26.1 Doppler assessment of the circulatory system. The type waveform observed on pulse-wave Doppler ultrasound will correspond to the sub-sections examined

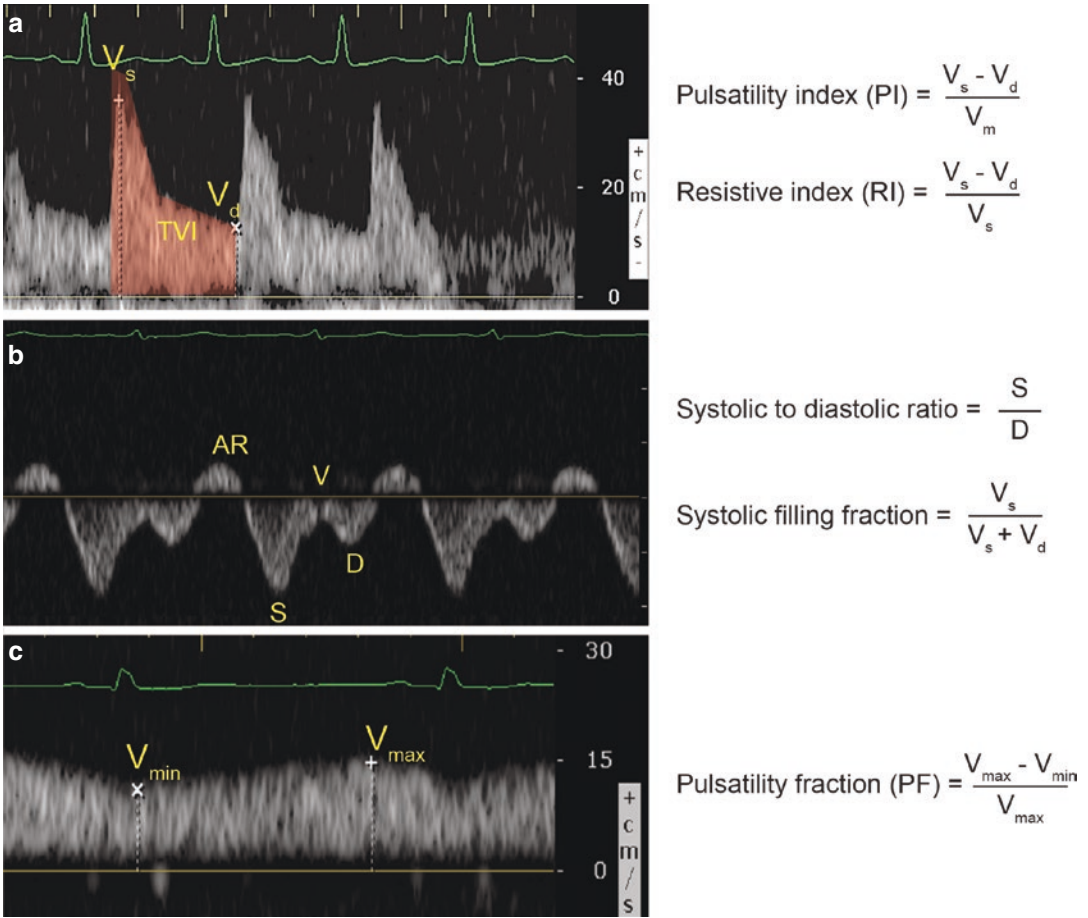


Fig. 26.2 Analysis of the (a) arterial, (b) venous, and (c) portal venous waveform. Indices for each type of waveforms can be calculated from measured absolute velocity values. AR atrial reversal, S systole, D diastole, TVI time

velocity integral, V_s systolic velocity, V_d diastolic velocity, V_m mean velocity, V_{\max} maximal velocity during the cardiac cycle, V_{\min} minimal velocity during the cardiac cycle

The Arterial Doppler Waveform

The indices derived from the arterial waveform are affected by multiple factors. For PI, these can be summarized using this equation (Adamson 1999):

$$PI_{\text{Doppler}} = PI_{\text{Pressure}} \times \frac{\text{Resistance}}{\text{Impedance}}$$

The pulsatility index of arterial pressure (PI_{Pressure}) is dependent upon upstream factors (cardiac, aortic, main arteries). Figure 26.3a, b shows modification of the arterial waveform by severe aortic stenosis and intra-aortic

balloon pump counter-pulsation. Resistance represents the opposition of the downstream vascular bed to steady (continuous) blood flow. This understanding explains why the Doppler waveform of the external carotid artery is different from that of the internal carotid artery (Fig. 26.3c, d). The external carotid artery supplies the facial muscles which are a high resistance circulation. This results in reduced or absent diastolic velocities. In contrast, the internal carotid artery supplies the cerebral circulation which is a low resistance circulation. As is case with other low resistance vascular beds such as renal and hepatic vascular beds, diastolic velocities are higher. Impedance is a complex concept that can be sim-

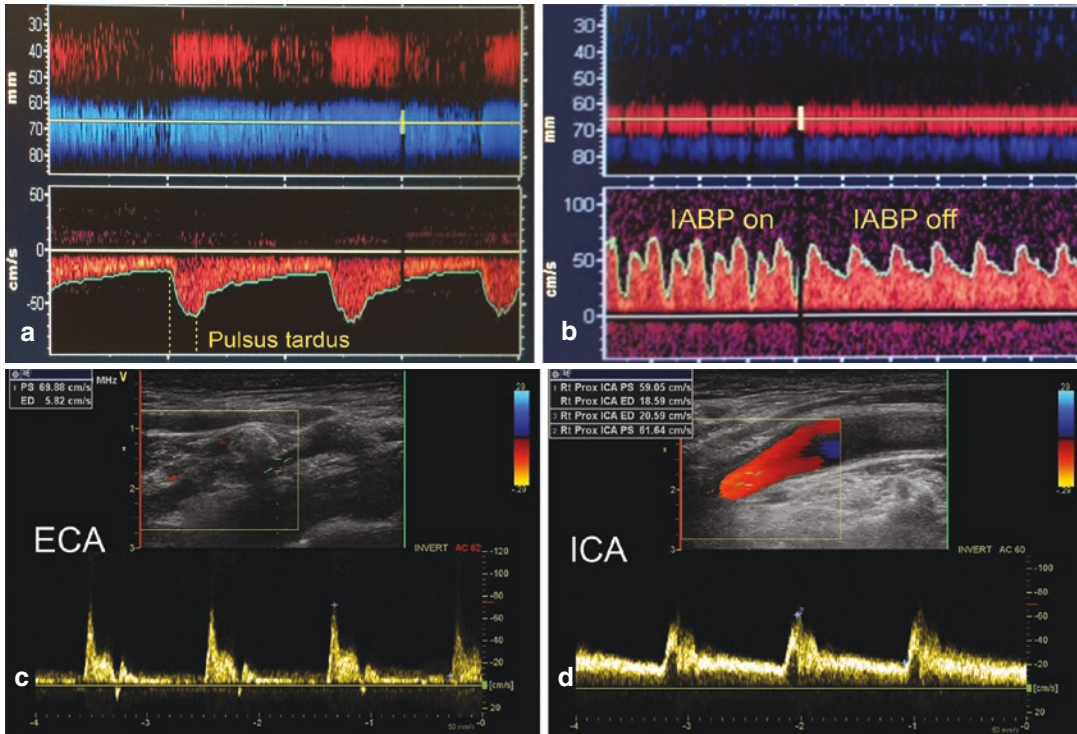


Fig. 26.3 Examples of factors affecting the arterial pressure waveform. (a) Delayed systolic upstroke observed on transcranial Doppler in a patient with severe aortic stenosis. (b) Modification of the transcranial Doppler waveform in a patient with an intra-aortic counterpulsation balloon pump (IABP). (c) Doppler waveform of the external carotid artery (ECA) compared with the (d) internal

carotid artery (ICA). The diastolic velocities are lower in the ECA due to the high resistance of the downstream circulation. (Adapted from Basic Transesophageal and Critical Care Ultrasound©, Denault et al. (Denault et al. 2017), reproduced with permission of Taylor and Francis Group, a division of Informa plc)

plified as the opposition to pulsatile blood flow or the resistance of a pulsatile system (Adamson 1999; Vlachopoulos et al. 2011). It depends upon the attributes of the vessel being assessed including its compliance, vessel dimension, and pulse wave reflections from downstream vascular beds. Therefore, impedance is also partially related to the resistance in this equation, although the relationship is complex and varies depending upon the location within the circulatory system at which it is measured. Hence, reflected waves from a high resistance circulation produce a lower diastolic velocity on Doppler assessment. This concept commonly is to diagnose intracranial hypertension with transcranial Doppler (Hassler et al. 1989).

The clinical factors that can commonly affect the PI_{Pressure} , resistance and impedance are pre-

sented in Table 26.1. Contrary to what is often believed, the PI and the RI are not direct measures of blood flow or resistance of the downstream vascular bed and there can be important variations within these parameters without any significant changes in the Doppler indices (Adamson 1999). Experiments in animals have shown that when vascular resistance is increased by infusion of vasoactive agents and organ blood flow modified, changes in RI and PI were not correlated with organ blood flow (Wan et al. 2008) and were only correlated with vascular resistance when impedance was integrated into the model (Adamson 1999). Notwithstanding that the interpretation of these indices is complex, the arterial pulse wave Doppler still can be informative for the following reasons: (1) assessment at multiple sites may potentially identify specific organs with

Table 26.1 Common clinical factors influencing the arterial Doppler waveform in critically ill patients

	Parameters
Pulse pressure (upstream factors)	Vascular rigidity: age, atherosclerosis
	Aortic valve disease
	Stroke volume
	Heart rate
	Stenosis of main arteries
	Mechanical circulatory support
Resistance (downstream factors)	Physiologic characteristic of the downstream capillary bed
	Vasoconstriction
	Occlusion: e.g., emboli, thrombotic microangiopathy
	External compression: e.g., compartment syndrome
	Venous hypertension
	Atherosclerosis of the downstream circulation
Impedance (local factors)	Characteristics of the vessel Compliance Cross-sectional area Vasoconstriction/dilatation
	Reflected secondary pressure wave ^a

^aAffected by downstream and local characteristics

ongoing pathological processes; (2) repeated assessment can identify important hemodynamic changes and provide insights about the effect of interventions.

The Venous Doppler Waveform

The venous waveform is determined by a different set of factors. Blood flow exiting the systemic capillary network is non-pulsatile. However, pressure variations in the right atrium during the cardiac cycle produces a “venous pulse” that is biphasic, with systolic and diastolic components corresponding to periods of right atrial filling and emptying. Consequently, there is a variable pressure difference to venous return during the cardiac cycle. These phases can be observed during pulse wave Doppler examination of large veins including the inferior and superior vena cava and large proximal veins such as the hepatic, femoral and jugular veins (Chavhan et al. 2008). However, the variations of blood flow velocities in these regions are dampened or completely absent when Doppler

signals are obtained in peripheral veins. This is explained by the high compliance of these venous compartments as presented in Fig. 26.4a, b.

The analysis venous waveform thus can be informative for the following reasons. (1) The appearance of pulsatile venous flow in the peripheral venous system is consistent with a non-physiologic decrease in venous compliance and can be used to indicate significantly increased venous pressure (Tang and Kitai 2016). This assessment complements the interpretation of the central venous pressure (CVP) waveform (Fig. 26.4c, d). (2) The absence of variations in proximal venous vessels indicates that there likely is an obstruction between the segment being assessed and the right atrium (Ko et al. 2003). (3) The relative proportion of the components (systolic and diastolic) of the venous waveform offer insights about cardiac function (Rudski et al. 2010) which can be assessed by using the ratio of the maximal venous velocity in systole and diastole (V_s/V_d) (Nagueh et al. 1996).

The Portal Doppler Waveform

The portal system is isolated from the systemic circulation by the splanchnic capillary bed and by the liver sinusoids. Physiologic blood flow in portal veins and its tributaries should therefore neither be pulsatile nor greatly affected by the pressure variations in the right atrium during the cardiac cycle (McNaughton and Abu-Yousef 2011). The main determinants of portal flow velocity include arterial blood flow to the splanchnic and splenic capillary networks, the vessel diameter at the site of assessment, and the trans-hepatic pressure difference which is due to intrahepatic resistance. Under normal conditions, the Doppler waveform of the portal vein is antegrade with minimal variations of velocity during the cardiac cycle. The maximal velocity occurs at the end of diastole and the nadir occurring in systole. These components correspond to the slightly delayed effect of the atrial or “a” wave and the diastolic or “D” wave of the systemic venous waveform presented earlier. Doppler assessment of the portal circulation can be informative for

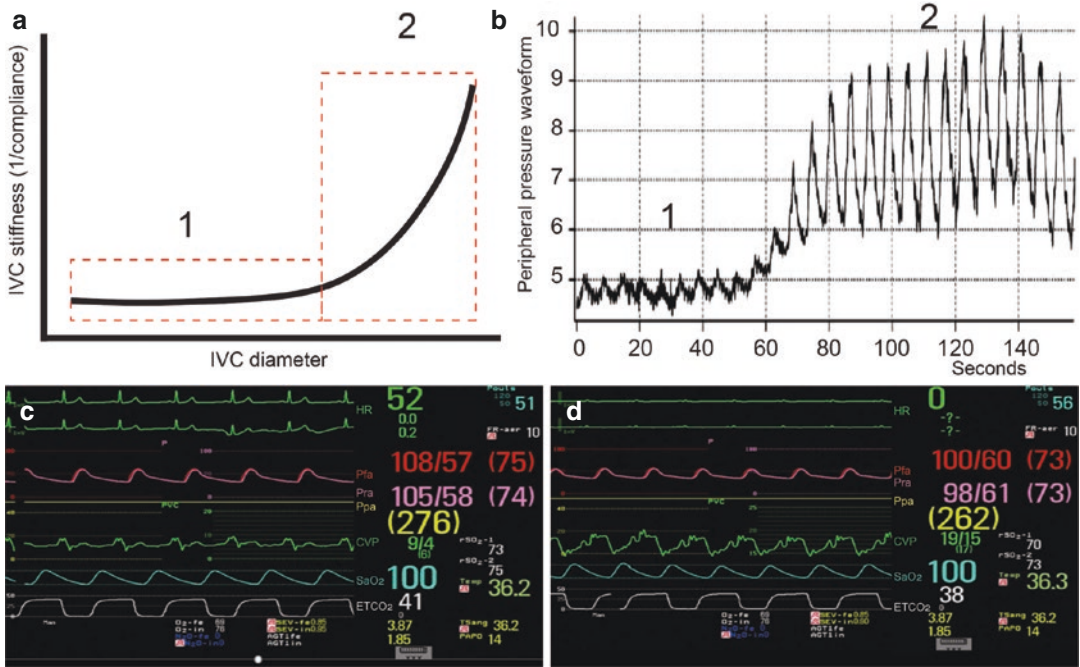


Fig. 26.4 Peripheral venous pulse pressure, venous compliance, and central venous pressure (CVP) waveform. (a) Relationship between inferior vena cava (IVC) compliance with increasing diameter. At low pressure, change in IVC diameter will have minimal effect on IVC stiffness (Abu-Yousef et al. 1990). However, at higher pressure, a small increase in IVC diameter will have an important increase in stiffness (Adamson 1999). (b) Peripheral venous pressure waveform illustrating the effect of a sudden decrease of downstream venous compliance with an increase in peripheral venous pulse pressure. (Adamson 1999) compared to minimal transmission of pressure vari-

ations when venous compliance is normal (Abu-Yousef et al. 1990). (Adapted from (Wardhan and Shelley 2009) with permission of Wolters Kluwer Health, Inc.) (c) Normal CVP waveform tracing before heart positioning during off-pump coronary revascularization. (d) Abnormal CVP with prominent “v” waves after heart positioning in the same patient. A concomitant decrease in cerebral regional oxygen saturation (rSO2) oximetry was also observed. ETCO2 end-tidal carbon dioxide, HR heart rate, Pfa femoral arterial blood pressure, Pra radial arterial pressure, Ppa pulmonary artery pressure, SaO2 oxygen saturation

the following reasons: (1) Increased pulsatility is observed when abnormal pressure is transmitted to the portal circulation. This is most often observed when CVP is increased and the venous pressure from the systemic circulation is transmitted to the liver and produces a cardiogenic-induced portal hypertension (Ikeda et al. 2018; Styczynski et al. 2016). (2) Very slow (<10 cm/s) or absent portal flow can be seen for multiple reasons including mesenteric hypoperfusion in the context of cardiogenic or hypovolemic shock, portal vein thrombosis, and cirrhosis with portal hypertension (McNaughton and Abu-Yousef 2011). However, elevated velocities can be seen in distributive shock and in patients with trans-intrahepatic portal shunts (Ricci et al. 2007).

Clinical Application of Doppler Ultrasound in Critically Ill Patients

The goal of POCUS is to acquire information in a timely manner that will lead to a better understanding of the patient’s current physiology to personalize management. This information must be integrated into the clinical context including history, physical examination, and laboratory information. Most of this area is still in development and clinicians must be cautious on how these findings will affect their decisions. In the following section, we explore how Doppler ultrasound assessment can inform decision at the bedside by presenting selected examples and references.

Differential Diagnosis of Undifferentiated Shock

In the setting of hemodynamic instability, the rapid identification of the offending mechanism is of critical importance. Shock can be categorized based on the concept of venous return to the heart (Guyton et al. 1957) integrating the use of POCUS (Guyton et al. 1957; Denault et al. 2014a; Vegas et al. 2014; Denault et al. 2014b). A decrease in effective vascular volume as occurs in hemorrhagic and distributive shock states results in a decrease in CVP. In septic shock, however, if associated with myocardial depression, elevated CVP can be present (Kimchi et al. 1984; Parker et al. 1990; Pulido et al. 2012; Vallabhajosyula et al. 2017). In cardiogenic shock, CVP are elevated.

Finally, in obstructive shock, there will be resistance to venous return or raised downstream pressure depending on the offending mechanism. Shock mechanism and then etiology can be rapidly identified at the bedside using POCUS as previously reported (Vegas et al. 2014; Denault et al. 2014b).

Ultrasound of the inferior vena cava (IVC) and hepatic vein act as a surrogate of CVP. This can

be performed easily at the bedside of an unstable patient by using several views, the most common of which is a coronal view of the liver in the mid-axillary position (Vegas et al. 2014). The size of the IVC is assessed in its intra-hepatic portion, usually at the junction of the hepatic veins, and is evaluated both in its longitudinal axis and in its transverse axis (Huguet et al. 2018). Combining information from the 2D ultrasound of the IVC and hepatic vein Doppler can provide insights into the mechanism involved as presented in Fig. 26.5. A large, non-compliant IVC can be caused by a cardiac dysfunction or obstruction to venous return. Assessment of the hepatic veins by Doppler can differentiate between these two possibilities; a monophasic Doppler or absent hepatic venous flow is suggestive of obstruction while a predominance of diastolic flow ($V_s/V_d < 1$) is suggestive of elevated right ventricular filling pressure (Rudski et al. 2010; Nagueh et al. 1996). Collapse of the IVC can be observed in hemorrhagic/distributive shock, but it can also be present when an extrinsic compression of the IVC impairs venous return. However, in the latter case, hepatic veins flow will be monophasic and greatly reduced on Doppler examination whereas it still will be pulsatile in the former. In such a

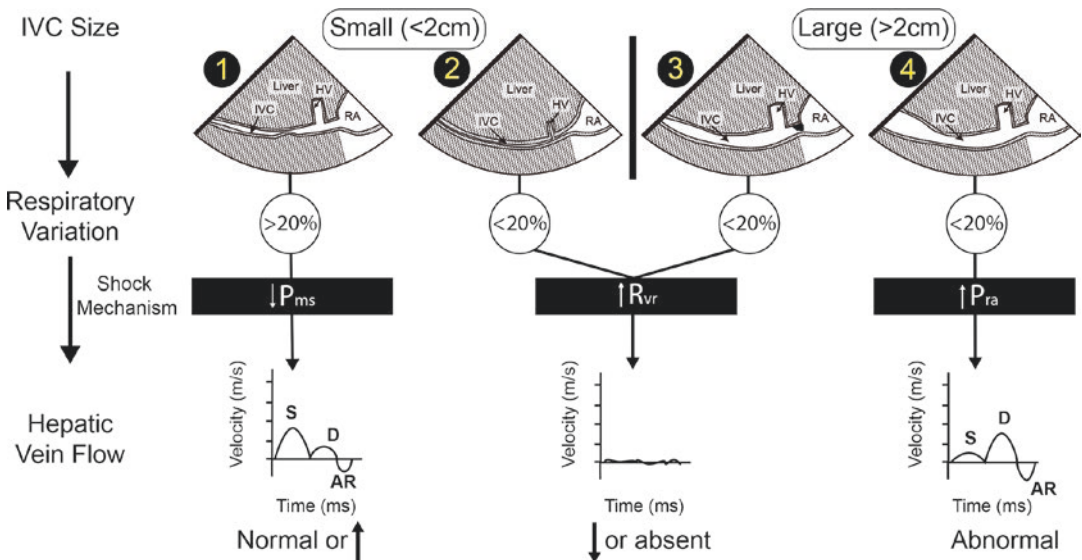


Fig. 26.5 Algorithm integrating inferior vena cava (IVC) and hepatic vein (HV) ultrasound to investigate hemodynamic instability. S systolic, D diastolic, AR atrial reversal, P_{ms} mean systemic venous pressure, P_{ra} right atrial

pressure, R_{vr} resistance to venous return, RA right atrium. (Adapted from Vegas et al. (Vegas et al. 2014) with permission of Springer Nature)

context, these findings should prompt the measurement of intra-abdominal pressure to exclude an abdominal compartment syndrome (Hulin et al. 2016).

Assessment of Fluid Responsiveness, Fluid Status, and Hemodynamic Management

Optimizing organ perfusion at the bedside is a complex task, and extra-cardiac Doppler can complement the assessment. As presented earlier, a compliant IVC with a normal hepatic vein waveform suggestive of hemorrhagic or distributive shock can indicate that the patient’s status

is likely to improve with fluid administration. Nevertheless, fluid administration in this setting should be guided by the clinical context and dynamic markers of fluid responsiveness (Marik and Lemson 2014; Toupin et al. 2013). This often requires invasive monitoring, which is sometimes not available, especially during the early management of hemodynamic instability. Pulse-wave Doppler ultrasound of the left ventricular outflow tract can be used to measure cardiac output and the change in response to interventions and provide a method to assess fluid responsiveness non-invasively (Godfrey et al. 2014). The technique is presented in Fig. 26.6. An increase of 10–15% with the passive leg raise manoeuvre can identify patients who are fluid responsive. By the same

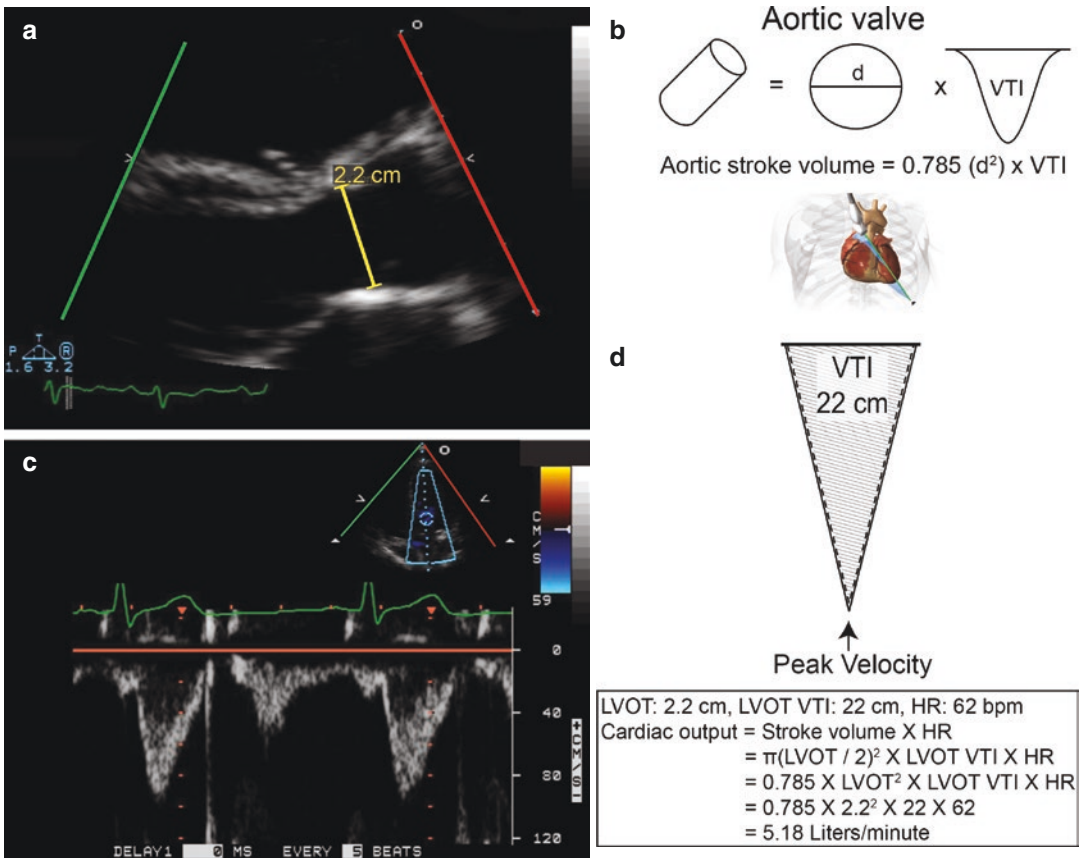


Fig. 26.6 Cardiac output (CO). Calculation of CO involves (a) measurements of the annulus diameter (d) in a zoom of the left ventricular outflow tract (LVOT) from the parasternal long axis view. (b) Formula to calculate CO is shown (c, d) the velocity of the LVOT is obtained from the apical five-chamber view. (d) Tracing the outline

of the velocity trace gives the time integral of the LVOT. HR heart rate, VTI velocity-time integral. (From Basic Transesophageal and Critical Care Ultrasound©, Denault et al (Denault et al. 2017), reproduced with permission of Taylor and Francis Group, a division of Informa plc)

principle, measuring change in carotid flow time-velocity integral (TVI) may be used as a surrogate for change in cardiac output if an adequate cardiac assessment is not possible (Sidor et al. 2018; Jalil et al. 2018). However, significant variability in VTI measurements can occur due to the angle of insonation. Alternatively, measuring the change in the duration of systolic flow from the beginning of the upstroke to the trough of the incisural notch on a pulse waveform with correction for heart rate (carotid corrected flow time) might be a more reproducible method to assess fluid responsiveness. In a recent study, a 7 ms increase in carotid corrected flow time in response to passive leg raising was associated with a 97% positive predictive value in detecting fluid responsiveness (Barjaktarevic et al. 2018). Another simple method in patients who are mechanically ventilated is to evaluate the diameter changes of the superior vena cava using TEE that occur during positive-pressure ventilation (Vieillard-Baron et al. 2001). Those changes will be associated with venous Doppler variations which can be diagnosed easily with a linear probe positioned at the confluence of the internal jugular vein and the superior vena cava (Fig. 26.7).

As discussed earlier, peripheral arterial Doppler velocity waveform indices such as RI do not correlate well with blood flow in animal models (Wan et al. 2008). However, monitoring changes in RI in response to interventions might be useful to guide the optimization organ perfusion is still largely unknown. In an exploratory study, Deruddre et al. observed a reduction of the renal RI in response to an increase of mean arterial pressure from 65 mmHg to 75 mmHg achieved by titrating norepinephrine infusion in critically ill patients (Deruddre et al. 2007). Similarly, we observed a reduction of RI in response to the passive leg raise manoeuvre in cardiac surgery patients who also had a concomitant increase in cardiac output measured by the thermodilution method (Beaubien-Souligny et al. 2018a). (Fig. 26.8) A decrease in RI in response to fluid administration also has been demonstrated in healthy volunteers (Bude et al. 1994; Boddi et al. 1996), but a decrease was not observed in two of three studies that included

critically ill patients (Schnell et al. 2013; Lahmer et al. 2016; Moussa et al. 2015). However, most of the included patients in that study already had established severe acute kidney injury or were septic, which are known to be associated with alterations in renal blood flow autoregulation (Langenberg et al. 2006; Langenberg et al. 2005). Consequently, further research is needed to determine what arterial Doppler indices can be used to optimize organ perfusion is warranted.

Excess fluid administration can lead to adverse consequences in critically ill patients, particularly in patients with impaired cardiac function (Prowle et al. 2010). High venous pressure can directly impair organ perfusion and increases interstitial edema in patients who have increased vascular permeability (Woodcock and Woodcock 2012). Bedside ultrasound, especially portal and peripheral venous Doppler, can provide a non-invasive Echo-Doppler way to monitor CVP changes.

Pulsatile blood flow in the portal vein, as presented in Fig. 26.9, is a sign of post-hepatic portal hypertension and has been demonstrated to be a measure of severity of disease in patients with congestive heart failure (Rengo et al. 1998; Catalano et al. 1998). In decompensated heart failure, a portal pulsatility of more than 50% was the best predictor of increased serum bilirubin compared with hemodynamic parameters such as CVP and echocardiographic measurements of right ventricular function such as tricuspid annular plane systolic excursion (TAPSE) (Styczynski et al. 2016), and portal congestion was independently associated with adverse outcomes (Ikeda et al. 2018). In two recent prospective cohort studies in cardiac surgery patients, detection of portal flow pulsatility after cardiac surgery was associated with an increase in the risk of major complications including severe acute kidney injury, delirium and prolonged duration of stay in the ICU and hospital (Beaubien-Souligny et al. 2018b; Eljaiek et al. 2019; Benkreira et al. 2019). Furthermore, the addition of this parameter improved risk prediction compared with intra-operative assessment of systolic right ventricular function and/or pre-operative risk assessment (Beaubien-Souligny et al. 2018b; Benkreira

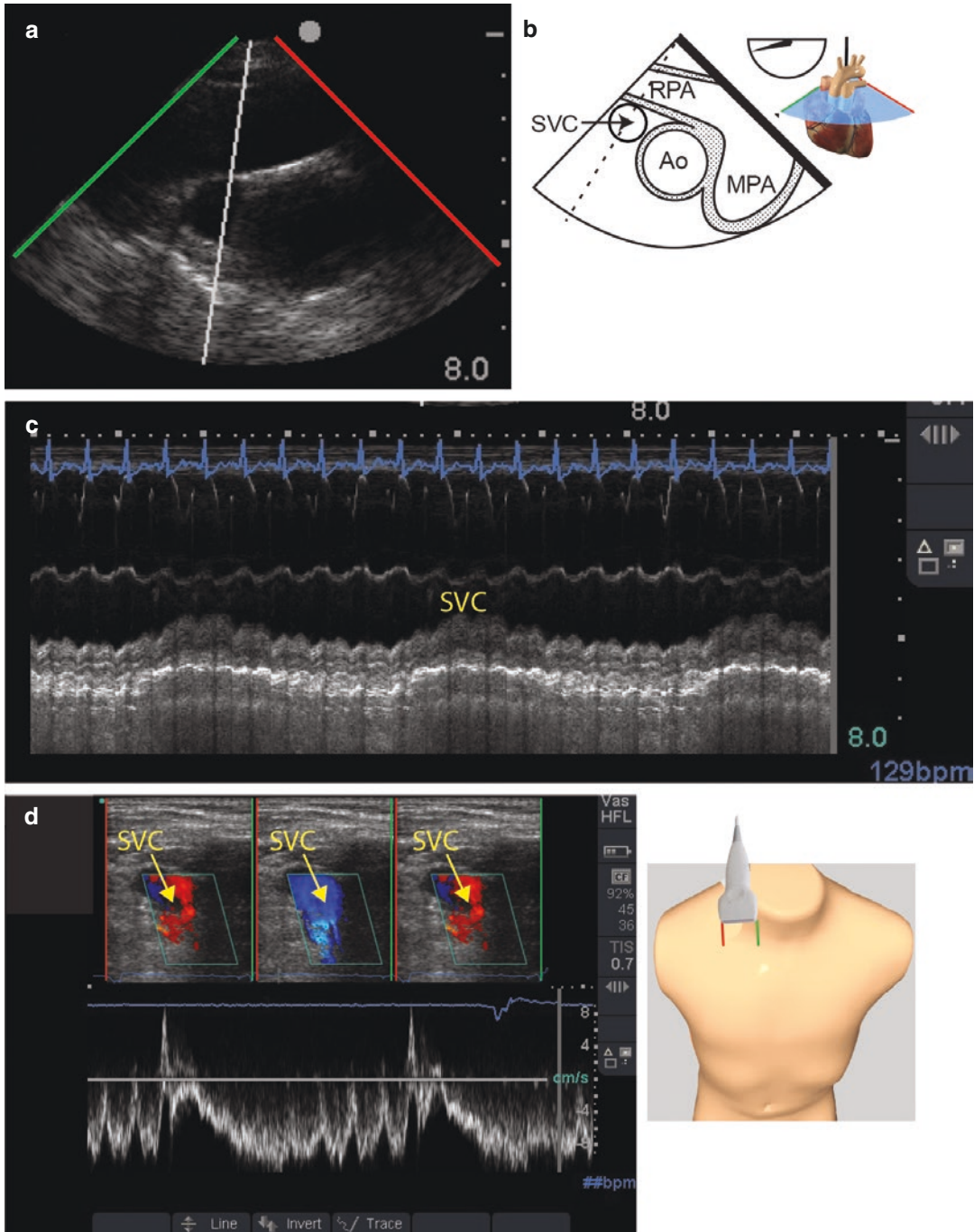


Fig. 26.7 Respiratory variations of the superior vena cava (SVC). A 76-year-old male in the intensive care unit is dialyzed with planned fluid removal of 1.8 L. (a, b) The transesophageal mid-esophageal ascending aorta (Ao) short-axis view with (c) M-mode of the SVC shows significant respiratory variation of the SVC diameter. (d) With a linear probe positioned in the right cervical region

over the distal internal jugular the phasic respiratory changes in Doppler signals can be appreciated. MPA main pulmonary artery, RPA right pulmonary artery. (From Basic Transesophageal and Critical Care Ultrasound©, Denault et al (Denault et al. 2017), reproduced with permission of Taylor and Francis Group, a division of Informa plc)

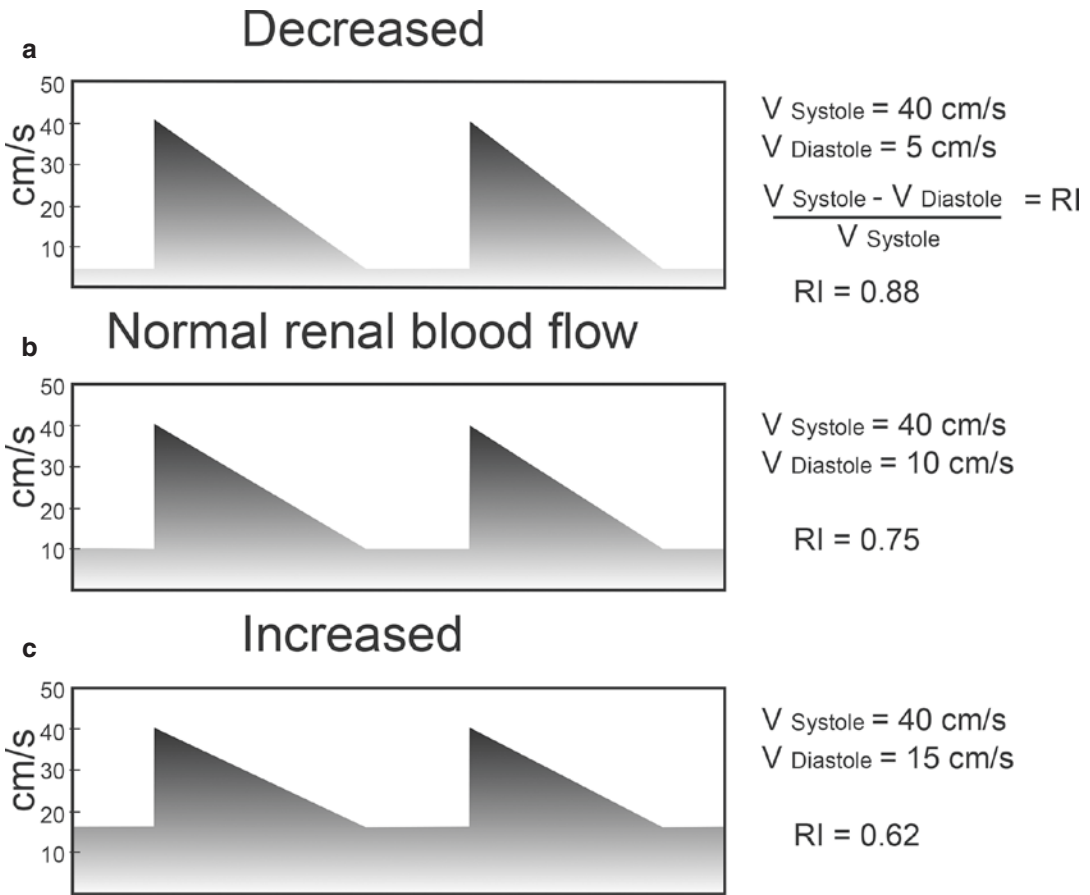


Fig. 26.8 Proposed relationship between rapid changes in renal blood flow and the renal resistive index (RI). In response to a change in cardiac output resulting in an increase in renal blood flow, the change in both the systolic (V_{Systole}) and diastolic (V_{Diastole}) velocities should be modified assuming that both the intra-renal

resistance and the central arterial compliance remain constant. (a) A decrease in cardiac output should result in an increase of the RI compared to (b) the baseline before the intervention while (c) an increase in cardiac output should result in a decrease of the RI

et al. 2019). However, some caution is advised. A PF of more than 50% has also been reported in some individuals with low body mass index and normal cardiac function (Gallix et al. 1997). Consequently, this finding should be supported by other signs of elevated CVP such an abnormal hepatic vein flow waveform. Furthermore, severe symptomatic tricuspid regurgitation is almost invariably associated with portal pulsatility (Abu-Yousef et al. 1990). Whether the prognostic implications of portal flow pulsatility are different in this sub-group of patients is unknown.

The pattern of Doppler velocity observed in the interlobar veins of the kidney, too, are

affected by central venous compliance and by the function of the right ventricle as shown in Fig. 26.10a–c (Beaubien-Souligny and Denault 2018). Abnormal patterns of intra-renal venous flow are associated with a higher risk of death and hospitalization in congestive heart failure patients (Iida et al. 2016). Furthermore, the administration of intra-venous fluids in congestive heart failure patients can lead to the transition from normal to abnormal intra-renal venous flow and a reduced diuretic response (Nijst et al. 2017). Abnormal patterns of intra-renal venous flow have been documented in cardiac surgery (Beaubien-Souligny and Denault 2018). In a

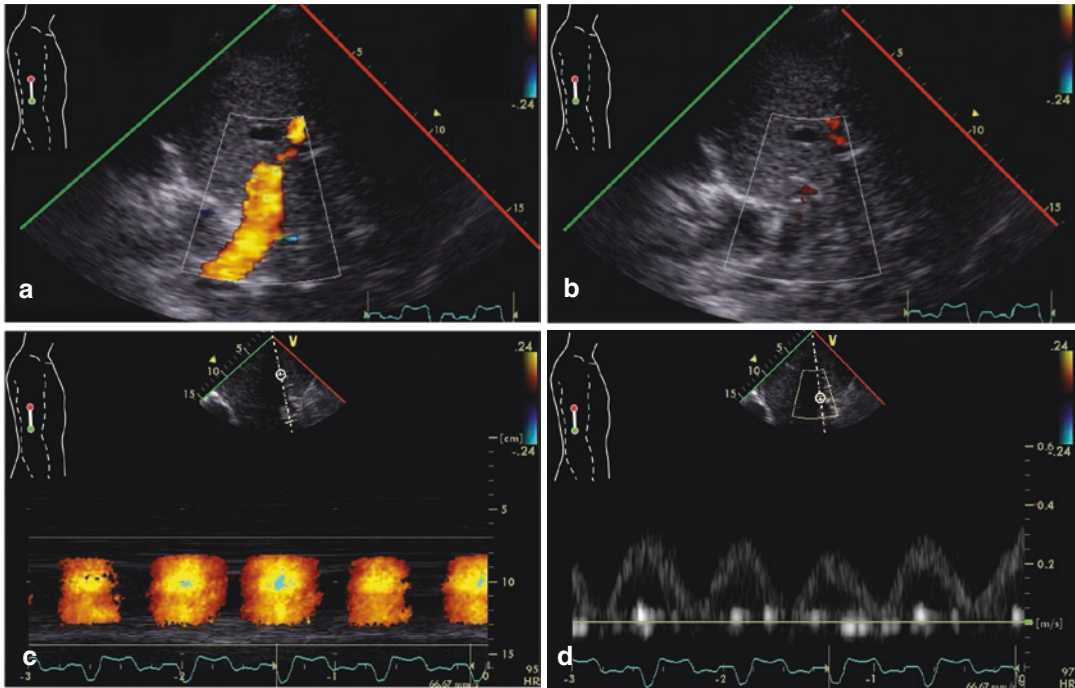


Fig. 26.9 Abnormal portal vein velocity in a 23-year-old female with right ventricular failure and fluid overload after a Ross procedure. Right posterior-axillary coronal view with color Doppler of the right portal vein in (a) systole and (b) diastole and the corresponding (c) color M-mode and (d) pulsed-wave Doppler are shown. The patient had renal dysfunction and increased liver enzymes

which resolved with important diuresis. HR heart rate. (From *Basic Transesophageal and Critical Care Ultrasound*©, Denault et al. (Denault et al. 2017), reproduced with permission of Taylor and Francis Group, a division of Informa plc.)

prospective cohort study in 145 cardiac surgery patients, the detection of a severe alteration in intra-renal venous flow was associated with an increased risk of acute kidney injury as shown in Fig. 26.10d.

Evaluation of Organ Injury

Different mechanisms of injury occur in critically ill patients including ischemia-reperfusion, cytokine-mediated, and inflammatory/auto-immune processes. Although these differ in a number of ways, they have a common pathway which leads to microvascular dysfunction. Endothelial injury upstream from the microcirculation leads to inappropriate vasoconstriction (Conger et al. 1991; Sutton et al. 2002; De Backer et al. 2002), a reduction in the capillary surface area of the vascular

bed by thrombosis (De Backer et al. 2014), and an alteration in vascular permeability due to the damage of endothelial glycocalyx on the surface of the vascular endothelium (Lelubre and Vincent 2018). Increased permeability leads to interstitial edema which is especially deleterious in organs for which volume expansion is limited by rigid or semi-rigid structures such as the brain, liver, and the kidney. All those elements of vascular injury contribute to increased vascular resistance in the injured organ which can be detected by arterial Doppler assessment as shown in Fig. 26.11. An elevated renal RI is predictive of acute kidney injury after cardiac surgery (Bossard et al. 2011) and can discriminate between temporary and persistent alteration in renal function (Guinot et al. 2013; Platt et al. 1991; Darmon et al. 2011; Ninet et al. 2015). As previously discussed, an increase in the PI or the RI may be produced by systemic

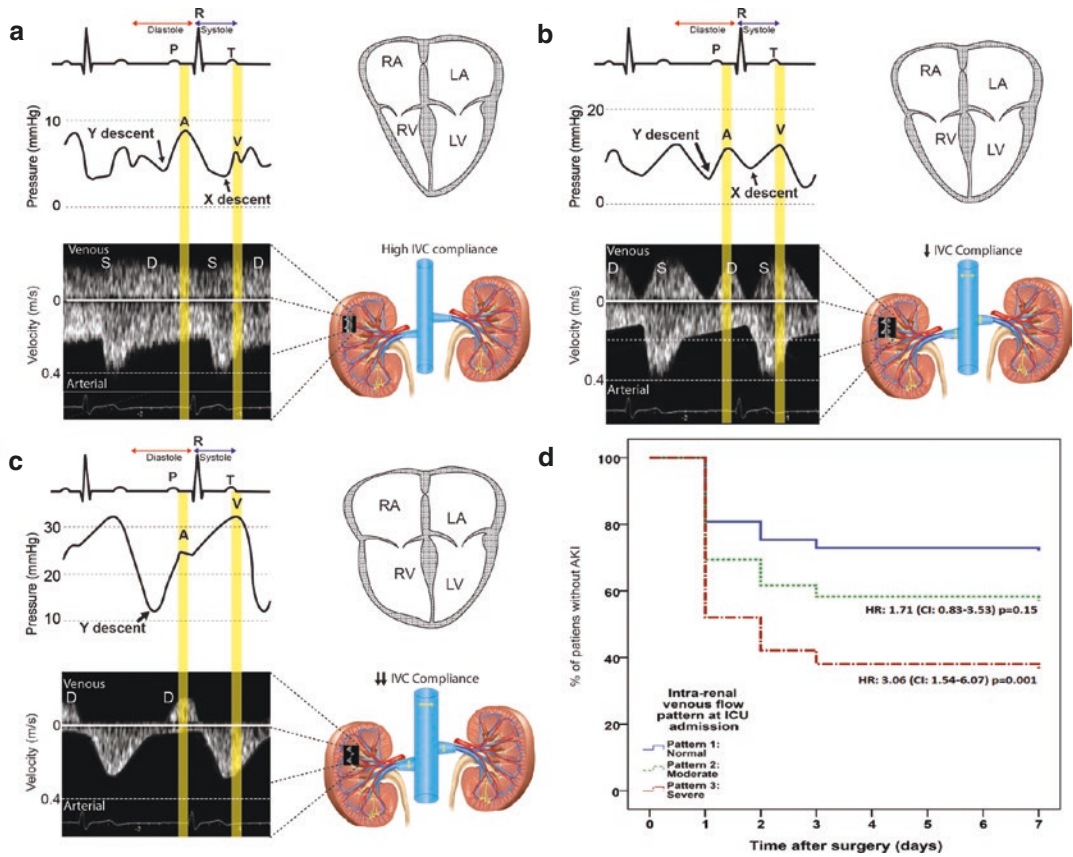


Fig. 26.10 Patterns of intra-renal venous flow (a) Continuous monophasic venous flow suggestive of a compliant venous system resulting in an absence of transmission of right atrial pressure. (b) Discontinuous pattern with flow both in systole and diastole suggestive of decreased central venous compliance. (c) Discontinuous pattern with flow detectable only in diastole suggestive of diastolic right ventricular dysfunction. (d) Acute kidney

injury after cardiac surgery according to venous Doppler patterns after surgery. CI confidence interval, HR hazard ratio, IVC inferior vena cava, ICU intensive care unit, LA left atrium, LV left ventricle, RA right atrium, RV right ventricle. (Adapted from Beaubien-Souligny et al. (Beaubien-Souligny and Denault 2018) with permission of Wolters Kluwer Health, Inc.)

hemodynamic parameters and are not necessarily specific to the characteristic to the downstream vascular bed. However, assessing these parameters in multiple locations help identify specific organ injuries as shown in Figs. 26.12 and 26.13. This approach has been used in outpatients to improve the accuracy of renal Doppler for identification of structural kidney damage (Grun et al. 2012). The presence of an “asymmetric” pattern should prompt the search for a reversible cause, such as venous thrombosis or extrinsic compression from abdominal compartment syndrome or hemorrhage. If this pattern is present after an initial period of hemodynamic instability, it sug-

gests ischemic acute tubular necrosis and the dysfunction will persist despite hemodynamic optimization.

Analysis of Doppler arterial waveforms also can inform about the severity of organ injury. In the brain, trans-cranial Doppler has been used to non-invasively assess intra-cranial hypertension and to identify cerebral circulatory arrest (Ducrocq et al. 1998a, b). The latter was defined as the appearance of diastolic reversal on the arterial Doppler waveform (oscillating flow). Likewise, diastolic reversal is a sign of severe pathology following renal transplantation including acute rejection, ischemia-reperfusion injury, renal vein

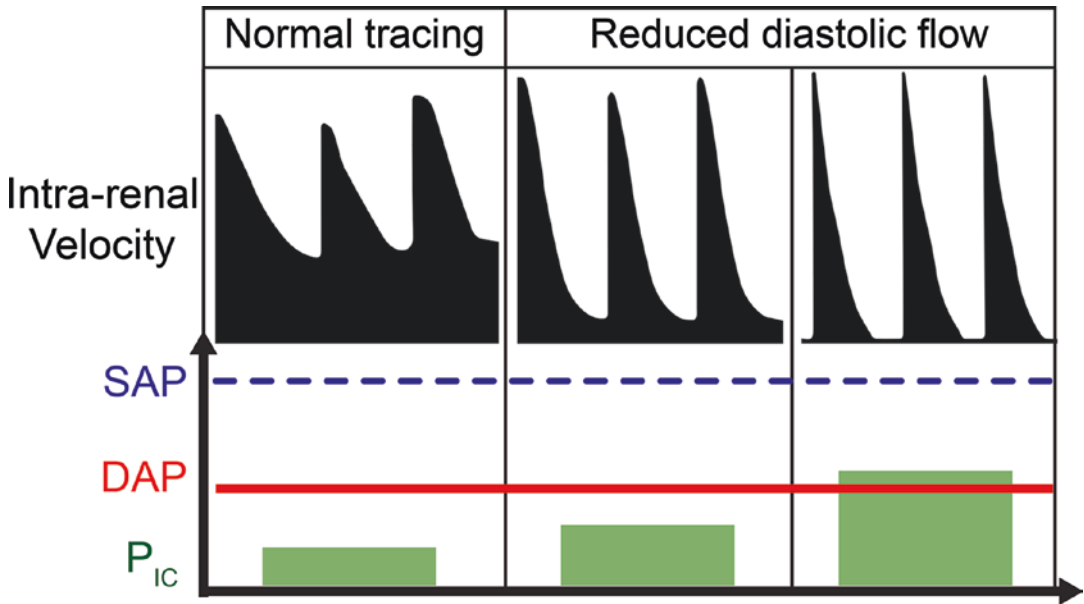


Fig. 26.11 Interpretation of an acute increase in the arterial resistive index (RI) illustrating the relationship between renal intra-renal pressure and the arterial RI. SAP systolic arterial pressure, DAP diastolic arterial pressure,

P_{IC} intra-capsular pressure. (Adapted from Basic Transesophageal and Critical Care Ultrasound©, Denault et al (Denault et al. 2017), reproduced with permission of Taylor and Francis Group, a division of Informa plc)

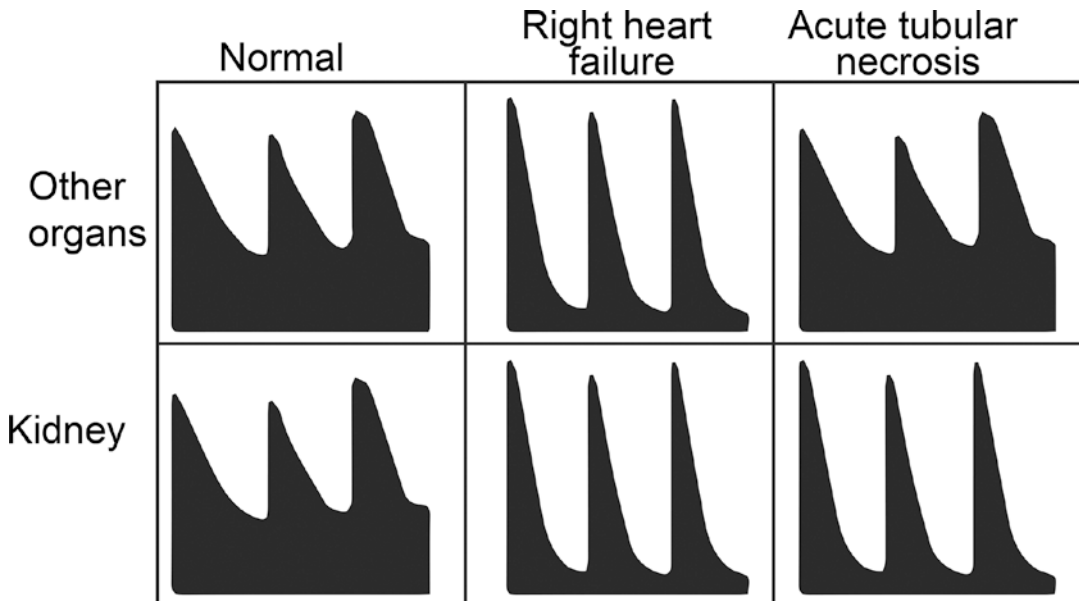


Fig. 26.12 A concurrent increase in the resistive index (RI) in all organs (symmetric) is the hallmark of a systemic process such as heart failure, while an isolated

change in the RI is suggestive of an increase in process specific to the organ assessed

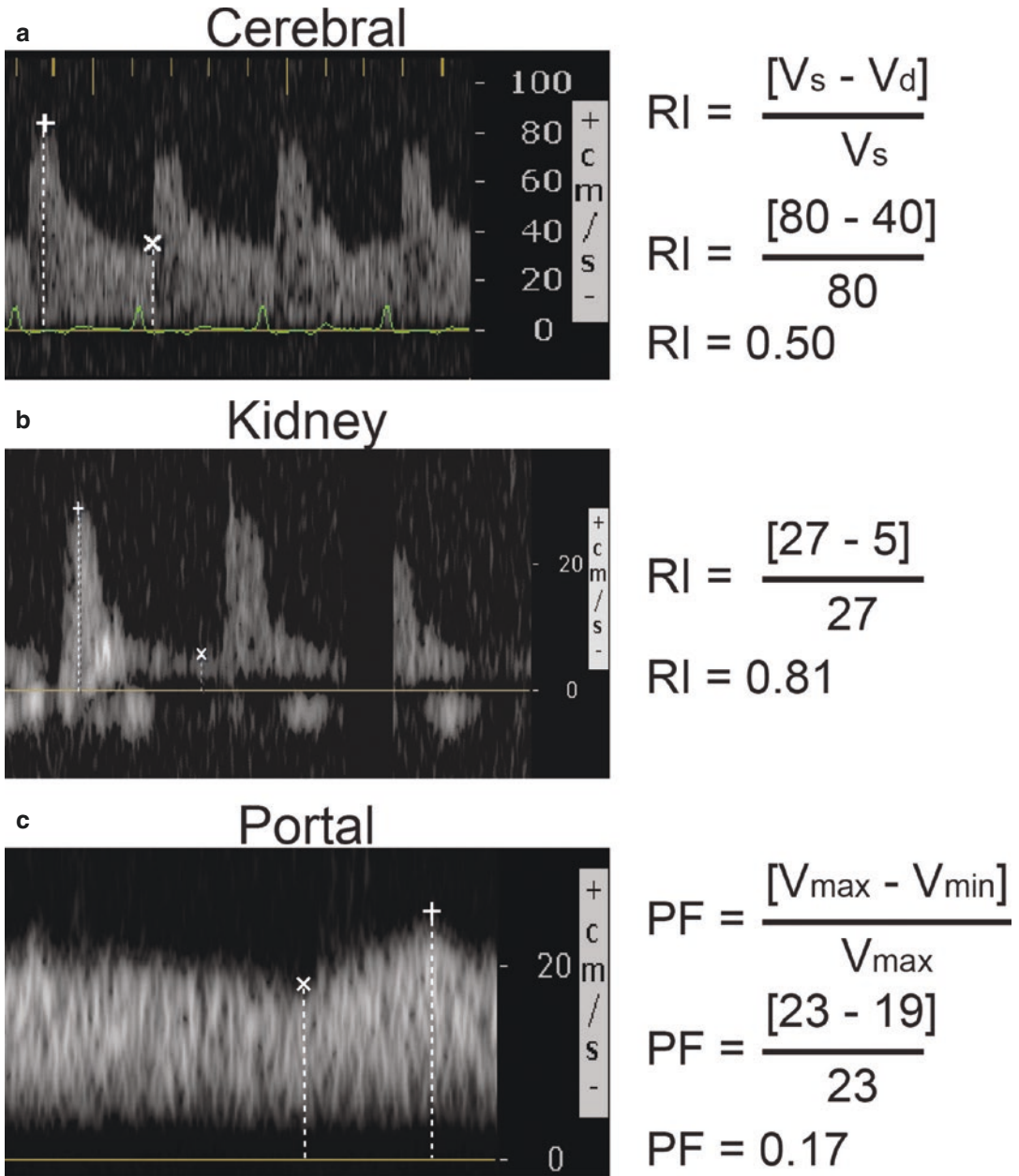


Fig. 26.13 Arterial Doppler obtained using surface ultrasound in a 67-year-old man following prolonged and complicated surgery for mitral valve replacement and tricuspid repair showing (a) normal resistance index (RI) in the

middle cerebral artery but (b) elevated RI on renal Doppler and (c) normal portal vein waveform. PF portal pulsatility fraction, V_s systolic velocity, V_d diastolic velocity, V_{max} maximal velocity, V_{min} , minimal velocity

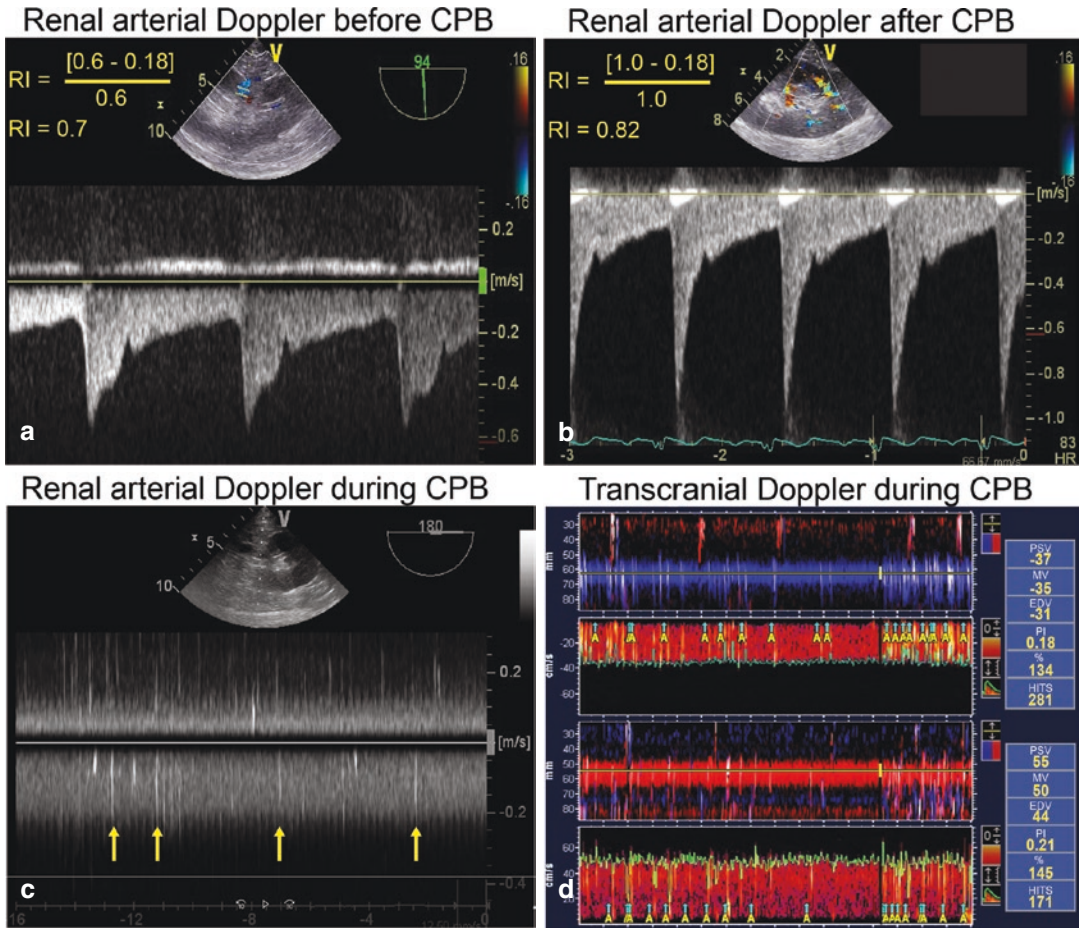


Fig. 26.14 Arterial renal Doppler signal before (a) and after (b) cardiopulmonary bypass (CPB). Signals compatible with air embolism were seen on transesophageal echocardiography monitoring (c) and transcranial Doppler (d) during CPB. The renal resistive index increases from

0.73 before CPB to 0.83 after CPB separation. EDV end diastolic velocity, HITS high intensity transient signals, HR heart rate, MV mean velocity, PSV peak systolic velocity, PI pulsatility index, RI resistance index

thrombosis, or sub-capsular hemorrhage compressing the renal parenchyma (Lockhart et al. 2008; Araújo and Suassuna 2016). Finally, arterial Doppler can be used to identify signals compatible with emboli as presented in Fig. 26.14.

Conclusions

As presented in this chapter, extra-cardiac arterial and venous Doppler ultrasound offers windows into the hemodynamic characteristics of

the patient. Use of this modality at the bedside is still in its infancy, and many uncertainties with its use still persist, especially the specificity and predictability of the findings. Assessment of Doppler waveform is likely to be of limited use when observed in isolation, and the information should always be interpreted in the light of the clinical context. The rapid adoption of POCUS offers the opportunity to develop this modality, both by stimulating research and by permitting the clinicians to develop their own experience.

References

- Abu-Yousef MM, Milam SG, Farner RM. Pulsatile portal vein flow: a sign of tricuspid regurgitation on duplex Doppler sonography. *AJR Am J Roentgenol*. 1990;155(4):785–8.
- Adamson SL. Arterial pressure, vascular input impedance, and resistance as determinants of pulsatile blood flow in the umbilical artery. *Eur J Obstet Gynecol Reprod Biol*. 1999;84(2):119–25.
- Araújo NC, Suassuna JHR. Reversed diastolic flow in page kidney following native kidney biopsy. *J Diagn Med Sonography*. 2016;32(6):371–4.
- Barjaktarevic I, Toppen WE, Hu S, Aquije Montoya E, Ong S, Buhr R, et al. Ultrasound assessment of the change in carotid corrected flow time in fluid responsiveness in undifferentiated shock. *Crit Care Med*. 2018;46(11):e1040–e6.
- Beaubien-Souligny W, Denault AY. Real-time assessment of renal venous flow by transesophageal echography during cardiac surgery. *A&A Pract*. 2018;12:30.
- Beaubien-Souligny W, Huard G, Bouchard J, Lamarche Y, Denault A, Albert M. Doppler renal resistance index for the prediction of response to passive leg-raising following cardiac surgery. *J Clin Ultrasound*. 2018a;46:455.
- Beaubien-Souligny W, Benkreira A, Robillard P, Bouabdallaoui N, Chasse M, Desjardins G, et al. Alterations in portal vein flow and intrarenal venous flow are associated with acute kidney injury after cardiac surgery: a prospective observational cohort study. *J Am Heart Assoc*. 2018b;7(19):e009961.
- Benkreira A, Beaubien-Souligny W, Mailhot T, Bouabdallaoui N, Robillard P, Desjardins G, et al. Portal hypertension is associated with congestive encephalopathy and delirium after cardiac surgery. *Can J Cardiol*. 2019; (In Press).
- Boddi M, Sacchi S, Lammel RM, Mohseni R, Sernerri GG. Age-related and vasomotor stimuli-induced changes in renal vascular resistance detected by Doppler ultrasound. *Am J Hypertens*. 1996;9(5):461–6.
- Bossard G, Bourgoin P, Corbeau JJ, Huntzinger J, Beydon L. Early detection of postoperative acute kidney injury by Doppler renal resistive index in cardiac surgery with cardiopulmonary bypass. *Br J Anaesth*. 2011;107(6):891–8.
- Bude RO, DiPietro MA, Platt JF, Rubin JM. Effect of furosemide and intravenous normal saline fluid load upon the renal resistive index in nonobstructed kidneys in children. *J Urol*. 1994;151(2):438–41.
- Catalano D, Caruso G, DiFazio S, Carpinteri G, Scalisi N, Trovato GM. Portal vein pulsatility ratio and heart failure. *J Clin Ultrasound*. 1998;26(1):27–31.
- Chavhan GB, Parra DA, Mann A, Navarro OM. Normal Doppler spectral waveforms of major pediatric vessels: specific patterns. *Radiographics*. 2008;28(3):691–706.
- Conger JD, Robinette JB, Hammond WS. Differences in vascular reactivity in models of ischemic acute renal failure. *Kidney Int*. 1991;39(6):1087–97.
- Darmon M, Schortgen F, Vargas F, Liazydi A, Schlemmer B, Brun-Buisson C, et al. Diagnostic accuracy of Doppler renal resistive index for reversibility of acute kidney injury in critically ill patients. *Intensive Care Med*. 2011;37(1):68–76.
- De Backer D, Creteur J, Preiser JC, Dubois MJ, Vincent JL. Microvascular blood flow is altered in patients with sepsis. *Am J Respir Crit Care Med*. 2002;166(1):98–104.
- De Backer D, Orbegozo Cortes D, Donadello K, Vincent JL. Pathophysiology of microcirculatory dysfunction and the pathogenesis of septic shock. *Virulence*. 2014;5(1):73–9.
- Denault A, Lamarche Y, Rochon A, Cogan J, Liszkowski M, Lebon JS, et al. Innovative approaches in the perioperative care of the cardiac surgical patient in the operating room and intensive care unit. *Can J Cardiol*. 2014a;30(12 Suppl):S459–77.
- Denault A, Vegas A, Royse C. Bedside clinical and ultrasound-based approaches to the management of hemodynamic instability--part I: focus on the clinical approach: continuing professional development. *Can J Anaesth*. 2014b;61(9):843–64.
- Denault AYCP, Lamarche Y, Tardif JC, Vegas A. Basic transesophageal and critical care ultrasound. CRC Press; 2017.
- Derudder S, Cheisson G, Mazoit JX, Vicaut E, Benhamou D, Duranteau J. Renal arterial resistance in septic shock: effects of increasing mean arterial pressure with norepinephrine on the renal resistive index assessed with Doppler ultrasonography. *Intensive Care Med*. 2007;33(9):1557–62.
- Ducrocq X, Braun M, Debouverie M, Junges C, Hummer M, Vespignani H. Brain death and transcranial Doppler: experience in 130 cases of brain dead patients. *J Neurol Sci*. 1998a;160(1):41–6.
- Ducrocq X, Hassler W, Moritake K, Newell DW, von Reutern GM, Shiohagi T, et al. Consensus opinion on diagnosis of cerebral circulatory arrest using Doppler-sonography: Task Force Group on cerebral death of the Neurosonology Research Group of the World Federation of Neurology. *J Neurol Sci*. 1998b;159(2):145–50.
- Eljaiek R, Cavayas YA, Rodrigue E, Desjardins G, Lamarche Y, Toupin F, et al. High postoperative portal venous flow pulsatility indicates right ventricular dysfunction and predicts complications in cardiac surgery patients. *Br J Anaesth*. 2019;122(2):206–14.
- Gallix BP, Taourel P, Dauzat M, Bruel JM, Lafortune M. Flow pulsatility in the portal venous system: a study of Doppler sonography in healthy adults. *AJR Am J Roentgenol*. 1997;169(1):141–4.
- Godfrey GE, Dubrey SW, Handy JM. A prospective observational study of stroke volume responsiveness to a passive leg raise manoeuvre in healthy non-starved volunteers as assessed by transthoracic echocardiography. *Anaesthesia*. 2014;69(4):306–13.
- Grun OS, Herath E, Weihrauch A, Flugge F, Rogacev KS, Fliser D, et al. Does the measurement of the difference of resistive indexes in spleen and kidney allow a selec-

- tive assessment of chronic kidney injury? *Radiology*. 2012;264(3):894–902.
- Guinot PG, Bernard E, Abou Arab O, Badoux L, Diouf M, Zogheib E, et al. Doppler-based renal resistive index can assess progression of acute kidney injury in patients undergoing cardiac surgery. *J Cardiothorac Vasc Anesth*. 2013;27(5):890–6.
- Guyton AC, Lindsey AW, Abernathy B, Richardson T. Venous return at various right atrial pressures and the normal venous return curve. *Am J Phys*. 1957;189(3):609–15.
- Hassler W, Steinmetz H, Pirschel J. Transcranial Doppler study of intracranial circulatory arrest. *J Neurosurg*. 1989;71(2):195–201.
- Huguet R, Fard D, d’Humieres T, Brault-Meslin O, Faivre L, Nahory L, et al. Three-dimensional inferior vena cava for assessing central venous pressure in patients with cardiogenic shock. *J Am Soc Echocardiogr*. 2018;31:1034.
- Hulin J, Aslanian P, Desjardins G, Belaidi M, Denault A. The critical importance of hepatic venous blood flow Doppler assessment for patients in shock. *A & A Case Rep*. 2016;6(5):114–20.
- Iida N, Seo Y, Sai S, Machino-Ohtsuka T, Yamamoto M, Ishizu T, et al. Clinical implications of intrarenal hemodynamic evaluation by Doppler ultrasonography in heart failure. *JACC Heart Fail*. 2016;4(8):674–82.
- Ikeda Y, Ishii S, Yazaki M, Fujita T, Iida Y, Kaida T, et al. Portal congestion and intestinal edema in hospitalized patients with heart failure. *Heart Vessel*. 2018;33(7):740–51.
- Jalil B, Thompson P, Cavallazzi R, Marik P, Mann J, El-Kersh K, et al. Comparing changes in carotid flow time and stroke volume induced by passive leg raising. *Am J Med Sci*. 2018;355(2):168–73.
- Kimchi A, Ellrodt AG, Berman DS, Riedinger MS, Swan HJ, Murata GH. Right ventricular performance in septic shock: a combined radionuclide and hemodynamic study. *J Am Coll Cardiol*. 1984;4(5):945–51.
- Ko EY, Kim TK, Kim PN, Kim AY, Ha HK, Lee MG. Hepatic vein stenosis after living donor liver transplantation: evaluation with Doppler US. *Radiology*. 2003;229(3):806–10.
- Lahmer T, Rasch S, Schnappauf C, Schmid RM, Huber W. Influence of volume administration on Doppler-based renal resistive index, renal hemodynamics and renal function in medical intensive care unit patients with septic-induced acute kidney injury: a pilot study. *Int Urol Nephrol*. 2016;48(8):1327–34.
- Langenberg C, Bellomo R, May C, Wan L, Egi M, Morgera S. Renal blood flow in sepsis. *Crit Care*. 2005;9(4):R363–74.
- Langenberg C, Wan L, Egi M, May CN, Bellomo R. Renal blood flow in experimental septic acute renal failure. *Kidney Int*. 2006;69(11):1996–2002.
- Lelubre C, Vincent JL. Mechanisms and treatment of organ failure in sepsis. *Nat Rev Nephrol*. 2018;14(7):417–27.
- Lockhart ME, Wells CG, Morgan DE, Fineberg NS, Robbin ML. Reversed diastolic flow in the renal transplant: perioperative implications versus transplants older than 1 month. *AJR Am J Roentgenol*. 2008;190(3):650–5.
- Marik PE, Lemson J. Fluid responsiveness: an evolution of our understanding. *Br J Anaesth*. 2014;112(4):617–20.
- McNaughton DA, Abu-Yousef MM. Doppler US of the liver made simple. *Radiographics*. 2011;31(1):161–88.
- Moussa MD, Scolletta S, Fagnoul D, Pasquier P, Brasseur A, Taccone FS, et al. Effects of fluid administration on renal perfusion in critically ill patients. *Crit Care*. 2015;19:250.
- Nagueh SF, Kopelen HA, Zoghbi WA. Relation of mean right atrial pressure to echocardiographic and Doppler parameters of right atrial and right ventricular function. *Circulation*. 1996;93(6):1160–9.
- Narula J, Chandrashekar Y, Braunwald E. Time to add a fifth pillar to bedside physical examination: inspection, palpation, percussion, auscultation, and insonation. *JAMA Cardiol*. 2018;3(4):346–50.
- Nijst P, Martens P, Dupont M, Tang WHW, Mullens W. Intrarenal flow alterations during transition from euvolemia to intravascular volume expansion in heart failure patients. *JACC Heart Fail*. 2017;5(9):672–81.
- Ninet S, Schnell D, Dewitte A, Zeni F, Meziani F, Darmon M. Doppler-based renal resistive index for prediction of renal dysfunction reversibility: a systematic review and meta-analysis. *J Crit Care*. 2015;30(3):629–35.
- Parker MM, McCarthy KE, Ognibene FP, Parrillo JE. Right ventricular dysfunction and dilatation, similar to left ventricular changes, characterize the cardiac depression of septic shock in humans. *Chest*. 1990;97(1):126–31.
- Platt JF, Rubin JM, Ellis JH. Acute renal failure: possible role of duplex Doppler US in distinction between acute prerenal failure and acute tubular necrosis. *Radiology*. 1991;179(2):419–23.
- Prowle JR, Echeverri JE, Ligabo EV, Ronco C, Bellomo R. Fluid balance and acute kidney injury. *Nat Rev Nephrol*. 2010;6(2):107–15.
- Pulido JN, Afessa B, Masaki M, Yuasa T, Gillespie S, Herasevich V, et al. Clinical spectrum, frequency, and significance of myocardial dysfunction in severe sepsis and septic shock. *Mayo Clin Proc*. 2012;87(7):620–8.
- Rengo C, Brevetti G, Sorrentino G, D’Amato T, Imparato M, Vitale DF, et al. Portal vein pulsatility ratio provides a measure of right heart function in chronic heart failure. *Ultrasound Med Biol*. 1998;24(3):327–32.
- Ricci P, Cantisani V, Lombardi V, Alfano G, D’Ambrosio U, Menichini G, et al. Is color-Doppler US a reliable method in the follow-up of transjugular intrahepatic portosystemic shunt (TIPS)? *J Ultrasound*. 2007;10(1):22–7.
- Rudski LG, Lai WW, Afilalo J, Hua L, Handschumacher MD, Chandrasekaran K, et al. Guidelines for the echocardiographic assessment of the right heart in adults: a report from the American Society of Echocardiography endorsed by the European Association of Echocardiography, a registered branch of the European Society of Cardiology, and the Canadian Society of Echocardiography. *J Am Soc Echocardiogr*. 2010;23(7):685–713; quiz 86–8

- Schnell D, Camous L, Guyomarc'h S, Duranteau J, Canet E, Gery P, et al. Renal perfusion assessment by renal Doppler during fluid challenge in sepsis. *Crit Care Med.* 2013;41(5):1214–20.
- Sidor M, Premachandra L, Hanna B, Nair N, Misra A. Carotid flow as a surrogate for cardiac output measurement in hemodynamically stable participants. *J Intensive Care Med.* 2018;885066618775694.
- Styczynski G, Milewska A, Marczevska M, Sobieraj P, Sobczynska M, Dabrowski M, et al. Echocardiographic correlates of abnormal liver tests in patients with exacerbation of chronic heart failure. *J Am Soc Echocardiogr.* 2016;29(2):132–9.
- Sutton TA, Fisher CJ, Molitoris BA. Microvascular endothelial injury and dysfunction during ischemic acute renal failure. *Kidney Int.* 2002;62(5):1539–49.
- Tang WH, Kitai T. Intrarenal venous flow: a window into the congestive kidney failure phenotype of heart failure? *JACC Heart Fail.* 2016;4(8):683–6.
- Toupin F, Denault A, Lamarche Y, Deschamps A. Hemodynamic instability and fluid responsiveness. *Can J Anaesth.* 2013;60(12):1240–7.
- Vallabhajosyula S, Kumar M, Pandompam G, Sakhuja A, Kashyap R, Kashani K, et al. Prognostic impact of isolated right ventricular dysfunction in sepsis and septic shock: an 8-year historical cohort study. *Ann Intensive Care.* 2017;7(1):94.
- Vegas A, Denault A, Royse C. A bedside clinical and ultrasound-based approach to hemodynamic instability – part II: bedside ultrasound in hemodynamic shock: continuing professional development. *Can J Anaesth.* 2014;61(11):1008–27.
- Vieillard-Baron A, Augarde R, Prin S, Page B, Beauchet A, Jardin F. Influence of superior vena caval zone condition on cyclic changes in right ventricular outflow during respiratory support. *Anesthesiology.* 2001;95(5):1083–8.
- Vlachopoulos C, O'Rourke M, Nichols WW. McDonald's blood flow in arteries: theoretical, experimental and clinical principles. CRC Press; 2011.
- Wan L, Yang N, Hiew CY, Schelleman A, Johnson L, May C, et al. An assessment of the accuracy of renal blood flow estimation by Doppler ultrasound. *Intensive Care Med.* 2008;34(8):1503–10.
- Wardhan R, Shelley K. Peripheral venous pressure waveform. *Curr Opin Anaesthesiol.* 2009;22(6):814–21.
- Woodcock TE, Woodcock TM. Revised Starling equation and the glycocalyx model of transvascular fluid exchange: an improved paradigm for prescribing intravenous fluid therapy. *Br J Anaesth.* 2012;108(3):384–94.



Measurements of Fluid Requirements with Cardiovascular Challenges

27

Xavier Monnet and Jean-Louis Teboul

Introduction

Since it has become clear that patients with circulatory failure inconstantly respond to volume expansion by increasing cardiac output (Bentzer et al. 2016), a whole vein of intensive care research has been dug to develop tests that predict “fluid responsiveness” (Monnet et al. 2016a). In fact, these test use various challenges of the cardiovascular system to predict the effects of a fluid infusion on cardiac output. This gold rush has been greatly enhanced by the growing evidence that fluid overload is deleterious in critically ill patients, especially with acute respiratory distress syndrome (ARDS) and septic shock (Sakr et al. 2017). The most recent recommendations in septic shock suggest managing the fluid strategy by using these “dynamic” tests of fluid responsiveness (Rhodes et al. 2017).

X. Monnet (✉) · J.-L. Teboul
Université Paris-Saclay, AP-HP, Service de médecine intensive-réanimation, Hôpital de Bicêtre, DMU CORREVE, Inserm UMR S_999, FHU SEPSIS, Groupe de recherche clinique CARMAS, Le Kremlin-Bicêtre, France
e-mail: xavier.monnet@aphp.fr;
jean-louis.teboul@aphp.fr

In this chapter, we review these indices, explain the pathophysiological principles that are behind them, state their advantages and limitations, and explain how they might be used in clinical practice.

Static Indices of Cardiac Preload

It has been shown over and over again that the observation of “static” markers of cardiac preload, i.e. absolute values of preload measurements, fail to reliably detect preload dependence (Bentzer et al. 2016; Marik and Cavallazzi 2013). The essential reason is physiology. By observing the Frank-Starling curve (Fig. 27.1), it is obvious that the variability of the slope of the curve explains why a given cardiac preload value may correspond to a state of preload dependence as to a state of preload independence.

In this respect, no static cardiac preload measurement is superior to another for detecting preload dependence. Central venous pressure, diameter of the inferior vena cava, pulmonary artery occlusion pressure, echocardiographic indices used to estimate it (E/A or E/e' waves ratio), end-diastolic dimensions of the left ventricle, corrected flow time at oesophageal Doppler, etc., are, except for extreme values, incapable of predicting the response of cardiac output to volume expansion (Monnet et al. 2016a).

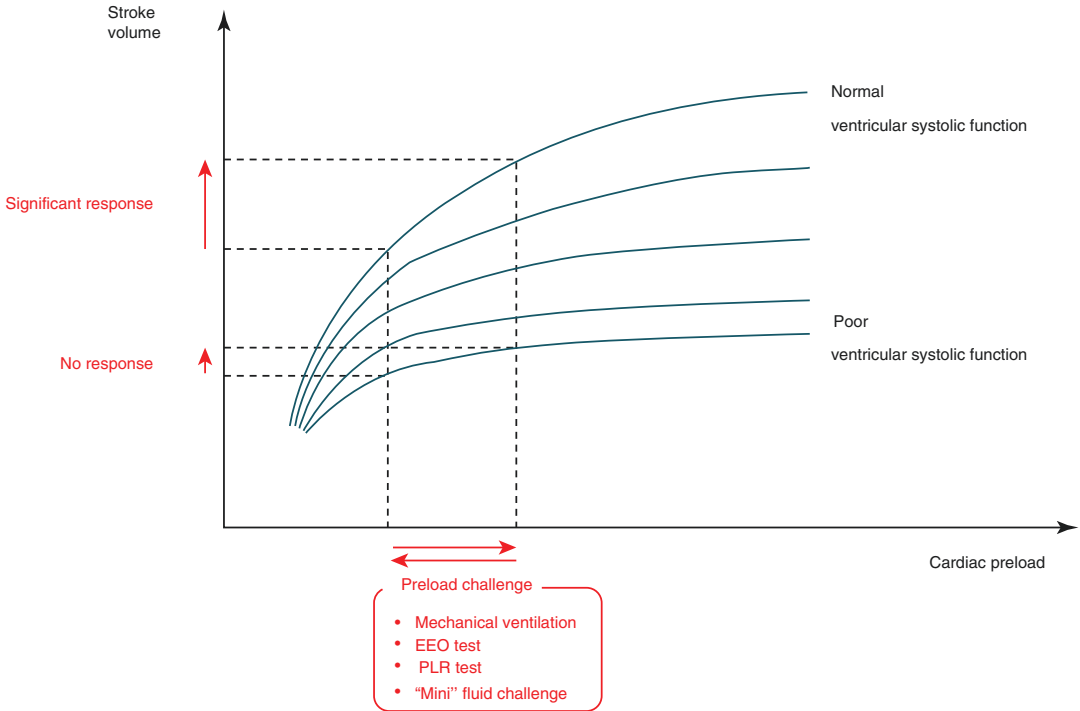


Fig. 27.1 Frank-Starling relationship. The slope of the Frank-Starling curve depends on the ventricular systolic function. Then, one given level of cardiac preload does not help in predicting fluid responsiveness. By contrast, dynamic tests include a preload challenge (either spontaneous, induced by mechanical ventilation or provoked, by

passive leg raising, end-expiratory occlusion or fluid infusion). Observing the resulting effects on stroke volume allows for the detection of preload responsiveness. EEO end-expiratory occlusion, PLR passive leg raising. (Adapted from (Monnet et al. 2016a) (Open Access Journal))

Fluid Challenge

Standard Fluid Challenge

The most obvious way to detect preload dependence dynamically is to administer fluid and measure the response of cardiac output. De facto, the method of injecting 300–500 mL of fluid to guide fluid strategy has been used for many years (Vincent and Weil 2006). Nevertheless, the fluid “challenge” is not a therapeutic test, but the treatment itself. It is not certain that a patient who has just responded to a fluid challenge by a significant increase in cardiac output will still do so during the next one since the 300 or 500 mL of the first challenge may have made the patient already preload independent.

Another disadvantage of the fluid challenge is that it requires a direct measurement of the cardiac output. Indeed, if its effects are assessed by simply measuring the blood pressure, the estimation of its effects on cardiac output is poorly reliable (Monnet et al. 2011) or even not reliable at all (Pierrakos et al. 2012). From this point of view, the fluid challenge is not different from the passive leg raising (PLR) test that we will see later.

Finally, the major disadvantage of the fluid challenge is that it is not reversible. Repeated use in a patient with multiple hypotensive episodes can only contribute to fluid overload. From this point of view, it is probably necessary to bear in mind the particular risk of fluid challenge in patients for whom fluid overload is particularly deleterious.

Mini Fluid Challenge

To circumvent this latter problem, some authors have developed a “mini” fluid challenge with 100 mL of starch only. They showed that the response to a subsequent volume expansion (500 mL) was predicted by the increase in velocity-time integral (VTI) of the left ventricular outflow tract, a reflection of stroke volume measured by echocardiography, induced by the infusion of this small amount of fluid (Muller et al. 2011).

In our opinion, the main limitation of the “mini” fluid challenge is that it induces only small changes in cardiac output so that the technique used to measure these changes must be very precise. In this regard, echocardiography is probably not the most suitable tool. Pulse contour analysis, which provides a very accurate measurement of cardiac output (Jozwiak et al. 2018), is likely more appropriate (Biais et al. 2017a; Smorenberg et al. 2018).

It has been suggested that the prediction of the response to volume expansion was less good when not 100 mL but 50 mL was used to practice fluid flush (Biais et al. 2017a). This suggests that the volume is too small to generate sufficient preload changes to test preload responsiveness. The minimum volume of fluid to cause a significant haemodynamic effect has been demonstrated to be 4 mL/kg (Aya et al. 2017). Finally, not only the volume of fluid but also the timing of administration is important to consider. It has been shown that the longer the duration of the fluid challenge, the lower the proportion of fluid responders (Toscani et al. 2017).

Pulse Pressure Variation, Stroke Volume Variation

Principle

The method that has historically been the first to be described for detecting preload dependence without administering fluid is the arterial pulse

pressure variation (PPV). This index is based on the principle that mechanical ventilation induces changes in the loading conditions of the two ventricles which ultimately lead to increased changes in stroke volume and, consequently, to increased arterial pulse pressure changes in case of preload dependence (Teboul et al. 2019).

In more detail, positive pressure insufflation induces an increase in intrathoracic pressure (Fig. 27.2). This is transmitted to the right atrium, and the resulting increase in right atrial pressure decreases the pressure gradient of venous return and reduces the right cardiac preload (Teboul et al. 2019). If the right ventricle is preload-dependent, this preload decrease is transmitted to the left ventricle. If the left ventricle is also preload-dependent, its stroke volume decreases in turn. Due to the time that is required by the “preload bolus” to cross the pulmonary circulation, this decrease in stroke volume occurs during expiration. In addition to decreasing the right cardiac preload, positive pressure insufflation increases the transpulmonary pressure. This stretches the pulmonary vessels, increases their resistance, and finally increases the right ventricular afterload. This contributes to the decrease in right ventricular stroke volume but may not indicate volume responsiveness (Teboul et al. 2019) (Fig. 27.2).

In addition, the increase in intrathoracic pressure at inspiration leads to a decrease in the transmural pressure of the left ventricle, which decreases its afterload. This afterload increase causes an increase in left ventricular stroke volume that occurs during inspiration. Also, the inspiratory increase of the transpulmonary pressure, by compressing the pulmonary vessels, propels their contents towards the left ventricle, contributing to increasing stroke volume at inspiration (Teboul et al. 2019).

In total, all of these phenomena contribute to the appearance, in case of preload dependence, of an increase in stroke volume at inspiration and a decrease of it at the expiration. This stroke volume variation (SVV) is reflected by the variation of pulse pressure, the amplitude of which reflects stroke volume (Teboul et al. 2019) (Fig. 27.2).

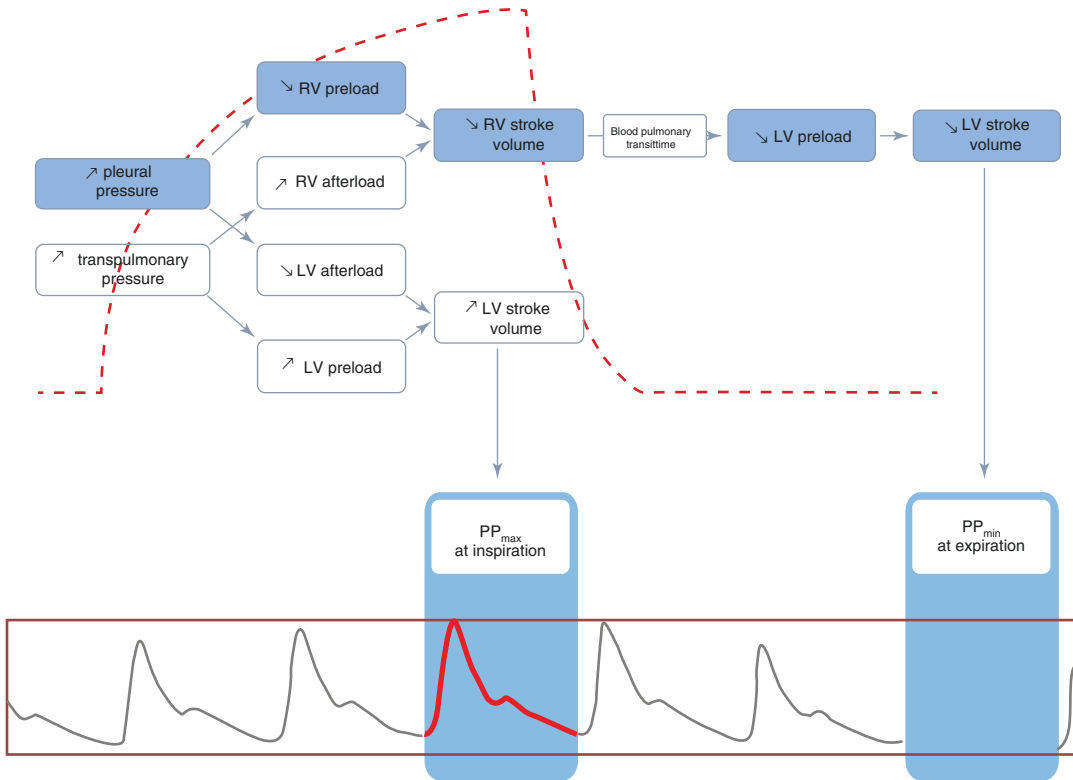


Fig. 27.2 Mechanisms of heart–lung interactions explaining pulse pressure variation. Top: airway pressure tracing; bottom: arterial pressure tracing. LV left ventricle, PP

pulse pressure, RV right ventricle. (Adapted from (Teboul et al. 2019) with permission of the American Thoracic Society. Copyright © 2019 American Thoracic Society)

Demonstration

A large number of studies and some meta-analyses conducted in adults have shown that PPV can predict the response to volume expansion with good reliability (Bentzer et al. 2016; Yang and Du 2014; Marik et al. 2009). This has also been demonstrated with all estimates of stroke volume that can be used clinically: the respiratory variability of the stroke volume measured by pulse contour analysis, the maximum velocity in the left ventricular outflow tract measured in echocardiography, the amplitude of the plethysmography signal, and of the carotid flow also. The amplitude of respiratory changes of all these indices showed a diagnostic reliability roughly comparable to that of PPV (Monnet et al. 2016a).

Limitations

These indices of preload responsiveness are those with the most restrictive conditions of validity. The circumstances generating false positives and false negatives of PPV and SVV are numerous, especially in critically ill patients (Fig. 27.3).

Among these circumstances, mechanical ventilation with a low tidal volume is one of the most common. To circumvent this limit, a “tidal volume challenge” has been developed (Myatra et al. 2017), which consists in increasing tidal volume from 6 to 8 mL/kg for a few minutes. If PPV increases $\geq 3.5\%$ (in absolute value) during the test, preload responsiveness is likely (Myatra et al. 2017). The test has the advantage of not requiring a direct measurement of cardiac output (Myatra et al. 2017). Sometimes, even during

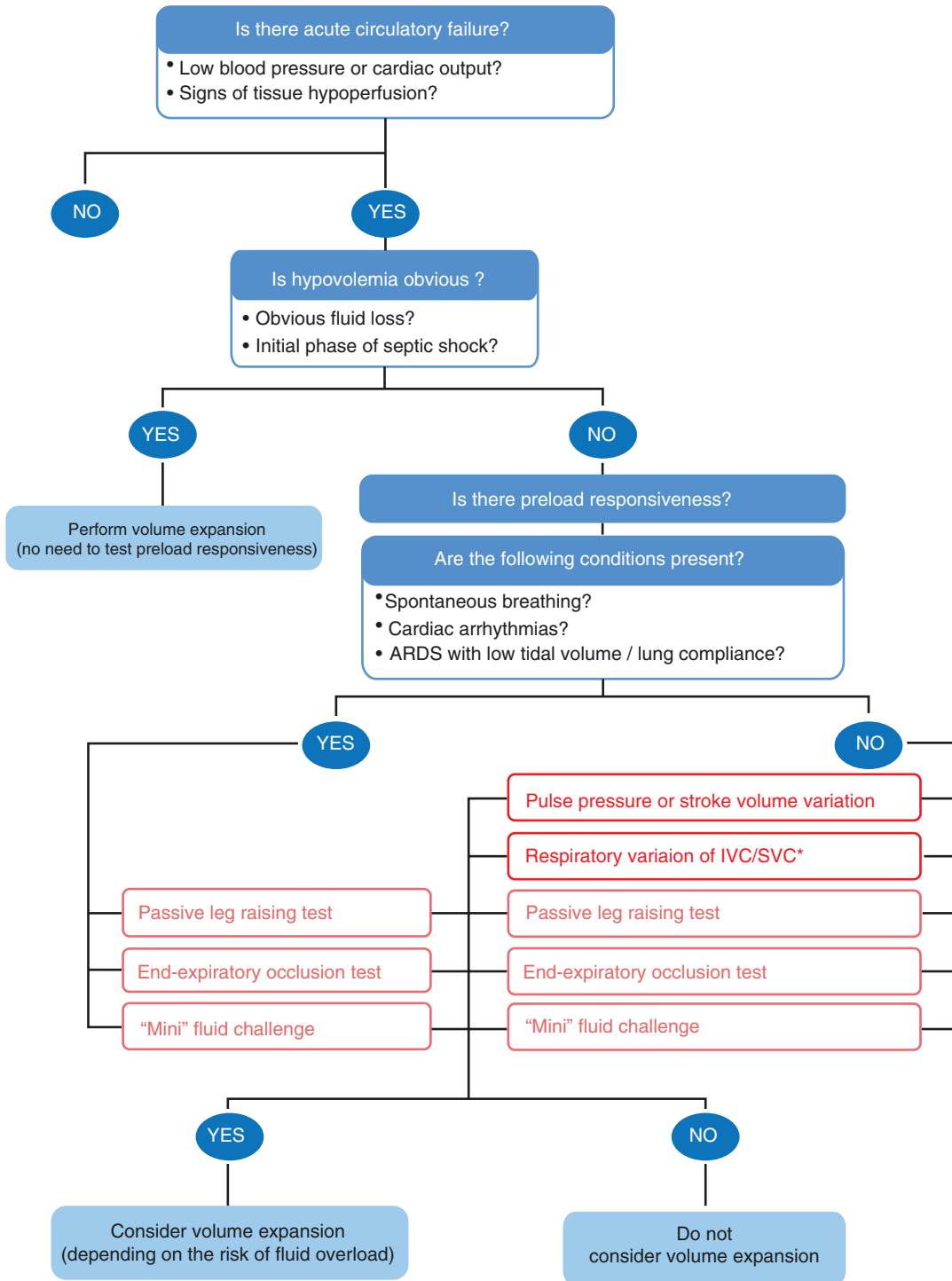


Fig. 27.3 Fluid strategy. *The variation in inferior/superior vena cava diameters can be used in case of cardiac arrhythmias. ARDS: acute respiratory distress syndrome, IVC: inferior vena cava, PCO₂ gap: veno-arterial differ-

ence in carbon dioxide tension, SVC: superior vena cava. (Adapted from (Monnet et al. 2016a) (Open Access Journal))

normal tidal volume ventilation, it can be difficult to interpret PPV, when its value lies in a zone of uncertainty (between 9% and 13%) described by Cannesson et al. as a “gray zone” (Cannesson et al. 2011). A study showed that in such a situation, the increase in PPV predicted fluid responsiveness when tidal volume was increased from 8 to 12 mL/kg (Min et al. 2017).

It should be kept in mind that during ARDS, the false negatives encountered for PPV and SVV are explained not only by the low tidal volume but also by the decreased lung compliance (Monnet et al. 2012; Liu et al. 2016). Another way to circumvent the limitation of PPV in case of low tidal volume that has been investigated consisted in indexing it with the changes in pleural pressure, assessed by an oesophageal catheter (Liu et al. 2016). The method performs much better than indexation by tidal volume. Nevertheless, this method requires an oesophageal pressure catheter in place, which is still uncommon at the bedside.

Another way to use PPV in circumstances generating false positives and false negatives would be to use it instead of cardiac output to judge the effects of a preload challenge. One study showed that the decrease in PPV during a PLR test predicted the response to volume expansion as well as concurrent changes in cardiac output. Nevertheless, these results are questioned by a recent study that showed that PPV did not track the changes in cardiac output during a fluid challenge in patients with septic shock (De la Puente-Diaz de Leon et al. 2017).

Variability of the Diameter of Vena Cava

Principle

The use of variability in the vena cava diameter to predict fluid responsiveness is based on a principle a little different than that of PPV/SVV (Vieillard-Baron et al. 2004). This variability, which appears in case of preload dependence, is probably explained on the one hand by a respi-

ratory variability of the central venous pressure as a reflection of a change in the surrounding pleural pressure (Magder et al. 1992) and, on the other hand, a more distensible vena cava in hypovolemic patients, which makes the diameter more sensitive to changes in external pressure (intra-abdominal for inferior vena cava, intrathoracic for superior vena cava). The contribution of these two components in the variability of the vena cava is not well characterized.

Measurement Method

The variability of the inferior vena cava diameter is easily measured by transthoracic echocardiography but the superior vena cava can be performed only transoesophageally. Variability is calculated as the difference between maximum and minimum vein diameter over a respiratory cycle divided by either the average of the two or the minimum diameter value. Both methods theoretically lead to different thresholds.

It has been reported that the respiratory variability of the right internal jugular vein predicts the response to volume expansion, even though the diagnostic threshold was lower than that of the inferior vena cava (Ma et al. 2018).

Limitations

The variability of cave vein diameter shares many of the limitations of PPV/SVV. During spontaneous ventilation, the irregularity of the intrathoracic pressure variations prevents the definition of any diagnostic threshold (Bentzer et al. 2016; Corl et al. 2012). A study showed that in case of spontaneous breathing, only the very high values of the inferior vena cava diameter variation were of diagnostic value (Airapetian et al. 2015). In case of low tidal volume and, probably also, in case of low lung compliance, false negatives are likely to appear. In other words, apart from the cardiac arrhythmias, the conditions in which the variability of the vena cava diameter cannot be

used are the same as for PPV/SVV (Fig. 27.3). For the superior vena cava, it must be added that it can only be measured by transoesophageal echography.

Overall, the reliability of vena cava diameter variability for predicting fluid responsiveness is probably lower than that of PPV. In a meta-analysis that included eight studies, sensitivity was only 76% and specificity was 86% (Zhang et al. 2014). In a study in 540 patients, the area under the Receiver Operating Characteristic Curve was only 0.755 for the variability of the superior vena cava and 0.635 for that of the inferior vena cava, whereas a diagnostic method is considered reliable when the area under this curve is greater than 0.75 (Vignon et al. 2017). This was also the case in a multi-centre clinical study, although it is true that reliability of PPV in this study was also poor, which casts doubt on the quality with which these different indices were collected in this “pragmatic” study (Vignon et al. 2017).

Passive Leg Raising Test

Principle

The transition from the semi-recumbent position to a position in which the lower limbs are raised to 30–45 ° and the trunk is horizontal induces the transfer of venous blood from the lower limbs, and also from the splanchnic territory, toward the heart chambers. This results in a significant increase in mean systemic filling pressure, the upstream systemic venous return pressure (Guerin et al. 2015), and right and left cardiac preload (Boulain et al. 2002). Therefore, PLR can be used as a preload dependence challenge. If cardiac output increases in response to the preload increase, both ventricles are likely preload-dependent and fluid responsiveness is likely. It has been shown that a PLR test was equivalent to about 300 mL of fluid challenge (Jabot et al. 2009), but this is an average value as this volume might highly vary depending on the patient.

Reliability

Many studies have shown that the PLR test can reliably detect preload dependence. The diagnostic threshold is a PLR-induced increase in cardiac output higher than 10% (Monnet et al. 2016b). A great advantage of the test is that it remains valid even in clinical circumstances where PPV/SVV cannot be used. In particular, the PLR test retains all its diagnostic value in case of spontaneous breathing, cardiac arrhythmia (Monnet et al. 2012), and ventilation at low tidal volume or low lung compliance (Monnet et al. 2012).

Two meta-analyses confirmed the diagnostic value of the PLR test (Monnet et al. 2016b; Cherpwsqanath et al. 2016). It has been included in the most recent version of the Surviving Sepsis Campaign’s guidelines (Rhodes et al. 2017) and in a consensus conference of the European Society of Intensive Care Medicine (Cecconi et al. 2014).

Cardiac Output Measurement Technique

The effects of the PLR test should be measured directly on cardiac output (Monnet and Teboul 2015) (Fig. 27.4). Indeed, if these effects are assessed on arterial pressure, even pulse pressure, the sensitivity of the test is lower, and the number of false negatives is greater (Monnet et al. 2016b; Cherpanath et al. 2016). From this point of view, the PLR test is similar to the fluid challenge, the effects of which can only be reliably assessed by directly measuring cardiac output (Monnet et al. 2011; Pierrakos et al. 2012).

Several cardiac output measurement techniques can be used for this purpose. They must meet the requirement to measure flow continuously and in real time, in order to capture the maximum effect of the test. In fact, when the PLR test is positive, the increase in cardiac output occurs during the first minute (Monnet et al. 2006). Nevertheless, it may occur that cardiac output decreases after reaching this maximum. This effect is particularly observed in patients

with severe septic shock, whose vasodilatation is marked. This is, for example, not possible with thermodilution, neither classic pulmonary nor transpulmonary.

Oesophageal Doppler, calibrated or non-calibrated pulse wave contour analysis can be used (Monnet et al. 2006). With echocardiography, one must look for the increase in the velocity-time integral in the left ventricular outflow tract. The changes in the amplitude of the plethysmographic signal, assessed by the perfusion index, reflects stroke volume changes, provided that the vascular tone remains constant. It has been shown that a PLR-induced increase in this perfusion index could reflect the simultaneous changes in cardiac output (Beurton et al. 2019a). This needs to be confirmed, but this opens the possibility of an easy and non-invasive assessment of the test. Another interesting technique is capnography (Young et al. 2013; Monnet et al. 2013; Monge Garcia et al. 2012). In fact, if the ventilation conditions are perfectly stable, changes in end-tidal carbon dioxide are proportional to changes in cardiac output. It was shown that if this end-tidal carbon dioxide value increased by more than 5%

during the PLR test, fluid responsiveness could be reliably predicted (Monnet et al. 2013; Monge Garcia et al. 2012).

Other Practical Aspects

The position from which the PLR test is started is of great importance (Fig. 27.4). Indeed, if the test is started from the semi-recumbent position, in which the trunk is elevated by 45°, the test mobilizes not only the volume of the venous blood contained in the lower limbs but also the volume of blood contained in the vast splanchnic reservoir. The test is more sensitive (Jabot et al. 2009).

The PLR test should ideally be performed using the automatic movements of the bed. Indeed, the “manual” embodiment, which involves holding the patient’s heels, can cause discomfort, or even pain, which could distort the analysis of changes in cardiac output (Monnet and Teboul 2015).

Finally, it is important to measure cardiac output after performing the test, when the patient has been returned to the semi-recumbent position, in

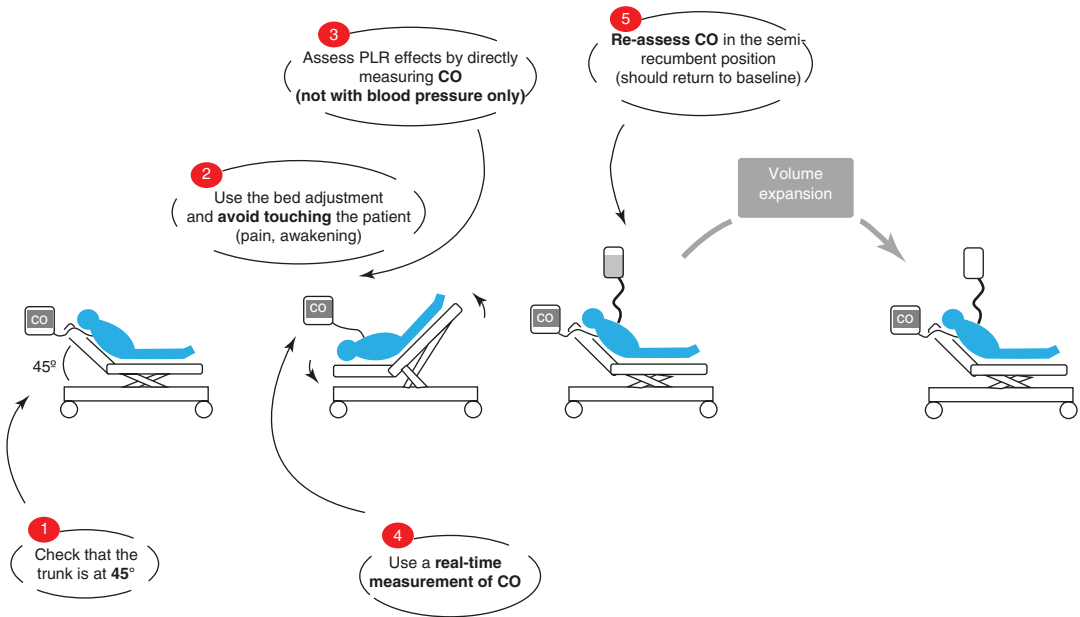


Fig. 27.4 Five rules to respect when performing the passive leg raising test. CO cardiac output. (Adapted from (Monnet and Teboul 2015) (Open Access Journal))

order to verify that it has returned to its baseline value, and that the changes observed during PLR were only attributable to the test (Monnet and Teboul 2015) (Fig. 27.4).

Limitations

As stated above, the essential limitation of the PLR test is that it requires a direct measurement of cardiac output. Also, the test is difficult or impossible to use during a surgical procedure and is reasonably contra-indicated in case of intracranial hypertension. In case of intra-abdominal hypertension, it has been demonstrated that some false negatives to the PLR test may appear (Beurton et al. 2019b). This might be due to the compression of the splanchnic compartment in this condition. Finally, the PLR test is probably less sensitive in patients with venous compression stocking.

Respiratory Occlusion Tests

Principle

As stated above, during mechanical ventilation, each insufflation increases the intrathoracic pressure and, consequently, the right atrial pressure, which opposes the systemic venous return. When mechanical ventilation is interrupted by end-expiration for a few seconds, the cyclical decrease in cardiac preload is interrupted. Cardiac preload increases transiently. If, in response, cardiac output increases, it means that both ventricles are preload-dependent. Conversely, an end-inspiratory pause should decrease cardiac output in case of preload-dependence. Importantly, the duration of the ventilator occlusion should be long enough for the “preload bolus” to pass through the pulmonary circulation. Five seconds is insufficient (Monnet et al. 2009), and the studies reported a reliable test when occlusions of 12 to 30 sec were performed (Monnet et al. 2009; Georges et al. 2018; Biais et al. 2017b).

End-Expiratory Occlusion Test

It has been shown that if cardiac output increases by more than 5% in the last few seconds of an expiratory pause of at least 12 seconds, the response to volume expansion could be predicted with good reliability (Biais et al. 2017a; Monnet et al. 2012; Monnet et al. 2009; Silva and Teboul 2011). The test has the advantage of being simple to perform.

An important practical point is that the technique used to measure cardiac output must be a real-time measurement, and also that it must be precise enough to measure small amplitude changes. From this point of view, the analysis of the contour of the pulse wave is well suited (Jozwiak et al. 2017a).

Association of End-Inspiratory and End-Expiratory Occlusions

The increase in the velocity-time integral of the sub-aortic flow measured by echocardiography during an end-expiratory occlusion allows one to predict the response to volume expansion (Georges et al. 2018; Jozwiak et al. 2017b). Nevertheless, the diagnostic threshold might be low compared to the accuracy of echocardiography. This is why, in a clinical study, we associated a 15-second end-inspiratory pause with a 15-second end-expiratory pause, a few seconds before the first one (Jozwiak et al. 2017b). We have shown that end-inspiratory occlusion decreased the sub-aortic velocity-time integral more in preload dependent patients than in those who are not. Interestingly, if we considered the sum of the effects on the velocity-time integral of the end-expiratory and the end-inspiratory occlusions, the prediction of fluid responsiveness was made with sensitivity and a specificity identical to those obtained with end-expiratory occlusion alone, but with a diagnostic threshold of 15%, which is more compatible with the precision of the echocardiography (Jozwiak et al. 2017b).

The method is somewhat restrictive, since it imposes a careful measurement of the velocity-

time integral during two successive respiratory breaks, but it could be an alternative when no other technique than echocardiography is available to estimate the cardiac output. Nevertheless, when cardiac output is measured by a technique that cannot reliably detect changes in cardiac output less than 5%, it seems interesting to associate the end-expiratory and end-inspiratory occlusions.

Limitations

Respiratory occlusion tests can only be performed, of course, in patients under mechanical ventilation. In addition, patients must be able to support relatively long breathing occlusions. This is not a problem in the operating room for anaesthetized patients but may be a significant limitation in some critically ill patients.

It has been shown that the diagnostic value of the end-expiratory occlusion test does not depend on the level of positive expiratory pressure at which it was performed, at least between 5 and 15 cmH₂O (Silva and Teboul 2011). Finally, some studies have suggested that the test is less reliable if tidal volume is at 6 mL/kg rather than at 8 mL/kg (Myatra et al. 2017; Messina et al. 2019a).

Other Tests Using Heart–Lung Interactions

An increase in the level of positive expiratory pressure from 5 to 10 cmH₂O induces a decrease in cardiac preload that can be used to detect preload-dependence. This was shown in a study where the effects of the manoeuvre were measured on expired carbon dioxide, used as an estimate of cardiac output, in patients who were stably ventilated (Tusman et al. 2015).

In the patients with ARDS in whom it is indicated, recruitment manoeuvres induce an increase in intrathoracic pressure with similar haemodynamic effects. Concomitant cardiac output changes can predict the response to volume expansion (Biais et al. 2017c). Sigh

manoeuvres might even be useful in selected patients under pressure support ventilation (Messina et al. 2019b). The Respiratory Systolic Variation Test consists of measuring the effects on the systolic blood pressure of a series of three respiratory cycles performed with increasing airway pressure. The essential advantage of the test is that it does not depend on the tidal volume (Preisman et al. 2005). It can be done automatically by some ventilators during anaesthesia.

Nobody Is Perfect!

None of the indices of preload responsiveness has shown to predict fluid responsiveness with absolute sensitivity and specificity. Moreover, the interpretation of these tests has an intrinsic limit. For the purpose of statistical analysis, the status of fluid responsiveness has been dichotomously described: present or absent. In fact, the response to fluid administration is conventionally defined by an increase in cardiac output of more than 15%, while it is a continuous variable. Is a patient with a 14% increase so different from another in whom fluid increases cardiac output by 16%? In practice, this limit must be taken into account at the bedside. The predictive certainty is all the more established as the observed changes are remote from the diagnostic threshold.

It is to our advantage today that we have at our disposal many of these tests (Monnet et al. 2016a) (Fig. 27.2). In patients in whom it is considered critically necessary to detect preload responsiveness or unresponsiveness, for example in patients with circulatory failure and ARDS, one should use several tests when the response of cardiac output is close to thresholds described by the literature.

Finally, a reasoned fluid strategy should not be based only on fluid responsiveness indices. The decision to administer fluid should also take into account the risk of fluid administration. It should be evaluated for instance on the degree of lung impairment, the level of extravascular lung water (Monnet and Teboul 2017) or of the left ventricu-

lar filling pressure. The relative weight of this risk must be compared with the advantage of increasing cardiac output.

Conclusion

The literature devoted to the tests and indices of preload responsiveness has been abundant and a review like this one can obviously not report it entirely. These markers are now available at the bedside to make sure that the volume expansion that one is about to perform will be effective. They are even more useful for detecting preload unresponsiveness, avoiding unnecessary and dangerous fluid administration. Although limited for the moment, there are today some studies telling us that using these tests reduces fluid administration in critically ill patients (Rameau et al. 2017; Latham et al. 2017). A recent meta-analysis even suggested that it may decrease mortality (Bednarczyk et al. 2017). They are helpful for guiding fluid administration, and also for guiding fluid removal, which can be safely performed when tests have verified that there is no preload responsiveness (Monnet et al. 2016a; Honore and Spapen 2017).

Conflicts of Interest Profs. Monnet and Teboul are members of the Medical Advisory Board of Pulsion Medical Systems, member of Getinge. They gave lectures for Baxter and for Masimo.

References

- Airapetian N, Maizel J, Alyamani O, Mahjoub Y, Lorne E, Levrard M, Ammenouche N, Seydi A, Tinturier F, Lobjoie E, et al. Does inferior vena cava respiratory variability predict fluid responsiveness in spontaneously breathing patients? *Crit Care*. 2015;19:400.
- Aya HD, Rhodes A, Chis Ster I, Fletcher N, Grounds RM, Cecconi M. Hemodynamic effect of different doses of fluids for a fluid challenge: a quasi-randomized controlled study. *Crit Care Med*. 2017;45(2):e161–8.
- Bednarczyk JM, Fridfinnson JA, Kumar A, Blanchard L, Rabbani R, Bell D, Funk D, Turgeon AF, Abou-Setta AM, Zarychanski R. Incorporating dynamic assessment of fluid responsiveness into goal-directed therapy: a systematic review and meta-analysis. *Crit Care Med*. 2017;45(9):1538–45.
- Bentzer P, Griesdale DE, Boyd J, MacLean K, Sirounis D, Ayas NT. Will this Hemodynamically unstable patient respond to a bolus of intravenous fluids? *JAMA*. 2016;316(12):1298–309.
- Beurton A, Teboul JL, Gavelli F, Gonzalez FA, Giroto V, Galarza L, Anguel N, Richard C, Monnet X. The effects of passive leg raising may be detected by the plethysmographic oxygen saturation signal in critically ill patients. *Crit Care*. 2019a;23(1):19.
- Beurton A, Teboul JL, Giroto V, Galarza L, Anguel N, Richard C, Monnet X. Intra-abdominal hypertension is responsible for false negatives to the passive leg raising test. *Crit Care Med*. 2019b; in press.
- Biais M, de Courson H, Lanchon R, Pereira B, Bardonneau G, Griton M, Sesay M, Nouette-Gaulain K. Mini-fluid challenge of 100 ml of crystalloid predicts fluid responsiveness in the operating room. *Anesthesiology*. 2017a;127(3):450–6.
- Biais M, Larghi M, Henriot J, de Courson H, Sesay M, Nouette-Gaulain K. End-expiratory occlusion test predicts fluid responsiveness in patients with protective ventilation in the operating room. *Anesth Analg*. 2017b;125(6):1889–95.
- Biais M, Lanchon R, Sesay M, Le Gall L, Pereira B, Futier E, Nouette-Gaulain K. Changes in stroke volume induced by lung recruitment maneuver predict fluid responsiveness in mechanically ventilated patients in the operating room. *Anesthesiology*. 2017c;126(2):260–7.
- Boulain T, Achard JM, Teboul JL, Richard C, Perrotin D, Ginies G. Changes in BP induced by passive leg raising predict response to fluid loading in critically ill patients. *Chest*. 2002;121(4):1245–52.
- Cannesson M, Le Manach Y, Hofer CK, Goarin JP, Lehot JJ, Vallet B, Tavernier B. Assessing the diagnostic accuracy of pulse pressure variations for the prediction of fluid responsiveness: a “Gray zone” approach. *Anesthesiology*. 2011;115(2):231–41.
- Cecconi M, De Backer D, Antonelli M, Beale R, Bakker J, Hofer C, Jaeschke R, Mebazaa A, Pinsky MR, Teboul JL, et al. Consensus on circulatory shock and hemodynamic monitoring. Task force of the European Society of Intensive Care Medicine. *Intensive Care Med*. 2014;40(12):1795–815.
- Cherpanath TG, Hirsch A, Geerts BF, Lagrand WK, Leeftang MM, Schultz MJ, Groeneveld AB. Predicting fluid responsiveness by passive leg raising: a systematic review and meta-analysis of 23 clinical trials. *Crit Care Med*. 2016;44(5):981–91.
- Corl K, Napoli AM, Gardiner F. Bedside sonographic measurement of the inferior vena cava caval index is a poor predictor of fluid responsiveness in emergency department patients. *Emerg Med Australas*. 2012;24(5):534–9.
- De la Puente-Diaz de Leon V, de Jesus J-RV, Teboul JL, Garcia-Miranda S, Martinez-Guerra BA, Dominguez-Cherit G. Changes in radial artery pulse pressure during a fluid challenge cannot assess fluid responsiveness in patients with septic shock. *J Intensive Care Med*. 2017;885066617732291

- Georges D, de Courson H, Lanchon R, Sesay M, Nouette-Gaulain K, Biais M. End-expiratory occlusion maneuver to predict fluid responsiveness in the intensive care unit: an echocardiographic study. *Crit Care*. 2018;22(1):32.
- Guerin L, Teboul JL, Persichini R, Dres M, Richard C, Monnet X. Effects of passive leg raising and volume expansion on mean systemic pressure and venous return in shock in humans. *Crit Care*. 2015;19:411.
- Honore PM, Spapen HD. Passive leg raising test with minimally invasive monitoring: the way forward for guiding septic shock resuscitation? *J Intensive Care*. 2017;5:36.
- Jabot J, Teboul JL, Richard C, Monnet X. Passive leg raising for predicting fluid responsiveness: importance of the postural change. *Intensive Care Med*. 2009;35(1):85–90.
- Jozwiak M, Monnet X, Teboul JL. Pressure waveform analysis. *Anesth Analg*. 2017a;126:1930.
- Jozwiak M, Depret F, Teboul JL, Alphonsine JE, Lai C, Richard C, Monnet X. Predicting fluid responsiveness in critically ill patients by using combined end-expiratory and end-inspiratory occlusions With echocardiography. *Crit Care Med*. 2017b;45(11):e1131–8.
- Jozwiak M, Monnet X, Teboul JL. Pressure waveform analysis. *Anesth Analg*. 2018;126(6):1930–3.
- Latham HE, Bengtson CD, Satterwhite L, Stites M, Subramaniam DP, Chen GJ, Simpson SQ. Stroke volume guided resuscitation in severe sepsis and septic shock improves outcomes. *J Crit Care*. 2017;42:42–6.
- Liu Y, Wei LQ, Li GQ, Yu X, Li GF, Li YM. Pulse pressure variation adjusted by respiratory changes in pleural pressure, rather than by tidal volume, reliably predicts fluid responsiveness in patients with acute respiratory distress syndrome. *Crit Care Med*. 2016;44(2):342–51.
- Ma GG, Hao GW, Yang XM, Zhu DM, Liu L, Liu H, Tu GW, Luo Z. Internal jugular vein variability predicts fluid responsiveness in cardiac surgical patients with mechanical ventilation. *Ann Intensive Care*. 2018;8(1):6.
- Magder S, Georgiadis G, Cheong T. Respiratory variations in right atrial pressure predict the response to fluid challenge. *J Crit Care*. 1992;1992(7):76–85.
- Marik PE, Cavallazzi R. Does the central venous pressure predict fluid responsiveness? An updated meta-analysis and a plea for some common sense. *Crit Care Med*. 2013;41(7):1774–81.
- Marik PE, Cavallazzi R, Vasu T, Hirani A. Dynamic changes in arterial waveform derived variables and fluid responsiveness in mechanically ventilated patients: a systematic review of the literature. *Crit Care Med*. 2009;37(9):2642–7.
- Messina A, Montagnini C, Cammarota G, De Rosa S, Giuliani F, Muratore L, Della Corte F, Navalesi P, Cecconi M: Tidal volume challenge to predict fluid responsiveness in the operating room: a prospective trial on neurosurgical patients undergoing protective ventilation. *Eur J Anaesthesiol*. 2019a.
- Messina A, Colombo D, Barra FL, Cammarota G, De Mattei G, Longhini F, Romagnoli S, DellaCorte F, De Backer D, Cecconi M, et al. Sigh maneuver to enhance assessment of fluid responsiveness during pressure support ventilation. *Crit Care*. 2019b;23(1):31.
- Min JJ, Gil NS, Lee JH, Ryu DK, Kim CS, Lee SM. Predictor of fluid responsiveness in the ‘grey zone’: augmented pulse pressure variation through a temporary increase in tidal volume. *Br J Anaesth*. 2017;119(1):50–6.
- Monge Garcia MI, Gil Cano A, Gracia Romero M, Monterroso Pintado R, Perez Madueno V, Diaz Monrove JC. Non-invasive assessment of fluid responsiveness by changes in partial end-tidal CO₂ pressure during a passive leg-raising maneuver. *Ann Intensive Care*. 2012;2:9.
- Monnet X, Teboul JL. Passive leg raising: five rules, not a drop of fluid! *Crit care*. 2015;19(1):18.
- Monnet X, Teboul JL. Transpulmonary thermomodulation: advantages and limits. *Crit Care*. 2017;21(1):147.
- Monnet X, Rienzo M, Osman D, Anguel N, Richard C, Pinsky MR, Teboul JL. Passive leg raising predicts fluid responsiveness in the critically ill. *Crit Care Med*. 2006;34(5):1402–7.
- Monnet X, Osman D, Ridel C, Lamia B, Richard C, Teboul JL. Predicting volume responsiveness by using the end-expiratory occlusion in mechanically ventilated intensive care unit patients. *Crit Care Med*. 2009;37(3):951–6.
- Monnet X, Letierce A, Hamzaoui O, Chemla D, Anguel N, Osman D, Richard C, Teboul JL. Arterial pressure allows monitoring the changes in cardiac output induced by volume expansion but not by norepinephrine*. *Crit Care Med*. 2011;39:1394–9.
- Monnet X, Bleibtreu A, Ferré A, Dres M, Gharbi R, Richard C, Teboul JL. Passive leg raising and end-expiratory occlusion tests perform better than pulse pressure variation in patients with low respiratory system compliance. *Crit Care Med*. 2012;40:152–7.
- Monnet X, Bataille A, Magalhaes E, Barrois J, Le Corre M, Gosset C, Guerin L, Richard C, Teboul JL. End-tidal carbon dioxide is better than arterial pressure for predicting volume responsiveness by the passive leg raising test. *Intensive Care Med*. 2013;39(1):93–100.
- Monnet X, Marik PE, Teboul JL. Prediction of fluid responsiveness: an update. *Ann Intensive Care*. 2016a;6(1):111.
- Monnet X, Marik P, Teboul JL. Passive leg raising for predicting fluid responsiveness: a systematic review and meta-analysis. *Intensive Care Med*. 2016b;42(12):1935–47.
- Muller L, Toumi M, Bousquet PJ, Riu-Poulenc B, Louart G, Candela D, Zoric L, Suehs C, de La Coussaye JE, Molinari N, et al. An increase in aortic blood flow after an infusion of 100 ml colloid over 1 minute can predict fluid responsiveness: the mini-fluid challenge study. *Anesthesiology*. 2011;115(3):541–7.
- Myatra SN, Prabu NR, Divatia JV, Monnet X, Kulkarni AP, Teboul JL. The changes in pulse pressure variation or stroke volume variation after a “tidal volume

- challenge” reliably predict fluid responsiveness during low tidal volume ventilation. *Crit Care Med.* 2017;45(3):415–21.
- Pierrakos C, Velissaris D, Scolletta S, Heenen S, De Backer D, Vincent JL. Can changes in arterial pressure be used to detect changes in cardiac index during fluid challenge in patients with septic shock? *Intensive Care Med.* 2012;38(3):422–8.
- Preisman S, Kogan S, Berkenstadt H, Perel A. Predicting fluid responsiveness in patients undergoing cardiac surgery: functional haemodynamic parameters including the Respiratory Systolic Variation Test and static preload indicators. *Br J Anaesth.* 2005;95(6):746–55.
- Rameau A, de With E, Boerma EC. Passive leg raise testing effectively reduces fluid administration in septic shock after correction of non-compliance to test results. *Ann Intensive Care.* 2017;7(1):2.
- Rhodes A, Evans LE, Alhazzani W, Levy MM, Antonelli M, Ferrer R, Kumar A, Sevransky JE, Sprung CL, Nunnally ME, et al. Surviving sepsis campaign: international guidelines for management of sepsis and septic shock: 2016. *Intensive Care Med.* 2017;43(3):304–77.
- Sakr Y, Rubatto Birri PN, Kottfis K, Nanchal R, Shah B, Kluge S, Schroeder ME, Marshall JC, Vincent JL. Intensive care over nations I: higher fluid balance increases the risk of death from sepsis: results from a large international audit. *Crit Care Med.* 2017;45(3):386–94.
- Silva S, Teboul JL. Defining the adequate arterial pressure target during septic shock: not a ‘micro’ issue but the microcirculation can help. *Crit Care.* 2011;15(6):1004.
- Smorenberg A, Cherpanath TGV, Geerts BF, de Wilde RBP, Jansen JRC, Maas JJ, Groeneveld ABJ. A mini-fluid challenge of 150mL predicts fluid responsiveness using Modelflow(R) pulse contour cardiac output directly after cardiac surgery. *J Clin Anesth.* 2018;46:17–22.
- Teboul JL, Monnet X, Chemla D, Michard F. Arterial pulse pressure variation with mechanical ventilation. *Am J Respir Crit Care Med.* 2019;199(1):22–31.
- Toscani L, Aya HD, Antonakaki D, Bastoni D, Watson X, Arulkumaran N, Rhodes A, Cecconi M. What is the impact of the fluid challenge technique on diagnosis of fluid responsiveness? A systematic review and meta-analysis. *Crit Care.* 2017;21(1):207.
- Tusman G, Groisman I, Maidana GA, Scandurra A, Arca JM, Bohm SH, Suarez-Sipmann F. The sensitivity and specificity of pulmonary carbon dioxide elimination for noninvasive assessment of fluid responsiveness. *Anesth Analg.* 2015;122:1404–11.
- Vieillard-Baron A, Chergui K, Rabiller A, Peyrouset O, Page B, Beauchet A, Jardin F. Superior vena caval collapsibility as a gauge of volume status in ventilated septic patients. *Intensive Care Med.* 2004;30(9):1734–9.
- Vignon P, Repesse X, Begot E, Leger J, Jacob C, Bouferrache K, Slama M, Prat G, Vieillard-Baron A. Comparison of echocardiographic indices used to predict fluid responsiveness in ventilated patients. *Am J Respir Crit Care Med.* 2017;195(8):1022–32.
- Vincent JL, Weil MH. Fluid challenge revisited. *Crit Care Med.* 2006;34(5):1333–7.
- Yang X, Du B. Does pulse pressure variation predict fluid responsiveness in critically ill patients? A systematic review and meta-analysis. *Crit Care.* 2014;18(6):650.
- Young A, Marik PE, Sibole S, Grooms D, Levitov A. Changes in end-tidal carbon dioxide and volumetric carbon dioxide as predictors of volume responsiveness in hemodynamically unstable patients. *J Cardiothorac Vasc Anesth.* 2013;27:681–4.
- Zhang Z, Xu X, Ye S, Xu L. Ultrasonographic measurement of the respiratory variation in the inferior vena cava diameter is predictive of fluid responsiveness in critically ill patients: systematic review and meta-analysis. *Ultrasound Med Biol.* 2014;40(5):845–53.



CO₂-Derived Indices to Guide Resuscitation in Critically Ill Patients

Francesco Gavelli, Jean-Louis Teboul,
and Xavier Monnet

Introduction

In acute circulatory failure, the first-line treatment is aimed at increasing cardiac output. By improving oxygen delivery, this intervention is expected to correct the mismatch between oxygen demand and supply, which is the hallmark of shock (Vincent and De Backer 2004). However, no absolute value of cardiac output or oxygen delivery is recommended to be reached during resuscitation. As a matter of fact, the “good value” of cardiac output is the one that ensures a flow of oxygen that meets the metabolic demands (Gattinoni et al. 1995; Monnet and Teboul 2018). Thus, any treatment aimed at changing cardiac

output, such as fluids or inotrope administration, should be given according to the assessment of the adequacy between oxygen demand and supply.

This adequacy cannot be reliably detected by clinical examination, as signs of skin hypoperfusion do not precisely correlate with the degree of tissue hypoxia (Londoño et al. 2018). Urine output, although reflecting, to some extent, kidney perfusion, is altered by many factors during shock and cannot be used as an indicator of kidney perfusion in the case of acute tubular necrosis (Legrand and Payen 2011). Blood lactate concentration, which depends on the balance between lactate production and clearance, cannot be used as a real-time marker of tissue metabolism, due to the delay required for its metabolism (Vincent et al. 2016). Moreover, its levels may augment for processes unrelated to tissue hypoxia, giving false positives (Hernandez et al. 2019). Finally, the alteration of tissue oxygen extraction and/or utilisation in septic shock makes the evaluation of the central ($S_{c_v}O_2$) or mixed ($S_{\bar{v}}O_2$) venous oxygen saturation unable to detect anaerobic metabolism, these values being often in the normal range in such a condition (Monnet et al. 2013).

Many of these limitations for detecting the adequacy between oxygen demand and supply may be overcome by indices derived from the partial tension in carbon dioxide (CO₂) in the

F. Gavelli
Université Paris-Saclay, AP-HP, Service de médecine,
intensive-réanimation, Hôpital de Bicêtre, DMU
CORREVE, Inserm UMR S_999, FHU SEPSIS,
Groupe de recherche clinique CARMAS,
Le Kremlin-Bicêtre, France

Emergency Medicine Unit, Department of
Translational Medicine, Università degli Studi del
Piemonte Orientale, Novara, Italy
e-mail: francesco.gavelli@uniupo.it

J.-L. Teboul · X. Monnet (✉)
Université Paris-Saclay, AP-HP, Service de médecine
intensive-réanimation, Hôpital de Bicêtre, DMU
CORREVE, Inserm UMR S_999, FHU SEPSIS,
Groupe de recherche clinique CARMAS,
Le Kremlin-Bicêtre, France
e-mail: jean-louis.teboul@aphp.fr;
xavier.monnet@aphp.fr

arterial and the central or mixed venous blood (Zhang and Vincent 1993).

The Meaning of PCO₂ Gap

What Is the PCO₂ Gap?

The difference between the mixed venous blood content ($C_v\text{CO}_2$) and the arterial content ($C_a\text{CO}_2$) of CO₂ reflects the balance between its production by the tissues and its elimination through the lungs. This venoarterial difference in CO₂ content (CCO_2) can be estimated at the bedside by the venoarterial difference in PCO₂ ($P_v\text{CO}_2 - P_a\text{CO}_2$), named PCO₂ gap or ΔPCO_2 .

However, it is not possible to understand its clinical value without understanding how CO₂ is produced, transported, and eliminated, in aerobic and anaerobic conditions.

CO₂ Production

Under conditions of *normoxia*, CO₂ is produced in the cells during oxidative metabolism. The CO₂ production ($V\text{CO}_2$) is directly related to the global O₂ consumption ($V\text{O}_2$) by the relation:

$$V\text{CO}_2 = R \times V\text{O}_2$$

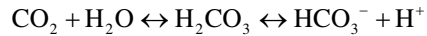
where R is the respiratory quotient. R may vary from 0.7 to 1 depending on the predominant energetic substrate (0.7 for lipids, 1 for carbohydrates). Therefore, under aerobic conditions, CO₂ production should increase either because the aerobic metabolism increases or, for a given $V\text{O}_2$, because more carbohydrates are used as energetic substrates.

Under conditions of *hypoxia*, CO₂ is produced in the cells through buffering of excessively produced protons by local bicarbonate ions (HCO_3^-). Protons are generated by two mechanisms (Randall and Cohen 1966). First, CO₂ increases because of the hydrolysis of adenosine triphosphate and of adenosine diphosphate, which occurs in anaerobic conditions. Second, another potential but minor source of CO₂ production under anaerobic conditions is the decarboxyl-

ation of some substrates produced by intermediate metabolism (α -ketoglutarate or oxaloacetate) (Randall and Cohen 1966).

How Is CO₂ Transported?

CO₂ is transported in the blood in three forms: dissolved (10%), carried in bicarbonate ions (60%), and associated with proteins as carbamino compounds (30%). Compared to what happens for O₂, the dissolved form of CO₂ plays a more significant role in its transport because CO₂ is approximately 20–30 times more soluble than O₂. However, the main proportion of CO₂ is carried in bicarbonates, which result from the reaction of CO₂ and water molecules:



From the tissues, CO₂ diffuses into the red blood cells, where erythrocytic carbonic anhydrase catalyzes CO₂ hydration, converting most CO₂ and H₂O to HCO_3^- and H^+ (Jensen 2004). In red blood cells, dissolved CO₂ can also be fixed by haemoglobin, according to its oxidation state, since CO₂ has a greater affinity for reduced than for oxygenated haemoglobin (Geers and Gros 2000). This is called the “Haldane effect” (Teboul and Scheeren 2017). In the peripheral capillaries, this phenomenon facilitates the loading of CO₂ by the blood, while O₂ is delivered to the tissues. By contrast, in the lungs, the Haldane effect promotes the unloading of CO₂ while O₂ is transferred to haemoglobin.

Finally, the carbamino compounds are formed by combining the CO₂ with the terminal NH₂ groups of proteins, especially with the globin of haemoglobin. This reaction is also favoured by haemoglobin deoxygenation.

How Is CO₂ Eliminated?

The three forms of CO₂ are carried by the blood flow to the pulmonary circulation and eliminated by ventilation. Passive diffusion from the capillaries to the alveoli eliminates CO₂, depending on the difference in the gas tension between both spaces.

What Is the Relationship Between CCO₂ and PCO₂?

Whilst the formula for calculating the content of oxygen is quite straightforward

$$1.34 \times \text{SO}_2 \times \text{Hb} + 0.034 \times \text{PO}_2$$

and can be obtained at the bedside, CCO₂ is determined by the combination of the three forms by which CO₂ is transported. As a consequence, the formula to calculate CCO₂ is complex and not practical for clinical purposes (Douglas et al. 1988):

$$\text{CCO}_2 = 2.226 \times s \times \text{PCO}_2 (1 + 10^{\text{pH} - \text{pK}'})$$

where *s* is the solubility coefficient of plasma CO₂, pK' the apparent pK of the CO₂-bicarbonate system, and 2.226 the conversion factor from mM to mL/100 mL (Douglas et al. 1988).

In this regard, the possibility to derive CCO₂ from one single component, notably the PCO₂, is useful:

$$\text{PCO}_2 = k \times \text{CCO}_2$$

The *k* value, which encompasses the inverse of all the coefficients of the previous equation, is influenced by the degree of blood pH, haemato-

crit, and arterial oxygen saturation (Jensen 2001; McHardy 1967) (Fig. 28.1). From a practical point of view, the relationship between CCO₂ and PCO₂ is almost linear over the physiological range (Fig. 28.1). Thus, in clinical practice, the PCO₂ gap can give an estimate of the difference between venous and arterial CO₂ content (C_{v-a}CO₂).

What Are the Determinants of the PCO₂ Gap?

According to the Fick equation applied to CO₂, the CO₂ excretion (which equals CO₂ production – VCO₂ – in a steady state) equals the product of cardiac output by the difference between mixed venous CCO₂ (C_vCO₂) and arterial CCO₂ (C_aCO₂):

$$\text{VCO}_2 = \text{Cardiac output} \times (C_v \text{CO}_2 - C_a \text{CO}_2).$$

As mentioned above, under physiological conditions, CCO₂ can be substituted by PCO₂ (PCO₂ = *k* × CCO₂), so that:

$$\Delta \text{PCO}_2 = k \times (C_v \text{CO}_2 - C_a \text{CO}_2)$$

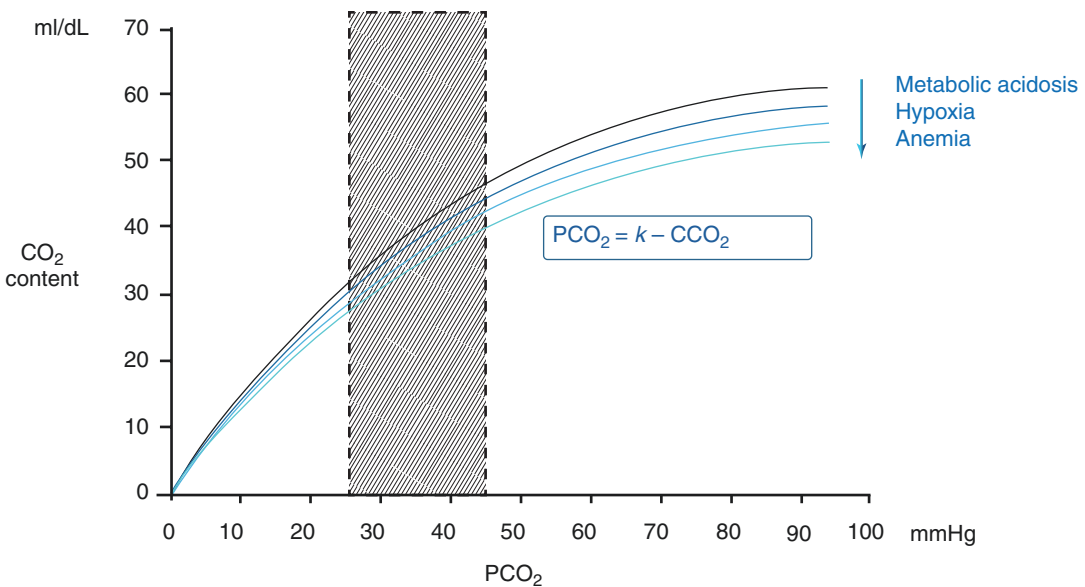


Fig. 28.1 Relationship between content (CCO₂) and partial pressure (PCO₂) of carbon dioxide

and

$$VCO_2 = \text{Cardiac output} \times \Delta PCO_2 / k.$$

Thus, ΔPCO_2 can be calculated from a modified Fick equation:

$$\Delta PCO_2 = (k \times VCO_2) / \text{Cardiac output}$$

where k is the factor cited above in the relationship between PCO_2 and CCO_2 .

The relationship between ΔPCO_2 and the cardiac output shows that if the cardiac output is low, the CO_2 clearance decreases, CO_2 stagnates at the venous side, and P_vCO_2 increases relatively to P_aCO_2 at the venous level; this leads to an increase in the PCO_2 gap.

In other words, for a given VCO_2 , a decrease in cardiac output results in an increased PCO_2 gap and vice versa. This was found by experimental studies in which, when cardiac output was gradually reduced under conditions of stable VO_2 , the PCO_2 gap was observed to concomitantly increase (Zhang and Vincent 1993; Groeneveld et al. 1991). Conversely, in a clinical study performed in normolactatemic patients with cardiac failure, the increase in cardiac index induced by dobutamine was associated with a decrease in the PCO_2 gap, while VO_2 was unchanged (Teboul et al. 1998).

What Is the Place of the PCO_2 Gap in Clinical Practice?

It is a common belief that ΔPCO_2 acts as a marker of tissue hypoxia. This might have been suggested by some old studies performed during cardiac arrest, in which a large increase in ΔPCO_2 has been observed (Grundler et al. 1986; Weil et al. 1986). However, the pathophysiologic elements explained above help in understanding why it is in fact not the case. Indeed, in the case of tissue hypoxia, ΔPCO_2 can increase, decrease, or remain unchanged, as the determinant of CO_2 production can vary in all directions.

First, since during hypoxia, tissues have a lesser quantity of oxygen for their metabolic needs and the principal source of CO_2 production comes from the oxidative metabolism, VCO_2

decreases. This situation leads to a decrease in the PCO_2 gap.

Second, it should be always kept in mind that PCO_2 is only an estimation of CCO_2 , and this approximation is mainly determined by the k factor. So, all the conditions that influence the k factor have a repercussion on the estimation of $C_{v-a}CO_2$ through the PCO_2 gap. As a matter of fact, the relationship is linear only in the case of physiological values of PCO_2 and becomes curvilinear for the extreme CO_2 values. Moreover, it also may be subjected to lower displacement in case of anaemia, metabolic acidosis, and hypoxia (Fig. 28.1). As a result, for the same content, in these situations, PCO_2 overestimates CCO_2 , leading to an artefactual increase in the PCO_2 gap.

So, since during tissue hypoxia, VCO_2 must decrease ($\searrow \Delta PCO_2$) and k must increase ($\nearrow \Delta PCO_2$), the resultant effect on ΔPCO_2 will mainly depend on cardiac output ($\Delta PCO_2 = (k \times VCO_2) / \text{cardiac output}$) (Dres et al. 2012).

Therefore, two situations should be distinguished: tissue hypoxia with reduced cardiac output and tissue hypoxia with preserved or high cardiac output (Fig. 28.2).

In cases of tissue hypoxia with *reduced cardiac output*, P_vCO_2 increases relatively to P_aCO_2 due to the venous stagnation phenomenon, which increases ΔPCO_2 . In this regard, in experimental studies where tissue hypoxia was induced by reducing blood flow, high values of ΔPCO_2 were found (Groeneveld et al. 1991; Van der Linden et al. 1995).

On the other hand, in the case of tissue hypoxia with *maintained or high cardiac output*, ΔPCO_2 should be normal or even reduced. The high efferent venous blood flow should be sufficient to wash out the CO_2 produced by the tissues, preventing CO_2 stagnation and ΔPCO_2 increase.

All the experimental (Nevière et al. 2002; Dubin et al. 2002; Vallet et al. 2000) and clinical (Bakker et al. 1992; Mecher et al. 1990; Wendon et al. 1991) studies conducted on this subject have confirmed that, during tissue hypoxia, ΔPCO_2 can be either high or normal depending on cardiac output. For example, Bakker et al. (Bakker et al. 1992) found that most patients with septic shock had a $\Delta PCO_2 \leq 6$ mmHg. The cardiac index obtained in

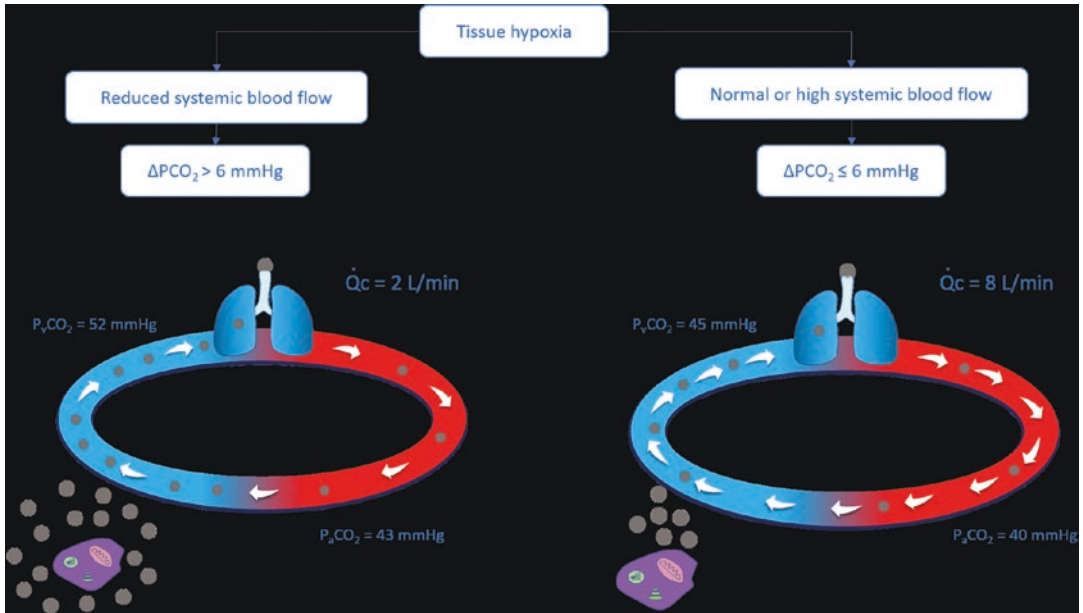


Fig. 28.2 Illustration of the influence of cardiac output on the amplitude of the venoarterial difference of carbon dioxide partial pressure. P_aCO_2 arterial partial pressure in

carbon dioxide P_vCO_2 venous partial pressure in carbon dioxide Q_c cardiac output ΔPCO_2 veno-arterial difference of carbon dioxide partial pressure

this subgroup of patients was significantly higher than the one obtained in the subgroup of patients with $\Delta PCO_2 > 6$ mmHg. Interestingly, the two subgroups did not differ in terms of blood lactate. Although VCO_2 and VO_2 were not directly measured, these data suggest that differences in CO_2 production did not account for differences in ΔPCO_2 . In other words, many patients had a normal ΔPCO_2 despite tissue hypoxia, probably because their high blood flow had easily removed the PCO_2 produced by the tissues.

Thus, a normal ΔPCO_2 cannot exclude the absence of tissue hypoxia in high blood flow states. On the other hand, ΔPCO_2 can be elevated in cases of low cardiac output, even in the absence of tissue hypoxia.

How to Interpret the PCO_2 Gap in Practice?

Once the patient has been confirmed to have acute circulatory failure, in the case of increased

S_vO_2 and increased lactate levels, the evaluation of the PCO_2 gap might be helpful to assess the efficacy of the cardiac output in regard to the metabolic conditions (Figure 28.3).

An increased PCO_2 gap (> 6 mmHg) suggests that *cardiac output is not high enough* with respect to the global metabolic conditions:

- In cases of shock (e.g. increased blood lactate), a high PCO_2 gap could prompt clinicians to increase cardiac output with the aim of reducing tissue hypoxia.
- In the absence of shock, a high PCO_2 gap can be associated with an increased oxygen demand.

On the other hand, a *normal PCO_2 gap* (≤ 6 mmHg) suggests that *cardiac output is high enough* to wash out the amount of CO_2 produced from the peripheral tissues (Fig. 28.2). Thus, increasing cardiac output has little chance to improve global oxygenation, and such a strategy cannot be a priority (Fig. 28.3).

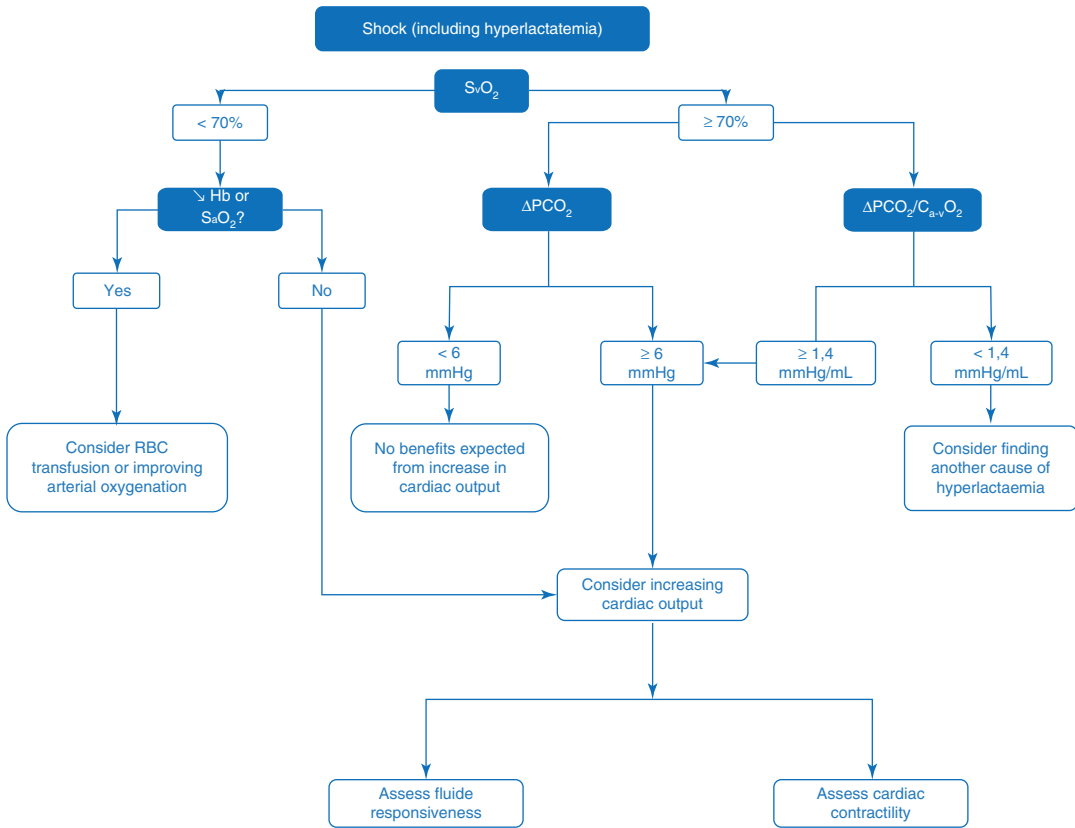


Fig. 28.3 Interpretation of indices of tissue oxygenation. Hb haemoglobin, S_{vO_2} venous oxygen saturation, S_{aO_2} arterial oxygen saturation, $C_{a-v}O_2$ arteriovenous difference

in oxygen content, ΔPCO_2 venoarterial difference in carbon dioxide partial pressure

Combination of ΔPCO_2 and Oxygen-Derived Variables

Even though ΔPCO_2 cannot directly identify the presence of anaerobic metabolism, its combination with oxygen-derived variables has been suggested to overcome this issue. The rationale comes from physiology. As mentioned above, during aerobic metabolism, CO_2 production is related to the O_2 consumption through the respiratory quotient ($VCO_2 = R \times VO_2$). Depending on the metabolic substrate, the respiratory quotient can vary among values below the unit, which means that the ratio between CO_2 produced and O_2 consumed does not exceed 1. In other words, in aerobic conditions, the amount of CO_2 produced cannot be larger than the amount of O_2 consumed. During tissue hypoxia, VO_2 and VCO_2

decrease, but VCO_2 decreases to a lesser extent due to the generation of CO_2 through anaerobic pathways. At the same time, k decreases. Then, indexing VCO_2 by VO_2 should help detect the excess CO_2 produced due to the occurrence of anaerobic metabolism. In other words, dividing VCO_2 by VO_2 may help detect the production of CO_2 which is not due to VO_2 , as a surrogate of the respiratory quotient. The issue is then to estimate the VCO_2/VO_2 ratio at the bedside. As shown in Fig. 28.4, using the Fick equation and substituting CCO_2 by PCO_2 , as suggested above, this ratio can be estimated by the $\Delta PCO_2/C_{a-v}O_2$ ratio, where $C_{a-v}O_2$ stands for the arteriovenous difference in O_2 content. In studies in which it has been evaluated, both the mixed venous (Mekontso-Dessap et al. 2002) and the central venous blood (Monnet et al. 2013) could be used to calculate

$$\text{Respiratory quotient} = \frac{\text{CO}_2 \text{ produced}}{\text{O}_2 \text{ consumed}} = \frac{\text{VCO}_2 - k}{\text{VO}_2} = \frac{\text{Cardiac output} - \text{CO}_{v-a}\text{CO}_2}{\text{Cardiac output} - \text{C}_{a-v}\text{O}_2} = \frac{\text{Cardiac output} - \text{P}_{v-a}\text{CO}_2}{\text{Cardiac output} - \text{C}_{a-v}\text{O}_2} = \frac{\text{PCO}_2 \text{ gap}}{\text{C}_{a-v}\text{O}_2}$$

Fig. 28.4 Estimation of the respiratory quotient from the ratio between venoarterial difference in carbon dioxide partial pressure and arteriovenous difference in oxygen content. C_{a-v}O₂ arteriovenous difference in oxygen content, CO₂ carbon dioxide, C_{v-a}CO₂ venoarterial difference in carbon dioxide content, P_{v-a}CO₂ venoarterial difference

in carbon dioxide partial pressure. (All figures are original drawings of the authors that were published in a previous article that appeared in the Journal of Thoracic Disease (<http://jtd.amegroups.com/about>), an Open-Access Journal. From Gavelli et al. (2019))

this ratio, providing a significant correlation with blood lactate levels.

Thus, an increase in the $\Delta\text{PCO}_2/\text{C}_{a-v}\text{O}_2$ ratio above 1.4 mmHg/mL (Mekontso-Dessap et al. 2002; Mesquida et al. 2015) should be considered as a marker of global anaerobic metabolism (Fig. 28.3). Its normalisation during resuscitation has been suggested as a therapeutic target (Ospina-Tascón et al. 2015). Interestingly, in the latter study, among a series of haemodynamic variables in septic shock, only lactate and the $\Delta\text{PCO}_2/\text{C}_{a-v}\text{O}_2$ ratio were independently associated with mortality at multivariate analysis. Moreover, mortality was significantly higher among patients with an increase in both lactate and $\Delta\text{PCO}_2/\text{C}_{a-v}\text{O}_2$ ratio compared to patients with elevated lactate levels but normal $\Delta\text{PCO}_2/\text{C}_{a-v}\text{O}_2$ ratio.

S_vO₂ vs. PCO₂-Derived Indices

An advantage of the PCO₂ gap over S_vO₂ is that it remains a valid marker of the adequacy of cardiac output to the metabolic conditions even if the microcirculation is injured and the oxygen extraction is impaired. This may be due to the fact that CO₂ is about 20 times more soluble than O₂ (Vallet et al. 2013). The microcirculatory impairment, with large venoarterial shunts, impedes the diffusion of O₂ between cells and red blood cells, while the diffusion of CO₂ remains unaltered (Vallet et al. 2013). Confirmations have been provided by some studies, in which ΔPCO_2 alone or in combination with S_{cv}O₂ was better both in identifying patients who still remained

inadequately resuscitated and in predicting outcome, compared to S_{cv}O₂ alone (Vallée et al. 2008; Du et al. 2013). In addition, in a series of septic patients in which volume expansion induced an increase in cardiac output, ΔPCO_2 was shown to be able to follow the changes in cardiac output. However, in patients in which VO₂ was increased after fluid expansion, this VO₂ increase was detected by changes in the $\Delta\text{PCO}_2/\text{C}_{a-v}\text{O}_2$ ratio but not by the changes in ΔPCO_2 or S_{cv}O₂ (Monnet et al. 2013). Lactate was also able to detect the changes in VO₂ but with a delay of some hours (Monnet et al. 2013).

Thus, in the case of septic shock with O₂ extraction impairment, in contrast with S_vO₂ or S_{cv}O₂, the ΔPCO_2 remains a reliable marker of the adequacy of cardiac output with the metabolic condition, and the $\Delta\text{PCO}_2/\text{C}_{a-v}\text{O}_2$ ratio is a valid indicator of the adequacy between O₂ delivery and VO₂. Moreover, compared to lactate, the CO₂-derived variables have the advantage to change without delay and to follow the metabolic condition in real time.

Errors and Pitfalls of the PCO₂ Gap

Despite the pathophysiological basis on which both ΔPCO_2 and its combination with oxygen-derived parameters stand, some technical aspects should be kept in mind when these indices are used in clinical practice. First, some errors in the PCO₂ gap measurements may occur when sampling the venous blood: incorrect sample container, contaminated sample by air or venous blood, or catheter fluid (d'Ortho et al. 2001).

Second, a too long delay of transport of blood sampling may significantly change the blood gas content at the venous and the arterial site (Wan et al. 2018).

Third, it is important to remind that variations in both ΔPCO_2 and the $\Delta\text{PCO}_2/\text{C}_{a-v}\text{O}_2$ ratio are submitted to a certain degree of variability. In this regard, on a series of 192 patients, Mallat et al. showed that the smallest detectable difference of ΔPCO_2 was ± 1.8 mmHg, corresponding to a least significant change of 32%. For the $\Delta\text{PCO}_2/\text{C}_{a-v}\text{O}_2$ ratio, the smallest detectable difference was ± 0.57 mmHg/mL, corresponding to a least significant change of 38% (Mallat et al. 2015).

Conclusion

A proper analysis of the physiology of CO_2 metabolism reveals that the PCO_2 gap indicates the adequacy of cardiac output with the metabolic condition, while the adequacy between O_2 delivery and O_2 consumption is better indicated by the $\Delta\text{PCO}_2/\text{C}_{a-v}\text{O}_2$ ratio in critically ill patients. The CO_2 -derived indices seem to be quite reliable when measured in the central venous blood. In contrast to S_vO_2 or S_{cv}O_2 , they remain useful in septic shock patients with an impaired O_2 extraction.

Conflicts of Interest Profs. Monnet and Teboul are members of the Medical Advisory Board of Pulsion Medical Systems, member of Getinge. They gave lectures for Baxter and for Masimo. Dr. Gavelli has no conflict of interest to declare.

References

- Bakker J, Vincent JL, Gris P, Leon M, Coffernils M, Kahn RJ. Venous-arterial carbon dioxide gradient in human septic shock. *Chest*. 1992;101(2):509–15.
- d'Ortho MP, Delclaux C, Zerach F, Herigault R, Adnot S, Harf A. Use of glass capillaries avoids the time changes in high blood PO_2 observed with plastic syringes. *Chest*. 2001;120(5):1651–4.
- Douglas AR, Jones NL, Reed JW. Calculation of whole blood CO_2 content. *J Appl Physiol* (1985). 1988;65(1):473–7.
- Dres M, Monnet X, Teboul J-L. Hemodynamic management of cardiovascular failure by using PCO_2 venous-arterial difference. *J Clin Monit Comput*. 2012;26(5):367–74.
- Du W, Liu D-W, Wang X-T, Long Y, Chai W-Z, Zhou X, et al. Combining central venous-to-arterial partial pressure of carbon dioxide difference and central venous oxygen saturation to guide resuscitation in septic shock. *J Crit Care*. 2013;28(6):1110.e1–5.
- Dubin A, Murias G, Estenssoro E, Canales H, Badie J, Pozo M, et al. Intramucosal-arterial PCO_2 gap fails to reflect intestinal dysoxia in hypoxic hypoxia. *Crit Care*. 2002;6(6):514–20.
- Gattinoni L, Brazzi L, Pelosi P, Latini R, Tognoni G, Pesenti A, et al. A trial of goal-oriented hemodynamic therapy in critically ill patients. SvO2 Collaborative Group. *N Engl J Med*. 1995;333(16):1025–32.
- Gavelli F, Teboul J-L, Monnet X. How can CO_2 -derived indices guide resuscitation in critically ill patients? *J Thorac Dis*. 2019;11:S1528–37. <https://doi.org/10.21037/jtd.2019.07.10>.
- Geers C, Gros G. Carbon dioxide transport and carbonic anhydrase in blood and muscle. *Physiol Rev*. 2000;80(2):681–715.
- Groeneveld AB, Vermeij CG, Thijs LG. Arterial and mixed venous blood acid-base balance during hypoperfusion with incremental positive end-expiratory pressure in the pig. *Anesth Analg*. 1991;73(5):576–82.
- Grundler W, Weil MH, Rackow EC. Arteriovenous carbon dioxide and pH gradients during cardiac arrest. *Circulation*. 1986;74(5):1071–4.
- Hernandez G, Bellomo R, Bakker J. The ten pitfalls of lactate clearance in sepsis. *Intensive Care Med*. 2019;45(1):82–5.
- Jensen FB. Comparative analysis of autoxidation of haemoglobin. *J Exp Biol*. 2001;204:2029–33.
- Jensen FB. Red blood cell pH, the Bohr effect, and other oxygenation-linked phenomena in blood O_2 and CO_2 transport. *Acta Physiol Scand*. 2004;182(3):215–27.
- Legrand M, Payen D. Understanding urine output in critically ill patients. *Ann Intensive Care*. 2011;1(1):13.
- Londoño J, Niño C, Díaz J, Morales C, León J, Bernal E, et al. Association of clinical hypoperfusion variables with lactate clearance and hospital mortality. *Shock*. 2018;50(3):286–92.
- Mallat J, Lazkani A, Lemyze M, Pepy F, Meddour M, Gasan G, et al. Repeatability of blood gas parameters, PCO_2 gap, and PCO_2 gap to arterial-to-venous oxygen content difference in critically ill adult patients. *Medicine (Baltimore)*. 2015;94(3):e415.
- McHardy GJ. The relationship between the differences in pressure and content of carbon dioxide in arterial and venous blood. *Clin Sci*. 1967;32(2):299–309.
- Mecher CE, Rackow EC, Astiz ME, Weil MH. Venous hypercarbia associated with severe sepsis and systemic hypoperfusion. *Crit Care Med*. 1990;18(6):585–9.
- Mekontso-Dessap A, Castelain V, Anguel N, Bahloul M, Schavuliege F, Richard C, et al. Combination of venoarterial PCO_2 difference with arteriovenous O_2 content difference to detect anaerobic metabolism in patients. *Intensive Care Med*. 2002;28(3):272–7.

- Mesquida J, Saludes P, Gruartmoner G, Espinal C, Torrents E, Baigorri F, et al. Central venous-to-arterial carbon dioxide difference combined with arterial-to-venous oxygen content difference is associated with lactate evolution in the hemodynamic resuscitation process in early septic shock. *Crit Care*. 2015;19:126.
- Monnet X, Teboul J-L. My patient has received fluid. How to assess its efficacy and side effects? *Ann Intensive Care*. 2018;8(1):54.
- Monnet X, Julien F, Ait-Hamou N, Lequoy M, Gosset C, Jozwiak M, et al. Lactate and venoarterial carbon dioxide difference/arterial-venous oxygen difference ratio, but not central venous oxygen saturation, predict increase in oxygen consumption in fluid responders. *Crit Care Med*. 2013;41(6):1412–20.
- Nevière R, Chagnon J-L, Teboul J-L, Vallet B, Wattel F. Small intestine intramucosal PCO₂ and microvascular blood flow during hypoxic and ischemic hypoxia. *Crit Care Med*. 2002;30(2):379–84.
- Ospina-Tascón GA, Umaña M, Bermúdez W, Bautista-Rincón DF, Hernandez G, Bruhn A, et al. Combination of arterial lactate levels and venous-arterial CO₂ to arterial-venous O₂ content difference ratio as markers of resuscitation in patients with septic shock. *Intensive Care Med*. 2015;41(5):796–805.
- Randall HM, Cohen JJ. Anaerobic CO₂ production by dog kidney in vitro. *Am J Phys*. 1966;211(2):493–505.
- Teboul J-L, Scheeren T. Understanding the Haldane effect. *Intensive Care Med*. 2017;43(1):91–3.
- Teboul JL, Mercat A, Lenique F, Berton C, Richard C. Value of the venous-arterial PCO₂ gradient to reflect the oxygen supply to demand in humans: effects of dobutamine. *Crit Care Med*. 1998;26(6):1007–10.
- Vallée F, Vallet B, Mathe O, Parraguette J, Mari A, Silva S, et al. Central venous-to-arterial carbon dioxide difference: an additional target for goal-directed therapy in septic shock? *Intensive Care Med*. 2008;34(12):2218–25.
- Vallet B, Teboul JL, Cain S, Curtis S. Venoarterial CO₂ difference during regional ischemic or hypoxic hypoxia. *J Appl Physiol* (1985). 2000;89(4):1317–21.
- Vallet B, Pinsky MR, Cecconi M. Resuscitation of patients with septic shock: please « mind the gap »! *Intensive Care Med*. 2013;39(9):1653–5.
- Van der Linden P, Rausin I, Deltell A, Bekrar Y, Gilbert E, Bakker J, et al. Detection of tissue hypoxia by arteriovenous gradient for PCO₂ and pH in anesthetized dogs during progressive hemorrhage. *Anesth Analg*. 1995;80(2):269–75.
- Vincent J-L, De Backer D. Oxygen transport-the oxygen delivery controversy. *Intensive Care Med*. 2004;30(11):1990–6.
- Vincent J-L, Quintairo E, Silva A, Couto L, Taccone FS. The value of blood lactate kinetics in critically ill patients: a systematic review. *Crit Care*. 2016;20(1):257.
- Wan X-Y, Wei L-L, Jiang Y, Li P, Yao B. Effects of time delay and body temperature on measurements of central venous oxygen saturation, venous-arterial blood carbon dioxide partial pressures difference, venous-arterial blood carbon dioxide partial pressures difference/arterial-venous oxygen difference ratio and lactate. *BMC Anesthesiol*. 2018;18(1):187.
- Weil MH, Rackow EC, Trevino R, Grundler W, Falk JL, Griffel MI. Difference in acid-base state between venous and arterial blood during cardiopulmonary resuscitation. *N Engl J Med*. 1986;315(3):153–6.
- Wendon JA, Harrison PM, Keays R, Gimson AE, Alexander G, Williams R. Arterial-venous pH differences and tissue hypoxia in patients with fulminant hepatic failure. *Crit Care Med*. 1991;19(11):1362–4.
- Zhang H, Vincent JL. Arteriovenous differences in PCO₂ and pH are good indicators of critical hypoperfusion. *Am Rev Respir Dis*. 1993;148:867–71.



Microcirculatory Monitoring to Assess Cardiopulmonary Status

29

Goksel Guven and Can Ince

Abbreviations

AU	Arbitrary unit
CCD	Charge-coupled device
HVM	Handheld vital microscope
IDF	Incident dark field
LDF	Laser Doppler flowmetry
LDPI	Laser Doppler perfusion imaging
LSCI	Laser speckle contrast imaging
NIRS	Near-infrared spectroscopy
OPS	Orthogonal polarization spectral
RBC	Red blood cell
SDF	Sidestream dark field

Introduction

Since the first discovery of microvessels by Marcello Malpighi in 1661 and the subsequent first visualization of microcirculatory blood by John Marshall in the eighteenth century, there has been a continuing quest for further insight into the microcirculation as an organ (Hwa and Aird 2007). Various microcirculatory monitoring techniques have come into preclinical and

clinical use for further assessment of microcirculatory function in different disease states. Over the last two decades, new discoveries and bedside clinical use of handheld vital microscopes (HVM) have advanced the field (Ince et al. 2018). Furthermore, the realization that microcirculatory dysfunction is associated with adverse outcome and can occur in the presence of normalized systemic hemodynamics, a condition referred to as loss of coherence between the micro- and macrocirculation, has underscored the importance of the assessment of the microcirculation in critically ill and perioperative patients (Ince 2015). The repeated failure of large randomized controlled clinical trials to demonstrate the benefit of conventional treatment modalities has encouraged clinicians toward a more personalized and physiological approach. The current availability of devices aimed at monitoring the microcirculation has increased the interest in this physiological compartment as an alternative treatment target for the critically ill and perioperative patient (Ince 2017).

This chapter aims to provide a comprehensive summary of the most commonly used microcirculatory monitoring techniques describing their fundamental principles, strengths, and weaknesses. Prior to a description of the operating principles of the various devices, a brief discussion of the physiology of the microcirculation and tissue oxygenation will be given.

G. Guven · C. Ince (✉)

Department of Intensive Care, Erasmus MC
University Medical Centre,
Rotterdam, The Netherlands
e-mail: c.ince@erasmusmc.nl

Microcirculation and Tissue Oxygenation

Oxygen is the terminal acceptor molecule of the electron transport chain responsible for energy production within the mitochondrial inner membrane. The circulatory system consists of the macro- and microcirculation and is designed to ensure the survival of living tissues by delivering oxygen by red blood cell (RBC) transport to the parenchymal cells. Providing the cells with an optimal amount of oxygen is essential and involves a multifaceted and coordinated microcirculatory perfusion by ensuring optimal convection of RBCs through the capillaries in combination with ensuring an optimal diffusion distance between the RBCs and the oxygen requiring parenchymal cells (den Uil et al. 2008).

The heart, lungs, and large vessels form the macrocirculation and are responsible for the convective transport of oxygen. The destination of the blood flowing through the macrocirculation is the microcirculation which consists of vessels less than 100 μm in diameter. This includes arterioles which are resistance vessels lined with smooth muscle cells that control vasotone), capillaries which are where oxygen leaves the circulation and diffuses passively to the parenchymal cells, and the collecting venules, which eventually enter the veins and returns blood to the heart. The microcirculation plays a crucial role in both convective and diffusive transport of oxygen (Ince et al. 2018).

The convection of oxygen through the capillaries and its diffusion into the mitochondria involve complex microhemodynamics due to the heterogeneous flow of RBCs through the capillary system. Furthermore, heterogeneity in the functional morphology of the microcirculation and the metabolic requirements of the cells influence the amount of oxygen transport to the tissues. The convective flow of oxygen in each capillary is described by the equation $QO_2^c = Q[O_2] = \pi R^2 v SO_2 [Hb] C_{Hb}$, where the R is inner radius, v is the average blood velocity, SO_2 is the oxygen saturation, and C_{Hb} is the oxygen-carrying capacity of hemoglobin. Fick's law of diffusion can be used to describe the dif-

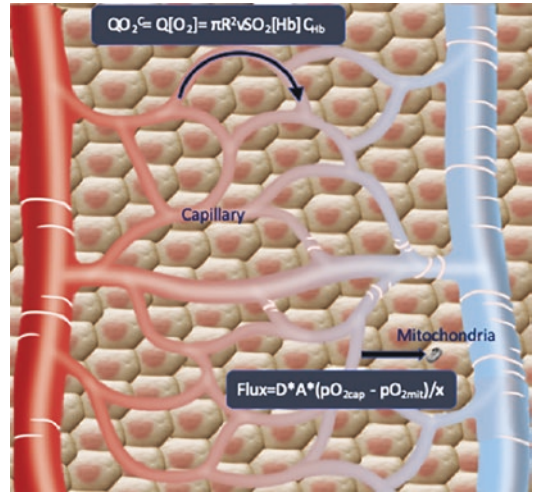


Fig. 29.1 Diffusion and convection of the oxygen in the microcirculation

O_2 flow rate in each capillary is estimated by the equation “ $QO_2C = Q[O_2] = \pi R^2 v SO_2 [Hb] C_{Hb}$ ”. Diffusion of the oxygen from the capillary to the mitochondria is estimated by the equation “ $Flux = D * A * (pO_{2cap} - pO_{2mit}) / x$ ”

QO_2^c , oxygen flow in the capillary; R , inner radius; v , average blood velocity; SO_2 , oxygen saturation; CHb , oxygen-carrying capacity of hemoglobin; D , constant; A , capillary surface area; pO_{2cap} , pO_{2mit} capillary and mitochondrial partial oxygen pressure difference; x , the distance between the capillary and mitochondria

fusion of oxygen from the capillary to mitochondria where the flux of oxygen depends on the diffusion constant (D), capillary surface area (A), capillary and mitochondrial partial oxygen pressure difference ($pO_{2cap} - pO_{2mit}$), and the distance between the capillary and mitochondria (x) ($Flux = D * A * (pO_{2cap} - pO_{2mit}) / x$) (Pittman 2005) (Fig. 29.1).

Microcirculatory Monitoring Techniques

An ideal microcirculatory monitoring device requires several technical features. It should provide real-time, quantitative, reproducible, and precise physiological data regarding the functional properties of the microcirculation. In addition, it should be cost effective and noninvasive and not require the administration of indicator dyes (e.g., fluorescent dyes) (Goedhart et al.

2007). Currently, several types of microcirculatory monitoring devices have been proposed to assess the blood flow and oxygenation of the microcirculation.

The preferred monitoring device should be able to distinguish between the different determinants of microcirculatory oxygen transport such as convection, diffusion, or oxygen utilization. The most used technologies currently include handheld vital microscopes (HVMs), laser-based techniques, and near-infrared spectroscopy (NIRS) (Table 29.1). Over the last years however, HVMs have developed as the gold standard for monitoring the microcirculation since they enable quantification and direct observation of both the convective and the diffusive components of the microcirculation as well as functional capillary density, RBC and leukocyte veloc-

ity, and flow heterogeneity (Ince et al. 2018). However, HVMs can by definition only visualize a small tissue area (e.g., 0–0.4 mm depth with a maximum 1.55×1.16 mm field of view). Laser-based techniques can evaluate tissue perfusion by estimating the blood flux of large tissue surfaces but do not provide functional microcirculatory parameters and do not provide quantitative information. NIRS is also a promising technique due to its noninvasive nature but provides no information regarding the nature of microcirculatory alterations and is not quantitative. NIRS and the laser-based techniques can be used to assess the dynamic response of the microcirculation to a provocation (Allen and Howell 2014).

Considering the physiologic basis of providing the tissues with adequate amounts of oxygen, each step of oxygen transport and utilization must

Table 29.1 Overview of microcirculatory monitoring tools

	OPS/SDF/IDF	LDPI	LSCI	NIRS
Wavelength	530–548	633 nm	785 nm	700–900
Measured parameter	RBC velocity Leukocyte kinetics Blood flow index FCD Capillary hematocrit Heterogeneity index	Blood flux	Blood flux Vascular reactivity	Hb/HbO ₂ Cytochrome aa3
Info for diffusion	+	–	–	+
Info for convection	+	+	+	+
Measurement depth	0–0.4 mm	~1–1.5 mm	~0.3 mm	~4 cm
Advantage	Direct visualization Quantitative output	Noncontact High SR Good reproducibility	Noncontact High SR High TR Excellent reproducibility Available for a provocation test	Good reproducibility A measure of oxidative metabolism (O ₂ delivery/ utilization) Available for a provocation test
Limitation	Pressure artifact Movement artifact Need contact	Movement artifact Use AU Brownian motion Low TR Takes longer time	Movement artifact Use AU Brownian motion	Unknown contribution of skin pigmentation, bone, myoglobin, adipose tissue, etc. Blood pressure fluctuations can affect the output Need contact

OPS orthogonal polarization spectral imaging, SDF sidestream dark-field imaging, IDF incident dark-field imaging, NIRS near-infrared spectroscopy, FCD functional capillary density, TR temporal resolution, SR spatial resolution, AU arbitrary units, Hb hemoglobin, mm millimeter

be monitored by a target for a microcirculatory monitoring device. In this chapter, the microcirculatory monitoring devices will be reviewed in relation to microcirculatory perfusion, oxygen metabolism, and microvascular function.

Assessment of Microcirculatory Perfusion

Videomicroscopic Techniques

Capillaroscopy

Capillaroscopy is a noninvasive imaging technique used to visualize microvessels at tissue surfaces. It is composed of a digital camera system, a microscope with a magnification lens, and a light source that can use both green and white light. From a technical point of view, the construction of a capillaroscopy looks simple; however, it provides valuable information in the setting of clinical practice. The nail fold is the most frequently examined area with this technique, but the mouth, lips, and tongue also can be visualized. The microvessels within a few millimeters depth can be investigated by capillaroscopy revealing the capillary density, RBC velocity, capillary pressure (if used with micro pressure devices and micropipettes), and transcapillary diffusion (with intravenous sodium fluorescein). Capillaroscopy is a popular clinical measurement tool in rheumatology and vascular medicine for the diagnosis and follow-up of patients with scleroderma, mixed connective tissue disease, and Raynaud's phenomenon (De Angelis et al. 2009).

Handheld Vital Microscopes (HVM)

HVM devices also are used to visualize the microcirculation of tissue surfaces. Although the sublingual area is the most commonly preferred region due to its easy approachability, many other organ surfaces have been monitored using HVM. Over the years, three generations of HVMs have been developed including orthogonal polarization spectral imaging (OPS), sidestream dark-field imaging (SDF), and incident dark-field imaging (IDF). These devices are based on optical techniques allowing epi-illumination

described by Goedhart et al., Slaaf et al., and Cook et al., respectively (Goedhart et al. 2007; Slaaf et al. 1987; Sherman et al. 1971). Although there are some minor differences between these techniques, they share common physical principles. All HVMs use green light for absorption by hemoglobin in the RBCs, thereby allowing visualization RBC as dark globules on a white background. A wavelength with an isosbestic wavelength for hemoglobin is used such that there is equal absorption by both oxy and deoxy forms of hemoglobin. Therefore, all RBCs absorb the light irrespective of the oxygenation status of their hemoglobin and become visible as black/gray dots. The leukocytes and plasma gaps appear as white. The microvessels that include RBC appear visible (Ince et al. 2018).

Analysis of the temporal and spatial alterations in moving cells and microvessel density provides a unique perspective for quantifying the functional activity of the microcirculation. These include quantitative measurement of RBC velocity, functional capillary density, and a heterogeneity of flow index described in the recent international consensus on the use of HVM (Ince et al. 2018). In addition to the identification of RBCs, the HVM technique have also been developed by us to visualize and quantify leukocyte kinetics (Uz et al. 2018). Figure 29.2 shows how to calculate these parameters (Dobbe et al. 2008; Boerma et al. 2005; De Backer et al. 2002).

Since the first clinical use of an HVM during a brain operation by our group using OPS imaging (Mathura et al. 2001a), there has been an increasing interest in the clinical application of HVMs. The growing clinical evidence on the clinical use of HVMs incorporated the experts of the cardiovascular dynamic section of ESICM to create a consensus paper for the standardization and interpretation of microcirculatory monitoring (Ince et al. 2018). In parallel, significant technical progress has been achieved in the development of novel devices. The HVMs are classified based on their illumination basics as shown in Table 29.2.

The OPS device is known as the first-generation HVM and uses an incident green light with a wavelength of 548 nm. A polarizer linearly polarizes the light and projects the light

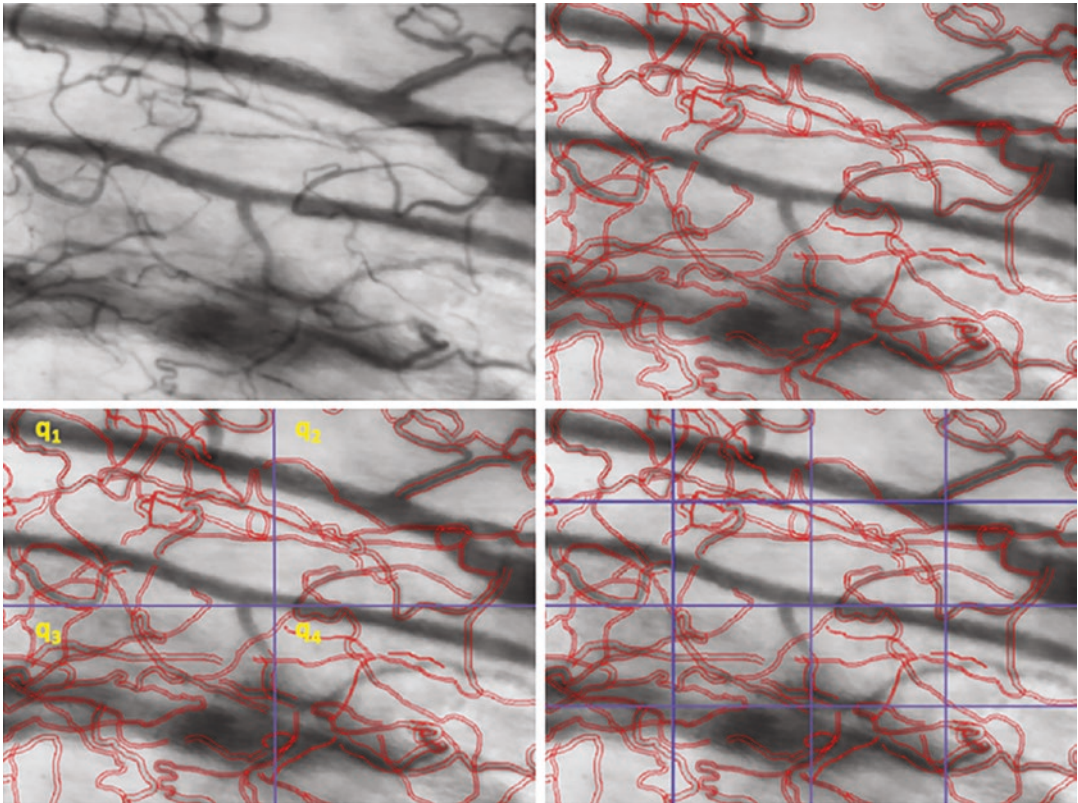


Fig. 29.2 Calculation of the microcirculatory parameters
Right upper: A healthy sublingual microcirculation image obtained by IDF imaging
Left upper: Microcirculation image after manual drawing the microvessels with the software AVA 3.2 (Dobbe et al. 2008)
Right down: Microcirculatory image with Boerma grids (Boerma et al. 2005). In order to calculate the microvascular flow index, each capillary flow is scored with a number (0: no flow, 1: intermittent flow, 2: sluggish flow, 3: continuous flow). The predominant flow in each quadrant defines the MFI score of that quadrant. Total MFI score is equal to $[(MFI_{q_1} + MFI_{q_2} + MFI_{q_3} + MFI_{q_4})/4]$. An alter-

native MFI scoring system is based on the average MFI of all the each microvessels. Heterogeneity index is calculated as the difference between the highest and lowest MFI divided by mean MFI (Ince et al. 2018).
Left down: Microcirculatory image with de Backer grids (De Backer et al. 2002)
 Total vessel density = (length of the microvessels)/(total surface area of the field of view) mm/mm²
 Perfused vessel density = percentage of perfused vessels * total vessel density
 Proportion of perfused vessels: (perfused vessels crossings/total number of vessel crossings) * 100

Table 29.2 Classification of handheld vital microscopes

First-generation OPS	Cytoscan (Cytometrics, Philadelphia, PA, USA)
Second-generation SDF	Microscan (MicroVision Medical B.V., Amsterdam, the Netherlands)
	CapiScope HVCS (KK Technology, Honiton, United Kingdom)
	CapiScope HVCS-HR (KK Technology, Honiton, United Kingdom)
Third-generation IDF	CytoCam (Braedius Medical B.V., Huizen, the Netherlands)

OPS orthogonal polarization spectral imaging, SDF side-stream dark-field imaging, IDF incident dark-field imaging

through a beam splitter onto the tissue of interest. A certain amount of the penetrated light scatters several times inside the tissue and becomes depolarized. An orthogonally constructed polarized analyzer reflects the light that keeps its polarization and allows only the depolarized light to pass through to the camera system to form the image of the microcirculatory field (Fig. 29.3a). OPS device was validated with conventional capillary microscopy and intravital fluorescence microscopy (Mathura et al. 2001b; Groner et al. 1999). Although easy accessibility to the sublingual

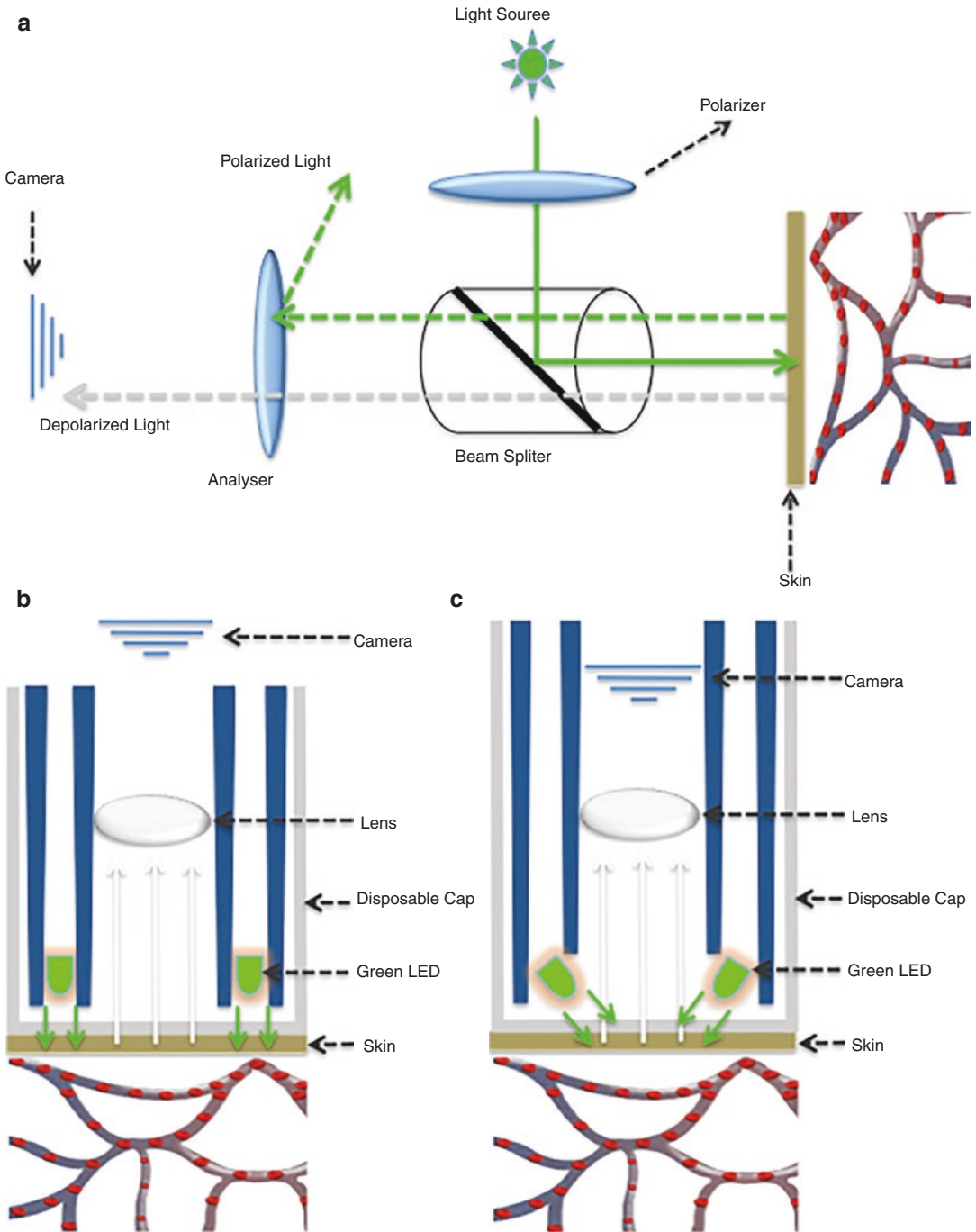


Fig. 29.3 Handheld vital microscopes. (a) OPS imaging. (b) SDF imaging. (c) IDF imaging

area, ability to assess the inner organ surfaces, not requiring fluorescence dyes, and transillumination are the main advantages over OPS device, this device is no longer commercially available since the technique has limited image quality and low power light sources required for bedside use. OPS imaging has been replaced by SDF imaging (Goedhart et al. 2007).

The SDF device was launched as the second-generation HVM to overcome the limitations of OPS device. In this technique, a central light guide is concentrically surrounded by the light-emitting diodes (LEDs) with a green light (530 nm wavelength) to provide a sidestream dark-field illumination. A magnification lens resides in the core of the light guide and becomes optically isolated from the illuminating outer ring so that the lens is protected from tissue surface reflections (Fig. 29.3b). In contrast to OPS imaging, the use of pulsed LEDs helped overcome the motion-induced blurring of moving RBCs. Overall, the SDF device provided a higher image quality and capillary contrast compared with the OPS device (Goedhart et al. 2007). Importantly, the incorporation of a battery made the device more mobile than its predecessor and paved the way for bedside clinical use especially in critically ill patients.

IDF imaging is the latest generation HVM. It uses incident dark-field illumination. In this technique, the green light (530 nm wavelength) is synchronized with high-brightness LEDs, which includes a rapid pulse time of 2 milliseconds. In this way, the blurring problem seen in previous HVMs was mostly solved by these short-pulsed LEDs. A further improvement was that the IDF device contains a high-resolution optic lens and a 3.5-megapixel high-resolution sensor with an optical magnification factor ($\times 4$) (Fig. 29.3c). Differently, the OPS and SDF devices have resolution between 0.36 and 1.3 megapixel resolution (Lindert et al. 2002; Ince et al. 2018). These features provide a significant improvement on image quality with a view of 1.55×1.16 mm that corresponds to three times larger field of view

compared with previous HVMs (Aykut et al. 2015). The IDF device also contains a quantitative focusing mechanism realized by a piezo linear motor with an integrated depth measuring system. This system enables precise focusing microvessel by adjusting the focus depth by 2 micrometers and recently has been validated (Kastelein et al. 2019).

The OPS and the SDF devices use an analog video camera system that needs an external analog-to-digital converting apparatus for analyzing the output. This conversion from analog to a digital decreases the image quality. Conversely, the IDF imaging has a fully digital camera system in which the images are recorded and analyzed digitally. The low weight and easy-to-handle feature of the IDF device (120 gr) minimizes the pressure artifact problem distinctively from OPS (500 gr) and SDF (320 gr) devices. Improvement in the optics of the IDF device has resulted in the visualization of 30% more capillaries with higher image quality compared with the SDF device (Aykut et al. 2015; Gilbert-Kawai et al. 2016).

Directly monitoring the microcirculation with HVM offers real-time quantitative information and has been used in a wide range of clinical and experimental scenarios (Ince et al. 2018). HVM devices have been mostly used in critically ill patients suffering from shock or hemodynamic compromise. The growing clinical evidence obtained from these patient groups have shown that persistent microcirculatory deterioration is associated with adverse outcome and organ dysfunction independently from the status of microcirculation (De Backer et al. 2010). From this and several other studies, it is now recognized that normalization of the macrocirculation does not always result in a normalization of the microcirculation. The term loss of hemodynamic coherence was coined for this phenomenon and raised interest in the use of HVMs for identifying the presence of microcirculatory alterations in individual patients (Ince 2015).

Although bedside use of HVMs provides valuable information regarding the functional state of

the microcirculation, the main obstacle for the routine use of HVMs at the bedside has been the need for offline analysis of the HVM images with time-consuming software to obtain quantitative data. Recently, a novel software package has been developed and validated by our group called Micro Tools, which enables automated quantification of capillary density and RBC velocity obtained by HVM (Hilty et al. 2019). It is expected that this innovative development in the field of microcirculatory monitoring will start a new era on the bedside microcirculatory-based diagnosis and treatment modalities in the future.

Laser-based Techniques

Laser Doppler Techniques

Laser Doppler Flowmetry (LDF)

LDF is a noninvasive technique that is used to estimate the blood flux of the tissue surfaces. This technique involves use of a single probe placed on the skin surface. It consists of two optical fibers for transmitting and receiving the coherent laser light. In theory, the transmitted laser light is scattered after hitting the static and dynamic particles inside the tissue. Once the laser light hits the dynamic particles (e.g., RBCs), a certain amount of the laser light backscatters, and a Doppler shift in frequency occurs. The amount of this shift is correlated with the laser wavelength, velocity, and concentration of the particles (Rajan et al. 2009). The backscattered light is received by an optic fiber and collected by a photodetector in which the signal is converted, expressed as flux in arbitrary units (AU) and displayed on a monitor.

The range of the penetration depth of laser light depends on the distance between the transmitting and the receiving fibers and the wavelength of the laser. For this reason, measurement depth is limited to 1–1.5 mm which allows microcirculatory blood flux to be monitored in superficial structures. LDF records blood flux at a single point only, which is approximately between 0.5 and 1 mm³. Since the estimated blood volume and concentration are not quantitative, the LDF technique, as well as other laser-based tech-

niques, gives a mean value of blood flux rather than blood flow in real units. Conductance (blood flux AU/arterial blood pressure mmHg) is sometimes also used instead of AU to express the data to consider differences and variations in blood pressure (Basak et al. 2012).

The LDF technique has several limitations when compared with the HVMs. This technique estimates blood flux in a range of blood volumes, and it is not possible to assess blood flux in each blood vessel and discriminate blood flux based on the vessel type such as arteriole, venules, and capillaries. Besides this limitation, LDF does not provide information regarding tissue microvascular blood flow heterogeneity. The other main limitation of this technique is its limited reproducibility. The use of integrating probes, however, including several collecting fibers can overcome this limitation by averaging the outputs from different regions. Nevertheless, LDF is a useful technique to detect and quantify the rapid changes in blood flux, which allows the use of physiological tests to assess vessel functionality.

Laser Doppler Perfusion Imaging (LDPI)

LDPI is a noncontact laser-based technique that is used to assess perfusion of larger surfaces that are up to 50*50 cm. The main difference from LDF imaging is the noncontact nature of LDPI. This removes the likelihood of pressure artifacts. In addition, measurement of a larger area results in a good spatial resolution and good reproducibility. Unlike the LDF technique, LDPI consists of a computer-driven mirror system which helps scan the coherent laser beam to illuminate the field of interest. The laser light interacts with the mobile RBCs and induces a Doppler shift. The depth measured with LDPI ranges between 1 and 1.5 mm depending on the laser wavelength and the structure of the tissue. Similar to the LDF technique, LDPI does not have an absolute unit and uses AU to define the output. The main limitation of the LDPI technique is the relatively slow scanning procedure; it can take a relatively long time to acquire images, which causes low temporal resolution and makes it difficult to use with functional provocation tests (Daly and Leahy 2013).

LDPI has been extensively studied in clinical and experimental studies. Currently, LDPI has a proven clinical utility for the estimation of burn depth and has an essential role in deciding the appropriate treatment modality to be applied to burn patients (Park et al. 2013). Besides this application, LSPI is also used in the field of dermatology, plastic surgery, rheumatology, and endocrinology to assess skin flap viability, wound healing, microvascular flow alterations in patients with psoriasis, Raynaud's phenomenon, connective tissue disease, and diabetic ulcers and to evaluate the effect of treatment modalities such as hyperbaric oxygen (Allen and Howell 2014; Anderson et al. 2004).

Laser Speckle Contrast Imaging (LSCI)

LSCI is a noninvasive and noncontact technique that can be used to assess the blood flux at tissue surfaces. When the coherent laser light illuminates an optically rough object, a fraction of the light backscatters and generates an interference pattern, which consists of bright and dark

spots, so-called speckles. If the particles are moving, the speckle contrast changes over time due to the phase difference in the backscattered light. The change in speckle pattern is recorded by a charge-coupled device (CCD) camera which has an integration time and speckle decorrelation time. Since the decorrelation time of the speckle is shorter than the integration time of the CCD camera, the speckle is recorded as a blurred screen. The speckle contrast represents the mean velocity and the concentration of the particles and quantifies the level of the blurring. High blood flow increases the image blurring by decreasing the contrast. Based on the speckle contrast, the blood flux received is given a value in AUs (Fig. 29.4).

LSCI technique combines the advantages of LDF and LDPI imaging by having a high spatial and temporal resolution and excellent reproducibility. Because of the fact that the LSCI technique does not use scanning as in the LDPI technique, the imaging process takes a very short time. The investigated depth varies depending

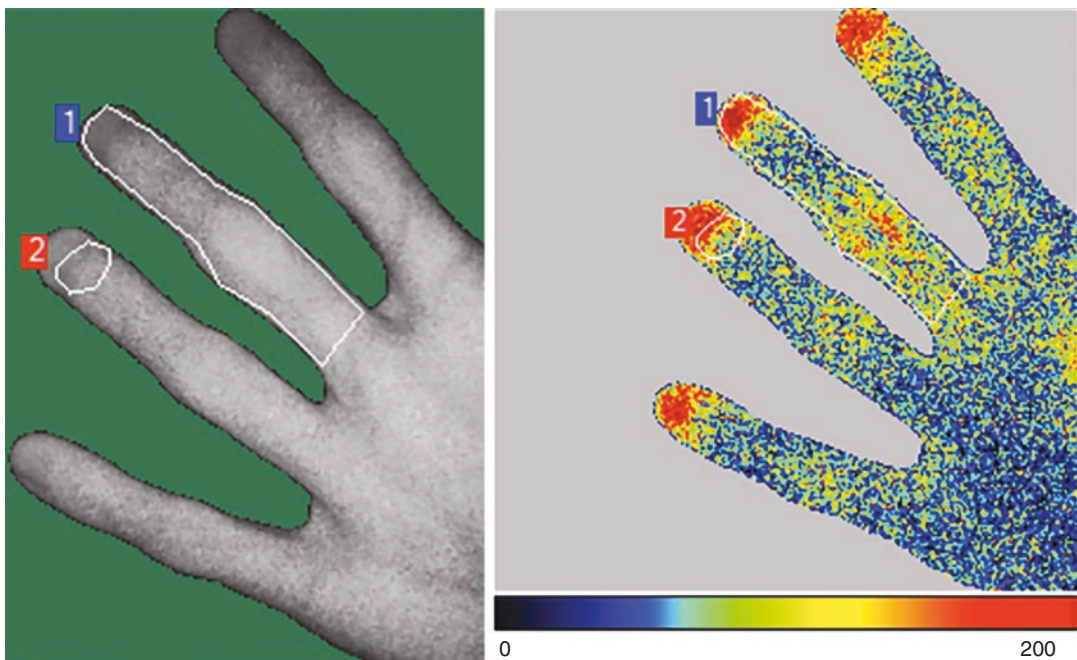


Fig. 29.4 Monitoring of hand with laser speckle contrast imaging

The color code indicates that the blood flux decreases from red to dark blue. This technique also allows the mea-

surement of a specific region of interest, for example, 1 and 2

on the type of laser-based technique. LSCI measures the depth around 300 μm ; however, LDF and LDPI measure around 1–1.5 mm. So, while the LSCI estimates blood flux in nutritional capillaries, the LDF and LDPI techniques estimate blood flux of thermoregulatory capillaries of the skin. LSCI technique has been compared with microcirculatory monitoring techniques and has a good correlation with LDPI technique (Mahe et al. 2012) and SDF imaging (Bezemer et al. 2010); however, inconsistent results have been found with the LDF technique (Tew et al. 2011; Binzoni et al. 2013).

Main advantages of the LSCI technique are its noncontact nature, having both high temporal and spatial resolution, measuring the large tissue surfaces, and having good reproducibility (Roustit et al. 2010). Conversely, its main weakness is that the technique is sensitive to movement artifact and that the skin should remain stable during recordings. Besides, similar to other laser-based techniques, LSCI does not have an absolute perfusion unit, has a biologic zero due to Brownian motion, and is not able to generate information about the heterogeneity of microvascular perfusion and quantitative findings such as total/perfused vessel density, perfusion of each capillary, and velocity of blood components.

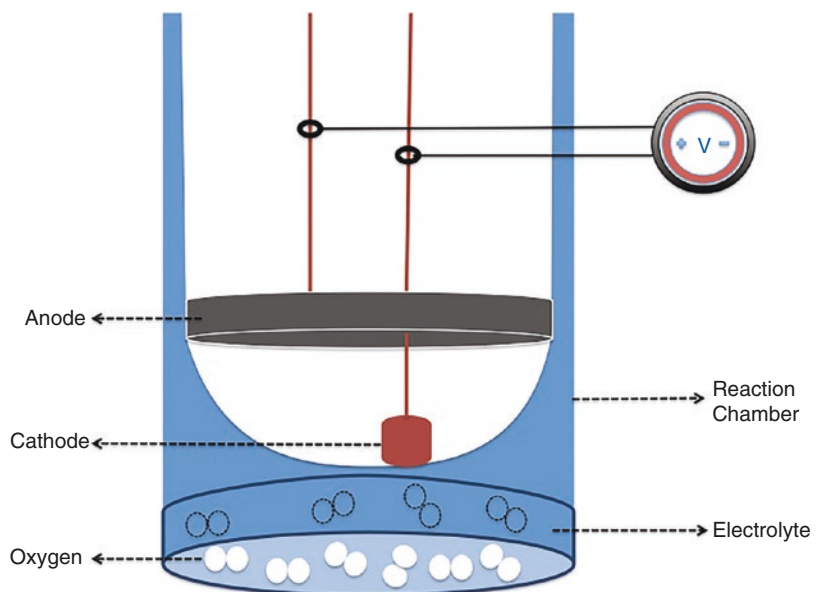
Assessment of Microcirculatory Function

Oxygen Electrodes and Optode Sensors

This technique measures the tissue PO_2 by using Clark-type electrodes. These electrodes can be very small with tips in the range of 15 μm . They conventionally are made from gold, silver, or platinum. The gold cathode and silver anode electrodes are located in a reaction chamber and surrounded by an electrolyte. An oxygen-permeable membrane separates the reaction chamber (Fig. 29.5). Oxygen crosses the membrane and is exposed to a chemical reaction at the cathode, which causes a potential difference (current difference) between the electrodes. The recorded current is directly proportional to the PO_2 at a single point (Hopf and Hunt 1994). The electrodes can also be used to penetrate the tissue although such measurements cause a tissue damage and can give artifactual values.

This technique has limitations. The discordance of oxygen content between tissue and vessels in high FiO_2 patient group leads to misinterpretation of tissue oxygen level (Sinaasappel and van Iterson 1999). Besides, the small size of

Fig. 29.5 Oxygen electrodes



the electrodes means the oxygen content is measured only in a small portion of tissue. The technique measures only average PO_2 . Heterogeneity of PO_2 in the tissue sample cannot be evaluated, which is a limitation in, for example, septic patients although multi-arrayed oxygen sensors have been used for this purpose (Hopf and Hunt 1994).

Optode sensors are used to estimate oxygen concentrations by using the principle of oxygen-dependent fluorescence quenching. The optode consists of light-emitting or laser dioxides, a photodiode covered by an oxygen-permeable layer. Inside the layer, there are oxygen-dependent fluorescent dyes which take a role as an indicator (e.g., ruthenium). Changes in the oxygen concentration cause an altered fluorescence or absorbance of these indicators. The alteration over time creates a decay time, which quantitatively estimates the amount of oxygen by using the Stern-Volmer relationship (Sinaasappel and van Iterson 1999). This time-resolved technique thus allows oxygen concentration to be measured quantitatively. This technique is a more straightforward, stable, and reliable technique when compared with Clark electrodes (Hopf and Hunt 1994; Opitz and Lubbers 1987). Both the oxygen electrodes and the optode sensors are mainly used in experimental studies, and so far there is limited clinical use.

Near-infrared Spectroscopy (NIRS)

NIRS is a continuous noninvasive microcirculatory imaging technique used for the assessment of tissue oxygenation. It takes advantage of the relatively penetrability of near infrared to the tissue and the differential absorption of this light by oxy- and deoxyhemoglobin. NIRS can yield real-time information about regional perfusion and oxygen utilization by measuring the oxygenated and deoxygenated hemoglobin or cytochrome aa3 (Jobsis 1977). In this technique, a modified Beer-Lambert law is used to estimate the relative concentration of oxygenated hemoglobin. Fick's law then can be used for assessing the blood flow

of the microvessels; however, a detectable tracer is required such as indocyanine green (Scheeren et al. 2012; Simonson and Piantadosi 1996). The NIRS technique has been around for many decades but has not gained a routine use in clinical medicine other than in pediatric medicine.

Hemoglobin largely exists in two forms as oxyhemoglobin and deoxyhemoglobin, where both have a distinctive absorption spectrum and can be distinguished from each other based on analysis. Light of wavelength between 700 and 1100 nm can penetrate tissue, the amount of which is dependent on the oxygen status of the hemoglobin in the (micro)vasculature. By measuring the absorption of a number of oxygen-dependent wavelengths of near-infrared light, oxyhemoglobin and deoxyhemoglobin levels can be determined. Moreover, the presence of copper in the central part of the cytochrome aa3 shows different absorption bands from other cytochromes (800–900 nm). Monitoring of the cytochrome aa3 can be helpful to assess the cellular oxidative metabolism and tissue dysoxia although its accuracy is contentious (Scheeren et al. 2012).

Most commonly, NIRS has been used for the monitoring of cerebral and muscle oxygenation during cardiothoracic surgery (Nagdyman et al. 2005; Nagdyman et al. 2008; Creteur et al. 2007). NIRS monitoring also has been applied in critically ill patients, peripheral vascular disease, cancer, and urologic disease, as well as in trauma and prehospital emergency settings (De Backer et al. 2012). NIRS has also been extensively used to test the microvascular reactivity when combined with a provocation test (Creteur et al. 2007). Although the NIRS technique has been continuously modified over the years, a number of limitations still persist. Firstly, the extent to which other factors (myoglobin, skin pigmentation, scatter of light) have an impact on the NIRS signal is not yet clear. Secondly, much of the signal returns from the deeper tissues such as muscle, bone, and fat, the effect of which is not known. For example, tissue oxygenation can be overestimated if there is a large muscle in the chosen area since the oxygen affinity of myoglobin is markedly higher than that of hemoglobin.

Conclusion

In this brief review we have discussed the prominent clinical techniques currently being used to functionally monitor the microcirculation during surgery and the intensive care unit. Although each technique has its pros and cons, it is evident that the introduction of HVM to direct observation of red and white cell flow in the microcirculation can provide deep insight into underlying mechanisms and importance of microcirculatory alterations as prime determinants of cardiovascular dysfunction at the bedside. The recent introduction and validation of automatic quantitative software for extracting quantitative functional data from HVM-generated image sequences (De Backer et al. 2010) have made microcirculatory monitoring at the bedside as point-of-care technique for microcirculation goal-directed target therapy a reality.

References

- Allen J, Howell K. Microvascular imaging: techniques and opportunities for clinical physiological measurements. *Physiol Meas*. 2014;35(7):R91–R141.
- Anderson ME, Moore TL, Lunt M, Herrick AL. Digital iontophoresis of vasoactive substances as measured by laser Doppler imaging—a non-invasive technique by which to measure microvascular dysfunction in Raynaud's phenomenon. *Rheumatology (Oxford)*. 2004;43(8):986–91.
- Aykut G, Veenstra G, Scorcea C, Ince C, Boerma C. Cytocam-IDF (incident dark field illumination) imaging for bedside monitoring of the microcirculation. *Intensive Care Med Exp*. 2015;3(1):40.
- Basak K, Manjunatha M, Dutta PK. Review of laser speckle-based analysis in medical imaging. *Med Biol Eng Comput*. 2012;50(6):547–58.
- Bezemer R, Klijn E, Khalilzada M, Lima A, Heger M, van Bommel J, et al. Validation of near-infrared laser speckle imaging for assessing microvascular (re)perfusion. *Microvasc Res*. 2010;79(2):139–43.
- Binzoni T, Humeau-Heurtier A, Abraham P, Mahe G. Blood perfusion values of laser speckle contrast imaging and laser Doppler flowmetry: is a direct comparison possible? *IEEE Trans Biomed Eng*. 2013;60(5):1259–65.
- Boerma EC, Mathura KR, van der Voort PH, Spronk PE, Ince C. Quantifying bedside-derived imaging of microcirculatory abnormalities in septic patients: a prospective validation study. *Crit Care*. 2005;9(6):R601–6.
- Creteur J, Carollo T, Soldati G, Buchele G, De Backer D, Vincent JL. The prognostic value of muscle StO₂ in septic patients. *Intensive Care Med*. 2007;33(9):1549–56.
- Daly SM, Leahy MJ. 'Go with the flow': a review of methods and advancements in blood flow imaging. *J Biophotonics*. 2013;6(3):217–55.
- De Angelis R, Grassi W, Cutolo M. A growing need for capillaroscopy in rheumatology. *Arthritis Rheum*. 2009;61(3):405–10.
- De Backer D, Creteur J, Preiser JC, Dubois MJ, Vincent JL. Microvascular blood flow is altered in patients with sepsis. *Am J Respir Crit Care Med*. 2002;166(1):98–104.
- De Backer D, Ospina-Tascon G, Salgado D, Favory R, Creteur J, Vincent JL. Monitoring the microcirculation in the critically ill patient: current methods and future approaches. *Intensive Care Med*. 2010;36(11):1813–25.
- De Backer D, Donadello K, Cortes DO. Monitoring the microcirculation. *J Clin Monit Comput*. 2012;26(5):361–6.
- den Uil CA, Klijn E, Lagrand WK, Brugs JJ, Ince C, Spronk PE, et al. The microcirculation in health and critical disease. *Prog Cardiovasc Dis*. 2008;51(2):161–70.
- Dobbe JG, Streekstra GJ, Atasever B, van Zijderveld R, Ince C. Measurement of functional microcirculatory geometry and velocity distributions using automated image analysis. *Med Biol Eng Comput*. 2008;46(7):659–70.
- Gilbert-Kawai E, Coppel J, Bountziouka V, Ince C, Martin D, Caudwell Xtreme E, et al. A comparison of the quality of image acquisition between the incident dark field and sidestream dark field video-microscopes. *BMC Med Imaging*. 2016;16:10.
- Goedhart PT, Khalilzada M, Bezemer R, Merza J, Ince C. Sidestream Dark Field (SDF) imaging: a novel stroboscopic LED ring-based imaging modality for clinical assessment of the microcirculation. *Opt Express*. 2007;15(23):15101–14.
- Groner W, Winkelman JW, Harris AG, Ince C, Bouma GJ, Messmer K, et al. Orthogonal polarization spectral imaging: a new method for study of the microcirculation. *Nat Med*. 1999;5(10):1209–12.
- Hilty MP, Guerci P, Ince Y, Toraman F, Ince C. MicroTools enables automated quantification of capillary density and red blood cell velocity in handheld vital microscopy. *Commun Biol*. 2019;2:217.
- Hopf HW, Hunt TK. Comparison of Clark electrode and optode for measurement of tissue oxygen tension. *Adv Exp Med Biol*. 1994;345:841–7.
- Hwa C, Aird WC. The history of the capillary wall: doctors, discoveries, and debates. *Am J Physiol Heart Circ Physiol*. 2007;293(5):H2667–79.
- Ince C. Hemodynamic coherence and the rationale for monitoring the microcirculation. *Crit Care*. 2015;19(Suppl 3):S8.
- Ince C. Personalized physiological medicine. *Crit Care*. 2017;21(Suppl 3):308.

- Ince C, Boerma EC, Cecconi M, De Backer D, Shapiro NI, et al. Second consensus on the assessment of sublingual microcirculation in critically ill patients: results from a task force of the European Society of Intensive Care Medicine. *Intensive Care Med.* 2018;44(3):281–99.
- Jobsis FF. Noninvasive, infrared monitoring of cerebral and myocardial oxygen sufficiency and circulatory parameters. *Science.* 1977;198(4323):1264–7.
- Kastelein AW, Diedrich CM, Jansen C, Zwolsman SE, Ince C, JWR R. Validation of noninvasive focal depth measurements to determine epithelial thickness of the vaginal wall. *Menopause.* 2019;26(10):1160–16.
- Lindert J, Werner J, Redlin M, Kuppe H, Habazettl H, Pries AR. OPS imaging of human microcirculation: a short technical report. *J Vasc Res.* 2002;39(4):368–72.
- Mahe G, Humeau-Heurtier A, Durand S, Leftheriotis G, Abraham P. Assessment of skin microvascular function and dysfunction with laser speckle contrast imaging. *Circ Cardiovasc Imaging.* 2012;5(1):155–63.
- Mathura KR, Bouma GJ, Ince C. Abnormal microcirculation in brain tumours during surgery. *Lancet.* 2001a;358(9294):1698–9.
- Mathura KR, Vollebregt KC, Boer K, De Graaff JC, Ubbink DT, Ince C. Comparison of OPS imaging and conventional capillary microscopy to study the human microcirculation. *J Appl Physiol (1985).* 2001b;91(1):74–8.
- Nagdyman N, Fleck T, Schubert S, Ewert P, Peters B, Lange PE, et al. Comparison between cerebral tissue oxygenation index measured by near-infrared spectroscopy and venous jugular bulb saturation in children. *Intensive Care Med.* 2005;31(6):846–50.
- Nagdyman N, Ewert P, Peters B, Miera O, Fleck T, Berger F. Comparison of different near-infrared spectroscopic cerebral oxygenation indices with central venous and jugular venous oxygenation saturation in children. *Paediatr Anaesth.* 2008;18(2):160–6.
- Opitz N, Lubbers DW. Theory and development of fluorescence-based optochemical oxygen sensors: oxygen optodes. *Int Anesthesiol Clin.* 1987;25(3):177–97.
- Park YS, Choi YH, Lee HS, Moon DJ, Kim SG, Lee JH, et al. The impact of laser Doppler imaging on the early decision-making process for surgical intervention in adults with indeterminate burns. *Burns.* 2013;39(4):655–61.
- Pittman RN. Oxygen transport and exchange in the microcirculation. *Microcirculation.* 2005;12(1):59–70.
- Rajan V, Varghese B, van Leeuwen TG, Steenbergen W. Review of methodological developments in laser Doppler flowmetry. *Lasers Med Sci.* 2009;24(2):269–83.
- Roustit M, Millet C, Blaise S, Dufournet B, Cracowski JL. Excellent reproducibility of laser speckle contrast imaging to assess skin microvascular reactivity. *Microvasc Res.* 2010;80(3):505–11.
- Scheeren TW, Schober P, Schwarte LA. Monitoring tissue oxygenation by near infrared spectroscopy (NIRS): background and current applications. *J Clin Monit Comput.* 2012;26(4):279–87.
- Sherman H, Klausner S, Cook WA. Incident dark-field illumination: a new method for microcirculatory study. *Angiology.* 1971;22(5):295–303.
- Simonson SG, Piantadosi CA. Near-infrared spectroscopy. Clinical applications. *Crit Care Clin.* 1996;12(4):1019–29.
- Sinaasappel M, van Iterson M. Can Ince. Microvascular oxygen pressure in the pig intestine during haemorrhagic shock and resuscitation. *J Physiol.* 1999;514:245–53.
- Slaaf DW, Tangelder GJ, Reneman RS, Jager K, Bollinger A. A versatile incident illuminator for intravital microscopy. *Int J Microcirc Clin Exp.* 1987;6(4):391–7.
- Tew GA, Klonizakis M, Crank H, Briers JD, Hodges GJ. Comparison of laser speckle contrast imaging with laser Doppler for assessing microvascular function. *Microvasc Res.* 2011;82(3):326–32.
- Uz Z, van Gulik TM, Aydemirli MD, Guerci P, Ince Y, Cuppen D, et al. Identification and quantification of human microcirculatory leukocytes using handheld video microscopes at the bedside. *J Appl Physiol (1985).* 2018;124(6):1550–7.



Clinical Assessment and Monitoring of Peripheral Circulation During Shock and Resuscitation

30

Bernardo Lattanzio and Vanina Kanoore Edul

Introduction

Shock is a life-threatening disorder, best defined as the inability of the cardiovascular system to sustain tissue oxygen demand. As a consequence, cellular dysfunction and anaerobic metabolism ensue (Cecconi et al. 2014). Interestingly, resuscitation targeted to normalize systemic hemodynamic variables such as cardiac output (CO) and blood pressure (BP) often fails to correct tissue hypoxia and hypoperfusion. Over the last decades, a large body of scientific evidence has linked microcirculatory alterations to the pathogenesis of shock states and multiple organ failure (Ellis et al. 2002; Ince and Sinaasappel 1999). Although septic shock is the most emblematic example of microcirculatory failure, every type of shock can eventually evolve to distributive shock as a result of a persistent inflammatory response and endothelial dysfunction (Vallet

2002). Recently, we defined microcirculatory shock as a condition in which microcirculation fails to support tissue oxygenation despite normalized systemic hemodynamics (Kanoore Edul et al. 2015). Therefore, microcirculatory alterations and tissue hypoperfusion can persist even though global variables of oxygenation have been corrected. Hence, it is important to have bedside tools for the detection of tissue dysoxia.

Although there are a number of new technologies that have evolved to analyze tissue perfusion, much information can be obtained by examining the patient. Examination of the skin, in particular, can give useful information to guide therapy with minimal need for technologies. In this chapter we will discuss the relevance of peripheral perfusion evaluation in shock states both before and after resuscitation, its impact on outcome of critically ill patients, and how to use them in clinical practice.

B. Lattanzio
Facultad de Ciencias Médicas, Universidad Nacional de La Plata, Cátedra de Farmacología Aplicada, La Plata, Argentina

Critical Care Unit, Clínica Bazterrica y Santa Isabel, Buenos Aires, Argentina

V. K. Edul (✉)
Facultad de Ciencias Médicas, Universidad Nacional de La Plata, Cátedra de Farmacología Aplicada, La Plata, Argentina

Intensive Care Department, Hospital Juan A. Fernández, Buenos Aires, Argentina

Skin Blood Flow Regulation

Although the skin of humans has an average area of 1.8 m², it only accounts for 5% of total body weight. Its main function is to protect the surface of the body, and, thanks to its ability to produce sweat, it has a major role in thermoregulation. Changes in skin blood flow, especially during exposure to cold or heat stress, are sensed by its special innervation and microcirculation (Roddie

2011). Blood vessels in the skin and subcutaneous tissues have multiple arteriovenous anastomoses, particularly in the hands, feet, and ears. Skin vessels can function as heat exchangers. For instance, when blood flow is low, temperature of the blood flowing through capillaries equilibrates with temperature of the skin.

Physiologically, skin has a low metabolic rate which is easily supplied by the low fraction of CO directed to this region. Except for special inflammatory states, changes in skin blood flow are not a consequence of changes in skin metabolism (Borici-Mazi et al. 1999). Under normal circumstances, skin vessels are constricted. When core temperature rises, skin's blood flow increases due to loss of vasoconstrictor tone and activation of vasodilator fibers. Conversely, cooling a subject leads to a decrease in blood flow due to activation of vasoconstrictor fibers. Nevertheless, changes in skin temperature are not linear. Skin temperature is influenced by both environmental temperature and cutaneous blood flow. Exposure to ambient temperatures below 10 °C causes intermittent cold vasodilation of cutaneous vessels due to impaired smooth muscle constriction (Roddie 2011). The physiological behavior of cutaneous circulation, and its determinants, is especially relevant for the assessment of peripheral perfusion variables as we will discuss in following sections.

Rationale for Monitoring Peripheral Perfusion During Shock

The evaluation of cutaneous circulation during physical examination should be a first step for clinicians in the assessment of peripheral perfusion (Lima and Bakker 2015). This simple observation allows simultaneous evaluation of the relationship between systemic hemodynamics, regional blood flow distribution, and microcirculatory perfusion.

During shock, organ perfusion becomes heterogeneous, and blood flow to some systems is jeopardized at the onset of sepsis. For example, splanchnic hypoperfusion and subsequent mucosa ischemic injury occur early in shock

(Marshall et al. 1993). This was the rationale for the introduction of gastric tonometry into the clinical practice, a tool that can detect occult shock in patients who look well-resuscitated (Gutierrez et al. 1992).

Skin perfusion can vary broadly during shock. Due to its limited autoregulatory capacity, early vasoconstriction of cutaneous vessels mediated by sympathetic neuro-activation redistributes blood flow away from cutaneous tissue to vital organs. This drop in perfusion results in a drop in skin temperature. Accordingly, skin has been proposed as one of the windows that can be used to assess severity of shock (Vincent et al. 2012) and could become one of the first approaches for assessment of overall tissue perfusion (Fig. 30.1).

Two types of responses have been described during resuscitation of circulatory shock. One is characterized by a new physiological concept called hemodynamic coherence, which is used to explain the condition in which resuscitation maneuvers targeted to correct systemic hemodynamics also correct tissue oxygenation. The second is the opposite and is characterized by a loss of coherence. The point is that normalization of global variables does not necessarily result in parallel improvements of perfusion and oxygenation (Ince 2015). It is during *loss of coherence* that evaluation of peripheral perfusion and microcirculation may help clinical management.

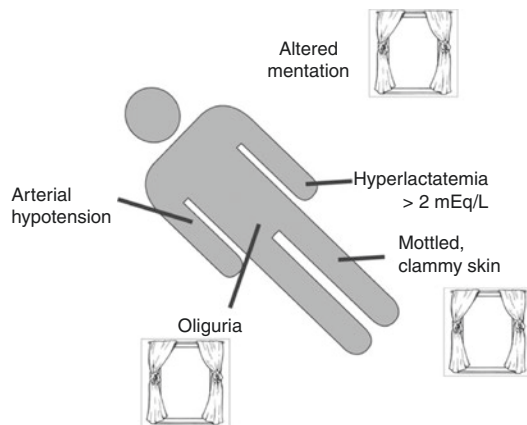


Fig. 30.1 The three windows of shock (Vincent et al. 2012). Skin is one of the three “windows” to assess shock. (Reproduced with permission of Springer Nature)

In the following sections we will discuss the scientific evidence supporting assessment of peripheral perfusion:

- To detect the subgroup of higher risk for a worse outcome
- To monitor the response to therapy
- To redefine a target of resuscitation
- To unmask persistent shock in apparently well-resuscitated patients
- To guide therapy as a target of resuscitation

In addition, we will discuss the shortcomings of studies and the methods of evaluation.

Assessment of Peripheral Perfusion

There are a number of methods for evaluating peripheral perfusion (Table 30.1). Clinical assessment is the least invasive and should be the first approach. Simple subjective evaluation of skin temperature (feeling warm or cold to hand touch), inspection of skin color, and measurement of capillary refill time (CRT) are the most commonly used methods. In addition, temperature of extremities (finger, great toe) or temperature gradients between two sites of the body (central-to-toe temperature) were proposed

Table 30.1 Methods for assessment of peripheral perfusion available in clinical practice

Clinical evaluation
Subjective assessment of skin temperature (warm/cold)
Capillary refill time (s)
Mottling score (0–5)
Temperature evaluation
Toe temperature (°C)
Central (rectal/pulmonary artery) to toe T° gradient (°C)
Skin difference temperature (forearm-to-fingertip) (°C)
Optical methods
Peripheral perfusion index (PPI) (%)
Near-infrared spectroscopy (NIRS)
Laser Doppler flow (LDF)
Videomicroscopy (SDF, IDF)

SDF sidestream dark field imaging, IDF incident dark field illumination imaging

almost 50 years ago and recently have regained interest. More sophisticated methods use optical properties of hemoglobin for evaluation of oxygenation and perfusion. Peripheral perfusion index (PPI) derived from the pulse oximetry and near-infrared spectroscopy (NIRS) are currently available in different clinical scenarios (van Genderen et al. 2012a). Finally, videomicroscopes bring microvascular imaging to the bedside (Ince et al. 2018).

Clinical Assessment of Peripheral Perfusion

Subjective Assessment and Skin Temperature Gradients

Blood flow in the cutaneous circulation is the main determinant of skin temperature. Hence, it is advocated that *skin is a flow-sensitive organ* (Dubin et al. 2018). Based on this close relationship, skin temperature is often considered a surrogate of cutaneous perfusion in patients with shock. However, a strong limitation of this association is that a drop in skin perfusion and temperature is also the physiologic response in states of central hypothermia which is the body's physiological attempt to prevent heat loss and to defend central temperature (Brock et al. 1975). Therefore, skin temperature needs to be interpreted in the context of systemic hemodynamic status and environment temperature.

However, a fall in CO has the opposite effect on body temperature. Peripheral temperature decreases, whereas central temperature is maintained, or even is increased, due to less blood flowing through peripheral capillaries and thus decreased exposure to the environment. This is the rationale behind the use of body temperature gradients as an objective assessment of peripheral perfusion (Rubinstein and Sessler 1990). The most widespread body gradients, measured between two different sites, are (1) central-to-toe, which is the difference between rectal or pulmonary artery temperature and great toe; (2) central-to-index finger; and (3) forearm-to-fingertip (Tskin-diff) (Ait-Oufella and Bakker 2016). A difference of up to 7 °C is accepted as normal

for central-to-toe gradient, and values above this represent a major decrease in cutaneous blood flow. Because skin is influenced by the environmental temperature, whereas core temperature is less affected, $T_{\text{skin-diff}}$ seems to be a more reliable indicator for patients in the operating room or in the critical care unit where ambient temperature is often low. $T_{\text{skin-diff}}$ normally should be 0 °C, because both forearm and finger are exposed to the same ambient temperature. Any value above this is considered pathologic, and a difference >4 °C is a marker of severe vasoconstriction (Table 30.2).

In 1969, Joly and Weil were the first to investigate whether quantitative changes in skin temperature would provide an objective proof of the severity of shock. In a mix cohort of critically ill patients ($n = 100$), skin temperature was measured at various sites of the body. Measurements obtained at early (within 3 hours of admission) and late stages (3 hours before discharge or death) were compared with simultaneous changes in several hemodynamic variables and metabolic parameters. There was a predictable relationship between change in toe temperature and cardiac index (CI) ($r = 0.71$). When CI was below $2 \text{ L min}^{-1} \cdot \text{m}^2$, temperature of the toe was below 27 °C in 95% of cases. Conversely, increases in toe temperature were related to improvement in CI and patients' outcome. Measurements taken at a late stage had a better prognostic ability than measurement taken immediately after admission. Interestingly, there was no correlation with arterial pressure ($r = 0.28$, $p = \text{NS}$), suggesting once again that in some tissues, pressure and flow are poorly related. Due to the availability, the non-invasive nature, and low cost in instrumentation, measurement of great toe temperature was proposed as a useful tool for the assessment of shock severity and prediction of outcome. It is worth mentioning, however, that the patient sample included many subjects with cardiovascular disease and with very low CI ($<2 \text{ L min}^{-1} \cdot \text{m}^2$) and few had a hyperdynamic pattern (CI $>4 \text{ L min}^{-1} \cdot \text{m}^2$) (Joly and Weil 1969).

More recently, a retrospective study assessed the usefulness of the subjective evaluation of skin temperature for the identification of patients

in a surgical ICU who have occult hypoperfusion. Patients' extremities were categorized as "warm" or "cold" on a subjective manner, and comparisons were made between the two groups and more objective variables. Patients with cool extremities were more likely to be hypoperfused (Kaplan et al. 2001). Interestingly, there were no differences in blood pressure, hemoglobin concentration, heart rate, or arterial oxygen saturation between cohorts, but patients with warm extremities had higher CI, central venous oxygen saturation (ScvO_2), lower lactate levels, and higher pH values. This study highlighted the role of subjective assessment of skin temperature for discriminating the subgroup of patients who would benefit from further invasive monitoring. Nevertheless, several limitations should be mentioned, including the retrospective nature, the lack of room temperature control, patient's temperature, use of vasopressor therapy, and lack of interobserver and intraobserver variability in subjective assessment.

Other researchers also have found that physical examination performed at an early stage is an independent predictor of 30-day mortality in patients with cardiogenic shock (Hasdai et al. 1999) and in pediatric patients with meningococcal disease (Brent et al. 2011). In a prospective study in general ICU patients, Alexander Lima and Jan Bakker assessed the role of physical exam and its impact on outcome when performed after initial resuscitation. Simple subjective assessment of peripheral perfusion could predict organ dysfunction as expressed by high Sequential Organ Failure Assessment (SOFA) score and lactate levels (Lima et al. 2009). Peripheral perfusion was defined as abnormal if there was an increase in CRT (≥ 4.5 s) or if the extremities felt cool to the examiner's hands. In addition, this subjective assessment was compared with more objective variables of perfusion such as skin temperature differences, including $T_{\text{skin-diff}}$, $T_{\text{c-toe}}$, and peripheral perfusion index (PPI). The latter is an index derived from the oximeter pulse wave (see below). Almost 50% of the cohort had abnormal peripheral perfusion despite systemic hemodynamic stabilization and finalization of initial resuscitation. Individual SOFA score and

Table 30.2 Advantages, limitations, and references values for peripheral perfusion indexes

Method	Variable	Advantages	Limitations	Normal values	Cutoff values related to poor outcomes
Clinical assessment	Subjective temperature evaluation	Available No cost	Interobserver variability Affected by environment temperature	Warm/cold	Cold extremities after initial resuscitation are associated with hyperlactatemia, an increase risk of multiple organ failure, and low cardiac index (Kaplan et al. 2001; Lima et al. 2009)
	Capillary refill time (s)	Accessible No cost Quantitative Relative simplicity Rapid changes in response to therapy	Interobserver variability (Espinoza et al. 2014) Modified by environmental and body temperature, sex, and age (Schriger and Baraff 1988; Anderson et al. 2008) Heterogeneity in normal values	Schriger and Baraff (1988) ULN 95% Male adults: 1.6 s Female adults: 2.9 s Elderly: 4.5 s Anderson et al. (2008) ULN 95% Overall: 3.5 s Lima et al. (2009) ULN 95% Overall: 4.5 s	>4.5 s (Lima et al. 2009) >2.4 s AUROC 0.84 (Ait-OUfella et al. 2014) >3 s (Hernandez et al. 2014) >4 s (Lara et al. 2017) >4.5 s AUROC 0.91 (van Genderen et al. 2014)
Temperature gradients	Mottling score (score 0–5)	Good reproducibility (kappa 0.87) (Ait-OUfella et al. 2011)	Dark skin	0–1 (Ait-OUfella et al. 2011)	Mortality: Score 2–3 OR 16 (4–81) Score 4–5 OR 74 (11–1568) (Ait-OUfella et al. 2011)
	Toe-to-ambient (°C)	Objective measurement	Influenced by ambient temperature (John et al. 2018)		<2 °C (Joly and Weil 1969) <1.75 °C at 24 hours AUROC 0.84 (Bourcier et al. 2016)
	Central-to-toe (Tc-toe) (°C)	Objective measurement	Influenced by ambient temperature	3–7 °C	>7 °C (Hernandez et al. 2014; Levy et al. 2008)
	Forearm-finger (Tskin-diff) (°C)	Less influenced by environmental temperature	Slower response compared with other perfusion parameters (Rubinstein and Sessler 1990)	0 °C (Rubinstein and Sessler 1990)	>2 °C day 2 AUROC 0.79 (van Genderen et al. 2014) >4°severe vasoconstriction (Rubinstein and Sessler 1990)

(continued)

Table 30.2 (continued)

Method	Variable	Advantages	Limitations	Normal values	Cutoff values related to poor outcomes
Optical monitoring	<p><i>Peripheral perfusion index (PPI)</i> $PPI = \text{pulsatile/nonpulsatile blood flow} (\%)$ <i>Pleth variability index (PVI)</i> $PVI = (PPI_{\text{max}} - PPI_{\text{min}}) / PPI_{\text{max}} \times 100$</p> <p><i>Near-infrared spectroscopy (NIRS)</i> $StO_2 (\%)$ THI $R_{\text{des}} (\%/s)$ $R_{\text{res}} (\%/s)$</p>	<p>Early changes in hypovolemia (van Genderen et al. 2013) Functional hemodynamic variable to assess fluid responsiveness through PVI (Feissel et al. 2007)</p>	<p>Wide distribution of normal values (Lima et al. 2002)</p> <p>Influenced by other peripheral perfusion parameters (Lima et al. 2011) Static NIRS variables have overlap between sick and healthy population (Creteur et al. 2007)</p>	<p>Median 1,4 (0.3–10) (Lima et al. 2002)</p> <p>StO_2 $R_{\text{res}} > 4\%/s$ (Creteur et al. 2007)</p>	<p><0.6 (He et al. 2015) AUC for fluid responders 0.85 [95% (CI) 0.79–0.92] (Feissel et al. 2007)</p> <p>Recovery slope 2.55%/s (Creteur et al. 2007)</p>

ULN upper limits of normality, *AUROC* area under receiving operating curve, *R_{des}* rate of desaturation, *R_{res}* rate of resaturation (recovery slope)

the proportion of patients with unfavorable outcome were higher in the subgroup of patients with abnormal peripheral perfusion. This study demonstrated that after initial resuscitation, daily physical examination, focused on evaluation of peripheral perfusion, could help to identify the subgroup at high risk of dying.

There are, however, some controversies related to the relationship of temperature gradients and hemodynamic variables. The relationship between central-to-peripheral temperature gradient and CI was not predictive of outcome in the first 24 hours after cardiac surgery. This possibly could have been because patients started hypothermic and thermoregulatory responses in that context is cutaneous hypoperfusion. Interestingly, once central temperature recovered normal values, the correlation between temperature gradients and CI became significant (Bailey et al. 1990). On the other side, in pediatric patients after cardiac surgery, correlation between CI and temperature gradients was poor ($r = 0.28$) (Ryan and Soder 1989). Woods et al. found the same lack of correlation between temperature gradients and macrohemodynamic variables in a cohort of adult patients with shock (Woods et al. 1987). Children with sepsis, unlike adults, have a low CI before receiving resuscitation with fluids.

Whether body temperature gradients correlate with other microcirculatory territories is still a matter of debate. In patients with sepsis and septic shock, Boerma explored the relationship between sublingual microcirculation, assessed with videomicroscopy, and central-to-peripheral temperature gradients. There was neither a correlation between these microcirculatory territories nor with global hemodynamic variables (Boerma et al. 2008).

In a cohort of septic patients, toe-to-room temperature gradient correlated with other tissue perfusion variables and illness severity. The study collected hemodynamic data, CRT, mottling score, and several temperature gradients during the first 24 hours. Tissue perfusion parameters were significantly different between patients with sepsis and septic shock. There was no correlation with macrohemodynamic variables (Bourcier

et al. 2016). In postoperative patients undergoing abdominal surgery, temperature gradients increased on the second and third days after surgery and showed good sensitivity and specificity for the prediction of severe complications (van Genderen et al. 2014).

Several external factors might distort assessment of temperature gradients (John et al. 2018). Altered perfusion indexes may reflect peripheral vasoconstriction due to low skin temperature and have no relationship to hemodynamic changes. A study performed in 8 volunteers showed that surface cooling without changing central temperature resulted in skin vasoconstriction and significant changes in CRT, PI, T_{skin-diff}, and NIRS-derived parameters (John et al. 2018). Therefore, under resting conditions, the impact of peripheral perfusion alterations can be magnified as the skin temperature decreases (Gorelick et al. 1993).

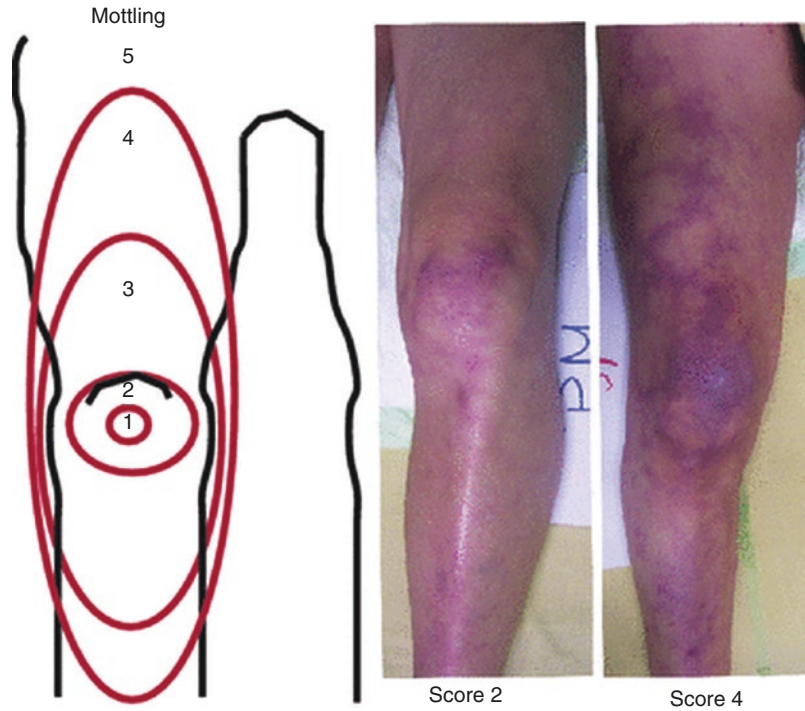
In summary, body temperature gradients seem to be a valuable complementary tool to the clinical assessment in critically ill patients. When confounding factors such as core or ambient temperature are controlled, temperature gradient augments the odds of detecting the subgroup of patients who will evolve with worse outcome.

Skin Mottling

Skin mottling is a common clinical sign in critically ill patients. It consists of an irregular, patchy, red-bluish discoloration of the skin, frequently located at the knee, elbows, and more distal extremities areas. Ait-Oufella et al. developed a six-degree semiquantitative score to quantify the extension of skin discoloration around the knee (Ait-Oufella et al. 2011). This “mottling score” ranges from 0 to 5, with 0 indicating no mottling and 5 corresponding to severe discoloration area that goes beyond the fold of the groin (Fig. 30.2).

The prognostic value of the mottling score has been assessed in several studies. In 60 septic shock patients, 14-day mortality increased in parallel with increases in mottling score at 6 hours (13% for a score of 0–1 to 70% for a score of 2–3 and 92% for a score of 4–5, $X^2 p < 0.001$). Moreover, the higher the degree of mottling, the shorter the survival (Ait-Oufella et al. 2011).

Fig. 30.2 The mottling score (Ait-Oufella et al. 2011). On the left, grading of the score. For details, see text. On the right, two pictures illustrating two different grades of score. (Reproduced with permission of Springer Nature)



In addition, an increase in the mottling score, from admission to 6 hours, was associated with increasing lactate levels ($p < 0.0001$), decreasing urinary output ($p < 0.0001$), and increasing SOFA score ($p = 0.0002$). Conversely, an improvement in skin perfusion denoted better outcome. These findings were confirmed in a larger study; in 791 critically ill patients, almost 29% had at least one episode of mottling during ICU stay (Coudroy et al. 2015). This percentage increased among patients with shock (43%) and especially those with septic shock (49%). In addition to increased mortality, skin mottling was associated with more organ dysfunctions, ICU length of stay, mechanical ventilation, vasopressor dose, and renal replacement therapy.

The pathophysiological alteration behind mottling is not known. Recently, the evaluation of the knee area with laser Doppler flowmetry (LDF), a technique that measures blood flow in regional microvessels, showed an inverse correlation between skin perfusion and extension of mottling (Ait-Oufella et al. 2013). In another study, mottling also was associated with low tissue oxygen saturation levels (Ait-Oufella et al.

2012). In summary, this easy-to-learn, simple score can add prognostic value to assessment of ICU patients. Its presence is a strong predictor of increased risk of morbidity and mortality.

Capillary Refill Time (CRT)

Capillary refill time is defined as the time required for a distal capillary bed to recover its color once the pressure applied to cause blanching has been released (King et al. 2014). It was first described during World War II as a parameter for grading shock; the categories were normal, definitive slowing, and very sluggish (Beecher et al. 1947). In 1981, Champion proposed adding it into the five elements of the trauma score (Champion et al. 1981). Since then, it has been introduced rapidly into the clinical practice as a tool during physical exam for prompt assessment of the status of the circulation, particularly in children (King et al. 2014). Furthermore, it is taught worldwide in medical schools.

Ait-Oufella et al. conducted the first study to demonstrate the prognostic value of CRT in septic shock patients. Persistent alterations in CRT concomitantly measured at the knee and a finger had

high accuracy for predicting 14-day mortality. Measurement of CRT at the knee area had better accuracy and reproducibility than the finger area (knee AUC: 90, index AUC: 84). Assessment of CRT after resuscitation was proposed as an integrative variable to evaluate improvement of tissue perfusion (Ait-Oufella et al. 2014).

The value of CRT for the prediction of postoperative complications was studied in a population of patients undergoing major abdominal surgery (van Genderen et al. 2014). In 111 patients, hemodynamic, metabolic, and peripheral perfusion parameters were recorded one day before (baseline), immediately after surgery (D0) and then over the first three postoperative days (D1–D3). Prolonged CRT (>4.5 s) at D0 predicted severe complications. This predictive value continued until the third day and increased from the first to the second day. Peripheral perfusion assessment after surgery improved the discriminatory power to stratify patients at high risk for developing severe complications.

Peripheral perfusion parameters and sublingual microcirculation were evaluated at ICU admission, during therapeutic hypothermia, after passive rewarming and 24 hours after hospital admission in patients who had suffered an out-of-hospital cardiac arrest. CRT was more prolonged at ICU admission in nonsurvivors than in survivors (11.5 s (SD 1.0) vs. 5.4 s (0.6) respectively, $p < 0.05$). Sublingual microcirculation had a similar behavior, with nonsurvivors having worse parameters than survivors at baseline ($p < 0.05$). There were no differences between nonsurvivors and survivors during hypothermia. However, after rewarming, these parameters again showed the divergent behavior detected at baseline. Survivors had a rapid improvement toward normalization, whereas the abnormalities persisted in nonsurvivors (van Genderen et al. 2012b). Key messages from this study are that abnormal sublingual microcirculation and peripheral perfusion indexes are predictors of unfavorable outcome both at baseline and after rewarming. Thus, monitoring peripheral perfusion after cardiac arrest could underscore patients with persistent hypoperfusion. Nevertheless, whether these

alterations are an epiphenomenon or a cause/consequence relationship is not clear.

The association between CRT and very short-term mortality (day 1 and day 7) was prospectively assessed in 1931 patients in the emergency department. An increasing CRT was an independent predictor of 1-day and 7-day mortality, OR 1.69 (95% CI 1.20–2.39, $p = 0.003$) and 1.38 (95% CI 1.12–1.69, $p = 0.002$), respectively. Notwithstanding the value of this parameter, it is worth noting that heart rate, age, and body temperature were better predictors of mortality than CRT (Mrgan et al. 2014). On the other hand, during conditions of low intravascular volume, CRT performed worse as an identifier of mild hypovolemia than classic orthostatic vital signs (Schriger and Baraff 1991).

CRT is measured by applying an external pressure to a distal capillary bed, usually the nail or finger pulp, until blanching of the area develops. After a variable amount of seconds, the pressure is released, and the time required for skin recoloring is recorded with a wristwatch or chronometer. Unfortunately, there are great disparities in the way this test is performed which accounts for the contradictory results related to its usefulness. Normal CRT has been traditionally considered as less than 2 s, (Champion et al. 1981) but unfortunately, without appropriate validation. One study that was performed in volunteers reported that CRT is affected by age, sex, and temperature. The value of 2 s was maintained for children and young men, while in women it was defined as 3 s and in elderly people it was extended to 4.5 s (Jubran 1998). In addition, CRT is prolonged with a decrease in temperature. A more recent study confirmed the upper limit of normality to be 3.5 s (Chan et al. 2013) (Table 30.2).

There is no agreement on the definition of an abnormal CRT in critically ill patients. Cutoff values of 2.4, 3.0, 4.5, and 5.0 s have been used to discriminate normal from abnormal states and when tested as predictors of poor outcome. After initial resuscitation, a CRT >5.0 s is definitely a marker of poor outcome and increased risk of multiple organ failure. In addition, multiple evaluations might improve its prognostic power

(Lima et al. 2009; van Genderen et al. 2014). The environmental temperature should be between 22 and 24 °C, while the skin's temperature needs careful evaluation.

Optical Methods

Optical methods use physical principles related to illumination of a tissue with light of different wavelengths. Methods available in clinical practice are:

1. Videomicroscopy (discussed in other sections of this book) (C Ince)
2. Pulse oximetry waveform analysis with its derived indexes
3. Near infrared spectroscopy with tissue oxygen derived parameters

Peripheral Perfusion Index

Oximetry measures hemoglobin oxygen saturation based on spectrophotometric principles. The physics behind this method relies on the Beer-Lambert law which states that the concentration of a solute is directly proportional to the intensity of the light transmitted through a solution (Jubran 1998).

The oximeter probe has two LEDs with two known wavelengths: 660 nm (red) and 940 nm (infrared). Hemoglobin species have different absorption spectra, and therefore, it is possible to quantify the proportion of hemoglobin bound to oxygen (Chan et al. 2013). In addition, this method can discriminate light absorption due to pulsatile arterial blood from absorption of nonpulsatile blood, that is, venous and capillary blood. A ratio between the pulsatile and all nonpulsatile components allows calculation of arterial oxygen saturation and the *peripheral perfusion index (PPI)*, expressed as percentages. During peripheral hypoperfusion, the pulsatile component (i.e., arterial component) decreases, while the nonpulsatile component stays stable. Accordingly, the ratio decreases.

Lima and colleagues proposed use of this index as a noninvasive marker of perfusion in

critically ill patients (Lima et al. 2002). In healthy persons, PPI's distribution was skewed with a median value of 1.4 (IQR 0.7–3.0), and the range was wide (0.3–10.0). There were neither intrasubject (before/after meal) nor differences between smokers, subjects with cardiovascular disease, and completely healthy volunteers. In critically ill patients, mean and median PPI values were 2.2 (SD 0.22) and 1.8 (IQR 0.5–3.3), respectively. Surprisingly, it was higher in the ill population than in healthy volunteers. Nevertheless, when PPI was evaluated during conditions of abnormal peripheral perfusion, defined as a CRT > 2 s and T^c-toe > 7 °C, mean values were significantly lower in the critically ill group. ROC curve identified a cutoff value of 1.4 for prediction of abnormal peripheral perfusion (AUC 0.91) (Table 30.2).

A prospective observational study in critically ill patients evaluated the combination of PPI and central venous oxygen saturation (ScvO₂) for predicting outcome before and after resuscitation (He et al. 2015). In multivariate logistic regression analysis, PPI measured 8 hours after initial resuscitation was an independent predictor of mortality, but basal values did not correlate with outcome. In addition, only critical values, that is, < 0.6, were related to 30-day mortality. These values, however, were poorly correlated with lactate, venous-to-arterial CO₂ difference, and ScvO₂. Interestingly, PPI had a better discriminative value than lactate.

In healthy volunteers, PPI was more sensitive for the detection of hypovolemia induced by lower body negative pressure than stroke volume and heart rate. The negative pressure was applied in a stepwise manner. PPI decreased in the first step of the protocol, demonstrating that it is an early indicator of peripheral vasoconstriction due to sympathetic activation. Heart rate and stroke volume were altered in the second step, but cardiac output and blood pressure did not change (van Genderen et al. 2013).

Pleth Variability Index

Variability of the perfusion index (PVI) is a dynamic parameter that can be automatically derived by analysis of changes in the plethys-

mographic curve during a respiratory cycle. It is computed as the difference between the maximum and minimum PI over the maximum value, multiplied by 100 and expressed as a percentage: $[(PI_{max} - PI_{min}) / PI_{max}] \times 100$. This is the same way that pulse pressure variation (PPV) is calculated from arterial pressure (Michard et al. 2000). This index was proposed more than 10 years ago as a new parameter for the prediction of fluid responsiveness, and it rapidly raised interest because pulse oximetry is broadly available and because of its non-invasive nature. Although plethysmographic waveform measures volume and not pressure, there was good agreement between plethysmographic and PPV derived from the arterial pressure waveform (Cannesson et al. 2005). In mechanically ventilated hemodynamic unstable patients, both PPV and PVI showed moderate accuracy at predicting a lack of fluid responsiveness (ROC curve area between 0.64 and 0.74) when measured by an increase in CI after a fluid challenge (Natalini et al. 2006). Correct classification of patients as responders was good with both indexes, but they were inaccurate for discrimination between responders and nonresponders at low values. This result is in contrast with previous observational studies that found a better performance for PVI as predictor of fluid responsiveness (94% sensitivity and 80% specificity) (Feissel et al. 2007). Differences in tidal volume and hemodynamic profiles likely explain the discrepancies between these two studies. A systematic review and meta-analysis (Sandroni et al. 2012) found that the PVI was a reliable predictor of fluid responsiveness in mechanically ventilated patients who received large bolus of fluids (>500 ml) and who were ventilated with a tidal volume of at least 8 ml/kg. Importantly, the quality of the plethysmographic signal is critically dependent on peripheral perfusion.

NearInfrared Spectroscopy (NIRS) of the Thenar Eminence

Near-infrared spectroscopy provides noninvasive monitoring of oxy- and deoxyhemoglobin through the emission of wavelength of approxi-

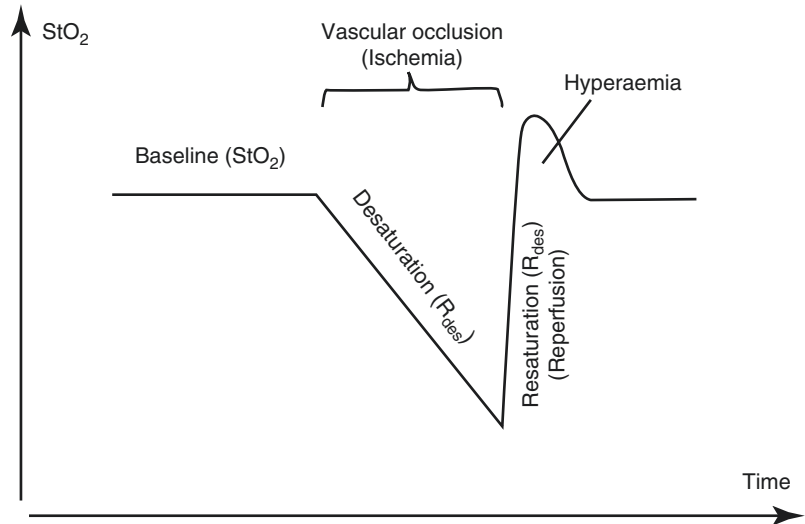
mately 700–850 nm at the measured area. NIRS can be applied to different organs such as brain, kidneys, and extremities. The thenar eminence is the most commonly used area in the intensive care because it has a thin fat layer and allows light to penetrate into the subcutaneous tissue. Tissue oxygen saturation (StO_2) is calculated by the ratio of oxy- and deoxyhemoglobin (Lipcsey et al. 2012).

The most interesting application of NIRS in critically ill patients is related to the measurement of dynamic changes that arise after a vascular occlusion test (VOT). Usually, a pneumatic cuff placed in the arm is inflated to a pressure above systolic arterial pressure to stop flow (ischemia). A sensor placed at the thenar eminence detects the decrease in StO_2 from the basal level. This allows measurement of the lowest StO_2 and the rate of desaturation ($R_{des}: \% \times sec$). After cuff deflation, there is reperfusion and reactive hyperemia which are accompanied by an increase in StO_2 and the rate of resaturation (StO_2 upslope, $R_{res}: \% \times sec$) (Fig. 30.3). The velocity of the increase in StO_2 increase gives a quantitative measurement of reactive hyperemia and represents microcirculatory recruitment. It was proposed as a test to assess microcirculatory response and a potential predictor of outcome in septic patients (Creteur et al. 2007). In an initial study, StO_2 recovery slope was lower in septic than in control patients and volunteers and was a better predictor of outcome than basal StO_2 which had a large overlap between septic patients and healthy volunteers. These findings have been reproduced in similar studies (Leone et al. 2009; Doerschug et al. 2007).

Dynamic NIRS-derived parameters can be used to assess the response to therapy during resuscitation of shock. In non-resuscitated patients who had MAP below the threshold for autoregulation-increasing BP caused an improvement in StO_2 . Noteworthy, in this study, StO_2 recovery slope remained low in 50% of the population, despite normalization of MAP and other global hemodynamic variables (Georger et al. 2010).

Alterations in local vasomotor tone can profoundly alter NIRS-derived parameter at the thenar

Fig. 30.3 NIRS-derived parameters (Lipcsey et al. 2012). Schematic illustration of the StO_2 changes during VOT. (Reproduced with permission of Springer Nature)



eminence. Lima and colleagues correlated NIRS measurements with CRT and temperature gradient ($T_{skin-diff}$) as well as subjective physical examination, from admission to the ICU until the third day. Almost 50% of this population had an abnormal peripheral circulation, defined by CRT >4.5 s or by $T_{skin-diff} >4$ °C. Basal StO_2 and StO_2 recovery slope were significantly different between patients with normal versus those with abnormal peripheral circulation. However, StO_2 , StO_2 desaturation, and recovery slopes were similar between patients with and without shock, including septic patients, and thus only in those with decreased peripheral indicators. In addition, values did not correlate with vasopressor dose and mortality. Of importance, a worse outcome was better predicted by abnormal CRT or skin temperature gradients than by StO_2 -derived parameters. Consequently, the status of peripheral circulation should be taken into account to correctly interpret NIRS-derived variables (Lima et al. 2011), and its usefulness is dubious.

Peripheral Perfusion Indexes During Shock and Resuscitation

Correlation of Peripheral Perfusion Indexes with Perfusion of Internal Organs

A key relevant question is, does cutaneous perfusion indicate a parallel alteration in internal

organs? Patients with septic shock usually exhibit dissociation between macro- and microhemodynamic variables. After correction of relative or absolute hypovolemia by fluid resuscitation, a significant proportion of patients have a hyperdynamic pattern. Despite the increase in systemic blood flow, sublingual microcirculation frequently is hypoperfused (Edul et al. 2016), and these derangements are more severe in nonsurvivors.

In experimental studies the relationship between changes in the sublingual microcirculation compared to other microvascular beds is contradictory. In early sepsis and septic shock, there was no correlation in simultaneous measurements of perfusion in the sublingual microcirculation and Tc-toe difference (Boerma et al. 2008). In postoperative patients with abdominal sepsis, we found that the sublingual response was dependent on both the magnitude of the increase in cardiac output and the basal state of the microcirculation. The sublingual microvascular bed responded in patients who started with a profound disturbance in the microcirculation at baseline and who had a positive response to fluids. Villous microcirculation behaved as an isolated territory; it was not influenced by changes in cardiac output, and its status did not correlate with sublingual or cutaneous perfusion. Sublingual microcirculation status and central-to-finger temperature differences were not correlated at baseline or on the second day, but changes in these parameters in response

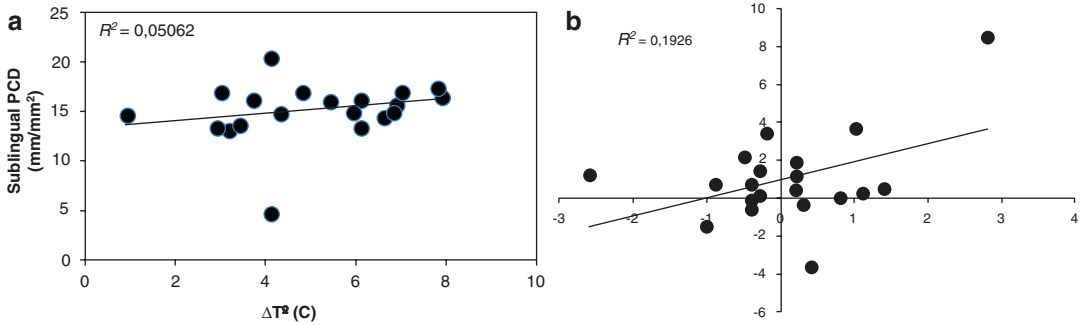


Fig. 30.4 Effects of a fluid challenge on sublingual microcirculation and central-to-finger temperature difference. **Panel A** Correlation between sublingual perfused capillary density (PCD) and central-to-finger temperature gradient (ΔTc -finger) at baseline. There is no correlation

between two territories. **Panel B** Correlation between sublingual perfused capillary density (PVD) and central-to-finger temperature gradient (ΔTc -finger) in response to volume expansion. After fluid loading, both changes in both variables showed a moderate correlation

to fluid loading were correlated. This means that while it is not possible to predict the state of the sublingual microcirculation from evaluation of the skin, both territories behaved similarly when preload is optimized. Dissociation of these two microvascular beds is a dynamic process (Fig. 30.4) (Edul et al. 2014).

The relationship between skin and visceral organ perfusion was recently studied in patients with septic shock. Perfusion in the hepatosplanchnic region was assessed by the pulsatility index, a Doppler sonographic measure of the variability of blood velocity in regional arterioles. Normalization of CRT correlated with improvement in the pulsatility index of the mesenteric artery (Spearman correlation coefficient = 0.325, $P = 0.007$), whereas improvements in the mottling score correlated with improvement in the vascular tone of the renal artery (Spearman correlation coefficient = 0.396, $P = 0.006$). As a conclusion, in early septic shock patients, a prolonged CRT or mottling of the skin points toward visceral organ vasoconstriction (Brunauer et al. 2016).

Peripheral Perfusion Indexed During Resuscitation

Because skin is a flow sensitive variable, it would seem to be reasonable to presume that monitoring changes in skin perfusion during fluid resuscita-

tion should give an indication of the status of organ perfusion during resuscitation. Based on this reasoning, Hernandez and colleagues evaluated temporal changes in peripheral perfusion parameters during resuscitation of patients with sepsis and septic shock. Peripheral perfusion was assessed by CRT (normal <4 s), Tc-toe (normal < 7°), Tskin-diff (normal = 0), and subjective assessment of skin temperature and livedo reticularis. These were followed at different time points during the first 24 hours. They also were compared to metabolic parameters such as ScvO₂, central venous-to-arterial CO₂ difference (Pcv-aCO₂), and lactate. Changes in metabolic and peripheral perfusion parameters over time were different. CRT normalized as early as 2 hours after start of resuscitation. By 6 hours, lactate and CRT were significantly decreased, whereas ScvO₂ and the Pcv-aCO₂ difference improved only at 24 hours. Normal values of CRT and Tc-toe at 6 hours were independently associated with a successful resuscitation. Nonetheless, persistent hyperlactatemia was the only parameter associated with 28-day mortality (Hernandez et al. 2012).

In patients with sepsis-induced-hyperlactatemia (lactate >2 mg/dL), only 30% of the population had abnormal CRT (>3 s). In this highly selected population, basal CRT did not predict outcome, but persistence of abnormal CRT after fluid resuscitation did discriminate patients with an augmented risk of an adverse outcome (88% vs. 20% $p < 0.001$; RR 4.4 [2.7 ± 7.4]) and increased

hospital mortality (63% vs. 9% $p < 0.001$; RR 6.7 [2.9 ± 16]). This study showed the dynamic behavior of CRT and the feasibility of using it to evaluate the success of resuscitation (Lara et al. 2017). It seems to have high specificity but low sensitivity.

Recently, the kinetics of recovery of macrohemodynamic, metabolic, and peripheral perfusion variables were evaluated in septic shock (Hernandez et al. 2014). Normalization rates markedly differed during the first 24 hours of resuscitation for all variables. Changes in lactate, P(cv-a)CO₂ difference, and CRT were biphasic with a prompt improvement during the first 6 hours, followed by a slower normalization. The majority of patients had normal ScvO₂ at ICU admission, as has previously been shown (van Beest et al. 2008). If the endpoints of resuscitation had been based solely in this parameter, resuscitation would only have been continued in 10% of patients. Nearly 70% of patients had normal CRT 3 hours after fluid resuscitation, whereas only 15% had normal lactate. Traditionally, persistent hyperlactatemia has been interpreted as a result of anaerobic metabolism secondary to tissue hypoperfusion. However, there are other non-hypoxic sources of lactate, such as stress-related or decreased hepatic clearance, that also can contribute to delayed lactate clearance (Levy et al. 2008). If all hyperlactatemia is not related to hypoperfusion, guiding therapy based on this parameter could be misleading. These observations thus pose an interesting debate about when to stop resuscitation of patients with septic shock. If the ultimate goal of resuscitation is to correct tissue dysoxia, sublingual microcirculation and peripheral perfusion indexes perhaps are better reflections of tissue perfusion than global parameters, and these parameters may more accurately assess reperfusion than ScvO₂ or lactate. Since they are earlier, their use could help prevent fluid overload (Hernandez et al. 2014).

Peripheral Perfusion Indexes as a Target of Resuscitation

Some clinical data suggest that targeting peripheral perfusion during resuscitation of septic shock might improve outcome. In a small RCT, patients who were resuscitated according to a protocol aimed at improving peripheral circulation received less fluids and had shorter hospital stays than the traditional treatment (van Genderen et al. 2015).

Recently, a larger study, the ANDROMEDA-SHOCK TRIAL, randomized 424 patients with early septic shock to two alternative 8-hour strategies: one based on resuscitation guided by peripheral perfusion (PPTR), assessed by serial measurements of CRT, and the other based on serum lactate levels (LTR). Resuscitation protocol was stratified in assessing fluid responsiveness, vasopressor, and inodilator needs. The clinical improvement with both lactate and CRT from baseline to 72 hours was biphasic. Improvement was faster at the beginning and then more slowly. There was a 9% difference in mortality that favored PPTR, but it was not statistically significant (HR 0.75 95CI 0.55–1.02, $p = 0.07$). Patients in the PPTR group received less fluid during the first 8 hours of resuscitation than LTR group (2359 ± 1344 vs. 2767 ± 1748, $p = 0.01$). A predefined subgroup analysis showed that patients with a lower SOFA score (<10) had an almost 20% decrease in mortality if they were assigned to PPTR branch (20.4 vs. 39.3, $p = 0.03$). Although the primary outcome was not reached, there is an important message from these results. Resuscitation guided by peripheral perfusion indexes is feasible and non-inferior to a lactate clearance strategy. This is especially important for places with low incomes and resource limitations (Hernández et al. 2019). Currently ongoing trials should bring more insight into this approach (Pettilä et al. 2016).

Limitations

Measurement of peripheral perfusion is an attractive tool because it is noninvasive, relative simple, available in low resource settings and responds rapidly to therapy. However, before these indexes turn into new targets of resuscitation, we should carefully consider several factors and technical difficulties inherent in the measurements. These include factors related to the subjects, environment, unclear reference values, and reproducibility of standard procedures (Schriger and Baraff 1988; Anderson et al. 2008).

Mottling score and CRT have limited value in burns, in amputations, and in subjects with dark skin or vascular peripheral disease. Body temperature gradients are affected by hypothermia and room temperature. Optical methods require expensive equipment and probes.

Another major issue is the operator dependency of the procedures. Interobserver reproducibility is an unresolved problem. It has been evaluated in studies with small sample size and produced conflicting results. Several studies in pediatric population have found that marked interobserver variability is very common (Gorelick et al. 1993; Lobos et al. 2012). Conversely, both Ait-Oufella et al. and van Genderen et al. reported a good overall agreement between observers (van Genderen et al. 2014; Ait-Oufella et al. 2014). Nevertheless, proper evaluation of CRT with a chronometer and agreement between different methods and observers was performed in only one study (Espinoza et al. 2014). In this study, CRT was recorded with a chronometer under direct visualization and video-recorded. The procedures were as analyzed by two observers. The Bland and Altman analysis showed poor agreement both between observers and different methods. It is expected that training, education, and standardization of the methods with a focus on reducing the impact of subject and environmental factors might improve reproducibility and imple-

mentation of the indexes into the clinical practice (Hernández et al. 2019; Shavit et al. 2006).

Summary and Conclusions

Resuscitation of patients with circulatory shock has been traditionally centered on invasive parameters and targeted to correction of systemic hemodynamic variables. During the last years, however, the role of clinical assessment of peripheral perfusion during shock and resuscitation has regained interest. One obvious question is related to what is the usefulness of evaluating a nonvital organ such as the skin. The answer is that cutaneous perfusion is affected early during shock and undergoes large changes in flow because of its limited autoregulation. Observing these changes gives an estimation of shock severity and recovery. It also is possible to quantify the response.

Clinical assessment of peripheral perfusion should be incorporated into the algorithms of therapeutic strategies. It can be performed by simple methods such as examination of the skin, measurement of temperature, or CRT or by using more sophisticated optical techniques. Before resuscitation, evaluation of peripheral perfusion indexes, especially CRT and mottling score, can help the assessment of the severity of shock. After initial resuscitation, persistence of alterations is associated with increased morbidity and mortality. Probably the most interesting information from these variables comes from the evaluation of kinetics of recovery. Since skin is a flow-sensitive organ, it is possible to assess response to treatments by the cutaneous windows. In addition, the absence of cost of CRT and mottling score, and the noninvasiveness nature of these indexes, makes them into attractive tools, especially in resource-limiting settings. Reliability and reproducibility are challenged by factors related to the subject, environment, and

technical aspects of measurement, but the significance of these can be reduced by integrating the test results into the whole clinical picture. Some studies have reported wide limits of agreement between different observers, but this variability potentially could be overcome with training and education and by choosing the correct cut-off value. In addition, development of devices that allow automatic evaluation may be possible in the future. Finally, in a medical specialty that is so much based on invasive technology, these approaches demonstrate that the value of physical exam performed by intensivist is still fundamental for daily clinical practice in the ICU.

References

- Ait-Oufella H, Bakker J. Understanding clinical signs of poor tissue perfusion during septic shock. *Intensive Care Med.* 2016;42(12):2070–2.
- Ait-Oufella H, Lemoine S, Boelle PY, Galbois A, Baudel JL, Lemant J, Joffre J, Margetis D, Guidet B, Maury E, Offenstadt G. Mottling score predicts survival in septic shock. *Intensive Care Med.* 2011;37:801–7.
- Ait-Oufella H, Joffre J, Boelle PY, Galbois A, Bourcier S, Baudel JL, Margetis D, Alves M, Offenstadt G, Guidet B, Maury E. Knee area tissue oxygen saturation is predictive of 14-day mortality in septic shock. *Intensive Care Med.* 2012;38:976–83.
- Ait-Oufella H, Bourcier S, Alves M, Galbois A, Baudel JL, Margetis D, Bige N, Offenstadt G, Maury E, Guidet B. Alteration of skin perfusion in mottling area during septic shock. *Ann Intensive Care.* 2013;3(1):31.
- Ait-Oufella H, Bige N, Boelle PY, Pichereau C, Alves M, Bertinchamp R, Baudel JL, Galbois A, Maury E, Guidet B. Capillary refill time exploration during septic shock. *Intensive Care Med.* 2014;40(7):958–64.
- Anderson B, Kelly AM, Kerr D, Clooney M, Jolley D. Impact of patient and environmental factors on capillary refill time in adults. *Am J Emerg Med.* 2008;26(1):62–5.
- Bailey JM, Levy JH, Kopel MA, Tobia V, Grabenkort WR. Relationship between clinical evaluation of peripheral perfusion and global hemodynamics in adults after cardiac surgery. *Crit Care Med.* 1990;18(12):1353–6.
- Beecher HK, Simeone FA, Burnett CH, Shapiro SL, Sullivan ER, Mallory TB. The internal state of the severely wounded man on entry to the most forward hospital. *Surgery.* 1947;22(4):672–711.
- Boerma EC, Kuiper MA, Kingma WP, Egbers PH, Gerritsen RT, Ince C. Disparity between skin perfusion and sublingual microcirculatory alterations in severe sepsis and septic shock: a prospective observational study. *Intensive Care Med.* 2008;34(7):1294–8.
- Borici-Mazi R, Kouridakis S, Kontou-Fili K. Cutaneous responses to substance P and calcitonin gene-related peptide in chronic urticaria: the effect of cetirizine and dimethindene. *Allergy.* 1999;54(1):46–56.
- Bourcier S, Pichereau C, Boelle PY, Nemlaghi S, Dubée V, Lejour G, Baudel JL, Galbois A, Lavillegrand JR, Bigé N, Tahiri J, Leblanc G, Maury E, Guidet B, Ait-Oufella H. Toe-to-room temperature gradient correlates with tissue perfusion and predicts outcome in selected critically ill patients with severe infections. *Ann Intensive Care.* 2016;6(1):63.
- Brent AJ, Lakhampaul M, Ninis N, Levin M, MacFaul R, Thompson M. Evaluation of temperature-pulse centile charts in identifying serious bacterial illness: observational cohort study. *Arch Dis Child.* 2011;96(4):368–73.
- Brock L, Skinner JM, Manders JT. Observations on peripheral and central temperatures with particular reference to the occurrence of vasoconstriction. *Br J Surg.* 1975;62(8):589–95.
- Brunauer A, Koköfer A, Bataar O, Gradwohl-Matis I, Dankl D, Bakker J, Dünser MW. Changes in peripheral perfusion relate to visceral organ perfusion in early septic shock: a pilot study. *J Crit Care.* 2016;35:105–9.
- Cannesson M, Besnard C, Durand PG, Bohé J, Jacques D. Relation between respiratory variations in pulse oximetry plethysmographic waveform amplitude and arterial pulse pressure in ventilated patients. *Crit Care.* 2005;9(5):R562–8.
- Cecconi M, De Backer D, Antonelli M, Beale R, Bakker J, Hofer C, Jaeschke R, Mebazaa A, Pinsky MR, Teboul JL, Vincent JL, Rhodes A. Consensus on circulatory shock and hemodynamic monitoring. Task force of the European Society of Intensive Care Medicine. *Intensive Care Med.* 2014;40(12):795–815.
- Champion HR, Sacco WJ, Carnazzo AJ, Copes W, Fouty WJ. Trauma score. *Crit Care Med.* 1981;9(9):672–6.
- Chan ED, Chan MM, Chan MM. Pulse oximetry: understanding its basic principles facilitates appreciation of its limitations. *Respir Med.* 2013;107(6):789–99.
- Coudroy R, Jamet A, Frat JP, Veinstein A, Chatellier D, Goudet V, Cabasson S, Thille AW, Robert R. Incidence and impact of skin mottling over the knee and its duration on outcome in critically ill patients. *Intensive Care Med.* 2015;41(3):452–9.
- Creteur J, Carollo T, Soldati G, Buchele G, De Backer D, Vincent JL. The prognostic value of muscle StO₂ in septic patients. *Intensive Care Med.* 2007;33(9):1549–56.
- Doerschug KC, Delsing AS, Schmidt GA, Haynes WG. Impairments in microvascular reactivity are related to organ failure in human sepsis. *Am J Physiol Heart Circ Physiol.* 2007;293(2):H1065–71.
- Dubin A, Henriquez E, Hernández G. Monitoring peripheral perfusion and microcirculation. *Curr Opin Crit Care.* 2018;24(3):173–80.

- Edul VS, Ince C, Navarro N, Previgliano L, Risso-Vazquez A, Rubatto PN, Dubin A. Dissociation between sublingual and gut microcirculation in the response to a fluid challenge in postoperative patients with abdominal sepsis. *Ann Intensive Care*. 2014;4:39.
- Edul VS, Ince C, Vazquez AR, Rubatto PN, Espinoza ED, Welsh S, Enrico C, Dubin A. Similar microcirculatory alterations in patients with normodynamic and hyperdynamic septic shock. *Ann Am Thorac Soc*. 2016;13(2):240–7.
- Ellis CG, Bateman RM, Sharpe MD, Sibbald WJ, Gill R. Effect of a maldistribution of microvascular blood flow on capillary O₂ extraction in sepsis. *Am J Physiol Heart Circ Physiol*. 2002;282(1):H156–64.
- Espinoza ED, Welsh S, Dubin A. Lack of agreement between different observers and methods in the measurement of capillary refill time in healthy volunteers: an observational study. *Rev Bras Ter Intensiva*. 2014;26(3):269–76.
- Fissel M, Teboul JL, Merlani P, Badie J, Faller JP, Bendjelid K. Plethysmographic dynamic indices predict fluid responsiveness in septic ventilated patients. *Intensive Care Med*. 2007;33(6):993–9.
- Georger JF, Hamzaoui O, Chaari A, Maizel J, Richard C, Teboul JL. Restoring arterial pressure with norepinephrine improves muscle tissue oxygenation assessed by near-infrared spectroscopy in severely hypotensive septic patients. *Intensive Care Med*. 2010;36(11):1882–9.
- Gorelick MH, Shaw KN, Baker MD. Effect of ambient temperature on capillary refill in healthy children. *Pediatrics*. 1993;92(5):699–702.
- Gutierrez G, Palizas F, Doglio G, Wainsztein N, Gallezio A, Pacin J, Dubin A, Schiavi E, Jorge M, Pusajo J, et al. Gastric intramucosal pH as a therapeutic index of tissue oxygenation in critically ill patients. *Lancet*. 1992;339(8787):195–9.
- Hasdai D, Holmes DR Jr, Califf RM, Thompson TD, Hochman JS, Pfisterer M, Topol EJ. Cardiogenic shock complicating acute myocardial infarction: predictors of death. GUSTO Investigators. Global Utilization of Streptokinase and Tissue-Plasminogen Activator for Occluded Coronary Arteries. *Am Heart J*. 1999;138(1 Pt 1):21–31.
- He H, Long Y, Liu D, Wang X, Zhou X. Clinical classification of tissue perfusion based on the central venous oxygen saturation and the peripheral perfusion index. *Crit Care*. 2015;19:330.
- Hernandez G, Pedreros C, Veas E, Bruhn A, Romero C, Rovegno M, Neira R, Bravo S, Castro R, Kattan E, Ince C. Evolution of peripheral vs metabolic perfusion parameters during septic shock resuscitation. A clinical-physiologic study. *J Crit Care*. 2012;27(3):283–8.
- Hernandez G, Luengo C, Bruhn A, Kattan E, Friedman G, Ospina-Tascón GA, Fuentealba A, Castro R, Regueira T, Romero C, Ince C, Bakker J. When to stop septic shock resuscitation: clues from a dynamic perfusion monitoring. *Ann Intensive Care*. 2014;4:30.
- Hernández G, Ospina-Tascón GA, Damiani LP, Estenssoro E, Dubin A, Hurtado J, Friedman G, Castro R, Alegría L, Teboul JL, Cecconi M, Ferri G, Jibaja M, Pairumani R, Fernández P, Barahona D, Granda-Luna V, Cavalcanti AB, Bakker J, ANDROMEDA-SHOCK Investigators and the Latin America Intensive Care Network (LIVEN). Effect of a resuscitation strategy targeting peripheral perfusion status vs serum lactate levels on 28-day mortality among patients with septic shock: The ANDROMEDA-SHOCK Randomized Clinical Trial. *JAMA*. 2019;321(7):654–64.
- Ince C. Hemodynamic coherence and the rationale for monitoring the microcirculation. *Crit Care*. 2015;19:S8.
- Ince C, Sinaasappel M. Microcirculatory oxygenation and shunting in sepsis and shock. *Crit Care Med*. 1999;27(7):1369–77.
- Ince C, Boerma EC, Cecconi M, De Backer D, Shapiro NI, Duranteau J, Pinsky MR, Artigas A, Teboul JL, Reiss IKM, Aldecoa C, Hutchings SD, Donati A, Maggiorini M, Taccone FS, Hernandez G, Payen D, Tibboel D, Martin DS, Zarbock A, Monnet X, Dubin A, Bakker J, Vincent JL, Scheeren TWL, Cardiovascular Dynamics Section of the ESICM. Second consensus on the assessment of sublingual microcirculation in critically ill patients: results from a task force of the European Society of Intensive Care Medicine. *Intensive Care Med*. 2018;44(3):281–99.
- John RT, Henricson J, Junker J, Jonson CO, Nilsson GE, Wilhelms D, Anderson CD. A cool response-The influence of ambient temperature on capillary refill time. *J Biophotonics*. 2018;11(6):e201700371.
- Joly HR, Weil MH. Temperature of the great toe as an indication of the severity of shock. *Circulation*. 1969;39(1):131–8.
- Jubran A. Pulse oximetry. In: Tobin MJ, editors. *Principles and practices of intensive care monitoring*. McGraw-Hill; 1998. ISBN 0-07-065094-2. p. 261–87.
- Kanoore Edul VS, Ince C, Dubin A. What is microcirculatory shock? *Curr Opin Crit Care*. 2015;21(3):245–52.
- Kaplan LJ, McPartland K, Santora TA, Trooskin SZ. Start with a subjective assessment of skin temperature to identify hypoperfusion in intensive care unit patients. *J Trauma*. 2001;50(4):620–7.
- King D, Morton R, Bevan C. *Arch Dis Child Educ Pract Ed*. 2014;99:111–6.
- Lara B, Enberg L, Ortega M, Leon P, Kripper C, Aguilera P, Kattan E, Castro R, Bakker J, Hernandez G. Capillary refill time during fluid resuscitation in patients with sepsis-related hyperlactatemia at the emergency department is related to mortality. *PLoS One*. 2017;12(11):e0188548.
- Leone M, Bliidi S, Antonini F, Meyssignac B, Bordon S, Garcin F, Charvet A, Blasco V, Albanèse J, Martin C. Oxygen tissue saturation is lower in nonsurvivors than in survivors after early resuscitation of septic shock. *Anesthesiology*. 2009;111(2):366–71.
- Levy B, Desebbe O, Montemont C, Gibot S. Increased aerobic glycolysis through beta2 stimulation is a com-

- mon mechanism involved in lactate formation during shock states. *Shock*. 2008;30(4):417–21.
- Lima A, Bakker J. Clinical assessment of peripheral circulation. *Curr Opin Crit Care*. 2015;21(3):226–31.
- Lima AP, Beelen P, Bakker J. Use of a peripheral perfusion index derived from the pulse oximetry signal as a noninvasive indicator of perfusion. *Crit Care Med*. 2002;30(6):1210–3.
- Lima A, Jansen TC, van Bommel J, Ince C, Bakker J. The prognostic value of the subjective assessment of peripheral perfusion in critically ill patients. *Crit Care Med*. 2009;37(3):934–8.
- Lima A, van Bommel J, Sikorska K, van Genderen M, Klijn E, Lesaffre E, Ince C, Bakker J. The relation of near-infrared spectroscopy with changes in peripheral circulation in critically ill patients. *Crit Care Med*. 2011;39(7):1649–54.
- Lipcey M, Woinarski NC, Bellomo R. Near infrared spectroscopy (NIRS) of the thenar eminence in anesthesia and intensive care. *Ann Intensive Care*. 2012;2(1):11.
- Lobos AT, Lee S, Menon K. Capillary refill time and cardiac output in children undergoing cardiac catheterization. *Pediatr Crit Care Med*. 2012;13(2):136–40.
- Marshall JC, Christou NV, Meakins JL. The gastrointestinal tract. The “undrained abscess” of multiple organ failure. *Ann Surg*. 1993;218(2):111–9.
- Michard F, Boussat S, Chemla D, Anguel N, Mercat A, Lecarpentier Y, Richard C, Pinsky MR, Teboul JL. Relation between respiratory changes in arterial pulse pressure and fluid responsiveness in septic patients with acute circulatory failure. *Am J Respir Crit Care Med*. 2000;162:134–8.
- Mrgan M, Rytter D, Brabrand M. Capillary refill time is a predictor of short-term mortality for adult patients admitted to a medical department: an observational cohort study. *Emerg Med J*. 2014;31:954–8.
- Natalini G, Rosano A, Taranto M, Faggian B, Vittorielli E, Bernardini A. Arterial versus plethysmographic dynamic indices to test responsiveness for testing fluid administration in hypotensive patients: a clinical trial. *Anesth Analg*. 2006;103:1478–84.
- Pettilä V, Merz T, Wilkman E, Perner A, Karlsson S, Lange T, Hästbacka J, Hjortrup PB, Kuitunen A, Jakob SM, Takala J. Targeted tissue perfusion versus macrocirculation-guided standard care in patients with septic shock (TARTARE-2S): study protocol and statistical analysis plan for a randomized controlled trial. *Trials*. 2016;17:384.
- Roddie IC. Circulation to skin and adipose tissue. *Compr Physiol* 2011, Supplement 8: Handbook of physiology, the cardiovascular system, peripheral circulation and organ blood flow. p. 285–317.
- Rubinstein EH, Sessler DI. Skin-surface temperature gradients correlate with fingertip blood flow in humans. *Anesthesiology*. 1990;73(3):541–5.
- Ryan CA, Soder CM. Relationship between core/peripheral temperature gradient and central hemodynamics in children after open heart surgery. *Crit Care Med*. 1989;17(7):638–40.
- Sandroni C, Cavallaro F, Marano C, Falcone C, De Santis P, Antonelli M. Accuracy of plethysmographic indices as predictors of fluid responsiveness in mechanically ventilated adults: a systematic review and meta-analysis. *Intensive Care Med*. 2012;38(9):1429–37.
- Schriger DL, Baraff L. Defining normal capillary refill: variation with age, sex, and temperature. *Ann Emerg Med*. 1988;17(9):932–5.
- Schriger DL, Baraff LJ. Capillary refill: is it a useful predictor of hypovolemic states? *Ann Emerg Med*. 1991;20(6):601–5.
- Shavit I, Brant R, Nijssen-Jordan C, Galbraith R, Johnson DW. A novel imaging technique to measure capillary-refill time: improving diagnostic accuracy for dehydration in young children with gastroenteritis. *Pediatrics*. 2006;118(6):2402–8.
- Vallet B. Endothelial cell dysfunction and abnormal tissue perfusion. *Crit Care Med*. 2002;30(5):S229–34.
- van Beest PA, Hofstra HH, Schultz MJ, Boerma EC, Spronk PE, Kuiper MA. The incidence of low venous oxygen saturation on admission to the intensive care unit: a multi-centre observational study in The Netherlands. *Crit Care*. 2008;12:R33.
- van Genderen ME, van Bommel J, Lima A. Monitoring peripheral perfusion in critically ill patients at the bedside. *Curr Opin Crit Care*. 2012a;18(3):273–9.
- van Genderen ME, Lima A, Akkerhuis M, Bakker J, van Bommel J. Persistent peripheral and microcirculatory perfusion alterations after out-of-hospital cardiac arrest are associated with poor survival. *Crit Care Med*. 2012b;40(8):2287–94.
- van Genderen ME, Bartels SA, Lima A, Bezemer R, Ince C, Bakker J, van Bommel J. Peripheral perfusion index as an early predictor for central hypovolemia in awake healthy volunteers. *Anesth Analg*. 2013;116(2):351–6.
- van Genderen ME, Paaauw J, de Jonge J, van der Valk RJ, Lima A, Bakker J, van Bommel J. Clinical assessment of peripheral perfusion to predict postoperative complications after major abdominal surgery early: a prospective observational study in adults. *Crit Care*. 2014;18(3):R114.
- van Genderen ME, Engels N, van der Valk RJ, Lima A, Klijn E, Bakker J, van Bommel J. Early peripheral perfusion-guided fluid therapy in patients with septic shock. *Am J Respir Crit Care Med*. 2015;191(4):477–80.
- Vincent JL, Ince C, Bakker J. Clinical review: circulatory shock – an update: a tribute to Professor Max Harry Weil. *Crit Care*. 2012;16(6):239.
- Woods I, Wilkins RG, Edwards JD, Martin PD, Faragher EB. Danger of using core/peripheral temperature gradient as a guide to therapy in shock. *Crit Care Med*. 1987;15(9):850–2.



Optimizing Oxygen Delivery in Clinical Practice

31

Marat Slessarev and Claudio M. Martin

Abbreviations

[Hb]	Hemoglobin concentration in blood
CaO ₂	Arterial oxygen content
DO ₂	Oxygen delivery
FiO ₂	Fractional concentration of inspired oxygen
HR	Heart rate
OEF	Oxygen extraction fraction
PaO ₂	Partial pressure of oxygen in arterial blood
PCO ₂	Partial pressure of CO ₂
PEEP	Positive end-expiratory pressure
pRBC	Packed red blood cells
Q	Cardiac output
SaO ₂	Arterial oxygen saturation
SV	Stroke volume
VO ₂	Oxygen consumption

carbon dioxide. Oxygen delivery is the product of the amount of blood flow from the lungs to various organs (i.e., cardiac output) and the blood's capacity to carry oxygen (arterial oxygen content) (McLellan and Walsh 2004). While this describes global oxygen delivery, the organ-specific oxygen delivery varies both between (van der Laan et al. 2016) and within organs (Pittman 2013). During the early stage of resuscitating patients in shock, restoration of appropriate global oxygen delivery for tissue needs is the primary goal (Vincent and De Backer 2013; Gidwani and Gómez 2017). Once global oxygen delivery is restored, focus can shift to optimizing organ-specific oxygen delivery (Dünser et al. 2013). In this chapter, we consider practical aspects of optimizing oxygen delivery with emphasis on the relative effect of manipulating individual factors that affect oxygen delivery.

Introduction

The main function of the cardiovascular system is to deliver oxygen and other nutrients to tissues and remove products of metabolism, including

Oxygen Delivery Equation

Global oxygen delivery (DO₂) is a product of cardiac output (Q) and arterial oxygen content (CaO₂, Eq. 31.1).

$$DO_2 = Q \times CaO_2 \quad (31.1)$$

Cardiac output is the product of heart rate and stroke volume (Vincent 2008), which in turn is a function of preload, contractility, and afterload (Eq. 31.2). Similarly, the arterial oxygen content

M. Slessarev (✉) · C. M. Martin
Division of Critical Care Medicine, Department of
Medicine, University of Western Ontario,
London, ON, Canada
e-mail: marat.slessarev@lhsc.on.ca;
cmartin1@uwo.ca

is a function of hemoglobin concentration ($[Hb]$), arterial oxygen saturation (SaO_2), and partial pressure of oxygen in arterial blood (PaO_2 , Eq. 31.3). Each gram of hemoglobin can carry 1.39 ml of oxygen, but given the presence of other forms of hemoglobin in human blood (e.g., methemoglobin), this constant (known as Hufner's constant) in the first part of Eq. 31.4 may be closer to 1.31 ml O_2 /g (McLellan and Walsh 2004). We have chosen 1.34 ml O_2 /g in this chapter although the value is arbitrary. The

second part of Eq. 31.4 accounts for oxygen directly dissolved in plasma, but this component is small because of the poor solubility of oxygen in plasma (McLellan and Walsh 2004).

$$Q = SV \times HR \quad (31.2)$$

where $SV =$

$$\int (\text{preload, contractility, afterload}) \quad (31.3)$$

$$CaO_2 = 1.34 \times [Hb] \times SaO_2 + 0.003 \times PaO_2 \quad (31.4)$$

$$DO_2 = (SV \times HR) \times (1.34 \times [Hb] \times SaO_2 + 0.003 \times PaO_2) \quad (31.5)$$

Equations 31.2 and 31.4 can be substituted into Eq. 31.1 to illustrate primary determinants of global oxygen delivery (Eq. 31.5). These include stroke volume, heart rate, hemoglobin concentration, oxygen saturation, and, to a small extent, partial pressure of O_2 . It is useful to examine the effect of clinical interventions on each of these parameters.

Optimizing Cardiac Output

Commonly used therapeutic interventions that can affect cardiac output in critically ill patients include fluid administration, administration of vasoactive agents, and positive pressure ventilation.

Fluid Administration

The main goal of fluid administration is to increase cardiac output by optimizing preload (Magder 2016). Cardiac output only increases with increasing preload if the heart remains on the steep part of the Frank-Starling curve. Furthermore, too much fluid can decrease cardiac output by overdistending the right ventricle and bulging of the interventricular septum into the left ventricle (Cecconi et al. 2006), impairing its filling and preload. As a result, fluids are best administered as small volume predefined boluses with concurrent objective monitoring of cardiac output (or its proxy) to ensure that each bolus

leads to increase in cardiac output (Magder 2016), thereby preventing fluid overload and its associated morbidity (Finfer et al. 2018).

The choice of fluid for increasing cardiac output remains controversial. In theory, colloids should have a greater impact on preload than crystalloids per volume of fluid infused (László et al. 2017), since only a third of crystalloid remains in intravascular space 30 minutes after infusion (Ueyama and Yoshiya 1999). However, in the SAFE trial which compared albumin to saline for resuscitation of ICU patients, the ratio of the volumes of albumin to the volumes of saline administered to achieve hemodynamic resuscitation endpoints was 1:1.4 (Finfer et al. 2004). Furthermore, the excess use of synthetic colloids is associated with increased mortality (Perner et al. 2012) and renal replacement therapy use in septic patients (Perner et al. 2012; Myburgh et al. 2012), with no apparent improvement in short-term hemodynamic resuscitation endpoints or colloid-crystalloid volume ratio (1:1.3 in these trials). Regardless of the choice of fluid, the effect of bolus infusion on cardiac output should be assessed, ideally using dynamic, rather than static, measures (Cherpanath et al. 2013).

Vasoactive Medications

Inotropic and chronotropic agents can be used to increase contractility and thus stroke volume and heart rate, respectively (Hollenberg 2011; Overgaard and Dzavík 2008; Bangash et al. 2012),

but these should be carefully titrated to prevent tachyarrhythmias that can increase myocardial oxygen demand, shorten diastolic filling time, and impair preload. Furthermore, vasoactive agents with peripheral pressor activity can increase left ventricular afterload, reducing overall stroke volume and cardiac output. Ideally, titration of vasoactive drugs should occur with continuous monitoring of their effect on cardiac output (McGuinness and Parke 2015). Since cardiac function can vary during the course of critical illness (Parker et al. 1984), decision to initiate inotropic support should be guided by a point-of-care echocardiographic assessment of ventricular function (Arntfield and Millington 2012).

Mechanical Ventilation

Positive pressure ventilation can have opposing effects on stroke volume. Increase in intrathoracic pressure reduces venous return, right ventricular preload, and stroke volume. Depending on the respiratory system compliance, the use of high levels of positive end-expiratory pressure (PEEP) to increase oxygenation and optimize lung compliance may worsen the O_2 delivery and result in decreased by decreasing cardiac output. As a result, clinicians should be cautious when initiating positive pressure ventilation in hypovolemic patients and employ the lowest PEEP level for optimizing the pulmonary status and ensuring adequate preload using fluid resuscitation prior to intubation. On the other hand, positive pressure ventilation can reduce left ventricular afterload, although the effect is small, and reduce wasted preload in patients with heart failure (Jiang et al. 2016) (see Chap. 50 on “cardiogenic shock”). The relative effects of positive pressure on stroke volume therefore depend on the patient’s preload conditions, which can be assessed using a range of noninvasive methods (Monnet and Teboul 2018).

Optimizing Arterial Oxygen Content

From Eq. 31.4, we can see that hemoglobin concentration and arterial oxygen saturation are the

primary determinants of arterial oxygen content. Although PaO_2 determines the amount of dissolved oxygen, at normal barometric pressure, this volume is negligible due to the low solubility of oxygen in plasma. Clinically, hemoglobin concentration is increased by the administration of packed red blood cells (pRBCs) or whole blood, while arterial oxygen saturation is optimized using supplemental oxygen delivered noninvasively or using mechanical ventilation.

Transfusion of one unit of pRBCs will on average increase hemoglobin concentration by 10 g/L, but this number will vary depending on the patient’s total blood volume, ongoing bleeding, and co-administration of RBC-free fluids. Since hemoglobin concentration is affected by hemoglobin mass and the volume of plasma that it is dissolved in, the infusion of crystalloids or colloids other than blood as part of a large-volume resuscitation in shock patients will increase the volume of plasma with no effect on the hemoglobin mass and cause hemodilution (Perel 2017) and thus reduce arterial oxygen content. However, since afterload is dependent on hematocrit, hemodilution can increase cardiac output (Shah et al. 1980). The net effect of these interventions on oxygen delivery therefore requires repeated measurement of these parameters. While using RBC transfusion to increase oxygen carrying capacity appears to be an appealing and efficient treatment, clinical trials failed to demonstrate the benefit of liberal transfusion strategies (Ripollés Melchor et al. 2016), and transfusion may even be associated with harm (Gong et al. 2005). The reason for this may lie in the microcirculation and oxygen delivery at the tissue level.

Increasing the fraction of inspired oxygen (FiO_2) is the primary mechanism of increasing arterial oxygen saturation. This can be achieved by using a nasal cannula or face masks or via noninvasive or invasive positive pressure ventilation. The net FiO_2 delivered via nasal cannula or face mask depends on the patient’s ventilatory drive, as higher-peak inspiratory flows will result in proportional dilution of inspired oxygen and lowering of effective FIO_2 (Slessarev and Fisher 2006). Positive pressure ventilation can improve lung aeration by recruiting an atelectatic lung.

Increasing PEEP reduces lung cyclic recruitment-derecruitment and improves oxygenation (Caironi et al. 2010), but higher PEEP levels can adversely affect cardiac output in hypovolemic patients by reducing venous return and ventricular preload. Therefore, PEEP levels need to be carefully titrated to ensure optimal oxygen saturation without compromising cardiac output. In certain conditions, such as carbon monoxide poisoning, achieving 100% oxygen saturation does not guarantee adequate DO_2 , as the mass of hemoglobin available to carry oxygen is reduced with resultant decrease in arterial oxygen content. In this situation, increasing FIO_2 , alveolar ventilation (Fisher et al. 1999), or barometric pressure (using hyperbaric chamber) can significantly shorten the half-life of carbon monoxide elimination and restore normal DO_2 (Takeuchi et al. 2000).

Oxygen Delivery to Tissues

At the tissue level, DO_2 is affected by additional factors that can be manipulated clinically. At a given global cardiac output, the flow through individual organ capillary beds is tightly regulated by a multitude of factors, including metabolic milieu. Local changes in tissue partial pressure of CO_2 (PCO_2) or pH can significantly impact blood flow, especially in the brain (Battisti-Charbonney et al. 2011). These changes can be a direct result of increase in tissues metabolic activity, for example, due to an increase in neuronal firing as used in functional MRI (Gore 2003) or due to a global increase in arterial CO_2 , as is used in studies of cerebrovascular reactivity (Fisher et al. 2018). In healthy people, an increase in metabolism is usually met with increase in organ-specific blood flow and DO_2 . In shock states, however, these compensatory mechanisms may be exhausted, and this may lead to an imbalance between oxygen demand and delivery and lead to ischemia and tissue injury. To counteract this, clinicians may consider reducing tissue-specific metabolic demand, for example, by hypothermia (Luscombe and Andrzejowski

2006) or by supporting ventilation mechanically (Hussain et al. 1986; Magder 2009).

Increases in PCO_2 , acidity (lower pH), and temperature can affect the affinity of hemoglobin for oxygen by shifting the oxygen dissociation curve to the right, resulting in a lower hemoglobin saturation at a given PaO_2 (Collins et al. 2015). This mechanism (known as the Bohr effect) improves oxygen off-loading from hemoglobin in tissues. Systemic reduction in PCO_2 or temperature can therefore lead to reduced oxygen off-loading at the same PaO_2 level, leading to tissue hypoxia.

Compartment pressure is another factor that may influence tissue DO_2 (Cheatham 2009). Increase in compartment pressure above capillary perfusion pressure can obstruct capillary blood flow (Lawendy et al. 2011). Clinically, this can occur as a result of intracranial pathology, limb trauma, or intra-abdominal catastrophe that leads to increased pressure in intracranial, limb, or abdominal compartments, respectively. Decrease or complete cessation of capillary blood flow through these compartments would result in tissue ischemia despite preserved global hemodynamic parameters including cardiac output and arterial blood pressure. Clinicians should therefore be cognizant of compartment pressures during resuscitation efforts to restore global DO_2 , since certain interventions (e.g., massive transfusion or fluid resuscitation) can compromise capillary blood flow via increased compartment pressure, contributing to tissue injury.

In summary, clinicians should always consider the impact of their interventions on tissue DO_2 . For example, hyperventilation is sometimes employed to treat refractory intracranial pressure in traumatic brain injury (Marion et al. 1995). However, the associated reduction in PCO_2 can lead to significant decrease in brain DO_2 via reduction in cerebral blood flow, as well as reduction in oxygen off-loading at the tissue level via a leftward shift of the oxygen dissociation curve. Similarly, increasing PEEP may improve arterial oxygenation while also lowering cardiac output by the same proportion, which will result in no change in DO_2 despite improvement in oxygen-

ation saturation seen on the monitor. It is therefore always necessary to consider the secondary effects of seemingly beneficial interventions, especially as they relate to tissue DO_2 .

Relative Effects of DO_2 Variables on Oxygen Delivery

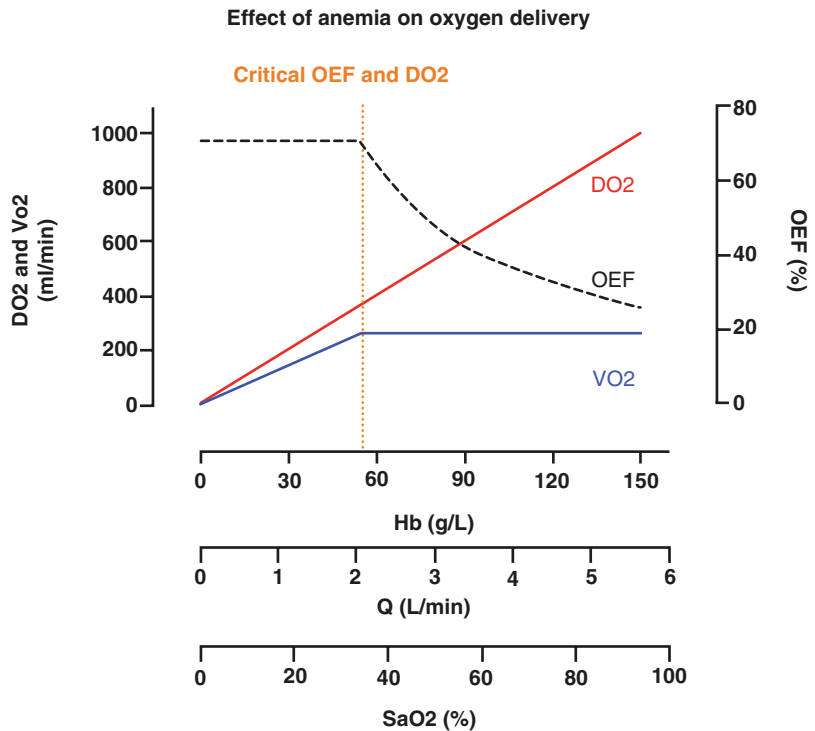
Transfusion of pRBCs, optimization of cardiac output via fluids and vasoactive agents, and optimization of SaO_2 via titration of FIO_2 and PEEP are commonly used at the bedside to improve global oxygen delivery. Figure 31.1 illustrates the relative effect of changes in these variables on oxygen delivery.

Initially, tissues counteract a decrease in DO_2 by increasing oxygen extraction fraction (OEF) in order to maintain constant oxygen consumption (VO_2). However, once OEF reaches approximately 70% (critical OEF), VO_2 becomes dependent on DO_2 and decreases proportionally with the fall in DO_2 . This is known as flow-dependent oxygen consumption, and it is associ-

ated with tissue ischemia and lactate production. Note that once arterial oxygen saturation is restored, the OEF threshold corresponds approximately to a hemoglobin concentration of 60 g/L or cardiac output of 2 L/min. Optimizing these parameters in a shock patient is therefore a priority during the initial stages of resuscitation.

Fluid resuscitation is the cornerstone of shock management and is usually the first intervention that is considered by a bedside clinician. The choice of fluid is often dictated by the type of shock (e.g., hemorrhagic vs. septic), local stock (e.g., saline vs. Ringer’s), and clinician’s prior experience. However, the relative effect of different fluid types on global DO_2 should be considered. Although a given volume of colloid solution should have a greater impact on intravascular volume and preload than a comparable volume of crystalloid solution, results of multiple trials (Finfer et al. 2004; Perner et al. 2012; Myburgh et al. 2012) suggest that these assumptions may be exaggerated, and the real colloid-crystalloid volume ratio is close to 1:1.3. Taking this into account, as well as the higher cost and risk of renal injury

Fig. 31.1 The relative effects of changes in hemoglobin concentration (Hb), cardiac output (Q), and arterial oxygen saturation (SaO_2) on oxygen delivery (DO_2), oxygen consumption (VO_2), and oxygen extraction fraction (OEF). This graph illustrates that as DO_2 falls due to decrease in hemoglobin concentration, cardiac output, or oxygen saturation, VO_2 is initially maintained by increase in the OEF. However, once OEF reaches approximately 70% (critical OEF), VO_2 becomes dependent on DO_2 and decreases proportionally with it



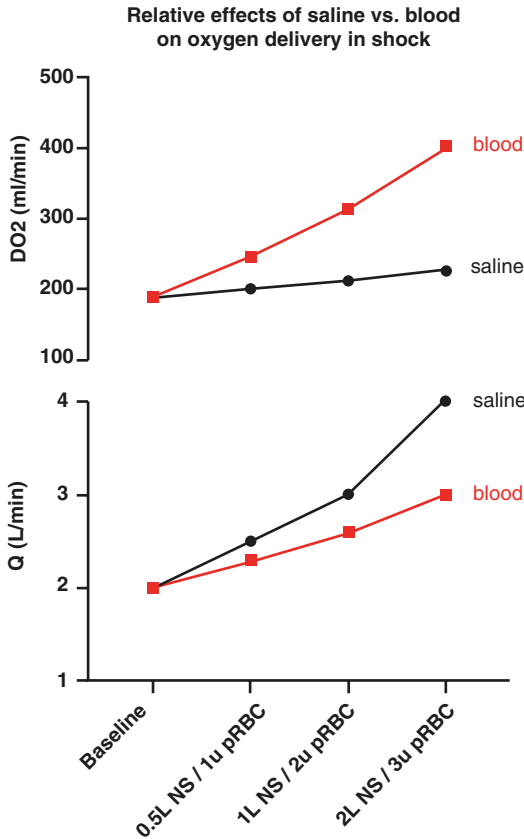


Fig. 31.2 Relative effects of resuscitation with saline versus packed red blood cells (pRBC) on oxygen delivery (DO₂) and cardiac output (Q). Note that although the administration of saline leads to a greater increase in cardiac output, it also causes reduces blood's oxygen carrying capacity by hemodilution, leading to a slower rate of increase in DO₂ than resuscitation with packed red blood cells. This is why resuscitation with reconstituted whole blood is preferred in hemorrhagic shock

with synthetic colloids, most clinical guidelines favor crystalloid resuscitation (Dellinger et al. 2013; Cecconi et al. 2014). Whether a colloid or crystalloid is used to try and restore cardiac output, there will always be a component of hemodilution, which will attenuate relative increase in global DO₂. If the hemodilution is greater than the increase in cardiac output, the DO₂ will actually decrease. For this reason, resuscitation with pRBCs has the potential for a greater impact on DO₂ than resuscitation with saline, despite saline having a great impact on cardiac output, although this too can be modified by changes in viscosity and the quality of the red cells (Fig. 31.2).

This effect becomes even more apparent when we consider the effect of adding positive pressure ventilation to resuscitation of a patient with hemorrhagic shock. Figure 31.3 illustrates changes in DO₂ and cardiac output as a function of increasing PEEP in a shock patient resuscitated with saline or pRBCs. In all instances, progressive increase in PEEP causes reduction in preload and a proportional fall in cardiac output and DO₂. Administration of 2 L of saline almost doubles cardiac output but has little impact on DO₂. In contrast, administration of 3 units of pRBCs almost doubles baseline DO₂, although its effect on cardiac output is half

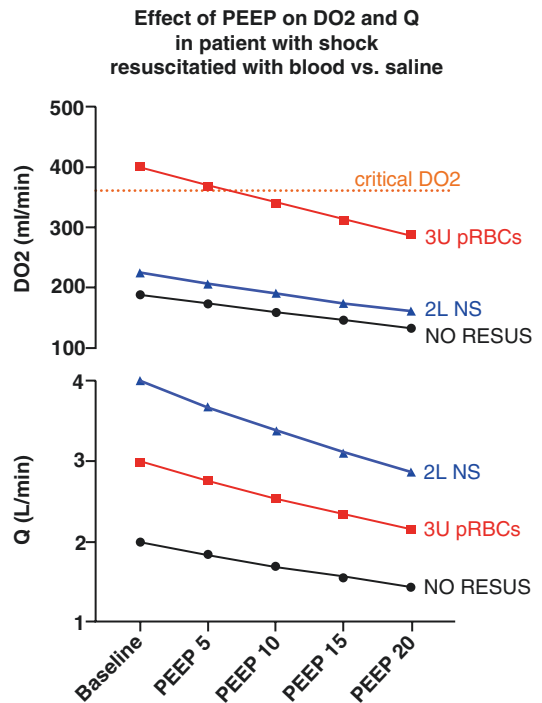


Fig. 31.3 The effect of increasing positive end-expiratory pressure (PEEP) on oxygen delivery and cardiac output in a patient with hemorrhagic shock. Increase in PEEP in non-resuscitated patients (NO RESUS, black line) leads to a progressive decrease in both DO₂ and Q. Although resuscitation with 2 liters of normal saline (NS, blue line) almost doubles cardiac output, it has little impact on DO₂, which again worsens with increasing PEEP. Administration of 3 units of packed red blood cells (pRBCs, red line) increases DO₂ above the critical DO₂ threshold, but PEEP levels higher than 5 cmH₂O will cause it to decrease below this critical DO₂ threshold, leading to tissue hypoxia. Clinicians, therefore, should carefully consider their choice of resuscitation fluid and delay positive pressure ventilation or at least use lower PEEP levels until the patient is fully resuscitated

that of 2 L of saline bolus. However, this increase in baseline DO_2 restores its value above critical DO_2 threshold, even if PEEP is raised to 5 cm of H_2O , avoiding flow-dependent oxygen consumption and ischemia. This example illustrates why clinicians should carefully consider their choice of resuscitation fluid, especially in the context of anemia from any source, and assess potential impact of intervention that may impact preload and ultimately DO_2 (such as positive pressure ventilation).

Maximizing Oxygen Delivery in the Critically Ill

Several studies have attempted to improve clinical outcomes by achieving supraphysiologic hemodynamic and oxygen transport targets. In 1988, Shoemaker et al. (Shoemaker et al. 1988) showed that targeting higher cardiac output, DO_2 , and VO_2 resulted in shorter duration of mechanical ventilation and ICU stay in high-risk general surgical patients. His results were supported by two other studies that demonstrated reduced mortality in septic (Tuchschmidt et al. 1992) and high-risk surgical patients (Boyd et al. 1993). However, other studies in more heterogeneous groups of critically ill patients (Gattinoni et al. 1995; Yu et al. 1993; Hayes et al. 1994) failed to show any clinical benefit, instead demonstrating that aiming for supraphysiologic DO_2 may lead to higher dose of vasoactive medications and increase in mortality (Hayes et al. 1994). Overall, although early studies suggested that there is a benefit to supranormal DO_2 and there was trend towards lower mortality (Heyland et al. 1996), methodological limitations of these trials including lack of blinding, selection bias, control for interventions, high rate of crossover between control and treatment groups, and variability in timing of the intervention prevent drawing definitive conclusions with respect to DO_2 -targeted resuscitation. Given that a large proportion of patients in these studies achieved supranormal cardiac output, DO_2 , and VO_2 on their own, it is

possible that the ability of patients to meet supranormal cardiac output and DO_2 goals is predictive of prognosis, but does not affect it (i.e., patients who are able to increase their DO_2 to supranormal levels have the adequate reserve to survive, while those that do not die). Since pulmonary artery catheter has fallen out of favor (Vincent 2012), clinicians are less likely to target resuscitation to supraphysiologic DO_2 goals. However, understanding the principles behind optimizing DO_2 remains important for anyone who takes care of patients with shock states. While the restoration of systemic hemodynamics is of paramount importance in shock resuscitation, once global DO_2 is restored, microcirculatory failure may persist and contribute to ongoing tissue injury (Dubin et al. 2009; De Backer et al. 2010). In this situation, further optimization of global DO_2 via ongoing fluid administration or transfusions may be deleterious by further impairing microcirculatory function and tissue oxygen delivery.

Summary and Conclusions

In summary, oxygen delivery is an important concept that should be considered when resuscitating patients with shock. In the early stages of shock, the focus should be on restoring global oxygen delivery. Later, and in specific situations such as traumatic brain injury, factors that affect organ-specific oxygen delivery should be taken into account. For the clinician at the bedside, the interventions that can be used to optimize oxygen delivery include the optimization of (1) preload by means of fluid or blood product administration; (2) cardiac contractility, afterload, heart rate, and vascular resistance by means of vasoactive agents and manipulation of PCO_2 and pH; (3) preload and afterload by PEEP; and (4) oxygen carrying capacity by means of transfusions, PO_2 , and PCO_2 . Careful consideration of the competing effects of these variables on the overall and organ-specific oxygen delivery is the cornerstone of effective resuscitation.

References

- Arntfield RT, Millington SJ. Point of care cardiac ultrasound applications in the emergency department and intensive care unit—a review. *Curr Cardiol Rev*. 2012;8(2):98–108.
- Bangash MN, Kong M-L, Pearse RM. Use of inotropes and vasopressor agents in critically ill patients: inotropes and vasopressors in the critically ill. *Br J Pharmacol*. 2012;165(7):2015–33.
- Battisti-Charbonney A, Fisher J, Duffin J. The cerebrovascular response to carbon dioxide in humans. *J Physiol*. 2011;589(Pt 12):3039–48.
- Boyd O, Grounds RM, Bennett ED. A randomized clinical trial of the effect of deliberate perioperative increase of oxygen delivery on mortality in high-risk surgical patients. *JAMA*. 1993;270(22):2699–707.
- Caironi P, Cressoni M, Chiumello D, Ranieri M, Quintel M, Russo SG, et al. Lung opening and closing during ventilation of acute respiratory distress syndrome. *Am J Respir Crit Care Med*. 2010;181(6):578–86.
- Ceccconi M, Johnston E, Rhodes A. What role does the right side of the heart play in circulation? *Crit Care*. 2006;10:7.
- Ceccconi M, De Backer D, Antonelli M, Beale R, Bakker J, Hofer C, et al. Consensus on circulatory shock and hemodynamic monitoring. Task force of the European Society of Intensive Care Medicine. *Intensive Care Med*. 2014;40(12):1795–815.
- Cheatham ML. Abdominal compartment syndrome. *Curr Opin Crit Care*. 2009;15(2):154–62.
- Cherpanath TGV, Geerts BF, Lagrand WK, Schultz MJ, Groeneveld ABJ. Basic concepts of fluid responsiveness. *Neth Hear J*. 2013;21(12):530–6.
- Collins J-A, Rudenski A, Gibson J, Howard L, O’Driscoll R. Relating oxygen partial pressure, saturation and content: the haemoglobin–oxygen dissociation curve. *Breathe (Sheff)*. 2015;11(3):194–201.
- De Backer D, Ortiz JA, Salgado D. Coupling microcirculation to systemic hemodynamics. *Curr Opin Crit Care*. 2010;16(3):250–4.
- Dellinger RP, Levy MM, Rhodes A, Annane D, Gerlach H, Opal SM, et al. Surviving sepsis campaign: international guidelines for management of severe sepsis and septic shock: 2012. *Crit Care Med*. 2013;41(2):580–637.
- Dubin A, Pozo MO, Casabella CA, Pálizas F, Murias G, Moseinco MC, et al. Increasing arterial blood pressure with norepinephrine does not improve microcirculatory blood flow: a prospective study. *Crit Care*. 2009;13(3):R92.
- Dünser MW, Takala J, Brunauer A, Bakker J. Re-thinking resuscitation: leaving blood pressure cosmetics behind and moving forward to permissive hypotension and a tissue perfusion-based approach. *Crit Care*. 2013;17(5):326.
- Finfer S, Bellomo R, Boyce N, French J, Myburgh J, Norton R, et al. A comparison of albumin and saline for fluid resuscitation in the intensive care unit. *N Engl J Med*. 2004;350(22):2247–56.
- Finfer S, Myburgh J, Bellomo R. Intravenous fluid therapy in critically ill adults. *Nat Rev Nephrol*. 2018;14(9):541–57.
- Fisher JA, Rucker J, Sommer LZ, Vesely A, Lavine E, Greenwald Y, et al. Isocapnic hyperpnea accelerates carbon monoxide elimination. *Am J Respir Crit Care Med*. 1999;159(4 Pt 1):1289–92.
- Fisher JA, Venkatraghavan L, Mikulis DJ. Magnetic resonance imaging-based cerebrovascular reactivity and hemodynamic reserve: a review of method optimization and data interpretation. *Stroke*. 2018;49(8):2011–8.
- Gattinoni L, Brazzi L, Pelosi P, Latini R, Tognoni G, Pesenti A, et al. A trial of goal-oriented hemodynamic therapy in critically ill patients. SvO2 Collaborative Group. *N Engl J Med*. 1995;333(16):1025–32.
- Gidwani H, Gómez H. The crashing patient: hemodynamic collapse. *Curr Opin Crit Care*. 2017;23(6):533–40.
- Gong MN, Thompson BT, Williams P, Pothier L, Boyce PD, Christiani DC. Clinical predictors of and mortality in acute respiratory distress syndrome: potential role of red cell transfusion. *Crit Care Med*. 2005;33(6):1191–8.
- Gore JC. Principles and practice of functional MRI of the human brain. *J Clin Invest*. 2003;112(1):4–9.
- Hayes MA, Timmins AC, Yau EH, Palazzo M, Hinds CJ, Watson D. Elevation of systemic oxygen delivery in the treatment of critically ill patients. *N Engl J Med*. 1994;330(24):1717–22.
- Heyland DK, Cook DJ, King D, Kernerman P, Brun-Buisson C. Maximizing oxygen delivery in critically ill patients: a methodologic appraisal of the evidence. *Crit Care Med*. 1996;24(3):517–24.
- Hollenberg SM. Vasoactive drugs in circulatory shock. *Am J Respir Crit Care Med*. 2011;183(7):847–55.
- Hussain SN, Graham R, Rutledge F, Roussos C. Respiratory muscle energetics during endotoxic shock in dogs. *J Appl Physiol*. 1986;60(2):486–93.
- Jiang H, Han Y, Xu C, Pu J, He B. Noninvasive positive pressure ventilation in chronic heart failure. *Can Respir J*. 2016;2016:3915237.
- László I, Demeter G, Óveges N, Érces D, Kaszaki J, Tánczos K, et al. Volume-replacement ratio for crystalloids and colloids during bleeding and resuscitation: an animal experiment. *Intensive Care Med Exp [Internet]*. 2017 [cited 2018 Sep 12];5(1). Available from: <https://icm-experimental.springeropen.com/articles/10.1186/s40635-017-0165-y>.
- Lawendy A-R, Sanders DW, Bihari A, Parry N, Gray D, Badhwar A. Compartment syndrome–induced microvascular dysfunction: an experimental rodent model. *Can J Surg*. 2011;54(3):194–200.
- Luscombe M, Andrzejowski JC. Clinical applications of induced hypothermia. *Contin Educ Anaesth Crit Care Pain*. 2006;6(1):23–7.
- Magder S. Bench-to bedside review: ventilatory abnormalities in sepsis. *Crit Care*. 2009;13(1):202.

- Magder S. Volume and its relationship to cardiac output and venous return. *Crit Care*. 2016;20:271.
- Marion DW, Firlirk A, McLaughlin MR. Hyperventilation therapy for severe traumatic brain injury. *New Horiz*. 1995;3(3):439–47.
- McGuinness S, Parke R. Using cardiac output monitoring to guide perioperative haemodynamic therapy. *Curr Opin Crit Care*. 2015;21(4):364–8.
- McLellan SA, Walsh TS. Oxygen delivery and haemoglobin. *Continuing Educ Anaesth Crit Care Pain*. 2004;4(4):123–6.
- Monnet X, Teboul J-L. Assessment of fluid responsiveness: recent advances. *Curr Opin Crit Care*. 2018;24(3):190–5.
- Myburgh JA, Finfer S, Bellomo R, Billot L, Cass A, Gattas D, et al. Hydroxyethyl starch or saline for fluid resuscitation in intensive care. *N Engl J Med*. 2012;367(20):1901–11.
- Overgaard CB, Dzavík V. Inotropes and vasopressors: review of physiology and clinical use in cardiovascular disease. *Circulation*. 2008;118(10):1047–56.
- Parker MM, Shelhamer JH, Bacharach SL, Green MV, Natanson C, Frederick TM, et al. Profound but reversible myocardial depression in patients with septic shock. *Ann Intern Med*. 1984;100(4):483–90.
- Perel A. Iatrogenic hemodilution: a possible cause for avoidable blood transfusions? *Crit Care* [Internet]. 2017; [cited 2018 Sep 12];21. Available from: <https://www.ncbi.nlm.nih.gov/pmc/articles/PMC5702064/>.
- Perner A, Haase N, Guttormsen AB, Tenhunen J, Klemenzson G, Åneman A, et al. Hydroxyethyl starch 130/0.42 versus Ringer's acetate in severe sepsis. *N Engl J Med*. 2012;367(2):124–34.
- Pittman RN. Oxygen transport in the microcirculation and its regulation. *Microcirculation*. 2013;20(2):117–37.
- Ripollés Melchor J, Casans Francés R, Espinosa Á, Martínez Hurtado E, Navarro Pérez R, Abad Gurumeta A, et al. Restrictive versus liberal transfusion strategy for red blood cell transfusion in critically ill patients and in patients with acute coronary syndrome: a systematic review, meta-analysis and trial sequential analysis. *Minerva Anesthesiol*. 2016;82(5):582–98.
- Shah DM, Prichard MN, Newell JC, Karmody AM, Scovill WA, Powers SR. Increased cardiac output and oxygen transport after intraoperative isovolemic hemodilution. A study in patients with peripheral vascular disease. *Arch Surg*. 1980;115(5):597–600.
- Shoemaker WC, Appel PL, Kram HB, Waxman K, Lee TS. Prospective trial of supranormal values of survivors as therapeutic goals in high-risk surgical patients. *Chest*. 1988;94(6):1176–86.
- Slessarev M, Fisher J. Oxygen administration in the emergency department: choosing the appropriate dosage and the technology. 2006 [cited 2014 Dec 10]; Available from: http://www.cerotecmed.com/Slessarev_Hi-Ox_in_the_ER_IJEM_2006.pdf.
- Takeuchi A, Vesely A, Rucker J, Sommer LZ, Tesler J, Lavine E, et al. A simple “new” method to accelerate clearance of carbon monoxide. *Am J Respir Crit Care Med*. 2000;161(6):1816–9.
- Tuchschmidt J, Fried J, Astiz M, Rackow E. Elevation of cardiac output and oxygen delivery improves outcome in septic shock. *Chest*. 1992;102(1):216–20.
- Ueyama H, Yoshiya I. Effects of crystalloid and colloid preload on blood volume in the parturient undergoing spinal anesthesia for elective cesarean section. *Anesthesiology*. 1999;91(6):6.
- van der Laan ME, Roofthoof MTR, Fries MWA, Schat TE, Bos AF, Berger RMF, et al. Multisite tissue oxygenation monitoring indicates organ-specific flow distribution and oxygen delivery related to low cardiac output in preterm infants with clinical sepsis. *Pediatr Crit Care Med*. 2016;17(8):764–71.
- Vincent J-L. Understanding cardiac output. *Crit Care*. 2008;12(4):174.
- Vincent J-L. The pulmonary artery catheter. *J Clin Monit Comput*. 2012;26(5):341–5.
- Vincent J-L, De Backer D. Circulatory shock. *N Engl J Med*. 2013;369(18):1726–34.
- Yu M, Levy MM, Smith P, Takiguchi SA, Miyasaki A, Myers SA. Effect of maximizing oxygen delivery on morbidity and mortality rates in critically ill patients: a prospective, randomized, controlled study. *Crit Care Med*. 1993;21(6):830–8.

Part V

The Tools: Respiratory



Measuring Volume, Flow, and Pressure in the Clinical Setting

32

Jason H. T. Bates

List of symbols and acronyms

A, B, K	Parameters of the exponential PV relationship	P_{ip}	Transpulmonary pressure
E_L	Lung elastance	r	Radius
E_{rs}	Respiratory system elastance	R_{aw}	Airway resistance
E_w	Chest wall elastance	R_L	Lung resistance
f	Frequency in Hertz (Hz)	R_{rs}	Respiratory system resistance
FEV ₁	Volume of air expired in the first second of a maximal forced expiration	RV	Residual volume
FRC	Functional residual capacity	V	Volume
FVC	Forced vital capacity	ΔV	Change in volume
g	Acceleration due to gravity	\dot{V}	Flow
i	Square root of -1	\ddot{V}	Volume acceleration
I_{aw}	Inertance due to airways gas	\dot{V}_{max}	Maximum expiratory flow
P	Pressure	V_{tg}	Thoracic gas volume
P_0	Baseline pressure pertaining when both volume and flow are zero	Z_{rs}	Respiratory system impedance
ΔP	Change in pressure	β	Flow velocity profile factor in Bernoulli equation
P_A	Alveolar pressure	ρ	Gas density
P_{ao}	Airway opening pressure		
P_{atm}	Atmospheric pressure		
ΔP_B	Bernoulli effect pressure		
P_{chamb}	Gas pressure inside a body plethysmograph		
P_{es}	Esophageal pressure		
P_{pl}	Pleural pressure		

J. H. T. Bates (✉)

Department of Medicine, Larner College of
Medicine, University of Vermont,
Burlington, VT, USA
e-mail: Jason.h.bates@uvm.edu

Introduction

The volumes, flows, and pressures of gas impinging upon or emanating from the lung reflect its mechanical properties. These properties are critical determinants of the lung's ability to function normally and are often compromised in disease. For example, a lung with narrowed airways requires a larger than normal inflation pressure to maintain a given inspiratory flow. Conversely, a lung suffering from the tissue destruction characteristic of advanced emphysema requires a lower than normal pressure to maintain a given level of

inflation. Measurements of lung mechanics can thus provide important diagnostic information about the nature of lung disease and the progress of therapy. Sudden alterations in lung mechanics can even signal acute life-threatening events that may arise in the intensive care unit or operating theater, such as a kinked or blocked airway, sudden bronchospasm, or the onset of pulmonary edema. Indeed, lung compliance is routinely measured in patients receiving mechanical ventilation, while periodic assessment of lung function via spirometry continues to be the principal diagnostic platform for managing patients with asthma.

The lung comprises a very large number of components interacting in a highly complex way. We can never hope to understand this behavior in all its details because the scale of the task is simply too great. It is possible, however, to understand the important global features of lung mechanics, at least to the extent that they characterize health versus disease. We gain this understanding by probing the lung in various mechanical ways and observing what mechanical consequences result (Bates 2009). In engineering terms, this amounts to applying controlled inputs to the lung and measuring the resultant outputs. Such an exercise can be purely empirical in the sense that observed relationships between input and output are viewed solely in terms of what they portend for treatment and prognosis. Indeed, since treatment and prognosis represent the bottom line in patient care, the empiricism of this kind characterizes much of clinical medicine. The scientific study of lung mechanics, however, rests on using input-output relationships to infer how observed function is linked to the internal structure. This linkage is formalized in terms of mathematical models that are necessarily vastly more simple than the real organ but nevertheless capture its important global attributes (Bates 2009).

Using measurements of lung mechanics to diagnose and monitor lung disease in the clinical setting is appealing because the measurements are typically sensitive to abnormalities in lung physiology, and they can be obtained continuously in real time. Furthermore, the equipment

required to make the measurements is convenient and cheap compared to, say, advanced imaging modalities such as x-ray computed tomography. The instrumentation and data acquisition technology required to measure and record respiratory volumes, flows, and pressures are also well established and available in a variety of off-the-shelf forms. The principal challenge therefore lies in knowing how to interpret measurements of lung mechanics in a way that aids diagnosis and, if possible, to interpret them in a way that links anatomic structure and physiologic function.

Spirometry

Most lung function assessment in the clinic is performed by *spirometry* (Irvin 2005), which rests on the phenomenon of *expiratory flow limitation*. This causes the rate of exhalation to be limited to a maximum value that is a function of lung volume but is independent of expiratory effort above a level easily achieved by most people greater than about 5 years of age. The general physical principles behind expiratory flow limitation are well known (Bates 2009; Wilson et al. 1986) and are of two types that can each be understood by viewing the lung as a single alveolar compartment connected to the airway opening by a single airway conduit, with both structures encased in a pressurized chamber representing the pleural space surrounded by the thorax (Fig. 32.1).

One mechanism of flow limitation arises from the viscous pressure loss along the airway that begins at the pressure in the alveolus (P_A) and ends at the pressure at the airway opening (P_{ao}) which is zero (gas pressures being expressed relative to atmospheric pressure). The pressure in the pleural space (P_{pl}) differs from P_A by the elastic pressure drop across the parenchymal tissue, which itself is expressed as the product of lung volume (V , expressed relative to functional residual capacity, FRC) and lung elastance (E_L). The airway itself is embedded in parenchymal tissue, and so, the parenchymal attachments to the outside of the airway wall serve to transmit transpulmonary pressure across the wall in this simple model (Fig. 32.1).

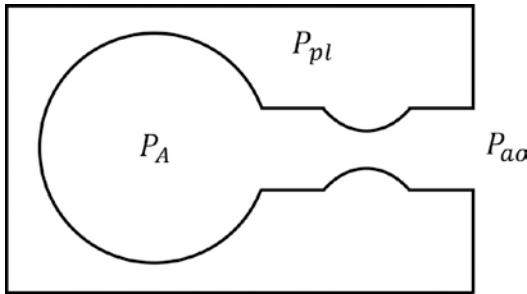


Fig. 32.1 Model of the respiratory system showing the lung as a single alveolar compartment connected to the atmosphere by a single airway, both encased in the chest wall. The airway opening pressure (P_{ao}) is atmospheric. Pleural pressure (P_{pl}) is generated by the expiratory muscles, which then increases alveolar pressure (P_A) to drive gas out of the lungs. At some point along the airways, the pressure falls to equal P_{pl} at the so-called equal pressure point beyond which the airways will narrow if they do not have stiff enough walls to resist collapse

Expiratory effort increases P_{pl} , which cause commensurate increases in P_A according to

$$P_{pl} = P_A - E_L V \quad (32.1)$$

During normal breathing, P_{pl} at FRC is negative, and it becomes even more negative during inspiration. During forced expiration, however, P_{pl} becomes positive and therefore greater than P_{ao} . Nevertheless, as Eq. 32.1 shows, P_{pl} still remains less than P_A . This means that there is a point somewhere along the airway where pressure falls to a value equal to P_{pl} . This is known as the *equal pressure point* (Mead et al. 1967). If the walls of the airways were completely rigid then the equal pressure point would have no particular functional significance, but the airways of the lung are not rigid. Even the trachea and central airways with their supporting cartilage will collapse at physiological pressures, and the small distal airways are highly collapsible. The result is that somewhere downstream of the equal pressure point, where intra-airway pressure has fallen sufficiently, the airway wall will start to narrow and thus restrict flow. This narrowing will increase with effort-dependent increases in P_{pl} such that one reaches a point of diminishing returns; further increases in effort are met with further airway narrowing, so the net flow that passes along the airway remains unchanged. The

position of the equal pressure point depends on the resistive pressure drop along the airways, and thus on airway resistance (R_{aw}). R_{aw} depends on gas viscosity when the flow is low enough to be purely laminar flow, but gains a dependency on gas density as flow increases and becomes turbulent.

The other potential mechanism for flow limitation depends solely on gas density and can be understood in terms of the *Bernoulli effect* whereby the pressure exerted laterally by a flowing stream of gas decreases as flow increases. This is a manifestation of the principle of conservation of energy; when a freely flowing body of gas gains velocity and thus kinetic energy due to geometric constraints, it compensates by losing potential energy due to pressure. The Bernoulli effect is a widely important phenomenon and is involved, for example, in the lift of airplane wings and the Venturi effect used in vacuum pumps. In terms of the airways, the magnitude of the Bernoulli effect can be expressed as the reduction in lateral pressure, ΔP_B , produced by a gas of density ρ moving along an airway of diameter r at a flow of \dot{V} thus (Bates et al. 1992):

$$\Delta P_B = \frac{\beta \rho \dot{V}^2}{2\pi^2 g r^4} \quad (32.2)$$

where g is the acceleration due to gravity and β is a factor that depends on the way in which the linear velocity of the gas varies across the diameter of the airway (e.g., $\beta = 1$ when the radial velocities are all equal, and $\beta = 2$ when the flow velocity is parabolic as in fully developed Poiseuille flow). ΔP_B represents the amount by which the air in the airway lumen reduces the pressure it exerts on the airway wall. Since the pressure on the outside of the airway wall is unaffected, and the wall itself is compliant, the difference between outside and inside pressures may become great enough to push the wall inward.

Equation 32.2 shows that the reduction in lumen pressure increases with the square of \dot{V} , so once flow becomes large enough for the pressure difference across the wall to begin to overwhelm its ability to resist compression, further increases will rapidly bring about the dramatic narrowing of lumen area. Eq. 32.2 also shows

that ΔP_B depends inversely on the fourth power of r , which means that airway collapse due to the Bernoulli effect can very rapidly become a major problem, for a given \dot{V} , when airways become pathologically narrowed as occurs in asthma. However, once narrowing occurs to the point that \dot{V} is significantly reduced, the magnitude of ΔP_B will fall to the point that airway compression is relieved allowing flow to build up again. The Bernoulli effect thus leads to rapid cycles of airway collapse and reopening that can manifest as a clinically detectable flutter characteristic of obstructive lung disease. A simplified analysis of a single airway (Bates 2009) gives the maximum expiratory flow as

$$\dot{V}_{\max} = \pi r^2 \sqrt{\frac{\pi r^2}{\rho} E_w} \quad (32.3)$$

where E_w is the elastance of the airway wall given by the change in transmural pressure for a unit change in A . This equation shows that expiratory flow is more severely limited when the ability of the airway wall to resist collapse is reduced, such as occurs in emphysema due to the reduction in outward tethering afforded by damaged parenchymal attachments. Equation 32.3 also shows that flow limitation is more severe when A is reduced, an obvious consequence of a reduction in r .

The limitation of expiratory flow is also often attributed to what is known as *wave speed*, which refers to the speed at which elastic waves in the wall of an airway move axially in much the same way that water waves move toward the beach in the ocean. This phenomenon is straightforward to understand intuitively; because airways are not completely rigid, when an aliquot of air enters an airway at its upstream end due to an increase in upstream pressure, the aliquot is initially accommodated by an outward bulging of the proximal section of the airway wall that then moves distally as a traveling wave. The velocity of this wave depends on the stiffness of the airway wall, which provides the elastic force driving the wave forward, as well as on the mass of the aliquot of gas that is being transported. In fact, analysis of the situation based on Newton's laws of motion for a single idealized airway leads

to exactly the same expression for \dot{V}_{\max} as found for the Bernoulli effect, namely, Eq. 32.3 above (Bates 2009). The Bernoulli effect and wave speed explanations of expiratory flow limitation can thus be thought of as alternate but identical ways of accounting for the same phenomenon.

Flow limitation in a real lung may involve any or all of the theoretical considerations given above, which likely manifest during a forced expiration in a distributed and time-varying manner throughout the airway tree. The overall limiting expiratory flow that results would thus be extremely difficult to calculate exactly even if all the necessary information, such as individual airway dimensions and compliance values, was at hand. Consequently, while we have a good understanding of the fundamental physical principles behind expiratory flow limitation, usefully linking abnormalities in \dot{V}_{\max} to pathological alterations in lung structure is generally not possible. Accordingly, the clinical applications afforded by the phenomenon of expiratory flow limitation remain empirical and are largely limited to two parameters known as FEV₁ and FVC (Fig. 32.2). Both FEV₁ (the volume of air

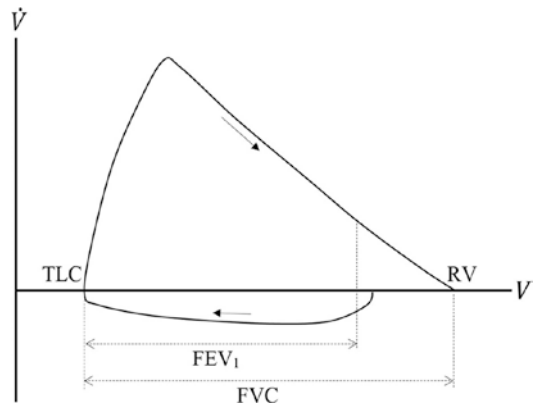


Fig. 32.2 The flow-volume loop during a maximal forced expiration. Following an inspiration to total lung capacity (TLC), the expiratory flow (\dot{V}) rapidly reaches a peak value that is determined by the physical properties of the airways and lung parenchyma. Maximal expiratory flow then decreases progressively with decreasing volume as expiration proceeds to residual volume (RV). The volume of gas expired in the first second of the expiration (FEV₁) and the total volume expired (FVC) are the two key parameters used to evaluate lung function clinically

expelled from the lung during the first second of a maximal forced expiration starting at total lung capacity) and FVC (forced vital capacity, the total volume of air expelled over the entire course of expiration) depend strongly on demographic characteristics such as age, height and sex, and to some extent ethnicity (Bates et al. 2011). As a result of numerous studies in large populations that have determined normal values for these two parameters, measurements of FEV₁ and FVC in patients are invariably expressed in terms of percent predicted value.

Generally speaking, an abnormally low value of FEV₁ is a reflection of reduced \dot{V}_{\max} , which itself indicates the presence of narrowed airways for the reasons outlined above and is thus indicative of obstructive pulmonary disease. Conversely, an abnormally low-value FVC may reflect a reduction in the ability of the lungs to expand and thus indicate restrictive pulmonary disease. The situation in any given patient, however, is invariably not this straightforward. For example, FVC will also be reduced if the airways become completely occluded by mucus plugs during the course of expiration, trapping air that cannot be exhaled. This occurs in the classic obstructive disease of asthma. A disease such as emphysema that has its primary manifestation in the alveolar parenchyma typically presents with a decreased FEV₁ because reduced mechanical support of the airway wall reduces \dot{V}_{\max} . Nevertheless, this ideal picture of the relative diagnostic roles of FEV₁ and FVC is almost never cleanly realized in practice, making these two parameters sensitive but nonspecific biomarkers of lung disease (Mead 1979). Their inestimable clinical utility arises from their sensitivity to the presence of lung disease of some kind as well as their practical utility in terms of ease and convenience of use.

Body Plethysmography

The other widely used clinical approach to the assessment of lung mechanical function in the outpatient setting is *body plethysmography*, which involves having a subject perform various breathing maneuvers while sealed inside

a chamber with rigid walls. The utility of body plethysmography arises from *Boyle's law*, which tells us how the volume of an isolated aliquot of gas will change when its pressure is altered by a given amount. This principle can be used to estimate the total volume of gas in the thorax, V_{tg} . This makes body plethysmography an important adjunct to spirometry since the latter can only measure a change in lung volume by observing the volume of gas entering or leaving the mouth. The method of measuring V_{tg} in a body plethysmograph is as follows.

If the subject is apneic with an open glottis, the pressure of the gas in their lungs is that of the atmosphere, P_{atm} . If the subject then the subject tries to breathe through an occluded mouthpiece, the volume of gas distal to the occlusion (i.e., V_{tg}) will change its pressure everywhere by the same amount ΔP because there will be no flow of gas and hence no pressure difference anywhere throughout the system. Boyle's law states that the resulting change in the total volume of the gas, ΔV , satisfies the relation

$$P_{\text{atm}} V_{tg} = (P_{\text{atm}} + \Delta P)(V_{tg} + \Delta V) \quad (32.4)$$

provide that the gas remains at the same temperature. Note that ΔV will be negative if ΔP is positive, and vice versa.

P_{atm} is obviously a known quantity, and ΔP can be readily determined by connecting a pressure transducer to the mouthpiece distal to the occlusion. This leaves V_{tg} and ΔV as the only unknown quantities in Eq. 32.4. Recall, however, that the subject is inside a sealed chamber while this maneuver is being performed. Consequently, as the gas in the thorax is cyclically compressed and decompressed during the attempts at breathing, the volume of the subject's entire body undergoes the same changes. This causes the gas that is inside the chamber, but outside the subject, to experience equal and opposite changes in volume that are reflected in corresponding changes in chamber pressure, P_{chamb} (Fig. 32.3). A separate calibration maneuver provides the relationship that links a change in P_{chamb} to a change in its gas volume, which then leaves V_{tg} as the only unknown in Eq. 32.4, thus allowing it to be evaluated from the remaining known quantities. (Note that the above analysis assumes that the only gas in the body is in the thorax, which may not be

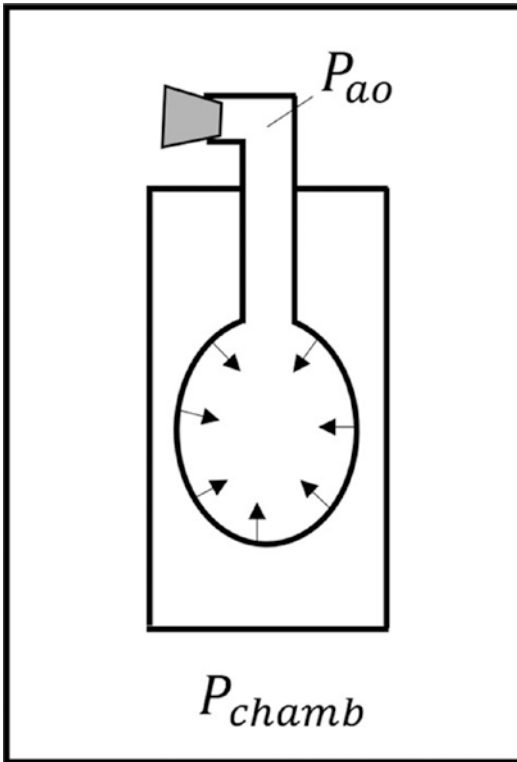


Fig. 32.3 When a subject sits inside a sealed chamber and attempts to expire against a closed airway, mouth pressure (P_{ao}) increases and so compresses the gas in the lungs. This causes an equal and opposite expansion of the gas in the chamber around the subject. Measuring the change in chamber pressure (P_{chamb}) that results provides the compressive change in the volume of the gas in the lungs via knowledge of the compressibility of the gas in the chamber

the case since the bowels can also contain significant volumes of gas.)

Once V_{lg} has been determined, body plethysmography permits the flow resistance of the airway tree, R_{aw} , to be measured. Here, the subject breathes freely from the air in the chamber while \dot{V} is measured at the mouth. During this maneuver P_A differs from P_{chamb} by an amount ΔP due to a compressive or expansive change, ΔV , in the volume of the thoracic gas. As before, ΔV is determined from the corresponding change in P_{chamb} , and Eq. 32.4 is invoked once again. This time, however, the only unknown is ΔP , which can thus be evaluated. Finally, R_{aw} is calculated as the ratio of ΔP to \dot{V} .

The use of body plethysmography to assess lung function is based on a particularly simple

model of the respiratory system in which all alveoli are represented as a single-compartment and all airways are represented as a single conduit. This model is obviously a gross oversimplification of the real system, but within the limits imposed by its sweeping assumptions, it allows the structure to be linked to function. For example, a change in a measured value of V_{lg} can be reasonably taken to reflect an actual change in the volume of gas in the lungs, which might then be linked to a pathological process such as gas trapping in asthma or parenchymal restriction in pulmonary fibrosis. Similarly, R_{aw} can be reasonably related to the caliber of the airways in a general overall sense, so an elevation in R_{aw} can be a useful indicator of the degree of bronchoconstriction occurring in asthma or following a methacholine challenge.

Resistance and Elastance

The single-compartment model of the respiratory system (Fig. 32.4) also provides the conceptual basis for a general approach to the assessment of lung mechanics in which the pressure drop across the system is related to the flow entering

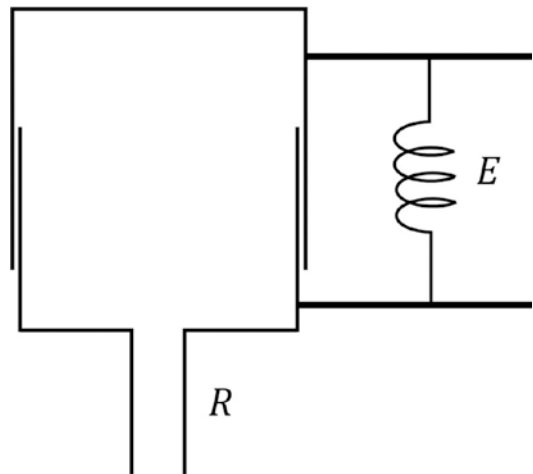


Fig. 32.4 The single-compartment model of the respiratory system. A pair of telescoping canisters accommodate changes in the volume of gas that flows in through a single airway conduit. A spring with elastance E becomes stretched according to this volume change and thus generates a proportional elastic recoil pressure inside the alveolar compartment

it. This approach has a number of instantiations depending on exactly which pressures are being measured and under what circumstances. If the mechanical properties of the lung alone are of interest, independent of the influence of the chest wall, then it is necessary to measure pleural pressure (P_{pl}) because this allows the pressure drop across the lung (transpulmonary pressure, P_{ip}) to be calculated as

$$P_{ip} = P_{ao} - P_{pl} \quad (32.5)$$

where P_{ao} is the pressure at the airway opening. P_{ip} is responsible for inflating the lung tissue and driving flow along the airways. P_{pl} is not easily measured in human subjects, but fortunately, the pressure in the esophagus (P_{es}) provides a useful surrogate that can be measured with the use of an esophageal balloon catheter (Baydur et al. 1982). The equation of motion describing how the single-compartment model of the lung behaves is then

$$P_{ip}(t) = P_{ao}(t) - P_{es}(t) = E_L V(t) + R_L \dot{V}(t) + P_0 \quad (32.6)$$

where \dot{V} is flow entering the airway opening, and the variables P_{ip} , P_{ao} , P_{es} , V , and \dot{V} vary with time (t). The three parameters of the equation are *lung elastance* (E_L), *lung resistance* (R_L), and the baseline pressure (P_0) that accounts for the fact that P_{ip} is typically negative when V and \dot{V} are both zero.

Equation 32.6 is the only useful formulation of the single-compartment model that can be applied to spontaneously breathing subjects because P_{es} is the only variable that carries useful pressure information (P_{ao} is always zero relative to atmospheric pressure), but it requires that subjects have an esophageal balloon catheter in place. However, Eq. 32.6 is equally applicable in mechanically ventilated subjects where P_{ao} reflects the driving pressure supplied by the ventilator. If subjects are completely passive during mechanical ventilation, meaning that they make no spontaneous breathing efforts at all, then P_{ao} equals the pressure drop across the respiratory system and Eq. 32.6 becomes

$$P_{ao}(t) = E_{rs} V(t) + R_{rs} \dot{V}(t) + P_0 \quad (32.7)$$

where the parameters are now respiratory system elastance (E_{rs}), respiratory system resistance (R_{rs}), and P_0 represents any positive end-expiratory pressure that has been applied. A corresponding equation can be written for the chest wall alone by replacing P_{ip} with P_{es} .

The advantages of using the above equations of motion might appear to center around the apparently straightforward physiological interpretations of the model parameters, but here some

caution is required. In particular, it is tempting to equate the parameter R_L in Eq. 32.6 with the flow resistance of the pulmonary airways, if for no other reason than the single-compartment model (Fig. 32.4) would seem to compel such an interpretation. In fact, R_L varies inversely with the frequency at which flow is oscillated into and out of the lungs (Sato et al. 1991). Over the range of normal breathing frequencies, the viscous nature of these properties is substantial, with the result that R_L carries a significant component due to tissue resistance (Fig. 32.5) (Ludwig et al. 1987).

Both the airway and tissue components of R_L also depend to a certain extent on the magnitude of \dot{V} , although during regular quiet breathing or mechanical ventilation the assumption of flow independence is usually reasonable. A much more important nonlinear effect is seen in the parameter E_L , which increases dramatically at high lung volumes. Indeed, the increase in lung tissue stiffness with lung volume is readily apparent in the pressure-volume (PV) relationship of the lung which can be determined by either cycling lung volume very slowly over the vital capacity range or by inflating and deflating the lungs in steps and recording pressure at the end of each volume plateau. A popular empirical description of the nonlinear PV curve of the lung for volumes above normal function residual capacity is the exponential expression (32.11)

$$V = A - B e^{-KP} \quad (32.8)$$

where A , B , and K are constants (Salazar and Knowles, 1964). These constants are not directly

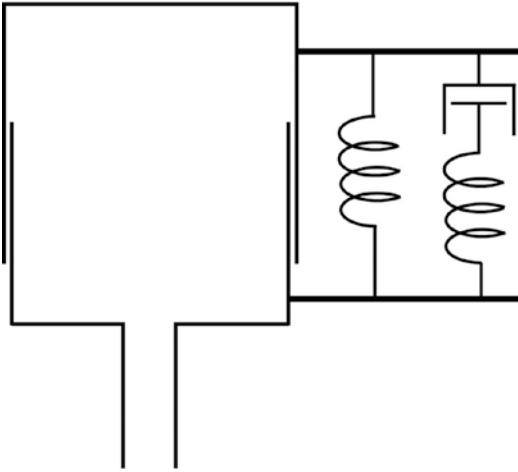


Fig. 32.5 The viscoelastic model of the respiratory system. This model is an extension of that shown in Fig. 32.4 by the inclusion of a spring and a resistor connected in series between the two telescoping canisters. A sudden increase in lung volume initially stretches both springs, but only the spring that spans the two horizontal connectors remains stretched. The other spring relaxes by moving the resistive element. This model accounts in a simple way for the frequency dependence of resistance and elastance; when flow is oscillated into the airway at low frequency, the second spring does not have a chance to stretch much before this is compensated for by sliding of the resistive element, so total tissue elastance is low and resistance is high. Conversely, at high oscillation frequencies, the resistive element has little chance to move before the force exerted by the second spring changes direction, so total tissue elastance is high and resistance tends toward zero

interpretable in anatomic or physiologic terms, although the parameter K has received some attention as an empirical marker of overall PV curve shape that changes characteristically with age and in certain lung diseases (Colebatch et al. 1979). This equation also makes explicit the fact that lung elastance is not a single invariant quantity in any particular lung, but rather increases progressively as the lung tissues stiffen with progressive stretch.

Oscillometry and Impedance

The way that resistance and elastance change with oscillation frequency has received a great deal of attention because these changes are typically accentuated in obstructive lung disease and thus have diagnostic value (Bates et al. 2011). In

a healthy lung, these dependencies on frequencies below about 2 Hz are due largely to the viscoelastic properties of the lung and chest wall tissues. In disease, however, these dependencies are increased and extended to higher frequencies by regional heterogeneities in lung mechanical properties that cause different regions of the lung to have different time-constants of emptying (Bates 2009). Obviously, regional heterogeneity in an organ as complex as the lung can have innumerable manifestations, but much of it can be usefully captured by considering the lung to become segregated into a small number of communicating compartments. At the simplest level, there can be two such compartments, although whether they are most appropriately arranged in series or parallel cannot be determined solely from measurements of pressure flow made at the airway opening (Similowski and Bates 1991), so which should be invoked depends on the circumstances and on what appears to make the most sense physiologically.

In any case, the way that resistance and elastance vary with frequency is encapsulated in a function of frequency, f , known as the *input impedance of the respiratory system*, $Z_{rs}(f)$. Clinically, $Z_{rs}(f)$ is measured by *oscillometry*, also known as the *forced oscillation technique*, in which an oscillating $\dot{V}(t)$ signal containing multiple frequencies is applied to the airway opening while the $P_{ao}(t)$ generated by these oscillations is measured. $Z_{rs}(f)$ is calculated and expressed using the algebra of complex numbers, so it is a complex function of frequency that has both a real part and an imaginary part. These two parts reflect the components of $\dot{V}(t)$ that are in-phase and out-of-phase, respectively, with $P_{ao}(t)$, and are known as *resistance* and *reactance*, respectively.

The impedance of the single-compartment model (Fig. 32.4) is illustrated in Fig. 32.6. It is calculated by taking the Fourier transform of Eq. 32.7 to yield (Bates 2009).

$$Z_{rs}(f) = R_{rs} - i \frac{E_{rs}}{2\pi f} \quad (32.9)$$

where $i = \sqrt{-1}$. This illustrates why the real part, R_{rs} , is called resistance; in the single-compartment model, it is equal simply to the resistance of the

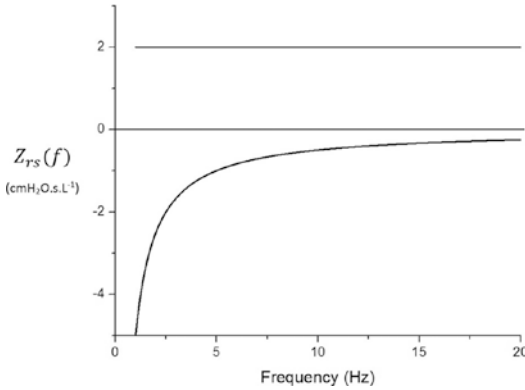


Fig. 32.6 Impedance (Z_{rs}) of the single-compartment model shown in Fig. 32.4. The real part (R_{rs}), known as resistance, is constant with frequency (f). The imaginary part (X_{rs}), known as reactance, is a negative hyperbolic function of f

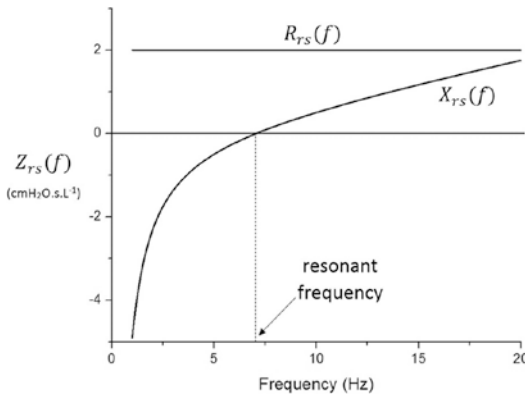


Fig. 32.7 Impedance (Z_{rs}) of the single-compartment model shown in Fig. 32.4 with the addition of airway inertia, I_{aw} . R_{rs} remains unchanged, but X_{rs} now crosses zero at the resonant frequency

model. The reactance is a negative hyperbolic function of f scaled by E_{rs} .

There are a number of models that have been used to model the inverse relationship between R_{rs} and f that is observed experimentally (Bates 2009). In the low-frequency range, typically below 2–4 Hz, these models incorporate descriptions of tissue viscoelasticity, while at higher frequencies, the frequency dependence of R_{rs} is attributed to regional heterogeneities of ventilation throughout the lung. At these higher frequencies, it is also necessary to account for the acceleration of components in the system that have mass. The principle such component relevant to frequencies up to 30 Hz or so is the gas in

the central airways. In this case, Eq. 32.7 must be modified to include an extra term accounting for this airway inertia, I_{aw} , and so becomes (Bates 2009; Bates et al. 2011).

$$P_{ao}(t) = E_{rs}V(t) + R_{rs}\dot{V}(t) + I_{aw}\ddot{V}(t) + P_0 \tag{32.10}$$

where \ddot{V} is volume acceleration (the time-derivative of \dot{V}). The Fourier transform of this equation leads to

$$Z_{rs}(f) = R_{rs} + i\left(2\pi fI_{aw} - \frac{E_L}{2\pi f}\right) \tag{32.11}$$

$Z_{rs}(f)$ from Eq. 32.11 is illustrated in Fig. 32.7 and shows that the reactance changes sign at the resonant frequency which, in a normal adult human, is around 8 Hz.

$Z_{rs}(f)$ can be measured in human subjects over a wide range of frequencies from that of normal breathing (Lutchen et al. 1993a, 1994) to the acoustic range of hundreds of Hertz (Dorkin et al. 1988). Measuring $Z_{rs}(f)$ below about 5 Hz, which covers the range of breathing frequencies and their first few harmonics, requires that the subject be apneic or else an unknown portion of the oscillations in $\dot{V}(t)$ are generated by the subject’s respiratory musculature. Above 5 Hz subjects may breathe freely. The information gained from oscillometry about the respiratory system (or lung alone, if P_{ip} is measured) depends very much on the range of frequencies employed. $Z_{rs}(f)$ below about 2 Hz is strongly reflective of the viscoelastic properties of the tissues (Lutchen et al. 1993a, 1994) and, depending on disease state, regional heterogeneities of lung function (Bates 2009; Bates et al. 2011). Variations in $Z_{rs}(f)$ with f above this range are more reflective of the extent to which the imposed oscillations in flow reach the distal regions of the lung as opposed to being confined to more proximal upper airways. This confinement is greatly accentuated when the peripheral airway constricts (Kaczka et al. 1997). Similarly, the most appropriate model of $Z_{rs}(f)$ will depend on the frequency range over which $Z_{rs}(f)$ is measured and on the particular lung pathology involved.

These complications can be avoided by taking a purely empirical approach to the analysis

of $Z_{rs}(f)$. A particularly common such approach is to focus on the values of R_{rs} at specific frequencies such as 5, 15, or 20 Hz and their difference (Goldman et al. 2002; Lipworth and Jabbal 2018), the idea being that elevations in these quantities indicate a general constriction of the airways while an elevation in their difference indicates narrowing predominately in the lung periphery. Similarly, the magnitude of the area under the reactance curve from its lowest value to the resonant frequency has proven to be a robust metric of lung derecruitment which often accompanies obstructive lung disease, particularly after the methacholine challenge (Goldman et al. 2002; Lipworth and Jabbal 2018).

Measuring lung mechanics can also provide clinically useful information in mechanical ventilation patients in whom direct access to the airway provides ideal conditions for applying controlled flows into the lungs while measuring the driving pressures generated at the mouth. Indeed, mechanical ventilation can be considered a form of oscillometry device for which the fundamental frequency of flow oscillation is the number of breaths applied per minute. The higher harmonics of the ventilator waveform may be used for determining $Z_{rs}(f)$ over a range of frequencies, although the spectral content of conventional ventilator waveforms is not generally ideal for this. However, it is possible to use specially designed waveforms that have spectra designed for determining $Z_{rs}(f)$ over specified frequency ranges while still applying effective ventilation to the patient (Lutchen et al. 1993b).

Clinical Applications

Lung mechanics can be measured in any situation in which respiratory volumes, flow, and pressures can be measured (in practice, it is only ever necessary to measure either V or \dot{V} because one can be calculated from the other by differentiation or integration, respectively). All the approaches to lung function assessment discussed above can be applied in an outpatient setting by merely having the subject perform the appropriate maneuver with the appropriate equipment. In the case of spirometry, this means exhaling forcefully through a flow meter. With plethysmography, it means sit-

ting inside a closed chamber while breathing (or attempting to breathe) through a mouthpiece. With oscillometry, it means either breathing through a mouthpiece or remaining apneic for a few seconds, while small-amplitude flow oscillations are directed into the mouth. A nose clip is invariably employed with each technique to ensure that the mouth provides the only access to the lungs. In the case of oscillometry, it is also usual to have the subject support their cheeks with their hands so that as much of the imposed flow oscillations as possible travel into the lungs rather than oscillating structures proximal to the larynx (Bates et al. 2011). If the mechanics of the lungs are required independent of the chest wall then an esophageal balloon must be installed, but even that is relatively innocuous as medical procedures go, so measuring lung mechanics is not particularly arduous for the patient. Importantly, lung mechanics can be measured repeatedly with minimal risk.

Lung mechanics assessment has also found applications during sleep, although obviously, measurements cannot rely on subject cooperation. Oscillometry (Farre et al. 2001) and plethysmography (Bates et al. 2011) have both been successfully used in this application.

Summary

In summary, respiratory volumes, flows, and pressures comprise the fundamental signals from which parameters reflecting respiratory mechanical function are derived. The mainstay of lung function measurement continues to be spirometry which provides the empirical parameters FEV_1 and FVC. These parameters are sensitive to the presence of lung disease but are rather non-specific about the disease itself. Body plethysmography exploits the physics of gases inherent in Boyle's law to provide estimates of the total volume of gas in the lungs and the flow resistance of the airways. These parameters are both directly relatable to physical structures within the lungs and thus begin to link structure to function based on the notion of the lungs behaving like a single alveolar compartment served by a single airway. The single-compartment model also provides the conceptual basis for tissue elas-

tance and resistance that can be determined by fitting a simple equation of motion (Eqs. 32.6 and 32.7) to measurements of volume, pressure, and flow made during cyclic breathing or mechanical ventilation. When the imposed oscillations contain multiple frequencies simultaneously one can determine a function of frequency known as impedance with a real part expressing the apparent resistance of the system and an imaginary part expressing the combined contributions of elastic and inertive components of the system. Interestingly, although spirometry and body plethysmography have been in regular clinical use for decades while oscillometry has remained largely confined to the research arena thus far, all three techniques were introduced to the pulmonary community at roughly the same time (Fry et al. 1954; Dubois et al. 1956a, b).

References

- Bates JHT. Lung mechanics. An inverse modeling approach. Cambridge: Cambridge University Press; 2009.
- Bates JH, Sly PD, Sato J, Davey BL, Suki B. Correcting for the Bernoulli effect in lateral pressure measurements. *Pediatr Pulmonol.* 1992;12(4):251–6.
- Bates JH, Irvin CG, Farre R, Hantos Z. Oscillation mechanics of the respiratory system. *Compr Physiol.* 2011;1(3):1233–72.
- Baydur A, Behrakis PK, Zin WA, Jaeger M, Milic-Emili J. A simple method for assessing the validity of the esophageal balloon technique. *Am Rev Respir Dis.* 1982;126(5):788–91.
- Colebatch HJ, Ng CK, Nikov N. Use of an exponential function for elastic recoil. *J Appl Physiol Respir Environ Exerc Physiol.* 1979;46(2):387–93.
- Dorkin HL, Lutchen KR, Jackson AC. Human respiratory input impedance from 4 to 200 Hz: physiological and modeling considerations. *J Appl Physiol (1985).* 1988;64(2):823–31.
- Dubois AB, Botelho SY, Bedell GN, Marshall R, Comroe JH Jr. A rapid plethysmographic method for measuring thoracic gas volume: a comparison with a nitrogen washout method for measuring functional residual capacity in normal subjects. *J Clin Invest.* 1956a;35(3):322–6.
- Dubois AB, Brody AW, Lewis DH, Burgess BF Jr. Oscillation mechanics of lungs and chest in man. *J Appl Physiol.* 1956b;8(6):587–94.
- Farre R, Rigau J, Montserrat JM, Ballester E, Navajas D. Evaluation of a simplified oscillation technique for assessing airway obstruction in sleep apnoea. *Eur Respir J.* 2001;17(3):456–61.
- Fry DL, Ebert RV, Stead WW, Brown CC. The mechanics of pulmonary ventilation in normal subjects and in patients with emphysema. *Am J Med.* 1954;16(1):80–97.
- Goldman MD, Carter R, Klein R, Fritz G, Carter B, Pachucki P. Within- and between-day variability of respiratory impedance, using impulse oscillometry in adolescent asthmatics. *Pediatr Pulmonol.* 2002;34(4):312–9.
- Irvin CG. Guide to the evaluation of pulmonary function. In: Hamid Q, Shannon J, Martin JG, editors. *Physiologic basis of respiratory disease.* Hamilton: BC Dekker; 2005. p. 649–57.
- Kaczka DW, Ingenito EP, Suki B, Lutchen KR. Partitioning airway and lung tissue resistances in humans: effects of bronchoconstriction. *J Appl Physiol (1985).* 1997;82(5):1531–41.
- Lipworth BJ, Jabbal S. What can we learn about COPD from impulse oscillometry? *Respir Med.* 2018;139:106–9.
- Ludwig MS, Dreshaj I, Solway J, Munoz A, Ingram RH Jr. Partitioning of pulmonary resistance during constriction in the dog: effects of volume history. *J Appl Physiol (1985).* 1987;62(2):807–15.
- Lutchen KR, Kaczka DW, Suki B, Barnas G, Cevenini G, Barbini P. Low-frequency respiratory mechanics using ventilator-driven forced oscillations. *J Appl Physiol (1985).* 1993a;75(6):2549–60.
- Lutchen KR, Yang K, Kaczka DW, Suki B. Optimal ventilation waveforms for estimating low-frequency respiratory impedance. *J Appl Physiol (1985).* 1993b;75(1):478–88.
- Lutchen KR, Suki B, Zhang Q, Petak F, Daroczy B, Hantos Z. Airway and tissue mechanics during physiological breathing and bronchoconstriction in dogs. *J Appl Physiol (1985).* 1994;77(1):373–85.
- Mead J. Problems in interpreting common tests of pulmonary mechanical function. In: Macklem PT, Permutt S, editors. *The lung in transition between health and disease.* New York: Marcell Dekker; 1979. p. 43–52.
- Mead J, Turner JM, Macklem PT, Little JB. Significance of the relationship between lung recoil and maximum expiratory flow. *J Appl Physiol.* 1967;22(1):95–108.
- Salazar E, Knowles JH. An analysis of pressure-volume characteristics of the lungs. *J Appl Physiol.* 1964;19:97–104.
- Sato J, Davey BL, Shardonofsky F, Bates JH. Low-frequency respiratory system resistance in the normal dog during mechanical ventilation. *J Appl Physiol (1985).* 1991;70(4):1536–43.
- Similowski T, Bates JH. Two-compartment modelling of respiratory system mechanics at low frequencies: gas redistribution or tissue rheology? *Eur Respir J.* 1991;4(3):353–8.
- Wilson T, Rodarte J, Butler J. Wave-speed and viscous flow limitation. In: Macklem P, Mead J, editors. *Handbook of physiology section 3: the respiratory system.* Bethesda: American Physiological Society; 1986. p. 55–61.



Measurement of Pleural Pressure

33

Nadia Corcione, Francesca Dalla Corte,
and Tommaso Mauri

Esophageal Pressure as an Estimate of Pleural Pressure

In 1949, Buytendijk introduced the method of esophageal pressure measurement for studying the mechanics of active breathing (Buytendijk 1949). Being a collapsible empty cavity between the lungs and chest wall, the esophagus was thought to reflect pressures similar to the pleural cavity. Subsequent experimental findings confirmed that changes in pleural pressure (Ppl) were closely correlated to changes in esophageal pressure (Pes) (Dornhorst and Leathart 1952; Cherniack et al. 1955). Absolute values of pressures in the pleural space are often lower than in those measured in the esophagus, especially for gravitationally nondependent regions, but Pes measurements give good estimates of the effective Ppl in healthy, upright subjects (Washko et al. 2006; Fry et al. 1952). Moreover, recent studies have shown that Pes accurately reflects absolute Ppl values of the collapsed dependent lung regions in experimental acute lung injury and in cadavers (Yoshida et al. 2018).

Positioning of the Esophageal Balloon

Pes is measured with an air-filled catheter that terminates in a 1.5 ml balloon. The catheter is introduced through the nose or mouth and advanced until it reaches the stomach (approximately 50–55 cm from the nares in an adult). Then, the balloon is filled with a standard volume of air according to the manufacturer's recommendations. This usually is 1–2 ml for smaller balloons and 3–4 ml for larger ones. The intragastric position of the esophageal balloon is confirmed by a positive pressure deflection during gentle external manual compression of the abdomen. The balloon then is withdrawn until cardiac artifacts appear, and there are negative inspiratory swings on the pressure tracings. This corresponds to placement in the lower third of the esophagus. Standard balloons are 10 cm long, and the catheter has multiple side holes within the balloon (Mauri et al. 2016).

Calibration

In 1982, Baydur and Colleagues described “the occlusion test” procedure for correct positioning of the esophageal balloon in active subjects (Baydur et al. 1982). The occlusion test allows subjects to perform static voluntary inspiratory efforts (glottis open) against a closed airway, and

N. Corcione · F. D. Corte · T. Mauri (✉)
Department of Anesthesia, Critical Care and
Emergency, Fondazione IRCCS Ca' Granda Ospedale
Maggiore Policlinico, University of Milan,
Milan, Italy
e-mail: francesca.dallacorte@student.unife.it;
tommaso.mauri@unimi.it

a comparison is made between the change in esophageal pressure (ΔP_{es}) and the corresponding change in airway pressure (ΔP_{aw}). In the lower third of the esophagus, approximately 10 cm above the gastroesophageal junction, and in the absence of airflow and change in lung volume, the ratio $\Delta P_{es}/\Delta P_{aw}$ should be close to unity (1.0 ± 0.2). If $\Delta P_{es}/\Delta P_{aw}$ is between 0.8 and 1.2, measurements of lung mechanics based on esophageal pressure changes are considered accurate and valid (Brochard 2014; Yoshida and Brochard 2018). It must be noted that esophageal balloon inflation plays an important role. When the balloon is inflated with too little air, the positive pressure in the esophagus on inspiration will empty the balloon, and the measured pressure will be an underestimate of Ppl. Conversely, if the balloon is inflated with too much air, it will distend the esophagus and stress the balloon so that the measured pressure will overestimate Ppl. The minimal non-stressed balloon volume should be used to measure P_{es} accurately; the range of appropriate filling volumes is catheter-specific and should be carefully checked before catheter positioning (Brochard 2014).

Technical Pitfalls

Many factors can cause artifactual differences between P_{es} and regional Ppl. These include variations unrelated to Ppl, depending on postural artifacts, on the position of the balloon in the esophagus, or on the volume of air inside the balloon. Moreover, due to the effect of gravity, in an upright individual, Ppl at the base of the lung is greater (less negative) than at the apex. In the supine position, lung volume is decreased in the dependent zones, and the abdominal contents compress the dependent lung, resulting in an increased gravitational Ppl gradient (Hubmayr et al. 1983; Mead and Gaensler 1959). At low lung volumes, Ppl can even be locally positive (Washko et al. 2006). Furthermore, in the supine position, the esophagus is compressed by the overlying mediastinal structures, which potentially can increase P_{es} values. As reported by physiological studies, in the upright and prone positions, the lung's inherent shape is close to

that of its container, the gravitational Ppl gradient is low, and the lung compliance (C_L) is high. Neither prone nor upright positions cause the compression of the dependent lung by the heart that occurs in the supine position. In summary, the pleural cavity is characterized by differences in regional pressures, while P_{es} reflects the pressure only corresponding to one region of the pleural space (Plataki and Hubmayr 2011).

Clinically Relevant Measures

The main clinical applications of P_{es} measurement are (Mauri et al. 2016):

1. To estimate the transpulmonary pressure (P_L)
2. To assess patient's effort when the respiratory muscles are active
3. To monitor patient-ventilator interaction

Transpulmonary Pressure

Mechanical ventilation can, per se, cause lung injury. The so-called ventilator-induced lung injury (VILI) is a dysregulated inflammatory response due to an excessive volume and pressure load imposed on ventilated lung regions along with the cyclic opening and closing of distal airways and collapsed alveoli during tidal ventilation. VILI can result in worsening hypoxemia and multi-organ dysfunction, which increases the mortality of patients affected by hypoxemic respiratory failure (Grieco et al. 2017). Reducing VILI is a key goal in the management of acute respiratory distress syndrome (ARDS) ventilatory management. In a pioneering single-center study, Amato and Colleagues were the first to show a reduction in mortality in patients with ARDS when using a strategy based on achieving low tidal volume (V_t) (6 mL/Kg), high positive end-expiratory (PEEP), and low inspiratory driving pressures (< 20 cmH₂O) (Amato et al. 2015). Driving pressure (DP) is the difference between the static airway pressure at the end of inspiration (plateau pressure, P_{plat}) and total positive end-expiratory pressure (PEEP). In turn, static compliance of the respiratory system (C_{RS}) is the ratio between V_t and DP:

$$C_{RS} = Vt / P_{plat} - PEEP \gg C_{RS} = Vt / DP \gg DP = Vt / C_{RS}$$

Thus, DP represents the Vt corrected for the patient's C_{RS} , and using DP as a safety limit may be more accurate than Vt to decrease VILI in ARDS patients. However, DP reflects a force acting on two different structures: lung and chest wall. Thus, because airway pressure (Paw) is the sum of pressures across both the lung and chest wall, the portion of the pressure applied to the lung varies widely, depending on chest wall characteristics. Lungs inflate and deflate in response to changes in transpulmonary pressure (P_L), which is the pressure difference between the airway opening (Pao) and the pleural space:

$$P_L = +Pao - Ppl$$

In the absence of flow (i.e., during an end-inspiratory occlusion maneuver to obtain Pplat or an end-expiratory occlusion maneuver to measure total PEEP), Pao corresponds to the Paw measured by the ventilator at airway opening, which in turn is equal to the pressure inside the alveoli. The potential for damage to the lungs caused by mechanical ventilation depends on the magnitude of P_L . (Mauri et al. 2016) The measurement of Pes as an estimate of Ppl can represent the only way to distinguish what fraction of Paw is applied to the lung and chest wall (Keller and Fessler 2014). In critically ill patients, chest wall elastance (E_{CW}) is often increased by many factors including obesity, increased intra-abdominal pressure, the effect of drugs, and fluid overload, which cause chest wall edema (Brochard 2014; Gattinoni et al. 2004); in the presence of these alterations, Paw overestimates the pressure applied to the lungs and can limit optimal lung recruitment.

Two different methods have been proposed to estimate P_L from Pes (Mauri et al. 2016). The first method is based on the absolute value of Pes as a surrogate for absolute Ppl. By this method, P_L is directly calculated as follows:

$$P_L = Paw - Ppl$$

That is,

$$P_L = P_{plat} - P_{es}$$

This “static” P_L decreases progressively from nondependent to dependent lung region in the supine position, because of gravitational edema and reduction of lung volume. At very low lung volume, such as what occurs in ARDS, Ppl can be locally positive in the dependent lung, and thus, P_L can be a negative value. This phenomenon exposes the unstable, collapsed alveoli that needs to be repeatedly opened and re-collapsed with each tidal breath and an increased shunt fraction. In the presence of closed airway and flooded or atelectatic lung, raising PEEP until P_L becomes positive at end-expiration could avoid cyclic alveolar recruitment and de-recruitment and assure that airways remain open. In a phase-2 randomized controlled trial, Talmor et al. assigned patients with ARDS to undergo mechanical ventilation with PEEP adjusted to obtain positive end-expiratory absolute P_L values (intervention group) or according to the ARDS Network PEEP/FiO₂ titration tables (control group) (Talmor et al. 2008). The primary endpoint was the improvement in oxygenation. The intervention group had both significantly improved oxygenation and respiratory system compliance. Moreover, these improvements were achieved without elevating transpulmonary pressure at end-inspiration above the physiologic range. P_L during end-inspiratory occlusion never exceeded 24 cmH₂O. More recently, the same group conducted a larger multicenter randomized controlled trial comparing PEEP set by positive transpulmonary pressure at end-expiration vs. a high PEEP/FiO₂ table method. The study enrolled 200 patients, but the results weren't as encouraging: the mortality and ventilation days didn't differ as well as most secondary endpoints. However, the average PEEP and end-expiratory transpulmonary pressure were similar in the two groups, questioning whether the study really compared two different strategies for PEEP titration (Beitler et al. 2019). Moreover, P_L measured from absolute Pes does not assure that VILI is prevented in lung regions that are not near to the

esophagus. This is particularly true in ARDS in which the lung involvement is heterogeneous and not symmetric. In ARDS, it's reasonable to expect that in lung regions below the level of esophageal balloon, Ppl will be underestimated, whereas in lung regions above the level of esophageal balloon, Ppl will be lower than Pes. Even if PEEP is titrated to optimize the lung volume at the level of the esophagus, lung regions elsewhere likely are under- or overinflated (Talmor and Fessler 2010).

The second method is based on the assumption that the ratio of lung elastance (E_L) to respiratory system elastance (E_{RS}) determines the fraction of DP needed to expand the lung. Physiologically, E_L/E_{RS} is around 0.5, but in ARDS, it ranges from 0.2 to 0.8. The ratio of lung elastance to respiratory system elastance (E_L/E_{RS}) may be used to calculate transpulmonary pressure and guide the “open lung” ventilation approach. In this method, P_L is calculated as follows:

$$\Delta P_L = P_{aw} \times E_L / E_{RS}$$

where E_{RS} is calculated as the DP/Vt in liter ratio at the set PEEP level and ΔP_L is the true indicator of inspiratory lung stress (Fig. 33.1). In a case series of patients with severe ARDS and who were candidates for ECMO, Grasso et al.

increased end-inspiratory P_L as calculated by the elastance ratio method up to the physiologic threshold of 25 cmH₂O, and this improved oxygenation and prevented the use of ECMO without signs of barotrauma (Grasso et al. 2012).

Patient's Effort When the Respiratory Muscles Are Active

The main goal of assisted mechanical ventilation is to permit spontaneous breathing but with a reduction of the patient's work of breathing (WOB). Compared to controlled mechanical ventilation, spontaneous breathing has some advantages: oxygenation is generally better because of recruitment of the juxta-diaphragmatic lung region, respiratory muscle atrophy is avoided, and the breathing pattern is variable (“noisy”), unlike the monotonous ventilator pattern. However, uncontrolled patient efforts which correspond to negative Pes deflections (Fig. 33.2) can cause additional lung injury. This is known as patient self-inflicted lung injury (P-SILI). (Li et al. 2017) Because of the large variability in the negative inspiratory Ppl that can occur with large variability in patient efforts, airway pressure delivered by the ventilator is a poor indicator of the inspiratory stress determined by the ΔP_L .

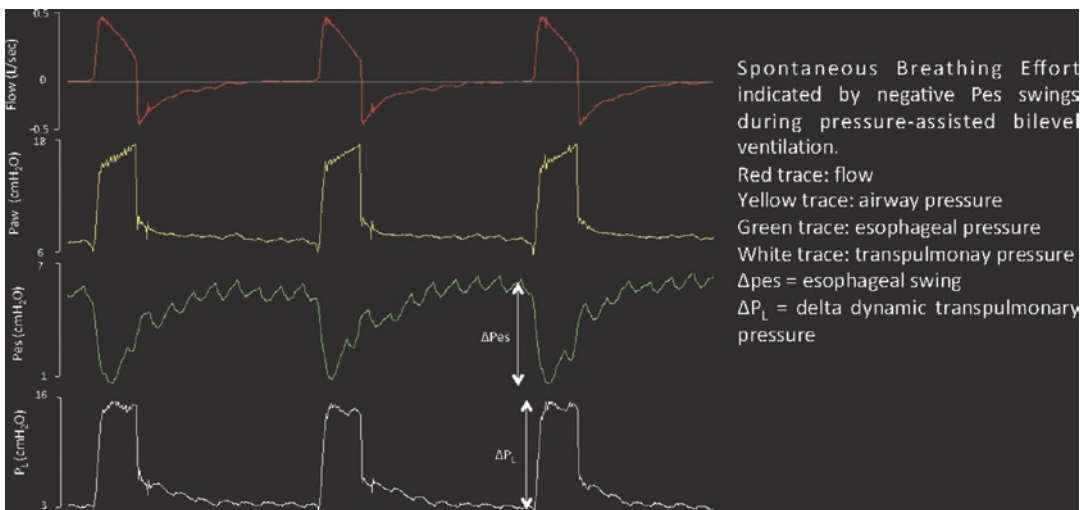


Fig. 33.1 Esophageal pressure monitoring and relevant derived measures during controlled ventilation

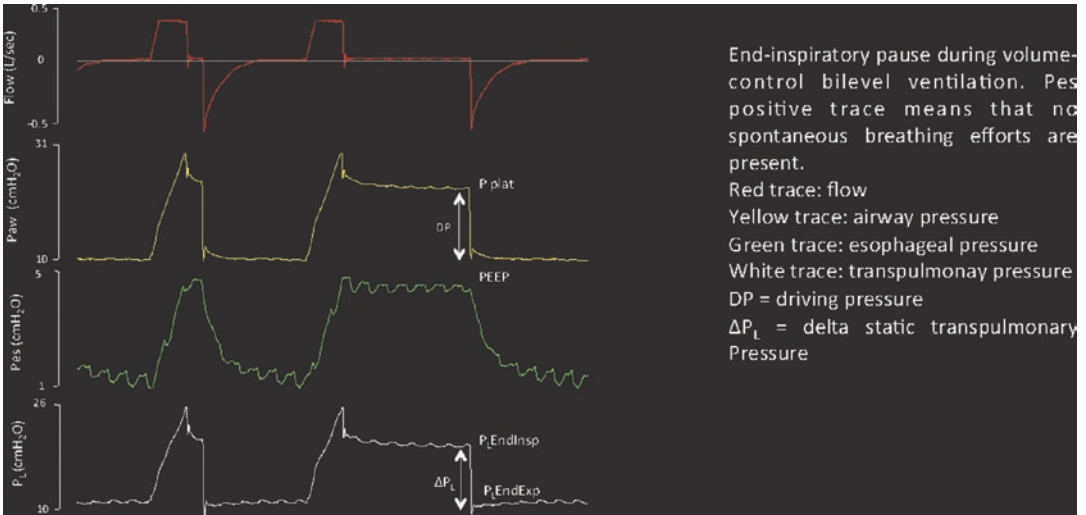


Fig. 33.2 Esophageal pressure monitoring and relevant derived measures during assisted ventilation

$$\Delta P_L = DP \times +E_L / E_{is}$$

For this reason, the difference between peak airway pressure and PEEP in pressure-target mode with active triggering cannot be taken as an approximation of driving pressure. Furthermore, in the injured, “solid-like” lung, the inspiratory Ppl swing is localized more in dependent regions and with the higher regional stress can damage lung tissues (Yoshida et al. 2013, 2016). Negative, vigorous Ppl swings increase transmural vascular pressure and favor lung edema and worse hypoxemia. Hence, monitoring Pes swings in ARDS patients with assisted mechanical ventilation is highly recommended. According to the PLUG working group recommendations in these patients, end-inspiratory dynamic P_L should be less than 20–25 cmH₂O with inspiratory P_{eo} from muscle effort in the 5–10 cmH₂O range (Mauri et al. 2016).

Patient-Ventilator Interaction

As widely reported in literature, poor patient-ventilator interaction worsens lung injury, causes discomfort and dyspnea, increases the need for sedative and paralytic agents, prolongs mechanical ventilation and intensive care unit length of

stay, and increases the likelihood of respiratory muscle injury and the need for a tracheostomy (Murias et al. 2016). As reported by Blanch et al., in a large, prospective, non-interventional observational study, respiratory asynchronies are associated with mortality, although further studies are needed to know whether an elevated asynchrony index is just a marker of the severity or whether it constitutes a cause of higher mortality (Blanch et al. 2015).

Major asynchronies can be classified as follows (Mellott et al. 2014):

1. Diaphragmatic muscle contractions triggered by ventilator insufflations constitute a form of patient-ventilator interaction referred to as “entrainment.” This phenomenon is frequent in deeply sedated patients, and it is called reverse triggering, because the insufflation triggers respiratory muscle contraction. Reverse triggering results in breath stacking and high V_t and increased oxygen consumption. It is usually very difficult to recognize in critically ill patients, but it becomes easy to recognize if respiratory muscle activity is monitored by the measurement of Pes.
2. Ineffective efforts are recognized by a negative Pes swing without ventilator pressurization. It can be caused by the presence of

auto-PEEP and/or excessive support, and it is aggravated by the trigger setting being set too low (if pressure-based) or too high (if flow-based).

3. Double triggering is the result of the ventilator inspiratory time (T_i) being shorter than the patient's inspiratory time. The patient's effort then continues after the first cycle and can trigger a second ventilator breath. In this case, a single Pes deflection can persist for two or even three breaths delivered by the ventilator.
4. Auto-triggering is defined as a cycle delivered by the ventilator without inspiratory effort by the patient. It is often due to an air leak, cardiac artifacts, or secretions. Auto-triggering is recognized by the absence of negative Pes swing preceding a mechanical breath.
5. Premature cycling is defined as a cycle in which the ventilator's inspiratory time, T_i , is shorter than the neural T_i . This is seen as the duration of Pes deflection being longer than the ventilator's inspiratory time.
6. Delayed cycling occurs when the machine T_i is longer than the neural T_i (i.e., longer than the duration of Pes deflection).

Understanding how to place an esophageal balloon, the limitations of the measurements, and potential artifacts can lead to the improved matching of ventilator settings to patient's physiology and safer management of ventilated patients. Monitoring Pes allows the early detection of asynchronies, which can help physicians optimize ventilatory settings and to titrate sedation. Esophageal pressure allows better titration of PEEP by identifying positive transpulmonary pressure at the end of expiration and/or excessive transpulmonary pressure at end-inspiration. Finally, it may especially have a value by avoiding potentially large transpulmonary pressures due to uncontrolled patient efforts.

Authors' Contribution NC, FDC, and TM conceived and drafted the text; all authors approved the final draft of the report.

Conflicts of Interest None

References

- Amato MB, Meade MO, Slutsky AS, Brochard L, Costa EL, Schoenfeld DA, Stewart TE, Briel M, Talmor D, Mercat A, Richard JC, Carvalho CR, Brower RG. Driving pressure and survival in the acute respiratory distress syndrome. *N Engl J Med*. 2015;372(8):747–55.
- Baydur A, Behrakis PK, Zin WA, Jaeger M, Milic-Emili J. A simple method for assessing the validity of the esophageal balloon technique. *Am Rev Respir Dis*. 1982;126(5):788–91.
- Beitler JR, Sarge T, Banner-Goodspeed VM, Gong MN, Cook D, Novack V, Loring SH, Talmor D. EPVent-2 Study Group. Effect of titrating positive end-expiratory pressure (PEEP) with an esophageal pressure-guided strategy vs an empirical high PEEP-Fio₂ strategy on death and days free from mechanical ventilation among patients with acute respiratory distress syndrome: a randomized clinical trial. *JAMA*. 2019. <https://doi.org/10.1001/jama.2019.0555>.
- Blanch L, Villagra A, Sales B, Montanya J, Lucangelo U, Luján M, García-Esquirol O, Chacón E, Estruga A, Oliva JC, Hernández-Abadía A, Albaiceta GM, Fernández-Mondejar E, Fernández R, Lopez-Aguilar J, Villar J, Murias G, Kacmarek RM. Asynchronies during mechanical ventilation are associated with mortality. *Intensive Care Med*. 2015;41(4):633–41.
- Brochard L. Measurement of esophageal pressure at bedside: pros and cons. *Curr Opin Crit Care*. 2014;20(1):39–46.
- Buytendijk JH. Intraesophageal pressure and lung elasticity [thesis]. Groningen: University of Groningen; 1949.
- Cherniack RM, Farhi LE, Armstrong BW, Proctor DF. A comparison of esophageal and intrapleural pressure in man. *J Appl Physiol*. 1955;8(2):203–11.
- Dornhorst AC, Leathart GL. A method of assessing the mechanical properties of lungs and air-passages. *Lancet*. 1952;2(6725):109–11.
- Fry DL, Stead WW, Ebert RV, Lunin RI, Wells HS. The measurement of intraesophageal pressure and its relationship to intrathoracic pressure. *J Lab Clin Med*. 1952;40:664–73.
- Gattinoni L, Chiumello D, Carlesso E, Valenza F. Bench-to-bedside review: chest wall elastance in acute lung injury/acute respiratory distress syndrome patients. *Crit Care*. 2004;8(5):350–5.
- Grasso S, Terragni P, Birocco A, Urbino R, Del Sorbo L, Filippini C, Mascia L, Pesenti A, Zangrillo A, Gattinoni L, Ranieri VM. ECMO criteria for influenza a (H1N1)-associated ARDS: role of transpulmonary pressure. *Intensive Care Med*. 2012;38(3):395–403.
- Grieco DL, Chen L, Brochard L. Transpulmonary pressure: importance and limits. *Ann Transl Med*. 2017;5(14):285.
- Hubmayr RD, Walters BJ, Chevalier PA, Rodarte JR, Olson LE. Topographical distribution of regional lung volume in anesthetized dogs. *J Appl Physiol*. 1983;54:1048–56.

- Keller SP, Fessler HE. Monitoring of oesophageal pressure. *Curr Opin Crit Care*. 2014;20(3):340–6.
- Li HL, Chen L, Brochard L. Protecting lungs during spontaneous breathing: what can we do? *J Thorac Dis*. 2017;9(9):2777–81.
- Mauri T, Yoshida T, Bellani G, Goligher EC, Carreaux G, Rittayamai N, Mojoli F, Chiumello D, Piquilloud L, Grasso S, Jubran A, Laghi F, Magder S, Pesenti A, Loring S, Gattinoni L, Talmor D, Blanch L, Amato M, Chen L, Brochard L, Mancebo J, PLeUral pressure working Group (PLUG—Acute Respiratory Failure section of the European Society of Intensive Care Medicine). Esophageal and transpulmonary pressure in the clinical setting: meaning, usefulness and perspectives. *Intensive Care Med*. 2016;42(9):1360–73.
- Mead J, Gaensler EA. Esophageal and pleural pressures in man, upright and supine. *J Appl Physiol*. 1959;14:81–3.
- Mellott KG, Grap MJ, Munro CL, Sessler CN, Wetzel PA, Nilsestuen JO, Ketchum JM. Patient ventilator asynchrony in critically ill adults: frequency and types. *Heart Lung*. 2014;43(3):231–43.
- Murias G, Lucangelo U, Blanch L. Patient-ventilator asynchrony. *Curr Opin Crit Care*. 2016;22(1):53–9.
- Plataki M, Hubmayr RD. Should mechanical ventilation be guided by esophageal pressure measurements? *Curr Opin Crit Care*. 2011;17(3):275–80.
- Talmor DS, Fessler HE. Are esophageal pressure measurements important in clinical decision-making in mechanically ventilated patients? *Respir Care*. 2010;55(2):162–72; discussion 172–4.
- Talmor D, Sarge T, Malhotra A, O'Donnell CR, Ritz R, Lisbon A, Novack V, Loring SH. Mechanical ventilation guided by esophageal pressure in acute lung injury. *N Engl J Med*. 2008;359(20):2095–104.
- Washko GR, O'Donnell CR, Loring SH. Volume-related and volume-independent effects of posture on esophageal and transpulmonary pressures in healthy subjects. *J Appl Physiol* (1985). 2006;100(3):753–8.
- Yoshida T, Brochard L. Esophageal pressure monitoring: why, when and how? *Curr Opin Crit Care*. 2018;24(3):216–22.
- Yoshida T, Torsani V, Gomes S, De Santis RR, Beraldo MA, Costa EL, Tucci MR, Zin WA, Kavanagh BP, Amato MB. Spontaneous effort causes occult pendelluft during mechanical ventilation. *Am J Respir Crit Care Med*. 2013;188(12):1420–7.
- Yoshida T, Roldan R, Beraldo MA, Torsani V, Gomes S, De Santis RR, Costa EL, Tucci MR, Lima RG, Kavanagh BP, Amato MB. Spontaneous effort during mechanical ventilation: maximal injury with less positive end-expiratory pressure. *Crit Care Med*. 2016;44(8):e678–88.
- Yoshida T, Amato MBP, Grieco DL, Chen L, Lima CAS, Roldan R, Morais CCA, Gomes S, Costa ELV, Cardoso PFG, Charbonney E, Richard JM, Brochard L, Kavanagh BP. Esophageal manometry and regional transpulmonary pressure in lung injury. *Am J Respir Crit Care Med*. 2018;197(8):1018–26.



Ultrasound Assessment of the Lung

34

Alberto Goffi, Emanuele Pivetta,
and Richelle Kruisselbrink

Abbreviations

ARDS	Acute respiratory distress syndrome
CT	Computed tomography
CXR	Chest radiography
HRCT	High-resolution CT
ILDs	Interstitial lung diseases
LUS	Lung ultrasound
MHz	Millions of cycles/sec

A. Goffi (✉)

Interdepartmental Division of Critical Care Medicine,
University of Toronto, Toronto, ON, Canada

Department of Medicine and Department of Critical
Care Medicine, St. Michael's Hospital,
Toronto, ON, Canada

Li Ka Shing Knowledge Institute, St. Michael's
Hospital, Toronto, ON, Canada
e-mail: alberto.goffi@uhn.ca

E. Pivetta

Division of Emergency Medicine and High
Dependency Unit, Department of Medical Sciences,
University of Turin, Turin, Italy

Cancer Epidemiology Unit and CRPT U, Department
of Medical Sciences, University of Turin, Turin, Italy
e-mail: emanuele.pivetta@unito.it

R. Kruisselbrink

Department of Anesthesia, Grand River Hospital and
St. Mary's General Hospital, Kitchener, ON, Canada

Department of Anesthesia, McMaster University,
Hamilton, ON, Canada
e-mail: Richelle.kruisselbrink@medportal.ca

Introduction

Lung ultrasound (LUS) is a point-of-care modality that can be effectively used at the bedside for patients with respiratory signs and symptoms, in both diagnostic and monitoring roles (Volpicelli et al. 2012; Kendall et al. 2007; Kruisselbrink et al. 2017; Goffi et al. 2018). When performed in an organized and protocol-based fashion, LUS is accurate, reproducible and repeatable.

Principles

Basic Physics of Ultrasound

Ultrasound systems are devices that generate and receive high-frequency (MHz - i.e., millions of cycles/sec) sound waves by activating piezoelectric materials contained within ultrasound transducers. Upon leaving the transducer, these high-frequency waves propagate through biological tissues in straight lines until they encounter tissues with different acoustic properties (i.e., acoustic impedance). When such a boundary between tissues of different acoustic impedance is reached, a fraction of the ultrasound energy is reflected back to the transducer (“*reflection*”), while the remainder continues to travel. As ultrasound waves travel, they undergo loss of energy due to absorption and scattering (“*attenuation*”), and therefore gradually disappear as

they propagate linearly through the tissues. The degree of attenuation depends both on ultrasound frequency (e.g., higher-frequency attenuated more than lower-frequency ultrasounds) and characteristics of the conducting medium (e.g., greatest attenuation in air and bone) (Bertrand et al. 2016; Goffi et al. 2018; Aldrich 2007; Edelman 2012) (Fig. 34.1a). Finally, the speed at which ultrasound waves travel is determined only by the insonated medium and not affected by the frequency or other characteristics of the ultrasounds. In biological tissues, ultrasound propagation speeds range between 500 and 3000 m/sec; however, except for aerated lungs and bone, the average speed of sounds in soft tissues is very similar, approximately 1540 m/sec.

The image generated when a reflected ultrasound wave returns to the transducer depends

mainly on the total travel time and the intensity of reflection. (1) The elapsed time from ultrasound generation to reception (“*time of flight*”) depends on propagation speed (that in diagnostic ultrasound is essentially constant at approximately 1540 m/s) and the tissue depth at which the waves are reflected. The greater the elapsed time (or tissue depth), the lower the returning echo will appear on the screen. (2) The intensity of reflection depends on the angle at which the sound wave encounters a tissue boundary and the relative impedance of both tissues. Reflection intensity determines the brightness of the generated image, with weaker reflections appearing as darker gray pixels (hypoechoic structures) and stronger reflections as white pixels (hyperechoic structures). Areas that do not reflect ultrasound (i.e., no difference in acoustic impedance) will

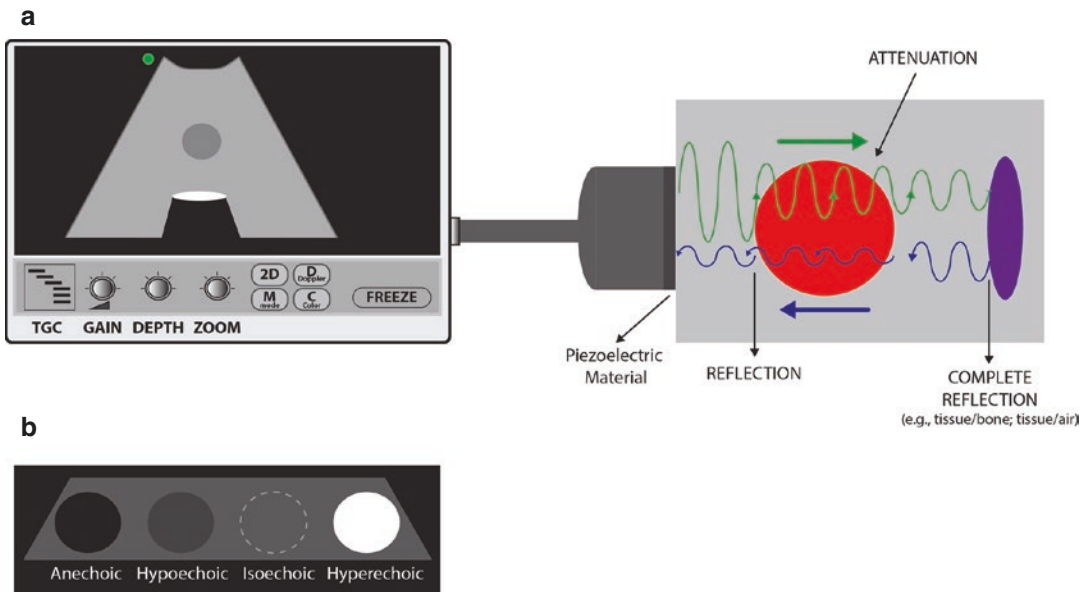


Fig. 34.1 (a, b) Physics of Ultrasound. (a) High-frequency sound waves (ultrasounds) are generated by activating piezoelectric materials contained inside ultrasound transducers. Upon leaving the transducer, these high-frequency waves propagate through biologic tissues in straight lines until they encounter a tissue with different acoustic impedance. When such a boundary between tissues of different acoustic impedance is reached, a fraction of the ultrasound energy is reflected back to the transducer (“*reflection*”), while the remainder continues to travel further. As ultrasound waves travel, they undergo loss of energy due to absorption and scattering (“*attenuation*”),

and therefore gradually disappear as they propagate linearly through the tissues. (b) The intensity of reflection that occurs at a tissue interface determines the brightness of the generated image: areas that do not reflect ultrasound appear black on the ultrasound screen (anechoic structures); areas with weaker reflections appear as darker gray pixels (hypoechoic structures), while areas with similar reflection as surrounding structures appear of the same gray intensity (isoechoic structures). Finally, stronger reflections are represented as increasingly white pixels (hyperechoic structures)

appear black on the ultrasound screen (anechoic structures) (Bertrand et al. 2016; Goffi et al. 2018; Edelman 2012) (Fig. 34.1b).

Erroneous images may be generated due to interactions of ultrasound waves with tissues, physical properties of the ultrasound beam, and specific image reconstruction algorithms. These ultrasound artifacts affect quality of images and, if not recognized, may lead to misinterpretation (Bertrand et al. 2016; Feldman et al. 2009; Edelman 2012). Most ultrasound modalities aim at avoiding these artifacts, with newer ultrasound systems designed to minimize them as much as possible. However, in LUS, as discussed below, artifacts are a valuable source of information and should be systematically analyzed together with more anatomical images (Kruisselbrink et al. 2017; Volpicelli et al. 2012; Goffi et al. 2018).

Ultrasound Systems

Although ultrasound machines can vary in appearance with respect to size, apparatus design, and available system controls, all of them share three key components: transducer, micro-processor, and screen.

The transducer, containing the piezoelectric material, is the gateway allowing tissue evaluation; it is essential not only for the generation and propagation of waves but also for the acquisition of information coming from the returning echoes. Many types of transducers are available, varying primarily in footprint size, frequency of vibration of the piezoelectric material and overall shape (allowing access to different body structures, including intracavitary applications such as transesophageal echocardiography). Three transducers are typically used for LUS, depending on the clinical question (Alrajab et al. 2013). Linear probes use higher frequencies (usually 13–8 MHz) and generate rectangular-shaped high-resolution images that are limited in depth. These transducers are used to evaluate superficial structures such as the chest wall, pleural line, and subpleural space, especially when

high-resolution details are needed. By contrast, curvilinear and phased-array transducers use lower frequencies (5–2 and 3–1 MHz, respectively) and generate triangular-shaped images with increased depth but decreased resolution. With these transducers, superficial structures are still recognizable but with fewer details than provided by linear probes. Low-frequency transducers are used when information regarding deeper structures is needed, such as characterization of large pulmonary consolidations, assessment and quantification of pleural effusion, and interstitial syndrome (see below).

Effectiveness of bedside ultrasonography is closely related to the quality of images obtained. Every ultrasound machine allows the operator to optimize the image by performing several system adjustments. Two key modifications are scanning depth and gain adjustment. Modifying the depth of the insonated area allows better visualization of specific regions of interest. For example, to rule out pneumothorax with LUS, adequate visualization of the pleural line is essential (see below); therefore, depth should be adjusted (often reduced) to best visualize the pleura and minimize visualization of deeper structures. On the other hand, adequate characterization of a large pleural effusion will require setting an appropriately deep field to allow identification of the entire effusion and the underlying consolidated lung. The gain control modulates the intensity of returned echoes as shown on the screen. By increasing the gain, images displayed on the screen appear brighter, while decreasing the gain causes the image display to darken. Gain adjustment facilitates identification of structures and boundaries; for example, adequate gain adjustment may facilitate identification of two key movements of the pleural line, sliding and pulse.

Lung Ultrasound Findings

Normal and pathologic findings are summarized in Table 34.1.

Table 34.1 Lung Ultrasound Findings

Sonographic Findings	Definition	Clinical significance
Lung Sliding	Shimmering movement synchronous with respiration at the pleural line indicating sliding of the visceral pleura against the parietal pleura.	<p><i>Present in normal lung</i> or in <i>pathological conditions that do not affect ventilation</i></p> <p><i>Absent</i> or <i>reduced</i> when visceral pleura does <i>not slide</i> against parietal pleura: apnea, inflammatory adherences, loss of lung expansion (over-inflation/distension or severe bullous disease), decrease in lung compliance, airway obstruction/atelectasis, pleural symphysis, selective intubation</p> <p><i>Absent</i> when visceral and parietal pleura are <i>separated</i> (i.e., pneumothorax)</p>
Lung Pulse	Subtle, rhythmic movement of the lung parenchyma at the cardiac frequency from transmission of heartbeat vibrations through the lung tissue.	<p><i>Present in normal lung</i> and conditions with minimal effect on lung aeration (e.g., pulmonary embolism)</p> <p><i>Absent</i> or <i>reduced</i> when <i>lung aeration is significantly increased</i> (e.g., bullous disease, over-inflation/distension)</p> <p><i>Absent</i> when visceral and parietal pleura are <i>separated</i> (i.e., pneumothorax)</p> <p><i>Increased</i> in conditions associated with <i>increased lung density</i> (see B-lines and interstitial syndrome)</p> <p><i>Note:</i> Identification of lung pulse in the context of absent lung sliding is considered a <i>sign of lack of ventilation</i> as seen in apnea, selective intubation, airway obstruction (foreign body, mucous plugging, etc.)</p>
A-lines	Hyperechoic horizontal lines at increasing depth separated by same distance as that between the probe and the pleural line. Considered reverberation artifacts arising from the strongly reflective interfaces of the probe and pleural line.	<p><i>Present when air is homogeneously distributed below the pleural line:</i></p> <ul style="list-style-type: none"> Normally aerated lung Pneumothorax Pathological conditions with minimal effect on lung aeration (e.g., acute pulmonary embolism, asthma/acute COPD exacerbation, early phases of airway obstruction/atelectasis) <p><i>Absent</i> or <i>reduced</i> when:</p> <ul style="list-style-type: none"> Increased lung density and nonhomogeneous distribution of air Nonperpendicular angulation of the ultrasound beam with the pleural line

Table 34.1 (continued)

Sonographic Findings	Definition	Clinical significance
B-lines and Interstitial Syndrome	<p>Discrete laser-like, vertical, hyperechoic artifacts that arise from the pleural line, extend to the bottom of the screen without fading, and move synchronously with lung sliding (Volpicelli et al. 2012). Three or more B-lines/intercostal space (sagittal scan) represent a positive region of increased lung density (Volpicelli et al. 2012):</p> <p><i>Normal aeration</i>: presence of ≤ 2 isolated B-lines/intercostal space; <i>Moderate loss of lung aeration (B1 pattern)</i>: presence of ≥ 3 well-defined spaced B-lines/intercostal space; <i>Severe loss of lung aeration (B2 pattern)</i>: multiple coalescent B-lines/intercostal space (Bouhemad et al. 2011; Soummer et al. 2012).</p> <p>Vertical artifacts at the transition from consolidated to normally aerated lung (“shred sign”) represent the same physical and pathophysiological phenomenon as B lines, although not defined as such (Volpicelli et al. 2012).</p>	<p><i>Present</i> in conditions associated with <i>increased lung density</i> and involvement of alveolar units in close relationship with visceral pleura such as: <i>Lung deflation</i> (i.e., atelectasis)</p> <p>Normal pattern (if isolated at lung bases)</p> <p><i>Increased lung weight</i>:</p> <p>Extra Vascular Lung Water (EVLW) (e.g., cardiogenic or nonhydrostatic pulmonary edema – ARDS, idiopathic interstitial pneumonias, lung consolidation, pneumonitis, pulmonary infarct)</p> <p>Pus (e.g., infection, pneumonitis, lung consolidation)</p> <p>Blood (e.g., alveolar hemorrhage)</p> <p>Protein/Collagen (e.g., idiopathic interstitial pneumonias, alveolar proteinosis, lung consolidation, pulmonary infarct)</p> <p>Cells (e.g., primary or metastatic lung cancer)</p> <p>Lipids (e.g., lipoid pneumonia)</p> <p><i>Absent</i> when visceral and parietal pleura are <i>separated</i> (i.e., pneumothorax) and <i>in normally aerated lung</i></p>
Short vertical artifacts (also known as Z lines or comet tails)	Vertical artifacts that originate from and move with the pleural line but fade quickly; do not obscure A-lines.	<p><i>Present</i> in <i>normal lungs</i></p> <p><i>Absent</i> when visceral and parietal pleura are <i>separated</i> (i.e., pneumothorax)</p>
Lung Point	Presence of lung sliding, pulse and/or vertical artifacts on one side of an image with the absence of these findings on the other side.	<p><i>Present</i> and <i>very specific</i> in <i>pneumothorax</i>, representing transition point at which partially collapsed lung contacts the parietal pleura during respiration.</p> <p><i>Absent</i> in presence of <i>large pneumothorax</i> causing complete lung collapse (not a highly sensitive finding)</p>
Pleural line abnormalities	Any deviation from the normally appearing thin, smooth and continuous hyperechoic line including thickening, coarse irregularities, and the presence of small subpleural consolidations.	<p><i>Present</i> in association with several <i>inflammatory conditions</i> (e.g., ARDS, infection, pneumonitis, idiopathic interstitial pneumonia and other interstitial lung diseases)</p> <p><i>Note</i>: False positive pleural line abnormalities when ultrasound beam not perpendicular to the pleural line</p>
Lung consolidation	Anechoic or tissue-like image (hepatisation) arising from the pleural line that is limited in depth by an irregular border (shred sign). Represents severely increased lung density with (almost) complete loss of aeration.	<i>Present</i> in same conditions associated with B-lines and interstitial syndrome, as the extreme spectrum of increased lung density.
Air bronchogram	Hyperechoic spots or branch-like structures seen within consolidated lung: static air bronchograms dynamic air bronchograms (moving with the respiratory cycle).	<i>Present</i> within areas of lung consolidation (dynamic air bronchograms) or atelectasis (if obstruction atelectasis, static air bronchograms)

(continued)

Table 34.1 (continued)

Sonographic Findings	Definition	Clinical significance
Spine sign	Discontinuation of the transverse processes of the spine above the diaphragm from the presence of normally aerated lung tissue preventing their visualization (negative spine sign).	<i>Negative spine sign:</i> Present in normally aerated supra-diaphragmatic lung <i>Positive spine sign:</i> visualization of the transverse processes of the spine above the diaphragm; Present in pleural effusion and/or supra-diaphragmatic lung consolidation
Curtain sign	Phenomenon at the lung base, where diaphragm, liver/spleen, and spine disappear on inspiration due to lung descent and reappear on expiration as the lung ascends.	Present in normally aerated supra-diaphragmatic lung Absent in the presence of pleural effusion and/or supra-diaphragmatic lung consolidation
Pleural Effusion	Anechoic (fluid) collection between the parietal and visceral pleura. Associated with positive spine sign and absent curtain sign.	Present most often in supra-diaphragmatic regions; complex or loculated collections may be elsewhere. <i>Note:</i> Ultrasound cannot differentiate the nature of the pleural effusion (e.g., hemothorax, transudate, exudate) although visualization of mobile echoic particles or septa is highly suggestive of complex effusion (e.g. empyema)

Table reproduced with permission from Wolters Kluwer: Kruisselbrink et al. (Kruisselbrink et al. 2017). Promotional and commercial use of the material in print, digital, or mobile device format is prohibited without the permission of the publisher Wolters Kluwer. Please contact healthpermissions@wolterskluwer.com for further information.

Normal Lung Ultrasound (Figs. 34.2 and 34.3; Table 34.1)

Normally aerated lungs almost completely reflect ultrasound waves at the interface between the visceral pleura and aerated lung tissue. On the ultrasound display, this generates a hyperechoic (i.e., white) horizontal homogenous line, representing the pleural line. When the transducer is placed in a sagittal orientation, this line is regularly interrupted by the shadow artifacts created by the ribs. Deep to the pleural line, multiple regularly spaced horizontal reverberation artifacts are usually seen (“A lines”). In addition, short bright vertical artifacts (formerly called Z lines) originating from the pleural line and fading almost immediately are commonly identified; these are thought to represent areas of focal increased lung density at the subpleural level (i.e., interlobular septa, micro-atelectasis) (Soldati and Demi 2017; Soldati et al. 2016). Finally, two important lung movements can be identified with LUS: the gliding of visceral pleura against parietal pleura during breathing (“lung sliding”) and the pulsation of the pleural line as a result of conduction

of cardiac contractions (“lung pulse”) (Volpicelli et al. 2012) (Fig. 34.2 and Table 34.1). For visualization of normally aerated lungs, transducers of low or high frequency may be used.

Several additional structures and artifacts are seen when examining the supradiaphragmatic region of normally aerated lungs: (1) the diaphragm, identified as a hyperechoic homogenous curved line between the lung and abdomen; (2) abdominal organs: liver/spleen and kidney; (3) vertebral column with posterior acoustic shadowing. An important finding related to the vertebral column is that it is not visualized above the diaphragm in normally aerated lungs (“negative spine sign”). This is due to the presence of air causing near complete reflection of the ultrasound beam. Identification of a negative spine sign is also important to confirm that the beam is insonating the most dependent part of the pleural cavity, the posterior costo-phrenic angle (assuming a semi-recumbent patient position). Finally, in normal lungs another dynamic sign should be seen, the *curtain sign*, characterized by the descent of the lung and diaphragm during inspiration to obscure the liver/spleen previously seen to the right of the image (Fig. 34.3 and Table 34.1).

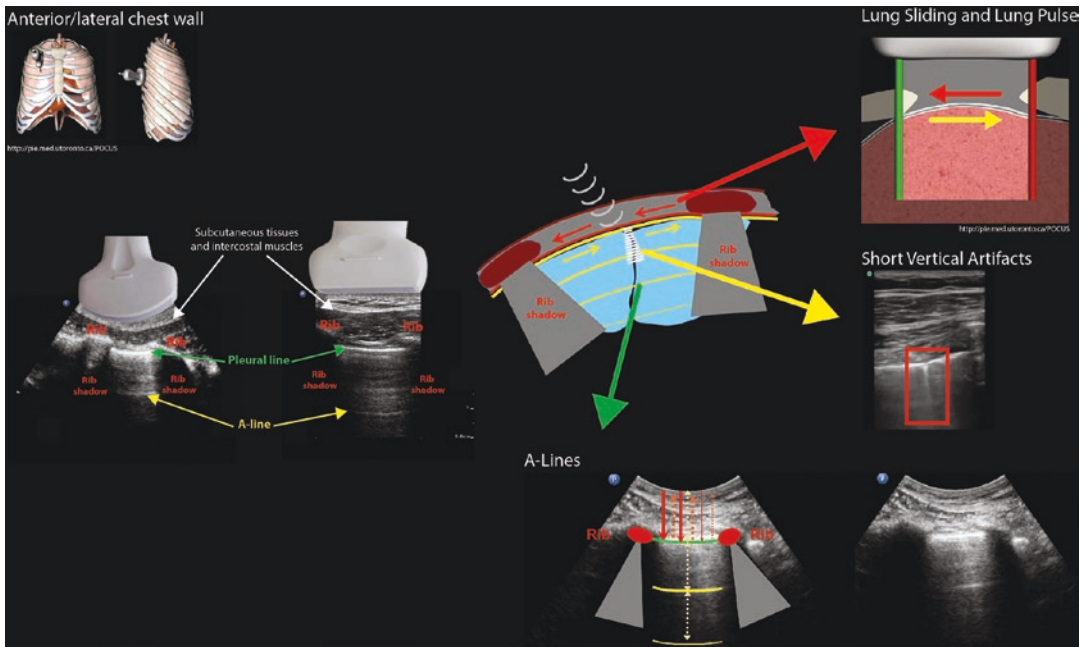


Fig. 34.2 Normal lung ultrasound findings: anterior and lateral chest. In normal lungs, when a transducer is placed sagittally on the chest wall over any intercostal space projecting over aerated lung (e.g., 2nd to 7th), the following structures and artifacts may be identified: (1) subcutaneous tissues and intercostal muscles; (2) ribs with posterior acoustic shadowing; (3) hyperechoic horizontal pleural line at the interface between pleura and aerated lung tissue; (4) hyperechoic horizontal A-line artifacts below the pleural line at multiples of the distance between the probe

and the pleural line (5) Short vertical artifacts (formerly called Z lines) originating from and moving with the pleural line (6) Two dynamic LUS findings: lung sliding and lung pulse, generated by the movement of the lung surface (visceral pleura) with respect to the innermost chest wall (parietal pleura). (Image reproduced with permission from Springer Nature: Goffi et al. [4]. Promotional and commercial use of the material in print, digital, or mobile device format is prohibited without the permission of the publisher Springer Nature)

The abdominal organs reappear on expiration when the lung and diaphragm ascend. For visualization of the supradiaphragmatic region of the lungs, a low frequency (curvilinear or phased-array) transducer is required for adequate depth penetration.

Interstitial Syndrome (Fig. 34.4 and Table 34.1)

Conditions causing loss of aerated lung tissue (i.e., increased lung density), either due to increased lung weight (e.g., increased extravascular lung water as seen in ARDS or cardiogenic pulmonary edema, deposition of collagen and fibrotic tissue, accumulation of blood, lipids, pus or proteins) or lung de-aeration (i.e., atelectasis),

affect the type of interactions generated between lung tissue and ultrasound waves (Soldati et al. 2016; Goffi et al. 2018; Volpicelli et al. 2012). A partially de-aerated lung presents an abnormally elevated tissue–air ratio (i.e., lung density) that can be either diffuse (e.g., pulmonary edema) or focal (e.g., pneumonia, lung contusion). On LUS, such abnormal tissue–air ratios are associated with the appearance of B-lines, sonographic artifacts defined as “laser-like, vertical, hyperechoic artifacts that arise from the pleural line, extend to the bottom of the screen without fading, and move synchronously with lung sliding” (Volpicelli et al. 2012; Lichtenstein and Mezière 2008; Lichtenstein et al. 1997; Soldati et al. 2016). Three or more B-lines in an intercostal space represent a positive region of loss of lung aeration (i.e., interstitial syndrome) (Volpicelli

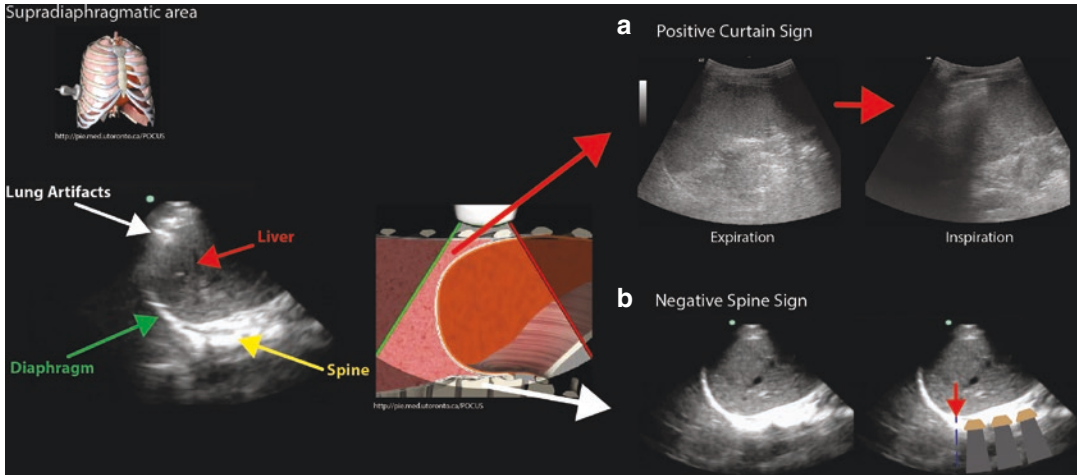


Fig. 34.3 Normal lung ultrasound findings: supradiaphragmatic area. In the postero-lateral and supradiaphragmatic regions of normal lung, when a low-frequency transducer is placed at the 8th-9th /9th-10th intercostal spaces, in a cephalo-caudal orientation and directed posteriorly, the following structures and artifacts can be identified: (1) hyperechoic homogenous curved line of the diaphragm between the lung artifacts cephalad and abdomen caudad; (2) abdominal organs: liver/spleen and potentially kidney; (3) vertebral column with posterior acoustic shadowing. (4) The *curtain sign* should be observed (top right panel A): at full inspiration, the

descent of the lung and diaphragm obscures the liver/spleen previously seen to the right of the image and with expiration these organs reappear. (5) Also, a “negative” *spine sign* should be observed (bottom right panel B): in a normally aerated lung the vertebral column is not visualized above the diaphragm due to the presence of air causing near complete reflection of the ultrasound beam. (Image reproduced with permission from Springer Nature: Goffi et al. [4]. Promotional and commercial use of the material in print, digital, or mobile device format is prohibited without the permission of the publisher Springer Nature)

et al. 2012). Several characteristics of B-lines should be highlighted:

- B-lines appear very early in the course of diseases that cause loss of lung aeration and are thus an extremely sensitive marker of lung injury. For example, in an experimental model of acid-induced lung injury, B-lines appear even before gas exchange deterioration and correlate with changes in lung compliance (Gargani et al. 2007).
- The temporal profile (appearance and resolution) of B-lines can be followed in real time as lung density changes, making them very useful in clinical monitoring applications (Pichette and Goffi 2018; Noble et al. 2009; Liteplo et al. 2010; Via et al. 2010).
- B-lines are affected by gravitational and hydrostatic forces. Therefore, their distribu-

tion with respect to gravity (i.e., patient position) should be considered when performing and interpreting LUS findings (Kruisselbrink et al. 2017; Bouhemad et al. 2015).

- The absolute number of B-lines correlates with severity of disease, loss of lung aeration (Via et al. 2010) and extravascular lung water, when the interstitial syndrome is caused by fluid accumulation (e.g., pulmonary edema) (Volpicelli et al. 2014; Agricola et al. 2005; Jambrik et al. 2004; Enghard et al. 2015). Several methods have been used to quantify interstitial syndrome (Anderson et al. 2013; Bedetti et al. 2006; Cardinale et al. 2009; Liteplo et al. 2009). The most commonly used method is a semi-quantitative score that correlates moderate loss of aeration with ≥ 3 well-defined spaced B-lines/intercostal space (“B1 pattern”) and severe

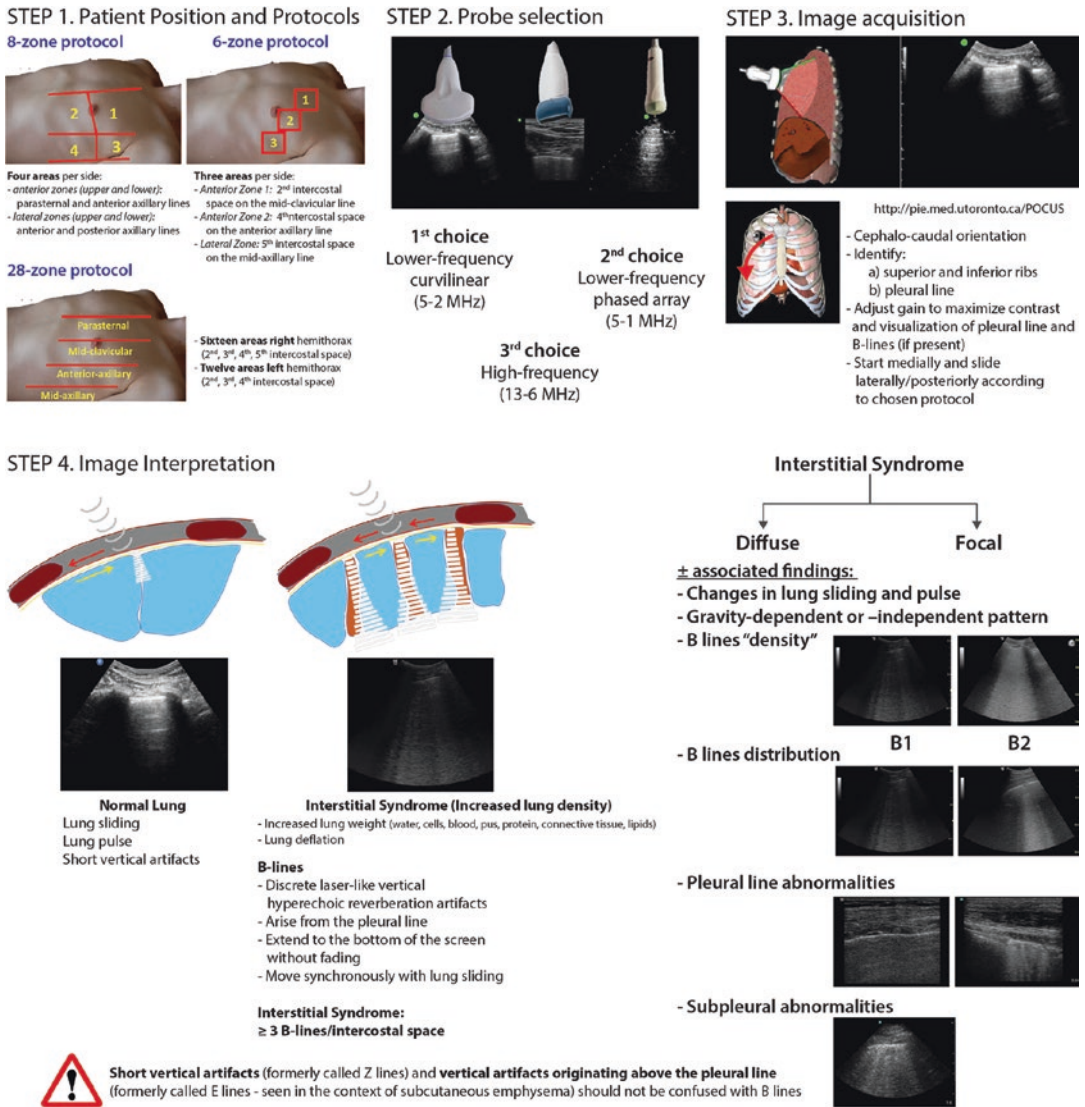


Fig. 34.4 Step-by-step approach to lung ultrasound for the diagnosis of interstitial syndrome. (Image reproduced with permission from Springer Nature: Goffi et al. [4].

Promotional and commercial use of the material in print, digital, or mobile device format is prohibited without the permission of the publisher Springer Nature)

loss of aeration with multiple coalescent B-lines/intercostal space ("B2 pattern") (Bouhemad et al. 2011; Soummer et al. 2012; Silva et al. 2017).

- B-lines are very sensitive for increased lung density, but they lack specificity, being caused by several different conditions (Soldati et al.

2016). Integration with the clinical context and identification of additional sonographic findings (e.g., B-line distribution, B-line density, gravity-dependent vs. -independent pattern, associated changes in lung sliding and pulse, presence of pleural line and subpleural abnormalities, identification of fluid or air

bronchograms) can be used to narrow the differential diagnosis and increase specificity (Goffi et al. 2018; Pivetta et al. 2015; Copetti et al. 2008).

Low-frequency probes (5–1 MHz) are preferred for diagnosing interstitial syndrome as they allow visualization of the vertical extent of artifacts, thereby avoiding the error of misreading short vertical artifacts as B-lines. Nevertheless, high-frequency (13–6 MHz) transducers can also be used.

Alveolar Syndrome (Fig. 34.5 and Table 34.1)

When the tissue–air ratio in an injured lung is extremely high (i.e., complete or near-complete disappearance of alveolar air as seen in lung consolidations, atelectasis, pulmonary infarcts, tumors, and contusions), an anatomical tissue-like pattern, termed “alveolar syndrome,” can be seen on LUS (Volpicelli et al. 2012; Goffi et al. 2018; Volpicelli 2013). Three characteristic

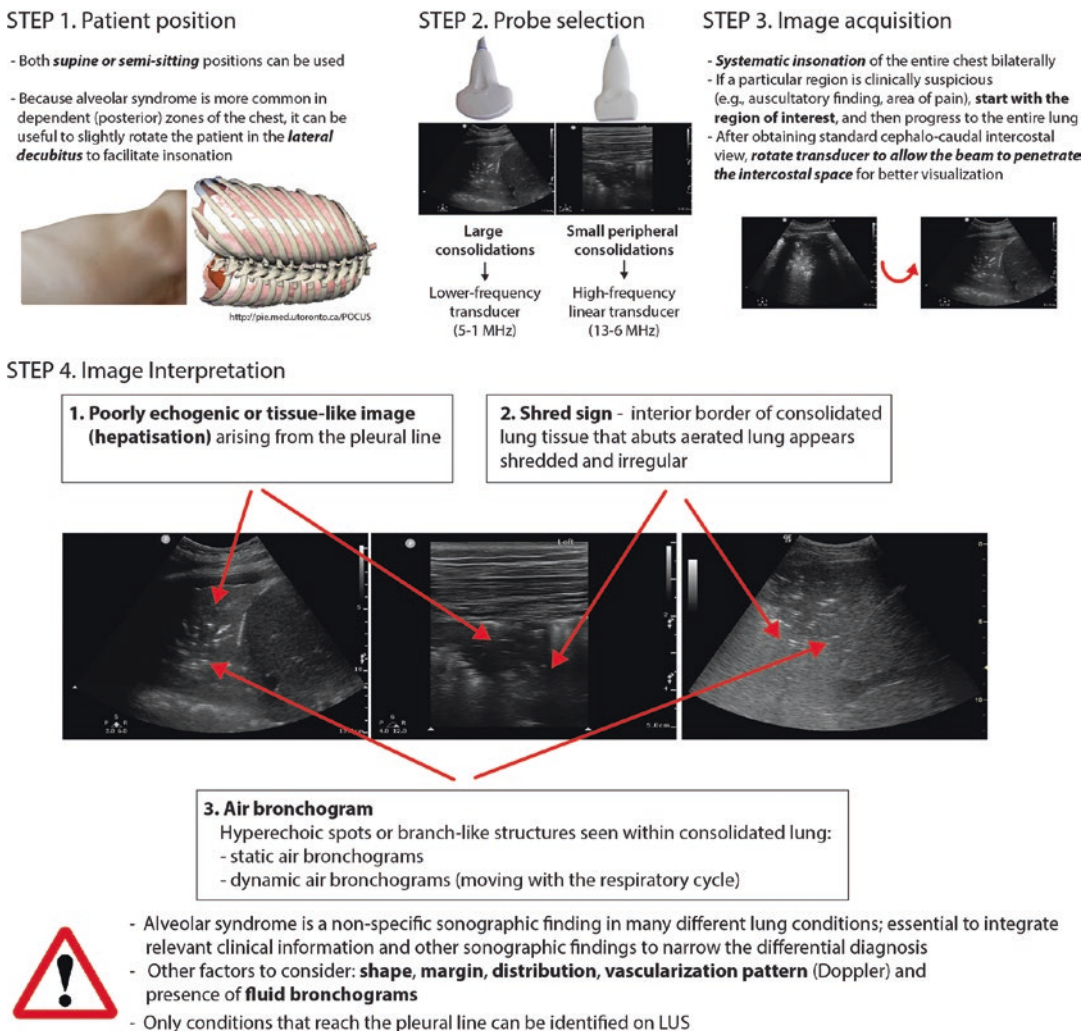


Fig. 34.5 Step-by-step approach to lung ultrasound for the diagnosis of alveolar syndrome. (Image reproduced with permission from Springer Nature: Goffi et al. [4].

Promotional and commercial use of the material in print, digital, or mobile device format is prohibited without the permission of the publisher Springer Nature)

sonographic patterns may be found when alveolar consolidation is present:

- Presence of a poorly echogenic or tissue-like image (hepatization) extending below the pleural line (Volpicelli et al. 2012; Goffi et al. 2018; Kruisselbrink et al. 2017). Note that only conditions (both interstitial and alveolar syndromes) abutting the pleural line can be identified on LUS, thus creating potential for false negative results when the condition does not reach the pleural line (Goffi et al. 2018; Volpicelli 2013; Reissig et al. 2012).
- “Shredded” and irregular interior border of consolidated lung tissue (“shred sign”), at the transition zone with more aerated areas (usually characterized by interstitial syndrome);
- Hyperechoic spots or branch-like structures (air bronchograms) within the consolidated lung representing residual air in lung tissue (likely bronchial structures). Air bronchograms can be static or dynamic (moving with the respiratory cycle).

Like interstitial syndrome, alveolar syndrome is a sensitive but nonspecific sonographic finding that can be seen in many different lung conditions. Other sonographic findings (e.g., shape, margin, distribution, vascularization pattern on Doppler imaging and presence of air and fluid bronchograms), together with clinical information, may help to narrow the differential diagnosis (Reissig et al. 2012; Mathis et al. 2005; Lichtenstein et al. 2004; Lichtenstein et al. 2009; Nazerian et al. 2015).

Both low- and high-frequency transducers can be used to identify alveolar syndrome, although one type may be preferable depending on the size of the consolidation. For large consolidations, low-frequency (5–1 MHz) transducers facilitate assessment of the extension of the consolidation (Reissig et al. 2012), whereas for small peripheral consolidations and in children, high-frequency (13–6 MHz) transducers are preferred.

Lung Ultrasound for the Diagnosis and Monitoring of Lung Pathologies

Use of LUS for the assessment of patients with respiratory deterioration and/or clinical findings suggestive of lung pathology is extremely attractive. LUS is easy to learn, can be applied at the bedside, and does not require radiation exposure (Kendall et al. 2007; Reissig et al. 2012; Rouby et al. 2018). Further, its routine use has been shown to have substantial diagnostic impact (with a net reclassification index of 85%) and therapeutic impact (management change in 47% of patients as a result of LUS findings) (Xirouchaki and Georgopoulos 2014). Use of LUS for monitoring purposes is also effective. Daily bedside LUS in critically ill patients can detect real-time changes in aeration patterns and has been shown to reduce the number of CXR and computed tomography (CT) scans performed in this population (Peris et al. 2010).

We will now review the sonographic findings and current available evidence for the most common lung pathologies (Table 34.2). We also recommend the online educational resource available at http://pie.med.utoronto.ca/POCUS/POCUS_content/lungUS.html

Pneumothorax. (Fig. 34.6; Tables 34.1 and 34.2)

- *Ultrasound findings.* The sonographic findings for pneumothorax on LUS are actually the absence of the normal LUS findings: absent lung sliding, lung pulse, and vertical artifacts. In other words, identification of either lung sliding, lung pulse, or vertical artifacts allows immediate exclusion of a pneumothorax at the level of the insonated area (Lichtenstein and Mezière 2008). Conversely, when both lung movements and pleural vertical artifacts are not detectable, pneumothorax is highly likely,

Table 34.2 Lung Pathologies and Associated Sonographic Findings

Condition	Lung sliding	Lung Pulse	A-Lines pattern	B-Lines / Vertical artifacts	Consolidation(s)	Pattern of distribution	Pleural line characteristics	Other(s)
Normal lung	Present	Present	Present	Absent (Rare B-lines possible in dependent areas)	Absent	Bilateral and Homogenous	Thin, homogenous appearance	-
Bullous diseases	Reduced/ Absent	Reduced/ Absent	Present	Possible in the context of focal increased lung density	Absent	Focal or diffuse	May appear thick and irregular	-
Lung hyper-inflation	Reduced/ (Absent)*	Reduced/ (Absent)	Present			More prominent in non-dependent zones	Thin, homogenous appearance	-
Pneumothorax	Absent	Absent	Present	Absent	Absent	Unilateral (bilateral rare)	Visceral pleural not visible	Lung point
Asthma/COPD exacerbation	Present (Reduced)	Present (Reduced)	Present	Absent, unless associated infection/atelectasis	Absent, unless associated infection/atelectasis	Bilateral	Thin, homogenous appearance	-
Pulmonary embolism (± pulmonary infarcts)	Present	Present	Present	Absent, unless evolving pulmonary infarct(s)	Absent, unless pulmonary infarct(s) peripheral consolidations)	Bilateral or unilateral	Pleural line may be “interrupted” by small peripheral consolidations	-
Cardiogenic (hydrostatic) pulmonary edema	Present	Present/ Increased	Usually abolished	Present (B1 or B2 pattern) Regularly spaced	Possible in dependent areas (especially if associated pleural effusion)	Bilateral and Homogenous: gravity-dependent pattern	Thin, homogenous appearance	-
Nonhydrostatic pulmonary edema (e.g. ARDS)	Present (Often reduced)	Present/ Increased	Preserved in some areas	Present (B1 or B2 pattern) Irregularly spaced	Present (mostly in dependent areas)	Bilateral and Heterogeneous (“spared” areas): non-gravity-dependent pattern	Pleural line abnormalities (thick, fragmented with small peripheral consolidations)	-
Idiopathic interstitial pneumonias and other interstitial lung diseases (ILDs)	Present (Reduced)	Present/ Increased	Preserved in some areas	Present Irregularly spaced	Not typically present	Bilateral but not necessarily homogenous distribution (disease-specific)	Pleural line abnormalities (thick, fragmented with small peripheral consolidations)	-

Alveolar hemorrhage/ alveolar proteinosis/diffuse pneumonitis	Present (Reduced)	Present/ Increased	Preserved in some areas (if not diffuse)	Usually present (B1 or B2 pattern)	Can be present	Bilateral, more homogeneous than ARDS	In inflammatory processes, pleural line abnormalities (thick, fragmented with small peripheral consolidations)	-
Focal infection/inflammation (e.g., pneumonia, aspiration pneumonitis)	Reduced/ (Absent)	Present/ Increased	Absent in affected area	It can present as irregularly spaced B-lines pattern (initial or resolution phase, or interstitial pneumonia) or as large consolidation (with irregular margins)		Focal (or multifocal)	If vertical artifacts present, usually associated with pleural line abnormalities (thick, fragmented with small peripheral consolidations)	- Often presence of dynamic air bronchograms or fluid - Sonographic findings only evident if lesion reaching pleural line
Atelectasis (absorption or compression)	Reduced/ Absent (if obstruction present)	Present/ Increased	Present in initial phases, then absent with increased lung density	Initially absent, then present with increased lung density	Initially absent, then present with increased lung density (more regular borders compared to pneumonia)	Usually focal (often dependent areas)	Thin, homogenous appearance	Absence of dynamic air bronchograms (in absorption atelectasis)
Pulmonary contusion	Present (Reduced)	Present/ Increased	Absent in affected area	It can present as irregularly spaced B-lines pattern (initial or resolution phase) or as consolidation (peak evolution)		Focal (or multifocal)	If vertical artifacts present, usually associated with pleural line abnormalities (thick, fragmented with small peripheral consolidations)	-
Primary lung cancer/tumor or metastasis	Present	Present/ Increased	Absent in affected area	Vertical artifacts often present at the periphery of the lesion	If peripheral lesion, detection of consolidation-like area	Focal	If vertical artifacts present, usually associated with pleural line abnormalities (thick and fragmented)	Sonographic findings only evident if lesion reaching pleural line

*The terms in parentheses in column 2 and 3 indicate that the finding described can be observed but occurs less often. Table reproduced with permission from Wolters Kluwer: Kruijselbrink et al. (Kruijselbrink et al. 2017). Promotional and commercial use of the material in print, digital, or mobile device format is prohibited without the permission of the publisher Wolters Kluwer. Please contact healthpermissions@wolterskluwer.com for further information.

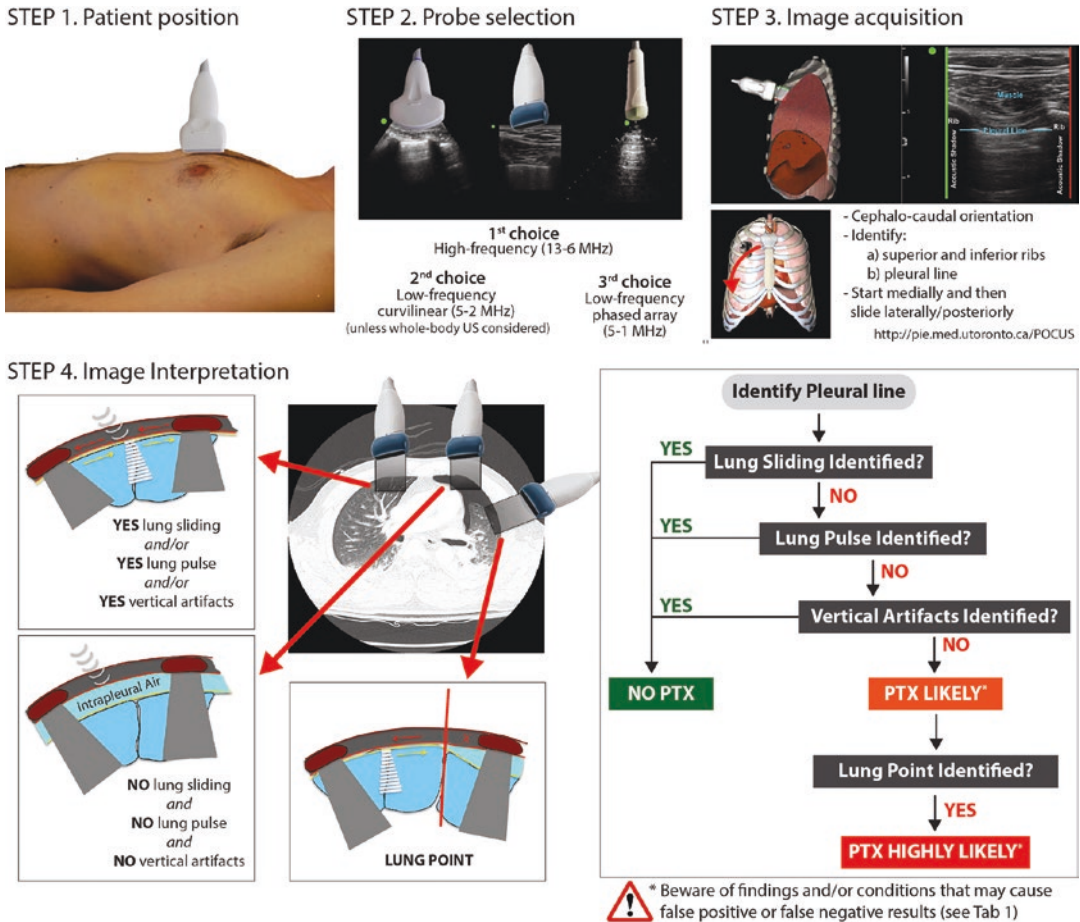


Fig. 34.6 Step-by-step approach to lung ultrasound for the diagnosis of pneumothorax. (Image reproduced with permission from Springer Nature: Goffi et al. [4].

Promotional and commercial use of the material in print, digital, or mobile device format is prohibited without the permission of the publisher Springer Nature)

though not definite (false positive results might be generated by other conditions that reduce lung sliding and pulse such as severe COPD or lung overdistension). In order to confirm a suspected pneumothorax, one should visualize the “lung point,” or the transition between intrapleural air (no sliding, no pulse, and no vertical artifacts) and a normally aerated area (sliding, pulse and/or vertical artifacts). The lung point is a highly specific finding for pneumothorax (Lichtenstein et al. 2000). However, in some cases, the lung point may not be visible as it can be hidden behind osseous structures (ribs and scapula) or may not be present at all, as in a complete pneumothorax. When using LUS to assess for pneumothorax, it is important to

recall that intrapleural air will collect in the least dependent area of the thorax (except in the presence of loculated pneumothorax) with the exact location depending on patient position. In most studies, patients have been imaged in the supine position with the head of the bed at zero degrees. In this position, the least dependent area of the chest is identified at the second-fourth intercostal space between the parasternal and midclavicular lines. In patients unable to lie completely flat (e.g., non-intubated patients in respiratory distress), pleural air will accumulate in the apical regions, making the examination more challenging due to the presence of the clavicles (Kruisselbrink et al. 2017; Goffi et al. 2018; Alrajab et al.

2013; Volpicelli 2010). If possible, a high-frequency transducer is preferred.


- *The Evidence.* When performed by expert providers and in patients with a high pretest probability (e.g., respiratory distress, dyspnea or chest pain post-trauma or central line insertion), the accuracy of LUS for pneumothorax is superior to chest radiography (CXR). In particular, the sensitivity of LUS is higher than supine CXR [79% (95% CI 68–89%) versus 40% (95% CI 29–50%), respectively], whereas specificity is equally very high for both [98% (95% CI 97–99%) versus 99% (95% CI 98–100%)] (Alrajab et al. 2013).

However, as most studies on the diagnostic accuracy of LUS for pneumothorax are in trauma or post-procedural patients, these numbers may overestimate LUS performance in other settings (e.g. nontrauma patients with preexistent conditions such as emphysema) (Alrajab et al. 2013; Staub et al. 2018).

Pleural Effusion (Fig. 34.7; Tables 34.1 and 34.2)

- *Ultrasound findings.* The primary sonographic finding is the presence of an anechoic region

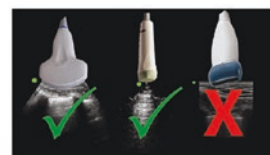
STEP 1. Patient position



1st choice
Semi-sitting position maximizes effect of gravity and sensitivity of scan

2nd choice
Supine position

STEP 2. Probe selection



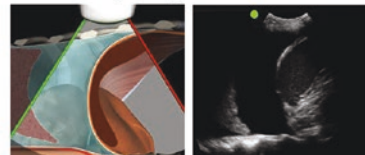
YES

- Low-frequency curvilinear (5-2 MHz)
- Low-frequency phased array (5-1 MHz)

NO

- High-frequency linear

STEP 3. Image acquisition

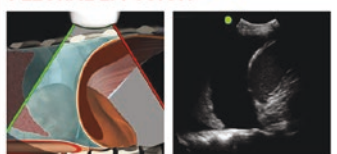


Probe at the mid-axillary line in a cephalo-caudal orientation with slight counterclockwise rotation

- Beam directed posteriorly towards the vertebral column
- Identify lung artifacts, diaphragm, liver/spleen and vertebral column
- Visualization of the spine is essential


STEP 4. Image Interpretation

PLEURAL EFFUSION



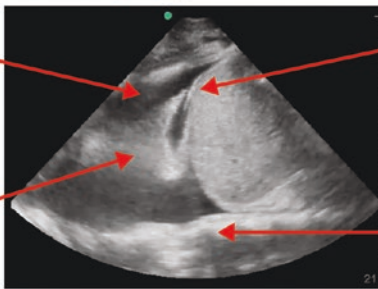
NO CURTAIN SIGN & POSITIVE SPINE SIGN

NO PLEURAL EFFUSION



CURTAIN SIGN NEGATIVE SPINE SIGN

1. Anechoic region above the diaphragm between the visceral and parietal pleura.



2. Absent curtain sign
Lung artifacts and diaphragm do not descend with inspiration and the abdominal organs remain visible throughout

4. Lung consolidation/collapse within effusion

3. Positive spine sign
The spine is visualized above as well as below the diaphragm because the fluid conducts the ultrasound beam

! Beware of findings and/or conditions that may cause false positive or false negative results (e.g. free fluid below the diaphragm) - see Tab 1

Fig. 34.7 Step-by-step approach to lung ultrasound for the diagnosis of pleural effusion. (Image reproduced with permission from Springer Nature: Goffi et al. [4].

Promotional and commercial use of the material in print, digital, or mobile device format is prohibited without the permission of the publisher Springer Nature)

(fluid) above the diaphragm between the visceral and parietal pleura, displacing the lung upwards. Within the anechoic area, hyperechoic regions of collapsed lung are often present. Respiratory movements within the hyperechoic regions (i.e., sinusoid sign) (Volpicelli et al. 2012) may or may not be seen. Additional internal echoes may also be seen within the anechoic effusion; if present, these suggest the presence of complicated effusions (e.g., exudates, empyemas, hemorrhage), although thoracentesis is required for a definite diagnosis. Due to the presence of fluid above the diaphragm, a positive *spine sign* is seen, where the vertebral column is visible above the diaphragm. The *curtain sign* is usually absent, with the abdominal organs remaining visible throughout the respiratory cycle. Note that the ultrasound findings in nonoculated pleural effusions are affected by gravity and therefore dependent on patient position. All of the previously mentioned findings assume the patient is in a supine or semi-sitting position. In this position the posterior costophrenic angle is the most dependent region of the pleural space.

- *Evidence.* The diagnostic accuracy of LUS for the diagnosis of pleural effusion is excellent and superior to that of conventional CXR. A recent meta-analysis, combining results of over 1500 patients found the sensitivity and specificity of LUS to be 94% (95% CI 88–97%) and 98% (95% CI 92–100%) respectively. In the same analysis, the specificity of CXR was comparable at 91% (95% CI 68–98%) but the sensitivity was much lower at 51% (95% CI 33–68%) (Yousefifard et al. 2016). There is also evidence suggesting that the use of LUS to guide thoracentesis results in a lower rate of complications, especially that of pneumothorax (Gordon et al. 2010; Sikora et al. 2012).

Diffuse Lung Diseases

- *Cardiogenic (Hydrostatic) Pulmonary Edema* (Table 34.2).
 - *Ultrasound findings.* The hallmark finding is a diffuse bilateral interstitial syndrome. B-lines are regularly spaced and present in a homogenous and gravity-dependent pattern (characteristic of hydrostatic pathophysiology). Consolidations (i.e., alveolar syndrome) in dependent areas can be associated, especially when a pleural effusion is also present (usually a marker of accompanying right ventricular failure). Lung sliding and lung pulse are preserved, and the pleural line appears thin and homogeneous. The absolute number of B-lines correlates with the extravascular lung water content (Volpicelli et al. 2014; Agricola et al. 2005; Jambrik et al. 2004; Enghard et al. 2015).
 - *Evidence.* LUS is more useful and accurate for the diagnosis of acute decompensated heart failure than routinely used tests, such as CXR and natriuretic peptides (Pivetta et al. 2015; Volpicelli et al. 2006; Liteplo et al. 2009; Al Deeb et al. 2014; Cibinel et al. 2012; Gargani et al. 2008). Remember that B-lines lack specificity (Soldati et al. 2016), thus integration with the clinical context is an essential component of an effective diagnostic approach (Pivetta et al. 2015). In patients with increased extravascular lung water, serial LUS exams allow monitoring of changes in lung aeration and effectiveness of interventions such as heart failure treatment (Strnad et al. 2016; Frassi et al. 2007; Liteplo et al. 2010) and dialysis (Mallamaci et al. 2010; Noble et al. 2009). Finally, the presence and amount of interstitial syndrome may have a prognostic role for conditions such as heart failure and

end-stage renal disease (Platz et al. 2017; Zoccali et al. 2013; Gargani et al. 2015).

- *Acute Respiratory Distress Syndrome (ARDS)* (Table 34.2).

- *Ultrasound findings.* ARDS has been defined as “a type of acute diffuse, inflammatory lung injury, leading to increased pulmonary vascular permeability, increased lung weight, and loss of aerated lung tissue” (The Berlin Definition) (Definition Task Force 2012). It is therefore not surprising that findings of diffuse interstitial (B-lines) and alveolar syndromes on LUS have been associated with the diagnosis of ARDS. However, these findings can be seen in multiple conditions (e.g., cardiogenic pulmonary edema) and lack specificity for ARDS. Therefore additional LUS findings must be sought to increase the specificity of LUS for the diagnosis of ARDS (Copetti et al. 2008; Kruisselbrink et al. 2017; Volpicelli et al. 2012). These include:

- lung heterogeneity [areas of focal interstitial syndrome alternate with areas of normal lung (A-line pattern); non-gravity-dependent distribution];
- irregularly spaced B-lines;
- pleural and subpleural line abnormalities (thick, fragmented pleural line with small consolidations);
- reduction or absence of lung sliding;
- increased transmission of lung pulse;
- presence of large alveolar syndrome in gravity-dependent areas.

- *Evidence.*

A. *ARDS Diagnosis.* B-lines have been shown to appear very early in the course of ARDS. In an experimental model of oleic acid-induced lung injury, Gargani et al. demonstrated that B-lines appear even before gas exchange deterioration

and correlate with changes in lung compliance (Gargani et al. 2007). Integration of LUS findings with cardiac ultrasound and/or clinical characteristics may help differentiate ARDS, pulmonary edema, and other causes of acute hypoxemic respiratory failure (Sekiguchi et al. 2015; Riviello et al. 2016; See et al. 2018). Recently, LUS has been proposed as an alternative to CXR for the diagnosis of ARDS. Riviello et al. used LUS in a modified version of the ARDS Berlin definition (Kigali modification) and demonstrated its feasibility to diagnose ARDS in resource-limited settings (Riviello et al. 2016). In addition, in a retrospective cohort study, See et al., analyzed clinical outcomes of patients admitted with hypoxemic respiratory failure and diagnosed with ARDS according to the original Berlin definition (using CXR) or a modified definition that uses LUS as an alternative imaging method. Among 456 patients admitted with respiratory failure, 216 met CXR-Berlin criteria, 229 LUS-Berlin criteria, and 295 either CXR- or LUS-Berlin criteria. Intensive care unit and hospital mortality did not differ significantly among these three groups; rather, simply having ARDS was associated with significantly higher mortality independent of the diagnostic criteria used (hospital mortality 34.2% vs 24.2%, $P = 0.027$) (See et al. 2018). These studies suggest that LUS may be an alternative (or complementary) tool to assess and risk-stratify patients admitted with hypoxemic respiratory failure.

B. *ARDS Monitoring.* LUS can be used to monitor changes in lung aeration in

response to recruitment maneuvers or changes in PEEP (Tusman et al. 2003; Tusman et al. 2016; Stefanidis et al. 2011; Song et al. 2017; Chiumello et al. 2018), during tidal breaths (Tusman et al. 2015), and during extracorporeal membrane oxygenation (ECMO) (Mongodi et al. 2017). However, although LUS seems to reliably assess lung aeration, its role in determining PEEP-induced lung recruitment seems to be limited (Chiumello et al. 2018). With regard to predicting the oxygenation response during prone positioning for ARDS, the role of LUS is unclear (Haddam et al. 2016; Prat et al. 2016). Current literature suggests that aeration changes in the first hour after initiation of prone positioning may be a better predictor of response to treatment than the initial LUS pattern in the supine position (Wang et al. 2016; Persona et al. 2016).

- *Interstitial lung diseases (ILDs)* (Table 34.2).
 - *Ultrasound findings.* The family of interstitial lung diseases (ILDs) encompass a heterogeneous group of conditions (e.g., chronic hypersensitivity pneumonitis; idiopathic interstitial pneumonia, especially idiopathic pulmonary fibrosis; pulmonary sarcoidosis, and connective tissue disease-associated ILDs) characterized by interstitial (e.g., within the alveolar wall) inflammation and/or fibrosis, not due to infection or cancer (Lederer and Martinez 2018; Rosas et al. 2014). Interstitial lung involvement can be suspected on LUS by the detection of multiple B-lines in a diffuse and nonhomogenous distribution (Volpicelli et al. 2012). Pleural line abnormalities (thickened ≥ 3 mm, irregular, fragmented pleural line) and subpleural abnormalities (small hypoechoic areas immediately below the pleural line and subpleural cysts) are also often present (Volpicelli et al. 2012; Manolescu et al. 2018). ILDs associated with the presence

of ground glass opacities on high-resolution CT (HRCT), as seen in fibrotic nonspecific interstitial pattern, demonstrate areas of B2 pattern (“white lung”) on LUS, associated with a thickened and fragmented pleural line (Manolescu et al. 2018). Subpleural fibrosis may also cause a reduction in lung sliding (Sperandeo et al. 2009).

- *Evidence.* Distribution of B-lines, severity of interstitial involvement and other associated LUS findings correlate well with HRCT findings and scores (e.g., Warrick score) (Sperandeo et al. 2009; Barskova et al. 2013; Gargani et al. 2009). LUS is highly sensitive (91.5%; 95% CI 84.5–96%) for the diagnosis of ILDs, though its specificity is not as high (81.3%; 95% CI 74.6–86.9%). This lack of specificity is not surprising as B-lines appear in other diffuse lung conditions, such as ARDS and pulmonary edema, and in the presence of superimposed infective processes (Song et al. 2016).

Focal Lung Diseases (Table 34.2)

- *Pneumonia*
 - *Ultrasound findings.* The main LUS finding is alveolar syndrome. Lobar consolidations appear as large areas of alveolar syndrome with irregular margins displaying vertical artifacts (representing the transition from densely consolidated areas to areas still retaining some degree of aeration). Dynamic air bronchograms are frequently present within the areas of large consolidation. Small peripheral consolidations can also be seen, especially in multifocal pneumonia. Irregularly spaced B-lines associated with pleural line abnormalities (thick and fragmented pleural line) may be seen in interstitial/viral pneumonia or during the initial/resolution phase of alveolar consolidation. Note that all of these sonographic findings are only evident if the infection is reaching the pleura abut-

ting the chest wall (i.e., mediastinal or deep consolidations will not be detected on LUS).

- *Evidence.* Several meta-analyses comparing LUS to CXR for the diagnosis of pneumonia have been published (Ye et al. 2015; Chavez et al. 2014; Alzahrani et al. 2017; Orso et al. 2018). Despite differences in the reference tests used (e.g. hospital discharge diagnosis, CT, mixed gold standard using laboratory, microbiology and imaging data) and the large spectrum of diseases evaluated in the studies collected (i.e. community-, ventilator-, and hospital-acquired pneumonia), LUS seems to accurately diagnose pneumonia, with sensitivities ranging between 82% and 95% and specificities of 72–95%. However, one should be cautious in ruling out pneumonia using LUS in patients with moderate/high pre-test probability, as the largest published observational study of patients with suspected pneumonia (n = 362) showed a significant number of false-negative LUS results (7.9%) (Reissig et al. 2012).
- *Pulmonary Embolism*
 - *Ultrasound findings.* Patients with acute pulmonary embolism usually present with a sonographic pattern typical of normal lung. Patients with pulmonary infarcts may show areas of small peripheral consolidations associated with focal B-lines.
 - *Evidence.* In pulmonary embolism, LUS does not perform well, with a sensitivity of 85% (95% CI 78–90%) and specificity of 83% (95% CI 73–90%) (Jiang et al. 2015). However, in situations where a CT cannot be performed or is contraindicated, LUS could be considered as one of the elements in an alternative diagnostic algorithm combining pre-test probability, laboratory tests (i.e., d-dimer), and multi-organ ultrasound scanning (Mathis et al. 2005). Such a multi-organ approach, including lung, focused cardiac, and venous ultrasonography, has been shown to achieve acceptable diagnostic accuracy for pulmonary embolism (sensitivity 90%, specificity 86.2%) (Nazerian et al. 2014).
- *Obstructive/Absorption Atelectasis*
 - *Ultrasound findings.* In cases of bronchial obstruction, the initial finding will be reduction or disappearance of lung sliding with preservation of the lung pulse. If the obstruction does not resolve, air reabsorption from the alveoli will lead to increased lung density and the appearance of B-lines (interstitial syndrome). As the de-aeration process continues, interstitial syndrome will progress to alveolar syndrome, with borders that will appear more regular than in pneumonia. Often, static air or fluid bronchograms can be observed (Mathis 1997).
 - *Evidence.* There are no studies evaluating the diagnostic characteristics of LUS for the diagnosis of atelectasis. A few studies have described the sonographic findings in atelectasis but their sample size is small (Lichtenstein et al. 2009; Lichtenstein et al. 2003; Xirouchaki et al. 2014).
- *Pulmonary Contusion*
 - *Ultrasound findings.* Traumatic injuries to the lung lead to increased vascular and epithelial permeability with a resulting increase in lung density. Therefore, on LUS, pulmonary contusions will vary in presentation depending on the relative time of the scan, with focal B-lines during the initial and resolution phases and alveolar consolidation at the time of peak loss of aeration. Pleural abnormalities are often associated and pleural effusion (usually hemothorax) can also be seen. Lung sliding and pulse are maintained.
 - *Evidence.* In trauma patients, LUS has shown high diagnostic accuracy for pulmonary contusion (sensitivity 94.6%, specificity 96.1%) (Soldati et al. 2006; Volpicelli et al. 2008a; Reissig et al. 2011), even in extremely early phases such as the pre-hospital setting (Scharonow and Weilbach 2018).

- *Primary lung cancer/tumor or metastasis*
 - *Ultrasound findings.* Peripheral lesions may appear as a consolidation-like area surrounded by focal B-lines.
 - *Evidence.* Little evidence is available on the use of LUS for detection of lung tumor or metastasis. The nonspecific LUS pattern (i.e. consolidation-like area) means that further testing is required to characterize the identified lesion (Volpicelli et al. 2008a; Volpicelli et al. 2008b; Volpicelli et al. 2010). Typical Color Doppler findings (irregular blood flow, increased flow, and the “corkscrew” sign at the periphery of the lesion) have been described in primary lung cancer and metastatic lesions (Mathis 1997).

Diagnostic Approach

Several diagnostic approaches to LUS have been described, varying primarily with respect to the patient’s characteristics and goals of the LUS examination (e.g., emergency scan versus comprehensive study) (Volpicelli et al. 2012; Kruisselbrink et al. 2017; Lichtenstein and Mezière 2008; Bouhemad et al. 2011; Martindale et al. 2017). We favor the I-AIM (Indication, Acquisition, Interpretation, Medical decision-making) model, an intuitive framework and cognitive aid that provides a standardized approach to LUS (Kruisselbrink et al. 2017; Bahner et al. 2012) (Fig. 34.8).

The first step when considering a LUS exam should always be the INDICATION for the study. Common indications for LUS are unexplained respiratory symptoms or signs, unclear CXR findings (both diagnostic indications) (Lichtenstein and Mezière 2008; Zanobetti et al. 2017; Laursen et al. 2014), or monitoring of the evolution/response to treatment of previously identified LUS findings (monitoring indication) (Mongodi et al. 2017; Bouhemad et al. 2011; Haddam et al. 2016).

The second step regards the ACQUISITION of the best possible image and includes adjusting the patient position (if necessary), choosing the most suitable transducer and scanning protocol,

and optimizing the ultrasound settings (especially gain, depth and focus adjustments). The probe should always be held over an intercostal space in a cephalo-caudal orientation, and at least two ribs with the pleural line between should be identified.

Even when the indication is very specific (e.g., identification of pleural effusion), one should always systematically insonate the entire chest. However, the LUS assessment may start with the clinically suspicious chest region and then progress to the entire lung. Several scanning protocols have been described (Fig. 34.9):

- eight-zone or twelve-zone protocols, most commonly used in acute care settings in patients with acute respiratory failure. The twelve-zone protocol (including posterior zones of the chest) is recommended for the assessment of alveolar syndrome and monitoring of lung aeration in critically ill patients (Pivetta et al. 2015; Lichtenstein and Mezière 2008; Bouhemad et al. 2011);
- twenty-eight-zone protocol, used for monitoring interstitial syndrome in patients with chronic heart failure (Miglioranza et al. 2013);
- abbreviated six-zone protocol used in emergency situations to rapidly diagnose or exclude life-threatening causes of respiratory failure (anterior zone for pneumothorax, lateral zone for interstitial syndrome and postero-inferior zone for hemothorax/massive pleural effusion; Volpicelli et al. 2012; Kruisselbrink et al. 2017).

The third stage of the I-AIM framework, INTERPRETATION of the LUS scan, can be divided into 4 steps: (1) assessment of image quality and adequacy for interpretation; (2) identification of the presence or absence of specific LUS findings; (3) integration of findings from all lung zones and generation of a sonographic differential diagnosis; (4) performance of additional point-of-care exams (e.g., focused cardiac ultrasound, vascular ultrasound, diaphragmatic or abdominal ultrasound) if needed.

After ensuring the image is adequate, we begin our assessment of LUS findings with an

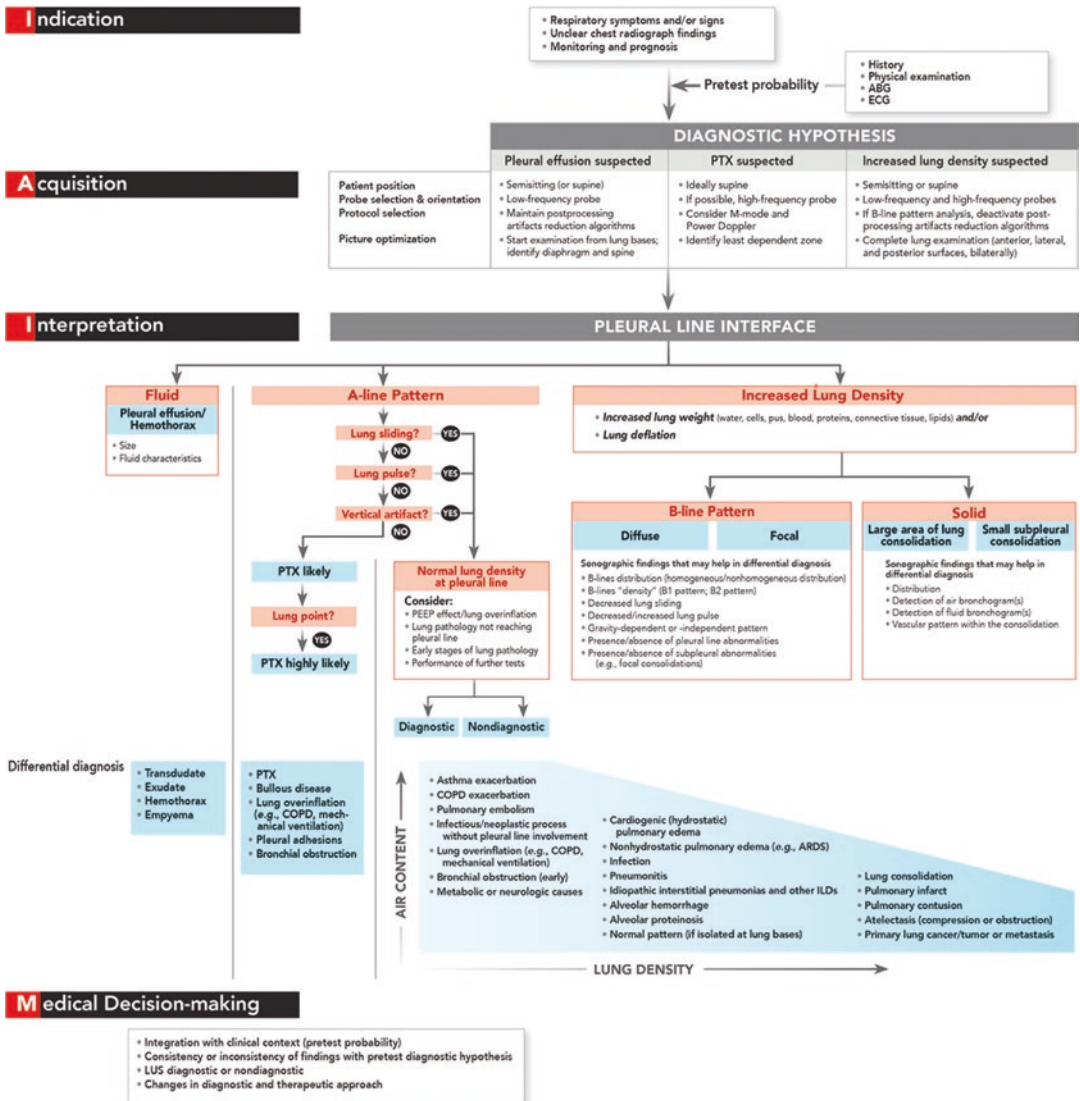


Fig. 34.8 Clinical application of the I-AIM framework for lung ultrasound. ABG arterial blood gas. ARDS acute respiratory distress syndrome; COPD chronic obstructive pulmonary disease; ECG electrocardiogram; ILDs interstitial lung diseases; LUS lung ultrasound; PEEP positive end-expiratory pressure; PTX pneumothorax. (Image

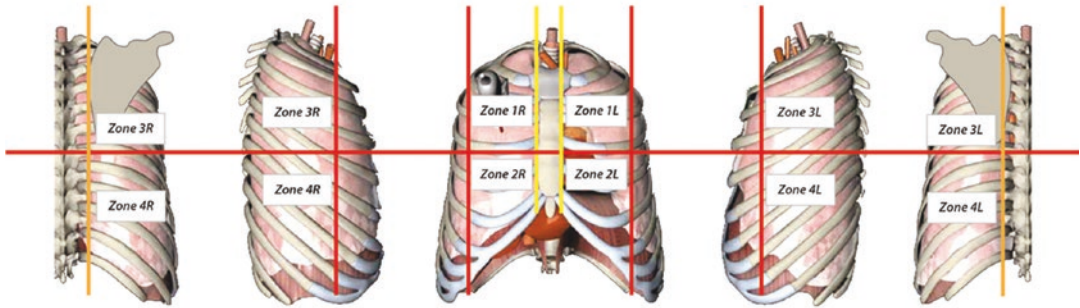
reproduced with permission from Wolters Kluwer: Kruiesselbrink et al. [3]. Promotional and commercial use of the material in print, digital or mobile device format is prohibited without the permission of the publisher Wolters Kluwer. Please contact healthpermissions@wolterskluwer.com for further information)

analysis of the pleural line, where three different patterns can be observed:

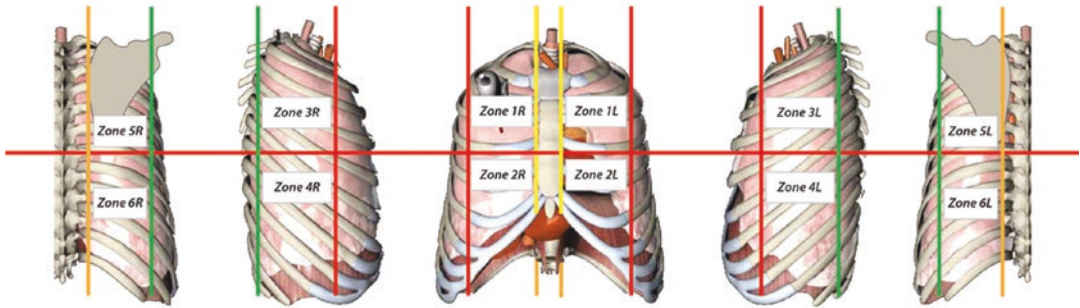
1. A-line pattern (i.e., normally aerated lung or presence of intrapleural air);
2. Anechoic pattern (i.e., pleural fluid);
3. Interstitial (B-lines) or alveolar syndrome (i.e., increased lung density).

When an A-line pattern is identified, one should immediately assess for pneumothorax by noting the presence or absence of pleural line movements (lung sliding and/or pulse) and vertical artifacts. Absence of all of these findings is highly suggestive of pneumothorax, whereas the presence of any or all of these findings excludes the diagnosis at the scanning

8-ZONE PROTOCOL



12-ZONE PROTOCOL



6-ZONE "EMERGENCY" PROTOCOL

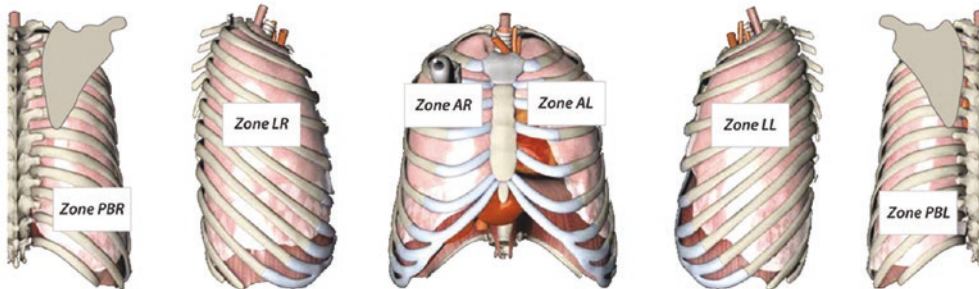


Fig. 34.9 Lung Ultrasound Scanning Protocols. AL anterior left, AR anterior right, LL lateral left, LR lateral right, PBL postero-basal left, PBR postero-basal right. (Image reproduced with permission from Wolters Kluwer: Kruiesselbrink et al. (Kruiesselbrink et al. 2017).

Promotional and commercial use of the material in print, digital or mobile device format is prohibited without the permission of the publisher Wolters Kluwer. Please contact healthpermissions@wolterskluwer.com for further information)

location. An A-line pattern with pleural line movements and few to no B-lines suggests normal lung density immediately below the visceral pleura; this pattern is seen in normal lung and also in pathologies not easily recognized by LUS (e.g., lung over-inflation, pathologies not reaching the pleural line, pulmonary vascular diseases).

Increased lung density can be caused by either (1) lung deflation (atelectasis) or (2) increased lung weight due to accumulation of water (edema), cells, pus, blood, proteins, connective tissue, or lipids. As previously mentioned, the distribution of B-lines/consolidation as well as additional sonographic findings may help to narrow the broad list of possible diagnoses:

- Diffuse versus focal B-line pattern;
- Large areas of lung consolidation versus small subpleural consolidations;
- B-lines distribution (homogeneous/nonhomogeneous);
- B-lines density (B1, B2 patterns);
- Decreased lung sliding;
- Decreased/increased lung pulse;
- Gravity-dependent or -independent pattern;
- Presence/absence of pleural line abnormalities;
- Presence/absence of subpleural abnormalities.
- Detection of air and/or fluid bronchograms;
- Doppler pattern within the consolidation.

The final step requires integration of LUS with the clinical context for appropriate MEDICAL DECISION-MAKING. LUS is rarely the sole answer in a diagnostic conundrum, and four possible outcomes should always be considered to avoid medical errors (Kruisselbrink et al. 2017):

1. LUS findings corroborate and support pre-test hypothesis;
2. LUS findings are mistakenly interpreted and mislead clinical decision-making (e.g., normal LUS in a patient with pneumonia not reaching pleural line);
3. LUS findings are inconsequential, neither supporting or changing initial hypothesis/plan.
4. LUS findings completely change the pre-test hypothesis (e.g., identification of pneumothorax in patient being assessed for COPD exacerbation).

Training

The operator dependency of LUS is a real concern, especially with its use expanding beyond select research centers and becoming commonplace in clinical practice. Adequate training (See et al. 2016; Rouby et al. 2018) and use of standardized protocols (Brandli 2007; Kruisselbrink et al. 2017) are extremely important to limit diagnostic error and variability in scanning and inter-

pretation. Approximately 25 supervised LUS examinations has been suggested as an adequate number of studies to achieve competency (Rouby et al. 2018).

Future Directions

Technology evolution will further facilitate the use of LUS in nontraditional scenarios, such as remote, limited-resource locations, ambulatory/community medicine settings, and emergency pre-hospital services. Development of tele-ultrasound in particular will certainly play a role in the expansion of LUS use in remote and/or under-resourced settings (Pian et al. 2013). Artificial intelligence and deep learning algorithms may further increase LUS use in research and clinical settings, leading to more precise diagnosis and quantification of lung injury. Finally, there is potential for LUS to be used not only as a diagnostic but also as a therapeutic tool. It has been recently demonstrated that commercially available microbubbles (currently used as a contrast agent), when exposed to ultrasounds, cause transient formation of pores and enhanced endocytosis of biological membranes increasing local uptake of drugs or genes (Fekri et al. 2016; Cao et al. 2015). In a murine experimental model of gram-negative pneumonia, Sugiyama et al. used LUS and microbubbles to increase gentamicin delivery to injured lungs enhancing bacterial killing (Sugiyama et al. 2018). If confirmed, this new application could create new therapeutic options for the treatment of lung diseases.

Conclusion

LUS is very useful in the initial assessment and subsequent monitoring of patients presenting with several respiratory conditions. Because of the unique interactions between ultrasound waves and aerated lung tissue, only a thorough and systematic approach focusing on correct indications, proper image acquisition and careful interpretation of both artifacts and anatomical findings allows accurate sonographic diagnosis and integration with clinical data.

Acknowledgements We would like to thank Jean YiChun Lin, Gordon Tait and Massimiliano Meineri from the Toronto General Hospital Department of Anesthesia Perioperative Interactive Education (<http://pie.med.utoronto.ca/index.htm>) for the generous sharing of their educational material.

References

- Agricola E, Bove T, Oppizzi M, Marino G, Zangrillo A, Margonato A, et al. "Ultrasound comet-tail images": a marker of pulmonary edema: a comparative study with wedge pressure and extravascular lung water. *Chest*. 2005;127(5):1690–5.
- Al Deeb M, Barbic S, Featherstone R, Dankoff J, Barbic D. Point-of-care ultrasonography for the diagnosis of acute cardiogenic pulmonary edema in patients presenting with acute dyspnea: a systematic review and meta-analysis. *Acad Emerg Med*. 2014;21(8):843–52.
- Aldrich JE. Basic physics of ultrasound imaging. *Crit Care Med*. 2007;35(5 Suppl):S131–7.
- Alrajab S, Youssef A, Akkus N, Caldito G. Pleural ultrasonography versus chest radiography for the diagnosis of pneumothorax: review of the literature and meta-analysis. *Crit Care*. 2013;17(5):R208.
- Alzaharani SA, Al-Salamah MA, Al-Madani WH, Elbarbary MA. Systematic review and meta-analysis for the use of ultrasound versus radiology in diagnosing of pneumonia. *Crit Ultrasound J*. 2017;9(1):6.
- Anderson KL, Fields JM, Panebianco NL, Jenq KY, Marin J, Dean AJ. Inter-rater reliability of quantifying pleural B-lines using multiple counting methods. *J Ultrasound Med*. 2013;32(1):115–20.
- Bahner DP, Hughes D, Royall NA. I-AIM: a novel model for teaching and performing focused sonography. *J Ultrasound Med*. 2012;31(2):295–300.
- Barskova T, Gargani L, Guiducci S, Randone SB, Bruni C, Carnesecchi G, et al. Lung ultrasound for the screening of interstitial lung disease in very early systemic sclerosis. *Ann Rheum Dis*. 2013;72(3):390–5.
- Bedetti G, Gargani L, Corbisiero A, Frassi F, Poggianti E, Mottola G. Evaluation of ultrasound lung comets by hand-held echocardiography. *Cardiovasc Ultrasound*. 2006;4(1):34.
- Bertrand PB, Levine RA, Isselbacher EM, Vandervoort PM. Fact or artifact in two-dimensional echocardiography: avoiding misdiagnosis and missed diagnosis. *J Am Soc Echocardiogr*. 2016;29(5):381–91.
- Bouhemad B, Brisson H, Le-Guen M, Arbelot C, Lu Q, Rouby JJ. Bedside ultrasound assessment of positive end-expiratory pressure-induced lung recruitment. *Am J Respir Crit Care Med*. 2011;183(3):341–7.
- Bouhemad B, Mongodi S, Via G, Rouquette I. Ultrasound for "lung monitoring" of ventilated patients. *Anesthesiology*. 2015;122(2):437–47.
- Brandli L. Benefits of protocol-driven ultrasound exams. *Radiol Manage*. 2007;29(4):56–9.
- Cao WJ, Rosenblat JD, Roth NC, Kuliszewski MA, Matkar PN, Rudenko D, et al. Therapeutic angiogenesis by ultrasound-mediated MicroRNA-126-3p delivery. *Arterioscler Thromb Vasc Biol*. 2015;35(11):2401–11.
- Cardinale L, Volpicelli G, Binello F, Garofalo G, Priola SM, Veltri A, et al. Clinical application of lung ultrasound in patients with acute dyspnea: differential diagnosis between cardiogenic and pulmonary causes. *Radiol Med*. 2009;114(7):1053–64.
- Chavez MA, Shams N, Ellington LE, Naithani N, Gilman RH, Steinhoff MC, et al. Lung ultrasound for the diagnosis of pneumonia in adults: a systematic review and meta-analysis. *Respir Res*. 2014;15(1):50.
- Chiumello D, Mongodi S, Algieri I, Vergani GL, Orlando A, Via G, et al. assessment of lung aeration and recruitment by CT scan and ultrasound in acute respiratory distress syndrome patients. *Crit Care Med*. 2018. [Epub ahead of print].
- Cibinel GA, Casoli G, Elia F, Padoan M, Pivetta E, Lupia E, et al. Diagnostic accuracy and reproducibility of pleural and lung ultrasound in discriminating cardiogenic causes of acute dyspnea in the Emergency Department. *Intern Emerg Med*. 2012;7(1):65–70.
- Copetti R, Soldati G, Copetti P. Chest sonography: a useful tool to differentiate acute cardiogenic pulmonary edema from acute respiratory distress syndrome. *Cardiovasc Ultrasound*. 2008;6(1):16.
- Definition Task Force ARDS. Acute respiratory distress syndrome: The Berlin Definition. *JAMA*. 2012;307(23):2526–33.
- Edelman SK. Understanding ultrasound physics. 4th ed. Woodlands: ESP Inc; 2012. p. 567.
- Engard P, Rademacher S, Nee J, Hasper D, Engert U, Jörres A, et al. Simplified lung ultrasound protocol shows excellent prediction of extravascular lung water in ventilated intensive care patients. *Crit Care*. 2015;19(1):36.
- Fekri F, Delos Santos RC, Karshafian R, Antonescu CN. Ultrasound microbubble treatment enhances clathrin-mediated endocytosis and fluid-phase uptake through distinct mechanisms. *PLoS One*. 2016;11(6):e0156754.
- Feldman MK, Katyal S, Blackwood MS. US artifacts. *Radiographics*. 2009;29(4):1179–89.
- Frassi F, Gargani L, Tesorio P, Raciti M, Mottola G, Picano E. Prognostic value of extravascular lung water assessed with ultrasound lung comets by chest sonography in patients with dyspnea and/or chest pain. *J Card Fail*. 2007;13(10):830–5.
- Gargani L, Lionetti V, Di Cristofano C, Bevilacqua G, Recchia FA, Picano E. Early detection of acute lung injury uncoupled to hypoxemia in pigs using ultrasound lung comets. *Crit Care Med*. 2007;35(12):2769–74.
- Gargani L, Frassi F, Soldati G, TESORIO P, GHEORGHIAD E M, Picano E. Ultrasound lung comets for the differential diagnosis of acute cardiogenic dyspnoea: a comparison with natriuretic peptides. *Eur J Heart Fail*. 2008;10(1):70–7.
- Gargani L, Doveri M, D'Errico L, Frassi F, Bazzichi ML, Sedie AD, et al. Ultrasound lung comets in

- systemic sclerosis: a chest sonography hallmark of pulmonary interstitial fibrosis. *Rheumatology*. 2009;48(11):1382–7.
- Gargani L, Pang PS, Frassi F, Miglioranza MH, Dini FL, Landi P, et al. Persistent pulmonary congestion before discharge predicts rehospitalization in heart failure: a lung ultrasound study. *Cardiovasc Ultrasound*. 2015;13(1):40.
- Goffi A, Krusselbrink R, Volpicelli G. The sound of air: point-of-care lung ultrasound in perioperative medicine. *Can J Anesth*. 2018;65(4):399–416.
- Gordon CE, Feller-Kopman D, Balk EM, Smetana GW. Pneumothorax following thoracentesis: a systematic review and meta-analysis. *Arch Intern Med*. 2010;170(4):332–9.
- Haddam M, Zieleskiewicz L, Perbet S, Baldovini A, Guervilly C, Arbelot C, et al. Lung ultrasonography for assessment of oxygenation response to prone position ventilation in ARDS. *Intensive Care Med*. 2016;42(10):1546–155.
- Jambrik Z, Monti S, Coppola V, Agricola E, Mottola G, Miniati M, et al. Usefulness of ultrasound lung comets as a nonradiologic sign of extravascular lung water. *Am J Cardiol*. 2004;93(10):1265–70.
- Jiang L, Ma Y, Zhao C, Shen W, Feng X, Xu Y, et al. Role of transthoracic lung ultrasonography in the diagnosis of pulmonary embolism: a systematic review and meta-analysis. *PLoS One*. 2015;10(6):e0129909.
- Kendall JL, Hoffenberg SR, Smith RS. History of emergency and critical care ultrasound: the evolution of a new imaging paradigm. *Crit Care Med*. 2007;35(5 Suppl):S126–30.
- Krusselbrink R, Chan V, Cibinel GA, Abrahamson S, Goffi A. I-AIM (indication, acquisition, interpretation, medical decision-making) framework for point of care lung ultrasound. *Anesthesiology*. 2017;127(3):568–82.
- Laursen CB, Sloth E, Lassen AT, Christensen R, de Pont LJ, Madsen PH, et al. Point-of-care ultrasonography in patients admitted with respiratory symptoms: a single-blind, randomised controlled trial. *Lancet Respir Med*. 2014;2(8):638–46.
- Lederer DJ, Martinez FJ. Idiopathic pulmonary fibrosis. *N Engl J Med*. 2018;379(8):797–8.
- Lichtenstein DA, Mezière GA. Relevance of Lung Ultrasound in the Diagnosis of Acute Respiratory Failure. *Chest*. 2008;134(1):117–25.
- Lichtenstein D, Mézière G, Biderman P, Gepner A, Barré O. The comet-tail artifact. An ultrasound sign of alveolar-interstitial syndrome. *Am J Respir Crit Care Med*. 1997;156(5):1640–6.
- Lichtenstein D, Mezière G, Biderman P, Gepner A. The “lung point”: an ultrasound sign specific to pneumothorax. *Intensive Care Med*. 2000;26(10):1434–40.
- Lichtenstein DA, Lascols N, Prin S, Mezière G. The “lung pulse”: an early ultrasound sign of complete atelectasis. *Intensive Care Med*. 2003;29(12):2187–92.
- Lichtenstein DA, Lascols N, Mezière G, Gepner A. Ultrasound diagnosis of alveolar consolidation in the critically ill. *Intensive Care Med*. 2004;30(2):276–81.
- Lichtenstein D, Mezière G, Seitz J. The dynamic air bronchogram. A lung ultrasound sign of alveolar consolidation ruling out atelectasis. *Chest*. 2009;135(6):1421–5.
- Liteplo AS, Marill KA, Villen T, Miller RM, Murray AF, Croft PE, et al. Emergency thoracic ultrasound in the differentiation of the etiology of shortness of breath (ETUDES): sonographic B-lines and N-terminal pro-brain-type natriuretic peptide in diagnosing congestive heart failure. *Acad Emerg Med*. 2009;16(3):201–10.
- Liteplo AS, Murray AF, Kimberley HH, Noble VE. Real-time resolution of sonographic B-lines in a patient with pulmonary edema on continuous positive airway pressure. *Am J Emerg Med*. 2010;28(4):541.e5–8.
- Mallamaci F, Benedetto FA, Tripepi R, Rastelli S, Castellino P, Castellino P, et al. Detection of pulmonary congestion by chest ultrasound in dialysis patients. *JACC Cardiovasc Imaging*. 2010;3(6):586–94.
- Manolescu D, Davidescu L, Traila D, Oancea C, Tudorache V. The reliability of lung ultrasound in assessment of idiopathic pulmonary fibrosis. *Clin Interv Aging*. 2018;13:437–49.
- Martindale JL, Secko M, Kilpatrick JF, de Souza IS, Paladino L, Aherne A, et al. Serial Sonographic Assessment of Pulmonary Edema in Patients With Hypertensive Acute Heart Failure. *J Ultrasound Med*. 2017;2(4):269.
- Mathis G. Thoraxsonography—part II: peripheral pulmonary consolidation. *Ultrasound Med Biol*. 1997;23(8):1141–53.
- Mathis G, Blank W, Reissig A, Lechleitner P, Reuss J, Schuler A, et al. Thoracic ultrasound for diagnosing pulmonary embolism: a prospective multicenter study of 352 patients. *Chest*. 2005;128(3):1531–8.
- Miglioranza MH, Gargani L, Sant’Anna RT, Rover MM, Martins VM, Mantovani A, et al. Lung ultrasound for the evaluation of pulmonary congestion in outpatients: a comparison with clinical assessment, natriuretic peptides, and echocardiography. *JACC Cardiovasc Imaging*. 2013;6(11):1141–51.
- Mongodi S, Pozzi M, Orlando A, Bouhemad B, Stella A, Tavazzi G, et al. Lung ultrasound for daily monitoring of ARDS patients on extracorporeal membrane oxygenation: preliminary experience. *Intensive Care Med*. 2017;42(Suppl 1):682–6.
- Nazerian P, Vanni S, Volpicelli G, Gigli C, Zanobetti M, Bartolucci M, et al. Accuracy of point-of-care multi-organ ultrasonography for the diagnosis of pulmonary embolism. *Chest*. 2014;145(5):950–7.
- Nazerian P, Volpicelli G, Vanni S, Gigli C, Betti L, Bartolucci M, et al. Accuracy of lung ultrasound for the diagnosis of consolidations when compared to chest computed tomography. *Am J Emerg Med*. 2015;33(5):620–5.
- Noble VE, Murray AF, Capp R, Sylvia-Reardon MH, Steele DJR, Liteplo A. Ultrasound assessment for extravascular lung water in patients undergoing hemodialysis. Time course for resolution. *Chest*. 2009;135(6):1433–9.

- Orso D, Guglielmo N, Copetti R. Lung ultrasound in diagnosing pneumonia in the emergency department. *Eur J Emerg Med.* 2018;25(5):312–21.
- Peris A, Tutino L, Zagli G, Batacchi S, Cianchi G, Spina R, et al. The use of point-of-care bedside lung ultrasound significantly reduces the number of radiographs and computed tomography scans in critically ill patients. *Anesth Analg.* 2010;111(3):687–92.
- Persona P, De Cassai A, Franco M, Facchin F, Ori C, Rossi S, et al. Prone position and lung ultrasound (PROPLUS) in ARDS. *Intensive Care Med Exp. Milan, Italy.* 2016;4(Suppl 1):27.
- Pian L, Gillman LM, McBeth PB, Xiao Z, Ball CG, Blaivas M, et al. Potential use of remote teleultrasonography as a transformational technology in underresourced and/or remote settings. *Emerg Med Int.* 2013;2013:986160.
- Pichette M, Goffi A. A 45-year-old man with severe respiratory failure after cardiac arrest. *Chest.* 2018;153(6):e133–7.
- Pivetta E, Goffi A, Lupia E, Tizzani M, Porrino G, Ferreri E, et al. Lung ultrasound-implemented diagnosis of acute decompensated heart failure in the ED: a SIMEU multicenter study. *Chest.* 2015;148(1):202–10.
- Platz E, Merz AA, Jhund PS, Vazir A, Campbell R, McMurray JJ. Dynamic changes and prognostic value of pulmonary congestion by lung ultrasound in acute and chronic heart failure: a systematic review. *Eur J Heart Fail.* 2017;19(9):1154–63.
- Prat G, Guinard S, Bizien N, Nowak E, Tonnelier J-M, Alavi Z, et al. Can lung ultrasonography predict prone positioning response in acute respiratory distress syndrome patients? *J Crit Care.* 2016;32:36–41.
- Reissig A, Copetti R, Kroegel C. Current role of emergency ultrasound of the chest*. *Crit Care Med.* 2011;39(4):839–45.
- Reissig A, Copetti R, Mathis G, Mempel C, Schuler A, Zechner P, et al. Lung ultrasound in the diagnosis and follow-up of community-acquired pneumonia: a prospective, multicenter, diagnostic accuracy study. *Chest.* 2012;142(4):965–72.
- Riviello ED, Kiviri W, Twagirumugabe T, Mueller A, Banner-Goodspeed VM, Officer L, et al. Hospital incidence and outcomes of the acute respiratory distress syndrome using the Kigali modification of the Berlin definition. *Am J Respir Crit Care Med.* 2016;193(1):52–9.
- Rosas IO, Dellaripa PF, Lederer DJ, Khanna D, Young LR, Martinez FJ. Interstitial lung disease: NHLBI workshop on the primary prevention of chronic lung diseases. *Ann Am Thorac Soc.* 2014;11(Suppl 3):S169–77.
- Rouby J-J, Arbelot C, Gao Y, Zhang M, Lv J, An Y, et al. Training for lung ultrasound score measurement in critically ill patients. *Am J Respir Crit Care Med.* 2018; [Epub ahead of print].
- Scharonow M, Weilbach C. Prehospital point-of-care emergency ultrasound: a cohort study. *Scand J Trauma Resusc Emerg Med.* 2018;26(1):49.
- See KC, Ong V, Wong SH, Leanda R, Santos J, Taculod J, et al. Lung ultrasound training: curriculum implementation and learning trajectory among respiratory therapists. *Intensive Care Med.* 2016;42(1):63–71.
- See KC, Ong V, Tan YL, Sahagun J, Taculod J. Chest radiography versus lung ultrasound for identification of acute respiratory distress syndrome: a retrospective observational study. *Crit Care.* 2018;22(1):203.
- Sekiguchi H, Schenck LA, Horie R, Suzuki J, Lee EH, McMenomy BP, et al. Critical care ultrasonography differentiates ARDS, pulmonary edema, and other causes in the early course of acute hypoxemic respiratory failure. *Chest.* 2015;148(4):912–8.
- Sikora K, Perera P, Mailhot T, Mandavia D. Ultrasound for the detection of pleural effusions and guidance of the thoracentesis procedure. *Emerg Med.* 2012;2012(4):1–10.
- Silva S, Ait Aissa D, Cocquet P, Hoarau L, Ruiz J, Ferre F, et al. Combined thoracic ultrasound assessment during a successful weaning trial predicts Postextubation distress. *Anesthesiology.* 2017;127(4):666–74.
- Soldati G, Demi M. The use of lung ultrasound images for the differential diagnosis of pulmonary and cardiac interstitial pathology. *J Ultrasound.* 2017;20(2):91–6.
- Soldati G, Testa A, Silva FR, Carbone L, Portale G, Silveri NG. Chest ultrasonography in lung contusion. *Chest.* 2006;130(2):533–8.
- Soldati G, Demi M, Inchingolo R, Smargiassi A, Demi L. On the physical basis of pulmonary sonographic interstitial syndrome. *J Ultrasound Med.* 2016;35(10):2075–86.
- Song GG, Bae S-C, Lee YH. Diagnostic accuracy of lung ultrasound for interstitial lung disease in patients with connective tissue diseases: a meta-analysis. *Clin Exp Rheumatol.* 2016;34(1):11–6.
- Song I-K, Kim E-H, Lee J-H, Ro S, Kim H-S, Kim J-T. Effects of an alveolar recruitment manoeuvre guided by lung ultrasound on anaesthesia-induced atelectasis in infants: a randomised, controlled trial. *Anaesthesia.* 2017;72(2):214–22.
- Soummer A, Perbet S, Brisson H, Arbelot C, Constantin J-M, Lu Q, et al. Ultrasound assessment of lung aeration loss during a successful weaning trial predicts postextubation distress. *Crit Care Med.* 2012;40(7):2064–7.
- Sperandeo M, Varriale A, Sperandeo G, Filabozzi P, Piattelli ML, Carnevale V, et al. Transthoracic ultrasound in the evaluation of pulmonary fibrosis: our experience. *Ultrasound Med Biol.* 2009;35(5):723–9.
- Staub LJ, Biscaro RRM, Kaszubowski E, Maurici R. Chest ultrasonography for the emergency diagnosis of traumatic pneumothorax and haemothorax: a systematic review and meta-analysis. *Injury.* 2018;49(3):457–66.
- Stefanidis K, Dimopoulos S, Tripodaki E-S, Vintzilaios K, Politis P, Piperopoulos P, et al. Lung sonography and recruitment in patients with early acute respiratory distress syndrome - a pilot study. *Crit Care.* 2011;15(4):R185.
- Strnad M, Prosen G, Borovnik LV. Bedside lung ultrasound for monitoring the effectiveness of prehospital treatment with continuous positive airway pressure in acute decompensated heart failure. *Eur J Emerg Med.* 2016;23(1):50–5.

- Sugiyama MG, Mintsopoulos V, Raheel H, Goldenberg NM, Batt JE, Brochard L, et al. Lung ultrasound and microbubbles enhance aminoglycoside efficacy and delivery to the lung in *Escherichia coli*-induced pneumonia and acute respiratory distress syndrome. *Am J Respir Crit Care Med*. 2018;198(3):404–8.
- Tusman G, Böhm SH, Tempra A, Melkun F, García E, Turchetto E, et al. Effects of recruitment maneuver on atelectasis in anesthetized children. *Anesthesiology*. 2003;98(1):14–22.
- Tusman G, Acosta CM, Nicola M, Esperatti M, Bohm SH, Suárez-Sipmann F. Real-time images of tidal recruitment using lung ultrasound. *Crit Ultrasound J*. 2015;7(1):19.
- Tusman G, Acosta CM, Costantini M. Ultrasonography for the assessment of lung recruitment maneuvers. *Crit Ultrasound J*. 2016;8(1):8.
- Via G, Lichtenstein D, Mojoli F, Rodi G, Neri L, Storti E, et al. Whole lung lavage: a unique model for ultrasound assessment of lung aeration changes. *Intensive Care Med*. 2010;36(6):999–1007.
- Volpicelli G. Sonographic diagnosis of pneumothorax. *Intensive Care Med*. 2010;37(2):224–32.
- Volpicelli G. Lung sonography. *J Ultrasound Med*. 2013;32(1):165–71.
- Volpicelli G, Mussa A, Garofalo G, Cardinale L, Casoli G, Perotto F, et al. Bedside lung ultrasound in the assessment of alveolar-interstitial syndrome. *Am J Emerg Med*. 2006;24(6):689–96.
- Volpicelli G, Caramello V, Cardinale L, Mussa A, Bar F, Frascisco MF. Detection of sonographic B-lines in patients with normal lung or radiographic alveolar consolidation. *Med Sci Monit*. 2008a;14(3):CR122–8.
- Volpicelli G, Caramello V, Cardinale L, Cravino M. Diagnosis of radio-occult pulmonary conditions by real-time chest ultrasonography in patients with pleuritic pain. *Ultrasound Med Biol*. 2008b;34(11):1717–23.
- Volpicelli G, Silva F, Radeos M. Real-time lung ultrasound for the diagnosis of alveolar consolidation and interstitial syndrome in the emergency department. *Eur J Emerg Med*. 2010;17(2):63–72.
- Volpicelli G, Elbarbary M, Blaivas M, Lichtenstein DA, Mathis G, Kirkpatrick AW, et al. International evidence-based recommendations for point-of-care lung ultrasound. *Intensive Care Med*. 2012;38(4):577–91.
- Volpicelli G, Skurzak S, Boero E, Carpinteri G, Tengattini M, Stefanone V, et al. Lung ultrasound predicts well extravascular lung water but is of limited usefulness in the prediction of wedge pressure. *Anesthesiology*. 2014;121(2):320–7.
- Wang X, Ding X, Zhang H, Chen H, Su L, Liu D. Lung ultrasound can be used to predict the potential of prone positioning and assess prognosis in patients with acute respiratory distress syndrome. *Crit Care*. 2016;20(1):385.
- Xirouchaki N, Georgopoulos D. Impact of lung ultrasound on clinical decision making in critically ill patients: response to O'Connor et al. *Intensive Care Med*. 2014;40(7):1063.
- Xirouchaki N, Kondili E, Prinianakis G, Malliotakis P, Georgopoulos D. Impact of lung ultrasound on clinical decision making in critically ill patients. *Intensive Care Med*. 2014;40(1):57–65.
- Ye X, Xiao H, Chen B, Zhang S. Accuracy of lung ultrasonography versus chest radiography for the diagnosis of adult community-acquired pneumonia: review of the literature and meta-analysis. *PLoS One*. 2015;10(6):e0130066.
- Yousefifard M, Baikpour M, Ghelichkhani P, Asady H, Shahsavari Nia K, Moghadas Jafari A, et al. Screening performance characteristic of ultrasonography and radiography in detection of pleural effusion; a meta-analysis. *Emergency*. 2016;4(1):1–10.
- Zanobetti M, Scorpiniti M, Gigli C, Nazerian P, Vanni S, Innocenti F, et al. Point-of-care ultrasonography for evaluation of acute dyspnea in the ED. *Chest*. 2017;151(6):1295–301.
- Zoccali C, Torino C, Tripepi R, Tripepi G, D'Arrigo G, Postorino M, et al. Pulmonary congestion predicts cardiac events and mortality in ESRD. *J Am Soc Nephrol*. 2013;24(4):639–46.



Diaphragm Ultrasound: Physiology and Applications

35

Ewan C. Goligher

Introduction

Diaphragm ultrasound permits direct visual assessment of diaphragm structure and function. First described in the 1980s, the technique has become an invaluable physiological tool for research and clinical practice in both outpatient and critical care settings. The complex structure and function of the diaphragm must be appreciated to correctly interpret diaphragm sonographic data. This chapter provides an overview of the anatomical and physiological basis for diaphragm ultrasound imaging, the techniques used to evaluate the diaphragm by ultrasound, and the applications of these techniques in research and clinical practice.

Physiological Basis of Diaphragm Ultrasound

Basic Functional Anatomy of the Diaphragm

The diaphragm is a thin, dome-shaped muscular structure separating the thoracic and abdominal cavities. It is composed of three separate segments: the central tendon (a noncontractile structure through which major blood vessels transit; the costal diaphragm, which has fibers projecting onto the rib cage and xiphoid process; and the crural diaphragm, the fibers of which insert into the first three lumbar vertebrae (Fig. 35.1). Given this anatomical arrangement, crural diaphragmatic contractions tend to lower the dome of the diaphragm, while costal diaphragmatic contractions both lower the dome of the diaphragm and expand the lower rib cage (the latter depending on opposition from the abdominal contents) (Fig. 35.1). The outer aspect of the costal diaphragm is apposed to the rib cage, covering approximately 1/3 of the lower rib cage surface at functional residual capacity in health (Mead 1979). The thickness of the diaphragm is variable over its surface, with tapering from the anterior to posterior costal regions, and from its costal insertions to the central tendon (Poole et al. 1997).

E. C. Goligher (✉)
Interdepartmental Division of Critical Care Medicine,
University of Toronto, Toronto, ON, Canada

Department of Medicine, Division of Respiriology,
University Health Network, Toronto, ON, Canada

Toronto General Hospital Research Institute,
Toronto, ON, Canada
e-mail: ewan.goligher@mail.utoronto.ca

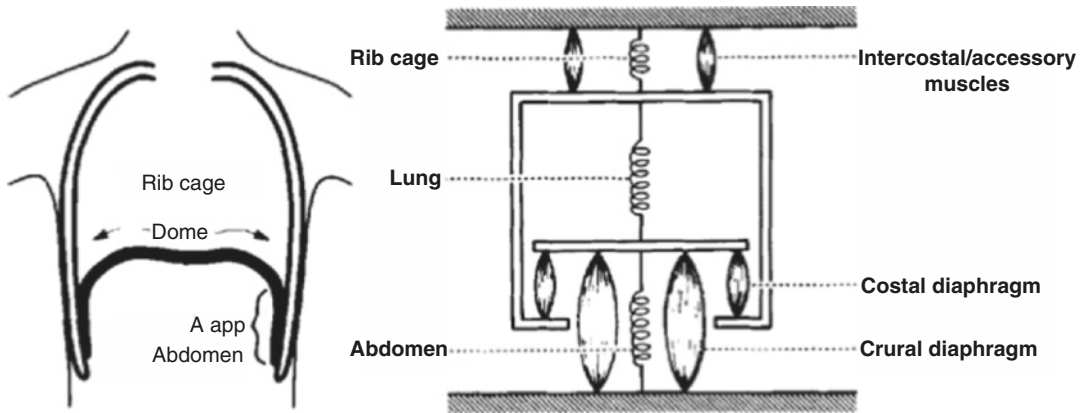


Fig. 35.1 Functional anatomy of the diaphragm. The diaphragm is a dome-shaped muscle with a substantial proportion of its surface area apposed to the chest wall (the zone of apposition). The crural diaphragm inserts into the spine; crural diaphragmatic contractions lower the dome

of the diaphragm. The costal diaphragm inserts into the rib cage; costal diaphragmatic contractions lower the dome and elevate and expand the lower rib cage. (Figure from Loring and De Troyer 1986. Used with permission of Wiley)

Basic Mechanics of Diaphragm Contraction

Under normal conditions, the diaphragm moves within the chest much like a piston within a cylinder, generating flow as its dome descends within the thoracic cavity, displacing the abdominal contents beneath and expanding the lower rib cage. During contractile shortening, the shape of the diaphragm changes relatively little in the coronal plane (Gauthier et al. 1994); rather, the shortening translates into axial descent. The shape of the dome flattens, to some extent, in the sagittal plane as the diaphragm shortens posteriorly more than it does anteriorly.

The pressure gradient generated across the dome between the thoracic and abdominal cavities, the transdiaphragmatic pressure (P_{di} , quantified as the gradient between the gastric pressure, P_{ga} , and the esophageal pressure, P_{es} (Agostoni and Rahn 1960)), is proportional to the tension developed within the muscle fibers and inversely proportional to the cross-sectional area of the thoracic cavity at the level of the dome (Troyer and Loring 1986; Braun et al. 1982). The geometric configuration of the dome (i.e. its radius of curvature) exerts relatively minor influence on transdiaphragmatic pressure generation except at high lung volumes (Troyer and Loring 1986).

The relations between diaphragmatic shortening and transdiaphragmatic pressure generation are complex, influenced by the length-tension relationship and the force-velocity relationship. These factors are in turn determined by the respiratory mechanics and by the action of other inspiratory and expiratory muscles.

The length-tension relation, a feature of muscle function arising from myosin-actin filament interactions during myofibril excitation-contraction coupling, entails that as muscle is passively lengthened prior to contraction (until some optimal length is obtained), the force generated in response to a given stimulus progressively increases (Braun et al. 1982). Given the diaphragm's unique anatomical situation, resting length also modifies diaphragm force generation by changing the surface area of the zone of apposition which determines the force applied to expand the lower rib cage. As a consequence, diaphragmatic force generation varies considerably with its resting length—and therefore with end-expiratory lung volume.

The force-velocity relation is closely related to the length-tension relation: the more rapidly a muscle shortens during contraction, the lower the force generated during contraction (Coirault et al. 1995). Consequently, greater transdiaphragmatic pressure will be generated for a given

degree of diaphragmatic shortening if diaphragmatic descent is resisted by the simultaneous activation of rib cage inspiratory muscles (which “pull” the diaphragm upward) or if increased airways resistance or lung elastance impede diaphragmatic descent. The overall pattern of thoracoabdominal motion therefore influences the relationship between muscular shortening and force generation. These relationships are fundamental to understanding the relationship between sonographic measurements of diaphragm function and diaphragmatic force generation.

Sonographic Correlates of Diaphragm Structure and Function

Structure

Transthoracic ultrasound permits visualization of the diaphragm in cross-section in the zone of apposition (Matamis et al. 2013) (Fig. 35.2). This permits direct measurement of diaphragm muscle thickness; the validity of these measurements has been directly confirmed in autopsy studies (Wait et al. 1989; Cohn et al. 1997). Because the thickness of the diaphragm is small relative to its radius of curvature, changes in muscle cross-sectional area are directly proportional to changes in thickness. Ultrasound has been used to moni-

tor changes in diaphragm thickness over time, for example, in patients with idiopathic diaphragmatic paralysis (Summerhill et al. 2008), during long-term diaphragm pacing (Ayas et al. 1999), or during mechanical ventilation (Goligher et al. 2015a). Because diaphragm thickness varies across its surface, thickness measurements should be referenced to the exact location of the ultrasound probe (Goligher et al. 2015b). In healthy subjects, right hemidiaphragm thickness measured at the eighth or ninth intercostal space at the anterior axillary line is approximately 3.3 mm (range 1.3–7.6 mm) (Boon et al. 2013), and left hemidiaphragm thickness at the same location on the left chest wall is similar: 3.4 mm (range 1.2–12 mm) (Boon et al. 2013). Diaphragm thickness is slightly lower in women than in men (Boon et al. 2013) and is correlated with height and weight (McCool et al. 1997) but is independent of age or smoking status (Boon et al. 2013). Physical training such as weight-lifting increases diaphragm thickness (McCool et al. 1997). In cardiopulmonary disease, diaphragm thickness may be atrophic, increased, or relatively spared (de Bruin et al. 1997a, b; Pinet et al. 2003).

Changes in muscle quality can be detected on ultrasound by measurement of echodensity (the “brightness” of the ultrasound region relative to a standard image). Muscle echodensity increases in a variety of acute and chronic muscle disease states (Sarwal et al. 2014, 2015), signifying

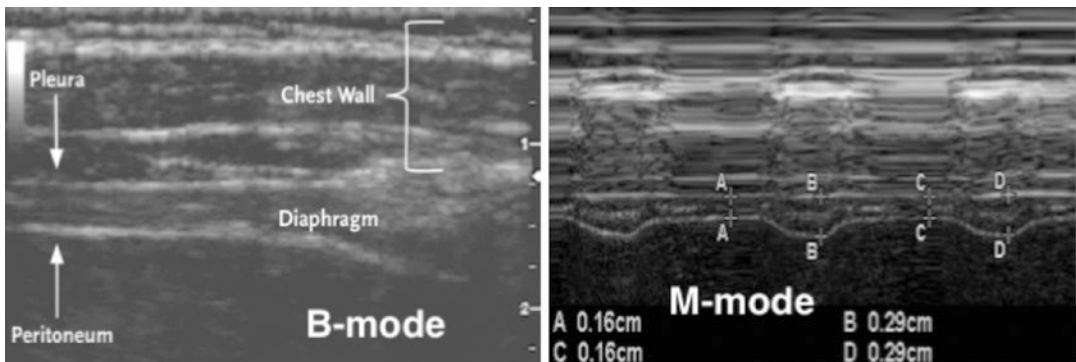


Fig. 35.2 B-mode and M-mode images of diaphragm thickness and thickening. Viewed in cross-section in the zone of apposition, the diaphragm is demarcated as the relatively hypoechoic region between the echogenic pleural and peritoneal lines. During M-mode imaging, the

thickening of the diaphragm during its contractions may be visualized and quantified. Markers A and C indicate the thickness of the diaphragm at end-expiration; markers B and D indicate the thickness of the diaphragm at peak inspiration

muscle inflammation, necrosis, and/or connective tissue deposition (Sarwal et al. 2013; Boussuges et al. 2009). A method for quantifying echodensity of the diaphragm was recently reported (Sarwal et al. 2015), but the physiological and clinical import of changes in diaphragm echodensity have not yet been established.

Motion

Diaphragmatic motion can be assessed by visualizing the dome of the diaphragm on ultrasound (Fig. 35.3). The downward excursion of the dome during inspiration can be easily quantified using M-mode ultrasound (details below) (Matamis et al. 2013; Sarwal et al. 2013). This technique provides a method of assessing diaphragm function analogous to conventional fluoroscopy: normal values of diaphragm excursion during various inspiratory maneuvers have been published (Boussuges et al. 2009), and the reproducibility of this technique is excellent (Boussuges et al. 2009) (Table 35.1 for normal values).

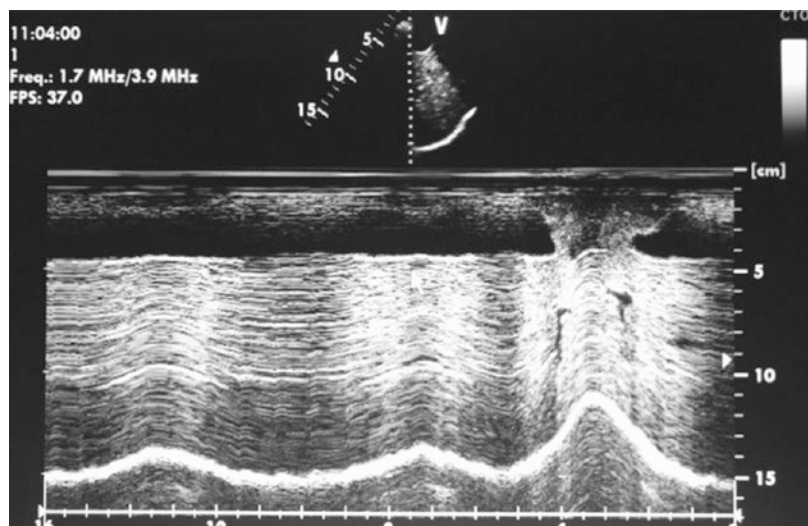
Because the diaphragm primarily functions by shortening within the thorax like a piston within a cylinder, diaphragm excursion can be used to assess muscle performance. Diminished diaphragm excursion has been shown to be diagnostic of diaphragm dysfunction (Lerolle et al. 2009). This technique can also visualize the paradoxical motion of the diaphragm (upward move-

ment of the hemidiaphragm during inspiration) which may be seen in the context of severe diaphragmatic weakness (Nason et al. 2012) or from “inversion” of the muscle due to massive pleural effusion (Cooper and Elliott 1995).

In non-ventilated subjects, downward motion of the diaphragm during inspiration can be attributed to diaphragmatic contraction (though some downward motion may also result from pre-inspiratory abdominal muscle relaxation) (Lessard et al. 1995). In ventilated subjects, the downward inspiratory motion may also result from passive insufflation of the chest by the ventilator. Consequently, diaphragmatic motion cannot be used to assess inspiratory effort or diaphragm function in ventilated patients unless inspiratory pressure support is temporarily withdrawn (Fig. 35.4); even CPAP may support the diaphragmatic motion (Umbrello et al. 2015). Inferences about diaphragm function from sonographic measurements of diaphragm motion are only valid when these measurements are obtained during a T-piece trial in these patients.

Because muscle relaxation is an energy-dependent process, the development of muscle fatigue leads to the slowing of muscle relaxation following each contractile effort (Esau et al. 1983). This slowing has traditionally detected by assessing changes in the rate of Pdi decay during expiration; by visualizing diaphragm motion in M-mode, the maximal rate of expiratory dia-

Fig. 35.3 Diaphragm excursion visualized by M-mode ultrasound. The B-mode image is shown at the top of the figure. The subject takes two tidal breaths and then inhales to total lung capacity, increasing diaphragm excursion on the final breath



phragm relaxation can also be measured noninvasively to detect the development of fatigue (Matamis et al. 2013).

Shortening

While respiratory muscle activity and function are generally evaluated in terms of pressure gen-

eration (i.e. for the diaphragm, Pdi), the diaphragm’s primary function is to shorten so as to generate inspiratory flow and volume. As a muscle shortens, its cross-sectional area increases due to the increasing overlap of actin-myosin filaments within sarcomeres (Wait et al. 1989). Increases in diaphragm cross-sectional area are readily visualized as increases in muscle thickness during inspiration. These dynamic changes in thickness during inspiration have been measured as the thickening ratio (peak thickness/end-expiratory thickness) or thickening fraction ($[\text{peak thickness} - \text{end-expiratory thickness}] / \text{end-expiratory thickness}$). We will employ the latter quantity throughout this discussion.

Table 35.1 Reference range for diaphragm ultrasound measurements

Measurement	Reference range Mean (5th–95th percentile)
End-expiratory right hemidiaphragm thickness	3.3 mm (0.17 mm–0.53 mm) (Boon et al. 2013)
Diaphragm thickening fraction during resting breathing	20% (5%–50%) (Harper et al. 2013)
Maximal diaphragm thickening fraction	80% (20%–180%) (Boon et al. 2013; Gottesman and McCool 1997)
Diaphragm excursion during resting breathing	1.7 cm (1.0–2.5 cm)
Diaphragm excursion during sniffing	2.7 cm (1.6–4.4 cm)
Diaphragm excursion during inspiratory capacity maneuver	6.5 cm (3.6–9.2 cm)

Diaphragm Thickening: Relation to Inspiratory Volume

The relationship between changes in the thickness of the diaphragm during inspiration and its physiological action has been explored in considerable detail. The relationship between thickness and fiber length is complex. Assuming that the volume of the diaphragm muscle remains constant as it shortens, muscle thickness will vary inversely with muscle length. The thickness of the diaphragm increases with lung volume

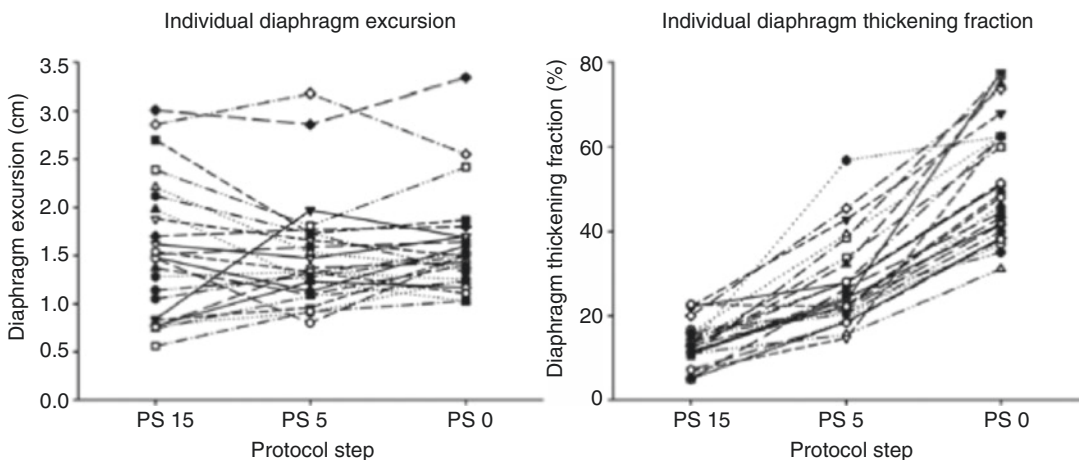


Fig. 35.4 The influence of reducing ventilator support on patient respiratory effort is reflected by changes in diaphragm thickening fraction (right) signifying an increase in contractile activation; because the increase in diaphragmatic effort counterbalances the reduction in ventilator support, overall diaphragm motion (reflecting thoracic

volume changes) is unaffected by changes in ventilator support (left). (Figure from Umbrello et al. 2015. © Umbrello et al.; licensee BioMed Central. 2015. Permission granted under the Creative Commons License. <https://ccforum.biomedcentral.com/articles/10.1186/s13054-015-0894-9>)

during inspiration (Wait et al. 1989; Cohn et al. 1997) although the slope of this relation varies considerably between subjects. The unique geometric arrangements of diaphragm muscle fibers (with fibers arranged cylindrically arising from the central tendon in the dome) probably modify this relationship because sarcomeres may “enter” the zone of apposition as the dome descends (Wait and Johnson 1997). Thus, some observations suggest that diaphragm thickness increases out of proportion to changes in muscle length as lung volume increases (Wait and Johnson 1997) while others suggest that increases in thickness are consistent with what would be expected for changes in muscle length (Cohn et al. 1997).

The relationship between muscle thickness and lung volume also depends on whether increases in lung volume result from active inspi-

ration or passive insufflation. Smaller increases in lung volume (<50% of inspiratory capacity) do not increase diaphragm thickness in the absence of diaphragm contractile activation, whereas larger increases in lung volume increase diaphragm thickness even in the absence of contractile activity (Goligher et al. 2015b) (Fig. 35.5). Smaller increases in lung volume may therefore primarily be accommodated by changes in the shape of the diaphragm apart from changes in muscle length. This finding suggests that diaphragm thickening during mechanical ventilation can be used to make inferences about contractile activation in the usual range of tidal volumes employed in the clinical setting (<50% of inspiratory capacity in health).

Finally, the relationship between diaphragm thickness and lung volume depends on the nature

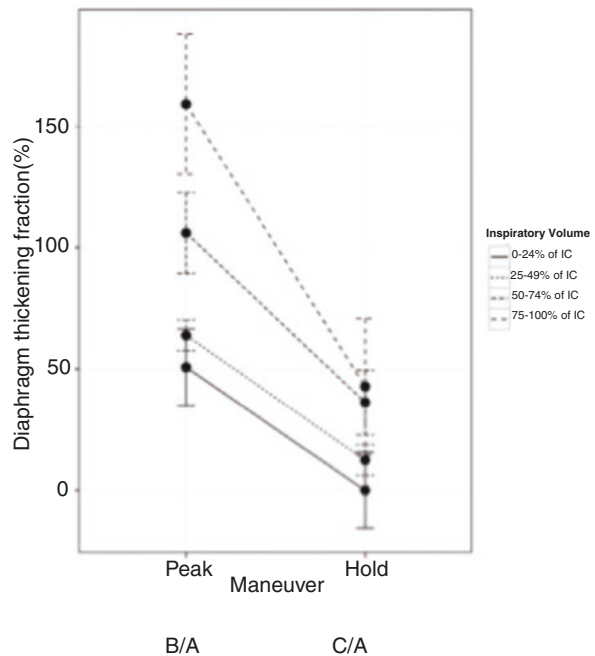
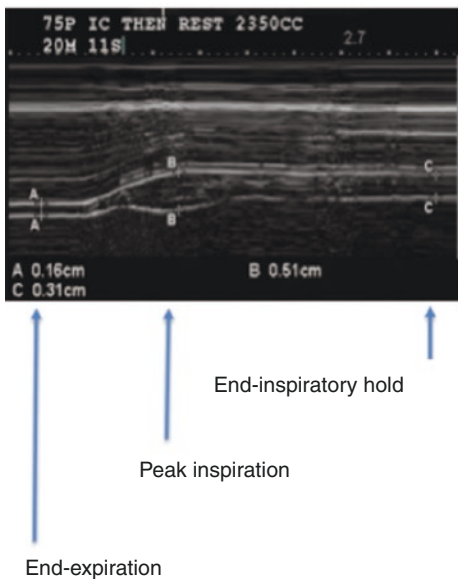


Fig. 35.5 Influence of effort and lung volume on diaphragm thickness. Healthy subjects were instructed to inspire from the functional residual capacity (point A) to a series of progressively greater target inspiratory volumes. Upon reaching the target volume (point B), subjects were instructed to close the glottis while relaxing the inspiratory muscles to maintain lung volume in the absence of inspiratory effort (point C) so as to isolate the influence of lung volume on diaphragm thickness. At lower inspiratory volumes below 50% of inspiratory capacity, diaphragm

thickness returned to a value similar to that obtained at functional residual capacity after muscle relaxation suggesting that thickening was entirely attributable to muscle activation. At higher lung volumes, diaphragm thickness remained elevated after relaxation, suggesting that changes in diaphragm length at higher volumes contribute to diaphragm thickening during inspiration apart from the inspiratory effort. (Figure modified from Goligher et al. 2015b. Used with permission of Springer Nature)

of thoracoabdominal motion. Increases in thickness are greater for a given increase in lung volume if changes in lung volume primarily arise from the descent of the diaphragm rather than expansion of the ribcage (Wait and Johnson 1997).

Diaphragm Thickening: Relation to Inspiratory Pressure

The relationship between thickening and transdiaphragmatic pressure generation is similarly complex. The diaphragm generates transdiaphragmatic pressure either by shortening or by preventing lengthening to oppose rib cage expansion by parasternal and accessory muscle activation (or some combination between these extremes)—consequently, the relation between transdiaphragmatic pressure generation and diaphragm shortening (and thickening) depends on thoracoabdominal motion. The transdiaphragmatic pressure resulting from a given degree of diaphragmatic shortening (and thickening) will also depend on lung, chest wall, and abdominal elastances. This relation, although diaphragm thickening and transdiaphragmatic pressure generation or diaphragm electrical activity are correlated, varies considerably within and between subjects (between subjects $R^2 = 0.28$ and 0.32 , respectively; within-subjects $R^2 = 0.6$ for both) (Goligher et al. 2015b). Nevertheless, changes in diaphragm thickening in response to varying loading conditions (i.e. changes in ventilator support) reliably reflect changes in transdiaphragmatic pressure generation (Umbrello et al. 2015; Vivier et al. 2012) (Fig. 35.4); under a given loading condition (i.e., during airway occlusion), diaphragm thickening is directly related to inspiratory pressure (Ueki et al. 1995). Because high loading conditions may influence thoracoabdominal motion and respiratory elastance (Tobin et al. 1987), the relation between thickening and inspiratory pressure likely varies with the loading condition.

Diaphragm Strain

Diaphragm shortening might be assessed more directly by means of sonographic speckle tracking. The displacement of small groups of echogenic pixels ('kernels') are tracked over time and

changes in distance between kernels are used to quantify muscle deformation ('strain'). This technique, already employed in echocardiography (Nesbitt and Mankad 2009), has been used to assess diaphragm shortening in the zone of apposition in healthy subjects. During inhalation to 60% of inspiratory capacity, diaphragmatic strain is approximately -40% (Orde et al. 2016); the diaphragmatic strain was correlated with diaphragm thickening ($R^2 = 0.44$). During progressive inspiratory threshold loading, strain and strain rate are correlated with transdiaphragmatic pressure and diaphragm electrical activity.³⁶ It remains unclear whether speckle tracking analysis offers any advantages in assessing diaphragm contractile activity over measurements of thickening fraction. To date, diaphragmatic strain measurements have not been reported in mechanically ventilated patients.

Technical Approach to Diaphragm Ultrasound

Diaphragm Excursion

To quantify diaphragm excursion, a low frequency (3.5–5 MHz) phased array transducer is employed to visualize the dome of each hemidiaphragm. The dome may be visualized in the coronal plane by placing the probe on the lateral chest wall or in the sagittal plane by placing the probe below the costal margin at either the right or left mid-clavicular line. The overall motion of the dome can be visualized in 2D (B) mode. After identifying the point of maximal excursion on the diaphragm, an M mode line can be placed to quantify excursion (Fig. 35.4). Care should be taken that the M mode line is perpendicular to the dome and angled in the plane of the diaphragm's motion, otherwise, the dome will be foreshortened, leading to overestimates of excursion.

Diaphragm excursion measurements obtained in this manner are quite precise, with limits of agreement for interobserver and intraobserver reproducibility of approximately 10–15% of mean measurement value (Boussuges et al. 2009; Lerolle et al. 2009).

Diaphragm Thickness and Thickening

Diaphragm thickness and tidal thickening fraction are measured using a 13 MHz transducer placed on the chest wall in the eighth, ninth, or tenth intercostal space, mid-way between the anterior and mid-axillary line. The probe is held perpendicular to the chest wall and angled along the intercostal space. The patient should be semi-recumbent. In this location, the diaphragm is identified as a three-layered structure just superficial to the liver, consisting of a relatively non-echogenic muscular layer bound by the echogenic membranes of the diaphragmatic pleura and peritoneum (Fig. 35.2). The distance between the leading edge of the diaphragmatic pleura and the leading edge of the peritoneum is taken as the thickness of the diaphragm. Because the thickness of the diaphragm varies somewhat across its surface, the location of the probe must be marked on the skin if repeated measurements are planned to ensure adequate measurement reproducibility. End-expiratory thickness measurements are highly reproducible within and between observers (coefficient of reproducibility 0.2–0.4, ~10–15% of mean value). Thickening fraction measurements exhibit greater variability because this quantity combines the errors of both end-expiratory and peak inspiratory thickness measurements (coefficient of reproducibility 16–18%) (Goligher et al. 2015b).

Diaphragm thickening fraction during inspiration is calculated as the percentage change in thickness between end-expiration (i.e. minimum muscle thickness) and peak inspiration (i.e. maximal muscle thickness) visualized in M-mode.

Maximal diaphragm thickening fraction is a measure of the diaphragm's capacity to shorten (thicken) during a maximal inspiratory effort, a means of assessing muscle function. Maximal thickening fraction is measured during an attempted inspiratory capacity maneuver; coaching may enhance volitional effort. In ventilated patients, the mode of ventilation can be transiently changed to CPAP to increase respiratory effort. If ventilated patients are unable to

follow instructions, significant increases in the inspiratory effort can be stimulated by transiently occluding the endotracheal tube (Truwin and Marini 1992). Maximal thickening fraction is then measured immediately after the occlusion is released while the patient effort is increased is released to allow for maximal diaphragmatic shortening. The highest value obtained for thickening fraction during 3–5 repeated inspiratory efforts can be taken as the best measurement.

Diaphragm Echodensity

Echodensity is measured by quantifying the distribution of greyscale pixel values in the region bounded by the pleural and peritoneal lines in a two-dimensional B mode ultrasound image of the costal diaphragm in cross-section collected as described above. Such analysis can be performed on images using freely available image analysis software (e.g., ImageJ, National Institutes of Health, Bethesda MD, <https://imagej.nih.gov/ij/>). Changes in sonographic contrast and image settings strongly influence the greyscale distribution in ultrasound images, so great care must be taken to standardize the settings at which images are acquired. Given the lack of standardized reference values, echodensity is currently only assessable in terms of changes within patients over time.

Diaphragm Speckle Tracking

Specialized commercially available image analysis software enables speckle-tracking analysis on B mode clips of diaphragm contractions visualized in cross-section (as described for measurement of diaphragm thickness above). Careful selection of the region of interest for analysis is necessary to ensure reliable results (Oppersma et al. 2017). A standardized technique for speckle tracking analysis in images acquired in patients has not yet been described.

Clinical and Research Applications of Diaphragm Ultrasound

Detecting Structural Changes in the Diaphragm

Ultrasound can detect structural changes in the diaphragm associated with a variety of acute and chronic disease states. Chronic asthma and Duchenne muscular dystrophy are associated with increased resting diaphragm thickness compared to healthy controls (de Bruin et al. 1997a, b), whereas resting diaphragm thickness is significantly decreased in patients with chronic diaphragmatic paralysis (Summerhill et al. 2008; Gottesman and McCool 1997). Diaphragm ultrasound studies in acute mechanical ventilation have demonstrated the development of diaphragm atrophy (Goligher et al. 2015a; Grosu et al. 2012; Schepens et al. 2015; Zambon et al. 2016) and changes in diaphragm echodensity (Riegler et al. 2017). Ultrasound has also been used to demonstrate recovery from atrophy with the use of neuromuscular stimulation techniques (Ayas et al. 1999; Reynolds et al. 2017).

Facilitating Nerve Conduction and Electromyography Studies

Ultrasound has been used in the outpatient setting to evaluate patients presenting with possible neuromuscular causes of respiratory symptoms with high sensitivity and specificity (Boon et al. 2014). The use of ultrasound increases the accuracy of needle placement for diaphragm electromyography and phrenic nerve conduction testing (Boon et al. 2011).

Evaluating Diaphragm Function

Diaphragm weakness is an important clinical problem in the context of neuromuscular disease, respiratory disease, and mechanical ventilation. Assessing diaphragm function by ultrasound can provide diagnostic or prognostic data and guide therapy in these patients.

Diaphragm excursion has been employed to assess diaphragm function in studies of mechanically ventilated patients (Valette et al. 2015; Kim et al. 2011), stroke patients (Choi et al. 2017; Park et al. 2015), and patients with acute dyspnea presenting to the emergency department (Bobbia et al. 2016). Visualizing diaphragm motion can also detect paradoxical motion due to pleural effusions—drainage is likely to strongly improve the mechanics of breathing in such cases (Cooper and Elliott 1995; Goligher and Ferguson 2012). Threshold values of excursion with different inspiratory maneuvers diagnostic for diaphragm weakness have been published (Table 35.1). These threshold values have been validated against various reference standards including the Gilbert index (ratio of gastric to transdiaphragmatic pressure swings during inspiration) (Lerolle et al. 2009) and twitch airway pressure during phrenic nerve magnetic stimulation (Dubé et al. 2017). Reduced diaphragm excursion predicts prolonged mechanical ventilation and hospitalization (Kim et al. 2011).

Diaphragm thickening (shortening) on ultrasound can also be used as a measure of diaphragmatic function. Maximal diaphragm thickening fraction measurements have been used to diagnose diaphragm weakness in patients with idiopathic diaphragm paralysis or hemidiaphragm paralysis (Summerhill et al. 2008; Gottesman and McCool 1997), neuromuscular disease (de Bruin et al. 1997a), and mechanically ventilated patients (Ferrari et al. 2014; Goligher et al. 2018). Maximal thickening fraction below 20% is diagnostic for severe diaphragm weakness. This approach has been validated in patients with hemidiaphragm paralysis, where maximal thickening on the unaffected side was always greater than 20% and always less than 20% of the affected side (Gottesman and McCool 1997). In mechanically ventilated patients, maximal thickening is correlated with maximal inspiratory pressure (Ferrari et al. 2014), and maximal thickening below 20% strongly predicted prolonged mechanical ventilation and an increased risk of reintubation and tracheostomy (Goligher et al. 2018).

In mechanically ventilated patients, tidal thickening fraction (i.e. diaphragm thickening

during tidal breathing) measured under pressure support ventilation (titrated to target tidal volume of 6–8 ml/kg predicted body weight) is strongly correlated with diaphragm strength as measured by twitch airway pressures during magnetic twitch stimulation of the phrenic nerves (Dubé et al. 2017). Indeed, tidal thickening predicts weaning failure with the same discrimination as twitch airway pressure (Dres et al. 2018). This is somewhat surprising since tidal thickening reflects both muscle function and muscle loading/unloading under assisted ventilation. The relation between tidal thickening and diaphragm function might be attributable to the fact that patient inspiratory effort (P_{mus}) under assisted ventilation is strongly correlated with maximal inspiratory pressure (Marini et al. 1986).

In theory, diaphragm thickening should provide a more reliable measure of diaphragm performance than excursion because excursion measurements are likely to be more heavily influenced by the mechanical conditions of the lung and chest wall. However, no studies have specifically examined this question to date.

Given the mounting evidence of iatrogenic injury to the diaphragm due to inappropriately titrated mechanical ventilation, there is widespread interest in developing diaphragm-protective strategies for mechanical ventilation. Central to this paradigm is the notion that titrating ventilator support to achieve an optimal level of inspiratory effort avoiding both insufficient and excessive diaphragm loading will minimize diaphragm atrophy and injury (Heunks and Ottenheijm 2018; Tobin et al. 2010). Previous clinical studies using ultrasound have shown that changes in diaphragm thickness during ventilation are minimized when thickening fraction is in the range of 20–40% (Goligher et al. 2015a) and that a thickening fraction value in the range of 15–30% is associated with the shortest duration of ventilation (Goligher et al. 2018). These data suggest that titrating ventilator support to achieve a level of diaphragm activation and shortening consistent with a thickening fraction between 15% and 30% might prevent diaphragm atrophy or injury and accelerate liberation from ventilation. This hypothesis suggests an important

potential therapeutic application of diaphragm ultrasound to guide the titration of mechanical ventilation.

Predicting Weaning Outcomes

Given the crucial role of diaphragm performance in successful liberation from mechanical ventilation and the high stakes dilemma of deciding to attempt liberation from ventilation (choosing whether to accept prolonged ventilation vs. the risk of potential reintubation), there has been widespread interest in using diaphragm ultrasound measurements to predict whether patients will require re-intubation after extubation. Diaphragm excursion, tidal diaphragm thickening fraction, and maximal diaphragm thickening fraction measured during the spontaneous breathing predict successful liberation from ventilation with the same or better discriminative performance than the conventional rapid-shallow breathing index (Kim et al. 2011; Ferrari et al. 2014; Dres et al. 2018; DiNino et al. 2014; Jiang 2004; Yoo et al. 2018). In general, the diaphragm thickening fraction appears to have superior performance characteristics to diaphragm excursion (Llamas-Álvarez et al. 2017). The optimal cut-off of tidal or maximal diaphragm thickening fraction to predict successful liberation ranges from 25% to 30% in studies; patients with thickening fraction values below 25% during spontaneous breathing trials are much more likely to fail extubation. It should be noted that the use of inspiratory pressure augmentation during the spontaneous breathing trial may reduce the thickening fraction and reduce the specificity of the test for extubation failure (DiNino et al. 2014).

References

- Agostoni E, Rahn H. Abdominal and thoracic pressures at different lung volumes. *J Appl Physiol.* 1960;15:1087–92.
- Ayas NT, McCool FD, GORE R, LIEBERMAN SL, Brown R. Prevention of human diaphragm atrophy with short periods of electrical stimulation. *Am J Respir Crit Care Med.* 1999;159(6):2018–20.

- Bobbia X, Clément A, Claret PG, et al. Diaphragmatic excursion measurement in emergency patients with acute dyspnea: toward a new diagnostic tool? *Am J Emerg Med.* 2016;34(8):1653–7.
- Boon AJ, Oney-Marlow TM, Murthy NS, Harper CM, McNamara TR, Smith J. Accuracy of electromyography needle placement in cadavers: non-guided vs. ultrasound guided. *Muscle Nerve.* 2011;44(1):45–9.
- Boon AJ, Harper CJ, Ghahfarokhi LS, Strommen JA, Watson JC, Sorenson EJ. Two-dimensional ultrasound imaging of the diaphragm: quantitative values in normal subjects. *Muscle Nerve.* 2013;47(6):884–9.
- Boon AJ, Sekiguchi H, Harper CJ, et al. Sensitivity and specificity of diagnostic ultrasound in the diagnosis of phrenic neuropathy. *Neurology.* 2014;83(14):1264–70.
- Boussuges A, Gole Y, Blanc P. Diaphragmatic motion studied by M-mode ultrasonography: methods, reproducibility, and normal values. *Chest.* 2009;135(2):391–400.
- Braun NM, Arora NS, Rochester DF. Force-length relationship of the normal human diaphragm. *J Appl Physiol Respir Environ Exerc Physiol.* 1982;53(2):405–12.
- Choi Y-M, Park G-Y, Yoo Y, Sohn D, Jang Y, Im S. Reduced diaphragm excursion during reflexive citric acid cough test in subjects with subacute stroke. *Respir Care.* 2017;62(12):1571–81.
- Cohn D, Benditt JO, Eveloff S, McCool FD. Diaphragm thickening during inspiration. *J Appl Physiol.* 1997;83(1):291–6.
- Coirault C, Chemla D, Pery-Man N, Suard I, Lecarpentier Y. Effects of fatigue on force-velocity relation of diaphragm. Energetic implications. *Am J Respir Crit Care Med.* 1995;151(1):123–8.
- Cooper JC, Elliott ST. Pleural effusions, diaphragm inversion, and paradox: new observations using sonography. *AJR Am J Roentgenol.* 1995;164(2):510.
- de Bruin PF, Ueki J, Bush A, Khan Y, Watson A, Pride NB. Diaphragm thickness and inspiratory strength in patients with Duchenne muscular dystrophy. *Thorax.* 1997a;52(5):472–5.
- de Bruin PF, Ueki J, Watson A, Pride NB. Size and strength of the respiratory and quadriceps muscles in patients with chronic asthma. *Eur Respir J.* 1997b;10(1):59–64.
- DiNino E, Gartman EJ, Sethi JM, McCool FD. Diaphragm ultrasound as a predictor of successful extubation from mechanical ventilation. *Thorax.* 2014;69(5):423–7.
- Dres M, Goligher EC, Dubé B-P, et al. Diaphragm function and weaning from mechanical ventilation: an ultrasound and phrenic nerve stimulation clinical study. *Ann Intensive Care.* 2018;8(1):1–7.
- Dubé B-P, Dres M, Mayaux J, Demiri S, Similowski T, Demoule A. Ultrasound evaluation of diaphragm function in mechanically ventilated patients: comparison to phrenic stimulation and prognostic implications. *Thorax.* 2017;72(9):811–8. <https://doi.org/10.1136/thoraxjnl-2016-209459>.
- Esau SA, Bellemare F, Grassino A, Permutt S, Roussos C, Pardy RL. Changes in relaxation rate with diaphragmatic fatigue in humans. *J Appl Physiol Respir Environ Exerc Physiol.* 1983;54(5):1353–60.
- Ferrari G, De Filippi G, Elia F, Panero F, Volpicelli G, Aprà F. Diaphragm ultrasound as a new index of discontinuation from mechanical ventilation. *Crit Ultrasound J.* 2014;6(1):8.
- Gauthier AP, Verbanck S, Estenne M, Segebarth C, Macklem PT, Paiva M. Three-dimensional reconstruction of the in vivo human diaphragm shape at different lung volumes. *J Appl Physiol.* 1994;76(2):495–506.
- Goligher EC, Ferguson ND. Utility of draining pleural effusions in mechanically ventilated patients. *Curr Opin Pulm Med.* 2012;18:359–65.
- Goligher EC, Fan E, Herridge MS, et al. Evolution of diaphragm thickness during mechanical ventilation. Impact of inspiratory effort. *Am J Respir Crit Care Med.* 2015a;192(9):1080–8.
- Goligher EC, Laghi F, Detsky ME, et al. Measuring diaphragm thickness with ultrasound in mechanically ventilated patients: feasibility, reproducibility and validity. *Intensive Care Med.* 2015b;41(4):642–9.
- Goligher EC, Dres M, Fan E, et al. Mechanical ventilation-induced diaphragm atrophy strongly impacts clinical outcomes. *Am J Respir Crit Care Med.* 2018;197(2):204–13.
- Gottesman E, McCool FD. Ultrasound evaluation of the paralyzed diaphragm. *Am J Respir Crit Care Med.* 1997;155(5):1570–4.
- Grosu HB, Lee YI, Lee J, Eden E, Eikermann M, Rose KM. Diaphragm muscle thinning in patients who are mechanically ventilated. *Chest.* 2012;142(6):1455–60.
- Harper CJ, Shahgholi L, Cieslak K, Hellyer NJ, Strommen JA, Boon AJ. Variability in diaphragm motion during normal breathing, assessed with B-mode ultrasound. *J Orthop Sports Phys Ther.* 2013;43(12):927–31.
- Heunks L, Ottenheijm C. Diaphragm-protective mechanical ventilation to improve outcomes in ICU patients? *Am J Respir Crit Care Med.* 2018;197(2):150–2.
- Jiang JR. Ultrasonographic evaluation of liver/spleen movements and extubation outcome. *Chest.* 2004;126(1):179–85.
- Kim WY, Suh HJ, Hong S-B, Koh Y, Lim C-M. Diaphragm dysfunction assessed by ultrasonography: influence on weaning from mechanical ventilation. *Crit Care Med.* 2011;39(12):2627–30.
- Lerolle N, Guerot E, Dimassi S, et al. Ultrasonographic diagnostic criterion for severe diaphragmatic dysfunction after cardiac surgery. *Chest.* 2009;135(2):401–7.
- Lessard MR, Lofaso F, Brochard L. Expiratory muscle activity increases intrinsic positive end-expiratory pressure independently of dynamic hyperinflation in mechanically ventilated patients. *Am J Respir Crit Care Med.* 1995;151(2 Pt 1):562–9.
- Llamas-Álvarez AM, Tenza-Lozano EM, Latour-Pérez J. Diaphragm and lung ultrasound to predict weaning outcome: systematic review and meta-analysis. *Chest.* 2017;152(6):1140–50.
- Marini JJ, Rodriguez RM, Lamb V. The inspiratory workload of patient-initiated mechanical ventilation. *Am Rev Respir Dis.* 1986;134(5):902–9.
- Matamis D, Soilemezi E, Tsagourias M, et al. Sonographic evaluation of the diaphragm in critically ill patients.

- Technique and clinical applications. *Intensive Care Med.* 2013;39(5):801–10.
- McCool FD, Benditt JO, Conomos P, Anderson L, Sherman CB, Hoppin FG. Variability of diaphragm structure among healthy individuals. *Am J Respir Crit Care Med.* 1997;155(4):1323–8.
- Mead J. Functional significance of the area of apposition of diaphragm to rib cage [proceedings]. *Am Rev Respir Dis.* 1979;119(2 Pt 2):31–2.
- Nason LK, Walker CM, McNealey MF, Burivong W, Fligner CL, Godwin JD. Imaging of the diaphragm: anatomy and function. *Radiographics.* 2012;32(2):E51–70.
- Nesbitt GC, Mankad S. Strain and strain rate imaging in cardiomyopathy. *Echocardiography.* 2009;26(3):337–44.
- Oppersma E, Hatam N, Doorduyn J, et al. Functional assessment of the diaphragm by speckle tracking ultrasound during inspiratory loading. *J Appl Physiol.* 2017;123(5):1063–70.
- Orde SR, Boon AJ, Firth DG, Villarraga HR, Sekiguchi H. Diaphragm assessment by two dimensional speckle tracking imaging in normal subjects. *BMC Anesthesiol.* 2016;16(1):43.
- Park G-Y, Kim S-R, Kim YW, et al. Decreased diaphragm excursion in stroke patients with dysphagia as assessed by M-mode sonography. *Arch Phys Med Rehabil.* 2015;96(1):114–21.
- Pinet C, Cassart M, Scillia P, et al. Function and bulk of respiratory and limb muscles in patients with cystic fibrosis. *Am J Respir Crit Care Med.* 2003;168(8):989–94.
- Poole DC, Sexton WL, Farkas GA, Powers SK, Reid MB. Diaphragm structure and function in health and disease. *Med Sci Sports Exerc.* 1997;29(6):738–54.
- Reynolds SC, Meyyappan R, Thakkar V, et al. Mitigation of ventilator-induced diaphragm atrophy by transvenous phrenic nerve stimulation. *Am J Respir Crit Care Med.* 2017;195(3):339–48.
- Riegler S, Lee M, Vorona S, et al. Diaphragm echogenicity in mechanically ventilated patients: measurement precision and preliminary findings. *Am J Resp Crit Care Med.* 2017;195:A3702.
- Sarwal A, Walker FO, Cartwright MS. Neuromuscular ultrasound for evaluation of the diaphragm. *Muscle Nerve.* 2013;47(3):319–29.
- Sarwal A, Cartwright MS, Walker FO, et al. Ultrasound assessment of the diaphragm: preliminary study of a canine model of X-linked myotubular myopathy. *Muscle Nerve.* 2014;50(4):607–9.
- Sarwal A, Parry SM, Berry MJ, et al. Interobserver reliability of quantitative muscle sonographic analysis in the critically ill population. *J Ultrasound Med.* 2015;34(7):1191–200.
- Schepens T, Verbrugge W, Dams K, Corthouts B, Parizel PM, Jorens PG. The course of diaphragm atrophy in ventilated patients assessed with ultrasound: a longitudinal cohort study. *Crit Care.* 2015;19(1):422.
- Summerhill EM, El-Sameed YA, Glidden TJ, McCool FD. Monitoring recovery from diaphragm paralysis with ultrasound. *Chest.* 2008;133(3):737–43.
- Tobin MJ, Perez W, Guenther SM, Lodato RF, Dantzker DR. Does rib cage-abdominal paradox signify respiratory muscle fatigue? *J Appl Physiol.* 1987;63(2):851–60.
- Tobin MJ, Laghi F, Jubran A. Narrative review: ventilator-induced respiratory muscle weakness. *Ann Intern Med.* 2010;153(4):240–5.
- Troyer A, Loring SH. Chapter 26. Action of the respiratory muscles. In: Macklem PT, Mead J, editors. *American Physiological Society handbook of physiology: respiratory system, vol. 3.* Lippincott Williams and Wilkins; 1986.
- Truwit JD, Marini JJ. Validation of a technique to assess maximal inspiratory pressure in poorly cooperative patients. *Chest.* 1992;102(4):1216–9.
- Ueki J, de Bruin PF, Pride NB. In vivo assessment of diaphragm contraction by ultrasound in normal subjects. *Thorax.* 1995;50(11):1157–61.
- Umbrello M, Formenti P, Longhi D, et al. Diaphragm ultrasound as indicator of respiratory effort in critically ill patients undergoing assisted mechanical ventilation: a pilot clinical study. *Crit Care.* 2015;19:161.
- Valette X, Seguin A, Daubin C, et al. Diaphragmatic dysfunction at admission in intensive care unit: the value of diaphragmatic ultrasonography. *Intensive Care Med.* 2015;41(3):557–9.
- Vivier E, Mekontso Dessap A, Dimassi S, et al. Diaphragm ultrasonography to estimate the work of breathing during non-invasive ventilation. *Intensive Care Med.* 2012;38(5):796–803.
- Wait JL, Johnson RL. Patterns of shortening and thickening of the human diaphragm. *J Appl Physiol.* 1997;83(4):1123–32.
- Wait JL, Nahormek PA, Yost WT, Rochester DP. Diaphragmatic thickness-lung volume relationship in vivo. *J Appl Physiol.* 1989;67(4):1560–8.
- Yoo J-W, Lee SJ, Lee JD, Kim HC. Comparison of clinical utility between diaphragm excursion and thickening change using ultrasonography to predict extubation success. *Korean J Intern Med.* 2018;33(2):331–9.
- Zambon M, Beccaria P, Matsuno J, et al. Mechanical ventilation and diaphragmatic atrophy in critically ill patients: an ultrasound study. *Crit Care Med.* 2016;44(7):1347–52.



Monitoring Respiratory Muscle Function

36

Franco Laghi and Martin J. Tobin

Problems with the respiratory muscles arise in varying degrees in patients with almost every respiratory disorder. Abnormalities in the respiratory neuromuscular system may originate at several levels: decreased motor output from the respiratory centers, intrinsic weakness of the respiratory muscles, and increased load that the muscles cannot meet. Despite the frequency of suboptimal respiratory muscle performance, the quotidian approach to monitoring of the respiratory muscles is rudimentary.

Clinical Assessment

The symptoms of respiratory muscle dysfunction are subtle and the condition frequently goes undetected until late in its natural evolution

Supported by grants from the Veterans Administration Research Service.

F. Laghi
Division of Pulmonary and Critical Care Medicine,
Hines Veterans Administration Hospital,
Hines, IL, USA

Loyola University of Chicago Stritch School of
Medicine, Maywood, IL, USA
e-mail: flaghi@lumc.edu

M. J. Tobin (✉)
Division of Pulmonary and Critical Care Medicine,
Hines Veterans Administration Hospital,
Hines, IL, USA
e-mail: mtobin2@lumc.edu

(Laghi and Tobin 2003). Coexisting impairment of other skeletal muscles may prevent patients from exceeding their limited ventilatory capacity and, as a result, they may not develop dyspnea (Smith et al. 1987; Buyse et al. 1997). The critical step in making a diagnosis of respiratory muscle dysfunction is for the clinician to suspect a muscle problem when the presentation is camouflaged by obscuring features.

Orthopnea often develops immediately upon laying supine in bilateral diaphragmatic paralysis (McCool and Tzelepis 2012) and contrasts with the more gradual onset of orthopnea in patients with congestive heart failure (Tobin and Laghi 1998). Orthopnea occurs when maximal transdiaphragmatic pressure ($P_{di,max}$) is less than 30 cm H₂O (Tobin and Laghi 1998) or with a supine drop in vital capacity (VC) of more than 30% (Howard 2016).

Cough may be impaired in patients with respiratory muscle dysfunction secondary to a patient's inability to take a deep inspiration and because of poor expulsive forces. Cough-induced dynamic airway compression is consequently lost with a reduction in the velocity of airflow (Laghi et al. 2017).

Physical examination may reveal evidence of chest-wall deformity or features of generalized neuromuscular disease (Tobin and Laghi 1998). Evidence of increased patient effort is reflected by nasal flaring, increased sternomastoid activity (Fig. 36.1), tracheal tug, and recession of the



Fig. 36.1 Assessment of sternomastoid activity. When gauging sternomastoid activity, the examiner must not rely on inspection only. Patients with minimal adipose tissue exhibit prominence of the sternomastoids without increased contractile activity (sculpting). Assessment requires placing the index finger – gently, barely touching – on the body of the sternomastoid, to judge the presence of phasic contraction and qualitatively determine its magnitude (mild, moderate, marked). The examiner needs to focus solely on phasic muscle activity; tonic activity is used for posture and has no respiratory significance. (From Tobin (2019), with permission of Elsevier Science & Technology Journals)

suprasternal, supraclavicular, and intercostal spaces (Tobin 2019).

P_{aCO_2} may be reduced early in the disease (Rimmer et al. 1993), but hypercapnia is likely when respiratory muscle strength falls to 25% of predicted (Braun et al. 1983). Reduction in strength, however, does not consistently predict alveolar hypoventilation because factors such as elastic load and breathing pattern also contribute (Misuri et al. 2000). Abnormalities in respiratory muscle performance and alveolar ventilation may be evident initially only during exercise (Sinderby et al. 1996a) or sleep (Arnulf et al. 2000; White et al. 1995). When inspiratory strength and VC are 50% of predicted, hypoventilation can occur with minor upper respiratory tract infections.

Pulmonary Function Testing

Severe weakness of the inspiratory muscles produces a restrictive pattern with decreases in VC, total lung capacity (TLC), and functional residual

capacity (FRC), while the ratio of forced expiratory volume in 1 second to vital capacity (FEV_1/VC) remains relatively normal. Provided the expiratory muscles are not weak, residual volume (RV) remains relatively normal.

Generation of a VC maneuver requires maximal voluntary recruitment of the inspiratory muscles, followed by maximal voluntary recruitment of the expiratory muscles. Although VC is affected by impairments of the inspiratory and expiratory muscles, VC remains normal, or only minimally reduced, if respiratory muscle strength is more than 50% of predicted (De Troyer et al. 1980). This finding results from the sigmoid shape of the pressure–volume relationship of the respiratory system. When strength is less than 50% of predicted, the loss in VC is greater than expected (De Troyer et al. 1980; Estenne et al. 1993). The decrease is secondary to the associated decrease in compliance of the chest-wall and lungs (Misuri et al. 2000; Estenne et al. 1993). The latter has been attributed to diffuse microatelectasis – purported mechanisms include infrequent sighs and rapid shallow breathing (Laghi et al. 2019).

VC in healthy adults is approximately 50–60 mL/kg. VC less than 30 mL/kg is associated with a weak cough, impaired elimination of secretions, and development of macro atelectasis (Laghi et al. 2019). In patients with Guillain-Barre' syndrome, a decline in VC of less than 1 L or 10–15 mL/kg portends ventilatory failure with need for mechanical ventilation (Chevrolet and Deleamont 1991). In contrast, serial measurements of VC in patients with myasthenia gravis do not reliably predict the need for intubation and mechanical ventilation probably secondary to the erratic course of this disease, which involves sudden deterioration (Rieder et al. 1995).

Respiratory Muscle Pressure Output

The pressure output of the respiratory muscles can be monitored in terms of strength and effort.

Respiratory Muscle Pressure Output: Strength

Respiratory muscle strength can be assessed by recording pressure signals elicited during maximal voluntary or evoked maneuvers.

Voluntary Maneuvers: Airway Pressures

Measurements of maximal static respiratory pressures during forceful efforts against an occluded airway reflect global respiratory muscle strength (Rohrer 1925; Rahn et al. 1946; Agostoni and Mead 1964; Rochester 1988; Bellemare 1995; Gibson 1995; Clanton and Diaz 1995; Harik-Khan et al. 1998). Maximal inspiratory pressure ($P_{I\max}$) is usually measured after exhalation to RV (Fig. 36.2); maximal expiratory pressure ($P_{E\max}$) is measured at TLC, where expiratory muscles are maximally stretched (Black and Hyatt 1969).

Mouth pressure during maximal efforts includes a contribution from the passive recoil pressure of the total respiratory system. At vol-

umes above relaxation volume, recoil pressure assists the expiratory muscles and opposes the inspiratory muscles, while the reverse is true at lower volumes (Rahn et al. 1946).

Maximal pressure is measured as the largest absolute numerical value that can be generated (Larson et al. 1993; American Thoracic Society/European Respiratory Society 2002; Fiz et al. 1989). To avoid glottic closure, a small leak is introduced in the mouthpiece (Ringqvist 1966). Although this is often considered to be a static maneuver, diaphragmatic length and configuration change substantially during measurement of $P_{I\max}$ (Gandevia et al. 1992); thus, it is not a true isometric contraction.

In a research setting, complete (or virtually complete) activation of phrenic motor units has been documented in some but not all $P_{I\max}$ and $P_{di\max}$ maneuvers (Bellemare and Bigland-Ritchie 1987; Gandevia and McKenzie 1985; Similowski et al. 1991, 1993, 1996; Allen et al. 1993; Laghi et al. 2003). Because it is effort dependent, maximal activation of diaphragmatic motor units is less likely to occur in a routine

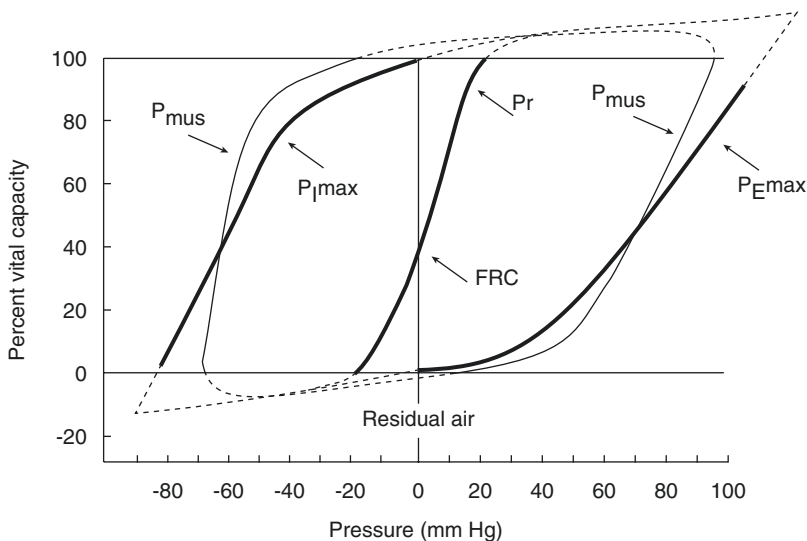


Fig. 36.2 The pressure–volume diagram of breathing. Maximal inspiratory ($P_{I\max}$) and maximal expiratory airway pressure ($P_{E\max}$) developed at the mouth during maximal voluntary efforts against a closed airway at different lung volumes. The thick solid black line in the center is the passive recoil pressure (relaxation pressure, P_r) of the total respiratory system (lung plus chest wall). The

net pressures developed by contraction of the respiratory muscles during maximum static voluntary efforts (P_{mus}) (thin black lines) are obtained by subtracting P_r from the measured maximal inspiratory and expiratory airway pressures (thick black lateral lines). (Modified from Rahn et al. (1946), with permission of American Physiological Society)

clinical setting (Fiz et al. 1989). It is commonly assumed that achievement of a reproducible $P_{I\max}$ (less than 5% variation) with multiple efforts signifies maximal efforts. Unfortunately, reproducibility is not a reliable guide to validity (Aldrich and Spiro 1995). This means a low $P_{I\max}$, even if reproducible, cannot be considered diagnostic of inspiratory muscle weakness.

Measurements of $P_{I\max}$ and $P_{E\max}$ in healthy subjects have been collected by several investigators. The normal range is very wide (Table 36.1), and the coefficient of variation is about 25%, with a range of 8 – 37% in different studies (Rochester 1988). In both sexes, the values decline linearly with age, decreasing by 0.8–2.7 cm H₂O per year between the ages of 65 and 85 (Enright et al. 1994). Weakness has been defined using specific predictive equations (Rodrigues et al. 2017).

$P_{I\max}$ is commonly listed as one of the measurements that guides the decision of whether or not to institute mechanical ventilation. In reality, it is rarely performed for this purpose and its accuracy in this regard has not been subjected to systematic research. Once mechanical ventilation has been instituted, however, $P_{I\max}$ values are commonly obtained (Yang and Tobin 1991).

In an effort to make measurements of $P_{I\max}$ reliable in intubated patients, Marini et al. (1986) used a one-way valve attached to the airway to ensure that inspiratory efforts were made at a low lung volume. The period of occlusion was maintained for 20 seconds. Values were one-third more negative than without the valve (Fig. 36.3) (Tobin et al. 1994). Multz et al. (1990) examined the reproducibility of this method in 14 patients. Triplicate measurements were obtained by five experienced investigators who encouraged the

Table 36.1 Reference equations for normal maximal inspiratory airway and expiratory pressures

Population (age)	$P_{I\max}$ reference equation (cm H ₂ O) ^a	Lower limit of normal (cm H ₂ O)	Group mean ± S.D. (cm H ₂ O)	Study
Adult men (20–65)	$-143 + 0.55 (\text{age})$	-75	-124 ± 44	Black and Hyatt (1969)
Adult women (20–65)	$-104 + 0.51 (\text{age})$	-50	-87 ± 32	Black and Hyatt (1969)
Adult men (20–90)	$-126 + 1.028 (\text{age}) - 0.343 (\text{wt})$	-37	-101.2 ± 29.4	Harik-Khan et al. (1998)
Adult women (20–90)	$-171 + 0.694 (\text{age}) - 0.861 (\text{wt}) + 0.743 (\text{ht})$	-32	-72.4 ± 23.3	Harik-Khan et al. (1998)
Elderly men (65–85)	$-153 + 1.27 (\text{age}) - 0.289 (\text{wt})$	Ref + 41	-83 ± 27	Enright et al. (1994)
Elderly women (65–85)	$-96 + 0.805 (\text{age}) - 0.293 (\text{wt})$	Ref + 32	-58 ± 22	Enright et al. (1994)
Population (age)	$P_{E\max}$ reference equation (cm H ₂ O) ^a	Lower limit of normal (cm H ₂ O)	Group mean ± S.D. (cm H ₂ O)	Study
Adult men (20–65)	$268 - 1.03 (\text{age})$	140	233 ± 84	Black and Hyatt (1969)
Adult women (20–65)	$170 - 0.53 (\text{age})$	95	152 ± 54	Black and Hyatt (1969)
Elderly men (65–85)	$347 - 2.95 (\text{age}) + 0.551 (\text{wt})$	Ref - 71	175 ± 46	Enright et al. (1994)
Elderly women (65–85)	$219 - 2.12 (\text{age}) + 0.758 (\text{wt})$	Ref - 52	118 ± 37	Enright et al. (1994)

Modified from Tobin and Laghi (1998), with permission of McGraw Hill

Key: $P_{I\max}$ maximal inspiratory pressure, $P_{E\max}$: maximal expiratory pressure, *wt* weight in kilograms, *Ref* pressure derived from reference equation, *ht* height in centimeters. Predicted values for $P_{I\max}$ are at residual volume and for $P_{E\max}$ at total lung capacity

^aTo calculate approximate values at functional residual capacity, decrease $P_{I\max}$ by 14% and $P_{E\max}$ by 19% (Ringqvist 1966) assuming that the functional residual capacity–total lung capacity ratio is about 55%

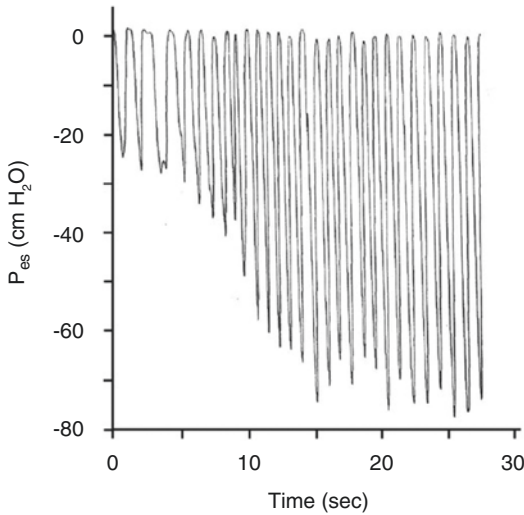


Fig. 36.3 Measurement of maximal inspiratory pressure in a ventilator-supported patient. Note that the pressures become progressively more negative over a period of about 20 seconds and show little change thereafter. Although esophageal pressure (P_{es}) is shown in this tracing, similar information can be obtained by measurement of airway pressure. (From Tobin et al. (1994), with permission of McGraw Hill LLC)

patients to make vigorous inspiratory efforts. Measurements of $P_{I\max}$ obtained at a single sitting by a single investigator showed good reproducibility: coefficient of variation $12 \pm 1\%$. Significant variation among $P_{I\max}$ measurements was observed by different investigators studying the same patient on the same day: coefficient of variation, $32 \pm 4\%$.

Sniff pressures are usually greater than $P_{I\max}$ (Nava et al. 1993), suggesting that the mechanical disadvantage of the maneuver is outweighed by greater activation of the respiratory muscles (Fig. 36.4). Originally, sniff pressures were recorded using esophageal pressure (P_{es}) signals (Laroche et al. 1988). The clinical application of sniff P_{es} , however, is limited by its invasive nature, requiring an esophageal balloon catheter. Subsequent investigators reported that sniff nasal pressure (sniff P_n) provides a reliable estimate of sniff P_{es} in the absence of severe nasal congestion (Heritier et al. 1994; Laveneziana et al. 2019; Lofaso et al. 2006; Araujo et al. 2012; Kamide et al. 2009; Uldry and Fitting 1995; Huang et al. 2014).

Uldry and Fitting (1995) developed the following equations to predict sniff P_n :

- Sniff P_n (cm H₂O), men: $-0.42 \text{ age} + 126.8$; residual standard deviation, 23.8
- Sniff P_n (cm H₂O), women: $-0.22 \text{ age} + 94.9$; residual standard deviation, 17.1

Values of sniff P_n were higher than $P_{I\max}$ in about two-thirds of the subjects.

Sniff P_n and $P_{I\max}$ measurements complement each other (Steier et al. 2007; Fitting 2006). Because $P_{I\max}$ is easier to perform, it remains the measurement of choice (Tobin and Laghi 1998). If a normal value is obtained, no further testing is necessary. If a low $P_{I\max}$ is obtained, sniff P_n helps in differentiating true inspiratory muscle weakness from an unsatisfactory maneuver. P_{es} recordings are preferred for sniff measurements in patients with COPD (Tobin and Laghi 1998; Uldry et al. 1997).

Patients with severe weakness of facial muscles (bulbar amyotrophic lateral sclerosis) have difficulty in performing $P_{E\max}$ maneuvers (Suarez et al. 2002). Provided bulbar dysfunction is not severe, maximal expiratory flow during a cough (peak cough flow) (Suarez et al. 2002; Tzani et al. 2014) offers an alternative to $P_{E\max}$. In the absence of bronchial obstruction peak cough flow reflects the expiratory muscle force.

Voluntary Maneuvers:

Transdiaphragmatic Pressure

Measurements of $P_{I\max}$, $P_{E\max}$, sniff, and peak cough flow do not directly reflect the function of the diaphragm. Simultaneous measurements of P_{es} and gastric pressure (P_{ga}) permit calculation of transdiaphragmatic pressure: $P_{di} = P_{ga} - P_{es}$ (Agostoni and Rahn 1960). P_{di} is not a direct reflection of diaphragm strength because it depends on multiple factors governing the transformation of force into pressure. Such factors include lung volume, thoracic and abdominal compliance, and thoracoabdominal configuration (Chen et al. 2000).

Measurement of P_{di} is especially helpful in diagnosing severe weakness or paralysis of the diaphragm, where approaches such as fluoroscopy

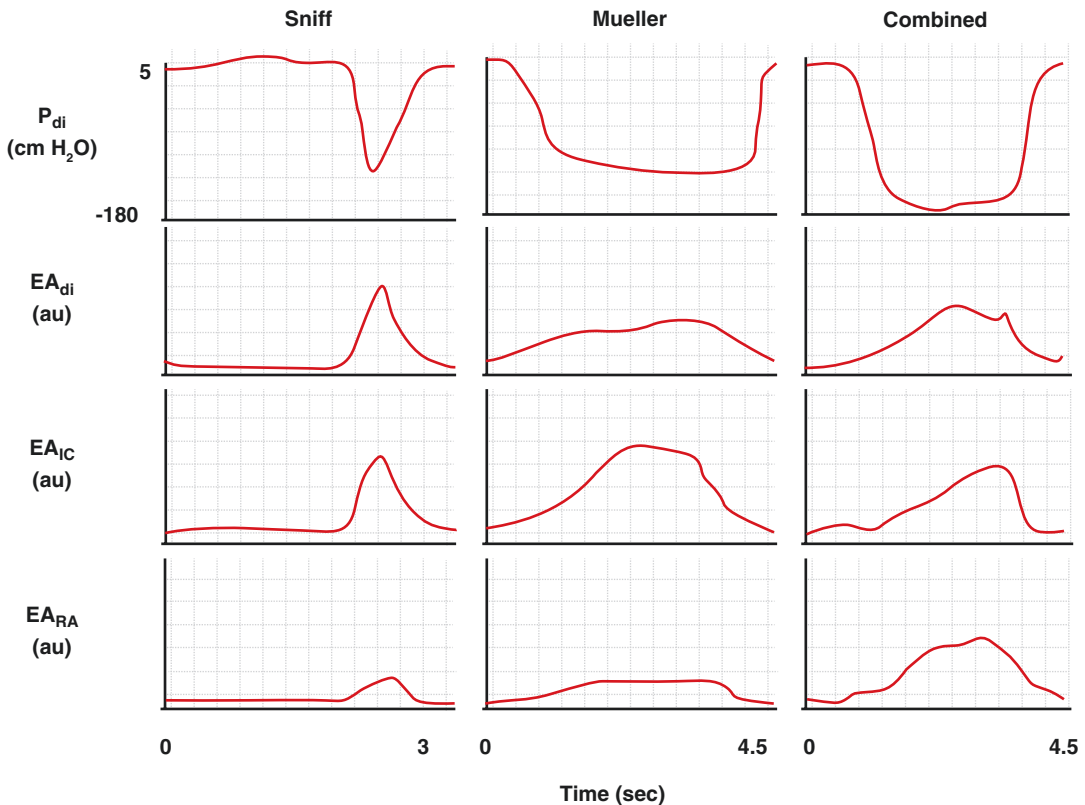


Fig. 36.4 Recordings of transdiaphragmatic pressure (P_{di}) and electromyographic activity of the diaphragm (EA_{di}), intercostal muscles (EA_{IC}) and rectus abdominis (EA_{RA}) in a healthy subject performing a sniff maneuver, a Mueller maneuver, and a combined Muller plus maxi-

mal expiratory maneuver (combined maneuver). Peak diaphragmatic EMG activity, expressed in arbitrary units (au), was highest during the sniff maneuver (Based on Nava et al. (1993))

are misleading (Davis et al. 1976) (Fig. 36.5). Because of considerable variability in the values of $P_{di,max}$, (Braun et al. 1982; Bellemare and Grassino 1982; De Troyer and Estenne 1981; Gibson et al. 1981; Miller et al. 1985; Hershenson et al. 1988; Ueki et al. 1995) it is important to scrutinize the method of measurement. Maximal inspiratory efforts against a closed airway (Mueller maneuver), maximal inspiratory efforts combined with maximal expiratory effort (Mueller-expulsive maneuver), and maximal sniffs are three maneuvers that quantify inspiratory muscle strength.

Mueller Maneuver

Measuring P_{di} during a maximal static inspiratory effort against an occluded airway is the usual

method of measuring $P_{di,max}$. When patients are not given specific instructions or provided with a visual display of pressure tracings, maximal static measurements of P_{di} have enormous variability (De Troyer and Estenne 1981).

Mueller-Expulsive Maneuver

The highest and most reproducible $P_{di,max}$ values are obtained with the Mueller-expulsive maneuver (Laporta and Grassino 1985). P_{es} and P_{ga} are displayed on a storage oscilloscope and the patient is instructed to combine an abdominal expulsive maneuver with a Mueller maneuver. Visual feedback enhances a subject's control over the degree to which the diaphragm is activated. Unlike the simple Muller maneuver, the feedback maneuver results in higher and consistently

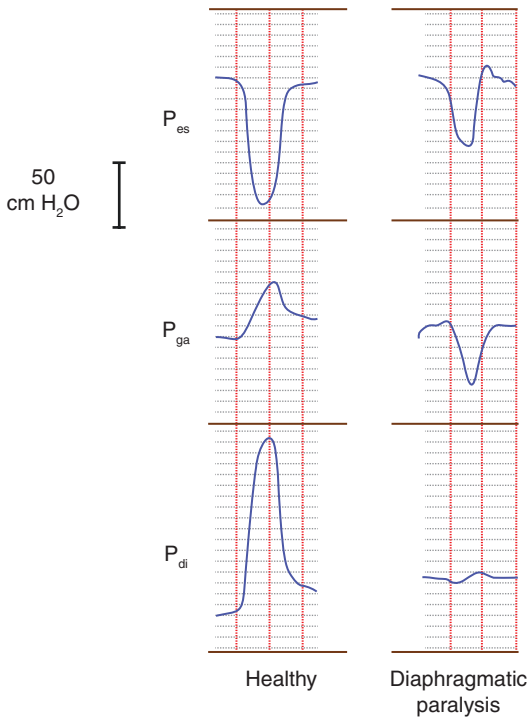


Fig. 36.5 Esophageal pressure (P_{es}), gastric pressure (P_{ga}), and transdiaphragmatic pressure (P_{di}) in a healthy subject and in a patient with bilateral diaphragmatic paralysis. When a patient with diaphragmatic paralysis makes a maximal inspiratory effort, the negative P_{es} generated by the other inspiratory muscles pulls the flaccid diaphragm cephalad, thereby resulting in a fall in P_{ga} .

positive P_{ga} values; it has no effect on P_{es} values (Laporta and Grassino 1985).

Even in well-trained patients, $P_{di,max}$ during a Mueller-expulsive maneuver is higher than that obtained with a Mueller maneuver (Hershenson et al. 1988). Several investigators have demonstrated that maximal diaphragmatic recruitment can be attained during a simple Mueller maneuver (Gandevia and McKenzie 1985; Similowski et al. 1991, 1993; Similowski et al. 1996; Allen et al. 1993). Therefore, mechanisms other than submaximal diaphragmatic recruitment may be responsible for the lower $P_{di,max}$ values during the Mueller versus the Mueller-expulsive maneuver (Gandevia et al. 1990; McKenzie et al. 1994). During a Mueller maneuver, the diaphragm is displaced downward towards the abdominal cav-

ity, decreasing its length (Gandevia et al. 1990) and thus reducing pressure generation. During an expulsive maneuver, the diaphragm initially shortens a small amount and then lengthens (Gandevia et al. 1990; McKenzie et al. 1994). In other words, an eccentric (pliometric) contraction (Hillman et al. 1990) produces greater tension than an isometric contraction secondary to the force-generating reserve of the abdominal muscles (Laghi et al. 2014a).

Sniff P_{di}

While many patients find it difficult to perform the Mueller-expulsive maneuver, most can perform a sniff (Fig. 36.5). Miller et al. (1985) found that sniff P_{di} values were higher than $P_{di,max}$ values in 92% of 64 healthy subjects – suggesting that most performed the Mueller-expulsive maneuver suboptimally. Luo et al. (2002) assessed the reproducibility of sniff P_{di} in 32 healthy volunteers by repeating the measurements on two to eight occasions over 1–5 years. The within-subject coefficient of variation was 11%.

In patients with bilateral diaphragmatic paralysis, sniff P_{es} may underestimate diaphragmatic dysfunction (Mills et al. 1997) because patients increasingly recruit rib cage and neck muscles during the maneuver. Patients with unilateral diaphragmatic paresis experience a significant reduction in sniff P_{es} (Verin et al. 2006). This reduction correlates with the time elapsed from onset of symptoms to respiratory muscle testing (Verin et al. 2006).

Pressure Relaxation Rate

As a skeletal muscle fatigues, there is the slowing of rate at which the muscle relaxes from a stimulated or voluntary contraction (Edwards et al. 1975). Slowing of the relaxation rate is considered an early consequence of excessive muscle loading, and it precedes the failure of force generation (Esau et al. 1983; Mador and Kufel 1992). Despite great interest in the 1980s and 1990s, measurements of the relaxation phase of respiratory muscle contraction has not significantly impacted clinical practice.

Voluntary Maneuvers: Cough P_{ga}

$P_{E\max}$ is a well-established test to assess expiratory muscle strength. Low $P_{E\max}$ values are difficult to interpret particularly in patients with facial muscle weakness (Laveneziana et al. 2019). Another approach is to measure P_{ga} during a cough (Man et al. 2003). Complementing $P_{E\max}$ with cough P_{ga} recordings decreases false-positive diagnosis of expiratory muscle weakness by 30–42% (Steier et al. 2007; Man et al. 2003).

Voluntary Maneuvers: Clinical Usefulness of Transdiaphragmatic Pressure Measurements

A decrease in VC on switching from the upright to horizontal position (Allen et al. 1985) arouses suspicion of inspiratory muscle weakness, and $P_{I\max}$ should be checked. A $P_{I\max}$ more negative than -80 cm H₂O in men and -70 cm H₂O in women excludes clinically important muscle weakness (Polkey et al. 1995). A less negative value could result from poor technique. The addition of sniff P_n to $P_{I\max}$ helps in this situation, reducing false-positive diagnosis of inspiratory muscle weakness by 20% (Steier et al. 2007). Sniff P_n more negative than -70 cm H₂O in men and more negative than -60 cm H₂O in women excludes clinically significant weakness (Polkey et al. 1995). With less negative pressures, clinicians should measure P_{di} , using voluntary maneuvers and/or stimulation of the phrenic nerves. Sniff P_{di} is useful when sniff P_n yields suspiciously low values, such as with upper airway obstruction (hypertrophy of the adenoids, rhinitis, polyps) or lower airway obstruction (Laveneziana et al. 2019). When bilateral diaphragmatic paralysis is suspected, fluoroscopy can be misleading (Davis et al. 1976). Alternatively, diaphragm ultrasound can be used to identify diaphragmatic paresis or paralysis.

Evoked Maneuvers

Non-volitional evaluation of the diaphragm can be achieved by measuring changes in P_{di} elicited by phrenic nerve stimulation. Non-volitional evaluation of the abdominal muscles is likewise achieved measuring changes in P_{ga} elicited by stimulation of thoracic nerve roots.

Evoked Maneuvers: Phrenic Nerve Stimulation

Phrenic nerve stimulation has the advantage of being independent of patient motivation. Activation was formerly achieved with an electrical stimulator whereas magnetic stimulation is now gaining popularity (Laghi et al. 2014b).

Electrical Stimulation

The phrenic nerve is accessible for electrical stimulation as it descends over the anterior surface of the anterior scalene muscle (McKenzie and Gandevia 1995). An inaccessible ectopic branch of the phrenic nerve (Sarnoff et al. 1951) (found in up to 20% of autopsies (Rajanna 1947)) can make it difficult (even impossible) to stimulate the entire phrenic nerve. Because of the high impedance of the skin, less electrical current is required for phrenic nerve stimulation using percutaneous stimulation than using surface transcutaneous stimulation (Bellemare 1995; McKenzie and Gandevia 1995; MacLean and Mattioni 1981; Aubier et al. 1985; Hubmayr et al. 1989). In expert hands, this system provides stable stimulating conditions for several hours despite vigorous contractions of the inspiratory muscles (McKenzie and Gandevia 1995).

Magnetic Stimulation

Although electrical stimulation of the phrenic nerves has yielded important information, it has several limitations. Use of needle electrodes poses a hazard of phrenic nerve injury (Al-Shekhlee et al. 2003) and pneumothorax (Laghi et al. 2014b). For transcutaneous stimulation, the high voltage required to overcome skin resistance is painful (Mier et al. 1989). Locating the phrenic nerves can be difficult or even impossible in over one quarter of patients with respiratory disease (Mills et al. 1994). Maintaining a constant symmetrical maximal stimulus can be difficult, and repetitive twitch stimulations are commonly performed (Bellemare and Bigland-Ritchie 1984). The approach produces artifactual increases in twitch pressure: so-called staircase potentiation (an increase in muscle contractility after a series of low-frequency stimulations) (Vandenboom et al. 2013). Consequently, pressure tracings are

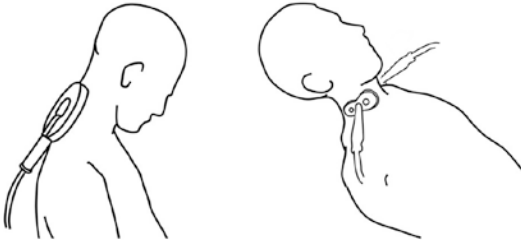


Fig. 36.6 Magnetic stimulation of the phrenic nerves. (*Left panel*) Posterior approach: A circular magnetic probe is centered over the spinous process of the seventh cervical vertebra. When activated, the probe generates a broad magnetic field that causes bilateral stimulation of the phrenic nerve roots. (*Right panel*) Anterolateral approach: Two figure-of-eight probes are positioned adjacent to the posterior border of the sternomastoid muscle at the level of the cricoid cartilage. (From Laghi et al. (2014b), with permission of Springer Nature BV)

distorted and rendered uninterpretable. Because of these problems, phrenic nerve stimulation with electrical electrodes (needle or transcutaneous) is a difficult technique to use – and not feasible in the intensive care unit (ICU).

To overcome technical limitations of electrical stimulation, industry developed magnetic stimulation of the phrenic nerves (Fig. 36.6) (Mills et al. 1996; Similowski et al. 1989). This approach has a number of attractions. It creates brief intense magnetic fields that (in contrast with electrical currents) are only slightly attenuated by natural barriers (skin, bone) (Laghi et al. 2014b). Rapidly changing magnetic fields can reach deep nervous structures, inducing electrical fields and in situ stimulation. Locating the phrenic nerves is not a problem and intact nerves are stimulated invariably because the magnetic probe generates a broad field of activity over the neck – in contrast with the need to precisely position an electric probe over the phrenic nerve. The likelihood of inducing staircase potentiation is lessened because locating the area of maximal stimulation requires only a few stimulations. Magnetic stimulation is considerably less painful than electrical stimulation (Laghi et al. 2014b; Hamnegård et al. 1996). Reproducibility of P_{di} tw (when measured on different occasions) is better with magnetic than electrical stimulation: coefficients of variation of 6.6 and 8.8%, respectively (Wragg et al. 1994a).

Comparison of Electrical and Magnetic Stimulation

Magnetic stimulation of the phrenic nerves evokes greater P_{di} tw at FRC than does electrical stimulation (Wragg et al. 1994a; Laghi et al. 1996; Mador et al. 1996), typical values being 37.7 ± 1.9 (S.E.) and 32.3 ± 2.2 cm H₂O, respectively (Laghi et al. 1996); this difference is solely the consequence of larger P_{es} tw. The larger P_{es} tw results from recruitment of the sternomastoid, trapezius, parasternal, and pectoral muscles, whereas electrical stimulation causes only diaphragmatic depolarization (Laghi et al. 1996). Contraction of rib cage muscles is known to decrease rib cage compliance, which achieves a greater P_{es} tw for a given diaphragmatic contraction (Laghi et al. 1996). Laghi et al. (1996) compared the ability of the two techniques to detect changes in diaphragmatic contractility after induction of fatigue. Decreases in P_{di} tw were closely correlated ($r = 0.96$), indicating that relative nonselectivity of magnetic stimulation does not undermine its ability to detect diaphragmatic fatigue (Fig. 36.7).

Paired stimulations with different inter-stimulus intervals have been used to construct a

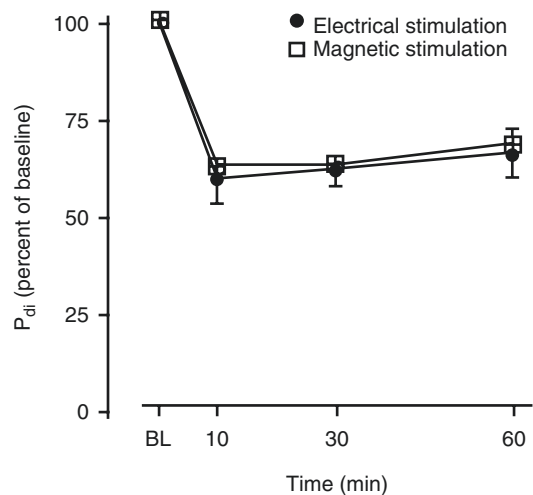


Fig. 36.7 Transdiaphragmatic twitch pressure (P_{di}) at baseline and the percentage decrease at 10, 30, and 60 min after induction of diaphragmatic fatigue. The decreases were similar for magnetic and electrical stimulation of the phrenic nerves. (From Laghi et al. (1996), with permission of American Physiological Society)

surrogate force-frequency curve to discriminate between low-frequency and high-frequency fatigue (Yan et al. 1993a). Low-frequency fatigue, signified by a decrease in force occurring at stimulation frequencies between 10 and 20 Hz, is thought to be caused by irreversible disruption of calcium release in the cytoplasm and muscle damage (Laghi and Tobin 2003; Verburg et al. 2009); it has a slow rate of recovery. High-frequency fatigue, signified by a decrease in force at stimulation frequencies between 50 and 100 Hz (Aubier et al. 1981a), results from various mechanisms related to intracellular concentrations of calcium and inorganic phosphate; it has a rapid rate of recovery (Allen et al. 2008). During normal regular breathing, the peak frequency of motor neurons for the phrenic nerves is 7–14 Hz (De Troyer et al. 1997); thus, low-frequency fatigue is judged to have greater clinical importance than high-frequency fatigue (Mador and Acevedo 1991; Yan et al. 1993b; Laghi et al. 1998a). Magnetic stimulation can also be used to detect abdominal muscle fatigue (Kyroussis et al. 1996).

Given the considerable logistical difficulty involved in performing tetanic stimulations needed to generate full force–frequency curves, increasing attention has focused on measuring the response to isolated single supramaximal nerve stimulations (Fig. 36.8) (Laghi et al. 2014b; Laghi 2014). The pressure response is termed twitch pressure. Twitch pressure provides a reliable means of detecting low-frequency fatigue – the type of greatest clinical significance (Laghi and Tobin 2003; Babcock et al. 1995; Ferguson 1994).

Unilateral stimulation is appropriate when assessing the integrity of a phrenic nerve (Tobin and Laghi 1998). It is not reliable for assessing diaphragmatic contractile properties (Bellemare et al. 1986); the peak amplitude of $P_{di,tw}$ in response to bilateral supramaximal stimulation exceeds the sum of left and right pressure responses by $32 \pm 6\%$ (S.D.) (Fig. 36.9) (Bellemare et al. 1986). This difference is caused by the degree of mechanical distortion induced by the two types of stimulation.

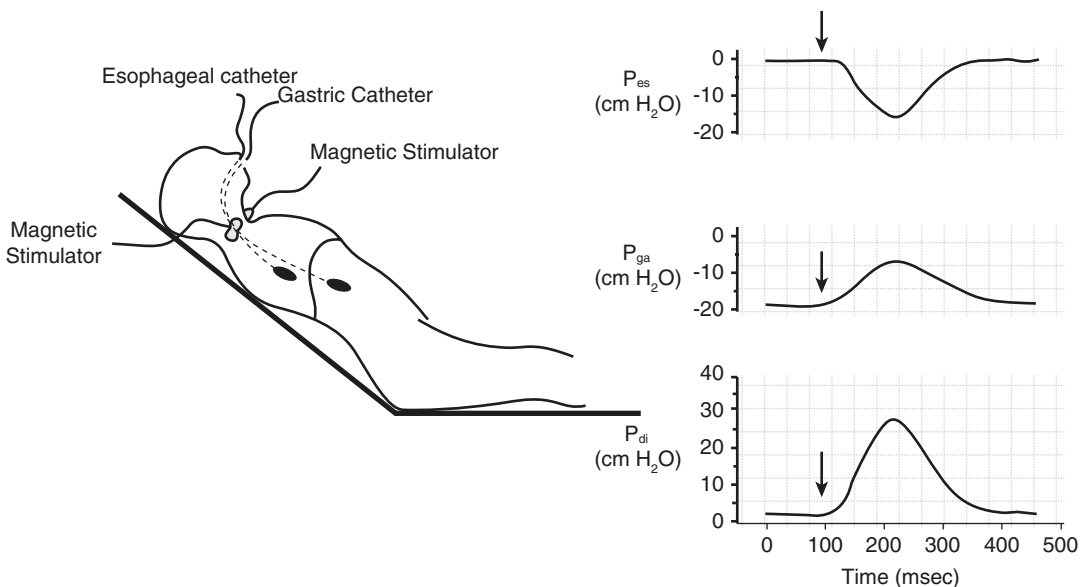


Fig. 36.8 Recording of transdiaphragmatic twitch pressure. (Left panel) An esophageal balloon and a gastric balloon are passed through the nares. Magnetic stimulation of the phrenic nerves elicits diaphragmatic contraction. (Right panel) Continuous recordings of esophageal (P_{es}) and gastric pressures (P_{ga}) and transdiaphragmatic pres-

sure (P_{di}). Phrenic nerve stimulation (arrows) results in contraction of the diaphragm with consequent fall in P_{es} and rise in P_{ga} . These swings in pressure are responsible for the transdiaphragmatic twitch pressure. (From Laghi (2014), with permission of Elsevier Science & Technology Journals)

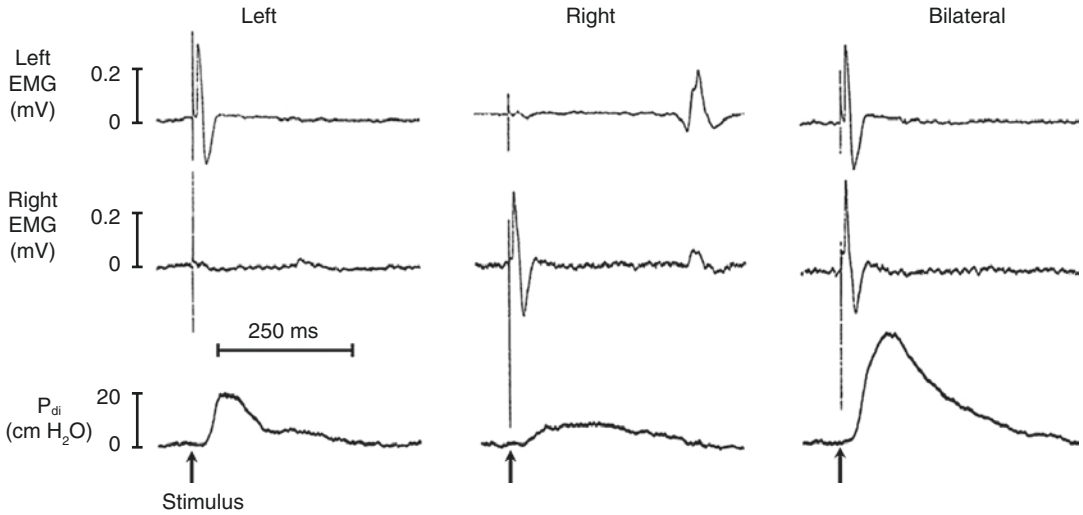


Fig. 36.9 Electromyograms (EMG) of the right and left hemidiaphragms and transdiaphragmatic pressure twitches ($P_{di,tw}$) in response to unilateral (*right, left*) and bilateral supramaximal phrenic nerve stimulations in a healthy subject. The shape and amplitude of the ipsilateral compound action potentials remain unaltered regardless

of whether one or both phrenic nerves are stimulated, indicating that each hemidiaphragm is maximally activated under both conditions. The amplitude of the $P_{di,tw}$ response during bilateral stimulation exceeds the sum of left and right responses. (From Bellemare et al. (1986), with permission of American Physiological Society)

It is imperative to carefully monitor the lung volume at which stimulation is performed (Hubmayr et al. 1989; Laghi et al. 1996; Yan et al. 1992a; Hamnegard et al. 1995; Polkey et al. 1996). Rigid binding of the abdomen and lower rib cage produce a 20–40% increase in $P_{di,tw}$ (Bellemare and Bigland-Ritchie 1984; Koulouris et al. 1989; Wilcox et al. 1988), probably by causing an increase in the initial muscle fiber length, reducing diaphragmatic shortening, and decreasing the radius of diaphragmatic curvature. Because a binding technique is difficult to standardize, it is better to leave the abdomen unbound.

Pressure resulting from twitch stimulation is influenced by the history of preceding muscle contractions. A forceful voluntary muscle contraction causes an increase in the muscle tension that is subsequently elicited during twitch stimulation, termed post-activation potentiation (Mador et al. 1994; Laghi et al. 1995; Wragg et al. 1994b). The mechanism has not been completely elucidated; it may result from an increase in extracellular potassium consequent to vigorous muscle contractions (Mador et al. 1994;

Holmberg and Waldeck 1980) or to reversible phosphorylation of myosin P light-chain units (Manning and Stull 1982). Potentiation decays in a monoexponential manner (Mador et al. 1994), and $P_{di,tw}$ values return to baseline 10–20 min after a vigorous contraction. To correctly quantify a change in diaphragmatic contractility, 10–20 min should elapse after a fatigue-inducing protocol before twitch stimulation is employed.

Normal values of $P_{di,tw}$ elicited by bilateral electrical stimulation have a wide range; 8.8–49.8 cm H₂O among individuals; group mean values, 20.7 – 32.3 cm H₂O (Table 36.2). With bilateral magnetic stimulation, normal values range from 18 to 49.7 cm H₂O, and group mean values from 26.5 to 38.9 cm H₂O. Some of the wide variation may be caused by failure to carefully control for twitch potentiation.

Reproducibility of $P_{di,tw}$ measurements is good (Tobin and Laghi 1998): between-occasion coefficients of variation are 7–11.5% for electrical stimulation and 6.6–10.7% for magnetic stimulation. In 32 healthy subjects, Luo et al. (2002) recorded $P_{di,tw}$ on 2 to 14 occasions over 1–5 years. The within-subject coefficient

Table 36.2 Transdiaphragmatic twitch pressure in healthy subjects^a

	Range	Mean \pm S.D.	Controlled for potentiation	<i>N</i>
Electrical stimulation technique				
Mier et al. (1989)	8.8–33.1	20.7 \pm 5.3	No	20
Hubmayr et al. (1989)	19–36	31.4 \pm 6.4	No	6
Wragg et al. (1994a)	22–40	29.7	No	9
Mador et al. (1996)	–	28.1 \pm 6.3	Yes	10
Mills et al. (1996)	24.7–2.1	28.1	Yes	6
Laghi et al. (1996)	20.4–49.8	32.2 \pm 7.0	Yes	10
Magnetic stimulation technique				
Similowski et al. (1989)	26.6–49.7	33.4 \pm 23.8	No	6
Wragg et al. (1994a)	27–48	36.5	Yes	9
Laghi et al. (1995)	32.8–42.1	38.9 \pm 3.1	Yes	8
Hamnegard et al. (1995)	–	31.6	Yes	6
Mills et al. (1996)	20.2–30.6	26.7	Yes	6
Laghi et al. (1996)	23.0–52.3	37.7 \pm 7.6	Yes	16
Mador et al. (1996)	–	37.2 \pm 8.3	Yes	10
Hamnegård et al. (1996)	18–45	31 \pm 28.7	Yes	23
Luo et al. (2002)	18–42	28 \pm 5	Yes	32

Modified from Tobin and Laghi (1998), with permission of McGraw Hill

^aValues are in centimeters of water

of variation was 11%. The limits of agreement between $P_{di,tw}$ measurements over time were ± 7 cm H₂O.

Because need for balloon catheters limits the clinical application of $P_{di,tw}$ measurements, investigators have evaluated mouth twitch pressures ($P_{mo,tw}$) as a means for estimating $P_{di,tw}$. $P_{mo,tw}$ provides a useful noninvasive estimate of $P_{di,tw}$ in healthy subjects (Yan et al. 1992b; Hamnegard et al. 1995; Laghi and Tobin 1997; Ju et al. 2014; Kabitz et al. 2007) and in patients (Similowski et al. 1991, 1993; Hamnegard et al. 1995; Ju et al. 2014; Kabitz et al. 2007; Topeli et al. 1999).

Twitch Pressure: Airway Twitch Pressure

In ventilated patients, twitch airway pressures ($P_{aw,tw}$) and $P_{di,tw}$ are well correlated (Fig. 36.10) (Cattapan et al. 2003; Watson et al. 2001), but the limits of agreement are wide, meaning that a particular $P_{aw,tw}$ is a poor predictor of $P_{di,tw}$. Because $P_{aw,tw}$ values are extremely reproducible, they appear useful in tracking changes in diaphragmatic contractility (Cattapan et al. 2003).

$P_{aw,tw}$ pressures in intubated patients (Cattapan et al. 2003; Watson et al. 2001) are a fraction of

those in healthy volunteers (Kabitz et al. 2007; Maillard et al. 1998), suggesting fatigue or weakness. Fatigue is an implausible mechanism because patients have received mechanical ventilation for days before the measurements (Tobin et al. 2012). Muscle weakness is a more plausible mechanism raising the possibility of ventilator-induced respiratory muscle injury and atrophy (Levine et al. 2008; Vassilakopoulos 2013; Supinski et al. 2018; Hooijman et al. 2015; Jaber et al. 2011).

Whether duration of mechanical ventilation, sepsis, and severity of underlying disease are risk factors for diaphragmatic weakness is controversial (Laghi et al. 2003; Jaber et al. 2011; Dres et al. 2017; Hermans et al. 2010; Supinski and Callahan 2013; Demoule et al. 2013). Whether diaphragmatic weakness impacts weaning outcome and duration of mechanical ventilation is also controversial (Laghi et al. 2003; Jaber et al. 2011; Dres et al. 2017; Hermans et al. 2010; Supinski and Callahan 2013; Demoule et al. 2013; Jung et al. 2016). Lack of standardization of twitch recordings impedes ability to judge the clinical impact of diaphragmatic weakness in ventilated patients.

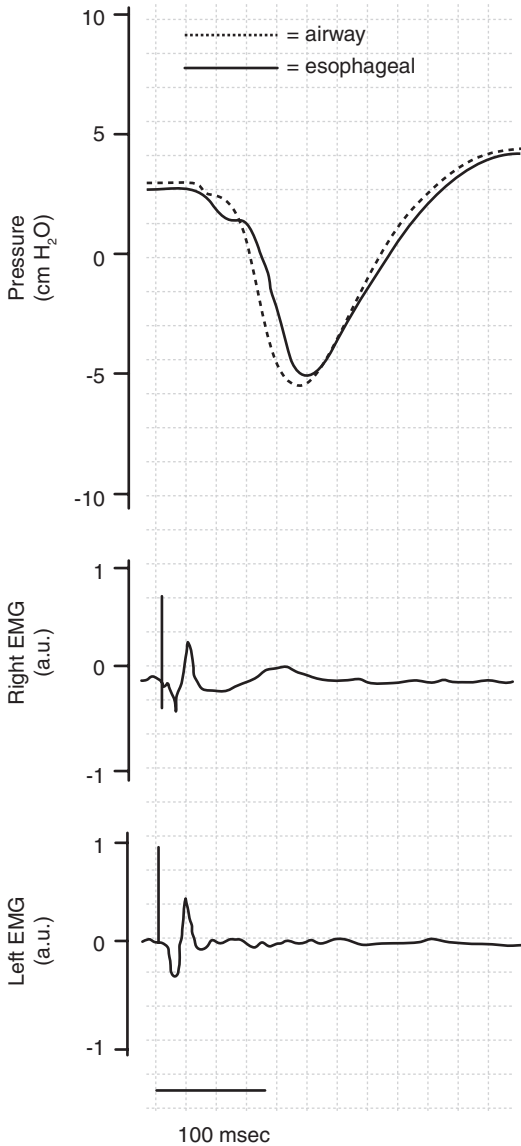


Fig. 36.10 Airway pressures and electromyographic (EMG) signals of the right and left hemidiaphragm in an intubated patient. Following phrenic nerve stimulation, muscle depolarization produces compound motor action potentials which are followed by the equivalent falls in airway pressure (broken line) and esophageal pressure (continuous line). (From Laghi et al. (2014b), with permission of Springer Nature BV)

Twitch Interpolation Technique: General Concepts

When a supramaximal (electrical or magnetic) stimulus is applied to peripheral nerves during a voluntary contraction, the motor units that have

not already been recruited respond by generating a twitch response (Belanger and McComas 1981). Motor units firing at submaximal rates (and whose motoneurons are not in a refractory state) respond with a twitch increment in force (Belanger and McComas 1981). As neural output to the muscle increases, fewer units are available for recruitment and the twitch increment in force diminishes. Consequently, the superimposed twitch is eventually undetectable (Shield and Zhou 2004). Performing a twitch stimulation during a voluntary effort allows indirect assessment of both the maximal strength of a muscle and its relative degree of activation (by the central nervous system) (Fig. 36.11) (Bellemare and Bigland-Ritchie 1984; Merton 1954).

In healthy subjects performing graded voluntary contractions, Bellemare and Bigland-Ritchie (Bellemare and Bigland-Ritchie 1984) detected no

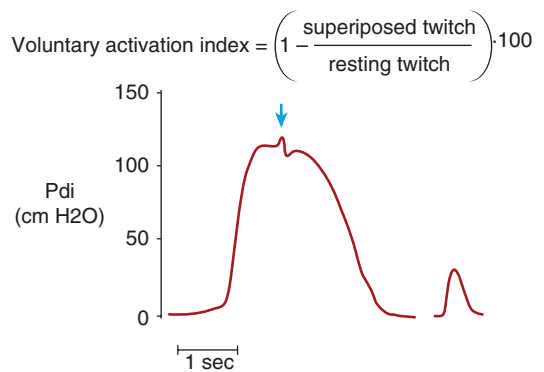


Fig. 36.11 Tracings of transdiaphragmatic pressure during bilateral phrenic nerve stimulation in a patient with COPD. During a forceful Mueller maneuver, stimulation produced a superimposed twitch pressure (arrow). On the right is a twitch pressure achieved by stimulation during resting breathing just after the Mueller maneuver. The ratio of the amplitude of superimposed twitch pressure to resting twitch pressure measures the extent that muscle is not recruited by the central nervous system during the Mueller maneuver. Muscle recruitment (by voluntary effort) is commonly expressed as voluntary activation index, calculated as: $1 - \frac{\text{superimposed twitch}}{\text{resting twitch}} \cdot 100$. In the example, the amplitude of the superimposed twitch pressure is 19% of the amplitude of resting twitch pressure, yielding a voluntary activation index of 81%; if the superimposed stimulus had evoked no increase in pressure, the activation index would have been 100%. (Based on Tobin et al. (2012))

superimposed twitches during $P_{di,max}$ contractions, indicating that the central nervous system was capable of recruiting all diaphragmatic motor units. The ratio of the twitch amplitude superimposed on a voluntary contraction to the twitch response of relaxed muscle between the contractions yields an estimate of maximum muscle strength without necessarily requiring a maximal voluntary effort: twitch interpolation. Bellemare and Bigland-Ritchie (Bellemare and Bigland-Ritchie 1984) observed a linear decline in the amplitude of superimposed $P_{di,tw}$ as a function of voluntary P_{di} in the range of 0–70% of $P_{di,max}$ (Fig. 36.12). A quasi-asymptotic decline was observed for P_{di} values above 70% of $P_{di,max}$. The result is that extrapolation of the relationship between evoked and voluntary force during submaximal contractions underestimated true $P_{di,max}$ by about 10%. Mechanism that may contribute to the asymptotic decline include decreased dissipation of twitch force in the in-series compliant compartment of muscle fibers (Loring and Hershenson 1992) and alterations in upper rib cage distortability (Similowski et al. 1996).

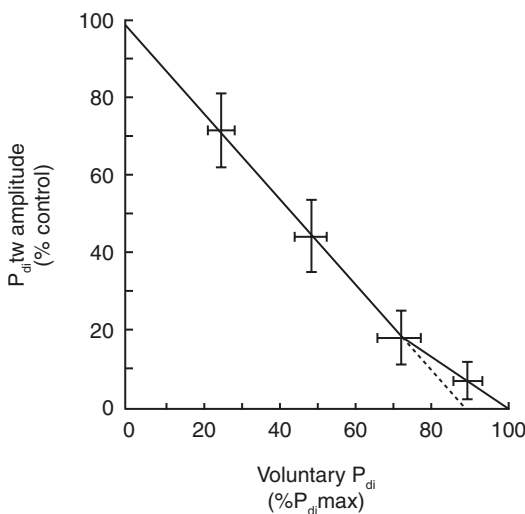


Fig. 36.12 The amplitude of transdiaphragmatic twitch pressure ($P_{di,tw}$), expressed as a percentage of the twitch amplitude from the relaxed muscle, versus voluntary P_{di} of up to 70% of maximum resulted in a decrease in the amplitude of the superimposed $P_{di,tw}$. A slight nonlinearity in the relationship was observed during voluntary contractions above 70% of $P_{di,max}$. (From Bellemare and Bigland-Ritchie (1984), with permission of Elsevier Science & Technology Journals)

Twitch Interpolation Technique: Central Fatigue

Bellemare and Bigland-Ritchie (1987) used the twitch interpolation method to quantify the separate contributions of central and peripheral components to the development of diaphragmatic fatigue in healthy volunteers. In five subjects in whom they induced diaphragmatic fatigue about 50% of the reduction in voluntary $P_{di,max}$ resulted from decreased central motor output; the rest resulted from peripheral muscle contractile failure (Bellemare and Bigland-Ritchie 1987). The purported mechanisms for the failure to maximally activate the diaphragm include the depressant effect of rising endorphin concentrations (Scardella et al. 1986), increased discharge of group III and IV muscle afferents in forcefully contracting inspiratory muscles (Gandevia 2001) and nociceptive phrenic afferents (Road et al. 1987). Additional factors that can trigger inhibition of central activation include failing cardiovascular response to increased metabolic demand and decreased perfusion of the central nervous system (Gandevia 2001; Viires et al. 1983).

Allen et al. (1993) used this approach to compare the degree of voluntary activation of the diaphragm in 11 stable patients with asthma and 10 healthy control subjects. All of the healthy subjects were capable of near complete activation (>95%) of the diaphragm during repeated voluntary $P_{i,max}$ maneuvers, and only 1 subject had less than 60% activation. In contrast, 5 of the patients with asthma had less than 60% activation of the diaphragm and 4 of them had occasional values below 30%. Such an inability to achieve full neural activation of the diaphragm may be an important contributor to the rapid development of ventilatory failure and death in some patients with acute severe asthma. They subsequently showed that impaired reflex excitation of inspiratory motoneurons in patients with asthma contributes to their reduced ability to fully activate the diaphragm during volitional efforts (Butler et al. 1996).

Topeli et al. (2001) used the twitch interpolation technique to investigate the role of voluntary activation of the diaphragm in patients with COPD and chronic hypercapnia. Voluntary acti-

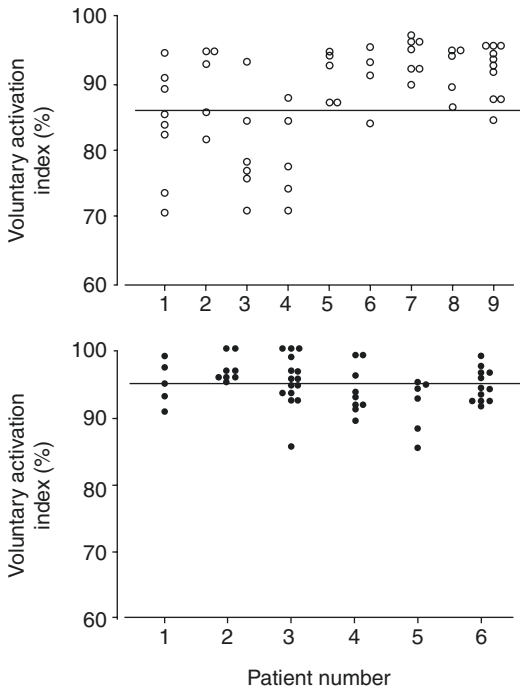


Fig. 36.13 Voluntary activation index of the diaphragm during maximal voluntary inspiratory efforts in normocapnic (upper panel) and hypercapnic patients (lower panel) with severe COPD. The mean value of the voluntary activation index (horizontal line) was higher in the hypercapnic patients than in the normocapnic patients ($p = 0.01$). (From Topeli et al. (2001), with permission of European Respiratory Society)

vation was higher in six hypercapnic patients than in nine normocapnic patients: 95 versus 89% (Fig. 36.13). The value in normocapnic patients was equivalent to that in healthy subjects (88%) (Allen et al. 1993). The extent of voluntary activation of the diaphragm and $P_a\text{CO}_2$ were both positively correlated with inspiratory muscle load (Topeli et al. 2001), suggesting that patients with a high load may have learned to fully activate their diaphragm (Topeli et al. 2001). The ability to mount an increase in voluntary motor output to the diaphragm could be especially important during an acute exacerbation. If patients have a low baseline level of voluntary activation, they may be unable to generate sufficient inspiratory pressure to avoid alveolar hypoventilation. The situation is analogous to patients with prior poliomyelitis who exhibit greater-than-normal fatigability of limb muscles, partly because of impaired voluntary activation of the limb muscles (Allen et al.

1994). In contrast to COPD patients with chronic hypercapnia (Topeli et al. 2001), (induction of) acute hypercapnia in healthy subjects had no effect on the voluntary neural output to the diaphragm (Wan et al. 2018).

It is not known if patients who fail a weaning trial experience reflex inhibition of central activation. It is extremely difficult to assess the extent of diaphragmatic recruitment in such patients. It is virtually impossible to assess diaphragmatic recruitment because twitch interpolation requires precise timing of phrenic-nerve stimulation at the zenith of an inspiratory effort (that is maintained steady during stimulation) and also supramaximal recruitment of the phrenic nerve throughout the stimulation (Laghi et al. 2003; Gandevia 2001). Twitch interpolation is also limited by its insensitivity to changes in diaphragmatic motor-unit firing rate (an important component of central activation) (Gandevia 2001).

Evoked Maneuvers: $P_{ga\ tw}$

Non-volitional assessment of expiratory muscle strength can be obtained by stimulating the thoracic nerve roots that innervate the abdominal muscles (Kyroussis et al. 1996). Following placement of a gastric balloon, the operator applies the stimulating probe over the tenth thoracic vertebra (Fig. 36.14) (Kyroussis et al. 1996). In healthy

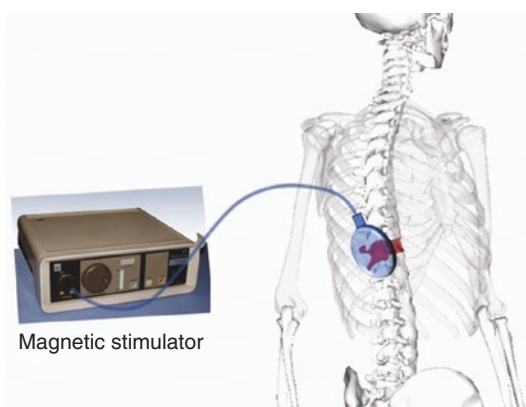


Fig. 36.14 Schematic representation of magnetic stimulation of the thoracic nerve roots to assess non-volitionally expiratory muscle strength. Following placement of a gastric balloon (not shown), the operator applies the center of the stimulating probe (blue circle) over the tenth thoracic vertebra (red vertebral body). Stimulations can be delivered while the patient is seated, prone, or supine

subjects, the median $P_{\text{ga,tw}}$ is 39.4 cm H₂O (interquartile range 26.6 cm H₂O)(Steier et al. 2007) and within-session coefficient of variation is 10% (Wuthrich et al. 2015).

A $P_{\text{E,max}}$ less than +80 cm H₂O in men and less than +60 cm H₂O in women arouses suspicion of expiratory muscle weakness (Steier et al. 2007), and cough P_{ga} should be checked. Cough P_{ga} greater than 132 cm H₂O in men and 97 cm H₂O in women excludes clinically important muscle weakness (Steier et al. 2007). A smaller value could result from poor technique. The addition of $P_{\text{ga,tw}}$ to $P_{\text{E,max}}$ helps in this situation, reducing false-positive diagnosis of expiratory muscle weakness by 56.4% (Steier et al. 2007). Caution must be taken when interpreting low $P_{\text{ga,tw}}$ values as they may result from submaximal stimulation of the thoracic nerve roots and not because of weakness or fatigue (Kyroussis et al. 1996; Verges et al. 2010). $P_{\text{ga,tw}}$ has also been used to detect expiratory muscle fatigue in healthy subjects and in patients (Kyroussis et al. 1996; Wuthrich et al. 2015; Verges et al. 2006; Elia et al. 2013; Bachasson et al. 2013).

Respiratory Muscle Pressure Output: Effort

Respiratory muscle effort can be computed in terms of work of breathing, pressure–time product, and tension–time index.

Work of Breathing

Work of breathing is commonly increased in critically ill patients, and many patients have a decreased capacity to perform work (Marini et al. 1985; Ward et al. 1988; Sassoon et al. 1988). Mechanical work is performed when a force moves its point of application through a distance (Tobin and Van de Graff 1994). In the case of a three-dimensional fluid system, work is done when a pressure (P) changes the volume (V) of the system.

$$W = P \cdot V = \int_0^V P \cdot dV$$

When a muscle contracts, mechanical work is performed only if displacement takes place. During an *isometric* contraction, no displacement takes place; therefore no mechanical work is performed – there is, of course, a metabolic cost for exerting the force.

Mechanical work of breathing can be calculated by measuring the generation of intrathoracic pressure secondary to contraction of the respiratory muscles (or a ventilator substituting for them) and the displacement of gas volume. Changes in pressure and volume can be analyzed graphically, and the area enclosed within a volume–pressure loop has the units of mechanical work.

Measurements of respiratory work in spontaneously breathing patients require an estimate of pleural pressure (P_{pl}), usually achieved by means of P_{es} . P_{es} can be viewed as the sum of the pressure developed by the respiratory muscles in expanding the chest-wall (P_{mus}) and the static pressure of the chest-wall (P_{cw}). Thus, P_{mus} can be expressed as $P_{\text{mus}} = P_{\text{es}} - P_{\text{cw}}$. The graphical approach to the analysis of P_{es} -volume loops introduced by Campbell (Campbell 1958; Agostoni et al. 1970) allows work to be separated into several components.

To quantitate work performed in distending the lungs alone, the relevant transstructural pressure is transpulmonary pressure (P_{L}), which is equal to $P_{\text{aw}} - P_{\text{es}}$. During spontaneous breathing, P_{aw} is zero, and, thus, inspiratory work can be calculated from P_{es} and volume recordings alone (Simmons 1989). In a patient connected to a ventilator circuit, P_{aw} is not zero; consequently, measurement of P_{es} alone does not permit calculation of work performed on the lung, although it allows calculation of work performed by the patient. Work imposed on the patient by the breathing apparatus, external circuit, and endotracheal tube is determined from the integral of the change in pressure at the carinal end of the endotracheal tube and the change in volume. Measurements of total work during spontaneous efforts while a patient is attached to a ventilator requires measurements of both P_{es} and P_{aw} (as well as volume).

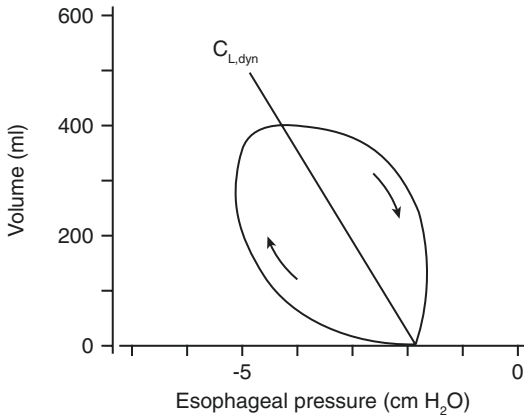


Fig. 36.15 A plot of esophageal pressure versus volume during a respiratory cycle. The line between the points of zero flow, the dynamic pulmonary compliance line ($C_{L,dyn}$), partitions resistive work into its inspiratory and expiratory components. Note the clockwise direction in which actively generated esophageal pressure–volume curves are formed. (From Tobin and Van de Graff (1994), with permission of McGraw Hill LLC)

During unassisted breathing, the total resistive work done on the lungs in each breath is obtained by integrating the area subtended by P_{es} and lung volume during a complete respiratory cycle (Fig. 36.15). Work is partitioned into its inspiratory and expiratory resistive components by drawing a line between points of zero flow: the dynamic pulmonary compliance line.

During unassisted breathing, work performed by the inspiratory muscles against the elastic recoil of the lungs and chest-wall can be calculated by constructing a Campbell diagram. This method requires measurement of the static compliance of the chest-wall (C_{cw}), which can be closely estimated by recording P_{es} and volume during controlled ventilation while the respiratory muscles are completely relaxed (Fig. 36.16). Subtraction of P_{es} from P_{cw} indicates the pressure developed by the respiratory muscles in expanding the chest-wall (P_{mus}) (see above).

Elastic inspiratory work is measured as the area between the line of dynamic pulmonary compliance ($C_{L,dyn}$) and the line of static chest-wall compliance (C_{cw}) within the tidal volume range (Fig. 36.17). In patients with elevated end-expiratory volume and intrinsic positive end-expiratory pressure (PEEPi) (Fig. 36.18), the P_{es} -

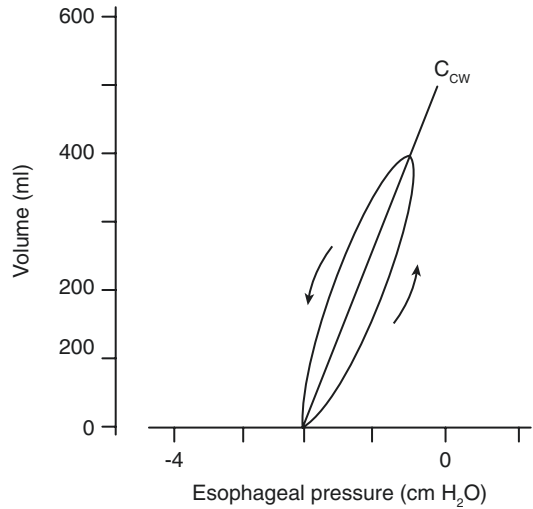


Fig. 36.16 A plot of esophageal pressure versus volume during passive ventilation. The line connecting the points of zero flow is the static chest wall compliance line (C_{cw}). Note the counterclockwise direction in which passively generated esophageal pressure–volume curves are formed. (From Tobin and Van de Graff (1994), with permission of McGraw Hill LLC)

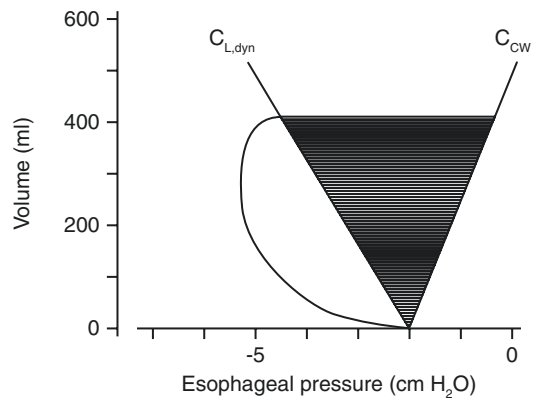


Fig. 36.17 A plot of esophageal pressure versus volume during unassisted ventilation. The static chest wall compliance line (C_{cw}) is fitted at the end-expiratory elastic recoil pressure of the chest wall. Inspiratory elastic work is calculated as the cross-hatched area of the pressure–volume curve subtended by the C_{cw} line and the dynamic pulmonary compliance line ($C_{L,dyn}$). See Fig. 36.15 and 36.16. (From Tobin and Van de Graff (1994), with permission of McGraw Hill LLC)

volume loop is displaced upward as compared with Fig. 36.17 and has a prominent flat base formed as PEEPi is overcome at the start of an

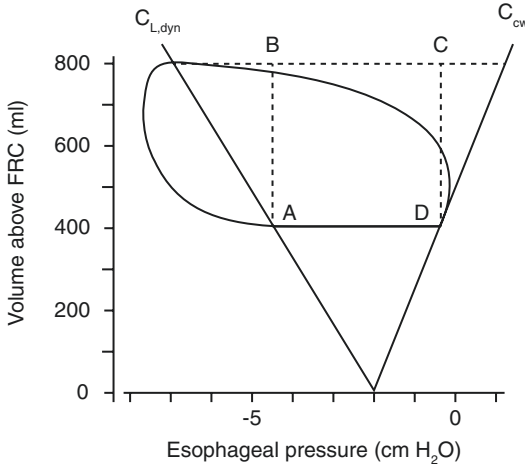


Fig. 36.18 A plot of esophageal pressure versus volume in a patient with intrinsic positive end-expiratory pressure (PEEPi). The end-expiratory elastic recoil pressure of the chest-wall no longer coincides with zero flow. End-expiratory lung volume is elevated (here, by 400 mL) above relaxed functional residual capacity (FRC). The distance between the static chest-wall compliance line (C_{cw}) and the dynamic lung compliance line ($C_{L,dyn}$) is equal to the level of PEEPi. Given the presence of PEEPi, the amount of work has been increased from that shown in Fig. 36.17 by an amount proportional to the area enclosed by the rectangle ABCD. (From Tobin and Van de Graff (1994), with permission of McGraw Hill LLC)

inspiratory effort. Inspiratory work is increased because the added pressure change required to initiate flow must be continued throughout inspiration (Fig. 36.18).

During quiet breathing, expiration is passive and the work of breathing is usually performed entirely by the inspiratory muscles. About 50 percent of inspiratory work is dissipated as heat in overcoming flow-resistive forces (Nunn 1977). The remaining 50 percent of inspiratory work is stored as potential energy in the deformed tissues of the lung and chest-wall and is used during expiration. When ventilatory demands increase or expiratory resistance is markedly increased, the expiratory muscles are recruited. Such expiratory muscle activity increases P_{es} , producing P_{es} -volume values to the right of the chest-wall relaxation line and outside the elastic work area on a Campbell diagram: P_{es} is higher than the static elastic recoil pressure of the chest-wall (Agostoni et al. 1970; Fleury et al. 1985). This

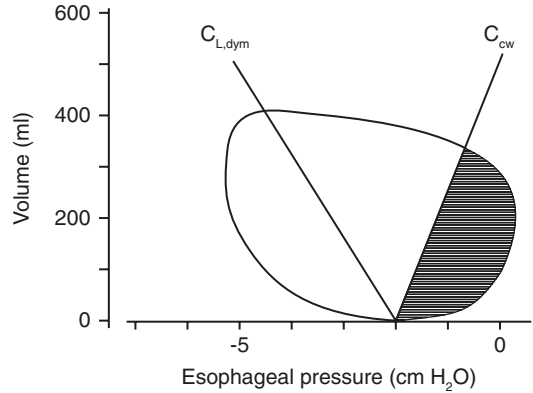


Fig. 36.19 A plot of esophageal pressure versus volume in a patient exhibiting expiratory muscle activity. The chest-wall compliance line is measured and fitted to the pressure volume curve as described in Figs. 36.16 and 36.17. Expiratory work is quantitated as the cross-hatched area enclosed by the portion of the pressure-volume loop lying to the right of the static chest-wall compliance line (C_{cw}). (From Tobin and Van de Graff (1994), with permission of McGraw Hill LLC)

can be quantitated as the area enclosed by the expiratory portion of the P_{es} -volume loop to the right of the chest-wall relaxation line (Van de Graaff et al. 1991) (Fig. 36.19).

During the expiratory phase of the respiratory cycle, some of the elastic energy stored in the tissues deformed during inspiration is used to overcome flow resistances of the lung and chest-wall; the remainder is used to overcome the persistent activity of inspiratory muscles during expiration (Laghi and Shaikh 2017; Roussos 1986). This postinspiratory activity represents negative (plometric) work by the inspiratory muscles as they lengthen. During normal resting ventilation, this negative work is substantial (Petit et al. 1960; Milic-Emili 1991), but it becomes relatively small with increasing ventilation (Petit et al. 1960). Negative inspiratory work can be calculated by subtracting expiratory-flow resistive work from the elastic work of inspiration (Fig. 36.20) (Fleury et al. 1985).

Pressure-Time Product

Measurements of mechanical work of breathing can substantially underestimate oxygen consumption by the respiratory muscles, being totally insensitive to energy expenditure during

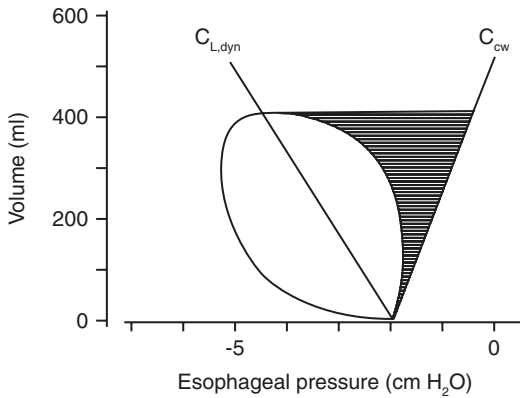


Fig. 36.20 A plot of esophageal pressure versus volume during a respiratory cycle. The dynamic pulmonary compliance line ($C_{L,dyn}$) and the static chest-wall compliance line (C_{cw}) are calculated and fitted to the curves as shown in Figs. 36.15, 36.16, and 36.17. Negative inspiratory work shown with cross-hatching is calculated by subtracting expiratory-flow resistive work from the elastic work of inspiration. (From Tobin and Van de Graff (1994), with permission of McGraw Hill LLC)

an isometric contraction. Mechanical work also fails to account for the duration of a muscle contraction. Two breaths may have the same tidal volume and intrathoracic pressure excursion but differ in inspiratory duration. Because pressure–volume relationships are the same, mechanical work of breathing will be identical. Energy requirements, however, will be greater for the breath with the longer inspiratory time. Under loaded conditions, the efficiency of respiratory muscle contraction decreases considerably and oxygen consumption increases for a given amount of work (Field et al. 1984).

Pressure–time product (PTP) circumvents these problems (Fig. 36.21) and several investigators have shown that a measurement of the magnitude and duration of pressure generation is more closely related to respiratory muscle oxygen consumption than is mechanical work (Field et al. 1984; McGregor and Becklake 1961; Rochester and Bettini 1976; Robertson et al. 1977). PTP is an important determinant of energy supply, because blood flow to the diaphragm is a unique function of the tension–time index of the diaphragm, the equivalent of PTP (Bellemare and Grassino 1982; Bellemare et al. 1983a).

Jubran and Tobin (1997) obtained measurements of PTP product in 17 ventilator-supported patients with COPD who failed a trial of spontaneous breathing and 14 patients who tolerated a trial and were extubated. At the onset of the trial, PTP was not different between the failure and success groups, 255 ± 59 and 158 ± 23 (S.E.) $\text{cmH}_2\text{O}\cdot\text{s}/\text{min}$, respectively. Both these values were higher than PTP of 94 ± 12 $\text{cmH}_2\text{O}\cdot\text{s}/\text{min}$ recorded in 7 healthy subjects using the same methodology. Throughout the course of the trial, PTP was higher in the weaning failure group, increasing to 388 ± 68 $\text{cmH}_2\text{O}\cdot\text{s}/\text{min}$ at the end of the trial. Partitioning of PTP into its resistive, PEEPi, and non-PEEPi elastic components revealed increases in all three components at the end of the trial (Fig. 36.22).

Tension–Time Index of the Diaphragm

Tension–time index of the diaphragm is an alternative to pressure–time product for quantifying the magnitude and duration of respiratory muscle contractions. Bellemare and Grassino (1982) reasoned that because the diaphragm contracts mainly during inspiration, the relative duration of inhalation (T_I) to the duration of the total respiratory cycle (T_{TOT}) should be an important determinant of diaphragmatic fatigue. In subjects breathing against resistive loads, they examined the relative importance of mean P_{di} (\bar{P}_{di}) and T_I/T_{TOT} in determining endurance time. The ratios of $\bar{P}_{di}/P_{di,max}$ and T_I/T_{TOT} were equally important determinants. They combined these factors into a tension–time index of the diaphragm (TTdi), calculated as

$$\text{TTdi} = \bar{P}_{di} / P_{di,max} \times T_I / T_{TOT}$$

During inspiratory resistive loading, endurance time progressively decreases as TTdi increases. Below a critical TTdi value of 0.15, breathing can be sustained indefinitely. Healthy subjects breathing at rest have a TTdi value of 0.02, indicating approximately an eightfold reserve.

Laghi et al. (2003) measured the TTdi in nine weaning-failure patients and seven weaning-success patients. Over the course of the trial, TTdi was higher in the failure group than in the

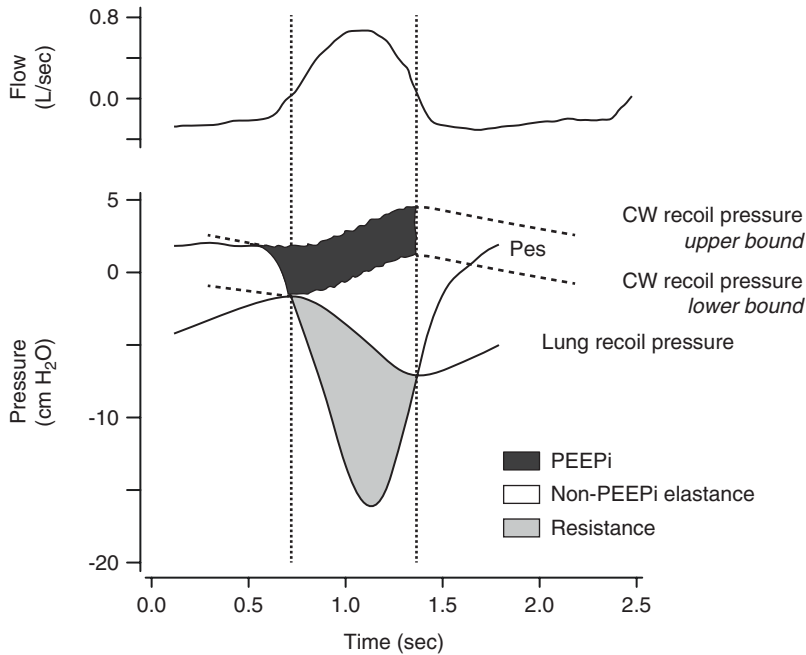


Fig. 36.21 Flow (inspiration upward) and pressure tracings during spontaneous breathing. Recoil pressures of chest-wall (CW) and lung are calculated from dynamic elastances of chest-wall and lung, respectively, and lung volume. Upper bound inspiratory pressure–time product (PTP) is integral of difference between P_{es} and upper bound CW recoil pressure from onset of rapid P_{es} decrease to inspiratory-to-expiratory flow transition. Component of PTP secondary to intrinsic positive end-expiratory pressure (PEEPi) is computed using the integral of the difference between upper and lower bound of CW recoil pressure from rapid decrease in P_{es} to inspiratory-to-

expiratory flow transition. Component of PTP secondary to non-PEEPi elastance is the integral of difference between lung recoil pressure and lower bound CW recoil pressure from onset of inspiratory flow to inspiratory-to-expiratory flow transition. Resistive fraction of PTP is the integral of the difference between P_{es} and lung recoil pressure. The vertical interrupted lines represent points of zero flow. (Reprinted with permission of the American Thoracic Society. Copyright © 2020 American Thoracic Society. All rights reserved. Jubran and Tobin (1997). The American Journal of Respiratory and Critical Care Medicine is an official journal of the American Thoracic Society)

success group (Fig. 36.23). Of the nine failure patients, seven had a TTdi at or above 0.15 yet none developed diaphragmatic fatigue (no patient experienced a decrease in $P_{di,tw}$). This finding was the result of several concurrent factors: greater recruitment of rib cage and expiratory muscles, development of clinical signs of distress (mandating the reinstatement of mechanical ventilation) before the development of fatigue, and overestimation of TTdi (Laghi et al. 2003).

Interpretation of tension–time index values is confounded by several factors. During inspiratory loading, progressive diaphragmatic fatigue develops before the occurrence of task failure

(Laghi et al. 1998a). In the laboratory, endurance time has been determined while subjects generate square-wave breathing pattern (Bellemare and Grassino 1982). The latter results in very low flow rates and minimal velocity of muscle shortening. This contrasts with tachypnea commonly observed in critically ill patients (Clanton et al. 1985; McCool et al. 1986). Patients commonly develop dynamic hyperinflation (Tobin et al. 2012), which decreases pressure-generating capacity as a result of inspiratory muscle shortening (Laghi et al. 1996). In turn, muscle shortening increases susceptibility to fatigue (Fitch and McComas 1985).

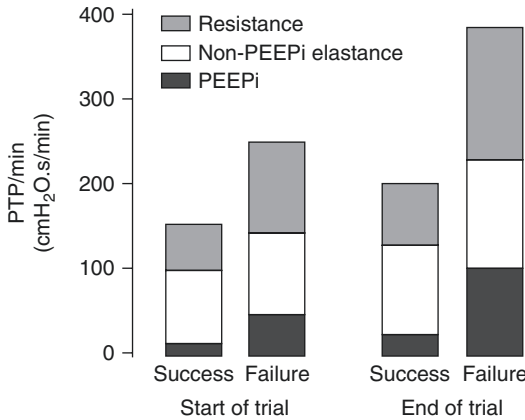


Fig. 36.22 Partitioning of pressure–time product (PTP/min) into intrinsic positive end-expiratory pressure (PEEPi), non-PEEPi elastic, and resistive components at the start and end of a weaning trial in 17 patients who failed the trial and 14 patients who were successfully weaned. At the end of the trial, increase in PTP/min in failure group resulted from increases in the PEEPi component by 111% ($p < 0.0001$), non-PEEPi elastic component by 33 percent ($p < 0.0001$), and resistive component by 42 percent ($p < 0.0001$). The increase in PTP/min at end of the trial in success group resulted from an increase in non-PEEPi elastic component by 23 percent ($p < 0.02$) and in resistive component by 26 percent ($p < 0.01$), while the PEEPi fraction did not change. (Reprinted with permission of the American Thoracic Society. Copyright © 2020 American Thoracic Society. All rights reserved. Jubran and Tobin (1997). The American Journal of Respiratory and Critical Care Medicine is an official journal of the American Thoracic Society)

Esophageal and Gastric Pressure Tracings

Pleural Pressure–Abdominal Pressure Diagram

The plot of swings in P_{ga} and P_{es} against each other provides qualitative information on the relative contributions of the diaphragm, rib cage inspiratory muscles, and abdominal muscles to breathing and conveys how these muscles are coordinated (Table 36.3) (Tobin and Laghi 1998). The $P_{es} - P_{ga}$ diagram and related ratios represent useful means of assessing respiratory muscle function in critically ill patients.

Excursions in P_{es} and P_{ga} are referred to the relaxation line (P_{es} and P_{ga} during a relaxed exhalation from TLC), and departures from this rela-

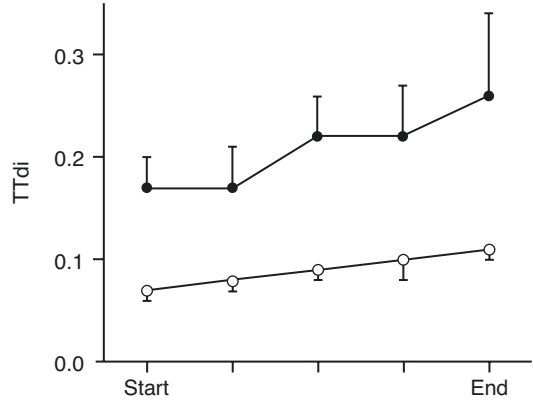


Fig. 36.23 Tension–time index of the diaphragm (TTdi) during a weaning trial in the failure (closed symbols) and success (open symbols) groups. Between the onset and the end of the trial, increases TTdi ($p < 0.005$) occurred in both groups. Over the course of the trial, the failure group had higher values of TTdi ($p = 0.01$) than did the success group. Bars represent SE. (Reprinted with permission of the American Thoracic Society. Copyright © 2020 American Thoracic Society. All rights reserved. Laghi et al. (2003). The American Journal of Respiratory and Critical Care Medicine is an official journal of the American Thoracic Society)

Table 36.3 Effect of major muscle groups on directional change in pressures and dimensions

Muscle	Activity	P_{es}	P_{ga}	V_{RC}	V_{Ab}
Diaphragm	Contraction	↓	↑	↑ ^a	↑
	Relaxation	↑	↓	↓	↓
Inspir RC	Contraction	↓	↓	↑	↓
	Relaxation	↑	↑	↓	↑
Expir RC	Contraction	↑	↑	↓	↑
	Relaxation	↓	↓	↑	↓
Abdominals	Contraction	↑	↑	↓	↓
	Relaxation	↓	↓	↑	↑

^aAlthough overall V_{RC} and lower V_{RC} increase, upper V_{RC} decreases

Key: P_{es} esophageal pressure, P_{ga} gastric pressure, V_{RC} rib cage volume or dimensions, V_{Ab} abdominal volume or dimension, ↑ = upgoing (more positive or less negative) signal, ↓ = downgoing signal

Modified from Tobin and Laghi (1998), with permission of McGraw Hill

tionship are used to infer the recruitment of various respiratory muscle groups. In addition to plotting the point-by-point course of P_{es} and P_{ga} throughout a breath, diagrams of $P_{es} - P_{ga}$ are sometimes generated by plotting only the values during zero flow at the onset and end of a breath

(Laghi et al. 1998a; Criner and Celli 1988; Martinez et al. 1990; Epstein et al. 1995; Hillman and Finucane 1988; Yan et al. 1993c; Sliwinski et al. 1996). The latter approach is useful when the pressure contour makes it difficult to pick off the peak inspiratory and peak expiratory points with confidence (Sliwinski et al. 1996).

During inhalation, P_{es} becomes progressively more negative as a result of the combined action of the diaphragm, parasternal intercostal muscles, and scalene muscles. When ventilation is challenged, recruitment of the sternocleidomastoid and other accessory muscles contributes to the decrease in P_{es} (Parthasarathy et al. 2007); a decrease in P_{es} during early inhalation may also result from relaxation of the expiratory muscles (Parthasarathy et al. 1998). Abdominal pressure (P_{ab}) is estimated from measurement of P_{ga} .

The diaphragm is the only muscle that simultaneously lowers P_{es} and increases P_{ga} when it contracts; thus, ΔP_{di} during tidal breathing is considered to represent the force achieved by diaphragmatic contraction. In isolation, recordings of ΔP_{di} can result in overestimation or underestimation of diaphragmatic activity (Clergue et al. 1995). Recruitment of the expiratory muscles can stretch the diaphragm with resultant increase in P_{di} . At the completion of an active exhalation, relaxation of the expiratory muscles causes P_{di} to move in a negative direction. A subsequent active contraction of the diaphragm will cause P_{di} to move in a positive direction only after it first makes up for this loss of the tension. In this situation, measurement of ΔP_{di} will underestimate the degree of active diaphragmatic contraction (Clergue et al. 1995).

During normal quiet inhalation, the diaphragm contracts and descends, P_{es} becomes more negative, and P_{ga} becomes more positive. The increase in P_{ga} causes outward movements of the abdomen and rib cage. The changes in P_{es} and P_{ga} fall very close to the relaxation line (Fig. 36.24) indicating that normal breathing involves the generation of little additional pressure over that needed to inflate the system pas-

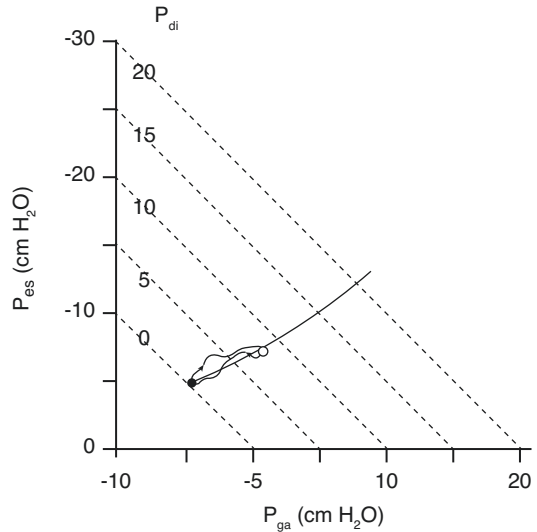


Fig. 36.24 A plot of negative esophageal pressure (P_{es}) against positive gastric pressure (P_{ga}) during quiet breathing; the slight irregularities the tracings are secondary to cardiogenic oscillations. *Closed circle*: Onset of inspiratory flow. *Open circle*: Onset of expiratory flow. The curvilinear line in the background is the relaxation line. Isopleths for different levels of transdiaphragmatic pressure (P_{di}) are shown as dashed diagonal lines. The downward 45° slope signifies that the change in P_{es} is accompanied by equal and opposite (in sign) change in P_{ga} . (From Tobin and Laghi (1998), with permission of McGraw Hill LLC)

sively (Macklem 1985). At the start of normal exhalation, relaxation of the diaphragm is accompanied by a decrease in P_{ga} and inward motion of the abdomen. When the diaphragm is stretched (abdominal muscle contraction), the $P_{es} - P_{ga}$ plot will be displaced to the right of the isopleth for $P_{di} = 0$ in proportion to the associated increase in P_{di} (Fig. 36.25).

Figures 36.26, 36.27, and 36.28 are $P_{es} - P_{ga}$ plots recorded during isolated contraction of the rib cage muscles, tonic contraction of the inspiratory rib cage muscles during inhalation, and isolated contraction of the abdominal muscles during exhalation followed by their abrupt relaxation with resultant passive inhalation. Critically ill patients commonly contract several respiratory muscle groups during a single respiratory cycle, which produce $P_{es} - P_{ga}$ diagrams

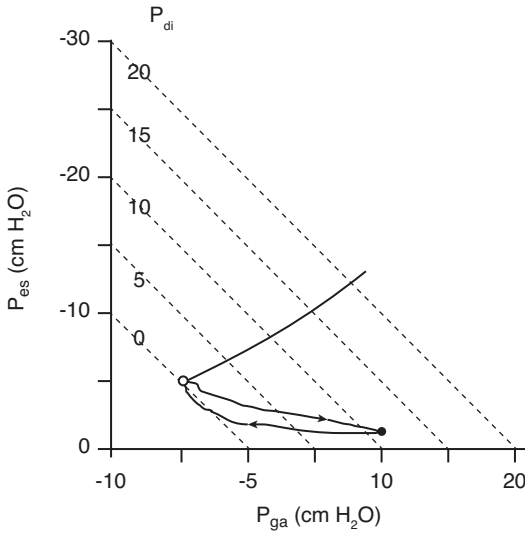


Fig. 36.25 Abdominal muscle contraction produces an increase in gastric pressure (P_{ga}) and a less negative esophageal pressure (P_{es}), as indicated by displacement of $P_{es} - P_{ga}$ plot down and to the right. The associated passive stretching of the diaphragm results in an increase in P_{di} . *Closed circle*: Onset of inspiratory flow. *Open circle*: Onset of expiratory flow. (From Tobin and Laghi (1998), with permission of McGraw Hill LLC)

that can be more difficult to decipher. Figure 36.29 illustrates the activity of the diaphragm and expiratory muscles at different stages of a respiratory cycle.

Ratio of Change in Gastric-to-Esophageal Pressure

To properly employ $P_{es} - P_{ga}$ diagrams, patients must first perform a relaxation maneuver. This maneuver is challenging to many patients. To simplify the $P_{es} - P_{ga}$ diagram, some investigators calculate the ratio of tidal swing in P_{ga} to tidal swing in P_{es} or $\Delta P_{ga}/\Delta P_{es}$ ratio (Moreno et al. 1981). The ratio reflects the relative contributions of the diaphragm and other respiratory muscles to quiet breathing. A $P_{es} - P_{ga}$ loop that shifts to the left (Fig. 36.26) is associated with a $\Delta P_{ga}/\Delta P_{es}$ ratio becoming less negative. The range of potential values of the $\Delta P_{ga}/\Delta P_{es}$ ratio and their significance are listed in Table 36.4.

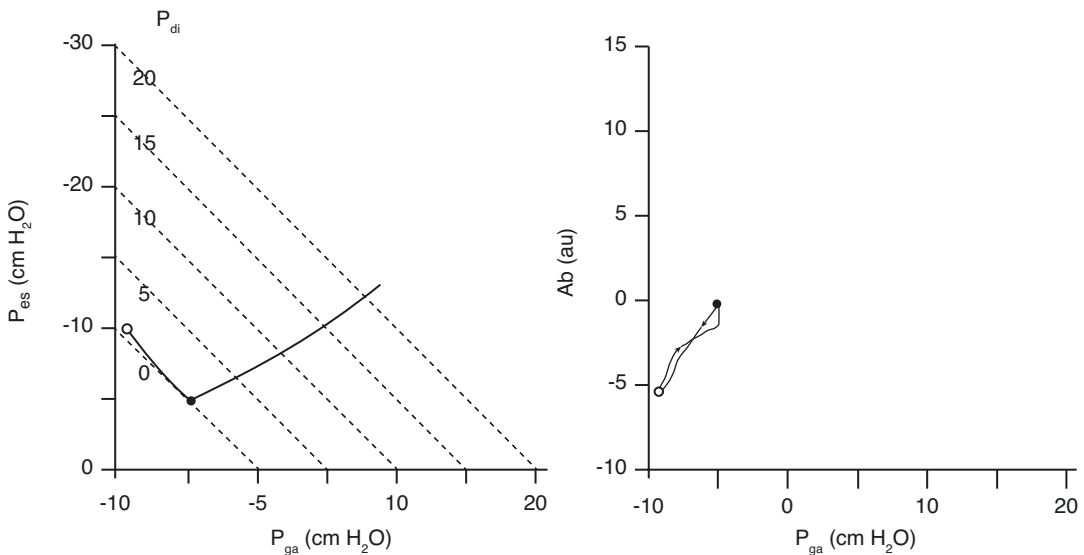


Fig. 36.26 *Left panel*: A plot of esophageal pressure (P_{es}) versus gastric pressure (P_{ga}) during isolated contraction of rib-cage muscles. The plot moves up and to the left along the isopleth for $P_{di} = 0$. *Right panel*: A simultaneous recording of abdominal cross-sectional area (in arbitrary

units) shows the abdomen moving inward as P_{ga} becomes less positive during inspiration. *Closed circle*: Onset of inspiratory flow. *Open circle*: Onset of expiratory flow. (From Tobin and Laghi (1998), with permission of McGraw Hill LLC)

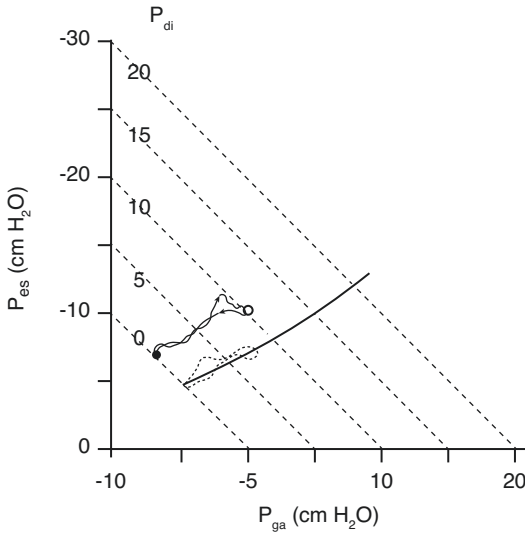


Fig. 36.27 Tonic activity of the inspiratory rib cage muscles. The esophageal pressure–gastric pressure ($P_{es} - P_{ga}$) loop is parallel to that of quiet breathing (shown as a ghost plot). Inspiration commences from a higher end-expiratory lung volume, as indicated by the higher transpulmonary pressure. *Closed circle*: Onset of inspiratory flow. *Open circle*: Onset of expiratory flow. (From Tobin and Laghi (1998), with permission of McGraw Hill LLC)

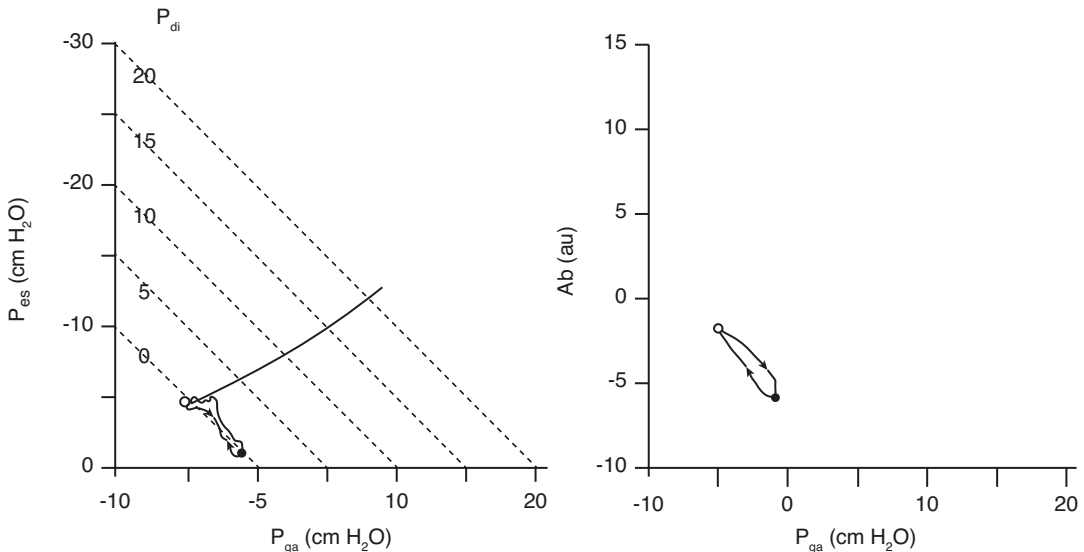


Fig. 36.28 *Left panel*: A plot of esophageal pressure (P_{es}) versus gastric pressure (P_{ga}) during isolated abdominal muscle contraction. During exhalation, the plot moves down and to the right along the isopleth for $P_{di} = 0$. *Right panel*: A simultaneous recording of abdominal cross-

In 8 patients with COPD (FEV_1 : 0.71 ± 0.06 (SE) L) undergoing lung volume reduction surgery, Laghi et al. (2004) found that the $\Delta P_{ga}/\Delta P_{es}$ ratio changed from -0.6 ± 0.1 before surgery to -1.2 ± 0.3 three months after surgery ($p < 0.01$) suggesting an increased diaphragmatic contribution to tidal breathing.

A shift in the $\Delta P_{ga}/\Delta P_{es}$ ratio to a less negative value was originally considered pathognomonic of impaired diaphragmatic activity. It is now recognized that a less negative ratio may also result from proportionally greater activity of the intercostal-accessory muscles, which will reduce the magnitude of an increase in P_{ga} achieved by diaphragmatic contraction (Parthasarathy et al. 2007; Clergue et al. 1995).

Ratio of Change in Gastric-to-Transdiaphragmatic Pressure

The $\Delta P_{ga}/\Delta P_{di}$ ratio provides qualitative information on the contribution of the diaphragm to tidal

sectional area shows that the abdomen moves inward as P_{ga} becomes more positive during exhalation. *Closed circle*: Onset of inspiratory flow. *Open circle*: Onset of expiratory flow. (From Tobin and Laghi (1998), with permission of McGraw Hill LLC)

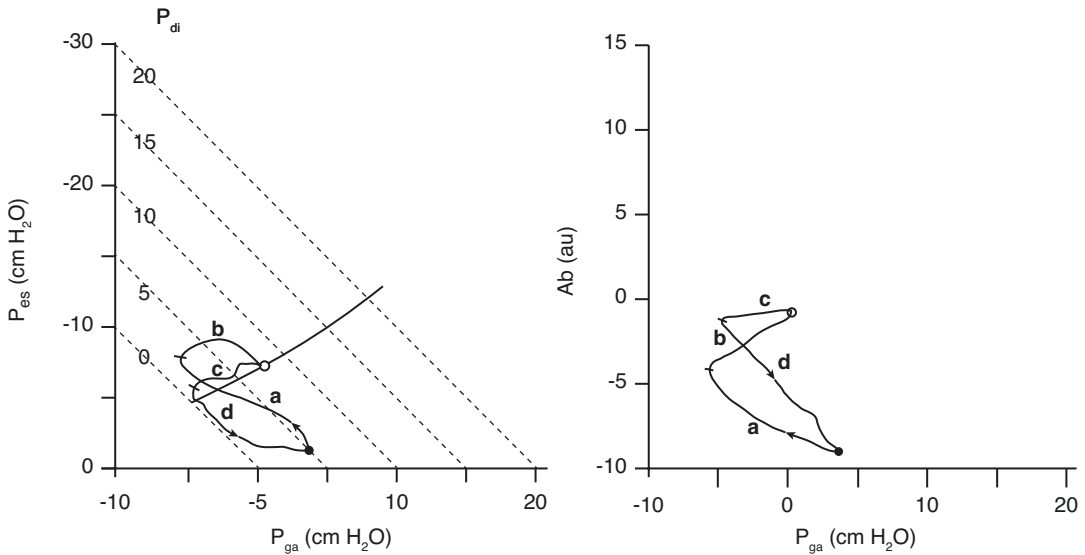


Fig. 36.29 *Left panel:* Segment a, commencing with onset of inspiratory flow (closed circle), represents expiratory muscle relaxation, with both gastric pressure (P_{ga}) and esophageal pressure (P_{es}) becoming less positive. Segment b represents diaphragmatic contraction, with P_{ga} becoming more positive and P_{es} becoming initially more negative. Segment c, commencing with onset of expiratory flow (open circle), represents diaphragmatic relaxation, signaled by P_{ga} becoming less positive and P_{es} becoming less negative. Segment d (final portion of expiratory flow) represents expiratory muscle contraction, signaled by P_{ga} becoming more positive and P_{es} also becoming more positive. *Right panel:* A simultaneous plot of abdominal cross-sectional area against P_{ga} shows in segment a that the onset of inspiratory flow (closed circle)

is associated with P_{ga} becoming less positive; the accompanying increase in abdominal cross-sectional area indicates that this is caused by relaxation of the abdominal muscles. Diaphragmatic contraction in segment b causes P_{ga} to become more positive and abdominal cross-sectional area to further increase. Diaphragmatic relaxation in segment c causes P_{ga} to become less positive and abdominal cross-sectional area to decrease. During the final portion of expiratory flow, segment d, P_{ga} becomes more positive; the accompanying decrease in abdominal cross-sectional area indicates that the expiratory muscle activity originates in the expiratory muscles of the rib cage. (From Tobin and Laghi (1998), with permission of McGraw Hill LLC)

Table 36.4 Abdominal–pleural pressure ratio

$\Delta P_{ga}/\Delta P_{es}$	Significance
≤ -1	Normal
-1 to 0	Inspiratory increase in P_{ga} is less than the decrease in P_{es}
0	Diaphragm acts as a fixator, preventing transmission of P_{es} to abdomen
>0	P_{ga} falls during inspiration
+1	Totally ineffective diaphragm

Modified from Tobin and Laghi (1998), with permission of McGraw Hill

breathing (Gilbert et al. 1981, 1983). The ratio has been used to assess the contribution of the diaphragm to breathing in healthy subjects (Gilbert et al. 1981), in patients with midcervical

cord lesions and intercostal paralysis (Gilbert et al. 1983), patients with COPD following lung volume reduction surgery (Laghi et al. 1998b), and difficult-to-wean patients (Diehl et al. 1994).

Electromyography

The basic functional unit of the neuromuscular system is the motor unit, which consists of an anterior horn cell in the spinal cord, its axon, and all muscle fibers innervated by the axon (Fig. 36.30, left panel) (Liddell and Sherrington 1925). Neural signals from the spinal cord are transmitted along the axon to all muscle fibers innervated by the axon. This transmission of

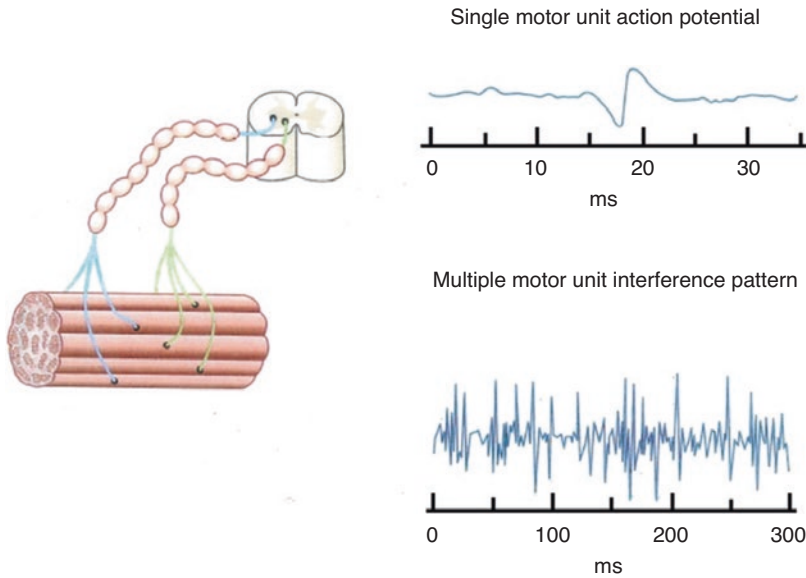


Fig. 36.30 Skeletal muscle structure and the origin of the interference-pattern electromyogram (EMG). *Left side:* Representation of the structure of skeletal muscle and motor units. Two motor units are demonstrated for simplicity. A motor unit is a single motor neuron and all of the muscle fibers it innervates. Electrical activation of a single motor unit produces a motor unit action potential (*top*

right). A spatial and/or temporal summation of the motor-unit action potentials, resulting in an interference-pattern EMG signal (*bottom right*), occurs when several motor units are recruited and/or their firing rate increases. (Modified from Sinderby and Beck (2013), with permission of McGraw Hill LLC)

neural signals triggers a movement of ions across the sarcolemma with resultant depolarization and then contraction. Single-fiber action potentials are activated in groups because a single nerve fiber innervates multiple muscle fibers (Sinderby and Beck 2013). These action potentials summate to form a composite motor unit action potential, which can be recorded as the electromyogram (EMG) (Fig. 36.30, *right upper panel*) (Sharp and Hyatt 1986; O'Brien and Van Eykern 1989). Neural breathing modulates motor-unit firing rate and recruitment. This means that the resulting motor unit action potentials are summated in time (temporally) and space (spatially). The cumulative motor unit action potential activity (the interference pattern EMG) yields a signal where individual motor unit action potentials can no longer be distinguished (Fig. 36.30, *right lower panel*) (Sinderby and Beck 2013).

When a nerve is activated by a supramaximal stimulation (electrical or magnetic), all fibers in the innervated muscle generate almost

synchronous action potentials that summate to produce a compound muscle action potential (CMAP) (Daube 1986) (Fig. 36.31). The size and configuration of the CMAP is determined by the number of muscle fibers activated; the size of the muscle fibers (bigger fibers produce larger amplitude); synchronization of firing; the distance between the discharging fiber and recording electrode (as distance increases, amplitude decreases); the resistive and capacitive properties of intervening tissues, which can act as a low-pass filter, with the result that high frequencies are attenuated as distance between the fiber and electrode increases (Sharp et al. 1993) temperature of the muscle (Sharp and Hyatt 1986; Daube 1986).

Activity of the diaphragm can be recorded with surface electrodes placed at the level of the seventh and eighth intercostal spaces and the anterior axillary line (Laghi et al. 1995; Fitting and Grassino 1987). This approach has several disadvantages. The EMG signal can be contaminated by electrical activity from adjacent muscles (Luo

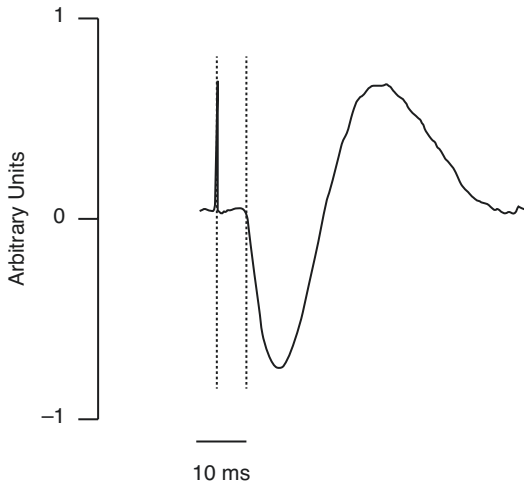


Fig. 36.31 Measurement of phrenic nerve conduction time. Surface electrodes placed in the seventh intercostal space record the diaphragmatic action potential following a single twitch stimulation of phrenic nerve in the neck. Conduction time (latency) is measured as the time between vertical cursors located at stimulus artifact and onset of action potential. (From Tobin and Laghi (1998), with permission of McGraw Hill LLC)

et al. 1999a, b; 1998; Sinderby et al. 1996b) (Fig. 36.32), rendering the EMG power spectrum unreliable (Sinderby et al. 1996b). Subcutaneous fat significantly reduces signal strength because of muscle-to-electrode filtering effects (Beck et al. 1995). Because no standardized method exists for placing chest-wall electrodes (Luo et al. 2008), data comparisons are difficult. To circumvent these problems, ring-shaped metal electrodes can be incorporated into an esophageal catheter (positioned just above the gastroesophageal junction) to record activity of the crural diaphragm (Onal et al. 1981; Sinderby et al. 1997). This EMG signal is less affected by obesity, power line artifact, and cross-talk signals (Luo et al. 1999a, b; 1998; Sinderby et al. 1996b; Beck et al. 1995).

Esophageal electrodes to record the diaphragmatic EMG were introduced in the late 1950s (Petit et al. 1959) and early 1960s (Petit et al. 1960; Agostoni et al. 1960). Early esophageal electrode catheters contained only a single elec-

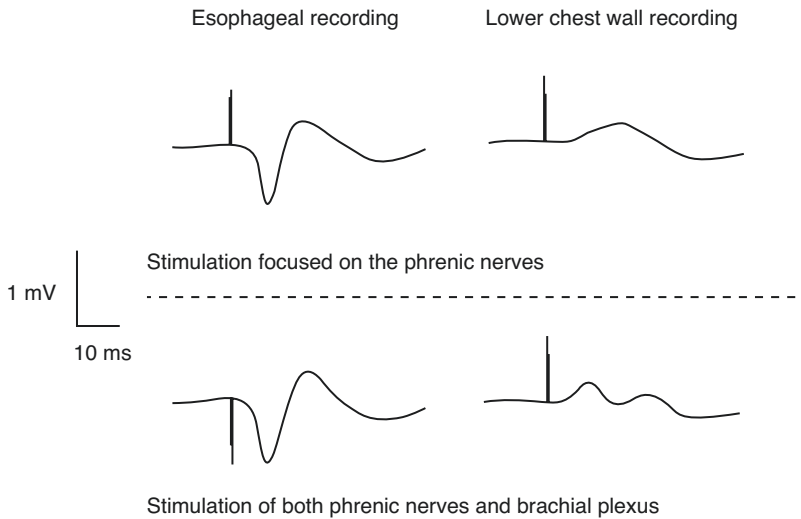


Fig. 36.32 Diaphragm compound muscle action potential (CMAP) recorded simultaneously from esophageal electrodes (*left panels*) and lower chest-wall electrodes (*right panels*) during stimulation of the phrenic nerve alone (*upper panels*) and stimulation of both the brachial plexus and phrenic nerve (*lower panels*). Latency and CDAP waveforms recorded with esophageal electrodes (*upper and lower left panels*) were similar. This result indicates that the EMG signal recorded by the esophageal

electrodes is not cross-contaminated by recruitment of the brachial plexus. With the lower chest-wall recordings, latency of the CMAP is shorter when stimulation coactivates the brachial plexus (*right lower panel*); amplitude of the CMAP is also reduced (*right lower panel*). This finding indicates that the EMG signal recorded by lower chest-wall electrodes is cross-contaminated by recruitment of the brachial plexus. (Based on Luo et al. (2008))

trode pair (Petit et al. 1960; Agostoni et al. 1960). An esophageal electrode with three pairs of electrodes was introduced in 1979 (Onal et al. 1979). In 1989, Daubenspeck et al. (1989) developed an array of seven sequential electrode pairs at 1-cm spacing to cover the span of diaphragmatic excursion. Later, Beck et al. (1995) used a similar system to measure the EMG power spectrum and its center frequency. They selected the electrode pair along the array that was closest to the diaphragm. Center frequency measured from this pair was not influenced by chest-wall configuration and/or diaphragmatic length (Sinderby et al. 1998; Beck et al. 1996, 1997).

Esophageal electrodes record electrical activity from the crural diaphragm while surface electrodes record the costal component (Luo et al. 2008). EMGs recorded from the costal and crural diaphragm have synchronous activation and similar time course during respiratory tasks (Sinderby et al. 1998; Kim et al. 1978; Lourenco et al. 1966; Sharshar et al. 2005; San'Ambrogio et al. 1963; Van et al. 1985; Pollard et al. 1985)

(Fig. 36.33). Differential activation of selective portions of the diaphragm are observed with the following tasks: repetitive alterations in posture (Hodges and Gandevia 2000), control of the gastroesophageal sphincter during coughing (Leith et al. 1986) and vomiting, micturition, parturition, and defecation (Luo et al. 2008; Monges et al. 1978; Agostoni 1964).

Intramuscular electrodes can be constructed to facilitate recording voluntary potentials of a muscle fiber from an area of only a few millimeters in diameter (Daube 1986; Bruce and Loring 1985). Needle electrodes can be used to record diaphragmatic, intercostal, and abdominal muscle activity (Laghi et al. 2003; McKenzie and Gandevia 1995; Parthasarathy et al. 1998, 2007; Laghi et al. 1998b; Demoule et al. 2003; Gorman et al. 2005; De Troyer and Estenne 1984, 1990; De Troyer et al. 1990; Ninane et al. 1992), but are problematic because of the risk of pneumothorax.

Several factors interfere with the ability to obtain accurate EMG recordings. These include interference from power lines (60 Hz in the

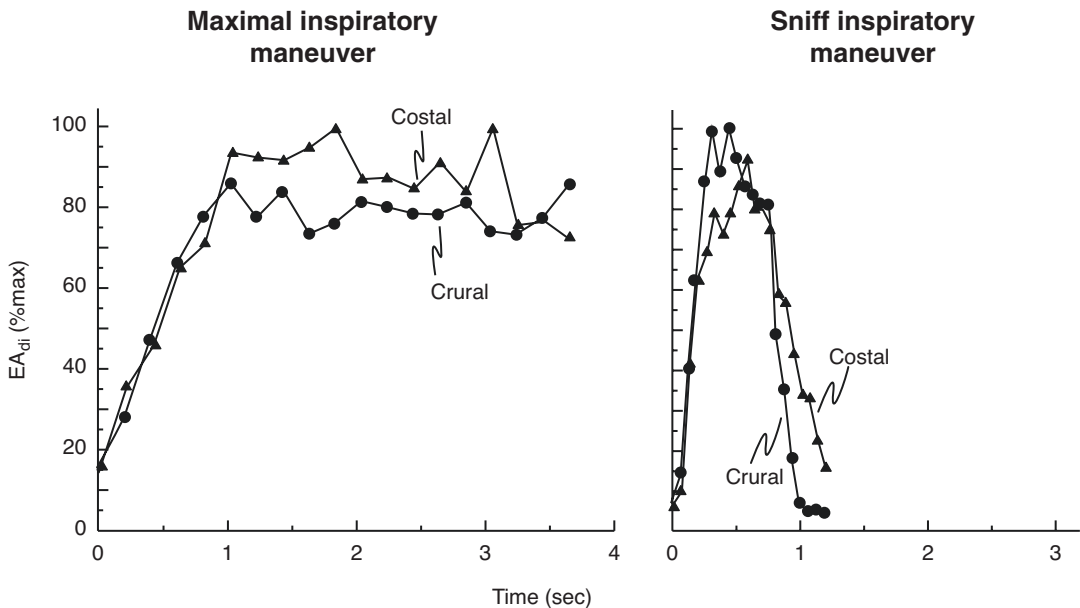


Fig. 36.33 Synchronous activation of costal and crural diaphragm during maximal inspiration to total lung capacity (*left panel*) and a maximal sniff (*right panel*) in a patient with COPD. Electrical activity of the diaphragm (EA_{di}) was calculated as the root-mean-square value of the crural and costal diaphragm EMG signal. Overlap

between the costal and crural EA_{di} signals indicates that both costal and crural diaphragm were concurrently recruited during both maneuvers. (From in Sinderby et al. (1998), with permission of American Physiological Society)

United States, 50 Hz in Europe), electrode motion during voluntary contractions and esophageal peristalsis, and ECG. Interference from power lines can be reduced by using proper ground connections and differential amplifiers with a high common mode rejection ratio (greater than 100 dB) (Luo et al. 1999c; Sinderby et al. 1995). Interference from electrode motion can be reduced by using a high-pass-filter setting at 10 or 20 Hz (Sinderby et al. 1995; Schweitzer et al. 1979; Luo and Moxham 2005; Luo et al. 2001). Various methods have been used to reduce ECG contamination (McKenzie and Gandevia 1995; Schweitzer et al. 1979; Levine et al. 1986; Bartolo et al. 1996; Sarlabous et al. 2015; Lozano-García et al. 2019). Maneuvers that alter lung volume, thoracoabdominal configuration, or posture can produce substantial artifactual changes in the diaphragmatic EMG (Gandevia and McKenzie 1986).

Analysis of EMG Signals

Time-domain and frequency domain analysis of the EMG signals are used in the assessment of the diaphragm and of other respiratory muscles.

Frequency-Domain Analysis

Any complex waveform can be regarded as being constituted of an infinite number of sine waves, each having a different frequency, amplitude, and phase (Tobin and Laghi 1998). When a fast-Fourier transform is performed on this complex waveform, a graphic plot is obtained in which power is related to the frequency content of the signal (Fig. 36.34) (Tobin 1991). In the healthy diaphragm, most of the power is distributed between 20 and 250 Hz. (The frequency content of the diaphragmatic EMG signal bears *no* relationship to the frequency of phrenic nerve depolarization.)

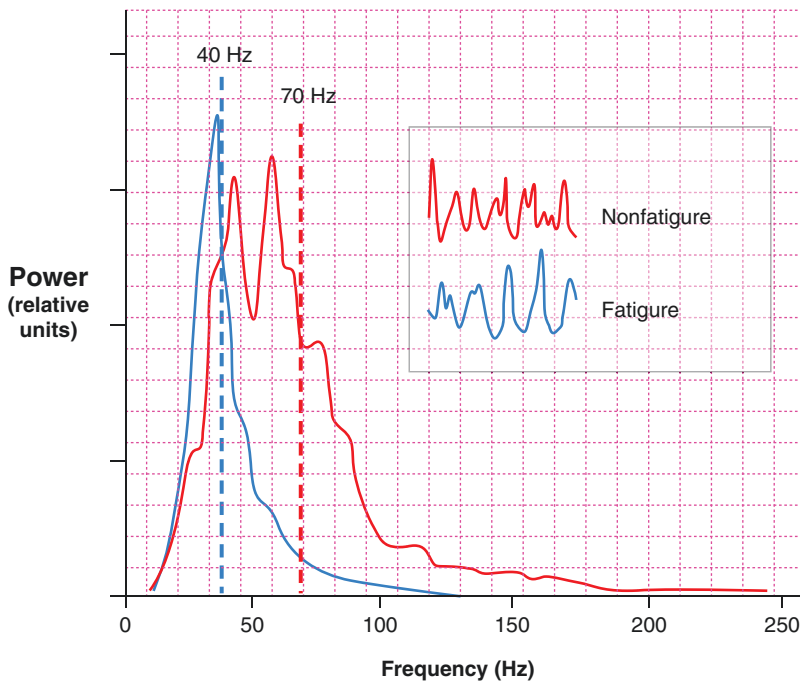


Fig. 36.34 The raw EMG (*inset*) and the associated power spectra of a nonfatigued and fatigued muscle. Fatigue was induced by maintaining a constant increased load. Note the generalized slowing of the raw EMG that occurs with fatigue. Second, there is a leftward shift of the power spectrum representing an increase in low fre-

quency and a decrease in high frequency components. Thirdly, the spectrum itself is characterized by its mean frequency, which decreases with fatigue. The mean frequency (*vertical line*) of nonfatigued muscle is 70 Hz, whereas it is only 40 Hz in the fatigued muscle. (Based on Tobin (1991))

When a skeletal muscle fatigues, total power (area under the curve) in the EMG signal is unchanged, but it is redistributed: power decreases at high frequencies (150–350 Hz) and increases at low frequencies (20–47 Hz) (Gross et al. 1979). This redistribution is referred to as a *fall in the high-to-low (H/L) ratio* (Gross et al. 1979; Cohen et al. 1982). The alteration in the power spectrum with fatigue is thought to result from slowing of conduction velocity of the action potential along the muscle membrane (Lindstrom et al. 1970; Kranz et al. 1983), a reduction in the firing frequencies of motor units (Bellemare et al. 1983b), and alterations in their recruitment pattern and synchronization (McKenzie and Gandevia 1995; Sharp and Hyatt 1986; Sharp et al. 1993). Changes in the EMG power spectrum occur early with onset of fatiguing contractions. As such, alterations in the power spectrum signify that muscles are contracting in a fatiguing manner, rather than indicating the presence of overt fatigue. In healthy subjects who developed diaphragmatic fatigue, Moxham et al. (1982) found that the H/L ratio had returned to 90% of control values within 1 min of completing a fatiguing task. This indicates that alterations in the power spectrum cannot be used to detect low-frequency (long-lasting) fatigue – a fact that has dampened the enthusiasm for the use of the H/L ratio in the assessment of diaphragmatic fatigue

(Luo et al. 2008). Other limitations include the confounding factor of muscle temperature (Doud and Walsh 1993), and length (Doud and Walsh 1995). This technique cannot detect fatigue at a single moment in time, and it requires a control value in the nonfatigue state for comparison.

Time-Domain Analysis

Time-domain analysis focuses on the relationship between EMG strength and time (Luo et al. 2008), the product of the amplitude of the EMG signal and its duration.

Quantification of EMG activity (in terms of amplitude) is obtained by rectification and integration of the electrical signal (Onal et al. 1981; Gross et al. 1979; Lourenco and Miranda 1968; Juan et al. 1984) or through the calculation of the moving time average (Lopata et al. 1977). The integrated EMG can quantify changes in both phasic and tonic inspiratory muscle activity (Fig. 36.35) (Luo and Moxham 2005; Luo et al. 2001; Beck et al. 2001; Sinderby et al. 2007; Sieck and Fournier 1990). Phasic activity is usually measured as the difference in EMG activity between the peak and end of expiration (Meessen et al. 1994), and it can be also measured as the area under the curve (Dres et al. 2012).

When electrical activity of the diaphragm (EA_{di}) persists after inhalation, the amplitude of the tonic EA_{di} signal can be quantified and

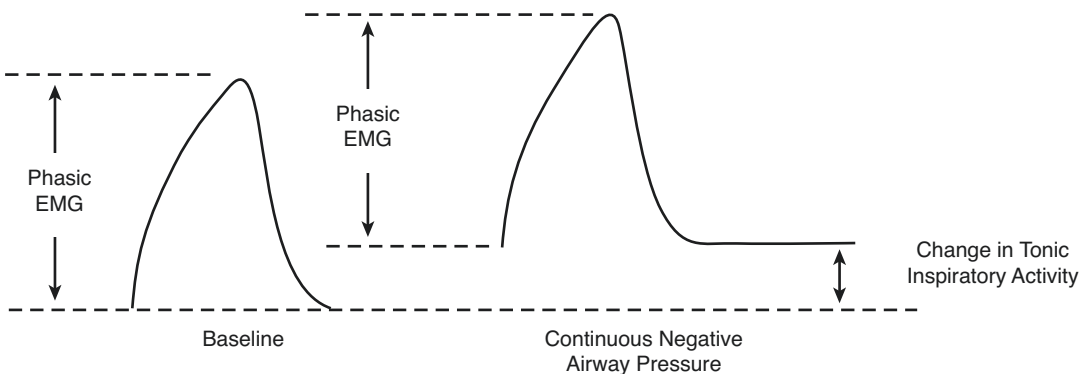


Fig. 36.35 Quantification of changes in phasic and tonic EMG activity during use of continuous negative airway pressure compared with a control state. Phasic activity is measured as the difference between peak activity and the end-expiratory signal. The change in tonic inspiratory

activity is measured as the difference in the end-expiratory signal between continuous negative airway pressure and the control state. (Modified from Meessen et al. (1994), with permission of American Physiological Society)

expressed in absolute values (μV) or as percentage of the mean inspiratory EA_{di} (Emeriaud et al. 2006; Larouche et al. 2015). Tonic EA_{di} indicates continuous activation of the diaphragm between respiratory cycles (Fig. 36.36). Tonic EA_{di} can represent a reflex response induced by lung derecruitment (Emeriaud et al. 2006; D'Angelo et al. 2002; Allo et al. 2006; Pellegrini et al. 2017). Experimental vagotomy abolishes this reflex (D'Angelo et al. 2002; Allo et al. 2006). Adult mechanically ventilated patients show little, if any, tonic EA_{di} activity (Sinderby et al. 1998; Passath et al. 2010; Brander et al. 2009).

During voluntary contraction of a muscle, the integrated EMG signal is proportional to the tension developed by the muscle, its oxygen consumption, and force output (Bigland and Lippold

1954; Lippold 1952; Bigland-Ritchie and Woods 1974). The diaphragmatic EMG directly reflects changes in phrenic motor activity (Lourenco et al. 1966). The integrated EMG signal is not influenced by mechanical problems in the respiratory system, unlike other techniques of assessing neuromuscular output. A major drawback is the inability to standardize and calibrate the integrated EMG signal. Thus, EMG recordings are of limited value in studies *between* patients (Sinderby and Beck 2013), although they are of value when studying changes in respiratory motor output over a short period of time in a single patient. EA_{di} signals during breathing can be normalized to EA_{di} during maximal voluntary efforts ($P_{\text{I,max}}$ or maximal sniffs maneuvers), and inhalation to TLC (Sinderby et al. 1998).

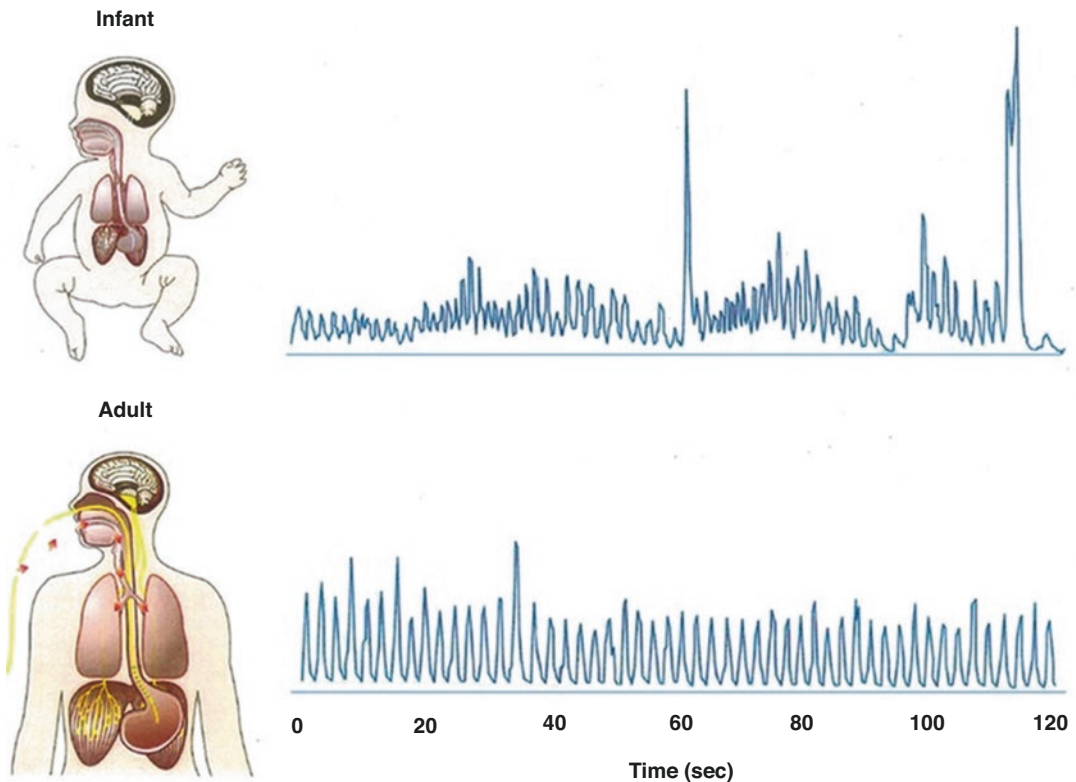


Fig. 36.36 Examples of the diaphragmatic electrical activity (EA_{di}) waveform in a premature neonate and in an adult patient. *Top panel:* processed EA_{di} waveform obtained in a nonintubated premature infant. *Bottom panel:* processed EA_{di} waveform obtained in an intubated adult. The EA_{di} waveform in infants is characterized by

larger variability in timing and amplitude, with a distinct amount of changes in the baseline, the so-called tonic activity of diaphragm. The EA_{di} waveform in adults is generally less variable with minimal tonic EA_{di} . (Modified from Sinderby and Beck (2013), with permission of McGraw Hill LLC)

(The amplitude of EA_{di} usually ranges between few μV during resting breathing to more than 100 μV during maximal inspiratory efforts (Sinderby and Beck 2013)).

Neuromechanical Coupling

Quantification of EA_{di} derived from time-domain analysis has been used in the evaluation of neuromuscular coupling (Laghi et al. 2014a; Dres et al. 2012; Aubier et al. 1981b; Jensen et al. 2011; Doorduyn et al. 2012; Di et al. 2016; Bellani et al. 2013) and neuroventilatory coupling (Dres et al. 2012; Jensen et al. 2011; Di et al. 2016; He et al. 2017; Liu et al. 2012; Barwing et al. 2013; Roze et al. 2013; Ramsook et al. 2017).

Neuromuscular Coupling

Neuromuscular coupling is the ability of the diaphragm to convert EA_{di} into inspiratory pressure (Laghi et al. 2014a; Dres et al. 2012; Aubier et al. 1981b; Jensen et al. 2011; Doorduyn et al. 2012; Di et al. 2016; Bellani et al. 2013). A quasi-linear relationship exists between P_{di} and EA_{di} (Bazzy and Haddad 1984; Beck et al. 1998). Diaphragmatic neuromuscular coupling can be calculated as the ratio of tidal P_{di} to tidal EA_{di} ($\Delta P_{di}/\Delta EA_{di}$) (Laghi et al. 2014a; Abdallah et al. 2017, 2018; Doorduyn et al. 2018), the ratio of mean inspiratory P_{di} to mean inspiratory EA_{di} ($\bar{P}_{di}/\bar{EA}_{di}$) (Doorduyn et al. 2012), or the ratio of PTP_{di} to the corresponding EA_{di} -time product of the EA_{di} signal ($P_{di,AUC}/EA_{di,AUC}$) (Dres et al. 2012). In a preliminary study, Morales et al. (2012) calculated diaphragmatic neuromuscular coupling in 12 healthy subjects sustaining an incremental inspiratory threshold loading until task failure. Neuromuscular coupling increased during loading. This pattern was similar whether neuromuscular coupling was calculated as $\Delta P_{di}/\Delta EA_{di}$ or $P_{di,AUC}/EA_{di,AUC}$.

The same investigators (Laghi et al. 2014a) recorded $\Delta P_{di}/\Delta EA_{di}$ in 18 healthy subjects while sustaining progressive inspiratory threshold loading. As expected (Morales et al. 2012), neuromuscular coupling increased *pari passu* with the increase in loading, but was insufficient to prevent alveolar hypoventilation and task failure. At task failure, mean ΔEA_{di} was $74.9 \pm 4.9\%$ of

maximum, indicating that the primary mechanism of hypercapnia was submaximal diaphragmatic recruitment. The investigators concluded that hypercapnia during acute loading primarily resulted from central-output inhibition of the diaphragm. They also reasoned that acute loading responses are controlled by the cortex rather than bulbopontine centers.

Investigators have recorded neuromuscular coupling in patients with COPD at rest and during exercise (Jensen et al. 2011; Abdallah et al. 2018) and in critically ill patients during trials of weaning from mechanical ventilation (Doorduyn et al. 2018). Computation of the neuromuscular coupling of the diaphragm requires placement of a multipair esophageal electrode catheter and placement of esophageal and gastric balloons (Laghi et al. 2014a). To avoid this invasive approach, investigators have estimated muscle pressure signals (P_{mus}) as the difference between P_{es} and chest-wall elastic recoil (Bellani et al. 2013) or using P_{aw} signals (Liu et al. 2012). The major limitation of calculating neuromuscular coupling as the ratio of P_{mus} to EA_{di} or P_{aw} to EA_{di} is that P_{mus} and P_{aw} can result from the contraction of a host of respiratory muscles other than the diaphragm. In contrast, EA_{di} is a diaphragm-specific signal.

Neuroventilatory Coupling

Neuroventilatory coupling is the ability of the diaphragm to convert EA_{di} into inspired volume (Dres et al. 2012; Jensen et al. 2011; Di et al. 2016; He et al. 2017; Liu et al. 2012; Barwing et al. 2013; Roze et al. 2013; Ramsook et al. 2017). Investigators have used this approach to gain insights into pathophysiological mechanisms in healthy subjects (dyspnea) (Ramsook et al. 2017), patients with COPD (Langer et al. 2018; Jolley et al. 2015; Qin et al. 2015), sleep-related hypoventilation (He et al. 2017), and weaning failure (Dres et al. 2012; Liu et al. 2012; Barwing et al. 2013).

During weaning from mechanical ventilation, neuroventilatory coupling is inferior in weaning failure patients than in weaning success patients (Liu et al. 2012). Compared to neuroventilatory coupling in weaning success patients, inferior

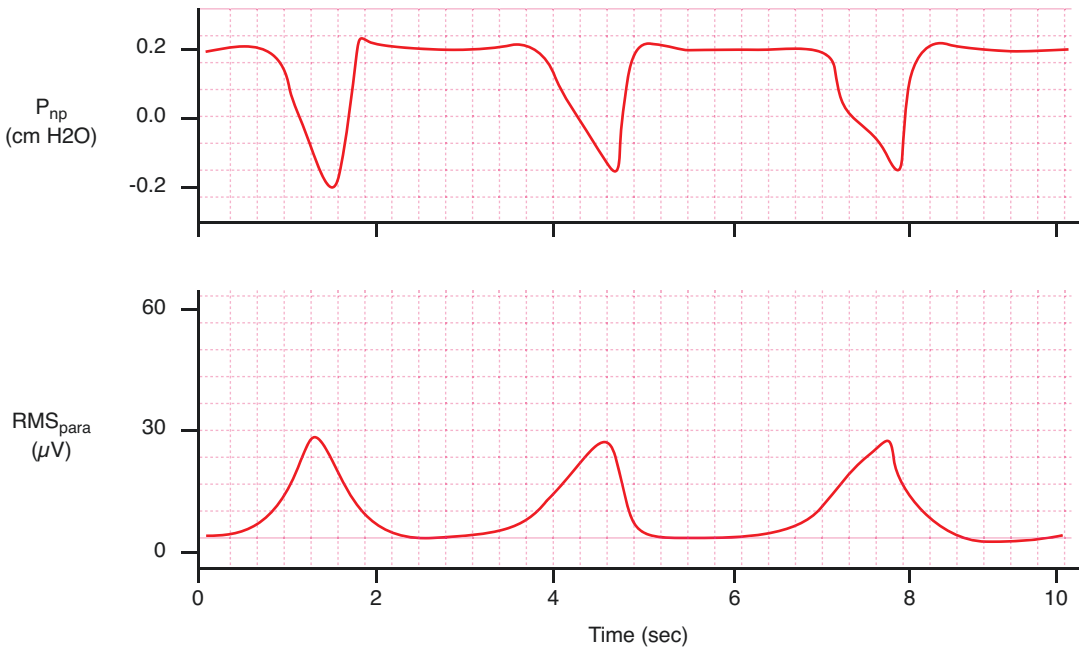


Fig. 36.37 Representative trace of nasal pressure (P_{np}) and root mean square of the parasternal electromyogram signal (RMS_{para}) during tidal breathing in a patient with COPD during an exacerbation. (Based on Suh et al. (2015))

neuroventilatory coupling in weaning failure patients results from greater EA_{di} that does not translate to increased tidal volume (V_T) (Dres et al. 2012; Liu et al. 2012; Barwing et al. 2013). Neuroventilatory coupling is not superior than the respiratory frequency (f) to V_T (f/V_T) ratio in predicting weaning outcome (Dres et al. 2012). Like neuromechanical coupling calculated using P_{aw} or P_{mo} signals (Liu et al. 2012), the major limitation of neuroventilatory coupling ($V_T/\Delta EA_{di}$) is that V_T can be achieved by respiratory muscles other than the diaphragm.

Clinical Applications of Electromyography

EMG signals from the intercartilaginous portion of the internal intercostals (parasternal intercostals) (De Troyer et al. 2005) have a direct relationship with respiratory muscle load (Duiverman et al. 2004; Maarsingh et al. 2002; Maarsingh et al. 2006). Suh et al. (2015) assessed whether parasternal EMG signals predicted early readmission in 120 patients treated for a COPD ex-

acerbation (Fig. 36.37). Sixteen (13.3%) patients were readmitted or died within 14 days of discharge. Changes in parasternal EMG between admission and discharge predicted readmission with greater accuracy than did changes in FEV_1 and inspiratory capacity. During 3.6 years (median) of follow-up, 69 (57.5%) patients died (Patout et al. 2019). Parasternal EMG was independently associated with increased mortality (Patout et al. 2019).

EA_{di} signals can be used to deliver ventilator assistance in proportion to a patient's central respiratory command: *neurally adjusted ventilator assist* (NAVA) (Sinderby et al. 1999). Whether delivered invasively (Navalesi and Longhini 2015) or noninvasively (Longhini et al. 2019), EA_{di} signals during NAVA are obtained through a dedicated nasogastric (or orogastric) tube containing a distal array of electrodes (Sinderby and Beck 2013). Applied inspiratory support (P_{aw} above PEEP) is determined by the magnitude of both EA_{di} and the NAVA level (cm $H_2O/\mu V$), a proportionality constant set by the clinician. Whether the increase in respiratory motor output that accompanies most cases of

acute respiratory failure causes overassistance during NAVA remains controversial (Coisel et al. 2010; Spahija et al. 2010; Blankman et al. 2013; Assy et al. 2019; Karagiannidis et al. 2010; Terzi et al. 2010; Patroniti et al. 2012). In eleven French ICUs (Demoule et al. 2016), investigators reported that the probability of ventilator-free days on day 14 and day 28, successful extubation, and mortality were similar in patients receiving NAVA and patients receiving pressure support ventilation.

Imaging

Several imaging methods are used to assess the function and dimensions of the diaphragm (Nason et al. 2012). These include chest radiography (Tanaka 2016), fluoroscopy (Leal et al. 2017), computed tomography (Li et al. 2015), magnetic resonance imaging (Takazakura et al. 2004), and ultrasonography (Sarwal et al. 2013).

Chest X-ray and Fluoroscopy

An elevated hemidiaphragm suggests unilateral phrenic nerve paralysis, but it is nonspecific because it occurs also with atelectasis, pneumonia, and other conditions. Detecting diaphragmatic elevation in patients with bilateral diaphragmatic paralysis can be difficult unless x-rays before paralysis are available (Tobin and Laghi 1998). On fluoroscopy, the diaphragm normally descends during a sniff, whereas a paralyzed diaphragm paradoxically ascends. Fluoroscopy can be misleading. Patients with bilateral diaphragmatic paralysis sometimes contract their abdominal muscles during expiration, displacing the abdomen inward and the diaphragm into the rib cage. At the onset of inspiration, relaxation of the abdominal muscles causes outward recoil of the abdominal wall and diaphragmic descent, which can be misinterpreted as normal diaphragmatic activation (Newsom-Davis et al. 1976). Paradoxical motion of one hemidiaphragm has been observed in 6% of healthy subjects (Alexander 1966).

Computed Tomography

Using computed tomography (CT), investigators (Cassart et al. 1997) observed that patients with COPD have marked reductions in total surface area of the diaphragm and the area of the zone of apposition (at FRC). At similar absolute lung volumes, diaphragmatic dimensions are similar in patients and healthy subjects. CT measurements of diaphragmatic volume are smaller in septic than in nonseptic patients (Fig. 36.38) (Jung et al. 2014).

Magnetic Resonance Imaging

Magnetic resonance imaging has been used to examine the stabilizing function of the diaphragm during limb movement (Kolar et al. 2010). In 30 subjects, investigators (Kolar et al. 2010) reported that the position of the diaphragm at end exhalation was lower (more caudal) during lower extremity contraction versus relaxed conditions, suggesting greater tonic (diaphragmatic) activity. This tonic activity suggests that the diaphragm contributes to stabilizing the spine with variation of posture. Attractive aspects of magnetic resonance imaging include the ability to image the entire thorax, absence of radiation, three-dimensional information of diaphragm dimension (Paiva et al. 1992) and motion (Takazakura et al. 2004; Kolar et al. 2010; Gierada et al. 1995; Kiryu et al. 2006; Ūnal et al. 2000), and estimation of volumes displaced by the rib cage and diaphragm (Cluzel et al. 2000).

Diaphragm Ultrasonography

Ultrasonography is used to measure thickness, strength, recruitment, and motion of the diaphragm.

Ultrasound Measurement of Diaphragm Thickness (Zone of Apposition)

Diaphragmatic thickness is quantified using linear probes (Sarwal et al. 2013). These probes use

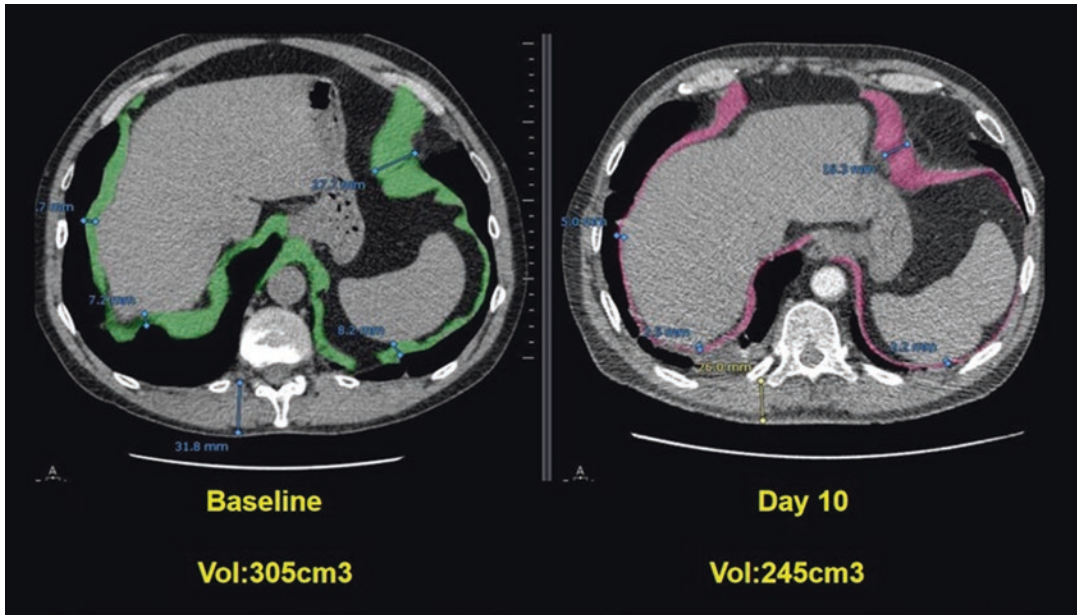


Fig. 36.38 Computed tomography measurements of diaphragmatic volume in a critically ill, septic patient on admission to the intensive care unit (*left panel*) and 10 days later (*right panel*). Sepsis was associated with a

decrease in diaphragmatic volume. (Images provided by Drs. Boris Jung, Stephanie Nougaret and Samir Jaber, University Hospital of Montpellier, France)

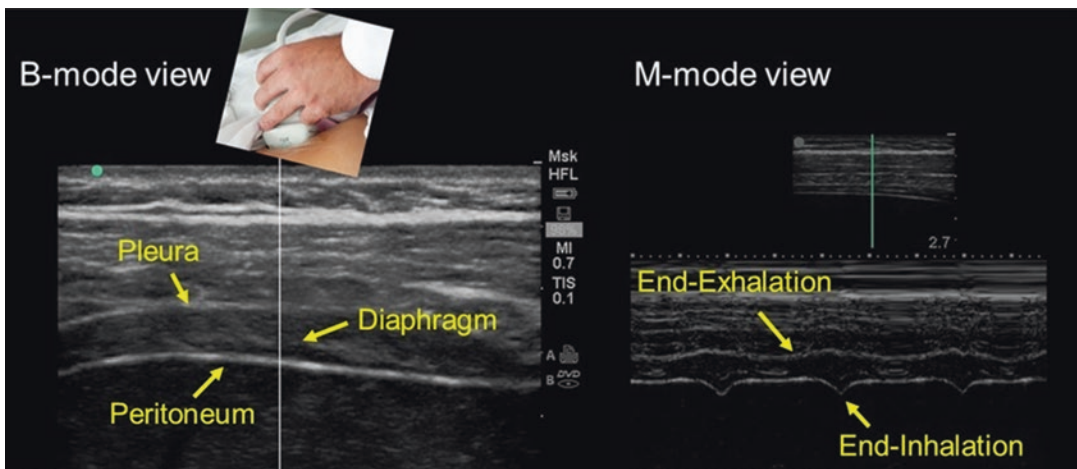


Fig. 36.39 Ultrasound image of the zone of apposition of the diaphragm. In bright-mode (B-mode; *left panel*), the diaphragm appears as a three-layer structure. In motion-mode (M-mode; *right panel*), the diaphragm is thinnest at end-exhalation and thickest at end-inhalation;

stronger diaphragmatic inspiratory efforts are associated with greater tidal thickening of the diaphragm. (Modified from Laghi and Shaikh (2019), with permission of Daedalus Enterprises Inc.)

high-frequency ultrasound waves (7–18 Hz) to create high-resolution images (0.1 mm) of structures near the body surface (Sarwal et al. 2013; Zamboni et al. 2016). With this approach, the dia-

phragm is identifiable as a three-layer structure: two echogenic layers of peritoneum and pleura sandwiching a more hypoechoic layer of the muscle itself (Fig. 36.39, *left panel*) (Shaikh

2019). Images are easier to obtain of the right than of the left hemidiaphragm (Zambon et al. 2016; Goligher et al. 2015).

Diaphragmatic thickness ranges from 1.2 to 11.8 mm among healthy individuals resting at FRC (Carrillo-Esper et al. 2016; Boon et al. 2013; Cardenas et al. 2018; Scarlata et al. 2019; Wait et al. 1989; Gottesman and McCool 1997; Orde et al. 2015). Intra- and interobserver agreement of measurements obtained at a single sitting in healthy adults and ventilated patients is high (Goligher et al. 2015; Boon et al. 2013; Scarlata et al. 2019). To ensure reproducible recordings, it is imperative to mark the site on which the probe is placed and record all subsequent images from that spot (Goligher et al. 2015). This step is critical because diaphragmatic thickness is highly variable, changing by up to 6 mm from one inter-

costal space to the next (Boon et al. 2013). The lower limit of normal of diaphragm thickness is 0.80–1.60 mm (Carrillo-Esper et al. 2016; Boon et al. 2013; Cardenas et al. 2018; Scarlata et al. 2019).

Diaphragmatic paralysis is associated with decreased muscle thickness and decreased thickening on inhaling from FRC to TLC (Gottesman and McCool 1997); thickness of less than 2 mm at resting FRC combined with a less than 20% increase in thickness during inhalation discriminates between a paralyzed and normal diaphragm (Fig. 36.40).

Investigators have reported decreases, increases, and no change in thickness of the diaphragm in mechanically ventilated patients (Zambon et al. 2016; Goligher et al. 2018; Grosu et al. 2012; Schepens et al. 2015; Moury et al.

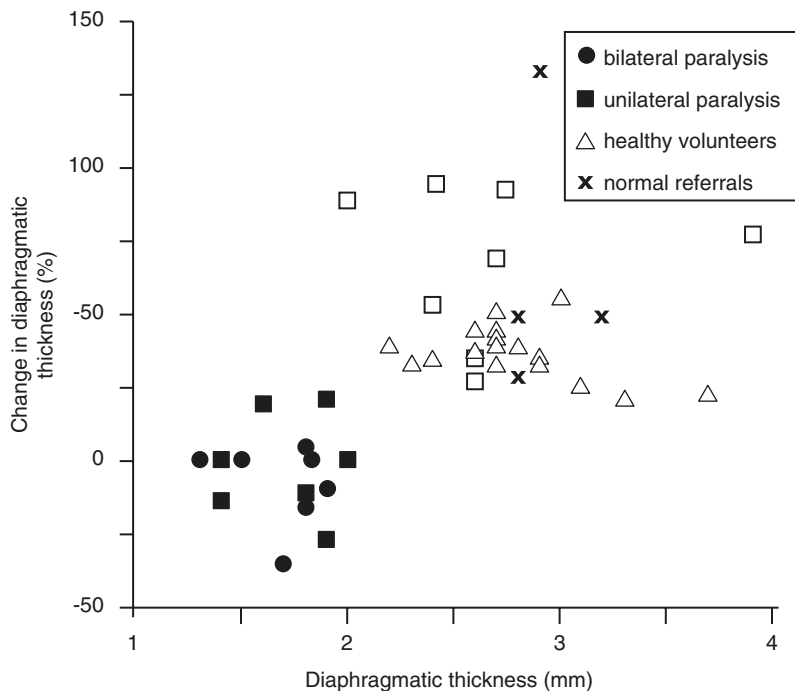


Fig. 36.40 Values of diaphragmatic thickness at resting functional residual capacity (FRC) and percentage increase in thickness on inhaling from FRC to total lung capacity (TLC) in 5 patients with bilateral diaphragmatic paralysis, in 7 patients with unilateral diaphragmatic paralysis, 3 patients with normal function, and 15 healthy volunteers. A paralyzed diaphragm (*solid symbols*) could be distinguished from a functioning diaphragm (*open*

symbols) by a resting thickness of less than 2 mm and a less than 20 percent increase in thickening on inhaling to TLC. (Reprinted with permission of the American Thoracic Society. Copyright © 2020 American Thoracic Society. All rights reserved. Gottesman and McCool (1997). The American Journal of Respiratory and Critical Care Medicine is an official journal of the American Thoracic Society)

2019). These changes are not predictive of diaphragmatic strength ($P_{aw,tw}$) (Dubé et al. 2017) or risk of death (Goligher et al. 2018; Vivier et al. 2019). Change in diaphragmatic thickness has been reported to predict worse weaning outcome (Goligher et al. 2018), better weaning outcome (Grosu et al. 2017), and no impact (Vivier et al. 2019).

Ultrasound Estimation of Diaphragm Strength and Recruitment (Zone of Apposition)

Diaphragmatic strength and recruitment during voluntary contractions is estimated by recordings of contraction-associated thickening, two-dimensional speckle tracking, and shear-wave elastography.

Diaphragm Thickening

Measurements of diaphragmatic thickening upon contraction (Fig. 36.39, right panel) (Shaikh 2019) have been recorded in critically ill patients

during noninvasive (Vivier et al. 2012; Marchioni et al. 2018; Cammarota et al. 2019; Antenora et al. 2017) and invasive ventilation (Goligher et al. 2015, 2018; Umbrello et al. 2015; Ferrari et al. 2014). Employing post hoc analysis, investigators have reported an association between diaphragmatic thickening of 26–36% and duration of mechanical ventilation (Dubé et al. 2017), weaning outcome (Moury et al. 2019; Ferrari et al. 2014; DiNino et al. 2014; Pirompianich and Romsaiyut 2018) and mortality (Dubé et al. 2017), but these thresholds have not been prospectively tested.

Measurements of diaphragmatic thickening are marred by many limitations. Measurements of diaphragmatic thickening explain as little as one-third of the variability in inspiratory effort (Goligher et al. 2015; Vivier et al. 2012; Umbrello et al. 2015) (Fig. 36.41). Within-session reproducibility of diaphragmatic thickening is weak (Goligher et al. 2015). Ultrasound recordings of diaphragmatic thickening are obtained over a

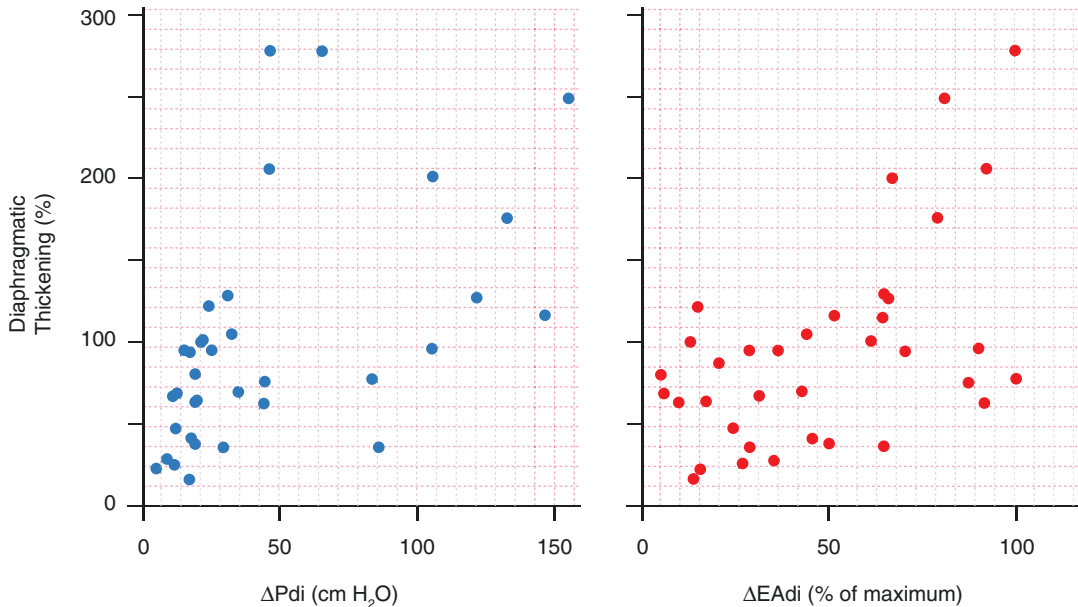


Fig. 36.41 Relationship between the thickening of the diaphragm recorded with ultrasonography and changes in transdiaphragmatic pressure (ΔP_{di} ; left panel) and diaphragmatic electrical activity (ΔEA_{di} ; right panel) in five healthy subjects during a series of inspiratory maneuvers. Diaphragmatic thickening increased as transdiaphrag-

matic pressure (left panel) and electrical activity of the diaphragm (right panel) increased. The correlation was weak ($r^2 = 0.32$ and 0.28 , respectively, $p < 0.01$). (Modified from Goligher et al. (2015), with permission of Springer Nature BV)

limited time (Goligher et al. 2018), yet patient-ventilator interaction is repeatedly changing (Vaporidi et al. 2017).

Two-Dimensional Speckle Tracking Imaging

Ultrasound images inherently contain speckle artifacts, consisting of a granular appearance (Huang and Orde 2013). Speckles do not represent any anatomical structures but are composite echoes resulting from reflection of anatomical structures positioned closer than the resolution limit of the ultrasound system (Huang and Orde 2013). A cluster of speckles is known as a kernel (Orde et al. 2015). A speckle-tracking software measures the displacement of kernels in relation to one another (deformation) (Huang and Orde 2013; Oppersma et al. 2017) (Fig. 36.42). The extent of deformation is known as strain. Negative

strain indicates speckles coming closer together: a strain of -30% indicates 30% fiber shortening. During loaded breathing, strain is closely correlated with P_{di} ($r^2 = 0.72$) and EA_{di} ($r^2 = 0.60$), whereas diaphragmatic thickening is not (Oppersma et al. 2017).

Shear-Wave Elastography

Ultrasound shear-wave elastography permits real-time quantification of tissue mechanics (Gennisson et al. 2013) through use of ultrasonic focused beams. It is possible to estimate the shear modulus of a contracting muscle (Bachasson et al. 2019; Nowicki and Dobruch-Sobczak 2016; Chino et al. 2018) as the ratio of shear stress to shear strain, where stress refers to the deforming force applied on an object and strain refers to the change in size or shape of that object. The shear modulus of the diaphragm cor-

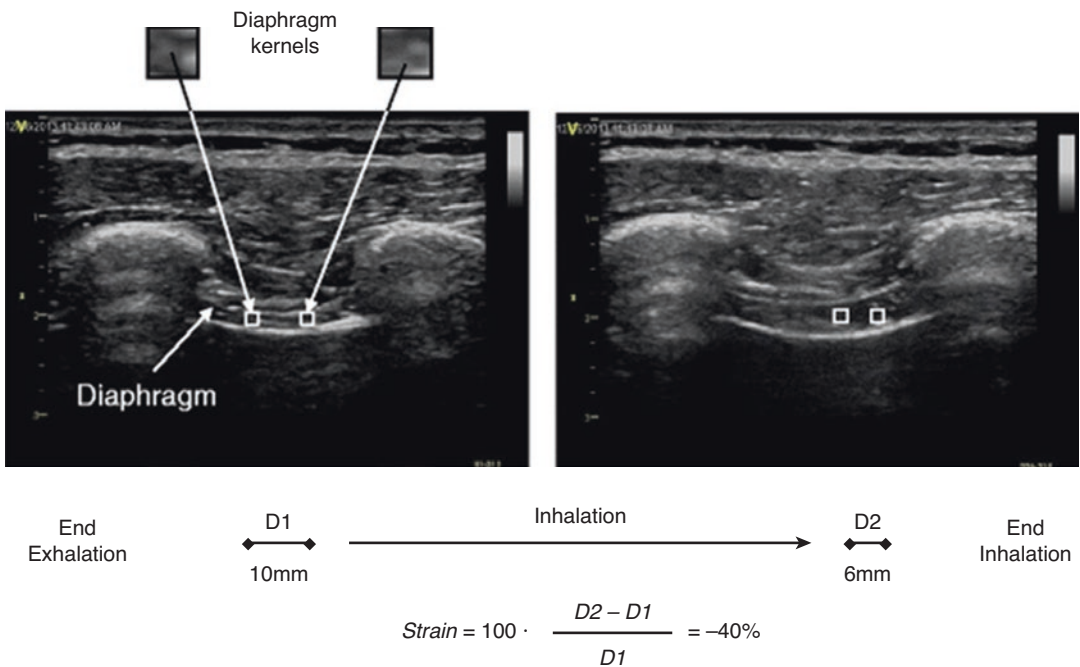


Fig. 36.42 Ultrasound of the zone of apposition at end-exhalation (*left panel*) and end-inhalation (*right panel*). The image of the diaphragm has a granularity caused by an inherent ultrasound artifact known as speckle. A cluster of speckles form a kernel. The stronger the contraction of the diaphragm, the closer kernels come together (strain). With speckle-tracking software, it is possible to quantify the strain of the diaphragm as: 100 multiplied the differ-

ence of the distance between two representative kernels at end-inhalation (D2) minus the distance between the same kernels at end-exhalation (D1) divided by D1. Here, the distance between two representative kernels at end-exhalation (*left panel*) is 10 mm (D1) and at end-inhalation (*right panel*) 6 mm (D2), yielding a strain of -40% . (Modified from Orde et al. (2015), open access)

relates with changes in P_{di} during loading (Bachasson et al. 2019). Problems with the technique include limited acquisition frequency (2 Hz), misalignment between transducer and diaphragm fascicles, and frequent inability to record shear modulus during maximal inspiratory efforts (Bachasson et al. 2019).

Ultrasound Measurement of Diaphragm Motion (Dome)

Cranio-caudal movement of the dome of the diaphragm during quiet breathing (Cardenas et al. 2018; Scarlata et al. 2018; Boussuges et al. 2009, 2019) and forceful inspiratory efforts (Scarlata et al. 2018; Boussuges et al. 2009; Gerscovich et al. 2001) is quantified using curvilinear probes (Fig. 36.43) (Sarwal et al. 2013; Shaikh 2019). These probes use low-frequency ultrasound waves (2–6 Hz) that penetrate deeply giving a wide depth of field (Sarwal et al. 2013). It is impossible to record maximal diaphragmatic excursions using M-mode ultrasonography in up to 28% of patients (Scott et al. 2006).

During quiet breathing, mean diaphragmatic motion varies between 14.1 and 20.3 mm (Cardenas et al. 2018; Scarlata et al. 2018; Boussuges et al. 2009, 2019; Gerscovich et al. 2001). During inspiration from FRC to TLC, mean diaphragm motion varies between 25.0 and

84.0 mm (Cardenas et al. 2018; Scarlata et al. 2018; Boussuges et al. 2009, 2019; Gerscovich et al. 2001; Kantarci et al. 2004). Intra- and interobserver agreement (intra-class correlation coefficients) of measurements obtained at a single sitting in healthy adults and ventilated patients range from 0.60 to 0.99 (Scarlata et al. 2018; Koo and Li 2016; Lerolle et al. 2009). The association between diaphragmatic excursion and diaphragmatic thickening and between diaphragmatic excursions and diaphragmatic pressure output is weak (Cardenas et al. 2018; Orde et al. 2015; Dubé et al. 2017; Umbrello et al. 2015).

Measurements of diaphragmatic excursions have been recorded in critically ill patients during noninvasive (Cammarota et al. 2019) and invasive ventilation (Dubé et al. 2017; Lerolle et al. 2009; Kim et al. 2011; Palkar et al. 2018a; Jiang et al. 2004; Palkar et al. 2018b). Employing post hoc analysis, investigators have reported association between diaphragmatic excursions and failure of noninvasive ventilation (Cammarota et al. 2019), duration of (invasive) mechanical ventilation (Lerolle et al. 2009), weaning outcome (Dubé et al. 2017; Kim et al. 2011; Palkar et al. 2018a; Jiang et al. 2004), and length of stay (Kim et al. 2011), but the thresholds put forward have not been prospectively tested.

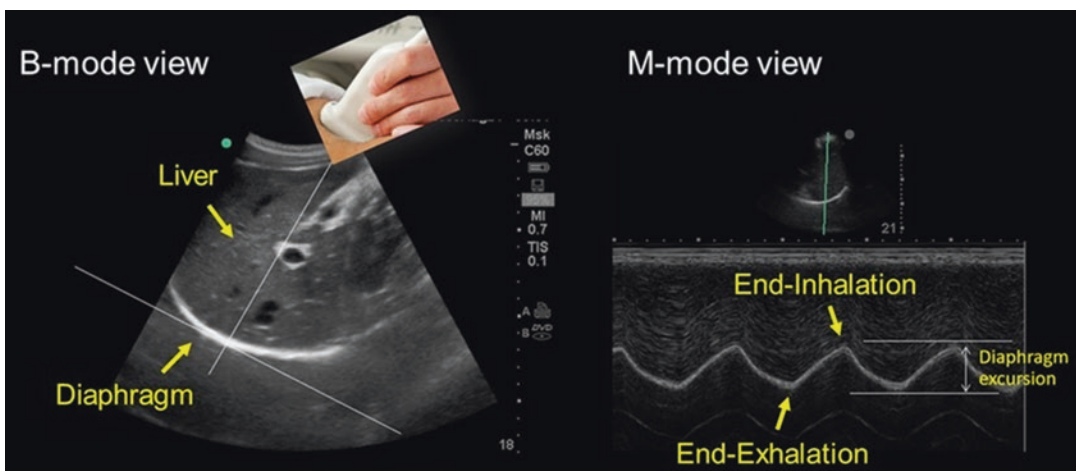


Fig. 36.43 Ultrasound image of the dome of the diaphragm in bright-mode (B-mode; left panel) and motion-mode (M-mode; right panel). As the diaphragm contracts, the dome moves towards the ultrasound probe. The larger

the caudal displacement of the diaphragm, the greater the diaphragmatic contribution to tidal breathing. (Modified from Laghi and Shaikh (2019), with permission of Daedalus Enterprises Inc.)

Assessment of Muscle Fiber Vibration

Diaphragmatic fibers vibrate during contractions elicited by stimulation of the phrenic nerves (Petitjean and Bellemare 1994) and voluntary efforts (Lozano-Garcia et al. 2018). The vibrations can be recorded using surface microphones (phonomyography) (Petitjean and Bellemare 1994; Barry 1987) or accelerometers (mechanomyography) placed over the zone of apposition (Sarlabous et al. 2014, 2015, 2017). Phonomyography and mechanomyography provide a noninvasive index of the magnitude of P_{di} (Lozano-Garcia et al. 2018; Petitjean et al. 1997), and neuromechanical coupling (Petitjean and Bellemare 1994; Lozano-Garcia et al. 2018; Sarlabous et al. 2017).

Surface Phonomyography

The amplitude of the diaphragmatic phonomyogram signal is proportional to P_{di} during graded diaphragmatic contractions elicited by electrical phrenic nerve stimulation (Petitjean and Bellemare 1994). Diaphragmatic fatigue produces a decrease in the phonomyogram as well as a decrease in P_{di} . Some investigators claim that the phonomyogram elicited by submaximal unilateral

phrenic nerve stimulations is a reliable measure of impaired diaphragmatic contractility caused by fatigue (Petitjean et al. 1997). Problems with the technique include variable effect of lung volume (Petitjean et al. 1996), high interindividual variability (Petitjean et al. 1996), contamination by chest-wall and abdominal muscle vibration, lack of proportionality between maximum instantaneous frequency of the diaphragm phonomyogram and maximum P_{di} (Chen et al. 1997), and unknown reproducibility of the signals.

Surface Mechanomyography

Like surface EMG, the surface mechanomyogram of the diaphragm is contaminated by cardiac artifact. This artifact can be reduced using the nonlinear multistate Lempel-Ziv index (Sarlabous et al. 2017) or fixed sample entropy (Sarlabous et al. 2015; Lozano-García et al. 2019) (Fig. 36.44). Unlike surface EMG, surface mechanomyogram is not influenced by skin bioimpedance, bioelectrical interference from other muscles, or by power-line interference (Lozano-Garcia et al. 2018). The mechanomyogram of the diaphragm strongly correlates with changes in P_{aw} and P_{di} during loading (Lozano-Garcia et al. 2018; Sarlabous et al. 2017) (Fig. 36.44).

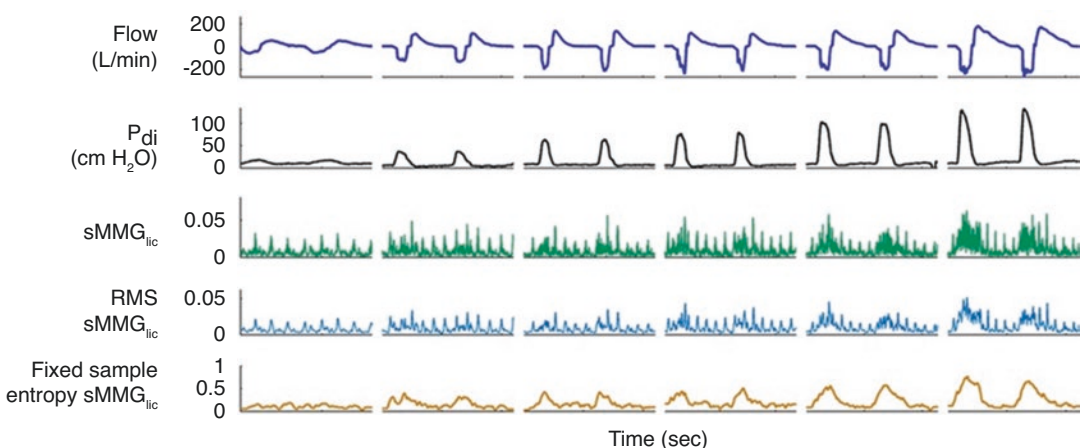


Fig. 36.44 Flow, transdiaphragmatic pressure (P_{di}), surface mechanomyogram of the diaphragm recorded from lower intercostal spaces ($sMMG_{ic}$), root-mean-square (RMS) of $sMMG_{ic}$, and fixed sample entropy of $sMMG_{ic}$ signal during inspiratory threshold loading in a healthy

subject. Fixed-sample entropy successfully reduced the cardiac artifact that contaminated the raw and RMS mechanomyogram signals. Amplitude of the mechanomyogram increased *pari passu* with increase in P_{di} . (Modified from Manuel Lozano-García et al. (2018), open access)

The strong relationship between mechanomyogram and P_{di} (Lozano-Garcia et al. 2018; Sarlabous et al. 2017) and an enhanced signal in inpatients with COPD (Sarlabous et al. 2017), suggest that mechanomyography might provide a useful measure of inspiratory effort. Problems with the technique include contamination by chest-wall and abdominal muscles, challenges in controlling for variable muscle-to-electrode distance (Lozano-Garcia et al. 2018), and muscle shortening (Sarlabous et al. 2017).

Conclusion

More than 20 years ago, we wrote a chapter on monitoring of respiratory muscle function and remarked that few monitoring tools had been introduced into clinical practice (Tobin et al. 1994). In the intervening period, several approaches have been developed although research has largely focused on the delineating the capabilities and limitations of preexisting techniques. Knowledge among bedside physicians has not kept pace with these advances. All the machines in the world will not improve patient care if intensivists do not possess sufficient understanding of physiology to employ the machines wisely (Tobin 2019). The state of affairs is exemplified by recurring triumphalist claims for a minor new index derived from ultrasound or airway pressure recordings without acknowledgment of the limited reproducibility of a measurement or rigorous validation of supposedly discriminating threshold value. Physician knowledge of the basic science underlying ICU monitoring – physiology – is the critical stumbling block. That is why diligent reading of books like the present one remains the foundation for improvements in clinical care (Tobin 2014).

References

Abdallah SJ, Chan DS, Glicksman R, et al. Abdominal binding improves neuromuscular efficiency of the human diaphragm during exercise. *Front Physiol.* 2017;8:345.

- Abdallah SJ, Smith BM, Wilkinson-Maitland C, et al. Effect of abdominal binding on diaphragmatic neuromuscular efficiency, exertional breathlessness, and exercise endurance in chronic obstructive pulmonary disease. *Front Physiol.* 2018;9:1618.
- Agostoni E. Action of the respiratory muscles. In: Fenn WO, Rahn H, editors. *Handbook of physiology.* Washington: American Physiological Society; 1964. p. 377–86.
- Agostoni P, Mead J. Statics of the respiratory system. In: Fenn WO, Rahn H, editors. *Handbook of physiology.* Washington, DC: American Physiological Society; 1964. p. 387–409.
- Agostoni P, Rahn H. Abdominal and thoracic pressures at different lung volumes. *J Appl Physiol.* 1960;15:1087–92.
- Agostoni E, Sant'Ambrogio G, Del Portillo Carrasco H. Electromyography of the diaphragm in man and transdiaphragmatic pressure. *J Appl Physiol.* 1960;15:1093–7.
- Agostoni E, Campbell E, Freedman S. Energetics. In: EJM C, Agostoni E, Newsom-Davis J, editors. *The respiratory muscles.* Philadelphia: Saunders; 1970. p. 115–37.
- Aldrich TK, Spiro P. Maximal inspiratory pressure: does reproducibility indicate full effort? *Thorax.* 1995;50:40–3.
- Alexander C. Diaphragm movements and the diagnosis of diaphragmatic paralysis. *Clin Radiol.* 1966;17:79–83.
- Allen SM, Hunt B, Green M. Fall in vital capacity with posture. *Br J Dis Chest.* 1985;79:267–71.
- Allen GM, McKenzie DK, Gandevia SC, Bass S. Reduced voluntary drive to breathe in asthmatic subjects. *Respir Physiol.* 1993;93:29–40.
- Allen GM, Gandevia SC, Neering IR, et al. Muscle performance, voluntary activation and perceived effort in normal subjects and patients with prior poliomyelitis. *Brain.* 1994;117(Pt 4):661–70.
- Allen DG, Lamb GD, Westerblad H. Skeletal muscle fatigue: cellular mechanisms. *Physiol Rev.* 2008;88:287–332.
- Allo JC, Beck JC, Brander L, et al. Influence of neurally adjusted ventilatory assist and positive end-expiratory pressure on breathing pattern in rabbits with acute lung injury. *Crit Care Med.* 2006;34:2997–3004.
- Al-Shekhlee A, Shapiro BE, Preston DC. Iatrogenic complications and risks of nerve conduction studies and needle electromyography. *Muscle Nerve.* 2003;27:517–26.
- American Thoracic Society/European Respiratory Society. ATS/ERS statement on respiratory muscle testing. *Am J Respir Crit Care Med.* 2002;166:518–624.
- Antenora F, Fantini R, Iattoni A, et al. Prevalence and outcomes of diaphragmatic dysfunction assessed by ultrasound technology during acute exacerbation of COPD: a pilot study. *Respirology.* 2017;22:338–44.
- Araujo PR, Resqueti VR, Nascimento JJ, et al. Reference values for sniff nasal inspiratory pressure in healthy subjects in Brazil: a multicenter study. *J Bras Pneumol.* 2012;38:700–7.

- Arnulf I, Similowski T, Salachas F, et al. Sleep disorders and diaphragmatic function in patients with amyotrophic lateral sclerosis. *Am J Respir Crit Care Med.* 2000;161:849–56.
- Assy J, Mauriat P, Tafer N, et al. Neurally adjusted ventilatory assist for children on veno-venous ECMO. *J Artif Organs.* 2019;22:118–25.
- Aubier M, Farkas G, De Troyer A, et al. Detection of diaphragmatic fatigue in man by phrenic stimulation. *J Appl Physiol.* 1981a;50:538–44.
- Aubier M, Trippenbach T, Roussos C. Respiratory muscle fatigue during cardiogenic shock. *J Appl Physiol.* 1981b;51:499–508.
- Aubier M, Murciano D, Lecocguic Y, et al. Bilateral phrenic stimulation: a simple technique to assess diaphragmatic fatigue in humans. *J Appl Physiol.* 1985;58:58–64.
- Babcock M, Pegelow D, McClaran S, et al. Contribution of diaphragmatic power output to exercise-induced diaphragm fatigue. *J Appl Physiol.* 1995;78:1710–9.
- Bachasson D, Wuyam B, Pepin JL, et al. Quadriceps and respiratory muscle fatigue following high-intensity cycling in COPD patients. *PLoS One.* 2013;8:e83432.
- Bachasson DDM, N  rat MC, Gennisson JL, Hogrel JY, Doorduyn J, Similowski T. Diaphragm shear modulus reflects transdiaphragmatic pressure during isovolumetric inspiratory efforts and ventilation against inspiratory loading. *J Appl Physiol.* 2019;126:699–707.
- Barry DT. Acoustic signals from frog skeletal muscle. *Biophys J.* 1987;51:769–73.
- Bartolo A, Roberts C, Dzwonczyk RR, Goldman E. Analysis of diaphragm EMG signals: comparison of gating vs. subtraction for removal of ECG contamination. *J Appl Physiol.* 1996;80:1898–902.
- Barwing J, Pedroni C, Olgemoller U, et al. Electrical activity of the diaphragm (EAdi) as a monitoring parameter in difficult weaning from respirator: a pilot study. *Crit Care.* 2013;17:R182.
- Bazzy AR, Haddad GG. Diaphragmatic fatigue in unanesthetized adult sheep. *J Appl Physiol.* 1984;57:182–90.
- Beck J, Sinderby C, Weinberg J, Grassino A. Effects of muscle-to-electrode distance on the human diaphragm electromyogram. *J Appl Physiol.* 1995;79:975–85.
- Beck J, Sinderby C, Lindstrom L, Grassino A. Influence of bipolar esophageal electrode positioning on measurements of human crural diaphragm electromyogram. *J Appl Physiol.* 1996;81:1434–49.
- Beck J, Sinderby C, Lindstrom L, Grassino A. Diaphragm interference pattern EMG and compound muscle action potentials: effects of chest wall configuration. *J Appl Physiol.* 1997;82:520–30.
- Beck J, Sinderby C, Lindstrom L, Grassino A. Effects of lung volume on diaphragm EMG signal strength during voluntary contractions. *J Appl Physiol.* 1998;85:1123–34.
- Beck J, Gottfried SB, Navalesi P, et al. Electrical activity of the diaphragm during pressure support ventilation in acute respiratory failure. *Am J Respir Crit Care Med.* 2001;164:419–24.
- Belanger AY, McComas AJ. Extent of motor unit activation during effort. *J Appl Physiol.* 1981;51:1131–5.
- Bellani G, Mauri T, Coppadoro A, et al. Estimation of patient's inspiratory effort from the electrical activity of the diaphragm. *Crit Care Med.* 2013;41:1483–91.
- Bellemare F. Strength of the respiratory muscles. In: Roussos C, editor. *The thorax.* New York: Marcel Dekker; 1995. p. 1161–97.
- Bellemare F, Bigland-Ritchie B. Assessment of human diaphragm strength and activation using phrenic nerve stimulation. *Respir Physiol.* 1984;58:263–77.
- Bellemare F, Bigland-Ritchie B. Central components of diaphragmatic fatigue assessed by phrenic nerve stimulation. *J Appl Physiol.* 1987;62:1307–16.
- Bellemare F, Grassino A. Effect of pressure and timing of contraction on human diaphragm fatigue. *J Appl Physiol.* 1982;53:1190–5.
- Bellemare F, Wight D, Lavigne CM, Grassino A. Effect of tension and timing of contraction on the blood flow of the diaphragm. *J Appl Physiol.* 1983a;54:1597–606.
- Bellemare F, Woods JJ, Johansson R, Bigland-Ritchie B. Motor-unit discharge rates in maximal voluntary contractions of three human muscles. *J Neurophysiol.* 1983b;50:1380–92.
- Bellemare F, Bigland-Ritchie B, Woods JJ. Contractile properties of the human diaphragm in vivo. *J Appl Physiol.* 1986;61:1153–61.
- Bigland B, Lippold OJC. The relation between force, velocity and integrated electrical activity in human muscles. *J Physiol Lond.* 1954;123:214–24.
- Bigland-Ritchie B, Woods JJ. Integrated EMG and oxygen uptake during dynamic contractions of human muscles. *J Appl Physiol.* 1974;36:475–9.
- Black LF, Hyatt RE. Maximal respiratory pressures: normal values and relationship to age and sex. *Am Rev Respir Dis.* 1969;99:696–702.
- Blankman P, Hasan D, van Mourik MS, Gommers D. Ventilation distribution measured with EIT at varying levels of pressure support and Neurally adjusted Ventilatory assist in patients with ALI. *Intensive Care Med.* 2013;39:1057–62.
- Boon AJ, Harper CJ, Ghahfarokhi LS, et al. Two-dimensional ultrasound imaging of the diaphragm: quantitative values in normal subjects. *Muscle Nerve.* 2013;47:884–9.
- Boussuges A, Gole Y, Blanc P. Diaphragmatic motion studied by m-mode ultrasonography: methods, reproducibility, and normal values. *Chest.* 2009;135:391–400.
- Boussuges A, Br  geon F, Blanc P, et al. Characteristics of the paralysed diaphragm studied by M-mode ultrasonography. *Clin Physiol Funct Imaging.* 2019;39:143–9.
- Brander L, Leong-Poi H, Beck J, et al. Titration and implementation of neurally adjusted ventilatory assist in critically ill patients. *Chest.* 2009;135:695–703.
- Braun NM, Arora NS, Rochester DF. Force-length relationship of the normal human diaphragm. *J Appl Physiol Respir Environ Exerc Physiol.* 1982;53:405–12.

- Braun NM, Arora NS, Rochester DF. Respiratory muscle and pulmonary function in polymyositis and other proximal myopathies. *Thorax*. 1983;38:616–23.
- Bruce EN, Loring SH. Methods for assessing chest wall behavior. In: Roussos C, Macklem PT, editors. *The thorax*. New York: Marcell Dekker; 1985. p. 235–55.
- Butler JE, McKenzie DK, Gandevia SC. Impaired reflex responses to airway occlusion in the inspiratory muscles of asthmatic subjects. *Thorax*. 1996;51:490–5.
- Buyse B, Demedts M, Meekers J, et al. Respiratory dysfunction in multiple sclerosis: a prospective analysis of 60 patients. *Eur Respir J*. 1997;10:139–45.
- Cammarota G, Sguazzotti I, Zanoni M, et al. Diaphragmatic ultrasound assessment in subjects with acute hypercapnic respiratory failure admitted to the emergency department. *Respir Care*. 2019;64:1469–77.
- Campbell EJM. *The respiratory muscles and the mechanics of breathing*. London: Lloyd-Luke; 1958.
- Cardenas LZ, Santana PV, Caruso P, et al. Diaphragmatic ultrasound correlates with inspiratory muscle strength and pulmonary function in healthy subjects. *Ultrasound Med Biol*. 2018;44:786–93.
- Carrillo-Esper R, Perez-Calatayud AA, Arch-Tirado E, et al. Standardization of sonographic diaphragm thickness evaluations in healthy volunteers. *Respir Care*. 2016;61:920–4.
- Cassart M, Pettiaux N, Gevenoix PA, et al. Effect of chronic hyperinflation on diaphragm length and surface area. *Am J Respir Crit Care Med*. 1997;156:504–8.
- Cattapan SE, Laghi F, Tobin MJ. Can diaphragmatic contractility be assessed by airway twitch pressure in mechanically ventilated patients? *Thorax*. 2003;58:58–62.
- Chen D, Durand LG, Bellemare F. Time and frequency domain analysis of acoustic signals from a human muscle. *Muscle Nerve*. 1997;20:991–1001.
- Chen R, Kayser B, Yan S, Macklem PT. Twitch transdiaphragmatic pressure depends critically on thoracoabdominal configuration. *J Appl Physiol*. 2000;88:54–60.
- Chevrolet JC, Deleamont P. Repeated vital capacity measurements as predictive parameters for mechanical ventilation need and weaning success in the Guillain-Barre syndrome. *Am Rev Respir Dis*. 1991;144:814–8.
- Chino K, Ohya T, Katayama K, Suzuki Y. Diaphragmatic shear modulus at various submaximal inspiratory mouth pressure levels. *Respir Physiol Neurobiol*. 2018;252:52–7.
- Clanton TL, Diaz PT. Clinical assessment of the respiratory muscles. *Phys Ther*. 1995;75:983–95.
- Clanton TL, Dixon GF, Drake J, Gadek JE. Effects of breathing pattern on inspiratory muscle endurance in humans. *J Appl Physiol*. 1985;59:1834–41.
- Clergue F, Whitelaw WA, Charles JC, et al. Inferences about respiratory muscle use after cardiac surgery from compartmental volume and pressure measurements. *Anesthesiology*. 1995;82:1318–27.
- Cluzel P, Similowski T, Chartrand-Lefebvre C, et al. Diaphragm and chest wall: assessment of the inspiratory pump with MR imaging—preliminary observations. *Radiology*. 2000;215:574–83.
- Cohen CA, Zagelbaum G, Gross D, et al. Clinical manifestations of inspiratory muscle fatigue. *Am J Med*. 1982;73:308–16.
- Coisel Y, Chanques G, Jung B, et al. Neurally adjusted ventilatory assist in critically ill postoperative patients: a crossover randomized study. *Anesthesiology*. 2010;113:925–35.
- Criner GJ, Celli BR. Effect of unsupported arm exercise on ventilatory muscle recruitment in patients with severe chronic airflow obstruction. *Am Rev Respir Dis*. 1988;138:856–61.
- D'Angelo E, Pecchiari M, Acocella F, et al. Effects of abdominal distension on breathing pattern and respiratory mechanics in rabbits. *Respir Physiol Neurobiol*. 2002;130:293–304.
- Daube JR. Electrodiagnosis of muscle disorders. In: Engel AG, Banker BQ, editors. *Myology: basic and clinical*. New York: McGraw Hill; 1986. p. 1081–121.
- Daubenspeck JA, Leiter JC, McGovern JF, et al. Diaphragmatic electromyography using a multiple electrode array. *J Appl Physiol*. 1989;67:1525–34.
- Davis J, Goldman M, Loh L, Casson M. Diaphragm function and alveolar hypoventilation. *Q J Med*. 1976;45:87–100.
- De Troyer A, Estenne M. Limitations of measurement of transdiaphragmatic pressure in detecting diaphragmatic weakness. *Thorax*. 1981;36:169–74.
- De Troyer AD, Estenne M. Coordination between rib cage muscles and diaphragm during quiet breathing in humans. *J Appl Physiol*. 1984;57:899–906.
- De Troyer A, Estenne M. Chest wall motion in paraplegic subjects. *Am Rev Respir Dis*. 1990;141:332–6.
- De Troyer A, Borenstein S, Cordier R. Analysis of lung volume restriction in patients with respiratory muscle weakness. *Thorax*. 1980;35:603–10.
- De Troyer A, Estenne M, Ninane V, et al. Transversus abdominis muscle function in humans. *J Appl Physiol*. 1990;68:1010–6.
- De Troyer A, Leeper JB, McKenzie DK, Gandevia SC. Neural drive to the diaphragm in patients with severe COPD. *Am J Respir Crit Care Med*. 1997;155:1335–40.
- De Troyer A, Kirkwood PA, Wilson TA. Respiratory action of the intercostal muscles. *Physiol Rev*. 2005;85:717–56.
- Demoule A, Verin E, Locher C, et al. Validation of surface recordings of the diaphragm response to transcranial magnetic stimulation in humans. *J Appl Physiol*. 2003;94:453–61.
- Demoule A, Jung B, Prodanovic H, et al. Diaphragm dysfunction on admission to the intensive care unit. Prevalence, risk factors, and prognostic impact—a prospective study. *Am J Respir Crit Care Med*. 2013;188:213–9.
- Demoule A, Clavel M, Rolland-Debord C, et al. Neurally adjusted ventilatory assist as an alternative to pressure support ventilation in adults: a French multicentre randomized trial. *Intensive Care Med*. 2016;42:1723–32.

- Di MR, Spadaro S, Mirabella L, et al. Impact of prolonged assisted ventilation on diaphragmatic efficiency: NAVA versus PSV. *Crit Care*. 2016;20:1.
- Diehl JL, Lofaso F, Deleuze P, et al. Clinically relevant diaphragmatic dysfunction after cardiac operations. *J Thorac Cardiovasc Surg*. 1994;107:487–98.
- DiNino E, Gartman EJ, Sethi JM, McCool FD. Diaphragm ultrasound as a predictor of successful extubation from mechanical ventilation. *Thorax*. 2014;69:431–5.
- Doorduyn J, Sinderby CA, Beck J, et al. The calcium sensitizer levosimendan improves human diaphragm function. *Am J Respir Crit Care Med*. 2012;185:90–5.
- Doorduyn J, Roesthuis LH, Jansen D, et al. Respiratory muscle effort during expiration in successful and failed weaning from mechanical ventilation. *Anesthesiology*. 2018;129:490–501.
- Doud JR, Walsh JM. Muscle temperature alters the EMG power spectrum of the canine diaphragm. *Respir Physiol*. 1993;94:241–50.
- Doud JR, Walsh JM. Muscle fatigue and muscle length interaction: effect on the EMG frequency components. *Electromyogr Clin Neurophysiol*. 1995;35:331–9.
- Dres M, Schmidt M, Ferre A, et al. Diaphragm electromyographic activity as a predictor of weaning failure. *Intensive Care Med*. 2012;38:2017–25.
- Dres M, Dube BP, Mayaux J, et al. Coexistence and impact of limb muscle and diaphragm weakness at time of liberation from mechanical ventilation in medical intensive care unit patients. *Am J Respir Crit Care Med*. 2017;195:57–66.
- Dubé B-P, Dres M, Mayaux J, et al. Ultrasound evaluation of diaphragm function in mechanically ventilated patients: comparison to phrenic stimulation and prognostic implications. *Thorax*. 2017;72:811–8.
- Duiverman ML, Van Eykern LA, Vennik PW, et al. Reproducibility and responsiveness of a noninvasive EMG technique of the respiratory muscles in COPD patients and in healthy subjects. *J Appl Physiol*. 2004;96:1723–9.
- Edwards RH, Hill DK, Jones DA. Metabolic changes associated with the slowing of relaxation in fatigued mouse muscle. *J Physiol*. 1975;251:287–301.
- Elia D, Kelly JL, Martolini D, et al. Respiratory muscle fatigue following exercise in patients with interstitial lung disease. *Respiration*. 2013;85:220–7.
- Emeriaud G, Beck J, Tucci M, et al. Diaphragm electrical activity during expiration in mechanically ventilated infants. *Pediatr Res*. 2006;59:705–10.
- Enright PL, Kronmal RA, Manolio TA, et al. Respiratory muscle strength in the elderly. Correlates and reference values. Cardiovascular health study research group. *Am J Respir Crit Care Med*. 1994;149:430–8.
- Epstein SK, Celli BR, Williams J, et al. Ventilatory response to arm elevation. Its determinants and use in patients with chronic obstructive pulmonary disease. *Am J Respir Crit Care Med*. 1995;152:211–6.
- Esau SA, Bellemare F, Grassino A, et al. Changes in relaxation rate with diaphragmatic fatigue in humans. *J Appl Physiol*. 1983;54:1353–60.
- Estenne M, Gevenois PA, Kinnear W, et al. Lung volume restriction in patients with chronic respiratory muscle weakness: the role of microatelectasis. *Thorax*. 1993;48:698–701.
- Ferguson GT. Use of twitch pressures to assess diaphragmatic function and central drive. *J Appl Physiol*. 1994;77:1705–15.
- Ferrari G, De Filippi G, Elia F, et al. Diaphragm ultrasound as a new index of discontinuation from mechanical ventilation. *Crit Ultrasound J*. 2014;6:8.
- Field S, Sanci S, Grassino A. Respiratory muscle oxygen consumption estimated by the diaphragm pressure-time index. *J Appl Physiol*. 1984;57:44–51.
- Fitch S, McComas A. Influence of human muscle length on fatigue. *J Physiol*. 1985;362:205–13.
- Fitting JW. Sniff nasal inspiratory pressure: simple or too simple? *Eur Respir J*. 2006;27:881–3.
- Fitting JW, Grassino A. Diagnosis of diaphragmatic dysfunction. *Clin Chest Med*. 1987;8:91–103.
- Fiz JA, Montserrat JM, Picado C, et al. How many manoeuvres should be done to measure maximal inspiratory mouth pressure in patients with chronic airflow obstruction? *Thorax*. 1989;44:419–21.
- Fleury B, Murciano D, Talamo C, et al. Work of breathing in patients with chronic obstructive pulmonary disease in acute respiratory failure. *Am Rev Respir Dis*. 1985;131:822–7.
- Gandevia SC. Spinal and supraspinal factors in human muscle fatigue. *Physiol Rev*. 2001;81:1725–89.
- Gandevia SC, McKenzie DK. Activation of the human diaphragm during maximal static efforts. *J Physiol*. 1985;367:45–56.
- Gandevia SC, McKenzie DK. Human diaphragmatic EMG: changes with lung volume and posture during supramaximal phrenic stimulation. *J Appl Physiol*. 1986;60:1420–8.
- Gandevia SC, McKenzie DK, Plassman BL. Activation of human respiratory muscles during different voluntary manoeuvres. *J Physiol*. 1990;428:387–403.
- Gandevia SC, Gorman RB, McKenzie DK, Southon FC. Dynamic changes in human diaphragm length: maximal inspiratory and expulsive efforts studied with sequential radiography. *J Physiol*. 1992;457:167–76.
- Gennisson J-L, Deffieux T, Fink M, Tanter M. Ultrasound elastography: principles and techniques. *Diagn Interv Imaging*. 2013;94:487–95.
- Gerscovich EO, Cronan M, McGahan JP, et al. Ultrasonographic evaluation of diaphragmatic motion. *J Ultrasound Med*. 2001;20:597–604.
- Gibson GJ. Measurement of respiratory muscle strength. *Respir Med*. 1995;89:529–35.
- Gibson GJ, Clark E, Pride NB. Static transdiaphragmatic pressures in normal subjects and in patients with chronic hyperinflation. *Am Rev Respir Dis*. 1981;124:685–9.
- Gierada DS, Curtin JJ, Erickson SJ, et al. Diaphragmatic motion: fast gradient-recalled-echo MR imaging in healthy subjects. *Radiology*. 1995;194:879–84.

- Gilbert R, Auchincloss JH Jr, Peppi D. Relationship of rib cage and abdomen motion to diaphragm function during quiet breathing. *Chest*. 1981;80:607–12.
- Gilbert R, Auchincloss JH, Peppi D. Significance of relative rib cage and abdomen motion in patients with chronic obstructive pulmonary disease. *Lung*. 1983;161:77–85.
- Goligher EC, Laghi F, Detsky ME, et al. Measuring diaphragm thickness with ultrasound in mechanically ventilated patients: feasibility, reproducibility and validity. *Intensive Care Med*. 2015;41:642–9.
- Goligher EC, Dres M, Fan E, et al. Mechanical ventilation-induced diaphragm atrophy strongly impacts clinical outcomes. *Am J Respir Crit Care Med*. 2018;197:204–13.
- Gorman RB, McKenzie DK, Butler JE, et al. Diaphragm length and neural drive after lung volume reduction surgery. *Am J Respir Crit Care Med*. 2005;172:1259–66.
- Gottesman E, McCool FD. Ultrasound evaluation of the paralyzed diaphragm. *Am J Respir Crit Care Med*. 1997;155:1570–4.
- Gross D, Grassino A, Ross WR, Macklem PT. Electromyogram pattern of diaphragmatic fatigue. *J Appl Physiol*. 1979;46:1–7.
- Grosu HB, Im Lee Y, Lee J, et al. Diaphragm muscle thinning in patients who are mechanically ventilated. *Chest*. 2012;142:1455–60.
- Grosu HB, Ost DE, Im Lee Y, et al. Diaphragm muscle thinning in subjects receiving mechanical ventilation and its effect on extubation. *Respir Care*. 2017;62:904–11.
- Hamnegaard CH, Wragg S, Kyroussis D, et al. Mouth pressure in response to magnetic stimulation of the phrenic nerves. *Thorax*. 1995;50:620–4.
- Hamnegard CH, Wragg S, Mills G, et al. The effect of lung volume on transdiaphragmatic pressure. *Eur Respir J*. 1995;8:1532–6.
- Hamnegård C, Wragg SD, Mills GH, et al. Clinical assessment of diaphragm strength by cervical magnetic stimulation of the phrenic nerves. *Thorax*. 1996;51:1239–42.
- Harik-Khan RI, Wise RA, Fozard JL. Determinants of maximal inspiratory pressure. The Baltimore longitudinal study of aging. *Am J Respir Crit Care Med*. 1998;158:1459–64.
- He BT, Lu G, Xiao SC, et al. Coexistence of OSA may compensate for sleep related reduction in neural respiratory drive in patients with COPD. *Thorax*. 2017;72:256–62.
- Heritier F, Rahm F, Pasche P, Fitting JW. Sniff nasal inspiratory pressure. A noninvasive assessment of inspiratory muscle strength. *Am J Respir Crit Care Med*. 1994;150:1678–83.
- Hermans G, Agten A, Testelmans D, et al. Increased duration of mechanical ventilation is associated with decreased diaphragmatic force: a prospective observational study. *Crit Care*. 2010;14:R127.
- Hershenson MB, Kikuchi Y, Loring SH. Relative strengths of the chest wall muscles. *J Appl Physiol*. 1988;65:852–62.
- Hillman DR, Finucane KE. Respiratory pressure partitioning during quiet inspiration in unilateral and bilateral diaphragmatic weakness. *Am Rev Respir Dis*. 1988;137:1401–5.
- Hillman DR, Markos J, Finucane KE. Effect of abdominal compression on maximum transdiaphragmatic pressure. *J Appl Physiol*. 1990;68:2296–304.
- Hodges PW, Gandevia SC. Activation of the human diaphragm during a repetitive postural task. *J Physiol*. 2000;522(Pt 1):165–75.
- Holmberg E, Waldeck B. On the possible role of potassium ions in the action of terbutaline on skeletal muscle contractions. *Acta Pharmacol Toxicol (Copenh)*. 1980;46:141–9.
- Hooijman PE, Beishuizen A, Witt CC, et al. Diaphragm muscle fiber weakness and ubiquitin-proteasome activation in critically ill patients. *Am J Respir Crit Care Med*. 2015;191:1126–38.
- Howard RS. Respiratory failure because of neuromuscular disease. *Curr Opin Neurol*. 2016;29:592–601.
- Huang SJ, Orde S. From speckle tracking echocardiography to torsion: research tool today, clinical practice tomorrow. *Curr Opin Crit Care*. 2013;19:250–7.
- Huang CH, Yang GG, Chen TW. Sniff nasal inspiratory pressure does not decrease in elderly subjects. *J Phys Ther Sci*. 2014;26:1509–13.
- Hubmayr RD, Litchy WJ, Gay PC, Nelson SB. Transdiaphragmatic twitch pressure. Effects of lung volume and chest wall shape. *Am Rev Respir Dis*. 1989;139:647–52.
- Jaber S, Petrof BJ, Jung B, et al. Rapidly progressive diaphragmatic weakness and injury during mechanical ventilation in humans. *Am J Respir Crit Care Med*. 2011;183:364–71.
- Jensen D, O'Donnell DE, Li R, Luo YM. Effects of dead space loading on neuro-muscular and neuro-ventilatory coupling of the respiratory system during exercise in healthy adults: implications for dyspnea and exercise tolerance. *Respir Physiol Neurobiol*. 2011;179:219–26.
- Jiang J-R, Tsai T-H, Jerng J-S, et al. Ultrasonographic evaluation of liver/spleen movements and extubation outcome. *Chest*. 2004;126:179–85.
- Jolley CJ, Luo YM, Steier J, et al. Neural respiratory drive and breathlessness in COPD. *Eur Respir J*. 2015;45:355–64.
- Ju C, Liu W, Chen RC. Twitch mouth pressure and disease severity in subjects with COPD. *Respir Care*. 2014;59:1062–70.
- Juan G, Calverley P, Talamo C, et al. Effect of carbon dioxide on diaphragmatic function in human beings. *N Engl J Med*. 1984;310:874–9.
- Jubran A, Tobin MJ. Pathophysiologic basis of acute respiratory distress in patients who fail a trial of weaning from mechanical ventilation. *Am J Respir Crit Care Med*. 1997;155:906–15.

- Jung B, Nougaret S, Conseil M, et al. Sepsis is associated with a preferential diaphragmatic atrophy: a critically ill patient study using tridimensional computed tomography. *Anesthesiology*. 2014;120:1182–91.
- Jung B, Moury PH, Mahul M, et al. Diaphragmatic dysfunction in patients with ICU-acquired weakness and its impact on extubation failure. *Intensive Care Med*. 2016;42:853–61.
- Kabitiz HJ, Waltersbacher S, Walker D, Windisch W. Inspiratory muscle strength in chronic obstructive pulmonary disease depending on disease severity. *Clin Sci (Lond)*. 2007;113:243–9.
- Kamide N, Ogino M, Yamashina N, Fukuda M. Sniff nasal inspiratory pressure in healthy Japanese subjects: mean values and lower limits of normal. *Respiration*. 2009;77:58–62.
- Kantarci F, Mihmanli I, Demirel MK, et al. Normal diaphragmatic motion and the effects of body composition: determination with M-mode sonography. *J Ultrasound Med*. 2004;23:255–60.
- Karagiannidis C, Lubnow M, Philipp A, et al. Autoregulation of ventilation with neurally adjusted ventilatory assist on extracorporeal lung support. *Intensive Care Med*. 2010;36:2038–44.
- Kim MJ, Druz WS, Danon J, et al. Effects of lung volume and electrode position on the esophageal diaphragmatic EMG. *J Appl Physiol*. 1978;45:392–8.
- Kim WY, Suh HJ, Hong S-B, et al. Diaphragm dysfunction assessed by ultrasonography: influence on weaning from mechanical ventilation. *Crit Care Med*. 2011;39:2627–30.
- Kiryu S, Loring SH, Mori Y, et al. Quantitative analysis of the velocity and synchronicity of diaphragmatic motion: dynamic MRI in different postures. *Magn Reson Imaging*. 2006;24:1325–32.
- Kolar P, Sulc J, Kyncl M, et al. Stabilizing function of the diaphragm: dynamic MRI and synchronized spirometric assessment. *J Appl Physiol*. 2010;109:1064–71.
- Koo TK, Li MY. A guideline of selecting and reporting intraclass correlation coefficients for reliability research. *J Chiropr Med*. 2016;15:155–63.
- Koulouris N, Mulvey DA, Laroche CM, et al. The effect of posture and abdominal binding on respiratory pressures. *Eur Respir J*. 1989;2:961–5.
- Kranz H, Williams AM, Cassell J, et al. Factors determining the frequency content of the electromyogram. *J Appl Physiol*. 1983;55:392–9.
- Kyroussis D, Mills GH, Polkey MI, et al. Abdominal muscle fatigue after maximal ventilation in humans. *J Appl Physiol*. 1996;81:1477–83.
- Laghi F. Hypoventilation and respiratory muscle dysfunction. In: Parrillo JE, Dellinger RP, editors. *Critical care medicine: principles of diagnosis and management in the adult*. 4th ed. St. Louis: Mosby, Inc; 2014. p. 674–91.
- Laghi F, Shaikh H. Expiratory diaphragmatic recruitment in acute respiratory distress syndrome. A happy coincidence or much more? *Am J Respir Crit Care Med*. 2017;195:1548–50.
- Laghi F, Tobin MJ. Relationship between transdiaphragmatic and mouth twitch pressures at functional residual capacity. *Eur Respir J*. 1997;10:530–6.
- Laghi F, Tobin MJ. Disorders of the respiratory muscles. *Am J Respir Crit Care Med*. 2003;168:10–48.
- Laghi F, D'Alfonso N, Tobin MJ. Pattern of recovery from diaphragmatic fatigue over 24 hours. *J Appl Physiol*. 1995;79:539–46.
- Laghi F, Harrison MJ, Tobin MJ. Comparison of magnetic and electrical phrenic nerve stimulation in assessment of diaphragmatic contractility. *J Appl Physiol*. 1996;80:1731–42.
- Laghi F, Topeli A, Tobin MJ. Does resistive loading decrease diaphragmatic contractility before task failure? *J Appl Physiol*. 1998a;85:1103–12.
- Laghi F, Jubran A, Topeli A, et al. Effect of lung volume reduction surgery on neuromechanical coupling of the diaphragm. *Am J Respir Crit Care Med*. 1998b;157:475–83.
- Laghi F, Cattapan SE, Jubran A, et al. Is weaning failure caused by low-frequency fatigue of the diaphragm? *Am J Respir Crit Care Med*. 2003;167:120–7.
- Laghi F, Jubran A, Topeli A, et al. Effect of lung volume reduction surgery on diaphragmatic neuromechanical coupling at 2 years. *Chest*. 2004;125:2188–95.
- Laghi F, Shaikh HS, Morales D, et al. Diaphragmatic neuromechanical coupling and mechanisms of hypercapnia during inspiratory loading. *Respir Physiol Neurobiol*. 2014a;198:32–41.
- Laghi F, D'Alfonso N, Tobin MJ. A paper on the pace of recovery from diaphragmatic fatigue and its unexpected dividends. *Intensive Care Med*. 2014b;40:1220–6.
- Laghi F, Maddipati V, Schnell T, et al. Determinants of cough effectiveness in patients with respiratory muscle weakness. *Respir Physiol Neurobiol*. 2017;240:17–25.
- Laghi F, Shaikh H, Radovanovic D. Pathophysiology of respiratory failure in neuromuscular diseases. In: Elliott MW, Nava S, Schnhofer B, editors. *Non-invasive ventilation and weaning. Principles and practice*. London: CRC Press. Taylor & Francis Group; 2019. p. 364–74.
- Langer D, Ciavaglia C, Faisal A, et al. Inspiratory muscle training reduces diaphragm activation and dyspnea during exercise in COPD. *J Appl Physiol*. 2018;125:381–92.
- Laporta D, Grassino A. Assessment of transdiaphragmatic pressure in humans. *J Appl Physiol*. 1985;58:1469–76.
- Laroche CM, Mier AK, Moxham J, Green M. The value of sniff esophageal pressures in the assessment of global inspiratory muscle strength. *Am Rev Respir Dis*. 1988;138:598–603.
- Larouche A, Massicotte E, Constantin G, et al. Tonic diaphragmatic activity in critically ill children with and without ventilatory support. *Pediatr Pulmonol*. 2015;50:1304–12.
- Larson JL, Covey MK, Vitalo CA, et al. Maximal inspiratory pressure. Learning effect and test-retest reliability in patients with chronic obstructive pulmonary disease. *Chest*. 1993;104:448–53.

- Laveneziana P, Albuquerque A, Aliverti A, et al. ERS statement on respiratory muscle testing at rest and during exercise. *Eur Respir J*. 2019;53:1801214.
- Leal BE, Gonçalves MA, Lisboa LG, et al. Validity and reliability of fluoroscopy for digital radiography: a new way to evaluate diaphragmatic mobility. *BMC Pulm Med*. 2017;17:62.
- Leith DE, Butler JP, Sneddon SL, Brain JD. Cough. In Macklem PT, Mead J (eds): *Handbook of physiology*. Washington: American Physiological Society 1986; 315–336.
- Lerolle N, Guérot E, Dimassi S, et al. Ultrasonographic diagnostic criterion for severe diaphragmatic dysfunction after cardiac surgery. *Chest*. 2009;135:401–7.
- Levine S, Gillen J, Weiser P, et al. Description and validation of an ECG removal procedure for EMGdi power spectrum analysis. *J Appl Physiol*. 1986;60:1073–81.
- Levine S, Nguyen T, Taylor N, et al. Rapid disuse atrophy of diaphragm fibers in mechanically ventilated humans. *N Engl J Med*. 2008;358:1327–35.
- Li G, Wei J, Huang H, et al. Automatic assessment of average diaphragm motion trajectory from 4DCT images through machine learning. *Biomed Phys Eng Express*. 2015;1:045015.
- Liddell EGT, Sherrington CS. Recruitment and some other factors of reflex inhibition. *Proc R Soc Lond Ser B*. 1925;97:488–517.
- Lindstrom L, Magnusson R, Petersen I. Muscular fatigue and action potential conduction velocity changes studied with frequency analysis of EMG signals. *Electromyography*. 1970;10:341–56.
- Lippold OCJ. The relationship between force-velocity and integrated electrical activity in human muscles. *J Physiol Lond*. 1952;117:492–9.
- Liu L, Liu H, Yang Y, et al. Neuroventilatory efficiency and extubation readiness in critically ill patients. *Crit Care*. 2012;16:R143.
- Lofaso F, Nicot F, Lejaille M, et al. Sniff nasal inspiratory pressure: what is the optimal number of sniffs? *Eur Respir J*. 2006;27:980–2.
- Longhini F, Liu L, Pan C, et al. Neurally-adjusted ventilatory assist for noninvasive ventilation via a helmet in subjects with COPD exacerbation: a physiologic study. *Respir Care*. 2019;64:582–9.
- Lopata M, Evanich MJ, Lourenco RV. Quantification of diaphragmatic EMG response to CO₂ rebreathing in humans. *J Appl Physiol*. 1977;43:262–70.
- Loring SH, Hershenson MB. Effects of series compliance on twitches superimposed on voluntary contractions. *J Appl Physiol*. 1992;73:516–21.
- Lourenco RV, Miranda JM. Drive and performance of the ventilatory apparatus in chronic obstructive lung disease. *N Engl J Med*. 1968;279:53–9.
- Lourenco RV, Cherniack NS, Malm JR, Fishman AP. Nervous output from the respiratory center during obstructed breathing. *J Appl Physiol*. 1966;21:527–33.
- Lozano-Garcia M, Sarlabous L, Moxham J, et al. Surface mechanomyography and electromyography provide non-invasive indices of inspiratory muscle force and activation in healthy subjects. *Sci Rep*. 2018;8:16921.
- Lozano-García M, Estrada L, Jané R. Performance evaluation of fixed sample entropy in Myographic signals for inspiratory muscle activity estimation. *Entropy*. 2019;21:183.
- Luo YM, Moxham J. Measurement of neural respiratory drive in patients with COPD. *Respir Physiol Neurobiol*. 2005;146:165–74.
- Luo YM, Polkey MI, Johnson LC, et al. Diaphragm EMG measured by cervical magnetic and electrical phrenic nerve stimulation. *J Appl Physiol*. 1998;85:2089–99.
- Luo YM, Polkey MI, Lyall RA, Moxham J. Effect of brachial plexus co-activation on phrenic nerve conduction time. *Thorax*. 1999a;54:765–70.
- Luo YM, Johnson LC, Polkey MI, et al. Diaphragm electromyogram measured with unilateral magnetic stimulation. *Eur Respir J*. 1999b;13:385–90.
- Luo YM, Lyall RA, Lou HM, et al. Quantification of the esophageal diaphragm electromyogram with magnetic phrenic nerve stimulation. *Am J Respir Crit Care Med*. 1999c;160:1629–34.
- Luo YM, Hart N, Mustfa N, et al. Effect of diaphragm fatigue on neural respiratory drive. *J Appl Physiol*. 2001;90:1691–9.
- Luo YM, Hart N, Mustfa N, et al. Reproducibility of twitch and sniff transdiaphragmatic pressures. *Respir Physiol Neurobiol*. 2002;132:301–6.
- Luo YM, Moxham J, Polkey MI. Diaphragm electromyography using an oesophageal catheter: current concepts. *Clin Sci (Lond)*. 2008;115:233–44.
- Maarsingh EJ, Van Eykern LA, de Haan RJ, et al. Airflow limitation in asthmatic children assessed with a non-invasive EMG technique. *Respir Physiol Neurobiol*. 2002;133:89–97.
- Maarsingh EJ, Oud M, Van Eykern LA, et al. Electromyographic monitoring of respiratory muscle activity in dyspneic infants and toddlers. *Respir Physiol Neurobiol*. 2006;150:191–9.
- Macklem PT. Inferring the actions of the respiratory muscles. In: Roussos C, editor. *The thorax*. New York: Marcel Dekker; 1985. p. 531–8.
- MacLean IC, Mattioni TA. Phrenic nerve conduction studies: a new technique and its application in quadriplegic patients. *Arch Phys Med Rehabil*. 1981;62:70–3.
- Mador MJ, Acevedo FA. Effect of respiratory muscle fatigue on subsequent exercise performance. *J Appl Physiol*. 1991;70:2059–65.
- Mador MJ, Kufel TJ. Effect of inspiratory muscle fatigue on inspiratory muscle relaxation rates in healthy subjects. *Chest*. 1992;102:1767–73.
- Mador MJ, Magalang UJ, Kufel TJ. Twitch potentiation following voluntary diaphragmatic contraction. *Am J Respir Crit Care Med*. 1994;149:739–43.
- Mador JM, Rodis A, Diaz J. Diaphragmatic fatigue following voluntary hyperpnea. *Am J Respir Crit Care Med*. 1996;154:63–7.
- Maillard JO, Burdet L, van Melle G, Fitting JW. Reproducibility of twitch mouth pressure, sniff

- nasal inspiratory pressure, and maximal inspiratory pressure. *Eur Respir J*. 1998;11:901–5.
- Man WD, Kyroussis D, Fleming TA, et al. Cough gastric pressure and maximum expiratory mouth pressure in humans. *Am J Respir Crit Care Med*. 2003;168:714–7.
- Manning DR, Stull JT. Myosin light chain phosphorylation-dephosphorylation in mammalian skeletal muscle. *Am J Phys*. 1982;242:C234–41.
- Marchioni A, Castaniere I, Tonelli R, et al. Ultrasound-assessed diaphragmatic impairment is a predictor of outcomes in patients with acute exacerbation of chronic obstructive pulmonary disease undergoing noninvasive ventilation. *Crit Care*. 2018;22:109.
- Marini JJ, Capps JS, Culver BH. The inspiratory work of breathing during assisted mechanical ventilation. *Chest*. 1985;87:612–8.
- Marini JJ, Smith TC, Lamb V. Estimation of inspiratory muscle strength in mechanically ventilated patients: the measurement of maximal inspiratory pressure. *J Crit Care*. 1986;1:32–8.
- Martinez FJ, Couser JI, Celli BR. Factors influencing ventilatory muscle recruitment in patients with chronic airflow obstruction. *Am Rev Respir Dis*. 1990;142:276–82.
- McCool FD, Tzelepis GE. Dysfunction of the diaphragm. *N Engl J Med*. 2012;366:932–42.
- McCool FD, McCann DR, Leith DE, Hoppin FG Jr. Pressure-flow effects on endurance of inspiratory muscles. *J Appl Physiol*. 1986;60:299–303.
- McGregor M, Becklake MR. The relationship of oxygen cost of breathing to respiratory mechanical work and respiratory force. *J Clin Invest*. 1961;40:971–80.
- McKenzie DK, Gandevia SC. Electrical assessment of respiratory muscles. In: Roussos C, editor. *The thorax*. New York: Marcel Dekker; 1995. p. 1029–48.
- McKenzie DK, Gandevia SC, Gorman RB, Southon FC. Dynamic changes in the zone of apposition and diaphragm length during maximal respiratory efforts. *Thorax*. 1994;49:634–8.
- Meessen NE, van der Grinten CP, Luijendijk SC, Folgering HT. Continuous negative airway pressure increases tonic activity in diaphragm and intercostal muscles in humans. *J Appl Physiol*. 1994;77:1256–62.
- Merton PA. Voluntary strength and fatigue. *J Physiol*. 1954;123:553–64.
- Mier A, Brophy C, Moxham J, Green M. Twitch pressures in the assessment of diaphragm weakness. *Thorax*. 1989;44:990–6.
- Milic-Emili J. Work of breathing. In: Crystal RG, West JB, editors. *The lung: scientific foundations*. New York: Raven Press; 1991. p. 1065–75.
- Miller JM, Moxham J, Green M. The maximal sniff in the assessment of diaphragm function in man. *Clin Sci (Lond)*. 1985;69:91–6.
- Mills G, Kyroussis D, Hamnegard CH, et al. Evaluation of hemidiaphragmatic contractility by unilateral magnetic phrenic nerve stimulation. *Eur Respir J*. 1994;8:339s.
- Mills GH, Kyroussis D, Hamnegard CH, et al. Bilateral magnetic stimulation of the phrenic nerves from an anterolateral approach. *Am J Respir Crit Care Med*. 1996;154:1099–105.
- Mills GH, Kyroussis D, Hamnegard CH, et al. Cervical magnetic stimulation of the phrenic nerves in bilateral diaphragm paralysis. *Am J Respir Crit Care Med*. 1997;155:1565–9.
- Misuri G, Lanini B, Gigliotti F, et al. Mechanism of CO₂ retention in patients with neuromuscular disease. *Chest*. 2000;117:447–53.
- Monges H, Salducci J, Naudy B. Dissociation between the electrical activity of the diaphragmatic dome and crura muscular fibers during esophageal distension, vomiting and eructation. An electromyographic study in the dog. *J Physiol Paris*. 1978;74:541–54.
- Morales D, Khan U, Shaikh H, et al. Mechanical advantage of the diaphragm during inspiratory threshold loading. *Am J Respir Crit Care Med*. 2012;185:A5304.
- Moreno R, Pertuze J, Giugliano C, et al. Respiratory muscles in pulmonary emphysema. *Rev Med Chil*. 1981;109:393–400.
- Moury P-H, Cuisinier A, Durand M, et al. Diaphragm thickening in cardiac surgery: a perioperative prospective ultrasound study. *Ann Intensive Care*. 2019;9:50.
- Moxham J, Edwards RH, Aubier M, et al. Changes in EMG power spectrum (high-to-low ratio) with force fatigue in humans. *J Appl Physiol*. 1982;53:1094–9.
- Multz AS, Aldrich TK, Prezant DJ, et al. Maximal inspiratory pressure is not a reliable test of inspiratory muscle strength in mechanically ventilated patients. *Am Rev Respir Dis*. 1990;142:529–32.
- Nason LK, Walker CM, McNealey MF, et al. Imaging of the diaphragm: anatomy and function. *Radiographics*. 2012;32:E51–70.
- Nava S, Ambrosino N, Crotti P, et al. Recruitment of some respiratory muscles during three maximal inspiratory manoeuvres. *Thorax*. 1993;48:702–7.
- Navalesi P, Longhini F. Neurally adjusted ventilatory assist. *Curr Opin Crit Care*. 2015;21:58–64.
- Newsom-Davis JG, M., Loh L, Casson M. Diaphragm function and alveolar hypoventilation. *Q J Med*. 1976;177:87–100.
- Ninane V, Rypens F, Yernault JC, De Troyer A. Abdominal muscle use during breathing in patients with chronic airflow obstruction. *Am Rev Respir Dis*. 1992;146:16–21.
- Nowicki A, Dobruch-Sobczak K. Introduction to ultrasound elastography. *J Ultrason*. 2016;16:113–24.
- Nunn JF. *Applied respiratory physiology*. Boston: Butterworths; 1977.
- O'Brien MJ, Van Eykern LA. Respiratory muscle EMG monitoring. *Probl Respir Care*. 1989;2:176–90.
- Onal E, Lopata M, Evanich MJ. Effects of electrode position on esophageal diaphragmatic EMG in humans. *J Appl Physiol*. 1979;47:1234–8.
- Onal E, Lopata M, Ginzburg AS, O'Connor TD. Diaphragmatic EMG and transdiaphragmatic pressure measurements with a single catheter. *Am Rev Respir Dis*. 1981;124:563–5.
- Oppersma E, Hatam N, Doorduyn J, et al. Functional assessment of the diaphragm by speckle tracking

- ultrasound during inspiratory loading. *J Appl Physiol.* 2017;123:1063–70.
- Orde SR, Boon AJ, Firth DG, et al. Diaphragm assessment by two dimensional speckle tracking imaging in normal subjects. *BMC Anesthesiol.* 2015;16:43.
- Paiva M, Verbanck S, Estenne M, et al. Mechanical implications of in vivo human diaphragm shape. *J Appl Physiol.* 1992;72:1407–12.
- Palkar A, Mayo P, Singh K, et al. Serial diaphragm ultrasonography to predict successful discontinuation of mechanical ventilation. *Lung.* 2018a;196:363–8.
- Palkar A, Narasimhan M, Greenberg H, et al. Diaphragm excursion-time index: a new parameter using ultrasonography to predict extubation outcome. *Chest.* 2018b;153:1213–20.
- Parthasarathy S, Jubran A, Tobin MJ. Cycling of inspiratory and expiratory muscle groups with the ventilator in airflow limitation. *Am J Respir Crit Care Med.* 1998;158:1471–8.
- Parthasarathy S, Jubran A, Laghi F, Tobin MJ. Sternomastoid, rib cage, and expiratory muscle activity during weaning failure. *J Appl Physiol.* 2007;103:140–7.
- Passath C, Takala J, Tuchscherer D, et al. Physiologic response to changing positive end-expiratory pressure during neurally adjusted ventilatory assist in sedated, critically ill adults. *Chest.* 2010;138:578–87.
- Patout M, Meira L, D’Cruz R, et al. Neural respiratory drive predicts long-term outcome following admission for exacerbation of COPD: a post hoc analysis. *Thorax.* 2019;74:910–3.
- Patroniti N, Bellani G, Saccavino E, et al. Respiratory pattern during neurally adjusted ventilatory assist in acute respiratory failure patients. *Intensive Care Med.* 2012;38:230–9.
- Pellegrini M, Hedenstierna G, Roneus A, et al. The diaphragm acts as a brake during expiration to prevent lung collapse. *Am J Respir Crit Care Med.* 2017;195:1608–16.
- Petit JM, Milic-Emili J, Delhez L. New technic for the study of functions of the diaphragmatic muscle by means of electromyography in man. *Boll Soc Ital Biol Sper.* 1959;35:2013–4.
- Petit JM, Milic-Emili J, Delhez I. Role of the diaphragm in breathing in conscious normal man: an electromyographic study. *J Appl Physiol.* 1960;15:1101–6.
- Petitjean M, Bellemare F. Phonomyogram of the diaphragm during unilateral and bilateral phrenic nerve stimulation and changes with fatigue. *Muscle Nerve.* 1994;17:1201–9.
- Petitjean M, Ripart TJ, Couture J, Bellemare F. Effects of lung volume and fatigue on evoked diaphragmatic phonomyogram in normal subjects. *Thorax.* 1996;51:705–10.
- Petitjean M, Ripart J, Couture J, Bellemare F. Diaphragmatic fatigue investigated by phonomyography. *Am J Respir Crit Care Med.* 1997;155:1162–6.
- Pirompanich P, Romsaiyut S. Use of diaphragm thickening fraction combined with rapid shallow breathing index for predicting success of weaning from mechanical ventilator in medical patients. *J Intensive Care.* 2018;6:6.
- Polkey MI, Green M, Moxham J. Measurement of respiratory muscle strength. *Thorax.* 1995;50:1131–5.
- Polkey MI, Kyroussis D, Hamnegard CH, et al. Diaphragm strength in chronic obstructive pulmonary disease. *Am J Respir Crit Care Med.* 1996;154:1310–7.
- Pollard MJ, Megirian D, Sherrey JH. Unity of costal and crural diaphragmatic activity in respiration. *ExpNeurol.* 1985;90:187–93.
- Qin YY, Li RF, Wu GF, et al. Effect of tiotropium on neural respiratory drive during exercise in severe COPD. *Pulm Pharmacol Ther.* 2015;30:51–6.
- Rahn H, Otis AB, Chadwick LE, Fenn WO. The pressure-volume diagram of the thorax and lung. *Am J Phys.* 1946;146:161–78.
- Rajanna MJ. Anatomical and surgical considerations of the phrenic and accessory phrenic nerves. *J Int Call Surg.* 1947;10:42–52.
- Ramsook AH, Molgat-Seon Y, Schaeffer MR, et al. Effects of inspiratory muscle training on respiratory muscle electromyography and dyspnea during exercise in healthy men. *J Appl Physiol.* 2017;122:1267–75.
- Rieder P, Louis M, Jolliet P, Chevrolet JC. The repeated measurement of vital capacity is a poor predictor of the need for mechanical ventilation in myasthenia gravis. *Intensive Care Med.* 1995;21:663–8.
- Rimmer KP, Golar SD, Lee MA, Whitelaw WA. Myotonia of the respiratory muscles in myotonic dystrophy. *Am Rev Respir Dis.* 1993;148:1018–22.
- Ringqvist T. The ventilatory capacity in healthy subjects. An analysis of causal factors with special reference to the respiratory forces. *Scand J Clin Lab Invest Suppl.* 1966;88:5–179.
- Road JD, West NH, Van Vliet BN. Ventilatory effects of stimulation of phrenic afferents. *J Appl Physiol.* 1987;63:1063–9.
- Robertson CH, Foster GH, Johnson RL. The relationship of respiratory failure to the oxygen consumption of, lactate production by, and distribution of blood flow among respiratory muscles during increasing inspiratory resistance. *J Clin Invest.* 1977;59:31–42.
- Rochester DF. Tests of respiratory muscle function. *Clin Chest Med.* 1988;9:249–61.
- Rochester DF, Bettini G. Diaphragmatic blood flow and energy expenditure in the dog. Effects of inspiratory airflow resistance and hypercapnia. *J Clin Invest.* 1976;57:661–72.
- Rodrigues A, Da Silva ML, Berton DC, et al. Maximal inspiratory pressure: does the choice of reference values actually matter? *Chest.* 2017;152:32–9.
- Rohrer F. Physiologie der Atembewegung. In: Bethe A, von Bergmann G, Embden G, Ellinger A, editors. *Handbuch der normalen und pathologischen Physiologie.* Berlin: Springer; 1925. p. 70–127.
- Roussos CCE. *Handbook of physiology.* Bethesda: American Physiological Society; 1986.
- Roze H, Repusseau B, Perrier V, et al. Neuro-ventilatory efficiency during weaning from mechanical ventila-

- tion using neurally adjusted ventilatory assist. *Br J Anaesth.* 2013;111:955–60.
- San'Ambrogio G, Frazier DT, Wilson MF, Agostoni E. Motor innervation and pattern of activity of cat diaphragm. *J Appl Physiol.* 1963;18:43–6.
- Sarlabous L, Torres A, Fiz JA, Jane R. Evidence towards improved estimation of respiratory muscle effort from diaphragm mechanomyographic signals with cardiac vibration interference using sample entropy with fixed tolerance values. *PLoS One.* 2014;9:e88902.
- Sarlabous L, Torres A, Fiz JA, et al. Efficiency of mechanical activation of inspiratory muscles in COPD using sample entropy. *Eur Respir J.* 2015;46:1808–11.
- Sarlabous L, Torres A, Fiz JA, et al. Inspiratory muscle activation increases with COPD severity as confirmed by non-invasive mechanomyographic analysis. *PLoS One.* 2017;12:e0177730.
- Sarnoff SJ, Sarnoff LC, Wittenberger JL. Electrophrenic respiration. VII. The motor point of the phrenic nerve in relation to external stimulation. *Surg Gynecol Obstet.* 1951;93:190–6.
- Sarwal A, Walker FO, Cartwright MS. Neuromuscular ultrasound for evaluation of the diaphragm. *Muscle Nerve.* 2013;47:319–29.
- Sassoon CS, Mahutte CK, Te TT, et al. Work of breathing and airway occlusion pressure during assist-mode mechanical ventilation. *Chest.* 1988;93:571–6.
- Scardella AT, Parisi RA, Phair DK, et al. The role of endogenous opioids in the ventilatory response to acute flow-resistive loads. *Am Rev Respir Dis.* 1986;133:26–31.
- Scarlata S, Mancini D, Laudisio A, et al. Reproducibility and clinical correlates of supine diaphragmatic motion measured by M-mode ultrasonography in healthy volunteers. *Respiration.* 2018;96:259–66.
- Scarlata S, Mancini D, Laudisio A, Raffaele AI. Reproducibility of diaphragmatic thickness measured by M-mode ultrasonography in healthy volunteers. *Respir Physiol Neurobiol.* 2019;260:58–62.
- Schepens T, Verbrugge W, Dams K, et al. The course of diaphragm atrophy in ventilated patients assessed with ultrasound: a longitudinal cohort study. *Crit Care.* 2015;19:422.
- Schweitzer TW, Fitzgerald JW, Bowden JA, Lynne-Davies P. Spectral analysis of human inspiratory diaphragmatic electromyograms. *J Appl Physiol.* 1979;46:152–65.
- Scott S, Fuld JP, Carter R, et al. Diaphragm ultrasonography as an alternative to whole-body plethysmography in pulmonary function testing. *J Ultrasound Med.* 2006;25:225–32.
- Shaikh H, Laghi F. Role of diaphragm ultrasound when NIV fails in COPD exacerbations. *Respir Care.* 2019; [in press].
- Sharp JT, Hyatt RE. Mechanical and electrical properties of respiratory muscles. In *handbook of Physiology.* Bethesda: American Physiological Society; 1986. p. 389–414.
- Sharp JT, Hammond MD, Aranda AU, Rocha RD. Comparison of diaphragm EMG centroid frequencies: esophageal versus chest surface leads. *Am Rev Respir Dis.* 1993;147:764–7.
- Sharshar T, Hopkinson NS, Ross ET, et al. Motor control of the costal and crural diaphragm—insights from transcranial magnetic stimulation in man. *Respir Physiol Neurobiol.* 2005;146:5–19.
- Shield A, Zhou S. Assessing voluntary muscle activation with the twitch interpolation technique. *Sports Med.* 2004;34:253–67.
- Sieck GC, Fournier M. Changes in diaphragm motor unit EMG during fatigue. *J Appl Physiol.* 1990;68:1917–26.
- Similowski T, Fleury B, Launois S, et al. Cervical magnetic stimulation: a new painless method for bilateral phrenic nerve stimulation in conscious humans. *J Appl Physiol.* 1989;67:1311–8.
- Similowski T, Yan S, Gauthier AP, et al. Contractile properties of the human diaphragm during chronic hyperinflation. *N Engl J Med.* 1991;325:917–23.
- Similowski T, Gauthier AP, Yan S, et al. Assessment of diaphragm function using mouth pressure twitches in chronic obstructive pulmonary disease patients. *Am Rev Respir Dis.* 1993;147:850–6.
- Similowski T, Duguet A, Straus C, et al. Assessment of the voluntary activation of the diaphragm using cervical and cortical magnetic stimulation. *Eur Respir J.* 1996;9:1224–31.
- Simmons DH. Assessing the work of breathing. *Chest.* 1989;95:482–3.
- Sinderby C, Beck J. Neurally adjusted ventilatory assist. In: Tobin MJ, editor. *Principles and practice of mechanical ventilation.* New York: Mc Graw Hill; 2013. p. 351–75.
- Sinderby C, Lindstrom L, Grassino AE. Automatic assessment of electromyogram quality. *J Appl Physiol.* 1995;79:1803–15.
- Sinderby C, Weinberg J, Sullivan L, et al. Electromyographical evidence for exercise-induced diaphragm fatigue in patients with chronic cervical cord injury or prior poliomyelitis infection. *Spinal Cord.* 1996a;34:594–601.
- Sinderby C, Friberg S, Comtois N, Grassino A. Chest wall muscle cross talk in canine costal diaphragm electromyogram. *J Appl Physiol.* 1996b;81:2312–27.
- Sinderby CA, Beck JC, Lindstrom LH, Grassino AE. Enhancement of signal quality in esophageal recordings of diaphragm EMG. *J Appl Physiol.* 1997;82:1370–7.
- Sinderby C, Beck J, Spahija J, et al. Voluntary activation of the human diaphragm in health and disease. *J Appl Physiol.* 1998;85:2146–58.
- Sinderby C, Navalesi P, Beck J, et al. Neural control of mechanical ventilation in respiratory failure. *Nat Med.* 1999;5:1433–6.
- Sinderby C, Beck J, Spahija J, et al. Inspiratory muscle unloading by neurally adjusted ventilatory assist during maximal inspiratory efforts in healthy subjects. *Chest.* 2007;131:711–7.

- Sliwinski P, Yan S, Gauthier AP, Macklem PT. Influence of global inspiratory muscle fatigue on breathing during exercise. *J Appl Physiol.* 1996;80:1270–8.
- Smith PE, Calverley PM, Edwards RH, et al. Practical problems in the respiratory care of patients with muscular dystrophy. *N Engl J Med.* 1987;316:1197–205.
- Spahija J, de Marchie M, Albert M, et al. Patient-ventilator interaction during pressure support ventilation and neurally adjusted ventilatory assist. *Crit Care Med.* 2010;38:518–26.
- Steier J, Kaul S, Seymour J, et al. The value of multiple tests of respiratory muscle strength. *Thorax.* 2007;62:975–80.
- Suarez AA, Pessolano FA, Monteiro SG, et al. Peak flow and peak cough flow in the evaluation of expiratory muscle weakness and bulbar impairment in patients with neuromuscular disease. *Am J Phys Med Rehabil.* 2002;81:506–11.
- Suh ES, Mandal S, Harding R, et al. Neural respiratory drive predicts clinical deterioration and safe discharge in exacerbations of COPD. *Thorax.* 2015;70:1123–30.
- Supinski GS, Callahan LA. Diaphragm weakness in mechanically ventilated critically ill patients. *Crit Care.* 2013;17:R120.
- Supinski GS, Morris PE, Dhar S, Callahan LA. Diaphragm dysfunction in critical illness. *Chest.* 2018;153:1040–51.
- Takazakura R, Takahashi M, Nitta N, Murata K. Diaphragmatic motion in the sitting and supine positions: healthy subject study using a vertically open magnetic resonance system. *J Magn Reson Imaging.* 2004;19:605–9.
- Tanaka R. Dynamic chest radiography: flat-panel detector (FPD) based functional X-ray imaging. *Radiol Phys Technol.* 2016;9:139–53.
- Terzi N, Pelieu I, Guittet L, et al. Neurally adjusted ventilatory assist in patients recovering spontaneous breathing after acute respiratory distress syndrome: physiological evaluation. *Crit Care Med.* 2010;38:1830–7.
- Tobin MJ. *Respiratory monitoring.* New York: Churchill Livingstone; 1991.
- Tobin MJ. Put down your smartphone and pick up a book. *BMJ.* 2014;349:g4521.
- Tobin MJ. Why physiology is critical to the practice of medicine: a 40-year personal perspective. *Clin Chest Med.* 2019;40:243–57.
- Tobin MJ, Laghi F. Monitoring respiratory muscle function. In: Tobin MJ, editor. *Principles and practice of intensive care monitoring.* New York: McGraw-Hill Co; 1998. p. 497–544.
- Tobin MJ, Van de Graff WB. Monitoring of lung mechanics and work of breathing. In: Tobin MJ, editor. *Principles and practice of mechanical ventilation.* 1st ed. New York: McGraw-Hill; 1994. p. 967–1003.
- Tobin MJ, Walsh JM, Laghi F. Monitoring of respiratory neuromuscular function. In: Tobin MJ, editor. *Principles and practice of mechanical ventilation.* New York: McGraw-Hill Co; 1994. p. 945–66.
- Tobin MJ, Laghi F, Jubran A. Ventilatory failure, ventilator support, and ventilator weaning. *Compr Physiol.* 2012;2:2871–921.
- Topeli A, Laghi F, Tobin MJ. Can diaphragmatic contractility be assessed by twitch airway pressures in patients with chronic obstructive pulmonary disease? *Am J Respir Crit Care Med.* 1999;160:1369–74.
- Topeli A, Laghi F, Tobin MJ. The voluntary drive to breathe is not decreased in hypercapnic patients with severe COPD. *Eur Respir J.* 2001;18:53–60.
- Tzani P, Chiesa S, Aiello M, et al. The value of cough peak flow in the assessment of cough efficacy in neuromuscular patients. A cross sectional study. *Eur J Phys Rehabil Med.* 2014;50:427–32.
- Ueki J, de Bruin PF, Pride NB. In vivo assessment of diaphragm contraction by ultrasound in normal subjects. *Thorax.* 1995;50:1157–61.
- Uldry C, Fitting JW. Maximal values of sniff nasal inspiratory pressure in healthy subjects. *Thorax.* 1995;50:371–5.
- Uldry C, Janssens JP, de Muralt B, Fitting JW. Sniff nasal inspiratory pressure in patients with chronic obstructive pulmonary disease. *Eur Respir J.* 1997;10:1292–6.
- Umbrello M, Formenti P, Longhi D, et al. Diaphragm ultrasound as indicator of respiratory effort in critically ill patients undergoing assisted mechanical ventilation: a pilot clinical study. *Crit Care.* 2015;19:161.
- Ünal Ö, Arslan H, Uzun K, et al. Evaluation of diaphragmatic movement with MR fluoroscopy in chronic obstructive pulmonary disease. *Clin Imaging.* 2000;24:347–50.
- Van de Graaff WB, Gordey K, Dornseif SE, et al. Pressure support: changes in ventilatory pattern and components of the work of breathing. *Chest.* 1991;100:1082–9.
- Van LE, Haxhiu MA, Cherniack NS, Goldman MD. Differential costal and crural diaphragm compensation for posture changes. *J Appl Physiol* (1985). 1985;58:1895–900.
- Vandenboom R, Gittings W, Smith IC, et al. Myosin phosphorylation and force potentiation in skeletal muscle: evidence from animal models. *J Muscle Res Cell Motil.* 2013;34:317–32.
- Vaporidi K, Babalis D, Chytas A, et al. Clusters of ineffective efforts during mechanical ventilation: impact on outcome. *Intensive Care Med.* 2017;43:184–91.
- Vassilakopoulos T. Ventilator induced diaphragmatic dysfunction. In: Tobin MJ, editor. *Principles and practice of mechanical ventilation.* New York: McGraw Hill; 2013. p. 1025–40.
- Verburg E, Murphy RM, Richard I, Lamb GD. Involvement of calpains in Ca²⁺-induced disruption of excitation-contraction coupling in mammalian skeletal muscle fibers. *Am J Physiol Cell Physiol.* 2009;296:C1115–22.
- Verges S, Schulz C, Perret C, Spengler CM. Impaired abdominal muscle contractility after high-intensity exhaustive exercise assessed by magnetic stimulation. *Muscle Nerve.* 2006;34:423–30.

- Verges S, Bachasson D, Wuyam B. Effect of acute hypoxia on respiratory muscle fatigue in healthy humans. *Respir Res.* 2010;11:109.
- Verin E, Marie JP, Tardif C, Denis P. Spontaneous recovery of diaphragmatic strength in unilateral diaphragmatic paralysis. *Respir Med.* 2006;100:1944–51.
- Viies N, Sillye G, Aubier M, et al. Regional blood flow distribution in dog during induced hypotension and low cardiac output. Spontaneous breathing versus artificial ventilation. *J Clin Invest.* 1983;72:935–47.
- Vivier E, Dessap AM, Dimassi S, et al. Diaphragm ultrasonography to estimate the work of breathing during non-invasive ventilation. *Intensive Care Med.* 2012;38:796–803.
- Vivier E, Roussey A, Doroszewski F, et al. Atrophy of diaphragm and pectoral muscles in critically ill patients. *Anesthesiology.* 2019;131:569–79.
- Wait JL, Nahormek PA, Yost WT, Rochester DP. Diaphragmatic thickness-lung volume relationship in vivo. *J Appl Physiol.* 1989;67:1560–8.
- Wan HY, Stickford JL, Kitano K, et al. Acute hypercapnia does not alter voluntary drive to the diaphragm in healthy humans. *Respir Physiol Neurobiol.* 2018;258:60–8.
- Ward ME, Corbeil C, Gibbons W, et al. Optimization of respiratory muscle relaxation during mechanical ventilation. *Anesthesiology.* 1988;69:29–35.
- Watson AC, Hughes PD, Louise HM, et al. Measurement of twitch transdiaphragmatic, esophageal, and endotracheal tube pressure with bilateral anterolateral magnetic phrenic nerve stimulation in patients in the intensive care unit. *Crit Care Med.* 2001;29:1325–31.
- White JE, Drinnan MJ, Smithson AJ, et al. Respiratory muscle activity and oxygenation during sleep in patients with muscle weakness. *Eur Respir J.* 1995;8:807–14.
- Wilcox PG, Eisen A, Wiggs BJ, Pardy RL. Diaphragmatic relaxation rate after voluntary contractions and unilateral and bilateral phrenic stimulation. *J Appl Physiol.* 1988;65:675–82.
- Wragg S, Aquilina R, Moran J, et al. Comparison of cervical magnetic stimulation and bilateral percutaneous electrical stimulation of the phrenic nerves in normal subjects. *Eur Respir J.* 1994a;7:1788–92.
- Wragg S, Hamnegard C, Road J, et al. Potentiation of diaphragmatic twitch after voluntary contraction in normal subjects. *Thorax.* 1994b;49:1234–7.
- Wuthrich TU, Marty J, Benaglia P, et al. Acute effects of a respiratory sprint-interval session on muscle contractility. *Med Sci Sports Exerc.* 2015;47:1979–87.
- Yan S, Similowski T, Gauthier AP, et al. Effect of fatigue on diaphragmatic function at different lung volumes. *J Appl Physiol.* 1992a;72:1064–7.
- Yan S, Gauthier AP, Similowski T, et al. Evaluation of human diaphragm contractility using mouth pressure twitches. *Am Rev Respir Dis.* 1992b;145:1064–9.
- Yan S, Gauthier AP, Similowski T, et al. Force-frequency relationships of in vivo human and in vitro rat diaphragm using paired stimuli. *Eur Respir J.* 1993a;6:211–8.
- Yan S, Lichros I, Zakyntinos S, Macklem PT. Effect of diaphragmatic fatigue on control of respiratory muscles and ventilation during CO₂ rebreathing. *J Appl Physiol.* 1993b;75:1364–70.
- Yan S, Sliwinski P, Gauthier AP, et al. Effect of global inspiratory muscle fatigue on ventilatory and respiratory muscle responses to CO₂. *J Appl Physiol.* 1993c;75:1371–7.
- Yang KL, Tobin MJ. A prospective study of indexes predicting the outcome of trials of weaning from mechanical ventilation. *N Engl J Med.* 1991;324:1445–50.
- Zambon M, Beccaria P, Matsuno J, et al. Mechanical ventilation and diaphragmatic atrophy in critically ill patients: an ultrasound study. *Crit Care Med.* 2016;44:1347–52.



Basics of Electrical Impedance Tomography and Its Application

37

Christian Putensen, Benjamin Hentze,
and Thomas Muders

Abbreviations

AC	Alternating electric current	SPECT	Single-photon emission computed tomography
CoV	Center of ventilation	TIV	Tidal impedance variation
CRS	Cardiac-related signal	UIP	Upper inflection point
C_{RS}	Respiratory system compliance	VRS	Ventilation-related signal
CT	Computer tomography	V_T	Tidal volume
EBCT	Electron-beam computed tomography	Z	Impedance
EELI	End-expiratory lung impedance	Ω	Ohm
EELV	End-expiratory lung volume		
EIT	Electrical impedance tomography		
fEIT	Functional EIT		
FEM	Finite element method		
GI	Index global inhomogeneity index		
GREIT	Graz consensus reconstruction algorithm for EIT		
IBS	Indicator-based signal		
ICS	Intercostal spaces		
ITV	Intratidal gas distribution		
LIP	Lower inflection point		
MRI	Magnetic resonance tomography		
ODCL	Alveolar overdistension and collapse		
PEEP	Positive end-expiratory pressure		
ROI	Region of interest		
RVD	Regional ventilation delay		
RVDI	Regional ventilation delay index		

Introduction

Electrical impedance tomography (EIT) is a non-invasive and radiation-free functional imaging modality that can be used to monitor regional lung ventilation and perfusion at the bedside. Recently, the commercial availability of EIT devices has introduced this technique for clinical application. Thoracic EIT has been used safely in adult and pediatric patients including neonates (Leonhardt and Lachmann 2012; Frerichs et al. 2017).

Basics of Bioimpedance

Bioimpedance is the voltage response of a living tissue to an externally applied alternating electric current (AC). Thoracic EIT is designed to measure intrathoracic bioimpedance. Electrical impedance, or simply “impedance,” is a mea-

C. Putensen (✉) · B. Hentze · T. Muders
Department of Anesthesiology and Intensive Care
Medicine, University Hospital Bonn, Bonn, Germany
e-mail: Christian.Putensen@ukbonn.de;
hentze@hia.rwth-aachen.de;
Thomas.Muders@ukbonn.de

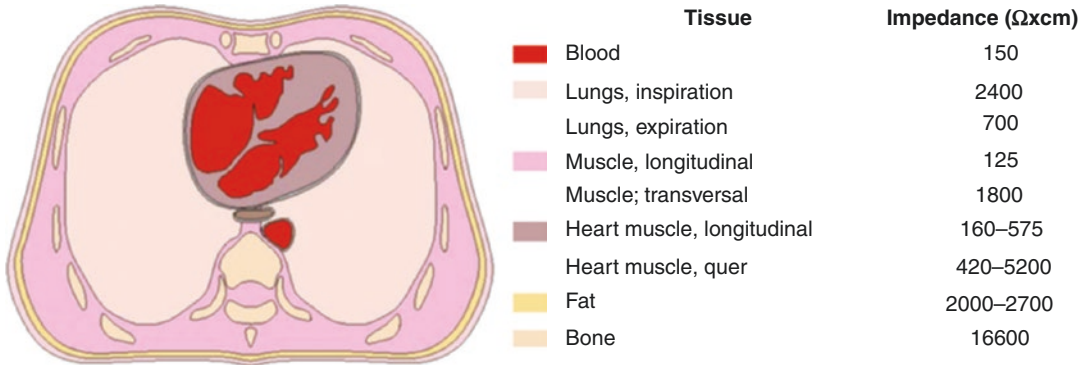


Fig. 37.1 Bioimpedance of different tissues

sure of the opposition to the flow of a sinusoidal AC through materials or tissues, the inverse of electrical conductivity. Dimensionally, impedance (Z) is the same as resistance; the SI unit is the Ohm (Ω). From an electrical point of view, impedance is a more general term for resistance that also includes reactance. Pure resistance does not change with frequency, and is considered with direct current but not AC. Reactance is a measure of the type of opposition to AC due to capacitance or inductance.

Whereas capacitance depends on the biomembranes' characteristics of the tissue such as ion channels, fatty acids, and gap junctions, resistance is mainly determined by the composition and amount of the extracellular fluid (Leonhardt and Lachmann 2012; Frerichs et al. 2017). At frequencies below 5 kHz, electrical current flows only through extracellular fluid and is primarily dependent on the resistive characteristics of the tissues. At higher frequencies up to 50 kHz electrical currents, there is slight deflection at cell membranes, and capacitive tissue properties increase. A decrease in the capacitive component is observed at frequencies above 100 kHz and the electrical current can pass through cell membranes (Leonhardt and Lachmann 2012; Frerichs et al. 2017). Thus, impedance is sensitive to changes in the electrical conductivity of tissues at the stimulation frequency. Conductivity is a bulk property of tissues and is measured in Siemens per meter and ranges from 0.042 (inflated lung), 0.11 (deflated lung), 0.48 (heart) to 0.60 (blood) (Leonhardt and Lachmann 2012;

Frerichs et al. 2017). Resistivity (in $\Omega\text{-m}$) is the inverse of conductivity (Fig. 37.1). In general, tissue conductivity depends on fluid content and ion concentration, whereas in the case of the lung, it also strongly depends on the amount of air in the alveoli.

EIT Measurements and Image Reconstruction

EIT measurements require the placement of electrodes around the thorax in a transverse plane. Electrode placement in the fifth to sixth intercostal spaces (ICS) at the parasternal line is usually used and allows measurement of impedance changes in the lower lobes of the right and left lungs as well as in the heart region (Leonhardt and Lachmann 2012; Frerichs et al. 2017). Placement of the electrodes below the sixth ICS is not recommended because the diaphragm and abdominal content periodically enter the measurement plane. An electrode plane in the third to fourth ICS has been used to reduce heart-induced impedance changes. EIT measurements using two and three transverse planes for 3D imaging have been investigated. However, 3D EIT imaging is not available for routine clinical use in commercial devices yet.

Electrodes are either single self-adhesive electrodes (e.g., ECG electrodes) that are placed individually with equal spacing or integrated with electrode belts or self-adhesive stripes for a user-friendly application (Leonhardt and Lachmann 2012; Frerichs et al. 2017). Chest wounds, chest

tubes, nonconductive bandages or conductive wire sutures may preclude or significantly affect EIT measurements.

Commercially available EIT devices usually use 16 electrodes, although EIT systems with 8 or 32 electrodes are available (Leonhardt and Lachmann 2012; Frerichs et al. 2017) (Table 37.1). Potential advantages of a higher number of electrodes are an improved spatial resolution and redundancy of data. Thus, the reconstruction algorithm can reject weak signals from poorly adherent electrodes.

During an EIT measurement, small AC are applied through pairs of electrodes, and result-

ing voltages are measured using the remaining electrodes (Bodenstein et al. 2009). The bioelectrical impedance between injecting and measuring electrode pairs is calculated from the known applied current and the measured voltages. Most commonly, an adjacent electrode pair is used for AC application, while the resulting voltages are measured using the remaining electrodes. Thus, to obtain a full EIT data set of bioelectrical measurements, the injecting and measuring electrode pairs are successively rotated around the entire thorax (Fig. 37.2). Other patterns of AC supply and potential measurements such as an adjustable or three-electrode skip have been

Table 37.1 Commercially available EIT devices

Manufacturer	EIT System	Electrode		Measurement and data acquisition	Image reconstruction algorithm
		number	Configuration		
CareFusion	Goe-MF II	16	Individual electrodes	Pair drive (adjacent) Serial measurement	Sheffield back-projection
Dräger Medical	PulmoVista 500	16	Electrode belt	Pair drive (adjacent) Serial measurement	Finite element method-based Newton-Raphson method
Maltron Inc	Mark 1 Mark 3.5	16	Individual electrodes	Pair drive (adjacent) Serial measurement	Sheffield back-projection
		8	Individual electrodes		
Swisstom AG	BB ²	32	Electrode belt	Pair drive (adjustable skip) Serial measurement	Graz consensus reconstruction algorithm for EIT (GREIT)
Timpel SA	Enlight	32	Electrode stripes	Pair drive (3-electrode skip) Parallel measurement	Finite element method-based Newton-Raphson method

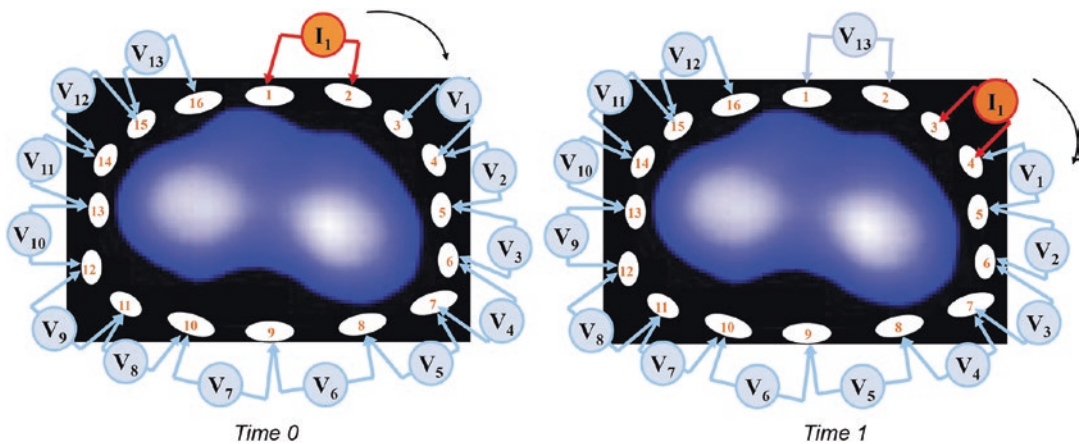


Fig. 37.2 Current application and voltage measurements around the thorax using an EIT system with 16 electrodes. Within a few milliseconds, both the current electrodes and

the active voltage electrodes are repeatedly rotated around the thorax

described and may offer technical advantages (Adler et al. 2011).

Although, AC used during EIT (e.g., 5 mA at a frequency of 50 kHz) are not noticeable and safe for body surface application, the use of EIT in patients with electrically active implants such as cardiac pacemakers or cardioverter-defibrillators is not recommended.

The EIT data set recorded during one cycle of AC applications and voltage measurements is called a frame. An EIT frame contains the voltage measurements and is used to generate the raw EIT image. The scan rate (or frame rate) gives the number of EIT frames or raw EIT images recorded per second. Scan rates of at least 10 images/s are recommended to monitor ventilation and 25 images/s to monitor cardiac function or perfusion. Currently, available EIT devices use maximum scan rates between 40 and 50 images/s (Frerichs et al. 2017).

Generating an image from the measured impedance is called “image reconstruction.” EIT images comparable to a two-dimensional computer tomography (CT) image are conventionally rendered so that the view is from caudal to cranial. Hence, the right chest side is on the left side of the image and vice versa, while anterior in the image is the patient’s anterior and vice versa. However, EIT does not display a “slice” such as CT images

but an “EIT sensitivity region” (Rabbani and Kabir 1991). The “EIT sensitivity region” is a lens-shaped intrathoracic volume whose impedance changes contribute to the EIT image generation (Rabbani and Kabir 1991; Teschner et al. 2015). Thickness and shape of the EIT sensitivity region depend on the dimensions, the bioelectric properties, and the shape of the thorax as well as the morphological structures inside the thorax. Depending on the electrode size, the thickness of the EIT sensitivity region near the skin is about 30–40 mm and increases towards the center of the body (Teschner et al. 2015).

Typically, time-difference imaging is used for EIT reconstruction which displays changes in conductivity rather than the absolute conductivity levels. A time-difference EIT image compares the change in impedance referenced to a baseline frame and allows tracing of time-varying physiological phenomena such as lung ventilation and perfusion (Frerichs et al. 2017). Currently, frequency-difference imaging is under investigation and might enable the reconstruction of absolute EIT images of bioelectric tissue properties (Menden et al. 2019). However, it is not yet robust enough to be applied in routine clinical thoracic EIT yet. Color coding of EIT images is not unified and displays the change in impedance to a reference level (Fig. 37.3). A common color coding

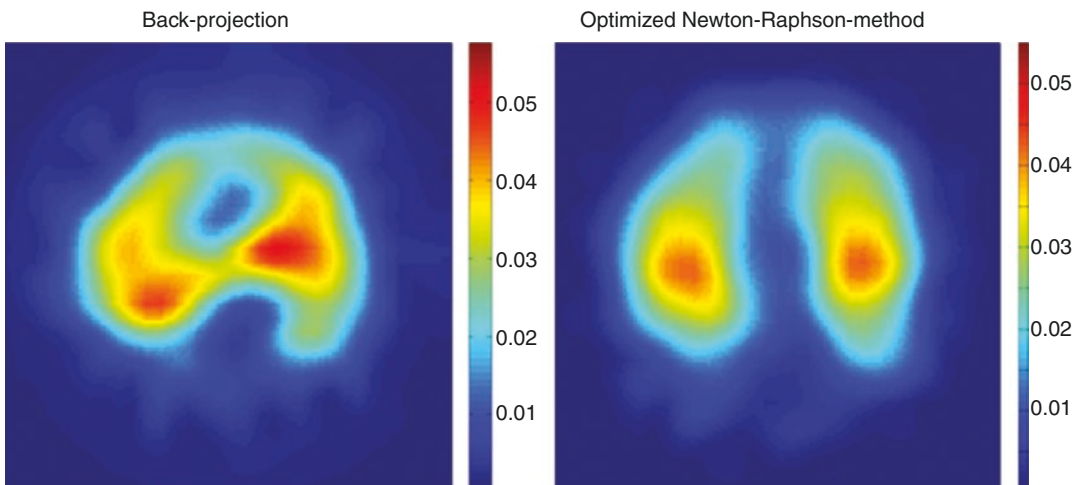


Fig. 37.3 An EIT image either reconstructed with the Sheffield backprojection or with the finite element method based linearized Newton-Raphson algorithm

of EIT images is to use a rainbow-color scheme with red indicating the highest relative impedance (e.g., during inspiration), green a medium relative impedance, and blue the lowest relative impedance (e.g., during expiration). Newer color scales use instead black (no impedance change), blue (intermediate impedance change), and white (strong impedance change) for ventilation or black, red, and white for perfusion.

Reconstruction algorithms aim to solve the so-called “inverse problem” of EIT, which is recovering the conductivity distribution inside the thorax based on the voltage measurements obtained at the electrodes on the thorax boundary. Initially, EIT reconstruction assumed that electrodes were placed on a circular or ellipsoid plane, whereas newer algorithms can use information about the anatomical shape of the thorax. Currently, the Sheffield backprojection algorithm (Barber and Brown 1986), the finite element method (FEM)-based linearized Newton-Raphson algorithm (Yorkey et al. 1987), and the Graz consensus reconstruction algorithm for EIT (GREIT) (Adler et al. 2009) are most commonly used. The Sheffield backprojection has been widely applied but assumes a circular electrode plain and thorax; it tends to display streak-like artifacts that point towards the boundary and requires a fixed sequence of AC injections and voltage measurements (Barber and Brown 1986). The linearized Newton-Raphson algorithm uses an FEM mesh of triangular elements to model the thorax shape often simplified as an ellipsoid. The FEM is employed to solve the forward problem, whereas the regularized Newton-Raphson iterative method is used for the inverse problem (Yorkey et al. 1987). GREIT tries to improve image reconstruction by optimizing the algorithm towards specific quality criteria (called “figures of merit”) such as uniform amplitude response, small and uniform position error, high and uniform resolution, small ringing artifacts, low noise amplification, low shape deformation, high resolution, and small sensitivity to electrode and boundary movement (Adler et al. 2009). However, optimization of the algorithm is a trade-off, and it is not possible to achieve optimum performance with respect to all of the aforementioned criteria.

Functional Imaging and EIT Waveform Analysis

Analysis of EIT data is based on EIT waveforms that are formed in individual image pixels in a series of raw EIT images over time. A region of interest (ROI) can be defined in an image and has a minimum size of one pixel. In each ROI, the waveform displays periodic changes in regional impedance over time resulting from ventilation (*ventilation-related signal*, VRS) or cardiac action (*cardiac-related signal*, CRS). The CRS is present in both the cardiac and lung regions and can be partly attributed to lung perfusion. However, its exact origin and composition is not yet completely understood (Adler et al. 2017). Furthermore, electrically conductive contrast agents (such as hypertonic saline) can be used to obtain an EIT waveform (*indicator-based signal*, IBS) which can be clearly linked to lung perfusion. Frequency spectrum analysis is often used to discriminate between ventilation- and cardiac-related impedance changes. Nonperiodic changes in impedance may result, e.g., from changes in gas volume due to increasing or decreasing positive end-expiratory pressure (PEEP) during mechanical ventilation.

Functional EIT (fEIT) images are generated by applying a mathematical operation on a sequence of raw images and the corresponding pixel EIT waveforms (Hahn et al. 1995). Because the mathematical operation is applied to calculate a physiologically relevant parameter for each pixel, regional physiological characteristics such as respiratory system compliance can be measured and displayed. Using pixel EIT waveforms and simultaneously registered airway pressure allows the use of changes of pressure and impedance (volume) to calculate, e.g., compliance as well as lung opening and closing for each pixel. Comparable EIT measurements during stepwise inflation and deflation of the lungs allow the display of pressure-volume curves on a pixel level. Thus, depending on the mathematical operation, different types of fEIT images, addressing different functional characteristics of the respiratory and cardio-circulatory system, can be generated from a single EIT examination.

Ventilation Monitoring Using EIT

Validation of EIT Measurements

Global Ventilation

Global ventilation has been shown to correlate well with ΔZ_{global} resulting from sequential EIT measurements in animals and humans with normal or injured lungs by using a super-syringe technique (Adler et al. 1997), plethysmography (Marquis et al. 2006), or spirometry (Hinze et al. 2003a). Tidal impedance variation (TIV) represents ΔZ generated during a tidal breath and is calculated as the difference of the maximum and minimum impedance at end-inspiration and end-expiration. Global TIV can be scaled and converted to volume (ml) with sufficient accuracy using spirometric measurements of tidal volume (V_T).

Global Changes in End-Expiratory Lung Volume (EELV) and Impedance (EELI)

Changes in EELV (ΔEELV) and EELI (ΔEELI) were investigated during lung inflation using a super-syringe in an animal model or based on different PEEP-trial or recruitment maneuvers in animals and patients with normal and injured lungs. Global ΔEELI has been found to correlate well ($R^2 = 0.92\text{--}0.95$) with global ΔEELV determined by spirometric measurements of V_T (Hinze et al. 2003a; Grivans et al. 2011), multi-breath nitrogen-washout technique (Bikker et al. 2009), computed tomography (CT) (Wrigge et al. 2008), and electron-beam computed tomography (EBCT) (Frerichs et al. 2002a). Data from patients with acute respiratory distress syndrome (ARDS) indicate that the linear relationship between global ΔEELI and ΔEELV may be weaker in heterogeneous lung injury due to atelectasis and end-inspiratory alveolar overdistension (Bikker et al. 2009). For clinical purposes, ΔEELI can be scaled and converted to volume (ml) with sufficient accuracy by using the global tidal variation resulting from a change in PEEP. However, alterations in thoracic impedance by PEEP-induced changes in intrathoracic blood volume must be taken into account.

Regional Changes in Lung Ventilation or Volume

Regional ventilation as assessed by regional impedance changes ($\Delta Z_{\text{regional}}$) measured by EIT correlation well with data (derived by EBCT $R = 0.81\text{--}0.93$). In patients with ARDS, an excellent correlation ($R^2 = 0.96$) was observed between $\Delta Z_{\text{regional}}$ and regional air content changes determined by CT during slow inflation maneuvers (Wrigge et al. 2008). Other studies have reported a good correlation between $\Delta Z_{\text{regional}}$ and regional air content changes or ventilation using dynamic X-ray CT (Wrigge et al. 2008), single-photon emission computed tomography (Hinze et al. 2003b), and positron emission tomography (Frerichs et al. 2002a).

In summary, all these data suggest that changes in relative impedance measured by EIT can be used to quantify regional ventilation and lung volumes with sufficient accuracy in homogeneously and inhomogeneously ventilated lungs.

EIT Measures for Analyzing Spatial Distribution of Ventilation

Subtracting fEIT Images

Changes in lung function can be measured and visualized by a pixel-by-pixel subtraction of an fEIT image from a previous fEIT image. To obtain an approximation for changes in regional V_T , the difference is normalized to the V_T divided by ΔZ_{global} (see Fig. 37.4).

Subtracting fEIT images allows the visualization and measurement of regional gain or loss of ventilation and lung volume caused by changes in ventilator settings (e.g. PEEP) or maneuvers (e.g., recruitment maneuvers, prone positioning). Subtracting fEIT images can thus localize and quantify recruitment and derecruitment indicated by an increase or decrease in $\Delta Z_{\text{regional}}$ (see Fig. 37.4).

Impedance Ratio

The impedance ratio divides the ventilation activity of the ventral (upper) region by the dorsal ventilation activity of the fEIT images, and the

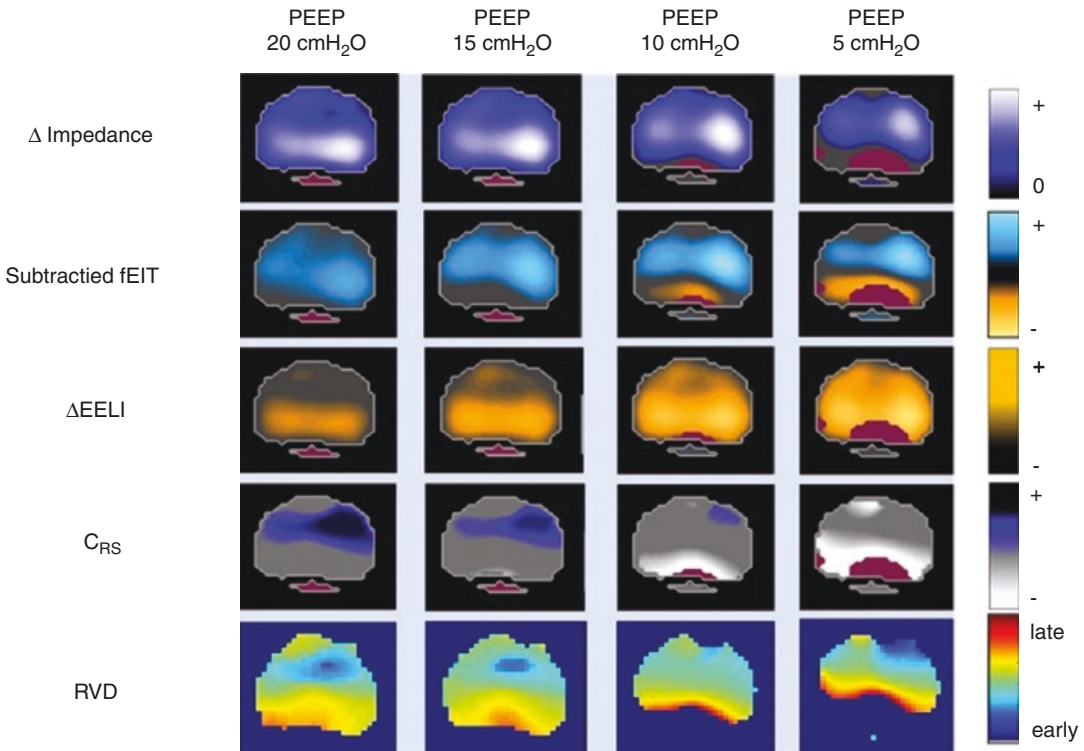


Fig. 37.4 Change in impedance (Δ impedance), subtracted fEIT, end-expiratory lung impedance (Δ EELI), regional respiratory system compliance (C_{RS}), and regional ventilation delay (RVD) at different PEEP levels

ratio has been suggested to indicate recruitment and derecruitment (Kunst et al. 2000a).

Regional Respiratory System Compliance (C_{RS})

C_{RS} can be calculated during mechanical ventilation dividing V_T by driving pressure. Comparably, using EIT with simultaneously registered airway pressures, global and regional C_{RS} can be measured and visualized in fEIT images by dividing pixel-by-pixel TIV by global driving pressure (see Fig. 37.4) (Bikker et al. 2011; Dargaville et al. 2010). Regional C_{RS} has been suggested to be helpful to localize and quantify regional alveolar collapse and overdistension during ventilation. In an animal lung injury model, EIT-derived regional C_{RS} correlated well to regional C_{RS} calculated from CT data (Bikker et al. 2011; Dargaville et al. 2010).

Regional Pressure–Volume (P/V) Curves

Global quasi-static P/V curves have been recorded during low-flow inspiratory and expi-

ratory maneuvers to identify the airway pressure required to open collapsed (lower inflection point; LIP) and overdistended lung units (upper inflection point, UIP). Similarly, regional quasi-static P/V curves can be generated during low-flow inspiratory and expiratory maneuvers ΔZ in a pixel or ROI when global airway pressure is registered simultaneously. The resulting opening pressures (LIP) varied significantly and were highest in the dorsal lung regions. The visualized regional distribution of LIP and UIP in different lung regions using fEIT images has been suggested to be helpful to individually select or titrate PEEP (Kunst et al. 2000b; Hinz et al. 2006).

Alveolar Overdistension and Collapse (ODCL)

ODCL is based on the monitoring of pixel C_{RS} during a decremental PEEP trial with a fixed driving pressure (Costa et al. 2009). This maneuver is used to identify the highest compliance and

the best pixel compliance for a specific PEEP level. Lung collapse is assumed if a reduction PEEP results in a lower pixel C_{RS} . In contrast, lung overdistention is assumed if increased PEEP results in a lower pixel C_{RS} (Costa et al. 2009). Lung collapse or overdistention in percent is calculated for each pixel by subtracting a C_{RS} at a given PEEP level from the best C_{RS} and referencing it to the best C_{RS} . Accumulated collapse/overdistention for the entire lung at each PEEP step is calculated as a weighted average summed up for all collapsed/overdistended pixels, where the weighting factor is the best pixel compliance (Costa et al. 2009). In an fEIT image, ODCL allows one to display and quantify collapse/overdistention at the pixel level and could help titration of PEEP and help prevent alveolar collapse and overdistention.

Center of Ventilation (CoV)

The center of ventilation (CoV) describes variations of the pulmonary ventilation distribution in the ventral–dorsal direction and is defined as a vertical coordinate that marks the point where the sum of the regional ventilation (ventral and dorsal) divides the lung into two equal parts (Frerichs et al. 2006). CoV is expressed as a percent of the vertical diameter ranging from 0% (ventral) to 100% (dorsal). A CoV of 50% indicates equal ventilation distribution between ventral and dorsal lung regions, whereas lower values indicate a shift of ventilation distribution towards ventral lung regions, which may be observed during derecruitment due to alveolar collapse in the dependent lung regions. CoV has been used in many experimental and clinical investigations to evaluate recruitment or derecruitment of the lungs (Frerichs et al. 2006).

Global Inhomogeneity Index (GI Index)

The GI index was introduced to quantify V_T distribution within the lungs and aims to summarize the complex pulmonary impedance distribution pattern using a single numeric value (Zhao et al. 2009a, b). Calculation of the GI index and modifications to adapt to a low-flow inflation have been described (Zhao et al. 2009a, b) and require an image of EIT scans at two selected time points.

Then, the median impedance value within an ROI is calculated. The differences in impedance variation between each pixel and median value of all pixels are calculated and normalized to the sum of impedance values, in order to make the GI index universal and inter-patient comparable (Zhao et al. 2009a, b). The GI index has been used to titrate PEEP, to investigate changes in ventilation distribution, and for the progression of obstructive lung disease (Zhao et al. 2009a, b). During a PEEP trial, increase in PEEP resulted in a parabolic curve of the GI index. The PEEP level at which the GI value was minimal corresponded to the highest global dynamic compliance and lowest ventilator inhomogeneity and was suggested to indicate the optimal PEEP level (Zhao et al. 2009a, b).

EIT Measures for Analyzing Temporal Distribution of Ventilation

Regional Ventilation Delay (RVD): Regional Ventilation Delay Index (RVDI)

In an inhomogeneous lung with atelectasis formation, higher airway pressure is required to open and ventilate the collapsed lung regions. Thus, ventilation of these initially collapsed and recruited alveolar regions is delayed. The high temporal resolution of EIT allows the analysis of aeration and ventilation time courses. The regional ventilation delay (RVD) is an EIT measure that can show a temporal delay in regions of the lung and thus the temporal heterogeneity occurring in the ventilated lung by the relationship between ΔZ and the ventilation time course in each pixel (Wrigge et al. 2008; Muders et al. 2012). The RVD is the delay time needed for a regional impedance-time curve to reach a certain threshold of its maximal impedance change, which is normally set between 30% and 40% of its maximal impedance value during a low-flow inflation (Wrigge et al. 2008; Muders et al. 2012). RVDI is the standard deviation of RVD in all pixels (Wrigge et al. 2008; Muders et al. 2012). A small RVDI indicates a more homogeneous, a high RVDI an inhomogeneous regional

ventilation delay distribution. In an fEIT image, RVD pixel values can be localized and quantified by color coding (see Fig. 37.4).

Intratidal Gas Distribution (ITV)

ITV analyzes the ventilation homogeneity during the inspiration (Lowhagen and Lundin 2010). ITV describes the amount of impedance distributed to a predefined ROI within one inspiration. To calculate ITV, the inspiratory part of the global impedance curve is divided into eight equal volume sections (12.5% of the entire inspiration). Then, sequential corresponding time points of the eight iso-volume steps are translated to the regional ITV curves. Thus, ITV gives the percentile contribution of the inspired air distributed to the selected lung region at a certain time point. During spontaneous breathing, ITV could demonstrate that gas distributes more to the dorsal region, resulting from the diaphragm contraction in the early phase of inspiration, showing a more than 50% contribution in the dorsal region to the global ITV.

Clinical Application

EIT can generate regional measures that allow the localization and quantification of ventilation heterogeneity under dynamic conditions. Thus, EIT has the potential to monitor heterogeneities in regional ventilation in diseases such as ARDS (Victorino et al. 2004), chronic obstructive lung disease (Frerichs et al. 2016), lung cancer (Serrano et al. 2002), or cystic fibrosis (Zhao et al. 2013). In addition, EIT has been used to guide mechanical ventilation and pulmonary therapy. Being a noninvasive and radiation-free technique that allows ventilator monitoring independent of an endotracheal tube, EIT offers particular advantages in neonatal and pediatric patients.

Estimation of Lung Collapse and Overdistension

Experimental studies have shown that continuous registration of ΔZ_{global} and $\Delta Z_{\text{regional}}$ or EIT-derived parameters, such as C_{RS} , P/V curves, GI

index ODCL, RVDI, and ITV, can be helpful for maximizing lung recruitment and reducing alveolar overdistension using recruiting maneuvers, PEEP-trials, or V_T adjustment.

Bikker et al. (2010) observed that during a decremental PEEP trial in patients with and without ARDS, ventilation distribution change maps (Δ fEIT maps) can visualize improvements or loss of regional ventilation in dependent and nondependent lung areas at the bedside in the individual patient. Δ fEIT and regional C_{RS} maps during stepwise decrease in PEEP were significantly different between patients with and without ARDS, indicating a different PEEP dependency between these two groups and between individual patients. By using a recruitment maneuver and a decremental PEEP trial, Lowhagen and Lundin (2010) demonstrated that ITV and Δ EELI offer additional information on recruitability and optimal PEEP in patients with ARDS. Zick et al. (2013) showed that ventilation distribution, regional C_{RS} , and Δ EELI can be used to assess tidal recruitment and end-inspiratory overinflation in patients with ARDS. In patients with and without ARDS, Zhao et al. (2014) demonstrated that the GI index is a reliable measure of ventilation heterogeneity and highly correlates with recruitment determined using EIT. Cinnella et al. (2015) described patients who have diffuse loss in aeration ROIvenral/dorsal impedance tidal variation ratio detected lung recruitment using open lung ventilator strategy. Yun et al. (2016) suggested that EIT has the potential to evaluate if ARDS patients respond to a recruitment.

Mauri et al. (2013) showed a more homogeneous ventral-to-dorsal ventilation distribution during assisted ventilation with high PEEP when compared with control mechanical ventilation. Karsten et al. used EIT to study V_T distribution on a regional basis in patients undergoing general anesthesia for laparoscopic cholecystectomy. Nestler et al. (2017) observed in anesthetized, morbidly obese patients during laparoscopic surgery observed the restoration of EELI and a significantly better regional ventilation distribution and oxygenation when PEEP was titrated according to the lowest RVDI when compared to a fixed PEEP level of 5 cm H_2O .

Pneumothorax Detection

EIT has been shown to reliably detect the development of a pneumothorax at the bedside in real time (Hahn et al. 2006). Initially, the EIT scan displays a clear rapid increase in regional impedance with an associated decrease in ΔEELI at the side of the pneumothorax. The change in aeration images showed a similar clear increase. About 30 seconds after onset, an increase in EELI is observed at the side of the pneumothorax, which is explained by ongoing increasing pleural gas accumulation (Costa et al. 2008). In an experimental model, EIT has been shown to detect a pneumothorax within three ventilator cycles with 100% sensitivity (Costa et al. 2008). EIT has been found to be useful for bedside early detection of a pneumothorax occurring during a lung recruitment maneuver in a patient with ARDS (Morais et al. 2017).

Monitoring Lung Volumes During Endotracheal Suctioning

Investigations indicate that EIT may be helpful for localizing and quantifying loss of lung volume caused by open endotracheal suctioning (Lindgren et al. 2007) or after the disconnection of the endotracheal during cardiac surgery (Corley et al. 2012). In addition, EIT allows the titration of recruitment maneuvers to restore ventilation distribution between the ventral and dorsal lung regions (Lindgren et al. 2007; Corley et al. 2012).

Monitoring Positioning of Endotracheal Tubes

Asymmetrical distribution of ventilation measured by EIT allows early detection of one-lung ventilation caused by inadvertent malpositioning of the endotracheal tube. On the other side, EIT has been used intraoperatively for correct positioning of double-lumen endotracheal tubes to assure one-lung ventilation during thoracic surgery (Steinmann et al. 2008).

Monitoring Ventilatory Dyssynchrony

During assisted spontaneous breathing, the EIT plethysmogram may assist in the early identification of potentially harmful dyssynchronies, such

as breath stacking and pendelluft (Pohlman et al. 2008; Yoshida et al. 2013).

Breath stacking is usually caused by reverse triggering or double-triggering and results in consecutive inspiratory cycles delivered by the ventilator on top of an incomplete exhalation (Pohlman et al. 2008). During breath stacking, EIT may detect potential harmful inspired end-inspiratory lung volumes even if regular monitoring only indicates a moderate increase in V_T .

Pendelluft describes an intrapulmonary dyssynchrony caused by gas movement between different pulmonary regions resulting in alveolar de-inflation and inflation. Using EIT, it was possible to monitor a pendelluft phenomenon due to a movement of gas within the lung from nondependent to dependent regions without change in V_T (Yoshida et al. 2013). This phenomenon can be caused by intense diaphragmatic contraction during excessive spontaneous efforts in volume-assisted modes of ventilation. Pendelluft has been suggested to cause unsuspected overstretch of the dependent lung during early inflation and can only be visualized by EIT and not by conventional monitoring of flow, volume, or pressure curves (Yoshida et al. 2013).

Perfusion Monitoring Using EIT

Measurement Principle

EIT has been shown useful for monitoring regional lung perfusion as well as stroke volume estimation. In principle, continuous and noninvasive monitoring can be performed based on the EIT waveforms resulting from cardiac activity (cardiac-related signal, CRS) in both the heart and lung region, whereas intermittent and invasive monitoring is possible using contrast agents (indicator-based signal, IBS) injected through a central venous line.

Perfusion Monitoring Using Cardiac Activity

In the EIT waveform, cardiac activity is observed in the heart as well as in the lung region (Vonk Noordegraaf et al. 1998). Impedance changes

in both the heart and lung region can mainly be attributed to localized changes in blood volume. As blood has a higher conductivity (and thus lower impedance) than tissue, an impedance decrease or increase can be observed when blood enters or leaves a region, respectively. In the heart region, an impedance increase is observed during systole, whereas an impedance decrease results during diastole. In the lung region, a similar, however, delayed behavior is observed. During systole, an impedance decrease results, whereas an impedance increase is found during diastole (Grant et al. 2011). The impedance changes are likely to result from volume changes induced by the arterial pulse-wave traveling from the heart into the pulmonary vascular tree. However, the exact origin and composition of the impedance changes are not yet fully understood and can only partly be attributed to lung perfusion. Most probably, the flow speed of blood as well as mechanic deformation and movement of organs resulting from a cardiac activity are also causing alterations in regional impedance.

In order to enable real-time analysis of regional perfusion, techniques to separate cardiac- and ventilation-related EIT waveforms are of great importance. A major difficulty is a difference in amplitude of the two signals, because the CRS is an order of magnitude smaller than the VRS (Leonhardt et al. 2012). Several methods exist, including short-time apnea, ECG gating, frequency filtering, as well as more advanced signal processing techniques. While setting the mechanical ventilator on short-time apnea is not an actual separation technique, it is a very efficient way to obtain a clear recording of the CRS free of disturbance from the VRS. However, repeated periods of apnea might be problematic in some patients. For ECG gating (Eyüboğlu and Brown 1988; Braun et al. 2018a), the QRS complex of a synchronously recorded ECG is used as a trigger to successively average a high number (e.g., 200) of heart cycles from the EIT waveform. Assuming that VRS and CRS are uncorrelated, this operation will amplify the CRS and suppress (or say, “average out”) the VRS. While this method provides a very good separation, it has the disadvantage of delaying the EIT waveform

as a result of the averaging process, which makes it unsuitable for real-time analysis. Frequency filtering (Frerichs et al. 2009; Zadehkoochak et al. 1992) is based on the assumption that the VRS and CRS span different ranges in the frequency spectrum. Specifically designed digital filters can be used to efficiently separate the CRS from the combined EIT waveform in real time. However, problems arise when there is a high breathing rate or low heart rate because the frequency spectra of VRS and CRS might overlap. In these cases, only frequency filtering provides insufficient separation. Highly promising results have been achieved with more advanced signal processing techniques. Specifically, principal component analysis (PCA) has proven to be useful for extracting cardiac template functions from combined EIT waveforms (Deibele et al. 2008). Linear fitting of these template functions can achieve the capability of efficient, real-time separation of VRS and CRS.

Regional perfusion based on the CRS has been compared to radionuclide scintigraphy (Kunst et al. 1998), magnetic resonance imaging (MRI) (Vonk Noordegraaf et al. 1998), and single-photon emission computed tomography (SPECT) (Borges et al. 2012). Further investigations of pulmonary perfusion using the CRS involved the modification of pulmonary perfusion using a balloon catheter (Fagerberg et al. 2009), one-lung ventilation (Frerichs et al. 2009), and repositioning of the EIT belt and patient (Grant et al. 2011). Stroke volume estimation using the CRS has been explored in animal (Pikkemaat et al. 2014) and human (Braun et al. 2018a; Vonk Noordegraaf et al. 2000) studies. Recently, interesting simulative studies have shown limitations and challenges (Braun et al. 2018b) as well as the influence of heart motion (Proença et al. 2015) on stroke volume estimation using the CRS.

Perfusion Monitoring Using Contrast Agents

A promising technique for perfusion monitoring with EIT involves the application of conductive or resistive contrast agents, such as hypertonic saline (e.g., NaCl 5.85%, 10 ml), to obtain an EIT waveform (indicator-based signal, IBS). The

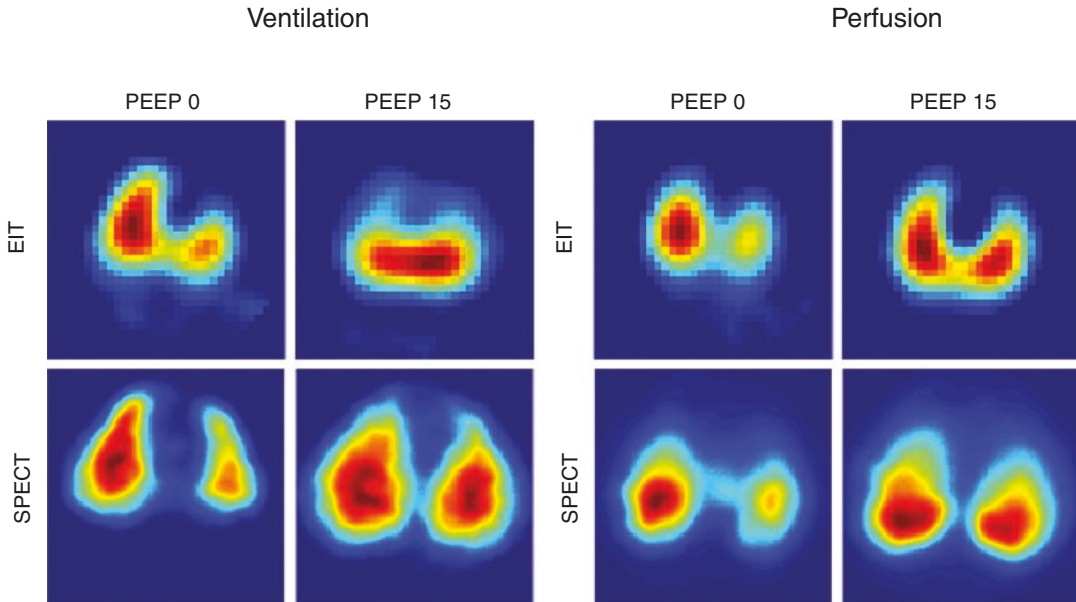


Fig. 37.5 Functional EIT image reconstructed with the GREIT algorithm. Regional lung ventilation and perfusion obtained by EIT compared to single-photon emission computed tomography (SPECT) using a comparable framework

contrast agent is injected into the bloodstream as a bolus through a central venous line under short-time apnea (Borges et al. 2012; Hentze et al. 2018). It follows the blood flow through the cardio-pulmonary system from the right heart, to the lung, to the left heart, and exits the EIT region through the aorta. Since the conductivity of the bolus is different from that of blood, it leaves a trace of impedance change in the EIT waveform, which can be directly linked to regional perfusion. Disadvantages are increased invasiveness resulting from the need for a central venous line as well as the possibility of hemolysis due to the use of contrast agents. Owing to its invasiveness, the method is currently only used as a research tool in animal trials. However, successive lowering of contrast agent concentration might enable clinical application.

In order to extract lung perfusion, curve-fitting techniques, similar to the ones known from indicator dilution theory, can be employed (Borges et al. 2012). Recently, an approach based on a gamma-variate model has been used to achieve a complete separation of the IBS into right-heart, lung, and left-heart components (Fagerberg et al. 2009). Using the technique, a strong agreement

of regional perfusion from EIT with single-photon emission tomography (SPECT) is found (see Fig. 37.5). Furthermore, a method based on wavelet filters that eliminates the need for short-time apnea during the recording of the IBS has shown promising results (Nguyen et al. 2014). Thus, regional lung perfusion monitoring under ongoing mechanical ventilation might become possible at the bedside.

An initial self-study, using isotonic saline injection in an arm vein, introduced the concept to the research community (Brown et al. 1992). Regional perfusion based on the IBS has since then been compared with electron-beam computed tomography (EBCT) (Frerichs et al. 2002b) and SPECT (Borges et al. 2012; Hentze et al. 2018).

Conclusion

EIT creates noninvasively and radiation-free images of the regional ventilation and arguably lung perfusion distribution at the bedside. Functional EIT images are generated by applying a mathematical operation on a sequence of raw

images and the corresponding pixel EIT waveforms and allow to address different functional characteristics of the respiratory and cardio-circulatory system. Thus, EIT can be combined with other signals, such as airway pressure, enabling the assessment of regional respiratory system compliance (C_{RS}) or regional pressure/volume (P/V) curves. Changes in lung ventilation and EELV, compliance, C_{RS} , P/V curves, as well as alveolar overdistension and collapse can be assessed by EIT dynamically on a regional level. The high temporal resolution of EIT allows the analysis of aeration and ventilation time courses and to determine the temporal ventilation heterogeneity. Clinical and experimental studies suggest that EIT-based lung function monitoring may help to guide mechanical ventilation. Recently, EIT has been shown useful for monitoring regional lung perfusion as well as stroke volume estimation. Continuous and noninvasive perfusion monitoring can be performed based on the EIT waveforms resulting from cardiac activity in both heart and lung regions, whereas intermittent and invasive monitoring is possible using contrast agents such as hypertonic saline injected through a central venous line. Ongoing experimental and clinical studies evaluate regional lung perfusion and V/Q matching monitoring under ongoing mechanical ventilation might become possible at the bedside.

References

- Adler A, Amyot R, Guardo R, Bates JH, Berthiaume Y. Monitoring changes in lung air and liquid volumes with electrical impedance tomography. *J Appl Physiol.* 1997;83:1762–7.
- Adler A, Arnold JH, Bayford R, Borsic A, Brown B, Dixon P, Faes TJ, Frerichs I, Gagnon H, Gärber Y, Grychtol B, Hahn G, Lionheart WR, Malik A, Patterson RP, Stocks J, Tizzard A, Weiler N, Wolf GK. GREIT: a unified approach to 2D linear EIT reconstruction of lung images. *Physiol Meas.* 2009;30:S35–55.
- Adler A, Gaggero PO, Maimaitijiang Y. Adjacent stimulation and measurement patterns considered harmful. *Physiol Meas.* 2011;32:731–44.
- Adler A, Proença M, Braun F, Brunner J, Sola J. Origins of cardiosynchronous signals in EIT. In: 18th international conference on biomedical applications of electrical impedance tomography. Dartmouth, Hanover, New Hampshire, USA; 2017. p. 73.
- Barber DC, Brown BH. Recent developments in applied potential tomography-APT. In: Bacharach SL, Nijhoff M, editors. Proceedings of 9th conference on information processing in medical imaging. Dordrecht; 1986. p. 106–21.
- Bikker IG, Leonhardt S, Bakker J, Gommers D. Lung volume calculated from electrical impedance tomography in ICU patients at different PEEP levels. *Intensive Care Med.* 2009;35:1362–7.
- Bikker IG, Leonhardt S, Reis Miranda D, Bakker J, Gommers D. Bedside measurement of changes in lung impedance to monitor alveolar ventilation in dependent and non-dependent parts by electrical impedance tomography during a positive end-expiratory pressure trial in mechanically ventilated intensive care unit patient. *Crit Care.* 2010;14:R100.
- Bikker IG, Preis C, Egal M, Bakker J, Gommers D. Electrical impedance tomography measured at two thoracic levels can visualize the ventilation distribution changes at the bedside during a decremental positive endexpiratory lung pressure trial. *Crit Care.* 2011;15:R193.
- Bodenstein M, David M, Markstaller K. Principles of electrical impedance tomography and its clinical application. *Crit Care Med.* 2009;37:713–24.
- Borges JB, Suarez-Sipmann F, Böhm SH, Tusman G, Melo A, Maripuu E, Sandström M, Park M, Costa EL, Hedenstierna G, Amato M. Regional lung perfusion estimated by electrical impedance tomography in a piglet model of lung collapse. *J Appl Physiol.* 2012;112:225–36.
- Braun F, Proença M, Adler A, Riedel T, Thiran JP, Solà J. Accuracy and reliability of noninvasive stroke volume monitoring via ECG-gated 3D electrical impedance tomography in healthy volunteers. *PLoS One.* 2018a;13:e0191870.
- Braun F, Proença M, Lemay M, Bertschi M, Adler A, Thiran JP, Solà J. Limitations and challenges of EIT-based monitoring of stroke volume and pulmonary artery pressure. *Physiol Meas.* 2018b;39:014003.
- Brown BH, Leathard A, Sinton A, McArdle FJ, Smith RW, Barber DC. Blood flow imaging using electrical impedance tomography. *Clin Phys Physiol Meas.* 1992;13(Suppl A):175–9.
- Cinnella G, Grasso S, Raimondo P, D’Antini D, Mirabella L, Rausedo M, Rausedo M, Dambrosio M. Physiological effects of the open lung approach in patients with early, mild, diffuse acute respiratory distress syndrome: an electrical impedance tomography study. *Anesthesiology.* 2015;123:1113–2.
- Corley A, Spooner AJ, Barnett AG, Caruana LR, Hammond NE, Fraser JF. Endexpiratory lung volume recovers more slowly after closed endotracheal suctioning than after open suctioning: a randomized crossover study. *J Crit Care.* 2012;27:742.e1–7.
- Costa ELV, Chaves CN, Gomes S, Beraldo MA, Volpe MS, Tucci MR, et al. Real-time detection of pneumo-

- thorax using electrical impedance tomography. *Crit Care Med.* 2008;36:1230–8.
- Costa ELV, Borges JB, Melo A, Suarez-Sipmann F, Toufen C, Bohm SH, Amato MB. Bedside estimation of recruitable alveolar collapse and hyperdistension by electrical impedance tomography. *Intensive Care Med.* 2009;35:1132–7.
- Dargaville PA, Rimensberger PC, Frerichs I. Regional tidal ventilation and compliance during a step-wise vital capacity manoeuvre. *Intensive Care Med.* 2010;36:1953–61.
- Deibele JM, Luepschen H, Leonhardt S. Dynamic separation of pulmonary and cardiac changes in electrical impedance tomography. *Physiol Meas.* 2008;29:S1–14.
- Eyüboğlu BM, Brown BH. Methods of cardiac gating applied potential tomography. *Clin Phys Physiol Meas.* 1988;9(Suppl A):43–8.
- Fagerberg A, Stenqvist O, Aneman A. Monitoring pulmonary perfusion by electrical impedance tomography: an evaluation in a pig model. *Acta Anaesthesiol Scand.* 2009;53:152–8.
- Frerichs I, Hinz J, Herrmann P, Weisser G, Hahn G, Dudykevych T, Quintel M, Hellige G. Detection of local lung air content by electrical impedance tomography compared with electron beam CT. *J Appl Physiol.* 2002a;93:660–6.
- Frerichs I, Hinz J, Herrmann P, Weisser G, Hahn G, Quintel M, Hellige G. Regional lung perfusion as determined by electrical impedance tomography in comparison with electron beam CT imaging. *IEEE Trans Med Imaging.* 2002b;21:646–52.
- Frerichs I, Dargaville PA, Van Genderingen H, Morel DR, Rimensberger PC. Lung volume recruitment after surfactant administration modifies spatial distribution of ventilation. *Am J Respir Crit Care Med.* 2006;174:772–9.
- Frerichs I, Pulletz S, Elke G, Reifferscheid F, Schadler D, Scholz J, Weiler N. Assessment of changes in distribution of lung perfusion by electrical impedance tomography. *Respiration.* 2009;77:282–91.
- Frerichs I, Zhao Z, Becher T, Zabel P, Weiler N, Vogt B. Regional lung function determined by electrical impedance tomography during bronchodilator reversibility testing in patients with asthma. *Physiol Meas.* 2016;37:698–712.
- Frerichs I, Amato MB, van Kaam AH, Tingay DG, Zhao Z, Grychtol B, Bodenstein M, Gagnon H, Böhm SH, Teschner E, Stenqvist O, Mauri T, Torsani V, Camporota L, Schibler A, Wolf GK, Gommers D, Leonhardt S, Adler A, TREND Study Group. Chest electrical impedance tomography examination, data analysis, terminology, clinical use and recommendations: consensus statement of the TRanslational EIT developmeNt stuDy group. *Thorax.* 2017;72:83–93.
- Grant CA, Pham T, Hough J, Riedel T, Stocker C, Schibler A. Measurement of ventilation and cardiac related impedance changes with electrical impedance tomography. *Crit Care.* 2011;15(1):R37.
- Grivans C, Lundin S, Stenqvist O, Lindgren S. Positive endexpiratory pressure-induced changes in end-expiratory lung volume measured by spirometry and electric impedance tomography. *Acta Anaesthesiol Scand.* 2011;55:1068–77.
- Hahn G, Sipinková I, Baisch F, Hellige G. Changes in the thoracic impedance distribution under different ventilatory conditions. *Physiol Meas.* 1995;16:A161–73.
- Hahn G, Just A, Dudykevych T, Frerichs I, Hinz J, Quintel M, Hellige G. Imaging pathologic pulmonary air and fluid accumulation by functional and absolute EIT. *Physiol Meas.* 2006;27:S187–98.
- Hentze B, Muders T, Luepschen H, Maripuu E, Hedenstierna G, Putensen C, Walter M, Leonhardt S. Regional lung ventilation and perfusion by electrical impedance tomography compared to single-photon emission computed tomography. *Physiol Meas.* 2018;39:065004.
- Hinz J, Hahn G, Neumann P, Sydow M, Mohrenweiser P, Hellige G, Burchardi H. End-expiratory lung impedance change enables bedside monitoring of end-expiratory lung volume change. *Intensive Care Med.* 2003a;29:37–43.
- Hinz J, Neumann P, Dudykevych T, Andersson LG, Wrigge H, Burchardi H, Hedenstierna G. Regional ventilation by electrical impedance tomography: a comparison with ventilation scintigraphy in pigs. *Chest.* 2003b;124:314–22.
- Hinz J, Moerer O, Neumann P, Dudykevych T, Frerichs I, Hellige G, Quintel M. Regional pulmonary pressure volume curves in mechanically ventilated patients with acute respiratory failure measured by electrical impedance tomography. *Acta Anaesthesiol Scand.* 2006;50:331–9.
- Kunst PW, Vonk Noordegraaf A, Hoekstra OS, Postmus PE, de Vries PM. Ventilation and perfusion imaging by electrical impedance tomography: a comparison with radionuclide scanning. *Physiol Meas.* 1998;19:481–90.
- Kunst PW, Vazquez de Anda G, Boehm SH, Faes TJ, Lachmann B, Postmus PE, de Vries PM. Monitoring of recruitment and derecruitment by electrical impedance tomography in a model of acute lung injury. *Crit Care Med.* 2000a;28:3891–5.
- Kunst PW, Bohm SH, Vazquez de Anda G, Amato MB, Lachmann B, Postmus PE, de Vries PM. Regional pressure volume curves by electrical impedance tomography in a model of acute lung injury. *Crit Care Med.* 2000b;28:178–83.
- Leonhardt S, Lachmann B. Electrical impedance tomography: the holy grail of ventilation and perfusion monitoring? *Intensive Care Med.* 2012;38:1917–29.
- Leonhardt S, Pikkemaat R, Stenqvist O, Lundin S. Electrical impedance tomography for hemodynamic monitoring. *Conf Proc IEEE Eng Med Biol Soc.* 2012;2012:122–5.
- Lindgren S, Odenstedt H, Olegård C, Söndergaard S, Lundin S, Stenqvist O. Regional lung derecruitment after endotracheal suction during volume- or pressure-

- controlled ventilation: a study using electric impedance tomography. *Intensive Care Med.* 2007;33:172–80.
- Lowhagen K, Lundin SSO. Regional intratidal gas distribution in acute lung injury and acute respiratory distress syndrome assessed by electric impedance tomography. *Minerva Anesthesiol.* 2010;76:1024–35.
- Marquis F, Coulombe N, Costa R, Gagnon H, Guardo R, Skrobik Y. Electrical impedance tomography's correlation to lung volume is not influenced by anthropometric parameters. *J Clin Monit Comput.* 2006;20:201–7.
- Mauri T, Bellani G, Confalonieri A, Tagliabue P, Turella M, Coppadoro A, Coppadoro A, Citerio G, Patroniti N, Pesenti A. Topographic distribution of tidal ventilation in acute respiratory distress syndrome. *Crit Care Med.* 2013;41:1664–73.
- Menden T, Orschulik J, Dambun S, Matuszczyk J, Aguiar Santos S, Leonhardt S, Walter M. Reconstruction algorithm for frequency-differential EIT using absolute values. *Physiol Meas.* 2019;40:034008.
- Morais CCA, De Santis Santiago RR, de Oliveira Filho JRB, Hirota AS, PHD P, Ferreira JC, Camargo ED, Amato MB, Costa EL. Monitoring of pneumothorax appearance with electrical impedance tomography during recruitment maneuvers. *Am J Respir Crit Care Med.* 2017;195:1070–3.
- Muders T, Luepschen H, Zinserling J, Greschus S, Fimmers R, Guenther U, Buchwald M, Grigutsch D, Leonhardt S, Putensen C, Wrigge H. Tidal recruitment assessed by electrical impedance tomography and computed tomography in a porcine model of lung injury. *Crit Care Med.* 2012;40:903–11.
- Nestler C, Simon P, Petroff D, Hammermüller S, Kamrath D, Wolf S, Dietrich A, Camilo LM, Beda A, Carvalho AR, Giannella-Neto A, Reske AW, Wrigge H. Individualized positive end-expiratory pressure in obese patients during general anaesthesia. A randomized controlled clinical trial using electrical impedance tomography. *Br J Anaesth.* 2017;119:1194–205.
- Nguyen DT, Thiagalingam A, Bhaskaran A, Barry MA, Pouliopoulos J, Jin C, McEwan AL. Electrical impedance tomography for assessing ventilation/perfusion mismatch for pulmonary embolism detection without interruptions in respiration. *Conf Proc IEEE Eng Med Biol Soc.* 2014;2014:6068–71.
- Pikkemaat R, Lundin S, Stenqvist O, Hilgers RD, Leonhardt S. Recent advances in and limitations of cardiac output monitoring by means of electrical impedance tomography. *Anesth Analg.* 2014;119:76–83.
- Pohlman MC, McCallister KE, Schweickert WD, Pohlman AS, Nigos CP, Krishnan JA, Charbeneau JT, Gehlbach BK, Kress JP, Hall JB. Excessive tidal volume from breath stacking during lungprotective ventilation for acute lung injury. *Crit Care Med.* 2008;36:3019–23.
- Pronça M, Braun F, Rapin M, Solà J, Adler A, Grychtol B, Bohm SH, Lemay M, Thiran JP. Influence of heart motion on cardiac output estimation by means of electrical impedance tomography: a case study. *Physiol Meas.* 2015;36:1075–91.
- Rabbani KS, Kabir AM. Studies on the effect of the third dimension on a two-dimensional electrical impedance tomography system. *Clin Phys Physiol Meas.* 1991;12:393–402.
- Serrano RE, de Lema B, Casas O, Feixas T, Calaf N, Camacho V, Carrió I, Casan P, Sanchis J, Riu PJ. Use of electrical impedance tomography (EIT) for the assessment of unilateral pulmonary function. *Physiol Meas.* 2002;23:211–20.
- Steinmann D, Stahl CA, Minner J, Schumann S, Loop T, Kirschbaum A, Priebe HJ, Guttman J. Electrical impedance tomography to confirm correct placement of double-lumen tube: a feasibility study. *Br J Anaesth.* 2008;101:411–8.
- Teschner E, Michael I, Leonhardt S. Electrical impedance tomography: the realisation of regional ventilation monitoring. 2nd ed. Draeger GmbH; 2015.
- Victorino JA, Borges JB, Okamoto VN, Matos GF, Tucci MR, Carames MP, Tanaka H, Sipmann FS, Santos DC, Barbas CS, Carvalho CR, Amato MB. Imbalances in regional lung ventilation: a validation study on electrical impedance tomography. *Am J Respir Crit Care Med.* 2004;169:791–800.
- Vonk Noordegraaf A, Kunst PW, Janse A, Marcus JT, Postmus PE, Faes TJ, de Vries PM. Pulmonary perfusion measured by means of electrical impedance tomography. *Physiol Meas.* 1998;19:263–73.
- Vonk-Noordegraaf A, Janse A, Marcus JT, Bronzwaer JG, Postmus PE, Faes TJ, De Vries PM. Determination of stroke volume by means of electrical impedance tomography. *Physiol Meas.* 2000;21:285–93.
- Wrigge H, Zinserling J, Muders T, Varelmann D, Günther U, vd Groeben C, Magnusson A, Hedenstierna G, Putensen C. Electrical impedance tomography compared with thoracic computed tomography during a slow inflation maneuver in experimental models of lung injury. *Crit Care Med.* 2008;36:903–9.
- Yorkey TJ, Webster JG, Tompkins WJ. Comparing reconstruction algorithms for electrical impedance tomography. *EEE Trans Biomed Eng.* 1987;34:843–52.
- Yoshida T, Torsani V, Gomes S, De Santis RR, Beraldo MA, ELV C, Costa EL, Tucci MR, Zin WA, Kavanagh BP, Amato MB. Spontaneous effort causes occult pendelluft during mechanical ventilation. *Am J Respir Crit Care Med.* 2013;188:1420–7.
- Yun L, He H, Möller K, Frerichs I, Liu D, Zhao Z. Assessment of lung recruitment by electrical impedance tomography and oxygenation in ARDS patients. *Medicine (Baltimore).* 2016;95:e3820.
- Zadehkoochak M, Blott BH, Hames TK, George RF. Pulmonary perfusion and ventricular ejection imaging by frequency domain filtering of EIT (electrical impedance tomography) images. *Clin Phys Physiol Meas.* 1992;13(Suppl A):191–6.
- Zhao Z, Möller K, Steinmann D, Frerichs I, Guttman J. Evaluation of an electrical impedance tomography-based global inhomogeneity index for pulmo-

- nary ventilation distribution. *Intensive Care Med.* 2009a;35:1900–6.
- Zhao Z, Steinmann D, Guttman J. Global and local inhomogeneity indices of lung ventilation based on electrical impedance tomography. *IFMBE Proc.* 2009b;22:256–9.
- Zhao Z, Müller-Lisse U, Frerichs I, Fischer R, Möller K. Regional airway obstruction in cystic fibrosis determined by electrical impedance tomography in comparison with high resolution CT. *Physiol Meas.* 2013;34:N107–14.
- Zhao Z, Pulletz S, Frerichs I, Müller-Lisse U, Möller K. The EIT-based global inhomogeneity index is highly correlated with regional lung opening in patients with acute respiratory distress syndrome. *BMC Res Notes.* 2014;7:82.
- Zick G, Elke G, Becher T, Schädler D, Pulletz S, Freitag-Wolf S, Weiler N, Frerichs I. Effect of PEEP and tidal volume on ventilation distribution and end-expiratory lung volume: a prospective experimental animal and pilot clinical study. *PLoS One.* 2013;8:e72675.



Clinical Monitoring by Volumetric Capnography

38

Gerardo Tusman and Stephan H. Bohm

Carbon dioxide (CO₂) is a biological gas closely related to global cardiorespiratory physiology. The kinetic of CO₂ in the body involves basic biological processes such as cellular metabolism, lung perfusion, gas exchange, and ventilation (Breen 1998). These processes begin with the cellular production of CO₂ by aerobic and anaerobic metabolism, which creates a CO₂ gradient from mitochondria to alveoli (Wiklund 1996; Folch et al. 2005). This “CO₂ cascade” and the corresponding partial pressure of CO₂ in venous and arterial blood is continuously and strictly controlled by local/global blood flow, buffer systems in blood and tissues (stores of CO₂), and the chemical control of ventilation (Farhi and Rahn 1955; Cherniack and Longobardo 1970). Cardiopulmonary diseases can alter such homeostasis in many ways by activating compensatory mechanisms that change the kinetics of CO₂ stores and alveolar ventilation in order to keep blood pH within the normal range (Gluck 1998; Kellum 2000). When the system fails and cannot maintain adequate blood CO₂ values, patients require cardiorespiratory support until the causes

and mechanisms responsible for such disturbances are removed or controlled.

Capnography refers to the measurement of the concentration of CO₂ within the breathing gas that represents the whole-body CO₂ recovered at the opening of the airways during the ventilatory cycle (Huttman et al. 2014; Carlon et al. 1988; Anderson and Breen 2000). Therefore, capnography is attractive for monitoring many important aspects of mechanically ventilated patients. A relevant feature of capnography is that the information is obtained noninvasive breath-by-breath at the bedside by using a robust and accurate technology. This chapter describes the role of volumetric capnography (VCap) as a monitoring tool for the assessment of cardiopulmonary function in mechanically ventilated patients.

Time-Based and Volume-Based Capnography

The graphical representation of the tidal elimination of CO₂ is called a *capnogram*, and the device that measures it is called a *capnograph*. This device measures CO₂ by spectrometry, especially by the absorption of infrared light by breathing gases. It is expressed as a fraction (%) or partial pressure (mmHg). There are two kinds of capnographs which are classified according to the way the CO₂ measurement is performed (Block and McDonald 1992). *Side-stream* capnographs take

G. Tusman (✉)
Department of Anesthesiology, Hospital Privado de
Comunidad, Mar del Plata, Buenos Aires, Argentina

S. H. Bohm
Department of Anesthesiology and Intensive Care
Medicine, Rostock University Medical Center,
Rostock, Germany

samples of breathing gases at the opening of the airways and transport them by a vacuum system to the analysis unit within the device. The side-stream gadget has low weight and instrumental dead space. The slow gas transport within the sample line caused a delay in CO₂ signal related to flow that needs a precise synchronization between these two signals for proper VCap analysis. *Main-stream* capnographs, on the other hand, measure CO₂ by a sensor placed between the endotracheal tube and the “Y” piece of the ventilatory circuit. The flow sensor is commonly integrated into the same main-stream device, which gives good coordination between signals for adequate VCap analysis but at the cost of a heavier and bigger gadget when compared than side-stream ones (Huttman et al. 2014; Carlon et al. 1988; Anderson and Breen 2000; Block and McDonald 1992; Jaffe 2008; Orr and Jaffe 1994).

Capnography is clinically represented as *time-based* (standard capnography) or *volume-based*

(volumetric capnography – VCap) (Bhavani-Shankar and Philip 2000; Jaffe 2014; Siobal 2016). Time and volume-based capnography are different ways to present and analyze the CO₂ signal. Standard capnography is depicted as a temporal series like the flow, volume, and pressure signals in mechanically ventilated patients. The visualization of the CO₂ tracing helps detect not only ventilatory problems but also hemodynamics deteriorations continuously and in real-time. VCap, on the other hand, provides “volumetric” information like dead space, alveolar ventilation, the elimination of CO₂ per breath, and the calculation of the pulmonary blood flow. As opposed to standard capnography, VCap is limited to the analysis of one breath at a time since the CO₂ is displayed over the tidal volume.

Figure 38.1 shows standard capnography and VCap with their respective main parameters (Tusman et al. 2013; Suarez Sipmann et al. 2014). While standard capnography shares with VCap

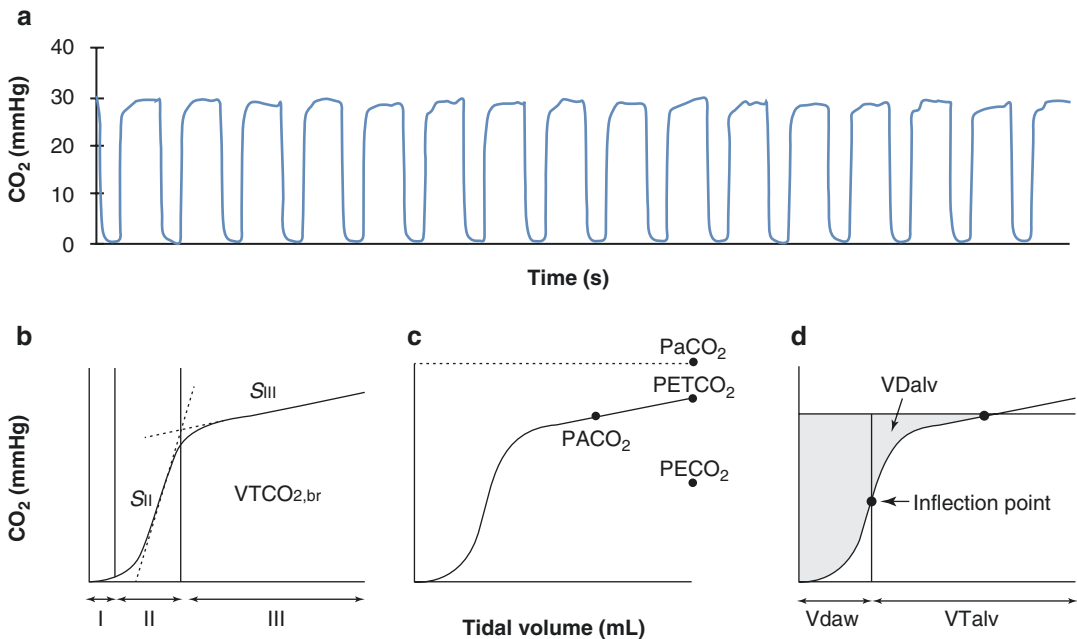


Fig. 38.1 Time- and volume-based capnography. (a) Standard capnography presented as a continuous temporal series. (b) Volumetric capnography showing the three phases of the capnogram, where phase I and II represent gas within the conducting airways while phase III represents pure alveolar gas. Phases II and III have corresponding slopes (S) the intersection of which defines the alpha angle. The area under the curve ($VTCO_{2,br}$) is the amount of CO₂ eliminated in one breath. (c) The partial pressures

of CO₂ are depicted on the volumetric capnogram. $P\bar{E}CO_2$, $PACO_2$, $PETCO_2$, and $PaCO_2$ are the mixed expired, alveolar, end-tidal, and arterial partial pressure of CO₂, respectively. (d) Graphical representation of the airway (VD_{aw}) and alveolar (VD_{alv}) dead space. The gray area represents the global or physiological dead space (VD_{phys}). According to the principles described by Fowler, the mathematical inflection point of the capnogram marks the limit between airway dead space and alveolar tidal volume (VT_{alv}).

the same nomenclature as phases and partial pressures of CO₂, it cannot measure volumetric variables.

Time- and volume-based capnography show complementary information and must be analyzed simultaneously (Fig. 38.2). Both types of

capnography are analog to the monitoring of respiratory mechanics where pressure, flow, and volume/time waveforms give visual online information, while the combination of these parameters (volume/pressure – flow/volume loops) expands the monitoring capabilities of the pri-

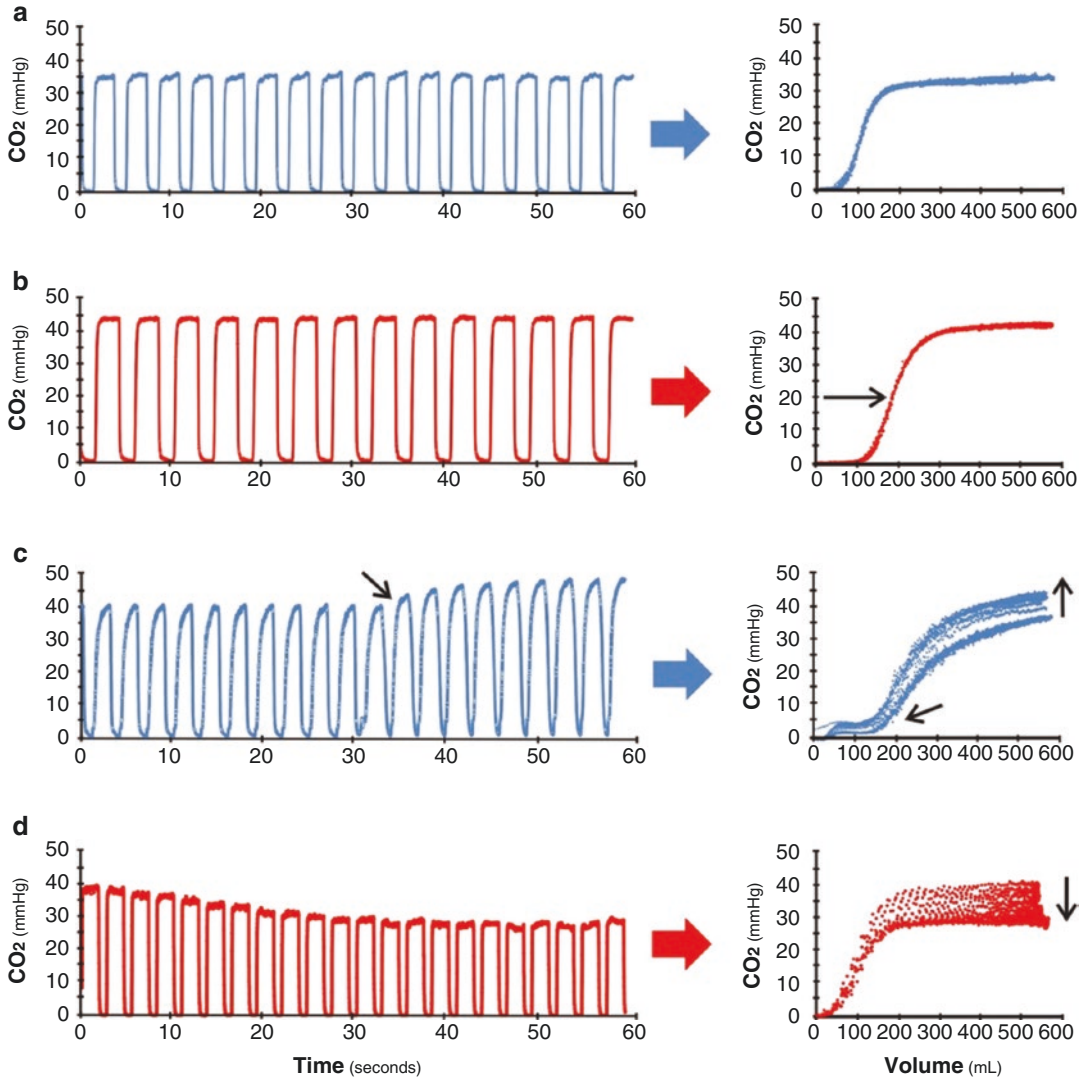


Fig. 38.2 Examples of monitoring by both time-based and volume-based capnography. *Left hand:* time-based capnography. *Right hand:* volumetric capnography of the same breaths depicted on the left. **(a)** Capnograms in an anesthetized patient at fixed ventilatory settings during the steady-state condition. **(b)** The same patient as in “a” but minutes after placing a passive heat moisture exchanger (HME) between the mainstream sensor and the endotracheal tube. This additional instrumental dead space increased PETCO₂ and PaCO₂. The black arrow indicates

the increase in airway dead space by the added volume of the HME (80 mL). **(c)** A rebreathing caused by the malfunction of the anesthesia machine’s expiratory valve. Arrow marks the time when CO₂ started to be re-inhaled, subsequent increases in baseline CO₂, alveolar PCO₂ indicated by rising VCap curves. **(d)** An episode of sudden arterial hypotension and low cardiac output at fixed ventilatory settings. Both time- and volume-based capnograms decrease

mary outcome signals. Figure 38.2 shows a few examples of the monitoring capabilities of capnography.

CO₂ kinetics are *context-sensitive*, which means that its proper interpretation depends on the understanding of how a particular patient's clinical situation (the context) affects the CO₂ kinetics. Suppose, for example, a ventilated patient who is fighting the ventilator. In this chaotic scenario, modifications in metabolism, hemodynamics, and breathing pattern render analysis by capnography useless (but also that of respiratory mechanics) because all components of the CO₂ kinetics are changing at the same time and in different directions. Let us suppose now a ventilated patient with stable metabolism and ventilation, who presents a sudden decrease in the elimination of CO₂. This change can only be explained by a diminution in lung perfusion, and in this particular clinical context, diagnosing a hemodynamic problem based purely on the expired CO₂ is quite easy, quick, and feasible (Fig. 38.2d).

These illustrative examples don't imply that the analysis of CO₂ kinetics is useful only during "steady-states," but on the contrary, CO₂ signals can unmask any non-steady-state conditions by changing one parameter of its kinetics at a time (Breen et al. 2000).

Respiratory Monitoring

Standard monitoring of mechanically ventilated patients is based on respiratory mechanics using pressure, flow, and volume waveforms with their derived variables like compliance, airways resistance, and driving pressure, among others. Respiratory mechanics evaluates how the delivered tidal volume interacts physically with the respiratory system, detecting inappropriate ventilatory settings causing exaggerated stress and strain of the lung tissue (Protti et al. 2013). This mechanistic analysis of ventilation, however, does not contemplate the effect on the lung's main function, and therefore, gas exchange must be evaluated intermittently by analyzing PO₂ and PCO₂ in blood samples. The development of

pulse oximetry and capnography allowed a non-invasive assessment of those biological gases, decreasing the number of blood sample analyses and promoting the real-time adjustment of ventilatory settings (Anderson and Vann 1988; Duncan and Cohen 1991; Roizen et al. 1993).

Monitoring ventilation by VCap

The first step to start controlled mechanical ventilation is to select the minute volume ventilation (VE) related to a patient's anthropometric features and therapeutic concepts such as lung-protective ventilation with low tidal volumes (VT). VE is calculated as VT times the respiratory rate followed by the adjustment of the I:E ratio, PEEP, FiO₂, and any other ventilatory parameter like trigger threshold and alarms.

The next obligatory step should be to determine the *efficiency/inefficiency* of such selected ventilatory settings (Tusman et al. 2011a). This approach uses the following formula:

$$VE = VA + VD$$

where VA is the alveolar ventilation or the *effective* portion of VE. Dead space (VD) is *ineffective* ventilation because this part does not get in contact with the pulmonary capillaries and therefore does not participate in gas exchange (Tusman et al. 2011a). VD can be calculated using tracer gases provided that an external gas source and the corresponding sensor placed at the opening of the airways are available (Bartels et al. 1954). However, the body's own carbon dioxide is the best option for the clinical measurement of VD because of the following: (1) CO₂ is a biological gas, and an external source is not needed. (2) CO₂ is a good tracer of ventilation due to its particular kinetics with its obligatory elimination by the lungs. (3) Infrared CO₂ sensors are small, robust, precise, and accurate for bedside assessment. (4) Dead space induces hypercapnia with hardly any effect or no effect at all on arterial oxygenation. VD measured by VCap evaluates not only the efficiency of particular ventilatory settings but also the complete kinetics of CO₂, which in most cases reveal the cause of hypercapnia.

In general, VD is constituted by any artificial airways placed proximally to the Y piece and by lung tissue that have no contact with the pulmonary capillary blood flow (Siobal 2016; Tusman et al. 2011a; Sinha et al. 2011). It is formed by the airways (VD_{aw}) and alveolar (VD_{alv}) dead spaces, and their sum comprises the global or physiological dead space (VD_{phys}) (Fig. 38.1d). In mechanically ventilated patients, we must take into account the instrumental dead space (VD_{inst}) (Tusman et al. 2015), which is an additional gadget placed between the Y piece and the patient's airways like elbows, mainstream sensors, connectors, heat moisture exchangers, and facial mask. (see Fig. 38.2a and b). The smaller the patient's body size, the higher will be the impact of VD_{inst} on the arterial partial pressure of CO_2 ($PaCO_2$).

Two mechanisms are involved in the genesis of dead space (Tusman et al. 2015). On the one hand, the inhaled fresh gas containing no CO_2 mixes with gases filling the FRC at the end of inspiration, thereby causing a dilution of the alveolar CO_2 in well-ventilated zones (high V/Q areas), reaching its maximum expression within the alveolar dead space units where the alveolar gas has similar composition than the inspired air. This dilution effect explains why the mean alveolar partial pressure of CO_2 ($PACO_2$) remains below the level of the arterial value. On the other hand, the airways and instrumental dead spaces are filled with CO_2 from the previous expiration, which is re-inhaled in the next inspiration and then retained within the lungs. Both *dilution* and *rebreathing* have "dead space effects" which impair the lung's efficiency for the elimination of CO_2 .

VD is measured in a noninvasive fashion with volumetric capnography using both *Fowler's concept* and *Bohr's formula* (Fowler 1948; Bohr 1891). The Fowler concept is based on the slope of phase II of the capnograms, which represents the expiratory volume of CO_2 stemming from lung units with different rates of emptying. As lungs are fractal asymmetric structures, each lung unit has its own transition zone between gas transported by convection and by diffusion that is placed close to the boundary between conducted

airways and alveoli at end-inspiration (Horsfield and Cumming 1968; Crawford et al. 1985). During expiration, those gas interfaces move proximally and reach the mainstream CO_2 sensor at different moments, explaining the origin of phase II and its corresponding slope. Thus, Fowler's concept separates the airways compartment (convective transport) from the alveolar compartment (diffusive transport) at the midpoint of the slope of phase II. This *mean airway-alveolar interface* defines the VD_{aw} (Fig. 38.1d) (Tusman et al. 2011a). There are many techniques to determine this midpoint of phase II, but all of them refer to the concept initially described by Fowler (Hatch et al. 1953; Langley et al. 1975; Olsson et al. 1980; Fletcher and Jonson 1981; Cumming and Guyatt 1982; Wolff et al. 1989; Tusman et al. 2009).

Bohr's formula is a mass balance equation that calculates the physiological dead space ratio (VD/VT or VD_{phys}/VT) using both the alveolar ($PACO_2$), inspired ($PICO_2$), and mixed expired partial pressures of CO_2 ($\bar{P}E_{CO_2}$) as:

$$VD/VT = \left(PACO_2 - \bar{P}E_{CO_2} \right) / \left(PACO_2 - PICO_2 \right)$$

$PICO_2$ is assumed to be zero because fresh breathing gas mixtures should not have CO_2 . However, some CO_2 re-inhalation from the circuit "Y" piece and from instrumental dead space must be taken into account at times to do proper dead space measurements.

$PACO_2$ expresses the averaged partial pressure of CO_2 that comes from the entire population of ventilated alveoli (Tusman et al. 2011a). $PACO_2$ is affected by phenomena that take place within alveoli and depends on the balance between the amount of CO_2 supplied to the lungs by blood and its elimination by ventilation. $PACO_2$ is difficult to measure because the composition of alveolar gas varies during the respiratory cycle and because each lung unit has its own value depending on the local V/Q ratio. A solution to get a representative $PACO_2$ is to determine the mean value in a breath at the midpoint of the slope of phase III (Tusman et al. 2009; Fletcher and Jonson 1984; Tusman et al. 2011b). The

rationale of this concept is based on the certainty to get a pure alveolar gas sample with the phase III of volumetric capnograms, once the CO₂-free inspired gases within non-alveolated airways are expired.

$\bar{P}\bar{E}CO_2$ is the mixed partial pressure of CO₂ that is caused by the dilution effect of gas free of CO₂ (inspired VT) within the resident gas in the lungs rich in CO₂. $\bar{P}\bar{E}CO_2$ is influenced by the dilution effect of the whole VT including not only the alveolar but also the airway and instrumental dead spaces. $\bar{P}\bar{E}CO_2$ derives from the mixed expired fraction of CO₂ ($F\bar{E}CO_2 = VT_{CO_2,br}/VT$) originally obtained by breathing into Douglas's bag. Nowadays, $\bar{P}\bar{E}CO_2$ measured by VCap has been validated and can be easily calculated in one breath as follow (Tusman et al. 2011a, b):

$$\bar{P}\bar{E}CO_2 = \bar{F}\bar{E}CO_2 * (\text{barometric pressure} - \text{vapor pressure})$$

The absolute VD_{phys} value is calculated by multiplying VD/VT by VT , and then, VD_{alv} is obtained by subtracting VD_{aw} from VD_{phys} . All dead spaces are clinically expressed in relation to the expired volume because VD is highly dependent on the size of VT (Fletcher and Jonson 1984).

Nowadays, dead space calculations using Bohr's original formula are possible ever since the breath-by-breath measurements of $PACO_2$ and $\bar{P}\bar{E}CO_2$ by VCap became feasible. Such measurements were validated against reference values calculated by the alveolar gas equation using information from the multiple inert gas elimination technique (MIGET) (Tusman et al. 2011b).

The inability to obtain $PACO_2$ at the bedside forced physicians to use Enghoff's alternative to Bohr's equation for many years (Enghoff 1938):

$$VD / VT = (PaCO_2 - \bar{P}\bar{E}CO_2) / PaCO_2$$

$PACO_2$ was replaced by the $PaCO_2$ value obtained by arterial blood analysis, making this calculation intermittent and invasive in nature. The main pitfall of this formula is the fact that $PaCO_2$ is systematically higher than the $PACO_2$

due to the effect of the shunt. This means that the high venous PCO_2 of low V/Q and shunting areas is not eliminated by ventilation and will thus reach the systemic side of the circulation. This shunt-related increase in $PaCO_2$ relative to $PACO_2$ results in an overestimation of the actual VD/VT value (Suarez Sipmann et al. 2014; Tusman et al. 2011a; Sinha et al. 2011). The "fictitious" dead space created by the shunt effect is a virtual alveolar VD that does not represent any real gas volume (Fletcher and Jonson 1981). This is the reason why we postulated that Enghoff's equation represents an index of V/Q inequalities and should not be considered a surrogate of dead space because it includes all kinds caused by V/Q mismatch (Suarez Sipmann et al. 2014; Tusman et al. 2011a). Figure 38.3 clearly shows the differences between the equations proposed by Bohr and by Enghoff in mechanically ventilated patients with ARDS (Gogniat et al. 2018). Sicker patients with worse lung mechanics presented higher dead spaces and Enghoff's indices, which are suggestive of more overdistension and shunt in these patients than in the ones with better lung mechanics. Therefore, both formulas are of clinical importance, but they represent different aspects of lung physiology and their difference corresponds to the amount of shunt.

For the clinical application of the dead space concept, it is mandatory to know the normal values (Table 38.1). We described that the physiological dead space is close to 1/5 or 1/4 of the tidal volume in healthy volunteers during spontaneous breathing. The value increases to 1/3 when mechanical ventilation is established (Tusman et al. 2013). These values were similar to the ones obtained by Åström et al. in volunteers with VD/VT values of 0.24 ± 0.4 , VD_{aw}/VT of 0.19 ± 0.4 , and VD_{alv}/VT of 0.09 ± 0.3 (Åström et al. 2000). It is common to observe VD/VT values ≥ 0.30 in anesthetized and ≥ 0.40 in critically ill patients. This is caused by the known effect of positive pressure ventilation on dead space as well as by the influence of surgical technics (capnoperitoneum, one-lung ventilation), body positions (Trendelenburg, lateral), and cardiopulmonary diseases. In ARDS patients, Bohr's VD/VT values are higher than 0.50 (Gogniat et al. 2018;

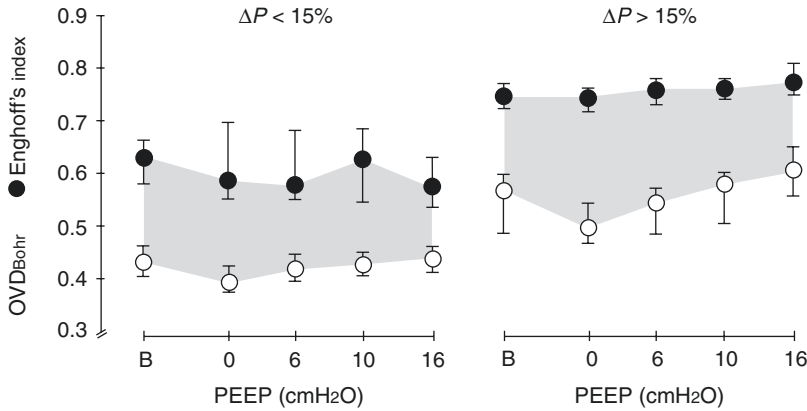


Fig. 38.3 Differences between Bohr’s and Enghoff’s formulas. Data of 14 mechanically ventilated patients with ARDS (Tusman et al. 2011b). Patients were ventilated with fixed ventilatory settings at baseline (B) and at four randomized PEEP steps. Bohr’s physiological dead space (VD_{Bohr}) and Enghoff’s index were calculated at the end of each PEEP step. Two kinds of responses to PEEP can be

observed: a group of patients in whom driving pressure did not surpass 15% of baseline values ($\Delta P < 15\%$, $n = 7$) and another group of patients in whom driving pressure exceeded 15% of baseline values ($\Delta P > 15\%$, $n = 7$). The gray area represents the shunt effect. Data presented as median and first to third quartiles

Table 38.1 Reference values of dead space parameters in adults

Patient	Ventilation	VD/VT	VD_{aw}/VT	VD_{alv}/VT_{alv}
Healthy volunteer	Spontaneous breathing	0.23 ± 0.08	0.17 ± 0.09	0.07 ± 0.06
Healthy anesthetized	VT 6 mL/kg PEEP 6 cmH ₂ O	0.28 ± 0.07	0.18 ± 0.08	0.09 ± 0.07
Critically ill anesthetized	VT 6 mL/kg PEEP 8 cmH ₂ O	0.41 ± 0.07	0.23 ± 0.07	0.23 ± 0.08
Critically ill ARDS	VT 6 mL/kg PEEP 12 cmH ₂ O	0.55 ± 0.11	0.33 ± 0.09	0.29 ± 0.10

From Tusman et al. (2013)

Different dead space parameters: Bohr’s physiological (VD/VT), airway (VD_{aw}), and alveolar (VD_{alv}/VT_{alv}) dead spaces observed in spontaneously breathing volunteers and in mechanically ventilated patients

Blanch et al. 1999) and Enghoff’s index reaching even higher values due to the effect of the right-to-left shunt (Beydon et al. 2002; Kallet et al. 2017; Doorduyn et al. 2016).

Monitoring dead space in mechanically ventilated patients transcends the evaluation of alveolar ventilation and the fine-tuning of baseline ventilatory settings. Dead space was found to be useful when conducting lung recruitment maneuvers at the bedside in experimental models (Tusman et al. 2006, 2010), in morbidly obese patients (Tusman et al. 2014), and in ARDS patients (Fengmei et al. 2012; Rodriguez et al. 2013). Recently, we described how dead space measurements in ARDS patients could be used to

evaluate different patterns in the response to PEEP (Gogniat et al. 2018). Those patients whose response to PEEP was positive based on a decrease in driving pressure (plateau minus PEEP) $\leq 15\%$ of baseline values showed much lower physiological and alveolar dead space ratios compared to non-responders (Fig. 38.3). These findings are in line with the findings of Suter et al. who found the lowest VD value at “best” PEEP (Suter et al. 1975). This best PEEP was also associated with lower shunt, higher respiratory compliance, and better cardiac output and oxygen delivery. In contrast, VD increased at low and high PEEP levels, probably because of lung collapse and overdistension, respectively. In

addition, Enghoff's index calculated by VCap has an important value as a predictor of mortality in ARDS (Nuckton et al. 2002; Kallet et al. 2004). This index is an independent variable related to death in ARDS patients during the early and late evolution of the syndrome.

Monitoring Gas Exchange by VCap

Gas exchange occurs by diffusion, a passive mechanism in which O₂ and CO₂ molecules move along a concentration or partial pressure gradient across the alveolar-capillary membrane. Diffusion is a process contemplated in Fick's law (Brogioli and Vailati 2001), where the amount of CO₂ molecules that cross the membrane per unit of time (Dg/Dt) is directly proportional to the solubility of CO₂ in blood (λ), the area available for gas exchange (A), the partial pressure gradient of CO₂ across the membrane (ΔP), and inversely proportional to membrane width (w):

$$Dg / Dt = \lambda * A * \Delta P / w$$

The almost 20 times higher λ of CO₂ compared to that of O₂ in blood is responsible for the fact that neither the erythrocyte capillary transit time (i.e., anemia, exercise) nor any increment in w (i.e., interstitial pulmonary diseases) exerts any clinically relevant influence on CO₂'s passage to the alveolar compartment. This means that these factors per se do not cause clinically important hypercapnia.

However, the remaining two factors of Fick's law affect the elimination of this gas more profoundly. The A is reduced not only by problems at the alveolar side (atelectasis, airways closure, mucus, pneumonia, etc.) but also by deficient pulmonary perfusion (embolism, excess of PEEP, or any global hemodynamic deterioration). In mechanically ventilated patients, A can be modified dynamically by changes in the underlying disease and changes in ventilator settings, both of which affect the V/Q ratio. Temporal and spatial V/Q inhomogeneities decrease the functional area of gas exchange and thereby reduce the amount of CO₂ that can be eliminated by ventilation per minute (VCO₂), which results in the retention of CO₂ in the arterial side.

The remaining factor of Fick's law that can affect CO₂ diffusion is ΔP or the CO₂ gradient between the pulmonary capillaries and the alveoli. While similar to the alveolar-to-arterial oxygen partial pressure gradient, the $P(A - a)O_2$, CO₂ elimination relies on a diffusion gradient across the alveolar-capillary membrane in the opposite direction which is abbreviated as $P(a - A)CO_2$ (Tusman et al. 2011a). The clinical meaning of both parameters is roughly the same as both reflect all factors that affect the exchange of these gases across the membrane. In the past, PACO₂ could not be measured at the bedside, and thus, for practical purposes, this index was replaced by the difference between PaCO₂ and the end-tidal partial pressure of CO₂ (PETCO₂) obtained by standard capnography. The P(a-ET)CO₂ difference in healthy patients during anesthesia is between 3–5 mmHg; any V/Q mismatch increases this value (Nunn and Hill 1960). Nowadays, PACO₂ can be accurately measured by VCap which makes P(a-A)CO₂ available at the bedside; normal values are between 5–8 mmHg (Tusman et al. 2011b). This latter index makes more physiological sense than the often used $P(a - ET)CO_2$ because PETCO₂ represents lung units with a high expiratory-time constant that emptied later during the breath and therefore have more time to receive CO₂ molecules from the capillary side. PACO₂, on the other hand, represents all lung units with different expiratory time constants and V/Q ratios thereby constituting the average CO₂ value within the alveolar compartment in the same way that PaCO₂ represents an average value within the arterial blood (Tusman et al. 2011a).

Considering the above thoughts about CO₂ exchange, the elimination of CO₂ can be manipulated clinically in two ways. One is by increasing alveolar ventilation (VA) at constant A , by augmenting tidal volume and/or respiratory rate, or by decreasing dead space. VD can be reduced by eliminating any unnecessary instrumental dead space, by adding an inspiratory hold, by limiting plateau pressure and PEEP, or by avoiding autoPEEP.

The other way to improve the removal of CO₂ is to increase A at constant VA. This can be done by reducing inflammation in alveoli by the use of antibiotics in pneumonia or by recruiting atelec-

tatic lungs. The increased area of gas exchange then allows more CO₂ molecules per unit of time to cross the membrane, thereby decreasing not only the partial pressure of CO₂ on both sides of the membrane but also the gradient (Fig. 38.4). In this context, $P(a - A)CO_2$ becomes a surrogate for the size of A and resembles a more commonly used $P(A - a)O_2$ gradient.

Figure 38.4 shows how decreases in A , documented as lung collapse in CT images, alter the shape of capnograms and reduce the amount of CO₂ eliminated per breath. The worse the V/Q ratio, the more the capnogram is deformed, and

the higher the difference between arterial and alveolar PCO₂.

Hemodynamic Monitoring

Pulmonary perfusion transports CO₂ molecules into the lungs to be eliminated by ventilation. The elimination of CO₂ (VCO₂) per minute is calculated by multiplying the area under the VCap curve ($VT_{CO_2,br}$ = amount of CO₂ eliminated per breath) by the respiratory rate (Fig. 38.1b). There is a direct relationship between pulmonary perfu-

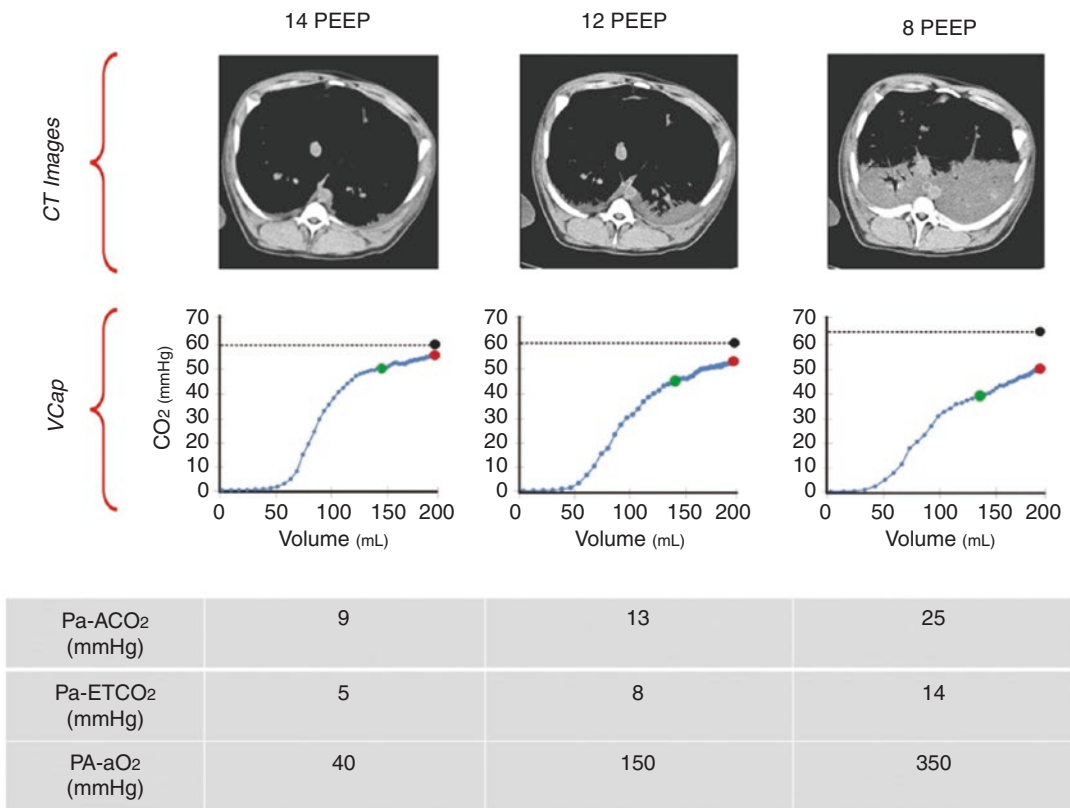


Fig. 38.4 Monitoring the diffusion of CO₂ by volumetric capnography. Data belongs to a mechanically ventilated pig with ARDS after lung recruitment and PEEP titration. PEEP titration was performed in a volume-controlled mode of ventilation using fixed settings and the same alveolar ventilation. The *open lung* PEEP – the minimum amount of PEEP that keeps the lung without collapse – was found at 14 cmH₂O (left). The first dependent lung atelectasis appears at PEEP 12 cmH₂O (middle), while almost half the lungs are collapsed at PEEP 8 cmH₂O

(right). Looking at the CT findings, the corresponding changes in the area of gas exchange (A) become evident and are associated with characteristic modifications of the shape of the VCap and of the arterial (black dot), the end-tidal (red dot), and the mean alveolar (green dot) partial pressures of CO₂. Corresponding differences between arterial and alveolar, between arterial and end-tidal PCO₂, as well as between alveolar and arterial O₂ are provided in the table below the curves

sion and $\dot{V}CO_2$, which was clearly demonstrated in mathematical models (Schwardt et al. 1994; Schwardt et al. 1991), in animals (Tusman et al. 2010), and in humans during the weaning of cardiopulmonary bypass (Tusman et al. 2005, 2012). This close dependency is clinically useful for monitoring pulmonary blood flow noninvasively on a breath-by-breath basis. Such clinical monitoring can be conducted in a *qualitative* way simply by observing the real-time changes in expired CO_2 during an acute hemodynamic problem. Typical examples are the sudden decrease of $PETCO_2$ and $\dot{V}CO_2$ values during surgery resulting from low cardiac output states of any cause (Fig. 38.2d).

Quantitative monitoring utilizes VCap to calculate effective pulmonary blood flow (EPBF) by applying a partial CO_2 rebreathing and the capnodynamic method (Capek and Roy 1988; Peyton et al. 2006). But what exactly is EPBF? This parameter is the portion of right heart cardiac output (CO) that comes in contact with ventilated alveoli and thus participates in gas exchange. Therefore, right heart cardiac output (CO) is nothing else but the sum of blood flowing through the effective (CO_{EPBF}) and shunted (CO_{SHUNT}) portions of the lungs per unit of time. CO_{EPBF} can be measured noninvasively by applying the inverse Fick principle and by using CO_2 instead of O_2 :

$$CO_{EPBF} = \dot{V}CO_2 / (CvCO_2 - CaCO_2),$$

$CvCO_2$ and $CaCO_2$ are venous and arterial contents of carbon dioxide, respectively.

In order to make the CO_{EPBF} calculation noninvasive, the kinetics of CO_2 needed to be disturbed either by a short rebreathing maneuver (adding an instrumental dead space or adding CO_2 to the inspired gases) or by a temporary change in alveolar ventilation (Capek and Roy 1988; Peyton et al. 2006). The following is the differential Fick equation applied before (b) and after (a) CO_2 alteration:

$$CO_{EPBF} = (\dot{V}CO_2 [b] - \dot{V}CO_2 [a]) / S_{CO_2} * (PACO_2 [a] - PACO_2 [b])$$

where S_{CO_2} is the coefficient of solubility of CO_2 in blood introduced in the equation to transform the alveolar partial pressure (mmHg) into a concentration (L_{gas}/L_{blood}) of CO_2 . The differential Fick equation assumes that the mixed venous CO_2 concentration remains constant and that the capillary fraction of CO_2 is similar to the $FACO_2$ measured by VCap.

The NICO monitor (Respironics, Murrysville, PA, US) calculates CO_{EPBF} using the partial CO_2 -rebreathing technique intermittently throughout an additional instrumental dead space (Capek and Roy 1988; Gedeon et al. 1980; Jaffe 1999). This additional dead space is a short circuit placed in parallel at the “Y” piece of the patient’s circuit. This parallel tubing makes contact with the main ventilatory circuit when an automatic valve is open. Thus, breathing gases that comes into this special tube are re-inhaled during 50 seconds. After a total time of 3 minutes and after CO_2 concentration reaches the baseline values, the CO_{EPBF} is calculated. Shunt fraction is estimated from the SpO_2 and FiO_2 values entered into the device by using the iso-shunt plot and adding this to the CO_{EPBF} to obtain the global CO (Gedeon et al. 1980). The NICO performance was compared to standard measurements of CO by thermodilution in many experimental and clinical studies with variable results (Gama de Abreu et al. 1997; Nilsson et al. 2001; Rocco et al. 2004; Allardet-Servent et al. 2009). In general, good agreement with the reference CO was found in healthy lungs, and limited agreement was observed in sick lungs with high shunt fractions.

The capnotracking method described by Peyton et al. calculates CO_{EPBF} based on brief modifications of tidal volume (Peyton et al. 2008; Peyton 2012; Peyton 2013). A complete 12-breaths sequence of six low VTs followed by six high VTs induces a change in alveolar ventilation and the corresponding CO_2 balance from which CO_{EPBF} is derived. A series of equations, called *calibration*, *capacitance*, and *continuous* formulas, are applied to get the final CO_{EPBF} value (Peyton et al. 2008; Peyton 2012, 2013). The global CO is calculated by adding CO_{EPBF} to the CO_{SHUNT} value estimated by the shunt equation,

taking into account pulse oximetry (SpO₂) and by assuming a mixed venous saturation of 70%. Thus, the system delivers fully automated and quasi-continuous CO_{EPBF} using Fick's principle and avoids any additional rebreathing loop within the ventilator's circuit.

The capnotracking method showed good accuracy and agreement with the standard right heart thermodilution technique and transesophageal echocardiography (Peyton 2012). The authors have recently improved the technique in a second-generation capnotracking prototype which was tested in 50 patients undergoing cardiac and liver surgeries (Peyton and Kozub 2018). Compared to thermodilution, the bias was -0.3 L/min, the percentage of error $\pm 38\%$, concordance in the measurement of changes at least 15% in CO of 81%, and intra-class correlation coefficient of 0.91.

Albu et al. described another solution of the capnodynamic equation to obtain CO_{EPBF} and the effective lung volume (ELV) by using a mole balance equation for the carbon dioxide content in the lung (Albu et al. 2013). The equation can be implemented in a ventilatory algorithm which changes alveolar ventilation by inspiratory or expiratory holds maintaining VT stability. This pattern alters the alveolar fraction (FACO₂) and the amount of expired (VCO₂) carbon dioxide, including 3 unknown values in the formula – ELV, EPBF, and CvCO₂:

$$\text{ELV} * (\text{FACO}_2^n - \text{FACO}_2^{n-1}) = \text{EPBF} * \Delta t^n * (\text{CvCO}_2 - \text{CaCO}_2) - \text{VTCO}_2$$

where n is the current breath, $n - 1$ is the previous breath and Δt^n is the current breath cycle time. The left-hand side of the equation represents the difference in CO₂ content in the lungs between two breaths, while the right-hand side expresses the circulatory supply of CO₂ into the lung. The equation compares the content and elimination of CO₂ during pause-induced fluctuations in alveolar ventilation without altering airway pressures or lung volumes. This approach avoids the impact of increases in VT or airways pressure on hemodynamics.

The actual algorithm includes a sequence of 6 normal breaths followed by 3 breaths with an expiratory hold of 5 seconds. This breathing pattern is controlled by software within the ventilator (Servoi, Maquet, Sweden) which cyclically varies the PETCO₂ between 4–8 mmHg. The above formula is applied continuously, whenever a new breath replaces the previous one in the formula thereby outputting one CO_{EPBF} value per breath.

Sander et al. compared the performance of the capnodynamic method and thermodilution with the reference ultrasonic flow probe placed around the pulmonary artery trunk in pigs (Sander et al. 2014). Different hemodynamic states were created by hemorrhage, fluid overload, infusions of vasoactive drugs, and occlusion of the vena cava. They found a bias (limits of agreement) of 0.2 (-1.0 to -1.4) L/min⁻¹ and a percentage error (PE) for CO_{EPBF} of 47%. The trending ability of CO_{EPBF} was assessed by calculating delta values from CO readings before and during each intervention. The correlation between delta-CO_{EPBF} and delta-CO by ultrasound was high ($r = 0.96$, $P < 0.0001$). The concordance was 97% assessed by the four-quadrant plot and 97% ($+30^\circ$ radial limits) using the polar plot method, with 15% exclusion zones applied. These authors showed in the same model and setup that the presence of high shunt impaired the performance of the capnodynamic method (Sander et al. 2015). This indicates that a correction of CO_{EPBF} for shunt effects is needed anytime a global CO is needed.

Similar preliminary data were obtained in cardiac surgery patients when CO_{EPBF} was compared with thermodilution (unpublished personal data). We found a bias of 0.63 L/min⁻¹, a trending ability of 81% with a percentage error of 34%, and an inherent precision of 8%. The system was reliable during relevant moments of the surgery. The method does not need calibration (beyond CO₂ and flow sensors calibration), is easy to use and its rapid response allows detection of acute hemodynamic events. Figure 38.5 shows the high time-resolution of the capnodynamic method to get CO_{EPBF} in one of these cardiac surgery patients. Further evaluation of improved capno-

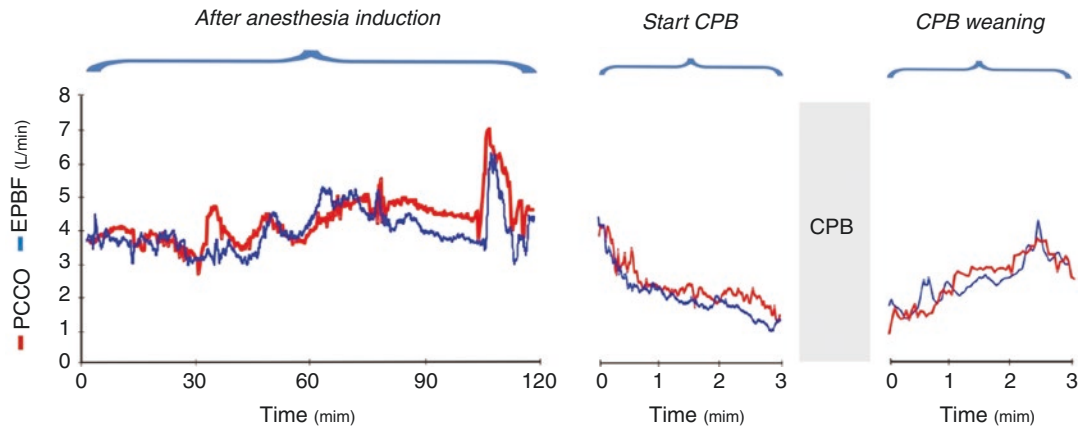


Fig. 38.5 Effective pulmonary blood flow calculated from volumetric capnography. Data belongs to a patient undergoing cardiac surgery. The figure shows the time course of the effective pulmonary blood flow (CO_{EPBF}) calculated breath-by-breath using the capnodynamic method. Calibrated cardiac output derived from analysis

of the contour of the femoral arterial pulse wave (PCCO) was used as a reference (red line). Note the good trending between signals and the high time-resolution of CO_{EPBF} during the start and weaning from the cardiopulmonary bypass (CPB)

dynamic systems with shunt corrections is guaranteed in the next years.

Preload Assessment by VCap

The first section of this book describes cardiovascular pathophysiology and how heart-lung interaction can alter hemodynamics in mechanically ventilated patients. The origins of such hemodynamic instability are multiple although one of the most common causes is an inadequate preload. Thus, 50% of critically ill patients in ICU and similar percentages of cardiac surgery patients in the operating room present with some deficit in preload (Michard and Teboul 2002; Kim et al. 2011). This preload-dependency does not mean that the patient actually needs fluids. The attending physician will have to decide whether to treat with fluids or not taking into consideration other important clinical aspects and the historical evolution of the patient's disease or clinical condition. Physicians are thus immersing in a crucial dilemma because intravenous fluids can improve survival in selected critically ill patients (Rivers et al. 2001), while fluid overload, on the other

hand, can impair outcome due to hemodilution, cardiovascular overload, and tissue edema (Vincent et al. 2006; Boyd et al. 2011; Payen et al. 2008; Jozwiak et al. 2013; Kirkpatrick et al. 2013). Therefore, the important question is how to identify patients who really need treatment with intravenous fluids.

Fluid responsiveness refers to the ability of the heart to increase cardiac output after fluid infusions. Many techniques have been developed to predict fluid responsiveness in a reversible manner without having to challenge the patient with intravenous fluids. Those techniques stress the cardiovascular system for a brief moment to unmask any preload dependency. Examples of such dynamic maneuvers are passive leg-rising (PLR), Trendelenburg position, and addition of PEEP or inspiratory-expiratory holds (Monnet et al. 2006, 2009; Geerts et al. 2011). The response to these maneuvers is evaluated by observing changes in cardiac output by dynamic parameters like variation in pulse pressure, stroke volume, plethysmography, vena cava diameter, central venous pressure, pre-ejection period, or aortic blood velocity to name but a few (Preisman et al. 2005; Cavallaro et al. 2008).

Capnography is an attractive option to test fluid responsiveness in mechanically ventilated patients. As described before, CO_2 elimination is highly dependent on right heart cardiac output and particularly sensitive to changes in hemodynamics caused by cardiopulmonary problems (Tusman et al. 2005, 2012). Therefore, CO_2 has all the features of a parameter that can suitably detect changes in cardiac output induced by a dedicated challenge of the cardiovascular system. A few studies have evaluated this hypothesis. Monnet et al. described in critically ill patients that a change $\geq 5\%$ in PETCO_2 had a sensitivity of 71% (95% CI, 48–89%) and specificity of 100% (95% CI, 82–100%) to predict fluid responsiveness during a PLR maneuver (Monnet et al. 2013). Along the same research line, Monge et al. showed similar results in patients with respiratory failure during PLR: an increase $\geq 5\%$ in PETCO_2 showed a sensitivity of 91% (95% CI, 70–99%) and a specificity of 94% (95% CI, 70–100%) (Monge García et al. 2012).

We have proposed another approach using a brief increment in PEEP to unmask any hidden preload dependency in cardiac surgery patients (Tusman et al. 2016). This challenge is based on the known cardio-respiratory interaction in patients undergoing positive-pressure ventilation (Geerts et al. 2011). The PEEP maneuver makes the patient's heart move temporarily and reversibly from the flat to the steep portion of the Frank-Starling curve. We evaluated by VCap the changes in the amount of CO_2 eliminated during this PEEP challenge. We hypothesized that VCO_2 is a good and reliable noninvasive surrogate of cardiac output because both share the dimension of flow (L/min). Our hypothesis was derived from the good correlation we found between VCO_2 and cardiac output in previous studies (Schwardt et al. 1991, 1994; Tusman et al. 2005, 2012).

Our results showed that a decrease $\geq 11\%$ in VCO_2 predicted preload dependency with a sensitivity of 92% (95% CI, 85–97%), a specificity of 94% (95% CI, 91–96%), and an accuracy of

99% (95% CI, 96–99%) (Tusman et al. 2016). As opposed to the results of Monnet et al. and Monge et al. (Monnet et al. 2013; Monge García et al. 2012), our study revealed that a decrease $\geq 5\%$ in PETCO_2 showed only low sensitivity (63%; 95% CI, 49–75%) and specificity (74%; 95% CI, 67–80%) for the detection of preload-dependency. Figure 38.6 depicts an example of a preload-dependent patient during the PEEP challenge. Note how hemodynamic parameters and VCO_2 decreased at the end of a 1-minute ventilation period at 10 cmH_2O of PEEP. This particular cardiac surgery patient showed a decrease $\geq 11\%$ in VCO_2 and a $\geq 15\%$ fall in CO identifying him as a “responder” to intravenous fluids. The strategy is simple, noninvasive, reversible, and not affected by arrhythmias or the size of the tidal volume used.

However, as a method for preload-dependency assessment, the PEEP maneuver has its own pitfalls and limitations. For example, VCO_2 could increase with the application of 10 cmH_2O of PEEP because of the potential recruitment of small airways and atelectasis, thereby mitigating the PEEP-induced decrement in VCO_2 in responders (Tusman et al. 2016). Besides, the transmission of PEEP to the pleural space is variable and depends on lung compliance, extravascular lung water, and autoPEEP among other factors (Magder et al. 2001). Thus, the effect on cardiac output would be also variable giving some false-negative results. As similar to the leg-rising maneuver for preload assessment, the PEEP maneuver should be evaluated in less than 1 minute to avoid any potential activation of compensatory neuro-humoral reflex (De Backer 2006).

These limitations can be solved by normalizing lung volume history before the maneuver, measuring and taking into account autoPEEP, adding more PEEP to stiff lungs, and limiting the maneuver to less than 1 minute. New studies should be done testing these limitations and looking for improvement in this PEEP maneuver for the assessment of fluid responsiveness using the expired CO_2 signal.

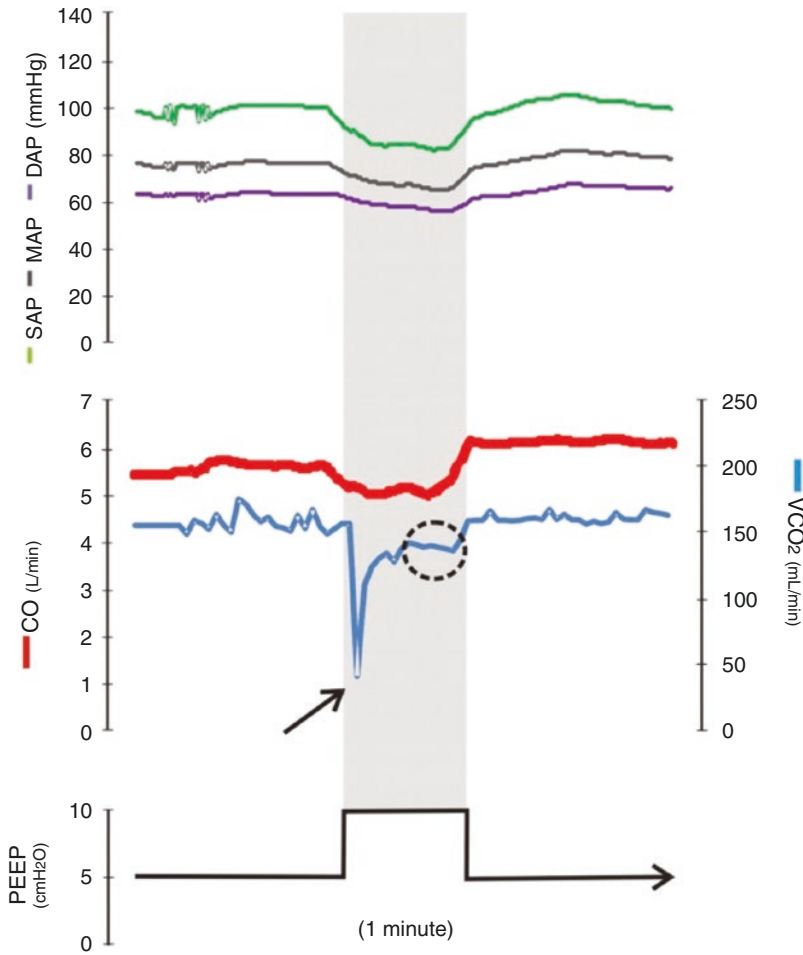


Fig. 38.6 Preload assessment by volumetric capnography. Data of a patient scheduled for cardiac surgery obtained immediately after the induction of anesthesia. The PEEP challenge, from 5 to 10 cmH₂O for 1 minute, induced a change >14% in minute elimination of CO₂ (VCO₂) and >15% in cardiac output (CO) compared to the values immediately before the maneuver. Similar changes were observed in systolic (SAP), diastolic (DAP), and

mean (MAP) arterial pressures (upper curves). By definition, this patient was preload-dependent and should respond positively to intravenous fluids. The arrow indicates the effect of a decreased expiratory tidal volume on VCO₂ at the very moment PEEP was increased. The VCO₂ is evaluated during the last breaths (dotted circle) and compared to previous values with 5 cmH₂O of PEEP (more details in Monnet et al. 2013)

Summary

Vcap possesses all features of an ideal noninvasive monitoring methodology providing important clinical insights into gas exchange and hemodynamics breath-by-breath. Although VCap can be used to evaluate steady-state conditions such as the metabolic production of CO₂, it also

has great potential to provide information during unsteady-state conditions. This will allow the assessment of many of the individual components of cardiorespiratory functions at the bedside. However, the context sensitivity of CO₂ kinetics must always be considered to avoid false conclusions.

References

- Albu G, Wallin M, Hallbäck M, Emtell P, Wolf A, Lönnqvist PA, Habre W. Comparison of static end-expiratory and effective lung volumes for gas exchange in healthy and surfactant-depleted lungs. *Anesthesiology*. 2013;119:101–10.
- Allardet-Servent J, Forel JM, Roch A, Chiche L, Guerville C, Bouzana F, Papazian L. Pulmonary capillary blood flow and cardiac output measurement by partial carbon dioxide rebreathing in patients with acute respiratory distress syndrome receiving lung protective ventilation. *Anesthesiology*. 2009;111:1085–92.
- Anderson CT, Breen PH. Carbon dioxide kinetics and capnography during critical care. *Crit Care*. 2000;4:207.
- Anderson JA, Vann WF. Respiratory monitoring during pediatric sedation: pulse oximetry and capnography. *Pediatr Dent*. 1988;10:94–101.
- Aström E, Niklason L, Drefeldt B, Bajc M, Jonson B. Partitioning of dead space – a method and reference values in the awake human. *Eur Respir J*. 2000;16:659–64.
- Bartels J, Severinghaus JW, Forster RE, Briscoe WA, Bates DV. The respiratory dead space measured by single breath analysis of oxygen, carbon dioxide, nitrogen or helium. *J Clin Invest*. 1954;33:41–8.
- Beydon L, Uttman L, Rawal R, Jonson B. Effects of positive end-expiratory pressure on dead space and its partitions in acute lung injury. *Intensive Care Med*. 2002;28:1239–45.
- Bhavani-Shankar K, Philip JH. Defining segments and phases of a time capnogram. *Anesth Analg*. 2000;91:973–7.
- Blanch L, Lucangelo U, Lopez-Aguilar J, Fernandez R, Romero PV. Volumetric capnography in patients with acute lung injury: effects of positive end-expiratory pressure. *Eur Respir J*. 1999;13:1048–54.
- Block FE Jr, McDonald JS. Sidestream versus mainstream carbon dioxide analyzers. *J Clin Monit*. 1992;8:139–41.
- Bohr C. Über die Lungeatmung. *Skand Arch Physiol*. 1891;2:236–8.
- Boyd JH, Forbes J, Nakada TA, Walley KR, Russell JA. Fluid resuscitation in septic shock: a positive fluid balance and elevated central venous pressure are associated with increased mortality. *Crit Care Med*. 2011;39:259–65.
- Breen PH. Carbon dioxide kinetics during anesthesia. *Anesthesiol Clin*. 1998;16:259–93.
- Breen PH, Isserles SA, Taitelman UZ. Non-steady state monitoring by respiratory gas exchange. *J Clin Monit Comput*. 2000;16:351–60.
- Broglioli D, Vailati A. Diffusive mass transfer by nonequilibrium fluctuations: Fick's law revisited. *Phys Rev E*. 2001;63(1–4):012105. [arXiv:cond-mat/0006163](https://arxiv.org/abs/cond-mat/0006163).
- Capek JM, Roy RJ. Noninvasive measurement of cardiac output using partial CO₂ rebreathing. *IEEE Trans Biomed Eng*. 1988;35:653–61.
- Carlson GC, Ray C, Miodownik S, Kopec I, Groeger JS. Capnography in mechanically ventilated patients. *Crit Care Med*. 1988;16:550–6.
- Cavallaro F, Sandroni C, Antonelli M. Functional hemodynamic monitoring and dynamic indices of fluid responsiveness. *Minerva Anestesiol*. 2008;74:123–35.
- Cherniack NS, Longobardo GS. Oxygen and carbon dioxide gas stores of the body. *Physiol Rev*. 1970;50:197–243.
- Crawford ABH, Makowska M, Paiva M, Engel LA. Convection- and diffusion-dependent ventilation misdistribution in normal subjects. *J Appl Physiol*. 1985;59:838–46.
- Cumming G, Guyatt AR. Alveolar gas mixing efficiency in the human lung. *Clin Sci (Lond)*. 1982;62:541–7.
- De Backer D. Can passive leg raising be used to guide fluid administration? *Crit Care*. 2006;10:170.
- Doorduyn J, Nollet JL, Vugts MPAJ, et al. Assessment of dead-space ventilation in patients with acute respiratory distress syndrome: a prospective observational study. *Crit Care*. 2016;20:121.
- Duncan PG, Cohen MM. Pulse oximetry and capnography in anaesthetic practice: an epidemiological appraisal. *Can J Anesth*. 1991;38:619–25.
- Enghoff H. Volumen inefficax. Bemerkungen zur Frage des schädlichen Raumes. *Uppsala Läkareforen Forhandl*. 1938;44:191–218.
- Farhi LE, Rahn H. Gas stores of the body and the unsteady state. *J Appl Physiol*. 1955;7:472–84.
- Fengmei G, Jin C, Songqiao L, Congshan Y, Yi Y. Dead space fraction changes during PEEP titration following lung recruitment in patients with ARDS. *Respir Care*. 2012;57:1578–85.
- Fletcher R, Jonson B. The concept of deadspace with special reference to the single breath test for carbon dioxide. *Br J Anaesth*. 1981;53:77–88.
- Fletcher R, Jonson B. Dead-space and the single breath test for carbon dioxide during anaesthesia and artificial ventilation. Effects of tidal volume and frequency of respiration. *Br J Anaesth*. 1984;56:109–19.
- Folch N, Peronnet F, Pean M, Massicotte D, Lavoie C. Labeled CO₂ production and oxidative vs nonoxidative disposal of labeled carbohydrate administered at rest. *Metabolism*. 2005;54:1428–34.
- Fowler WS. Lung function studies II. The respiratory dead space. *Am J Phys*. 1948;154:405–16.
- Gama de Abreu M, Quintel M, Ragaller M, Albrecht M. Partial carbon dioxide rebreathing: a reliable technique for noninvasive measurement of nonshunted pulmonary capillary blood flow. *Crit Care Med*. 1997;25:675–83.
- Gedeon A, Forslund L, Hedenstierna G, Romano E. A new method for noninvasive bedside determination of pulmonary blood flow. *Med Bio Eng Comput*. 1980;18:411–8.
- Geerts BF, Aarts LPH, Groeneveld AB, Jansen JRC. Predicting cardiac output responses to passive leg rising by PEEP-induced increase in central venous pressure, in cardiac surgery patients. *Br J Anaesth*. 2011;107:150–6.

- Gluck S. Acid-base. *Lancet*. 1998;352:474–9.
- Gogniat E, Ducey M, Dianti J, Madorno M, Roux N, Midley A, Raffo J, Giannasi S, San Roman E, Suarez-Sipmann F, Tusman G. Dead space analysis at different levels of positive end-expiratory pressure in acute respiratory distress syndrome patients. *J Crit Care*. 2018;45:231–8.
- Hatch T, Cook KM, Palm PE. Respiratory dead space. *J Appl Physiol*. 1953;5:341–7.
- Horsfield K, Cumming G. Functional consequences of airway morphology. *J Appl Physiol*. 1968;24:384–90.
- Huttman SE, Windisch W, Storre JH. Techniques for the measurement and monitoring of carbon dioxide in the blood. *Ann Am Thorac Soc*. 2014;11:645–52.
- Jaffe MB. Partial CO₂ rebreathing cardiac output – operating principles of the NICO™ system. *J Clin Monit Comput*. 1999;15:387–401.
- Jaffe MB. Infrared measurement of carbon dioxide in the human breath: “breathe through” devices from Tyndall to the present day. *Anesth Analg*. 2008;107:890–904.
- Jaffe MB. Time and volumetric capnography. In: Ehrenfeld J, Cannesson M, editors. *Monitoring technologies in acute care environments*. New York: Springer; 2014.
- Jozwiak M, Silva S, Persichini R, Anguel N, Osman D, Richard C, et al. Extravascular lung water is an independent prognostic factor in patients with acute respiratory distress syndrome. *Crit Care Med*. 2013;41:472–80.
- Kallet RH, Alonso JA, Pittet JF, Matthay MA. Prognostic value of the pulmonary dead space fraction during the first 6 days of acute respiratory distress syndrome. *Respir Care*. 2004;49:1008–14.
- Kallet RH, Zhuo H, Ho K, Lipnick MS, Gomez A, Matthay MA. Lung injury and other factors influencing the relationship between dead space fraction and mortality in ARDS. *Respir Care*. 2017; <https://doi.org/10.4187/respcare.05589>.
- Kellum J. Determinant of blood pH in health and disease. *Crit Care*. 2000;4:6–14.
- Kim B, Bellomo R, Fealy N, Baldwin I. A pilot study of the epidemiology and associations of pulse pressure variation in cardiac surgery patients. *Crit Care Resusc*. 2011;13:17–23.
- Kirkpatrick AW, Roberts DJ, De Waele J, Jaeschke R, Malbrain ML, De Keulenaer B, et al. Intra-abdominal hypertension and the abdominal compartment syndrome: updated consensus definitions and clinical practice guidelines from the World Society of the Abdominal Compartment Syndrome. *Intensive Care Med*. 2013;39:1190–206.
- Langley F, Even P, Duroux P, Nicolas RL, Cumming G. Ventilatory consequences of unilateral pulmonary artery occlusion. *Les colloques de L'Institut National de la Santé et de la Recherche Medicale*. 1975;51:209–14.
- Magder S, Lagonidis D, Erice F. The use of respiratory variations in right atrial pressure to predict the cardiac output response to PEEP. *J Crit Care*. 2001;16:108–14.
- Michard F, Teboul JL. Predicting fluid responsiveness in ICU patients. A critical analysis of evidence. *Chest*. 2002;121:2000–8.
- Monge García IM, Gil Cano A, García Romero M, Monteroso Pintado R, Pérez Madueño V, Díaz Monrové JC. Non-invasive assessment of fluid responsiveness by changes in partial end-tidal CO₂ pressure during passive leg-raising maneuver. *Ann Intensive Care*. 2012;2:9.
- Monnet X, Rienzo M, Osman D, Anguel N, Richard C, Pinsky MR, et al. Passive leg raising predicts fluid responsiveness in the critically ill. *Crit Care Med*. 2006;34:1402–7.
- Monnet X, Osman D, Ridet C, Lamia B, Richard C, Teboul JL. Predicting volume responsiveness by using the end-expiratory occlusion in mechanically ventilated intensive care unit patients. *Crit Care Med*. 2009;37:951–6.
- Monnet X, Bataille A, Magalhaes E, Barrois J, Le Corre M, Gosset C, Guerin L, Richard C, Teboul JL. End-tidal carbon dioxide is better than arterial pressure for predicting volume responsiveness by the passive leg raising test. *Intensive Care Med*. 2013;39:93–100.
- Nilsson LB, Eldrup N, Berthelsen PG. Lack of agreement between thermodilution and carbon dioxide-rebreathing cardiac output. *Acta Anaesthesiol Scand*. 2001;45:680–5.
- Nuckton TJ, Alonso JA, Kallet RH, Daniel BM, Pittet JF, Eisner MD, Matthay MA. Pulmonary dead-space fraction as a risk factor for death in the acute respiratory distress syndrome. *N Engl J Med*. 2002;346:1281–6.
- Nunn JF, Hill DW. Respiratory dead space and arterial to end-tidal CO₂ difference in anesthetized man. *J Appl Physiol*. 1960;15:383–9.
- Olsson SG, Fletcher R, Jonson B, Nordstroem L, Prakash O. Clinical studies of gas exchange during ventilatory support – a method using the Siemens-Elema CO₂ analyzer. *Br J Anaesth*. 1980;52:491–8.
- Orr JA, Jaffe MB. Combining flow and carbon dioxide, Chapter 39. In: Gravenstein, et al., editors. *Capnography*. 2nd ed. Cambridge University Press; 1994. p. 407–11.
- Payen D, de Pont AC, Sakr Y, Spies C, Reinhart K, Vincent JL, et al. A positive fluid balance is associated with a worse outcome in patients with acute renal failure. *Crit Care*. 2008;12:R74.
- Peyton PJ. Continuous minimally invasive peri-operative monitoring of cardiac output by pulmonary capnography: comparison with thermodilution and transesophageal echocardiography. *J Clin Monit Comput*. 2012;26:121–32.
- Peyton PJ. Pulmonary carbon dioxide elimination for cardiac output monitoring in peri-operative and critical care patients: history and current status. *J Health Eng*. 2013;4:203–22.
- Peyton PJ, Kozub M. Performance of a second generation pulmonary capnography system for continuous monitoring of cardiac output. *J Clin Monit Comput*. 2018;32:1057–64.
- Peyton PJ, Venkatesan Y, Hood SG, Junor P, May C. Noninvasive, automated and continuous cardiac output monitoring by pulmonary capnodynamics: breath-by-breath comparison with ultrasonic flow probe. *Anesthesiology*. 2006;105:72–80.

- Peyton PJ, Thompson D, Junor P. Non-invasive automated measurement of cardiac output during stable cardiac surgery using a fully integrated differential CO₂ Fick method. *J Clin Monit Comput.* 2008;22:285–92.
- Preisman S, Kogan S, Berkenstadt H, Perel A. Predicting fluid responsiveness in patients undergoing cardiac surgery: functional haemodynamic parameters including the respiratory systolic variation test and static preload indicators. *Br J Anaesth.* 2005;95:746–55.
- Protti A, Andreis DT, Monti M, Santini A, Sparacino C, et al. Lung stress and strain during mechanical ventilation: any difference between statics and dynamics? *Crit Care Med.* 2013;41:1046–55.
- Rivers E, Nguyen B, Havstad S, Ressler J, Muzzin A, Knoblich B, et al. Early goal-directed therapy in the treatment of severe sepsis and septic shock. *N Engl J Med.* 2001;345:1368–77.
- Rocco M, Spadetta G, Morelli A, Dell'Utri D, Porzi P, Conti G, Pietrapaoli P. A comparative evaluation of thermodilution and partial CO₂ rebreathing techniques for cardiac output assessment in critically ill patients during assisted ventilation. *Intensive Care Med.* 2004;30:82–7.
- Rodriguez PO, Bonelli I, Setten M, Attie S, Madorno M, Maskin LP, Valentini R. Transpulmonary pressure and gas exchange during decremental PEEP titration in pulmonary ARDS patients. *Respir Care.* 2013;58:754–63.
- Roizen MF, Schreider B, Austin W, Polk S. Pulse oximetry, capnography, and blood gas measurements: reducing cost and improving the quality of care with technology. *J Clin Monit.* 1993;9:237–40.
- Sander CH, Hallböck M, Wallin M, Emtell P, Oldner A, Björne H. Novel continuous capnodynamic method for cardiac output assessment during mechanical ventilation. *Br J Anaesth.* 2014;112:824–31.
- Sander CH, Hallböck M, Suarez Sipmann F, Wallin M, Oldner A, Björne H. A novel continuous capnodynamic method for cardiac output assessment in a porcine model of lung lavage. *Acta Anaesthesiol Scand.* 2015; <https://doi.org/10.1111/aas.12559>.
- Schwardt JD, Gobran SR, Neufeld GR, Aukburg SJ, Scherer PW. Sensitivity of CO₂ washout to changes in acinar structure in a single-path model of lung airways. *Ann Biomed Eng.* 1991;19:679–97.
- Schwardt JD, Neufeld GR, Baumgardner JE, Scherer PW. Noninvasive recovery of acinar anatomic information from CO₂ expirograms. *Ann Biomed Eng.* 1994;22:293–306.
- Sinha P, Flower O, Soni N. Dead-space ventilation: a waste of breath! *Intensive Care Med.* 2011;37:735–46.
- Siobal MS. Monitoring exhaled carbon dioxide. *Respir Care.* 2016;61:1397–416.
- Suarez Sipmann F, Bohm SH, Tusman G. Volumetric capnography: the time has come. *Curr Opin Crit Care.* 2014;20:333–9.
- Suter PM, Fairley HB, Isenberg MD. Optimum end-expiratory airway pressure in patients with acute pulmonary failure. *N Engl J Med.* 1975;292:284–9.
- Tusman G, Areta M, Climente C, Plit R, Suarez-Sipmann F, Rodríguez-Nieto MJ. Effect of pulmonary perfusion on the slopes of single-breath test of CO₂. *J Appl Physiol.* 2005;99:650–5.
- Tusman G, Suarez-Sipmann F, Bohm SH, Pech T, Reissmann H, Meschino G, et al. Monitoring dead space during recruitment and PEEP titration in an experimental model. *Intensive Care Med.* 2006;32:1863–71.
- Tusman G, Scandurra A, Bohm SH, Suarez Sipmann F, Clara F. Model fitting of volumetric capnograms improves calculations of airway dead space and slope of phase III. *J Clin Monitor Comput.* 2009;23:197–206.
- Tusman G, Bohm SH, Suarez-Sipmann F, Scandurra A, Hedenstierna G. Lung recruitment and positive end-expiratory pressure have different effects on CO₂ elimination in healthy and sick lungs. *Anesth Analg.* 2010;111:968–77.
- Tusman G, Suarez Sipmann F, Bohm SH. Rationale of dead space measurement by volumetric capnography. *Anesth Analg.* 2011a;114:866–74.
- Tusman G, Suarez Sipmann F, Borges JB, Hedenstierna G, Bohm SH. Validation of Bohr dead space measured by volumetric capnography. *Intensive Care Med.* 2011b;37:870–4.
- Tusman G, Suarez-Sipmann F, Paez G, Alvarez J, Bohm SH. States of low pulmonary blood flow can be detected non-invasively at the bedside measuring alveolar dead space. *J Clin Monit Comput.* 2012;26:183–90.
- Tusman G, Gogniat E, Bohm SH, Scandurra A, et al. Reference values for volumetric capnography-derived non-invasive parameters in healthy individuals. *J Clin Monit Comput.* 2013;27:281–8.
- Tusman G, Groisman I, Fiolo FE, Scandurra A, Martinez Arca J, Krumrick G, Bohm SH, Suarez SF. Noninvasive monitoring of lung recruitment maneuvers in morbidly obese patients: the role of pulse oximetry and volumetric capnography. *Anesth Analg.* 2014;118:137–44.
- Tusman G, Bohm SH, Suarez SF. Dead space during one-lung ventilation. *Curr Opin Anesthesiol.* 2015;28:10–7.
- Tusman G, Groisman I, Maidana GA, Scandurra A, Arca JM, Bohm SH, Suarez-Sipmann F. The sensitivity and specificity of pulmonary carbon dioxide elimination for noninvasive assessment of fluid responsiveness. *Anesth Analg.* 2016;122:1404–11.
- Vincent JL, Sakr Y, Sprung CL, Ranieri VM, Reinhart K, Gerlach H, et al. Sepsis in European intensive care units: results of the SOAP study. *Crit Care Med.* 2006;34:344–53.
- Wiklund L. Carbon dioxide formation and elimination in man: recent theories and possible consequences. *Ups J Med Sci.* 1996;101:35–67.
- Wolff G, Brunner JX, Weibel W, Bowes CL, Muchenberger R, Bertschmann W. Anatomical and series dead space volume: concept and measurement in clinical praxis. *ACP Appl Cardiopulm Pathophysiol.* 1989;2:299–307.



MRI in the Assessment of Cardiopulmonary Interaction

39

Ritu R. Gill and Samuel Patz

Introduction

Pulmonary functional imaging combining anatomical and morphological evaluation is being actively explored both in research and clinical practice (Matsuoka et al. 2009). Functional assessment of the lungs can be achieved with several techniques such as dual energy computed tomography (CT), lung scintigraphy, 18-FDG-PETCT, and MRI, each with its own advantages and limitations. MRI of the lung offers a unique advantage over other modalities, as it allows us to map cardiopulmonary interactions without the use of ionizing radiation. However, MRI of lung can be challenging due to the inherent lack of protons in the lung parenchyma, magnetic field inhomogeneity due to susceptibility differences between air and tissues, and artifacts from cardiac and respiratory motion (Biederer et al. 2012a). Novel MR techniques based on proton imaging (described below) such as arterial spin labeling, Fourier decomposition, and hyperpolarized gas can be combined with routine clinical

sequences to enhance the signal from the lung parenchyma and assess cardiopulmonary interactions (Guimaraes et al. 2014; Van Beek et al. 2004; van Beek and Hoffman 2008; Nakai et al. 2008).

In the current clinical practice, comprehensive cardiopulmonary imaging evaluation cannot be achieved with a single modality. The convention is to perform serial exams in varying physiological and disease states, using a combination of imaging techniques with and without ionizing radiation and intravenous contrast. However, due to increasing concern over exposure to ionizing radiation and intravenous contrast, repeat examinations over time to assess treatment response, map pathophysiology and cardiopulmonary interactions may not be a viable strategy. Alternatively, single comprehensive MR scans combining both anatomical imaging and functional components potentially could be used to provide all the information. The latter approach would comprise of a generic protocol, which could take 10 times longer to perform as compared to a CT scan and could result in image degradation due to subject motion secondary to fatigue. Therefore, it is vital that the information needed from an MRI be clearly defined, thus allowing for optimal sequence and protocol selection.

In order to image cardiopulmonary interactions and to allow simultaneous evaluation of the lungs during a routine cardiac or thoracic evaluation (Cheng et al. 2017) the MRI workflow

R. R. Gill (✉)
Department of Radiology, Beth Israel Deaconess
Medical Center, Harvard Medical School,
Boston, MA, USA
e-mail: rgill@bidmc.harvard.edu

S. Patz
Department of Radiology, Harvard Medical School,
Brigham & Women's Hospital, Boston, MA, USA
e-mail: patz@bwh.harvard.edu

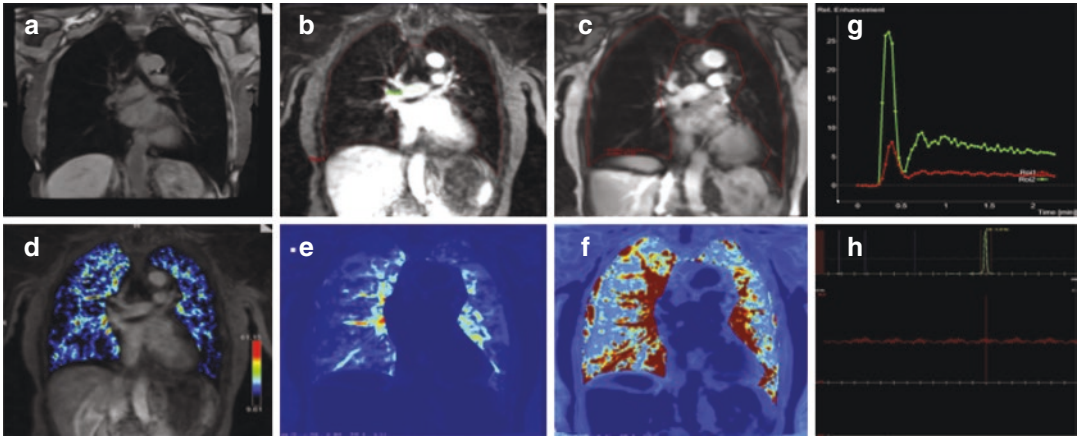


Fig. 39.1 (a) Pre-contrast coronal VIBE, post-contrast coronal TWIST and coronal FD TrueFISP respectively. Corresponding ROIs are indicated in (b) and (c) to indicate that the same region of interest was evaluated in both the cases. An additional ROI (green) was placed in the pulmonary artery to acquire the AIF in the DCE acquisition. (d–f) Calculated blood volume map (iAUC) from the dynamic TWIST acquisition, perfusion and ventilation maps from the FD TrueFISP sequence, respectively. (g) Time course curves for the two ROIs in (b) and (h) show the components of the Fourier Decomposition for the ROI in (c)

will need to be optimized to include sequences that can be combined with contrast-enhanced volumetric cardiac-resolved flow imaging (4D flow). Pulmonary functional assessment using MRI can map perfusion, ventilation, and measure gas exchange with and without intravenous and inhalational contrast agents. Dynamic contrast enhanced (DCE) MRI utilizes gadolinium-based vascular contrast agents tracked over time to generate pharmacokinetic indices that can be used to assess the pathophysiology of a disease process. Inhaled agents, such as hyperpolarized gases, can measure regional ventilation as well as gas exchange (Nakai et al. 2008). Novel techniques that do not rely on any contrast material such as arterial spin labeling, Fourier decomposition, and Ultra short turbo spin echo techniques also can be used to map function in the lung (Guimaraes et al. 2014; Bauman et al. 2016; Körzdörfer et al. 2019; Biederer et al. 2012b) (Fig. 39.1).

Techniques for Mapping Cardiopulmonary Interaction

Mapping cardiopulmonary interactions in the lung is challenging due to respiratory and cardiac motion. Several sequences are available for thoracic imaging that depend on the clinical indication

and include strategies to minimize or eliminate motion artifacts from cardiac and respiratory motion. This includes cardiac gating synchronization of the MR acquisition with the ECG tracing; this is more reliable in normal sinus rhythm. Respiratory motion can be highly problematic. Apart from artifacts, it affects the reproducibility of pharmacokinetic parameters; hence breath-hold acquisition may be needed for short sequences. For longer sequences, however, other techniques such as reordering of phase-encoding steps are recommended. Bellows and respiratory triggering can be used in patients with regular respiratory rates. Some sequences provide a navigator to measure the position of the diaphragm. The pulse sequence is then programmed to limit the data acquisition to a narrow range of diaphragm positions. The navigator typically uses a fast line-scan (one dimensional readout) to monitor diaphragmatic position at the beginning of each radiofrequency (RF) excitation pulse of the nuclei.

Dynamic Contrast Enhanced (DCE) MRI

DCE MRI is used to map perfusion of the lungs, by injecting gadolinium-based contrast agents and tracking the contrast over time (Gill et al.

2015). This is achieved by acquiring a three-dimensional acquisition of the whole chest over a 2–5 minute period during shallow breathing. Traditionally, sequences such as Fast low angle shot (FLASH) or time-resolved angiography with interleaved stochastic trajectories (TWIST) were used to map perfusion, but these sequences require motion correction prior to pharmacokinetic evaluation, and depending on the type of motion correction technique, the reproducibility of the pharmacokinetic parameters may be adversely affected (Tokuda et al. 2011). Motion robust sequences, such as Radial Acquisition of Volumetric Interpolated Breath-hold Examination (RADIAL-VIBE) and Controlled Aliasing in Parallel Imaging Results in Higher Acceleration (CAIPIRINHA-VIBE), can obviate the need for motion correction and improve the reproducibility of the pharmacokinetics (Ng 2020; Kim et al. 2016). Another strategy is to acquire timed runs through the chest using short breath-hold gradi-

ent echo sequences but these can be cumbersome as the patient needs to hold still in the same position for a period of 5 minutes, and also requires precision to align all the contrast enhanced sequences, prior to calculating pharmacokinetics. Additionally, time-resolved MR angiography using techniques such as TWIST can be used to evaluate pulmonary vascular flow with high temporal resolution. The acquired data is then post-processed using softwares such as Osirix (Bernex, Switzerland) /Matlab (Boston, US) to generate the pharmacokinetic parameters (Yamamuro et al. 2007; Mamata et al. 2011; Ingrisich et al. 2014; Scheffler et al. 2010a). The arterial input function can be obtained by placing a region of interest (ROI) in the aorta at peak arterial enhancement and another ROI on the lungs or the area to be assessed and then using a Toft's model or extended Toft's model to generate permeability parameters (Tofts 1997; Duan et al. 2017) (Fig. 39.2).

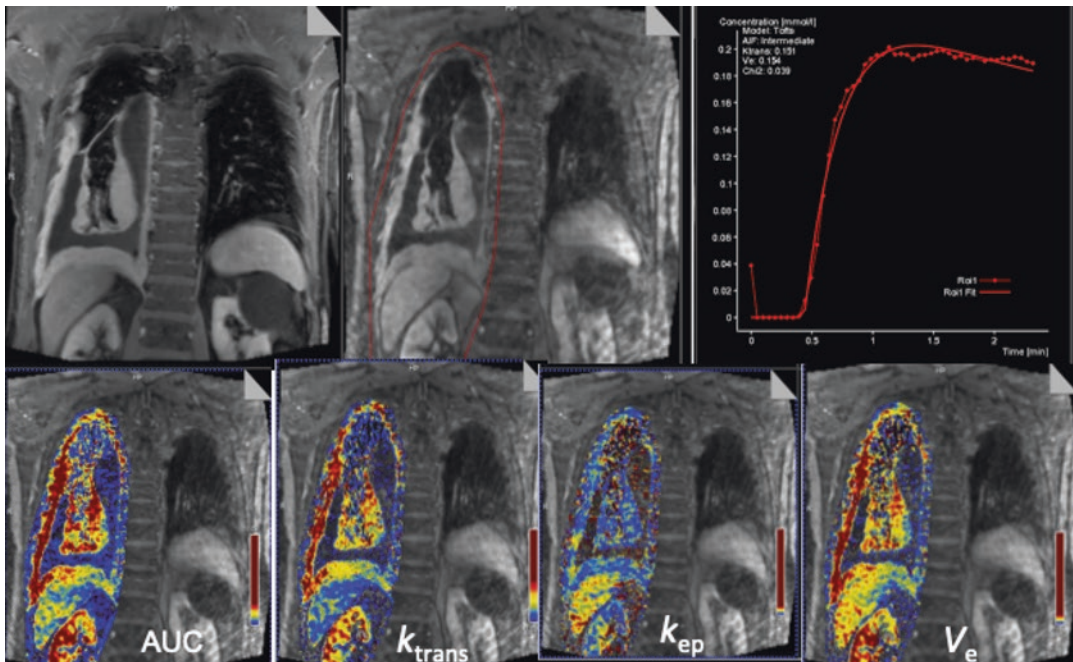


Fig. 39.2 A 48-year-old man with right-sided epithelial mesothelioma who underwent MRI for surgical planning. Coronal post-contrast and multiparametric maps depicting perfusion parameters of the tumor. MR-determined pharmacokinetic parameters: AUC area under the curve and represents blood volume, k_{trans} transfer constant

(min^{-1}), k_{ep} rate constant (min^{-1}), V_e elimination constant (dimensionless). 3D FLASH sequence (TR/TE: 2.02/0.84 ms; flip angle: 10 degrees; acquisition matrix: 256×135 ; slab thickness: 168–200 mm; 42–56 slice encoding

Proton Imaging

Proton imaging is acquired without the administration of intravenous or oral contrast. Two main techniques are used in proton imaging of the lung: arterial spin labeling (ASL), and Fourier Decomposition (FD); these techniques are used to quantify regional perfusion (ASL and FD) and ventilation (FD) (Bauman et al. 2013; Lederlin et al. 2013; Miller et al. 2014). These are free breathing non-contrast techniques based on mathematical modeling of vascular delivery and exchange within tissues (ASL) and spectral decomposition (using a Fourier decomposition) to determine time-dependent modulation in the parenchyma signal either at the heart rate or breathing rate (FD) to determine perfusion or ventilation dependent signal respectively. The imaging data is acquired while the patient is breathing and then postprocessed to derive ventilation and perfusion maps (Kjørstad et al. 2014; Buxton et al. 1998).

Oxygen Enhanced MRI

Oxygen can be used to enhance the signal from the lung by using a fast imaging sequence such as single-shot fast spin echo with an inversion recovery pre-pulse to introduce T1 contrast (Miller et al. 2014; Biederer et al. 2014). Oxygen enhances the magnitude of the microscopic fluctuations of the local magnetic field that each water molecule experiences and thereby enhances the longitudinal magnetization (T1) recovery process. This technique allows comparison of the difference in lung parenchyma during breathing normal air vs breathing higher concentrations and generate a qualitative map of parenchymal oxygen concentration; the differential subtraction maps can help in evaluating diffuse lung disease, such as emphysema and interstitial lung disease (Nakai et al. 2008; Biederer et al. 2014; Kruger et al. 2016; Ohno et al. 2014). The signal-to-noise ratio (SNR) provided by oxygen is lower when compared to hyperpolarized noble gases, but its cost is much less. However due to the low SNR, this technique has had limited clinical impact.

Hyperpolarized Gases

MRI imaging using hyperpolarized Nobel gases requires special RF coils and typically a polarizer on site. For ^3He , the lifetime can be many days if properly stored. However, for ^{129}Xe , the polarization is very short lived with relaxation times on the order of an hour. Nobel gases such as ^3He and ^{129}Xe can be hyperpolarized using a laser, and when inhaled during a MR exam can amplify the signal by a factor of 100,000 beyond thermal equilibrium (Van Beek et al. 2004; Fain et al. 2010). ^3He is relatively easier to polarize compared to ^{129}Xe , and has a stronger signal. Because of these reasons it was initially more popular of the two. Xenon polarizers, however, have improved and because the price of a liter of He gas is now ~\$3000, ^{129}Xe , whose price is at least 10 times less, is the gas of choice. ^{129}Xe is soluble both in septal tissue and blood. In particular, it is lipid soluble, which allows diffusion into blood. The T1 for both ^3He and ^{129}Xe is highly sensitive to the concentration of oxygen. Hence, before the gas is inhaled, it is kept in an oxygen-free container. The T1 for both ^3He and ^{129}Xe once inhaled is on the order of 10–20 seconds. Thus, for each inhalation of hyperpolarized gas, one must complete the imaging acquisition very rapidly because the hyperpolarization decays quickly. Normally, this would be a great impediment to imaging because one normally relies on waiting time TR between each excitation of the nuclei to allow for T1 relaxation. When using hyperpolarized gas, however, one can repeatedly excite the nuclei much faster because there is no need to wait for T1 recovery. Instead, a small fraction of the nonrenewable hyperpolarization is used for each excitation of the nuclei. The gyromagnetic ratio of ^{129}Xe is approximately 1/3 that of ^3He and therefore its inherent sensitivity is less by that factor compared to ^3He . Besides the lower cost of ^{129}Xe compared to ^3He , a great advantage of ^{129}Xe is its solubility in tissue and blood. Further, the different tissue compartments, i.e. parenchyma, RBC's and plasma, all have different chemical shifts. This has led to the development of very elegant methods to measure the

dynamics of the signal in each compartment and then with the use of various models of diffusion, use the data to calculate a number of very useful pulmonary function parameters (Van Beek et al. 2004; Miller et al. 2014; Fain et al. 2010; Albert et al. 2000).

Fluorine Gas MRI

Fluorine-19 (^{19}F) MRI with inhaled inert fluorinated gases can provide functional images of the lungs. Fluorine-19 (^{19}F) MRI is typically performed in humans by using a gas mixture containing 79% perfluoropropane (PFP) or sulfur hexafluoride (SF_6) and 21% oxygen. It is relatively inexpensive and can be performed on any MRI scanner with broadband multinuclear imaging capabilities (Schmieder et al. 2016; Adolphi and Kuethe 2008; Couch et al. 2019; Schreiber et al. 2001). Imaging with ^{19}F can be acquired in a single breath-hold, or in a time-resolved multiple breath fashion, to measure ventilation defect percent (VDP), or quantify gas replacement (i.e., fractional ventilation), and map the kinetics of gas exchange (Schreiber et al. 2001).

Applications of MR Imaging in Cardiopulmonary Interactions

MRI can be used to assess cardiopulmonary interactions in a variety of diseases and clinical states both as a primary modality and as an adjunct to other modalities.

Pulmonary Perfusion

Pulmonary perfusion can be mapped in a variety of lung diseases, such as emphysema, interstitial lung disease, asthma, tumors, and in primary and secondary pulmonary vascular pathologies. The most commonly used technique for mapping perfusion is dynamic contrast enhanced MRI. The pharmacokinetics derived from the perfusion maps can be used to predict histology, angiogenesis, compare pre- and posttreatment scans to

assess response and compare with outcome measures, to identify disease-specific imaging biomarkers (Mamata et al. 2011; Ingrisich et al. 2014; Scheffler et al. 2010a; Coolen et al. 2012; Tao et al. 2016; Hochegger et al. 2011; Swift et al. 2014).

The pulmonary arteries can also be simultaneously assessed using Magnetic resonance angiography, which consists of a heavily T1 weighted gradient echo sequence after injection of gadolinium-based contrast. Time-resolved MR angiography using techniques such as TWIST help evaluate pulmonary vascular flow with high temporal resolution. This enables evaluation of not only pulmonary vascular anatomy but can also assess pulmonary hemodynamics, including pulmonary perfusion. 3D whole heart navigator gated SSFP sequence is a non-contrast alternative to evaluate the pulmonary artery, especially in patients with severe renal dysfunction (Swift et al. 2014). Additionally, the pulmonic valve can also be evaluated by using cine SSFP images in the short axis plane and sagittal view during a focused MR exam for assessment of the heart and lungs. A flow quantification sequence is used for evaluating and quantifying pulmonic valvular and flow abnormalities.

Quantitative pulmonary perfusion can be combined with magnetic resonance angiography (MRA) to enhance the accuracy of detection of pulmonary emboli and also assess the functional consequences of pulmonary emboli on the heart and the lung parenchyma and assess the degree of the resulting hemodynamic abnormality. Arterial spin labeling (also known as arterial spin tagging) also can be used for mapping perfusion abnormalities and can be a very powerful tool for mapping interventions after detection of pulmonary pathology because it does not need contrast, and the images can be acquired during free breathing at multiple time points.

Pulmonary hypertension is characterized by abnormally elevated pulmonary arterial pressures and increased pulmonary vascular resistance. Primary or idiopathic pulmonary hypertension presents in the first or second decade. Secondary causes of pulmonary hypertension are cardiac disorders, chronic lung disease, chronic pulmo-

nary emboli and shunts. MRI can be used to depict the anatomic changes of pulmonary hypertension including dilated central pulmonary arteries, tapered or pruned peripheral pulmonary arteries, right ventricular hypertrophy, and systolic bowing of the interventricular septum. A comprehensive cardiac MR exam is indicated to evaluate the valves and the chambers.

Features suggestive of pulmonary hypertension include dilatation of the main pulmonary artery >2.8 cm or greater than the size of ascending aorta, and features suggestive of right heart strain. The severity of pulmonary hypertension has been correlated with increased intraluminal signal intensity in the pulmonary arteries on spin-echo images (Swift et al. 2014), and can be characterized by high signal intensity in the lumen of the pulmonary artery in systole and early diastole due to slow blood flow in diastole as compared to signal void in both systole and diastole in normal individuals. RV function, including stroke volume, end diastolic volume and ejection fraction, can be assessed from MR images and provide important prognostic value (Peacock and Noordegraaf 2013). Additionally there may be decreased myocardial perfusion reserve, which inversely correlates with RV workload and ejection fraction and reduced biventricular regional function associated with increased RV load (Peacock and Noordegraaf 2013). Perfusion imaging of the lungs can identify abnormalities in pulmonary perfusion, such as infarcts and mosaic perfusion suggestive of chronic thromboembolic disease. Delayed mid-myocardial enhancement at the RV insertion points of interventricular septum can be seen in patients with pulmonary hypertension due to increased stress. Altered hemodynamics detected with time-resolved MRA has been shown to correlate with pulmonary arterial pressure and pulmonary vascular resistance (Peacock and Noordegraaf 2013). Therefore a carefully planned cardiopulmonary MRI exam can provide both anatomical and functional imaging and illustrate the cardiopulmonary interaction and guide management.

Pulmonary embolism is the third most common acute cardiovascular disease and can be acute or chronic. CT is the most commonly used

imaging modality in the evaluation of acute pulmonary embolism, MRI shows comparable diagnostic accuracy but has low specificity. A meta-analysis of studies using MRI for evaluating pulmonary embolism has shown that MRI has a sensitivity of 100% for detecting PE in central and lobar arteries, 84% in segmental arteries and 40% in subsegmental arteries (Oudkerk et al. 2002). There is limited sensitivity for distal PE and results can be inconclusive in up to 30–50% patients (Revel et al. 2012).

Pulmonary perfusion can be assessed by non-contrast sequences such as ASL and FD before and after treatment to ensure perfusion abnormalities have resolved. However, these techniques are currently only qualitative; they show patterns of abnormality but cannot give the quantitative information provided by DCE MRI and nuclear medicine. Nevertheless, they can be combined with cardiac perfusion scans as they can be performed in 2–5 minutes during free breathing without contrast administration and can provide disease-specific functional information.

Lung Parenchyma (Diffuse Lung Disease)

CT is the modality of choice for evaluating lung parenchyma, and MR imaging of lung parenchyma is limited by low intrinsic proton density of the lung parenchyma and is further limited by magnetic susceptibility mismatch at air/tissue interfaces that creates gradients that cause intravoxel dephasing and signal loss (Wild et al. 2012). Novel MR techniques including short echo times, ultrafast turbo-spin-echo acquisitions, projection reconstruction techniques, breath-hold imaging, ECG triggering, contrast agents (perfusion imaging, aerosols, oxygen), and hyperpolarized noble gas imaging allow both anatomical and functional imaging of the lung parenchyma.

Several studies have explored the potential of MR to image (a) acute alveolar processes in chronic infiltrative lung disease, (b) detection and characterization of pulmonary nodules, (c) detection, characterization, and follow-up of pneumo-

nia, (d) differentiation of obstructive atelectasis from non-obstructive atelectasis and infarctions, (e) measure the lung water content (f) assess progression of interstitial lung disease, and (g) evaluate inflammation and infection in cystic fibrosis (Nakai et al. 2008; Fain et al. 2010; Hochegger et al. 2011; Capaldi et al. 2015; Mamata et al. 2012; Voskrebenezov et al. 2018; Altes et al. 2007; Bannier et al. 2010; Horak et al. 2007; Wielpütz et al. 2013; Mathew et al. 2011). Carefully chosen sequences can provide anatomical detail with enhanced tissue characterization. When combined with perfusion imaging, MR can provide information at the molecular level that can help differentiate between inflammation and infection and has the potential to assess treatment response earlier than CT scans (Voskrebenezov et al. 2018). The pharmacokinetic parameters combined with structural imaging and enhancement characteristics can help differentiate inflammation, infection, and malignancy (Tao et al. 2016; Altes et al. 2007; Horn et al. 2010; Koyama et al. 2008). These techniques can also be used to image chronic bronchitis, bronchiectasis, asthma, and emphysema (Wild et al. 2012; Eichinger et al. 2010).

Novel techniques such as Fourier Decomposition, Arterial Spin Labelling and proton imaging are under investigation for evaluation of pulmonary ventilation and perfusion without the administration of contrast (Bauman et al. 2013). These techniques combine static and dynamic MR imaging without the use of intravenous contrast and enable repeat imaging over time which can provide functional imaging of the lung, and the potential to provide information about regional lung function, including ventilation, perfusion, V/Q ratio, intrapulmonary oxygen partial pressure (PO_2), gas exchange, and spirometric and biomechanical parameters at a lobar and alveolar level. They also have the ability to quantify disease processes, identify imaging phenotypes, help identify disease early and can aid in monitoring therapeutic interventions (Kjørstad et al. 2014; Capaldi et al. 2017; Kaireit et al. 2018). They can potentially be used to identify imaging signatures that could correlate to phenotypes and help develop disease-specific biomarkers.

Ventilation (Gas Exchange)

Conventional MR imaging has limited value in evaluating lung parenchyma due to the paucity of protons (1H) in lung parenchyma; however, by the inhalation of hyperpolarized gases (3He or ^{129}Xe) the signal can be enhanced many fold allowing for evaluation of pulmonary ventilation and alveolar microstructure. Alveolar microstructure is evaluated by measuring restrictions in 3He diffusion that depend on the alveolar size. The size and exchange rate of different pulmonary compartments, alveoli, septal tissue, and RBC, can be evaluated by examining the kinetics of different chemical shift components in the ^{129}Xe spectrum. Most of these measurements are possible from a single inhalation of hyperpolarized gas. This technique requires the use of a polarizer, special coils, and software modifications to conventional scanners (Matsuoka et al. 2009; Biederer et al. 2014; Fain et al. 2010).

Laser-polarized 3He MR images have very high SNR with superb images of ventilation and ventilation defects. ^{129}Xe on the other hand due to lipid solubility and transmission across blood barrier allows imaging of all three compartments of the lung (airspace, septa, and red blood cells) and thus can map both ventilation and perfusion. This feature makes it attractive to image lung parenchymal abnormalities and assess progression and response to treatment (Fain et al. 2010; Mathew et al. 2011; Kirby et al. 2014). The hyperpolarized gases require a well-practiced and well-defined workflow in combination with special coils and ultrafast MR sequences, as there is relatively fast in vivo depolarization of hyperpolarized nuclei (on the order of 10–20 seconds) and lack of magnetization recovery.

Ventilation also can be mapped using noncontrast techniques such as Fourier decomposition and ASL; however, these techniques are not currently quantitative, but can be repeated multiple times, which makes them desirable to assess treatment and interventions (Kjørstad et al. 2014; Capaldi et al. 2017; Guo et al. 2017).

Quantitative ventilation can be assessed by calculating apparent diffusion coefficient value, which is a measure of gas diffusion across the

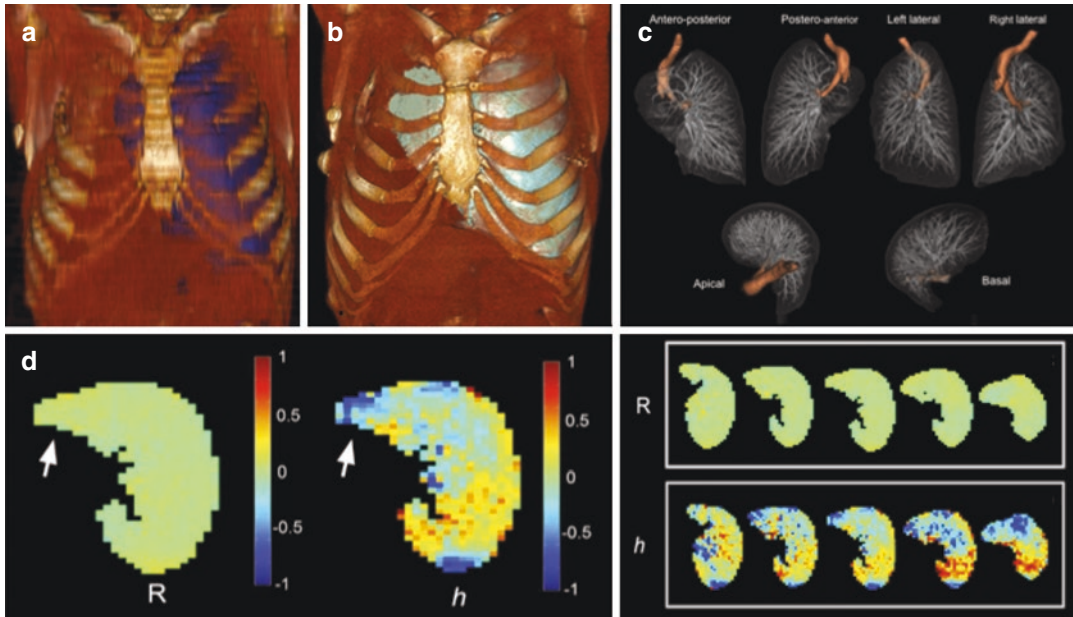


Fig. 39.3 Volume rendered CT scan images (a) 1 year after right pneumonectomy, (b) 5 years after pneumonectomy showing left lung increase in volume, (c) volume rendered CT scan images showing equal distribution of

vascularity, (d) acinar airway dimensions obtained from hyperpolarized ^3He study, demonstrating uniformity of the acinar radius, representing lung growth

alveolar capillary membrane and serves as a surrogate for gas distribution that is altered by changes in the lung microstructure and thus indirectly gives information about changes in function. The average distance traveled by the hyperpolarized gas in a given time is determined by the diffusion coefficient D , and is specific to that gas or gas mixture. For example the D of ^3He gas under standard conditions (and without restricting wall and barriers), D is $2.05 \text{ cm}^2/\text{sec}$ and approximately $0.88 \text{ cm}^2/\text{sec}$ in an atmospheric concentration. However D is much smaller than predicted from free diffusion due to diffusion hindrance by the lung microstructure itself. ADC appears to be a sensitive and reproducible marker for early detection and progression of disease and other processes affecting the size of alveoli and small airways. It thus can be used to calculate pulmonary microstructure (alveolar size and wall thickness), regional oxygen partial pressure, regional oxygen uptake, and V/Q matching in patients with emphysema, interstitial lung disease, and lung regeneration after

pneumonectomy or partial resection (Van Beek et al. 2004; Fain et al. 2010; Butler et al. 2012) (Figs. 39.3 and 39.4).

Oxygen-sensitive imaging can be used in conjunction with ^3He MR to destroy its signal as it shortens the T_1 of ^3He . Therefore areas of lung with high PO_2 will lose signal more rapidly than those with lower oxygen concentrations. This function can then be used to indirectly map oxygen partial pressures quantitatively in the lungs and also assess regional oxygen uptake and V/Q Alveolar–capillary transfer of oxygen. Interrupted uptake of oxygen from the alveoli into the blood due to either pulmonary arterial obstruction or a significant diffusion defect can be detected as an area of abnormally high V/Q using the oxygen-sensitive ^3He MR technique (Kirby et al. 2014).

Molecular oxygen, which is weakly paramagnetic, can be used as an MR agent to assess ventilation in proton MRI. The diffusion of oxygen from the alveoli into the capillary blood and binding to hemoglobin results in a reduction in

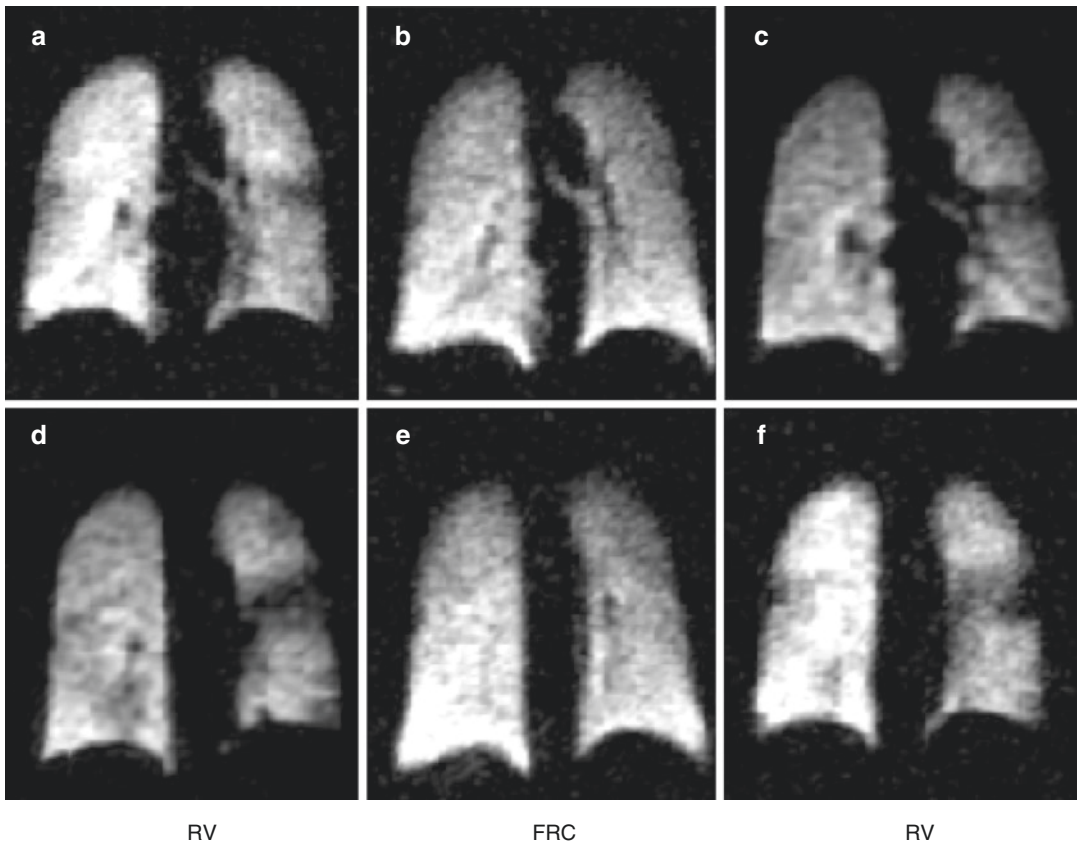


Fig. 39.4 Demonstration of “opening volume” effects (a–c). A ventilation defect is seen when inhalation is started from a low lung volume (RV) and reverses after

starting the ^{129}Xe inhalation from a higher lung volume (FRC). This ventilation defect was reproducible 1 week after the initial scan (d–f)

the T_1 of the blood and thus an increase in lung signal on a T_1 -weighted sequence. By subtracting an image acquired with room air from one acquired with 100% oxygen, oxygen-enhanced MR lung scans are obtained. Unlike hyperpolarized ^3He , in which the signal is obtained directly from the gas itself, the signal obtained using molecular oxygen as a ventilation agent results from its paramagnetic effect on the alveolar capillary blood and interstitial water.

Hyperpolarized ^{129}Xe readily diffuses into interstitial tissues and alveolar blood, therefore MR spectroscopic techniques can be used to measure separately the ^{129}Xe signal in alveolar gas, interstitial parenchyma, and alveolar capillary blood. By following the diffusion of the gas from the alveoli into the blood and/or the intersti-

tium, the hyperpolarized ^{129}Xe scans have the potential to map regional ventilation, perfusion, and V/Q all within a single examination. Moreover, the kinetics of gas transfer from air-space to capillary could potentially be used to calculate a host of other parameters, including alveolar wall thickness, capillary blood volume, mean alveolar transit time, and pulmonary perfusion. These techniques are still in the research arena and translation to clinical care will need improvement in workflow and improved patient compliance.

In lung diseases, such as asthma, chronic obstructive pulmonary disease (COPD), and cystic fibrosis (CF), ventilation defects are apparent in regions that the inhaled gas cannot access (Fain et al. 2010).

Heart Disease

MRI is a valuable complementary imaging modality to echocardiography in the evaluation of both congenital and acquired heart disease. MR protocols for evaluation of valves include velocity-encoded sequences targeted towards the valve of interest. Cine SSFP images are utilized to evaluate morphology and valvular regurgitation/stenosis and quantify ventricular function and volumes. Delayed enhancement can be used to evaluate myocardial scar or cardiomyopathies. Velocity-encoded phase contrast imaging can quantify both regurgitation and stenosis. On MRI, regurgitation is graded as mild (<15%), moderate (16–25%), moderate severe (25–45%) and severe (>45%). The velocity of stenotic jet is measured, and using this the pressure gradient can be calculated using modified Bernoulli equation, $\Delta p = 4v^2$.

Aortic stenosis is characterized by restricted systolic opening of the leaflets, with systolic flow acceleration. The leaflets are thickened and calcified. The valve morphology is also exquisitely demonstrated using MRI, including abnormalities such as bicuspid, quadricuspid, and unicuspid valves. Aortic regurgitation is seen as a regurgitant jet in diastole. Pulmonic stenosis is identified during systole and regurgitation in diastole. MRI is the most valuable imaging modality for the quantification of pulmonary valvular abnormalities, mitral, and tricuspid stenosis. MRI also evaluates the consequences of valvular abnormalities such as ventricular hypertrophy, dilation, and systolic dysfunction (Revel et al. 2012; Stein et al. 2008). MRI is the modality of choice for evaluation of congenital cardiac abnormalities and is especially useful for adults who had pediatric congenital heart surgery (Hsiao et al. 2012). MRI is superior to echocardiography for evaluation of right ventricular volumes. It also is useful in the evaluation of surgically placed shunts in these patients including aortopulmonary shunts (Blalock-Taussing, modified Blalock-Taussing, Potts, Waterston), Glenn shunt (SVC to right pulmonary artery), and Fontan shunt (IVC to right pulmonary artery). MRI is a

good imaging modality in the evaluation of coronary artery abnormalities, both congenital anomalies and also atherosclerotic disease. It also allows functional assessment of the myocardium.

Lung imaging can be added to the cardiac sequences, which allows mapping of cardiopulmonary interactions both in congenital valvular disease and also in acquired heart disease.

Imaging of Lung Mechanics

Chest wall and lung mechanics can be assessed by MRI. The high temporal and spatial resolution of the volumetric MR image data sets can be used to obtain regional rather than global spirometric parameters and other measures of lung mechanics. Potential uses include the mapping of abnormal regional compliance in patients with pulmonary fibrosis or emphysema (Biederer et al. 2012b; Scheffler et al. 2010b). Two MR approaches have been used to quantify tissue deformation and localized lung inflation: tissue tagging to track lung motion and displacement of vector maps derived from the registration of serial images acquired during breathing by using the pulmonary vasculature and parenchymal structures as inherent spatial markers. Mapping of regional lung mechanics using these new techniques can add unique, previously unavailable functional information beyond anatomy and structure.

Summary

Imaging of cardiopulmonary interactions can be high yield and provide vital prognostic information that can help design management strategies. Imaging can be accomplished by the administration of contrast agents by using DCE-MRI, or non-contrast images, such as ASL, FD, and inhaled hyperpolarized gases. Translation to clinical care needs optimization of MR protocols to include functional sequences, optimized to disease states and well-defined workflow.

References

- Adolphi NL, Kueth DO. Quantitative mapping of ventilation-perfusion ratios in lungs by ¹⁹F MR imaging of T1 of inert fluorinated gases. *Magn Reson Med*. 2008;59(4):739–46.
- Albert MS, Balamore D, Kacher DF, Venkatesh AK, Jolesz FA. Hyperpolarized ¹²⁹XE T1 in oxygenated and deoxygenated blood. *NMR Biomed*. 2000;13(7):407–14.
- Altes TA, Eichinger M, Puderbach M. Magnetic resonance imaging of the lung in cystic fibrosis. *Proc Am Thorac Soc*. 2007;4(4):321–7.
- Bannier E, Cieslar K, Mosbah K, Aubert F, Duboeuf F, Salhi Z, et al. Hyperpolarized ³He MR for sensitive imaging of ventilation function and treatment efficiency in young cystic fibrosis patients with normal lung function. *Radiology* [Internet] 2010;255(1):225–232. Available from: <https://doi.org/10.1148/radiol.09090039>
- Bauman G, Scholz A, Rivoire J, Terekhov M, Friedrich J, De Oliveira A, et al. Lung ventilation- and perfusion-weighted Fourier decomposition magnetic resonance imaging: in vivo validation with hyperpolarized ³He and dynamic contrast-enhanced MRI. *Magn Reson Med*. 2013;69(1):229–37.
- Bauman G, Pusterla O, Bieri O. Ultra-fast steady-state free precession pulse sequence for Fourier decomposition pulmonary MRI. *Magn Reson Med*. 2016;75(4):1647–53.
- Biederer J, Beer M, Hirsch W, Wild J, Fabel M, Puderbach M, et al. MRI of the lung (2/3). Why ... when ... how? *Insights Imaging* [Internet]. 2012a [cited 2014 Oct 2];3(4):355–71.
- Biederer J, Mirsadraee S, Beer M, Molinari F, Hintze C, Bauman G, et al. MRI of the lung (3/3)-current applications and future perspectives. *Insights Imaging* [Internet]. 2012b [cited 2014 Oct 2];3(4):373–86.
- Biederer J, Heussel CP, Puderbach M, Wielpuetz MO. Functional magnetic resonance imaging of the lung. *Semin Respir Crit Care Med*. 2014;35(1):74–82.
- Butler JP, Loring SH, Patz S, Tsuda A, Yablonskiy DA, Mentzer SJ. Evidence for adult lung growth in humans. *N Engl J Med*. 2012;367(3):244–7.
- Buxton RB, Frank LR, Wong EC, Siewert B, Warach S, Edelman RR. A general kinetic model for quantitative perfusion imaging with arterial spin labeling. *Magn Reson Med*. 1998;40(3):383–96.
- Capaldi DPI, Sheikh K, Guo F, Svenningsen S, Etemad-Rezai R, Coxson HO, et al. Free-breathing pulmonary ¹H and hyperpolarized ³He MRI: comparison in COPD and bronchiectasis. *Acad Radiol*. 2015;22(3):320–9.
- Capaldi DPI, Sheikh K, Eddy RL, Guo F, Svenningsen S, Nair P, et al. Free-breathing functional pulmonary MRI: response to bronchodilator and bronchoprovocation in severe asthma. *Acad Radiol*. 2017;24(10):1268–76.
- Cheng JY, Zhang T, Alley MT, Uecker M, Lustig M, Pauly JM, et al. Comprehensive Multi-Dimensional MRI for the Simultaneous Assessment of Cardiopulmonary Anatomy and Physiology. *Sci Rep*. 2017;13;7(1):5330. <https://doi.org/10.1038/s41598-017-04676-8>. PMID: 28706270; PMCID: PMC5509743.
- Coolen J, De Keyzer F, Naftoux P, De Wever W, Dooms C, Vansteenkiste J, et al. Malignant pleural disease: diagnosis by using diffusion-weighted and dynamic contrast-enhanced MR imaging--initial experience. *Radiology*. 2012;263:884–92.
- Couch MJ, Ball IK, Li T, Fox MS, Biman B, Albert MS. ¹⁹F MRI of the lungs using inert fluorinated gases: challenges and new developments. *J Magn Reson Imaging*. 2019;49:343–54.
- Duan C, Kallehauge JF, Bretthorst GL, Tanderup K, Ackerman JJH, Garbow JR. Are complex DCE-MRI models supported by clinical data? *Magn Reson Med*. 2017;77(3):1329–39.
- Eichinger M, Heussel CP, Kauczor HU, Tiddens H, Puderbach M. Computed tomography and magnetic resonance imaging in cystic fibrosis lung disease. *J Magn Reson Imaging*. 2010;32:1370–8.
- Fain S, Schiebler ML, McCormack DG, Parraga G. Imaging of lung function using hyperpolarized helium-3 magnetic resonance imaging: review of current and emerging translational methods and applications. *J Magn Reson Imaging*. 2010;32:1398–408.
- Gill RR, Patz S, Muradyan I, Seethamraju RT. Novel MR imaging applications for pleural evaluation. *Magn Reson Imaging Clin North Am*. 2015;23:179–95.
- Guimaraes MD, Schuch A, Hochegger B, Gross JL, Chojniak R, Marchiori E. Functional magnetic resonance imaging in oncology : state of the art *. 2014;47(5):101–11.
- Guo F, Capaldi DPI, Di Cesare R, Fenster A, Parraga G. Registration pipeline for pulmonary free-breathing ¹H MRI ventilation measurements. In: *Medical imaging 2017: biomedical applications in molecular, structural, and functional imaging*; 2017. p. 101370A.
- Hochegger B, Ley-Zaporozhan J, Marchiori E, Irion K, Soares Souza A, Moreira J, et al. Magnetic resonance imaging findings in acute pulmonary embolism. *Br J Radiol*. 2011;84:282–7.
- Horak F Jr, Moeller A, Singer F, Straub D, Höller B, Helbich TH et al. Longitudinal monitoring of pediatric cystic fibrosis lung disease using nitrite in exhaled breath condensate. *Pediatr Pulmonol*. 2007;42(12):1198–206. <https://doi.org/10.1002/ppul.20719>. PMID: 17968999.
- Horn M, Oechsner M, Gardarsdottir M, Köstler H, Müller MF. Dynamic contrast-enhanced MR imaging for differentiation of rounded atelectasis from neoplasm. *J Magn Reson Imaging* [Internet]. 2010 [cited 2014 Oct 2];31(6):1364–70.
- Hsiao A, Lustig M, Alley MT, Murphy MJ, Vasanawala SS. Evaluation of Valvular insufficiency and shunts

- with parallel-imaging compressed-sensing 4D phase-contrast MR imaging with stereoscopic 3D velocity-fusion volume-rendered visualization. *Radiology*. 2012;265(1):87–95.
- Ingrisch M, Maxien D, Schwab F, Reiser MF, Nikolaou K, Dietrich O. Assessment of pulmonary perfusion with breath-hold and free-breathing dynamic contrast-enhanced magnetic resonance imaging: quantification and reproducibility. *Investig Radiol*. 2014;49(6):382–9.
- Kaireit TF, Gutberlet M, Voskrebenez A, Freise J, Welte T, Hohlfeld JM, et al. Comparison of quantitative regional ventilation-weighted fourier decomposition MRI with dynamic fluorinated gas washout MRI and lung function testing in COPD patients. *J Magn Reson Imaging*. 2018;47(6):1534–41.
- Kim B, Lee CK, Seo N, Lee SS, Kim JK, Choi Y, et al. Comparison of CAIPIRINHA-VIBE, Radial-VIBE, and conventional VIBE sequences for dynamic contrast-enhanced (DCE) MRI: a validation study using a DCE-MRI phantom. *Magn Reson Imaging*. 2016;34(5):638–44.
- Kirby M, Ouriadov A, Svenningsen S, Owrangi A, Wheatley A, Etemad-Rezai R, et al. Hyperpolarized ³He and ¹²⁹Xe magnetic resonance imaging apparent diffusion coefficients: physiological relevance in older never-and ex-smokers. *Physiol Rep*. 2014; 16;2(7):e12068. <https://doi.org/10.14814/phy2.12068>. PMID: 25347853; PMCID: PMC4187551.
- Kjørstad Å, Corteville DMR, Fischer A, Henzler T, Schmid-Bindert G, Zöllner FG, et al. Quantitative lung perfusion evaluation using fourier decomposition perfusion MRI. *Magn Reson Med*. 2014;72(2):558–62.
- Körzdörfer G, Jiang Y, Speier P, Pang J, Ma D, Pfeuffer J, et al. Magnetic resonance field fingerprinting. *Magn Reson Med*. 2019;81(4):2347–59.
- Koyama H, Ohno Y, Kono A, Takenaka D, Maniwa Y, Nishimura Y, et al. Quantitative and qualitative assessment of non-contrast-enhanced pulmonary MR imaging for management of pulmonary nodules in 161 subjects. *Eur Radiol [Internet]*. 2008 [cited 2014 Oct 2];18(10):2120–31.
- Kruger SJ, Nagle SK, Couch MJ, Ohno Y, Albert M, Fain SB. Functional imaging of the lungs with gas agents. *J Magn Reson Imaging*. 2016;43:295–315.
- Lederlin M, Bauman G, Eichinger M, Dinkel J, Brault M, Biederer J, et al. Functional MRI using Fourier decomposition of lung signal: reproducibility of ventilation- and perfusion-weighted imaging in healthy volunteers. *Eur J Radiol*. 2013;82(6):1015–22.
- Mamata H, Tokuda J, Gill RR, Padera RF, Lenkinski RE, Sugarbaker DJ, et al. Clinical application of pharmacokinetic analysis as a biomarker in solitary pulmonary nodules : dynamic contrast enhanced MR imaging. *Magn Reson Med*. 2011;19:1–9.
- Mamata H, Tokuda J, Gill RR, Padera RF, Lenkinski RE, Sugarbaker DJ, et al. Clinical application of pharmacokinetic analysis as a biomarker of solitary pulmonary nodules: dynamic contrast-enhanced MR imaging. *Magn Reson Med*. 2012;68(5):1614–22. <https://doi.org/10.1002/mrm.24150>. Epub 2012 Jan 9. PMID: 22231729; PMCID: PMC3335927.
- Mathew L, Kirby M, Etemad-Rezai R, Wheatley A, McCormack DG, Parraga G. Hyperpolarized ³He magnetic resonance imaging: preliminary evaluation of phenotyping potential in chronic obstructive pulmonary disease. *Eur J Radiol*. 2011;79(1):140–6.
- Matsuoka S, Patz S, Albert MS, Sun Y, Rizi RR, Gefter WB, et al. Hyperpolarized gas MR imaging of the lung: current status as a research tool. *J Thorac Imaging*. 2009:181–8.
- Miller GW, Mugler JP, Sá RC, Altes TA, Prisk GK, Hopkins SR. Advances in functional and structural imaging of the human lung using proton MRI. *NMR Biomed*. 2014;27:1542–56.
- Nakai A, Koyama T, Fujimoto K, Togashi K. Functional MR imaging of the uterus. *Magn Reson Imaging Clin N Am*. 2008;16(4):673–84.
- Ohno Y, Nishio M, Koyama H, Seki S, Yoshikawa T, Matsumoto S, et al. Asthma: comparison of dynamic oxygen-enhanced MR imaging and quantitative thin-section CT for evaluation of clinical treatment. *Radiology*. 2014;273(3):907–16.
- Oudkerk M, Van Beek EJR, Wielopolski P, Van Ooijen PMA, Brouwers-Kuyper EMJ, Bongaerts AHH, et al. Comparison of contrast-enhanced magnetic resonance angiography and conventional pulmonary angiography for the diagnosis of pulmonary embolism: a prospective study. *Lancet*. 2002;359(9318):1643–7.
- Peacock AJ, Noordegraaf AV. Cardiac magnetic resonance imaging in pulmonary arterial hypertension. *Eur Respir Rev*. 2013;22:526–34.
- Revel MP, Sanchez O, Couchon S, Planquette B, Hernigou A, Niarra R, et al. Diagnostic accuracy of magnetic resonance imaging for an acute pulmonary embolism: results of the “IRM-EP” study. *J Thromb Haemost*. 2012;10(5):743–50.
- Scheffler M, Ullrich R, Wetzel T, Nogova L, Zander T, Mattonet C, et al. Feasibility of dynamic contrast-enhanced MRI (DCE-MRI) based angiogenesis biomarker assessment in advanced NSCLC treated with erlotinib and bevacizumab [Internet]. *Onkologie*. 2010a;33:284.
- Scheffler M, Ullrich R, Wetzel T, Nogova L, Zander T, Mattonet C, et al. Feasibility of dynamic contrast-enhanced MRI (DCE-MRI) based angiogenesis biomarker assessment in advanced NSCLC treated with erlotinib and bevacizumab. *Onkologie*. 2010b.
- Schmieder AH, Caruthers SD, Keupp J, Wickline SA, Lanza GM. Recent advances in ¹⁹F fluorine magnetic resonance imaging with perfluorocarbon emulsions. *Engineering*. 2016;1(4):475–89.
- Schreiber WG, Eberle B, Laukemper-Ostendorf S, Markstaller K, Weiler N, Scholz A, et al. Dynamic ¹⁹F-MRI of pulmonary ventilation using sulfur hexafluoride (SF₆) gas. *Magn Reson Med*. 2001;45(4):605–13.
- Stein PD, Gottschalk A, Sostman HD, Chenevert TL, Fowler SE, Goodman LR, et al. Methods of prospec-

- tive investigation of pulmonary embolism diagnosis III (PIOPED III). *Semin Nucl Med.* 2008;38(6):462–70.
- Swift AJ, Wild JM, Nagle SK, Roldán-Alzate A, François CJ, Fain S, et al. Quantitative magnetic resonance imaging of pulmonary hypertension. *J Thorac Imaging* [Internet]. 2014;29(2):68–79.
- Tao X, Wang L, Hui Z, Liu L, Ye F, Song Y, et al. DCE-MRI Perfusion and Permeability Parameters as predictors of tumor response to CCRT in Patients with locally advanced NSCLC. *Sci Rep.* 2016;20;6:35569. <https://doi.org/10.1038/srep35569>. PMID: 27762331; PMCID: PMC5071875.
- Thomas S. C. Ng, Ravi T. Seethamraju, Raphael Bueno, Ritu R. Gill, (2020) Clinical Implementation of a Free-Breathing, Motion-Robust Dynamic Contrast-Enhanced MRI Protocol to Evaluate Pleural Tumors. *American Journal of Roentgenology* 215 (1):94–104.
- Tofts PS. Modeling tracer kinetics in dynamic Gd-DTPA MR imaging. *J Magn Reson Imaging.* 1997;7:91–101.
- Tokuda J, Mamata H, Gill RR, Hata N, Kikinis R, Padera RF, et al. Impact of nonrigid motion correction technique on pixel-wise pharmacokinetic analysis of free-breathing pulmonary dynamic contrast-enhanced MR imaging. *J Magn Reson Imaging.* 2011;33:968–73.
- van Beek EJ, Hoffman EA. Functional imaging: CT and MRI. *Clin Chest Med.* 2008;29(1):195–vii.
- Van Beek EJR, Wild JM, Kauczor HU, Schreiber W, Mugler JP, De Lange EE. Functional MRI of the lung using hyperpolarized 3-helium gas. *J Magn Reson Imaging.* 2004;20:540–54.
- Voskrebenezv A, Gutberlet M, Klimeš F, Kaireit TF, Schönfeld C, Rotärmel A, et al. Feasibility of quantitative regional ventilation and perfusion mapping with phase-resolved functional lung (PREFUL) MRI in healthy volunteers and COPD, CTEPH, and CF patients. *Magn Reson Med.* 2018;79(4):2306–14.
- Wielpütz MO, Eichinger M, Puderbach M. Magnetic resonance imaging of cystic fibrosis lung disease. In: *J Thoracic Imaging.* 2013. p. 151–9.
- Wild JM, Marshall H, Bock M, Schad LR, Jakob PM, Puderbach M, et al. MRI of the lung (1/3): methods. *insights imaging* [Internet]. 2012 [cited 2014 Oct 2];3(4):345–53. Available from: <http://www.pubmedcentral.nih.gov/articlerender.fcgi?artid=3481083&tool=pmcentrez&rendertype=abstract>
- Yamamuro M, Gerbaudo VH, Gill RR, Jacobson FL, Sugarbaker DJ, Hatabu H. Morphologic and functional imaging of malignant pleural mesothelioma. *Eur J Radiol.* 2007;64(3):356–66. <https://doi.org/10.1016/j.ejrad.2007.08.010>. Epub 2007 Oct 22. PMID: 17954021.

Part VI

The Tools: Interaction



Respiratory Function of Hemoglobin: From Origin to Human Physiology and Pathophysiology

Connie C. W. Hsia

Abbreviations

2,3-BPG	2,3-bisphosphoglycerate	Hb(II)	Hemoglobin containing iron in the reduced ferrous (Fe^{+2}) state
AE-1	Anion exchanger-1	Hb(II) O_2	Oxyhemoglobin containing iron in the reduced ferrous (Fe^{+2}) state
ATP	adenosine triphosphate	Hb(III)	Methemoglobin containing iron in the oxidized ferric (Fe^{+3}) state
BYA	Billion years ago	Hb(III)NO	Heme-nitrosylated methemoglobin with its iron in the oxidized ferric (Fe^{+3}) state
CA	Carbonic anhydrase	HbCO	Carboxyhemoglobin
CarHb	Carbamylated hemoglobin	HCO_3^-	Bicarbonate anion
CO	Carbon monoxide	HIF	Hypoxia-inducible factor
CO_2	Carbon dioxide	NADP+	Nicotinamide adenine dinucleotide phosphate (oxidized form)
Epo	Erythropoietin	NADPH	Nicotinamide adenine dinucleotide phosphate (reduced form)
Fe^{+2}	Ferrous cation, a reduced state of iron	NHE	Sodium-proton (Na^+/H^+) exchanger
Fe^{+3}	Ferric cation, an oxidized state of iron	NO	Nitric oxide
G6PD	Glucose-6-phosphate dehydrogenase	NO_2	Nitrite
H^+	Proton, hydrogen ion	NO_3	Nitrate
H_2S	Hydrogen sulfide	O_2	Oxygen
HA	High altitude	ODC	Oxyhemoglobin dissociation curve
Hb A	Human adult hemoglobin	P_{50}	Partial pressure of oxygen at 50% saturation of the heme-binding sites on hemoglobin
Hb F	Human fetal hemoglobin	PCO_2	Partial pressure of carbon dioxide
Hb M	Hemoglobin variant associated with methemoglobinemia	PO $_2$	Partial pressure of oxygen
Hb S	Sickle cell hemoglobin	ROS	Reactive oxygen species
Hb	Hemoglobin	SNO	S-nitrosothiol

C. C. W. Hsia (✉)

Department of Internal Medicine, Pulmonary and Critical Care Medicine, University of Texas Southwestern Medical Center, Dallas, TX, USA
e-mail: Connie.Hsia@utsouthwestern.edu

Introduction

Hemoglobin is much more than an oxygen (O₂) carrier. Hemoglobin packaged inside erythrocytes stores, delivers, coordinates and actively regulates the exchange of multiple gases including O₂, carbon dioxide (CO₂) and nitric oxide (NO) among distant sites of uptake, production, utilization and elimination. Hemoglobin traces its origin to the earliest anaerobic prokaryote that ingested metals from rocks to produce hemoproteins and facilitate non-O₂-based cellular respiration, only later acquiring O₂-binding ability as atmospheric O₂ concentration rose. In multicellular organisms, some hemoprotein-producing cells either extruded their product or detached to enter the circulation, becoming erythrocytes and co-evolving with the microvascular system. Over time, hemoglobins acquired features favored by natural selection (*adaptation*), co-opted existing features for purposes other than originally intended (*exaptation*), shed useless features via negative selection (*disaptation*) and struck compromises to satisfy competing environmental and organismal constraints (*trade-off*). The sheer diversity of hemoproteins across species and human hemoglobin variants directly reflects the selection pressures for facilitated gas transport. This article surveys the anaerobic origin and natural selection of hemoglobin as an O₂ carrier, the sequestration of hemoglobin within erythrocytes allowing a multitude of interactions within and among subunits, with erythrocyte metabolism, and with the microvasculature to enhance gas transport efficiency, and how the evolutionary history of hemoglobin informs its integrated respiratory function in human physiology, adaptation to exercise and hypoxia, and clinical medicine in terms of understanding the pathophysiological disturbances in hemoglobin quantity, quality and regulation of its function.

Anaerobic Origin of Hemoproteins

The ancestral cell (so-called Last Universal Common Ancestor) appeared ~4 billion years ago (BYA) in an anoxic Earth. These organisms lived

in extreme environments similar to the modern *extremophiles* found near geothermal vents and the *methanogens* found in marine sediments and the Earth's crust (Gribaldo and Brochier-Armanet 2006). These ancient *lithotrophs* ("rock-eaters") utilized inorganic electron donors including hydrogen, carbon monoxide (CO), ammonia, nitrite, sulfide (H₂S) and iron in chemiosmosis to generate transmembrane electrochemical gradients and produce adenosine triphosphate (ATP). Eventually, a molecular cage, the *porphyrin ring*, evolved to trap these ions. A porphyrin ring containing a central iron molecule became *heme*; one that contained a central magnesium molecule became *chlorophyll* (Fig. 40.1). Polypeptides became associated with heme in order to modify its function, producing *hemoproteins*. Ancestral hemoproteins were cytochromes that reduced nitrite, NO and H₂S (Hsia et al. 2013).

Hemoglobin as Oxygen Carrier

The enduring *cyanobacteria* were initially anaerobic H₂S oxidizers (de Wit and van Gernerden 1987) that formed enormous fossil colonies (*stromatolite*) near shallow water. Around 3.5 BYA, cyanobacteria acquired chlorophyll for photosynthesis, producing water and O₂. The O₂ was scavenged by ferrous iron in Earth's crust, producing the iron oxides seen in the geologic strata called *banded iron formations*, while free O₂ entered the atmosphere, causing the first and possibly the greatest mass extinction ~2 BYA, termed the *Oxygen Holocaust* (de Duve 1996). Species survived by: (a) hiding under deep sea, soil or rock while remaining anaerobic, (b) developing mechanisms to detoxify and eliminate O₂ and (c) co-opting O₂ for energy production.

Detoxification of O₂ is seen in anaerobic worms that possess an ultrahigh-affinity hemoglobin (P₅₀ 0.0001 Torr) as an O₂ scavenger and a deoxygenase (Minning et al. 1999). After binding O₂, the Fe⁺² in hemoglobin is oxidized to Fe⁺³ methemoglobin in reaction with endogenous NO; the bound O₂ is converted to nitrite (NO₂) and nitrate (NO₃⁻) and excreted or used to regenerate NO via reverse reducing reaction with

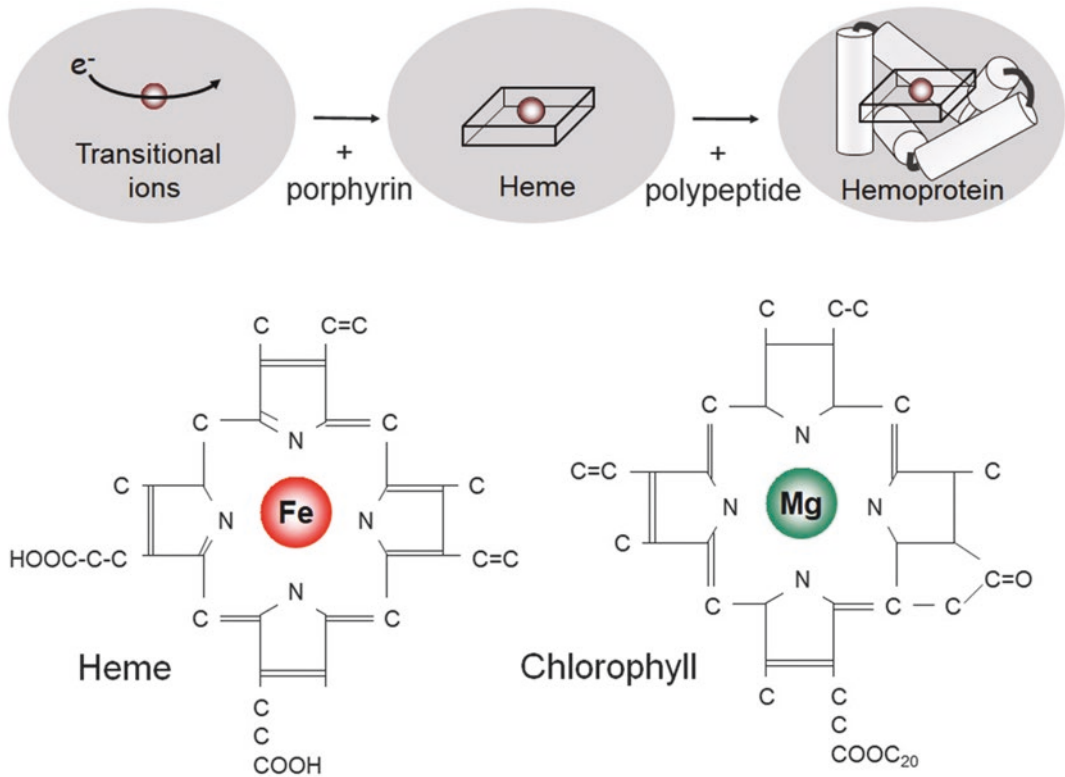


Fig. 40.1 Upper: Cellular respiration in ancient bacteria harnesses chemical energy from electron transfer via transitional metals. A porphyrin-based molecular cage traps an iron molecule to produce heme. Polypeptides modify

the function of heme, producing hemoproteins. Lower: A porphyrin ring containing a central iron molecule became heme; one that contains a central magnesium molecule became chlorophyll. (Adapted from Hsia et al. 2013)

methemoglobin. Other cytochromes developed to utilize O_2 as an electron acceptor. This evolutionary shift is deduced from extant hemoglobin variants in bacteria and yeast that support both aerobic and non-aerobic (nitrogen-based) respiration (Weber and Vinogradov 2001), the multifunctional hemoglobins in deep sea tubeworms living near thermal vents that reversibly bind both H_2S and O_2 , (Zal et al. 1998), and the *protoglobins* of *archaea* species that reversibly bind O_2 , CO and NO (Pesce et al. 2013). Several amino acid residues that covalently bind heme, and cysteine residues that form thermostable disulfide bridges (Freitas et al. 2004), are highly conserved and responsible for O_2 detoxification coupled to NO. Thus, ancestral hemoglobins are highly flexible in their mode of redox energy production and in cross-protection against a combination of thermal, nitrosative and oxidative stress. The basic

motif of hemoglobin-binding sites is universally adaptable to different gas molecules. As ambient oxygenation increased, the inherent capacity for O_2 binding by hemoglobin was preferentially exploited.

Hemoglobins consist of monomers or oligomers of a basic single-domain O_2 -binding subunit (M.W. 15–17 kDa), with 153 residues, 8 α -helices and a hydrophobic interior. Variants of the subunit exist in muscle (myoglobin), nerve (neuroglobin) and cells (cytoglobin). Single-chain hemoglobins exist in bacteria, algae, protozoa and plants, while giant hemoglobin complexes exist in nematodes, mollusks, crustaceans and earthworms (Terwilliger 1980). The O_2 -binding metal may be iron (hemoglobin) or copper (hemocyanin). From an ancestral globin gene, hemoglobin diverged from cytoglobin and neuroglobin ~800 million years ago. Later, it diverged from myoglobin,

and the α - and β -globin genes segregated onto separate chromosomes (Pesce et al. 2002). Most mutations occur on the β -chain, while the α -chain is more stable. All known aerobic respiratory pigments are sensitive to hypoxia under regulation by hypoxia-inducible factor (HIF)-erythropoietin (Epo) signaling (Jelkmann 2007).

Erythrocytes as Hemoglobin Carrier

As organisms became larger and ventilatory and circulatory systems evolved, some hemoglobin-producing cells extruded their products into the circulation while other became mobile erythrocytes to sustain the delivery function. Free hemoglobin circulates in the hemolymph of invertebrate species. Large free hemoglobin molecules increase plasma osmotic pressure and viscosity (Snyder 1977). Giant invertebrate hemoproteins (>100 subunits) exhibit high O₂ affinity and act as an O₂ reservoir but are incapable of regulating tissue O₂ exchange (Mangum 1998). As O₂ demands increased, smaller more versatile hemoglobins with fewer subunits, lower blood viscosity and higher O₂ transport capacity were favored by natural selection. However, small hemoglobins are poorly retained; intravascular half-life of free human hemoglobin tetramers (2 α - and 2 β -subunits) is only ~4 hr (Bleeker et al. 1992). Retention of high concentrations of small hemoglobin was achieved by packaging it within mobile erythrocytes. The postulated origins of erythrocytes include fat cells lining the hemolymph channel, osmoregulatory epithelial cells and peritoneal endothelial cells (Glomski and Tamburlin 1989, 1990; Glomski et al. 1992, 1997; Paul et al. 2004).

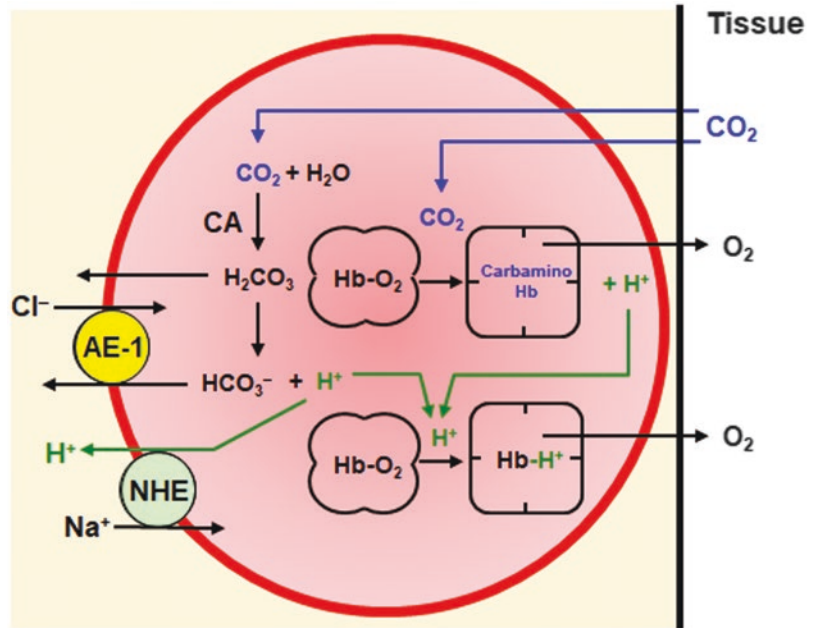
Confining hemoglobin within erythrocytes also facilitates interactions among subunits and with the erythrocyte membrane and blood; these interactions optimize not just O₂ transport but also transport of CO₂ and NO. Mechanisms for regulating O₂-binding kinetics include: *co-operativity* (O₂ binding to one heme group alters the molecular conformation of the hemoglobin tetramer and increases the likelihood of O₂ binding to the

remaining heme groups), *Bohr and Haldane shifts* (sensitivity to pH and CO₂) (Sterner and Decker 1994), *allosterism* (altered O₂ affinity due to conformational changes brought about by the binding of another molecule to a site on hemoglobin other than the heme-binding site) (Strand et al. 2004), and *high thermostability* (Mangum 1998).

Bohr and Haldane Effects

Increasing blood CO₂ concentration (lower pH) reduces hemoglobin affinity for O₂, leading to a higher P₅₀ (right shift of oxyhemoglobin dissociation curve, ODC), i.e., the *Bohr effect* that favors O₂ unloading. Reciprocally, increasing blood oxygenation reduces hemoglobin affinity for CO₂, i.e., the *Haldane effect* that favors CO₂ release. Both effects arise from interactions with the erythrocyte (Fig. 40.2) (Hsia et al. 2016): CO₂ from tissue diffuses into capillary erythrocytes and is converted via carbonic anhydrase (CA) to carbonic acid (H₂CO₃) that dissociates into bicarbonate (HCO₃⁻) and proton (H⁺); the latter binds histidine residues on globin chain to stabilize the deoxyhemoglobin (Tense state) conformation, thereby facilitating unloading of O₂. CO₂ also directly binds oxyhemoglobin forming carbaminohemoglobin, a reaction that also facilitates O₂ release. While H₂CO₃ can diffuse across the cell membrane, excess HCO₃⁻ anions are shuttled out of the cell via the membrane anion exchanger-1 (AE-1) in exchange with chloride (Cl⁻) (McMurtrie et al. 2004), and excess H⁺ ions are shuttled out of the cell via the sodium (Na⁺)/proton (H⁺) exchanger (NHE) (Pedersen and Cala 2004; Matteucci and Giampietro 2007). The reverse reactions occur in pulmonary capillaries where CO₂ diffuses along its pressure gradient into alveolar air; the decrease in PCO₂ facilitates O₂ loading onto heme, which stabilizes the oxyhemoglobin (Relaxed state) configuration and in turn favors unloading of CO₂ from hemoglobin for elimination. Thus, changes in blood PCO₂ and PO₂ are reciprocally coupled; binding of one ligand regulates binding and release of the other.

Fig. 40.2 Coupling of O_2 and CO_2 exchange within erythrocytes. AE-1 anion exchanger-1, CA carbonic anhydrase, CarbaminoHb carbamino-hemoglobin, Cl^- chloride anion, H^+ proton, $Hb-O_2$ oxyhemoglobin, Hb deoxyhemoglobin, H_2CO_3 carbonic acid, HCO_3^- bicarbonate anion, NHE Sodium/proton (Na^+/H^+) exchanger. See text for explanation (under *Erythrocytes as hemoglobin carrier: Bohr and Haldane effects*). (Adapted from Hsia et al. 2016)



2,3-Bisphosphoglycerate

Oxygen affinity is expressed by its partial pressure at which half of the heme-binding sites are saturated (P_{50}) (Fig. 40.3a). As reviewed previously (Hsia 1998), at a given alveolar O_2 tension, the pressure gradient from alveolar air to blood drives O_2 loading onto hemoglobin, while the pressure gradient from blood to tissue mitochondria drives O_2 unloading from hemoglobin. Shifting P_{50} alters the balance between loading and unloading. Erythrocytic glycolysis produces the intermediary compound 2,3-bisphosphoglycerate (2,3-BPG) that binds deoxyhemoglobin between α -1 and β -2 globins stabilizing the deoxy-(tense) conformation, thereby increasing P_{50} and favoring O_2 unloading. Metabolic stress (e.g., increased temperature, hypermetabolism, moderate hypoxia) increases erythrocytic glycolysis and in turn 2,3-BPG production and O_2 unloading (Fig. 40.3a). Alkalosis, reduced metabolism and extreme hypoxia have the opposite effects that favor O_2 loading (Fig. 40.3b). By coupling cellular metabolic state to function, erythrocytes effectively act as an O_2 sensor that utilizes their glycolytic by-product to gauge and optimize regional O_2 delivery.

Effects of Temperature

Circulating blood is exposed to large temperature changes from baseline core temperature ($37^\circ C$) to skin temperature ($33^\circ C$ and lower especially in cold air or water without insulation), and rising to $>39.5^\circ C$ in strenuously exercising muscles and with fever. An elevated temperature favors O_2 unloading (higher P_{50}) to meet tissue metabolic demands. In hypothermia, O_2 is bound more tightly to hemoglobin (lower P_{50}) and O_2 unloading is reduced, matched by a corresponding reduction in metabolic activity and O_2 demand (Mairbaurl and Weber 2012).

Erythrocyte as a Source of Bioactive NO

Beyond the classical concept of hemoglobin as NO scavenger due to a high NO -binding affinity of heme, erythrocytes possess intrinsic NO synthase activity (Kleinbongard et al. 2006) and nitrite reductase activity (Fens et al. 2014). Nitrite-hemoglobin reactions preserve and modulate NO bioactivity under hypoxia (Sun et al. 2019; Schmidt and Feelisch 2019; Huang

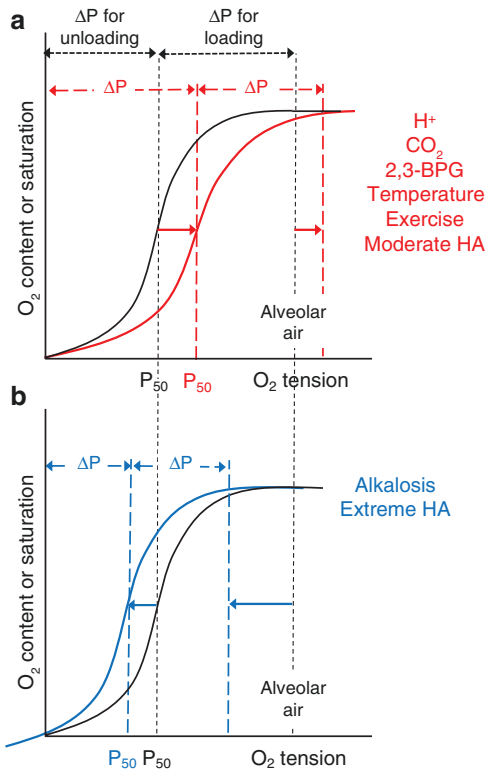


Fig. 40.3 Regulation of O₂ loading and unloading via adjustment of the oxyhemoglobin dissociation curve. (a) The P₅₀ (O₂ tension at 50% saturation of heme-binding sites) balances partial pressure gradients (ΔP) for O₂ loading from alveolar air onto hemoglobin and O₂ unloading from hemoglobin to tissue mitochondria (PO₂ < 1 mmHg) (baseline shown in black). Acidosis (H⁺), CO₂, the intermediary product of erythrocyte glycolysis 2,3-BPG, elevated temperature, exercise and moderate high altitude (HA) exposure increase P₅₀ and the mean ΔP for unloading O₂ from hemoglobin, while hyperventilation increases alveolar PO₂ and ΔP for O₂ loading in the lung (shown in red). (b) Alkalosis and exposure to extreme HA have the opposite effects by reducing alveolar PO₂, causing a reduction in P₅₀ that favors loading of O₂ onto hemoglobin (shown in blue).

et al. 2005; Nagababu et al. 2003a) (Fig. 40.4): Nitric oxide synthesized in endothelium diffuses to nearby smooth muscle cells and mediates vasomotor relaxation. Some NO diffuses into blood and rapidly reacts with O₂-forming nitrite (NO₂⁻), which may enter erythrocytes via the anion exchanger-1 (AE-1) or diffuse directly as nitrous acid (HNO₂) and react with both oxy- and deoxyhemoglobin. Reaction of nitrite with oxyhemoglobin (Hb(II)O₂ with ferrous heme)

oxidizes Fe⁺² to Fe⁺³ forming methemoglobin (Hb(III) with ferric heme) and converting nitrite to stable inert nitrate (NO₃⁻). Reaction of nitrite with deoxyhemoglobin (Hb(II)) rapidly produces heme-nitrosylated methemoglobin (Hb(III)NO), a labile intermediate that more slowly converts to a stable heme-nitrosylated hemoglobin (Hb(II)NO). Hypoxia favors nitrite reaction of with Hb(II), leading to accumulation of the labile intermediate (Hb(III)NO) which constitutes a reservoir capable of dissociating and releasing bioactive NO into microcirculation. Additional non-hemoglobin intra-erythrocyte nitrite reductases also contribute to the NO reservoir (Schmidt and Feelisch 2019). Maximal erythrocyte nitrite reductase activity occurs at ~50% O₂ saturation, i.e., near the *in vivo* P₅₀ (Huang et al. 2005).

An earlier hypothesis, that NO reversibly binds a sulfhydryl group on β 93 cysteine forming S-nitroso (SNO)-hemoglobin coupled to O₂ loading (Gow and Stamler 1998), was later disproved as a major source of NO bioavailability; instead, the β 93 cysteine is critical in sustaining heme-heme subunit interactions for cooperative O₂ binding and for protecting tissue from oxidative stress (Sun et al. 2019; Schmidt and Feelisch 2019).

Antioxidation

Erythrocytes are both a source and a sink for reactive oxygen and nitrogen species. Erythrocytes generate superoxide anions via autooxidation. The Fe⁺² heme is a target of reactive O₂ species (ROS). Oxidative stress damages erythrocyte membrane and impairs cell deformability and blood rheology. In defense, erythrocytes contain numerous antioxidants, including glutathione, thioredoxin, ascorbic acid, vitamin E, catalase, superoxide dismutase, membrane oxidoreductases, and the methemoglobin reductase-NADH-glycolysis system (Minetti et al. 2007; Nagababu et al. 2003b). Erythrocytes regenerate redox equivalents via glutathione reductase and the pentose phosphate pathway. Because of their excess antioxidative capacity, erythrocytes effectively constitute a mobile antioxidant sink for the whole body. Erythrocyte oxidant scaveng-

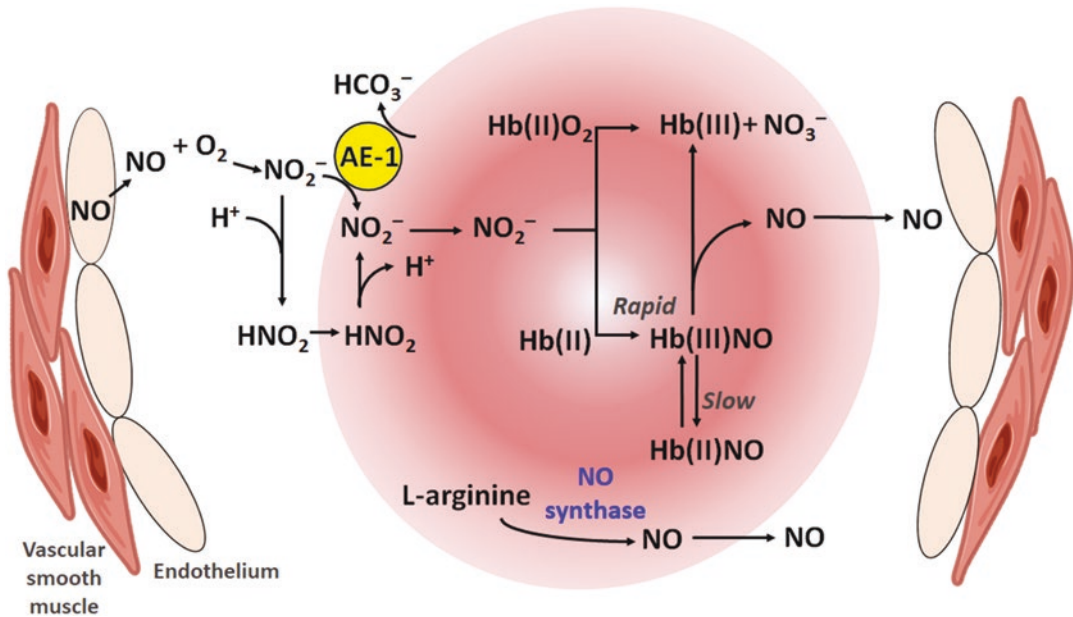


Fig. 40.4 Hemoglobin-mediated interactions between NO and O₂ exchange. AE-1 anion exchanger-1, H⁺ proton, Hb(II) deoxyhemoglobin (ferrous heme), Hb(II)NO nitrosylated deoxyhemoglobin (ferrous heme), Hb(II)O₂ oxyhemoglobin (ferrous heme), Hb(III) methemoglobin

(ferric heme), Hb(III)NO nitrosylated methemoglobin, NO₂⁻ Nitrite, HNO₂ nitrous acid, NO₃⁻ nitrate. See text for explanation (under *Erythrocytes as hemoglobin carrier: Erythrocyte as a source of bioactive NO*)

ing has been implicated in lymphocyte activation, endothelial cell signaling and anti-inflammation (Minetti et al. 2007). As NO can react directly with superoxide in addition to its reactions with heme, elimination of superoxide by intracellular superoxide dismutase effectively increases yield of NO-bound hemoglobin (Gow et al. 1999), leading to enhanced allosteric NO–O₂ interactions and vasoregulatory capability.

Adaptation of Erythrocytes for Oxygen Transport

Despite their favorable characteristics, erythrocytes also represent a trade-off as they impart unfavorable characteristics, i.e., higher resistance to flow and gas diffusion, compared to cell-free hemoglobin (Betticher et al. 1995). Mechanical stress and strain experienced by circulating erythrocytes mandate cells that are sturdy yet flexible, thereby creating selection pressures on cell size, shape and elasticity.

Size

Mammalian microvasculature is characterized by small capillary diameter and high capillary density to reduce diffusion distance. Correspondingly, erythrocytes also downsize (~70 μm in amphibians, ~7 μm in humans and 2 μm in deer mice). Eliminating the rigid nucleus and excess organelles not needed for gas transport allows cell downsizing, increases gas exchange capacity per cell, improves cell deformability and minimizes energy expenditure. Most vertebrate species possess nucleated erythrocytes, while mammals possess non-nucleated erythrocytes. Mammalian erythroblasts extrude their nuclei and organelles during maturation (Lee et al. 2004). Reticulocytes retain some ribosomal and mitochondrial material. Mature erythrocytes have stripped most metabolic machinery except that for glycolysis and pentose phosphate shunt; waste products are packaged into cell membrane vesicles and expelled (Gifford et al. 2006). Aging erythrocytes gradually lose membrane and cyto-

plasm, becoming smaller. Age-related changes such as glycation render key proteins, e.g., AE-1, immunogenic (Kay 2005), and mark the cell for destruction in the reticulo-endothelial system. Oxidative stress hastens erythrocyte senescence and apoptosis by modifying surface antigens or disrupting the cytoskeleton, leading to loss of plasticity and susceptibility to elimination.

Shape

Erythrocyte shape is determined by membrane elasticity, surface area and cell volume. Most mammalian erythrocytes are oval or spindle-shaped. The biconcavity of human erythrocyte increases surface-to-volume ratio allowing greater deformation without altering surface area, minimizes total cellular electrostatic energy and promotes mechanical stability (Adams 1973). Since biconcavity distributes more cell mass to the periphery and increases the moment of inertia compared to spherocytes, biconcave cells can better resist rotation during flow, which in turn minimizes turbulence, platelet scatter and induction of inflammation (Uzoigwe 2006).

Across vertebrates, average erythrocyte diameter is 25–30% larger than the corresponding capillary diameter, suggesting beneficial effects of cell deformation (Snyder and Sheafor 1999). Compared to spheres, distortion of flowing erythrocytes minimizes flow resistance and maximizes the membrane area in close proximity to capillary endothelium (Betticher et al. 1995). Human erythrocytes can elongate threefold in linear dimension without changing surface area. Membrane bending and shear elasticity are attributed to *spectrin*, the principal cytoskeletal protein that associates with actin to form a hexagonal lattice (Mohandas and Chasis 1993). Deformation causes spectrin tetramers to dissociate into dimers, allowing some molecules to uncoil and extend, while others fold and compress; dynamic tetramer dissociation–association permits reversible cell shape change as in a viscoelastic solid (An et al. 2002). Prolonged shear stress induces spectrin re-organization leading to irreversibly deformed cells, while supra-physiological shear stress causes membrane failure.

Distribution

Reaction velocity between O₂ and hemoglobin is much faster in cell-free hemoglobin solutions than whole blood; lungs perfused with hemoglobin solutions exhibit higher diffusing capacity than those perfused with erythrocyte suspensions (Geiser and Betticher 1989). The higher diffusion resistance of erythrocyte suspension is attributed to (a) the erythrocyte membrane, plasma layer and a dynamic unstirred boundary layer surrounding the erythrocyte, and (b) sub-optimal diffusion–perfusion matching along the erythrocyte–capillary interface. Capillary erythrocytes flow at a slower rate than plasma, and their transit time is influenced by perfusion pressure, vessel diameter and leukocyte traffic, leading to heterogeneous distribution of hemoglobin with respect to capillary surface and a lower efficiency of gas exchange (Hsia et al. 1999). At baseline, all lung capillaries are perfused by plasma (König et al. 1993), but in regions where alveolar pressure exceeds intra-capillary pressure (zone 1), partially collapsed capillaries admit few erythrocytes; regional heterogeneity is worsened by local hypoxic vasoconstriction and leukocyte margination (Hogg et al. 1988). Gas exchange limitations due to regional heterogeneity can be overcome only by local vasomotor regulation such as the intra-erythrocytic O₂–NO interactions as described above.

Production, Storage and Release

In lower vertebrates, erythropoiesis occurs mainly in pre-splenic tissue, spleen and kidney. In higher vertebrates, erythropoiesis shifts to liver and bone marrow, while the spleen increasingly assumes lymphoid functions (Glomski and Tamburlin 1990; Glomski et al. 1992; Glomski et al. 1997). Competing pressures for O₂ transport and immune defenses drove these shifts as demands for hematopoiesis exceed splenic capacity. Hepatic erythropoiesis normally occurs in human fetuses, while extramedullary erythropoiesis occurs in liver, spleen and kidney when bone marrow production is compro-

mised (Fan et al. 2018). Multiple production sites increase the versatility and reserve capacity of O₂ transport. Benefits of a large erythrocyte mass are limited by the attendant increases in vascular resistance and blood viscosity and risks of endothelial cell injury and thrombogenicity. Athletic mammals (dogs, horses, diving seals) adapt to these competing selection pressures by evolving both a high vascular capacity and a dynamic hemoglobin reservoir in a large spleen that sequesters ~13% of total blood volume at a hematocrit of 80–90% (Cabanac et al. 1997). Under sympathetic and catecholamine stimulation imposed by hypoxia, ischemia or exercise, splenic contraction reversibly augments circulating hemoglobin mass and O₂-carrying capacity while avoiding resting polycythemia (Hsia et al. 2007). *Demand-driven reversible autologous blood doping* contributes to the exceptional aerobic capacity and hypoxia tolerance of athletic mammals. In contrast, persistent erythrocytosis in polycythemia rubra vera (Podoltsev et al. 2018) and the artificially augmented blood volume and hemoglobin mass by autologous transfusion in athletes (Cacic et al. 2013) incur risks of thromboembolism.

Adaptation to Life Without Hemoglobin

Fish living in frigid oceans possess a low hematocrit (15–18%) to counter the cold-induced increase in blood viscosity. Some Antarctic icefish species have lost their hemoglobin as a result of large-scale gene deletion (Sidell and O'Brien 2006); erythrocytes are absent or defunct. Myoglobin gene may also be inactivated in independent mutation events, resulting in pale blood and tissue (Sidell et al. 1997). Adaptation relies on a low metabolic rate, high O₂ solubility in freezing water, antifreeze glycoproteins and wide-ranging compensatory responses including large gills, scaleless skin, hypervolemia, cardiac hypertrophy, high capillary density, large capillary lumens and elevated NO synthase lev-

els to facilitate vasodilatation and angiogenesis (Sidell and O'Brien 2006; Garofalo et al. 2009). Mammalian hemoglobin knockout is lethal; however, myoglobin-deficient mice exhibit a parallel set of cardiovascular compensation for maintaining O₂ transport, including upregulation of HIF's, stress proteins, vascular endothelial growth factor and NO synthase (Meeson et al. 2001).

Clinical Physiology and Pathophysiology

Baseline P₅₀ of human adult hemoglobin (Hb A, 26.7 mmHg) represents a trade-off among all O₂ transport steps from pulmonary uptake to cardiovascular delivery and peripheral utilization (Hsia 2001). An increase in P₅₀ (lower affinity) occurs when tissue O₂ demands predominate over that for pulmonary O₂ uptake. A decrease in P₅₀ (higher affinity) occurs when demands for pulmonary O₂ uptake predominate over tissue O₂ demands.

Increased Metabolic Demand

During heavy exercise, elevated muscle temperature, lactate and CO₂ production predominate, raising erythrocyte 2,3-BPG and shifting the ODC to a higher P₅₀ favoring O₂ unloading, while hyperventilation increases alveolar PO₂; consequently, pressure gradients (ΔP) for both O₂ loading and unloading are balanced and O₂ transport is maintained (Fig. 40.3a). In healthy volunteers, infusion of bisphosphonate reproduces the increase in P₅₀ and lowers cardiac work during exercise (Farber et al. 1984). In elite athletes at maximal exercise, cardiovascular O₂ delivery and muscle utilization may exceed pulmonary capacity for O₂ uptake, and the higher P₅₀ may not be enough to offset tissue O₂ deficit leading to exercise-induced arterial hypoxemia (Hopkins 2006). Diverse pathological conditions causing fever, tissue hypoxia, ischemia and hypermetabolism are also associated with elevated P₅₀ to satisfy tissue O₂ demands.

Adaptation to Ambient Hypoxia

Ambient hypoxia limits pulmonary O_2 uptake. In response, hyperventilation increases alveolar PO_2 but only to a limited degree; acidosis and elevated 2,3-BPG favor an increase in P_{50} , while hypocapnia and alkalosis favor a reduction in P_{50} (Fig. 40.3b). The net result of opposing responses depends on the severity and duration of hypoxia and the robustness of the overall O_2 transport cascade. In lowlanders during acclimation to moderate HA, hyperventilation increases alveolar PO_2 , while acidosis and 2,3-BPG increase P_{50} ; these adjustments maintain sufficient ΔP 's for both O_2 loading and unloading (Hsia 1998). Serum erythropoietin increases transiently; iron utilization and reticulocyte counts also increase (Mairbaurl et al. 1990). At extreme HA (>4000 m), excessive hyperventilation leads to severe respiratory alkalosis that increases O_2 affinity (lower P_{50}) (West, 1983). In healthy fit subjects during a simulated ascent to Mt. Everest (barometric pressure 253 mmHg) (Wagner et al. 2007), standard P_{50} (at pH 7.40, 37 °C) increased from sea level to the summit; the effect was balanced by progressive hypocapnia and alkalosis such that *in vivo* P_{50} remained unchanged. The reduced O_2 saturation was balanced by an increased O_2 extraction.

In chronic HA exposure, upregulated erythropoiesis leads to polycythemia and susceptibility to chronic mountain sickness in lowlanders living at HA and native Andean highlanders whose ancestors migrated to HA ~15,000 years ago (Gassmann et al. 2019). In contrast, hemoglobin concentration in Tibetans is often within the normal sea-level range (Simonson et al. 2015) accompanied by higher ventilatory and exercise capacities at HA, brisk hypoxic ventilatory responses, larger lung volumes, higher O_2 saturation and lung diffusing capacities, higher offspring survival at HA and a lower incidence of chronic mountain sickness compared to Han lowlanders (Simonson et al. 2015; Wu et al. 2005; Beall 2007). There is continuing debate as to whether the superior phenotypic adap-

tation in Tibetans is inherited or acquired. Animals indigenous to HA typically possess high O_2 affinity hemoglobins (lower P_{50}) (Sillau et al. 1976; Snyder 1985; Jurgens et al. 1988). A low P_{50} and absence of polycythemia or chronic mountain sickness are considered hallmarks of genotypic adaptation (Beall 2007). The P_{50} is typically normal in Andeans and either normal or lower in Tibetans compared to ethnically matched lowlanders (Beall 2007; Simonson et al. 2014). A large genome-wide association study found no preferential selection of HA adaptive genes among native Andeans (Gazal et al. 2019). In contrast, Tibetans inherited beneficial HIF pathway genes from archaic Denisovans who lived in Siberia ~40,000 years ago, including a gain-of-function mutation in *EGLN1* associated with higher O_2 affinity (lower hypoxia sensitivity), an *EPAS1* haplotype favoring anaerobic metabolism, and a *PPARA* haplotype favoring reduced fat oxidation (Simonson et al. 2012; Ge et al. 2015). As the descendants of Denisovans migrated to the Tibetan Plateau, these favorable traits were preferentially retained and likely contributed to their superior phenotypic features at HA.

Hemoglobinopathy

More than 1,000 human hemoglobin mutations exist involving insertion, deletion or substitution of amino acids on the globin chain; most of these are asymptomatic. Clinically significant mutations are classified into hereditary or acquired disorders of hemoglobin production, structure and/or function (Table 40.1). The major hereditary forms are (a) sickle cell syndromes (Hb S), (b) α - and β -thalassemias, (c) unstable hemoglobins, (d) high O_2 affinity and (e) low O_2 affinity variants.

Sickle cell, thalassemia and unstable hemoglobins accelerate erythrocyte destruction leading to hemolytic anemia. Sickle cells with impaired deformability can obstruct microvessels, causing tissue hypoxia, acidosis and necro-

Table 40.1 Clinical alterations of hemoglobin structure and function and related erythrocyte abnormalities

Disorder	Etiology	Manifestations
<i>Reduced production</i>		
α -Thalassemia	Deletion/mutation of α -globin genes	Anemia, hemolysis, splenomegaly, iron overload, bone deformities, heart failure Increased 2,3-BPG and P ₅₀
β -Thalassemia minor	Heterozygous mutation/deletion of β -globin genes	
β -Thalassemia major	Homozygous mutation/deletion of β -globin Destruction of bone marrow erythroid progenitors	
Myelodysplastic syndromes	Acquired reduction in α -globin gene expression	Anemia, neutropenia, thrombocytopenia
<i>Excess production</i>		
Polycythemia	Polycythemia rubra vera, hematological malignancy	Elevated blood viscosity, thromboembolism
	Acquired—chronic hypoxemia, blood transfusion	
<i>Abnormal structure</i>		
Sickle cell anemia (Hb S disease)	Amino acid substitution causing hemoglobin polymerization, erythrocyte distortion and rigidity	Hemolytic anemia, tissue necrosis, vaso-occlusive crises, increased 2,3-BPG and P ₅₀
Spherocytosis	Hereditary spherocytosis Southeast Asian ovalocytosis Acquired autoimmune hemolytic diseases	Hemolytic anemia Increased 2,3-BPG and P ₅₀
Schistocytosis	Microangiopathic hemolysis Infection Hematologic malignancy	Erythrocyte fragmentation
<i>Altered function</i>		
Unstable hemoglobin variants	Heinz body hemolytic anemia G6PD deficiency	Hemolysis due to globin precipitation or oxidant and drug exposure
High O ₂ affinity variants	Hereditary persistence of fetal hemoglobin (Hb F)	Often associated with sickle cell disease and thalassemia
	Various amino acid substitutions that stabilize oxyhemoglobin conformation	Erythrocytosis, normal O ₂ saturation
Low O ₂ affinity variants	Various amino acid substitutions that stabilize deoxyhemoglobin conformation	Cyanosis, low O ₂ saturation Normal hemoglobin level
Methemoglobinemia	Congenital hemoglobin M or Cytochrome b5 reductase deficiency Acquired—drug and toxin exposure	Cyanosis, normal hemoglobin level or mild anemia, responds to methylene blue
Carboxyhemoglobinemia	Increased endogenous CO production, smoking, CO poisoning	O ₂ deficit, headache, dizziness, confusion, dyspnea
Post-translational modification of hemoglobin	Non-enzymatic glycation, e.g., Hemoglobin A1c	Marker of glycemic control
	Deamination, e.g., hemoglobin Providence	Reduced P ₅₀ , erythrocytosis
	Amino-terminal acylation by aspirin-like diacyl esters	Reduced P ₅₀ , no significant clinical manifestation
	Amino-terminal carbamylation by cyanate	Marker of uremia and adequacy of dialysis

sis. Erythrocyte deformability is also impaired in hereditary spherocytosis and ovalocytosis where abnormal cell shapes and mechanics predispose to hemolysis. Schistocytes are seen in microangiopathic hemolysis due to infection or malignancy. In all hemolytic conditions, acidosis and increased erythrocyte 2,3-BPG reduce hemoglobin O₂ affinity (higher P₅₀) to preserve O₂ unloading in the periphery.

Several hemoglobinopathies, e.g., sickle cell trait, hemoglobins C, E, F, thalassemias, and mutations that alter erythrocyte cytoskeleton or membrane surface proteins, confer survival advantage and protection from severe malaria infection; this is an important example of coevolution and trade-off between the *Plasmodium falciparum* parasite and the human hosts native to malaria-endemic regions. Numerous mechanisms of protection have been proposed, including accelerated hemolysis and splenic phagocytosis of infected erythrocytes, inhibition of intra-erythrocytic parasite growth by O₂-dependent hemoglobin polymerization (Archer et al. 2018), induction of hemoxygenase-1 to catabolize heme and produce CO which protects the endothelium and preserves microvascular and blood–brain barrier integrity (Weinberg et al. 2008; Ferreira et al. 2011) and acquired antimalaria immunity (Williams et al. 2005), among others.

Unstable Hemoglobins

Unstable hemoglobins predispose to erythrocyte oxidative damage and hemolysis. In the rare congenital Heinz body hemolytic anemia (Gallagher 2015), globin chain mutations cause structural alterations, leading to altered solubility and intracellular precipitates (Heinz bodies) that bind to erythrocyte membrane, impair membrane deformability, increase permeability and predispose to hemolysis. More common is the X-linked recessive glucose-6-phosphate dehydrogenase (G6PD) deficiency (Frank 2005). G6PD mediates the first reaction in the pentose phosphate pathway that reduces NADP⁺ to NADPH; the latter prevents intra-erythrocyte ROS buildup. As erythrocytes lack other NADPH-producing

enzymes, mutations that cause G6PD deficiency promote ROS-induced damage to hemoglobin and hemolysis upon exposure to infection, certain drugs, toxins and fava beans. G6PD deficiency also weakens erythrocyte membrane and shortens erythrocyte life span, rendering the cell an unsuitable host for the life cycle of *P. falciparum*, thereby conferring malaria resistance to individuals native to malaria-endemic regions (Cappadoro et al. 1998).

Hemoglobin Variants with Altered O₂ Affinity

Human fetal hemoglobin (Hb F, P₅₀ 19.7 mmHg) is adapted to uterine hypoxia; Hb F also resists polymerization and sickling. Patients with sickle cell anemia and thalassemia often exhibit elevated Hb F, a hereditary trait that attenuates the complications of tissue hypoxia resulting from recurrent hemolytic crises (Akinsheye et al. 2011). Almost 100 hereditary high-affinity hemoglobin variants are known, involving amino acid substitutions that stabilize oxyhemoglobin, leading to full O₂ saturation but reduced tissue O₂ supply, which can stimulate Epo production with secondary erythrocytosis (Wajcman and Galacteros 2005).

Nearly 70 low-affinity hemoglobin variants are known, involving amino acid substitutions that stabilize deoxyhemoglobin. As pulmonary O₂ loading is impaired and tissue O₂ delivery is enhanced, patients can be asymptomatic or present with cyanosis, arterial O₂ desaturation, secondary reduction in erythropoiesis and chronic normocytic anemia (Yudin and Verhovsek 2019). Animal studies of low-affinity hemoglobin demonstrate gain-of-function physiology with reduced left ventricular work, enhanced tissue oxygenation and utilization, and increased exercise capacity (Berlin et al. 2002; Shirasawa et al. 2003).

Carboxyhemoglobinemia

Carbon monoxide (CO), a normal product of heme breakdown, binds heme with an affinity ~200 times that of O₂, forming carboxyhemoglobin.

globin (HbCO) and competitively displacing O₂ from heme-binding sites. In addition, CO binding to one heme increases O₂ affinity of the remaining heme-binding sites (Hlastala et al. 1976). CO poisoning causes tissue anoxia, nausea, vomiting, dyspnea, chest pain, confusion, seizures, loss of consciousness and death. Hyperbaric O₂ therapy is often necessary to replace CO with O₂ on hemoglobin.

Methemoglobinemia

An increase in methemoglobin containing non-O₂-binding oxidized iron (Fe⁺³) may be hereditary or acquired. Hereditary forms may result from deficiency of cytochrome b5 reductase enzyme in erythrocytes only (Type I) or in all cells (Type II) (Lorenzo et al. 2011) or from Hemoglobin M disease, a variant methemoglobin that stabilizes oxidized Fe⁺³ (Mansouri and Lurie 1993). Having one Fe⁺³ heme also increases O₂ affinity of the remaining Fe⁺² hemes in the same hemoglobin tetramer, further reducing O₂ delivery and resulting in “functional anemia” even when blood hemoglobin concentration is normal. Acquired methemoglobinemia is more common and associated with exposure to oxidant drugs and chemicals, including dapsone and other sulfonamides, chloroquine, nitrates, nitrite, inhaled NO, local anesthetics and aniline dyes. Patients appear cyanotic and may be asymptomatic or suffer manifestations of tissue hypoxia. O₂ saturation should be verified with blood gas analysis (Stucke et al. 2006) as pulse oximetry values are falsely high and fail to improve following supplemental O₂ administration. Methylene blue, ascorbic acid and riboflavin are the standard treatment for methemoglobinemia >30% or patients who remain symptomatic despite supplemental O₂ therapy (Cefalu et al. 2020).

Post-translational Modification of Hemoglobin

(a) *Glycation*: Glucose non-enzymatically reacts with the free amino group of globin produc-

ing glycated hemoglobin (HbA1c), a widely adopted marker of glycemic control in diabetic subjects. HbA1c has a higher intrinsic O₂ affinity (lower standard P₅₀ at pH 7.40) than Hb A (Coletta et al. 1988); HbA1c also alters erythrocyte metabolism to increase 2,3-BPG which tends to increase P₅₀ (Solomon and Cohen 1989). These counterbalancing actions result in little net change of baseline *in vivo* P₅₀ among diabetic patients. An elevated HbA1c level can also lead to overestimation of arterial O₂ saturation by pulse oximetry (Pu et al. 2012).

- (b) *Deamination*: Hemoglobin Providence is a rare hereditary variant where a β-chain asparagine substitutes for lysine and is later deaminated to aspartic acid *in vivo* during the life span of the erythrocyte. These changes reduce hemoglobin affinity for 2,3-BPG, leading to high O₂ affinity and secondary erythrocytosis. Hemoglobin Providence and several other hemoglobin variants interfere with HbA1c immunoassay, yielding falsely low values (Newman et al. 2017). Presence of hemoglobin variants should be suspected in diabetic subjects when HbA1c level is inconsistent with other measures of glycemic control.
- (c) *Acylation*: Aspirin and similar diacyl esters can transfer the acyl group to the amino terminal of hemoglobin resulting in increased O₂ affinity (Bridges et al. 1975). In the presence of a high glucose concentration, aspirin also inhibits glycation of hemoglobin and prevents the associated conformational changes (Bakhti et al. 2007). Functional impact of these interactions is considered minimal.
- (d) *Carbamylation*: Carbamylated hemoglobin (CarHb) is formed by non-enzymatic reaction of hemoglobin with cyanate, a product of *in vivo* urea dissociation. CarHb level is dependent upon blood urea concentration and duration of urea exposure; higher levels are seen in chronic than acute renal failure (Stim et al. 1995). CarHb hinders hemoglobin binding to 2,3-BPG and increases O₂ affinity. However, urea also directly alters hemoglobin structure by stabilizing

2,3-BPG-hemoglobin, which reduces O₂ affinity. Owing to the opposing effects, uremic patients do not exhibit increased hemoglobin O₂ affinity (Monti et al. 1995). CarHb is a marker for the adequacy of hemodialysis and correlates with neuropathic complications (Abdelwhab and Ahmed 2008). Carbamylation and glycation both involve free amino groups. In diabetic uremic patients, glycation of hemoglobin reduces CarHb at a given urea concentration, likely by decreasing the available free amino groups (Hammouda and Mady 2001).

Conclusions

Ancestral hemoproteins arose to harness chemical energy from nitrogen- and sulfur-based redox reactions and only later pivoted to O₂ detoxification and eventually aerobic respiration. As organismal O₂ demands increased, intricate molecular interactions permit dynamic regulation of O₂ uptake, storage and delivery by hemoglobin, coupled to that of CO₂ and NO. Erythrocytes greatly enhance the respiratory function of hemoglobin; both co-evolved with the microvasculature. The astounding number of hemoglobin variants attests to robust selection pressures for meeting the demands of O₂ transport while minimizing trade-offs under various organismal and environmental constraints. Knowledge of the origin and physiology of hemoglobin facilitates understanding of its respiratory functions, pathophysiological disturbances and the compensatory responses to guide clinical management of disease and provide a robust foundation for therapeutic explorations, e.g., to correct specific mutations in hemoglobinopathies, manipulate allosterism to optimize O₂ uptake and delivery in accordance with metabolic needs, develop effective hemoglobin or erythrocyte substitutes, or engineer hematopoietic stem cells into mature erythrocytes with normal hemoglobin function.

Acknowledgment The author acknowledges the support by National Heart, Lung and Blood Institute grant R01

HL134373. The content of this manuscript is solely the author's responsibility and does not necessarily represent the official views of the funding agency.

References

- Abdelwhab S, Ahmed H. Carbamylated Hemoglobin as an Indicator of Hemodialysis adequacy and complications. *Kidney*. 2008;17(4):178–84.
- Adams KH. A theory for the shape of the red blood cell. *Biophys J*. 1973;13(10):1049–53.
- Akinsheye I, Alsultan A, Solovieff N, Ngo D, Baldwin CT, Sebastiani P, et al. Fetal hemoglobin in sickle cell anemia. *Blood*. 2011;118(1):19–27.
- An X, Lecomte MC, Chasis JA, Mohandas N, Gratzer W. Shear-response of the spectrin dimer-tetramer equilibrium in the red blood cell membrane. *J Biol Chem*. 2002;277(35):31796–800.
- Archer NM, Petersen N, Clark MA, Buckee CO, Childs LM, Duraisingh MT. Resistance to Plasmodium falciparum in sickle cell trait erythrocytes is driven by oxygen-dependent growth inhibition. *Proc Natl Acad Sci U S A*. 2018;115(28):7350–5.
- Bakhti M, Habibi-Rezaei M, Moosavi-Movahedi AA, Khazaei MR. Consequential alterations in haemoglobin structure upon glycation with fructose: prevention by acetylsalicylic acid. *J Biochem*. 2007;141(6):827–33.
- Beall CM. Detecting natural selection in high-altitude human populations. *Respir Physiol Neurobiol*. 2007;158(2–3):161–71.
- Berlin G, Challoner KE, Woodson RD. Low-O(2) affinity erythrocytes improve performance of ischemic myocardium. *J Appl Physiol* (1985). 2002;92(3):1267–76.
- Betticher DC, Reinhart WH, Geiser J. Effect of RBC shape and deformability on pulmonary diffusing capacity and resistance to flow in rabbit lungs. *J Appl Physiol*. 1995;78(3):778–83.
- Bleeker WK, Berbers GA, den Boer PJ, Agterberg J, Rigter G, Bakker JC. Effect of polymerization on clearance and degradation of free hemoglobin. *Biomater Artif Cell Immobil Biotechnol*. 1992;20(2–4):747–50.
- Bridges KR, Schmidt GJ, Jensen M, Cerami A, Bunn HF. The acetylation of hemoglobin by aspirin. *In vitro and in vivo*. *J Clin Invest*. 1975;56(1):201–7.
- Cabanac A, Folkow LP, Blix AS. Volume capacity and contraction control of the seal spleen. *J Appl Physiol*. 1997;82(6):1989–94.
- Cacic DL, Hervig T, Seghatchian J. Blood doping: the flip side of transfusion and transfusion alternatives. *Transfus Apher Sci*. 2013;49(1):90–4.
- Cappadoro M, Giribaldi G, O'Brien E, Turrini F, Mannu F, Ulliers D, et al. Early phagocytosis of glucose-6-phosphate dehydrogenase (G6PD)-deficient erythrocytes parasitized by Plasmodium falciparum may explain malaria protection in G6PD deficiency. *Blood*. 1998;92(7):2527–34.

- Cefalu JN, Joshi TV, Spalitta MJ, Kadi CJ, Diaz JH, Eskander JP, et al. Methemoglobinemia in the operating room and intensive care unit: early recognition, pathophysiology, and management. *Adv Ther*. 2020;37(5):1714–23.
- Coletta M, Amiconi G, Bellelli A, Bertolini A, Carsky J, Castagnola M, et al. Alteration of T-state binding properties of naturally glycosylated hemoglobin, HbA1c. *J Mol Biol*. 1988;203(1):233–9.
- de Duce C. The birth of complex cells. *Sci Amer*. 1996:50–7.
- de Wit R, van Gernerden H. Oxidation of sulfide to thiosulfate by microcoleus chthonoplastes. *FEMS Microbiol Letters*. 1987;45(1):7–13.
- Fan N, Lavu S, Hanson CA, Tefferi A. Extramedullary hematopoiesis in the absence of myeloproliferative neoplasm: Mayo Clinic case series of 309 patients. *Blood Cancer J*. 2018;8(12):119.
- Farber MO, Sullivan TY, Fineberg N, Carlone S, Manfredi F. Effect of decreased O₂ affinity of hemoglobin on work performance during exercise in healthy humans. *J Lab Clin Med*. 1984;104(2):166–75.
- Fens MH, Larkin SK, Oronsky B, Scicinski J, Morris CR, Kuypers FA. The capacity of red blood cells to reduce nitrite determines nitric oxide generation under hypoxic conditions. *PLoS One*. 2014;9(7):e101626.
- Ferreira A, Marguti I, Bechmann I, Jeney V, Chora A, Palha NR, et al. Sickle hemoglobin confers tolerance to Plasmodium infection. *Cell*. 2011;145(3):398–409.
- Frank JE. Diagnosis and management of G6PD deficiency. *Am Fam Physician*. 2005;72(7):1277–82.
- Freitas TA, Hou S, Dioum EM, Saito JA, Newhouse J, Gonzalez G, et al. Ancestral hemoglobins in Archaea. *Proc Natl Acad Sci U S A*. 2004;101(17):6675–80.
- Gallagher PG. Diagnosis and management of rare congenital nonimmune hemolytic disease. *Hematology Am Soc Hematol Educ Program*. 2015;2015:392–9.
- Garofalo F, Amelio D, Cerra MC, Tota B, Sidell BD, Pellegrino D. Morphological and physiological study of the cardiac NOS/NO system in the Antarctic (Hb-/Mb-) icefish *Chaenocephalus aceratus* and in the red-blooded *Trematomus bernacchii*. *Nitric Oxide*. 2009;20(2):69–78.
- Gassmann M, Mairbaurl H, Livshits L, Seide S, Hackbusch M, Malczyk M, et al. The increase in hemoglobin concentration with altitude varies among human populations. *Ann NY Acad Sci*. 2019;1450(1):204–20.
- Gazal S, Espinoza JR, Austerlitz F, Marchant D, Macaralup J, Rodriguez J, et al. The genetic architecture of chronic mountain sickness in Peru. *Front Genet*. 2019;10:690.
- Ge RL, Simonson TS, Gordeuk V, Prchal JT, McClain DA. Metabolic aspects of high-altitude adaptation in Tibetans. *Exp Physiol*. 2015;100(11):1247–55.
- Geiser J, Betticher DC. Gas transfer in isolated lungs perfused with red cell suspension or hemoglobin solution. *Respir Physiol*. 1989;77(1):31–9.
- Gifford SC, Derganc J, Shevkopyas SS, Yoshida T, Bitensky MW. A detailed study of time-dependent changes in human red blood cells: from reticulocyte maturation to erythrocyte senescence. *Br J Haematol*. 2006;135(3):395–404.
- Glomski CA, Tamburlin J. The phylogenetic odyssey of the erythrocyte. I. Hemoglobin: the universal respiratory pigment. *Histol Histopathol*. 1989;4(4):509–14.
- Glomski CA, Tamburlin J. The phylogenetic odyssey of the erythrocyte. II. The early or invertebrate prototypes. *Histol Histopathol*. 1990;5(4):513–25.
- Glomski CA, Tamburlin J, Chainani M. The phylogenetic odyssey of the erythrocyte. III. Fish, the lower vertebrate experience. *Histol Histopathol*. 1992;7(3):501–28.
- Glomski CA, Tamburlin J, Hard R, Chainani M. The phylogenetic odyssey of the erythrocyte. IV. The amphibians. *Histol Histopathol*. 1997;12(1):147–70.
- Gow AJ, Stamler JS. Reactions between nitric oxide and haemoglobin under physiological conditions. *Nature*. 1998;391(6663):169–73.
- Gow AJ, Luchsinger BP, Pawloski JR, Singel DJ, Stamler JS. The oxyhemoglobin reaction of nitric oxide. *Proc Natl Acad Sci U S A*. 1999;96(16):9027–32.
- Gribaldo S, Brochier-Armanet C. The origin and evolution of Archaea: a state of the art. *Philos Trans R Soc Lond Ser B Biol Sci*. 2006;361(1470):1007–22.
- Hammouda AM, Mady GE. Correction formula for carbamylated haemoglobin in diabetic uraemic patients. *Ann Clin Biochem*. 2001;38(Pt 2):115–9.
- Hlastala MP, McKenna HP, Franada RL, Deter JC. Influence of carbon monoxide on hemoglobin-oxygen binding. *J Appl Physiol*. 1976;41(6):893–9.
- Hogg JC, McLean T, Martin BA, Wiggs B. Erythrocyte transit and neutrophil concentration in the dog lung. *J Appl Physiol*. 1988;65(3):1217–25.
- Hopkins SR. Exercise induced arterial hypoxemia: the role of ventilation-perfusion inequality and pulmonary diffusion limitation. *Adv Exp Med Biol*. 2006;588:17–30.
- Hsia CCW. Respiratory function of hemoglobin. *N Engl J Med*. 1998;338:239–47.
- Hsia CC. Coordinated adaptation of oxygen transport in cardiopulmonary disease. *Circulation*. 2001;104(8):963–9.
- Hsia CC, Johnson RL Jr, Shah D. Red cell distribution and the recruitment of pulmonary diffusing capacity. *J Appl Physiol* (1985). 1999;86(5):1460–7.
- Hsia CC, Johnson RL Jr, Dane DM, Wu EY, Estrera AS, Wagner HE, et al. The canine spleen in oxygen transport: gas exchange and hemodynamic responses to splenectomy. *J Appl Physiol*. 2007;103(5):1496–505.
- Hsia CC, Schmitz A, Lambert M, Perry SF, Maina JN. Evolution of air breathing: oxygen homeostasis and the transitions from water to land and sky. *Compr Physiol*. 2013;3(2):849–915.
- Hsia CC, Hyde DM, Weibel ER. Lung structure and the intrinsic challenges of gas exchange. *Compr Physiol*. 2016;6(2):827–95.
- Huang Z, Shiva S, Kim-Shapiro DB, Patel RP, Ringwood LA, Irby CE, et al. Enzymatic function of hemoglobin as a nitrite reductase that produces NO under allosteric control. *J Clin Invest*. 2005;115(8):2099–107.

- Jelkmann W. Erythropoietin after a century of research: younger than ever. *Eur J Haematol*. 2007;78(3):183–205.
- Jurgens KD, Pietschmann M, Yamaguchi K, Kleinschmidt T. Oxygen binding properties, capillary densities and heart weights in high altitude camelids. *J Comp Physiol B*. 1988;158(4):469–77.
- Kay M. Immunoregulation of cellular life span. *Ann NY Acad Sci*. 2005;1057:85–111.
- Kleinbongard P, Schulz R, Rassaf T, Lauer T, Dejam A, Jax T, et al. Red blood cells express a functional endothelial nitric oxide synthase. *Blood*. 2006;107(7):2943–51.
- König MF, Lucocq JM, Weibel ER. Demonstration of pulmonary vascular perfusion by electron and light microscopy. *J Appl Physiol*. 1993;75(4):1877–83.
- Lee JC, Gimm JA, Lo AJ, Koury MJ, Krauss SW, Mohandas N, et al. Mechanism of protein sorting during erythroblast enucleation: role of cytoskeletal connectivity. *Blood*. 2004;103(5):1912–9.
- Lorenzo FR, Phillips JD, Nussenzeig R, Lingam B, Koul PA, Schrier SL, et al. Molecular basis of two novel mutations found in type I methemoglobinemia. *Blood Cells Mol Dis*. 2011;46(4):277–81.
- Mairbaurl H, Schobersberger W, Oelz O, Bartsch P, Eckardt KU, Bauer C. Unchanged in vivo P50 at high altitude despite decreased erythrocyte age and elevated 2,3-diphosphoglycerate. *J Appl Physiol* (1985). 1990;68(3):1186–94.
- Mairbaurl H, Weber RE. Oxygen transport by hemoglobin. *Compr Physiol*. 2012;2(2):1463–89.
- Mangum CP. Major events in the evolution of the oxygen carriers. *Amer Zool*. 1998;38(1):1–13.
- Mansouri A, Lurie AA. Concise review: methemoglobinemia. *Am J Hematol*. 1993;42(1):7–12.
- Matteucci E, Giampietro O. Electron pathways through erythrocyte plasma membrane in human physiology and pathology: potential redox biomarker? *Biomark Insights*. 2007;2:321–9.
- McMurtrie HL, Cleary HJ, Alvarez BV, Loiselle FB, Sterling D, Morgan PE, et al. The bicarbonate transport metabolon. *J Enzyme Inhib Med Chem*. 2004;19(3):231–6.
- Meeson AP, Radford N, Shelton JM, Mammen PP, DiMaio JM, Hutcheson K, et al. Adaptive mechanisms that preserve cardiac function in mice without myoglobin. *Circ Res*. 2001;88(7):713–20.
- Minetti M, Agati L, Malorni W. The microenvironment can shift erythrocytes from a friendly to a harmful behavior: pathogenetic implications for vascular diseases. *Cardiovasc Res*. 2007;75(1):21–8.
- Minning DM, Gow AJ, Bonaventura J, Braun R, Dewhirst M, Goldberg DE, et al. Ascaris haemoglobin is a nitric oxide-activated 'deoxygenase'. *Nature*. 1999;401(6752):497–502.
- Mohandas N, Chasis JA. Red blood cell deformability, membrane material properties and shape: regulation by transmembrane, skeletal and cytosolic proteins and lipids. *Semin Hematol*. 1993;30(3):171–92.
- Monti JP, Brunet PJ, Berland YF, Vanuxem DC, Vanuxem PA, Crevat AD. Opposite effects of urea on hemoglobin-oxygen affinity in anemia of chronic renal failure. *Kidney Int*. 1995;48(3):827–31.
- Nagababu E, Ramasamy S, Abernethy DR, Rifkind JM. Active nitric oxide produced in the red cell under hypoxic conditions by deoxyhemoglobin-mediated nitrite reduction. *J Biol Chem*. 2003a;278(47):46349–56.
- Nagababu E, Chrest FJ, Rifkind JM. Hydrogen-peroxide-induced heme degradation in red blood cells: the protective roles of catalase and glutathione peroxidase. *Biochim Biophys Acta*. 2003b;1620(1–3):211–7.
- Newman CN, Litwin CM, Bowlby DA, Lewis KA, Paulo RC. Hemoglobin Providence (beta82 Lys > Asn, Asp) and lower-than-expected HbA1c in a nonadherent teenager with type 1 diabetes: a case report and literature review. *Clin Case Rep*. 2017;5(12):2000–2.
- Paul RJ, Zeis B, Lamkemeyer T, Seidl M, Pirov R. Control of oxygen transport in the microcrustacean *Daphnia*: regulation of haemoglobin expression as central mechanism of adaptation to different oxygen and temperature conditions. *Acta Physiol Scand*. 2004;182(3):259–75.
- Pedersen SF, Cala PM. Comparative biology of the ubiquitous Na⁺/H⁺ exchanger, NHE1: lessons from erythrocytes. *J Exp Zool A Comp Exp Biol*. 2004;301(7):569–78.
- Pesce A, Bolognesi M, Bocedi A, Ascenzi P, Dewilde S, Moens L, et al. Neuroglobin and cytoglobin. Fresh blood for the vertebrate globin family. *EMBO Rep*. 2002;3(12):1146–51.
- Pesce A, Bolognesi M, Nardini M. Protoglobin: structure and ligand-binding properties. *Adv Microb Physiol*. 2013;63:79–96.
- Podoltsev NA, Zhu M, Zeidan AM, Wang R, Wang X, Davidoff AJ, et al. The impact of phlebotomy and hydroxyurea on survival and risk of thrombosis among older patients with polycythemia vera. *Blood Adv*. 2018;2(20):2681–90.
- Pu LJ, Shen Y, Lu L, Zhang RY, Zhang Q, Shen WF. Increased blood glycohemoglobin A1c levels lead to overestimation of arterial oxygen saturation by pulse oximetry in patients with type 2 diabetes. *Cardiovasc Diabetol*. 2012;11:110.
- Schmidt H, Feelisch M. Red blood cell-derived nitric oxide bioactivity and hypoxic vasodilation. *Circulation*. 2019;139(23):2664–7.
- Shirasawa T, Izumizaki M, Suzuki Y, Ishihara A, Shimizu T, Tamaki M, et al. Oxygen affinity of hemoglobin regulates O₂ consumption, metabolism, and physical activity. *J Biol Chem*. 2003;278(7):5035–43.
- Sidell BD, O'Brien KM. When bad things happen to good fish: the loss of hemoglobin and myoglobin expression in Antarctic icefishes. *J Exp Biol*. 2006;209(Pt 10):1791–802.
- Sidell BD, Vayda ME, Small DJ, Moylan TJ, Londraville RL, Yuan ML, et al. Variable expression of myoglobin among the hemoglobinless Antarctic icefishes. *Proc Natl Acad Sci U S A*. 1997;94(7):3420–4.

- Sillau AH, Cueva S, Valenzuela A, Candela E. O₂ transport in the alpaca (*Lama pacos*) at sea level and at 3,300 m. *Respir Physiol*. 1976;27(2):147–55.
- Simonson TS, McClain DA, Jorde LB, Prchal JT. Genetic determinants of Tibetan high-altitude adaptation. *Hum Genet*. 2012;131(4):527–33.
- Simonson TS, Wei G, Wagner HE, Wuren T, Bui A, Fine JM, et al. Increased blood-oxygen binding affinity in Tibetan and Han Chinese residents at 4200 m. *Exp Physiol*. 2014;99(12):1624–35.
- Simonson TS, Wei G, Wagner HE, Wuren T, Qin G, Yan M, et al. Low haemoglobin concentration in Tibetan males is associated with greater high-altitude exercise capacity. *J Physiol*. 2015;593(14):3207–18.
- Snyder GK. Blood corpuscles and blood hemoglobins: a possible example of coevolution. *Science*. 1977;195(4276):412–3.
- Snyder GK, Sheafor BA. Red blood cells: centerpiece in the evolution of the vertebrate circulatory system. *Amer Zool*. 1999;39:189–98.
- Snyder LR. Low P50 in deer mice native to high altitude. *J Appl Physiol* (1985). 1985;58(1):193–9.
- Solomon LR, Cohen K. Erythrocyte O₂ transport and metabolism and effects of vitamin B6 therapy in type II diabetes mellitus. *Diabetes*. 1989;38(7):881–6.
- Sterner R, Decker H. Inversion of the Bohr effect upon oxygen binding to 24-meric tarantula hemocyanin. *Proc Natl Acad Sci U S A*. 1994;91(11):4835–9.
- Stim J, Shaykh M, Anwar F, Ansari A, Arruda JA, Dunea G. Factors determining hemoglobin carbamylation in renal failure. *Kidney Int*. 1995;48(5):1605–10.
- Strand K, Knapp JE, Bhyravhatla B, Royer WE Jr. Crystal structure of the hemoglobin dodecamer from *Lumbricus erythrocytorin*: allosteric core of giant annelid respiratory complexes. *J Mol Biol*. 2004;344(1):119–34.
- Stucke AG, Riess ML, Connolly LA. Hemoglobin M (Milwaukee) affects arterial oxygen saturation and makes pulse oximetry unreliable. *Anesthesiology*. 2006;104(4):887–8.
- Sun CW, Yang J, Kleschyov AL, Zhuge Z, Carlstrom M, Pernow J, et al. Hemoglobin beta93 cysteine is not required for export of nitric oxide bioactivity from the red blood cell. *Circulation*. 2019;139(23):2654–63.
- Terwilliger RC. Structure of invertebrate hemoglobins. *Amer Zool*. 1980;20:53–67.
- Uzoigwe C. The human erythrocyte has developed the biconcave disc shape to optimise the flow properties of the blood in the large vessels. *Med Hypotheses*. 2006;67(5):1159–63.
- Wagner PD, Wagner HE, Groves BM, Cymerman A, Houston CS. Hemoglobin P(50) during a simulated ascent of Mt. Everest, operation Everest II. *High Alt Med Biol*. 2007;8(1):32–42.
- Wajcman H, Galacteros F. Hemoglobins with high oxygen affinity leading to erythrocytosis. New variants and new concepts. *Hemoglobin*. 2005;29(2):91–106.
- Weber RE, Vinogradov SN. Nonvertebrate hemoglobins: functions and molecular adaptations. *Physiol Rev*. 2001;81(2):569–628.
- Weinberg JB, Lopansri BK, Mwaikambo E, Granger DL. Arginine, nitric oxide, carbon monoxide, and endothelial function in severe malaria. *Curr Opin Infect Dis*. 2008;21(5):468–75.
- West JB. Climbing Mt. Everest without oxygen: an analysis of maximal exercise during extreme hypoxia. *Respir Physiol*. 1983;52(3):265–79.
- Williams TN, Mwangi TW, Roberts DJ, Alexander ND, Weatherall DJ, Wambua S, et al. An immune basis for malaria protection by the sickle cell trait. *PLoS Med*. 2005;2(5):e128.
- Wu T, Li S, Ward MP. Tibetans at extreme altitude. *Wilderness Environ Med*. 2005;16(1):47–54.
- Yudin J, Verhovsek M. How we diagnose and manage altered oxygen affinity hemoglobin variants. *Am J Hematol*. 2019;94(5):597–603.
- Zal F, Leize E, Lallier FH, Toulmond A, Van Dorsselaer A, Childress JJ. S-Sulfohemoglobin and disulfide exchange: the mechanisms of sulfide binding by Riftia pachyptila hemoglobins. *Proc Natl Acad Sci U S A*. 1998;95(15):8997–9002.



Sheldon Magder and Raghu R. Chivukula

Introduction

Hydrogen (H^+) ion concentration $[H^+]$ in biological solutions is a very small number. In normal arterial blood, $[H^+]$ is 0.00000004, or better written as 40×10^{-9} . Because it is such a small number, $[H^+]$ traditionally is given as a negative inverted logarithm which gives $pH = 7.4$. The advantage of the pH notation is that the very small $[H^+]$ is easier to visualize over the very large range of possible values in chemical reactions. Furthermore, the electrodes that are used to measure $[H^+]$ have a logarithmic output. However, in the clinical setting, the range of changes in $[H^+]$ is linear, and the pH notation can obscure significant changes of $[H^+]$ that occur in the small range of biological values. The normal pH of human blood at body temperature is 7.40 ± 0.02 , and values between ~ 6.80 and ~ 7.80 are compatible with life at least transiently. These observations highlight both how low and how

tightly blood normal $[H^+]$ is controlled. If $[H^+]$ is used instead of pH , the concentration varies from 0.00000038 mM to 0.00000042 mM, which is orders of magnitude less than most of the commonly measured serum electrolytes, although it is still in the range of vasoactive active peptides. By convention, blood pH values greater than 7.42 are defined as an alkalemia and those below 7.38 as an acidemia, although as will be seen, biological solutions are mainly alkaline solutions. In contrast to the terms acidemia and alkalemia, the terms acidosis and alkalosis refer to the process that created the acidemia or alkalemia.

Despite being such a small number, the $[H^+]$, with the odd exception, is maintained in a relatively constant range in all living organisms extending from bacteria to humans. The reason why this is important biologically is that H^+ only has a proton and no neutron in its nucleus and thus has the greatest charge density and field effect of any atom. Because of this, H^+ has strong effects on surrounding charged substances. Thus, $[H^+]$ affects the binding of organic molecules as well as the function of many proteins by altering their tertiary structures. To deal with this, nature has evolved many processes to regulate $[H^+]$ in a tight range, but these processes often are disturbed in the critically ill. To understand what can disturb $[H^+]$ in disease, it is important to understand the normal determinants of $[H^+]$ in biological solutions and how therapies can restore normal $[H^+]$. This topic usually is discussed as acid–base

S. Magder (✉)
Royal Victoria Hospital (McGill University
Health Centre), Departments of Critical Care and
Physiology McGill University, Montreal, QC, Canada
e-mail: sheldon.magder@mcgill.ca

R. R. Chivukula
Harvard Medical School, Massachusetts General
Hospital, Division of Pulmonary and Critical Care
Medicine, Department of Medicine,
Boston, MA, USA
e-mail: rchivukula@partners.org

disorders, but from a physical–chemical point of view, it really is about regulation of $[H^+]$. As already noted, biological solutions are almost always alkaline. Disease is just about more or less alkalinity.

Traditionally, pH and $[H^+]$ in biology have been analyzed based on the equilibrium equation for carbon dioxide (CO_2) dissolved in water, the formation of carbonic acid (H_2CO_3), and its dissociation into H^+ and HCO_3^- (Adrogué et al. 2009). When written in the logarithmic form of the Henderson–Hasselbalch equation and grouping of the constant that accounts for the solubility of CO_2 in its gas form in water with the dissociation constants of the components of the reactions, the equilibrium of this system can be written as:

$$pH = K \times \log \left[\frac{PCO_2}{[HCO_3^-]} \right]$$

where K is the grouped constants. Based on this equation, an increase or decrease in PCO_2 indicates a respiratory acidosis or alkalosis, respectively, and an increase or decrease in HCO_3^- indicates a metabolic alkalosis or acidosis, respectively. Empiric equations have been derived to determine whether the process is acute or chronic, compensated or uncompensated (Schwartz and Relman 1963). This equation is valid, and this approach describes the system. However, its limitation is that just examining the CO_2/HCO_3^- equilibrium fails to take into account other components of the solution that affect this equilibrium, as well as the role of other components of the solution including the spontaneous ionization (i.e., dissociation) of water, a

potentially very large source of H^+ . This classical approach thus does not lead to a physiological and physical–chemical understanding of the underlying chemical processes.

The late Peter Stewart went back to basic physical chemistry and identified the components of biological solutions that need to be taken into account to predict $[H^+]$ balance (Stewart 1978, 1981, 1983; Magder and Emami 2015). In his analysis, $[H^+]$ is a dependent variable, and its value is determined by the composition of the fluid being studied. H^+ is not an independent variable that can be moved from compartment to compartment. Instead, movement of other components determines $[H^+]$. The three independent determinants of $[H^+]$ are as follows: (1) the differences in concentrations of strong positive and negative ions, which is called the strong ion difference [SID] (Fig. 41.1); (2) PCO_2 and the weak volatile acid that it forms as in the standard approach; and (3) the concentration of non-volatile weak acids, of which the dominant one in plasma is albumin (Fig. 41.2). The effect of each of these components is based on not only their total mass in the body but also their concentrations so that the total amount of water in the body also has an impact.

Importance of Water

To understand the significance of $[H^+]$, it is best to start with pure water at standard temperature. The concentration of water molecules, i.e., $[H_2O]$ in “water”, is 55.3 moles. Compare this concen-

Fig. 41.1 Strong ions. Strong ions in water are almost completely dissociated. Thus, putting NaCl in water gives equal Na^+ and Cl^-

- Strong electrolytes are always completely dissociated in solution, $km > 4.0 \times 10^{-4}$ Eq/l

POSITIVE: Na^+ , K^+ , Ca^{2+} , Mg^{2+}

NEGATIVE: Cl^- , SO_4^{2-} , lactate, β -hydroxy butarate, formate, oxalate

NaCl does not exist in solution; there is only Na^+ and Cl^-

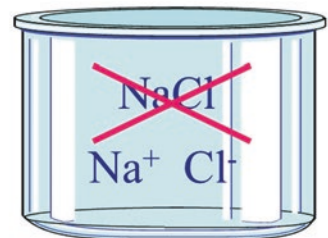
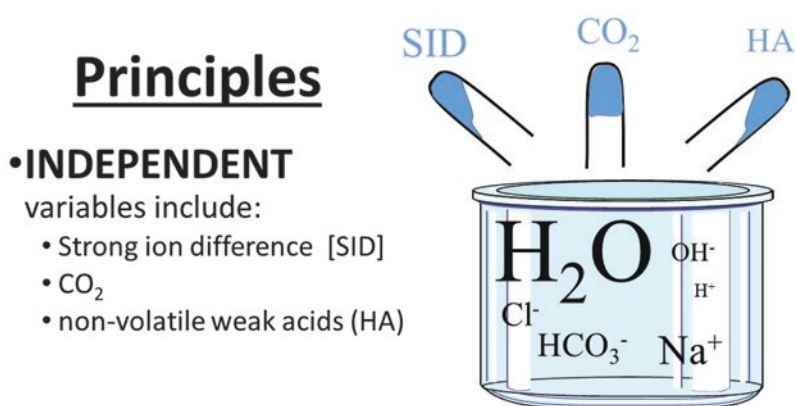


Fig. 41.2 The three independent determinants of $[H^+]$ and HCO_3^- . The three independent factors are the SID, CO_2 , and weak acids (HA) which in blood is primarily albumin. H^+ and HCO_3^- are dependent variables



tration to that of $[Na^+]$ which is 0.140 moles in normal serum. Thus, water has a large amount of H^+ atoms, but only a very small amount of the H_2O dissociates into H^+ and OH^- . The dissociation constant of H_2O at standard temperature and pressure is 14×10^{-9} , and $[H^+]$ is 100×10^{-7} (pH 7.0). If a beaker of pure water is heated to body temperature, $36.7^\circ C$, pH decreases to ~ 6.8 . One might ask, is this solution acidic? The answer to this question is central to an understanding of $[H^+]$ and acid–balance and discussed next.

Acids have been defined as electron acceptors or proton donors; these definitions were created to deal with $[H^+]$ in all types of solutions. However, the solvent in biology is water and thus the behavior of $[H^+]$ in water is what needs to be understood. This allows for the much simpler, and biologically useful, definition, created by Arrhenius in the eighteenth century. He defined an acid solution as one in which $[H^+]$ is greater than $[OH^-]$, a neutral solution as one in which $[H^+] = [OH^-]$, and an alkaline solution as one in which $[OH^-]$ is $> [H^+]$. Thus, even though at a temperature of $36.6^\circ C$, pure water has a pH of 6.8, it still is a neutral solution because $[H^+]$ equals $[OH^-]$. What happened is that the dissociation of H_2O increased at the higher temperature, and both $[H^+]$ and $[OH^-]$ increased equally. This had to occur to maintain conservation of mass and electrical neutrality, i.e., all positives need to match all negatives, and there are no other substances to allow the positive and

negative charges to differ. This is called the principle of electrical neutrality. The message here is that the values of $[H^+]$ or pH do not indicate whether the solution is acidic. As already noted, all bodily solutions, with exception of the fasting stomach and lysozymes, are alkaline, and when we say that the blood is acidic, it really is just less alkaline. This is true down to a pH of around 6.6. In Arrhenius' definitions, an acid is a substance that increases the $[H^+]$ of the solution and base in one that decreases $[H^+]$. Despite the point that acid–base disorders are really about more or less alkalinity, this is too cumbersome a usage and goes against the long historically used terminology. Accordingly, we still will continue to describe a pH less than 7.4 as being acidic, and a pH greater than 7.4 as being alkaline for biological purposes.

Importance of Strong Ions

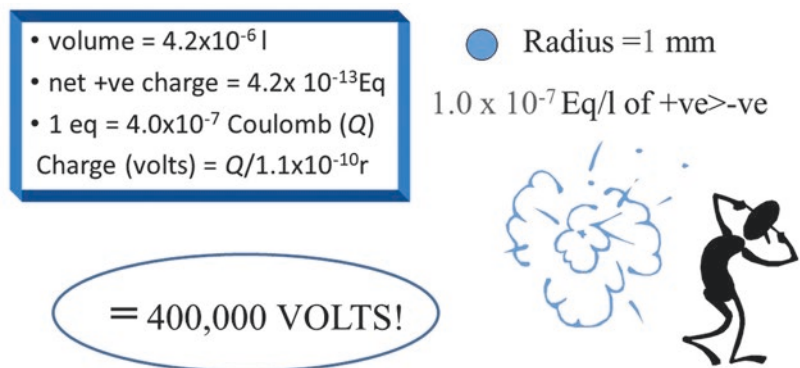
A key factor was introduced in the last paragraph and that is the principle of electrical neutrality. This says that in a macro-solution, the concentration of all positive and negative charges must be equal. This is because a small difference between positive and negative charges creates a large electrical force that can change the dissociation of substances that are weakly associated such as carbonic acid, albumin, phosphate, and importantly, even H_2O .

A quantitative example of this force will help illustrate its importance (Fig. 41.3). Consider a sphere that has a radius of 1 mm and contains a solution with an ionic concentration difference of 1×10^{-7} Eq/L. Also remember that $[\text{Na}^+]$ and $[\text{Cl}^-]$ in normal blood are in the 10^{-3} range or 1000 times greater than this. The volume of the sphere is 4.2×10^{-6} L, and the net positive charge is thus $4.2 \times 10^{-6} \times 10^{-7} = 4.2 \times 10^{-13}$. One Eq is 96,500 coulombs (coul) so that the charge on the sphere is $4.2 \times 10^{-13} \times 96,500 = 4.0 \times 10^{-8}$ coul. The electrical potential of a sphere of radius r (in meters) carrying a charge of Q (coul) is given by $Q/1.1 \times 10^{-10}r$ (volts), which results in 400,000 volts! The value is huge, and thus, even this small difference in charge cannot be sustained in solution and must be discharged by changing the equilibrium of weaker ionic substances. This means that the concentrations of ions that are strongly dissociated in the solution must be matched by the concentration of weaker charged ions. Strong positive ions include Na^+ , K^+ , Ca^{2+} , and Mg^{2+} , and strong negative ions include Cl^- and SO_4^- . The addition of NaCl to a beaker of pure water results in Na^+ and Cl^- ions but no NaCl (Fig. 41.1). The solution still is neutral because $[\text{Na}^+]$ and $[\text{Cl}^-]$ are equal. However, if the solution is made from solutions in which $[\text{Na}^+]$ and $[\text{Cl}^-]$ are not equal, $[\text{H}^+]$ and pH must change. The difference in concentration is called the strong ion difference [SID]. This occurs because the electrical force created by the difference in charge of the $[\text{Na}^+]$ and $[\text{Cl}^-]$ must be accommodated by a change in the balance of dissociation of water. If the $[\text{Na}^+]$

increases relative to the $[\text{Cl}^-]$, the solution must have more $[\text{OH}^-]$ to balance the charge from Na^+ , and it will have a lower $[\text{H}^+]$ (Fig. 41.4); the new solution thus will be less acidic (or more alkaline). If $[\text{Cl}^-]$ increases relative to the $[\text{Na}^+]$, the solution will need to have a higher $[\text{H}^+]$ to balance the Cl^- and a lower $[\text{OH}^-]$, and the solution will be more acidic (less alkaline) (Fig. 41.4). The change in $[\text{H}^+]$ with a change in [SID] of this simple system that only has strong ions requires a quadratic equation to solve two equations for the two unknown values ($[\text{H}^+]$ and $[\text{OH}^-]$), i.e., the electrical neutrality equation and the water equilibrium equation. As already noted, almost all bodily solutions are alkaline, i.e., $[\text{OH}^-]$ is greater than $[\text{H}^+]$. This primarily is because [SID] always is positive, i.e., $[\text{Na}^+]$ is greater than $[\text{Cl}^-]$ (Fig. 41.4). The advantage of having a positive [SID] is that it means changes in $[\text{H}^+]$ are much smaller for any change in [SID], and thus there is smaller effects from changes in $[\text{OH}^-]$ on molecular structures while the concentrations of ionic elements can be regulated to maintain normal osmolality.

To appreciate the contribution of positive and negative ions in blood, it is useful to examine “Gamblegrams”, developed by the American physiologist James Gamble (Harvey 1979). In these figures, the concentrations of cations and anions are plotted as individual stacked columns (Fig. 41.5). Because of the principle of electrical neutrality, the cation and anion column heights must be identical. It is evident that strong cations are higher than strong anions, and the normal

Fig. 41.3 Significance of electrical neutrality. See text for calculations. A charge difference between strong positive and negative ions of only 1×10^{-7} Eq in a sphere with a radius of 1 mm is 400,000 volts and must be quickly discharged



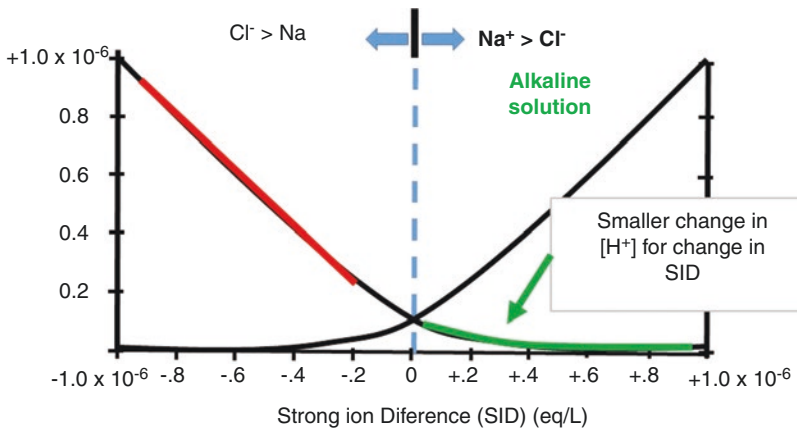


Fig. 41.4 Changes in H^+ and OH^- with change in concentration of Na^+ relative to Cl^- (strong ion difference). When the SID is negative, changes in Cl^- match changes in H^+ , but when SID is positive, changes in H^+ are much smaller than changes in Cl^- (or Na^+). The solution is also

alkaline which is the case for almost all bodily solutions. To be able to display the changes, the SID is presented only for differences of 1×10^{-6} (micromolar), whereas in plasma, the difference in 40×10^{-3} (millimolar) and not seen on this scale

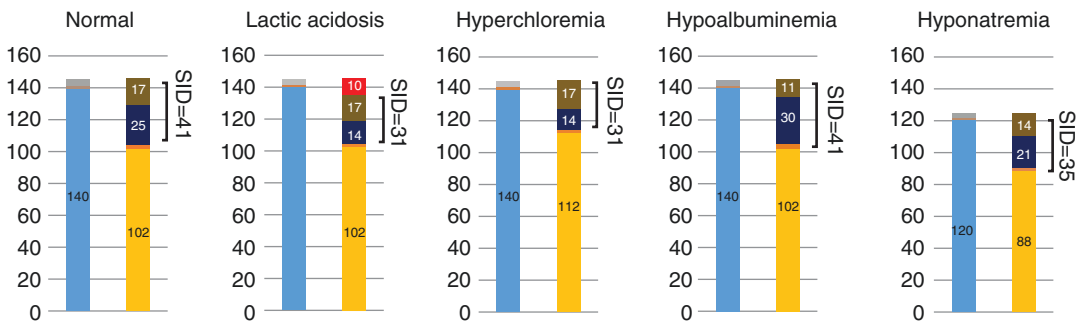


Fig. 41.5 Gambelgrams of normal blood, lactic acidosis, hyperchloremia, hypoalbuminemia, and hyponatremia. Cations are on the left of each set and anions on the right. The $[Na^+]$ (light blue) is 140 mEq in all but the hyperhydration (hyponatremia example). $[Cl^-]$ is in yellow. The standard is 102, and it is increased to 112 in the hyperchloremia example and 88 in the hyperhydration example.

The baseline $[HCO_3^-]$ is 25 mEq/L, it is 14 in the lactic acidosis (increase of 10 mEq/L) and in the hyperchloremic example, 30 mEq/L in hypoalbuminemia and 21 mEq/L with the hyponatremia. The SID is 41 in the baseline, 31 in the hyperchloremia, 41 in the hypoalbuminemia, and 35 mEq/L in hyponatremia

[SID] is approximately 40 mEq/L in plasma. The difference in strong ions is primarily made up of HCO_3^- and the ionic effect of weak acids, which is primarily albumin in plasma. $[H^+]$ and $[OH^-]$ are not seen on this graph because their concentrations are so much smaller. Under normal conditions, the $[SID] \sim [A^-] + [HCO_3^-]$ in which A^- is the concentration of the charge due to dissociated weak acid. Two common clinical conditions illustrate the significance of the [SID]. There currently is a lot of discussion about the hyperchloremic

acidosis that is seen when too much normal saline is given (Magder 2014). What simply is happening is that a solution with equal $[Na^+]$ and $[Cl^-]$ is being added to plasma which normally has a $[Na^+]$ that is around 40 meq/L greater than $[Cl^-]$ (i.e., $[SID] = 40$) (Fig. 41.5). We normally consume $[Na^+]$ and $[Cl^-]$ in almost equal amounts, and our bodies can handle it. However, when an excess load of $[Na^+]$ and $[Cl^-]$ is given, the kidney can rapidly excrete Na^+ , but the mechanisms for excreting Cl^- are much slower. The [SID] thus is

narrowed and $[H^+]$ is increased (actually, less of a difference from $[OH^-]$), and there is a metabolic acidosis (actually less alkalosis). The simple solution is to give less Cl^- . As a simple quick guideline, a narrowing of the difference between $[Na^+]$ and $[Cl^-]$ is an acidifying process, and a widening of the difference between $[Na^+]$ and $[Cl^-]$ is an alkalizing process.

A second example is a dilutional acidosis. When the amount of pure water is doubled in a solution with different concentrations of Na^+ and Cl^- , the $[Na^+]$ and $[Cl^-]$ are equally diluted (Fig. 41.6). As a result, the $[SID]$ is decreased and the solution becomes more acidic (or less alkaline) because not as much $[OH^-]$ and other weak negative ions are needed to balance $[Na^+]$. The same occurs in plasma when plasma is diluted by an increase in water, and a metabolic acidemia is the result. In the opposite direction, a loss of water and hemoconcentration produces an alkalemia. These occur without any action required by the kidney. As long as PCO_2 remains constant as regulated by the brain, the HCO_3^- will also go down with the dilution and increase with the hemoconcentration simply by the interaction of all the elements in the system and the need for electrical neutrality.

As noted, Na^+ and Cl^- are the dominant strong ions in plasma, but under pathological conditions, other relatively strong ions can become important.

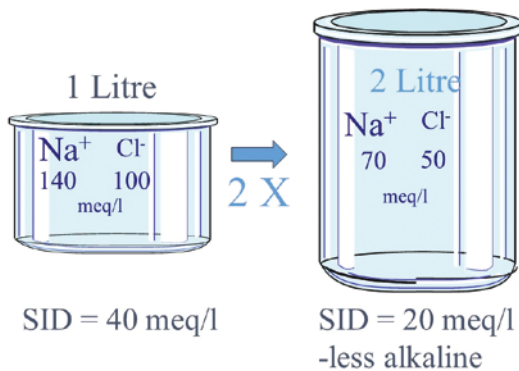


Fig. 41.6 Dilutional effect on the SID . Doubling the amount of water reduces the concentration of Na^+ and Cl^- by half and thus the SID is half which will reduce the alkalinity of the solution (i.e., make it more acidic)

These are almost always negative ions. The two most common ones are lactate and the ketones, acetoacetate, and beta-hydroxy-butyrate, but there are many others, which are the well-known causes of the traditional wide-anion gap acidosis. These include salicylate, formate (derived from methyl alcohol), glycolate (from ethylene glycol), some amino acids, sulfates (renal failure), and iron (which acts by binding OH^-). The effect on $[H^+]$ of any of the strong anions that cause a wide anion gap acidosis is the same as an increase in $[Cl^-]$.

Importance of CO_2

The amount of CO_2 in the blood is a balance between production and clearance by the lungs (Jones 2008). The lungs can eliminate CO_2 as fast as it is delivered by the circulatory system so that the concentration of CO_2 remains in tight limits and the body normally is an open system for CO_2 . Furthermore, CO_2 in the blood is directly proportional to PCO_2 in the gas phase so that PCO_2 in blood can be used as an indication of dissolved CO_2 and therefore indicates how fast and which way CO_2 will move between two solutions. Thus, it can be said that when the cardiorespiratory systems are intact, CO_2 is a controlled or independent variable, and the total amounts of the concentration of all the other components of the CO_2 equilibrium are fixed by PCO_2 . It is worth noting, however, that reaction time of dissolved CO_2 with H_2O or OH^- to form H_2CO_3 is slow, in the order of 30 seconds, but this is reduced to milliseconds in the presence of the enzyme carbonic anhydrase, which is widely available in the body, but importantly, not everywhere.

The role of CO_2 in the determination of $[H^+]$ is the same as in the classical approach, but it is important to consider how its equilibrium is altered by the $[SID]$. H_2CO_3 is a weak acid. Unlike Na^+ and Cl^- , it is equilibrium with multiple forms including PCO_2 , HCO_3^- , and CO_3^{2-} , although by far, HCO_3^- is the dominant form by a ratio of ~ 24 to 1 at normal pH. The differentiation of the activity of a strong and weak acid can be appreciated by considering the effect of

creating a negative [SID] on the equilibrium of the CO_2 system; all carbamate forms are driven to CO_2 . This property is the basis for the electrode measurement of $[\text{HCO}_3^-]$ in plasma; what actually is measured is “total” CO_2 , but because most of the total is in the form of HCO_3^- , total PCO_2 is a close approximation of HCO_3^- . On a blood gas sample, HCO_3^- actually is not measured but calculated based on the measurement of PCO_2 and $[\text{H}^+]$ and the known equilibrium constants. Significantly, when [SID] is negative, adding CO_2 has no effect on $[\text{H}^+]$ (or pH) of a solution because carbonic acid does not dissociate.

As long as central mechanisms keep PCO_2 constant, adding HCO_3^- , for example in the form of NaHCO_3^- , only very briefly increases plasma $[\text{HCO}_3^-]$ because the CO_2 form is quickly blown off. However, if CO_2 is given in the form of NaHCO_3^- , the Na^+ is left behind, widens the [SID], and alkalinizes the blood. This, too, will not last long. Because $[\text{Na}^+]$ in the body is a major determinant of the body’s osmolality, its concentration is tightly regulated and the Na^+ is quickly excreted (if the kidneys are working). On the other hand, when CO_2 is added to a solution with a positive [SID], and cannot be cleared by ventilation, $[\text{H}^+]$ always increases.

Importance of Albumin

The third independent determinant of $[\text{H}^+]$ is the concentration of non-volatile weak acids (Fig. 41.7). To know the effect of a weak acid on the solution, it is necessary to know the total concentration of all species of the substance, including the un-dissociated and dissociated species, the dissociation constant, and the most difficult part for a large molecule, its ionic activity (Fig. 41.8). It has been shown empirically by Figge and coworkers that weak acid activity in blood is dominated by albumin (Figge et al. 1991; Figge et al. 1992). They performed titration studies by adding different amounts of albumin to blood samples and derived a linear equation that describes the ionic effect of a total concentration of albumin depending upon the $[\text{H}^+]$ (or pH). The consequence of a decrease in [albumin] is an alkalinizing effect, and an increase in [albumin] is an acidifying effect. Thus, a decrease in [albumin] can off-set the acidifying effect of an elevated lactate. On the other side, hemoconcentration due to excess water loss can produce an acidemia by increasing [albumin] (Wang et al. 1986).

Fig. 41.7 Properties of weak ions

- Substances that are only partly dissociated
($10^{-4} < K_m > 10^{-12}$ Eq/l)
- Volatile weak acid
 - $\text{H}_2\text{CO}_3/\text{PCO}_2$
- Non-volatile
 - Proteins (mainly albumin [Halb])

Important variables include
concentration of substance,
its dissociation
($\alpha_A = [\text{A}^-]/[\text{A}_{\text{TOTAL}}]$),
& its “ionic” equivalent

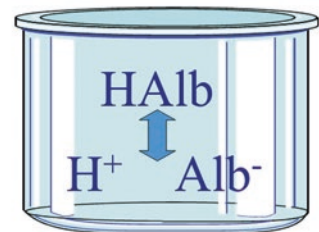
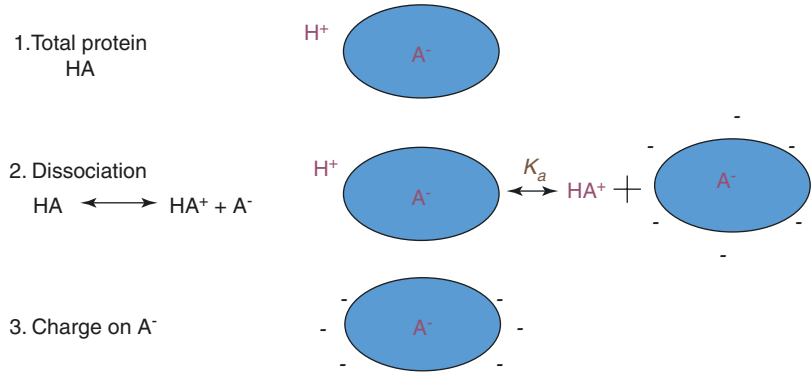


Fig. 41.8 Factors that determine the charge related to a weak acid (the major A^- is from albumin). The factors include (1) the total protein in all its form, (2) the dissociation constant, and (3) the ionic equivalent of the charged ion



Approach to Identifying the Cause of a Disturbance of Blood $[H^+]$ (pH)

Stewart and others after him (Kellum et al. 1995; Jones 1990) presented a physical–chemical approach to determining the cause of a deviation of $[H^+]$ from normal reference values by calculating the difference in all major strong positive ions in blood, which include $[Na^+]$, $[K^+]$, $[Ca^{2+}]$, and $[Mg^{2+}]$ and the strong negative ions $[Cl^-]$, and $[lactate^-]$ and comparing the difference in positive and negative charge to the charge accounted for by $[HCO_3^-]$, albumin (with the charge obtained from the Figge equation (Figge et al. 1992), and phosphate (with the charge, too, determined by a Figge equation) (Figge et al. 1992)). They called this difference the strong ion gap [SIG]. If [SIG] is greater than [SID], there must be unmeasured anions which are the known substances in a wide anion gap. However, this approach is more complicated than necessary. The contributions of $[K^+]$, $[Ca^{2+}]$, and $[Mg^{2+}]$ are very small because their baseline values are low, and large deviations in their concentrations are fatal. The [SIG] approach also does not readily identify the contribution of changes in [SID] due to dilution or concentration of electrolytes, changes in albumin, nor the change just related to $[Cl^-]$ and thus does not allow quantitative insight into the underlying pathological process and allow for targeted therapy. An alternative pragmatic bedside approach involves use of the base excess (BE) which that is calculated with all blood gas machines, but first this concept of BE needs to be explained.

Base Excess: Direct Estimation of Metabolic Derangements in Acid–Base Status

Driven in part by the recognition during the Danish polio epidemic of 1952 that an isolated measurement of total CO_2 in the blood could not distinguish between such processes as a metabolic alkalosis and a respiratory acidosis, in the early 1950s, there was an interest in developing a way to separate these two processes, which led to the concept of base excess (BE), described first by Ole Siggaard-Anderson working in the laboratory of Poul Astrup (Siggaard-Andersen 1962, 1966). These investigators took blood samples from patients and fixed the value of PCO_2 in the samples by inserting a tonometer to maintain a PCO_2 of 40 mmHg. They then measured the pH at a PCO_2 of 40 mmHg and titrated the solutions with a strong acid or base to bring the pH back to 7.4. This was essentially a titration of the [SID] back to the normal value (i.e., eliminating any [SIG]). As such, BE is a direct measure of the net metabolic component of an acid–base disorder, independent of the effect of ventilation through control of pCO_2 . BE should be 0 under physiological conditions of pH 7.40, temperature $37^\circ C$, and pCO_2 40 mmHg. Samples with a pH > than 7.4 after PCO_2 correction were said to have a base excess (BE) because an acid was necessary to bring the pH back to 7.4. Samples with a pH < 7.4 after PCO_2 correction were called a base deficit. Rather than using two terms, just BE is used, and when the solution has a metabolic acidosis and a base deficit, it is called a negative

BE, which is the way we use it in this chapter. Siggaard-Anderson created a nomogram based on the PCO_2 , pH, and bicarbonate of the samples they studied, which is still what is used in blood gas machines today (Siggaard-Andersen 1962). Some confusion arises around the term standard base excess versus base excess. This arose because of two misconceptions. It was initially thought that because only a blood sample was analyzed in a test tube, and without the interactions with the larger interstitial space factors that could affect blood pH, adjustments needed to be made for the potential effect of electrolytes in the interstitial space. However, the $[\text{H}^+]$ in a solution only is affected by the substances in that solution at that time. The interstitial space has a different [SID] and only can alter the [SID] and $[\text{H}^+]$ of blood by movement of substances over time, which would be a new condition. In the steady state, they can have different values. For example, $[\text{HCO}_3^-]$ is lower in the interstitial space because the [Albumin] is lower than in plasma even though the [SID] is similar. Secondly, Siggaard-Anderson used hemolyzed red cells because he wanted to include the buffering effect of hemoglobin. However, the effect of hemoglobin on the SID is minimal because binding of strong ions to hemoglobin is minimal, and its own dissociation has a very small effect. Furthermore, when whole blood is tested, it is inside red cells and thus not part of the plasma space. There also is confusion of the term “standard” base excess which was used to avoid the need to have a hemoglobin value and instead used an assumed standard value. When examining the equations for BE, it can be seen that the hemoglobin effect on BE is very small and beyond the accuracy needed for use of BE for practical clinical purposes (Schlichtig 1997).

BE Approach to Evaluation of Acid-Base Disorders (Table 41.1)

The initial approach to analyzing an abnormal pH in blood starts the same way as the traditional approach (Magder and Emami 2015; Fencl and Leith 1991). If pH is less than the normal reference value of 7.4, there is an acidemia, and if it

Table 41.1 Step-wise acid-base analysis

1. Assess the pH. $\text{pH} > 7.42 =$ acidemia and $\text{pH} < 7.38 =$ alkalemia.
2. Assess the respiratory component of pH regulation. If PCO_2 is greater than 42 mmHg, there is a respiratory acidosis. If PCO_2 is less than 38, there is a respiratory alkalosis. .
3. Assess the metabolic component of pH regulation. This is done by examining the BE. If BE is >0 mEq/L, there is a metabolic alkalosis. If BE is <0 , there is a metabolic acidosis.
4. Examine the causes of a metabolic disturbance by first looking for a $\text{Water}_{\text{effect}}$, $[\text{Cl}^-]_{\text{effect}}$, and $\text{albumin}_{\text{effect}}$.
 - (a) $\text{Water}_{\text{effect}} = 0.3 \times ([\text{Na}^+] - 140)$.
 - (b) $[\text{Cl}^-]_{\text{effect}}$. First correct $[\text{Cl}^-]$ for hydration effect which already was accounted for in 4a by calculating the “effective” $[\text{Cl}^-] = [\text{Cl}^-] \times 140 / [\text{Na}^+]$. The $[\text{Cl}^-]_{\text{effect}}$ then = $102 - [\text{Cl}^-]_{\text{effective}}$
 - (c) $\text{Albumin}_{\text{effect}}$. This is done by using the equation for the difference of [Albumin] based on the equation by Figge et al. (Figge et al. 1992) from the reference value of 42 g/L. $[\text{Albumin}]_{\text{effect}} = (42 - [\text{Albumin}]) \times 25$.
5. Determine the presence of missing ions. Subtract the sum of the $\text{Water}_{\text{effect}}$, $[\text{Cl}^-]_{\text{effect}}$, and $\text{Albumin}_{\text{effect}}$ from the calculated BE obtained from the blood gas report. If BE is negative, there are missing anions which the standard wide anion gap acidosis. If BE is positive, there are unexplained cations, which currently are not well defined. This analysis does not include the initial lactate or normal phosphate because these would have been incorporated in the blood samples that were analyzed by Siggaard-Anderson (Siggaard-Andersen 1962). The contribution of abnormal lactate is obtained by simply examining the serum lactate value, and the phosphate value can be obtained by another empiric equation derived by Figge et al. (Siggaard-Andersen 1962). These can be calculated by a free APP called acid-base calculator (Magder).

is greater than 7.4, there is an alkalemia. The next step is to determine what processes are active, that is, the “-osis”. This, too, continues as with the traditional approach by determining if there is a respiratory component, metabolic component, or both. Evaluation of the respiratory component is based on the PCO_2 . If PCO_2 is elevated, there is a respiratory acidosis; if the PCO_2 is decreased, there is a respiratory alkalosis. These are processes and are independent of the actual pH. It is with the metabolic component that the physical-chemical approach differs from the traditional. Rather than

using $[\text{HCO}_3^-]$ to determine if there is a metabolic acidosis or alkalosis, the BE is used as first introduced by Fencl and Leith (Fencl and Leith 1991). If BE is a positive value, there is a metabolic alkalosis, and if BE is negative, there is a metabolic acidosis. The terms compensated and uncompensated are not used. Instead, the effects of dilution of electrolytes and the deviations of $[\text{Cl}^-]$ and [albumin] from their reference values are quantitated to determine if they can account for a deviation of BE from 0. If after accounting for these factors the BE still is negative, this indicates there are unmeasured anions. The differential diagnosis then is the same as for the classical wide anion gap acidosis. These also could be called a BE gap. There is surprisingly not a close correlation between BE gap and the anion gap because BE was produced by a titration with strong ions (Gilfix et al. 1993). The advantage of BE over the traditional use of $[\text{HCO}_3^-]$ to a metabolic acidosis is that it removes any effect from the change in PCO_2 on $[\text{HCO}_3^-]$ and changes of [albumin] on the anion gap. We have chosen to leave $[\text{lactate}^-]$ out of initial assessment because the measurement may not always be available on the blood gas device, and the normal concentration of 1 mmol/L would have been included in Siggaard-Anderson's initial studies as component of normal blood. This approach, too, allows the clinician to think of this component relative to others. We also do not include phosphate in the initial analysis but evaluate it after when there are missing anions. It can be a significant contributor in patients with renal failure.

How Are the "Water" (i.e., Dilutional Effects), $[\text{Cl}^-]$ Effects, and [Albumin] Evaluated?

Water Effect

1. As already discussed (Fig. 41.6), the effects of strong ions are dependent upon their concentrations. Accordingly, an increase in hydration, i.e., more water relative to solutes, or dehydration, less water relative to solute, changes [SID] and thus changes $[\text{H}^+]$. To

illustrate the importance of this effect, consider the effects of a sudden 1 liter bolus of D5W on a 4 liter blood volume prior to any equilibration. The concentrations of all ionic species will fall acutely by 20%; $[\text{Na}^+]$ would fall from 140 mmol/L to 112, $[\text{K}^+]$ from 4 to 3.2, $[\text{Cl}^-]$ from 105 to 84, and the SID would fall from ~39 mmol/L to ~31 mmol/L and result in an acidemia from a metabolic acidosis which was caused just by the addition of water. Importantly, this change is driven entirely by chemical equilibria and would occur identically even in a beaker. Serum sodium concentration reflects total body water status. As such, the hydration (water) effect can be calculated by using the equation $\text{Water}_{\text{effect}} = (0.3) * ([\text{Na}^+] - 140)$.

Chloride_{effect}

2. Chloride_{effect} refers to a change in $[\text{Cl}^-]$ relative to $[\text{Na}^+]$ when there is either an increase or decrease in [SID] (Fig. 41.5). If $[\text{Na}^+]$ deviates from the reference value as evaluated under the $\text{Water}_{\text{effect}}$, the first step is to account for hydration change on measured $[\text{Cl}^-]$ by assessing effective $[\text{Cl}^-]$ independent of the already considered dilutional component by the equation $[\text{Cl}^-]_{\text{effective}} = [\text{Cl}^-] * (140/[\text{Na}^+])$. The effect of a deviation of $[\text{Cl}^-]$ from the normal reference (we use 102 mEq/L) then can be calculated as $[\text{Cl}^-]_{\text{effect}} = 102 - [\text{Cl}^-]_{\text{effective}}$. The combined effects of hydration and actual change in the amount of Cl^- effects can be rapidly estimated using the rule of thumb that $[\text{Na}^+] - [\text{Cl}^-] = 40 \text{ mmol/L}$. Departures from this value indicate a change in hydration, change in actual $[\text{Cl}^-]$, or mixed effects on [SID]. As a clinical point, the importance of recognizing and avoiding hyperchloremic acidosis has recently been highlighted in several large observational studies in which hyperchloremia is associated with renal injury and possibly even death (Magder 2014) as well as a randomized trial suggesting increased renal injury (Self et al. 2018).

Protein_{effect}

- Changes in the Protein_{effect}, which is dominated by albumin, alter the weak acid component. To determine the effect of the ionic form of albumin on $[H^+]$, it is necessary to know the total concentration of ionized and non-ionized albumin, the dissociation constant of albumin, and the resulting ionic effect. The last two could only be derived empirically. This was done by Figge and coworkers who derived an equation to account for the ionic effect of albumin (Figge et al. 1992). The potential effect of a deviation of BE from normal to a deviation in [Albumin] can be estimated by $\text{Albumin}_{\text{effect}} = 25 * (42 - [\text{albumin}])^{11}$. As we already have seen, this relationship indicates that hypoalbuminemia produces an alkalosis and, conversely, that “correction” of hypoalbuminemia produces a relative acidosis (Fig. 41.5).

“Other Effects”

- The final step is to sum the Water_{effect}, $[Cl^-]_{\text{effect}}$ and $[\text{albumin}]_{\text{effect}}$ and compare the sum to the calculated BE. If all the BE is not accounted for, there are unmeasured ions. Occasionally, positive ions are identified, especially in chronic obstructive lung disease (COPD) patients, and it is not clear what these are. Changes in the values of $[Ca^{2+}]$, $[Mg^{2+}]$, and $[K^+]$ usually are too low to explain this (Gilfix et al. 1993). More commonly, there is an unexplained negative BE in which case there are unmeasured anions. These are the same as the standard wide anion gap acidosis and include ketoacids, methanol-derived formate, ethylene glycol-derived glycolate, acetaminophen-associated pyroglutamic acid, salicylate, uremic toxins such as hippurate, and SO_4^{3-} . Accumulation of plasma weak acids can occur with paraproteinemias and with hyperphosphatemia. In this way, renal failure contributes to metabolic acidosis both through SID and Protein_{effect} effects. As a general rule, the presence of a significant residual BE should prompt evaluation for the offending species by

toxicology screen, osmolar gap calculation, and/or specific assays as indicated by the clinical situation.

To understand the significance of “others”, it is worthwhile considering the example of a lactic acidosis, especially because it is such a common problem in the ICU. Lactic acid has a dissociation constant, pKa, of 3.8 and thus is almost completely dissociated in body solutions, and it acts as a strong anion. Accumulation of lactate⁻ by increased production and/or decreased clearance narrows the [SID] and increases $[H^+]$ (Fig. 41.5). As an example, an increase of [lactate⁻] to 11 mmol/L decreases [SID] to 30 mmol/L and, as a result, decreases $[HCO_3^-]$ to 14 mmol/L because not as much HCO_3^- is needed to balance the charge on Na^+ . The same would occur if $[Cl^-]$ rose from 105 to 115 mmol/L (Fig. 41.5). Yet, a magnitude of rise in $[Cl^-]$ of 10 mmol/L often is ignored clinically $[Cl^-]$ even though it has an equivalent effect on $[H^+]$ as a relatively severe lactic acidosis. It is not uncommon for clinicians seeing the fall in $[HCO_3^-]$ with a lactic acidosis, or for that matter with a $[Cl^-]$ acidosis, to try to correct the acidemia by giving $NaHCO_3$, but this does not alter the acidosis and does not even affect the acidemia very much. The only way that an infusion of $NaHCO_3$ can reduce $[H^+]$ (i.e., increase pH) is by raising the $[Na^+]$ by the same amount as the increase in [lactate⁻] and thereby restore the normal [SID]. If [lactate⁻] increased by 10 mmol/L and $[Na^+]$ starts at 140 mmol/L, the $[Na^+]$ would have to increase to 150 mmol/L for this to work. Thus, the increase in $[Na^+]$ can become toxic. Furthermore, if the kidneys are working, they will excrete the Na^+ to maintain normal osmolality. The answer to the clinical problem is to treat the cause of the lactic acidosis.

It also is worth considering the quantitative effect of a change in [Albumin] to that of [lactate⁻]. If the serum [Albumin] concentration falls from 4.5 g/dL to 2.0 g/dL (Fig. 41.1d), the amount of weak acid decreases from 11 mmol/L to 5 mmol/L, which the resulting alkalosis is associated with a rise in bicarbonate to 30 mmol/L. This magnitude of a fall [Albumin] would negate the effect of an increase in [lactate⁻] of 7 mmol/L.

Summary

The advantage of the physical–chemical BE approach is that it identifies processes that are involved in an alteration in pH and $[H^+]$. This can lead to targeted management, or in some cases, help avoid potentially unnecessary therapies, such as the frequently use of $NaHCO_3$ infusion for a wide anion gap acidosis, dilutional acidosis, or hyperchloremic acidosis unless it was used to avoid use of Cl^- . A dilutional acidosis is treated by restricting water. Acute hyperchloremic acidosis is treated by avoiding solutions that are high in $[Cl^-]$. A hypo-albuminemic alkalosis should only be treated by correcting the underlying catabolic state. Lactic and ketoacidosis are treated

by reversing the underlying metabolic process. H^+ and HCO_3^- are dependent variables in bodily solutions and are determined by the $[SID]$, PCO_2 , and weak acids of which albumin is the primary player. H^+ and HCO_3^- by themselves cannot be “added” to the solution.

Case Examples

Case 1

A 39-year-old man with type I diabetes presents with a 1-day history of abdominal pain and fatigue. He has been non-compliant with insulin therapy. Blood chemistry analysis gives the following:

pH	pCO ₂ mmHg	HCO ₃ ⁻ mEq/L	BE mEq/L	Albumin g/L	Na ⁺ mEq/L	Cl ⁻ mEq/L
6.80	12	2	-30	42	140	103

Applying the above steps, the patient is found to be profoundly acidemic. pCO₂ is <38 so that there is a respiratory alkalosis. BE is negative, indicating a metabolic acidosis. The components of the metabolic acidosis are $Water_{effect} = 0$, $[Cl^-]_{effect} = -1$, $[Albumin]_{effect} = 0$, and “other effects” = -29 mEq/L. In this case, the most likely cause of the “other” is ketoacids, but there also could be a lactate component, and if renal function is decreased, strong ions as a result of decreased renal clearance.

The patient is resuscitated aggressively with normal saline and treated with intravenous insulin. The following day, blood chemistries reveal the following:

pH	pCO ₂	HCO ₃	SBE	Albumin	Na	Cl
7.23	28	12	-13	40	152	130

Again, applying a stepwise approach, we find the patient has an acidemia. There still is

a respiratory alkalosis and a metabolic acidosis. The components of the metabolic acidemia are $Water_{effect} = +3.6$, $[Cl^-]_{effect} = -17.7$, $[Albumin]_{effect} = +0.5$, other effects = ~0. The data now indicate that the ketoacidosis has resolved, and the acidosis is explained but hyperchloremia which is a result of the resuscitation with a large volume of normal saline administration. There is also a minor metabolic alkalosis due to dehydration (increase in $[Na^+]$).

Case 2

A 55-year-old male presented to the emergency department with hepatic failure due to cirrhosis and respiratory failure. He was hypotensive and unresponsive. He was intubated and mechanically ventilated, and 2 L of normal saline were administered for the hypotension. Blood chemistry revealed the following:

pH	pCO ₂	[HCO ₃ ⁻]	BE	[Albumin]	[Na ⁺]	[Cl ⁻]	[lactate ⁻]
6.95	47	10	-22	22	128	115	5

The patient is acidemic. The elevated PCO₂ indicates a respiratory acidosis; his ventilator settings need to be adjusted. Of note, cirrhosis patients more often have a respiratory alkalosis, but in this case, he was unresponsive and has a depressed drive. There is a profound metabolic acidosis based on the negative BE. Partitioning the BE, we find a Water_{effect} = -3.60, [Cl⁻]_{effect} = -23.8, and [Albumin]_{effect} = +4.2. There is 1.2 unexplained ion. The high [Cl⁻] is the dominant factor. The elevated value is much higher than can be explained by 2 L of saline and indicates that he likely has had a long-standing renal tubular problem. The elevated [lactate⁻] adds -4 the BE that leaves 9 unexplained. It previously has been shown that in liver failure patients, there can be unmeasured anions but is matched by the decrease in [Albumin] so that there is only 1 unaccounted for anion which in this case was due to an elevated phosphate. Given the very high [Cl⁻], if further fluid resuscitation was needed, it would be best to use a solution of NaHCO₃ in 5% dextrose in water to avoid giving any more Cl⁻.

References

- Adroque HJ, Gennari FJ, Galla JH, Madias NE. Assessing acid-base disorders. *Kidney Int.* 2009;76(12):1239-47.
- Fencl V, Leith DE. Stewart's quantitative acid-base chemistry: applications in biology and medicine. *Respir Physiol.* 1991;91:1-16.
- Figge J, Rosling TH, Fencl V. The role of serum proteins in acid-base equilibria. *J Lab Clin Med.* 1991;117:453-67.
- Figge J, Mydosh T, Fencl V. Serum proteins and acid-base equilibria: a follow-up. *J Lab Clin Med.* 1992;120:713-9.
- Gilfix BM, Bique M, Magder SA. A physiological approach to the analysis of acid-base balance in the clinical setting. *J Crit Care.* 1993;8:187-97.
- Harvey AM. Classics in clinical science: James L. Gamble and "Gamblegrams". *Am J Med.* 1979;66(6):904-6.
- Jones NL. A quantitative physicochemical approach to acid-base physiology. *Clin Biochem.* 1990;23:189-95.
- Jones NL. An obsession with CO₂. *Appl Physiol Nutr Metab.* 2008;33(4):641-50.
- Kellum JA, Kramer DJ, Pinsky MR. Strong ion gap: a methodology for exploring unexplained anions. *J Crit Care.* 1995;10(2):51-5.
- Magder S. Balanced versus unbalanced salt solutions: what difference does it make? *Best Pract Res Clin Anaesthesiol.* 2014;28:235-47.
- Magder S, Emami A. Practical approach to physical-chemical acid-base management. *Stewart at the bedside. Ann Am Thorac Soc.* 2015;12(1):111-7.
- Schlichtig R. [Base excess] and [strong ion difference] during O₂-CO₂ exchange. *Adv Exp Med Biol.* 1997;411:97-102.
- Schwartz WB, Relman AS. A critique of the parameters used in the evaluation of acid-base disorders. *N Engl J Med.* 1963;268(25):1382-8.
- Self WH, Semler MW, Wanderer JP, Wang L, Byrne DW, Collins SP, et al. Balanced crystalloids versus saline in noncritically ill adults. *N Engl J Med.* 2018;378(9):819-28.
- Siggaard-Andersen OS. The pH-log PCO₂ blood acid-base nomogram revised. *Scandinav J Clin & Lab Invest.* 1962;14:598-604.
- Siggaard-Andersen O. Titratable acid or base of body fluids. *Ann N Y Acad Sci.* 1966;133(1):41-58.
- Stewart PA. Independent and dependent variables of acid-base control. *Respir Physiol.* 1978;33(1):9-26.
- Stewart PA. How to understand acid-base. A quantitative acid-base primer for biology and medicine. New York: Elsevier North Holland; 1981.
- Stewart PA. Modern quantitative acid-base chemistry. *Can J Physiol Pharmacol.* 1983;61(12):1444-61.
- Wang F, Butler T, Rabbani GH, Jones PK. The acidosis of cholera. Contributions of hyperproteinemia, lactic acidemia, and hyperphosphatemia to an increased serum anion gap. *N Engl J Med.* 1986;315(25):1591-5.

Part VII
Applications



Use of Maintenance and Resuscitation Fluids

42

Sheldon Magder

Introduction

The basics of the fluid physiology are discussed in Chap. 10 (Magder, Basics of Fluid Physiology). This chapter deals with the administration of intravenous fluids. This is divided between use of fluids for maintenance needs and use of fluids for resuscitation. The parallel that I like to use is that of having a checking account and a savings account. Maintenance fluids are like a checking account and deal with the intake and output of fluids and electrolytes for normal daily needs. Resuscitation fluids are used to replenish stores that were lost during acute illness or to add to the reserve capacity of the system. I will begin with daily requirements of water and electrolytes and then discuss how these should be administered intravenously when oral intake is not possible. I then will discuss the characteristics and potential problems with the different solutions that can be used for resuscitation. Next, I will discuss some practical approaches. Finally, I will discuss important limits to what fluid administration can accomplish. Use of intravenous infusions of fluids to patients is common, but it is important to respect their use because it is

increasingly evident that excess use of fluids, and fluids with incorrect compositions, can be harmful (Boyd et al. 2011; Vincent et al. 2006; Santry and Alam 2010; Hjortrup et al. 2016; Kelm et al. 2015; Perner et al. 2012; Wiedemann et al. 2006); equally important, inadequate administration of fluids, too, is harmful.

The approach taken in this chapter differs considerably from a recent review published in the NEJM on maintenance intravenous fluids in the critically ill (Moritz and Ayus 2015). The authors considered the contents of the various solutions and their impact on the electrolyte balance of plasma. They emphasized the importance of the sodium ion (Na^+) concentration in the infused fluid and the potential danger of producing hyponatremia with solutions that have concentrations of Na^+ less than normal, especially in critically ill patients who often have disordered regulation of concentration of Na^+ . I take the opposite approach. I first consider the daily requirements of water, Na^+ , potassium (K^+), and glucose (minimal amount) and consider these needs in the daily prescription of infused fluids. Adjustments are then made for individual patients when electrolyte values are abnormal. The basic argument is that it is not the specific composition of the infused solutions that is important but rather the effect of the components of the infused fluid on the total amount of the substance in the appropriate amount of total body water. The volume of fluid infusion is usually small compared to

S. Magder (✉)

Royal Victoria Hospital (McGill University Health Centre), Departments of Critical Care and Physiology McGill University, Montreal, QC, Canada
e-mail: sheldon.magder@mcgill.ca

overall body water which thus dilutes whatever substance that is infused. Furthermore, the body has many regulatory mechanisms that control the contents of infused substances, although these can fail. A key part of intravenous fluid management is thus monitoring the composition of the essential components of body water and making adjustments to the infused water and the electrolytes it contains.

Volume and the Generation of Blood Flow

As emphasized in Chap. 2 (Magder, Volume), under normal conditions almost 70% of blood volume simply rounds out vessel walls. Only approximately 30% of blood volume stretches the walls of vessels and produces the elastic recoil force that drives blood back to the heart. The portion of total blood volume stretching vascular walls is called stressed volume. In a standard size male, with a total blood volume of approximately 5.5 L, stressed volume is in the range of 1.3–1.4 L (Magder and De Varennes 1998). Furthermore, with a hematocrit of 45%, plasma volume only is about 3–3.5 L; the rest of the blood volume is made up by the mass of red cells. A key point is that a volume an intravenous bolus of more than 1–1.5 L is not likely to remain in the vascular space because the accompanying marked increase in capillary hydrostatic pressures will increase fluid filtration out of the vasculature (Table 42.1). Furthermore, if the fluid were not leaked, it would markedly decrease hemoglobin concentration. For example, if the total blood volume is 5.5 L, and the hematocrit (Hct) is 45%, an increase of plasma volume by a fluid infusion of 2 L would decrease the Hct to 33, a 26% decrease. Assuming a systemic vascular compliance of 150 ml/mmHg, mean systemic filling pressure (MSFP) would go from 9 to 22 mmHg.

Stressed volume can be increased rapidly without the addition of exogenous volume by two important mechanisms. Vascular smooth muscle in the walls of small veins and venules can contract and convert unstressed volume into

Table 42.1 Key clinical points

- | |
|---|
| 1. Na ⁺ maintains water in the body and, consequently, fluid balance is really about Na ⁺ balance |
| 2. Always consider the total amount of Na ⁺ given and total body Na ⁺ status and not the actual concentration of the fluid given |
| 3. Monitoring electrolyte concentrations and making adjustments to the infused water and its contained electrolytes are critical components of intravenous fluid management |
| 4. An infusion of a volume bolus of more than 1–1.5 L the volume is unlikely to stay in the vascular space |
| 5. Unstressed vascular volume cannot be measured in an intact person because it does not create a measurable force; the reserve only can be predicted by considering the patient's volume history |
| 6. Only stressed volume produces the force that drives fluid around the circulation |
| 7. Fluid responsiveness does not indicate fluid need |

stressed volume and thereby increase MSFP (Magder and De Varennes 1998; Deschamps and Magder 1992). Shortening vessel circumference occurs without a change in the vessel wall compliance and is called a decrease in capacitance (Rothe 1983a). In animal studies, up to 18 ml/kg of unstressed volume can be converted into stressed volume (Rothe 1983b), although 10 ml/kg is likely a more common achievable upper value. This recruited volume is directly added to the stressed volume component in seconds. There are limits to the amount of recruitable volume, and these reserves frequently are depleted in the critically ill. Unfortunately, the unstressed reserve cannot be measured in an intact person because it does not create a measurable force; the reserve only can be predicted by considering the patient's volume history.

A second intrinsic regulator of plasma volume is the interstitial space (Bhave and Neilson 2011). This, too, can provide a rapid increase in plasma volume. Equally quickly, volume can be lost from the plasma space into the interstitial space and deplete plasma volume when capillary permeability is increased, as is the case in sepsis and SIRS, or when albumin is decreased as in nephrotic syndrome. To appreciate how large and rapid volume shifts can be, consider a patient who comes for outpatient dialysis and 4 L are

ultra-filtrated in 3–4 hours. This volume is greater than normal plasma volume, yet the patient can get up after dialysis and leave the hospital. The normal exchange between the plasma and interstitial spaces is dependent upon adjustment in tone of resistance vessels upstream and downstream from the capillaries, capillary surface area, the permeability of the walls of capillaries, the hydrostatic pressure across the walls, differences in oncotic pressure inside and outside the vessel, and the characteristics of the interstitial space (Levick and Michel 2010; Michel 1997).

Clinical Administration of Fluids

Assessment of Hydration, Na⁺ Balance, and Vascular Volume

Fluid management should start with an assessment of three components of volume status: hydration, total body Na⁺, and intravascular volume (Table 42.1). Hydration is the simplest to assess once the definition of hydration is understood, but this term frequently is misused (Fortes et al. 2015; Hooper et al. 2015; Gorelick et al. 1997; McGee et al. 1999; Mange et al. 1997). Hydration is defined as the amount of solute relative to solvent. In biological systems, the solvent always is water. For pragmatic bedside management, assessment of hydration is made simply by measuring the serum Na⁺ concentration, because as discussed in Chap. 10 (Magder, Fluid Physiology), Na⁺ is the major element used by the body to regulate volume. If Na⁺ concentration is elevated relative to the normal reference value, there is more Na⁺ than water and the patient is dehydrated, whatever the total body volume. If Na⁺ concentration is less than the normal reference value, the patient is over-hydrated. Hydration has nothing to do with intravascular volume, interstitial volume, or total body Na⁺; it only indicates the relationship of solute, i.e., Na⁺, to solvent, i.e., water.

The next step is assessment of total body Na⁺. Excess total body Na⁺ is evaluated by examining the patient for edema, ascites, pleural effusions, or expanded intravascular volume. If any of these are present, all the extra water has approximately

the same concentration of Na⁺ as in the serum, and thus total body Na⁺ is elevated. Na⁺ balance is not determined by the concentration of Na⁺; that is hydration. A reduction in total body Na⁺ is harder to assess. A decrease in a patient's skin turgor can help, especially if it is followed serially (Laron 1957). The best test likely is knowing the patient's volume history and whether there has been a process that could have depleted the interstitial volume. Of importance, the status of interstitial volume does not indicate the status of intravascular volume; intravascular volume can be normal with either an excess or deficiency of extracellular volume.

The third step is assessment of intravascular volume, more specifically stressed vascular volume because that is what stretches vascular wall. This usually is what most concerns clinicians because of its importance as a determinant of cardiac output. Unfortunately, there are very limited tools to determine the adequacy of intravascular volume (Hooper et al. 2015; McGee et al. 1999). When intravascular volume is in excess, jugular venous pressure should be elevated and pulmonary veins prominent on a chest X-ray, and possibly, there should be a third heart sound. There is not much more to help. The best test for identifying reduced intravascular volume is a postural increase in heart rate and decrease in blood pressure (McGee et al. 1999), but this requires having the person sit up with at least their feet over the side of the bed, or preferably stand up, which is not feasible in most critically ill patients. Neck veins should be flat. Heart rate and blood pressure are poor indicators (Hamilton-Davies et al. 1997). The person might also complain of thirst (Vivanti et al. 2008). Importantly, fluid responsiveness does not indicate reduced intravascular volume and fluid need (Table 42.1). Fluid responsiveness is the normal state, especially in the upright posture in which central venous pressure usually is below atmospheric pressure.

Maintenance and Daily Needs

The dominant components of daily maintenance fluids for someone with no oral intake are water, Na⁺, K⁺, and glucose. All numbers in the following discussion are adjusted for a 70 kg

Table 42.2 Composition of basic fluid needs: daily requirements (70 kg man)

Substance	Per kg	Daily	D5W in ½ NS At 80 cc/hr
Water	30 ml/kg	2 L	2 L
Na ⁺	<2 meq/kg	140 meq	154 meq
K ⁺	1.7 meq/kg	120 meq	40 meq
Glucose (for brain)		100 g	100 g

The per kg and daily numbers are approximations based on food guides. This is provided pretty closely by 80 cc/hr of 2 L of ½ N saline in 5% dextrose in water (D%W). The Na⁺ is slightly higher and the K⁺ is much lower but safer for continuous infusion

male but easily can be scaled up or down based on body size (Table 42.2). With at least moderate kidney function, the precise amounts are not critical because the kidney will make the fine adjustments.

Water Water is lost daily by evaporation from the skin, expiration of air that was humidified by the upper airway on inspiration, by urine which is used to get rid of wastes and regulates the concentrations of elements, and normally, by a small amount of loss from the gastrointestinal tract. Under normal conditions, without excess heat stress, high rates of ventilation, and in the absence of liquid stool, approximately 400 ml of water are lost through the skin and lungs per day in what are called insensible losses. With a urine output of approximately 60–70 ml/hr, another 1600 ml is lost, for a total of around 2 L or ~30 ml/kg in a 70 kg male. In the average patient without any oral intake, but functioning kidneys, this amounts to approximately 80 ml/hr of water per day. The requirement for water frequently needs to be adjusted based on hydrations status (Moritz and Ayus 2015), which is discussed below.

Sodium As already indicated in Chap. 10 (Magder, Fluid Physiology), Na⁺ concentration is the major regulator of water in the extracellular space; K⁺ plays the same role in the intracellular space. However, because Na⁺ is in the extracellular space, and easily can be absorbed and excreted from the body, it has evolved as the

major determinant of the overall osmolality of the body. Thus total body water and total body K⁺ follow total body Na⁺. The key clinical point is that Na⁺ maintains water in the body and, consequently, fluid balance is really about Na⁺ balance (Table 42.1).

International food guides recommend a daily intake of 2.3–3 g of Na⁺ per day, although most people eat a lot more. To put this in perspective, 1 teaspoon of salt has 2.3 grams (g) of Na⁺. Grams are converted to mEq¹ by dividing the of the weight in grams by the molecular weight of Na⁺, which is 23, and multiplying by 1000 to convert grams to milligram; 2.3 g is thus 100 mEq. An intake of 3 g per day equals 130 mEq or close to 2 mEq/kg per day (Table 42.2). A 1 liter bag of normal saline contains 154 mEq/L so that the equivalent of a bag of normal saline gives between 18% and 50% more than the daily recommended Na⁺. Thus, 80 ml/hr of 0.45% saline (“half normal”) provides the daily water need and greater than normal need for Na⁺. Use of a saline solution less concentrated than 0.45% can result in clinically significant hyponatremia, especially in children (Halberthal et al. 2001; McNab 2016). If Na⁺ is especially low, it could cause hemolysis because it is too hypotonic. It is worth noting that the frequently used maintenance fluid of 100 ml/hr of normal saline gives close to 8.5 g of Na⁺ per day, which is more than three times the recommended daily requirement of Na⁺. It is the equivalent of giving a bottle of salted dill pickles with the juice!

When over-hydration or dehydration is present, the total amount of infused Na⁺ and water needs to be modified by considering to the total Na⁺ balance and total body water. If a patient has a marked excess of Na⁺, as evidenced by edema, ascites, or pleural effusions, and is undergoing diuresis, daily Na⁺ intake should be reduced accordingly. Limiting Na⁺ intake is as important

¹A mole indicates the amount of a substance but what is important in chemical reactions is how much the substance reacts, which is called equivalents. The values are close but equivalents are actually measured and the values reported in tests. mEq is 1000th of an equivalent.

as giving a diuretic to reduce excess Na^+ and to create negative Na^+ balance (Bihari et al. 2012, 2013). If edema is present, and Na^+ concentration is elevated, free water still must be given to correct the osmolality and allow excretion of Na^+ . If Na^+ concentration is low because of a water retaining process, it may be necessary to use 0.9% normal saline instead 0.45% saline to avoid worsening hyponatremia, but in this case the infusion should be reduced to ≤ 30 ml/hr to be consistent with daily Na^+ need. A diuretic also is needed to excrete the excess Na^+ because the edema indicates that there is excess total body Na^+ ; it is just diluted by an even greater excess of water. The message is to always consider the total amount of Na^+ given and total body Na^+ status and not the actual concentration in the given fluid. It also is worth noting that the diet of a normal healthy individual is always “hyponatremic.” Enteric formula feeds, too, given in the 1.8–2 L per day range, usually only provide 60–80 mEq of Na^+ per day and are thus “hyponatremic” solutions. That is the biological norm.

Potassium The daily requirement of K^+ is 4.7 g which is close to 120 mEq per day. However, this is based on oral intake and functioning regulatory systems in the gastrointestinal tract and kidneys. It is very risky to give this amount intravenously in maintenance fluids in critically ill patients because normal renal function is so often compromised. A safer amount is 20 mEq/L of maintenance fluid. K^+ then can be supplemented either orally or intravenously as needed based on the serum concentration of K^+ . Although K^+ only is about 4 mEq/L in serum, the concentration of K^+ inside cells is in the range of 120–140 mEq/L, and there is twice as much intracellular water compared to the extracellular water. There thus is at least 60 times more K^+ inside than outside cells. When major tissue necrosis occurs, the large amount of released K^+ must pass through the extracellular space to be excreted from the plasma. This is a major clinical problem when the kidneys are not working efficiently.

Chloride There are no specific guidelines for intake of Cl^- . Intake of Cl^- generally follows Na^+ in the form of NaCl . However, the extracellular concentration of Cl^- is about 2/3 that of Na^+ . This is accomplished in the body by regulation of Cl^- intake in the gastrointestinal tract and by renal excretion of more Cl^- than Na^+ . There thus needs to be a concern about excess Cl^- intake when the kidneys are not functioning normally and NaCl is given intravenously. Although not known, from the above discussion it is likely that the amount of Cl^- given is more important than the concentration of Cl^- in the administered solution. Accordingly, use of 0.45% saline with only 77 mEq/L of Na^+ and Cl^- may not produce as large a stress to the system when used for maintenance fluids as 0.9% saline or even lactated Ringer’s solution, which has a Cl^- concentration of 109 mEq/L (Table 42.3) (Magder 2014).

To excrete Cl^- in the urine, a strong positive ion must be excreted with it to balance its negative charge and to maintain electrical neutrality (Magder and Emami 2015). Since Cl^- and Na^+ usually are absorbed in equal amounts, more Cl^- needs to be excreted than Na^+ to maintain the normal difference of almost 40 mEq/L in plasma, and thus Na^+ cannot be the cation to solve this problem. The serum concentration of K^+ is far too low, and H^+ has a million-fold lower concentration than Cl^- so that it cannot perform this role. The problem is solved by enzymatic production of ammonium (NH_3) primarily from the amino acid glutamine in renal tubular cells and the subsequent formation of the strong cation, NH_4^+ (Pitts 1968; Sartorius et al. 1949; Weiner and Verlander 2013). There are two consequences of this. An enzymatic process is needed to make $\text{NH}_3/\text{NH}_4^+$. For this reason, excretion of Cl^- is slower than excretion of Na^+ , which can occur rapidly by channels and exchangers. When the enzymatic processes for cleaving NH_3 are not active, excretion of Cl^- is greatly impaired and results in renal tubular acidosis.

Glucose The last major component of daily fluid needs is glucose (Table 42.2). The brain derives

Table 42.3 Composition of common intravenous solutions

		Normal saline	Lactated Ringer	Hartman's	Plasma-Lyte-148
Cations	Sodium	154	130	131	140
	Potassium	–	4	5	5
	Calcium	–	3	4	–
	Magnesium	–	–	–	3
Anions	Chloride	154	109	111	98
	Lactate	–	28	29	–
	Acetate	–	–	–	27
	Gluconate	–	–	–	23
	Osmolality	308	274	280	293

All values are mEq/L except osmolality which is mOsm/L

energy primarily from glucose. It requires in the range of 100 g of glucose per day for this purpose. When glucose is not available, the body must break down proteins for gluconeogenesis. Two liters of 5% dextrose in water satisfies the brain's daily need and can reduce protein breakdown by over 50% (Tredget and Burke 1988; Gomez-Izquierdo et al. 2017; Long et al. 1976; Schricker et al. 2005). This still leaves a large gap for other bodily needs of proteins and glucose which must be met by enteral or parental nutrition. Of note, in sepsis, the benefit derived by providing glucose does not occur (Long et al. 1976). Giving more sugar without the presence of appropriate hormones to metabolize it just leads to hyperglycemia and water loss by osmotic diuresis.

Use of Fluids for Resuscitation

Goals

As in any clinical action, it always is essential to start by asking: what is the objective of the therapeutic action? Volume is given in resuscitation to restore lost reserves and to improve tissue perfusion by increasing venous return and consequently cardiac output.

When vascular volume is lost by hemorrhage, diarrhea, vomiting, or excess evaporative losses, as well as by aggressive diuresis or inadequate volume intake, volume reserves in the interstitial space and unstressed volume are recruited to restore MSFP. This occurs by baroreceptor-induced activation of sympathetic nerve activity

which results in contraction of splanchnic veins (Deschamps and Magder 1992; Rothe 1983a; Caldini et al. 1974; Mitzner and Goldberg 1975) in response to the decrease in blood pressure. An infusion of exogenous catecholamines, too, can recruit these reserves. If sympathetic tone is removed, capacitance increases and MSFP again falls. Cardiac output and blood pressure then fall too. The supply of vascular reserves is limited, and when reserves are sufficiently depleted, the body can no longer defend itself. Any further loss of volume results in a decrease in MSFP, cardiac output, and blood pressure. As already noted, loss of unstressed volume cannot be measured in an intact person and only can be predicted by the clinical history. In sepsis, even without an actual loss of total volume, capacitance increases because of relaxation of the venous vascular compartment in the same way that there is arterial vasodilation (Magder and Vanelli 1996). This, too, reduces the stressed component of total vascular volume and lowers MSFP. The consequence of a loss of unstressed reserves is greater in mechanically ventilated patients because recruitment of unstressed volume is required to increase MSFP to overcome the increase in pleural pressure (Nanas and Magder 1992) (Chap. 18). Thus, a first step in resuscitation is to restore reserves in unstressed volume and interstitial volume. It would be unusual for more than 10 ml/kg of unstressed volume to be lost due to an increase in capacitance, so that no more than 1 liter of fluid, and likely less, is needed to restore this vascular loss. A volume infusion of greater than 1 L likely is filling interstitial reserves, but

this is important, too, because it allows a more normal autoregulatory adaptation in the microcirculation. It also is likely that even an extra 1 L of fluid in the large interstitial space will not have major negative consequences. I say this without evidence, but anyone who has had a weight gain of 1 kg after a meal with a high Na⁺ content has retained 1 L of water with no consequences (unless they have congestive heart failure!). Of note, although restoration of reserves occurs in association with expansion of vascular volume, just filling reserves will not be associated with a change in central venous pressure, cardiac output, or blood pressure and therefore not measurable.

The second part of volume resuscitation is what most people think of as resuscitation, and that is, infusion of volume to increase cardiac output and to improve tissue perfusion. The only way that volume can do this is by increasing cardiac output, and thus assessment of a change in cardiac output needs to be a major component of managing volume resuscitation. It is important to appreciate the limit of what volume can do to increase cardiac output. To repeat, only the stressed component of total blood volume creates the force that drives blood around the circulation (Table 42.1). In a 70 kg male, stressed volume is in the range of 1.3–1.4 L. Even at peak exercise, with cardiac output in the 20–25 L/min range, stressed volume likely only increases by about 6 ml/kg. Thus, increasing normal blood volume by 500 ml should provide a very large increase in MSFP; with a venous compliance of 150 ml/mmHg, the increase in MSFP would be in the order of 6 to 7 mmHg, which is more than 50% above the normal value. It is unlikely that volume infusions of greater than this amount remain in the vasculature because the inevitable increase in capillary pressures will increase filtration from the vasculature. This especially is a problem in patients with distributive shock because they usually have increased capillary permeability, and the infused fluid is rapidly lost from the vascular compartment. The infused volume likely just is keeping up with the losses and actually driving increased losses to the interstitial space. The decreased arterial resistance in distributive

shock also means that a greater proportion of the arterial pressure is transmitted to capillaries (Mellander and Johansson 1968), and increasing MSFP by volume infusions means that the downstream venous pressure is increased too. Both of these factors further increase fluid filtration. Even worse, in septic shock the oncotic pressure of blood usually is decreased due to loss of albumin, and this, too, reduces the forces opposing the increased hydrostatic pressure. As discussed in Chap. 10 (Magder, Fluid Physiology), the interstitial space normally has a low compliance, and because of this, the interstitial pressure quickly rises with increased fluid filtration. This decreases the hydrostatic pressure gradient for filtration and filtration slows. However, with about a 50% increase in interstitial volume, and an interstitial pressure above 4 mmHg, the interstitial compliance markedly falls and capillary filtration occurs much more easily, and then there is a much more rapid loss of vascular volume (Bhave and Neilson 2011). More intravenous fluids are then needed to maintain vascular volume and a vicious cycle is created. Furthermore, as also discussed in Chap. 10 (Magder, Fluid Physiology), Na⁺ distributes throughout the whole extracellular space. This means that as the extracellular space increases, the distribution space for Na⁺ and other elements increase proportionally, and a progressively smaller portion of infused crystalloid remains in the vascular space. Fluid filtered into the pulmonary interstitial space worsens oxygenation, and excessive filtration into the abdominal compartment can produce an abdominal compartment syndrome.

There is an important limit to what volume can do. Once the flat part of the cardiac function curve is reached, further volume loading does not increase cardiac output and cannot alter tissue perfusion. The fluid infusion then only raises central venous pressure, and the rise in pressure congests upstream organs such as the liver, gut, and kidney. A critical part of use of fluids for resuscitation is recognition of the limit of cardiac filling and knowing when to stop the giving volume because more volume only will do harm. A simple indication of a volume limited right heart is the lack of an inspiratory fall in right

atrial pressure with a negative pressure inspiratory effort (Magder et al. 1992); similarly this can be identified by loss of inspiratory variations of the vena cava although primarily with the superior vena cava which requires transesophageal echocardiography (Charron et al. 2006). Another approach is to observe the response to a small volume bolus, or the equivalent, by lifting the legs up and determining whether there is a change in cardiac output (Monnet et al. 2006). It is important to emphasize that the limit to right ventricular filling is sharp and in normal persons occurs at central venous pressures below 10 mmHg when the transducer is leveled at 5 cm below the sternal angle or 12–14 mmHg when leveled at the mid-axillary line (Bafaqeeh and Magder 2004). Furthermore, although some patients may have an increase in cardiac output at higher values of central venous pressure, filtration will markedly increase with consequent congestion of upstream organs and tissues.

These complex interactions seem to create an unsolvable problem which sometimes is the case. Management requires carefully dosed use of fluids combined with pharmacological therapy to restore vascular tone and maintain cardiac function. A number of studies are currently underway that are trying to determine the role of fluids versus norepinephrine, but it should be clear that just indiscriminately giving volume to septic patients is not beneficial and likely harmful (Boyd et al. 2011). An important part of any protocol for fluid management in sepsis should include a determination of whether right heart function is volume limited, in which case giving more volume will not help and only can do harm.

What Types of Fluids?

If the loss of volume is due to hemorrhage, the obvious resuscitation “fluid” should be blood, which most often is packed red blood cells with some crystalloid to account for the interstitial fluid that was recruited to maintain blood volume. When blood is not immediately available, and arterial pressure is very low, the temptation often is to infuse large amounts of other types of

fluid. This must be avoided and the oxygen delivery equation must be considered. Oxygen delivery is the product of cardiac output, hemoglobin concentration, and arterial oxygenation (Chap. 31). Once again, the way that a volume infusion corrects hypotension is by increasing cardiac output. An infusion of a non-red cell solutions will decrease effective hemoglobin concentration by dilution. If the percent decrease in hemoglobin concentration is greater than the percent increase in cardiac output, O₂ delivery will be decreased, despite an increase in arterial pressure. Second, the limit of the cardiac function curve must be remembered because once it is reached, a volume infusion cannot increase cardiac output and only can dilute the hemoglobin concentration. It thus has no place in the management because it only can make the patient worse.

Crystalloid Solutions

The interstitial volume is primarily a crystalloid solution, and crystalloids should be used for resuscitating this compartment (Table 42.3). It is important to avoid increasing the interstitial oncotic pressure for this will increase fluid filtration by decreasing the oncotic pressure gradient across the vascular wall.

In distributive shock the equivalent of a crystalloid solution leaks from the vascular space into the interstitial space. This is due to increased vascular permeability and decreased colloid osmotic pressure because albumin is consumed as an acute phase reactant. Excessive loading of vascular volume also can contribute by increasing the capillary hydrostatic pressure. The crystalloid options for resuscitation include 0.9% isotonic “normal” saline, lactated Ringer’s solution, or what are called “balanced” salt solutions, which have compositions close to that of normal serum (Table 42.3). Normal saline is inexpensive and readily available and still is the most widely used solution. The primary concern with normal saline is that it has a Cl⁻ concentration equal to that of Na⁺. When used in large amounts, it creates a metabolic acidemia. There currently is a lot of discussion of how harmful this is and is

discussed next (Magder 2014; Kellum and Shaw 2015; Kellum et al. 1998).

Because of the concerns of hyper-Cl⁻ induced acidemia, it has been proposed to use crystalloid solutions that have reduced Cl⁻. Reduction of Cl⁻ concentration requires replacing it with another anion to maintain electrical neutrality. The most common solution is lactated Ringer's solution in which Na⁺ is reduced to 130 mEq/L and Cl⁻ is reduced to 109 mEq/L (Table 42.3). There also are 4 mEq/L of K and 1.5 mEq/L of Ca²⁺ and 28 mEq/L of lactate to provide the missing anions. The lactate is quickly metabolized to CO₂ and water leaving behind a 28 mEq/L difference between positive and negative strong cation compared to zero with normal saline. However, this initially still is an acidifying solution because the normal strong ion difference is around 40 mEq/L (see Chap. 41 acid base). When the lactate is metabolized to water and CO₂ and the CO₂ is blow off, the lactate has an alkalinizing effect. This solution also is a relatively hyponatremic solution which reduces the benefit of the lower Cl⁻ concentration because what counts for pH is the difference between Na⁺ and Cl⁻ (Traverso et al. 1986). The hyponatremia of the solution can be an issue in patients with excess antidiuretic hormone or salt wasting in neurosurgical patients. The Ca²⁺ in lactated Ringer solution has raised concern in patients receiving citrate or blood transfusions. Finally, concerns have been raised about the presence of K⁺ in patients with elevated K⁺ or renal failure, but this is not an issue because it is the concentration that counts and the K⁺ in lactated Ringer's is in the normal range and will not increase the serum K⁺ above 4 mEq/L and the increase in total body K⁺ is very modest considering the very large intracellular amounts of K⁺. If anything, K⁺ has been found to increase more with the use of NaCl likely due to the effect of the high Cl⁻ on renal function (O'Malley et al. 2005; Khajavi et al. 2008). On the positive side, there is evidence that the lactate in lactated Ringer's solution can have an anti-inflammatory effect in patients with pancreatitis, but the mechanism is not obvious (Wu et al. 2011).

A third approach is to use solutions that are designed to match the components of normal

serum. These are called balanced salt solutions. A common one is Plasma-Lyte which has a Na⁺ of 140, Cl⁻ of 98, and Mg²⁺ of 1.5 mEq/L and makes up the anion difference with 23 mEq/L gluconate and 27 mEq/L acetate (Table 42.3). It may be asked why lactate, gluconate, and acetate are used rather than HCO₃⁻ which is the normal anion that plays this role in plasma. The reason is that HCO₃⁻ is in equilibrium with PCO₂ which leaches out of plastic bags unless the plastic is very thick as is the case for bags used for continuous renal replacement therapy. However, use of these would make the bags prohibitively expensive for regular use.

The question arises as to whether the rise in serum Cl⁻ concentration is clinically significant and is it worth using these other crystalloid solutions. In observational studies on critically ill patients, the incidence of renal dysfunction was higher with Cl⁻ rich solutions ((Shaw et al. 2012, 2015; McCluskey et al. 2013; Yunos et al. 2012). In other studies, large amounts of saline solutions in patients undergoing abdominal surgery were associated with slower recovery of bowel function (Moretti et al. 2003; Chowdhury et al. 2012; Chowdhury and Lobo 2011).

More recently there has been a few randomized controlled trial which compared balanced salt solutions to normal saline for general management. SPLIT was a double-blind cluster randomized cross-over design that was carried out in four hospitals in New Zealand (Young et al. 2015). During each block all patients in the hospital received either normal saline or Plasma-Lyte® for a 7-week periods. The primary endpoint was a doubling of serum creatinine or a serum level greater than 3.96 mg/dL with an increase of ≥0.5 mg/dL from baseline. There was no difference between groups, and a larger trial is now being conducted, but I would predict that it is unlikely to show much difference because the amounts of fluid given are not large enough to have an effect and there is no stratification by risk factors for renal or bowel dysfunction (Kellum and Shaw 2015).

The SALT group performed two studies. SALT-ED studied patients not admitted to the intensive care, whereas SMART studied patients

admitted to the intensive care unit. The endpoints were different. In SALT-ED, the primary endpoint was hospital free days at 28 days; in SMART the endpoint was a composite measure of renal dysfunction. In SALT-ED use of solutions other than saline did not alter hospital stay. There was a small decrease in markers of renal dysfunction, which was a secondary outcome. In SMART there was a significant reduction of markers of renal dysfunction. It is important to appreciate that these studies were not blinded. Even more important was that the protocol required that the control patients receive normal saline for all intravenous fluid needs. As described above under maintenance fluids, use of only normal saline at the rates used would have resulted in a marked excess of Na^+ as well as Cl^- and protocol essentially forced clinicians to continue using a Cl^- rich solution even when Cl^- was elevated. These studies thus may be more of an indication of the need to monitor Cl^- use, as well as Na^+ use and make intelligent individualized decisions at the bedside rather than indicating that these solutions should always be used.

From my perspective, it seems that the consequences of Cl^- are minimal in most people when the volumes of normal saline are ≤ 2 L, but the risk likely is greater in those that have a reduced capacity to excrete Cl^- such as patients with renal dysfunction from diabetes or hypertension. Patients receiving very large amounts of normal saline likely also are at greater risk because of the size of the Cl^- load. Perhaps the evidence would be clearer if just these higher-risk patients were studied in randomized trials. The kidney and the gut all are particularly at risk because the excess Cl^- must pass through their walls to be excreted. It has been noted in an editorial by Kellum and Shaw that greatest risk from the elevated Cl^- and consequent acidemia is that it induces inappropriate clinical responses because the clinicians do not appreciate that only the Cl^- is producing the acidemia and there is nothing more sinister (Kellum and Shaw 2015).

When patients have had a high Cl^- load, and a significant acidemia, an approach to reducing Cl^- concentration is to make a solution with NaHCO_3 in dextrose and water. The HCO_3^- com-

ponent is in equilibrium with CO_2 , and as long as there is spontaneous ventilation, the brain regulates CO_2 , and the HCO_3^- is blown off leaving the Na^+ to widen the strong ion difference and to be excreted with the Cl^- and to restore the normal $\text{Na}^+ \text{Cl}^-$ difference.

Colloids

In patients who have increased capillary filtration, preserving or even increasing colloid osmotic pressure is of major interest so as to try to maintain intravascular volume. The hope is that these substances stay in the vasculature and do not leak out. This can be done with the body's natural primary colloid, albumin, or with synthetic colloids.

Albumin comes in two general forms: 4 or 5% solutions that have an oncotic pressure close to that of normal plasma or in concentrated solutions of 20 or 25% that are hyperoncotic relative to normal plasma. The solvents are either normal saline or another crystalloid including balanced salt solutions. As discussed in Chap. 10 (Magder, Fluid Physiology), the hemodynamic actions of 5% and 25% are very different and should not be lumped together. The 5% solution expands intravascular volume, whereas the 25% solution increases plasma oncotic pressure and either reduces capillary filtration or actually draws fluid from the interstitial space back into the vasculature. Despite an initial meta-analysis that indicated major harm (Offringa 1998), albumin has been shown to be safe (Finfer et al. 2004), except in patients with head trauma (Myburgh et al. 2007), and it is not associated with renal injury. The hyper-oncotic form of albumin has been shown to be especially useful in patients who have cirrhosis and spontaneous bacterial peritonitis (Sort et al. 1999). This study was designed to determine if giving albumin would reduce renal failure but ended up demonstrating a reduction in mortality. It also has been shown that addition of doses of hyper-oncotic albumin to a continuous intravenous infusion of furosemide in volume overloaded patients with acute respiratory distress syndrome reduced time on the ventilator (Martin et al. 2005).

There also are a number of synthetic colloids including dextrans, gelatins, and starches. The primary ones that are still used, but to a much smaller extent than previously, are hydroxyethyl starches. These come in many molecular sizes, concentrations, and with many differences in the substitutions of the glucose molecules which have significant impacts on their actions (Treib et al. 1999), but these differences will not be discussed here. An important limitation to their use is that they can cause renal injury and increase bleeding if used inappropriately. They also are associated with pruritus post use (Myburgh et al. 2012). Three large randomized trials in septic patients have shown that they cause harm or at least no mortality benefit, and their use has greatly decreased (Perner et al. 2012; Myburgh et al. 2012; Brunkhorst et al. 2008). The reputation of starches also was sullied by the falsification of data by a major investigator in the field (Wiedermann and Joannidis 2018). However, there has been an important misleading component to this story in the literature. The three large studies that showed harm were all in septic patients who have a large capillary leak component (Perner et al. 2012; Myburgh et al. 2012; Brunkhorst et al. 2008). The quantities of starch given were very large. In the study that showed the greatest harm, the fifth quintile group received 250 ml/kg. This works out to 17 L in a 70 kg male (Brunkhorst et al. 2008)! Since the rationale for use of a starch is to give something that will stay in the vasculature, and stressed volume normally only is about 1.3–1.5 L, clearly these solutions at high volumes are not staying in the vasculature. Likely, only a maximum of 1 L should be used to avoid harm and maximize benefit. These starch studies all were done with septic patients, most likely because septic patients have a high enough mortality to allow for sufficient power to identify a change in deaths, which is a hard endpoint, and produce a higher profile publication. However, this also produced an important publication bias because the potential for harm is greater in septic patients. Septic patients have increased vascular leak, and it is more likely that the starch would leak into the interstitial space. The more effective increase in vascular pressure would actually

increase filtration. As these studies have shown, there is no value for use of starch solutions in patients with distributive shock. Thus, these large trials do not inform us on the use of starches in non-septic patients. It would have made far more sense to study routine operative patients with intact capillary function and who require smaller amounts of volume. However, these patients have a low mortality, which makes it difficult to find a hard clinical endpoint to demonstrate a convincing benefit.

A pilot, randomized, double-blind, nurse-driven study in patients following cardiac surgery found that use of a pentastarch reduced use of catecholamines the morning after surgery by over 60% with no increase in bleeding and no difference in renal function between treated and non-treated patients (Magder et al. 2010). Of importance, in the study, the amount of the starch solution was limited to 1 L, and fluid was given based on a strict flow-directed protocol in which more fluid was not given if a previous bolus failed to increase measured cardiac output. Half the subjects only required a total of 500 ml of the colloid. There are little other randomized trials of adequate size in non-septic subjects.

Managing Hydration Status

Osmolality of body solutions normally is tightly regulated because it needs to be relatively constant to avoid swelling or shrinking of cells. This is reflected in the state of hydration, which is defined as the relationship of amount of solute to the amount of solvent, which is water. As previously indicated, Na^+ is the primary solute used by the body to regulate normal osmolality. Thus, deviations of Na^+ concentration from the normal value indicate a deviation in the hydration state and need to be corrected. However, abnormalities in Na^+ concentration should not be corrected too quickly because this can lead to cell damage, especially in the delicate neurons in the midbrain that are involved in regulating osmolality (Ayus et al. 1987; Adrogue and Madias 2000). The recommended rate of change is not more than 0.5 mEq per hour unless there are severe consequences from the dis-

order such as seizures in which case the value can be lowered by 1–2 mEq/h for 2–3 hours.

For someone who is hypernatremic and has a functioning gastrointestinal tract, the simplest approach is to give pure water enterally, which could be by the patient drinking water, but more often through a gastric tube. If the enteral route cannot be used, the situation is more complicated. Infusion of a solution of 5% dextrose in water does not work in most patients because they become hyperglycemic, and once blood sugar is above 10 mmol/L, the kidney starts to spill the sugar, which increases water loss and further dehydrates the patient. Insulin can be added to control the blood glucose, but in practice this is hard to regulate. A better approach is to give ½ normal saline with a diuretic such as furosemide to maintain a diuresis. This is slower than giving oral water but will gradually correct the Na⁺ concentration. Whichever therapeutic approach is used, the patient most often will have a positive fluid balance, but it needs to be appreciated that the water is only correcting the Na⁺ concentration. If it is considered that total body Na⁺ is in excess, a diuretic should be given to produce a natriuresis to lower total body Na⁺.

For someone who has a Na⁺ concentration lower than normal, the first question should be: Is Na⁺ concentration low because of too much water or is it low due to too little Na⁺? If the patient is thought to be total body Na⁺ depleted, the deficit in Na⁺ should be corrected with boluses of saline, and the maintenance fluid should be changed to normal saline instead of half-normal saline. However, the amount of Na⁺ should be based on daily needs. If the patient is hyponatremic, but has signs of increased total body Na⁺ as indicated by the presence of edema or fluid collections in the pleural or abdominal spaces, the primary approach is to restrict free water, both orally and in all intravenous solutions. Unless Na⁺ concentration is critically low, hypertonic solutions should be avoided because there already is an excess of Na⁺ in the body and especially if the patient has central nervous symptoms. In that case, a hypertonic solution of Na⁺ is required and, again, administered carefully to avoid too rapid a correction.

Summary

The major points covered in this review are that the total amount of Na⁺ in the body dictates the amount of water in the body. Fluid balance thus is about Na⁺ balance. Elements such as Na⁺, K⁺ and Cl⁻ only can be absorbed or excreted, and thus intake and output of Na⁺ in particular need to be followed. It is important to consider the fluid reserves in unstressed vascular volume and in interstitial space when planning fluid management; they often need to be repleted. All fluid-filled compartments are connected in a dynamic equilibrium so that movement of fluids and electrolytes across all spaces need to be considered when managing fluid balance. It is important to distinguish between the concentration and the total amount of substances. Finally, responses to fluid boluses only can be in the realm of the physiologically possible.

References

- Adrogue HJ, Madias NE. Hyponatremia. *N Engl J Med*. 2000;342(21):1581–9.
- Ayus JC, Krothapalli RK, Arief AI. Treatment of symptomatic hyponatremia and its relation to brain damage. A prospective study. *N Engl J Med*. 1987;317(19):1190–5.
- Bafaqeh F, Magder S. CVP and volume responsiveness of cardiac output. *Am J Respir Crit Care Med*. 2004;169(7):A344.
- Bhave G, Neilson EG. Body fluid dynamics: back to the future. *J Am Soc Nephrol*. 2011;22(12):2166–81.
- Bihari S, Ou J, Holt AW, Bersten AD. Inadvertent sodium loading in critically ill patients. *Crit Care Resusc*. 2012;14(1):33–7.
- Bihari S, Peake SL, Seppelt I, Williams P, Bersten A. Sodium administration in critically ill patients in Australia and New Zealand: a multicentre point prevalence study. *Crit Care Resusc*. 2013;15(4):294–300.
- Boyd JH, Forbes J, Nakada TA, Walley KR, Russell JA. Fluid resuscitation in septic shock: a positive fluid balance and elevated central venous pressure are associated with increased mortality. *Crit Care Med*. 2011;39(2):259–65.
- Brunkhorst FM, Engel C, Bloos F, Meier-Hellmann A, Ragaller M, Weiler N, et al. Intensive insulin therapy and pentastarch resuscitation in severe sepsis. *N Engl J Med*. 2008;358(2):125–39.
- Caldini P, Permutt S, Waddell JA, Riley RL. Effect of epinephrine on pressure, flow, and volume relation-

- ships in the systemic circulation of dogs. *Circ Res*. 1974;34:606–23.
- Charron C, Caille V, Jardin F, Vieillard-Baron A. Echocardiographic measurement of fluid responsiveness. *Curr Opin Crit Care*. 2006;12(3):249–54.
- Chowdhury AH, Lobo DN. Fluids and gastrointestinal function. *Curr Opin Clin Nutr Metab Care*. 2011;14(5):469–76.
- Chowdhury AH, Cox EF, Francis ST, Lobo DN. A randomized, controlled, double-blind crossover study on the effects of 2-L infusions of 0.9% saline and plasma-lyte(R) 148 on renal blood flow velocity and renal cortical tissue perfusion in healthy volunteers. *Ann Surg*. 2012;256(1):18–24.
- Deschamps A, Magder S. Baroreflex control of regional capacitance and blood flow distribution with or without alpha adrenergic blockade. *J Appl Physiol*. 1992;263:H1755–H63.
- Finfer S, Bellomo R, Boyce N, French J, Myburgh J, Norton R. A comparison of albumin and saline for fluid resuscitation in the intensive care unit. *N Engl J Med*. 2004;350(22):2247–56.
- Fortes MB, Owen JA, Raymond-Barker P, Bishop C, Elghenzai S, Oliver SJ, et al. Is this elderly patient dehydrated? Diagnostic accuracy of hydration assessment using physical signs, urine, and saliva markers. *J Am Med Dir Assoc*. 2015;16(3):221–8.
- Gomez-Izquierdo JC, Trainito A, Mirzakandov D, Stein BL, Liberman S, Charlebois P, et al. Goal-directed fluid therapy does not reduce primary postoperative ileus after elective laparoscopic colorectal surgery: a randomized controlled trial. *Anesthesiology*. 2017;127(1):36–49.
- Gorelick MH, Shaw KN, Murphy KO. Validity and reliability of clinical signs in the diagnosis of dehydration in children. *Pediatrics*. 1997;99(5):E6.
- Halberthal M, Halperin ML, Bohn D. Lesson of the week: acute hyponatraemia in children admitted to hospital: retrospective analysis of factors contributing to its development and resolution. *BMJ*. 2001;322(7289):780–2.
- Hamilton-Davies C, Mythen MD, Salmon JB, Jacobson D, Shukla A, Webb AR. Comparison of commonly used clinical indicators of hypovolaemia with gastrointestinal tonometry. *Intensive Care Med*. 1997;23:276–81.
- Hjortrup PB, Haase N, Bundgaard H, Thomsen SL, Winding R, Pettilä V, et al. Restricting volumes of resuscitation fluid in adults with septic shock after initial management: the CLASSIC randomised, parallel-group, multicentre feasibility trial. *Intensive Care Med*. 2016;42(11):1695–705.
- Hooper L, Abdelhamid A, Attreed NJ, Campbell WW, Channell AM, Chassagne P, et al. Clinical symptoms, signs and tests for identification of impending and current water-loss dehydration in older people. *Cochrane Database Syst Rev*. 2015;(4).
- Kellum JA, Shaw AD. Assessing toxicity of intravenous crystalloids in critically ill patients. *JAMA*. 2015;314(16):1695–7.
- Kellum JA, Bellomo R, Kramer DJ, Pinsky MR. Etiology of metabolic acidosis during saline resuscitation in endotoxemia. *Shock*. 1998;9(5):364–8.
- Kelm DJ, Perrin JT, Cartin-Ceba R, Gajic O, Schenck L, Kennedy CC. Fluid overload in patients with severe sepsis and septic shock treated with early goal-directed therapy is associated with increased acute need for fluid-related medical interventions and hospital death. *Shock*. 2015;43(1):68–73.
- Khajavi MR, Etezadi F, Moharari RS, Imani F, Meysamie AP, Khashayar P, et al. Effects of normal saline vs. lactated ringer's during renal transplantation. *Ren Fail*. 2008;30(5):535–9.
- Laron Z. Skin turgor as a quantitative index of dehydration in children. *Pediatrics*. 1957;19(5):816–22.
- Levick JR, Michel CC. Microvascular fluid exchange and the revised Starling principle. *Cardiovasc Res*. 2010;87(2):198–210.
- Long CL, Kinney JM, Geiger JW. Nonsuppressability of gluconeogenesis by glucose in septic patients. *Metabolism*. 1976;25(2):193–201.
- Magder S. Balanced versus unbalanced salt solutions: what difference does it make? *Best Pract Res Clin Anaesthesiol*. 2014;28:235–47.
- Magder S, De Varennes B. Clinical death and the measurement of stressed vascular volume. *Crit Care Med*. 1998;26:1061–4.
- Magder S, Emami A. Practical approach to physical-chemical acid-base management. *Stewart at the bedside*. *Ann Am Thorac Soc*. 2015;12(1):111–7.
- Magder S, Vanelli G. Circuit factors in the high cardiac output of sepsis. *J Crit Care*. 1996;11(4):155–66.
- Magder SA, Georgiadis G, Cheong T. Respiratory variations in right atrial pressure predict response to fluid challenge. *J Crit Care*. 1992;7:76–85.
- Magder S, Potter BJ, Varennes BD, Doucette S, Fergusson D. Fluids after cardiac surgery: a pilot study of the use of colloids versus crystalloids. *Crit Care Med*. 2010;38(11):2117–24.
- Mange K, Matsuura D, Cizman B, et al. Language guiding therapy: the case of dehydration versus volume depletion. *Ann Intern Med*. 1997;127(9):848–53.
- Martin GS, Moss M, Wheeler AP, Mealer M, Morris JA, Bernard GR. A randomized, controlled trial of furosemide with or without albumin in hypoproteinemic patients with acute lung injury. *Crit Care Med*. 2005;33(8):1681–7.
- McCluskey SA, Karkouti K, Wijeyesundera D, Minkovich L, Tait G, Beattie WS. Hyperchloremia after noncardiac surgery is independently associated with increased morbidity and mortality: a propensity-matched cohort study. *Anesth Analg*. 2013;117(2):412–21.
- McGee S, Abernethy WB III, Simel DL. Is this patient hypovolemic? *J Am Med Assoc*. 1999;281(11):1022–9.

- McNab S. Intravenous maintenance fluid therapy in children. *J Paediatr Child Health*. 2016;52(2):137–40.
- Mellander S, Johansson B. Control of resistance, exchange, and capacitance functions in the peripheral circulation. *Pharmacol Rev.: The Williams & Wilkins Co*. 1968;20:117–96.
- Michel CC. Starling: the formulation of his hypothesis of microvascular fluid exchange and its significance after 100 years. *Exp Physiol*. 1997;82(1):1–30.
- Mitzner W, Goldberg H. Effects of epinephrine on resistive and compliant properties of the canine vasculature. *J Appl Physiol*. 1975;39(2):272–80.
- Monnet X, Rienzo M, Osman D, Anguel N, Richard C, Pinsky MR, et al. Passive leg raising predicts fluid responsiveness in the critically ill. *Crit Care Med*. 2006;34(5):1402–7.
- Moretti EW, Robertson KM, El-Moalem H, Gan TJ. Intraoperative colloid administration reduces postoperative nausea and vomiting and improves postoperative outcomes compared with crystalloid administration. *Anesth Analg*. 2003;96(611):617.
- Moritz ML, Ayus JC. Maintenance intravenous fluids in acutely ill patients. *N Engl J Med*. 2015;373(14):1350–60.
- Myburgh J, Cooper DJ, Finfer S, Bellomo R, Norton R, Bishop N, et al. Saline or albumin for fluid resuscitation in patients with traumatic brain injury. *N Engl J Med*. 2007;357(9):874–84.
- Myburgh JA, Finfer S, Bellomo R, Billot L, Cass A, Gattas D, et al. Hydroxyethyl starch or saline for fluid resuscitation in intensive care. *N Engl J Med*. 2012;367(20):1901–11.
- Nanas S, Magder S. Adaptations of the peripheral circulation to PEEP. *Am Rev Respir Dis*. 1992;146:688–93.
- O'Malley CM, Frumento RJ, Hardy MA, Benvenisty AI, Brentjens TE, Mercer JS, et al. A randomized, double-blind comparison of lactated Ringer's solution and 0.9% NaCl during renal transplantation. *Anesth Analg*. 2005;100(5):1518–24, table.
- Offringa M. Excess mortality after human albumin administration in critically ill patients. *BMJ*. 1998;317:223–4.
- Perner A, Haase N, Guttormsen AB, Tenhunen J, Klemenzson G, Aneman A, et al. Hydroxyethyl starch 130/0.4 versus ringer's acetate in severe sepsis. *N Engl J Med*. 2012;367:124–34.
- Pitts RF. Renal regulation of acid-base balance. In: Robert FP, editor. *Physiology of the kidney and body fluids*. 2nd ed. Chicago: Year Book Medical Publishers Incorporated; 1968. p. 179–212.
- Rothe C. Venous system: physiology of the capacitance vessels. In: Shepherd JT, Abboud FM, editors. *Handbook of physiology. The cardiovascular system*. Section 2. III. Bethesda: American Physiological Society; 1983a. p. 397–452.
- Rothe CF. Reflex control of veins and vascular capacitance. *Physiol Rev*. 1983b;63(4):1281–95.
- Santry HP, Alam HB. Fluid resuscitation: past, present, and the future. *Shock*. 2010;33(3):229–41.
- Sartorius OW, Roemmelt JC, Pitts RF. The renal regulation of acid-base balance in man; the nature of the renal compensations in ammonium chloride acidosis. *J Clin Invest*. 1949;28(3):423–39.
- Schricker T, Lattermann R, Carli F. Intraoperative protein sparing with glucose. *J Appl Physiol* (1985). 2005;99(3):898–901.
- Shaw AD, Bagshaw SM, Goldstein SL, Scherer LA, Duan M, Schermer CR, et al. Major complications, mortality, and resource utilization after open abdominal surgery: 0.9% saline compared to Plasma-Lyte. *Ann Surg*. 2012;255(5):821–9.
- Shaw AD, Schermer CR, Lobo DN, Munson SH, Khangulov V, Hayashida DK, et al. Impact of intravenous fluid composition on outcomes in patients with systemic inflammatory response syndrome. *Crit Care*. 2015;19:334.
- Sort P, Navasa M, Arroyo V, Aldeguer X, Planas R, Ruizdel-Arbol L, et al. Effect of intravenous albumin on renal impairment and mortality in patients with cirrhosis and spontaneous bacterial peritonitis. *N Engl J Med*. 1999;341:403–9.
- Traverso LW, Lee WP, Langford MJ. Fluid resuscitation after an otherwise fatal hemorrhage: I. Crystalloid solutions. *J Trauma*. 1986;26(2):168–75.
- Tredget EE, Burke JF. In: Clowes Jr GHA, editor. *Calorie and substrate requirements in trauma and sepsis*. New York: Marcel Dekker, Inc; 1988.
- Treib J, Baron JF, Grauer MT, Strauss RG. An international view of hydroxyethyl starches. *Intensive Care Med*. 1999;25(3):258–68.
- Vincent JL, Sakr Y, Sprung CL, Ranieri VM, Reinhart K, Gerlach H, et al. Sepsis in European intensive care units: results of the SOAP study. *Crit Care Med*. 2006;34(2):344–53.
- Vivanti A, Harvey K, Ash S, Battistutta D. Clinical assessment of dehydration in older people admitted to hospital: what are the strongest indicators? *Arch Gerontol Geriatr*. 2008;47(3):340–55.
- Weiner ID, Verlander JW. Renal ammonia metabolism and transport. *Compr Physiol*. 2013;3(1):201–20.
- Wiedemann HP, Wheeler AP, Bernard GR, Thompson BT, Hayden D, de Boisblanc B, et al. Comparison of two fluid-management strategies in acute lung injury. *N Engl J Med*. 2006;354(24):2564–75.
- Wiedemann CJ, Joannidis M. The Boldt scandal still in need of action: the example of colloids 10 years after initial suspicion of fraud. *Intensive Care Med*. 2018;44(10):1735–7.
- Wu BU, Hwang JQ, Gardner TH, Repas K, Delee R, Yu S, et al. Lactated Ringer's solution reduces sys-

- temic inflammation compared with saline in patients with acute pancreatitis. *Clin Gastroenterol Hepatol*. 2011;9(8):710–7.
- Young P, Bailey M, Beasley R, Henderson S, Mackle D, McArthur C, et al. Effect of a buffered crystalloid solution vs saline on acute kidney injury among patients in the intensive care unit: the SPLIT randomized clinical trial. *JAMA*. 2015;314(16):1701–10.
- Yunos NM, Bellomo R, Hegarty C, Story D, Ho L, Bailey M. Association between a chloride-liberal vs chloride-restrictive intravenous fluid administration strategy and kidney injury in critically ill adults. *J Am Med Assoc*. 2012;308(15):1566–72.



Identifying and Applying Best PEEP in Ventilated Critically Ill Patients

Takeshi Yoshida, Lu Chen, Remi Coudroy,
and Laurent J. Brochard

Introduction

Positive end-expiratory pressure (PEEP) is an essential, life-saving component of the management of acute respiratory distress syndrome (ARDS). In their first description of ARDS, Ashbaugh and colleagues in 1967 reported the benefits of positive end-expiratory pressure (PEEP) on oxygenation in patients with refractory hypoxemia (Ashbaugh et al. 1967). PEEP can improve oxygenation through alveolar recruitment (Falke et al. 1972) and can reduce atelectrauma (Webb and Tierney 1974), but it can

also generate adverse events such as barotrauma (subcutaneous emphysema or pneumothorax) (Kumar et al. 1970), increase dead space (Suter et al. 1975), or increase right heart load and cause acute cor pulmonale (Mekontso Dessap et al. 2016). According to the current American and European guidelines, PEEP should be set at high rather than low values in patients with moderate to severe ARDS (Fan et al. 2017). PEEP is undoubtedly life-saving in ARDS as demonstrated in experimental studies, and all recommendations indicate that PEEP should be used in (all) patients with ARDS. Remarkably, PEEP also has been consistently shown to protect against ventilator-induced lung injury (Dreyfuss et al. 1988; Tremblay et al. 1997). However, after many years of experimental and clinical research, the best method to set PEEP is still debated, however, and different strategies have been tested to set PEEP based on a balance between alveolar recruitment and overdistension.

The lungs in patients with acute respiratory distress syndrome (ARDS) can be considered as having three compartments from non-dependent to dependent lung regions in a gravitational direction: aerated lung available for ventilation, also classically referred to as the baby lung; recruitable lung regions that are collapsed during expiration, but potentially can be reopened during expiration with PEEP; and non-recruitable lung regions that do not even with high PEEP (Fig. 43.1). In the next section, we will discuss

T. Yoshida
Osaka University Graduate School of Medicine,
Department of Anesthesiology and Intensive Care
Medicine, Yamadaoka, Suita, Osaka, Japan

Interdepartmental Division of Critical Care Medicine,
University of Toronto, St. Michael's Hospital,
Toronto, ON, Canada

Keenan Research Centre for Biomedical Science,
Li Ka Shing Knowledge Institute, St. Michael's
Hospital, Unity Health Toronto, Toronto, ON, Canada
e-mail: takeshiyoshida@hp-icu.med.osaka-u.ac.jp

L. Chen · R. Coudroy · L. J. Brochard (✉)
Interdepartmental Division of Critical Care Medicine,
University of Toronto, St. Michael's Hospital,
Toronto, ON, Canada

Keenan Research Centre for Biomedical Science,
Li Ka Shing Knowledge Institute, St. Michael's
Hospital, Unity Health Toronto, Toronto, ON, Canada
e-mail: lu.chen@unityhealth.to;
Laurent.brochard@unityhealth.to

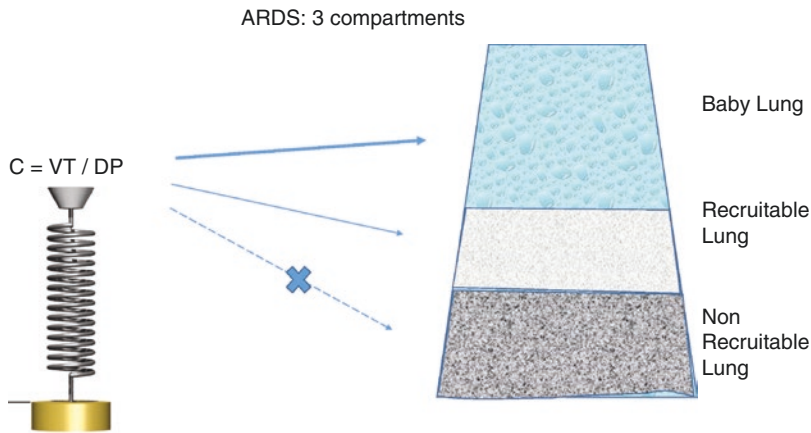


Fig. 43.1 Three compartments of lung regions in ARDS. Typically, ARDS has three compartments from non-dependent to dependent lung regions in a gravitational direction: the aerated lung is available for ventilation, i.e., the baby lung, the recruitable lung regions are usually collapsed/partially aerated during expiration, but can be potentially be reopened during expiration with

PEEP, and non-recruitable lung regions where the lung is hardly recruited with any PEEP. Compliance of the two lungs is like springs attached in series, and the relative “stiffness” of each part will explain the distribution of ventilation when PEEP is increased. *Abbreviations:* ARDS acute respiratory distress syndrome, PEEP positive end-expiratory pressure

how best to describe the relative magnitude of these three compartments.

Classical Methods to Set PEEP: Compliance and PEEP-FiO₂ Tables

The Best Respiratory System Compliance

One of the first methods proposed to set PEEP was based on the compliance of the respiratory system (Suter et al. 1975). The static compliance of the respiratory system (Crs) can be calculated at the bedside as follows:

$$\frac{\text{Tidal volume}}{\text{Plateau pressure} - \text{total PEEP}}$$

It can also be

measured using a low-flow inflation pressure–volume (PV) curve which shows the evolution of the quasistatic elastic pressure of the respiratory system (corresponding to the alveolar pressure when airways are open) over volume. Importantly, Crs is not linear throughout all lung volumes but rather has a sigmoid shape. Indeed, at low pressure and low volume, Crs is low and the slope is flat until pressure reaches a so-called “lower

inflection point”. Crs then increases abruptly with a steep slope until pressure reaches an “upper inflection point” at which Crs again decreases. The “lower inflection point” was initially thought to indicate the opening pressure of compressed alveoli. Therefore, setting PEEP above this point, i.e., in the steeper part of the slope where the compliance is higher, was proposed to avoid repeated opening and closure of alveoli and to decrease ventilator-induced lung injury. We will see later in this chapter that this interpretation is now debated (see airway closure).

In 1975, Suter and colleagues found that the PEEP associated with the best oxygen transport (necessitating measurement of cardiac output) coincided with the best Crs (Suter et al. 1975). PEEP set according to the best Crs was associated with better oxygenation and better Crs as compared to conventional ventilation settings in the 1990s (Amato et al. 1995). Different studies used a somewhat similar approach to set PEEP, and clinical trials found lower risk for barotrauma, shorter duration of mechanical ventilation, and better survival (Villar et al. 2006; Amato et al. 1998). However, the precise way PEEP was set was not always the same, and more impor-

tantly, these studies tested multiple interventions, making difficult to know what was the specific effect of PEEP. Since then, a number of important physiological points have been raised cautioning the use of Crs to titrate PEEP. This includes intratidal recruitment influencing the value of Crs (Jonson et al. 1999) and the recent description of airway closure as described later in this chapter (Chen et al. 2018). In addition, a recent large randomized trial reported higher mortality when a high PEEP was set according to the best Crs compared to a lower PEEP strategy (Writing Group for the Alveolar Recruitment for Acute Respiratory Distress Syndrome Trial I et al. 2017).

It is important to move away from a simplistic view of Crs. First, the belief that recruitment did not occur above the “lower inflection point” of the *PV* curve (Maggiore et al. 2001) is not true, as alveolar recruitment occurs above this threshold along the whole *PV* curve. Second, Crs varies with PEEP but also varies with tidal volume (Suter et al. 1978). In some positive trials, tidal volume was lower in the best Crs arm than in the conventional ventilation arm (Amato et al. 1995, 1998; Villar et al. 2006). As low tidal volume ventilation is associated with better outcomes than large tidal volume ventilation (ARDSnet 2000), it is not clear whether benefits reported depended on the PEEP level or the low tidal volume ventilation. Third, the best Crs may be associated with tidal hyperinflation and may lead to alveolar overdistension, consequently increasing lung injury (McKown et al. 2018). Fourth, intratidal recruitment “improves” compliance by adding “infinite” compliance values of newly recruited values during the insufflation. If tidal recruitment must be avoided, then the best Crs may be very misleading. For example, ventilating a patient at zero end-expiratory pressure may achieve the highest tidal compliance due to a large amount of ongoing tidal recruitment during the insufflation (Jonson et al. 1999; Hickling 1998, 2001). Last, Crs may be influenced by the chest wall. In the current era of low tidal volume ventilation, setting PEEP according to the best Crs does not seem to be an ideal strategy. However, some of the problems discussed can be

mitigated by ensuring that the improvement in compliance is not due to overdistention and by ensuring that it is not due to opening airways. Combination with EIT, which is discussed below, could serve this purpose.

PEEP-FiO₂ Tables and EXPRESS Approach

The PEEP-FiO₂ table was initially designed as a compromise between the harmful effects of high FiO₂ (Nash et al. 1967) and high PEEP. It allows keeping PEEP in a low range as long as FiO₂ is below 60%, and increasing PEEP when FiO₂ requirements are higher. PEEP and FiO₂ are both adjusted to maintain adequate oxygenation (ARDSnet 2000). PEEP-FiO₂ tables were proposed as a way to standardize PEEP settings in clinical trials (Brower et al. 2004). A high PEEP-FiO₂ table was created to try to limit atelectrauma (Brower et al. 2004; Meade et al. 2008). Interestingly, PEEP levels from the high PEEP-FiO₂ table have been found to increase according to ARDS severity (Chiumello et al. 2014) and recently were found to be very similar to values that were required to reach a positive esophageal pressure at end-expiration (Beitler et al. 2019). Although high PEEP-FiO₂ tables were associated with better oxygenation than the low PEEP-FiO₂ table, duration of ventilation and mortality rates were not found to be improved in trials using this approach to set PEEP (Brower et al. 2004; Meade et al. 2008). A rationale for this table can be found in the fact that there is some relationship between oxygenation and recruitment (Maggiore et al. 2001; Ranieri et al. 1991). An important limitation of the PEEP-FiO₂ table approach is that it does not take into account the interaction of the response to PEEP and oxygenation: i.e., an unresponsive patient (potentially non recruitable) will receive higher PEEP. Response to PEEP in terms of oxygenation seems, however, to predict a favorable response to high PEEP in terms of outcome (Goligher et al. 2014). An improvement of PaO₂/FiO₂ > 25 mmHg after an increase in PEEP among patients with baseline PaO₂/FiO₂ ≤ 150 mmHg was associated with better

survival in a post-hoc analysis of two PEEP trials, and this could potentially guide high or low PEEP setting (Goligher et al. 2014).

Oxygenation is influenced by lung recruitability but also can be greatly modified by changes in cardiac output induced by PEEP and/or by a *patent foramen ovale* with intracardiac shunting, which is present in 20% of the patients (Suter et al. 1975; Dantzker et al. 1980; Mekontso Dessap et al. 2010). Also important is that the link between oxygenation and VILI/mortality is not unidirectional. In large randomized controlled trials, groups using more aggressive ventilation strategies can have better oxygenation with worse outcome (Writing Group for the Alveolar Recruitment for Acute Respiratory Distress Syndrome Trial I et al. 2017; ARDSnet 2000).

Another approach has been proposed in the EXPRESS study, setting PEEP independently of oxygenation (Mercat et al. 2008). In order to “safely” maximize recruitment, PEEP was adjusted based on airway pressure and was kept as high as possible without increasing the maximal inspiratory plateau pressure above 28–30 cmH₂O, a value shown to limit the risk of distension-related lung injury. PEEP was therefore individually titrated based on plateau pressure, regardless of its effect on oxygenation, which makes this method very simple to use at the bedside. The EXPRESS approach was shown to be associated with improved ventilator and organ-failure free days but did not alter mortality.

Finally, none of the RCTs that have compared high PEEP versus low PEEP with all these different methods have been able to demonstrate a mortality benefit (Brower et al. 2004; Meade et al. 2008; Mercat et al. 2008). This absence of a difference in survival across the RCTs testing two PEEP strategies may be explained by inclusion of patients who have varying degree of hypoxemia in the above-mentioned trials but having different needs for PEEP (Brower et al. 2004; Meade et al. 2008). In an individual-patient data meta-analysis including the first three trials comparing high to low PEEP (Brower et al. 2004; Meade et al. 2008; Mercat et al. 2008), outcomes differed according to baseline hypoxemia (Briel

et al. 2010). Only patients with a PaO₂/FiO₂ ≤ 200 mmHg had shorter duration of mechanical ventilation and lower mortality (in the range of 5% absolute difference) with higher than lower PEEP, whereas those with a PaO₂/FiO₂ > 200 mmHg had longer duration of mechanical ventilation with higher PEEP (Briel et al. 2010). Importantly, none of the above-mentioned trials considered lung recruitability. Indeed, whereas high PEEP can increase oxygenation and Crs in recruitable patients, oxygenation remained unchanged and Crs decreased in non-recruiters (Grasso et al. 2005). Unfortunately, the bedside reference method to assess recruitability remains to be determined, as discussed below. A more recent large multicenter trial found a worse outcome with use of high PEEP (Writing Group for the Alveolar Recruitment for Acute Respiratory Distress Syndrome Trial I et al. 2017). Four important points are worth noticed about this trial: (1) the low PEEP arm used values close to the high PEEP arm in other trials; the high PEEP arm was thus substantially higher than in other trials; (2) the use of aggressive recruitment maneuvers in the high PEEP arm was significantly associated with side effects, which may have contributed to a worse outcome; (3) the PEEP titration of the high arm was based on the best Crs (or lowest driving pressure), which, as we mentioned, may be misleading; (4) there was no control of patient-ventilator asynchrony, which may have introduced noise in the results, especially at high PEEP.

Airway Closure: A Major Confounding Factor

As mentioned above, it may be important to understand the phenomenon of airway closure in ARDS because (1) it has been the source of errors in calculations of respiratory mechanics (Crs, driving pressure, etc.), and (2) it should be part of the measurements required to set PEEP. In a seminal study by Muscedere et al. in the 1990s, significant injury of small airways and alveoli was found when PEEP was set at lower than the so-called “lower inflection point” (Muscedere

et al. 1994). These injuries, in excised rat lungs without the effect of perfusion, were interpreted as a consequence of repeated opening and closure of airways and alveoli during tidal breaths at low PEEP (≤ 4 cmH₂O). This study also showed that applying a PEEP above the “lower inflection point” greatly reduced lung injuries. The presence of small airway injury and alveolar injury was confirmed by autopsy in ARDS patients who were ventilated at clinical PEEP level (~ 11 cmH₂O) (Rouby et al. 1993; Morales et al. 2011). Setting a PEEP slightly above the “lower inflection point” to reopen small airways and alveoli was then proposed as the “open lung” strategy by Amato et al. in the mid of 1990s (Amato et al. 1995, 1998). The challenges were recognized soon. Firstly, the so-called “lower inflection point” could not be identified in many ARDS patients (Vieira et al. 1999), and a subjective definition frequently was used (Harris et al. 2000; Gattinoni et al. 1987). Secondly, as mentioned earlier, alveolar recruitment “continues” above the “lower inflection point” (Jonson et al. 1999). These findings, along with concerns about risk of overdistension, probably encumbered the application of the “open lung” strategy.

Recently, to our surprise, we found that approximately one-third of ARDS patients present a complete airway closure requiring an airway opening pressure (AOP) greater than 5 cmH₂O, which was previously misinterpreted as “lower inflection point”. An example is given on Fig. 43.2. The average AOP was around 13 cmH₂O (Chen et al. 2018). We showed that the pressure volume behavior was explained by a complete occlusion of the airways, based on three findings: (1) the initial part of the low-flow (5 L/min) pressure-volume (*P-V*) curve (i.e., before reaching the AOP) in these patients was entirely superimposed with a *P-V* curve of a blocked ventilator circuit; (2) the absence of fluctuation at the initial part of *P-V* curve indicates a lack of communication with alveoli (Fig. 43.2); (3) the esophageal pressure (a surrogate of pleural pressure) at the initial part of *P-V* curve did not rise when airway pressure increased dramatically (Chen et al. 2018). In

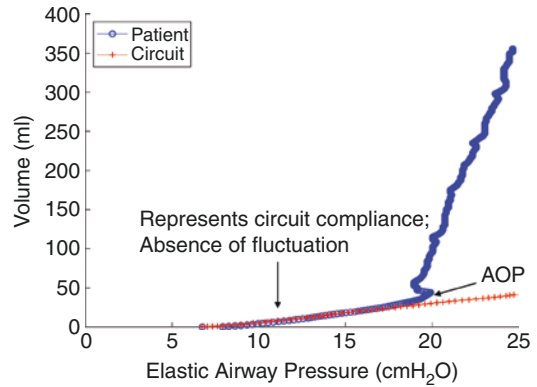


Fig. 43.2 Airway closure and lower inflection point in *P-V* curve. Complete airway closure and AOP at the airway *P-V* curve. A low-flow (5 L/min) inflation was performed to minimize the resistive pressure. In this case, the airway pressure represents the elastic pressure. The blue line is the *P-V* curve obtained in a patient, whereas the red line is the *P-V* curve obtained in a blocked circuit. The initial part of patient’s *P-V* curve completely superimposed with the circuit *P-V* curve and does not have any fluctuation. This suggests a complete occlusion of airways. When airway pressure exceeded about 20 cmH₂O, the lungs started to inflate with the presence of fluctuations. AOP is identified as the elastic airway pressure at which gas volume delivered to a patient became 4 mL greater than the volume compressed in an occluded circuit, and 1 cmH₂O greater than PEEP. *Abbreviations:* AOP airway opening pressure, *P-V* curve pressure-volume curve, PEEP positive end-expiratory pressure

addition, chest X-ray or computer tomography (CT) had shown that these patients still have “baby lung” which remained aerated below this pressure level. A question unresolved is the site of this complete airway closure. In healthy subjects, airway closure occurs in small airways in which cartilage is absent (during a forced expiration to reach residual volume, small airways diffusely close preventing a complete empty of lungs). In patients with ARDS, functional residual capacity can be remarkably reduced. Two potential mechanisms can facilitate diffuse airway closure in small airways. First, both alveoli and airways can be flooded by liquid with less functional surfactant. The surface tension increases, promoting the formation of liquid plugs in small airways (based on the Laplace Law). Indeed, a recent analysis showed that airway closure was associated with surfactant depletion (Coudroy et al. 2018). Second, pleural

pressure can be increased due to increased intra-abdominal pressure for instance, leading to lung compression. Therefore, it is likely, but not yet conclusively proven, that the complete airway closure occurs in small airways. Setting PEEP above the AOP can eliminate this phenomenon. Several studies confirmed the high prevalence of complete airway closure (Coudroy et al. 2018; Yonis et al. 2018), which might explain the observations of the diffuse bronchiolar injury found in ARDS as aforementioned. The detection of airway closure is thus potentially important for reducing the repeated airway closure and reopening for each individual patient. Moreover, identifying airway closure is also important for respiratory mechanics measurements. For example, estimating alveolar pressure from airway pressure would be misleading when airway closure blocks the communication between alveoli and airway opening. Measurement of AOP at the bedside only requires performing a low-flow inflation maneuver (i.e., use volume control mode with constant flow at 5 L/min) at 0–5 cmH₂O of PEEP. One can then identify AOP from either the *P-V* curve (Fig. 43.1) or from pressure-time curve displayed on the ventilator by comparing with circuit compliance (see our video demonstration at <https://rec.coemv.ca>).

Esophageal Manometry

Estimating Transpulmonary Pressure with Esophageal Pressure

Esophageal pressure manometry has been shown to be useful for more than 50 years of research. A clinical application of esophageal pressure manometry is estimation of pleural pressure (P_{pl}) and using it to calculate transpulmonary pressure (P_L), which is the distending pressure of the lungs. Esophageal pressure manometry is thus the reference technique to estimate the distending pressure of the lung at the bedside.

During positive-pressure mechanical ventilation (i.e., no active spontaneous effort), pressure applied to the respiratory system by a ventilator

both inflates the lung and moves the chest wall. The lung distending pressure, i.e., transpulmonary pressure or P_L , is calculated as follows:

$$P_L = P_{aw} - P_{pl}$$

Two different methods have been proposed to estimate P_{pl} and thus P_L : by it with use of directly measured esophageal pressure (P_{es}) (Talmor et al. 2008) or by using the product of the airway plateau pressure and the elastance ratio of chest wall to respiratory system (Chiumello et al. 2014; Staffieri et al. 2012). The latter technique does not directly use the absolute value of P_{es} but only the relative changes (elastance and ratio of elastances). Both techniques are thus derived from esophageal pressure manometry, but it was recently shown that they do not measure the same thing.

Guiding PEEP with Esophageal Pressure

1. Absolute esophageal pressure

The lung collapse predominantly occurs in dependent lung along a gravitational direction (when supine), and the dependent collapsed lung contributes to intrapulmonary shunting and poor oxygenation. PEEP theoretically maintains positive transpulmonary lung distending pressure, i.e., PEEP minus P_{pl} , which should minimize collapse in dependent regions.

The first method is based on the measured “absolute” value of P_{es} (Talmor et al. 2008). This method has an assumption that absolute P_{es} *per se* is used as a surrogate of P_{pl} and that P_L then is directly calculated as follows:

$$P_L = P_{aw} - P_{es}$$

Using this measurement, PEEP can be simply titrated to make P_L positive. Indeed, patients with ARDS exhibit high values of P_{es} at end expiration, and values higher than PEEP are likely to be associated with persisting lung collapse. However, in a heterogeneous, injured lung, a large vertical gradient of P_{pl} (i.e., higher P_{pl} in more dependent lung) exists (Pelosi et al. 2001;

Yoshida et al. 2018). It was recently shown that if properly calibrated (i.e., minimal non-stressed volume), the absolute P_{es} accurately reflects local P_{pl} in the middle to dependent lung regions, adjacent to the esophageal balloon, independently of the mediastinal structures (Yoshida et al. 2018). Since collapse usually predominates in the mid to dependent lung regions in ARDS, setting PEEP using expiratory absolute P_{es} to prevent dependent lung collapse is theoretically reasonable. A clinical trial (small, single-center) showed that setting PEEP to maintain a positive value of P_L with esophageal pressure manometry had physiological benefits in patients with ARDS (Talmor et al. 2008), but a larger multicenter phase 2 study showed no superiority of setting PEEP with esophageal pressure manometry over empirical PEEP setting according to high PEEP/FiO₂ table. Again, the lack of assessment of recruitability may be an important limitation of this appealing technique used alone.

2. Elastance Ratio of Chest Wall to Respiratory System

A second use of the esophageal pressure is based on the calculation of the elastance ratio of chest wall to respiratory system (Staffieri et al. 2012). This method has two assumptions: (1) the ratio of lung elastance to respiratory system elastance (E_L/E_{RS}) determines the fraction of airway driving pressure consumed to inflate lung and (2) P_{pl} is zero at functional residual capacity. At functional residual capacity, lung is neither expanding nor collapsing, and thus P_L must be zero: since P_{aw} is zero, P_{pl} must be zero for P_L being zero. Thus, P_L is calculated as follows:

$P_L = P_{aw} \times [E_L/E_{RS}]$, and this method can be used to calculate the “lung plateau” pressure.

A recent study revealed that P_L calculated from elastance ratio can serve as a good surrogate for inspiratory P_L in the non-dependent lung regions where the lung is most vulnerable to ventilator-induced lung injury (Yoshida et al. 2018). This happens because the assumptions are true only in these regions, considering P_{pl} in non-dependent lung (but not in other lung regions) was the closest to zero at low PEEP levels (close

to functional residual capacity). Thus, PEEP can be elevated until inspiratory P_L calculated from elastance ratio (i.e., inspiratory P_L in non-dependent lung) reaches a physiological limit around 25 cmH₂O. In a cohort study, setting PEEP with P_L calculated from elastance ratio resulted in better oxygenation and avoided escalation of care from conventional mechanical ventilation to ECMO (Grasso et al. 2012).

Electrical Impedance Tomography

Guiding PEEP with EIT

Electrical impedance tomography (EIT) is a non-invasive, radiation-free monitoring tool that enables real-time, cross-sectional imaging of tidal ventilation at the bedside. Reconstructed EIT images represent relative impedance changes for each pixel (delta Z), compared to a convenient reference value taken at the beginning of data acquisition. The majority of impedance changes in a thorax is caused by an increase/decrease in intrapulmonary gas volume so that EIT is a proper tool to evaluate the distribution of ventilation.

Decremental PEEP Steps

Delta Z in a region of interest represents regional tidal volume during tidal breaths, and therefore, regional (pixel) compliance can be measured in EIT as delta Z /driving pressure, assuming that driving pressure is equally distributed in the lung. By using regional compliance calculated with EIT, the amount of collapsed lung (and overdistension) can be assessed at the bedside.

During decremental PEEP step following lung recruitment (e.g., PEEP 24 cmH₂O to 4 cmH₂O), lung collapse can be estimated by comparing regional (pixel) compliance at different PEEP levels to the lung after recruitment (Costa et al. 2009). At each pixel, the best (pixel) compliance is achieved at the PEEP level where neither collapse nor overdistension is present. A decrease in compliance at higher PEEP levels (before reach-

ing best compliance) is assumed to be caused by overdistension, and a decrease in compliance at lower PEEP levels (after passing best compliance) is assumed to be caused by collapse. Cumulative lung collapse at each PEEP level is reported as the averaged sum of collapse of each pixel. This method can be helpful to set PEEP to minimize the amount of lung collapse and overdistension by choosing the value where lung collapse and overdistension curves cross-over.

Center of Ventilation

Lung collapse in ARDS predominantly occurs in dependent lung regions and therefore the size of aerated lung available for ventilation, i.e., baby lung is usually limited to non-dependent lung regions. EIT can provide a functional information of lung aeration and ventilation. Clinicians can easily visualize this inhomogeneous distribution of lung aeration at the bedside. PEEP, by recruiting the lung, shifts ventilation to non-dependent lung regions in EIT.

The center of ventilation can be used as an index to visualize the shifts in regional tidal ventilation in the ventro-dorsal direction (Yoshida et al. 2019). Here, the center of ventilation is defined as

$$\text{COV}(\%) = \frac{(\Delta Z \text{ in the dorsal half of lung})100}{(\Delta Z \text{ in the whole lung})}$$

Where ΔZ represents change in impedance (Yoshida et al. 2019).

The center of ventilation has been defined differently by different groups. Perhaps the best term could be the dorsal fraction of ventilation (using the calculation as mentioned above) (Yoshida et al. 2019; Frerichs et al. 2006; Blankman et al. 2014).

The range available for ventilation was defined as from 0% (most ventral) to 100% (most dorsal), such that homogeneous ventilation is represented as the bulk of the imaged ventilation at the axis mid-point (i.e., a 50% center of ventilation or 50% of dorsal fraction) (Fig. 43.3) (Yoshida et al. 2019). A simple visual

tool based on the ventral-to-dorsal distribution of ventilation can alert the clinician about potentially excessive as well as insufficient PEEP (Yoshida et al. 2019). At low PEEP, the center of ventilation/dorsal fraction reflects ventilation to non-dependent lung regions because of the lung collapse predominating in the dependent lung regions. PEEP will re-equilibrate the distribution of ventilation. When PEEP is excessive, overinflation occurs in non-dependent lung regions, and ventilation is shifted predominantly to dependent lung regions because the non-dependent regions become hyperinflated, and the value of this dorsal fraction of ventilation increases (Yoshida et al. 2019). A recent study showed that when the center of ventilation/dorsal fraction indicates a shift to predominantly dorsal ventilation, in the context of ARDS with relatively high PEEP, this strongly suggests that the PEEP level is excessive and should be reduced (Yoshida et al. 2019). It constitutes an easy incentive to decrease PEEP.

Direct Assessment of Lung Recruitability

Rationale

Instead of focusing on gas exchange, the modern rationale for using PEEP is or should be to keep the lung as recruited as possible in order to minimize repeated alveolar (and airways) repeated opening and collapse to prevent VILI. This rationale can be achieved only if the lungs are recruitable within a reasonable range of pressure. This is essential because the less that lung is recruitable, the higher the risk of lung injury when increasing PEEP.

CT Scan

By using CT scan images, researchers have visualized the lung recruitment and recognized the importance of lung recruitability—reaeration in the non-aerated/poorly aerated lung tissue (Vieira et al. 1999; Gattinoni et al. 1986, 2006;

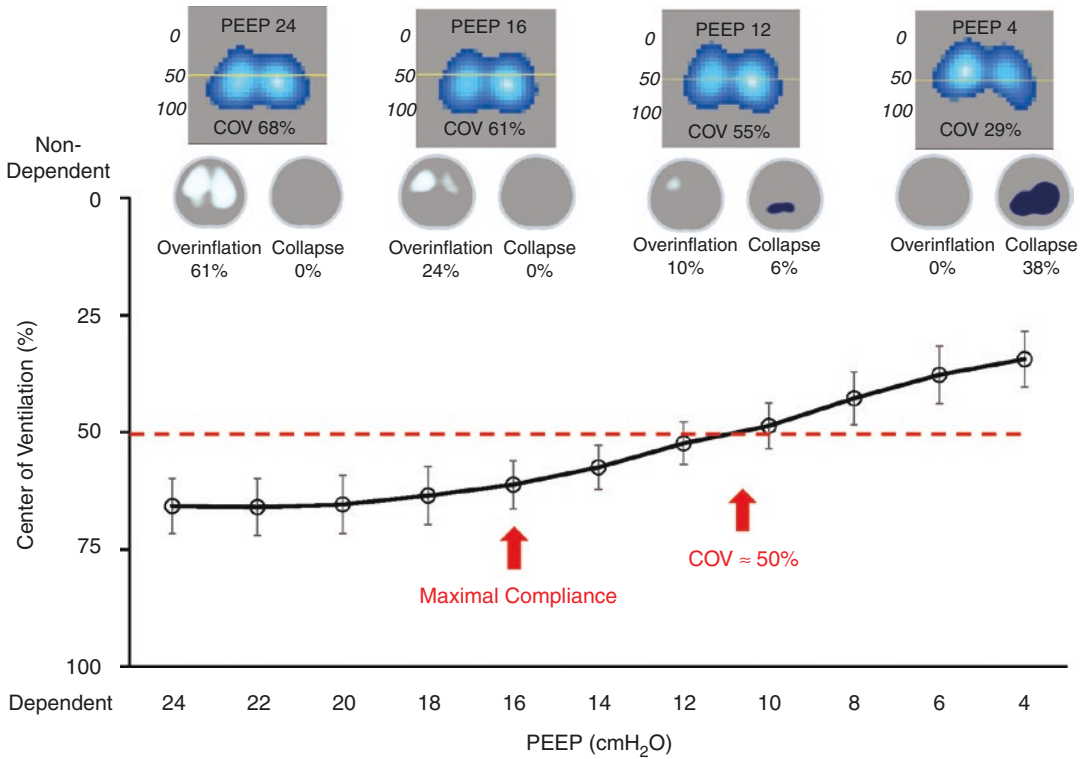


Fig. 43.3 The distribution of lung aeration and center of ventilation in ARDS. Representative EIT images describing COV and distribution of overinflation and collapse were presented. COV was shifted to dependent lung at higher PEEP levels due to overinflation in non-dependent lung. Decreasing PEEP to 12 cmH₂O was associated with homogeneous distributions (centered at approximately midpoint between dependent and non-dependent limits), corresponding to decreasing lung hyperinflation. Further decreases in PEEP (below PEEP 12 cmH₂O) resulted in a progressive shift of ventilation into more non-dependent lung because lung collapse was progressively increased. Red dot line indicates 50% of COV. Note that at PEEP of 16 cmH₂O where respiratory system compliance reached its maximum, COV was still shifted to dependent lung due

to overinflation in non-dependent lung. *Abbreviations:* COV center of ventilation, EIT electrical impedance tomography, PEEP positive end-expiratory pressure. (Adapted with permission of the American Thoracic Society. Copyright © 2020 American Thoracic Society. All rights reserved. From Yoshida et al. (2019). The American Journal of Respiratory and Critical Care Medicine is an official journal of the American Thoracic Society. Readers are encouraged to read the entire article for the correct context at [<https://www.atsjournals.org/doi/abs/10.1164/rccm.201904-0797LE?journalCode=ajrccm>]. The authors, editors, and The American Thoracic Society are not responsible for errors or omissions in adaptations)

Malbouisson et al. 2001)—in the setting of PEEP. Applying a high PEEP in poorly recruitable lungs may not effectively reduce the “atelectrauma” in collapsed lung tissues and simply hyperinflate already opened lung tissue; by contrast, a similar level of PEEP can result in large recruitment without significant hyperinflation in highly recruitable lungs. In the first case, PEEP will increase the strain without any benefit, whereas in the second case, PEEP will minimize

repeated opening and closure and prevent VILI (Caironi et al. 2010).

Despite its potential usefulness, lung recruitability has never been assessed in clinical practice. The barrier is the lack of reliable and feasible tool for assessing lung recruitability at the bedside. The CT scan technique is a powerful tool for quantitative analysis on regional aeration in lung tissue, but the analysis is extremely time consuming, needs repeated measurements at two

fixed airway pressures, and increases radioactivity and transport risks for patients (Chen and Brochard 2015). Moreover, it remains controversial on how to define lung recruitment using CT scan (Chen et al. 2016). For example, it has been debated whether one should include or exclude poorly aerated lung tissue (i.e., radiodensity within 100–500 Hounsfield Units) for quantitating lung recruitment and whether one should use “voxel-by-voxel” method or use “anatomically delineated” method (Chen et al. 2016; Chiumello et al. 2015; Amato and Santiago 2016).

Alternatively, oxygenation (such as $\text{PaO}_2/\text{FiO}_2$) and compliance, which are available for every patient, are poor surrogate for the assessment of lung recruitability and as a guide to setting PEEP settings as already discussed. Therefore, it is necessary to have reliable but still feasible tools to measure lung recruitment directly.

Pressure-Volume Curves, Lung Volume, and a Simplified Method

So far, the multiple pressure-volume curves technique remains the most feasible way to quantify recruited volume and differentiate lung recruitability at the bedside (Chen et al. 2017). This method is based on the quantification of the hysteresis-like behavior of the lungs. Briefly, by plotting two pressure-volume curves starting at different PEEP levels together, an upward shift in volume for a given elastic pressure is defined as lung recruitment. This technique was validated against CT scan (Lu et al. 2006). Ideally, this technique can be used with measurements of lung volume (Dellamonica et al. 2011) to test whether the increase in lung volume is predicted by the compliance. Increase in lung volume in itself can suggest if recruitment occurs when the increase in end-expiratory lung volume obtained is very large, suggesting recruitment (Dellamonica et al. 2011).

Because plotting multiple *PV* curves is still complex, we have recently described a simplified tool to assess alveolar recruitment at the bedside and validated it against the multiple pressure-

volume curves: the recruitment to inflation ratio (R/I) (Chen et al. 2017). This simple tool requires only a one-breath maneuver with PEEP reduction and can be done within 10–15 seconds. Firstly, PEEP is reduced by 10 cmH_2O in one breath, and the actual lung volume loss by reducing PEEP is measured as the difference in expiratory tidal volumes between the breath with PEEP reduction and the preceding breath. In parallel, the lung volume loss (assuming a linear recoil process) that would occur in the complete absence of recruitment with PEEP can be easily predicted: it is estimated by the product of respiratory system compliance at lower PEEP and the effective change in PEEP. The effective change in pressure is thus the change in PEEP (10 cmH_2O) in patients without airway closure; and is the difference between higher PEEP and AOP in patients with airway closure (see above). When the actual lung volume loss is greater than the predicted one, the difference is taken as the recruited volume gained by higher PEEP. By knowing the recruited volume, one can then estimate that, for a given change in PEEP, the proportion of gas volume distributed into collapsed lung (recruitment) and “baby lung” (inflation/hyperinflation) (Chen et al. 2019). In this way, one is able to balance the benefit of lung recruitment and the risk of lung hyperinflation at the bedside. A video demonstration and detailed calculations can be found in an academic website (<https://rec.coemv.ca>).

This method is able to separate patients who, on average, will improve oxygenation and reduce dead space with higher PEEP, from patients who will not or much less improve oxygenation or worsen dead space and hemodynamics. No study, however, has so far used this technique to assess the effects on outcome.

Global Integrative Clinical Approach

PEEP is an essential component in the management of ARDS, but when too high, it also can be harmful. Therefore, clinicians need to be aware of the different aspects of the physiology of PEEP on gas exchange, mechanics, lung volume, and

circulation and should use all these parameters to carefully titrate PEEP at the bedside.

A few points must be highlighted. Any increase in PEEP will increase lung volume and increase plateau pressure, whether recruitment occurs or not. However, the lower the recruitment for a given increase in pressure, the higher will be the negative hemodynamic effects of PEEP. This will manifest as a drop in systolic and mean blood pressure, and often as an increase in PaCO₂ by increasing dead space due to a reduction in alveolar perfusion under high alveolar pressure. These effects however will be more or less pronounced depending on the fluid status and the presence of right ventricular dysfunction. Before testing the effects of PEEP, checking that the patient is not fluid responsive is therefore clinically important, as it will facilitate the interpretation of hemodynamic changes with PEEP. This can be easily obtained by transiently increasing tidal volume and following pulse pressure variation for instance (Teboul et al. 2019). Hyperinflation will usually manifest with substantial increases in driving pressure, but a small increase in driving pressure can be also present with recruitment, whether it is due to the chest wall or to minimizing tidal recruitment.

The PEEP level will depend on the severity of ARDS assessed by oxygenation and the amount of alveolar infiltrates. The more diffuse are the infiltrates, the higher is the loss of aeration and the higher is, *a priori*, the benefit of high PEEP.

Last, a factor playing a role in compressing the lung is the load represented by a fatty chest wall and represented by a high Body Mass Index (BMI) in obese patients. Obesity is associated with higher intrathoracic pressure and may require higher PEEP to counteract (Fumagalli et al. 2019; Coudroy et al. 2019).

Recommendations for titrating PEEP include the following: (1) always try to test PEEP at two (or three) different levels without changing another factor influencing oxygenation (FiO₂, ventilation, vasopressor, fluids) and ten minutes at each step is sufficient (Taskar et al. 1995). (2) Check the fluid volume status first, to be able to interpret changes in oxygenation, blood pressure,

and CO₂. (3) When assessing the effects of PEEP, assess the effects on oxygenation, PaCO₂, driving pressure (ideally lung driving pressure), and blood pressure at the same time. (4) Add a specific simplified measurement of recruitability. (5) Adapt the levels of PEEP tested according to the patient's severity of illness, BMI, and pleural (esophageal) pressure.

This general assessment can give a consistent response (recruitment, respiratory mechanics, oxygenation, PaCO₂, blood pressure) either in favor of high PEEP or against high PEEP. In the first case, PEEP should be increased using small tidal volumes, and higher limits should be dictated by plateau pressure of the lung (transpulmonary pressure) or driving pressure (ideally lung driving pressure). Again, morbidly obese patients may require higher PEEP because of the additional load on the chest wall (independently of the degree of lung injury). In a case against PEEP, PEEP should be set as low as possible (<10 cmH₂O) based on acceptable oxygenation. When not all effects are consistent, clinical judgment is needed and the decision on PEEP titration may depend on the context and the tolerance of PEEP. In all cases, proning the patient must also be considered as an alternative method of recruitment (Guerin et al. 2013).

References

- Amato MB, Santiago RR. The recruitability paradox. *Am J Respir Crit Care Med.* 2016;193(11):1192–5.
- Amato MB, Barbas CS, Medeiros DM, Schettino Gde P, Lorenzi Filho G, Kairalla RA, et al. Beneficial effects of the “open lung approach” with low distending pressures in acute respiratory distress syndrome. A prospective randomized study on mechanical ventilation. *Am J Respir Crit Care Med.* 1995;152(6 Pt 1):1835–46.
- Amato MB, Barbas CS, Medeiros DM, Magaldi RB, Schettino GP, Lorenzi-Filho G, et al. Effect of a protective-ventilation strategy on mortality in the acute respiratory distress syndrome. *N Engl J Med.* 1998;338(6):347–54.
- ARDSnet. Ventilation with lower tidal volumes as compared with traditional tidal volumes for acute lung injury and the acute respiratory distress syndrome. The Acute Respiratory Distress Syndrome Network. *New Engl J Med.* 2000;342(18):1301–8.

- Ashbaugh DG, Bigelow DB, Petty TL, Levine BE. Acute respiratory distress in adults. *Lancet* (London, England). 1967;2(7511):319–23.
- Beitler JR, Sarge T, Banner-Goodspeed VM, Gong MN, Cook D, Novack V, et al. Effect of titrating positive end-expiratory pressure (PEEP) with an esophageal pressure-guided strategy vs an empirical high PEEP-Fio2 strategy on death and days free from mechanical ventilation among patients with acute respiratory distress syndrome: a randomized clinical trial. *JAMA*. 2019;321(9):846–57.
- Blankman P, Hasan D, Erik GJ, Gommers D. Detection of 'best' positive end-expiratory pressure derived from electrical impedance tomography parameters during a decremental positive end-expiratory pressure trial. *Crit Care*. 2014;18(3):R95.
- Briel M, Meade M, Mercat A, Brower RG, Talmor D, Walter SD, et al. Higher vs lower positive end-expiratory pressure in patients with acute lung injury and acute respiratory distress syndrome: systematic review and meta-analysis. *JAMA*. 2010;303(9):865–73.
- Brower RG, Lanken PN, MacIntyre N, Matthay MA, Morris A, Ankiewicz M, et al. Higher versus lower positive end-expiratory pressures in patients with the acute respiratory distress syndrome. *N Engl J Med*. 2004;351(4):327–36.
- Caironi P, Cressoni M, Chiumello D, Ranieri M, Quintel M, Russo SG, et al. Lung opening and closing during ventilation of acute respiratory distress syndrome. *Am J Respir Crit Care Med*. 2010;181(6):578–86.
- Chen L, Brochard L. Lung volume assessment in acute respiratory distress syndrome. *Curr Opin Crit Care*. 2015;21(3):259–64.
- Chen L, Sklar M, Dres M, Goligher EC. Different definitions of lung recruitment by computed tomography scan. *Am J Respir Crit Care Med*. 2016;193(11):1314–5.
- Chen L, Chen GQ, Shore K, Shklar O, Martins C, Devenyi B, et al. Implementing a bedside assessment of respiratory mechanics in patients with acute respiratory distress syndrome. *Crit Care*. 2017;21(1):84.
- Chen L, Del Sorbo L, Grieco DL, Shklar O, Junhasavasdikul D, Telias I, et al. Airway closure in acute respiratory distress syndrome: an underestimated and misinterpreted phenomenon. *Am J Respir Crit Care Med*. 2018;197(1):132–6.
- Chen L, Del Sorbo L, Grieco DL, Junhasavasdikul D, Rittayamai N, Soliman I, et al. Recruitment-to-inflation ratio in acute respiratory distress syndrome. *Am J Respir Crit Care Med*. 2019;Revised.
- Chiumello D, Cressoni M, Carlesso E, Caspani ML, Marino A, Gallazzi E, et al. Bedside selection of positive end-expiratory pressure in mild, moderate, and severe acute respiratory distress syndrome. *Crit Care Med*. 2014;42(2):252–64.
- Chiumello D, Marino A, Brioni M, Cigada I, Menga F, Colombo A, et al. Lung recruitment assessed by respiratory mechanics and by CT scan: what is the relationship? *Am J Respir Crit Care Med*. 2015.193(11):1254–63.
- Costa EL, Borges JB, Melo A, Suarez-Sipmann F, Toufen C Jr, Bohm SH, et al. Bedside estimation of recruitable alveolar collapse and hyperdistension by electrical impedance tomography. *Intensive Care Med*. 2009;35(6):1132–7.
- Coudroy R, Lu C, Chen L, Demoule A, Brochard L. Mechanism of airway closure in acute respiratory distress syndrome: a possible role of surfactant depletion. *Intensive Care Med*. 2018.45(2):290–91.
- Coudroy R, Vimperc D, Aissaoui N, Younan R, Bailleul C, Couteau-Chardon A, Lancelot A, Guerot E, Chen L, Brochard L, Diehl JL. Prevalence of Complete Airway Closure According to Body Mass Index in Acute Respiratory Distress Syndrome. *Anesthesiology*. 2019;133(4):867–78.
- Dantzker DR, Lynch JP, Weg JG. Depression of cardiac output is a mechanism of shunt reduction in the therapy of acute respiratory failure. *Chest*. 1980;77(5):636–42.
- Dellamonica J, Lerolle N, Sargentini C, Beduneau G, Di Marco F, Mercat A, et al. PEEP-induced changes in lung volume in acute respiratory distress syndrome. Two methods to estimate alveolar recruitment. *Intensive Care Med*. 2011;37(10):1595–604.
- Dreyfuss D, Soler P, Basset G, Saumon G. High inflation pressure pulmonary edema. Respective effects of high airway pressure, high tidal volume, and positive end-expiratory pressure. *Am Rev Respir Dis*. 1988;137(5):1159–64.
- Falke KJ, Pontoppidan H, Kumar A, Leith DE, Geffin B, Laver MB. Ventilation with end-expiratory pressure in acute lung disease. *J Clin Investig*. 1972;51(9):2315–23.
- Fan E, Del Sorbo L, Goligher EC, Hodgson CL, Munshi L, Walkey AJ, et al. An Official American Thoracic Society/European Society of Intensive Care Medicine/Society of Critical Care Medicine clinical practice guideline: mechanical ventilation in adult patients with acute respiratory distress syndrome. *Am J Respir Crit Care Med*. 2017;195(9):1253–63.
- Frerichs I, Dargaville PA, van Genderingen H, Morel DR, Rimensberger PC. Lung volume recruitment after surfactant administration modifies spatial distribution of ventilation. *Am J Respir Crit Care Med*. 2006;174(7):772–9.
- Fumagalli J, Santiago RRS, Teggia Droghi M, Zhang C, Fintelmann FJ, Trotschel FM, et al. Lung recruitment in obese patients with acute respiratory distress syndrome. *Anesthesiology*. 2019;130(5):791–803.
- Gattinoni L, Mascheroni D, Torresin A, Marcolin R, Fumagalli R, Vesconi S, et al. Morphological response to positive end expiratory pressure in acute respiratory failure. Computerized tomography study. *Intensive Care Med*. 1986;12(3):137–42.
- Gattinoni L, Pesenti A, Avalli L, Rossi F, Bombino M. Pressure-volume curve of total respiratory system in acute respiratory failure. Computed tomographic scan study. *Am Rev Respir Dis*. 1987;136(3):730–6.
- Gattinoni L, Caironi P, Cressoni M, Chiumello D, Ranieri VM, Quintel M, et al. Lung recruitment in patients

- with the acute respiratory distress syndrome. *N Engl J Med.* 2006;354(17):1775–86.
- Goligher EC, Kavanagh BP, Rubenfeld GD, Adhikari NKJ, Pinto R, Fan E, et al. Oxygenation response to positive end-expiratory pressure predicts mortality in acute respiratory distress syndrome. A secondary analysis of the LOVS and ExPress trials. *Am J Respir Crit Care Med.* 2014;190(1):70–6.
- Grasso S, Fanelli V, Cafarelli A, Anaclerio R, Amabile M, Ancona G, et al. Effects of high versus low positive end-expiratory pressures in acute respiratory distress syndrome. *Am J Respir Crit Care Med.* 2005;171(9):1002–8.
- Grasso S, Terragni P, Birocco A, Urbino R, Del Sorbo L, Filippini C, et al. ECMO criteria for influenza A (H1N1)-associated ARDS: role of transpulmonary pressure. *Intensive Care Med.* 2012;38(3):395–403.
- Guerin C, Reignier J, Richard JC, Beuret P, Gacouin A, Boulain T, et al. Prone positioning in severe acute respiratory distress syndrome. *N Engl J Med.* 2013;368(23):2159–68.
- Harris RS, Hess DR, Venegas JG. An objective analysis of the pressure-volume curve in the acute respiratory distress syndrome. *Am J Respir Crit Care Med.* 2000;161(2 Pt 1):432–9.
- Hickling KG. The pressure-volume curve is greatly modified by recruitment. A mathematical model of ARDS lungs. *Am J Respir Crit Care Med.* 1998;158(1):194–202.
- Hickling KG. Best compliance during a decremental, but not incremental, positive end-expiratory pressure trial is related to open-lung positive end-expiratory pressure: a mathematical model of acute respiratory distress syndrome lungs. *Am J Respir Crit Care Med.* 2001;163(1):69–78.
- Jonson B, Richard JC, Straus C, Mancebo J, Lemaire F, Brochard L. Pressure-volume curves and compliance in acute lung injury: evidence of recruitment above the lower inflection point. *Am J Respir Crit Care Med.* 1999;159(4 Pt 1):1172–8.
- Kumar A, Falke KJ, Geffin B, Aldredge CF, Laver MB, Lowenstein E, et al. Continuous positive-pressure ventilation in acute respiratory failure: effects on hemodynamics and lung function. *N Engl J Med.* 1970;283(26):1430–6.
- Lu Q, Constantin JM, Nieszkowska A, Elman M, Vieira S, Rouby JJ. Measurement of alveolar derecruitment in patients with acute lung injury: computerized tomography versus pressure-volume curve. *Crit Care.* 2006;10(3):R95.
- Maggiore SM, Jonson B, Richard JC, Jaber S, Lemaire F, Brochard L. Alveolar derecruitment at decremental positive end-expiratory pressure levels in acute lung injury: comparison with the lower inflection point, oxygenation, and compliance. *Am J Respir Crit Care Med.* 2001;164(5):795–801.
- Malbouisson LM, Muller JC, Constantin JM, Lu Q, Puybasset L, Rouby JJ, et al. Computed tomography assessment of positive end-expiratory pressure-induced alveolar recruitment in patients with acute respiratory distress syndrome. *Am J Respir Crit Care Med.* 2001;163(6):1444–50.
- McKown AC, Semler MW, Rice TW. Best PEEP trials are dependent on tidal volume. *Crit Care.* 2018;22(1):115.
- Meade MO, Cook DJ, Guyatt GH, Slutsky AS, Arabi YM, Cooper DJ, et al. Ventilation strategy using low tidal volumes, recruitment maneuvers, and high positive end-expiratory pressure for acute lung injury and acute respiratory distress syndrome: a randomized controlled trial. *JAMA.* 2008;299(6):637–45.
- Mekontso Dessap A, Boissier F, Leon R, Carreira S, Campo FR, Lemaire F, et al. Prevalence and prognosis of shunting across patent foramen ovale during acute respiratory distress syndrome. *Crit Care Med.* 2010;38(9):1786–92.
- Mekontso Dessap A, Boissier F, Charron C, Bégot E, Repessé X, Legras A, et al. Acute cor pulmonale during protective ventilation for acute respiratory distress syndrome: prevalence, predictors, and clinical impact. *Intensive Care Med.* 2016;42(5):862–70.
- Mercat A, Richard J-CM, Vielle B, Jaber S, Osman D, Diehl J-L, et al. Positive end-expiratory pressure setting in adults with acute lung injury and acute respiratory distress syndrome: a randomized controlled trial. *JAMA.* 2008;299(6):646–55.
- Morales MM, Pires-Neto RC, Inforsato N, Lancas T, da Silva LF, Saldiva PH, et al. Small airway remodeling in acute respiratory distress syndrome: a study in autopsy lung tissue. *Crit Care.* 2011;15(1):R4.
- Muscledere JG, Mullen JB, Gan K, Slutsky AS. Tidal ventilation at low airway pressures can augment lung injury. *Am J Respir Crit Care Med.* 1994;149(5):1327–34.
- Nash G, Blennerhassett JB, Pontoppidan H. Pulmonary lesions associated with oxygen therapy and artificial ventilation. *N Engl J Med.* 1967;276(7):368–74.
- Pelosi P, Goldner M, McKibben A, Adams A, Eccher G, Caironi P, et al. Recruitment and derecruitment during acute respiratory failure: an experimental study. *Am J Respir Crit Care Med.* 2001;164(1):122–30.
- Ranieri VM, Eissa NT, Corbeil C, Chasse M, Braidy J, Matar N, et al. Effects of positive end-expiratory pressure on alveolar recruitment and gas exchange in patients with the adult respiratory distress syndrome. *Am Rev Respir Dis.* 1991;144(3 Pt 1):544–51.
- Rouby JJ, Lherm T, Martin de Lassale E, Poete P, Bodin L, Finet JF, et al. Histologic aspects of pulmonary barotrauma in critically ill patients with acute respiratory failure. *Intensive Care Med.* 1993;19(7):383–9.
- Staffieri F, Stripoli T, De Monte V, Crovace A, Sacchi M, De Michele M, et al. Physiological effects of an open lung ventilatory strategy titrated on elastance-derived end-inspiratory transpulmonary pressure: study in a pig model*. *Crit Care Med.* 2012;40(7):2124–31.
- Suter PM, Fairley B, Isenberg MD. Optimum end-expiratory airway pressure in patients with acute pulmonary failure. *N Engl J Med.* 1975;292(6):284–9.
- Suter PM, Fairley HB, Isenberg MD. Effect of tidal volume and positive end-expiratory pressure on compliance during mechanical ventilation. *Chest.* 1978;73(2):158–62.

- Talmor D, Sarge T, Malhotra A, O'Donnell CR, Ritz R, Lisbon A, et al. Mechanical ventilation guided by esophageal pressure in acute lung injury. *N Engl J Med*. 2008;359(20):2095–104.
- Taskar V, John J, Larsson A, Wetterberg T, Jonson B. Dynamics of carbon dioxide elimination following ventilator resetting. *Chest*. 1995;108(1):196–202.
- Teboul JL, Monnet X, Chemla D, Michard F. Arterial pulse pressure variation with mechanical ventilation. *Am J Respir Crit Care Med*. 2019;199(1):22–31.
- Tremblay L, Valenza F, Ribeiro SP, Li J, Slutsky AS. Injurious ventilatory strategies increase cytokines and c-fos mRNA expression in an isolated rat lung model. *J Clin Invest*. 1997;99(5):944–52.
- Vieira SR, Puybasset L, Lu Q, Richecoeur J, Cluzel P, Coriat P, et al. A scanographic assessment of pulmonary morphology in acute lung injury. Significance of the lower inflection point detected on the lung pressure-volume curve. *Am J Respir Crit Care Med*. 1999;159(5 Pt 1):1612–23.
- Villar J, Kacmarek RM, Perez-Mendez L, Aguirre-Jaime A. A high positive end-expiratory pressure, low tidal volume ventilatory strategy improves outcome in persistent acute respiratory distress syndrome: a randomized, controlled trial. *Crit Care Med*. 2006;34(5):1311–8.
- Webb HH, Tierney DF. Experimental pulmonary edema due to intermittent positive pressure ventilation with high inflation pressures. Protection by positive end-expiratory pressure. *Am Rev Respir Dis*. 1974;110(5):556–65.
- Writing Group for the Alveolar Recruitment for Acute Respiratory Distress Syndrome Trial I, Cavalcanti AB, Suzumura EA, Laranjeira LN, Paisani DM, Damiani LP, et al. Effect of lung recruitment and titrated positive end-expiratory pressure (PEEP) vs low PEEP on mortality in patients with acute respiratory distress syndrome: a randomized clinical trial. *JAMA*. 2017;318(14):1335–45.
- Yonis H, Mortaza S, Baboi L, Mercat A, Guerin C. Expiratory flow limitation assessment in patients with acute respiratory distress syndrome. A reappraisal. *Am J Respir Crit Care Med*. 2018;198(1):131–4.
- Yoshida T, Amato MBP, Grieco DL, Chen L, Lima CAS, Roldan R, et al. Esophageal manometry and regional transpulmonary pressure in lung injury. *Am J Respir Crit Care Med*. 2018;197(8):1018–26.
- Yoshida T, Piraino T, Lima CAS, Kavanagh BP, MBP A, Brochard L. Regional ventilation displayed by electrical impedance tomography as an incentive to decrease PEEP. *Am J Respir Crit Care Med*. 2019;200:933–7.



Cardiopulmonary Monitoring in the Prone Patient

44

Hernan Aguirre-Bermeo and Jordi Mancebo

Abbreviations

ARDS	Acute respiratory distress syndrome
EELV	End-expiratory lung volume (residual lung volume at PEEP)
FRC	Functional residual capacity (residual lung volume at zero end-expiratory pressure)
PaCO ₂	Arterial partial pressure of carbon dioxide
PaO ₂	Arterial partial pressure of oxygen
PEEP	Positive end-expiratory pressure
PP	Prone position
SP	Supine position

Introduction

Prone position (PP) for acute respiratory distress syndrome (ARDS) in humans was first described in 1976 by Piehl et al. (Piehl and Brown 1976). Those authors found that this position increased the arterial partial pressure of oxygen (PaO₂) and made it easier to suction respiratory secre-

tions, although several subsequent studies failed to show a survival benefit for this maneuver (Gattinoni et al. 2001; Guerin et al. 2004; Taccone et al. 2009; Voggenreiter et al. 2005). In 2006, a multicenter trial (Mancebo et al. 2006) evaluated the early application of PP in ARDS patients and found that PP was a safe and feasible maneuver and also showed a trend toward improved survival when applied early. The heterogenous results reported in the aforementioned studies could be related to variability in disease severity, the duration of the PP sessions, and the time interval from diagnosis to the application of PP. To better understand the effect of PP on survival outcomes, Sud et al. (2010) performed a meta-analysis, which showed that PP reduces mortality in patients with severe hypoxemia. This finding suggests that the correct and early application of PP in a well-defined group of patients could improve survival outcomes. Finally, in 2014, Guerin et al. (2013) evaluated a group of patients with severe ARDS (PaO₂/FiO₂ index <150) who received PP in the early phases of the syndrome and relative prolonged time in PP (16 hours). In that study, this approach was associated with improved survival. Those findings have been confirmed by two recent meta-analyses (Beitler et al. 2014; Munshi et al. 2017). Despite the strong evidence demonstrating the survival benefit for PP, two recently published epidemiological studies found that PP remains underutilized in routine clinical practice (Bellani et al. 2016; Guerin et al. 2018). To

H. Aguirre-Bermeo
Intensive Care Unit, Hospital Santa Inés,
Cuenca, Ecuador

J. Mancebo (✉)
Intensive Care Unit, Hospital de la Santa Creu i Sant
Pau, Barcelona, Spain
e-mail: jmancebo@santpau.cat

better understand how PP improves survival, it is important to evaluate and monitor the physiological changes in the cardiopulmonary system that take place during PP. A better understanding of these changes could encourage a wider use of PP in clinical practice for the specific group of ARDS patients who would most benefit from this maneuver. The main objectives of this chapter are to explain the cardiopulmonary changes that occur during PP.

Prone Position and Hemodynamics

In patients with ARDS, several factors including hypoxic vasoconstriction, vessel obliteration, and extrinsic vessel compression alter the distribution of pulmonary blood flow (Gattinoni et al. 2006). However, when patients are placed in PP, the vertical perfusion gradient may disappear, and perfusion to the dorsal regions seems to increase relative to the ventral regions (Glenny et al. 1991). Wiener et al. (1990) evaluated PP in animal models of ARDS, finding that regional perfusion in the lungs was more uniformly distributed in PP, mainly in nondependent regions. This finding suggests a redistribution of blood flow. Pappert et al. (1994) found that the improvement in oxygenation in patients with ARDS was associated with an improvement in ventilation/perfusion matching, suggesting that mechanisms other than gravity or hypoxic pulmonary vasoconstriction may be involved in influencing the redistribution of blood flow in PP (Gattinoni et al. 2006; Rialp and Mancebo 2002).

PP has several beneficial effects on hemodynamics. Bull et al. (2010) found that pulmonary vascular dysfunction is independently associated with poor outcomes in ARDS patients; however, this dysfunction can be improved by placing patients in PP, which reduces the pulmonary vascular resistance (Guerin et al. 2014; Jozwiak et al. 2013). In patients with severe ARDS, PP improves right ventricle failure by decreasing afterload while increasing preload (Vieillard-Baron et al. 2007; Jozwiak et al. 2016). Systemic venous return increases in PP due to (1) the transfer of blood volume from the splanchnic compart-

ment and (2) higher intra-abdominal pressure, which increases the mean systemic pressure (Jozwiak et al. 2013, 2016). Other reported benefits of PP on hemodynamics include an increase in cardiac output, with higher left ventricular afterload and improved oxygen transportation (Jozwiak et al. 2013, 2016; Hering et al. 2001, 2002; Blanch et al. 1997). However, these potential benefits must be analyzed cautiously due to the potential influence of confounding factors (mainly positive end-expiratory pressure [PEEP] levels and volume status) (Guerin et al. 2014; Jozwiak et al. 2013).

Lim et al. (1999) conducted an experimental study in an animal model of ARDS and compared gas exchange and the hemodynamic effects of lower versus higher PEEP in supine and prone positions. These authors found that higher PEEP levels decreased cardiac output in the supine position (SP). However when the animals were placed in PP, cardiac output increased by the same amount (or more) than obtained with SP at lower PEEP.

PP may also have adverse effects on hemodynamics. The slight increase in mean arterial blood pressure due to compression of the abdominal arterial system in PP could negatively affect left ventricular afterload (Jozwiak et al. 2013; Hering et al. 2001, 2002). Decreased splanchnic perfusion and higher renal vascular resistance secondary to an increase of intra-abdominal pressure have been described in patients in PP, although the effect on the organs does not appear to be harmful (Guerin et al. 2014; Hering et al. 2001).

Prone Position and the Lung

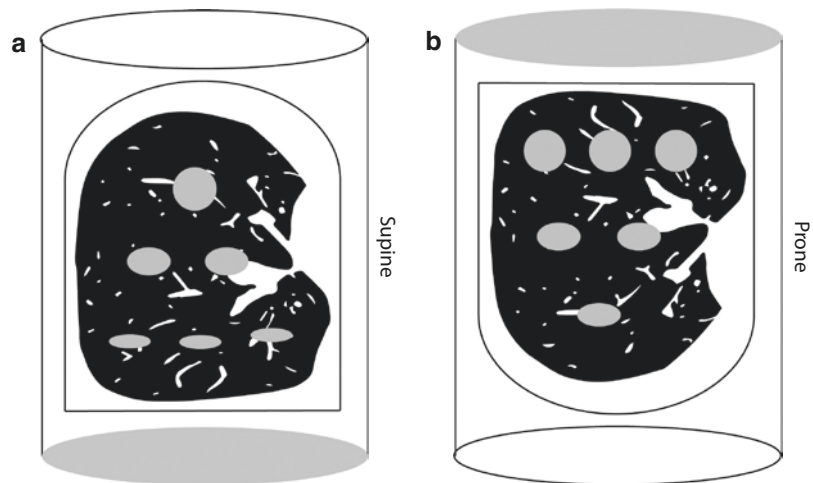
Effects on Ventilation In ARDS patients, the distribution of altered alveolar tissue is heterogeneous and located preferentially in dependent lung regions (dorsal lung regions). In SP, the inflation decreases along the vertical axis from nondependent to dependent regions (Pelosi et al. 1994; Gattinoni et al. 2013). In supine paralyzed patients, the cephalic displacement of the diaphragm by intra-abdominal pressure primarily affects the dependent regions, leading to worse

dorsal lung ventilation. In addition, in SP, the shape of the lung (a cone) must adapt to match the cylindrical form of the chest wall, thus generating a large amount of distension in nondependent (ventral) regions. At the same time, gravitational forces compress the dependent regions (Gattinoni et al. 2013) (Fig. 44.1). By contrast, in PP, the distribution of aeration is more homogeneous (Pelosi et al. 2001; Valenza et al. 2005), and these two factors (gravity and lung shape) act in opposing directions (Fig. 44.1), leading to a more uniform alveolar inflation and more homogeneous distribution of stress and strain (Gattinoni et al. 2013). Vieillard-Baron et al. found that PP improves homogenization of tidal ventilation by reducing time-constant inequalities (Vieillard-Baron et al. 2005). The diaphragm also plays an important role in PP, as the migration of the diaphragm secondary to the effect of the abdomen is more uniform and the dorsal portion of the diaphragm also moves better in the nondependent region of the lung (Rialp and Mancebo 2002). These effects improve ventilation of the dorsal lung zones. However, intra-abdominal pressure could counteract the beneficial effects of PP. In an experimental animal model, Mure et al. (1998) found that PP caused a significant decrease in both the alveolo-arterial PaO_2 gradient and ventilation/perfusion heterogeneity in the presence of abdominal distension.

Effects on Respiratory Mechanics The respiratory system is composed of two structures (lung and chest wall). Several studies have shown decreases in chest wall compliance in PP as compared to SP (Pelosi et al. 1998; Guerin et al. 1999; Mentzelopoulos et al. 2005a) due to an increase in abdominal pressure and/or a cranial diaphragm displacement in patients with high intra-abdominal pressure. When the patient is in PP, and recruitment in dependent zones is higher than the decrease in compliance of the thoracic cage, then overall respiratory system compliance will improve. However if pulmonary recruitment is lower in PP and there is still a decrease in the compliance of the thoracic cage, the overall compliance of the respiratory system may remain unchanged or even decrease (Pelosi et al. 1998).

The effect of PP on transpulmonary pressure is still not clear. Mezidi et al. (2018) evaluated the influence of PEEP and patient positioning on transpulmonary pressure but did not find any variation in transpulmonary pressure due to the position change, regardless of the specific PEEP strategy used (PEEP/ FiO_2 table vs PEEP titrated to reach a plateau pressure around 28 cmH_2O). More studies are needed to explore variations in transpulmonary pressure in PP and the importance of this variation.

Fig. 44.1 Distribution of alveolar size according to shape matching of the lung to the chest wall and gravity. Alveolar units are compressed by the weight of the pulmonary units from the levels above. (a) In supine position, both forces (matching shape and gravity) act in the same direction; (b) in prone position, the forces act in opposite directions



Effects on Lung Volumes In ARDS patients, resting lung volume at zero end-expiratory pressure (the functional residual capacity (FRC)) and the resting lung volume at PEEP (the end-expiratory lung volume (EELV)) are decreased (Chiumello et al. 2008). Two studies found significant increases in FRC in ARDS patients placed in PP (Mentzelopoulos et al. 2005a, b). However, reported data on variations in EELV when switching from supine to prone position are inconsistent (Pelosi et al. 1998; Mentzelopoulos et al. 2005a, b; Pelosi et al. 2003; Reutershan et al. 2006). These findings could be explained by differences in lung recruitability, the extent of lung volume alterations, differences in chest wall compliance, the influence of abdominal weight, and heart compression (Gattinoni et al. 2013; Galiatsou et al. 2006; Albert et al. 2014; Nieszkowska et al. 2004). Recently, Aguirre-Bermeo et al. (2018) evaluated variation in lung volumes with position switching using the nitrogen washout/washin technique. In that study, both EELV and FRC increased significantly (by 18% in FRC and 17% in EELV) when the position was switched from supine to prone. These increases in lung volumes could be due to a redistribution of aeration in PP (a minor decrease in non-aerated lung tissue, a major decrease in poorly aerated tissue, and a major increase in well-aerated tissue). The variation of aeration in lung zones is thus considered to reflect better gas distribution within the lung and not recruitment per se (Chiumello et al. 2016).

Effects on Strain and Stress Considering the aforementioned modifications in respiratory mechanics and volumes in PP, it seems safe to presume that PP homogenizes lung strain and reduces lung stress. Aguirre-Bermeo et al. (2018) found that increases in lung volumes are accompanied by a significant decrease in dynamic lung strain, which could be another protective mechanism provided by PP against ventilator-induced lung injury.

Effects on Gas Exchange The improvement in gas exchange in PP is associated with two main physiological effects: (1) a reduction in intrapul-

monary shunt due to aeration distribution (as described in the preceding paragraph). As a result, either perfusion is redirected to well-ventilated lung areas or lung ventilation increases in well-perfused lung areas. In both cases, the ventilation/perfusion ratio improves, thus potentially modifying the gas exchange; and (2) there is a reduction in intrapulmonary shunt due to gravity. The effect of gravity increases along the dorsal to ventral gradient, reaching its maximum effect in ventral zones (exactly the opposite of what occurs in SP). This effect should decrease the intrapulmonary shunt in dorsal lung regions, which are now nondependent (Guerin et al. 2014; Roche-Campo et al. 2011). However, improved oxygenation alone does not imply a lower death rate in ARDS patients. Albert et al. (2014) retrospectively analyzed data collected in the multicenter study carried out by Guerin et al. (2013) and found that the better survival outcome among severe ARDS patients placed in PP was not associated with improved oxygenation. In fact, 39 of 43 patients (91%) in whom the $\text{PaO}_2/\text{FiO}_2$ index decreased 1 hour after prone positioning survived.

A decrease in arterial partial pressure of carbon dioxide (PaCO_2) in PP could indicate lung recruitment, especially if this decrease is accompanied by a decrease in dead space. Gattinoni et al. (2003) performed a multicenter, retrospective analysis of patients with ARDS and found out that patients whose PaCO_2 decreased in PP had better survival at 28 days.

Prone Position Maneuver

Before considering the use of PP, the mechanical ventilator settings must first be optimized. The use of protective ventilation (low tidal volume and moderate PEEP levels to achieve plateau pressure ≤ 28 cmH₂O) is essential given the published evidence demonstrating that the combination of protective ventilation and PP improves outcomes (Munshi et al. 2017). However, PP is not appropriate for all ARDS patients. Guerin et al. (2013) found that PP improved survival only

in patients with a $\text{PaO}_2/\text{FiO}_2$ ratio < 150 mmHg in whom PP was applied early (within 24 hours from the ARDS diagnosis) and for a prolonged time (≥ 16 hours). The influence of early application in the outcomes could be because the increase in lung volumes is accompanied by a decrease in lung strain only in the early stages (< 72 hours) of the diagnosis of ARDS, but not in late stages of ARDS (Aguirre-Bermeo et al. 2018).

In some cases, the decision to apply PP should be carefully considered and individualized according to the patient's specific clinical characteristics. Factors to consider include (1) conditions that make it difficult to turn the patient to the prone position, such as external fixators, multiple pleural tubes, pericardial drainage, tracheotomy, and morbid obesity, and (2) clinical conditions that are contraindications for PP: spinal cord injury with unstable vertebral fractures, pelvic fractures, open abdominal cavity, hemodynamic instability, traumatic brain injury with intracranial hypertension, pregnancy, severe burns, and facial lesions.

The experience level of the clinical team may be important in preventing complications during and after the maneuver. The entire process (preparation and turning) typically takes about 10 minutes. To perform the turning procedure safely, it is advisable to carefully follow the recommendations described below:

1. Pre-maneuver: It is advisable to perform the following: (1) interrupt enteral nutrition, (2) perform preoxygenation, (3) ensure that all necessary materials are available and readily accessible, (4) hydrate the eyes and skin, (5) protect the eyes from erosion, and (6) apply skin protections. In addition, the mouth should be aspirated and bronchial secretions carefully suctioned.
2. Performing the maneuver: each step should be initiated only when indicated by the coordinator (i.e., the person standing at the head of the bed). The first step is to move the patient to the side of the bed. While either side can be used, the choice will depend on the location of

the catheters, the mechanical ventilator, the dialysis machine, etc. To perform the maneuver, the people assigned to the upper and lower limbs should lock their hands together beneath the patient's body. Next, the patient should be placed in the lateral position. Then, the patient should be turned to the prone position and moved to the center of the bed, after which the electrodes and the other monitoring cables and medical instruments should be reconnected.

3. Post-maneuver. Protective cushions (face, chest, knees, feet) should be placed. Then, the patient should be put into reverse Trendelenburg (30°) with the arms placed in one of the following two positions: (a) swimmer's (crawl) position (one arm raised with the head rotated toward the raised arm and the other arm positioned alongside the body) (Fig. 44.2) or (b) both arms positioned alongside the body. After



Fig. 44.2 Patient in prone position with swimmer's (crawl) position (one arm raised with the head rotated toward the raised arm and the other arm positioned alongside the body)

turning the patient, the position (arms, head, neck) should be alternated (i.e., right to left or left to right) every 2 hours. It is important to take special care to monitor pressure points and to check the eyes. Supine positioning should be performed following the same steps and the same precautions and care.

hypoxemia, arrhythmias, etc.), we recommend the following:

- Develop an institutional protocol and checklist for PP.
- Designate a coordinator (the person at the head of the bed) who is responsible for assigning the responsibilities and positions of the other team members.
- Apply continuous peripheral oxygen saturation monitoring using a finger pulse oximeter throughout the whole maneuver process.
- Reconnect electrodes and monitoring cables as soon as possible.

Phase 2: Monitor the effects of prone positioning: the main objectives of monitoring patients in PP are described in detail in Table 44.1.

Monitoring in Prone Position

Monitoring can be divided into two phases.

Phase 1: Monitoring the maneuver: The level of experience of the clinical teams (physicians and nurses) with the maneuver directly influences the likelihood of complications occurring during maneuver. To avoid maneuver-related complications (extubation, drainage tube loss,

Table 44.1 Summary of the effects of prone position and monitoring techniques

Physiologic variable(s)	Effect of prone position	Monitoring technique	Interpretation
Right ventricle	Improves failure	Echocardiography, thermodilution catheter.	Decrease in afterload and increase in preload.
Systemic venous return	Increase	Echocardiography, thermodilution catheter, central venous catheter	Redistribution of splanchnic volume Higher intra-abdominal pressure
Cardiac output	Improvement	Echocardiography, thermodilution catheter	Higher ventricular afterload
Intra-abdominal pressure	Increase	Foley urinary catheter	Affects left ventricular afterload Alteration of splanchnic and renal perfusion (non-dangerous) effect
Lung ventilation	Redistribution of aeration	Thoracic computed tomography, electrical impedance tomography	Minor decrease in non-aerated lung tissue, a major decrease in poorly aerated tissue, and a major increase in well-aerated tissue
Respiratory system elastance	Increase or decrease	Ventilatory values, esophageal balloon catheter (transpulmonary pressure)	The variation depends on the effect of PP on lung elastance
Lung volumes (FRC and EELV)	Either no variation or an increase	Nitrogen washout/washin technique	Lung volumes vary depending on the time interval from ARDS diagnosis (increase in early phase)
Stress and strain	Decrease	Pressure-volume curve, nitrogen washout/washin technique.	Could decrease depending on changes in lung volumes
Gas exchange	Increase in PaO ₂ and decrease in PaCO ₂	Blood gases	Could increase PaO ₂ and decrease PaCO ₂ (if there is a decrease in dead space)

Abbreviations: *ARDS* Acute respiratory distress syndrome, *EELV* end-expiratory lung volume, *FRC* functional residual capacity, *PaCO₂* arterial partial pressure of carbon dioxide, *PaO₂* arterial partial pressure of oxygen, *PP* prone position

Summary

The use of prone position in patients with severe ARDS has been shown to increase survival. Prone position has several beneficial effects on the cardiopulmonary system, which may explain the better survival outcomes obtained with this technique. It is important to monitor the cardiopulmonary changes induced by prone position to better understand the beneficial effects of this maneuver and to use these data to adjust the mechanical ventilation settings.

References

- Aguirre-Bermeo H, Turella M, Bitondo M, Grandjean J, Italiano S, Festa O, et al. Lung volumes and lung volume recruitment in ARDS: a comparison between supine and prone position. *Ann Intensive Care*. 2018;8:25.
- Albert RK, Keniston A, Baboi L, Ayzac L, Guerin C, Proseva I. Prone position-induced improvement in gas exchange does not predict improved survival in the acute respiratory distress syndrome. *Am J Respir Crit Care Med*. 2014;189:494–6.
- Beitler JR, Shaefi S, Montesi SB, Devlin A, Loring SH, Talmor D, et al. Prone positioning reduces mortality from acute respiratory distress syndrome in the low tidal volume era: a meta-analysis. *Intensive Care Med*. 2014;40:332–41.
- Bellani G, Laffey JG, Pham T, Fan E, Investigators LS, the ETG. The LUNG SAFE study: a presentation of the prevalence of ARDS according to the Berlin Definition! *Crit Care*. 2016;20:268.
- Blanch L, Mancebo J, Perez M, Martinez M, Mas A, Betbese AJ, et al. Short-term effects of prone position in critically ill patients with acute respiratory distress syndrome. *Intensive Care Med*. 1997;23:1033–9.
- Bull TM, Clark B, McFann K, Moss M. Pulmonary vascular dysfunction is associated with poor outcomes in patients with acute lung injury. *Am J Respir Crit Care Med*. 2010;182:1123–8.
- Chiumello D, Carlesso E, Cadringer P, Caironi P, Valenza F, Polli F, et al. Lung stress and strain during mechanical ventilation for acute respiratory distress syndrome. *Am J Respir Crit Care Med*. 2008;178:346–55.
- Chiumello D, Marino A, Brioni M, Cigada I, Menga F, Colombo A, et al. Lung recruitment assessed by respiratory mechanics and computed tomography in patients with acute respiratory distress syndrome. What is the relationship? *Am J Respir Crit Care Med*. 2016;193:1254–63.
- Galiatsou E, Kostanti E, Svarna E, Kitsakos A, Koulouras V, Efremidis SC, et al. Prone position augments recruitment and prevents alveolar overinflation in acute lung injury. *Am J Respir Crit Care Med*. 2006;174:187–97.
- Gattinoni L, Tognoni G, Pesenti A, Taccone P, Mascheroni D, Labarta V, et al. Effect of prone positioning on the survival of patients with acute respiratory failure. *N Engl J Med*. 2001;345:568–73.
- Gattinoni L, Vagginielli F, Carlesso E, Taccone P, Conte V, Chiumello D, et al. Decrease in PaCO₂ with prone position is predictive of improved outcome in acute respiratory distress syndrome. *Crit Care Med*. 2003;31:2727–33.
- Gattinoni L, Taccone P, Mascheroni D, Valenza F, Pelosi P. Prone positioning in acute respiratory failure. In: Tobin MJ, editor. *Principles & practice of mechanical ventilation*. New York: McGraw-Hill; 2006. p. 1169–81.
- Gattinoni L, Taccone P, Carlesso E, Marini JJ. Prone position in acute respiratory distress syndrome. Rationale, indications, and limits. *Am J Respir Crit Care Med*. 2013;188:1286–93.
- Glenny RW, Lamm WJ, Albert RK, Robertson HT. Gravity is a minor determinant of pulmonary blood flow distribution. *J Appl Physiol* (1985). 1991;71:620–9.
- Guerin C, Badet M, Rosselli S, Heyer L, Sab JM, Langevin B, et al. Effects of prone position on alveolar recruitment and oxygenation in acute lung injury. *Intensive Care Med*. 1999;25:1222–30.
- Guerin C, Gaillard S, Lemasson S, Ayzac L, Girard R, Beuret P, et al. Effects of systematic prone positioning in hypoxemic acute respiratory failure: a randomized controlled trial. *JAMA*. 2004;292:2379–87.
- Guerin C, Reignier J, Richard JC, Beuret P, Gacouin A, Boulain T, et al. Prone positioning in severe acute respiratory distress syndrome. *N Engl J Med*. 2013;368:2159–68.
- Guerin C, Baboi L, Richard JC. Mechanisms of the effects of prone positioning in acute respiratory distress syndrome. *Intensive Care Med*. 2014;40:1634–42.
- Guerin C, Beuret P, Constantin JM, Bellani G, Garcia-Olivares P, Roca O, et al. A prospective international observational prevalence study on prone positioning of ARDS patients: the APRONET (ARDS Prone Position Network) study. *Intensive Care Med*. 2018;44:22–37.
- Hering R, Wrigge H, Vorwerk R, Brensing KA, Schroder S, Zinserling J, et al. The effects of prone positioning on intraabdominal pressure and cardiovascular and renal function in patients with acute lung injury. *Anesth Analg*. 2001;92:1226–31.
- Hering R, Vorwerk R, Wrigge H, Zinserling J, Schroder S, von Spiegel T, et al. Prone positioning, systemic hemodynamics, hepatic indocyanine green kinetics, and gastric intramucosal energy balance in patients with acute lung injury. *Intensive Care Med*. 2002;28:53–8.
- Jozwiak M, Teboul JL, Anguel N, Persichini R, Silva S, Chemla D, et al. Beneficial hemodynamic effects of prone positioning in patients with acute respiratory distress syndrome. *Am J Respir Crit Care Med*. 2013;188:1428–33.

- Jozwiak M, Monnet X, Teboul JL. Optimizing the circulation in the prone patient. *Curr Opin Crit Care*. 2016;22:239–45.
- Lim CM, Koh Y, Chin JY, Lee JS, Lee SD, Kim WS, et al. Respiratory and haemodynamic effects of the prone position at two different levels of PEEP in a canine acute lung injury model. *Eur Respir J*. 1999;13:163–8.
- Mancebo J, Fernandez R, Blanch L, Rialp G, Gordo F, Ferrer M, et al. A multicenter trial of prolonged prone ventilation in severe acute respiratory distress syndrome. *Am J Respir Crit Care Med*. 2006;173:1233–9.
- Mentzelopoulos SD, Roussos C, Zakynthinos SG. Prone position reduces lung stress and strain in severe acute respiratory distress syndrome. *Eur Respir J*. 2005a;25:534–44.
- Mentzelopoulos SD, Roussos C, Zakynthinos SG. Static pressure volume curves and body posture in acute respiratory failure. *Intensive Care Med*. 2005b;31:1683–92.
- Mezidi M, Parrilla FJ, Yonis H, Riad Z, Bohm SH, Waldmann AD, et al. Effects of positive end-expiratory pressure strategy in supine and prone position on lung and chest wall mechanics in acute respiratory distress syndrome. *Ann Intensive Care*. 2018;8:86.
- Munshi L, Del Sorbo L, Adhikari NKJ, Hodgson CL, Wunsch H, Meade MO, et al. Prone position for acute respiratory distress syndrome. A systematic review and meta-analysis. *Ann Am Thorac Soc*. 2017;14:S280–S8.
- Mure M, Glenn RW, Domino KB, Hlastala MP. Pulmonary gas exchange improves in the prone position with abdominal distension. *Am J Respir Crit Care Med*. 1998;157:1785–90.
- Nieszkowska A, Lu Q, Vieira S, Elman M, Fetita C, Rouby JJ. Incidence and regional distribution of lung overinflation during mechanical ventilation with positive end-expiratory pressure. *Crit Care Med*. 2004;32:1496–503.
- Pappert D, Rossaint R, Slama K, Gruning T, Falke KJ. Influence of positioning on ventilation-perfusion relationships in severe adult respiratory distress syndrome. *Chest*. 1994;106:1511–6.
- Pelosi P, D'Andrea L, Vitale G, Pesenti A, Gattinoni L. Vertical gradient of regional lung inflation in adult respiratory distress syndrome. *Am J Respir Crit Care Med*. 1994;149:8–13.
- Pelosi P, Tubiolo D, Mascheroni D, Vicardi P, Crotti S, Valenza F, et al. Effects of the prone position on respiratory mechanics and gas exchange during acute lung injury. *Am J Respir Crit Care Med*. 1998;157:387–93.
- Pelosi P, Caironi P, Taccone P, Brazzi L. Pathophysiology of prone positioning in the healthy lung and in ALI/ARDS. *Minerva Anesthesiol*. 2001;67:238–47.
- Pelosi P, Bottino N, Chiumello D, Caironi P, Panigada M, Gamberoni C, et al. Sigh in supine and prone position during acute respiratory distress syndrome. *Am J Respir Crit Care Med*. 2003;167:521–7.
- Piehl MA, Brown RS. Use of extreme position changes in acute respiratory failure. *Crit Care Med*. 1976;4:13–4.
- Reutershan J, Schmitt A, Dietz K, Unertl K, Fretschner R. Alveolar recruitment during prone position: time matters. *Clin Sci (Lond)*. 2006;110:655–63.
- Rialp G, Mancebo J. Prone positioning in patients with acute respiratory distress syndrome. *Respir Care Clin N Am*. 2002;8:237–45, vi–vii.
- Roche-Campo F, Aguirre-Bermeo H, Mancebo J. Prone positioning in acute respiratory distress syndrome (ARDS): when and how? *Presse Med*. 2011;40:e585–94.
- Sud S, Friedrich JO, Taccone P, Polli F, Adhikari NK, Latini R, et al. Prone ventilation reduces mortality in patients with acute respiratory failure and severe hypoxemia: systematic review and meta-analysis. *Intensive Care Med*. 2010;36:585–99.
- Taccone P, Pesenti A, Latini R, Polli F, Vagginielli F, Mietto C, et al. Prone positioning in patients with moderate and severe acute respiratory distress syndrome: a randomized controlled trial. *JAMA*. 2009;302:1977–84.
- Valenza F, Guglielmi M, Maffioletti M, Tedesco C, Maccagni P, Fossali T, et al. Prone position delays the progression of ventilator-induced lung injury in rats: does lung strain distribution play a role? *Crit Care Med*. 2005;33:361–7.
- Vieillard-Baron A, Rabiller A, Chergui K, Peyrouset O, Page B, Beauchet A, et al. Prone position improves mechanics and alveolar ventilation in acute respiratory distress syndrome. *Intensive Care Med*. 2005;31:220–6.
- Vieillard-Baron A, Charron C, Caille V, Belliard G, Page B, Jardin F. Prone positioning unloads the right ventricle in severe ARDS. *Chest*. 2007;132:1440–6.
- Voggenreiter G, Aufmkolk M, Stiletto RJ, Baacke MG, Waydhas C, Ose C, et al. Prone positioning improves oxygenation in post-traumatic lung injury—a prospective randomized trial. *J Trauma*. 2005;59:333–41; discussion 41–3.
- Wiener CM, Kirk W, Albert RK. Prone position reverses gravitational distribution of perfusion in dog lungs with oleic acid-induced injury. *J Appl Physiol* (1985). 1990;68:1386–92.



Cardiopulmonary Interactions in the Management of Acute Obstructive Disease

45

Charles Corey Hardin and Julian Solway

Introduction

Respiratory illness is frequently accompanied by a derangement of the normal mechanics of the respiratory system. In this circumstance, coupling of the cardiovascular and respiratory systems can, in turn, precipitate additional, sometimes profound, alterations in circulatory function. Interventions such as mechanical ventilation undertaken to stabilize respiratory function can either attenuate or further exaggerate adverse interactions between the cardiovascular and respiratory systems. In this chapter, we review some aspects of normal respiratory mechanics, describe how they may be altered in obstructive lung disease, discuss the coupling of cardiovascular and respiratory function, and briefly consider implications of the above for clinical management.

C. C. Hardin (✉)
Division of Pulmonary and Critical Care Medicine,
Massachusetts General Hospital, Boston, MA, USA
e-mail: Charles.Hardin@mgh.harvard.edu

J. Solway
Department of Medicine, Section of Pulmonary/
Critical Care, University of Chicago,
Chicago, IL, USA
e-mail: jsolway@uchicago.edu

Normal Respiratory Mechanics

In the normal lung during tidal breathing, it frequently suffices to use a single compartment, linear model of respiratory mechanics (Bates 2009). Within this approximation, lung inflation is achieved by applying a total pressure, P_T , across the respiratory system that instantaneously reflects the sum of an elastic component (the increase in volume, V , above functional residual capacity divided by respiratory system compliance C) and a flow-resistive component (the flow rate, \dot{V} , times airflow resistance, R), as described by the classical equation of motion (Marini and Crooke 3rd. 1993):

$$P_T = \frac{V}{C} + \dot{V}R \quad (45.1)$$

When flow is zero (for example, at end-inspiration), the pressure across the respiratory system (the trans-respiratory system pressure) will be due solely to elastic distension with no flow-resistive component. Therefore, during mechanical ventilation, if a pause is instituted at end-inspiration, the pressure decreases from the peak inspiratory pressure (PIP), which reflects both flow-resistive and elastic components, to a lower, steady-state value called the plateau pressure (P_{plat}), which reflects only the elastic component (Dhand et al. 1995). The difference between PIP and P_{plat} therefore reflects the contribution of

the resistive term ($R \cdot \dot{V}$) in Eq. 45.1 (Hess and Kacmarek 2002):

$$\text{PIP} - P_{\text{plat}} = R \cdot \dot{V} \quad (45.2)$$

Airflow Limitation in Obstructive Lung Diseases

Equations 45.1 and 45.2 suppose a simple linear relationship between flow and flow-related pressure (i.e., a fixed resistance). While this is a reasonable approximation for normal lungs and low flows, dynamic airflow limitation is often observed during the expiratory phase of tidal breathing in patients with obstructive lung diseases. During airflow limitation, expiratory flow is not determined simply by the pressure driving flow (alveolar gas pressure, P_{alv} , minus airway opening pressure, P_{ao}) and a constant resistance to airflow (as might be measured during inspiration) because the bronchial airways are collapsible and can become sucked partially shut by a lowering of intraluminal gas pressure due to the Bernoulli effect. While this effect in principle could happen in normal lungs, the flow rates during passive exhalation are almost never high enough for this dynamic flow limitation phenomenon to occur. However, in obstructive lung diseases, the smaller airway diameters result in faster velocities for a given airflow rate, that in turn exacerbate the Bernoulli-related lowering of intraluminal pressure and worsen airway collapse. Intraluminal pressure may be even further lowered below P_{alv} by frictional pressure loss due to the narrowed airways and, in the cases of emphysema or even asthma, by reduced alveolar pressure for a given lung volume due to loss of lung parenchymal elastic recoil. All these phenomena conspire together to limit maximal expiratory flow below that which might have been anticipated from the alveolar-to-airway opening pressure difference and inspiratory airflow resistance. The resultant inability to exhale quickly can lead to incomplete exhalation and consequent dynamic lung hyperinflation with elevated alveolar gas pressure, as discussed below. Because the Bernoulli effect

also depends upon gas density, sometimes respiratory gas mixtures containing a high proportion of helium are used to mitigate expiratory airflow limitation. Pedersen et al. (Pedersen and Butler 2011) provide a good overview of the quantitative relationships among flow, airway distensibility, gas density, lung elastic recoil pressure, and frictional pressure losses during flow limitation and are summarized for any single airway as follows:

$$\dot{V}(P_{\text{tm}}) = A \sqrt{\frac{2 \cdot (P_{\text{el}}(V_{\text{L}}) - P_{\text{fr}} - P_{\text{tm}})}{\rho}} \quad (45.3)$$

$$\dot{V}_{\text{max}}(P_{\text{tm}}) = A \sqrt{\frac{A}{\rho C_{\text{aw}}}} \quad (45.4)$$

where A is the airway area; $\dot{V}(P_{\text{tm}})$ is the expiratory flow through the airway; $P_{\text{el}}(V_{\text{L}})$ is the lung elastic recoil, which is a function of lung volume (V_{L}); P_{fr} is the frictional pressure loss between the alveoli and the airway being sucked shut, which is a complex function of the airflow pathways upstream of that site and the maximal flow in Eq. 45.4, $\dot{V}_{\text{max}}(P_{\text{tm}})$, is determined by setting the derivative of Eq. 45.3 with respect to P_{tm} equal to zero and solving for the flow. C_{aw} ,

the airway compliance, is $\frac{\partial A}{\partial P_{\text{tm}}}$ (Pedersen and Butler 2011). In addition, there is heterogeneity of severity of airflow obstruction among differentially obstructed pathways (typical of most obstructive lung diseases) that contribute to non-uniform ventilation. In all, \dot{V}_{max} results from the interactions across multiple pathways upon lung elastic recoil (a function of regional lung inflation), frictional pressure loss (determined by local flow and airway caliber), bronchial wall compliance (which varies widely throughout the respiratory tree), and gas density.

Heart-Lung Interaction in Health

The anatomic relationships that contribute to the coupling of pulmonary and cardiovascular function are outlined in Fig. 45.1.

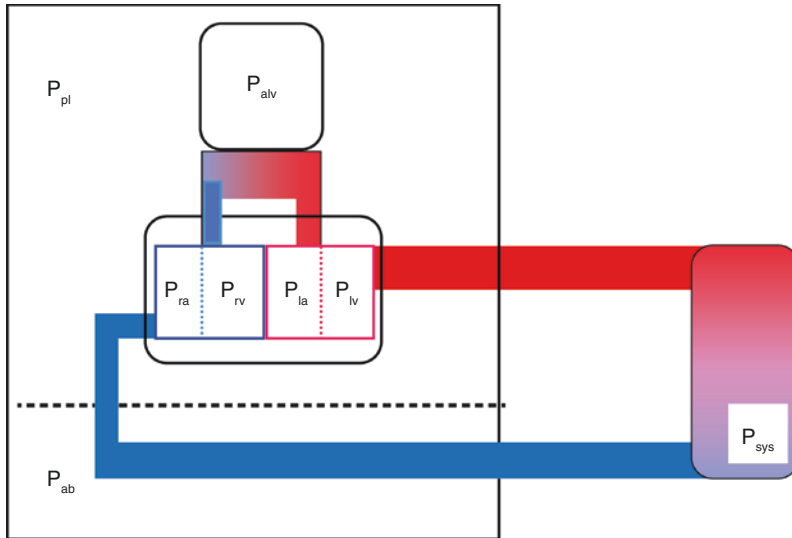


Fig. 45.1 Simplified model of heart-lung mechanical coupling. The heart and great vessels are exposed to pleural pressure (P_{pl}). Intra-alveolar vessels of the pulmonary circulation are exposed to alveolar pressure (P_{alv}). The return of blood from the systemic veins to the right atrium is driven by the pressure difference between the mean systemic pressure (P_{sys}) and the right atrial pressure P_{ra} , but

blood return is via vessels exposed on their outer surface to abdominal pressure (P_{ab}). Extra-thoracic systemic vessels are not exposed to P_{pl} . P_{la} is the left atrial pressure, P_{rv} the right ventricular pressure, P_{lv} the left ventricular pressure, and the right and left heart volumes are constrained by the pericardium (rounded rectangle)

Pleural Pressure and the Right Heart

Under normal circumstances, the heart pumps blood from the left ventricle into the systemic arterial circulation from where it drains into the systemic veins. The difference in pressure between the systemic veins (P_{sys}) and the right atrium (P_{ra}) drives the venous return (VR) – the passive return of blood to the heart. Over the normal range of P_{ra} (Guyton et al. 1957), the venous return will be proportional to the pressure gradient between the systemic veins and the right atrium and inversely proportional to the venous resistance (R_v):

$$VR = \frac{(P_{sys} - P_{ra})}{R_v} \quad (45.5)$$

The upstream pressure driving venous return, the pressure in the systemic veins, varies by location in the vascular tree, but it can be summarized in practice by a single value which is in most circumstances close to the pressure experienced in the large abdominal veins (Fessler 1997) (see also Chap. 2). P_{sys} is a func-

tion of the volume of blood in the venous system, the venous compliance, and the pressure surrounding the veins (such as the abdominal pressure, P_{ab}). In health, the downstream pressure opposing venous return, P_{ra} , is kept quite low (0–5 mmHg) by the action of the right ventricle. Like the airways, veins are compliant and their diameter is a function of the transmural pressure. At sufficiently low P_{ra} (and thus low pressure in the vena cava draining into the right atrium), the veins can close resulting in a situation in which further reductions in P_{ra} do not augment flow (Guyton et al. 1957). In this regime, venous return is flow-limited and the phenomenon is analogous to airflow limitation in the airways. As P_{ra} decreases during inspiration, venous return reaches a maximum flow (Fessler 1997).

The outer surfaces of intra-thoracic structures such as the heart are exposed to the pleural pressure. Changes in pleural pressure therefore affect transmural pressures across the heart and intra-thoracic vessels. During spontaneous inspiration, the increasingly negative pleural pressure will

result in an increase in right heart transmural pressure and a lower right atrial pressure which will augment venous return (up to the point of flow limitation) and right heart diastolic filling (Fessler 1997; Duke 1999).

Increases in P_{ra} at a constant P_{sys} decrease venous return so that the increase in P_{pl} associated with positive pressure ventilation will decrease venous return. However, the clinical importance of this is somewhat tempered by the fact that increases in P_{ra} often occur when P_{sys} is not constant. For example, increases in the pleural pressure (P_{pl}) are transmitted to the surface of the heart and thereby increase P_{ra} , but increased P_{pl} also results in displacement of the diaphragm and activation of various reflex mechanisms, all of which (Magder et al. 1983) act to increase P_{sys} (Nanas and Magder 1992) to some extent (Fessler et al. 1991). Even if increases in P_{ra} occur at a constant ($P_{sys} - P_{ra}$), there may still be a decrease in venous return, and thus a decrease in cardiac output, which may be attributed to an increase in venous resistance from decreases in the radius of the vena cava (Fessler 1997).

Pleural Pressure and the Left Heart

The left heart and proximal aorta are also exposed on their outer surfaces to pleural pressure. The increasingly negative pleural pressure associated with lung inflation during spontaneous breathing will increase the transmural pressure across the left ventricular wall (Magder et al. 1983) and increase the left heart afterload, thus increasing the left ventricular wall stress (which is proportional to the left heart transmural pressure according to the law of Laplace). Conversely, increases in pleural pressure, for example as caused by positive pressure mechanical ventilation or the further addition of PEEP, will lower the left heart afterload by raising the pressure level of the heart and intrathoracic aorta relative to the systemic circulation and decreasing the left ventricular transmural pressure and wall stress (Cassidy et al. 1979; Cherpanath et al. 2013).

Intra-pulmonary Vessels

In addition to the effect of changing pleural pressure on venous return, lung inflation impacts the pressure on intra-pulmonary vessels. Increasing lung volume has opposite effects on extra-alveolar and alveolar vessels (see chapter on pulmonary circulation by W. Mitzner in this volume). In the extra-alveolar vessels, diameter increases with increased lung volume due to parenchymal tethering; therefore, vascular resistance decreases. The behavior of the intra-alveolar vessels is opposite. Since the intra-alveolar vessels are exposed to the alveolar pressure, the transmural pressure (and thus the radius) will decrease with lung inflation and the resistance will increase. The net effect is a U-shaped dependence of total pulmonary vascular resistance on lung volume with the minimum occurring at functional residual capacity and increasing with lung volume thereafter.

In addition to changes in vessel diameter, alveolar pressure may directly impact right heart afterload in a manner determined by the relationship between the pulmonary arterial pressure, the alveolar pressure (P_{alv}), and the left atrial pressure P_{la} (see Mitzner). In many circumstances, it is accurate to treat the flow in the pulmonary circulation, the right heart cardiac output, as being determined by the difference in pressure between the mean pulmonary artery pressure, the left atrial pressure, and the pulmonary vascular resistance. But the downstream pressure is the left atrial pressure only if that pressure is greater than the alveolar pressure. If alveolar pressure exceeds pulmonary venous pressure, it is the alveolar pressure that determines pulmonary vascular flow. The circumstance in which P_{la} no longer affects pulmonary vascular flow has been termed a “vascular waterfall” (Permutt et al. 1962). The waterfall analogy is based on the fact that flow over the top of a waterfall is independent of the height of the riverbed downstream. Under waterfall conditions, increases in P_{alv} will directly decrease right heart cardiac output. This is yet another example of a flow limitation-like phenomenon.

In sum, in a spontaneously breathing patient, lung inflation will increase venous return to the right heart and decrease the resistance of the extra-alveolar vessels while increasing the resistance of the intra-alveolar vessels and, above FRC, increasing total pulmonary vascular resistance. Inflation will also increase the left heart afterload. In a mechanically ventilated patient, the positive intrathoracic pressure may result in a decrease in venous return to the right heart and a decrease in left heart afterload.

Heart-Lung Interaction in Obstructive Disease – The Spontaneously Breathing Patient

In the setting of obstructive lung disease, reduced expiratory flow related to abnormal airways resistance, lung compliance, or airflow limitation may prolong the time required for complete exhalation of each breath. When airflow obstruction is substantial, the allowed expiratory time (T_E) may be insufficient for complete exhalation (Leatherman et al. 2004). In this circumstance, there will be a residual pressure gradient between the alveolus and the airway opening at end-expiration; the positive alveolar pressure at end-expiration is referred to as auto-PEEP, distinct from any extrinsic or set PEEP that may be delivered as part of mechanical ventilation (Marini and Crooke 3rd. 1993). The risk of auto-PEEP will thus be determined by the tidal volume (V_T), the expiratory time (T_E), and the factors determining expiratory flow rate discussed above (Pride et al. 1967; Dawson and Elliott 1977; Mead et al. 1967). The presence or absence of flow limitation and attendant auto-PEEP has significant consequences for cardiovascular function.

Auto-PEEP and Hyperinflation

An underlying contributor to respiratory failure in obstructive lung disease is the increased tendency to airway closure. Airway closure, usu-

ally limited to small airways when it occurs, is promoted by a combination of increased smooth muscle tone (in the case of asthma) (Austen and Lichtenstein 1974), inflammation, increased mucus production, and decreased lung elastic recoil (Calverley 2003). Airway closure or narrowing will decrease the maximal expiratory flow and increase the time required for complete exhalation and thus the risk of auto-PEEP and attendant dynamic hyperinflation. Hyperinflation counteracts the threat of airway closure by increasing parenchymal traction on airways (providing outward radial pull), but this occurs at the cost of decreased inspiratory capacity, decreased respiratory system compliance, and positioning of the inspiratory muscles into a geometrically unfavorable arrangement (Loring et al. 2009). The consequent mechanical disadvantage can lead to increased respiratory effort – larger negative inspiratory pleural pressure – and a greater tendency to inspiratory muscle fatigue (Pedersen and Butler 2011; Calverley 2003; Permutt 1973).

In the setting of very severe obstructive lung disease or during exacerbations of milder disease, the maximal expiratory flow can be reached during tidal breathing (Pellegrino and Brusasco 1997). Resultant auto-PEEP presents an inspiratory load in so much as pleural pressure must be lowered below the positive end-expiratory alveolar pressure in order to initiate inspiratory flow. This inspiratory load increases the work of breathing and may result in respiratory distress. Hyperinflation also increases pulmonary vascular resistance, which increases right ventricular afterload, and if auto-PEEP exceeds left atrial pressure, it further increases right heart afterload. Despite the increasingly negative pleural pressure required during inspiration, there is a net increase in mean intrathoracic pressure and thus a decrease in venous return. The decrease in venous return and increase in right heart afterload are the major hemodynamic derangements during acute obstructive disease. The primary intervention for spontaneous breathing patients is to reduce airflow obstruction with pharmacotherapy.

Pulsus Paradoxus

Under normal circumstances, cardiac output and blood pressure are slightly lower during inspiration than during expiration. This effect of the negative intrathoracic pressure associated with spontaneous inspiration arises from the increase in left heart afterload during inspiration and, to a lesser extent, from the increase in right ventricular volume and ventricular interdependence. Left ventricular afterload is best described as intraventricular pressure relative to pleural pressure (Magder et al. 1983; Buda et al. 1979) so that increasingly negative pleural pressure directly increases afterload. The transmission of negative pleural pressure to the right atrium will increase the gradient for venous return and thus can increase right ventricular volume which may impede left ventricular filling due to the constraint of the pericardium (Duke 1999). In exacerbations of obstructive lung disease, respiratory effort can increase leading to an increase in the amplitude of pleural pressure cycles and an exaggeration of the normal inspiratory fall in cardiac output, a phenomenon termed pulsus paradoxus (Hamzaoui et al. 2013). Pulsus paradoxus is an exaggeration of the normal hemodynamic effect of inspiration. Increasingly negative inspiratory pleural pressure results in an increase in left ventricular transmural pressure and thus its afterload which results in a decrease in LV stroke volume (Magder et al. 1983). In addition, the increasingly negative pleural pressure when transmitted to the right atrium leads to an exaggerated increase in venous return. At the same time, the large lung volumes typically encountered will increase right ventricular afterload (Burton and Patel 1958). The simultaneous increase in venous return and right ventricular afterload can lead to an exaggerated increase in right ventricular volume (RV), which may limit left ventricular (LV) stroke volume due to the pericardial constraint and shift of the interventricular septum. The degree to which this occurs, and the magnitude of the associated decrease in LV stroke volume, will depend on the degree of pleural pressure lowering (and thus augmentation of venous return) as well as the ability of the

LV to expand in the pericardial space. The ability of the LV to expand will depend on starting ventricular volumes and the compliance of the pericardium (Hamzaoui et al. 2013).

Heart-Lung Interaction in Severe Obstructive Disease – The Mechanically Ventilated Patient

During positive pressure mechanical ventilation, alveolar pressure remains above atmospheric pressure throughout the respiratory cycle. The positive alveolar pressure will directly increase right heart afterload in regions of the lung in which P_{alv} exceeds the pulmonary venous pressure (Howell et al. 1961). Hyperinflation is present in lung regions (Gattinoni and Pesenti 2006) with regional lung volume above the regional functional residual capacity resulting in a net increase in pulmonary vascular resistance. For both reasons, mechanical ventilation may result in an increase in right heart afterload. In addition to the effects on right heart afterload, mechanical ventilation can exaggerate the effects of alveolar hyperinflation on venous return. During a mechanically supported inspiration, the intrathoracic pressure increases resulting in an increase in P_{ra} and potentially a decrease in the gradient between the P_{sys} and the P_{ra} [13]. The combination of decreased preload and increased afterload may lead to drastically reduced cardiac output and hemodynamic compromise.

Therapeutic Strategy

Minimization of hyperinflation and consequent reduction of cardiac output are the primary hemodynamic objectives in ventilation of the patient with severe obstructive disease (Leatherman 2015). This can, of course, be accomplished by attempts to reverse the airflow obstruction by treatment with bronchodilators, steroids, and potentially bronchoscopy to minimize mucus plugging. However, an immediate intervention is to decrease the respiratory rate – even at the cost of some decrease in minute ventilation and

thus increase in hypercarbia. Indeed, reductions in hyperinflation and auto-PEEP may, paradoxically, reduce dead space (as P_{alv} is lowered below the pulmonary venous pressure). Hyperinflation may also be lessened by decreasing the inspiratory time (and thus increasing the expiratory time). In volume-controlled ventilation, this may be accomplished by increasing the inspiratory flow rate, though this does come at the cost of increased peak inspiratory pressures (Tuxen and Lane 1987).

In contrast to the situation in hypoxemic respiratory failure, extrinsic positive end-expiratory pressure is of lesser importance in the management of acute obstructive disease (Davidson et al. 2016). External PEEP may reduce the inspiratory load presented by hyperinflation and auto-PEEP (Marini and Dynamic 2011). This is less relevant in ventilated patients who are not spontaneously initiating breaths. Other than the possibility of offsetting the inspiratory threshold load, PEEP has variable effects (Caramez et al. 2005) on hyperinflation which depends on the degree of flow limitation. External PEEP below the level of auto-PEEP should not affect expiratory flow, as in the presence of flow limitation the expiratory flow will be, by definition, independent of the downstream pressure. In the absence of the flow limitation, pressure applied at the airway opening should be rapidly transmitted to the alveolar level and therefore should still not affect expiratory flow but may contribute to worsening hyperinflation (Tuxen 1989). Classically, then there is a threshold effect of PEEP on hyperinflation. As long as the extrinsic PEEP is set below the auto-PEEP, there should be no effect on lung volume. Once extrinsic PEEP exceeds auto-PEEP, however, it can worsen hyperinflation and its attendant hemodynamic effects.

Conclusion

The normal interaction of the heart and respiratory system includes the effects of intrathoracic pressure on venous return, the consequence of lung inflation for extra-alveolar and intra-alveolar vessels, the effect of intrathoracic pressure on

right and left heart afterloads, and the effects of all of the above on ventricular interaction. During airflow obstruction, the combination of hyperinflation and auto-PEEP results in exaggeration of these normal interactions with the effect of limiting cardiac output. The therapeutic strategy in acute obstructive disease therefore prioritizes reduction of hyperinflation in order to minimize hemodynamic compromise.

References

- Austen KF, Lichtenstein LM. Asthma: physiology, immunopharmacology, and treatment. *Q Rev Biol.* 1974;49:383.
- Bates JHT. Lung mechanics: an inverse modeling approach. Cambridge: Cambridge University Press; 2009.
- Buda AJ, et al. Effect of intrathoracic pressure on left ventricular performance. *N Engl J Med.* 1979;301:453–9.
- Burton AC, Patel DJ. Effect on pulmonary vascular resistance of inflation of the rabbit lungs. *J Appl Physiol.* 1958;12:239–46.
- Calverley PMA. Respiratory failure in chronic obstructive pulmonary disease. *Eur Respir J Suppl.* 2003;47:26s–30s.
- Caramez MP, et al. Paradoxical responses to positive end-expiratory pressure in patients with airway obstruction during controlled ventilation. *Crit Care Med.* 2005;33:1519–28.
- Cassidy SS, et al. Cardiovascular effects of positive-pressure ventilation in normal subjects. *J Appl Physiol.* 1979;47:453–61.
- Cherpanath TGV, Lagrand WK, Schultz MJ, Groeneveld ABJ. Cardiopulmonary interactions during mechanical ventilation in critically ill patients. *Neth Heart J.* 2013;21:166–72.
- Davidson AC, et al. BTS/ICS guideline for the ventilatory management of acute hypercapnic respiratory failure in adults. *Thorax.* 2016;71 Suppl 2:ii1–35.
- Dawson SV, Elliott EA. Wave-speed limitation on expiratory flow—a unifying concept. *J Appl Physiol.* 1977;43:498–515.
- Dhand R, Jubran A, Tobin MJ. Bronchodilator delivery by metered-dose inhaler in ventilator-supported patients. *Am J Respir Crit Care Med.* 1995;151:1827–33.
- Duke GJ. Cardiovascular effects of mechanical ventilation. *Crit Care Resusc.* 1999;1:388–99.
- Fessler HE. Heart-lung interactions: applications in the critically ill. *Eur Respir J.* 1997;10:226–37.
- Fessler HE, Brower RG, Wise RA, Permutt S. Effects of positive end-expiratory pressure on the gradient for venous return. *Am Rev Respir Dis.* 1991;143:19–24.
- Gattinoni L, Pesenti A. The concept of ‘baby lung’. In: Pinsky MR, Brochard L, Mancebo J, editors. *Applied physiology in intensive care medicine.* Berlin Heidelberg: Springer; 2006. p. 303–11.

- Guyton AC, Lindsey AW, Abernathy B, Richardson T. Venous return at various right atrial pressures and the normal venous return curve. *Am J Physiol.* 1957;189:609–15.
- Hamzaoui O, Monnet X, Teboul J-L. Pulsus paradoxus. *Eur Respir J.* 2013;42:1696–705.
- Hess D, Kacmarek R. *Essentials of mechanical ventilation.* 2nd ed. McGraw Hill Professional, New York; 2002.
- Howell JB, Permutt S, Proctor DF, Riley RL. Effect of inflation of the lung on different parts of pulmonary vascular bed. *J Appl Physiol.* 1961;16:71–6.
- Leatherman J. Mechanical ventilation for severe asthma. *Chest.* 2015;147:1671–80.
- Leatherman JW, McArthur C, Shapiro RS. Effect of prolongation of expiratory time on dynamic hyperinflation in mechanically ventilated patients with severe asthma. *Crit Care Med.* 2004;32:1542–5.
- Loring SH, Garcia-Jacques M, Malhotra A. Pulmonary characteristics in COPD and mechanisms of increased work of breathing. *J Appl Physiol.* 2009;107:309–14.
- Magder SA, Lichtenstein S, Adelman AG. Effect of negative pleural pressure on left ventricular hemodynamics. *Am J Cardiol.* 1983;52:588–93.
- Marini JJ, Crooke PS 3rd. A general mathematical model for respiratory dynamics relevant to the clinical setting. *Am Rev Respir Dis.* 1993;147:14–24.
- Marini J, Dynamic J. Hyperinflation and auto-positive end-expiratory pressure: lessons learned over 30 years. *Am J Respir Crit Care Med.* 2011;184:756–62.
- Mead J, Turner JM, Macklem PT, Little JB. Significance of the relationship between lung recoil and maximum expiratory flow. *J Appl Physiol.* 1967;22:95–108.
- Nanas S, Magder S. Adaptations of the peripheral circulation to PEEP1-4. *Am Rev Respir Dis.* 1992;146:688–93.
- Pedersen OF, Butler JP. Expiratory flow limitation. *Compr Physiol.* 2011. <https://doi.org/10.1002/cphy.c100025>.
- Pellegrino R, Brusasco V. On the causes of lung hyperinflation during bronchoconstriction. *Eur Respir J.* 1997;10:468–75.
- Permutt S. Relation between pulmonary arterial pressure and pleural pressure during the acute asthmatic attack. *Chest.* 1973;63, Suppl:25S–8S.
- Permutt S, Bromberger-Barnea B, Bane HN. Alveolar pressure, pulmonary venous pressure, and the vascular waterfall. *Med Thorac.* 1962;19:239–60.
- Pride NB, Permutt S, Riley RL, Bromberger-Barnea B. Determinants of maximal expiratory flow from the lungs. *J Appl Physiol.* 1967;23:646–62.
- Tuxen DV. Detrimental effects of positive end-expiratory pressure during controlled mechanical ventilation of patients with severe airflow obstruction. *Am Rev Respir Dis.* 1989;140:5–9.
- Tuxen DV, Lane S. The effects of ventilatory pattern on hyperinflation, airway pressures, and circulation in mechanical ventilation of patients with severe air-flow obstruction. *Am Rev Respir Dis.* 1987;136:872–9.



Evaluation and Management of Ventilator-Patient Dyssynchrony

46

Enrico Lena, José Aquino-Esperanza,
Leonardo Sarlabous, Umberto Lucangelo,
and Lluís Blanch

Introduction

In order to effectively unload inspiratory muscles and provide a safe ventilation (enhancing gas exchange and protecting the lungs), the ventilator should be in synchrony with patient's respiratory rhythm. The complexity of such interplay leads to several concerning issues that clinicians should be aware and able to recognize. Patient-ventilator dyssynchrony may induce several deleterious effects ranging from dyspnea, anxiety and delirium, and potential cognitive alterations to prolonged mechanical ventilation, diaphragm injury, and patient self-inflicted lung

injury (P-SILI) due to vigorous inspiratory effort leading to high stress (elevated transpulmonary pressure) and strain (global or regional lung overdistension) (Teliás et al. 2018).

Research has shown that patients ventilated for more than 24 h who are able to trigger the ventilator have a high incidence of asynchrony during assisted mechanical ventilation (Thille et al. 2006). Asynchronies are common throughout mechanical ventilation, occur in all mechanical ventilation modes, and might be associated with outcome (Blanch et al. 2015) especially when they occur in clusters (Vaporidi et al. 2017).

E. Lena · U. Lucangelo
Department of Perioperative Medicine, Intensive Care and Emergency, Cattinara Hospital, Trieste University, Trieste, Italy

J. Aquino-Esperanza (✉)
Critical Care Center, Hospital Universitari Parc Taulí, Institut d'Investigació i Innovació Parc Taulí I3PT, Sabadell, Spain

Universitat de Barcelona, Facultat de Medicina, Barcelona, Spain

Biomedical Research Networking Center in Respiratory Diseases (CIBERES), Instituto de Salud Carlos III, Madrid, Spain
e-mail: jaquino@tauli.cat

L. Sarlabous
Critical Care Center, Hospital Universitari Parc Taulí, Institut d'Investigació i Innovació Parc Taulí I3PT, Sabadell, Spain

Biomedical Research Networking Center in Bioengineering, Biomaterials and Nanomedicine (CIBER-BBN), Instituto de Salud Carlos III, Madrid, Spain
e-mail: lsarlabous@tauli.cat

L. Blanch
Critical Care Center, Hospital Universitari Parc Taulí, Institut d'Investigació i Innovació Parc Taulí I3PT, Sabadell, Spain

Biomedical Research Networking Center in Respiratory Diseases (CIBERES), Instituto de Salud Carlos III, Madrid, Spain
e-mail: Lblanch@tauli.cat

Table 46.1 Classification of asynchronies according to the phase of respiratory cycle

Inspiratory period	During the transition from inspiration to expiration	Expiratory period
Trigger delay	Double triggering	Ineffective inspiratory effort
Inspiratory flow mismatching	due to short cycling or reverse triggering	Auto-triggering
Short cycling	Expiratory muscle contraction due to prolonged cycling	Expiratory muscle contraction
Prolonged cycling		
Reverse triggering		

From Subirá et al. (2018). Reproduced with permission of the American Association for Respiratory Care.

For educational and research purpose, asynchronies have been classified according to the phase of the respiratory cycle in which they occur and are as follows: inspiratory or pressurization phase, cycling off to the expiratory phase, and during expiration phase. Table 46.1, reproduced with permission of Subirá et al. (2018), shows this approach. Nevertheless, from a clinical point of view (Aquino Esperanza et al. 2020; Pham et al. 2018), an approach centered on the condition that leads to the mismatch between the patient and the ventilator may help better understand the underlying mechanism and help design new treatment strategies. We will focus primarily on this classification but also will describe others, such as reverse triggering, separately.

Classification

During mechanical ventilation, the control of breathing becomes complex with feedback signals from chemoreceptors (central and peripheral) and mechanoreceptors with vagal and free afferent inputs from the lung, chest wall, and respiratory muscles (Georgopoulos and Roussos 1996). Additionally, pain, anxiety, or endotoxins can directly influence respiratory centers. A high respiratory drive can result from increased metabolic demands, altered gas exchange, and/or intense mechanical stimuli through lung recep-

tors (Brochard et al. 2017). On the contrary, a low respiratory drive can be due to either a primarily depressed central nervous system, by high levels of sedation, or an excessive ventilatory support (Aquino Esperanza et al. 2020; Pham et al. 2018).

Based on the appropriateness of the level of assistance provided by the ventilator, asynchronies could be considered as over-assistance, when the respiratory drive is low, or insufficient assistance, when the patient’s respiratory drive is high.

Over-Assistance (Low Respiratory Drive)

Ineffective Efforts

Ineffective triggering (IE) is the most frequent type of dyssynchrony (Thille et al. 2006; de Wit 2011). It is defined as an inspiratory muscle effort that is not followed by a ventilator breath. This asynchrony occurs when the patient’s attempt to initiate a breath does not reach the ventilator’s trigger threshold. In other words, the ventilator fails to detect the patient’s inspiratory efforts and the patient’s breathing frequency is different from that of the ventilator. These patients often seem calm and not dyspneic. The main causes are delayed cycling, over-assistance, and hyperinflation. All of these lead to intrinsic positive end-expiratory pressure (PEEPi). Decreased respiratory drive by other mechanisms such as sedation increases the occurrence of IE. Of note, a deeper level of sedation with propofol has been associated with higher frequency of IE during pressure support ventilation (Vaschetto et al. 2014). For diagnostic purposes, a decrease in airway pressure (Paw) waveform in association with an increase in flow during expiration is highly suggestive (Figs. 46.1 and 46.2). Confirmatory evidence can be obtained with the use of esophageal pressure (Pes) measurement or a catheter dotted with electrodes to measure the electromyographic activity of the diaphragm (EAdi). These can show a negative deflection in Pes or an increase in the EAdi signal that is not followed by a mechanical breath.

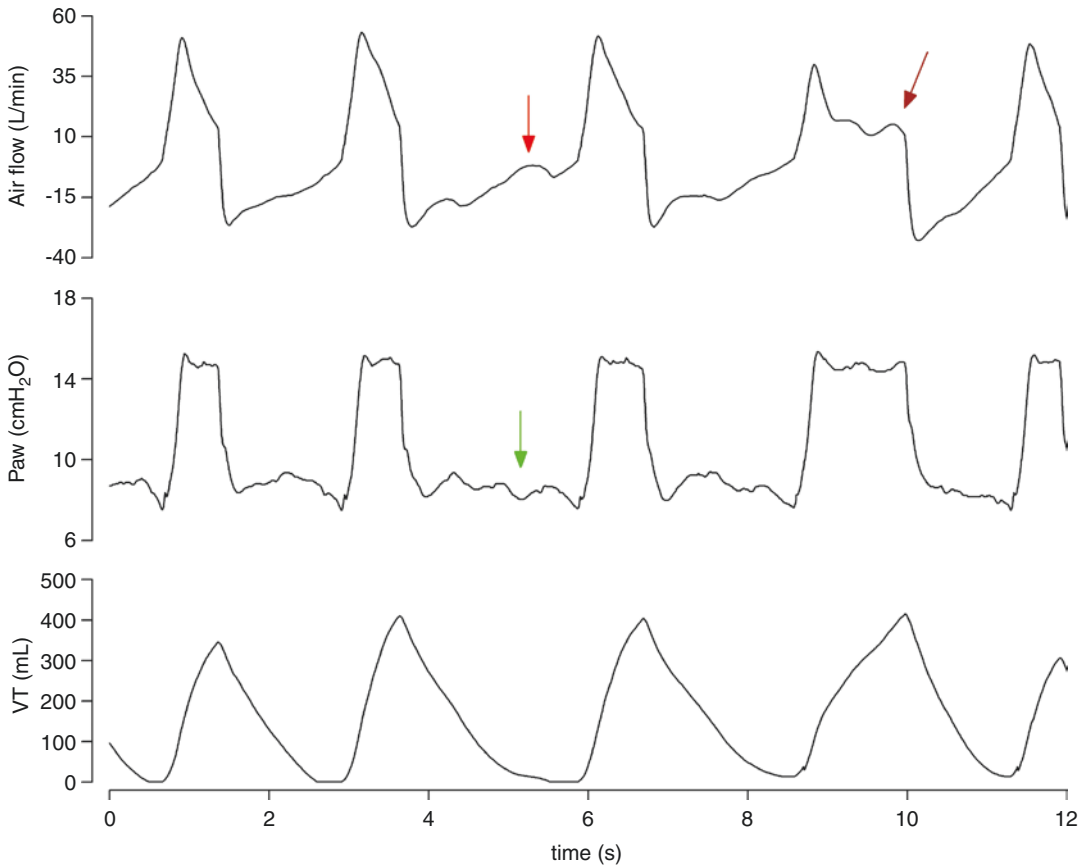


Fig. 46.1 Ineffective effort: tracings of airflow, airway pressure, and tidal volume in a mechanically ventilated patient on pressure support ventilation mode. Ineffective inspiratory efforts are present during expiratory periods. A decrease in airway pressure (green arrow) together with an increase in airflow (red arrow) not followed by a venti-

lator breath during expiration is suggestive of an ineffective inspiratory effort. This asynchrony occurs when the patient's attempt to initiate a breath does not reach the ventilator's trigger threshold. An example of prolonged cycling (see Fig. 46.3 for further details) could also be observed (brown arrow)

Delayed or Prolonged Cycling

Delayed cycling occurs when mechanical insufflation continues after neural inspiration has ceased or even during active expiration. If the ventilator breath is longer than the patient's neural inspiratory time, the patient may actually fight the ventilator, recruiting expiratory muscles in an attempt to force expiration.

In pressure support ventilation mode (PSV), the ventilator cycles to expiration when flow decreases to a set percentage of peak inspiratory flow. Insufflation tends to be longer with higher levels of pressure support and with increased airflow resistance. Additionally, higher levels of

pressure support result in a higher peak flow that may shorten neural inspiratory time (Fernandez et al. 1999) further contributing to a mismatch between a long mechanical insufflation and a short neural inspiratory time. In this scenario, delivered inspiratory flow decreases very slowly with mechanical inspiratory time (T_i) potentially exceeding neural T_i due to the flow cycling mechanism. This over-insistence results in hyperventilation, hypocapnia, respiratory alkalosis, and reduced respiratory drive which leads to further dyssynchrony and perpetuates the mechanism (Gilstrap and Davies 2016). It also needs to be appreciated that non-respiratory mechanisms

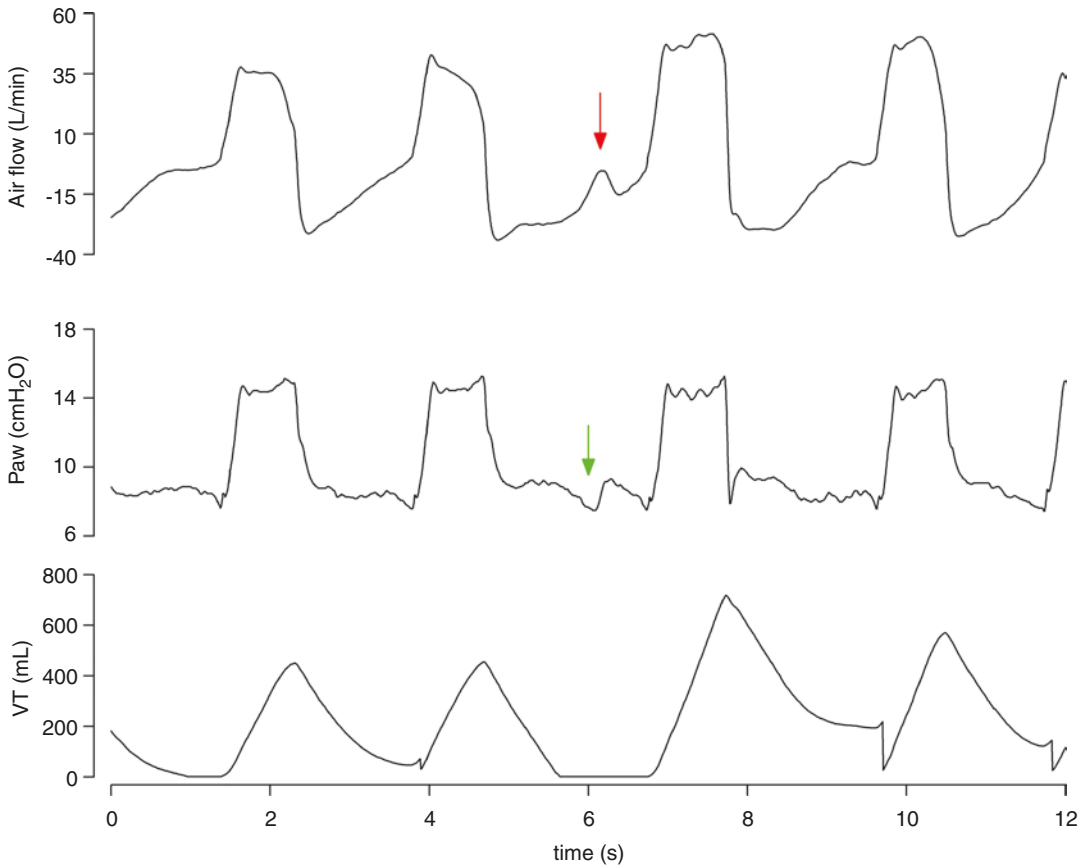


Fig. 46.2 Ineffective effort: tracings of airflow, airway pressure, and tidal volume in a mechanically ventilated patient on pressure support ventilation mode. Other examples of ineffective inspiratory efforts are present during expiratory periods. A decrease in airway pressure (green

arrow) together with an increase in airflow (red arrow) not followed by a ventilator breath during expiration is suggestive of an ineffective inspiratory effort. This type of asynchrony occurs when the patient's attempt to initiate a breath does not reach the ventilator's trigger threshold

such as airway leaks can induce prolonged cycling. Thus, attention should be paid to the cuff, the mechanical circuit, and the integrity of the endotracheal or tracheostomy tube.

Detection of prolonged cycling can be quite problematic when only ventilator waveforms are used (Fig. 46.3), but it can be easily detected by comparing mechanical insufflation with the duration of inspiratory effort as assessed by *Peso* or *EAdi*.

Insufficient Assistance (High Respiratory Drive)

Flow Starvation

Inspiratory flow mismatching occurs when the ventilator fails to meet the patient's flow

demand. Inadequate flow delivery is most common when ventilator flow delivery is set inappropriately low, or the combination of tidal volume (VT) and *Ti* does not result in adequate flow during acute respiratory failure, or when inspiratory flow demands are high and vary from breath to breath (Flick et al. 1989; Marini et al. 1986). Inspiratory flow mismatching is more frequent in modalities in which it is impossible for the patient to modify the flow, such as volume control-continuous mandatory ventilation (Gilstrap and Davies 2016). MacIntyre et al. (1997) demonstrated that inspiratory flow mismatching could be improved by increasing ventilator flow delivery or, when subjects were ventilated with a flow limited strategy, by using the variable flow pressure-limited breath. It is particularly impor-

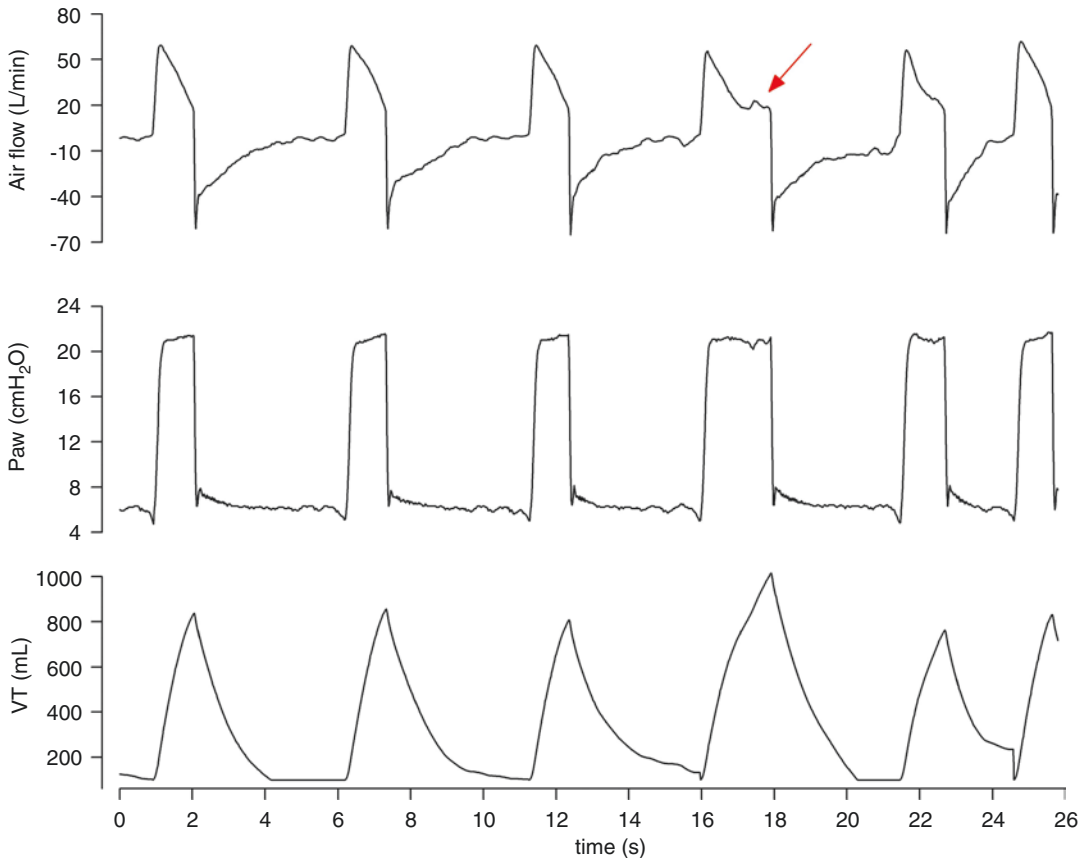


Fig. 46.3 Delayed or prolonged cycling: tracings of air-flow, airway pressure, and tidal volume in a mechanically ventilated patient on pressure support ventilation mode. In this mode, each breath is patient triggered and the cycling from inspiration to expiration occurs when airflow decreases to a set percentage of peak inspiratory airflow. Prolonged or delayed cycling (red arrow) occurs when

mechanical insufflations continue after neural inspiration has ceased or even during active expiration. High levels of pressure support, increased airflow resistance, and airways leaks are predisposing factors. Persistence of mechanical inflation during neural expiration is uncomfortable and patients may exhibit expiratory muscle activity

tant to track inspiratory flow mismatching during lung-protective ventilation because vigorous inspiratory efforts could promote pulmonary edema by increasing the transvascular pressure gradient (Kallet et al. 1999), tidal recruitment associated with pendelluft flow (lung volume redistribution), and consequent regional lung over-distention, which can occur in flow- and pressure-limited breaths in volume control-continuous mandatory ventilation and volume control decelerated flow, as well as in pressure control-continuous mandatory ventilation (Yoshida et al. 2017). Sometimes, if the effort made by the patient is high enough, a second

mechanical breath can be triggered (double trigger and breath stacking) (Figs. 46.4 and 46.5).

Short or Premature Cycling

Premature or short cycling occurs when the neural time is greater than the ventilator's inspiratory time.

The ventilator ends flow delivery, but the patient's inspiratory effort continues. If the patient's effort exceeds the trigger threshold, it can activate another breath, generating a double trigger (Fig. 46.6). Activation of inspiratory muscles during mechanical deflation (lengthening) results in an eccentric contraction of the dia-

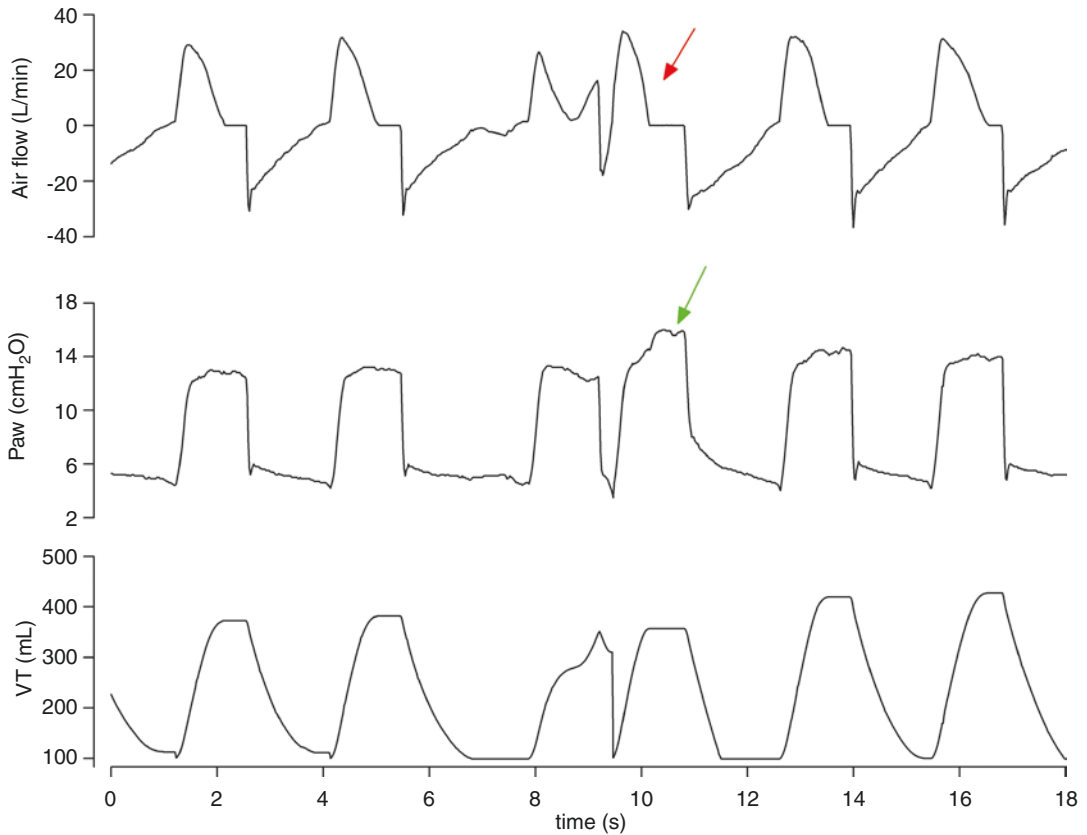


Fig. 46.4 Flow starvation: tracings of airflow, airway pressure, and tidal volume in a mechanically ventilated patient on pressure-limited ventilation mode. Example of inspiratory flow mismatching (also named flow starvation) which occurs when the ventilator fails to meet the patient's flow demand. In this case, ventilator airflow is set inappropriately too low to fulfill the patient's high

inspiratory flow demands. Inspiratory effort continues during mechanical insufflation and it is strong enough to trigger a second mechanical breath (red arrow), which occurs without expiration and leads to breath stacking (green arrow). Notice that the tidal volume in breath stacking is almost double with associated elevated airway pressure

phragm (Gea et al. 2009) which is potentially injurious to the respiratory muscles.

Double Trigger and Breath Stacking

Double triggering consists of a sustained inspiratory effort that persists beyond the ventilator inspiratory time, cessation of inspiratory flow, or the beginning of mechanical expiration. A second ventilator breath consequently is triggered, which may or may not be followed by a short expiration, in which all or part of the volume of the first breath is added to the second breath, a phenomenon called breath stacking (Fig. 46.7) (Blanch et al. 2015; de Wit 2011; Gilstrap and MacIntyre 2013; Kallet et al. 2006). The delivered volume accumulated

during the two breaths without normal exhalation is very high and can potentially double VT of normal breaths in volume-targeted modes (de Haro et al. 2018). Therefore, high VT from double triggering might result in hyperinflation and high transpulmonary pressures leading to pulmonary barotrauma, excessive stress and strain, and increased inflammatory response (Yoshida et al. 2017).

Importantly, double triggering can originate from different underlying conditions, such as those where a high respiratory drive exists (flow starvation and premature cycling) or when a reverse trigger occurs with a diaphragmatic contraction strong enough to trigger a second mechanical breath.

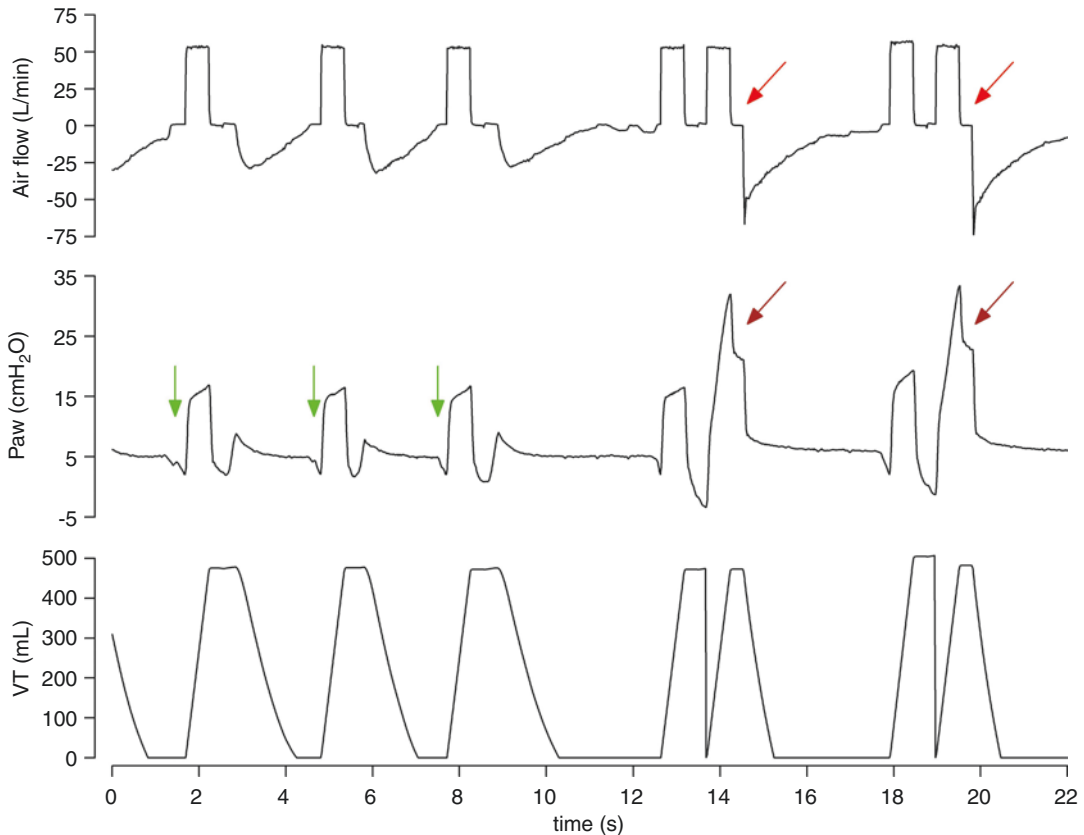


Fig. 46.5 Flow starvation: tracings of airflow, airway pressure, and tidal volume in a mechanically ventilated patient on volume assist-control ventilation mode. Inspiratory flow mismatching (also named flow starvation) occurs when the ventilator fails to meet the patient's flow demand. Inspiratory flow is set inappropriately low to fulfill patient's demand. Inspiratory effort continues

during mechanical insufflation (green arrow in airway pressure waveform) in each breath, and sometimes it is strong enough to trigger a second mechanical insufflation (red arrow) without expiration and consequent breath stacking (brown arrows). Notice that the tidal volume in breath stacking is almost double with associated elevated airway pressure

The Entrainment Phenomenon: Reverse Triggering

Reverse triggering (RT) is a recently identified type of dyssynchrony, in which ventilator insufflations trigger diaphragmatic muscle contractions through activation of the patient's respiratory center in response to passive insufflation of the lungs. It is a consequence of respiratory entrainment which occurs when the patient's respiratory center is harmonized with the rhythm of the ventilator. Entrainment most often occurs when tidal volumes and respiratory rates are similar to the subject's own respiratory rate and tidal volume (Flick et al. 1989). The possible explanation is

that flow and pressure applied by the ventilator activate stretch receptors in the upper airways, lungs, and chest wall. Feedback from these receptors causes the respiratory control center to match the phase and frequency of the external stimulus, producing a repetitive respiratory pattern (de Vries et al. 2019). The ventilator seemingly "triggers" the patient. The resulting neural and muscular activity is a "reverse-triggered" effort.

During reverse triggering, the patient's inspiratory effort starts after and usually persists beyond the machine breath. Because the patient's inspiratory muscles are still active at the beginning of expiration, they impede the elastic recoil of the

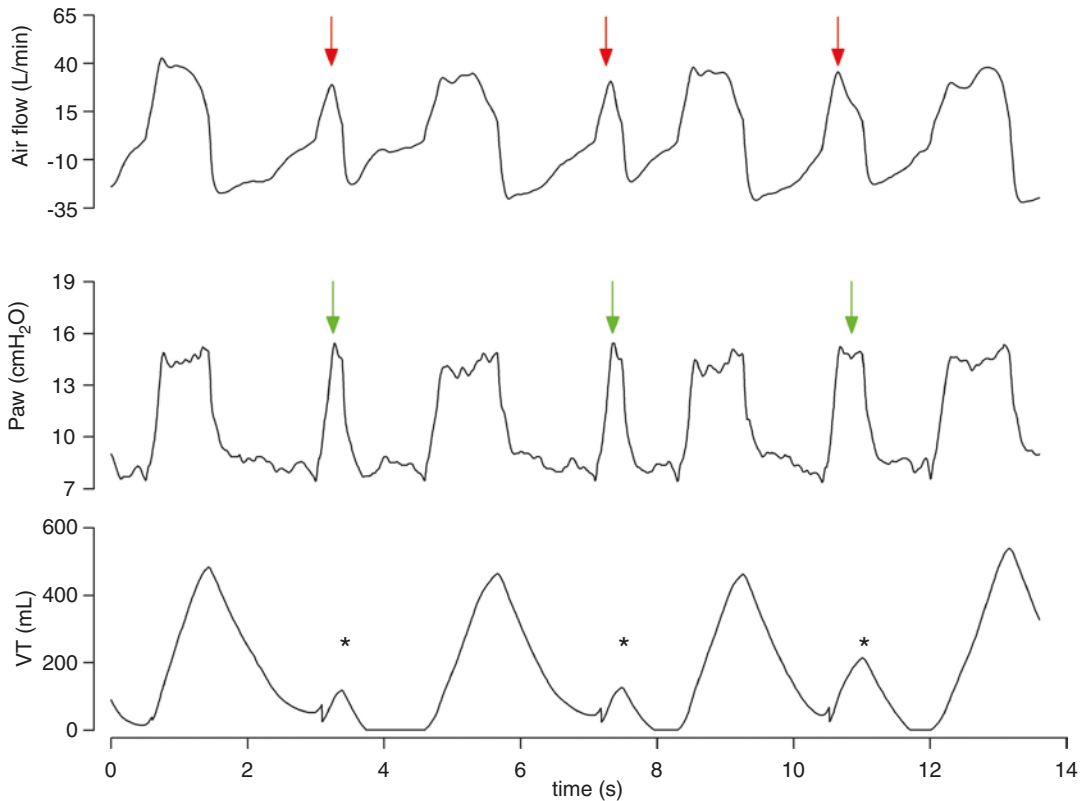


Fig. 46.6 Short or premature cycling: tracings of airflow, airway pressure, and tidal volume in a mechanically ventilated patient on pressure support ventilation mode. In this mode, each breath is patient triggered and cycling from inspiration to expiration occurs when airflow decreases to a set percentage of peak inspiratory airflow. Short or premature cycling ensues when mechanical insufflations end before neural inspiration. Therefore, patient's inspiratory muscles are still active at the beginning of expiration and impede the elastic recoil of the

respiratory system. A short cycle is identified as an inspiratory time less than one-half the mean inspiratory time (red arrow in flow waveform and green arrow in airway pressure waveform). Identification of short-cycled breaths sometimes requires monitoring the esophageal pressure or electrical activity of the diaphragm. Notice the small delivered tidal volume during the short-cycled breath, which is added to the previous delivered breath because of an insufficient expiration time (asterisk)

respiratory system from increasing the alveolar pressure that is needed for expiration, and the peak expiratory flow is reduced (Fig. 46.8) (Murias et al. 2016). When the patient's effort is sufficiently deep and long, the decrease in airway pressure can trigger a second ventilator breath with a nil or very short expiratory time (Akoumianaki et al. 2013; Delisle et al. 2016) (Fig. 46.9).

Assessment of Asynchronies

Detection of asynchronies can be made by different techniques. These include analysis of waveforms provided on the ventilator screen of flow

time, pressure time, and integrated volume; the addition of esophageal tracings obtained by an esophageal balloon-tipped catheter; diaphragmatic electromyography, which is commercially available on some ventilators; and, more recently, automated algorithms (Subirà et al. 2018).

The inspection of waveforms can provide clues for the existence of dyssynchrony. It is noteworthy that the ability of clinicians to properly identify them by visual inspection is partially influenced by their expertise and the type of dyssynchrony. Moreover, the sole analysis of breath-to-breath waveforms shows a very low sensitivity and a low positive predictive value (22% and 32% respectively). Even trained physicians were able

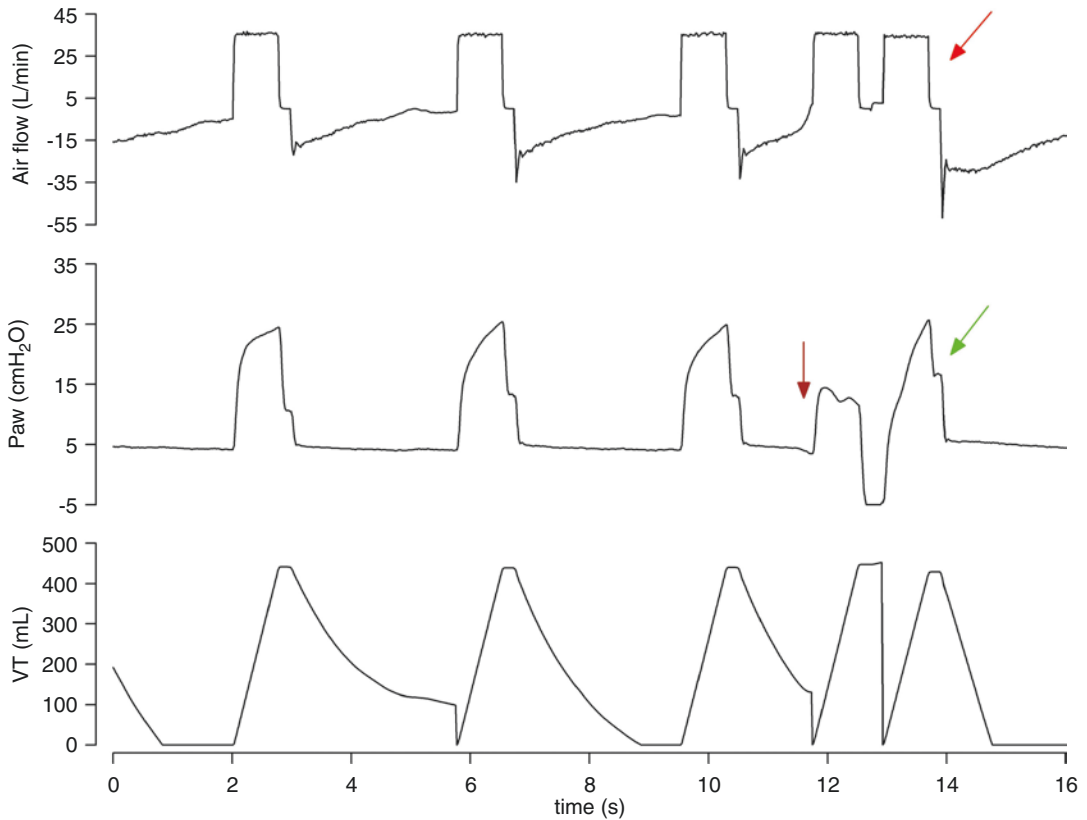


Fig. 46.7 Double cycling: tracings of airflow, airway pressure, and tidal volume in a mechanically ventilated patient on volume assisted-control ventilation mode. In this mode, each breath is either machine triggered or patient triggered, and the cycling from inspiration to expiration occurs when the tidal specified volume is delivered.

Double cycling (red arrow in flow waveform and green arrow in airway pressure waveform) develops when a sustained effort (brown arrow in airway pressure) persists beyond ventilator's inspiratory time and reaches a defined trigger threshold inducing a second mechanical breath

to recognize less than one-third of asynchronies. By contrast, negative predictive values by this method were high and were achieved in over 90% of cases. Addition of the esophageal pressure tracings can help ameliorate the process and favor a better recognition. Unfortunately, this minimal invasive manoeuvre is not routinely utilized in mechanical ventilated patients and it requires experience for properly placing and understanding how to interpret the tracing.

EAdi is commercially available in Servo I (Maquet, Sweden) ventilators in Neurally Adjusted Ventilatory Assist (NAVA) mode and provides a reliable insight into patient's inspiratory and expiratory time and can be used to detect asynchronies. Supporting ventilation based on

EAdi signal should improve the response of the ventilator and synchrony, given that the signal reflects closely the neural time of the control of breathing. Moreover, a direct comparison of asynchronies detections in patients of intensive care unit using waveforms analysis or EAdi during the weaning phase showed that double, premature, and late cyclings, as well as asynchrony index, were more frequently detected utilizing EAdi (Rolland-Debord et al. 2017). Unfortunately, NAVA is only available in Servo I ventilators, and careful adjustments for correct positioning must be made by periodically checking for catheter displacement.

More recently, automated detection algorithms have been developed and validated utiliz-

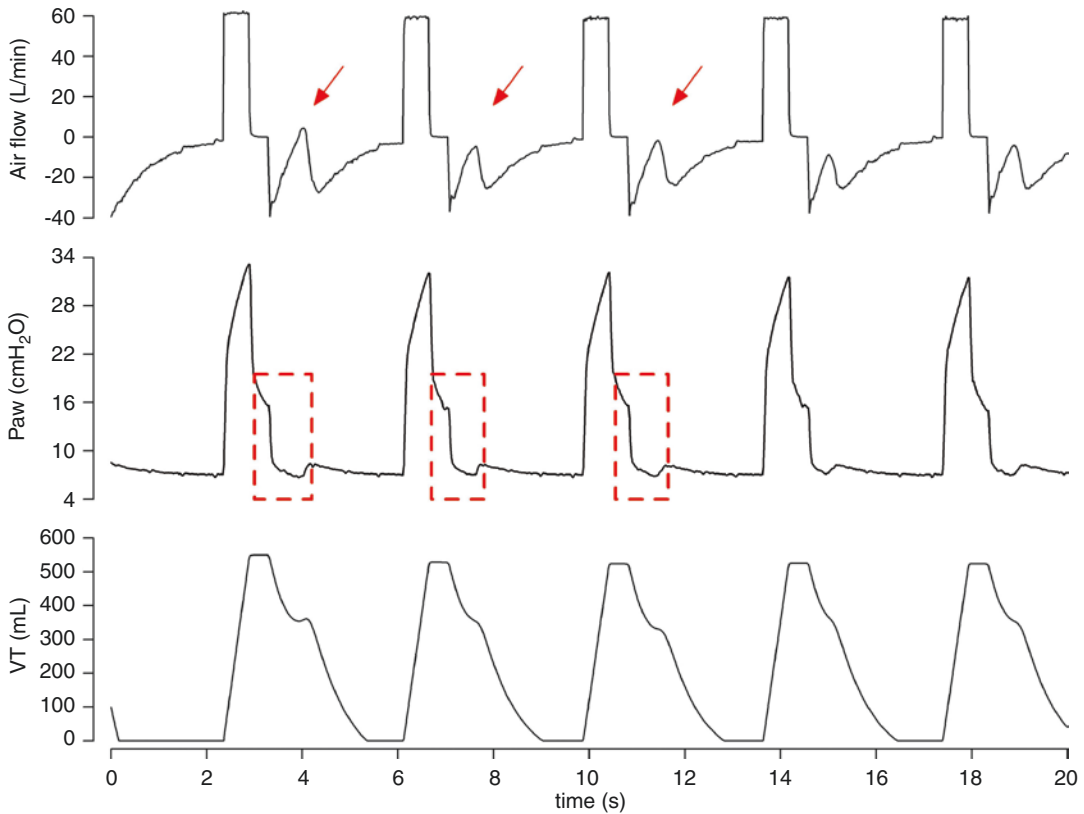


Fig. 46.8 Reverse triggering: tracings of airflow, airway pressure, and tidal volume in a mechanically ventilated patient on volume assisted-control ventilation mode. Reverse triggering results in an ineffective effort. Ventilator insufflations trigger diaphragmatic muscle contractions in response to passive insufflations of the lungs.

In the absence of the esophageal pressure or electrical activity of the diaphragm monitoring, an increase in expiratory flow (red arrows) or decrease in inspiratory airway pressure later in the respiratory cycle (box in dotted lines) can indicate the event

ing the continuous analysis of the flow-time and pressure-time tracings in order to detect asynchronies. There are several different algorithms that have different performances. BetterCare™ system is one which can be adapted to any ventilator. It has been validated for the automated detection of ineffective efforts during expiration with high positive and negative predictive values compared either to expert's judgment or to physiological measurements obtained by EAdi (Blanch et al. 2015; de Haro et al. 2018; Blanch et al. 2012). There are many other programs such as VentMAP platform, NeuroSync index, and others. We believe that, given the pattern of appearance of patient-ventilator asynchronies over time which recently have been shown to occur in clusters rather than fixed time intervals, automated

software detection and prediction, as well as intelligent alarms, will be more helpful and more accurate for improving patients care during mechanical ventilation than visual inspection of the waveforms at fixed periods. Visual inspections are time-consuming and the absence of events during the observational period does not mean that they do not appear at other times.

Management – A Clinical Approach

Identifying asynchronies requires careful attention to patients and their ventilator waveforms. Table 46.2, from Subirá et al. (2018), summarizes the different approaches that can be used to correct each type of asynchrony. Although sedation

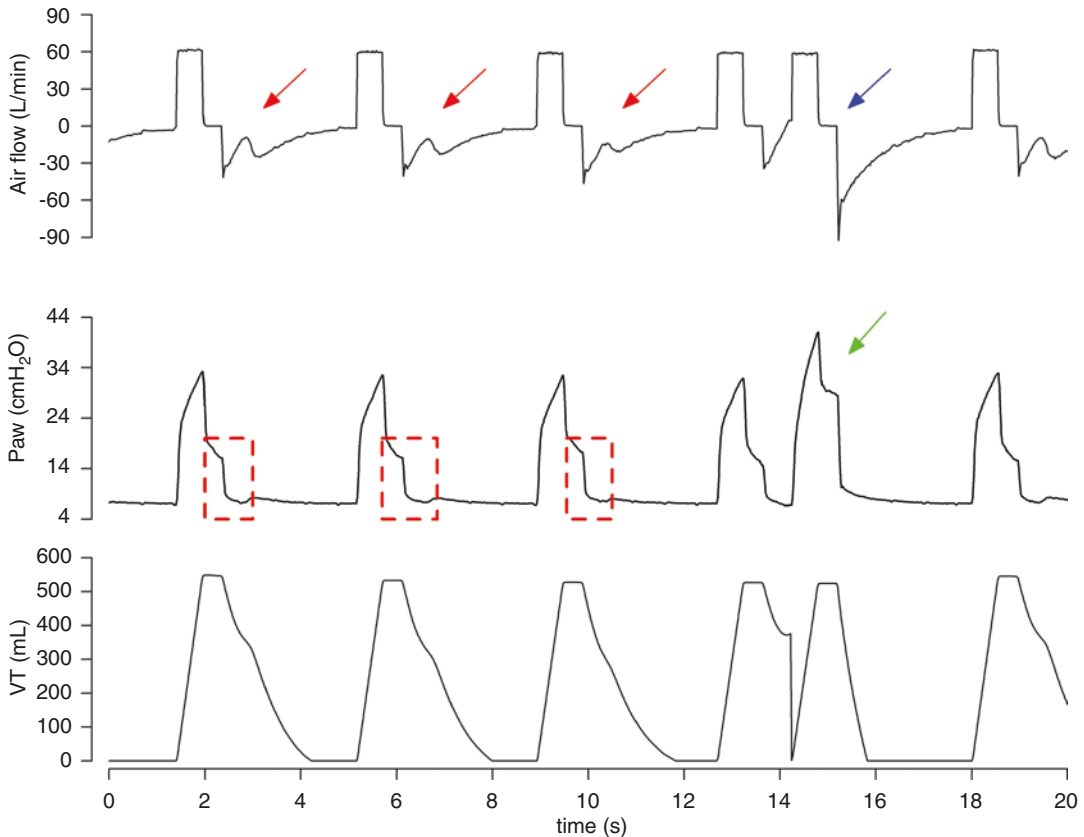


Fig. 46.9 Reverse triggering: tracings of airflow, airway pressure, and tidal volume in a mechanically ventilated patient on volume assisted-control ventilation mode. Reverse triggering results in an ineffective effort (red arrow in flow waveform and dotted lines in airway pressure). Ventilator insufflations trigger diaphragmatic mus-

cle contractions in response to passive insufflations of the lungs; if patient's inspiratory effort is greater than the trigger threshold, a second breath (double cycling) could be developed (blue arrow) with associated breath stacking (green arrow) due to high tidal volumes

and analgesia are often used to treat asynchronies, this approach raises various concerns. Deep sedation is actually an independent risk factor for ineffective inspiratory efforts (Chanques et al. 2013). Furthermore, deep sedation is associated with longer mechanical ventilation duration and ICU stays (Barr et al. 2013). Importantly, a recent investigation has shown that sedatives, whether alone or combined with opioids, do not result in better patient-ventilator interaction than opioids alone, in any ventilatory mode, and that opioid administration in elevated doses (alone or with sedatives) with lowered the Asynchrony Index without depressing consciousness (de Haro et al. 2019). Adjusting ventilator settings seems to be a better approach than use of narcotics.

Chanques et al. (2013) found that in subjects with asynchronies who were treated with increased sedation-analgesia and either adjustments or no adjustments in ventilator settings, asynchronies only significantly decreased in those who had ventilator setting adjustments. Opioids can help bring about better patient-ventilator interaction because they can reduce active expiration, reduce the activity of the respiratory control center, and reduce the central perception of dyspnea and anxiety. It is essential to detect dyspnea caused by low assistance and to adjust the breathing frequency to ensure that each inspiratory effort is followed by a ventilator breath, while at the same time evaluating the potential for lung injury and newly elevated TV.

Table 46.2 Summary of various approaches to correct each type of asynchrony

Asynchrony	Action
Inspiratory flow mismatching	Increase gas flow; decrease respiratory drive, and assess adequacy of analgesia and sedation; check for dyspnea
Short or prolonged cycling	Increase or decrease inspiratory period; check cycling off in pressure support; use proportional modes
Double triggering	Increase ventilator inspiratory time; try pressure support, titrating flow termination criteria to improve synchrony, or proportional modes; consider paralyzing agents if tidal volume is too elevated (> 8 mL/kg) in ARDS or in patients with risk factors for developing lung injury
Double triggering due to reverse triggering	Decrease sedation; check breathing frequency; consider paralyzing agents if tidal volume is too elevated (> 8 mL/kg) in ARDS or in patients with risk factors for developing lung injury
Expiratory muscle contraction due to prolonged cycling	Reduce inspiratory period by checking cycling off and tidal volume; check for comfort
Ineffective inspiratory efforts	Check trigger sensitivity and excessive air trapping; check for excessive assistance (excessive set frequency and/or inspiratory time during controlled modes or excessive pressure support ventilation level); counterbalance auto-PEEP by using external PEEP; check for dyspnea; consider proportional modes
Auto-triggering	Check trigger sensitivity; check for leaks and water in the ventilator circuit
Expiratory muscle contraction during expiration	Check for excessive assistance; check for air trapping and auto-PEEP

From Subirá et al. (2018). Reproduced with permission of the American Association for Respiratory Care.

Clinical Consequences

Some studies (Thille et al. 2006; Blanch et al. 2015; Vaporidi et al. 2017; Beitler et al. 2016) have reported that asynchronies are more common than expected and are associated with poor prognosis. In one study, subjects with an ineffective triggering index greater than 10% required longer duration of mechanical ventilation (De Wit et al. 2009). Moreover, Thille et al. (2006) reported that mechanical ventilation duration and incidence of tracheostomy were greater in subjects who had an asynchrony index greater than 10%. Furthermore, in a recent analysis of ventilator waveforms that covered more than 80% of total ventilatory time, ICU and hospital mortality were higher in subjects who had an asynchrony index greater than 10% (Blanch et al. 2015). Excessive effort and discomfort often are treated with sedatives or even neuromuscular blockers. However, avoiding patient-ventilator interactions by these approaches is not necessarily helpful because both of these increase the risk of respiratory muscle weakness and atrophy (Powers et al. 2009; Levine et al. 2008), which can lead to prolongation of weaning, increased dependence on the ventilator, and a longer ICU stay. The average proportion of asynchronies dur-

ing mechanical ventilation may be less important for outcomes than the intensity or period in which they occur. Recently, Vaporidi and colleagues (2017) pointed out the importance of clusters of ineffective inspiratory efforts compared to global incidence over a long period of time. By analyzing 24-h recordings obtained from 110 subjects on the first day of PSV or PAV, they found that clusters of IE (more than 30 in a 3-min period) were often present. Unlike the overall incidence, the duration and power of clusters were associated with prolonged mechanical ventilation and increased mortality. This investigation highlights the importance of variability of ineffective efforts over time within patients and underscores the need for continuous monitoring of airway pressure and air flow.

Conclusion

Mechanical ventilation is a life-saving supportive treatment in critically ill patients. However, adverse effects associated with mechanical ventilation can also prolong ICU stay and affect outcome. Asynchronies can inflict lung injury, cause discomfort, increase dyspnea, prolong ventilator use and ICU stay, and even increase mortality.

The evidence suggests that increasing sedation is not the answer, and even the use of proportional modes of ventilation does not provide a definitive solution to fully synchronizing ventilator breaths with the patient's respiratory activity. To improve patient-ventilator interaction, we must deepen our understanding of the principles of respiratory physiology and respiratory system mechanics and improve our ability to apply these concepts in individual patients.

References

- Akoumianaki E, Lyazidi A, Rey N, Matamis D, Perez-Martinez N, Giraud R, et al. Mechanical ventilation-induced reverse-triggered breaths: a frequently unrecognized form of neuromechanical coupling. *Chest*. 2013;143(4):927–38.
- Aquino Esperanza J, Sarlabous L, de Haro C, Magrans R, Lopez-Aguilar J, Blanch L. Monitoring asynchrony during invasive mechanical ventilation. *Respir Care*. 2020;65(6):847–69. <https://doi.org/10.4187/respcare.07404>.
- Barr J, Fraser GL, Puntillo K, Ely EW, Gélinas C, Dasta JF, et al. Clinical practice guidelines for the management of pain, agitation, and delirium in adult patients in the intensive care unit: executive summary. *Am J Heal Pharm*. 2013;70(1):53–8.
- Beitler JR, Sands SA, Loring SH, Owens RL, Malhotra A, Spragg RG, et al. Quantifying unintended exposure to high tidal volumes from breath stacking dyssynchrony in ARDS: the BREATHE criteria. *Intensive Care Med*. 2016;42(9):1427–36.
- Blanch L, Sales B, Montanya J, Lucangelo U, Oscar GE, Villagra A, et al. Validation of the better care® system to detect ineffective efforts during expiration in mechanically ventilated patients: a pilot study. *Intensive Care Med*. 2012;38(5):772–80.
- Blanch L, Villagra A, Sales B, Montanya J, Lucangelo U, Luján M, et al. Asynchronies during mechanical ventilation are associated with mortality. *Intensive Care Med*. 2015;41(4):633–41.
- Brochard L, Slutsky A, Pesenti A. Mechanical ventilation to minimize progression of lung injury in acute respiratory failure. *Am J Respir Crit Care Med*. 2017;195:438–42.
- Chanques G, Kress JP, Pohlman A, Patel S, Poston J, Jaber S, et al. Impact of ventilator adjustment and sedation-analgesia practices on severe asynchrony in patients ventilated in assist-control mode. *Crit Care Med*. 2013;41(9):2177–87.
- de Haro C, López-Aguilar J, Magrans R, Montanya J, Fernández-Gonzalo S, Turon M, et al. Double cycling during mechanical ventilation: frequency, mechanisms, and physiological implications. *Crit Care Med*. 2018;46(9):1385–92.
- de Haro C, Magrans R, López-aguilar J, Montanya J, Lena E, Subirà C, et al. Effects of sedatives and opioids on trigger and cycling asynchronies throughout mechanical ventilation: an observational study in a large dataset from critically ill patients. *Crit Care*. 2019;23(1):245.
- de Vries HJ, Jonkman AH, Tuinman PR, Girbes ARJ, Heunks LMA. Respiratory entrainment and reverse triggering in a mechanically ventilated patient. *Ann Am Thorac Soc*. 2019;16(4):499–505.
- de Wit M. Monitoring of patient-ventilator interaction at the bedside. *Respir Care*. 2011;56(1):61–72.
- De Wit M, Miller KB, Green DA, Ostman HE, Gennings C, Epstein SK. Ineffective triggering predicts increased duration of mechanical ventilation. *Crit Care Med*. 2009;37(10):2740–5.
- Delisle S, Charbonney E, Albert M. Patient-ventilator asynchrony due to reverse triggering occurring in brain-dead patients: clinical implications and physiological meaning. *Am J Respir Crit Care Med*. 2016;194(9):1166–8.
- Fernandez R, Mendez M, Younes M. Effect of ventilator flow rate on respiratory timing in normal humans. *Am J Respir Crit Care Med*. 1999;159:710–9.
- Flick GR, Bellamy PE, Simmons DH. Diaphragmatic contraction during assisted mechanical ventilation. *Chest*. 1989;96(1):130–5.
- Gea J, Zhu E, Gáldiz JB, Comtois N, Salazkin I, Antonio Fiz J, et al. Functional consequences of eccentric contractions of the diaphragm. *Arch Bronconeumol*. 2009;45(2):68–74.
- Georgopoulos D, Roussos C. Control of breathing in mechanically ventilated patients. *Eur Respir J*. 1996;9(10):2151–60.
- Gilstrap D, Davies J. Patient-ventilator interactions. *Clin Chest Med*. 2016;37(4):669–81.
- Gilstrap D, MacIntyre N. Patient-ventilator interactions implications for clinical management. *Am J Respir Crit Care Med*. 2013;188(9):1058–68.
- Kallet RH, Alonso JA, Luce JM, Matthay MA. Exacerbation of acute pulmonary edema during assisted mechanical ventilation using a low-tidal volume, lung-protective ventilator strategy. *Chest*. 1999;116(6):1826–32.
- Kallet RH, Campbell AR, Dicker RA, Katz JA, Mackersie RC. Effects of tidal volume on work of breathing during lung-protective ventilation in patients with acute lung injury and acute respiratory distress syndrome. *Crit Care Med*. 2006;34(1):8–14.
- Levine S, Nguyen T, Taylor N, Friscia M, Budak MT, Rothenberg P, et al. Rapid disuse atrophy of diaphragm fibers in mechanically ventilated humans. *N Engl J Med*. 2008;358(13):1327–35.
- MacIntyre NR, McConnell R, Cheng K, Sane A. Patient-ventilator flow dyssynchrony: flow-limited versus pressure-limited breaths. *Crit Care Med*. 1997;25:161–7.

- Marini JJ, Rodriguez RM, Lamb V. The inspiratory workload of patient-initiated mechanical ventilation. *Am Rev Respir Dis.* 1986;134(5):902–9.
- Murias G, Lucangelo U, Blanch L. Patient-ventilator asynchrony. *Curr Opin Crit Care.* 2016;22(1):53–9.
- Pham T, Telias I, Piraino T, Yoshida T, Brochard LJ. Asynchrony consequences and management. *Crit Care Clin.* 2018;34(3):325–41.
- Powers SK, Kavazis AN, Levine S. Prolonged mechanical ventilation alters diaphragmatic structure and function. *Crit Care Med.* 2009;37(Suppl. 10):347–53.
- Rolland-Debord C, Bureau C, Poitou T, Belin L, Clavel M, Perbet S, et al. Prevalence and prognosis impact of patient – ventilator asynchrony in early phase of weaning according to two detection methods. *Anesthesiology.* 2017;127:989–97.
- Subirà C, de Haro C, Magrans R, Fernández R, Blanch L. Minimizing asynchronies in mechanical ventilation: current and future trends. *Respir Care.* 2018;63(4):464–78.
- Telias I, Brochard L, Goligher EC. Is my patient's respiratory drive (too) high? *Intensive Care Med.* 2018;44(11):1936–9.
- Thille AW, Rodriguez P, Cabello B, Lellouche F, Brochard L. Patient-ventilator asynchrony during assisted mechanical ventilation. *Intensive Care Med.* 2006;32(10):1515–22.
- Vaporidi K, Babalis D, Chytas A, Lilitsis E, Kondili E, Amargianitakis V, et al. Clusters of ineffective efforts during mechanical ventilation: impact on outcome. *Intensive Care Med.* 2017;43(2):184–91.
- Vaschetto R, Cammarota G, Colombo D, Longhini F, Grossi F, Giovanniello A, et al. Effects of propofol on patient-ventilator synchrony and interaction during pressure support ventilation and neurally adjusted ventilatory assist. *Crit Care Med.* 2014;42(1):74–82.
- Yoshida T, Fujino Y, Amato MBP, Kavanagh BP. Fifty years of research in ARDS spontaneous breathing during mechanical ventilation risks, mechanisms, and management. *Am J Respir Crit Care Med.* 2017;195(8):985–92.



Cardiopulmonary Monitoring in the Patient with an Inflamed Lung

Tommaso Tonetti and V. Marco Ranieri

ARDS as an Inflammatory Disease

The acute respiratory distress syndrome (ARDS) is a complex and high-mortality disease, which is invariably characterized by three main elements: (a) lung inflammation, (b) diffuse alveolar damage (edema, hemorrhage, hyaline membranes), and (c) severe impairment of gas exchange (Thompson et al. 2017). Since its original description in 1967 (Ashbaugh et al. 1967), four different (and partly conflicting) definitions have been used, but in the present decade, the current Berlin definition has gained widespread consensus (ARDS Definition Task Force et al. 2012). It defined ARDS based on the ratio of the arterial partial pressure of oxygen to the fraction of inspired oxygen ($\text{PaO}_2/\text{FiO}_2$ ratio, with the former measured in mmHg) measured at the clinical level of positive end-expiratory pressure (PEEP). The level of hypoxemia defines three mutually exclusive categories of ARDS: mild ($200 < \text{PaO}_2/\text{FiO}_2 \leq 300$), moderate ($100 < \text{PaO}_2/\text{FiO}_2 \leq 200$),

and severe ($\text{PaO}_2/\text{FiO}_2 \leq 100$) (ARDS Definition Task Force et al. 2012). ARDS can be considered primary if the pathogenic insult is directed to the lung (e.g., infective pneumonia, aspiration of gastric content) or secondary if it develops as a consequence of other conditions (e.g., sepsis, trauma).

Pathophysiology of ARDS

Exudative Phase

Whatever the initial causative disease, the lung-damaging chain of events starts with the activation of alveolar macrophages through the TLR pathways (or similar pattern recognition receptors), leading to the so-called exudative phase of ARDS (Thompson et al. 2017). This phase is mainly characterized by damage of epithelial and endothelial monolayers, causing barrier function loss, exudative flooding of the alveoli, and formation of hyaline membranes.

In particular, activated alveolar macrophages release proinflammatory mediators and cytokines, such as complement proteins, tumor necrosis factor (TNF), transforming growth factor (TGF)- β , interleukin (IL)-1 β , IL-6, IL-8, and IL-17. These recruit neutrophils and monocytes to the alveolar and interstitial spaces. The accumulation of inflammatory cells further increases epithelial damage and starts a positive feedback circuit that further increases mediator produc-

T. Tonetti · V. M. Ranieri (✉)
Alma Mater Studiorum – Università di Bologna,
Dipartimento di Scienze Mediche e Chirurgiche,
Anesthesia and Intensive Care Medicine, IRCCS
Policlinico di Sant'Orsola, Bologna, Italy
e-mail: tommaso.tonetti@unibo.it; m.ranieri@unibo.it

tion and cell recruitment. Moreover, neutrophils in the alveolar space release reactive oxygen species, elastases, and other proteinases, which increase cell damage and basement membrane degradation.

Epithelial cells are particularly damaged during neutrophil-mediated inflammation, not only due to the release of the abovementioned mediators, but also due to damage of intercellular tight junctions. Indeed, massive neutrophil activation in the alveolar space leads to the onset of widespread epithelial injury which is caused by separation of previously adjacent monolayer cells (Fanelli and Ranieri 2015). Moreover, the epithelial cell monolayer has the important function of stabilizing the alveolar content, by producing surfactant and ensuring an active resorption process, known as alveolar fluid clearance (AFC). This process is particularly impaired in ARDS lungs, due to different mechanisms: on one hand, hypoxia and hypercapnia lead to endocytosis of the basolateral Na/K ATPases; on the other hand, two of the previously listed inflammatory mediators, TGF- β and IL-8, specifically inhibit AFC by inducing internalization of membrane sodium channels (ENaC) (Peters et al. 2014) and by desensitization/deregulation of the β_2 -adrenergic receptor (β_2 -AR) (Roux et al. 2013), respectively. Moreover, viral proteins of some strains of influenza virus which are important causative agents of pneumonia and ARDS also can inhibit (directly and indirectly) the activity of ENaC (Lazrak et al. 2009).

On the other side of the basement membrane lie the second leading “actors” of alveolar function and stability: the endothelial cells. The alveolar capillary endothelium constitutes the first barrier against fluid extravasation. Endothelial activation by TNF, vascular endothelial growth factor (VEGF), histamine, and other mediators causes structural alterations in vascular endothelial cadherins (VE-cadherins), which lose part of their inter-cellular adhesive properties and thus favor paracellular fluid transfer and leukocyte diapedesis. Other leukocyte mediators can even induce VE-cadherin endocytosis, thus creating inter-endothelial cell gaps that further increase edema formation and leukocyte transfer into

the alveolar space (Fanelli and Ranieri 2015). Moreover, endothelial activation and expression of tissue factor favor platelet adhesion and coagulative pathway activation, with increasing microvascular injury, subsequent microthrombi formation, intra-alveolar coagulation, and hyaline membrane formation (Thompson et al. 2017). Recently, the renin-angiotensin system has been put under scrutiny as a relevant pathway mediating pulmonary vascular permeability, epithelial cell survival, and activation of fibroblasts. The angiotensin-converting enzyme 2 (ACE2) reduced lung injury in several experimental models of ARDS, and it has been identified as a receptor for severe acute respiratory syndrome coronavirus (SARS-CoV) (Kuba et al. 2005).

The activation of the abovementioned mechanisms results in alveolar flooding and capillary obstruction/disruption, which in turn leads to increased alveolar dead space and/or right-to-left venous admixture, producing the hallmark alterations of gas exchange found in ARDS.

Proliferative Phase

In order for the host to survive ARDS, the exudative phase must be followed by a proliferative phase, usually beginning approximately 72 hours after the initial insult and lasting for about 7 days. In this process, fibroblasts replace the already disrupted basement membrane with a provisional matrix mainly composed of fibrin and fibronectin (Thompson et al. 2017). Progenitor cells of mesenchymal, epithelial, and endothelial lineage provide new cellular elements for all the components of the alveolar structures. The new epithelial cells again provide AFC, while the new endothelial cells restore capillary integrity. Key actors in these processes are again the neutrophils, which activate β -catenin signaling in epithelial cells, leading to expression of genes involved in cell proliferation. (Fanelli and Ranieri 2015; Zemans et al. 2011)

Fibrotic Phase

In some ARDS patients, the “healing” proliferative phase may be followed by an “injurious” fibrotic phase; this transition has been linked to prolonged mechanical ventilation and increased

mortality (Thompson et al. 2017; Cabrera-Benitez et al. 2014). Since this phase is usually a direct consequence of ventilator-induced lung injury, it will be discussed in the next paragraph.

ARDS Phenotypes: The “Hyperinflammation”

Analysis of biological subphenotypes recently offered new insights into the inflammatory response in ARDS. Indeed, a retrospective analysis of two randomized clinical trials (the ARMA (Acute Respiratory Distress Syndrome Network et al. 2000) and the ALVEOLI (Brower et al. 2004) trials) showed the existence of two distinct subphenotypes in ARDS: a less-inflammatory one and the so-called “hyperinflammatory” phenotype, characterized by higher plasma concentrations of IL-6, IL-8, soluble TNF receptor-1, and plasminogen activator inhibitor-1; moreover, this phenotype is associated with increased needs for mechanical ventilation (higher total minute ventilation) and signs of shock (higher heart rate, lower systolic blood pressure, lower bicarbonate, and lower coagulative protein C concentration) (Calfee et al. 2014). By analyzing the receiver-operator characteristic curve, the authors further determined that the hyperinflammatory phenotype can be predicted with just three variables (IL-6, soluble TNF receptor-1, vasopressor use), thus suggesting a possible way of monitoring and prognosticating ARDS. Interestingly, phenotypes were strongly associated with prognostic markers, such as ventilator-free days, organ failure-free days, and mortality. Moreover, the authors found that patients with the hyperinflammatory phenotype who were treated with higher PEEP tended to have a lower mortality than those treated with lower PEEP, whereas higher PEEP exerted the opposite effect (i.e., higher mortality) in patients with low-inflammatory phenotype (Calfee et al. 2014). More recently, the same group tried the same subphenotypes in the populations of another randomized clinical trial, the FACCT trial on fluid and catheter strategies in ARDS (Wiedemann et al. 2006; Louise et al. 2006); in that study they were able to show differences in

mortality based on the fluid management strategy; patients with the hyperinflammatory phenotype had higher mortality when treated with a conservative fluid strategy, whereas patients with the less inflammatory phenotype showed higher mortality with a liberal fluid strategy (Famous et al. 2017).

In summary, present evidence on ARDS subphenotypes underlines not only the wide phenotypic variability of the syndrome but also the great importance of inflammation (and its intensity) in determining the prognosis and the response to therapy of ARDS patients.

Ventilator-Induced Lung Injury and Inflammation

ARDS, especially in its moderate and severe forms, usually requires considerable ventilatory support, which normally is delivered in the form of invasive mechanical ventilation. Despite being one of the most important and effective supportive therapies practiced in intensive care units, mechanical ventilation also is responsible for at least a part of the lung damage occurring in ARDS patients.

Indeed, at least since the 1970s, mechanical ventilation has been associated with collateral effects, ranging from macroscopic lung ruptures to more subtle, but equally dangerous, lesions that develop more slowly in the course of the disease.

The terminology “ventilator-induced lung injury” (VILI) was first introduced in 1993, and it has since gained a wide consensus. It indicates a complex pathophysiological entity, characterized by histologic alterations similar to those found in the ARDS lungs: inflammatory cell infiltrates, hyaline membranes, increased vascular permeability, and pulmonary edema. Although this type of damage was first described in ARDS, several experimental studies have shown that injurious ventilatory regimens may damage epithelial and endothelial cells and induce lung inflammation and edema (by altering the alveolar-capillary barrier) even in previously healthy lungs (Slutsky and Ranieri 2013; de Prost et al. 2011).

Evolving Definitions and Pathophysiology of VILI: From “Barotrauma” to “Ergotrauma”

The terminology used in the VILI literature has evolved since the 1970s, paralleling new discoveries in the etiology and pathophysiology. This evolution is summarized in Table 47.1. As shown, the first described entity was barotrauma, or “damage due to excessive pressure” (Kumar et al. 1973). Typical manifestations of barotrauma were different forms of gas leaks inside the body (pneumothorax, pneumomediastinum, subcutaneous emphysema, and gas embolism) (Zimmerman et al. 1974; Marini and Culver 1989). Since the most used ventilator mode was volume control, and normocapnia was the absolute target of mechanical ventilation, pneumothorax was a very frequent and deadly complication.

During the 1980s, the focus progressively shifted toward volutrauma, or “damage due to excessive volume.” This was based on a series of experiments in which rats were ventilated with

the same high airway pressures (45 cmH₂O) but with either high or low volumes which were obtained by ventilating the animals with or without the chest and abdomen strapped. These experiments showed that damage developed only in the rats ventilated with high volume and high pressure, whereas those ventilated with low volume and high pressure did not show signs of lung damage (Dreyfuss et al. 1988).

Barotrauma and volutrauma and their relationship can be explained in more modern terms by the concepts of transpulmonary pressure (also known as lung stress) and lung strain (Tonetti et al. 2017). Indeed, only a part of the total airway pressure delivered by a ventilator is needed to inflate the lungs (the transpulmonary pressure), while the rest is used to lift the chest wall. The relationship between transpulmonary pressure and total airway pressure is linear in an individual subject, but the slope of this relationship is widely variable inter-individually; it averages 0.7 (i.e., on average the transpulmonary pressure is 70% of the airways pressure), but it ranges in

Table 47.1 Historical perspective on VILI

Definition	Years	Experimental evidence	Clinical evidence	References
Barotrauma	1970s	Rats ventilated with peak pressures up to 45 cmH ₂ O developed pulmonary edema within 20 minutes; ventilation at 30 cmH ₂ O induced edema within 60 minutes	High incidence of pneumothoraces and other forms of gas leaks in ventilated ARDS patients	de Prost et al. (2011), Kumar et al. (1973), Zimmerman et al. (1974), Marini and Culver (1989)
Volutrauma	1980s	High pressure ventilation (45 cmH ₂ O) is harmless if the volume is low (chest strapping), while it causes lung damage if the volume is high (no strapping)	Ventilating ARDS patients with tidal volume of 6 ml/kg IBW reduces mortality by ~9% compared to 12 ml/kg	Acute Respiratory Distress Syndrome Network et al. (2000), Dreyfuss et al. (1988)
Atelectrauma/ biotrauma	Late 1990s– early 2000s	Ventilation of rat lungs with zero PEEP and high volume causes abnormal release of inflammatory cytokines; PEEP application causes less cytokine liberation	Patients treated with lung protective ventilation (higher PEEP and low tidal volume) had lower inflammatory cytokines in BAL and plasma compared to patients ventilated with conventional strategies	Tremblay et al. (1997), Ranieri et al. (1999)
Ergotrauma	2010s	Respiratory rate, inspiratory flow, and PEEP can cause VILI per se and synergistically with inspiratory pressure and volume	Only retrospective evidence: correlation of mechanical power with worse outcome	Cressoni et al. (2016), Collino et al. (2019), Serpa Neto et al. (2018), Zhang et al. (2019)

the population from 0.2 to 0.8, making it very difficult to predict lung stress from airway pressure readings (Chiumello et al. 2008). Moreover, volume is more precisely defined in terms of lung strain, i.e., normalized to the functional residual capacity (the lung resting volume). Lung stress and strain are related by a proportionality constant called lung-specific elastance, which corresponds to the transpulmonary pressure needed to double the lung volume from its resting position; this pressure seems to be species-specific and corresponds to 12 cmH₂O in humans (Chiumello et al. 2008).

The clinical relevance of volutrauma was definitely proved by the ARMA trial, in which ARDS patients were randomly assigned to ventilation with lower (6 ml/kg) or higher (12 ml/kg) tidal volume; tidal volume was normalized to a surrogate measure of lung dimensions (the ideal body weight), and the results showed an almost 10% difference in mortality favoring the lower tidal volume group (Acute Respiratory Distress Syndrome Network et al. 2000).

During the 1990s, the focus of VILI research shifted to a new mechanism of lung injury, which can be possibly active at low lung volumes: the atelectrauma, or “damage due to cyclic opening and closing of lung units.” The theoretical foundations of atelectrauma lie in the model of stress and strain amplification at the interfaces of different elasticity regions (Mead et al. 1970). This theoretical model found experimental confirmation in a rat model in which ventilation with moderate tidal volume and high PEEP was less injurious (in terms of inflammation and cytokine release) when compared to low or even zero PEEP (Tremblay et al. 1997). Similar results were obtained in a clinical study that compared lung protective ventilation (based on higher PEEP and lower tidal volumes) and conventional ventilation (higher volumes and lower PEEP); patients in the lung protective ventilation group had significantly lower levels of cytokines and other inflammation markers both in plasma and in the bronchoalveolar lavage (Ranieri et al. 1999). Nevertheless, the hypothesis was subsequently tested in a number of randomized clinical of patients with ARDS patients, but they failed to show any benefit in

survival from high recruitment strategies in comparison to low recruitment (i.e., high cyclic opening and closing) (Brower et al. 2004; Meade et al. 2008; Mercat et al. 2008). The debate on the relevance of atelectrauma in the framework of VILI is still open, and more compelling evidence is needed (Gattinoni et al. 2018; Del Sorbo et al. 2019).

In the last few years, the theory of ergotrauma, or “damage through excessive energy/power,” is gaining consensus. The ergotrauma theory starts from experimental and clinical evidence that not only pressure and volume but also other “basic elements” of mechanical ventilation such as respiratory rate (Hotchkiss et al. 2000), strain rate (i.e., the inspiratory flow) (Prutti et al. 2016), and PEEP (Dreyfuss and Saumon 1993) can be lung-damaging factors. By conceptually and mathematically combining all these elements, it appears evident that the energy per unit of time (i.e., the mechanical power) delivered by the ventilator to the lung parenchyma may explain VILI, in the same way as repeated delivery of energy cycles can cause fatigue and ruptures in other materials (Gattinoni et al. 2016). Interestingly, in different series of animal experiments, a threshold value of mechanical power for the onset of VILI in healthy lungs (i.e., ~13 Joules/minute) has been identified (Cressoni et al. 2016; Collino et al. 2019); moreover, recent retrospective clinical data show that mechanical power is associated with mortality and other outcome variables in ventilated patients (Serpa Neto et al. 2018; Zhang et al. 2019). Although conceptually compelling and of interest, prospective evidence on ergotrauma is still lacking, and more robust trials are needed to confirm whether mechanical power is the root cause of VILI.

Mechanotransduction and Ventilator-Induced Lung Injury

Whichever the root physical mechanism of VILI (barotrauma, volutrauma, atelectrauma, ergotrauma), the second important element to clarify is how the physical stimulus causes biological damage. As already stated, very high

pressure and volume can simply rip off lung tissue from the supportive matrix and lead to the typical barotrauma epiphenomena such as gas leaks, pneumothorax, and pneumomediastinum.

Lower intensity forces, especially if cyclically repeated, do not usually cause macroscopic lesions; however, they can directly injure epithelial and endothelial cells at the microscopic level. This includes stress failure of plasma membranes and their junctions, eventually leading to necrosis and consequent inflammation and neutrophil infiltration.

Another even more subtle mechanism takes place only in intact cells and involves the indirect transduction (hence the term “mechanotransduction”) of physical forces into biological signals through the mediation of intracellular biochemical pathways (Uhlir 2002). These pathways are very complex and have not been completely described. As explained in detail below, activation of these pathways tends to favor inflammation and cell apoptosis, in comparison to the direct cellular injury that usually causes cell death by necrosis (see above).

Lung epithelial cells have at least three “mechanosensors”: integrins, cytoskeleton proteins, and ion channels (Gattinoni et al. 2003); one of the most studied pathways is the one involving Ca^{2+} channels. Experimental stretching of alveolar epithelial cells yields an increase in the intracellular Ca^{2+} concentration, both from extracellular influx and by liberation from intracellular reservoirs (Frick et al. 2004); increased Ca^{2+} intracellular concentrations can activate transcription pathways and mediate epithelial cell contraction (Dudek and Garcia 2001). Moreover, stretch-induced Ca^{2+} signaling also has been observed in lung endothelial cells (Winston et al. 1993); an intracellular Ca^{2+} increase in endothelial cells can alter vascular permeability by inducing contractile elements and alter intercellular gaps. Indeed, inhibiting stretch-activated ionic channels or prevention of contraction of actin/myosin complexes reduced endothelial permeability (Parker et al. 1998; Parker 2000).

Other mechanosensors, such as integrins and cytoskeleton proteins, when stretched, can indirectly activate genetic transcription through the

NF- κ B pathway or through protein kinases of the MAPK family (such as ERK1-2) (Correa-Meyer et al. 2002). Both alveolar macrophages and alveolar epithelial cells, when subjected to unphysiological strain, can release IL-8 and metalloproteinases (Gattinoni et al. 2003). The latter are involved in extracellular matrix remodeling, whereas IL-8 is the most potent chemokine for attraction of neutrophils. The MAPK kinases also are essential in cell death/survival pathways (Lionetti et al. 2006); the importance of MAPK pathways has been shown in experimental settings, where protective ventilation was related to less activation of MAPKs and significant decrease in apoptotic cells (Fanelli et al. 2009).

Another mechanism activated by high inspiratory pressure is related to the impairment of nitric oxide production, which in turn impairs cAMP-dependent alveolar fluid clearance (see also the first paragraph) (Frank et al. 2003).

Biotrauma and Inflammation

As described above, physical stimuli lead to inflammation and immune system activation, either directly through microscopic cellular tears or indirectly by mechanotransduction. The theory of biotrauma or “damage through excessive mediator release and immune system overactivation” developed in the 1990s and built on previous observations that ventilation with high inspiratory pressures induced neutrophil infiltration in the lung (Tsuno et al. 1991) and that animals with neutrophil depletion had less severe lung injury (Kawano et al. 1987).

The first experimental study explicitly investigating the biotrauma hypothesis was performed on excised and un-perfused rat lungs in 1997 (Tremblay et al. 1997). The authors were able to show a significant increase in TNF- α , IL-1 β , and IL-6 in bronchoalveolar lavage and macrophage inflammatory protein-2 (MIP-2) in the lungs ventilated with high tidal volume (40 ml/kg) and zero PEEP, when compared to lungs ventilated with more “protective” settings (Tremblay et al. 1997).

Two years later, a randomized clinical trial showed that patients ventilated with a strategy of low tidal volume and PEEP titration based on the pressure-volume curve had lower bronchoalveolar lavage concentrations of polymorphonuclear cells, TNF- α , IL-1 β , soluble TNF- α receptor 55, and IL-8; moreover, they had lower concentrations of IL-6 and IL-1 receptor antagonist both in plasma and bronchoalveolar lavage (Ranieri et al. 1999). Further, in a post hoc analysis of the trial, the authors showed a significant correlation between the plasma concentration of inflammatory markers and the development of multisystem organ failure (Ranieri et al. 2000).

Consequently, the biologic alterations encountered in VILI are very similar to those described in the exudative phase of ARDS. Although the specific mechanisms that recruit leukocytes during the early phases of VILI have not been clearly elucidated, alveolar macrophages certainly play a fundamental role in activating inflammation by releasing TGF- β and IL-8, and there is clear evidence that type II alveolar epithelial cells can produce chemokines such as MIP-2 (Vanderbilt et al. 2003). The resulting polymorphonucleated cell recruitment into the alveolar space further increases inflammation and the release of other mediators (such as TNF- α , IL-6, and IL-1 β).

The increased alveolar-capillary permeability (inherent to ARDS or caused by VILI) allows for systemic dissemination of mediators that can lead to multiorgan failure through multiple mechanisms such as increased apoptosis and may favor the dissemination of bacteria and endotoxin into the circulation (Nahum et al. 1997; Murphy et al. 2000).

VILI, Inflammation and Fibrosis

An important complication of ventilated ARDS patients is the development of lung fibrosis. This process usually happens late in the course of ARDS (Thompson et al. 2017; Thille et al. 2013) and is probably a consequence of VILI (Slutsky and Ranieri 2013). Nevertheless, there is evi-

dence that the fibrotic process may start earlier during inflammation (Marshall et al. 2000).

The biochemical cascade leading eventually to fibrosis can be initiated by mechanical stretch (another example of mechanotransduction) or by the release of matrix-metalloproteinases and chemotactic factors by neutrophils (Cabrera-Benitez et al. 2014). Cyclic mechanical stretch seems to be a key factor. Stretched murine alveolar type II epithelial cells increase their production of the short fragment hyaluronan (sHA), which in turn activates signaling pathways that lead to epithelial-mesenchymal transition (EMT) (Heise et al. 2011). EMT is the cellular phenotypical switch from epithelial to mesenchymal cells (fibroblasts and myofibroblasts) and is fundamental for the development of VILI-associated lung fibrosis (Cabrera-Benitez et al. 2012). Other mechanisms involve the activation and proliferation of resident alveolar fibroblasts and the recruitment to the lung of circulating fibrocytes (Cabrera-Benitez et al. 2014). Together with neutrophils, macrophages may also play a role, especially when their phenotype shifts to M2 (Cabrera-Benitez et al. 2014).

Already in the 1990s, pulmonary fibrosis was recognized as an important complication of ARDS, and it was linked to mortality and worse outcome (Martin et al. 1995). Subsequent clinical studies underlined the importance of TGF- β and procollagen type III (PCIII) levels in lung lavage in determining the evolution toward fibrosis and death (Marshall et al. 2000; Madtes et al. 1998; Steinberg et al. 2006). In this respect, some authors talk about a “fibrosis paradox,” in that fibrosis is part of the repair process and it leads to increased duration of ARDS and worsens outcome; indeed patients who die of ARDS almost always show signs of fibrosis, whereas survivors usually do not show any signs of it (Cabrera-Benitez et al. 2014). For all these reasons, fibroproliferation may be a relevant biomarker of VILI and may become a target for future therapies.

In Fig. 47.1, we schematically represent the mechanical and biological pathways leading to VILI.

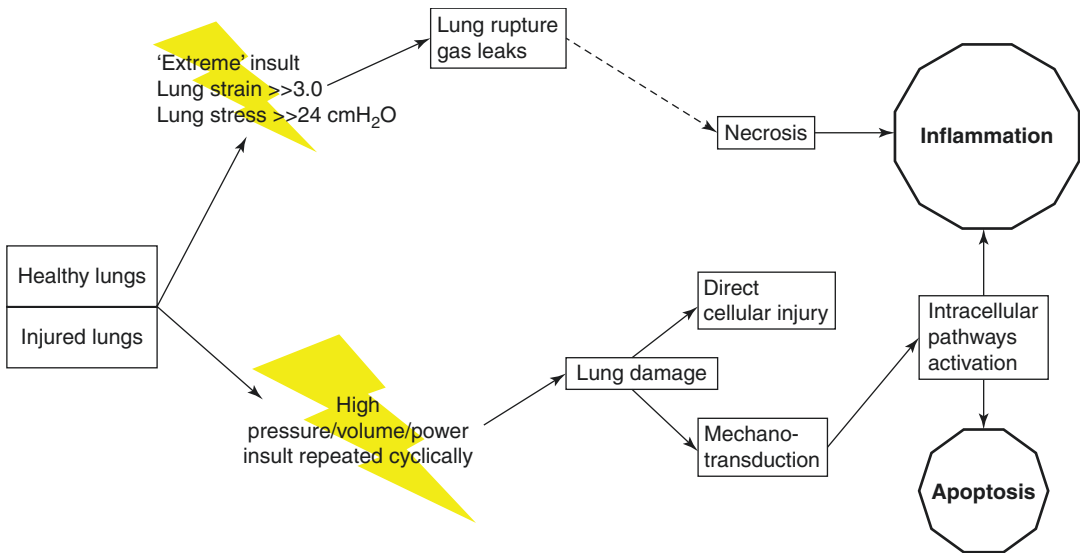


Fig. 47.1 Schematic representation of the mechanical and biological pathways leading to VILI

Biological Modulation of the Inflamed Lung

Present treatment of ARDS is based on ventilatory strategies aimed at minimizing VILI: “gentle” ventilation with low tidal volumes, moderate levels of PEEP, avoidance of patient-ventilator dys-synchronies, and minimization of lung inhomogeneity through the use of prone positioning are all recommended interventions (Fan et al. 2017). A conservative fluid management strategy also has proved to be of benefit (Wiedemann et al. 2006). In the most severe cases, the use of extracorporeal gas exchange techniques may be useful to further reduce the burden of mechanical ventilation and to ensure viable gas exchange (Fan et al. 2016; Rozenchwajg et al. 2019).

Instead, modulation of the immune system, although very intriguing and promising from a conceptual point of view, to date has failed to deliver significant results. Indeed, use of glucocorticoids in ARDS has shown no benefit for the reduction of mortality and only has resulted in moderate improvements in oxygenation, airway pressures, and radiological presentation (Steinberg et al. 2006). Many other treatments aimed at modulating the inflammatory response such as neutrophil elastase inhibitors, statins,

nonsteroidal anti-inflammatories, angiotensin-converting enzyme inhibitors, β -agonists, and antioxidants have been tested in different clinical trials in the last decade, with disappointing results (Boyle et al. 2013).

At the beginning of the 2010s, recombinant interferon- 1β proved to be safe and effective in reducing mortality in phase I and II trials on ARDS patients. The anti-inflammatory effects of IFN- 1β seem to be related to increased expression of the enzyme CD73 on several cell types; this in turn increases the conversion of adenosine monophosphate to adenosine, a potent anti-inflammatory molecule which favors stability of the alveolar epithelial-endothelial barrier and thus limits edema formation. More recently, however, a phase III trial of this molecule failed to deliver the expected results in terms of mortality reduction, and the trial was prematurely interrupted (Bellingan et al. 2017).

Future Perspectives

A promising treatment, though still under evaluation, is based on infusion of mesenchymal stromal cells (MSCs). Several mechanisms have been advocated to explain the lung-protective

role of MSCs. It may include secretion of soluble factors, such as keratinocyte growth factor, angiotensin-1, IL-1 receptor antagonist, IL-10, prostaglandin E2, and antimicrobial peptide LL-37; moreover, MSCs can interact with injured cells, thus promoting edema clearance and reparative processes (Fanelli and Ranieri 2015). Indeed, preclinical data show that infusion or tracheal instillation of this type of cell reduces vascular and alveolar permeability, increases clearance of edema, and shows anti-inflammatory and antimicrobial properties (Thompson et al. 2017). A recent published phase IIa trial confirmed safety of a single intravenous dose of MSCs in moderate and severe ARDS patients (Matthay et al. 2019), but more trials are underway, and results are expected in the next few years.

Finally, in the recent observation that ARDS patients can be classified into two phenotypes with very different natural histories, degrees of inflammation, outcome, and response to treatment should inspire researchers in targeting future trials to patients who are more likely to respond to the tested treatment, thus reducing the possibility of a “negative” trial (Calfee et al. 2014; Famous et al. 2017). Moreover, at least theoretically, this approach should help design innovative therapies that target mediators and mechanisms that are significantly more activated in the worse outcome group of patients.

References

- Acute Respiratory Distress Syndrome Network, Brower RG, Matthay MA, Morris A, Schoenfeld D, Thompson BT, Wheeler A. Ventilation with lower tidal volumes as compared with traditional tidal volumes for acute lung injury and the acute respiratory distress syndrome. *N Engl J Med*. 2000;342:1301–8.
- ARDS Definition Task Force, Ranieri VM, Rubenfeld GD, Thompson BT, Ferguson ND, Caldwell E, Fan E, Camporota L, Slutsky AS. Acute respiratory distress syndrome: the Berlin Definition. *JAMA*. 2012;307:2526–33.
- Ashbaugh DG, Bigelow DB, Petty TL, Levine BE. Acute respiratory distress in adults. *Lancet (London, England)*. 1967;2:319–23.
- Bellingan G, Brealey D, Mancebo J, et al. Comparison of the efficacy and safety of FP-1201-lyo (intravenously administered recombinant human interferon beta-1a) and placebo in the treatment of patients with moderate or severe acute respiratory distress syndrome: study protocol for a randomized co. *Trials*. 2017;18:1–9.
- Boyle AJ, Sweeney RM, McAuley DF. Pharmacological treatments in ARDS: a state-of-the-art update. *BMC Med*. 2013;11:166.
- Brower RG, Lanken PN, MacIntyre N, Matthay MA, Morris A, Ancukiewicz M, Schoenfeld D, Thompson BT, National Heart, Lung and BIACTN. Higher versus lower positive end-expiratory pressures in patients with the acute respiratory distress syndrome. *N Engl J Med*. 2004;351:327–36.
- Cabrera-Benítez NE, Parotto M, Post M, et al. Mechanical stress induces lung fibrosis by epithelial–mesenchymal transition. *Crit Care Med*. 2012;40:510–7.
- Cabrera-Benitez NE, Laffey JG, Parotto M, Spieth PM, Villar J, Zhang H, Slutsky AS. Mechanical ventilation-associated lung fibrosis in acute respiratory distress syndrome: a significant contributor to poor outcome. *Anesthesiology*. 2014;121:189–98.
- Calfee CS, Delucchi K, Parsons PE, Thompson BT, Ware LB, Matthay MA. Subphenotypes in acute respiratory distress syndrome: latent class analysis of data from two randomised controlled trials. *Lancet Respir Med*. 2014;2:611–20.
- Chiumello D, Carlesso E, Cadringer P, et al. Lung stress and strain during mechanical ventilation for acute respiratory distress syndrome. *Am J Respir Crit Care Med*. 2008;178:346–55.
- Collino F, Rapetti F, Vasques F, et al. Positive end-expiratory pressure and mechanical power. *Anesthesiology*. 2019;130:119–30.
- Correa-Meyer E, Pesce L, Guerrero C, Sznajder JI. Cyclic stretch activates ERK1/2 via G proteins and EGFR in alveolar epithelial cells. *Am J Physiol Lung Cell Mol Physiol*. 2002;282:L883–91.
- Cressoni M, Gotti M, Chiurazzi C, et al. Mechanical power and development of ventilator-induced lung injury. *Anesthesiology*. 2016;124:1100–8.
- de Prost N, Ricard J-D, Saumon G, Dreyfuss D. Ventilator-induced lung injury: historical perspectives and clinical implications. *Ann Intensive Care*. 2011;1:28.
- Del Sorbo L, Tonetti T, Ranieri VM. Alveolar recruitment in acute respiratory distress syndrome: should we open the lung (no matter what) or may accept (part of) the lung closed? *Intensive Care Med*. 2019;45(10):1436–39.
- Dreyfuss D, Saumon G. Role of tidal volume, FRC, and end-inspiratory volume in the development of pulmonary edema following mechanical ventilation. *Am Rev Respir Dis*. 1993;148:1194–203.
- Dreyfuss D, Soler P, Basset G, Saumon G. High inflation pressure pulmonary edema: respective effects of high airway pressure, high tidal volume, and positive end-expiratory pressure. *Am Rev Respir Dis*. 1988;137:1159–64.
- Dudek SM, Garcia JGN. Cytoskeletal regulation of pulmonary vascular permeability. *J Appl Physiol*. 2001;91:1487–500.

- Famous KR, Delucchi K, Ware LB, Kangelaris KN, Liu KD, Thompson BT, Calfee CS. Acute respiratory distress syndrome subphenotypes respond differently to randomized fluid management strategy. *Am J Respir Crit Care Med.* 2017;195:331–8.
- Fan E, Gattinoni L, Combes A, et al. Venovenous extracorporeal membrane oxygenation for acute respiratory failure: a clinical review from an international group of experts. *Intensive Care Med.* 2016;42:712–24.
- Fan E, Del Sorbo L, Goligher EC, et al. An official American Thoracic Society/European Society of Intensive Care Medicine/Society of Critical Care Medicine clinical practice guideline: mechanical ventilation in adult patients with acute respiratory distress syndrome. *Am J Respir Crit Care Med.* 2017;195:1253–63.
- Fanelli V, Ranieri VM. Mechanisms and clinical consequences of acute lung injury. *Ann Am Thorac Soc.* 2015;12:S3–8.
- Fanelli V, Mascia L, Puntorieri V, et al. Pulmonary atelectasis during low stretch ventilation: “open lung” versus “lung rest” strategy. *Crit Care Med.* 2009;37:1046–53.
- Frank JA, Pittet JF, Lee H, Godzich M, Matthay MA. High tidal volume ventilation induces NOS2 and impairs cAMP-dependent air space fluid clearance. *Am J Physiol Lung Cell Mol Physiol.* 2003;284:791–8.
- Frick M, Bertocchi C, Jennings P, Haller T, Mair N, Singer W, Pfaller W, Ritsch-Marte M, Dietl P. Ca²⁺ entry is essential for cell strain-induced lamellar body fusion in isolated rat type II pneumocytes. *Am J Physiol Lung Cell Mol Physiol.* 2004;286:L210–20.
- Gattinoni L, Carlesso E, Cadringer P, Valenza F, Vagginelli F, Chiumello D. Physical and biological triggers of ventilator-induced lung injury and its prevention. *Eur Respir J.* 2003;22:15s–25s.
- Gattinoni L, Tonetti T, Cressoni M, et al. Ventilator-related causes of lung injury: the mechanical power. *Intensive Care Med.* 2016;42:1567–75.
- Gattinoni L, Quintel M, Marini JJ. Volutrauma and atelectrauma: which is worse? *Crit Care.* 2018;22:264.
- Heise RL, Stober V, Cheluvraju C, Hollingsworth JW, Garantziotis S. Mechanical stretch induces epithelial-mesenchymal transition in alveolar epithelia via hyaluronan activation of innate immunity. *J Biol Chem.* 2011;286:17435–44.
- Hotchkiss JR, Blanch L, Murias G, Adams AB, Olson DA, Wangenstein OD, Leo PH, Marini JJ. Effects of decreased respiratory frequency on ventilator-induced lung injury. *Am J Respir Crit Care Med.* 2000;161:463–8.
- Kawano T, Mori S, Cybulsky M, Burger R, Ballin A, Cutz E, Bryan AC. Effect of granulocyte depletion in a ventilated surfactant-depleted lung. *J Appl Physiol.* 1987;62:27–33.
- Kuba K, Imai Y, Rao S, et al. A crucial role of angiotensin converting enzyme 2 (ACE2) in SARS coronavirus-induced lung injury. *Nat Med.* 2005;11:875–9.
- Kumar A, Pontoppidan H, Falke KJ, Wilson RS, Laver MB. Pulmonary barotrauma during mechanical ventilation. *Crit Care Med.* 1973;1:181–6.
- Lazrak A, Iles KE, Liu G, Noah DL, Noah JW, Matalon S. Influenza virus M2 protein inhibits epithelial sodium channels by increasing reactive oxygen species. *FASEB J.* 2009;23:3829–42.
- Lionetti V, Lisi A, Patrucco E, et al. Lack of phosphoinositide 3-kinase- γ attenuates ventilator-induced lung injury. *Crit Care Med.* 2006;34:134–41.
- Louise C, Powell JT, Simon G, Sculpher MJ. Pulmonary-artery versus central venous catheter to guide treatment of acute lung injury. *N Engl J Med.* 2006;354:2213–24.
- Madtes DK, Rubenfeld G, Klima LD, Milberg JA, Steinberg KP, Martin TR, Raghu G, Hudson LD, Clark JG. Elevated transforming growth factor- α levels in bronchoalveolar lavage fluid of patients with acute respiratory distress syndrome. *Am J Respir Crit Care Med.* 1998;158:424–30.
- Marini JJ, Culver BH. Systemic gas embolism complicating mechanical ventilation in the adult respiratory distress syndrome. *Ann Intern Med.* 1989;110:699–703.
- Marshall RP, Bellingan G, Webb S, Puddicombe A, Goldsack N, McNulty RJ, Laurent GJ. Fibroproliferation occurs early in the acute respiratory distress syndrome and impacts on outcome. *Am J Respir Crit Care Med.* 2000;162:1783–8.
- Martin C, Papazian L, Payan M-J, Saux P, Gouin F. Pulmonary fibrosis correlates with outcome in adult respiratory distress syndrome. *Chest.* 1995;107:196–200.
- Matthay MA, Calfee CS, Zhuo H, et al. Treatment with allogeneic mesenchymal stromal cells for moderate to severe acute respiratory distress syndrome (START study): a randomised phase 2a safety trial. *Lancet Respir Med.* 2019;7:154–62.
- Mead J, Takishima T, Leith D. Stress distribution in lungs: a model of pulmonary elasticity. *J Appl Physiol.* 1970;28:596–608.
- Meade MO, Cook DJ, Guyatt GH, et al. Ventilation strategy using low tidal volumes, recruitment maneuvers, and high positive end-expiratory pressure for acute lung injury and acute respiratory distress syndrome: a randomized controlled trial. *JAMA.* 2008;299:637–45.
- Mercat A, Richard JM, Vielle B, et al. Positive end-expiratory pressure setting in adults with acute lung injury and acute respiratory distress syndrome: a randomized controlled trial. *JAMA.* 2008;299:646–55.
- Murphy DB, Cregg N, Tremblay L, Engelberts D, Laffey JG, Slutsky AS, Romaschin A, Kavanagh BP. Adverse ventilatory strategy causes pulmonary-to-systemic translocation of endotoxin. *Am J Respir Crit Care Med.* 2000;162:27–33.
- Nahum A, Hoyt J, Schmitz L, Moody J, Shapiro R, Marini JJ. Effect of mechanical ventilation strategy on dissemination of intratracheally instilled *Escherichia coli* in dogs. *Crit Care Med.* 1997;25:1733–43.
- Parker JC. Inhibitors of myosin light chain kinase and phosphodiesterase reduce ventilator-induced lung injury. *J Appl Physiol.* 2000;89:2241–8.
- Parker JC, Ivey CL, Tucker JA. Gadolinium prevents high airway pressure-induced permeability increases in isolated rat lungs. *J Appl Physiol.* 1998;84:1113–8.

- Peters DM, Vadász I, Wujak Ł, et al. TGF- β directs trafficking of the epithelial sodium channel ENaC which has implications for ion and fluid transport in acute lung injury. *Proc Natl Acad Sci U S A*. 2014;111:E374–83.
- Protti A, Maraffi T, Milesi M, et al. Role of strain rate in the pathogenesis of ventilator-induced lung edema*. *Crit Care Med*. 2016;44:e838–45.
- Ranieri VM, Suter PM, Tortorella C, De Tullio R, Dayer JM, Brienza A, Bruno F, Slutsky AS. Effect of mechanical ventilation on inflammatory mediators in patients with acute respiratory distress syndrome: a randomized controlled trial. *JAMA*. 1999;282:54–61.
- Ranieri VM, Giunta F, Suter PM, Slutsky AS. Mechanical ventilation as a mediator of multisystem organ failure in acute respiratory distress syndrome. *JAMA*. 2000;284:43–4.
- Roux J, McNicholas CM, Carles M, Goolaerts A, Houseman BT, Dickinson DA, Iles KE, Ware LB, Matthay MA, Pittet JF. IL-8 inhibits cAMP-stimulated alveolar epithelial fluid transport via a GRK2/PI3K-dependent mechanism. *FASEB J*. 2013;27:1095–106.
- Rozencwajg S, Guihot A, Franchineau G, et al. Ultra-protective ventilation reduces biotrauma in patients on venovenous extracorporeal membrane oxygenation for severe acute respiratory distress syndrome. *Crit Care Med*. 2019;47:1505.
- Serpa Neto A, Deliberato RO, Johnson AEW, et al. Mechanical power of ventilation is associated with mortality in critically ill patients: an analysis of patients in two observational cohorts. *Intensive Care Med*. 2018;44:1914–22.
- Slutsky AS, Ranieri VM. Ventilator-induced lung injury. *N Engl J Med*. 2013;369:2126–36.
- Steinberg KP, Hudson LD, Goodman RB, Hough CL, Lanken PN, Hyzy R, Thompson BT, Ancukiewicz M, National Heart, Lung and BIARDS (ARDS) CTN. Efficacy and safety of corticosteroids for persistent acute respiratory distress syndrome. *N Engl J Med*. 2006;354:1671–84.
- Thille AW, Esteban A, Fernández-Segoviano P, Rodriguez J-M, Aramburu J-A, Vargas-Errázuriz P, Martín-Pellicer A, Lorente JA, Frutos-Vivar F. Chronology of histological lesions in acute respiratory distress syndrome with diffuse alveolar damage: a prospective cohort study of clinical autopsies. *Lancet Respir Med*. 2013;1:395–401.
- Thompson BT, Chambers RC, Liu KD. Acute respiratory distress syndrome. *N Engl J Med*. 2017;377:562–72.
- Tonetti T, Vasques F, Rapetti F, et al. Driving pressure and mechanical power: new targets for VILI prevention. *Ann Transl Med*. 2017;5:286.
- Tremblay L, Valenza F, Ribeiro SP, Li J, Slutsky AS. Injurious ventilatory strategies increase cytokines and c-fos m-RNA expression in an isolated rat lung model. *J Clin Invest*. 1997;99:944–52.
- Tsuno K, Miura K, Takeya M, Kolobow T, Morioka T. Histopathologic pulmonary changes from mechanical ventilation at high peak airway pressures. *Am Rev Respir Dis*. 1991;143:1115–20.
- Uhlir S. Ventilation-induced lung injury and mechanotransduction: stretching it too far? *Am J Physiol Lung Cell Mol Physiol*. 2002;282:L892–6.
- Vanderbilt JN, Mager EM, Allen L, Sawa T, Wiener-Kronish J, Gonzalez R, Dobbs LG. CXC chemokines and their receptors are expressed in type II cells and upregulated following lung injury. *Am J Respir Cell Mol Biol*. 2003;29:661–8.
- Wiedemann HP, Wheeler AP, Bernard GR, Thompson BT, Hayden D, DeBoisblanc B, Connors AF, Hite RD, Harabin AL. Comparison of two fluid-management strategies in acute lung injury. *N Engl J Med*. 2006;354:2564–75.
- Winston FK, Thibault LE, Macarak EJ. An analysis of the time-dependent changes in intracellular calcium concentration in endothelial cells in culture induced by mechanical stimulation. *J Biomech Eng*. 1993;115:160–8.
- Zemans RL, Briones N, Campbell M, et al. Neutrophil transmigration triggers repair of the lung epithelium via β -catenin signaling. *Proc Natl Acad Sci U S A*. 2011;108:15990–5.
- Zhang Z, Zheng B, Liu N, Ge H, Hong Y. Mechanical power normalized to predicted body weight as a predictor of mortality in patients with acute respiratory distress syndrome. *Intensive Care Med*. 2019;45:856–64.
- Zimmerman JE, Dunbar BS, Klingenstein CH. Pneumothorax during respirator therapy. *Med Ann Dist Columbia*. 1974;43:107–9.



Ventilation During Venovenous Extracorporeal Membrane Oxygenation

48

Jacopo Fumagalli, Eleonora Carlesso,
and Tommaso Mauri

Introduction

Veno-venous extracorporeal membrane oxygenation (VV-ECMO) is an advanced medical support that is being increasingly used in patients with severe hypercapnic and/or hypoxic respiratory failure. VV-ECMO can replace the ventilatory and/or the oxygenation function of the native lung. ECMO currently is being used as rescue therapy when it is believed that the underlying pathology is potentially reversible.

In 1979, following initial enthusiasm derived from the development of the technology necessary to allow gas exchange through an external biocompatible membrane, the National Institute of Health (NIH, Bethesda, MD, USA) endorsed the first randomized clinical trial to compare ECMO treatment to conventional mechanical ventilation in patients with severe hypoxemic

respiratory failure (Zapol et al. 1979). Technological limitations of the extracorporeal devices limited the benefit of the technique (90% mortality in both ECMO and conventional mechanical ventilation groups). In this pivotal NIH trial, a high fraction of inspired oxygen ($F_{I}O_2$) was considered one of the iatrogenic causes of direct lung injury in patients undergoing mechanical ventilation. For this reason, the only real difference in ventilator management between the ECMO and control group was magnitude of $F_{I}O_2$. Other ventilator parameters were not different between the groups. Furthermore, the tidal volumes were high, 10–15 mL/Kg IBW, as were the inspiratory pressures of 40–50 cmH₂O.

Around that time, the first evidence of the potential injurious effects of mechanical ventilation appeared (Kolobow et al. 1987), and the concept of ventilator-induced lung injury (VILI) was introduced. From then on, there were large efforts to identify the causes and to prevent VILI. During that time, a pioneering group at the NIH led by Dr. Kolobow proposed taking advantage of ECMO to reduce respiratory rate, tidal volume, and airway pressure, and thereby minimizing lung damage (Gattinoni et al. 1979). Today, the concept that patients treated with VV-ECMO might benefit from ultra-protective ventilation seems more obvious; however, data supporting the proper management of mechanical ventilation during ECMO are limited and clear rationale

J. Fumagalli · E. Carlesso
Dipartimento di Fisiopatologia Medico-Chirurgica e
dei Trapianti, Università degli Studi di Milano,
Milan, Italy
e-mail: eleonora.carlesso@unimi.it

T. Mauri (✉)
Dipartimento di Fisiopatologia Medico-Chirurgica e
dei Trapianti, Università degli Studi di Milano,
Milan, Italy

Dipartimento di Anestesia, Rianimazione ed
Emergenza, Fondazione IRCCS Ca' Granda Ospedale
Maggiore Policlinico, Milan, Italy
e-mail: Tommaso.mauri@unimi.it

frequently missing. This chapter focuses on current mechanical ventilation settings adopted during ECMO support, the rationale behind different approaches, and the potential use of ECMO to allow ultra-protective mechanical ventilation and an early transfer to spontaneous breathing.

Principles of Gas Exchange During VV-ECMO in Acute Respiratory Failure

During VV-ECMO (Combes et al. 2014), blood is drawn from the patient's venous system by a venous cannula and then driven by a mechanical pump through an artificial lung, which oxygenates the blood and removes the carbon dioxide (CO₂). The arterialized blood is then returned to the patient central venous system and flows through the patient's lungs. Thus, gas exchange occurs in series in the membrane lung (ML) first and subsequently in the natural lung (NL).

Blood oxygenation by the extracorporeal system is dependent on the intrinsic characteristics of the ML, the ratio between extracorporeal flow and native cardiac output, the hemoglobin concentration, and the hemoglobin oxygen saturation in the venous blood. Potential technical shortcomings such as recirculation need to be considered. Therefore, VV-ECMO requires a high enough extracorporeal blood flow to match the total oxygen demand of the patient. Conversely, CO₂ removal by the artificial lung is relatively independent from extracorporeal blood flow, but it is tightly correlated with the gas flow ventilating the artificial lung. Venous blood contains about 55 mL of CO₂ per 100 mL of blood, which is mainly in the form of bicarbonate ions. This implies that 500 mL of blood contains the total minute CO₂ production of an adult. By maintaining an adequate pCO₂ gradient between blood flowing through the artificial lung and the sweep gas flow, removal of a significant proportion of venous CO₂ content is achieved. Thus, CO₂ removal is controlled by sweep gas flow settings; the higher the sweep gas flow and the CO₂ tension in the incoming ECMO blood flow, the higher the CO₂ clearance.

The NL can be approximated to a three-compartment model characterized by high, normal, and low (or nil) ventilation/perfusion (VA/Q) ratio, following gravitational distribution (Gattinoni and Pesenti 2005). The compartment with high VA/Q ratio is usually located in the non-dependent part of the lung and includes over- and normally inflated alveoli, presence of microthrombi, and vasoconstriction. In the middle part of the lung, regions with normal and low VA/Q ratios coexist; percentages of alveoli with lower VA/Q increase progressively to the dependent regions. The most dependent lung regions are characterized by compressed, virtually recruitable regions that can be kept open by an adequate amount of positive end-expiratory pressure (PEEP) and collapsed, unrecruitable, alveoli. Dead space and shunt coexist and are strictly bonded: the higher the shunt, the higher the VA/Q ratio of the ventilated regions and the higher the dead space. In this setting, ECMO can reduce hypoxemia by increasing the oxygen content of the mixed venous blood and thus reducing the effect of shunted blood, and at the same time, by allowing decreased minute ventilation by the mechanical removal of CO₂. Thus, gas exchange is dissociated from the ventilator requirement of the NL, and this can allow the clinician to apply the most protective ventilatory strategy to the patient lung. Although ventilation is virtually not required any more to remove CO₂, lung inflation still might be required to contribute to oxygenation which could decrease the requirement for extracorporeal blood flow, which in turn directly influences cannula size and negative drainage pressure.

Thus, ECMO might be considered not only as a technique to rescue moribund patients but also as the only therapy that, in patients with the most severe respiratory distress, can dramatically decrease the load of mechanical ventilation in the NL, and minimizing VILI in all of its aspects (Slutsky and Ranieri 2013) including barotrauma (injury due to high pressure), volutrauma (high volume), atelectrauma (cyclic opening and closing), biotrauma (inflammation secondary to mechanical injury), and the recently introduced ergotrauma (injury due to the mechanical power

applied to the lung, including volume, pressure, respiratory rate, and inspiratory flow) (Gattinoni et al. 2016).

Mechanical Ventilation Strategies During VV-ECMO

Ventilatory Strategy During the Early Phase of VV-ECMO

The optimal lung management of the natural lung during VV-ECMO is controversial with many different approaches being described (see Table 48.1). In a recent survey, only 30% of the centers participating reported an explicit mechanical ventilation protocol (Marhong et al. 2014).

Controlled ventilation modes are indicated in patients with severe ARDS in order to closely control tidal volume and inspiratory pressure and to reduce self-inflicted lung injury secondary to patients' uncontrolled respiratory drive (Brochard et al. 2017). Volume or pressure targeted assist-control ventilation are the most frequently used modes used in ARDS patients (Esteban et al. 2002). Some authors suggest use of pressure controlled ventilation (PCV) during the first days of ECMO support and use of predefined threshold values of plateau and driving pressures not to be exceeded (Camporota et al. 2015). Moreover, during PCV, lung recruitment and de-recruitment can be easily monitored by continuously monitoring increases or decreases in tidal volume.

There is general agreement for the benefit of reducing tidal volume, and driving pressure, plateau pressure, and $F_{I}O_2$ after starting VV-ECMO. In an international retrospective analysis from high volume ECMO centers, during the first 3 day of ECMO, Schmidt et al. reported that tidal volume was decreased from 6.3 (before ECMO) to 3.9 mL/kg, plateau pressure from 32.2 to 26.6 cmH₂O, and driving pressure from 19.0 to 13.7 cmH₂O (Schmidt et al. 2015). In an international survey from all ELSO-registered centers, medical directors, and ECMO program coordinators, 66% of centers had adopted controlled ventilatory modes as initial ventilatory management of ECMO patients

(Marhong et al. 2014). Tidal volume was usually limited to less than 4 mL/kg PBW in 34% of the centers, whereas 47% used tidal volumes between 4 and 6 mL/kg PBW. Serpa Neto et al., in a pooled individual patient analysis from nine observational studies (545 patients), reported that during the first day of ECMO, tidal volume was reduced from 6.0 to 4.0 mL/kg PBW, plateau pressure from 31.1 to 26.2 cmH₂O, and $F_{I}O_2$ from 0.9 to 0.7. Driving pressure, too, was reduced from 17.7 to 13.7 cmH₂O; this was the only ventilation parameter that showed an independent association with in-hospital mortality (Serpa Neto et al. 2016). The value of tight limitation of inspiratory plateau pressure during the first days of ECMO is supported by evidence of increased mortality risk at increasing levels of plateau pressure in A(H1N1) ARDS patients undergoing ECMO (Pham et al. 2013). Based on this observational evidence, a large randomized clinical trial comparing ECMO to conventional mechanical ventilation was undertaken to determine if there is a survival benefit with use of ECMO by prevention of VILI (EOLIA study) (Combes et al. 2018). This recently published trial took 9 years to complete and participation of 100 centers and enrollment of 240 patients. Use of VV-ECMO in the treatment group allowed a decrease in minute ventilation from 12 to less than 5 L/min, primarily due to a reduction of tidal volume (from \approx 6.0 to \approx 3.4 mL/kg). This was associated with a reduction in plateau pressure from 30 to 24.5 cmH₂O and thus a reduction of the driving pressure by \approx 5 cmH₂O because PEEP was unchanged. With use of these settings, there was a trend toward reduction of mortality in ECMO patients compared to conventional mechanical ventilation. Interestingly, in the control group, a large percentage (28%) underwent ECMO as rescue support with similar reduction of ventilation.

There is less agreement on the appropriate PEEP setting during ECMO. The basic debate is between use of a strategy that gives complete lung rest by applying low levels of PEEP and allowing the lung to collapse, or applying an open lung strategy with higher PEEP levels (15–20 cmH₂O) to maintain open recruitable lung regions combined with very low tidal volumes to

Table 48.1 Ventilation parameters before and after ECMO initiation in published studies

	Study type & Number of patients	Tidal volume (mL/kg PBW)		Plateau pressure (cmH ₂ O)		PEEP (cmH ₂ O)		FiO ₂ (%)		RR (breath/min)	
		Pre ECMO	During ECMO	Pre ECMO	During ECMO	Pre ECMO	During ECMO	Pre ECMO	During ECMO	Pre ECMO	During ECMO
Peek et al. Lancet 2009	National Multicenter Randomized Clinical Trial 90 pts	NA	NA	NA	Peak airways Pressure 20–25	13.7 ± 9.6	10–15	NA	30	NA	10
Holzgraefe et al. Minerva Anest 2010	Single Center Observational study 13 pts	6.2 (4.6–7.0)	7.7 (5.1–9.0)	25 (21–26)	12 (10–13)	17 (15–20)	5 (5–8)	1	60 (46–63)	NA	NA
Marhong et al. Int Care Med 2015	Systematic Review 42 studies 2042 pts	6.2 (5.9–6.7) 12 studies	4.0 (3.0–6.0) 19 studies	32.0 (30.0–33.7) 12 studies	26.0 (22.0–30.0) 18 studies	13.0 (12.0–15.0) 33 studies	12.0 (9.6–14.5) 40 studies	99 (80–100) 18 studies	40 (35–50) 31 studies	NA	NA
Schmidt et al. Crit Care Med 2016	Retrospective International Multicenter Observational Study 168 pts	6.3 ± 1.5	3.9 ± 1.6	32.2 ± 4.7	26.4 ± 3.5	13 ± 4	12 ± 3	NA	NA	NA	NA
Serpa Neto et al. Int Care Med 2016	Pooled Individual Patient Data Meta-analysis 9 studies 545 pts	6.0 ± 1.9	4.0 ± 1.7	31.1 ± 5.7	26.2 ± 4.6	13.7 ± 4.3	12.9 ± 3.4	90 ± 17	69 ± 24	21.9 ± 7.9	17.8 ± 8.0
Combes et al. N Engl J Med 2018	International Multicenter Randomized Clinical Trial 44 pts	6.0 ± 1.3	≈3.34	29.8 ± 5.5	≈24.5	11.7 ± 3.9	Unchanged	96 ± 10	NA	30.4 ± 4.7	NA

Pts patients, PBW Predicted Body Weight, PEEP Positive End-Expiratory Pressure, FiO₂ Fraction of Inspired Oxygen, RR respiratory rate

Table 48.2 Potential advantages and disadvantages of a total rest vs. open lung ventilatory strategy during ECMO

Total rest strategy	Open lung strategy
<i>PRO:</i> Minimize overdistention Lower airway plateau pressure	<i>PRO:</i> Minimize atelectrauma Lower $V_t/EELV$ ratio
<i>CON:</i> Atelectrauma Right ventricular failure Higher intrapulmonary shunt	<i>CON:</i> Overdistention Lower venous return

V_t Tidal Volume, $EELV$ End-Expiratory Lung Volume

prevent over-stretching the lung (Table 48.2). Low tidal volume ventilation adopted during ECMO might produce reabsorption atelectasis of regions with a low VA/Q ratio, since, despite a high oxygen saturation of mixed venous blood, a positive PO_2 gradient remains at the alveolar-capillary interface. Patients managed with low tidal volume ventilation and low PEEP levels during ECMO might develop a progressive decrease in respiratory system compliance attributable to this reabsorption atelectasis (Gattinoni et al. 1980). In the opposite direction, high levels of PEEP could be adopted during ECMO to maintain static aeration with minimal ventilation, or slightly lower PEEP might be sufficient if a plateau pressure of 25–28 cmH₂O is reached during residual tidal ventilation. Such open lung strategies during ECMO could be particularly useful when the ratio of extracorporeal flow to the patient's own cardiac output is not enough to achieve the desired degree of mixed venous and, consequently, arterial oxygenation. On the other hand, the open lung strategy could be associated with higher risk of barotrauma and right heart failure and need to be converted from VV to VA ECMO to unload the right ventricle. By contrast, adopting a lung rest strategy, the native lung does not contribute to gas exchange, and higher extracorporeal blood flow is required, and it might require insertion of a second drainage cannula or tolerating very high negative drainage pressure that could induce hemolysis, cavitation, and air embolisms. Moreover, in ARDS patients, increased pulmonary arterial pressure is com-

mon, and diffuse alveolar collapse might result in further loading of the right heart and lead to right heart failure with the need to convert to VA-ECMO. The Extracorporeal Life Support Organization recommends a PEEP of 10 cmH₂O during ECMO support (Extracorporeal Life Support Organization 2017). In the CESAR trial, which showed survival and cost benefits of referral to an ECMO center for severe ARDS patients, the ventilation protocol targeted a lung rest strategy (Peek et al. 2009). For patients enrolled in the ECMO group, PEEP was progressively decreased to 10 cmH₂O, respiratory rate to 10 breath/min, F_{iO_2} at 30%, and tidal volume to reach a maximum peak inspiratory pressure of 20 cmH₂O. However, detailed ventilation parameters were not reported in the study. In the EOLIA trial, the PEEP levels adopted in both the treatment and control group were in the intermediate range (10–12 cmH₂O) and were not changed substantially between before and after ECMO initiation (Combes et al. 2018). The Karolinska workgroup during the 2009 influenza A/H1N1 severe respiratory failure pandemic reported an approach that shifted toward the total lung rest strategy (Holzgraefe et al. 2010). At arrival to the ECMO referral center, VV-ECMO was promptly started and mechanical ventilation was set with a PEEP between 5 and 10 cmH₂O, F_{iO_2} below 50%, and pressure control ventilation with a maximum peak airway pressure of 25 cmH₂O. Despite maximal extracorporeal support in this approach, they had to accept a median arterial oxygen saturation around 85% which likely was similar to the patients' mixed venous oxygen saturation. Hypoxic pulmonary vasoconstriction in 4 patients was treated by switching to VA-ECMO. This approach however did not avoid barotrauma, which occurred in 3 of the 4 patients. Reviewing the pragmatic approaches proposed by different study protocols and the heterogeneous reported PEEP values, it seems reasonable to translate knowledge deriving from research in ARDS patients to severe ARDS treated by ECMO. Titrating PEEP according to improved oxygenation or to minimize lung collapse according to electrical impedance tomography or the CT scan represents a valuable option in order to

minimize lung stress and strain and to maximize the contribution of NL to gas exchange (Franchineau et al. 2017). Furthermore, although there is still insufficient evidence, Schmidt et al. reported a higher survival rate among patients treated with higher PEEP levels during VV-ECMO support (Schmidt et al. 2015).

Setting of respiratory rate during VV-ECMO is another controversial issue. Natural lung contributes minimally to CO₂ clearance during ECMO, for this reason, and to minimize dynamic strain rate, during the early phase of extracorporeal support, very low respiratory rates are usually adopted. Furthermore, low respiratory rate might contribute to the protection from excessive mechanical power. However, trials generally have reported only a slight decrease in respiratory rate after ECMO institution, and values between 15 and 25 breath/min are frequent. This approach does not have a clear rationale and might be attributable to the attempt to maintain mean airways pressure when applying a low PEEP strategy.

Whether to perform or the timing for tracheostomy in patients with severe ARDS is another unanswered question. Compared to oro/nasal-tracheal intubation, tracheostomy decreases airways resistance and dead space, improves patient comfort, and allows a decrease of sedatives. However, similar to setting high respiratory rate, optimization of airway dead space and resistance contribute minimally to optimization of ventilation. Still, use of tracheostomy is very high in ECMO patients (about 37%) (Combes et al. 2018), and its timing is extremely variable among centers, usually being occurring between days 6 and 10 from initiation of mechanical ventilation.

Limiting F_IO₂ during ECMO to reduce direct oxygen toxicity on the lung and generation of reabsorption atelectasis was one of the original hypotheses for the potential advantage of ECMO compared to conventional mechanical ventilation (Kobayashi et al. 2001). All ECMO trials have reported a substantial reduction of F_IO₂ after institution of the extracorporeal support. A marked F_IO₂ reduction implies that when the native lung is still contributing to arterial oxygenation, high extracorporeal blood flows is neces-

sary. This would support the argument that an open lung strategy might provide adequate oxygen delivery from the NL with lower F_IO₂ fraction as compared to a total lung rest strategy.

The pathophysiological rationale for prone positioning of patients with ARDS, was that it allowed more homogenous distribution of aeration, (Langer et al. 1988) and the prone position was eventually shown to decrease mortality (Guérin et al. 2013). Prone positioning during ECMO has been used to improve ventilation perfusion matching in the NL, and thus improving arterial oxygenation as well as possibly reducing the extent and the duration of extracorporeal support (Kimmoun et al. 2015; Masuda et al. 2014). Moreover, in patients with extremely low compliance values, prone position could reduce regional lung stress associated with the minimal residual ventilation during ECMO. A recent descriptive study (Lucchini et al. 2018) reported no displacements of vascular lines nor other complications (dislodgment or compression) related to the maneuver. However, this approach only should be considered in centers with adequate training.

Monitoring of the NL function during VV-ECMO is of paramount importance to assess the clinical course of the lung disease. However, arterial blood gas analysis is strongly affected by the presence of the ML and NL in series and may not always be accurate. Some authors suggest that improvement of intrapulmonary shunt of the NL strongly predicts the weaning success from ECMO. In a large cohort of ARDS patients treated with VV-ECMO, Mols et al. reported successful weaning from ECMO when at least 80% of total oxygen delivery was provided by the patient NL (Mols et al. 2000). However, to assess intrapulmonary shunt, a pulmonary artery catheter is required and F_IO₂ must be set at 100% on both supports temporarily to minimize the contribution of regions with very low VA/Q value (Zanella et al. 2016). A pulmonary artery catheter also can be useful to assess the ratio of cardiac output to extracorporeal flow which during ECMO is one of the main determinants of arterial oxygenation. Daily assessment of respiratory mechanics and repeated lung imaging studies

(ultrasound, electrical impedance tomography, CT scan, or chest X-rays) also can add useful information on the course of the patient undergoing ECMO to the clinician.

Assisted Mechanical Ventilation During VV-ECMO

During the earliest phase of ARDS, controlled mechanical ventilation with high levels of sedation and muscle paralysis might cause diaphragmatic atrophy due to inactivity (Levine et al. 2008). Muscles wasting and un-physiology of controlled ventilation can prolong mechanical ventilation and cause difficult weaning from the respiratory support. Early application of assisted ventilation modes might decrease the degree of muscle atrophy and favor patient reconditioning to spontaneous breathing. However, in contrast to controlled ventilator modes, achieving *protective* assisted mechanical ventilation setting may represent a real challenge for the intensive care physician and the respiratory therapist. High tidal volume and high levels of transpulmonary pressure due to uncontrolled inspiratory effort are frequent in ARDS patients breathing spontaneously. Similarly, the high respiratory rate and severely impaired lung mechanics make it difficult to obtain a good patient–ventilator interaction, and multiple asynchronies might be present. To identify the optimal timing to switch the severe ARDS patient undergoing ECMO from controlled to assisted ventilation mode is crucial. Lung function has been traditionally used as guide. It has been proposed not to change to a spontaneous mode when intrapulmonary shunt fraction is >40% and/or respiratory system compliance is below 20 mL/cmH₂O. The risk of worsening lung injury up to plasma leak and intra-alveolar bleeding has been described (Yoshida et al. 2017). Moreover, during switch from controlled to assisted ventilation, hemodynamics should be carefully monitored because volume overload with left heart failure or increased workload to right heart with consequent right ventricular failure are not uncommon (Lemaire et al. 1988). However, the Karolinska ECMO group reported

a case series of severe ARDS patients managed with minimal sedation and pressure support ventilation with low tidal volumes throughout the whole period of extracorporeal support with a low mortality rate (24%) (Lindén et al. 2000).

It has been recommended to use appropriate short acting sedatives after a period of clearance of long-lasting drugs that accumulate in the system. Heunks et al. also proposed a partial muscle paralysis protocol to decrease pharmacologically patient's muscle effort during mechanical ventilation (Doorduyn et al. 2017) albeit not in a population treated by ECMO.

In terms of monitoring, esophageal manometry can be useful during spontaneous breathing to assess patient's inspiratory effort and intrinsic PEEP level and easily detect the presence of asynchronies (Mauri et al. 2016a). Electrical impedance tomography can reveal occult pendelluft phenomenon that could increase injury as well as asynchronies (Yoshida et al. 2013). The use of monitoring tools together with a careful knowledge of the intensive care unit mechanical ventilator settings (trigger level, cycling criteria, inspiratory ramp, etc.) are helpful for adapting the ventilator settings to the patient's requirement and minimizing potential injurious ventilation pattern.

Closed loop-ventilation modes, automatically adjusting some ventilator settings to the patient's respiratory drive, might minimize asynchronies and increase successful switch to assisted mode. Neurally adjusted ventilator assist (NAVA) has been suggested as a useful option for closed loop assisted ventilation and as a monitoring tool of patients' neural respiratory drive and effort. During NAVA, because the inspiratory trigger based on diaphragm electromyography is highly accurate, risk of missed efforts and auto-triggering is minimized. Moreover, ARDS patients can develop double-triggering when pressure support ventilation is applied, because the cycling-off criteria are reached very early during inspiration due to the low lung compliance and increased airways resistance. During NAVA, cycling-off criteria are independent of the patient's lung mechanics, and this should promote patient–ventilator synchrony, reduce

double-triggering, and early and delayed cycling (Mauri et al. 2011). It could also be used as a monitoring tool to assess patient's response to decreasing sweep gas flow during the ECMO weaning process (Karagiannidis et al. 2010). Manipulation of CO₂ elimination by regulating sweep gas flow acts as an external modulator of the patient's respiratory drive. In the pivotal study on extracorporeal CO₂ removal by Kolobow and Gattinoni, incremental rates of CO₂ removal in awake healthy lambs led to progressively decreasing minute ventilation up to complete apnea (Kolobow et al. 1977). Recently, our group reported that in patients recovering from ARDS undergoing ECMO, modulating the amount of CO₂ removed from the artificial lung, it is possible to decrease patient's respiratory drive and effort (Mauri et al. 2016b). Indeed, extracorporeal CO₂ removal might be considered as a strategy to modulate patient respiratory effort during the weaning from respiratory support (Scaravilli et al. 2016).

The newest frontier of application of VV ECMO is for the treatment of awake spontaneously breathing patients and avoidance of intubation and mechanical ventilation. This approach has been proposed for use in both patients with acute on chronic respiratory failure as a bridge to lung transplant or for chronic obstructive pulmonary disease, and in pure acute respiratory failure (ARDS) (Crotti et al. 2017) with around a 50% clinical success rate. However, the effect of CO₂ removal on a patient's respiratory drive is not always predictable, especially in ARDS patients, in whom factors other than the plasma CO₂ levels, such as afferent signaling arising from inflamed pulmonary parenchymal, can increase respiratory drive. In these cases, extracorporeal CO₂ removal with full ECMO support is not sufficient to reduce inspiratory effort and to keep transpulmonary pressure within a safe range (Mauri et al. 2016c). Furthermore, spontaneous breathing activity of awake patients responds to multiple conditions such as wakefulness, sleep, fever, and changes in sedation which result in variable respiratory patterns in the presence of a constant ECMO support (Crotti et al. 2018). Based on these considerations, this approach

likely should be reserved for highly selected candidates and only performed in experienced centers.

Authors' Contribution JF, EC, and TM conceived and drafted the text; all authors approved the final draft of the report.

Conflicts of Interest Jacopo Fumagalli: none; Eleonora Carlesso: none; Tommaso Mauri: none.

References

- Brochard L, Slutsky A, Pesenti A. Mechanical ventilation to minimize progression of lung injury in acute respiratory failure. *Am J Respir Crit Care Med.* 2017;195:438–42.
- Camporota L, Nicoletti E, Malafronte M, De Neef M, Mongelli V, Calderazzo MA, Caricola E, Glover G, Meadows C, Langrish C, Ioannou N, Wyncoll D, Beale R, Shankar-Hari M, Barrett N. International survey on the management of mechanical ventilation during ECMO in adults with severe respiratory failure. *Minerva Anesthesiol.* 2015;81:1170–83, 77 p following 1183.
- Combes A, Brodie D, Bartlett R, Brochard L, Brower R, Conrad S, De Backer D, Fan E, Ferguson N, Fortenberry J, Fraser J, Gattinoni L, Lynch W, MacLaren G, Mercat A, Mueller T, Ogino M, Peek G, Pellegrino V, Pesenti A, Ranieri M, Slutsky A, Vuylsteke A, International ECMO Network (ECMONet). Position paper for the organization of extracorporeal membrane oxygenation programs for acute respiratory failure in adult patients. *Am J Respir Crit Care Med.* 2014;190:488–96.
- Combes A, Hajage D, Capellier G, Demoule A, Lavoué S, Guervilly C, Da Silva D, Zafrani L, Tirot P, Veber B, Maury E, Levy B, Cohen Y, Richard C, Kalfon P, Bouadma L, Mehdaoui H, Beduneau G, Lebreton G, Brochard L, Ferguson ND, Fan E, Slutsky AS, Brodie D, Mercat A, EOLIA Trial Group, REVA, and ECMONet. Extracorporeal membrane oxygenation for severe acute respiratory distress syndrome. *N Engl J Med.* 2018;378:1965–75.
- Crotti S, Bottino N, Ruggeri GM, Spinelli E, Tubiolo D, Lissoni A, Protti A, Gattinoni L. Spontaneous breathing during extracorporeal membrane oxygenation in acute respiratory failure. *Anesthesiology.* 2017;126:678–87.
- Crotti S, Bottino N, Spinelli E. Spontaneous breathing during veno-venous extracorporeal membrane oxygenation. *J Thorac Dis.* 2018;10:S661–9.
- Doorduyn J, Nollet JL, Roesthuis LH, van Hees HWH, Brochard LJ, Sinderby CA, van der Hoeven JG, Heunks LMA. Partial neuromuscular blockade during partial ventilatory support in sedated patients

- with high tidal volumes. *Am J Respir Crit Care Med*. 2017;195:1033–42.
- Esteban A, Anzueto A, Frutos F, Alía I, Brochard L, Stewart TE, Benito S, Epstein SK, Apezteguía C, Nightingale P, Arroliga AC, Tobin MJ, Mechanical Ventilation International Study Group. Characteristics and outcomes in adult patients receiving mechanical ventilation: a 28-day international study. *JAMA*. 2002;287:345–55.
- Extracorporeal Life Support Organization. Extracorporeal Life Support Organization (ELSO) guidelines for adult respiratory failure. 2017. https://www.else.org/Portals/0/ELSO%20Guidelines%20For%20Adult%20Respiratory%20Failure%201_4.pdf.
- Franchineau G, Bréchet N, Lebreton G, Hekimian G, Nieszowska A, Trouillet J-L, Leprince P, Chastre J, Luyt C-E, Combes A, Schmidt M. Bedside contribution of electrical impedance tomography to setting positive end-expiratory pressure for extracorporeal membrane oxygenation-treated patients with severe acute respiratory distress syndrome. *Am J Respir Crit Care Med*. 2017;196:447–57.
- Gattinoni L, Pesenti A. The concept of “baby lung”. *Intensive Care Med*. 2005;31:776–84.
- Gattinoni L, Kolobow T, Agostoni A, Damia G, Pelizzola A, Rossi GP, Langer M, Solca M, Citterio R, Pesenti A, Fox U, Uziel L. Clinical application of low frequency positive pressure ventilation with extracorporeal CO₂ removal (LFPPV-ECCO₂R) in treatment of adult respiratory distress syndrome (ARDS). *Int J Artif Organs*. 1979;2:282–3.
- Gattinoni L, Agostoni A, Pesenti A, Pelizzola A, Rossi GP, Langer M, Vesconi S, Uziel L, Fox U, Longoni F, Kolobow T, Damia G. Treatment of acute respiratory failure with low-frequency positive-pressure ventilation and extracorporeal removal of CO₂. *Lancet Lond Engl*. 1980;2:292–4.
- Gattinoni L, Tonetti T, Cressoni M, Cadringer P, Herrmann P, Moerer O, Protti A, Gotti M, Chiurazzi C, Carlesso E, Chiumello D, Quintel M. Ventilator-related causes of lung injury: the mechanical power. *Intensive Care Med*. 2016;42:1567–75.
- Guérin C, Reigner J, Richard J-C, Beuret P, Gacouin A, Boulain T, Mercier E, Badet M, Mercat A, Baudin O, Clavel M, Chatellier D, Jaber S, Rosselli S, Mancebo J, Sirodot M, Hilbert G, Bengler C, Richecoeur J, Gannier M, Bayle F, Bourdin G, Leray V, Girard R, Baboi L, Ayzac L, PROSEVA Study Group. Prone positioning in severe acute respiratory distress syndrome. *N Engl J Med*. 2013;368:2159–68.
- Holzgraefe B, Broomé M, Kalzén H, Konrad D, Palmér K, Frenckner B. Extracorporeal membrane oxygenation for pandemic H1N1 2009 respiratory failure. *Minerva Anestesiol*. 2010;76:1043–51.
- Karagiannidis C, Lubnow M, Philipp A, Riegger GAJ, Schmid C, Pfeifer M, Mueller T. Autoregulation of ventilation with neurally adjusted ventilatory assist on extracorporeal lung support. *Intensive Care Med*. 2010;36:2038–44.
- Kimmoun A, Roche S, Bridey C, Vanhuyse F, Fay R, Girerd N, Mandry D, Levy B. Prolonged prone positioning under VV-ECMO is safe and improves oxygenation and respiratory compliance. *Ann Intensive Care*. 2015;5:35.
- Kobayashi H, Hataishi R, Mitsufuji H, Tanaka M, Jacobson M, Tomita T, Zapol WM, Jones RC. Antiinflammatory properties of inducible nitric oxide synthase in acute hyperoxic lung injury. *Am J Respir Cell Mol Biol*. 2001;24:390–7.
- Kolobow T, Gattinoni L, Tomlinson TA, Pierce JE. Control of breathing using an extracorporeal membrane lung. *Anesthesiology*. 1977;46:138–41.
- Kolobow T, Moretti MP, Fumagalli R, Mascheroni D, Prato P, Chen V, Joris M. Severe impairment in lung function induced by high peak airway pressure during mechanical ventilation. An experimental study. *Am Rev Respir Dis*. 1987;135:312–5.
- Langer M, Mascheroni D, Marcolin R, Gattinoni L. The prone position in ARDS patients. A clinical study. *Chest*. 1988;94:103–7.
- Lemaire F, Teboul JL, Cinotti L, Giotto G, Abrouk F, Steg G, Macquin-Mavier I, Zapol WM. Acute left ventricular dysfunction during unsuccessful weaning from mechanical ventilation. *Anesthesiology*. 1988;69:171–9.
- Levine S, Nguyen T, Taylor N, Friscia ME, Budak MT, Rothenberg P, Zhu J, Sachdeva R, Sonnad S, Kaiser LR, Rubinstein NA, Powers SK, Shrager JB. Rapid disuse atrophy of diaphragm fibers in mechanically ventilated humans. *N Engl J Med*. 2008;358:1327–35.
- Lindén V, Palmér K, Reinhard J, Westman R, Ehrén H, Granholm T, Frenckner B. High survival in adult patients with acute respiratory distress syndrome treated by extracorporeal membrane oxygenation, minimal sedation, and pressure supported ventilation. *Intensive Care Med*. 2000;26:1630–7.
- Lucchini A, De Felippis C, Pelucchi G, Grasselli G, Patroniti N, Castagna L, Foti G, Pesenti A, Fumagalli R. Application of prone position in hypoxaemic patients supported by venovenous ECMO. *Intensive Crit Care Nurs* 2018. <https://doi.org/10.1016/j.iccn.2018.04.002>.
- Marhong JD, Telesnicki T, Munshi L, Del Sorbo L, Detsky M, Fan E. Mechanical ventilation during extracorporeal membrane oxygenation. An international survey. *Ann Am Thorac Soc*. 2014;11:956–61.
- Masuda Y, Tatsumi H, Imaizumi H, Gotoh K, Yoshida S, Chihara S, Takahashi K, Yamakage M. Effect of prone positioning on cannula function and impaired oxygenation during extracorporeal circulation. *J Artif Organs Off J Jpn Soc Artif Organs*. 2014;17:106–9.
- Mauri T, Bellani G, Foti G, Grasselli G, Pesenti A. Successful use of neurally adjusted ventilatory assist in a patient with extremely low respiratory system compliance undergoing ECMO. *Intensive Care Med*. 2011;37:166–7.
- Mauri T, Yoshida T, Bellani G, Goligher EC, Carreaux G, Rittayamai N, Mojoli F, Chiumello D, Piquilloud L, Grasso S, Jubran A, Laghi F, Magder S, Pesenti A,

- Loring S, Gattinoni L, Talmor D, Blanch L, Amato M, Chen L, Brochard L, Mancebo J, PLeUral pressure working Group (PLUG—Acute Respiratory Failure section of the European Society of Intensive Care Medicine). Esophageal and transpulmonary pressure in the clinical setting: meaning, usefulness and perspectives. *Intensive Care Med.* 2016a;42:1360–73.
- Mauri T, Grasselli G, Suriano G, Eronia N, Spadaro S, Turrini C, Patroniti N, Bellani G, Pesenti A. Control of respiratory drive and effort in extracorporeal membrane oxygenation patients recovering from severe acute respiratory distress syndrome. *Anesthesiology.* 2016b;125:159–67.
- Mauri T, Langer T, Zanella A, Grasselli G, Pesenti A. Extremely high transpulmonary pressure in a spontaneously breathing patient with early severe ARDS on ECMO. *Intensive Care Med.* 2016c;42:2101–3.
- Mols G, Loop T, Geiger K, Farthmann E, Benzing A. Extracorporeal membrane oxygenation: a ten-year experience. *Am J Surg.* 2000;180:144–54.
- Peek GJ, Mugford M, Tiruvoipati R, Wilson A, Allen E, Thalanany MM, Hibbert CL, Truesdale A, Clemens F, Cooper N, Firmin RK, Elbourne D, CESAR Trial Collaboration. Efficacy and economic assessment of conventional ventilatory support versus extracorporeal membrane oxygenation for severe adult respiratory failure (CESAR): a multicentre randomised controlled trial. *Lancet Lond Engl.* 2009;374:1351–63.
- Pham T, Combes A, Rozé H, Chevret S, Mercat A, Roch A, Mourvillier B, Ara-Somohano C, Bastien O, Zogheib E, Clavel M, Constan A, Marie Richard J-C, Brun-Buisson C, Brochard L, Research Network REVA. Extracorporeal membrane oxygenation for pandemic influenza A(H1N1)-induced acute respiratory distress syndrome: a cohort study and propensity-matched analysis. *Am J Respir Crit Care Med.* 2013;187:276–85.
- Scaravilli V, Kreyer S, Belenkiy S, Linden K, Zanella A, Li Y, Dubick MA, Cancio LC, Pesenti A, Batchinsky AI. Extracorporeal carbon dioxide removal enhanced by lactic acid infusion in spontaneously breathing conscious sheep. *Anesthesiology.* 2016;124:674–82.
- Schmidt M, Stewart C, Bailey M, Nieszkowska A, Kelly J, Murphy L, Pilcher D, Cooper DJ, Scheinkestel C, Pellegrino V, Forrest P, Combes A, Hodgson C. Mechanical ventilation management during extracorporeal membrane oxygenation for acute respiratory distress syndrome: a retrospective international multicenter study. *Crit Care Med.* 2015;43:654–64.
- Serpa Neto A, Schmidt M, LCP A, Bein T, Brochard L, Beutel G, Combes A, ELV C, Hodgson C, Lindskov C, Lubnow M, Lueck C, Michaels AJ, Paiva J-A, Park M, Pesenti A, Pham T, Quintel M, Marco Ranieri V, Ried M, Roncon-Albuquerque R, Slutsky AS, Takeda S, Terragni PP, Vejen M, Weber-Carstens S, Welte T, Gama de Abreu M, Pelosi P, et al. Associations between ventilator settings during extracorporeal membrane oxygenation for refractory hypoxemia and outcome in patients with acute respiratory distress syndrome: a pooled individual patient data analysis : Mechanical ventilation during ECMO. *Intensive Care Med.* 2016;42:1672–84.
- Slutsky AS, Ranieri VM. Ventilator-induced lung injury. *N Engl J Med.* 2013;369:2126–36.
- Yoshida T, Torsani V, Gomes S, De Santis RR, Beraldo MA, Costa ELV, Tucci MR, Zin WA, Kavanagh BP, Amato MBP. Spontaneous effort causes occult pendelluft during mechanical ventilation. *Am J Respir Crit Care Med.* 2013;188:1420–7.
- Yoshida T, Fujino Y, Amato MBP, Kavanagh BP. Fifty Years of Research in ARDS. Spontaneous breathing during mechanical ventilation. Risks, mechanisms, and management. *Am J Respir Crit Care Med.* 2017;195:985–92.
- Zanella A, Salerno D, Scaravilli V, Giani M, Castagna L, Magni F, Carlesso E, Cadringer P, Bombino M, Grasselli G, Patroniti N, Pesenti A. A mathematical model of oxygenation during venovenous extracorporeal membrane oxygenation support. *J Crit Care.* 2016;36:178–86.
- Zapol WM, Snider MT, Hill JD, Fallat RJ, Bartlett RH, Edmunds LH, Morris AH, Peirce EC, Thomas AN, Proctor HJ, Drinker PA, Pratt PC, Bagniewski A, Miller RG. Extracorporeal membrane oxygenation in severe acute respiratory failure. A randomized prospective study. *JAMA.* 1979;242:2193–6.



Vasopressor Support for Patients with Cardiopulmonary Failure

49

Daniel De Backer and Pierre Foulon

Introduction

Vasopressors are an essential part of our resuscitation strategies. The rationale for their use is based on the preservation of perfusion pressure to the organs. For most organs, blood flow is considered to be constant over a broad range of pressures, but it is only when blood pressure decreases below a critical threshold (autoregulation threshold) that perfusion becomes dependent on inflow pressure. Organs can become dependent on inflow pressure at different autoregulation thresholds, and this autoregulation threshold is affected by age and disease. In addition, while most organs are dependent on mean arterial pressure (MAP), the heart also depends on diastolic pressure. For the left ventricle, coronary artery pressure equals left ventricular parietal pressure during systole so that perfusion of the left ventricle only depends on diastolic arterial pressure (DAP). For the right ventricle, the situation is more complex as its coronary perfusion depends upon the instantaneous pressure difference between systemic arterial pressure, on the one hand, and pulmonary artery pressure during systole and right atrial pressure during diastole, on the other. Accordingly, it is difficult to determine a universal autoregulation threshold.

There are numerous observations reporting that both the severity and duration of hypotension are associated with organ dysfunction and increased risk of death (Maheshwari et al. 2018; Vincent et al. 2018; Dunser et al. 2009a). However, the determination of the target blood pressure for a given patient condition is far from easy. Indeed, there are a lot of factors that interfere with tissue perfusion including arterial pressure, organ interstitial pressure, and venous outflow pressure. In addition, vasopressors do not uniformly affect organ perfusion pressure due to the variable density of receptors across the vascular beds. Finally, when considering the optimal target pressure, one should also consider that vasopressor agents are associated with adverse effects that are often dose dependent (Dunser et al. 2009b; Auchet et al. 2017). Targeting higher (or “more normal”) levels of blood pressure may expose the patient to higher doses of vasopressors and hence to higher risks of adverse events (Asfar et al. 2014). Finally, blood pressure is only one of the components of organ perfusion, and sometimes raising blood pressure may be associated with a decrease in cardiac output due to the increase in left ventricular afterload. Accordingly, the target blood pressure should be individually estimated, taking into account indices of organ perfusion (including the heart and brain!) and the risks of adverse events associated with vasopressor therapy.

D. De Backer (✉) · P. Foulon
Department of Intensive Care, CHIREC Hospitals,
Université Libre de Bruxelles, Brussels, Belgium
e-mail: ddebacke@ulb.ac.be

Differences Between Various Agents

Vasopressors can be categorized as adrenergic and non-adrenergic vasopressor agents.

Adrenergic Vasopressor Agents

Adrenergic vasopressor agents exert their pressive effect through stimulation of alpha-adrenergic receptors present on endothelial cells. Differences between adrenergic agents arise due to the additional stimulation of beta-adrenergic and dopaminergic receptors. Beta-adrenergic receptor stimulation increases not only cardiac inotropy but also chronotropy and improves not only splanchnic perfusion but also increases cellular metabolism (accelerated glycolysis through stimulation of NaKATPase, thermogenic effects, etc.). Phenylephrine is a pure alpha-adrenergic agent and results in an increase in blood pressure and also in a slight decrease in cardiac output due to the uncompensated increase in left ventricular afterload. Norepinephrine combines strong alpha stimulation with a weak beta stimulation so that cardiac output is usually preserved or slightly increased together with the pressive effect. Epinephrine is a strong alpha- and also beta-adrenergic agent. While, at a first glance, this combined increase in arterial pressure and cardiac output may appear attractive, the excessive beta stimulation often results in increased heart workload (Ducrocq et al. 2012), arrhythmias, and even hyperlactatemia (Myburgh et al. 2008).

Finally dopamine is a less potent agent having combined alpha- and beta-adrenergic effects. This agent also stimulates dopaminergic receptors. The beneficial effects of dopaminergic stimulation on splanchnic and renal circulations seem to be relatively limited (De Backer et al. 2003), but the central effects should not be neglected as it may downregulate some aspects of the hypothalamo-pituitary axis (van den Berghe and de Zegher 1996). The excessive beta-stimulation is also associated with tachycardia and an excess in arrhythmic events (De Backer et al. 2010).

Non-adrenergic Vasopressor Agents

Non-adrenergic vasopressors include vasopressin derivatives and angiotensin. Interestingly, although the receptors at endothelial surface differ from the alpha receptor, the downstream intracellular mechanisms are quite similar. Accordingly, differences between the various vasopressor agents arise due to the sensitivity of the surface receptors (downregulation may occur for one but not another subtype, especially after exposure to a vasopressor agent of that type), density of receptors along the vascular system, which determines the regional effects of these agents, and concomitant stimulation of other receptors such as beta receptors for adrenergic vasopressors, V2 receptors for vasopressin derivatives, AG 1–7 receptors for angiotensin II.

Vasopressin Derivatives

Vasopressin derivatives exert their pressor effect through stimulation of the V1 receptor. V2 receptor stimulation results in various actions. On the renal collecting duct, it results in an antidiuretic action which is a cAMP-dependent process; on endothelial cells, it results in vasodilation through generation of nitric oxide (NO); and on platelets, it results in platelet aggregation. Stimulation of other vasopressin receptors (V3 and octreotide) usually is not relevant with vasopressin derivatives used as vasopressors.

Arginine vasopressin, often referred to as vasopressin, has been the most investigated. It acts on V1 and V2 receptors and results in potent arteriolar and venular constriction. The hemodynamic profile is relatively similar to that of norepinephrine, except that it has no inotropic effect. However, at high doses, vasopressin results in significant splanchnic vasoconstriction and sometimes even ischemia so that doses higher than 0.04 are usually not recommended.

Terlipressin has a higher V1 affinity compared to vasopressin, but it still exerts some V2 agonist effect. Given its long half-life (6 h), this agent is more difficult to manipulate and is given either as a bolus of 0.5–1 mg every 6–8 hours or as continuous infusion of 20–160 µg/h. Selepressin is a

selective V1 agonist, still currently in its experimental phase.

Vasopressin derivatives have interesting properties on the kidney. Due to their higher density on efferent than afferent arterioles, vasopressin derivatives result in improved glomerular filtration pressure (independently of the effect on systemic pressure). Accordingly, urine output often increases, despite the intrinsic antidiuretic effect of the agent (Patel et al. 2002). Being deprived of V2 stimulation, selepressin may even result in a more negative fluid balance (Russell et al. 2017). Vasopressin derivatives may improve renal function in patients with vasodilatory shock (McIntyre et al. 2018). Vasopressin seems also to be associated with less episodes of atrial fibrillation but may increase the risk of digital necrosis (McIntyre et al. 2018).

Angiotensin II

Angiotensin II is a potent vasopressor agent (Udhoji and Weil 1964) which was recently reintroduced for the therapy of hypotensive patients (Senatore et al. 2019). Angiotensin constricts arterioles and venules. The higher distribution of its receptors in the splanchnic area also carries a risk of splanchnic hypoperfusion, especially in hypovolemic states (Aneman et al. 1997). The absence of inotropic capacity may also be of concern in patients with cardiac dysfunction. On the other hand, angiotensin can improve renal perfusion. It also may blunt the increase in vascular permeability (Victorino et al. 2002).

The effects of angiotensin administration on tissue perfusion are far from obvious. While it can increase perfusion pressure to the organs by increasing MAP, angiotensin impairs microvascular perfusion by direct vasoconstriction and by increasing adhesion of circulating cells to the endothelium (Piqueras et al. 2000). Of note, administration of angiotensin-converting enzyme inhibitors improved microcirculation in experimental sepsis (Salgado et al. 2011) and in patients with cardiogenic shock (Salgado et al. 2013). In a small-sized randomized trial, administration of angiotensin II was associated with an increase in MAP (Khanna et al. 2017), and clinical experience within strict inclusion crite-

ria did not demonstrate obvious detrimental effects (Busse et al. 2017).

Impact on Outcome

In patients with septic shock, norepinephrine was associated with an improved outcome compared to dopamine (De Backer et al. 2012). Similar results were observed in patients with cardiogenic shock (De Backer et al. 2010). In the perioperative period, continuous intravenous infusion of norepinephrine was associated with lower occurrence of postoperative organ dysfunction compared to ephedrine boluses (Futier et al. 2017). Compared to epinephrine, norepinephrine administration was associated with a trend to a lower mortality in patients with cardiogenic shock (Levy et al. 2018). Confirmatory data were obtained during a shortage of norepinephrine in the United States (Vail et al. 2017). Substitution of norepinephrine by other vasopressor agents was associated with a transient increase in mortality rate in septic shock patients which resolved after return to the preferential use of norepinephrine in these units (Vail et al. 2017).

Vasopressin derivatives have been mostly investigated as an add-on to adrenergic vasopressors (mostly norepinephrine) in order to limit the potential adverse effects observed at high doses of norepinephrine. Two large-scale randomized trials were performed in patients with septic shock, and none of these reported an improvement in outcome with vasopressin compared to norepinephrine (Russell et al. 2008; Gordon et al. 2016). Similar results were observed with terlipressin, a more selective V1 agonist (Liu et al. 2018). In a meta-analysis that incorporated lower quality trials, there was nevertheless a signal that addition of vasopressin derivatives may improve outcome compared to norepinephrine (McIntyre et al. 2018). Interestingly, the incidence of arrhythmias and acute kidney injury was lower with vasopressin derivatives, but incidence of digital necrosis was higher. The impact of vasopressin derivatives on outcome has not been investigated in other types of shock, nor as the first-line agent in septic shock.

To date, there has been no adequately powered study to evaluate the impact of angiotensin on outcome. The ATHOS-3 trial compared the addition of angiotensin to placebo in patients with distributive shock who were mostly septic and were already receiving adrenergic vasopressors (mostly norepinephrine) with or without vasopressin (Khanna et al. 2017). As expected, angiotensin was more effective than placebo to raise MAP up to 75 mmHg. However, this trial did not test whether increasing the doses of ongoing vasopressors would have allowed patients to reach the target MAP. This trial also was not powered to evaluate differences in patient relevant outcomes. However, there was a non-significant trend toward a decreased mortality at day 28 (46% in angiotensin vs 54% in placebo, $p = 0.12$) that deserves confirmation in a phase III trial. Similarly, a post-hoc analysis of the patients with acute kidney injury requiring renal replacement therapy at inclusion indicated that angiotensin was associated with a better renal recovery compared to placebo-treated patients (Tumlin et al. 2018). There are at this stage no recent data on the use of angiotensin in other types of shock.

Altogether, these data suggest that norepinephrine is the vasopressor of choice, in septic shock (Rhodes et al. 2017) as well as in cardiogenic shock (van Diepen et al. 2017). Vasopressin derivatives may safely be considered as a second-line agent in patients with septic shock (Rhodes et al. 2017).

Effects of Vasopressors on Left Ventricular Function

The effects of vasopressors on left ventricular function are multiple.

On the one hand, cardiac output and function may be impaired by vasopressor administration. Cardiac output decreases mostly as a result of the increase in left ventricular afterload. This is mostly observed in patients with impaired cardiac function. A nice illustration of this phenomenon is the observation that some patients demonstrate signs of sepsis-associated myocardial dysfunction only after blood pressure correc-

tion (Vieillard-Baron et al. 2008; Boissier et al. 2017). Another potential mechanism is an adrenergic cardiomyopathy, which results from excessive beta-adrenergic stimulation. In a recent trial in patients with cardiogenic shock, epinephrine was associated with an increased incidence of refractory shock and rescue use of extracorporeal life support compared to norepinephrine (Levy et al. 2018).

On the other hand, vasopressors may exert beneficial effects on cardiac function (De Backer and Pinsky 2018; Foulon and De Backer 2018). Adrenergic agents that combine some beta-adrenergic properties to their alpha-adrenergic actions improve myocardial contractility. In addition to this effect, other effects may also increase myocardial contractility (Hamzaoui et al. 2018). First the restoration of coronary perfusion pressure can be useful in cardiogenic shock, especially when it is of ischemic origin, but even also in septic shock. Another mechanism is the Anrep effect, which represents the increase in contractility in response to an increase in arterial pressure. Finally, the increase in vascular tone is associated with an increase in arterial elastance, which in turn may improve ventriculo-arterial coupling (Guarracino et al. 2014). Administration of norepinephrine was associated with an increase in stroke volume only in patients who had impaired ventriculo-arterial coupling at baseline and who improved their ventriculo-arterial coupling with the correction of hypotension (Guinot et al. 2018).

Finally, vasopressors also induce venular constriction. This results in an increase in mean systemic pressure and hence, potentially, results in the gradient for venous return. This effect is also associated with an increased resistance to venous return. The net effect on cardiac output is variable and depends on cardiac function and the presence of preload responsiveness.

Differences between agents on left ventricular function have not been well studied. It is likely that most effects, including an increase in venous return due to venular constriction, an increase in resistance to venous return, and an increase in left ventricular afterload, are shared by most vasopressors, but adrenergic agents that exert beta

effects can contribute to beneficial effects on contractility and also some adverse effects including an increase in myocardial oxygen consumption and an increased risk of arrhythmias. Finally, it is likely that the beta effects vanish over time with desensitization of adrenergic receptors, while most of the other effects remain. Nevertheless, great caution should be applied when considering angiotensin II in patients with ventricular dysfunction. In a systematic review of the clinical experience with this agent, the most common serious side effect was exacerbation of left ventricular dysfunction, and it was sometimes fatal (Busse et al. 2017).

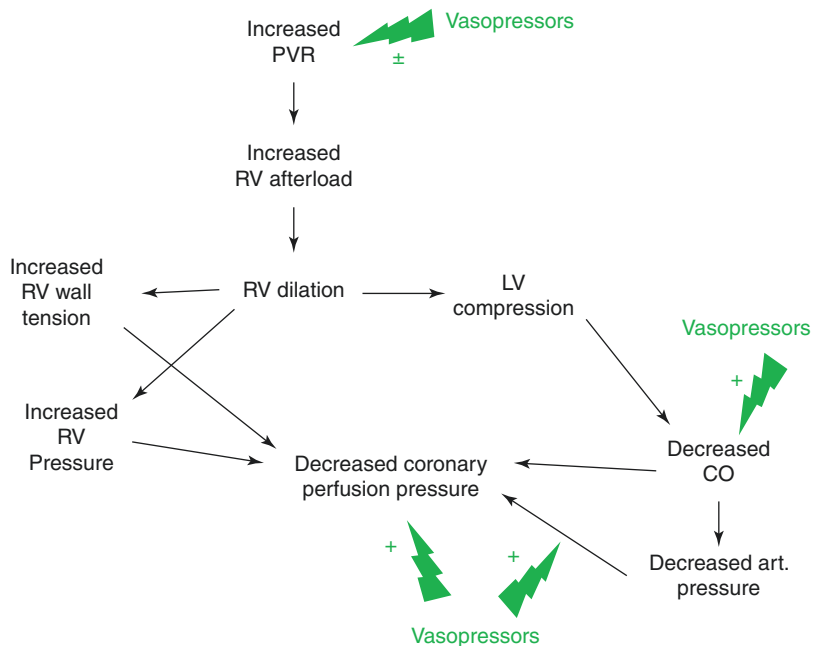
Altogether, the effects of vasopressors on left ventricular function are very variable. In patients with severely impaired cardiac function, vasopressors can further compromise cardiac function predominantly through the increase they induce in left ventricular afterload. This may lead to a decrease in cardiac output. In patients with relatively preserved cardiac function, vasopressors may increase cardiac output and even contractility, but this effect is expected to occur primarily at initiation of their use, but later on, the impact of their increase in left ventricular afterload may predominate.

Accordingly, in patients treated with vasopressors, one should always cautiously follow left ventricular function and keep in mind that initial beneficial response does not guarantee a sustained positive effect.

Effects of Vasopressors in Right Heart Failure: (Fig. 49.1)

In patients with right heart failure (RHF), whatever its cause, the maintenance of right coronary artery perfusion is critical. Right ventricular perfusion can indeed be impaired by several mechanisms. First, right ventricular dilation leads to an increase in right ventricular tension which can impair right ventricular perfusion. Second, the decrease in arterial pressure combined with the increase in right atrial/ventricular pressures decreases right ventricular coronary perfusion pressure. This effect is even more crucial in patients with pulmonary hypertension as right ventricular pressure increases in parallel to pulmonary artery pressure. Accordingly, the systolic contribution of right coronary artery perfusion will decrease proportionally to the increase in pulmonary artery pressure (van Wolferen et al.

Fig. 49.1 Mechanisms leading to impaired coronary perfusion in the right ventricular failure. The potential impact of vasopressors is indicated with green arrow. RV right ventricle, LV left ventricle, CO cardiac output



2008). Finally, the decrease in cardiac output also contributes to the decrease in coronary artery blood flow.

In these conditions, it may appear worthwhile to increase systemic arterial pressure in order to restore coronary artery perfusion pressure. The use of vasopressors can nevertheless be associated with two important drawbacks. First, some adrenergic vasopressors increase pulmonary artery pressure (PAP) and hence right ventricular afterload. Second, most vasopressor agents also constrict the venular system. This may be associated with an increase in preload which may not be well tolerated in an already-dilated right ventricle. The consequent increase in right atrial pressure could potentially limit the improvement in coronary artery perfusion pressure from the systemic constriction. Finally, the vasoconstricting actions of the drugs could decrease venous return and thereby decrease cardiac output.

Large-scale randomized trials addressing these issues are lacking. A landmark experimental trial nevertheless provided a lot of information. In canine experimental pulmonary embolism, randomized to volume expansion, isoproterenol, and norepinephrine when systemic blood pressure fell to 70 mmHg. All control animals, as well as all animals treated with volume expansion or isoproterenol died. All animals treated with norepinephrine survived and remained hemodynamically stable for 1 h (Molloy et al. 1984). Longer-term outcome was not evaluated. Based on that study, guidelines suggest the use of norepinephrine to support blood pressure in patients with right heart failure (Price et al. 2010). Norepinephrine improved right ventricular performance by increasing blood pressure and improving right ventricular perfusion and/or by a direct increase in contractility. We thus conclude that in a canine model of pulmonary embolism and shock, norepinephrine may be the drug of choice for acute resuscitation. Nevertheless, there are concerns about adrenergic vasopressors that may raise pulmonary vascular resistances more than systemic vascular resistances. Interestingly, this effect disappears when these agents are infused directly into the

left atrium, suggesting a direct effect on pulmonary circulation rather than an indirect effect due to blood redistribution between left and right circulations (Pearl et al. 1987). Vasopressin derivatives may be associated with less impact on the pulmonary circulation (Price et al. 2010). In a recent trial in patients after cardiac surgery, norepinephrine and terlipressin increased MAP to the similar extent, but terlipressin was associated with a lower MAP compared to norepinephrine (Abdelazziz and Abdelhamid 2019). However, these effects may be model dependent as other studies have failed to report differences in pulmonary vascular resistance (Leather et al. 2002). In the subset of patients in the VASST study that compared vasopressin and norepinephrine in septic shock, PAP remained unchanged with norepinephrine infusion as well as with vasopressin (Gordon et al. 2012).

Accordingly, the main focus should be preservation of perfusion pressure of the right ventricle, differences between agents being perhaps overstated.

Conclusions

Vasopressor agents should be used to correct hypotension in patients with shock, but the exact target pressure level needs to be individualized. Norepinephrine is the first-line vasopressor agent but vasopressin derivatives can be considered in vasodilatory shock as well as in patients with right heart failure. Angiotensin II appears to be a promising agent but more data are needed to better position this agent.

References

- Abdelazziz MM, Abdelhamid HM. Terlipressin versus norepinephrine to prevent milrinone-induced systemic vascular hypotension in cardiac surgery patient with pulmonary hypertension. *Ann Card Anaesth.* 2019;22(2):136–42.
- Aneman A, Pettersson A, Eisenhofer G, Friberg P, Holm M, von Bothmer C, et al. Sympathetic and renin-angiotensin activation during graded hypovolemia in pigs: impact on mesenteric perfusion and duodenal mucosal function. *Shock.* 1997;8:378–84.

- Asfar P, Meziani F, Hamel JF, Grelon F, Megarbane B, Anguel N, et al. High versus low blood-pressure target in patients with septic shock. *N Engl J Med*. 2014;370(17):1583–93.
- Auchet T, Regnier MA, Girerd N, Levy B. Outcome of patients with septic shock and high-dose vasopressor therapy. *Ann Intensive Care*. 2017;7(1):43.
- Boissier F, Razazi K, Seemann A, Bedet A, Thille AW, de Prost N, et al. Left ventricular systolic dysfunction during septic shock: the role of loading conditions. *Intensive Care Med*. 2017;43(5):633–42.
- Busse LW, Wang XS, Chalikhonda DM, Finkel KW, Khanna AK, Szerlip HM, et al. Clinical experience with IV angiotensin II administration: a systematic review of safety. *Crit Care Med*. 2017;45(8):1285–94.
- De Backer D, Pinsky M. Norepinephrine improves cardiac function during septic shock, but why? *Br J Anaesth*. 2018;120(3):421–4.
- De Backer D, Creteur J, Silva E, Vincent JL. Effects of dopamine, norepinephrine, and epinephrine on the splanchnic circulation in septic shock: which is best? *Crit Care Med*. 2003;31:1659–67.
- De Backer D, Biston P, Devriendt J, Madl C, Chochrad D, Aldecoa C, et al. Comparison of dopamine and norepinephrine in the treatment of shock. *N Engl J Med*. 2010;362(9):779–89.
- De Backer D, Aldecoa C, Njimi H, Vincent J-L. Dopamine versus norepinephrine in the treatment of septic shock: a metaanalysis. *Crit Care Med*. 2012;40:725–30.
- Ducrocq N, Kimmoun A, Furmaniuk A, Hekalo Z, Maskali F, Poussier S, et al. Comparison of equipressor doses of norepinephrine, epinephrine, and phenylephrine on septic myocardial dysfunction. *Anesthesiology*. 2012;116(5):1083–91.
- Dunser MW, Takala J, Ulmer H, Mayr VD, Luckner G, Jochberger S, et al. Arterial blood pressure during early sepsis and outcome. *Intensive Care Med*. 2009a;35(7):1225–33.
- Dunser MW, Ruokonen E, Pettila V, Ulmer H, Torgersen C, Schmittinger CA, et al. Association of arterial blood pressure and vasopressor load with septic shock mortality: a post hoc analysis of a multicenter trial. *Crit Care*. 2009b;13(6):R181.
- Foulon P, De Backer D. The hemodynamic effects of norepinephrine: far more than an increase in blood pressure! *Ann Transl Med*. 2018;6(Suppl 1):S25.
- Futier E, Lefrant JY, Guinot PG, Godet T, Lorne E, Cuvillon P, et al. Effect of individualized vs standard blood pressure management strategies on postoperative organ dysfunction among high-risk patients undergoing major surgery: a randomized clinical trial. *JAMA*. 2017;318(14):1346–57.
- Gordon AC, Wang N, Walley KR, Ashby D, Russell JA. The cardio-pulmonary effects of vasopressin compared to norepinephrine in septic shock. *Chest*. 2012;142:593–605.
- Gordon AC, Mason AJ, Thirunavukkarasu N, Perkins GD, Ceconi M, Cepkova M, et al. Effect of early vasopressin vs norepinephrine on kidney failure in patients with septic shock: the VANISH randomized clinical trial. *JAMA*. 2016;316(5):509–18.
- Guarracino F, Ferro B, Morelli A, Bertini P, Baldassarri R, Pinsky MR. Ventriculararterial decoupling in human septic shock. *Crit Care*. 2014;18(2):R80.
- Guinot PG, Longrois D, Kamel S, Lorne E, Dupont H. Ventriculo-arterial coupling analysis predicts the hemodynamic response to norepinephrine in hypotensive postoperative patients: a prospective observational study. *Crit Care Med*. 2018;46(1):e17–25.
- Hamzaoui O, Jozwiak M, Geffriaud T, Szymf B, Prat D, Monnet X, et al. Norepinephrine exerts an inotropic effect at the early phase of human septic shock. *Br J Anaesth*. 2018;120(3):517–24.
- Khanna A, English SW, Wang XS, Ham K, Tumlin J, Szerlip H, et al. Angiotensin II for the treatment of vasodilatory shock. *N Engl J Med*. 2017;377(5):419–30.
- Leather HA, Segers P, Berends N, Vandermeersch E, Wouters PF. Effects of vasopressin on right ventricular function in an experimental model of acute pulmonary hypertension. *Crit Care Med*. 2002;30(11):2548–52.
- Levy B, Clere-Jehl R, Legras A, Morichau-Beauchant T, Leone M, Frederique G, et al. Epinephrine versus norepinephrine for cardiogenic shock after acute myocardial infarction. *J Am Coll Cardiol*. 2018;72(2):173–82.
- Liu ZM, Chen J, Kou Q, Lin Q, Huang X, Tang Z, et al. Terlipressin versus norepinephrine as infusion in patients with septic shock: a multicentre, randomised, double-blinded trial. *Intensive Care Med*. 2018;44(11):1816–25.
- Maheshwari K, Nathanson BH, Munson SH, Khangulov V, Stevens M, Badani H, et al. The relationship between ICU hypotension and in-hospital mortality and morbidity in septic patients. *Intensive Care Med*. 2018;44:857–67.
- McIntyre WF, Um KJ, Alhazzani W, Lengyel AP, Hajjar L, Gordon AC, et al. Association of vasopressin plus catecholamine vasopressors vs catecholamines alone with atrial fibrillation in patients with distributive shock: a systematic review and meta-analysis. *JAMA*. 2018;319(18):1889–900.
- Molloy WD, Lee KY, Girling L, Schick U, Prewitt RM. Treatment of shock in a canine model of pulmonary embolism. *Am Rev Respir Dis*. 1984;130(5):870–4.
- Myburgh JA, Higgins A, Jovanovska A, Lipman J, Ramakrishnan N, Santamaria J. A comparison of epinephrine and norepinephrine in critically ill patients. *Intensive Care Med*. 2008;34(12):2226–34.
- Patel BM, Chittock DR, Russell JA, Walley KR. Beneficial effects of short-term vasopressin infusion during severe septic shock. *Anesthesiology*. 2002;96:576–82.
- Pearl RG, Maze M, Rosenthal MH. Pulmonary and systemic hemodynamic effects of central venous and left atrial sympathomimetic drug administration in the dog. *J Cardiothorac Anesth*. 1987;1(1):29–35.
- Piqueras L, Kubes P, Alvarez A, O'Connor E, Issekutz AC, Esplugues JV, et al. Angiotensin II induces leukocyte-endothelial cell interactions in vivo via

- AT(1) and AT(2) receptor-mediated P-selectin upregulation. *Circulation*. 2000;102:2118–23.
- Price LC, Wort SJ, Finney SJ, Marino PS, Brett SJ. Pulmonary vascular and right ventricular dysfunction in adult critical care: current and emerging options for management: a systematic literature review. *Crit Care*. 2010;14(5):R169.
- Rhodes A, Evans LE, Alhazzani W, Levy MM, Antonelli M, Ferrer R, et al. Surviving sepsis campaign: international guidelines for management of sepsis and septic shock: 2016. *Intensive Care Med*. 2017;43(3):304–77.
- Russell JA, Walley KR, Singer J, Gordon AC, Hebert PC, Cooper DJ, et al. Vasopressin versus norepinephrine infusion in patients with septic shock. *N Engl J Med*. 2008;358(9):877–87.
- Russell JA, Vincent JL, Kjolbye AL, Olsson H, Blemings A, Spapen H, et al. Selepressin, a novel selective vasopressin V1A agonist, is an effective substitute for norepinephrine in a phase IIa randomized, placebo-controlled trial in septic shock patients. *Crit Care*. 2017;21(1):213.
- Salgado DR, He X, Su F, de Sousa DB, Penaccini L, Maciel LK, et al. Sublingual microcirculatory effects of enalaprilat in an ovine model of septic shock. *Shock*. 2011;35(6):542–9.
- Salgado DR, Favory R, Rocco JR, Silva E, Ortiz JA, Donadello K, et al. Microcirculatory effects of angiotensin II inhibitors in patients with severe heart failure. *Clin Hemorheol Microcirc*. 2013;54(1):87–98.
- Senatore F, Jagadeesh G, Rose M, Pillai VC, Hariharan S, Liu Q, et al. FDA approval of angiotensin II for the treatment of hypotension in adults with distributive shock. *Am J Cardiovasc Drugs*. 2019;19(1):11–20.
- Tumlin JA, Murugan R, Deane AM, Ostermann M, Busse LW, Ham KR, et al. Outcomes in patients with vasodilatory shock and renal replacement therapy treated with intravenous angiotensin II. *Crit Care Med*. 2018;46(6):949–57.
- Udhoji VN, Weil MH. Circulatory effects of angiotensin, levarterenol and metaraminol in the treatment of shock. *N Engl J Med*. 1964;270:501–5.
- Vail E, Gershengorn HB, Hua M, Walkey AJ, Rubenfeld G, Wunsch H. Association between US norepinephrine shortage and mortality among patients with septic shock. *JAMA*. 2017;317(14):1433–42.
- van den Berghe G, de Zegher F. Anterior pituitary function during critical illness and dopamine treatment. *Crit Care Med*. 1996;24:1580–90.
- van Diepen S, Katz JN, Albert NM, Henry TD, Jacobs AK, Kapur NK, et al. Contemporary management of cardiogenic shock: a scientific statement from the American Heart Association. *Circulation*. 2017;136(16):e232–e68.
- van Wolferen SA, Marcus JT, Westerhof N, Spreuwenberg MD, Marques KM, Bronzwaer JG, et al. Right coronary artery flow impairment in patients with pulmonary hypertension. *Eur Heart J*. 2008;29(1):120–7.
- Victorino GP, Newton CR, Curran B. Effect of angiotensin II on microvascular permeability. *J Surg Res*. 2002;104:77–81.
- Vieillard-Baron A, Caille V, Charron C, Belliard G, Page B, Jardin F. Actual incidence of global left ventricular hypokinesia in adult septic shock. *Crit Care Med*. 2008;36(6):1701–6.
- Vincent JL, Nielsen ND, Shapiro NI, Gerbasi ME, Grossman A, Doroff R, et al. Mean arterial pressure and mortality in patients with distributive shock: a retrospective analysis of the MIMIC-III database. *Ann Intensive Care*. 2018;8:107.



Cardiogenic Shock Part 1: Epidemiology, Classification, Clinical Presentation, Physiological Process, and Nonmechanical Treatments

Sheldon Magder

The heart has a central role in maintaining normal body function, and, when it fails, and cardiogenic shock develops, the consequences are devastating. Even after many years of new innovations, and improvement in-hospital mortality, the death rate from cardiogenic shock over the past two decades remains high. Overall survival at 1 year still only is around 50–60% in many studies (Vahdatpour et al. 2019; Hochman et al. 1999), although it is somewhat lower in some recent studies (Goldberg et al. 2016). In the SHOCK-IABP 2 trial, approximately 65% of patients were alive at 6 years (Thiele et al. 2018). However, in a recent report from the CathPCI registry, which dealt specifically with re-vascularized patients, in-hospital mortality actually increased from 27.6% in 2005 to 30.6% in 2013 (Katz and Sabe 2019). The mortality was accounted for by more patients having diabetes, hypertension, dyslipidemias, previous percutaneous balloon angioplasty, and dialysis. An indication that we are doing things better comes from a decade-long population study which reported 10-year trends in outcomes of patients hospitalized with ischemic heart disease. Although there was no reduction of the incidence of cardiogenic shock, mortality decreased (Goldberg et al. 2016). The improved outcome

was associated with earlier identification and aggressive therapy.

Definition

A general definition of shock is that it is a condition in which cardiac output is inadequate for the metabolic needs of tissues resulting in tissue dysfunction and multiorgan failure. In cardiogenic shock, the specific cause of inadequate organ perfusion is impairment of the ability of the heart to eject the blood returning to it. Precise definitions of cardiogenic shock have varied in large therapeutic clinical trials on the management of cardiogenic shock, but in general, the definitions include a cardiac index (CI) <2.2 L/min per m^2 , systolic pressure <90 mmHg for ≥ 30 minutes, or use of pharmacological and/or mechanical devices to maintain a systolic pressure ≥ 90 mmHg. Usually, signs of organ dysfunction are required and include arterial lactate >2 mMol/L, urine output <30 ml/h, altered mental status, and cool extremities. Based on the criteria of inadequate tissue perfusion, it is possible to have cardiogenic shock with a systolic pressure >90 mmHg; this occurred in approximately 5% of patients in the SHOCK registry (Menon et al. 2000a).

A problem when discussing cardiogenic shock is that almost all of the large randomized intervention studies and registries dealing with cardiogenic shock have involved primarily patients

S. Magder (✉)
Royal Victoria Hospital (McGill University Health Centre), Departments of Critical Care and Physiology
McGill University, Montreal, QC, Canada
e-mail: sheldon.magder@mcgill.ca

with ischemic heart disease and, more specifically, left ventricular (LV) dysfunction (Hochman et al. 1999; Goldberg et al. 2016; Menon et al. 2000b; Berg et al. 2019; Harjola et al. 2016; Jeger et al. 2008). Furthermore, in more than 80% of cases, the cause of cardiogenic shock was an acute myocardial infarction (AMI) (Vahdatpour et al. 2019; Thiele et al. 2019). Accordingly, statistics derived from these studies are affected by the management of the underlying coronary artery disease in cardiac care units. The studies thus heavily involve treatments that are specific to myocardial ischemia and its primary treatment, which is restoration of coronary flow by early revascularization of a culprit coronary artery lesion.

CardShock was a prospective observational study by a consortium of European centers. It aimed at providing a more general picture of patients presenting with cardiogenic shock by identifying differences in patients presenting with an acute coronary syndrome versus those without (Harjola et al. 2015). They observed 219 patients over 15 months. Of these, 81% still had an acute coronary syndrome, but shock was due to a ST elevation myocardial infarction (STEMI) in only 148 (68%). In another 19 patients (9%), the cause of shock was a mechanical complication of an AMI including myocardial rupture, severe mitral insufficiency, or ventricular septal defect, and the rest were due to other causes. Thus, although this study tried to obtain a broader view of cardiogenic shock by including general intensive care units and emergency department patients, the population still was biased toward acute coronary syndromes because the majority of the data came primarily from the coronary care units and catheterization laboratories of the nine tertiary care referral hospitals in the study. In CardioShock, in-hospital mortality was 37% compared with >50% in SHOCK (Harjola et al. 2016; Hochman et al. 2006) indicating how the selection criteria affect outcome statistics. Mortality was higher in patients without an acute coronary syndrome, likely because of the contribution to this group of patients with mechanical cardiac complications that are hard to repair. In a recent survey of 16 centers with more generalized cardiac care units in the USA and Canada, only 30% of patients with cardiogenic shock had an acute coronary

syndrome (Berg et al. 2019). In this study, mortality related to mixed shock was 39%, shock related to an acute myocardial infarct (AMI) was 36%, and shock that was not related to an acute ischemic event was 31%. The percentage of cases of shock with AMI also has been decreasing, and, importantly, mortality in the patients without AMI is lower (Shah et al. 2018). Caution thus must be used when generalizing outcomes from studies that predominantly have patients with acute ischemic events. However, these patients still make up a large proportion of the patients with cardiogenic shock, and they are well characterized. It thus is worthwhile discussing these patients in greater detail, which is done in the next section.

Cardiogenic Shock with Acute Coronary Syndromes

It was estimated that in 2006 there were 500,000 ST-segment elevation AMI in the USA, and an even greater number was observed in a European study (Westaby et al. 2011). It has been estimated further that the incidence of cardiogenic shock among patients hospitalized with an AMI is 5–10% (Hochman et al. 1999), which gives a prediction of over 50,000 cases of cardiogenic shock per year from an AMI in the USA (Westaby et al. 2011). It now is well accepted that early revascularization improves outcome in patients with cardiogenic shock. The primary evidence comes from the *Should we emergently vascularize Occluded Coronaries in cardiogenic Shock* (SHOCK) trial (Hochman et al. 1999). The rationale for this study was that ischemia becomes a self-perpetuating syndrome in that acute deterioration of cardiac pump function results in further ongoing myocardial ischemia due to increasing myocardial wall tension as the heart dilates because it fails to adequately eject. This increases myocardial oxygen (O₂) demand and also decreases coronary perfusion, which decreases O₂ supply. The result is further oxygen-supply imbalance and increased myocardial damage unless perfusion is reestablished. The median time to revascularization in SHOCK was 1.4 hours from time of randomization. It is worth noting that the primary outcome, which was 30-day mortality,

was not significantly reduced by revascularization, so by a strict evidence-based definition, the study was negative. However mortality was significantly decreased at 6 months from 63.1% to 50.3%. Furthermore, hospital mortality has decreased steadily since the SHOCK trial, and this is believed to be due to early revascularization, which has become the standard of care.

Subsequent observations support the SHOCK trial hypothesis that early revascularization improves outcome by preventing further cardiac deterioration. In a US National Hospital Discharge Survey with data from 1979 to 2003 (Fang et al. 2006), the incidence of cardiogenic shock associated with an AMI decreased by 50% (3.9–1.7), whereas primary percutaneous coronary intervention (PPCI) increased from 0% to 28%. Importantly, the in-hospital mortality from cardiogenic shock decreased from 84% to 43% (Fang et al. 2006). The implication of these observations is that early revascularization reduces the number of patients with an AMI who would subsequently go into shock and those who develop shock have a better outcome than previously. Another important observation was that patients who survived the initial cardiogenic shock had a similar long-term prognosis as those who had an AMI without shock (Hochman et al. 2006; Singh et al. 2007).

Further insight into the importance of early revascularization comes from a Swiss registry called the Acute Myocardial Infarction in Switzerland (AMIS). They collected 10-year data on 23,696 patients who had an acute coronary syndrome from 1997 to 2006 (Jeger et al. 2008). In 70% of cases, shock occurred after admission; this indicates that there is time to try to prevent shock after patient arrival at the hospital. The overall incidence of cardiogenic shock was 12.9% at the start of the study but decreased to 5.5% by the end. How this occurred provides insight into what likely was happening and what can be done. In the first years of the study, 30% of all cases of cardiogenic shock occurred at the time of admission, but of significance, in those with an acute coronary syndrome, shock only was present in 2.3% of cases on admission, and eventually 10.6% had shock during their hospital stay. Of importance, over the course of the study, approximately the same percent presented with

cardiogenic shock, but the number of AMI patients who developed shock after admission dramatically dropped. Consequently the incidence of shock dropped from 10.6% to 2.7% indicating that there were few cases of shock after admission. The overall shock mortality, too, dropped from 62.8% to 47.7%. Also of significance, over this period, primary percutaneous coronary intervention (PPCI) use rose from 7.6% to 65.9% of patients. Together these data support the argument that the early revascularization prevents later cardiogenic shock. It also is noteworthy that shock-related mortality seemingly was paradoxically higher, although only moderately, in non-STEMI patients than in the STEMI patients (58.0% versus 52.5%). This perhaps was due to less use of PPCI in these patients because of the lack of ST elevations (Westaby et al. 2011). In summary, these studies indicate that in patients with shock from an acute coronary artery event, revascularization greatly reduces mortality and improves long-term outcomes. The data even suggests that if cardiogenic shock is present, revascularization should be attempted even without ST elevations, as long as other factors have been ruled out. However, an important caveat is that patients >75 years of age did not benefit from early revascularization in SHOCK, and this reasoning should not necessarily apply to them.

Despite these advances, the mortality in patients with cardiogenic shock in association with an acute coronary syndrome remains high. This partially can be attributed to a distinction between two types of patients. One type can be called “acute transient” ischemia. These patients respond to reperfusion, and stunned myocardium rapidly recovers. They also respond to vasopressors and inotropes after PPCI. In contrast, the second type has refractory ischemia, likely because there is a larger area of injury that cannot easily be re-vascularized. These patients do not recover sufficient cardiac muscle function to maintain adequate cardiac function. Refractory ischemia is more likely to occur when there is a left main stenosis, three-vessel disease, a previous myocardial infarction, a large anterior myocardial infarct, or previous aorto-coronary bypass surgery (John et al. 2007). Another term that has been used is “profound shock.” It is characterized

by a systolic arterial pressure <75 mmHg despite support with inotropes and/or use of an IABP, cerebral dysfunction, and respiratory failure. In one non-randomized study, patients with profound shock who required ECMO had a mortality of 22% compared to 74% in those who did not receive ECMO, although selection bias likely was a factor for the differences in mortality (Sheu et al. 2010). Improved strategies are needed to more quickly identify these patients at greater risk and consideration of earlier mechanical support (Singh et al. 2019).

Cardiogenic Shock Without an Acute Coronary Syndrome

In CardioShock, 9% of patients had shock in association with an AMI, but the primary cause of shock was thought to be a mechanical problem and not the coronary artery occlusion (Harjola et al. 2016). Causes of shock in the 28% of patients who did not have an acute coronary syndrome were worsening chronic heart failure (11%), nonischemic mechanical problems (6%), stress-induced cardiomyopathy (Tako-Tsubo; 2%), and a viral cardiomyopathy (2%). It is noteworthy that the clinical presentation was similar in patients with an acute coronary syndrome and without.

In a report from the Critical Care Cardiology Trials group, 25% of cases had biventricular failure, and 9% had right ventricular (RV) failure. In 19% of cases, shock was not related primarily to myocardial ischemia but was due to an uncontrolled arrhythmia, a severe valve problem, and in 7% the cause was known. This study specified a group whom the authors called “mixed” shock. These patients had both a low CI and distributive shock based on an inappropriately low systemic vascular resistance (SVR) (Berg et al. 2019). The mixed group had the highest hospital mortality. Of note, their cardiovascular comorbidities were similar to the other cardiogenic shock patients. The distributive shock group is especially difficult to manage and likely will need different strategies than patients with a normal or elevated SVR. Furthermore, early revascularization may not be a good approach in this group because they may be at increased risk from intravascular interventions, such as infection of a stent or a mechanical support device if the distributive hemodynamics is due to a bacterial infection. Because of their special nature, they are discussed in detail below.

It recently has been recommended that cardiogenic shock be viewed as a continuum (Baran et al. 2019) with the hope that this will allow earlier recognition and treatment of people at risk (Fig. 50.1). It also is hoped that this approach will

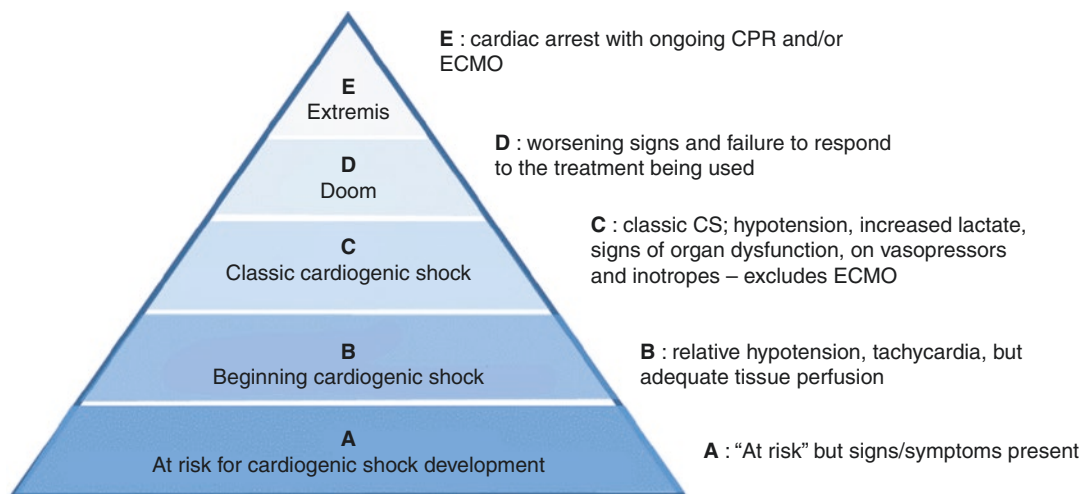


Fig. 50.1 Pyramid of stages of cardiogenic shock. (Based on Baran et al. (Baran et al. 2019); see text for discussion)

provide better classification of subjects in clinical trials. Based on this classification, the first stage is “At Risk”; it describes patients who do not yet have signs or symptoms of cardiogenic shock but who have had a large AMI, a prior infarction, or have acute on chronic heart failure symptoms. The second is “Beginning cardiogenic shock”; this includes patients who have relative hypotension and tachycardia but still do not have signs of tissue hypoperfusion. The third is “Classic cardiogenic shock”; it describes patients who are hypoperfused and require pharmacological or mechanical support, including extracorporeal membrane oxygenation (ECMO), to prevent further deterioration. The fourth is “Deteriorating/doom”; these patients have the criteria for “Classic cardiogenic shock,” but it is getting worse. The fifth is “Extremis”; these patients require multiple interventions for the ongoing cardiopulmonary resuscitation.

A number of scoring systems have been developed for predicting outcomes in cardiogenic shock. These have the potential to guide early interventions and to allow comparisons of subjects among clinical trials. Currently, the ORBI score is considered to be the best for predicting the development of in-hospital cardiogenic shock for those in Stages A and B (Thiele et al. 2019). The score was developed from 6838 patients in the Observatoire Regional Breton sur l’infarctus registry (Auffret et al. 2018, 2016) and gives a prediction that subsequently was validated from 2208 patients in the RICO database (observatoire des Infarctus de Côte d’Or) (Zeller et al. 2004) (Table 50.1). The score can be calculated with an online calculator (<https://www.orbiriskscore.com/>).

Currently, only one score has been validated for survival of patients with developed cardiogenic shock (Stages C to E) (Pöss et al. 2017). It is based on patients in the IABP-SHOCK II trial (Thiele et al. 2012) and was validated with the IABP SHOCK II registry and CardShock (Harjola et al. 2015). The score is based on six variables and divides patients into low-, intermediate-, and high-risk groups with predicted 30-mortality of 20–30%, 40–60%, and 70–90%, respectively (Fig. 50.2).

Table 50.1 Orbi score

Variable	Points	
Age >70 years old	2	
Previous stroke/TIA	2	
Presentation with cardiac arrest	3	
Anterior AMI	1	
>90 min from medical contact to pPCI	2	
Killip class II on admission	2	
Killip class III on admission	6	
Heart rate >90/min on admission	3	
SBP <125 and PP <45 mmHg on admission	4	
Glycemia >10 mmol/l on admission	3	
Left main is the culprit lesion	5	
Post PCI TMI flow <3	5	
Risk category		
Category	Score	Observed CS incidence
Low	0–7	1.3
Low to intermediate	8–10	6.6
Intermediate to high	11–12	11.7
High	>13	31.8

Based on the ORBI risk score by Auffret et al. CS cardiogenic shock, pPCI primary percutaneous coronary intervention, TIA transient ischemic attack (<https://www.orbiriskscore.com/>)

A validated score called SAVE score has been developed for outcome with ECMO (Schmidt et al. 2015). It is based on the European Life Support Organization (ELSO) registry with 3846 patients (Wengenmayer et al. 2019) and was validated with an Australian database of VA-ECMO patients. An online calculator also is available for this scoring system (<http://www.save-score.com/>) (Table 50.2). Another ECMO score was developed at single center but with no external validation. It uses only three variables: pH, lactate, and HCO_3^- . It is called PREDIT-VA-ECMO and uses an online calculator based on the variables from the logistical regression analysis (<https://www.predict-va-ecmo.org/>). Of note, when normal pH, lactate, and HCO_3^- at 6 hours are put into the calculator, the mortality is 32%.

A term that overlaps with cardiogenic shock, but is useful clinically, is acute heart failure. This can be divided further into “forward failure” or “backward failure”; these classifications allow more targeted therapy for the primary pathophysiological presentation. In forward fail-

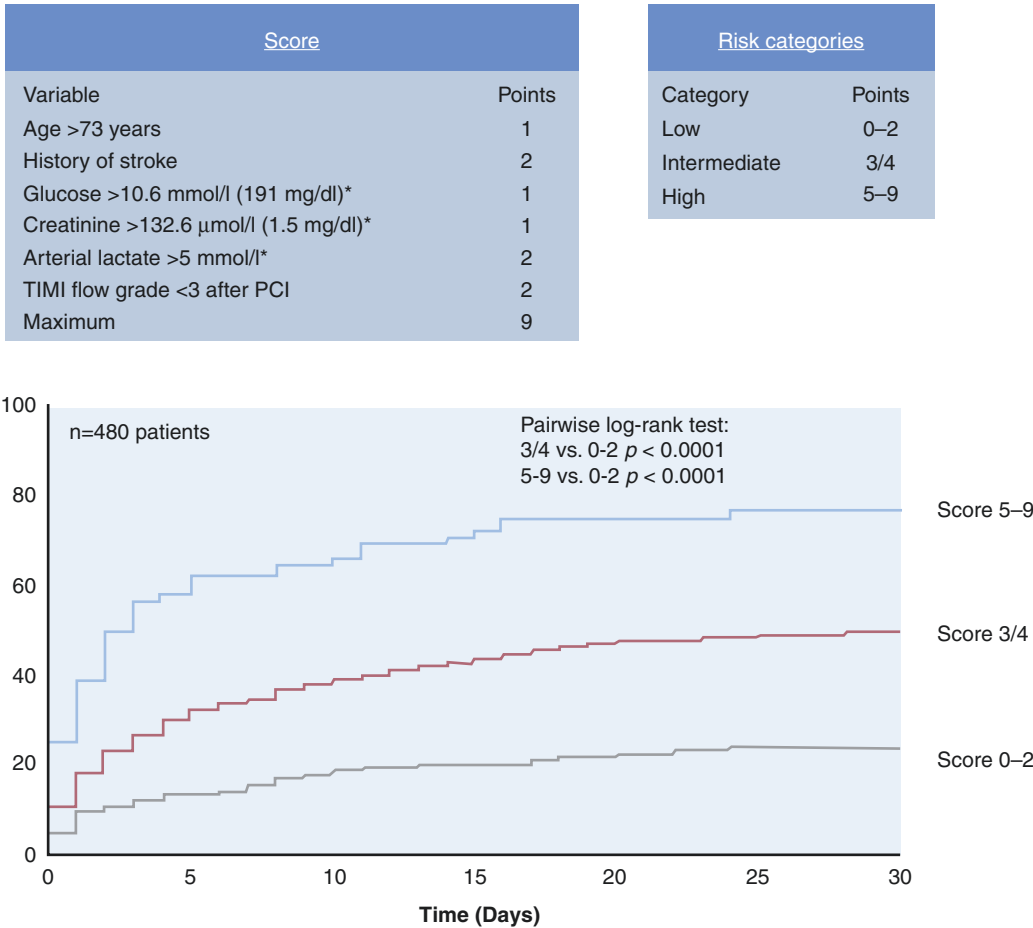


Fig. 50.2 IABP Shock II Risk Score and survival prediction. (From Pöss et al. (2017). See text for details. Used with permission of Elsevier)

ure, the dominant signs and symptoms are related to a low cardiac output. These include decreased sensorium, lack of energy, cool clammy and cyanotic extremities, decreased renal function, and, at the extreme, rising lactate, which are a criteria for cardiogenic shock. In backward failure, the dominant signs and symptoms are related to failure of the heart to keep up with the rate of returning blood and consequent congestion of proximal tissues. This can occur with a normal or at least adequate forward flow but also can occur with decreased forward flow. When the primary problem is in the left heart, the patient has dyspnea on exertion and, when more severe, dyspnea at rest, orthopnea, paroxysmal nocturnal dyspnea, signs of pulmonary edema on examination and on

chest X-ray, and, eventually, hypoxemia, hypercarbia, and acidemia. On the right side, the signs are peripheral edema, ascites, hepatic dysfunction, and renal failure. Renal failure and hepatic failure are common to both forward and backward failure. With forward failure, splanchnic organs fail because the heart does not provide adequate blood flow. In backward failure, the high venous pressures congest these organs and eventually compromise their arterial inflow, and then forward and backward components merge.

A recent consensus classification of cardiogenic shock tried to take these aspects of forward and backward failure into account by classifying cardiogenic shock based on volume status and peripheral perfusion by introducing the terms

Table 50.2 Survival after veno-arterial ECMO score (SAVE score)

Parameter	Score	
Diagnostic cause		
Myocarditis	3	
Refractory VT/VF	2	
Post heart or lung transplant	3	
Congenital heart disease	-3	
Other causes leading to shock	0	
Age		
18-38	7	
39-52	4	
53-62	3	
≥63	0	
Weight (Kg)		
<65	1	
65-89	2	
≥90	0	
Acute organ failure pre-ECMO (can be more than one)		
Liver failure	-3	
Renal failure	-3	
Central nervous system dysfunction	-3	
Chronic renal failure	-6	
Duration of intubation prior to initial of ECMO (hr)		
≤10	0	
11-29	-2	
>30	-4	
Peak inspiratory pressure ≤20 cmH ₂ O	3	
Pre-ECMO cardiac arrest	-2	
Diastolic pressure before ECMO ≤ 40 mmHg	3	
HCO ₃ ⁻ before ECMO ≤15	-3	
Constant value to add to all SAVE scores	-7	
Total SAVE scores	-35-17	
Hospital survival by risk class		
Score	Risk class	Survival (%)
>5	I	75
1 to 5	II	58
-4 to 0	III	42
-9 to -5	IV	30
≤ -10	V	18

Based on the SAVE score (<http://www.save-score.com/>)

warm and cold shock and euvoletic and hyper-voletic shock in a 2 × 2 (Baran et al. 2019).

Cold-dry shock indicates that the patient is euvoletic and filling pressures are low. A potential limit to this definition is that it likely implies RV limitation because pure LV failure should always have a wet component if it is the cause of

the low cardiac output and RV limitation (see Chap. 3 on RV function). When LV filling pressure (left ventricular end-diastolic, left atrial, or pulmonary artery occlusion pressure [Ppao]) is elevated, the condition is called cold-wet shock; this is said to be classic cardiogenic shock. Warm cardiogenic shock has been recognized more recently (Hochman 2003). Again, there are dry and wet types of warm cardiogenic shock. In warm-dry shock, there are no signs of excess volume, systemic vascular resistance is low, and CI is increased, but flow likely still is not adequate for tissue needs; cardiac filling pressures are normal or decreased. These findings likely are a consequence of inadequate tissue perfusion and consequent tissue injury, which leads to the release of cytokines and a generalized inflammatory state. It is not clear whether this should really be classified as cardiogenic shock. In reality, it is a distributive shock with an inadequate cardiac response. This specific group will be discussed in more detail later. The inflammatory response to shock also can contribute to myocardial depression as seen in sepsis (Chap. 52) (Parillo 1993; Parker et al. 1987). The warm-wet group is a mixed group with a low CI, low systemic vascular resistance, but an elevated left ventricular end-diastolic pressure. They have what was called above backward failure plus a distributive picture.

These definitions likely do not add much to the simple forward/backward designation used above. In a review of the hemodynamic profiles of patients in the SHOCK registry, Ppao was the same in all four subtypes of patients with LV failure identified in the study (Menon et al. 2000b). This suggests that it is more likely that there was a failure to recognize increased pulmonary venous pressures as discussed latter under “congestion.” Part of the problem, too, likely was failure to distinguish primary RV failure from RV limitation that was a result of the primary LV failure. Another group that may not have been recognized is generalized cardiac failure due to a global cardiac process; this too would have spared the lungs. In the latter two groups, the RV becomes the limiting factor for cardiac output, and marked LV failure can be hidden because the

RV does not provide enough flow to raise the LV end-diastolic pressure sufficiently to produce pulmonary congestion. The LV also looks small on an echocardiogram so that its dysfunction is not appreciated.

This chapter primarily deals with failure of the LV, either from a primary LV process, or in the context of a global cardiomyopathy; primary failure of RV is discussed in Chap. 3. However, it is important to remember that cardiac output is determined by the interaction of cardiac function and return function (Chap. 2), and this interaction occurs at the right atrium. Thus a low cardiac output in cardiogenic shock eventually must always involve elevation of right atrial and RV diastolic pressures.

Presentation of Shock

As already noted, shock only is present at admission in approximately 2% of patients who develop cardiogenic from an acute ischemic event. In the SHOCK trial, the time from the onset of symptoms to the development of shock criteria was 5.0 hours (interquartile 2.2–12.0 hours), and in 36% of cases, shock was not yet evident at 24 hours. Similarly, in the SHOCK registry, median onset was 6.0 hours after presentation of symptoms and 4.0 hours after admission; shock on admission only was present in 10–15% of STEMI. Mortality was higher in patients who presented <24 hours than in those who presented >24 hours (63% vs. 54%), although both rates still were high. The median time to shock in patients with left main stenosis only was 1.7 hours, right coronary lesions 3.5 hours, and circumflex occlusions 3.9 hours, but somewhat surprisingly, it was 11 hours in those with left anterior descending occlusions. Perhaps the later presentation of shock in those with left anterior descending (LAD) occlusions is because it is an easier condition to identify so that these patients got treated before shock developed. If shock then develops, this may indicate that there likely is an additional process. Another possibility is that right coronary and circumflex obstructions have a greater effect on RV and thus LV output, whereas the LAD

lesion produces greater pulmonary edema as the presenting problem. Patients with non-STEMI present with shock much later than those with STEMI. In GUSTO-IIIb, the average presentation of shock in non-STEMI was 76 hours (Global Use of Strategies to Open Occluded Coronary Arteries in Acute Coronary Syndromes (GUSTO IIIb) Angioplasty Substudy Investigators 1997), and in PURSUIT, it was 94 hours (Hasdai et al. 2000a). This data supports the hypothesis that the initial occlusion is compensated for a while and then there is a progressive decrease in the patient's status as organ dysfunction develops. This fits with the underlying premise of the SHOCK trials that ischemia becomes a self-perpetuating syndrome of deteriorating pump function. The inadequate forward flow leads to multiorgan dysfunction and injury with subsequent hormonal and cytokine release, which negatively feed back on the heart. The larger the initial damage, the faster the deterioration. It also makes it clear that early stabilization of the hemodynamics is critical. In patients with coronary occlusions, this means early revascularization, and in those without them, it may mean that mechanical support should be started as soon as there is evidence of shock, or even if the shock risk score is high. However, it also is worth considering the alternative hypothesis. The progressive deterioration could be because of over-treatment, including too much fluid, excessive inotropes, and excessive use of vasopressors in an attempt to “normalize” hemodynamic values.

Congestive Component

Menon et al. performed a detailed analysis of the clinical presentation of patients presenting with cardiogenic shock that was based primarily on LV failure in the SHOCK registry (Menon et al. 2000b). They identified four groups: group A had no hypoperfusion or pulmonary congestion; B had no hypoperfusion but had pulmonary congestion; C had hypoperfusion but no congestion; D had both hypoperfusion and pulmonary congestion; this group represents the more classical picture of cardiogenic shock and accounted for 64% of patients. These groups are similar to

the cold/wet classification described above and the forward-backward failure classification. Somewhat surprisingly, although they were able to identify four different patterns of patient presentations, there only were small differences in the hemodynamics among the four groups, including cardiac index (CI) and Ppao (Menon et al. 2000b). Group C, which made up 28% of subjects, is particularly noteworthy. This group was said to have no pulmonary congestions based on chest X-ray and lack of rales on auscultation, but 50% of the group had a Ppao of at least 20 mmHg. Mortality also was highest in this group. The authors appropriately argue that the elevated Ppao makes it less likely that the lungs were “spared” by failure of the RV to produce adequate forward flow. No information on arterial blood gases was provided, but 73% were mechanically ventilated. My takeaway from this is that chest X-ray and physical exam were poor indicators of the pulmonary congestion that likely was present.

Distributive Component

The expected physiological response to a fall in cardiac output with primary LV dysfunction is peripheral vasoconstriction and an increase in systemic vascular resistance (SVR). Yet, of the 210 out of 302 patients in SHOCK in whom SVR could be measured, half had a low SVR (Kohsaka et al. 2005). In the SHOCK registry, the small group that maintained their arterial pressure despite having signs of hypoperfusion had the best outcome. This indicates that maintenance of appropriate normal vasomotor tone is associated with a better outcome (Menon et al. 2000a) and presence of a low SVR is a predictor of worse outcome (Kohsaka et al. 2005). A normal or lower than normal SVR in shock, or “distributive” hemodynamics, is becoming increasingly recognized in patients with cardiogenic shock and indicates that there not infrequently is a generalized systemic inflammatory response syndrome (SIRS). Manifestations include temperature abnormalities (both high and low), elevated white cell count, complement activation,

and increased C reactive protein. The presence of these impacts 90-day outcomes (Berg et al. 2019; van Diepen et al. 2013, 2017). Some of the inflammatory states could have been induced by cardiac arrest before the onset of the shock state. In the SHOCK study, 33% of revascularized patients were resuscitated before randomization (Hochman et al. 1999). A significant proportion of patients also had clear signs of infection. The incidence of an inflammatory state was related to prolonged use of an IABP and multiple central venous catheters (Kohsaka et al. 2005). It is hard to know if this was causal or just associative. In many patients, the distributive state likely was due to tissue injury from the low flow state.

The expression of components of a generalized inflammatory process explains why the original paradigm that cardiogenic shock only occurs when there is greater than 40% loss of the myocardium (Hasdai et al. 2000b; Hochman Judith et al. 1995) is not consistent with observations from recent shock trials (Hochman 2003). For example, in SHOCK mean EF was in the 30% range. This still should have been adequate for tissue needs. Many patients also often have further recovery of cardiac function over time, and 85% of survivors in SHOCK were New York Heart Class 1 or 2 by 1 year (Hochman et al. 2001).

Nitric oxide (NO) released from the inducible form of the enzyme NO synthase has been proposed to be a mediator of the vasodilation in the cases of cardiogenic shock that have a distributive hemodynamic pattern (Russell 2006). Interest in NO evolved from the hypothesis that NO has a major role in septic shock based on studies in rats and mice. However, there is no good evidence that NO plays a role in human sepsis (see Septic Shock, Chap. 52). Indeed, a clinical trial in which septic patients were randomized to receive an NO synthase (NOS) inhibitor (the enzyme responsible for producing NO) was stopped prematurely because of evidence of harm (Lopez et al. 2004). In a small pilot study in patients with cardiogenic shock, use of the NOS inhibitor N^G-nitro-L-arginine methyl ester (L-NAME) dramatically increased arterial pressure and produced a marked reduction in mortality (Cotter et al. 2003). This

was followed by a large, multicenter, double-blind, randomized trial called TRIUMPH in which the NO synthase inhibitor L-N^G-monomethyl arginine (L-NMMA; tilarginine) was given to patients with cardiogenic shock (Alexander et al. 2007). Despite the obstructed coronary arteries being successfully opened, mortality remained high, and if anything, mortality was higher in the L-NMMA group. A lesson learned from this study is that raising blood pressure should not by itself be a target for therapy. Of importance, there are two constitutive forms of NOS that regulate normal distribution of blood flow, inhibit platelet aggregation, and play a role in neuro-regulation and a third form of NOS that is induced during inflammation (Moncada and Higgs 1993). Nonspecific NOS inhibitors block all three isoforms of NOS and thus likely interfere with normal blood flow regulation. NO also decreases coagulation, and thus NOS inhibitors are pro-coagulants. Probably most importantly, it is likely that inducible NOS does not have a significant role in larger animals and humans, and use of a nonspecific NOS inhibitor just blocked the beneficial constitutive forms of NOS (Mehta et al. 1999). This is discussed in more detail in the Septic Shock chapter (Chap. 52).

Physiology and Pathophysiology

Under normal conditions, there is a tight relationship between output from the heart (cardiac output) and the energy needs of the body. O₂ is the final electron receptor in the extraction of energy from food sources, and, as such, there is a tight relationship between cardiac output and O₂ consumption (VO₂). VO₂ is dependent upon how much blood is delivered to tissues and how much O₂ is extracted. VO₂ can be calculated from the product of cardiac output and the amount of extracted O₂ (Fig. 50.3). Delivery of O₂ to tissues is dependent upon the concentration of hemoglobin (Hb) available to carry O₂ and the Hb saturation. The O₂-carrying capacity of Hb sets the upper limit for the amount of O₂ that can be extracted in the peripheral circulation and thus limits the maximum amount of O₂ that can be extracted to compensate for decreased blood flow. There is a physiological limit, though, to how much increasing Hb can be helpful because at hematocrit values much above 55–60% blood viscosity increases exponentially. This increases vascular resistance and the risk of thrombosis in small vessels. To obtain a quantitative sense for the role of O₂ extraction, it is worthwhile consider-

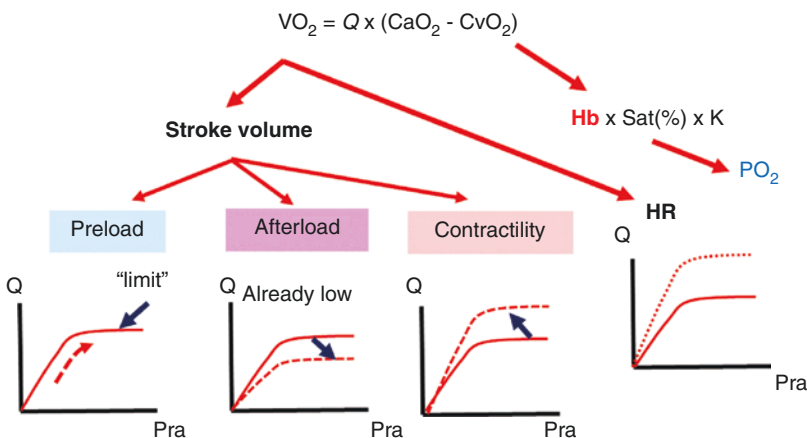


Fig. 50.3 Variables that can potentially improve oxygen delivery to tissues. (Based on the Fick principle, oxygen (O₂) consumption (VO₂) equals the product of cardiac output (Q) and difference between the arterial (CaO₂) and venous O₂ content (CvO₂). O₂ content is the product of the hemoglobin (Hb) concentration, Hb saturation, and a con-

stant for the amount of O₂ bound to each Hb molecule. Saturation is determined by the partial pressure of O₂ (PO₂). Cardiac output is determined by stroke volume and heart rate. Stroke volume is determined by preload, afterload, and contractility. Cardiac function curves are shown below each variable and indicate how they improve Q)

ing the normal ranges of cardiac output and extraction. In healthy young males of normal body size, cardiac output can go from 5 L/min to 20 to 25 L/min at peak exercise, a four- to fivefold increase. At rest, Hb is ~ 150 g/L and Hb O₂-carrying capacity is about 190 mlO₂/L. Resting O₂ extraction is about 25%, which gives a mixed venous O₂ saturation in the range of 70–75% of the Hb O₂ capacity and a mixed venous O₂ content of 142 mlO₂/L. At peak exercise, mixed venous O₂ content can be as low as 25 mlO₂/L. The reserves for O₂ extraction thus normally are very large. Yet, an AMI can severely compromise O₂ delivery to organs. If cardiac output falls to 2.5 L/min, and Hb is only 100 g/L, the mixed venous saturation would have to fall to 22 mlO₂/L to maintain a normal resting VO₂. This value is lower than the mixed venous O₂ content at peak exercise in a normal young male. This also is an average extraction value from all tissues, which during exercise is driven by working muscles. Other tissues may not be able to extract enough O₂ to reach this level. Thus, a decrease of cardiac output in this range cannot be tolerated for long, especially if Hb is compromised.

The two determinants of output from the heart are the amount of volume put out per beat, which is stroke volume, and the number of ejections per minute, which is heart rate (Fig. 50.3). The heart rate component is easy to evaluate and remedy but with a few caveats (Chap. 7). If the patient has a sinus bradycardia, simply pacing the ventricle will usually not work unless the sinus rate is very low. This is because the patient's own atrial beats march through the paced ventricular beats, and when atrial contraction occurs during ventricular systole, cannon "a" waves are produced. These atrial contractions pump blood in a retrograde direction and interfere with RV and LV filling. This does not occur with atrial triggered pacing because the presystolic atrial contractions maintain normal presystolic filling. On the other hand, if the heart rate is too fast, diastolic filling is reduced, which compromises the stroke return and forward stroke volume. It is very important to distinguish two conditions. One needs to whether the tachycardia is caused by the heart failing to generate an adequate stroke

volume and the resultant inadequate tissue perfusion triggering a reflex increase in sympathetic activation of heart rate? Or, is the tachycardia caused by a primary rhythm problem which reduced diastolic filling time and reduced cardiac filling (and ejection time) and that is what lowered cardiac output? In the former case, it is very risky to lower the heart rate; the CVP also likely is elevated. In the latter case, the CVP is more likely not elevated because the rapid rate is inhibiting filling and lowering heart rate might be helpful (Magder 2012a).

The most significant clinical problem in cardiogenic shock is failure to generate an adequate LV stroke volume. The three determinants of the stroke volume are preload, contractility, and afterload. By definition, in cardiogenic shock, LV filling pressures are elevated, afterload is most often decreased (but not always), and the primary problem is inadequate contractile function. I say primarily, because cardiac failure also can occur from inefficient mechanical function as a result of tricuspid, mitral, or aortic valve insufficiencies, valvular stenosis, shunting as occurs with a ruptured ventricular septum, or the development of dyskinetic-aneurysmal regions of the heart that balloon out during systole. However, the primary problem in forward cardiogenic failure most often is inadequate contractile force.

The best way to understand failure of the development of contractile force in cardiogenic shock is by the use of Sagawa's concept that the ventricles generate systolic pressure by what he called a time-varying elastance (Fig. 50.4). This is discussed for the LV in Chap. 4 and for the RV in Chap. 3. Elastance is a measure of the stiffness of a substance. Its units are force per length. In the heart, the force is given by pressure and the length by the volume so that the units are pressure per volume. The inverse of elastance is compliance, i.e., change in volume for a change in pressure. (Compliance is sometime referred to as capacitance because this is the equivalent electrical term. However, in a "hydraulic" analysis, the term capacitance is used for total volume at a given pressure and includes stressed and unstressed volume, which does not exist in an electrical system (Chap. 2).

In the Sagawa concept, the heart walls cycle from resting state with a low elastance during diastole to a high elastance state during systole. The changing elastance can be studied with a pressure-volume graph in which the slope of a line is elastance. The rise in elastance during systole increases the pressure in the volume contained in the ventricle (Fig. 50.4). If the aorta is clamped, and volume is not ejected, the final pressure for a starting volume is the corresponding pressure-volume point on the final elastance line in the cardiac cycle. The greater the initial volume, the greater the final pressure point. When the aortic valve can open, pressure initially rises without a change in volume until LV pressure is greater than aortic pressure. Ejection then occurs and continues to the maximal end-systolic line (Fig. 50.5). When systole ends, elastance of the cardiac muscle relaxes back to the resting dia-

stolic elastance. The aortic valve closes and the mitral valve is not yet open, so that the pressure falls with no change in volume; this volume is the end-systolic volume.

The increase in ventricular elastance during systole occurs when calcium ion (Ca^{2+}) is released into the cytoplasm and activates the interaction of actin and myosin. It ends when the cytoplasmic Ca^{2+} is taken up again by the sarcoplasmic reticulum. The Ca^{2+} release occurs during the plateau (phase 3) of the ventricular action potentials (Chap. 7), and thus the cycle time for the changing systolic ventricular elastance is fixed by the length of the plateau phase of the LV action potential plateau. The maximum elastance reached in this fixed cycle time is determined by how quickly the elastance can increase. This in turn is dependent upon how much and how fast calcium ion (Ca^{2+}) can be released into the cyto-

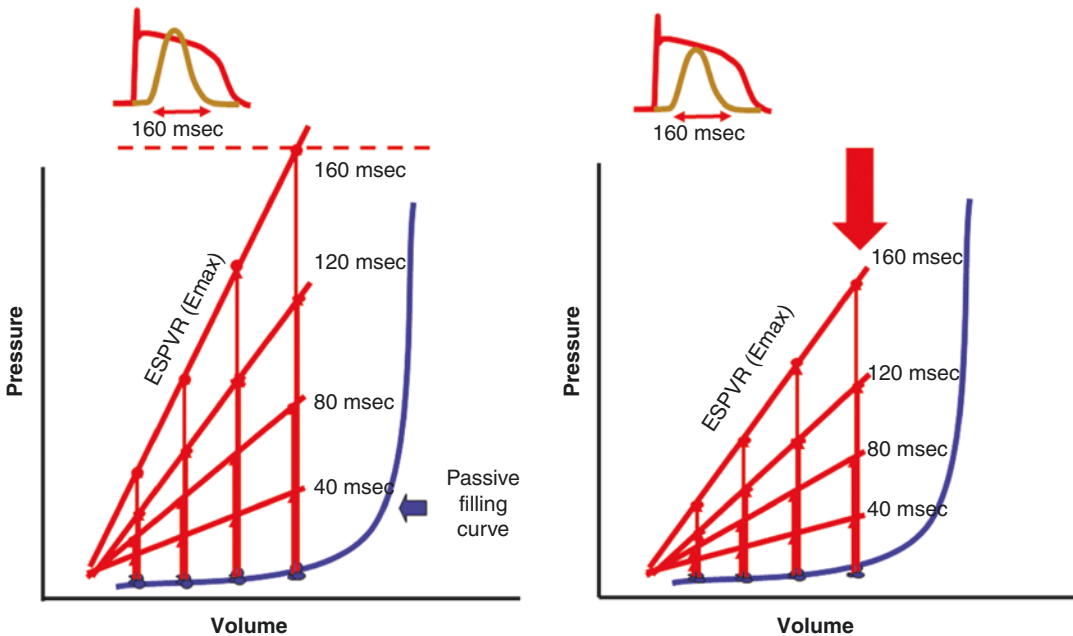


Fig. 50.4 Sagawa's concept of time-varying elastance of the left ventricle with no ejection. Pressure is plotted against volume. In this example from a dog heart, the aorta is clamped and contractions are isovolumetric. Contractions are initiated from different diastolic volumes. After the onset of contraction, at any given time, the pressures always fall on a straight pressure-volume line. Times in msec are marked for each line. The final line, in this example at 160 msec, indicates the end-systolic pressure-volume relationship (ESPVR) which

indicates the maximum elastance (E_{max}) during the time available for systole. The passive filling curve gives the elastance during diastole. The left side shows normal LV function. The right side shows depressed LV function. At a lower ESPVR (i.e., flatter curve), a lower pressure is reached in the time available. The top shows the timing of tension development (brown, peaked curve) during the plateau of the action potential. The time is the same in both cases, but the peak elastance is lower with the reduced function

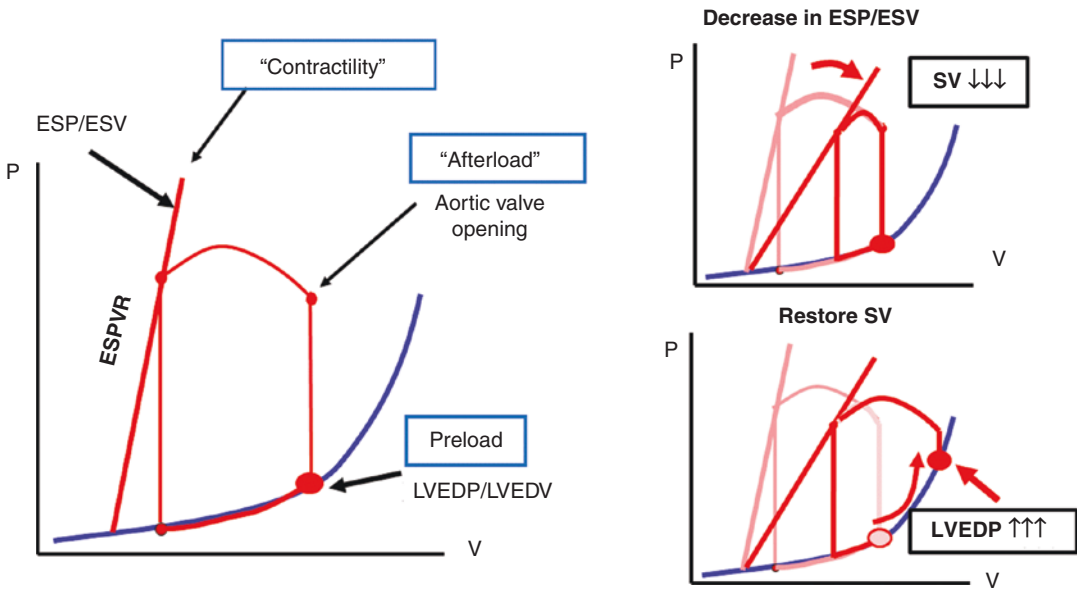


Fig. 50.5 Pressure volume loop of the ejecting heart with normal and depressed cardiac function. The left shows a normal pressure vs volume relationship. Preload, effective afterload, and the end-systolic pressure (ESP) versus volume (ESV) relationship (ESPVR) are marked. See text for details. The right side shows the initial effect of a decrease

in the ESPVR because of an ischemic injury. The stroke volume falls and ESP and ESV rise. On the subsequent beats, volume accumulates in the ventricle so that the LV end-diastolic pressure (LVEDP) markedly rises especially when it is on the steep part of diastolic filling curve

plasm in the available time, and the velocity of stiffening of the sarcomeres, which is dependent upon the rate of turnover of actin-myosin binding sites. This process can be modified by neuro-humeral mechanisms that modify the phosphorylation states of intracellular enzymes which regulate these mechanisms. Based on this analysis, a decrease in the contractile force generated by the heart can be considered essentially as failure to generate a sufficient maximal elastance during the time available for systole.

At low LV diastolic volumes, the slope of the LV pressure-volume relationship (diastolic elastance) is low, although it is steeper than that of the RV. The diastolic slope becomes exponentially steeper at higher diastolic volumes, meaning that the chamber becomes less compliant. In the body, the steep portion of the diastolic filling curve for the whole heart usually is determined by the pericardium, which limits right heart output and thus LV output, but even without a pericardium, the ventricular walls become stiffer at

higher volumes. Passive diastolic stretch of cardiac muscle differs from the length-tension curve of skeletal muscle. Muscles generate maximal force at the length at which the overlap of actin and myosin is optimal. Skeletal muscle can be stretched beyond this optimal length, and when that happens, the generated force during contraction decreases. This would not be a great characteristic for cardiac muscle because it would mean that, after some peak filling pressure, the force generated by the ventricles would decrease and cause volume to back up. In the LV this would result in pulmonary edema. Thus, cardiac muscle evolved so as not to stretch beyond the optimal length of its length-tension relationship, at the single sarcomere level. This occurs because of the characteristics of the sarcomere structures; a primary factor for this likely is the titin content (Granzier et al. 1997).

On the pressure-volume graph (Fig. 50.5), systole starts at the end-diastolic volume and pressure; this represents the preload. There is a

period of isovolumetric contraction until the aortic valve opens. The pressure at which the valve opens gives a good indication of the afterload on the LV. Afterload is related to the tension faced by the ventricle after it begins to shorten. During systolic ejection, arterial pressure rises, but the LV radius decreases so that tension stays approximately constant. This can be considered a quasi-isotonic contraction. Ejection continues until the volume reaches the end-systolic elastance relationship (ESPVR), which, as already indicated, is the maximum elastance (E_{max}) that can be reached during the cardiac cycle. The slope of ESPVR is the best indicator of the contractile state of the LV. When measurements are made in situ with high-precision instruments in non-ejecting isolated hearts, the relationship is linear (Sagawa 1978). The significance of this relationship is that the pressure for a given volume can never be greater than the values on this elastance line. Unfortunately, ESPVR cannot be evaluated easily in intact persons because of a number of technical reasons, and it should only be used for a conceptual framework. A key technical factor is that a change made in *in vivo* studies, such as occlusions of the vena cava to obtain different preloads, also affects the right heart and its diastolic interaction with the LV. The change in blood return to the left heart also is out of synch with what is happening hemodynamically in the right heart because of “buffering” by the pulmonary venous compartment which can continue to supply additional volume to the LV for a few beats. This can affect septal motion (Magder and Guerard 2012). Other technical problems are the difficulty of accurately measuring LV volume, that the real stress is total energy and not just lateral pressure which does not include kinetic energy, and inertial components that can be significant as the flow accelerates (Honda et al. 1994; Beyar and Sideman 1984). These factors can make the end-systolic elastance line appear curvilinear at higher pressures, but in reality this does not represent what is occurring at the sarcomere level (Kass et al. 1987). Despite these limits to the precise clinical measurement of E_{max} , the concept E_{max} still indicates the limit to what the heart can do, and the small differences from lin-

earity have small effects on measured stroke volumes. I will use the term end-systolic pressure-volume relationship (ESPVR) to differentiate what is measured from the true theoretical term E_{max} . The implication of E_{max} line is that a decrease in contractile function is really a failure to reach a normal E_{max} in the time available in the cardiac cycle. When that happens, cardiac output only can increase by an increase in preload if ventricular filling is not limited, an increase in heart rate, or a decrease in afterload.

Because of the difficulty in obtaining the pressure-volume plot, cardiac function is most often considered in terms of a Starling cardiac function curve. This plot treats all the pulmonary vascular structures as one unit and plots the output from the whole unit at the aorta in relationship to the preload of the unit which is defined as right atrial pressure (P_{ra}). The derivation from the pressure-volume relationship is shown in Fig. 50.6. Note the sharp plateau of this function curve which is due to reaching the limit of RV filling. An increase in heart rate or contractility or a decrease in afterload shifts the curve upward, and a decrease in heart rate or contractility or an increase in afterload shifts it upward (Fig. 50.6); they all look the same. The advantage of this plot is that P_{ra} and cardiac output can be fairly easily obtained at the bedside, but pressure volume points cannot.

The pressure-volume analysis illustrates the importance of Starling’s law, which is that the initial stretch of the myocardium determines the amount ejected. In the pressure-volume plot, it can be seen that whatever volume was ejected by a ventricle has to be exactly the same as the volume that filled the ventricle as long as there is no change in heart rate, contractility, or afterload (Fig. 50.5). The importance of this can be appreciated by considering the following. If the RV puts out a stroke volume of 101 ml per beat, and the LV 100 ml, a 1% error, at a heart rate of 70 b/min a total blood volume of 5 L, would be in the lungs in one and half hours. The matching of the two ventricles therefore must be perfect over time. I will come back to this issue when I discuss the use of inotropic therapies with mechanical cardiac assist devices.

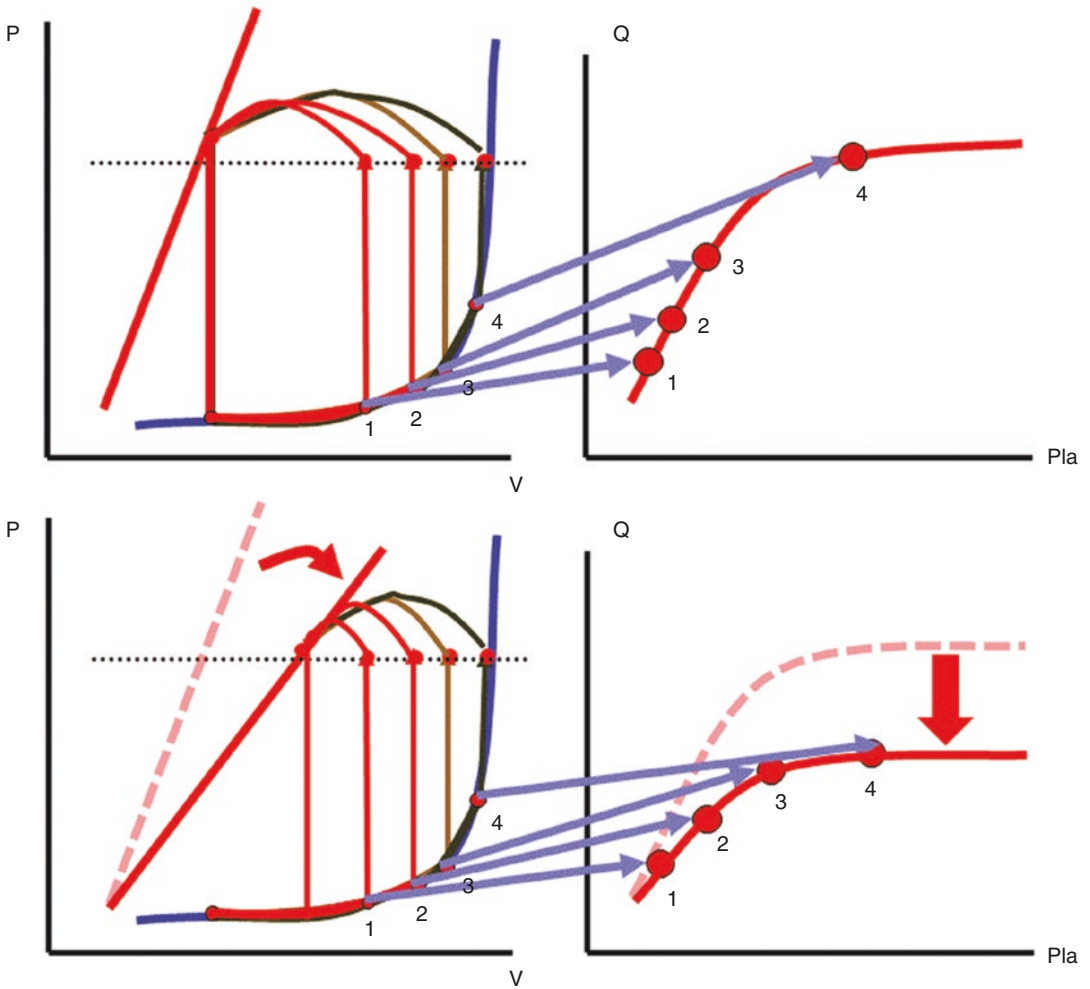


Fig. 50.6 Derivation of left ventricular cardiac function curve from the pressure-volume relationship. The top shows a normal LV pressure-volume (P-V) relationship. Heart rate, afterload (dotted line), and contractility (ESPVR) are kept constant, and preload (end-diastolic pressure – numbers 1–4) is progressively increased. Each increase in end-diastolic volume is exactly matched by the increase in stroke volume as per Starling’s law. The right side shows the Starling function curve for the left heart

with cardiac output (Q) plotted against left atrial pressure (Pla). (Most often this function is plotted as Q versus right atrial pressure, but Pla is used here to understand the direct link.) When the steep part of the diastolic P-V curve is reached, increasing Pla no longer increases Q because there is no change in diastolic volume. The bottom shows what happens when ESPVR is depressed. The function curve is shifted downward and the plateau occurs at lower cardiac output

On the pressure-volume relationship, a decrease in contractile function is seen as a decrease in the slope of the ESPVR (Figs. 50.4 and 50.5) and indicates that the rate of rise to E_{max} is decreased. As already pointed out, the consequence is that, for the same preload, i.e., end-diastolic pressure-volume value, stroke volume is reduced unless there is a decrease in afterload or an increase in heart rate. Consequently,

the end-systolic volume increases. Because the next cycle starts from a higher end-systolic volume, on the subsequent beat, the return of blood raises the end-diastolic pressure-volume value to a higher value.

A decrease in the slope of ESPVR has important consequences for changes in afterload. When the slope of ESPVR is flatter than normal, an increase in the pressure at aortic valve opening,

i.e., an increase in afterload, produces a greater reduction of stroke volume. On the other hand, it also means that a reduction in LV afterload produces a greater increase in stroke volume (Fig. 50.5).

Limitation to Filling

An increase in preload increases stroke volume because there is more time to get to E_{max} . However, the consequence is an increase in LV end-diastolic pressure; the magnitude of the increase in LV end-diastolic pressure depends upon the slope of the LV passive filling curve and the starting volume at the onset of diastole (i.e., end-systolic volume), because the passive filling curve is curvilinear and gets steeper at higher volumes. If the patient starts off with decreased diastolic compliance (i.e., a steeper diastolic filling curve), the rise in diastolic filling pressure with an increase in volume is greater and so is the risk of pulmonary congestion. On the other hand, it also means that a decrease in LV afterload produces a greater decrease in LV end-diastolic pressure.

When just examining the pressure-volume relationship, it would seem that if there is a sudden decrease in stroke volume because of a decrease in the slope of the ESPVR, and the stroke return does not change on the next beat, end-diastolic volume will increase by the same amount as with the previous stroke return, and the stroke volume would be back to the same value that it had before the rise in afterload. However, the same amount of blood does not return. To understand why, it is necessary to consider Guyton's plot of the venous return and cardiac function curves (Magder 2012b; Guyton 1955), which was discussed in Chap. 2.

To review some basic points, this graph plots two functions: cardiac and return functions. The cardiac function describes a set of cardiac outputs from the LV for a given P_{ra} at a constant heart rate, constant afterload, and constant contractility. The return function describes the return of blood back to the heart from the large peripheral venous reservoir. It gives a set of venous

returns for a given set of P_{ra} at a constant stressed volume, constant venous compliance, and constant venous resistance. The venous return is related to the blood flow through the tissues which, as discussed previously, is related to metabolic activity. P_{ra} is common to both functions so that the working cardiac output, working venous return, and working P_{ra} are given by the intersection of the two functions.

To emphasize again, the primary event in cardiogenic shock is depression of E_{max} (Figs. 50.5 and 50.6) (Kass et al. 1989). The consequence of the decrease in cardiac function is that, for the same venous return function (note "function" not flow), cardiac output is lower and P_{ra} higher. This is true whether the problem is a pure LV problem, RV problem, or both because the cardiac function curve considers the heart as a whole beginning at the right atrium and ejecting from the aorta. The pattern also would be the same if there were a decrease in heart rate or an increase in afterload. However, the magnitude of the depression of the cardiac function curve with these other processes is much less than what is seen with the major loss of contractility (E_{max}) in cardiogenic shock, except for extreme bradycardia. Heart rate and afterload also can be more readily corrected by reflex adjustments in the circulation, but the ischemic heart has minimal reserves.

Venous return can be separated into venous return-cardiac function for the RV and LV (Fig. 50.7). In this case, the volume reservoir for the LV is the stressed volume in the pulmonary venous compartment, and the return flow to the LV is based upon the pulmonary venous compliance, pulmonary venous resistance, and left atrial pressure. However, this does not add much to the overall understanding of how the whole system works because the systemic venous compliance is seven times greater than that of the pulmonary circuit (Lindsey et al. 1957), and thus the systemic vascular volume dominates the overall process. More importantly, separating the two ventricles misses the key role of the RV in determining the filling of the pulmonary venous reservoir for the stroke return to the LV. However, this relationship is of importance in the generation of pulmonary

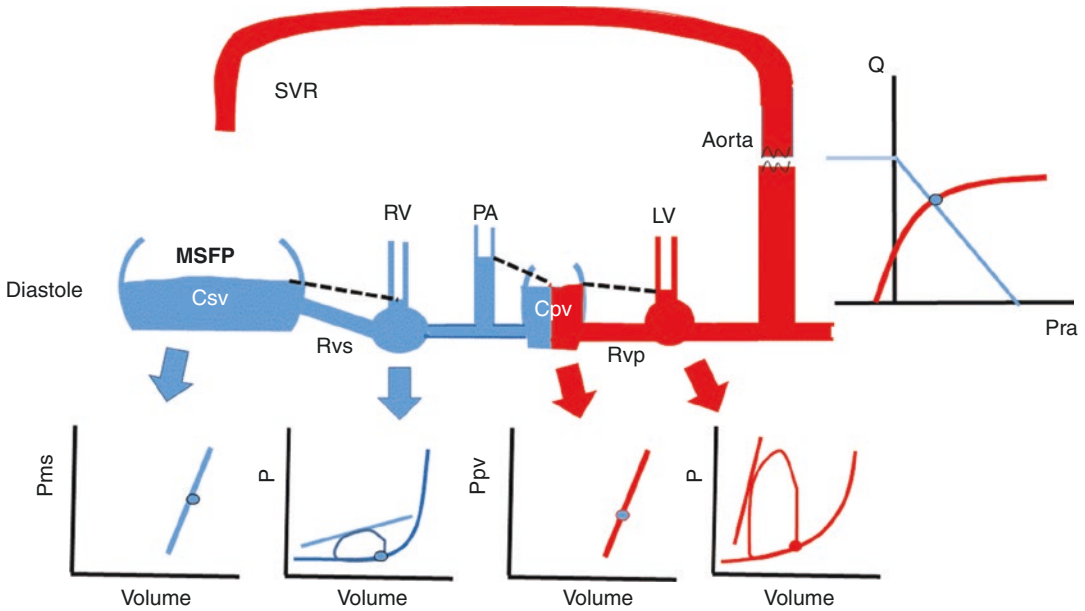


Fig. 50.7 General model of the circulation at the end of diastole with normal function. The pressure in the systemic venous compliant region (Cvs) is MSFP. This pressure drives volume through the venous resistance (Rvs) to the RV which actively pumps blood into the pulmonary artery (PA) and thereby lowers Pra for the next cycle. The PA blood is emptied into the pulmonary venous compliant

region (Cvp), which empties into the LV, which actively pumps the blood into the aorta. The blood returns to the Cvs through the systemic vascular resistance. The left side figure shows the interaction of the return function and cardiac function which give the working cardiac output and right atrial pressure (Pra)

edema because just as a decrease in cardiac function increases Pra, a primary decrease in LV function must be associated with an increase left atrial pressure, and the effect on left atrial pressure is greater than the increase in Pra because the LV diastolic compliance is much lower than that of the RV (Sylvester et al. 1983a).

It now is possible to explain why the return of blood per beat and, consequently, why the stroke volume are lower, when ESPVR suddenly decreases or afterload increases (Fig. 50.8). The rise in LV end-diastolic pressure reduces the pressure difference from pulmonary veins to the LV. Volume accumulates in pulmonary veins, and pulmonary venous pressure rises. By the same reasoning, pulmonary arterial pressure increases which increases RV afterload. This increases RV end-diastolic pressure, which increases Pra. The rise in Pra decreases the pressure difference for venous return, and a new steady state flow occurs with a lower venous return and lower cardiac output as seen in the Guyton plot of cardiac function

and venous return (see Chap. 2). The effect is greater when RV filling is limited already and the heart is functioning on the flat part of the cardiac function curve.

Clinical Consequences of the Above Analysis

The fall in cardiac output with a pure LV event tends to be milder than that of a right-sided or combined RV and LV process, at least in the initial stages (Sylvester et al. 1983a). The previous analysis indicates why a fall in cardiac output due to a fall in cardiac function ultimately requires a rise in Pra to reduce venous return. Thus, for a pure left-sided event, the sequence is as follows. Enough volume must accumulate in the compliant pulmonary vessels to raise the afterload on the RV sufficiently to raise Pra, which decreases venous return. The amount of volume that needs to accumulate in the pulmonary veins to suffi-

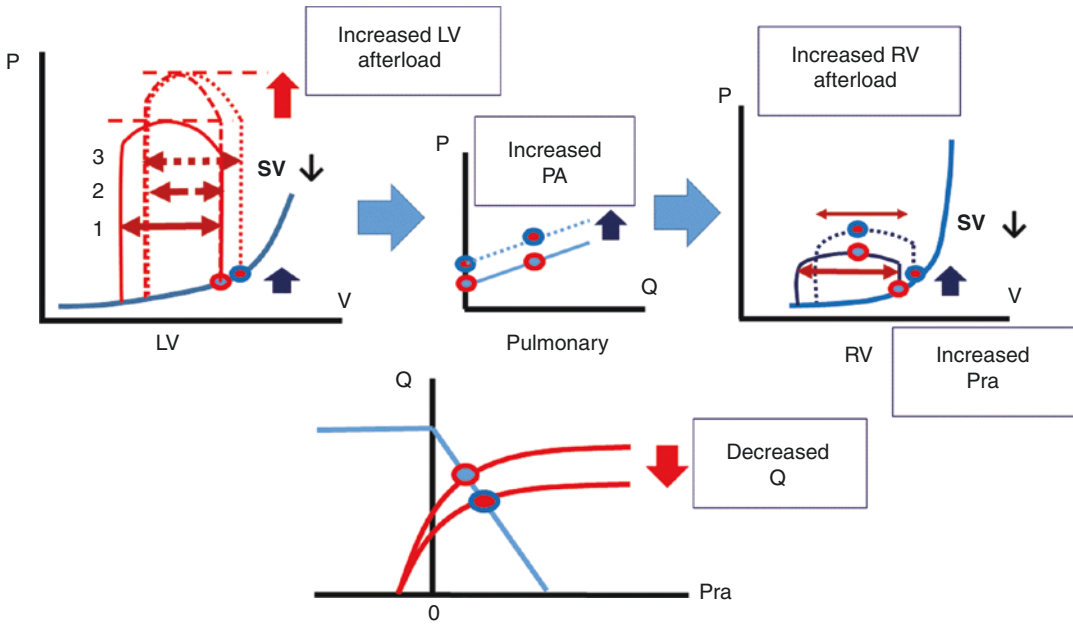


Fig. 50.8 Explanation of why an increase in afterload or decrease in contractility reduces steady state stroke volume. The top left starts with the LV P-V relationship with (#1) the starting stroke volume (SV). The afterload (opening pressure of aorta) is abruptly increased; on the first beat, end-systolic volume is increased because there is less time to reach the ESPVR and SV is decreased (#2). On the next beat, the LV diastolic pressure increases because the return starts from a higher diastolic pressure, but the return to the LV from the pulmonary vasculature is reduced due to the higher downstream pressure and SV is

still reduced from the starting value (#3). The rise in LV ESP also increases left atrial pressure and shifts the pulmonary pressure versus flow (Q) curve upward (pulmonary = pulmonary vasculature, PA = pulmonary artery). The third panel on the top shows the P-V of the RV. The rise in PA increases the afterload on the RV and decreases its SV. The bottom shows the cardiac function-venous return curve. The increase in afterload depressed the cardiac function curve so that it intersects the venous return curve at a higher Pra and lower Q

ciently to lower cardiac output by a rise in Pra generally will produce severe pulmonary edema before Pra increases sufficiently to lower venous return and cardiac output (Fig. 50.7). It thus is likely that the person starts to effectively “drown” first and the disturbance of gas exchange and burden on the respiratory muscles cause the cardiovascular collapse. Hypoxic pulmonary vasoconstriction also might increase the load on the RV and further contribute to the fall in cardiac output (Sylvester et al. 1983b).

There are useful clinical lessons from this analysis. A patient who presents acutely with a very low cardiac output and high Pra likely has one of the following: right-sided ventricular dysfunction (e.g., RV infarct), chronic heart failure with chronic renal retention of volume, or a ruptured ventricular septum that is shunting LV

blood to the RV. Myocardial rupture and tamponade also should be considered; they could be increasing pericardial pressure.

In modeling studies of decreased ventricular function, but without reflexes, another cause of a decrease in cardiac output with just a severe decrease in E_{max} of the left heart became apparent (Magder et al. 2009). The volume that must inevitably accumulate in the pulmonary circuit because of the high LV diastolic pressure reduces total systemic stressed volume. This can be physiologically significant because stressed volume normally only is 1.3–1.4 L (Magder and De Varennes 1998). The decrease in MSFP decreases venous return. In the modeling study, Pra actually fell as did RV and consequently LV stroke volume (Magder et al. 2009). In the intact person, recruitment of unstressed into stressed volume

and other reflex adjustments (Deschamps and Magder 1992) make this less likely, but a fall in MSFP still could happen in someone with minimal unstressed volume reserves. Giving volume though likely is not a good solution because it will just increase pulmonary flooding.

Guyton’s venous return-cardiac function plot also brings up a point that was first identified by Ernest Starling in his studies on cardiac responses to filling and loading of the LV (Patterson et al. 1914; Starling 1918). An arrested heart is the extreme of cardiac dysfunction, and in this state, because there is no flow, Pra equals MSFP; it never can be higher. Thus, Pra (and central venous pressure) higher than the normal range of MSFP, which is 8–10 mmHg, only can occur if there has been an expansion of intravascular volume, either by retention of fluid over time by the kidneys or by iatrogenic administration of fluid.

As an example, we recently observed a patient who presented with severe cardiogenic shock, likely from a viral cardiomyopathy in association with a severe diarrheal disease. His clinical status deteriorated very rapidly over a few days, and he presented to another hospital in extremis. He was transferred to our institution for implantation of an LV assist device (Impella CP®– 3.5 L/min) and a possible RV assist device. On presentation his RV was massively dilated, and the LV was moderately dilated with an ejection fraction <15% (Fig. 50.9). Pra was over 20 mmHg and Ppao equaled Pra. The chest X-ray showed mild pulmonary edema, and

he only had mild hypoxemia. Based on the previous discussion, we assumed that he must have received a large amount of intravenous fluids as part of his initial resuscitation to account for the high Pra (Fig. 50.10). However, the initial managing physicians were adamant that they had not given a lot of intravenous fluids and the records supported their claim. The patient himself was a physician and confirmed that not a lot of fluid had been given. However, he then informed us that he was at fault! Because of the diarrhea, he had consumed 4 L of Gatorade®, which combined with his renal shutdown explained the expanded vascular volume and right ventricular distention. With the increase in his LV forward flow by the support from the Impella®, his kidneys quickly began to work; he had a vigorous dialysis and lost over 5 L within hours. His Pra fell and so did his Ppao. Shortly after insertion of the Impella®, the normal septal curvature returned and RV volume decreased. An RV assist device never ended up being necessary. The Impella® was removed after 5 days, and he made an excellent recovery.

Management

Monitoring

A patient-centered approach to management of shock requires feedback of responses to therapeutic choices. Good monitoring tools are nec-

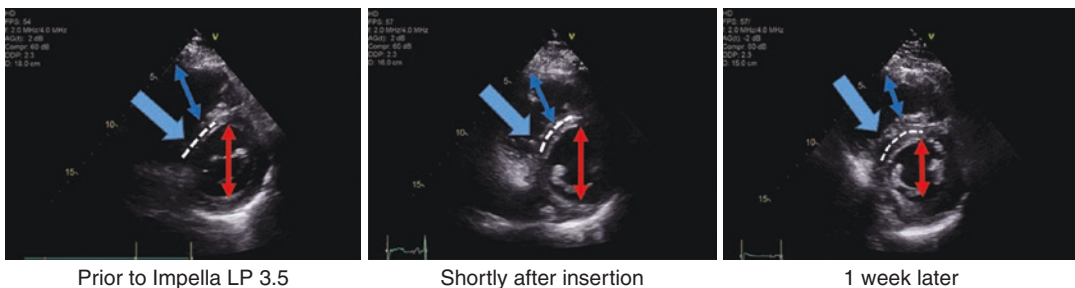


Fig. 50.9 Trans-echocardiograms (short axis) from the case in the text demonstrating LV failure from cardiomyopathy. The first panel is before insertion of the Impella®. The septum is flattened (large blue arrow), the RV is markedly enlarged (double headed blue arrow), and the LV is dilated (double-headed red arrow). The middle

panel shows the same view shortly after insertion of the Impella®. The normal septal curvature has returned, the RV size is reduced, and so is the LV. The third panel is 1 week later. There is further reduction of the RV and reduction in the end-systolic LV indicates the improved ejection fraction. See text for further details

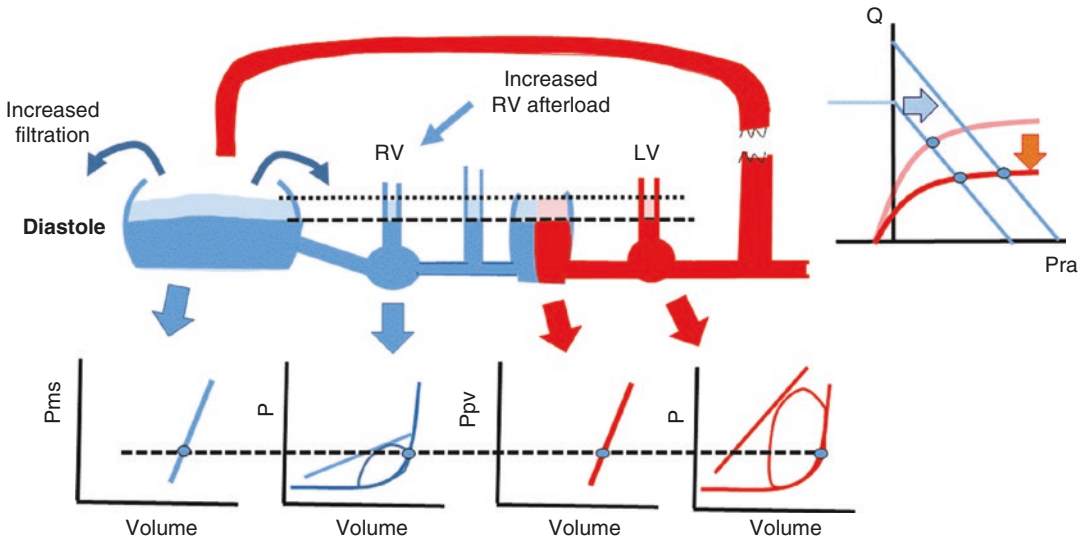


Fig. 50.10 General model of the circulation at the end of diastole with RV and LV limitation—the link between LV failure and RV failure. The compartments are the same as in Fig. 50.7. In this example, LV function is markedly depressed much as was the situation for the case in Fig. 50.9. Consequently, LV diastolic pressure (LVEDP) is increased, as is pulmonary venous pressure, PA dia-

stolic (and systolic) pressure, and RV diastolic pressure. The RV becomes volume limited, and in diastole, the pressures are the same in all regions. Adding volume only increases MSFP, but does not change RV output, and does not change forward cardiac output. The added volume only increases capillary filtration and worsens organ congestion

essary to accomplish this. This should include an intra-arterial catheter and a central venous line because infusion of vasoactive drugs usually is required acutely. In moderate, or “pre-cardiogenic shock” cases, a central venous O_2 saturation measurement ($ScvO_2$) can be helpful if Hb is close to normal and there is not a peripheral distributive state. A $ScvO_2$ of $>55\%$ indicates that it is very likely that the cardiac index is >2.2 L/min/ m^2 (Jain et al. 1991). In more complex cases, a cardiac output measurement becomes important considering that the primary problem is a lack of peripheral perfusion. The more critically ill the patient, the more reliable the device needs to be, and the more reliable the device, the more invasive it tends to be. Although use of a pulmonary artery (PA) catheter remains controversial (Baran et al. 2019), its use in cardiogenic shock still is recommended in most reviews (Vahdatpour et al. 2019; Thiele et al. 2019; Westaby et al. 2011; Baran et al. 2019; van Diepen et al. 2017), and it still is widely used (Allen et al. 2008; Hernandez et al. 2019; Pandey et al.

2016; Basir et al. 2019). The limitation of previous studies of its use is that the studies either were just observational (Connors Jr. et al. 1996) or just examined the presence of the catheter rather than studying an algorithm that required use of a PA catheter.

Use of a PA catheter can be considered under two categories: (1) diagnostic and classification and (2) management of hemodynamic drugs and fluids. The recently identified very important group of patients who have cardiogenic shock and a low SVR and distributive picture cannot be identified without a flow measurement. There currently are noninvasive devices for the measurement of cardiac output, but the more critical the condition, the less accurate they become; thus outside of trending, these devices are not adequate for obtaining an accurate cardiac output, and the PA catheter remains the gold standard. The basic PA catheter also is the cheapest device. The PICO® device placed in a femoral artery is a reasonable alternative choice, but the space available in the groin may be limited in patients assisted with mechanical devices.

Diagnostic value of PA catheter

Diagnostic value of the PA catheter was the basis for the development of the original floatation catheter by Swan and Ganz (Swan et al. 1970; Forrester et al. 1971). They noted that patients with an AMI could be in pulmonary edema because of an elevated Ppao as an indicator of elevated left atrial pressure but have a normal Pra/CVP. Furthermore, the chest X-ray alone is not a good indicator for the presence of an elevated left atrial pressure, because resolution of the chest X-ray pattern often lags behind changes in pulmonary capillary pressure and, sometimes, because of the quality of the image. Thus, the classification of the “dry” and “wet” cardiogenic shock cannot be made reliably without a Ppao measurement.

The second diagnostic value of the PA catheter as already noted is determination of a low-resistance distributive component to the shock. In the face of decreased blood pressure, if the cardiac output is normal or, even more so, elevated, the systemic vascular resistance must be decreased, and it is not even necessary to calculate the resistance value. Thus, this state too requires a flow measurement to make the diagnosis, to monitor its evolution, and to adjust vasoactive and inotropic therapies. Intelligent management of a low cardiac output in which the central problem is cardiogenic shock, requires a measurement of cardiac output!

A third diagnostic value of the PA catheter is measurement of the pulmonary artery pressure and the relationship of the pulmonary diastolic pressure to the Ppao. This is especially important in nonischemic cardiogenic shock such as post-cardiac surgery. A minimal pressure drop from the pulmonary diastolic pressure to Ppao indicates that pulmonary vascular resistance is not elevated (except for some possible precapillary increase from hypoxic vasoconstriction), and the LV dysfunction likely is the major cause of the elevated PA pressure. In severe cases, right atrial pressure and Ppao often are equal as occurred in the case discussed above. This occurs because the increased pulmonary pressure and backup of volume in the lungs drive the

RV to the steep part of its passive diastolic filling curve and result in right heart limitation (Fig. 50.10). The RV then becomes the limiting factor for cardiac output. This is seen as the flat part of the cardiac function curve (Fig. 50.6). In this situation, lowering Pra does not decrease cardiac output until the ascending part of the cardiac function curve is reached (Fig. 50.6). Often, paradoxically, reduction in vascular volume increases cardiac output. This can occur because RV wall stress is decreased and also because the reduction of the high Pra decreases left atrial pressure, which decreases pulmonary artery pressure and the afterload on the RV. The improvement in oxygenation also might contribute further by reducing hypoxic vasoconstriction. If pulmonary arterial systolic pressure is elevated, and there is a significant pressure gradient from the pulmonary diastolic pressure to the Ppao, pulmonary vascular resistance must be elevated, and there likely is a chronic component. If the cardiac output is low, it also is likely that there is limitation of RV filling. Use of inotropes and an attempt at RV volume reduction should be tried first, but an LV mechanical assist might be necessary. The RV should be decompressed before an RV assist device is implanted because otherwise the RV device might just worsen pulmonary edema.

Management value of PA catheter

In an analysis of patients with cardiogenic shock who were enrolled in the CardShock, observational, prospective, multicenter European registry, the PA catheter provided no survival benefit although patients receiving a catheter had more interventions (Sionis et al. 2019). The problem with this study, as well as many studies before it, is the lack of a protocol with a physiologically based algorithm for the management of patients with cardiogenic shock. As for specific examples, the studies fail to consider different management plans for patients with distributive shock, fail to indicate when to stop giving fluids based upon reaching the plateau of the cardiac function curve, and fail to track responses of cardiac output to drug therapies and alter therapy accordingly.

The PA catheter has great potential for guiding fluid management as also discussed in Chap. 22 on hemodynamic monitoring. CVP values that are in the normal upper range of greater than 10 mmHg (assuming leveling 5 cm below the sternal angle) (Magder and Bafaqeeh 2007) make it unlikely that more fluid will help, and there is a greater likelihood of harm, such as hepatic, bowel, and renal dysfunction. However, the catheter is best used with a “responsive” approach (Magder 2012b, 2016; Potter et al. 2013). If the clinician hypothesizes that fluids may increase cardiac output, the next step should be to observe whether the fluid bolus actually increased cardiac output. If it did not, and there was evidence of an adequate fluid bolus based on a rise in CVP, giving more volume will not be helpful, and the added volume only will contribute to the overloading of the patient. Similarly, if the physician hypothesizes that giving an inotrope, such as dobutamine, might improve the clinical situation by increasing cardiac output, it behooves the clinician to determine whether cardiac output actually rises when dobutamine is given. If it does not, either the dose should be increased or another drug tried.

Volume

Current treatment recommendations for cardiogenic shock start with giving a fluid bolus (Thiele et al. 2019; Shah et al. 2019). However, fluid should be used with caution in cardiogenic shock (Vahdatpour et al. 2019) and are likely not needed as the first step for a number of reasons. First, normal physiological increases in cardiac output do not occur through the addition of exogenous volume. Instead, cardiac output occurs by increases in heart rate and contractility. Second, most people presenting with cardiogenic shock should not be volume depleted. The shock most often is caused by an acute ischemic event, and their volume status likely is normal at the onset. One group presenting with cardiogenic shock are those who have decompensated chronic heart failure (Lee et al. 2011). They are even more likely to already be overloaded. The recommen-

ation for giving fluids may come from the management of septic shock, because in that condition there is significant capillary leak and intravascular volume depletion. Accordingly, some fluid might be considered in patients who present with “mixed” shock, but this should only be done with small aliquots, perhaps 250 ml at a time, and careful monitoring. It is worth emphasizing that in SHOCK Ppao in the 20 mmHg plus range was present in all groups. CVP also was in the 12–14 mmHg range, which is on the higher side, especially because patients with RV dysfunction were excluded. Once the sharp break of the diastolic pressure-volume relationship of the RV is reached, the RV diastolic pressure rises steeply with more volume, and the consequent septal shift can further compromise LV as was shown in the case above. This is particularly important when the infarct affects the septum. One could even go as far as to say that volume given to patients in shock may have contributed to increased morbidity and mortality some studies. Others, too, have suggested the same (Hochman 2003). It is noteworthy that, as already discussed, pulmonary congestion seemed to not have been always recognized (Menon et al. 2000b).

There is evidence that “decompressing” the RV can be beneficial. Atherton et al. applied lower body negative pressure to normal subjects, a group of patients with compensated (treated) heart failure, and a group with uncompensated heart failure (Atherton et al. 1997a, b). The lower body negative pressure decreased LV volume in the normal subjects and patients with compensated heart failure but increased LV size in those with decompensated heart failure, indicating that they had RV interference with left-sided filling. The implication of these studies is that early use of diuretics to bring Pra into a more normal range can be useful early in shock. Monitoring cardiac output can be very useful for guiding this therapy and avoiding a decrease in cardiac output by excessive fluid removal. Once again, if the heart is functioning on the flat part of its function curve, decreasing the wasted preload should not decrease cardiac output (Westaby et al. 2011).

Pharmacological Approaches

The primary management of cardiogenic shock is the judicious use of pharmacological agents to increase cardiac and circulatory performance. However, there are only limited physiological processes that can be targeted to increase circulatory performance. These include increasing cardiac contractility and heart rate, altering systemic vascular resistance, and lowering pulmonary vascular resistance when there is a need to assist the RV. It also is important to make sure that Hb and O₂ saturation are adequate. One must always remember that pressure is not flow, and the primary clinical objective in shock is to provide adequate flow to the tissues. I purposely use the word “adequate” rather than normal. It is possible that overzealous attempts to increase flow and pressure may have caused harm. As a comparison, no physician would try to restore Hb to the normal value after a large hemorrhage; the same likely should apply to hemodynamic parameters. Adequacy of blood flow should be assessed by following measures of tissue perfusion, which include blood lactate, venous saturation, wakefulness, and renal function. It likely also is important to provide an adequate perfusion pressure to appropriately match flow to tissue needs, but the appropriate value for pressure is still not well established. Raising arterial pressure raises the afterload on an already weakened LV and also raises myocardial O₂ demand in patients who likely have limited coronary reserves for O₂ delivery. Furthermore, a rise in arterial pressure without a rise in cardiac output only can be clinically helpful if the flow becomes redistributed to areas of greater metabolic need, but this also means that flow to some other areas must decrease (Magder 2014).

Epinephrine (Epi)

Epinephrine (Epi) is a catecholamine that has almost equal effects on alpha- and beta-adrenergic receptors with some variability in receptor affinity that is dependent upon the dose used (Russell 2019). It has potent effects on cardiac output and arterial resistance. Its half-life is short, and thus it is used generally as an infusion. It is the primary

agent used to revive an arrested heart. In that situation, it is given as a bolus, usually of 200–1000 mc intravenously. Boluses often are given as well when flow and pressure are drifting down and the patient is pre-arrest, but one must be cautious about causing myocardial damage (contraction-band necrosis) and inducing arrhythmias. When used as an infusion, a low to moderate dose is 0.14 mcg/kg/min (~10 mcg/min) and a high dose is 0.60 mcg/kg/min (~40 mcg/min). Higher doses often are given, but it is hard to know what these large doses are doing, or if they even are causing harm (Levy et al. 2018). Epi is best used with a measurement of cardiac output or at least a surrogate of flow, which should be the primary determinant of the rate of infusion. More often, only pressure is monitored and the appropriate targets for this are not currently established. Epi is a very effective agent, but it gives course adjustments rather than fine tuning. It also causes metabolic disturbances such as a rise in lactate, a fall in potassium, and hyperglycemia. It also can be very arrhythmogenic. The rise in lactate can sometime confuse physicians and lead to unnecessary increases in therapy. In the markedly depressed heart, it likely is the best agent in the short run, although a prospective study which is discussed further below showed harm when it was the primary agent (Levy et al. 2018). This was also seen in meta-analysis on the use of Epi although the analysis was primarily based on observational data (Léopold et al. 2018).

An observation by the author is that Epi in some patients seems to have a greater effect on the RV than the LV, especially in the presence of an LV assist device. In this situation, if the output from the LV assist device is not increased, the infusion of Epi can result in pulmonary edema because the LV does not keep up with increased filling from a better functioning RV. Although mechanical devices have a “preload” response (Lim et al. 2017), they do not have the precise match of inflow to outflow that occurs with the Frank-Starling mechanism.

Norepinephrine (NE)

Norepinephrine (NE) has a dominant alpha-adrenergic effect, but it still has a significant

beta-adrenergic component and thus also can increase cardiac output. This is in contrast to phenylephrine which has no beta-adrenergic activity and thus likely is not useful in cardiogenic shock because it does not increase cardiac function (Thiele et al. 2011a, b; Magder 2011). Furthermore, phenylephrine increases venous resistance, and if it fails to recruit unstressed volume into stressed volume, it decreases venous return and cardiac output (Thiele et al. 2011b). Of interest, it was observed that mortality increased in patients with septic shock when there was a shortage of norepinephrine and phenylephrine was substituted as the primary vasopressor (Vail et al. 2017). Phenylephrine can be helpful in the rare situation of someone who has an ischemic LV but who also has dynamic outflow tract obstruction. In this situation, it might be necessary to add phenylephrine to Epi or NE to increase the arterial pressure which increases LV volume and thereby reduce the dynamic outflow tract obstruction.

An underappreciated effect of NE, as well as Epi, is that they decrease vascular capacitance and thus raise MSFP. This increases venous return and cardiac output if the heart is functioning on the ascending part of the cardiac function curve. The beta-agonist component also decreases venous resistance, which increases venous return and contributes to their effect on cardiac output. Dobutamine, too, decreases venous resistance and produces a small reduction on venous capacitance, which contributes to its effect on cardiac output.

In the past, an expression evolved for use of NE that was a play-on-words of its old trade name which was levophed®. It was said: “levophed leaves then dead.” This was based on the use of high doses of NE in patients in cardiogenic shock in whom the low blood pressure is due to a low cardiac output and increased SVR. Clearly, raising the resistance more cannot help. To emphasize the point again, pressure is not flow and if only pressure is increased without a change in flow, it is unlikely that increasing the NE dose has any clinical benefit. In that situation, NE only is acting as phenylephrine. NE has a less potent effect on cardiac output compared to Epi, and if

used alone, and it does not increase cardiac output, the patient will not survive (Annane et al. 2007). However, as already discussed, it is becoming increasingly evident that many patients in cardiogenic shock have a distributive state with a low SVR. In these cases, NE is the ideal agent. The maximal useful dose of NE is not known. Just because it raised pressure is not a useful indicator of outcome. It is quite likely that high doses interfere with the distribution of blood flow and compromise flow to vital regions. Of note, NE has a minimal effect on pulmonary vascular resistance (Datta and Magder 1999). I have begun to limit norepinephrine doses to 50–60 mcg/min, but I know of no data to back up this statement!

Epi versus NE

There have been ongoing debates about the advantages of Epi versus NE for the treatment of cardiogenic shock. Currently, NE is the favored drug. However, most of the comparative studies are in patients with heart failure (Bayram et al. 2005) or multiple types of shock (Russell 2019; De et al. 2010; Myburgh et al. 2008). There only is one small, but frequently referenced, randomized trial that compared the use of Epi to NE in cardiogenic shock (Levy et al. 2018). It took place over 4 years, and only 57 patients were recruited before the study was stopped because of concerns of a higher rate of refractory shock in the Epi group. Despite its small size, this study will be reviewed in detail because it gives important insights into the problems doing these kinds of studies and whether it is the agent or a protocol that is the cause of the problem.

In this blinded randomized study, the endpoint was CI over the first 24 hours, but the clinical target for titration of the drugs was blood pressure. Mean blood pressures were identical in both groups and hovered a little above 70 mmHg; this is a tribute to the effectiveness of bedside nurses. There was no difference in CI over the 24 hours, although CI was higher at 2 and 4 hours from the onset of the study in the Epi group. This occurred because heart rate was higher in the Epi group, but stroke volume was the same. A rather striking observation was that CI rose in both groups in

parallel at 12 hours likely indicating that the process was resolving. Death rate at 28 days was 48% in the Epi group and 24% in the NE group, which not surprisingly was not significant given the small numbers, but the results do raise concerns. A major safety concern raised by the study was development refractory shock based on echocardiographic findings (not defined), a rise in lactate, and worsening of SOFA-based organ dysfunction which occurred in 37% of the Epi group but only in 7% of those receiving NE. However, the difference in this score was solely determined by the difference in lactate, and, as the authors of the study had previously shown, the lactate rise with Epi is due to its action on skeletal muscle $\text{Na}^+\text{-K}^+$ ATP pump and not due to ischemia. The lactate actually may have the advantage of providing fuel for the heart and in this setting does not require treatment (Brooks 2020).

What should we learn from this study? First, studies like this are hard to do – 4 years for 57 patients. A larger study in sepsis did not show evidence of differences between Epi alone versus NE plus dobutamine, or Epi alone versus NE in a group of mixed shock patients, but with a low percentage of patients with ischemic heart disease. Perhaps the difference is that patients with ischemic heart disease are more sensitive to the O_2 supply-delivery balance than nonischemic patients, and Epi may worsen this balance in some patients. However, a more important issue might be that this kind of study uses a fixed drug protocol. It did not take into account the therapeutic goal of the therapy and did not readily allow adaptations to the patient's condition such as tapering Epi down when cardiac output was adequate. There also likely were unfortunate clinical reactions to the Epi-induced rise in lactate, which by itself was harmless. Epi gives a quick response, which can be critical in the early stages. The patients in this study were beyond that phase. It also is important to know if the primary clinical decision was based on a need to have more flow or a higher arterial pressure. Cardiac output was measured but was not included in the clinical algorithm. A proper clinical approach should start by first considering

whether the primary problem is the pump (i.e., heart) or the SVR, especially because of the increasing recognition of a distributive component in many patients with cardiogenic shock. NE is a better drug for a low SVR, whereas Epi has stronger pump effects as was seen in the Levy trial (Levy et al. 2018). Dobutamine often is less effective when the CI index is severely depressed, and Epi may be needed at that early stage to improve pump function, but it then can be switched to dobutamine as heart function improves. When perfusion is restored, NE likely is a better choice because it does not have the metabolic effects of Epi and allows for a gentler titration. This type of individualized care is very difficult to put into a randomized trial, and the fixed required regiment likely exacerbated differences between the drugs. Other important individual characteristics that should affect the choice of drugs include how resistant the patient is to the agent being used. Another important issue is whether the protocol pushed for too high a blood pressure. A higher pressure could help coronary flow to obstructed regions, but it also increases the afterload on the heart and increases the myocardial O_2 demand of the wounded ventricle. Long-term management likely will involve afterload reduction. As suggested above, perhaps the best approach is not to aim for “normal” values but rather “adequate” values based on overall organ function. Does it matter that the patient still needs some support after the first 24 hours? It was quite striking that CI at 24 hours was almost identical with Epi and NE. This seems to indicate that the venous return and cardiac output were being regulated according to metabolic need as the patients stabilized, whether or not they were on a drug and whichever agent was used.

Dobutamine

Dobutamine is primarily a beta-agonist that acts on both beta-1 and beta-2 receptors. Its D-isomer also has some alpha effects (Ruffolo Jr. and Messick 1985). Its primary role should be to increase an inappropriately low cardiac output. If it fails to do so, its peripheral dilating effect may decrease arterial pressure, and it often needs to be combined with NE to maintain a chosen blood

pressure target. It acts directly on beta-adrenergic receptors. This differs from the action of dopamine which acts by increasing the release of NE from sympathetic nerve terminals (Nash et al. 1968; Maekawa et al. 1983). Thus dopamine requires that there be adequate NE stores to be released but dobutamine does not. It also means that dopamine increases myocardial NE, which can increase myocardial ischemia, whereas dobutamine decreases myocardial NE because there is less need for sympathetic activity (Maekawa et al. 1983).

Dobutamine's effects on cardiac output tend to be milder and more variable than that of Epi and changes in doses usually are made in larger steps. In some patients, it has minimal effects. Its half-life also is short so that if its effects are undesirable, it wears off quickly. An approach for the patient in cardiogenic shock is to start with 2.5–5 mcg/kg/min and reassess cardiac output, if measured, in 10 min. If cardiac output does not increase by at least 10%, the dose can be doubled and the response reassessed. If the response still is not satisfactory, double the dose again (now 20 mcg/kg/min), and if the response is not adequate, discontinue the dobutamine and choose another agent (most likely Epi). If the patient is stabilizing but still requires inotropic support, this agent is likely better than Epi because of its more moderate metabolic effects, but this is not established with data.

Dopamine

Dopamine is a drug with mixed and complicated effects because it has five different receptors and also can interact with adrenergic receptors (Marinosci et al. 2012). As indicated above, it can release NE from sympathetic fibers in the heart and worsen ischemia (Nash et al. 1968). At low doses, ≤ 2.5 mcg/kg/min dopamine acts on dopaminergic receptors. These primarily are in the kidney where dopamine can increase natriuresis in a volume replete patient, but it does not alter renal function (i.e., creatinine clearance) (Kellum and Decker 2001). From 2.5 to 10 mcg/kg/min, it has mixed beta- and alpha-adrenergic properties, and above 10 mcg/kg/min, it has more dominant alpha properties, but these ranges are not precise,

which makes it a difficult drug to use. Importantly, in a multicenter randomized trial of the use of dopamine versus NE, side effects were more frequent and mortality was higher in the cardiogenic shock subgroup treated with dopamine (De et al. 2010).

Milrinone

Milrinone is a phosphodiesterase inhibitor that inhibits the breakdown of cyclic AMP and thereby increases intracellular Ca^{2+} and myocardial contractility. It also produces vasodilation peripherally. Because it has a half-life in the 4–5-hour range, typically a bolus is given which should be in the range of 50 mcg/kg, but less should be used if the patient's blood pressure is low. An infusion is then given in the range of 0.25–0.75 mcg/kg/min. It has been argued that the beneficial effect of milrinone and its predecessor, amrinone, on cardiac output only is due to its vasodilatory effect and the reduction of ventricular afterload (Wilmshurst et al. 1983). Accordingly, it has been called an inodilator. However, it has potent direct effects on the heart, and this effect can be seen at doses that do not decrease blood pressure (Jaski et al. 1985). Some patients even respond with an increase in arterial pressure, but most often arterial pressure falls, and NE may be necessary to support arterial pressure. Another important component of its action is that it decreases pulmonary vascular resistance and thus reduces the afterload on the RV. This is especially important when the RV is volume limited, and the only way to increase RV output is by increasing cardiac contractility or decreasing pulmonary artery pressures. Milrinone does both. It likely decreases venous resistance and thereby increases the venous return function (Hirakawa et al. 1992). Milrinone is less arrhythmogenic than Epi, but it still can increase arrhythmias. A retrospective two-center cohort study found that both dobutamine and Epi increased in-hospital mortality in patients with septic shock, whereas milrinone did not (Sato et al. 2019).

Milrinone is primarily cleared by the kidney, and thus caution must be exercised in patients in renal failure. In general, higher blood concentrations are well tolerated, but they can result in

persistent hypotension, and doses should be reduced in the presence of renal failure (Chong et al. 2018).

Vasopressin is a small peptide hormone (9 amino acids) that acts on two receptors. It is primarily secreted in response to a low osmolality, and at concentrations of 0.9–6.5 pmol/L, it acts on V2 receptors to regulate the permeability to water in the kidney's collecting ducts (Landry and Oliver 2001). It also is secreted in response to a decrease in the pressure of the carotid baroreceptor at higher concentrations, 9–187 pmol/L, and by acting on V1 receptors it induces contraction of vascular smooth muscle (Landry and Oliver 2001). The effect of exogenous vasopressin is markedly increased in patients with hemorrhagic and septic shock, but it has little effect on normal subjects; it seems to require decreased baroreceptor activity for its vasopressor effects (Cowley Jr. et al. 1974; Braunwald and Wagner Jr. 1956). It initially was thought that it would not have much effect in cardiogenic shock, but clinical experience shows that it is very effective in distributive shock post-cardiac surgery (Hajjar et al. 2017). Although there are no direct confirmatory studies of its efficacy in patients with cardiogenic shock, it still commonly is used. As with phenylephrine, it has no significant effect on cardiac output. Importantly, vasopressin increases the response to NE (Landry and Oliver 2001). Although a randomized trial that tested the use of vasopressin versus NE in septic shock failed to find a benefit, in a secondary analysis there was a benefit in subjects who were receiving lower concentrations of NE (≤ 15 mcg/min) (Russell et al. 2008). Perhaps vasopressin is acting through an NE “sparing” effect by reducing the need for very high doses of NE and making the NE that is being given more effective. The normal vascular response to a decrease in baroreceptor pressure is peripheral vasoconstriction, which is greater in the peripheral muscle beds compared to the splanchnic bed (Deschamps and Magder 1992; Hainsworth and Karim 1976). High doses of exogenous NE reduce this specificity, and use of vasopressin reduces the need for these high doses. Typically vasopressin is infused at doses in the range of 0.01–0.04 units per min; larger

does should not be used because of the risk of bowel ischemia.

Sodium bicarbonate (NaHCO₃)

Sodium bicarbonate (NaHCO₃) is often infused when patients are severely acidemic based on the belief that acidemia reduces vascular responsiveness to catecholamines. The evidence for this is poor, and the decrease in vascular response is likely a result of the underlying process producing the acidemia. For example, there is no evidence of reduced catecholamine responsiveness in patients who are acidemic from hypercapnia. There now have been two randomized trials that have shown that infusion of NaHCO₃ in patients with severe acidemia does not alter catecholamine responsiveness nor outcome and thus NaHCO₃ has little place in the management of cardiogenic shock (Cooper et al. 1990; Jaber et al. 2018; Magder and Samoukovic 2019). The reasons why it likely is ineffective are given in Chap. 41 on acid-base.

Role of Ventilation in Cardiogenic Shock

The details of heart-lung interaction are discussed in Chap. 18. Here we discuss issues directly relevant to cardiogenic shock. Spontaneous inspiratory efforts with negative pleural pressure swings normally produce an inspiratory increase in venous return to the RV and then to the lungs. The amount that can return is limited by the collapse of the vena cava at around atmospheric pressure where they enter the thoracic cavity. This collapse occurs because when the pressure inside floppy veins becomes less than the pressure surrounding them, outflow becomes limited (Permutt and Riley 1963). This has a protective action for the lungs because it limits inspiratory overfilling of the LV and production of excessive pulmonary capillary hydrostatic pressures. The greater the CVP before the onset of inspiration, the greater the potential “bolus” that can be delivered to the lungs with each breath. Thus elevation of CVP increases the potential venous return with inspiration.

Secondly, respiratory drive is typically increased in shock because of lactate acidemia, hypoxemia, and central drive from activation of pulmonary afferents from an increase in pulmonary water. The increased respiratory effort creates a greater reduction in pleural pressure with each breath, and more breaths per minute, which further can increase the inspiratory fluid bolus to the lungs. The lungs become increasingly more congested, work of breathing goes up, and respiratory failure can ensue. Negative pleural pressure also increases the afterload on the LV (Magder et al. 1983), and the more marked the inspiratory fall in pleural pressure with increasing pulmonary congestion, the greater the effect. The increased LV diameter with dilation from the inspiratory afterload also increases myocardial oxygen demand.

If spontaneous breathing with negative pleural pressure swings can exacerbate pulmonary edema in cardiogenic shock, it should be evident that the positive pressure breathing could be therapeutic, mainly because it will decrease this inspiratory increase. This indeed was demonstrated by Bersten et al. who applied a continuous positive pressure mask (CPAP) to patients with acute heart failure and reduced the time to stabilization (Bersten et al. 1991). The most likely major effect of the positive pressure is that it shifts the heart to the right relative of the venous return function and thus decompresses the right heart. It might be thought that this would decrease venous return, but in someone who is in shock with pulmonary edema, most often the venous return curve intersects the flat part of the cardiac function curve, in what can be called wasted preload (i.e., steep part of the diastolic passive filling curve or plateau of the cardiac function curve). Thus the positive pressure inflations decrease diastolic wall tension without necessarily changing stroke volume. In a sense, the positive pleural pressure acts like the historical rotating tourniquets or phlebotomy. The positive pressure also recruits atelectatic lungs, which improves lung compliance, and reduces the inspiratory effort. It thereby decreases the inspiratory increase in right heart filling and inspiratory afterload on the LV. The assist component likely is better when an inspiratory assist is combined with positive end-expiratory pressure (i.e., BiPAP versus just CPAP). Reduction

of atelectasis and the consequent improvement in oxygenation also can decrease hypoxic vasoconstriction. Finally, the improvement in ventilation and decrease in PCO_2 decrease patient anxiety, and the decrease in the work of breathing decreases the blood flow needs of the respiratory muscles. This has been shown to result in an increase in blood flow to other parts of the body (Rutledge et al. 1985; Hussain et al. 1990a, b).

Although positive pressure ventilation has benefits in cardiogenic shock, there is the potential for harm. Use of excessive transpulmonary pressure can potentially produce nonzone III conditions in the lung in which case alveolar pressure becomes the load on the RV. If excessive, this reduces RV function and worsens the shock. To avoid this, tidal volume should be kept in the 6 ml/kg range, and the driving pressure should be less than 15 cmH₂O. Another potential problem is that if the pleural pressure is increased too much, vascular volume needs to increase to maintain the needed pressure difference from peripheral veins to the right atrium, and the consequent rise in venous pressures can compromise upstream organs such as the kidney, bowel, and liver. The excess volume also can be a potential problem when weaning positive pressure ventilation (Lemaire et al. 1988). In these cases, positive pressure ventilation must be reduced in steps to give time for the excess volume to be excreted because otherwise the depressed LV will have trouble handling the rise in venous return with the decrease in pleural pressure.

Summary

The primary problem in cardiogenic shock is that delivery of O_2 and metabolites and the clearance of the products of metabolism are insufficient for normal organ function. The fundamental requirement in cardiogenic shock is to restore a sufficient cardiac output for tissue needs. This does not necessarily mean that the flow has to be normal; flow just needs to be enough to prevent progressive deterioration. It is even possible that efforts to try to restore complete normality, at least in the acute phase, are harmful. It needs to

be remembered that pressure is not flow and that too much emphasis on an arterial pressure target can lead to increased stress on the injured heart, as well as increase the heart's energy requirements when the delivery of this energy already is compromised. Careful hemodynamic monitoring, especially with some measurement of cardiac output, should be an essential part of the rational management and choice of therapeutic devices in patients with cardiogenic shock. This approach allows for individualized treatment of patients based on the details of their own pathophysiology.

References

- Alexander JH, Reynolds HR, Stebbins AL, Dzavik V, Harrington RA, Van de Werf F, et al. Effect of tilarginine acetate in patients with acute myocardial infarction and cardiogenic shock: the TRIUMPH randomized controlled trial. *JAMA*. 2007;297(15):1657–66.
- Allen LA, Rogers JG, Warnica JW, DiSalvo TG, Tasissa G, Binanay C, et al. High mortality without ESCAPE: the registry of heart failure patients receiving pulmonary artery catheters without randomization. *J Card Fail*. 2008;14(8):661–9.
- Anname D, Vignon P, Renault A, Bollaert PE, Charpentier C, Martin C, et al. Norepinephrine plus dobutamine versus epinephrine alone for management of septic shock: a randomised trial. *Lancet*. 2007;370(9588):676–84.
- Atherton JJ, Thomson HL, Moore TD, Wright KN, Muehle GWF, Fitzpatrick LE, et al. Diastolic ventricular interaction. A possible mechanism for abnormal vascular responses during volume unloading in heart failure. *Circulation*. 1997a;96:4273–9.
- Atherton JJ, Moore TD, Lele SS, Thomson HL, Galbrath AJ, Belenkie I, et al. Diastolic ventricular interaction in chronic heart failure. *Lancet*. 1997b;349:1720–4.
- Auffret V, Loirat A, Leurent G, Martins RP, Filippi E, Coudert I, et al. High-degree atrioventricular block complicating ST segment elevation myocardial infarction in the contemporary era. *Heart*. 2016;102(1):40–9.
- Auffret V, Cottin Y, Leurent G, Gilard M, Beer JC, Zabalawi A, et al. Predicting the development of in-hospital cardiogenic shock in patients with ST-segment elevation myocardial infarction treated by primary percutaneous coronary intervention: the ORBI risk score. *Eur Heart J*. 2018;39(22):2090–102.
- Baran DA, Grines CL, Bailey S, Burkhoff D, Hall SA, Henry TD, et al. SCAI clinical expert consensus statement on the classification of cardiogenic shock: this document was endorsed by the American College of Cardiology (ACC), the American Heart Association (AHA), the Society of Critical Care Medicine (SCCM), and the Society of Thoracic Surgeons (STS) in April 2019. *Catheter Cardiovasc Interv*. 2019;94(1):29–37.
- Basir MB, Kapur NK, Patel K, Salam MA, Schreiber T, Kaki A, et al. Improved outcomes associated with the use of shock protocols: updates from the National Cardiogenic Shock Initiative. *Catheter Cardiovasc Interv*. 2019;93(7):1173–83.
- Bayram M, De Luca L, Massie MB, Gheorghide M. Reassessment of dobutamine, dopamine, and milrinone in the management of acute heart failure syndromes. *Am J Cardiol*. 2005;96(6A):47G–58G.
- Berg DD, Bohula EA, van Diepen S, Katz JN, Alviar CL, Baird-Zars VM, et al. Epidemiology of shock in contemporary cardiac intensive care units. *Circ Cardiovasc Qual Outcomes*. 2019;12(3):e005618.
- Bersten AD, Holt AW, Vedig AE, Skowronski GA, Baggoley CJ. Treatment of severe cardiogenic pulmonary edema with continuous positive airway pressure delivered by face mask. *N Engl J Med*. 1991;325(26):1825.
- Beyar R, Sideman S. Model for left ventricular contraction combining the force length velocity relationship with the time varying elastance theory. *Biophys J*. 1984;45(6):1167–77.
- Braunwald E, Wagner HN Jr. The pressor effect of the antidiuretic principle of the posterior pituitary in orthostatic hypotension. *J Clin Invest*. 1956;35(12):1412–8.
- Brooks GA. The tortuous path of lactate shuttle discovery: from cinders and boards to the lab and ICU. *J Sport Health Sci*. 2020;9(5):446–60.
- Chong LYZ, Satya K, Kim B, Berkowitz R. Milrinone dosing and a culture of caution in clinical practice. *Cardiol Rev*. 2018;26(1):35–42.
- Connors AF Jr, Speroff T, Dawson NV, Thomas C, Harrell FE Jr, Wagner D, et al. The effectiveness of right heart catheterization in the initial care of critically ill patients. SUPPORT Investigators. *JAMA*. 1996;276(11):889–97.
- Cooper DJ, Walley KR, Wiggs BR, Russell JA. Bicarbonate does not improve hemodynamics in critically ill patients who have lactic acidosis. A prospective, controlled clinical study. *Ann Intern Med*. 1990;112(7):492–8.
- Cotter G, Kaluski E, Milo O, Blatt A, Salah A, Hendler A, et al. LINCOS: L-NAME (a NO synthase inhibitor) in the treatment of refractory cardiogenic shock: a prospective randomized study. *Eur Heart J*. 2003;24(14):1287–95.
- Cowley AW Jr, Monos E, Guyton AC. Interaction of vasopressin and the baroreceptor reflex system in the regulation of arterial blood pressure in the dog. *Circ Res*. 1974;34(4):505–14.
- Datta P, Magder S. Hemodynamic response to norepinephrine with and without inhibition of nitric oxide synthase in porcine endotoxemia. *Am J Resp Crit Care Med*. 1999;160(6):1987–93.
- De BD, Biston P, Devriendt J, Madl C, Chochrad D, Aldecoa C, et al. Comparison of dopamine and nor-

- epinephrine in the treatment of shock. *N Engl J Med.* 2010;362(9):779–89.
- Deschamps A, Magder S. Baroreflex control of regional capacitance and blood flow distribution with or without alpha adrenergic blockade. *J Appl Physiol.* 1992;263:H1755–H63.
- Fang J, Mensah GA, Alderman MH, Croft JB. Trends in acute myocardial infarction complicated by cardiogenic shock, 1979–2003, United States. *Am Heart J.* 2006;152(6):1035–41.
- Forrester JS, Diamond G, McHugh TJ, Swan HJ. Filling pressures in the right and left sides of the heart in acute myocardial infarction. A reappraisal of central-venous-pressure monitoring. *N Engl J Med.* 1971;285(4):190–3.
- Global Use of Strategies to Open Occluded Coronary Arteries in Acute Coronary Syndromes (GUSTO IIb) Angioplasty Substudy Investigators. A clinical trial comparing primary coronary angioplasty with tissue plasminogen activator for acute myocardial infarction. *N Engl J Med.* 1997;336(23):1621–8.
- Goldberg RJ, Makam RC, Yarzelski J, McManus DD, Lessard D, Gore JM. Decade-long trends (2001–2011) in the incidence and hospital death rates associated with the in-hospital development of cardiogenic shock after acute myocardial infarction. *Circ Cardiovasc Qual Outcomes.* 2016;9(2):117–25.
- Granzier H, Kellerermayer M, Helmes M, Trombitás K. Titin elasticity and mechanism of passive force development in rat cardiac myocytes probed by thin-filament extraction. *Biophys J.* 1997;73(4):2043–53.
- Guyton AC. Determination of cardiac output by equating venous return curves with cardiac response curves. *Physiol Rev.* 1955;35:123–9.
- Hainsworth R, Karim F. Responses of abdominal vascular capacitance in the anaesthetized dog to changes in the carotid sinus pressure. *J Physiol London.* 1976;262:659–77.
- Hajjar LA, Vincent JL, Barbosa Gomes Galas FR, Rhodes A, Landoni G, Osawa EA, et al. Vasopressin versus norepinephrine in patients with vasoplegic shock after cardiac surgery: the VANCS randomized controlled trial. *Anesthesiology.* 2017;126(1):85–93.
- Harjola VP, Lassus J, Sionis A, Køber L, Tarvasmäki T, Spinar J, et al. Clinical picture and risk prediction of short-term mortality in cardiogenic shock. *Eur J Heart Fail.* 2015;17(5):501–9.
- Harjola VP, Mebazaa A, Celutkiene J, Bettex D, Bueno H, Chioncel O, et al. Contemporary management of acute right ventricular failure: a statement from the Heart Failure Association and the Working Group on Pulmonary Circulation and Right Ventricular Function of the European Society of Cardiology. *Eur J Heart Fail.* 2016;18(3):226–41.
- Hasdai D, Harrington RA, Hochman JS, Califf RM, Battler A, Box JW, et al. Platelet glycoprotein IIb/IIIa blockade and outcome of cardiogenic shock complicating acute coronary syndromes without persistent ST-segment elevation. *J Am Coll Cardiol.* 2000a;36(3):685–92.
- Hasdai D, Topol EJ, Califf RM, Berger PB, Holmes DR Jr. Cardiogenic shock complicating acute coronary syndromes. *Lancet.* 2000b;356(9231):749–56.
- Hernandez GA, Lemor A, Blumer V, Rueda CA, Zalawadiya S, Stevenson LW, et al. Trends in utilization and outcomes of pulmonary artery catheterization in heart failure with and without cardiogenic shock. *J Card Fail.* 2019;25(5):364–71.
- Hirakawa S, Ito H, Sahashi T, Takai K, Wada H. Effects of milrinone on systemic capacitance vessels in relation to venous return and right ventricular pump function. *J Cardiovasc Pharmacol.* 1992;19(1):96–101.
- Hochman JS. Cardiogenic shock complicating acute myocardial infarction: expanding the paradigm. *Circulation.* 2003;107(24):2998–3002.
- Hochman Judith S, Boland J, Sleeper Lynn A, Porway M, Brinker J, Col J, et al. Current spectrum of cardiogenic shock and effect of early revascularization on mortality. *Circulation.* 1995;91(3):873–81.
- Hochman JS, Sleeper LA, Webb JG, Sanborn TA, White HD, Talley JD, et al. Early revascularization in acute myocardial infarction complicated by cardiogenic shock. SHOCK Investigators. Should we emergently revascularize occluded coronaries for cardiogenic shock. *N Engl J Med.* 1999;341(9):625–34.
- Hochman JS, Sleeper LA, White HD, Dzavik V, Wong SC, Menon V, et al. One-year survival following early revascularization for cardiogenic shock. *JAMA.* 2001;285(2):190–2.
- Hochman JS, Sleeper LA, Webb JG, Dzavik V, Buller CE, Aylward P, et al. Early revascularization and long-term survival in cardiogenic shock complicating acute myocardial infarction. *JAMA.* 2006;295(21):2511–5.
- Honda H, Kinbara K, Tani J, Ogimura T, Koiwa Y, Takishima T. Simulation study on heart failure: effects of contractility on cardiac function. *Med Eng Phys.* 1994;16(1):39–46.
- Hussain S, Magder S, Chatillon A, Roussos C. Chemical activation of thin-fibre phrenic afferents: 1) The respiratory responses. *J Appl Physiol.* 1990a;69(3):1002–11.
- Hussain S, Chatillon A, Comtois A, Roussos C, Magder SA. Chemical activation of thin-fiber phrenic afferents: the vascular responses. *Am Rev Respir Dis.* 1990b;141:A64.
- Jaber S, Paugam C, Futier E, Lefrant J-Y, Lasocki S, Lescot T, et al. Sodium bicarbonate therapy for patients with severe metabolic acidemia in the intensive care unit (BICAR-ICU): a multicentre, open-label, randomised controlled, phase 3 trial. *Lancet (London, England).* 2018;392(10141):31–40.
- Jain A, Shroff SG, Janicki JS, Reddy HK, Weber KT. Relation between mixed venous oxygen saturation and cardiac index. Nonlinearity and normalization for oxygen uptake and hemoglobin. *Chest.* 1991;99(6):1403–9.
- Jaski BE, Fifer MA, Wright RF, Braunwald E, Colucci WS. Positive inotropic and vasodilator actions of milrinone in patients with severe congestive heart failure. Dose-response relationships and comparison to nitroprusside. *J Clin Invest.* 1985;75(2):643–9.

- Jeger RV, Radovanovic D, Hunziker PR, Pfisterer ME, Stauffer JC, Erne P, et al. Ten-year trends in the incidence and treatment of cardiogenic shock. *Ann Intern Med.* 2008;149(9):618–26.
- John R, Liao K, Lietz K, Kamdar F, Colvin-Adams M, Boyle A, et al. Experience with the Levitronix CentriMag circulatory support system as a bridge to decision in patients with refractory acute cardiogenic shock and multisystem organ failure. *J Thorac Cardiovasc Surg.* 2007;134(2):351–8.
- Kass DA, Maughan WL, Guo ZM, Kono A, Sunagawa K, Sagawa K. Comparative influence of load versus inotropic states on indexes of ventricular contractility: experimental and theoretical analysis based on pressure-volume relationships. *Circulation.* 1987;76(6):1422–36.
- Kass DA, Marino P, Maughan WL, Sagawa K. Determinants of end-systolic pressure-volume relations during acute regional ischemia in situ. *Circulation.* 1989;80(6):1783–94.
- Katz DH, Sabe MA. Mechanical circulatory support. In: Askari AT, Messerli AW, editors. *Cardiovascular hemodynamics: an introductory guide.* Cham: Springer International Publishing; 2019. p. 117–33.
- Kellum JA, Decker JM. Use of dopamine in acute renal failure: a meta-analysis. *Crit Care Med.* 2001;29(8):1526–31.
- Kohsaka S, Menon V, Lowe AM, Lange M, Dzavik V, Sleeper LA, et al. Systemic inflammatory response syndrome after acute myocardial infarction complicated by cardiogenic shock. *Arch Intern Med.* 2005;165(14):1643–50.
- Landry DW, Oliver JA. The pathogenesis of vasodilatory shock. *N Engl J Med.* 2001;345(8):588–95.
- Lee DS, Gona P, Albano I, Larson MG, Benjamin EJ, Levy D, et al. A systematic assessment of causes of death after heart failure onset in the community: impact of age at death, time period, and left ventricular systolic dysfunction. *Circ Heart Fail.* 2011;4(1):36–43.
- Lemaire F, Teboul JL, Cinotti L, Giotto G, Arbrout F, Steg G, et al. Acute left ventricular dysfunction during unsuccessful weaning from mechanical ventilation. *Anesthesiology.* 1988;69:171–9.
- Léopold V, Gayat E, Pirracchio R, Spinar J, Parenica J, Tarvasmäki T, et al. Epinephrine and short-term survival in cardiogenic shock: an individual data meta-analysis of 2583 patients. *Intensive Care Med.* 2018;44(6):847–56.
- Levy B, Clere-Jehl R, Legras A, Morichau-Beauchant T, Leone M, Frederique G, et al. Epinephrine versus norepinephrine for cardiogenic shock after acute myocardial infarction. *J Am Coll Cardiol.* 2018;72(2):173–82.
- Lim HS, Howell N, Ranasinghe A. The physiology of continuous-flow left ventricular assist devices. *J Card Fail.* 2017;23(2):169–80.
- Lindsey AW, Banahan BF, Cannon RH, Guyton AC. Pulmonary blood volume of the dog and its changes in acute heart failure. *Am J Phys.* 1957;190(1):45–8.
- Lopez A, Lorente JA, Steingrub J, Bakker J, McLuckie A, Willatts S, et al. Multiple-center, randomized, placebo-controlled, double-blind study of the nitric oxide synthase inhibitor 546C88: effect on survival in patients with septic shock. *Crit Care Med.* 2004;32(1):21–30.
- Maekawa K, Liang CS, Hood WB Jr. Comparison of dobutamine and dopamine in acute myocardial infarction. Effects of systemic hemodynamics, plasma catecholamines, blood flows and infarct size. *Circulation.* 1983;67(4):750–9.
- Magder S. Phenylephrine and tangible bias. *Anesth Analg.* 2011;113(2):211–3.
- Magder SA. The ups and downs of heart rate. *Crit Care Med.* 2012a;40(1):239–45.
- Magder S. An approach to hemodynamic monitoring: Guyton at the bedside. *Crit Care.* 2012b;16:236–43.
- Magder SA. The highs and lows of blood pressure: toward meaningful clinical targets in patients with shock. *Crit Care Med.* 2014;42(5):1241–51.
- Magder S. Flow-directed vs. goal-directed strategy for management of hemodynamics. *Curr Opin Crit Care.* 2016;22(3):267–73.
- Magder S, Bafaqeeh F. The clinical role of central venous pressure measurements. *J Intensive Care Med.* 2007;22(1):44–51.
- Magder S, De Varennes B. Clinical death and the measurement of stressed vascular volume. *Crit Care Med.* 1998;26:1061–4.
- Magder S, Guerard B. Heart-lung interactions and pulmonary buffering: lessons from a computational modeling study. *Respir Physiol Neurobiol.* 2012;182(2–3):60–70.
- Magder S, Samoukovic G. Sodium bicarbonate for severe metabolic acidemia. *Lancet (London, England).* 2019;393(10179):1414.
- Magder SA, Lichtenstein S, Adelman AG. Effects of negative pleural pressure on left ventricular hemodynamics. *Am J Cardiol.* 1983;52(5):588–93.
- Magder S, Veerassamy S, Bates JH. A further analysis of why pulmonary venous pressure rises after the onset of LV dysfunction. *J Appl Physiol.* 2009;106(1):81–90.
- Marinosci GZ, De Robertis E, De Benedictis G, Piazza O. Dopamine use in intensive care: are we ready to turn it down? *Transl Med UniSa.* 2012;4:90–4.
- Mehta S, Javeshghani D, Datta P, Levy RD, Magder S. Porcine endotoxaemic shock is associated with increased expired nitric oxide. *Crit Care Med.* 1999;27(2):385–93.
- Menon V, Slater JN, White HD, Sleeper LA, Cocke T, Hochman JS. Acute myocardial infarction complicated by systemic hypoperfusion without hypotension: report of the SHOCK trial registry. *Am J Med.* 2000a;108(5):374–80.
- Menon V, White H, LeJemtel T, Webb JG, Sleeper LA, Hochman JS. The clinical profile of patients with suspected cardiogenic shock due to predominant left ventricular failure: a report from the SHOCK Trial Registry. Should we emergently revascularize Occluded Coronaries in cardiogenic shock? *J Am Coll Cardiol.* 2000b;36(3 Suppl A):1071–6.
- Moncada S, Higgs A. The L-arginine-nitric oxide pathway. *N Engl J Med.* 1993;329(27):2002–12.

- Myburgh JA, Higgins A, Jovanovska A, Lipman J, Ramakrishnan N, Santamaria J, et al. A comparison of epinephrine and norepinephrine in critically ill patients. *Intensive Care Med.* 2008;34(12):2226–34.
- Nash CW, Wolff SA, Ferguson BA. Release of tritiated noradrenaline from perfused rat hearts by sympathomimetic amines. *Can J Physiol Pharmacol.* 1968;46(1):35–42.
- Pandey A, Khera R, Kumar N, Golwala H, Girotra S, Fonarow GC. Use of pulmonary artery catheterization in US patients with heart failure, 2001–2012. *JAMA Intern Med.* 2016;176(1):129–32.
- Parillo JE. Pathogenetic mechanisms of septic shock. *N Engl J Med.* 1993;328(20):1471–7.
- Parker MM, Shelhamer JH, Natanson C, Alling DW, Parillo JE. Serial cardiovascular variables in survivors and nonsurvivors of human septic shock: heart rate as an early predictor of prognosis. *Crit Care Med.* 1987;15:923–9.
- Patterson SW, Piper H, Starling EH. The regulation of the heart beat. *J Physiol.* 1914;48(6):465–513.
- Permutt S, Riley S. Hemodynamics of collapsible vessels with tone: the vascular waterfall. *J Appl Physiol.* 1963;18(5):924–26.
- Pöss J, Köster J, Fuernau G, Eitel I, de Waha S, Ouarrak T, et al. Risk stratification for patients in cardiogenic shock after acute myocardial infarction. *J Am Coll Cardiol.* 2017;69(15):1913–20.
- Potter BJ, Deverenne B, Doucette S, Fergusson D, Magder S. Cardiac output responses in a flow-driven protocol of resuscitation following cardiac surgery. *J Crit Care.* 2013;28(3):265–9.
- Ruffolo RR Jr, Messick K. Effects of dopamine, (+)-dopamine and the (+) and (-)-enantiomers of dobutamine on cardiac function in pithed rats. *J Pharmacol Exp Ther.* 1985;235(3):558–65.
- Russell JA. Management of sepsis. *N Engl J Med.* 2006;355(16):1699–713.
- Russell JA. Vasopressor therapy in critically ill patients with shock. *Intensive Care Med.* 2019;45(11):1503–17.
- Russell JA, Walley KR, Singer J, Gordon AC, Hébert PC, Cooper DJ, et al. Vasopressin versus norepinephrine infusion in patients with septic shock. *N Engl J Med.* 2008;358(9):877–87.
- Rutledge F, Hussain S, Roussos C, Magder SA. Diaphragmatic blood flow and oxygen delivery in pulmonary edema and hypotension. *Clin Invest Med.* 1985;8:183.
- Sagawa K. The ventricular pressure-volume diagram revisited. *Circ Res.* 1978;43:677–87.
- Sato R, Ariyoshi N, Hasegawa D, Crossey E, Hamahata N, Ishihara T, et al. Effects of inotropes on the mortality in patients with septic shock. *J Intensive Care Med.* 2019. <https://doi.org/10.1177/885066619892218>.
- Schmidt M, Burrell A, Roberts L, Bailey M, Sheldrake J, Rycus PT, et al. Predicting survival after ECMO for refractory cardiogenic shock: the survival after veno-arterial-ECMO (SAVE)-score. *Eur Heart J.* 2015;36(33):2246–56.
- Shah M, Patnaik S, Patel B, Ram P, Garg L, Agarwal M, et al. Trends in mechanical circulatory support use and hospital mortality among patients with acute myocardial infarction and non-infarction related cardiogenic shock in the United States. *Clin Res Cardiol.* 2018;107(4):287–303.
- Shah AH, Puri R, Kalra A. Management of cardiogenic shock complicating acute myocardial infarction: a review. *Clin Cardiol.* 2019;42(4):484–93.
- Sheu JJ, Tsai TH, Lee FY, Fang HY, Sun CK, Leu S, et al. Early extracorporeal membrane oxygenator-assisted primary percutaneous coronary intervention improved 30-day clinical outcomes in patients with ST-segment elevation myocardial infarction complicated with profound cardiogenic shock. *Crit Care Med.* 2010;38(9):1810–7.
- Singh M, White J, Hasdai D, Hodgson PK, Berger PB, Topol EJ, et al. Long-term outcome and its predictors among patients with ST-segment elevation myocardial infarction complicated by shock: insights from the GUSTO-I trial. *J Am Coll Cardiol.* 2007;50(18):1752–8.
- Singh T, Samson R, Ayinapudi K, Motwani A, Le Jemtel TH. Precardiogenic shock: a new clinical entity. *Cardiol Rev.* 2019;27(4):198–201.
- Sionis A, Rivas-Lasarte M, Mebazaa A, Tarvasmäki T, Sans-Roselló J, Tolppanen H, et al. Current use and impact on 30-day mortality of pulmonary artery catheter in cardiogenic shock patients: results from the CardShock study. *J Intensive Care Med.* 2019. <https://doi.org/10.1177/885066619828959>.
- Starling EH. The Linacre lecture of the law of the heart. London: Longmans, Green & Co.; 1918.
- Swan HJC, Ganz W, Forrester J, Marcus H, Diamond G, Chonette D. Catheterization of the heart in man with use of a flow-directed balloon-tipped catheter. *N Engl J Med.* 1970;282(9):447–51.
- Sylvester JT, Goldberg HS, Permutt S. The role of the vasculature in the regulation of cardiac output. *Clin Chest Med.* 1983a;4(2):111–25.
- Sylvester JT, Mitzner W, Ngeow Y, Permutt S. Hypoxic constriction of alveolar and extra-alveolar vessels in isolated pig lungs. *J Appl Physiol Respir Environ Exerc Physiol.* 1983b;54(6):1660–6.
- Thiele RH, Nemergut EC, Lynch C III. The physiologic implications of isolated alpha 1 adrenergic stimulation. *Anesth Analg.* 2011a;113(2):284–96.
- Thiele RH, Nemergut EC, Lynch C III. The clinical implications of isolated alpha 1 adrenergic stimulation. *Anesth Analg.* 2011b;113(2):297–304.
- Thiele H, Zeymer U, Neumann F-J, Ferenc M, Olbrich H-G, Hausleiter J, et al. Intraaortic balloon support for myocardial infarction with cardiogenic shock. *N Engl J Med.* 2012;367(14):1287–96.
- Thiele H, Zeymer U, Thelemann N, Neumann F-J, Hausleiter J, Abdel-Wahab M, et al. Intraaortic balloon pump in cardiogenic shock complicating acute myocardial infarction: long-term 6-year outcome of the randomized IABP-SHOCK II

- Trial. *Circulation*. 2018. <https://doi.org/10.1161/CIRCULATIONAHA.118.038201>.
- Thiele H, Ohman EM, de Waha-Thiele S, Zeymer U, Desch S. Management of cardiogenic shock complicating myocardial infarction: an update 2019. *Eur Heart J*. 2019;40(32):2671–83.
- Vahdatpour C, Collins D, Goldberg S. Cardiogenic shock. *J Am Heart Assoc*. 2019;8(8):e011991.
- Vail E, Gershengorn HB, Hua M, Walkey AJ, Rubenfeld G, Wunsch H. Association between US norepinephrine shortage and mortality among patients with septic shock. *JAMA*. 2017;317(14):1433–42.
- van Diepen S, Vavalle JP, Newby LK, Clare R, Pieper KS, Ezekowitz JA, et al. The systemic inflammatory response syndrome in patients with ST-segment elevation myocardial infarction. *Crit Care Med*. 2013;41(9):2080–7.
- van Diepen S, Katz JN, Albert NM, Henry TD, Jacobs AK, Kapur NK, et al. Contemporary management of cardiogenic shock: a scientific statement from the American Heart Association. *Circulation*. 2017;136(16):e232–e68.
- Wengenmayer T, Duerschmied D, Graf E, Chiabudini M, Benk C, Muhlschlegel S, et al. Development and validation of a prognostic model for survival in patients treated with venoarterial extracorporeal membrane oxygenation: the PREDICT VA-ECMO score. *Eur Heart J Acute Cardiovasc Care*. 2019;8(4):350–9.
- Westaby S, Kharbanda R, Banning AP. Cardiogenic shock in ACS. Part 1: prediction, presentation and medical therapy. *Nat Rev Cardiol*. 2011;9(3):158–71.
- Wilmshurst PT, Thompson DS, Jenkins BS, Coltart DJ, Webb-Peploe MM. Haemodynamic effects of intravenous amrinone in patients with impaired left ventricular function. *Br Heart J*. 1983;49(1):77–82.
- Zeller M, Cottin Y, Brindisi MC, Dentan G, Laurent Y, Janin-Manificat L, et al. Impaired fasting glucose and cardiogenic shock in patients with acute myocardial infarction. *Eur Heart J*. 2004;25(4):308–12.



Cardiogenic Shock Part 2: Mechanical Devices for Cardiogenic Shock

51

Sheldon Magder and Gordan Samoukovic

Introduction

For many years use of mechanical support devices for cardiogenic shock was largely confined to the intra-aortic balloon pump (IABP) and large paracorporeal devices implanted centrally through a sternotomy or thoracotomy (Kirklin and Naftel 2008). Over the last two decades, there has been rapid development of more portable devices for both shorter- and longer-term management. There also has been increasing development of techniques for peripheral implantation of devices, which allow rapid insertion for rescue therapy and early support. These devices have the potential to make major changes in the approach to cardiogenic shock although it also must be emphasized that this potential is not yet established by major studies.

There are four general physiological approaches to the use of mechanical circulatory devices for supporting the circulation in cardiogenic shock (Fig. 51.1) (Burkhoff et al. 2015; Mandawat and Rao 2017). (1) The device can decrease the left

ventricle (LV) afterload and thereby ease LV ejection while at the same time increasing diastolic pressure and coronary perfusion; this is done with the IABP (Fig. 51.1 #1). (2) The device can decompress or off-load the LV by propelling blood out of the ventricle. These devices are considered left ventricular assist devices (LVADs). One such system is Impella Recover® micro-axial devices (Abiomed, Aachen, Germany) in which a pump is positioned across the aortic valve; it draws blood from the LV and injects it into the aorta (Fig. 51.1 #2a). These devices can be inserted percutaneously or by cutdown on a vessel and positioned with fluoroscopic and echocardiographic guidance depending upon the size of the device. The other approach is to surgically implant a conduit in the LV and drain blood into an external device such as the CentriMag® (Levitronix, Waltham, MA, USA) that pumps the blood back into the aorta (Fig. 51.1 #2b). (3) The device can decompress the LV by reducing its filling. This is accomplished by advancing a catheter through a large vein to the right atrium and then puncturing the intra-atrial septum to pass the catheter into the left atrium (Fig. 51.1 #3). Blood is drawn from the left atrium by an external pump and returned to the arterial vasculature through a peripheral arterial cannula; this is the basis of TandemHeart® p-VAD (CardiacAssist Inc., Pittsburgh, PA, USA). (4) The device can take over the total function of the heart and lungs and maintain systemic perfusion and oxygenation by draining blood from the venous circulation, passing it through an extracorporeal circuit with a

S. Magder (✉)

Royal Victoria Hospital (McGill University Health Centre), Departments of Critical Care and Physiology McGill University, Montreal, QC, Canada
e-mail: sheldon.magder@mcgill.ca

G. Samoukovic

Department of Critical Care, Royal Victoria Hospital – McGill University and McGill University Health Centre, Montreal, QC, Canada
e-mail: gordan.samoukovic@mcgill.ca

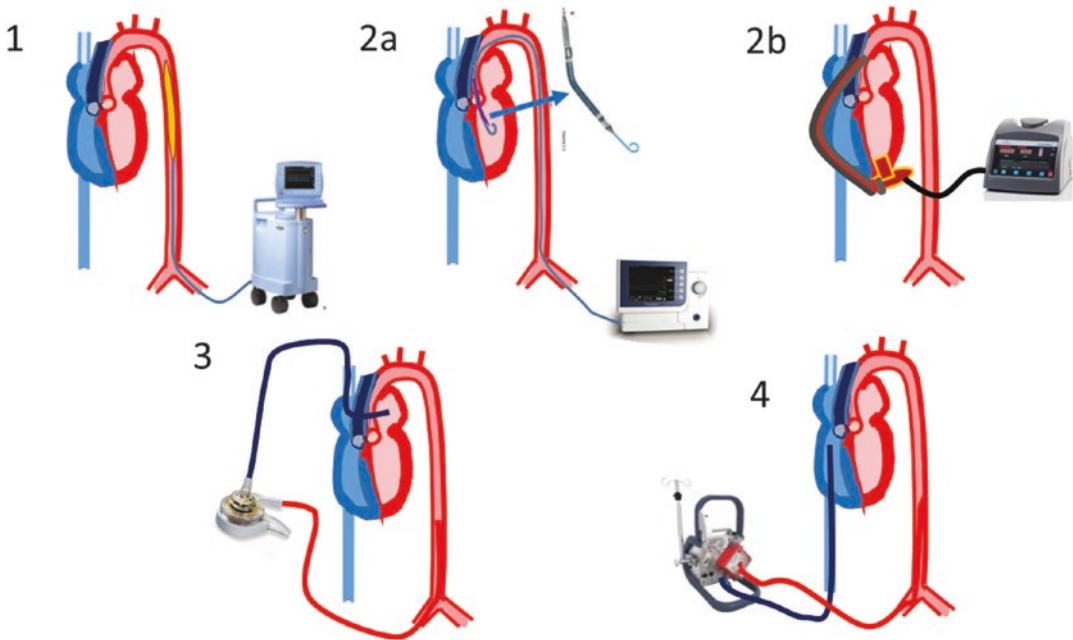


Fig. 51.1 Four main types of left ventricular support. 1. Intra-aortic balloon pump. 2a. Trans-aortic LV pump (Impella®) – percutaneous or vascular cutdown. 2b. Pump surgically implanted directly on the ventricle with return of blood to the aorta. 3. Withdrawal of blood from percutaneously inserted catheter in the left atrium and returned

to peripheral artery (TandemHeart®). 4. Complete cardiac support with extracorporeal membrane oxygenator. Blood is withdrawn from a catheter placed centrally, passed through an oxygenator, and returned to the distal aortal through a femoral cannula. See text for more details

membrane oxygenator, and then returning the blood back into the arterial system through either central or peripheral cannulation (ECMO) (Fig. 51.1 #4). This has become much more feasible with the development of the compact Maquet Cardiohelp® system (Maquet Cardiopulmonary AG, Hirrlingen, Germany) hybrid pump oxygenator. In addition, RV support can be added to the LV devices. To do this the device draws blood from the right atrium and pumps it into a cannula positioned in the pulmonary artery (TandemHeart RA-PA, LivaNova, London, UK) or by Impella RP® device (Abiomed, Danvers, MA, USA) which is inserted through a large vein and positioned across the pulmonary artery.

IABP

The earliest cardiac support device (Scheidt et al. 1973; Kantrowitz 1990; Mouloupoulos et al. 1962) was the IABP, and it still is widely used (Khera

et al. 2015; Khera et al. 2016; Kapur and Esposito 2015). It is not difficult to insert, unless the patient has significant peripheral vascular disease. It also is much less costly than the other devices discussed later. Its use markedly decreased following the IABP-SHOCK 2 trial, which failed to demonstrate any benefit with the addition of an IABP to standard care (Thiele et al. 2012). To appreciate the potential clinical role of IABP, it is necessary to understand what it actually does physiologically. The IABP consists of an inflatable balloon that surrounds a catheter inserted through a femoral artery and is advanced to just below the takeoff of the left subclavian artery. In this position the device is below the takeoff of vessels perfusing the brain, thus theoretically (but never studied) reducing stroke risk, but it also is high enough in the aorta avoiding obstruction of renal blood flow. The balloon typically has a volume of 40 ml, which is less than the normal stroke volume. Inflation is synchronized to either the “T” wave of the ECG or

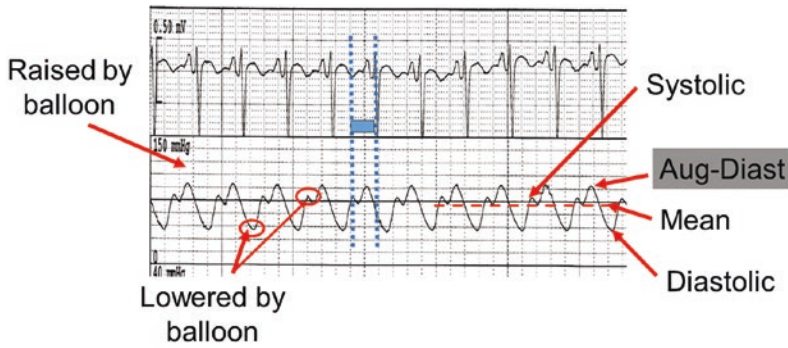


Fig. 51.2 Example of arterial pressure and proper pressure measurement with IABP. The dotted lines and box indicate the period of balloon inflation (note that there is a time delay between fluid-based pressure measurement and the electrical ECG signal). The augmented diastolic pressure is raised by the balloon, and systolic and end-

diastolic pressures are lowered. It is thus preferable to titrate vasopressor therapy to the augmented diastolic pressure than the mean (dashed line) as long as the augmented diastolic pressure is greater than the systolic pressure as in this example. If not, the mean needs to be used because the augmented is not adding much

the diastolic notch of the aortic pulse pressure so that the IABP augments diastolic pressure and potentially increases coronary perfusion (Fig. 51.2). Deflation of the balloon occurs just before the onset of systole and thereby increases the “volume-space” available in the aorta. This transiently decreases the aortic pressure just before the onset of LV ejection and consequently reduces LV afterload, which potentially can increase the ejected stroke volume. Timing of inflation and deflation can be manipulated to maximize the effect of the IABP. No pharmacological agent can do the same as the IABP, that is, decrease LV afterload, but at the same time increase diastolic coronary perfusion pressure. Why then is there limited proven clinical benefit of the IABP (Thiele et al. 2013)?

First, consider the potential range of coronary flow. Coronary flow reserves are the largest of all vascular regions in the body, and so is the myocardial ability to extract O_2 as demonstrated by low hemoglobin O_2 saturations in the coronary sinus (Magder 1986); coronary flow can increase almost fivefold from the coronary flow at resting cardiac output to the flow at maximal exercise. However, the increase in coronary flow cannot occur when epicardial coronary arteries are severely narrowed. Thus, when a proximal coronary artery stenosis is present, augmenting diastolic pressure with an IABP has the potential to maintain coronary perfusion and reduce myocar-

dial ischemia in a failing heart. By the same argument, the IABP is unlikely to have a benefit when the proximal coronary stenosis has been relieved as was the case in SHOCK-IABP. Over 90% of patients were successfully revascularized before insertion of IABP, and thus they had no need for an increased coronary perfusion pressure (Thiele et al. 2012). Furthermore, if mean blood pressure is low in cardiogenic shock, and especially if there is a distributive component to the shock, the diastolic augmentation usually is small, and there likely is little IABP augmentation of coronary flow in these patients (Kolyva et al. 2010).

The second potential benefit from an IABP is reduction of LV afterload and an increase in stroke volume. However, in general, the IABP has a minimal effect on stroke volume. The afterload reduction on stroke volume is very dependent upon the slope of the LV end-systolic pressure-volume relationship, which generally is steep, even in moderate shock. Another limitation is that deflation of the balloon typically decreases the end-diastolic pressure only by 5–10 mmHg, which is a very small reduction compared to normal variations in systolic arterial pressure (Kapur et al. 2015). Consequently, stroke volume is only increased by a few mL on each beat, if at all. Larger balloons have been used, but they only produce a small further decrease in afterload and are associated with more peripheral complications (Kapur et al. 2015).

It is also worth considering how a left-sided device can increase cardiac output. In the steady state, the heart only can pump out what comes back to it. Therefore, there must be either an increase in the upstream mean systemic filling pressure (MSFP) or a decrease in right atrial pressure (Pra) (see cardiogenic shock part 1). Inflation of the balloon essentially adds a transient 40 mL to increase in arterial volume, but this volume rapidly becomes distributed throughout all vascular compartments and would add very little to MSFP which is determined by the large volume in the compliant veins. Furthermore, during balloon deflation, the volume is essentially “lost.” Any potential increase in stroke volume thus must occur from a decrease in Pra (Fig. 51.3). This only can occur if there is a decrease in LV diastolic pressure, leading to a subsequent decrease in left atrial pressure, and pulmonary artery pressure and finally increased RV output and a reduction in Pra. It is more likely that when an IABP increases stroke volume, this occurs because of an increase in coronary perfusion through a tight coronary arterial stenosis and thereby improves overall cardiac contractile function, and that is what lowered Pra.

The afterload reducing effect from the IABP often is further limited because vasopressors are titrated to maintain a mean arterial pressure, which was reduced by the IABP. The vasopressor infusion then offsets the potential benefit of the afterload reduction from balloon deflation. For this reason, in patients with an IABP, as long as the diastolic augmented pressure is greater than the systolic pressure, vasopressors should be titrated based on the augmented diastolic pressure and not the mean arterial pressure (Fig. 51.2).

Although the IABP has little benefit in patients without a major limitation to coronary flow, it can be very effective in patients who have severe acute mitral insufficiency or rupture of the intraventricular septum following an acute myocardial infarction. In these patients, the LV afterload reducing effect can be very significant. From the reasoning above, the benefit is likely more related to the reduction of LV end-diastolic pressure (LVEDP) and the consequent reduction in pulmonary edema than any increase in stroke vol-

ume. This is because at higher LVEDP, the LV diastolic pressure-volume relationship becomes very steep (Fig. 51.3). In that situation, a very small reduction in end-diastolic volume potentially can have a very large effect on LVEDP and thus on pulmonary capillary pressure.

Devices that Support Ventricular Outflow

General Principles

Devices supporting cardiac output can either act as volume displacement pumps, in which case the device provides an alternating vacuum to fill the device and a pressure to eject the blood from the ventricle, or a continuous flow device, which has a constant pressure difference between the inflow and outflow. Currently, 98% of devices are continuous flow pumps. This is because they can be more compact and have lower energy consumption, a lower hemolytic risk, and lower costs (Hosseinipour et al. 2017). There are three types of continuous flow devices: centrifugal, axial, and combined (Fig. 51.4). The advantage of axial pumps is that they can be smaller, but a disadvantage is their relationship of the pressure differences to flow as discussed below. Axial pumps usually have higher rotations per minute (RPM), which can result in more hemolysis, especially when compared to the new magnetically levitating centrifugal pump such as the HeartMate III™³ (St. Jude Medical, Minnesota, USA). However, these are primarily implanted for long-term use (Mehra et al. 2019). Small-sized micro-axial pumps such as the Impella® family inserted percutaneously are the most commonly used pumps for the short-term acute usage.

The interaction of mechanical devices with the native circulation and the heart itself is very complex. It is highly dependent upon design features of the pump but also on the functional status of the patient's heart and circulation. Much of the literature on flow dynamics of mechanical devices is based on isolated models under controlled conditions, often without inclusion of a right heart and the equivalent of the vasculature's large venous compliance. Furthermore, to obtain

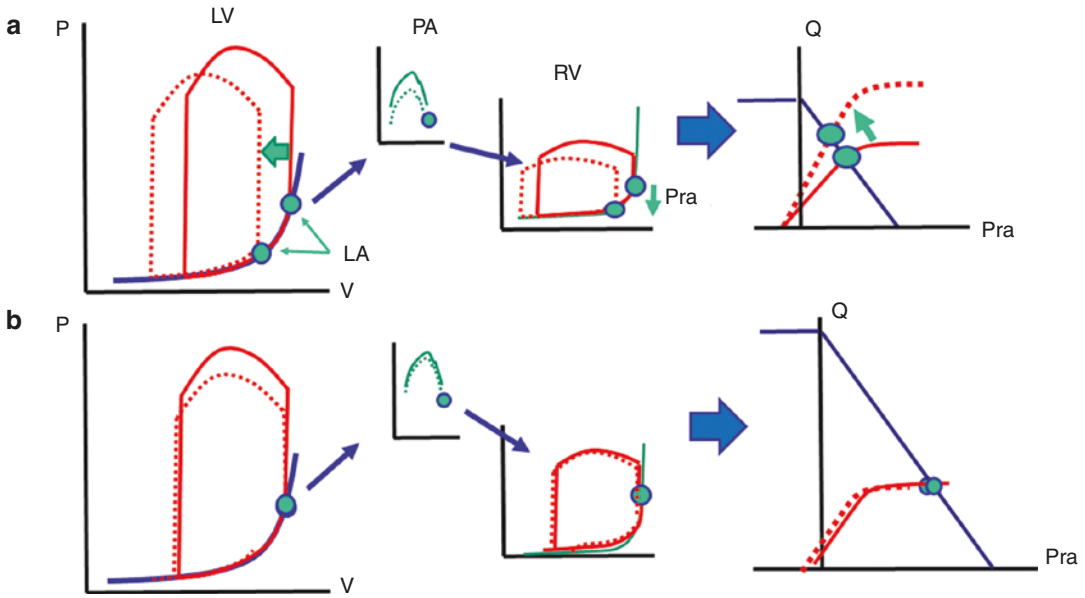


Fig. 51.3 An increase in cardiac output (Q) with an improvement in LV function ultimately requires a decrease in Pra (right atrial pressure or CVP). In (a) reduction in LV afterload, for example, by an IABP requires a fall in left atrial pressure (LA); a fall in PA (pulmonary artery pressure), which decreases RV afterload; a fall in RV end-systolic pressure; and a decrease in Pra. On the venous return-cardiac function curve, the improved pump function shifts the cardiac function upward, and it intersects the venous return curve at a lower Pra. The same

would occur with an increase in heart rate or contractility. In (b), the RV is working on the flat part of its function curve, and Pra is high. Pra is transmitted to the LV so that Pra and LA are the same. Lowering LV afterload or increasing LV output cannot increase stroke volume because more blood cannot come back to the LV. This is because LA pressure is determined by the Pra and Pra does not change because the PA is not reduced because the LA is not reduced. Thus, RV stroke volume does not change, nor can that of the LV

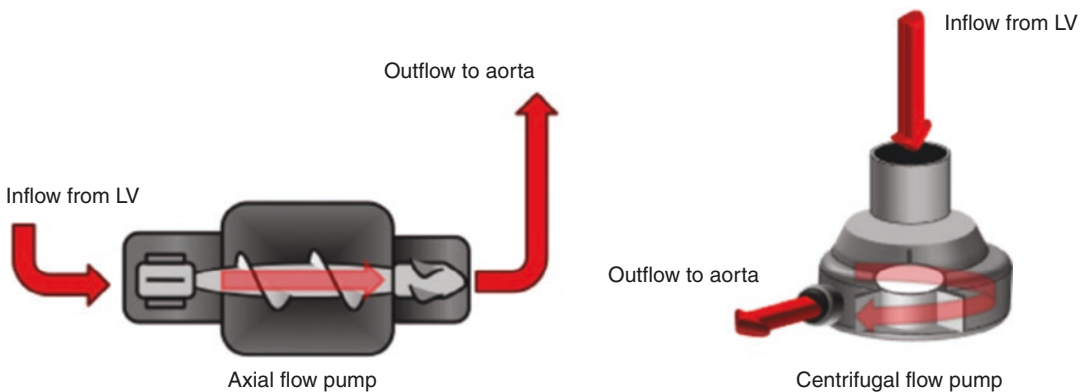


Fig. 51.4 Principle of axial flow pump (left) versus centrifugal. In the axial pump, flow comes out in a straight line. In the centrifugal pump it comes off the side. See text

for details. (From Lim et al. (Lim et al. 2017) Used with permission of Elsevier)

consistent results, studies on patients supported with mechanical devices usually are done when patients are in a relatively stable hemodynamic

state. However, in acute cardiogenic shock the patient’s circulation is constantly changing as the patients intrinsic function improves or worsens.

The device settings, the patient’s blood volume, intrinsic vascular tone, use of exogenous vasoactive drugs, and even the level of sedation and its effect on the patient’s metabolic activity all constantly change.

It is important to begin with a fundamental feature of continuous flow pumps and to first consider the condition in which there is no LV contraction. These pumps generate flow by creating kinetic energy and torque. The energy produced by the pump produces flow that is inversely related to the pressure difference across the pump. To produce the continuous flow, this pressure difference is always present, even when the ventricle is not contracting. However, even though flow is continuous, fluctuations in the pressure across the pump still exist. Some of this is because a beating RV returns blood to the LV with pulsatility, but even without RV activity, small pulsations in the pressure generation by the pump still occur. To understand why, it is important to understand the inverse relationship of flow to the pressure difference across the

pump (Hosseinipour et al. 2017). In axial pumps, the relationship of the pressure difference, also called the pressure head, versus flow generated by the device, is almost a straight line with a negative slope (Fig. 51.5). The greater the pressure difference, the lesser the flow. Centrifugal pumps have a flatter pressure head, which means that at lower values of flow, flows can increase with little change in the pressure difference (Fig. 51.5). For the device to pump, it draws blood from the LV and displaces it into the aorta so that the proximal pressure must decrease and the distal pressure, that is, the pressure in the aorta, must increase. As the pressure difference increases, flow decreases, and the proximal pressure increases. This again increases the flow these actions result in flow oscillations that are relative to rates of emptying and filling of the LV. The pump is programed to compensate for changes in the pressure difference by changing the power (Watts) driving the pump. This is displayed on the monitor and is used to calculate an estimate of the pump flow based on the known

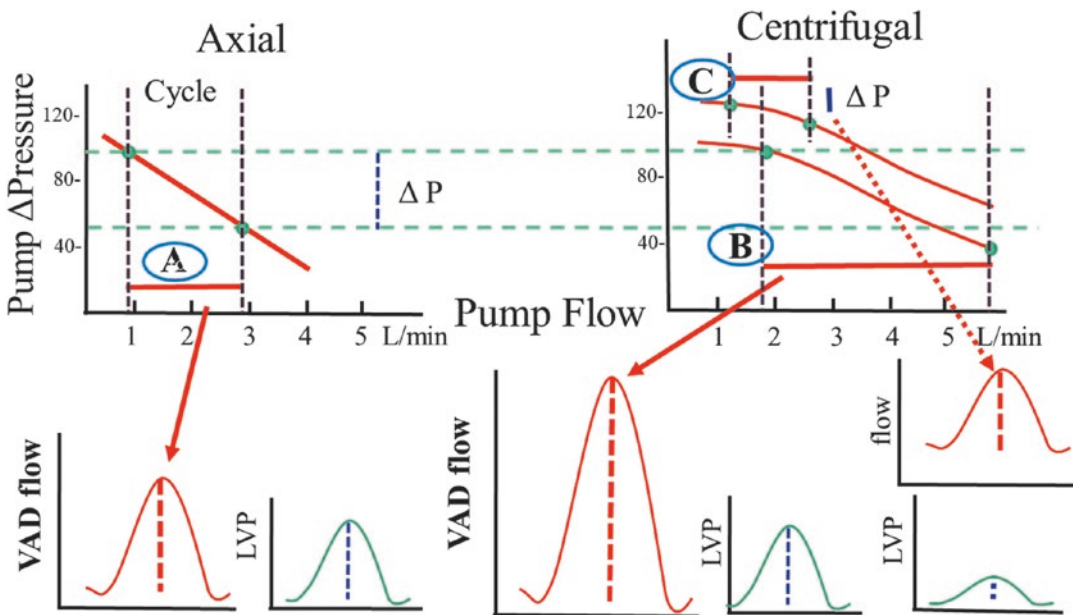


Fig. 51.5 Comparison of axial (left) and centrifugal (right) pumps. The relationship of pressure difference (ΔP) to pump flow (x -axis) is linear in an axial pump but has an initial “flat head” in a centrifugal pump. As a consequence for the same ΔP , a centrifugal pump has a

higher flow variation (circled B) than the axial pump (circled A). Increasing the pump RPM shifts the ΔP relationship upward so that there is a greater mean flow. See text for more details (Lim et al. 2017)

flow-RPM relationship to the pressure difference for each device. However, this estimate is less accurate at lower levels of flow, especially in axial devices. Even though electrical fluctuations are seen on the monitor, there may be no observable fluctuation in the arterial pressure because the fluctuating current is compensating for a range of pressure differences.

When the heart begins to contract, things get much more complicated. During ventricular diastole, the LV pressure is low compared to aortic pressure. Because of the large pressure flow from the pump is low. Because the device crosses the aortic valve, unlike the native LV, the distal end of the device senses arterial pressure throughout the cardiac cycle, thus including diastolic pressure. As arterial pressure falls during diastole, pump flow increases (Fig. 51.6). The magnitude of this increase depends on the magnitude of the aortic pulse pressure. With the onset of systole, the LV cavity pressure rises rapidly, and the pressure difference between the LV and aorta decreases, and pump flow increases. The pump flow adds to the aortic pressure. This offsets some of the increase in flow from the pump because of the now small but increasing pressure difference from the LV to the aorta (Fig. 51.7). There only should be a small effect from the further increase in afterload on the native ventricular flow, and

this only exists after the aortic valve opens, unless the native heart is providing most of the flow, and the maximum end-systolic pressure-volume line is very flattened. If the aortic valve does not open, the rise in aortic pressure only affects the flow from the device. Because of its flatter pressure head, a centrifugal pump produces greater variation in its outflow than an axial pump. This is because the flat pressure head allows more flow over the same pressure difference (Figs. 51.5 and 51.6). It has been argued that arterial pressure fluctuations are important for organ function, especially in the case of durable mechanical devices (Mehra et al. 2019), but this is not well established, and it does not seem to be an issue with short-term use.

The pressure sensitivity of axial versus centrifugal pumps is potentially important when LV diastolic volume is low. Because of its steep pressure difference versus flow relationship, at low LV diastolic pressures, an axial pump may greatly increase suction in the LV to try to maintain flow. This can potentially produce collapse of the ventricular walls around the inflow to the device, which is called latching, and produce hemolysis, arrhythmia, and transient limitation of flow. This is much less of a problem with centrifugal pumps because their flat pressure head does not result in these abrupt suction events. However, this also

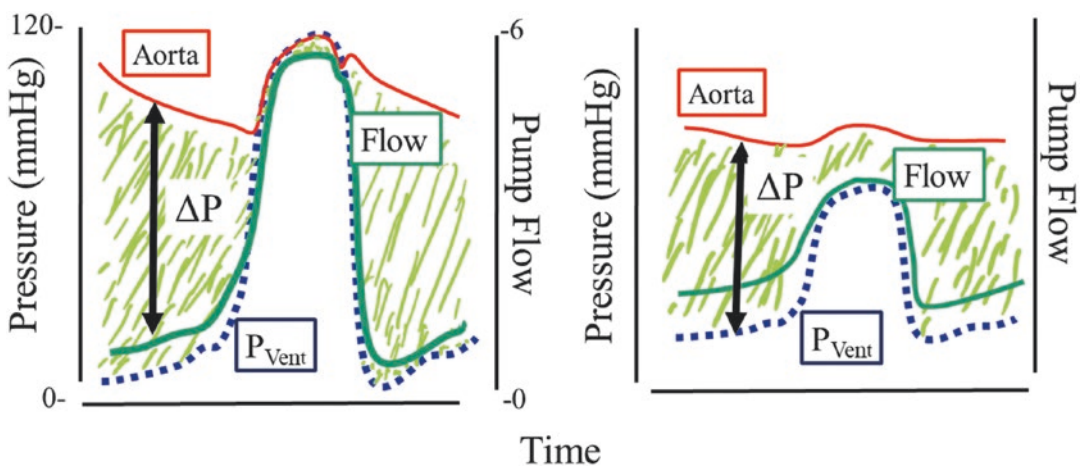


Fig. 51.6 Theoretical ventricular pressure, aortic pressure, pressure head, and pump flow over time. On the left there is enough developed LV pressure (P_{Vent}) to open the

aortic valve. On the right the aortic valve does not open, and there is minimal aortic pulsatility

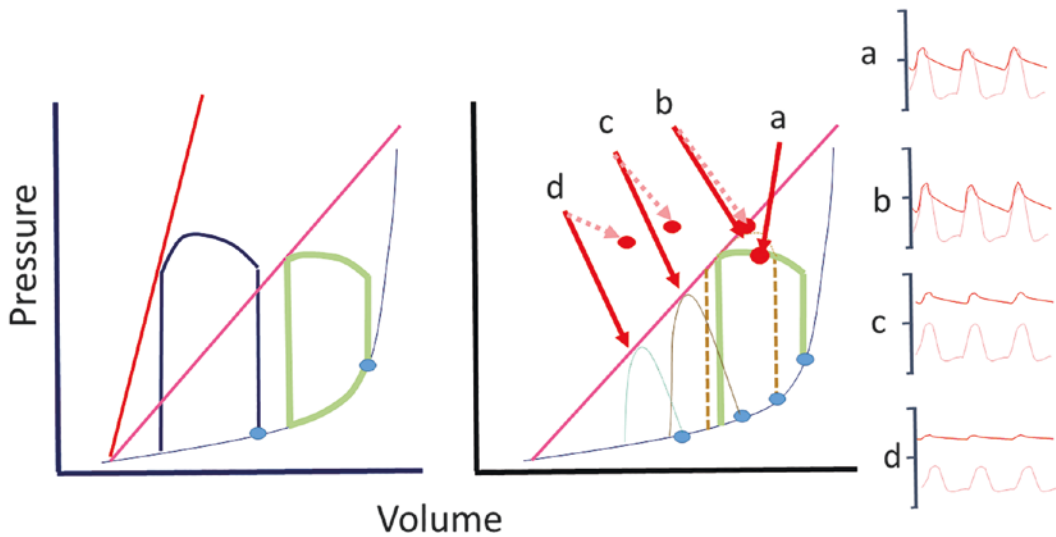


Fig. 51.7 Effect of mechanical assist device on the pressure-volume loop. The left side shows a normal ESPVR and P-V loop and that of a patient with cardiogenic shock and a markedly depressed ESPVR. There is a marked rise in end-diastolic pressure, a moderate decrease in stroke volume. The right side shows the same cardiogenic P-V curve without support (a) and then with progressively increasing LV support with a pump (b to d) (not IABP). The initial support (b) slightly raised arterial pres-

sure and kept the same P-V shape. The closed represent the peak arterial pressure produced by the LV and the pump flow. In C the support has increased sufficiently to lower the generated pressure of the LV below aortic pressure (i.e., valve does not open), and LV isovolumetric contraction no longer produces a perpendicular line because volume is already being ejected. The effect is greater in d. With increasing LV support, the LVEDP decreases indicating reduced LV volume (i.e., LV decompression)

may imply that centrifugal pumps are less effective at decompressing a dilated LV, which is important when there is an acutely injured myocardial because decompression of the heart has been shown to reduce infarct size (Saku et al. 2016, 2018; Kapur et al. 2019).

High arterial pressure reduces flow from the devices because the isovolumetric phase is longer and the time before the pressure gradient is minimized and shortened as a result of LV ejection. The effect of variations in arterial pressure on flow when there are native LV contractions is milder with centrifugal pumps because of their flatter pressure head; this can lead to higher systolic pressures because they continue to eject with the same force despite the pressure rise. The effect of afterload on forward flow from LVADs has been estimated to be three to four times greater than for ejection by the native heart (Lim et al. 2017), and when present, the native heart needs to increase its output to maintain the same cardiac output. This afterload effect on the native

LV function likely is much more significant for patients with long-term use of LVADs. Because these patients are ambulatory, they have greater needs for variations in their native cardiac outputs and potential for greater pressure swing. In the intensive care unit, high arterial pressures can be easily managed because the patient is continuously monitored and SVR can be manipulated with intravenous or oral vasodilators. However, elevated pressures can be also easily missed in the ICU, and these principles must always be considered when acutely managing patients on an LVAD. The 13th International Society for Heart and Lung Transplantation guideline for mechanical circulatory support recommends treatment of a mean arterial pressure greater than 90 mmHg and less than 65 mmHg, although the evidence for this is limited (level C) (Feldman et al. 2013) and is based on chronic and not acute use. Finally, it must be remembered that it is flow and not pressure that matters for the tissues, so

the emphasis should be on keeping the pressure controlled.

The LV diastolic pressure is a complex variable in the function of mechanical hearts. First, diastolic pressure does not indicate volume. The curvilinear diastolic pressure-volume relationship implies that a low diastolic pressure does indicate a low volume; the heart may just be on the normal compliant part of the passive diastolic filling curve (Fig. 51.7). A high diastolic pressure also does not imply that diastolic volume is high; LV compliance could be low and LV diastolic pressure high because the LV is compressed by a very distended RV or other mediastinal structure or because of significant aortic or mitral regurgitation. For the purpose of flow generation by mechanical hearts, diastolic pressure and not volume is what matters because flow is determined by the pressure difference between the LV and the aorta. An increase in LV diastolic pressure reduces the pressure difference between the LV and the aorta, which should increase flow just as happens with the normal Starling function. The devices indeed have a “preload” response, meaning that a higher diastolic filling pressure increases output, but the effect is very small and is only in the range of 0.02–0.1 L/min/mmHg (Khalil et al. 2008). In contrast, the preload response in the native human heart is greater than 0.5 L/min/mmHg at rest and as much as 20 L/min/mmHg at peak exercise in a young male (Magder 2017).

The effect of an elevated LV diastolic pressure on the LV to outflow pressure difference is complicated and potentially is more of an issue when arterial pressure is low. A rise in LV diastolic pressure reduces the pressure difference for the pump and should therefore increase flow. This is the way the pump has somewhat of a “preload” effect. The high end-diastolic pressure and low arterial pressure, though, indicate that the pump is not effective at decompressing the LV. The higher end-diastolic pressure means that the pressure difference for ejection will more rapidly decrease with the onset of systole. This aids ejection and lower LV diastolic pressure at the start of diastolic which decreases output from the device

in the early part of diastole and allows greater volume buildup in the LV.

Another issue which often is neglected is the volume flowing into the LV (Fig. 51.3). An elevated LV diastolic pressure indicates that the LV is failing to keep up with what is coming back. The elevated LV diastolic pressure reduces the already small pressure difference for inflow from the pulmonary veins to the LV. Less flow into the LV must mean less flow out in the steady state. The high LVEDP does not mean that cardiac output is low. It could be because the rate of return is higher than normal as occurs with distributive physiology. However, this still means that the LV and the assist device are not keeping up with the return and the power setting of the device needs to be increased if possible.

In all these situations, it may appear that RV dysfunction is the problem, because the backup of pulmonary volume loads the RV and increases the CVP, but the real problem is inadequate emptying of the blood returning to the LV. This situation only can be properly evaluated by measuring left-sided filling pressures with a pulmonary artery catheter. As will be discussed later, there is no advantage to adding a RV assist device if the LV cannot decrease its diastolic volume at maximal RPM settings of the assist device.

The pressure head is not the only factor regulating output from the LV and the mechanical device. There is an important interaction between the function of the venous circuit and cardiac function which includes the native heart and the mechanical device. Before discussing this interaction, it is first necessary to review some basic physiological principles that regulate normal cardiac output. First, under normal physiological conditions, cardiac output is tightly related to the metabolic needs of tissues. Second, the heart only can put out what comes back to it, and that return of blood is directly related to tissue metabolism. Third, because of the large venous compliance (see Chap. 2), the mechanical device does not determine its return flow by pumping more out. It only determines what comes back to it, ultimately by lowering P_{ra} and allowing more to come back. The pump (in this case meaning the heart plus mechanical device) does not have the

volume to add to the venous compliant region to change MSFP. As per the discussion with the IABP (Fig. 51.2), for a mechanical device on the LV, this means lowering left atrial pressure, which lowers pulmonary venous pressure, which lowers pulmonary arterial pressure, and which eventually must lower Pra (Fig. 51.3), can occur even without RV contractions, but it is greatly aided if the RV can further lower Pra and allow more venous blood to come back to the heart.

What then are the controllable factors on the pump that can affect its output beyond the pressure difference? Clearly, a primary one is the function of the RV, because this determines what comes back and fills the LV. An enlarged RV also can compromise the mediastinal space available for LV filling. A key issue for the RV is to avoid reaching its volume limitation because once that happens, a rise in Pra creates “wasted preload” which does not change sarcomere length, the critical factor in the Starling relationship. Furthermore, when RV filling is limited, and its diastolic pressure is high, Pra is largely dependent upon how high the pressure in upstream venous compliant region can be increased. The high Pra also can end up determining the left atrial pressure because of the high pressure in the common pericardial space. When this happens, blood displacement by the mechanical device does not effectively lower left atrial pressure because it is being determined by Pra. The consequence is that unless LV emptying increases sufficiently to off-load the RV and lower Pra, left atrial pressure will not fall. Furthermore, without a fall in Pra, RV stroke volume cannot increase nor can cardiac output. The primary solution then is to decrease vascular volume with diuretics, or in the critical state, by using continuous ultrafiltration. Increasing the effective output by the native heart or the mechanical device might also help if the output is sufficient to lower left atrial pressure and RV afterload. However, if the LV is already small, despite the high pressure, this likely will not work.

Second, RV function may have to be improved so that Pra is decreased and venous return increased. RV output and then LV output then can increase and meet metabolic demands. This can be achieved by using inotropes such as dobuta-

mine, milrinone, and epinephrine and, perhaps, by using nitric oxide to decrease pulmonary vascular resistance and the RV afterload. As discussed below, an RV assist device should not be used until all these are considered.

The primary factor that can be altered to change output from mechanical devices is a change in the devices' rotational speed which is expressed in revolutions per minute (RPM). An increase in RPM shifts the pressure head to flow relationship upward, and usually in parallel, so that the same pressure head gives a greater flow (Fig. 51.5). The diastolic volume is thus decreased because more volume is pumped out of the LV, and this allows more volume to come back to the RV because it then has a lower diastolic pressure. Without a change in SVR, mean arterial pressure will increase when more blood is pumped out, depending upon what happens with the native heart. The peak systolic pressure should be smaller because of the decrease in stroke volume at higher-rate pumping, but the mean may not change. Some of the gain in total flow could be offset by an increase in arterial pressure, but cardiac output also is regulated according to tissue needs by the body's normal regulatory pathways. If the support is high enough, and the native LV function is weak enough, the aortic valve may not open during systole so that flow from the device is in series with the LV, rather than being in parallel, as occurs when the native LV also is ejecting through the aortic valve (Figs. 51.6 and 51.7). This “resting” of the LV likely is beneficial after acute ischemic injury, because at a minimum, it should greatly decrease myocardial O_2 demand. It may even be of benefit in non-ischemic failure by decreasing LV wall tension and allowing myofibers to recover, although clinical benefits are not yet established, nor is it known how much and for how long decompression should be applied.

Increased support by a mechanical heart reduces the slope of isovolumetric contraction of the LV which takes on a more lopsided pyramidal appearance of the pressure-volume loop (Fig. 51.7). An increase in the patient's heart rate also should affect the peak pressures produced by the mechanical device. The decrease in systolic time reduces stroke volume but maintains the

same cardiac output unless venous return increases. The decrease in stroke volume will decrease peak systolic pressure which could result in an increase output by the mechanical device, depending upon what happens to the response of native heart. A decrease in pump RPM will increase LV diastolic pressure, which potentially may increase outflow from the native LV because of the increased LV preload depending upon the contractile status of the LV. A greater swing in native LV systolic pressure, even without ejection, will increase aortic pulsatility because of the pressure difference across the mechanical device. Again, the final blood pressure response will depend upon the baroreceptor adjustments of SVR and the arteriolar critical closing pressure.

A major issue that comes up with long-term management of continuous flow devices is the risk of stroke. In the HeartWare Ventricular Assist System as Destination Therapy of Advanced Heart Failure (ENDURANCE) trial, the stroke risk was 30% at 1 year in the group that got HeartWare® LVAD (Rogers et al. 2017). An important risk factor for stroke was hypertension defined as a mean arterial pressure greater than 80 mmHg and systolic pressure greater than 100 mmHg (Saeed et al. 2015). Current guidelines recommend hypertensive treatment for long-term management when the mean arterial pressure exceeds 90 mmHg.

In longer-term studies of patients with advanced heart failure, a centrifugal pump was superior to an axial flow pump in stroke-free survival and need for reoperation to remove or replace a malfunctioning device (Mehra et al. 2019). This was believed to be because at lower LV diastolic pressures, the flatter pressure head reduced clots by producing less suction events. In larger devices, the pressure head of axial pumps can be modified by changing the design of the rotor, which may lead to important future technological developments (Frazier et al. 2010).

An important problem with blood pressure management is that standard techniques for measuring blood pressure require a pulse pressure, but pulse pressure often is too small to be detected by auscultation or with automated devices. Thus,

an arterial catheter is recommended for initial management following insertion of a mechanical assist device. However, it still can be difficult to assess the validity of the observed value when it is just a flat line on a monitor. The pressure in the line can be confirmed by occluding the arm with a cuff and observing the pressure at which the signal returns. When an arterial line cannot be used, the only approach is to make a Doppler measurement. This, too, is difficult because there is no pulse. The best approach in this situation is to use the opening pressure with continuous flow Doppler. This correlates best with the mean arterial blood pressure (Li et al. 2019).

LV Off-loading by Percutaneous Micro-axial Trans-aortic Devices (Impella®)

Devices that unload the LV can be surgically placed directly on the LV apex. Blood is drained into an external pump and returned to the ascending aorta. In the acute state, percutaneous devices are most frequently used.

The first of the Impella® family of cardiac assist devices was approved by the FDA in 2008 for selected needs of cardiac support, which was primarily high-risk percutaneous angioplasty and stenting (Seyfarth et al. 2008; Sarkar and Kini 2010). The device contains a micro-axial flow turbine that evolved from a previous device called the Hemopump. The rotor of the pump was based on the principle Archimedes' screw that is still used to pump water in the fields of Egypt (Frazier and Jacob 2007; Glazier and Kaki 2019). These devices can be inserted percutaneously through a femoral or axillary artery or by a cutdown on an artery depending upon the size of the device used. The miniaturized pump consists of an incorporated levitated magnetic rotor motor that is positioned across the aortic valve by echocardiographic or fluoroscopic guidance. A hydrodynamic purging system reduces clotting within the device. Blood is aspirated from an inflow cannula in the LV cavity, and pulseless flow is expelled into the ascending aorta. Pump performance depends on rotary speed, which has

a maximum of 32,000 RPM, the pressure head faced by the pump which as discussed above is the pressure difference between the LV cavity and the aorta, and the size of the rotor. Contraindications to its use include the presence of aortic stenosis, an aortic dissection, a mechanical aortic valve, a LV thrombus, or a ventricular septal defect (now a relative contraindication) (Ergle et al. 2016).

Because flow is based on the inverse of the pressure difference as with all LVADs, flow is reduced by elevated arterial pressures. Clinically, there needs to be a balance in arterial pressure that is adequate to allow proper distribution of blood flow, especially to the kidneys (Flaherty et al. 2020), but not so high that flow from the heart is reduced below a level that is critical for tissue needs. A lower arterial pressure also means that the native LV can eject more easily.

Impella® LP 2.5 is 9 Fr housing catheter at the insertion site but is 12 Fr at the level of the pump where it transverses the aortic valve. Because these devices cross the aortic valve, there is inevitable aortic insufficiency of varying degrees, but it is usually clinically insignificant. The larger the device, the larger the potential aortic insufficiency. At maximum RPM the flow in water for the 2.5 device can be as high as 4.5 L/min, but in the body, flow is limited to a maximum of 2.5 L/min because blood viscosity reduces the flow, and hemolysis becomes a major issue at higher RPM need for higher flows; flow most often is less than 2.5 L/min, and this device is not sufficient to support a markedly depressed cardiac output, especially in patients with a large body mass index (BMI). The 2.5 device primarily has been used to support cardiac output during complicated revascularization procedures in the catheterization laboratory and in the operating room to off-load the LV during “off-pump” revascularization (Glazier and Kaki 2019; Isgro et al. 2003).

No survival advantage has been found between Impella® LP 2.5 and IABP (Schrage et al. 2019; Ouweneel et al. 2017; Thiele et al. 2017) although the studies were small, the populations were mixed, the pump capacity likely was too small for some patients, and patients were randomized only

in a few of the studies. In a study in which percutaneous ventricular assist devices were used in patients with congestive heart failure, mortality actually was higher in those receiving a device, but there likely was a significant selection bias that contributed to worse outcome in Impella® group who warranted the device because they were sicker (this retrospective analysis included Impella® and TandemHeart® and did not separate them in the analysis) (Ogunbayo et al. 2018).

Flows of up to 5 L/min can be provided by Impella® LP 5.0. However, to do so the diameter at the level of the pump needs to be 21 Fr, and the device has to be implanted surgically through a femoral or axillary artery cutdown. In most centers, this necessitates involvement of a surgeon. This reduces the potential for rapid insertion of the device in patients who are failing acutely. Hemolysis is less with Impella® 5.0, but there tends to be more bleeding complications and limb ischemia. Anticoagulation is essential for the prevention of clotting of the rotor; this can be difficult to manage when patients also have received potent platelet inhibitors after a revascularization procedure. The 5.0 device has been shown to improve outcomes in patients with cardiogenic shock post-cardiac surgery (Griffith et al. 2013), but it is worth noting that patients with RV dysfunction were excluded from the trial.

Impella CP® was an improvement over the smaller 2.5 device. The rotor size and its efficiency were increased and allow for flows of up to 3.5 L/min. The diameter at the level of the aortic valve is 14 Fr, so that percutaneous implantation is possible, although with more difficulty than with the 2.5 device. This device provides adequate support for patients who are not too large, including children, and those who still have residual LV stroke volumes. However, in a retrospective study, Scharage et al. found that Impella® did not provide a better outcome than use of an IABP; this was true with Impella® CP as well as Impella® LP 2.5 (Schrage et al. 2019). Limitations of this study are that there were no prospective rules for selecting the devices, and selection bias again could have been an important factor because Impella® patients might have been more hemodynamically compromised.

Impella® was first approved by the US Food and Drug Administration (FDA) for 6 h, but European regulatory bodies approved it for 5 days (Anusionwu et al. 2012) and subsequently in the USA for 4 days for Impella 2.5® and CP and 6 days for Impella 5.0®. In May of 2019, use of Impella 5.0® and Impella LD® was extended to 14 days. Limitation of these devices is that they often have to be repositioned because the placement across the valve needs to be precise and the positioning can be unstable. If delivered through the femoral artery, the patient must remain supine and cannot be mobilized; however, patients in whom the device was inserted through an axillary vessel can be mobilized (Gilotra and Stevens 2015). Impella® devices are primarily used for early support. If shock persists, a more durable device is required. Although the rotor pump of the device is continuously purged, the devices still require systemic anticoagulation to prevent strokes and thrombosis of the device itself. Anticoagulation can be problematic if there was a lot of bleeding at the insertion site and/or if the patient was loaded with anti-platelet drugs during a revascularization procedure. Bleeding rates have been shown to be greater with Impella® devices than with IABP, as are ischemic leg episodes (Wernly et al. 2019).

Physiological Considerations with Micro-axial LVAD Support

Impella® devices unload the LV by decreasing the force needed by the heart to eject the appropriate amount of blood for tissue needs (Valgimigli et al. 2005). The larger-sized 5.0 device can even take over the full role of the LV. Assessment of the actual output from the LV with the addition of an assist device is more complicated than might initially be thought and gives good insight into the normal regulation of cardiac output.

Once again, the LV only can eject what comes back to it from the venous return and the right heart. When RV flow is limited, a mechanical pump cannot increase total flow unless there is a sufficient decrease in pulmonary artery pressure

that unloads the RV and allows its output to increase. As already indicated, when the RV is markedly overloaded, this may require actively removing blood volume.

By decreasing LV end-diastolic pressure, LV preload is reduced, which reduces native outflow by the LV. Again, because of the Starling mechanism, if more blood does not come back to the heart, more cannot go out. Thus, the native contribution by the LV goes down, and the flow from the pump contributes a greater proportion of the total cardiac output (Fig. 51.7). A greater output from the LV by itself cannot increase the return to the heart because it cannot add sufficient volume to significantly change MSFP, the force determining return of blood to the RV. Based on all these factors, it is hardly surprising that the new cardiac output with the LVAD does not equal the sum of the initial cardiac output plus Impella® flow.

Decompressing the left heart allows left atrial, and subsequently, pulmonary capillary pressure to decrease and reduces pulmonary edema if present. Because of the reduction of the downstream pressure (i.e., left atrium), pulmonary arterial pressure also decreases. The decrease in pulmonary congestion improves oxygenations and reduces pulmonary hypoxic vasoconstriction. These factors decrease the load on the RV, which in turn lowers P_{ra} and allows increased venous return. Right heart output then increases, and subsequently left heart output can increase. Systemic organ congestion also is decreased because of the decreased venous pressure. Furthermore, reduction of ventricular wall tension decreases myocardial O_2 consumption and the coronary blood flow requirements and reduces the compression of blood flow in the myocardial walls.

Depending upon the rate of rise of LV pressure with the onset of systole, the continuous flow from the LVAD pump can eliminate the isovolumetric phase at the start of ventricular systole and potentially lead to a more triangular shaped pressure-volume relationship instead of the usual loop with an isovolumetric onset and offset (Burkhoff et al. 2015) (Fig. 51.7). On the other hand, if the LV afterload is effectively off-loaded by the paral-

lel flow from the LVAD pump, native ejection can increase for the same preload. When the LV contractile function (i.e., the end-systolic pressure-volume relationship, ESPVR) is severely depressed, it is not uncommon to observe a peak ventricular pressure that is less than the peak arterial systolic pressure because arterial systolic pressure is determined by the combination of the output from the native LV and the LVAD pump contribution that continues through systole and diastole (Stoliński et al. 2002). The increase in arterial pressure combined with reduced diastolic pressure in the ventricle, and potentially the increase coronary perfusion, reduces ischemia and thereby improves LV contractile function (Kapur et al. 2019). There is evidence that this can lead to a reduction in infarct size and improved LV systolic function (Saku et al. 2018; Ouweneel et al. 2017; Briceno et al. 2019; Ishikawa and Meyns 2018; Garatti et al. 2007).

Most of the studies on use of these devices have emphasized outcome measures and have not reported hemodynamic consequences, but a few reports offer some insights. Before and after hemodynamic parameters were reported in the randomized ISAR-Shock study which compared Impella® LP 2.5 and IABP (Seyfarth et al. 2008). As expected, there was minimal change in hemodynamic parameters with use of IABP. Impella® LP 2.5 increased cardiac output on average by 0.9 L/min (3.2–4.1 L/min) and decreased the pulmonary artery occlusion pressure (Ppao) by 3 mmHg (22–19 mmHg) and CVP by 1 mmHg (from 13 to 12 mmHg). In comparison, use of Impella® LP 5.0 device for patients in shock following cardiac surgery (Griffith et al. 2013) increased CI on average from 1.7 to 2.7 L/min/m², a 58% increase. Flow by the device was given in L/min and indexed, but assuming an average body surface area of 1.9, the average LVAD pump flow would have been 2.4 L/min/m², and the pump accounted for the majority of the increase in cardiac output. The results from these two studies show that use of the LVAD pump decreases native LV output but total flow increases as determined by metabolic needs.

Thus, simple changes in CI and hemodynamic parameters cannot be used as markers of success. Rather, success should be based on clearance of multi-organ dysfunction and, more importantly, functional survival.

The flow produced by Impella® and other contemporary paracorporeal or axial devices is non-pulsatile. There initially was a concern that this might depress organ function. Theoretically, the non-pulsatile pressure could affect the distribution of organ function between areas with faster versus slower time constants of arterial drainage (i.e., lower resistance) and lower versus higher critical closing pressure because of the loss of selectivity from different pressure heads during the cardiac cycle. Differences in myogenic tone in vascular beds also could be an issue when the pressure is always the same. However, this does not seem to have been a problem, likely because metabolic controls are the most significant and ensure that the most metabolically active beds preferentially get the flow that they need. Regions such as the kidney, heart, and brain are well auto-regulated and can limit excess flow to their region, too.

Besides the risk of bleeding, limb ischemia, and strokes (Wernly et al. 2019), a problem arises when patients develop a distributive state and require cardiac outputs that are higher than the usual normal which is the range of 5 L/min. If the native heart cannot provide the additional output, progressive tissue ischemia occurs, and a device with a greater flow capacity is required.

In summary, smaller devices provide only partial circulatory support. Larger devices can provide full support for normal blood flow needs, but these only can be used for limited periods of time before risk of complications and device failure increase. It is likely that the benefit occurs by maintaining adequate tissue perfusion and thereby preventing ischemic tissue injury. By decompressing the heart and supporting arterial pressure, the devices appear to improve myocardial perfusion and allow recovery of ischemic regions. Their primary use is thus as a bridge to recovery.

Surgically Implantable Devices for LV Decompression

The circulation can be maintained by surgically implanted devices that drain blood either from the LV apex or the left atrium and return the blood to the ascending aorta. Because surgical implantation is required, they are no longer used to treat acute shock states except for failure to separate from cardiopulmonary bypass. Generally, these devices are used when support is expected to be needed for prolonged periods. The physiological implications of implanted devices are similar to micro-axial systems except that because larger catheters are inserted surgically, they can produce flows of up to 10 L/min. They also have less vascular complications than occur with percutaneous catheter-based approaches, although there can be significant bleeding associated with the required sternotomy, especially if patients have pre-existing liver congestion and/or a coagulopathic state. Surgically implanted devices are much more durable than percutaneous devices, but for same reason, they are significantly more expensive. For patients with acute shock, it is thus best to first to determine the patient's long-term survival potential while supporting the patient with a percutaneous short-term peripheral device.

Surgically implanted LVAD can be classified as those designed for temporary use, which usually means about a month, or those designed for expected prolonged support as a bridge to heart transplantation or destination therapy. We only discuss short-term devices here.

CentriMag® (Levitronix, Waltham, MA, USA) has a magnetically levitated rotor that spins at 500–5500 rpm and can generate flows up to 10 L/min (Westaby et al. 2012). It has no mechanical bearings and no contact between the rotor and the pump housing. This eliminates wear on the rotor and reduces hemolysis and clots in the pump. Consequently, anticoagulation with heparin can be withheld for up to 72 h if the patient is coagulopathic at the time of implantation. A large number of these units have been implanted. In a report of patients with post-infarction shock, mean duration of support was 17 days with a range from 1 to 60 day; 50% survived to hospital discharge (John et al. 2007).

Based on the registry for the Abiomed AB5000 (Danvers, MA, USA) paracorporeal external pulsatile system, the pump was implanted more than 24 h after the onset of shock in 52% of patients. The mean time of insertion was 26.5 h. Mortality was much less when implantation occurred within 6 h. Urgent implantation during cardiac arrest occurred in 7% of patients, and 44% had undergone cardiac massage (Anderson et al. 2010). The duration of support was 25 ± 22 days. Although in this very sick population most patients had high doses of inotropes, mechanical ventilation (82%), an IABP (91%), life-threatening arrhythmia, and multiple organ dysfunctions, survival was 40% at 30 days. Importantly, ventricular function recovered in 63% of survivors (Anderson et al. 2010).

An important contribution to our understanding of the potential future directions for use of these devices is retrospective review of patients with and without cardiogenic shock post-myocardial infarction and who were treated with a variety of implanted devices at the Hospital of the University of Pennsylvania (Leshnower et al. 2006). This discussion only deals with the patients who had an acute myocardial infarction. The mean time from the acute myocardial infarction was 6.4 days so that this generally was not an early intervention. An IABP already was in place in 88% of the patients. The patients were very sick; for example, 31% required renal replacement therapy. The mean duration of support was 56 ± 54 days indicating that treating teams should be prepared for a long course when these devices are implanted. Despite being very ill, the in-hospital survival was 67%, and 78% of the 49 patients ultimately received a heart transplant. It is worth noting that at this experienced center, 57% of patients had to be re-operated, most commonly for bleeding. There has been concern about cannulating the LV apex in patients with a recent myocardial infarction, but this did not pose a problem in this series in which the drainage cannula was inserted into the apex in almost all patients. The authors recommended that the apex should be used as the standard approach because it is safe, provided superior cardiac decompression, and reduced the risk of stroke

compared to atrial cannulation. Others have found the same (Dang et al. 2005; Tayara et al. 2006). A cautionary note was that outcome was worse when coronary artery surgery was performed before insertion of the LV assist device (Dang et al. 2005). This argues for its use as a planned approach rather than a salvage approach.

Left Atrial Decompression of the LV: TandemHeart® p-VAD

Another percutaneous device that is available for LV support is TandemHeart® p-VAD (previously known as AB-180). The largest experience comes from the Texas Heart Institute in a mixed patient population with ischemic and non-ischemic cardiogenic shock (Kar et al. 2011). This, too, is a percutaneous system. A 21 French catheter is inserted through a femoral vein and advanced to the right atrium and then across the atrial septum into the left atrium. Blood is drawn through an external centrifugal pump with fluid dynamic hydraulic bearings at rotational speeds of 2500–4500 rpm. Blood is returned through a 21 French catheter to the right femoral artery (Thiele et al. 2001). Flows of up to 4 l/min are possible. Because the pump is continuously purged, a lower degree of anticoagulation is permissible.

In a series from the Texas Heart Institute, the changes in hemodynamics were striking. Over 80% of patients already had an IABP. The average CI increased from 0.5 l/min/m² prior to insertion of the device to 3.0 l/min/m², and systolic arterial pressure rose from 75 to 100 mmHg. In the almost 50% of patients who had a cardiac arrest, the mean duration from cardiac arrest to implantation was 65 ± 41 min, and it took only from 15 to 65 min to insert the device. In those who presented with an STEMI, the 30 day survival was 60%.

Despite these dramatic results, there are important limitations to this system. There were many complications, including distributive shock in 30%, frequent coagulopathies, gastrointestinal hemorrhage in 20%, limb ischemia in 3%, and strokes in 7%. The catheter across the septum often is not stable, and if it springs back into the right atrium, cardiac output rapidly drops, which

can be lethal. The need to cross the atrial septum also constrains potential catheter size. In one patient the device perforated the left atrium and led to subsequent death. Finally, the atrial transseptal approach requires an advanced technical skill that not all interventional cardiologists have. Two randomized trials failed to find any benefit for the use of TandemHeart® p-VAD compared to use of an IABP (Thiele et al. 2005; Burkhoff et al. 2006), which itself has not been found to have any survival benefit (Thiele et al. 2018). One advantage of TandemHeart® p-VAD is that arterial and venous catheters are in place, and, if the patient deteriorates, it is not difficult to convert to ECMO.

Physiological Considerations Related to Devices Based on LA Drainage

Flows of up to 4 L/min can be achieved with these devices, which is on the lower side of normal tissue requirements. To understand the fundamental limits to flow with all systems requiring catheters for outflow and inflow, it is necessary to review principles that determine flow through catheters. These principles are true for all devices, but they are especially important for percutaneous devices because blood is withdrawn and returned through catheters in vessels rather than by withdrawal of blood directly through a large cannula on the ventricle.

Flow in a tube (i.e., a cannula) is based on the pressure difference between the inflow and outflow of the system and resistance to flow between them. Resistance is primarily determined by the cross-sectional area (i.e., radius of the tube) as discussed in Chap. 8 on blood pressure. The narrower the tube, the greater the force that is needed to give the same volume flow per minute. The velocity (volume per distance) also must be greater. Above a certain force required to generate blood flow, red cell hemolysis increases significantly and limits the maximum flow that can be used. Increasing the catheter size and modifications in the pumping device allow greater flow with less hemolysis. However, arterial and venous vessel sizes create anatomical constraints for

catheter placement. The greater the catheter size, the greater the difficulty of catheter insertion, risk of vessel injury, limitations of access sites, and increased costs. On the arterial side, use of larger catheters results in increased risk of distal limb ischemia and bleeding. Accordingly, the need for a transeptal catheter which for technical regions requires a smaller catheter greatly limits the possible flow with TandemHeart® p-VAD.

A second issue with this device is the impact of the returning arterial blood. With Impella®, blood flow to the aorta is in the antegrade direction, whereas with TandemHeart® p-VAD, arterial flow returns in a retrograde direction, which increases the load on the ejecting ventricle. This can result in ventricular distention and diminished output from the native LV (Rajagopal 2019). The effect is less if arterial blood flow is returned more distally (Geier et al. 2017). On the other hand, a potential advantage of TandemHeart® p-VAD system is that arterial blood can be returned through an axillary artery instead of a femoral artery and thus allows mobilization (Abrams et al. 2014). This configuration likely is worse for the LV because it imposes a higher LV afterload (Geier et al. 2017). Ventricular distention with TandemHeart® is less amendable to decompression procedures that often are used with ECMO. For example, it would make no sense to add an Impella® device to decompress the LV!

Comparison of Hemodynamic Profile of TandemHeart Versus Impella®

The hemodynamics of TandemHeart® p-VAD and Impella® LP LVAD were compared in a porcine model of an acute myocardial infarction and in which volume conductance catheters were inserted to obtain pressure-volume loops (Weil et al. 2016). The authors concluded that TandemHeart® p-VAD had a better hemodynamic profile than Impella CP® based on a greater reduction in stroke work with TandemHeart® p-VAD. First, it is worth noting that the predicted non-perpendicular isovolumetric slope of the P-V loop (Burkhoff et al. 2015) with both device did not occur indicating that the native heart still had strong function and that

there was not complete unloading of the LV with either device. The more important point, though, is that this study illustrates the limitation of the usefulness of stroke work as an indicator of improved cardiac function. As seen in Fig. 51.8, Impella® markedly reduced LV end-diastolic volume and end-systolic volume, and to a milder extent, LV end-diastolic pressure, which already was low. In contrast, TandemHeart® p-VAD produced only a moderate decrease in LV end-diastolic volume and increased end-systolic volume, which resulted in a smaller stroke volume. The peak systolic pressure was the same with both devices as was the heart rate, likely because these value are regulated by the baroreceptors. Stroke work is calculated as the product of the pressure difference between the aorta and ventricular diastolic pressure and stroke volume. Since the pressure difference was similar with both devices, the improved stroke work resulted from a smaller stroke volume with TandemHeart p-VAD, which hardly is a benefit for tissue perfusion. This occurred because TandemHeart failed to decompress LV volume, which is known to lead to worse outcomes (Rajagopal 2019). It is also noteworthy that the end-systolic elastance line was curved in Impella®-supported animals, indicating that there was continuous off-loading during ejection as volume fell off the maximum elastance line, which is what is desired.

Extracorporeal Membrane Oxygenation (ECMO)

ECMO provides full cardiopulmonary support with flows typically in the 4–5 L/min range, which is adequate for normal baseline O₂ demands (Keller 2019). Cannulation can be central through a sternotomy, but most often it is performed by peripheral cannulation especially in emergency situations. For peripheral cannulation, blood is drawn from the venous compartment, from either a femoral or jugular vein, passed through a membrane oxygenator and returned to the femoral artery. This allows complete substitution of the functions of the failing heart and lungs that are compromised because of pulmonary

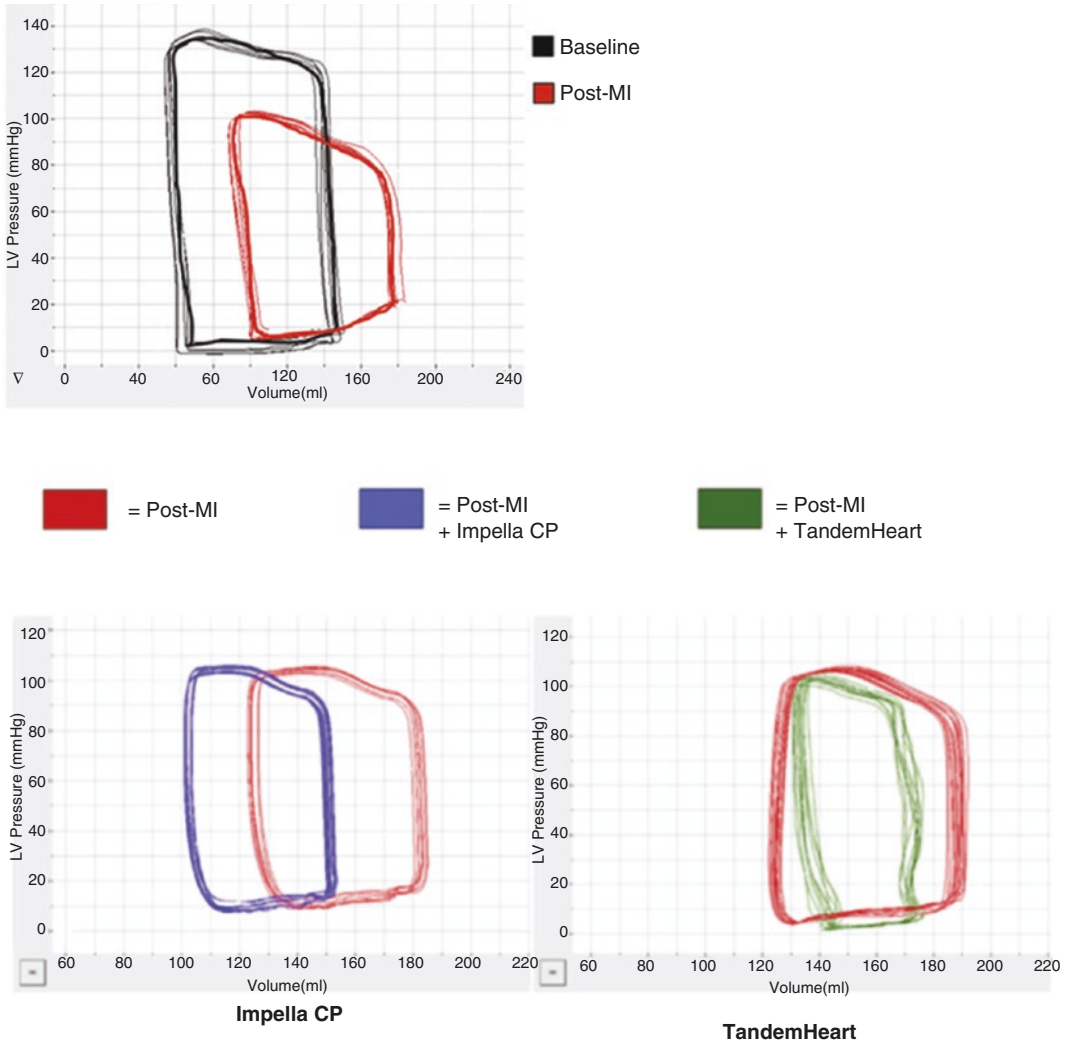


Fig. 51.8 Comparison of P-V following production of myocardial infarction in pig supported by Impella CP (bottom left) or TandemHeart® (bottom right). The top shows the baseline P-V loop of the LV and the P-V loop post-infarction. Following the infarct, the peak systolic pressure is lower, and the diastolic pressure is increased and also follows the same diastolic passive filling curve. In this case the stroke volume is not decreased. With Impella®, the end-diastolic volume and end-systolic volume are decreased. There is a small change in stroke volume (heart not given). The LV end-diastolic and end-systolic volume are not decreased as much with

TandemHeart®. The stroke volume was considerably reduced, and there was a small decrease in the LVEDP. The authors concluded that there was an advantage to TandemHeart® because it lowered stroke work (SW, $SV \times$ systolic-diastolic pressure). This to us indicates the lack of usefulness of using SW as a marker of improved function because Impella® decompressed the heart which would have lowered LV wall stress and LVEDP which should have better decreased pulmonary capillary pressure. (From Weil et al. (Weil et al. 2016) Used with permission of Elsevier)

edema and abnormal gas exchange. The heart thus requires only baseline metabolic activity which is less than 30% of its normal energy needs. As discussed above, the larger the catheter,

the higher the possible flow, but once again, a larger catheter increases the risks of complications, especially distal leg ischemia and bleeding. To reduce this, it is recommended to always

insert an auxiliary catheter to directly perfuse the femoral artery distal to the arterial cannula insertion site (Juo et al. 2017). It is also advisable to continuously monitor transcutaneous tissue oxygenation with near infrared spectroscopy.

Physiological Considerations with ECMO

Although ECMO provides total circulatory support, it does not unload the heart and actually increases the load on the LV. Venous flow still returns to the heart and must be injected. The amount of venous return to the heart increases as RV function improves. This lowers the right atrial pressure, and the RV competes with the draining venous catheter. As with TandemHeart® p-VAD, the returning arterial blood increases the load on LV ejection, which frequently results in left ventricular distention (Rajagopal 2019). The distention can produce further LV ischemia, increase pulmonary venous pressure, worsen aortic regurgitation, and even induce pulmonary venous hemorrhage. There are a number of solutions to this problem (Cevasco et al. 2019; Jayaraman et al. 2017; Xie et al. 2019). Some centers insert an IABP to decrease LV end-diastolic pressure and make it easier for the LV to eject. This benefit may not actually be derived through the production of a negative pressure in the aorta at the onset of systolic, but rather by preventing the retrograde flow from the arterial cannula reaching the ascending aorta, which is not necessarily beneficial. The IABP also aids coronary flow as discussed above although this effect would be lost if the balloon inhibits the retrograde aortic flow of fully oxygenated blood from the arterial cannula reaching the coronary arteries and brain. A better, but more expensive, approach is to add an Impella® system to truly decompress the LV; both Impella® LP 2.5 and Impella® CP have been used for this purpose. This approach allows for a smoother transition when weaning off the ECMO. In a propensity-matched retrospective analysis, use of ECMO combined with Impella® markedly increased survival (Pappalardo et al. 2017). However, there was a greater need for

renal replacement therapy and more hemolysis in the combined group. The authors attributed the increased incidence of renal failure to their longer survival. Considering the frequent need for another mechanical assist device when using ECMO, it likely only should be used as a first-line therapy when the lungs are severely compromised or during a cardiac arrest. Current ECMO devices allow rapid insertion in a crisis and thus are ideal for rescue therapy or when overall status is not clear. This is called a “bridge to decision.” An important clinical problem can arise with ECMO when cardiac function begins to recover and an increasing proportion of blood goes through the lungs. When the alveolar-arterial O₂ gradient is increased because of pulmonary shunting and ventilation/perfusion mismatching, the O₂ saturation of blood coming from the native heart is reduced. As native heart function improves, and the fraction of total cardiac output coming from the native heart increases, an increasing amount of deoxygenated blood is transmitted to the systemic circulation. Even more concerning, this poorly oxygenated blood coming from the heart preferentially goes to vessels that come off the proximal aorta, including the innominate and potentially the right and left cerebral arteries and the coronary arteries, whereas the rest of the body preferentially gets the fully oxygenated blood arriving retrograde in the aorta from the ECMO circuit. This difference in the oxygenation of the right arm, head, and heart compared to the rest of the body is called Harlequin syndrome indicating the difference in color (more bluish in deoxygenated area) due to the differences in oxygenated blood. The consequence can be severe including unsuspected brain hypoxemia and myocardial ischemia (Sorokin et al. 2017). To detect this potentially dangerous situation, it is important to monitor O₂ saturation in both the right and left arms. Lower O₂ saturation in the right arm compared to the left indicates presence of Harlequin syndrome but also indicates a recovering heart. This problem can be treated by increasing ECMO flow so that more of the returning blood is “shunted” to the ECMO circuit. Other more aggressive approaches include pharmacologically or electrically suppressing the native cardiac output or by branching off another arterial

catheter from the ECMO circuit to deliver well-oxygenated blood to the right atrium (Sorokin et al. 2017). On the other hand, if the heart is working adequately, it may be preferable to just convert to venovenous ECMO. This is especially the case if Impella® device is in place.

Right Ventricular Failure

Mechanical support for the RV is frequent in patients with left-sided mechanical support devices. In the US registry of the first 100 patients to receive the AB5000, 45% were judged to require biventricular support (Anderson et al. 2010), and in the retrospective analysis for the Hospital of the University of Pennsylvania, 39% received biventricular support because of what was identified as RV dysfunction (Leshnower et al. 2006). A high CVP and low arterial pressure were deemed to be predictors of RV failure. Risk factors for this state included a history of pulmonary hypertension, hypoxic pulmonary vasoconstriction, female sex, and cytokine-induced myocardial dysfunction (Lahm et al. 2010; Ochiai et al. 2002; Drakos et al. 2010; Morgan et al. 2004). Somewhat surprisingly, in one study, elevated Ppao or pulmonary vascular resistance was not a risk factor for RV failure after LVAD insertion (Ochiai et al. 2002).

To better understand what is happening to the RV, it is important to review the meaning of RV dysfunction. In Chap. 3, three terms were introduced: RV limitation, RV dysfunction, and RV failure. RV limitation indicates that further volume loading will not increase cardiac output because the diastolic limit of RV filling has been reached. This limit can occur with excessive vascular volume and a normal functioning RV, or because of a decrease in the contractile state of the RV, in which case a higher right-sided filling pressure is needed for a normal stroke volume. In the latter case, RV limitation occurs at a lower than normal cardiac index. RV failure means that the RV output is inadequate for tissue needs, and when it occurs with a lower than expected CI, there is also RV dysfunction. Furthermore, an elevated CVP is never normal and always indicates that there is excess intravascular volume.

This must come from either fluid retention because of recent decreased renal function or more commonly in the acute state because of excessive use of volume during resuscitation. The implication of a high CVP was the basis of Ernest Starling's studies (Starling 1918). He realized that, even when the heart is at a standstill, Pra/CVP only can rise to MSFP (Patterson and Starling 1914) (see Chap. 2). Use by Leshnower et al. of an elevated CVP and low arterial pressure to predict RV failure (Leshnower et al. 2006) is actually a definition for RV failure. Unless there is distributive shock, a low blood pressure most likely indicates that cardiac output is low, and the elevated CVP most likely indicates RV limitation. As was noted in Chap. 3, people born without a RV can perform high levels of exercise and generate cardiac outputs greater than 15 L/min, so why should a non-working RV matter? The answer is that patients without an RV are functional as long as pulmonary arterial pressure is not elevated. Pulmonary pressure elevation can occur either because of an increase in pulmonary vascular resistance or because of a rise in left atrial pressure, which is what occurs in cardiogenic shock with LV failure. When the RV is intact, the effect of increased pulmonary pressure is even greater than the absence of an RV. This is because the pulsatility of RV output fixes the time available for it to fill, and its intrinsic structural size limits the maximum RV diastolic volume. Together these properties of the RV set the limit for its stroke volume on each beat. Furthermore, when the RV dilates, tricuspid regurgitation occurs, and the contracting RV then sends more blood backward which interferes with venous return. Finally, when the RV filling limit is reached, an increase in pulmonary artery pressure always will decrease RV stroke volume and cardiac output, unless heart rate or RV contractility is increased pharmacologically or augmented by mechanical RV support.

The question in RV limitation and RV failure in cardiogenic shock then becomes, what keeps Pra higher than normal? There are two possible processes: either the downstream left atrial pressure is elevated or the pulmonary vascular resistance is elevated, both of which increase the load

on the ejecting RV. If both of these are low as is the normal case, even lack of any RV function would not limit the left-sided flow. If the left atrial pressure is elevated in the presence of a mechanical assist device, the primary problem is insufficient emptying of the LV by the assist device. This supports the observation by Morgan et al. that a CVP that is high and equal to Ppao is a bad prognostic sign (Morgan et al. 2004). The size of the LV on echocardiography is not adequate for assessment of this state because the pericardium and other mediastinal structures can limit the space for the LV to enlarge. This is especially the case when the RV is very dilated. The LV then may not look enlarged only because it cannot dilate, and the LV diastolic pressure still can be very high. Proper determination of this state requires measurement of the left-sided fill-

ing pressures by obtaining Ppao. When the right and left diastolic pressures are equal, and there is no tamponade, overfilling of the vasculature likely is the problem, as was indicated in the clinical example in Cardiogenic Shock part A. As discussed above, the diastolic pressure in an excessively filled RV is transmitted to the LV and directly increases left atrial pressure (Fig. 51.9 Part A). This then increases the pulmonary artery pressure, and the concept is that RV preload becomes RV afterload. As shown by Atherton and co-workers in patients with heart failure, decompression of the venous system by lower body negative pressure can result in increased LV filling and a rise in cardiac output (Atherton et al. 1997a; Atherton et al. 1997b).

A potential cause of RV dysfunction with application of an LVAD is decreased load toler-

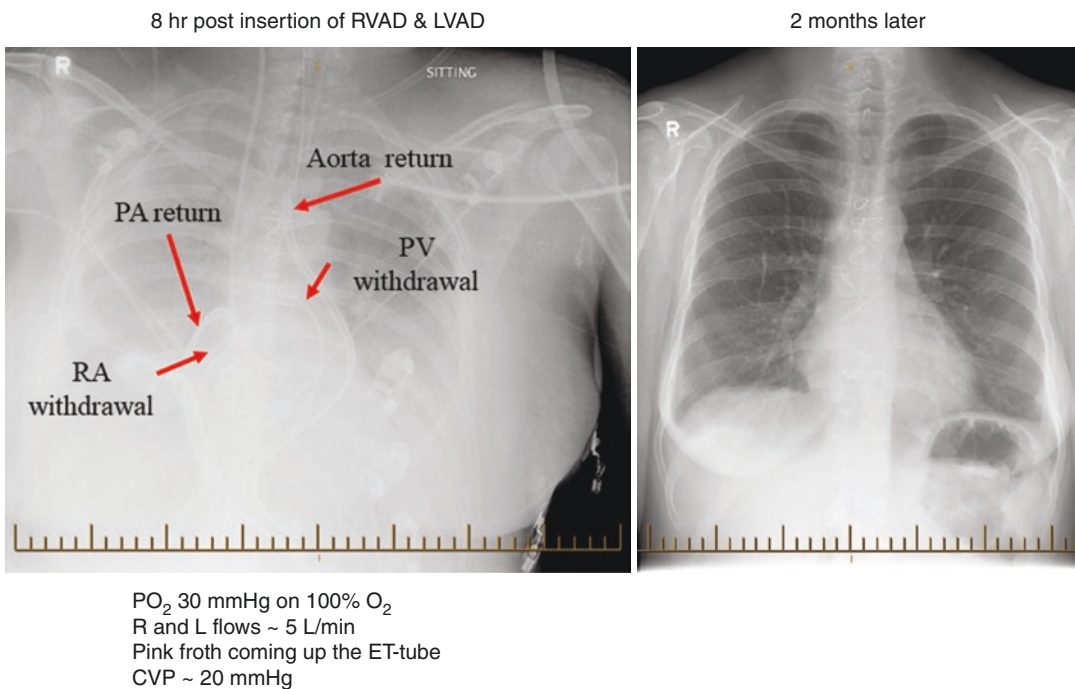


Fig. 51.9 Example of RV LV mismatch in 42 y/o woman with influenza A-induced cardiogenic shock. She was transferred from another hospital with almost no arterial pulsations. Right and left Thoratec ventricular assist devices were implanted. Her flows were ~5 L.min, but 8 h later she could not be oxygenated. She was taken to the operating room to insert an oxygenator, but upon opening the chest oxygenation rapidly improved. The cannula draining pulmonary venous flow was kinked, and this was

relieved when the chest was opening. Although RV and LV flows were similar, even an unmeasurable difference overwhelms the volume of pulmonary vasculature in a short time. She rapidly improved over the next few days. The RVAD was removed after 1 week and the LVAD about a week later. She returned home largely intact after 2 months, although she lost tips of extremities likely from high doses of vasopressors. PA, pulmonary artery; PV, pulmonary vein/left atrium; RA, right atrium

ance of the RV caused by unloading of the LV (Pavie and Leger 1996; Santamore and Dell'Italia 1998; Santamore et al. 1990; Damiano Jr. et al. 1991; Scharf et al. 1986). The basis for this is that the intraventricular septum plays a role in RV force production. When systemic arterial pressure is reduced, septal contractions are reduced, and this potentially can decrease RV performance. It has been demonstrated in animal studies that increasing systemic arterial pressure can increase RV load tolerance, independent of an effect on coronary circulation (Page et al. 1992; Belenkie et al. 1989). Increasing systemic arterial pressure with vasoconstrictors allowed for a higher pulmonary artery pressure before the RV failed. It has been proposed that the opposite effect could occur when the LV is unloaded by an LVAD; the decrease in LV force production could reduce RV force production. However, this effect should likely be much less in cardiogenic shock. To begin, decreasing LV diastolic volume should decrease pulmonary artery pressure and ease the load on the RV. As indicated above, if pulmonary vascular resistance is not elevated, left atrial pressure is the major determinant of outflow from the RV (Pavie and Leger 1996). A number of studies have carefully investigated the role of the LV portion of septum on RV function in animals. Only very minor effects of the LV contraction on RV systolic pressure generation and cardiac output were demonstrated by rapidly unloading the LV in animal studies (Santamore et al. 1976; Santamore and Gray Jr. 1996; Moon et al. 1993). However, a significant effect was observed in animals which had a pacing-induced cardiomyopathy (Chow and Farrar 1992; Farrar et al. 1993). These animals have a marked depression of the pressure-volume curves of RV indicating marked depression of the RV end-systolic elastance curve. This would have made the animals very susceptible to developing RV limitation with volume loading. Furthermore, the LV systolic pressure was reduced from 92 to 11 mmHg, a degree of reduction in LV systolic pressure that is never seen clinically and likely contributed to a major right-to-left shift of the septum. Importantly, the authors indicated that reduction of the pulmonary pressure likely overrode any interaction effect. In another study by the same investigators, 2 min-

utes of occlusion of the right coronary artery greatly increased the effect of unloading the LV indicating that any effect would also depend upon the initial RV function, although this might be because when RV limitation is in place, the RV cannot compensate by an increased in end-diastolic volume (Farrar et al. 1991).

In summary, these studies indicate that in most cases, unloading the LV by an LVAD should have a minimal effect on RV systolic function. Furthermore, evidence for a lack of clinical significance of the importance of LV contractions for support of RV pressure generation comes from the observation that large pulmonary artery pulse pressures often can be seen in patients that have no LV systolic pulsations. Finally, these studies were performed with pulsatile mechanical devices. When an LVAD provides continuous flow, which currently is the standard, there is even less likelihood that LV-RV interaction is a significant clinical issue.

Understanding this pathophysiology should allow a more systematic approach to RV limitation or failure and use of RV assist devices. If the LV end-diastolic pressure is high, and CVP/Pra is not excessive, output from the LV needs to be increased if the limits of the LVAD have not been reached. If CVP is high, and especially if it is equal to the left atrial pressure, the first step should be to decompress the RV by use of intravenous diuretics if the kidneys are still functioning, as was illustrated in the case study in Cardiogenic shock part A, or by active ultrafiltration if the kidneys are not functioning. Adding an RV assist device to someone with elevated left atrial pressure is not a solution and is quite likely harmful because it will just pump more volume into the lungs due to the inability of the LV to eject it. This may explain why overall, patients with biventricular VADS do worse (Westaby et al. 2012). Many of these patients likely needed volume depletion rather than an RV assist device. These overfilled patients also likely have hepatic congestion and are at a much greater risk of bleeding, which occurs in 50% of patients implanted with BiVADs.

It is worth noting the magnitude of changes in CVP that potentially can be hemodynamically significant. The normal gradient for venous return is

in the range 4–8 mmHg. Accordingly, an increase in CVP of 10 mmHg, without an equivalent rise in MSFP by the same amount, would reduce cardiac output to zero. If a patient has a CVP of 20 mmHg, the MSFP must be at least 25 mmHg or perhaps even 30 mmHg in order to allow effective venous return to the heart. Even worse, the capillaries are upstream from the MSFP so that the raising venous pressure further will greatly increase fluid filtration, even in the heart.

A very difficult situation arises when a patient with cardiogenic shock develops distributive hemodynamics. When this happens, not only is arterial resistance decreased but so is venous resistance. Venous return increases, and cardiac output may need to be greater than 8–10 L/min to maintain a normal arterial pressure and tissue perfusion, but this value is well beyond the capacity of most devices. Furthermore, if the RV is functioning better than the LV, this can lead to progressively worsening of pulmonary edema, especially because capillary permeability usually also is increased in distributive physiology because of an associated inflammatory condition. The only treatments are broad-spectrum antibiotics, especially with good gram positive activity to treat the most likely infectious causes, use of vasoconstrictors to try to restore normal tone, and very careful use of fluids.

If the rise in pulmonary pressure is not due to increased LV diastolic filling pressures, the increased RV afterload must be due to a rise in pulmonary vascular resistance or an increase in pulmonary vascular critical closing pressures (Chap. 5 on pulmonary vascular resistance). Causes for these include hypoxic vasoconstriction due to pulmonary edema or lung injury, a ventilator-induced load on the RV from high trans-pulmonary pressure and creation of non-Zone III conditions in the pulmonary vasculature (Permutt et al. 1962; Vieillard-Baron et al. 1999), obstruction of pulmonary venous drainage by a cannula draining the left atrium, or because of a chronic process that has created pulmonary vascular disease. The hypoxic vasoconstriction might be resolved by removing fluid and maneuvers that increase oxygenation; ventilator-induced loads can be improved by ventilator adjustments; and an obstructing atrial cannula

can be fixed by repositioning it. A dramatic case of this is shown in Fig. 51.9. A chronic increase in pulmonary vascular resistance though is dire, and survival is unlikely without a right ventricular assist device (Pavie and Leger 1996). This, though, must be considered cautiously. If the increase in pulmonary vascular resistance is unlikely to be resolved by pulmonary vascular remodeling, cardiac transplant will not be a long-term solution. A destination LVAD alone also will not be possible, and the patient will require permanent biventricular support. In these cases, the overall status of the patient's survivability should be carefully reviewed.

Given the above discussion, the need for right heart support for acute cardiogenic shock should be low. Careful management of volume should eliminate the need in a large proportion of cases. RV support should not be considered without a careful invasive hemodynamic assessment with a pulmonary artery catheter and demonstration of elevated pulmonary vascular resistance. If the resistance is not elevated, the problem is the elevated LV and RV filling pressures, which should be dealt with by volume removal or increasing LV systolic pumping capacity. The primary role of RV support likely is in elective patients with chronic processes and who have elevated pulmonary vascular resistance.

Right Heart Support

From the above discussion, it is likely that RV support is used too often. However, there are patients with elevated pulmonary vascular resistances who need the added systolic pressure to overcome this increased RV load. One approach is to percutaneously insert a large gauge venous catheter that has two lumens (TandemLife Protect Duo®, CardiacAssist Inc., Pittsburgh, PA, USA) (Schmack et al. 2016). One lumen is positioned in the right atrium and draws venous blood through a pump and returns the blood through the second lumen which is positioned in the pulmonary artery. This also can be done with two separate venous catheters.

An increasingly popular approach is use of Impella® RP which is a minimally invasive 22

FR FA, catheter-based percutaneous micro-axial pump. The device needs to be positioned under fluoroscopic guidance (Pieri and Pappalardo 2018). It is advanced antegrade from a femoral vein across the tricuspid and pulmonary valves so that the outflow end is positioned in the pulmonary artery. The pump inflow is positioned in the inferior vena cava. The device can provide flows up to 4.0 L/min. Use of this device increased significantly after publication of the RECOVER RIGHT which was a prospective cohort study that evaluated safety and efficacy of Impella® RP from (Anderson et al. 2015). It included 30 patients, 18 of whom had RV failure after an LVAD implantation and 12 whose RV failure occurred after cardiac surgery or a myocardial infarction. The pump quickly increased CI index from a mean of 1.8 to 3.3 L/min/m² and lowered the CVP from 19.2 to 12.6 mmHg. Hospital survival in this higher-risk group was 73.3%, and importantly, all discharged patients still were alive at 3 months. The series was expanded in a subsequent report called the RP CAP study which combined three data sets that used the same screening criteria (Anderson et al. 2018). Results were similar to the original data set. Some details are worth noting. There were 376 patients screened, but only 60 patients enrolled; 116 were excluded because they were not deemed to be in RV failure, 8 because they had profound shock, and 24 because they already were on an RV assist device. An additional 12 were excluded because CVP was less than 15 mmHg, but perhaps if their CI was low, these patients still might have benefited as per the previous discussion. Arterial lactate and mixed venous O₂ saturation were not reported so it is difficult to know the extent of the metabolic compromise of tissues and the severity of their condition. The cardiac output before insertion of Impella RP was 3.86 L/min, and the average estimated Impella RP flow was 3.19 L/min. However, the cardiac output post insertion was 6.4 L/min with a flow on the LVAD device that went from 4.0 to 4.6. The high cardiac output would suggest a distributive state. It would also indicate a major increase in native LV-sided output. However it is likely that the post implanta-

tion measurements of CI were invalid. Details were not given, but if the outputs were made with thermodilution pulmonary artery catheter, the results would have been artificially elevated. The bolus for the measurement would have been in the right atrium, but the pump takes blood from the IVC and ejects it in the pulmonary artery. Thus, there would have been mixed sources of blood being evaluated at the PA, and this violates the need to have conservation of mass to make the thermodilution measurement. Perhaps much of the enthusiasm of the increase in CI should be tempered. It was also noteworthy that despite adding an RV assist device, CVP still was elevated at 13 mmHg indicating that there likely was excess vascular volume. Information on the change in fluid balance would have been very helpful.

Khalid et al. reported on the incidence of the most common complications and failure modes from the post-marketing surveillance data from the Food and Drug Administration (FDA) Manufacturer and User Facility Device Experience (MAUDE) database (Khalid et al. 2019). The authors could not comment on incidence because reporting was voluntary so that there was no denominator. For example, there were 5 deaths reported under complications, but the data set indicated 11. Of the events reported, the most common was bleeding, which accounted for 42.9% of events. Significant vascular complications were reported in eight patients, and five of these required surgical repairs. Of the 35 device complications with Impella RP, only 16 devices were returned to the manufacturer for analysis. Of these 34.2% were structural damage of components. Others included thrombus in the device, device detachment, and malfunction. When a RV assist device is combined with a LV device, an important concern is that the output from the LV device must be greater than that of the RV device. This is not an issue with normal ventricles because they adapt their output to their input based on the Starling mechanism, but mechanical devices do not. This also can occur when the RV responds to an inotrope better than the LV with a mechanical device.

Summary

Use of mechanical devices for support of the circulation in patients with cardiogenic shock is expanding rapidly. Proper large-scale studies are needed to better understand their role and proper use. The initial short-term benefit can be obvious and satisfying, but it is important to know the long-term outcomes, especially because these devices are not without significant complications and costs. We need to know the best timing for initiation of these devices; should they be started at an early stage to prevent deterioration, or should they be started only when a patient is in extremis? What is the appropriate duration of treatment? When should the patient be transitioned to a longer-term device? In making these decisions and planning prospective trials, it will be critical to understand the physiological implications of the various devices and their impact on LV recovery. Finally, an ongoing question is that of the role of the RV in cardiogenic shock and how this should best be managed because it is clear that when RV function is limited, clinical outcomes are much worse.

References

- Abrams D, Javidfar J, Farrand E, Mongero LB, Agerstrand CL, Ryan P, et al. Early mobilization of patients receiving extracorporeal membrane oxygenation: a retrospective cohort study. *Crit Care*. 2014;18(1):R38–R.
- Anderson M, Smedira N, Samuels L, Madani M, Naka Y, Acker M, et al. Use of the AB5000 ventricular assist device in cardiogenic shock after acute myocardial infarction. *Ann Thorac Surg*. 2010;90(3):706–12.
- Anderson MB, Goldstein J, Milano C, Morris LD, Kormos RL, Bhama J, et al. Benefits of a novel percutaneous ventricular assist device for right heart failure: the prospective RECOVER RIGHT study of the Impella RP device. *J Heart Lung Transplant*. 2015;34(12):1549–60.
- Anderson M, Morris DL, Tang D, Batsides G, Kirtane A, Hanson I, et al. Outcomes of patients with right ventricular failure requiring short-term hemodynamic support with the Impella RP device. *J Heart Lung Transplant*. 2018;37(12):1448–58.
- Anusionwu O, Fischman D, Cheriya P. The duration of impella 2.5 circulatory support and length of hospital stay of patients undergoing high-risk percutaneous coronary interventions. *Cardiol Res*. 2012;3(4):154–7.
- Atherton JJ, Moore TD, Lele SS, Thomson HL, Galbrath AJ, Belenkie I, et al. Diastolic ventricular interaction in chronic heart failure. *Lancet*. 1997a;349:1720–4.
- Atherton JJ, Thomson HL, Moore TD, Wright KN, Muehle GWF, Fitzpatrick LE, et al. Diastolic ventricular interaction. A possible mechanism for abnormal vascular responses during volume unloading in heart failure. *Circulation*. 1997b;96:4273–9.
- Belenkie I, Dani R, Smith ER, Tyberg JV. Effects of volume loading during experimental acute pulmonary embolism. *Circulation*. 1989;80:178–88.
- Briceno N, Annamalai SK, Reyelt L, Crowley P, Qiao X, Swain L, et al. Left ventricular unloading increases the coronary collateral flow index before reperfusion and reduces infarct size in a Swine model of acute myocardial infarction. *J Am Heart Assoc*. 2019;8(22):e013586.
- Burkhoff D, Cohen H, Brunckhorst C, O'Neill WW, TandemHeart Investigators G. A randomized multicenter clinical study to evaluate the safety and efficacy of the TandemHeart percutaneous ventricular assist device versus conventional therapy with intraaortic balloon pumping for treatment of cardiogenic shock. *Am Heart J*. 2006;152(3):469.e1–8.
- Burkhoff D, Sayer G, Doshi D, Uriel N. Hemodynamics of mechanical circulatory support. *J Am Coll Cardiol*. 2015;66(23):2663–74.
- Cevasco M, Takayama H, Ando M, Garan AR, Naka Y, Takeda K. Left ventricular distension and venting strategies for patients on venoarterial extracorporeal membrane oxygenation. *J Thorac Dis*. 2019;11(4):1676–83.
- Chow E, Farrar DJ. Right heart function during prosthetic left ventricular assistance in a porcine model of congestive heart failure. *J Thorac Cardiovasc Surg*. 1992;104(3):569–78.
- Damiano RJ Jr, La Follette P Jr, Cox JL, Lowe JE, Santamore WP. Significant left ventricular contribution to right ventricular systolic function. *Am J Phys*. 1991;261(5 Pt 2):H1514–24.
- Dang NC, Topkara VK, Leacche M, John R, Byrne JG, Naka Y. Left ventricular assist device implantation after acute anterior wall myocardial infarction and cardiogenic shock: a two-center study. *J Thorac Cardiovasc Surg*. 2005;130(3):693–8.
- Drakos SG, Janicki L, Horne BD, Kfoury AG, Reid BB, Clayson S, et al. Risk factors predictive of right ventricular failure after left ventricular assist device implantation. *Am J Cardiol*. 2010;105(7):1030–5.
- Ergle K, Parto P, Krim SR. Percutaneous ventricular assist devices: a novel approach in the management of patients with acute cardiogenic shock. *Ochsner J*. 2016;16(3):243–9.
- Farrar DJ, Chow E, Compton PG, Foppiano L, Woodard J, Hill JD. Effects of acute right ventricular ischemia on ventricular interactions during prosthetic left ventricular support. *J Thorac Cardiovasc Surg*. 1991;102(4):588–95.

- Farrar DJ, Woodard JC, Chow E. Pacing-induced dilated cardiomyopathy increases left-to-right ventricular systolic interaction. *Circulation*. 1993;88(2):720–5.
- Feldman D, Pamboukian SV, Teuteberg JJ, Birks E, Lietz K, Moore SA, et al. The 2013 International Society for Heart and Lung Transplantation guidelines for mechanical circulatory support: executive summary. *J Heart Lung Transplant*. 2013;32(2):157–87.
- Flaherty MP, Moses JW, Westenfeld R, Palacios I, O'Neill WW, Schreiber TL, et al. Impella support and acute kidney injury during high-risk percutaneous coronary intervention: the Global cVAD Renal Protection Study. *Catheter Cardiovasc Interv*. 2020;95(6):1111–21.
- Frazier OH, Jacob LP. Small pumps for ventricular assistance: progress in mechanical circulatory support. *Cardiol Clin*. 2007;25(4):553–vi.
- Frazier OH, Khalil HA, Benkowski RJ, Cohn WE. Optimization of axial-pump pressure sensitivity for a continuous-flow total artificial heart. *J Heart Lung Transplant*. 2010;29(6):687–91.
- Garatti A, Russo C, Lanfranchi M, Colombo T, Bruschi G, Trunfio S, et al. Mechanical circulatory support for cardiogenic shock complicating acute myocardial infarction: an experimental and clinical review. *ASAIO J*. 2007;53(3):278–87.
- Geier A, Kunert A, Albrecht G, Liebold A, Hoenicka M. Influence of cannulation site on carotid perfusion during extracorporeal membrane oxygenation in a compliant human aortic model. *Ann Biomed Eng*. 2017;45(10):2281–97.
- Gilotra NA, Stevens GR. Temporary mechanical circulatory support: a review of the options, indications, and outcomes. *Clin Med Insights Cardiol*. 2015;8(Suppl 1):75–85.
- Glazier JJ, Kaki A. The impella device: historical background, clinical applications and future directions. *Int J Angiol*. 2019;28(2):118–23.
- Griffith BP, Anderson MB, Samuels LE, Pae WE Jr, Naka Y, Frazier OH. The RECOVER I: a multicenter prospective study of Impella 5.0/LD for postcardiotomy circulatory support. *J Thorac Cardiovasc Surg*. 2013;145(2):548–54.
- Hosseini-pour M, Gupta R, Bonnell M, Elahinia M. Rotary mechanical circulatory support systems. *J Rehabil Assist Technol Eng*. 2017;4:2055668317725994.
- Isgro F, Kiessling AH, Rehn E, Lang J, Saggau W. Intracardiac left ventricular support in beating heart, multi-vessel revascularization. *J Card Surg*. 2003;18(3):240–4.
- Ishikawa K, Meyns B. Acute mechanical LV unloading in ischemia reperfusion injury: be prepared. *J Am Coll Cardiol*. 2018;72(5):515–7.
- Jayaraman AL, Cormican D, Shah P, Ramakrishna H. Cannulation strategies in adult veno-arterial and veno-venous extracorporeal membrane oxygenation: techniques, limitations, and special considerations. *Ann Card Anaesth*. 2017;20(Supplement):S11–8.
- John R, Liao K, Lietz K, Kamdar F, Colvin-Adams M, Boyle A, et al. Experience with the Levitronix CentriMag circulatory support system as a bridge to decision in patients with refractory acute cardiogenic shock and multisystem organ failure. *J Thorac Cardiovasc Surg*. 2007;134(2):351–8.
- Juo Y-Y, Skancke M, Sanaiha Y, Mantha A, Jimenez JC, Benharash P. Efficacy of distal perfusion cannulae in preventing limb ischemia during extracorporeal membrane oxygenation: a systematic review and meta-analysis. *Artif Organs*. 2017;41(11):E263–E73.
- Kantrowitz A. Origins of intraaortic balloon pumping. *Ann Thorac Surg*. 1990;50(4):672–4.
- Kapur NK, Esposito M. Hemodynamic support with percutaneous devices in patients with heart failure. *Heart Fail Clin*. 2015;11(2):215–30.
- Kapur NK, Paruchuri V, Majithia A, Esposito M, Shih H, Weintraub A, et al. Hemodynamic effects of standard versus larger-capacity intraaortic balloon counterpulsation pumps. *J Invasive Cardiol*. 2015;27(4):182–8.
- Kapur NK, Alkhouli MA, DeMartini TJ, Faraz H, George ZH, Goodwin MJ, et al. Unloading the left ventricle before reperfusion in patients with anterior ST-segment-elevation myocardial infarction. *Circulation*. 2019;139(3):337–46.
- Kar B, Gregoric ID, Basra SS, Idelchik GM, Loyalka P. The percutaneous ventricular assist device in severe refractory cardiogenic shock. *J Am Coll Cardiol*. 2011;57(6):688–96.
- Keller SP. Management of peripheral venoarterial extracorporeal membrane oxygenation in cardiogenic shock. *Crit Care Med*. 2019;47(9):1235–42.
- Khalid N, Rogers T, Shlofmitz E, Chen Y, Musallam A, Khan JM, et al. Adverse events and modes of failure related to Impella RP: insights from the manufacturer and user facility device experience (MAUDE) database. *Cardiovasc Revasc Med*. 2019;20(6):503–6.
- Khalil HA, Cohn WE, Metcalfe RW, Frazier OH. Preload sensitivity of the Jarvik 2000 and HeartMate II left ventricular assist devices. *ASAIO J*. 2008;54(3):245–8.
- Khera R, Cram P, Lu X, Vyas A, Gerke A, Rosenthal GE, et al. Trends in the use of percutaneous ventricular assist devices: analysis of national inpatient sample data, 2007 through 2012. *JAMA Intern Med*. 2015;175(6):941–50.
- Khera R, Cram P, Vaughan-Sarrazin M, Horwitz PA, Girotra S. Use of mechanical circulatory support in percutaneous coronary intervention in the United States. *Am J Cardiol*. 2016;117(1):10–6.
- Kirklin JK, Naftel DC. Mechanical circulatory support: registering a therapy in evolution. *Circ Heart Fail*. 2008;1(3):200–5.
- Kolyva C, Pantalos GM, Pepper JR, Khir AW. How much of the intraaortic balloon volume is displaced toward the coronary circulation? *J Thorac Cardiovasc Surg*. 2010;140(1):110–6.
- Lahm T, McCaslin CA, Wozniak TC, Ghumman W, Fadl YY, Obeidat OS, et al. Medical and surgical treatment of acute right ventricular failure. *J Am Coll Cardiol*. 2010;56(18):1435–46.
- Leshnowar BG, Gleason TG, O'Hara ML, Pochettino A, Woo YJ, Morris RJ, et al. Safety and efficacy of left ventricular assist device support in postmyocar-

- dial infarction cardiogenic shock. *Ann Thorac Surg.* 2006;81(4):1365–71.
- Li S, Beckman JA, Welch NG, Bjelkengren J, Masri SC, Minami E, et al. Accuracy of Doppler blood pressure measurement in continuous-flow left ventricular assist device patients. *ESC Heart Fail.* 2019;6(4):793–8.
- Lim HS, Howell N, Ranasinghe A. The physiology of continuous-flow left ventricular assist devices. *J Card Fail.* 2017;23(2):169–80.
- Magder SA. Pressure-flow relations of diaphragm and vital organs with nitroprusside-induced vasodilation. *J Appl Physiol.* 1986;61:409–16.
- Magder S. Right atrial pressure in the critically ill: how to measure, what is the value, what are the limitations. *Chest.* 2017;151(4):908–16.
- Mandawat A, Rao SV. Percutaneous mechanical circulatory support devices in cardiogenic shock. *Circ Cardiovasc Interv.* 2017;10(5):e004337.
- Mehra MR, Uriel N, Naka Y, Cleveland JC Jr, Yuzefpolskaya M, Salerno CT, et al. A fully magnetically levitated left ventricular assist device – final report. *N Engl J Med.* 2019;380(17):1618–27.
- Moon MR, Castro LJ, DeAnda A, Tomizawa Y, Daughters GT 2nd, Ingels NB Jr, et al. Right ventricular dynamics during left ventricular assistance in closed-chest dogs. *Ann Thorac Surg.* 1993;56(1):54–67.
- Morgan JA, John R, Lee BJ, Oz MC, Naka Y. Is severe right ventricular failure in left ventricular assist device recipients a risk factor for unsuccessful bridging to transplant and post-transplant mortality. *Ann Thorac Surg.* 2004;77(3):859–63.
- Mouloupoulos SD, Topaz S, Kolff WJ. Diastolic balloon pumping (with carbon dioxide) in the aorta—a mechanical assistance to the failing circulation. *Am Heart J.* 1962;63:669–75.
- Ochiai Y, McCarthy PM, Smedira NG, Banbury MK, Navia JL, Feng J, et al. Predictors of severe right ventricular failure after implantable left ventricular assist device insertion: analysis of 245 patients. *Circulation.* 2002;106(12 Suppl 1):I198–202.
- Ogunbayo GO, Ha LD, Ahmad Q, Misumida N, Elbadawi A, Olorunfemi O, et al. In-hospital outcomes of percutaneous ventricular assist devices versus intra-aortic balloon pumps in non-ischemia related cardiogenic shock. *Heart Lung.* 2018;47(4):392–7.
- Ouweneel DM, Eriksen E, Sjaun KD, van Dongen IM, Hirsch A, Packer EJS, et al. Percutaneous mechanical circulatory support versus intra-aortic balloon pump in cardiogenic shock after acute myocardial infarction. *J Am Coll Cardiol.* 2017;69(3):278–87.
- Page RD, Harringer W, Hodakowski GT, Guerrero JL, LaRaia PJ, Austen WG, et al. Determinants of maximal right ventricular function. *J Heart Lung Transplant.* 1992;11(1 Pt 1):90–8.
- Pappalardo F, Schulte C, Pieri M, Schrage B, Contri R, Soeffker G, et al. Concomitant implantation of Impella® on top of veno-arterial extracorporeal membrane oxygenation may improve survival of patients with cardiogenic shock. *Eur J Heart Fail.* 2017;19(3):404–12.
- Patterson SW, Starling EH. On the mechanical factors which determine the output of the ventricles. *J Physiol.* 1914;48(5):357–79.
- Pavie A, Leger P. Physiology of univentricular versus biventricular support. *Ann Thorac Surg.* 1996;61(1):347–9; discussion 57–8.
- Permutt S, Bromberger-Barnea B, Bane HN. Alveolar pressure, pulmonary venous pressure, and the vascular waterfall. *Med Thorac.* 1962;19:239–60.
- Pieri M, Pappalardo F. Impella RP in the treatment of right ventricular failure: what we know and where we go. *J Cardiothorac Vasc Anesth.* 2018;32(5):2339–43.
- Rajagopal K. Left ventricular distension in veno-arterial extracorporeal membrane oxygenation: from mechanics to therapies. *ASAIO J.* 2019;65(1):1–10.
- Rogers JG, Pagani FD, Tatooles AJ, Bhat G, Slaughter MS, Birks EJ, et al. Intraoperative left ventricular assist device for advanced heart failure. *N Engl J Med.* 2017;376(5):451–60.
- Saeed O, Jermyn R, Kargoli F, Madan S, Mannem S, Gunda S, et al. Blood pressure and adverse events during continuous flow left ventricular assist device support. *Circ Heart Fail.* 2015;8(3):551–6.
- Saku K, Kakino T, Arimura T, Sakamoto T, Nishikawa T, Sakamoto K, et al. Total mechanical unloading minimizes metabolic demand of left ventricle and dramatically reduces infarct size in myocardial infarction. *PLoS One.* 2016;11(4):e0152911.
- Saku K, Kakino T, Arimura T, Sunagawa G, Nishikawa T, Sakamoto T, et al. Left ventricular mechanical unloading by total support of impella in myocardial infarction reduces infarct size, preserves left ventricular function, and prevents subsequent heart failure in dogs. *Circ Heart Fail.* 2018;11(5):e004397.
- Santamore WP, Dell'Italia LJ. Ventricular interdependence: significant left ventricular contributions to right ventricular systolic function. *Prog Cardiovasc Dis.* 1998;40(4):289–308.
- Santamore WP, Gray LA Jr. Left ventricular contributions to right ventricular systolic function during LVAD support. *Ann Thorac Surg.* 1996;61(1):350–6.
- Santamore WP, Lynch PR, Heckman JL, Bove AA, Meier GD. Left ventricular effects on right ventricular developed pressure. *J Appl Physiol.* 1976;41(6):925–30.
- Santamore WP, Shaffer T, Papa L. Theoretical model of ventricular interdependence: pericardial effects. *Am J Phys.* 1990;259(1 Pt 2):H181–9.
- Sarkar K, Kini AS. Percutaneous left ventricular support devices. *Cardiol Clin.* 2010;28(1):169–84.
- Scharf SM, Warner KG, Joseph M, Khuri SF, Brown R. Load tolerance of the right ventricle: effect of increased aortic pressure. *J Crit Care.* 1986;1(3):163–72.
- Scheidt S, Wilner G, Mueller H, Summers D, Lesch M, Wolff G, et al. Intra-aortic balloon counterpulsation in cardiogenic shock. Report of a co-operative clinical trial. *N Engl J Med.* 1973;288(19):979–84.
- Schmack B, Weymann A, Popov A-F, Patil NP, Sabashnikov A, Kremer J, et al. Concurrent left ventricular assist device (LVAD) implantation and percu-

- aneous temporary RVAD support via CardiacAssist Protek-Duo TandemHeart to Preempt Right Heart Failure. *Med Sci Monit Basic Res.* 2016;22:53–7.
- Schrage B, Ibrahim K, Loehn T, Werner N, Sinning JM, Pappalardo F, et al. Impella support for acute myocardial infarction complicated by cardiogenic shock. *Circulation.* 2019;139(10):1249–58.
- Seyfarth M, Sibbing D, Bauer I, Fröhlich G, Bott-Flügel L, Byrne R, et al. A randomized clinical trial to evaluate the safety and efficacy of a percutaneous left ventricular assist device versus intra-aortic balloon pumping for treatment of cardiogenic shock caused by myocardial infarction. *J Am Coll Cardiol.* 2008;52(19):1584–8.
- Sorokin V, MacLaren G, Vidanapathirana PC, Delnoij T, Lorusso R. Choosing the appropriate configuration and cannulation strategies for extracorporeal membrane oxygenation: the potential dynamic process of organ support and importance of hybrid modes. *Eur J Heart Fail.* 2017;19(S2):75–83.
- Starling EH. The Linacre lecture of the law of the heart. London: Longmans, Green & Co.; 1918.
- Stoliński J, Rosenbaum C, Flameng W, Meyns B. The heart-pump interaction: effects of a microaxial blood pump. *Int J Artif Organs.* 2002;25(11):1082–8.
- Tayara W, Starling RC, Yamani MH, Wazni O, Jubran F, Smedira N. Improved survival after acute myocardial infarction complicated by cardiogenic shock with circulatory support and transplantation: comparing aggressive intervention with conservative treatment. *J Heart Lung Transplant.* 2006;25(5):504–9.
- Thiele H, Lauer B, Hambrecht R, Boudriot E, Cohen HA, Schuler G. Reversal of cardiogenic shock by percutaneous left atrial-to-femoral arterial bypass assistance. *Circulation.* 2001;104(24):2917–22.
- Thiele H, Sick P, Boudriot E, Diederich K-W, Hambrecht R, Niebauer J, et al. Randomized comparison of intra-aortic balloon support with a percutaneous left ventricular assist device in patients with revascularized acute myocardial infarction complicated by cardiogenic shock. *Eur Heart J.* 2005;26(13):1276–83.
- Thiele H, Zeymer U, Neumann FJ, Ferenc M, Olbrich HG, Hausleiter J, et al. Intraaortic balloon support for myocardial infarction with cardiogenic shock. *N Engl J Med.* 2012;367(14):1287–96.
- Thiele H, Zeymer U, Neumann FJ, Ferenc M, Olbrich HG, Hausleiter J, et al. Intra-aortic balloon counterpulsation in acute myocardial infarction complicated by cardiogenic shock (IABP-SHOCK II): final 12 month results of a randomised, open-label trial. *Lancet.* 2013;382(9905):1638–45.
- Thiele H, Jobs A, Ouweneel DM, Henriques JPS, Seyfarth M, Desch S, et al. Percutaneous short-term active mechanical support devices in cardiogenic shock: a systematic review and collaborative meta-analysis of randomized trials. *Eur Heart J.* 2017;38(47):3523–31.
- Thiele H, Zeymer U, Thelemann N, Neumann F-J, Hausleiter J, Abdel-Wahab M, et al. Intraaortic balloon pump in cardiogenic shock complicating acute myocardial infarction: long-term 6-year outcome of the randomized IABP-SHOCK II trial. *Circulation.* 2018. <https://doi.org/10.1161/CIRCULATIONAHA.118.038201>.
- Valgimigli M, Steendijk P, Sianos G, Onderwater E, Serruys PW. Left ventricular unloading and concomitant total cardiac output increase by the use of percutaneous Impella Recover LP 2.5 assist device during high-risk coronary intervention. *Catheter Cardiovasc Interv.* 2005;65(2):263–7.
- Veillard-Baron A, Loubieres Y, Schmitt JM, Page B, Dubourg O, Jardin F. Cyclic changes in right ventricular output impedance during mechanical ventilation. *J Appl Physiol.* 1999;87(5):1644–50.
- Weil BR, Konecny F, Suzuki G, Iyer V, Cauty JM Jr. Comparative hemodynamic effects of contemporary percutaneous mechanical circulatory support devices in a porcine model of acute myocardial infarction. *JACC Cardiovasc Interv.* 2016;9(22):2292–303.
- Wernly B, Seelmaier C, Leistner D, Stahl BE, Pretsch I, Lichtenauer M, et al. Mechanical circulatory support with Impella versus intra-aortic balloon pump or medical treatment in cardiogenic shock—a critical appraisal of current data. *Clin Res Cardiol.* 2019;108(11):1249–57.
- Westaby S, Anastasiadis K, Wieselthaler GM. Cardiogenic shock in ACS. Part 2: role of mechanical circulatory support. *Nat Rev Cardiol.* 2012;9(4):195–208.
- Xie A, Forrest P, Loforte A. Left ventricular decompression in veno-arterial extracorporeal membrane oxygenation. *Ann Cardiothorac Surg.* 2019;8(1):9–18.



Pathophysiology of Sepsis and Heart-Lung Interactions: Part 1, Presentation and Mechanisms

52

Sheldon Magder

Introduction

Sepsis is a frequent clinical problem in intensive care units (Angus and van der Poll 2013). It can be difficult to treat and it occupies a considerable amount of an intensivist's time. It is the final factor in the death of many critically ill patients (Rhee et al. 2019). Survival from sepsis has improved considerably over the past two decades (Thompson et al. 2019; Angus et al. 2001) but mortality still remains high, it is costly to treat, and it results in considerable long-term morbidity (Buchman et al. 2020a, b). The management of sepsis also is an evolving subject. Newer approaches to sepsis management and further improvements in survival require an understanding of the macro- and micro-physiological processes that lead to septic patients being in extremis. Many of the reviews on sepsis have dealt with the variabilities in immune responses over prolonged periods (Hotchkiss and Karl 2003). The emphasis in this chapter, though, is on hemodynamics and the early approaches to the treatment of severe sepsis and septic shock. When treatments are started quickly, and appropriate antibiotics are given, sepsis often largely resolves in a few days. When it does not, the course is pro-

longed, mortality is much higher, and the associated multi-organ injury and failure do not respond to simple hemodynamic management and lead to a prolonged course of recovery (Thompson et al. 2019). The management of this later phase is quite different than the acute (i.e., less than 5 days) phase and involves a smaller proportion of the total sepsis population. Accordingly, this chapter concentrates on patients in the acute phase with marked hemodynamic instability. It has become clear that early hemodynamic and respiratory stabilization is an important factor for a positive outcome.

Definition

The term systemic inflammatory response (SIRS) indicates the generalization of the inflammatory process to include the whole body as is manifest by a number of non-specific symptoms and signs that include pyrexia, tachycardia, tachypnea, and neutrophilia, but the cause is not believed to be an infection. Classic examples include pancreatitis, cytokine chemotherapies (Oved et al. 2019; Abboud et al. 2016; Crayne et al. 2019), and cardiogenic shock when it is accompanied by vasodilation and a distributive shock (Kohsaka et al. 2005; Hochman Judith et al. 1995; van Diepen et al. 2013, 2017). Initially, sepsis was based on the definition of SIRS with the addition of a suspected infection (Bone et al. 1989). There have

S. Magder (✉)
Royal Victoria Hospital (McGill University Health Centre), Departments of Critical Care and Physiology
McGill University, Montreal, QC, Canada
e-mail: sheldon.magder@mcgill.ca

been updates on the definition. The third international consensus definitions of sepsis and septic shock (Sepsis 3) defined sepsis as (Singer et al. 2016):

a life-threatening organ dysfunction caused by a dysregulated host response to infection. This new definition emphasizes the primacy of the non-homeostatic host response to infection, the potential lethality that is considerably in excess of a straightforward infection, and the need for urgent recognition. As described later, even a modest degree of organ dysfunction when infection is first suspected is associated with an in-hospital mortality in excess of 10%. Recognition of this condition thus merits a prompt and appropriate response.

The new definition incorporated the SOFA score and defined organ dysfunction as a change from baseline values of \geq two points in the organ SOFA score. Septic shock is considered a subset of sepsis and is defined as persisting hypotension requiring vasopressors to maintain mean arterial pressure \geq 65 mmHg and a lactate $>$ 2 mmol/l, despite adequate volume resuscitation. These criteria are believed to represent profound underlying circulatory and cellular metabolism abnormalities that substantially increase mortality. The task force preferred the newer definition of septic shock over the 2001 task force definition of septic shock as “a state of acute circulatory failure” because the new definition includes the cellular abnormalities in the condition discussed below.

The quick SOFA score (eSOFA) was added to indicate the “state of acute circulatory failure” group (Singer et al. 2016; Seymour et al. 2016) and defined it as:

- Respiratory rate \geq 22/min
- Altered mentation
- Systolic blood pressure \leq 100 mmHg.

Limitations of these new definitions were covered well in the editorial that accompanied the publication of the new definitions (Abraham 2016). The major concern was that all definitions of sepsis describe a syndrome and not a specific biological entity that has discriminat-

ing biochemical markers as have evolved for cancers. Another criticism was that the eSOFA score was developed from retrospective analyses and needs to be validated prospectively. However, the score provides a quick indicator at the bedside of patients who need close observation.

Clinical Presentation

I only will highlight key points on the clinical presentation because this subject is extensively covered elsewhere (Angus and van der Poll 2013). The clinical presentation depends upon whether the patient presents with sepsis in the emergency department (ER) or becomes septic in the hospital. Patients presenting in the ER can be in shock when they arrive in the ER, but frequently they arrive looking ill and rapidly deteriorate in the ER. In ProCESS (Protocol Based Care for Early Sepsis) (Yealy et al. 2014) patients were randomized on average within 3 h after arrival in the ER, and around 1 h after they met the criteria for shock. This indicates that there likely was a period in the ER before the onset of shock in many patients. Sepsis most often starts with a depressed blood pressure, but blood pressure many not initially have reached shock levels. Respecting this, the new definition is based on a pressure of \leq 100 mmHg. Fever is a key indicator but it can be absent in the elderly and patients on steroids. Some patients even are initially hypothermic, which easily can be missed if the starting temperature of the probe is not sufficiently lowered before use. A strong clinical indicator of shock is an alteration in the patient’s mental status. This can vary from complete coma to loss of spontaneity in speech, decreased concentration, drowsiness, or even frank delirium, in which case a toxic cause must be ruled out. Tachycardia and tachypnea are common and are part of the SIRS criteria. The tachypnea often produces a primary respiratory alkalosis, which can be an early warning sign of evolving sepsis. A history of chills and rigors, combined with general body aches, especially in the back, strongly suggest the pres-

ence of bacteria in the blood. Based on observations on patients admitted to studies on early management of sepsis in the ER (Yealy et al. 2014; Rivers et al. 2001; Mouncey et al. 2015), the lung is the most frequent source and accounts for between 30% and 40% of cases, followed by urinary tract at 20–27%, and the abdomen at 4–13%. Accordingly, the history and exam need to especially focus on these systems for the typical presentations. In ProCESS (Yealy et al. 2014) and the Rivers' trial (Early Goal Directed in the Treatment of Sepsis and Septic Shock), (Rivers et al. 2001) between 30% and 36% of patients respectively had a positive blood culture, and Rivers reported that 76% had a positive culture from somewhere (Rivers et al. 2001). Thus, the absence of positive cultures does not rule out sepsis.

Sepsis in hospitalized patients is generally more insidious and the causes are different. The lung still is the most common site of infection and is even a more frequent cause than in the ER studies; as examples, the lung was the primary site in 43% in VASST (Vasopressin Versus Norepinephrine Infusion in Patients with Septic Shock) (Russell et al. 2008) and 51% PROWESS (Efficacy and Safety of Recombinant Human Activated Protein C for Severe Sepsis) (Bernard et al. 2001). Abdominal processes are more common in hospital-acquired cases than in the ER and accounted for 20% and 26% of cases in PROWESS and VASST respectively; urinary tract infections were about half as common as in the ER. It was not stated in the studies, but catheter and wound infections are also likely more common in hospitalized patients. Early common warning signs are altered mental status, initially low-grade then higher-grade fevers, decreasing urine output, and decreasing arterial pressure. Increasing heart rate and respiratory rate should always raise the suspicion of sepsis as should a rising neutrophil count. If blood gases are obtained for some other clinical reason, a primary respiratory alkalosis should raise the suspicion of sepsis. Another subtle indicator can be a rising cardiac output in someone whose cardiac output is being monitored for some other reason.

Epidemiology

Sepsis is a common clinical problem and is likely to become even more common because of the increasingly aging population, the increasing survival with complex chronic diseases, and the increasing number of immune-compromised patients. As such, sepsis is a major public health concern; it accounted for more than \$20 billion (5.2%) of total US hospital costs in 2011 (Singer et al. 2016) and in 2018 it accounted for \$22.4 billion cost for USA Medicare, a rise from \$17.8 billion in 2012 (Buchman et al. 2020b). The incidence of sepsis is common. Some have suggested that it is the leading cause of mortality and critical illness worldwide (Vincent et al. 2014; Sakr et al. 2018). It also is clear that many who survive sepsis have long-term physical, psychological, and cognitive disabilities with significant health care and social implications (Iwashyna et al. 2010, 2012). However, a complicating factor in these statistics is that death from sepsis is often an end consequence of another condition and as such more a mode of death. When deaths have been attributed to the primary condition in the adjudication of deaths in large studies, attributable mortality solely due to sepsis is very low (McGarvey et al. 2012). Another important consideration is that mortality from sepsis has significantly decreased. This could be because more people have been identified with sepsis. However, in the large randomized trials on goal-directed therapy, the death rate decreased by half with similar entrance criteria compared to older studies (Rivers et al. 2001; Russell et al. 2008; Hayes et al. 1994; Gattinoni et al. 1995). Finally, in some countries, sepsis coding favors reimbursement which perhaps also favored a higher incidence (Rhee et al. 2014, 2019; Gohil et al. 2016).

Presentation in Experimental Inflammatory Syndromes

Human Data

The evolution of the sepsis syndrome was elegantly studied by Suffredini et al. (1989) in

normal human volunteers. They gave a small bolus of endotoxin to 6 normal subjects and recorded their hemodynamic and biochemical responses for 24 h. Endotoxin is the lipopolysaccharide (LPS) envelope of gram-negative organisms. A control group of 3 subjects received an equal volume bolus of normal saline. LPS activates the innate immune system by binding to Toll-like receptor 4 (TLR4). This triggers a cytokine cascade which is discussed further below (Fig. 52.1) (Suffredini et al. 1989). Even though no bacteria were given, the LPS infusion reproduced typical features seen in most patients with bacteria-induced sepsis including fever, chills, nausea, headaches, arthralgia, myalgia, tachycardia, tachypnea, and hypotension. This indicates that the septic response is due to the activation of cell receptors that are part of the innate immune response and, for the most part, the process does not require an invading live organism. Innate immune cells include dendritic cells, macrophages, and neutrophils, but also endothelial and

epithelial cells that line all body cavities. The presence of activators allows the process to continue. In the normal human study, it took more than 8 h for the activation to wear-off and it is likely that counter-regulatory mechanisms need to be induced to stop the process (van der Poll et al. 1997).

The subjects in the Suffredini study (Suffredini et al. 1989) were instrumented with an arterial line and a pulmonary artery catheter and hemodynamics were followed for 8 h (Figs. 52.2 and 52.3). A strong point of this study is that, unlike the clinical situation, time zero is precisely known. An increase in temperature was evident by 1 h after LPS, peaked by 3 h, and was not back to baseline at 8 h post dose. Cardiac output increased slightly at 1 h, but by 3 h it had increased to 50% above the baseline. This indicates that cardiac output can increase in sepsis without fluid being given. At the 3 h mark, saline was infused at 44 ml/h for 2 h. This further increased cardiac output to over 70% of the

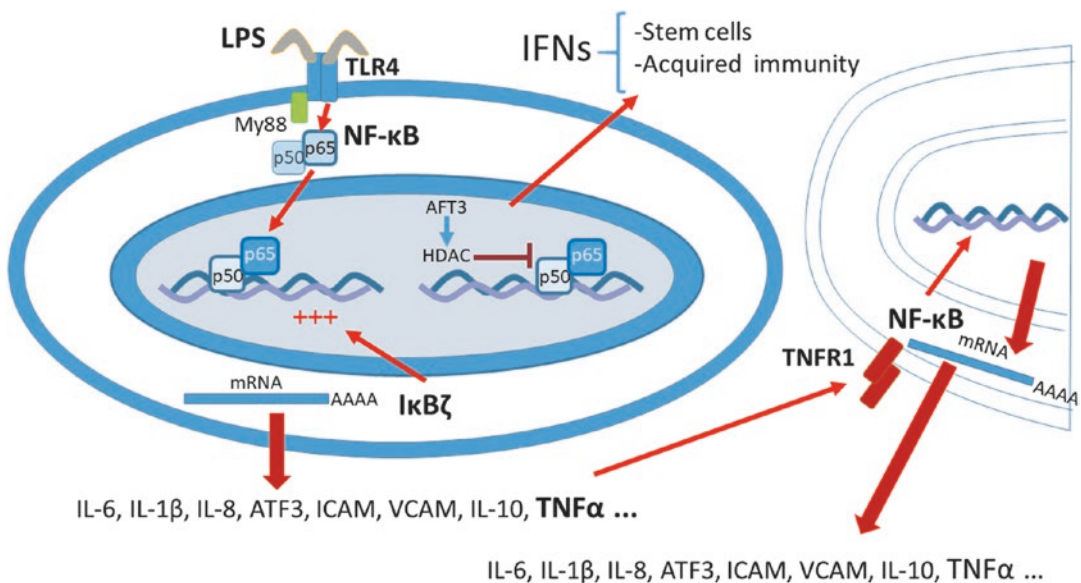


Fig. 52.1 Initiation of septic response through toll-like (TLR4) signaling. The lipopolysaccharide (LPS) coating of gram-negative bacteria activate the TLR4 receptor. TLR4 acts through My88 and other proteins to activate the nuclear factor NF-κB which then moves to the nucleus and drives the transcription of a large number of cytokines, adhesion molecules, and many other proteins involved in the septic response. TNF-α is an especially

important product. It as well as other products signal innate immune cells that also signal through NF-κB to amplify the process. At the same time, pathways are activated such as AFT3 which act on HDAC to inhibit the transcriptional action of NFκB. TLR4 also produces cytokines such as IL-10 that can inhibit the inflammatory process

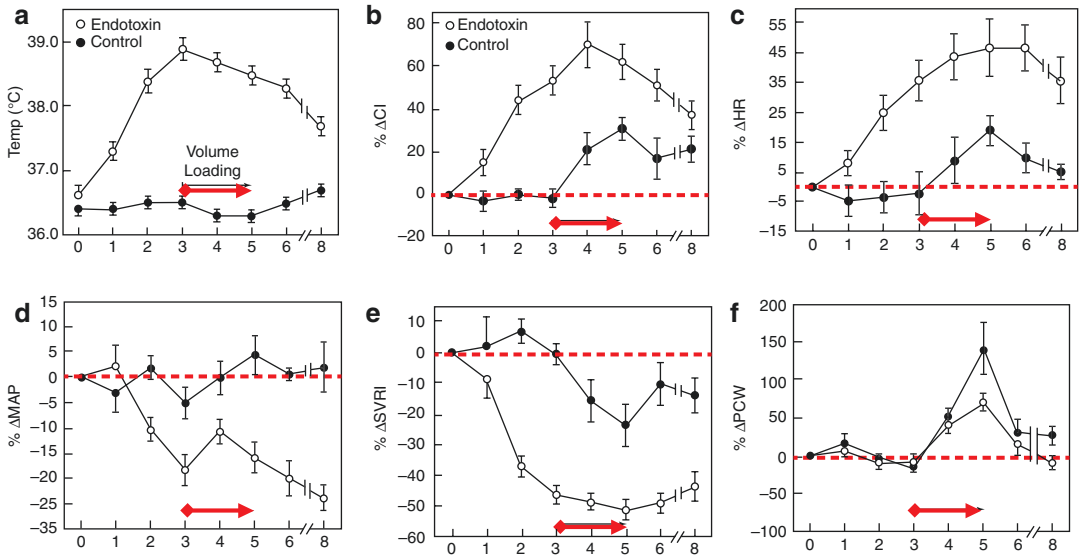


Fig. 52.2 Response of human volunteers to injection of LPS (endotoxin). Responses for 8 h are shown for (a) Temperature, and percent change for (b) cardiac index (CI), (c) heart rate (HR), (d) mean arterial pressure (MAP), (e) systemic vascular resistance (SVR), and (f) pulmonary capillary wedge pressure (PCW). The dark circles are

controls ($n = 3$) and open circles are LPS ($n = 6$). The arrow marks infusion of volume. The dotted lines indicate the baseline value. Data are mean \pm SD. Details are in the text. (From Suffredini et al. (Suffredini et al. 1989). Used with permission of the Massachusetts Medical Society)

baseline value, but the increase in cardiac output with the bolus in the LPS group was less than the increase in the control group. At 8 h, the cardiac output in the LPS group still was higher than in the controls.

The blood pressure did not change at 1 h post LPS infusion, even though the cardiac output had increased. By 3 h the blood pressure fell by 20%, and fell further by 8 h despite the volume infusion. Although systemic vascular resistance (SVR) began to improve by a small amount at the start of volume infusion, it then continued to decline to 25% of the baseline value by 5 h and then moderately improved despite the still falling blood pressure. These observations indicate the limited effect of volume on blood pressure and that there is a dissociation between arterial pressure and systemic vascular resistance that only can be recognized by measuring cardiac output. It also indicates that an increase in cardiac output can be an early sign of impending sepsis.

The pulmonary capillary wedge pressure (Ppcw) and pulmonary arterial pressure (PAP) increased in both groups after the volume infu-

sion; values peaked at 5 h. By 8 h the rise in PAP normalized in the control group but still remained moderately increased in the LPS group.

There was a small initial 5% increase in left ventricular (LV) end-diastolic volume at 1 h, with a return to baseline at 3 h and an associated 5% increase in the EF. Following the volume infusion, LV end-diastolic volume increased by 15% and the EF fell by 10%. At 24 and 48 h after the infusion of LPS all echocardiographic parameters had returned to normal. This quick reversibility indicates that cytokine-induced depression of cardiac function does not produce direct damage to myocytes. It is of interest that the increase in LV volume only occurred after the volume infusion. This might suggest that volume infusion, which was not given for a clinical reason but rather as part of the protocol, “caused the dilatation”. I would prefer to think that the volume infusion just made the LV dysfunction apparent and the volume given allowed for a higher venous return and the maintenance of a higher cardiac output, which was necessary for normal function because of the maldistribution of flow.

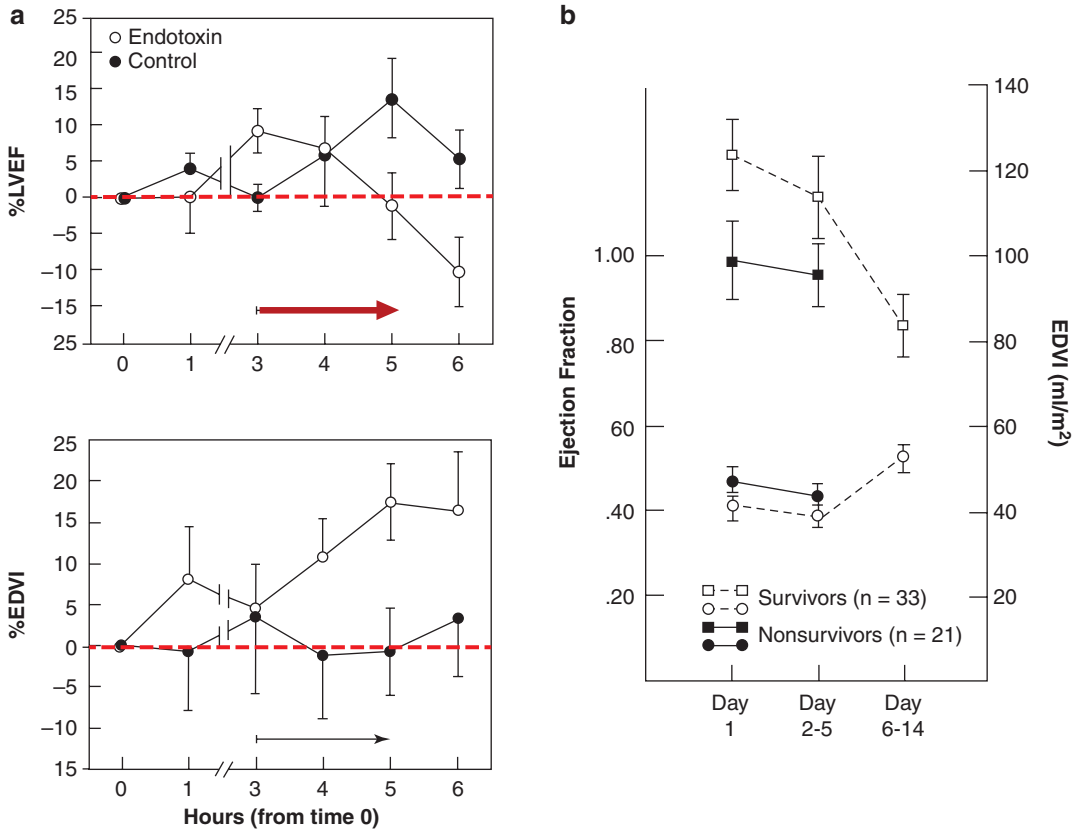


Fig. 52.3 Changes in cardiac volumes in response to LPS. (a) shows percent change in left ventricular ejection fraction (LVEF) and end-diastolic volume indexed (EDVI) from the subjects in Fig. 52.2. (b) shows changes in EF and EDVI in survivor (open symbol) and non-survivors

(closed symbols) over 3 days. (a: From Suffredini et al. (Suffredini et al. 1989). Used with permission of the Massachusetts Medical Society; b: from Parker et al. (Parker et al. 1989). Used with permission of Elsevier)

A striking case report gives further insight into activation of the sepsis syndrome and because of the nature of the event, it is included here under “experimental”. Two and half hours before presentation, a middle-aged laboratory worker injected herself with 1500 ng/kg of *Salmonella minnesota* endotoxin in an attempt to treat her newly discovered malignancy (Taveira Da Silva et al. 1993). For comparison, the usual dose of LPS used in normal human volunteers is 4 ng/kg of *E. coli* endotoxin. The woman had the typical increase in cardiac output, tachycardia, hypotension, and severe hypotension related to a marked

fall in SVR. She also had an initial fall in her neutrophil (PMN) count to $1.6 \times 10^6/L$. Her PMN rose to a peak of $37 \times 10^6/L$ at 24 h. Her liver enzymes rose, her serum creatinine doubled, and she had a mild acidemia. The cytokines TNF- α , interleukins IL-6 and IL-8, and granulocyte colony-stimulating factors all were markedly elevated. By 72 h her signs and symptoms had resolved. Lessons from these two studies are that bacteria are not needed for the process, cytokines drive the septic process, and if the inciting signal is no longer present, the severe process turns off fairly quickly.

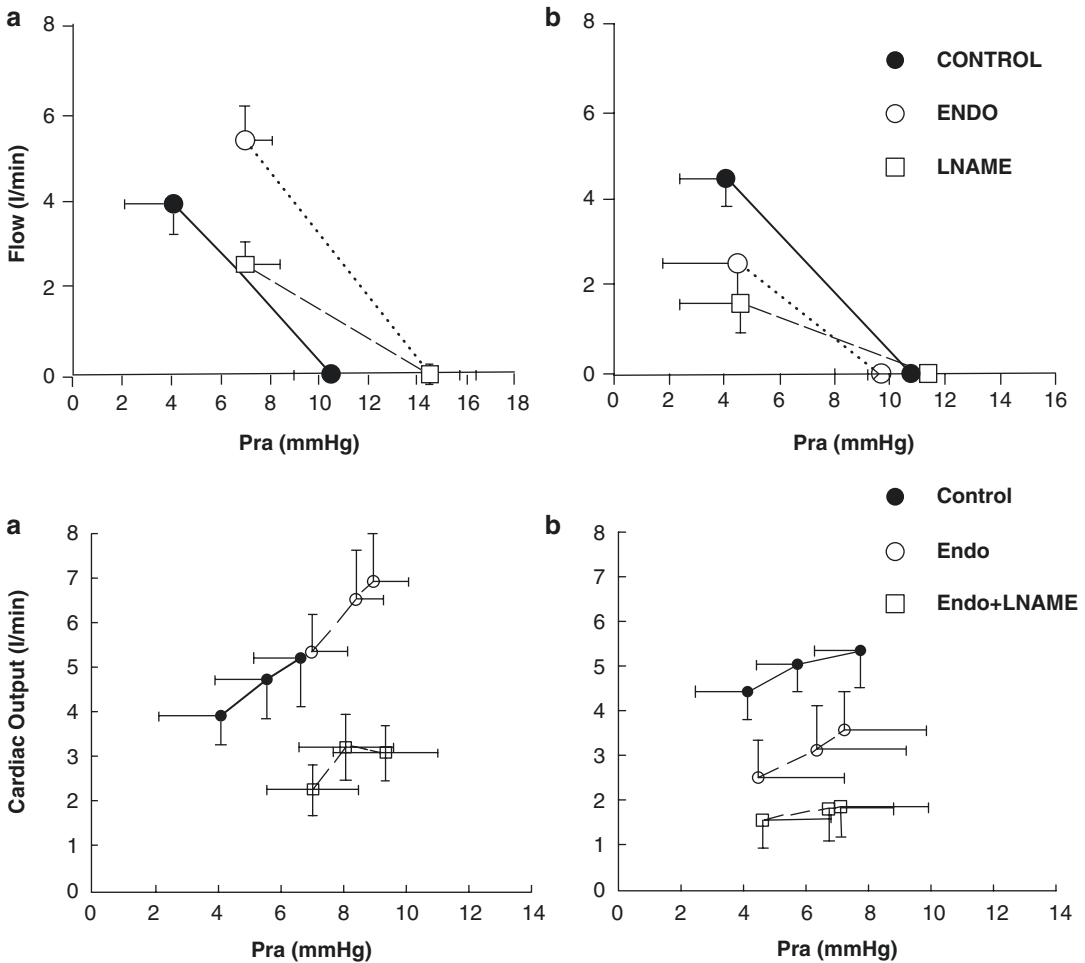


Fig. 52.4 On the left side (a) Venous return and cardiac function curves from pigs under baseline condition, after 2 h of treatment with endotoxin (endo), and then with nitric oxide synthase inhibitor L-NAME. On the left side, the animals were given volume to maintain the baseline Pra (right atrial pressure). In the right panels (b) In the right panels volume was not given. See text for details. Note that with volume and Endo, the venous return curve shifted to the right (control close circle, endo open) and the slope slightly increased (i.e., lower resistance to venous

return – RVR). The cardiac function curve shifted upward suggesting improved function. When no volume was given, RVR increased and MSFP (x-intercept) decreased indicating an increase in vascular capacitance. There was the striking depression of the cardiac function curve when the volume was not given. Application of L-NAME (open square) depressed cardiac function and markedly lowered its plateau; the effect was even greater without volume as was the effect on RVR. (From Magder and Vanelli (Magder and Vanelli 1996). Used with permission of Elsevier)

Animal Data

Pigs treated with a low-dose endotoxin infusion had similar responses to those observed in the human studies but with some notable differences (Figs. 52.4, 52.5, 52.6, and 52.7) (Magder and Vanelli 1996). Cardiac output fell in the first hour and then rose by about 20% by 2 h, which is less than the rise in cardiac output seen in the human

studies. This occurred with what appeared to be an increase in the cardiac function curve (Fig. 52.4). Arterial pressure fell after 1 h and, as in the human studies, this was due to a fall in systemic vascular resistance (Fig. 52.5). In the porcine studies, there was a large increase in PAP in the first hour and it remained elevated at a more moderate level (Mehta et al. 1999a), but there was minimal change in PAP in the human study.

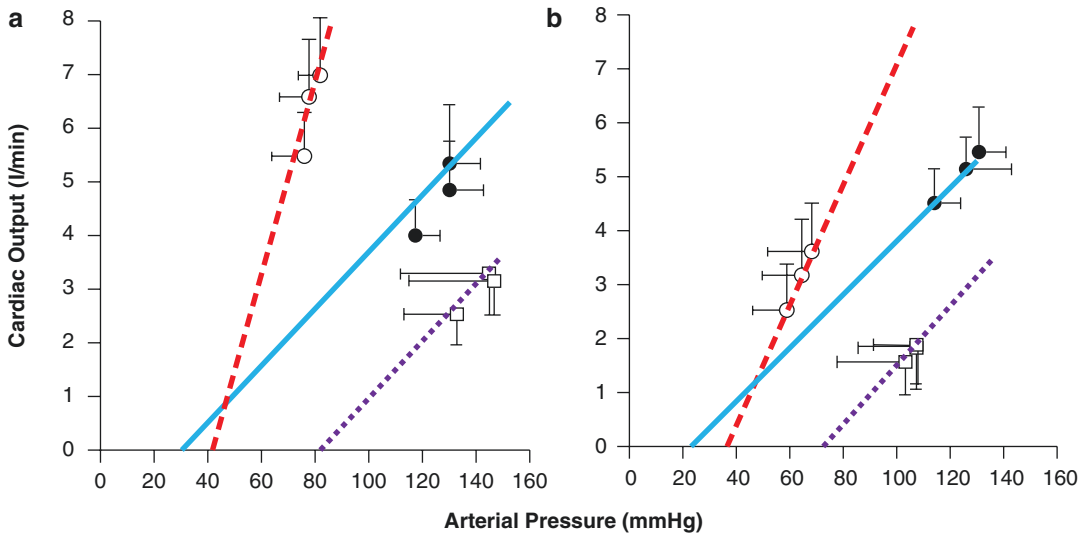


Fig. 52.5 Arterial flow versus pressure curves ($1/\text{resistance}$) for the same animals as in Fig. 52.5. The lines drawn through the mean points indicate the approximate average slopes. Volume-treated animals are on the left (**a**) and no volume on the right (**b**). Symbols are the same as in Fig. 52.5. In both groups, after LPS the arterial flow versus pressure curve became much steeper (decreased

resistance) and there was a small increase in the x-intercept (arterial critical closing pressure). L-NAME restored the resistance to the baseline value but markedly increased the arterial critical closing pressure in both conditions. (From Magder and Vanelli (Magder and Vanelli 1996). Used with permission of Elsevier)

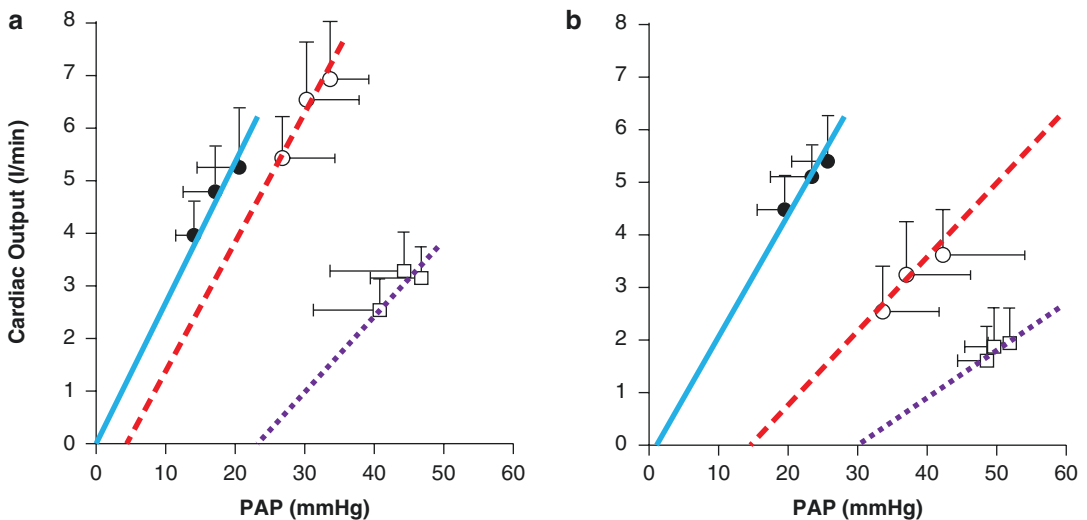


Fig. 52.6 Pulmonary artery flow (cardiac output) versus pulmonary artery pressure (PAP) curves ($1/\text{resistance}$) for the same animals as in Fig. 52.5. Volume-treated animals are on the left (**a**) and no volume on the right (**b**). Symbols are the same as in Figs. 52.5 and 52.6. In volume-treated animals the flow vs pressure curve had a small parallel shift to the right and no change in slope (i.e., $1/\text{resistance}$); this indicates a small increase in pulmonary vascular criti-

cal closing pressure. When no volume was given, there was a moderate increase in pulmonary vascular resistance but a very marked increase in the pulmonary critical closing pressure so that PAP was markedly elevated. These effects were greatly increased with L-NAME. (From Magder and Vanelli (Magder and Vanelli 1996). Used with permission of Elsevier)

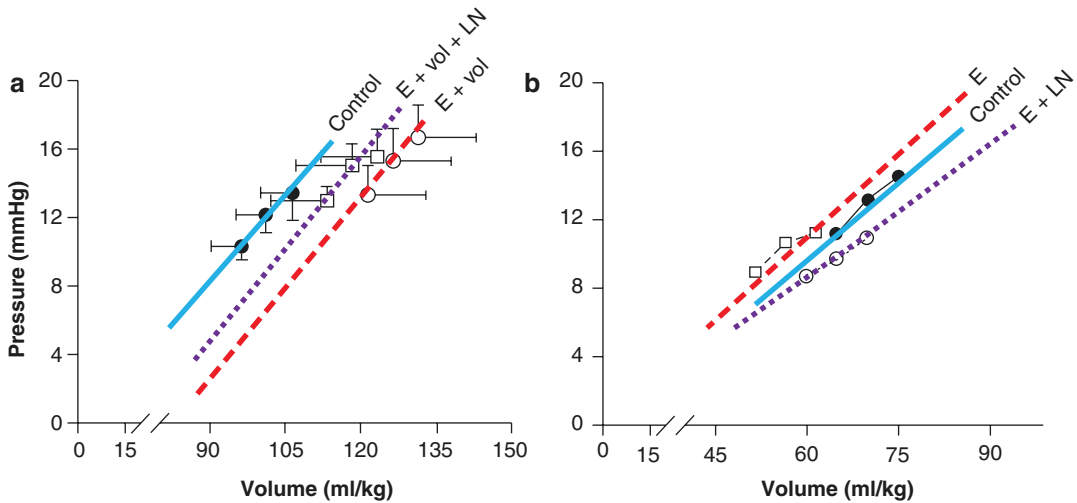


Fig. 52.7 MSFP versus total vascular volume for the same animals as in Figs. 52.5, 52.6, and 52.7. The slope of this relationship is $1/\text{compliance}$. Volume-treated animals are on the left (**a**) and no volume on the right (**b**). Symbols are the same as in Figs. 52.5, 52.6, and 52.7. In volume-treated animals, LPS shifted the line in parallel to the right indicating an increase in vascular capacitance (shift of stressed into unstressed volume). In animals not given

volume, there was a slight decrease in capacitance. In volume-treated animals given L-NAME after LPS, there was a partial return to the left of the compliance curve in volume-treated animals but in non-volume-treated animals there was a small rightward shift (i.e., increase in capacitance). (From Magder and Vanelli (Magder and Vanelli 1996). Used with permission of Elsevier)

The pressure-flow relationship of the pulmonary vasculature was evaluated after 2 h with three repeated rapid boluses of blood. What was apparent was that the pulmonary artery resistance (i.e., slope of the pressure-flow relationship) was unchanged from baseline but the pressure intercept (i.e., x -intercept) increased indicating the development of non-zone III conditions in the pulmonary vasculature (Fig. 52.6). Another observation was that when the volume was given, vascular capacitance increased (i.e., the total vascular pressure-volume curve shifted to the right), which is consistent with the generalized decrease in vascular tone. However, the mean systemic filling pressure (MSFP) still was higher than baseline because of the infused volume (Fig. 52.7).

Sepsis has been studied in an extensive series of studies by Natanson and co-workers who implanted an infected clot in the abdomen of dogs to create a model of abdominal sepsis. Results from their work will be referred to throughout this review (Karzai et al. 1995; Natanson et al. 1990; Natanson 1990; Natanson et al. 1989a; Natanson et al. 1989b; Natanson

et al. 1988; Natanson et al. 1986). The time course of changes in LV and EF was very similar to the pattern seen in humans given LPS (Natanson et al. 1986). A limitation of their studies was that cardiac output did not rise with sepsis as it does in humans. Another large series of animal studies were performed by Traber and co-workers (Talke et al. 1985; Pittet et al. 2000; Traber 2000) as well as Pittet et al. who used an ovine model of sepsis with a slow infusion of endotoxin in awake lambs over a few days. About half the animals developed an increased cardiac output and a distributive state but they did not address the underlying mechanical changes in the circulation to account for it.

Vascular Mechanics Required for the High Cardiac Output State

A striking feature of patients in septic shock is that cardiac output is increased in the majority of patients but yet they have severe hypotension which responds poorly to vasopressors. How can

these two be reconciled? It is best to start with a basic relationship:

$$BP \sim \text{cardiac output} \times \text{SVR} \quad (52.1)$$

It becomes obvious that since cardiac output is elevated in most cases of sepsis and as was seen in the study by Suffredini et al. (Suffredini et al. 1989) and the self-poisoning case report, the primary cause of the hypotension in sepsis is a decrease in SVR, and not a fall but actually a rise in cardiac output. As reviewed in Chap. 2, cardiac output is determined by the interaction of cardiac function, as described in the Frank-Starling relationship, and the venous return function, as described by Arthur Guyton (Guyton 1955). A higher cardiac output indicates that more blood must be coming back to the heart so that more can go out. It at first might be considered that this occurs because the low SVR decreases LV afterload and allows a higher cardiac output. However, this only can account for a small increase in cardiac output because, as discussed in Chap. 2, the cardiac function does not determine what comes back to the heart, except by lowering right atrial pressure, which usually is not low in sepsis. It also needs to be appreciated that in normal physi-

ology, blood pressure is tightly regulated by the arterial baroreceptors and does not normally increase when cardiac output increases. This dissociation was clearly evident in the Suffredini study (Suffredini et al. 1989). This means that a significant proportion of the decrease in SVR could be because the increased cardiac output triggers a baroreceptor decrease in SVR rather than the SVR producing the increase in cardiac output, although the lower arterial pressure does help the rise in cardiac output. Furthermore, PAP often is increased in sepsis, which means that right ventricular (RV) afterload actually is increased. The answer must be that the venous return function increased. It is important to appreciate that in the Suffredini study (Suffredini et al. 1989) (Fig. 52.2), cardiac output increased before exogenous fluid was given. This could have happened two ways. There could have been a decrease in vascular capacitance and recruitment of unstressed volume into stressed volume (Rothe 1983a; Rothe 1983b); this would have increased MSFP and shifted the venous return curve to the right (Fig. 52.8). Alternatively, there could have been a decrease in venous resistance. These two possibilities are discussed next.

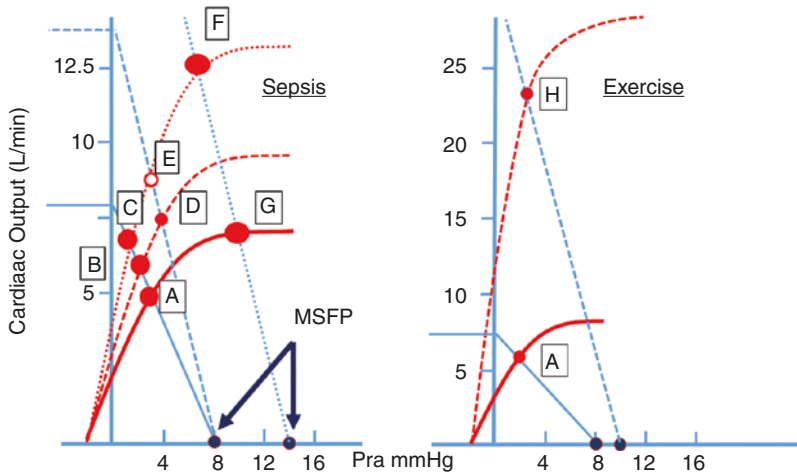


Fig. 52.8 Theoretical comparison of the changes in venous return and cardiac function required to reach the elevated cardiac outputs in a septic patient (left) and a normal young male maximally exercising (right). Note that the y-axis scale on the right is double that of the left. In sepsis, despite depression of myocardial function, the compensating release of catecholamines and vagal withdrawal increase heart rate and contractility and the function curve moves up (A–C) with a fall in Pra (right atrial pressure). If venous resistance decreases, there can be

further increases in cardiac output (D, E) with little rise in Pra. An increase in vascular volume by volume infusion, or by constriction of vascular capacitance by NE, shifts the venous return curve to the right (increase in MSFP) and produce a much larger rise in cardiac output (F, G). On the right, during exercise, the cardiac output and CVP start the same but the rise is markedly greater because of the much larger increase in cardiac function, decrease in venous resistance, with a smaller increase in MSFP (H)

Sepsis is associated with a generalized loss of vascular tone. Accordingly, in animal models of sepsis without volume resuscitation, MSFP falls. This indicates that vascular capacitance increases along with the general loss of vascular tone and cannot account for a rise in MSFP (Figs. 52.4 and 52.7) (Magder and Vanelli 1996; Rastegarpanah and Magder 1998). Volume resuscitation thus likely restores intravascular volume and increases MSFP. This then would produce the further increase in cardiac output with volume infusion observed by Suffredini et al. in humans (Suffredini et al. 1989).

The other possibility is that there was a decrease in venous resistance. Given the very large increases in cardiac output that can occur in septic patients, this must be the case (Fig. 52.8). Venous resistance could decrease by dilation of venous resistance vessels as part of the generalized loss of vascular tone that also occurs in arterial resistance vessels and even in the ventricles. It also could occur through a decrease in the tone of a sphincter-like mechanism that controls the venous outflow from the splanchnic circulation; this is known to occur by the action of beta agonists in response to decreased baroreceptor tone (Deschamps and Magder 1992; Greenway 1983; Green 1977). Unfortunately, it has not been possible to demonstrate a decrease in venous resistance in septic animals. This is because, in contrast to what happens in septic humans, cardiac output generally is decreased and SVR increased in most animal models of sepsis, and especially in studies with rats and mice. Of interest, SVR is frequently increased in children (Wheeler and Wong 2016; Ceneviva et al. 1998). The reasons given for this in children are that children are more sensitive to changes in afterload, their endothelium tends to respond to stress by sending vaso-constricting signals instead of vasodilatory signals, they have a greater dependency on Ca^{2+} and beta adrenergic activity, and there is less total cardiac muscle mass to sufficiently increase contractility in response to the stress (Wheeler and Wong 2016). Some of these factors may also be true in small mammals.

An effective decrease in venous resistance also occurs if there is redistribution of blood flow

to the muscle vasculature because of its faster time constant of drainage than the splanchnic circulation (Deschamps and Magder 1992; Green 1977; Mitzner and Goldberg 1975). This is known to occur through baroreceptor signaling and infusion of beta-agonists. This redistribution has not been shown in septic animal models, but as already noted, they do not mimic the usual distributive shock seen in the human condition, and the experimental conditions needed to measure these changes are very complex (Deschamps and Magder 1992). A final mechanism could be congestion of the liver because liver congestion decreases the venous compliance of splanchnic vasculature and a decrease in compliance (not capacitance) decreases the time constant of drainage of a vascular bed (Magder and Quinn 1991). This would effectively appear as a decrease in the resistance to venous return because the time constant of drainage of the splanchnic vasculature would become faster.

Cardiac output can increase without an increase in cardiac function by the Frank-Starling mechanism when venous return increases (Patterson and Starling 1914). However, the increase in cardiac output by this mechanism is modest and cannot explain the high cardiac output observed in septic patients. This is because of the normal limit of right heart filling. Thus, there also must be an increase in cardiac function. Yet, it is widely accepted that myocardial function is depressed in septic patients (Parker et al. 1989, 1990) and animals (Magder and Vanelli 1996; Natanson et al. 1986; Ognibene et al. 1988). This most commonly is identified by dilatation of the LV and a decrease in the ejection fraction (Fig. 52.3). This seeming contradiction can be understood by appreciating that in vivo there are competing factors. First, the increase in diastolic size can allow stroke volume to be maintained or even increased at the same heart rate and LV end-systolic pressure volume relationship (LVESPV). The decrease in systemic arterial pressure decreases LV afterload and shifts the cardiac function curve upward. Increased sympathetic drive also increases heart rate and restores some of the loss of contractility as represented by an increase in the LV end-systolic elastance, which

further shifts the cardiac function curve upward. The combination of all these factors allows for a higher cardiac output and improvement in the cardiac function curve despite the intrinsic function of the heart being depressed. The depression would be evident if the cardiac output was driven to its maximum capacity, but is not evident at sub-maximum conditions (Fig. 52.8). Thus, a distinction needs to be made between an increase in cardiac output and a decrease in cardiac function that could still be pushed by other factors to give a higher cardiac output than normal.

Another somewhat surprising observation is that non-surviving septic patients have less dilatation of the LV than surviving patients (Fig. 52.3) (Parker et al. 1987, 1989). This might be explained by their being more RV dysfunction when sepsis is worse. The depressed RV then cannot pass sufficient volume to the LV to allow it to dilate. This could be a direct effect on RV myocardium or due to increased PAP compromising the RV output as in the porcine study shown in Fig. 52.7.

PAP commonly increases in sepsis and this can potentially compromise overall cardiac function by increasing RV afterload (Suffredini et al. 1989; Parker et al. 1987). It also rises in the hyperdynamic sheep studies (Talke et al. 1985; Pittet et al. 2000). Of note, in Suffredini et al. (Suffredini et al. 1989) on normal subject treated with LPS, PAP only increased after volume was given, and the increase in cardiac output was the same in the control subjects except that their PAP fell after the fluid infusion but it did not fall in the LPS subjects. An increase in PAP can be due to increased pulmonary vascular resistance as well as an increase in non-zone III lung, lung injury which produces loss of effective lung tissue and thus loss of vascular cross-sectional vascular area, hypoxic vasoconstriction, and by the often required mechanical ventilator support. As discussed in Chap. 3, the RV does not tolerate pressure loads well. The tolerance is even worse in sepsis because of the intrinsic compromise of cardiac muscle and increased volume returning per minute. The rise in PAP in response to an infusion of LPS has two phases in animal studies which were identified by the use of pharmacological inhibitors (Javeshghani

and Magder 2001a; Yamamoto et al. 1997). There is an early marked rise due to the release of thromboxane A2 and a later phase with a smaller increase in PAP which was due to endothelin-1 (Yamamoto et al. 1997).

Coronary Blood Flow and Myocardial Ischemia

A rise in troponins is frequent in patients with septic shock. The increase is generally in proportion to the degree of myocardial depression and thus correlates with mortality. This raises the question as to whether the myocardial injury in septic shock patients is due to impaired coronary blood flow and ischemic myocardium. To address the issue, Cunnion et al. (Cunnion et al. 1986) placed catheters in the coronary sinus of patients with septic shock and measured coronary blood flow and extraction of lactate. Coronary blood flow was increased in all subjects and the increase was greatest in those who died. Fractional O₂ extraction was decreased, as has been observed in other tissues (Duff et al. 1969; MacLean et al. 1967), and there was no decrease in lactate extraction. Similar studies were performed by Dhainaut et al. (Dhainaut 1987). They, too, found that coronary flow was increased in septic patients and the coronary flow was even higher in those that died. It thus is evident that the low blood pressure in septic shock does not compromise coronary flow. The coronary arteries dilate as part of the generalized vasodilation and according to the metabolic needs of the heart. Coronary reserves are very large and are sufficient for the heart's needs even in shock (Magder 1986). The authors also found that lactate extraction was not decreased but rather increased, and there was a marked reduction in the extraction of free fatty acids. These results indicate that the primary problem is the distribution of flow and the uptake of substrates by myofibres. It also is unlikely that the troponin indicates irreversible ischemic damage and that it indicates a failure to deal with the turnover and degradation of proteins as part of normal recycling processes (Weil et al. 2018; White 2011).

In further studies in his septic dog model, Natanson and co-workers found that a catecholamine challenge doubled myocardial O₂ consumption without any abnormality in O₂ extraction, lactate production, or intracellular concentrations of high-energy phosphate compounds, further confirming that myocardial dysfunction in sepsis is not due to impaired O₂ delivery or utilization (Solomon et al. 1994).

Basic Cellular Mechanisms

Triggering the Process: Cytokine Cascade

The sepsis syndrome begins with activation of the innate immune system when pathogen-associated molecular patterns (PAMPS) in blood or tissues are recognized by pattern-recognition receptors (PRRs) (Bianchi 2007; Takeuchi and Akira 2010). This initiates a highly complex and coordinated transcriptional process that results in a large variety of proteins involved in the inflammatory process of which only key factors are highlighted here (Fig. 52.1). PAMPS include LPS, lipoteichoic acid, flagellin, mannan in fungi, DNA in bacteria, and double- or single-strand RNA in viruses. There are four classes of PRRs. Two are transmembrane proteins which include the 10 Toll-like receptors (TLR) (Takeda et al. 2003; Akira et al. 2001) and C-type lectin receptors. The other two are cytoplasmic proteins and include the Retinoic acid-inducible gene-1-like receptors (RLRs) and the NOD-like receptors (NLRs), which are parts of inflammasomes (Takeuchi and Akira 2010). When tissue injury develops, endogenous damage-associated molecules (DAMPs or Alarmins) are released and also can bind to PRRs and further perpetuate the inflammatory state (Takeuchi and Akira 2010).

Once PAMPS bind to PRRs, intracellular signaling pathways are activated. These most often cause the translocation of nuclear factor- κ B (NF κ B) and the transcription of cytokine mRNA (Takeuchi and Akira 2010; Bohrer et al. 1997). Bacterial infections primarily activate TLR2 and TLR4 (Fig. 52.1). One of the first cytokines to be

produced in the pathway is tumor necrosis factor- α (TNF α) (Angus and van der Poll 2013; Thiemeermann et al. 1993a; Beutler and Cerami 1986; Dinarello et al. 1986; Tracey et al. 1986; Beutler et al. 1985; Ziegler 1988). It then feeds back on its own cellular receptors and drives further cytokine production. At the same time that pro-inflammatory cytokines are being produced, there also is the expression of anti-inflammatory cytokines, such as IL-10, which begin to dampen the process (Cavaillon et al. 1994). As well, transcriptional processes are negatively regulated by simultaneous activation of such factors as transcription factor-3 (ATF3) which acts by increasing histone deacetylase activity (Takeuchi and Akira 2010) which inhibits transcriptional processes. There also is the activation of the acquired immune system that can both amplify and turn down the inflammatory pathway (Angus and van der Poll 2013; Hotchkiss and Karl 2003; van der Poll et al. 1997; Opal and DePalo 2000).

Because TNF α is produced so early in the septic process, and because it triggers the transcription of a host of other cytokines, it was considered to be a good target to silence, and thereby turn down the inflammatory state (Tracey et al. 1987). However, this rational failed in clinical trials (Abraham et al. 1995, 1997, 1998). This naive thought has been repeated many times with drugs targeted against multiple mediators of the septic response (Marshall 2014). The signaling by TNF α does start early in the process, and it is at the top of the cytokine cascade, but there are other redundant pathways that have the same intracellular signaling pathways. For example, in endothelial cells, the transcriptional profile of LPS and TNF α are almost identical except for some extra mRNA induced or suppressed by TNF α which has two receptors (Magder et al. 2006). It also is a common mistake to think that the inflammatory process is not active when TNF α is not evident. This simply could mean that its time of expression has passed and other downstream cytokines are active. As an example, in the study by Suffredini et al. (Suffredini et al. 1989), TNF α expression was almost gone by 3 h after the LPS bolus and also in the case report of the overdose of LPS (Taveira Da Silva et al.

1993). In the overdose case report, there was no expression of IL-6 at 1 h and but IL-6 peaked at 6 h. A very similar pattern was found in endothelial cells grown in culture and treated with endotoxin (Magder et al. 2006). Thus, when trying to understand the evolution of pathological processes, the timing of cytokine measurements from a known starting point is very important (Werner et al. 2005), but it is not possible to precisely know this time of onset in most human diseases.

Drivers of the Clinical Manifestations

In a large percentage of patients with sepsis, and even septic shock, the onset of symptoms is relatively fast, but if treatment is started promptly, marked recovery can be seen as early as 8–10 h after the onset, and supportive therapies can be de-escalated rapidly. The implication of this observation is that tissues must not be irreparably damaged by the initial septic process, but instead, they have alterations in their normal metabolic functions and transcriptional profile. In support of this, autopsy studies have shown a marked discordance between histological findings and the degree of clinical organ dysfunction (Hotchkiss and Karl 2003). Little cell death is seen in the heart, kidney, liver, and lung (Singer 2014). The main two cell types dying are lymphocytes and gastrointestinal epithelial cells. The question then becomes what is producing this reversible disruption of normal homeostatic mechanisms (Hotchkiss and Karl 2003).

Vascular Failure in Sepsis

An important early step in the understanding of the pathophysiology of sepsis was the observation by McClean and co-workers that the venous O₂ saturation in septic patients was normal or higher than normal even though serum lactate concentration was elevated (Duff et al. 1969; MacLean et al. 1967; Wright et al. 1971). This indicated that the problem was not an inadequate supply of O₂ to tissues, but rather a failure of tis-

ues to use the delivered O₂ in normal metabolism. They hypothesized that this was because blood flow bypassed the capillary beds through alternative shunt-like channels that dilated as part of the septic process. The problem also could have been because the microcirculation became obstructed by micro-thrombi, which diverted the blood (Russell 2006). These processes produce an ischemic hypoxemia. An alternative hypothesis also emerged that the problem is not related to blood flow, but rather to the failure of the mitochondria to extract the O₂ in what is called cytotoxic hypoxia (Singer 2007; Fink 2001). Likely both occur.

Mechanisms of Vascular Dysfunction

A major challenge for clinicians dealing with septic patients is how to maintain adequate cardiovascular system performance that can maintain the perfusion needs of the tissues. Even though inadequate flow may not be the primary process, adequate distribution of blood flow is necessary to deliver antibiotics as well as the body's immune cells and agents that are needed to reverse the septic process. The primary vascular problem is the failure of vascular smooth muscle to maintain appropriate vascular tone. The consequence is loss of a steady perfusion pressure, maldistribution of blood flow on a global level and at a microcirculatory level, and failure to maintain adequate vascular filling pressures for the return of blood to the heart in the time available for each cardiac cycle. The second major problem is a change in the expression profile of normal endothelium to a phenotype that is prothrombotic, pro-inflammatory, and has diminished barrier function (Russell 2006; Engelmann and Massberg 2013; Singla and Machado 2018). Currently, there are no therapies directed specifically at endothelial dysfunction except possible manipulations of the coagulation system (Bernard et al. 2001). This chapter thus will primarily discuss vascular smooth muscle dysfunction.

As a brief background, a fundamental principle for understanding vascular smooth muscle

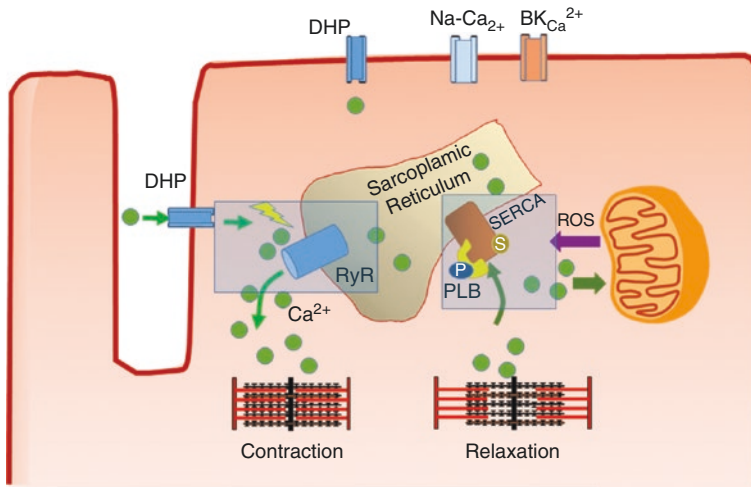


Fig. 52.9 General outline of calcium regulation of cytoplasm in sarcomeres (myocardial cells). Increased cytoplasmic Ca²⁺ is the key factor for activation of actin-myosin sliding filaments and force production. During the plateau of the action potential Ca²⁺ enters the cell through L-type Ca²⁺ channels (i.e., dihydropyridine – DHP). This triggers a larger release in Ca²⁺ from the sarcoplasmic reticulum (SR) via the Ryanodine receptor (RyR), which increases intracellular [Ca²⁺] and activates contraction. When the

action potential repolarizes, the sarco-endoplasmic reticulum Ca²⁺-ATPase (SERCA) pumps cytoplasmic Ca²⁺ back into the SR and ends contraction. Activities of both of pumps are altered by changes in the redox state and for SERCA, by alterations in sulfhydryl through the action of nitrotyrosine which derives from nitric oxide (NO). Alterations in the handling of Ca²⁺ by these two pumps are potentially important targets for the loss of vascular tone and decreased myocardial function in sepsis

tone is that the tone is determined by the concentration of cytoplasmic calcium ions ([Ca²⁺]) which acts through the action of Ca²⁺ on proteins that regulate the activity contractile proteins. Ca²⁺ enters the cytoplasm from extracellular and intracellular stores (sarcoplasmic reticulum) (Fig. 52.9). An increase in cytoplasmic [Ca²⁺] increases muscle tone and a decrease in cytoplasmic [Ca²⁺] decreases muscle tone in all muscle types. The primary action of Ca²⁺ is on the kinase calmodulin which when phosphorylated increases the activity of the regulatory component of the light chain of myosin. This allows actin to activate myosin ATPase and contraction to occur. A counter-regulatory mechanism also exists. Activation of cyclic guanosine monophosphate (cGMP) activates a phosphatase that removes the phosphate and decreases the activity of the regulatory component of the myosin light chain and thereby reduces the force of muscle contraction (Landry and Oliver 2001).

Role of Potassium ATP Channel

The activation of intracellular processes is very dependent upon the electrical charge (i.e., transmembrane potential) across the cell membrane because the transmembrane potential controls the influx of Ca²⁺. Potassium ion (K⁺) is the primary determinant of transmembrane potential. Of the four known K⁺ channels, the K⁺-ATP channel (K_{ATP}) has been of particular interest because it is linked to metabolism (Landry and Oliver 2001; Landry and Oliver 1992; Lange et al. 2008). This discussion involves the role of this channel in vascular smooth muscle. An increase in H⁺ and lactate, as would exist with muscle activity and increased energy needs, activates this channel. K⁺ is extruded from the cell, and the membrane becomes hyperpolarized (more negative) relative to the outside. Less Ca²⁺ enters the smooth muscle cells and they relax. Under physiological conditions, this allows tissue blood flow to increase

in relation to metabolic demand. It was hypothesized that the increase in H^+ and lactate during sepsis activates this channel and thereby decreases vascular smooth muscle tone. If true, an inhibitor of K_{ATP} such as the sulfonylurea drugs used in diabetes could potentially restore vascular tone. This indeed was demonstrated in controlled animal studies. However, it failed in human studies (Lange et al. 2008; Morelli et al. 2007; Chan et al. 2012; Warrillow et al. 2006). There are a number of reasons why this might have happened (Dünser and Brunauer 2012). First, the many other regulatory systems likely over-rode the importance of K_{ATP} channels under pathological conditions. However, a more important argument may be that the hypothesis required the inhibitor prevent the hyperpolarization of the cell membrane by the K_{ATP} . Maintenance of membrane potential is an energy-expensive activity that takes up a lot of an organism's resting energy needs. Under septic conditions, and when there are abnormal metabolic processes and disordered energy use, it is more likely that the transmembrane potential is already decreased because of the failure of systems required to maintain it. At cell death, there is no transmembrane potential! The real problem thus is more likely that intracellular regulation of the phosphorylation status of the myosin is already altered and that it is no longer simply regulated by the transmembrane potential and external factors. For example, methylene blue, which inhibits the intracellular mediator cGMP, can increase arterial pressure when adrenergic agents fail, but unfortunately, this effect is short lived as other intracellular factors likely counter act it (Preiser et al. 1995; Keaney et al. 1994; Schneider et al. 1992).

Nitric Oxide and Superoxide

In the 1980s the gas nitric oxide (NO), and the enzymes that make it, nitric oxide synthases (NOS), were identified as new regulators of intracellular $[Ca^{2+}]$ and vascular tone (Petros et al. 1991a; Moncada 1992; Furchgott and Zawadzki 1980). NOS enzymes are found in endothelial

cells, neutrophils and macrophages, cardiac cells, and neuronal cells. When discovered, these enzymes created a revolution in vascular biology and many other physiological processes. There are three types of NOS: endothelial NOS (eNOS), neuronal NOS (nNOS), and an inducible NOS (iNOS), which is primarily found in inflammatory cells. There was particular interest in iNOS because its transcription is markedly increased as part of the inflammatory response, whereas transcription of eNOS and bNOS are only moderately regulated. Instead, the production of NO by eNOS and bNOS is regulated by membrane regulators of intracellular $[Ca^{2+}]$ (Preiser et al. 1995; Keaney et al. 1994) and thus their production of NO is regulated and responsive to physiological demands. In contrast, NO production by iNOS is not regulated by intracellular $[Ca^{2+}]$, and the amount of NO produced is dependent upon how much iNOS protein is produced. As a result, iNOS can produce large amounts of NO without counter-regulatory processes and can cause major vascular vasodilation in septic animals. It thus was hypothesized that production of iNOS is the major player in the vasodilation in septic shock (Hom et al. 1995; Thiernemann and Vane 1990) as well as in severe hemorrhagic shock (Landry and Oliver 2001; Thiernemann et al. 1993b), and that blocking NOS production of NO would be a useful therapeutic tool for patients with refractory septic shock (Petros et al. 1991a; Szabo et al. 1993). Indeed, in small early series of patients with septic shock, an NOS inhibitor restored arterial pressure (Petros et al. 1991b; Nava et al. 1992). However, a subsequent large, multicenter, double-blind randomized study was stopped prematurely because of increased harm in the NOS inhibitor group (Lopez et al. 2004). What went wrong? The answer to this is informative for many of the other treatments that have been tried but have failed in sepsis.

First, in the preliminary study by Petros et al., the NOS inhibitor raised blood pressure but did not change or even decrease cardiac output (Petros et al. 1991b). It is important to remember that pressure is not flow, and it is blood flow that counts for tissue function. The second problem is that NO from eNOS plays a very important role

in vascular health, including regulation of downstream resistances by flow-mediated dilation and maintenance of an antithrombotic and anti-inflammatory endothelial phenotype and that NO from nNOS is important for normal neuronal and even cardiac function. These functions were inhibited by the non-specific NOS inhibition. More importantly, though, is that the original studies were done in rats and mice. These species have a robust induction of iNOS (Stewart et al. 1995) in response to cytokines and LPS, but this is not the case in larger animals and humans. Although iNOS messenger RNA (mRNA) has been identified in a number of human tissues, including vascular smooth muscle (MacNaul and Hutchinson 1993), macrophages (Weinberg et al. 1995; Reiling et al. 1994), hepatocytes (Geller et al. 1995), synovial cells of inflamed joints (Sakurai et al. 1995), thyroid cells in culture (Kasai et al. 1995), breast cancer cells (Thomsen et al. 1995), squamous cell carcinoma (Rosbe et al. 1995), and renal tubular cells (McLay et al. 1994), the only evidence for iNOS protein was obtained by immunostaining which is not specific. None of these studies showed protein by western blotting, the definitive marker of iNOS protein, whereas the protein is very easy to identify in rodents (Thiemermann and Vane 1990). The one exception is the detection of significant amounts of iNOS protein expressed in the nares and upper airways of human and it is associated with measurable constitutive NO production. This is thought to have a protective role in regulating airway tone. iNOS also has been found in the hearts of patients with end-stage heart failure in some studies (Haywood et al. 1996), but not in others (Stein et al. 1998) although in the study that claimed to find iNOS protein, the protein was a different size than the reference sample on the western blot (Haywood et al. 1996). We, too, found induction of iNOS mRNA in pigs treated with LPS but failed to find iNOS protein by western blot in multiple tissues (Javeshghani and Magder 2001b; Mehta et al. 1999b). iNOS has been found in human neutrophils by enrichment techniques (Javeshghani and Magder 2001b; Wheeler et al. 1997) and we, too, were able to use such an approach to verify that there was a very

low detectable level of iNOS protein and that our antibody was working. Natanson and coworkers also found limited evidence of increased NO metabolites in the acute stage of sepsis in dogs (Quezado et al. 1998). An interesting report of iNOS in human neuronal and ocular tissues showed that there are two isoforms of iNOS in humans and one isoform produces little NO (Park et al. 1996). Thus, although iNOS induction frequently is cited as a mechanism for the loss of vascular tone in septic shock in humans, it is unlikely that iNOS plays a significant role. Zhang et al. showed that the difficulty in inducing iNOS in human tissues may be related to a mutation in the human iNOS promoter which results in an inactivating nucleotide substitution in the enhancer element that responds in rats to interferon δ . There also is the absence of a nuclear factor that is induced in rats (Zhang et al. 1996). Based on all this evidence, it is hardly surprising that the clinical trial of an NOS inhibitor for septic shock not only failed, but actually produced harm (Lopez et al. 2004). This likely was because there was limited pathological iNOS to act on and the inhibitor then only inhibited physiological NO production from eNOS and nNOS. To my mind, there, thus, is little value for pursuing newer agents to deal with iNOS for human sepsis.

Despite the absence of significant iNOS in humans, dogs and pigs, inhibition of NO had profound effects in porcine LPS studies. This indicates that constitutive sources NO, likely primarily from eNOS, but also possibly from nNOS (Javeshghani and Magder 2001b), play an important positive role in sepsis. In pigs, infusion of a non-specific NOS inhibitor, N-methyl-L-arginine (L-NAME) produced marked depression of cardiac function, and importantly, markedly reduced the plateau of the cardiac function curve (Magder and Vanelli 1996) (Fig. 52.4). This was associated with a marked increase in the resistance to venous return (Fig. 52.4). These effects were much greater when the animal was not volume resuscitated; this will be discussed further under the section on the use of volume for resuscitation in Part 2. L-NAME decreased the LPS-induced increase in capacitance,

indicating that L-NAME produced constriction of veins in the capacitance region (Fig. 52.7). The effect of L-NAME on arterial pressure was unexpected and only was detected because arterial pressure-flow lines were constructed (Fig. 52.5). The relationship was shifted to the right with no change in the slope. This indicates that its effect was primarily on the arterial critical closing pressure (Magder 1990) rather than the actual resistance as has been previously observed in the hind limbs of normal dogs (Shrier and Magder 1993). Its most striking effect was on the pulmonary vascular flow versus pressure relationships (Fig. 52.6). It only had a moderate effect on the slope of the arterial flow versus pressure relationship, which represents pulmonary vascular resistance, but it produced a striking increase in the pulmonary arterial outflow pressure (i.e., critical closing pressure) which markedly increased the load on the RV and likely was an important factor in the marked decrease in RV function.

A surprising observation in the porcine sepsis model was that although only a minimal amount of iNOS was induced, there still was a moderate increase in NO production from constitutive NOSs as indicated by increased expired NO, nitrates in the blood, and increased mRNA expression of these proteins (Mehta et al. 1999b). There also was increased expression of nitrotyrosine in tissues. This strong reactive oxygen species is produced when NO reacts with superoxide (Beckman and Koppenol 1996; Liu et al. 1994; Ischiropoulos et al. 1991) and it is thought to be one of the factors responsible for tissue damage from NO (Javeshghani and Magder 2001a). Thus, we hypothesized that the increased production of nitrotyrosine occurred because of the moderate increase in constitutive NO from eNOS and bNOS combined with increased production of superoxide. Two potential sources for increased superoxide production are the mitochondria (Galley 2011) and the enzyme complex nicotinamide-adenine-dinucleotide phosphate (NADPH) oxidase (Griendling et al. 2000; De Keulenaer et al. 1998; Brandes and Kreuzer 2005; Brandes et al. 1999). Pharmacological blockers of mitochondrial superoxide produc-

tion had little effect on the increased superoxide production, but blockers of NADPH oxidase reduced it.

NADPH oxidase has an important role in bacterial killing activity by phagocytic cells but it also exists in vascular smooth muscle and endothelial cells and accounts for a large proportion of superoxide production in these cells and has a regulatory role (Al Ghouleh and Magder 2008; Griendling and Ushio-Fukai 1997). The issue then was that it may not be the NO that counts but the company that it keeps (Javeshghani and Magder 2001a) in that a mild increase in NO combined with a significant increase in superoxide could account for the production of toxic nitrotyrosine. In further studies, it was shown that superoxide produced by NADPH oxidase has an important regulatory role in the transcription of important molecules involved in the regulation of the septic response including vascular adhesion molecules and the cytokines interleukin-8 (IL-8) and IL-6 (Al Ghouleh and Magder 2008; Al Ghouleh and Magder 2012). IL-8 has a particularly important role in bacterial sepsis because it regulates the attraction of polymorphonuclear cells (PMN) to sights of inflammation. One way that PMN kills bacteria is by producing superoxide. Superoxide has been shown to reduce the IL-8 mRNA stability (Al Ghouleh and Magder 2012). By this process, the superoxide produced by PMN could reduce IL-8 protein production and thus help moderate the extent of PMN infiltration (Al Ghouleh and Magder 2012). On the other hand, the stability of IL-6 and ICAM mRNA was stabilized by superoxide indicating the very complicated interactions of signaling pathways and why it is unlikely that a single intervention can reduce the overall sepsis process.

Mitochondrial Dysfunction

Another potential cause for the metabolic disruption in sepsis is depression, or even uncoupling, of mitochondrial function. Mitochondria are the central energy generator of the body through their production of ATP, the body's major source

of energy (Singer 2007, 2014; Fink 2001; Brealey et al. 2004). In this process, mitochondrial metabolism accounts for 98% of total body O_2 consumption (Singer 2014). It also is worth noting that mitochondria are believed to have derived from bacteria which are the primary foreign invader in septic shock. It may thus not be surprising that many of body's host defense mechanisms may also act on mitochondrial function. Many abnormalities in mitochondrial function have been documented in sepsis and will not be repeated here. In general, it can be said that mitochondrial respiration is impaired in sepsis. It is most likely not simply due to inadequate O_2 supply (Fink 2001). Proposed causes of mitochondrial dysfunction in sepsis have included inhibition of their function by excess production NO, carbon monoxide, hydrogen sulfide, and reactive oxygen species such as peroxynitrite, hormonal perturbations, and morphological changes from oxidative injury (Galley 2011; Puthuchery et al. 2018). All these could be altering the fundamental membrane stability of the mitochondrial outer lining. A limitation of the mitochondrial hypothesis is that cellular dysfunction is necessary for all these potential "causes" to be active so that this still leaves the question as to what started the original process that resulted in mitochondrial dysfunction. The argument then might be made that mitochondrial dysfunction is just an epi-phenomenon but when it occurs, it is a key factor perpetuating the process (Fink 2015).

Intracellular Calcium Regulation

As already discussed, smooth muscle tone and cardiac muscle contractions are highly dependent upon intracellular $[Ca^{2+}]$. This is regulated by two sources of Ca^{2+} (Fig. 52.9). One is Ca^{2+} that comes in through cell walls and the other is Ca^{2+} that is taken up and released from the sarcoplasmic reticulum (SR). Ca^{2+} entering across the cell membrane sets the overall intracellular Ca^{2+} content. This Ca^{2+} enters sarcomeres primarily through L-type calcium channels when sarcomere membranes depolarize. The total intracellular $[Ca^{2+}]$ content also is regulated by a number of exchange-

ers that primarily extrude Ca^{2+} but also can allow its entry. These include the Na^+/H^+ exchanger and K- Ca^{2+} ATPase. Rapid entry of Ca^{2+} through L-type Ca^{2+} channels triggers the release of Ca^{2+} from the SR, which sets the cytoplasmic Ca^{2+} concentration ($[Ca^{2+}]$), and thereby regulates activation of myosin-actin interaction and muscle force production. Ca^{2+} is released from the SR through its Ryanodine receptors (RyR) and $[Ca^{2+}]$ is taken back up by the SR by sarco/endoplasmic reticulum Ca^{2+} ATPase (SERCA). The activity of these proteins can be modified by other proteins and their function in turn is altered by oxidation from reactive species (ROS). The RyR normally leaks out some Ca^{2+} . This plays a role in relating muscle contractions to metabolic and transcriptional processes. In patients with heart failure, the leak is increased and thought to be a factor in myocardial failure (George 2008) and could potentially play a similar role in the septic heart. This process seems to be redox sensitive and SERCA activity is especially highly regulated by the redox status (Fig. 52.10). Activity of both the RyR and SERCA is increased by beta-agonists. Moderate amounts of oxidation of sulfhydryl groups increase SERCA activity, whereas higher amounts produce irreversible oxidation and inhibit contractile function (Adachi et al. 2004) (Fig. 52.10). NO has been shown to contribute to the oxidation of SERCA through the producing of peroxynitrite (Adachi et al. 2004) by the interaction of NO and superoxide. At low concentrations, peroxynitrite increases re-uptake of Ca^{2+} by SERCA and improves contractile function but at higher concentrations, peroxynitrite irreversibly oxidizes SERCA and reduces Ca^{2+} re-uptake and contractile function. The combination of increased leak of Ca^{2+} from the SR and impaired uptake because of decreased SERCA function results in a failure of the contractile activity of cardiac myocytes and vascular smooth muscle. Because these processes occur at the very level of contractile function in sepsis, they would then make these cells refractory to inotropes and vasoconstrictors as is observed clinically. As discussed above, the NO for this does not have to come from iNOS. A moderate increased production by eNOS or nNOS as seen in the porcine studies, combined with increased

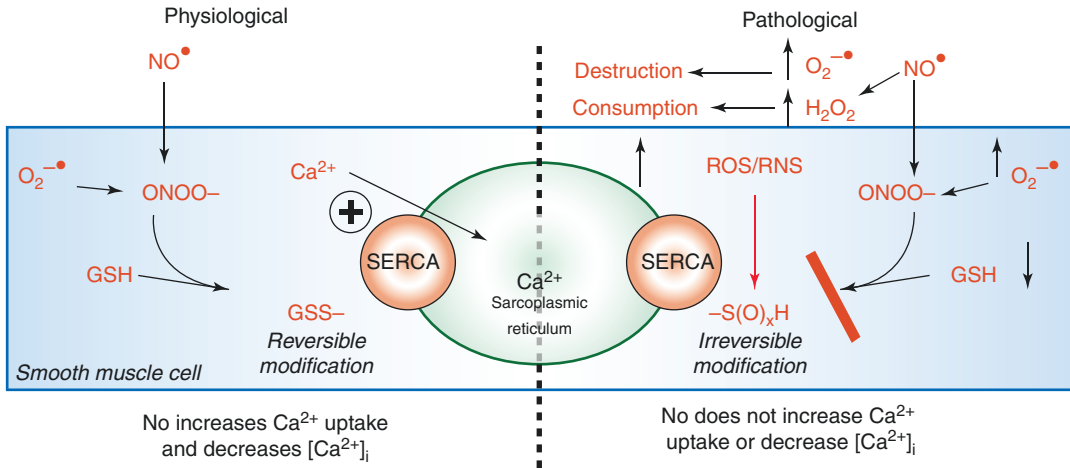


Fig. 52.10 Oxidative regulation of the sarco-endoplasmic Ca^{2+} ATPase in heart muscle. Under physiological conditions with basal levels of endogenously produced NO and superoxide ($\text{O}_2^{\cdot-}$), a low level of the potent oxidant peroxynitrite (ONOO^-) is formed and oxidizes glutathione (GSH) to GSS- in a reversible reaction with sulfhydryl groups on SERCA. This increases its uptake of Ca^{2+} . The ratio of the potent anti-oxidant GSH to GSS- is an indicator of the redox-balance. Faster removal and an increased

amount of Ca^{2+} in the SR allows faster and greater turnover of actin-myosin and stronger cardiac contractions. However, higher levels of ONOO^- , because of more NO or more $\text{O}_2^{\cdot-}$ produces sulfhydryl bonds that irreversibly oxidize SERCA and inhibit its function. This indicates the fine balance between appropriate and excessive oxidation and that it is not appropriate to try to just block all reactive species. (From Adachi et al. (Adachi et al. 2004). Used with permission of Springer Nature)

superoxide production, also can do this. It likely will be very difficult to directly prevent this activity because it is occurring at such a basic regulatory level and NOS inhibition or the high amount of anti-oxidant activity required to alter this activity, likely will interfere with many other homeostatic mechanisms.

Both extracellular histones and high-mobility group box 1 (HMGB1) have been shown to be endogenous DAMPs that can alter intracellular Ca^{2+} . Aggregation of neutrophils in the vasculature can activate complement (C5a) by producing extracellular traps (NET). This results in the appearance of histones. Cardiomyocytes exposed to histones have increased intracellular Ca^{2+} , a reduced redox state, and mitochondrial dysfunction because of increased membrane permeability (Kakihana et al. 2015, 2016). The concentration of these circulation histones closely correlates with elevated troponin in septic patients. This is potentially a more reversible process.

HMGB1 has been shown to mediate LPS mortality (Zhang et al. 2014). It increases intracellular ROS by an interaction of HMGB and TLR4.

The consequent oxidative stress alters the calmodulin phosphorylation of RyR2. This enhances the Ca^{2+} spark mediated leak from RyR2, which depletes SR Ca^{2+} . This leads to decreased myocardial contractility. The effect in animals can be reduced by inhibiting TLR4 signaling or by adding antioxidants but the doses are high and unlikely to be feasible in patients.

Permeable Barriers

A major component of the normal homeostasis of all complex organisms is the preservation of cellular barrier functions that keep fluids and proteins in their proper compartments. This function in the body primarily is provided by endothelial and epithelial cells. A fundamental feature of the septic syndrome is the loss of this barrier function. Examples of this are the movement of fluid, solutes, and proteins from the vascular space into the interstitial space, leakage of fluid from pulmonary vessels into alveoli, and movement of bacteria and their toxins from the gut into the

blood. Loss of volume from the vascular space contributes to inadequate tissue perfusion both by reducing cardiac output and the delivery of nutrients to tissues, as well as by the creation of tissue edema which decreases diffusion in tissues. This leakage of fluid from the vascular to interstitial space creates one of the greatest clinical challenges in the management of the septic patient. Administration of too little fluid to maintain vascular volume results in worsening shock (Figs. 52.4, 52.5, 52.6, and 52.7), but giving too much fluid leads to increasing tissue edema and pulmonary edema with a failure of gas exchange. The increase in interstitial fluid also changes the mechanical characteristics of the vascular space which accelerate the vascular leak and limits the value of infusing more crystalloid solutions (Bhave and Neilson 2011) (See Chap. 10).

The barrier function of endothelial and epithelial cells is provided by cell-cell junctions. Dysfunction of these results in para-cellular leak (Goldenberg et al. 2011). Variations in the protein components of these junctions provide widely different permeabilities in different tissues which is important for normal variations in their physiological function. For example, permeability across the blood-brain barrier is very low, whereas permeability across the kidney, intestine, pancreas, and liver sinusoids is very high. These junctions provide what is termed “selective” permeability and this activity can be regulated to allow adaptation to different physiological needs. Unfortunately, the function also can be altered, or even dismantled in disease states (Vermette et al. 2018). Increased barrier permeability has some adaptive advantages because it allows immune cells and signaling proteins to pass from the blood to the underlying cells. However, the regulating processes can be subverted by invading organisms. This is especially the case in many viruses that use this approach to invade tissues and become uncontrolled (Vestweber 2008). Regulation of the processes that regulate cellular barrier function is an evolving area of study. An extensive number of proteins, with multiple targets for intervention, have been identified (Goldenberg et al. 2011; Vestweber 2008; Rahimi 2017; Darwish and

Liles 2013; Gavard 2009, 2014). These pathways only will be described here in general terms, but clinicians will need to become increasingly aware of these pathways because of the numerous therapeutic tools that are being considered as treatments for the vascular leak. To date, many of these have been shown to be effective in animal studies, but at the time of writing this chapter, none have shown any clinical outcome benefit.

There are two major types of junctions – tight junctions and adherens junctions. Tight junctions have a major role in controlling monolayer permeability by forming a semi-permeable connection between cells lining corporeal compartments (Vermette et al. 2018). They also act as signaling platforms that establish cell polarity, send signals to the nucleus, and modulate gene expression. These structures are very complex and have more than 40 proteins. They all have three types of transmembrane proteins: claudins, MARVEL domain proteins, and junctional molecules (JAMs) (Vermette et al. 2018). The claudins are the main regulators of permeability. MARVEL domain proteins regulate the recruitment of signaling complex proteins to the tight junction. JAMS are similar to immunoglobulins and are involved in signaling circulating cells.

The adherens junctions have more diverse roles. These include maintenance of cell-cell adhesion, interaction with actin for cytoskeleton remodeling, and signal transduction and transcriptional regulation (Goldenberg et al. 2011; Rahimi 2017). The dominant component of vascular endothelial cells is vascular endothelial cadherin (VE-cadherin) (Goldenberg et al. 2011; Rahimi 2017; Darwish and Liles 2013). These structures are especially important for regulating permeability in venules, which are thought to be the major sight of vascular leakage in sepsis. The endothelial cells in this region express receptors for many of the mediators of inflammation in sepsis including TNF- α , IL-1, and vascular endothelial growth factor (VEGF) (Darwish and Liles 2013). Numerous inflammatory mediators can produce internalization of VE-cadherin, which leads to increased vascular leak. These include VEGF, thrombin, histamine, LPS, and ROS which can come from many sources. Attempts

have been made to stabilize and prevent the internalization of VE-cadherin with agents such as angiotensin-1(Ang1), which is an endogenous VE-cadherin stabilizer. These agents work in animals but so far have not been shown to be effective in humans (Gavard 2014; Gavard et al. 2008), likely because of the difficulty of targeting areas of need and because in the clinical setting they inevitably have to be given after the process has occurred.

In summary, although barrier permeability is a central part of the pathogenesis of the septic syndrome, and the great advances in our understanding of the complex underlying biology, and despite many hopeful forays (Goldenberg et al. 2011; Darwish and Liles 2013; Lee and Slutsky 2010; Riedemann et al. 2003), the solution to this problem remains elusive. One aspect is likely. Animal studies, or even more so, in vitro studies, do not replicate the complex interactions of multiple and diverse proteins that exist in the patient. It also is likely that a molecule that provides a benefit in one region may be counter-productive in a different region because of the normal diversity of the regulation of permeability among organs. This contrasts with the use of these agents as newer cancer treatments because in cancer treatment only one cell type needs to be targeted.

Synthesis of Mechanisms

It does not seem that inadequate O₂ delivery by itself is the cause vascular collapse and multi-organ failure in sepsis, but it also is clear that adequate cardiac output and its distribution to tissues of need is essential for allowing counter active and reparatory processes (Natanson et al. 1990). It also is clear that no single agent is responsible for the global organ failure in sepsis, and a comprehensive approach to patient management is required. An early and important component of the septic syndrome is profound vascular leak. Transmembrane potentials across cells, and even across mitochondrial walls, seem to be decreased. This indicates that there is a general loss of barrier functions and an inability to maintain electrical gradients across cell walls.

These processes suggest that perhaps a key component of the septic process may be the disruption of cell and organelle membranes by cytokines and other mediators, which leads to disruption of the normally tightly regulated intracellular and also intra-mitochondrial milieu and this leads to the generalized organ dysfunction. On the basis of this mechanism, the most vulnerable tissues would be those that start with an already low electrical resistance barrier, such as intestinal epithelial cells, or cells that are highly dependent upon a tightly regulated transmembrane potentials such as the heart, brain, and vascular smooth muscle (Fink 2015).

From this discussion, it should be evident that current therapeutic options are limited to maintaining adequate perfusion, ensuring that there is adequate vascular volume to provide for the increased preload needs of the heart, and for the loss of fluid through increased filtration. At the same time, strategies are needed that do not overload the system with too much fluid because this will increase capillary fluid filtration and tissue congestion. The therapeutic options for dealing with these issues are discussed in Sepsis Part 2.

References

- Abboud R, Keller J, Slade M, DiPersio JF, Westervelt P, Rettig MP, et al. Severe cytokine-release syndrome after T cell-replete peripheral blood haploidentical donor transplantation is associated with poor survival and anti-IL-6 therapy is safe and well tolerated. *Biol Blood Marrow Transplant.* 2016;22(10):1851–60.
- Abraham E. New definitions for sepsis and septic shock: continuing evolution but with much still to be done. *JAMA.* 2016;315(8):757–9.
- Abraham E, Wunderink R, Silverman H, Perl TM, Nasraway S, Levy H, et al. Efficacy and safety of monoclonal antibody to human tumor necrosis factor alpha in patients with sepsis syndrome. A randomized, controlled, double-blind, multicenter clinical trial. TNF-alpha MAb Sepsis Study Group. *JAMA.* 1995;273(12):934–41.
- Abraham E, Glauser MP, Butler T, Garbino J, Gelmont D, Laterre PF, et al. p55 Tumor necrosis factor receptor fusion protein in the treatment of patients with severe sepsis and septic shock. A randomized controlled multicenter trial. Ro 45-2081 Study Group. *JAMA.* 1997;277(19):1531–8.

- Abraham E, Anzueto A, Gutierrez G, Tessler S, San Pedro G, Wunderink R, et al. Double-blind randomised controlled trial of monoclonal antibody to human tumour necrosis factor in treatment of septic shock. NORASEPT II Study Group. *Lancet*. 1998;351(9107):929–33.
- Adachi T, Weisbrod RM, Pimentel DR, Ying J, Sharov VS, Schöneich C, et al. S-Glutathiolation by peroxynitrite activates SERCA during arterial relaxation by nitric oxide. *Nat Med*. 2004;10(11):1200–7.
- Akira S, Takeda K, Kaisho T. Toll-like receptors: critical proteins linking innate and acquired immunity. *Nat Immunol*. 2001;2(8):675–80.
- Al Ghoulah I, Magder S. Nicotinamide adenine dinucleotide phosphate (reduced form) oxidase is important for LPS-induced endothelial cell activation. *Shock*. 2008;29(5):553–9.
- Al Ghoulah I, Magder S. NADPH oxidase-derived superoxide destabilizes lipopolysaccharide-induced interleukin 8 mRNA via p38, extracellular signal-regulated kinase mitogen-activated protein kinase, and the destabilizing factor tristetraprolin. *Shock*. 2012;37(4):433–40.
- Angus DC, van der Poll T. Severe sepsis and septic shock. *N Engl J Med*. 2013;369(9):840–51.
- Angus DC, Linde-Zwirble WT, Lidicker J, Clermont G, Carcillo J, Pinsky MR. Epidemiology of severe sepsis in the United States: analysis of incidence, outcome, and associated costs of care. *Crit Care Med*. 2001;29(7):1303–10.
- Beckman JS, Koppenol WH. Nitric oxide, superoxide, and peroxynitrite: the good, the bad, and the ugly. *Am J Physiol*. 1996;271(5 Pt 1):C1424–C37.
- Bernard GR, Vincent JL, Laterre PF, LaRosa SP, Dhainaut JF, Lopez-Rodriguez A, et al. Efficacy and safety of recombinant human activated protein C for severe sepsis. *N Engl J Med*. 2001;344(10):699–709.
- Beutler B, Cerami A. The endogenous mediator of endotoxic shock. *Clin Res*. 1986;35:192–7.
- Beutler B, Greenwald D, Hulmes JD, Chang M, Pan YCE, Mathison J, et al. Identity of tumor necrosis factor and the macrophage-secreted factor cachectin. *Nature*. 1985;316:552–4.
- Bhave G, Neilson EG. Body fluid dynamics: back to the future. *J Am Soc Nephrol*. 2011;22(12):2166–81.
- Bianchi ME. DAMPs, PAMPs and alarmins: all we need to know about danger. *J Leukoc Biol*. 2007;81(1):1–5.
- Bohrer H, Qiu F, Zimmermann T, Zhang Y, Jllmer T, Mannel D, et al. Role of NFκB in the mortality of sepsis. *J Clin Invest*. 1997;100:972–85.
- Bone RC, Fisher CJ, Clemmer TP, Slotman GJ, Metz CA, Balk RA. Sepsis syndrome: a valid clinical entity. *Crit Care Med*. 1989;17:389–93.
- Brandes RP, Kreuzer J. Vascular NADPH oxidases: molecular mechanisms of activation. *Cardiovasc Res*. 2005;65(1):16–27.
- Brandes RP, Koddenberg G, Gwinner W, Kim DY, Kruse HJ, Busse R, et al. Role of increased production of superoxide anions by NAD(P)H oxidase and xanthine oxidase in prolonged endotoxemia. *Hypertension*. 1999;33:1243–9.
- Brealey D, Karyampudi S, Jacques TS, Novelli M, Stidwill R, Taylor V, et al. Mitochondrial dysfunction in a long-term rodent model of sepsis and organ failure. *Am J Physiol Regul Integr Comp Physiol*. 2004;286(3):R491–R7.
- Buchman TG, Simpson SQ, Sciarretta KL, Finne KP, Sowers N, Collier M, et al. Sepsis among medicare beneficiaries: 2. The trajectories of sepsis, 2012–2018. *Crit Care Med*. 2020a;48(3):289–301.
- Buchman TG, Simpson SQ, Sciarretta KL, Finne KP, Sowers N, Collier M, et al. Sepsis among medicare beneficiaries: 1. The burdens of sepsis, 2012–2018. *Crit Care Med*. 2020b;48(3):276–88.
- Cavaillon J, Pitton C, Fitting C. Endotoxin tolerance is not a LPS-specific phenomenon: partial mimicry with IL-1, IL-10 and TGFβ. *J Endotoxin Res*. 1994;1:21–9.
- Ceneviva G, Paschall JA, Maffei F, Carcillo JA. Hemodynamic support in fluid-refractory pediatric septic shock. *Pediatrics*. 1998;102(2):e19.
- Chan YL, Orie NN, Dyson A, Taylor V, Stidwill RP, Clapp LH, et al. Inhibition of vascular adenosine triphosphate-sensitive potassium channels by sympathetic tone during sepsis. *Crit Care Med*. 2012;40(4):1261–8.
- Crayne CB, Albeituni S, Nichols KE, Cron RQ. The immunology of macrophage activation syndrome. *Front Immunol*. 2019;10:119.
- Cunha RE, Schaer GL, Parker MM, Natanson C, Parrillo JE. The coronary circulation in human septic shock. *Circulation*. 1986;73(4):637–44.
- Darwish I, Liles WC. Emerging therapeutic strategies to prevent infection-related microvascular endothelial activation and dysfunction. *Virulence*. 2013;4(6):572–82.
- De Keulenaer GW, Alexander RW, Ushio-Fukai M, Ishizaka N, Griendling KK. Tumour necrosis factor alpha activates a p22phox-based NADH oxidase in vascular smooth muscle. *Biochem J*. 1998;329:653–7.
- Deschamps A, Magder S. Baroreflex control of regional capacitance and blood flow distribution with or without alpha adrenergic blockade. *J Appl Physiol*. 1992;263:H1755–H63.
- Dhainaut JFJ. Coronary hemodynamics and myocardial metabolism of lactate, free fatty acids, glucose, and ketones in patients with septic shock. *Circulation*. 1987;75(3):533–41.
- Dinarello CA, Cannon JG, Wolfe SM, Bernheim HA, Beutler B, Cerami A, et al. Tumor necrosis factor (cachectin) is an endogenous pyrogen and induces production of interleukin 1. *J Exp Med*. 1986;163:1433–50.
- Duff JH, Groves AC, McLean APH, LaPointe R, MacLean LD. Defective oxygen consumption in septic shock. *Surg Gynecol Obstet*. 1969;128:1051–60.
- Dünser MW, Brunauer A. One step back for adenosine triphosphate-sensitive potassium channel inhibition in sepsis but progress in the quest for the optimum vasopressor. *Crit Care Med*. 2012;40(4):1377–8.

- Engelmann B, Massberg S. Thrombosis as an intravascular effector of innate immunity. *Nat Rev Immunol*. 2013;13(1):34–45.
- Fink MP. Cytopathic hypoxia. Mitochondrial dysfunction as mechanism contributing to organ dysfunction in sepsis. *Crit Care Clin*. 2001;17(1):219–37.
- Fink MP. Cytopathic hypoxia and sepsis: is mitochondrial dysfunction pathophysiologically important or just an epiphenomenon. *Pediatr Crit Care Med*. 2015;16(1):89–91.
- Furchgott RF, Zawadzki JV. The obligatory role of endothelial cells in the relaxation of arterial smooth muscle by acetylcholine. *Nature*. 1980;288:373–6.
- Galley HF. Oxidative stress and mitochondrial dysfunction in sepsis. *Br J Anaesth*. 2011;107(1):57–64.
- Gattinoni L, Brazzi L, Pelosi P, Latini R, Tognoni G, Pesenti A, et al. A trial of goal-oriented hemodynamic therapy in critically ill patients. SvO₂ Collaborative Group. *N Engl J Med*. 1995;333(16):1025–32.
- Gavard J. Breaking the VE-cadherin bonds. *FEBS Lett*. 2009;583(1):1–6.
- Gavard J. Endothelial permeability and VE-cadherin. *Cell Adh Migr*. 2014;8(2):158–64.
- Gavard J, Patel V, Gutkind JS. Angiopoietin-1 prevents VEGF-induced endothelial permeability by sequestering Src through mDia. *Dev Cell*. 2008;14(1):25–36.
- Geller DA, de Vera ME, Russell DA, Shapiro RA, Nussler AK, Simmons RL, et al. A central role for IL-1 beta in the in vitro and in vivo regulation of hepatic inducible nitric oxide synthase. IL-1 beta induces hepatic nitric oxide synthesis. *J Immunol*. 1995;155(10):4890–8.
- George CH. Sarcoplasmic reticulum Ca²⁺ leak in heart failure: mere observation or functional relevance? *Cardiovasc Res*. 2008;77(2):302–14.
- Gohil SK, Cao C, Phelan M, Tjoa T, Rhee C, Platt R, et al. Impact of policies on the rise in sepsis incidence, 2000–2010. *Clin Infect Dis*. 2016;62(6):695–703.
- Goldenberg NM, Steinberg BE, Slutsky AS, Lee WL. Broken barriers: a new take on sepsis pathogenesis. *Sci Transl Med*. 2011;3(88):88ps25.
- Green JF. Mechanism of action of isoproterenol on venous return. *Am J Physiol*. 1977;232(2):H152–H6.
- Greenway CV. Role of splanchnic venous system in overall cardiovascular homeostasis. *Fed Proc*. 1983;42:1678–84.
- Griendling KK, Ushio-Fukai M. NADH/NADPH oxidase and vascular function. *Trends Cardiovasc Med*. 1997;7:301–7.
- Griendling KK, Sorescu D, Ushio-Fukai M. NAD(P)H oxidase. Role in cardiovascular biology and disease. *Circ Res*. 2000;86:494–501.
- Guyton AC. Determination of cardiac output by equating venous return curves with cardiac response curves. *Physiol Rev*. 1955;35:123–9.
- Hayes M, Timmins AC, Yau EHS, Palazzo M, Hinds CJ, Watson D. Elevation of systemic oxygen delivery in the treatment of critically ill patients. *N Engl J Med*. 1994;330:1717–22.
- Haywood GA, Tsao PS, von der Leyen HE, Mann MJ, Keeling PJ, Trindade PT, et al. Expression of inducible nitric oxide synthase in human heart failure. *Circulation*. 1996;93:1087–94.
- Hochman Judith S, Boland J, Sleeper Lynn A, Porway M, Brinker J, Col J, et al. Current spectrum of cardiogenic shock and effect of early revascularization on mortality. *Circulation*. 1995;91(3):873–81.
- Hom GJ, Grant SK, Wolfe G, Bach TJ, MacIntyre DE, Hutchinson NI. Lipopolysaccharide-induced hypotension and vascular hyporeactivity in the rat: tissue analysis of nitric oxide synthase mRNA and protein expression in the presence and absence of dexamethasone, N G-monomethyl-L-arginine or indomethacin. *J Pharmacol Exp Ther*. 1995;272:452–9.
- Hotchkiss RS, Karl IE. The pathophysiology and treatment of sepsis. *N Engl J Med*. 2003;348(2):138–50.
- Ischiropoulos H, Zhu L, Beckman J. Peroxynitrite formation from macrophage-derived nitric oxide. *Arch Int Physiol Biochim*. 1991;298:446–51.
- Iwashyna TJ, Ely EW, Smith DM, Langa KM. Long-term cognitive impairment and functional disability among survivors of severe sepsis. *JAMA*. 2010;304(16):1787–94.
- Iwashyna TJ, Cooke CR, Wunsch H, Kahn JM. Population burden of long-term survivorship after severe sepsis in older Americans. *J Am Geriatr Soc*. 2012;60(6):1070–7.
- Javeshghani D, Magder S. Presence of nitrotyrosine with minimal iNOS induction in LPS treated pigs. *Shock*. 2001a;16(4):304–11.
- Javeshghani D, Magder S. Regional changes in constitutive nitric oxide synthase and the hemodynamic consequences of its inhibition in lipopolysaccharide-treated pigs. *Shock*. 2001b;16(3):232–8.
- Kakahana Y, Ito T, Nakahara M, Yamaguchi K, Yasuda T. Sepsis-induced myocardial dysfunction: pathophysiology and management. *J Intensive Care*. 2016;4:22.
- Kalbitz M, Graier JJ, Fattahi F, Jajou L, Herron TJ, Campbell KF, et al. Role of extracellular histones in the cardiomyopathy of sepsis. *FASEB J*. 2015;29(5):2185–93.
- Karzai W, Reilly JM, Hoffman WD, Cunnion RE, Danner RL, Banks SM, et al. Hemodynamic effects of dopamine, norepinephrine, and fluids in a dog model of sepsis. *Am J Physiol*. 1995;268(2 Pt 2):H692–702.
- Kasai K, Hattori Y, Nakanishi N, Manaka K, Banba N, Motohashi S, et al. Regulation of inducible nitric oxide production by cytokines in human thyrocytes in culture. *Endocrinology*. 1995;136(10):4261–70.
- Keaney JF, Puyana JC, Francis S, Loscalzo JF, Stamler JS, Loscalzo J. Methylene blue reverses endotoxin-induced hypotension. *Circ Res*. 1994;74:1121–5.
- Kohsaka S, Menon V, Lowe AM, Lange M, Dzavik V, Sleeper LA, et al. Systemic inflammatory response syndrome after acute myocardial infarction complicated by cardiogenic shock. *Arch Intern Med*. 2005;165(14):1643–50.

- Landry DW, Oliver JA. The ATP-sensitive K⁺ channel mediates hypotension in endotoxemia and hypoxic lactic acidosis in dog. *J Clin Invest.* 1992;89:2071–4.
- Landry DW, Oliver JA. The pathogenesis of vasodilatory shock. *N Engl J Med.* 2001;345(8):588–95.
- Lange M, Morelli A, Westphal M. Inhibition of potassium channels in critical illness. *Curr Opin Anaesthesiol.* 2008;21(2):105–10.
- Lee WL, Slutsky AS. Sepsis and endothelial permeability. *N Engl J Med.* 2010;363(7):689–91.
- Liu S, Beckman JS, Ku DD. Peroxynitrite, a product of superoxide and nitric oxide, produces coronary vasorelaxation in dogs. *J Pharmacol Exp Ther.* 1994;268(3):1114–21.
- Lopez A, Lorente JA, Steingrub J, Bakker J, McLuckie A, Willatts S, et al. Multiple-center, randomized, placebo-controlled, double-blind study of the nitric oxide synthase inhibitor 546C88: effect on survival in patients with septic shock. *Crit Care Med.* 2004;32(1):21–30.
- MacLean LD, Mulligan WG, McLean APH, Duff JH. Patterns of septic shock in man – a detailed study of 56 patients. *Ann Surg.* 1967;166:543–62.
- MacNaul KL, Hutchinson NI. Differential expression of iNOS and cNOS mRNA in human vascular smooth muscle cells and endothelial cells under normal and inflammatory conditions. *Biochem Biophys Res Commun.* 1993;196(3):1330–4.
- Magder SA. Pressure-flow relations of diaphragm and vital organs with nitroprusside-induced vasodilation. *J Appl Physiol.* 1986;61:409–16.
- Magder S. Starling resistor versus compliance. Which explains the zero-flow pressure of a dynamic arterial pressure-flow relation? *Circ Res.* 1990;67:209–20.
- Magder S, Quinn R. Endotoxin and the mechanical properties of the canine peripheral circulation. *J Crit Care.* 1991;6:81–8.
- Magder S, Vanelli G. Circuit factors in the high cardiac output of sepsis. *J Crit Care.* 1996;11(4):155–66.
- Magder S, Neculcea J, Neculcea V, Sladek R. Lipopolysaccharide and TNF- α produce very similar changes in gene expression in human endothelial cells. *J Vasc Res.* 2006;43(5):447–61.
- Marshall JC. Why have clinical trials in sepsis failed? *Trends Mol Med.* 2014;20(4):195–203.
- McGarvey LP, Magder S, Burkhart D, Kesten S, Liu D, Manuel RC, et al. Cause-specific mortality adjudication in the UPLIFT[®] COPD trial: findings and recommendations. *Respir Med.* 2012;106(4):515–21.
- McLay JS, Chatterjee P, Nicolson AG, Jardine AG, McKay NG, Ralston SH, et al. Nitric oxide production by human proximal tubular cells: a novel immunomodulatory mechanism? *Kidney Int.* 1994;46(4):1043–9.
- Mehta S, Javeshghani D, Datta P, Levy RD, Magder S. Porcine endotoxemic shock is associated with increased expired nitric oxide. *Crit Care Med.* 1999a;27(2):385–93.
- Mehta S, Javeshghani D, Datta P, Levy RD, Magder S. Porcine endotoxaemic shock is associated with increased expired nitric oxide. *Crit Care Med.* 1999b;27(2):385–93.
- Mitzner W, Goldberg H. Effects of epinephrine on resistive and compliant properties of the canine vasculature. *J Appl Physiol.* 1975;39(2):272–80.
- Moncada S. The L-arginine: nitric oxide pathway. *Acta Physiol Scand.* 1992;145:201–27.
- Morelli A, Lange M, Ertmer C, Broeking K, Van Aken H, Orecchioni A, et al. Glibenclamide dose response in patients with septic shock: effects on norepinephrine requirements, cardiopulmonary performance, and global oxygen transport. *Shock.* 2007;28(5):530–5.
- Mouncey PR, Osborn TM, Power GS, Harrison DA, Sadique MZ, Grieve RD, et al. Trial of early, goal-directed resuscitation for septic shock. *N Engl J Med.* 2015;372(14):1301–11.
- Natanson C. Studies using a canine model to investigate the cardiovascular abnormality of and potential therapies for septic shock. *Clin Res.* 1990;38:206–14.
- Natanson C, Fink MP, Ballantyne HK, MacVittie TJ, Conklin JJ, Parrillo JE. Gram-negative bacteremia produces both severe systolic and diastolic cardiac dysfunction in a canine model that stimulates human septic shock. *J Clin Invest.* 1986;78:259–70.
- Natanson C, Danner RL, Fink MP, MacVittie TJ, Walker RI, Conklin JJ, et al. Cardiovascular performance with *E. coli* challenges in a canine model of human sepsis. *Am J Physiol.* 1988;254:H558–H69.
- Natanson C, Danner RL, Elin RJ, Hosseini JM, Peart KW, Banks SM, et al. Role of endotoxemia in cardiovascular dysfunction and mortality. *J Clin Invest.* 1989a;83:243–51.
- Natanson C, Eichenholz PW, Danner RL, Eichacker PQ, Hoffman WD, Kuo GC, et al. Endotoxin and tumor necrosis factor challenges in dogs simulate the cardiovascular profile of human septic shock. *J Exp Med.* 1989b;169:823–32.
- Natanson C, Danner RL, Reilly JM, Doerfler ML, Hoffman WD, Akin GL, et al. Antibiotics versus cardiovascular support in a canine model of human septic shock. *Am J Physiol.* 1990;259:H1440–H7.
- Nava E, Palmer RMJ, Moncada S. The role of nitric oxide in endotoxic shock: effects of N^G-monomethyl-L-arginine. *J Cardiovasc Pharmacol.* 1992;20:S132–S4.
- Ognibene FP, Parker MM, Natanson C, Shelhamer JH, Parrillo JE. Depressed left ventricular performance. Response to volume infusion in patients with sepsis and septic shock. *Chest.* 1988;93(5):903–10.
- Opal SM, DePalo VA. Anti-inflammatory cytokines. *Chest.* 2000;117(4):1162–72.
- Oved JH, Barrett DM, Teachey DT. Cellular therapy: immune-related complications. *Immunol Rev.* 2019;290(1):114–26.
- Park CS, Park R, Krishna G. Constitutive expression and structural diversity of inducible isoform of nitric oxide synthase in human tissues. *Life Sci.* 1996;59(3):219–25.
- Parker MM, Shelhamer JH, Natanson C, Alling DW, Parrillo JE. Serial cardiovascular variables in survivors and nonsurvivors of human septic shock: heart

- rate as an early predictor of prognosis. *Crit Care Med.* 1987;15:923–9.
- Parker MM, Suffredini AF, Natanson C, Ognibene P, Shelhamer JH, Parillo JE. Responses of left ventricular function in survivors and nonsurvivors of septic shock. *J Crit Care.* 1989;4(1):19–25.
- Parker MM, McCarthy KE, Ognibene FP, Parillo JE. Right ventricular dysfunction and dilatation, similar to left ventricular changes, characterize the cardiac depression of septic shock in humans. *Chest.* 1990;97:126–31.
- Patterson SW, Starling EH. On the mechanical factors which determine the output of the ventricles. *J Physiol.* 1914;48(5):357–79.
- Petros AJ, Hewlett AM, Bogle RG, Pearson JD. L-Arginine-induced hypotension. *Lancet.* 1991a;337:1044–5.
- Petros A, Bennett D, Vallance P. Effect of nitric oxide synthase inhibitors on hypotension in patients with septic shock. *Lancet.* 1991b;338:1557–8.
- Pittet JF, Pastor CM, Morel DR. Spontaneous high systemic oxygen delivery increases survival rate in awake sheep during sustained endotoxemia. *Crit Care Med.* 2000;28(2):496–503.
- Preiser JC, Lejeune P, Roman A, Carlier E, De Backer D, Leeman M, et al. Methylene blue administration in septic shock: a clinical trial. *Crit Care Med.* 1995;23(2):259–64.
- Puthucherry ZA, Astin R, McPhail MJW, Saeed S, Pasha Y, Bear DE, et al. Metabolic phenotype of skeletal muscle in early critical illness. *Thorax.* 2018;73(10):926–35.
- Quezado ZMN, Karzai W, Danner RL, Freeman BD, Yan L, Eichacker PQ, et al. Effects of L-NMMA and fluid loading on TNF-induced cardiovascular dysfunction in dogs. *Am J Respir Crit Care Med.* 1998;157(5):1397–405.
- Rahimi N. Defenders and challengers of endothelial barrier function. *Front Immunol.* 2017;8:1847.
- Rastegarpanah M, Magder S. Role of sympathetic pathways in the vascular response to sepsis. *J Crit Care.* 1998;13(4):169–76.
- Reiling N, Ulmer AJ, Ernst M, Flad HD, Hauschildt S. Nitric oxide synthase: mRNA expression of different isoforms in human monocytes/macrophages. *Eur J Immunol.* 1994;24(8):1941–4.
- Rhee C, Gohil S, Klompas M. Regulatory mandates for sepsis care--reasons for caution. *N Engl J Med.* 2014;370(18):1673–6.
- Rhee C, Jones TM, Hamad Y, Pande A, Varon J, O'Brien C, et al. Prevalence, underlying causes, and preventability of sepsis-associated mortality in US acute care hospitals. *JAMA Netw Open.* 2019;2(2):e187571.
- Riedemann NC, Guo RF, Ward PA. Novel strategies for the treatment of sepsis. *Nat Med.* 2003;9(5):517–24.
- Rivers E, Nguyen B, Havstad S, Ressler J, Muzzin A, Knoblich B, et al. Early goal-directed therapy in the treatment of severe sepsis and septic shock. *N Engl J Med.* 2001;345(19):1368–77.
- Rosbe KW, Prazma J, Petrusz P, Mims W, Ball SS, Weissler MC. Immunohistochemical characterization of nitric oxide synthase activity in squamous cell carcinoma of the head and neck. *Otolaryngol Head Neck Surg.* 1995;113(5):541–9.
- Rothe C. Venous system: physiology of the capacitance vessels. In: Shepherd JT, Abboud FM, editors. *Handbook of physiology. The cardiovascular system. Section 2. III.* Bethesda: American Physiological Society; 1983a. p. 397–452.
- Rothe CF. Reflex control of veins and vascular capacitance. *Physiol Rev.* 1983b;63(4):1281–95.
- Russell JA. Management of sepsis. *N Engl J Med.* 2006;355(16):1699–713.
- Russell JA, Walley KR, Singer J, Gordon AC, Hébert PC, Cooper DJ, et al. Vasopressin versus norepinephrine infusion in patients with septic shock. *N Engl J Med.* 2008;358(9):877–87.
- Sakr Y, Jaschinski U, Wittebole X, Szakmany T, Lipman J, Namendys-Silva SA, et al. Sepsis in intensive care unit patients: worldwide data from the intensive care over nations audit. *Open Forum Infect Dis.* 2018;5(12):ofy313.
- Sakurai H, Kohsaka H, Liu MF, Higashiyama H, Hirata Y, Kanno K, et al. Nitric oxide production and inducible nitric oxide synthase expression in inflammatory arthritides. *J Clin Invest.* 1995;96(5):2357–63.
- Schneider F, Lutun P, Hasselmann M, Stoclet JC, Temp JD. Methylene blue increases systemic vascular resistance in human septic shock. Preliminary observations. *Intensive Care Med.* 1992;18(5):309–11.
- Seymour CW, Liu VX, Iwashyna TJ, Brunkhorst FM, Rea TD, Scherag A, et al. Assessment of clinical criteria for sepsis: for the third international consensus definitions for sepsis and septic shock (Sepsis-3). *JAMA.* 2016;315(8):762–74.
- Shrier I, Magder S. L-nitro-arginine and phenylephrine have similar effects on the vascular waterfall, arterial resistance and venous resistance in the canine hindlimb. *FASEB J.* 1993;7(4):A761.
- Singer M. Mitochondrial function in sepsis: acute phase versus multiple organ failure. *Crit Care Med.* 2007;35(9 Suppl):S441–S8.
- Singer M. The role of mitochondrial dysfunction in sepsis-induced multi-organ failure. *Virulence.* 2014;5(1):66–72.
- Singer M, Deutschman CS, Seymour CW, Shankar-Hari M, Annane D, Bauer M, et al. The third international consensus definitions for sepsis and septic shock (Sepsis-3). *JAMA.* 2016;315(8):801–10.
- Singla S, Machado RF. Death of the endothelium in sepsis: understanding the crime scene. *Am J Respir Cell Mol Biol.* 2018;59(1):3–4.
- Solomon MA, Correa R, Alexander HR, Koev LA, Cobb JP, Kim DK, et al. Myocardial energy metabolism and morphology in a canine model of sepsis. *Am J Physiol.* 1994;266(2 Pt 2):H757–68.
- Stein B, Eschenhagen T, Rüdiger J, Scholz H, Förstermann U, Gath I. Increased expression of constitutive nitric

- oxide synthase III, but not inducible nitric oxide synthase II, in human heart failure. *J Am Coll Cardiol*. 1998;32(5):1179–86.
- Stewart TE, Valenza F, Ribeiro SP, Wener AD, Volgyesi G, Mullen JB, et al. Increased nitric oxide in exhaled gas as an early marker of lung inflammation in a model of sepsis. *Am J Respir Crit Care Med*. 1995;151(3):713–8.
- Suffredini AF, Fromm RE, Parker MM, Brenner M, Kovacs JA, Wesley RA, et al. The cardiovascular response of normal humans to the administration of endotoxin. *N Engl J Med*. 1989;321(5):280–7.
- Szabo C, Thiemermann C, Vane JR. Inhibition of the production of nitric oxide and vasodilator prostaglandins attenuates the cardiovascular response to bacterial endotoxin in adrenalectomized rats. *Proc R Soc Lond B*. 1993;253:233–8.
- Takeda K, Kaisho T, Akira S. Toll-like receptors. *Annu Rev Immunol*. 2003;21:335–76.
- Takeuchi O, Akira S. Pattern recognition receptors and inflammation. *Cell*. 2010;140(6):805–20.
- Talke P, Dunn A, Lawlis L, Sziebert L, White A, Herndon D, et al. A model of ovine endotoxemia characterized by an increased cardiac output. *Circ Shock*. 1985;17(2):103–8.
- Taveira Da Silva AM, Kaulbach FS, Chuidian FS, Lambert DR, Suffredini AF, Danner RL. Brief report: shock and multiple-organ dysfunction after self-administration of salmonella endotoxin. *N Engl J Med*. 1993;328(20):1457–60.
- Thiemermann C, Vane J. Inhibition of nitric oxide synthesis reduces the hypotension induced by bacterial lipopolysaccharides in the rat in vivo. *Eur J Pharmacol*. 1990;182:591–5.
- Thiemermann C, Wu CC, Szabo C, Perretti M, Vane JR. Role of tumor necrosis factor in the induction of nitric oxide synthase in a rat model of endotoxin shock. *Br J Pharmacol*. 1993a;110:177–82.
- Thiemermann C, Szabo C, Mitchell JA. Vascular hyporeactivity to vasoconstrictor agents and hemodynamic decompensation in hemorrhagic shock is mediated by nitric oxide. *Proc Natl Acad Sci U S A*. 1993b;90:267–71.
- Thompson K, Venkatesh B, Finfer S. Sepsis and septic shock: current approaches to management. *Intern Med J*. 2019;49(2):160–70.
- Thomsen LL, Miles DW, Happerfield L, Bobrow LG, Knowles RG, Moncada S. Nitric oxide synthase activity in human breast cancer. *Br J Cancer*. 1995;72(1):41–4.
- Traber DL. Animal models: the sheep. *Crit Care Med*. 2000;28(2):591–2.
- Tracey KJ, Beutler B, Lowry SF, Merryweather J, Wolpe S, Milsark IW, et al. Shock and tissue injury induced by recombinant human cachectin. *Science*. 1986;234:470–4.
- Tracey KJ, Fong Y, Hesse DG, Manogue KR, Lee AT, Kuo GC, et al. Anti-cachectin/TNF monoclonal antibodies prevent septic shock during lethal bacteraemia. *Nature*. 1987;330:662–4.
- van der Poll T, de Waal Malefyt R, Coyle SM, Lowry SF. Antiinflammatory cytokine responses during clinical sepsis and experimental endotoxemia: sequential measurements of plasma soluble interleukin (IL)-1 receptor type II, IL-10, and IL-13. *J Infect Dis*. 1997;175:118–22.
- van Diepen S, Vavalle JP, Newby LK, Clare R, Pieper KS, Ezekowitz JA, et al. The systemic inflammatory response syndrome in patients with ST-segment elevation myocardial infarction. *Crit Care Med*. 2013;41(9):2080–7.
- van Diepen S, Katz JN, Albert NM, Henry TD, Jacobs AK, Kapur NK, et al. Contemporary management of cardiogenic shock: a scientific statement from the American Heart Association. *Circulation*. 2017;136(16):e232–e68.
- Vermette D, Hu P, Canarie MF, Funaro M, Glover J, Pierce RW. Tight junction structure, function, and assessment in the critically ill: a systematic review. *Intensive Care Med Exp*. 2018;6(1):37.
- Vestweber D. VE-cadherin: the major endothelial adhesion molecule controlling cellular junctions and blood vessel formation. *Arterioscler Thromb Vasc Biol*. 2008;28(2):223–32.
- Vincent JL, Marshall JC, Namendys-Silva SA, François B, Martin-Loeches I, Lipman J, et al. Assessment of the worldwide burden of critical illness: the intensive care over nations (ICON) audit. *Lancet Respir Med*. 2014;2(5):380–6.
- Warrillow S, Egi M, Bellomo R. Randomized, double-blind, placebo-controlled crossover pilot study of a potassium channel blocker in patients with septic shock. *Crit Care Med*. 2006;34(4):980–5.
- Weil BR, Suzuki G, Young RF, Iyer V, Canty JM Jr. Troponin release and reversible left ventricular dysfunction after transient pressure overload. *J Am Coll Cardiol*. 2018;71(25):2906–16.
- Weinberg JB, Misukonis MA, Shami PJ, Mason SN, Sauls DL, Dittman WA, et al. Human mononuclear phagocyte inducible nitric oxide synthase (iNOS): analysis of iNOS mRNA, iNOS protein, biopterin and nitric oxide production by blood monocytes and peritoneal macrophages. *Blood*. 1995;86:1184–95.
- Werner SL, Barken D, Hoffmann A. Stimulus specificity of gene expression programs determined by temporal control of IKK activity. *Science*. 2005;309(5742):1857–61.
- Wheeler DS, Wong HR. Sepsis in pediatric cardiac intensive care. *Pediatr Crit Care Med*. 2016;17(8 Suppl 1):S266–71.
- Wheeler MA, Smith SD, Garcia-Cardena G, Nathan CF, Weiss RM, Sessa WC. Bacterial infection induces nitric oxide synthase in human neutrophils. *J Clin Invest*. 1997;99:110–6.
- White HD. Pathobiology of troponin elevations: do elevations occur with myocardial ischemia as well as necrosis? *J Am Coll Cardiol*. 2011;57(24):2406–8.
- Wright CJ, Duff JH, McLean APH, MacLean LD. Regional capillary blood flow and oxygen uptake in severe sepsis. *Surg Gynecol Obstet*. 1971;132:637–44.

- Yamamoto S, Burman HP, O'Donnell CP, Cahill PA, Robotham JL. Endothelin causes portal and pulmonary hypertension in porcine endotoxemic shock. *Am J Physiol.* 1997;272:H1239–H49.
- Yealy DM, Kellum JA, Huang DT, Barnato AE, Weissfeld LA, Pike F, et al. A randomized trial of protocol-based care for early septic shock. *N Engl J Med.* 2014;370(18):1683–93.
- Zhang X, Laubach VE, Alley EW, Edwards KA, Sherman PA, Russell SW, et al. Transcriptional basis for hyporesponsiveness of the human inducible nitric oxide synthase gene to lipopolysaccharide/interferon- γ . *J Leukoc Biol.* 1996;59:575–85.
- Zhang C, Mo M, Ding W, Liu W, Yan D, Deng J, et al. High-mobility group box 1 (HMGB1) impaired cardiac excitation-contraction coupling by enhancing the sarcoplasmic reticulum (SR) Ca(2+) leak through TLR4-ROS signaling in cardiomyocytes. *J Mol Cell Cardiol.* 2014;74:260–73.
- Ziegler EJ. Tumor necrosis factor in humans. *N Engl J Med.* 1988;318(23):1533–5.



Pathophysiology of Sepsis and Heart-Lung Interactions: Part 2, Treatment

53

Sheldon Magder and Margaret McLellan

The presentation of the septic syndrome was discussed in Part 1 with particular emphasis on the response of normal human subjects who were injected with endotoxin as well as studies of animals. The advantage of these experimental studies is that the precise time of onset of the sepsis syndrome is known. They also provide a homogeneous cause for the sepsis response in all subjects. Neither of these are true in the clinical setting. However, these experimental studies help us to develop an understanding of the potential benefits, but also the limits of current treatment options. In this chapter, only therapies aimed at hemodynamic abnormalities are discussed. A discussion of antibiotic choices, immunotherapies, and hematological therapies is beyond the scope of this review.

Treatments

Since the septic response is triggered by the presence of invading agents, the obvious first objec-

tive is the initiation of appropriate antimicrobial agents and ensuring that the source of the invading agents is controlled (Kumar et al. 2006; Paul et al. 2010; Bochud et al. 2004). The sooner this is achieved, the better the outcome. Initial antimicrobial coverage needs to start broadly, but can be narrowed when a specific offending agent is identified. It is unlikely that short-term use of antibiotics (24–48 h) will induce resistance in the ICU population or the patient, but failing to initiate the right antibiotic worsens the outcome (Bochud et al. 2004; Leibovici et al. 1995). The second objective is to deal with the generalized consequences of the septic syndrome (Fig. 53.1). These include hypoxemia due to the inflammatory lung injury, loss of vascular volume due to the major increase in capillary permeability, hypotension due to the loss of vascular tone, loss of volume, and decreased cardiac function, all of which lead to inadequate O₂ delivery to tissues. Basic measures for these, such as supplemental O₂ and a fluid bolus may need to be started immediately, even while still evaluating the situation, because of the need to maintain hemodynamic stability and often to prevent death.

The landmark study by Rivers and co-workers at a single center gave us hope that a systematic approach to managing these hemodynamic abnormalities in sepsis could produce a marked reduction in mortality (Rivers et al. 2001). Their approach to the hypotensive septic patient started by giving intravenous volume to target a value of

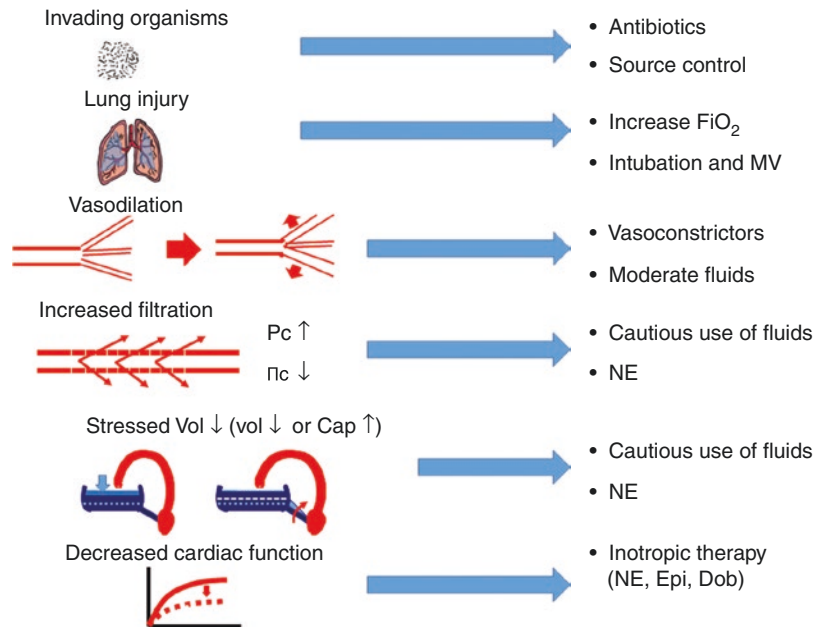
S. Magder (✉)

Royal Victoria Hospital (McGill University Health Centre), Departments of Critical Care and Physiology
McGill University, Montreal, QC, Canada
e-mail: sheldon.magder@mcgill.ca

M. McLellan

Department of Anesthesia and Critical Care, McGill University and McGill University Health Centre,
Montreal, QC, Canada

Fig. 53.1 Summary of general derangements in the early stages of sepsis that need immediate responses. Each of these topics is covered in the text. Pc capillary pressure, Π_c plasma oncotic pressure, Vol volume, Cap capacitance, NE nor-epinephrine, Epi epinephrine, Dob dobutamine



CVP that was presumed to ensure adequate vascular filling; giving norepinephrine (NE) to target a desired arterial pressure after the CVP target was reached; monitoring and targeting a central venous O_2 saturation value as an indicator of adequate tissue perfusion by giving an inotrope to treat values of cardiac output below a designated target and transfusions of red cells to maintain a designated value of hemoglobin. The program seemed rational, the designated end-points were widely used, and the results in the initial report were inspiring. Unfortunately, three large multi-center trials that tried to reproduce the findings failed to show a benefit when compared to clinicians' own choices and the specific protocol has gone out of favor (Angus et al. 2015; Peake et al. 2014; Yealy et al. 2014; Mouncey et al. 2015).

The disappointment from these studies, however, misses the real important contribution of Rivers and co-workers (Rivers et al. 2001). The mortality in the control groups in the subsequent three trials was half that in the original Rivers trial and other studies from the same time period. The question has been raised whether this is simply because the patients in the later trials were at lower risk, but this is unlikely. The entry criteria were not different from the Rivers trial and it is reasonable to surmise populations were equivalent (Iwashyna et al. 2012; Kaukonen et al. 2014).

It is more likely that the change in outcomes over the past years is because the Rivers trial changed practice patterns. The real message from the Rivers trial is not that the dramatic improvement in outcome was based on specific targets that have never been validated, but rather was because of early identification of septic patients, early supportive care, and then continuously closely following these patients until the septic process has resolved. A concern has been raised that we may have traded improved short-term outcomes for more longitudinal morbidity (Iwashyna et al. 2012; Shankar-Hari et al. 2020). However, it is our general impression that patients who recover quickly in the first hours of treatment seem to remain more functional. Furthermore, a systematic review found no association of sepsis with a higher risk of death post-hospitalization when underlying conditions were taken into account (Shankar-Hari et al. 2016).

What then are the key parts of supportive therapy? Organ dysfunction in sepsis is the consequence of a cytokine storm, which results in a miss-match between O_2 delivery and tissue needs. As indicated in Part 1, cardiac output most often is increased in septic patients. Thus, the problem is either that the flow does not get to the right places, or that the tissues are not able to adequately use the delivered O_2 . Part of this likely is

due to mitochondrial dysfunction and failure to extract O_2 which produces cytopathic hypoxia (Fink 2001), and another part likely is due to maldistribution of flow and effective shunting in the microcirculation due to loss of normal local regulation of flow with consequent ischemic hypoxemia (Wright et al. 1971; Duff et al. 1969). There currently are no treatments for either of these. The only thing that can be done is to maintain adequate O_2 delivery when the circulation fails because of cardiac dysfunction, loss of volume, and loss of vascular tone. Based on past studies, it is evident that supplying supra-normal levels of O_2 does not improve outcome and is actually harmful (Gattinoni et al. 1995; Hayes et al. 1994). Instead of aiming for supra-normal values of O_2 delivery, the goal-directed protocol of Rivers et al. (2001) tried to target hemodynamic values that were potentially normal, but as already indicated, even that is a problem as these values never have been validated in terms of outcome benefits. Rather than aiming for precise measured values that likely vary largely in the normal population, perhaps a better strategy is to just maintain enough hemodynamic function to avoid tissue ischemia. This can be guided with the use of falling lactate and other clinical markers such as wakefulness, skin perfusion, and renal function as indicators of the success of the applied treatments (Jansen et al. 2010; Chertoff et al. 2015, 2016). In other words, perhaps the physicians managing the control groups in the three large trials that tested the validity of the Rivers' protocol, began tailoring their therapy when the patients started to "look" better rather than pushing for an arbitrary target. This general approach can be called a responsive therapy in that it reacts to the patient's response to the treatment that was given to fix something rather than targeting a specific value (Magder 2016).

Management of O_2 Delivery

Since the only hemodynamic factor that can be manipulated clinically is O_2 delivery (DO_2), it is important to consider what can be done based on the O_2 delivery equation:

$$DO_2 = \text{cardiac output} \times \text{arterial } O_2 \text{ content}$$

$$\text{and } O_2 \text{ content is } = [\text{Hb}] \times \text{Sat}_a \times K,$$

where $[\text{Hb}]$ is the concentration of hemoglobin (in this case g/L), Sat_a is the arterial O_2 saturation, and K is a constant that indicates the amount of ml O_2 per gram of Hb (range from 1.34 to 1.39) and cardiac output is L/min.

O_2 content is based on $[\text{Hb}]$ and partial pressure of O_2 (PO_2). Cardiac output is dependent upon heart rate and stroke volume, and stroke volume is dependent upon the vascular volume, the ventricular afterloads and contractility. The DO_2 equation indicates that there only are limited therapeutic options. PO_2 usually is easily corrected by supplemental inspired O_2 , although intubation often is required to make sure that O_2 saturation is adequate, or because of failure of the respiratory muscles, which has been identified as a primary cause of death in septic animals (see Chap. 16) (Hussain et al. 1985a, 1986). $[\text{Hb}]$ usually is not very low, at least initially. Heart rate most often is already elevated. The blood pressure already is low as part of the shock state so that lowering the arterial pressure to decrease LV afterload is not an option. This only leaves giving volume to try to restore the intravascular volume that has been lost through the capillary leak and an increase in vascular capacitance, giving vasoconstrictors to restore vascular tone and hopefully providing a more physiological pattern for the distribution of flow, and giving inotropic agents when cardiac output is inappropriately normal or worse, low. The use of each these and their merits are discussed next.

Role of Volume

The standard initial management of septic shock is the administration of fluid (Levy et al. 2018a), but it often is not considered what that volume can do. As indicated in Chap. 2, blood volume is relatively constant in the steady state. Under normal physiological conditions, cardiac output increases because of an increase in cardiac function and a consequent decrease in right atrial pressure. This occurs primarily by an increase in

heart rate, with some additional benefit from an increase in contractility. Cardiac output also can increase without a change in cardiac function by an increase in the venous return function. This can occur through the recruitment of unstressed into stressed volume, and by a decrease in the resistance to venous return. The study by Suffredini et al. (Suffredini et al. 1989) discussed in detail in Part 1 in which LPS was given to normal subjects gives useful insight into what happens when septic patients are given fluid boluses. Importantly, the major rise in cardiac output occurred before fluids were given, and before the major fall in blood pressure and SVR. The rise in cardiac output occurred primarily because of the rise in heart rate, although there also was an increase in stroke volume (based on a greater change in cardiac output than heart rate). When the fluid was given at the 3 h mark (Figs. 52.2 and 52.3 in Part 1), cardiac output rose further, but the increase in cardiac output with fluids was smaller than in normal subjects given the same amount of volume. The volume infusion produced a small, transient increase in arterial pressure, but the pressure continued to fall because of a progressive decrease in SVR. Of interest, CVP and Ppao did not increase until the volume was given. The change in CVP with the volume infusion also was the same in both LPS-treated and normal subjects. The increase in cardiac output without a change CVP during the initial phase indicates that cardiac function must have increased during this phase because a pure change in cardiac output from a fluid bolus should be associated with an increase in CVP because it acts through the Starling mechanism (Chap. 2). It also indicates that in the septic heart, an increase in heart rate is a key determinant of the rise in cardiac output and that changes in cardiac output are not necessarily reflected in changes of arterial pressure, which is more related to vascular tone. Therefore, volume infusions have limited utility for correcting hypotension. This also raises the question as to whether cardiac output or blood pressure should be the target for volume therapy. Since volume only acts by increasing cardiac output, it would seem that cardiac output should be the indicator of the

success of this therapy or at least a surrogate of an increase in cardiac output.

A notable observation in the Suffredini study (Suffredini et al. 1989) is that blood pressure fell as cardiac output rose and that the volume infusion only produced a small brief rise in arterial pressure. Temperature subsided by 6 h, but arterial pressure and SVR did not improve indicating that temperature is not a good indicator of hemodynamic responses. Two factors likely contributed to the persistent hypotension. The vascular leak likely increased over time, and volume was being steadily lost from the vascular space. Secondly, there may have been an increase in the myocardial depression as evidenced by the increase in end-diastolic volume and decrease in EF after 5 h.

The role of volume has been studied in a porcine model of sepsis produced by a low-dose infusion of LPS (Magder and Vanelli 1996). Unlike rats and mice which in response to LPS or TNF- α have a fall in cardiac output and rise in SVR (Thiemermann et al. 1993; Thiemermann and Vane 1990; Stewart et al. 1995), the pigs in this model, as is the case in humans, have a modest increase in cardiac output and a fall in SVR when fluids are administered. In this study, when the blood pressure started to fall, one group was randomized to receive an infusion of saline (to maintain a CVP of 5 mmHg referenced to the mid-point of the right atrium), whereas in the other group intravenous fluids only were infused at the baseline maintenance rate and the CVP was allowed to fall. In both groups, a balloon was transiently inflated in the right atrium to stop the flow and allow measurements of MSFP and the resistance to venous return. After 2 h, two boluses of 5 ml/kg of blood were given rapidly and then removed to obtain cardiac function curves, a measure of vascular compliance, and systemic arterial and pulmonary pressure-flow relationships (vascular resistance). The hemodynamic patterns were strikingly different between the fluid-treated and non-fluid-treated animals (Septic Shock Part 1, Figs. 52.5, 52.6, and 52.7). In the animals that received volume, cardiac output increased by 38% and the cardiac function curve was higher and somewhat steeper than in the control condi-

tion. This was associated with an apparent decrease in venous resistance (the value of 18% was not significant in the small sample size with a lot of variance), and an increase in stressed volume with an increase in MSFP despite an increase in vascular capacitance (dilation, or rightward shift of venous pressure versus volume curve). The arterial pressure fell to a mean of 76 mmHg. In the animals that did not receive fluid, all hemodynamic components were dramatically different. Cardiac output fell by almost 50% and the cardiac function curve was markedly flattened. The venous resistance doubled, MSFP fell because of a decrease in stressed volume despite a decrease in vascular capacitance. After 2 h the animals were given the NOS inhibitor L-nitro-arginine methyl ester (L-NAME). Blood pressure rose in both groups but cardiac function and cardiac output markedly decreased, venous resistance markedly increased and so did venous capacitance from the state following volume. The negative effects from L-NAME were much greater in the group that did not receive volume. From these animal studies, it appears that infused volume counters the large loss of fluid from the vasculature to the interstitial space, as well as the increase in venous capacitance due to loss of venous tone. Vascular volume thereby is maintained and can actually increase cardiac output and blood pressure, improve tissue perfusion, and prevent multi-organ dysfunction. This only is true as long as cardiac output can increase with the volume, i.e., the heart is on ascending part of its function curve.

The changes in the pulmonary vascular pressure-flow relationship were strikingly different in the volume versus no volume resuscitation groups (Part 1, Fig. 52.7). In the volume group, there was a small increase in the critical closing pressure of the pulmonary circuit with little change in pulmonary vascular resistance. However, when the volume was not given, there was a marked increase in both the pulmonary vascular resistance and the critical closing pressure. This suggests a reaction to increased tissue injury from the inflammatory response that might

have been related to the failure to maintain an adequate cardiac output.

Synthesis of the Defects

Putting the human and animal studies together, it seems that infused volume helps mitigate the loss of volume from the vasculature. This allows maintenance of an increased cardiac output which is necessary to match the decreased SVR and allows for better distribution of blood flow. As a consequence, tissue injury is reduced, which reduces further production of cytokines and other endogenous damaging molecular species that can perpetuate the septic process (Chan et al. 2012). Evidence for this comes from studies on LPS infusions into normal human volunteers. Initial loading with fluid before giving LPS significantly dampened the cytokine response, although it did not alter the hemodynamics in these normal subjects (Dorresteijn et al. 2005). The argument then might be that if cardiac output is adequate, and lactate is not increasing, there is not much value to continue infusing large amounts of fluid. Giving excess volume even seems to cause harm (Boyd et al. 2011). Increasing intravascular pressures always increases capillary filtration and the increase in filtration always will be much greater in septic patients because their capillary permeability is increased. As discussed in Chap. 10, after a critical value, the extra fluid might just be feeding the leak because the compliance of the interstitial space increases when the interstitial pressure reaches a high enough value. This produces the equivalent of a decrease in the resistance to filtration across the capillary bed and it then becomes much easier for trans-capillary filtration to occur. Furthermore, as also discussed in Chap. 10, when the interstitial volume expands, further infusions of a crystalloid solution become progressively less effective because an increasingly larger proportion of the infused volume goes into the interstitial space and proportionally increases the edema more than it expands the intravascular space.

Norepinephrine

One of the central hemodynamic problems in sepsis is the loss of vascular tone. Thus, norepinephrine (NE) with its potential to restore vascular tone through its potent effect on alpha-adrenergic receptors, as well as its effect on cardiac contractility through its action on beta-adrenergic receptors, is an ideal choice for initial pharmacological management of sepsis. In a classic prospective observational cohort study, Martin et al. found that NE was strongly associated with survival in septic patients and the outcome with NE was significantly better than seen with other hemodynamic drugs (Martin et al. 2000). However, in a later study, they also showed that excessive doses of NE were associated with worse outcome (Martin et al. 2015).

The most obvious effect of NE is the rise in arterial pressure due to constriction of arterial resistance vessels (Table 53.1). In moderate

doses, the rise in arterial pressure with NE can reverse an oliguric state (Desjars et al. 1989; Martin et al. 1990). Of importance, at least at moderate doses, NE has a greater effect on the efferent arterioles of the glomerulus than on the afferent arterioles, and thus can increase glomerular filtration rate (Mills et al. 1960). However, the effects of NE are much more coordinated than simply the effect on SVR (Fig. 53.2). NE constricts vascular smooth muscle in the venous capacitance beds which recruits unstressed into stressed volume; this provides the equivalent of an auto-transfusion (Rothe 1983; Deschamps and Magder 1992) (Fig. 53.2). In someone who has adequate volume reserves, based on animal data this can increase stressed volume by around 10 ml/kg, and even up to about 18 ml/kg with a major stress, although increases of this magnitude are less likely in most patients. This response is very dependent upon the reserves of unstressed volume which cannot be measured.

Table 53.1 Cardiovascular responses to major drugs used in sepsis

	NE	Epi	Dobut	Vaso	Phenyl	Milrinone
Arterial P	↑↑↑	↑↑↑	↑	↑↑↑	↑↑	↓
Q	↑	↑↑↑	↑↑	↓, ↔	↓, ↔, ↑	↑↑
Pra	↓	↓	↓↓	↑	↑	↓↓
Contract	↑	↑↑	↑↑	↔	↔	↑↑
HR	↑	↑↑	↑↑	↔	↔, ↓	↑
SVR	↑↑	↑	↓	↑↑	↑	↓↓
RVR	↓, ↔	↓	↓	↑	↑	↓
MSFP	↑↑	↑↑	↑	↑	↑	↔
Capacitance	↓↓	↓↓	↓	↓	↓	↔
PAP	↔	↑	↓	↔	↔	↓↓
Pro-arrhythmic	+	+++	+			+
Receptors	α, β	α, β	β, α	V1 (vascl), V2 (water)	α	phospho III

Details and references are given in the text. The strengths of the activities either increasing or decreasing the variable are given by arrows and the pro-arrhythmic effects with + signs. The data are general patterns based a variety of studies but it is important to appreciate that the actual action in an individual patient will be highly variable. Note, for example, the responses to NE under normal conditions and after LPS in Fig. 53.3. It thus is not difficult to obtain data from in vitro studies or under very controlled conditions in vivo, most often in the normal conditions but it is hard to get dependable information on what happens in the septic patient. Responses also depend upon the patient's status. For example, phenylephrine is marked as possibly giving an increase in cardiac output. This can occur if a patient's vascular volume is increased and the volume recruitment from venous constriction overrides an increase in RVR and thereby increases cardiac output. As such, the authors have added a subjective component based on their experience. The values indicate responses that are most likely. The table should thus be viewed as a guide but not as a dogmatic statement. The best principle is to always monitor the hemodynamic response and determine if the agent did what was desired. If not, try a higher dose or choose a different agent

NE norepinephrine, Epi epinephrine, Dobut dobutamine, Vaso vasopressin, Phenyl Phenylephrine, P pressure, Q cardiac output, Pra right atrial pressure, HR heart rate, SVR systemic vascular resistance, RVR resistance to venous return, MSFP mean systemic filling pressure, PAP pulmonary artery pressure, α alpha-adrenergic receptor, β beta-adrenergic receptor, phospho phosphodiesterase III inhibitor

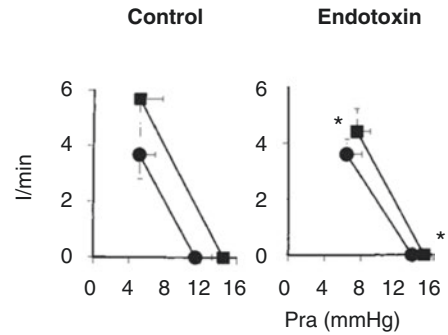
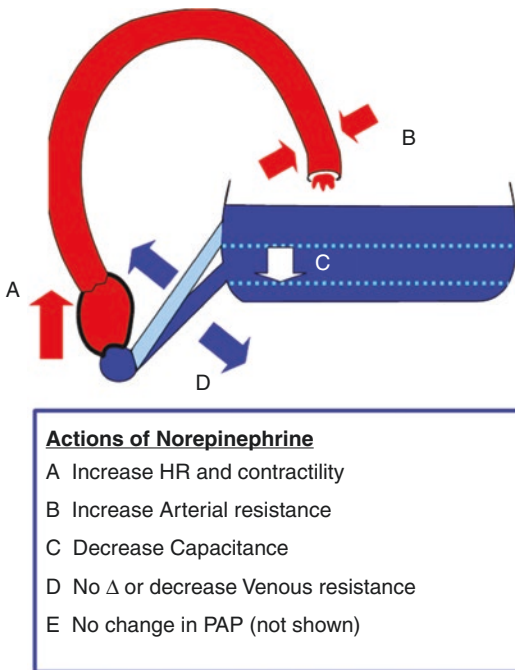


Fig. 53.2 The multiple sites of action of NE on the vasculature. The left side shows a general model of the circulation and sites of action by NE. The right side shows the effect of NE infusion (27 mcg) on the return function with and without endotoxin. NE shifted the control venous return curve to the right, indicating a decrease in vascular capacitance and an increase in MSFP; there was a negli-

gible effect on venous resistance (RVR); this led to an increase in cardiac output. In LPS-treated animals the decrease in capacitance and RVR were smaller, which led to a smaller increase in cardiac output. (From Datta and Magder (Datta and Magder 1999). Reprinted with permission of the American Thoracic Society)

This action of NE is supported by qualitative data in septic humans (Persichini et al. 2012). It is important to remember that normal stressed volume only is about 1.4 L so that an increase in 10 ml/kg in a 70 kg male would increase stressed volume by 700 ml, which would be a 50% increase. Importantly, this effect occurs almost immediately. The consequent rise in MSFP produces a major increase in the driving force from the veins back to the heart. It also is important to appreciate that the vasoconstrictor effect of NE is primarily on venous capacitance vessels. Although alpha-adrenergic agonists can constrict the downstream veins that provide the resistance to venous return, at moderate doses of NE this does not occur (Fig. 53.2) (Datta and Magder 1999). A likely explanation is that the effect of NE on alpha-adrenergic receptors in the venous resistance vessels is off-set by the action of NE on beta-adrenergic receptors in the venous resistance vessels not present in venous capaci-

tance vessels. The decrease in capacitance is well described for the venous drainage from the splanchnic circulation, but seems to be less significant in muscle beds (Deschamps and Magder 1992; Green 1977). It must be remembered that the effect of an increase in the return function on cardiac output is minimal if RV filling is already limited. In this situation, the clinical prediction is that NE only will increase arterial pressure by increasing SVR and cardiac output, the critical variable for O₂ delivery, will not increase, or possibly even decrease, unless the NE also increases cardiac function. This, though, is the fourth effect of NE. NE can moderately increase cardiac contractility and cardiac function, which will allow the heart to pump out increased venous return (Fig. 53.3). The final effect of NE is really a lack of effect; NE has minimal effects on pulmonary vascular resistance and thus does not increase the afterload on the right ventricle (Fig. 53.3) (Datta and Magder 1999).

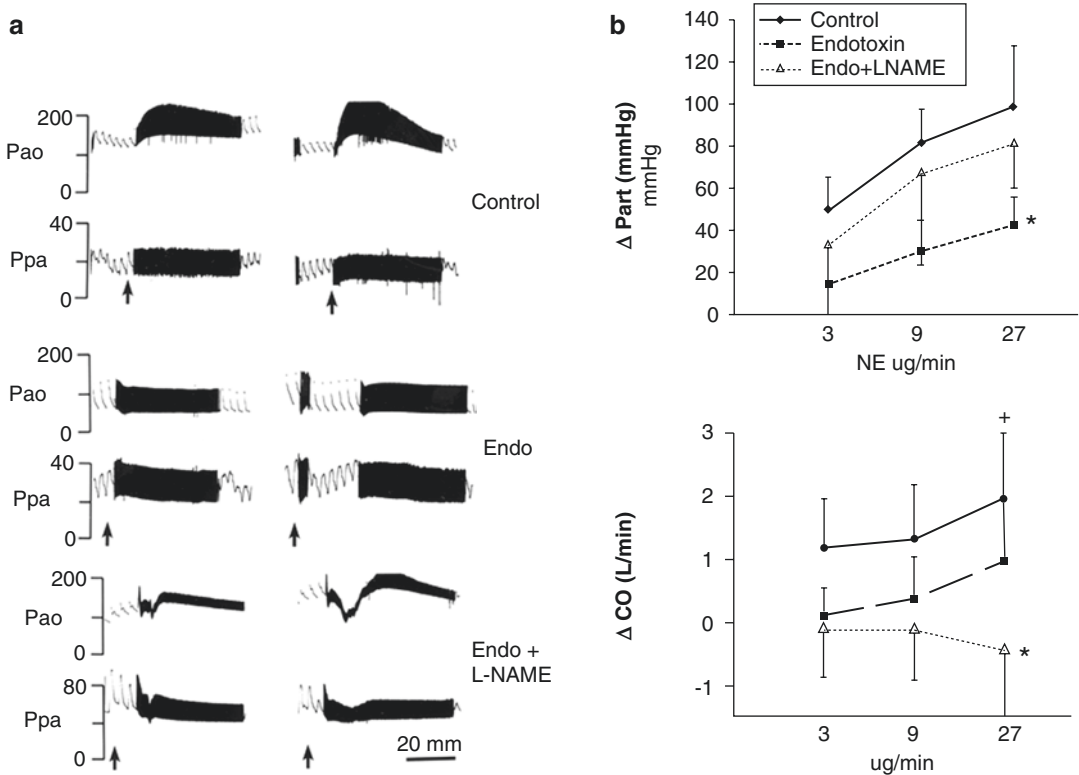


Fig. 53.3 Cardiovascular responses to different doses of norepinephrine (NE) at baseline (control), after infusion of endotoxin, and then with the addition of L-NAME. Panel (a) shows the responses in the pig of arterial pressure (Pao) and pulmonary artery pressure (Ppa) to a 30 min infusion of 9 mcg/min (left side) and 27 mcg/min (right side). At baseline, there was a brisk rise in Pao with a strong dose response and no effect on Ppa. In this animal, after infusion of endotoxin for 2 h, there was almost no response in Pao to the two doses of NE. There was a mild increase in Ppa at the higher dose. After the addition of L-NAME, NE produced a transient increase in Pao and marked increase in Ppa but it was not sustained. The

response was similar with both doses. Panel (b) shows the average peak changes in Pao and cardiac output at 3 doses of NE, from 8 animals. L-NAME almost restored the peak response to NE but as the example in Panel (a) shows, this occurred with an unsustained and variable response. Notice the large standard deviations. NE increased cardiac output in the baseline condition and there was a dose response. In the endotoxin group, there was no effect at the lower dose. L-NAME blocked any response in cardiac output to NE. (From Datta and Magder (Datta and Magder 1999). Reprinted with permission of the American Thoracic Society)

Typical dose ranges for NE are from 8 mcg/min (~ 0.1 mcg/kg/min) and up to 60 mcg/min (~ 0.85 mcg/kg/min). Higher doses than these are often used and might still increase arterial pressure. However, it is not known whether this is of medical utility or if it is just increasing harm. It is evident that at autopsy, large doses of catecholamines can produce clumping and disorganization of cardiac myofibrils and this can evolve into degenerative changes in the cell cytoplasm and mineralization of mitochondria (Reichenbach and Benditt 1970). In the initial

study by Martin et al., the highest dose of NE was 2.27 ± 2.10 mcg/kg/min (Martin et al. 2000). Indeed, higher doses of NE are associated with an increase in mortality, but this obviously may simply represent patients in more extremis (Martin et al. 2015). There is physiological rationale, though, for why higher doses of NE might be harmful. When a baroreceptor-mediated response to systemic hypotension is activated, the increase in arterial resistance is greater in peripheral muscle beds than in the splanchnic vasculature (Deschamps and Magder

1992; Hainsworth et al. 1983). This increases the fraction of cardiac output that goes to the splanchnic vasculature while decreasing flow to the periphery. The consequence is a potential survival benefit because there is less compromise of flow to more delicate and metabolically active abdominal organs. It is quite likely that very high doses of NE override this selectivity and compromise flow to the vital abdominal organs. At higher doses of NE, the alpha-adrenergic component might over-ride the dilating effect of NE on venous drainage, thus raising venous resistance, and decreasing venous return and cardiac output. The answer to what is a high dose of NE will be very difficult to determine with a rigorous randomized approach because of the desperate state of these patients. To comment on our own experience, we generally have been limiting NE to 50–60 mcg/min, but admittedly without data.

An important question currently being tested in the management of septic shock is when to stop using fluids to raise blood pressure and to shift to the use of NE. The limits of the usefulness of fluids have already been discussed as well as their potential to do harm, and that increasing total body volume is not a physiological way to increase cardiac output. However, there is an additional factor (Fig. 53.4). When arterial pressure is increased by expanding vascular volume, capillary hydrostatic pressure always increases, too, and colloid oncotic pressure is reduced due to dilution of plasma proteins; both of these contribute to increased capillary fluid filtration. This effect on filtration is even greater in sepsis because vascular permeability is increased. On the other hand, increasing arterial pressure by increasing SVR with NE likely results in either no change or even a decrease in capillary hydrostatic pressure, especially if the NE increases cardiac function and decreases the CVP (Fig. 53.4) (Tatara 2016; Fishel et al. 2003).

Some insight into the debate about the use of fluid versus NE can be found in an older study that compared the effects of fluid infusions versus NE on hemodynamics and distribution of organ perfusion in an LPS animal model of sepsis (Hussain et al. 1988a). In this study, perfusion of

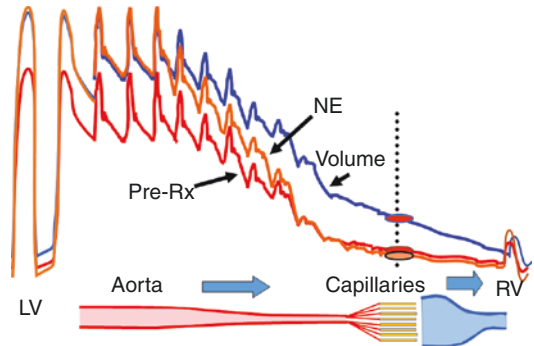


Fig. 53.4 Schematic diagram of the effect of NE compared to a volume effusion on the vascular pressure profile. The pressures start from the LV and go to the RV. In the large arterial vessel, there is little pressure drop. Resistance increases markedly in small arteries and arterioles (400–100 microns). There is little pressure drop across the capillaries and a small drop from the veins back to the heart (in the range of 4–8 mmHg). The same increase in arterial pressure is presumed to be produced by NE and volume. Because of the greater pressure drop with NE, and the lower right atrial pressure because of increased cardiac function, the pressure in the capillaries likely is the same or as normal or even less with NE than with volume

multiple organs was assessed simultaneously with radio-labeled microspheres. As already indicated, a limitation of animal studies is that LPS most often produces a low cardiac output with a high SVR rather than the high cardiac output low SVR most commonly observed in humans and this was the case in this study too. However, in this case, this limitation helps us understand the importance of considering cardiac output during resuscitation. LPS alone decreased cardiac output to about a third of the control value, and mean arterial pressure decreased to less than 60 mmHg. Infusion of either fluid (normal saline) or NE restored the arterial pressure to the baseline level, although large amounts of both agents were required. How they did this, though, is most informative. The saline mildly increased cardiac output from the baseline value, whereas cardiac output did not rise with NE (Fig. 53.5). The consequences were evident when organ perfusions were examined. Coronary blood flow fell with LPS and only moderately increased with NE. On the other hand, coronary blood flow increased when saline was given (even though the heart rate

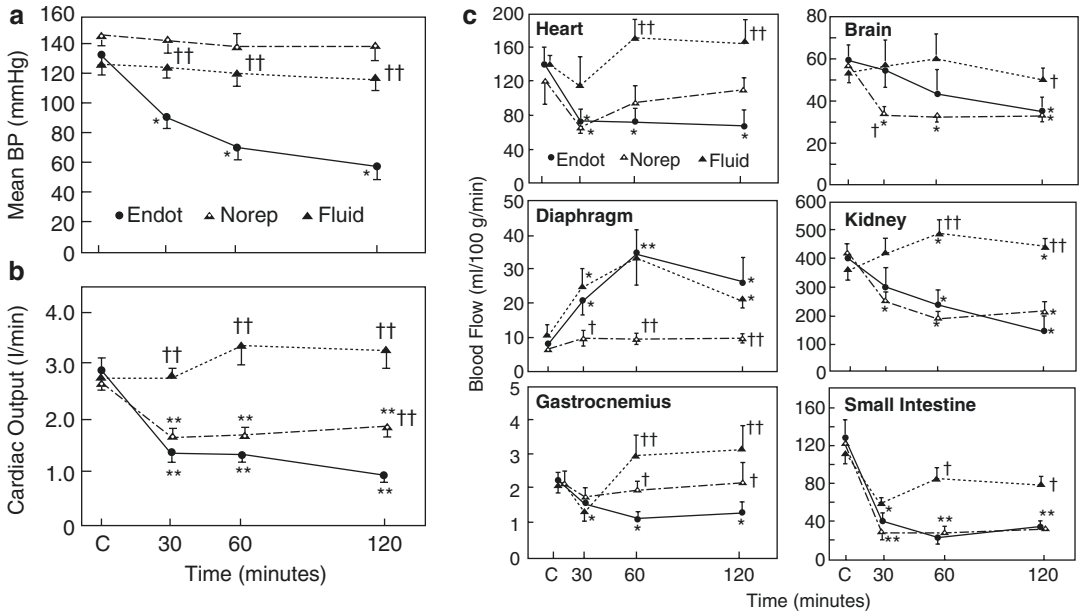


Fig. 53.5 Comparison of hemodynamic responses to raising arterial pressure with volume (fluid) or norepinephrine (NE) in dogs given endotoxin (Endot). (a) Mean arterial blood pressure (BP) over 2 h. With Endot alone, BP fell to 60 mmHg. By design, BP remained at baseline levels with NE and fluid. (b) cardiac output. With Endot alone, cardiac output fell to about 1/3 of baseline and fell almost the same with NE except for some mild recovery (or less fall) by 2 h cardiac output was maintained with fluid. (c) blood flow in ml/100 g/min to the heart, brain, diaphragm, kidney, gastrocnemius, and small intestine. Legends as in (a) and (b). With Endot blood flow fell to all

regions except the diaphragm. With volume, blood flow to the heart increased by a small amount, had the same increase in the diaphragm as with Endo, remained at baseline in the brain, increased in the gastrocnemius and fell in the intestine but less than in the other groups. With NE there was an initial fall in blood flow to the heart and then a moderate increase compared to endotoxin, it fell more than with Endot alone in the initial stages, fell in the kidney and intestine and changed little in the gastrocnemius. See text for more details. (From Hussain et al. 1988b). <https://journals.physiology.org/author-info/permissions>)

decreased). Intestinal blood flow fell markedly with LPS and was partially restored with saline but not at all with NE. The pattern in the kidney was similar, except that NE did not restore renal blood flow at all. Blood flow to the diaphragm and the gastrocnemius muscle are worth noting. The animals were breathing spontaneously so that diaphragmatic blood flow increased with LPS. This increased diaphragmatic blood flow stayed the same when saline was given, but diaphragmatic blood flow did not increase from baseline in the NE group, despite the ventilation pattern being similar in all three groups. In contrast, blood flow to a sample muscle, the gastrocnemius, fell with LPS as expected with the decrease in cardiac output, although the muscle still took a greater percentage of cardiac output than under control conditions. This indicates a

failure of the peripheral vasculature to constrict as much as other tissues and thus there is a failure to redirect blood flow to other areas of need, especially the intestine. The saline infusion increased blood flow to the muscle and maintained the percentage of total blood flow seen with LPS alone. NE kept the gastrocnemius blood flow constant and prevented the increase in blood flow seen with LPS alone or with the fluid infusion. It is worth noting that resting muscle blood flow is very low and thus cannot decrease much more. Brain blood flow decreased the most in the NE group.

The lessons from this study are that if cardiac output is low, and there is inadequate blood volume to recruit or redistribute, NE does not increase cardiac output and has little benefit; it can actually further compromise flow to vital

organs. A limitation of the study, though, is that there was not a fourth group which received fluid and NE. When NE has been given in volume resuscitated animals, NE increased cardiac output, which would be expected to improve tissue perfusion (Fig. 53.3) (Villablanca et al. 2002). The important point to take away is that volume status must be addressed first and knowledge of the cardiac output, either with a direct measure or through clinical indicators, should be a key factor in making decisions on the supportive therapy for patients in septic shock, especially cases in extremis. These results might also explain some of the variable results in the literature on the effects of catecholamines on splanchnic flow. If the NE only produces vasoconstriction, and there is a failure to increase cardiac output, blood flow to normally low resistance regions such as the gut, most likely only will decrease. The other side of this story is that if the plateau of the cardiac function curve has been reached, fluid cannot help either; only increasing in cardiac performance can help. The ideal is to use volume therapy and NE in a coordinated approach by following the cardiac output and blood pressure responses.

The role of fluid and catecholamines also was addressed by Natanson and co-workers with their peritonitis model of sepsis (Natanson et al. 1990). Four groups of animals with an implanted *E. coli*-infected clot were randomized to receive one of four treatments: (1) nothing; (2) NE alone to sustain arterial pressure; (3) fluid infusion to try to maintain arterial pressure; or (4) combination of NE and fluid boluses. All animals received the appropriate antibiotics. Only the group with combined NE and volume had a successful outcome. This implies that supportive care is necessary to give time for antibiotics to work and that this is best done with combined pharmacological and fluid therapy, although how much of each is still not known. This animal data are supported by benefits of at least early therapy, if not goal-directed therapy.

A limitation to the use of NE is that there often is a failure of vascular smooth muscle to respond as evidenced by intrinsic catecholamine concentrations being markedly elevated in sepsis (Natanson et al. 1990). In their peritonitis model

of sepsis, Natanson and co-workers found that catecholamine dose-response curves were shifted downward (Karzai et al. 1995). One factor for the decrease in sensitivity to catecholamines is that the increased oxidation with sepsis alters cell membrane signaling processes of catecholamines (Macarthur et al. 2000). It has been proposed that NO plays a role in this process. In a porcine model of sepsis, we found that LPS produced a profound decrease in the arterial pressure response to NE (Fig. 53.3) (Datta and Magder 1999). Inhibiting NO production with an NOS inhibitor partially restored the vascular response, but the response pattern was very different than in the control state (Fig. 53.3). There was an initial transient increase in the pressure response, then a loss of response, and then a small increase in pressure. The short effect on constriction is similar to what is seen with an infusion of methylene blue (Preiser et al. 1995; Keaney et al. 1994; Schneider et al. 1992); it too often produces a transient increase in vascular responsiveness but this usually does not last longer than 20–30 minutes. These types of responses are consistent with the failure of the uptake and release in of Ca^{2+} from oxidative changes in RyR2 and SERCA discussed in the mechanisms section (Figs. 52.9 and 52.10, Part 1).

Phenylephrine

Phenylephrine acts primarily on alpha-adrenergic receptors and produces some of the same effects as NE but is much less potent (Table 53.1). It can increase arterial resistance, decrease vascular capacitance and potentially increase cardiac output by recruiting unstressed volume (Magder 2011; Thiele et al. 2011a, b). However, it lacks beta-adrenergic activity. This means that unlike NE, it increases the resistance to venous return, which in most cases, negates the effect of the decrease in capacitance and venous return decreases. It also has no significant effect on cardiac function and can even decrease cardiac output because of the increase in arterial afterload with no increase in contractility. The overall effect of all these actions is that phenylephrine

usually results in a decrease in cardiac output (Thiele et al. 2011b). An advantage for phenylephrine over NE is that if it goes interstitial when given through a peripheral vessel, the risk of limb ischemia is much less than occurs with the more potent NE. Thus, it can be useful during short-term urgent interventions such as during intubation and maintenance of arterial pressure when central access is being obtained. Other specialized uses can be in patients with a dynamic outflow tract obstruction, loss of alpha-adrenergic tone because of spinal injury, or in patients with expanded intravascular volume such as during pregnancy. A positive aspect of phenylephrine is that it does not increase pulmonary vascular resistance (Tanaka and Dohi 1994). In Table 53.1, it is indicated that phenylephrine can decrease heart rate. This occurs because it triggers a baroreflex reaction from the sudden rise in pressure that comes without any beta-adrenergic activation and can be quite significant when a bolus is given. It also is associated with vagal tone withdrawal. This can be put to good use when it is used to convert a supraventricular re-entry arrhythmia. In contrast to beta blocker and calcium channel blockers, it increases vagal tone with a rise in arterial pressure. Dose for a bolus range from 200 to 1000 mcg.

Vasopressin

A role for the administration of exogenous vasopressin in septic shock was first proposed by Landry who noted that plasma vasopressin is inappropriately low in septic shock (Landry and Oliver 2001; Landry et al. 1997). Vasopressin is a peptide hormone produced in the thalamus and stored and secreted from the pituitary gland in response to hypovolemia or increased plasma osmolality. It acts on its V1 receptor to constrict vascular smooth muscle, but importantly, also increases the responsiveness of adrenergic receptors to their agonists (Hollenberg 2011). It has potent effects on systemic vascular resistance (Table 53.1). It also has been shown to constrict capacitance vessels in the splanchnic region and thereby recruit unstressed into stressed volume

(Welt and Rutlen 1991). The vasopressin V2 receptors result in water retention. It has subsequently been found that vasopressin infusion increases blood pressure even in patients with a normal concentration of plasma vasopressin and thus works as a pharmacological agent rather than hormone replacement.

The role of vasopressin was studied in a large randomized double-blind controlled trial that compared the effect on survival of NE alone to NE plus vasopressin for septic shock (VASST) (Russell et al. 2008). An initial concern was that vasopressin would produce bowel ischemia but this did not occur at the doses used which were in the range of 0.01–0.04 u/min. However, no survival benefit was observed. An important limitation of the study was that it was significantly underpowered because the original estimate of the 28 day mortality for the power calculation was 50%, but mortality only was 39% in the NE control group. A somewhat surprising finding in a predefined subgroup analysis was that vasopressin seemed to have a benefit in patients who received a lower dose of NE, which was defined as ≤ 15 mcg/min. This might be related to the potential harmful effect of higher doses of NE (Martin et al. 2015) and the sensitization adrenergic receptors to NE by vasopressin. Although there is no further data on its usefulness, vasopressin still is very commonly used in septic shock. Our own practice is to start it when NE doses are greater than 20 mcg/min.

Epinephrine

Epinephrine (Epi) is released from chromaffin cells in the adrenal medulla. It has potent alpha and beta-adrenergic effects and tends to produce much more abrupt changes in hemodynamics than NE and for that reason, it has a specific role as a “rescue” drug when patients are in a death spiral with shock (Table 53.1). Typical doses are in the 1–20 mcg/min range, although higher doses often are used, but the efficacy, and the ultimate effect on mortality of these higher doses, are not known. During cardiac arrest, boluses in the 250–1000 mcg range are used. Although epi-

nephrine is potent, and gives a rapid and comforting response for the clinician, it is associated with complicating features including an increased risk of atrial and ventricular arrhythmia, increased lactate (Levy et al. 2005), possible gut ischemia, and hypoglycemia (Hollenberg 2011). In patients with a critical coronary stenosis, the associated tachycardia could trigger myocardial ischemia.

Despite these concerns, three studies have shown little increased harm when Epi was compared to NE (Myburgh et al. 2008) for shock in general, or NE plus dobutamine for septic shock (Annane et al. 2007; Levy et al. 1997). Myburgh and coworkers (Myburgh et al. 2008) found that the time to achieve the arterial pressure goal and the 28 day and 90 day mortality rates were similar with Epi and NE, although 13% of patients in the Epi group were withdrawn from the study prematurely because of tachycardia or increased lactate. Annane and coworkers found no difference in outcomes with either drug and no patients were withdrawn from their study (Annane et al. 2007). Levy et al., too, found no survival difference between Epi and NE, although lactate levels were greater with Epi. A worrisome observation was decreased perfusion of the gut mucosa by gastric tonometry in the Epi group. This last study was the only one to have reported cardiac output values; it is noteworthy that the mean cardiac outputs were above normal in both groups before being given the assigned treatments.

A synthesis of these observations is as follows. Because of its mixed alpha and beta-adrenergic activity, Epi has a great potential to increase cardiac output. However, it does not make a lot of sense to use this “course” drug when cardiac output is already adequate. NE is then the better choice because the primary need in that case is to restore vascular tone. On the other hand, the reasons for stopping Epi in the Myburgh study were the increase in lactate and tachycardia. These might not have been a valid reason for stopping it because the rise in lactate in most cases is due to a benign increase in lactate metabolism directly by Epi. It is noteworthy that the outcome was not worse when Epi was compared to NE in sepsis, although there was a tendency for worse survival with the use of Epi in a

small study in cardiogenic shock, perhaps because of the increase in myocardial O₂ demand in persons with limited reserves (Levy et al. 2018b). Epi likely has an important role in the management of septic shock patients who have inappropriately normal or low cardiac outputs, but its use, as well as the next two drugs, should best be followed with cardiac output monitoring. The argument is that Epi should be considered when the goal is to increase cardiac output whereas NE should be titrated for blood pressure targets. The validity of this approach will not be easy to address in randomized trials, but the principle still needs to be considered clinically. It may be possible to follow surrogates of cardiac output such as a decreasing lactate and an improving central venous saturation. Clinical signs of better perfusion such as increased wakefulness, improvement in urine production, and resolving skin signs of inadequate perfusion also should be helpful (Chap. 30).

Dobutamine

Dobutamine is made up of a D-isomer, that has beta-1 and beta-2 adrenergic activity, and an L-isomer that has beta-1 and alpha-1 activity. It increases cardiac output by both increasing cardiac contractility and heart rate through its beta-1 activity and by causing some vasodilation through the beta-2 receptor activity (Pollard et al. 2015; Ruffolo Jr. and Messick 1985) (Table 53.1). The net effect on blood pressure depends upon how much cardiac output increases relative to the fall in SVR. Because both isomers have beta-1 activity, its effect on heart rate tends to be greater than other agents. The alpha-1 activity is overshadowed by the stronger beta-2 effect in the arterial vasculature so that the net effect is a decrease in SVR. In an unpublished study, we found that dobutamine increases MSFP, likely through its α activity, indicating that it decreased vascular capacitance, and at the same time through its β activity it also decreased venous resistance in non-septic animals. The net effect of these two processes is an increase in venous return. Typical doses of dobutamine range from 2.5 to 20 mcg/

kg/min. The half-life is short so that a bolus is not needed. It also means that the effect wears off quickly, usually in less than 15–20 minutes.

In our personal experience, we have found that the cardiac output response to dobutamine is not always predictable and less consistent than with Epi. Post cardiac surgery patients can be very sensitive and can have a marked rise in cardiac output with only 2.5 mcg/kg/min, whereas patients with an acute myocardial infarct may not respond at doses of 20 mcg/kg/min; we have not gone higher and when dobutamine fails at this level, our default would be to use Epi. As discussed with Epi, the use of dobutamine in sepsis should be reserved for patients with a lower than expected cardiac output and preferably with cardiac output monitoring.

Milrinone

Milrinone increases myocardial contractility and decreases SVR (Table 53.1). It does this by acting as a type III phosphodiesterase inhibitor which reduces the breakdown of cyclic adenosine monophosphate (cAMP), the major secondary messenger that promotes Ca^{2+} entry into cardiomyocytes. The rise in cytoplasmic Ca^{2+} in cardiomyocytes increases inotropy, but in vascular smooth muscle it decreases cytoplasmic Ca^{2+} and produces vasodilation (Chong et al. 2018). Milrinone has a half-life of 4–5 h so that an initial bolus of 50 mcg/kg usually is recommended. Typical infusion rates are 0.25–0.5 mcg/kg/min (Chong et al. 2018). Given its long half-life, it is important to appreciate that the effect lasts for 4–5 h. Milrinone is excreted primarily by the kidney; 90% of the drug can be recovered from the urine within 8 h. Doses thus must be adjusted when creatinine is elevated and it needs to be appreciated that the effect will last longer (Chong et al. 2018).

A primary regulator of cAMP activity is the beta-1-adrenergic receptor. Because the action of milrinone is downstream from the receptor, it has been thought that milrinone still could be effective in individuals who are beta-blocked (Chong et al. 2018). However, this only is true if some-

thing else is stimulating cAMP production. We have found the opposite; often it is the case that the action of milrinone is not very strong if there also is not some beta-adrenergic activity, either intrinsic or exogenously administered. Milrinone can be a potent inotropic agent and has less proarrhythmic effects than dobutamine and Epi (Hollenberg 2011). However, it also can produce a significant decrease in SVR. This likely contributes to the increase in cardiac output, especially in patients with heart failure, but it also can be a problem in patients who are hypotensive to start with and it is not uncommon to have to add NE to stabilize the arterial pressure.

Milrinone has been studied primarily in heart failure and cardiogenic shock (reviewed in reference (Chong et al. 2018)). It also is used frequently following cardiac surgery in children (Angela et al. 2016). However, there are very limited data on its use in septic shock. There only is one small (six patients per group), short, blinded, randomized trial in septic children who were not initially hyperdynamic (Barton et al. 1996). Milrinone increased cardiac output, decreased SVR, and decreased pulmonary vascular resistance, all as expected from its known hemodynamic profile. Most adults have hyperdynamic sepsis and thus it is unlikely that milrinone is of much use in the majority of septic patients, but it does have potential value in patients with an inappropriately low cardiac output. The great concern with its use is that if milrinone fails to increase cardiac output, and only further lowers the already low SVR, there could be an uncontrollable drop in arterial pressure. The authors have used milrinone on occasion (off-label) in septic patients who have lower than expected cardiac outputs and have observed positive hemodynamic results with no hypotensive crises. A loading dose still is given, but it is broken up into aliquots of 0.5 mg which are repeated every 10 minutes until the target loading dose is reached as long as there is not a critical drop in arterial pressure. This only should be done with monitoring of cardiac output. Milrinone is a treatment that is directed at increasing cardiac output and if it fails to do so it should be stopped.

Miscellaneous Therapies

There are numerous therapies that have been tried over the years to try to regulate the cytokine response, block NOS, reduce inflammation with steroids, and attempts at altering the vascular leak. To date, all of these have failed and are not discussed further here.

Heart-Lung Component

Heart-lung interactions become greatly exaggerated in septic patients (Figs. 53.6 and 53.7, Table 53.2). An early component of the sepsis syndrome, indeed a part of the definition, is tachypnea. When a patient is breathing without mechanical support, the more frequent inspira-

tory efforts and stronger respiratory drive produce more frequent and stronger inspiratory increases in venous return to the RV. The increased cycling of pulmonary blood flow increases the shear stress on an already injured endothelium. If the lungs become congested because of ARDS, and the capillary leak is increased, or if there is a primary pneumonia, the stiffer lungs require greater inspiratory swings in pleural pressure (Ppl) to maintain an appropriate tidal volume. This will further increase cyclic changes in venous return and cyclic increases in LV afterload. These effects can be exaggerated further if the increased respiratory drive includes active recruitment of expiratory muscles, because this further amplifies the swings in pulmonary blood flow (Magder et al. 2018). These respiratory-induced swings in pulmonary flow in

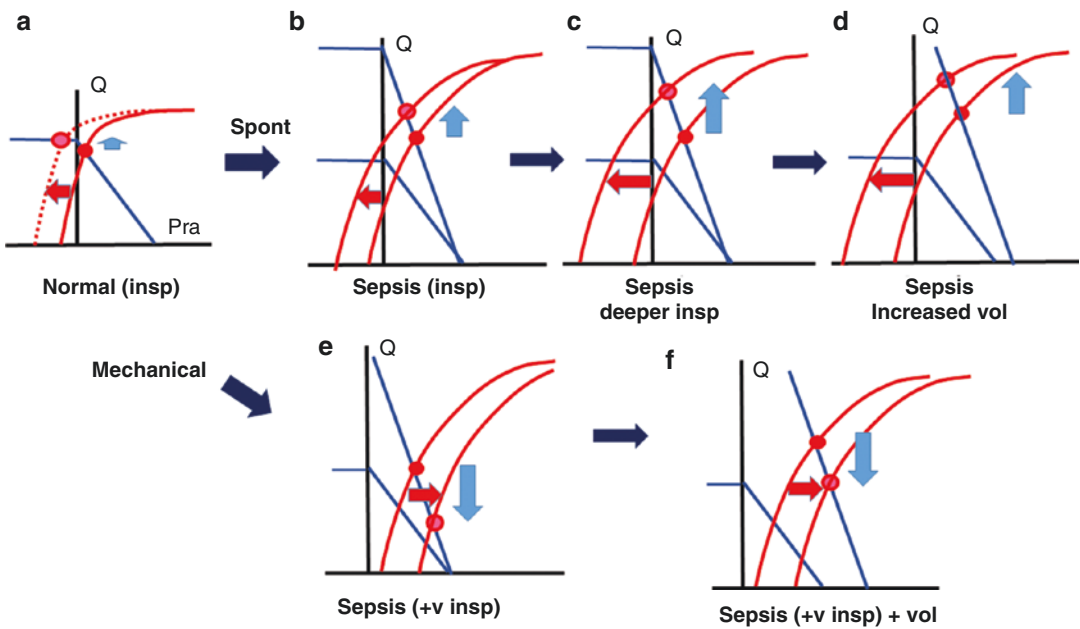


Fig. 53.6 Consequences of spontaneous (spont) and mechanical (mech) ventilation for heart-lung interaction in sepsis. Graphs show the interaction of venous return function (blue lines) and cardiac function (red lines) during ventilation. The upper left, (a), shows baseline conditions in a normal person. With each spontaneous inspiration (insp) the cardiac function curve shifts to the left (dotted line) of the venous return curve (red arrow), right atrial pressure (Pra) falls, and RV filling increases. In sepsis (b), the slopes of the return function are steeper and the cardiac function curve is less steep; the inspiratory increase in RV filling is increased (blue arrow). A deeper

inspiration (c) produces a greater increase RV filling. Increasing blood volume with fluids (d) shifts the venous return curve further to the right and, in this example, decreased the inspiratory increase because it moved the venous return closer to the plateau of the cardiac function curve. However, Pra also was already higher. The bottom half shows the effect of mechanical (positive Ppl) breaths. With inspiration (e) the cardiac function curve shifts to the right and there is a large decrease in RV filling but an increase in Pra relative to the atmosphere. The effect is the same when the stressed volume is increased (f), however, the swings in Pra are at higher values

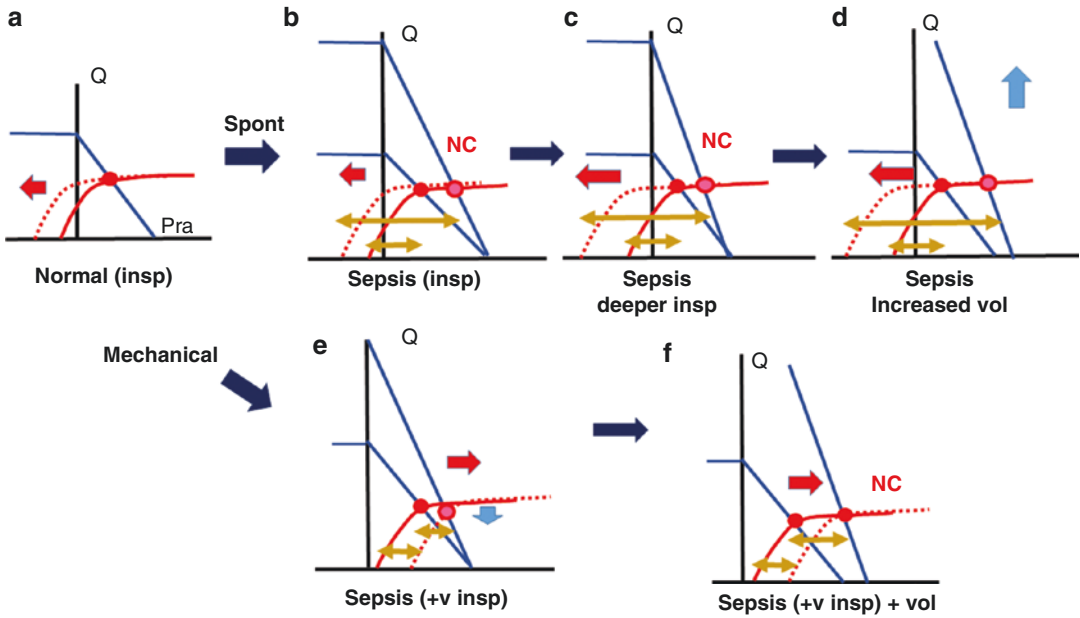


Fig. 53.7 Spontaneous (spont) and mechanical (mech) ventilation when venous return intersects the cardiac plateau of the cardiac function curve. Conditions are the same as in Fig. 53.4 except that venous return function starts with an intersection on the plateau of the cardiac function curve. During spontaneous inspiration (a–d) there is no change in cardiac output with inspiration. However, the change in diastolic wall tension (double arrows) is increased by sepsis (b), deeper inspiration (c), and by giving more volume. The bottom (e and f) shows mechanical breaths with sepsis. In (e) there is a small fall in cardiac output with inspiration because the venous return curve is no longer on the flat part of cardiac function curve. In (f), volume is given and there this no fall in cardiac output with the breath because the venous return curve is again on the plateau of the cardiac function curve. With mechanical breaths, the diastolic wall tension decreases in (e) but not in (f) because of the increased volume

Table 53.2 Factors increasing heart-lung interactions in sepsis

<i>(A) Spontaneous respiratory efforts</i>	
1. Increased drive to breath and deeper inspiratory effort (more negative Ppl)	Larger inspiratory increase in RV filling Increased left atrial transmural pressure (afterload effect) increases pulmonary edema especially because of increased capillary permeability
2. Increased respiratory rate	More frequent increases in RV filling per minute
3. Lung edema produces stiffer lungs	Greater fall in Ppl per breath and increased inspiratory RV filling
4. Steeper slopes of venous return and cardiac function curves	Greater increase in RV filling per breath
5. Greater demands on respiratory muscles.	Weaker muscle and greater potential for failure
<i>(B) Mechanical breath</i>	
<i>Beneficial effects</i>	
1. Decreased drive to breath	Reduced inspiratory fall in Ppl
2. Positive pressure on each breath	Positive pressure inhibits return to the RV Decompresses RV (reduced transmural pressure) Removes inspiratory increase in afterload on LV
3. Maintains ventilation	Prevents death from respiratory arrest
<i>Negative effects</i>	
1. Higher MSFP required to maintain venous return	Increased peripheral congestion Excess volume needs to be removed when weaning
2. Greater swings in RV filling and output	Increase pulmonary arterial shear stress and damage the pulmonary endothelium
3. Increase transpulmonary pressure beyond critical value	Produces non-zone III condition and increases RV afterload

a septic patient can have an even greater effect than in patients with just ARDS. This is because the resistance to venous return is reduced and a greater amount of volume comes back on each breath (Fig. 53.6[B]). The swings in venous return can be further exaggerated when large volumes of resuscitation are given, although the effect is variable (Fig. 53.6). If the heart is on the steep part of the curve there is a greater potential increase before venous flow limitation occurs, but if the cardiac function curve is close to or on its plateau, the inspiratory increase in RV volume is reduced there will be no change in cardiac output or pulmonary flow (Fig. 53.7). However, there still will be a large increase in the wall tension of the RV (Fig. 53.7). The rapid heart rate that usually occurs in septic subjects may dampen the respiratory swing in the ventricular filling because of the reduced time for blood to come back and smaller stroke volumes on each beat.

As discussed previously, the LV most often dilates in sepsis because its function is decreased. If this decrease in function is associated with an elevated left atrial pressure, this too will contribute to pulmonary capillary leak and worsens pulmonary edema. Depressed LV function also makes the LV more susceptible to the increased afterload effect from the inspiratory fall in pleural pressure with strong inspiratory efforts as discussed in Chap. 18 (Heart Lung). Somewhat ironically, if the RV fails, the pulmonary capillaries are protected unless excess fluid continues to be given and raises right-sided filling pressure sufficiently to be transmitted to the LV, raise left atrial pressure, and again contribute to pulmonary edema.

Mechanical ventilation has potentially both beneficial and harmful effects (Figs. 53.6 and 53.7 and Table 53.2). If the patient is volume overloaded, or even if not but still has lung edema, positive pleural pressure can potentially reduce pulmonary edema. On the other hand, the positive pleural pressure also could decrease cardiac output and worsen tissue perfusion. The net effect depends on whether or not the RV is on the flat part of the cardiac function curve (Fig. 53.7) and how big the increase in positive pressure. If the intersection of cardiac and venous return

function is not on the plateau of the cardiac function curve, MSFP needs to be increased, either by the patient recruiting unstressed into stressed volume (Nanas and Magder 1992) (see Chap. 2) or by the physician giving volume to maintain adequate venous return for an adequate cardiac output. The consequence, though, is a rise in right atrial pressure relative to the atmosphere and a further increase in upstream capillary pressures which contributes to tissue edema, especially if high PEEP values are required. Furthermore, this volume will need to be removed when the patient is being weaned and extubated, especially if there is decreased LV function.

Higher levels of positive end-expiratory pressure and higher transpulmonary pressures can produce non-zone III conditions in the pulmonary vasculature. This increases the load on the already compromised RV. Under non-zone III conditions, alveolar pressure becomes the outflow pressure for the RV which can add a considerable load on the already compromised RV. An increase in pulmonary vascular resistance because of sepsis or hypoxic vasoconstriction will increase the pressure drop across the pulmonary vasculature and potentially increase the development of non-zone III conditions. As was discussed in Part 1, septic pigs appeared to have developed a marked increase in non-zone III conditions based on the shift of the x-intercept of the volume versus pressure plot (Fig. 52.7 in Part 1) (Magder and Vanelli 1996). This could have been due to changes in the ventilator pattern but also could have been due to hypoxic vasoconstriction or a direct effect of cytokines on pulmonary vessels. If it was due to direct effects and not ventilation, the choice of ventilator settings will not have a significant effect.

It should be evident from this discussion that there are conflicting pulmonary and vascular needs that can be very difficult to manage clinically. The prudent physician must be careful to balance the needs of all components and avoid excess use of both the pulmonary and systemic vascular interventions by using careful monitoring to respond to changes in the wrong direction and to then modify the therapies being used.

Another component of heart-lung interaction in sepsis occurs with the blood flow needs of the respiratory muscles (see Chap. 16). The work of breathing is increased in sepsis and there must be an appropriate increase in respiratory muscle blood flow. If cardiac output is increased there is likely plenty of blood flow for the respiratory muscles. However, when the cardiac output is not increased, or more importantly, decreased, there may be inadequate blood flow for the needs of the respiratory muscles. This may lead to respiratory failure. As the respiratory muscles start to fail, the work of breathing can increase because of atelectasis and decreasing lung compliance, as well as hypoxemia. The actively working diaphragm also increases sympathetic drive through afferent nerves in the working muscle that alters the normal distribution of blood flow and also increases the drive to breathe (Hussain et al. 1991). This creates a vicious cycle of increased energy needs for the muscle with worsening supply which then leads to respiratory arrest (Hussain et al. 1985b). The solution is mechanical ventilator support which should be instituted with signs of distress and before respiratory failure (Teitelbaum et al. 1992). The motto should be “ensure balance and enough but not too much” of any treatment.

Summary

Based on this discussion, we propose these principles for the hemodynamic management of patients in septic shock. By definition, sepsis is due to an invasive organism. Therefore, of primary importance is the treatment of the infection and stopping the trigger for the cytokine storm. The aim of cardio-pulmonary resuscitation should be to ensure an adequate O₂ delivery that stabilizes the patient but does not necessarily restore hemodynamic values to normal levels and certainly not to supernormal levels. There needs to be a careful balance between using enough fluid to ensure that there are volume reserves in the system to allow normal cardiac adaptations to metabolic needs, but at the same time, it is important to not overload the vascular system and to

avoid tissue edema. It is important to keep in mind that once the plateau of the cardiac function curve is reached, giving more volume will not improve, and may even worsen O₂ delivery. To support the cardiac function and arterial pressure and to avoid fluid overload, likely requires earlier use of vasopressors and inotropes. In the mechanically ventilated patient, ventilator settings need to be adjusted carefully to avoid excessive RV load and a decrease in O₂ delivery. Finally, be wary of new magical therapies; to date, they all have failed. What would be especially useful is the development of new therapies that reduce the capillary leak. Tissue perfusion is all about cardiac output and thus following the response of a therapy to cardiac output, either by direct or indirect means, should be a central factor in the management of septic patients.

References

- Angela F-B, Iria G-R, Victor B-H. Inodilators in the management of low cardiac output syndrome after pediatric cardiac surgery. *Curr Vasc Pharmacol*. 2016;14(1):48–57.
- Angus DC, Barnato AE, Bell D, Bellomo R, Chong CR, Coats TJ, et al. A systematic review and meta-analysis of early goal-directed therapy for septic shock: the ARISE, ProCESS and ProMISe Investigators. *Intensive Care Med*. 2015;41(9):1549–60.
- Annane D, Vignon P, Renault A, Bollaert PE, Charpentier C, Martin C, et al. Norepinephrine plus dobutamine versus epinephrine alone for management of septic shock: a randomised trial. *Lancet*. 2007;370(9588):676–84.
- Barton P, Garcia J, Kouatli A, Kitchen L, Zorka A, Lindsay C, et al. Hemodynamic effects of i.v. milrinone lactate in pediatric patients with septic shock. A prospective, double-blinded, randomized, placebo-controlled, interventional study. *Chest*. 1996;109(5):1302–12.
- Bochud PY, Bonten M, Marchetti O, Calandra T. Antimicrobial therapy for patients with severe sepsis and septic shock: an evidence-based review. *Crit Care Med*. 2004;32(11 Suppl):S495–512.
- Boyd JH, Forbes J, Nakada TA, Walley KR, Russell JA. Fluid resuscitation in septic shock: a positive fluid balance and elevated central venous pressure are associated with increased mortality. *Crit Care Med*. 2011;39(2):259–65.
- Chan JK, Roth J, Oppenheim JJ, Tracey KJ, Vogl T, Feldmann M, et al. Alarmins: awaiting a clinical response. *J Clin Invest*. 2012;122(8):2711–9.
- Chertoff J, Chisum M, Garcia B, Lascano J. Lactate kinetics in sepsis and septic shock: a review of the literature

- and rationale for further research. *J Intensive Care*. 2015;3:39.
- Chertoff J, Chisum M, Simmons L, King B, Walker M, Lascano J. Prognostic utility of plasma lactate measured between 24 and 48 h after initiation of early goal-directed therapy in the management of sepsis, severe sepsis, and septic shock. *J Intensive Care*. 2016;4:13.
- Chong LYZ, Satya K, Kim B, Berkowitz R. Milrinone dosing and a culture of caution in clinical practice. *Cardiol Rev*. 2018;26(1):35–42.
- Datta P, Magder S. Hemodynamic response to norepinephrine with and without inhibition of nitric oxide synthase in porcine endotoxemia. *Am J Respir Crit Care Med*. 1999;160(6):1987–93.
- Deschamps A, Magder S. Baroreflex control of regional capacitance and blood flow distribution with or without alpha adrenergic blockade. *J Appl Physiol*. 1992;263:H1755–H63.
- Desjars P, Pinaud M, Bugnon D, Tasseau F. Norepinephrine therapy has no deleterious renal effects in human septic shock. *Crit Care Med*. 1989;17:426.
- Dorresteijn MJ, van Eijk LT, Netea MG, Smits P, van der Hoeven JG, Pickkers P. Iso-osmolar prehydration shifts the cytokine response towards a more anti-inflammatory balance in human endotoxemia. *J Endotoxin Res*. 2005;11(5):287–93.
- Duff JH, Groves AC, McLean APH, LaPointe R, MacLean LD. Defective oxygen consumption in septic shock. *Surg Gynecol Obstet*. 1969;128:1051–60.
- Fink MP. Cytopathic hypoxia. Mitochondrial dysfunction as mechanism contributing to organ dysfunction in sepsis. *Crit Care Clin*. 2001;17(1):219–37.
- Fishel RS, Are C, Barbul A. Vessel injury and capillary leak. *Crit Care Med*. 2003;31(8 Suppl):S502–11.
- Gattinoni L, Brazzi L, Pelosi P, Latini R, Tognoni G, Pesenti A, et al. A trial of goal-oriented hemodynamic therapy in critically ill patients. SvO₂ Collaborative Group. *N Engl J Med*. 1995;333(16):1025–32.
- Green JF. Mechanism of action of isoproterenol on venous return. *Am J Physiol*. 1977;232(2):H152–H6.
- Hainsworth R, Karim F, McGregor KH, Rankin AJ. Effects of stimulation of aortic chemoreceptors on abdominal vascular resistance and capacitance in anesthetized dogs. *J Physiol*. 1983;334:421–31.
- Hayes M, Timmins AC, Yau EHS, Palazzo M, Hinds CJ, Watson D. Elevation of systemic oxygen delivery in the treatment of critically ill patients. *N Engl J Med*. 1994;330:1717–22.
- Hollenberg SM. Vasoactive drugs in circulatory shock. *Am J Respir Crit Care Med*. 2011;183(7):847–55.
- Hussain SNA, Simkus G, Roussos C. Respiratory muscle fatigue: a cause of ventilatory failure in septic shock. *J Appl Physiol*. 1985a;58:2033–40.
- Hussain SNA, Simkus G, Roussos C. Ventilatory muscle fatigue: a cause of hypercapnic respiratory failure during endotoxic shock in dogs. *J Appl Physiol*. 1985b;58:2033–40.
- Hussain SNA, Graham R, Rutledge F, Roussos C. Respiratory muscle energetics during endotoxic shock in dogs. *J Appl Physiol*. 1986;60:486–93.
- Hussain S, Rutledge F, Roussos C, Magder SA. Effects of norepinephrine and fluid administration on the selective blood flow distribution in endotoxic shock. *J Crit Care*. 1988a;3:32–42.
- Hussain SNA, Rutledge F, Magder S, Roussos C. Effects of norepinephrine and fluid infusion on selective blood distribution in septic shock. *J Crit Care*. 1988b;3(1):32–42.
- Hussain S, Chatillon A, Comtois A, Roussos C, Magder S. The chemical activation of thin-fiber phrenic afferents: cardiovascular responses. *J Appl Physiol*. 1991;70:77–86.
- Iwashyna TJ, Cooke CR, Wunsch H, Kahn JM. Population burden of long-term survivorship after severe sepsis in older Americans. *J Am Geriatr Soc*. 2012;60(6):1070–7.
- Jansen TC, van Bommel J, Schoonderbeek FJ, Sleswijk Visser SJ, van der Klooster JM, Lima AP, et al. Early lactate-guided therapy in intensive care unit patients: a multicenter, open-label, randomized controlled trial. *Am J Respir Crit Care Med*. 2010;182(6):752–61.
- Karzai W, Reilly JM, Hoffman WD, Cunnion RE, Danner RL, Banks SM, et al. Hemodynamic effects of dopamine, norepinephrine, and fluids in a dog model of sepsis. *Am J Physiol*. 1995;268(2 Pt 2):H692–702.
- Kaukonen KM, Bailey M, Suzuki S, Pilcher D, Bellomo R. Mortality related to severe sepsis and septic shock among critically ill patients in Australia and New Zealand, 2000–2012. *JAMA*. 2014;311(13):1308–16.
- Keaney JF, Puyana JC, Francis S, Loscalzo JF, Stamler JS, Loscalzo J. Methylene blue reverses endotoxin-induced hypotension. *Circ Res*. 1994;74:1121–5.
- Kumar A, Roberts D, Wood KE, Light B, Parrillo JE, Sharma S, et al. Duration of hypotension before initiation of effective antimicrobial therapy is the critical determinant of survival in human septic shock. *Crit Care Med*. 2006;34(6):1589–96.
- Landry DW, Oliver JA. The pathogenesis of vasodilatory shock. *N Engl J Med*. 2001;345(8):588–95.
- Landry DW, Levin HR, Gallant EM, Ashton RC Jr, Seo S, D'Alessandro D, et al. Vasopressin deficiency contributes to the vasodilation of septic shock. *Circulation*. 1997;95(5):1122–5.
- Leibovici L, Samra Z, Konigsberger H, Drucker M, Ashkenazi S, Pitlik SD. Long-term survival following bacteremia or fungemia. *JAMA*. 1995;274(10):807–12.
- Levy B, Bollaert PE, Charpentier C, Nace L, Audibert G, Bauer P, et al. Comparison of norepinephrine and dobutamine to epinephrine for hemodynamics, lactate metabolism, and gastric tonometric variables in septic shock: a prospective, randomized study. *Intensive Care Med*. 1997;23(3):282–7.
- Levy B, Gibot S, Franck P, Cravoisy A, Bollaert PE. Relation between muscle Na⁺K⁺ ATPase activity and raised lactate concentrations in septic shock: a prospective study. *Lancet*. 2005;365(9462):871–5.

- Levy MM, Evans LE, Rhodes A. The surviving sepsis campaign bundle: 2018 update. *Intensive Care Med.* 2018a;44(6):925–8.
- Levy B, Clere-Jehl R, Legras A, Morichau-Beauchant T, Leone M, Frederique G, et al. Epinephrine versus norepinephrine for cardiogenic shock after acute myocardial infarction. *J Am Coll Cardiol.* 2018b;72(2):173–82.
- Macarthur H, Westfall TC, Riley DP, Misko TP, Salvemini D. Inactivation of catecholamines by superoxide gives new insights on the pathogenesis of septic shock. *Proc Natl Acad Sci.* 2000;97(17):9753–8.
- Magder S. Phenylephrine and tangible bias. *Anesth Analg.* 2011;113(2):211–3.
- Magder S. Flow-directed vs. goal-directed strategy for management of hemodynamics. *Curr Opin Crit Care.* 2016;22(3):267–73.
- Magder S, Vanelli G. Circuit factors in the high cardiac output of sepsis. *J Crit Care.* 1996;111(4):155–66.
- Magder S, Serri K, Verscheure S, Chauvin R, Goldberg P. Active expiration and the measurement of central venous pressure. *J Intensive Care Med.* 2018;33(7):430–5.
- Martin C, Eon B, Saux P, Aknin P, Gouin F. Renal effects of norepinephrine used to treat septic shock patients. *Crit Care Med.* 1990;18(3):282–5.
- Martin C, Viviani X, Leone M, Thirion X. Effect of norepinephrine on the outcome of septic shock. *Crit Care Med.* 2000;28(8):2758–65.
- Martin C, Medam S, Antonini F, Alingrin J, Haddam M, Hammad E, et al. Norepinephrine: not too much, too long. *Shock.* 2015;44(4):305–9.
- Mills LC, Moyer JH, Handley CA. Effects of various sympathicomimetic drugs on renal hemodynamics in normotensive and hypotensive dogs. *Am J Physiol.* 1960;198:1279–83.
- Mouncey PR, Osborn TM, Power GS, Harrison DA, Sadique MZ, Grieve RD, et al. Trial of early, goal-directed resuscitation for septic shock. *N Engl J Med.* 2015;372(14):1301–11.
- Myburgh JA, Higgins A, Jovanovska A, Lipman J, Ramakrishnan N, Santamaria J, et al. A comparison of epinephrine and norepinephrine in critically ill patients. *Intensive Care Med.* 2008;34(12):2226–34.
- Nanas S, Magder S. Adaptations of the peripheral circulation to PEEP. *Am Rev Respir Dis.* 1992;146:688–93.
- Natanson C, Danner RL, Reilly JM, Doerfler ML, Hoffman WD, Akin GL, et al. Antibiotics versus cardiovascular support in a canine model of human septic shock. *Am J Physiol.* 1990;259:H1440–H7.
- Paul M, Shani V, Mughtar E, Kariv G, Robenshtok E, Leibovici L. Systematic review and meta-analysis of the efficacy of appropriate empiric antibiotic therapy for sepsis. *Antimicrob Agents Chemother.* 2010;54(11):4851–63.
- Peake SL, Delaney A, Bailey M, Bellomo R, Cameron PA, Cooper DJ, et al. Goal-directed resuscitation for patients with early septic shock. *N Engl J Med.* 2014;371(16):1496–506.
- Persichini R, Silva S, Teboul JL, Jozwiak M, Chemla D, Richard C, et al. Effects of norepinephrine on mean systemic pressure and venous return in human septic shock. *Crit Care Med.* 2012;40(12):3146–53.
- Pollard S, Edwin SB, Alaniz C. Vasopressor and inotropic management of patients with septic shock. *P T.* 2015;40(7):438–50.
- Preiser JC, Lejeune P, Roman A, Carlier E, De Backer D, Leeman M, et al. Methylene blue administration in septic shock: a clinical trial. *Crit Care Med.* 1995;23(2):259–64.
- Reichenbach DD, Benditt EP. Catecholamines and cardiomyopathy: the pathogenesis and potential importance of myofibrillar degeneration. *Hum Pathol.* 1970;1(1):125–50.
- Rivers E, Nguyen B, Havstad S, Ressler J, Muzzin A, Knoblich B, et al. Early goal-directed therapy in the treatment of severe sepsis and septic shock. *N Engl J Med.* 2001;345(19):1368–77.
- Rothe CF. Reflex control of veins and vascular capacitance. *Physiol Rev.* 1983;63(4):1281–95.
- Ruffolo RR Jr, Messick K. Effects of dopamine, (+)-dopamine and the (+) and (–)-enantiomers of dobutamine on cardiac function in pithed rats. *J Pharmacol Exp Ther.* 1985;235(3):558–65.
- Russell JA, Walley KR, Singer J, Gordon AC, Hébert PC, Cooper DJ, et al. Vasopressin versus norepinephrine infusion in patients with septic shock. *N Engl J Med.* 2008;358(9):877–87.
- Schneider F, Lutun P, Hasselmann M, Stoclet JC, Temp JD. Methylene blue increases systemic vascular resistance in human septic shock. Preliminary observations. *Intensive Care Med.* 1992;18(5):309–11.
- Shankar-Hari M, Ambler M, Mahalingasivam V, Jones A, Rowan K, Rubinfeld GD. Evidence for a causal link between sepsis and long-term mortality: a systematic review of epidemiologic studies. *Crit Care.* 2016;20:101.
- Shankar-Hari M, Saha R, Wilson J, Prescott HC, Harrison D, Rowan K, et al. Rate and risk factors for rehospitalisation in sepsis survivors: systematic review and meta-analysis. *Intensive Care Med.* 2020;46(4):619–36.
- Stewart TE, Valenza F, Ribeiro SP, Wener AD, Volgyesi G, Brendan J, et al. Increased nitric oxide in exhaled gas as an early marker of lung inflammation in a model of sepsis. *Am J Respir Crit Care Med.* 1995;151:713–8.
- Suffredini AF, Fromm RE, Parker MM, Brenner M, Kovacs JA, Wesley RA, et al. The cardiovascular response of normal humans to the administration of endotoxin. *N Engl J Med.* 1989;321(5):280–7.
- Tanaka M, Dohi S. Effects of phenylephrine and ephedrine on pulmonary arterial pressure in patients with cervical or lumbar epidural anesthesia, or enflurane anesthesia. *J Anesth.* 1994;8(2):125–31.
- Tatara T. Context-sensitive fluid therapy in critical illness. *J Intensive Care.* 2016;4:20.

- Teitelbaum JS, Magder SA, Roussos C, Hussain SNA. Effects of diaphragmatic ischemia on the inspiratory motor drive. *J Appl Physiol.* 1992;72:447–54.
- Thiele RH, Nemergut EC, Lynch C III. The physiologic implications of isolated alpha 1 adrenergic stimulation. *Anesth Analg.* 2011a;113(2):284–96.
- Thiele RH, Nemergut EC, Lynch C III. The clinical implications of isolated alpha 1 adrenergic stimulation. *Anesth Analg.* 2011b;113(2):297–304.
- Thiemermann C, Vane J. Inhibition of nitric oxide synthesis reduces the hypotension induced by bacterial lipopolysaccharides in the rat in vivo. *Eur J Pharmacol.* 1990;182:591–5.
- Thiemermann C, Wu CC, Szabo C, Perretti M, Vane JR. Role of tumor necrosis factor in the induction of nitric oxide synthase in a rat model of endotoxin shock. *Br J Pharmacol.* 1993;110:177–82.
- Villablanca AC, Lewis KA, Rutledge JC. Time- and dose-dependent differential upregulation of three genes by 17 beta-estradiol in endothelial cells. *J Appl Physiol.* 2002;92(3):1064–73.
- Welt FG, Rutlen DL. Effect of vasopressin on systemic capacity. *Am J Physiol.* 1991;261(5 Pt 2):H1494–8.
- Wright CJ, Duff JH, McLean APH, MacLean LD. Regional capillary blood flow and oxygen uptake in severe sepsis. *Surg Gynecol Obstet.* 1971;132:637–44.
- Yealy DM, Kellum JA, Huang DT, Barnato AE, Weissfeld LA, Pike F, et al. A randomized trial of protocol-based care for early septic shock. *N Engl J Med.* 2014;370(18):1683–93.



Cardiopulmonary Monitoring of Patients with Pulmonary Hypertension and Right Ventricular Failure

Ryan A. Davey, Ahmed Fathe A. Alohali, Sang Jia, and Sanjay Mehta

Introduction

Pulmonary hypertension (PH) is a hemodynamically defined condition that is characterized by alterations in pulmonary vascular physiology that results in disturbed cardiopulmonary function and interactions. The clinical presentation and severity of PH are linked to these pathophysiologic disturbances. The primary manifestations in patients with PH include dyspnea and exercise limitation, which results in functional limitations and impaired health-related quality of life (HRQoL).

The hypertensive state in the pulmonary circulation imposes an elevated afterload on the right

ventricle (RV), which relies on several compensatory mechanisms to adapt to the PH state to maintain cardiopulmonary function. Eventually, these mechanisms are overwhelmed, and RV failure ensues, which is the main determinant of symptoms and reduced functional capacity. Moreover, the pathophysiologic cardiopulmonary perturbations, including RV failure, significantly contribute to the risk of adverse clinical outcomes in patients with PH, including premature mortality.

Rigorous initial clinical assessment, accurate diagnosis, and appropriate treatment choices are key to mitigating the risks of poor clinical outcomes. There now are numerous medical and

R. A. Davey
St. Josephs Hospital PH Clinic, London, ON, Canada

Heart Failure Service, Division of Cardiology,
London Health Sciences Centre and St. Josephs
Healthcare Centre, London, ON, Canada
e-mail: ryan.davey@lhsc.on.ca

A. F. A. Alohali
Southwest Ontario PH Clinic, Division of
Respirology, London Health Sciences Centre,
London, ON, Canada

Department of Medicine, Schulich School of
Medicine, Western University, London, ON, Canada

Internal Medicine, Adult Pulmonary Medicine and
Pulmonary Hypertension, Adult Critical Care and
Cardiovascular Critical Care, King Fahad Medical
City Hospital, Critical Care Services Administration,
Riyadh, Kingdom of Saudi Arabia
e-mail: Afalohali@kfmc.med.sa

S. Jia
Department of Medicine, University of Manitoba,
Winnipeg, MB, Canada
e-mail: jias1@myumanitoba.ca

S. Mehta (✉)
Southwest Ontario PH Clinic, Division of
Respirology, London Health Sciences Centre,
London, ON, Canada

Department of Medicine, Schulich School of
Medicine, Western University, London, ON, Canada

Pulmonary Hypertension Association (PHA) of
Canada, Vancouver, BC, Canada

Western University, London Health Sciences Centre,
Department of Medicine/Respirology, Victoria
Hospital, London, ON, Canada
e-mail: sanjay.mehta@lhsc.on.ca

surgical treatment choices for patients with different kinds of PH, but initial management, subsequent modification, and/or intensification of treatment for individual patients must be guided by an appropriate assessment of their status.

A comprehensive assessment of an individual PH patient requires understanding the severity of their disease, and perhaps more importantly, their risk for poor clinical outcomes, including premature death. This should not only be done at the time of initial diagnosis and initial therapy but is even more important during follow-up after the institution of therapy in order to maximally improve clinical outcomes. Risk assessment in an individual patient requires a multi-modality approach with both invasive and non-invasive investigations to obtain multiple clinical parameters that capture a holistic picture of the patient's disease state. This includes clinical assessment, functional assessments, biochemical markers, invasive hemodynamic measurements, and targeted imaging.

The World Symposium on Pulmonary Hypertension (WSPH) 6th Session held in 2018, refined the diagnostic classification of PH and its subtypes (Table 54.1) (Simonneau et al. 2019). Our focus will be on WHO Group 1 pulmonary arterial hypertension (PAH). In the sections below, we will outline available methods for cardiopulmonary monitoring based on a review of relevant pathophysiologic features, and provide a practical approach that clinicians can use for optimal assessment of PAH patients.

Pulmonary Pathophysiology

Cardiopulmonary Hemodynamics

Normal Pulmonary Circulation

The pulmonary circulation is a low resistance circuit that accommodates the entire cardiac output at a low pressure, even when cardiac output is increased in conditions such as exercise. The pulmonary circulation's low pressure is the result of the structural anatomy of pulmonary arteries, which are more thin-walled than vessels in other

Table 54.1 WHO 2019 PH classification system

WHO Group	Subgroups
<i>Group 1:</i> PAH	Idiopathic PAH
	Heritable PAH
	Drug- and toxin-induced PAH
	PAH associated with: connective tissue disease, HIV infection, portal hypertension, congenital heart disease, schistosomiasis
	Long-term responders to calcium channel blockers
	PAH with prominent venous (PVOD) and/or capillary (PCH) involvement
	Persistent PH of the newborn
<i>Group 2:</i> PH due to left heart disease (post-capillary PH)	Heart failure with preserved LVEF
	Heart failure with reduced LVEF
	Valvular heart disease
	Congenital/acquired cardiovascular conditions
<i>Group 3:</i> PH due to lung diseases and/ or hypoxia	Obstructive lung disease
	Restrictive lung disease
	Lung disease with mixed restrictive/obstructive pattern
	Hypoxia without lung disease (e.g., sleep apnea)
	Developmental lung disorders
<i>Group 4:</i> PH due to pulmonary artery obstructions	Chronic thromboembolic PH
	Other pulmonary artery obstructions
<i>Group 5:</i> PH with unclear and/or multifactorial mechanisms	Hematological disorders (e.g., hemolytic anemia)
	Systemic and metabolic disorders (e.g., sarcoid)
	Complex congenital heart disease

Data compiled from Simonneau et al. (Simonneau et al. 2019)

regions and have more limited smooth muscle. This makes them more easily distensible than other vessels. Moreover, gravity-dependent zones of low or no perfusion allow recruitment when the flow is higher and also helps maintain a low pressure. The normal human pulmonary hemodynamics and cardiac output have been established in a systematic review of supine right-heart catheterization studies in healthy subjects (Table 54.2) (Kovacs et al. 2009).

Table 54.2 Resting cardiopulmonary hemodynamic indices in 882 healthy volunteers in supine position

sPAP	dPAP	mPAP	PAWP	CO	CI	PVR	PVR
mmHg	mmHg	mmHg	mmHg	L/min	L/min/m ²	dyn·s·cm ⁻⁵	Wood units
20.8 ± 4.4	8.8 ± 3.0	14.0 ± 3.3	8.0 ± 2.9	7.3 ± 2.3	4.1 ± 1.3	74 ± 30	0.95 ± 0.38

Data compiled from Kovacs et al. (2009)

Data are mean ± SEM

Abbreviations: *sPAP* systolic pulmonary arterial pressure, *dPAP* diastolic pulmonary arterial pressure, *mPAP* mean pulmonary arterial pressure, *PAWP* pulmonary arterial wedge pressure, *CO* cardiac output, *CI* cardiac index, *PVR* pulmonary vascular resistance

Table 54.3 Hemodynamic definitions of pulmonary hypertension (PH)

Definition	Hemodynamic criteria	WHO PH group(s)
PH	mPAP >20 mmHg	All
Pre-capillary PH	mPAP >20 mmHg PAWP ≤15 mmHg PVR ≥3 Wood U	WHO group 1 PAH WHO group 3 PH (lung diseases/hypoxia) WHO group 4 CTEPH WHO group 5 PH (unclear/multifactorial)
Post-capillary PH	mPAP >20 mmHg PAWP >15 mmHg	WHO group 2 PH (left heart disease)
(i) Isolated post-capillary	PVR <3 WU (and/or DPG <7 mmHg)	No additional pre-capillary PH component
(ii) Combined pre- and post-capillary	PVR ≥3 Wood U (and/or DPG >7 mmHg)	Additional pre-capillary PH component due to: Contribution of WHO group 1, 3, 4, or 5 PH Remodelling due to chronic post-capillary PH

Data compiled from Simonneau et al. (Simonneau et al. 2019)

Abbreviations: *DPG* diastolic pressure gradient (diastolic PAP – mean PAWP)

Pulmonary Hypertension (PH)

PH has traditionally been defined as an elevation of mean pulmonary artery pressure (mPAP) ≥25 mmHg at rest. This definition was revised at the 6th World PH Symposium in Nice in 2018 and now emphasizes that mPAP should not exceed 20 mmHg in healthy subjects (Table 54.3) (Simonneau et al. 2019). Furthermore, hemodynamic characterization of PH allows differentiation between pre-capillary PH and post-capillary PH, primarily through measurement of the pulmonary artery wedge pressure (PAWP). Conditions characterized by pre-capillary PH are hemodynamically defined by PAWP ≤15 mmHg and pulmonary vascular resistance (PVR) ≥3 Wood units (WU). Pre-capillary PH is typical of WHO Group 1 PAH but the same hemodynamic pattern of PH is also seen in patients with hypoxia from lung

diseases (WHO Group 3), chronic thromboembolic PH (CTEPH; WHO Group 4), and some conditions in WHO Group 5, such as those with sarcoidosis and pulmonary vasculitis (Table 54.3).

Increased PVR and the resulting load on the RV in PAH can arise from a broad range of distinct pulmonary vascular pathophysiological processes which primarily are due to proliferative remodeling of the vascular wall and a variable degree of vasoconstriction. Collectively, these result in the narrowing of pulmonary arteries and reductions in the normal compliance which can affect the pulse-pressure and capacitance of these vessels. Moreover, rarefaction of the lung micro-circulation and loss of small arteries has become a more commonly recognized pathologic changes in pulmonary capillaries and venous system (Humbert et al. 2019).

Other Pulmonary Vascular Physiologic Parameters

Introduction

Calculation of PVR assumes a simple linear pulmonary circulation and ignores two key physiologic aspects: (i) normal pulsatile pulmonary arterial flow, and (ii) the presence of a non-zero downstream pressure, as per the “vascular waterfall” hypothesis of in vivo vascular function (Vonk-Noordegraaf et al. 2013; Permutt et al. 1962; Naeije et al. 2013). As such, there are other parameters of pulmonary artery function which can be measured and better reflect the pulsatile nature of pulmonary artery blood flow. These parameters include compliance (and its inverse, elastance), as well as impedance (Table 54.4) (Thenappan et al. 2016; Murgo and Westerhof 1984; McCabe et al. 2014; Lankhaar et al. 2006).

Pulmonary Vascular Compliance

The compliance of the entire pulmonary circulation reflects the ability of all arteries, capillaries, and veins to accommodate blood ejected by the RV during systole and is defined as the change in volume for a given change in pressure ($\Delta V/\Delta P$). In contrast, capacitance includes two volumes, the “unstressed” volume that fills a cylindrical vessel and makes it round but does not create a pressure, and the “stressed” volume that creates the change in pressure. These two terms are often incorrectly and interchangeably used. For example, pulmonary circulation angiographic imaging

techniques including magnetic resonance imaging report total volume at a single or changing pressure but cannot differentiate stressed and unstressed volumes. The situation is also complicated by vascular recruitment which increases total cross-sectional area and thus compliance.

During right heart catheterization, pulmonary vascular compliance can be estimated, based on the assumption that the pulmonary circulation is closed at the distal venous end, from the increase in pulmonary artery pressure (pulse pressure [PP] = sPAP – dPAP) due to the stroke volume (SV) during a single cardiac systole, such that $\Delta V/\Delta P$ can be approximated by SV/PP. Pulmonary vascular compliance has an inverse hyperbolic relationship with PVR in the normal pulmonary circulation (Lankhaar et al. 2008; Saouti et al. 2010; Vonk Noordegraaf et al. 2017; Ghio et al. 2015). However, it should be appreciated that this measurement is in reality a “dynamic” compliance which incorporates resistance because of blood flow at the venous end.

Pulmonary Artery Elastance

Elastance (or stiffness) is the inverse of pulmonary vascular compliance, and thus is subject to the same issues discussed above for compliance. Increased elastance captures the important concept of loss of vascular distensibility. Elastance is most commonly estimated from the dicrotic notch pressure of the PAP waveform, which reflects mPAP at rest (McCabe et al. 2014; Chemla et al. 1996).

Table 54.4 Other pulmonary vascular physiologic parameters related to the pulsatile nature of pulmonary artery (PA) blood flow

Parameter Units	Physiologic definition	Normal range	Reference
PA compliance (C) mm ² /mmHg	Change in PA cross-sectional lumen area for a given change in PAP	3.2–7.9	(Thenappan et al. 2016)
PA capacitance (Ca) mm ³ /mmHg	Change in pulmonary circulation volume for a given change PAP	7.9 ± 4.1	(Murgo and Westerhof 1984)
PA impedance (PVZ) dynes s/cm ⁵	Relationship between pulsatile PA blood flow and pressure	20 ± 1	(McCabe et al. 2014)
PA elastance (Ea) mmHg/ml	Relationship between end-systolic PAP and RV stroke volume	0.3 ± 0.1	(Lankhaar et al. 2006)

Although both two-dimensional compliance and three-dimensional capacitance are static measures independent of flow, and thus not affected by vascular resistance, the common clinical measurements are done under conditions of flow, such that resulting “dynamic” values inherently include the element of resistance

Pulmonary Artery Impedance

Impedance is a measure of the relationship between pulsatile blood flow and pressure. As such, pulmonary vascular impedance reflects the time-dependent continuous variation of the PAP waveform and the blood flow waveform over an entire cardiac cycle. Calculation of impedance requires synchronized, high-fidelity recordings of PAP and pulmonary artery flow, spectral analysis of pressure and flow waveforms, and mathematical Fourier analysis of the relationship between these two parameters to derive an impedance spectrum (Ghio et al. 2015).

Pulmonary Hypertension

Introduction

PH is characterized by increased PA stiffness (reduced compliance) and decreased capacitance, which are the result of several potential mechanisms, including PA distension-related strain in larger pulmonary arteries, as well as pulmonary macro- and microvascular arterial wall thickening due to both remodeling of the extracellular matrix and smooth muscle cell hyperplastic/hypertrophic responses (Humbert et al. 2019; Schäfer et al. 2016). Increased impedance (which incorporates reduced compliance and increased resistance) as well as enhanced pulmonary arterial vasoconstrictor reactivity of medium- and small-sized pulmonary arterioles all worsen pulmonary gas-exchange, as well as increase RV afterload (Naeije 2013).

Dynamic PA elastance provides the most comprehensive assessment of the pulmonary vascular load on the RV, incorporating resistive, pulsatile, and passive components (Vonk Noordegraaf et al. 2017; Schäfer et al. 2016). Increased PA elastance in PH decreases the capacity of the proximal PAs to accommodate RV stroke volume and also enhances arterial pressure wave reflection. Along with the predominant contribution of increased resistance to RV load, increased elastance can further increase the load on the RV, both of which contribute to progressive RV failure and risk of death (Thenappan et al. 2016; Naeije 2013; Castelain et al. 2001).

Relationship Between Pulmonary Vascular Physiologic Parameters

There is an uncertain relationship between alterations in pulmonary vascular compliance and pulmonary hemodynamics in PH. In the most robust study of the relationship between PA compliance and pulmonary hemodynamics in 719 patients with incident IPAH, dynamic PA compliance was only modestly related to mPAP (Chemla et al. 2018) although it previously had been suggested that vascular stiffness and resistance were directly related, i.e., PA compliance has an inverse hyperbolic relationship with PVR such that the product of PVR and compliance (RC-time) was constant in health and PH (Lankhaar et al. 2006, 2008; Saouti et al. 2010; Vonk Noordegraaf et al. 2017). As mentioned above, the clinical measurement of compliance (and sometimes even capacitance) fails to appreciate the dynamic nature of the measurement which is likely dominated by resistance.

It has become clear that the PVR-compliance relationship is disturbed in PH, and is significantly different from that observed in the normal pulmonary circulation (Hadinnapola et al. 2015; Chemla et al. 2015). PVR and PA compliance are inversely related in PH, in large part because of the use of dynamic compliance. However, PA compliance is poorly correlated with PVR, so that it cannot be estimated from PVR alone, which may indicate that PAH differentially affects PA stiffness and PVR (Chemla et al. 2018). Early stages of pulmonary vascular disease can result in a marked loss in PA compliance with only minimal increases in PVR, because of both pulmonary circulatory distension and recruitment. Increasingly severe pulmonary vascular disease is characterized by significant increases in PVR with only minimal further decline in PA compliance (Ghio et al. 2017).

Clinical Significance of Altered Pulmonary Vascular Physiology

The changes in pulmonary vascular physiology discussed above all result in an increase in the RV afterload and likely contribute to the risk of progressive RV failure and death, although there is

limited direct clinical evidence that the altered pulmonary vascular physiologic parameters play a role. Specifically, the term PA capacitance, which was already discussed is a combination of PA compliance and more importantly resistance, has been shown to correlate with clinical severity of PH and was an independent predictor of mortality in patients with idiopathic PAH in some studies (Ghio et al. 2017; Mahapatra et al. 2006; Gan et al. 2007; Stevens et al. 2012), but not in the largest study of ($n = 719$) treatment-naïve incident IPAH patients (Chemla et al. 2018). It is noteworthy that PH-targeted therapy increases PA capacitance in proportion to the reduction of PVR, which confirms the important contribution of PVR to such dynamic measurements (Lankhaar et al. 2008; Ghio et al. 2017).

Other Aspects of Pulmonary Physiology

Pulmonary Gas Exchange

Hypoxemia at rest and/or during exercise are common findings in patients with IPAH, due to ventilation:perfusion mismatch, impaired diffusion, and increased shunt fraction (Hoepfer et al. 2007; Khirfan et al. 2018). For example, 20% of 292 patients with IPAH/HPAH had hypoxemia at rest, and 31% had exertional desaturation during 6MWT, and these individuals had worse long-term survival when compared to subjects without hypoxemia (Khirfan et al. 2018).

Hyperventilation resulting in mild-to-moderate resting and exercise hypocapnia is common in patients with IPAH, and low P_{aCO_2} is an independent prognostic marker (Hoepfer et al. 2007; Yasunobu et al. 2005).

Pulmonary Diffusing Capacity (DLco)

A large majority (~75%) of PAH patients have reduced DLco, and the decrease in DLco correlates significantly with worse PAH disease severity and poor prognosis (Sun et al. 2003; Jing et al. 2009). The fall in DLco relates largely to a reduction of pulmonary capillary blood volume, which

is driven by the rarefaction of the pulmonary microcirculation typical of PAH. Severely reduced DLco (typically <50%) is less common in PAH and is more typically associated with a history of smoking, underlying emphysema or interstitial lung disease (e.g., scleroderma), and left-sided cardiac disease (Trip et al. 2013; Olsson et al. 2017).

Reduced DLco has been identified as an early marker of pulmonary vascular disease in some patients at risk for PAH, e.g., scleroderma. Thus, regular monitoring of DLco is recommended as part of a screening algorithm for early detection of PH in scleroderma (Coghlan et al. 2014; Galiè et al. 2015).

Airway Function

Many patients with PAH have normal spirometry, suggesting minimal airway disease or obstruction (Sun et al. 2003). However, other physiologic measures do suggest airway narrowing, including reduced mid-expiratory flow (MEF50%) and dynamic hyperinflation (Jing et al. 2009; Meyer 2002; Laveneziana et al. 2013). The pathophysiology of airway obstruction in PAH is uncertain, but the pulmonary artery inflammatory process may result in adjacent airway bronchospasm and fibrosis.

Pulmonary Compliance/Volumes

A minority of patients with PAH have a total lung capacity (TLC) that is less than 80% of predicted (Sun et al. 2003; Romano et al. 1993; Low et al. 2015). This restriction is most common in PAH associated with congenital heart disease (CHD), in the presence of parenchymal lung disease in CTD-PAH, and quite uncommon in IPAH. The physiologic basis of lung restriction is multifactorial and can be related to previous cardiothoracic surgery and lack of full respiratory development (e.g., CHD-PAH), cardiomegaly in the setting of RV failure, as well as reduced lung compliance due to less distensible, fibrotic/hypertrophied intrapulmonary arteries in PAH (Sun et al. 2003; Low et al. 2015).

Pathophysiology of RV Failure in PAH

Normal RV Function

Introduction

The function of the RV was noted by the early anatomist William Harvey (1578–1657) in that it “may be said to be made for the sake of transmitting blood through the lungs, not for nourishing them”; therefore, the RV can best be thought of as adding efficiency for oxygen exchange. It should be able to deliver all the blood it receives and then transmit that blood to the lungs without any rise in the right atrial pressure (Pinsky 2016).

Normally, the pulmonary vasculature has sufficient adaptability through distention of the large arteries or recruitment of closed vessels that result in a decrease in PVR and allow only a minimal increase in PAP. Since the RV is thinner-walled and more heavily trabeculated than the left ventricle, it is less able to manage significant increases in these parameters. Even more importantly, as discussed in Chap. 3, the RV end-systolic elastance is much less than that of the LV, so that the RV cannot produce a high systolic pressure unless there is a major adaptation of an increase in RV contractility, reflected by increased end-systolic elastance.

The geometry of the RV is more complex than that of the LV, and longitudinal shortening of the RV myocardial fibers plays a greater role in contractility than short-axis shortening. In the LV, the lateral free wall is felt to have a greater contribution to output than the septum, whereas in the RV, both septum and free wall significantly contribute to overall ventricular function.

Finally, the blood supply to the RV comes mainly from the right coronary artery and, since there is a significant coronary-RV myocardial pressure differential during systole and diastole, coronary perfusion to the RV occurs relatively equally throughout the cardiac cycle (Van Wolferen et al. 2008). This is in stark contrast to the LV which, by virtue of the inherently higher systolic myocardial pressures generated, is largely only perfused during ventricular diastole.

This unique feature of the RV becomes important in the presence of elevated pulmonary pressures.

RV Failure

Introduction

The pulmonary vascular physiologic effects of PH (increased PA impedance and resistance, and reduced compliance) all contribute to increased afterload on the RV. Because of its anatomy and normal low-pressure function, the RV is poorly adapted to act as an efficient pump in the setting of increased PAP and PVR. Although both the RV and LV are sensitive to changes in preload, the RV is particularly sensitive to even small increases in afterload, which significantly reduce RV output (Vonk-Noordegraaf et al. 2013).

After some typically prolonged period of increased RV afterload, which is often clinically asymptomatic, RV function begins to decline. It is at this point that symptoms worsen and clinical signs of RV failure develop. Typical symptoms include worsening dyspnea, increasing peripheral and abdominal edema, and eventually, exertional chest pain and syncope. Signs of RV failure include jugular venous distension, hepatomegaly, and lower extremity edema. These clinical features should alert the astute practitioner to the presence of RV failure before the onset of worsening end-organ function, e.g., renal failure, which is associated with a high risk of mortality.

RV Failure: RV-PA Coupling Versus Decoupling

In the initial stages of PH, when the RV is faced with mild-moderate increases in PAP and PVR, the RV can compensate for the increased afterload with early remodeling changes, including myocyte hypertrophy and mild fibrosis (Seo and Lee 2018). RV decompensation in the face of persistent afterload is characterized by progressive loss of myocyte mass and fibrotic changes progress. These pathologic changes are functionally important. They negatively affect diastolic RV function first with prolongation of the isovolumic phase of relaxation, and then with a similar increase in the duration of isovolumic

contraction; therefore, there is a concomitant increase in right ventricular end-diastolic volume.

However, with persistent and progressive increases in afterload, the RV is unable to compensate and further, maladaptive increases in ventricular dimensions result. This has multiple effects including a drop in cardiac output and distortion of perivalvular geometry (especially in the tricuspid apparatus) with further increases in RV end-diastolic pressure/right atrial pressure (Vonk-Noordegraaf et al. 2013). As the process continues, there is a drop in sPAP and pulmonary circulation pulse pressure, as the RV becomes increasingly unable to generate an adequate stroke volume. This late-stage clinical finding is known as ventricular-arterial decoupling (Tello et al. 2019). In some patients in whom the RV has had early and chronic exposure to high PAP (e.g., in certain types of CHD), the compensated RV can maintain reasonably intact function for many decades. In contrast, in patients with most types of PAH other than CHD-PAH (e.g., IPAH, CTD-PAH), the presence of more significant or more sustained elevations in PAP and PVR typically have a fairly rapid and progressively deleterious effect on RV function. This is commonly termed “decoupling” between increasing RV load and falling RV pressure generation because of impaired contractility (falling end-systolic elastance), with a resultant decrement in stroke volume and impaired cardiac output.

RV Failure: RV Ischemia

The normal myocardial mass of the RV is considerably less than of the LV. When the RV mass increases to adapt to the increased RV load in PH, microvascular growth fails to match myocyte hypertrophy and as well microvascular dysfunction develops (Crystal and Pagel 2018). The rising RV systolic pressure also can inhibit the RV systolic coronary flow and thereby cause a “systemic ventricularization” of the RV. Changes in myocardial oxygen demand during a state of heightened afterload then can result in ischemia which further worsens RV function (Haddad et al. 2008). Ongoing RV dysfunction results in an inability to offload its volume and causes further ventricular distension. This sets up a cycle of

worsening ischemia and leads to worsening signs of clinical RV failure (peripheral and abdominal congestion along with poor forward flow).

RV Failure: Ventricular Interdependence

The failing RV has multiple adverse effects on the LV, through multiple mechanisms, including changes in RV size/shape and common pericardial constraint. Firstly, with ongoing increases in afterload, the normal crescentic shape of the RV becomes more spherical and exerts an additional leftward force on the septum which in turn alters LV geometry to become narrower and more conical (Kind et al. 2010).

Since the total cardiac volume is constrained by the compliance of the pericardium, increases in RV size begins to limit LV size. This negative geometric change is known as ventricular interdependence (Peluso et al. 2014). This change can further reduce cardiac output by decreasing LV distensibility, preload, and ventricular elastance, thereby adversely affecting LV diastolic filling. Somewhat paradoxically in PAH, the increasing constraint can elevate the left atrial pressure and further impair pulmonary vascular unloading. This sets up a deleterious cycle whereby worsening pulmonary artery pressures cause worsening biventricular function which increase vascular resistance and further decrease overall cardiac output. At this stage, pump failure is imminent. It is crucial, therefore, both to recognize when patients are at this point, and perhaps more importantly, attempt to avoid it through careful and particular attention to all of their antecedent hemodynamic parameters.

Cardiopulmonary Monitoring of the PAH Patient

Introduction

Pulmonary arterial hypertension is an uncommon but progressive disease associated with significant morbidity and eventual mortality. Although there are many therapies that are now available to clinicians which have helped mitigate these negative outcomes, their appropriate usage remains a

challenge. These therapies comprise a spectrum of complexity ranging from oral formulations, to parenteral administrations, and to surgical options such as lung transplantation. Inherently, these therapies have adverse effects that range from being mild and just a nuisance to being very disabling, and so both under-treatment and inappropriate intensification of treatment can result in poor patient outcomes. It is therefore crucial for the treating practitioner to appropriately assess the patient’s clinical status and determine where the patient sits on this continuum. This can allow for appropriate therapeutic choices at the appropriate time in a given patient’s clinical course.

There are many parameters that are likely relevant in the assessment of a patient with PAH and these include clinical, laboratory, imaging, and hemodynamic variables. It should be noted that no single parameter can accurately indicate progression or improvement of the disease state (Benza et al. 2010). As a result, multiple risk assessment and stratification approaches have been proposed in the PH literature, some are detailed and some are abbreviated, some include only variable parameters while others are fixed. In the sections below we will endeavor to outline the most relevant investigations for a clinician treating PAH and provide a workable approach to integrating them into practice.

Cardiopulmonary Monitoring of the PAH Patient: Clinical Parameters

Symptomatic/Functional Classification

One of the most important clinical effects of PH is reduced ability to be physically active, to exercise, and to perform activities of daily living. As such, the specific determination of a patient’s abilities to perform everyday activity and tasks with or without symptoms is a key part of the initial assessment of patients with PH and during long-term monitoring. Moreover, this is one key component of assessment of how patients are affected by the disease, or their health-related quality of life (HRQoL).

Since PH and resulting RV failure manifest signs and symptoms similar to left-sided heart failure, the New York Heart Association’s (NYHA) functional classification (FC), first published in 1928, has also been used to functionally classify patients with PH. However, due to the recognition of subtle but relevant differences in clinical features, the NYHA FC was modified (mNYHA) at the 1993 World Health Organization (WHO)-sponsored World Symposium on PH to be a more PH-specific FC system (Table 54.5); this specifically highlights the significance of pre-syncope, syncope and chest pain in the assessment and monitoring of these patients.

At the time of the initial diagnosis, baseline NYHA FC reflects the clinical severity of PH as

Table 54.5 Functional classification of PH

WHO (Modified NYHA) FC (PH)	NYHA FC (Heart failure)
I. Patients without limitation of physical activity. Ordinary physical activity does not cause undue dyspnea or fatigue, chest pain or near syncope.	1. No limitation of physical activity. Ordinary physical activity does not cause undue fatigue, palpitation, dyspnea.
II. Patients with a slight limitation of physical activity. They are comfortable at rest. Ordinary physical activity causes undue dyspnea or fatigue, chest pain or near syncope.	2. Slight limitation of physical activity. Comfortable at rest. Ordinary physical activity results in fatigue, palpitation, dyspnea.
III. Patients with marked limitation of physical activity. They are comfortable at rest. Less than ordinary activity causes undue dyspnea or fatigue, chest pain or near syncope.	3. Marked limitation of physical activity. Comfortable at rest. Less than ordinary activity causes fatigue, palpitation, or dyspnea.
IV. Patients with inability to carry out any physical activity without symptoms. These patients manifest signs of right heart failure. Dyspnea and/or fatigue may even be present at rest. Discomfort is increased by any physical activity.	4. Unable to carry on any physical activity without discomfort. Symptoms of heart failure at rest.

well as the burden of living with PH. FC is also one of the most robust and consistent prognostic markers in PH in general and importantly, specifically in PAH (Brenot 1994; Boucly et al. 2017). Moreover, a significant correlation between baseline NYHA FC and survival was found in the first US NIH registry of idiopathic IPAH patients, several single-center cohorts from many countries, and in the US REVEAL, the largest registry ever of 2716 PAH patients of all subtypes (Benza et al. 2010).

FC is a responsive measure of the severity of PH and its effect on patients, as FC has been shown to improve in PAH patients treated with PH-targeted medications (Galiè et al. 2009; Farber et al. 2015). Moreover, after the institution of effective PAH therapy, a clinical improvement from initial FC III/IV to FC II is associated with improved prognosis.

Most importantly, there is strong evidence that the improvement in NYHA FC in treated PAH patients strongly predicts improved clinical outcomes, including a lower risk of disease progression and better long-term survival. For example, in the REVEAL registry, patients who improved from FC III to FC I/II, regardless of PAH cause, had better survival compared with patients who remained in FC III or worsened to FC IV (Barst et al. 2013; Nickel et al. 2012). Although this has only been demonstrated in open-label or retrospective analyses (Boucly et al. 2017; Hoeper et al. 2017; Kylhammar et al. 2017), the consistency of the prognostic importance of changes in FC across multiple clinical registries from various countries/regions supports the strength of this association.

Recommendations for Clinical Practice

WHO/mNYHA FC is the most commonly used parameter in clinical practice to assess dyspnea and functional ability in PAH patients, and it provides important information regarding the severity of PAH and the effect of the illness on a patient's everyday life. Furthermore, all current PH clinical practice guidelines (e.g., ESC/ERS PH guidelines) (Galiè et al. 2015) and PH risk stratification systems (e.g., WSPH 2019 (Galiè et al. 2019), REVEAL registry 2.0 (Benza et al.

2019)) emphasize the critical importance of monitoring FC in determining prognosis in individual patients. Limitations in the reliability of FC assessment are recognized, including in subjects of older age and with comorbid conditions, as well as poor inter-/intra-observer reproducibility.

Nevertheless, mNYHA FC is a simple, reproducible, and clinically important assessment tool and prognostic measure in PAH patients at the time of diagnosis and especially during follow-up assessment of treated PAH patients. Repeated assessment of FC reflects the response to therapy, and strongly predicts the prognosis for long-term clinical wellbeing and survival. The simple, practical goal is for each patient to achieve better daily functional capacity, specifically mNYHA FC 1 or 2.

We endorse the regular use of WHO/mNYHA FC assessments but recommend caution in the over-reliance on FC as a singular determinant of patient clinical status and prognosis.

Health-Related Quality of Life (HRQoL)

Patient-reported outcomes (PROs) can include physical symptom scores (e.g., Borg dyspnea index), psychological wellbeing vs distress, and formal measures of a patient's HRQoL. Most importantly, PROs such as HRQoL measures are increasingly important clinical assessment tools, as they provide a direct, holistic reflection of a patient's perspective of their own clinical status. PROs may also be considered important potential endpoints for clinical trials. Ancillary benefits include enhanced patient engagement, improved medication and lifestyle adherence, as well as greater patient satisfaction (Anker et al. 2014; Howard et al. 2014; McGoan et al. 2019).

A number of HRQoL measures have been studied in patients with PH. Initially, the Short Form-36 (SF-36) and Nottingham Health Profile (NHP) were used but these are not PH specific questionnaires. Additionally, the Minnesota Living with Heart Failure Questionnaire (MLHFQ) has been used to assess PH patients, sometimes in a modified form to account for specific aspects in the PH patient population (Reis et al. 2018). More recently, the CAMPHOR (McCabe et al. 2013), emPHasis-10 (Yorke et al.

Table 54.6 PH-specific patient-reported outcome (PRO) tools

Domains	CAMPHOR	emPHasis-10	PAH-SYMPACT
Baseline symptoms	Yes (25 questions)	Yes (4 questions)	Yes (11 questions)
Activity tolerance	Yes (15 questions)	Yes (1 question)	
Quality of life	Yes (25 questions)	Yes (5 questions)	Yes (11 questions)

2014), and PAH-SYMPACT (McCollister et al. 2016) scores have been developed to directly assess PH-specific HRQoL. Both CAMPHOR and PAH-SYMPACT are somewhat intricate, being developed for use in clinical research trials and have been validated in large clinical trials of PAH medications. By contrast, emPHasis-10 is designed as a PRO that can be more readily integrated into a standard clinic visit. Table 54.6 below lists specific aspects of and different domains assessed by the 3 PH-specific PROs.

Recommendations for Clinical Practice

We recommend the use of a PH-specific PRO in the routine clinical assessment of PAH patients, e.g., emPHasis-10. We also recommend that all future PH clinical trials should include a PH-specific PRO, and that expectation of an improvement in a patient's perceived HRQoL should be an expectation of the drug approval process.

Physical Examination

The physical examination of a patient with suspected PH can detect the presence of PH and assess the degree of fluid overload which reflects the severity of RV failure. Although the findings of PH on physical exam are often subtle and difficult to confidently ascertain, a careful physical exam helps monitor PH patients during regular follow-up.

The most common finding on physical exam suggestive of PH is an accentuated pulmonary component of the second heart sound (P2). Other findings commonly include jugular venous distension with a large V wave indicative of tricuspid regurgitation (TR), peripheral edema, and less commonly a left parasternal RV heave, a

pansystolic murmur of TR, and a diastolic murmur of pulmonary insufficiency. In more advanced states of RV failure, PH patients may manifest systemic hypotension, a third or fourth heart sound originating in the RV, hepatomegaly, and abdominal bloating due to ascites.

Additionally, patients with PH in association with underlying medical conditions can have specific physical exam findings. Examples include patients with congenital heart disease and right-to-left shunting (e.g., clubbing and central cyanosis), connective tissue disease associated PAH (e.g., cutaneous manifestations such as sclerodactyly and telangiectasia), and portopulmonary hypertension (e.g., sequelae of cirrhosis such as palmar erythema and spider angiomas).

There is only weak evidence to support the clinical utility of the physical examination in the detection of the presence of PH. Historically, the most specific and greatest predictive finding of PH was a loud P2 (positive likelihood ratio 56.4, 95% CI 7.9–401.7) (Sutton et al. 1968). However, more recent studies have found more modest likelihood ratios for the presence of PH in patients with a loud P2. For example, one study reported a positive likelihood ratio of 1.9, but this did not improve the overall ability of physicians to accurately diagnose PH (Colman et al. 2014). The largest, most rigorous prospective study of physical exam findings assessed 116 patients pre-RHC, of whom 87% were confirmed to have PH based on mPAP ≥ 25 mmHg (Braganza et al. 2019). Although no single finding reliably diagnosed or excluded PH, the combination of elevated JVP >3 cm above the sternal angle and RV heave best discriminated the presence of PH. The combination of RV heave, JVP >3 cm above the sternal angle and peripheral edema were 100% predictive of having a severely elevated mPAP ≥ 45 mmHg. Presence of a loud P2 was not shown to be independently predictive of PH (Braganza et al. 2019).

Recommendations for Clinical Practice

Overall, the physical exam can suggest the presence of PH, but cannot be used to reliably diagnose or exclude the presence of PH. Furthermore, the accuracy and utility of

regular physical examination of PH patients in order to monitor the severity of PH or RV failure has not been formally studied. Given the poorer reliability of physical exam prediction of PH in newer versus older studies, we suspect that decreased sensitivity and specificity is a result of the deterioration of modern physical exam skills.

We recommend that clinicians not rely on the presence or absence of a loud P2 to suspect or exclude PH. We recommend regular physical examination of all PH patients for evidence of RV failure (elevated JVP, RV heave, peripheral edema), which is of particularly worrying clinical concern. If signs of RV failure are present or worsening, thorough investigation for contributing factors as well as appropriate management should be promptly undertaken.

Cardiopulmonary Monitoring of the PAH Patient: Exercise Capacity

Introduction

PH is typically associated with symptoms on exertion, and many patients experience reduced activity tolerance to the point of functional limitation and disability. As such, objective assessment of specific functional capacity is an important aspect of the assessment of disease severity in PH patients. This is most commonly done with two specific exercise testing methods, 6-minute walk test (6MWT) and treadmill or cycle cardiopulmonary exercise testing (CPET).

6-Minute Walk Test (6MWT)

Introduction

This is a simple, safe, reproducible test which assesses submaximal functional capacity of patients using the most common daily activity, walking. 6MWT is typically performed according to recommended technical standards, including physical space, procedure, and monitored variables (Crapo et al. 2002). The 6MWT distance (6MWD) walked by a patient is typically reported as an absolute value in meters. Normative values have been established in a single study of

290 subjects including 173 females, resulting in sex-specific reference equations (Enright and Sherrill 1998). Reporting of individual patient data as % predicted has not yet been considered by guidelines, as prognostic ability does not appear superior to that of absolute 6MWD (Lee et al. 2010). A simpler weight-adjusted 6MWD (6MWD [m] × weight [kg]) has also been proposed (Oudiz et al. 2006).

Effects of PH on 6MWT

Registry data from studies in France, United States, China, and Spain have reported reduced 6MWD in patients with many subtypes of PAH, which is proportional to the clinical severity of PH as assessed by NYHA FC (Benza et al. 2010; Brenot 1994; Miyamoto et al. 2000). Moreover, there is an association between reduced 6MWD and lower CPET V_{O2PEAK} (Miyamoto et al. 2000), although the correlation between weight-adjusted 6MWD and V_{O2PEAK} appears to be significantly stronger than for the unadjusted 6MWD (Oudiz et al. 2006). 6MWD is importantly related to health-related quality of life (HRQoL) in individual patients. For example, 6MWD correlated with seven of eight subscales of the SF-36 (Halank et al. 2013). Although 6MWD is reduced in most patients with PH, it is generally only modestly correlated with hemodynamic PH severity, including some cardiopulmonary parameters (e.g., CO, RAP, and TPR), but typically not with mPAP (Miyamoto et al. 2000).

Effects of PH-Targeted Therapy on 6MWT

In PAH patients who are treated with PH-targeted medical therapy, 6MWD typically improves significantly, with a range from 15 to 90 m depending on the specific PH-targeted medication (Galiè et al. 2009). Improvement is usually less marked following the addition of a 2nd medication in monotherapy-treated PAH patients (Lajoie et al. 2016). Functional capacity of PH patients, including those with PAH, also improves significantly following exercise rehabilitation therapy. This includes slight increases in V_{O2PEAK} (e.g., 2.2 mL/kg/min; 95% CI 0.4–3.9) and more marked increases in 6MWD (e.g., 73 m; 95% CI 46–99 m) (Buys et al. 2015).

The improvement in 6MWD in PAH patients treated with PH-targeted medications is inversely correlated with the decline in PVR (Savarese et al. 2012). Moreover, improved NYHA FC in PAH patients treated with current PH-targeted medications was associated with greater increases in 6MWD as compared to patients with unchanged NYHA FC (Barst et al. 2013). However, a minimal clinically important difference (MCID) for improvement in 6MWD has not been clearly defined in PH. A statistical minimal important difference (MID) was identified at approximately 33 m, using both distributional and anchor-based methods in PAH patients treated with the PDE-5 inhibitor tadalafil (Mathai et al. 2012). Similarly, in sildenafil-treated PAH patients, a MID of 42 m corresponded to a statistically significant reduction in clinical events (Gilbert et al. 2009).

Prognostic Value of 6MWT in PH

Many studies support the strong negative prognostic value of poor baseline 6MWD in newly diagnosed PAH patients. For example, IPAH patients with baseline 6MWD less than the median value (332 m) had a significantly lower survival rate than those walking farther than the median (Miyamoto et al. 2000). Similarly, there was a significant difference in survival ($p = 0.002$) based on a baseline 6MWD >330 m vs <330 in a single-center study from France (Provencher et al. 2006). In contrast, in a cohort of 178 French patients with more severe IPAH (required treatment with IV epoprostenol), there was a 2.2-fold increased risk of death with baseline 6MWD less than the median (250 m) (Sitbon et al. 2002). Patients with a significantly reduced 6MWT (<165 m) or marked deterioration (e.g., >70 m, $>15\%$ reduction from baseline) are at high risk; a cut-off value of 165 m performed best in prognostication of mortality, whereas patients above 440 m appear to be at low risk of death in 1-year (Zelniker et al. 2018).

Cardiopulmonary Exercise Test (CPET)

Introduction

Treadmill or cycle ergometer, incremental, symptom-limited CPET provides the most com-

prehensive non-invasive assessment of integrated exercise responses involving the pulmonary, cardiovascular, hematologic, and neuromuscular systems. Technical aspects of CPET are critical for safe assessment of PH patients and to obtain clinically relevant data, but will not be reviewed here as they are well-summarized elsewhere (Ross et al. 2001). CPET has proven value in the evaluation of patients with symptoms such as dyspnea and exertion intolerance, based on classic patterns of dynamic abnormalities suggestive of respiratory, cardiac, or other conditions including unfitnes (Ferrazza et al. 2009).

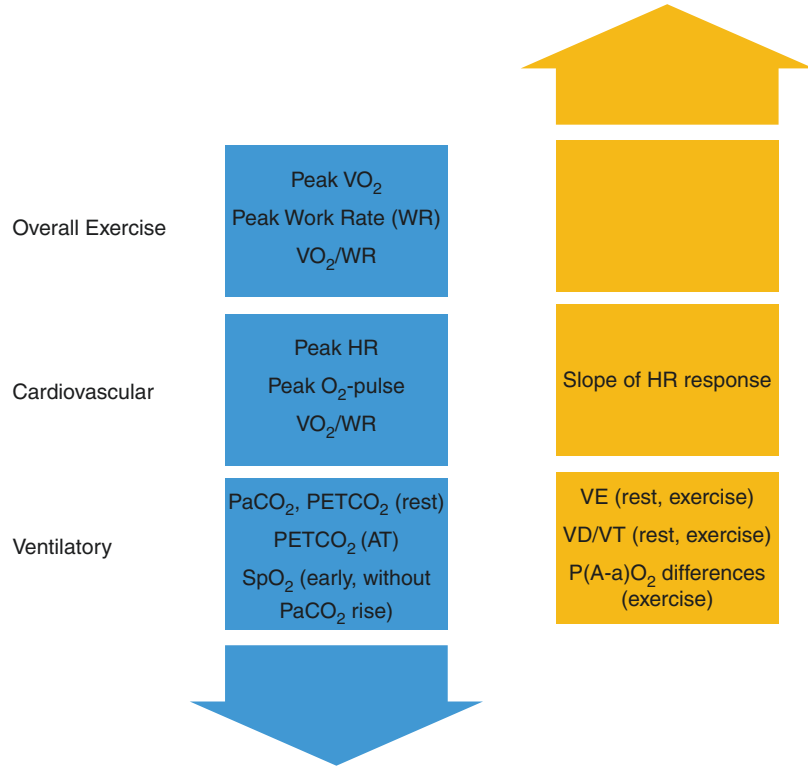
CPET Patterns in PAH

In patients with PH, a panel of characteristic sub-maximal and peak exercise CPET abnormalities have been consistently described which may identify the presence of significant pulmonary vascular disease. As well, CPET's comprehensive assessment of dyspnea and exercise limitation, key clinical features of PH, can categorize the functional severity of PH and associated RV failure (Sun et al. 2001a; Arena et al. 2010; Weatherald et al. 2017; Farina et al. 2018a). Moreover, classic cardiopulmonary abnormalities may be prognostic in individual patients and may also be responsive to PH-targeted therapy (Groepenhoff et al. 2013).

Several large case series have reported findings on incremental, symptom-limited, maximal CPET in PH patients, most commonly idiopathic PAH patients (Sun et al. 2001a; Wensel et al. 2002). It is clear that CPET parameters typically are markedly abnormal in most PAH patients compared to healthy control subjects. The classic CPET pattern is characterized by a marked reduction in overall exercise capacity, as reflected by reduced work rate (WR) and $V_{O_{2PEAK}}$, with a blunted V_{O_2}/WR relationship, associated with evidence of impairment of both cardiovascular and ventilatory responses (Fig. 54.1).

Cardiac abnormalities largely specific to the RV are central to the symptoms and exercise limitation in patients with PH. RV output is normally inversely correlated with PAP, such that PH results in a decreased ability of the RV to increase stroke volume (as reflected by the impaired increase in oxygen pulse) and cardiac output. In

Fig. 54.1 Characteristic disturbances in CPET parameters in patients with PAH vs healthy controls. Abbreviations. VO_2 oxygen uptake, WR work rate. PaCO_2 arterial carbon dioxide tension. $\text{P}_{\text{ET}}\text{CO}_2$ end-tidal carbon dioxide tension. AT anaerobic threshold. SpO_2 arterial oxygen saturation by pulse oximetry. V_E minute ventilation, V_D dead space volume. V_T tidal volume, $\text{P}(\text{A-a})\text{O}_2$ alveolar–arterial oxygen tension difference



addition, based on principles of ventricular interdependence, RV enlargement and resulting septal flattening or leftward shift can result in important alterations in LV geometry, diastolic function, and systemic perfusion.

The consequence of impaired cardiac function and reduced CO/CI is inadequate tissue O_2 delivery and early-onset lactic acidosis (Weatherald et al. 2017; Groepenhoff et al. 2010; Holverda et al. 2006), resulting in lower AT, and a resulting excessive HR response for any WR, which is also driven in part by sympathetic hyperactivity. Moreover, cardiac responses at the onset of exercise appear to be delayed in PAH patients, as CO may actually transiently decline, possibly due to increased venous return resulting in RV distension and reduced stroke volume (Lador et al. 2016). Overall, there is a less efficient coupling of O_2 delivery and V_{O_2} , contributing to impaired V_{O_2} kinetics in PAH and blunted V_{O_2}/WR relationship.

In healthy subjects, normal levels of V_E , V_E/V_{CO_2} , and PaCO_2 ($\text{P}_{\text{ET}}\text{CO}_2$) reflect the appro-

priate matching of ventilation and perfusion at rest and exercise. In PAH patients, the ventilatory pattern is characterized by increased V_E at rest and at any exercise WR (Hoepfer et al. 2007; Velez-Roa et al. 2004; Farina et al. 2018b). This excessive ventilation is a function of several stimuli, including: (i) the above cardiovascular abnormalities which result in early lactic acidosis due to impaired CO, (ii) arterial hypoxemia and carotid body chemoreceptor stimulation, (iii) high levels of physiologic (total) dead space (V_D/V_T) characterized functionally by areas of either absent or markedly impaired perfusion with relative over-ventilation, as well as (iv) increased chemosensitivity of peripheral chemoreceptors (driven by hypoxia, catecholamines, as well as lactic acid and lower pH), potentiated by neural sensing of central pulmonary artery and right atrial/ventricular stretch (Velez-Roa et al. 2004; Farina et al. 2018b; Naeije and Van De Borne 2009).

Importantly, despite the increased total V_D/V_T , the increase in V_E in PAH is typically excessive

and inefficient, resulting in a reduction of resting PaCO₂ and often a further decrease during exercise. This ventilatory inefficiency is best reflected by an increased V_E/V_{CO₂} ratio (and less reliably by increased V_E/V_{O₂} ratio), which is most evident at specific exercise levels (e.g., anaerobic or ventilatory threshold), as well as the increased slope of the overall, continuous V_E/V_{CO₂} relationship (Hoepfer et al. 2007; Velez-Roa et al. 2004; Farina et al. 2018b). Moreover, this ventilatory inefficiency is reflected by a widened difference between PaCO₂ and P_{ET}CO₂; specifically, P_{ET}CO₂ is even more dramatically reduced than PaCO₂ at rest and declines further during exercise. Hypoxemia in PAH is common, typically only mild at rest but commonly significantly worse on exercise. Hypoxemia is the result of multiple cardiopulmonary physiologic disturbances most prominent on exercise, including lower SvO₂ (impaired cardiac output), impaired alveolar-arterial O₂ diffusion, as well as increased right-to-left shunting which can be both intrapulmonary as well as through a patent foramen ovale (Hoepfer et al. 2007; Dantzker et al. 1984; Sun et al. 2002).

In summary, PH is characterized by marked abnormalities of V/Q matching resulting in excessive VE and higher V_E/V_{CO₂}, due both to increased V_D/V_T as well as hyperventilation and reduced PaCO₂ (and P_{ET}CO₂) both at rest and during exercise compared to normal subjects (Velez-Roa et al. 2004; Farina et al. 2018b). Such ventilatory abnormalities are clinically important, as the reduction in P_{ET}CO₂ correlates inversely with the elevation in mPAP, and is proportional to the impairment of V_{O₂PEAK} (Yasunobu et al. 2005).

Correlation of CPET Parameters with Severity of PAH

The degree of abnormal CPET cardiopulmonary responses are strongly associated with the severity of PAH (Yasunobu et al. 2005; Sun et al. 2001b; Correale et al. 2017). Worsening PAH, especially in association with RV failure, is associated with progressively worse overall exercise capacity (e.g., WR, V_{O₂PEAK}), lower VO₂/WR ratio, as well as greater abnormalities in cardiovascular (e.g., lower exercise HR_{PEAK}, lower O₂-pulse_{PEAK}, earlier AT) and ventilatory responses

(e.g., higher V_D/V_T at rest and exercise, higher V_E/V_{CO₂} at AT and overall slope, lower P_{ET}CO₂ at AT) (Arena et al. 2010). For example, exercise cardiac index correlated with V_{O₂PEAK}, and furthermore, was the only independent predictor of V_{O₂PEAK} in multivariate stepwise linear regression analyses (Blumberg et al. 2013). In addition, the reduction in P_{ET}CO₂ correlates inversely with the elevation in mPAP, and is proportional to the impairment of V_{O₂PEAK} (Yasunobu et al. 2005).

Prognostic Value of CPET Parameters in PAH

CPET parameters correlate importantly with the severity of PAH and RV failure, and correspondingly, may have clinical utility as markers of prognosis in individual PAH patients. One of the strongest predictors of worse survival in PAH remains an impairment of overall exercise capacity, as reflected by reduced V_{O₂PEAK}. In various studies, different threshold values of V_{O₂PEAK} have been identified, e.g., 10.4, 11.5, and 13.2 ml/min/kg, below which mortality is increased (Wensel et al. 2002; Deboeck et al. 2012; Groepenhoff et al. 2008). Similarly, PAH patients with V_{O₂PEAK} more than 65% predicted have a good prognosis for 5-year survival (Wensel et al. 2013). Similarly, other markers of impaired overall exercise capacity are also associated with worse survival, e.g., lower HR_{PEAK} (Groepenhoff et al. 2013). Aerobic capacity can improve following treatment of PAH patients with PH-targeted medications; a greater change in V_{O₂PEAK} was associated with better survival, and this change in aerobic capacity was significantly related to changes in RVEF (Groepenhoff et al. 2013).

Other CPET parameters also appear to be important prognostic markers in PAH patients, particularly markers of impaired cardiac function (e.g., lower peak sBP, reduced O₂-pulse) and ventilatory inefficiency (higher V_E/V_{CO₂}, reduced P_{ET}CO₂) (Groepenhoff et al. 2013; Wensel et al. 2002; Groepenhoff et al. 2008). For example, increased V_E/V_{CO₂} slope (e.g., greater than 48) is associated with worse survival (Groepenhoff et al. 2008, 2013). Similarly, another study found worse survival with V_E/V_{CO₂} slope >62, as well as poor prognosis with V_E/V_{CO₂} >54 specifically at

AT (Deboeck et al. 2012). Impaired oxygenation on exercise also appears to be an important prognostic marker. Indeed, exercise-induced right-to-left shunt strongly predicts death or transplantation in PAH patients, independently of hemodynamics and other exercise parameters including $V_{O_{2PEAK}}$ (Oudiz et al. 2010).

Following exercise, post-exercise HR recovery (1 min) response, which is delayed in PH patients vs controls, appears to be a marker of poor prognosis (Ramos et al. 2012). Indeed, patients with more rapid HR recovery had better NYHA FC, resting hemodynamics and 6MWT distance. It is unclear whether all parameters are responsive to treatment. For example, the change in O₂-pulse following PH-targeted therapy predicted survival whereas changes in V_E/V_{CO_2} slope did not (Groepenhoff et al. 2013).

Rather than using individual CPET parameters, the prognosis may be better predicted by using either combinations of several CPET parameters, or a combination of CPET and other parameters, e.g., hemodynamic. For example, in multivariate analysis, reduced $V_{O_{2PEAK}}$ and low sBP at peak exercise were both independent predictors of survival; specifically, patients with combined lower $V_{O_{2PEAK}}$ (<10.4 mL/kg/min) and peak sBP (<120 mmHg) had the worst survival rates at 12 months (Wensel et al. 2002).

Similarly, combining CPET abnormalities (e.g., low $V_{O_{2PEAK}}$, and low ΔHR) and resting hemodynamic abnormalities (e.g., high PVR) or RV dysfunction by imaging may improve the ability to predict prognosis in PAH patients (Wensel et al. 2013). For example, 10-year survival was best (up to 75%) in patient with both high $V_{O_{2PEAK}}$ and low PVR. In addition, a risk prediction model performed better when incorporating both exercise O₂-pulse_{PEAK} and echo RV systolic function (using fractional area change), indeed better than traditional clinical, 6MWD, and invasive hemodynamic parameters (Badagiacca et al. 2016).

Summary

CPET is not currently widely used globally, even in major PH centers, largely because of a lack of medical expertise in the test, and a result-

ing lack of comfort in the safety, reliability, and usefulness of testing. Indeed, the STRIDE-1 randomized clinical trial of sitaxsentan was the only trial to use $V_{O_{2PEAK}}$ as a co-primary endpoint (along with 6MWD); despite improved 6MWD, the trial was widely perceived as negative because of a lack of change in $V_{O_{2PEAK}}$, largely because of lack of clinical expertise and inadequate technical standardization of CPETs (Barst et al. 2006).

Nevertheless, rigorously performed and carefully monitored CPET is a safe and sensitive tool for the detection of PH, as well as characterization of the severity.

Recommendations for Clinical Practice

Diagnosis of PH

CPET can serve as a diagnostic tool in patient with exertional dyspnea of unknown origin and in those with echocardiographic findings of suspected PH. Impaired exercise capacity (reduced $V_{O_{2PEAK}}$) is common in many patients with dyspnea and exercise intolerance, and is not sufficient to suggest the presence of PAH. Rather, disturbances of ventilatory parameters appear to be most specific in identifying a potential diagnosis of PAH. Among these, the most robust are P_{ETCO_2} and V_E/V_{CO_2} , especially at AT. The combination of an increase in V_E/V_{CO_2} slope with reduced values of end-tidal carbon dioxide tension (P_{ETCO_2}) has high diagnostic accuracy, identifying the likelihood of pulmonary vasculopathy (Yasunobu et al. 2005; Sun et al. 2001b). For example, threshold values have been identified for reductions in P_{ETCO_2} , such that $P_{ETCO_2} < 30$ mmHg at AT suggests PAH is possible, but < 20 mmHg indicates a strong likelihood of PAH (Yasunobu et al. 2005). Combined analysis of both P_{ETCO_2} and V_E/V_{CO_2} ratio at AT permitted even more precise estimates of the risk of PAH (e.g., unlikely, suspect, likely, or very likely). For example, increased V_E/V_{CO_2} slope along with reduced P_{ETCO_2} was found to accurately identify the presence of PAH in patients with unexplained dyspnea (Sun et al. 2001b) and in subjects with echo-suspected PH (Ferrazza et al. 2009).

The presence of increasing numbers of CPET abnormalities, especially combinations of cardiovascular and ventilatory parameters, is a stronger marker of the presence of PH. For example, the combination of increased V_E/V_{CO_2} slope and early AT had a specificity of 95% and a sensitivity of 92.6% for the identification of PAH (Zhao et al. 2017). Although CPET parameters predict an increased risk of the presence of pulmonary vascular disease, there is no pattern that can confirm a diagnosis of PAH. Most importantly, CPET abnormalities should support a clinical indication for a right heart catheterization.

Assessment of PH Severity/Prognosis

CPET is an emerging tool with high potential for clinical utility, based on several parameters which could serve as novel prognostic markers in the serial assessment and cardiopulmonary monitoring of PAH patients. Specific patterns of abnormalities may be suitable for establishing and guiding therapeutic management in PAH patients. A number of CPET variables have been shown to be consistently altered in patients with PAH (Schwaiblmair et al. 2012). These include $V_{O_{2PEAK}}$ as well as V_E/V_{CO_2} absolute value (e.g., at AT) and slope. Although many of these variables provide prognostic information, $V_{O_{2PEAK}}$ is most widely used for therapeutic decision making (Arena et al. 2010; Wensel et al. 2002, 2013; Diller et al. 2005).

Further studies on PAH are needed to allow for a more valid, comprehensive, and defined integration of CPET parameters into guidelines for monitoring of PH patients (Galiè et al. 2015). Based on some robust evidence from multivariate analyses, specific CPET parameters (e.g., V_E/V_{CO_2} , O_2 -pulse) may provide added value in combination with common clinical and hemodynamic variables in the modern treatment context (Deboeck et al. 2012; Wensel et al. 2013). CPET may be most useful in specific PAH subgroups; e.g., worsening CPET abnormalities during follow-up may be more sensitive in young patients with excellent 6MWD in whom disease progression may be quite significant before 6MWD falls to less than 440 m.

Cardiopulmonary Monitoring of the PAH Patient: Invasive Hemodynamics

Right Heart Catheterization (RHC)

Introduction

Since the diagnosis and differentiation of pulmonary hypertension relies on accurate pressure measurements, to date there is no test which has been shown superior to that of direct pressure transduction via insertion of a right heart catheter. Not only does RHC document pulmonary pressures, it also helps determine RV function, LV function, pericardial parameters and valvular function.

Performing pressure measurements in the right heart was first undertaken by Forssmann in the 1920s using himself as a subject (Chatterjee 2009; Nossaman et al. 2010). However, it was not until 1970 that the balloon-tipped Swan-Ganz catheter was developed and allowed for easier measurements in a clinical laboratory setting but also at the bedside. This catheter has become the most widely used tool for RHC, because it permits multiple functions: pressure transduction, measurement of temperature for thermodilution cardiac output, and ability to sample blood as well as infuse through multiple ports.

The technical procedure and relevant issues have been described in detail (Rosenkranz and Preston 2015). In brief, required venous access is typically accessed via the right internal jugular, brachial, or femoral veins. The SG catheter is advanced into the pulmonary artery using continuous pressure transduction, but fluoroscopy can also aid in appropriate catheter positioning, especially in cases where right-heart chamber sizes are increased. Potential pitfalls include the appropriate placement of the transducer or “zero-level” and effects of respiratory cycle and effort. Pressures that should be routinely measured include PAP, PAWP, right atrial pressure (RAP) and right ventricular pressure, as well as CO and mixed venous oxygen saturation (SvO_2). Parameters calculated from these measurements include the transpulmonary pressure gradient,

diastolic pressure gradient, PVR, and CI. Cardiac output is most commonly measured via the thermodilution method, the Fick method, or both.

RHC in PH Patients

RHC is a critical tool in the assessment of every patient with suspected, clinically significant PH. Diagnosis of PAH depends on the identification of pre-capillary hemodynamics, principally characterized by appropriately low left-heart filling pressures, e.g., PAWP and/or LVEDP. In the presence of more severe PH, especially with significant pulmonary vascular remodeling (e.g., PAH), the compliance of the pulmonary artery may be decreased and accurate PAWP measurement requires more attention to appropriate balloon positioning. Careful review of the characteristic PA wedged balloon waveform may help accurately measure PAWP, but in some patients with suspected LV diastolic dysfunction, transaortic LV pressure tracing may be required to determine LVEDP.

A number of functional tests can then be performed if indicated (Table 54.7). In some patients

who appear to have pre-capillary PH but are volume contracted (normal/low RAP), the presence of left-sided cardiac contribution to PH may be masked by over-diuresis and resulting “normal” PAWP. In such patients with co-morbid conditions associated with LV dysfunction (especially diastolic dysfunction) and post-capillary PH (e.g., obesity, coronary disease, atrial fibrillation, systemic hypertension, presence of diabetes mellitus) and the finding of apparent pre-capillary PH, consideration should be given to a fluid challenge in order to unmask abnormal LV function associated with increased PAWP and important contribution of post-capillary PH (Fujimoto et al. 2013).

Care must be taken when measuring the mixed venous O₂ saturation at the pulmonary artery level (SvO₂) so as not to miss a possible left-to-right shunt. This may have clinical implications for diagnosis and treatment. In general, SvO₂ ≥75% with a normal hemoglobin (>130 g/L) should alert the clinician to the presence of a possible left-right shunt. In this case, additional O₂ saturation readings should be taken at all points

Table 54.7 Potential provocative tests during RHC in PH patients

Provocative test	Purpose	Method	Interpretation
Pulmonary vasoreactivity	To identify potential therapeutic use of CCB (selectively IPAH, HPAH, Drug/Toxin-PAH)	Preferred: Inhaled nitric oxide (10–40 ppm via nasal prongs) for 5–10 min	Positive acute vasodilator test: mPAP decreases ≥10 to <40 mmHg AND Stable/increased CO
Exercise	To identify the presence of exercise-induced PH	Steady-state exercise for 5–10 min e.g., Recumbent cycle at 25W, arm exercise with saline bags	No consensus but concern when: mPAP >30 mmHg AND CO <10 L/min AND TPR >3 WU ^a
Fluid challenge	To identify the presence of “masked” post-capillary PH in patients with pre-capillary PH hemodynamics	Rapid administration of IV normal saline e.g., 500 mL over 5 min	Positive fluid challenge: Post-bolus PAWP >15 mmHg, with initial RAP <5–10 mmHg (Fujimoto et al. 2013)
Systemic vasodilator	To identify the presence of pre-capillary component in patients with post-capillary PH hemodynamics	Sublingual NTG 0.4–0.8 mg Milrinone 50 mcg/kg IV over 5 min Nitroprusside 1–5 mcg/kg/min for 5–10 min	Positive response: Increased CO AND reduction in PAWP ≤15 mmHg AND either (i) Reduction in mPAP ≤20 mmHg OR (ii) Reduction in PVR <3 WU

^aTotal pulmonary resistance (TPR) is defined as mPAP/CO in Wood Units (WU)

along the venous return including superior and inferior vena cavae, RA and RV. Multiple points in each chamber may be helpful in localizing the shunt but imaging should also be performed which allows for sufficient visualization of all possible anomalous connections (Lilly and Section 2012).

Clinical Importance of Pulmonary Hemodynamics in PH

Baseline abnormalities in cardiopulmonary hemodynamics are essential to the diagnosis of PH and the definition of the hemodynamic cause (e.g., pre-capillary vs post-capillary), and are also prognostically important in each individual patient. The initial report of the NIH Registry of Primary Pulmonary Hypertension (PPH; currently labelled IPAH) first suggested that the hemodynamic severity of PH was prognostically important (D'Alonzo et al. 1991). Specifically, higher mPAP and RAP, as well as lower CI were independent predictors of mortality. Many other reports have confirmed the fundamental nature of abnormal cardiopulmonary hemodynamics in PH, and the important contribution to morbidity and mortality (Benza et al. 2010; Sitbon et al. 2002; McLaughlin et al. 2002). The most consistently validated parameters include measures of the severity of pulmonary vascular disease, as reflected by PVR, as well as of right ventricular adaptation to the increased load in PH, as reflected specifically by RAP, cardiac index (CI), and mixed venous O₂ saturation (SvO₂) (Galie et al. 2019). Despite its central importance to the diagnosis of PH, mPAP is not consistently associated with prognosis, as mPAP initially increases with progression of pulmonary vascular disease, but in the setting of advanced RV failure often with markedly elevated RAP, a falling mPAP is a bad prognostic sign (Sitbon et al. 2002; McLaughlin et al. 2002).

Although baseline cardiopulmonary hemodynamics are prognostically important in each individual patient, the severity of cardiopulmonary hemodynamic abnormalities are of even greater prognostic importance during ongoing clinical monitoring following institution or modification of PH-targeted therapy (Nickel et al. 2012). For

example, initial follow-up data on IV epoprostenol-treated IPAH patients reported better survival with lower TPR (>30% decline from baseline) and mean RAP (<10 mm Hg), as well as higher SvO₂ (≥62%) and CI (>0.5 l/min/m² increase from baseline) (Sitbon et al. 2002; McLaughlin et al. 2002).

Most of the evidence in support of the prognostic role of cardiopulmonary hemodynamics in PAH comes from open-label, observational studies. This idea has importantly been confirmed with data from a post hoc, sub-group analysis of a blinded RCT (Galie et al. 2017). Specifically, baseline hemodynamic parameters (mPAP, RAP, PVR, CI, SvO₂) were prognostic of adverse future clinical outcomes over 3 years, but values observed after 6 months of follow-up were more highly prognostic, especially CI >2.5 L/min/m² and RAP <8 mmHg.

Recommendations for Clinical Practice

RHC remains essential in the initial assessment of every patient with suspected clinically significant PH and may also be useful in the ongoing monitoring of patients with confirmed PAH. In general, it is a well-tolerated test and an experienced operator should allow for a relatively comfortable patient experience with a serious complication rate that should be below 1 in 1000 cases. However, not all newly diagnosed patients receive RHC as part of their diagnostic work-up, even in PH expert centers (Deaño et al. 2013; Zuckerman et al. 2013).

Cardiopulmonary Monitoring of the PAH Patient: Echocardiography

Introduction

The primary imaging modality for nearly all cardiovascular diagnosis is the echocardiogram. Its use of two-dimensional, and increasingly three-dimensional, imaging along with its Doppler functions and the more recent advancement of speckle-tracked strain imaging, provides a powerful tool to delineate cardiovascular structures and determine their function. Although traditionally valvular structures and left ventricular func-

tion have formed the basis of echocardiographic analysis, the increased recognition of the importance of right ventricular function has helped to focus the field on improving the accuracy of imaging this structure. Additionally, echo analysis is heavily favored in clinical guidelines for the initial recognition of pulmonary hypertension (Galiè et al. 2015).

Echocardiography in PH

Overall Approach

Echocardiography provides the principal screening tool for the presence or absence of PH. It is important however not to rely on a single echo measurement to either rule in or rule out the presence of significantly elevated pulmonary pressures but to rather take into account a number of different parameters that echo can assess. Guidelines recommend that a detailed echo evaluation of all patients with suspected PH be performed (Galiè et al. 2019; Hirani et al. 2020). Although systolic PAP can be approximated from the calculated RVSP through Doppler measure-

ment of the tricuspid regurgitant velocity (TRV), this measurement alone is equally likely to both underestimate and overestimate the presence of PH (Fisher et al. 2009). For example, underestimated TRV results from an insufficient Doppler envelope or eccentric TR jet. It is therefore essential to adopt a more complete approach to the analysis of echo images in evaluating the possible presence of PH (Table 54.8) (Rudski et al. 2010). In addition to parameters reflective of elevated PAP, a qualitative analysis of the RV adds important details such as regional wall motion abnormalities and a global impression of overall ventricular function (Fig. 54.2).

2-D Evaluation

There are three standard echocardiographic views that are routinely used. Below we detail the important structures visualized in each view as they relate to the right heart and PH (Grapsa et al. 2011).

- *Parasternal views*

This view is best for visualization of the interventricular septum as most right heart

Table 54.8 Typical echocardiographic parameter abnormalities in PH

Modality	Parameter	Abnormal value	Relevance
2-D/m-mode analysis	RV size ^a	≥41 mm	Multiple uses including RV function, chronicity and severity of disease
	RVFAC	≤31%	RV systolic function
	TAPSE	<17 mm	RV systolic function
	RA area	>18 cm ²	RV diastolic function
	LA volume index	>34 mL/m ²	LV diastolic function
	IVC width	≥20 mm	RA pressure, RV diastolic function
Continuous-wave and pulse-wave Doppler analysis	Tricuspid regurgitant velocity (TRV)	>2.9 m/s	PA systolic pressure; single most useful value in determining presence of PH by echo.
	Pulmonary regurgitant velocity (PRV)	No recognized value	End-diastolic PA regurgitant Doppler velocity may aid in determining PA diastolic pressure.
Tissue Doppler analysis	Tricuspid S'	<11 cm/s	RV systolic function
	Tei index	>40 (PW) >55 (TD)	RV systolic and diastolic function
Strain imaging	RV strain ^b	≥45%	RV contractility

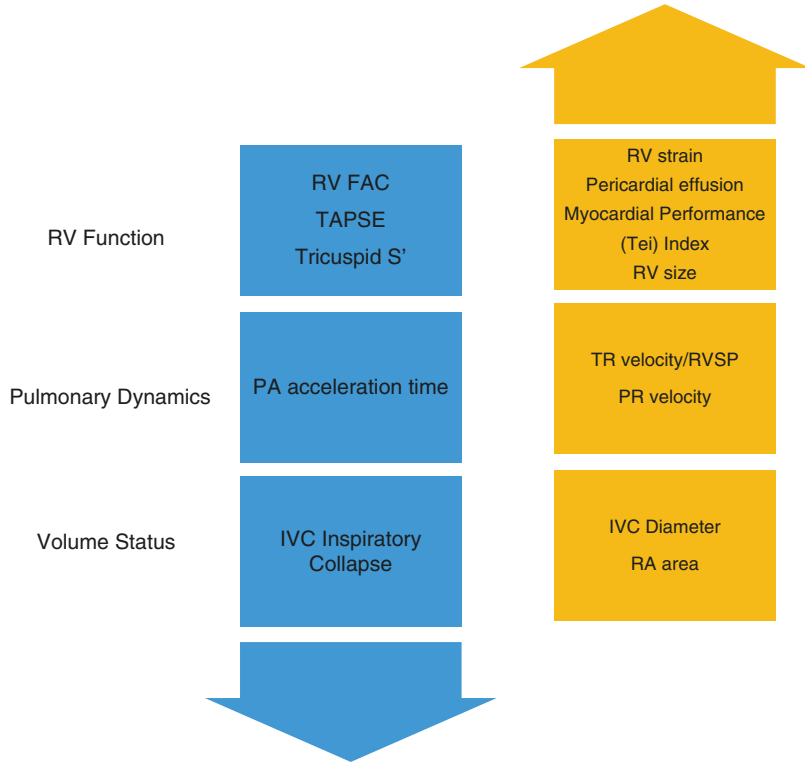
Data compiled from Rudski et al. (Rudski et al. 2010)

Abbreviations: *RVFAC* RV fractional area change, *TAPSE* tricuspid annular plane systolic excursion, *PW* pulse-wave, *TD* tissue Doppler

^aAs measured in 4-chamber view at the RV base

^bDetermined by Doppler peak strain at the RV base (best validated method)

Fig. 54.2 Characteristic changes in /rt parameters in PAH vs healthy controls. Abbreviations: RVFAC (Right ventricular fractional area change), TAPSE (tricuspid annular plane systolic excursion), PA (pulmonary artery), IVC (inferior vena cava), TR (tricuspid regurgitation), RVSP (right ventricular systolic pressure), PR (pulmonary regurgitation), RA (right atrium)



structures are either not seen or incompletely seen at this level. In the long-axis view, the moderator band is usually seen close to the interventricular septum traversing the RV and care should be taken not to include the moderator band in the measurement of the septal structure and function. Additionally, the long-axis view allows for partial visualization of the RV inflow tract. The tricuspid regurgitant jet can usually be visualized in this view but the accurate quantitation may not be possible.

In both the short-axis and long-axis views, the RV outflow tract can be visualized, and in some patients, this allows for quantification of the main pulmonary artery diameter and even the main pulmonary branches. Pulmonary regurgitation can also be seen best in these views.

- *Apical views*

This view provides for the best visualization of the right ventricle along with both qualitative and quantitative evaluation of size and function. Additional care should be given

to the examination of the apex which is often hypertrophic and/or akinetic – a scenario that can predispose to the formation of thrombus formation. Opening of the tricuspid leaflets during diastole can also be assessed in this view which may appear restricted as PA pressures rise and RV function continues to decline.

- *Subcostal view*

This view can be helpful in patients where parasternal or apical window views are difficult to image, such as those with pulmonary disease/WHO Group III PH. It also provides the best view for the measurement of RV inferior wall thickness and allows for imaging of the atrial septum to assess for a patent foramen ovale or other septal defects.

The inferior vena cava is also imaged from this view to allow for an estimate of right atrial pressure. By convention, both the diameter of the IVC (with a cut-off of less 20 mm) and its collapsibility during sharp inspiration (with a cut-off of greater than 50%) should be normal

in order to report normal right atrial pressure, estimated at approximately 3 mmHg. When both are abnormal, right atrial pressure is estimated at least 15 mmHg with intermediate values usually estimated at 8 mmHg (Rudski et al. 2010).

Doppler Examination

Doppler analysis is the additional complement to 2-D analysis and provides important functional information in echo analysis (Fisher et al. 2009). This analysis can generally be grouped in pulsed-wave, continuous-wave, and tissue Doppler analyses. The details of these evaluations are outside the scope of this section. However, continuous-wave Doppler analysis of the tricuspid regurgitant jet, as mentioned above provides the single most utilized value for the diagnosis of PH. The calculation of RVSP can be supplemented with continuous-wave analysis of the pulmonary regurgitant jet to help determine pulmonary diastolic pressures. These values are all dependent on the determination of the best location to sample the regurgitant jet and, as a result, are susceptible to underestimation.

Right-Heart Chamber Evaluation

It is well documented that right heart chamber size and function are important predictors of symptom severity, morbidity, and mortality (Galiè et al. 2015). In echocardiographic analysis, size determinations of the right atrium and ventricle are key parameters in the PH patients along with functional assessment of the right ventricle, both qualitative and quantitative. Traditionally this was done using only 2-D imaging techniques, but more modern analysis now incorporates Doppler parameters and speckle tracking to assess for myocardial strain.

Current guidelines suggest using RA area and a cut-off of 18cm² as measured in the standard apical four-chamber view. More recently, right atrial volume has been put forth as a more accurate assessment of right heart function. Right atrial volume is usually indexed to body surface area and is calculated from the apical four-chamber view or from the subcostal view and is

measured at maximum atrial volume at end-systole. The single plane area-length method is used and right atrium volume is measured using the area and the long-axis length of the atrium using the formula: $RAVI = (0.85 A^2/L)/BSA$, where A is the atrium area in any view (cm²), L is the long-axis atrium length (cm), and BSA is body surface area (Wang et al. 1984).

Functional assessment of the RV can be undertaken either qualitatively or quantitatively. On the basis of the parameters of RV dilation, hypertrophy and contractility, an experienced echocardiographer will be able to make a good qualitative assessment of RV function and will be able to grade it as mild, moderate, or severe impairment. However, the addition of quantitative measures can aid in further refinement of the qualitative assessment and also allow for values which the clinician can follow over time. Overall RV function can be commonly assessed by fractional area change from diastole to systole known as RVFAC, by measuring the excursion of the tricuspid annulus during systole known as TAPSE, and by assessing the systolic wave velocity (S') of the RV lateral wall using tissue Doppler analysis. Although RV ejection fraction is technically possible, especially with the advent of 3-D imaging, it is often laborious due to the geometry of the RV and as a consequence, is not well validated in any large patient population. The Myocardial Performance (or Tei) Index combines Doppler data taken during systole and diastole and, despite lack of wide adoption, may provide for an excellent global analysis of RV function (Tei et al. 1995).

Newer echocardiographic techniques such as exercise evaluation for early detection in at-risk populations has been proposed but clear clinical cut-offs have yet to be accepted (Grünig et al. 2009). Using speckle-tracking technology to examine myocardial strain and strain rate in the deformation and rate of deformation, respectively, of the myocardial segment and, in PH, RV systolic strain and strain rate has been shown to predict morbidity and mortality (Sachdev et al. 2011). In one study of a cohort diagnosed with PAH, all patients had a depressed RV systolic strain ($-15\% \pm 5\%$) and strain rate

($-0.80 \pm 0.29 \text{ s}^{-1}$). Of the parameters assessed, average RV free wall systolic strain worse than -12.5% identified a cohort with greater severity of disease (82% were FC III/IV), greater RV systolic dysfunction (RV stroke volume index $26 \pm 9 \text{ mL/m}^2$), and higher right atrial pressure ($12 \pm 5 \text{ mm Hg}$). Patients with a RV free wall strain worse than -12.5% were associated with a greater degree of disease progression within 6 months, a greater requirement for loop diuretics, and/or a greater degree of lower extremity edema, and it also predicted 1-, 2-, 3-, and 4-year mortality (unadjusted 1-year hazard ratio, 6.2; 2.1–22.3). After adjusting for age, sex, PH cause, and FC, patients had a 2.9-fold higher rate of death per 5% absolute decline in RV free wall strain at 1 year (Sachdev et al. 2011).

Recommendations for Clinical Practice

Although echo provides a widely accessible, non-invasive assessment of PH, accurate and clinically useful information depends upon image analysis by a cardiologist specializing in echocardiography at a center with a high volume of PH patients.

We agree that all echocardiographic reports should include measurements, descriptions of all valves, the proximal great arteries, the heart chambers, the pericardium, and Doppler findings. But, when PH is the reason for the referral, we encourage special emphasis to be put on pulmonary pressures, right heart chamber size and function and any finding that may indicate a secondary cause (e.g., LV dysfunction, left heart valve disease, or congenital heart disease). Furthermore, when a diagnosis of PH is already confirmed, the report should also include the various parameters that provide prognostic information (e.g., right atrial volume index, inferior vena cava diameter, eccentricity index, presence of pericardial effusion, and TAPSE).

Although not all centers have the access and training to perform more advanced techniques such as Tei Index or strain imaging, we recommend that where possible, these are used preferentially in PH analyses so as to help prognosticate outcomes.

Cardiopulmonary Monitoring of the PAH Patient: Cardiac MR

Introduction

Cardiac magnetic resonance imaging has been in use for many years to aid in the description of both structural and functional abnormalities. Specifically, CMR has been particularly valuable in congenital heart disease for the characterization of shunts and anatomic vascular and structural variants. Additionally, in coronary disease it has been used to assess for myocardial viability along with the characterization of many different types of infiltrative and inflammatory conditions. At this point, it can also be considered to be the gold standard for assessment of RV metrics including size and function, that is, ventricular volume, ejection fraction, and presence of regional wall motion abnormalities. Additionally, the use of gadolinium contrast can aid in determining myocardial characteristics such as the presence of fibrosis.

CMR is non-invasive, can image in three dimensions, and has an excellent temporal resolution. It unfortunately lacks spatial resolution as compared with other imaging modalities such as CT or echocardiography and is very sensitive to motion artefact. Additionally, patient-related factors such as long scan times, claustrophobia and the presence of metal fragment and/or medical devices can limit or preclude its use.

Cardiac MR in PH

The use of CMR in the diagnosis and follow-up of patients with PH has continued to evolve. There are data that directly correlates CMR measurements with clinical parameters.

Stroke volumes obtained by CMR in patients with PH correlate well with 6MWD; specifically, a change in SV of approximately 10 mL (range: 8–12 mL) was highly associated with a statistical change in 6MWD (van Wolferen et al. 2011).

Changes in RVEF also appear to relate to overall mortality in patients with PAH. Specifically, a cohort of patients that showed preserved RVEF by CMR preserved their mortality rates over time as compared with those

who showed a decline in RVEF. The same cohort also demonstrated that a baseline reduction in indexed LV and RV end-diastolic volumes (LVEDVI and RVEDVI) had worse outcomes with a significant cut-point of LVEDVI <40 mL/m² and RVEDVI <84 mL/m² (Peacock and Noordegraaf 2013).

The presence of late gadolinium enhanced at the so-called RV insertion point also has been shown to be clinically relevant (see Fig. 54.3). Approximately 40% of PAH patients with this abnormality had an event associated with clinical worsening at 1 year (Peacock and Noordegraaf 2013).

Despite these powerful findings, CMR has yet to supplant traditional invasive methods such as right heart catheterization for the overall diagnosis and risk modeling in PAH (Benza et al. 2008; Grunig and Peacock 2015) as there are still only limited studies of acceptably large patient populations to promote this approach. Additionally, the availability and expertise in this approach is still lacking even at most academic centers.

Recommendations for Clinical Practice

We recognize both the diagnostic and predictive power of CMR in patient with PH. Although still not in wide use at most centers for the ongoing

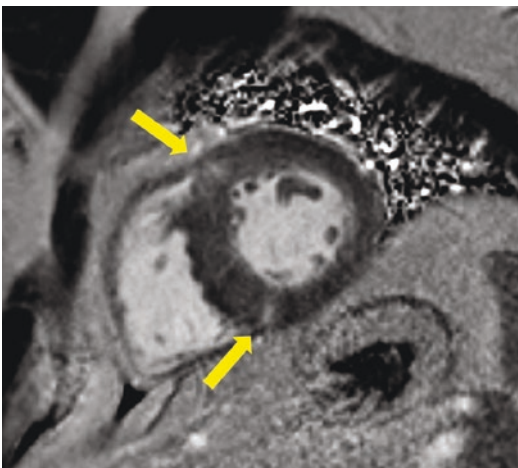


Fig. 54.3 Short-axis MR image of right ventricle showing gadolinium enhancement (fibrosis) of right ventriculo-septal insertion point (see arrows). (Courtesy: Nikolaos Tzemos, MD)

follow-up of these patients, we would recommend the implementation of CMR, wherever possible, at centers that specialize in the treatment of PH. Although the routine follow-up may not be feasible due to resource allocation and/or patient preference, we recommend that CMR be used in the initial evaluation of the stable outpatient population so as to further refine clinical decision-making via the use of CMR-derived parameters like RV ejection fraction, stroke volume, and indexed end-diastolic volumes.

Cardiopulmonary Monitoring of the PAH Patient: Biomarkers

Introduction: PAH Vascular Biology

The pathobiology of each of the different types of PH is quite distinct, although there are areas of commonality including endothelial cell (EC) injury and dysfunction. Changes in pulmonary vascular physiology are strongly related to structural and functional alterations in the entire pulmonary circulation, especially the pulmonary arteries. These biologic changes can be driven by a genetic predisposition. More than 30 genes have been identified which may contribute to the pathobiology of PAH, including many with strong evidence of a causal role (Garcia-Rivas et al. 2017; Morrell et al. 2019). Specific mutations in some of these genes contribute to a risk of hereditary PAH in individual patients, the most frequent of which are Bone Morphogenetic Receptor type 2 (*BMPR2*) in adults and T-box 4 (*TBX4*) in children (Morrell et al. 2019). In most PAH patients, pulmonary vascular injury is most likely initiated by a second, acquired, extrinsic insult including infection (HIV), inflammatory-fibrotic disease process such as the connective tissue disease scleroderma, or high pulmonary arterial blood flow as seen in CHD with left-right shunt.

Pulmonary arterial pathology is characterized by remodeling of all layers of the arterial wall, including intima, media, and adventitia (Humbert et al. 2019). Intimal lesions account for most of the reduction of luminal area of small pulmonary arteries and largely explain the increased

PVR. These lesions consist of both concentric and eccentric intimal fibrosis, inflammatory cell infiltration, as well as endothelial proliferative plexiform and dilation/angiomatoid lesions. In situ thrombosis also contributes to luminal narrowing. Medial changes include inflammatory cell infiltration, as well as smooth muscle cell hypertrophy, hyperplasia, and distal arterialization of smaller pulmonary arteries. There are increasingly appreciated pathologic changes in the pulmonary capillaries and veins, typically to a lesser degree than arterial abnormalities, but in individual patients, these capillary and venous changes can be predominant.

Regardless of the underlying genetic and extrinsic insult-driven mechanisms of injury, the most common result is pulmonary arterial EC injury and dysfunction, which results in dysregulation of multiple pathobiologic pathways, which have been recognized to contribute to PH pulmonary vascular pathophysiology (Humbert et al. 2019).

Biomarkers Which Reflect the Pathobiology of PAH

There is no specific marker for the pulmonary vascular remodeling of PAH, although a vast number of potential biomarkers continue to be investigated (Table 54.9) (Galiè et al. 2015; Sitbon and Morrell 2012; Foris et al. 2013; Al-Naamani et al. 2016). Potential biomarkers in PAH include markers of vascular dysfunction and inflammation, as well as of the resulting RV strain and dysfunction, including markers of myocardial stress, impaired tissue perfusion, and secondary organ dysfunction. One of the first pathobiologic abnormalities identified in PH was an imbalance of circulating vasoconstrictor and vasodilator mediators. This includes increased production of the vasoconstrictors endothelin, thromboxane, and serotonin, and reduced synthesis of vasodilators prostacyclin and nitric oxide (Sitbon and Morrell 2012).

Blood levels of many of these biomolecules can be measured; however, few have been confirmed as adequately robust diagnostically or clinically useful in biologically phenotyping patients. For example, soluble levels of endothe-

Table 54.9 Cardiopulmonary monitoring: Potential biomarkers in PAH

Pathobiologic feature	Potential biomarkers
Pulmonary vascular dysfunction	Nitric oxide (NO) and related metabolites
	Asymmetric dimethylarginine (ADMA)
	Endothelin-1
	Angiopoietins
	Von Willebrand factor
	Platelet-derived growth factor (PDGF)
	Basic fibroblast growth factor (bFGF)
	5-hydroxy-tryptamine (5-HT)
Inflammation	VEGF
	C-reactive protein
	Interleukins (e.g., 1B, 6)
	Chemokines (e.g., CCL21)
	TNF α
	Soluble urokinase plasminogen activator receptor (suPAR)
Myocardial stress	Matrix metalloproteinases (e.g., MMP9)
	Atrial natriuretic peptide
	Brain natriuretic peptide (BNP)/NT-proBNP
	Troponins
	Heart type fatty acid binding protein (H-FABP)
	Soluble suppression of tumorigenicity 2 (sST2)
	Uric acid
Low CO and/or tissue hypoxia	Growth differentiation factor 15 (GDF-15)
	Osteopontin
	Creatinine
Markers of secondary organ damage	Bilirubin
	Creatinine

lin are elevated in many patients with PAH; however, there is no evidence to support routine measurement of endothelin at either baseline or during follow-up in PAH patients.

At present, many potential biomarkers of PAH pathobiology have been identified, but very few are recommended for routine clinical use, as most have not been validated for any clinical utility in the diagnosis or management of an individual patient with PAH. There is great excitement about the potential future utility of biomarkers in

a precision medicine approach, whereby an assessment of the underlying PAH pathobiology in each individual patient guides clinical decisions regarding the most effective or safest PH-targeted medical therapy or more effectively assess prognosis.

Natriuretic Peptides (ANP, BNP, NT-proBNP)

Introduction

Natriuretic peptides (NPs) consist of four groups of hormones, including atrial type, B-type natriuretic peptide (BNP), C-type, and dendroaspis D-type, each with its own characteristic functions. The most studied and clinically useful in PH are BNP and NT-proBNP (Foris et al. 2013). In response to RV and/or LV wall stretch or tension, BNP is synthesized as a prohormone proBNP (108 amino acid polypeptide), which is secreted intact and subject to cleavage in the bloodstream yielding the N-terminal 76 amino acid fragment (termed NT-proBNP) and a bioactive C-terminal 32 amino acid fragment (termed BNP-32) (Yeo et al. 2003). BNP and NT-proBNP have many systemic biological effects, specifically diuresis (including natriuresis and kaliuresis), systemic vasodilatation, inhibition of renin/aldosterone production, cardiac, and vascular myocyte growth (Hall 2004).

Plasma BNP correlates with the severity of PH, specifically the degree of RV failure (Nagaya et al. 1998; Tulevski 2001; Mauritz et al. 2011), and specifically RV wall stress (Uchiyama et al. 2019). BNP also correlates significantly with clinical severity (e.g., NYHA FC) and hemodynamic severity (e.g., mPAP, CO, RAP) of idiopathic PAH (Nagaya et al. 2000). Similarly, NT-proBNP also correlates with clinical (e.g., NYHA FC) and hemodynamic severity of PAH (e.g., RAP, mPAP, PVR, heart rate, CI, SvO₂) (Mauritz et al. 2011; Andreassen et al. 2006). Moreover, NT-proBNP was inversely correlated with V_{O2PEAK} on CPET (Andreassen et al. 2006). Plasma NT-proBNP levels were also found to correlate with PAH severity specifically in scleroderma patients (Mukerjee et al. 2003).

Prognostic Role of BNP and NT-proBNP

There is strong evidence to support a prognostic role for the measurement of BNP and/or NT-proBNP levels in individual patients (Benza et al. 2010; Mauritz et al. 2011; Nagaya et al. 2000; Fijalkowska et al. 2006). For example, higher plasma levels of BNP (>150 pg/mL at baseline) and after initiation of PH-targeted therapy (>180 pg/mL) were associated with worse survival (Nagaya et al. 2000). Similarly, higher NT-proBNP levels (≥ 1400 pg/mL) identified patients with poor long-term prognosis (Fijalkowska et al. 2006). A similar level (≥ 1256 pg/mL) was identified as the optimal NT-proBNP threshold for predicting a higher risk of mortality at the time of diagnosis in PAH patients (Mauritz et al. 2011).

There also is evidence that both BNP and NT-proBNP are responsive to PH-targeted medical treatment. Indeed, levels of both BNP and NT-proBNP decline in PAH patients treated with PH-targeted medications (Uchiyama et al. 2019; Nagaya et al. 2000; Andreassen et al. 2006; Fijalkowska et al. 2006). Moreover, an annual decrease in NT-pro-BNP (>15% /year) was associated with better survival in treated PAH patients (Mauritz et al. 2011).

Recommendations for Clinical Practice

At present, one of the most critical aspects in the management of PAH patients is the assessment of RV dysfunction for risk stratification and assessment of response to treatment. Current guidelines recommend multi-parameter assessment of RV function vs dysfunction, including clinical assessment of RV failure, RV imaging (e.g., echocardiography, CMR), and assessment of blood levels of BNP/NT-proBNP.

Blood levels of BNP or NT-proBNP should be assessed at diagnosis, regularly during follow-up, e.g., 3–6 months intervals, specifically at the time of any clinical deterioration, and also after any changes in medical therapy. Although guidelines recommend monitoring of blood levels of BNP and/or NT-proBNP in PAH patients in order to assess the degree of RV failure, it should be recognized that these natriuretic peptides are not

specific for PH, but can be elevated in many other cardiac conditions associated with both RV and LV dysfunction.

The major goal of management of PAH patients is improvement in RV failure, which is reflected in achieving lower and possibly normal levels of BNP/NT-proBNP. Normal levels of BNP and NT-proBNP are age- and sex-dependent, such that values tend to rise with increasing age. It is yet unclear if BNP values should be normalized to age- and sex-specific predicted. In addition, although BNP and NT-proBNP tend to be concordant, there is an increasing discrepancy in the presence of renal impairment, which tends to elevate NT-ProBNP levels more than BNP (Farnsworth et al. 2018). Although plasma levels of NT-ProBNP are more sensitive to changes in renal function than BNP, potentially reducing the diagnostic accuracy of NT-proBNP for RV dysfunction in patients with impaired renal function, NT-proBNP may actually be superior to BNP as a mortality marker in PH patients with renal insufficiency (Leuchte et al. 2007).

Cardiopulmonary Monitoring of the PAH Patient: Summary

Multiple parameters can be assessed which reflect the clinical status of PAH patients. Some of these may be useful at the time of initial diagnosis and especially during ongoing follow-up in order to determine individual patient-specific risk for worsening and poor clinical outcomes. The major outcome that has typically been assessed is mortality, and it is clear that no single assessment parameter reliably and reproducibly predicts the risk of death in PAH patients. Therefore, PH physicians commonly use a panel of parameters – some variable and some fixed – in an attempt to predict patient mortality. Clinicians rely on these variables to not only to help guide the intensity of initial and subsequent therapy but also, perhaps just as important, to inform and engage patients in understanding the severity of their disease process at diagnosis and following institution of treatment (Table 54.10) (Gan et al. 2007; van de Veerdonk et al. 2011; van Wolferen et al. 2007).

Table 54.10 Cardiopulmonary monitoring of the PAH Patient: Practical vs complete assessment

Parameter	Low risk	Specific goal
<i>Practical assessment</i>		
History	No or only mild limitation	mNYHA FC 1 or 2
HRQoL	Good – excellent	EmPHasis-10 score <15
Physical exam	No or only mild RV failure	JVP <5 cm ASA
		No/minimal peripheral edema
		Absence of: RV heave, hepatomegaly
Functional (6MWT)	Very good – excellent	6MWD >440 m 6MWD >80% predicted ^a
Imaging (Echo)	No or only mild RV failure	No/mild RV dilation and/or systolic dysfunction
		TAPSE >18 mm
		IVC diameter <2.0 cm RA area <18 cm ²
Metabolic	No or only mild RV failure	NT-pro-BNP <300 pg/mL
		BNP <50 pg/mL
<i>Complete assessment</i>		
Functional (CPET)	Very good – excellent	$V_{O_{2PEAK}} > 65\%$ predicted
	No/mild ventilatory inefficiency	$V_E/V_{CO_2} < 45$
Hemodynamic	Normal or only mild PH	mPAP <35 mmHg
	Normal RV function	RAP <8 mmHg AND CI >2.5 L/min/m ² AND SvO ₂ > 65%
Imaging (CMR)	No or only mild RV failure	RAC >16% (Gan et al. 2007) RVEF >35% (van de Veerdonk et al. 2011) RVEDVI <84 mL/m ² (van Wolferen et al. 2007)

Abbreviations. RAC relative area change, RVEDVI RV end-diastolic volume index, RVEF RV ejection fraction
^aSpecific populations in which 440 m may not be an appropriate goal, e.g., young, elderly, SSc-PAH

The most commonly used sets of parameters are derived from the ERS/ESC guidelines on PH (Galiè et al. 2015) and those from the REVEAL registry (Benza et al. 2010, 2019). Common parameters that were most predictive include, WHO/mNYHA FC (I or II), 6MWD (≥ 440 m), BNP (< 50 pg/ml)/NT-proBNP (< 300 pg/ml), and CI (≥ 2.5 l/min/m²). Future risk of mortality over time can be calculated and predicted for each individual patient. For example, patients meeting low-risk criteria for WHO/mNYHA FC, 6MWD, and BNP/NT-proBNP at first follow-up following institution of initial therapy had a 1-year survival rate of 97% in the French registry, 95% in the COMPERA registry, and 93% in REVEAL (Boucly et al. 2017; Hoepfer et al. 2017; Benza et al. 2019; Hoepfer et al. 2018).

There is no current model that perfectly predicts the risk of individual PAH patients, and as such, there is a lack of international consensus on a recommended model. Moreover, there continues to be detailed analyses comparing different models, as well as modifications of all models, as new data emerge such as the inclusion of renal dysfunction and hospitalization. For example, a preliminary c-index analysis (Benza et al. 2018) reported that revised risk models using the original REVEAL registry, colloquially referred to as REVEAL 2.0 and mini-REVEAL scores, maintain very good discriminative ability (c-index ≥ 0.7) compared to the ESC/ERS models.

With increasing access to high-powered computing and machine learning, risk modeling appears ready to make a quantum leap forward. The NIH-funded PHora project (<https://myphora.org>) seeks to use Bayesian statistical methods to further elucidate individual patient risk via complex assessment of multiple pathways and their interactions. We see great promise in this method and eagerly await the results of this endeavor.

References

- Al-Naamani N, Palevsky HI, Lederer DJ, Horn EM, Mathai SC, Roberts KE, et al. Prognostic significance of biomarkers in pulmonary arterial hypertension. *Ann Am Thorac Soc*. 2016;13(1):25–30.
- Andreassen AK, Wergeland R, Simonsen S, Geiran O, Guevara C, Ueland T. N-terminal pro-B-type natriuretic peptide as an indicator of disease severity in a heterogeneous group of patients with chronic precapillary pulmonary hypertension. *Am J Cardiol*. 2006;98(4):525–9.
- Anker SD, Agewall S, Borggrefe M, Calvert M, Jaime Caro J, Cowie MR, et al. The importance of patient-reported outcomes: a call for their comprehensive integration in cardiovascular clinical trials. *Eur Heart J*. 2014;35(30):2001–9.
- Arena R, Lavie CJ, Milani RV, Myers J, Guazzi M. Cardiopulmonary exercise testing in patients with pulmonary arterial hypertension: an evidence-based review. *J Heart Lung Transplant*. 2010;29(2):159–73.
- Badagliacca R, Papa S, Valli G, Pezzuto B, Poscia R, Manzi G, et al. Echocardiography combined with cardiopulmonary exercise testing for the prediction of outcome in idiopathic pulmonary arterial hypertension. *Chest*. 2016;150(6):1313–22.
- Barst RJ, Langleben D, Badesch D, Frost A, Lawrence EC, Shapiro S, et al. Treatment of pulmonary arterial hypertension with the selective endothelin-A receptor antagonist sitaxsentan. *J Am Coll Cardiol*. 2006;47(10):2049–56.
- Barst RJ, Chung L, Zamanian RT, Turner M, McGoan MD. Functional class improvement and 3-year survival outcomes in patients with pulmonary arterial hypertension in the REVEAL registry. *Chest*. 2013;144(1):160–8.
- Benza R, Biederman R, Murali S, Gupta H. Role of cardiac magnetic resonance imaging in the management of patients with pulmonary arterial hypertension. *J Am Coll Cardiol*. 2008;52(21):1683–92.
- Benza RL, Miller DP, Gomberg-Maitland M, Frantz RP, Foreman AJ, Coffey CS, et al. Predicting survival in pulmonary arterial hypertension: insights from the registry to evaluate early and long-term pulmonary arterial hypertension disease management (REVEAL). *Circulation*. 2010;122(2):164–72.
- Benza RL, Gomberg-Maitland M, Elliott CG, Farber HW, Foreman AJ, Frost AE, et al. Comparison of three risk assessment strategies as predictors of one-year survival in US pulmonary arterial hypertension (PAH) patients. In: *A27 you got another thing coming: diagnosis and prognostication in pulmonary hypertension*. American Thoracic Society; 2018. p. A7649. (American Thoracic Society International Conference Abstracts) 2019;156(2):323–37.
- Benza RL, Gomberg-Maitland M, Elliott CG, Farber HW, Foreman AJ, Frost AE, et al. Predicting survival in patients with pulmonary arterial hypertension: the REVEAL risk score calculator 2.0 and comparison with ESC/ERS-based risk assessment strategies. *Chest*. 2019:1–15.
- Blumberg FC, Arzt M, Lange T, Schroll S, Pfeifer M, Wensel R. Impact of right ventricular reserve on exercise capacity and survival in patients with pulmonary hypertension. *Eur J Heart Fail*. 2013;15(7):771–5.

- Boucly A, Weatherald J, Savale L, Jaïs X, Cottin V, Prevot G, et al. Risk assessment, prognosis and guideline implementation in pulmonary arterial hypertension. *Eur Respir J*. 2017;50(2):1–10.
- Braganza M, Shaw J, Solverson K, Vis D, Janovcik J, Varughese RA, et al. A prospective evaluation of the diagnostic accuracy of the physical examination for pulmonary hypertension. *Chest*. 2019;155(5):982–90.
- Brenot F. Primary pulmonary hypertension: case series from France. *Chest*. 1994;105(2 Suppl):33S–6S.
- Buys R, Avila A, Cornelissen VA. Exercise training improves physical fitness in patients with pulmonary arterial hypertension: a systematic review and meta-analysis of controlled trials. *BMC Pulm Med*. 2015;15(1):40.
- Castelain V, Hervé P, Lecarpentier Y, Duroux P, Simonneau G, Chemla D. Pulmonary artery pulse pressure and wave reflection in chronic pulmonary thromboembolism and primary pulmonary hypertension. *J Am Coll Cardiol*. 2001;37(4):1085–92.
- Chatterjee K. The Swan-Ganz catheters: past, present, and future: a viewpoint. *Circulation*. 2009;119(1):147–52.
- Chemla D, Hebert JL, Coirault C, Salmeron S, Zamani K, Lecarpentier Y. Matching dirotic notch and mean pulmonary artery pressures: implications for effective arterial elastance. *Am J Physiol Circ Physiol*. 1996;271(4):H1287–95.
- Chemla D, Lau EMT, Papelier Y, Attal P, Hervé P. Pulmonary vascular resistance and compliance relationship in pulmonary hypertension. *Eur Respir J*. 2015;46(4):1178–89.
- Chemla D, Weatherald J, Lau EMT, Savale L, Boucly A, Attal P, et al. Clinical and hemodynamic correlates of pulmonary arterial stiffness in incident, untreated patients with idiopathic pulmonary arterial hypertension. *Chest*. 2018;154(4):882–92.
- Coghlan JG, Denton CP, Grünig E, Bonderman D, Distler O, Khanna D, et al. Evidence-based detection of pulmonary arterial hypertension in systemic sclerosis: the DETECT study. *Ann Rheum Dis*. 2014;73(7):1340–9.
- Colman R, Whittingham H, Tomlinson G, Granton J. Utility of the physical examination in detecting pulmonary hypertension. A mixed methods study. *PLoS One*. 2014;9(10):e108499.
- Correale M, Tricarico L, Ferraretti A, Monaco I, Concilio M, Padovano G, et al. Cardiopulmonary exercise test predicts right heart catheterization. *Eur J Clin Invest*. 2017;47(12):1–8.
- Crapo RO, Casaburi R, Coates AL, Enright PL, MacIntyre NR, McKay RT, et al. American Thoracic Society ATS statement: guidelines for the six-minute walk test. *Am J Respir Crit Care Med*. 2002;166:111–7.
- Crystal GJ, Pagel PS. Right ventricular perfusion: physiology and clinical implications. *Anesthesiology*. 2018;128(1):202–18.
- D'Alonzo GE, Barst RJ, Ayres SM, Bergofsky EH, Brundage BH, Detre KM, et al. Survival in patients with primary pulmonary hypertension. Results from a national prospective registry. *Ann Intern Med*. 1991;115(5):343–9.
- Dantzker DR, D'Alonzo GE, Bower JS, Popat K, Crevey BJ. Pulmonary gas exchange during exercise in patients with chronic obliterative pulmonary hypertension. *Am Rev Respir Dis*. 1984;130(3):412–6.
- Deaño RC, Glassner-Kolmin C, Rubenfire M, Frost A, Visovatti S, McLaughlin VV, et al. Referral of patients with pulmonary hypertension diagnoses to tertiary pulmonary hypertension centers: the multicenter RePHerral study. *JAMA Intern Med*. 2013;173(10):887–93.
- Deboeck G, Scoditti C, Huez S, Vachiéry JL, Lamotte M, Sharples L, et al. Exercise testing to predict outcome in idiopathic versus associated pulmonary arterial hypertension. *Eur Respir J*. 2012;40(6):1410–9.
- Diller GP, Dimopoulos K, Okonko D, Li W, Babu-Narayan SV, Broberg CS, et al. Exercise intolerance in adult congenital heart disease: comparative severity, correlates, and prognostic implication. *Circulation*. 2005;112(6):828–35.
- Enright PL, Sherrill DL. Reference equations for the six-minute walk in healthy adults. *Am J Respir Crit Care Med*. 1998;161(4 Pt 1):1396.
- Farber HW, Miller DP, McGoon MD, Frost AE, Benton WW, Benza RL. Predicting outcomes in pulmonary arterial hypertension based on the 6-minute walk distance. *J Heart Lung Transplant*. 2015;34(3):362–8.
- Farina S, Correale M, Bruno N, Paolillo S, Salvioni E, Badagliacca R, et al. The role of cardiopulmonary exercise tests in pulmonary arterial hypertension. *Eur Respir Rev*. 2018a;27(148):1–10.
- Farina S, Bruno N, Agalbatto C, Contini M, Cassandro R, Elia D, et al. Physiological insights of exercise hyperventilation in arterial and chronic thromboembolic pulmonary hypertension. *Int J Cardiol*. 2018b;259:178–82.
- Farnsworth CW, Bailey AL, Jaffe AS, Scott MG. Diagnostic concordance between NT-proBNP and BNP for suspected heart failure. *Clin Biochem*. 2018;59(April):50–5.
- Ferrazza AM, Martolini D, Valli G, Palange P. Cardiopulmonary exercise testing in the functional and prognostic evaluation of patients with pulmonary diseases. *Respiration*. 2009;77(1):3–17.
- Fijalkowska A, Kurzyna M, Tobicki A, Szewczyk G, Florczyk M, Pruszczyk P, et al. Serum N-terminal brain natriuretic peptide as a prognostic parameter in patients with pulmonary hypertension. *Chest*. 2006;129(5):1313–21.
- Fisher MR, Forfia PR, Chamera E, Houston-Harris T, Champion HC, Girgis RE, et al. Accuracy of doppler echocardiography in the hemodynamic assessment of pulmonary hypertension. *Am J Respir Crit Care Med*. 2009;179(7):615–21.
- Foris V, Kovacs G, Tscherner M, Olschewski A, Olschewski H. Biomarkers in pulmonary hypertension: what do we know? *Chest*. 2013;144(1):274–83.
- Fujimoto N, Borlaug BA, Lewis GD, Hastings JL, Shafer KM, Bhella PS, et al. Hemodynamic responses to rapid saline loading: the impact of age, sex, and heart failure. *Circulation*. 2013;127(1):55–62.

- Galiè N, Manes A, Negro L, Palazzini M, Bacchi-Reggiani ML, Branzi A. A meta-analysis of randomized controlled trials in pulmonary arterial hypertension. *Eur Heart J*. 2009;30(4):394–403.
- Galiè N, Humbert M, Vachiery J-L, Gibbs S, Lang I, Torbicki A, et al. 2015 ESC/ERS guidelines for the diagnosis and treatment of pulmonary hypertension. *Eur Heart J*. 2015;46(4):903–75.
- Galiè N, Jansa P, Pulido T, Channick RN, Delcroix M, Ghofrani HA, et al. SERAPHIN haemodynamic sub-study: the effect of the dual endothelin receptor antagonist macitentan on haemodynamic parameters and NT-proBNP levels and their association with disease progression in patients with pulmonary arterial hypertension. *Eur Heart J*. 2017;38(15):1147–55.
- Galiè N, Channick RN, Frantz RP, Grünig E, Jing ZC, Moiseeva O, et al. Risk stratification and medical therapy of pulmonary arterial hypertension. *Eur Respir J*. 2019;53(1):1801889.
- Gan CTJ, Lankhaar JW, Westerhof N, Marcus JT, Becker A, Twisk JWR, et al. Noninvasively assessed pulmonary artery stiffness predicts mortality in pulmonary arterial hypertension. *Chest*. 2007;132(6):1906–12.
- Garcia-Rivas G, Jerjes-Sánchez C, Rodriguez D, Garcia-Pelaez J, Trevino V. A systematic review of genetic mutations in pulmonary arterial hypertension. *BMC Med Genet*. 2017;18(1):1–10.
- Ghio S, Schirinzì S, Pica S. Pulmonary arterial compliance: how and why should we measure it? *Glob Cardiol Sci Pract*. 2015;2015(4):58.
- Ghio S, D'Alto M, Badagliacca R, Vitulo P, Argiento P, Mulè M, et al. Prognostic relevance of pulmonary arterial compliance after therapy initiation or escalation in patients with pulmonary arterial hypertension. *Int J Cardiol*. 2017;230:53–8.
- Gilbert C, Brown MCJ, Cappelleri JC, Carlsson M, McKenna SP. Estimating a minimally important difference in pulmonary arterial hypertension following treatment with sildenafil. *Chest*. 2009;135(1):137–42.
- Grapsa J, Dawson D, Nihoyannopoulos P. Assessment of right ventricular structure and function in pulmonary hypertension. *J Cardiovasc Ultrasound*. 2011;19(3):115.
- Groepenhoff H, Vonk-Noordegraaf A, Boonstra A, Spreeuwenberg MD, Postmus PE, Bogaard HJ. Exercise testing to estimate survival in pulmonary hypertension. *Med Sci Sports Exerc*. 2008;40(10):1725–32.
- Groepenhoff H, Westerhof N, Jacobs W, Boonstra A, Postmus PE, Vonk-Noordegraaf A. Exercise stroke volume and heart rate response differ in right and left heart failure. *Eur J Heart Fail*. 2010;12(7):716–20.
- Groepenhoff H, Vonk-Noordegraaf A, van de Veerdonk MC, Boonstra A, Westerhof N, Bogaard HJ. Prognostic relevance of changes in exercise test variables in pulmonary arterial hypertension. *PLoS One*. 2013;8(9):1–11.
- Grünig E, Peacock AJ. Imaging the heart in pulmonary hypertension: an update. *Eur Respir Rev*. 2015;24(138):653–64.
- Grünig E, Weissmann S, Ehlken N, Fijalkowska A, Fischer C, Fourme T, et al. Stress doppler echocardiography in relatives of patients with idiopathic and familial pulmonary arterial hypertension results of a multi-center European analysis of pulmonary artery pressure response to exercise and hypoxia. *Circulation*. 2009;119(13):1747–57.
- Haddad F, Doyle R, Murphy DJ, Hunt SA. Right ventricular function in cardiovascular disease, part II: pathophysiology, clinical importance, and management of right ventricular failure. *Circulation*. 2008;117(13):1717–31.
- Hadinnapola C, Li Q, Su L, Pepke-Zaba J, Toshner M. The resistance-compliance product of the pulmonary circulation varies in health and pulmonary vascular disease. *Physiol Rep*. 2015;3(4):1–9.
- Halank M, Einsle F, Lehman S, Bremer H, Ewert R, Wilkens H, et al. Exercise capacity affects quality of life in patients with pulmonary hypertension. *Lung*. 2013;191(4):337–43.
- Hall C. Essential biochemistry and physiology of (NT-pro) BNP. *Eur J Heart Fail*. 2004;6(3):257–60.
- Hirani N, Brunner N, Kapasi A, Chandy G, Rudski L, Paterson I, et al. Canadian Cardiovascular Society/Canadian Thoracic Society position statement on pulmonary hypertension. *Can J Cardiol*. 2020;36(7):977–92.
- Hoepfer MM, Pletz MW, Golpon H, Welte T. Prognostic value of blood gas analyses in patients with idiopathic pulmonary arterial hypertension. *Eur Respir J*. 2007;29(5):944–50.
- Hoepfer MM, Kramer T, Pan Z, Eichstaedt CA, Spiesshoefer J, Benjamin N, et al. Mortality in pulmonary arterial hypertension: prediction by the 2015 European pulmonary hypertension guidelines risk stratification model. *Eur Respir J*. 2017;50(2):1–10.
- Hoepfer MM, Pittrow D, Opitz C, Gibbs JSR, Rosenkranz S, Grünig E, et al. Risk assessment in pulmonary arterial hypertension. *Eur Respir J*. 2018;16(9–10):342–4.
- Holverda S, Gan CTJ, Marcus JT, Postmus PE, Boonstra A, Vonk-Noordegraaf A. Impaired stroke volume response to exercise in pulmonary arterial hypertension. *J Am Coll Cardiol*. 2006;47(8):1732–3.
- Howard LS, Ferrari P, Mehta S. Physicians' and patients' expectations of therapies for pulmonary arterial hypertension: where do they meet? *Eur Respir Rev*. 2014;23(134):458–68.
- Humbert M, Guignabert C, Bonnet S, Dorfmueller P, Klinger JR, Nicolls MR, et al. Pathology and pathobiology of pulmonary hypertension: state of the art and research perspectives. *Eur Respir J*. 2019;53(1):1801887.
- Jing ZC, Xu XQ, Badesch DB, Jiang X, Wu Y, Liu JM, et al. Pulmonary function testing in patients with pulmonary arterial hypertension. *Respir Med*. 2009;103(8):1136–42.
- Khirfan G, Naal T, Abuhalimeh B, Newman J, Heresi GA, Dweik RA, et al. Hypoxemia in patients with idiopathic or heritable pulmonary arterial hypertension. *PLoS One*. 2018;13(1):1–11.

- Kind T, Mauritz G-J, Marcus JT, van de Veerdonk M, Westerhof N, Vonk-Noordegraaf A. Right ventricular ejection fraction is better reflected by transverse rather than longitudinal wall motion in pulmonary hypertension. *J Cardiovasc Magn Reson.* 2010;12:35.
- Kovacs G, Berghold A, Scheidl S, Olschewski H. Pulmonary arterial pressure during rest and exercise in healthy subjects: a systematic review. *Eur Respir J.* 2009;34(4):888–94.
- Kylhammar D, Kjellström B, Hjalmarsson C, Jansson K, Nisell M, Söderberg S, et al. A comprehensive risk stratification at early follow-up determines prognosis in pulmonary arterial hypertension. *Eur Heart J.* 2017;39(47):4175–81.
- Lador F, Bringard A, Bengueddache S, Ferretti G, Bendjelid K, Soccal PM, et al. Kinetics of cardiac output at the onset of exercise in precapillary pulmonary hypertension. *Biomed Res Int.* 2016pf: <https://doi.org/10.1155/2016/6050193>.
- Lajoie AC, Lauzière G, Lega JC, Lacasse Y, Martin S, Simard S, et al. Combination therapy versus monotherapy for pulmonary arterial hypertension: a meta-analysis. *Lancet Respir Med.* 2016;4(4):291–305.
- Lankhaar JW, Westerhof N, Faes TJC, Marques KMJ, Marcus JT, Postmus PE, et al. Quantification of right ventricular afterload in patients with and without pulmonary hypertension. *Am J Physiol Heart Circ Physiol.* 2006;291(4):1731–7.
- Lankhaar JW, Westerhof N, Faes TJC, Tji-Joong Gan C, Marques KM, Boonstra A, et al. Pulmonary vascular resistance and compliance stay inversely related during treatment of pulmonary hypertension. *Eur Heart J.* 2008;29(13):1688–95.
- Laveneziana P, Garcia G, Joureau B, Nicolas-Jilwan F, Brahimi T, Laviolette L, et al. Dynamic respiratory mechanics and exertional dyspnoea in pulmonary arterial hypertension. *Eur Respir J.* 2013;41(3):578–87.
- Lee WTN, Peacock AJ, Johnson MK. The role of per cent predicted 6-min walk distance in pulmonary arterial hypertension. *Eur Respir J.* 2010;36(6):1294–301.
- Leuchte HH, El Nounou M, Tuerpe JC, Hartmann B, Baumgartner RA, Vogeser M, et al. N-terminal pro-brain natriuretic peptide and renal insufficiency as predictors of mortality in pulmonary hypertension. *Chest.* 2007;131(2):402–9.
- Lilly LS. Section I. Fundamentals of cardiovascular disease; genetics and personalized medicine; evaluation of the patient. In: Miller A, Soukoulis V, LL, editor. Braunwald's heart disease review and assessment. 9th ed. Elsevier, Philadelphia; 2012. p. 1–86.
- Low AT, Medford ARL, Millar AB, Tulloh RMR. Lung function in pulmonary hypertension. *Respir Med.* 2015;109(10):1244–9.
- Mahapatra S, Nishimura RA, Oh JK, McGoon MD. The prognostic value of pulmonary vascular capacitance determined by doppler echocardiography in patients with pulmonary arterial hypertension. *J Am Soc Echocardiogr.* 2006;19(8):1045–50.
- Mathai SC, Puhon MA, Lam D, Wise RA. The minimal important difference in the 6-minute walk test for patients with pulmonary arterial hypertension. *Am J Respir Crit Care Med.* 2012;186(5):428–33.
- Mauritz GJ, Rizopoulos D, Groepenhoff H, Tiede H, Felix J, Eilers P, et al. Usefulness of serial N-terminal ProB-type natriuretic peptide measurements for determining prognosis in patients with pulmonary arterial hypertension. *Am J Cardiol.* 2011;108(11):1645–50.
- McCabe C, Bennett M, Doughty N, MacKenzie Ross R, Sharples L, Pepke-Zaba J. Patient-reported outcomes assessed by the CAMPHOR questionnaire predict clinical deterioration in idiopathic pulmonary arterial hypertension and chronic thromboembolic pulmonary hypertension. *Chest.* 2013;144(2):522–30.
- McCabe C, White PA, Hoole SP, Axell RG, Priest AN, Gopalan D, et al. Right ventricular dysfunction in chronic thromboembolic obstruction of the pulmonary artery: a pressure-volume study using the conductance catheter. *J Appl Physiol.* 2014;116(4):355–63.
- McCollister D, Shaffer S, Badesch DB, Filusch A, Hunsche E, Schuler R, et al. Development of the Pulmonary Arterial Hypertension-Symptoms and Impact (PAH-SYMPACT(R)) questionnaire: a new patient-reported outcome instrument for PAH. *Respir Res.* 2016;17(1):72.
- McGoon MD, Ferrari P, Armstrong I, Denis M, Howard LS, Lowe G, et al. The importance of patient perspectives in pulmonary hypertension. *Eur Respir J.* 2019;53(1):1801919.
- McLaughlin VV, Shillington A, Rich S. Survival in primary pulmonary hypertension: the impact of epoprostenol therapy. *Circulation.* 2002;106(12):1477–82.
- Meyer FJ. Peripheral airway obstruction in primary pulmonary hypertension. *Thorax.* 2002;57(6):473–6.
- Miyamoto S, Nagaya N, Satoh T, Kyotani S, Sakamaki F, Fujita M, et al. Clinical correlates and prognostic significance of six-minute walk test in patients with primary pulmonary hypertension. *Am J Respir Crit Care Med.* 2000;161(2):487–92.
- Morrell NW, Aldred MA, Chung WK, Elliott CG, Nichols WC, Soubrier F, et al. Genetics and genomics of pulmonary arterial hypertension. *Eur Respir J.* 2019;53(1):1801899.
- Mukerjee D, Yap LB, Holmes AM, Nair D, Ayrton P, Black CM, et al. Significance of plasma N-terminal pro-brain natriuretic peptide in patients with systemic sclerosis-related pulmonary arterial hypertension. *Respir Med.* 2003;97(11):1230–6.
- Murgo JP, Westerhof N. Input impedance of the pulmonary arterial system in normal man. Effects of respiration and comparison to systemic impedance. *Circ Res.* 1984;54(6):666–73.
- Naeije R. Physiology of the pulmonary circulation and the right heart. *Curr Hypertens Rep.* 2013;15(6):623–31.
- Naeije R, Van De Borne P. Clinical relevance of autonomic nervous system disturbances in pulmonary arterial hypertension. *Eur Respir J.* 2009;34(4):792–4.
- Naeije R, Vachiery JL, Yerly P, Vanderpool R. The transpulmonary pressure gradient for the diagno-

- sis of pulmonary vascular disease. *Eur Respir J*. 2013;41(1):217–23.
- Nagaya N, Nishikimi T, Okano Y, Uematsu M, Satoh T, Kyotani S, et al. Plasma brain natriuretic peptide levels increase in proportion to the extent of right ventricular dysfunction in pulmonary hypertension. *J Am Coll Cardiol*. 1998;31(1):202–8.
- Nagaya N, Satoh T, Kyotani S, Sakamaki F, Kakishita M, Fukushima K, et al. Plasma brain natriuretic peptide as a prognostic indicator in patients with primary pulmonary hypertension. *Circulation*. 2000;102(8):865–70.
- Nickel N, Golpon H, Greer M, Knudsen L, Olsson K, Westerkamp V, et al. The prognostic impact of follow-up assessments in patients with idiopathic pulmonary arterial hypertension. *Eur Respir J*. 2012;39(3):589–96.
- Nossaman BD, Scruggs BA, Nossaman VE, Murthy SN, Kadowitz PJ. History of right heart catheterization: 100 years of experimentation and methodology development. *Cardiol Rev*. 2010;18(2):94–101.
- Olsson KM, Fuge J, Meyer K, Welte T, Hoepfer MM. More on idiopathic pulmonary arterial hypertension with a low diffusing capacity. *Eur Respir J*. 2017;50(2):0–3.
- Oudiz RJ, Barst RJ, Hansen JE, Sun XG, Garofano R, Wu X, et al. Cardiopulmonary exercise testing and six-minute walk correlations in pulmonary arterial hypertension. *Am J Cardiol*. 2006;97(1):123–6.
- Oudiz RJ, Midde R, Hovenesyan A, Sun XG, Roveran G, Hansen JE, et al. Usefulness of right-to-left shunting and poor exercise gas exchange for predicting prognosis in patients with pulmonary arterial hypertension. *Am J Cardiol*. 2010;105(8):1186–91.
- Peacock AJ, Noordegraaf AV. Cardiac magnetic resonance imaging in pulmonary arterial hypertension. *Eur Respir Rev*. 2013;22(130):526–34.
- Peluso D, Tona F, Muraru D, Romeo G, Cucchini U, Marra M, et al. Right ventricular geometry and function in pulmonary hypertension: non-invasive evaluation. *Diseases*. 2014;2(3):274–95.
- Permutt S, Bromberger-Barnea B, Bane HN. Alveolar pressure, pulmonary venous pressure, and the vascular waterfall. *Med Thorac*. 1962;19:239–60.
- Pinsky MR. The right ventricle: interaction with the pulmonary circulation. *Crit Care*. 2016;20:266.
- Provencher S, Sitbon O, Humbert M, Cabrol S, Jaïs X, Simonneau G. Long-term outcome with first-line bosentan therapy in idiopathic pulmonary arterial hypertension. *Eur Heart J*. 2006;27(5):589–95.
- Ramos RP, Arakaki JSO, Barbosa P, Treptow E, Valois FM, Ferreira EVM, et al. Heart rate recovery in pulmonary arterial hypertension: relationship with exercise capacity and prognosis. *Am Heart J*. 2012;163(4):580–8.
- Reis A, Santos M, Vicente M, Furtado I, Cruz C, Melo A, et al. Health-related quality of life in pulmonary hypertension and its clinical correlates: a cross-sectional study. *Biomed Res Int*. 2018;2018:3924517.
- Romano AM, Tomaselli S, Gualtieri G, Zoia MC, Fanfulla F, Berrayah L, et al. Respiratory function in precapillary pulmonary hypertension. *Monaldi Arch Chest Dis*. 1993;48:201–4.
- Rosenkranz S, Preston IR. Right heart catheterisation: best practice and pitfalls in pulmonary hypertension. *Eur Respir Rev*. 2015;24(138):642–52.
- Ross RM, Beck KC, Casaburi R, Johnson BD, Marciniuk DD, Wagner PD, et al. ATS/ACCP statement on cardiopulmonary exercise testing (multiple letters). *Am J Respir Crit Care Med*. 2001;167(10):1451.
- Rudski LG, Lai WW, Afilalo J, Hua L, Handschumacher MD, Chandrasekaran K, et al. Guidelines for the echocardiographic assessment of the right heart in adults: a report from the American Society of Echocardiography. Endorsed by the European Association of Echocardiography, a registered branch of the European Society of Cardiology, and the Canadian Society of Echocardiography. *J Am Soc Echocardiogr*. Elsevier. 2010;23(7):685–713.
- Sachdev A, Villarraga HR, Frantz RP, McGoon MD, Hsiao JF, Maalouf JF, et al. Right ventricular strain for prediction of survival in patients with pulmonary arterial hypertension. *Chest*. 2011;139(6):1299–309.
- Saouti N, Westerhof N, Postmus PE, Vonk-Noordegraaf A. The arterial load in pulmonary hypertension. *Eur Respir Rev*. 2010;19(117):197–203.
- Savarese G, Paolillo S, Costanzo P, D'Amore C, Cecere M, Losco T, et al. Do changes of 6-minute walk distance predict clinical events in patients with pulmonary arterial hypertension?: a meta-analysis of 22 randomized trials. *J Am Coll Cardiol*. 2012;60(13):1192–201.
- Schäfer M, Myers C, Brown RD, Frid MG, Tan W, Hunter K, et al. Pulmonary arterial stiffness: toward a new paradigm in pulmonary arterial hypertension pathophysiology and assessment. *Curr Hypertens Rep*. 2016;18(1):1–13.
- Schwaiblmair M, Faul C, von Scheidt W, Berghaus TM. Ventilatory efficiency testing as prognostic value in patients with pulmonary hypertension. *BMC Pulm Med*. 2012;12(1):1.
- Seo HS, Lee H. Assessment of right ventricular function in pulmonary hypertension with multimodality imaging. *J Cardiovasc Imaging*. 2018;26(4):189–200.
- Simonneau G, Montani D, Celermajer DS, Denton CP, Gatzoulis MA, Krowka M, et al. Haemodynamic definitions and updated clinical classification of pulmonary hypertension. *Eur Respir J*. 2019;53(1):1801913.
- Sitbon O, Morrell NW. Pathways in pulmonary arterial hypertension: the future is here. *Eur Respir Rev*. 2012;21(126):321–7.
- Sitbon O, Humbert M, Nunes H, Parent F, Garcia G, Hervé P, et al. Long-term intravenous epoprostenol infusion in primary pulmonary hypertension. *J Am Coll Cardiol*. 2002;40(4):780–8.
- Stevens GR, Garcia-Alvarez A, Sahni S, Garcia MJ, Fuster V, Sanz J. RV dysfunction in pulmonary hypertension is independently related to pulmonary artery stiffness. *JACC Cardiovasc Imaging*. 2012;5(4):378–87.
- Sun XG, Hansen JE, Oudiz RJ, Wasserman K. Exercise pathophysiology in patients with primary pulmonary hypertension. *Circulation*. 2001a;104(4):429–35.
- Sun XG, Hansen JE, Oudiz RJ, Wasserman K. Exercise pathophysiology in patients with primary hypertension. *5-Minute Anesth Consult*. 2001b:429–35.

- Sun XG, Hansen JE, Oudiz RJ, Wasserman K. Gas exchange detection of exercise-induced right-to-left shunt in patients with primary pulmonary hypertension. *Circulation*. 2002;105(1):54–60.
- Sun XG, Hansen JE, Oudiz RJ, Wasserman K. Pulmonary function in primary pulmonary hypertension. *J Am Coll Cardiol*. 2003;41(6):1028–35.
- Sutton G, Harris A, Leatham A. Second heart sound in pulmonary hypertension. *Br Heart J*. 1968;30(6):743–56.
- Tei C, Ling LH, Hodge DO, Bailey KR, Oh JK, Rodeheffer RJ, et al. New index of combined systolic and diastolic myocardial performance: a simple and reproducible measure of cardiac function—a study in normals and dilated cardiomyopathy. *J Cardiol*. 1995;26(6):357–66.
- Tello K, Dalmer A, Axmann J, Vanderpool R, Ghofrani HA, Naeije R, et al. Reserve of right ventricular-arterial coupling in the setting of chronic overload. *Circ Heart Fail*. 2019;12(1):e005512.
- Thenappan T, Prins KW, Pritzker MR, Scandurra J, Volmers K, Weir EK. The critical role of pulmonary arterial compliance in pulmonary hypertension. *Ann Am Thorac Soc*. 2016;13(2):276–84.
- Trip P, Nossent EJ, De Man FS, Van Den Berk IAH, Boonstra A, Groepenhoff H, et al. Severely reduced diffusion capacity in idiopathic pulmonary arterial hypertension: patient characteristics and treatment responses. *Eur Respir J*. 2013;42(6):1575–85.
- Tulevski II. Increased brain and atrial natriuretic peptides in patients with chronic right ventricular pressure overload: correlation between plasma neurohormones and right ventricular dysfunction. *Heart*. 2001;86(1):27–30.
- Uchiyama N, Yuasa T, Miyata M, Horizoe Y, Chaen H, Kubota K, et al. Correlation of right ventricular wall stress with plasma B-type natriuretic peptide levels in patients with pulmonary hypertension. *Circ J*. 2019;83(6):1278–85.
- van de Veerdonk MC, Kind T, Marcus JT, Mauritz G-J, Heymans MW, Bogaard H-J, et al. Progressive right ventricular dysfunction in patients with pulmonary arterial hypertension responding to therapy. *J Am Coll Cardiol*. 2011;58(24):2511–9.
- van Wolferen SA, Marcus JT, Boonstra A, Marques KMJ, Bronzwaer JGF, Spreeuwenberg MD, et al. Prognostic value of right ventricular mass, volume, and function in idiopathic pulmonary arterial hypertension. *Eur Heart J*. 2007;28(10):1250–7.
- Van Wolferen SA, Marcus JT, Westerhof N, Spreeuwenberg MD, Marques KMJ, Bronzwaer JGF, et al. Right coronary artery flow impairment in patients with pulmonary hypertension. *Eur Heart J*. 2008;29(1):120–7.
- van Wolferen SA, van de Veerdonk MC, Mauritz G-J, Jacobs W, Marcus JT, Marques KMJ, et al. Clinically significant change in stroke volume in pulmonary hypertension. *Chest*. 2011;139(5):1003–9.
- Velez-Roa S, Ciarka A, Najem B, Vachieri JL, Naeije R, Van De Borne P. Increased sympathetic nerve activity in pulmonary artery hypertension. *Circulation*. 2004;110(10):1308–12.
- Vonk Noordegraaf A, Westerhof BE, Westerhof N. The relationship between the right ventricle and its load in pulmonary hypertension. *J Am Coll Cardiol*. 2017;69(2):236–43.
- Vonk-Noordegraaf A, Haddad F, Chin KM, Forfia PR, Kawut SM, Lumens J, et al. Right heart adaptation to pulmonary arterial hypertension: physiology and pathobiology. *J Am Coll Cardiol*. 2013;62(25 Suppl):22–33.
- Wang Y, Gutman JM, Heilbron D, Wahr D, Schiller NB. Atrial volume in a normal adult population by two-dimensional echocardiography. *Chest*. 1984;86(4):595–601.
- Weatherald J, Farina S, Bruno N, Laveneziana P. Cardiopulmonary exercise testing in pulmonary hypertension. *Ann Am Thorac Soc*. 2017;14(July):S84–92.
- Wensel R, Opitz CF, Anker SD, Winkler J, Höffken G, Kleber FX, et al. Assessment of survival in patients with primary pulmonary hypertension: importance of cardiopulmonary exercise testing. *Circulation*. 2002;106(3):319–24.
- Wensel R, Francis DP, Meyer FJ, Opitz CF, Bruch L, Halank M, et al. Incremental prognostic value of cardiopulmonary exercise testing and resting haemodynamics in pulmonary arterial hypertension. *Int J Cardiol*. 2013;167(4):1193–8.
- Yasunobu Y, Oudiz RJ, Sun XG, Hansen JE, Wasserman K. End-tidal Pco₂ abnormality and exercise limitation in patients with primary pulmonary hypertension. *Chest*. 2005;127(5):1637–46.
- Yeo KTJ, Wu AHB, Apple FS, Kroll MH, Christenson RH, Lewandrowski KB, et al. Multicenter evaluation of the Roche NT-proBNP assay and comparison to the Biosite Triage BNP assay. *Clin Chim Acta*. 2003;338(1–2):107–15.
- Yorke J, Corris P, Gaine S, Gibbs JSR, Kiely DG, Harries C, et al. emPHasis-10: development of a health-related quality of life measure in pulmonary hypertension. *Eur Respir J*. 2014;43(4):1106–13.
- Zelniker TA, Huscher D, Vonk-Noordegraaf A, Ewert R, Lange TJ, Klose H, et al. The 6MWT as a prognostic tool in pulmonary arterial hypertension: results from the COMPERA registry. *Clin Res Cardiol*. 2018;107(6):460–70.
- Zhao QH, Wang L, Pudasaini B, Jiang R, Yuan P, Gong SG, et al. Cardiopulmonary exercise testing improves diagnostic specificity in patients with echocardiography-suspected pulmonary hypertension. *Clin Cardiol*. 2017;40(2):95–101.
- Zuckerman WA, Turner ME, Kerstein J, Torres A, Vincent JA, Krishnan U, et al. Safety of cardiac catheterization at a center specializing in the care of patients with pulmonary arterial hypertension. *Pulm Circ*. 2013;3(4):831–9.



Monitoring and Management of Acute Pulmonary Embolism

55

Jenna McNeill and Richard N. Channick

Introduction

Acute pulmonary embolism (PE) is a commonly encountered medical condition that contributes up to 15% of total hospital mortality (Lehnert et al. 2018; Scarvelis et al. 2010). In the United States, PE has been associated with 200,000 deaths annually and the incidence of PE has been quoted to be between 600,000 to slightly less than one million annually (Dalen and Alpert 1975; Bell and Simon 1982). The true incidence of PE might be underestimated because it can go undiagnosed, with up to one-third of fatal PEs being identified post-mortem (Goldhaber et al. 1982; Stein and Henry 1995). The mortality associated with PE is linked to the categorization of disease severity: massive, sub-massive, or low-risk PE. Early recognition and treatment of massive PE is vital, as massive PE is associated with a mortality rate that can exceed 50% (Goldhaber et al. 1999). To combat the rapid clinical deterioration that can occur with PE, it is important to understand the natural history, pathophysiology,

and therapeutic options in acute PE, changes in hemodynamics that occur in the right ventricle (RV), and options for treatment.

Pathophysiology

Pulmonary embolism at a fundamental level derives from clot formation in peripheral veins which dislodge and then pass to the pulmonary vasculature with consequent clinical and laboratory abnormalities. Increased patient risk for pulmonary embolism is based on the principles of Virchow's triad which involve alterations in blood flow, vascular endothelial injury, or inherited or acquired hypercoagulable states. Inherited risk factors for clot formation include factor V leiden mutation, prothrombin gene mutation, protein S deficiency, protein C deficiency, and antithrombin deficiency. Acquired risk factors for clot formation include malignancy, trauma, surgery, immobilization, drugs (e.g., hormonal therapy, tamoxifen, steroids), pregnancy, tobacco use, and chronic obstructive lung disease. Most PEs arise from proximal lower extremity veins and commonly PEs occur in conjunction with deep venous thrombosis. The mortality and hemodynamic compromise that is associated with high-risk PE arise secondary to acute increase in pulmonary vascular resistance (PVR) and RV failure. The proposed mechanism for the increase in PVR involves both mechanical

J. McNeill (✉)

Massachusetts General Hospital, Department of Pulmonary and Critical Care, Boston, MA, USA
e-mail: Jmcneill2@partners.org

R. N. Channick

UCLA Medical Center, UCLA David Geffen School of Medicine, Pulmonary and Critical Care Division, Los Angeles, CA, USA
e-mail: Rchannick@mednet.ucla.edu

obstructions from the emboli as well as vasoconstrictive mediators.

In patients without underlying cardiac or pulmonary conditions, RV pressure elevation occurs when 25–30% of the pulmonary vasculature is occluded. RV failure is associated with 50–75% of pulmonary vasculature occlusion (McIntyre and Sasahara 1971; McIntyre and Sasahara 1977). The emboli create ventilation and perfusion mismatch. Dead space, ventilation without perfusion, is created in areas of the lungs distal to the clot. In acute PE, the total dead space will increase which will cause a rise in arterial PCO₂. This rise in PCO₂ is sensed by the medullary chemoreceptors and in response patients will have a rise in total minute ventilation (Goldhaber and Elliott 2003). By increasing total minute ventilation, acute PE patients can present with normal to below normal PCO₂ (Goldhaber and Elliott 2003). There is also shunting as vascular compromise reduces surfactant production which results in atelectasis in parts of the lungs. Hypoxemia can also be seen in the setting of acute PE secondary to the low partial pressure of oxygen within the venous system (Goldhaber and Elliott 2003). In the setting of low cardiac output, oxygen is extracted by the tissues at a higher rate. When the oxygen content in the venous system is low there is an enhanced effect of ventilation and perfusion mismatch as it moves through areas of atelectatic lung.

The notion pulmonary vasculature occlusion is the sole cause for elevated PVR and RV failure has been challenged by cases where clot burden less than 25% has caused a significant elevation in mean pulmonary artery pressure (Miller et al. 1998; Bshouty 2012; Alpert et al. 1978). This has raised further investigation into the role of vasoconstrictive mediators in the setting of acute PE. The most commonly discussed vasoconstrictive mediators include thromboxane-A₂ (TxA₂), serotonin, and endothelin-1.

Vasoconstrictive Mediators

Thromboxane-A₂(TxA₂) is a potent vasoconstrictor that is one of the end products of arachidonic acid metabolism (Smulders 2000). The

primary source of TxA₂ production is platelets which aggregate in the setting of clot formation (Utsonomiya et al. 1982). Many studies have examined the serum concentration of TxA₂ or its degradation product thromboxane B₂ in the setting of PE and have found that TxA₂ rises acutely after embolus formation and higher levels are associated with greater mortality (Reeves et al. 1983). The inhibition of cyclooxygenase (COX), which is the upstream enzyme for the formation of TxA₂ in arachidonic acid metabolism, can reduce the increase in PVR and pulmonary artery pressure which is associated with a PE (Todd et al. 1983; Weidner 1979).

Serotonin has been associated with the formation of increased pulmonary artery pressures in both the acute and chronic PE. The role of serotonin as a pulmonary vasoconstrictor in PE was first described by Comroe in 1952 and he proposed that platelets were the source of serotonin release and the consequent pulmonary hypertension, bronchoconstriction and eventually bradycardia, hypotension, and apnea (Daily and Moulder 1966). A number of animal studies have examined the role of serotonin as the cause of the elevated PVR in patients with PE. Depletion of serotonin by agents such as reserpine or cyprohepatine reduces the PE-induced rise in PVR whereas serotonin reuptake inhibitors, such as fluoxetine, worsen PVR and lead to hypotension (Chou and Canning 2011; Utsonomiya et al. 1981; Rosoff et al. 1971).

Endothelin-1 is produced when there is endothelial vascular injury induced by clot and is released by thrombin activation. Endothelin levels have been noted to be elevated in patients with acute PE in comparison to healthy matched controls (Sofia et al. 1997). In animal models in which endothelin receptor antagonists have been used in the setting of acute PE, there has been lower PA pressures and PVR (Lee et al. 2001).

The Role of the Right Ventricle

The RV is structurally very different than the left ventricle (LV) and in particular, has a much lower pressure tolerance. Thus, the acute pulmonary pressure rise can result in dramatic changes in

RV function. The RV has fibers that are arranged in series while the LV has fibers that are arranged in parallel (Matthews and McLaughlin 2008). The RV is crescentic in shape, with a thin free wall that allows a three to four-fold increase in stroke volume without a significant increase in pressure (RV compliance is high). While the RV is able to handle large alterations in preload, it does not handle significant changes in afterload without hemodynamic consequences.

In the setting of acute PE, the sudden increase in RV afterload results in acute RV dilation and increased RV end-diastolic volume (Miller et al. 1998). This increase in RV end-diastolic volume creates more wall stress on the RV leading to decreased stroke volume of the RV. Unlike the LV which can handle large amounts of increased afterload with only small declines in stroke volume, the RV can have a significant decline in stroke volume for only small changes in afterload (Fig. 55.1) (Chin et al. 2005; Braunwald 1980). The higher wall stress applied secondary to greater end-diastolic volumes in the RV also creates an increased myocardial oxygen demand (Crystal and Pagel 2018). Unlike the LV, the normal RV receives coronary blood flow in both systole and diastole. However, when the RV needs to generate a higher systolic pressure it behaves more like the left ventricle and only is perfused during systole. When the RV systolic pressure exceeds coronary perfusion pressure the RV will

become ischemia. This results in a decrease in RV output and thus LV output and further drop in coronary perfusion pressure and more myocardial ischemia (Vlahakes et al. 1981; Konstantinides et al. 2014). If this cycle is not reversed, cardiovascular collapse and death will ensue (Fig. 55.2).

Besides the link between the RV and LV in the maintenance of coronary perfusion to the right heart and development in patients with PE of RV ischemia, interventricular dependence between the RV and LV also plays a significant role in the

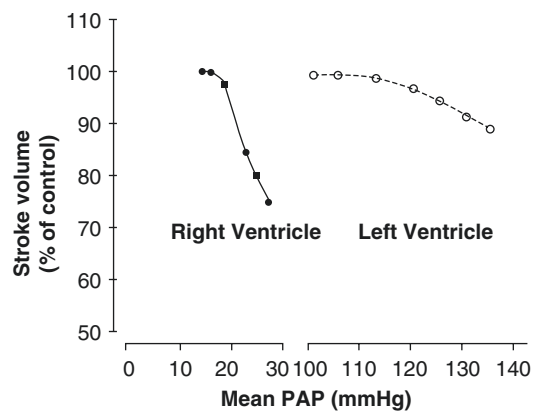
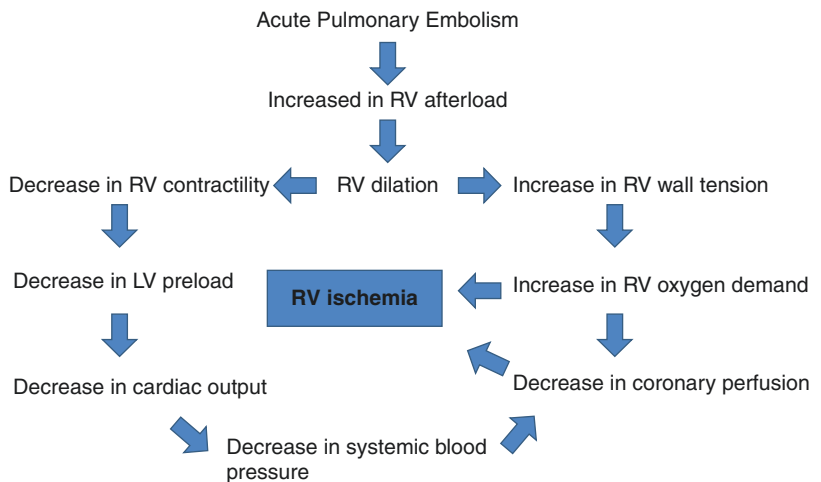


Fig. 55.1 Impact on right ventricle (RV) and left ventricle (LV) stroke volumes with increased afterload. Acute increases in RV afterload lead to significant decreases in RV stroke volume with a much lesser effect seen with elevations in LV afterload. (Reproduced with permission of Elsevier (Ref. (Braunwald 1980)))

Fig. 55.2 Pathophysiology of right ventricle (RV) collapse in the setting of acute PE. Abbreviations: RV right ventricle, LV left ventricle



production of hemodynamic instability. Under normal conditions during systole, the LV contracts and the septum is shifted towards the RV. In the setting of high-risk PE, the increase in RV volume and right ventricular diastolic pressure causes the interventricular septum to intrude into the LV. This presents as septal flattening or the “D sign” on transthoracic echocardiography (TTE). Compression of the LV can alter its compliance, decrease its volume, and thus reduce LV stroke volume and cardiac output. The LV cardiac output can further be reduced as RV stroke volume decreases resulting in a decrease in stroke volume within the LV.

Categorization of Pulmonary Embolism

It is important to identify the severity of the PE because the potential for hemodynamic compromise and outcome are dependent on the severity. Deterioration can occur quickly; two out of three patients who eventually die from PE succumb to death within the initial 2 h of presentation (Belohlavek et al. 2013a). The major classification of PE is based on hemodynamic stability. Massive PE or high-risk PE is defined as sustained hypotension (SBP < 90 mmHg for at least 15 minutes or requiring inotropic support), pulselessness, or persistent profound bradycardia (heart rate < 40 bpm with signs and symptoms of shock) (Jaff et al. 2011). Submassive PE or intermediate risk is defined as the presence of RV dysfunction or myocardial necrosis without the presence of systemic hypotension (SBP > 90 mmHg) (Jaff et al. 2011). Low-risk PE has no evidence of RV dysfunction, myocardial necrosis, or systemic hypotension (Jaff et al. 2011). The prevalence of high-risk PE is 5% and the mortality rate is 30% and can increase to greater than 70% if associated with cardiac arrest (Abrahams-van Doorn and Hartmann 2011; Becattini and Agnelli 2008). Submassive or intermediate risk PE has a prevalence of 10–25% and a mortality rate between 3% and 10% (Becattini and Agnelli 2008). Low-risk PE is the most com-

mon presentation and has a mortality rate within 1–3% (Becattini and Agnelli 2008).

Diagnosis of Acute PE

The diagnosis of acute PE is aided by laboratory testing, clinical imaging, and scoring systems that assess the clinical likelihood such as Wells criteria and revised Geneva score (Table 55.1).

Laboratory Testing

Cardiac troponins (troponin I and T) and brain natriuretic peptide (BNP) have been used as markers of cardiac necrosis as well as volume

Table 55.1 Scoring systems for grading PE: Wells Score and Revised Geneva Score (Penalzoza et al. 2011)

<i>Wells score</i>	
<i>Variable</i>	<i>Points</i>
Previous deep vein thrombosis (DVT) or PE	1.5
Recent surgery or immobilization	1.5
Cancer	1
Hemoptysis	1
Heart rate > 100 beats/min	1.5
Clinical signs of DVT	3
Alternative diagnosis less likely than PE	3
<i>Clinical probability</i>	
Low	0–1
Intermediate	2–6
High	>7
<i>Revised Geneva score</i>	
<i>Variable</i>	<i>Points</i>
Age 65 or over	1
Previous DVT or PE	3
Surgery or fracture within 1 month	2
Active malignant condition	2
Unilateral lower limb pain	3
Hemoptysis	2
Heart rate 75–94 beats per minute	3
Heart rate > 95 beats per minute	5
Pain on deep palpation of lower limb and unilateral edema	4
<i>Clinical probability</i>	
Low	0–3
Intermediate	4–10
High	≥11

overload. Troponin elevation is thought to be related to subendocardial ischemia created from a mismatch of increased cardiac demand and decreased coronary perfusion. Cardiac troponin has been used as a prognostication tool, with patients presenting with elevated troponin and PE having a higher odds ratio for death of 15.2–21.0 in comparison to the patient with no elevation (Giannitsis et al. 2000). Similarly, BNP elevation has been associated with between a six and nine- fold increase in the risk of death from PE and is thought to reflect the degree of RV afterload experienced secondary to the PE (Kostrubiec et al. 2007).

Presence of elevated plasma d-dimer unlike troponin or BNP does not help categorization of the severity of the PE but does aid in the diagnosis. In the setting of an acute clot, the fibrinolysis system is activated and d-dimer is elevated as a reflection of fibrin degradation. Plasma d-dimer elevation is not specific to PE and can also be elevated in infection, malignancy, inflammation, and aortic dissection. A typical abnormal cut-off for a d-dimer is greater than 500 ng/mL; however, adjustments for the cutoff should be increased in the setting of advanced age (Urban et al. 2014).

Transthoracic Echocardiography

TTE has become a very useful tool in the diagnosis of massive and submassive PE. The presence of RV dysfunction found on TTE in the setting of normotensive patients has been associated with a higher rate of developing shock and increased hospital mortality in comparison to normotensive patients without RV dysfunction (Grifoni et al. 2000). RV dysfunction on TTE can present as RV to LV ratio greater than 1 in an apical four-chamber view, global hypokinesis of the RV free wall also known as McConnell's sign, reduced inferior vena cava collapse with inspiration (less than 40%), right atrium pressure elevation, elevation in the RV end-diastolic diameter, increased tricuspid regurgitation and deviation of the inter-ventricular septum creating a "D-sign" in the parasternal short axis (Fig. 55.3) (Matthews and

McLaughlin 2008). On a TTE, right ventricular systolic pressures (RVSP) are estimated by observing the tricuspid regurgitant jet velocity (TRV) and using the formula $RVSP = 4TRV^2 + RA$ pressure. When a patient has an RVSP greater than 40 mmHg, tricuspid jet velocity > 3.7 m/s or RV wall thickness > 5 mm there should be suspicion of an underlying chronic component to their RV dysfunction (Matthews and McLaughlin 2008). With chronic RV afterload, remodeling occurs resulting in hypertrophy of the RV. As the RV becomes thicker its shape changes, losing its typical triangular shape resulting in tricuspid annular dilation. With the change in the shape of the RV, the TRV increases and therefore the RVSP increases (Gerges et al. 2014).

Computed Tomography Angiography (CTA)

Computed tomography angiography (CTA) is the imaging modality of choice to help with the diagnosis of PE. CTA can identify the degree of thrombus load as well as identify the presence of both acute and chronic thrombi formation. There are multiple scores, such as the Miller, which quantify the degree of pulmonary vasculature obstruction by reviewing the number of segments involved and the degree of obstruction in each lung zone on a four-point scale (Yu et al. 2011). While it is helpful to understand the level of clot burden, at the current time there is no established association between clot burden and mortality (Abrahams-van Doorn and Hartmann 2011). Similar to TTE, CTA when viewed in the axial cuts can display the RV to LV ratio. A RV/LV ratio > 0.9 has been proposed as an indication of right ventricle dysfunction and a higher likelihood for decompensation (Gibson et al. 2005).

Management

The management of hemodynamic comprising PE should focus on initially stabilizing the patient with supportive measures including oxygen therapy, blood pressure support in the form of vaso-

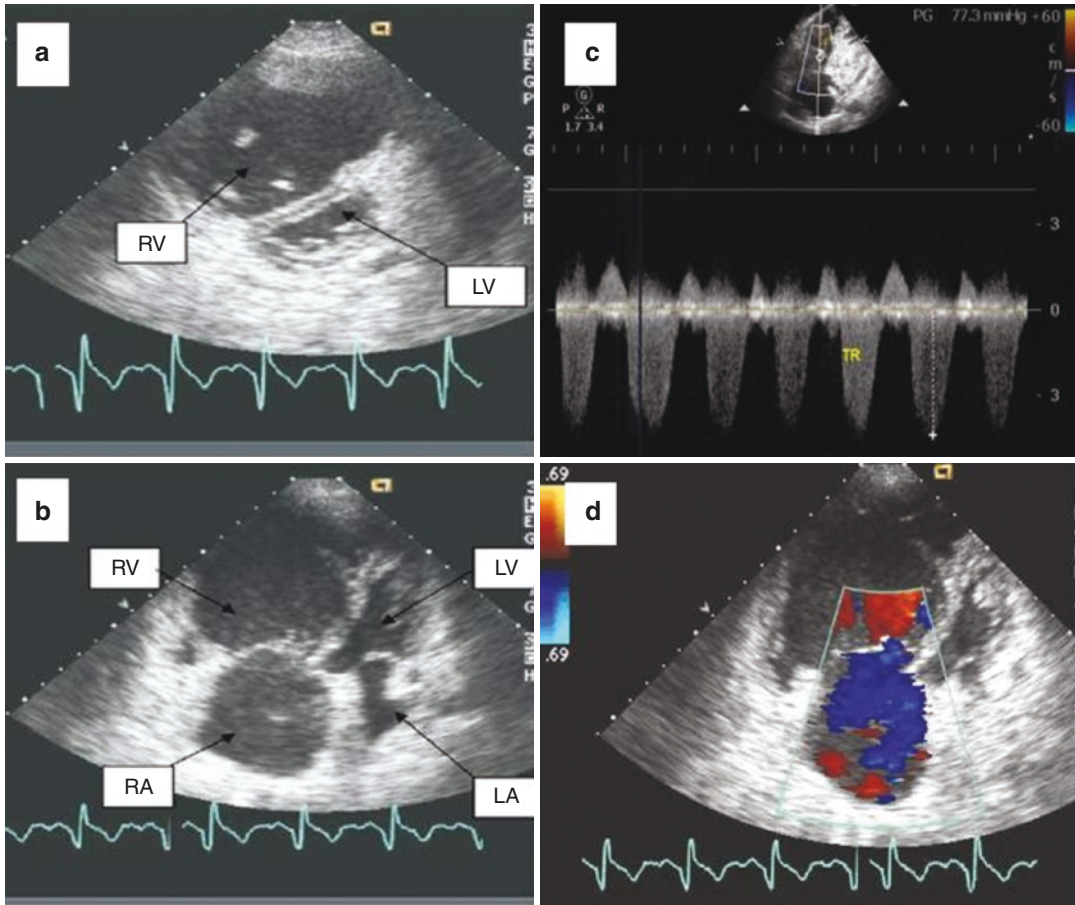


Fig. 55.3 Classical echocardiographic signs of massive and submassive pulmonary embolisms. (a) “D-Shape” of the left ventricle (LV). Thrombus formation in the right ventricle (RV). (b) Dilation of the right atrium (RA) and

right ventricle (RV). (c) Jet of tricuspid regurgitation corresponding with pulmonary hypertension. (d) Abnormal tricuspid regurgitation

pressors, and/or inotropy and then move on to consideration of definitive treatment which can include anticoagulation, thrombolytics (pharmacological, catheter-directed, surgical embolectomy) or mechanical circulatory support (extracorporeal membrane oxygenation).

Anticoagulation and Thrombolytics

Anticoagulation has been the foundation of PE management. Anticoagulation in the form of low molecular weight heparin, unfractionated heparin, or direct oral anti-coagulants (DOACs) is a first line therapy for patients with low-risk PE; however,

it may not be the therapy of choice for hemodynamically unstable patients (Leentjens et al. 2017).

For patients who present with intermediate and high-risk PE, systemic thrombolysis at the earliest time point can be the key to reduction in pulmonary vascular bed obstruction and restoring stability. There are numerous medication options for systemic thrombolysis which include alteplase (tPA), streptokinase, urokinase, reteplase, and tenecteplase (Belohlavek et al. 2013b). Alteplase has been the most widely studied and frequently used in clinical practice. Alteplase is typically given in one of two forms. Alteplase is bolused 50 mg over

2 minutes and can be rebolused 50 mg after 15 minutes or alteplase is administered with a 10 mg IV bolus over 1–2 minutes followed by 90 mg IV over the course of 2 h. Although alteplase thrombolysis can be performed in combination with a heparin infusion, many providers will choose to start heparin after the alteplase infusion has discontinued.

The role of systemic thrombolysis in the setting of intermediate risk or submassive PE is still debated. The PEITHO trial evaluated the role of heparin alone versus heparin plus systemic thrombolysis (Meyer et al. 2014). Patients were randomly assigned to receive heparin plus tenecteplase or heparin plus placebo. The heparin plus tenecteplase group had a reduced likelihood for hemodynamic decompensation (1.6% vs. 5.0%; $P = 0.002$); however, there was no statistically significant difference in mortality at 7 days (1.2% vs. 1.8%; $P = 0.42$) which was the primary end-point. The heparin plus tenecteplase group was associated with a higher risk of major extracranial bleeding (6.3% vs. 1.2%; $P < 0.001$) as well as stroke risk (2.4% vs. 0.2%; $P = 0.003$). Absolute contraindications to thrombolytic therapy include active internal bleeding, ischemic stroke within 6 months, brain tumor, history of intracranial hemorrhage, gastrointestinal bleeding within the past 4 weeks or recent extensive trauma or surgery within 3 weeks (Belohlavek et al. 2013b).

Catheter-directed thrombolysis (CDT) is an increasingly utilized option for patients with acute PE. CDT involves the placement of infusion catheters into the pulmonary artery and direct infusion of a thrombolytic agent. Lower doses of thrombolytics (12–24 mg tPA) have been utilized in CDT studies. Although there are several favorable reports reporting on the benefits of CDT, including a reduction in RV dilatation and pulmonary artery pressure, to date there are very limited controlled data. One method of CDT, ultrasound enhanced thrombolysis, has been studied in a small randomized controlled trial that demonstrated improved RV/LV ratio at 24 h in patients receiving this treatment compared to heparin alone (Kucher et al. 2014).

In addition to CDT, there are several extraction devices that fragment the clot and allow aspiration of thrombi. Extraction is typically performed with concurrent intravenous unfractionated heparin (Zarghouni et al. 2016; Kuo et al. 2015; Jaber et al. 2016). These methods can create significant reductions in RV afterload even with only partial clot removal.

In patients who have life-threatening PE (e.g., shock, cardiac arrest) and are unable to receive thrombolytic therapy, open surgical embolectomy is an option. The mortality of surgical embolectomy ranges from 3% to greater than 60%, with the greatest predisposing factor being cardiac arrest prior to embolectomy. When surgical embolectomy has been compared to repeat systemic thrombolytics in patients who initially failed thrombolysis, embolectomy has been associated with reduced mortality as well as reduced recurrence of PE (Yavuz et al. 2014). Recent studies have looked the usefulness of RV/LV ratio to determine which patients may fail systemic thrombolysis. Patients with an initial RV/LV ratio >1.5 on CT imaging were more likely to fail systemic thrombolysis and convert to surgical embolectomy as definitive treatment (Aymard et al. 2013).

Mechanical circulatory support in the form of venous-arterial extracorporeal membrane oxygenation (VA-ECMO) has been used to provide clinical stability or to allow for a bridge until definitive therapy can be performed in patients with sustained hemodynamic instability. VA ECMO can off-load the RV as deoxygenated blood is removed from the inferior vena cava via femoral vein cannulation site. This can cause the reduction of preload in the RV, decrease the pulmonary artery pressures, and bypass the obstruction within the pulmonary vasculature (Belohlavek et al. 2010). Deoxygenated blood from the venous cannula is then passed through an external oxygenator and returned to the arterial system via the femoral artery into the aorta. Of note, it is important to closely monitor for pulmonary edema in the setting of VA ECMO (Baran 2017; Burkhoff et al. 2015). As flows are increased in the circuit, LV afterload is increased and LV volume can also increase. This can create

an increase in pulmonary capillary wedge pressure and the formation of pulmonary edema (Baran 2017; Burkhoff et al. 2015). Management of this requires some process to decompress the left ventricle which can include performing a septal puncture or using another mechanical device to off-load the LV. There have been several case series reporting the use of VA ECMO for massive PE. In a retrospective review of 78 patients who received VA ECMO for acute massive PE, the mean duration of VA ECMO support was 4.47 ± 2.98 days (Yusuff et al. 2015). Forty-three patients had a cardiac arrest prior to initiation of VA ECMO and cardiac arrest significantly increased the risk of death with an odds ratio of 16.71 (Yusuff et al. 2015). The overall mortality was 29.9% for all patients who received VA ECMO with the leading cause of death being multi-organ dysfunction (Yusuff et al. 2015).

The decision to attempt systemic anticoagulation, CDT, surgical embolectomy, or VA ECMO in the setting of high-risk PE can be challenging. Given the complexity of submassive and massive PE cases, a Pulmonary Embolism Response Team (PERT) was first created at Massachusetts General Hospital. The PERT is a multidisciplinary rapid response team comprised of physicians in cardiovascular medicine and surgery, emergency medicine, hematology, pulmonary/critical care, and radiology. The adoption of the PERT approach has expanded to numerous institutions across the country and even worldwide.

Vasoactive Medications

Supportive treatment of shock and hypoperfusion in massive PE is challenging, but is critical for maintaining organ function and, hopefully preventing the “death spiral.”

Fluid resuscitation, although tempting in the setting of hypotension, is rarely beneficial and may, in fact be harmful (Ducas and Prewitt 1987). The already elevated right atrial pressure and RV volume overload seen in massive PE indicates that RV filling is limited and more fluid cannot increase cardiac output and more volume only worsens RV function by bulging the septum into the LV. Thus, avoiding volume challenges should be stressed.

The selection of vasopressor medication to help support the blood pressure in a hemodynamically unstable patient with a PE can vary across institutions. The main goal of vasopressors is simply to achieve a high enough mean arterial pressure to maintain adequate coronary and systemic perfusion. Given that the right coronary fills throughout the cardiac cycle, when there is high right ventricular pressure, coronary perfusion pressure must be adequate or RV ischemia can result.

Several pressors are available (Table 55.2). Norepinephrine acts on alpha-1 and beta-1 receptors. It acts on alpha-1 causing vasoconstriction leading to increases in mean systemic pressures. With high systemic pressures, there is better coronary perfusion to the RV which helps prevent or

Table 55.2 Vasopressor and inotropy mechanism of action for hemodynamically unstable PE

Receptor of action	α 1	β 1	β 2	D	V1	Other
Norepinephrine	++	+				
Epinephrine	++	++	+			
Vasopression					+	
Dopamine <5 μ g/kg/min		+		++		
Dopamine 5–10 μ g/kg/min	+	++		++		
Dopamine >10 μ g/kg/min	++	++		++		
Dobutamine		++	+			
Milrinone						Phosphodiesterase-3 inhibitor

Abbreviations: *D* dopaminergic receptor, *V1* vasopressin receptor, + low effect, ++ moderate to high effect

reduce myocardial ischemia (Ventetuolo and Klinger 2014). Norepinephrine also acts on beta-1 receptors creating inotropic support. Epinephrine acts on alpha-1, beta-1, and beta 2 receptors. Similar to norepinephrine it promotes vasoconstriction causing increases in systemic blood pressure, however has larger effects on beta-1 which can promote arrhythmia which can be detrimental to perfusion. By acting on beta-2 receptors it may produce a slight reduction in pulmonary vascular resistance (Ventetuolo and Klinger 2014). Dopamine has a dose-dependent effect on receptors. At doses less than 5 µg/kg/min it acts mainly on dopaminergic receptors, from 5 to 10 µg/kg/min on beta-1 receptors and >10 µg/kg/min alpha 1 receptors. Dopamine shares similar risks to epinephrine at higher doses for arrhythmias (Ventetuolo and Klinger 2014). Vasopressin acts on V1 receptors and has been associated with pulmonary vasodilation via stimulation of endothelial nitric oxide at low doses. Inotropic agents can be used when additional support is necessary to maintain adequate perfusion. Prior to using inotropic agents, it is imperative that the mean systemic blood pressure is high enough to maintain perfusion as these agents can cause a drop in blood pressure which could precipitate RV failure if used in isolation. Dobutamine acts on beta-1 and beta-2 receptors. At doses of 5–10 µg/kg/min, dobutamine has been demonstrated to reduce PVR as it acts on beta-2 receptors (Ventetuolo and Klinger 2014). At higher doses, there is concern it can cause increased vasodilation and potentially lead to systemic hypotension (Ventetuolo and Klinger 2014). Milrinone is a phosphodiesterase-3 inhibitor and has been used in biventricular failure as it has been demonstrated to improve cardiac output while also reducing PVR (Ventetuolo and Klinger 2014). A relatively newer inotropic agent, levosimendan, improves cardiac contractility by increasing the sensitization of Troponin C to calcium (Ventetuolo and Klinger 2014). It has been demonstrated to act independently of cyclic-AMP, therefore may cause less ventricular arrhythmias as it does not use intracellular calcium. Levosimendan has vasodilating properties by a proposed mechanism of activating potas-

sium channels within the vascular smooth muscle cells. When studied in the setting of acute PE, levosimendan reduced PVR and increased RV contractility, and when compared to dobutamine in animal models levosimendan reduced RV afterload to a greater extent (Kerbaul et al. 2007; Kerbaul et al. 2006). At the current time, there is not a general consensus on what vasopressor or inotropic support is ideal for hypotension in the setting of PE; however, the goal should be to maintain mean arterial pressures (MAP) >65 to reduce RV ischemia.

Selective pulmonary vasodilators such as inhaled nitric oxide (iNO) or inhaled epoprostenol can be used to counteract the vasoconstriction that can occur in acute PE. These agents are potentially ideal given their selectivity to the pulmonary vascular bed and their selectivity within the lung that may improve V/Q matching and oxygenation (Ventetuolo and Klinger 2014). Although numerous case reports describe the benefits of inhaled NO in acute PE, to date there are no randomized control trials (Kline et al. 2017; Bhat et al. 2015).

Airway Management in PE

Intubation should ideally be avoided in patients with hemodynamically compromising PEs. In a hypotensive patient, the transition from negative pressure to positive pressure ventilation can increase intrathoracic pressure and subsequently reduce RV preload. A further reduction in preload can compromise cardiac output which could further worsen a patient's hypotension. If a patient does need intubation, assuring adequate mean arterial pressure with the use of vasopressors (discussed above) is key to prevent cardiac arrest.

If a patient is intubated it is important to consider transpulmonary pressures, and lung volumes for these patients are at high risk for RV failure. Increased transpulmonary pressures can increase the load on the right ventricle by creating non-west zone III condition during lung inflations as discussed in Chap. 5 (Mitzner). When this occurs the downstream pressure for the RV is

the alveolar pressure and not the left atrial pressure. Pulmonary vascular resistance changes with alterations in lung volumes secondary to compression of intra (arterioles, capillaries, and venules) and extra alveolar vessels (pulmonary arteries and veins) (Ventetuolo and Klinger 2014; Murray 1986) The ideal lung volume thus is likely around functional residual capacity. This is important to consider in ventilated patients, as FRC may not reflect lung-protective volumes in each patient.

Conclusion

Submassive and massive PEs can lead to hemodynamic compromise, therefore early recognition and treatment is key. Diagnosis of RV dysfunction can be aided through troponin, BNP, and TTE. Management can range from anticoagulation, CDT, surgical embolectomy, and VA ECMO. Treatment should focus on the resolution of the clot while also maintaining mean arterial pressure and cardiac output with the utilization of vasopressors and inotropy. Given the challenging nature of many PE cases, PERT can be a valuable resource to determine the best course of action.

References

- Abrahams-van Doorn PJ, Hartmann IJ. Cardiothoracic CT: one-stop-shop procedure? Impact on the management of acute pulmonary embolism. *Insights Imaging*. 2011;2(6):705–15. PubMed PMID: 23100045. Pubmed Central PMCID: 3289035.
- Alpert JS, Godtfredsen J, Ockene IS, Anas J, Dalen JE. Pulmonary hypertension secondary to minor pulmonary embolism. *Chest*. 1978;73(6):795–7. PubMed PMID: 657852.
- Aymard T, Kadner A, Widmer A, Basciani R, Tevæarai H, Weber A, et al. Massive pulmonary embolism: surgical embolectomy versus thrombolytic therapy--should surgical indications be revisited? *Eur J Cardiothorac Surg*. 2013;43(1):90–4; discussion 4. PubMed PMID: 22466693.
- Baran DA. Extracorporeal membrane oxygenation (ECMO) and the critical cardiac patient. *Curr Transplant Rep*. 2017;4(3):218–25. PubMed PMID: 28932651. Pubmed Central PMCID: 5577059.
- Beattini C, Agnelli G. Predictors of mortality from pulmonary embolism and their influence on clinical management. *Thromb Haemost*. 2008;100(5):747–51. PubMed PMID: 18989514.
- Bell WR, Simon TL. Current status of pulmonary thromboembolic disease: pathophysiology, diagnosis, prevention, and treatment. *Am Heart J*. 1982;103(2):239–62. PubMed PMID: 7034515.
- Belohlavek J, Rohn V, Jansa P, Tosovsky J, Kunstyr J, Semrad M, et al. Venous-arterial ECMO in severe acute right ventricular failure with pulmonary obstructive hemodynamic pattern. *J Invasive Cardiol*. 2010;22(8):365–9. PubMed PMID: 20679672.
- Belohlavek J, Dytrych V, Linhart A. Pulmonary embolism, part I: epidemiology, risk factors and risk stratification, pathophysiology, clinical presentation, diagnosis and nonthrombotic pulmonary embolism. *Exp Clin Cardiol*. 2013a;18(2):129–38. PubMed PMID: 23940438. Pubmed Central PMCID: 3718593.
- Belohlavek J, Dytrych V, Linhart A. Pulmonary embolism, part II: management. *Exp Clin Cardiol*. 2013b;18(2):139–47. PubMed PMID: 23940439. Pubmed Central PMCID: 3718594.
- Bhat T, Neuman A, Tantary M, Bhat H, Glass D, Mannino W, et al. Inhaled nitric oxide in acute pulmonary embolism: a systematic review. *Rev Cardiovasc Med*. 2015;16(1):1–8. PubMed PMID: 25813791.
- Braunwald E. Pathophysiology of heart failure. In: Braunwald E, editor. *Heart disease: a textbook of cardiovascular medicine*. Philadelphia: Saunders; 1980. p. 453–71.
- Bshouty Z. Vascular compromise and hemodynamics in pulmonary arterial hypertension: model predictions. *Can Respir J*. 2012;19(3):e15–7. PubMed PMID: 22679616. Pubmed Central PMCID: 3418098.
- Burkhoff D, Sayer G, Doshi D, Uriel N. Hemodynamics of mechanical circulatory support. *J Am Coll Cardiol*. 2015;66(23):2663–74. PubMed PMID: 26670067.
- Chin KM, Kim NH, Rubin LJ. The right ventricle in pulmonary hypertension. *Coron Artery Dis*. 2005;16(1):13–8. PubMed PMID: 15654194.
- Chou Y, Canning BJ. Serotonin regulates the cardiopulmonary effects of pulmonary embolism through vagal C-fiber activation. *FASEB J*. 2011;25(1_Suppl):1077.2–2.
- Crystal GJ, Pagel PS. Right ventricular perfusion: physiology and clinical implications. *Anesthesiology*. 2018;128(1):202–18. PubMed PMID: 28984631.
- Daily PO, Moulder PV. Serotonin and pulmonary embolism. *Arch Surg*. 1966;93(2):348–54. PubMed PMID: 5913573.
- Dalen JE, Alpert JS. Natural history of pulmonary embolism. *Prog Cardiovasc Dis*. 1975;17(4):259–70. PubMed PMID: 1089991.
- Ducas J, Prewitt RM. Pathophysiology and therapy of right ventricular dysfunction due to pulmonary embolism. *Cardiovasc Clin*. 1987;17(2):191–202. PubMed PMID: 3536103.
- Gerges C, Skoro-Sajer N, Lang IM. Right ventricle in acute and chronic pulmonary embolism (2013 Grover conference series). *Pulm Circ*. 2014;4(3):378–86.

- PubMed PMID: 25621151. Pubmed Central PMCID: 4278597.
- Giannitsis E, Muller-Bardorff M, Kurowski V, Weidtmann B, Wiegand U, Kampmann M, et al. Independent prognostic value of cardiac troponin T in patients with confirmed pulmonary embolism. *Circulation*. 2000;102(2):211–7. PubMed PMID: 10889133.
- Gibson NS, Sohne M, Buller HR. Prognostic value of echocardiography and spiral computed tomography in patients with pulmonary embolism. *Curr Opin Pulm Med*. 2005;11(5):380–4. PubMed PMID: 16093809.
- Goldhaber SZ, Elliott CG. Acute pulmonary embolism: part I: epidemiology, pathophysiology, and diagnosis. *Circulation*. 2003;108(22):2726–9. PubMed PMID: 14656907.
- Goldhaber SZ, Hennekens CH, Evans DA, Newton EC, Godleski JJ. Factors associated with correct antemortem diagnosis of major pulmonary embolism. *Am J Med*. 1982;73(6):822–6. PubMed PMID: 7148876.
- Goldhaber SZ, Visani L, De Rosa M. Acute pulmonary embolism: clinical outcomes in the International Cooperative Pulmonary Embolism Registry (ICOPER). *Lancet*. 1999;353(9162):1386–9. PubMed PMID: 10227218.
- Grifoni S, Olivetto I, Cecchini P, Pieralli F, Camaiti A, Santoro G, et al. Short-term clinical outcome of patients with acute pulmonary embolism, normal blood pressure, and echocardiographic right ventricular dysfunction. *Circulation*. 2000;101(24):2817–22. PubMed PMID: 10859287.
- Jaber WA, Fong PP, Weisz G, Lattouf O, Jenkins J, Rosenfield K, et al. Acute pulmonary embolism: with an emphasis on an interventional approach. *J Am Coll Cardiol*. 2016;67(8):991–1002. PubMed PMID: 26916490.
- Jaff MR, McMurtry MS, Archer SL, Cushman M, Goldenberg N, Goldhaber SZ, et al. Management of massive and submassive pulmonary embolism, iliofemoral deep vein thrombosis, and chronic thromboembolic pulmonary hypertension: a scientific statement from the American Heart Association. *Circulation*. 2011;123(16):1788–830. PubMed PMID: 21422387.
- Kerbaul F, Rondelet B, Demester JP, Fesler P, Huez S, Naeije R, et al. Effects of levosimendan versus dobutamine on pressure load-induced right ventricular failure. *Crit Care Med*. 2006;34(11):2814–9. PubMed PMID: 16971854.
- Kerbaul F, Gariboldi V, Giorgi R, Mekkaoui C, Guieu R, Fesler P, et al. Effects of levosimendan on acute pulmonary embolism-induced right ventricular failure. *Crit Care Med*. 2007;35(8):1948–54. PubMed PMID: 17568324.
- Kline JA, Hall CL, Jones AE, Puskarich MA, Mastouri RA, Lahm T. Randomized trial of inhaled nitric oxide to treat acute pulmonary embolism: The iNOPE trial. *Am Heart J*. 2017;186:100–10. PubMed PMID: 28454823. Pubmed Central PMCID: 5412723.
- Konstantinides SV, Torbicki A, Agnelli G, Danchin N, Fitzmaurice D, Galie N, et al. 2014 ESC guidelines on the diagnosis and management of acute pulmonary embolism. *Eur Heart J*. 2014;35(43):3033–69, 69a–69k. PubMed PMID: 25173341.
- Kostrubiec M, Pruszczyk P, Kaczynska A, Kucher N. Persistent NT-proBNP elevation in acute pulmonary embolism predicts early death. *Clin Chim Acta*. 2007;382(1–2):124–8. PubMed PMID: 17507005.
- Kucher N, Boekstegers P, Muller OJ, Kupatt C, Beyer-Westendorf J, Heitzer T, et al. Randomized, controlled trial of ultrasound-assisted catheter-directed thrombolysis for acute intermediate-risk pulmonary embolism. *Circulation*. 2014;129(4):479–86. PubMed PMID: 24226805.
- Kuo WT, Banerjee A, Kim PS, DeMarco FJ Jr, Levy JR, Facchini FR, et al. Pulmonary embolism response to fragmentation, embolectomy, and catheter thrombolysis (PERFECT): initial results from a prospective multicenter registry. *Chest*. 2015;148(3):667–73. PubMed PMID: 25856269.
- Lee JH, Chun YG, Lee IC, Tuder RM, Hong SB, Shim TS, et al. Pathogenic role of endothelin 1 in hemodynamic dysfunction in experimental acute pulmonary thromboembolism. *Am J Respir Crit Care Med*. 2001;164(7):1282–7. PubMed PMID: 11673223.
- Leentjens J, Peters M, Esselink AC, Smulders Y, Kramers C. Initial anticoagulation in patients with pulmonary embolism: thrombolysis, unfractionated heparin, LMWH, fondaparinux, or DOACs? *Br J Clin Pharmacol*. 2017;83(11):2356–66. PubMed PMID: 28593681. Pubmed Central PMCID: 5651323.
- Lehnert P, Lange T, Moller CH, Olsen PS, Carlsen J. Acute pulmonary embolism in a National Danish Cohort: increasing incidence and decreasing mortality. *Thromb Haemost*. 2018;118(3):539–46. PubMed PMID: 29536465.
- Matthews JC, McLaughlin V. Acute right ventricular failure in the setting of acute pulmonary embolism or chronic pulmonary hypertension: a detailed review of the pathophysiology, diagnosis, and management. *Curr Cardiol Rev*. 2008;4(1):49–59. PubMed PMID: 19924277. Pubmed Central PMCID: 2774585.
- McIntyre KM, Sasahara AA. The hemodynamic response to pulmonary embolism in patients without prior cardiopulmonary disease. *Am J Cardiol*. 1971;28(3):288–94. PubMed PMID: 5155756.
- McIntyre KM, Sasahara AA. The ratio of pulmonary arterial pressure to pulmonary vascular obstruction: index of preembolic cardiopulmonary status. *Chest*. 1977;71(6):692–7. PubMed PMID: 862439.
- Meyer G, Vicaut E, Danays T, Agnelli G, Becattini C, Beyer-Westendorf J, et al. Fibrinolysis for patients with intermediate-risk pulmonary embolism. *N Engl J Med*. 2014;370(15):1402–11. PubMed PMID: 24716681.
- Miller RL, Das S, Anandarangam T, Leibowitz DW, Alderson PO, Thomashow B, et al. Association between right ventricular function and perfusion abnormalities in hemodynamically stable patients with acute pulmonary embolism. *Chest*. 1998;113(3):665–70. PubMed PMID: 9515840.

- Murray JF. The normal lung: the basis for diagnosis and treatment of pulmonary disease. 2nd ed. Philadelphia: Saunders; 1986. xi, 377 p.
- Penalzo A, Melot C, Motte S. Comparison of the Wells score with the simplified revised Geneva score for assessing pretest probability of pulmonary embolism. *Thromb Res.* 2011;127(2):81–4. PubMed PMID: 21094985.
- Reeves WC, Demers LM, Wood MA, Skarlatos S, Copenhaver G, Whitesell L, et al. The release of thromboxane A2 and prostacyclin following experimental acute pulmonary embolism. *Prostaglandins Leukot Med.* 1983;11(1):1–10. PubMed PMID: 6348800.
- Rosoff CB, Salzman EW, Gurewich V. Reduction of platelet serotonin and the response to pulmonary emboli. *Surgery.* 1971;70(1):12–9. PubMed PMID: 4326431.
- Scarvelis D, Anderson J, Davis L, Forgie M, Lee J, Petersson L, et al. Hospital mortality due to pulmonary embolism and an evaluation of the usefulness of preventative interventions. *Thromb Res.* 2010;125(2):166–70. PubMed PMID: 19647292.
- Smulders YM. Pathophysiology and treatment of haemodynamic instability in acute pulmonary embolism: the pivotal role of pulmonary vasoconstriction. *Cardiovasc Res.* 2000;48(1):23–33. PubMed PMID: 11033105.
- Sofia M, Faraone S, Alifano M, Micco A, Albinini R, Maniscalco M, et al. Endothelin abnormalities in patients with pulmonary embolism. *Chest.* 1997;111(3):544–9. PubMed PMID: 9118685.
- Stein PD, Henry JW. Prevalence of acute pulmonary embolism among patients in a general hospital and at autopsy. *Chest.* 1995;108(4):978–81. PubMed PMID: 7555172.
- Todd MH, Forrest JB, Cragg DB. The effects of aspirin and methysergide on responses to clot-induced pulmonary embolism. *Am Heart J.* 1983;105(5):769–76. PubMed PMID: 6405602.
- Urban K, Kirley K, Stevermer JJ. PURLs: it's time to use an age-based approach to D-dimer. *J Fam Pract.* 2014;63(3):155–8. PubMed PMID: 24701602. Pubmed Central PMCID: 4042909.
- Utsonomiya T, Krausz MM, Levine L, Shepro D, Hechtman HB. Thromboxane mediation of cardiopulmonary effects of embolism. *J Clin Invest.* 1982;70(2):361–8. PubMed PMID: 6284801. Pubmed Central PMCID: 371244.
- Utsonomiya T, Krausz MM, Shepro D, Hechtman HB. Prostaglandin control of plasma and platelet 5-hydroxytryptamine in normal and embolized animals. *Am J Phys.* 1981;241(5):H766–71. PubMed PMID: 7030086.
- Ventetuolo CE, Klingler JR. Management of acute right ventricular failure in the intensive care unit. *Ann Am Thorac Soc.* 2014;11(5):811–22. PubMed PMID: 24828526. Pubmed Central PMCID: 4225807.
- Vlahakes GJ, Turley K, Hoffman JI. The pathophysiology of failure in acute right ventricular hypertension: hemodynamic and biochemical correlations. *Circulation.* 1981;63(1):87–95. PubMed PMID: 7438411.
- Weidner WJ. Effects of indomethacin on pulmonary hemodynamics and extravascular lung water in sheep after pulmonary microembolism. *Prostaglandins Med.* 1979;3(2):71–80. PubMed PMID: 552101.
- Yavuz S, Toktas F, Goncu T, Eris C, Gucu A, Ay D, et al. Surgical embolectomy for acute massive pulmonary embolism. *Int J Clin Exp Med.* 2014;7(12):5362–75. PubMed PMID: 25664045. Pubmed Central PMCID: 4307492.
- Yu T, Yuan M, Zhang Q, Shi H, Wang D. Evaluation of computed tomography obstruction index in guiding therapeutic decisions and monitoring percutaneous catheter fragmentation in massive pulmonary embolism. *J Biomed Res.* 2011;25(6):431–7. PubMed PMID: 23554721. Pubmed Central PMCID: 3596723.
- Yusuff HO, Zochios V, Vuylsteke A. Extracorporeal membrane oxygenation in acute massive pulmonary embolism: a systematic review. *Perfusion.* 2015;30(8):611–6. PubMed PMID: 25910837.
- Zarghouni M, Charles HW, Maldonado TS, Deipolyi AR. Catheter-directed interventions for pulmonary embolism. *Cardiovasc Diagn Ther.* 2016;6(6):651–61. PubMed PMID: 28123985. Pubmed Central PMCID: 5220195.



Clinical Neurologic Issues in Cerebrovascular Monitoring

56

Thomas P. Bleck

The relationship between cerebral blood flow and the oxygen demands of the brain is frequently disrupted by disease. Focal disorders of blood flow occur acutely as a consequence of arterial disorders, most commonly ischemic stroke but also in the tissue adjacent to an intracerebral hematoma (primary, such as a hypertensive hemorrhage, or due to trauma or hemorrhage from a tumor). Cerebral venous occlusion also affects oxygen delivery, as venous stasis will prevent oxygenated blood from entering the affected tissue. Multifocal ischemia commonly occurs in the setting of cerebral vasospasm after aneurysmal subarachnoid hemorrhage, and may also be seen as a consequence of head trauma. Global cerebral ischemia is typically a consequence of cardiac arrest, but may also be seen in conditions such as drowning, hanging, or asphyxiation (physical or chemical). In addition to such primary injuries, any condition increasing intracranial pressure can impair cerebral perfusion. This relationship is discussed in detail in (Chaps. 11 and 23).

In any setting, clinical evaluation of the patient often suffices to determine that global cerebral perfusion is adequate. If the patient is sufficiently

conscious to make appropriate verbal responses, or to protect against noxious stimuli, perfusion at that time is adequate, and invasive pressure monitoring is not indicated for clinical management. However, since many causes of brain swelling will progress over hours, placement of an ICP monitor is often prudent based either on the likelihood of clinical worsening, or imaging findings that may presage such a decline. The choice of a monitoring device depends on many factors; parenchymal monitors are less invasive than external ventricular drains, but the latter allow removal of cerebrospinal fluid to reduce pressure as well as monitor it.

Intracranial pressure monitoring allows the clinician to determine the cerebral perfusion pressure (CPP); CPP management is one of the cornerstones of acute brain trauma care for moderately or severely injured patients (Carney et al. 2017). Monitoring CPP requires an arterial line as well as an ICP monitor. The arterial line should be leveled at the level of the foramen of Monro for calculation of CPP, rather than at the phlebostatic axis, since when the head of the patient is elevated, the arterial pressure experienced by the brain will be reduced by the height of the column of blood above the heart (Thomas et al. 2015). Practically, this is accomplished by keeping the transducer near the tragus of the ear, so that changes in head elevation are automatically applied to the arterial line.

T. P. Bleck (✉)
Division of Stroke and Neurocritical Care, Davee
Department of Neurology, Northwestern University
Feinberg School of Medicine, Chicago, IL, USA
Rush Medical College, Chicago, IL, USA

The optimal value of CPP is a subject of debate. In general, a CPP of 60 mmHg is the typical goal in adults, with age-dependent lower values in children. As discussed below, there are circumstances in which a higher CPP may be tolerated in order to improve cerebral oxygenation.

Many therapeutic modalities are applied to improve CPP. Raising the MAP with vasopressors is often required, and is usually the most rapidly effective. Lowering the ICP can be accomplished in several ways. If a mass lesion is responsible for elevating the ICP, its expeditious removal is usually an important component of treatment, but this may not be possible, or other therapeutic approaches may be required in order for the patient to survive long enough to get to the operating room. Table 56.1 presents a history of modern attempts to treat intracranial hypertension.

Monitoring and management of CPP does not predict or prevent all problems with intracranial pressure; it is most useful when the cause of the ICP elevation is global. Herniation from one intracranial compartment to another occurs because of a pressure gradient, but even the higher pressure driving herniation may not exceed the commonly accepted upper limit of normal (e.g., 22 mmHg). Physical signs of herniation (e.g., pupillary or eye movement changes, or the development of asymmetric weakness or posturing) may also require therapies to lower ICP in order to decrease such gradients.

Jugular venous oxygen measurements (of either saturation, which can be monitored continuously, or partial pressure, or content) were some of the earliest approaches to studying cere-

bral oxygenation in trauma. The mixing of venous blood in the confluence of sinuses is rarely complete, however, and the values obtained when both jugular veins are studied may be quite disparate. Finding diminished oxygen in jugular venous blood is a reliable marker of inadequate delivery for demand, and thus indicates cerebral ischemia. A minority of patients, especially young patients, have had increased oxygen in their jugular veins; this was previously thought to indicate hyperemia, which might be safely treated with hyperventilation. However, this circumstance more likely indicates the inability to utilize the oxygen being delivered, either because of mitochondrial dysfunction or impaired diffusion (vide infra). This is not to say that true hyperemia never occurs, but recent measurements with better time resolution than the older studies often reveal that hyperemia may occur as a consequence of spikes in MAP, as the arterial pressure rise precedes the increase in CBF (Akbik et al. 2016).

The major factors controlling cerebral arterial caliber are the extracellular pH and the extravascular concentrations of potassium and nitric oxide; carbon dioxide itself plays a minor role, but is crucial because of its effect on pH. CO₂ is freely diffusible across the blood-brain barrier, whereas buffers such as bicarbonate and phosphate are not. Thus, alterations in PaCO₂ almost immediately change the cerebral extracellular pH; hyperventilation produces vasoconstriction, decreasing the caliber of arterioles (and possibly of venous structures), decreasing cerebral blood volume and thus ICP. This effect is very rapid, a drop in ICP occurring in less than 1 minute after hyperventilation begins.

Once the increase in minute ventilation leads to a new PaCO₂ steady state, it is common to see that the ICP slowly begins to rise. This is often interpreted as a failure of hyperventilation. However, the arteriolar response to the rise in pH does not appear to fatigue. Instead, three factors mitigate against a sustained effect on ICP. First, the choroid plexus begins to export bicarbonate when the CSF pH exceeds its normal value of 7.3 (Christensen et al. 2018). (Another explanation based on the strong-ion difference to acid-base

Table 56.1 Therapeutic approaches to intracranial hypertension

1918: Tentorial incision (Cushing)
1923: Osmotic diuretics (Fay)
1955: Hypothermia (Sedzimir)
1957: Hyperventilation (Furness)
1960: Ventricular drainage (Lundberg)
1961: Steroids (Gailich and French)
1971: Decompressive craniectomy (lateral: Ransohoff; bifrontal: Kjellberg)
1973: Barbiturates (Shapiro)

balance is that Na^+ is extruded which will lower the bicarbonate concentration – see acid-base Chap. 41.) This compensation is complete within 6 hours in normal subjects, but appears to be slower in patients with brain injuries. Second, the cause of the ICP elevation is usually progressive, so the decreased blood volume will be counteracted by the pathologic process at work. Third, as the minute ventilation is further increased in subsequent attempts to control the ICP, the increases in tidal volume and respiratory rate will eventually result in increasing intrathoracic pressure to the point that jugular venous return is impaired, which itself will elevate the ICP.

In the 1970s, investigators became concerned that excessive hyperventilation might produce cerebral ischemia. Mechanistically one might expect that the acidosis accompanying ischemia would counteract the vasoconstrictive effect, but it seemed prudent to examine whether hyperventilation might have an effect on outcome. Muizelaar et al. compared severely head injured patients who were randomized to PaCO_2 partial pressures of 30–35 mmHg with those ventilated to PaCO_2 partial pressures between 24 and 28 mmHg (Muizelaar et al. 1991). The value of 30–35 was chosen as the control because these patients often maintained themselves in that range when not controlled. Interim analyses at 3 and 6 months suggested that the more severely hyperventilated group had poorer outcomes as measured by the Glasgow Outcome Scale score, leading to premature termination of the trial. This difference was no longer present at 12 months, but this study is frequently invoked as an indication to avoid hyperventilation for ICP control. More recent work suggests that hyperventilation in the range of 30–35 mmHg does not adversely affect cerebral metabolism.

Global insults such as head trauma can produce both generalized and localized abnormalities in blood flow. One technique to assess regional blood flow abnormalities is “cold” (non-radioactive) xenon CT scanning. A 1992 study of severely head-injured patients found that a substantial minority had diminished CBF, even in the absence of intracranial hematomata (Bouma et al. 1992). This study found no patients with

hyperemia; those with diffuse swelling had the worst CBF.

Positron emission tomographic (PET) studies of hyperventilation using ^{15}O -labeled water to measure CBF with high spatial resolution have yielded results with conflicting interpretations. The Cambridge neurocritical care group reported that hyperventilation increased the volume of hypoperfused tissue, although they noted that the response varied among patients and that no PaCO_2 threshold for ischemia could be established (Coles et al. 2002). They also noted that hyperemia was rare. The same group later showed that the oxygen extraction fraction (OEF) increased, in some regions to levels that the investigators considered critically high. Using similar techniques, the Washington University neurocritical care team obtained similar results, but considered that the increase in OEF represented successful compensation for diminished regional cerebral blood flow (Diringer et al. 2002). This disagreement remains unresolved.

One of the principles underlying CPP management is pressure autoregulation. Under normal conditions, CBF remains constant over a range of MAP extending from about 50 to 150 mmHg; this is accomplished by progressive constriction of arteriolar sphincters. However, pressure autoregulation may fail in pathologic situations. Studies in head trauma patients, using transcranial Doppler flow velocity measurements as a surrogate for actual CBF measurements, suggest that pressure autoregulation fails in about 55% of patients, resulting in CBF that increases passively as MAP increases through the normally autoregulated range (Lang et al. 2003; Oertel et al. 2002). A few studies using CT perfusion measurements suggest that this phenomenon may be less common, perhaps occurring in 24% (Peterson and Chesnut 2009). The slope of the increase in MAP appears to be steeper than the slope of CBF increase, indicating that raising the MAP can still increase the CPP, but not to the extent that would occur if pressure autoregulation was intact.

Oxygen-derived free radicals are generated when previously underperfused areas experience a return of blood supply, especially when iron is

available to catalyze the Fenton reaction. Studies of free radical scavengers such as tirilazad mesylate, or substances to reduce free radical concentrations such as superoxide dismutase, have failed to improve outcome in brain injuries of various types. The largest such study, MRC CRASH, which used a dose of methylprednisolone that was a very effective free radical scavenger, actually had higher mortality in the active treatment group (Edwards et al. 2005). Chelating iron has similarly been ineffective. Improved strategies for dealing with oxygen-derived free radicals are in development (Ma et al. 2017; Frati et al. 2017).

In the mid-1990s, deoxyglucose PET studies indicated the presence of hyperglycolysis in areas of severe injury, suggesting that mitochondria were unable to use the oxygen being delivered (Bergsneider et al. 1997). This finding correlated with microdialytic studies suggesting the same problem. Studies of mitochondria in resected tissue specimens indicated a defect in the function of mitochondrial transition pores, which could be partially corrected with cyclosporin (Yokobori et al. 2014). However, initial human studies with cyclosporin were discouraging, and research into its use in the treatment of this problem has stagnated (Mazzeo et al. 2009).

More recent studies by the Cambridge neurocritical care group have underscored another potential cause of mitochondrial metabolic difficulty after trauma. Electronic microscopic analysis of tissue resected in the management of increased intracranial pressure suggests a substantial degree of impairment of oxygen diffusion from the capillaries to the mitochondria because of endothelial swelling, microvascular collapse, and perivascular edema (Menon et al. 2004).

The finding that mitochondria may not be receiving adequate oxygen to supply the energy needs of the brain suggests that attempts to improve oxygen delivery may be useful. Tissue brain oxygen monitors, discussed in (Chap. 23), allow the clinician to introduce therapies to restore brain oxygen delivery to more normal levels. Early attempts to do so in head trauma (Spiotta et al. 2010) and subarachnoid hemorrhage (Ramakrishna et al. 2008) appear promising. A phase 2 trial comparing conventional ICP/

Table 56.2 Techniques for improving brain oxygen delivery

Goal	Technique
Increase blood oxygen carrying capacity	RBC transfusion
Increase oxygen dissolved in plasma	Increase FiO ₂ Increase PEEP
Increase cerebral blood flow	Raise MAP with vasopressors Increase collateral blood flow by raising cardiac output with inotropes Allow modest vasodilation by slightly decreasing minute ventilation

CPP management to brain oxygen optimization showed that the techniques proposed for improving brain oxygen delivery were successful in accomplishing this goal safely (Okonkwo et al. 2017). Although clinical outcomes were not the object of the study, both mortality and poor outcomes were lower in the brain oxygen group. Techniques used to improve brain oxygen are listed in Table 56.2. A phase 3 study has been funded to determine whether this strategy improves clinical outcomes.

The future of cerebrovascular monitoring will depend in part on its inclusion as a component of multimodality monitoring. The most important additional techniques are surface and cortical electroencephalographic monitoring to detect sustained depolarizations, which appear to play an important role in secondary injury in both trauma and cerebrovascular disorders (Eriksen et al. 2019). Originally described in 1944 by Leão as “spreading depression,” (Leão 1944) this phenomenon is capable of producing ischemia at sites removed from the original injury and helps to explain many potentially destructive phenomena such as delayed ischemic damage after subarachnoid hemorrhage.

References

- Akbik OS, Carlson AP, Krasberg M, Yonas H. The utility of cerebral blood flow assessment in TBI. *Curr Neurol Neurosci Rep.* 2016;16:72.

- Bouma GJ, Muizelaar JP, Stringer WA, Choi SC, Fatouros P, Young HF. Ultra-early evaluation of regional cerebral blood flow in severely head-injured patients using xenon-enhanced computerized tomography. *J Neurosurg.* 1992;77:360–8.
- Carney N, Totten AM, O'Reilly C, et al. Guidelines for the management of severe traumatic brain injury, fourth edition. *Neurosurgery.* 2017;80:6–15.
- Christensen HL, Barbuskaite D, Rojek A, et al. The choroid plexus sodium-bicarbonate cotransporter NBCe2 regulates mouse cerebrospinal fluid pH. *J Physiol.* 2018;596:4709–28.
- Coles JP, Minhas PS, Fryer TD, et al. Effect of hyperventilation on cerebral blood flow in traumatic head injury: clinical relevance and monitoring correlates. *Crit Care Med.* 2002;30:1950–9.
- Diringer MN, Videen TO, Yundt K, et al. Regional cerebrovascular and metabolic effects of hyperventilation after severe traumatic brain injury. *J Neurosurg.* 2002;96:103–8.
- Edwards P, Arango M, Balica L, et al. Final results of MRC CRASH, a randomised placebo-controlled trial of intravenous corticosteroid in adults with head injury—outcomes at 6 months. *Lancet.* 2005;365:1957–9.
- Frati A, Cerretani D, Fiaschi AI, et al. Diffuse axonal injury and oxidative stress: a comprehensive review. *Int J Mol Sci.* 2017;18:E2600.
- Lang EW, Lagopoulos J, Griffith J, et al. Cerebral vasomotor reactivity testing in head injury: the link between pressure and flow. *J Neurol Neurosurg Psychiatry.* 2003;74:1053–9.
- Ma MW, Wang J, Zhang Q, et al. NADPH oxidase in brain injury and neurodegenerative disorders. *Mol Neurodegener.* 2017;12(1):7.
- Muizelaar JP, Marmarou A, Ward JD, et al. Adverse effects of prolonged hyperventilation in patients with severe head injury: a randomized clinical trial. *J Neurosurg.* 1991;75:731–9.
- Oertel M, Kelly DF, Lee JH, et al. Efficacy of hyperventilation, blood pressure elevation, and metabolic suppression therapy in controlling intracranial pressure after head injury. *J Neurosurg.* 2002;97:1045–53.
- Peterson E, Chesnut RM. Static autoregulation is intact in majority of patients with severe traumatic brain injury. *J Trauma.* 2009;67:944–9.
- Thomas E, Czosnyka M, Hutchinson P. Calculation of cerebral perfusion pressure in the management of traumatic brain injury: joint position statement by the councils of the Neuroanaesthesia and critical Care Society of Great Britain and Ireland (NACCS) and the Society of British Neurological Surgeons (SBNS). *Br J Anaesthesia.* 2015;115:457–88.
- Bergsneider M, Hovda DA, Shalmon E, et al. Cerebral hyperglycolysis following severe traumatic brain injury in humans: a positron emission tomography study. *J Neurosurg.* 1997;86:241–51.
- Yokobori S, Mazzeo AT, Gajavelli S, Bullock MR. Mitochondrial neuroprotection in traumatic brain injury: rationale and therapeutic strategies. *CNS Neurol Disord Drug Targets.* 2014;13:606–19.
- Mazzeo AT, Brophy GM, Gilman CB, et al. Safety and tolerability of cyclosporin a in severe traumatic brain injury patients: results from a prospective randomized trial. *J Neurotrauma.* 2009;26:2195–206.
- Menon DK, Coles JP, Gupta AK, et al. Diffusion limited oxygen delivery following head injury. *Crit Care Med.* 2004;32:1384–90.
- Spiotto AM, Stiefel MF, Gracias VH, et al. Brain tissue oxygen-directed management and outcome in patients with severe traumatic brain injury. *J Neurosurg.* 2010;113:571–80.
- Ramakrishna R, Stiefel M, Udoetuk J, et al. Brain oxygen tension and outcome in patients with aneurysmal subarachnoid hemorrhage. *J Neurosurg.* 2008;109:1075–82.
- Okonkwo DO, Shutter LA, Moore C, et al. Brain Oxygen Optimization in Severe Traumatic Brain Injury Phase-II: A Phase II Randomized Trial. *Crit Care Med.* 2017;45:1907–14.
- Eriksen N, Rostrup E, Fabricius M, et al. Early focal brain injury after subarachnoid hemorrhage correlates with spreading depolarizations. *Neurology.* 2019;92:e326–41.
- Leão AAP. Spreading depression of activity in the cerebral cortex. *J Neurophysiol.* 1944;7:359–90.



Alex K. Pearce, Jamie Labuzetta, Atul Malhotra,
and Biren B. Kamdar

Introduction: ICU Delirium and its Consequences

The Diagnostic and Statistical Manual of Mental disorders (DSM-5) defines delirium as “a disturbance of consciousness characterized by acute onset and fluctuating course of inattention accompanied by either a change in cognition or a perceptual disturbance, so that a patient’s ability to receive, process, store, and recall information is impaired” (American Psychiatric 2013). This disturbance is acute, typically developing over hours to days, and a stark deviation from the patient’s baseline. Moreover, this change in consciousness cannot be explained by another cause such as intoxication or an underlying medical condition (e.g., dementia).

A. K. Pearce (✉) · B. B. Kamdar
Division of Pulmonary, Critical Care, Sleep Medicine
and Physiology, University of California San Diego,
La Jolla, CA, USA
e-mail: apearce@ucsd.edu; bkamdar@ucsd.edu

J. Labuzetta
Division of Neurocritical Care, Department of
Neurosciences, University of California San Diego,
La Jolla, CA, USA
e-mail: jlubuzetta@ucsd.edu

A. Malhotra
UC San Diego, Department of Medicine,
La Jolla, CA, USA
e-mail: amalhotra@ucsd.edu

Delirium is common in the intensive care unit (ICU). Various studies have demonstrated that at least one-third of critically ill patients will develop delirium over the course of their ICU stay (Ely et al. 2007; Ely et al. 2004; van den Boogaard et al. 2012; Salluh et al. 2015). Incidence of delirium is even higher among mechanically ventilated patients (Ely et al. 2007; Ely et al. 2004; van den Boogaard et al. 2012; Salluh et al. 2015). Delirium is associated with increased mortality and length of hospital admission (Ely et al. 2004; Ely et al. 2001a). A recent meta-analysis demonstrated that the development of delirium in the ICU was associated with a two-fold increased relative risk of in-hospital mortality (Salluh et al. 2015).

An episode of delirium can have severe, lasting consequences extending beyond the index hospitalization. Patients experiencing ICU delirium have increased mortality up to 12 months following hospital discharge (Pisani et al. 2009). Delirium has been identified as an independent predictor of cognitive impairment 3 and 12 months following hospital discharge (Girard et al. 2010a; Pandharipande et al. 2013). Additionally, increased duration of delirium was associated with impairment in activities of daily living and motor sensory function (Brummel et al. 2014). To date, delirium has not been associated with an increased risk of mental health problems such as anxiety, depression, or post-traumatic stress (Wolters et al. 2016).

Established tools have been validated for bedside detection of delirium in the ICU (Ely et al. 2001b). Identification of risk factors and evaluation of non-pharmacological and pharmacological management strategies are ongoing areas of investigation. Emphasis on identification, prevention, and treatment of delirium is vital in improving outcomes in critically ill patients. This chapter discusses the pathophysiology and risk factors for delirium in the ICU, along with management approaches.

Delirium Definition and Epidemiology

Delirium is described as an acute disturbance of consciousness, characterized by fluctuating levels of inattention and disorganized thinking. While the clinical presentation of delirium is variable, it typically develops early during ICU admission, with the majority of afflicted patients developing delirium within the first 48 hours of their ICU stay (Peterson et al. 2006). Clinical manifestations of delirium in the ICU are diverse and vary from patient to patient. Patients often experience impairments in memory and orientation, accompanied by difficulty with language and thought processes. Other frequently observed symptoms include sleep-wake cycle disruption, motor disturbances (hyperactive or hypoactive), mood changes, and hallucinations and/or delusions. Sleep-wake cycle disruption is often the earliest manifestation of delirium, characterized by insomnia, daytime sleepiness, and/or complete sleep-wake reversal. Inattention is also often present in the early stages of delirium. Patients can suffer from hallucinations, described as simple, visual, or somatic in comparison to more complex hallucinations associated with other major psychotic disorders (Meagher 2009).

Delirium is categorized into three subtypes: (American Psychiatric 2013) hyperactive (agitated); (Ely et al. 2007) hypoactive; and (Ely et al. 2004) mixed. Hypoactive delirium is characterized by lethargy, slowed speech, and psychomotor slowing (Liptzin and Levkoff 1992). Hypoactive delirium can be difficult to differenti-

ate from acute metabolic encephalopathy, and for this reason is often missed by clinicians (Pandharipande et al. 2007a). Hyperactive delirium is easier to recognize as patients are overtly agitated and often require pharmacologic or physical interventions.

In critically ill patients, hypoactive and mixed delirium subtypes predominate, comprising 27–55% and 36–44% of delirium episodes in the ICU, respectively (Peterson et al. 2006; Rood et al. 2019). Older patients (e.g., ≥ 65 years old) have a higher rate of hypoactive delirium as compared to younger patients (Peterson et al. 2006). As compared to hyperactive delirium, hypoactive and mixed delirium have been associated with higher mortality; however, further research is needed to evaluate this association (Rood et al. 2019; Meagher et al. 2000).

Delirium Pathophysiology

Though its mechanisms are complex and poorly understood, the high prevalence and adverse consequences of ICU delirium have motivated a growing body of research aimed at disentangling causal pathways. Several pathways have been proposed, including those involving neurotransmitter imbalance, inflammation, hypoxia, sleep disruption, and circadian rhythm disturbance. In critically ill patients exposed to a complex ICU environment, these pathways co-exist, rarely acting independently (Maldonado 2013). The theories underlying the pathogenesis of delirium provide a framework for studies focused on the identification, treatment, and prevention of delirium in the ICU.

Neurotransmitter imbalance during acute illness, specifically acetylcholine (ACh) and dopamine, are linked to delirium. Acetylcholine plays an important role in attention and consciousness (Hshieh et al. 2008). Increased serum anticholinergic levels are often seen in patients with delirium (Flacker et al. 1998). The involvement of ACh is reinforced by the observation that anticholinergic medications are associated with delirium and hyperactivity (Han et al. 2001; Meagher 2001). Despite these observations, delirium prevention trials evaluating the use of medications that oppose

anticholinergic activity, such as one involving the anticholinesterase inhibitor donepezil in the post-operative setting, have been largely unsuccessful (Liptzin et al. 2005).

Dopamine excess has also been cited as a contributor to delirium development (Trzepacz 2000). The importance of the dopaminergic system is reflected clinically in the pharmacological approach to delirium management. Dopamine antagonism serves as a key target for delirium prevention, although most trials to date have been inconclusive (discussed in more detail in “Prevention and Treatment” below).

Abnormalities in GABA and glutamate are also identified as participants in the delirium pathway. GABA levels vary based on different clinical scenarios (Maldonado 2013). For example, elevated GABA is thought to play a role in the development of hepatic encephalopathy (Maldonado 2013; Ahboucha and Butterworth 2004; Ahboucha et al. 2004). Additionally, this mechanism has been linked with the observed association of benzodiazepine sedative infusions and incident delirium (Pandharipande et al. 2006).

A neuro-inflammatory mechanism is also implicated in ICU delirium. A systemic inflammatory state is common in patients admitted to the ICU. Elevation in inflammatory cytokines such as IL-8 is seen in patients with delirium (van den Boogaard et al. 2011). Pro-inflammatory cytokines have been linked with decreased cholinergic activity (Eikelenboom et al. 2002). Hypoxia, oxidative stress, and disruption in oxidative metabolism contribute to cerebral dysfunction (Seaman et al. 2006). Furthermore, the pro-inflammatory state experienced by many ICU patients can lead to disruption in the blood-brain barrier/endothelium allowing pathogens and cytokines to penetrate the brain, causing neuronal dysfunction leading to delirium (Slooter et al. 2017). Hence, delirium is considered by some to be the central nervous system (CNS) manifestation of systemic inflammation (Maldonado 2008).

Finally, sleep-wake and circadian rhythm disruption are implicated in the development of delirium (Jacobson et al. 2008). As discussed in “Definition and Epidemiology” above, sleep-

wake disturbance is often an early sign of delirium. Melatonin is intricately tied to the sleep-wake regulation. Primarily synthesized in the pineal gland, melatonin release is suppressed by light and promotes a new cycle of melatonin synthesis (which peaks at night). Darkness then prompts melatonin release. Melatonin exerts considerable influence over the suprachiasmatic nucleus, which is responsible for maintaining circadian rhythms. Delirious patients often exhibit low levels of melatonin (Mo et al. 2015). For example, irregular and low levels of melatonin are seen in the patients who develop delirium (Miyazaki et al. 2003). The irregular melatonin secretion alters the homeostatic circadian sleep-wake rhythm (BaHamam 2006). The association between melatonin, sleep-wake rhythm disturbance, and delirium is clear; however, a causal relationship has not been established. The relationship of melatonin, sleep-wake disturbance, and delirium represents intriguing areas of research.

Delirium Identification

Recognition of delirium is a critical first step in management. Early studies showed that delirium is generally under-identified in real-world ICU settings (van den Boogaard et al. 2012). Several widely available delirium screening tools have been developed, and two, the Confusion Assessment Method-Intensive Care Unit (CAM-ICU) and Intensive Care Delirium Screening Checklist (ICDSC), are recommended in the Society of Critical Care Medicine Clinical Practice Guidelines (Ely et al. 2001a). The CAM was initially introduced for screening delirium in non-ICU hospitalized patients (Inouye et al. 1990); a modified “ICU” version was subsequently developed for use in the critical care setting. The CAM-ICU is simple to perform, requiring <2 minutes, and can easily be performed by any member of the medical team (Table 57.1). Both CAM-ICU and ICDSC are simple and efficient screening tools specifically intended for the critical care environment.

As part of standard ICU delirium screening, a standardized sedation evaluation is required,

Table 57.1 Delirium screening methods

The confusion assessment method for the intensive care unit	The intensive care delirium screening check list
CAM-ICU	ICDSC
1. Acute onset and/or fluctuating mental status ^a	1. Altered level of consciousness ^d
2. Inattention ^b	2. Inattention
3. Altered level of consciousness (RASS \neq 0) ^c	3. Disorientation
4. Disorganized thinking	4. Hallucination delusion or psychosis
<u>Interpretation:</u> Positive CAM-ICU (indicating delirium): Criterion 1 and 2 <u>both</u> positive AND Either 3 <u>or</u> 4 positive	5. Psychomotor agitation or retardation
	6. Inappropriate speech or mood
	7. Sleep-wake cycle disturbance
	8. Symptom fluctuation
	<u>Scoring (1 point for each item present)</u>
	0: No delirium
	1–3: Subsyndromal delirium
	4–8: Delirium

CAM-ICU and ICDSC are two methods commonly used to screen for delirium in the ICU. Both screening methods require RASS score (–) 2 to (+)4. CAM-ICU and ICDSC cannot be performed on deeply sedated or comatose patients (RASS –4, –5) (Ely et al. 2001a; Ely et al. 2001b; Bergeron et al. 2001; Ouimet et al. 2007).

^aAcute change in mental status or fluctuation from baseline within the past 24 hours

^bInattention is evaluated using either visual or auditory components of attention screening examination (ASE)

^cPositive if RASS score is any value other than 0

^dAssessed based on number of errors in answering a pre-defined set of yes or no questions, or if patient is nonverbal, errors in completing 2 step commands

most often utilizing the Richmond Agitation-Sedation Scale (RASS) (Table 57.2) or Riker Sedation Agitation Scale (SAS) (Sessler et al. 2002; Riker et al. 1999). RASS scores range from minus-5 (comatose) to plus-4 (combative, violent, danger to staff), and corresponding SAS scores range from 1 to 7, with RASS = 0 and SAS = 4 indicating a calm and cooperative patient. For a patient to be evaluated for delirium, they must have a RASS of minus-3 (SAS = 3) or higher, denoting moderate sedation-movement or eye-opening to voice, but no eye contact. These sedation scales further delineate hyperactive versus hypoactive delirium. For example, if a patient

Table 57.2 Richmond Agitation-Sedation Scale (RASS)

4	Combative	Overly combative, violent, immediate danger to staff
3	Very agitated	Pulls or removes tubes or catheters
2	Agitated	Frequent non-purposeful movement, fighting ventilator
1	Restless	Anxious but movements not aggressive or vigorous
0	Alert and calm	Alert and calm
(–)1	Drowsy	Not fully alert, but has sustained awakening (eye-opening or eye-contact) in response to voice (>10 seconds)
(–)2	Light sedation	Briefly awakens with eye contact to voice (<10 seconds)
(–)3	Moderate sedation	Movement or eye opening to voice, but no eye contact
(–)4	Deep sedation	No response to voice, but movement or eye opening to physical stimulation
(–)5	Unarousable	No response to voice or physical stimulation

Reprinted with permission of the American Thoracic Society. Copyright © 2019 American Thoracic Society. Sessler et al. (2002)

is identified as delirious by the CAM-ICU assessment, a corresponding positive RASS score would indicate hyperactive delirium, while a negative score would indicate a hypoactive subtype.

Importantly, several novel strategies are currently under investigation such as the Edinburgh Delirium Test Box (EDTB-ICU), which incorporates computerized, objective, graded assessment of delirium that can be monitored over time (Green et al. 2017). Additional research is aimed at creating prediction models to identify high-risk patients to provide targeted, intensive, preventative strategies. (van den Boogaard et al. 2012)

Risk Factors

The risk of developing ICU delirium rises in the presence of predisposing factors, such as older age and pre-existing cognitive impairments, and precipitating factors such as critical illness and

Table 57.3 Delirium risk factors (Pandharipande et al. 2006; Zaal et al. 2015; Miyazaki et al. 2011; Van Rompaey et al. 2009)

Predisposing	Precipitating
Older age	<i>Non-modifiable</i>
Alcohol use	Emergency surgery
Baseline hypertension	Metabolic acidosis
Baseline cognitive impairment	Illness severity
Genetics (e.g., apolipoprotein E4 polymorphism)	Anemia
Nicotine use	Organ failure
	<i>Modifiable</i>
	Benzodiazepine infusions
	Mechanical ventilation
	Immobilization
	Unwanted sounds
	Lack of daylight
	Disrupted sleep-wake cycles
	Physical restraints

medications. Risk factors for ICU delirium can be categorized into non-modifiable versus modifiable, and predisposing as well as precipitating (Table 57.3).

Delirium Prevention and Treatment

PADIS Guidelines and the ABCDEF Bundle

In 2018, the Society of Critical Care Medicine appended their 2013 Clinical Practice Guidelines for the Prevention and Management of Pain, Agitation/Sedation, Delirium (PAD) in Adult Patients in the ICU, adding Immobility and Sleep Disruption (PADIS) to provide an up-to-date, comprehensive framework for use in all adult ICU settings (Devlin et al. 2018). Implementation of these guidelines requires an interdisciplinary, multicomponent approach such as the “ABCDEF” bundle, referring to complementary actions to (A) assess, prevent, and manage pain; promote (B)oth spontaneous awakening and breathing trials; (C)hoose Analgesia and Sedation; assess, prevent, and manage (D)elirium; promote (E)arly mobility and exercise; and encourage (F)amily engagement and empowerment (Table 57.4) (Marra et al. 2017). Notably, each implemented component of

Table 57.4 ABCDEF Critical Care Bundle

Bundle component	Description
(A) Assess, prevent, and manage pain	Understand pain and its triggers and utilize screening tools to determine the best analgesia only or analgesodation strategy for the patient
(B) Both SAT and SBT	Light sedation is preferred in mechanically ventilated patients. Pair interruptions in sedation with spontaneous breathing trials
(C) Choice of analgesia and sedation	Choose the right sedative for the patient’s clinical picture. Avoid benzodiazepines when able
(D) Delirium: Assess, prevent, and manage	Routinely screen for delirium with a validated tool. Promote early mobilization and sleep. Avoid benzodiazepines. Pharmacologic prophylaxis is not recommended
(E) Early mobility and exercise	Early (within 48 hours) mobility and exercise is necessary for all patients, even those who are mechanically ventilated
(F) Family engagement	Family involvement in decision making and treatment can improve recovery

The ABCDEF critical care bundle has evolved over time with the addition of additional components to optimize care of critically ill patients (Devlin et al. 2018; Marra et al. 2017; Balas et al. 2014)

the ABCDEF bundle has been shown to produce step-wise improvements in clinical outcomes, including incremental decreases in duration of mechanical ventilation and hospital length of stay (Hsieh et al. 2019). While delirium is a specific domain of this implementation bundle, each bundle element influences the other, with all elements playing a role in delirium management. The key delirium-focused elements of PADIS and ABCDEF are discussed below.

Nonpharmacological Interventions

The optimal approach for delirium prevention must be tailored based on barriers and opportunities unique to each ICU. As a rule of thumb, non-pharmacological interventions are the cornerstone and first step of delirium prevention and treatment.

Environment

Because the interventions are often low cost, common sense, easy to perform, and of minimal risk to patients, environmental optimization should be considered “first line” in the management of ICU delirium. Such interventions include critical evaluation of the patient environment and delivery of familiar devices or aids (i.e., glasses, hearing aids, time outdoors, pets, music) or minimization of noxious stimuli, including unwanted sounds and lights (see Sleep below).

Early Rehabilitation and Mobilization

Immobility is common in critical illness and associated with adverse outcomes including critical illness myopathy, pressure ulcers, and delirium. While prolonged bed rest was once considered essential to recovery (Brower 2009), numerous studies over the past decade have flipped this paradigm, demonstrating that early and frequent rehabilitation and mobilization interventions are safe, with minimal adverse events observed, and associated with improved ICU outcomes (Devlin et al. 2018; Nydahl et al. 2017). These findings were supported by a landmark randomized controlled trial (Schweickert et al. 2009; Schweickert and Kress 2011) which evaluated early exercise and mobilization combined with daily sedation interruption (within the first 72 hours of intubation) versus usual care in mechanically ventilated patients. As compared with the usual care arm, patients in the intervention arm experienced a shorter duration of delirium (4 versus 2 days), ventilator-free days (23.5 versus 21.1 days), and increased return to independent functional status at discharge (59% versus 35%) (Schweickert et al. 2009; Schweickert and Kress 2011). Additionally, a pre-post quality improvement study demonstrated that a multidisciplinary early rehabilitation intervention decreased ICU and hospital length of stay by 2.1 and 3.1 days, respectively. Finally, a recent systematic review evaluating 22,351 mobility sessions in 7546 critically ill patients demonstrated that potential safety events (i.e., hemodynamic changes) were rare, occurring in fewer than 3.8 of every 1000 mobilization/rehabilitation sessions (Nydahl et al. 2017). Hence, early rehabili-

tation and mobilization are safe, vital to patient outcomes, and, importantly, should occur early during ICU admission, within the first 48 hours. Early rehabilitation and mobilization interventions should be considered a cornerstone of modern ICU care.

Sleep

Sleep disruption in the ICU also likely has implications in the development of delirium. Numerous studies have demonstrated that critically ill patients commonly experience poor sleep quality (Elliott et al. 2013; Cooper et al. 2000). While the association of poor sleep quality and delirium remains unclear and methodologically complicated to evaluate, a correlation has been shown between REM deprivation and delirium, and between lack of N2 sleep, delirium severity, and increased odds of death (Trompeo et al. 2011). Despite a paucity of clear causative data, the majority of intensivists feel poor sleep adversely affects ICU outcomes and is a contributor to delirium (Kamdar et al. 2016a). While poor sleep is gaining attention as a problem in the ICU, protocolized sleep-promoting interventions are generally lacking (Kamdar et al. 2016a). Initial efforts to improve sleep should include the formation of a multidisciplinary team (Kamdar et al. 2014; Kamdar et al. 2016b) and identification of feasible intervention targets, such as discontinuation of unnecessary medications that may interfere with sleep and minimization of unwanted noise (i.e., staff conversations, alarms, and squeaky shoes) in the ICU (Freedman et al. 2001). Although noise levels in the ICU can be problematic, the abrupt changes in noise level may be particularly disruptive to sleep in the ICU patient (Stanchina et al. 2005). Non-pharmacological interventions such as ear plugs and eye masks may also play a role in sleep improvement (Demoule et al. 2017). Music therapy, another example of nonpharmacologic intervention, showed a significant decrease in patient anxiety, and a greater reduction in sedative exposure (Chlan et al. 2013). Finally, increased attention is being paid to the promotion of daytime wakefulness, including out of bed activities and provision of bright light, as methods to promote

sleep and prevent sleep-wake rhythm misalignment (Oldham et al. 2016; Danielson et al. 2018).

Pharmacological Interventions

Individual drugs (e.g., benzodiazepines), drug-drug interactions, and withdrawal from drugs have been associated with delirium in the ICU. Thus, medication lists should be reviewed frequently and modified, if possible, if potentially deliriogenic medications have been prescribed. Recent literature has highlighted the potential role of medications for delirium prophylaxis and treatment, with mixed results.

Drugs for Delirium Prophylaxis and Treatment

Several studies have evaluated the efficacy of pharmacologic prophylaxis for delirium (Wang et al. 2012; Su et al. 2016; Prakanrattana and Prapaitrakool 2007). Specific drugs have been targeted based on the pathophysiological pathways implicated in the development of delirium such as typical and atypical antipsychotics. For example, haloperidol is a dopamine antagonist that targets the dopaminergic system, a pathway often upregulated in delirium (Trzepacz 2000). Dexmedetomidine is another drug of interest and specifically activates alpha-2 receptors and is involved in neurotransmitter regulation, although its exact mechanism is not entirely understood (Gertler et al. 2001).

Early studies evaluated the use of haloperidol, dexmedetomidine, and risperidone in a prophylactic role (Wang et al. 2012; Su et al. 2016; Prakanrattana and Prapaitrakool 2007). For example, two early studies evaluated pharmacologic prophylactic strategies, in non-cardiac post-operative patients using haloperidol and dexmedetomidine (Wang et al. 2012; Su et al. 2016). Both studies showed decreased incidence of delirium in the first seven days following surgery in the pharmacologic intervention group. Similarly, atypical antipsychotics such as risperidone were also trialed in post-operative cardiac patients, with similar results (Prakanrattana and Prapaitrakool 2007); however, these studies were limited in their enrollment of

mostly post-operative patients who were less vulnerable to delirium (Wang et al. 2012; Su et al. 2016; Prakanrattana and Prapaitrakool 2007). Two subsequent larger trials evaluated pharmacologic interventions in general ICU populations, with equivocal results (Kamdar et al. 2014; Kamdar et al. 2016b). First, the REDUCE randomized clinical trial, which enrolled 1789 patients examined haloperidol in a prophylactic role and showed no improvement in delirium prevention or overall mortality (van den Boogaard et al. 2018). Another recent study evaluated the administration of low-dose dexmedetomidine at night for delirium prevention and sleep promotion (Skrobik et al. 2018). Although nocturnal low-dose dexmedetomidine showed a reduction in incident delirium, it did not lead to improved sleep; additional studies are needed in this area (Skrobik et al. 2018).

Overall, based on current evidence, there is no recommendation for pharmacologic prophylaxis of delirium in the ICU (Devlin et al. 2018). Similarly, pharmacologic treatment of delirium, once it has occurred, has not been shown to improve outcomes (Devlin et al. 2010; Girard et al. 2010b; Page et al. 2013; Girard et al. 2018). Specifically, the MIND-USA trial evaluated the administration of haloperidol or ziprasidone versus placebo in critically ill patients with hypoactive and hyperactive delirium (Girard et al. 2018). The primary outcome was median days alive without delirium or coma, with no difference demonstrated when comparing the intervention and control groups (Girard et al. 2018). While many studies are underway, including studies evaluating haloperidol for delirium treatment, the influence of dexmedetomidine or propofol on ICU delirium ([ClinicalTrials.gov](https://clinicaltrials.gov) ID NCT02807467), ramelteon (NCT02807467), as well as ketamine for delirium prevention in post-surgical patients (NCT02807467), there are currently no compelling data to support the use of medications to either prevent or treat delirium. Hence, the mainstay of delirium management involves non-pharmacologic interventions, including avoidance of deliriogenic medications and interventions involving the promotion of early mobility/rehabilitation and aligned sleep-wake cycles.

Analgesia and Sedation Management

Analgesia and sedation are often considered concurrently, and play an important role in ICU delirium. Pain assessment and management should be prioritized before adding sedative agents (Devlin et al. 2018). Control of pain is particularly important not only for patient comfort but for preventing delirium precipitated by uncontrolled pain (Chanques et al. 2010). The PADIS guidelines suggest regularly assessing for pain in the ICU and initiating appropriate treatment (Devlin et al. 2018). Although vital sign changes can often clue providers to uncontrolled pain, particularly in mechanically ventilated patients, their role as a proxy for pain is largely inconsistent and therefore should be interpreted with caution (Arbour and Gelinas 2010). The PADIS guidelines recommend a multimodal approach to pain: use of both opioid and non-opioid analgesics as well as non-pharmacologic interventions. Regarding opioid therapy, the lowest effective dose to achieve analgesia is recommended. Adjunctive non-opioid and non-pharmacologic therapies are emphasized to facilitate opioid-sparing management.

After addressing analgesia, some patients will also require sedation, especially those receiving mechanical ventilation. Sedation targeted to a specific level, with a thoughtful selection of sedative agents, is vital to minimize sedation-induced delirium and associated adverse outcomes.

In general, critically ill mechanically ventilated patients should be maintained on as little sedation as possible, e.g., with a RASS target of minus-2 to plus-1 (Devlin et al. 2018). This concept stemmed from the introduction of the spontaneous awakening trial (SAT) (Kress et al. 2000), where mechanically ventilated patients were randomized to daily sedation interruption versus usual care. As compared to usual care, this study demonstrated a significant association with daily sedation interruption with decreased length of mechanical ventilation (4.9 versus 7.3 days) and ICU length of stay (6.4 versus 9.9 days) (Kress et al. 2000). Building on the daily sedation holiday concept, experts now recommend minimal/light sedation throughout the day instead of a single daily interruption (Devlin et al. 2018). Although light sedation has not been shown to

decrease incident delirium or mortality, (Pandharipande et al. 2007b; Shehabi et al. 2013) minimal sedation practices decrease time to extubation, need for tracheostomy (Tanaka et al. 2014), and facilitate rehabilitation and mobilization interventions (Devlin et al. 2018). When considering ventilator liberation, sedation interruption should be paired with spontaneous breathing trials with the goal of having an awake and alert patient breathing comfortably on minimum ventilator settings.

Sedative choice is also important to minimize delirium risk. In 2006, a landmark study of mechanically ventilated ICU patients demonstrated an independent association of continuous benzodiazepine infusions with incident delirium, with a dose-dependent effect (Pandharipande et al. 2006). Alternatives such as propofol and dexmedetomidine are used preferentially for sedation in critically ill patients (Schweickert et al. 2009; Schweickert and Kress 2011). This recommendation is based on various studies, including the multicenter SEDCOM RCT which demonstrated that mechanically ventilated patients randomized to receive dexmedetomidine versus continuous midazolam infusions, with as-needed fentanyl and haloperidol boluses in both arms, experienced less delirium (54% versus 77%) and had a shorter time to extubation (3.7 versus 5.9 days) (Riker et al. 2009). A subsequent randomized controlled trial examining dexmedetomidine versus midazolam or propofol infusions demonstrated that patients in the dexmedetomidine arm had a shorter duration of mechanical ventilation; however, they experienced increased adverse effects, specifically hypotension (Jakob et al. 2012). Large retrospective analyses comparing patients receiving propofol- versus benzodiazepine-based sedative infusions demonstrated that patients receiving propofol had significantly shorter ICU lengths of stay and decreased risk of ICU (RR \approx 0.70) and hospital (RR \approx 0.77) mortality (Lonardo et al. 2014). Notably, while each of these sedation studies evaluated continuous benzodiazepine infusions, they did not examine the effect of benzodiazepines administered intermittently as needed or scheduled in bolus form. Limited data exist regarding delirium risk and bolus-dosed

sedation, a compelling area of ongoing investigation.

Choice of sedative agents should take into account patient specifics in addition to medication side effects. Bradycardia and hypotension occasionally occur with dexmedetomidine (Jakob et al. 2012). Additionally, because dexmedetomidine is intended for light to moderate and not deep sedation, it should not be administered as monotherapy for patients requiring neuromuscular blockade. Alternatively, propofol also carries the risk of propofol infusion syndrome, which typically occurs when on high doses of propofol for >48 hours and traditionally is associated with elevated triglycerides, hepatomegaly, and refractory bradycardia (Kam and Cardone 2007). There is also rising interest in the use of ketamine for ICU sedation, although additional studies are needed. Currently, propofol and dexmedetomidine are preferred for sedation in the ICU; however, overall sedation strategy should be determined based on individual patient characteristics.

Conclusion

Delirium presents a complex pathophysiologic phenomenon that frequently occurs in the intensive care environment and poses a challenge to clinicians and health care staff. It is associated with adverse patient outcomes both during the index hospitalization and months to years later. A multifaceted approach is required to identify and manage this common ICU phenomenon, including frequent identification of modifiable risk factors, optimization of the patient environment, sedation minimization, early mobilization/rehabilitation, and promotion of sleep-wake alignment.

References

Ahboucha S, Butterworth RF. Pathophysiology of hepatic encephalopathy: a new look at GABA from the molecular standpoint. *Metab Brain Dis.* 2004;19(3–4):331–43.

Ahboucha S, Pomier-Layrargues G, Butterworth RF. Increased brain concentrations of endogenous

(non-benzodiazepine) GABA-A receptor ligands in human hepatic encephalopathy. *Metab Brain Dis.* 2004;19(3–4):241–51.

American Psychiatric Association DSM-5. *Diagnostic and statistical manual of mental disorders: DSM-5.* 5th ed. Washington, D.C.: American Psychiatric Association; 2013. 947 p.

Arbour C, Gelinas C. Are vital signs valid indicators for the assessment of pain in postoperative cardiac surgery ICU adults? *Intensive Crit Care Nurs.* 2010;26(2):83–90.

BaHammam A. Sleep in acute care units. *Sleep Breath.* 2006;10(1):6–15.

Balas MC, Vasilevskis EE, Olsen KM, Schmid KK, Shostrom V, Cohen MZ, et al. Effectiveness and safety of the awakening and breathing coordination, delirium monitoring/management, and early exercise/mobility bundle. *Crit Care Med.* 2014;42(5):1024–36.

Bergeron N, Dubois MJ, Dumont M, Dial S, Skrobik Y. Intensive Care Delirium Screening Checklist: evaluation of a new screening tool. *Intens Care Med.* 2001;27(0342–4642; 0342–4642; 5):859.

van den Boogaard M, Kox M, Quinn KL, van Achterberg T, van der Hoeven JG, Schoonhoven L, et al. Biomarkers associated with delirium in critically ill patients and their relation with long-term subjective cognitive dysfunction; indications for different pathways governing delirium in inflamed and noninflamed patients. *Crit Care.* 2011;15(6):R297.

van den Boogaard M, Pickkers P, Slooter AJ, Kuiper MA, Spronk PE, van der Voort PH, et al. Development and validation of PRE-DELIRIC (PREdiction of DELIRium in ICU patients) delirium prediction model for intensive care patients: observational multicentre study. *BMJ.* 2012;344:e420.

van den Boogaard M, Slooter AJC, Bruggemann RJM, Schoonhoven L, Beishuizen A, Vermeijden JW, et al. Effect of haloperidol on survival among critically ill adults with a high risk of delirium: the REDUCE randomized clinical trial. *JAMA.* 2018;319(7):680–90.

Brower RG. Consequences of bed rest. *Crit Care Med.* 2009;37(10 Suppl):S422–8.

Brummel NE, Jackson JC, Pandharipande PP, Thompson JL, Shintani AK, Dittus RS, et al. Delirium in the ICU and subsequent long-term disability among survivors of mechanical ventilation. *Crit Care Med.* 2014;42(2):369–77.

Chanques G, Viel E, Constantin JM, Jung B, de Lattre S, Carr J, et al. The measurement of pain in intensive care unit: comparison of 5 self-report intensity scales. *Pain.* 2010;151(3):711–21.

Chlan LL, Weinert CR, Heiderscheid A, Tracy MF, Skaar DJ, Guttormson JL, et al. Effects of patient-directed music intervention on anxiety and sedative exposure in critically ill patients receiving mechanical ventilatory support: a randomized clinical trial. *JAMA.* 2013;309(22):2335–44.

Cooper AB, Thornley KS, Young GB, Slutsky AS, Stewart TE, Hanly PJ. Sleep in critically ill patients requiring mechanical ventilation. *Chest.* 2000;117(3):809–18.

- Danielson SJ, Rappaport CA, Loher MK, Gehlbach BK. Looking for light in the din: an examination of the circadian-disrupting properties of a medical intensive care unit. *Intensive Crit Care Nurs*. 2018;46:57–63.
- Demoule A, Carreira S, Lavault S, Pallanca O, Morawiec E, Mayaux J, et al. Impact of earplugs and eye mask on sleep in critically ill patients: a prospective randomized study. *Crit Care*. 2017;21(1):284.
- Devlin JW, Roberts RJ, Fong JJ, Skrobik Y, Riker RR, Hill NS, et al. Efficacy and safety of quetiapine in critically ill patients with delirium: a prospective, multicenter, randomized, double-blind, placebo-controlled pilot study. *Crit Care Med*. 2010;38(2):419–27.
- Devlin JW, Skrobik Y, Gelinas C, Needham DM, Slooter AJC, Pandharipande PP, et al. Clinical practice guidelines for the prevention and Management of Pain, agitation/sedation, delirium, immobility, and sleep disruption in adult patients in the ICU. *Crit Care Med*. 2018;46(9):e825–e73.
- Eikelenboom P, Hoogendijk WJ, Jonker C, van Tilburg W. Immunological mechanisms and the spectrum of psychiatric syndromes in Alzheimer's disease. *J Psychiatr Res*. 2002;36(5):269–80.
- Elliott R, McKinley S, Cistulli P, Fien M. Characterisation of sleep in intensive care using 24-hour polysomnography: an observational study. *Crit Care*. 2013;17(2):R46.
- Ely EW, Margolin R, Francis J, May L, Truman B, Dittus R, et al. Evaluation of delirium in critically ill patients: validation of the confusion assessment method for the intensive care unit (CAM-ICU). *Crit Care Med*. 2001a;29(7):1370–9.
- Ely EW, Inouye SK, Bernard GR, Gordon S, Francis J, May L, et al. Delirium in mechanically ventilated patients: validity and reliability of the confusion assessment method for the intensive care unit (CAM-ICU). *JAMA*. 2001b;286(21):2703–10.
- Ely EW, Shintani A, Truman B, Speroff T, Gordon SM, Harrell FE Jr, et al. Delirium as a predictor of mortality in mechanically ventilated patients in the intensive care unit. *JAMA*. 2004;291(14):1753–62.
- Ely EW, Girard TD, Shintani AK, Jackson JC, Gordon SM, Thomason JW, et al. Apolipoprotein E4 polymorphism as a genetic predisposition to delirium in critically ill patients. *Crit Care Med*. 2007;35(1):112–7.
- Flacker JM, Cummings V, Mach JR Jr, Bettin K, Kiely DK, Wei J. The association of serum anticholinergic activity with delirium in elderly medical patients. *Am J Geriatr Psychiatry*. 1998;6(1):31–41.
- Freedman NS, Gazendam J, Levan L, Pack AI, Schwab RJ. Abnormal sleep/wake cycles and the effect of environmental noise on sleep disruption in the intensive care unit. *Am J Respir Crit Care Med*. 2001;163(2):451–7.
- Gertler R, Brown HC, Mitchell DH, Silvius EN. Dexmedetomidine: a novel sedative-analgesic agent. *Proc (Bayl Univ Med Cent)*. 2001;14(1):13–21.
- Girard TD, Jackson JC, Pandharipande PP, Pun BT, Thompson JL, Shintani AK, et al. Delirium as a predictor of long-term cognitive impairment in survivors of critical illness. *Crit Care Med*. 2010a;38(7):1513–20.
- Girard TD, Pandharipande PP, Carson SS, Schmidt GA, Wright PE, Canonic AE, et al. Feasibility, efficacy, and safety of antipsychotics for intensive care unit delirium: the MIND randomized, placebo-controlled trial. *Crit Care Med*. 2010b;38(2):428–37.
- Girard TD, Exline MC, Carson SS, Hough CL, Rock P, Gong MN, et al. Haloperidol and ziprasidone for treatment of delirium in critical illness. *N Engl J Med*. 2018;379(26):2506–16.
- Green C, Hendry K, Wilson ES, Walsh T, Allerhand M, MacLulich AMJ, et al. A novel computerized test for detecting and monitoring visual attentional deficits and delirium in the ICU. *Crit Care Med*. 2017;45(7):1224–31.
- Han L, McCusker J, Cole M, Abrahamowicz M, Primeau F, Elie M. Use of medications with anticholinergic effect predicts clinical severity of delirium symptoms in older medical inpatients. *Arch Intern Med*. 2001;161(8):1099–105.
- Hshieh TT, Fong TG, Marcantonio ER, Inouye SK. Cholinergic deficiency hypothesis in delirium: a synthesis of current evidence. *J Gerontol A Biol Sci Med Sci*. 2008;63(7):764–72.
- Hsieh SJ, Otusanya O, Gershengorn HB, Hope AA, Dayton C, Levi D, et al. Staged implementation of awakening and breathing, coordination, delirium monitoring and management, and early mobilization bundle improves patient outcomes and reduces hospital costs. *Crit Care Med*. 2019;47(7):885–93.
- Inouye SK, van Dyck CH, Alessi CA, Balkin S, Siegel AP, Horwitz RI. Clarifying confusion: the confusion assessment method. A new method for detection of delirium. *Ann Intern Med*. 1990;113(12):941–8.
- Jacobson SA, Dwyer PC, Machan JT, Carskadon MA. Quantitative analysis of rest-activity patterns in elderly postoperative patients with delirium: support for a theory of pathologic wakefulness. *J Clin Sleep Med*. 2008;4(2):137–42.
- Jakob SM, Ruokonen E, Grounds RM, Sarapohja T, Garratt C, Pocock SJ, et al. Dexmedetomidine vs midazolam or propofol for sedation during prolonged mechanical ventilation: two randomized controlled trials. *JAMA*. 2012;307(11):1151–60.
- Kam PC, Cardone D. Propofol infusion syndrome. *Anaesthesia*. 2007;62(7):690–701.
- Kamdar BB, Yang J, King LM, Neufeld KJ, Bienvenu OJ, Rowden AM, et al. Developing, implementing, and evaluating a multifaceted quality improvement intervention to promote sleep in an ICU. *Am J Med Qual*. 2014;29(6):546–54.
- Kamdar BB, Knauert MP, Jones SF, Parsons EC, Parthasarathy S, Pisani MA, et al. Perceptions and practices regarding sleep in the intensive care unit. A survey of 1,223 critical care providers. *Ann Am Thorac Soc*. 2016a;13(8):1370–7.
- Kamdar BB, Martin JL, Needham DM, Ong MK. Promoting sleep to improve delirium in the ICU. *Crit Care Med*. 2016b;44(12):2290–1.

- Kress JP, Pohlman AS, O'Connor MF, Hall JB. Daily interruption of sedative infusions in critically ill patients undergoing mechanical ventilation. *N Engl J Med*. 2000;342(20):1471–7.
- Liptzin B, Levkoff SE. An empirical study of delirium subtypes. *Br J Psychiatry*. 1992;161:843–5.
- Liptzin B, Laki A, Garb JL, Fingerroth R, Krushell R. Donepezil in the prevention and treatment of post-surgical delirium. *Am J Geriatr Psychiatry*. 2005;13(12):1100–6.
- Lonardo NW, Mone MC, Nirula R, Kimball EJ, Ludwig K, Zhou X, et al. Propofol is associated with favorable outcomes compared with benzodiazepines in ventilated intensive care unit patients. *Am J Respir Crit Care Med*. 2014;189(11):1383–94.
- Maldonado JR. Pathoetiological model of delirium: a comprehensive understanding of the neurobiology of delirium and an evidence-based approach to prevention and treatment. *Crit Care Clin*. 2008;24(4):789–856. ix
- Maldonado JR. Neuropathogenesis of delirium: review of current etiologic theories and common pathways. *Am J Geriatr Psychiatry*. 2013;21(12):1190–222.
- Marra A, Ely EW, Pandharipande PP, Patel MB. The ABCDEF bundle in critical care. *Crit Care Clin*. 2017;33(2):225–43.
- Meagher D. Delirium episode as a sign of undetected dementia among community dwelling elderly subjects. *J Neurol Neurosurg Psychiatry*. 2001;70(6):821.
- Meagher D. Motor subtypes of delirium: past, present and future. *Int Rev Psychiatry*. 2009;21(1):59–73.
- Meagher DJ, O'Hanlon D, O'Mahony E, Casey PR, Trzepacz PT. Relationship between symptoms and motoric subtype of delirium. *J Neuropsychiatry Clin Neurosci*. 2000;12(1):51–6.
- Miyazaki T, Kuwano H, Kato H, Ando H, Kimura H, Inose T, et al. Correlation between serum melatonin circadian rhythm and intensive care unit psychosis after thoracic esophagectomy. *Surgery*. 2003;133(0039–6060); 0039–6060; 6:662.
- Miyazaki S, Yoshitani K, Miura N, Irie T, Inatomi Y, Ohnishi Y, et al. Risk factors of stroke and delirium after off-pump coronary artery bypass surgery. *Interact Cardiovasc Thorac Surg*. 2011;12(3):379–83.
- Mo Y, Scheer CE, Abdallah GT. Emerging role of melatonin and melatonin receptor agonists in sleep and delirium in intensive care unit patients. *J Intensive Care Med*. 2015;
- Nydahl P, Sricharoenchai T, Chandra S, Kundt FS, Huang M, Fischill M, et al. Safety of patient mobilization and rehabilitation in the intensive care unit. Systematic review with meta-analysis. *Ann Am Thorac Soc*. 2017;14(5):766–77.
- Oldham MA, Lee HB, Desan PH. Circadian rhythm disruption in the critically ill: an opportunity for improving outcomes. *Crit Care Med*. 2016;44(1):207–17.
- Ouimet S, Riker R, Bergeron N, Cossette M, Kavanagh B, Skrobik Y. Subsyndromal delirium in the ICU: evidence for a disease spectrum. *Intensive Care Med*. 2007;33(6):1007–13.
- Page VJ, Ely EW, Gates S, Zhao XB, Alce T, Shintani A, et al. Effect of intravenous haloperidol on the duration of delirium and coma in critically ill patients (Hope-ICU): a randomised, double-blind, placebo-controlled trial. *Lancet Respir Med*. 2013;1(7):515–23.
- Pandharipande P, Shintani A, Peterson J, Pun BT, Wilkinson GR, Dittus RS, et al. Lorazepam is an independent risk factor for transitioning to delirium in intensive care unit patients. *Anesthesiology*. 2006;104(1):21–6.
- Pandharipande P, Cotton BA, Shintani A, Thompson J, Costabile S, Truman Pun B, et al. Motoric subtypes of delirium in mechanically ventilated surgical and trauma intensive care unit patients. *Intensive Care Med*. 2007a;33(10):1726–31.
- Pandharipande PP, Pun BT, Herr DL, Maze M, Girard TD, Miller RR, et al. Effect of sedation with dexmedetomidine vs lorazepam on acute brain dysfunction in mechanically ventilated patients: the MENDS randomized controlled trial. *JAMA*. 2007b;298(22):2644.
- Pandharipande PP, Girard TD, Jackson JC, Morandi A, Thompson JL, Pun BT, et al. Long-term cognitive impairment after critical illness. *N Engl J Med*. 2013;369(14):1306–16.
- Peterson JF, Pun BT, Dittus RS, Thomason JW, Jackson JC, Shintani AK, et al. Delirium and its motoric subtypes: a study of 614 critically ill patients. *J Am Geriatr Soc*. 2006;54(3):479.
- Pisani MA, Kong SY, Kasl SV, Murphy TE, Araujo KL, Van Ness PH. Days of delirium are associated with 1-year mortality in an older intensive care unit population. *Am J Respir Crit Care Med*. 2009;180(11):1092–7.
- Prakanrattana U, Prapaitrakool S. Efficacy of risperidone for prevention of postoperative delirium in cardiac surgery. *Anaesth Intensive Care*. 2007;35(5):714–9.
- Riker RR, Picard JT, Fraser GL. Prospective evaluation of the sedation-agitation scale for adult critically ill patients. *Crit Care Med*. 1999;27(7):1325–9.
- Riker RR, Shehabi Y, Bokesch PM, Ceraso D, Wisemandle W, Koura F, et al. Dexmedetomidine vs midazolam for sedation of critically ill patients: a randomized trial. *JAMA*. 2009;301(5):489.
- Rood PJT, van de Schoor F, van Terhollen K, Pickkers P, van den Boogaard M. Differences in 90-day mortality of delirium subtypes in the intensive care unit: a retrospective cohort study. *J Crit Care*. 2019;53:120–4.
- Salluh JI, Wang H, Schneider EB, Nagaraja N, Yenokyan G, Damluji A, et al. Outcome of delirium in critically ill patients: systematic review and meta-analysis. *BMJ*. 2015;350:h2538.
- Schweickert WD, Kress JP. Implementing early mobilization interventions in mechanically ventilated patients in the ICU. *Chest*. 2011;140(6):1612–7.
- Schweickert WD, Pohlman MC, Pohlman AS, Nigos C, Pawlik AJ, Esbrook CL, et al. Early physical and occupational therapy in mechanically ventilated, critically ill patients: a randomised controlled trial. *Lancet*. 2009;373(9678):1874–82.
- Seaman JS, Schillerstrom J, Carroll D, Brown TM. Impaired oxidative metabolism precipitates delir-

- ium: a study of 101 ICU patients. *Psychosomatics*. 2006;47(1):56–61.
- Sessler CN, Gosnell MS, Grap MJ, Brophy GM, O'Neal PV, Keane KA, et al. The Richmond agitation-sedation scale: validity and reliability in adult intensive care unit patients. *Am J Respir Crit Care Med*. 2002;166(10):1338–44.
- Shehabi Y, Bellomo R, Reade MC, Bailey M, Bass F, Howe B, et al. Early goal-directed sedation versus standard sedation in mechanically ventilated critically ill patients: a pilot study*. *Crit Care Med*. 2013;41(8):1983–91.
- Skrobik Y, Duprey MS, Hill NS, Devlin JW. Low-dose nocturnal Dexmedetomidine prevents ICU delirium. A randomized, placebo-controlled trial. *Am J Respir Crit Care Med*. 2018;197(9):1147–56.
- Slooter AJ, Van De Leur RR, Zaal IJ. Delirium in critically ill patients. *Handb Clin Neurol*. 2017;141:449–66.
- Stanchina ML, Abu-Hijleh M, Chaudhry BK, Carlisle CC, Millman RP. The influence of white noise on sleep in subjects exposed to ICU noise. *Sleep Med*. 2005;6(5):423–8.
- Su X, Meng ZT, Wu XH, Cui F, Li HL, Wang DX, et al. Dexmedetomidine for prevention of delirium in elderly patients after non-cardiac surgery: a randomised, double-blind, placebo-controlled trial. *Lancet*. 2016;388(10054):1893–902.
- Tanaka LM, Azevedo LC, Park M, Schettino G, Nassar AP, Rea-Neto A, et al. Early sedation and clinical outcomes of mechanically ventilated patients: a prospective multicenter cohort study. *Crit Care*. 2014;18(4):R156.
- Trompeo AC, Vidi Y, Locane MD, Braghiroli A, Mascia L, Bosma K, et al. Sleep disturbances in the critically ill patients: role of delirium and sedative agents. *Minerva Anesthesiol*. 2011;77(6):604–12.
- Trzepacz PT. Is there a final common neural pathway in delirium? Focus on acetylcholine and dopamine. *Semin Clin Neuropsychiatry*. 2000;5(2):132–48.
- Van Rompaey B, Elseviers MM, Schuurmans MJ, Shortridge-Baggett LM, Truijzen S, Bossaert L. Risk factors for delirium in intensive care patients: a prospective cohort study. *Crit Care*. 2009;13(3):R77.
- Wang W, Li HL, Wang DX, Zhu X, Li SL, Yao GQ, et al. Haloperidol prophylaxis decreases delirium incidence in elderly patients after noncardiac surgery: a randomized controlled trial*. *Crit Care Med*. 2012;40(3):731–9.
- Wolters AE, Peelen LM, Welling MC, Kok L, de Lange DW, Cremer OL, et al. Long-term mental health problems after delirium in the ICU. *Crit Care Med*. 2016;44(10):1808–13.
- Zaal IJ, Devlin JW, Peelen LM, Slooter AJ. A systematic review of risk factors for delirium in the ICU. *Crit Care Med*. 2015;43(1):40–7.



Kathryn A. Hibbert and Atul Malhotra

Introduction

With the rising prevalence of obesity (McTigue and Kuller 2008; McTigue et al. 2006), a nuanced understanding of the physiologic impact and clinical implications of obesity in the critically ill are integral to clinical practice (Malhotra and Hillman 2008). In the United States, recent data show that roughly one-third of the population have a normal BMI, one-third are overweight, and one-third are obese (BMI >30 kg/m²) (McTigue and Kuller 2008; McTigue et al. 2006). In some areas of the country, the prevalence of obesity reaches >40%. In addition, morbid obesity (BMI >35–40 kg/m²) is on the rise, and these patients are increasingly prevalent in the intensive care setting. Across Europe, obesity prevalence varies by country but ranges from 9% to 30% and is also steadily increasing. These data emphasize the importance of obesity and related conditions in patient care. Even in a state of relative health, obesity has major effects on cardiopulmonary physiology, and some of these are

exacerbated by critical illness. Additionally, obese patients can be challenging to manage due to issues including line placement, transportation, drug dosing, and imaging. Of note, morbidly obese patients are often excluded from major clinical trials and therefore reliance on physiological principles is generally required to guide management.

Changes in Baseline Physiology

Obese patients experience a number of changes in their baseline physiology (i.e., before critical illness) compared to lean controls (Owens et al. 2012). Baseline alterations in respiratory mechanics of obese patients include a decrease in total lung capacity (TLC), functional residual capacity (FRC), and vital capacity (VC), as well as increases in pleural pressure, and increased upper and lower airway resistance (Malhotra and Hillman 2008) (Fig. 58.1).

The decreased TLC, FRC, and VC are due to an overall decrease in respiratory system compliance, which in turn is secondary to the increased weight of the chest wall and increased abdominal pressure due to obesity (Malbrain and Cheatham 2011; Malbrain et al. 2007). In studies that have carefully measured lung and chest wall compliance, measured compliance of the chest wall is relatively normal, but the position of the pressure volume curve is shifted to the right

K. A. Hibbert (✉)
Division of Pulmonary and Critical Care Medicine,
Massachusetts General Hospital, Boston, MA, USA
Harvard Medical School, Boston, MA, USA
e-mail: kahibbert@mgh.harvard.edu

A. Malhotra
UC San Diego, Department of Medicine,
La Jolla, CA, USA
e-mail: amalhotra@health.ucsd.edu

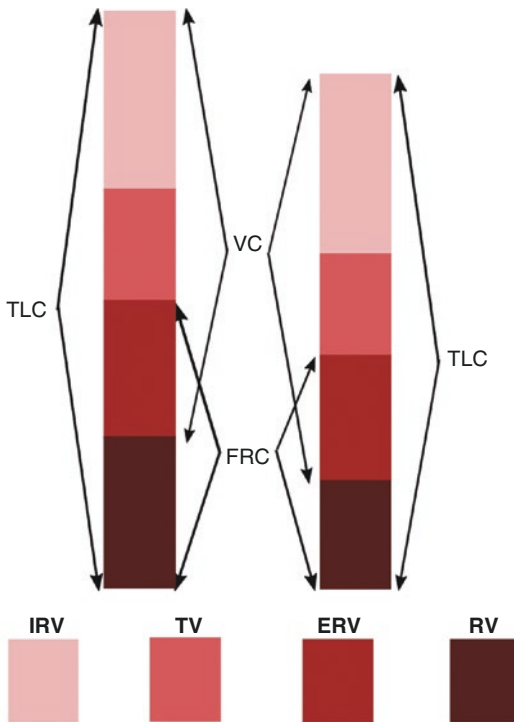


Fig. 58.1 Impact of obesity on lung volumes. In the setting of increased chest wall weight and increased pleural pressure, patients with obesity often have decreased tidal volume (TV), expiratory reserve volume (ERV), and residual volume (RV). These result in a lower vital capacity (VC), functional residual capacity (FRC), and total lung capacity (TLC)

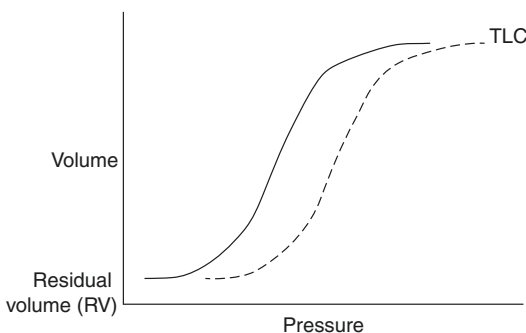


Fig. 58.2 Pressure volume curve of the respiratory system in obesity. Although the measured respiratory system compliance in patients with obesity is often low, the pressure volume curve is typically shifted to the right but has a similar compliance (slope)

(Behazin et al. 2010) (Fig. 58.2). In contrast, measured lung compliance is often low, likely due to atelectasis, and thus the measured value of

compliance varies with recruitment along the pressure volume curve (Owens et al. 2008). A key physiological parameter in obese patients is transpulmonary pressure, which is the distending pressure across the lung (i.e., airway opening pressure minus pleural pressure) and which is distinguished from trans-chest wall pressure (the difference between pleural and atmospheric pressures) (Mead et al. 1970). With the increased pleural pressure in obesity, transpulmonary pressure becomes less positive (or more negative during a spontaneous breath) and the lung parenchyma experiences less distending (and more collapsing) pressure. The increase in pleural pressure, and resultant decrease in transpulmonary pressure, varies with gravitational position. Obese patients therefore have considerable atelectasis in some regions (e.g., dependent on the lung), whereas other regions remain well aerated (e.g., non-dependent on the lung) (Schetz et al. 2019). Atelectasis in obesity results in both impaired gas exchange and decreased compliance (Pelosi et al. 1996, 1997, 1998).

Some authors have questioned the occurrence of negative transpulmonary pressures in obesity, i.e. pleural pressure in excess of pressure measured at the airway opening (Bernard 2008). However, such pleural pressure elevations without complete lung collapse are commonly observed during forced exhalation, when expiratory muscle activity raises pleural pressure and airway opening pressure remains atmospheric (Loring et al. 2010). Other situations in which pleural pressure elevations are common are expiratory flow limitation and airway closure, in which high pleural pressure, which is the pressure outside of the major airways, leads to airway narrowing or collapse, thereby allowing alveolar pressures to exceed those at the airway opening. Negative transpulmonary pressures are therefore commonly seen clinically even if not directly measured, and as described above, the resultant atelectasis is an important consideration in obese patients, even in the absence of additional lung pathology.

FEV1 and FVC are reduced in proportion to each other in obese patients, but small airways dysfunction has also been observed in obese patients, and in some, expiratory flow limitation (Dixon and Peters 2018; Dixon and Poynter 2016;

Dixon and Suratt 2017; Shore 2008, 2013, 2017). This phenomenon can result in the development of intrinsic PEEP at rest. During exercise, it can cause air trapping and a dynamic increase in end-expiratory lung volume. Even in the absence of increased end-expiratory lung volume, alveolar pressure may be elevated at end-exhalation secondary to the increased intra-abdominal pressure observed in obesity. These changes, combined with the intrinsic mechanical loading of inspiratory muscles in obesity, increase the work and oxygen cost of breathing both at rest and during exercise (Pankow et al. 1998).

A decrease in lung compliance and increase in airway resistance have been observed in sedated, paralyzed, and morbidly obese patients without underlying lung pathology (Pelosi et al. 1996; Suratt et al. 1984a; Cherniack 1958; Naimark and Cherniack 1960). As stated above, this decrease in compliance is likely due to atelectasis and a shift of the pressure-volume curve of the lung rather than alteration of the underlying parenchyma. Obese patients frequently have arterial hypoxemia and an elevated alveolar to arterial oxygen (A-a) gradient. These changes are hypothesized to be secondary to a combination of atelectasis with shunting and V/Q mismatch due to airway narrowing and variations in lung perfusion.

Obesity has many important effects on non-pulmonary physiology, including vascular physiology and endocrine function, and it is accompanied by comorbidities that complicate critical illness. These issues are complex – for example, measured vascular pressures are higher in obese patients, which reflect both issues of accurate measurement and actual physiologic changes – and are reviewed extensively elsewhere in the literature (Malhotra and Hillman 2008; Pelosi et al. 1996).

Obesity and the Abdomen

When considering chest wall compliance in obesity, the role of the abdomen is frequently underappreciated, particularly in critically ill patients. Abdominal compartment syndrome is well recognized by trauma surgeons, but the recognition of its high prevalence in medical ICUs has been less well appreciated. Malbrain et al. performed

an observational study in mixed ICUs across Europe and demonstrated a remarkably high prevalence of raised intra-abdominal pressure in unselected ICU patients (Malbrain et al. 2007, 2006a, b). Based on an elevated intra-abdominal pressure >20 mmHg, 8% of patients had evidence of abdominal compartment syndrome. Recognizing that normal intra-abdominal pressure is typically atmospheric, the authors reported that 58% of medical ICU patients had an intra-abdominal pressure of >12 mmHg. In multivariate analysis, body mass index (BMI) was the only independent predictor of intra-abdominal pressure, emphasizing the critical importance of obesity in the ICU. Of note, obesity rates are much greater in the United States than in Europe, suggesting that the incidence may be even higher depending on the geographic setting and demographics.

Raised intra-abdominal pressure has multiple consequences, particularly in the ICU. First, the elevated pressure can affect visceral organ function. For example, when IAP is sufficiently elevated, renal failure is thought to occur by compression of renal veins and the subsequent reduction in perfusion. Second, elevated intra-abdominal pressure can contribute to raised intrathoracic pressure since some pressure is transmitted across the diaphragm. The extent to which IAP is transmitted to the thorax is variable and likely depends upon patient position, chronicity, and other individual chest wall mechanical characteristics and, as discussed above, can have important implications for transpulmonary pressure. Increased abdominal weight also increases diaphragmatic loading, which increases the work of breathing in spontaneously breathing patients (Cherniack and Guenter 1961). These effects are especially important in the supine position and should not be underestimated in the obese and critically ill patient.

Obesity Control of Breathing/ OSA/ OHS

Obstructive sleep apnea (OSA) is a common condition with major neurocognitive and cardiovascular sequelae. Recent estimates suggest that at

least 13% of men and 6% of women have clinically important OSA, with up to 1 billion people affected worldwide (Benjafield et al. 2019; Peppard et al. 2013; Heinzer et al. 2015). Obesity is a major risk factor for OSA, although up to 30% of OSA patients are not obese. OSA is characterized by intermittent hypoxemia and recurrent surges in catecholamines, which contribute to its clinical manifestations.

OSA is now thought to be a complex disease with multiple underlying endotypes (Jordan et al. 2014). Anatomical compromise of the upper airway is a common underlying feature as measured by the critical closing pressure (Pcrit) of the airway (i.e., the pressure that must be overcome to keep the airway open) (Gold et al. 1996). A positive value for the Pcrit reflects a “floppy” airway that requires positive intraluminal pressure to restore patency (Strohl et al. 2012). On the other hand, a negative Pcrit value reflects a “sturdy” airway that requires subatmospheric pressure to promote collapse. Alterations in transmural pressure of the upper airway are particularly important for non-intubated patients, including post-extubation (Epstein 2002). In addition to anatomy, pharyngeal dilator muscle function is thought to be affected in some patients. This dysfunction in upper airway muscles can be further exacerbated with sedative medications including benzodiazepines and propofol (Malhotra et al. 2000, 2001; Genta et al. 2011; Eastwood et al. 2002). Lastly, instability in ventilatory control (elevated loop gain) also plays an important role in a subset of OSA patients (Khoo 2000a, b, 2001; Younes et al. 2001; Wellman et al. 2003, 2004, 2007). Unstable ventilatory control may promote patient/ventilator asynchrony, although data in this context are sparse (Beitler et al. 2016a; Meza et al. 1998).

Obesity hypoventilation syndrome (OHS) occurs in a subset of patients with OSA (and rarely in the absence of OSA) and has several important implications in critical illness (Nowbar et al. 2004; Berger et al. 2001). OHS is defined by elevated PaCO₂ in the context of obesity without major parenchymal lung disease and is thought to result from the combination of a low central ventilatory drive and abnormal respira-

tory mechanics (O’donnell et al. 1999). In aggregate, the data suggest that at least 10–20% of obese patients being evaluated for OSA have OHS, although the diagnosis is still proportionately infrequent and may be under-diagnosed (Mokhlesi 2010; Mokhlesi and Tulaimat 2007). Indeed, data suggest that roughly 30% of patients with a BMI of 40 kg/m² will have evidence of OHS if appropriately evaluated (Mokhlesi et al. 2019). Second, several studies suggest that even though OHS is a chronic condition, OHS commonly comes to clinical fruition in the ICU (Esquinas and BaHammam 2013; Sequeira et al. 2017). That is, patients with respiratory infection may arrive with an unexplained elevation in bicarbonate or, in some cases, they are misdiagnosed as acute exacerbations of chronic obstructive pulmonary disease based on assumptions in the setting of an acute or chronic hypercapnia. Thus, an appropriate level of clinical suspicion is required for this diagnosis to optimize management of these patients. Third, considerable data have shown that a diagnosis of OHS changes management not only in the ICU but also during follow-up. Although newer strategies are available for non-invasive ventilation of these patients, including volume-assured pressure support modes, the bulk of the recent data suggests that nasal CPAP (continuous positive airway pressure) provides good long-term results (Masa et al. 2019).

The impact of OSA and OHS on critical illness is complex and incompletely studied. Potential implications include management considerations for non-intubated patients who have vulnerable upper airways and the potential for abnormal breathing patterns including ventilator asynchrony and spontaneous breathing patterns. Chronic intermittent hypoxia and hypercapnia also have metabolic sequelae that affect the critically ill (Xue et al. 2017). These factors can contribute to cardiovascular risk and also may include a protective effect in some ICU patients through ischemic preconditioning (Sanchez-de-la-Torre et al. 2018). Lastly, the clinician must understand these effects in order to return patients to their baseline physiology and a state of relative health.

Obesity as a Risk Factor for Critical Illness

In addition to the changes in respiratory mechanics, obese patients experience chronic alterations in circulating inflammatory mediators derived from adipose tissue (collectively known as adipocytokines) (Mantzoros et al. 2011). Obese patients have increased circulating levels of cytokines (including TNF- α and IL-6), increased chemokine production (including IL-8), and altered levels of hormones produced by adipocytes such as leptin and adiponectin. A causal link between this inflammatory milieu in obese patients and asthma or airway hyper-responsiveness has been more thoroughly explored than the potential link with other critical illnesses (Dixon and Peters 2018; Dixon and Poynter 2016; Shore 2010). Additionally, in the setting of the baseline changes in physiology described above, obese patients may be more likely to have acute respiratory failure and even to meet criteria for acute respiratory distress syndrome (ARDS) without true lung injury, given their propensity to atelectasis and subsequent hypoxemia (Pepper et al. 2014, 2016, 2017, 2019).

Airway Management

Airway management is a key issue in critically ill obese patients. Even relatively healthy obese patients who undergo surgery have an increased risk of complications and respiratory failure peri-operatively. There is ongoing discussion about the degree to which obesity predicts difficult endotracheal intubation. Other predictive tools such as Mallampati scale may outperform body mass index (BMI) as a prognostic tool (De Cassai et al. 2020; Moon et al. 2019). Obese patients often have anatomical changes to head and neck regions that can make intubation difficult. These include increased soft tissue mass in the neck, decreased airway diameter, and increased airway collapsibility (Shore 2017; Pankow et al. 1998). When sedation and paralytics are given, the critical closing pressure (Pcrit) of the upper airway increases as muscle tone decreases and also is

affected by other factors such as airway structure. Thus, complete airway closure is common during intubation of obese patients following muscle relaxation (Suratt et al. 1984a; Cherniack 1958; Naimark and Cherniack 1960; Suratt et al. 1984b).

Based on the known effects on respiratory mechanics, obesity results in reduced end-expiratory lung volume and the subsequent atelectasis, and ventilation/perfusion mismatch can yield rapid desaturation during intubation, despite pre-oxygenation. There is also an increased prevalence of gastroesophageal reflux disease (GERD) in obese patients that can complicate intubation by increasing risk of aspiration. Although many patients will do well with the standard practice of “rapid sequence intubation” (with use of short-acting neuromuscular blockade, short-acting sedatives, and standard technique of pre-oxygenation), if there are additional issues that may lead to difficult intubation, then it is reasonable to pursue an awake fiberoptic intubation (Brodsky et al. 2002).

There are also additional considerations when extubating obese patients, especially those with OSA who are predisposed to airway collapse and who have increased risk of re-intubation. Residual effects of sedatives and muscle relaxants may be more pronounced in obese patients given their unique pharmacodynamics. In addition to decreased wakefulness drive to breathe as sedatives wear off, the presence of an endotracheal tube can blunt upper airway reflexes that normally help maintain airway patency (Benumof 2001; Brown et al. 2010). Non-invasive positive pressure ventilation can assist in successful extubation and can help prevent reintubation in high-risk patients (de Larminat et al. 1995). Notably, use of non-invasive ventilation after the development of post-extubation respiratory failure has been shown to delay, but not prevent, reintubation and is also associated with high mortality (Nava et al. 2005; Esteban et al. 2004). Conversely, pre-emptive non-invasive ventilation at the time of extubation of high-risk patients has been shown to shorten the duration of invasive mechanical ventilation without increasing the risk of reintubation, ICU length of stay, or mor-

tality. These data suggest that non-invasive ventilation may be useful in patients who are at high risk of extubation failure, though this strategy is not specific to obese patients. We recommend extubation to non-invasive ventilation in patients with known OSA and history of failed extubation, as well as patients in whom there is co-existing CO₂ retention due to either obstructive airways disease or obesity hypoventilation syndrome. Although the role of tracheostomy in the ICU has been debated, it does represent definitive therapy for OSA. Thus, we consider tracheostomy in our ICU patients with variable CNS status and complex cardiopulmonary disease, particularly with underlying OSA or control of breathing abnormalities.

Ventilator Management in Obese Patients

When obesity is coincident with respiratory failure, there are specific issues for mechanical ventilation and management. With increased abdominal pressure and concomitant elevated pleural pressure, obese patients develop atelectasis and therefore have a more heterogeneous lung at baseline, with some areas of lung being well aerated and other areas being relatively collapsed. This heterogeneity may be compounded in the acute respiratory distress syndrome (ARDS), in which increased pleural pressure is combined with increased surface tension due to surfactant dysfunction. Obese patient with ARDS can thus experience considerable atelectasis with resultant gas exchange abnormalities and potential risk of additional lung injury. Atelectasis in ARDS predisposes to ventilator-associated lung injury (VALI) in multiple ways. Cyclic opening and closing of lung units can result in shear stress, the so-called atelectrauma (Slutsky and Drazen 2002; Slutsky and Ranieri 2013). There are also concentrations of stress at the intersection of open and closed alveoli (i.e., junctions between normal and abnormal lungs). On conventional ventilator settings, the effective pressures generated in these heterogeneous areas are estimated theoretically to exceed 100 cmH₂O, which greatly

surpasses the generally accepted “safe” maximum transpulmonary pressure of 25 cmH₂O (Mead et al. 1970). Lastly, atelectasis results in a small functional lung and so even a “low tidal volume” ventilation strategy may result in high regional strain, the so-called volutrauma (Beitler et al. 2016b).

These mechanisms of lung injury have led to an “open lung” strategy of ventilation, in which attempts are made to create parenchymal homogeneity. Strategies to achieve this end have included recruitment maneuvers (e.g., applying sustained high airway pressures (40 cmH₂O) for brief periods) and PEEP titration to optimize respiratory mechanics (Hubmayr and Malhotra 2014). This “open lung” strategy has traditionally been balanced with attempts to minimize airway pressures, which are also thought to contribute to ventilator-associated lung injury (the so-called barotrauma). The relevant distending pressure to the lung parenchyma is the transpulmonary pressure, and thus in theory reducing transpulmonary pressure may be a desirable target to reduce lung injury. In the setting of obesity with raised pleural pressure, high plateau airway pressures can be applied without lung overdistention since transpulmonary pressures <25 cmH₂O at end-inspiration are generally considered safe. By extension, high PEEP is often required in the context of obesity to prevent end-expiratory collapse, and the concomitant elevation in plateau pressure on fixed tidal volume is generally well tolerated. Recent data suggest that driving pressure is better associated with outcomes in ARDS than plateau pressure, and this finding may be especially true in patients with obesity in whom elevated plateau pressure can be misleading (i.e., a function of elevated pleural pressure rather than of elevated transpulmonary pressure) (Meier et al. 2020; Amato et al. 2015; Loring and Malhotra 2015).

Failure to account for increased pleural pressure, which is rarely measured directly, can result in under-titration of PEEP and increased shear stress and lung injury. In contrast, empiric titration to a high PEEP may result in lung overdistention and hemodynamic compromise. In theory, esophageal manometry, which estimates a pleural pressure, allows titration of ventilator settings

based on the physiological requirements of the specific patient, i.e., to achieve a positive transpulmonary pressure at end-exhalation.

Clinical data on the use of esophageal manometry have shown mixed results. An initial study by Talmor et al. showed improved gas exchange and a trend toward improved survival as compared to standard mechanical ventilation based on the ARDSNET protocol (Talmor et al. 2008). However, a subsequent recent study by Beitler et al. that used higher PEEP in the control group failed to show important benefits to esophageal balloon-guided therapy (Beitler et al. 2019). Nonetheless, we still find the concept of esophageal pressure a useful one at the bedside even if not directly measured routinely – for example, it offers the unique advantage of separating the mechanics of the chest wall from that of the lungs. One study that compared different PEEP titration strategies in obese patients (BMI >35 kg/m²) did not demonstrate a physiological benefit to PEEP titration by esophageal manometry compared to titration to optimal respiratory system compliance. In the absence of compelling data to suggest improved outcomes with any specific titration strategy, we recommend titration of PEEP based on local expertise and individual responses. Methods may include use of esophageal balloons, analysis of airway pressure-time curve profiles (stress index), and titration of PEEP to optimize tidal compliance, recognizing that the individual response to therapy may be an important consideration.

Importantly, even though higher airway pressures can be tolerated in obesity, the strategy of low tidal volume ventilation is still paramount, and tidal volumes should be based on *ideal body weight* (Malhotra 2007). This recommendation is because as body weight increases, lung size does not increase concomitantly and, therefore, individuals of the same height and different weights should receive the same tidal volume (approximately 6 ml/kg ideal body weight (IBW)). It must be noted that this low tidal volume strategy is frequently accompanied by hypercapnia, which in obese patients may reflect both the acute illness and chronic hypoventilation.

In addition to the titration of PEEP, prone positioning may be an important recruitment

strategy in obese patients with lung injury. Prone positioning allows the weight of mediastinal tissue to be supported by the sternum, and thus less lung tissue may be susceptible to collapsing forces (Scholten et al. 2017). These issues are especially relevant in obese patients. Prone positioning in the obese patient may offer the same putative benefits as in lean patients, including more homogeneous distribution of perfusion, recruitment of atelectatic lung in the non-dependent position, and improved oxygenation through reduction of shunt and improved ventilation/perfusion matching. Small case-controlled clinical studies have demonstrated the safety of prone positioning in patients with obesity (BMI ≥ 35 kg/m²) and a greater improvement in oxygenation compared to leaner patients, perhaps reflecting a greater fraction of atelectatic lung that is recruitable. Intra-abdominal pressures may increase in the prone position, and that increased IAP may be transmitted across the diaphragm to the pleural space leading to atelectasis. This effect may depend on whether the abdomen is suspended (e.g., in a specialty bed) or is lain upon by the patient in the prone position. Additionally, the impact of obesity and fat distribution with resulting influences on position-induced changes in abdominal pressure has not yet been studied, and it may be a critical variable explaining some of the variance in clinical trials. Additionally, there may be logistic concerns for transitioning very obese patients between the supine and prone positions. However, there are no data to suggest reduced benefit of prone positioning in obese patients with ARDS.

These important physiological considerations are also relevant to the liberation of patients from mechanical ventilation. A study of obese patients without lung injury and also of patients with ascites demonstrated that a reverse Trendelenburg position at 45 degrees facilitated liberation from the ventilator. This finding is presumably due to a reduction in trans-diaphragmatic pressure, decreased atelectasis, and improved gas exchange with the postural change. Such benefit may also be seen prior to ventilator liberation in patients with a large fraction of recruitable lung (Richard et al. 2006).

Additional Considerations

There are multiple additional considerations in the care of critically ill obese patients. Many critical care trials have excluded patients with a weight greater than 1 kg/cm of height (approximately BMI of 45 kg/m²), and even those studies without an exclusion for obese patients have had a relatively moderate mean BMI in their study population leading to perhaps limited ability to extrapolate to the morbidly obese population (Guerin et al. 2013). At many institutions, some therapies such as extra corporeal membrane oxygenation (ECMO) remain available only to patients below a threshold BMI (e.g., 40–45 kg/m²), and so experience and data to guide use are limited.

Special considerations are required for interventions such as central line placement in morbidly obese patients. Variations in fat distribution and underlying anatomy may make one site preferred over another (e.g., avoiding subclavian site if the clavicle is not palpable). The length of the central line is also important since anecdotes have shown that infusions can extravasate into the soft tissues even when the distal tip of the line is in the lumen of the vessel. In addition, the femoral site may be associated with risk of deep venous thrombosis, which may be a particular concern in obese patients. Appropriate prophylaxis is recommended in all ICU patients particularly among the obese. We typically recommend both anticoagulant therapy and sequential compression devices (SCDs) if there are no contraindications in morbidly obese patients, even though recent data have not supported the use of SCDs for this purpose in general ICU patients (Arabi et al. 2019). Pharmacokinetics in obesity is also unique. There can be delayed clearance of lipophilic drugs, which can lead to extended sedation. Drugs that are dosed by weight may also be optimally dosed by ideal body weight (IBW) or by lean body weight (LBW), while others should be dosed by total body weight (TBW) based on volume of distribution (Bernard et al. 2001).

Obesity and Outcomes

The clinical literature regarding obesity and outcomes in the ICU has produced somewhat mixed results and is in need of further study. In several cohort studies, obesity has been associated with improved outcomes, although the mechanism underlying this observation is unclear. Several potential theories have been proposed but no definitive answer has emerged. In theory, obese patients may be less susceptible to iatrogenic injury since they are subject to fewer procedures and less transport for radiology assessments. In addition, some have suggested a survivor effect in surgical intensive care units (i.e., the sickest patients with morbid obesity are unlikely to undergo elective surgery). Obesity effects on the chest wall may also have a protective role from the standpoint of overdistension since the elevated pleural pressure associated with obesity results in lower transpulmonary pressure compared to lean individuals. Patients with obesity may also be more likely to qualify as having moderate or severe ARDS due to underlying atelectasis and not true lung injury and, therefore, may have a higher chance of survival. Thus, further work is clearly needed in this area (Pepper et al. 2014, 2017, 2019).

Conclusion

The many alterations in baseline physiology with obesity and the impact of obesity on critical illness are increasingly important as the prevalence of obesity continues to increase. A thorough understanding of the physiological considerations related to obese patients with lung injury is becoming essential for optimal patient care given the obesity pandemic and ongoing prevalence of ARDS. An individualized approach to the care of these patients can be invaluable, since a “one-size-fits-all” approach may be problematic for some patients. We support further clinical trials using individual patient measurements and response to guide therapy rather than overly simplified algorithms that are likely to provide heterogeneous results.

References

- Amato MB, Meade MO, Slutsky AS, Brochard L, Costa EL, Schoenfeld DA, Stewart TE, Briel M, Talmor D, Mercat A, Richard JC, Carvalho CR, Brower RG. Driving pressure and survival in the acute respiratory distress syndrome. *N Engl J Med*. 2015;372(8):747–755. Epub 2015/02/19. <https://doi.org/10.1056/NEJMsa1410639>. PubMed PMID: 25693014.
- Arabi YM, Al-Hameed F, Burns KEA, Mehta S, Alsalamy SJ, Alshahrani MS, Mandourah Y, Almekhlafi GA, Almaani M, Al Bshabshe A, Finfer S, Arshad Z, Khalid I, Mehta Y, Gaur A, Hawa H, Buscher H, Lababidi H, Al Aithan A, Abdukahil SAI, Jose J, Afesh LY, Al-Dawood A, Saudi Critical Care Trials G. Adjunctive intermittent pneumatic compression for venous thromboprophylaxis. *N Engl J Med*. 2019;380(14):1305–1315. Epub 2019/02/20. <https://doi.org/10.1056/NEJMoa1816150>. PubMed PMID: 30779530.
- Behazin N, Jones SB, Cohen RI, Loring SH. Respiratory restriction and elevated pleural and esophageal pressures in morbid obesity. *J Appl Physiol* (1985). 2010;108(1):212–8. <https://doi.org/10.1152/jap-physiol.91356.2008>. Epub 2009/11/17. PubMed PMID: 19910329; PMCID: PMC2885073.
- Beitler JR, Majumdar R, Hubmayr RD, Malhotra A, Thompson BT, Owens RL, Loring SH, Talmor D. Volume delivered during recruitment maneuver predicts lung stress in acute respiratory distress syndrome. *Crit Care Med*. 2016b;44(1):91–9. Epub 2015/10/17. <https://doi.org/10.1097/CCM.0000000000001355>. PubMed PMID: 26474111; PMCID: PMC5224862.
- Beitler JR, Sands SA, Loring SH, Owens RL, Malhotra A, Spragg RG, Matthay MA, Thompson BT, Talmor D. Quantifying unintended exposure to high tidal volumes from breath stacking dyssynchrony in ARDS: the BREATHE criteria. *Intensive Care Med*. 2016a;42(9):1427–36. Epub 2016/06/28. <https://doi.org/10.1007/s00134-016-4423-3>. PubMed PMID: 27342819; PMCID: PMC4992404.
- Beitler JR, Sarge T, Banner-Goodspeed VM, Gong MN, Cook D, Novack V, Loring SH, Talmor D, Group EP-S. Effect of titrating Positive End-Expiratory Pressure (PEEP) with an esophageal pressure-guided strategy vs an empirical high peep-fio2 strategy on death and days free from mechanical ventilation among patients with acute respiratory distress syndrome: a randomized clinical trial. *JAMA*. 2019;321(9):846–57. Epub 2019/02/19. <https://doi.org/10.1001/jama.2019.0555>. PubMed PMID: 30776290; PMCID: PMC6439595.
- Benjafield AV, Ayas NT, Eastwood PR, Heinzer R, Ip MSM, Morrell MJ, Nunez CM, Patel SR, Penzel T, Pepin JL, Peppard PE, Sinha S, Tufik S, Valentine K, Malhotra A. Estimation of the global prevalence and burden of obstructive sleep apnoea: a literature-based analysis. *Lancet Respir Med*. 2019;7(8):687–98. [https://doi.org/10.1016/S2213-2600\(19\)30198-5](https://doi.org/10.1016/S2213-2600(19)30198-5). Epub 2019/07/14. PubMed PMID: 31300334.
- Benumof JL. Obstructive sleep apnea in the adult obese patient: implications for airway management. *J Clin Anesth*. 2001;13(2):144–56.
- Berger KI, Ayappa I, Chatr-Amontri B, Marfatia A, Sorkin IB, Rapoport DM, Goldring RM. Obesity hypoventilation syndrome as a spectrum of respiratory disturbances during sleep. *Chest*. 2001;120(4):1231–1238. Epub 2001/10/10. <https://doi.org/10.1378/chest.120.4.1231>. PubMed PMID: 11591566.
- Bernard GR. PEEP guided by esophageal pressure--any added value? *N Engl J Med*. 2008;359(20):2166–2168. Epub 2008/11/13. <https://doi.org/10.1056/NEJMe0806637>. PubMed PMID: 19001506.
- Bernard GR, Vincent JL, Laterre PF, LaRosa SP, Dhainaut JF, Lopez-Rodriguez A, Steingrub JS, Garber GE, Helterbrand JD, Ely EW, Fisher CJ, Jr., Recombinant human protein CWEiSSg. Efficacy and safety of recombinant human activated protein C for severe sepsis. *N Engl J Med*. 2001;344(10):699–709. Epub 2001/03/10. <https://doi.org/10.1056/NEJM200103083441001>. PubMed PMID: 11236773.
- Brodsky JB, Lemmens HJ, Brock-Utne JG, Vierra M, Saidman LJ. Morbid obesity and tracheal intubation. *Anesth Analg*. 2002;94(3):732–6; table of contents. Epub 2002/02/28. <https://doi.org/10.1097/00005539-200203000-00047>. PubMed PMID: 11867407.
- Brown EN, Lydic R, Schiff ND. General anesthesia, sleep, and coma. *N Engl J Med*. 2010;363(27):2638–50. Epub 2010/12/31. <https://doi.org/10.1056/NEJMr0808281>. PubMed PMID: 21190458; PMCID: 3162622.
- Cherniack RM. Respiratory effects of obesity. *Can Med Assoc J*. 1958;80(8):613–6. Epub 1958/04/15. PubMed PMID: 13638925; PMCID: PMC1830796.
- Cherniack RM, Guenter CA. The efficiency of the respiratory muscles in obesity. *Can J Biochem Physiol*. 1961;39:1215–22. <https://doi.org/10.1139/o61-127>. Epub 1961/08/01. PubMed PMID: 13692840.
- De Cassai A, Boscolo A, Rose K, Carron M, Navalesi P. Predictive parameters of difficult intubation in thyroid surgery: a meta-analysis. *Minerva Anestesiol*. 2020. Epub 2020/01/11. <https://doi.org/10.23736/S0375-9393.19.14127-2>. PubMed PMID: 31922378.
- de Larminat V, Montravers P, Dureuil B, Desmots JM. Alteration in swallowing reflex after extubation in intensive care unit patients. *Crit Care Med*. 1995;23(3):486–490. Epub 1995/03/01. <https://doi.org/10.1097/00003246-199503000-00012>. PubMed PMID: 7874899.
- Dixon AE, Peters U. The effect of obesity on lung function. *Expert Rev Respir Med*. 2018;12(9):755–67. Epub 2018/07/31. <https://doi.org/10.1080/17476348.2018.1506331>. PubMed PMID: 30056777; PMCID: PMC6311385.
- Dixon AE, Poynter ME. Mechanisms of asthma in obesity: pleiotropic aspects of obesity produce distinct asthma phenotypes. *Am J Respir Cell Mol Biol*. 2016;54(5):601–8. Epub 2016/02/18. <https://doi.org/10.1165/ajrcmb.1506331>.

- [org/10.1165/rcmb.2016-0017PS](https://doi.org/10.1165/rcmb.2016-0017PS). PubMed PMID: 26886277; PMCID: PMC4942199.
- Dixon AE, Suratt BT. Chair's summary: obesity and associated changes in metabolism, implications for lung diseases. *Ann Am Thorac Soc*. 2017;14(Suppl_5):S314–S5. Epub 2017/11/22. <https://doi.org/10.1513/AnnalsATS.201702-116AW>. PubMed PMID: 29161083; PMCID: PMC5711266.
- Eastwood PR, Szollosi I, Platt PR, Hillman DR. Comparison of upper airway collapse during general anesthesia and sleep. *Lancet*. 2002;359:1207–9.
- Epstein SK. Extubation. *Respir Care*. 2002;47(4):483–92; discussion 93-5. Epub 2002/04/04. PubMed PMID: 11929619.
- Esquinas AM, BaHammam AS. The emergent malignant obesity hypoventilation syndrome: a new critical care syndrome. *J Intensive Care Med*. 2013;28(3):198–199. Epub 2013/05/16. <https://doi.org/10.1177/0885066612464340>. PubMed PMID: 23674510.
- Esteban A, Frutos-Vivar F, Ferguson ND, Arabi Y, Apezteguia C, Gonzalez M, Epstein SK, Hill NS, Nava S, Soares MA, D'Empaire G, Alia I, Anzueto A. Noninvasive positive-pressure ventilation for respiratory failure after extubation. *N Engl J Med*. 2004;350(24):2452–2460. Epub 2004/06/11. <https://doi.org/10.1056/NEJMoa032736350/24/2452> [pii]. PubMed PMID: 15190137.
- Genta PR, Eckert DJ, Gregorio MG, Danzi NJ, Moriya HT, Malhotra A, Lorenzi-Filho G. Critical closing pressure during midazolam-induced sleep. *J Appl Physiol*. 2011;111(5):1315–1322. Epub 2011/08/20. doi: japplphysiol.00508.2011 [pii]. <https://doi.org/10.1152/japplphysiol.00508.2011>. PubMed PMID: 21852408.
- Gold AR, et al. The pharyngeal critical pressure. The whys and hows of using nasal continuous positive airway pressure diagnostically. *Chest*. 1996;110(4):1077–88. Review.
- Guerin C, Reignier J, Richard JC. Prone positioning in the acute respiratory distress syndrome. *N Engl J Med*. 2013;369(10):980–981. Epub 2013/09/06. <https://doi.org/10.1056/NEJMc1308895>. PubMed PMID: 24004127.
- Heinzer R, Vat S, Marques-Vidal P, Marti-Soler H, Andries D, Tobback N, Mooser V, Preisig M, Malhotra A, Waeber G, Vollenweider P, Tafti M, Haba-Rubio J. Prevalence of sleep-disordered breathing in the general population: the HypnoLaus study. *Lancet Respir Med*. 2015;3(4):310–8. Epub 2015/02/16. [https://doi.org/10.1016/S2213-2600\(15\)00043-0](https://doi.org/10.1016/S2213-2600(15)00043-0). PubMed PMID: 25682233; PMCID: PMC4404207.
- Hubmayr RD, Malhotra A. Still looking for best PEEP. *Anesthesiology*. 2014;121(3):445–6. <https://doi.org/10.1097/ALN.0000000000000374>. PubMed PMID: 25050574; PMCID: 4165827.
- Jordan AS, McSharry DG, Malhotra A. Adult obstructive sleep apnoea. *Lancet*. 2014;383(9918):736–47. [https://doi.org/10.1016/S0140-6736\(13\)60734-5](https://doi.org/10.1016/S0140-6736(13)60734-5). PubMed PMID: 23910433; PMCID: 3909558.
- Khoo M. Determinants of ventilatory instability and variability. *Respir Physiol*. 2000a;122:167–82.
- Khoo M. Theoretical models of periodic breathing. In: Bradley T, Floras J, editors. *Sleep apnea implications in cardiovascular and cerebrovascular disease*. New York: Marcel Dekker; 2000b. p. 355–84.
- Khoo MC. Using loop gain to assess ventilatory control in obstructive sleep apnea. *Am J Respir Crit Care Med*. 2001;163(5):1044–5.
- Loring SH, Malhotra A. Driving pressure and respiratory mechanics in ARDS. *N Engl J Med*. 2015;372(8):776–7. Epub 2015/02/19. <https://doi.org/10.1056/NEJMe1414218>. PubMed PMID: 25693019; PMCID: PMC4356532.
- Loring SH, O'Donnell CR, Behazin N, Malhotra A, Sarge T, Ritz R, Novack V, Talmor D. Esophageal pressures in acute lung injury: do they represent artifact or useful information about transpulmonary pressure, chest wall mechanics, and lung stress? *J Appl Physiol*. 2010;108(3):515–22. Epub 2009/12/19. doi: 00835.2009 [pii] <https://doi.org/10.1152/jap-physiol.00835.2009>. PubMed PMID: 20019160; PMCID: 2838644.
- Malbrain ML, Cheatham ML. Definitions and pathophysiological implications of intra-abdominal hypertension and abdominal compartment syndrome. *Am Surg*. 2011;77(Suppl 1):S6–11. Epub 2011/10/14. PubMed PMID: 21944445.
- Malbrain ML, Cheatham ML, Kirkpatrick A, Sugrue M, De Waele J, Ivatury R. Abdominal compartment syndrome: it's time to pay attention! *Intensive Care Med*. 2006a;32(11):1912–4. <https://doi.org/10.1007/s00134-006-0303-6>. Epub 2006/08/10. PubMed PMID: 16896853.
- Malbrain ML, Cheatham ML, Kirkpatrick A, Sugrue M, Parr M, De Waele J, Balogh Z, Leppaniemi A, Olivera C, Ivatury R, D'Amours S, Wendon J, Hillman K, Johansson K, Kolkman K, Wilmer A. Results from the international conference of experts on intra-abdominal hypertension and abdominal compartment syndrome. I. Definitions. *Intensive Care Med*. 2006b;32(11):1722–32. <https://doi.org/10.1007/s00134-006-0349-5>. Epub 2006/09/13. PubMed PMID: 16967294.
- Malbrain ML, De Laet I, Cheatham M. Consensus conference definitions and recommendations on intra-abdominal hypertension (iah) and the abdominal compartment syndrome (acs) - the long road to the final publications, how did we get there? *Acta Clin Belg*. 2007;62(Suppl 1):44–59. <https://doi.org/10.1179/acb.2007.62.s1.007>. Epub 2007/01/01. PubMed PMID: 24881700.
- Malhotra A. Low-tidal-volume ventilation in the acute respiratory distress syndrome. *N Engl J Med*. 2007;357(11):1113–20. Epub 2007/09/15. 357/11/1113 [pii] <https://doi.org/10.1056/NEJMct074213>. PubMed PMID: 17855672; PMCID: 2287190.

- Malhotra A, Hillman D. Obesity and the lung: 3. Obesity, respiration and intensive care. *Thorax*. 2008;63(10):925–31. <https://doi.org/10.1136/thx.2007.086835>. Epub 2008/09/30. doi: 63/10/925 [pii]. PubMed PMID: 18820119; PMCID: 2711075.
- Malhotra A, Pillar G, Fogel R, Beauregard J, White D. Genioglossal but not palatal muscle activity relates closely to pharyngeal pressure. *Am J Respir Crit Care Med*. 2000;162(3):1058–62.
- Malhotra A, Pillar G, Fogel R, Edwards J, Beauregard J, White DP. Upper airway collapsibility: measurement and sleep effects. *Chest*. 2001;120:156–61.
- Mantzoros CS, Magkos F, Brinkoetter M, Sienkiewicz E, Dardeno TA, Kim SY, Hamnvik OP, Koniaris A. Leptin in human physiology and pathophysiology. *Am J Physiol Endocrinol Metab*. 2011;301(4):E567–84. <https://doi.org/10.1152/ajpendo.00315.2011>. PubMed PMID: 21791620; PMCID: 3191548.
- Masa JF, Mokhlesi B, Benitez I, Gomez de Terreros FJ, Sanchez-Quiroga MA, Romero A, Caballero-Eraso C, Teran-Santos J, Alonso-Alvarez ML, Troncoso MF, Gonzalez M, Lopez-Martin S, Marin JM, Marti S, Diaz-Cambriles T, Chiner E, Egea C, Barca J, Vazquez-Polo FJ, Negrin MA, Martel-Escobar M, Barbe F, Corral J, Spanish Sleep N. Long-term clinical effectiveness of continuous positive airway pressure therapy versus non-invasive ventilation therapy in patients with obesity hypoventilation syndrome: a multicentre, open-label, randomised controlled trial. *Lancet*. 2019;393(10182):1721–32. Epub 2019/04/03. [https://doi.org/10.1016/S0140-6736\(18\)32978-7](https://doi.org/10.1016/S0140-6736(18)32978-7). PubMed PMID: 30935737.
- McTigue K, Kuller L. Cardiovascular risk factors, mortality, and overweight. *JAMA*. 2008;299(11):1260–1261. <https://doi.org/10.1001/jama.299.11.1260-c>. author reply 1. Epub 2008/03/20. doi: 299/11/1260-b [pii]. PubMed PMID: 18349086.
- McTigue K, Larson JC, Valoski A, Burke G, Kotchen J, Lewis CE, Stefanick ML, Van Horn L, Kuller L. Mortality and cardiac and vascular outcomes in extremely obese women. *JAMA*. 2006;296(1):79–86. <https://doi.org/10.1001/jama.296.1.79>. Epub 2006/07/06. doi: 296/1/79 [pii]. PubMed PMID: 16820550.
- Mead J, Takishima T, Leith D. Stress distribution in lungs: a model of pulmonary elasticity. *J Appl Physiol*. 1970;28(5):596–608. Epub 1970/05/01. PubMed PMID: 5442255.
- Meier A, Sell RE, Malhotra A. Driving pressure for ventilation of patients with acute respiratory distress syndrome. *Anesthesiology*. 2020. Epub 2020/02/27. <https://doi.org/10.1097/ALN.0000000000003195>. PubMed PMID: 32101980.
- Meza S, Mendez M, Ostrowski M, Younes M. Susceptibility to periodic breathing with assisted ventilation during sleep in normal subjects. *J Appl Physiol* (1985). 1998;85(5):1929–40. Epub 1998/11/06. <https://doi.org/10.1152/jappl.1998.85.5.1929>. PubMed PMID: 9804601.
- Mokhlesi B. Obesity hypoventilation syndrome: a state-of-the-art review. *Respir Care*. 2010;55(10):1347–62; discussion 63–5. Epub 2010/09/30. PubMed PMID: 20875161.
- Mokhlesi B, Masa JF, Brozek JL, Gurubhagavatula I, Murphy PB, Piper AJ, Tulaimat A, Afshar M, Balachandran JS, Dweik RA, Grunstein RR, Hart N, Kaw R, Lorenzi-Filho G, Pamidi S, Patel BK, Patil SP, Pepin JL, Soghier I, Tamae Kakazu M, Teodorescu M. Evaluation and management of obesity hypoventilation syndrome. an official american thoracic society clinical practice guideline. *Am J Respir Crit Care Med*. 2019;200(3):e6–e24. Epub 2019/08/02. <https://doi.org/10.1164/rccm.201905-1071ST>. PubMed PMID: 31368798; PMCID: PMC6680300.
- Mokhlesi B, Tulaimat A. Recent advances in obesity hypoventilation syndrome. *Chest*. 2007;132(4):1322–1336. Epub 2007/10/16. <https://doi.org/10.1378/chest.07-0027>. PubMed PMID: 17934118.
- Moon TS, Fox PE, Somasundaram A, Minhajuddin A, Gonzales MX, Pak TJ, Ogunnaike B. The influence of morbid obesity on difficult intubation and difficult mask ventilation. *J Anesth*. 2019;33(1):96–102. Epub 2019/01/09. <https://doi.org/10.1007/s00540-018-2592-7>. PubMed PMID: 30617589.
- Naimark A, Cherniack RM. Compliance of the respiratory system and its components in health and obesity. *J Appl Physiol*. 1960;15:377–82. <https://doi.org/10.1152/jappl.1960.15.3.377>. Epub 1960/05/01. PubMed PMID: 14425845.
- Nava S, Gregoretti C, Fanfulla F, Squadrone E, Grassi M, Carlucci A, Beltrame F, Navalesi P. Noninvasive ventilation to prevent respiratory failure after extubation in high-risk patients. *Crit Care Med*. 2005;33(11):2465–2470. Epub 2005/11/09. 00003246-200511000-00003 [pii]. PubMed PMID: 16276167.
- Nowbar S, Burkart KM, Gonzales R, Fedorowicz A, Gozansky WS, Gaudio JC, Taylor MR, Zwillich CW. Obesity-associated hypoventilation in hospitalized patients: prevalence, effects, and outcome. *Am J Med*. 2004;116(1):1–7. Epub 2004/01/07. <https://doi.org/10.1016/j.amjmed.2003.08.022>. PubMed PMID: 14706658.
- O'donnell CP, Schaub CD, Haines AS, Berkowitz DE, Tankersley CG, Schwartz AR, Smith PL. Leptin prevents respiratory depression in obesity. *Am J Respir Crit Care Med*. 1999;159:1477–84.
- Owens RL, Campana LM, Hess L, Eckert DJ, Loring SH, Malhotra A. Sitting and supine esophageal pressures in overweight and obese subjects. *Obesity* (Silver Spring). 2012; <https://doi.org/10.1038/oby.2012.120>oby2012120. Epub 2012/06/15 [pii]. PubMed PMID: 22695479.
- Owens RL, Hess DR, Malhotra A, Venegas JG, Harris RS. Effect of the chest wall on pressure-volume curve analysis of acute respiratory distress syndrome lungs. *Crit Care Med*. 2008;36(11):2980–5. <https://doi.org/10.1097/CCM.0b013e318186afcb>. Epub 2008/10/01. PubMed PMID: 18824918.

- Pankow W, Podszus T, Gutheil T, Penzel T, Peter J, Von Wichert P. Expiratory flow limitation and intrinsic positive end-expiratory pressure in obesity. *J Appl Physiol* (1985). 1998;85(4):1236–43. Epub 1998/10/07. <https://doi.org/10.1152/jappl.1998.85.4.1236>. PubMed PMID: 9760311.
- Pelosi P, Croci M, Ravagnan I, Cerisara M, Vicardi P, Lissoni A, Gattinoni L. Respiratory system mechanics in sedated, paralyzed, morbidly obese patients. *J Appl Physiol* (1985). 1997;82(3):811–8. <https://doi.org/10.1152/jappl.1997.82.3.811>. Epub 1997/03/01. PubMed PMID: 9074968.
- Pelosi P, Croci M, Ravagnan I, Tredici S, Pedoto A, Lissoni A, Gattinoni L. The effects of body mass on lung volumes, respiratory mechanics, and gas exchange during general anesthesia. *Anesth Analg*. 1998;87(3):654–660. Epub 1998/09/05. <https://doi.org/10.1097/0000539-199809000-00031>. PubMed PMID: 9728848.
- Pelosi P, Croci M, Ravagnan I, Vicardi P, Gattinoni L. Total respiratory system, lung, and chest wall mechanics in sedated-paralyzed postoperative morbidly obese patients. *Chest*. 1996;109(1):144–151. Epub 1996/01/01. <https://doi.org/10.1378/chest.109.1.144>. PubMed PMID: 8549177.
- Peppard PE, Young T, Barnett JH, Palta M, Hagen EW, Hla KM. Increased prevalence of sleep-disordered breathing in adults. *Am J Epidemiol*. 2013. Epub 2013/04/17. kws342 [pii] <https://doi.org/10.1093/aje/kws342>. PubMed PMID: 23589584; PMCID: 3639722.
- Pepper DJ, Brewer M, Koch CA. About obese adults admitted to hospital. *J Miss State Med Assoc*. 2014;55(1):11–2. Epub 2014/03/20. PubMed PMID: 24640064.
- Pepper DJ, Demirkale CY, Sun J, Rhee C, Fram D, Eichacker P, Klompas M, Suffredini AF, Kadri SS. Does obesity protect against death in sepsis? A retrospective cohort study of 55,038 adult patients. *Crit Care Med*. 2019;47(5):643–50. Epub 2019/02/23. <https://doi.org/10.1097/CCM.0000000000003692>. PubMed PMID: 30789403; PMCID: PMC6465121.
- Pepper DJ, Sun J, Suffredini AF, Kadri S. Body-mass index and all-cause mortality. *Lancet*. 2017;389(10086):2284. Epub 2017/06/15. [https://doi.org/10.1016/S0140-6736\(17\)31436-8](https://doi.org/10.1016/S0140-6736(17)31436-8). PubMed PMID: 28612743.
- Pepper DJ, Sun J, Welsh J, Cui X, Suffredini AF, Eichacker PQ. Increased body mass index and adjusted mortality in ICU patients with sepsis or septic shock: a systematic review and meta-analysis. *Crit Care*. 2016;20(1):181. Epub 2016/06/17. <https://doi.org/10.1186/s13054-016-1360-z>. PubMed PMID: 27306751; PMCID: PMC4908772.
- Richard JC, Maggiore SM, Mancebo J, Lemaire F, Jonson B, Brochard L. Effects of vertical positioning on gas exchange and lung volumes in acute respiratory distress syndrome. *Intensive Care Med*. 2006;32(10):1623–1626. Epub 2006/08/10. <https://doi.org/10.1007/s00134-006-0299-y>. PubMed PMID: 16896856.
- Sanchez-de-la-Torre A, Soler X, Barbe F, Flores M, Maisel A, Malhotra A, Rue M, Bertran S, Aldoma A, Woner F, Valls J, Lee CH, Turino C, Galera E, de Batlle J, Sanchez-de-la-Torre M, Spanish Sleep N. Cardiac troponin values in patients with acute coronary syndrome and sleep apnea: a pilot study. *Chest*. 2018;153(2):329–38. Epub 2017/07/25. <https://doi.org/10.1016/j.chest.2017.06.046>. PubMed PMID: 28736306; PMCID: PMC6026229.
- Schetz M, De Jong A, Deane AM, Druml W, Hemelaar P, Pelosi P, Pickkers P, Reintam-Blaser A, Roberts J, Sakr Y, Jaber S. Obesity in the critically ill: a narrative review. *Intensive Care Med*. 2019;45(6):757–69. <https://doi.org/10.1007/s00134-019-05594-1>. Epub 2019/03/20. PubMed PMID: 30888440.
- Scholten EL, Beitler JR, Prisk GK, Malhotra A. Treatment of ARDS with prone positioning. *Chest*. 2017;151(1):215–224. Epub 2016/07/13. <https://doi.org/10.1016/j.chest.2016.06.032>. PubMed PMID: 27400909; PMCID: PMC6026253.
- Sequeira TCA, BaHammam AS, Esquinas AM. Noninvasive ventilation in the critically ill patient with obesity hypoventilation syndrome: a review. *J Intensive Care Med*. 2017;32(7):421–428. Epub 2016/08/18. <https://doi.org/10.1177/0885066616663179>. PubMed PMID: 27530511.
- Shore SA. Obesity and asthma: possible mechanisms. *J Allergy Clin Immunol*. 2008;121(5):1087–93. <https://doi.org/10.1016/j.jaci.2008.03.004>. quiz 94–5. Epub 2008/04/15.
- Shore SA. Obesity, airway hyperresponsiveness, and inflammation. *J Appl Physiol* (1985). 2010;108(3):735–43. Epub 2009/10/31. <https://doi.org/10.1152/japplphysiol.00749.2009>. PubMed PMID: 19875711; PMCID: PMC2838631.
- Shore SA. Obesity and asthma: location, location, location. *Eur Respir J*. 2013;41(2):253–4. Epub 2013/02/02. doi: <https://doi.org/10.1183/09031936.00128812>. PubMed PMID: 23370797; PMCID: PMC3966106.
- Shore SA. Mechanistic Basis for Obesity-related Increases in Ozone-induced Airway Hyperresponsiveness in Mice. *Ann Am Thorac Soc*. 2017;14(Supplement_5):S357–S62. Epub 2017/11/22. <https://doi.org/10.1513/AnnalsATS.201702-140AW>. PubMed PMID: 29161088; PMCID: PMC5711270.
- Slutsky AS, Drazen JM. Ventilation with small tidal volumes. *N Engl J Med*. 2002;347(9):630–631. Epub 2002/08/30. <https://doi.org/10.1056/NEJMp020082347/9/630> [pii]. PubMed PMID: 12200549.
- Slutsky AS, Ranieri VM. Ventilator-induced lung injury. *N Engl J Med*. 2013;369(22):2126–2136. Epub 2013/11/29. <https://doi.org/10.1056/NEJMra1208707>. PubMed PMID: 24283226.
- Strohl K, Butler J, Malhotra A. Mechanical properties of the upper airway. *Comprehens Physiol*. 2012;2:1–20.
- Suratt PM, Wilhoit SC, Cooper K. Induction of airway collapse with subatmospheric pressure in awake patients with sleep apnea. *J Appl Physiol*. 1984b;57(1):140–6.

- Suratt PM, Wilhoit SC, Hsiao HS, Atkinson RL, Rochester DF. Compliance of chest wall in obese subjects. *J Appl Physiol Respir Environ Exerc Physiol* 1984a;57(2):403–407. <https://doi.org/10.1152/jappl.1984.57.2.403>. Epub 1984/08/01. PubMed PMID: 6469810.
- Talmor D, Sarge T, Malhotra A, O'Donnell CR, Ritz R, Lisbon A, Novack V, Loring SH. Mechanical ventilation guided by esophageal pressure in acute lung injury. *N Engl J Med*. 2008;359(20):2095–2104. Epub 2008/11/13. doi: NEJMoa0708638 [pii] <https://doi.org/10.1056/NEJMoa0708638>. PubMed PMID: 19001507.
- Wellman A, Jordan AS, Malhotra A, Fogel RB, Katz E, Schory KE, Edwards JK, White DP. Ventilatory control and airway anatomy in obstructive sleep apnea. *Am J Respir Crit Care Med*. 2004;170:1225–32.
- Wellman A, Malhotra A, Fogel R, Schory KE, Edwards JK, White DP. Respiratory system loop gain in normal men and women measured with proportional assist ventilation. *J Appl Physiol*. 2003;94:205–12.
- Wellman A, Malhotra A, Jordan AS, Schory K, Gautam S, White DP. Chemical control stability in the elderly. *J Physiol*. 2007;581(Pt 1):291–8. Epub 2007/02/24. doi: jphysiol.2006.126409 [pii]. <https://doi.org/10.1113/jphysiol.2006.126409>. PubMed PMID: 17317747; PMCID: 2075232.
- Xue J, Zhou D, Poulsen O, Imamura T, Hsiao YH, Smith TH, Malhotra A, Dorrestein P, Knight R, Haddad GG. Intermittent hypoxia and hypercapnia accelerate atherosclerosis, partially via trimethylamine-oxide. *Am J Respir Cell Mol Biol*. 2017;57(5):581–8. Epub 2017/07/06. <https://doi.org/10.1165/rcmb.2017-0086OC>. PubMed PMID: 28678519; PMCID: PMC5705907.
- Younes M, Ostrowski M, Thompson W, Leslie C, Shewchuk W. Chemical control stability in patients with obstructive sleep apnea. *Am J Respir Crit Care Med*. 2001;163(5):1181sss1180. . Epub 2001/04/24. PubMed PMID: 11316657.

Part VIII

Epilogue



Sheldon Magder, Charles C. Hardin,
Kathryn A. Hibbert, and Atul Malhotra

Speculations on the future must inevitably be a mixture of fears and hopes, anticipating new challenges but also adopting new ways of dealing with them. We will begin with the fears to get the depressing side out of the way before dealing with our positive hopes for the future.

Populations are aging, and although many older individuals are increasingly functional, when ill they have little reserves. Aging also is associated with a progressive loss of immune capacity, in what is called immune senescence (Weyand and Goronzy 2016; Goronzy and Weyand 2013). Because of the many newer life-preserving therapies, patients who would have died at an early stage from their disease are now living longer but the therapies prolonging their lives often increase their vulnerability to other diseases, compromise their immune systems, and decrease their overall functional status. These

therapies also often are extremely expensive and are putting an increasing burden on the already high costs of health care. As the world increasingly becomes a global village, the old challenges of viral illnesses, such as the COVID-19 pandemic, are likely to become more common. Yet, besides vaccines, we still have minimal direct therapies for most viral illnesses that compare to the direct actions of antibacterial agents. Our current management of patients who are seriously ill from a viral infection is limited to providing life-sustaining therapies while waiting for host defenses to deal with the invading organism. Therapies that effectively direct attack viruses thus will need to be a major goal for the future.

We also can expect an ongoing escalation of the negative health effects of climate change, including its impact on infectious diseases, air quality-related lung disease, and potential negative health consequences from global warming. Worsening economic inequity will exacerbate these issues, as we have seen during the COVID-19 pandemic in which the concentration of resources often has been away from the most heavily impacted communities (Danziger 2020).

With modern critical care, even very frail individuals can be supported through acute illnesses, but considerable resources are frequently required to do so. This demand will further aggravate the already very large variations in health care distribution which is heavily affected by where one lives and socio-economic status. Because of

S. Magder (✉)

Royal Victoria Hospital (McGill University Health Centre), Departments of Critical Care and Physiology McGill University, Montreal, QC, Canada
e-mail: sheldon.magder@mcgill.ca

C. C. Hardin · K. A. Hibbert

Division of Pulmonary and Critical Care Medicine, Massachusetts General Hospital, Boston, MA, USA
e-mail: Charles.hardin@mgh.harvard.edu;
KAHIBBERT@mgh.harvard.edu

A. Malhotra

UC San Diego, Department of Medicine, La Jolla, CA, USA
e-mail: amalhotra@health.ucsd.edu

impending limits on available support, it is likely that physicians will have to deal with the difficult task of balancing the needs of the patient in front of them with the impact on society as a whole. Labor issues also likely will become worse because the population is aging and there will be fewer individuals of working age to provide the needed care, especially long-term care for the elderly and incapacitated. These issues, while distinct, are closely related to the ever present need to judge the appropriateness of increasingly sophisticated and invasive therapies with the goals, values, and prognosis of the individual in a patient-centered approach to care.

The availability of increasingly specialized interventions, such as Extra Corporal Membrane Oxygenation (ECMO), also will present new demands on the organization of care. We will need to consider what structures should be put into place to facilitate the transfer of patients from smaller facilities to centers that have the structures, experience, budget, and economy of scale to provide these more sophisticated therapies while still maintaining equitable access to these therapies. Indeed, as critical care matures as a field, it may be important to explore whether formal triage and transfer systems, similar to those in place for trauma centers, are required.

On the other hand, there is a lot of hope for the future. Life expectancy around the world has steadily increased, and even more importantly, the aged are living more functionally. In the last two decades, there has been an important decrease in the mortality of patients presenting with sepsis despite aging and sicker patients. What is even more striking is that these improvements in sepsis outcomes have occurred despite the failure to show survival benefits in almost all major randomized trials of new therapeutic approaches in the critically ill. It can be said that in recent years, the major theme in critical care research has been the extreme rarity of positive trials. Importantly, many studies included innovative therapies that had strong basic science rationale, but still failed to show clinical benefits. A major priority in the near term will be sorting out the reasons for these failures. Importantly, we must ask if failure was a result of inadequate understanding of the biology,

the heterogeneity of patient populations, or was it simply because of the technical challenges involved in performing clinical trials in the ICU.

In the meantime, it seems fair to say that improvements in outcomes of critically ill patients have largely come from a better understanding of the underlying pathophysiological processes and the course of diseases, as well as the widespread adoption of relatively simple supportive interventions. Two of the most significant advances likely have been the appreciation that early identification and treatment of patients in shock prevents a downhill spiral to death, and that less intervention is better than more! Surgical outcomes, too, have dramatically improved over the past decades. In the 1990s mortality in reports from studies that attempted to augment oxygen delivery with high-risk surgery was 20% (Boyd et al. 1993) but it was down to less than 2% in the control group 20 years later in a study by the same investigators (Pearse et al. 2014). This change is likely because clinicians now have a better understanding of what matters and what does not. A remarkable example has been the shortening of hospital stay for colorectal surgery from 10 to 12 days to the current 2 days and in some cases, same day; and this has come with a marked reduction in surgical mortality (Gustafsson et al. 2019; Ljungqvist et al. 2017). The increasing use of less invasive approaches with laparoscopy and radiological guidance likely have had a major impact on outcomes, and the use of these approaches continues to expand. Greater use of simulation for education likely also has helped across critical care. This technology has allowed clinicians to gain more hands-on and technical experiences and to develop a systematic approach to management, even with a declining number of actual cases. Further refinement of basic clinical skills and more rational, physiologically based therapies likely will continue to improve outcomes even without elaborate new technological developments.

The rapidly expanding capacity to collect, store, and analyze bedside data likely will provide additional insights into ways to improve patient outcomes (Seymour et al. 2019a; Knaus and Marks 2019) but this, too, will come with its

own set of challenges. Big data approaches already have been used to describe different patient phenotypes that are indicative of which patients are expected to respond to a specific therapy versus those who will not (Knaus and Marks 2019). Currently, this information is largely only available retrospectively (Seymour et al. 2019b), but with improved computing capacities, and artificial intelligence techniques, this type of information likely will be available in real time and could provide prospective insights. This information still may not be useful in individual patients because data are collected with tight restrictions that are needed to allow population-based statistics. However, insights gained should allow us to further refine therapies by providing constant feedback about the patient's potential outcome. It should also strengthen the use of Bayesian approaches to support decision-making (Browner and Newman 1987). Given the intense interest in machine learning and big data approaches, it seems safe to predict widespread availability of decision support of this nature in the future. However, it also is worth sounding a note of caution. The fields of phenotyping and data analysis will face a crucial fork in the road in the near future. Do we content ourselves with outcome associations and purely statistical knowledge, or do we use the insights available from data analysis to formulate and test the mechanistic hypothesis? we still contend that bedside medicine is about formulating a hypothesis about the cause of a patient's condition and a hypothesis of how to treat it. With this construct, the data given to the clinician only can be used to further strengthen the probability of the hypotheses and support the continuation of the same clinical approach, or it could indicate inconsistencies which should trigger re-evaluation of the hypotheses and the potential need to develop new ones.

A tremendous advance over the past decade has been the immediate access to medical information. Gone are the days when it was necessary to go to a library to find an article on a specific subject. The world literature is now available at the bedside to any physician who has a modern cell phone. It will be important to make sure that

this essential information remains accessible to all. A down side to our access to so much information is that the amount of information can become overwhelming and indiscriminant. This is already an issue with patients and families who regularly come to us with advice from Dr. Internet! In the future it will be essential that the organization, prioritization, and evaluation of new evidence become more efficient. Individual journals will continue to provide a general format for special interests and detailed analysis but there likely will be the expansion of the "encyclopedic" approaches which already have developed links to the supporting evidence on their sites. These are necessary to allow clinicians to make critical evaluations for the benefit of the patient in front of them rather than just considering the "mean" population-based response. With easy access to summary information, it will be important to encourage medical professionals making decisions that have major clinical implications to go back to the original data and assess the strength behind the recommendations. There thus needs to be a component of the personalized physician and not just personalized medicine. This philosophy also will need to impact on medical education. Curriculums are moving more and more to management driven by guidelines and formulaic treatments and so is the evaluation of trainees. Less time is spent in the curriculum on developing the scientific skills, as well as statistical skills, to evaluate the evidence that guidelines are based upon. It will be important to make sure that physicians of the future obtain the capacity to deal with the rapid increase in medical knowledge.

Increased understanding of the pathophysiological pathways in critical illness has offered up many potential therapeutic targets. However, despite these insights into the basic biochemical pathways, there have been few therapeutic advancements. This likely is because of the complexity and redundancy of the pathophysiology of critical illness, and caution is warranted rather than enthusiastic early adoption. A common factor in many failed clinical trials in the critically ill is that a single therapeutic agent was thought to be able to reverse a complex and multifactorial process that has many redundant effectors such

as septic shock. Classic examples of this simplistic reasoning were the targeting of single signaling proteins such as tumor necrosis factor (Abraham et al. 1995; Abraham et al. 1997) and other cytokines, use of antibodies to block endotoxin (McCloskey et al. 1994; Cross 1994), and inhibition of nitric oxide production (Lopez et al. 2004). While these mediators are key factors in the inflammatory process, none of them are solely responsible for the inflammatory cascade in critical illness, and each also is involved in normal physiological functions, including activation of anti-inflammatory processes. Many other potentially important targets likely will emerge, but in the future, we will need to avoid the temptation of targeting a single molecule and plan more coordinated or personalized approaches.

Decoding the human genome had promised a great potential for individualizing care. Identification of genetic polymorphisms explains in part why some patients have worse outcomes with the same disease and the same therapy (Rautanen et al. 2015). Faster identification of an individual's genetic code could therefore provide better patient-centered care. However, although decoding of the genetic code has given insights into many new biochemical pathways, to date, it has added very little to therapeutic outcomes in the critically ill. It is worth paraphrasing Edmund Burke: "Those who don't know history are destined to repeat it" (Burke n.d.). Just as targeting single agents in the pathophysiologic pathways of critical illness failed to yield powerful therapeutic approaches, the promise of so-called personalized medicine based on more precise knowledge of a patient's genetic profile has failed to deliver outcome improvements and likely will not provide a simple solution. Biological systems are complex. They are composed of pathways with multiple interactions that act across a spectrum that seeks to develop thermodynamic equilibrium and not with a dichotomous response. It will be difficult, therefore, to precisely titrate therapy in an individual patient based only on a genetic code. Furthermore, identifying the genetic code responsible for proteins production is just the first step. In addition to the transcriptional and translational controls that determine

actual protein production, other variables usually increase or decrease protein activity so that it is very difficult to predict what will happen in an individual patient under all conditions. On the other hand, the use of a specific therapy in all patients should occur with constant assessment of the responses and adjustments as necessary in what we have called "responsive" management. This part of patient-centered care is essential.

Another molecular approach being considered is the manipulation of the epigenetic processes that regulate protein expression (Browner and Newman 1987). This approach has been used with success for cancer treatments, but the abnormal processes in cancers are in specific cell types and persist over long periods of time. In contrast, in critically ill patients processes are more complex and acute. The pathological process effect multiple organs, and each one has its own varying expression profile. Furthermore, processes are constantly and rapidly changing with a time scale of minutes to hours. A patient with severe sepsis can go from being in refractory shock to being awake, stable, and recovering within 12 hours if the offending invasive agent is rapidly identified and treated.

A better use of molecular tools may be to expand the phenotypic description of critically ill patients. Current monitoring is largely limited to heart rate, blood pressure, temperature, urine output, lactate and white blood cell count, and perhaps cardiac output. A rapid deeper biochemical profile obtained with modern molecular tools at the bedside could provide more detailed insights into underlying processes. The same way that a falling lactate, falling creatinine, and rising urine output indicate that a patient is responding to therapy, more specific biochemical markers could add more sensitive and rapid insights into underlying processes and allow an adaptive approach to therapy. For example, perhaps there could be a detector of the ongoing activity of nuclear factor- κ B (NF κ B), a central transcriptional regulator of many molecules in the inflammatory cascade, or ongoing monitoring of the redox state in blood, or perhaps even in tissues of critically ill patients. In this approach, these disturbed biochemical processes would be used as indicators

of the course of disease and not as targets of therapy similar to the way that lactate currently is used, but hopefully with more precision and more insights into underlying processes. Readily available, and more detailed phenotyping and endotyping of critical illness, perhaps even at the organ level, also will allow more efficient and high yield clinical trials, either through predictive enrichment (including only those patients most likely to benefit from a therapy) or through a responsive trial design that adapts the interventions based on patient responses. Importantly, these tools will have to have a proven benefit compared to standard bedside evaluation. For example, one of the best indicators of a patient's state is wakefulness. If a previously comatose patient is awake and talking, or at least interacting spontaneously and coherently, it likely does not matter what the value is of any other indicators! Bedside assessment likely will remain a cornerstone of patient evaluation and care. An important limitation on the utility of newer biomarkers will likely not be the assay of biomarkers but rather the knowledge that it is necessary to interpret the significance of the level of the biomarker in the appropriate context.

Genetic and molecular techniques have great potential for the treatment of infectious agents, but here the greatest benefit likely will be derived from the genetics of the invading organism rather than the host's genetics. Recent experience with the COVID-19 pandemic illustrates the potential of these techniques to rapidly identify the organism as well as to track its epidemiology by detailed genetic analysis. Rapid genetic identification of pathogenic organisms can allow rapid identification of potential resistance to current standard treatments. This approach would be a major breakthrough because we have learned that the faster and more precise the treatment of an invading organism, the better the outcome. Better genetic profiling of invading organisms potentially also can help us understand the transmission of resistant organisms and strengthen public health policies. In addition, the rapid definition of the genetics of novel pathogens is a prerequisite for the development of novel therapies, to say nothing of vaccines.

An area in which there have been tremendous advances is in patient imaging technologies. Improvements in ultrasonography have allowed rapid bedside evaluation of patient's interior structures. Tissue tracking approaches are enhancing evaluations of cardiac muscle function, and likely will provide new insights into other organ pathologies. Increasing use of Doppler signals allows non-invasive evaluation of regional blood flows. In the future, it is likely that these tools will be combined with challenges to the system that tests the limit of responses and the reserves in the system in the same way that exercise testing is regularly used to evaluate cardiac limitation, and glucose is infused to test insulin responses. The future likely will provide more portable and less expensive devices that can be kept at the bedside of critically ill patients and provide dynamic information as the disease course evolves. An example is electrical impedance tomography. Techniques are beginning to evolve that will allow real-time assessment of ventilation-perfusion matching in the lung. This potentially will be used to adjust ventilator settings and would allow the clinician to better take into account heart-lung interactions, which is a major theme of this book. In the future, we should expect newer technologies that will expand on computed tomography and nuclear magnetic resonance by providing bedside approaches to patient investigations and more rapid processing. Resolution will also likely continue to improve as technology advances. Lastly, metabolic monitoring and profiling is another area ripe for development. It has long been said that "death begins in radiology" so the ability to obtain quality cross-sectional imaging without the need to transport critically ill patients will be an unalloyed good.

Mitochondrial dysfunction is considered to be a major component of multi-organ failure. Currently, evaluation of mitochondrial function only can be done in vitro or in genetically modified animals, but perhaps newer imaging techniques will evolve that will allow assessment in vivo. We would then be able to evaluate how therapies affect mitochondrial function. It is unlikely that mitochondria could be a simple target of a single therapy because their dysfunction

is most likely organ-specific, but this information would lead to a greater understanding of disease processes and the consequences of our overall treatments.

Membrane dysfunction is likely also a major component of critical illness. It leads to vascular leak and the loss of blood volume, which is one of the greatest challenges in managing patients with distributive shock. It also leads to the failure of organs that require maintenance of a strong transmembrane potential such as the heart, smooth and skeletal muscles, the brain, and perhaps even mitochondria. Potential agents to improve this function currently are being studied, mainly at the cellular level, but hopefully in the future agents will be developed that will allow moderation of these processes in patients (Gavard 2014).

With the increasing availability of extracorporeal membrane oxygenation and CO₂ removal, we have the ability to maintain life and provide time for organ recovery. A future concept may be to use these devices to “rest” injured tissues, i.e., heart and lungs, while they recover. For example, such advanced support could be important for avoiding ventilator-induced lung injury or for decompressing a distended left heart, thereby protecting the lungs from high vascular pressures. However, caution will be required because these aggressive approaches may lead to tissue injuries themselves by removing normal functions. In addition, before broadly applying such intensive therapy, better predictive tools will be necessary to identify patients who may benefit so that life is prolonged instead of just prolonging dying. To date, this hypothesis of organ rest has not been supported by available data.

As we get better at improving early survival, we will need better approaches to the long road to recovery (Herridge et al. 2011). It is evident that patients with post-intensive care syndrome (PICS) are left with multi-organ dysfunction and functional impairment. They most often have long-term disabilities in muscle, joints, and sensory functions. They frequently suffer from depression, post-traumatic stress disorder, and chronic pain syndromes (Herridge et al. 2011). There also are major disruptions in their social

structures, and in many health care systems, the financial toxicity of critical illness is increasingly recognized (Cameron et al. 2016). We will need to learn what we can do at early stages to prevent, or at least reduce, these complications. Early mobilization and nutritional support have improved functional outcomes to a degree, but a very large burden of chronic disease during ICU recovery remains. This issue is especially problematic in patients over 50 years of age (Herridge et al. 2003). It will be a major challenge to find therapeutic interventions that alleviate the burden in these individuals who make up the increasing proportion of critically ill patients.

Ultimately, one of the best ways to treat the critically ill is the prevention of the factors that endanger patients. Thus, a better understanding of risk factors, and better preventive approaches in those at risk, should be a major priority in future management. Important measures should include improved hospital design with greater use of single rooms, improved surfaces for better cleaning and prevention of contamination, and advancements in hospital ventilations systems. As technologies advance, and our potential to sustain life improves, it will be important to evaluate how effectively new life-prolonging therapies provide a meaningful chance of recovery and an acceptable quality of life. Failure to consider this, the indiscriminant use of aggressive new technologies, and an increasing number of potential patient candidates, could overwhelm our health care systems without providing tangible benefits to patients.

In summary, in some ways, the future is here. Outcomes of critically ill patients, and those undergoing complex surgical procedures, have improved dramatically. Further improvements will continue to require close and continuous attention to each patient’s clinical course, but more importantly, there needs to be an ongoing evolution of our understanding of the underlying physiological and pathophysiological processes. In addition, better bedside management will continue to require a skilled and well-trained workforce, which currently often is challenged by fragmented management and over-reliance on new technologies. The values obtained with new

devices only can be as good as the questions asked of them by the treating team. When evaluating new technologies, it is worthwhile considering the words of the late Neil Postman, who was an expert in the social consequences of technologies (Postman 1992). What is the problem that this new technology solves? Whose problem is it? What new problems do we create by solving this problem? Which people and institutions will be most impacted by a technological solution?

To end, we had some fun speculating on primary predictions and will finish with our list of favorites:

1. Technology: real time, non-invasive readout of intravascular volume and cardiac output.
2. Predictive analytics: use of big data to predict individual outcomes by using deep learning with iterative algorithms that improve with experience.
3. Smart pharmacology: Some drugs can help and some may hurt subgroups of patients; use of genomics and physiology may help us move past the one-size-fits-all approach by indicating who is most likely to respond.
4. Real-time lung imaging: This could help titrate PEEP and peak transpulmonary pressure in order to minimize atelectasis and over-distension.
5. Immunomodulation: better understanding of immune system dynamics may lead to more targeted approaches to immune modulation, for example, suppression of the response at some stage and stimulating the response at another time during the course of the illness. Humoral, T cell and neutrophil function are all different, some patients need more, some need less, and in some circumstances perhaps patients at risk should be vaccinated with endotoxin prior to sepsis.
6. Anti-infection: bedside, rapid genetic characterization of invading organisms will provide more rapid identification of the appropriate therapeutic agent.
7. Development of active antiviral agents that have comparable therapeutic effects as antibacterial and antifungal agents.
8. Development of drugs that stabilize vascular permeability and prevent the marked increase in fluid loss in sepsis.
9. Prevention and recovery – Better understanding of the mechanism of post-intensive care syndrome will lead to changes in care delivery and therapies to prevent the long-term sequelae of critical illness.
10. Understanding of the microbiome: a better understanding of the role of the microbiome will lead to both smarter use of antibiotics to avoid ablation of the host flora, but also will direct therapeutic manipulation of the microbiome itself.
11. Targeted therapies for common comorbidities; much intensive care unit mortality is related to underlying conditions but rapidly developing, targeted molecular therapies for common medical illness (heart failure, cancer) will lead to greater patient resilience in the face of critical illness.
12. Monitoring: as the use of single rooms with isolation capacity increase, alarms hopefully will finally be removed from around the patient's head and moved to a control panel outside the patient's room. Remote facilities will be established so that ventilators, pumps, and other controls can be managed remotely outside the room especially when patients are isolated for infection control.

Maybe we will be right, maybe we will be wrong, or maybe the future will outshine the best of any predictions that we came up with and all our current thoughts will just seem naïve!

References

- Abraham E, Wunderink R, Silverman H, Perl TM, Nasraway S, Levy H, et al. Efficacy and safety of monoclonal antibody to human tumor necrosis factor alpha in patients with sepsis syndrome. A randomized, controlled, double-blind, multicenter clinical trial. TNF-alpha MAb Sepsis study group. *J Am Med Assoc.* 1995;273(12):934–41.
- Abraham E, Glauser MP, Butler T, Garbino J, Gelmont D, Laterre PF, et al. p55 tumor necrosis factor receptor fusion protein in the treatment of patients with severe sepsis and septic shock. A randomized controlled

- multicenter trial. Ro 45-2081 study group. *JAMA*. 1997;277(19):1531–8.
- Boyd O, Grounds RM, Bennett ED. A randomized clinical trial of the effect of deliberate perioperative increase of oxygen delivery on mortality in high-risk surgical patients. *J Am Med Assoc*. 1993;270(22):2699–707.
- Browner WS, Newman TB. Are all significant P values created equal? The analogy between diagnostic tests and clinical research. *JAMA*. 1987;257(18):2459–63.
- Burke E. Edmund Burke quotes [quote-coyote.com](https://www.quote-coyote.com/quotes/authors/b/edmund-burke/). (Available from: <https://www.quote-coyote.com/quotes/authors/b/edmund-burke/>).
- Cameron JI, Chu LM, Matte A, Tomlinson G, Chan L, Thomas C, et al. One-year outcomes in caregivers of critically ill patients. *N Engl J Med*. 2016;374(19):1831–41.
- Cross AS. Antiendotoxin antibodies: a dead end? *Ann Intern Med*. 1994;121(1):58–60.
- Danziger J, Ángel Armengol de la Hoz M, li W, Komorowski M, Deliberato RO, rush BNM, et al. temporal trends in critical care outcomes in U.S. minority-serving hospitals. *Am J Respir Crit Care Med*. 2020;201(6):681–7.
- Gavard J. Endothelial permeability and VE-cadherin. *Cell Adhes Migr*. 2014;8(2):158–64.
- Goronzy JJ, Weyand CM. Understanding immunosenescence to improve responses to vaccines. *Nat Immunol*. 2013;14(5):428–36.
- Gustafsson UO, Scott MJ, Hubner M, Nygren J, Demartines N, Francis N, et al. Guidelines for perioperative Care in Elective Colorectal Surgery: enhanced recovery after surgery (ERAS®) society recommendations: 2018. *World J Surg*. 2019;43(3):659–95.
- Herridge MS, Cheung AM, Tansey CM, Matte-Martyn A, Diaz-Granados N, Al-Saidi F, et al. One-year outcomes in survivors of the acute respiratory distress syndrome. *N Engl J Med*. 2003;348(8):683–93.
- Herridge MS, Tansey CM, Matté A, Tomlinson G, Diaz-Granados N, Cooper A, et al. Functional disability 5 years after acute respiratory distress syndrome. *N Engl J Med*. 2011;364(14):1293–304.
- Knaus WA, Marks RD. New phenotypes for Sepsis: the promise and problem of applying machine learning and artificial intelligence in clinical research. *JAMA*. 2019;321(20):1981–2.
- Ljungqvist O, Scott M, Fearon KC. Enhanced recovery after surgery: a review. *JAMA Surg*. 2017;152(3):292–8.
- Lopez A, Lorente JA, Steingrub J, Bakker J, McLuckie A, Willatts S, et al. Multiple-center, randomized, placebo-controlled, double-blind study of the nitric oxide synthase inhibitor 546C88: effect on survival in patients with septic shock. *Crit Care Med*. 2004;32(1):21–30.
- McCloskey RV, Straube RC, Sanders C, Smith SM, Smith CR. Treatment of septic shock with human monoclonal antibody HA-1A. A randomized, double-blind, placebo-controlled trial. CHESST trial study group. *Ann Intern Med*. 1994;121(1):1–5.
- Pearse RM, Harrison DA, MacDonald N, Gillies MA, Blunt M, Ackland G, et al. Effect of a perioperative, cardiac output-guided hemodynamic therapy algorithm on outcomes following major gastrointestinal surgery: a randomized clinical trial and systematic review. *JAMA*. 2014;311(21):2181–90.
- Postman N. Technopoloy: the surrender of culture to technology. New York: Vintage books; 1992.
- Rautanen A, Mills TC, Gordon AC, Hutton P, Steffens M, Nuamah R, et al. Genome-wide association study of survival from sepsis due to pneumonia: an observational cohort study. *Lancet Respir Med*. 2015;3(1):53–60.
- Seymour CW, Kennedy JN, Wang S, Chang C-CH, Elliott CF, Xu Z, et al. Derivation, validation, and potential treatment implications of novel clinical phenotypes for Sepsis. *JAMA*. 2019a;321(20):2003–17.
- Seymour CW, Kennedy JN, Wang S, Chang CH, Elliott CF, Xu Z, et al. Derivation, validation, and potential treatment implications of novel clinical phenotypes for Sepsis. *JAMA*. 2019b;321(20):2003–17.
- Weyand CM, Goronzy JJ. Aging of the immune system. mechanisms and therapeutic targets. *Ann Am Thorac Soc*. 2016;13(Suppl 5):S422–s8.

Index

A

- Abdominal pressure (P_{ab}), 554
- ABiomed AB5000, 807
- Absolute esophageal pressure, 690, 691
- Acid-base disorders, 654
 - base excess, 660, 661
 - chloride effect, 662
 - evaluation of, 661–662
 - protein effect, 663
 - water effect, 662
- Action potential duration (APD)
 - immediate change, 94, 95
 - steady-state, 95
 - transient change, 95
- Acute cor pulmonale, 685
- Acute Myocardial Infarction in Switzerland (AMIS), 761
- Acute obstructive disease
 - airflow limitation, 708
 - heart-lung interaction
 - intra-pulmonary vessels, 710–711
 - pleural pressure, 709–710
 - mechanical ventilation, 707
 - normal respiratory mechanics, 707–708
 - spontaneously breathing patient, 711–712
 - therapeutic strategy, 712–713
 - ventilated patient, 712
- Acute pulmonary embolism (PE)
 - categorization of, 908
 - CTA, 909
 - incidence, 905
 - laboratory testing, 908
 - management, 909
 - airway management, 913, 914
 - anticoagulation and thrombolytics, 910–912
 - vasoactive medications, 912, 913
 - mortality, 905
 - pathophysiology, 905, 906
 - right ventricle, 906–908
 - TTE, 909, 910
 - vasoconstrictive mediators, 906
 - Wells criteria and revised Geneva score, 908
- Acute respiratory distress syndrome (ARDS), 172, 200, 375, 486, 509, 590, 685, 699
 - biological modulation, 736
 - definition, 729
 - hyperinflammation, 731
 - pathophysiology of
 - exudative phase, 729, 730
 - fibrotic phase, 730
 - proliferative phase, 730
- VILI
 - biotrauma and inflammation, 734, 735
 - etiology and pathophysiology, 732, 733
 - histologic alterations, 731
 - historical perspective, 732
 - inflammation and fibrosis, 735
 - mechanical and biological pathways, 735, 736
 - mechanotransduction, 733, 734
- Aging, 951
- Airway opening pressure (AOP), 689
- Airway pressure (ΔP_{aw}), 486
- Airway pressures and electromyographic (EMG) signals, 545
- Airway resistance, 250
- Alternating electric current (AC), 585
- Alveolar-arterial difference (AaDO₂), 193, 194
- Alveolar overdistension and collapse (ODCL), 591–592
- Alveolar pressure, 254
- Alveolar syndrome, 502–503
- Ambient hypoxia, 644
- Amplitude of oscillations, 276
- Aortic stenosis, 628
- Apnea, 214, 215
- Arginine vasopressin, 752
- Arterial blood pressure
 - critical closing pressure, 117, 118
 - elastic energy, 108, 109
 - gravitational energy, 111, 112
 - impedance, 120
 - kinetic energy, 109–111
 - mammals, 112, 113
 - measurement, 120, 121
 - physical principles, 107, 108
 - pulse pressure, 119, 120
 - regional distribution of flow, 113–117
- Arterial cannulation, monitoring of BP, 273
- Arterial doppler waveform, 388, 389
- Arterial wall properties, 124–126

- Arterial wave reflections, 129–131
 Asynchronies, mechanical ventilation, 715, 716
 ATHOS-3 trial, 754
 Auscultatory method, 275
- B**
- Bainbridge reflex, 99, 100
 Barbiturates, 160
 Barotrauma, 172
 Base excess (BE), 660, 661
 Bedside management, 956
 Beginning cardiogenic shock, 763
 Benzodiazepines, 159
 Bernoulli effect, 475, 476
 Big data approaches, 953
 Bioimpedance, 585, 586
 Bisphosphoglycerate, 639
 Blood chemistry analysis, 664
 24-hour blood pressure assessment, 276
 Blood pressure measurement, 278, 279
 - innovative sensor technology developments, 278
 - intermittent non-invasive, 273, 274
 - invasive arterial, 273–275
 - nanocomposites, 278
 - non-invasive continuous arterial, 276–278
- Body plethysmography, 477, 478
 Bohr and Haldane effects, 638–639
 Bohr's and Enghoff's formulas, 607
 Bohr's formula, 605
 Brain monitoring, 337
 Bronchial C-fibers, 213
- C**
- Cabamylation, 648
 Calcium-clock, 90, 91
 Campbell diagram, 549
 Capnography, 613
 Capsaicin, 229
 Carbamylated hemoglobin (CarHb), 647, 648
 Carbon dioxide (CO₂), 601
 Carbon monoxide (CO), 646
 Cardiac output, 283
 - analytic problem, 292, 293
 - bath tub concept, 11, 12
 - capacitance, 9
 - closed circuit, 7
 - compliance, 10, 11
 - compliant region, 10–12
 - continuous thermodilution technique, 293
 - echocardiographic techniques, 299–301
 - errors, 286
 - esophageal doppler, 298, 299
 - fick method, 287
 - foreign gas method, 295, 296
 - Guyton's analysis, 13, 14
 - Guyton's, graphical approach, 14, 17
 - capacitance, 16, 17
 - cardiac function, 14–18
 - Starling's cardiac function curve, 13
 - stressed volume, 16
 - vascular capacitance, 16
 - venous return curve, 14–18
 - x-intercept, 14
 - hydraulic and electrical models, 12, 13
 - indicator dilution methods, 288, 289
 - injectate, 290, 291
 - intrathoracic volume, 303, 304
 - Krogh's two compartment model, 18, 19
 - LiDCO Plus®, 297
 - measurement method, 309–311
 - multicellular organisms, 7
 - normalization, 284
 - pathophysiologic factors, 292
 - physiologic factors, 291, 292
 - PiCCO system, 297
 - potential problems, 294
 - pressure-flow relationship, 10
 - pressure-volume relationship, 8–10
 - procedures, 313–318
 - pulse contour analysis, 296
 - rebreathing method, 294
 - reliability, 293
 - respiration, 287
 - single breath technique, 295
 - sources of variability, 290
 - specific quality criteria, 311, 313
 - stressed volume, 7
 - thermodilution technique, 289, 290
 - transoesophageal echocardiography, 302, 303
 - transthoracic echocardiography, 302
 - Vigileo™, 297
- Cardiac-related signal (CRS), 589
 Cardiogenic (hydrostatic) pulmonary edema, 508
 Cardiogenic shock
 - with acute coronary syndromes, 760–762
 - without acute coronary syndromes, 762–766
 - cardiac and return functions, 774
 - CathPCI registry, 759
 - clinical consequences, 775–778
 - congestive component, 766, 767
 - definition, 759, 760
 - depression of E_{max}, 774
 - diastolic filling pressure, 774
 - distributive component, 767
 - GUSTO-IIb, 766
 - Guyton's plot, 774, 775
 - in-hospital mortality, 759
 - left anterior descending (LAD) occlusions, 766
 - LV passive filling curve, 774
 - mechanical support devices
 - Centrimag®, 793
 - ECMO, 809, 811, 812
 - general principles, 796–803
 - IABP, 793–797
 - Impella®, 793, 803–806
 - left ventricular support, 794
 - para-corporal devices, 793
 - physiological approaches, 793, 809

Colloids, 678–679
 Colorectal surgery, 952
 Compound muscle action potential (CMAP), 558, 559
 Computed tomography angiography (CTA), 909
 Connective tissue disease-associated ILDs, 510
 Control of breathing
 arterial P_{O_2} , P_{CO_2} , and pH
 arterial chemoreceptors, 210, 211
 central chemoreceptors, 209, 210
 chemoreflex, mechanoreflex, and negative feedback, 207, 208
 clinical implications
 apnea, 214, 215
 chronic hypercapnia, 216, 217
 dyspnea, 215, 216
 patient/ventilator dyssynchrony, 215
 CNS-processed signal targeting effector respiratory muscles, 208, 209
 definition, 205
 limitations, 206
 lungs and airways
 autonomic nervous system, 213, 214
 bronchial C-fibers, 213
 juxtacapillary receptors, 213
 lungs and lower airways, 212
 nose and upper airways, 211, 212
 pulmonary stretch receptors, 212
 respiratory rhythm generation, 206
 Cranio-caudal movement, 571
 Curtain sign, 498, 508
 Cystic fibrosis (CF), 627

D

Delirium
 bedside detection, 923
 definition and epidemiology, 924
 Diagnostic and Statistical Manual of Mental disorders (DSM-5) definition, 923
 identification, 925, 926
 incidence, 923
 nonpharmacological interventions, 927, 928
 PADIS guidelines and ABCDEF bundle, 927
 pathophysiology, 924, 925
 pharmacological interventions, 929–931
 analgesia and sedation management, 930, 931
 drugs, 929
 risk factors, 923, 926, 927
 Deteriorating/doom, 763
 Dexmedetomidine, 160
 Dialysis disequilibrium syndrome, 143
 Diaphragm
 echodensity, 528
 electrical resistance of, 274
 excursion, 524, 529
 speckle tracking, 528
 thickening fraction, 525
 thickness and tidal thickening fraction, 528
 ultrasonography, 566–571
 ultrasound

 clinical and research applications, 529–530
 diaphragm excursion, 527
 diaphragm strain, 527
 echodensity, 528
 functional anatomy of, 521–522
 influence of effort and lung volume, 526
 mechanics of, 522–523
 motion, 524
 reference range for, 525
 relation to inspiratory pressure, 527
 relation to inspiratory volume, 525–527
 shortening, 525–527
 speckle tracking, 528
 structure and function, 523–527
 thickness and tidal thickening fraction, 523, 528
 Diaphragmatic motion, 524
 Diastolic compliance, right heart function, 24, 25, 28, 39, 40
 Diffuse lung disease, 624–625
 Dilutional effect, 658
 Dipalmitoylphosphatidylcholine(DPPC), 236
 Dopamine, 925
 Doppler measurements, 363
 Doppler ultrasound
 clinical application, 391–394, 396–398
 principles, 386, 388–391
 Duty cycle, 220
 Dynamic contrast enhanced (DCE) MRI, 620, 621
 Dyspnea, 215, 216

E

Echocardiography
 cardiogenic shock, 367, 368
 classical hemodynamical parameters, 363, 365
 clinical conditions, 365, 366
 education, 370
 pitfalls and limitations, 369, 370
 transthoracic technique, 371
 TTE imaging, 359–362
 Effective arterial elastance (E_a), 32
 Effective lung volume (ELV), 611
 Efficacy and Safety of Recombinant Human Activated Protein C for Severe Sepsis (PROWESS), 823
 Elastance, 769
 Elastic energy, 108, 109
 Elastic recoil, 8, 12
 Electrical impedance, 585
 Electrical impedance tomography (EIT), 587, 691, 692, 955
 bioimpedance, 585, 586
 clinical application, 593–594
 measurements and image reconstruction, 586–589
 perfusion monitoring, 594–596
 Sheffield backprojection, 588
 spatial distribution of ventilation, 590–592
 temporal distribution of ventilation, 592–593
 ventilation monitoring, 590–594
 voltage measurements, 587
 waveform analysis, 589

- Electromyograms (EMG), 543
 Embedding oscillometric techniques, 274
 Encyclopedic approaches, 953
 Endocardial endothelial cells (EEC), 23
 Endothelial glycocalyx, 72
 Endotracheal suctioning, 594
 Endotracheal tubes, 594
 End-systolic elastance relationship (ESPVR), 772
 End-systolic left ventricular pressure-volume (Es-Lv), 26
 End-systolic pressure-volume line (Es-Rv), 26
 End-systolic pressure volume relationship (ESPVR), 51–53
 Epipharynx, 211
 Epithelial-endothelial fluid reabsorption
 intestinal mucosa, 79
 in kidney, 78, 79
 lymph nodes, 79
 Equal pressure point, 475
 Esophageal balloon, 485
 Esophageal Doppler, 298
 Esophageal pressure (ΔP_{es}), 486, 490, 539
 auto-triggering, 490
 clinical applications of, 486
 delayed cycling, 490
 diaphragmatic muscle contractions, 489
 double triggering, 490
 estimate of pleural pressure, 485
 ineffective efforts, 489
 occlusion test, 485
 patient's effort, 488–489
 patient-ventilator interaction, 489–490
 positioning of, 485
 premature cycling, 490
 supine position, 486
 transpulmonary pressure, 486–488
 upright and prone positions, 486
 Esophageal pressure monitoring, 488, 489
 European Life Support Organization (ELSO)
 registry, 763
 Expiratory reflex, 212
 Extra corporal membrane oxygenation (ECMO), 952
 Extracellular fluid, 586
- F**
 Fick principle, 285
 sources of error, 286
 Figge equation, 660
 Finger cuff technology, *see* Volume clamp method
 Fluid filled system, 273
 Fluid filtration
 blood loss and saline infusion, 80, 81
 endothelial glycocalyx
 components, 82
 optical methods, 82, 83
 whole body glycocalyx volume, 83
 epithelial-endothelial fluid reabsorption
 intestinal mucosa, 79
 in kidney, 78, 79
 lymph nodes, 79
 fluid exchange, 81
 interstitial pressure, 80
 lung fluid balance, 81
 microvascular pressures, 79–81
 microvessel pressure and colloid osmotic pressure, 76, 78
 plasma proteins, 81
 plasma volume, 71
 revised Starling principle, 72
 classical Starling principle, 73, 74
 endothelial glycocalyx, 72
 filtration rate, 74–77
 fluid exchange, 75
 sub-glycocalyx space, 72, 73
 Fluid physiology
 body water and electrolytes, 139, 140
 compartments, 139
 extracellular fluid dynamics, 144, 145
 hyper-oncotic solutions, 148, 149
 hypertonic sodium chloride solutions, 147, 148
 iso-oncotic colloids, 148
 movement and distribution, 145, 146
 normal saline, 146, 147
 osmoles
 albumin molecules, 143
 analbuminemia, 144
 definition, 140
 diffusive permeability and reflection coefficient, 142, 143
 Gibbs-Donnan relationship, 143
 glucose, 142
 membrane, 141
 osmotic pressure, 140, 141, 143
 plasma volume, 144
 positive elements, 141, 142
 water movement, 141
 principles, 137
 pure water and dextrose, 146
 role of water, 137, 138
 sodium bicarbonate solution, 149
 volume and generation of blood flow, 138, 139
 Fluid-responsiveness, 366, 369
 fluid challenge, 406, 407
 heart-lung interactions, 414
 passive leg raising test, 411–413
 pulse pressure variation, 407
 respiratory occlusion tests, 413, 414
 static indices, 405
 stroke volume variation, 408, 410
 vena cava, 410, 411
 Fluorine gas MRI, 623
 Focal disorders, 917
 Focal lung diseases, 510–512
 Force balance, 171
 Forced oscillation technique, 480
 Force-velocity relation, 522
 Fourier transform analysis, 128
 Frank-Starling curve, 613
 Frequency-domain analysis, 561–562

- Fluid responsiveness, 414
 Functional EIT (fEIT) images, 589
 Functional residual capacity (FRC), 474, 534
- G**
 Gambelgrams, 657
 Gamblegrams, 656
 Gas exchange, 625–627
 Gastric pressure (P_{ga}), 539
 Gastric-to-esophageal pressure, 555–556
 Gatorade®, 777
 Genetic and molecular techniques, 955
 Gibbs-Donnan effect, 146
 Global cerebral ischemia, 917
 Global inhomogeneity index (GI index), 592
 Global ventilation, 590
 Glucose, 673
 Glycocalyx-cleft model, 77
 Glycocalyx-junction model, 77
 Gravitational energy, 111, 112
 Guillain-Barre' syndrome, 534
 Guyton's analysis, 13, 14, 100
- H**
 Heart disease, 628
 Heart lung interactions, 243, 244, 267
 active expiration, 264
 clinical implications, 244
 Guyton's graphical, 246–248
 HJR, 264
 inverse pulsus paradoxus, 263
 lung inflation, 255
 mueller maneuver, 265, 266
 Ppl, 249, 251–254
 pulsus paradoxus, 260, 262
 respiratory variations, 256–260
 transpulmonary pressure, 255–257
 Valsalva, 267
 Heart-lung mechanical coupling, 709
 Heart rate
 action potential, 87
 Bainbridge reflex, 99, 100
 beta-blockers and ejection fraction, 98, 99
 diastolic limitation, 101
 during exercise, 96–98
 Guyton analysis, 100
 intrinsic heart rate, 95, 96
 periodicity, 87
 rhythmicity
 APD, 94, 95
 SAN (*see* Sinoatrial node (SAN))
 stroke return, 87
 supply-demand of, 101, 102
 tachycardia and hypovolemia, 99
 time constants and volume constraints, 87–89
 Hemodynamic measurements, 319
 CVP, 329–332
 frequency response, 328, 329
 measuring pressures, 321–324
 Ppao, 333, 334
 pulmonary artery pressure, 334, 335
 transmural pressure, 324–327
 understanding pressure measurements, 320, 321
 volume vs. pressure measurements, 319, 320
 Hemoglobin-mediated interactions, 641
 Hemoglobin respiratory function
 adaptation of erythrocytes, 641–643
 adaptation to life, 643
 anaerobic origin of hemoproteins, 636
 clinical alterations of, 645
 clinical physiology and pathophysiology
 acylation, 647
 ambient hypoxia, 644
 carboxyhemoglobinemia, 646–647
 CarHb, 647, 648
 deamination, 647
 hemoglobinopathy, 644–646
 human fetal hemoglobin, 646
 increased metabolic demand, 643
 methemoglobinemia, 647
 post-translational modification, 647–648
 unstable hemoglobins, 646
 coupling of O₂ and CO₂ exchange, 639
 erythrocytes, 638–641
 oxygen carrier, 636–638
 Henderson-Hasselbalch equation, 654
 Hepatojugular reflux, 264
 Heat moisture exchanger (HME), 603
 Hooke's assessment, 9
 Hospital design, 956
 Hydrogen (H⁺) ion
 acidemia or alkalemia, 653
 albumin, 659–660
 CO₂, 658, 659
 empiric equations, 654
 Henderson-Hasselbalch equation, 654
 serum electrolytes, 653
 strong ions, 655–658
 water, 654, 655
 Hydrostatic pressure, 140, 143, 144
 Hydrostatic zero reference point, 275
 Hypercapnia, 196
 Hyperinflation, 695
 Hyperpolarisation-activated cyclic nucleotide-gated (HCN), 89
 Hypertonic saline, 158
 Hyperventilation, 156
 Hypovolemia, 99
 Hypoxic pulmonary vasoconstriction (HPV), 196
- I**
 IABP Shock II registry, 763
 IABP Shock II risk score, 764
 Idiopathic pulmonary fibrosis, 510
 Impedance ratio, 590
 Impella®, 777, 793
 Indicator-based signal (IBS), 589
 Inferior vena cava (IVC), 392
 Innovative non-invasive technologies, 278

- Input impedance, 127–129
 Inspiratory and expiratory intercostal muscle, 208
 Intensive care unit (ICU), 2
 Intensive therapy, 956
 Intermittent non-invasive arterial blood pressure measurement, 275, 276
 Interstitial lung diseases (ILDs), 510
 Interstitial pressure, 80
 Interstitial space, 138, 139, 142–144
 Interstitial syndrome, 499–503
 Intestinal mucosa, 79
 Intra-aortic balloon pump (IABP), 793–797
 Intracardiac nervous system (ICNS), 92
 Intracellular spaces, 142, 143, 148
 Intracranial monitoring, 337
 cerebral oxygenation, 347, 348
 cerebral perfusion pressure, 345, 346
 clinical application, 342–345
 electrophysiology, 351
 history, 339
 indications, 345
 modes of measurement, 341
 pressure, 338
 techniques, 342
 waveform analysis, 339–341
 Intramuscular electrodes, 560
 Intra-thoracic bioimpedance, 585
 Intratidal gas distribution (ITV), 593
 Intravenous fluids
 assessment of hydration, 671
 blood flow, 670–671
 colloids, 678–679
 crystalloid solutions, 676–678
 fluid infusion, 669
 intravenous solutions, 674
 maintenance and daily needs, 672
 chloride, 673
 glucose, 673
 potassium, 673
 sodium, 672, 673
 water, 672
 managing hydration status, 679–680
 Na⁺ balance and vascular volume, 671
 for resuscitation, 669, 674–676
 types of, 676
 Intrinsic positive end-expiratory pressure (PEEPi), 550
 Invasive arterial blood pressure measurement (arterial catheter), 273–275
 Ischemia, 155
 Iso-oncotic colloids, 148
- J**
 Jugular venous bulb oximetry (JVBO), 348
 Juxtacapillary receptors, 213
- K**
 Kigali modification, 509
 Kinetic energy, 109–111
 Krogh's two compartment model, 18, 19
 Kussmaul's sign, 265
- L**
 Labor issues, 952
 Larynx, 212
 Laser Doppler flowmetry (LDF), 436
 Laser Doppler perfusion imaging, 436
 Left heart function
 cardiac muscle characteristics, 49, 50
 contractility, 55
 ESPVR, 51–53
 maximum elastance (E_{max}), 53, 54
 myocardial oxygen consumption, 57
 pressure-volume relationships, 51, 52, 57, 58
 tension-length relationships, 50, 51
 time-varying elastance, 53, 54
 ventricular energetics, 55, 56
 Lempel-Ziv index, 572
 Length-tension relation, 522
 Life expectancy, 952
 Life-sustaining therapies, 951
 Lorazepam, 159
 Lower inflection point, 686, 687
 Low-frequency probes (5-1 MHz), 502
 Lung
 barotrauma and volutrauma, 172
 collapse and overdistension, 593
 edema, 184
 inflation, 68, 69, 167, 169, 170
 injury, 227
 mechanical ventilation, 167
 prestress and shear modulus, 170
 stress and strain
 non-uniform inflation, 172
 pressure and volume, 168, 169
 transmission, 170, 171
 viscoelasticity, respiratory rate and mechanical power, 172–174
 Lung elastance (E_L), 479
 Lung resistance (R_L), 479
 Lung ultrasound (LUS) assessment
 alveolar syndrome, 502–503
 anterior and lateral chest, 499
 ARDS, 509, 510
 cardiogenic (hydrostatic) pulmonary edema, 508
 clinical application of, 513
 diagnosis and monitoring, 503, 512–515
 of alveolar syndrome, 502
 of interstitial syndrome, 501
 of pneumothorax, 506
 focal lung diseases, 510–512
 ILDs, 510
 interstitial syndrome, 499–502
 lung ultrasound scanning protocols, 514
 normal lung ultrasound, 498–500
 physics of, 493–495
 pleural effusion, 507–508
 pneumothorax, 503–507
 training, 515
 ultrasound systems, 495
 LUS-Berlin criteria, 509
 Lymph nodes, 79

M

Magnetic stimulation, 540–541
 Main-stream capnographs, 602
 Mannitol, 157, 158
 Manufacturer and User Facility Device Experience (MAUDE) database, 816
 Maximal diaphragm thickening fraction, 528
 Maximal expiratory airway pressure ($P_{E\max}$), 535
 Maximal inspiratory pressure ($P_{I\max}$), 535
 Maximal transdiaphragmatic pressure ($P_{d\max}$), 533
 Maximum elastance (E_{\max}), 51, 53, 54
 Mean airways-alveolar interface, 605
 Mean circulatory filling pressure (MCFP), 12
 Mean systemic filling pressure (MSFP), 12, 25, 670
 Measurement precision, 310, 311
 Measurement trueness, 309
 Measurement uncertainty, 311
 Mechanoreceptors monitor, 208
 Melatonin, 925
 Membrane-clock, 89, 90
 Membrane dysfunction, 956
 Mesenchymal stromal cells (MSCs), 736
 Methemoglobinemia, 647
 Microcirculation, 429

- capillaroscopy, 432
- function, 438, 439
- hand-held vital microscopes, 432, 433, 435, 436
- laser-based techniques, 436
- LDPI, 436, 437
- LSCI, 437, 438
- monitoring techniques, 430, 431
- tissue oxygenation, 430

 Microvascular pressure, 79, 80
 Midazolam, 159
 Mild hypoxemia, 198
 Mitochondria, 156
 Mitochondrial dysfunction, 955
 Mitral annular plane systolic excursion (MAPSE), 369
 Mobile biomonitoring, 278
 Mobile health monitoring, 278
 Mueller-expulsive maneuver, 265, 266, 538–539
 Multifocal ischemia, 917
 Multiple inert gas elimination technique (MIGET), 194, 195
 Myocardial oxygen consumption (MVO_2), 56, 57, 101
 Myogenic peptides, 92, 93
 Myosin, 49

N

Nanocomposites, 278
 Near-infrared spectroscopy (NIRS), 439, 453
 Nephrotic syndrome, 145
 Neural breathing modulates, 558
 Neurally adjusted ventilator assist (NAVA), 565
 Neurocritical care, 337, 339, 348
 Neuromuscular coupling, 564
 Neuromuscular junction blockers, 160
 Neuroventilatory coupling, 564, 565
 Newton's laws of motion, 476

Newton-Raphson algorithm, 589
 Non-invasive continuous arterial blood pressure measurement, 276–278
 Nuclear factor- κ B (NF κ B), 954

O

Obesity

- and abdomen, 937
- additional considerations, 942
- airway management, 939, 940
- baseline physiology changes, 935–937
- control of breathing/OSA/OHS, 937, 938
- and outcomes, 942
- physiologic impact and clinical implications, 935
- prevalence, 935
- risk factor, 939
- ventilator management, 940, 941

 Observatoire Regional Breton sur l'infarctus registry, 763
 Occlusion test, 485
 Ohm's law, 61
 Oncotic pressure, 143
 "Open lung" strategy, 689
 Opioids, 159, 160
 Oscillometry, 275, 482
 Osmoles

- albumin molecules, 143
- analbuminemia, 144
- definition, 140
- diffusive permeability and reflection coefficient, 142, 143
- Gibbs-Donnan relationship, 143
- glucose, 142
- membrane, 141
- osmotic pressure, 140, 141, 143
- plasma volume, 144
- positive elements, 141, 142
- water movement, 141

 Osmotherapy

- hypertonic saline, 158
- mannitol, 157, 158

 Oxygen delivery

- critically ill, 467
- DO_2 , 465–467
- equation, 461, 462
- fluid administration, 462
- mechanical ventilation, 463
- optimizing arterial oxygen content, 463, 464
- tissues, 464
- vasoactive medications, 463

 Oxygen electrodes, 438
 Oxygen enhanced MRI, 622
 Oxygen extraction fraction (OEF), 155

P

Packed red blood cells, 463, 466
 Palpatory method, 275
 P_aO_2/F_iO_2 ratio ("P/F ratio"), 195
 Partial pressure of carbon dioxide ($PaCO_2$), 702

- Passive leg raising test, 366, 369, 411
- Patient self-inflicted lung injury (P-SILI), 488
- Patient's work of breathing (WOB), 488
- PCO₂ gap, 420–422
 - clinical practice, 422, 423
 - errors, 425, 426
 - oxygen-derived variables, 424, 425
 - SvO₂, 425
- Pendelluft, 594
- Peripheral perfusion indexes, 447–448
- Personalized medicine, 954
- Pharynx, 211
- Phospholipid, 235, 236
- PiCCO system, 297
- PICO® device, 778
- Plethysmography, 482
- Pleural effusion, 507–508
- Pleural line abnormalities, 510
- Pleural pressure (Ppl), 247, 485
- Pneumonia, 510, 511
- Pneumothorax detection, 594
- Point-of-care ultrasound (POCUS), 299, 386
- Poiseuille's law, 10, 61, 108
- Portal doppler waveform, 390, 391
- Positive end-expiratory pressure (PEEP), 173, 463, 464, 466, 486, 549, 552, 553, 700
 - airway closure, 688–690
 - airway P-V curve, 689
 - alveolar recruitment, 685
 - auto-PEEP, 185–187
 - baby lung, 685
 - “braking” effect, 184
 - cardiopulmonary effects, 184, 185
 - clinical applications, 185
 - definition, 177
 - dynamic hyperinflation, 185–187
 - EIT, 691, 692
 - esophageal pressure manometry
 - absolute esophageal pressure, 690, 691
 - chest wall to respiratory system, 691
 - estimating transpulmonary pressure, 690
 - EXPRESS study, 688
 - hemodynamic monitoring, 185
 - left ventricular afterload, 182
 - lung edema, 184
 - lung recruitability
 - CT scan images, 692–694
 - global integrative clinical approach, 694–695
 - lung volume and simplified method, 694
 - pressure-volume curves, 694
 - rationale, 692
 - mean airway pressure and hemodynamics, 180
 - myocardial contractility and compliance, 181, 183, 184
 - PEEP-FiO₂ table, 687, 688
 - recruitable lung regions, 685
 - regional heterogeneity, 179, 180
 - respiratory system compliance, 686–687
 - right ventricular afterload, 182, 183
 - spontaneous vs. passive inflation, 184, 185
 - transmural pressure, 177–179, 182
 - venous return and Starling curves, 180, 181
 - ventilation/perfusion abnormalities, 200
- Post-intensive care syndrome (PICS), 956
- Potassium, 673
- Pressure–time index (PTI), 220
- Pressure–time product (PTP), 551
- Pressure volume, 236
- Pressure–volume–area (PVA), 56
- Primary lung cancer, 512
- Primary percutaneous coronary intervention (PPCI), 761
- Principal component analysis (PCA), 595
- Prone position (PP), 197, 200
 - ARDS, 699, 700
 - distribution of alveolar size, 701
 - hemodynamics, 700
 - lung, 700–702
 - maneuver, 702–704
 - monitoring, 704
 - Swimmer's position, 703
- Prone position maneuver, 702–704
- Propofol, 159
- Protein effect, 663
- Protocol based care for early sepsis (ProCESS), 822
- Proton imaging, 622
- Pulmonary artery occlusion pressure (Ppao), 325, 335
- Pulmonary artery pressure (Ppa), 64, 65, 365, 370
- Pulmonary capillary wedge pressure (PCWP), 67
- Pulmonary contusion, 511
- Pulmonary embolism, 511, 624
- Pulmonary functional imaging, 619
- Pulmonary hypertension (PH), 623, 624
 - airway function, 876
 - apical views, 891
 - biomarkers, 894–896
 - cardiac magnetic resonance imaging, 893, 894
 - cardiopulmonary hemodynamics
 - definition, 873
 - hemodynamic characterization, 873
 - normal pulmonary circulation, 872–873
 - pre-capillary PH, 873
 - pulmonary vascular resistance, 873
 - cardiopulmonary monitoring
 - adverse effects, 879
 - HRQoL, 880–881
 - morbidity and mortality, 878
 - risk assessment and stratification, 879
 - symptomatic/functional classification, 879, 880
 - clinical practice, 889
 - clinical presentation and severity, 871
 - comprehensive assessment, 872
 - definition, 871
 - diagnosis, 886–887
 - diagnostic classification, 872
 - echocardiography, 889–893
 - ERS/ESC guidelines, 898
 - exercise capacity, 882
 - 6-minute walk test (6MWT), 882–883
 - cardiopulmonary exercise test (CPET), 883–887

- Pulmonary hypertension (PH) (*cont.*)
 natriuretic peptides (NPs), 896, 897
 normal RV function, 877
 PA elastance, 875
 parasternal views, 890
 PA stiffness, 875
 physical examination, 881–882
 practical vs. complete assessment, 897
 preliminary c-index analysis, 898
 pulmonary arterial vasoconstrictor reactivity, 875
 pulmonary artery elastance, 874
 pulmonary artery impedance, 875
 pulmonary compliance/volumes, 876
 pulmonary diffusing capacity (DLco), 876
 pulmonary gas exchange, 876
 pulmonary hemodynamics, 875, 889
 pulmonary vascular compliance, 874, 875
 pulmonary vascular physiology, 875, 876
 PVR calculation, 874
 PVR-compliance relationship, 875
 right heart catheterization (RHC), 887, 888
 risk assessment, 872
 RV failure, 877, 878
 RV-PA coupling Versus decoupling, 877, 878
 severity/prognosis assessment, 887
 subcostal view, 891, 892
 ventricular interdependence, 878
- Pulmonary perfusion, 609, 623, 624
- Pulmonary sarcoidosis, 510
- Pulmonary stability, 171
- Pulmonary stretch receptors, 212
- Pulmonary vascular resistance (PVR)
 compliance, 65–67
 definition, 61, 62
 interpretation, 67, 68
 lung inflation, 68, 69
 starling resistors, 63–65
 vascular distensibility, 62, 63
- Pulmonary wedge pressure (PWP), 67
- Pulsatile haemodynamics, 124–126
 and central aortic pressure, 132–134
 and ventricular arterial coupling, 134, 135
- Pulsatility index of arterial pressure (PI_{Pressure}), 388
- Pulse pressure respiratory variation (PPV), 379, 381
- Pulsed wave Doppler (PWD), 376
- Pulsus paradoxus, 712
- Q**
- Quantitative pulmonary perfusion, 623
- R**
- Reconstruction algorithm for EIT (GREIT), 589
- Regional pressure–volume (P/V) curves, 591
- Regional ventilation delay (RVD), 592–593
- Regional ventilation delay index (RVDI), 592–593
- Relative workload, 97
- Remifentanyl, 160
- Resistance and reactance, 480
- Resistive loading, 221
- Respiratory muscle function monitoring
 abdominal–pleural pressure ratio, 557
 airway and expiratory pressures, 536
 clinical assessment, 533, 534
 electromyography
 clinical applications of, 565–566
 esophageal electrodes, 559, 560
 frequency-domain analysis, 561–562
 intramuscular electrodes, 560
 left panel, 557
 neuromuscular coupling, 564
 neuroventilatory coupling, 564, 565
 right lower panel, 558
 right upper panel, 558
 time-domain analysis, 562–564
 esophageal and gastric pressure tracings
 gastric-to-esophageal pressure, 555–556
 gastric-to-transdiaphragmatic pressure, 556–557
 pleural pressure–abdominal pressure diagram,
 553–555
- imaging
 chest x-ray and fluoroscopy, 566
 computed tomography, 566
 diaphragm ultrasonography, 566–571
 magnetic resonance imaging, 566
- muscle fiber vibration assessment
 surface mechanomyography, 572–573
 surface phonomyography, 572
- output (*see* Respiratory muscle pressure output)
- pulmonary function testing, 534
- transdiaphragmatic twitch pressure, 544
- Respiratory muscle pressure output
 effort
 pressure–time product, 550–551
 tension–time index, 551, 552
 work of breathing, 548–550
- strength
 airway pressures, 535–537
 airway twitch pressure, 544
 cough P_{ga}, 540
 electrical and magnetic stimulation, 540–544
 evoked maneuvers, 547–548
 magnetic stimulation, 540–541
 Mueller-expulsive maneuver, 538–539
 phrenic nerve stimulation, 540–547
 pressure relaxation rate, 539
 sniff P_{di} values, 539
 transdiaphragmatic pressure, 537–539
 twitch interpolation technique, 545–547
 voluntary maneuvers, 540
- Respiratory muscles
 anatomy, 219, 220
 blood flow
 animal models, 228
 cardiogenic shock, 226–228
 diaphragm, 221, 222
 E coli, 226
 fatigue, 223, 224
 mechanical ventilation, 224–226
 O₂ consumption, 222, 223
 PCO₂, 224, 225
 principles, 221–223
 pulmonary edema, 227, 228

respiratory rate, 222
 sepsis, 226, 227
 septic shock, 226
 efferent fibres, 228–230
 energetics and mechanics, 220, 221
 Respiratory quotient, 420, 424, 425
 Respiratory system elastance (E_{rs}), 479
 Respiratory system resistance (R_{rs}), 479
 Respiratory volumes, flows and pressures
 body plethysmography, 477, 478
 clinical applications, 482
 input-output relationships, 474
 kinked/blocked airway, 474
 onset of pulmonary edema, 474
 oscillometry and impedance, 480–482
 resistance and elastance, 478–480
 spirometry
 Bernoulli effect, 475, 476
 equal pressure point, 475
 expiratory flow limitation, 474
 FEV₁ and FVC, 476
 forced expiration, 475
 intra-airway pressure, 475
 low value of FEV₁, 477
 Poiseuille flow, 475
 transmit transpulmonary pressure, 474
 wave speed, 476
 sudden bronchospasm, 474
 x-ray computed tomography, 474
 Responsive management, 954
 Responsive therapy, 2
 Revised Starling principle, 72
 vs. classical Starling principle, 73, 74
 endothelial glycocalyx, 72
 filtration rate, 74–77
 fluid exchange, 75
 sub-glycocalyx space, 72, 73
 Richmond agitation-sedation scale (RASS), 926
 Right heart function
 acute processes, 21
 aerobic function, 40, 41
 origins of, 21, 22
 right ventricular and left ventricular
 afterload, 37
 clinical and physiological significance, 37
 compartment model, 35
 consistent response, 40
 coronary blood flow, 41–43
 diastolic pressure, 36–38, 43
 diastolic-volume interaction, 35
 dysfunction, 34, 35
 EEC, 23
 electrophysiological differences, 23
 embryological development, 22
 failure, 34, 35
 limitation, 34
 Mueller maneuver, 36
 pharmacological differences, 23, 24
 pressure load vs. volume load, 33, 34
 pressure-volume loops, 28–33
 principles, 24–28
 properties, 23

pulmonary arterial compliance, 32, 33
 pulmonary hypertension, 40
 P-V plots, 37, 38
 septal shift, 36
 shape and load differences, 24–26
 systolic pressure, 39
 tetralogy of Fallot, 38, 39
 volume effects, 35, 36

S

Sagawa's concept, 769, 770
 SAVE score, 763, 765
 Sepsis, 226, 227, 952, 954
 animal data, 827–830
 antibiotics, 821
 capillary permeability, 853
 cardiovascular responses to major drugs, 854
 clinical manifestations, 834
 clinical presentation, 822–823
 coronary flow and myocardial ischemia, 832, 833
 definition, 822
 dobutamine, 861, 862
 epidemiology, 823
 epinephrine (Epi), 860, 861
 examples, 821
 experimental studies, 849
 heart-lung component, 863–866
 human data, 823–826
 intracellular calcium regulation, 839, 840
 intracellular signaling pathways, 833
 intravascular pressures, 853
 management, 821
 mechanical requirements, 829–832
 milrinone, 862
 mitochondria, 838
 mortality, 821
 myocardial depression, 852
 nitric oxide and superoxide, 836–838
 norepinephrine, 854–859
 O₂ delivery management, 851
 pathogen-associated molecular patterns (PAMPS), 833
 permeable barriers, 840–842
 phenylephrine, 859, 860
 potassium ATP channel, 835, 836
 quick SOFA score (eSOFA), 822
 role of volume, 851–853, 855, 856
 SOFA score, 822
 standard initial management, 851
 survival, 821
 symptoms and signs, 821
 systemic inflammatory response (SIRS), 821
 therapeutic options, 842
 transcription factor-3 (ATF3), 833
 treatments, 849–851
 tumour necrosis factor- α (TNF α), 833
 vascular collapse and multi-organ failure, 842
 vascular dysfunction, 834, 835
 vascular failure, 834
 vascular leak, 852
 vasopressin, 860
 volume infusions, 852

Shear-wave elastography, 570
 Side-stream capnographs, 601
 Single-compartment model, 478, 480, 481
 Single-photon emission computed tomography (SPECT), 596
 Sinoatrial node (SAN)
 calcium-clock, 90, 91
 definition, 88
 extrinsic control, 89
 central nervous system, 90, 91
 circulating factors, 91, 92
 function, 89
 intrinsic control, 89
 ICNS, 92
 myogenic peptides, 92, 93
 tissue stretch, 93
 membrane-clock, 89, 90
 Skeletal muscle structure, 558
 Sodium, 672, 673
 Spine sign, 508
 Starling resistors, 63–65
 Starling's cardiac function curve, 13, 14
 Step-wise acid-base analysis, 661
 Sternomastoid activity, 534
 Stressed volume, 9
 Strong ion difference (SID), 654
 Strong ion gap (SIG), 660
 Strong ions, 654
 Subtracting fEIT images, 590
 Surface mechanomyography, 572–573
 Surface phonomyography, 572
 Swallowing reflex, 211
 Swimmer's position, 703
 Systemic vascular resistance (SVR), 118
 Systolic overshoot, 275

T

Tachycardia, 99
 TandemHeart® p-VAD, 808–810, 813
 Tension-time index, 551–553
 Tension time index of the diaphragm (TTdi), 220
 Terlipressin, 752
 Thoracic EIT, 585
 Thoracocardiography, 304
 Tidal impedance variation (TIV), 590
 Time and volume-based capnography, 602, 603
 Time-based and volume based capnography, 603
 Time-domain analysis, 562–564
 Time-varying elastance, 10, 27
 Tissue hypoxia, 419, 422, 424
 Tissue tracking approaches, 955
 Tissue stretch, 93
 Total lung capacity (TLC), 476, 534
 Transdiaphragmatic twitch pressure ($P_{\text{di}tw}$), 538, 539, 541, 542, 546, 569, 572
 Transesophageal echocardiography (TEE), 359, 375–377
 clinical applications, 379–383
 monitoring cardiac flows, 377, 378
 2-D TEE, 378, 379

Transmural pressure, 325
 Transpulmonary pressure, 235, 237, 253, 254, 479
 Transthoracic echocardiography (TTE), 377, 909, 910
 Transthoracic ultrasound, 523
 Tricuspid annular plane systolic excursion (TAPSE), 362
 Troponin/tropomyosin, 49

U

Ultrasonography, 955
 Ultrasound systems, 495
 Unstable hemoglobins, 646
 Unstressed volume, 9

V

Valsalva, 266, 267
 Van't Hoff equation, 140
 Vascular compliance, 65–67
 Vascular distensibility, 62, 63
 Vascular impedance
 arterial resistance, 127
 arterial wave reflections, 129–131
 changes of waveforms, 131, 132
 characteristic impedance, 127
 frequency domain assessments, 127
 history, 126
 implications, 126
 input impedance, 127–129
 time domain assessments, 127
 Vascular smooth muscle, 670
 Vascular unloading technology, *see* Volume clamp method
 Vasoactive intestinal polypeptide (VIP), 92
 Vasopressin vs. Norepinephrine Infusion in Patients with Septic Shock (VASST), 823
 Vasopressors
 adrenergic vasopressor agents, 752
 adverse effects, 751
 angiotensin II, 753
 autoregulation threshold, 751
 on left ventricular function, 754, 755
 non-adrenergic vasopressor agents, 752
 outcomes, 753, 754
 in right heart failure (RHF), 755, 756
 vasopressin derivatives, 752
 Venous Doppler waveform, 390
 Venous return (VR), 709
 Veno-venous extracorporeal membrane oxygenation (VV-ECMO)
 advantage, 741
 assisted mechanical ventilation, 747, 748
 description, 741
 principles of gas exchange, 742, 743
 technological limitations, 741
 total rest vs. open lung ventilatory strategy, 745
 ventilation parameters, 744
 ventilator management, 741
 ventilatory strategy during early phase, 743, 745–747

- Ventilation/perfusion abnormalities
aging, 198
ARDS, 200
clinical assessment, 195, 196
gas exchange
 AaDO₂, 193, 194
 alveolar gas approach, 191
 alveolar gas concentrations and Va/Q ratio, 190
 Bohr dead space, 193
 Bohr effect, 191
 mass balance, 190, 191
 oxygen concentration, 191
 shunt, 192
gravity and posture, 196–199
healthy young subjects, 196
lung disease, 190, 199
MIGET, 194, 195
obesity, 198
positive airway pressure, 200
pulmonary gas exchange, 189
tidal volume, ventilation mode, and cardiac output, 200, 201
V_A/Q ratio, 189, 190
- Ventilation-perfusion matching, 955
- Ventilation-related signal (VRS), 589
- Ventilator induced lung injury (VILI), 486
biotrauma and inflammation, 734, 735
etiology and pathophysiology, 732, 733
histologic alterations, 731
historical perspective, 732
inflammation and fibrosis, 735
mechanical and biological pathways, 735, 736
mechanotransduction, 733, 734
- Ventilator-patient dyssynchrony
assessment, 722–724
clinical consequences, 726
entrainment phenomenon, reverse triggering, 721, 724, 725
insufficient assistance (high respiratory drive)
 double trigger and breath stacking, 720, 723
 flow starvation, 718–721
 premature/short cycling, 719, 720, 722
management, 724–726
over-assistance (low respiratory drive)
 delayed cycling, 717–719
 ineffective triggering (IE), 716–718
- Venturi effect, 475
- Vigileo™-FloTrac system, 297
- Viscoelastic model, 480
- Volume clamp method, 276, 277
- Volumetric capnography, 609, 612, 614
definition, 601
hemodynamic monitoring
 capnodynamic method, 611
 capnography, 613
 capnotracking method, 610, 611
 fluid responsiveness, 612
 Frank-Starling curve, 613
 NICO monitor, 610
 preload assessment, 612–613
 preload-dependency assessment, 613
 quantitative monitoring, 610
 thermodilution, 611
main-stream capnographs, 602
respiratory monitoring monitoring gas exchange, 608–609
respiratory monitoring monitoring ventilation, 604–608
side-stream capnographs, 601
time and volume-based capnography, 602
- Voluntary activation index, 547
- Volutrauma, 172
- W**
- Water, 654, 655, 663, 664, 672
- Wave reflection, 129, 131
- Wave speed, 476
- Weak acids, 660
- Windkessel model, 123, 124
- Work of breathing, 548–550
- World Symposium on Pulmonary Hypertension (WSPH), 872
- Z**
- Zeroing, 335